Sat. Jun 5, 2021

[E] Oral | U (Union)：Union

9:00 AM - 10:30 AM JST | 12:00 AM - 1:30 AM UTC | Ch.01 Zoom Room 01

[U-13] Advanced understanding of Quaternary and Anthropocene hydroclimate changes in East Asia:

convener:Li Lo(Department of Geosciences, National Taiwan University), Kaoru Kubota(Graduate School of Human Development and Environment, Kobe University), Chuan-Chou Shen(National Taiwan University), Yusuke Yokoyama(Atmosphere and Ocean Research Institute, University of Tokyo), Chairperson:Li Lo(Department of Geosciences, National Taiwan University), Kaoru Kubota(Graduate School of Human Development and Environment, Kobe University), Yusuke Yokoyama(Atmosphere and Ocean Research Institute, University of Tokyo), Chuan-Chou Shen(National Taiwan University)

9:00 AM - 9:15 AM JST | 12:00 AM - 12:15 AM UTC

[U13-01] Insight to Western Pacific circulation from coral skeletal radiocarbon during the Anthropocene and Holocene

★Invited Papers

*Shoko Hirabayashi[1,2,3], Yusuke Yokoyama[2], Atsushi Suzuki[4], Tezer Esat[5], Yosuke Miyairi[2], Takahiro AZE[2], Fernando Siringan [6], Yasuo Maeda[7], Hironobu Kan[3] (1.Faculty of Geo-Environmental Science, Rissho University, 2.Atmosphere and Ocean Research Institute, The University of Tokyo, 3.Department of Environmental Changes, Graduate School of Social and Cultural Studies, Kyushu University, 4.Geological Survey of Japan, National Institute of Advanced Industrial Science and Technology (AIST), 5.Research School of Physics and Engineering, The Australian National University, 6.Marine Science Institute, University of the Philippines, 7.Institute of Natural and Environmental Sciences, University of Hyogo)

9:15 AM - 9:30 AM JST | 12:15 AM - 12:30 AM UTC

[U13-02] **Increased soil erosion since Southeast Asia economic boom recorded in *Porites* corals**

★Invited Papers

*Xiaohua Li[1], Zhen Zeng[2], Yi Liu[3], Ching-Chih Chang[4], Hong-Wei Chiang[4], Xuan-Ce Wang[5], Weidong Sun[1], Hui-Min Yu[2], Fang Huang[2], Chung-Che Wu[4], Tsai-Luen Yu[4], Chun-Yuan Huang[4], Chuan-Chou Shen[4] (1.Institute of Oceanology, Chinese Academy of Sciences, 2.University of Science and Technology of China, 3.Tianjin University, 4.National Taiwan University, 5.Yunnan University)

9:30 AM - 9:45 AM JST | 12:30 AM - 12:45 AM UTC

[U13-03] **Upper ocean temperatures over the last glacial in the low-to-mid latitude Western Pacific based on a systematic multiproxy approach**

★Invited Papers

*Sze Ling Ho[1], Yuan-Pin Chang[2], Min-Te Chen[3], Jeroen Groeneveld[4], Kuo-Fang Huang[5], Pei-Ting Lee[1], Shih-Yun Lin[1], Maria Makarova[1], Nele Meckler[6], Mahyar Mohtadi[7], Ren Yi Ooi[1], Chuan-Chou Shen[8], Liang-Jian Shiau[3,9], Raul Tapia[1], Masanobu Yamamoto[10] (1.Institute of Oceanography, National Taiwan University, Taipei, Taiwan, 2.Department of Oceanography, National Sun Yat-sen University, Kaohsiung, Taiwan., 3.Institute of Applied Geosciences, National Taiwan Ocean University, Keelung, Taiwan., 4.Department of Geosciences, Hamburg University, Germany. , 5.Institute of Earth Sciences, Academia Sinica, Taipei, Taiwan., 6.Bjerknes Centre for Climate Research and Department of Earth Science, University of Bergen, Norway., 7.MARUM-Center for Marine Environmental Sciences, University of Bremen, Germany. , 8.High-Precision Mass Spectrometry and Environment Change Laboratory (HISPEC), Department of Geosciences, National Taiwan University, Taipei, Taiwan., 9.Exploration and Development Research Institute, CPC Corporation, Miaoli, Taiwan., 10.Faculty of Environmental Earth Science, Hokkaido University, Sapporo, Japan.)

9:45 AM - 10:00 AM JST | 12:45 AM - 1:00 AM UTC

[U13-04] Ultra-high resolution oxygen isotope records from the Chiba Composite Section ratified as the Chibanian GSSP

★Invited Papers

*Yuki Haneda[1], Makoto Okada[2], Yoshimi Kubota[3], Yusuke Suganuma[4,5] (1.Geological Survey of Japan, AIST, 2.Department of Environmental Science, Ibaraki University, 3.National Museum of Nature and Science, 4.National Institute of Polar Research, 5.The Graduate University for Advanced Studies)

10:00 AM - 10:15 AM JST | 1:00 AM - 1:15 AM UTC

[U13-05] Sub-surface water mass exchanges around the eastern equatorial Indian Ocean during the last 50,000 years

★Invited Papers

*Hideko Takayanagi[1], Ryota Wako[1], Yuna Kimoto[1], Shigeyuki Wakaki[2], Azumi Kuroyanagi[1], Takeshige Ishiwa[3], Yusuke Yokoyama[4], Hitomi Uchimura Wakaki[5], Tsuyoshi Ishikawa[2], Yasufumi Iryu[1] (1.Tohoku Univ., 2.JAMSTEC, 3.NIPR, 4.Univ. of Tokyo, 5.Kochi Univ.)

10:15 AM - 10:30 AM JST | 1:15 AM - 1:30 AM UTC

[U13-06] **Methane, Monsoons, and Milankovitch Modulation of Millennial-Scale Climate**

★Invited Papers

*Kaustubh Thirumalai[1], Steven Clemens[2], Judson Partin[3] (1.The University of Arizona, 2.Brown University, 3.The University of Texas at Austin)

[E] Poster | U (Union)：Union

5:15 PM - 6:30 PM JST | 8:15 AM - 9:30 AM UTC | Ch.01_1

[U-13] Advanced understanding of Quaternary and Anthropocene hydroclimate changes in East Asia:

convener:Li Lo(Department of Geosciences, National Taiwan University), Kaoru Kubota(Graduate School of Human Development and Environment, Kobe University), Chuan-Chou Shen(National Taiwan University), Yusuke Yokoyama(Atmosphere and Ocean Research Institute, University of Tokyo)

[U13-P01] Sclerochronology and geochemistry of *Mercenaria stimpsoni* collected from the western North Pacific

*Kaoru Kubota[1], Kotaro Shirai[2], Naoko Sugihara[2], Koji Seike[3], Kazushige Tanabe[4], Masayo Minami[5], Toshio Nakamura[5] (1.Graduate School of Human Development and Environment, Kobe University, 2.Atmosphere and Ocean Research Institute, The University of Tokyo, 3.Geological Survey of Japan, National Institute of Advanced Industrial Science and Technology, 4.The University Museum, The University of Tokyo, 5.Institute for Space-Earth Environmental Research, Nagoya University)

[U13-P02] Radiocarbon Variability Recorded in Coral from Kikai Island to Understand Oceanography in the North Pacific Region

★Invited Papers

*Yuning Zeng[1], Yusuke Yokoyama[1], Yosuke Miyairi[1], Shoko Hirabayashi[2], Atsushi Suzuki[3] (1.Atmosphere and Ocean Research Institute, The University of Tokyo, 2.Faculty of Geo-Environmental Science, Rissho University, 3.Geological Survey of Japan, National Institute of Advanced Industrial Science and Technology (AIST))

[U13-P03] Anthropocene signals recorded as Plutonium isotopes and Cesium-137 in Beppu Bay marine sediments, Eastern Kyushu, Japan.

*Yusuke Yokoyama[1,2,3,4,5], Stephen Tims[5], Michaela Froehlich[5], Takahiro AZE[1], Keith Fifield[5], Shoko Hirabayashi[6], Dominik Knoll[5], Michinobu Kuwae[7], Yosuke Miyairi[1], Stefan Pavetich[5] (1.Atmosphere and Ocean Research Institute, University of Tokyo, 2.Department of Earth and Planetary Science, Graduate School of Science, The University of Tokyo, 3.Graduate Program on Environmental Sciences, Graduate School of Arts and Sciences, The University of Tokyo, 4.Biogeochemistry Program, Japan Agency for Marine-Earth Science and Technology, 5.Research School of Physics, The Australian National University, 6.Faculty Geo-Environmental Science, Rissho University, 7.Center for Marine Environmental Studies, Ehime University)

[U13-P04] High-resolution marine surface $\Delta^{14}C$ reconstructions using marine organisms produced carbonate attached to tetrapod ashored by high-wave in northern Pacific Coast of Japan.

*Kai Leggett[1], Yusuke Yokoyama[1], Yosuke Miyairi[1], Ota Kosuke[1], Yoshiki Shirahama[2] (1.Atmosphere and Ocean Research Institute, University of Tokyo, 2.Advanced Industrial Science and Technology, Geological Survey of Japan, Research Institute of Earthquake and Volcano Geology, Active Fault Research Group)

[U13-P05] Bronze age megadrought and Trans-Eurasian culture exchange

★Invited Papers

*Liangcheng Tan[1,2,3,4], Guanghui Dong[5], Zhisheng An[1,2,4], Lawrence R. Edwards[6,7], Haiming li[8], Dong Li[9], Robert Spengler[10], Yanjun Cai[3], Hai Cheng[3,1], Jianghu Lan[1,2], Rustam Orozbaev[11,12], Ruiliang Liu[13], Jianhui Chen[5], Hai Xu[14], Fahu Chen[15] (1. Institute of Earth Environment, Chinese Academy of Sciences, 2. Center for Excellence in Quaternary Science and Global Change, Chinese Academy of Sciences, 3.Institute of Global Environmental Change, Xi'an Jiaotong University, 4.Open Studio for Oceanic-Continental Climate and Environment Changes, Pilot National Laboratory for Marine Science and Technology (Qingdao), 5. College of Earth and Environmental Sciences, Lanzhou University, 6.Department of Earth and Environmental Sciences, University of Minnesota, 7. School of Geography, Nanjing Normal University, 8.Institution of Chinese Agricultural Civilization, Nanjing Agricultural University, 9.Library of Chang'an University, 10. Max Planck Institute for the Science of Human History, 11.Research Center for Ecology and Environment of Central Asia (Bishkek), Chinese Academy of Sciences, 12. Institute of Geology, National Academy of Sciences of Kyrgyz Republic, 13. School of Archaeology, University of Oxford, 14.Institute of Surface-Earth System Science, Tianjin University, 15.Key Laboratory of Alpine Ecology and Biodiversity, Institute of Tibetan Plateau Research, Chinese Academy of Sciences)

[U13-P06] A gradual transition into Greenland Interstadial 14 in southeastern China based on a sub-decadally-resolved stalagmite record

★Invited Papers

*Xin Zhang[1], Xiuyang Jiang[1,2], Haiyan Xiao[2], Binggui Cai[1,2], Tsai-Luen Yu[3,4], Chuan-Chou Shen[3,4,5] (1.Key Laboratory of Humid Subtropical Eco-geographical Processes, Ministry of Education, College of Geography Science, Fujian

Normal University, 2.Institute of Geography, Fujian Normal University, 3.High-Precision Mass Spectrometry and Environment Change Laboratory (HISPEC), Department of Geosciences, National Taiwan University, 4.Research Center for Future Earth, National Taiwan University, 5.Global Change Research Center, National Taiwan University)

[U13-P07] Beppu Bay stratigraphy records the timing of human-induced planetary-scale biological and environmental shift at the beginning of the Anthropocene

★Invited Papers

*Michinobu Kuwae[1], Narumi Tsugeki[2], Atsuko Amano[3], Testuro Agusa[4], Yoshiaki Suzuki[3], Jun Tsutsumi[7], Peter R. Leavitt[5], Kotaro Hirose[6] (1.Center for Marine Environmental Studies, 2. The Faculty of Law, Matsuyama Univesity, Matsuyama, 3.Geological Survey of Japan, National Institute of Advanced Industrial Science and Technology, 4.Faculty of Environmental & Symbiotic Sciences, Prefectural University of Kumamoto, 5.Department of Biology,University of Regina, 6.Faculty of Science & Engineering, Waseda University, 7.School of Life and Environmental Science, University of Tsukuba)

[U13-P08] The series of precious coral samples collected from off the southwest coast of Kochi Prefecture: one potential thousand-scale proxy for understanding subsurface ocean conditions.

★Invited Papers

*Tomoyo Okumura[1], Fujio Kumon[1], Tokuyama Hidekazu[1] (1.Center for Advanced Marine Core Research, Kochi University)

[U13-P09] Impact of human activities and natural hazards recorded in a subtropical mountain lake, northeastern Taiwan

★Invited Papers

*Tsai-wen Lin[1], Stefanie Kaboth-Bahr[2], Kweku Afrifa Yamoah[3], André Bahr[4], George Burr[1], Chih-Chieh Su[5], Liang-Chi Wang[6], Ludvig A Lowemark[1] (1.Dept. of Geosciences, NTU, 2.Institute for Geosciences, Univ. of Potsdam, 3.School of Geography, Earth & Environmental Sciences, Univ. of Birmingham, 4.Institute of Earth Sciences., Heidelberg Univ., 5.Institute of Oceanography, NTU, 6.Dept. of Earth and Environmental Sciences, NCCU)

[U13-P10] Reconstruction of ventilation ages of the Indian Ocean sector of the Southern Ocean using ^{14}C and U-Th ages of deep-sea isidid octocorals

★Invited Papers

*Yukiko Kozaka[1], Chuan-Chou (River) Shen[2], Hiroshi Sato[3], Masayo Minami[1], Yuki Tokuda[4], Minoru Ikehara[5] (1.Institute for Space-Earth Environmental Research, Nagoya University, 2.Department of Geosciences, National Taiwan University, 3.School of Business Administration, Senshu University, 4.Faculty of Environmental Studies, Tottori University of Environmental Studies, 5.Center for Advanced Marine Core Research, Kochi University)

[U13-P11] **North Atlantic cooling desiccated western India during Early Holocene: Evidence-based on clumped and stable oxygen isotope analysis of Gastropod**

*THAMIZHARASAN SAKTHIVEL[1,2], PROSENJIT GHOSH[1,2], YOGARAJ BANERJEE[1] (1.Centre for Earth Sciences, Indian Institute of Science, Bangalore, India -560012, 2.Divecha Centre for Climate Change, Indian Institute of Science, Bangalore, India -560012)

[J] Oral | U (Union)：Union

3:30 PM - 5:00 PM JST | 6:30 AM - 8:00 AM UTC | Ch.01 Zoom Room 01

[U-14] Current status and issues of the earth education necessary for living on the changing earth

convener:Hiroshi Ichikawa, Saori Nakai(kyoto koka womens university department of child education), Hidenori Kumagai(Japan Agency for Marine-Earth Science and Technology), Hiroshi Nishi(The Center for Academic Resources and Archives, The Tohoku Museum Tohoku University), Chairperson:Hiroshi Ichikawa(None)

3:30 PM - 3:45 PM JST | 6:30 AM - 6:45 AM UTC

[U14-01] The Essentials of Living on a Changing Planet

★Invited Papers

*Hiroshi Nishi[1] (1.Fukui Prefectural University, Institute of Dinosaur Research)

3:45 PM - 4:00 PM JST | 6:45 AM - 7:00 AM UTC

[U14-02] **Variations in the promotions of high schools offering Basic and Advanced Earth Science classes in Prefectures throughout Japan**

★Invited Papers

*Hideo Takagi[1], Kohei Yoshida[2] (1.Department of Earth Science, Faculty of Education and Integrated Arts and Sciences, Waseda University, 2.Higashi Fukuoka High School)

4:00 PM - 4:15 PM JST | 7:00 AM - 7:15 AM UTC

[U14-03] Global-Earth education in geography of high school

★Invited Papers

*Yoshiyasu Ida[1] (1.Faculty of Human Sciences,University of Tsukuba)

4:15 PM - 4:30 PM JST | 7:15 AM - 7:30 AM UTC

[U14-04] How to support elementary, junior high and high school teachers who are not familiar with Earth Science

★Invited Papers

*Hiroyuki Hoshi[1] (1.Department of Earth Sciences, Aichi University of Education)

4:30 PM - 4:45 PM JST | 7:30 AM - 7:45 AM UTC

[U14-05] Issues raised at the meeting for exchanging Information on the Earth Science Education in High Schools

★Invited Papers

*Iwata Makoto[1], Iida Kazuya[2], Satoshi Miyajima[3] (1.Hiroshima Prefectural Ogaki High School, 2.Komaba-Toho Junior and Senior High School, 3.Saitama Prefectural Kumagaya High School)

4:45 PM - 5:00 PM JST | 7:45 AM - 8:00 AM UTC

[U14-06] Discussion on the current status and issues of the earth education

★Invited Papers

*Hiroshi Ichikawa[1], Saori Nakai[2], Hidenori Kumagai[3], Hiroshi Nishi[4] (1.Education Committee, JpGU, 2.Kyoto Koka Women's University, 3.Japan Agency for Marine-Earth Science and Technology, 4.Fukui Prefectural University)

[J] Poster | U (Union)：Union

5:15 PM - 6:30 PM JST | 8:15 AM - 9:30 AM UTC | Ch.01_2

[U-14] Current status and issues of the earth education necessary for living on the changing earth

convener:Hiroshi Ichikawa, Saori Nakai(kyoto koka womens university department of child education), Hidenori Kumagai(Japan Agency for Marine-Earth Science and Technology), Hiroshi Nishi(The Center for Academic Resources and Archives, The Tohoku Museum Tohoku University)

[U14-P01] WG for Studying on Teacher Training System in JpGU

*Hidenori Kumagai[1], Saori Nakai[2], Teacher's training WG JpGU Education Comittee (1.Japan Agency for Marine-Earth Science and Technology, 2.Kyoto Koka Women's University)

[U14-P02] Current state of Geoscience education in primary school teacher training courses to obtain a Type II teacher’s license

*Hiroo Nemoto[1] (1.Ritsumeikan University)

[J] Oral | U (Union)：Union

1:45 PM - 3:15 PM JST | 4:45 AM - 6:15 AM UTC | Ch.01 Zoom Room 01

[U-15] JpGU's mission against giant earthquake and tsunami disasters: last 10 years and the future

convener:Koji Okumura(Graduate School of Letters, Hiroshima University), Yoshinori MIYACHI(Geological Survey of Japan, AIST), Hitoshi SAITO(College of Economics, Kanto Gakuin University), Chairperson:Koji Okumura(Graduate School of Letters, Hiroshima University), Yoshinori MIYACHI(Geological Survey of Japan, AIST), Hitoshi SAITO(College of Economics, Kanto Gakuin University)

1:45 PM - 2:05 PM JST | 4:45 AM - 5:05 AM UTC

[U15-01] JpGU's activities on gigantic earthquakes and tsunamis, 10 years since Great East Japan disasters

★Invited Papers

*Koji Okumura[1] (1.Graduate School of Humanities and Social Sciences, Hiroshima University)

2:05 PM - 2:25 PM JST | 5:05 AM - 5:25 AM UTC

[U15-02] The Decade of Progress of the Tohoku Geographical Association following the 2011 Great East Japan Earthquake

★Invited Papers

*ODA TAKASHI[1] (1.Miyagi University of Education)

2:25 PM - 2:45 PM JST | 5:25 AM - 5:45 AM UTC

[U15-03] Correspondence and the BCP (business continuity plan) maintenance situation of the commerce and industry establishment after the East Japan great earthquake disaster

★Invited Papers

*Toshio HATSUZAWA[1] (1.Fukushima University)

2:45 PM - 3:05 PM JST | 5:45 AM - 6:05 AM UTC

[U15-04] Ground motion characteristics during The 2011 off the Pacific coast of Tohoku Earthquake and The 2016 Kumamoto Earthquake

★Invited Papers

*Shinichi Matsushima[1] (1.Disaster Prevention Research Institute, Kyoto University)

3:05 PM - 3:15 PM JST | 6:05 AM - 6:15 AM UTC

[U15-05] Discussion

[E] Oral | P (Space and Planetary Sciences)：P-PS Planetary Sciences

1:45 PM - 3:15 PM JST | 4:45 AM - 6:15 AM UTC | Ch.04 Zoom Room 04

[P-PS03] Regolith Science

convener:Koji Wada(Planetary Exploration Research Center, Chiba Institute of Technology), Akiko Nakamura(Graduate School of Science, Kobe University), Patrick Michel(Universite Cote D Azur Observatoire De La Cote D Azur CNRS Laboratoire Lagrange), John Kevin Walsh(Southwest Research Institute Boulder), Chairperson:Naoya Sakatani(Department of Physics, Rikkyo University)

1:45 PM - 2:00 PM JST | 4:45 AM - 5:00 AM UTC

[PPS03-01] **Landing on an asteroid: Simulations and image analysis of the OSIRIS-REx spacecraft touch-down on (101955) Bennu**

★Invited Papers

*Ronald Ballouz[1], Kevin John Walsh[2], Patrick Michel[3], Yun Zhang[3], Paul Sánchez[4], Daniel Jay Scheeres[4], Michael C Nolan[1], Stephen R Schwartz[1], Derek C Richardson[5], Olivier S Barnouin[6], Edward B Bierhaus[7], Harold C Connolly[8,1], Dante S Lauretta[1] (1.Lunar and Planetary Lab, University of Arizona, Tucson, AZ, USA, 2.Southwest Research Institute, Boulder, CO, USA, 3.Université Côte d'Azur, Observatoire de la Côte d'Azur, CNRS, Laboratoire Lagrange, Nice, France, 4.University of Colorado Boulder, CO, USA,, 5.University of Maryland, College Park, MD, USA, 6.The Johns Hopkins University Applied Physics Laboratory, Laurel, MD, USA, , 7.Lockheed Martin Space, Littleton, CO, USA, , 8.Dept. of Geology, Rowan University, Glassboro, NJ, USA)

2:00 PM - 2:15 PM JST | 5:00 AM - 5:15 AM UTC

[PPS03-02] Dust cloud mass from OSIRIS-REx sample collection event at Bennu

★Invited Papers

*Bashar Rizk[1], Kevin J. Walsh[2], Ronald Ballouz[1], Brent Bos[3], Christian Drouet d'Aubigny[1] (1.University of Arizona, 2.Southwest Research Institute, 3.Goddard Space Flight Center)

2:15 PM - 2:30 PM JST | 5:15 AM - 5:30 AM UTC

[PPS03-03] Hayabusa2 sampling operation at Ryugu and the returned regolith samples

★Invited Papers

*Shogo Tachibana[1,2], Hayabusa2 Sampler Team (1.UTokyo Organization for Planetary and Space Science, University of Tokyo , 2.ISAS, JAXA)

2:30 PM - 2:45 PM JST | 5:30 AM - 5:45 AM UTC

[PPS03-04] Surface roughness and cohesion of impact fragments of meteorite targets

*Yuuya Nagaashi[1], Akiko Nakamura[1] (1.Kobe University)

2:45 PM - 3:00 PM JST | 5:45 AM - 6:00 AM UTC

[PPS03-05] Size and Spatial Distribution of Rock Particles on Small Bodies Revealed with CNN-based Algorithm

*Yuta Shimizu[1], Taisuke Suzuki[1], Ryodo Hemmi[1], Hideaki Miyamoto[1] (1.University of Tokyo)

3:00 PM - 3:15 PM JST | 6:00 AM - 6:15 AM UTC

[PPS03-06] **Experimental Study on the Relationship between Surface distributions and Vertical Structures of Rock Particles on Small bodies.**

*Taisuke Suzuki[1], Yuta Shimizu[1], Hideaki Miyamoto[1] (1.The University of Tokyo)

[E] Oral | P (Space and Planetary Sciences)：P-PS Planetary Sciences

3:30 PM - 5:00 PM JST | 6:30 AM - 8:00 AM UTC | Ch.04 Zoom Room 04

[P-PS03] Regolith Science

convener:Koji Wada(Planetary Exploration Research Center, Chiba Institute of Technology), Akiko Nakamura(Graduate School of Science, Kobe University), Patrick Michel(Universite Cote D Azur Observatoire De La Cote D Azur CNRS Laboratoire Lagrange), John Kevin Walsh(Southwest Research Institute Boulder), Chairperson:Yuri Shimaki(Institute of Space and Astronautical Science, Japan Aerospace Exploration Agency)

3:30 PM - 3:45 PM JST | 6:30 AM - 6:45 AM UTC

[PPS03-07] Deciphering the regolith properties of small bodies from numerical modeling

★Invited Papers

*Yun Zhang[1] (1.UCA, OCA, CNRS, Lagrange, Nice, France)

3:45 PM - 4:00 PM JST | 6:45 AM - 7:00 AM UTC

[PPS03-08] Charge Magnitude of Electrostatically Lofted Dust Grains over the Lunar Terminator

*Necmi Cihan Orger[1], Kazuhiro Toyoda[1], Mengu Cho[1] (1.Laboratory of Lean Satellite Enterprises and In-Orbit Experiments - Kyushu Institute of Technology)

4:00 PM - 4:15 PM JST | 7:00 AM - 7:15 AM UTC

[PPS03-09] High-velocity impact experiments in reduced gravity: The effect of cohesive strength of particle layers

*Masato Kiuchi[1], Takaya Okamoto[1], Yuuya Nagaashi[2], Sunao Hasegawa[1], Akiko Nakamura[2] (1.Japan aerospace exploration agency, Institute of space and astronautical science, 2.Graduate School of Science, Kobe UniversityKobe University)

4:15 PM - 4:30 PM JST | 7:15 AM - 7:30 AM UTC

[PPS03-10] Local variation in thermal inertia around the artificial impact crater on Ryugu

*Naoya Sakatani[1], Satoshi Tanaka[2], Tatsuaki Okada[2], Toru Kouyama[3], Akira Miura[2], Naru Hirata[4], Hiroki Senshu[5], Takehiko Arai[6], Yuri Shimaki[2], Hirohide Demura[4], Tomohiko Sekiguchi[7], Jun Takita[8], Tetsuya Fukuhara[1], Thomas Müller[9], Axel Hagermann[10], Jens Biele[11], Matthias Grott[11], Maximillian Hamm[11,12], Marco Delbo[13], Masahiko Arakawa[14], Kazunori Ogawa[15], Koji Wada[5], Toshihiko Kadono[16], Rie Honda[17], Kei Shirai[14], Takanao Saiki[2], Hiroshi Imamura[2], Yasuhiko Takagi[18], Hajime Yano[2], Masahiko Hayakawa[2], Hirotaka Sawada[2], Satoru Nakazawa[2], Seiji Sugita[19], Tomokatsu Morota[19], Manabu Yamada[5], Shingo Kameda[1], ERI TATSUMI[20], Yasuhiro Yokota[2], Hidehiko Suzuki[21], Kazuo Yoshioka[19], Moe Matsuoka[2], Yuichiro Cho[2] (1.Rikkyo University, 2.Institute of Space and Astronautical Science, Japan Aerospace Exploration Agency, 3.National Institute of Advanced Industrial Science and Technology, 4.University of Aizu, 5.Chiba Institute of Technology, 6.Ashikaga University, 7.Hokkaido University of Education, 8.Hokkaido Kitami Hokuto High School, 9.Max-Planck Institute for Extraterrestrial Physics, 10.Luleå University of Technology, 11.German Aerospace Center, 12.University of Potsdam, 13.Observatoire de la Côte d'Azur, CNRS, 14.Kobe University, 15.JAXA Space Exploration Center, Japan Aerospace Exploration Agency, 16.University of Occupational and Environmental Health, 17.Kochi University, 18.Aichi Toho University, 19.University of Tokyo, 20.Instituto de Astrofisica de Canarias, 21.Meiji University)

4:30 PM - 4:45 PM JST | 7:30 AM - 7:45 AM UTC

[PPS03-11] Brightness change of Hayabusa2 SCI crater ejecta observed by ONC-T and its implication to the surface status of asteroid Ryugu

*Rie Honda[1], Yasuhiro Yokota[2], Masahiko Arakawa[3], Seiji Sugita[4], Yuri Shimaki[2], Koji Wada[5], Toshihiko Kadono[6], Kei Shirai[3], Kazunori Ogawa[7], Naoya Sakatani[8], Ko Ishibashi[5], Takanao Saiki[2], Hiroshi Imamura[2], Satoru Nakazawa[2], Masahiko Hayakawa[2], Hajime Yano[2], Yasuhiko Takagi[9], Naru Hirata[10], Hirotaka Sawada[2], Tomokatsu Morota[4], Shingo Kameda[8], Eri Tatsumi[11], Manabu Yamada[5], Toru Kouyama[12], Yuichiro Cho[4], Moe Matsuoka[2], Kazuo Yoshioka[4], Hidehiko Suzuki[13], Chikatoshi Honda[10] (1.Department of Science and Technology, System of Natual Science, Kochi University, 2.Institute of Space and Astronautical Science, Japan Aerospace Exploration Agency, 3.Kobe University, 4.The University of Tokyo, 5.Planetary Exploration Research Center, Chiba Institute of Technology, 6.University of Occupational and Environmental Health, 7.JAXA Space Exploration Center, Japan Aerospace Exploration Agency, 8.Rikkyo University, 9.Aichi Toho University, 10.The University of Aizu, 11.Instituto de Astrofisica de Canarias, University of La Laguna, 12.National Institute of Advanced Industrial Science and Technology, 13.Meiji University)

4:45 PM - 5:00 PM JST | 7:45 AM - 8:00 AM UTC

[PPS03-12] Study of Hydrated Asteroids via Polarimetry: Correlation between Polarimetric Properties and Degree of Aqueous Alteration of Hydrated asteroids.

*Jooyeon Geem[1], Masateru Ishiguro[1], Hiroyuki Naito[2], Daisuke Kuroda[6], Koki Takahashi[3], Tomohiko Sekiguchi[3], Seiko Takagi[4], Tatsuharu Ono[4], Kiyoshi Kuramoto[4], Tomoki Nakamura[5] (1.Astronomy program, Dept of Physics and Astronomy, Seoul National University, 2.Nayoro Observatory, 3.Hokkaido University of Education, 4.Department of Cosmosciences, Graduate School of Science, Hokkaido University, 5.Department of Earth and Planetary Material Sciences, Faculty of Science, Tohoku University, 6.Okayama Observatory, Kyoto University)

[E] Poster | P (Space and Planetary Sciences)：P-PS Planetary Sciences

5:15 PM - 6:30 PM JST | 8:15 AM - 9:30 AM UTC | Ch.02_1

[P-PS03] Regolith Science

convener:Koji Wada(Planetary Exploration Research Center, Chiba Institute of Technology), Akiko Nakamura(Graduate School of Science, Kobe University), Patrick Michel(Universite Cote D Azur Observatoire De La Cote D Azur CNRS Laboratoire Lagrange), John Kevin Walsh(Southwest Research Institute Boulder)

[PPS03-P01] Disk-resolved photometric properties of local regions on asteroid 25143 Itokawa

*Naru Hirata[1,2], Kohei Kitazato[1,2], Eri Tatsumi[3], Shota Katahira[1], Takuma Furudate[1], Hiroshi Kikuchi[4], Hiroyuki Sato[4] (1.Dep. of Computer Science and Engineering, Univ. of Aizu, 2.ARC-Space, Univ of Aizu, 3.Instituto de Astrofisica de Canarias, 4.Japan Aerospace Exploration Agency)

[PPS03-P02] Experimental study on impact ejecta velocity scaling law for regolith layer composed of weak boulders

*Yuya Yamamoto[1], Masahiko Arakawa[1], Minami Yasui[1], Sunao Hasegawa[2], Yusaku Yokota[1], Hatsune Okawa[1], Ryo Sugimura[1] (1.Graduate School of Science, Kobe University, 2.institute of Space and Astronautical Science, JAXA)

[PPS03-P03] Particle size of Ryugu's subsurface layer inferred from observation of SCI crater's ejecta curtain.

*Koji Wada[1], Ko Ishibashi[1], Hiroshi Kimura[1], Masahiko Arakawa[2], Hirotaka Sawada[3], Kazunori Ogawa[4,2], Kei Shirai[2], Rie Honda[5], Yuichi Iijima[3], Toshihiko Kadono[6], Naoya Sakatani[7], Yuya Mimasu[3], Tomoaki Toda[3], Yuri Shimaki[3], Satoru Nakazawa[3], Hajime Hayakawa[3], Takanao Saiki[3], Yasuhiko Takagi[8], Hiroshi Imamura[3], Chisato Okamoto[2], Masahiko Hayakawa[3], Naru Hirata[9], Hajime Yano[3] (1.Planetary Exploration Research Center, Chiba Institute of Technology, 2.Department of Planetology, Kobe University, 3.Institute of Space and Astronautical Science, Japan Aerospace Exploration Agency, 4.JAXA Space Exploration Center, Japan Aerospace Exploration Agency, 5.Department of Science and Technology, Kochi University, 6.Department of Basic Sciences, University of Occupational and Environmental Health, 7.Department of Physics, Rikkyo University, 8.Aichi Toho University, 9.School of Computer Science and Engineering, The University of Aizu)

[PPS03-P04] Ryugu's surface change formed by SCI forward debris

*Yuri Shimaki[1], Yasuhiro Yokota[1], Rie Honda[2], Masahiko Arakawa[3], Koji Wada[4], Toshihiko Kadono[5], Kei Shirai[3], Kazunori Ogawa[6], Naoya Sakatani[7], Ko Ishibashi[4], Takanao saiki[1], Hiroshi Imamura[1], Satoru Nakazawa[1], Masahiko Hayakawa[1], Hajime Yano[1], Yasuhiko Takagi[8], Naru Hirata[9], Hirotaka Sawada[1], Seiji Sugita[10], Tomokatsu Morota[10], Shingo Kameda[7], Eri Tatsumi[11], Manabu Yamada[4], Toru Kouyama[12], Yuichiro Cho[10], Moe Matsuoka[1], Kazuo Yoshioka[10], Hidehiko Suzuki[13], Chikatoshi Honda[9] (1.Institute of Space and Astronautical Science, Japan Aerospace Exploration Agency, 2.Kochi University, 3.Kobe University, 4.Planetary Exploration Research Center, Chiba Institute of Technology, 5.University of Occupational and Environmental Health, 6.JAXA Space Exploration Center, Japan Aerospace Exploration Agency, 7.Rikkyo University, 8.Aichi Toho University, 9.The University of Aizu, 10.The University of Tokyo, 11.Instituto de Astrofisica de Canarias, University of La Laguna, 12.National Institute of Advanced Industrial Science and Technology, 13.Meiji University)

[PPS03-P05] Static and impact strength of brittle regolith analogs

*Akiko Nakamura[1], Sae Shigaki[1] (1.Graduate School of Science, Kobe University)

[J] Oral | P (Space and Planetary Sciences)：P-PS Planetary Sciences

9:00 AM - 10:30 AM JST | 12:00 AM - 1:30 AM UTC | Ch.04 Zoom Room 04

[P-PS07] Formation and evolution of planetary materials in the Solar System

convener:Megumi Matsumoto(Graduate School of Science, Tohoku University), Shin Ozawa(Department of Earth Science, Graduate School of Science, Tohoku University), Yuki Hibiya(Submarine Resources Research Center, Japan Agency for Marine-Earth Science and Technology), Noriyuki Kawasaki(Department of Earth and Planetary Sciences, Graduate School of Science, Hokkaido University), Chairperson:Yuki Hibiya(Submarine Resources Research Center, Japan Agency for Marine-Earth Science and Technology), Noriyuki Kawasaki(Department of Earth and Planetary Sciences, Graduate School of Science, Hokkaido University)

9:00 AM - 9:30 AM JST | 12:00 AM - 12:30 AM UTC

[PPS07-06] Novel approaches based on correlated short-lived and stable isotope variations for dating nucleosyntheses and early solar system events

★Invited Papers

*Tsuyoshi Iizuka[1], Yuki Hibiya[2], Mitsuru SUZUKI[1], Takehito Hayakawa[3] (1.University of Tokyo, 2.JAMSTEC, 3.National Institutes for Quantum and Radiological Science and Technology)

9:30 AM - 9:45 AM JST | 12:30 AM - 12:45 AM UTC

[PPS07-07] Oxygen and Al–Mg isotopic constraints on the cooling rate, age, and precursor of partial melting of an Allende Type B CAI, Golfball

*Noriyuki Kawasaki[1], Shoichi Itoh[2], Naoya Sakamoto[1], Steven B. Simon[3], Daiki Yamamoto[4], Hisayoshi Yurimoto[1] (1.Hokkaido University, 2.Kyoto University, 3.University of New Mexico, 4.JAXA)

9:45 AM - 10:00 AM JST | 12:45 AM - 1:00 AM UTC

[PPS07-08] Chemical and isotopic fractionation of Type B CAI caused by evaporation: An experimental study

*Michiru Kamibayashi[1], Shogo Tachibana[1,3], Noriyuki Kawasaki[2], Daiki Yamamoto[3], Hisayoshi Yurimoto[2] (1.The University of Tokyo, 2.Hokkaido University, 3.Institute of Space and Astronautical Science, Japan Aerospace Exploration Agency)

10:00 AM - 10:15 AM JST | 1:00 AM - 1:15 AM UTC

[PPS07-09] I-Xe ages of chondrites and its relevance for solar-wind derived noble gas concentrations

*Koharu Arai[1], Hirochika Sumino[1], Atsushi Takenouchi[2], Shogo Tachibana[1,3] (1.The University of Tokyo, 2.National Institute of Polar Research, 3.Institute of Space and Astronautical Science)

10:15 AM - 10:30 AM JST | 1:15 AM - 1:30 AM UTC

[PPS07-10] Requirement of turbulent nebula and dust grains for grain size coarsening in chondrule rims

*Hiroaki Kaneko[1], Sota ARAKAWA[2], Taishi Nakamoto[1] (1.Tokyo Institude of Technology, 2.National Astronomical Observatory of Japan)

[J] Oral | P (Space and Planetary Sciences)：P-PS Planetary Sciences

10:45 AM - 12:15 PM JST | 1:45 AM - 3:15 AM UTC | Ch.04 Zoom Room 04

[P-PS07] Formation and evolution of planetary materials in the Solar System

convener:Megumi Matsumoto(Graduate School of Science, Tohoku University), Shin Ozawa(Department of Earth Science, Graduate School of Science, Tohoku University), Yuki Hibiya(Submarine Resources Research Center, Japan Agency for Marine-Earth Science and Technology), Noriyuki Kawasaki(Department of Earth and Planetary Sciences, Graduate School of Science, Hokkaido University), Chairperson:Shin Ozawa(Department of Earth Science, Graduate School of Science, Tohoku University), Megumi Matsumoto(Graduate School of Science, Tohoku University)

10:45 AM - 11:00 AM JST | 1:45 AM - 2:00 AM UTC

[PPS07-11] Nanostructures of iron sulfides in lunar soils and implications for the behavior of sulfur on airless bodies.

*Toru Matsumoto[1], Takaaki Noguchi[1], Yu Tobimatsu[1], Dennis Harries[2], Falko Langenhorst[2], Akira Miyake[3], Hiroshi Hidaka[4] (1.Kyushu University, 2.Friedrich Schiller University Jena, 3.Kyoto University, 4.Nagoya University)

11:00 AM - 11:15 AM JST | 2:00 AM - 2:15 AM UTC

[PPS07-12] **Multiple sulfur isotope evidence for the formation of mesosiderite meteorites**

*Shun Mihira[1], Madhusoodhan Satish-Kumar[1], Akira Yamaguchi[2], Tomohiro Usui[3] (1.Department of Geology, Faculty of Science, Niigata University, 2.National Institute of Polar Research, 3.Institute of Space and Astronautical Science, Japan Aerospace Exploration Agency)

11:15 AM - 11:30 AM JST | 2:15 AM - 2:30 AM UTC

[PPS07-13] The shock pressure threshold for producing shock melt veins in basaltic rocks

*Haruka Oono[1], Kosuke Kurosawa[1], Takafumi Niihara[2], Takashi Mikouchi[3], Hidenori Genda[4], Naotaka Tomioka[7], Masahiro KAYAMA[5], Mizuho Koike[6], Yuji Sano[8], Wataru Satake[1], Takafumi Matsui[1] (1.Planetary Exploration Research Center, Chiba Institute of Technology, 2.Shool of Engineering, The University of Tokyo, 3.The University of Museum, The University of Tokyo, 4.Earth-Life Science Institute, Tokyo Institute of Technology, 5.Graduate School of Arts and Sciences, The University of Tokyo, 6.Graduate School of Advanced Science and Engineering, Hiroshima University, 7.Kochi Institute for Core Sample Research, Japan Agency for Marine-Earth Science and Technology , 8.Atmosphere and Ocean Research Institute, The University of Tokyo)

11:30 AM - 11:45 AM JST | 2:30 AM - 2:45 AM UTC

[PPS07-14] **Shock effects in silica minerals in eucrites**

*Rei Kanemaru[1], Akira Yamaguchi[2,1], Naoya Imae[2,1], Atsushi Takenouchi[2], Hirotsugu Nishido[3] (1.The Graduate University for Advanced Studyies (SOKENDAI), 2.National Institute of Polar Research (NIPR), 3.Okayama University of Science (OUS))

11:45 AM - 12:00 PM JST | 2:45 AM - 3:00 AM UTC

[PPS07-15] Effect of ultraviolet C irradiation on surface alteration of basalt due to evaporation of sulfuric acid

*Nobuo Komori[1] (1.The United Graduate School of Education Tokyo Gakugei University)

12:00 PM - 12:15 PM JST | 3:00 AM - 3:15 AM UTC

[PPS07-16] Discussion

[J] Poster | P (Space and Planetary Sciences)：P-PS Planetary Sciences

5:15 PM - 6:30 PM JST | 8:15 AM - 9:30 AM UTC | Ch.02_2

[P-PS07] Formation and evolution of planetary materials in the Solar System

convener:Megumi Matsumoto(Graduate School of Science, Tohoku University), Shin Ozawa(Department of Earth Science, Graduate School of Science, Tohoku University), Yuki Hibiya(Submarine Resources Research Center, Japan Agency for Marine-Earth Science and Technology), Noriyuki Kawasaki(Department of Earth and Planetary Sciences, Graduate School of Science, Hokkaido University)

[PPS07-P01] Study of porosity change of simulated chondrite materials by impact experiments

*Akiko Nakamura[1], Yuki Hanzawa[2], Tomomi Omura[3], Sunao Hasegawa[4] (1.Graduate School of Science, Kobe University, 2.Faculty of Science, Kobe University, 3.Osaka Sangyo University, 4.Japan Aerospace Exploration Agency)

[PPS07-P02] Formation process of a multi-layered chondrule rim and relationship of fine-grained rim and matrix in two LL chondrites

Yukina Hashimoto[1], *Tomoki Nakamura[1], Megumi Matsumoto[1] (1.Department of Earth and Planetary Materials Sciences, Faculty of Science, Tohoku University)

[PPS07-P03] Mineralogical variations of CM chondrites revealed from X-ray diffraction method: Application to the parent body evolution

*Naoya Imae[1,2], Makoto Kimura[1], Akira Yamaguchi[1,2] (1.Antarctic Meteorite Research Center, National Institute of Polar Research, 2.The Graduate University for Advanced Studies (SOKENDAI))

[PPS07-P04] **Combined XRD-XCT-FIB-TEM analysis of experimentally heated Murchison CM chondrite**

*Megumi Matsumoto[1], Junya Matsuno[2], Akira Tsuchiyama[2,3], Yuri Fujioka[1], Tomoki Nakamura[1], Akira Miyake[4], Masahiro YASUTAKE[5], Shota Okumura[4], Kentaro Uesugi[5], Akihisa Takeuchi[5] (1.Graduate School of Science, Tohoku University, 2.Research Organization of Science and Technology, Ritsumeikan University, 3.Guangzhou Institute of Geochemistry, Chinese Academy of Science GIG, CAS , 4.Graduate School of Science, Kyoto University, 5.Japan Synchrotron Radiation Research Institute/SPring-8)

[PPS07-P05] Variations in initial 26Al/27Al ratios among condensate CAIs from CV chondrites

*Noriyuki Kawasaki[1], Naoya Sakamoto[2], Hisayoshi Yurimoto[2] (1.Department of Earth and Planetary Sciences, Graduate School of Science, Hokkaido University, 2.Hokkaido University)

[PPS07-P06] Petrology and mineralogy of a coarse-grained CAI “TTA01” from Allende

*Tadakatsu Yamasaki[1], Noriyuki Kawasaki[1], Hisayoshi Yurimoto[1] (1.Hokkaido University)

[PPS07-P07] **Development of a chemical separation procedure for determining the initial niobium-92 abundance of chondritic components**

*Yuki Hibiya[1] (1.Submarine Resources Research Center, Japan Agency for Marine-Earth Science and Technology)

[PPS07-P08] Motion of silicate particles in protoplanetary disk

*Tamami Okamoto[1], Shigeru Ida[1] (1.Earth-Life Science Institute, Tokyo Institute of Technology)

[PPS07-P09] Thermal history of andesitic achondrite Erg Chech 002

*Akira Yamaguchi[1], Atsushi Takenouchi[1], Jean-Alix Barrat[2] (1.National Institute of Polar Research, 2.UBO-IUEM)

[PPS07-P10] Excess silica in plagioclase in some mesosiderites

*naoji sugiura[1], tomoko Arai[1] (1.Chiba Institute of Technology)

[PPS07-P11] The petrological and mineralogical descriptions of nakhlites NWA 6148 and NWA 10153

*Kakeru Kukihara[1], Masaaki Miyahara[1], Akira Yamaguchi[2], Yoshio Takahashi[3], Yasuo Takeichi[4], Naotaka Tomioka[5], Eiji Ohtani[6] (1.hiroshima university , 2.National Institute of Polar Research, 3.Tokyo university, 4.Institute of Materials Structure Science, High-Energy Accelerator Research Organization (KEK), 5.Kochi Institute for Core Sample Research, Japan Agency for Marine-Earth Science and Technology (JAMSTEC), 6.Tohoku university)

[E] Oral | P (Space and Planetary Sciences)：P-EM Solar-Terrestrial Sciences, Space Electromagnetism & Space Environment

9:00 AM - 10:30 AM JST | 12:00 AM - 1:30 AM UTC | Ch.06 Zoom Room 06

[P-EM08] Space Weather and Space Climate

convener:Ryuho Kataoka(National Institute of Polar Research), A Antti Pulkkinen(NASA Goddard Space Flight Center), Kanya Kusano(Institute for Space-Earth Environmental Research, Nagoya University), Kaori Sakaguchi(National Institute of Information and Communications Technology), Chairperson:Kanya Kusano(Institute for Space-Earth Environmental Research, Nagoya University), Kaori Sakaguchi(National Institute of Information and Communications Technology)

9:00 AM - 9:15 AM JST | 12:00 AM - 12:15 AM UTC

[PEM08-13] Statistical analysis of variations of geoelectric field during magnetic storms/substorms in Japan

*Tian Zhang[1], Yusuke Ebihara[1] (1.Kyoto University)

9:15 AM - 9:30 AM JST | 12:15 AM - 12:30 AM UTC

[PEM08-14] How do auroral substorms depend on Earth's dipole magnetic moment?

*Yusuke Ebihara[1], Takashi Tanaka[2] (1.Research Institute for Sustainable Humanosphere, Kyoto University, 2.International Center for Space Weather Science and Education, Kyushu University)

9:30 AM - 9:45 AM JST | 12:30 AM - 12:45 AM UTC

[PEM08-15] Direct numerical simulation of the Alfvénic solar wind: a theoretical origin of magnetic switchback

★Invited Papers

*Munehito Shoda[1] (1.National Astronomical Observatory of Japan)

9:45 AM - 10:00 AM JST | 12:45 AM - 1:00 AM UTC

[PEM08-16] Simulation study on the deformation of magnetic field in interplanetary CMEs

*Minami Mori[1], Daikou Shiota[2], Kanya Kusano[1] (1.Institute for Space-Earth Environmental Research, Nagoya University , 2.National Institute of Information and Communications Technology (NICT))

10:00 AM - 10:15 AM JST | 1:00 AM - 1:15 AM UTC

[PEM08-17] Onset Mechanism of the Successive M-class Solar Flares in the Solar Active Region 12673 Based on a Nonlinear Force-Free Modeling

*Daiki Yamasaki[1], Satoshi Inoue[2], Takako T. Ishii[1], Ayumi Asai[1], Shin'ichi Nagata[1], Kiyoshi Ichimoto[1] (1.Astronomical Observatory, Kyoto University, 2.Institute for Space-Earth Environmental Research)

10:15 AM - 10:30 AM JST | 1:15 AM - 1:30 AM UTC

[PEM08-18] Data-driven MHD simulation of successive solar plasma eruptions

*Takafumi Kaneko[1], Sung-Hong Park[1], Kanya Kusano[1] (1.Institute for Space-Earth Environmental Research, Nagoya University)

[E] Poster | P (Space and Planetary Sciences)：P-EM Solar-Terrestrial Sciences, Space Electromagnetism & Space Environment

5:15 PM - 6:30 PM JST | 8:15 AM - 9:30 AM UTC | Ch.03_1

[P-EM08] Space Weather and Space Climate

convener:Ryuho Kataoka(National Institute of Polar Research), A Antti Pulkkinen(NASA Goddard Space Flight Center), Kanya Kusano(Institute for Space-Earth Environmental Research, Nagoya University), Kaori Sakaguchi(National Institute of Information and Communications Technology)

[PEM08-P01] NASA Goddard Space Flight Center Space Weather Activities

*Antti A Pulkkinen[1] (1.NASA Goddard Space Flight Center)

[PEM08-P02] Relationship between X-ray and EUV solar flare emissions and the Dellinger phenomenon

*Kyoko Watanabe[1], Munechika Arao[1], Shohei Nishimoto[1], Chihiro Tao[2], Michi Nishioka[2] (1.National Defense Academy of Japan, 2.National Institute of Information and Communications Technology)

[PEM08-P03] A comparative study of the empirical and physics-based methods for solar flare predictions

*Kaho Kondo[1], Kanya Kusano[1] (1.Institute for Space-Earth Environmental Research, Nagoya University)

[PEM08-P04] Data-driven MHD Simulation of Solar Active Region NOAA 11283

*Yeongmin Kang[1], Takafumi Kaneko[1], Kanya Kusano[1] (1.Institute for Space-Earth Environmental Research)

[PEM08-P05] Unusual enhancement of ~30 MeV proton flux in an ICME sheath region

*Takahiro Obara[1], Mitsuo Oka[2], Nariaki V Nitta[3], Seiji Yashiro[4], Daikou Shiota[5], Kiyoshi Ichimoto[6] (1.Planetary Plasma and Atmospheric Research Center,Tohoku University, 2.University of California Berkeley, 3.Lockheed Martin Solar and Astrophysics Laboratory, 4.The Catholic University of America, 5.National Institute of Information and Communications Technology, 6.Kyoto University)

[PEM08-P06] Development of spectral riometer for observation of energetic electron precipitation at Syowa Station, Antarctica

*Yoshimasa Tanaka[1,2,3], Masayuki Yamamoto[4], Koji Nishimura[1,2,3], Hisao Yamagishi[1], Antti Kero[5], Akira Kadokura[1,2,3], Akira Mizuno[6], Akira Sessai Yukimatu[1,3], Herbert Akihito Uchida[3], Ryuho Kataoka[1,3], Yasunobu Ogawa[1,2,3], Takanori Nishiyama[1,3], Masaki Tsutsumi[1,3], Mitsunori Ozaki[7], Yoshizumi Miyoshi[6], Shin-ichiro Oyama[6], Fuminori Tsuchiya[8] (1.National Institute of Polar Research, 2.Polar Environment Data Science Center, Joint Support-Center for Data Science Research, Research Organization of Information and Systems, 3.The Graduate University for Advanced Studies, SOKENDAI, 4.National Institute of Information and Communications Technology, 5.Sodankyla Geophysical Observatory, 6.Institute for Space-Earth Environmental Research, Nagoya University, 7.Faculty of Electrical and Computer Engineering, Institute of Science and Engineering, Kanazawa University, 8.Planetary Plasma and Atmospheric Research Center, Graduate School of Science, Tohoku University)

[PEM08-P07] Auroral oval in the last 3000 years and future

*Ryuho Kataoka[1], Shin ya Nakano[2] (1.National Institute of Polar Research, 2.The Institute of Statistical Mathmatics)

[PEM08-P08] Solar cycles around the onset of the Maunder Minimum

*Hiroko Miyahara[1], Fuyuki Tokanai[2], Toru Moriya[2], Mirei Takeyama[2], Hirohisa Sakurai[2], Kazuho Horiuchi[3], Hideyuki Hotta[4] (1.College of Art and Design, Musashino Art University, 2.Faculty of Science, Yamagata University, 3.Graduate School of Science and Technology, Hirosaki University, 4.Graduate School of Science, Chiba University)

[PEM08-P09] Simultaneous observation of cosmic rays with muon detector and neutron monitor at the Syowa station in the Antarctic

*Chihiro Kato[1], Kazuoki Munakata[1], Akira Kadokura[2], Ryuho Kataoka[2], Shoko Miyake[3], Paul Evenson[4], Shunta Asano[1] (1.Shinshu University, 2.National Institute of Polar Research, 3.National Institute of Technology, Ibaraki College, 4.University of Delaware)

[PEM08-P10] Measurement of cosmogenic 10Be in endogenic travertine deposits at Baishuitai

*Hiroko Miyahara[1], Hongyang Xu[2], Limin Zhou[2], Kazuho Horiuchi[3], Hiroyuki Matsuzaki[4] (1.College of Art and Design, Musashino Art University, 2.East China Normal University, 3.Hirosaki University, 4.The University Museum, The Univ. of Tokyo)

[PEM08-P11] Be-7 in Japan, Iceland and Thailand during solar cycle 24 descent phase

*Hirohisa Sakurai[1], Youmei Kawamura[1], Souichiro Suzuki[1], Fuyuki Tokanai[1], Emiko Inui[1], Mirei Takeyama[1], Toru Moriya[1], Satosi Kikuchi[1], Fusa Miyake[2], Akira Kadokura[3], Natsuo Sato[3], Naoko Sugihara[6], Bjornsson Gunnlaugur[4], David Ruffolo[5], Warit Mitthumsiri[5], Ronald Macatangay[7] (1.Yamagata University, 2.ISEE, Nagoya University, 3.National Institute of Polar Research, 4.Science Institute, Iceland University, 5.Department of Physics, Mahidol University, 6.Department of Chemical Oceanography Atmosphere and Ocean Research Institute,The University of Tokyo, 7.National Astronomical Research Institute of Thailand)

[PEM08-P12] Forecast of energetic electron flux variations of the outer belt using the machine learning

*Satoshi Fukuoka[1], Yoshizumi Miyoshi[1], Daikou Shiota[2], Shinji Saito[4], Takefumi Mitani[3], Tomoaki Hori[1], Nana Higashio[3], Shun Imajo[1], Iku Shinohara[3] (1.Institute for Space-Earth Environmental Research, Nagoya University, 2.National Institute of Information and Communications Technology (NICT), 3.Japan Aerospace Exploration Agency, Institute of Space and Astronautical Science, 4.National Institute of Information and Communications Technology)

[PEM08-P13] Spacecraft surface charging environment in the medium earth orbit

*Masao Nakamura[1], Kosei Nagasawa[1] (1.Osaka Prefecture University)

[PEM08-P14] Active Region Detection in the HMI magnetograms using the Mask R-CNN technique

*Akito Komatsu[1], Yusuke Iida[1] (1.Niigata University)

[PEM08-P15] Operations of Solar Flare Prediction Model Using Deep Neural Networks

*Naoto Nishizuka[1], Yuki Kubo[1], Komei Sugiura[2], Mitsue Den[1], Mamoru Ishii[1] (1.National Institute of Information and Communications Technology, 2.Keio University)

[PEM08-P16] Empirical/physical-based modeling of three-dimensional outer radiation belt for real-time operation

*Shinji Saito[1], Kaori Sakaguchi[1], Yuki kubo[1] (1.National Institute of Information and Communications Technology)

[PEM08-P17] **Mid-term Research Plan of NICT Space Weather Monitoring and Forecast**

*Mamoru Ishii[1] (1.National Institute of Information and Communications Technology)

[PEM08-P18] Development of a prediction system of the sporadic E layer occurrence: Current status and future prospects

*Hiroyuki Shinagawa[1], Chihiro Tao[1], Hidekatsu Jin[1], Yasunobu Miyoshi[2], Hitoshi Fujiwara[3] (1.National Institute of Information and Communications Technology, 2.Kyushu University, 3.Seikei University)

[PEM08-P19] Economic impacts of atmospheric radiation storm on aircraft operations and potential use of space weather information

*Susumu Saito[1], Navinda Kithmal Wickramasinghe[1], Tatsuhiko Sato[2], Daikou Shiota[3] (1.Electronic Navigation Research Institute, National Institute of Maritime, Port, and Aviation Technology, 2.Japan Atomic Energy Agency, 3.National Institute of Information and Communications Technology)

[PEM08-P20] Status of the GEO-X (Geospace X-ray imager) mission

*Yuichiro Ezoe[1], Ryu Funase[2,6], Harunori Nagata[3], Yoshizumi Miyoshi[4], Hiroshi Nakajima[5], Ikuyuki Mitsuishi[4], Kumi Ishikawa[1], Munetaka UENO[6], Atsushi Yamazaki[6], Hiroshi Hasegawa[6], Makoto Mita[6], Masaki Fujimoto[6], Yasuhiro Kawakatsu[6], Takahiro Iwata[6], Kazuhisa Mitsuda[7], Junko Hiraga[8], Satoshi Kasahara[6], Hironori Sahara[1], Yoshiaki Kanamori[9], Kohei Morishita[10], Takefumi Mitani[6], Masaki Numazawa[11] (1.Tokyo Metropolitan University, 2.University of Tokyo, 3.Hokkaido University, 4.Nagoya University, 5.Kanto Gakuin University, 6.ISAS/JAXA, 7.NAOJ, 8.Kwansei Gakuin University, 9.Tohoku University, 10.Kyushu University, 11.RIKEN)

[PEM08-P21] Soft-X ray emissions from Geospace: Possible science objectives of GEO-X

*Yoshizumi Miyoshi[1], Yosuke Matsumoto[2], Yuichiro Ezoe[3] (1.Institute for Space-Earth Environmental Research, Nagoya University, 2.Chiba University, 3.Tokyo Metropolitan University)

[PEM08-P22] Effects of Solar Proton Event on Global Lightning Activity

*Mitsuteru Sato[1], Ryuho Kataoka[2] (1.Department of Cosmoscience, Hokkaido University, 2.National Institute of Polar Research)

[PEM08-P23] Atmospheric electric field measurement for the study of space and atmospheric climate changes

*Masashi Kamogawa[1], Yasuhiro Minamoto[2], Akira Kadokura[3], Mitsuteru Sato[4] (1.Global Center for Asian and Regional Research, University of Shizuoka, 2.Laboratory for Environmental Research at Mount Fuji, 3.National Institute of Polar Research, 4.Hokkaido University)

[PEM08-P24] Current status of the new multi-frequency millimeter-wave spectrometer installed at Showa Station and initial results of multi-line observations

*Akira Mizuno[1], Daichi Tsutsumi[1], Takahiko Kosegaki[1], Hiroyuki Iwata[1], Kouki Satani[1], Taku Nakajima[1], Kohei Haratani[1], Tomoo Nagahama[1], Syoki Iriyama[1], Genma Mizoguchi[1], Shixun Fan[1], Naoto Sekiya[2], Takuma Hayashi[2], Masaki Tsutsumi[3], Yoshihiro Tomikawa[3], Mitsumu K. Ejiri[3], Kaoru Sato[4] (1.ISEE, Nagoya University, 2.University of Yamanashi, 3.National Institute of Polar Research, 4.University of Tokyo)

[PEM08-P25] Antarctica-based future space weather research project since 2022

*Ryuho Kataoka[1] (1.National Institute of Polar Research)

[PEM08-P26] Development of real-time prediction system of CME arrival and magnetic field with ensemble SUSANOO-CME simulation 2

*Daikou Shiota[1,4], Seiji Yashiro[2], Ryuho Kataoka[3], Kazumasa Iwai[4], Yusuke Ebihara[5], Kaori Sakaguchi[1], Yuki Kubo[1] (1.National Institute of Information and Communications Technology (NICT), 2.Catholic University of America, 3.National Institute of Polar Research, 4.Institute for Space-Earth Environmental Research, Nagoya University, 5.Research Institute for Sustainable Humanosphere, Kyoto University)

[PEM08-P27] Ionospheric storms in GAIA under lower atmospheric and magnetospheric inputs

*Chihiro Tao[1], Hidekatsu Jin[1], Hiroyuki Shinagawa[1], Yasunobu Miyoshi[2], Hitoshi Fujiwara[3] (1.National Institute of Information and Communications Technology, 2.Kyushu University, 3.Seikei University)

[PEM08-P28] The relevance between cosmic ray and ozone depletion

*Kazuyoshi Yamashita[1] (1.The Open University of Japan)

[PEM08-P29] Geomagnetically induced currents observed around solar minimum of Cycle 24

*Shinichi Watari[1], Satoko Nakamura[2], Yusuke Ebihara[3], Aoi Nakamizo[1] (1.National Institute of Information and Communications Technology, 2.Institute for Space-Earth Environmental Research, Nagoya University, 3.Research Institute for Sustainable Humanosphere, Kyoto University)

[E] Oral | P (Space and Planetary Sciences)：P-EM Solar-Terrestrial Sciences, Space Electromagnetism & Space Environment

9:00 AM - 10:30 AM JST | 12:00 AM - 1:30 AM UTC | Ch.05 Zoom Room 05

[P-EM12] Dynamics of the Inner Magnetospheric System

convener:Kunihiro Keika(Department of Earth and Planetary Science, Graduate School of Science, The University of Tokyo), Yoshizumi Miyoshi(Institute for Space-Earth Environmental Research, Nagoya University), W Lauren Blum(University of Colorado Boulder), Yuri Shprits(Helmholtz Centre Potsdam GFZ German Research Centre for Geosciences), Chairperson:Lauren W Blum(University of Colorado Boulder), Kunihiro Keika(Department of Earth and Planetary Science, Graduate School of Science, The University of Tokyo)

9:00 AM - 9:05 AM JST | 12:00 AM - 12:05 AM UTC

[PEM12-01] Introduction

9:05 AM - 9:30 AM JST | 12:05 AM - 12:30 AM UTC

[PEM12-02] Convection in the Inner Magnetosphere: Effects on Plasmasphere and Ring Current

★Invited Papers

*Jerry Goldstein[1,4], B. R. Sandel[2], D. J. McComas[3], P. W. Valek[1], J. Redfern[1] (1.Southwest Research Institute, 2.The University of Arizona, 3.Princeton University, 4.University of Texas at San Antonio)

9:30 AM - 9:55 AM JST | 12:30 AM - 12:55 AM UTC

[PEM12-03] Changing Composition of the Ring Current Source Region During Storm Main Phase

★Invited Papers

*Lynn M Kistler[1,2], Christopher G Mouikis[1], Kazushi Asamura[3], Satoshi Kasahara[4], Yoshizumi Miyoshi[2], Kunihiro Keika[4], Steven M Petrinec[5], Tomoaki Hori[2], Shoichiro Yokota[6], Iku Shinohara[3] (1.University of New Hampshire Main Campus, 2.Institute for Space-Earth Environmental Research, Nagoya University, 3.JAXA, 4.Graduate School of Science, University of Tokyo, 5.Lockheed-Palo Alto, 6.Graduate School of Science, Osaka University)

9:55 AM - 10:10 AM JST | 12:55 AM - 1:10 AM UTC

[PEM12-04] Multisatellite observations of field-aligned low-energy O^+ ion flux enhancements in the inner magnetosphere: September 22, 2018, Event

*Masahito Nose[1], Ayako Matsuoka[2], Yoshizumi Miyoshi[1], Kazushi Asamura[3], Mariko Teramoto[4], Iku Shinohara[3], Masafumi Hirahara[1], C. A. Kletzing[5], C. W. Smith[6], R. J. MacDowall[7], H. E. Spence[6], G. D. Reeves[8] (1.Institute for Space-Earth Environmental Research, Nagoya University, 2.Graduate School of Science, Kyoto University, 3.Institute of Space and Astronautical Science, Japan Aerospace Exploration Agency, 4.Department of Space Systems Engineering, Kyushu Institute of Technology, 5.Department of Physics and Astronomy, University of Iowa, 6.Institute for the Study of Earth, Oceans, and Space, University of New Hampshire, 7.Solar System Exploration Division, Goddard Space Flight Center, 8.Space Sciences and Applications Group, Los Alamos National Laboratory)

10:10 AM - 10:30 AM JST | 1:10 AM - 1:30 AM UTC

[PEM12-05] Deflection of upflowing ion beams by a converging electric field in the auroral flux tube: Alternative explanation for mass-dependent beam width

★Invited Papers

*Shun Imajo[1], Yoshizumi Miyoshi[1], Kazushi Asamura[2], Iku Shinohara[2], Masahito Nose[1], Yoshiya Kasahara[3], Yasumasa Kasaba[4], Ayako Matsuoka[5], Tomoaki Hori[1], Masafumi Shoji[1], Satoko Nakamura[1], Mariko Teramoto[6] (1.Nagoya University, 2.Institute of Space and Astronautical Science, 3.Kanazawa University, 4.Tohoku University, 5.Kyoto University, 6.Kyushu Institute of Technology)

[E] Oral | P (Space and Planetary Sciences)：P-EM Solar-Terrestrial Sciences, Space Electromagnetism & Space Environment

10:45 AM - 12:10 PM JST | 1:45 AM - 3:10 AM UTC | Ch.05 Zoom Room 05

[P-EM12] Dynamics of the Inner Magnetospheric System

convener:Kunihiro Keika(Department of Earth and Planetary Science, Graduate School of Science, The University of Tokyo), Yoshizumi Miyoshi(Institute for Space-Earth Environmental Research, Nagoya University), W Lauren Blum(University of Colorado Boulder), Yuri Shprits(Helmholtz Centre Potsdam GFZ German Research Centre for Geosciences), Chairperson:Kazuhiro Yamamoto(Graduate School of Science, The University of Tokyo)

10:45 AM - 11:05 AM JST | 1:45 AM - 2:05 AM UTC

[PEM12-06] **Ion dynamics in the inner magnetosphere during Van Allen Probe Era**

★Invited Papers

*Chao Yue[1] (1.Peking University)

11:05 AM - 11:20 AM JST | 2:05 AM - 2:20 AM UTC

[PEM12-07] Multipoint measurements to understand the drivers and structure of EMIC waves in the inner magnetosphere

*Lauren W Blum[1] (1.University of Colorado Boulder)

11:20 AM - 11:35 AM JST | 2:20 AM - 2:35 AM UTC

[PEM12-08] Particles simulations of whistler-mode triggered emissions with subpacket structures

Takeshi Nogi[1], *Yoshiharu Omura[1] (1.Reserach Institute for Sustainable Humanosphere, Kyoto University)

11:35 AM - 11:55 AM JST | 2:35 AM - 2:55 AM UTC

[PEM12-09] Nonlinear wave-particles interaction in radiation belts: how can we include it to global models?

★Invited Papers

*Anton Artemyev[1,2], Anatoly Neishtadt[2,3], Alexei Vasiliev[2], Xiao-Jia Zhang[1], Didier Mourenas[4], Dmitri Vainchtein[5,2] (1.Institute of Geophysics and Planetary Physics, UCLA, Los Angeles, California 90095, USA, 2.Space Research Institute of the Russian Academy of Sciences (IKI), 84/32 Profsoyuznaya Str., Moscow 117997, Russia, 3.Department of Mathematical Sciences, Loughborough University, Loughborough LE11 3TU, United Kingdom, 4.Laboratoire Mati`ere sous Conditions Extremes, Paris-Saclay University, CEA, Bruy`eres-le-Chatel, France, 5.Nyheim Plasma Institute, Drexel University, Camden, NJ, USA)

11:55 AM - 12:10 PM JST | 2:55 AM - 3:10 AM UTC

[PEM12-10] Modeling of outer radiation belt electron dynamics associated with whistler mode chorus emissions via Green’s function method

*Yikai Hsieh[1], Yoshiharu Omura[1] (1.Reserach Institute for Sustainable Humanosphere, Kyoto University)

[E] Oral | P (Space and Planetary Sciences)：P-EM Solar-Terrestrial Sciences, Space Electromagnetism & Space Environment

1:45 PM - 3:15 PM JST | 4:45 AM - 6:15 AM UTC | Ch.05 Zoom Room 05

[P-EM12] Dynamics of the Inner Magnetospheric System

convener:Kunihiro Keika(Department of Earth and Planetary Science, Graduate School of Science, The University of Tokyo), Yoshizumi Miyoshi(Institute for Space-Earth Environmental Research, Nagoya University), W Lauren Blum(University of Colorado Boulder), Yuri Shprits(Helmholtz Centre Potsdam GFZ German Research Centre for Geosciences), Chairperson:Yikai Hsieh(Reserach Institute for Sustainable Humanosphere, Kyoto University)

1:45 PM - 2:00 PM JST | 4:45 AM - 5:00 AM UTC

[PEM12-11] **Statistical study on spatial distribution of plasma waves observed by PWE/OFA**

*Yoshiya Kasahara[1], Kengo Nakashima[1], Shoya Matsuda[2], Yoshizumi Miyoshi[3], Ayako Matsuoka[4], Jean-Francois Rippol[5], David M. Malaspina[6] (1.Kanazawa University, 2.ISAS/JAXA, 3.Nagoya University, 4.Kyoto University, 5.CEA/DAM/DIF, 6.University of Colorado Boulder)

2:00 PM - 2:15 PM JST | 5:00 AM - 5:15 AM UTC

[PEM12-12] Long period modulations of pulsating aurora and chorus waves

*Yoshizumi Miyoshi[1], Keisuke Hosokawa[2], Yasunobu Ogawa[3], Satoshi Kurita[4], Shin-ichiro Oyama[1], Mariko Teramoto[5], Shinji Saito[6], Yoshiya Kasahara[7], Shoya Matsuda[8], Satoshi Kasahara[9], Shoichiro Yokota[10], Kunihiro Keika[9], Tomoaki Hori[1], Fuminori Tsuchiya[11], Atsushi Kumamoto[11], Satoko Nakamura[1], Masahiro Kitahara[1], Masafumi Shoji[1], Ayako Matsuoka[4], Shun Imajo[1], Iku Shinohara[8] (1.Institute for Space-Earth Environmental Research, Nagoya University, 2.The University of Electro-Communications, 3.NIPR, 4.Kyoto University, 5.Kyushu Inst. of Technology, 6.NICT, 7.Kanazawa University, 8.JAXA, 9.University of Tokyo, 10.Osaka University, 11.Tohoku University)

2:15 PM - 2:30 PM JST | 5:15 AM - 5:30 AM UTC

[PEM12-13] Whistler Driven Electron Precipitation Measured by ELFIN CubeSat and Arase Spacecraft

*Xiaojia Zhang[1], Vassilis Angelopoulos[1], Anton V. Artemyev[1], Satoshi Kasahara[2], Colin Wilkins[1], Ethan Tsai[1], Shoichiro Yokota[3], Kunihiro Keika[2], Tomoaki Hori[4], Yoshizumi Miyoshi[4], Yoshiya Kasahara[5], Shoya Matsuda[6], Ayako Matsuoka[7], Mariko Teramoto[8], Shun Imajo[4], Iku Shinohara[9] (1.University of California Los Angeles, 2.The Univ. of Tokyo, 3.Osaka Univ., 4.Nagoya Univ., 5.Kanazawa Univ., 6.ISAS, 7.Kyoto Univ., 8.Kyushu Institute of Technology, 9.ISAS, JAXA)

2:30 PM - 2:45 PM JST | 5:30 AM - 5:45 AM UTC

[PEM12-14] A case study to estimate energy spectra of pulsating auroral electrons from cosmic noise absorption and auroral brightness

*Shin-ichiro Oyama[1,2], Miyamoto Taishiro[1,6], Tero Raita[3], Keisuke Hosokawa[4], Yoshizumi Miyoshi[1], Yasunobu Ogawa[2], Satoshi Kurita[5] (1.Institute for Space-Earth Environmental Research, Nagoya University, 2.National Institute of Polar Research, 3.Sodankyla Geophysical Observatory, University of Oulu, 4.University of Electro-Communications, 5.Research Institute for Sustainable Humanosphere, Kyoto University, 6.Nippon Steel Corporation Nagoya Works)

2:45 PM - 3:00 PM JST | 5:45 AM - 6:00 AM UTC

[PEM12-15] Statistical characteristics of the magnetic field variations observed by Arase

*Ayako Matsuoka[1], Masahito Nose[2], Yoshizumi Miyoshi[2], Mariko Teramoto[4], Reiko Nomura[3], Akiko Fujimoto[5], Yoshimasa Tanaka[6], Manabu Shinohara[7], Satoshi Kurita[8], Shun Imajo[2], Iku Shinohara[3] (1.Data Analysis Center for Geomagnetism and Space Magnetism, Graduate School of Science, Kyoto University, 2.Institute for Space-Earth Environmental Research, Nagoya University, 3.Institute of Space and Astronautical Science, JAXA, 4.Graduate School of Engineering, Kyushu Institute of Technology, 5.Graduate School of Computer Science and Systems Engineering, Kyushu Institute of Technology, 6.National Institute of Polar Research, 7.National Institute of Technology Kagoshima College, 8.Research Institute for Sustainable Humanosphere, Kyoto University)

3:00 PM - 3:15 PM JST | 6:00 AM - 6:15 AM UTC

[PEM12-16] Mode-coupling Pi2 pulsations on the off-equatorial plasmapause inferred from the Arase satellite observation

*Mariko Teramoto[1], Ayako Matsuoka[2], Yoshiya Kasahara[3], Yasumasa Kasaba[4], Atsushi Kumamoto[4], Fuminori Tsuchiya[4], Shoya Matsuda[6], Yoshizumi Miyoshi[5], Masahito Nose[5], Tomoko Nakagawa[7], Shun Imajo[5], Masafumi Shoji[5], Satoko Nakamura[5], Iku Shinohara[6] (1.Kyushu Institute of Technology, 2.Kyoto University, 3.Kanazawa University, 4.Tohoku University, 5.Nagoya University, 6.Japan Aerospace Exploration Agency, Institute of Space and Astronautical Science, 7.Tohoku Institute of Technology)

[E] Oral | P (Space and Planetary Sciences)：P-EM Solar-Terrestrial Sciences, Space Electromagnetism & Space Environment

3:30 PM - 5:00 PM JST | 6:30 AM - 8:00 AM UTC | Ch.05 Zoom Room 05

[P-EM12] Dynamics of the Inner Magnetospheric System

convener:Kunihiro Keika(Department of Earth and Planetary Science, Graduate School of Science, The University of Tokyo), Yoshizumi Miyoshi(Institute for Space-Earth Environmental Research, Nagoya University), W Lauren Blum(University of Colorado Boulder), Yuri Shprits(Helmholtz Centre Potsdam GFZ German Research Centre for Geosciences), Chairperson:Kunihiro Keika(Department of Earth and Planetary Science, Graduate School of Science, The University of Tokyo)

3:30 PM - 3:45 PM JST | 6:30 AM - 6:45 AM UTC

[PEM12-17] Controlling factors of the occurrence of multi-harmonic toroidal ULF waves: A statistical study of the Arase satellite observations

*Kazuhiro Yamamoto[1], Kanako Seki[1], Ayako Matsuoka[2], Shun Imajo[3], Mariko Teramoto[4], Yoshiya Kasahara[5], Atsushi Kumamoto[6], Fuminori Tsuchiya[6], Masafumi Shoji[3], Yoshizumi Miyoshi[3], Iku Shinohara[7] (1.Graduate School of Science, The University of Tokyo, 2.Graduate School of Science, Kyoto University, 3.Institute for Space-Earth Environmental Research, Nagoya University, 4.Kyushu Institute of Technology, 5.Graduate School of Natural Science and Technology, Kanazawa University, 6.Graduate School of Science, Tohoku University, 7.Japan Aerospace Exploration Agency)

3:45 PM - 4:08 PM JST | 6:45 AM - 7:08 AM UTC

[PEM12-18] Probing inner magnetosphere dynamics and radial transport via observations of electron flux oscillations

★Invited Papers

*Theodore E Sarris[1] (1.Democritus University of Thrace)

4:08 PM - 4:30 PM JST | 7:08 AM - 7:30 AM UTC

[PEM12-19] Radiation belt electron acceleration during periods of low plasma density

★Invited Papers

*Hayley J Allison[1], Yuri Y Shprits[1,2,3], Irina Zhelavskaya[1], Dedong Wang[1], Artem Smirnov[1,2] (1.Helmholtz Centre Potsdam GFZ German Research Centre for Geosciences, Potsdam, Germany, 2.University of Potsdam, Potsdam, Germany, 3.University of California, Los Angeles, CA, USA)

4:30 PM - 4:45 PM JST | 7:30 AM - 7:45 AM UTC

[PEM12-20] Parameterized Lifetime of Energetic Electrons due to Interactions with Chorus Waves

*Dedong Wang[1], Yuri Shprits[1,2,3] (1.Helmholtz Center Potsdam German Research Centre for Geosciences Potsdam, 2.University of Potsdam, 3.UCLA)

4:45 PM - 5:00 PM JST | 7:45 AM - 8:00 AM UTC

[PEM12-21] Statistical Comparisons of Spin-Averaged Electron Flux from ARASE and Van Allen Probes Instruments

*Matyas Szabo-Roberts[1,2], Yuri Shprits[1,2], Hayley J Allison[1], Artem Smirnov[1,2], Nikita Aseev[7], Ruggero Vasile[1], Yoshizumi Miyoshi[4], Takefumi Mitani[4,5,6], Nana Higashio[5], Satoshi Kasahara[3] (1.Helmholtz Centre Potsdam GFZ German Research Centre for Geosciences, 2.University of Potsdam, 3.Department of Earth and Planetary Science, School of Science, The University of Tokyo, 4.Nagoya University, 5.JAXA Japan Aerospace Exploration Agency, 6.ISAS Institute of Space and Aeronautical Science, 7.Huawei Technologies)

[E] Poster | P (Space and Planetary Sciences)：P-EM Solar-Terrestrial Sciences, Space Electromagnetism & Space Environment

5:15 PM - 6:30 PM JST | 8:15 AM - 9:30 AM UTC | Ch.04_1

[P-EM12] Dynamics of the Inner Magnetospheric System

convener:Kunihiro Keika(Department of Earth and Planetary Science, Graduate School of Science, The University of Tokyo), Yoshizumi Miyoshi(Institute for Space-Earth Environmental Research, Nagoya University), W Lauren Blum(University of Colorado Boulder), Yuri Shprits(Helmholtz Centre Potsdam GFZ German Research Centre for Geosciences)

[PEM12-P01] Modulation of chorus intensity and UHR frequency in the off equatorial regions observed by the Arase satellite.

*Yuri Ampuku[1], Fuminori Tsuchiya[1], Yasumasa Kasaba[1], Satoshi Kurita[2], Yoshiya Kasahara[3], Shoya Matsuda[4], Atsushi Kumamoto[5], Ayako Matsuoka[6] (1.Planetary Plasma and Atmospheric Research Center, Graduate School of Science, Tohoku University, 2.Research Institute for Sustainable Humanosphere, Kyoto University, 3.Graduate School of Natural Science and Technology, Kanazawa University, 4.Institute of Space and Astronautical Science, JAXA, 5.Graduate School of Science, Tohoku University, 6.Graduate School of Science, Kyoto University)

[PEM12-P02] Spatio-temporal characteristics of the precipitating electron energy of pulsating aurora and comparison with the numerical simulation

*Kohei Toyama[1], Satoshi Kurita[2], Yoshizumi Miyoshi[1], Keisuke Hosokawa[3], Yasunobu Ogawa[4], Shin-ichiro Oyama[1], Satonori Nozawa[1], Tetsuya Kawabata[1], Shinji Saito[5], Yoshiki Ito[1] (1.Institute for Space-Earth Environmental Research, Nagoya University, 2.Research Institute for Sustainable Humanosphere, 3.University of Electro-Communications, 4.National Institute of Polar Research, 5.National Institute of Information and Communications Technology)

[PEM12-P03] An error estimation for energetic electron flux measured by the high-energy electron experiments (HEP) onboard the Arase satellite.

*Tomoaki Hori[1], Takefumi Mitani[2], Takeshi Takashima[2], Yoshizumi Miyoshi[1], Iku Shinohara[2] (1.Institute for Space-Earth Environmental Research, Nagoya University, 2.Japan Aerospace Exploration Agency)

[PEM12-P04] **Relationship between polar cap potential and MLT distribution of ground delta H during geomagnetic storms using observations and RAM-SCB simulations**

*Sandeep Kumar[1], Yoshizumi Miyoshi[1], Vania Jordanova[2] (1.Institute for Space Earth Environmental Research, Nagoya University, 2.Los Alamos National Laboratory, US)

[PEM12-P05] Global characteristics of cold protons in the near-Earth magnetotail: MMS/HPCA observations

*Kunihiro Keika[1], Masahiro Hoshino[1], Ryuta Asami[1] (1.Graduate School of Science, The University of Tokyo)

[PEM12-P06] Interaction between whistler waves and electrons at Earth's magnetotail: Test particle simulation and THEMIS observation

*Fumiko Otsuka[1], Kaiti Wang[2], Kirolosse Mina GIRGIS[1], Tohru Hada[1] (1.Earth System Science and Technology, 2.Tamkang University)

[PEM12-P07] Case analysis of SAPS wave structure events observed by ERG, DMSP, and SuperDARN

*Takehiro Fukami[1], Atsushi Kumamoto[1], Yuto Katoh[1], Nozomu Nishitani[2], Tomoaki Hori[2], Yasumasa Kasaba[3], Fuminori Tsuchiya[3], Mariko Teramoto[4], Tomoki Kimura[5], Yoshiya Kasahara[6], Masafumi Shoji[2], Satoko Nakamura[2], Masahiro Kitahara[2], Ayako Matsuoka[7], Shun Imajo[2], Satoshi Kasahara[8], Shoichiro Yokota[9], Kunihiro Keika[8], Yoichi Kazama[10], Shiang-Yu Wang Wang[10], Jun Chae-Woo[2], Kazushi Asamura[11], Yoshizumi Miyoshi[2], Iku Shinohara[11], Simon G. Shepherd[12] (1.Department of Geophysics, Graduate School of Science, Tohoku University, 2.Institute for Space-Earth Environmental Research, Nagoya University, 3.Planetary Plasma and Atmospheric Research Center, Tohoku University, 4.Kyushu Institute of Technology, 5.The Frontier Research Institute for Interdisciplinary Sciences, 6.Information Media Center, Kanazawa University, 7.Data analysis Center for Geomagnetism and Space Magnetism, Graduate School of Science, Kyoto University, 8.The university of Tokyo, 9.Graduate School of Science, Osaka University, 10.Academia Sinica Institute of Astronomy & Astrophysics, 11.Institute of Space and Astronautical Science, Japan Aerospace Exploration Agency, 12.Dartmouth College)

[PEM12-P08] Energetic electron precipitations showing ULF modulation observed by VLF/LF transmitter signals

*Tanaka Kentaro[1], Hiroyo Ohya[1], Fuminori Tsuchiya[2], Kazuo Shiokawa[3], Yoshizumi Miyoshi[3], Nozomu Nishitani[3], Tomoaki Hori[3], Mariko Teramoto[4], Martin G Connors[5], Simon G Shepherd[6], Hiroyuki Nakata[1] (1.Graduate School of Engineering, Chiba University, 2.Planetary Plasma and Atmospheric Research Center, Graduate School of Science, Tohoku University, 3.Institute for Space-Earth Environmental Research, Nagoya University, 4.Kyushu Institute of Technology, 5.Athabasca University, 6.Dartmouth College)

[PEM12-P09] A statistical study on the detachment of arc from the main auroral oval using all-sky imaging observations at Athabasca, Canada

*Sneha Yadav[1], Kazuo Shiokawa[1], Yuichi Otsuka[1], Martin G Connors[2,3] (1.Institute for Space-Earth Environmental Research, Nagoya University, Nagoya, Japan, 2.Athabasca University Observatories, Athabasca University, Athabasca, Alberta, Canada, 3.Department of Physics and Astronomy, University of Calgary, Calgary, Alberta, Canada)

[PEM12-P10] SAPS electric field and particle observations by the Arase satellite and SuperDARN

*Tomoya Takada[1], Nozomu Nishitani[1], Tomoaki Hori[1], Yasumasa Kasaba[2], Atsushi Kumamoto[2], Yuto Katoh[2], Yoshiya Kasahara[3], Masafumi Shoji[1], Satoko Nakamura[1], Masahiro Kitahara[1], Fuminori Tsuchiya[2], Kazushi Asamura[4], Yoshizumi Miyoshi[1], Yoichi Kazama[5], S Y Wang[5], Shoichiro Yokota[6], Satoshi Kasahara[7], Kunihiro Keika[7], Ayako Matsuoka[8], Shun Imajo[1], Iku Shinohara[4], Chae-Woo Jun[1], Simon G Shepherd[9] (1.Institute for Space-Earth Environmental Research, 2.Tohoku University, 3.Kanazawa University, 4.JAXA, 5.Academia Sinica, 6.Osaka University, 7.The University of Tokyo, 8.Kyoto University, 9.Thayer School of Engineering)

[PEM12-P11] Properties of EMIC waves observed by Van Allen Probes and ground-based magnetometers during relativistic electron precipitation

*Asuka Hirai[1], Fuminori Tsuchiya[1], Takahiro Obara[1], Yasumasa Kasaba[1], Yuto Katoh[2], Hiroaki Misawa[1], Kazuo Shiokawa[3], Yoshizumi Miyoshi[3], Chae-Woo Jun[3], Satoshi Kurita[4], Martin G Connors[5], Aaron Hendry[6] (1.Planetary Plasma and Atmospheric Research Center, Graduate School of Science, Tohoku Univ. , 2.Department of Geophysics, Graduate School of Science, Tohoku University, 3.Institute for Space-Earth Environmental Research, Nagoya University, 4.Research Institute for Sustainable Humanosphere, Kyoto University, 5.Athabasca University, 6.Otago University)

[PEM12-P12] A Study on the Effect of the Number of Snapshots for Averaging and the Noise Level on the Estimation Accuracy in Direction Finding

*Yuji Tanaka[1], Yoshiya Kasahara[1] (1.Division of Electrical Engineering and Computer Science, Graduate School of Natural Science and Technology, Kanazawa University)

[PEM12-P13] Relative Contribution of ULF Waves and Whistler-mode Chorus to the Radiation Belt Variation during the May 2017 Storm

*Naoko Takahashi[1], Kanako Seki[1], Mei-Ching Fok[2], Yihua Zheng[2], Yoshizumi Miyoshi[3], Satoshi Kasahara[1], Kunihiro Keika[1], David Hartley[4], Yoshiya Kasahara[5], Yasumasa Kasaba[6], Nana Higashio[1,7], Ayako Matsuoka[8], Shoichiro Yokota[9], Tomoaki Hori[3], Masafumi Shoji[3], Satoko Nakamura[3], Shun Imajo[3], Iku Shinohara[10] (1.Graduate School of Science, The University of Tokyo, 2.NASA Goddard Space Flight Center, 3.Institute for Space-Earth Environmental Research, Nagoya University, 4.Department of Physics and Astronomy, University of Iowa, 5.Graduate School of Natural Science and Technology, Kanazawa University, 6.Graduate School of Science, Tohoku University, 7.Japan Aerospace Exploration Agency, 8. Data Analysis Center for Geomagnetism and Space Magnetism, Graduate School of Science, Kyoto University, 9.Graduate School of Science, Osaka University, 10.Institute of Space and Astronautical Science, Japan Aerospace Exploration Agency)

[PEM12-P14] Initial results on multi event analysis of the simultaneous observation of isolated proton auroras at subauroral latitudes by a highly sensitive all-sky camera and the Van Allen Probes satellites

*Kohki Nakamura[1], Kazuo Shiokawa[1], Masahito Nose[1], Tsutomu Nagatsuma[2], Kaori Sakaguchi[2], Harlan Spence[3], Geoff Reeves[4], Herbert Funsten[4], Craig Kletzing[5], Robert MacDowall[6], Charles Smith[3], John Wygant[7], John Bonnell[7] (1.Nagoya Univ., 2.National Institute of Information and Communications Technology, 3.New Hampshire Univ., 4.Los Alamos National Laboratory, 5.Iowa Univ., 6.Goddard Space Flight Center, 7.Minnesota Univ.)

[PEM12-P15] Study of the excitation mechanism of internally driven ULF waves by the drift-bounce resonance with ring current ions based on the Magnetosphere-Ionosphere coupled model

*Tomotsugu Yamakawa[1], Kanako Seki[1], Takanobu Amano[1], Naoko Takahashi[1], Yoshizumi Miyoshi[2], Aoi Nakamizo[3] (1.Department of Earth and Planetary Science, School of Science, The University of Tokyo, 2.Institute for Space-Earth Environmental Research, Nagoya University, 3.National Institute of Information and Communications Technology)

[PEM12-P16] Statistical Analysis of Latitudinal Electron Density Distribution in the Plasmasphere

*Ayano Hambara[1], Yuki Obana[2], Yukinaga Miyashita[3,4], Atsuki Shinbori[5], Yuichi Otsuka[5], Atsushi Kumamoto[6], Fuminori Tsuchiya[7], Shoya Matsuda[8], Ayako Matsuoka[9], Yoshiya Kasahara[10], Yoshizumi Miyoshi[5], Iku Shinohara[8], William S. Kurth[11], Craig A. Kletzing[11], Charles W. Smith[12], Robert J. MacDowall[13] (1.Advanced Science and Engineering Course, Graduate School of Engineering, Osaka Electro-Communication University, 2.Department of Engineering Science, Faculty of Engineering, Osaka Electro-Communication University, 3.Korea Astronomy and Space Science Institute, 4.Korea University of Science and Technology, 5.Institute for Space-Earth Environmental Research, Nagoya University, 6.Department of Geophysics, Graduate School of Science, Tohoku University, 7.Planetary Plasma and Atmospheric Research Center, Graduate School of Science, Tohoku University, 8.Institute of Space and Astronautical Science/Japan Aerospace Exploration Agency, 9.Data Analysis Center for Geomagnetism and Space Magnetism, Graduate School of Science, Kyoto University, 10.Information Media Center, Kanazawa University, 11.Department of Physics and Astronomy, University of Iowa, 12.Institute for the Study of Earth, Oceans, and Space, University of New Hampshire, 13. Solar System Exploration Division, Goddard Space Flight Center)

[PEM12-P17] A statistical study of longitudinal extent of Pc1 pulsations using seven PWING ground stations at subauroral latitudes

*Jie Liu[1], Kazuo Shiokawa[1], Shin-ichiro Oyama[1], Yuichi Otsuka[1], Chae-Woo Jun[1], Masahito Nose[1], Tsutomu Nagatsuma[2], Kaori Sakaguchi[2], Akira Kadokura[3], Mitsunori Ozaki[4], Martin G Connors[5], Dmitry Baishev[6], Nozomu Nishitani[1], Alexey Oinats[7], Vladimir Kurkin[7], Tero Reita[8] (1.Institude for Space-Earth Environmental Research, Nagoya University, 2.National Institute of Information and Communications Technology, Japan, 3.National Institute of Polar Research, Tokyo, Japan, 4.Kanazawa University, Kanazawa, Japan, 5.Athabasca University, Athabasca, Canada, 6.Yu.G.Shafer Institute of Cosmophysical Research and Aeronomy of Siberian Branch of the Russian Academy of Sciences, Yakutsk, Russia, 7.Institute of Solar-Terrestrial Physics, Siberian Branch of the Russian Academy of Sciences, Irkutsk, Russia, 8.Sodankyla Geophysical Observatory, University of Oulu, Oulu, Finland)

[PEM12-P18] Altitude profile of isolated proton aurora as estimated from digital camera observations from International Space Station

*Kazuteru Takahashi[1], Sota Nanjo[2], Yuta Hozumi[2], Keisuke Hosokawa[2], Yoshizumi Miyoshi[1] (1.Institute for Space–Earth Environmental Research, 2.The University of Electro-Communications)

[PEM12-P19] Development of ISEE_Wave; Interactive Plasma Wave Analysis Tool

*Shoya Matsuda[1], Yoshizumi Miyoshi[2], Satoko Nakamura[2], Masahiro Kitahara[2], Masafumi Shoji[2], Tomoaki Hori[2], Shun Imajo[2], Chae-Woo Jun[2], Satoshi Kurita[3], Yoshiya Kasahara[4], Ayako Matsuoka[5], Iku Shinohara[1] (1.Institute of Space and Astronautical Science/Japan Aerospace Exploration Agency, 2.Institute for Space-Earth Environmental Laboratory, Nagoya University, 3.Research Institute for Sustainable Humanosphere, Kyoto University, 4.Kanazawa University, 5.kyoto University)

[PEM12-P20] Radiation characteristics of upper-band and lower-band chorus emissions in the generation region deduced from the Arase observation

*Seigo Hayashi[1], Satoshi Kurita[2], Hirotsugu Kojima[2], Yoshiya Kasahara[3], Shoya Matsuda[4], Ayako Matsuoka[5], Iku Shinohara[4], Yoshizumi Miyoshi[6] (1.Undergraduate School of Electrical and Electronic Engineering, Kyoto University, 2.Research Institute for Sustainable Humanosphere, Kyoto University, 3.Graduate School of Natural Science and Technology, Kanazawa University, 4.ISAS/JAXA, 5.Graduate School of Science, Kyoto University, 6.Institute for Space-Earth Environmental Research, Nagoya University)

[PEM12-P21] Isolated Electrostatic Potentials Observed by the Arase Satellite

*Tomoe Taki[1], Satoshi Kurita[1], Hirotsugu Kojima[1], Yoshiya Kasahara[2], Yoshizumi Miyoshi[3], Ayako Matsuoka[4], Shoya Matsuda[5] (1.Research Institute for Sustainable Humanosphere, Kyoto University, 2.Information Media Center, Kanazawa University, 3.Institute Space-Earth Environmental Research, Nagoya University, 4.Data Analysis Center for Geomagnetism and Space Magnetism Graduate School of Science, Kyoto University, 5.Institute of Space and Astronautical Science/Japan Aerospace Exploration Agency)

[PEM12-P22] Statistical study of drifting electron holes associated with substorms observed by the Arase satellite

*Taku Namekawa[1,2], Iku Shinohara[1], Takefumi Mitani[1], Kazushi Asamura[1], Nagai Tsugunobu[1], Satoshi Kasahara[2], Shoichiro Yokota[3], Tomoaki Hori[4], Ayako Matsuoka[5], Yoshizumi Miyoshi[4] (1.ISAS / JAXA, 2.The University of Tokyo, 3.Osaka University, 4.Nagoya University, 5.Kyoto University)

[PEM12-P23] **The influence of EMIC (ElectroMagnetic Ion Cyclotron) wave-interaction on energetic protons in the magnetosphere using Arase observations**

*Chae-Woo Jun[1], Yoshizumi Miyoshi[1], Satoko Nakamura[1], Shun Imajo[1], Masafumi Shoji[1], Chao Yue[2], Jacob Bortnik[3], Larry Lyons[3], Yoshiya Kasahara[4], Yasumasa Kasaba[5], Fuminori Tsuchiya[5], Atsushi Kumamoto[5], Shoya Matsuda[6], Kazushi Asamura[6], Iku Shinohara[6], Ayako Matsuoka[7] (1.Institute for Space-Earth Environmental Research, Nagoya University, 2.Peking University, Beijing, China , 3.Atmospheric and Oceanic Sciences, University of California Los Angeles, Los Angeles, USA, 4.Kanazawa University, Kanazawa, Japan, 5.Tohoku University, Sendai, Japan, 6.Institute of Space and Astronautical Science, Japan Aerospace Exploration Agency, Sagamihara, Japan, 7.Kyoto University, Kyoto, Japan)

[PEM12-P24] A statistical study on high-energy electron injection events observed by Arase (ERG)

*JINGXUAN YANG[1], Iku Shinohara[2], Taku Namekawa[1], Takefumi Mitani[2], Kazushi Asamura[2], Satoshi Kasahara[3], Nana Higashio[4], Ayako Matsuoka[5] (1.Department of Earth and Planetary Science, Graduate School of Science, The University of Tokyo, 2.Institute of Space and Astronautical Science, Japan Aerospace Exploration Agency, 3.The University of Tokyo, 4.Japan Aerospace Exploration Agency, 5.Data Analysis Center for Geomagnetism and Space Magnetism, Graduate School of Science, Kyoto University)

[PEM12-P25] Development of a high-energy electron analyzer onboard CubeSats

*Iku Shinohara[1], Takefumi Mitani[1], Mariko Teramoto[2], Kazushi Asamura[1], Ryota Onogi[1], Takeshi Takashima[1] (1.Japan Aerospace Exploration Agency/Institute of Space and Astronautical Science, 2.Kyushu Institute of Technology)

[PEM12-P26] **An observational study on possible excitation of storm-time Pc5 waves**

*Kento Otani[1], Iku Shinohara[2], Mariko Teramoto[3], Tomotsugu Yamakawa[1], Kanako Seki[4], Satoshi Kasahara[4], Shoichiro Yokota[5], Kunihiro Keika[1], Naoko Takahashi[4], Takefumi Mitani[2], Nana Higashio[2], Ayako Matsuoka[6], Kazuhiro Yamamoto[4] (1.Tokyo University/Graduate School of Science, 2.JAXA, 3.Kyushu Institute of Technology, 4.Tokyo University, 5.Graduate school of Science, Osaka University, 6.Graduate school of Science, Kyoto University)

[PEM12-P27] A Novel Calibration Method of Short Time Waveform Signals and its Approcation for the PWE/WFC Data

*Masahiro Kitahara[1], Shoya Matsuda[2], Yuto Katoh[3], Yoshiya Kasahara[4], Hirotsugu Kojima[5], Yoshizumi Miyoshi[1], Mitsuru Hikishima[2] (1.Institute for Space-Earth Environmental Research, Nagoya University, 2.Institute of Space and Astronautical Science/Japan Aerospace Exploration Agency, 3.Department of Geophysics, Graduate School of Science, Tohoku University, 4.Information Media Center, Kanazawa University, 5.Research Institute for Sustainable Humanosphere, Kyoto University)

[PEM12-P28] Nitrogen and oxygen ions from the Earth's ionosphere observed by the Arase satellite

*Shoichiro Yokota[1], Koichiro Tsuda[1], Satoshi Kasahara[2], Tomoaki Hori[3], Kunihiro Keika[2], Yoshizumi Miyoshi[3], Iku Shinohara[4] (1.Osaka University, 2.University of Tokyo, 3.ISEE, Nagoya University, 4.ISAS/JAXA)

[PEM12-P29] Electron Energization during Dipolarization Events: Test Particle Simulations

*Kirolosse Mina Girgis[1], Tohru Hada[1], Fumiko Otsuka[1], Kaiti Wang[2] (1.Department of Earth System Science and Technology, Interdisciplinary Graduate School of Engineering Sciences, Kyushu University, Japan , 2.Department of Aerospace Engineering, University of Tamkang, Taiwan)

[PEM12-P30] Computer simulations of electron scatterings through chorus-wave particle interactions

Yoshiki Ito[1], *Yoshizumi Miyoshi[1], Shinji Saito[2] (1.Institute for Space-Earth Environmental Research, Nagoya University, 2.NICT)

[PEM12-P31] Statistical analyses of low energy ion heating by electromagnetic ion cyclotron waves via wave-particle interaction analyses: Arase observations

*Masafumi Shoji[1], Yoshizumi Miyoshi[1], Lynn M Kistler[1,2], Kazushi Asamura[3], Yasumasa Kasaba[4], Ayako Matsuoka[5], Yoshiya Kasahara[6], Shoya Matsuda[3], Fuminori Tsuchiya[4], Atsushi Kumamoto[4], Satoko Nakamura[1], Masahiro Kitahara[1], Shun Imajo[1], Chae-Woo Jun[1], Iku Shinohara[3] (1.Institute for Space-Earth Environmental Research, Nagoya Univ., 2.University of New Hampshire, 3.ISAS/JAXA, 4.Tohoku Univ., 5.Kyoto Univ., 6.Kanazawa Univ.)

[PEM12-P32] Plasma waves causing 20 Hz intensity modulation of pulsating aurora: High-speed Tjörnes-Arase-Syowa conjugate observation

*Herbert Akihito Uchida[1], Ryuho Kataoka[2,1], Kiyoka Murase[1], Shoya Matsuda[3], Yoshiya Kasahara[4], Masafumi Shoji[5], Yoshizumi Miyoshi[5], Iku Shinohara[3], Ayako Matsuoka[6], Satoshi Kurita[7], Keisuke Hosokawa[8], Shun Imajo[5] (1.The Graduate University for Advanced Studies, 2.National Institute of Polar Research, 3.Institute of Space and Astronautical Science, Japan Aerospace Exploration Agency, 4.Kanazawa University, 5.Institute for Space–Earth

Environmental Research, Nagoya University, 6.Kyoto University, 7.Research Institute for Sustainable Humanosphere, Kyoto University, 8.University of Electro-Communications)

[J] Oral | P (Space and Planetary Sciences)：P-EM Solar-Terrestrial Sciences, Space Electromagnetism & Space Environment

10:45 AM - 12:15 PM JST | 1:45 AM - 3:15 AM UTC | Ch.06 Zoom Room 06

[P-EM14] Heliosphere and Interplanetary Space

convener:Kazumasa Iwai(Institute for Space–Earth Environmental Research (ISEE), Nagoya University), Yasuhiro Nariyuki(Faculty of Education, University of Toyama), Ken Tsubouchi(University of Electro-Communications), N Masaki Nishino(Japan Aerospace Exploration Agency, Institute of Space and Astronautical Science), Chairperson:Kazumasa Iwai(Institute for Space–Earth Environmental Research (ISEE), Nagoya University)

10:45 AM - 11:00 AM JST | 1:45 AM - 2:00 AM UTC

[PEM14-01] Yearly variation of the Sun’s polar regions during Solar Cycle 24 observed with Hinode

*Daikou Shiota[1], Masumi Shimojo[2] (1.National Institute of Information and Communications Technology (NICT), 2.National Astronomical Observatory of Japan (NAOJ))

11:00 AM - 11:15 AM JST | 2:00 AM - 2:15 AM UTC

[PEM14-02] Improvement of the computer assisted tomography of interplanetary scintillation observations

*Munetoshi Tokumaru[1], Ken'ichi Fujiki[1], Masayoshi Kojima[1], Kazumasa Iwai[1] (1.Institute for Space-Earth Environmental Research, Nagoya University)

11:15 AM - 11:30 AM JST | 2:15 AM - 2:30 AM UTC

[PEM14-03] Physical properties of fast and slow solar wind studied by spacecraft radio scintillation

*Shota Chiba[1], Takeshi Imamura[1], Munetoshi Tokumaru[2], Daikou Shiota[3], Hiroki Ando[4] (1.Graduate School of Frontier Sciences, The University of Tokyo, 2.Institute for Space-Earth Environment Research, Nagoya University, 3.National Institute of Information and Communications Technology, 4.Kyoto Sangyo University)

11:30 AM - 11:45 AM JST | 2:30 AM - 2:45 AM UTC

[PEM14-04] Solar wind density distribution derived from DM measurements of Crab pulsar

*Maeda Ryuya[1], Munetoshi Tokumaru[1], Kaito Tawara[1], Toshio Terasawa[2] (1.Institute for Space-Earth Environmental Research, Nagoya University, 2.Institute for Cosmis Ray Research,The University of Tokyo)

11:45 AM - 12:00 PM JST | 2:45 AM - 3:00 AM UTC

[PEM14-05] Next generation solar wind observation system: science requirements and pathfinders.

*Kazumasa Iwai[1], Munetoshi Tokumaru[1], Ken'ichi Fujiki[1] (1.Institute for Space–Earth Environmental Research (ISEE), Nagoya University)

12:00 PM - 12:15 PM JST | 3:00 AM - 3:15 AM UTC

[PEM14-06] Discussion

[J] Oral | P (Space and Planetary Sciences)：P-EM Solar-Terrestrial Sciences, Space Electromagnetism & Space Environment

1:45 PM - 3:15 PM JST | 4:45 AM - 6:15 AM UTC | Ch.06 Zoom Room 06

[P-EM14] Heliosphere and Interplanetary Space

convener:Kazumasa Iwai(Institute for Space–Earth Environmental Research (ISEE), Nagoya University), Yasuhiro Nariyuki(Faculty of Education, University of Toyama), Ken Tsubouchi(University of Electro-Communications), N Masaki Nishino(Japan Aerospace Exploration Agency, Institute of Space and Astronautical Science), Chairperson:Yasuhiro Nariyuki(Faculty of Education, University of Toyama), Masaki N Nishino(Japan Aerospace Exploration Agency, Institute of Space and Astronautical Science)

1:45 PM - 2:00 PM JST | 4:45 AM - 5:00 AM UTC

[PEM14-07] Identification of solar wind regimes using the non-hierarchical cluster analysis

*Shinichi Watari[1] (1.National Institute of Information and Communications Technology)

2:00 PM - 2:15 PM JST | 5:00 AM - 5:15 AM UTC

[PEM14-08] Numerical simulation on invasion process of galactic cosmic rays into the heliosphere: Particle orbits and statistics

*Kotaro Yoshida[1], Shuichi Matsukiyo[2,3], Haruichi Washimi[3], Tohru Hada[2,3] (1.Department of Earth System Science and Technology, Interdisciplinary Graduate School of Engineering Sciences, Kyushu University, 2.Faculty of Engineering Sciences, Kyushu University, 3.International Center for Space Weather Science and Education, Kyushu University)

2:15 PM - 2:30 PM JST | 5:15 AM - 5:30 AM UTC

[PEM14-09] Kaguya Observations of Solar Wind Electron Modification by Electrostatic Waves Above the Lunar Day Side: Preliminary Results

*Yuki Harada[1], Yoshiya Kasahara[2], Masaki N Nishino[3], Satoshi Kurita[4], Yoshifumi Saito[3], Shoichiro Yokota[5], Futoshi Takahashi[6], Hisayoshi Shimizu[7] (1.Graduate School of Science, Kyoto University, 2.Information Media Center, Kanazawa University, 3.ISAS, JAXA, 4.Research Institute for Sustainable Humanosphere, Kyoto University, 5.Graduate School of Science, Osaka University, 6.Faculty of Sciences, Kyushu University, 7.Earthquake Research Institute, University of Tokyo)

2:30 PM - 2:45 PM JST | 5:30 AM - 5:45 AM UTC

[PEM14-10] Elliptically polarized 0.01-0.3 Hz magnetic field variation in the lunar wake

*Tomoko Nakagawa[1], Futoshi Takahashi[2], Hisayoshi Shimizu[3], Yoshifumi Saito[4] (1.Information and Communication Engineering, Tohoku Institute of Technology, 2.Department of Earth and Planetary Sciences, Faculty of Science, Kyushu University, 3.Earthquake Research Institute, University of Tokyo, 4.Institute of Space and Astronautical Science, Japan Aerospace Exploration Agency)

2:45 PM - 3:00 PM JST | 5:45 AM - 6:00 AM UTC

[PEM14-11] On the relationship between the cross-helicty and the residual energy in the solar wind MHD turbulence: A phenomenological approach

*Yasuhiro Nariyuki[1] (1.Faculty of Education, University of Toyama)

3:00 PM - 3:15 PM JST | 6:00 AM - 6:15 AM UTC

[PEM14-12] Discussion

[J] Poster | P (Space and Planetary Sciences)：P-EM Solar-Terrestrial Sciences, Space Electromagnetism & Space Environment

5:15 PM - 6:30 PM JST | 8:15 AM - 9:30 AM UTC | Ch.03_2

[P-EM14] Heliosphere and Interplanetary Space

convener:Kazumasa Iwai(Institute for Space–Earth Environmental Research (ISEE), Nagoya University), Yasuhiro Nariyuki(Faculty of Education, University of Toyama), Ken Tsubouchi(University of Electro-Communications), N Masaki Nishino(Japan Aerospace Exploration Agency, Institute of Space and Astronautical Science)

[PEM14-P01] Relationship between solar type III radio bursts and electron energy spectra in solar impulsive electron events

Tatsuya Fujimoto[1], *Hiroaki Misawa[1], Fuminori Tsuchiya[1], Takahiro Obara[1] (1.Planetary Plasma and Atmospheric Research Center, Graduate School of Science, Tohoku University)

[PEM14-P02] Occurrence dependence on solar activity cycle for ordinary type III bursts and micro-type III bursts

*Yuichiro Seki[1], Hiroaki Misawa[1], Takahiro Obara[1], Fuminori Tsuchiya[1] (1.Tohoku University)

[PEM14-P03] Simple Estimation of the Global Solar Wind Structure

*Ken'ichi Fujiki[1], Munetoshi Tokumaru[1], Kazumasa Iwai[1] (1.Institute for Space-Earth Environmental Research)

[E] Oral | A (Atmospheric and Hydrospheric Sciences)：A-OS Ocean Sciences & Ocean Environment

9:00 AM - 10:30 AM JST | 12:00 AM - 1:30 AM UTC | Ch.09 Zoom Room 09

[A-OS11] Ocean Mixing Frontiers

convener:Toshiyuki Hibiya(Department of Earth and Planetary Science, Graduate School of Science, University of Tokyo), Chairperson:Takashi Ijichi(The University of Tokyo)

9:00 AM - 9:15 AM JST | 12:00 AM - 12:15 AM UTC

[AOS11-01] Tide-topography interactions with a background sheared current: critical layers and asymmetric internal wave breaking

*Kevin Lamb[1] (1.University of Waterloo)

9:15 AM - 9:30 AM JST | 12:15 AM - 12:30 AM UTC

[AOS11-02] Small-scale topographic effects on the generation of along-shelf propagating internal solitary waves on the Amazon Shelf

*Xiaolin Bai[1], Kevin Lamb[1], Jose C. B. da Silva[2] (1.Department of Applied Mathematics, The University of Waterloo, Canada, 2.Department of Geosciences, Environment, and Spatial Planning, and Instituto Ciencias da Terra (ICT), Polo Porto, Porto, Portugal)

9:30 AM - 9:45 AM JST | 12:30 AM - 12:45 AM UTC

[AOS11-03] Energetic turbulence and internal waves in Tokara Strait

*Anne Takahashi[1], Ren-Chieh Lien[1], Eric Kunze[2] (1.Applied Physics Laboratory, University of Washington, 2.NorthWest Research Associates)

9:45 AM - 10:00 AM JST | 12:45 AM - 1:00 AM UTC

[AOS11-04] A parameterization of local and remote tidal mixing

*Casimir de Lavergne[1] (1.LOCEAN laboratory, Sorbonne University)

10:00 AM - 10:15 AM JST | 1:00 AM - 1:15 AM UTC

[AOS11-05] **A new parameterization of turbulent mixing enhanced over rough seafloor topography**

*Toshiyuki Hibiya[1] (1.Department of Earth and Planetary Science, Graduate School of Science, The University of Tokyo)

10:15 AM - 10:30 AM JST | 1:15 AM - 1:30 AM UTC

[AOS11-06] Turbulent mixing variability in an energetic standing meander of the Southern Ocean

*Ajitha Cyriac[1,2], Helen Phillips[1,3], Nathan Bindoff[1,3], Kurt Polzin[4] (1.IMAS, University of Tasmania, Hobart, Australia, 2.ARCCSS, Hobart, Australia, 3.AAPP, Hobart, Australia, 4.WHOI, Woods Hole, USA)

[E] Oral | A (Atmospheric and Hydrospheric Sciences)：A-OS Ocean Sciences & Ocean Environment

10:45 AM - 12:15 PM JST | 1:45 AM - 3:15 AM UTC | Ch.09 Zoom Room 09

[A-OS11] Ocean Mixing Frontiers

convener:Toshiyuki Hibiya(Department of Earth and Planetary Science, Graduate School of Science, University of Tokyo), Chairperson:Toshiyuki Hibiya(Department of Earth and Planetary Science, Graduate School of Science, University of Tokyo)

10:45 AM - 11:00 AM JST | 1:45 AM - 2:00 AM UTC

[AOS11-07] Enhanced turbulent mixing in the equatorial thermocline

*Kelvin John Richards[1], Andrei Natarov[1], Yanli Jia[1] (1.International Pacific Research Center, School of Ocean and Earth Science Technology, University of Hawaii)

11:00 AM - 11:15 AM JST | 2:00 AM - 2:15 AM UTC

[AOS11-08] **Convection enhances upper ocean mixing during a tropical cyclone**

*Devang Falor[1], Bishakhdatta Gayen[1,2], Debasis Sengupta[1], Dipanjan Chaudhuri[3,1] (1.Indian Institute of Science, Bangalore, 2.University of Melbourne, Australia, 3.University of Washington, Seattle)

11:15 AM - 11:30 AM JST | 2:15 AM - 2:30 AM UTC

[AOS11-09] Near-inertial wave modulated turbulence in a Kuroshio anticyclonic eddy east of Japan

*Sebastian Essink[1], Ren-Chieh Lien[1], Eric Kunze[2] (1.UW/APL, 2.NWRA)

11:30 AM - 11:45 AM JST | 2:30 AM - 2:45 AM UTC

[AOS11-10] Upper ocean turbulence in the Icelandic Basin under strong forcing

*Harper L Simmons[1], Sophia Merrifield[2], Eric Skyllingstad[3], Louis St. Laurent[4] (1.University of Alaska Fairbanks, 2.Scripps Institution of Oceanography, University of California San Diego, 3.Oregon State University, 4.Applied Physics Laboratory, University of Washington)

11:45 AM - 12:00 PM JST | 2:45 AM - 3:00 AM UTC

[AOS11-11] Observed spectral distortion of temperature microstructure

*Takashi Ijichi[1], Louis St. Laurent[2] (1.Department of Earth and Planetary Science, Graduate School of Science, The University of Tokyo, 2.Applied Physics Laboratory, University of Washington)

12:00 PM - 12:15 PM JST | 3:00 AM - 3:15 AM UTC

[AOS11-12] 2D Horizontal-Vertical Wavenumber Spectra of Density Finestructure from a towed CTD chain

*Anda Vladoiu[1], Ren-Chieh Lien[1], Eric L Kunze[2] (1.Applied Physics Laboratory, University of Washington, Seattle, WA, USA, 2.NorthWest Research Associates, Redmond, WA, USA)

[E] Oral | A (Atmospheric and Hydrospheric Sciences)：A-OS Ocean Sciences & Ocean Environment

1:45 PM - 3:15 PM JST | 4:45 AM - 6:15 AM UTC | Ch.09 Zoom Room 09

[A-OS11] Ocean Mixing Frontiers

convener:Toshiyuki Hibiya(Department of Earth and Planetary Science, Graduate School of Science, University of Tokyo), Chairperson:Taira Nagai(Graduate School of Science, The University of Tokyo)

1:45 PM - 2:00 PM JST | 4:45 AM - 5:00 AM UTC

[AOS11-13] Internal tide radiation and intensified mixing in the Philippine Sea

*Zhenhua Xu[1], Jia You[1], Yang Wang[1], Qun Li[1], Toshiyuki Hibiya[2], Robin Robertson[3] (1.Institute of Oceanology, CAS, 2.Department of Earth and Planetary Science, Graduate School of Science, The University of Tokyo, Japan, 3.Xiamen University Malaysia, Malaysia)

2:00 PM - 2:15 PM JST | 5:00 AM - 5:15 AM UTC

[AOS11-14] Tidal and Wind Mixing in the Arafura Sea

*Robin Robertson[1] (1.Xiamen University Malaysia)

2:15 PM - 2:30 PM JST | 5:15 AM - 5:30 AM UTC

[AOS11-15] Verifying the parameterization of vertical eddy viscosity and diffusivity in the bottom boundary layer

*Takahiro Endoh[1], Takuya Hirooka[1] (1.RIAM Research Institute for Applied Mechanics)

2:30 PM - 2:45 PM JST | 5:30 AM - 5:45 AM UTC

[AOS11-16] The role of double-diffusive convection in basal melting and mixed layer under Antarctic ice shelves

*Bishakhdatta Gayen[1,2], Madi Rosevear [3,5], Ben Galton-Fenzi[4] (1.The University of Melbourne, 2. Indian Institute of Science, 3.University of Tasmania , 4.Australian Antarctic Division, 5.University of Western Australia)

2:45 PM - 3:00 PM JST | 5:45 AM - 6:00 AM UTC

[AOS11-17] The Kuroshio nutrient stream, where the diapycnal mixing matters

*Takeyoshi Nagai[1], Gloria Silvana Duran Gomez[1] (1.Department of Ocean Sciences, Tokyo University of Marine Science and Technology)

3:00 PM - 3:15 PM JST | 6:00 AM - 6:15 AM UTC

[AOS11-18] Turbulent mixing and its contribution to oxygen flux in the northwestern boundary current region of the Japan/East Sea, April-October 2015

*Dmitry Stepanov[1], Alexander Ostrovskii[2], Dmitry Kaplunenko[1], Jae-Hun Park[3], Young-Gyu Park[4], Pavel Tishchenko[1] (1.Pacific Oceanological Institute, Russia, 2.Shirshov Institute of Oceanology, Russia, 3.Department of Ocean Sciences, Inha University, Korea, 4.Korea Institute of Ocean Science and Technology, Korea)

[E] Poster | A (Atmospheric and Hydrospheric Sciences)：A-OS Ocean Sciences & Ocean Environment

5:15 PM - 6:30 PM JST | 8:15 AM - 9:30 AM UTC | Ch.05_1

[A-OS11] Ocean Mixing Frontiers

convener:Toshiyuki Hibiya(Department of Earth and Planetary Science, Graduate School of Science, University of Tokyo)

[AOS11-P01] Sensitivity of the ocean state estimation to the vertical distribution of tidally induced far-field mixing

*Satoshi Osafune[1], Shinya Kouketsu[1], Toshimasa Doi[1], Nozomi Sugiura[1], Shuhei Masuda[1] (1.Japan Agency for Marine-Earth Science and Technology)

[AOS11-P02] Tracer distribution produced by an optimized physical field with an improved vertical mixing

*Toshimasa Doi[1], Shinya Kouketsu[1], Satoshi Osafune[1], Shuhei Masuda[1], Nozomi Sugiura[1] (1.Japan Agency for Marine-Earth Science and Technology)

[AOS11-P03] **Lagrangian Dispersion and Mixing in the Open-ocean convection**

*Ankit Bhadouriya[1,2], Bishakhdatta Gayen[1,3] (1.The University of Melbourne, Australia, 2.Indian Institute of Technology Kanpur, India, 3.Indian Institute of Science, India)

[AOS11-P04] Assessing the role of deep ocean mixing on carbon and nutrients cycles using an Earth System Model

*Michio Watanabe[1], Akitomo Yamamoto[1], Tomohiro Hajima[1], Hiroaki Tatebe[1] (1.Research Center for Environmental Modeling and Application, Japan Agency for Marine-Earth Science and Technology (JAMSTEC))

[AOS11-P05] Performance of microstructure measurements using a deep float with a fast-response thermistor

*Shuo Zhai[1], Ichiro Yasuda[1] (1.Atmosphere and Ocean Research Institute, The University of Tokyo)

[AOS11-P06] Seasonal variations in salinity of the North Pacific Intermediate Water and vertical mixing intensity over the Okinawa Trough

*Hirohiko Nakamura[1], Ryuichiro Inoue[2], Ayako Nishina[1], Toshiya NAKANO[3] (1.Kagoshima University, Faculy of Fisheries, 2.Japan Agency for Marine-Earth Science and Technology, 3.Nagasaki Meteorological Office)

[AOS11-P07] **Elevated nutrient supply caused by the approaching Kuroshio to the southern coast of Japan**

*Gloria Silvana Duran Gomez[1], Takeyoshi Nagai[2] (1.Graduate School of Tokyo University of Marine Science and Technology, 2.Tokyo University of Marine Science and Technology)

[AOS11-P08] Direct estimates of turbulent mixing in the Indonesian Archipelago and its role in the transformation of the ITF waters

*Taira Nagai[1], Toshiyuki Hibiya[1] (1.Graduate School of Science, The University of Tokyo)

[AOS11-P09] **Double diffusion in the Arabian Sea during winter and spring**

*Ashin Kuriakose[1,2], Girishkumar M S -[1], Jofia Joseph -[1], Eric D'Asaro -[3], Sureshkumar N -[1], Sherin V R -[1], Murali B -[1], Thangaprakash V P -[1], E Pattabhi Ram Rao[1], S. S. C. Shenoi (1.Indian National Centre for Ocean Information Services, 2.School of Ocean Science and Technology, Kerala University of Fisheries and Ocean Studies, 3.Applied Physics Laboratory and School of Oceanography, University of Washington, Seattle, Washington, USA)

[AOS11-P10] On widespread intensified thermocline turbulence in the seasonally stratified Yellow Sea

*Wei Yang[1] (1.Tianjin University)

[AOS11-P11] Observation of energy transfer from traveling typhoons to turbulent mixing in the ocean

*Aiqi Zhang[1], Ichiro Yasuda[1], Daigo Yanagimoto[1], Shinzou Fujio[1], Yusuke Sasaki[1] (1.the University of Tokyo)

[AOS11-P12] Can tidal forcing alone generate a GM-like internal wave spectrum?

*Zhiwu Chen[1], Shaomin Chen[1], Zhiyu Liu[2], Jiexin Xu[1], Jieshuo Xie[1], Yinghui He[1], Shuqun Cai[1] (1.South China Sea Institute of Oceanology, Chinese Academy of Sciences, 2.Department of Physical Oceanography, College of Ocean and Earth Sciences, Xiamen University)

[E] Oral | A (Atmospheric and Hydrospheric Sciences)：A-OS Ocean Sciences & Ocean Environment

3:30 PM - 5:00 PM JST | 6:30 AM - 8:00 AM UTC | Ch.11 Zoom Room 11

[A-OS12] Physical, biogeochemical, and ecological processes and variability in the Indian Ocean

convener:Yukio Masumoto(Graduate School of Science, The University of Tokyo), Hiroaki Saito(Atmosphere and Ocean Research Institute, The University of Tokyo), Chairperson:Yukio Masumoto(Graduate School of Science, The University of Tokyo), Hiroaki Saito(Atmosphere and Ocean Research Institute, The University of Tokyo)

3:30 PM - 3:45 PM JST | 6:30 AM - 6:45 AM UTC

[AOS12-01] Determination of nitrogen source for phytoplankton in the eastern Indian Ocean by $\delta^{15}N$ of chlorophyll *a* and divinylchlorophyll *a*

*Yuta Isaji[1], Chisato Yoshikawa[1], Nanako O. Ogawa[1], Kazuhiko Matsumoto[1], Naoto F. Ishikawa[1], Akiko Makabe[1], Hiroshi Ogawa[2], Hiroaki Saito[2], Makio Honda[1], Naohiko Ohkouchi[1] (1.Japan Agency for Marine-Earth Science and Technology, 2.Atmosphere and Ocean Research Institute, University of Tokyo)

3:45 PM - 4:00 PM JST | 6:45 AM - 7:00 AM UTC

[AOS12-02] **Temporary phytoplankton bloom induced by physical disturbances in the Eastern Indian Ocean**

*Siyu Jiang[1], Fuminori Hashihama[2], Hiroaki Saito[1] (1.Atmosphere and Ocean Research Institute, The University of Tokyo, 2.Tokyo University of Marine Science and Technology)

4:00 PM - 4:15 PM JST | 7:00 AM - 7:15 AM UTC

[AOS12-03] Intraseasonal variation of surface Chlorophyll-a associated with coastal upwelling along the southern coast of Java

*Takanori Horii[1], Eko Siswanto[2], Iskhaq Iskandar[3], Iwao Ueki[1] (1.Global Ocean Observation Research Center, Research Institute for Global Change, Japan Agency for Marine-Earth Science and Technology (JAMSTEC), 2.Earth Surface System Research Center, Research Institute for Global Change, Japan Agency for Marine-Earth Science and Technology (JAMSTEC), 3.Faculty of Mathematics and Natural Sciences, Sriwijaya University, Indonesia)

4:15 PM - 4:30 PM JST | 7:15 AM - 7:30 AM UTC

[AOS12-04] Interannual variability in sea surface temperature off Somalia
in boreal summer
– Similarities and differences between “Warm year” and “Cold year” –

*Kusumi Takahiro[1], Yukio Masumoto[1] (1.the Unversity of Tokyo)

4:30 PM - 4:45 PM JST | 7:30 AM - 7:45 AM UTC

[AOS12-05] Seasonal and Interannual Variations of Indian Ocean Subtropical Mode Water Based on the Argo Data

*Hanani Adiwira[1], Toshio Suga[1] (1.Tohoku University)

4:45 PM - 5:00 PM JST | 7:45 AM - 8:00 AM UTC

[AOS12-06] Distribution and movement of microplastics in the Indian Ocean

*Yukio Masumoto[1] (1.Graduate School of Science, The University of Tokyo)

[E] Poster | A (Atmospheric and Hydrospheric Sciences)：A-OS Ocean Sciences & Ocean Environment

5:15 PM - 6:30 PM JST | 8:15 AM - 9:30 AM UTC | Ch.05_2

[A-OS12] Physical, biogeochemical, and ecological processes and variability in the Indian Ocean

convener:Yukio Masumoto(Graduate School of Science, The University of Tokyo), Hiroaki Saito(Atmosphere and Ocean Research Institute, The University of Tokyo)

[AOS12-P01] **Nitrogen cycling in the primary nitrite maximum of the Indian Ocean**

*Shigenobu Takeda[1], Kunioki Hirata[1], Takuhei Shiozaki[2] (1.Nagasaki University, 2.The University of Tokyo)

[AOS12-P02] Coastal ecosystem study in the Indian Ocean and adjacent seas under international collaboration

*Hiroaki Saito[1], Yukio Masumoto[2], Zainal Arifin[3] (1.Atmosphere and Ocean Research Institute, The University of Tokyo, 2.Graduate School of Science, The University of Tokyo, 3.Research Centre for Oceanograph, Indonesian Institute of Sciences)

[AOS12-P03] Issues and future directions of the Indian Ocean researches

*Yukio Masumoto[1] (1.Graduate School of Science, The University of Tokyo)

[E] Oral | A (Atmospheric and Hydrospheric Sciences)：A-OS Ocean Sciences & Ocean Environment

9:00 AM - 10:30 AM JST | 12:00 AM - 1:30 AM UTC | Ch.11 Zoom Room 11

[A-OS13] Marine ecosystems and biogeochemical cycles: theory, observation and modeling

convener:Takafumi Hirata(Arctic Research Center, Hokkaido University), Shin-ichi Ito(Atmosphere and Ocean Research Institute, The University of Tokyo), E Eileen Hofmann(Old Dominion University), N Enrique Curchitser(Rutgers University New Brunswick), Chairperson:Shin-ichi Ito(Atmosphere and Ocean Research Institute, The University of Tokyo), Takafumi Hirata(Arctic Research Center, Hokkaido University), Eileen E Hofmann(Old Dominion University), Enrique N Curchitser(Rutgers University New Brunswick)

9:00 AM - 9:05 AM JST | 12:00 AM - 12:05 AM UTC

[AOS13-01] Introduction

9:05 AM - 9:30 AM JST | 12:05 AM - 12:30 AM UTC

[AOS13-02] Understanding Marine Ecosystems – A View to the Future

★Invited Papers

*Eileen E Hofmann[1] (1.Old Dominion University)

9:30 AM - 9:45 AM JST | 12:30 AM - 12:45 AM UTC

[AOS13-03] Marine Ecosystem Variations Over the North Pacific and Their Linkage to Large-Scale Climate Variability and Change

*Emi Yati[1], Shoshiro Minobe[2,3], Nathan Mantua[4], Shin-ichi Ito[5], Emanuele Di Lorenzo[6] (1.Remote Sensing Application Center, Indonesian National Institute of Aeronautics and Space, Jakarta, Indonesia, 2.Department of Natural History Sciences, Graduate School of Science, Hokkaido University, Sapporo, Japan, 3.Department of Earth and Planetary Sciences, Faculty of Science, Hokkaido University, Sapporo, Japan, 4.Fish Ecology Division, Southwest Fisheries Science Center, National Marine Fisheries Service, National Oceanographic and Atmospheric Administration, Santa Cruz, CA, United States, 5.Atmosphere and Ocean Research Institute, University of Tokyo, Kashiwa, Japan, 6.School of Earth and Atmospheric Sciences, Georgia Institute of Technology, Atlanta, GA, United States)

9:45 AM - 10:00 AM JST | 12:45 AM - 1:00 AM UTC

[AOS13-04] **Future biogeographic shifts of marine biodiversity in the Pacific Arctic**

*Irene Alabia[1], Jorge Garcia Molinos[1], Sei-Ichi Saitoh[1], Takafumi Hirata[1], Toru Hirawake[1], Franz Mueter[2] (1.Hokkaido University, 2.University of Alaska Fairbanks)

10:00 AM - 10:15 AM JST | 1:00 AM - 1:15 AM UTC

[AOS13-05] Instantaneous Acclimation allows computationally efficient modelling of the biogeochemical impacts of plankton ecophysiology

*S. Lan Smith[1], Onur Kerimoglu[2], Prima Anugerahanti[1], Yoshio Masuda[3], Yasuhiro Yamanaka[3], Yoshikazu Sasai[1] (1.Marine Ecosystem Dynamics Research Group, Research Institute for Global Change, Japan Agency for Marine-Earth Science and Technology, 2.ICBM, University of Oldenburg, Germany, 3.Faculty of Environmental Earth Science, Hokkaido University)

10:15 AM - 10:30 AM JST | 1:15 AM - 1:30 AM UTC

[AOS13-06] Interannual Variability in contributions of the Equatorial Undercurrent (EUC) to Peruvian Upwelling

*Gandy Maria Rosales Quintana[1], Robert Marsh[2], Luis Alfredo Icochea Salas[3] (1.Course of Applied Marine Environmental Studies, Tokyo University of Marine Science and Technology, 2.University of Southampton, UK, 3.Universidad Nacional Agraria La Molina, Peru)

[E] Oral | A (Atmospheric and Hydrospheric Sciences)：A-OS Ocean Sciences & Ocean Environment

10:45 AM - 12:15 PM JST | 1:45 AM - 3:15 AM UTC | Ch.11 Zoom Room 11

[A-OS13] Marine ecosystems and biogeochemical cycles: theory, observation and modeling

convener:Takafumi Hirata(Arctic Research Center, Hokkaido University), Shin-ichi Ito(Atmosphere and Ocean Research Institute, The University of Tokyo), E Eileen Hofmann(Old Dominion University), N Enrique Curchitser(Rutgers University New Brunswick), Chairperson:Takafumi Hirata(Arctic Research Center, Hokkaido University), Shin-ichi Ito(Atmosphere and Ocean Research Institute, The University of Tokyo), Eileen E Hofmann(Old Dominion University), Enrique N Curchitser(Rutgers University New Brunswick)

10:45 AM - 11:00 AM JST | 1:45 AM - 2:00 AM UTC

[AOS13-07] Influence of ENSO on surface chlorophyll-a in the Gulf of Thailand

*Dudsadee Leenawarat[1], Jutarak Luang-on[1], Anukul Buranapratheprat[2], Joji Ishizaka[3] (1.Graduate School of Environmental Studies, Nagoya University, 2.Department of Aquatic Science, Faculty of Science, Burapha University, Thailand, 3.Institute for Space-Earth Environmental Research, Nagoya University, Japan)

11:00 AM - 11:15 AM JST | 2:00 AM - 2:15 AM UTC

[AOS13-08] Nitrogen isotope mapping in the North Pacific using a marine nitrogen isotope model

*Chisato Yoshikawa[1], Masahito Shigemitsu[1], Akitomo Yamamoto[1], Akira Oka[2], Naohiko Ohkouchi[1] (1.JAMSTEC, 2.AORI)

11:15 AM - 11:30 AM JST | 2:15 AM - 2:30 AM UTC

[AOS13-09] **Interannual variations of the lower-trophic level ecosystem in the Harima-Nada, eastern Seto Inland Sea, Japan simulated by a plankton functional type model.**

*Naoki Yoshie[1], Ayaka Hiramine[1] (1.Center for Marine Environmental Studies, Ehime University)

11:30 AM - 11:45 AM JST | 2:30 AM - 2:45 AM UTC

[AOS13-10] **Occurrence of phytoplankton bloom as the Kuroshio passes an island**

*JIE GAO[1], Xinyu Guo[1] (1.Center for Marine Environmental Studies, Ehime University)

11:45 AM - 12:00 PM JST | 2:45 AM - 3:00 AM UTC

[AOS13-11] Long-term comparison between the Japanese sardine stock level and simulated zooplankton density around the Kuroshio axis

*Haruka Nishikawa[1], Hiroyuki Tsujino[2], Shiro Nishikawa[1], Hideyuki Nakano[2], Toru Sugiyama[1], Yoichi Ishikawa[1] (1.Japan Agency for Marine-Earth Science and Technology, 2.Meteorological Research Institute)

12:00 PM - 12:15 PM JST | 3:00 AM - 3:15 AM UTC

[AOS13-12] Changes in phytoplankton photophysiology during pre-bloom and bloom phases in the coastal Oyashio waters

*Tomonori Isada[1], Toru Hirawake[2], Koji Suzuki[3], Jun Nishioka[4], Hiromi Kasai[5] (1.Field Science Center for Northern Biosphere, Hokkaido University, 2.Faculty of Fisheries Sciences, Hokkaido University, 3.Faculty of Environmental Earth Science, Hokkaido University, 4.Institute of Low Temperature Science, Hokkaido University, 5.Japan fisheries research and education agency)

[E] Oral | A (Atmospheric and Hydrospheric Sciences)：A-OS Ocean Sciences & Ocean Environment

1:45 PM - 3:15 PM JST | 4:45 AM - 6:15 AM UTC | Ch.11 Zoom Room 11

[A-OS13] Marine ecosystems and biogeochemical cycles: theory, observation and modeling

convener:Takafumi Hirata(Arctic Research Center, Hokkaido University), Shin-ichi Ito(Atmosphere and Ocean Research Institute, The University of Tokyo), E Eileen Hofmann(Old Dominion University), N Enrique Curchitser(Rutgers University New Brunswick), Chairperson:Shin-ichi Ito(Atmosphere and Ocean Research Institute, The University of Tokyo), Takafumi Hirata(Arctic Research Center, Hokkaido University), Eileen E Hofmann(Old Dominion University), Enrique N Curchitser(Rutgers University New Brunswick)

1:45 PM - 2:05 PM JST | 4:45 AM - 5:05 AM UTC

[AOS13-13] Biogeochemical fingerprints of ocean migration of Pacific salmon

★Invited Papers

*Jun Matsubayashi[1] (1.Chuo University)

2:05 PM - 2:20 PM JST | 5:05 AM - 5:20 AM UTC

[AOS13-14] Vertical habitat shifts of juvenile Japanese jack mackerel (*Trachurus japonicus*) estimated by otolith microchemistry

*Megumi Enomoto[1], Shin-ichi Ito[1], Motomitsu Takahashi[2], Chiyuki Sassa[2], Tomihiko Higuchi[1], Kotaro Shirai[1] (1.Atmosphere and Ocean Research Institute, The University of Tokyo, 2.Fisheries Resource Institute, Japan Fisheries Research and Education Agency)

2:20 PM - 2:35 PM JST | 5:20 AM - 5:35 AM UTC

[AOS13-15] Retrospective time-series nitrogen isotope analysis of fish otoliths

*Yota Harada[1], Chisato Yoshikawa[1], Nanako O. Ogawa[1], Saburo Sakai[1], Shin-ichi Ito[2], Naohiko Ohkouchi[1] (1.Biogeochemistry Research Center, Japan Agency for Marine-Earth Science and Technology, 2.Atmosphere and Ocean Research Institute, The University of Tokyo)

2:35 PM - 2:55 PM JST | 5:35 AM - 5:55 AM UTC

[AOS13-16] Fish specialize their metabolic performance to maximize bioenergetic efficiency in their local environment

★Invited Papers

*Chenying Guo[1], Shin-ichi Ito[1], Michio Yoneda[2], Hajime Kitano[2], Hitoshi Kaneko[3], Megumi Enomoto[1], Tomoya Aono[1], Masahiro Nakamura[2], Takashi Kitagawa[1], Nicolas C Wegner[4], Emmanis Dorval[5] (1.Atmosphere and Ocean Research Institute, the University of Tokyo, 2.Japan Fisheries Research and Education Agency, 3.Japan Agency for Marine-Earth Science and Technology (JAMSTEC), 4.Southwest Fisheries Science Center, National Marine Fisheries Service, NOAA, 5.Lynker Technologies, LLC., under contract to Southwest Fisheries Science Center, NOAA)

2:55 PM - 3:10 PM JST | 5:55 AM - 6:10 AM UTC

[AOS13-17] Comparative study on environment experienced by jack mackerel in the East China Sea between 1960s and 2000s.

*Tomihiko Higuchi[1], Motomitsu Takahashi[2], Megumi Enomoto[1], Kotaro Shirai[1], Shin-ichi Ito[1] (1.Atmosphere and Ocean Research Institute, The University of Tokyo, 2.Fisheries Resources Institute, Japan Fisheries Research and Education Agency, Nagasaki, Japan)

3:10 PM - 3:15 PM JST | 6:10 AM - 6:15 AM UTC

[AOS13-18] Discussion

[E] Poster | A (Atmospheric and Hydrospheric Sciences)：A-OS Ocean Sciences & Ocean Environment

5:15 PM - 6:30 PM JST | 8:15 AM - 9:30 AM UTC | Ch.05_3

[A-OS13] Marine ecosystems and biogeochemical cycles: theory, observation and modeling

convener:Takafumi Hirata(Arctic Research Center, Hokkaido University), Shin-ichi Ito(Atmosphere and Ocean Research Institute, The University of Tokyo), E Eileen Hofmann(Old Dominion University), N Enrique Curchitser(Rutgers University New Brunswick)

[AOS13-P01] Marine fish distribution in the Kuroshio Extension area observed by OceanDNA

*ZESHU YU[1], Shin-ichi Ito[2], Marty Wong[2], Susumu Yoshizawa[2], Jun Inoue[2], Sachihiko Itoh[2], Susumu Hyodo[2] (1.Graduate School of Agricultural and Life Sciences, The University of Tokyo, 2. Atmosphere and Ocean Research Institute, The University of Tokyo)

[AOS13-P02] Introducing phytoplankton size structure in an ocean biogeochemical model OECO2

*Wenhui Sun[1], Ryota Shibano[1], Michio Watanabe[2], Sachihiko Itoh[1] (1.Atmosphere and Ocean Research Institute, The University of Tokyo, 2.Japan Agency for Marine-Earth Science and Technology)

[AOS13-P03] Origin of dissolved inorganic nitrogen in the Tsushima Strait and its seasonal and interannual variation

*Ryota Shibano[1], Akihiko Morimoto[2], Katsumi Takayama[3], Tetsutaro Takikawa[4], Joji Ishizaka[5], Xinyu Guo[2] (1.Atmosphere and Ocean Research Institute, The University of Tokyo, 2.Center for Marine Environmental Studies, Ehime University, 3.Research Institute for Applied Mechanics, Kyushu University, 4.Graduate School of Fisheries and Environmental Sciences, Nagasaki University, 5.Institute for Space-Earth Environmental Research, Nagoya University)

[AOS13-P04] Comparative study on respiration of Japanese anchovy (*Engraulis japonicus*) around Japan II.

*Shin-ichi Ito[1], Chenying Guo[1], Megumi Enomoto[1], Tomoya Aono[1], Michio Yoneda[2], Michiya Matsuyama[3], Takashi Kitagawa[1], Motomitsu Takahashi[2], Taketo Hashioka[4] (1.Atmosphere and Ocean Research Institute, The University of Tokyo, 2.Japan Fisheries Research and Education Agency, 3.Kyushu University, 4.Japan Agency for Marine-Earth Science and Technology)

[AOS13-P05] A state-space production model to analyze the impact of stock enhancement on population dynamics: a case study of Japanese flounder in the Seto Inland Sea

*LIN ZHEN[1], Toshihide Kitakado[2], Naoki Suzuki[2], Shin-ichi Ito[1] (1.Atmosphere and Ocean Research Institute, The University of Tokyo, 2.Tokyo University of Marine Science and Technology)

[AOS13-P06] Variability in phytoplankton Chlorophyll-a in the Kuroshio western boundary current: a result from 14-year observation by satellite remote sensing

*Takafumi Hirata[1], Keiko Sato[1], Satoshi Kitaoka (1.Arctic Research Center, Hokkaido University)

[J] Oral | A (Atmospheric and Hydrospheric Sciences)：A-OS Ocean Sciences & Ocean Environment

3:30 PM - 5:00 PM JST | 6:30 AM - 8:00 AM UTC | Ch.09 Zoom Room 09

[A-OS14] Coastal physical processes associated with mixing, eddies, internal waves

convener:Eisuke Tsutsumi(Atmosphere and Ocean Research Institute, The University of Tokyo), Eiji Masunaga(Ibaraki University), Taira Nagai(Graduate School of Science, The University of Tokyo), Chairperson:Eisuke Tsutsumi(Atmosphere and Ocean Research Institute, The University of Tokyo), Eiji Masunaga(Ibaraki University), Taira Nagai(Graduate School of Science, The University of Tokyo)

3:30 PM - 3:45 PM JST | 6:30 AM - 6:45 AM UTC

[AOS14-01] Enhancement of turbulent mixing over tidal sandwaves and formation of front: an observational study in Seto Inland Sea

*Eisuke Tsutsumi[1], Xinyu Guo[2], Naoki Yoshie[2], Takahiro Endoh[3], Takeshi Matsuno[3], Sachihiko Itoh[1] (1.Atmosphere and Ocean Research Institute, The University of Tokyo, 2.Center for Marine Environmental Studies, Ehime University, 3.Research Institute for Applied Mechanics, Kyushu University)

3:45 PM - 4:00 PM JST | 6:45 AM - 7:00 AM UTC

[AOS14-02] Dynamics of the upwelling at the upstream of the East Sakhalin Current (ESC)

*Nan Yuan[1] (1.Hokkaido University, the Institute of Low Temperature Science)

4:00 PM - 4:15 PM JST | 7:00 AM - 7:15 AM UTC

[AOS14-03] Numerical study of tide-induced deep-ocean mixing near the head of Suruga Trough

*Taira Nagai[1], Toshiyuki Hibiya[1] (1.Graduate School of Science, The University of Tokyo)

4:15 PM - 4:30 PM JST | 7:15 AM - 7:30 AM UTC

[AOS14-04] **Amplitude modulation of currents at tidal and inertial bands at the Otsuchi Bay mouth**

*Tongjun Sun[3,1], Sachihiko Itoh[3], Eisuke Tsutsumi[3], Miho Ishizu[2], Kiyoshi Tanaka[3] (1.Graduate School of Agricultural and Life Sciences/Faculty of Agriculture,The University of Tokyo, 2.Japan Agency for Marine-Earth Science and Technology, 3.Atmosphere and Ocean Research Institute, The University of Tokyo)

4:30 PM - 4:45 PM JST | 7:30 AM - 7:45 AM UTC

[AOS14-05] Water mass classification off the east coast of Japan mainland using Regional Ocean Modeling System (ROMS)

*Masashi Ikeda[1], Eiji Masunaga[1], Yusuke Uchiyama[2], Yota Suzue[4], Sachihiko Itoh[3] (1.Ibaraki University , 2.Kobe University, 3.The University of Tokyo, 4.CTI Engineering)

4:45 PM - 5:00 PM JST | 7:45 AM - 8:00 AM UTC

[AOS14-06] Vertical mixing and mass transport in a shallow lake, Lake Kasumingaura, Japan

*Eiji Masunaga[1], Tatsumi Kitamura[2], Sachihiko Itoh[3] (1.Ibaraki University, 2.Ibaraki Kasumigaura Environmental Science Center, 3.The University of Tokyo)

[J] Poster | A (Atmospheric and Hydrospheric Sciences)：A-OS Ocean Sciences & Ocean Environment

5:15 PM - 6:30 PM JST | 8:15 AM - 9:30 AM UTC | Ch.06_1

[A-OS14] Coastal physical processes associated with mixing, eddies, internal waves

convener:Eisuke Tsutsumi(Atmosphere and Ocean Research Institute, The University of Tokyo), Eiji Masunaga(Ibaraki University), Taira Nagai(Graduate School of Science, The University of Tokyo)

[AOS14-P01] Material transport and diffusion around Sagami Bay and Suruga Bay using a particle tracking model

*Takayoshi Inoue[1], Eiji Masunaga[1], Taichi Kosako[2], Yusuke Uchiyama[3] (1.Ibaraki University, 2.Port and Airport Research Institute, 3.Kobe University)

[AOS14-P02] Physical structure and mixing processes in the inner part of Tokyo Bay

*Haruki Itozu[1], Eiji Masunaga[1] (1.Ibaraki University)

[AOS14-P03] Secular variations of M_2 tide, its resonant amplification, and the associated energy dissipation in a semi-enclosed sea connected to the East China Sea (Ariake Sea, Japan), 1980–2019.

*Eisuke Tsutsumi[1], Matsuno Takeshi[2], Sachihiko Itoh[1] (1.Atmosphere and Ocean Research Institute, The University of Tokyo, 2.Research Institute for Applied Mechanics, Kyushu University)

[J] Oral | A (Atmospheric and Hydrospheric Sciences)：A-OS Ocean Sciences & Ocean Environment

3:30 PM - 5:00 PM JST | 6:30 AM - 8:00 AM UTC | Ch.07 Zoom Room 07

[A-OS16] Global ocean observing systems, their status, research results and future perspective

convener:Shigeki Hosoda(Japan Marine-Earth Science and Technology), Shuhei Masuda(Japan Agency for Marine-Earth Science and Technology), Yosuke Fujii(Meteorological Research Institute, Japan Meteorological Agency), Fujiki Tetsuichi(Japan Agency for Marine-Earth Science and Technology), Chairperson:Shuhei Masuda(Japan Agency for Marine-Earth Science and Technology), Yosuke Fujii(Meteorological Research Institute, Japan Meteorological Agency), Fujiki Tetsuichi(Japan Agency for Marine-Earth Science and Technology), Shigeki Hosoda(Japan Marine-Earth Science and Technology)

3:30 PM - 3:35 PM JST | 6:30 AM - 6:35 AM UTC

[AOS16-01] Introduction

3:35 PM - 3:55 PM JST | 6:35 AM - 6:55 AM UTC

[AOS16-02] Biogeochemical Argo: Significances and Challenges

★Invited Papers

*Masao Ishii[1] (1.Meteorological Research Institute, Japan Meteorological Agency)

3:55 PM - 4:15 PM JST | 6:55 AM - 7:15 AM UTC

[AOS16-03] Global deployment of Deep Argo floats toward accurate prediction of future climate and ecosystem changes

★Invited Papers

*Toshiyuki Hibiya[1] (1.Department of Earth and Planetary Science, Graduate School of Science, University of Tokyo)

4:15 PM - 4:30 PM JST | 7:15 AM - 7:30 AM UTC

[AOS16-04] Two-year seismic observation by hydrophone floats

*Masayuki Obayashi[1], Hiroko Sugioka[2], Junko Yoshimitsu[1] (1.Japan Agency for Marine-Earth Science and Technology, 2. Department of Planetology, Kobe University)

4:30 PM - 5:00 PM JST | 7:30 AM - 8:00 AM UTC

[AOS16-05] Discussion toward a New Global Ocean Observing System

*Shuhei Masuda[1] (1.Japan Agency for Marine-Earth Science and Technology)

[J] Poster | A (Atmospheric and Hydrospheric Sciences)：A-OS Ocean Sciences & Ocean Environment

5:15 PM - 6:30 PM JST | 8:15 AM - 9:30 AM UTC | Ch.06_2

[A-OS16] Global ocean observing systems, their status, research results and future perspective

convener:Shigeki Hosoda(Japan Marine-Earth Science and Technology), Shuhei Masuda(Japan Agency for Marine-Earth Science and Technology), Yosuke Fujii(Meteorological Research Institute, Japan Meteorological Agency), Fujiki Tetsuichi(Japan Agency for Marine-Earth Science and Technology)

[AOS16-P01] Spatiotemporal variability of vertical structures of temperature and salinity in the mid-latitude northwest Pacific Ocean based on unsupervised clustering

★Invited Papers

*Fumika Sambe[1], Toshio Suga[1,2] (1.Graduate School of Science, Tohoku University, 2.JAMSTEC)

[AOS16-P02] Temporal variations of Kuroshio transport based on a repeated hydrographic section along 137E

*Yuma Kawakami[1], Toshiya NAKANO[1], Atsushi Kojima[1], Kiyoshio Murakami[1], Shusaku Sugimoto[2] (1.Japan Meteorological Agency, 2.Tohoku University)

[AOS16-P03] Global distribution of 10-day differences of temperature and salinity around 2000 m depth observed with Argo floats

*Yoshimi Kawai[1] (1.Research Institute for Global Change, Japan Agency for Marine-Earth Science and Technology)

[AOS16-P04] GO-SHIP Easy Ocean: formatted and gridded ship-based hydrographic section data

*Katsuro Katsumata[1], Sarah Purkey[2], Rebecca Cowley[3], Bernadette Sloyan[3], Stephen Diggs[4], Thomas Moore, II[3], Lynne Talley[2], James Swift[4] (1.JAMSTEC, 2.Scripps Institution of Oceanography, 3.Oceans and Atmosphere, CSIRO, 4.CLIVAR and Carbon Hydrographic Data Office, Scripps Institution of Ocenaography)

[AOS16-P05] Salinity bias with negative pressure dependency caused by anisotropic deformation of CTD measuring cell under pressure examined with a dual-cylinder cell model

*Taiyo Kobayashi[1] (1.Japan Agency for Marine-Earth Science and Technology)

[AOS16-P06] pH measurement in the ocean

*Hajime Kayanne[1], Toshimasa Miyawaki[1], Nori Fujita[1], Kenta Suzuki[2], Hizuru Nakajima[2], Kazuhiro Morioka[3], Akihide Hemmi[4] (1.the University of Tokyo, 2.Tokyo Metropolitan Univ., 3.Tokyo Univ. Pharmacy Life Sci., 4.Möbius Advanced Tech.)

[AOS16-P07] Advances in the estimation of global surface net heat flux based on satellite observation: J-OFURO3 V1.1

*Hiroyuki Tomita[1], Kunio Kutsuwada[2], Masahisa Kubota[3], Tsutomu Hihara[4] (1.Institute for Space-Earth Environmental , Nagoya University, 2.School of Marine Science and Technology, Tokai University, 3.Institute of Ocean Research and Development, 4.Japan Fisheries Information Service Center)

[AOS16-P08] Keeping the PACE with the NASA Plankton, Aerosol, Cloud, ocean Ecosystem (PACE) mission

*Lachlan McKinna[1], Ivona Cetinić[2,3], Jeremy Werdell[3] (1.Go2Q Pty Ltd, 2.USRA, 3.NASA GSFC)

[J] Oral | A (Atmospheric and Hydrospheric Sciences)：A-OS Ocean Sciences & Ocean Environment

10:45 AM - 12:15 PM JST | 1:45 AM - 3:15 AM UTC | Ch.10 Zoom Room 10

[A-OS19] Physical Oceanography (General)

convener:Yoshimi Kawai(Research Institute for Global Change, Japan Agency for Marine-Earth Science and Technology), Kitade Yujiro(Tokyo University of Marine Science and Technology), Chairperson:Yoshimi Kawai(Research Institute for Global Change, Japan Agency for Marine-Earth Science and Technology)

10:45 AM - 11:00 AM JST | 1:45 AM - 2:00 AM UTC

[AOS19-01] Frontal waves in the east of the Tsugaru Strait revealed by the high-frequency radar observation

*Hitoshi Kaneko[1], Takahiro Tanaka[2], Hiroto Abe[1,3], Masahide Wakita[1], Ken'ichi Sasaki[1], Daisuke Hasegawa[2], Takeshi Okunishi[2], Shuichi Watanabe[1], Shoko Tatamisashi[1], Yoshiaki Sato[1] (1.Japan Agency for Marine-Earth Science and Technology, 2.Japan Fisheries Research and Education Agency, 3.Graduate School/Faculty of Fisheries Sciences, Hokkaido University)

11:00 AM - 11:15 AM JST | 2:00 AM - 2:15 AM UTC

[AOS19-02] 17 year observation of bottom water current on deep seafloor offshore of Tokachi in Hokkaido: Recovery of acoustic Doppler current profiler (ADCP) data of cabled observatory

*Ryoichi Iwase[1] (1.National Research and Development Agency, Japan Agency for Marine-Earth Science and Technology)

11:15 AM - 11:30 AM JST | 2:15 AM - 2:30 AM UTC

[AOS19-03] Winter large-scale atmospheric circulation during La Niña events: A comparison between the first year and second year of events

*Gaku Nishihira[1], Shusaku Sugimoto[1] (1.Graduate School of Science, Tohoku University)

11:30 AM - 11:45 AM JST | 2:30 AM - 2:45 AM UTC

[AOS19-04] Decadal variation of the asymmetry of SSTA in the tropical Atlantic and its relations with midlatitude atmosphere circulation

*Yoshinobu Furukawa[1], Shusaku Sugimoto[1] (1.Graduate School of Science, Tohoku University)

11:45 AM - 12:00 PM JST | 2:45 AM - 3:00 AM UTC

[AOS19-05] Nearshore wave–current interaction effects on wave power density near Japan

*Adrean Webb[1], Takuji Waseda[2] (1.Kyoto University, Disaster Prevention Research Institute, Coastal Disaster Research, 2.The University of Tokyo, Graduate School of Frontier Sciences, Department of Ocean Technology Policy and Environment)

12:00 PM - 12:15 PM JST | 3:00 AM - 3:15 AM UTC

[AOS19-06] Medium-term oceanic transport of microplastics in and around the South China Sea analyzed with climatological and synoptic models

*Kosei Matsushita[1], Yusuke Uchiyama[1], Naru Takaura[1], Taichi Kosako[2] (1.Kobe University, 2.Port and Airport Research Institute)

[J] Poster | A (Atmospheric and Hydrospheric Sciences)：A-OS Ocean Sciences & Ocean Environment

5:15 PM - 6:30 PM JST | 8:15 AM - 9:30 AM UTC | Ch.06_3

[A-OS19] Physical Oceanography (General)

convener:Yoshimi Kawai(Research Institute for Global Change, Japan Agency for Marine-Earth Science and Technology), Kitade Yujiro(Tokyo University of Marine Science and Technology)

[AOS19-P01] Long-term variability of summertime convective activity over the tropical northwestern Pacific and its influence on large-scale atmospheric circulation

*Shota Sera[1], Shusaku Sugimoto[1] (1.Graduate School of Science, Tohoku University)

[AOS19-P02] **Temporal variation of heat content within surface mixed layer in the western Arctic from Iridium-based autonomous thermistor strings**

*EunYae Son[1], Yusuke Kawaguchi[1] (1.University of Tokyo)

[AOS19-P03] Data and Sample Management for Marine Observation Cruises: Complaint can be Awareness

*Takayuki Tomiyama[1], Takako Sato[1], Kazuyo Fukuda[1], Hajime Kawakami[1], Makoto Ito[1], Chizuru Saito[1] (1.Japan Agency for Marine-Earth Science and Technology)

[AOS19-P04] Meridional heat transport in the North Pacific subtropical gyre -Analysis by ARMOR 3D-

*Yukina Fukaumi[1], Kazuyuki Uehara[1] (1.The Graduate School of Marine Science and Technology of Tokai University)

[E] Oral | A (Atmospheric and Hydrospheric Sciences)：A-HW Hydrology & Water Environment

9:00 AM - 10:30 AM JST | 12:00 AM - 1:30 AM UTC | Ch.12 Zoom Room 12

[A-HW20] Hydrology & Water Environment

convener:Takeshi Hayashi(Faculty of Education and Human Studies, Akita University), Keisuke Fukushi(Institute of Nature & Environmental Technology, Kanazawa University), Koichi Sakakibara(Department of Environmental Sciences, Faculty of Science, Shinshu University), Dai Yamazaki(Institute of Industrial Sciences, The University of Tokyo), Chairperson:Takeshi Hayashi(Faculty of Education and Human Studies, Akita University), Keisuke Fukushi(Institute of Nature & Environmental Technology, Kanazawa University), Koichi Sakakibara(Department of Environmental Sciences, Faculty of Science, Shinshu University), Dai Yamazaki(Institute of Industrial Sciences, The University of Tokyo)

9:00 AM - 9:05 AM JST | 12:00 AM - 12:05 AM UTC

[AHW20-01] Introduction

9:05 AM - 9:20 AM JST | 12:05 AM - 12:20 AM UTC

[AHW20-02] Behavior of pore-air entrapment in unsaturated soil layer in two small headwater catchments with different soil depth

*Sho Iwagami[1], Shoji Noguchi[2], Takanori Shimizu[1], Tayoko Kubota[1], Shin'ichi Iida[1] (1.Forestry and Forest Products Research Institute, Forest Research and Management Organization, National Research and Development Agency, 2.Kansai Research Center, Forestry and Forest Products Research Institute, Forest Research and Management Organization, National Research and Development Agency)

9:20 AM - 9:35 AM JST | 12:20 AM - 12:35 AM UTC

[AHW20-03] Developement of a 2D Eulerian SPH shallow water model for dam break flows

*Kao-Hua Chang[1] (1.National Taiwan Ocean University)

9:35 AM - 9:50 AM JST | 12:35 AM - 12:50 AM UTC

[AHW20-04] Investigating the validity of a meso scale constitutive equation using micro scale water dynamics simulations for hillslope rainfall-runoff processes

*Yutaka Ichikawa[1], Yuusuke Mori[1], Yasuto Tachikawa[1] (1.Graduate School of Engineering, Kyoto University)

9:50 AM - 10:05 AM JST | 12:50 AM - 1:05 AM UTC

[AHW20-05] A review of ensemble flood forecasting for operational warning

*Megumi Watanabe[1], Shunsuke Ito[2], Wenchao Ma[1], Dai Yamazaki[1] (1.Institute of Industrial Science, The University of Tokyo, Japan, 2.School of Engineering, The University of Tokyo, Japan)

10:05 AM - 10:20 AM JST | 1:05 AM - 1:20 AM UTC

[AHW20-06] ***Toward Downscaling Storage-Discharge Dynamics: Training Long Short-Term Memory (LSTM) model for Simulating Nonlinear Storage-Discharge Relation in HUC-8 Rum River Watershed, MN***

*Pai-Feng Victor Teng[1] (1.University of Minnesota)

10:20 AM - 10:30 AM JST | 1:20 AM - 1:30 AM UTC

[AHW20-07] Discussion

[E] Oral | A (Atmospheric and Hydrospheric Sciences)：A-HW Hydrology & Water Environment

10:45 AM - 12:15 PM JST | 1:45 AM - 3:15 AM UTC | Ch.12 Zoom Room 12

[A-HW20] Hydrology & Water Environment

convener:Takeshi Hayashi(Faculty of Education and Human Studies, Akita University), Keisuke Fukushi(Institute of Nature & Environmental Technology, Kanazawa University), Koichi Sakakibara(Department of Environmental Sciences, Faculty of Science, Shinshu University), Dai Yamazaki(Institute of Industrial Sciences, The University of Tokyo), Chairperson:Takeshi Hayashi(Faculty of Education and Human Studies, Akita University), Koichi Sakakibara(Department of Environmental Sciences, Faculty of Science, Shinshu University), Dai Yamazaki(Institute of Industrial Sciences, The University of Tokyo), Shin'ichi Iida(Department of Disaster Prevention, Meteorology and Hydrology, Forestry and Forest Products Research Institute)

10:45 AM - 10:50 AM JST | 1:45 AM - 1:50 AM UTC

[AHW20-08] Introduction

10:50 AM - 11:05 AM JST | 1:50 AM - 2:05 AM UTC

[AHW20-09] Distribution of Uranium and Arsenic in Surface Water around Alkaline-Hyposaline Lake from Valley of Gobi Lakes in Mongolia

*Baasansuren Gankhurel[1], Keisuke Fukushi[1], Davaadorj Davaasuren[2], Eigo Imai[1], TAKUMA KITAJIMA[1], Tuvshin Gerelmaa[2], Yasuhito Sekine[3], Yoshio Takahashi[4], Noriko Hasebe[1] (1.Kanazawa University, 2.National University of Mongolia, 3.Tokyo Institute of Technology, 4.The University of Tokyo)

11:05 AM - 11:20 AM JST | 2:05 AM - 2:20 AM UTC

[AHW20-10] Differences in nitrogen biogeochemical cycles of a reservoir with a hydraulic retention time of several days, before and after the dam was built

*Qingqing Sun[1] (1.Tianjin University)

11:20 AM - 11:35 AM JST | 2:20 AM - 2:35 AM UTC

[AHW20-11] **Plastic debris as a carrier of inorganic contaminants in the urban river of Mongolia**

*Batdulam Battulga[1], Masayuki Kawahigashi[1], Bolormaa Oyuntsetseg[2] (1.Department of Geography, Tokyo Metropolitan University, Tokyo, 192-0397, Japan , 2.Department of Chemistry, National University of Mongolia, Ulaanbaatar, 210646, Mongolia)

11:35 AM - 11:50 AM JST | 2:35 AM - 2:50 AM UTC

[AHW20-12] Geochemisty and environmental impact on groundwater in Eastern Serbia

*Dragana Adamovic[1,2], Daizo Ishiyama[1], Hiroshi Kawaraya[1], Yasumasa Ogawa[1] (1.Akita University, Japan, 2.MMI Bor, Serbia)

11:50 AM - 12:05 PM JST | 2:50 AM - 3:05 AM UTC

[AHW20-13] **Measurement of reactive oxygen species (ROS) and fluorescent organic matter in selected rivers in Hiroshima Prefecture, Japan.**

*Taiwo Tolulope Ayeni[1], Takashi Umeda[1], Yoko Iwamoto[1], Kazuhiko Takeda[1], Hiroshi M. G. Sakugawa[1], Khan M. G. Mostofa[2] (1.Hiroshima University Japan, 2.Tianjin University, China)

12:05 PM - 12:15 PM JST | 3:05 AM - 3:15 AM UTC

[AHW20-14] Discussion

[E] Poster | A (Atmospheric and Hydrospheric Sciences)：A-HW Hydrology & Water Environment

5:15 PM - 6:30 PM JST | 8:15 AM - 9:30 AM UTC | Ch.07_1

[A-HW20] Hydrology & Water Environment

convener:Takeshi Hayashi(Faculty of Education and Human Studies, Akita University), Keisuke Fukushi(Institute of Nature & Environmental Technology, Kanazawa University), Koichi Sakakibara(Department of Environmental Sciences, Faculty of Science, Shinshu University), Dai Yamazaki(Institute of Industrial Sciences, The University of Tokyo)

[AHW20-P01] Contribution of understory vegetation to evapotranspiration in a tropical dry forest, Cambodia

*Shin'ichi Iida[1], Takanori Shimizu[1], Koji Tamai[1], Naoki Kabeya[1], Akira Shimizu[1], Eriko Ito[1], Yasuhiro Ohnuki[1], Sophal Chann[2], Delphis F. Levia[3] (1.Forestry and Forest Products Research Institute, Japan, 2.Institute of Forest and Wildlife Research and Development, Cambodia, 3.University of Delaware, USA)

[AHW20-P02] Rainfall partitioning in two Japanese cedar stands with high stand densities as evidence of splash droplet evaporation hypothesis

*Shigeki Murakami[1], Kenzo Kitamura[1] (1.Kyushu Research Center, Forestry and Forest Products Research Institute)

[AHW20-P03] Vegetation response to soil moisture and groundwater in west-central Africa revealed by satellite observations

*Ryotaro Suzuki[1], Atsushi Higuchi[2] (1.Graduate School of Science and Engineering, Chiba University, Japan, 2.Center for Environmental Remote Sensing, Chiba University, Japan)

[AHW20-P04] An Efficient Surrogate Model for Extreme Hydrologic Predictions using Polynomial Chaos-Kriging

Vinh Ngoc Tran[1], *Jongho Kim[1] (1.University of Ulsan)

[AHW20-P05] **Hydrological Hindcasts and Parameterizations for Flash Floods Real-Time Forecasting in the Chugoku Region of Japan**

*Josko Troselj[1], Han Soo Lee[1] (1.Graduate School of Advanced Science and Engineering, Hiroshima University)

[AHW20-P06] Geochemical signature of trace elements in lake water at Lake Tazawa

*Arata Katamura[1], Daizo Ishiyama[1], Takeshi Hayashi[2], Yasumasa Ogawa[1] (1.Graduate School of International Resource Science, Akita University, 2.Faculty of Education and Human Studies, Akita University)

[E] Oral | A (Atmospheric and Hydrospheric Sciences)：A-HW Hydrology & Water Environment

9:00 AM - 10:30 AM JST | 12:00 AM - 1:30 AM UTC | Ch.13 Zoom Room 13

[A-HW21] Interdisciplinary approach to support climate change adaptation measures in regional scale

convener:TEBAKARI TAICHI(Toyama Prefectural University), Sompratana Ritphring(Kasetsart University), Masashi Kiguchi(University of Tokyo), weerakaset Suanpaga(Associate professor in Civil Engineering,Kasetsart University), Chairperson:TEBAKARI TAICHI(Toyama Prefectural University), Masashi Kiguchi(University of Tokyo)

9:00 AM - 9:15 AM JST | 12:00 AM - 12:15 AM UTC

[AHW21-01] ADAP-T for water-related adaptation to climate change and supporting its policy making

★Invited Papers

*Taikan Oki[1], Thanya Kiatiwat[2], Hiroaki Shirakawa[3], Weerakaset Suanpaga[2], Taichi Tebakari[4], Sompratana Ritphring[2], Masashi Kiguchi[5], Kyoko Matsumoto[4] (1.Graduate School of Engineering, The University of Tokyo, 2.Faculty of Engineering, Kasetsart University, 3.Granduate School of Environmental Studies, Nagoya University, 4.Department of Civil and Environmental Engineering, Toyama Prefectural University, 5.Institute of Industrial Science, The University of Tokyo)

9:15 AM - 9:30 AM JST | 12:15 AM - 12:30 AM UTC

[AHW21-02] The GEWEX Regional Hydroclimate Projects in High Mountainous Terrain in Asia

★Invited Papers

*Petrus J van Oevelen[1] (1.George Mason University)

9:30 AM - 9:45 AM JST | 12:30 AM - 12:45 AM UTC

[AHW21-03] **Effectiveness of Flood Diversion Canals and Retention Ponds as Adaptation Strategies in the Upper Chao Phraya River Basin**

*Saritha Padiyedath Gopalan[1], Naota Hanasaki[1] (1.National Institute for Environmental Studies)

9:45 AM - 10:00 AM JST | 12:45 AM - 1:00 AM UTC

[AHW21-04] **The impact of sensible heat and latent heat on monsoon onset over Indochina peninsula**

Tomohito Yamada[1], Ryosuke Kato[1], *Sourabh Shrivastava[1] (1.Hokkaido University)

10:00 AM - 10:15 AM JST | 1:00 AM - 1:15 AM UTC

[AHW21-05] S2S prediction challenge with deep learning in Thailand

*Kiyoharu Hasegawa[1], Shinjiro Kanae[1] (1.Toyko Institute of Technology)

10:15 AM - 10:30 AM JST | 1:15 AM - 1:30 AM UTC

[AHW21-06] Local knowledge: A comprehensive agricultural system and incremental drought adaptation strategy for Javanese society

*Muhamad Khoiru Zaki[1], Keigo Noda[1], Kengo Ito[1], Komariah Komariah[2], Sumani Sumani[2] (1.Gifu University, 2.Sebelas Maret University)

[E] Oral | A (Atmospheric and Hydrospheric Sciences)：A-HW Hydrology & Water Environment

10:45 AM - 12:15 PM JST | 1:45 AM - 3:15 AM UTC | Ch.13 Zoom Room 13

[A-HW21] Interdisciplinary approach to support climate change adaptation measures in regional scale

convener:TEBAKARI TAICHI(Toyama Prefectural University), Sompratana Ritphring(Kasetsart University), Masashi Kiguchi(University of Tokyo), weerakaset Suanpaga(Associate professor in Civil Engineering,Kasetsart University), Chairperson:Masashi Kiguchi(University of Tokyo), TEBAKARI TAICHI(Toyama Prefectural University)

10:45 AM - 11:00 AM JST | 1:45 AM - 2:00 AM UTC

[AHW21-07] **Climate change effect the relationship between land-use and poverty in major cities of Thailand.**

★Invited Papers

*weerakaset Suanpaga[1], Shirakawa Hiroaki[2], Nichanun Trakulphudphong [3], Wuthiporn Klinhom[3], Krittanut Thumsatsarn[3] (1.Associate professor in Civil Engineering,Kasetsart University,Thailand, 2.Associate professor in Graduate School of Engineering,Nagoya University,Japan, 3.Bachelor degree student in Civil Engineering,Kasetsart University,Thailand)

11:00 AM - 11:15 AM JST | 2:00 AM - 2:15 AM UTC

[AHW21-08] **Local adaptation strategy to climate change considering local context in Thailand**

★Invited Papers

*Kyoko Matsumoto[1], Sompratana Ritphring[2], Masashi Kiguchi[3], Taichi Tebakari[1], Taikan Oki[4] (1.Department of Civil and Environmental Engineering, Toyama Prefectural University, 2.Faculty of Engineering, Kasetsart University, 3.Institute of Industrial Science, The University of Tokyo, 4.School of Engineering, The University of Tokyo)

11:15 AM - 11:30 AM JST | 2:15 AM - 2:30 AM UTC

[AHW21-09] **Beach Nourishment to Mitigate the Impact of Beach Erosion and Sea Level Rise, Thailand**

*Sompratana Ritphring[1], Keiko Udo[2] (1.Department of Water Resources Engineering, Kasetsart University, 2.International Research Institute of Disaster Science, Tohoku University)

11:30 AM - 11:45 AM JST | 2:30 AM - 2:45 AM UTC

[AHW21-10] **Valuation of Sandy Beach Tourism Benefit with Respect to Hotel Room Rates by Using a Spatial Hedonic Model in Thailand**

*Chatuphorn Somphong[1], Keiko Udo[1], Sompratana Ritphring[2], Hiroaki Shirakawa[3] (1.International Research Institute of Disaster Science, Tohoku University, Japan, 2.Department of Water Resources Engineering, Kasetsart University, Thailand, 3.Graduate School of Environmental Studies, Nagoya University, Japan)

11:45 AM - 12:00 PM JST | 2:45 AM - 3:00 AM UTC

[AHW21-11] Impacts of urban flood and adapataion on traffic flow in Bangkok

*Shinichiro NAKAMURA[1], Horoyoshi Morita[4], Tsuyoshi Takano[4], Varameth Vichiensan[2], Sanit Wongsa[3], Napaporn Piamsa-nga[2] (1.Nagoya University, 2.Kasetsaet University, 3.King Mongkut's University of Technology Thonburi, 4.Nippon Engineering Consultants Co., Lld)

12:00 PM - 12:15 PM JST | 3:00 AM - 3:15 AM UTC

[AHW21-12] Effectiveness of crop calendar shift as an adaptation measure for climate change - Case study for rice production in Hokkaido, Japan

*Kenji Tanaka[1], Tomoki Yamada[2], Shigenobu Tanaka[1] (1.Disaster Prevention Research Institute, Kyoto University, 2.Faculty of Engineering, Kyoto University)

[E] Poster | A (Atmospheric and Hydrospheric Sciences)：A-HW Hydrology & Water Environment

5:15 PM - 6:30 PM JST | 8:15 AM - 9:30 AM UTC | Ch.07_2

[A-HW21] Interdisciplinary approach to support climate change adaptation measures in regional scale

convener:TEBAKARI TAICHI(Toyama Prefectural University), Sompratana Ritphring(Kasetsart University), Masashi Kiguchi(University of Tokyo), weerakaset Suanpaga(Associate professor in Civil Engineering,Kasetsart University)

[AHW21-P01] Attempt to separate factors to reduce locality of precipitation-elevation dependence in Japan

*Mayu Otsuki[1], Atsushi Higuchi[2], Hitoshi Hirose[3] (1.Chiba University, 2.Center for Environmental Remote Sensing Chiba University, 3.Japan Aerospace Exploration Agency)

[AHW21-P02] Prediction process in the seasonal forecast model of monthly precipitation by global climate data using deep learning

*Shingo Zenkoji[1], TEBAKARI TAICHI[1], SAKAKIBARA KAZUTOSHI[1] (1.Toyama Prefecural University)

[AHW21-P03] Regional climate change impacts on groundwater level in the Kurobe River alluvial fan, Japan

*Takuya Matsuura[1], TEBAKARI TAICHI[1] (1.Toyama prefectural University)

[AHW21-P04] Atmosphericfronts of the rainy season in kyushu region using an objective method

*Maki Miyamoto[1], Tomohito Yamada[1] (1.Hokkaido University)

[AHW21-P05] Climate Change Impact on Salt Affected Soil in Northeast Thailand

*KOSHI YOSHIDA[1], Supranee SRITUMBOON[2], Mallika SRISUTHAM[3], KOKI HOMMA[4], MASAYASU MAKI[5], KAZUO OKI[6] (1.The University of Tokyo, 2.Land Development Department, Thailand, 3.Khon Kaen University, Thailand, 4.Tohoku University, 5.Fukushima University, 6.Kyoto University of Advanced Science)

[AHW21-P06] Development of a numerical model to simulate the salinity distribution in the tidal area of the lower Chao Phraya Basin, Thailand

*Ryota Tsuji[1], TAICHI TEBAKARI[1], Keisuke Nakayama[2] (1.Toyama Prefectural University, 2.Kobe University)

[J] Poster | A (Atmospheric and Hydrospheric Sciences)：A-HW Hydrology & Water Environment

5:15 PM - 6:30 PM JST | 8:15 AM - 9:30 AM UTC | Ch.07_3

[A-HW24] Water Environment and Geology in Urban Areas

convener:Takeshi Hayashi(Faculty of Education and Human Studies, Akita University), Akinobu Miyakoshi(Geological Survey of Japan, AIST)

[AHW24-P01] Variability of land-use in the catchments of spring water in the western marginal area of Kanto Plain

*Takeshi Hayashi[1], Masaya Yasuhara[2], Takashi Nakamura[3] (1.Faculty of Education and Human Studies, Akita University, 2.Department of Environment Systems, Rissho University, 3.ICRE, University of Yamanashi)

[AHW24-P02] Evaluation of subsurface warming in the Tokyo metropolitan area, Japan: Effective application of groundwater observation wells for subsurface temperature monitoring

*Akinobu Miyakoshi[1], Takeshi Hayashi[2], Hideki Hamamoto[3], Shoichi Hachinohe[3] (1.Geological Survey of Japan, AIST, 2.Faculty of Education and Human Studies, Akita University, 3.Center for Environmental Science in Saitama)

[AHW24-P03] Demonstration of Ground Source Heat Pump systems and variations of the subsurface temperatures in Saitama Prefecture

*Hideki Hamamoto[1], Hidetaka Shiraishi[1], Masaki Nakayama[2], Shingo Uchiyama[2], Shuhei Ishiguro[3], Junya Takeshima[3] (1.Center for Environmental Science in Saitama, 2.Environmental Energy Division, Environment Department, Saitama Prefecture, 3.OYO Corporation)

[AHW24-P04] Examination of groundwater level measurement method by microtremor array exploration

*Yuji Miyashita[1], Hideki Hamamoto[2], Shigeki Senna[3] (1.Hot Springs Research Institute of Kanagawa Prefecture, 2.Center for Environmental Science in Saitama, 3.National Research Institute for Earth Science and Disaster Resilience)

[E] Oral | A (Atmospheric and Hydrospheric Sciences)：A-CG Complex & General

10:45 AM - 12:15 PM JST | 1:45 AM - 3:15 AM UTC | Ch.07 Zoom Room 07

[A-CG30] Multi-scale ocean-atmosphere interaction in the tropics

convener:Hiroki Tokinaga(Research Institute for Applied Mechanics, Kyushu University), Yu Kosaka(Research Center for Advanced Science and Technology, University of Tokyo), Ayako Seiki(Japan Agency for Marine-Earth Science and Technology), Tomoki Tozuka(Department of Earth and Planetary Science, Graduate School of Science, The University of Tokyo), Chairperson:Yu Kosaka(Research Center for Advanced Science and Technology, University of Tokyo), Ayako Seiki(Japan Agency for Marine-Earth Science and Technology)

10:45 AM - 11:00 AM JST | 1:45 AM - 2:00 AM UTC

[ACG30-01] The impact of North Pacific climate variability on historical ENSO and its mechanisms

★Invited Papers

*Dillon J Amaya[1,2], Yu Kosaka[3], Wenyu Zhou[4], Yu Zhang[5], Shang-Ping Xie[6], Arthur J Miller[6] (1.Cooperative Institute for Research in Environmental Sciences, 2.University of Colorado Boulder, 3.University of Tokyo, 4.Pacific Northwest National Laboratory, 5.Ocean University of China, 6.Scripps Institution of Oceanography)

11:00 AM - 11:15 AM JST | 2:00 AM - 2:15 AM UTC

[ACG30-02] Radiative impacts of low clouds on the subtropical North Pacific climate

*Ayumu Miyamoto[1], Hisashi Nakamura[1], Takafumi Miyasaka[2], Yu Kosaka[1], Shang-Ping Xie[3] (1.Research Center for Advanced Science and Technology,The University of Tokyo, 2.Japan Meteorological Business Support Center, 3.Scripps Institution of Oceanography, University of California San Diego)

11:15 AM - 11:30 AM JST | 2:15 AM - 2:30 AM UTC

[ACG30-03] Disparate Midlatitude Responses to El Niño/Southern Oscillation

*Shiozaki Masahiro[1], Takeshi Enomoto[2,3], Takaya Koutarou[4] (1.Research Institute for applied mechanics, Kyushu University, 2.Disaster Prevention Research Institute, Kyoto University, 3.Application Laboratory, Japan Agency for Marine-Earth Science and Technology, 4.Kyoto Sangyo University)

11:30 AM - 11:45 AM JST | 2:30 AM - 2:45 AM UTC

[ACG30-04] Formation of Barrier Layers and Temperature Inversions in the Eastern Tropical Pacific Detected by Mooring Observation

*Shota Katsura[1], Janet Sprintall[1], Thomas Farrar[2], Dongxiao Zhang[3,4], Meghan Cronin[3] (1.Scripps Institution of Oceanography, University of California, San Diego, 2.Department of Physical Oceanography, Woods Hole Oceanographic Institution, 3.NOAA Pacific Marine Environmental Laboratory, 4.Cooperative Institute for Climate, Ocean, and Ecosystem Studies, University of Washington)

11:45 AM - 12:00 PM JST | 2:45 AM - 3:00 AM UTC

[ACG30-05] The intraseasonal relationship between the boreal summer intraseasonal oscillation and the Pacific-Japan pattern

*Ayako Seiki[1], Yu Kosaka[2], Satoru Yokoi[1] (1.Japan Agency for Marine-Earth Science and Technology, 2.The University of Tokyo)

12:00 PM - 12:15 PM JST | 3:00 AM - 3:15 AM UTC

[ACG30-06] Why does convection weaken over Sumatra Island in an active phase of the MJO?

*Ning Zhao[1], Peiming Wu[1], Miki Hattori[1] (1.JAMSTEC Japan Agency for Marine-Earth Science and Technology)

[E] Oral | A (Atmospheric and Hydrospheric Sciences)：A-CG Complex & General

1:45 PM - 3:15 PM JST | 4:45 AM - 6:15 AM UTC | Ch.07 Zoom Room 07

[A-CG30] Multi-scale ocean-atmosphere interaction in the tropics

convener:Hiroki Tokinaga(Research Institute for Applied Mechanics, Kyushu University), Yu Kosaka(Research Center for Advanced Science and Technology, University of Tokyo), Ayako Seiki(Japan Agency for Marine-Earth Science and Technology), Tomoki Tozuka(Department of Earth and Planetary Science, Graduate School of Science, The University of Tokyo), Chairperson:Hiroki Tokinaga(Research Institute for Applied Mechanics, Kyushu University), Tomoki Tozuka(Department of Earth and Planetary Science, Graduate School of Science, The University of Tokyo)

1:45 PM - 2:00 PM JST | 4:45 AM - 5:00 AM UTC

[ACG30-07] Understanding tropical interbasin interaction using linear inverse modelling

*Shoichiro Kido[1], Ingo Richter[1], Tomoki Tozuka[2,1], Ping Chang[3] (1.JAMSTEC Application Lab, 2.Department of Earth and Planetary Science, University of Tokyo, 3.Texas A&M University)

2:00 PM - 2:15 PM JST | 5:00 AM - 5:15 AM UTC

[ACG30-08] **An assessment of the tropical Atlantic influence on El Niño-Southern Oscillation**

*Ingo Richter[1], Hiroki Tokinaga[2], Yu Kosaka[3], Takeshi Doi[1], Takahito Kataoka[1] (1.Japan Agency for Marine-Earth Science and Technology, Yokohama, Japan, 2.Kyushu University, Kasuga, Japan, 3.University of Tokyo, Tokyo, Japan)

2:15 PM - 2:30 PM JST | 5:15 AM - 5:30 AM UTC

[ACG30-09] **The roles of diabatic heating for the seasonality of the Atlantic Niño**

★Invited Papers

*Hyacinth C. Nnamchi[1], Mojib Latif[1], Noel S. Keenlyside[2,3], Joakim Kjellsson[1], Ingo Richter[4] (1.GEOMAR Helmholtz Centre for Ocean Research Kiel, 2.Geophysical Institute, University of Bergen, and Bjerknes Centre for Climate Research, Bergen, Norway, 3.Nansen Environmental and Remote Sensing Center, Bergen, Norway, 4.Application Laboratory, Research Institute for Value-Added-Information Generation, Japan Agency for Marine-Earth Science and Technology, Yokohama, Japan)

2:30 PM - 2:45 PM JST | 5:30 AM - 5:45 AM UTC

[ACG30-10] Simulated thermocline tilt over the tropical Indian Ocean and its influence on future sea surface temperature variability

★Invited Papers

*Guojian Wang[1,2], Wenju Cai[1,2], Agus Santoso[1,3] (1.Center for Southern Hemisphere Oceans Research (CSHOR), CSIRO Oceans and Atmosphere, 2.Key Laboratory of Physical Oceanography–Institute for Advanced Ocean Studies, Ocean University of China and Qingdao National Laboratory for Marine Science and Technology, 3.The University of New South Wales)

2:45 PM - 3:00 PM JST | 5:45 AM - 6:00 AM UTC

[ACG30-11] Asymmetry in sea surface temperature anomalies and atmospheric teleconnection associated with the Indian Ocean Dipole

Mai Nakazato[1], Shoichiro Kido[2], *Tomoki Tozuka[1,2] (1.Department of Earth and Planetary Science, Graduate School of Science, The University of Tokyo, 2.Application Laboratory, Research Institute for Value-Added-Information Generation, Japan Agency for Marine-Earth Science and Technology)

3:00 PM - 3:15 PM JST | 6:00 AM - 6:15 AM UTC

[ACG30-12] Investigation of interannual variability in the tropical Indian Ocean based on the transfer routes of wave energy

*Zimeng Li[1], Hidenori AIKI[2] (1.Graduate school of environmental studies, Nagoya university, 2.Institute for Space-Earth Environmental Research)

[E] Poster | A (Atmospheric and Hydrospheric Sciences)：A-CG Complex & General

5:15 PM - 6:30 PM JST | 8:15 AM - 9:30 AM UTC | Ch.08_1

[A-CG30] Multi-scale ocean-atmosphere interaction in the tropics

convener:Hiroki Tokinaga(Research Institute for Applied Mechanics, Kyushu University), Yu Kosaka(Research Center for Advanced Science and Technology, University of Tokyo), Ayako Seiki(Japan Agency for Marine-Earth Science and Technology), Tomoki Tozuka(Department of Earth and Planetary Science, Graduate School of Science, The University of Tokyo)

[ACG30-P01] Evaluation of externally forced component on interannual-scale SST anomalies over the tropical Indo-Pacific Ocean

*Takuya Hasegawa[1,2], Yuma Miyaji[1], Youichi Tanimoto[1,3] (1.Hokkaido University, 2.Tohoku University, 3.JAMSTEC)

[ACG30-P02] Potential predictability of regional extreme events associated with large-scale teleconnection from the tropical ocean

*Yukiko Imada[1], Hiroaki Kawase[1] (1.Meteorological Research Institute, Japan Meteorological Agency)

[ACG30-P03] **External and Internal forcings of the Indian Ocean Dipole**

*Lianyi Zhang[1,2], Yan Du[1,2], Tomoki Tozuka[3] (1.South China Sea Institute of Oceanology, Chinese Academy of Sciences, 2.Southern Marine Science and Engineering Guangdong Laboratory, 3.Dept. of Earth and Planetary Science Graduate School of Science, Univ. of Tokyo)

[ACG30-P04] Variations of sea surface temperature and salinity using coral Sr/Ca and $\delta^{18}O$ in the Java Sea and the Lombok Strait.

*Ai Genda[1], Ali Arman[2], Minoru Ikehara[3], Atsushi Suzuki[4], Mayuri Inoue[1] (1.Graduate School of National Science and Technology, Okayama University, 2.National Nuclear Energy Agency of Indonesia (BATAN), 3.Center of Advanced Marine Core Research, Kochi University, 4.Geological Survey of Japan, National Institute of Advanced Industrial Science and Technology)

[E] Oral | A (Atmospheric and Hydrospheric Sciences)：A-CG Complex & General

9:00 AM - 10:30 AM JST | 12:00 AM - 1:30 AM UTC | Ch.08 Zoom Room 08

[A-CG34] Global Carbon Cycle Observation and Analysis

convener:Kazuhito Ichii(Chiba University), Prabir Patra(Research Institute for Global Change, JAMSTEC), Akihiko Ito(National Institute for Environmental Studies), Chairperson:Prabir Patra(Research Institute for Global Change, JAMSTEC), Kazuhito Ichii(Chiba University)

9:00 AM - 9:15 AM JST | 12:00 AM - 12:15 AM UTC

[ACG34-01] Atmospheric inversions of greenhouse gas fluxes: A story of uneven development

★Invited Papers

*Peter J Rayner[1] (1.University of Melbourne)

9:15 AM - 9:30 AM JST | 12:15 AM - 12:30 AM UTC

[ACG34-02] **Decadal variability in land and ocean carbon fluxes by inverse modelling of atmospheric CO_2**

★Invited Papers

*Naveen Chandra[1,2], Prabir Patra[2] (1.National Institute for Environmental Studies, Japan, 2.Japan Agency for Marine-Earth Science and Technology)

9:30 AM - 9:45 AM JST | 12:30 AM - 12:45 AM UTC

[ACG34-03] **Changes in the atmospheric CO_2/CH_4 variability in the East Asian outflow region caused by plummet of fossil fuel-derived CO_2 in China due to COVID-19 outbreak**

*Yasunori Tohjima[1], Prabir Patra[2], Yosuke Niwa[1], Hitoshi Mukai[1], Motoki Sasakawa[1], Toshinobu Machida[1], Shin-ichiro Nakaoka[1] (1.National Institute for Environmental Studies, 2.Japan Agency for Marine-Earth Science and Technology)

9:45 AM - 10:00 AM JST | 12:45 AM - 1:00 AM UTC

[ACG34-04] Impact of anomalous high temperature anomaly in the 2020 spring-summer on terrestrial environment across Siberia

*Kazuhito Ichii[1], Riku Kawase[1], Yuhei Yamamoto[1], Shunji Kotsuki[1] (1.Chiba University)

10:00 AM - 10:15 AM JST | 1:00 AM - 1:15 AM UTC

[ACG34-05] CH_4 surface flux estimation based on local ensemble transform Kalman filter

*Jagat Bisht[1], Prabir Patra[1,2], Masayuki Takigawa[1], Takashi Sekiya[1], Yugo Kanaya[1], Naoko Saito[2] (1.Japan Agency for Marine-Earth Science and Technology , 2.Center for Environ. Remote Sensing, Chiba University)

10:15 AM - 10:30 AM JST | 1:15 AM - 1:30 AM UTC

[ACG34-06] Toward multi-scale greenhouse gas monitoring system for supporting global stock take

*Akihiko Ito[1,2], Yosuke Niwa[1], Tomohiro Hajima[2], Nobuko Saigusa[1] (1.National Institute for Environmental Studies, 2.Japan Agency for Marine-Earth Science and Technology)

[E] Oral | A (Atmospheric and Hydrospheric Sciences)：A-CG Complex & General

10:45 AM - 12:15 PM JST | 1:45 AM - 3:15 AM UTC | Ch.08 Zoom Room 08

[A-CG34] Global Carbon Cycle Observation and Analysis

convener:Kazuhito Ichii(Chiba University), Prabir Patra(Research Institute for Global Change, JAMSTEC), Akihiko Ito(National Institute for Environmental Studies), Chairperson:Kazuhito Ichii(Chiba University), Akihiko Ito(National Institute for Environmental Studies)

10:45 AM - 11:00 AM JST | 1:45 AM - 2:00 AM UTC

[ACG34-07] Co-evolution of carbon cycle and air quality fluxes constrained by CMS-Flux and MOMO-Chem assimilation systems

★Invited Papers

*Kevin W Bowman[1], Kazuyuki Miyazaki[1], Junjie Liu[1], Anthony Bloom[1] (1.Jet Propulsion Laboratory)

11:00 AM - 11:15 AM JST | 2:00 AM - 2:15 AM UTC

[ACG34-08] **Lower anthropogenic fossil CH_4 emissions inferred from multi-isotopic constraints on the global CH_4 budget**

★Invited Papers

*Ryo Fujita[1,2], Heather Graven[2] (1.Meteorological Research Institute, 2.Imperial College London)

11:15 AM - 11:30 AM JST | 2:15 AM - 2:30 AM UTC

[ACG34-09] The burned area extracting in Chernobyl Exclusion Zone using random forest

*JUN HU[1], Shunji Kotsuki[1], Yasunori IGARASHI[2], Mykola TALERKO[3], Kazuhito Ichii[1] (1.Center for Environmental Remote Sensing, Chiba University, Chiba, Japan, 2.Institute of Environmental Radioactivity, Fukushima University, Fukushima, Japan, 3.Institute for Safety Problems of Nuclear Power Plants, National Academy of Sciences of Ukraine, Kyiv, Ukraine)

11:30 AM - 11:45 AM JST | 2:30 AM - 2:45 AM UTC

[ACG34-10] Monitoring and evaluation of carbon absorption in pasture areas near Ulaanbaatar and far from cities

*Qinxue Wang[1], Tomohiro OKADERA[1], Masataka WATANABE[2], Ochirbat Batkhishig[3] (1.National Institute for Environmental Studies, 2.Research and Development Initiative, 3.Institute of Geography and Geoecology, Mongolian Academy of Sciences)

11:45 AM - 12:00 PM JST | 2:45 AM - 3:00 AM UTC

[ACG34-11] An observation-based reconstruction reveals progressive ocean acidification around Japan

*Yosuke Iida[1], Takashi Nakamura[1], Yoshikazu Fukuda[1], Masao Ishii[2] (1.Japan Meterological Agency, 2.Meteorological Research Institute)

12:00 PM - 12:15 PM JST | 3:00 AM - 3:15 AM UTC

[ACG34-12] Trend in Southern Ocean CO_2 sink – a review and outlook

*Prabir Patra[1], Naveen Chandra[2], Pedro S Monteiro[3], Masao Ishii[4] (1.Research Institute for Global Change, JAMSTEC, 2.National Institute for Environmental Studies, 3.CSIR-CHPC, South Africa, 4.Meteorological Research Institute)

[E] Poster | A (Atmospheric and Hydrospheric Sciences)：A-CG Complex & General

5:15 PM - 6:30 PM JST | 8:15 AM - 9:30 AM UTC | Ch.08_2

[A-CG34] Global Carbon Cycle Observation and Analysis

convener:Kazuhito Ichii(Chiba University), Prabir Patra(Research Institute for Global Change, JAMSTEC), Akihiko Ito(National Institute for Environmental Studies)

[ACG34-P01] Asian methane outflow captured by the CONTRAIL flask air samplings

*Yosuke Niwa[1,2], Toshinobu Machida[1], Taku Umezawa[1], Kazuhiro Tsuboi[2], Kentaro Ishijima[2], Ryo Fujita[2], Hidekazu Matsueda[3], Takuya Saito[1] (1.National Institute for Environmental Studies, 2.Meteorological Research Institute, 3.Dokkyo University)

[ACG34-P02] High-resolution mapping of anthropogenic CO_2 emissions in Japan

*Makoto Saito[1], Hiroko Yamada[1] (1.National Institute for Environmental Studies)

[ACG34-P03] Estimating solar-induced chlorophyll fluorescence using process-based ecosystem model VISIT-SIF

*Tatsuya Miyauchi[1], Makoto Saito[1], Hibiki M. Noda[1], Yukio Yoshida[1], Haruki Oshio[1], Akihiko Ito[1], Tsuneo Matsunaga[1] (1.National Institute for Environmental Studies)

[ACG34-P04] **Estimation of Aerosol Optical Characteristics of Wildfires in 2018 - 2020 with GCOM-C/SGLI**

*Kazuhisa Tanada[1], Hiroshi Murakami[1] (1.Earth Observation Research Center, Japan Aerospace Exploration Agency)

[ACG34-P05] **Satellite-data based monitoring of changes in the terrestrial carbon cycle in Mongolia: Synthesis analysis**

*ZAYA MART[1], Ichii Kazuhito [1], Tsolmon Renchin[2] (1.Chiba University , 2.National University of Mongolia)

[ACG34-P06] **Changes in terrestrial vegetation activities observed by satellite-based products across Eurasia**

*Da WANG[1], Kazuhito Ichii[1] (1.Chiba University)

[J] Oral | A (Atmospheric and Hydrospheric Sciences)：A-CG Complex & General

1:45 PM - 3:15 PM JST | 4:45 AM - 6:15 AM UTC | Ch.08 Zoom Room 08

[A-CG37] Biogeochemical cycles in Land Ecosystem

convener:Tomomichi Kato(Research Faculty of Agriculture, Hokkaido University), Kazuhito Ichii(Chiba University), Takeshi Ise(FSERC, Kyoto University), Munemasa Teramoto(Arid Land Research Center, Tottori University)

1:45 PM - 2:00 PM JST | 4:45 AM - 5:00 AM UTC

[ACG37-01] Temporal and spatial variation of soil CO_2/CH_4 fluxes in two cool-temperate forests in Japan

*Lifei Sun[1], Naishen Liang[1], Takashi Hirano[2], Yoshiyuki Takahashi [1], Munemasa Teramoto[3], Kentaro Takagi[2], Toshiaki Kondo[4], Jun Koarashi[5], Mariko Atarashi-Andoh[5], Reiko Ide[1], Xin Zhao[1], Sachinobu Ishida[6], Masahiro Takagi[7], Tomotsugu Yazaki[8] (1.National Institute for Environmental Studies Japan, 2.Hokkaido University, 3.Tottori University, 4.Japan International Research Center for Agricultural Sciences , 5.Japan Atomic Energy Agency , 6.Hirosaki University, 7.University of Miyazaki, 8.Meji University)

2:00 PM - 2:15 PM JST | 5:00 AM - 5:15 AM UTC

[ACG37-02] Decomposition of coarse woody debris produced through land conversion from a forest to an oil palm plantation

*Takashi Hirano[1], Shoko Murata[2], Guan Xhuan Wong[3], Joseph Wenceslaus Waili[3], Kim San Lo[3], Frankie Kiew[3], Edward Baran Aeries[3], Ryuichi Hirata[4], Tomohiro Shiraishi[4], Masato Hayashi[6], Masayuki Itoh[5], Lulie Melling[3] (1.Research Faculty of Agriculture, Hokkaido University, 2.Japan Science and Technology Agency, 3.Sarawak Tropical Peat Research Institute, 4.National Institute for Environmental Studies, 5.University of Hyogo, 6.Japan Aerospace Exploration Agency)

2:15 PM - 2:30 PM JST | 5:15 AM - 5:30 AM UTC

[ACG37-03] Anticipation of research development on the atmosphere-land interactions of the terrestrial nitrogen cycle

*Kentaro Hayashi[1] (1.Institute for Agro-Environmental Sciences, NARO)

2:30 PM - 2:45 PM JST | 5:30 AM - 5:45 AM UTC

[ACG37-04] Simulation of snow algal blooming in the global scale using a land surface model

*Yukihiko Onuma[1], Kei Yoshimura[1], Nozomu Takeuchi[2] (1.Institute of Industrial Science, The University of Tokyo, 2.Graduate School of Science, Chiba University)

2:45 PM - 3:00 PM JST | 5:45 AM - 6:00 AM UTC

[ACG37-05] Intercomparison of Data-Driven Estimation of Soil Respiration in Japan

*Hina Yamanuki[1], Kazuhito Ichii[1,2], Naishen Liang[2], Munemasa Teramoto[3], Yoshiyuki Takahashi[2], Jiye Zeng[2], Kentaro Takagi[4], Takashi Hirano[4], Sachinobu Ishida[5], Masahiro Takagi[6], Masaaki Naramoto[7], Kaneyuki Nakane[8], Toshiaki Kondo[9], Jun Koarashi[10], Mariko Atarashi-Andoh[10] (1.Center for Environmental Remote Sensing, Chiba University, 1-33 Yayoi-cho, Inage-ku, Chiba-shi, Chiba 263-8522, Japan, 2.Center for Global Environmental Research, National Institute for Environmental Studies, Tsukuba, Ibaraki 305- 8506, Japan, 3.Arid Land Research Center, Tottori University, 1390 Hamasaka, Tottori, Tottori 680-0001, Japan, 4.Hokkaido University, Kita 8, Nishi 5, Kita-ku, Sapporo, Hokkaido 060-0808, Japan, 5.Hirosaki University, 3 Bunkyo-cho, Hirosaki-shi, Aomori 036-8561, Japan, 6.University of Miyazaki, Gakuen-kibanadai-nishi-1-1, Miyazaki, Miyazaki 889-2192, Japan, 7.Shizuoka University, 836, Ohya, Suruga-ku, Shizuoka-Shi, Shizuoka 422-8529, Japan, 8.Hiroshima University, 1-3-2 Kagamiyama, Higashi-Hiroshima-Shi, Hiroshima 739-8511, Japan, 9.Japan International Research Center for Agricultural Sciences, 1-1 Ohwashi, Tsukuba, Ibaraki 305-8686, Japan, 10.Japan Atomic Energy Agency, 2-4 Shirakata, Tokai-mura, Naka-gun, Ibaraki 319-1195, Japan)

3:00 PM - 3:15 PM JST | 6:00 AM - 6:15 AM UTC

[ACG37-06] Overview of the Regional Carbon Budget Assessment and Processes (RECCAP2), and activities on Southeast Asia

*Masayuki Kondo[1] (1.Center for Global Environmental Research, National Institute for Environmental Studies)

[J] Oral | A (Atmospheric and Hydrospheric Sciences)：A-CG Complex & General

3:30 PM - 5:00 PM JST | 6:30 AM - 8:00 AM UTC | Ch.08 Zoom Room 08

[A-CG37] Biogeochemical cycles in Land Ecosystem

convener:Tomomichi Kato(Research Faculty of Agriculture, Hokkaido University), Kazuhito Ichii(Chiba University), Takeshi Ise(FSERC, Kyoto University), Munemasa Teramoto(Arid Land Research Center, Tottori University)

3:30 PM - 3:45 PM JST | 6:30 AM - 6:45 AM UTC

[ACG37-07] Influence of fire and drainage on evapotranspiration in a tropical ex-peat swamp forest

*Shinjiro Ohkubo[1], Takashi Hirano[1], Kitso Kusin[2] (1.National University Corporation, Hokkaido University, 2.University of Palangkaraya)

3:45 PM - 4:00 PM JST | 6:45 AM - 7:00 AM UTC

[ACG37-08] Ground-Based Measurement of Solar-Induced Chlorophyll Fluorescence in Wetland by High-Spectral Resolution

*Kitpanuwat TANATARAKEREE[1], Tomomichi Kato[2,3], Tomoki Morozumi[3], KANOKRAT BUAREAL[2], Masahito Ueyama[4], Naohisa Nakashima[3], Hideki Ninomiya[2], Lan Wu[5] (1.Graduate School of Agriculture, Hokkaido University, 2.Graduate School of Global Food Resources, Hokkaido University, 3.Research Faculty of Agriculture, Hokkaido University , 4.Graduate School of Life and Environmental Science, Osaka Prefecture University, 5.Hainan University)

4:00 PM - 4:15 PM JST | 7:00 AM - 7:15 AM UTC

[ACG37-09] Accounting for the emissions of tree stems in the methane budget of forests: upscaling chamber measurements to the stand

*Daniel EPRON[1], Ayaka Sakabe[1], Kenshi Takahashi[1], Takeshi Ise[1] (1.Kyoto University)

4:15 PM - 4:30 PM JST | 7:15 AM - 7:30 AM UTC

[ACG37-10] Estimation of non-photosynthetic vegetation amount in the northern Gobi Desert using MODIS satellite data

*Jing Wu[1], Yasunori Kurosaki[1], Gantsetseg Batdelger[2], Batjargal Buyantogtoh[1], Ishizuka Masahide[3], Thomas Sekiyama[4], Jiaqi Liu[1] (1. Arid Land Research Center, Tottori University, 2.Information and Research Institute of Meteorology, Hydrology and Environment, 3.Kagawa University, 4.Meteorological Research Institute)

4:30 PM - 4:45 PM JST | 7:30 AM - 7:45 AM UTC

[ACG37-11] **Mapping Peatland Fires in Indonesia Using a Drone Equipped with an Infrared Camera**

*Taishin Kameoka[1], Osamu Kozan[2,3] (1.Educational Unit for Studies on Connectivity of Hills, Humans and Oceans, Kyoto University, 2.Center for Southeast Asian Studies, Kyoto University, 3.Research Institute for Humanity and Nature)

4:45 PM - 5:00 PM JST | 7:45 AM - 8:00 AM UTC

[ACG37-12] Incorporating non-structural carbon dynamics in individual-based vegetation model SEIB-DGVM

*Hideki Ninomiya[1], Tomomichi Kato[1] (1.Hokkaido University)

[J] Poster | A (Atmospheric and Hydrospheric Sciences)：A-CG Complex & General

5:15 PM - 6:30 PM JST | 8:15 AM - 9:30 AM UTC | Ch.08_3

[A-CG37] Biogeochemical cycles in Land Ecosystem

convener:Tomomichi Kato(Research Faculty of Agriculture, Hokkaido University), Kazuhito Ichii(Chiba University), Takeshi Ise(FSERC, Kyoto University), Munemasa Teramoto(Arid Land Research Center, Tottori University)

[ACG37-P01] Change in soil respiration rate and soil organic matter for three years after clear-cutting in a *Cryptomeria japonica* plantation

*Yukiko Abe[1], Naishen Liang[2], Munemasa Teramoto[3], Takeshi Tange[1] (1.The University of Tokyo, 2.National Institute for Environmental Studies, 3.Tottori University)

[ACG37-P02] Continuous measurement of atmospheric methane mixing ratio at a cool-temperate deciduous forest site, Takayama, Japan

*Shohei Murayama[1], Shigeyuki Ishidoya[1], Tomoyuki Hori[1], Shinpei YOSHITAKE[2], Takahisa Maeda[1] (1.National Institute of Advanced Industrial Science and Technology, 2.Waseda University)

[ACG37-P03] Seasonal variation and controlling factors of stem methane emissions from *Alnus japonica* revealed by continuous measurements

*Ayaka Sakabe[1], Kenshi Takahashi[1], Wakana Azuma[2], Masayuki Itoh[3], Makiko Tateishi[1], Yoshiko Kosugi[1] (1.Kyoto University, 2.Kobe University, 3.University of Hyogo)

[ACG37-P04] **Spatio-temporal variation of soil respiration in coastal sand dunes and the mechanisms**

*Munemasa Teramoto[1], Toru Hamamoto[1], Naishen Liang[2], Takeshi Taniguchi[1], Takehiko Y. Ito[3], Richa Hu[4], Norikazu Yamanaka[1] (1.Arid Land Research Center, Tottori University, 2.Center for Global Environmental Research, National Institute for Environmental Studies, 3.International Platform for Dryland Research and Education, Tottori University, 4.The United Graduate School of Agricultural Sciences, Tottori University)

[ACG37-P05] Validation of Two Vegetation Indices: NDVI and PRI Derived from GCOM-C/SGLI

*Sasagawa Taiga[1], Tomoko Kawaguchi Akitsu[2], Kenlo Nishida Nasahara[2] (1.Graduate School of Science and Technology, University of Tsukuba, 2.Faculty of Life and Environmental Sciences, University of Tsukuba)

[ACG37-P06] **Seasonal variation in Solar Induced chlorophyll Fluorescence detected by multi-vertical layer spectroscopy in a canopy of cool-temperate deciduous broadleaf forest in Takayama, Gifu**

*Tomoki Morozumi[1], Tomomichi Kato[1], Katsuto Tsujimoto[2], KANOKRAT BUAREAL[3], Naohisa Nakashima[1], Yuma Sakai[4], Hideki Kobayashi[4], Kenlo Nasahara[5], Tomoko Akitsu[5], Shohei Murayama[6], Hibiki M Noda[7], Hiroyuki Muraoka[8] (1.Research Faculty of Agriculture, Hokkaido University, 2.Graduate School of Life Sciences, Tohoku University, 3.Graduate School of Global Food Resources, Hokkaido University, 4.Institute of Arctic Climate and Environment Research, Japan Agency for Marine-Earth Science and Technology, 5.Faculty of Life and Environmental Sciences, University of Tsukuba, 6.Environmental Management Research Institute, National Institute of Advanced Industrial Science and Technology, 7.Center for Global Environmental Research, National Institute for Environmental Studies, 8.River Basin Research Center, Gifu University)

[ACG37-P07] On the factors affecting reproducibility of GPP estimated by the Earth System Model MIROC-ES2L

*Akira Kurisu[1], Toru Nozawa[2], Manabu Abe[3], Tomohiro Hajima[3] (1.Faculty of Science, Okayama University, 2.Graduate School of Natural Science and Technology, Okayama University, 3.Japan Agency for Marine-Earth Science and Technology)

[ACG37-P08] Estimation of forest above ground biomass from PALSAR Data

*Hantao Li[1], Tomomichi Kato[2], Lan Wu[3], Masato Hayashi[4] (1.Graduate School of Agriculture, Hokkaido University, 2.Research Faculty of Agriculture, Hokkaido University, 3.College of Ecology and Environment, Hainan University, China, 4.Earth Observation Research Center, Japan Aerospace Exploration Agency)

[ACG37-P09] Development of process-based model for estimating wheat production MATCRO-Wheat

*Maki Nakaguki[1], Tomomichi Kato[2], Yuji Masutomi[3], Leilei Liu[4], Seiji Shimoda[5] (1.Hokkaido University, 2.Research Faculty of Agriculture, Hokkaido University, 3.National Institute for Environmental Studies, 4.National Engineering and Technology Center for Information Agriculture, Nanjing Agricultural University, 5.Hokkaido Agricultural Research Center, National Agriculture and Food Research Organization)

[J] Oral | H (Human Geosciences)：H-QR Quaternary research

9:00 AM - 10:30 AM JST | 12:00 AM - 1:30 AM UTC | Ch.16 Zoom Room 16

[H-QR04] Quaternary, Diachronic dynamics of human-environment interactions

convener:Mamoru Koarai(Earth Science course, College of Science, Ibaraki University), Yusuke Yokoyama(Atmosphere and Ocean Research Institute, University of Tokyo), Koji Okumura(Graduate School of Letters, Hiroshima University), Yasufumi Satoguchi(Lake Biwa Museum), Chairperson:Mamoru Koarai(Earth Science course, College of Science, Ibaraki University), Tsutomu Nakazawa(Geological Survey of Japan, AIST)

9:00 AM - 9:15 AM JST | 12:00 AM - 12:15 AM UTC

[HQR04-01] Distribution and classification of buried flat surfaces beneath the post-LGM deposits in central Tokyo

*Junko Komatsubara[1], Yoshinori Miyachi[1], Susumu Nonogaki[1], Toshio Nakayama[2] (1.National Institute of Advanced Industrial Science and Technology, 2.Civil Engineering Support and Training Center)

9:15 AM - 9:30 AM JST | 12:15 AM - 12:30 AM UTC

[HQR04-02] 240 ka Ata-Th tephra layer found in Tokyo and its geological significance

*Kunihiko Endo[1], Mari Sumita[2], Toshihiko Sugai[4], Hisashi Fujine[3], Masaaki Suzuki[5], Kyota Uemura[6], Yusuke Suginaka[7], Marie Noguchi[3], Shigeko Ishiwata[8], Reisuke Kondo[9], Takato Takemura[10] (1.Nihon University, 2.GEOMAR, 3.Paleo Labo, 4.Tokyo University , 5.Education Center of Bunkyo, 6.The Institute of Natural Sciences, College of Humanities and Sciences, Nihon University, 7.RCCM, 8.GaNT, 9.Atmosphere and Ocean Research Institute, The University of Tokyo, 10.Nihon University college of humanities and sciences)

9:30 AM - 9:45 AM JST | 12:30 AM - 12:45 AM UTC

[HQR04-03] Estimation of sedimentary condition in Kinu River and Kokai River lowland using micro tremor survey

*Mamoru Koarai[1], Kanaho Miki[1], Keiichi Takami[1], Shigeki Senna[2] (1.Earth Science course, College of Science, Ibaraki University, 2.National Research Insutitute of Earth Science and Disaster Resilience)

9:45 AM - 10:00 AM JST | 12:45 AM - 1:00 AM UTC

[HQR04-04] Ground-type classification based on Quaternary stratigraphy and sedimentary facies and the corresponding ground motion characteristics, with special reference to the 3D Urban Geological Map of Central Tokyo

★Invited Papers

*Tsutomu Nakazawa[1], Ikuo Cho[1], Junko Komatsubara[1], Tomonori Naya[1], Susumu Nonogaki[1], Yoshinori Miyachi[1], Masanori Ozaki[1], Kentaro Sakata[1], Hiroomi Nakazato[2], Takehiko Suzuki[3], Toshio Nakayama[4] (1.Geological Survey of Japan, AIST, 2.NIRE, NARO, 3.Tokyo Metropolitan University, 4.Civil Engineering Support and Training Center, Bureau of Construction, Tokyo Metropolitan Government)

10:00 AM - 10:15 AM JST | 1:00 AM - 1:15 AM UTC

[HQR04-05] Stratigraphic division, age and distribution pattern of the Middle to Upper Pleistocene Shimosa Group in central Tokyo area

*Tomonori Naya[1], Tsutomu Nakazawa[1], Susumu Nonogaki[1], Kentaro Sakata[1], Hiroomi Nakazato[2], Takehiko Suzuki[3], Toshio Nakayama[4] (1.Geological Survey of Japan, National Institute of Advanced Industrial Science and Technology, 2.Institute for Rural Engineering, NARO, 3.Tokyo Metropolitan University , 4.Civil Engineering Support and Training Center, Bureau of Construction, Tokyo Metropolitan Government)

10:15 AM - 10:30 AM JST | 1:15 AM - 1:30 AM UTC

[HQR04-06] Paleoenvironmental change in Paleo-Tokyo Bay during MIS 5e inferred from ostracode assemblages of the Pleistocene Kioroshi Formation, Shimosa Group, northern Chiba Prefecture, central Japan.

*Mai Harashima[1], Tsutomu Nakazawa[2], Hirokazu Ozawa[3], Minoru Kaneko, Hiroyuki Ishikawa, Masahiro Nomura[4], Sachiko Agematsu[1] (1.University of Tsukuba, 2.Geological Survey of Japan, AIST, 3.Nihon University, 4.Surugadai University)

[J] Oral | H (Human Geosciences)：H-QR Quaternary research

10:45 AM - 12:15 PM JST | 1:45 AM - 3:15 AM UTC | Ch.16 Zoom Room 16

[H-QR04] Quaternary, Diachronic dynamics of human-environment interactions

convener:Mamoru Koarai(Earth Science course, College of Science, Ibaraki University), Yusuke Yokoyama(Atmosphere and Ocean Research Institute, University of Tokyo), Koji Okumura(Graduate School of Letters, Hiroshima University), Yasufumi Satoguchi(Lake Biwa Museum), Chairperson:Koji Okumura(Graduate School of Letters, Hiroshima University), Yusuke Yokoyama(Atmosphere and Ocean Research Institute, University of Tokyo)

10:45 AM - 11:00 AM JST | 1:45 AM - 2:00 AM UTC

[HQR04-07] Middle Pleistocene terraces in the Chita Peninsula, near Nagoya, central Japan

*Taku Komatsubara[1], Misao Hongo[2], Yoshiki Sato[1] (1.Institute of Geology and Geoinformation, Advanced Industrial Science and Technology, 2.Alps Technical Research Laboratory Co., Ltd.)

11:00 AM - 11:15 AM JST | 2:00 AM - 2:15 AM UTC

[HQR04-08] **Unveiling the black box: monthly measurements on dissolved inorganic radiocarbon in Fuji Five lakes water to understand the lake specific reservoir ages**

*Ota Kosuke[1,2], Yusuke Yokoyama[1,2], Yosuke Miyairi[2], Shinya Yamamoto[3], Toshihiro Miyajima[2] (1.Earth and Planetary Science Department, Graduate school of Science, University of Tokyo, 2.Atmosphere and Ocean Research Institute, University of Tokyo, 3.Mount Fuji Research Institute, Yamanashi Prefectural Government)

11:15 AM - 11:30 AM JST | 2:15 AM - 2:30 AM UTC

[HQR04-09] Eventual sediments presumed in lake deposits of coastal lakes along the western coast of Kyushu Island, Japan

*Kaoru Kashima[1], Yu Fukumoto[2], Tsuyoshi Haraguchi[2] (1.Department of Earth and Planetary Sciences, Kyushu University, 2.Osaka City University)

11:30 AM - 11:45 AM JST | 2:30 AM - 2:45 AM UTC

[HQR04-10] Origin and evolution of a delta-margin mangrove in Can Gio, southern Vietnam

★Invited Papers

Daniel S Collins[1,6], Lap V Nguyen[2], Oanh TK Ta[2], Limi Mao[3], Yuji Ishii[1], Hiroyuki Kitagawa[4], Rei Nakashima[1], *Toru Tamura[1,5] (1.Geological Survey of Japan, AIST, 2.HCMC Institute of Resources Geography, Vietnamese Academy of Science and Technology, 3.Nanjing Institute of Geology and Palaeontology, Chinese Academy of Sciences, 4.Institute for Space-Earth Environmental Research, Nagoya University, 5.Graduate School of Frontier Science, The University of Tokyo, 6.Shell International Ltd)

11:45 AM - 12:15 PM JST | 2:45 AM - 3:15 AM UTC

[HQR04-11] Discussion

[J] Poster | H (Human Geosciences)：H-QR Quaternary research

5:15 PM - 6:30 PM JST | 8:15 AM - 9:30 AM UTC | Ch.09_1

[H-QR04] Quaternary, Diachronic dynamics of human-environment interactions

convener:Mamoru Koarai(Earth Science course, College of Science, Ibaraki University), Yusuke Yokoyama(Atmosphere and Ocean Research Institute, University of Tokyo), Koji Okumura(Graduate School of Letters, Hiroshima University), Yasufumi Satoguchi(Lake Biwa Museum)

[HQR04-P01] Formation age of mire on marine terraces in Nemuro Peninsula, Hokkaido, Japan

*Reisuke Kondo[1], Minoru Yokochi[2], Takashi Inoue[5], Kazuhiro Kaneko[4], Hiroko Fujita[3], Mari Sumita[6], Yosuke Miyairi[1], Yusuke Yokoyama[1] (1.Atmosphere and Ocean Research Institute, The University of Tokyo, 2.Graduate School of Global Food Resources, Hokkaido University, 3.The Field Science Center for Northern Biosphere, Hokkaido University, 4.Graduate School of Agriculture, Hokkaido University, 5.Research Faculty of Agriculture, Hokkaido University, 6.GEOMAR Helmholtz Centre for Ocean Research Kiel)

[HQR04-P02] **Changes in sedimentary environment during the Holocene in a wetland in Chanai area on Konsen plateau, eastern Hokkaido**

*Ren Tsuneoka[1], Yusuke Yokoyama[1], Reisuke Kondo[1], Kosuke Ota[1], Minoru Yokochi[2], Kazuhiro Kaneko[3], Hiroko Fujita[4], Takashi Inoue[5], Norio Kito[6], Mari Sumita[7], Kyota Uemura[8], Yosuke Miyairi[1], Arata Momohara[9] (1.Atmosphere and Ocean Research Institute, The University of Tokyo, 2.Graduate School of Global Food Resources, Hokkaido University, 3.Graduate School of Agriculture, Hokkaido University, 4.The Field Science Center for Northern Biosphere, Hokkaido University, 5.Research Faculty of Agriculture, Hokkaido University, 6.International and Regional Studies, Hokkaido University of Education, 7.GEOMAR Helmholtz Centre for Ocean Research Kiel, 8.College of Humanities and Sciences, Nihon University, 9.Faculty of Horticulture, Chiba University)

[HQR04-P03] Holocene coastal evolution and vertical deformation in the Hachinohe plain, NE Japan, inferred from sedimentary analyses

*Yuichi Niwa[1], Toshihiko Sugai[2] (1.Faculty of Science and Engineering, Chuo University, 2.Department of Natural Environmental Studies, Graduate School of Frontier Sciences, The University of Tokyo)

[HQR04-P04] Landform evolution and estimation of crustal movement since MIS 12 in the central-northern part of the Kanto Plain

*Tatsuki Miyamoto[1], Toshihiko Sugai[1], Yuichi Niwa[2], Toshimichi Nakanishi[3], Tetsuya Komatsu[4], Yuki Hiura[4] (1.Department of Natural Environmental Studies, Institute of Environmental Studies,Graduate School of Frontier Science, The University of Tokyo, 2.Chuo Univ., 3.Museum of Natural and Environmental History, Shizuoka, 4.JAEA)

[HQR04-P05] Rock surface dating of granodiorite cobbles obtained from fluvial terrace deposits in the Chichibu Basin, central Japan

*Yuji Ishii[1], Takayuki Takahashi[2], Kazumi Ito[1] (1.National Institute of Advanced Industrial Science and Technology, 2.Tohoku Univ.)

[HQR04-P06] Identification of reworked volcaniclastic deposits composing the upper Alluvium along the Moto-arakawa River, east part of the Saitama Prefecture, Central Japan

*Masanori Murata[1], Takayuki Takahashi[2], Kaori Aoki[1], Fumikatsu NISHIZAWA[3], Makoto Kobayashi[4], Takehiko Suzuki[1,5] (1.Research Center for Volcanic Hazards and Their Mitigation, Tokyo Metropolitan University, 2.International Research Institute of Disaster Science, Tohoku University, 3.Kanagawa Prefectural Museum of Natural History, 4.Mt. Fuji World Heritage Centre, Shizuoka, 5.Department of Geography, Tokyo Metropolitan University)

[HQR04-P07] Tephrostratigraphy during the past 30,000 years in the Jaishi Oike Moor, southern Izu Peninsula, Japan.

*Tatsuki Watanabe[1], Takehiko Suzuki[1], Daisuke Ishimura[1] (1.Department of Geography, Tokyo Metropolitan University)

[HQR04-P08] Landform evolution since the Middle Pleistocene estimated at the lower reaches of the Himekawa River, central Japan

*Jun Matsukaze[1], Masaaki Shirai[1] (1.Tokyo Metropolitan University)

[HQR04-P09] Radiocarbon dating using pollen fossils and its potential in Quaternary studies

*Keitaro Yamada[1], Takayuki Omori[2], Ikuko Kitaba[3], Takeshi Nakagawa[3] (1.Research Organization of Science and Technology, Ritsumeikan University, 2.The University Museum, The University of Tokyo, 3.Research Centre for

Palaeoclimatology, Ritsumeikan University)

[HQR04-P10] Identification of middle to late Pleistocene marine sediments inferred from electric conductivity analysis of the Bando observation well core in Tokushima Plain, western Japan

*Yoshiki Sato[1], Kiyohide Mizuno[1], Yuki Haneda[1], Koretaka Nakatani[1], Rei Nakashima[1] (1.Advanced Industrial Science and Technology, Geological Survey of Japan)

[E] Poster | H (Human Geosciences)：H-DS Disaster geosciences

5:15 PM - 6:30 PM JST | 8:15 AM - 9:30 AM UTC | Ch.10_1

[H-DS06] Natural hazard impacts on human society, economics, and technological systems

convener:ELENA PETROVA(Lomonosov Moscow State University, Faculty of Geography), Hajime Matsushima(Research Faculty of Agriculture, Hokkaido University)

[HDS06-P01] Introduction

[HDS06-P02] Effects of abandoned paddy field use for the conservation of threatened hydrophyte after the 2011 Tohoku-oki tsunami

★Invited Papers

*Korehisa Kaneko[1], Hiroshi Jinguji[2] (1.Hokuso Creature Association, 2.Fukushima University)

[HDS06-P03] Citizens' Awareness of Transmitting Information about Earthquake Experiences in the Areas Affected by the Great East Japan Earthquake: A Focus on the Use of Earthquake Ruins

*Ryo Nishisaka[1], Katsunori Furuya[1] (1.Chiba University)

[HDS06-P04] Location of the Visitor Centers of National Parks of Japan and their Adapt to Climate Change

*Satoshi Sasaki[1], Kiyotatsu Yamamoto[1], Kazuhiko W. Nakamura[1] (1.The University of Tokyo)

[HDS06-P05] **The Activity of Kamchatka Volcanoes and theirs Danger to Human Society**

*Olga Girina[1], Evgenii Loupian[2], Alexei Ozerov[1], Dmitry Melnikov[1], Alexander Manevich[1], Elena Petrova[3] (1.Institute of Volcanology and Seismology, Far East Division, Russian Academy of Sciences, Russia, 2.Space Research Institute, Russian Academy of Sciences, Russia, 3.Lomonosov Moscow State University, Geography Faculty, Russia)

[HDS06-P06] The impact of the reduction of beach width by seawall construction on the distribution of ground prowling insects

*Hinata Okoshi[1], Hajime Matsushima[1], Junjiro Negishi[2], Masahiro Ohara[3] (1.Graduate School of Agriculture, Hokkaido University, 2.Faculty of Environmental Earth Science, Hokkaido University, 3.The Hokkaido University Museum, Hokkaido University)

[HDS06-P07] Discussion

[J] Poster | H (Human Geosciences)：H-DS Disaster geosciences

5:15 PM - 6:30 PM JST | 8:15 AM - 9:30 AM UTC | Ch.10_2

[H-DS07] Seismic hazards on subduction earthquakes and active faults in the Central Japan

convener:Takashi Azuma(National Institute of Advanced Industrial Science and Technology), Yasuhiro Suzuki(Nagoya University)

[HDS07-P01] Issues for long-term evaluation of Byobu-yama/Ena-san fault zone

*Yasuhiro Suzuki[1] (1.Nagoya University)

[HDS07-P02] Paleoseismological trenching surveys on the Enasan-Sanageyamakita fault zone, Central Japan

*Takashi Azuma[1], Norio Shigematsu[1], Rei Nakashima[1], Ken-ichi Yasue[2], Ryo Tateishi[2], Daisuke Hirouchi[3] (1.National Institute of Advanced Industrial Science and Technology, 2.Toyama University, 3.Shinshu University)

[HDS07-P03] Questionnaire survey for experts on long-term evaluation of active faults and evaluation of ground motion (Part 1)

*Noa Mitsui[1], Takeshi Sagiya[1] (1.Disaster Mitigation Research Center, Nagoya University)

[J] Oral | H (Human Geosciences)：H-DS Disaster geosciences

1:45 PM - 3:15 PM JST | 4:45 AM - 6:15 AM UTC | Ch.16 Zoom Room 16

[H-DS10] Geohazards in humid, tectonically active countries and their precursors

convener:Satoru Kojima(Department of Civil Engineering, Gifu University), Taro Uchida(University of Tsukuba), Yoshihiko Kariya(Department of Environmental Geography, Senshu University), Chairperson:Yoshihiko Kariya(Department of Environmental Geography, Senshu University), Satoru Kojima(Department of Civil Engineering, Gifu University)

1:45 PM - 2:00 PM JST | 4:45 AM - 5:00 AM UTC

[HDS10-01] Weathering styles and landslide types of granite

*Masahiro Chigira[1], Yasuto Hirata[2] (1.Fukada Geological Institute, 2.Central Research Institute of Electric Power Industry)

2:00 PM - 2:15 PM JST | 5:00 AM - 5:15 AM UTC

[HDS10-02] Slope failures induced by the 2020 July heavy rain in the Chubu Region

*Hidehisa Nagata[1] (1.Fu-Sui-Do Company Limited)

2:15 PM - 2:30 PM JST | 5:15 AM - 5:30 AM UTC

[HDS10-03] **Landslides in humid-temperate mountainous areas in northwestern Vietnam perceived by satellite images**

*Takahisa Furuichi[1,2,3], Hiromu Daimaru[1], Wataru Murakami[1], Takashi Okamoto[1] (1.Forest and Forest Products Research Institute, 2.University of the Sunshine Coast, 3.Miyagi University of Education)

2:30 PM - 2:45 PM JST | 5:30 AM - 5:45 AM UTC

[HDS10-04] Estimation of subsurface structure in the linear depression spreading over the landslide crown

*Hikaru Osawa[1], Issei Doi[2], Noriyuki Arai[2], Yosuke Yamakawa[1], Takuma Watakabe[3] (1.Mountain Science Center, University of Tsukuba, 2.DPRI, Kyoto University, 3.Forestry and Forest Products Research Institute)

2:45 PM - 3:00 PM JST | 5:45 AM - 6:00 AM UTC

[HDS10-05] Study on the landslide mechanism of the Iya area where the deep-seated landslide occurred by Typhoon Talas in 2011 using Drone Airborne TEM

*Atsuhiko Kinoshita[1,2], Suguru Shibata[2], Takao Yamakoshi[1], Hiroaki Nakaya[1], Yasumasa Fujiwara[3], Hideki Nakano[3], Akira Jomori[4], Katsushi Kawato[5], Muneki Mitamura[6], Tamotsu Matsui[7] (1.National Institute for Land and Infrastructure Management, 2.Sediment Disaster Prevention Technology Center, 3.Eight-Japan Engineering Consultants Inc., 4.NEOSCIENCE CO.LTD., 5.NIPPON ENGINEERING CONSULTANTS CO.,LTD., 6.Osaka City University, 7.Osaka University)

3:00 PM - 3:15 PM JST | 6:00 AM - 6:15 AM UTC

[HDS10-06] Creating a Landslide risk map of the Nachi River basin

*Makoto Msatsuzawa[1], Tatsuya Ito[1], Chiyoshi Minami[1], Atsuhiko Kinoshita[2], Suguru Shibata[2], Taku Yamada[3], Toshiaki Kotake[3], Yasutaka Tanaka[4] (1.PACIFIC CONSULTANTS CO., LTD., 2. Sediment Disaster Prevention Technology Center, 3.Kiisankei sabo office, 4.HOKKAIDO UNIVERSITY)

[J] Oral | H (Human Geosciences)：H-DS Disaster geosciences

3:30 PM - 5:00 PM JST | 6:30 AM - 8:00 AM UTC | Ch.16 Zoom Room 16

[H-DS10] Geohazards in humid, tectonically active countries and their precursors

convener:Satoru Kojima(Department of Civil Engineering, Gifu University), Taro Uchida(University of Tsukuba), Yoshihiko Kariya(Department of Environmental Geography, Senshu University), Chairperson:Taro Uchida(University of Tsukuba), Satoru Kojima(Department of Civil Engineering, Gifu University)

3:30 PM - 3:50 PM JST | 6:30 AM - 6:50 AM UTC

[HDS10-07] Back analysis for landslide occurrence based on the relationship between the rain and the slope condition.

★Invited Papers

*Reiko AKIYAMA[1], Kuniaki MIYAMOTO[2] (1.Oriental Consultants Co., Ltd., 2.Nippon Koei Co., Ltd.)

3:50 PM - 4:05 PM JST | 6:50 AM - 7:05 AM UTC

[HDS10-08] Spatial Variability of Rainfall-runoff Characteristics in a Large-scale Landslide-prone Area Underlain by Accretionary Sedimentary Rocks

*Yosuke Yamakawa[1], Kouji Koshimizu[2], Taro Uchida[1] (1.Faculty of Life and Environmental Sciences, University of Tsukuba, 2.Graduate School of Science and Technology, University of Tsukuba)

4:05 PM - 4:20 PM JST | 7:05 AM - 7:20 AM UTC

[HDS10-09] Observation of an effect of interstitial water saturation and water quality on changes in formation resistivity

*Yamato SUZUKI[1], Hiroaki NAKAYA[1], Atsushi FUNAYAMA[2], Toshihiko SAKASHIMA[2], Koushiro TANAKA[2], Akira JOMORI[3], Tetsuya TOYAMA[3] (1.National Institute for Land and Infrastructure Management, 2.Pacific Consultants Co., Ltd., 3.Neo-science Co. Ltd.)

4:20 PM - 4:35 PM JST | 7:20 AM - 7:35 AM UTC

[HDS10-10] Valley floor environmental changes and disasters associated with glacial collapse of mountain glaciers
-A case study of the 2003, 04 and 2021 floods in the Himalayas -

*Jiro Komori[1] (1.Teikyo Heisei University)

4:35 PM - 4:50 PM JST | 7:35 AM - 7:50 AM UTC

[HDS10-11] Characteristics of slope disasters triggered by sudden topographic deformation in the Himalayan region

*Hiroshi YAGI[1], Daisuke Higaki[2], Ching-Ying Tsuo[3], Akihiko Wakai[4], Yusuke Yamamoto[5] (1.Faculty of Art, Science and Education, Yamagata University, 2.Nippon Koei Co.,Ltd., 3.Faculty of Agriculture and Life Science, Hirosaki University, 4.Graduate School of Polytechnics, Gunma University, 5.Geoscience Research Laboratory Co.,Ltd.)

4:50 PM - 5:00 PM JST | 7:50 AM - 8:00 AM UTC

[HDS10-12] Discussion

[J] Poster | H (Human Geosciences)：H-DS Disaster geosciences

5:15 PM - 6:30 PM JST | 8:15 AM - 9:30 AM UTC | Ch.10_3

[H-DS10] Geohazards in humid, tectonically active countries and their precursors

convener:Satoru Kojima(Department of Civil Engineering, Gifu University), Taro Uchida(University of Tsukuba), Yoshihiko Kariya(Department of Environmental Geography, Senshu University)

[HDS10-P01] Large-scale collapse of permafrost waste dump at Kumtor gold mine in Kyrgyz republic

*Ayano Aoki[1], Chiyuki Narama[1], Tsutomu Yamanokuchi[2], Murataly Duishonakunov[3] (1.Niigata university, 2.Remote Sensing Technology Center of Japan, 3.Kyrgyz National University)

[HDS10-P02] Relationship between landslide distribution and topographic feature and subsurface structure for the case of the 2018 Hokkaido Eastern Iburi Earthquake

*Junichiro Furuyama[1], Issei Doi[1], Toshitaka Kamai[1], Yuki Matsushi[1] (1.Kyoto University)

[HDS10-P03] Sediment movement on landslide slopes and river channel after the 2018 Hokkaido Eastern Iburi Earthquake

*Takashi Koi[1], Yasutaka Tanaka[1], Shin'ya Katsura[2], Norifumi Hotta[3] (1.Center for Natural Hazards Research, Hokkaido University, 2.Research Faculty of Agriculture, Hokkaido University, 3.Graduate School of Agricultural and Life Sciences, The University of Tokyo)

[HDS10-P04] Surface changes of Ganpei landslide in Joetsu region

*Yutaka Inoue[1], Chiyuki Narama[2], Chunxiang WANG[3], Eiji Takita[3] (1.Graduate Student,Niigata University, 2.Niigata University, 3.KITAK Corporation)

[HDS10-P05] **Surface changes of rock slopes in the Hakuba-Daisekkei Valley, northern Japanese Alps**

*Hirotaka Sugiyama[1], Chiyuki Narama[1], Hiroshi Inoue[2] (1.Niigata University, 2.NIED)

[HDS10-P06] Revisiting stratigraphy and age of so-called Otsukigawa debris avalanche deposits in the upper Otsukigawa and Yukawa Rivers on the eastern side of Yatsugatake Volcano in central Japan

*Takahiro Kurimoto[1], Yoshihiko Kariya[2] (1.Graduate School of Humanities, Senshu Univ., 2.Senshu Univ.)

[HDS10-P07] Relationship between a natural dam at the Yomogisawa River in the headwater area of the Abe River and the Oya-Kuzure rockslide with reference to new chronological information

*Keiju Kimura[1], Yoshihiko Kariya[2] (1.Graduate, Senshu Univ., 2.Senshu Univ.)

[HDS10-P08] Activities of landslides and their precursors: Case studies in Okutabora, Gujo, Gifu Prefecture and in Kuchisakamoto, Shizuoka Prefecture, central Japan

*Satoru Kojima[1], Kazuhide Sawada[1], Mizuki Tatekawa[1] (1.Department of Civil Engineering, Gifu University)

[E] Poster | H (Human Geosciences)：H-TT Technology & Techniques

5:15 PM - 6:30 PM JST | 8:15 AM - 9:30 AM UTC | Ch.11_1

[H-TT13] Environmental Remote Sensing

convener:Wei Yang(Chiba University), Akihiko Kondoh(Center for Environmental Remote Sensing, Chiba University)

[HTT13-P01] A study on the long-term dynamics and phenology of mangrove forests based on the narratives of inhabitants in western India using Landsat

*Kai Yamamoto[1], Nobuhito Ohte[1], Ranit Chatterjee[1], Kenlo Nasahara[2], Pankaj Joshi Sahjeevan[4], Lyla Mehta[3] (1.Graduate School of Informatics Kyoto University, 2.Faculty of Life and Environmental Sciences University of Tsukuba, 3. Institute of Development Studies, Brighton, United Kingdom, 4.Sahjeevan(NGO))

[HTT13-P02] **Mapping Paddy Rice Planting Areas on the Cloud: Is Spatio-Temporal Fusion Helpful or Not**

*Ziping Yang[1], Wei Yang[2], Akihiko Kondoh[2] (1.Graduate School of Science and Engineering, Chiba University, 2.Center of Environmental Remote Sensing, Chiba University)

[HTT13-P03] Removal of residual reflected skylight for accurate measurement of water-leaving reflectance

*Wei Yang[1], Bunkei Matsushita[2], Dalin Jiang[2] (1.Chiba University, 2.University of Tsukuba)

[HTT13-P04] Yield Estimation of Paddy Rice using High Spatial and Temporal Satellite Data in Indonesia

*Yuki Sofue[1], Chiharu Hongo[1], Naohiro Manago[1], Koki Homma[2], Gunardi Sigit[3], Budi Utoyo[4] (1.Chiba University, 2.Tohoku University, 3.West Java Food Crops and Horticultural Agency, 4.Bogor Agricultural University)

[HTT13-P05] **Random Forest for Estimating Soil Moisture Based on Remote Sensing Test**

*Jyun-Lin Chen[1], Hong-Ru Lin[1], Jet-Chau Wen[1] (1.National Yunlin University of Science and Technology)

[E] Oral | H (Human Geosciences)：H-TT Technology & Techniques

3:30 PM - 5:00 PM JST | 6:30 AM - 8:00 AM UTC | Ch.15 Zoom Room 15

[H-TT15] Non-destructive techniques applied to stone cultural heritage

convener:Celine Thomachot-Schneider(University of Reims-Champagne-Ardenne), Chiaki T. Oguchi(Institute for Environmental Science and Technology, Graduate School of Science and Engineering, Saitama University), Patricia vazquez(University of Reims Champagne Ardenne), Chairperson:Celine Thomachot-Schneider(University of Reims-Champagne-Ardenne), Patricia vazquez(University of Reims Champagne Ardenne)

3:30 PM - 3:45 PM JST | 6:30 AM - 6:45 AM UTC

[HTT15-01] Comparison of classic aging and realistic tests: study of the compatibility between limestones and restoration mortar

*Emilie Huby[1], Celine Thomachot-Schneider[1], Patricia vazquez[1], Gilles Fronteau[1] (1.Groupe d'etude des environnements naturels, anthropiques et archeologiques - Universite de Reims-Champagne-Ardenne (France))

3:45 PM - 4:00 PM JST | 6:45 AM - 7:00 AM UTC

[HTT15-02] Measurement of anisotropy of liquid water diffusivity of brittle tuff stone of Takase stone buddhas using X-ray

*Masaru Abuku[1], Shuya Hiranuma[2], Takayuki Fumoto[1], Soichiro Wakiya[3], Daisuke Ogura[4] (1.Kindai University, 2.SEKISUI HOUSE. LTD., 3.Nara National Research Institute for Cultural Properties, National Institutes for Cultural Heritage, 4.Kyoto University)

4:00 PM - 4:15 PM JST | 7:00 AM - 7:15 AM UTC

[HTT15-03] **Granite Characterisation of Three Asynchronous Quarries of the Archaeological Site of *Touças* (North of Portugal)**

*David Martin Freire-Lista[1,2], Patricia Vazquez[3], Gerardo Vidal Gonçalves[4] (1.Universidade de Tras-os-Montes e Alto Douro. Quinta de Prados. 5001-801 Vila Real, Portugal., 2.Centro de Geociências da Universidade de Coimbra. Rua Silvino Lima. Universidade de Coimbra - Polo II. 3030-790 Coimbra, Portugal., 3.Université Reims-Champagne-Ardenne 2, esplanade Roland Garros 51100 Reims, France. , 4.Centro de Investigação e Desenvolvimento em Ciências Humanas e Sociais. Universidade de Évora, Portugal.)

4:15 PM - 4:30 PM JST | 7:15 AM - 7:30 AM UTC

[HTT15-04] **Spatiotemporal evaluation of weathering-induced depressions in sandstone blocks by terrestrial laser scanning**

*Yuichi S. Hayakawa[1], Hisashi Aoki[2] (1.Faculty of Environmental Earth Science, Hokkaido University, 2.Faculty of Education, Tokyo Gakugei University)

4:30 PM - 4:45 PM JST | 7:30 AM - 7:45 AM UTC

[HTT15-05] From photogrammetric modelling of the built heritage to the evaluation of the durability of stones via GIS

*Sebastien LARATTE[1,2], Celine Thomachot-Schneider[1,2], Gilles FRONTEAU[1,2], Alexandra GUILLANEUF[1,2] (1.University of Reims-Champagne-Ardenne, 2.GEGENAA)

4:45 PM - 5:00 PM JST | 7:45 AM - 8:00 AM UTC

[HTT15-06] Discussion

[E] Poster | H (Human Geosciences)：H-TT Technology & Techniques

5:15 PM - 6:30 PM JST | 8:15 AM - 9:30 AM UTC | Ch.11_2

[H-TT15] Non-destructive techniques applied to stone cultural heritage

convener:Celine Thomachot-Schneider(University of Reims-Champagne-Ardenne), Chiaki T. Oguchi(Institute for Environmental Science and Technology, Graduate School of Science and Engineering, Saitama University), Patricia vazquez(University of Reims Champagne Ardenne)

[HTT15-P01] Ultrasonic velocity attempted to the various rocks - laboratory experiment and field measurement -

*Chiaki T. Oguchi[1], Keishin Takahashi[2], Sota Noshiro[2], Yukina Ikeda[1] (1.Institute for Environmental Science and Technology, Graduate School of Science and Engineering, Saitama University, 2.Faculty of civil Engineering, Saitama University)

[HTT15-P02] **Magnetic susceptibility of obsidian from Shirataki, Hokkaido, Japan, to identify the source of obsidian tools**

*Kyohei Sano[1] (1.Graduate School of Regional Resource Management, University of Hyogo)

[HTT15-P03] **Estimation of uniaxial compressive strength and water permeability from elastic waves measurements in sedimentary stones**

*David Benavente[1], Juan Jose Galiana-Merino [2], Concepcion Pla[3], Marli De Jongh[4], Noe Garcia-Martinez[1], Javier Martinez-Martinez[5] (1.Department of Earth and Environmental Sciences, University of Alicante, 2.Department of Physics, Systems Engineering and Signal Theory, University of Alicante, 3.Department of Civil Engineering, University of Alicante, 4.University of Glasgow, School of Geographical & Earth Sciences, 5.Spanish Geological Survey)

[HTT15-P04] **INFLUENCE OF POROSITY AND MINERALOGY ON INFRARED THERMOGRAPHY MEASUREMENTS**

*Patricia vazquez[1], Thomas Junique[1], Sesil Can[1], Lena Ageorges[1], Dania Benkara[1] (1.University of Reims Champagne Ardenne)

[J] Poster | H (Human Geosciences)：H-TT Technology & Techniques

5:15 PM - 6:30 PM JST | 8:15 AM - 9:30 AM UTC | Ch.11_3

[H-TT18] Environmental Remote Sensing

convener:Naoko Saitoh(Center for Environmental Remote Sensing), Hitoshi Irie(Center for Environmental Remote Sensing, Chiba University), Hiroto Shimazaki(National Institute of Technology, Kisarazu College), Teppei Ishiuchi(Miyagi University)

[HTT18-P01] Feasibility of observations of middle and upper tropospheric and lower stratospheric ozone concentrations by GOSAT/TANSO-FTS

*Eito Seki[1], Naoko Saitoh[1] (1.Center for Environmental Remote Sensing, Chiba University)

[HTT18-P02] Data quality of GOSAT-2/TANSO-FTS-2 GHG profile data retrieved from the V102.102 radiance spectra

*Naoko Saitoh[1], Ryoichi Imasu[2], kei Shiomi[3] (1.Center for Environmental Remote Sensing, Chiba University, 2.Atmosphere and Ocean Research Institute, The University of Tokyo, 3.Japan Aerospace Exploration Agency)

[HTT18-P03] Land use and land cover change of illegal settlements by landless peasants in the Brazilian Amazon

*Sayaka Yoshikawa[1,3], Kanae Ishimaru[2] (1.Ibaraki university , 2.Fukui Prefectural University, 3.Tokyo institute of technology)

[HTT18-P04] Evaluation of heterogeneity in growth of black pines planted for artificial coastal forests in the Sendai Plain

*Takuto Kajiwara[1], Masayuki Kawahigashi[2] (1.Graduate Student of Tokyo Metropolitan University, 2.Tokyo Metropolitan University)

[HTT18-P05] Accounting for atmospheric factors to estimate photosynthetically active radiation from surface solar irradiance

*YAJIE DAI[1], Hitoshi Irie[1], Alessandro Damiani[1] (1.chiba university)

[HTT18-P06] Data-assimilation-based Estimation of Infectivity Parameter of COVID-19 Epidemic Model and its Relation to NO2 satellite observation.

*Osamu Kabayama[1], Okazaki Atsushi[2], Shunji Kotsuki[1] (1.Centre for Environment Remote Sensing, Chiba University, 2.The Pennsylvania State University)

[HTT18-P07] Changes in the NO2 weekly cycle under COVID-19 pandemic

*Alessandro Damiani[1], Hitoshi Irie[1], Saito Hikaru[1], Ying Cai[1], Dmitry Belikov[1], Raul R. Cordero[2] (1.CEReS, Chiba University, 2.Santiago de Chile University)

[E] Poster | H (Human Geosciences)：H-CG Complex & General

5:15 PM - 6:30 PM JST | 8:15 AM - 9:30 AM UTC | Ch.12_1

[H-CG22] Nuclear Geoscience in Developing Countries

convener:Mohammad Rajib(Bangladesh Atomic Energy Commission)

[HCG22-P01] Radioactive waste disposal in Japan, especially focused on geological disposal of high-level radioactive waste

★Invited Papers

*Eiji Sasao[1] (1.Tono Geoscience Center, Japan Atomic Energy Agency)

[HCG22-P02] Effect of external radioactivity on the mineral grains from placer deposits of Bangladesh

*Mohammad Rajib[1,2,3], Mahmudul Hossain[1,4], Md. Fahad Hossain[1,5], Tumpa Saha[1,5] (1.Bangladesh Atomic Energy Commission, 2.Atomic Energy Research Establishment, 3.Institute of Nuclear Minerals, 4.Sterile Insect Technique Unit and INMAS, Cox's Bazar, 5.Beach Sand Minerals Exploitation Centre, Cox's Bazar)

[J] Oral | H (Human Geosciences)：H-CG Complex & General

9:00 AM - 10:30 AM JST | 12:00 AM - 1:30 AM UTC | Ch.17 Zoom Room 17

[H-CG23] Nuclear Energy and Geoscience

convener:Eiji Sasao(Tono Geoscience Center, Japan Atomic Energy Agency), Shinji Takeuchi(Department of Earth and Environmental Sciences, College of Humanities & Sciences, Nihon University), Takuma HASEGAWA(Central Research Institute of Electric Power Industry), Chairperson:Takuma HASEGAWA(Central Research Institute of Electric Power Industry)

9:00 AM - 9:15 AM JST | 12:00 AM - 12:15 AM UTC

[HCG23-01] Recent trends on long-term supply of uranium resources

*Eiji Sasao[1] (1.Tono Geoscience Center, Japan Atomic Energy Agency)

9:15 AM - 9:30 AM JST | 12:15 AM - 12:30 AM UTC

[HCG23-02] Geological Descriptive Model and AI Geo-Database of Coastal Area by Using Published data from National Public Research Institutes in Japan

*Atsunao Marui[1], Norikazu Imai[2], Teruhiko Suzuki[2], Akinari Honda[2] (1.Goelogical Survey of Japan, AIST, 2.GMLabo Co. LTD)

9:30 AM - 9:45 AM JST | 12:30 AM - 12:45 AM UTC

[HCG23-03] Attempt to identify the origin of deep-seated fluids in terms of hydrogeochemical characteristics

*Yuichi Tomioka[1], Hirofumi Kondo[1], Fumitake Kusuhara[1], Ayumi Sugiyama[1,2] (1.Central Research Institute of Electric Power Industry, 2.Asano Taiseikiso Engineering Co., Ltd.)

9:45 AM - 10:00 AM JST | 12:45 AM - 1:00 AM UTC

[HCG23-04] Characterization and Distribution of fractures in Granite, Ningyo-Toge, Okayama Pref., Japan

*Takesue Norito[1], Tsuyoshi Nohara[1] (1.Japan Atomic Energy Agency)

10:00 AM - 10:15 AM JST | 1:00 AM - 1:15 AM UTC

[HCG23-05] Study on the hydro-mechanical characterization of the calcareous concretion

*Shinji Takeuchi[1], Hidekazu Yoshida[2], Sachiko Nakamura[1] (1.Department of Earth and Environmental Sciences, College of Humanities & Sciences, Nihon University, 2.Nagoya University Museum)

10:15 AM - 10:30 AM JST | 1:15 AM - 1:30 AM UTC

[HCG23-06] Estimation of ^{137}Cs uptake from forest floor in Japanese cedar and Japanese konara oak stands of the Abukuma Mountains, Fukushima

*Tadafumi Niizato[1], Yoshito Sasaki[1], Satomi Ito[1], Takayoshi Watanabe[1], Hiroki Amamiya[2] (1.Japan Atomic Energy Agency, 2.QJ Science)

[J] Oral | H (Human Geosciences)：H-CG Complex & General

10:45 AM - 12:15 PM JST | 1:45 AM - 3:15 AM UTC | Ch.17 Zoom Room 17

[H-CG23] Nuclear Energy and Geoscience

convener:Eiji Sasao(Tono Geoscience Center, Japan Atomic Energy Agency), Shinji Takeuchi(Department of Earth and Environmental Sciences, College of Humanities & Sciences, Nihon University), Takuma HASEGAWA(Central Research Institute of Electric Power Industry), Chairperson:Shinji Takeuchi(Department of Earth and Environmental Sciences, College of Humanities & Sciences, Nihon University)

10:45 AM - 11:00 AM JST | 1:45 AM - 2:00 AM UTC

[HCG23-07] Relationship between velocities in a single fracture and retardation effects by sorption investigated with laboratory tracer experiments

*Shunichi Okamoto[1], Kotaro Nakata[1], Takuma Hasegawa[1], Yasuharu Tanaka[1] (1.Central Research Institute of Electric Power Industry)

11:00 AM - 11:15 AM JST | 2:00 AM - 2:15 AM UTC

[HCG23-08] Evaluation on isotope and component separation by diffusion experiment

*Takuma HASEGAWA[1], Kotaro NAKATA[1], Rhys Gwynne[2] (1.Central Research Institute of Electric Power Industry, 2.University of Waterloo)

11:15 AM - 11:30 AM JST | 2:15 AM - 2:30 AM UTC

[HCG23-09] A study of U(VI) sorption on illite under carbonate-rich environments: Batch experiments, TRLFS and modeling

*Huiyang Mei[1], Noboru Aoyagi[1], Takumi Saito[2], Naofumi Kozai[1], Yukio Tachi[3] (1.Advanced Science Research Center, Nuclear Science Research Institute, Japan Atomic Energy Agency, Ibaraki, 2-4 Shirakata, Tokai-mura, Ibaraki 319-1195, Japan, 2.Nuclear Professional School, School of Engineering, The University of Tokyo, 2-22 Shirakata Shirane, Tokai-mura, Ibaraki 319-1188, Japan, 3.Nuclear Fuel Cycle Engineering Laboratories, Japan Atomic Energy Agency, 4-33 Muramatsu, Tokai-mura, Ibaraki 319-1194, Japan)

11:30 AM - 11:45 AM JST | 2:30 AM - 2:45 AM UTC

[HCG23-10] **Immobilization of Iodide and Iodate in Layered Double Hydroxide, Magnesium oxide and Silver embedded into Metakaolin-Based Alkali Activated Materials**

*CHAERUN Raudhatul Islam[1], Manami ISHIMURA[1], Kanako TODA[1], Tsubasa OTAKE[1], Ryosuke KIKUCHI[1], John PROVIS[2], Yogarajah ELAKNESWARAN[1], Tsutomu SATO[1] (1.Hokkaido University, 2.The University of Sheffield)

11:45 AM - 12:00 PM JST | 2:45 AM - 3:00 AM UTC

[HCG23-11] **Evolution of reaction and alteration of mudstone with cement leachate: Flow experiments and reactive-transport modelling**

*Keith Bateman[1], Yuki Amano[1], Yukio Tachi[1] (1.Radionuclide Migration Research Group, Japan Atomic Energy Agency, 4-33 Muramatsu, Tokai-Mura, IBARAKI, 319-1194 Japan)

12:00 PM - 12:15 PM JST | 3:00 AM - 3:15 AM UTC

[HCG23-12] Discussion

[J] Poster | H (Human Geosciences)：H-CG Complex & General

5:15 PM - 6:30 PM JST | 8:15 AM - 9:30 AM UTC | Ch.12_2

[H-CG23] Nuclear Energy and Geoscience

convener:Eiji Sasao(Tono Geoscience Center, Japan Atomic Energy Agency), Shinji Takeuchi(Department of Earth and Environmental Sciences, College of Humanities & Sciences, Nihon University), Takuma HASEGAWA(Central Research Institute of Electric Power Industry)

[HCG23-P01] Modeling of Radial Dikes by Topographical Analysis using GIS for Quaternary Volcanoes

Yuki Hiura[1], *Makoto Kawamura[1], Umeda Koji[2], Masakazu Niwa[1] (1.Japan Atomic Energy Agency, 2.Hirosaki Univ.)

[HCG23-P02] Three-dimensional resistivity distribution by magnetotelluric survey to evaluate the distribution of fossil seawater

*Naomi Satoh[1], Akira Hayano[1], Minoru Teshima[2], Tateyuki Negi[2], Terumasa Yamane[3], Shinji Kawasaki[3] (1.Japan Atomic Energy Agency, 2.Nittetsu Mining Consultants Co., Ltd., 3.JGI, Inc.)

[HCG23-P03] Microbial community analysis of deep-seated fluids: Do microbes live in slab-derived fluid?

*Ayumi Sugiyama[1,2], Yuichi Tomioka[1], Shin-ichi Hirano[1], Tokihiro Kurita[1] (1.Central Research Institute of Electric Power Industry, 2.Asano Taiseikiso Engineering Co., Ltd.)

[HCG23-P04] Constructions of hydrogeological structure and mass transport model around hydraulic conductive fractures

*Ai Hamada[1], Kimio Miyakawa[1], Yasuharu Tanaka[1] (1.Central Research Institute of Electric Power Industry)

[HCG23-P05] Development of multi-scale modeling for estimation of inflow volume into tunnels of the geological disposal facility

*Naoki Katsumata[1], Satoru Suzuki[1], Hiromitsu Saegusa[1], Tatsuya Tanaka[2], Yoshito Kitagawa[1] (1.Nuclear Waste Management Organization of Japan, 2.OBAYASHI CORPORATION)

[HCG23-P06] Introduction of the “KiNa” international project of natural analogue studies of the long-term stability of bentonite

*Satoru Suzuki[1], Tsutomu Sato[2], Tsubasa Otake[2], Kikuchi Ryosuke[2], Fujimura Tatsuya[2], Takahiro Goto[1], Yusuke Ogawa[1], Patrik Sellin[3], Daniel Svensson[3], Albert H. Gilg[4], Ulf B. Andersson[5], Elizaveta Klein[6], Olivier X. Leupin[6], Simon Norris[9], Russell W. Alexander[10], Mehran Behazin[7], Nicolas Michau[8] (1.Nuclear Waste Management Organization of Japan , 2.Hokkaido University, 3.SKB, 4.TU Munich, 5.Luossavaara-Kiirunavaara AB, 6.Nagra, 7.NWMO, 8.ANDRA, 9.RWM, 10.Bedrock Geosciences)

[HCG23-P07] Interaction at the interface between compacted bentonite and carbon steel plate in artificial seawater

*Tatsuya Fujimura [1], Tsutomu Sato[2], Tsubasa Otake[2], Kikuchi Ryosuke[2], Satoru Suzuki[3], Takahiro Goto[3] (1.Graduate School of Engineering, Hokkaido University, 2.Faculty of Engineering, Hokkaido University, 3.Nuclear Waste Management Organization of Japan)

[J] Poster | H (Human Geosciences)：H-CG Complex & General

5:15 PM - 6:30 PM JST | 8:15 AM - 9:30 AM UTC | Ch.12_3

[H-CG24] Coastal wetlands: geomorphologic, biologic and anthropogenic processes

convener:Kiyoshi Fujimoto(Nanzan University)

[HCG24-P01] Mapping of mangrove species and communities using UAV photography and high-resolution satellite data to evaluate surface erosion induced by sea-level rise on Pohnpei Island, Micronesia

*Kiyoshi Fujimoto[1], Takeki Yaguchi[1], Yasumasa HIrata[2], Shin Watanabe[3], Kodai Hasada[4], Kenji Ono[2], Shingo Taniguchi[3], Keita Furukawa[5], Saimon Lihpai[6] (1.Nanzan University, 2.Forestry and Forest Products Research Institute, 3.University of the Ryukyus, 4.Hosei University, 5.Association for Shore Environment Creation , 6.Pohnpei State Government, FSM)

[HCG24-P02] **Consideration of sea level rise effect on sediment transport process in mangrove forest - preliminary attempt for long-term analysis-**

*Keita Furukawa[1,2], Kiyoshi Fujimoto[3], Kenji Ono[4], Shin Watanabe[5], Shingo Taniguchi[5], Yasumasa Hirata[4], Kodai Hasada[6], Renpei Suwa[7], Saimon Lihpai[8] (1.Association for Shore Environment Creation, 2.Ocean Policy Research Institute, Sasakawa Peace Foundation, 3.Nanzan University, 4.Forestry and Forest Products Research Institute, 5.Ryukyu University, 6.Hosei University, 7.Japan International Research Center for Agricultural Sciences, 8.Pohnpei State Government)

[HCG24-P03] Comparison of Fine Root Production among Several Types of Tropical Mangrove Stands in the Federated States of Micronesia using the Continuous Inflow Estimation Method

*Kenji Ono[1], Kiyoshi Fujimoto[2], Yasumasa Hirata[3], Ryuuichi Tabuchi[3], Shingo Taniguchi[4], Shin Watanabe[4], Keita Furukawa[5], Rempei Suwa[6], Saimon Lihpai[7] (1.Tohoku research center, Forestry and Forest Products Research Institute, 2.Nanzan Univ., 3.Forestry and Forest Products Research Institute, 4.Univ. of Ryukyu, 5.Association for Shore Enviromnent Creation, 6.Japan International Research Center for Agricultural Science, 7.Phonpei State Gov. FSM)

[J] Oral | H (Human Geosciences)：H-CG Complex & General

3:30 PM - 5:00 PM JST | 6:30 AM - 8:00 AM UTC | Ch.17 Zoom Room 17

[H-CG27] Nuclear Power and Geoscience in Japan: 10 years after the 3.11 complex disaster

convener:Daisuke Suetsugu(institute for Marine Geodynamics, Japan Agency for Marine-Earth Science and Technology), Kohta Juraku(Department of Humanities, Social and Health Sciences, School of Engineering, Tokyo Denki University), Satoshi Kaneshima(Department of Earth and Planetary Sciences, Kyushu University), Takeshi Sagiya(Disaster Mitigation Research Center, Nagoya University), Chairperson:Daisuke Suetsugu(institute for Marine Geodynamics, Japan Agency for Marine-Earth Science and Technology), Takeshi Sagiya(Disaster Mitigation Research Center, Nagoya University)

3:30 PM - 3:45 PM JST | 6:30 AM - 6:45 AM UTC

[HCG27-01] How was the long-term forecast of tsunami earthquake distorted?

★Invited Papers

*Kunihiko Shimazaki[1] (1.University of Tokyo)

3:45 PM - 4:00 PM JST | 6:45 AM - 7:00 AM UTC

[HCG27-02] Changes in the Treatment of Scientific Issues in Nuclear Power Plant Trials

★Invited Papers

*Kazuki Koketsu[1] (1.Earthquake Research Institute, University of Tokyo)

4:00 PM - 4:15 PM JST | 7:00 AM - 7:15 AM UTC

[HCG27-03] Human Capacity Building at The University of Tokyo towards Knowledge Base Development for Nuclear Risk Management

*Tatsuya Itoi[1], Naoto Sekimura[1], Tsuyoshi Takada[1,2], Takumi Saito[1], Kenji Satake[1] (1.The University of Tokyo, 2.Japan Atomic Energy Agency)

4:15 PM - 4:30 PM JST | 7:15 AM - 7:30 AM UTC

[HCG27-04] Scientific characteristics of high-level nuclear waste disposal site -Geological perspective at Suttsu and Kamoenai areas, Hokkaido -

★Invited Papers

*Satoshi Okamura[1] (1.Hokkaido Education University)

4:30 PM - 4:45 PM JST | 7:30 AM - 7:45 AM UTC

[HCG27-05] Selection of high-level radioactive waste disposal site in Japan

★Invited Papers

*Masahiro Chigira[1] (1.Fukada Geological Institute)

4:45 PM - 5:00 PM JST | 7:45 AM - 8:00 AM UTC

[HCG27-06] Discussion

*Daisuke Suetsugu[1] (1.institute for Marine Geodynamics, Japan Agency for Marine-Earth Science and Technology)

[J] Poster | H (Human Geosciences)：H-CG Complex & General

5:15 PM - 6:30 PM JST | 8:15 AM - 9:30 AM UTC | Ch.12_4

[H-CG27] Nuclear Power and Geoscience in Japan: 10 years after the 3.11 complex disaster

convener:Daisuke Suetsugu(institute for Marine Geodynamics, Japan Agency for Marine-Earth Science and Technology), Kohta Juraku(Department of Humanities, Social and Health Sciences, School of Engineering, Tokyo Denki University), Satoshi Kaneshima(Department of Earth and Planetary Sciences, Kyushu University), Takeshi Sagiya(Disaster Mitigation Research Center, Nagoya University)

[HCG27-P01] Nuclear Power and Geoscience in Japan

*Daisuke Suetsugu[1], Satoshi Kaneshima[2], Takeshi Sagiya[4], Kohta Juraku[3] (1.institute for Marine Geodynamics, Japan Agency for Marine-Earth Science and Technology, 2.Department of Earth and Planetary Sciences, Kyushu University, 3.Department of Humanities, Social and Health Sciences, School of Engineering, Tokyo Denki University, 4.Disaster Mitigation Research Center, Nagoya University)

[HCG27-P02] Model and “Unexpected”

*Manabu Hashimoto[1] (1.Disaster Prevention Research Institute, Kyoto University)

[HCG27-P03] Does science give us THE answer? (2) Issues centering on scientific advice

*Kohta Juraku[1] (1.Department of Humanities, Social and Health Sciences, School of Engineering, Tokyo Denki University)

[HCG27-P04] A personal summary of JPGU sessions about earth science and nuclear power plants in Japan

*Satoshi Kaneshima[1] (1.Department of Earth and Planetary Sciences, Kyushu University)

[HCG27-P05] Has the situation surrounding nuclear power generation and earth science changed during the last decade?

*Takeshi Sagiya[1] (1.Disaster Mitigation Research Center, Nagoya University)

[E] Poster | S (Solid Earth Sciences)：S-SS Seismology

5:15 PM - 6:30 PM JST | 8:15 AM - 9:30 AM UTC | Ch.13_1

[S-SS03] New insights in Earthquake predictability: modelling and forecasting

convener:Hiroshi Tsuruoka(Earthquake Research Institute, Tokyo Univ.), Jiancang Zhuang(Institute of Statistical Mathematics), Danijel Schorlemmer(GFZ German Research Centre for Geosciences), Naoshi Hirata(National Research Institute for Earth Science and Disaster Resilience)

[SSS03-P01] A spherical version of the space-time ETAS model

*Jiancang Zhuang[1], Ziyao Xiong[1], Yosihiko Ogata[1] (1.Institute of Statistical Mathematics)

[SSS03-P02] Nonstationary Renewal Model for Forecasting Repeating Earthquakes under Aftershock-Triggering Effects

*Shunichi Nomura[1], Masayuki Tanaka[2] (1.The Institute of Statistical Mathematics, 2.Meteorological Research Institute)

[SSS03-P03] Machine Learning Models for Earthquake Number Forecasting in the Kanto Region

*Hanyuan Huang[1], Hiroe Miyake[1], Hiroshi Tsuruoka[1] (1.Earthquake Research Institute, University of Tokyo)

[J] Oral | S (Solid Earth Sciences)：S-SS Seismology

9:00 AM - 10:30 AM JST | 12:00 AM - 1:30 AM UTC | Ch.18 Zoom Room 18

[S-SS09] Seismic wave propagation: Theory and Application

convener:Kaoru Sawazaki(National Research Institute for Earth Science and Disaster Resilience), Kiwamu Nishida(Earthquake Research Institute, University of Tokyo), Takao Nibe(JAPEX), Kyosuke Okamoto(National Institute of Advanced Industrial Science and Technology), Chairperson:Kaoru Sawazaki(National Research Institute for Earth Science and Disaster Resilience), Kurama Okubo(National Research Institute for Earth Science and Disaster Resilience)

9:00 AM - 9:15 AM JST | 12:00 AM - 12:15 AM UTC

[SSS09-01] **Estimation of the elastic wave velocity in rock fractures revealed by the digital rock physics and energy approach**

*Kazuki Sawayama[1], Osamu NISHIZAWA[2], Tatsunori Ikeda[3], Fei Jiang[4], Takeshi Tsuji[3], Yasuhiro Fujimitsu[3] (1.Department of Earth Resources Engineering, Graduate school of engineering, Kyushu University, 2.International Institute of Carbon Neutral Energy Research, Kyushu University, 3.Department of Earth Resources Engineering, Faculty of engineering, Kyushu University, 4.Department of Mechanical Engineering, Faculty of Engineering, Yamaguchi University)

9:15 AM - 9:30 AM JST | 12:15 AM - 12:30 AM UTC

[SSS09-02] SH-wave propagation through the random distribution of aligned line cracks

*Haruo Sato[1] (1.Tohoku Unvieristy)

9:30 AM - 9:45 AM JST | 12:30 AM - 12:45 AM UTC

[SSS09-03] **Continuous monitoring of seismic velocity change at Parkfield towards identifying the strain accumulation**

*Kurama Okubo[1,2], Brent Delbridge[2], Marine Denolle[3,2] (1.National Research Institute for Earth Science and Disaster Resilience, 2.Harvard University, 3.University of Washington)

9:45 AM - 10:00 AM JST | 12:45 AM - 1:00 AM UTC

[SSS09-04] Changes in attenuation and its anisotropy associated with seismic ground motion

*Shuhei Tsuji[1], Koshun Yamaoka[2], Ryoya Ikuta[3] (1.Graduate School of Environmental Studies, Nagoya University, 2.Earthquake and Volcano Research Center Graduate School of Environmental Studies, Nagoya University, 3.Department of Geosciences, Shizuoka University)

10:00 AM - 10:15 AM JST | 1:00 AM - 1:15 AM UTC

[SSS09-05] **Seismic velocity response to ground water level revealed by ACROSS and seismic array**

*hiromu oba[1], Ryoya Ikuta[1], Shuhei Tsuji[2], Chen Feng[2], Koshun Yamaoka[2], Toshiki Watanabe[2] (1.Shizuoka University, 2.Nagoya University)

10:15 AM - 10:30 AM JST | 1:15 AM - 1:30 AM UTC

[SSS09-06] On the relationship between the streamflow due to snowmelt flood and ambient seismic noise observed by Hi-net stations

*Kaoru Sawazaki[1], Shakti P.C.[1] (1.National Research Institute for Earth Science and Disaster Resilience)

[J] Oral | S (Solid Earth Sciences)：S-SS Seismology

10:45 AM - 12:15 PM JST | 1:45 AM - 3:15 AM UTC | Ch.18 Zoom Room 18

[S-SS09] Seismic wave propagation: Theory and Application

convener:Kaoru Sawazaki(National Research Institute for Earth Science and Disaster Resilience), Kiwamu Nishida(Earthquake Research Institute, University of Tokyo), Takao Nibe(JAPEX), Kyosuke Okamoto(National Institute of Advanced Industrial Science and Technology), Chairperson:Kyosuke Okamoto(National Institute of Advanced Industrial Science and Technology), Shunsuke Takemura(Earthquake Research Institute, the University of Tokyo)

10:45 AM - 11:00 AM JST | 1:45 AM - 2:00 AM UTC

[SSS09-07] Effects of subsurface heterogeneities and surface topography on long-period surface wave monitoring

*Shunsuke Takemura[1], Ryo Okuwaki[2], Takanori Matsuzawa[3] (1.Earthquake Research Institute, the University of Tokyo, 2.Moutain Science Center, Faculty of Life and Environmental Sciences, University of Tsukuba, 3.National Research Institute for Earth Science and Disaster Resilience)

11:00 AM - 11:30 AM JST | 2:00 AM - 2:30 AM UTC

[SSS09-08] Fracture detection and properties estimation using fiber optic sensors

★Invited Papers

*Keisuke Teranishi[1], Naoshi Aoki[1], Moeto Fujisawa[1], Hidehiko Shimizu[1], Shinya Onodera[2] (1.JGI, 2.JOGMEC)

11:30 AM - 11:45 AM JST | 2:30 AM - 2:45 AM UTC

[SSS09-09] Connection between the correlation of strain and rotation seismograms and Green's function: Surface-wave case

*Hisashi Nakahara[1] (1.Solid Earth Physics Laboratory, Department of Geophysics, Graduate School of Science, Tohoku University)

11:45 AM - 12:00 PM JST | 2:45 AM - 3:00 AM UTC

[SSS09-10] Ambient Noise Differential Adjoint Tomography Applied to a Linear Array in Los Angeles Basin

*Xin Liu[1,2], Gregory C Beroza[1] (1.Stanford Earth, 2.JAMSTEC)

12:00 PM - 12:15 PM JST | 3:00 AM - 3:15 AM UTC

[SSS09-11] Estimating finite fault slip distributions of large earthquakes based on time-reversal wave propagation simulation with data assimilation

*Yugo Shibata[1], Takashi Furumura[1], Takuto Maeda[2] (1.Earthquake Research Institute, the University of Tokyo, 2.Hirosaki University)

[J] Oral | S (Solid Earth Sciences)：S-SS Seismology

1:45 PM - 3:15 PM JST | 4:45 AM - 6:15 AM UTC | Ch.18 Zoom Room 18

[S-SS09] Seismic wave propagation: Theory and Application

convener:Kaoru Sawazaki(National Research Institute for Earth Science and Disaster Resilience), Kiwamu Nishida(Earthquake Research Institute, University of Tokyo), Takao Nibe(JAPEX), Kyosuke Okamoto(National Institute of Advanced Industrial Science and Technology), Chairperson:Kiwamu Nishida(Earthquake Research Institute, University of Tokyo), Takashi Hirose(National Research Institute for Earth Science and Disaster Resilience)

1:45 PM - 2:15 PM JST | 4:45 AM - 5:15 AM UTC

[SSS09-12] Imaging the solar interior using noise tomography

★Invited Papers

*Shravan Hanasoge[1] (1.Tata Institute of Fundamental Research)

2:15 PM - 2:30 PM JST | 5:15 AM - 5:30 AM UTC

[SSS09-13] Incorporating wind information in the inversion of co-located pressure and seismic data for shallow elastic structure

*Toshiro Tanimoto[1] (1.Department of Earth Science, University of California, Santa Barbara, CA93106, USA)

2:30 PM - 2:45 PM JST | 5:30 AM - 5:45 AM UTC

[SSS09-14] Study on Microseisms excited by Typhoons around Japan

*Hiroki Kawakami[1], Naoki Suda[1] (1.Hiroshima University)

2:45 PM - 3:00 PM JST | 5:45 AM - 6:00 AM UTC

[SSS09-15] Extraction of P-wave reflections of mantle discontinuities from ambient seismic noise beneath Japan

*Shota Kato[1], Kiwamu Nishida[1] (1.Earthquake Research Institute, the University of Tokyo)

3:00 PM - 3:15 PM JST | 6:00 AM - 6:15 AM UTC

[SSS09-16] A centroid catalog of P-wave microseisms

*Kiwamu Nishida[1], Ryota Takagi[2] (1.Earthquake Research Institute, University of Tokyo, 2.Research Center for Prediction of Earthquakes and Volcanic Eruptions, Graduate School of Science, Tohoku University)

[J] Poster | S (Solid Earth Sciences)：S-SS Seismology

5:15 PM - 6:30 PM JST | 8:15 AM - 9:30 AM UTC | Ch.13_2

[S-SS09] Seismic wave propagation: Theory and Application

convener:Kaoru Sawazaki(National Research Institute for Earth Science and Disaster Resilience), Kiwamu Nishida(Earthquake Research Institute, University of Tokyo), Takao Nibe(JAPEX), Kyosuke Okamoto(National Institute of Advanced Industrial Science and Technology)

[SSS09-P01] Temporal variation in seismic velocity at the shallow part of the overriding plate in the Japan Trench

*Takashi Tonegawa[1], Ryota Takagi[2], Kaoru Sawazaki[3], Katsuhiko Shiomi[3] (1.Japan Agency for Marine-Earth Science and Technology, 2.Tohoku University, 3.National Research Institute for Earth Science and Disaster Resilience)

[SSS09-P02] Estimation of instrumental clock errors at 46 active volcanoes in Japan based on seismic interferometry

*Takashi Hirose[1] (1.National Research Institute for Earth Science and Disaster Resilience)

[SSS09-P03] On the factors influencing ambient-noise passive seismic imaging

*Xin Guo[1], Zhihui Zou[1,2], Yongjun Rui[3], Qinghui Cui[3], Xinmin Shang[3] (1.College of Marine Geosciences, Key Lab of Submarine Geosciences and Prospecting Techniques. MOE, Ocean University of China, Qingdao 266100, China, 2.Evaluation and Detection Technology Laboratory of Marine Mineral Resources, Qingdao National Laboratory for Marine Science and Technology, Qingdao 266061, China, 3.Geophysical Research Institute of Shengli Oilfield, Sinopec, Dongying, China 257022)

[SSS09-P04] **Migration of fluid during oil recovery revealed by Reverse Time Imaging**

*Runbi Yuan[1], Zhihui Zou[2,1], Cui Qinghui[3], Rui Yongjun[3], Shang Xinmin[3] (1.College of Marine Geosciences, Key Lab of Submarine Geosciences and Prospecting Techniques. MOE, Ocean University of China, Qingdao 266100, China, 2.Evaluation and Detection Technology Laboratory of Marine Mineral Resources, Qingdao National Laboratory for Marine Science and Technology, Qingdao 266061, China, 3.Geophysical Research Institute of Shengli Oilfield, Sinopec, Dongying, China 257022)

[SSS09-P05] Effects of fine-scale heterogeneity distribution in the Pacific slab on the generation of anomalously large intensities from deep-focus earthquakes

*Takashi Furumura[1], Brian LN Kennett[2] (1.Earthquake Research Institute The University of Tokyo, 2.Research School of Earth Sciences The Australian National University)

[SSS09-P06] Scattering properties in Japanese volcanoes as inferred from the peak ratio analysis of teleseismic P waves using the JMA seismometer network data

*Gugi Aucklandi Ganefianto[1], Hisashi Nakahara[1], Takeshi Nishimura[1] (1.Tohoku University)

[SSS09-P07] Crack source and volcanic structural heterogeneity inferred from oscillatory waveforms of long-period seismic events: Application at Kusatsu-Shirane Volcano

*Nakano Masayuki[1], Hiroyuki Kumagai[1] (1.Nagoya University)

[SSS09-P08] Applying the shortest path method to anisotropic media in order to calculate ray paths

*Shoji Sekiguchi[1] (1.National Research Institute for Earth Science and Disaster Resilience)

[SSS09-P09] Numerical simulations of weak localization of scalar waves based on the finite difference method (2)

*Jun Kawahara[1], Masanobu Sato[1] (1.Graduate School of Science and Engineering, Ibaraki University)

[SSS09-P10] Observability of seismic radial anisotropy parameters by the analysis of surface waves and receiver functions based on the MCMC analysis

*Jumpei Maruyama[1], Hitoshi Kawakatsu[1], Nozomu Takeuchi[1] (1.University of Tokyo, Earthquake Research Institute)

[J] Oral | S (Solid Earth Sciences)：S-SS Seismology

3:30 PM - 5:00 PM JST | 6:30 AM - 8:00 AM UTC | Ch.18 Zoom Room 18

[S-SS11] Strong Ground Motion and Earthquake Disaster

convener:Kazuhiro Somei(Geo-Research Institute), Yasuhiro Matsumoto(Kozo Keikaku Engineering), Chairperson:Tomohisa Okazaki(RIKEN Center for Advanced Intelligence Project), Kentaro Emoto(Graduate School of Science, Tohokuk University)

3:30 PM - 3:45 PM JST | 6:30 AM - 6:45 AM UTC

[SSS11-01] High-density estimation of site amplification characteristics from DAS observation along Route 4

*Kentaro Emoto[1], Hisashi Nakahara[1], Takeshi Nishimura[1], Mare Yamamoto[1] (1.Graduate School of Science, Tohokuk University)

3:45 PM - 4:00 PM JST | 6:45 AM - 7:00 AM UTC

[SSS11-02] Long-term fluctuation of microtremor at a permanent observation site in Tottori University

*Takao Kagawa[1], Soma Nishigaki[1], Tatsuya Noguchi[1] (1.Tottori University, Faculty of Engineering)

4:00 PM - 4:15 PM JST | 7:00 AM - 7:15 AM UTC

[SSS11-03] Numerical elucidation of the Aso Caldera graben mechanism focusing on stratum irregularities, soft clay and two consecutive earthquakes

*Kentaro Nakai[1], Toshihiro Noda[2], Akira Asaoka[3], Shinya Fukuda[1] (1.Graduate School of Engineering, Nagoya University, 2.Disaster Mitigation Research Center, Nagoya University, 3.Association for The Development of Earthquake Prediction)

4:15 PM - 4:30 PM JST | 7:15 AM - 7:30 AM UTC

[SSS11-04] Estimation of site amplification and S-wave velocity structure in Kumamoto Prefecture based on spectral inversion analysis of strong motion records

*Tomomi IIDA[1], Hiroaki Yamanaka[1], Kosuke Chimoto[1], Daiki Shinoyama[2], Seiji Tsuno[3], Masahiro Korenaga[3], Nobuyuki Yamada[4], Hiroe Miyake[5], Tatsuo Kanno[6], Michiko Shigefuji[6], Masayuki Yoshimi[7], Shinichi Matsushima[8], Hiroshi Kawase[8], Kimiyuki Asano[8], Tomotaka Iwata[8] (1.Tokyo institute of Technology, 2.Central Research Institute of Electric Power Industry, 3.Railway Technical Research Institute, 4.Kochi University, 5.The University of Tokyo, 6. Kyushu University, 7.National Institute of Advanced Industrial Science and Technology, 8. Kyoto University)

4:30 PM - 4:45 PM JST | 7:30 AM - 7:45 AM UTC

[SSS11-05] Toward Development of Spectral Inversion Method Considering with Rupture Directivity

*Kazuhiro Somei[1,2], Kimiyuki Asano[3], Tomotaka Iwata[3] (1.Graduate School of Science, Kyoto University, 2.Geo-Research Institute, 3.Disaster Prevention Research Institute, Kyoto University)

4:45 PM - 5:00 PM JST | 7:45 AM - 8:00 AM UTC

[SSS11-06] **Broadband Ground Motion Synthesis Using Wasserstein Interpolation of Acceleration Envelopes**

*Tomohisa Okazaki[1], Hirotaka Hachiya[1,2], Asako Iwaki[3], Takahiro Maeda[3], Hiroyuki Fujiwara[3], Naonori Ueda[1] (1.RIKEN Center for Advanced Intelligence Project, 2.Wakayama University, 3.National Research Institute for Earth Science and Disaster Resilience)

[E] Oral | S (Solid Earth Sciences)：S-IT Science of the Earth's Interior & Techtonophysics

3:30 PM - 5:00 PM JST | 6:30 AM - 8:00 AM UTC | Ch.23 Zoom Room 23

[S-IT17] Property and role of liquids inside terrestrial planets

convener:Tatsuya Sakamaki(Department of Earth Science, Tohoku University), Yoichi Nakajima(Kumamoto University, Priority Organization for Innovation and Excellence), Chairperson:Tatsuya Sakamaki(Department of Earth Science, Tohoku University), Yoichi Nakajima(Kumamoto University, Priority Organization for Innovation and Excellence)

3:30 PM - 3:45 PM JST | 6:30 AM - 6:45 AM UTC

[SIT17-01] Pressure-induced structural change of basaltic glass up to 18 GPa

*Tomonori Ohashi[1], Tatsuya Sakamaki[1], Ken-ichi Funakoshi[2], Takanori Hattori[3], Naoki Hisano[1], Jun Abe[2], Akio Suzuki[1] (1.Department of Earth Science, Tohoku University, 2.Neutron Science and Technology Center, Comprehensive Research Organization for Science and Society (CROSS), 3.J-PARC Center, Japan Atomic Energy Agency)

3:45 PM - 4:00 PM JST | 6:45 AM - 7:00 AM UTC

[SIT17-02] Atomic structure of CO_2-bearing melts along the carbonatite-basalt join at high pressure and temperature

*Veronica Stopponi[1], Annalisa D'Arco[2,3], Rostislav Hrubiak[4], Yoshio Kono[5], Stefano Lupi[2,6], Craig E Manning[7], Manuela Nazzari[8], Brent T Poe[9], Claudia Romano[10], Vincenzo Stagno[1,8] (1.Department of Earth Sciences, Sapienza University of Rome, Rome, Italy, 2.INFN National Institute of Nuclear Physics, Rome, Italy, 3.SBAI Department of Basic and Applied Sciences for Engineering, Physics, Sapienza University of Rome, Rome, Italy, 4.High Pressure Collaborative Access Team (HPCAT), X-ray Science Division, Argonne National Laboratory, Argonne, IL, USA, 5.Geodynamic Research Center, Ehime University, Matsuyama, Japan, 6.Department of Physics, Sapienza University of Rome, Rome, Italy, 7.Department of Earth, Planetary and Space Sciences, University of California, Los Angeles, CA, USA, 8.Istituto Nazionale di Geofisica e Vulcanologia (INGV), Rome, Italy, 9.Department of Engineering and Geology, University of Chieti-Pescara, Chieti Scalo, Italy, 10.Department of Sciences, University of Studies Roma Tre, Rome, Italy)

4:00 PM - 4:15 PM JST | 7:00 AM - 7:15 AM UTC

[SIT17-03] ***In situ X-ray study of liquid geomaterials under extreme conditions using Free-Electron Lasers***

★Invited Papers

*Guillaume Morard[1] (1.ISTerre, UGA, CNRS)

4:15 PM - 4:30 PM JST | 7:15 AM - 7:30 AM UTC

[SIT17-04] Density and thermal expansion of liquid and solid iron at 1 atm determined using high-temperature furnace

★Invited Papers

*Hidenori Terasaki[1], Asaka Kamiya[2], Tadashi Kondo[2] (1.Department of Earth science, Okayama University, 2.Department of Earth and Space science, Osaka University)

4:30 PM - 4:45 PM JST | 7:30 AM - 7:45 AM UTC

[SIT17-05] Sound velocity measurements of liquid Fe-N up to 100 GPa

Asaki Iwamoto[1], *Yoichi Nakajima[1,2], Daisuke Kinoshita[1], Yasuhiro Kuwayama[3], Kei Hirose[3,5], Daisuke Ishikawa[2,4], Alfred Q.R. Baron[2,4] (1.Kumamoto Univ., 2.RIKEN MDL, 3.Univ. Tokyo, 4.JASRI, 5.Tokyo Tech. ELSI)

4:45 PM - 5:00 PM JST | 7:45 AM - 8:00 AM UTC

[SIT17-06] Density and Sound Velocity of Liquid Fe and FeO at High Pressure

*Yasuhiro Kuwayama[1], Kei Hirose[1,2], Yoichi Nakajima[3,4], Yuki Adachi[3], Alfred Q.R. Baron[4], Guillaume Morard[5], Saori I. Kawaguchi[6], Daisuke Ishikawa[6,4], Naohisa Hirao[6], Yasuo Ohishi[6] (1.The University of Tokyo, 2.Tokyo Institute of Technology, 3.Kumamoto University, 4.RIKEN MDR, 5.Laboratoire ISTERRE, Université Grenoble Alpes, 6.JASRI)

[E] Poster | S (Solid Earth Sciences)：S-IT Science of the Earth's Interior & Techtonophysics

5:15 PM - 6:30 PM JST | 8:15 AM - 9:30 AM UTC | Ch.14_1

[S-IT17] Property and role of liquids inside terrestrial planets

convener:Tatsuya Sakamaki(Department of Earth Science, Tohoku University), Yoichi Nakajima(Kumamoto University, Priority Organization for Innovation and Excellence)

[SIT17-P01] Viscosity of silicate melts under high pressures

*Tatsuya Sakamaki[1] (1.Department of Earth Science, Tohoku University)

[SIT17-P02] Elastic wave velocity of silicate glasses at high pressure

*Tatsuya Sakamaki[1] (1.Department of Earth Science, Tohoku University)

[SIT17-P03] Density of Fe_2O_3–bearing magma under high pressure

*Rintaro Ban[1], Akio Suzuki[1], Tatsuya Sakamaki[1] (1.Department of Earth Science, Graduate School of Science, Tohoku University)

[SIT17-P04] **Melting phase equilibrium relations in the $MgSiO_3$-SiO_2 system at 13.5 GPa**

*Takuya Moriguti[1], Yusuke Yachi[1], Akira Yoneda[1], Eiji Ito[1] (1.Institute for Planetary Materials, Okayama University)

[E] Oral | S (Solid Earth Sciences)：S-IT Science of the Earth's Interior & Techtonophysics

9:00 AM - 10:30 AM JST | 12:00 AM - 1:30 AM UTC | Ch.23 Zoom Room 23

[S-IT20] MAGMA, FLUID TRANSPORT, AND SEISMICITY IN THE EARTH'S INTERIOR

convener:Eiji Ohtani(Department of Earth and Planetary Materials Science, Graduate School of Science, Tohoku University), Saeko Kita(International Institute of Seismology and Earthquake Engineering, BRI), Michihiko Nakamura(Division of Earth and Planetary Materials Science, Department of Earth Science, Graduate School of Science, Tohoku University), Bjorn Mysen(Geophysical Laboratory, Carnegie Inst. Washington), Chairperson:Bjorn Mysen(Geophysical Laboratory, Carnegie Inst. Washington), Michihiko Nakamura(Division of Earth and Planetary Materials Science, Department of Earth Science, Graduate School of Science, Tohoku University)

9:00 AM - 9:15 AM JST | 12:00 AM - 12:15 AM UTC

[SIT20-07] HDAC experiments on silica solubility and speciation in Na_2CO_3–H_2O fluids at high pressure and temperature

*Naoko Takahashi[1], Tatsuki Tsujimori[1,2], Seiji Kamada[1,3], Michihiko Nakamura[1] (1.Department of Earth Science, Graduate School of Science, Tohoku University, 2.Center for Northeast Asian Studies, Tohoku University, 3.Frontier Research Institute for Interdisciplinary Sciences, Tohoku University)

9:15 AM - 9:30 AM JST | 12:15 AM - 12:30 AM UTC

[SIT20-08] Permeability determination from multi-anvil experiments: Implications for the fluid flux in subduction zones

★Invited Papers

*Lisa Eberhard[1], Philipp Eichheimer[1], Marcel Thielmann[1], Michihiko Nakamura[2], Gregor Golabek[1], Dan Frost[1] (1.Bayerisches Geoinstitut, University of Bayreuth, Germany, 2.Departement of Earth Science, Tohoku University, Japan)

9:30 AM - 9:45 AM JST | 12:30 AM - 12:45 AM UTC

[SIT20-09] Fluid segregation and chemical compaction through efficient solute transport along wet grain boundaries

*Wakana Fujita[1], Michihiko Nakamura[1], Kentaro Uesugi[2] (1.Graduate School of Science, Tohoku University, 2.Synchrotron Radiation Research Institute (JASRI/SPring-8))

9:45 AM - 10:00 AM JST | 12:45 AM - 1:00 AM UTC

[SIT20-10] Coupling between fluid flux and dynamical permeability evolution in the middle-lower crust, an example from Sør Rondane Mountains (SRM), East Antarctica.

*Diana Mindaleva[1], Masaoki Uno[1], Atsushi Okamoto[1], Noriyoshi Tsuchiya[1] (1.Graduate school of environmental studies, Tohoku University)

10:00 AM - 10:15 AM JST | 1:00 AM - 1:15 AM UTC

[SIT20-11] Attenuation contrast in mantle wedge across the volcanic front of NE Japan that controls propagations of high-frequency S-wave later phases

*Takahiro Shiina[1], Kei Katsumata[2], Kiyoshi Yomogida[2], Aitaro Kato[3] (1.National Institute of Advanced Industrial Science and Technology (AIST), 2.Graduate School of Science, Hokkaido University, 3.Earthquake Research Institute, the University of Tokyo)

10:15 AM - 10:30 AM JST | 1:15 AM - 1:30 AM UTC

[SIT20-12] The effect of water on energy dispersion of olivine and its implications for the origin of the sharp contrast of seismic observation at the lithosphere-asthenosphere boundary

*Chao Liu[1], Takashi Yoshino[1] (1.Institute for Planetary Materials, Okayama University)

[E] Poster | S (Solid Earth Sciences)：S-IT Science of the Earth's Interior & Techtonophysics

5:15 PM - 6:30 PM JST | 8:15 AM - 9:30 AM UTC | Ch.14_2

[S-IT20] MAGMA, FLUID TRANSPORT, AND SEISMICITY IN THE EARTH'S INTERIOR

convener:Eiji Ohtani(Department of Earth and Planetary Materials Science, Graduate School of Science, Tohoku University), Saeko Kita(International Institute of Seismology and Earthquake Engineering, BRI), Michihiko Nakamura(Division of Earth and Planetary Materials Science, Department of Earth Science, Graduate School of Science, Tohoku University), Bjorn Mysen(Geophysical Laboratory, Carnegie Inst. Washington)

[SIT20-P01] **Electrical conductivity in texturally equilibrated fluid-bearing forsterite aggregates at 800°C and 1 GPa: implications for the high electrical conductivity anomalies in mantle wedges**

*Yongsheng HUANG[1], Haihao Guo[2], Takayuki Nakatani[1,4], Kentaro Uesugi[3], Michihiko Nakamura[1], Hans Keppler[2] (1.Graduate School of Science, Tohoku University, 2.Bayerisches Geoinstitut, University of Bayreuth, 3.Spring-8, Japan Synchrotron Radiation Research Institute (JASRI), 4.Geological Survey of Japan)

[SIT20-P02] Role of water in subducting slabs: dry phase transformation kinetics in wet slabs

*Eiji Ohtani[1], Takayuki Ishii[2,3] (1.Department of Earth and Planetary Materials Science, Graduate School of Science, Tohoku University, 2.Bayeriches Geoinstitut, University of Bayreuth, 3.Center for High Pressure Science and Technology Advanced Research)

[SIT20-P03] Melting phase relation of hydrous peridotite at the top of the lower mantle

*Kayan Lau[1], Takashi Yoshino[1], Hideharu Kuwahara[1] (1.Institute for Planetary Materials, Okayama University)

[SIT20-P04] Completeness magnitude of earthquakes and spatial variations of b-VALUE in Myanmar

Ngun Za Iang[1], *Saeko Kita[2] (1.Department of Meteorology and Hydrology (DMH), Ministry of Transport and Communications, Naypyitaw, Myanmar, 2.Building Research Institute)

[J] Oral | S (Solid Earth Sciences)：S-GL Geology

9:00 AM - 10:30 AM JST | 12:00 AM - 1:30 AM UTC | Ch.24 Zoom Room 24

[S-GL23] Geologic structure and tectonic history of East Asia and Japanese Islands

convener:Makoto Otsubo(Geological Survey of Japan, Research Institute of Earthquake and Volcano Geology), Jun Hosoi(Geological Survey of Japan, Institute of Geology and Geoinformation, AIST), Chairperson:Makoto Otsubo(Geological Survey of Japan, Research Institute of Earthquake and Volcano Geology)

9:00 AM - 9:15 AM JST | 12:00 AM - 12:15 AM UTC

[SGL23-01] Age spectra of detrital zircons of Paleogene fore-arc sandstones in Japan and the irreversible major change in mid-Eocene relevant to the initiation of Median Tectonic Line.

*Yukio Isozaki[1], Yukiyasu Tsutsumi[2], Tomohito Nakano[1] (1.Department of Earth Science and Astronomy, Graduate School of Arts and Sciences, The University of Tokyo, 2.Deprtment of Geology and Paleontology, National Musem of Nature and Science)

9:15 AM - 9:30 AM JST | 12:15 AM - 12:30 AM UTC

[SGL23-02] Zircon U-Pb ages of Momonoki Subgroup in the Koma Mountains

*Takashi Hakomori[1], Kenichiro Tani[2], Junichiro Kuroda[1], Asuka Yamaguchi[1] (1.Atmosphere and Ocean Research Institute, The University of Tokyo, 2.National Museum of Nature and Science)

9:30 AM - 9:45 AM JST | 12:30 AM - 12:45 AM UTC

[SGL23-03] Tectonostratigraphic characterization of Maizuru back-arc basin during its closure: geochemical and U-Pb detrital geochronological approaches.

*Larissa NGOMBI MAVOUNGOU[1], Kaushik Das[1,2], Yasutaka Hayasaka[1,2], Haruna Kuriu[1], Kenta Kawaguchi[3] (1.Department of Earth and Planetary Systems Science, Graduate School of Science, Hiroshima University, 2.HiPeR, Hiroshima, 3.Chonbuk National University, Korea)

9:45 AM - 10:00 AM JST | 12:45 AM - 1:00 AM UTC

[SGL23-04] Southwest Japan rotated clockwise during opening of the Japan Sea: Evidence from Miocene sediments in the Outer Zone

*Hiroyuki Hoshi[1], Hideki Iwano[2], Tohru Danhara[2] (1.Department of Earth Sciences, Aichi University of Education, 2.Kyoto Fission-Track Co., Ltd.)

10:00 AM - 10:15 AM JST | 1:00 AM - 1:15 AM UTC

[SGL23-05] Provenance of sandstones from the Eocene Urahoro Group, Hokkaido, Northern Japan: Tectonic Implications

*Toru Takeshita[1], Hiromi Kaji[1,2] (1.Department of Natural History Sciences, Graduate School of Science, Hokkaido University, 2.Oyo Co. Ltd.)

10:15 AM - 10:30 AM JST | 1:15 AM - 1:30 AM UTC

[SGL23-06] Shallow structure and late Quaternary slip rate on the Osaka Bay Fault: Aspects of climate-tectonic interaction

*Mari Hamahashi[1], Hironori Otsuka[1], Yoshiaki Suzuki[2], Jun Arimoto[2], Tetsuo Matsuno[1,3], Nobukazu Seama[1,3], Satoshi Shimizu[1,4], Hikaru Iwamaru[1,4], Mamoru Sano[1,4], Keita Suzuki[1,4], Katsuya Kaneko[1,3], Kazuo Nakahigashi[5], Itsuko Hidaka[1], Yuzuru Yamamoto[1,3], Yoshiyuki Tatsumi[1] (1.Kobe University, Ocean-Bottom Exploration Center, 2.Geological Survey of Japan, National Institute of Advanced Industrial Science and Technology, 3.Department of Planetology, Graduate School of Science, Kobe University, 4.Nippon Marine Enterprises, Ltd. , 5.School of Marine Resources and Environment, Tokyo University of Marine Science and Technology)

[J] Poster | S (Solid Earth Sciences)：S-GL Geology

5:15 PM - 6:30 PM JST | 8:15 AM - 9:30 AM UTC | Ch.15_1

[S-GL23] Geologic structure and tectonic history of East Asia and Japanese Islands

convener:Makoto Otsubo(Geological Survey of Japan, Research Institute of Earthquake and Volcano Geology), Jun Hosoi(Geological Survey of Japan, Institute of Geology and Geoinformation, AIST)

[SGL23-P01] Estimation of fluid migration along the Out of Sequence Thrust from quartz vein geometric information
-Estuimation of permeability at Nobeoka Thrust in Kyushu, southwest Japan-

*Hinako Hosono[1], Takato Takemura[1], Makoto Otsubo[2] (1.Nihon University Colledge of Humanities and Sciences, 2.Geological Survey of Japan, Research Institute of Earthquake and Volcano Geology)

[SGL23-P02] Detrital zircon geochemistry in the Shimanto Accretionary Complex: Tectonic constraints on formations of the Jurassic to Cretaceous batholiths in the eastern Asian margin

*Shogo Aoki[1], Kazumasa Aoki[2], Mayuko Fukuyama[3], Masatsugu Ogasawara[4] (1.Graduate School of International Resource Sciences, Akita University, 2.Center For Fundamental Education, Okayama Univerisity of Science, 3.Graduate School of Engeneering Science, Akita University, 4.Institute of Geology and Geoinformation, Geological Survey of Japan, National Institute of Advanced Industrial Science and Technology)

[SGL23-P03] Itayama Nappe, meta-chert and gabbro in the Ryoke Belt of the Takato-Itayama area, central Japan

*Akira Ono

[SGL23-P04] Publication of the 1:50,000 geological map of the Ikeda District

*Atsushi Noda[1], Kazuhiro Miyazaki[1], Kiyohide Mizuno[1], Mitsuhiro Nagata[2] (1.National Institute of Advanced Industrial Science and Technology, 2.Japan Atomic Energy Agency)

[SGL23-P05] Tectonic slices at the Anko outcrop of Median Tectonic Line, Oshika Village, Nagano Prefecture, Japan

*RYOSUKE ISAJI[1], HIDEO TAKAGI[1] (1.Waseda University)

[SGL23-P06] Zircon U–Pb age of Paleoproterozoic granite gneiss from the Ogcheon Belt, Geumsan area and Paleoproterozoic leucogranite and quartzite from the Yeongnam Massif, Seolcheon area, South Korea

*Kenichiro Iwamizu[1,2], Yasutaka Hayasaka[1], Ji-Hoon Kang[3], Kosuke Kimura[1,4], Tomoyuki Shibata[1] (1.Hiroshima Univ., 2.The Univ. of Tokyo, 3.Andong National Univ., 4.National Inst. of Tech., Kure College)

[E] Oral | S (Solid Earth Sciences)：S-MP Mineralogy & Petrology

1:45 PM - 3:15 PM JST | 4:45 AM - 6:15 AM UTC | Ch.20 Zoom Room 20

[S-MP24] Supercontinents and Crustal Evolution

convener:Tomokazu Hokada(National Institute of Polar Research), Tetsuo Kawakami(Graduate School of Science, Kyoto University), Krishnan Sajeev(Centre for Earth Sciences, Indian Institute of Science), Madhusoodhan Satish-Kumar(Department of Geology, Faculty of Science, Niigata University), Chairperson:Tomokazu Hokada(National Institute of Polar Research), Madhusoodhan Satish-Kumar(Department of Geology, Faculty of Science, Niigata University)

1:45 PM - 2:00 PM JST | 4:45 AM - 5:00 AM UTC

[SMP24-01] Decompression *P-T* evolution recorded in a pelitic gneiss from Tangarden, Sør Rondane Mountains, East Antarctica

*Tetsuo Kawakami[1], Fumiko Higashino[2], Tatsuro ADACHI[3], Masaoki Uno[4] (1.Graduate School of Science, Kyoto University, 2.Okayama University of Science, 3.Advanced Asian Archaeological Research Center, Kyushu University, 4.Graduate School of Environmental Studies, Tohoku University)

2:00 PM - 2:15 PM JST | 5:00 AM - 5:15 AM UTC

[SMP24-02] Post-peak Cl- and CO_2-bearing fluids in a Grt-Sil-Bt gneiss from southern Perlebandet, Sør Rondane Mountains, East Antarctica

*Fumiko Higashino[1], Tetsuo Kawakami[2], Tatsuro ADACHI[3], Masaoki Uno[4] (1.Faculty of Science, Okayama University of Science, 2.Kyoto University, 3.Kyushu University, 4.Tohoku University)

2:15 PM - 2:30 PM JST | 5:15 AM - 5:30 AM UTC

[SMP24-03] **Contrasting chemical reactions and fluid transport by melt and aqueous fluids during middle crustal fracturing (Sør Rondane Mountains, East Antarctica)**

*Masaoki Uno[1], Tetsuo Kawakami[2], Tatsuro Adachi[3], Fumiko Higashino[4], Noriyoshi Tsuchiya[1] (1.Tohoku University, 2.Kyoto University, 3.Kyushu University, 4.Okayama University of Science)

2:30 PM - 2:45 PM JST | 5:30 AM - 5:45 AM UTC

[SMP24-04] Geochemical characterization of zircon for U-Pb age determination in Fyfe Hills of the Napier Complex, East Antarctica

*Mami Takehara[1], Kenji Horie[1,2], Tomokazu Hokada[1,2] (1.National Institute of Polar Research, 2.The Graduate University for Advanced Studies, SOKENDAI)

2:45 PM - 3:00 PM JST | 5:45 AM - 6:00 AM UTC

[SMP24-05] Petrology, metamorphic conditions, and monazite dating of metapelites of the Zambezi Belt supracrustal sequence, Zambia

*Kabangu Grace Sakuwaha[1], Toshiaki Tsunogae[1] (1.University of Tsukuba)

3:00 PM - 3:15 PM JST | 6:00 AM - 6:15 AM UTC

[SMP24-06] Petro-tectonic setting of the Karagwe–Ankole Belt (Rwanda) and implications for the amalgamation of Rodinia

*Claude Nambaje[1], Madhusoodhan Satish-Kumar[2], Ian S. Williams[3], Toshiro Takahashi[2], Krishnan Sajeev[1] (1.Indian Institute of Science, 2.Niigata University, 3.Australian National University)

[E] Oral | S (Solid Earth Sciences)：S-MP Mineralogy & Petrology

3:30 PM - 5:00 PM JST | 6:30 AM - 8:00 AM UTC | Ch.20 Zoom Room 20

[S-MP24] Supercontinents and Crustal Evolution

convener:Tomokazu Hokada(National Institute of Polar Research), Tetsuo Kawakami(Graduate School of Science, Kyoto University), Krishnan Sajeev(Centre for Earth Sciences, Indian Institute of Science), Madhusoodhan Satish-Kumar(Department of Geology, Faculty of Science, Niigata University), Chairperson:Krishnan Sajeev(Centre for Earth Sciences, Indian Institute of Science), Tetsuo Kawakami(Graduate School of Science, Kyoto University)

3:30 PM - 3:45 PM JST | 6:30 AM - 6:45 AM UTC

[SMP24-07] **A comparison between carbon isotope thermometry and Raman spectra of carbonaceous material (RSCM) thermometry in low-medium grade carbonate rocks from the Chitradurga Schist Belt, Dharwar Craton**

*Kiran Sasidharan[1], Madhusoodhan Satish-Kumar[1], Yoshihiro Nakamura[2], Hiroaki Ohfuji[3] (1.Niigata University, 2.Geological Survey of Japan, AIST, 3.Tohoku University)

3:45 PM - 4:00 PM JST | 6:45 AM - 7:00 AM UTC

[SMP24-08] Insights into failed rift processes in the Archean, evidence from the Western Dharwar Craton, southern India.

*Sreehari Lakshmanan[1], Tsuyoshi Toyoshima[2], Madhusoodhan Satish-Kumar[2] (1.Graduate School of Science and Technology, Niigata University, Niigata, Japan, 2.Department of Geology, Niigata University, Niigata, Japan)

4:00 PM - 4:15 PM JST | 7:00 AM - 7:15 AM UTC

[SMP24-09] **Trace and rare earth element geochemistry of the clinopyroxene of dolerite dykes from Western Dharwar craton, southern India**

*Silpa Ammini Sasidharan[1], Madhusoodhan Satish-Kumar[1], Eiichi TAKAZAWA[1], Krishnan Sajeev[2] (1.Faculty of Science Niigata University, 2.Indian Institute of Science, Bangalore, India)

4:15 PM - 4:30 PM JST | 7:15 AM - 7:30 AM UTC

[SMP24-10] Evidence of carbonic crustal fluid during deep to shallow crustal evolution of the interior of Eastern Ghats Belt India: Grenvillian to Kuunga orogenies

*Kaushik Das[1,6], Sankar Bose[2,6], Junji Torimoto[3], Yasutaka Hayasaka[1,6], Daniel Dunkley[4,5] (1.Hiroshima University, 2.Presidency University, 3.JAMSTEC, Yokotsuka, 4.NIPR, Tokyo, 5.IG-PAS, Poland, 6.HiPeR, Japan)

4:30 PM - 4:45 PM JST | 7:30 AM - 7:45 AM UTC

[SMP24-11] **Metasomatic Corundum-Sapphirine-Spinel-Clinozoisite assemblage Indications for Ca-Al rich fluid**

*Krishnan Sajeev[1], S Veni[1] (1.Centre for Earth Sciences, Indian Institute of Science)

4:45 PM - 5:00 PM JST | 7:45 AM - 8:00 AM UTC

[SMP24-12] A geochemical perspective on tectonic setting and depositional environment of Precambrian metacarbonate rocks in collisional orogenic belts

*Madhusoodhan Satish-Kumar[1] (1.Department of Geology, Faculty of Science, Niigata University)

[E] Poster | S (Solid Earth Sciences)：S-MP Mineralogy & Petrology

5:15 PM - 6:30 PM JST | 8:15 AM - 9:30 AM UTC | Ch.15_2

[S-MP24] Supercontinents and Crustal Evolution

convener:Tomokazu Hokada(National Institute of Polar Research), Tetsuo Kawakami(Graduate School of Science, Kyoto University), Krishnan Sajeev(Centre for Earth Sciences, Indian Institute of Science), Madhusoodhan Satish-Kumar(Department of Geology, Faculty of Science, Niigata University)

[SMP24-P01] Geochronology of the metamorphic rocks at the Oyayubi ridge of Brattnipene, Sør Rondane Mountains, East Antarctica.

*Tatsuro ADACHI[1], Tetsuo Kawakami[2], Masaoki Uno[3], Fumiko Higashino[4] (1.Kyushu University, 2.Kyoto University, 3.Tohoku University, 4.Okayama University of Science)

[SMP24-P02] **Evidence of Paleoproterozoic rift-to-drift transition in eastern margin of Singhbhum Craton, India from U-Pb zircon, Sr-Nd isotopic and geochemical study of dismembered gabbro-wehrlite of Bangriposi**

*Tushar Mouli Chakraborti[1,2], Kosuke Kimura[1,2], Arijit Ray[3], Ramananda Chakrabarti[4], Gautam Kumar Deb[3] (1.Earth and Planetary System Science program, Graduate School of Advanced Science and Engineering, Hiroshima University, Japan, 2.Hiroshima Institute of Plate Convergence Region Research (HiPeR), Hiroshima University, Japan, 3.Department of Geology, Presidency University, Kolkata, India, 4.Centre for Earth Sciences, Indian Institute of Science, Bangalore, India)

[SMP24-P03] Sulfur isotope study of high-grade metamorphic rocks in Highland Complex, Sri Lanka

*Tokuya Mitsubori[1], Madhusoodhan Satish-Kumar[2], Sanjeewa P.K. Malaviarachchi[3] (1.Graduate School of Science and Technology, Niigata University, 2.Department of Geology, Faculty of Science, Niigata University, 3.Department of Geology, Faculty of Science, University of Peradeniya)

[SMP24-P04] **Sulfur isotope study of metacarbonate rocks from Highland Complex, Sri Lanka**

*Aoi Yoshioka[1], Madhusoodhan Satish-Kumar[1] (1.Department of Geology, Faculty of Science, Niigata University)

[SMP24-P05] Preliminary reports of U-Pb zircon age of charnockites in Aker Peaks of the Napier Complex, East Antarctica

*Kenji Horie[1,2], Mami Takehara[1], Tomokazu Hokada[1,2], Allen Nutman[3] (1.National Institute of Polar Research, 2.The Graduate University for Advanced Studies, SOKENDAI, 3.University of Wollongong)

[SMP24-P06] **Microtextural, fluid inclusion and C-O stable isotope studies of sparry magnesite of Deoban group of Kumaun Lesser Himalayas**

*Prakash Chandra Arya[1], Sajeev Krishnan[1], Kiran S[2,3], Satish Kumar[2], Claude Nambaje[1] (1.Centre for Earth Science, Indian Institute of Science, Bangalore, India, 2.Department of Geology, Faculty of Science, Niigata University, Niigata, Japan, 3.Graduate School of Science and Technology, Niigata University, Niigata, Japan)

[SMP24-P07] **Petrography and progressive metamorphism of Chitradurga Schist Belt, Dharwar Craton, southern India**

*Tomokazu Hokada[1,2], Madhusoodhan Satish-Kumar[3], Yuichiro Ueno[4], Tsuyoshi Toyoshima[3], Kaoru Mishima[4], Abdulla Nasheeth[4,5], Chiaki Ikawa[2] (1.National Institute of Polar Research, 2.The Graduate University for Advanced Studies (SOKENDAI), 3.Niigata University, 4.Tokyo Institute of Technology, 5.Osaka City University)

[J] Oral | S (Solid Earth Sciences)：S-VC Volcanology

9:00 AM - 10:30 AM JST | 12:00 AM - 1:30 AM UTC | Ch.25 Zoom Room 25

[S-VC28] Active Volcanism

convener:Yuta Maeda(Nagoya University), Takahiro Miwa(National research institute for earth science and disaster prevention), Takeshi Matsushima(Institute of Seismology and Volcanology, Faculty of Science, Kyushu University), Chairperson:Taketo Shimano(Graduate School of Environment and Disaster Research, Tokoha University), Takahiro Miwa(National research institute for earth science and disaster prevention)

9:00 AM - 9:15 AM JST | 12:00 AM - 12:15 AM UTC

[SVC28-19] Temporal variation of conduit process during the 2018 eruptive activity at Shinmoedake volcano, Japan: Implications from a time series of ash characteristics

*Takahiro Miwa[1], Masashi NAGAI[1], Hideki Ueda[1], Taku Ozawa[1], Eisuke Fujita[1] (1.National research institute for earth science and disaster resilience)

9:15 AM - 9:30 AM JST | 12:15 AM - 12:30 AM UTC

[SVC28-20] An emplacement mechanism of submarine pyroclastic products: insight form the seismic studies on Kikai caldera

*Satoshi Shimizu[1,2], Nobukazu Seama[3,1], Reina Nakaoka[1], Keiko Suzuki-Kamata[1], Koji Kiyosugi[1], Katsuya Kaneko[3,1], Tetsuo Matsuno[1], Yoshiyuki Tatsumi[1] (1.Kobe Ocean-Bottom Exploration Center, Kobe University, 2.Nippon Marine Enterprises, Ltd., 3.Department of Planetology, Graduate School of Science, Kobe University)

9:30 AM - 9:45 AM JST | 12:30 AM - 12:45 AM UTC

[SVC28-21] Comparison of subaerial and submarine deposits from the Kikai Akahoya eruption

*Reina NAKAOKA[1], Keiko Suzuki-Kamata[1], Satoshi Shimizu[1], Katsuya Kaneko[2], Nobukazu Seama[2], Koji Kiyosugi[1], Takeshi Hanyu[3], Yoshiyuki Tatsumi[1], CK20-S01 Leg2 Cruise Scientists, KS19-17 Cruise Scientists, KR20-11 Cruise Scientists (1.Kobe Ocean-Bottom Exploration Center, Kobe University, 2.Department of Planetology, Kobe University, 3.Japan Agency for Marine-Earth Science and Technology)

9:45 AM - 10:00 AM JST | 12:45 AM - 1:00 AM UTC

[SVC28-22] Tephrostratigraphy of drilled core C9010E off the Boso Peninsula: Estimated source volcano for 9th century eruption events

*Kaori Aoki[1], Makoto Kobayashi[2,1], Masanori Murata[1], Takehiko Suzuki[1] (1.Research Center for Volcanic Hazards and Their Mitigation, Tokyo Metropolitan University, 2.Mt.Fuji World Heritage Centre, Shizuoka)

10:00 AM - 10:15 AM JST | 1:00 AM - 1:15 AM UTC

[SVC28-23] Caldera structure and formation at Atosanupuri and Akaigawa, Hokkaido, northern Japan: A comparison of analogue sandbox experiments and field data

*Ryuhei Sanjo[1] (1.Institute of Geography, Graduate School of Science, Tohoku University)

10:15 AM - 10:30 AM JST | 1:15 AM - 1:30 AM UTC

[SVC28-24] Current state evaluation and long-term prediction of volcanic activity based on historical tracking of volcanic ash deposits at Suwanosejima volcano

*Taketo Shimano[1], Atsushi Yasuda[2], Masato Iguchi[3] (1.Graduate School of Environment and Disaster Research, Tokoha University, 2.Earthquake Research Institute, University of Tokyo, 3.Sakurajima Volcano Research Center, Disaster Prevention Research Institute, Kyoto University)

[J] Oral | S (Solid Earth Sciences)：S-VC Volcanology

10:45 AM - 11:30 AM JST | 1:45 AM - 2:30 AM UTC | Ch.25 Zoom Room 25

[S-VC28] Active Volcanism

convener:Yuta Maeda(Nagoya University), Takahiro Miwa(National research institute for earth science and disaster prevention), Takeshi Matsushima(Institute of Seismology and Volcanology, Faculty of Science, Kyushu University), Chairperson:Urumu Tsunogai(Graduate School of Environmental Studies, Nagoya University), Takeshi Ohba(Department of chemistry, School of Science, Tokia University)

10:45 AM - 11:00 AM JST | 1:45 AM - 2:00 AM UTC

[SVC28-25] Behavior of magmatic components in fumarolic gases related to the 2018 phreatic eruption at Ebinokogen Ioyama volcano, Kirishima Volcanic Group, Kyushu, Japan

*Takeshi Ohba[1], Muga Yaguchi[2], Urumu Tsunogai[3], Masanori Ito[3], Ryo Shingubara[3] (1.Department of chemistry, School of Science, Tokia University, 2.Meteorol. Res. Inst., 3.Grad. School of Envir. Studies Nagoya University)

11:00 AM - 11:15 AM JST | 2:00 AM - 2:15 AM UTC

[SVC28-26] Time variation in the composition of volcanic gases at Mt Hakone (2018-2020)

*Seiya Toyoshima[1], Nozomi Numanami[1], Takeshi Ohba[1], Muga Yaguchi[2] (1.Tokai University, 2.Meteorological Research Institute, JMA)

11:15 AM - 11:30 AM JST | 2:15 AM - 2:30 AM UTC

[SVC28-27] **Development of an automatic volcanic plume sampler SelPS for UAS**

*Urumu Tsunogai[1], Ryo Shingubara[1], Masanori Ito[1], Yuhei Morishita[1], Fumiko Nakagawa[1], Shin Yoshikawa[2], Mitsuru Utsugi[2], Akihiko Yokoo[2] (1.Graduate School of Environmental Studies, Nagoya University, 2.Graduate School of Science, Kyoto University)

[J] Poster | S (Solid Earth Sciences)：S-VC Volcanology

5:15 PM - 6:30 PM JST | 8:15 AM - 9:30 AM UTC | Ch.16_1

[S-VC28] Active Volcanism

convener:Yuta Maeda(Nagoya University), Takahiro Miwa(National research institute for earth science and disaster prevention), Takeshi Matsushima(Institute of Seismology and Volcanology, Faculty of Science, Kyushu University)

[SVC28-P01] Local deformation at Mt.Tokachi detected by TS-InSAR

*Satoshi Okuyama[1], Shinobu Ando[1] (1.Meteorological Research Institute)

[SVC28-P02] Volcanic tremor source location at Tokachidake volcano from cross-correlation analysis of 2018-2020 seismic data

*Theodorus Permana[1], Hiroshi Aoyama[1] (1.Institute of Seismology and Volcanology, Faculty of Science, Hokkaido University.)

[SVC28-P03] Time-series of crustal deformation on Azuma volcano revealed by PALSAR-2 data

*Yuji Himematsu[1], Taku Ozawa[1] (1.National Research Institute for Earth Science and Disaster Resilience)

[SVC28-P04] Existence of deep pressure sources and its behaviors during recent volcanic activity at Azumayama, NE Japan

*Jun Okada[1], Yu Nihara[2], Yuji Miyagawa[3], Susumu Seki[3], Takuya Yamamura[2], Shin Chikasawa[3] (1.Volcanology Research Department, Meteorological Research Institute - Japan Meteorological Agency, 2.Regional Volcanic Observation and Warning Center, Sendai Regional Headquarters - Japan Meteorological Agency, 3.Seismology and Volcanology Division, Sendai Regional Headquarters - Japan Meteorological Agency)

[SVC28-P05] Amorphous silica coating on flank deposits of the 1783 CE (Tenmei) eruption at Asama volcano

*Takayuki Nakatani[1], Sarina Sugaya[2], Maya Yasui[3], Satoshi Okumura[2], Michihiko Nakamura[2] (1.Geological Survey of Japan, National Institute of Advanced Industrial Science and Technology, 2.Department of Earth Science, Graduate School of Science, Tohoku University, 3.Department of Earth and Environmental Sciences, College of Humanities and Sciences, Nihon University,)

[SVC28-P06] **Monitoring of underground temperature in Jigokudani, Midagahara volcano using LPWA devices**

*Tohru Watanabe[1] (1.Faculty of Sustainable Design, University of Toyama)

[SVC28-P07] Formation of N_3 member from the younger Ō-shima group distributed around the Habu area, southeastern part of Izu-Ō-shima Island.

*Ryota Uchiyama[1], Izumi Sakamoto[1] (1.School of Marine and Technology, Tokai University)

[SVC28-P08] Banded Tremors Activity at Miyakejima Volcano

*Yoshihiro Otsuka[1], Shinya Nagato[1] (1.Japan Meteorological Agency)

[SVC28-P09] Estimating the underground pressure source of Miyakejima volcano by integrated processing of GNSS and leveling data

*Haruna Watanabe[1], Takeshi Matsushima[2], Miyo Fukui, Atsushi Watanabe[3], Jun Oikawa[3], Takashi OKUDA[4], Taku Ozawa[5], Yosuke Miyagi[5] (1.Department of Earth and Planetary Sciences, Graduate School of Science, Kyushu University, 2.Institute of Seismology and Volcanology, Faculty of Sciences, Kyushu University, 3.Earthquake Research Institute, University of Tokyo, 4.Earthquake and Volcanology Research Center, 5.National Research Institute for Earth Science and Disaster Resilience)

[SVC28-P10] Three-Dimensional Crustal Structure beneath Hachijojima Island using dense seismic observation data

*Shotaro Kanke[1], Hiroyuki Azuma[1], Yoshiya Oda[1] (1.Tokyo Metropolitan Univ.)

[SVC28-P11] Ground deformation between eruptions at Nishinoshima Island using InSAR time series analysis

*Shinobu Ando[1], Satoshi Okuyama[1] (1.Volcanology Research Department, Meteorological Research Institute)

[SVC28-P12] Abrupt change in eruption style during the 2019-2020 eruption of Nishinoshima, Ogasawara

*Fukashi Maeno[1], Takayuki Kaneko[1], Natsumi Hokanishi[1], ATSUSHI YASUDA[1], Yoshihiko Tamura[2] (1.Earthquake Research Institute, University of Tokyo, 2.Japan Agency for Marine-Earth Science and Technology)

[SVC28-P13] The depth of the air-magma interface and the sound velocity in the shallow conduit of Aso volcano inferred from seismic and infrasound signals

*Kyoka Ishii[1], Akihiko Yokoo[1] (1.Graduate School of Science, Kyoto University)

[SVC28-P14] Estimation of source location of high-frequency tremor at Aso volcano by array analysis

*hirotaka tanaka[1], Takahiro Ohkura[2], Hiroyuki Inoue[2], Shin Yoshikawa[2] (1.kyoto university, 2.Aso Volcanological Laboratory)

[SVC28-P15] Debris avalanche deposits and the stratigraphy on the outcrop to north east from Mt.Unzen

*Daisuke Nagai[1] (1.Mt.Unzen disaster memorial hall)

[SVC28-P16] Vault-housed extensometers and tiltmeters recorded continuous crustal movement during the eruption of Kirishima Shinmoe-dake in 2018

*Koki Yoshinaga[1], Takeshi Matsushima[2], Hiroshi Shimizu[2], Yusuke Yamashita[3], Shintaro Komatsu[3], Ken'ichi Yamazaki[3] (1.Department of Earth and Planetary Sciences, Graduate School of Science, Kyushu University, 2.Institute of Seismology and Volcanology, Faculty of Sciences, Kyushu University, 3.Miyazaki Observatory, Disaster Prevention Research Institute, Kyoto University)

[SVC28-P17] Two experiments using a small-aperture infrasonic array at Kirishima

*Kazuya Yamakawa[1], Mie Ichihara[1], Dan Muramatsu[2], Takeshi Matsushima[2], Ruka Wada[3], Hideki Takahashi[3], Isao Shimoyama[4] (1.Earthquake Research Institute, University of Tokyo, 2.Institute of Seismology and Volcanology, Faculty of Science, Kyushu University, 3.Department of Mechanical Engineering, Faculty of Science and Technology, Keio University, 4.Department of Intelligent Robotics, Toyama Prefectural University)

[SVC28-P18] Estimating the source of volcanic earthquakes during eruption events at Kirishima Volcanos, in 2018, using spatial distribution of earthquake amplitude.

*Daiki Goshima[1], Satoshi Matsumoto[2], Ayaho Mitsuoka[1], Yuhei Yuasa[4], Yuta Kawamura[1], Mie Ichihara[3] (1.Department of Earth and Planetary Sciences, Graduate School of Science, Kyushu University, 2.Institute of Seismology and Volcanology, Faculty of Sciences, Kyushu University, 3.Earthquake Research Institute, University of Tokyo, 4.Osaka Regional Headquarters, Japan Meteorological Agency)

[SVC28-P19] S-wave attenuation structure of Mt.Kirishima estimated using coda of S-wave

*Takuji Watanabe[1], Ayaho Mitsuoka[1], Yuhei Yuasa[1], Yuta Kawamura[1], Daiki Goshima[1], Satoshi Matsumoto[2], Mie Ichihara[3] (1.Department of Earth and Planetary Sciences, Graduate School of Science, Kyushu University, 2.Institute of seismology and Volcanology, Faculty of Sciences, Kyushu University, 3.Earthquake Research Institute, University of Tokyo)

[SVC28-P20] Estimate of magma supply beneath Aira caldera during the last 10 years based on ground deformation observation and amount of volcanic ejecta

*Daisuke Miki[1], Tomoki Tsutsui[1], Masato Iguchi[1] (1.Sakurajima Volcano Research Center, Disaster Prevention Research Institute, Kyoto University)

[SVC28-P21] Temporal changes of seismic velocities and scattering properties at Suwanosejima volcano inferred from seismic interferometry

*Takashi Hirose[1], Hideki Ueda[1], Eisuke Fujita[1] (1.National Research Institute for Earth Science and Disaster Resilience)

[SVC28-P22] Development of volcano deformation calculation system using boundary element method (2)

*Ryohei Kawaguchi[1] (1.Meteorological Research Institute)

[SVC28-P23] Estimation of seismic scattering coefficients at active volcanoes

*Mare Yamamoto[1] (1.Research Center for Prediction of Earthquakes and Volcanic Eruptions, Graduate School of Science, Tohoku University)

[SVC28-P24] Temporal Change in Coda-Q at the upper East Rift Zone of Kīlauea volcano, Island of Hawai‘i

*Takuji Yamada[1], Paul G Okubo[2] (1.Faculty of Science, Graduate School of Science and Technology, Ibaraki University, 2.University of Hawai‘i at Mānoa)

[SVC28-P25] A prototype of advanced Multi-GAS for unmanned aircraft systems

*Masaaki Morita[1], Toshiya Mori[2] (1.Geological Survey of Japan, AIST, 2.Graduate School of Science, The University of Tokyo)

[J] Oral | S (Solid Earth Sciences)：S-VC Volcanology

1:45 PM - 3:15 PM JST | 4:45 AM - 6:15 AM UTC | Ch.25 Zoom Room 25

[S-VC31] Dynamics of volcanic eruptions and their physical and chemical processes

convener:Yujiro Suzuki(Earthquake Research Institute, The University of Tokyo), Atsuko Namiki(Graduate School of Environmental Studies, Nagoya University), Masatoshi Ohashi(Earthquake Research Institute, the University of Tokyo), Chairperson:Yujiro Suzuki(Earthquake Research Institute, The University of Tokyo), Masatoshi Ohashi(Earthquake Research Institute, the University of Tokyo)

1:45 PM - 2:15 PM JST | 4:45 AM - 5:15 AM UTC

[SVC31-01] Experimental constraint on redox evolution of magma during decompression

★Invited Papers

*Satoshi Okumura[1], Hidemi Ishibashi[2], Shoichi Itoh[3], Akimasa Suzumura[3], Yoshihiro Furukawa[1], Takahiro Miwa[4], Hiroyuki Kagi[5] (1.Division of Earth and Planetary Materials Science, Department of Earth Science, Graduate School of Science, Tohoku University, 2.Department of Geosciences, Fuculty of Science, Shizuoka University, 3.Division of Earth and Planetary Sciences, Graduate School of Science, Kyoto University, 4.National Research Institute for Earth Science and Disaster Resilience, 5.Geochemical Research Center, Graduate School of Science, The University of Tokyo)

2:15 PM - 2:30 PM JST | 5:15 AM - 5:30 AM UTC

[SVC31-02] Factors affecting the sequence of Asama volcano 1783 eruption inferred from rock texture

*Tatsuki Mizuno[1], Fukashi Maeno[1], Atsushi Yasuda[1] (1.Earthquake Research Institute, Department of Earth and Planetary Science, University of Tokyo)

2:30 PM - 2:45 PM JST | 5:30 AM - 5:45 AM UTC

[SVC31-03] Genesis of vesiculation in dolerite sills of the Shimokawa ophiolite in the northern Hidaka belt, Hokkaido: Genesis of trachyte in the MORB

*Kato Satomi[1], Sumio Miyashita[2] (1.Graduate School of Science and Technology, Niigata University, 2.Hokkaido Research Center of Geology)

2:45 PM - 3:15 PM JST | 5:45 AM - 6:15 AM UTC

[SVC31-04] Discussion time

*Yujiro Suzuki[1] (1.Earthquake Research Institute, The University of Tokyo)

[J] Oral | S (Solid Earth Sciences)：S-VC Volcanology

3:30 PM - 5:00 PM JST | 6:30 AM - 8:00 AM UTC | Ch.25 Zoom Room 25

[S-VC31] Dynamics of volcanic eruptions and their physical and chemical processes

convener:Yujiro Suzuki(Earthquake Research Institute, The University of Tokyo), Atsuko Namiki(Graduate School of Environmental Studies, Nagoya University), Masatoshi Ohashi(Earthquake Research Institute, the University of Tokyo), Chairperson:Atsuko Namiki(Graduate School of Environmental Studies, Nagoya University), Masatoshi Ohashi(Earthquake Research Institute, the University of Tokyo)

3:30 PM - 3:45 PM JST | 6:30 AM - 6:45 AM UTC

[SVC31-05] The run-out distance of large-scale pyroclastic density currents in magmatic and phreatomagmatic eruptions: Numerical simulations of a two-layer depth-averaged model

*Hiroyuki A. Shimizu[1], Takehiro Koyaguchi[2], Yujiro J. Suzuki[2] (1.National Research Institute for Earth Science and Disaster Resilience, 2.Earthquake Research Institute, The University of Tokyo)

3:45 PM - 4:00 PM JST | 6:45 AM - 7:00 AM UTC

[SVC31-06] Effects of the dynamics of conduit flow with a plug on pre-eruptive crustal deformation

*Tomofumi Kozono[1], Chihiro Matsuno[2] (1.Department of Geophysics, Graduate School of Science, Tohoku University, 2.IDAJ Co., LTD.)

4:00 PM - 4:15 PM JST | 7:00 AM - 7:15 AM UTC

[SVC31-07] Volcanic glow fluctuation prior to vulcanian eruptions at Showa Crater, Sakurajima volcano, Japan

*Dan Muramatsu[1], Koki Aizawa[2], Akihiko Yokoo[3], Masato Iguchi[4] (1.Department of Earth and Planetary Sciences, Graduate School of Science, Kyushu University, 2.Institute of Seismology and Volcanology, Faculty of Science, Kyushu University, 3.Aso Volcanological Laboratory, Institute for Geothermal Sciences, Kyoto University, 4.Sakurajima Volcano Research Center, Disaster Prevention Reserach Institute, Kyoto University)

4:15 PM - 4:45 PM JST | 7:15 AM - 7:45 AM UTC

[SVC31-08] Discussion time

*Atsuko Namiki[1] (1.Graduate School of Environmental Studies, Nagoya University)

4:45 PM - 5:00 PM JST | 7:45 AM - 8:00 AM UTC

[SVC31-09] Discussion

[J] Poster | S (Solid Earth Sciences)：S-VC Volcanology

5:15 PM - 6:30 PM JST | 8:15 AM - 9:30 AM UTC | Ch.16_2

[S-VC31] Dynamics of volcanic eruptions and their physical and chemical processes

convener:Yujiro Suzuki(Earthquake Research Institute, The University of Tokyo), Atsuko Namiki(Graduate School of Environmental Studies, Nagoya University), Masatoshi Ohashi(Earthquake Research Institute, the University of Tokyo)

[SVC31-P01] **PHENO-BUBBLE NUMBER DENSITY (PBND) AS INDICATOR OF OVERPRESSURE IN PRE-ERUPTIVE MAGMA CHAMBER**

*Indranova Suhendro[1], Atsushi Toramaru[1] (1.Department of Earth and Planetary Sciences, Graduate School of Sciences, Kyushu University)

[SVC31-P02] **Crystal Fracture in the Youngest Toba Tuff (74 ka) Pumices**

*Gabriela Nogo Retnaningtyas Bunga Naen[1], Atsushi Toramaru[1], Haryo Edi Wibowo[2] (1.Department of Earth and Planetary Science, Kyushu University, Fukuoka, Japan, 2.Geological Engineering Department, Universitas Gadjah Mada, Yogyakarta, Indonesia)

[SVC31-P03] **Textural study of the 7.3 ka caldera-forming eruption of Kikai Caldera: Correlating bulk density to bubble-size observations**

*Selvia Novianty[1], Masatoshi Ohashi[1], Atsushi Toramaru[1] (1.Department of Earth and Planetary Sciences, Graduate School of Science, Kyushu University)

[SVC31-P04] Factors controlling bulk density of pumice in explosive eruption deposits

*Atsushi Toramaru[1], Miki Ogata[1], Haruka Ino[1], Indranova Suhendro[1], Gabriela Bunga Naen[1] (1.Department of Earth and Planetary Sciences, Faculty of Sciences, Kyushu University)

[SVC31-P05] Eruptive style and sequence of the 1235 eruption of Ohachi volcano, Kirishima, Japan - constraints from distribution, shape, and texture of pyroclasts-

*Sayaka Shohata[1], Fukashi Maeno[2], Natsumi Hokanishi[2], ATSUSHI YASUDA[2] (1.Department of Earth and Planetary Science, School of Science, The University of Tokyo, 2.Earthquake Research Institute, The University of Tokyo)

[SVC31-P06] Conduit ascent process of mafic subplinian eruption: Constraints from plagioclase microlites in the 1235 scoria of Kirishima-Ohachi volcano, Japan.

*Yoshiharu Iwaki[1], Hidemi Ishibashi[1], Natsumi Hokanishi[2], ATSUSHI YASUDA[2], Toru Ishikawa[3], Taketo Shimano[4] (1.Shizuoka University Graduate School of Integrated Science and Technology, 2.Earthquake Research Institute, University of Tokyo, 3.Kirishima Geopark Council, 4.Graduate School of Environment and Disaster Reserch, Tokoha University)

[SVC31-P07] Texture of ejecta of summit eruptions in Izu-Oshima

*Yuya Ikenaga[1], Fukashi Maeno[1], ATSUSHI YASUDA[1] (1.Earthquake Research Institute, The University of Tokyo)

[SVC31-P08] Shallow conduit process of Strombolian eruption: A case study of Izu-Omuroyama monogenetic volcano, Japan

*Hidemi Ishibashi[1], Risako Hatakeyama[1], Ryuta Sakamoto[1], Natsumi Hokanishi[2], ATSUSHI YASUDA[2] (1.Faculty of Science, Shizuoka University, 2.Earthquake Research Institute, The University of Tokyo)

[SVC31-P09] **Parameters to control bubble - crystal interaction styles**

*Kyoko Ikeda[1], Atsushi Toramaru[2] (1.Department of Earth and Planetary Sciences, Graduate School of Science, Kyushu University, 2.Department of Earth and Planetary Sciences, Faculty of Science, Kyushu University)

[SVC31-P10] 3D crystal size distributions of pyroxene nanolites plotted against short-axis length reflect magma ascent dynamics

*Shota Okumura[1], Mayumi Mujin[2], Akira Tsuchiyama[3,4], Akira Miyake[1] (1.Department of Geology and Mineralogy, Graduate School of Science, Kyoto University, 2.Division of Earth and Planetary Materials Science, Department of Earth Science, Tohoku University, 3.Research Organization of Science and Technology, Ritsumeikan University, 4.Guangzhou Institute of Geochemistry, Chinese Academy of Sciences)

[SVC31-P11] Petrological characteristics of the Kawago-daira rhyolite lava, Izu Peninsula, Japan

*Hiroshi Oka[1], Motohiro Tsuboi[1], Kuniyuki Furukawa[2] (1.Kwansei Gakuin University, 2.Aichi University)

[SVC31-P12] Determination of water solubility in the rhyolitic melt at 650°C and its interpretation by "hydrogen bonding model"

*Mizuki Nishiwaki[1], Takahiro Miwa[2] (1.Department of Earth and Planetary Sciences, Graduate School of Sciences, Kyushu University, 2.National Research Institute for Earth Science and Disaster Resilience)

[SVC31-P13] Flowage of the 1991 Unzen lava: Discussion to Goto et al.(2020) Rigid migration of Unzen lava rather than flow. JVGR

*Hiroaki Sato[1], Shigeru Suto[2], Tadahide Ui[3], Toshitsugu Fujii[4], Takahiro Yamamoto[2], Shinji Takarada[2], Keiichi Sakaguchi[2] (1.Kobe Univ., 2.Geological Survey of Japan, 3.Hokkaido Univ., 4.Mount Fuji Research Institute)

[E] Oral | S (Solid Earth Sciences)：S-GC Geochemistry

10:45 AM - 12:15 PM JST | 1:45 AM - 3:15 AM UTC | Ch.23 Zoom Room 23

[S-GC32] Volatiles in the Earth - from Surface to Deep Mantle

convener:Takeshi Hanyu(Japan Agency for Marine-Earth Science and Technology, Research Institute for Marine Geodynamics), E Gray Bebout(Lehigh University), Yuji Sano(Division of Ocean and Earth Systems, Atmosphere and Ocean Research Institute, University of Tokyo), Hirochika Sumino(Department of General Systems Studies, Graduate School of Arts and Sciences, The University of Tokyo), Chairperson:Gray E Bebout(Lehigh University), Hirochika Sumino(Department of General Systems Studies, Graduate School of Arts and Sciences, The University of Tokyo)

10:45 AM - 11:00 AM JST | 1:45 AM - 2:00 AM UTC

[SGC32-01] Helium isotope analyses of volcanic gases and HESJ standard gas using a multi-turn time-of-flight mass spectrometer

*Yuki Hattori[1], Yoshihide Akiyama[1], Hirochika Sumino[1] (1.Graduate School of Arts and Science, The University of Tokyo)

11:00 AM - 11:15 AM JST | 2:00 AM - 2:15 AM UTC

[SGC32-02] Systematic depth variation of water in the lithosphere-asthenosphere boundary beneath Ichinomegata, NE Japan

*Yuto Sato[1], Eiichi Takahashi[1], Kazuhito Ozawa[2] (1.State Key Labolatory of Isotope Geochemistry, Guangzhou Institute of Geochemistry, CAS, 2.Department of Earth and Planetary Science, Graduate School of Science, The University of Tokyo)

11:15 AM - 11:45 AM JST | 2:15 AM - 2:45 AM UTC

[SGC32-03] **Impact of mantle hydration on the global carbon cycle**

★Invited Papers

*Ikuo Katayama[1] (1.Department of Earth and Planetary Systems Science, Hiroshima University)

11:45 AM - 12:15 PM JST | 2:45 AM - 3:15 AM UTC

[SGC32-04] **The story of Earth's volatile accretion and evolution**

★Invited Papers

*Sujoy Mukhopadhyay[1], Sandrine Peron[1] (1.Department of Earth and Planetary Sciences, University of California Davis, Davis, CA, USA)

[E] Oral | S (Solid Earth Sciences)：S-GC Geochemistry

1:45 PM - 3:15 PM JST | 4:45 AM - 6:15 AM UTC | Ch.23 Zoom Room 23

[S-GC32] Volatiles in the Earth - from Surface to Deep Mantle

convener:Takeshi Hanyu(Japan Agency for Marine-Earth Science and Technology, Research Institute for Marine Geodynamics), E Gray Bebout(Lehigh University), Yuji Sano(Division of Ocean and Earth Systems, Atmosphere and Ocean Research Institute, University of Tokyo), Hirochika Sumino(Department of General Systems Studies, Graduate School of Arts and Sciences, The University of Tokyo), Chairperson:Yuji Sano(Center for Advanced Marine Core Research, Kochi University), Takeshi Hanyu(Japan Agency for Marine-Earth Science and Technology, Research Institute for Marine Geodynamics)

1:45 PM - 2:15 PM JST | 4:45 AM - 5:15 AM UTC

[SGC32-05] H/D partitioning between forsterite, wadsleyite and ringwoodite : ab initio free energy calculation

★Invited Papers

*Jun Tsuchiya[1], Taku Tsuchiya[1] (1.Geodynamics Research Center, Ehime University)

2:15 PM - 2:45 PM JST | 5:15 AM - 5:45 AM UTC

[SGC32-06] **Volatile characteristics of Central American geothermal fluids**8.6.0

★Invited Papers

*Peter H Barry[1], David V Bekaert[1], J M de Moor[2], Jabrane Labidi[3], Esteban Gazel[4], M Nakagawa[5], Donato Giovannelli[6], Matt Schrenk[7], Karen G Lloyd[8] (1.Woods Hole Oceanographic Institution, 2.Observatorio Volcanológico y Sismológico de Costa Rica (OVSICORI), Universidad Nacional, Costa Rica, 3.Université de Paris, Institut de physique du globe de Paris, CNRS, Paris, France, 4.Department of Earth and Atmospheric Sciences, Cornell University, Ithaca, New York 14853, USA, 5.Earth-Life Science Institute, Tokyo Institute for Technology, Tokyo, Japan, 6.Department of Biology, University of Naples “Federico II”, Naples, Italy, 7.Department of Earth and Environmental Sciences, Michigan State University, MI, USA, 8.Department of Microbiology, University of Tennessee, TN, USA)

2:45 PM - 3:00 PM JST | 5:45 AM - 6:00 AM UTC

[SGC32-07] Halogen and noble gas compositions of mantle wedge and subducted sediment, recorded in metamorphic rocks from the Sanbagawa belt

*JIE REN[1], Hirochika Sumino[1], Yui Kouketsu[2], Simon Richard Wallis[3] (1.Graduate School of Arts and Sciences, The University of Tokyo , 2.Graduate School of Environmental Studies, Nagoya University, 3.Graduate School Sciences, The University of Tokyo)

3:00 PM - 3:15 PM JST | 6:00 AM - 6:15 AM UTC

[SGC32-08] Discussion

[E] Poster | S (Solid Earth Sciences)：S-GC Geochemistry

5:15 PM - 6:30 PM JST | 8:15 AM - 9:30 AM UTC | Ch.17_1

[S-GC32] Volatiles in the Earth - from Surface to Deep Mantle

convener:Takeshi Hanyu(Japan Agency for Marine-Earth Science and Technology, Research Institute for Marine Geodynamics), E Gray Bebout(Lehigh University), Yuji Sano(Division of Ocean and Earth Systems, Atmosphere and Ocean Research Institute, University of Tokyo), Hirochika Sumino(Department of General Systems Studies, Graduate School of Arts and Sciences, The University of Tokyo)

[SGC32-P01] Secular variation of helium isotope ratios in Izu Oshima: What will be observed in the next eruption?

*Hirochika Sumino[1], Kei Ikehata[2], Aya Shimizu[3], Kotaro Toyama[4], Tomoya Obase[1], Kenji Notsu[5] (1.Department of General Systems Studies, Graduate School of Arts and Sciences, The University of Tokyo, 2.Faculty of Life and Environmental Sciences, University of Tsukuba, 3.Tokyo Metropolitan Industrial Technology Research Institute, 4.Atmosphere and Ocean Research Institute, The University of Tokyo, 5.Geochemical Research Center, Graduate School of Science, University of Tokyo)

[SGC32-P02] Noble gas analysis and microstructure observation of the Finero phlogopite peridotite in Northern Italy to constrain the origin of deformation process of mantle wedge peridotite

*Nanae Fukushima[1], Hirochika Sumino[1], Jun-ichi Ando[2], DAS KAUSHIK[2], Masahiro Kobayashi[3], Hiroyuki Kagi[4], Takafumi Yamamoto[2] (1.Graduate School of Arts and Sciences, the University of Tokyo, 2.Graduate School of Advanced Science and Engineering, Hiroshima University, 3.Metropolitan Industrial Technology Research Institute, 4.Graduate School of Science, the University of Tokyo)

[SGC32-P03] Noble gas isotopic composition of directly ascending petit-spot from the northwest Pacific Ocean

*Kaishi Nakao[1], Naoto Hirano[2], Hirochika Sumino[3] (1.Department of Earth Science, Graduate School of Science, Tohoku University, 2.Center for Northeast Asian Studies, Tohoku University, 3.Graduate School of Arts and Sciences, The University of Tokyo)

[SGC32-P04] Fate of Subducting Organic Carbon: Evidence from HP/UHP Metasedimentary Suites and Implications for Isotopic Compositions of Arc Volcanic Gases

*Gray E Bebout[1], Kaylee H. Kraft[1], Jennie Pinho[2], Gabe S. Epstein[1] (1.Lehigh University, Dept. Earth and Environmental Sciences, Bethlehem, Pennsylvania, USA, 2.Lafayette College, Dept. Chemistry, Easton, Pennsylvania, USA)

[SGC32-P05] **Monitoring the magmatic activity and volatile fluxes of Wakamiko caldera in southern Japan**

*Ma. Teresa Escobar[1], Naoto Takahata[1], Kotaro Shirai[1], Takanori Kagoshima[1,2], Kentaro Tanaka[1], Hajime Obata[1], Yuji Sano[1] (1.Atmosphere and Ocean Research Institute University of Tokyo, 2.University of Toyama)

[SGC32-P06] Heterogeneous accretion of Earth's volatiles as constrained by nitrogen isotopes

*Lanlan Shi[2,1,3], Takanori Kagoshima[2], Yuji Sano[2] (1.State Key Laboratory of Isotope Geochemistry, Guangzhou Institute of 7 Geochemistry, Chinese Academy of Sciences, Guangzhou 510640, China, 2.Division of Ocean-Earth System Science, Atmosphere and Ocean Research Institute, University of Tokyo, Kashiwa, Chiba 277-8564, Japan, 3.University of Chinese Academy of Sciences, Beijing 100049, China)

[SGC32-P07] **Hydrogen isotope of the mantle source in Pitcairn Island**

*Takahiro Ozawa[1], Akira Ishikawa[1], Takeshi Hanyu[2], Kenji Shimizu[3], Takayuki Ushikubo[3], Morihisa Hamada[2], Hikaru Iwamori[4] (1.Department of Earth and Planetary Sciences, Tokyo Institute of Technology, 2.Japan Agency for Marine-Earth Science and Technology, 3.Kochi Core Center, Japan Agency for Marine-Earth Science and Technology, 4.Earthquake Research Institute, the University of Tokyo)

[SGC32-P08] Helium isotope heterogeneity recorded in different phenocrysts in Samoan lavas

*Takeshi Hanyu[1] (1.Japan Agency for Marine-Earth Science and Technology, Research Institute for Marine Geodynamics)

[J] Oral | S (Solid Earth Sciences)：S-GC Geochemistry

1:45 PM - 3:15 PM JST | 4:45 AM - 6:15 AM UTC | Ch.24 Zoom Room 24

[S-GC33] Solid Earth Geochemistry, Cosmochemistry

convener:Gen Shimoda(Geological Survey of Japan, AIST), Katsuhiko Suzuki(Submarine Resources Research Center, Japan Agency for Marine-Earth Science and Technology), Katsuyuki Yamashita(Graduate School of Natural Science and Technology, Okayama University), Akira Ishikawa(Department of Earth and Planetary Sciences, Tokyo Institute of Technology), Chairperson:Katsuhiko Suzuki(Submarine Resources Research Center, Japan Agency for Marine-Earth Science and Technology), Katsuyuki Yamashita(Graduate School of Natural Science and Technology, Okayama University), Akira Ishikawa(Department of Earth and Planetary Sciences, Tokyo Institute of Technology), Gen Shimoda(Geological Survey of Japan, AIST)

1:45 PM - 2:00 PM JST | 4:45 AM - 5:00 AM UTC

[SGC33-01] Highly siderophile elements in Earth's oldest rocks from Acasta Gniess Complex, Canada: an impact melt origin or not?

*Akira Ishikawa[1,2], Keiko Koshida, Katsuhiko Suzuki[2], Tetsuya Yokoyama[1], Tsuyoshi Komiya[3] (1.Department of Earth and Planetary Sciences, Tokyo Institute of Technology, 2.Submarine Resources Research Center, Japan Agency for Marine-Earth Science and Technology, 3.Graduate School of Arts and Sciences, The University of Tokyo)

2:00 PM - 2:15 PM JST | 5:00 AM - 5:15 AM UTC

[SGC33-02] Estimation of highly siderophile element abundances in the primitive mantle from the perspective of the pyrolite model

*Tetsu Kogiso[1], Akira Ishikawa[2], Norikatsu Akizawa[3] (1.Kyoto University, 2.Tokyo Institute of Technology, 3.The University of Tokyo)

2:15 PM - 2:30 PM JST | 5:15 AM - 5:30 AM UTC

[SGC33-03] Chromium and titanium stable isotope measurements for volcanic rocks derived from deep mantle

*Yuki Hibiya[1], Tsuyoshi Iizuka[2], Katsuhiko Suzuki[1], Shigekazu Yoneda[3] (1.Submarine Resources Research Center, Japan Agency for Marine-Earth Science and Technology, 2.The University of Tokyo, 3.National Museum of Nature and Science)

2:30 PM - 2:45 PM JST | 5:30 AM - 5:45 AM UTC

[SGC33-04] $^{182}W/^{184}W$ of the komatiites from Dharwar and Singhbhum cratons, India: implications for the early evolution of the mantle

*Katsuhiko Suzuki[1,5], Madhusoodhan Satish-Kumar[2], Trisrota Chaudhuri[3], M. Jayananda[4] (1.Submarine Resources Research Center, Japan Agency for Marine-Earth Science and Technology, 2.Department of Geology, Faculty of Science, Niigata University, 3.Department of Geology, University of Calcutta, 4.Centre Earth and Space Sciences, University of Hyderabad, 5.Department of Earth Sciences, Graduate School of Science, Tohoku University)

2:45 PM - 3:00 PM JST | 5:45 AM - 6:00 AM UTC

[SGC33-05] The magma generation process of the North Sredinny Range, Kamchatka – Insights from highly siderophile elements and Re-Os isotope system

Yuri Mitsude[1], *Tatsuji Nishizawa[2], Hitomi Nakamura[3], Tatiana Churikova[4], Boris Gordeychik[5], Akira Ishikawa[6], Hikaru Iwamori[1] (1.Earthquake Research Institute, The University of Tokyo, 2.Volcanic Fluid Research Center, School of Science, Tokyo Institute of Technology, 3.Institute of Earthquake and Volcano Geology, Geological Survey of Japan, AIST, 4.Institute of Volcanology and Seismology, Far East Branch, RAS, 5.Institute of Experimental Mineralogy, RAS, 6.Department of Earth and Planetary Sciences, School of Science, Tokyo Institute of Technology)

3:00 PM - 3:15 PM JST | 6:00 AM - 6:15 AM UTC

[SGC33-06] The characteristics of highly siderophile elements in the high-Mg andesite and basalts and its implications for the origin of the Quaternary arc magmatism in the forearc region, Kamchatka

*Tatsuji Nishizawa[1], Yuri Mitsude[2], Hitomi Nakamura[3], Tatiana Churikova[4], Boris Gordeychik[5], Akira Ishikawa[6], Hikaru Iwamori[2] (1.Volcanic Fluid Research Center, School of Science, Tokyo Institute of Technology, 2.Earthquake Research Institute, The University of Tokyo, 3.Institute of Earthquake and Volcano Geology, Geological Survey of Japan, AIST, 4.Institute of Volcanology and Seismology, Far East Branch, RAS, 5.Institute of Experimental Mineralogy, RAS, 6.Department of Earth and Planetary Sciences, School of Science, Tokyo Institute of Technology)

[J] Poster | S (Solid Earth Sciences)：S-GC Geochemistry

5:15 PM - 6:30 PM JST | 8:15 AM - 9:30 AM UTC | Ch.17_2

[S-GC33] Solid Earth Geochemistry, Cosmochemistry

convener:Gen Shimoda(Geological Survey of Japan, AIST), Katsuhiko Suzuki(Submarine Resources Research Center, Japan Agency for Marine-Earth Science and Technology), Katsuyuki Yamashita(Graduate School of Natural Science and Technology, Okayama University), Akira Ishikawa(Department of Earth and Planetary Sciences, Tokyo Institute of Technology)

[SGC33-P01] Origin of intra-plate magmatism in Kamchatka constrained by noble gas isotopes

*Masao Fukagawa[1], Hirochika Sumino[2], Anna O Volynets[3], Yuri Taran[3] (1.Department of Integrated Science, College of Arts and Science, the University of Tokyo, 2.Department of General Systems Studies Graduate School of Arts and Sciences, The University of Tokyo, 3.Russian Academy of Sciences)

[SGC33-P02] **Rare earth elements composition of carbonate concretion in the Miocene Morozaki Group, southwestern Japan**

*Ryosuke Kitanaka[1], Motohiro Tsuboi[1] (1.Kwansei Gakuin University)

[SGC33-P03] Investigation of Validity for Evaluation Particle numbers on Characterization of Soil Particle Morphology Using Automated Particle Image Analysis and Computed Simulations.

*Daisuke Sasakura[1] (1.Malvern Japan ,Div of Spectris Co.Ltd,.)

[SGC33-P04] Role of fluid rock reaction for the production of FOZO isotopic composition

*Gen Shimoda[1], Tetsu Kogiso[2], Katsuhiko Suzuki[3], Akira Ishikawa[4], Norikatsu Akizawa[5] (1.Geological Survey of Japan, AIST, 2.Kyoto University, 3.Japan Agency for Marine-Earth Science and Technology, 4.Tokyo Institute of Technology, 5.University of Tokyo)

[J] Oral | S (Solid Earth Sciences)：S-TT Technology & Techniques

9:00 AM - 10:30 AM JST | 12:00 AM - 1:30 AM UTC | Ch.22 Zoom Room 22

[S-TT36] Synthetic Aperture Radar and its application

convener:Yohei Kinoshita(University of Tsukuba), Takahiro Abe(Graduate School of Bioresources, Mie University), Shoko Kobayashi(Tamagawa University), Yuji Himematsu(National Research Institute for Earth Science and Disaster Resilience), Chairperson:Takahiro Abe(Graduate School of Bioresources, Mie University), Yohei Kinoshita(University of Tsukuba)

9:00 AM - 9:15 AM JST | 12:00 AM - 12:15 AM UTC

[STT36-01] Automatic error-term estimation approach for improving the accuracy of InSAR time-series analysis - Example on the Arima-Takatsuki Fault Zone, Japan

*Yo Fukushima[1] (1.International Research Institute of Disaster Science, Tohoku University)

9:15 AM - 9:30 AM JST | 12:15 AM - 12:30 AM UTC

[STT36-02] Correlation between surface displacement and groundwater level displacement in the periods before and after the 2018 Northern Osaka earthquake

*Yutaro Shigemitsu[1], Kazuya Ishitsuka[1], Weiren Lin[1] (1.Kyoto University Graduate School of Engineering)

9:30 AM - 9:45 AM JST | 12:30 AM - 12:45 AM UTC

[STT36-03] Landslide and its displacement along the Marsyangdi River, Nepal detected by differential interferometric SAR

*Seiya Usami[1], Hiroshi, P. Sato[2], Hiroshi YAGI[3] (1.Grad student, Graduate School of Science and Technology, Nihon University, 2.College of Humanities and Science, Nihon University, 3.Faculty of Art, Science and Education, Yamagata University)

9:45 AM - 10:00 AM JST | 12:45 AM - 1:00 AM UTC

[STT36-04] Road blockage detection due to landslides using Sentinel-1 intensity images

*Keisho Ito[1], Yohei Kinoshita[1] (1.Tsukuba University)

10:00 AM - 10:15 AM JST | 1:00 AM - 1:15 AM UTC

[STT36-05] Short-term glacier velocity changes in the Southern Patagonian Ice Field detected by the Sentinel-1 satellite

*Yuya Ito[1], Masato Furuya[2] (1.Graduate School of Science, Hokkaido University, 2.Department of Earth and Planetary Hokkaido University)

10:15 AM - 10:30 AM JST | 1:15 AM - 1:30 AM UTC

[STT36-06] Discussion of the colour map for SAR interferograms

*Morishita Yu[1] (1.Geospatial Information Authority of Japan)

[J] Oral | S (Solid Earth Sciences)：S-TT Technology & Techniques

10:45 AM - 12:15 PM JST | 1:45 AM - 3:15 AM UTC | Ch.22 Zoom Room 22

[S-TT36] Synthetic Aperture Radar and its application

convener:Yohei Kinoshita(University of Tsukuba), Takahiro Abe(Graduate School of Bioresources, Mie University), Shoko Kobayashi(Tamagawa University), Yuji Himematsu(National Research Institute for Earth Science and Disaster Resilience), Chairperson:Masatsugu otsuki(Institute of Space and Astronautical Science, Japan Aerospace Exploration Agency), Yuji Himematsu(National Research Institute for Earth Science and Disaster Resilience)

10:45 AM - 11:00 AM JST | 1:45 AM - 2:00 AM UTC

[STT36-07] Examination of extraction method of topographical change due to eruption of Nishinoshima using time series SAR

*Daiki Inano[1], Masanobu Shimada[2] (1.Tokyo Denki University, graduate school of science and engineering ,division of architectural, civil and environmental engineering, 2.Tokyo Denki University, division of architectural, civil and environmental engineering)

11:00 AM - 11:15 AM JST | 2:00 AM - 2:15 AM UTC

[STT36-08] Tropospheric Dispersive Phase Anomalies during Heavy Rain Detected by L-band InSAR and Their Interpretation

Naufal Setiawan[1], *Masato Furuya[1] (1.Department of Earth and Planetary Sciences Hokkaido University)

11:15 AM - 11:30 AM JST | 2:15 AM - 2:30 AM UTC

[STT36-09] Error level evaluation of L-Band InSAR Water Vapor Observation by Comparison with GNSS Observations

*Keita Matsuzawa[1], Yohei Kinoshita[1] (1.University of Tsukuba)

11:30 AM - 11:45 AM JST | 2:30 AM - 2:45 AM UTC

[STT36-10] **Comparison of atmospheric delay correction methods in InSAR: Case study in Japan**

*Sardila Nurulhikmah Sailellah[1], Yo Fukushima[2] (1.Geophysics Department, Graduate School of Science Tohoku University, 2.International Research Institute of Disaster Science, Tohoku University)

11:45 AM - 12:00 PM JST | 2:45 AM - 3:00 AM UTC

[STT36-11] Development of ground-based radar interferometer for volcano deformation monitoring

*Taku Ozawa[1], Yuji Himematsu[1] (1.National Research Institute for Earth Science and Disaster Resilience)

12:00 PM - 12:15 PM JST | 3:00 AM - 3:15 AM UTC

[STT36-12] Small SAR satellite development and solution services

★Invited Papers

*Shuji Fujimaru[1] (1.Synspective Inc.)

[J] Poster | S (Solid Earth Sciences)：S-TT Technology & Techniques

5:15 PM - 6:30 PM JST | 8:15 AM - 9:30 AM UTC | Ch.18_1

[S-TT36] Synthetic Aperture Radar and its application

convener:Yohei Kinoshita(University of Tsukuba), Takahiro Abe(Graduate School of Bioresources, Mie University), Shoko Kobayashi(Tamagawa University), Yuji Himematsu(National Research Institute for Earth Science and Disaster Resilience)

[STT36-P01] Long-term crustal deformation of domestic volcanoes detected by InSAR time series analysis

*Kano Mikihara[1], Takaaki Inukai[1], Nobuhiro Ishikura[1], Kumi Shimazaki[1], Masayoshi Ishimoto[1], Tomokazu Kobayashi[1] (1.GSI of Japan)

[STT36-P02] Surface displacement in Hachijojima Island since 2014 by InSAR analysis and GNSS

*yusei Hamamura[1], HIROYUKI AZUMA[1], Yoshiya Oda[1] (1.Tokyo Metropolitan University)

[STT36-P03] Observing Crustal Deformation Using Interferometric Synthesis Aperture Rader and Estimating Magma Chamber Associating with the 2018 Eruption of Shinmoedake of Kirishima Volcanoes, Japan.

*Takahisa Tashiro[1], Koichi Suzuki[2] (1.Cooperative Program for Resources Engineering, Graduate School of Engineering, Hokkaido University, 2.Research Group of Geoenvironmental Engineering, Division of Sustainable Resource Engineering, Faculty of Engineering, Hokkaido University)

[STT36-P04] **Using InSAR for evaluating the accuracy of earthquake location determination, Comparison of Iranian and Japanese cases**

*Nematollah Ghayournajarkar[1], Yo Fukushima[2] (1.Graduate School of Science, Tohoku University, 2.International Research Institute of Disaster Science, Tohuku University)

[STT36-P05] Progress on developing a GNSS-based InSAR atmospheric delay correction model

*Yohei Kinoshita[1] (1.University of Tsukuba)

[STT36-P06] **Ship Detection Using Synthetic Aperture Radar**

*Kengo Iwata[1], Masanobu Shimada[1] (1.Tokyo Denki University)

[J] Oral | S (Solid Earth Sciences)：S-TT Technology & Techniques

9:00 AM - 10:30 AM JST | 12:00 AM - 1:30 AM UTC | Ch.21 Zoom Room 21

[S-TT38] Creating future of solid Earth science with high performance computing (HPC)

convener:Takane Hori(R&D Center for Earthquake and Tsunami, Japan Agency for Marine-Earth Science and Technology), Yuji Yagi(Graduate School of Life and Environmental Sciences, University of Tsukuba, Tsukuba), Katsuhiko Shiomi(National Research Institute for Earth Science and Disaster Resilience), Ryoichiro Agata(Japan Agency for Marine-Earth Science and Technology), Chairperson:Takane Hori(R&D Center for Earthquake and Tsunami, Japan Agency for Marine-Earth Science and Technology), Ryoichiro Agata(Japan Agency for Marine-Earth Science and Technology)

9:00 AM - 9:15 AM JST | 12:00 AM - 12:15 AM UTC

[STT38-01] On large-scale numerical simulation of earthquake generation, wave propagation and soil amplification aiming for comprehensive earthquake damage estimation

Takane Hori[1], Tsuyoshi Ichimura[2,3,4], Kohei Fujita[2,3], *Ryoichiro Agata[1] (1.Japan Agency for Marine-Earth Science and Technology, 2.Earthquake Research Institute, 3.Riken Center for Computational Science, 4.Riken Center for Advance Intelligence Project)

9:15 AM - 9:30 AM JST | 12:15 AM - 12:30 AM UTC

[STT38-02] Large-scale earthquake simulation with supercomputing and data-learning

★Invited Papers

*Tsuyoshi Ichimura[1] (1.the University of Tokyo)

9:30 AM - 9:45 AM JST | 12:30 AM - 12:45 AM UTC

[STT38-03] Comparison of E-wave FEM and GMS in Calculation of Long-Period Ground Motion in 3D Heterogeneous Underground Structures

*Ryoichiro Agata[1], Yoshihisa Hiyoshi[1], Sayako Hirobe[1], Takahiro Maeda[2], Asako Iwaki[2], Kohei Fujita[3,4], Hiroyuki Fujiwara[2], Tsuyoshi Ichimura[3,4,5], Takane Hori[1] (1.Japan Agency for Marine-Earth Science and Technology, 2.National Research Institute for Earth Science and Disaster Resilience, 3.Earthquake Research Institute, 4.Riken Center for Computational Science, 5.Riken Center for Advance Intelligence Project)

9:45 AM - 10:00 AM JST | 12:45 AM - 1:00 AM UTC

[STT38-04] Three-dimensional thermal structure modeling in the Alaska subduction zone

*Kaya Iwamoto[1], Nobuaki Suenaga[2], Shoichi Yoshioka[2,1] (1.Department of Planetology, Graduate School of Science, Kobe University, 2. Research Center for Urban Safety and Security, Kobe University,)

10:00 AM - 10:15 AM JST | 1:00 AM - 1:15 AM UTC

[STT38-05] Sensitivity analysis with large-scale 3D finite element crust structure model for seafloor geodetic constraints on coseismic slip and interseismic slip-deficit distributions

*Sota Murakami[1], Tsuyoshi Ichimura[1], Kohei Fujita[1], Takane Hori[2], Yusaku Ohta[3] (1.Earthquake Research Institute, The University of Tokyo, 2.R&D Center for Earthquake and Tsunami, Japan Agency for Marine-Earth Science and Technology, 3.Research Center for Prediction of Earthquakes and Volcanic Eruptions, Graduate School of Science, Tohoku University)

10:15 AM - 10:30 AM JST | 1:15 AM - 1:30 AM UTC

[STT38-06] Discussion

[J] Poster | S (Solid Earth Sciences)：S-TT Technology & Techniques

5:15 PM - 6:30 PM JST | 8:15 AM - 9:30 AM UTC | Ch.13_3

[S-TT38] Creating future of solid Earth science with high performance computing (HPC)

convener:Takane Hori(R&D Center for Earthquake and Tsunami, Japan Agency for Marine-Earth Science and Technology), Yuji Yagi(Graduate School of Life and Environmental Sciences, University of Tsukuba, Tsukuba), Katsuhiko Shiomi(National Research Institute for Earth Science and Disaster Resilience), Ryoichiro Agata(Japan Agency for Marine-Earth Science and Technology)

[STT38-P01] CMT catalog based on a local 3D structure model for simulations of long-period ground motions in the Kanto region, Japan

*Kazuo Yoshimoto[1], Kosuke Minamihama[1], Shunsuke Takemura[2], Katsuhiko Shiomi[3] (1.Yokohama City University, 2.Earthquake Research Institute, The University of Tokyo, 3.NIED)

[STT38-P02] Coordinate Independent Visualization Method for Stress Tensor Field by Using Principal Axis Line

*Sayako Hirobe[1], Kenji Oguni[1], Muneo Hori[1] (1.Japan Agency for Marine-Earth Science and Technology)

[E] Oral | S (Solid Earth Sciences)：S-CG Complex & General

10:45 AM - 12:15 PM JST | 1:45 AM - 3:15 AM UTC | Ch.21 Zoom Room 21

[S-CG39] Science of slow earthquakes: Toward unified understandings of whole earthquake process

convener:Satoshi Ide(Department of Earth an Planetary Science, University of Tokyo), Hitoshi Hirose(Research Center for Urban Safety and Security, Kobe University), Kohtaro Ujiie(Faculty of Life and Environmental Sciences, University of Tsukuba), Takahiro Hatano(Department of Earth and Space Science, Osaka University), Chairperson:Kohtaro Ujiie(Faculty of Life and Environmental Sciences, University of Tsukuba)

10:45 AM - 11:00 AM JST | 1:45 AM - 2:00 AM UTC

[SCG39-01] The stabilizing effect of pore-fluid pressure along subduction megathrust faults: Evidence from experiments on Nankai Trough sediments

*John D Bedford[1,2], Daniel R Faulkner[2], Michael J Allen[2], Takehiro Hirose[1] (1.JAMSTEC, 2.Univ. of Liverpool)

11:00 AM - 11:15 AM JST | 2:00 AM - 2:15 AM UTC

[SCG39-02] **Depth-dependent deep-slow earthquakes controlled by temperature dependence of brittle-ductile transitional rheology**

*Ryosuke Ando[1], Kohtaro Ujiie[2], Naoki Nishiyama[2], Yasushi Mori[3] (1.Graduate School of Science, University of Tokyo, 2.Graduate School of Life and Environmental Sciences, University of Tsukuba, 3.Kitakyushu Museum of Natural History and Human History)

11:15 AM - 11:30 AM JST | 2:15 AM - 2:30 AM UTC

[SCG39-03] **Localized megathrust slip controlled by chemical reactions in subduction mélanges**

*Kohtaro Ujiie[1], Kazuya Noro[2], Norio Shigematsu[3], Ake Fagereng[4], Naoki Nishiyama[1], Christopher Tulley[4], Haruna Masuyama[2], Yasushi Mori[5] (1.Faculty of Life and Environmental Sciences, University of Tsukuba, 2.Graduate School of Life and Environmental Sciences, University of Tsukuba, 3.Geological Survey of Japan, National Institute of Advanced Industrial Science and Technology, 4.School of Earth and Environmental Sciences, Cardiff University, 5.Kitakyushu Museum of Natural History and Human Histor)

11:30 AM - 11:45 AM JST | 2:30 AM - 2:45 AM UTC

[SCG39-04] Lithological heterogeneity and fluid flow related to seamount subduction: an exhumed example from Amami-Oshima Island

*Madison Frank[1], Ginta Motohashi[1], Kohtaro Ujiie[2] (1.Graduate School of Life and Environmental Sciences, University of Tsukuba, 2.Faculty of Life and Environmental Sciences, University of Tsukuba)

11:45 AM - 12:00 PM JST | 2:45 AM - 3:00 AM UTC

[SCG39-05] Constraints on silica transport along subduction boundaries based on volume change estimates of metamorphic rocks

*Shogo Soejima[1], Simon Richard Wallis[1] (1.Department of Earth and Planetary Science, Graduate School of Science, The University of Tokyo)

12:00 PM - 12:15 PM JST | 3:00 AM - 3:15 AM UTC

[SCG39-06] Discussion

[E] Oral | S (Solid Earth Sciences)：S-CG Complex & General

1:45 PM - 3:15 PM JST | 4:45 AM - 6:15 AM UTC | Ch.21 Zoom Room 21

[S-CG39] Science of slow earthquakes: Toward unified understandings of whole earthquake process

convener:Satoshi Ide(Department of Earth an Planetary Science, University of Tokyo), Hitoshi Hirose(Research Center for Urban Safety and Security, Kobe University), Kohtaro Ujiie(Faculty of Life and Environmental Sciences, University of Tsukuba), Takahiro Hatano(Department of Earth and Space Science, Osaka University), Chairperson:Takahiro Hatano(Department of Earth and Space Science, Osaka University)

1:45 PM - 2:00 PM JST | 4:45 AM - 5:00 AM UTC

[SCG39-07] Systematic understanding of the slip-front-propagation velocity in terms of Linear Marginal Stability Hypothesis

*Takehito Suzuki[1] (1.Department of Physics and Mathematics, Aoyama Gakuin University)

2:00 PM - 2:15 PM JST | 5:00 AM - 5:15 AM UTC

[SCG39-08] Effects of periodic stress perturbations on earthquake nucleation

*Takuya Saito[1], Takahiro Hatano[2] (1.Aoyama Gakuin University, 2.Osaka University)

2:15 PM - 2:30 PM JST | 5:15 AM - 5:30 AM UTC

[SCG39-09] Feasibility of periodic solution in Rate-State friction Law

*Ryo Mizushima[1], Takahiro Hatano[1] (1.Department of Earth and Space Science, Osaka University)

2:30 PM - 2:45 PM JST | 5:30 AM - 5:45 AM UTC

[SCG39-10] **Slow earthquake signatures in the ratio between acoustic and internal gravity wave amplitudes in coseismic ionospheric disturbances**

*Kosuke Heki[1], Yuki Takasaka [1] (1.Department of Earth and Planetary Sciences, Faculty of Science, Hokkaido University)

2:45 PM - 3:00 PM JST | 5:45 AM - 6:00 AM UTC

[SCG39-11] Observation of shallow slow slip event propagating updip to the trough in the Nankai Trough.

*Eiichiro Araki[1], Takeshi Iinuma[1], Yojiro Yamamoto[1], Toshinori Kimura[1], Yuya Machida[1], Ryoichiro Agata[1], Keisuke Ariyoshi[1], Tsuyoshi Ichimura[2], Takane Hori[1], Shuichi Kodaira[1] (1.Japan Agency for Marine-Earth Science and Technology, 2.Earthquake Research Insitute, the University of Tokyo)

3:00 PM - 3:15 PM JST | 6:00 AM - 6:15 AM UTC

[SCG39-12] Discussion

[E] Oral | S (Solid Earth Sciences)：S-CG Complex & General

3:30 PM - 5:00 PM JST | 6:30 AM - 8:00 AM UTC | Ch.21 Zoom Room 21

[S-CG39] Science of slow earthquakes: Toward unified understandings of whole earthquake process

convener:Satoshi Ide(Department of Earth an Planetary Science, University of Tokyo), Hitoshi Hirose(Research Center for Urban Safety and Security, Kobe University), Kohtaro Ujiie(Faculty of Life and Environmental Sciences, University of Tsukuba), Takahiro Hatano(Department of Earth and Space Science, Osaka University), Chairperson:Hitoshi Hirose(Research Center for Urban Safety and Security, Kobe University)

3:30 PM - 3:45 PM JST | 6:30 AM - 6:45 AM UTC

[SCG39-13] Development of the detection method for short-term slow slip events using GNSS data and its application to the Nankai subduction zone

*Yutaro Okada[1], Takuya Nishimura[2], Takao Tabei[3], Takeshi Matsushima[4], Hitoshi Hirose[5] (1.Graduate School of Science, Kyoto University, 2.Disaster Prevention Research Institute, Kyoto University, 3.Faculty of Science and Technology, Kochi University, 4.Faculty of Science, Kyushu University, 5.Research Center for Urban Safety and Security, Kobe University)

3:45 PM - 4:00 PM JST | 6:45 AM - 7:00 AM UTC

[SCG39-14] Spatiotemporal slip distributions of the 2018-2019 Bungo Channel long-term slow slip event

*Yukinari Seshimo[1], Shoichi Yoshioka[2,1] (1.Department of Planetology, Graduate School of Science, Kobe University, 2.Research Center for Urban Safety and Security, Kobe University)

4:00 PM - 4:15 PM JST | 7:00 AM - 7:15 AM UTC

[SCG39-15] What controls along-strike variations in Long term SSE recurrence intervals in the Western Nankaui Subduction Zone?

*Takanari Ohata[1], SHINICHI MIYAZAKI[1], Kazuro Hirahara[2] (1.KYOTO UNIVERSITY, 2.KAGAWA UNIVERSITY)

4:15 PM - 4:30 PM JST | 7:15 AM - 7:30 AM UTC

[SCG39-16] Post-seismic to Co-seismic Moment Ratio: a Case Study of the 2016 Moderate Earthquakes along Chaman Fault Inferred from Sentinel-1 InSAR Time-Series

*Masato Furuya[1], Fumiko Matsumoto[2] (1.Department of Earth and Planetary Sciences Hokkaido University, 2.PASCO)

4:30 PM - 4:45 PM JST | 7:30 AM - 7:45 AM UTC

[SCG39-17] The moment release rate of short-term slow slip events in the northern Kii Peninsula from 2002 to 2015 based on NIED Hi-net tilt data

*Naoya Chujo[1], Hitoshi Hirose[2,1,3], Takeshi Kimura[3] (1.Department of Planetology, Graduate School of Science, Kobe University, 2.Research Center for Urban Safety and Security, Kobe University, 3.National Research Institute for Earth Science and Disaster Resilience)

4:45 PM - 5:00 PM JST | 7:45 AM - 8:00 AM UTC

[SCG39-18] Discussion

[J] Oral | S (Solid Earth Sciences)：S-CG Complex & General

9:00 AM - 10:30 AM JST | 12:00 AM - 1:30 AM UTC | Ch.19 Zoom Room 19

[S-CG45] Ocean Floor Geoscience

convener:Kyoko Okino(Atmosphere and Ocean Research Institute, The University of Tokyo), Chairperson:Yukari Kido(Japan Agency for Marine-Earth Science and Technology), Asuka Yamaguchi(Atomosphere and Ocean Research Institute, The University of Tokyo)

9:00 AM - 9:15 AM JST | 12:00 AM - 12:15 AM UTC

[SCG45-01] JAMSTEC Contribution to the NIPPON FOUNDATION-GEBCO SEABED2030 Project

*Yukari Kido[1], Mitsuko Hidaka[1], Daisuke Matsuoka[1], Tatsu Kuwatani[1], Junji Kaneko[1], Takafumi Kasaya[1], Yoichi Ishikawa[1], Eiichi Kikawa[1] (1.Japan Agency for Marine-Earth Science and Technology)

9:15 AM - 9:30 AM JST | 12:15 AM - 12:30 AM UTC

[SCG45-02] The new tectonic model between the Madagascar Ridge and the Del Cano Rise in the southern Indian Ocean

*Taichi Sato[1], Yoshifumi Nogi[2], Hiroshi Sato[3], Masakazu Fujii[2] (1.National Institute of Advanced Industrial Science and Technology, 2.National Institute of Polar Research, 3.Senshu University)

9:30 AM - 9:45 AM JST | 12:30 AM - 12:45 AM UTC

[SCG45-03] Sedimentation process at the South Shetland Trench in the Antarctic Ocean

*Asuka Yamaguchi[1] (1.Atomosphere and Ocean Research Institute, The University of Tokyo)

9:45 AM - 10:00 AM JST | 12:45 AM - 1:00 AM UTC

[SCG45-04] Highly refractory dunite formation in Gibbs Island and Bruce Bank, and its role in the evolution of the circum-Antarctic continent

*Norikatsu Akizawa[1], Asuka Yamaguchi[1], Chihiro Ohshima[1], Kenichiro Tani[2], Akira Ishikawa[3], Ryo Fujita[3], SUNG HI CHOI[4] (1.Atmosphere and Ocean Research Institute, The University of Tokyo, 2.National Museum of Nature and Science, 3.Tokyo Institute of Technology, 4.Chungnam National University)

10:00 AM - 10:15 AM JST | 1:00 AM - 1:15 AM UTC

[SCG45-05] Magmatic evolutions erupted on the Cretaceous seamount province, western Pacific Plate

*Naoto Hirano[1], Hirochika Sumino[2], Taisei Morishita[3] (1.Center for Northeast Asian Studies, Tohoku University, 2.Graduate School of Arts and Sciences, The University of Tokyo, 3.Hydrographic and Oceanographic Department, Japan Coast Guard)

10:15 AM - 10:30 AM JST | 1:15 AM - 1:30 AM UTC

[SCG45-06] **Pre-stack depth imaging and pore-fluid pressure estimation along the Nankai Trough subduction zone off the Kii Peninsula, SW Japan**

*YU FAN[1], Ehsan Jamali Hondori[1], Jin-Oh Park[1] (1.The University of Tokyo)

[J] Oral | S (Solid Earth Sciences)：S-CG Complex & General

10:45 AM - 12:15 PM JST | 1:45 AM - 3:15 AM UTC | Ch.19 Zoom Room 19

[S-CG45] Ocean Floor Geoscience

convener:Kyoko Okino(Atmosphere and Ocean Research Institute, The University of Tokyo), Chairperson:Ryuta Arai(Japan Agency for Marine-Earth Science and Technology), Masakazu Fujii(National Institute of Polar Research and SOKENDAI)

10:45 AM - 11:00 AM JST | 1:45 AM - 2:00 AM UTC

[SCG45-07] Marine and earth science surveys in the Okinawa Trough for the IODP Scientific Drilling: Hakuhomaru KH-21-3 cruise preliminary reports

*Makoto Otsubo[1], Yoshimi Kubota[2], Ayanori Misawa[1], Ken Ikehara[1], Saki Ishino[1], Masataka Kinoshita[3], Kenji Matsuzaki[4], Katsura Kameo[4], Chiori Tamura[4], Ryuta Arai[5], Tomohiro Toki[6], Yuki Mitsudome[6], Zhirong Cai[7], Keiko Takehara[8], Kodai Kato[8], Daisuke Kuwano[9], Koshiro Matsuo[10], Keita Suzuki[11], Misaki Horiuchi[11], Yohei Katayama[12], Satoshi Okumura[13] (1.Geological Survey of Japan, AIST, 2.National Museum of Nature and Science, 3.The University of Tokyo, ERI, 4.The University of Tokyo, AORI, 5.JAMSTEC, 6.University of Ryukyus, 7.Kyoto University, 8.Kochi University, 9.Chiba University, 10.Kyushu University, 11.Nippon Marine Enterprises, Ltd., 12.Marine Works Japan, Ltd., 13.MOL Marine Co., Ltd.)

11:00 AM - 11:15 AM JST | 2:00 AM - 2:15 AM UTC

[SCG45-08] Structure and seismicity in the southern part of the Okinawa Trough and their implications for rifting and volcanic processes

*Ryuta Arai[1], Ayanori Misawa[2], Makoto Otsubo[2], Saki Ishino[2], Masataka Kinoshita[3], KH-21-3 Shipboard Scientists (1.Japan Agency for Marine-Earth Science and Technology, 2.Geological Survey of Japan, National Institute of Advanced Industrial Science and Technology, 3.Earthquake Research Institute, The University of Tokyo)

11:15 AM - 11:30 AM JST | 2:15 AM - 2:30 AM UTC

[SCG45-09] Heat flow anomaly in the southern part of Okinawa Trough – A preliminary result from the KH-21-3 cruise-

*Masataka Kinoshita[1], Ryuta Arai[2], Chiori Tamura[3], Ayanori Misawa[4], Saki Ishino[4], Makoto Otsubo[4], Shipboard Scientists KH-21-3 (1.Earthquake Research Institute, The University of Tokyo, 2.Japan Agency for Marine-Earth Science and Technology, 3.Atmospheric and Ocean Research Institute, the University of Tokyo, 4.National Institute of Advanced Industrial Science and Technology)

11:30 AM - 11:45 AM JST | 2:30 AM - 2:45 AM UTC

[SCG45-10] GNSS/Acoustic geodetic measurement at the southern end of Ryukyu Trench 2014-2020

*Akihiro Nagaya[1], Ryoya Ikuta[2], Mamoru Nakamura[3], Masataka Ando[4] (1.Undergraduate school of department of Geoscience, Shizuoka University, 2.Faculty of Science, Shizuoka University, 3.Faculty of Science, University of the Ryukyu, 4.Center for Natural Hazards of Integrated Education and Research, Shizuoka University)

11:45 AM - 12:00 PM JST | 2:45 AM - 3:00 AM UTC

[SCG45-11] Fluid-flow simulation for clarifying ore generation processes in the Izena Hole hydrothermal field, Okinawa Trough

*Shohei Albert Tomita[1], Katsuaki Koike[1], Tada-nori Goto[2], Katsuhiko Suzuki[3], Takafumi Kasaya[3] (1.Graduate School of Engineering, Kyoto University, 2.Graduate School of Life Science, University of Hyogo, 3.Research and Development Center for Submarine Resources, Japan Agency for Marine-Earth Science and Technology (JAMSTEC))

12:00 PM - 12:15 PM JST | 3:00 AM - 3:15 AM UTC

[SCG45-12] Examining the origin and depositional process of turbidites in the southern part of Okinawa Trough based on cores from Expedition KH-21-3

*Cai Zhirong[1], Hajime Naruse[1], Ken Ikehara[2], KH-21-3 Shipboard Scientists - (1.Department of Geology and Mineralogy, Graduate School of Science, Kyoto University, 2.Institute of Geology and Geoinformation, National Institute of Advanced Industrial Science and Technology)

[J] Oral | S (Solid Earth Sciences)：S-CG Complex & General

1:45 PM - 3:15 PM JST | 4:45 AM - 6:15 AM UTC | Ch.19 Zoom Room 19

[S-CG45] Ocean Floor Geoscience

convener:Kyoko Okino(Atmosphere and Ocean Research Institute, The University of Tokyo), Chairperson:Motoyuki Kido(International Research Institute for Disaster Science, Tohoku University), Fumiaki Tomita(Japan Agency for Marine-Earth Science and Technology)

1:45 PM - 2:00 PM JST | 4:45 AM - 5:00 AM UTC

[SCG45-13] Preliminary results of ocean bottom pressure observation around Kikai submarine caldera, SW Japan

Yuko Asai[1], *Nobukazu Seama[1,2], Tomoko Hanyu[2], Tetsuo Matsuno[2,1], Hitoshi Hirose[3,1], Takuto Minami[1], Hiroko Sugioka[2,1] (1.Department of Planetology, Graduate School of Science, Kobe University, 2.Kobe Ocean Bottom Exploration Center, Kobe University, 3.Research Center for Urban Safety and Security, Kobe University)

2:00 PM - 2:15 PM JST | 5:00 AM - 5:15 AM UTC

[SCG45-14] Characteristic of depth dependence and annual variation of OBP time series in DONET

*Hideto Otsuka[1], Yusaku Ohta[1], Ryota Hino[1], Tatsuya Kubota[2], Daisuke Inazu[3] (1.Department of Geophysics, Graduate School of Science, Tohoku University, 2.National Research Institute for Earth Science and Disaster Resilience, 3.Department of Marine Resources and Energy, Tokyo University of Marine Science and Technology)

2:15 PM - 2:30 PM JST | 5:15 AM - 5:30 AM UTC

[SCG45-15] GNSS-Acoustic observations using a Wave Glider and their results

*Fumiaki Tomita[1], Takeshi Iinuma[1], Motoyuki Kido[2], Yusaku Ohta[3], Chie Honsho[3], Tatsuya Fukuda[1], Takane Hori[1] (1.Japan Agency for Marine-Earth Science and Technology, 2.International Research Institute of Disaster Science, Tohoku University, 3.Graduate School of Science, Tohoku University)

2:30 PM - 2:45 PM JST | 5:30 AM - 5:45 AM UTC

[SCG45-16] Semi-realtime transmission of GNSS-A data using a Wave Glider

*Motoyuki Kido[1], Tatsuya Fukuda[2], Yusaku Ohta[3], Fumiaki Tomita[2], Chie Honsho[3], Takeshi Iinuma[2] (1.IRIDeS, Tohoku University, 2.JAMSTEC, 3.Sci. Division, Tohoku University)

2:45 PM - 3:00 PM JST | 5:45 AM - 6:00 AM UTC

[SCG45-17] Operation experiment of the system for seafloor crustal deformation observation system using a buoy

*Keiichi Tadokoro[1], Natsuki Kinugasa[1], Teruyuki Kato[2], Yukihiro Terada[3], Kenjiro Matsuhiro[4], Haruno Koike[4] (1.Research Center for Seismology, Volcanology and Earthquake and Volcano Research Center, Nagoya University, 2.Hot Springs Research Institute of Kanagawa Prefectural Government, 3.National Institute of Technology, Kochi College, 4.Technical Center, Nagoya University)

3:00 PM - 3:15 PM JST | 6:00 AM - 6:15 AM UTC

[SCG45-18] Initial results of sea trials on bathymetric survey performance of “AUV-NEXT”: aiming to acquire higher-quality bathymetric data

*MASANAO SUMIYOSHI[1], Ryosuke Nagasawa[1], Takashi Hashimoto[1], Kenji Nagahashi[2], Takao Sawa[2], Tadahiro Hyakudome[2], Takeshi Nakatani[2], Tatsuya Aso[2], Yusuke Yokota[3] (1.Hydrographic and Oceanographic Department, Japan Coast Guard, 2.JAMSTEC, 3.Institute of Industrial Science, University of Tokyo)

[J] Poster | S (Solid Earth Sciences)：S-CG Complex & General

5:15 PM - 6:30 PM JST | 8:15 AM - 9:30 AM UTC | Ch.19_1

[S-CG45] Ocean Floor Geoscience

convener:Kyoko Okino(Atmosphere and Ocean Research Institute, The University of Tokyo)

[SCG45-P01] **Temporal variation of crustal accretion along the Vulcan Transform, the Southern Ocean: Preliminary results of KH-19-6 cruise**

*Kyoko Okino[1], Kenichiro Tani[2], Osamu Ishizuka[3], Hiroaki Koge[3], JINYU ZHOU[1] (1.Atmosphere and Ocean Research Institute, The University of Tokyo, 2.National Museum of Nature and Science, 3.National Institute of Advanced Industrial Science and Technology)

[SCG45-P02] S wave velocity structure at the Kairei Hydrothermal Vent Field near the Rodriguez Triple Junction in the Indian Ocean

*Ayato Morii[1], Toshinori Sato[1], Hiroyoshi Takata[1], Tomoaki Yamada[2], Masanao Shinohara[3] (1.Chiba Unv., 2.JMA, 3.ERI, Unv. Tokyo)

[SCG45-P03] **Deep-tow magnetics for 29–33 Myr seafloor of the Southeast Indian Ridge**

*Masakazu Fujii[1,2], Kyoko Okino[3], Chiori Tamura[3] (1.National Institute of Polar Research, 2.SOKENDAI (The Graduate University for Advanced Studies), 3.AORI, UTokyo)

[SCG45-P04] **Magnetic and gravity constraints on crustal structure of the Nosappu Fracture Zone, Northwestern Pacific**

*Mai Kintsu[1], Nobukazu Seama[1], Masakazu Fujii[2,3], Tomoko Hanyu[4] (1.Department of Planetology, Graduate School of Science, Kobe University, 2.National Institute of Polar Research, 3.SOKENDAI (The Graduate University for Advanced Studies), 4.Kobe Ocean-Bottom Exploration Center)

[SCG45-P05] Multibeam bathymetric and single-channel seismic surveys of the Mid-Slope Terrace off Sanriku in the northern Japan Trench

*Toshiya Fujiwara[1], Toshiya Kanamatsu[1], KanHsi Hsiung[1] (1.Research Institute for Marine Geodynamics, Japan Agency for Marine-Earth Science and Technology)

[SCG45-P06] Deformation of the upper plate within the Tohoku Region Pacific Coast analyzed by the top surface structure

*Hiroaki Koge[1], Ayanori Misawa[1], Toshiya Fujiwara[2], Yoshiaki Suzuki[1], Yusuke Sato[3], Ryosuke Komatsu[5], Chiori Tamura[4], Katsura Kameo[4] (1.AIST, 2.JAMSTEC, 3.Tokai Univ., 4.AORI. UTokyo, 5.MOL Marine Co., Ltd)

[SCG45-P07] Classification and estimation of petit-spot volcanos by multibeam backscatter data

*Matamura Yuki[1], Naoto Hirano[2], Masakazu Fujii[3,4] (1.Tohoku University, 2.Center for Northeast Asian Studies, Tohoku University, 3.National Institute of Polar Research, 4.SOKENDAI)

[SCG45-P08] Origin of Philippine Sea basins -Tectonic setting leading to subduction initiation of Izu-Bonin-Mariana arc-

*Osamu Ishizuka[1,2], Kenichiro Tani[3], Gen Shimoda[1], Yumiko Harigane[1], Taichi Sato[1], Rex Taylor[4], Susumu Umino[5], Tian Yu Ping[5], Izumi Sakamoto[6], Yuka Yokoyama[6], Sho Yatsuka[6], Ryota Uchiyama[6], Tomoaki Wakayama[6], Aimi Suzuki[6], Kana Narita[7], Chinatsu Ogawa[7], Yasuhiko Ohara[8,2,9], Chris Conway[1] (1.Geological Survey of Japan, AIST, 2.JAMSTEC, 3.NMNS, 4.University of Southampton, 5.Kanazawa University, 6.Tokai University, 7.Ehime University, 8.Japan Coast Guard, 9.Nagoya University)

[SCG45-P09] What happened to the seafloor around Nishinoshima volcano during deployment of OBEMs between September 2018 and December 2020?

*Noriko Tada[1], Kiyoshi Baba[2], Toshiya Fujiwara[1], Yoshihiko Tamura[1], Toshiya Kanamatsu[1], Kenta Yoshida[1], Akimichi Takagi[3], Fukashi Maeno[2] (1.Research Institute for Marine Geodynamics, Japan Agency for Marine-Earth Science and Technology, 2.Earthquake Research Institute, The University of Tokyo, 3.Japan Meteorological Agency)

[SCG45-P10] Estimation of the Active Faults from BSR-derived heat flow by Automated Velocity Analysis in the Nankai Trough, Japan

*Shuto Takenouchi[1], Kota Mukumoto[1], Takeshi Tsuji[1], Shuichi Kodaira[2], Gou Fujie[2], Yasuyuki Nakamura[2], Kazuya Shiraishi[2] (1.Kyushu-university, 2.Japan Agency for Marine-Earth Science and Technology)

[SCG45-P11] Precipitation process and early diagenesis after deposition of iron hydroxide in Nagahama Bay, Satsuma Iwo-Jima Island, Kagoshima, Japan.

*Koki Hori[1], Shoichi Kiyokawa[2], Minoru Ikehara[3] (1.Department of Earth and Planetary Sciences, Graduate School of Sciences, Kyushu University, 2.Department of Earth and Planetary Sciences Faculty of sciences, Kyuushu University, 3.Center for Advanced Marine Core Research, Kochi University)

[SCG45-P12] Geological structures in the southern part of the Okinawa Trough north off Ishigaki Island: Preliminary results of the KH-21-3 cruise

*Ayanori Misawa[1], Ryuta Arai[2], Masahiko Sato[3], Saki Ishino[1], Misaki Horiuchi[4], Keita Suzuki[4], Chiori Tamura[5], Katsura Kameo[5], Satoshi Okumura[6], Makoto Otsubo[1], KH-21-3 Shipboard Scientists (1.Geological Survey of Japan, National Institute of Advanced Industrial Science and Technology(AIST), 2.Research Institute for Marine Geodynamics, Japan Agency for Marine-Earth Science and Technology (JAMSTEC), 3.Department of Earth and Planetary Science, The University of Tokyo, 4.Nippon Marine Enterprises, Ltd., 5.Atmosphere and Ocean Research Institute, The University of Tokyo, 6.MOL Marine Co. Ltd.)

[SCG45-P13] **The link between volcanism and tectonics at back-arc rifting stage: analysis of three volcanic areas in the southern Okinawa Trough**

*JINYU ZHOU[1], Kyoko Okino[1], Masakazu Fujii[2,3] (1. Atmosphere and Ocean Research Institute, The University of Tokyo, 2.National Institute of Polar Research, 3.The Graduate University for Advanced Studies)

[SCG45-P14] Mineralogical and geochemical study of sediment cores collected from the Ieyama hydrothermal field in the Okinawa Trough

*Jun-ichiro Ishibashi[1], Takashi Miyamoto[1,3], Shuhei Totsuka[1,2], Kazuhiko Shimada[1], Toru Yamasaki[2], Ken Ikehara[2], Toshiro Nagase[4], Yutaro Takaya[5], Hideaki Machiyama[6], Koichi Iijima[6], Hirofumi Yamamoto[6], Hidenori Kumagai[6] (1.Department of Earth and Planetary Sciences, School of Science, Kyushu University, 2.National Institute of Advanced Industrial Science and Technology, 3.School of science, University of Tokyo, 4.Tohoku University Museum, 5.Waseda Research Institute for Science and Engineering, 6.Japan Agency for Marine-Earth Science and Technology)

[SCG45-P15] Geochemical and geochronological study of barite in sediment cores obtained from Higashi Izena hydrothermal field, Okinawa Trough

Yushi Itatani[1], *Jun-ichiro Ishibashi[1], Makiko Tomita[2], Shin Toyoda[2], Ryuichi Shinjo[3], Kazuno Arai[4], Taisei Fujiwara[5] (1.Department of Earth and Planetary Sciences, Graduate School of Science, Kyushu University, 2.Okayama University of Science, 3.Faculty of Science, University of Ryukyus, 4.Center for Advanced Marine Core Research, Kochi University, 5.Institute for Geology and Geochronology)

[SCG45-P16] Fin whale signals recorded by S-net

*Masashi Mochizuki[1], Takeshi Nakamura[2], Ryoichi Iwase[3], Kenji Uehira[1] (1.National Research Institute for Earth Science and Disaster Resilience, 2.Central Research Institute of Electric Power Industry, 3.Japan Agency for Marine-Earth Science and Technology)

[SCG45-P17] Effective removal of oceanic variation from ocean bottom pressure gauge data using the MSSA

*Kenta Shimizu[1], Toshinori Sato[1], Koichi Murata[1], Norihisa Usui[2], Hajime Shiobara[3], Tomoaki Yamada[4], Masanao Shinohara[3] (1.Chiba Univ., 2.MRI, 3.ERI. Univ. Tokyo, 4.JMA)

[SCG45-P18] Sampling process of seafloor sediments as a source of information on their rheology

*Nikita Dubinya[1,2], Sergey Tikhotskiy[1,2], Victor Nachev[1,3] (1.Moscow Institute of Physics and Technology, 2.Schmidt Institute of Physics of the Earth of the Russian Academy of Sciences, 3.Sadovsky Institute of Geosphere Dynamics of the Russian Academy of Sciences)

[SCG45-P19] Technical protocol for deep-sea environmental monitoring by the portable seafloor observation platform Edokko Mark 1

*Hiroyuki Yamamoto[1], Tetsuya Miwa[1], Shinsuke Kawagucci[1], Sangkyun Lee[2], Atsuo Oono[3], Kousuke Tsutsumi[3], Hideki Sugishima[3] (1.Japan Agency for Marine-Earth Science and Technology, 2.J-MARES/JGI, 3.J-MARES/idea)

[J] Oral | S (Solid Earth Sciences)：S-CG Complex & General

9:00 AM - 10:30 AM JST | 12:00 AM - 1:30 AM UTC | Ch.20 Zoom Room 20

[S-CG46] Rheology, fracture and friction in Earth and planetary sciences

convener:Shintaro Azuma(Department of Earth and Planetary Sciences, School of Science, Tokyo Institute of Technology), Ichiko Shimizu(Division of Earth and Planetary Sciences, Graduate School of Science, Kyoto University), Osamu Kuwano(Japan Agency for Marine-Earth Science and Technology), Miki Tasaka(Shizuoka University), Chairperson:Shintaro Azuma(Department of Earth and Planetary Sciences, School of Science, Tokyo Institute of Technology), Miki Tasaka(Shizuoka University)

9:00 AM - 9:15 AM JST | 12:00 AM - 12:15 AM UTC

[SCG46-01] Low stress power-law creep of olivine

★Invited Papers

*Kosuke Yabe[1], Kenta Sueyoshi[1], Takehiko Hiraga[1] (1.Earthquake Research Institute, the University of Tokyo)

9:15 AM - 9:30 AM JST | 12:15 AM - 12:30 AM UTC

[SCG46-02] Vickers indentation tests on olivine: grain size and indentation size effects

*Sanae Koizumi[1], Takehiko Hiraga[1] (1.Earthquake Research Institute,The University of Tokyo)

9:30 AM - 9:45 AM JST | 12:30 AM - 12:45 AM UTC

[SCG46-03] Extremely slow grain growth of albitic feldspar

*Norio Shigematsu[1], Masanori Kido[1], You Zhou[2], Hideki Hyuga[2], Yuichi Yoshizawa[2] (1.Research Institute of Earthquake and Volcano Geology, Geological Survey of Japan, National Institute of Advanced Industrial Science and Technology, 2.Multi-material Research Institute, National Institute of Advanced Industrial Science and Technology)

9:45 AM - 10:00 AM JST | 12:45 AM - 1:00 AM UTC

[SCG46-04] The effect of grain size and porosity on compaction localisation in high-porosity sandstones

*Elliot Rice-Birchall[1], Daniel R Faulkner[1], John D Bedford[1,2] (1.University of Liverpool, 2.Kochi Institute for Core Sample Research, Japan Agency for Marine-Earth Science and Technology (JAMSTEC))

10:00 AM - 10:15 AM JST | 1:00 AM - 1:15 AM UTC

[SCG46-05] Deformation of simulated quartz-feldspar faults at the brittle-ductile transition zone

*Miho Furukawa[1], Berend A. Verberne[2], Jun Muto[1], Miki Takahashi[2], Hiroyuki Nagahama[1] (1.Department of Earth Sciences, Tohoku University, 2.Geological Survey of Japan, The National Institute of Advanced Industrial Science and Technology (AIST))

10:15 AM - 10:30 AM JST | 1:15 AM - 1:30 AM UTC

[SCG46-06] Initial results on high Pc-Pp-T rock deformation experiments under drained conditions

★Invited Papers

*Keishi Okazaki[1], Jun Muto[2] (1.Japan Agency for Marine-Earth Science and Technology, 2.Department of Earth Sciences, Tohoku University)

[J] Oral | S (Solid Earth Sciences)：S-CG Complex & General

10:45 AM - 12:15 PM JST | 1:45 AM - 3:15 AM UTC | Ch.20 Zoom Room 20

[S-CG46] Rheology, fracture and friction in Earth and planetary sciences

convener:Shintaro Azuma(Department of Earth and Planetary Sciences, School of Science, Tokyo Institute of Technology), Ichiko Shimizu(Division of Earth and Planetary Sciences, Graduate School of Science, Kyoto University), Osamu Kuwano(Japan Agency for Marine-Earth Science and Technology), Miki Tasaka(Shizuoka University), Chairperson:Ichiko Shimizu(Division of Earth and Planetary Sciences, Graduate School of Science, Kyoto University), Osamu Kuwano(Japan Agency for Marine-Earth Science and Technology)

10:45 AM - 11:00 AM JST | 1:45 AM - 2:00 AM UTC

[SCG46-07] Dehydration experiments of antigorite serpentinite under slab-mantle conditions

Sakurako Okude[1], *Ichiko Shimizu[1] (1.Division of Earth and Planetary Sciences, Graduate School of Science, Kyoto University)

11:00 AM - 11:15 AM JST | 2:00 AM - 2:15 AM UTC

[SCG46-08] Variation of stick-slip behaviors controlled by dehydration kinetics of simulated gypsum gouges

*Mikihiro Kawabata[1], Rei Shiraishi[1], Jun Muto[1], Hiroyuki Nagahama[1], Yuto Sasaki[2] (1.Department of Earth Science, Graduate School of Science and Faculty of Science, Tohoku University, 2.Earthquake Research Institute, The University of Tokyo)

11:15 AM - 11:30 AM JST | 2:15 AM - 2:30 AM UTC

[SCG46-09] Experimental study on drainage process of liquid film between bubbles during bubble growth

★Invited Papers

*Masatoshi Ohashi[1], Atsushi Toramaru[1], Atsuko Namiki[2] (1.Department of Earth and Planetary Sciences, Graduate School of Science, Kyushu University, 2.Graduate School of Environmental Studies Department of Earth and Environmental Sciences)

11:30 AM - 11:45 AM JST | 2:30 AM - 2:45 AM UTC

[SCG46-10] Transition from viscous to inertial regime in dense frictional suspensions

*Franco Antonio Tapia[1], Olivier Pouliquen[3], Elisabeth Guazzelli[2] (1.Department of Mechanical Systems Engineering, Tokyo University of Agriculture and Technology, 2.Université de Paris, CNRS, Matière et Systèmes Complexes (MSC) UMR 7057, Paris, France, 3.Aix-Marseille Université, CNRS, IUSTI, Marseille, France)

11:45 AM - 12:00 PM JST | 2:45 AM - 3:00 AM UTC

[SCG46-11] Peridodic fluctation in a compressed dust-aggregate layer

*Hiroaki Katsuragi[1], Felipe Pacheco Vazquez[2], Tomomi Omura[3] (1.Department of Earth and Space Science, Osaka University, 2.BUAP, Mexico, 3.Osaka Sangyo University)

12:00 PM - 12:15 PM JST | 3:00 AM - 3:15 AM UTC

[SCG46-12] Elasto-plastic behavior of carbonate rocks under high strain rate deformation

★Invited Papers

*Kosuke Kurosawa[1], Hidenori Genda[2], Shintaro Azuma[3], Keishi Okazaki[4], Haruka Oono[1], Takafumi Niihara[5], Takashi Mikouchi[6], Naotaka Tomioka[4], Tatsuhiro Sakaiya[7], Tadashi Kondo[7], Masahiro KAYAMA[8], Mizuho Koike[9], Yuji Sano[10], Takuya Matsuzaki[11], Masafumi MURAYAMA[11], wataru Satake[1], Takafumi Matsui[1,12] (1.Planetary Exploration Research Center, Chiba Institute of Technology, 2.Earth–Life Science Institute, Tokyo Institute of Technology, 3.Department of Earth and Planetary Sciences, Tokyo Institute of Technology, 4.Kochi Institute for Core Sample Research, Japan Agency for Marine-Earth Science and Technology, 5.Department of Systems Innovation, School of Engineering, The University of Tokyo, 6.The University Museum, The University of Tokyo, 7.Department of Earth and Space Science, Graduate School of Science, Osaka University, 8.Department of General Systems Studies, Graduate School of Arts and Sciences, The Univ. of Tokyo, 9.Department of Earth and Planetary Systems Science, Graduate School of Science, Hiroshima University, 10.Atmosphere and Ocean Research Institute, The University of Tokyo, 11.Center for Advanced Marine Core Research, Kochi University, 12.Institute of Geo-Cosmology, Chiba Institute of Technology)

[J] Poster | S (Solid Earth Sciences)：S-CG Complex & General

5:15 PM - 6:30 PM JST | 8:15 AM - 9:30 AM UTC | Ch.18_2

[S-CG46] Rheology, fracture and friction in Earth and planetary sciences

convener:Shintaro Azuma(Department of Earth and Planetary Sciences, School of Science, Tokyo Institute of Technology), Ichiko Shimizu(Division of Earth and Planetary Sciences, Graduate School of Science, Kyoto University), Osamu Kuwano(Japan Agency for Marine-Earth Science and Technology), Miki Tasaka(Shizuoka University)

[SCG46-P01] Experimental investigation of the pyroxene-garnet and olivine-spinel transformations under shear deformation using synchrotron radiation and acoustic emission techniques

*Yuki Mori[1], Tomoaki Kubo[1], Rikuto Honda[1], Takuya Iwasato[2], Yuji Higo[3], Yoshinori Tange[3] (1.Kyushu Univ., 2.Shin-Nippon Nondestructive Inspection Co.,Ltd., 3.JASRI)

[SCG46-P02] Creep behavior during the post-spinel transformation in $(Mg, Fe)_2SiO_4$

*Yuta Goto[1], Tomoaki Kubo[1], Rikuto Honda[1], Yumiko Tsubokawa[1], Yuichiro Mori[2] (1.Kyushu Univ., 2.The University of Tokyo)

[SCG46-P03] SOR and AE study on the olivine-spinel transformation in $(Mg,Fe)_2SiO_4$ under uniaxial deformation with D111-type apparatus

*Rikuto Honda[1], Tomoaki Kubo[1], Yuichiro Mori[2], Goto Yuta[1], Yumiko Tsubokawa[1], Takuya Iwasato[3], Yuji Higo[4] (1.Kyushu University, 2.The University of Tokyo, 3.Shin-Nippon Nondestructive Inspection Co., Ltd., 4.JASRI)

[SCG46-P04] Frequency characteristics of acoustic emission in the fracture process of thermally cracked granite

*Sueyoshi Kazumasa[1], Manami Kitamura[2], Xinglin Lei[2], Ikuo Katayama[1] (1.Department of Earth and Planetary Systems Science, Hiroshima University, 2.National Institute of Advanced Industrial Science and Technology)

[SCG46-P05] Flow-to-fracture transition of linear Maxwell-type fluid by air injection

*Claudia Sanchez[1], Osamu Kuwano[2], Mie Ichihara[1] (1.Earthquake Research Institute, Tokyo University , 2.JAMSTEC)

[SCG46-P06] Role of lithology in deformation mechanisms of shallow-crustal active faults: Evidence from the Nahan thrust of Himalayas

*Dyuti Prakash Sarkar[1], Jun-ichi Ando[1], Kaushik Das[1], Gautam Ghosh[2], Prabir Dasgupta[3] (1.Hiroshima University, 2.Presidency University, 3.Durgapur Govt. College)

[SCG46-P07] Study of the mobile granular layer in bedload transport by laminar shearing flow in a tilted channel

*Chong-Wei Hong[1], Franco Tapia[2], Pascale Aussillous[3], Élisabeth Guazzelli[4], Chi-Yao Hung[1] (1.Department of Soil and Water Conservation, National Chung Hsing University, Taichung, Taiwan, 2.Department of Mechanical Engineering, Tokyo University of Agriculture and Technology, Tokyo, Japan, 3.Aix-Marseille Université, CNRS, IUSTI, Marseille, France, 4.Université de Paris, CNRS, Matière et Systèmes Complexes (MSC) UMR 7057, Paris, France)

[SCG46-P08] Fracture behavior of silicate network phase-separating from aqueous fluid

*Takehito Koyama[1] (1.Institute of Industrial Science, the University of Tokyo)

[SCG46-P09] Evolution of patterns of hydraulically conductive natural fractures during inelastic deformation of rocks

*Nikita Dubinya[1,2] (1.Moscow Institute of Physics and Technology, 2.Schmidt Institute of Physics of the Earth of the Russian Academy of Sciences)

[SCG46-P10] Theoretical study on rock anelasticity;
Extension of a grain-boundary sliding model to two dimensions

*Mitsuyoshi Kunugihara[1], Yasuko Takei[1] (1.Earthquake Research Institute,The University of Tokyo)

[SCG46-P11] A DEM model of uniaxial and triaxial compression test of rocks

*Mikito Furuichi[1], Daisuke Nishiura[1], Yuzuru Yamamoto[2] (1.Japan Agency for Marine-Earth Science and Technology, 2.Kobe University)

[SCG46-P12] Relaxation of the frictional force in a statistical mechanical model of magnetic friction

*Komatsu Hisato[1] (1.National Institute for Materials Science)

[E] Poster | M (Multidisciplinary and Interdisciplinary)：M-IS Intersection

5:15 PM - 6:30 PM JST | 8:15 AM - 9:30 AM UTC | Ch.20_1

[M-IS06] Human-environment Nexus from Pre-Historic to Modern Times

convener:F Harry Lee(The Chinese University of Hong Kong)

[MIS06-P01] The socio-hydrological interactions in modern China: a case study based on flood events in Yangtze River Basin

*CHANG LIU[1], Akiyuki Kawasaki[1], Tomoko Shiroyama[2] (1.Department of Civil Engineering, the University of Tokyo, 2.Graduate School of Economics, the University of Tokyo)

[MIS06-P02] Historical climate-war nexus in the eyes of geographers

*Harry F Lee[1] (1.The Chinese University of Hong Kong)

[E] Oral | M (Multidisciplinary and Interdisciplinary) : M-IS Intersection

10:45 AM - 12:15 PM JST | 1:45 AM - 3:15 AM UTC | Ch.03 Zoom Room 03

[M-IS07] Effects of lightning, severe weather and tropical storms

convener:Mitsuteru Sato(Department of Cosmoscience, Hokkaido University), Hisayuki Kubota(Hokkaido University), C. Glenn Vincent Lopez(- - -), Purwadi Purwadi(Department of Cosmosciences, Hokkaido University, Sapporo 0600810, Japan), Chairperson:Mitsuteru Sato(Department of Cosmoscience, Hokkaido University), Hisayuki Kubota(Hokkaido University)

10:45 AM - 11:00 AM JST | 1:45 AM - 2:00 AM UTC

[MIS07-01] Current status and prospects of ULAT/SATREPS

*Yukihiro Takahashi[1,2], Mitsuteru Sato[1,2], Hisayuki Kubota[1,2], Tetsuro Ishida[1,2], Ellison Castro[3], Loren Jay Estrebillo[3], Purwadi Purwadi[4], Meryl Algodon[1], Gay Perez[3], Joel Marciano[5], Jun Matsumoto[6], Jun-Ichi Hamada[6] (1.Department of Cosmosciences, Graduate School of Science, Hokkaido University, 2.Department of Earth and Planetary Sciences, Faculty of Science, Hokkaido University, 3.University of the Philippines, Diliman, 4.BPPT, Indonesia, 5.PhilSA, Phlippines, 6.Tokyo Metropolitan University)

11:00 AM - 11:15 AM JST | 2:00 AM - 2:15 AM UTC

[MIS07-02] The relationship between CG lightning detected by AVON V-POTEKA and thunderstorm parameters

*Purwadi Purwadi[1], Yukihiro Takahashi[2], Mitsuteru Sato[2], Hisayuki Kubota[2], Kozo Yamashita[3] (1.Agency for Assessment and Application for Technology, Jakarta 10340, Indonesia, 2.Faculty of Science, Hokkaido University, Sapporo 0600810, Japan, 3.Department of Electrical Engineering, Salesian Polytechnic, Tokyo, Japan)

11:15 AM - 11:30 AM JST | 2:15 AM - 2:30 AM UTC

[MIS07-03] Machine Learning Prediction of Precipitation in Metro Manila, Philippines

★Invited Papers

*Akira Noda[1], Yukihiro Takahashi[2], Hisayuki Kubota[2], Ken-ichi Fukui[3], Mitsuteru Sato[2] (1.Department of Earth and Planetary Sciences, School of Science, Hokkaido University., 2.Department of Cosmosciences, Graduate School of Science, Hokkaido University, 3.The Institute of Scientific and Industrial Research, Osaka University)

11:30 AM - 11:45 AM JST | 2:30 AM - 2:45 AM UTC

[MIS07-04] 3D Reconstruction of Typhoon Trami Eye Using Airborne Camera

★Invited Papers

*Meryl Regine Llenaresas Algodon[1], Yukihiro Takahashi[2], Mitsuteru Sato[2], Hisayuki Kubota[3], Tetsuro Ishida[3], Kozo Yamashita[4], Ellison Caparas Castro[5], Gay Jane Perez[6], Joel Joseph Marciano[7], Jun Matsumoto[8], Jun-Ichi Hamada[9], Kazuhisa Tsuboki[10], Hiroyuki Yamada[11] (1.Hokkaido University, Graduate School of Science, 2.Hokkaido University, 3.Hokkaido University, Faculty of Science, 4.Ashikaga University, 5.University of the Philippines Quezon City (Philippines), 6.NASA Goddard Space Flight Center Earth Science Division Greenbelt MD 20771-0000 (United States), 7.Advanced Science and Technology Institute Quezon City (Philippines), 8.Tokyo Metropolitan University Tokyo 192, 9.Tokyo Metropolitan University Hachioji, 10.Nagoya University, Institute for Space–Earth Environmental Research Nagoya 464, 11.University of the Ryukyus Nishihara)

11:45 AM - 12:00 PM JST | 2:45 AM - 3:00 AM UTC

[MIS07-05] Successive observation of atmospheric electric observation at Kakioka Geomagnetic Observatory

*Masashi Kamogawa[1], Tomoyuki Suzuki[1], Toshiyasu Nagao[3], Yasuhiro Minamoto[2] (1.Global Center for Asian and Regional Research, University of Shizuoka, 2.Laboratory for Environmental Research at Mount Fuji, 3.Institute of Oceanic Research and Development, Tokai University)

12:00 PM - 12:15 PM JST | 3:00 AM - 3:15 AM UTC

[MIS07-06] Observation of Elves and Transient Luminous Events from the International Space Station with the Mini-EUSO telescope

*Marco Casolino[1], Toshikazu Ebisuzaki[1], Yoshiyuki Takizawa[1], Naoto Sakaki[1], Satoshi Wada[1] (1.Riken)

[E] Poster | M (Multidisciplinary and Interdisciplinary)：M-IS Intersection

5:15 PM - 6:30 PM JST | 8:15 AM - 9:30 AM UTC | Ch.21_1

[M-IS07] Effects of lightning, severe weather and tropical storms

convener:Mitsuteru Sato(Department of Cosmoscience, Hokkaido University), Hisayuki Kubota(Hokkaido University), C. Glenn Vincent Lopez(- - -), Purwadi Purwadi(Department of Cosmosciences, Hokkaido University, Sapporo 0600810, Japan)

[MIS07-P01] Lightning bursts observed during the tropical cyclone genesis over the Philippine Sea

*Hisayuki Kubota[1], Yukihiro Takahashi[1], Mitsuteru Sato[1] (1.Hokkaido University)

[MIS07-P02] Spatial and temporal variations of heavy rainfall in the Metro Manila, Philippines in the dry-wet transitional season based on a dense surface meteorological observation network

*Jun-Ichi Hamada[1], Jun Matsumoto[1], Hisayuki Kubota[2], Mitsuteru Sato[2], Yukihiro Takahashi[2], Glenn Vincent[3] (1.Tokyo Metropolitan University, 2.Hokkaido University, 3.Advanced Science and Technology Institute, Philippines)

[MIS07-P03] Estimation of the relation between electrical properties of lightning and tropical cyclone intensity in the western north Pacific.

*Shunsuke Niwa[1], Mitsuteru Sato[1], Yukihiro Takahashi[1], Hisayuki Kubota[1] (1.Department of Cosmoscience, Hokkaido University)

[MIS07-P04] Lightning Activity in Western North Pacific Measured by the V-POTEKA Network and Its Relation to Typhoon Intensity

*Mitsuteru Sato[1], Yukihiro Takahashi[1], Hisayuki Kubota[1], Glenn Vincent C. Lopez[2] (1.Faculty of Science, Hokkaido University, 2.ASTI, DOST)

[E] Oral | M (Multidisciplinary and Interdisciplinary)：M-IS Intersection

1:45 PM - 3:15 PM JST | 4:45 AM - 6:15 AM UTC | Ch.15 Zoom Room 15

[M-IS09] Weathering and conservation of cultural heritage and geosites

convener:Luigi Germinario(University of Padova, Italy), Chiaki T. Oguchi(Institute for Environmental Science and Technology, Graduate School of Science and Engineering, Saitama University), Akos Torok(Budapest University of Technology and Economics), Tetsuya Waragai(Graduate School of Science and Engineering, Nihon University), Chairperson:Luigi Germinario(University of Padova, Italy), Chiaki T. Oguchi(Institute for Environmental Science and Technology, Graduate School of Science and Engineering, Saitama University)

1:45 PM - 2:00 PM JST | 4:45 AM - 5:00 AM UTC

[MIS09-01] Evaluation of the degradation state of dinosaur footprint based on 3D measurement.

*Nobuaki Kuchitsu[1], Shuji SAKAI[2], Masato FUJITA[3] (1.Tokyo National Research Institute for Cultural Properties, 2.Toppan Printing Co., Ltd., 3.Toyama Science Museum)

2:00 PM - 2:15 PM JST | 5:00 AM - 5:15 AM UTC

[MIS09-02] Study on relations between deterioration of tuff stone used as exteriors of a historical building and microenvironment factors

*Uno Tomoko[1], Chiemi Iba[2], Masaru Abuku[3] (1.Mukogawa Womens University, 2.Kyouto University, 3.Kinki University)

2:15 PM - 2:30 PM JST | 5:15 AM - 5:30 AM UTC

[MIS09-03] Changes in pore-size distribution of rocks induced by thermal cycles of low temperature

*Tetsuya Waragai[1] (1.Graduate School of Science and Engineering, Nihon University)

2:30 PM - 2:45 PM JST | 5:30 AM - 5:45 AM UTC

[MIS09-04] **Non-destructive strength tests of heritage buildings: an overview of Schmidt hammer and Duroskop tests**

*Akos Torok[1] (1.Budapest University of Technology and Economics)

2:45 PM - 3:00 PM JST | 5:45 AM - 6:00 AM UTC

[MIS09-05] Numerical analysis of heat, moisture, and salt transfer and deformation in porous materials under atmospheric conditions

*Masaru Abuku[1], Koichi Ishii[2] (1.Kindai University, 2.Research Center of Computational Mechanics, Inc.)

3:00 PM - 3:15 PM JST | 6:00 AM - 6:15 AM UTC

[MIS09-06] **HYPERION: understanding and quantifying the effects of climate change on cultural heritage**

*Chiara Coletti[1], Luigi Germinario[1], Fabrizio Antonelli[2], Renzo Bertoncello[3], Antonio Galgaro[1], Lara Maritan[1], Matteo Massironi[1], Jacopo Nava[1], Rebecca Piovesan[2], Raffaele Sassi[1], Elena Tesser[2], Claudio Mazzoli[1] (1.Department of Geosciences, University of Padova, Via Gradenigo 6, 35131 Padova, Italy, 2.LAMA - Laboratory for Analysing Materials of Ancient origin, University Iuav of Venice, San Polo 2468/B, 30125 Venice, Italy, 3.Department of Chemical Sciences, University of Padova, Via Marzolo 1, 35131 Padova, Italy)

[E] Poster | M (Multidisciplinary and Interdisciplinary)：M-IS Intersection

5:15 PM - 6:30 PM JST | 8:15 AM - 9:30 AM UTC | Ch.20_2

[M-IS09] Weathering and conservation of cultural heritage and geosites

convener:Luigi Germinario(University of Padova, Italy), Chiaki T. Oguchi(Institute for Environmental Science and Technology, Graduate School of Science and Engineering, Saitama University), Akos Torok(Budapest University of Technology and Economics), Tetsuya Waragai(Graduate School of Science and Engineering, Nihon University)

[MIS09-P01] Mineralogical and microclimatic control on the salt weathering of Oya stone

*Luigi Germinario[1,2], Chiaki T. Oguchi[2] (1.University of Padova, Italy, 2.Saitama University, Japan)

[MIS09-P02] Relationship between carbon dioxide concentration and temperature in the Taya cave

*Chiaki T. Oguchi[1], Rina Matsumoto[2], Yasuhiko TAMURA[3] (1.Institute for Environmental Science and Technology, Graduate School of Science and Engineering, Saitama University, 2.Faculty of civil Engineering, Saitama University, 3.Executive Committee for the Preservation of TAYA CAVERN)

[MIS09-P03] Material properties and durability of stone in a medieval fortress; lessons to learn: an example from Hungary

*Akos Torok[1], Benedek Lógó[1] (1.Budapest University of Technology and Economics)

[E] Poster | M (Multidisciplinary and Interdisciplinary)：M-IS Intersection

5:15 PM - 6:30 PM JST | 8:15 AM - 9:30 AM UTC | Ch.21_2

[M-IS10] Exploring Origin of Space, Galaxies, Earth, Moon, Solar System, Plate Tectonics, and Life

convener:Akira Taneko(SEED SCIENCE Lab.)

[MIS10-P01] **Investigating Origin and how to verify it-** Verification goes back to the past -make Hypothesis and explain of Evolution Resules ***in a unified manner,*** MIH as a sanple

★Invited Papers

*Akira Taneko[1] (1.SEED SCIENCE Lab.)

[MIS10-P02] Most Scientists **do not deny the existence of Plate Tectonics**, but ***cannot explain why Plate Tectonics happened.*** **"Multi-Impact Hypothesis"** ***can explain Origin of Plate Tectonics*** and also ***verify Origin of Moon and Solar System.***

★Invited Papers

*Akira Taneko[1] (1.SEED SCIENCE Lab.)

[MIS10-P03] Liquid Crystal Peptide/DNA Coacervates in the Context of Prebiotic Molecular Evolution

★Invited Papers

*Tony Z Jia[1,2], Tommaso P Fraccia[3] (1.Earth-Life Science Institute, Tokyo Institute of Technology, 2.Blue Marble Space Institute of Technology, 3.Institut Pierre-Gilles de Gennes, CBI, ESPCI Paris, Université PSL, CNRS)

[J] Oral | M (Multidisciplinary and Interdisciplinary)：M-IS Intersection

9:00 AM - 10:30 AM JST | 12:00 AM - 1:30 AM UTC | Ch.02 Zoom Room 02

[M-IS12] Planetary Volcanology

convener:Rina Noguchi(Faculty of Science, Niigata University), Nobuo Geshi(Geological Survey of Japan, The National Institute of Advanced Industrial Science and Technology), Tomokatsu Morota(Department of Earth and Planetary Science, The University of Tokyo), Chairperson:Rina Noguchi(Faculty of Science, Niigata University), Nobuo Geshi(Geological Survey of Japan, The National Institute of Advanced Industrial Science and Technology), Tomokatsu Morota(Department of Earth and Planetary Science, The University of Tokyo)

9:00 AM - 9:15 AM JST | 12:00 AM - 12:15 AM UTC

[MIS12-01] Structures and formation age of lunar linear gravity anomalies constrained by impact simulations

*Gaku Nishiyama[1], Noriyuki Namiki[2], Seiji Sugita[1] (1.University of Tokyo, 2.National Astronomical Observatory of Japan)

9:15 AM - 9:30 AM JST | 12:15 AM - 12:30 AM UTC

[MIS12-02] Laboratory investigations of salt precipitation upon decompression and degassing of volatile-containing brines: Implication for carbonate mineral formations on Solar system icy bodies

*Masahiro Yoda[1,2], Yasuhito Sekine[2,3] (1.Department of Earth and Planetary Science, The University of Tokyo, 2.Earth-Life Science Institute of Tokyo Tech, 3.Institute of Nature and Environmental Technology, Kanazawa University)

9:30 AM - 9:45 AM JST | 12:30 AM - 12:45 AM UTC

[MIS12-03] Rootless cones in the southwest of Emuruangogolak Volcano, Kenya

*Rina Noguchi[1] (1.Institute of Space and Astronautical Science, Japan Aerospace Exploration Agency)

9:45 AM - 10:00 AM JST | 12:45 AM - 1:00 AM UTC

[MIS12-04] Conditions for the formation of rootless cones on Mars and Earth

*Kei Kurita, Rina Noguchi[1] (1.ISAS/JAXA)

10:00 AM - 10:15 AM JST | 1:00 AM - 1:15 AM UTC

[MIS12-05] Development of an efficient geological survey method for volcanoes on extraterrestrial bodies

★Invited Papers

*Junichi Haruyama[1], Rina Noguchi[1], Nobuo Geshi[2], Motomaro Shirao[3], Keiichiro Fujimoto[1], Daigo Shoji[1] (1.Japan Aerospace Exploration Agency, 2.National Institute of Advanced Industrial Science and Technology, 3.Institute of Planetary Geology)

10:15 AM - 10:30 AM JST | 1:15 AM - 1:30 AM UTC

[MIS12-06] Discussion

[J] Poster | M (Multidisciplinary and Interdisciplinary)：M-IS Intersection

5:15 PM - 6:30 PM JST | 8:15 AM - 9:30 AM UTC | Ch.21_3

[M-IS12] Planetary Volcanology

convener:Rina Noguchi(Faculty of Science, Niigata University), Nobuo Geshi(Geological Survey of Japan, The National Institute of Advanced Industrial Science and Technology), Tomokatsu Morota(Department of Earth and Planetary Science, The University of Tokyo)

[MIS12-P01] Review of duration and spatial heterogeneity of mare volcanism on the Moon

*Tomokatsu Morota[1] (1.Department of Earth and Planetary Science, The University of Tokyo)

[MIS12-P02] **Possible existence of lava tube cave and pit/fissure cave in the Moon and Mars**

*Tsutomu Honda[1] (1.Vulcano-speleological Society)

[MIS12-P03] Geomorphological and geological study of the summit caldera of Olympus Mons on Mars.

*Mayuko Nakamura[1], Tomohiro Tsuji[1] (1.Division of Earth Science The Graduate School of Sciences and Technology for Innovation , Yamaguchi University)

[MIS12-P04] The extent of shallow underground water-ice in the Amazonian period on Mars inferred from the distribution of rootless cones

*Rina Noguchi[1] (1.Institute of Space and Astronautical Science, Japan Aerospace Exploration Agency)

[J] Oral | M (Multidisciplinary and Interdisciplinary)：M-IS Intersection

10:45 AM - 12:15 PM JST | 1:45 AM - 3:15 AM UTC | Ch.02 Zoom Room 02

[M-IS14] Aqua planetology

convener:Yasuhito Sekine(Earth-Life Science Insitute, Tokyo Institute of Technology), Takazo Shibuya(Japan Agency for Marine-Earth Science and Technology), Hidenori Genda(Earth-Life Science Institute, Tokyo Institute of Technology), Keisuke Fukushi(Institute of Nature & Environmental Technology, Kanazawa University), Chairperson:Takazo Shibuya(Japan Agency for Marine-Earth Science and Technology), Yasuhito Sekine(Earth-Life Science Insitute, Tokyo Institute of Technology), Keisuke Fukushi(Institute of Nature & Environmental Technology, Kanazawa University), Tomohiro Usui(Japan Aerospace Exploration Agency), Hidenori Genda(Earth-Life Science Institute, Tokyo Institute of Technology)

10:45 AM - 11:00 AM JST | 1:45 AM - 2:00 AM UTC

[MIS14-01] Internal heating of icy ocean worlds

*Shunichi Kamata[1], Kento Nakanishi[1], Kiyoshi Kuramoto[1] (1.Faculty of Science, Hokkaido University)

11:00 AM - 11:15 AM JST | 2:00 AM - 2:15 AM UTC

[MIS14-02] Field investigations on salt partitioning in frozen closed-basin lakes in Mongolia as terrestrial analogues of subsurface brine reservoirs on Solar System icy bodies

*Masahiro Yoda[1,2], Yasuhito Sekine[2,3], Keisuke Fukushi[3], Takuma Kitajima[4], Baasansuren Gankhurel[4], Davaadorj Davaasuren[5], Tuvshin Gerelmaa[5], Shuukhaaz Ganbat[4], Daigo Shoji[6], Yoshio Takahashi[1] (1.Department of Earth and Planetary Science, The University of Tokyo, 2.Earth-Life Science Institute of Tokyo Tech, 3.Institute of Nature and Environmental Technology, Kanazawa University, 4.Division of Earth and Environmental Sciences, Graduate School of Natural Science and Technology, 5.Department of Geography, The National University of Mongolia, 6.Institute of Space and Astronautical Science, Japan Astronautical Exploration Agency)

11:15 AM - 11:30 AM JST | 2:15 AM - 2:30 AM UTC

[MIS14-03] In-situ observation of gas hydrate formation as a simulation of the bottom of ice crust in icy bodies

*Atsushi Tani[1], Kenshiro Moriyama[1] (1.Department of Human Environmental Science, Graduate School of Human Development and Environment, Kobe University)

11:30 AM - 11:45 AM JST | 2:30 AM - 2:45 AM UTC

[MIS14-04] Evolution processes of asteroid Ryugu inferred from orbit and spin dynamics

*Masanori Kanamaru[1], Ryuki Hyodo[1], Tomohiro Usui[1], Tatsuaki Okada[1] (1.Japan Aerospace Exploration Agency)

11:45 AM - 12:00 PM JST | 2:45 AM - 3:00 AM UTC

[MIS14-05] Oxygen isotopic systematics of chondrules in Tagish Lake (C2) and implications of volatiles in the protoplanetary disk

*Takayuki Ushikubo[1], Makoto Kimura[2] (1.Kochi Institute for Core Sample Research, Japan Agency for Marine-Earth Science and Technology, 2.National Institute of Polar Research)

12:00 PM - 12:15 PM JST | 3:00 AM - 3:15 AM UTC

[MIS14-06] Development of a technique for a multi-isotopic analyses of asteroid materials (small amount samples ~ 30 mg) returned by the Hayabusa2 mission

*Tetsuya Yokoyama[1], Ikshu Gautam[1], Yusuke Ohkuma[1], Tsuyoshi Iizuka[2], The Hayabusa2 initial analysis team “Isotopes and Chemistry” (1.Department of Earth and Planetary Sciences, School of Science, Tokyo Institute of Technology, 2.Department of Earth and Planetary Science, School of Science, The University of Tokyo)

[J] Oral | M (Multidisciplinary and Interdisciplinary) : M-IS Intersection

1:45 PM - 3:15 PM JST | 4:45 AM - 6:15 AM UTC | Ch.02 Zoom Room 02

[M-IS14] Aqua planetology

convener:Yasuhito Sekine(Earth-Life Science Insitute, Tokyo Institute of Technology), Takazo Shibuya(Japan Agency for Marine-Earth Science and Technology), Hidenori Genda(Earth-Life Science Institute, Tokyo Institute of Technology), Keisuke Fukushi(Institute of Nature & Environmental Technology, Kanazawa University), Chairperson:Yasuhito Sekine(Earth-Life Science Insitute, Tokyo Institute of Technology), Takazo Shibuya(Japan Agency for Marine-Earth Science and Technology), Keisuke Fukushi(Institute of Nature & Environmental Technology, Kanazawa University), Tomohiro Usui(Japan Aerospace Exploration Agency), Hidenori Genda(Earth-Life Science Institute, Tokyo Institute of Technology)

1:45 PM - 2:00 PM JST | 4:45 AM - 5:00 AM UTC

[MIS14-07] Comparative metagenomic studies of diverse serpentinized ecosystems

★Invited Papers

*Shino Suzuki[1], Shunichi Ishii[2], Nealson H. Kenneth[3] (1.JAXA, 2.JAMSTEC, 3.USC)

2:00 PM - 2:15 PM JST | 5:00 AM - 5:15 AM UTC

[MIS14-08] Thioester synthesis through geoelectrochemical CO2 fixation on Ni and Mo sulfides.

*Norio Kitadai[1] (1.Japan Agency for Marine-Earth Science and Technology)

2:15 PM - 2:30 PM JST | 5:15 AM - 5:30 AM UTC

[MIS14-09] Effects of pH on the ribose synthesis in the formose reaction: implication for abiotic synthesis on ancient Mars

*Chinatsu Ono[1], Takeshi Kakegawa[1], Yoshihiro Furukawa[1] (1.Graduate School of Science, Tohoku University)

2:30 PM - 2:45 PM JST | 5:30 AM - 5:45 AM UTC

[MIS14-10] Elucidation of the mechanism of organic matter synthesis process by reducing reaction of clay minerals on the surface of the planet by STXM

*Takahiro Kawai[1], Hiroki Suga[2], Yasuo Takeichi[3], Yoshio Takahashi[1,3] (1.University of Tokyo, 2.JASRI, 3.KEK-PF)

2:45 PM - 3:00 PM JST | 5:45 AM - 6:00 AM UTC

[MIS14-11] Solubility of amorphous magnesium carbonate: rarity of Mg-carbonate on surface of closed-basin lakes that existed on early Mars

*TAKUMA KITAJIMA[1], Keisuke Fukushi[2], Yasuhito Sekine[2,3], Masahiro Yoda[3,4], Baasansuren Gankhurel[1], Davaadorj Davaasuren[5] (1.Kanazawa university, 2.The Institute of Nature and Environmental Technology, Kanazawa University, 3.Earth-Life Science Institute, Tokyo Institute of Technology, 4.Department of Earth and Planetary Science, The University of Tokyo, 5.Department of Environment and Forest Engineering, The National University of Mongolia)

3:00 PM - 3:15 PM JST | 6:00 AM - 6:15 AM UTC

[MIS14-12] **Parent body processes reproduce soluble organics in carbonaceous chondrites via geo-electrochemistry**

★Invited Papers

*LI Yamei[1], Yasuhito Sekine[1], Norio Kitadai[1,2] (1.Earth-Life science Institute, Tokyo Institute of Technology, 2.Japan Agency for Marine-Earth Science and Technology)

[J] Oral | M (Multidisciplinary and Interdisciplinary) : M-IS Intersection

3:30 PM - 5:00 PM JST | 6:30 AM - 8:00 AM UTC | Ch.02 Zoom Room 02

[M-IS14] Aqua planetology

convener:Yasuhito Sekine(Earth-Life Science Insitute, Tokyo Institute of Technology), Takazo Shibuya(Japan Agency for Marine-Earth Science and Technology), Hidenori Genda(Earth-Life Science Institute, Tokyo Institute of Technology), Keisuke Fukushi(Institute of Nature & Environmental Technology, Kanazawa University), Chairperson:Hidenori Genda(Earth-Life Science Institute, Tokyo Institute of Technology), Yasuhito Sekine(Earth-Life Science Insitute, Tokyo Institute of Technology), Tomohiro Usui(Japan Aerospace Exploration Agency), Keisuke Fukushi(Institute of Nature & Environmental Technology, Kanazawa University), Takazo Shibuya(Japan Agency for Marine-Earth Science and Technology)

3:30 PM - 3:45 PM JST | 6:30 AM - 6:45 AM UTC

[MIS14-13] Degassing history and the structural evolution of Martian mantle

★Invited Papers

*Masaki Ogawa[1] (1.Division of General Systems Studies, Graduate School of Arts and Sciences, University of Tokyo)

3:45 PM - 4:00 PM JST | 6:45 AM - 7:00 AM UTC

[MIS14-14] Effect of photo-oxidation reactions of ferrous iron on geochemical conditions required for redox stratification on early Gale lake

*Haruhisa Tabata[1,2], Yasuhito Sekine[2], Kazumi Ozaki[3] (1.Department of Earth and Planetary Science, University of Tokyo, 2.Earth-Life Science Institute, Tokyo Institute of Technology, 3.Department of Environmental Science, Toho University)

4:00 PM - 4:15 PM JST | 7:00 AM - 7:15 AM UTC

[MIS14-15] Water vapor vertical distributions on Mars: Results from three years of TGO/NOMAD science operations

*Shohei Aoki[1,2], Ann Carine Vandaele[2], Frank Daerden [2], Geronimo L. Villanueva [3], Giuliano Liuzzi [3], Ian R, Thomas [2], Justin T. Erwin [2], Loic Trompet [2], Lori Neary [2], Severine Robert [2,9], Sebastien Viscardy [2], Arianna Piccialli [2], R. Todd Clancy [4], Michael Smith[3], Matteo Crismani [5], Bojan Ristic [2], Miguel A. Lopez-Valverde[6], Adrian Brines [6], Manish R. Patel [7], James A. Holmes [7], Giancarlo Bellucci[8], Jose J. Lopez-Moreno[6] (1.Université de Liège, 2.Royal Belgian Institute for Space Aeronomy, 3.NASA Goddard Space Flight Center, 4.Space Science Institute, 5.California State University, 6.Instituto de Astrofísica de Andalucía, 7.Open University, 8.Istituto di Astrofisica e Planetologia, 9.Université catholique de Louvain)

4:15 PM - 4:30 PM JST | 7:15 AM - 7:30 AM UTC

[MIS14-16] Theoretic study of atmosphere and hydrological cycle with groundwater transportation on land planets

*Taniguchi Keigo[1,2], Yasuhito Sekine[1], Takanori Kodama[3], Natsumi Noda[4], Hidenori Genda[1], Ayako Abe-Ouchi[5] (1.Earth-Life Science Institute, Tokyo Institute of Technology, 2.Department of Earth & Planetary Sciences, Tokyo Institute of Technology, 3.The university of Tokyo, 4.Department of Earth and Planetary Science, Graduate School of Science, The University of Tokyo, 5.Atmosphere and Ocean Research Institute, The University of Tokyo)

4:30 PM - 4:45 PM JST | 7:30 AM - 7:45 AM UTC

[MIS14-17] Possibility of formation of local reductive environment by cometary impact on the early Earth

*Ryo Miyazaki[1], Hidenori Genda[1] (1.Earth Life Science Institute, Tokyo Institute of Technology)

4:45 PM - 5:00 PM JST | 7:45 AM - 8:00 AM UTC

[MIS14-18] Oceanic retention of ammonia and thermal stability of the atmosphere-ocean system on the primitive earth

*Kirara Arima[1], Kiyoshi Kuramoto[1] (1.Hokkaido university)

[J] Poster | M (Multidisciplinary and Interdisciplinary)：M-IS Intersection

5:15 PM - 6:30 PM JST | 8:15 AM - 9:30 AM UTC | Ch.22_1

[M-IS14] Aqua planetology

convener:Yasuhito Sekine(Earth-Life Science Insitute, Tokyo Institute of Technology), Takazo Shibuya(Japan Agency for Marine-Earth Science and Technology), Hidenori Genda(Earth-Life Science Institute, Tokyo Institute of Technology), Keisuke Fukushi(Institute of Nature & Environmental Technology, Kanazawa University)

[MIS14-P01] Experimental study of hypervelocity impact penetration of asteroids into the Ocean and benthic cratering

*Manabu Nishizawa[1] (1.Japan Agency for Marine-Earth Science and Technology)

[MIS14-P02] Experimental study on the growth process of iron rind in Fe-oxide concretions

*Hiroyuki Okamura[1], Sin-iti Sirono[1] (1.Department of Earth and Planetary Sciences, Nagoya University)

[MIS14-P03] **Redox change by coseismic water-rock reactions in the interior of planets**

*Takehiro Hirose[1], Ryoichi Nakada[1], Keishi Okazaki[1], Takazo Shibuya[1] (1.Japan Agency for Marine-Earth Science and Technology)

[MIS14-P04] Characterizations of mineralogy and infrared spectra of serpentinized samples in Oman ophiolite along with redox gradients in subsurface: Toward identification of redox gradients in Martian subsurface

*Takumi Sato[1], Yasuhito Sekine[1], Ikuo Katayama[2] (1.Tokyo Institute of Technology , 2.Hiroshima University)

[MIS14-P05] Experimental study of element dissolution to liquid CO_2 from artificial seawater and hydrothermal vent chimney

*Kaito Seo[1,2], Takazo Shibuya[2], Kosuke Fujishima[3], Ken Takai[2], Masaru Tomita[1,4] (1.Graduate School of Media and Governance, Keio Univ., 2.JAMSTEC, 3.ELSI, 4.IAB, Keio Univ.)

[MIS14-P06] Rocognition and classification of Martian chaos terrains using imagery marchine learning: Implications for groundwater distribution and hydrological cycles

Hiroki Shozaki[2], *Yasuhito Sekine[1], Nicholas Guttenberg[1] (1.Earth-Life Science Insitute, Tokyo Institute of Technology, 2.Dept. Earth Planetary Sci., Tokyo Institute of Technology)

[MIS14-P07] No effective oxychloride formations on Europa's surface inferred from UV/electron irradiation experiments onto salt-ice mixtures

*Shuya Tan[1], Yasuhito Sekine[1], Takashi Kikuchi[2], Hisayuki Suematsu[2], Tetsuya Hama[3], Yoshio Takahashi[4] (1.Earth-Life Science Institute, Tokyo Institute of Technology, 2.Nagaoka University of Technology, 3.Komaba Institute for Science, The University of Tokyo, 4.Department of Earth and Planetary Science, Graduate School of Science, The University of Tokyo)

[MIS14-P08] An experimental study on evaporite formation around the north pole of Titan

*Eito Hirai[1,2], Yasuhito Sekine[2], ZHANG NAIZHONG[2] (1.Department of Earth and Planetary Sciences, School of Science, Tokyo Institute of Technology, 2.Earth-Life Science Institute, Tokyo Institute of Technology)

[MIS14-P09] **Prediction of the composition of the primordial ocean just after its formation**

*Hisahiro Ueda[1], Takazo Shibuya[1] (1.JAMSTEC)

[MIS14-P10] **Formation conditions of magnetite and hematite in Sheepbed mudstone and bioavailable energies in lake water-groundwater mixing zone in Gale crater, Mars**

*Sakiko Kikuchi[1], Takazo Shibuya[1] (1.Japan Agency for Marine-Earth Science and Technology)

[MIS14-P11] Measurements of elastic wave velocity of mafic and ultramafic rocks below the freezing point: Consideration about reflectivity due to ice-water phase transition in Mars

*Haruna Wakabayashi[1], Ikuo Katayama[1] (1.Hiroshima University)

[MIS14-P12] Viscosity of aqueous MgSO4 solutions at high-pressure and low-temperature: implications for icy satellites

*Shunsuke Nozaki[1], Seiji Kamada[2,3], Akio Suzuki[2] (1.Division of Earth and Planetary Materials Science, Faculty of Science, Tohoku University , 2.Department of Earth Science, Graduate School of Science, Tohoku University,

3.Frontier Research Institute for Interdisciplinary Sciences, Tohoku University)

[MIS14-P13] Formation mechanism of spherical concretions in Tatsukushi area: Possible analogy with spherical nodule in Gale crater, Mars

*Saki Asai[1], Hitoshi Hasegawa[1], Hidekazu Yoshida[2], Minoru Ikehara[1], Nagayoshi Katsuta[3], Masakazu Nara[1], Yui Tomonao[1], Satoru Imai[4] (1.Kochi University, 2.Nagoya University, 3.Gifu University, 4.Tosashimizu GeoPark)

[MIS14-P14] Synthesis and reversible redox properties of iron-saponite

*Hiroshi Sakuma[1], Koki Morida[2], Keisuke Fukushi[2], Yoshio Takahashi[3], Natsumi Noda[3,4], Yasuhito Sekine[4], Kenji Tamura[1] (1.National Institute for Materials Science, 2.Kanazawa University, 3.University of Tokyo, 4.Tokyo Institute of Technology)

[MIS14-P15] Physical dependence of stable carbon and hydrogen isotopic ratio of methane gas in gas hydrate

*Kushi Kudo[1], Atsushi Tani[1], Keita Yamada[2], Naohiro Yoshida[3] (1.Graduate School of Human Development and Environment, Kobe University, 2.Department of Chemical Science and Engineering, School of Materials and Chemical Technology, Tokyo Institute of Technology, 3.Earth–Life Science Institute)

[MIS14-P16] **Clumped isotope signatures of abiotic methane formed via Fischer-Tropsch catalysis and their implications**

*ZHANG NAIZHONG[1], Yasuhito Sekine[1], Mayuko Nakagawa[1], Naohiro Yoshida[1] (1.Tokyo Institute of Technology)

[MIS14-P17] Possibilities of the rubidium stable isotope ratio as geochemical tools

*Rimi Konagaya[1], Hiroyuki Tsuboi[1], Takaaki Itai[1], Yoshio Takahashi[1] (1.The University of Tokyo)

[MIS14-P18] **Determination method of ^{13}C-labeled isotopomer ratio of dissolved organic acids by GC-MS analysis**

*Konomi Suda[1] (1.National Institute of Advanced Industrial Science and Technology)

[MIS14-P19] **Selectivity coefficient of Na^+-NH_4^+ exchange in saponite interlayer: Reconstruction of ammonium concentration in early ocean on Ceres**

*Hiroto Tokumon[1], Keisuke Fukushi[2], Yasuhito Sekine[3], Kosuke Inoue[1], Koki Morida[1] (1.Kanazawa University , 2.Institute of Nature and Environmental Technology Kanazawa University, 3.Tokyo institute of technology)

[J] Oral | M (Multidisciplinary and Interdisciplinary) : M-IS Intersection

9:00 AM - 10:30 AM JST | 12:00 AM - 1:30 AM UTC | Ch.26 Zoom Room 26

[M-IS16] Paleoclimatology and paleoceanography

convener:Yusuke Okazaki(Department of Earth and Planetary Sciences, Graduate School of Science, Kyushu University), Hitoshi Hasegawa(Faculty of Science and Technology, Kochi University), Atsuko Yamazaki(Faculty of Science, Kyushu University), Akitomo Yamamoto(Japan Agency for Marine-Earth Science and TechnologyAtmosphere and Ocean Research Institute), Chairperson:Akitomo Yamamoto(Japan Agency for Marine-Earth Science and TechnologyAtmosphere and Ocean Research Institute)

9:00 AM - 9:15 AM JST | 12:00 AM - 12:15 AM UTC

[MIS16-11] **Reconstruction of the ice sheet history since the Last Glacial Maximum based on field-based geomorphological observations and surface exposure ages along the southern Soya Coast, Lützow-Holm Bay, East Antarctica**

*Moto Kawamata[1], Yusuke Suganuma[2,1], Koichiro Doi[2,1], Keiji Misawa[2,1], Motohiro Hirabayashi[2], Akihisa Hattori[1], Takanobu Sawagaki[3] (1.Department of Polar Science, School of Multidisciplinary Science, SOKENDAI (The Graduate Unversity for Advanced Studies), 2.National Institute of Polar Research, 3.Hosei University)

9:15 AM - 9:30 AM JST | 12:15 AM - 12:30 AM UTC

[MIS16-12] Characteristic of radiocarbon dates in response to sea-level changes in the Bonaparte Gulf, Northwestern Australia

*Takeshige Ishiwa[1,2,3], Yusuke Yokoyama[2,3,4], Stephen Obrochta[5], Katsuto Uehara[6], Jun'ichi Okuno[1,7], Minoru Ikehara[8], Yosuke Miyairi[2] (1.National Institute of Polar Research, 2.Atmosphere and Ocean Research Institute, The University of Tokyo, 3.Department of Earth and Planetary Science, Graduate School of Science, The University of Tokyo, 4.Japan Agency for Marine-Earth Science and Technology, 5.Graduate School of International Resource Science, Akita University, 6.Research Institute for Applied Mechanics, Kyushu University, 7.Department of Polar Research Science, School of Multidisciplinary Science, The Graduate University for Advanced Studies (SOKENDAI), 8.Center for Advanced Marine Core Research, Kochi University)

9:30 AM - 9:45 AM JST | 12:30 AM - 12:45 AM UTC

[MIS16-13] Wind-wave changes in Tokyo Bay during the Holocene: impact of sea-level change and land configuration

*Katsuto Uehara[1] (1.Kyushu University)

9:45 AM - 10:00 AM JST | 12:45 AM - 1:00 AM UTC

[MIS16-14] Reconstruction of organic matter inflow fluctuations from the Bolling-Allerod interstadial to Late Holocene using Lake Baikal sediments

*Keiko Takehara[1], Masatoshi Nakakuni[2], Shuichi Yamamoto[3] (1.Kochi university Graduate School of Integrated Arts and Sciences, 2.Faculty of Agriculture, Kagawa University, 3.Department of Environmental Engineering for Symbiosis, Graduate School of Engineering, Soka University)

10:00 AM - 10:15 AM JST | 1:00 AM - 1:15 AM UTC

[MIS16-15] Reconstruction of Early Pleistocene sea-surface temperature in the Northwestern Pacific Ocean based on calcareous microfossils

*Daisuke Kuwano[1], Yuki Tsuchiya[2], Yuma Oura[1], Hiroki Hayashi[3], Yoshimi Kubota[4], Kanako Mantoku[5], Koji Kameo[1] (1.Chiba University, 2.Nagoya University, 3.Shimane University, 4.National Museum of Nature and Science, 5.National Institute for Environmental Studies)

10:15 AM - 10:30 AM JST | 1:15 AM - 1:30 AM UTC

[MIS16-16] Variation of the North Pacific Ocean circulation during the Late Pleistocene glacial-interglacial cycles

*Furukawa Keisuke[1], Osamu Seki[1], Masanobu Yamamoto[1], Tomohisa Irino[1] (1.Hokkaido University)

[J] Oral | M (Multidisciplinary and Interdisciplinary) : M-IS Intersection

10:45 AM - 12:15 PM JST | 1:45 AM - 3:15 AM UTC | Ch.26 Zoom Room 26

[M-IS16] Paleoclimatology and paleoceanography

convener:Yusuke Okazaki(Department of Earth and Planetary Sciences, Graduate School of Science, Kyushu University), Hitoshi Hasegawa(Faculty of Science and Technology, Kochi University), Atsuko Yamazaki(Faculty of Science, Kyushu University), Akitomo Yamamoto(Japan Agency for Marine-Earth Science and TechnologyAtmosphere and Ocean Research Institute), Chairperson:Hitoshi Hasegawa(Faculty of Science and Technology, Kochi University)

10:45 AM - 11:00 AM JST | 1:45 AM - 2:00 AM UTC

[MIS16-17] Reconstruction of the Mediterranean sulfur cycle during the Messinian salinity crisis using evaporites

*Takeru Kochi[1], Junichiro Kuroda[1], Nanako O. Ogawa[2], Toshihiro Yoshimura[2], Takashi Miyazaki[2], Bogdan Stefanov Vaglarov[2], Naohiko Ohkouchi[2] (1.the University of Tokyo, 2.Japan Agency for Marine–Earth Science and Technology)

11:00 AM - 11:15 AM JST | 2:00 AM - 2:15 AM UTC

[MIS16-18] Increased eolian dust in the Pacific since around the Eocene-Oligocene boundary estimated from a rock-magnetic study of red clay

*Toshitsugu Yamazaki[1], Wei Fu[1], Takaya Shimono[2], Yoichi Usui[3] (1.Atmosphere and Ocean Research Institute, The University of Tokyo, 2.Geological Survey of Japan, AIST, 3.Japan Agency for Marine-Earth Science and Technology)

11:15 AM - 11:30 AM JST | 2:15 AM - 2:30 AM UTC

[MIS16-19] **Authigenic and detrital Mg and Li isotopes as a tracer of Antarctic chemical silicate weathering across the EOT**

*Adam David Sproson[1,2,3], Toshihiro Yoshimura[1], Yusuke Yokoyama[1,3], Takahiro AZE[3], Tsuyoshi Ishikawa[4], Shigeyuki Wakaki[4], Naohiko Ohkouchi[1] (1.Department of Biogeochemistry, Japan Agency for Marine-Earth Science and Technology, 2-15 Natsushima, Yokosuka, Kanagawa 237-0061, Japan, 2.Submarine Resources Research Center, Japan Agency for Marine-Earth Science and Technology, 2-15 Natsushima, Yokosuka, Kanagawa 237-0061, Japan, 3.Atmosphere and Ocean Research Institute, University of Tokyo, 5-1-5 Kashiwanoha, Kashiwa, Chiba 277-8564, Japan, 4.Kochi Institute for Core Sample Research, Japan Agency for Marine-Earth Science and Technology 200 Monobe Otsu, Nankoku City, Kochi 783-8502, Japan)

11:30 AM - 11:45 AM JST | 2:30 AM - 2:45 AM UTC

[MIS16-20] Terrestrial environmental response to the global climate change during the early to middle Eocene (52.7-43.8 Ma): evidence from lacustrine deposits of the Green River Formation, Utah, USA

*Ryusei Kuma[1], Hitoshi Hasegawa[2], Koshi Yamamoto[1], Jessica H. Whiteside[3], Amy L. Elson[3], Hidekazu Yoshida[1], Koichi Mimura[1] (1.Nagoya University, 2.Kochi University, 3.University of Southampton)

11:45 AM - 12:00 PM JST | 2:45 AM - 3:00 AM UTC

[MIS16-21] C40-alkenone unsaturation index from the Cretaceous and paleothermometry in southern high latitude of Proto-Indian Ocean

*Takashi Hasegawa[1], Akiko S. Goto[2,1], Hiromichi Komiya[3], Shota Morikawa[3] (1.Faculty of Geoscience and Engineering, Institute of Science and Engineering, Kanazawa University, 2.Center of Ecological Research, Kyoto University, 3.Graduate School of Natural Science and Engineering, Kanazawa University)

12:00 PM - 12:15 PM JST | 3:00 AM - 3:15 AM UTC

[MIS16-22] Opposing responses in the hydrological cycle of the East Asia to climate warming related with the Tibetan Plateau

*Taro Higuchi[1], Ayako Abe-Ouchi[1], Wing-Le Chan[1] (1.Atmospheric and Ocean Research Institute, the University of Tokyo)

[J] Poster | M (Multidisciplinary and Interdisciplinary) : M-IS Intersection

5:15 PM - 6:30 PM JST | 8:15 AM - 9:30 AM UTC | Ch.23

[M-IS16] Paleoclimatology and paleoceanography

convener:Yusuke Okazaki(Department of Earth and Planetary Sciences, Graduate School of Science, Kyushu University), Hitoshi Hasegawa(Faculty of Science and Technology, Kochi University), Atsuko Yamazaki(Faculty of Science, Kyushu University), Akitomo Yamamoto(Japan Agency for Marine-Earth Science and TechnologyAtmosphere and Ocean Research Institute)

[MIS16-P01] Temperature effect on Japanese stalagmite $\delta^{18}O$ records from Hiroshima and Gifu

*Hirokazu Kato[1], Taiki Mori[2], Shota Amekawa[1], Akihiro Kano[1] (1.Department of Earth and Planetary Science, The University of Tokyo, 2.Chuo Kaihatsu Corporation)

[MIS16-P02] **Oxygen isotope equilibrium of the shallow-water benthic foraminifer *Hanzawaia nipponica* (Asano) in Tosa Bay, southwest Japan**

*Minoru Ikehara[1,2], Shigetaka Kita[2], SHUNGO KAWAGATA[3] (1.Center for Advanced Marine Core Research, Kochi University, 2.Graduate School of Integrated Arts and Sciences, Kochi University, 3.Faculty of Education, Yokohama National University)

[MIS16-P03] **Variations in shell morphology of the planktonic foraminifer *Globigerina bulloides* in the sediment off Kashima**

*Yuya Hashimoto[1], Takuya Sagawa[2] (1.Kanazawa University College of Science and Engineering, 2.Institute of Science and Engineering, Kanazawa University)

[MIS16-P04] Climate characteristics of Amami , Kagoshima , Japan over the past 200 years inferred from tree-ring cellulose oxygen isotope ratio data

*Akihiro Masuoka[1], Kenjiro Sho[1], Masafumi Ohata[2], Zhen Li[3], Takeshi Nakatsuka[3] (1.Nagoya Institute of Technology, 2.Taisei Corporation, 3.Nagoya University)

[MIS16-P05] Coral skeletal records reveal the relationship between Kuroshio variability and North Pacific climate

*Atsuko Yamazaki[1,2], Tsuyoshi Watanabe[2,3] (1.Kyushu University, 2.KIKAI institute for Coral Reef Sciences, 3.Hokkaido University)

[MIS16-P06] Reconstruction of environmental and flooding histories since AD1250 at Lake Kortta, an annually laminated lake at the Central Finland presumed by Diatom and Chrysophyceae assemblages

*Kaoru Kashima[1], Yu Fukumoto[2], Timo Saarinen[3] (1.Department of Earth and Planetary Sciences, Kyushu University, 2.Osaka City University, 3.University of Turku)

[MIS16-P07] **Sphagnum and grass cellulose oxygen isotopes in peat cores reveal climate changes in northern Japan over the past 4400 years and close relationship with human histories**

*Masanobu Yamamoto[1], Osamu Seki[2] (1.Faculty of Environmental Earth Science, Hokkaido University, 2.Insititute of Low Temperature Science)

[MIS16-P08] Can Sedimentary fish DNA track decadal to centennial scale fish abundance?

*Michinobu Kuwae[1], Hiromichi Tamai[1], Hideyuki Doi[2], Masayuki Sakata[3], Toshifumi Minamoto[3], Yoshiaki Suzuki[4] (1.Center for Marine Environmental Studies, 2.Graduate School of Simulation Studies, University of Hyogo, 3.Graduate School of Human Development and Environment, Kobe University, 4.Research Institute of Geology and Geoinformation, Geological Survey of Japan, National Institute of Advanced Industrial Science and Technology)

[MIS16-P09] Paleoenvironmental variations reconstructed by algal biomarker analysis of a sediment core from Lake Nakaumi, Japan

*Akiko Taneichi[1], Yuki Hattori[1], Ken Sawada[1], Takuto Ando[2], Hideto Nakamura[3], Kotaro Hirose[4] (1.Hokkaido Univ., 2.Shimane Univ., 3.Osaka City Univ., 4.Waseda Univ.)

[MIS16-P10] Paleoceanographic changes in the western part of the Arctic Sea based on ostracods

*Katsura Yamada[1], Kosuke Yamaguchi[1], Masao Uchida[2], Takuya Itaki[3], Kanako Mantoku[2] (1.Department of Geology, Faculty of Science, 2.National Institute for Environmental Studies, 3.National Institute of Advanced Industrial Science and Technology)

[MIS16-P11] **Mid- to late Holocene variability of the Aleutian Low Atmospheric Pressure Cell: Forcing by the Western Jet**

*Kana Nagashima[1], Jason Addison[2], Tomohisa Irino[3], Takayuki Omori[4], Kei Yoshimura[5], Naomi Harada[1] (1.Research Institute for Global Change, Japan Agency for Marine-Earth Science and Technology, 2.U.S. Geological Survey, 3.Faculty of Environmental Earth Science, Hokkaido University, 4.The University Museum, The University of Tokyo, 5.Institute of Industrial Science, The University of Tokyo)

[MIS16-P12] Sedimentary characteristics, age and event of a marine core collected from Uranouchi Bay, Kochi, Japan

*Masafumi MURAYAMA[1,3], Wataru Tanikawa[2], Akira Ijiri[2], Tatsuhiko Hoshino[2], Takehiro Hirose[2], Katsuya Nejigaki[3], Kazuno Arai[3], Go-Ichiro Uramoto[3], Kondo Yasuo[4], Hiromasa Ozaki[5], Minoru Yoneda[5] (1.Faculty of Agriculture and Marine Science, Kochi University, 2. Institute for Extra-cutting-edge Science and Technology Avant-garde Research, Kochi Institute for Core Sample Research, JAMSTEC, 3.Center for Advanced Marine Core Research, Kochi University, 4.Faculty of Science and Technology, Kochi University, 5.The University Museum,The University of Tokyo)

[MIS16-P13] Estimation of amount of meltwater discharge from the Laurentide to the Arctic Ocean during the MWP1a event

★Invited Papers

*Kenta Suzuki[1], Masanobu Yamamoto[1], Leonid Polyak[2], Tomohisa Irino[1] (1.Faculty of Environmental Earth Science, Hokkaido Univ., 2.Byrd Polar and Climate Research Center, The Ohio State Univ.)

[MIS16-P14] Millennial variability in precipitation in Papua New Guinea during the last deglaciation

*Gaku Sudo[1], Masanobu Yamamoto[1], Samantha Bova[2], Yair Rosenthal[2] (1.Faculty of Environmental Earth Science, Hokkaido Univ., 2.Rutgers Univ.)

[MIS16-P15] A paleoclimatic reconstruction of the southeastern Pacific last deglacial using geochemical proxies obtained from offshore Chile

*Karin Nemoto[1,2], Yusuke Yokoyama[1,2], Adam David Sproson[2], Yosuke Miyairi[2], Takahiro AZE[2], Hiroyuki Matsuzaki[3,4], Yair Rosentha[5], Samantha Bova[5] (1.Department of Earth and Planetary Science, The University of Tokyo, 2.Atmosphere and Ocean Research Institute, The University of Tokyo, 3.The University Museum,The University of Tokyo, 4.School of Engineering, The University of Tokyo, 5.Department of Marine and Coastal Sciences, School of Environmental and Biological Sciences, Rutgers University)

[MIS16-P16] Paleovegetation changes in the northern Mongolia since the last glacial

*Ryosuke Imaoka[1], Koji Shichi[2], Hitoshi Hasegawa[1], Niiden Ichinnorov[3], Nagayoshi Katsuta[4], Davaasuren Davaadorj[5], Masafumi MURAYAMA[1], Masao Iwai[1], masami izuho[6] (1.Kochi University, 2.Forestry and Forest Products Research Institute, 3.Paleontological Center of Mongolia, 4.Gifu University, 5.National University of Mongolia, 6.Tokyo Metropolitan University)

[MIS16-P17] Glacial–interglacial variations in the Leeuwin Current for the last 50,000 years based on Nd isotope records of benthic foraminifers

*Ryota Wako[1], Hideko Takayanagi[1], Shigeyuki Wakaki[2], Takeshige Ishiwa[4], Yusuke Yokoyama[5], Hitomi Uchimura Wakaki[3], Tsuyoshi Ishikawa[2], Yasufumi Iryu[1] (1.Department of earth science, Tohoku university , 2.Kochi Institute for Core Sample Research, JAMSTEC, 3.Center for Advanced Marine Core Research, Kochi University, 4.National Institute of Polar Research, 5.Atmosphere and Ocean Research Institute, University of Tokyo)

[MIS16-P18] Changes in carbonate dissolution and preservation in Southern Ocean sediment off Chilean margin during the last 140 kyrs based on fragmentation and size-normalized weight of planktic foraminiferal tests.

*Takuto Kasuya[1], Yusuke Okazaki[2], Shinya Iwasaki[3], IODP Expedition 383 Scientific Party (1.Department of Earth and Planetary Sciences, School of Science, Kyushu University , 2.Department of Earth and Planetary Sciences, Faculty of Science, Kyushu University, 3.MARUM Center for Marine Environmental Sciences and Department of Geosciences, University of Bremen)

[MIS16-P19] Examining MIS 5e Sea-Levels around Japan: 60+ Years of Sea-Level Proxy Analysis and Applied Dating Techniques

*Evan Tam[1,2], Yusuke Yokoyama[1,2] (1.University of Tokyo, Atmosphere and Ocean Research Institute, 2.University of Tokyo, Graduate Program on Environmental Science)

[MIS16-P20] Integrated stratigraphy of the sediment core retrieved from the Manihiki Plateau in the central Pacific and the paleotemperature change for the last 800 kyr

*MISAKI URAKAMI[1], Takuya Sagawa[2], Yoshimi Kubota[3] (1.College of Science and Engineering, Kanazawa University, 2.Institute of Science and Engineering, Kanazawa University, 3.National Museum of Nature and Science)

[MIS16-P21] Preliminary results of oxygen isotopic, paleomagnetic, and pollen analyses from a mid-Piacenzian marine succession in the Boso Peninsula, central Japan.

*Yuki Haneda[1] (1.Geological Survey of Japan, AIST)

[MIS16-P22] The mid-Pliocene Warm Period: climate sensitivity to atmospheric CO_2 levels and inclusion of dynamic vegetation in the MIROC4m model

*Wing-Le Chan[1], Ayako Abe-Ouchi[1,2] (1.Atmosphere and Ocean Research Institute, The University of Tokyo, 2.National Institute of Polar Research)

[MIS16-P23] Chemical weathering feedback during the early Paleogene hyperthermals based on osmium isotope analysis

*Kakeru Ikegami[1], Kazutaka Yasukawa[1,2], Erika Tanaka[1], Junichiro Ohta[1,2], Yusuke Kuwahara[1], Moei Yano[2,1], Koichiro Fujinaga[2,1], Yasuhiro Kato[1,2] (1.School of Engineering, The University of Tokyo, 2.ORCeNG, Chiba Institute of Technology)

[MIS16-P24] High latitude paleoenvironments in Southern Hemisphere during mid-Cretaceous

*Hiromichi Komiya[1], Takashi Hasegawa[1] (1.Kanazawa University)

[MIS16-P25] A study on the responses of the climate field in the Cretaceous to orbital parameter changes

★Invited Papers

*Taro Higuchi[1], Ayako Abe-Ouchi[1], Wing-Le Chan[1] (1.Atmospheric and Ocean Research Institute, the University of Tokyo)

[MIS16-P26] **Eccentricity paced increase in the continental weathering in the latest Hauterivian, Early Cretaceous**

★Invited Papers

*Hironao Matsumoto[1], Rodolfo Coccioni[2], Fabrizio Frontalini[2], Kotaro Shirai[1], Junichiro Kuroda[1] (1.Atmosphere and Ocean Research Institute, the University of Tokyo, 2.University of Urbino)

[MIS16-P27] Millennial-scale cyclicities recorded in the Cretaceous lacustrine core using Monte Carlo approach

*Hitoshi Hasegawa[1], Hirofumi Asahi[2] (1.Faculty of Science and Technology, Kochi University, 2.Center for Advanced Marine Core Research, Kochi University)

[J] Oral | M (Multidisciplinary and Interdisciplinary)：M-IS Intersection

1:45 PM - 3:15 PM JST | 4:45 AM - 6:15 AM UTC | Ch.03 Zoom Room 03

[M-IS17] Interface- and nano-phenomena on crystal growth and dissolution

convener:Yuki Kimura(Institute of Low Temperature Science, Hokkaido University), Hitoshi Miura(Graduate School of Science, Department of Information and Basic Science, Nagoya City University), Hisao Satoh(Low-Level Radioactive Waste Disposal Center, Japan Nuclear Fuel Limited), Chairperson:Yuki Kimura(Institute of Low Temperature Science, Hokkaido University)

1:45 PM - 2:00 PM JST | 4:45 AM - 5:00 AM UTC

[MIS17-01] Nucleation of water particles in the mesosphere

*Kyoko Kitakami Tanaka[1,2], Yuki Kimura[3], Ingrid Mann[4] (1.Tohoku University, 2.Nihon University, 3.ILTS, Hokkaido University, 4.UiT the Arctic University of Norway)

2:00 PM - 2:15 PM JST | 5:00 AM - 5:15 AM UTC

[MIS17-02] Possible new water on an ice III crystal in water

*Hiromasa Niinomi[1], Tomoya Yamazaki[2], Hiroki Nada[3], Tetsuya Hama[4], Akira Kouchi[2], Junpei Okada[1], Nozawa Jun[1], Satoshi Uda[1], Yuki Kimura[2] (1.Institute for Materials Research, Tohoku University, 2.Institute of Low Temperature Science, Hokkaido University, 3.National Institute of Advanced Industrial Science and Technology, 4.Komaba Institute for Science, The University of Tokyo)

2:15 PM - 2:30 PM JST | 5:15 AM - 5:30 AM UTC

[MIS17-03] HCl droplets induced bunched steps on ice crystal surfaces under atmospheric-concentration HCl gas

*Ken Nagashima[1], Ken-ichiro Murata[1], Gen Sazaki[1] (1.The Institute of Low Temperature Science, Hokkaido University)

2:30 PM - 2:45 PM JST | 5:30 AM - 5:45 AM UTC

[MIS17-04] Adsorption of nucleotides on clay induced by change in hydration structure by magnesium ion

*Yuki Araki[1], Yoshihiro Furukawa[2] (1.Ritsumeikan University, 2.Tohoku University)

2:45 PM - 3:15 PM JST | 5:45 AM - 6:15 AM UTC

[MIS17-05] Surface-Selective Vibrational Micro-Spectroscopy Unveils Physicochemical States and the History of Crystals

★Invited Papers

*Hiroharu Yui[1] (1.Tokyo University of Science)

[J] Oral | M (Multidisciplinary and Interdisciplinary)：M-IS Intersection

3:30 PM - 5:00 PM JST | 6:30 AM - 8:00 AM UTC | Ch.03 Zoom Room 03

[M-IS17] Interface- and nano-phenomena on crystal growth and dissolution

convener:Yuki Kimura(Institute of Low Temperature Science, Hokkaido University), Hitoshi Miura(Graduate School of Science, Department of Information and Basic Science, Nagoya City University), Hisao Satoh(Low-Level Radioactive Waste Disposal Center, Japan Nuclear Fuel Limited), Chairperson:Hitoshi Miura(Graduate School of Science, Department of Information and Basic Science, Nagoya City University)

3:30 PM - 3:45 PM JST | 6:30 AM - 6:45 AM UTC

[MIS17-06] Control of particles by electric field and its applicability in LC-TEM for observing crystallization and dissolution processes

*Tomoya Yamazaki[1], Hiromasa Niinomi[2], Yuki Kimura[1] (1.Institute of Low Temperature Science Hokkkaido University, 2.Institute for Materials Research, Tohoku University)

3:45 PM - 4:00 PM JST | 6:45 AM - 7:00 AM UTC

[MIS17-07] Time lapse imaging of pH/ionic concentration distribution for understanding the dissolution/formation process of minerals in aqueous solution

*Jun Kawano[1], Makoto Yazaki[2], Shinji Matsumoto[2], Takashi Toyofuku[3,4], Yukiko Nagai[3,5], Kazuya Ohno[2], Takaya Nagai[1] (1.Faculty of Science, Hokkaido Univ., 2.Graduate School of Science, Hokkaido Univ., 3.JAMSTEC, 4.TUMSAT, 5.NMNS)

4:00 PM - 4:15 PM JST | 7:00 AM - 7:15 AM UTC

[MIS17-08] Pore space property of clayey materials in the forms of gelled to compacted: a strategy for designing buffer materials

*Hisao Satoh[1], Yuki Araki[2] (1.Japan Nuclear Fuel Limited, 2.Ritsumeikan University)

4:15 PM - 4:30 PM JST | 7:15 AM - 7:30 AM UTC

[MIS17-09] Hidden stability of norsethite revealed by phase diagram

*Harutoshi Asakawa[1], Kaoru Isobe[1], Hiroshi Uneda[1], Itaru Echigo[1], Ryuichi Komatsu[1] (1.Graduate School of Sciences and Technology for Innovation Yamaguchi University)

4:30 PM - 5:00 PM JST | 7:30 AM - 8:00 AM UTC

[MIS17-10] Control of defect structure in functional bulk crystals

★Invited Papers

*Harada Shunta[1,2] (1.Nagoya University, 2.PRESTO JST)

[J] Poster | M (Multidisciplinary and Interdisciplinary)：M-IS Intersection

5:15 PM - 6:30 PM JST | 8:15 AM - 9:30 AM UTC | Ch.21_4

[M-IS17] Interface- and nano-phenomena on crystal growth and dissolution

convener:Yuki Kimura(Institute of Low Temperature Science, Hokkaido University), Hitoshi Miura(Graduate School of Science, Department of Information and Basic Science, Nagoya City University), Hisao Satoh(Low-Level Radioactive Waste Disposal Center, Japan Nuclear Fuel Limited)

[MIS17-P01] Toward for the developing the thermal storage materials utilizing the Electrostatic Levitation Furnace in "Kibo" in space

*Hidekazu Kobatake[1], Kazuki Tonooka[2], Shumpei Ozawa[2], Ken'ichi Sugioka[3], Suguru Shiratori[4], Ken Nagashima[5], Hirohisa Oda[6], Hideki Saruwatari [6], Chihiro Koyama[6], Takehiko Ishikawa[6] (1.Hirosaki University, 2.Chiba Institute of Technology, 3.Toyama Prefectural University, 4.Tokyo City University, 5.Hokkaido University, 6.JAXA)

[MIS17-P02] Heteroepitaxial growth mechanism in colloidal crystallization

*Jun Nozawa[1], Hiromasa Niinomi[1], Junpei Okada[1], Satoshi uda[1] (1.Tohoku University)

[MIS17-P03] Fabrication of evaluation model for adgesion mechanism between bone mineral and soft tissue

*Yuki Sugiura[1], Masahiro Okada[2], Ken Hirano[1], Takuya Matsumoto[2] (1.National Institute of Advanced Industrial Science and Technology, 2.Okayama University)

[MIS17-P04] Conversion from a stable crystal to a metastable crystal by grinding

*Hiroyasu Katsuno[1], Makio Uwaha[2] (1.Institute of Low Temperature Science, Hokkaido University, 2.Center for General Education, Aichi Institute of Technology)

[MIS17-P05] Improvement of transmission electron microscope images by neural network model

*Hiroyasu Katsuno[1], Shizuka Hirakawa[1], Tomoya Yamazaki[1], Ichigaku Takigawa[2], Yuki Kimura[1] (1.Institute of Low Temperature Science, Hokkaido University, 2.RIKEN, Center for Advanced Intelligence Project)

[MIS17-P06] Development of an early detection method of nucleation in in-situ liquid-cell TEM observation

*Yuki Kimura[1], Hiroyasu Katsuno[1], Tomoya Yamazaki[1], Ichigaku Takigawa[2,3] (1.Institute of Low Temperature Science, Hokkaido University, 2.AIP, RIKEN, 3.ICReDD, Hokkaido University)

[MIS17-P07] In-situ observation at the moments of bubble nucleation using a liquid-cell transmission electron microscope

*Yuki Kimura[1], Tomoya Yamazaki[1], Hiroyasu Katsuno[1], Shizuka Hirakawa[1] (1.Institute of Low Temperature Science, Hokkaido University)

[J] Oral | M (Multidisciplinary and Interdisciplinary) : M-IS Intersection

1:45 PM - 3:15 PM JST | 4:45 AM - 6:15 AM UTC | Ch.10 Zoom Room 10

[M-IS20] Ocean Plastics, an earth science perspective

convener:Atsuhiko Isobe(Research Institute for Applied Mechanics, Kyushu University), Kiichiro Kawamura(Yamaguchi University), Yusuke Okazaki(Department of Earth and Planetary Sciences, Graduate School of Science, Kyushu University), Masashi Tsuchiya(Research Institute for Global Change, Japan Agency for Marine-Earth Science and Technology), Chairperson:Atsuhiko Isobe(Research Institute for Applied Mechanics, Kyushu University)

1:45 PM - 2:00 PM JST | 4:45 AM - 5:00 AM UTC

[MIS20-01] Numerical model approach on the fate of pelagic plastics in the world's ocean

*Atsuhiko Isobe[1] (1.Research Institute for Applied Mechanics, Kyushu University)

2:00 PM - 2:15 PM JST | 5:00 AM - 5:15 AM UTC

[MIS20-02] Estimating vertical distribution of microplastic particles under wind-driven and Langmuir turbulence by Large Eddy Simulation

*Yoshimasa Matsumura[1], Shin-ichi Ito[1], Chiharu Sasaki[1] (1.Atmosphere and Ocean Research Institute, University of Tokyo)

2:15 PM - 2:30 PM JST | 5:15 AM - 5:30 AM UTC

[MIS20-03] Numerical experiment on vertical motion of microplastics with biological processes

*Miho Yoshitake[1], Atsuhiko Isobe[1] (1.Kyushu university)

2:30 PM - 2:45 PM JST | 5:30 AM - 5:45 AM UTC

[MIS20-04] Numerical model approach of macroplastic transport to find microplastic sources around the Indonesian archipelago

*Ryohei Kono[1], Atsuhiko Isobe[1] (1.Research Institute for Applied Mechanics, Kyushu University)

2:45 PM - 3:00 PM JST | 5:45 AM - 6:00 AM UTC

[MIS20-05] Quantifying the degree of pollution of beaches using an AI technique

*Mitsuko Hidaka[1], Daisuke Sugiyama[1], Daisuke Matsuoka[1], Fumiaki Araki[1], Masafumi Kamachi[1], Yoichi Ishikawa[1] (1.Japan Agency for Marine-Earth Science and Technology)

3:00 PM - 3:15 PM JST | 6:00 AM - 6:15 AM UTC

[MIS20-06] Estimation of plastic litter abundance in cities using big data associated with citizen science and deep learning

*Shinichiro Kako[1], Shintaro Kanno[2], Atsuhiko Isobe[3], Masato Kuki[4], Kotaro Yamamoto[4], Fujio Kojima[4] (1.Graduate School of Science and Engineering, Kagoshima University, 2.Faculty of engineering, Kagoshima University, 3.Research Institute for Applied Mechanics, Kyushu University, 4.Pirika, Inc. / Prika association)

[J] Oral | M (Multidisciplinary and Interdisciplinary)：M-IS Intersection

3:30 PM - 5:00 PM JST | 6:30 AM - 8:00 AM UTC | Ch.10 Zoom Room 10

[M-IS20] Ocean Plastics, an earth science perspective

convener:Atsuhiko Isobe(Research Institute for Applied Mechanics, Kyushu University), Kiichiro Kawamura(Yamaguchi University), Yusuke Okazaki(Department of Earth and Planetary Sciences, Graduate School of Science, Kyushu University), Masashi Tsuchiya(Research Institute for Global Change, Japan Agency for Marine-Earth Science and Technology), Chairperson:Kiichiro Kawamura(Yamaguchi University)

3:30 PM - 3:45 PM JST | 6:30 AM - 6:45 AM UTC

[MIS20-07] Large-scale distribution and composition of floating plastic debris in the transition region of the North Pacific

*Kentaro Miyazono[1], Rei Yamashita[2], Hiroomi Miyamoto[3], Kazuaki Tadokoro[4], Yugo Shimizu[5], Kazutaka Takahashi[1] (1.Graduate school of agricultural and life science, The University of Tokyo , 2.Atmosphere and Ocean Research Institute, The University of Tokyo , 3.Fisheries Research Agency, Hachinohe, 4.Fisheries Research Agency, Shiogama, 5.Fisheries Agency)

3:45 PM - 4:00 PM JST | 6:45 AM - 7:00 AM UTC

[MIS20-08] TARA-JAMBIO Microplastic Mission : Distributions of microplastics in water surface and sediment of Japanese coastal waters

*Kugako Sugimoto[1], JAMBIO Consortium[3], Tara Japan[2], Sylvain Agostini[1] (1.Shimoda Marine Research Center, University of Tsukuba, 2.Tara Océan Fondation, 3.Japanese Association for Marine Biology)

4:00 PM - 4:15 PM JST | 7:00 AM - 7:15 AM UTC

[MIS20-09] Distribution of Microplastics in the Deep-sea Sediments

*Tomo Kitahashi[1], Masashi Tsuchiya[1], Ryota Nakajima[1], Rie Matsui[1], Kazumasa Oguri[1,2], Kiichiro Kawamura[3], Yosaku Maeda[1], Sanae Chiba[1], Katsunori FUJIKURA[1] (1.Japan Agency for Marine-Earth Science and Technology, 2.University of Southern Denmark, 3.Yamaguchi University)

4:15 PM - 4:30 PM JST | 7:15 AM - 7:30 AM UTC

[MIS20-10] Chemical properties of film coatings developed on microplastics distributed on the urban river shore in Mongolia

*Masayuki Kawahigashi[1], Batdulam Battulga[1] (1.Tokyo Metropolitan University)

4:30 PM - 4:45 PM JST | 7:30 AM - 7:45 AM UTC

[MIS20-11] A trial of small microplastics collection by Neuston net

*Haodong XU[1], Haruka NAKANO[1], Tadashi TOKAI[1], Hisayuki ARAKAWA[1] (1.Tokyo University of Marine Science and Technology)

4:45 PM - 5:00 PM JST | 7:45 AM - 8:00 AM UTC

[MIS20-12] Non-contact real-time identification of microplastics in flow by combining holography and Raman spectroscopy

*Tomoko Takahashi[1,2,3], Zonghua Liu[2], Thangavel Thevar[4], Nicholas Burns[4], Dhugal Lindsay[1], John Watson[4], Sumeet Mahajan[3], Blair Thornton[2,3] (1.Japan Agency for Marine-Earth Science and Technology, 2.Institute of Industrial Science, The University of Tokyo, 3.University of Southampton, 4.University of Aberdeen)

[J] Poster | M (Multidisciplinary and Interdisciplinary)：M-IS Intersection

5:15 PM - 6:30 PM JST | 8:15 AM - 9:30 AM UTC | Ch.20_3

[M-IS20] Ocean Plastics, an earth science perspective

convener:Atsuhiko Isobe(Research Institute for Applied Mechanics, Kyushu University), Kiichiro Kawamura(Yamaguchi University), Yusuke Okazaki(Department of Earth and Planetary Sciences, Graduate School of Science, Kyushu University), Masashi Tsuchiya(Research Institute for Global Change, Japan Agency for Marine-Earth Science and Technology)

[MIS20-P01] Automatic detection for Nile Red-stained microplastic particles

*Masashi Tsuchiya[1], Tomo Kitahashi[1], Yosuke Taira[2], Hitoshi Saito[2], Kazumasa Oguri[1,3], Ryota Nakajima[1], Dhugal J. Lindsay[4], Katsunori FUJIKURA[1], Tomohiko Fukushima[1,5] (1.Research Institute for Global Change, Japan Agency for Marine-Earth Science and Technology, 2.NEC Corporation, 3.Danish Center for Hadal Research, University of Southern Denmark, 4.Institute for Extra-cutting-edge Science and Technology Avant-garde Research, Japan Agency for Marine-Earth Science and Technology, 5.Deep Ocean Resources Development Co., Ltd.)

[MIS20-P02] Deep sea Macro plastics in the Northwestern Pacific Ocean

*Tomoaki Kitayama[1], Takashi Hosono[1], Hideaki Saito[1] (1.Japan Agency for Marine-Earth Science and Technology)

[J] Oral | M (Multidisciplinary and Interdisciplinary) : M-IS Intersection

1:45 PM - 3:15 PM JST | 4:45 AM - 6:15 AM UTC | Ch.26 Zoom Room 26

[M-IS28] Evolution of Pelagic Realm

convener:Atsushi Matsuoka(Department of Geology, Faculty of Science, Niigata University), Toshiyuki Kurihara(Graduate School of Science and Technology, Niigata University), Junichiro Kuroda(Department of Ocean Floor Geoscience, Atmosphere and Ocean Research Institute, the University of Tokyo), XIN LI(State Key Laboratory of Palaeobiology and Stratigraphy, Nanjing Institute of Geology and Palaeontology, Chinese Academy of Sciences), Chairperson:Atsushi Matsuoka(Department of Geology, Faculty of Science, Niigata University), Junichiro Kuroda(Department of Ocean Floor Geoscience, Atmosphere and Ocean Research Institute, the University of Tokyo)

1:45 PM - 2:00 PM JST | 4:45 AM - 5:00 AM UTC

[MIS28-01] Toward a global correlation of the Jurassic–Cretaceous boundary among pelagic, neritic and terrestrial sequences in the Pacific and Asia

*Atsushi Matsuoka[1] (1.Department of Geology, Faculty of Science, Niigata University)

2:00 PM - 2:15 PM JST | 5:00 AM - 5:15 AM UTC

[MIS28-02] **Early Cretaceous anti-tropical radiolarians of from Tibet at the breakup timing of Gondwana**

*XIN LI[1], Noritoshi Suzuki[2], Peter Baumgartner[4], Atsushi Matsuoka[3] (1.State Key Laboratory of Palaeobiology and Stratigraphy, Nanjing Institute of Geology and Palaeontology, Chinese Academy of Sciences, 2.Institute of Geology and Paleontology, Gradute School of Science, Tohoku University, 3.Department of Geology, Faculty of Science, Niigata University, 4.Institut des sciences de la Terre, Université de Lausanne)

2:15 PM - 2:30 PM JST | 5:15 AM - 5:30 AM UTC

[MIS28-03] Repeated organic-rich deposition in Early Triassic pelagic deep Panthalassa and its relationship with global seafloor anoxia

*Shun Muto[1] (1.Geological Survey of Japan, National Institute of Advanced Industrial Science and Technology)

2:30 PM - 2:45 PM JST | 5:30 AM - 5:45 AM UTC

[MIS28-04] Marine Os isotope record from the uppermost Barremian to the lowest Turonian

*Hironao Matsumoto[1], Rodolfo Coccioni[2], Fabrizio Frontalini[2], Kotaro Shirai[1], Junichiro Kuroda[1] (1.Atmosphere and Ocean Research Institute, the University of Tokyo, 2.University of Urbino)

2:45 PM - 3:00 PM JST | 5:45 AM - 6:00 AM UTC

[MIS28-05] Depositional ages of multiple REY peaks in deep-sea sediments around Minamitorishima Island based on osmium isotope stratigraphy

*Yuta Oda[1], Junichiro Ohta[1,2], Erika Tanaka[1], Kazutaka Yasukawa[1,2], Yusuke Kuwahara[1], Moei Yano[2,1], Koichiro Fujinaga[2,1], Kentaro Nakamura[1], Yasuhiro Kato[1,2] (1.School of Engineering, The University of Tokyo, 2.ORCeNG, Chiba Institute of Technology)

3:00 PM - 3:15 PM JST | 6:00 AM - 6:15 AM UTC

[MIS28-06] Depositional environments of the Late Cretaceous REY-rich mud in the western North Pacific Ocean inferred from deep-water agglutinated foraminifers

*Kondo Yuta[1], Junichiro Ohta[1,2], Kazutaka Yasukawa[1,2], Kentaro Nakamura[1], Koichiro Fujinaga[2,1], Yasuhiro Kato[1,2] (1.School of Engineering, The University of Tokyo, 2.ORCeNG, Chiba Institute of Technology)

[E] Poster | M (Multidisciplinary and Interdisciplinary)：M-GI General Geosciences, Information Geosciences & Simulations

5:15 PM - 6:30 PM JST | 8:15 AM - 9:30 AM UTC | Ch.20_4

[M-GI32] Integration of Earth Observations and Multiple use for Earth Science and Benefits to Societies - GEO

convener:Kentaro Ando(Japan Agency for Marine and Earth Science and Technology), Hiroyuki Muraoka(River Basin Research Center), Osamu Ochiai(Japan Aerospace Exploration Agency), Shinichi Sobue(Japan Aerospace Exploration Agency)

[MGI32-P01] Developments of a new ocean data networking system for coastal ocean data sharing, and satellite data management system for Integrated Priority Study in AOGEO

*Kentaro Ando[1], Fumihiko Akazawa[1] (1.Japan Agency for Marine and Earth Science and Technology)

[MGI32-P02] Asia Pacific Biodiversity Observation Network (APBON) Strategic Plan 2030

*Hiroyuki Muraoka[1], Yayoi Takeuchi[2], Takehisa Yamakita[3], Yuichi Kano[4], Shin Nagai[3], Masahiro Nakaoka[5], Yongyut Trisurat[6], Runi Sylvester Pungga[7] (1.Gifu University, 2.National Institute for Environmental Studies, 3.Japan Agency for Marin-Earth Science and Technology, 4.Kyusyu University, 5.Hokkaido University, 6.Kasetsart University, 7.Forest Department Sarawak)

[MGI32-P03] Status of Global Forest Observation Initiative (GFOI) and its contribution to climate change monitoring

*Osamu Ochiai[1] (1.Japan Aerospace Exploration Agency)

[J] Oral | EVENT：EVENT

12:20 PM - 1:00 PM JST | 3:20 AM - 4:00 AM UTC | Ch.01 Zoom Room 01

[EV-22] Lunchtime Special Lecture

12:20 PM - 1:00 PM JST | 3:20 AM - 4:00 AM UTC

[E-11-24] Uncover the cryptic nitrogen flows in the terrestrial ecosystems

[E] Oral | EVENT：EVENT

9:00 AM - 9:45 AM JST | 12:00 AM - 12:45 AM UTC | Ch.07 Zoom Room 07

[EV-23] Exhibitors' Seminar

9:00 AM - 9:45 AM JST | 12:00 AM - 12:45 AM UTC

[E-11-23] Latest Application Developments from Picarro

[J] Oral | EVENT：EVENT

1:45 PM - 2:30 PM JST | 4:45 AM - 5:30 AM UTC | Ch.12 Zoom Room 12

[EV-24] Exhibitors' Seminar

1:45 PM - 2:30 PM JST | 4:45 AM - 5:30 AM UTC

[E-11-25] An introduction to Research Institute for Humanity Nature (RIHN)'s interdisciplinary researches on global environmental issues. Earth Scientists, join our Research Projects!

[E] Oral | U (Union) : Union

Sat. Jun 5, 2021 9:00 AM - 10:30 AM JST | Sat. Jun 5, 2021 12:00 AM - 1:30 AM UTC | Ch.01 Zoom Room 01

[U-13] Advanced understanding of Quaternary and Anthropocene hydroclimate changes in East Asia:

convener:Li Lo(Department of Geosciences, National Taiwan University), Kaoru Kubota(Graduate School of Human Development and Environment, Kobe University), Chuan-Chou Shen(National Taiwan University), Yusuke Yokoyama(Atmosphere and Ocean Research Institute, University of Tokyo), Chairperson:Li Lo(Department of Geosciences, National Taiwan University), Kaoru Kubota(Graduate School of Human Development and Environment, Kobe University), Yusuke Yokoyama(Atmosphere and Ocean Research Institute, University of Tokyo), Chuan-Chou Shen(National Taiwan University)



For the sustainability of biosphere and human society, it is crucial to in-depth understand Earth's climate system changes on different timescales. Anthropogenic forcing is also strongly affecting different aspects of human living environments, natural ecological through physical and chemical climatic perturbations, especially in East Asia with swift economic takeoff in the recent decades. We welcome climate and environmental reconstructions based on natural archives, proxy data, numerical simulations on the topics of monsoon, precipitation beef shifting, typhoon, and drought histories in Quaternary and Anthropocene. atmospheric and oceanic interactions, greenhouse gases radiative forcing and anthropogenic forcing impact from regional to global are also welcomed.

9:00 AM - 9:15 AM JST | 12:00 AM - 12:15 AM UTC

[U13-01] Insight to Western Pacific circulation from coral skeletal radiocarbon during the Anthropocene and Holocene

★Invited Papers

*Shoko Hirabayashi[1,2,3], Yusuke Yokoyama[2], Atsushi Suzuki[4], Tezer Esat[5], Yosuke Miyairi[2], Takahiro AZE[2], Fernando Siringan [6], Yasuo Maeda[7], Hironobu Kan[3] (1.Faculty of Geo-Environmental Science, Rissho University, 2.Atmosphere and Ocean Research Institute, The University of Tokyo, 3.Department of Environmental Changes, Graduate School of Social and Cultural Studies, Kyushu University, 4.Geological Survey of Japan, National Institute of Advanced Industrial Science and Technology (AIST), 5.Research School of Physics and Engineering, The Australian National University, 6.Marine Science Institute, University of the Philippines, 7.Institute of Natural and Environmental Sciences, University of Hyogo)

9:15 AM - 9:30 AM JST | 12:15 AM - 12:30 AM UTC

[U13-02] Increased soil erosion since Southeast Asia economic boom recorded in *Porites* corals

★Invited Papers

*Xiaohua Li[1], Zhen Zeng[2], Yi Liu[3], Ching-Chih Chang[4], Hong-Wei Chiang[4], Xuan-Ce Wang[5], Weidong Sun[1], Hui-Min Yu[2], Fang Huang[2], Chung-Che Wu[4], Tsai-Luen Yu[4], Chun-Yuan Huang[4], Chuan-Chou Shen[4] (1.Institute of Oceanology, Chinese Academy of Sciences, 2.University of Science and Technology of China, 3.Tianjin University, 4.National Taiwan University, 5.Yunnan University)

9:30 AM - 9:45 AM JST | 12:30 AM - 12:45 AM UTC

[U13-03] Upper ocean temperatures over the last glacial in the low-to-mid latitude Western Pacific based on a systematic multiproxy approach

★Invited Papers

*Sze Ling Ho[1], Yuan-Pin Chang[2], Min-Te Chen[3], Jeroen Groeneveld[4], Kuo-Fang Huang[5], Pei-Ting Lee[1], Shih-Yun Lin[1], Maria Makarova[1], Nele Meckler[6], Mahyar Mohtadi[7], Ren Yi Ooi[1], Chuan-Chou Shen[8], Liang-Jian Shiau[3,9], Raul Tapia[1], Masanobu Yamamoto[10] (1.Institute of Oceanography, National Taiwan University, Taipei, Taiwan, 2.Department of Oceanography, National Sun Yat-sen University, Kaohsiung, Taiwan., 3.Institute of Applied Geosciences, National Taiwan Ocean University, Keelung, Taiwan., 4.Department of Geosciences, Hamburg University, Germany. , 5.Institute of Earth Sciences, Academia

Sinica, Taipei, Taiwan., 6.Bjerknes Centre for Climate Research and Department of Earth Science, University of Bergen, Norway., 7.MARUM-Center for Marine Environmental Sciences, University of Bremen, Germany. , 8.High-Precision Mass Spectrometry and Environment Change Laboratory (HISPEC), Department of Geosciences, National Taiwan University, Taipei, Taiwan., 9.Exploration and Development Research Institute, CPC Corporation, Miaoli, Taiwan., 10.Faculty of Environmental Earth Science, Hokkaido University, Sapporo, Japan.)

9:45 AM - 10:00 AM JST | 12:45 AM - 1:00 AM UTC

[U13-04] Ultra-high resolution oxygen isotope records from the Chiba Composite Section ratified as the Chibanian GSSP

★Invited Papers

*Yuki Haneda[1], Makoto Okada[2], Yoshimi Kubota[3], Yusuke Suganuma[4,5] (1.Geological Survey of Japan, AIST, 2.Department of Environmental Science, Ibaraki University, 3.National Museum of Nature and Science, 4.National Institute of Polar Research, 5.The Graduate University for Advanced Studies)

10:00 AM - 10:15 AM JST | 1:00 AM - 1:15 AM UTC

[U13-05] Sub-surface water mass exchanges around the eastern equatorial Indian Ocean during the last 50,000 years

★Invited Papers

*Hideko Takayanagi[1], Ryota Wako[1], Yuna Kimoto[1], Shigeyuki Wakaki[2], Azumi Kuroyanagi[1], Takeshige Ishiwa[3], Yusuke Yokoyama[4], Hitomi Uchimura Wakaki[5], Tsuyoshi Ishikawa[2], Yasufumi Iryu[1] (1.Tohoku Univ., 2.JAMSTEC, 3.NIPR, 4.Univ. of Tokyo, 5.Kochi Univ.)

10:15 AM - 10:30 AM JST | 1:15 AM - 1:30 AM UTC

[U13-06] **Methane, Monsoons, and Milankovitch Modulation of Millennial-Scale Climate**

★Invited Papers

*Kaustubh Thirumalai[1], Steven Clemens[2], Judson Partin[3] (1.The University of Arizona, 2.Brown University, 3.The University of Texas at Austin)

Insight to Western Pacific circulation from coral skeletal radiocarbon during the Anthropocene and Holocene

*Shoko Hirabayashi[1,2,3], Yusuke Yokoyama[2], Atsushi Suzuki[4], Tezer Esat[5], Yosuke Miyairi[2], Takahiro AZE[2], Fernando Siringan [6], Yasuo Maeda[7], Hironobu Kan[3]

1. Faculty of Geo-Environmental Science, Rissho University, 2. Atmosphere and Ocean Research Institute, The University of Tokyo, 3. Department of Environmental Changes, Graduate School of Social and Cultural Studies, Kyushu University, 4. Geological Survey of Japan, National Institute of Advanced Industrial Science and Technology (AIST), 5. Research School of Physics and Engineering, The Australian National University, 6. Marine Science Institute, University of the Philippines, 7. Institute of Natural and Environmental Sciences, University of Hyogo

Coral skeletal radiocarbon ($\Delta^{14}C$) records can be used as a sensitive proxy of water mass mixing. Compiling coral skeletal $\Delta^{14}C$ datasets in the western Pacific will contribute to our understanding of the oceanography of the region and its relationship to climate change such as El Nino-Southern Oscillation.

In this study, high-resolution coral skeletal $\Delta^{14}C$ dataset during the Anthropocene and Holocene are reported from the western Pacific. Our $\Delta^{14}C$ data indicates the unusual, rapid $\Delta^{14}C$ increase (early bomb-^{14}C spikes) in the 1950s related to the “close-in fallout” found in the corals from Ishigaki and Luzon Island. The amplitude of the bomb-^{14}C spike in the Luzon Island was less than half that in Ishigaki, likely due to upwelling around Luzon Island and the Kuroshio intrusion into the South China Sea. We also calculated the local marine reservoir age (R) and the regional offset (ΔR) during the Holocene using paired analyses of $\Delta^{14}C$ and ^{230}Th in pristine corals. An abrupt ΔR shift occurred between 5.5 ka BP and 4.0 ka BP in the northwest Pacific. Compared with the previously reported data from the Tropical East Pacific and Great Barrier reef, the timing of the shift is different because the ^{14}C content of the northwestern Pacific was affected by not only the intensity of upwelling at the Peru-Chile coast, but also by the East Asian monsoon.

Keywords: Radiocarbon, U/Th dating, Local marine reservoir age, Corals, Kuroshio

©2021. Japan Geoscience Union. All Right Reserved.

Increased soil erosion since Southeast Asia economic boom recorded in *Porites* corals

*Xiaohua Li[1], Zhen Zeng[2], Yi Liu[3], Ching-Chih Chang[4], Hong-Wei Chiang[4], Xuan-Ce Wang[5], Weidong Sun[1], Hui-Min Yu[2], Fang Huang[2], Chung-Che Wu[4], Tsai-Luen Yu[4], Chun-Yuan Huang[4], Chuan-Chou Shen[4]

1. Institute of Oceanology, Chinese Academy of Sciences, 2. University of Science and Technology of China, 3. Tianjin University, 4. National Taiwan University, 5. Yunnan University

Soil erosion has raised public concern in Southeast Asia which has been poorly documented due to the lack of long, continuous records. Here we present two *Porites* coral records of monthly-resolved Ba/Ca ratios and monthly and yearly-resolved $\delta^{137/134}$Ba from the Nanwan (NW), southern Taiwan, and Son Tra Island (STI), central Vietnam, to explore the extent of soil erosion. Our major finding is that erosion and sediment transport have increase substantially since the regional economic boom and resulted in Ba/Ca ratios significantly elevated during 1987-1996 and 1992-2001 for NW and STI corals, respectively, principally due to increasing pressure on land use. Due to terrestrial inputs yield a homogeneous Ba isotope composition, the $\delta^{137/134}$Ba values of coral NW and STI show essentially constant with the mean isotope fractionation between coral and seawater $\Delta^{137/134}Ba_{coral - seawater}$ is -0.1‰, suggesting that *Porties* coral could be used to trace the Ba isotope composition in ambient seawater. Coupled Ba/Ca and Ba isotopes analysis on *Porites* coral has the potentially to provide new information about the historical soil erosion events.

Keywords: soil erosion, Porites coral, Ba/Ca, δ137/134Ba, Southeast Asia, economic boom

©2021. Japan Geoscience Union. All Right Reserved.

Upper ocean temperatures over the last glacial in the low-to-mid latitude Western Pacific based on a systematic multiproxy approach

*Sze Ling Ho[1], Yuan-Pin Chang[2], Min-Te Chen[3], Jeroen Groeneveld[4], Kuo-Fang Huang[5], Pei-Ting Lee[1], Shih-Yun Lin[1], Maria Makarova[1], Nele Meckler[6], Mahyar Mohtadi[7], Ren Yi Ooi[1], Chuan-Chou Shen[8], Liang-Jian Shiau[3,9], Raul Tapia[1], Masanobu Yamamoto[10]

1. Institute of Oceanography, National Taiwan University, Taipei, Taiwan, 2. Department of Oceanography, National Sun Yat-sen University, Kaohsiung, Taiwan., 3. Institute of Applied Geosciences, National Taiwan Ocean University, Keelung, Taiwan., 4. Department of Geosciences, Hamburg University, Germany. , 5. Institute of Earth Sciences, Academia Sinica, Taipei, Taiwan., 6. Bjerknes Centre for Climate Research and Department of Earth Science, University of Bergen, Norway., 7. MARUM-Center for Marine Environmental Sciences, University of Bremen, Germany. , 8. High-Precision Mass Spectrometry and Environment Change Laboratory (HISPEC), Department of Geosciences, National Taiwan University, Taipei, Taiwan., 9. Exploration and Development Research Institute, CPC Corporation, Miaoli, Taiwan., 10. Faculty of Environmental Earth Science, Hokkaido University, Sapporo, Japan.

Upper ocean (0-200 m) temperature reflects large-scale ocean circulation and the atmosphere-ocean heat exchange. It is therefore a useful metric in characterizing paleoclimate, including the roles played by the East Asian Monsoon and the Indo-Pacific Warm Pool in driving climate change in the low-to-mid latitude Western Pacific. Biomarker- and calcite-based geochemical proxies are widely used to reconstruct past ocean temperature, but may yield discrepant estimates due to chemical and ecological differences of the proxy carriers. Deriving temperature estimates from multiple proxies for the same site may shed light on proxy systematics and improve the robustness of ocean temperature reconstruction, yet there are few multiproxy temperature records spanning the upper water column in the aforementioned region. Therefore, we aim to fill in the gap by using a network of sediment cores from the South China Sea, Indo-Pacific Warm Pool and Okinawa Trough. We compile and generate for each site paleotemperature records of the sea surface and thermocline, inferred from proxies based on vastly different proxy carriers, namely planktic foraminifera-based Mg/Ca and clumped isotopes, haptophyte-based $U^{K'}_{37}$, and archaea-based TEX_{86}. Preliminary results show that the sea surface glacial cooling estimates inferred from clumped isotopes are stronger than the Mg/Ca-derived estimates, despite both proxies being based on the same proxy carriers. At several sites, the temporal patterns of planktic foraminifera Mg/Ca records differ for the mixed layer and thermocline, as the thermocline warms while the surface ocean cools during the last glacial. Thermocline glacial warming, however, is not replicated by TEX_{86} which is increasingly interpreted as shallow subsurface or thermocline temperature signal. Despite consistent glacial-interglacial patterns, the magnitude of change in TEX_{86} temperature records differ substantially across sites, in contrast to that suggested by $U^{K'}_{37}$ and Mg/Ca of mixed layer-dwelling planktic foraminifera. We discuss possible causes leading to the abovementioned proxy discrepancies. We envisage that such a systematic multiproxy approach will refine our understanding of past changes in the oceans surrounding East Asia as well as proxy interpretation in general.

Keywords: UK’37, Mg/Ca, TEX86, Clumped isotopes, South China Sea, Okinawa Trough

©2021. Japan Geoscience Union. All Right Reserved.

Ultra-high resolution oxygen isotope records from the Chiba Composite Section ratified as the Chibanian GSSP

*Yuki Haneda[1], Makoto Okada[2], Yoshimi Kubota[3], Yusuke Suganuma[4,5]

1. Geological Survey of Japan, AIST, 2. Department of Environmental Science, Ibaraki University, 3. National Museum of Nature and Science, 4. National Institute of Polar Research, 5. The Graduate University for Advanced Studies

Marine isotope stage (MIS) 19 has been suggested as one of the best orbital analogs for present interglacial, because of the similarity of the orbital configurations between both interglacial periods. Therefore, paleoenvironmental reconstructions of MIS 19 will provide valuable knowledge to evaluate the anthropogenic impacts for present and future climate changes. The Chiba composite section (CbCS) in the Boso Peninsula, central Japan, is a marine succession straddling the Early–Middle Pleistocene boundary, ranges from the late MIS 20 to early MIS 18. The Chiba section, a main portion of the CbCS, has been ratified as the Global Boundary Stratotype Section and Point (GSSP) of the Chibanian Stage/Age by the Executive Committiee of the International Union of Geological Science on January 17, 2020 (Suganuma et al., 2021). The subtropical Kuroshio and subpolar Oyashio currents generate the large latitudinal water temperature gradient off the Boso Peninsula, and strongly influence the East Asian climate. Therefore, the CbCS sensitively documents a behavior of the Kuroshio Current across the Early–Middle Pleistocene boundary. In this study, we reconstructed detailed oxygen isotope ($\delta^{18}O$) records using surface and subsurface planktonic, and benthic foraminifera from the CbCS to reveal paleoceanographic variation in the northwestern Pacific from the late MIS 20 to early MIS 18.

The age model of the CbCS was established by correlating the benthic $\delta^{18}O$ record to the sea level curve obtained from the southwestern Pacific (Elderfield et al., 2012). The resultant age interval of the $\delta^{18}O$ records is 747.6–801.1 ka on average temporal resolution of 160 yr with a chronological uncertainty of 5 kyr. MIS 19 (MIS 19a, 19b, and 19c) substages are assigned based on climatic variability proposed by Nomade et al. (2019). Vertical water temperature structure and their gradient (ΔT) exhibit latitudinal displacements of the Kuroshio Extension Front (KEF) on multi-millennial scale across the MIS 20–19 transition and during late MIS 19 (MIS 19b to 19a). Results of the spectral and wavelet analyses for the $\delta^{18}O$ records show periodicities of approximately 3,000–6,000 year from MIS 19b to 19a. Similarities of timing and periodicity between paleoceanographic records from the CbCS, North Atlantic, and Mediterranean indicate that disruption of the Atlantic meridional overturning circulation due to freshwater discharge into the North Atlantic caused the southward displacements of the KEF via atmospheric dynamic.

Keywords: Chibanian, Early–Middle Pleistocene boundary, Oxygen isotope ratio, Kuroshio Extension Front, Marine Isotope Stage 19

©2021. Japan Geoscience Union. All Right Reserved.

Sub-surface water mass exchanges around the eastern equatorial Indian Ocean during the last 50,000 years

*Hideko Takayanagi[1], Ryota Wako[1], Yuna Kimoto[1], Shigeyuki Wakaki[2], Azumi Kuroyanagi[1], Takeshige Ishiwa[3], Yusuke Yokoyama[4], Hitomi Uchimura Wakaki[5], Tsuyoshi Ishikawa[2], Yasufumi Iryu[1]

1. Tohoku Univ., 2. JAMSTEC, 3. NIPR, 4. Univ. of Tokyo, 5. Kochi Univ.

The eastern equatorial Indian Ocean (EEIO) is part of the Indo-Pacific Warm Pool and its oceanographic conditions change responding to that of the Indonesian Through Flow (ITF). The EEIO plays an important role in the global ocean overturning circulation. Therefore, it is crucial to unravel temporal variations in the interaction between the Pacific and Indian oceans and their relationships with local (around EEIO) and global paleoclimate and paleoceanography at various time scales. In this study, we studied neodymium (Nd) isotope composition (ε Nd) of bulk benthic foraminifers from a shallow-water to hemipelagic carbonate sediment core drilled at northwestern Australia (IODP Exp. 356, Hole U1464B) to understand changes in surface to sub-surface water mass structures induced probably by the strength of the ITF in the EEIO for the last 50,000 years.
Nd isotope results showed that ε Nd values of bulk benthic foraminifers fluctuated between −9.1 and −5.2, and its variations accord well with the phase and periodicity of the Earth's axial obliquity. The ε Nd values indicated that such variations were caused by exchanges of the source of sub-surface water masses between the Pacific and Indian oceans. Since an increased/decreased axial obliquity is known to result in a reduced/enhanced meridional gradient of solar insolation, respectively, our results indicate that such water mass exchanges in the sub-surface layer around the EEIO are caused by changes in atmospheric and oceanic circulation (including the ITF) as well as those in thermocline depths in the northwestern Pacific Ocean during the last 50,000 years.

Keywords: Eastern Indian Ocean, Thermocline, Water mass, Indonesian ThroughFlow

©2021. Japan Geoscience Union. All Right Reserved.

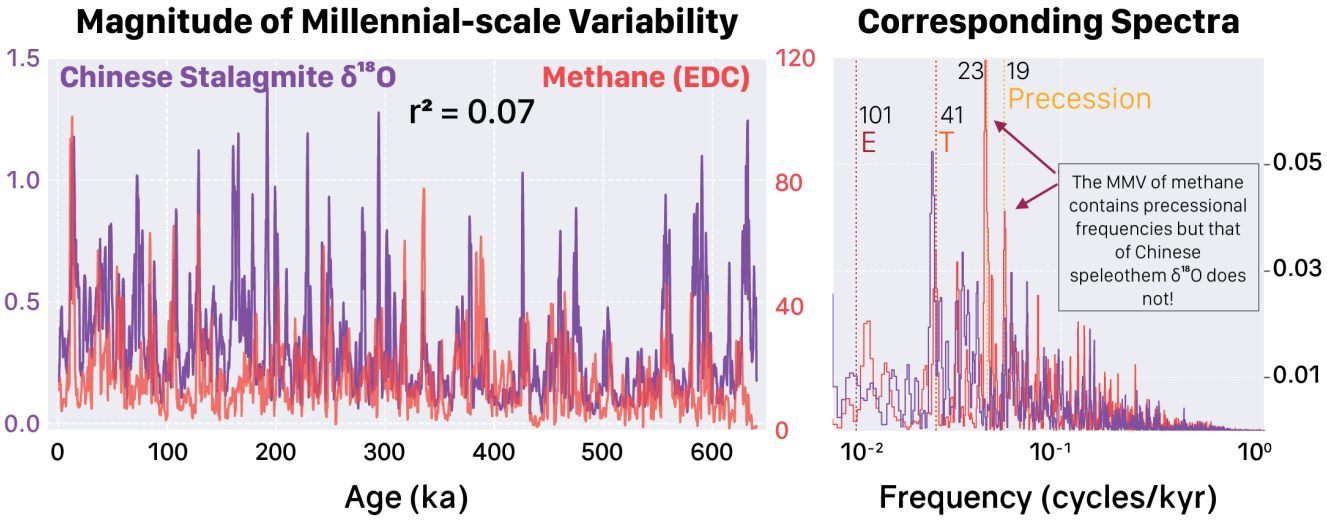
Methane, Monsoons, and Milankovitch Modulation of Millennial-Scale Climate

*Kaustubh Thirumalai[1], Steven Clemens[2], Judson Partin[3]

1. The University of Arizona, 2. Brown University, 3. The University of Texas at Austin

Earth's orbital geometry exerts a profound influence on climate by regulating changes in incoming solar radiation. Superimposed on orbitally paced climate change, Pleistocene records reveal substantial millennial-scale variability characterized by abrupt changes and rapid swings. However, the extent to which orbital forcing modulates the amplitude and timing of these millennial variations is unclear. Here we isolate the magnitude of millennial-scale variability (MMV) in two well-dated records, both linked to precession cycles (19,000- and 23,000-year periodicity): composite Chinese speleothem $\delta^{18}O$, commonly interpreted as a proxy for Asian monsoon intensity, and atmospheric methane. At the millennial timescale (1,000–10,000 years), we find a fundamental decoupling wherein precession directly modulates the MMV of methane but not that of speleothem $\delta^{18}O$, which is shown to be strikingly similar to the MMV of Antarctic ice core $\delta^{2}H$. One explanation is that the MMV of methane responds to changes in midlatitude to high-latitude insolation, whereas speleothem $\delta^{18}O$ is modulated by internal climate feedbacks.

Keywords: Millennial-scale climate, Methane, Monsoon, Paleomonsoon, Orbital Forcing



©2021. Japan Geoscience Union. All Right Reserved.

[E] Poster | U (Union) : Union

Sat. Jun 5, 2021 5:15 PM - 6:30 PM JST | Sat. Jun 5, 2021 8:15 AM - 9:30 AM UTC | Ch.01_1

[U-13] Advanced understanding of Quaternary and Anthropocene hydroclimate changes in East Asia:

convener:Li Lo(Department of Geosciences, National Taiwan University), Kaoru Kubota(Graduate School of Human Development and Environment, Kobe University), Chuan-Chou Shen(National Taiwan University), Yusuke Yokoyama(Atmosphere and Ocean Research Institute, University of Tokyo)



For the sustainability of biosphere and human society, it is crucial to in-depth understand Earth's climate system changes on different timescales. Anthropogenic forcing is also strongly affecting different aspects of human living environments, natural ecological through physical and chemical climatic perturbations, especially in East Asia with swift economic takeoff in the recent decades. We welcome climate and environmental reconstructions based on natural archives, proxy data, numerical simulations on the topics of monsoon, precipitation beef shifting, typhoon, and drought histories in Quaternary and Anthropocene. atmospheric and oceanic interactions, greenhouse gases radiative forcing and anthropogenic forcing impact from regional to global are also welcomed.

[U13-P01] Sclerochronology and geochemistry of *Mercenaria stimpsoni* collected from the western North Pacific

*Kaoru Kubota[1], Kotaro Shirai[2], Naoko Sugihara[2], Koji Seike[3], Kazushige Tanabe[4], Masayo Minami[5], Toshio Nakamura[5] (1.Graduate School of Human Development and Environment, Kobe University, 2.Atmosphere and Ocean Research Institute, The University of Tokyo, 3.Geological Survey of Japan, National Institute of Advanced Industrial Science and Technology, 4.The University Museum, The University of Tokyo, 5.Institute for Space-Earth Environmental Research, Nagoya University)

[U13-P02] Radiocarbon Variability Recorded in Coral from Kikai Island to Understand Oceanography in the North Pacific Region

★Invited Papers

*Yuning Zeng[1], Yusuke Yokoyama[1], Yosuke Miyairi[1], Shoko Hirabayashi[2], Atsushi Suzuki[3] (1.Atmosphere and Ocean Research Institute, The University of Tokyo, 2.Faculty of Geo-Environmental Science, Rissho University, 3.Geological Survey of Japan, National Institute of Advanced Industrial Science and Technology (AIST))

[U13-P03] Anthropocene signals recorded as Plutonium isotopes and Cesium-137 in Beppu Bay marine sediments, Eastern Kyushu, Japan.

*Yusuke Yokoyama[1,2,3,4,5], Stephen Tims[5], Michaela Froehlich[5], Takahiro AZE[1], Keith Fifield[5], Shoko Hirabayashi[6], Dominik Knoll[5], Michinobu Kuwae[7], Yosuke Miyairi[1], Stefan Pavetich[5] (1.Atmosphere and Ocean Research Institute, University of Tokyo, 2.Department of Earth and Planetary Science, Graduate School of Science, The University of Tokyo, 3.Graduate Program on Environmental Sciences, Graduate School of Arts and Sciences, The University of Tokyo, 4.Biogeochemistry Program, Japan Agency for Marine-Earth Science and Technology, 5.Research School of Physics, The Australian National University, 6.Faculty Geo-Environmental Science, Rissho University, 7.Center for Marine Environmental Studies, Ehime University)

[U13-P04] High-resolution marine surface $\Delta^{14}C$ reconstructions using marine organisms produced carbonate attached to tetrapod ashored by high-wave in northern Pacific Coast of Japan.

*Kai Leggett[1], Yusuke Yokoyama[1], Yosuke Miyairi[1], Ota Kosuke[1], Yoshiki Shirahama[2] (1.Atmosphere and Ocean Research Institute, University of Tokyo, 2.Advanced Industrial Science and Technology, Geological Survey of Japan, Research Institute of Earthquake and Volcano Geology, Active Fault Research Group)

[U13-P05] Bronze age megadrought and Trans-Eurasian culture exchange
★Invited Papers

*Liangcheng Tan[1,2,3,4], Guanghui Dong[5], Zhisheng An[1,2,4], Lawrence R. Edwards[6,7], Haiming li[8], Dong Li[9], Robert Spengler[10], Yanjun Cai[3], Hai Cheng[3,1], Jianghu Lan[1,2], Rustam Orozbaev[11,12], Ruiliang Liu[13], Jianhui Chen[5], Hai Xu[14], Fahu Chen[15] (1. Institute of Earth Environment, Chinese Academy of Sciences, 2. Center for Excellence in Quaternary Science and Global Change, Chinese Academy of Sciences, 3.Institute of Global Environmental Change, Xi'an Jiaotong University, 4.Open Studio for Oceanic-Continental Climate and Environment Changes, Pilot National Laboratory for Marine Science and Technology (Qingdao), 5. College of Earth and Environmental Sciences, Lanzhou University, 6.Department of Earth and Environmental Sciences, University of Minnesota, 7. School of Geography, Nanjing Normal University, 8.Institution of Chinese Agricultural Civilization, Nanjing Agricultural University, 9.Library of Chang'an University, 10. Max Planck Institute for the Science of Human History, 11.Research Center for Ecology and Environment of Central Asia (Bishkek), Chinese Academy of Sciences, 12. Institute of Geology, National Academy of Sciences of Kyrgyz Republic, 13. School of Archaeology, University of Oxford, 14.Institute of Surface-Earth System Science, Tianjin University, 15.Key Laboratory of Alpine Ecology and Biodiversity, Institute of Tibetan Plateau Research, Chinese Academy of Sciences)

[U13-P06] **A gradual transition into Greenland Interstadial 14 in southeastern China based on a sub-decadally-resolved stalagmite record**
★Invited Papers

*Xin Zhang[1], Xiuyang Jiang[1,2], Haiyan Xiao[2], Binggui Cai[1,2], Tsai-Luen Yu[3,4], Chuan-Chou Shen[3,4,5] (1.Key Laboratory of Humid Subtropical Eco-geographical Processes, Ministry of Education, College of Geography Science, Fujian Normal University, 2.Institute of Geography, Fujian Normal University, 3.High-Precision Mass Spectrometry and Environment Change Laboratory (HISPEC), Department of Geosciences, National Taiwan University, 4.Research Center for Future Earth, National Taiwan University, 5.Global Change Research Center, National Taiwan University)

[U13-P07] Beppu Bay stratigraphy records the timing of human-induced planetary-scale biological and environmental shift at the beginning of the Anthropocene
★Invited Papers

*Michinobu Kuwae[1], Narumi Tsugeki[2], Atsuko Amano[3], Testuro Agusa[4], Yoshiaki Suzuki[3], Jun Tsutsumi[7], Peter R. Leavitt[5], Kotaro Hirose[6] (1.Center for Marine Environmental Studies, 2. The Faculty of Law, Matsuyama Univesity, Matsuyama, 3.Geological Survey of Japan, National Institute of Advanced Industrial Science and Technology, 4.Faculty of Environmental & Symbiotic Sciences, Prefectural University of Kumamoto, 5.Department of Biology,University of Regina, 6.Faculty of Science & Engineering, Waseda University, 7.School of Life and Environmental Science, University of Tsukuba)

[U13-P08] The series of precious coral samples collected from off the southwest coast of Kochi Prefecture: one potential thousand-scale proxy for understanding subsurface ocean conditions.
★Invited Papers

*Tomoyo Okumura[1], Fujio Kumon[1], Tokuyama Hidekazu[1] (1.Center for Advanced Marine Core Research, Kochi University)

[U13-P09] Impact of human activities and natural hazards recorded in a subtropical mountain lake, northeastern Taiwan
★Invited Papers

*Tsai-wen Lin[1], Stefanie Kaboth-Bahr[2], Kweku Afrifa Yamoah[3], André Bahr[4], George Burr[1], Chih-Chieh Su[5], Liang-Chi Wang[6], Ludvig A Lowemark[1] (1.Dept. of Geosciences, NTU, 2.Institute for Geosciences, Univ. of Potsdam, 3.School of Geography, Earth & Environmental Sciences, Univ. of Birmingham, 4.Institute of Earth Sciences., Heidelberg Univ., 5.Institute of Oceanography, NTU, 6.Dept. of Earth and Environmental Sciences, NCCU)

[U13-P10] Reconstruction of ventilation ages of the Indian Ocean sector of the Southern Ocean using ^{14}C and U-Th ages of deep-sea isidid octocorals

★Invited Papers

*Yukiko Kozaka[1], Chuan-Chou (River) Shen[2], Hiroshi Sato[3], Masayo Minami[1], Yuki Tokuda[4], Minoru Ikehara[5] (1.Institute for Space-Earth Environmental Research, Nagoya University, 2.Department of Geosciences, National Taiwan University, 3.School of Business Administration, Senshu University, 4.Faculty of Environmental Studies, Tottori University of Environmental Studies, 5.Center for Advanced Marine Core Research, Kochi University)

[U13-P11] **North Atlantic cooling desiccated western India during Early Holocene: Evidence-based on clumped and stable oxygen isotope analysis of Gastropod**

*THAMIZHARASAN SAKTHIVEL[1,2], PROSENJIT GHOSH[1,2], YOGARAJ BANERJEE[1] (1.Centre for Earth Sciences, Indian Institute of Science, Bangalore, India -560012, 2.Divecha Centre for Climate Change, Indian Institute of Science, Bangalore, India -560012)

Sclerochronology and geochemistry of *Mercenaria stimpsoni* collected from the western North Pacific

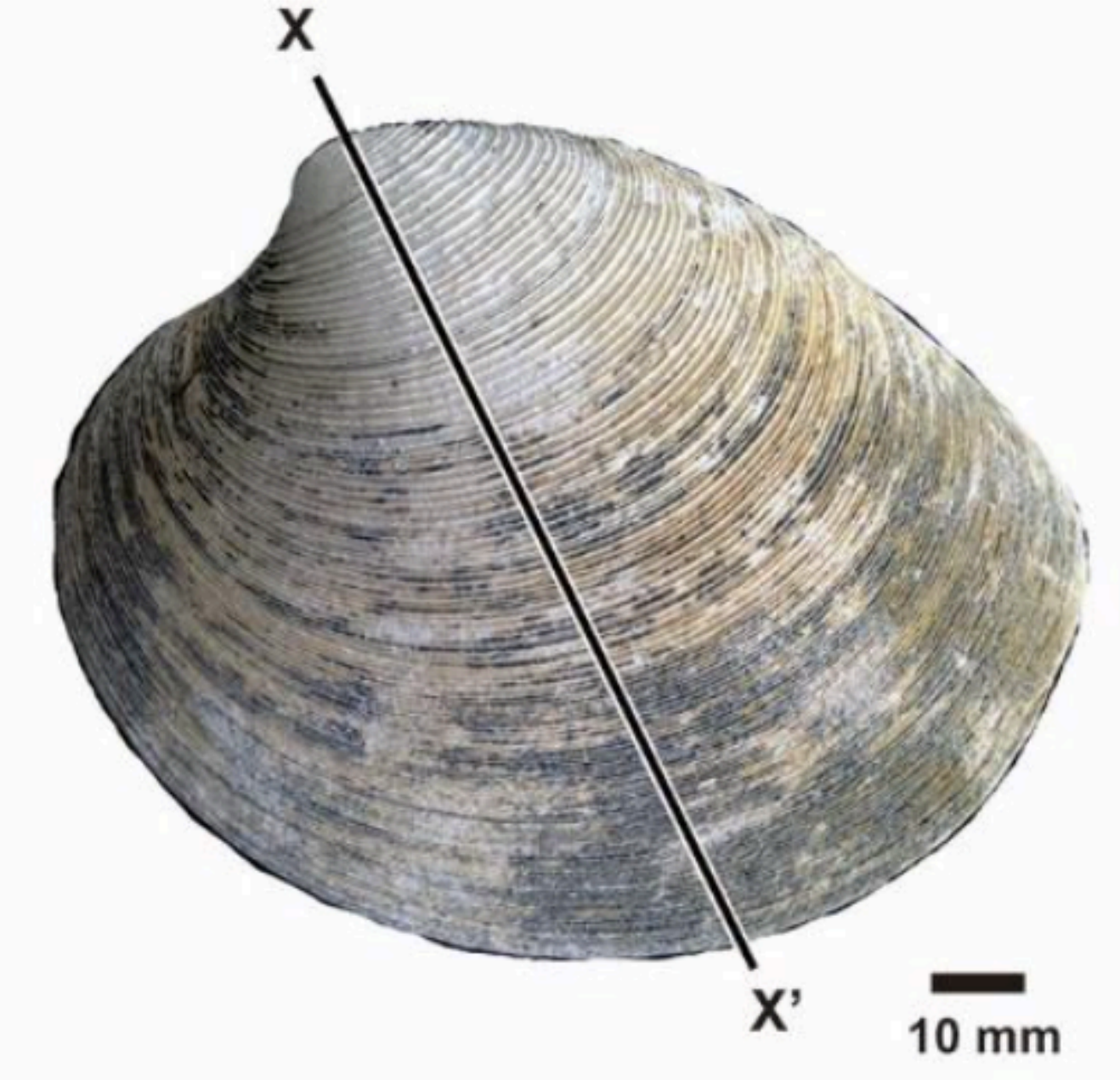
*Kaoru Kubota[1], Kotaro Shirai[2], Naoko Sugihara[2], Koji Seike[3], Kazushige Tanabe[4], Masayo Minami[5], Toshio Nakamura[5]

1. Graduate School of Human Development and Environment, Kobe University, 2. Atmosphere and Ocean Research Institute, The University of Tokyo, 3. Geological Survey of Japan, National Institute of Advanced Industrial Science and Technology, 4. The University Museum, The University of Tokyo, 5. Institute for Space-Earth Environmental Research, Nagoya University

Bivalve shell is one of the most important archives of past environmental changes because some species can live more than several decades and distribute broadly (e.g., from high to low latitude, fresh/brackish/sea water). We have investigated potential of long-lived cold water bivalve, *Mercenaria stimpsoni* (Stimpson's hard clam) living in the western North Pacific (especially, coastal area of North East Japan). In this presentation we will show sclerochlonological and geochemical records (e.g., oxygen isotopes and radiocarbon) of both live-caught and dead specimens collected from the seafloor of NE Japan (5–20 m). From both sclerochlonology and nuclear bomb-derived radiocarbon (bomb-^{14}C), it was found that this animal can live for more than 100 years, thus very useful for paleoeanograpic studies. It was also found that a lot of *M. stimpsoni* were killed by huge tsunami that hit NE Japan in March 2011, which is likely caused by disturbance of marine sediment, including seabed liquefaction.

Keywords: bivalve, radiocarbon, sclerochronology, oxygen isotope, tsunami, paleoeanography

©2021. Japan Geoscience Union. All Right Reserved.



©2021. Japan Geoscience Union. All Right Reserved.

Radiocarbon Variability Recorded in Coral from Kikai Island to Understand Oceanography in the North Pacific Region

*Yuning Zeng[1], Yusuke Yokoyama[1], Yosuke Miyairi[1], Shoko Hirabayashi[2], Atsushi Suzuki[3]

1. Atmosphere and Ocean Research Institute, The University of Tokyo, 2. Faculty of Geo-Environmental Science, Rissho University, 3. Geological Survey of Japan, National Institute of Advanced Industrial Science and Technology (AIST)

Atmospheric radiocarbon (^{14}C) rapidly increased after 1955 because of the nuclear test. This artificial ^{14}C called bomb-^{14}C is diffused into the surface ocean and taken up by coral skeletons from ambient seawater. However, the deep ocean is isolated from direct CO_2 exchange from the atmosphere. Therefore, bomb-^{14}C in coral can be used as a very sensitive indicator of vertical and horizontal advection of water masses, which contributes to the understanding of ocean circulation [1].

In this study, a challenge has made with a high vacuum gas treatment line that specially designed for small quantity of samples (ca.100 μg C). This experiment is aiming at obtaining seasonal-resolution ^{14}C data between 1940 and 1990 using the coral obtained from Kikai Island and revealing physical oceanographic information around Kuroshio region. The age model was based on high resolution Sr/Ca data determined by Kawakubo et al. (2017) [2].

At present, the contamination level during experimental steps of our method has been confirmed to be relatively low and constant by several repeated tests using standard samples distributed from International Atomic Energy Agency (IAEA). Besides, samples from the top part of coral corresponding to summer and winter shown by peaks of Sr/Ca data after 1975 has been measured. The trend and value of current bomb curve are similar to previous studies in Kikai Island and at other sampling sites in the Pacific, which proves the reliability of our data in high confidence. In this presentation, we will show the ^{14}C results and discuss the oceanographic implications inferred from the data.

[1] Hirabayashi, S., Yokoyama, Y., Suzuki, A., Miyairi, Y., Aze, T., Siringan, F., & Maeda, Y. (2019). Insight into Western Pacific Circulation from South China Sea Coral Skeletal Radiocarbon. *Radiocarbon*, 61(6), 1923-1937.

[2] Kawakubo, Y., Alibert, C., & Yokoyama, Y. (2017). A reconstruction of subtropical western North Pacific SST variability back to 1578, based on a Porites Coral Sr/Ca record from the northern Ryukyus, Japan. *Paleoceanography*, 32, 1352– 1370.

©2021. Japan Geoscience Union. All Right Reserved.

Anthropocene signals recorded as Plutonium isotopes and Cesium-137 in Beppu Bay marine sediments, Eastern Kyushu, Japan.

*Yusuke Yokoyama[1,2,3,4,5], Stephen Tims[5], Michaela Froehlich[5], Takahiro AZE[1], Keith Fifield[5], Shoko Hirabayashi[6], Dominik Knoll[5], Michinobu Kuwae[7], Yosuke Miyairi[1], Stefan Pavetich[5]

1. Atmosphere and Ocean Research Institute, University of Tokyo, 2. Department of Earth and Planetary Science, Graduate School of Science, The University of Tokyo, 3. Graduate Program on Environmental Sciences, Graduate School of Arts and Sciences, The University of Tokyo, 4. Biogeochemistry Program, Japan Agency for Marine-Earth Science and Technology, 5. Research School of Physics, The Australian National University, 6. Faculty Geo-Environmental Science, Rissho University, 7. Center for Marine Environmental Studies, Ehime University

Above ground nuclear weapon tests conducted between 1945 and 1980, have lead to the distribution of various anthropogenic radionuclides in the environment including Plutonium (Pu). It has been used as a time-marker of mid twentieth century in various geological archives similar to the ^{137}Cs fall out signature. Further, advancement of analytical techniques allows us to measure ^{239}Pu and ^{240}Pu accurately that can fingerprint the Pacific Pu signal that originated from the former Pacific Proving Grounds (PPG) in the Marshall Islands. Here we report the record of Pu isotopes between 1950 to 1990 for the sediments obtained from Beppu Bay, in Eastern Kyushu, Japan. Approximately 8m length of core was taken from 70m water depth and radiocarbon dates suggested the high sedimentation rate (2-3mm/yr) throughout (Kuwae et al., 2013). The record shows a clear Pu increase in 1950, which peaked during the1960s, followed by sharp decline in the section corresponding to the 1970s. A minor increase in the 1980s is also observed in the sediment, namely the sediment follows global fallout trends. However, a constantly higher isotope ratio between ^{239}Pu and ^{240}Pu suggest an additional contribution other than global fallout via ocean current. Further, distinguished higher points provided supportive evidence of close-in-fallout that are previously reported in open ocean environments.

Keywords: Anthropocene, Beppu Bay, Pu

©2021. Japan Geoscience Union. All Right Reserved.

High-resolution marine surface $\Delta^{14}C$ reconstructions using marine organisms produced carbonate attached to tetrapod ashored by high-wave in northern Pacific Coast of Japan.

*Kai Leggett[1], Yusuke Yokoyama[1], Yosuke Miyairi[1], Ota Kosuke[1], Yoshiki Shirahama[2]

1. Atmosphere and Ocean Research Institute, University of Tokyo, 2. Advanced Industrial Science and Technology, Geological Survey of Japan, Research Institute of Earthquake and Volcano Geology, Active Fault Research Group

Radiocarbon is produced in the upper atmosphere and distributed on the surface of the Earth via carbon cycles and has been used for radiometric dating and as a tracer of Earth surface processes including ocean current. Due to global ocean circulation, apparent radiocarbon ages ranging from ca. 400 to 2,000 years (eg., Servettaz et al., 2019), known as marine reservoir ages. Thus, continuous monitoring of radiocarbon concentrations, $\Delta^{14}C$, has been conducted commonly using annual bands of coral skeletons to reconstruct local oceanography (eg., Hirabayashi et al., 2019). Though, it has mainly been restricted in low latitude since warmer water (higher than 18 degrees C) is required to live for corals. One of the few studies that reconstruct the $\Delta^{14}C$ values in higher latitude, such as the Tohoku region, in Japan, Kubota et al. (2018) reported the $\Delta^{14}C$ values in the inner bay of the Otsuchi area using *M.stimposoni* shells. Yet the records could not cover recent $\Delta^{14}C$ variations. Additionally, the *M.stimposoni* samples used in this study are mostly collected from 20 m deep from the sea surface, only one sample collected from shallow water at around 5 m water depth thus more information at shallow water is needed. Ota et al. (2019) also reported high-resolution $\Delta^{14}C$ records using abalone shells. However, habitat differences for individual tests could not provide the reference of local marine water $\Delta^{14}C$. In this study, we reconstruct the $\Delta^{14}C$ of the sea surface by analyzing the calcium carbonate calcareous tubes of *Hydroides elegans*, which lives at ambient sea level. The samples were obtained from Iwate Prefecture and the carbonate tubes are found on tetrapods at an elevation of 7~8 m and were 30 m away from the nearest group of wave-dissipating blocks. According to the aerial photographs, we identified the exact timing when the tetrapods were dislodged. Eighteen samples of carbonate tubes of *Hydroides elegans* have filled the gap of the dataset previously published by Kubota et al. (2018). The oceanographic condition also seems to be overprinted to the signal and we will discuss it during the presentation.

Keywords: ΔC-14, Radiocarbon analysis, Hydroides Elegans, Aerial photographs, Accelerator Mass Spectrometer, Sanriku

©2021. Japan Geoscience Union. All Right Reserved.

Bronze age megadrought and Trans-Eurasian culture exchange

*Liangcheng Tan[1,2,3,4], Guanghui Dong[5], Zhisheng An[1,2,4], Lawrence R. Edwards[6,7], Haiming li[8], Dong Li[9], Robert Spengler[10], Yanjun Cai[3], Hai Cheng[3,1], Jianghu Lan[1,2], Rustam Orozbaev[11,12], Ruiliang Liu[13], Jianhui Chen[5], Hai Xu[14], Fahu Chen[15]

1. Institute of Earth Environment, Chinese Academy of Sciences, 2. Center for Excellence in Quaternary Science and Global Change, Chinese Academy of Sciences, 3. Institute of Global Environmental Change, Xi’ an Jiaotong University, 4. Open Studio for Oceanic-Continental Climate and Environment Changes, Pilot National Laboratory for Marine Science and Technology (Qingdao), 5. College of Earth and Environmental Sciences, Lanzhou University, 6. Department of Earth and Environmental Sciences, University of Minnesota, 7. School of Geography, Nanjing Normal University, 8. Institution of Chinese Agricultural Civilization, Nanjing Agricultural University, 9. Library of Chang’ an University, 10. Max Planck Institute for the Science of Human History, 11. Research Center for Ecology and Environment of Central Asia (Bishkek), Chinese Academy of Sciences, 12. Institute of Geology, National Academy of Sciences of Kyrgyz Republic, 13. School of Archaeology, University of Oxford, 14. Institute of Surface-Earth System Science, Tianjin University, 15. Key Laboratory of Alpine Ecology and Biodiversity, Institute of Tibetan Plateau Research, Chinese Academy of Sciences

Arid Central Asia (ACA), with its diverse landscapes of high mountains, oases, and deserts, hosted the central routes of the Silk Roads that linked trade centers from East Asia to the eastern Mediterranean. Ecological pockets and ecoclines in ACA are largely determined by local precipitation. However, little research has gone into the effects of hydroclimatic changes on trans-Eurasian cultural exchange. Here, we reconstruct precipitation changes in ACA, covering the mid-late Holocene with a U-Th dated, ~3 a resolution, multi-proxy time series of replicated stalagmites from the southeastern Fergana Valley, Kyrgyzstan. Our data reveal a 640-a megadrought between 5820 and 5180 a BP, which likely impacted cultural development in ACA and impeded the expansion of cultural traits along oasis routes. Instead, it may have diverted the earliest transcontinental exchange along the Eurasian steppe during the 5th millennium BP. With gradually increasing precipitation after the megadrought, settlement of peoples in the oases and river valleys may have facilitated the opening of the oasis routes, ‘ ‘prehistoric Silk Roads”, of trans-Eurasian exchange. By the 4th millennium BP, this process may have reshaped cultures across the two continents, laying the foundation for the organized Silk Roads.

Keywords: Megadrought, Trans-Eurasian exchange, Silk Roads, Arid Central Asia, Mid-Holocene

©2021. Japan Geoscience Union. All Right Reserved.

A gradual transition into Greenland Interstadial 14 in southeastern China based on a sub-decadally-resolved stalagmite record

*Xin Zhang[1], Xiuyang Jiang[1,2], Haiyan Xiao[2], Binggui Cai[1,2], Tsai-Luen Yu[3,4], Chuan-Chou Shen[3,4,5]

1. Key Laboratory of Humid Subtropical Eco-geographical Processes, Ministry of Education, College of Geography Science, Fujian Normal University, 2. Institute of Geography, Fujian Normal University, 3. High-Precision Mass Spectrometry and Environment Change Laboratory (HISPEC), Department of Geosciences, National Taiwan University, 4. Research Center for Future Earth, National Taiwan University, 5. Global Change Research Center, National Taiwan University

Greenland stadials and interstadials (GS and GIS) are prominent features in ice core records of the last glacial period and are characterized by millennial-scale climate oscillations with sub-decadal- to decadal-scale hydroclimatic shifts. Over the past two decades, studies of Chinese stalagmite records have revealed corresponding Chinese stadials/interstadials (CS/CIS). However, the CS/CIS shifts and their corresponding forcings across the Asian monsoon region are still not fully understood. In this study, we present a ^{230}Th-based sub-decadally-resolved stalagmite δ^{18}O record from Xianyun Cave in southeastern China covering the period 58.2–50.8 kyr BP (before 1950 AD) and including GIS (and CIS) 16–14. We used GIS (CIS) 15.1 (peak point) and 15.2 (first point) to chronologically link the high and low-latitude records. We found that the onset of GIS 14 in our record occurred earlier than in an ice core record from Greenland and stalagmite records from northern China. This finding implies that low-latitude tropical climate likely played a key role in triggering abrupt millennial-scale event. Moreover, the transition into GIS 14 lasted 1.49 kyr in our record, which is in contrast to the abrupt temperature rise observed in NGRIP (the North Greenland Ice Core Project, 0.02 kyr). Compared with previous stalagmite records, we identified two transitional patterns into GIS 14 in monsoonal China: 1) a rapid transition in northern China and 2) a gradual transition in southeastern China. The gradual transition in our Xianyun record is analogous to a sea surface temperature (SST) record in the western tropical Pacific, highlighting a possible inherent connection between the changes in western tropical Pacific SSTs and East Asian summer monsoon variability in southeastern China. Paleoclimate records in southeastern China are therefore critical for understanding the mechanisms of abrupt millennial-scale climate events, as they can act as a bridge between the high- and low-latitude records.

©2021. Japan Geoscience Union. All Right Reserved.

Beppu Bay stratigraphy records the timing of human-induced planetary-scale biological and environmental shift at the beginning of the Anthropocene

*Michinobu Kuwae[1], Narumi Tsugeki[2], Atsuko Amano[3], Testuro Agusa[4], Yoshiaki Suzuki[3], Jun Tsutsumi[7], Peter R. Leavitt[5], Kotaro Hirose[6]

1. Center for Marine Environmental Studies, 2. The Faculty of Law, Matsuyama Univesity, Matsuyama, 3. Geological Survey of Japan, National Institute of Advanced Industrial Science and Technology, 4. Faculty of Environmental & Symbiotic Sciences, Prefectural University of Kumamoto, 5. Department of Biology,University of Regina, 6. Faculty of Science & Engineering, Waseda University, 7. School of Life and Environmental Science, University of Tsukuba

The definition of the lower boundary of Anthropocene requires a global stratotype section showing a human-induced planetary-scale biological and environmental shift. However, such stratotype remains unclear. Here we present multiproxy records showing biological and environmental changes for the last multi-century or millennia using the sediment core samples from anoxic coastal marine basin, Beppu Bay, Japan. Biotic marker records showed an abrupt biological change as seen in algal communities due to eutrophication in 1960s, early Great Acceleration, which was unprecedented over the last 670 years. The remarkable biological changes reconstructed from Asian oceanic sediment imply that intensified coastal marine ecosystem degradation which started in Europe in 18th century extended over the northern hemisphere at the early Great Acceleration. Our results provide a geological evidence of the human-induced planetary-scale biological and environmental shift at the lower boundary of Anthropocene.

Keywords: GSSP, biostratigraphy, Beppu Bay

©2021. Japan Geoscience Union. All Right Reserved.

The series of precious coral samples collected from off the southwest coast of Kochi Prefecture: one potential thousand-scale proxy for understanding subsurface ocean conditions.

*Tomoyo Okumura[1], Fujio Kumon[1], Tokuyama Hidekazu[1]

1. Center for Advanced Marine Core Research, Kochi University

Radiocarbon dating was performed for various types of precious coral colony fragments collected from the Ashizuri fishing field, around 100 to 200 m deep, off the southwest coast of Kochi Prefecture as a first step for understanding the historical background of one of the largest precious coral fishing fields in Japan. The ^{14}C ages of the 55 specimens range from cal BC 5617–5411 to the modern and are broadly distributed over the past ~7500 years [1]. Most of the measured samples were older than 1871, when fishing activities of precious corals began in Kochi Prefecture. These results suggest that most of the deaths of the precious coral colonies were due to natural causes, such as natural mortality, predation, or various forms of environmental degradation, and not strictly related to destructive fishing practices. Additionally, precious corals started inhabiting the study area at least ~7500 years ago, when the marine condition became similar to that of today after the Last Glacial Period. The series of the measured samples have the potential to provide thousand-scale records of environmental conditions at deep waters. Preliminary measurements of Mg, Sr, S, Ba, $\delta^{13}C$, and $\delta^{18}O$ are underway by following previous studies [2, 3, 4, 5].

[1] Okumura et al. (2020) Radiocarbon, DOI:10.1017/RDC.2020.114
[2] Suzuki et al. (2010) In: A Biohistory of Precious corals –Scientific, Cultural and Historical Perspective, pp. 61-82.
[3] Tamenori et al. (2014) Journal of Structural Biology, 186 (2), 214-223.
[4] Yoshimura et al. (2015) Biogeoscience Discussions, 12, 413-444.
[5] Vielzeuf et al. (2013) Chemical Geology, 335, 13-27.

Keywords: precious corals, Octocorallia

©2021. Japan Geoscience Union. All Right Reserved.

Impact of human activities and natural hazards recorded in a subtropical mountain lake, northeastern Taiwan

*Tsai-wen Lin[1], Stefanie Kaboth-Bahr[2], Kweku Afrifa Yamoah[3], André Bahr[4], George Burr[1], Chih-Chieh Su[5], Liang-Chi Wang[6], Ludvig A Lowemark[1]

1. Dept. of Geosciences, NTU, 2. Institute for Geosciences, Univ. of Potsdam, 3. School of Geography, Earth & Environmental Sciences, Univ. of Birmingham, 4. Institute of Earth Sciences., Heidelberg Univ., 5. Institute of Oceanography, NTU, 6. Dept. of Earth and Environmental Sciences, NCCU

Alpine and subalpine lakes are sensitive to hydroclimate change in the catchment, making sediments from those lakes an ideal material to reconstruct terrestrial paleoclimate and paleoenvironment alteration. In addition to long-term climate change, natural hazards (e.g. forest fire and landslide) and human activities (e.g. logging, cultivation, and construction) also cause environmental changes recorded in the lake sediment. It is therefore important to differentiate between sediment geochemical signals induced by climate change, natural hazards, and human activity. Here we compare signals from a sediment core with historical records to understand how natural and artificial events affect the mountain environment and are recorded in the lake sediment. We used the most recent 300 years of record from a sediment core taken in Cueifong Lake, a mountain lake in northeastern Taiwan. The age model based on ^{210}Pb and ^{137}Cs indicates that the sediment environment in Cueifong Lake remained stable during the past 300 years. We use different parameters to make a multi-proxy reconstruction of environmental conditions in the sediment core, including TOC, C/N, δ^{13}C, charcoal, and element abundancy reconstructed from XRF core scanning. Historical documents and aerial photos were reviewed to assess forestry, constructions, and events in the catchment. Variations of organic matter and element abundancy indicate the sediment source changes before and after deforestation. Aerial photos can be used to capture the time and degree of deforestation surrounding the lake catchment. Our result could help to understand how human development might affect a mountainous closed-lake environment.

Keywords: deforestation, forest fire, aerial photo, XRF core scanning, mountain lake

©2021. Japan Geoscience Union. All Right Reserved.

Reconstruction of ventilation ages of the Indian Ocean sector of the Southern Ocean using ^{14}C and U-Th ages of deep-sea isidid octocorals

*Yukiko Kozaka[1], Chuan-Chou (River) Shen[2], Hiroshi Sato[3], Masayo Minami[1], Yuki Tokuda[4], Minoru Ikehara[5]

1. Institute for Space-Earth Environmental Research, Nagoya University, 2. Department of Geosciences, National Taiwan University, 3. School of Business Administration, Senshu University, 4. Faculty of Environmental Studies, Tottori University of Environmental Studies, 5. Center for Advanced Marine Core Research, Kochi University

Carbonaceous skeletons of the deep-sea corals are generally dated by uranium-series systematics. By combining the absolute ages obtained with radiocarbon, the past ocean ventilation rate has been estimated. This approach is particularly effective in the Southern Ocean, where carbonate compensation depths are shallow and carbonate rocks are not likely to remain. Previous studies performed on the Southern Ocean have mainly focused on corals from the Drake Passage and off Tasmania. In this study, we focused on deep-sea isidid octocorals (Bamboo coral) collected from the Conrad Rise, Indian sector of the Southern Ocean, and report the results of ^{14}C and U-Th ages in the presentation. The skeleton of deep-sea isidid octocorals is formed of very dense calcite material, which makes it difficult to dissolve even after the death of the coral polyp that cover it.

A characteristic of deep-sea isidid octocorals is that new skeletons may form to encapsulate the old coral skeleton. We performed both of uranium-series and radiocarbon measurements on two samples of old coral inclusions. The U-Th dating provided insight into the age distribution of coral skeletons collected by dredge from Conrad Rise. Periods of relatively high coral production frequency may indicate that the environment was conducive to coral growth.

Keywords: Deep-sea coral, Bamboo coral, U-Th dating, radiocarbon dating, Southern Ocean, Conrad Rise

©2021. Japan Geoscience Union. All Right Reserved.

North Atlantic cooling desiccated western India during Early Holocene: Evidence-based on clumped and stable oxygen isotope analysis of Gastropod

*THAMIZHARASAN SAKTHIVEL[1,2], PROSENJIT GHOSH[1,2], YOGARAJ BANERJEE[1]

1. Centre for Earth Sciences, Indian Institute of Science, Bangalore, India -560012, 2. Divecha Centre for Climate Change, Indian Institute of Science, Bangalore, India -560012

Last Glacial Period witnessed modulation of Indian Summer Monsoon (ISM) intensity due to its teleconnection with the North Atlantic climatology (Schulz et al.,1998). We investigated here the millennium scale record of Sea Surface Temperature (SST) and δ18O of seawater at coastal location during Early Holocene (12 to 7 kyr BP) based on clumped and stable oxygen isotope composition of well-preserved fossil specimen of Cerithium sp. These shells grow in the tidal environment and has potential to record upwelling process which controls the variation in water and air temperature (Yekta al., 2019). The raised paleo-gulf sedimentary sequence exposed adjoining the region of present-day Arabian Sea i.e., Great Rann of Kutch provided opportunity to study the coastal climate during the time interval when solar variability was minimal. The record of solar variability from the region was earlier studied from the offshore sedimentary archives from the Arabian Sea (Gupta et al., 2003). Our observation revealed variation of coastal apparent Sea Surface Temperature (SST) from 30 to 36˚C, which is negatively correlated with upwelling proxy G.bulloides abundance from the adjoining region of Eastern Arabian Sea (Naik et al., 2016). This suggests vertical entrainment of deep water due to wind strength variability drove the upwelling process and regional SST . The estimated equilibrium δ18O of water is consistent with the shift observed in the available record from the Indian Subcontinent (Dixit et al., 2014). We provided here fist evidence of intense monsoonal wind strength assessment at 12.2, 9.47, and 7.9 kyr BP. In contrast, our observation revealed weakening of ISM wind intensity at 9.86, 8.51, and 7.65 kyr BP, which is coherent sea ice variability in the North Atlantic (Bond et al., 2001). Therefore, we showed that North Atlantic climate has strong impact on ISM even during past as seen in the historical data and present day (Borah et al., 2020).

Keywords: Early Holocene , Clumped and Stable isotope of Gastropod, Indian Summer Monsoon, North Atlantic Teleconnection

©2021. Japan Geoscience Union. All Right Reserved.

[J] Oral | U (Union)：Union

Sat. Jun 5, 2021 3:30 PM - 5:00 PM JST | Sat. Jun 5, 2021 6:30 AM - 8:00 AM UTC | Ch.01 Zoom Room 01

[U-14] Current status and issues of the earth education necessary for living on the changing earth

convener:Hiroshi Ichikawa, Saori Nakai(kyoto koka womens university department of child education), Hidenori Kumagai(Japan Agency for Marine-Earth Science and Technology), Hiroshi Nishi(The Center for Academic Resources and Archives, The Tohoku Museum Tohoku University), Chairperson:Hiroshi Ichikawa(None)

A proposal entitled by "Importance of Earth Education in Elementary and Secondary School Education and Lifelong Education: for learning essential knowledge to live on a changing earth" was published by the Science Council of Japan on June 23, 2020. This proposal points out that, for all people living in the Japanese archipelago frequently attacked by severe natural disasters, it is important to increase the chances to acquire "the essential knowledge to live on a changing earth" in school learning of the nature, and learn it lifelong. Responding to this proposal, this session is held by WG for Studying on Teacher Training System, established for studying complex and diverse issues related to teacher training and others in May 2019 in the Education Committee, JpGU. This session aims to deepen discussions on the current situation and issues of elementary and secondary school teachers responsible for earth education in the fields of Geosciences and Geography regarding the teacher training and recruitment system and self-improvement of knowledge and skills.

3:30 PM - 3:45 PM JST | 6:30 AM - 6:45 AM UTC

[U14-01] The Essentials of Living on a Changing Planet

★Invited Papers

*Hiroshi Nishi[1] (1.Fukui Prefectural University, Institute of Dinosaur Research)

3:45 PM - 4:00 PM JST | 6:45 AM - 7:00 AM UTC

[U14-02] **Variations in the promotions of high schools offering Basic and Advanced Earth Science classes in Prefectures throughout Japan**

★Invited Papers

*Hideo Takagi[1], Kohei Yoshida[2] (1.Department of Earth Science, Faculty of Education and Integrated Arts and Sciences, Waseda University, 2.Higashi Fukuoka High School)

4:00 PM - 4:15 PM JST | 7:00 AM - 7:15 AM UTC

[U14-03] Global-Earth education in geography of high school

★Invited Papers

*Yoshiyasu Ida[1] (1.Faculty of Human Sciences,University of Tsukuba)

4:15 PM - 4:30 PM JST | 7:15 AM - 7:30 AM UTC

[U14-04] How to support elementary, junior high and high school teachers who are not familiar with Earth Science

★Invited Papers

*Hiroyuki Hoshi[1] (1.Department of Earth Sciences, Aichi University of Education)

4:30 PM - 4:45 PM JST | 7:30 AM - 7:45 AM UTC

[U14-05] Issues raised at the meeting for exchanging Information on the Earth Science Education in High Schools

★Invited Papers

*Iwata Makoto[1], Iida Kazuya[2], Satoshi Miyajima[3] (1.Hiroshima Prefectural Ogaki High School, 2.Komaba-Toho Junior and Senior High School, 3.Saitama Prefectural Kumagaya High School)

4:45 PM - 5:00 PM JST | 7:45 AM - 8:00 AM UTC

[U14-06] Discussion on the current status and issues of the earth education
★Invited Papers

*Hiroshi Ichikawa[1], Saori Nakai[2], Hidenori Kumagai[3], Hiroshi Nishi[4] (1.Education Committee, JpGU, 2.Kyoto Koka Women's University, 3.Japan Agency for Marine-Earth Science and Technology, 4.Fukui Prefectural University)

The Essentials of Living on a Changing Planet

*Hiroshi Nishi[1]

1. Fukui Prefectural University, Institute of Dinosaur Research

Japan faces many problems between the natural environment and human society, such as climate change, natural disasters and environmental pollution. We must be prepared to face the violence and prepare sufficient disaster prevention and mitigation measures. For that purpose, it is necessary to acquire the "discipline for living on a changing earth" that people living in this disaster-prone country should share through education in fields closely related to nature such as earth science and geography. As a result, each individual will have the ability to prepare for "saving lives" against the threat of nature, and will be able to live in harmony with nature.

There are two important points to acquire this background. One is to strengthen "learning the nature system" in school education. In particular, the perspective of "integration of literature and science" is important for this education. The other is to provide a place for learning during the lifetime. Examples of places to learn include museums and Geopark activities. Through learning in these school and lifelong educations, society will increase knowledge related to natural disasters and the global environment, and increase opportunities to learn countermeasures. In order to achieve this, it is need to establish human resources and organizations to support the activities. For that objectives, research institutes such as universities, academic societies, and local public organizations cooperate and collaborate, and citizens routinely work together. There should be many places where society can learn about the Earth.

Keywords: natural disaster, changing Earth, literacy for living

©2021. Japan Geoscience Union. All Right Reserved.

Variations in the promotions of high schools offering Basic and Advanced Earth Science classes in Prefectures throughout Japan

*Hideo Takagi[1], Kohei Yoshida[2]

1. Department of Earth Science, Faculty of Education and Integrated Arts and Sciences, Waseda University, 2. Higashi Fukuoka High School

The subject of science in Japanese high school is divided into physics, chemistry, biology and Earth science, and the number of credit is set to 2 for basic subjects and 4 for advanced subjects. With the change of courses based on the new course of study guidelines enforced by MEXT in 2012, the Earth science field has classes in Basic Earth Science (BES) and Advanced Earth Science (AES). However, the percentages of high schools that offer Earth science classes in each prefecture have not been reported. Therefore, we have estimated the proportion of high schools that offer BES and AES classes in a survey of more than 5,000 high schools in Japan. Data for the survey were collected from the curriculum listed in each high-school homepage and from a questionnaire distributed using the Google mail system. Survey results indicate that 43.7% of high schools offer BES, and only 8.8% of high schools offer AES nationwide. In addition, the proportion of high schools offering Earth science classes varies depending on the prefecture. The top prefectural percentage for AES is 48% (Okinawa) and then 38% (Chiba), but nine prefectures have no high schools that offer AES.The percentage of high school students who take Earth science classes is also estimated from the number of textbooks adopted by MEXT (26% for BES and 1.2-0.9% for AES). The proportion of high schools offering Earth science correlates with the number of teachers over the past 40 years employed in Earth science in each prefecture. However, some prefectures have records only of the total number of science teachers, therefore the numbers of teachers hired specifically for Earth science are unknown in these cases. The percentage of high schools offering Earth science classes is higher in prefectures for which only the total number of science teachers is known. Based on our results, for the promotion of high school geoscience education, supports should be provided through workshops in Earth science education, so that science teachers other than full-time Earth science can recognize the importance of Earth science and teach BES whose establishment rate has increased since 2012.
Reference: Yoshida, K. and Takagi, H., 2020, Journal of Geography (Chigaku Zasshi), 129, 337-354.

Keywords: high-school curriculum, establishment rate, Earth science subject

©2021. Japan Geoscience Union. All Right Reserved.

Global-Earth education in geography of high school

*Yoshiyasu Ida[1]

1. Faculty of Human Sciences,University of Tsukuba

The purpose of this presentation is to clarify the overview and issue of global-earth education in the compulsory subject "geography" in high school."Geography" can be said to be a subject that provides earth education that includes global citizenship education. While aiming for earth education from global perspective, it is also a subject that should foster awareness as citizen under nation of Japan. Teachers who teach "Geography" will be required the balance with global-earth citizenship education based on global natural phenomena, and global education based on tha country or identity of nation will be required. Training teachers who teach "Geography" is an one of urgent issues.

Keywords: Global-earth education, Geography in high school, citizenship education

©2021. Japan Geoscience Union. All Right Reserved.

How to support elementary, junior high and high school teachers who are not familiar with Earth Science

*Hiroyuki Hoshi[1]

1. Department of Earth Sciences, Aichi University of Education

School teachers who teach Earth Science and related subjects at elementary, junior high and high schools in Japan are not limited to those who majored in Earth Science at college or university. In fact, there are more teachers who do not know much about Earth Science than those who know well. Earth Science experts should strongly support such school teachers so that they raise the level of their knowledge, while making the teachers feel the fun and depth of Earth Science. This will greatly contribute to the improvement of the quality of Earth Science education in schools, which in turn will lead to the improvement of the Earth Science literacy of the people.

Keywords: Earth Science Education, Science Education, School Teacher

©2021. Japan Geoscience Union. All Right Reserved.

Issues raised at the meeting for exchanging Information on the Earth Science Education in High Schools

*Iwata Makoto[1], Iida Kazuya[2], Satoshi Miyajima[3]

1. Hiroshima Prefectural Ogaki High School, 2. Komaba-Toho Junior and Senior High School, 3. Saitama Prefectural Kumagaya High School

At the "the meeting for exchanging Information on the Earth Science Education in High Schools" held on November 23 and 24, 2019, the issues of geoscience education in high schools were the isolation and aging of earth science teachers, and teachers other than full-time earth science teachers. In order to solve these problems, "formation of a network that transcends schools and regions", "creation of a system that inherits know-how across generations", "dedicated to earth science" The need for "support for teachers other than" was proposed. In response to the proposal, the "the Online meeting for exchanging Information on the Earth Science Education in High Schools" was established as a place for online information exchange. The online information exchange meeting is a voluntary activity by junior high school, high school, university faculty members, research institutes, publishers, etc., and is mainly operated using apps called Slack and Zoom, and participants report on class practice. We have carried out various activities such as introduction of teaching materials, lectures on each specialized field by university faculty members and people from research institutes. Here, I would like to report on some of the issues that have emerged during the exchange of information.

The first is support for young earth science teachers. Many earth science teachers are often alone in school, and they are originally in an environment that tends to be isolated. In each prefecture, there are geoscience subcommittees and geoscience study groups that are active by high school teachers, and information exchange and exchanges have been carried out across schools. However, the number of young earth science faculty members who participate in these meetings is decreasing year by year, and in some prefectures, efforts are declining due to a shortage of people. In addition to supporting the activities of the earth science subcommittees and geoscience study groups in each prefecture, we also support students in the teacher training stage to continue learning earth science education even after becoming teachers, such as by introducing the efforts of these study groups.

The second is support for earth science education from outside the school. During the exchange of information, many high school teachers wanted to give students an opportunity to come into contact with earth science through lectures on the latest research by experts. There were also researchers and university officials looking for opportunities to outreach high school students. Despite the needs of both of these, there are still few practical examples that have been implemented. While online exchanges are seeing new forms of support for earth science education, it is necessary to consider how to increase opportunities for students to come into contact with earth science in the future.

©2021. Japan Geoscience Union. All Right Reserved.

Discussion on the current status and issues of the earth education

*Hiroshi Ichikawa[1], Saori Nakai[2], Hidenori Kumagai[3], Hiroshi Nishi[4]

1. Education Committee, JpGU, 2. Kyoto Koka Women's University, 3. Japan Agency for Marine-Earth Science and Technology, 4. Fukui Prefectural University

On June 23, 2020, the Earth and Planetary Science Committee, Earth and Planetary Science Human Resources Development Subcommittee, the Science Council of Japan, published a proposal "Importance of Earth Education in Elementary and Secondary Education and Lifelong Education: for learning essential knowledge to live on a changing earth". As a follow-up to this proposal, this session is convened by the WG for Studying on Teacher Training System, the Education Committee, JpGU, for the purpose of deepening discussions on the current status and issues regarding the training and recruitment system for primary and secondary school teachers in the fields of Geoscience and Geography, and self-improvement of knowledge and skills. We will discuss on what activities JpGU should carry out in the future in response to the proposal, what items should be intensively considered at the Science Council of Japan in the future, what proposal should be urgently published by the Science Council of Japan, and others. We look forward to the participation of many members who are interested in promoting and enhancing the earth education.

Keywords: Earth Education, Science Council of Japan, proposal, action plan

©2021. Japan Geoscience Union. All Right Reserved.

[J] Poster | U (Union)：Union

Sat. Jun 5, 2021 5:15 PM - 6:30 PM JST | Sat. Jun 5, 2021 8:15 AM - 9:30 AM UTC | Ch.01_2

[U-14] Current status and issues of the earth education necessary for living on the changing earth

convener:Hiroshi Ichikawa, Saori Nakai(kyoto koka womens university department of child education), Hidenori Kumagai(Japan Agency for Marine-Earth Science and Technology), Hiroshi Nishi(The Center for Academic Resources and Archives, The Tohoku Museum Tohoku University)

A proposal entitled by "Importance of Earth Education in Elementary and Secondary School Education and Lifelong Education: for learning essential knowledge to live on a changing earth" was published by the Science Council of Japan on June 23, 2020. This proposal points out that, for all people living in the Japanese archipelago frequently attacked by severe natural disasters, it is important to increase the chances to acquire "the essential knowledge to live on a changing earth" in school learning of the nature, and learn it lifelong. Responding to this proposal, this session is held by WG for Studying on Teacher Training System, established for studying complex and diverse issues related to teacher training and others in May 2019 in the Education Committee, JpGU. This session aims to deepen discussions on the current situation and issues of elementary and secondary school teachers responsible for earth education in the fields of Geosciences and Geography regarding the teacher training and recruitment system and self-improvement of knowledge and skills.

[U14-P01] WG for Studying on Teacher Training System in JpGU

*Hidenori Kumagai[1], Saori Nakai[2], Teacher's training WG JpGU Education Comittee (1.Japan Agency for Marine-Earth Science and Technology, 2.Kyoto Koka Women's University)

[U14-P02] Current state of Geoscience education in primary school teacher training courses to obtain a Type II teacher’s license

*Hiroo Nemoto[1] (1.Ritsumeikan University)

WG for Studying on Teacher Training System in JpGU

*Hidenori Kumagai[1], Saori Nakai[2], Teacher's training WG JpGU Education Comittee

1. Japan Agency for Marine-Earth Science and Technology, 2. Kyoto Koka Women's University

See abstract written in Japanese.

Keywords: Teacher Training System, limitation of lessons available for geology

©2021. Japan Geoscience Union. All Right Reserved.

Current state of Geoscience education in primary school teacher training courses to obtain a Type II teacher’ s license

*Hiroo Nemoto[1]

1. Ritsumeikan University

The purpose of this study is to clarify current state of Geoscience education in teacher training courses in order to obtain a teacher’ s license for primary schools or RIKA (natural science) and/or geoscience teachers at secondary schools in Japan. As the first step, I investigated the syllabi and its related system of primary school teacher training courses at junior colleges in Japan which can be obtained a Type II teacher’ s certificate for primary schools.

As a result, it was revealed that at least about 50 out of around 2,000 graduates in 2019 school year at these junior colleges became primary school teachers without learning RIKA or geoscience while they were junior college students. Moreover, about half of graduates who obtained its certificate had not learnt RIKA or geoscience while at the junior college.

Therefore, we need to discuss and to adopt opinions as below in order to make a recommendation toward reduce internal problems related to teacher training programmes at junior colleges:
- We should propose that “Type II teacher’ s certificate for primary schools” will be limited license such as its for pupils year 1 to 2 class only because there is not subject RIKA on year 1 and 2.
- Subjects which are related to RIKA will be compulsory subjects to obtain “Type II teacher’ s certificate for primary schools” at junior colleges.

Keywords: primary school teacher training courses, Type II teacher’ s certificate for primary schools, Type II TCPS, RIKA (Natural Science), Geoscience

©2021. Japan Geoscience Union. All Right Reserved.

[J] Oral | U (Union)：Union

Sat. Jun 5, 2021 1:45 PM - 3:15 PM JST | Sat. Jun 5, 2021 4:45 AM - 6:15 AM UTC | Ch.01 Zoom Room 01

[U-15] JpGU's mission against giant earthquake and tsunami disasters: last 10 years and the future

convener:Koji Okumura(Graduate School of Letters, Hiroshima University), Yoshinori MIYACHI(Geological Survey of Japan, AIST), Hitoshi SAITO(College of Economics, Kanto Gakuin University), Chairperson:Koji Okumura(Graduate School of Letters, Hiroshima University), Yoshinori MIYACHI(Geological Survey of Japan, AIST), Hitoshi SAITO(College of Economics, Kanto Gakuin University)

10 years have passed since the M9.0 2011 Tohoku Taiheiyo-Oki earthquake. Devastating disasters by strong and wide-spread ground motion, many fatalities and destruction of coastal area by huge tsunamis, and the accidents of the Fukushima Dai-ichi Nuclear Power Plant greatly impacted Japanese society and scientific community. Recovery from the damages is still under way. Meantime, the next giant earthquake from Nansai Trough is approaching. Researchers in earth and planetary sciences have been working hard on large earthquakes and tsunamis. In addition, researchers are obliged to contribute to the safe society from these disasters. 2011 great Tohoku disasters introduced collaboration of all disciplines in earth and planetary sciences together with related scientific communities. This session aims at first to summarize our scientific achievement with emphasis on the output to and the interaction with the society for disaster mitigation in these 10 years. Then we discuss about our missions against giant earthquakes and tsunamis in coming 10 years or before the next big one. The discussion will cover our contributions to national and local government efforts for disaster mitigation, risk management and hazard responses of individuals and organizations, and education on hazards and disasters.

1:45 PM - 2:05 PM JST | 4:45 AM - 5:05 AM UTC

[U15-01] JpGU's activities on gigantic earthquakes and tsunamis, 10 years since Great East Japan disasters

★Invited Papers

*Koji Okumura[1] (1.Graduate School of Humanities and Social Sciences, Hiroshima University)

2:05 PM - 2:25 PM JST | 5:05 AM - 5:25 AM UTC

[U15-02] The Decade of Progress of the Tohoku Geographical Association following the 2011 Great East Japan Earthquake

★Invited Papers

*ODA TAKASHI[1] (1.Miyagi University of Education)

2:25 PM - 2:45 PM JST | 5:25 AM - 5:45 AM UTC

[U15-03] Correspondence and the BCP (business continuity plan) maintenance situation of the commerce and industry establishment after the East Japan great earthquake disaster

★Invited Papers

*Toshio HATSUZAWA[1] (1.Fukushima University)

2:45 PM - 3:05 PM JST | 5:45 AM - 6:05 AM UTC

[U15-04] Ground motion characteristics during The 2011 off the Pacific coast of Tohoku Earthquake and The 2016 Kumamoto Earthquake

★Invited Papers

*Shinichi Matsushima[1] (1.Disaster Prevention Research Institute, Kyoto University)

3:05 PM - 3:15 PM JST | 6:05 AM - 6:15 AM UTC

[U15-05] Discussion

JpGU's activities on gigantic earthquakes and tsunamis, 10 years since Great East Japan disasters

*Koji Okumura[1]

1. Graduate School of Humanities and Social Sciences, Hiroshima University

The 2011 off the Pacific coast of Tohoku Earthquake and tsunamis, subsequent devastating damages, and the accidents of the Fukushima Daiichi Nuclear Power Plant were the most shocking severest natural hazards for the Japan Geoscience Union that was established in 2005. Before the great Tohoku disasters, the damages from natural hazards were not so severe and extensive as in 2011, so individual scientific organizations conducted researches by itself. However, the severity and the magnitude of the damages from the hazards and accidents in 2011 urged organized cooperative efforts of scientific organizations to study the hazards and disasters. The Japan Geoscience Union, as a unique organization consisted of most earth and planetary science societies in Japan, started to support these cooperative efforts immediately after the disasters. In the earliest days after the disasters, dissemination of information on the post earthquake investigation for better coordination of many groups through the internet was an important task of the Union. Information gathering and distribution have been carried out through the Union web pages, news letters, and scientific journals continuously. However, the most important activity of the Union is the annual meeting. For the advancement and promotion of the research on gigantic earthquakes and tsunamis, environmental effects of nuclear accidents, and disaster mitigation as well the sessions of the JpGU annual meetings have been the most important arena for scientists. Reviewing the activities in the past 10 years since the Great East Japan disasters, we will understand our missions to prepare for the future gigantic earthquakes and tsunamis.

Keywords: Great East Japan disaster, gigantic earthquake, tsunamis

©2021. Japan Geoscience Union. All Right Reserved.

The Decade of Progress of the Tohoku Geographical Association following the 2011 Great East Japan Earthquake

*ODA TAKASHI[1]

1. Miyagi University of Education

As an academic society located in a disaster-hit area, the Tohoku Geographical Association played an important role following the Great East Japan Earthquake of 2011. The member geographers conducted field studies to assess the damage, examine the recovery of lives of the affected people and discuss rebuilding of Tohoku. Wide range of related studies were conducted with a variety of topics including geomorphology, housing, migration and displacement, the impact of the Fukushima Daiichi Nuclear Power Plant accident, and welfares of affected people. It functioned as a hub of frontline researchers who were eager to draw lessons from the catastrophes that occurred in areas close to their fields of study.

Shortly after the earthquake, a special website was established to share geographic studies on this mega disaster and its lessons with the wider public in English and Japanese by the members. Based on the experience of the 2011 earthquake, the Association went on to build a framework to support members who conduct field research immediately after a disaster occurs. In February 2018, the "Internal Rules on Support for Emergency Disaster Investigations by Members of the Tohoku Geographical Society" was ratified to financially support the members. The rules applied recent disasters including the Hokkaido Eastern Iburi Earthquake of 2018, Western Japan Storms of 2018, and the Typhoon disasters of 2019.

There are great expectations for the role that studies of geography could play in disaster risk reduction and its education and enlightenment. One of such contributions include educating the school teachers and the students for topographic map and hazard map reading to raise awareness of the use of geographic information for disaster risk reduction. Hence, the Association in recent years began to hold a series of workshops for in-service high school teachers in collaboration with the Geospatial Information Authority of Japan to better understand geographic understanding of natural and social environments.

As described above, the academic society has developed various efforts in the wake of the catastrophe. By looking back on the trajectory of the decade of progress as local academic society, we discuss its contributions and interdisciplinary collaborations among the academic societies in earth and planetary science.

Keywords: Great East Japan Earthquake, disaster recovery, disaster risk reduction, education, academic society, geography

©2021. Japan Geoscience Union. All Right Reserved.

Correspondence and the BCP (business continuity plan) maintenance situation of the commerce and industry establishment after the East Japan great earthquake disaster

*Toshio HATSUZAWA[1]

1. Fukushima University

The Minamisoma-city Haramachi area is located in the Fukushima Beach street district central part and is located within the range of 20-30km from the first Fukushima nuclear power plant. At first I grasp the suffering situation of a commerce and industry establishment located in the Haramachi area and clarify it from the maintenance situation of BCP of each company after the earthquake disaster for disaster prevention. The reporter performed commerce and industry fact-finding after an earthquake disaster every year in cooperation with the Haramachi chamber of commerce. This report is based on the result.

The material damage was left to a small thing when I watched the damage situation at the time of the earthquake disaster. However, the influence of the nuclear plant accident was big, and the sales of 2011 decreased to 60% of manufacturing industry, 76% of construction industry, 45% of wholesale trade, 73% of retail trade, 63% of service industry compared with the previous year. The stop of the business by the suffering was big by the manufacturing industry. In the order of the manufacturing industry, the business partner of 39% in the city, 53% of Soma-Futaba area, 20% of prefecture except these areas, 29% of Tohoku districts except Fukushima were lost. The regional economy received an extremely big blow.

It is important that not only I merely strengthen the disaster prevention measures of the hard aspect, but also the software aspect including the security of a business partner and the circulation route takes measures to cope with a disaster. The development of BCP (business continuity plan) is the one.

The reporter investigated it over three times in the investigation that I performed in Minamisoma-city about BCP. From three investigations, the maintenance rate of BCP understands that it remain in the level for 10% of establishments which I maintain although it is in an upward trend. In the suffering company analysis of the East Japan typhoon of 2019, indirect damage exceeds direct damage greatly. This shows the importance of the measures of the software side, however, there is the disaster prevention correspondence of the establishment mainly on a hardware aspect. It is necessary to expand the disaster prevention of the software side including BCP.

Keywords: East Japan great earthquake disaster, BCP, Minami-Soma city Fukushima Prefecture

©2021. Japan Geoscience Union. All Right Reserved.

Ground motion characteristics during The 2011 off the Pacific coast of Tohoku Earthquake and The 2016 Kumamoto Earthquake

*Shinichi Matsushima[1]

1. Disaster Prevention Research Institute, Kyoto University

The 2011 off the Pacific coast of Tohoku Earthquake which caused the Great East Japan Earthquake Disaster, initiated on 14:46 of March 11th 2011. The epicenter was 130 km east of Sendai in the off Miyagi region and the focal depth was 24 km. As a result, the rupture spread to a length of 400 to 500 km and width of 150 to 200 km along the boundary between the Pacific plate and Eurasian plate and became moment magnitude (Mw) of 9.0. The relative slip close to the trench east of the epicenter was about 60 m and made a huge tsunami. On the other hand, it recorded the JMA seismic intensity of 7 in Tsukidate of City of Kurihara in Miyagi Prefecture. This earthquake counted 19,729 causalities, 2,559 missing and 6,233 injured, as of March 1st, 2020. There were 121,996 totally collapsed, 282,941 half destroyed and 748,416 partially damaged houses, and 14,527 public buildings and 92,059 of other structures suffered damage during the earthquake. This catastrophe was caused mainly by the huge tsunami along the shoreline. On the other hand, K-NET Tsukidate (MYG004) station of the Kyoshin Network (K-NET) operated by the National Research Institute for Earth Science and Disaster Resilience recorded JMA seismic intensity 7. Although it recorded a maximum acceleration of 2,700 cm/s/s for the north-south component (about 2.7 times of gravitational acceleration), there were hardly no building damage near the station. This was because the frequency content of the recorded ground motion was about 4 Hz. On the contrary, the K-NET Furukawa (MYG006) station recorded JMA seismic intensity of 6+, but there were collapsed houses because the dominant frequency of the ground motion was about 1 Hz (period of 1 sec). Despite the fact that the earthquake was the largest among the recorded earthquakes around Japan and the highest peak ground acceleration ever recorded, it was found by many researches that damage will not be caused depending on the characteristics of ground motions.

Furthermore, during the mainshock of the 2016 Kumamoto Earthquake, which was the largest JMA magnitude (Mjma) earthquake in this 10 years, JMA seismic intensity (JMA-SI) of 7 was recorded at two stations. Mjma 7.3 is the largest inland active fault earthquake that was recorded. Houses were damaged heavily in Mashiki town of Kumamoto Prefecture, one of the sites where JMA-SI 7 were recorded and the dominant frequency of the ground motion was about 1 Hz. The other site, Nishihara village had not suffered great damage in the central part of the village, but there where damage near the surface rupture of the fault. In Nishihara, the dominant period was about 3 seconds. It was re-recognized that the ground motion with dominant frequency of 1 Hz has the potential of causing great damage to houses. In addition, ground motion with dominant period of 3 seconds which may cause severe damage to base-isolated structures and high-rise buildings has been observed and it has raised a question concerning safety of these types of buildings.

Keywords: The 2011 off the Pacific coast of Tohoku Earthquake, The 2016 Kumamoto Earthquake, Ground motion, Period of 1 second, Building damage

©2021. Japan Geoscience Union. All Right Reserved.

[J] Oral | U (Union) | Union

[U-15] JpGU's mission against giant earthquake and tsunami disasters: last 10 years and the future

convener:Koji Okumura(Graduate School of Letters, Hiroshima University), Yoshinori MIYACHI(Geological Survey of Japan, AIST), Hitoshi SAITO(College of Economics, Kanto Gakuin University), Chairperson:Koji Okumura(Graduate School of Letters, Hiroshima University), Yoshinori MIYACHI(Geological Survey of Japan, AIST), Hitoshi SAITO(College of Economics, Kanto Gakuin University)

Sat. Jun 5, 2021 1:45 PM - 3:15 PM Ch.01 (Zoom Room 01)

10 years have passed since the M9.0 2011 Tohoku Taiheiyo-Oki earthquake. Devastating disasters by strong and wide-spread ground motion, many fatalities and destruction of coastal area by huge tsunamis, and the accidents of the Fukushima Dai-ichi Nuclear Power Plant greatly impacted Japanese society and scientific community. Recovery from the damages is still under way. Meantime, the next giant earthquake from Nansai Trough is approaching. Researchers in earth and planetary sciences have been working hard on large earthquakes and tsunamis. In addition, researchers are obliged to contribute to the safe society from these disasters. 2011 great Tohoku disasters introduced collaboration of all disciplines in earth and planetary sciences together with related scientific communities. This session aims at first to summarize our scientific achievement with emphasis on the output to and the interaction with the society for disaster mitigation in these 10 years. Then we discuss about our missions against giant earthquakes and tsunamis in coming 10 years or before the next big one. The discussion will cover our contributions to national and local government efforts for disaster mitigation, risk management and hazard responses of individuals and organizations, and education on hazards and disasters.

3:05 PM - 3:15 PM

[U15-05]Discussion

©Japan Geoscience Union

[E] Oral | P (Space and Planetary Sciences)：P-PS Planetary Sciences

Sat. Jun 5, 2021 1:45 PM - 3:15 PM JST | Sat. Jun 5, 2021 4:45 AM - 6:15 AM UTC | Ch.04 Zoom Room 04

[P-PS03] Regolith Science

convener:Koji Wada(Planetary Exploration Research Center, Chiba Institute of Technology), Akiko Nakamura(Graduate School of Science, Kobe University), Patrick Michel(Universite Cote D Azur Observatoire De La Cote D Azur CNRS Laboratoire Lagrange), John Kevin Walsh(Southwest Research Institute Boulder), Chairperson:Naoya Sakatani(Department of Physics, Rikkyo University)

Recent planetary explorations have revealed that almost all solid bodies in the solar system are covered with small particles, called regolith. The surface geology, especially regolith behavior on the surfaces of solid bodies, becomes increasingly more important as represented by Hayabusa mission and other on-going and planned sample-return missions such as Hayabusa2, OSIRIS-REx, and MMX.
For fully understanding the regolith science, it is required to know and compare the regolith conditions on various celestial bodies, from asteroids to planets, with various methods.
Therefore, this session welcomes broad topics related to regolith on various celestial bodies, such as asteroids, comets, the Moon, the martian moons, Mars, etc. Papers on the formation, evolution, and alteration processes of regolith particles and regolith systems on the surface of planetary bodies, remote and in-situ observational results and techniques, analyses and results of returned samples, and laboratory, numerical, and theoretical studies on the fundamental physical and chemical processes are all welcome.
Note that what we call regolith is not just fine grains: all kinds of materials (more or less loose) that lie on the surface, from cobbles to finer grains, are our targets.

1:45 PM - 2:00 PM JST | 4:45 AM - 5:00 AM UTC

[PPS03-01] Landing on an asteroid: Simulations and image analysis of the OSIRIS-REx spacecraft touch-down on (101955) Bennu

★Invited Papers

*Ronald Ballouz[1], Kevin John Walsh[2], Patrick Michel[3], Yun Zhang[3], Paul Sánchez[4], Daniel Jay Scheeres[4], Michael C Nolan[1], Stephen R Schwartz[1], Derek C Richardson[5], Olivier S Barnouin[6], Edward B Bierhaus[7], Harold C Connolly[8,1], Dante S Lauretta[1] (1.Lunar and Planetary Lab, University of Arizona, Tucson, AZ, USA, 2.Southwest Research Institute, Boulder, CO, USA, 3.Université Côte d'Azur, Observatoire de la Côte d'Azur, CNRS, Laboratoire Lagrange, Nice, France, 4.University of Colorado Boulder, CO, USA,, 5.University of Maryland, College Park, MD, USA, 6.The Johns Hopkins University Applied Physics Laboratory, Laurel, MD, USA, , 7.Lockheed Martin Space, Littleton, CO, USA, , 8.Dept. of Geology, Rowan University, Glassboro, NJ, USA)

2:00 PM - 2:15 PM JST | 5:00 AM - 5:15 AM UTC

[PPS03-02] Dust cloud mass from OSIRIS-REx sample collection event at Bennu

★Invited Papers

*Bashar Rizk[1], Kevin J. Walsh[2], Ronald Ballouz[1], Brent Bos[3], Christian Drouet d'Aubigny[1] (1.University of Arizona, 2.Southwest Research Institute, 3.Goddard Space Flight Center)

2:15 PM - 2:30 PM JST | 5:15 AM - 5:30 AM UTC

[PPS03-03] Hayabusa2 sampling operation at Ryugu and the returned regolith samples

★Invited Papers

*Shogo Tachibana[1,2], Hayabusa2 Sampler Team (1.UTokyo Organization for Planetary and Space Science, University of Tokyo , 2.ISAS, JAXA)

2:30 PM - 2:45 PM JST | 5:30 AM - 5:45 AM UTC

[PPS03-04] Surface roughness and cohesion of impact fragments of meteorite targets

*Yuuya Nagaashi[1], Akiko Nakamura[1] (1.Kobe University)

2:45 PM - 3:00 PM JST | 5:45 AM - 6:00 AM UTC

[PPS03-05] Size and Spatial Distribution of Rock Particles on Small Bodies Revealed with CNN-based Algorithm

*Yuta Shimizu[1], Taisuke Suzuki[1], Ryodo Hemmi[1], Hideaki Miyamoto[1] (1.University of Tokyo)

3:00 PM - 3:15 PM JST | 6:00 AM - 6:15 AM UTC

[PPS03-06] **Experimental Study on the Relationship between Surface distributions and Vertical Structures of Rock Particles on Small bodies.**

*Taisuke Suzuki[1], Yuta Shimizu[1], Hideaki Miyamoto[1] (1.The University of Tokyo)

Landing on an asteroid: Simulations and image analysis of the OSIRIS-REx spacecraft touch-down on (101955) Bennu

*Ronald Ballouz[1], Kevin John Walsh[2], Patrick Michel[3], Yun Zhang[3], Paul Sánchez[4], Daniel Jay Scheeres[4], Michael C Nolan[1], Stephen R Schwartz[1], Derek C Richardson[5], Olivier S Barnouin[6], Edward B Bierhaus[7], Harold C Connolly[8,1], Dante S Lauretta[1]

1. Lunar and Planetary Lab, University of Arizona, Tucson, AZ, USA, 2. Southwest Research Institute, Boulder, CO, USA, 3. Université Côte d'Azur, Observatoire de la Côte d'Azur, CNRS, Laboratoire Lagrange, Nice, France, 4. University of Colorado Boulder, CO, USA,, 5. University of Maryland, College Park, MD, USA, 6. The Johns Hopkins University Applied Physics Laboratory, Laurel, MD, USA, , 7. Lockheed Martin Space, Littleton, CO, USA, , 8. Dept. of Geology, Rowan University, Glassboro, NJ, USA

Spacecraft exploration of near-Earth asteroids (NEAs) has shown that their surfaces are composed of both fine regolith and larger meter-scale boulders. For asteroid sample-return missions, characterizing the geotechnical properties of the surface is critical for ensuring spacecraft safety and sampling success. Constraints on these geotechnical properties from remote observations can provide insight into their expected response from an interaction with a spacecraft; however, there is still a poor understanding of the behavior of granular materials in the low-gravity environment of NEAs. Here, we show direct simulations of the OSIRIS-REx spacecraft touching down on the NEA (101955) Bennu and compare them to images taken during the OSIRIS-REx sampling attempt on October 20, 2020. We discuss how these simulations, combined with observations of the surface and telemetry from spacecraft proximity operations, may provide insight into the behavior of granular materials in low gravity.

We discuss the results of varying the angle of friction, ϕ, and subsurface porosity as it is most pertinent for interpreting the data returned by OSIRIS-REx during the sampling maneuver. In our simulations, we found that the angle of friction of the material can strongly influence its response to an impact by a relatively massive spacecraft. We found that for low angles of friction, the OSIRIS-REx Touch and Go Sample Acquisition Mechanism (TAGSAM) is essentially unperturbed by the spacecraft. Past a friction angle of approximately 30 deg, the constant-force spring of TAGSAM engages. The porosity of the sub-surface can influence the manner in which the regolith resist the load of a spacecraft by changing the number of grain-to-grain contacts in the medium. These grain-to-grain contacts build a network of contacting particles known as a force chain, which we visualize in Fig. 1 for two different cases of regolith friction angle.

The value of ϕ for terrestrial granular materials typically ranges between approximately 20 and 40 deg and is controlled by the physical properties of individual grains such as size, shape, and roughness. We find that, for cases with high ϕ, the grains more strongly interlock in response to motion-loading from the spacecraft's intrusion. This allows the regolith to more readily resist penetration, leading to the spacecraft resting at shallower depths. For these same values of ϕ, a more porous bed may have a different response, as there would be fewer surfaces for particles to develop frictional contacts, allowing TAGSAM to penetrate deeper in to the bed.

Keywords: Asteroid, OSIRIS-REx, Regolith

©2021. Japan Geoscience Union. All Right Reserved.

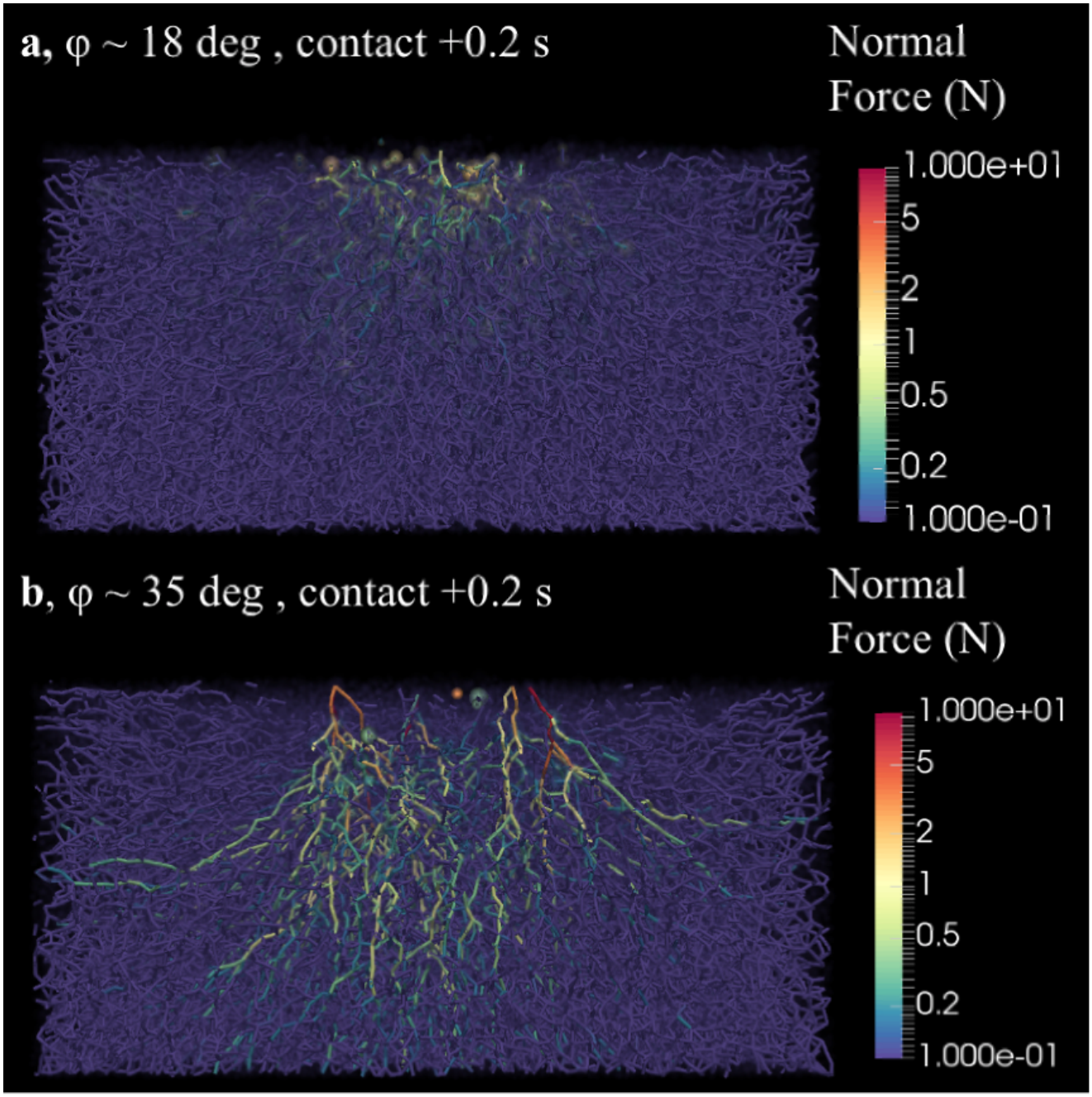


Figure 1. Snapshot of simulations showing the force-chain network for two simulation cases where the horizontal dimension is 120 cm, and the vertical dimension is 60 cm. The color represents the normal force (N) that each particle experiences 0.2 s after contact. **a**) For regolith with low φ, the force chains are relatively shallow and weak. **b**) For regolith with high φ, the force chains are relatively deep and strong.

©2021. Japan Geoscience Union. All Right Reserved.

Dust cloud mass from OSIRIS-REx sample collection event at Bennu

*Bashar Rizk[1], Kevin J. Walsh[2], Ronald Ballouz[1], Brent Bos[3], Christian Drouet d'Aubigny[1]

1. University of Arizona, 2. Southwest Research Institute, 3. Goddard Space Flight Center

The high-pressure gas released during the OSIRIS-REx sampling event, on 20 October 2020, lofted a cloud of sub-millimeter and smaller particles from the surface of asteroid Bennu . We attempted to determine the mass of this sub-millimeter dust cloud, and its initial layer thickness. The analysis relied on two images acquired before and after the event agitated Bennu’ s regolith at Nightingale, the sampling site. We measured the optical depth of the expanding cloud as a function of distance from the center of the expansion during the moment of sample acquisition. Specific values of mass and thickness relied on simplifying assumptions and varied with particle size. We integrated the imaged profile of radially varying optical depth to significantly narrow, or even collapse, the range of average optical depth. We recruited observations from other instruments and analyses to do the same for particle size. With our result, we hope to constrain the nature of the microphysical environment at and near the surface of Bennu’ s regolith by establishing the presence, or confirming the absence, of a population of sub-millimeter particles and measuring its magnitude.

Keywords: Regolith, Bennu, TAG, Dust, Sampling, Contamination

©2021. Japan Geoscience Union. All Right Reserved.

Hayabusa2 sampling operation at Ryugu and the returned regolith samples

*Shogo Tachibana[1,2], Hayabusa2 Sampler Team

1. UTokyo Organization for Planetary and Space Science, University of Tokyo , 2. ISAS, JAXA

C-type asteroids have been hypothesized to be parent bodies of carbonaceous chondrites that are primitive meteorites containing hydrated minerals and organic matter. The hydrated minerals and organics in carbonaceous chondrites could be a source of volatiles to the proto Earth. The JAXA's Hayabusa2 spacecraft explored the near Earth C-type asteroid (162173) Ryugu to return its surface regolith samples. During the seventeen-month proximity observation, Hayabusa2 discovered (1) Ryugu is a rubble pile body with a low albede, darker than typical carbonaceous chondrites (e.g., Watanebe et al., 2019; Sugita et al., 2019; Morota et al., 2020), (2) hydrated minerals are present ubiquitously on the surface (e.g., Kitazato et al., 2019, 2021), and (3) surface pebbles and boulders have lower thermal inertia than meteorites, implying the porous nature of Ryugu materials (e.g., Grott et al., 2019; Okada et al., 2020).

Hayabusa2 landed on Ryugu at two different surface locations for regolith sample collection in February and July, 2019. The second landing aimed at collecting sub-surface samples excavated by the artifical cratering experiment (Arakawa et al., 2020). The basic concept and design of the Hayabusa2 projectile-shooting sampling device are the same as those of the Hayabusa sampling device (Yano et al., 2006). A 5-gram tantalum projectile was successfully shot through a 1-m long sampler horn at an impact velocity 300 m/s at the timing of each touchdown (Sawada et al., 2017). Two landing operations of Hayabusa2 proved for the first time that the projectile-shooting sampling device works at the asteroid surface.

Hayabusa2 delivered its reentry capsule on December 6, 2020 to Woomera, South Australia. Numerous millimeter- to centimeter-sized particles were found in two separate chambers inside the sample container, which were used for two landing operations at Ryugu. The particles are black in color, consistent with the color of Ryugu boulders (e.g., Sugita et al., 2019; Morota et al., 2020). Centimeter-sized grains, close to the maximum collectible size with the sampler system (Sawada et al., 2017), are found in the sample obtained during the second landing operation. The total weight of the sample exceeds 5 g, which is far more than the mission requirement (100 mg) for scientific analysis (Tachibana et al., 2014). All the sample characteristics suggest that the Hayabusa2 sampler system worked efficiently and effectively to collect surface regoligh at the Ryugu surface.

The regolith sampling oreration and the characteristics of returned particles will be presented and discussed in detail at the meeting.

Keywords: Hayabusa2, asteroid, Solar System, sampling

©2021. Japan Geoscience Union. All Right Reserved.

Surface roughness and cohesion of impact fragments of meteorite targets

*Yuuya Nagaashi[1], Akiko Nakamura[1]

1. Kobe University

The shape and cohesive force of particles making up small bodies have significant effects on the physical properties of the bodies. The shape of particles affects the angle of internal friction and thus the porosity of the particle layer [1]. The cohesive force of particles would enable the fast rotation of small bodies [2]. Also, the deformation and failure modes of rubble piles depend on the angle of internal friction and the cohesive force [3]. We have measured the shape and cohesive force of meteorite particles ground with a pestle and mortar. We showed that the smaller the circularity C ($= 4\pi S/L^2$; S and L are the two-dimensional projected area and perimeter of the particle, respectively) and the larger the arithmetic mean roughness *Ra* (the average of the deviations from the mean surface), the smaller the cohesive force [4]. However, the ground meteorite particles have larger circularities than Itokawa rocks and basalt impact fragments, although they are different in size, and may also have different surface roughness. Therefore, we conducted impact experiments and collected tens of micron-sized particles ejected from meteorite targets to measure the circularity, surface roughness, and cohesion.
We collected the ejecta particles from impacts of a 1/8-inch stainless steel projectile and 1 mm aluminum projectiles to blocks of Allende at a speed of ~0.13 and ~2.9 km/s, respectively. We measured the circularity C and the axial ratio b/a (the ratios of the long-axis a and short-axis b lengths of the ellipsoidal approximation of the two-dimensional projection) of the ejecta using an optical microscope. We measured the roughness *Ra* of the ejecta using a confocal laser microscope.
The axial ratio b/a of the ejecta is 0.69–0.70 on average, similar to that of tens of micron-sized impact fragments of basalts and L5 chondrites (~0.7) [5] and the ground Allende particles (0.72 on average) [4]. The circularity C of the ejecta is 0.66–0.67 on average, similar to that of Itokawa rocks and basalt impact fragments (0.64–0.73 on average) [4], but smaller than that of the ground Allende particles (0.75 on average). Here, we compared the values of the circularity when the number of constituent pixels of each particle was corrected to 3000 pixels because the circularity depends on the number, i.e., image resolution [4]. The roughness *Ra* of the ejecta was ~500 nm, larger than that of the ground Allende particles (~300 nm) [4]. We will also compare the cohesive force of the Allende ejecta and ground particles, measured using a centrifugal method [4,6].

This research was supported by the Hypervelocity Impact Facility (former facility name: The Space Plasma Laboratory), ISAS, JAXA.

[1] Suzuki et al., 2003, *J. Soc. Powder Technol. Japan* **40**, 348-354. [2] Sánchez & Scheeres, 2014, *Meteorit. Planet. Sci* **49**, 788-811. [3] Sánchez & Scheeres, 2016, *Icarus* **271**, 453-471. [4] Nagaashi et al., in press, *Icarus*. [5] Michikami et al., 2018, *Icarus* **302**, 109-125. [6] Nagaashi et al., 2018, *Prog Earth Planet Sci* **5**, 52.

Keywords: impact fragment, surface roughness, cohesion

©2021. Japan Geoscience Union. All Right Reserved.

Size and Spatial Distribution of Rock Particles on Small Bodies Revealed with CNN-based Algorithm

*Yuta Shimizu[1], Taisuke Suzuki[1], Ryodo Hemmi[1], Hideaki Miyamoto[1]

1. University of Tokyo

As the number of small body exploration increases, the amount of science data obtained is expanding. Analyses of that data have yielded an unprecedented amount of knowledge about small bodies, and especially unexpected surfaces of small bodies covered by numerous rock particles have been revealed by high-resolution images [e.g., 1]. The size/shape/spatial distribution, sorting, and direction of rock particles have led us to discuss the origins and surface processes of small bodies [2, 3, 4]. Analysis of rock particles is also critical for landing missions to avoid hazardous objects [5], resulting in the growing demand for identifying countless rock particles. In many cases, the identification of particles has been manually conducted by fitting ellipses to the profile of particles. The profiles are generally blurred and difficult to be distinguished from the background due to irregular particle shapes, overlapping particles, image resolution limits, which makes the analysis time-consuming and difficult to be reconducted, leading to the lack of reproducibility. Therefore, a method to analyze a massive amount of rock particles with objectivity and reproducibility has to be established. Here, we develop the computational approach for the automated identifications of rock particles based on the image feature extraction algorithm, the convolutional neural networks (CNNs). We prepare images of the simulated surface of small bodies in a laboratory, and then carefully identified thousands of particles. Using the data of profiles, we trained the model, enabling nearly 90 % of profiles of particles to be correctly traced without the aid of manual analysis. Moreover, by using the model, rock particles on the global surface of asteroid Itokawa are mapped, revealing the size and spatial distribution of particles. The approach of this study can rapidly identify numerous particles, which can be a promising tool for analyzing countless images of the surface of small bodies taken by the current and future small body exploration missions.

References

[1] Lauretta et al., *Nature* **212**, 925-984 (2019). [2] Sugita et al., *Science* **364**, eaaw0422 (2019). [3] Miyamoto et al., *Science* **316**, 1011-1014 (2007) [4] Michikami et al., *Icarus* **331**, 179-191 (2019). [5] Yamaguchi et al., *Acta Astronautica* **151**, 217-227 (2018).

Keywords: Rock Particles, Automated Identification, Deep Learning

©2021. Japan Geoscience Union. All Right Reserved.

Experimental Study on the Relationship between Surface distributions and Vertical Structures of Rock Particles on Small bodies.

*Taisuke Suzuki[1], Yuta Shimizu[1], Hideaki Miyamoto[1]

1. The University of Tokyo

Small celestial bodies are covered by numerous rock particles. The distributions of rock particles on small bodies differ significantly from one body to another, reflecting the formation and evolution process of the body [1], and thus needs to be studied in detail. However, the information obtained by exploration is limited, and the distributions of rock particles are studied mostly by analyzing surface images, especially measuring cumulative size distributions (CSFD) of particles [2, 3, 4]. In general, the CSFD of small bodies can be fit by power-law, and the values of power-law index are compared between celestial bodies and different regions on the bodies. However, it is not clear to what extent the power-law indexes contain essential information. In fact, in order to understand the distributions of rock particles, it is necessary to focus not only on the surface but also on the subsurface. For example, layer structure and macroporosity of subsurface is fundamental for investigating the internal structure of small bodies[1]. However, the internal structures of small bodies have never been observed, and can only be inferred from gravity and grain density [5, 6]. Therefore, research has been conducted to infer the internal structures of celestial bodies from the results of image analyses [7, 8]. Such studies are based on the assumption that the particle size distributions obtained from surface images represent the interior, but this assumption has never been verified. Therefore, this study aims to verify the extent to which the information obtained from surface images of small bodies reflects the essential information including that of subsurface. Although such study can be performed by numerical simulation assuming spherical particles [9], reflecting the effects of the complex shapes of the rock particles of small bodies is extremely difficult. On the other hand, our approach is to conduct an experiment in a laboratory, where we use rock material made from fractured hornfels which are blended to have the power-law index of -3. When the rock material was laid out on a flat surface, the slopes of CSFD obtained from surface images were less steep than the actual value. In addition, when the material was placed in an acrylic container with an inner diameter of 140mm, the slopes of CSFD obtained from surface images got even less steep than when it was laid out on a flat surface. These results suggest that slope of the CSFD obtained from the images of the surfaces of the small bodies is less steep than the actual slope of the CSFD including the interior. Therefore, constraining the physical properties of the interior only from the surface images of small bodies is revealed to be challenging. Moreover, the material was vibrated in order to observe the effects of surface modifications. The result showed that the slope of the CSFD gradually got less steep. This suggests that the comparisons of the CSFD are important when we discuss surface modification processes of small bodies. Furthermore, the internal structure is visualized by micro-focus X-ray CT to understand how the CSFD on the surface relates to the subsurface structure. From the broad view and high contrast 3D images obtained, the values of macroporosity of the horizontal cross-sections are calculated, and we suggest that the macroporosity falls between 30% and 40%. These findings can be applied to image analyses and simulations to advance discussions on the geology of small bodies.

References

[1] Hirata et al., *Icarus* **200**, 486-502 (2009). [2] Saito et al., *Science (80-.).* (2006). [3] Michikami et al.,

©2021. Japan Geoscience Union. All Right Reserved.

Icarus **331**, 179-191 (2019). [4] DellaGuista et al., *Nat. Astron.* **3**, 341-351 (2019). [5] Fujiwara et al., *Science (80-.). **312**, 1330-1334* (2006). [6] Nakamura et al., *Science (80-.). **333***, 1113-1116 (2011). [7] Grott et al., *J. Geophys. Res. Planets* **125**, 1-15 (2020). [8] Cheng et al., *Nat. Astron.* (2020). [9] Tancredi et al., *Icarus* **247**, 279-290 (2015).

©2021. Japan Geoscience Union. All Right Reserved.

[E] Oral | P (Space and Planetary Sciences)：P-PS Planetary Sciences

Sat. Jun 5, 2021 3:30 PM - 5:00 PM JST | Sat. Jun 5, 2021 6:30 AM - 8:00 AM UTC | Ch.04 Zoom Room 04

[P-PS03] Regolith Science

convener:Koji Wada(Planetary Exploration Research Center, Chiba Institute of Technology), Akiko Nakamura(Graduate School of Science, Kobe University), Patrick Michel(Universite Cote D Azur Observatoire De La Cote D Azur CNRS Laboratoire Lagrange), John Kevin Walsh(Southwest Research Institute Boulder), Chairperson:Yuri Shimaki(Institute of Space and Astronautical Science, Japan Aerospace Exploration Agency)

Recent planetary explorations have revealed that almost all solid bodies in the solar system are covered with small particles, called regolith. The surface geology, especially regolith behavior on the surfaces of solid bodies, becomes increasingly more important as represented by Hayabusa mission and other on-going and planned sample-return missions such as Hayabusa2, OSIRIS-REx, and MMX.
For fully understanding the regolith science, it is required to know and compare the regolith conditions on various celestial bodies, from asteroids to planets, with various methods.
Therefore, this session welcomes broad topics related to regolith on various celestial bodies, such as asteroids, comets, the Moon, the martian moons, Mars, etc. Papers on the formation, evolution, and alteration processes of regolith particles and regolith systems on the surface of planetary bodies, remote and in-situ observational results and techniques, analyses and results of returned samples, and laboratory, numerical, and theoretical studies on the fundamental physical and chemical processes are all welcome.
Note that what we call regolith is not just fine grains: all kinds of materials (more or less loose) that lie on the surface, from cobbles to finer grains, are our targets.

3:30 PM - 3:45 PM JST | 6:30 AM - 6:45 AM UTC

[PPS03-07] Deciphering the regolith properties of small bodies from numerical modeling

★Invited Papers

*Yun Zhang[1] (1.UCA, OCA, CNRS, Lagrange, Nice, France)

3:45 PM - 4:00 PM JST | 6:45 AM - 7:00 AM UTC

[PPS03-08] Charge Magnitude of Electrostatically Lofted Dust Grains over the Lunar Terminator

*Necmi Cihan Orger[1], Kazuhiro Toyoda[1], Mengu Cho[1] (1.Laboratory of Lean Satellite Enterprises and In-Orbit Experiments - Kyushu Institute of Technology)

4:00 PM - 4:15 PM JST | 7:00 AM - 7:15 AM UTC

[PPS03-09] High-velocity impact experiments in reduced gravity: The effect of cohesive strength of particle layers

*Masato Kiuchi[1], Takaya Okamoto[1], Yuuya Nagaashi[2], Sunao Hasegawa[1], Akiko Nakamura[2] (1.Japan aerospace exploration agency, Institute of space and astronautical science, 2.Graduate School of Science, Kobe UniversityKobe University)

4:15 PM - 4:30 PM JST | 7:15 AM - 7:30 AM UTC

[PPS03-10] Local variation in thermal inertia around the artificial impact crater on Ryugu

*Naoya Sakatani[1], Satoshi Tanaka[2], Tatsuaki Okada[2], Toru Kouyama[3], Akira Miura[2], Naru Hirata[4], Hiroki Senshu[5], Takehiko Arai[6], Yuri Shimaki[2], Hirohide Demura[4], Tomohiko Sekiguchi[7], Jun Takita[8], Tetsuya Fukuhara[1], Thomas Müller[9], Axel Hagermann[10], Jens Biele[11], Matthias Grott[11], Maximillian Hamm[11,12], Marco Delbo[13], Masahiko Arakawa[14], Kazunori Ogawa[15], Koji Wada[5], Toshihiko Kadono[16], Rie Honda[17], Kei Shirai[14], Takanao Saiki[2], Hiroshi Imamura[2], Yasuhiko Takagi[18], Hajime Yano[2], Masahiko Hayakawa[2],

Hirotaka Sawada[2], Satoru Nakazawa[2], Seiji Sugita[19], Tomokatsu Morota[19], Manabu Yamada[5], Shingo Kameda[1], ERI TATSUMI[20], Yasuhiro Yokota[2], Hidehiko Suzuki[21], Kazuo Yoshioka[19], Moe Matsuoka[2], Yuichiro Cho[2] (1.Rikkyo University, 2.Institute of Space and Astronautical Science, Japan Aerospace Exploration Agency, 3.National Institute of Advanced Industrial Science and Technology, 4.University of Aizu, 5.Chiba Institute of Technology, 6.Ashikaga University, 7.Hokkaido University of Education, 8.Hokkaido Kitami Hokuto High School, 9.Max-Planck Institute for Extraterrestrial Physics, 10.Luleå University of Technology, 11.German Aerospace Center, 12.University of Potsdam, 13.Observatoire de la Côte d'Azur, CNRS, 14.Kobe University, 15.JAXA Space Exploration Center, Japan Aerospace Exploration Agency, 16.University of Occupational and Environmental Health, 17.Kochi University, 18.Aichi Toho University, 19.University of Tokyo, 20.Instituto de Astrofisica de Canarias, 21.Meiji University)

4:30 PM - 4:45 PM JST | 7:30 AM - 7:45 AM UTC

[PPS03-11] Brightness change of Hayabusa2 SCI crater ejecta observed by ONC-T and its implication to the surface status of asteroid Ryugu

*Rie Honda[1], Yasuhiro Yokota[2], Masahiko Arakawa[3], Seiji Sugita[4], Yuri Shimaki[2], Koji Wada[5], Toshihiko Kadono[6], Kei Shirai[3], Kazunori Ogawa[7], Naoya Sakatani[8], Ko Ishibashi[5], Takanao Saiki[2], Hiroshi Imamura[2], Satoru Nakazawa[2], Masahiko Hayakawa[2], Hajime Yano[2], Yasuhiko Takagi[9], Naru Hirata[10], Hirotaka Sawada[2], Tomokatsu Morota[4], Shingo Kameda[8], Eri Tatsumi[11], Manabu Yamada[5], Toru Kouyama[12], Yuichiro Cho[4], Moe Matsuoka[2], Kazuo Yoshioka[4], Hidehiko Suzuki[13], Chikatoshi Honda[10] (1.Department of Science and Technology, System of Natual Science, Kochi University, 2.Institute of Space and Astronautical Science, Japan Aerospace Exploration Agency, 3.Kobe University, 4.The University of Tokyo, 5.Planetary Exploration Research Center, Chiba Institute of Technology, 6.University of Occupational and Environmental Health, 7.JAXA Space Exploration Center, Japan Aerospace Exploration Agency, 8.Rikkyo University, 9.Aichi Toho University, 10.The University of Aizu, 11.Instituto de Astrofisica de Canarias, University of La Laguna, 12.National Institute of Advanced Industrial Science and Technology, 13.Meiji University)

4:45 PM - 5:00 PM JST | 7:45 AM - 8:00 AM UTC

[PPS03-12] Study of Hydrated Asteroids via Polarimetry: Correlation between Polarimetric Properties and Degree of Aqueous Alteration of Hydrated asteroids.

*Jooyeon Geem[1], Masateru Ishiguro[1], Hiroyuki Naito[2], Daisuke Kuroda[6], Koki Takahashi[3], Tomohiko Sekiguchi[3], Seiko Takagi[4], Tatsuharu Ono[4], Kiyoshi Kuramoto[4], Tomoki Nakamura[5] (1.Astronomy program, Dept of Physics and Astronomy, Seoul National University, 2.Nayoro Observatory, 3.Hokkaido University of Education, 4.Department of Cosmosciences, Graduate School of Science, Hokkaido University, 5.Department of Earth and Planetary Material Sciences, Faculty of Science, Tohoku University, 6.Okayama Observatory, Kyoto University)

Deciphering the regolith properties of small bodies from numerical modeling

*Yun Zhang[1]

1. UCA, OCA, CNRS, Lagrange, Nice, France

Surfaces of small bodies experience a wide range of processes that alter their local and global characteristics. Numerical modeling allows us to investigate these processes and decipher the history and physical properties of small bodies from their surface characteristics. I will present an overview of our recent investigations based on numerical modeling and give some examples below.
For objects whose surfaces have been characterized in detail by spacecrafts, e.g., Ryugu by Hayabusa2 (JAXA) and Bennu by OSIRIS-REx (NASA), comparisons with numerical modeling can be used to shed some light on the formation of these surface features. For instance, some surface local mass movement features in the downslope direction were detected on asteroid Bennu [1]. This direction and color variation analyses suggest that these mass movements occurred at times close to the current spin-period regime, which may result from YORP rotational accelerations. We carried out a numerical study using the soft-sphere discrete element modeling (SSDEM) to test Bennu’s structural evolution under the YORP spin-up effect. The current surface slope, the recent surface mass movement, and the old surface age of the equatorial bulge are used as constraints to shed some light on Bennu’s surface properties and internal structure.
Direct interaction with a small body surface is the most effective way to understand the regolith mechanical properties and behavior in the actual gravitational environment. The outcome also provides precious opportunities to interpret the results using numerical modeling. For instance, the experiment performed by the Hayabusa2 Small Carry-on Impactor (SCI) on asteroid Ryugu in April 2019 offers the first opportunity for a direct confrontation of cratering on small bodies with numerical modeling [2]. We conducted SCI-like cratering tests using a hybrid Smooth Particle Hydrodynamics (SPH) and SSDEM framework. The preliminary results show that regolith near the SCI-cratering region should have little cohesion in order to match the crater morphology.
In an indirect way, the regolith properties can also be inferred for some small bodies that are at the limit of maintaining their structural stability. For instance, there are dozens of fast-rotating asteroids that require material cohesion to keep their integrity. With comprehensive numerical exploration, we can derive the minimum required amount of cohesion of their regolith and the corresponding grain size distribution. Connecting the regolith properties with other observational data can help to reveal the formation mechanism of small bodies. For instance, our numerical modeling showed that the lack of apparent cometary activity of the interstellar object 1I/‘Oumuamua can be explained by the way its surface was built during its formation through a close encounter with its host star in another planetary system [3].

Reference: [1] Jawin et al. (2020) JGR: Planets, 125, e2020JE006475. [2] Arakawa M. et al. (2020) Science, 368: 67–71. [3] Zhang & Lin (2020) Nature Astronomy, 4, 852–860.

Acknowledgement: I acknowledge my collaborators (Ronald-L. Ballouz, Olivier S. Barnouin, Martin Jutzi, Douglas N. C. Lin, Patrick Michel, Derek C. Richardson, Stephen R. Schwartz, Kevin J. Walsh) for their contributions to these studies. I acknowledge funding from the Université Côte d'Azur “Individual grants for young researchers program of IDEX JEDI” and from the European Union’s Horizon 2020 research and innovation program under grant agreement No. 870377 (NEO-MAPP project).

©2021. Japan Geoscience Union. All Right Reserved.

Keywords: Small body formation and evolution, Regolith properties, Granular material, Numerical modeling

©2021. Japan Geoscience Union. All Right Reserved.

Charge Magnitude of Electrostatically Lofted Dust Grains over the Lunar Terminator

*Necmi Cihan Orger[1], Kazuhiro Toyoda[1], Mengu Cho[1]

1. Laboratory of Lean Satellite Enterprises and In-Orbit Experiments - Kyushu Institute of Technology

The interaction with the solar wind has several consequences on the lunar surface, and one of them can be described as electrostatic transportation of the lunar dust grains. It has been proposed that the emitted electrons within micro-cavities between the neighboring dust grains can produce strong repulsion to detach the dust particles from the loose upper layer of the lunar regolith, and this mechanism has been demonstrated in several laboratory experiments. In order to launch a charged dust particle from the lunar surface, the electrostatic repulsion should overcome the forces of contact and gravity. In this study, the charge magnitude requirement of the lofted dust particles in the range of 0.1 μm –10 μm in radius is investigated through a function of (1) specific gravity that is determined by the particle type such as agglutinates, basalt, or breccia, (2) inter-particle contact forces, (3) the surface electric field that is controlled by the solar wind, (4) the launch angle based on the experimental results, and (5) the characteristic size of micro-cavity that is related to the regolith configuration. It has been observed that the charge magnitude variation increases with the particle size, and the particles with 5-6 μm radius can gain sufficient charges to loft and produce the near-surface lunar horizon glow.

Keywords: lunar regolith, lunar dust charging, electrostatic dust lofting, lunar horizon glow

©2021. Japan Geoscience Union. All Right Reserved.

High-velocity impact experiments in reduced gravity: The effect of cohesive strength of particle layers

*Masato Kiuchi[1], Takaya Okamoto[1], Yuuya Nagaashi[2], Sunao Hasegawa[1], Akiko Nakamura[2]

1. Japan aerospace exploration agency, Institute of space and astronautical science, 2. Graduate School of Science, Kobe UniversityKobe University

The surfaces of small bodies are in a microgravity environment, and it is important to understand how gravity affects crater size to estimate the physical properties of the surface. Several studies have investigated the effect of gravity on crater size for low-velocity to high velocity (1 m s^{-1} to 6.6 km s^{-1}) impacts: the gravitational dependence of crater size was obtained in the low and high gravity range (Gault & Wedekind, 1977; Schmidt & Housen, 1987; Cintala et al., 1989; Takagi et al., 2007; Kiuchi et al., 2019). In most of the studies, the crater diameter was shown to be proportional to −0.165 ~ −0.19 power of the gravitational acceleration. However, in a microgravity environment such as the surface of small bodies, the effect of the cohesive strength of the regolith layer on crater formation may be more dominant than the effect of the gravity. The transition condition between the gravity regime and the strength regime is not well understood because the available laboratory data is limited.

We assembled a simple drop tower in the vacuum chamber of a two stage light gas gun at the Japan Aerospace Exploration Agency (JAXA) to conduct high velocity impact experiments in reduced gravity. We used quartz sand (particle size is ~425 μm) as the target material, and used a glass sphere of diameter 1 mm as the projectile. The target material was loosely filled in a stainless steel container with a diameter of 30 cm and a height of 10 cm. A projectile was impacted at a velocity of 1.2 km s^{-1}. As a result, the diameters of craters formed at 0.05 G was about 1.8 times larger than the one formed at 1 G and gravitational dependence of the crater diameter was clearly observed(Kiuchi et al., 2020, JpGU–AGU). We compiled the results using pi-scaling (e.g., Holsapple, 1994) and showed that our results in reduced gravity agreed well with the crater size scaling law for non–cohesive sand targets (Housen and Holsapple, 2011).

In addition, we used targets of fine glass beads (particle size is ~40 μm) and fused alumina particles (particle size is ~40 μm). As a result, the crater diameter formed at 0.05 G was not much different from the one formed at 1 G for both targets. We infer that the gravitational dependence of the crater diameter was reduced due to the effect of the cohesive strength of these targets. We constrained the transition condition between the gravity regime and the strength regime by estimating the tensile strength of the particle layers based on the measured cohesive force of the particles (Nagaashi et al., in press). From our experimental results, it was found that the effect of the target strength becomes dominant when the tensile strength of the particle layer is larger than $10\rho gD$, where ρ is the density of the particle layer, g is the gravitational acceleration, and D is the crater diameter. We will discuss the effect of the cohesive strength on the size frequency distribution of small craters on particle layers.

This research was supported by the Hypervelocity Impact Facility (former facility name: The Space Plasma Laboratory) of ISAS, JAXA, and JSPS KAKENHI Grant Number JP19K14824 and 18K03723.

Keywords: Impact crater formation experiments, Gravitational dependence of the crater diameter, Cohesive strength of particle layers

©2021. Japan Geoscience Union. All Right Reserved.

©2021. Japan Geoscience Union. All Right Reserved.

Local variation in thermal inertia around the artificial impact crater on Ryugu

*Naoya Sakatani[1], Satoshi Tanaka[2], Tatsuaki Okada[2], Toru Kouyama[3], Akira Miura[2], Naru Hirata[4], Hiroki Senshu[5], Takehiko Arai[6], Yuri Shimaki[2], Hirohide Demura[4], Tomohiko Sekiguchi[7], Jun Takita[8], Tetsuya Fukuhara[1], Thomas Müller[9], Axel Hagermann[10], Jens Biele[11], Matthias Grott[11], Maximillian Hamm[11,12], Marco Delbo[13], Masahiko Arakawa[14], Kazunori Ogawa[15], Koji Wada[5], Toshihiko Kadono[16], Rie Honda[17], Kei Shirai[14], Takanao Saiki[2], Hiroshi Imamura[2], Yasuhiko Takagi[18], Hajime Yano[2], Masahiko Hayakawa[2], Hirotaka Sawada[2], Satoru Nakazawa[2], Seiji Sugita[19], Tomokatsu Morota[19], Manabu Yamada[5], Shingo Kameda[1], ERI TATSUMI[20], Yasuhiro Yokota[2], Hidehiko Suzuki[21], Kazuo Yoshioka[19], Moe Matsuoka[2], Yuichiro Cho[2]

1. Rikkyo University, 2. Institute of Space and Astronautical Science, Japan Aerospace Exploration Agency, 3. National Institute of Advanced Industrial Science and Technology, 4. University of Aizu, 5. Chiba Institute of Technology, 6. Ashikaga University, 7. Hokkaido University of Education, 8. Hokkaido Kitami Hokuto High School, 9. Max-Planck Institute for Extraterrestrial Physics, 10. Luleå University of Technology, 11. German Aerospace Center, 12. University of Potsdam, 13. Observatoire de la Côte d'Azur, CNRS, 14. Kobe University, 15. JAXA Space Exploration Center, Japan Aerospace Exploration Agency, 16. University of Occupational and Environmental Health, 17. Kochi University, 18. Aichi Toho University, 19. University of Tokyo, 20. Instituto de Astrofisica de Canarias, 21. Meiji University

The Hayabusa2 spacecraft has completed the rendezvous phase around Cb-type asteroid Ryugu in 2019. From thermal infrared imaging by TIR, global temperature distribution of Ryugu is consistent with the thermal calculation with thermal inertia of 300±100 J m^{-2} K^{-1} $s^{-0.5}$ [1], and thermal inertia values of the floors of craters are in general roughly comparable with the global average [2]. On the other hand, few small and fresh craters show anomalously low thermal inertia less than 100 J m^{-2} K^{-1} $s^{-0.5}$, contributed from the highly porous nature of boulders exposed by the impact cratering [3]. On April 2019, Hayabusa2 performed an artificial impact (Small Carry-on Impactor or SCI) experiment [4], whereby a ~2 kg mass was fired at 2 km/s against the asteroid surface. As a result of the successful operation, an artificial crater (SCI crater) with diameter larger than 10 m was created on the asteroid.

In the preliminary analysis of TIR data of the SCI crater, we suggested no thermally-anomalous materials on the crater floor [3]. In other words, the SCI crater has similar thermal inertia with the global average, and physical properties of the subsurface materials are similar to that of the top surface, at least on the SCI impact site. However, regional difference in the thermal inertia inside and outside the SCI crater have not been discussed. We will present whether the regional variation of the thermophysical properties appears around the SCI craters.

References: [1] Okada et al. (2020), *Nature* 579, 518-522. [2] Shimaki et al. (2020), *Icarus* 348, 113835. [3] Sakatani et al. (2021), *LPSC* #1832, #2189. [4] Arakawa et al. (2020), Science 368, 67-71.

©2021. Japan Geoscience Union. All Right Reserved.

Brightness change of Hayabusa2 SCI crater ejecta observed by ONC-T and its implication to the surface status of asteroid Ryugu

*Rie Honda[1], Yasuhiro Yokota[2], Masahiko Arakawa[3], Seiji Sugita[4], Yuri Shimaki[2], Koji Wada[5], Toshihiko Kadono[6], Kei Shirai[3], Kazunori Ogawa[7], Naoya Sakatani[8], Ko Ishibashi[5], Takanao Saiki[2], Hiroshi Imamura[2], Satoru Nakazawa[2], Masahiko Hayakawa[2], Hajime Yano[2], Yasuhiko Takagi[9], Naru Hirata[10], Hirotaka Sawada[2], Tomokatsu Morota[4], Shingo Kameda[8], Eri Tatsumi[11], Manabu Yamada[5], Toru Kouyama[12], Yuichiro Cho[4], Moe Matsuoka[2], Kazuo Yoshioka[4], Hidehiko Suzuki[13], Chikatoshi Honda[10]

1. Department of Science and Technology, System of Natual Science, Kochi University, 2. Institute of Space and Astronautical Science, Japan Aerospace Exploration Agency, 3. Kobe University, 4. The University of Tokyo, 5. Planetary Exploration Research Center, Chiba Institute of Technology, 6. University of Occupational and Environmental Health, 7. JAXA Space Exploration Center, Japan Aerospace Exploration Agency, 8. Rikkyo University, 9. Aichi Toho University, 10. The University of Aizu, 11. Instituto de Astrofisica de Canarias, University of La Laguna, 12. National Institute of Advanced Industrial Science and Technology, 13. Meiji University

Introduction:
On April 5, 2019, Hayabusa2 Small Carry-on Impactor (SCI) experiment was conducted to form an artificial crater on the asteroid Ryugu. As a result, a crater with a rim diameter of 17.6 meters was successfully formed on the surface of Ryugu [1]. Comparison of the Hayabusa2 Telescopic Onboard Navigation Camera (ONC-T) [2] image data before and after the impact revealed that the brightness around the crater was darkened by 20% at the maximum due to ejecta rays [1]. Investigating the cause of this darkening and its temporal change will provide important insights into the weathering and alteration process on the asteroid's surface. We conducted a detailed analysis on the brightness of the SCI crater and its surrounding area by using the images of ONC-T v-band (0.55 μm) just before SCI impact and after SCI impact until the end of the proximity phase, Oct. 2019.

The analysis is conducted by two methods: (1) comparison of reflectance at the standard viewing geometry derived from images at a different time and phase angles and (2) evaluation of global phase-ratio map created by dividing two global mosaics at phase angle 31˚ and 1˚.

Analysis1. Comparison of images over 7 months:
High spatial resolution ONC-T images around the SCI crater was obtained just during the operations of the Hayabusa2 sampling (touchdown) and rehearsals. Thus we used images taken at an altitude of 20 km distance. This dataset contains various solar phase angle (1–33˚) observations. We used the photometrically corrected reflectance images (Level 2e product) for this analysis. In addition, we normalized each image by the average of a reference area defined far from the SCI crater.

From comparison around the SCI crater over 7 months, we found that the relative brightness of the ejecta and SCI crater varies with solar phase angle, rather than the elapsed time from SCI impact. Since the photometric correction for this Level 2e product did not concern the regional photometric difference, this residual dependency on the phase angle means that the photometric characteristic (surface roughness/texture) around the SCI crater is different from the reference area.

Analysis 2. Phase ratio image: To search the area of hidden ejecta around the natural crater similar to SCI crater ejecta, we made a global phase-ratio map by dividing two global mosaics (phase angle 31˚ / 1˚).

©2021. Japan Geoscience Union. All Right Reserved.

The ratio of two different phase angle images is often used as a method to identify the distribution of a characteristic surface roughness/texture area. In this map image, the SCI crater ejecta deposit is recognized as an area with a lower ratio than the surroundings. However, the results showed that there were no areas similar to the SCI crater ejecta deposit. This may suggest that the natural crater ejecta deposits have been smoothed out over a long time.

Summary:

It was found that the surface roughness/texture may play a major role in the darkening of the SCI crater ejecta deposit. The contribution of the intrinsic albedo is still unknown and needs to be studied in detail. It is also a future issue whether there was any change in roughness/texture or albedo during the 7-month period. However, observation of the natural craters on Ryugu suggests that the darkening area may fade over a long period of time.

References:

[1] Arakawa M. et al. (2020) Science 368, 67. [2] Sugita S., et al. (2019) Science 364, 252.

Keywords: Asteroid, Ryugu, Impact, Ejecta

©2021. Japan Geoscience Union. All Right Reserved.

Study of Hydrated Asteroids via Polarimetry: Correlation between Polarimetric Properties and Degree of Aqueous Alteration of Hydrated asteroids.

*Jooyeon Geem[1], Masateru Ishiguro[1], Hiroyuki Naito[2], Daisuke Kuroda[6], Koki Takahashi[3], Tomohiko Sekiguchi[3], Seiko Takagi[4], Tatsuharu Ono[4], Kiyoshi Kuramoto[4], Tomoki Nakamura[5]

1. Astronomy program, Dept of Physics and Astronomy, Seoul National University, 2. Nayoro Observatory, 3. Hokkaido University of Education, 4. Department of Cosmosciences, Graduate School of Science, Hokkaido University, 5. Department of Earth and Planetary Material Sciences, Faculty of Science, Tohoku University, 6. Okayama Observatory, Kyoto University

Hydrated asteroids have been attracting widespread interest due to the Hayabusa2 and OSIRIS-REx mission. These asteroids are considered as fragments that have experienced varying degrees of aqueous alteration in their parent bodies. Such aqueously altered asteroids have been extensively investigated by spectroscopic observations and laboratory experiments of carbonaceous chondrites. From spectroscopy, it is known that the spectral features in 0.7 μm or the 3 μm bands depend on the degree of aqueous alteration [2, 3]. On the other hand, mineralogical studies of chondrites found that the transition of composed minerals such as the cronstedtite converting to Mg-rich serpentine occurs as the alteration progressed [4]. While approaches via spectroscopy and meteoritics are widely employed, “polarimetry” has rarely been used to study hydrated asteroids.

Polarimetry has the advantage of being able to know the physical properties like albedo, particle size, and porosity of the target’s surface even without conducting space explorations [1]. The polarization degree (P) of reflected light from atmosphereless bodies exhibits the phase angle (α) dependence, where the α is the angle between Sun-Target-Observer. The $\alpha-P$ profile consists of several key parameters such as the minimum polarization degree (P_{min}) appearing at $\alpha \sim 10º$. The polarimetric parameters are useful diagnostic tools to estimate the surface properties. In this study, we examine “how the physical properties change depending on the degree of aqueous alteration” by utilizing polarimetry.

In 2020, we made the polarimetric observation for 35 nights with the visible Multi-Spectral Imager (MSI) attached on the 1.6m Pirka Telescope at the Nayoro Observatory. We observed 18 C-complex main-belt asteroids in the visible band, including Ch type asteroids (i.e., hydrated asteroids). These asteroids were observed at $\alpha \leqq 20º$, which allows us to obtain the P_{min} values of our targets. We also gathered archival data and derived the polarimetric parameters and spectral information of asteroids from the previous research.

As a result, we found that polarimetric parameters (e.g., the P_{min}) show a strong correlation with spectral features (e.g., the 0.7 μm and 3 μm range absorption). Because P_{min} is attributed to the physical properties (albedo, particle size, or porosity) of the surface materials, our observation suggests these physical properties changed as the aqueous alteration progressed. In this presentation, we will introduce our polarimetric observation, and discuss possible interpretations of these results.

[1] Cellino et al., 2015, MNRAS, 451,4.; [2] Fornasier et al., 2014, Icarus, 233, 163-178.; [3]Takir et al., 2013, Meteoritics and Planetary Science, 48, 9.; [4] Tomeoka et al., 1985, GCA, 49, 10.

©2021. Japan Geoscience Union. All Right Reserved.

Keywords: Asteroids, Polarimetry, Aqueous alteration process, Hydrated asteroids

©2021. Japan Geoscience Union. All Right Reserved.

[E] Poster | P (Space and Planetary Sciences)：P-PS Planetary Sciences

Sat. Jun 5, 2021 5:15 PM - 6:30 PM JST | Sat. Jun 5, 2021 8:15 AM - 9:30 AM UTC | Ch.02_1

[P-PS03] Regolith Science

convener:Koji Wada(Planetary Exploration Research Center, Chiba Institute of Technology), Akiko Nakamura(Graduate School of Science, Kobe University), Patrick Michel(Universite Cote D Azur Observatoire De La Cote D Azur CNRS Laboratoire Lagrange), John Kevin Walsh(Southwest Research Institute Boulder)

Recent planetary explorations have revealed that almost all solid bodies in the solar system are covered with small particles, called regolith. The surface geology, especially regolith behavior on the surfaces of solid bodies, becomes increasingly more important as represented by Hayabusa mission and other on-going and planned sample-return missions such as Hayabusa2, OSIRIS-REx, and MMX.
For fully understanding the regolith science, it is required to know and compare the regolith conditions on various celestial bodies, from asteroids to planets, with various methods.
Therefore, this session welcomes broad topics related to regolith on various celestial bodies, such as asteroids, comets, the Moon, the martian moons, Mars, etc. Papers on the formation, evolution, and alteration processes of regolith particles and regolith systems on the surface of planetary bodies, remote and in-situ observational results and techniques, analyses and results of returned samples, and laboratory, numerical, and theoretical studies on the fundamental physical and chemical processes are all welcome.
Note that what we call regolith is not just fine grains: all kinds of materials (more or less loose) that lie on the surface, from cobbles to finer grains, are our targets.

[PPS03-P01] Disk-resolved photometric properties of local regions on asteroid 25143 Itokawa

*Naru Hirata[1,2], Kohei Kitazato[1,2], Eri Tatsumi[3], Shota Katahira[1], Takuma Furudate[1], Hiroshi Kikuchi[4], Hiroyuki Sato[4] (1.Dep. of Computer Science and Engineering, Univ. of Aizu, 2.ARC-Space, Univ of Aizu, 3.Instituto de Astrofisica de Canarias, 4.Japan Aerospace Exploration Agency)

[PPS03-P02] Experimental study on impact ejecta velocity scaling law for regolith layer composed of weak boulders

*Yuya Yamamoto[1], Masahiko Arakawa[1], Minami Yasui[1], Sunao Hasegawa[2], Yusaku Yokota[1], Hatsune Okawa[1], Ryo Sugimura[1] (1.Graduate School of Science, Kobe University, 2.institute of Space and Astronautical Science, JAXA)

[PPS03-P03] Particle size of Ryugu's subsurface layer inferred from observation of SCI crater's ejecta curtain.

*Koji Wada[1], Ko Ishibashi[1], Hiroshi Kimura[1], Masahiko Arakawa[2], Hirotaka Sawada[3], Kazunori Ogawa[4,2], Kei Shirai[2], Rie Honda[5], Yuichi Iijima[3], Toshihiko Kadono[6], Naoya Sakatani[7], Yuya Mimasu[3], Tomoaki Toda[3], Yuri Shimaki[3], Satoru Nakazawa[3], Hajime Hayakawa[3], Takanao Saiki[3], Yasuhiko Takagi[8], Hiroshi Imamura[3], Chisato Okamoto[2], Masahiko Hayakawa[3], Naru Hirata[9], Hajime Yano[3] (1.Planetary Exploration Research Center, Chiba Institute of Technology, 2.Department of Planetology, Kobe University, 3.Institute of Space and Astronautical Science, Japan Aerospace Exploration Agency, 4.JAXA Space Exploration Center, Japan Aerospace Exploration Agency, 5.Department of Science and Technology, Kochi University, 6.Department of Basic Sciences, University of Occupational and Environmental Health, 7.Department of Physics, Rikkyo University, 8.Aichi Toho University, 9.School of Computer Science and Engineering, The University of Aizu)

[PPS03-P04] Ryugu's surface change formed by SCI forward debris

*Yuri Shimaki[1], Yasuhiro Yokota[1], Rie Honda[2], Masahiko Arakawa[3], Koji Wada[4], Toshihiko Kadono[5], Kei Shirai[3], Kazunori Ogawa[6], Naoya Sakatani[7], Ko Ishibashi[4], Takanao saiki[1], Hiroshi Imamura[1], Satoru

Nakazawa[1], Masahiko Hayakawa[1], Hajime Yano[1], Yasuhiko Takagi[8], Naru Hirata[9], Hirotaka Sawada[1], Seiji Sugita[10], Tomokatsu Morota[10], Shingo Kameda[7], Eri Tatsumi[11], Manabu Yamada[4], Toru Kouyama[12], Yuichiro Cho[10], Moe Matsuoka[1], Kazuo Yoshioka[10], Hidehiko Suzuki[13], Chikatoshi Honda[9] (1.Institute of Space and Astronautical Science, Japan Aerospace Exploration Agency, 2.Kochi University, 3.Kobe University, 4.Planetary Exploration Research Center, Chiba Institute of Technology, 5.University of Occupational and Environmental Health, 6.JAXA Space Exploration Center, Japan Aerospace Exploration Agency, 7.Rikkyo University, 8.Aichi Toho University, 9.The University of Aizu, 10.The University of Tokyo, 11.Instituto de Astrofisica de Canarias, University of La Laguna, 12.National Institute of Advanced Industrial Science and Technology, 13.Meiji University)

[PPS03-P05] Static and impact strength of brittle regolith analogs

*Akiko Nakamura[1], Sae Shigaki[1] (1.Graduate School of Science, Kobe University)

Disk-resolved photometric properties of local regions on asteroid 25143 Itokawa

*Naru Hirata[1,2], Kohei Kitazato[1,2], Eri Tatsumi[3], Shota Katahira[1], Takuma Furudate[1], Hiroshi Kikuchi[4], Hiroyuki Sato[4]

1. Dep. of Computer Science and Engineering, Univ. of Aizu, 2. ARC-Space, Univ of Aizu, 3. Instituto de Astrofisica de Canarias, 4. Japan Aerospace Exploration Agency

The photometric properties of asteroids reflect their surface compositions and conditions. Disk-integrated photometry of asteroid 25143 Itokawa was studied based on observations by AMICA on Hayabusa spacecraft (Tatsumi et al., 2018) and gave a global averaged surface properties. However, the surface of Itokawa shows a wide variety of terrains. Rough terrains are covered with numerous boulders of various sizes, while smooth terrains are covered with well-sorted pebbles. The degree of space weathering is also quite diverse over the surface. Disk-resolved photometry gives an opportunity to investigate local photometric properties of these interesting sites, but it requires considering the incidence angles and emission angles of observations at every pixel in observations. Our pixel database system stores individual pixel values with observation conditions such as incidence, emission, and phase angles extracted from observations, and enable us to make analysis using pixel values throughout all available images. We present results of disk-resolved photometric modeling at selected local regions on Itokawa using the pixel DB of AMICA images.

Keywords: Haybusa, Itokawa, light scattering property, asteroid

©2021. Japan Geoscience Union. All Right Reserved.

Experimental study on impact ejecta velocity scaling law for regolith layer composed of weak boulders

*Yuya Yamamoto[1], Masahiko Arakawa[1], Minami Yasui[1], Sunao Hasegawa[2], Yusaku Yokota[1], Hatsune Okawa[1], Ryo Sugimura[1]

1. Graduate School of Science, Kobe University, 2. institute of Space and Astronautical Science, JAXA

Impact cratering on solid bodies is one of the most important geological processes in our solar system. The excavation and ejection processes of sub-surface materials during the crater formation process are keys to understand the regolith formation and the escape of meteorite precursors from asteroids. Thus, it is essential to understand the ejecta velocity distribution regarding the crater formation process. Previous studies showed that both the size ratio of an impactor to surface boulders and the fracture strength of boulders would affect the final crater size, and they would also affect the ejecta velocity distribution. Then, in this study, we conducted impact experiments on granular targets composed of coarse-grains with low strength in order to study the effects of size and strength of target grains on the ejecta velocity distribution.

Cratering experiments were conducted by using a gas gun set at Kobe University and ISAS. Granular targets were prepared by using weathered tuff granules with the size of 1 to 4mm (small particle) and the size of 1 to 4cm (large particle). The crush strength of these tuff particles was measured to be about 60 kPa for small particles and 30 kPa for large particles. A spherical projectile with the size of 3mm (stainless steel, zirconia, alumina, glass, and nylon) was lunched at the impact velocity from 40 to 200m/s, and a spherical projectile with the size of 2mm (tungsten carbide, copper, stainless steel, zirconia, titan, aluminum, and nylon) was lunched at the impact velocity (U) from 1.2 to 4.5 km/s, and these two types of the projectile were impacted on the target surface at the normal direction. Impact cratering process was observed by a high-speed camera at 10^3-10^5 fps. We tracked positions of individual particles in the recorded high-speed images and tracked back initial positions of these tracked particles. Then, the ejection velocity and the ejection angle of these particles were calculated according to the ballistic trajectories.

As a result of the analysis for the high-speed images, we found that the large particles near the impact point were disrupted and the fractured particles were then ejected as a dust cloud immediately after the collision. After that, the intact large particles were ejected out of the crater slowly. The ejection velocity of the particles (v_e) decreased with the increase of the initial position (x), and we obtained the relationship between the normalized ejection velocity (v_e/U) and the normalized initial position (x/a), where a is a projectile radius. The slopes of these distributions were found to be dependent on the projectile density, so the conventional ejecta velocity scaling law was applied to these results. Then, we examined how the size and the strength of these particles affected the ejecta velocity distribution. All the data were clearly separated into two regions: One had large ejection velocities ($v_e/U > 10^{-3}$) and the other had small ejection velocities ($v_e/U < 10^{-3}$). The large normalized ejection velocities would represent those of disrupted particles around the impact point, thus we speculate that the ejection velocity could be scaled by the crushed strength scaled velocity of a particle. On the other hand, the small ejection velocities would show those of the intact particles, so the ejection velocities would be scaled by the gravity scaled velocity. Furthermore, the ejecta velocities at the crater wall were two to three times larger than those in the previous study, and the slope of the velocity distribution was gentler than those in previous studies. We obtained the relationship between the ejection angle and the normalized initial position (x/R), where

©2021. Japan Geoscience Union. All Right Reserved.

R is a crater radius, and the ejection angle was found to scatter from 20˚to 80˚depending on x/R, irrespective of the projectile density.

Keywords: ejecta velocity distribution, regolith, low-strength coarse grain, ejecta velocity scaling laws

©2021. Japan Geoscience Union. All Right Reserved.

Particle size of Ryugu's subsurface layer inferred from observation of SCI crater’ s ejecta curtain.

*Koji Wada[1], Ko Ishibashi[1], Hiroshi Kimura[1], Masahiko Arakawa[2], Hirotaka Sawada[3], Kazunori Ogawa[4,2], Kei Shirai[2], Rie Honda[5], Yuichi Iijima[3], Toshihiko Kadono[6], Naoya Sakatani[7], Yuya Mimasu[3], Tomoaki Toda[3], Yuri Shimaki[3], Satoru Nakazawa[3], Hajime Hayakawa[3], Takanao Saiki[3], Yasuhiko Takagi[8], Hiroshi Imamura[3], Chisato Okamoto[2], Masahiko Hayakawa[3], Naru Hirata[9], Hajime Yano[3]

1. Planetary Exploration Research Center, Chiba Institute of Technology, 2. Department of Planetology, Kobe University, 3. Institute of Space and Astronautical Science, Japan Aerospace Exploration Agency, 4. JAXA Space Exploration Center, Japan Aerospace Exploration Agency, 5. Department of Science and Technology, Kochi University, 6. Department of Basic Sciences, University of Occupational and Environmental Health, 7. Department of Physics, Rikkyo University, 8. Aichi Toho University, 9. School of Computer Science and Engineering, The University of Aizu

The particle size of subsurface layers of asteroids would result from the formation and the surface evolution processes of the asteroids. It is difficult, however, to reveal the properties of subsurface particles with remote sensing observations from spacecraft and telescopes. Hayabusa2, the second asteroid explorer mission led by Japan Aerospace Exploration Agency (JAXA), succeeded in forming an artificial crater on the asteroid Ryugu with Small Carry-on Impactor (SCI). In the course of the crater formation process, an ejecta curtain was observed by Deployable Camera 3 (DCAM3) that was separated from the spacecraft to take time-lapse optical images of the ejecta curtain. Since particles that compose the ejecta curtain emerged from a certain depth of the subsurface layer (~ 1 m deep), we are able to extract physical properties of the subsurface particles from the analysis of the ejecta curtain images.

We constructed a theoretical model of the ejecta curtain based on the crater scaling laws and compared it with the images in terms of optical depth. We found that the typical size of the ejecta particles lies in the range from several centimeters to decimeters, indicating a deficit of particles smaller than ~ 1 mm in the subsurface layer. The lack of minute particles suggests that Ryugu might have experienced some kind of surface flow process such as mass wasting to sink small particles into a deeper region or that small particles would have been eliminated by solar radiation pressure during the formation of a rubble pile asteroid Ryugu. We expect laboratory analysis of the size distribution and the interparticle adhesion of Ryugu returned samples to help elucidate the possibility of these processes.

Keywords: Hayabusa2, Small Carry-on Impctor, Impact crater, Subsurface particle size, Ryugu, Deployable Camera 3

©2021. Japan Geoscience Union. All Right Reserved.

Ryugu's surface change formed by SCI forward debris

*Yuri Shimaki[1], Yasuhiro Yokota[1], Rie Honda[2], Masahiko Arakawa[3], Koji Wada[4], Toshihiko Kadono[5], Kei Shirai[3], Kazunori Ogawa[6], Naoya Sakatani[7], Ko Ishibashi[4], Takanao saiki[1], Hiroshi Imamura[1], Satoru Nakazawa[1], Masahiko Hayakawa[1], Hajime Yano[1], Yasuhiko Takagi[8], Naru Hirata[9], Hirotaka Sawada[1], Seiji Sugita[10], Tomokatsu Morota[10], Shingo Kameda[7], Eri Tatsumi[11], Manabu Yamada[4], Toru Kouyama[12], Yuichiro Cho[10], Moe Matsuoka[1], Kazuo Yoshioka[10], Hidehiko Suzuki[13], Chikatoshi Honda[9]

1. Institute of Space and Astronautical Science, Japan Aerospace Exploration Agency, 2. Kochi University, 3. Kobe University, 4. Planetary Exploration Research Center, Chiba Institute of Technology, 5. University of Occupational and Environmental Health, 6. JAXA Space Exploration Center, Japan Aerospace Exploration Agency, 7. Rikkyo University, 8. Aichi Toho University, 9. The University of Aizu, 10. The University of Tokyo, 11. Instituto de Astrofisica de Canarias, University of La Laguna, 12. National Institute of Advanced Industrial Science and Technology, 13. Meiji University

The small carry-on impactor (SCI) on the Hayabusa2 spacecraft is designed to create an artificial crater on an asteroid surface for the collection of sub-surface materials and validation of crater scaling laws [1]. The SCI launches a hollow hemisphere copper liner with a diameter of 13 cm at a velocity of 2 km/s, accompanied by numerous debris [2]. In the ground tests, the SCI forward debris generated concentric damage on the target surface. The SCI successfully created an artificial crater on the surface of Ryugu in 2019 [3]. Besides the artificial crater, surface changes around the crater, such as rim formation, boulder movement, and the emergence of new boulders were observed by the optical navigation camera telescope (ONC-T) [4]. Additionally, concentric surface changes were observed ~70 m distance from the artificial crater, created by the SCI forward debris. Here we report the distribution of the surface changes formed by the SCI forward debris both in the ground test and Ryugu. Based on the SCI detonation position [5], we found that the polar angle of the forward debris in the ground tests is ~11˚, whereas that in Ryugu is ~15˚, probably due to the absence of ambient pressure.

[1] Arakawa et al. (2017), *Space Science Review* 208, 187–212. [2] Saiki et al. (2017), *Space Science Review* 208, 165–186. [3] Arakawa et al. (2020), *Science* 368, 67-71. [4] Honda et al., submitted to *Icarus* . [5] Saiki et al. (2020), *Astrodynamics* 4, 289–308.

Keywords: Hayabusa2, Crater formation, Asteroid Ryugu

©2021. Japan Geoscience Union. All Right Reserved.

Static and impact strength of brittle regolith analogs

*Akiko Nakamura[1], Sae Shigaki[1]

1. Graduate School of Science, Kobe University

Thermal observations showed that the surface rocks of the asteroid Ryugu have large porosity. Comparison of the porosity and strength of the returned samples with those of meteorites and terrestrial rocks is of interest in understanding the evolution of asteroid materials. Generally, a structure having a large porosity has a lower static strength than a structure having a dense structure even if the structure has the same composition. However, the relationship between static strength and porosity is not one-to-one. In addition, the relationship between impact strength and static strength also varies depending on the structure and material composition.

We have investigated static strength and impact strength of some natural brittle materials [1-4]. Samples were basalt, chondrules disassembled from meteorite specimens, dunite, pyrophyllite, pumice, and sandstones. Crushing strength was determined from compression test of spherical specimens and tensile strength was determined from compression test of disc specimens (Brazilian disc test). We obtained the Weibull parameter from the static strength measurement results of the samples, and the value range was 1.5 to 24. Two types of impact disruption experiments were conducted. One is the usual one using brittle targets and study the disruption threshold of the targets, and the other is the case of a small specimen using a brittle sample as a projectile. These results are discussed in comparison with the literature data of chondrites [5, 6].

[1] Nakamura, A. M., et al. (2007) J. Geophys. Res. 112, E02001.
[2] Nagaoka, H. et al. (2014) Meteorit. & Planet. Sci. 49, 69–79.
[3] Shigaki, S. (2016) (in Japanese) Master thesis. Kobe University.
[4] Murakami, Y. (2020) Planet. Space Sci. 182, 104819.
[5] Flynn, G. et al. (2018) Chemie der Erde 78, 269–298.
[6] Cotto-Figueroa, D. (2016) Icarus 277, 73-77.

Keywords: regolith, strength

©2021. Japan Geoscience Union. All Right Reserved.

[J] Oral | P (Space and Planetary Sciences)：P-PS Planetary Sciences

Sat. Jun 5, 2021 9:00 AM - 10:30 AM JST | Sat. Jun 5, 2021 12:00 AM - 1:30 AM UTC | Ch.04 Zoom Room 04

[P-PS07] Formation and evolution of planetary materials in the Solar System

convener:Megumi Matsumoto(Graduate School of Science, Tohoku University), Shin Ozawa(Department of Earth Science, Graduate School of Science, Tohoku University), Yuki Hibiya(Submarine Resources Research Center, Japan Agency for Marine-Earth Science and Technology), Noriyuki Kawasaki(Department of Earth and Planetary Sciences, Graduate School of Science, Hokkaido University), Chairperson:Yuki Hibiya(Submarine Resources Research Center, Japan Agency for Marine-Earth Science and Technology), Noriyuki Kawasaki(Department of Earth and Planetary Sciences, Graduate School of Science, Hokkaido University)

In this session, we will discuss the material evolution in the Solar System based on extraterrestrial sample analyses and experimental works. We will overlook recent knowledge from primitive materials such as chondrites, interplanetary dust particles, and returned samples by space missions. Research works on meteorite parent body processes such as aqueous alteration, thermal metamorphism, shock metamorphism, volcanic activity, and core-mantle-crust differentiation will also be discussed. The topics of this session include experimental studies which, together with meteorite studies, help us to understand the material formation/evolution in the Solar System as well as processes on meteorite parent bodies. Presentations on new innovative analytical and theoretical techniques in various research fields (chemistry, theoretical calculation, physical property) are highly welcome to improve future studies of the Solar System evolution. This session is J (Japanese) session but English talks are also welcomed.

9:00 AM - 9:30 AM JST | 12:00 AM - 12:30 AM UTC

[PPS07-06] Novel approaches based on correlated short-lived and stable isotope variations for dating nucleosyntheses and early solar system events

★Invited Papers

*Tsuyoshi Iizuka[1], Yuki Hibiya[2], Mitsuru SUZUKI[1], Takehito Hayakawa[3] (1.University of Tokyo, 2.JAMSTEC, 3.National Institutes for Quantum and Radiological Science and Technology)

9:30 AM - 9:45 AM JST | 12:30 AM - 12:45 AM UTC

[PPS07-07] Oxygen and Al–Mg isotopic constraints on the cooling rate, age, and precursor of partial melting of an Allende Type B CAI, Golfball

*Noriyuki Kawasaki[1], Shoichi Itoh[2], Naoya Sakamoto[1], Steven B. Simon[3], Daiki Yamamoto[4], Hisayoshi Yurimoto[1] (1.Hokkaido University, 2.Kyoto University, 3.University of New Mexico, 4.JAXA)

9:45 AM - 10:00 AM JST | 12:45 AM - 1:00 AM UTC

[PPS07-08] Chemical and isotopic fractionation of Type B CAI caused by evaporation: An experimental study

*Michiru Kamibayashi[1], Shogo Tachibana[1,3], Noriyuki Kawasaki[2], Daiki Yamamoto[3], Hisayoshi Yurimoto[2] (1.The University of Tokyo, 2.Hokkaido University, 3.Institute of Space and Astronautical Science, Japan Aerospace Exploration Agency)

10:00 AM - 10:15 AM JST | 1:00 AM - 1:15 AM UTC

[PPS07-09] I-Xe ages of chondrites and its relevance for solar-wind derived noble gas concentrations

*Koharu Arai[1], Hirochika Sumino[1], Atsushi Takenouchi[2], Shogo Tachibana[1,3] (1.The University of Tokyo, 2.National Institute of Polar Research, 3.Institute of Space and Astronautical Science)

10:15 AM - 10:30 AM JST | 1:15 AM - 1:30 AM UTC

[PPS07-10] Requirement of turbulent nebula and dust grains for grain size coarsening in chondrule rims

*Hiroaki Kaneko[1], Sota ARAKAWA[2], Taishi Nakamoto[1] (1.Tokyo Institude of Technology, 2.National Astronomical Observatory of Japan)

Novel approaches based on correlated short-lived and stable isotope variations for dating nucleosyntheses and early solar system events

*Tsuyoshi Iizuka[1], Yuki Hibiya[2], Mitsuru SUZUKI[1], Takehito Hayakawa[3]

1. University of Tokyo, 2. JAMSTEC, 3. National Institutes for Quantum and Radiological Science and Technology

Short-lived radionuclides (SLRs) present in the early solar system can be used to constrain the birth environment of our sun and serve as chronometers for nucleosyntheses and early solar system events. Their use as chronometers commonly rests on the assumption that they were uniformly distributed in the early solar system. However, this assumption has been challenged by the report of the heterogeneous distribution of the SLR ^{26}Al (e.g., Bollard et al., 2019 GCA). Such SLR heterogeneity is compatible to the results of high-precision isotope analyses of meteorites, showing that carbonaceous chondrites (CC) and non-carbonaceous (NC) meteorites exhibit fundamentally different nucleosynthetic anomalies with respect to stable isotopes, such as Ti isotopes (e.g., Kruijer et al., 2019 Nature Astronomy). In addition, we have recently found that the SLR ^{92}Nb was ~80% more abundant in CC than in NC reservoirs (Hibiya et al., 2019 LPSC). Because ^{92}Nb exclusively originates from supernovae, ^{92}Nb enrichment requires a biased distribution of ejecta from a supernova in the protoplanetary disk. These results call for establishment of new methodology for chronology of nucleosyntheses and early solar system events without assuming the homogeneous distribution of supernova-derived SLRs.
Here, we present novel chronological approaches coupling the SLR and nucleosynthetic stable isotope heterogeneities. In the chronology of early solar system events, the SLR heterogeneity leads to erroneous relative ages, which can be calibrated if the initial SLR abundance difference is known. We show that the ^{26}Al and ^{92}Nb clocks can be calibrated using the correlation with the nucleosynthetic Ti isotope heterogeneity, considering that these isotope variations are attributed to biased distribution of ejecta from a core-collapse supernova (CCSN) across the protoplanetary disk. Coupling the SLR and Ti isotope variations further allows us to estimate the timing of the CCSN. In the context of the heterogeneous distribution of CCSN ejecta, a difference in the initial abundance of a CCSN-derived SLR between two disk reservoirs is a function of two parameters: (i) the time interval from the CCSN to solar system formation and (ii) the difference in dilution factors of the ejecta in the disk reservoirs. Importantly, the latter can be independently estimated from the variation in the nucleosynthetic stable isotope heterogeneity, which in turn allows to date the CCSN. We combine the ^{26}Al and Ti isotope heterogeneities and estimate the timing of the CCSN explosion to be 0.4–1.5 Myr before the CAI formation. In addition, assuming that CAIs record the isotope composition of the molecular cloud core in which the CCSN ejecta were most efficiently trapped, we estimate the distance between the CCSN and cloud core to be ~1 parsec. These results imply that our sun was born in a stellar cluster containing massive stars and a nearby CCSN triggered the formation of the solar system. We will extend the cosmochronological approach proposed here to other nuclides, in particular proton-rich SLR ^{98}Tc and long-lived radionuclide ^{138}La. Because ^{98}Tc and ^{138}La as well as ^{92}Nb are produced by the same processes in CCSNe, combining these p-nuclides would potentially allows us to determine the timing of the last CCSN event more accurately than the combined ^{26}Al–Ti chronometer.

Keywords: supernova, short-lived radionuclide, nucleosynthesis, isotope dichotomy

©2021. Japan Geoscience Union. All Right Reserved.

Oxygen and Al–Mg isotopic constraints on the cooling rate, age, and precursor of partial melting of an Allende Type B CAI, Golfball

*Noriyuki Kawasaki[1], Shoichi Itoh[2], Naoya Sakamoto[1], Steven B. Simon[3], Daiki Yamamoto[4], Hisayoshi Yurimoto[1]

1. Hokkaido University, 2. Kyoto University, 3. University of New Mexico, 4. JAXA

Coarse-grained, igneous Ca-Al-rich inclusions (CAIs) in CV chondrites formed through multiple melting events (e.g., MacPherson and Davis, 1993; Yurimoto et al., 1998; Simon et al., 2005; Kawasaki et al., 2018). We conducted *in situ* O-isotope analysis and Al–Mg systematics by secondary ion mass spectrometry of relict and later-crystallized minerals from multiple melting events in an Allende Type B CAI, Golfball. Golfball has a type B CAI bulk composition (Simon and Grossman, 2004) and a unique structure (Simon et al., 2005): a fassaite-rich mantle enclosing a melilite-rich core. Blocky melilite crystals in the core often contain irregularly shaped Al-rich ($Åk_{5–12}$) grains enclosed in strongly zoned ($Åk_{15–70}$) overgrowths. Since the Al-rich melilite grains could not have formed from a melt of Golfball (Beckett et al., 1999), they are relict survived later melting events (Simon et al., 2005). The O-isotopic compositions of the blocky melilite crystals plot along the carbonaceous chondrite anhydrous mineral line, ranging between $\Delta^{17}O \sim -14‰$ and $-5‰$. The Al-rich relict melilite grains and their overgrowths exhibit the same O-isotopic compositions, while the O-isotopic variations for the melilite are spatially distributed. We found O-isotopic variations across several melilite crystals that gradually change within few tens of micrometers. The O-isotopic compositions of the melt could not have been homogenized during the partial melting in that scale and thus O-isotope exchange with the nebular gas was insufficient. Considering a timescale of O self-diffusion in the melt (Yamamoto et al., 2018), a cooling rate of partial melting would be $> \sim 10^4$ K/h. Al–Mg isotope data of relict and later-crystallized minerals perfectly plot on a straight line on an Al–Mg evolutionary diagram. A mineral isochron for Golfball gives initial $^{26}Al/^{27}Al$ of $(4.42 \pm 0.14) \times 10^{-5}$ and initial $^{26}Mg/^{24}Mg$ of $-0.020 \pm 0.047‰$. The O-isotopic compositions and initial values for Golfball are consistent with those for fluffy Type A (Kawasaki et al., 2019) and fine-grained CAIs (Kawasaki et al., 2020), implying its precursor contains fluffy Type A and/or fine-grained CAIs. The multiple melting events for Golfball occurred in very short order after the formation of the precursor.

©2021. Japan Geoscience Union. All Right Reserved.

Chemical and isotopic fractionation of Type B CAI caused by evaporation: An experimental study

*Michiru Kamibayashi[1], Shogo Tachibana[1,3], Noriyuki Kawasaki[2], Daiki Yamamoto[3], Hisayoshi Yurimoto[2]

1. The University of Tokyo, 2. Hokkaido University, 3. Institute of Space and Astronautical Science, Japan Aerospace Exploration Agency

CAIs are the oldest objects formed in the early Solar System, and some subsets of these inclusions show chemical and isotopic features that indicate their formation through high temperature events that resulted in partial melting and evaporation of relatively volatile elements such as Mg and Si. Many laboratory and theoretical studies have discussed evaporation and crystallization of CAI melts (e.g., Stolper and Paque, 1986; Grossman et al., 2002), but the circumstances that made their chemical and isotopic features have not yet been fully understood. These characteristics can be used as a cosmobarometry in the early solar system when appropriate interpretation is given. In this study, crystallization experiments of CAI-like composition melts in nebula-like low pressure hydrogen gas were conducted to investigate the effect of evaporation during crystallization of Type B CAIs and to constrain the nebular pressure during the CAI formation.

The starting material was prepared by mixing SiO_2, TiO_2, Al_2O_3, MgO, and $CaCO_3$ powders at a composition aiming at a precursor composition given on the condensation trajectory of Grossman et al. (2002). Premelted glassy spherical samples on Ir wire loop (2.5 mm in diameter) were used as starting materials. Cooling experiments were conducted using a vacuum furnace equipped with a hydrogen gas flow system. The experiments were conducted from 1420˚C to 1100-1277˚C at controlled cooling rates of 5-50˚C/hr and under three different pressures (P_{H2}=10, 1, 0.1 Pa) to examine the pressure dependence of compositional and textural change. Textural observation and quantitative analysis were conducted by FE-SEM-EDS. Magnesium isotopic analysis of melilite and pyroxene was conducted by SIMS (Cameca ims-1280HR at Hokkaido University).

All of the run products presented significant weight losses which can be attributed to the evaporation of volatile components, Mg and Si. Some of the experimental residues from experiments at P_{H2} = 1 and 10 Pa show their outer regions are enriched in melilite, which resembles the melilite mantle observed in natural Type B1 CAIs. The chemical composition of melilite is Mg-poor at the sample rim and becomes Mg-rich toward the inside, suggesting that these melilites crystallized inward from the melt droplet surface, as inferred from petrological studies of Type B1 (Wark and Lovering, 1982). Melilite composition at the rim is Mg-poor and as low as ~Åk10, which is more depleted in Mg than that expected for the melt of starting composition to crystallize (~Åk20). Such Mg-poor melilite can only crystallize from a melt which has lower Mg and Si concentrations.

For samples which exhibit a well-developed melilite mantle, elevated $d^{25}Mg$ values at the sample rim compared to the interior are observed. This can also be attributed to diffusion-limited evaporation of Mg and Si from the melt surface. Isotope fractionation in a vaporizing melt is controlled by the relative rates of evaporation and diffusion. At higher P_{H2} (e.g., 10 Pa), evaporation could occur faster than diffusive homogenization of the melt, because evaporation is enhanced by the presence of hydrogen (Mendybaev et al., 2021), while diffusion is not. The resulting consequence is preferential crystallization of melilite from the melt droplet surface enriched in Ca and Al. Despite many of the CAIs show lighter isotopic

©2021. Japan Geoscience Union. All Right Reserved.

composition at the margin or show homogeneous isotopic composition throughout the inclusion (e.g., Bullock et al., 2013), such increase in isotope fractionation at the margin of the inclusion is consistent with some of the natural existing CAIs (Goswami, 1994). Although one or more steps needs to be taken into account to explain the isotopic fractionation of the majority of natural CAIs, Type B1-like melilite mantle can indeed crystallize as a result of evaporation in relatively high P_{H2} condition.

Keywords: CAI, evaporation, protosolar disk

©2021. Japan Geoscience Union. All Right Reserved.

I-Xe ages of chondrites and its relevance for solar-wind derived noble gas concentrations

*Koharu Arai[1], Hirochika Sumino[1], Atsushi Takenouchi[2], Shogo Tachibana[1,3]

1. The University of Tokyo, 2. National Institute of Polar Research, 3. Institute of Space and Astronautical Science

The lifetime of protoplanetary disk gas ranges 1-10 million years, which depends on viscous dissipation and photo-evaporation of the disk gas. It is not clear how long the Sun’ s protoplanetary disk held its gas component, during which gas giants formed. Ca-, Al-rich inclusions and chondrules are considered to have formed in the presence of disk gas, but the timing of clearing of disk gas has not yet been tightly constrained [1]. Bajo [2] found a correlation between Solar-wind derived noble gas concentrations and I-Xe ages of brecciated chondrites. Bajo [2] hypothesized that the I-Xe ages, which could represent impact ages [3], of solar-wind-rich meteorites indicated the timing of disk-gas clearing because the solar wind reaches to the surface of small bodies only after the complete dissipation of disk gas. In this study, to test this hypothesis, I-Xe ages and solar-wind noble gas concentrations of Zag (H36), Northwest Africa 801 (CR2) (NWA 801), Ochansk (H4), Nuevo Mercurio (H5) meteorites were determined.

About 30 mg fragments of these meteorites, irradiated with neutrons at the Kyoto University research reactor, were heated in vacuum stepwisely in the temperatures range of 400-1800˚C to extract xenon. After purifying the noble gases extracted at each heating step, xenon isotope ratios were measured using a magnetic-sector-type mass spectrometer VG3600. The obtained $^{129}Xe/^{128}Xe$ ratios of the samples after corrections for low temperature alteration and trapped component were converted to relative I-Xe ages by comparing with $^{129}Xe/^{128}Xe$ ratio of the Shallowater meteorite with the absolute age of 4.5633±0.0004 billion years [4]. About 5 mg fragments of these meteorites were heated in vacuum at 800 and 1700℃ for noble gas analysis. We found that the solar-wind-poor portion of Zag was systematically older (4.551±0.008 and 4.558±0.013 billion years) than the solar-wind-rich portion (4.541±0.010 and 4.551±0.006 billion years) as shown in [2]. NWA 801 is also a solar wind rich meteorite Its I-Xe age is obtained as 4.529±0.016 billion years. The present dataset is broadly consistent with the hypothesis [2], but further data with lesser analytical uncertainties is surely required.

References: [1] I. Pascucci and S. Tachibana (2010) In Protoplanetary Dust (eds. D. Apai and D. S. Lauretta). [2] K. Bajo (2010) Ph.D thesis, Univ. Tokyo. [3] J. D. Gilmour and M. J. Filtness (2019) Nature Astronomy 3, 326. [4] J. D. Gilmour et al. (2006) Meteorit. Planet. Sci. 41, 19.

Keywords: I-Xe ages, solar-wind derived noble gases, chondrite

©2021. Japan Geoscience Union. All Right Reserved.

Requirement of turbulent nebula and dust grains for grain size coarsening in chondrule rims

*Hiroaki Kaneko[1], Sota ARAKAWA[2], Taishi Nakamoto[1]

1. Tokyo Institude of Technology, 2. National Astronomical Observatory of Japan

Chondrules are mm size objects in primitive chondrites. They are coated with fine-grained dust rim (FGRs). The origin of FGRs is still controversial. In a turbulent nebula, free floating chondrules can acquire FGRs through sweeping up dust grains. (nebula origin scenario)

Xiang et al. (2019) examined the internal structures of FGRs formed in such a turbulent nebula. They prepared two different dust populations; monomer grains or dust aggregates. When monomer grains accreted on chondrules, FGRs showed grain size coarsening from the bottom to the top. On the other hand, when aggregates accreted on chondrules, FGRs showed uniform structures. However, Xiang et al. (2019) did not consider dust aggregation and, in what kinds of nebular conditions monomer grains or dust aggregates accrete to form FGRs.

We simulate both aggregation of polydisperse monomer grains and their accretion on chondrules. Aggregate growth can be divided into two stages, monomer-aggregation stage and BCCA-like stage. In the monomer-aggregation stage, smaller monomer grains are incorporated into aggregates faster than larger ones. Most of the monomer grains larger than the average size of aggregates are isolated. In the BCCA-like stage, the evolution of aggregates is similar to the fractal evolution of single size monomer grains. We obtain the requirement for monomer grains to accrete on chondrules. When monomer grains population follows the same power-law size distribution as the Inter Stellar Medium (ISM), the maximum grain size of >1 μm is widely required in a moderately turbulent nebula ($\alpha < 10^{-3}$), while if turbulent intensity is very weak ($\alpha = 10^{-5}$), ~ 10 μm is required. Moreover, size distributions which weigh larger grains more than ISM may be preferable for effective grain size coarsening.

Keywords: chondrule, protoplanetary disk, fine-grained rims

©2021. Japan Geoscience Union. All Right Reserved.

[J] Oral | P (Space and Planetary Sciences)：P-PS Planetary Sciences

Sat. Jun 5, 2021 10:45 AM - 12:15 PM JST | Sat. Jun 5, 2021 1:45 AM - 3:15 AM UTC | Ch.04 Zoom Room 04

[P-PS07] Formation and evolution of planetary materials in the Solar System

convener:Megumi Matsumoto(Graduate School of Science, Tohoku University), Shin Ozawa(Department of Earth Science, Graduate School of Science, Tohoku University), Yuki Hibiya(Submarine Resources Research Center, Japan Agency for Marine-Earth Science and Technology), Noriyuki Kawasaki(Department of Earth and Planetary Sciences, Graduate School of Science, Hokkaido University), Chairperson:Shin Ozawa(Department of Earth Science, Graduate School of Science, Tohoku University), Megumi Matsumoto(Graduate School of Science, Tohoku University)

In this session, we will discuss the material evolution in the Solar System based on extraterrestrial sample analyses and experimental works. We will overlook recent knowledge from primitive materials such as chondrites, interplanetary dust particles, and returned samples by space missions. Research works on meteorite parent body processes such as aqueous alteration, thermal metamorphism, shock metamorphism, volcanic activity, and core-mantle-crust differentiation will also be discussed. The topics of this session include experimental studies which, together with meteorite studies, help us to understand the material formation/evolution in the Solar System as well as processes on meteorite parent bodies. Presentations on new innovative analytical and theoretical techniques in various research fields (chemistry, theoretical calculation, physical property) are highly welcome to improve future studies of the Solar System evolution. This session is J (Japanese) session but English talks are also welcomed.

10:45 AM - 11:00 AM JST | 1:45 AM - 2:00 AM UTC

[PPS07-11] Nanostructures of iron sulfides in lunar soils and implications for the behavior of sulfur on airless bodies.

*Toru Matsumoto[1], Takaaki Noguchi[1], Yu Tobimatsu[1], Dennis Harries[2], Falko Langenhorst[2], Akira Miyake[3], Hiroshi Hidaka[4] (1.Kyushu University, 2.Friedrich Schiller University Jena, 3.Kyoto University, 4.Nagoya University)

11:00 AM - 11:15 AM JST | 2:00 AM - 2:15 AM UTC

[PPS07-12] **Multiple sulfur isotope evidence for the formation of mesosiderite meteorites**

*Shun Mihira[1], Madhusoodhan Satish-Kumar[1], Akira Yamaguchi[2], Tomohiro Usui[3] (1.Department of Geology, Faculty of Science, Niigata University, 2.National Institute of Polar Research, 3.Institute of Space and Astronautical Science, Japan Aerospace Exploration Agency)

11:15 AM - 11:30 AM JST | 2:15 AM - 2:30 AM UTC

[PPS07-13] The shock pressure threshold for producing shock melt veins in basaltic rocks

*Haruka Oono[1], Kosuke Kurosawa[1], Takafumi Niihara[2], Takashi Mikouchi[3], Hidenori Genda[4], Naotaka Tomioka[7], Masahiro KAYAMA[5], Mizuho Koike[6], Yuji Sano[8], Wataru Satake[1], Takafumi Matsui[1] (1.Planetary Exploration Research Center, Chiba Institute of Technology, 2.Shool of Engineering, The University of Tokyo, 3.The University of Museum, The University of Tokyo, 4.Earth-Life Science Institute, Tokyo Institute of Technology, 5.Graduate School of Arts and Sciences, The University of Tokyo, 6.Graduate School of Advanced Science and Engineering, Hiroshima University, 7.Kochi Institute for Core Sample Research, Japan Agency for Marine-Earth Science and Technology , 8.Atmosphere and Ocean Research Institute, The University of Tokyo)

11:30 AM - 11:45 AM JST | 2:30 AM - 2:45 AM UTC

[PPS07-14] **Shock effects in silica minerals in eucrites**

*Rei Kanemaru[1], Akira Yamaguchi[2,1], Naoya Imae[2,1], Atsushi Takenouchi[2], Hirotsugu Nishido[3] (1.The Graduate University for Advanced Studyies (SOKENDAI), 2.National Institute of Polar Research (NIPR), 3.Okayama University of Science (OUS))

11:45 AM - 12:00 PM JST | 2:45 AM - 3:00 AM UTC

[PPS07-15] Effect of ultraviolet C irradiation on surface alteration of basalt due to evaporation of sulfuric acid

*Nobuo Komori[1] (1.The United Graduate School of Education Tokyo Gakugei University)

12:00 PM - 12:15 PM JST | 3:00 AM - 3:15 AM UTC

[PPS07-16] Discussion

Nanostructures of iron sulfides in lunar soils and implications for the behavior of sulfur on airless bodies.

*Toru Matsumoto[1], Takaaki Noguchi[1], Yu Tobimatsu[1], Dennis Harries[2], Falko Langenhorst[2], Akira Miyake[3], Hiroshi Hidaka[4]

1. Kyushu University, 2. Friedrich Schiller University Jena, 3. Kyoto University, 4. Nagoya University

Alteration of materials on airless bodies with time is referred to as space weathering. Extensive studies for space weathering have focused on silicate minerals, whereas the behavior of other minerals in space-exposed environments remains poorly investigated. Recent analysis of Itokawa samples revealed unique features of space weathered rims on iron sulfides, such as selective sulfur loss and the formation of metallic iron whiskers [1]. In this study [2], we investigated surface features of iron sulfides in lunar mature soil grains for the general understanding of sulfide space weathering. We used scanning electron microscopy (SEM) and transmission electron microscopy (TEM) for the observation of sulfides. SEM observations show that iron sulfides have vesicular textures and iron whiskers on their surfaces. Iron sulfides observed using TEM are composed of 2C troilite and NC-pyrrhotite. The space-weathered rim on the iron sulfides is characterized by crystallographic misorientations and the disappearance of superstructure reflections of 2C troilite in electron diffraction patterns. These crystallographic modifications are probably formed by solar wind irradiation. The rim contains opened vesicles that are aligned along the *c*-plane of the iron sulfides, as well as numerous tiny vesicles. The Fe/S ratio at the surface of the rim is higher than in non-altered regions, indicating that sulfur escaped from the sulfide surface. Iron whiskers protrude from the space weathered rim and consist of polycrystalline metallic iron. The sulfide rims and the iron whiskers are both coated with vapor-deposited materials rich in O and Si. The combined processes including the solar wind irradiation, heating during impact events, solar UV radiation, and the thermal cycling may cause vesicular textures, selective sulfur escape from the iron sulfides, and the formation of the iron whiskers. The structures of the space weathered rim support the notion that the enrichment of heavy sulfur isotopes in mature lunar soils is due to space weathering of iron sulfides [3]. The space weathered rims on lunar iron sulfides are similar to those observed in regolith particles from asteroid Itokawa. Therefore, alterations of iron sulfide might be common among airless bodies in the solar system.

[1]Matsumoto et al. 2020, *Nature Communications* 11, 1-8. [2] Matsumoto et al. 2021, *Geochimica Cosmochimica Acta*, accepted. [3] Kaplan and Smith 1970 *Science* 167, 541-543.

Keywords: Moon, iron sulfides, space weathering

©2021. Japan Geoscience Union. All Right Reserved.

Multiple sulfur isotope evidence for the formation of mesosiderite meteorites

*Shun Mihira[1], Madhusoodhan Satish-Kumar[1], Akira Yamaguchi[2], Tomohiro Usui[3]

1. Department of Geology, Faculty of Science, Niigata University, 2. National Institute of Polar Research, 3. Institute of Space and Astronautical Science, Japan Aerospace Exploration Agency

Mesosiderites and HED (howaldite, eucrite, diogenite) meteorites are considered to have a common origin, from the asteroid Vesta. However, the processes that led to the origin of mesosiderites and their relation with HED's are not clear yet. In this respect, multiple sulfur isotopic composition may track their petrological relationships and suggest genetic links of mesosiderites with other meteorites. In this study, multiple sulfur isotopic composition of selected mesosiderites were measured and a comparison with othermeteorites is attempt to constrain the formation process of mesosiderites.

Although Clayton et al. (1996) suggested genetic links between pallasites, IIIAB iron meteorites, and HED meteorites based on the $D^{17}O$ values, the $d^{34}S$ and $D^{33}S$ relationships of the pallasites and IIIAB iron meteorites indicate that they do not match with those of HED meteorites (Rai et al., 2005; Dottin et al., 2018). The sulfur isotopic composition of mesosiderites in this study indicates similarities with IIIAB iron meteorites and pallasites but not with HED. This suggests that the sulfur isotopic composition may not preserve their true parent body information, but probably represent information on some reactions or mixing during their formation.

A recent study suggests that the formation process of mesosiderites can be explained by a hit-and-run model (Haba et al., 2019). Rai et al. (2005) has reported Mass-Independent Fractionation (MIF) for HED meteorites, however in our study the mesosiderites are devoid of MIF. This indicates two possibilities, either mixing of Vesta with the impactor or there is no genetic links between HED and mesosiderites. In our presentation we will discuss about these two possibilities on the formation process of mesosiderites using sulfur isotopic composition in comparison with the existing data of HED meteorites.

References

1. Antonelli M. A., Kim S-T., Pters M., Labidi J., Cartigny P., Walker R. J., Lyons J. R., Hoek J., and Farquhar J., Early inner solar system origin for anomalous sulfur isotopes in differentiated protoplanets, PNAS, 111, 17749-17754, (2014).
2. Clayton R. N. and Mayeda T.K., Oxygen isotope studies of achondrites. Geochim. Cosmochim. Acta, 60, 1999-2017, (1996).
3. Dottin J. W., Farquhar J., and Labidi J., Multiple sulfur isotopic composition of main group pallasites support genetic links to IIIAB iron meteorites, Geochim. et Cosmochim. Acta, 224, 276-281, (2018).
4. Haba M. K., Wotzlaw J-F., Lai J-Y., Yamaguchi A., and Schonbachler M., Mesosiderite formation on asteroid 4 Vesta by a hit-and-run collision, Nature Geoscience, 12, 510-515, (2019).
5. Rai V. K., Jackson T. L., and Thiemens M. H., Photochemical mass-independent sulfur isotopes in achondritic meteorites, Science, 309, 1026-1065, (2005).

Keywords: Mesosiderite, Sulfur isotope

©2021. Japan Geoscience Union. All Right Reserved.

The shock pressure threshold for producing shock melt veins in basaltic rocks

*Haruka Oono[1], Kosuke Kurosawa[1], Takafumi Niihara[2], Takashi Mikouchi[3], Hidenori Genda[4], Naotaka Tomioka[7], Masahiro KAYAMA[5], Mizuho Koike[6], Yuji Sano[8], Wataru Satake[1], Takafumi Matsui[1]

1. Planetary Exploration Research Center, Chiba Institute of Technology, 2. Shool of Engineering, The University of Tokyo, 3. The University of Museum, The University of Tokyo, 4. Earth-Life Science Institute, Tokyo Institute of Technology, 5. Graduate School of Arts and Sciences, The University of Tokyo, 6. Graduate School of Advanced Science and Engineering, Hiroshima University, 7. Kochi Institute for Core Sample Research, Japan Agency for Marine-Earth Science and Technology , 8. Atmosphere and Ocean Research Institute, The University of Tokyo

Introduction

Shock metamorphic textures record the impact history of meteorite parent bodies. Shock features in meteorites have been classified into progressive stages (shock stages) based on petrological and mineralogical textures (e.g., Stöffler et al., 2018), and the classification has been used to decode the impact conditions, including projectile diameter and impact velocity. Stöffler et al., 2018 summarized the classifications for a variety of minerals and rocks as the table, which is known as “the Stöffler table”, by using a number of previous results of uniaxial-shock recovery experiments. Recently, Kanemaru et al. 2020 independently constructed a detailed shock metamorphic classification pertaining to basaltic eucrites. They showed that the shock stages of the Stöffler table for mafic rocks (Table M) could be further divided into a few shock degrees. In this study, we performed a shock recovery experiment with terrestrial basalt samples using decaying shock waves. We recovered the shocked sample which has experienced a wide range of shock pressures and temperatures. The shock textures in the recovered sample were compared with the previous study (Kanemaru et al., 2020). The peak pressures and temperatures depending on the initial locations in the target were estimated using numerical simulations under the same impact conditions.

Sample and Methods

We used terrestrial basalt samples (Inner Mongolia), which are composed mainly of plagioclase, pyroxene, and olivine, as a target. The sample was shaped to a cylinder (30 mm in diameter, 24 mm in height), and it was set in titanium (Ti) container. A polycarbonate sphere was used as a projectile. The impact velocity was 7.3 km s^{-1}. A thin section of the recovered sample was observed by optical microscopy and a Scanning Electron Microprobe (SEM). We estimated pressures and temperature in the sample based on petrological and mineralogical textures. In addition, peak pressures and temperatures in the target were also numerical estimated with the iSALE shock physics code (Amsden et al., 1980, Ivanov et al., 1997, Wünnemann et al., 2006). The results from the above two different estimations were compared with each other.

Results and Discussion

Plagioclase, pyroxene, and olivine in the shocked sample around the epicenter in the recovered sample showed a shock feature called undulatory extinction. Several shock melt veins (up to 4 μm in width) were identified around the epicenter. The presence of vesicles (~2 μm in diameter) in the melt veins would be evidence of volatile degassing due to melting. The plagioclase grains adjoining the shock melt veins exhibit undulatory extinction, but they do not exhibit planar deformation features (PDFs), mosaicism, and vitrification. According to the Stöffler table M, the recovered sample is classified into the shock stage S2 in terms of the shock features in plagioclase. The sample also belongs to the shock stage S3 based on the fact that shock melt veins are produced due to some local effects. In contrast, the textures observed in

©2021. Japan Geoscience Union. All Right Reserved.

our shocked sample uniquely correspond to the shock degree C proposed by Kanemaru et al. (2020). The iSALE simulations showed that the pressures and temperatures around shock melt veins were estimated to be up to 10 GPa and 600 K, respectively. Therefore, we recognized that the shock degree C (Kanemaru et al., 2020) was formed due to a shock compression to ~10 GPa, the local temperature could be about 800 K higher than the calculated temperature (the temperature is estimated from the solidus of dry basalt), and the Stöffler table does not predict such the temperature excess.

Conclusion

We performed a shock recovery experiment and determined the required pressure for producing shock melt veins in basaltic rocks to be ~10 GPa. The shock features in the collected sample are similar to the textures in basaltic eucrites at the shock degree C. The peak temperatures in the sample around the shock melt veins were estimated to be ~600 K, which is much lower than the solidus at the reference pressure. Thus, the local temperature could be much higher than the expected one from the conventional shock stage (Stöffler table).

Keywords: shock metamorphism, mafic rocks, basalt, shock experiment

©2021. Japan Geoscience Union. All Right Reserved.

Shock effects in silica minerals in eucrites

*Rei Kanemaru[1], Akira Yamaguchi[2,1], Naoya Imae[2,1], Atsushi Takenouchi[2], Hirotsugu Nishido[3]

1. The Graduate University for Advanced Studyies (SOKENDAI), 2. National Institute of Polar Research (NIPR), 3. Okayama University of Science (OUS)

Eucrite is a group of differentiated meteorites probably originated from the Vestan crust [1]. Recently, we defined the progressive shock degrees (A-E) of eucrites on the basis of petrographic and X-ray diffraction methods [2]. Here, we studied shock effects in eucrites of shock degrees C-E focusing on shock textures of silica minerals.

We studied polished thin sections of five eucrites, Y 980433 (shock degree: D), Y-792510 (C), A-881747 (C), Cachari (D), and A-87272 (E) using a micro-Raman spectrometer (Renishaw inVia), a Chroma CL (Gatan), and an energy dispersive spectrometer (Oxford Aztek Energy) attached to the JEOL JSM-7100 field emission scanning electron microscope at NIPR.

Eucrites studied here contain significant amounts (~10 vol%) of silica minerals. We identified tridymite, quartz, and silica glass in the host basaltic rocks, and quartz, coesite, stishovite in shock melt veins (Table 1). In eucrites with shock degree C, characterized by the absence of maskelynite, silica minerals do not show clear shock textures.

Eucrites with shock degree D, are characterized by the presence of maskelynite near shock veins, but these eucrites do not contain maskelynite in the basaltic host (unmelted portions). Maskelynite near shock veins was produced by shock under the heat from shock melt veins [e.g., 3]. Tridymite in the basaltic host in Cachari and Y 980433 is converted to glass (~50 vol%). Patches of remnant tridymite are heterogeneously distributed in silica glass. The tridymite (partly converted to glass) preserves original lath shape. In contrast, Y-790266 (D) contains quartz and cristobalite, and is not converted into glass. The facts indicate that the amorphization pressure of tridymite is lower than those of quartz, cristobalite, and calcic plagioclase. A-87272 (shock with shock degree: E) is characterized by the abundant maskelynite (>50 vol%). Most of the silica minerals (~90 vol%) in the host are converted to glass. We found traces of quartz and tridymite.

Shock veins are commonly observed in eucrites with shock degrees C or higher[2]. We found coesite and stishovite in Y-790266, quartz, stishovite, and coesite in Cachari, and silica glass in Y 980433. The occurrences of these silica minerals are controlled by local pressure-temperature paths in or near the shock melt veins [e.g., 4].

References

[1] Binzel R.P. and Xu S. (1993) *Science* 260, 186-191.
[2] Kanemaru R. et al. (2020) *Polar Science* 26, 100605.
[3] Yamaguchi A. et al. (2002) *High-Pressure Shock Compression of Solids V*. Springer, 29–44 chap. 2.
[4] Miyahara M. et al. (2014) *PNAS* 111, 30, 10939-10942.

Keywords: Eucrite, silica minerals, Shock metamorphism

©2021. Japan Geoscience Union. All Right Reserved.

Table 1. Silica minerals in studied eucrites.

Sample	Classification	Shock degree [2]	Silica minerals Lithology	
			Host	Shock vein
Y-792510	Basaltic	C	Trd, Qtz	-
A-881747	Basaltic	C	Trd, Qtz	Qtz
Y-790266	Basaltic	D	Qtz, Cri	Coe, Sti
Cachari	Basaltic	D	Trd, Qtz Glass (~50 vol%)	Qtz, Sti, Coe
Y 980433	Cumulate	D	Trd, Qtz,Glass (~50 vol%)	-
A-87272	Basaltic	E	Trd, Qtz, Glass (~90 vol%)	Qtz, Sti

Qtz: Quartz, Trd: Tridymite, Cri: Cristobalite, Sti: Stishovite, Coe: Coesite.

©2021. Japan Geoscience Union. All Right Reserved.

Effect of ultraviolet C irradiation on surface alteration of basalt due to evaporation of sulfuric acid

*Nobuo Komori[1]

1. The United Graduate School of Education Tokyo Gakugei University

A large amount of iron oxide, sulfate, chloride, etc. have been detected on the surface of Mars, which is the cause of the reddish-brown color of the surface of Mars. Also, much evidence has led to the belief that liquid water once existed widely.
As an research activity of the science club in the junior high school, the author has irradiated basalt and iron olivine soaked in water or an acidic aqueous solution with ultraviolet rays and investigated their changes (Komori, 2020). Studies related to weathering of the surface of Mars include Golden et al. (2005) and Cole (2015). No experimental research has been conducted to investigate changes in basalt in sulfuric acid while irradiating with ultraviolet rays.

Ⅰ Research purpose

In the process of drying basalt soaked in sulfuric acid aqueous solution, the effect of ultraviolet rays C on the alteration of basalt is investigated and compared with related studies.

Ⅱ Method

1 Immerse two shaped basalt samples in sulfuric acid for 24 hours. Sulfuric acid is a mixture of boiled purified water and a stock solution of sulfuric acid.
2 Take out the two basalt samples from sulfuric acid and put them in separate test tubes with the surface wet. Replace the air with nitrogen.
3 Set the two test tubes in the ultraviolet irradiator. The ultraviolet irradiator is a bundle of four 20W germicidal lamps, and irradiates the sample with ultraviolet C of about 20W / m2. One of the two test tubes was directly irradiated (UVC) and the other was covered with aluminum foil so that it was not irradiated (N).
4 Every few days after the ultraviolet irradiation, the test tube was taken out from the ultraviolet irradiator, and the basalt sample was visually observed and photographed. After that, the air in the test tube was replaced with nitrogen and returned to the ultraviolet irradiator.
5 After the experiment, the analysis of the brown powder generated on the sample surface was analyzed by XRD. The surface of the sample was photographed with a digital microscope.

Ⅲ Result

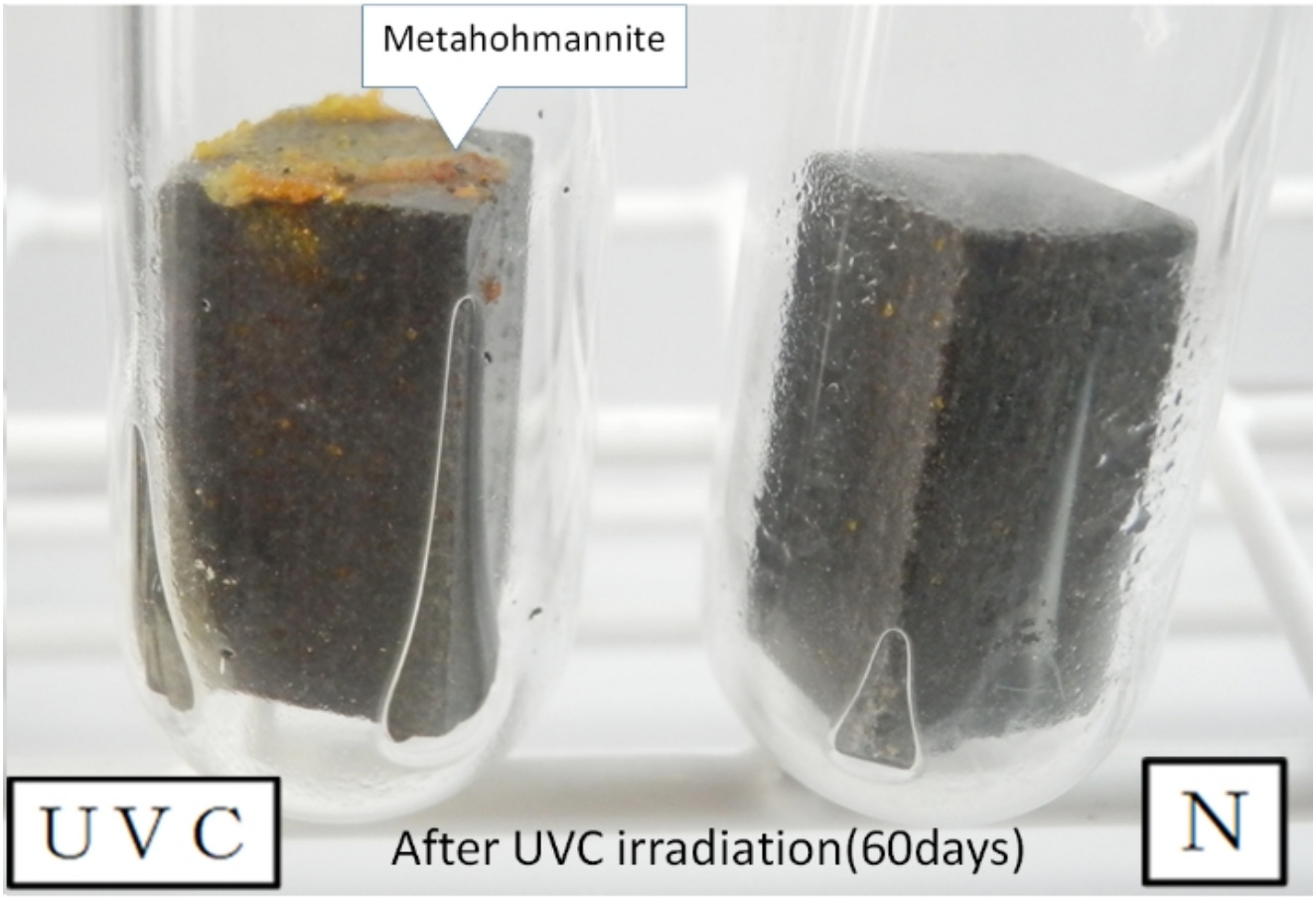
UVC produced a powdery substance on the surface of the basalt. XRD revealed that the brown powder formed on the sample UVC surface was ferric sulfate, mainly metahomanite, and the white powder was gypsum. In the sample N, it seems that a slight amount of gypsum was formed on the entire surface.

Ⅳ Discussions

On Mars in the past, it is possible that irradiation of ultraviolet C produced minerals containing Fe3+, such as metahomanite, in the process of drying basalt soaked in the sea of sulfuric acid due to regression.

Keywords: Mars, ultraviolet rays C, sulfuric acid, trivalent iron, evaporation

©2021. Japan Geoscience Union. All Right Reserved.



©2021. Japan Geoscience Union. All Right Reserved.

[J] Oral | P (Space and Planetary Sciences) | P-PS Planetary Sciences

[P-PS07] Formation and evolution of planetary materials in the Solar System

convener:Megumi Matsumoto(Graduate School of Science, Tohoku University), Shin Ozawa(Department of Earth Science, Graduate School of Science, Tohoku University), Yuki Hibiya(Submarine Resources Research Center, Japan Agency for Marine-Earth Science and Technology), Noriyuki Kawasaki(Department of Earth and Planetary Sciences, Graduate School of Science, Hokkaido University), Chairperson:Shin Ozawa(Department of Earth Science, Graduate School of Science, Tohoku University), Megumi Matsumoto(Graduate School of Science, Tohoku University)

Sat. Jun 5, 2021 10:45 AM - 12:15 PM Ch.04 (Zoom Room 04)

In this session, we will discuss the material evolution in the Solar System based on extraterrestrial sample analyses and experimental works. We will overlook recent knowledge from primitive materials such as chondrites, interplanetary dust particles, and returned samples by space missions. Research works on meteorite parent body processes such as aqueous alteration, thermal metamorphism, shock metamorphism, volcanic activity, and core-mantle-crust differentiation will also be discussed. The topics of this session include experimental studies which, together with meteorite studies, help us to understand the material formation/evolution in the Solar System as well as processes on meteorite parent bodies. Presentations on new innovative analytical and theoretical techniques in various research fields (chemistry, theoretical calculation, physical property) are highly welcome to improve future studies of the Solar System evolution. This session is J (Japanese) session but English talks are also welcomed.

12:00 PM - 12:15 PM

[PPS07-16]Discussion

©Japan Geoscience Union

[J] Poster | P (Space and Planetary Sciences)：P-PS Planetary Sciences

Sat. Jun 5, 2021 5:15 PM - 6:30 PM JST | Sat. Jun 5, 2021 8:15 AM - 9:30 AM UTC | Ch.02_2

[P-PS07] Formation and evolution of planetary materials in the Solar System

convener:Megumi Matsumoto(Graduate School of Science, Tohoku University), Shin Ozawa(Department of Earth Science, Graduate School of Science, Tohoku University), Yuki Hibiya(Submarine Resources Research Center, Japan Agency for Marine-Earth Science and Technology), Noriyuki Kawasaki(Department of Earth and Planetary Sciences, Graduate School of Science, Hokkaido University)

In this session, we will discuss the material evolution in the Solar System based on extraterrestrial sample analyses and experimental works. We will overlook recent knowledge from primitive materials such as chondrites, interplanetary dust particles, and returned samples by space missions. Research works on meteorite parent body processes such as aqueous alteration, thermal metamorphism, shock metamorphism, volcanic activity, and core-mantle-crust differentiation will also be discussed. The topics of this session include experimental studies which, together with meteorite studies, help us to understand the material formation/evolution in the Solar System as well as processes on meteorite parent bodies. Presentations on new innovative analytical and theoretical techniques in various research fields (chemistry, theoretical calculation, physical property) are highly welcome to improve future studies of the Solar System evolution. This session is J (Japanese) session but English talks are also welcomed.

[PPS07-P01] Study of porosity change of simulated chondrite materials by impact experiments

*Akiko Nakamura[1], Yuki Hanzawa[2], Tomomi Omura[3], Sunao Hasegawa[4] (1.Graduate School of Science, Kobe University, 2.Faculty of Science, Kobe University, 3.Osaka Sangyo University, 4.Japan Aerospace Exploration Agency)

[PPS07-P02] Formation process of a multi-layered chondrule rim and relationship of fine-grained rim and matrix in two LL chondrites

Yukina Hashimoto[1], *Tomoki Nakamura[1], Megumi Matsumoto[1] (1.Department of Earth and Planetary Materials Sciences, Faculty of Science, Tohoku University)

[PPS07-P03] Mineralogical variations of CM chondrites revealed from X-ray diffraction method: Application to the parent body evolution

*Naoya Imae[1,2], Makoto Kimura[1], Akira Yamaguchi[1,2] (1.Antarctic Meteorite Research Center, National Institute of Polar Research, 2.The Graduate University for Advanced Studies (SOKENDAI))

[PPS07-P04] **Combined XRD-XCT-FIB-TEM analysis of experimentally heated Murchison CM chondrite**

*Megumi Matsumoto[1], Junya Matsuno[2], Akira Tsuchiyama[2,3], Yuri Fujioka[1], Tomoki Nakamura[1], Akira Miyake[4], Masahiro YASUTAKE[5], Shota Okumura[4], Kentaro Uesugi[5], Akihisa Takeuchi[5] (1.Graduate School of Science, Tohoku University, 2.Research Organization of Science and Technology, Ritsumeikan University, 3.Guangzhou Institute of Geochemistry, Chinese Academy of Science GIG, CAS , 4.Graduate School of Science, Kyoto University, 5.Japan Synchrotron Radiation Research Institute/SPring-8)

[PPS07-P05] Variations in initial 26Al/27Al ratios among condensate CAIs from CV chondrites

*Noriyuki Kawasaki[1], Naoya Sakamoto[2], Hisayoshi Yurimoto[2] (1.Department of Earth and Planetary Sciences, Graduate School of Science, Hokkaido University, 2.Hokkaido University)

[PPS07-P06] Petrology and mineralogy of a coarse-grained CAI “TTA01” from Allende

*Tadakatsu Yamasaki[1], Noriyuki Kawasaki[1], Hisayoshi Yurimoto[1] (1.Hokkaido University)

[PPS07-P07] **Development of a chemical separation procedure for determining the initial niobium-92 abundance of chondritic components**

*Yuki Hibiya[1] (1.Submarine Resources Research Center, Japan Agency for Marine-Earth Science and Technology)

[PPS07-P08] Motion of silicate particles in protoplanetary disk

*Tamami Okamoto[1], Shigeru Ida[1] (1.Earth-Life Science Institute, Tokyo Institute of Technology)

[PPS07-P09] Thermal history of andesitic achondrite Erg Chech 002

*Akira Yamaguchi[1], Atsushi Takenouchi[1], Jean-Alix Barrat[2] (1.National Institute of Polar Research, 2.UBO-IUEM)

[PPS07-P10] Excess silica in plagioclase in some mesosiderites

*naoji sugiura[1], tomoko Arai[1] (1.Chiba Institute of Technology)

[PPS07-P11] The petrological and mineralogical descriptions of nakhlites NWA 6148 and NWA 10153

*Kakeru Kukihara[1], Masaaki Miyahara[1], Akira Yamaguchi[2], Yoshio Takahashi[3], Yasuo Takeichi[4], Naotaka Tomioka[5], Eiji Ohtani[6] (1.hiroshima university , 2.National Institute of Polar Research, 3.Tokyo university, 4.Institute of Materials Structure Science, High-Energy Accelerator Research Organization (KEK), 5.Kochi Institute for Core Sample Research, Japan Agency for Marine-Earth Science and Technology (JAMSTEC), 6.Tohoku university)

Study of porosity change of simulated chondrite materials by impact experiments

*Akiko Nakamura[1], Yuki Hanzawa[2], Tomomi Omura[3], Sunao Hasegawa[4]

1. Graduate School of Science, Kobe University, 2. Faculty of Science, Kobe University, 3. Osaka Sangyo University, 4. Japan Aerospace Exploration Agency

Primordial small bodies formed by the aggregation of matrix and chondrules have a porous structure that depends on the matrix fraction. Compression due to self-gravity alone is not sufficient for the reduction of porosity from those of the primordial small bodies to the porosity of chondrites [1, 2]. In addition to thermal evolution and aqueous alteration, compression by impact is considered to be a factor of porosity reduction. In a previous study, analogue materials of chondrite parent body consisting of dust and beads sealed in a cylindrical vessel was compressed by an impact of an aluminum cylinder to examine the degree of compaction due to impact [1]. In this study, we investigate the porosity change during the crater formation and material ejection process by impact on the surface of the chondrite parent body.

Samples were prepared by mixing 1.5 μm irregularly shaped silica particles and 4.3 μm fly-ash as matrix simulants, and glass beads of 220 μm in diameter as chondrules, adding water to the mixture, compressing the mixture at 7 -10 kPa, and then drying the mixture at 50 ˚C. The volume ratio of glass beads was 13% (Sample A) and 35% (Sample B). The porosity after drying was 62% (Sample A) and 38% (Sample B), respectively.

For these samples, SUS and aluminum spheres 3.2 mm in diameter were impacted at a speed of 4.5 km/s using a two-stage light gas-gun at the Institute of Space and Astronautical Science (ISAS). Flash X-ray transmission images were acquired at several timings during 6 ~ 3000 μs after the impact. In all samples, the growth of the crater cavity over time was captured. In Sample A, a compacted layer was formed just below the cavity, and it was observed that the compacted layer expanded after a lapse of time from the impact. It is considered that the porosity of the compacted layer depends on the distance from the impact point. However, assuming that it is constant for simplicity, the average porosity of the compacted layer was calculated to be 23 ~ 54%. On the other hand, in the sample B, the compacted layer could not be detected. This is considered to be because the spatial resolution and S/N of the flash X-ray image were not sufficient to capture the change in the porosity.

This research was supported by the Hypervelocity Impact Facility (former facility name: The Space Plasma Laboratory) of ISAS, JAXA.

[1] Beitz, et al., Icarus 225, 558-569, 2013.

[2] Omura, T. and Nakamura, A. M. Planetary Science Journal, accepted.

Keywords: chondrite, porosity, impact, compaction, small bodies

©2021. Japan Geoscience Union. All Right Reserved.

Formation process of a multi-layered chondrule rim and relationship of fine-grained rim and matrix in two LL chondrites

Yukina Hashimoto[1], *Tomoki Nakamura[1], Megumi Matsumoto[1]

1. Department of Earth and Planetary Materials Sciences, Faculty of Science, Tohoku University

Chondrules in primitive chondrites are commonly surrounded by two types of rims: coarse-grained rims and fine-grained rims. Many studies of CM chondrites suggest that fine-grained rims are formed by the accretion of dust onto chondrules in the solar nebula (e.g., Metzler et al., 1992). However, recent studies of CV chondrites show that fine-grained rims formed by parent-body process (e.g., Tomeoka and Ohnishi, 2015). No conclusions are obtained so far as to whether the rims were formed by the parent body process or the nebular process.

In this study, to uncover the origin of fine-grained rims and the relationship of fine-grained rim and matrix material in ordinary chondrites, we investigated mineralogy and chemical composition of coarse-grained rims, fine-grained rims and matrix material in Y-75273 (LL3.2) and Y-74660 (LL3.0) using an optical microscope, FE-SEM, and FE-EPMA.

Many chondrules in Y 75273 are surrounded by fine-grained rims. Among them, we found a multi-layered chondrule rim. The rim consists of five layers made up with four inner coarse-grained rims (1-4th layer) and one outermost fine-grained rim (5th layer). Mineral combination of 1-4th layer is similar, but relative mineral abundance, grain size, and chemical composition of the minerals differ among the four rims. The boundaries between the 3rd and 4th layer, between the 4th and 5th layer are distinct and smooth (no topographic depressions).

Defocused (10 μm diameter) electron beam analysis of each layer shows compositional variation in individual rims: in a Si–Mg–Fe ternary diagram, the 2nd layer data distribute close to the solar abundance and the 1st- and 2nd- layer data make a trend from solar toward the Si-apex suggestive of addition of Si-rich material such as silicate glass, while the 3rd and 4th layer data distribute from solar to the Fe-apex indicative of addition of Fe-rich material such as Fe sulfide and Fe–Ni metal. On the other hand, the 5th-layer data fall on the different compositional field in Fe-rich areas relative to solar. The compositional field of the 5th layer overlaps those of the single rims formed on many other chondrules in this meteorite and both rims show irregular-shape surface morphology, suggesting that they were produced by brecciation in the same meteorite parent body. Texture, mineralogy, and chemical compositions of the multi-layered rim in the Y-75273 suggest that the outermost fine-grained rim was formed by parent-body process after inner coarse-grained rims were formed by multiple heating in the solar nebula.

Defocused electron beam analysis of fine-grained rims and matrix shows compositional variation: in a Si–Mg–Fe ternary diagram, the fine-grained-rims fall on the Fe-rich areas relative to solar, while matrix falls on the Si-rich areas relative to solar, suggesting that the fine-grained rims and matrix are different material. The constituent minerals of the fine-grained rims and matrix, such as olivine and pyroxene, differ in the chemical composition. Olivine composition of the fine-grained rim (Fa_{77-80}) differs from matrix (Fa_{38-48}), indicating that these olivines are not chemically equilibrated during thermal metamorphism. The mesostasis glass of the chondrules which is the most susceptible to alteration, is clear and seems not to have altered, suggesting that aqueous alteration did not cause the exchange of elements between the chondrules and the fine-grained rims and between the chondrules and the matrix. This suggests that the

©2021. Japan Geoscience Union. All Right Reserved.

difference in chemical composition between the fine-grained rim and the matrix was not established by secondary alteration, rather they are originally different material.
This compositional difference between matrix and fine-grained rims is observed in both Y-75273 and Y-74660. This suggests that the fine-grained materials in the LL chondrite formation region could have changed over time or location, because earlier-formed fine-grained rims differ from later-formed matrix material.

Keywords: Chondrule rim, LL chondrites, Fine-grained rim

©2021. Japan Geoscience Union. All Right Reserved.

Mineralogical variations of CM chondrites revealed from X-ray diffraction method: Application to the parent body evolution

*Naoya Imae[1,2], Makoto Kimura[1], Akira Yamaguchi[1,2]

1. Antarctic Meteorite Research Center, National Institute of Polar Research, 2. The Graduate University for Advanced Studies (SOKENDAI)

Introduction
CM chondrites have been characterized by aqueous alteration in the parent body [e.g.,1,2], and subtypes have been identified [3,4]. Findings of dehydrated [5,6] and unaltered samples [7] added new views. We studied the significant variations. We newly modeled the parent body evolution.

Experiments
Samples are QUE 97990 (subtype, 2.6), Murchison (2.5), DOM 03183 (2.5), Y-791198 (2.4), QUE 99355 (2.3), SCO 06043 (2.0), MET 01070 (2.0), Y 980036 (2.4-2.5 and heating stage II), Y 980051 (2.4-2.5 II), and Jbilet Winselwan (2.4-2.7 II). Three types of equipment were mainly used: X-ray diffractometer (XRD), field emission scanning electron microscope, and electron probe microanalyzer. The measurement conditions for XRD are the same as [8]. Focused Miller indices for XRD are the same as [9].

Results and Discussion
Systematic change is observed for subtypes of unheated CMs: The intensities of olivine, pyroxenes, and kamacite plus troilite decrease with decreasing subtypes—instead, serpentines (antigorite and cronstedtite) increase. Tochilinite abundance is the highest at the intermediate subtype (2.5-2.3). The relative intensity of antigorite to cronstedtite increases with decreasing subtype. Y 980036 and Y 980051 are entirely dehydrated, and matrices are low-crystalline. The sulfide assemblages correspond to category B [10]. Chondrule phenocrysts of forsterite olivine, ferroan olivine, and clinoenstatite have not been altered. Although the mesostasis has been altered. Cronstedtite and tochilinite in Jbilet Winselwan are decomposed, but antigorite is partly survived. [11] also showed that Jbilet Winselwan is a regolith breccia. We also confirmed that textures and analyzed compositions are consistent with XRD.

Application to the parent body evolution
Based on the observed mineralogical variations of CM chondrites, we will consider the evolutional processes of the parent body, focusing on dehydration. The hydrous alteration degree may be related mainly to temperature, potential of hydrogen, and water/rock ratio [2,12]. On the other hand, after once hydrated, dehydration has been theoretically predicted in the early history of the parent body's interior in a few million years after the formation [13]. Due to the latent heat of water, the peak metamorphic temperature is limited to be 600-800 K for the hydrous parent body with 100 km diameter, lower than that of anhydrous parent body [13]. The textures and compositions for dehydrated CM should be controlled by the diffusion length of Mg-Fe diffusion of olivine. The diffusion feature between forsterite and ferroan olivines is not noticed from intermediately heated CM. The absence of the diffusion is consistent with the estimation that any significant diffusion for the intermediate depth is not expected within the cooling time scale of 1-10 million years from 600-700K. The present model on parent body evolution is seemingly consistent with our observations.

References
[1] Tomeoka K. and Buseck P. R. 1985. Geochim. Cosmochim. Acta 49:2149. [2] Zolensky M. et al. 1993.

©2021. Japan Geoscience Union. All Right Reserved.

Geochim. Cosmochim. Acta 57:3123. [3] Rubin A. 2007. Geochim. Cosmochim. Acta 71:2361. [4] Howard K. T. 2011. Geochim. Cosmochim. Acta 75:2735. [5] Nakamura T. 2005. J. Min. Pet. Sci. 100:260. [6] King A. et al. 2019. Meterit. Planet. Sci. 54:521. [7] Kimura M. et al. 2020. Polar Sci. 17:100565. [8] Imae N., et al. 2019. Meterit. Planet. Sci. 54:919. [9] Imae N. and Kimura M. 2020. Polar Science Symp. abstract. [10] Kimura M. et al. 2011. Meterit. Planet. Sci. 46:431. [11] Zolensky M., et al. 2016. 47th LPSC. #2148. [12] Brearley A. J. 2006. In Meteorites and the Early Solar System II. [13] Grimm R. E. and McSween H. Y. 1989. Icarus 82:244.

Keywords: CM chondrites, X-ray diffraction, hydrous minerals, Antarctic meteorites, meteorite parent body, metamorphism

©2021. Japan Geoscience Union. All Right Reserved.

Combined XRD-XCT-FIB-TEM analysis of experimentally heated Murchison CM chondrite

*Megumi Matsumoto[1], Junya Matsuno[2], Akira Tsuchiyama[2,3], Yuri Fujioka[1], Tomoki Nakamura[1], Akira Miyake[4], Masahiro YASUTAKE[5], Shota Okumura[4], Kentaro Uesugi[5], Akihisa Takeuchi[5]

1. Graduate School of Science, Tohoku University, 2. Research Organization of Science and Technology, Ritsumeikan University, 3. Guangzhou Institute of Geochemistry, Chinese Academy of Science GIG, CAS , 4. Graduate School of Science, Kyoto University, 5. Japan Synchrotron Radiation Research Institute/SPring-8

Hayabusa2 spacecraft succeeded to touchdown on the surface of C-type asteroid 162173 Ryugu and brought Ryugu surface materials to the earth in the last December. Spectroscopic observations [1] suggested that Ryugu surface consists of materials which are similar to partially dehydrated carbonaceous chondrites. This means that heated hydrous carbonaceous chondrites are the closest analogues to Ryugu surface material. Recently, we performed synchrotron radiation-based X-ray diffraction (SR-XRD) and X-ray computed nanotomography (SR-XCT) of unheated and experimentally heated (400 ˚C-50 hrs and 600 ˚C -50 hrs) Murchison CM chondrite particles (~50 μm in size) [2] as rehearsal analyses [3]. The SR-XCT results will be presented by Matsuno et al. and Sun et al. in this JpGU meeting. The synchrotron analyses revealed that hydrous phases, tochilinite-cronstedtite intergrowth (TCI) and Mg-rich serpentine, in the Murchison matrix were partially decomposed by 400 ˚C -50 hrs heating without significant changes in CT images. In this study, we extracted an ultrathin section from a 400 ˚C -50 hrs heated Murchison particle, which was previously analyzed by SR-XCT, using a focused ion beam system (FIB), and analyzed it by transmission electron microscopy (TEM) to investigate microstructural changes in the matrix caused by the heating.

The target slice section in the 400 ˚C -50 hrs heated Murchison particle for TEM observation was selected based on CT images. In the selection, we set a few mineral grains (0.5 to a few μm in size) in the CT images as specific phases which should be included in the ultrathin section. Then, the Murchison particle was mounted on the FIB sample stage appropriately and sliced carefully by comparing the FIB cutting surface images and the CT slice images one by one. Finally, we successfully obtained an ultrathin section (~20 ×20 μm) containing all the specific grains.

TEM observation revealed that the ultrathin section contains partially decomposed TCIs, which were replaced by relatively large (a few hundred of nm) Fe-Mg rich silicates and clusters of 10-20 nm sized magnetite. Previous SR-XRD analysis [3] suggested the presence of abundant magnetite in 400 ˚C -50 hrs heated Murchison samples, and is consistent with the TEM observation. The XRD peaks of magnetite were characteristic to 400 ˚C heated samples and were not found for unheated and 600 ˚C heated Murchison samples [3]. Therefore, the magnetite nano-grains replacing TCIs may be able to use as an indicator of relatively low degrees of heating for CM type chondrites. We will perform further FIB-TEM analysis and summarize microstructural changes in the Murchison matrix by 400 ˚C -50 hrs heating and other degrees of heating.

[1] Kitazato et al. (2019) *Science* **364**. [2] Mogi et al. (2017) *The 80th Annual Meeting of the Meteoritical Society*, Abstract #6225. [3] Matsumoto et al. (2020) *The JpGU-AGU joint meeting 2020*, Abstract PPS10-P09.

©2021. Japan Geoscience Union. All Right Reserved.

Keywords: heated CM chondrite, Hayabusa2 mission, synchrotron XCT, synchrotron XRD, FIB-TEM

©2021. Japan Geoscience Union. All Right Reserved.

Variations in initial 26Al/27Al ratios among condensate CAIs from CV chondrites

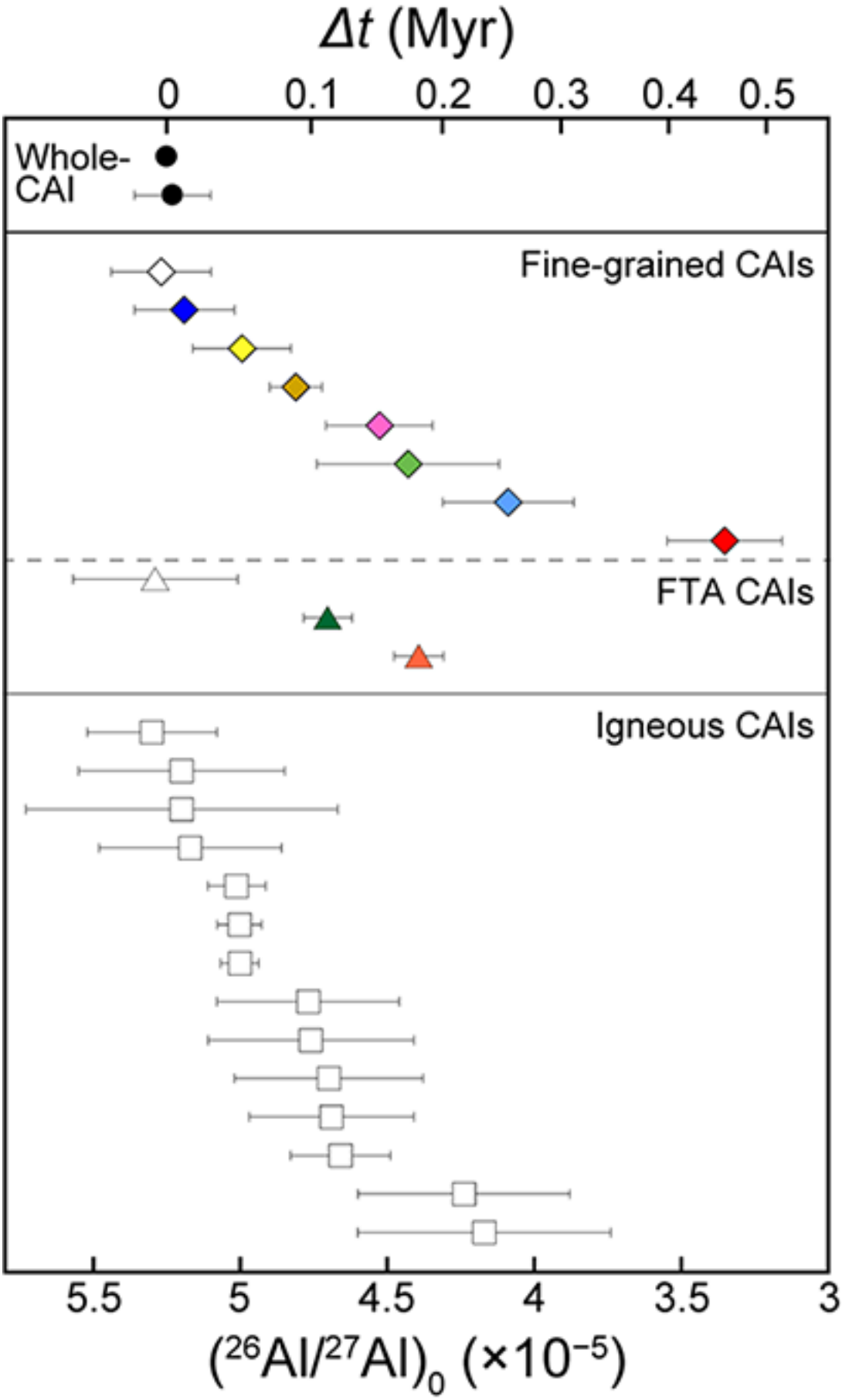
*Noriyuki Kawasaki[1], Naoya Sakamoto[2], Hisayoshi Yurimoto[2]

1. Department of Earth and Planetary Sciences, Graduate School of Science, Hokkaido University, 2. Hokkaido University

Fine-grained Ca-Al-rich inclusions (FGIs) and fluffy Type A CAIs (FTAs) in CV chondrites are suggested to be condensates formed directly from the solar nebular gas (e.g., MacPherson and Grossman, 1984; Krot et al., 2004). Al–Mg mineral isochrons of seven FGIs and two FTAs from reduced CV chondrites Efremovka, Vigarano, Thiel Mountains 07007, and Northwest Africa 8613 were obtained via in situ Al–Mg isotope measurements using secondary ion mass spectrometry (Cameca ims-1280HR at Hokkaido University). The slopes of the mineral isochrons for seven FGIs and two FTAs exhibit statistically significant variations in initial 26Al/27Al ratios, (26Al/27Al)0, ranging from (5.19 ±0.17) to (3.35 ±0.21) ×10^−5, which correspond to a relative age spread of 0.44 ±0.07 Myr. Inferred upper limit of (26Al/27Al)0 for them is identical to the Solar System (26Al/27Al)0 of ˜5.2 ×10^−5 as determined by whole-rock Al–Mg isochron studies for CAIs in CV chondrites. The intercepts of the mineral isochrons, the initial 26Mg/24Mg ratios, are consistent with Mg-isotope evolution path of a solar-composition nebular gas. The observed variations in (26Al/27Al)0 for condensate CAIs are essentially similar to those (˜5.2 to ˜4.2 × 10^−5) for coarse-grained, igneous CAIs of CV chondrites that are formed by melting and solidification (MacPherson et al., 2012, 2017). If 26Al was distributed homogeneously in the forming region, then our data indicate that thermal processes of condensation and melting for CAI formation occurred contemporaneously and continued for at least ˜0.4 Myr at the very beginning of the Solar System. Alternatively, the observed variations in (26Al/27Al)0 also indicate the possibility of heterogeneous distributions of 26Al in the forming region, corresponding to a range of over at least 3.4 ×10^−5 < (26Al/27Al)0 < 5.2 ×10^−5.

Fig. 1. Variations in initial 26Al/27Al ratios among CAIs in CV chondrites (after Kawasaki et al., 2020). Colored symbols indicate data from this study. Other data are from Jacobsen et al. (2008), Larsen et al. (2011), MacPherson et al. (2010, 2012, 2017), Kita et al. (2012), and Kawasaki et al. (2018).

©2021. Japan Geoscience Union. All Right Reserved.



©2021. Japan Geoscience Union. All Right Reserved.

Petrology and mineralogy of a coarse-grained CAI “TTA01” from Allende

*Tadakatsu Yamasaki[1], Noriyuki Kawasaki[1], Hisayoshi Yurimoto[1]

1. Hokkaido University

Ca-Al-rich inclusions (CAIs) in meteorites are the oldest objects formed in the Solar System (Connolly et al., 2012) and composed of high-temperature condensate minerals from a solar-composition gas (e.g., Grossman, 1972). Coarse-grained CAIs in CV chondrites are divided into Type A, Type B and Type C CAIs according to their petrography. Fine-grained inclusions and fluffy Type A CAI are suggested to be condensates from the solar nebular gas (e.g., MacPherson and Grossman, 1984), while compact Type A, Type B and Type C CAIs formed by melt crystallization (e.g., MacPherson and Grossman, 1981; Yurimoto et al., 1998). In this study, we conduct petrographic observations of a coarse-grained CAI from Allende, TTA01 (Imai and Yurimoto, 2000), which has two regions with distinct petrographic signatures, using FE-SEM-EDS system (JEOL JSM-7000F; Oxford X-Max 150) installed at Hokkaido University.

TTA01 has an elliptical shape with a size of ~3.5 x 2.5 mm on the polished section of Allende. It is mainly composed of spinel, melilite, anorthite, and fassaite and contains secondary minerals of sodalite, nepheline, grossular, and monticellite. TTA01 can be divided into two regions. “Region A” is enriched in fassaite and anorthite. Subhedral anorthite (~1 mm long) and anhedral melilite and fassaite poikilitically enclose spinel crystals. A bulk chemical composition of region A is Type C CAI-like and plotted on the spinel + anorthite area of the ternary phase diagram of CAIs by Stolper (1982). Åkermanite contents of melilite in region A are ~50-70 mol%.

“Region B” is enriched in melilite. Small melilite and spinel grains (5-50 μm) are poikilitically enclosed in anorthite and fassaite crystals. Melilite also contains finer spinel grains. A bulk chemical composition of region B is Type B CAI-like and plotted on the spinel + melilite area of the Stolper diagram. Åkermanite contents of melilite in region B are ~15-50 mol%. Small melilite crystals often contain Al-rich grains with åkermanite contents of < 25 mol% and they are surrounded by melilite with > 30 mol%.
According to the petrographic observations, crystallization orders for region A is from spinel, anorthite, to melilite + fassaite, while those for region B is from spinel, melilite to anorthite + fassaite. These crystallization orders are consistent with the bulk chemistry of each region. The bulk chemistry and distinct åkermanite contents of melilites in regions A and B suggest that the two regions could not have formed from a homogeneous, single melt. Type C CAI-like precursor and Type B CAI-like precursor may have been accreted together and then remelted to form TTA01. A liquids temperature of anorthite in region A is 1340℃ while that of melilite in region B is 1430℃ (Stolper, 1982). The melting of precursors of TTA01 at 1340-1430℃ is consistent with the above observations; spinel and a part of melilite in region B were relict of the melting event.

©2021. Japan Geoscience Union. All Right Reserved.

Development of a chemical separation procedure for determining the initial niobium-92 abundance of chondritic components

*Yuki Hibiya[1]

1. Submarine Resources Research Center, Japan Agency for Marine-Earth Science and Technology

Introduction

One of the long-standing issues in the study of material evolution in the early solar system is "where did the nuclides come from, when were they injected into the solar system, and how were they transported to form the planets?" The short-lived nuclide niobium-92 (^{92}Nb), which originated from core-collapse Type II supernovae (SNII) [1], holds the key to solving this issue.

In this study, I investigate the initial abundance of ^{92}Nb amongst the chondritic components and determine the distribution of SNII origin components in the early solar system. A special focus is on the oldest solid material Ca-Al-rich inclusion (CAI) which is likely to have existed over a wide area in the protoplanetary disk [2], and the initial abundance of ^{92}Nb including the genetic information of CAI is determined by combining the results from the high-precision Cr and Ti stable isotope measurements.

In order to clarify a detailed picture of the SNII-origin-material influx and transportation processes at the birth of the solar system by applying this method to various primitive components in the future, I develop here a chemical separation of Cr, Ti and Zr from a single digest for the high precision isotope measurements of chondritic components using mass spectrometry.

Results & Discussion

Samples were prepared by mixing terrestrial basalt (JB-1b) and peridotite (JP-1) in ratios that would yield the approximate compositions (for major elements and Zr) of chondrules and CAIs. The typical compositions of chondrules and CAIs were calculated based on the sizes and major element compositions reported in the previous studies [3, 4]. Following digestion with conc. HF-HNO_3, samples were dried down and re-dissolved in 6 M HCl for the first step of column chemistry. The chemical separation and purification of Cr, Ti and Zr from the samples were established based on the procedure described by [5-7].

The newly developed separation procedure comprises four steps: (i) Fe removal using AG1-X8 anion exchange resin; (ii) Zr separation using Ln-resin; (iii) Ti separation using TODGA resin; (iv) Cr separation using AG50W-X8 cation exchange resin. In the first step, Fe was separated using small resin volumes of ~0.5 mL. The recovery rates for Cr, Ti, and Zr were 93-100% for all studied samples. The elution was evaporated until the total volume reached ~1 mL and then converted to 3 mL of ~2 mol L^{-1} HCl solution by dilution with H_2O. Subsequently, Cr and Ti were separated from the column using 2 mol L^{-1} HNO_3 + 1 wt.% H_2O_2, followed by the elution of Zr in 0.5 mol L^{-1} HCl + 0.06 mol L^{-1} HF. The recovery rates for Cr and Ti were ~100%, and that for Zr was 97-98% for all the studied samples. The elution containing Cr and Ti was then evaporated to dryness and dissolved in 1 mL of 12 mol L^{-1} HNO_3 for the third separation step. In the third step, Ti was separated from Cr-fraction using the pre-packed 1 ml cartridges containing TODGA resin associated with the cartridge reservoirs. The recovery rates for Cr and Ti were 95-100% for

©2021. Japan Geoscience Union. All Right Reserved.

all the studied samples. Prior to the final step, I used a Cr pretreatment procedure [8] involving exposure to 1 mol L^{-1} HNO_3 + 1 wt.% H_2O_2 >3 days so that Cr(III) remained as the dominant species in the acid. In the final step, Cr was purified from matrix elements. The recovery rates of Cr were 98-100% for all the studied samples.

Hence, we can expect that the above new method separates Cr, Ti, and Zr with >88%, >93%, and >90%, respectively. I am now planning to apply this method to individual CAIs extracted from primitive meteorites and assess the nature of proto-planetary disk through the combined Cr, Ti, and Zr isotope analyses.

[1] Hibiya et al. (2019) *82nd Metsoc meeting, #6370*, [2] Hezel et al. (2008) *MAPS* **43** 1879–1894, [3] Goresy et al. (2002) *GCA* **66** 1459–1491, [4] Alexander et al. (2005) *Chondrites and the protoplanetary disk* **341** 972, [5] Iizuka et al. (2016) *EPSL* **439** 172–181, [6] Münker et al. (2001) *G-cube.* **2**, [7] Hibiya et al. (2019) *GGR* **43** 133–145, [8] Larsen et al. (2016)*J. Chromatogr. A* **1443** 162–174.

Keywords: niobium-92, Type II supernova, CAIs, column chromatography, mass spectrometry

©2021. Japan Geoscience Union. All Right Reserved.

Motion of silicate particles in protoplanetary disk

*Tamami Okamoto[1], Shigeru Ida[1]

1. Earth-Life Science Institute, Tokyo Institute of Technology

Forsterites are crystallized by annealing of amorphous precursors (~1000 K) or sublimation and recondensation (~1400 K) in inner protoplanetary disk. On the other hand, the observation showed that comets include crystalline forsterites. Therefore, there must be some mechanism that transports them from the inner area to the outer area in the disk. In this study, we investigate the motion of dusts in steady protoplanetary disk, considering that dusts stick to icy pebbles. From the result, we discuss the dependence of surface density of silicate dusts on the distance from the central star and compare a calculation result of the ratio of crystallized silicates to amorphous precursors to the observation result of comets.

©2021. Japan Geoscience Union. All Right Reserved.

Thermal history of andesitic achondrite Erg Chech 002

*Akira Yamaguchi[1], Atsushi Takenouchi[1], Jean-Alix Barrat[2]

1. National Institute of Polar Research, 2. UBO-IUEM

Petrologic and geochemical study of asteroidal achondrites is essential to understand the earliest volcanism on planetesimals and protoplanets. These differentiated bodies were likely covered by crust formed by the melting of the parent bodies. Such crustal rocks are divided into basaltic and andesitic types. The majority of basaltic types are eucrites. In contrast, the andesitic type is very rare. We present the petrology of a newly-found andesitic achondrite Erg Check 002 (EC 002) and discuss its petrogenesis and thermal history. We studied polished sections of EC 002 using an FE-SEM equipped with EDS/EBSD/CL system, an EPMA, and a Raman spectrometer.

The section of EC 002 is an unbrecciated rock with medium-grained groundmass with pores. It consists of lath-shaped feldspar, anhedral pyroxene, silica minerals, with minor minerals such as spinel, ilmenite, Ca-phosphate, troilite, and FeNi metal. Silica minerals are cristobalite and tridymite (PO), with no quartz, confirmed by Raman spectra and CL observations. Groundmass pyroxenes are partly equilibrated and consist of relict augite with fine exsolution lamellae of low-Ca pyroxene or relict low-Ca pyroxene with fine exsolution lamellae of augite. In addition, EC 002 also contains angular to rounded pyroxene or olivine xenocrysts. EC 002 is slightly shocked. Bulk groundmass pyroxene compositions are generally augitic (Wo27.7-33.0En36.9-38.5). Feldspars are albitic (Or2.0-7.1Ab75.8-87.4) and contain lamellae of K-rich feldspar. The pyroxene xenocryst has a chemically homogeneous core (Wo4.7En76.8) with zoned rims. There is no difference in the FeO/MnO ratios (~21) between the xenocryst and groundmass pyroxene. The texture of the second section is slightly different, which contains four xenocrysts (1-7 mm in size). One elongated xenocryst is surrounded by a fine-aggregate of pyroxene and feldspar. Compared to the first one, this section contains little amounts of pores. The textural difference may have resulted from the difference of local cooling rates. A further petrologic study of this sample is still in progress. The bulk major chemical compositions of the groundmass are andesitic (58 wt% SiO2 and 4.54 wt% Na2O and K2O). Other REE abundances are low and of the order of 5 or 6 times the chondritic reference.

The petrologic and geochemical data indicate that EC 002 experienced two-stage cooling history. The first stage is the crystallization from lava at ~1200 to ~1000 ˚C at ~5˚C/year, estimated from the compositional profile of Mg# in the pyroxene xenocryst. The second stage is the rapid cooling from ~900 ˚C, estimated from the occurrence of silica minerals. The sudden change of cooling rates can be explained by rapid cooling caused by impact excavation, consistent with the shock features. The presence of xenocrysts (olivine and pyroxene) gives an impression that EC 002 is an impact melt breccia. However, we do not have a definitive answer to this question. The identical FeO/MnO ratios may indicate the genetic linkage of the pyroxene and xenocryst. The groundmass compositions can only be explained by partial melting, not by impact melting unless the target was andesitic crust.

Keywords: achondrite, andesite, planetesimal, volcanism

©2021. Japan Geoscience Union. All Right Reserved.

Excess silica in plagioclase in some mesosiderites

*naoji sugiura[1], tomoko Arai[1]

1. Chiba Institute of Technology

Introduction: Excess silica in plagioclase has been reported in lunar rocks [1] and chondrules [2]. It is absent in terrestrial plagioclase and the presence of the excess is considered as evidence against metamorphism and/or slow cooling at temperatures where cations could move around. Here we report excess silica in plagioclase in some mesosiderites (Dong Ujimqin Qi (B1), NWA1878 (B0), NWA2924, NWA4747, Bondoc (B4)), and absence of the excess in Estherville(A3/4).

Instrumental: Plagioclase compositions were measured by SEM-EDS. The measurements were made without standards and normalized to 100%. Since excess silica is produced by vacancies [1] this is problematic, but until measurements with EPMA are made we have to abide this ambiguity. The differences in apparent excesses in mesosideritic plagioclase and those in other plagioclase (terrestrial and achondrites) at the same anorthite number (An#) are considered as true excess silica.

Results: Similar to lunar plagioclase, silica excesses in mesosideritic plagioclase increase with decreasing anorthite number [1]. The excess silica evaluated at the same An# varies considerably among the mesosiderites. It decreases in the order of, NWA1878 > Dong Ujimqin Qi > Bondoc > NWA2924 > NWA4747> Estherville. The excess is practically nil in Estherville, within the error (standard deviation) of the measurement (about +/- 1% which is not significantly larger than those reported for lunar rocks). A typical excess in NWA1878 is ~4.5 % at An90, which is significantly higher than those in lunar rocks [1].

Discussion: In the case of lunar rocks, the excess silica is explained as a result of a high silica activity during crystallization of increasingly Na-rich plagioclase from a melt. Most mesosiderites experienced brief reheating to near-solidus temperatures after the mixing of metal. Also, the silica activities in most mesosiderites were high during reheating as a result of phosphate formation reactions. (Note that this requires reheating after the formation of phosphates.) Therefore, the excess silica in mesosideritic plagioclase may be understood to have been produced by a mechanism similar to that in lunar rocks. The variation in the excess among mesosiderites could be due to difference in the thermal histories (cooling rate or multiple reheating). The higher excesses in mesosideritic plagioclase than those in lunar rocks may be due to difference in the thermal histories. Dissecting the mesosiderite data in detail, however, it is found that the vacancy corresponding to the silica excess seems to be mostly created by Na deficiency. Merrillite in mesosiderites is known to be deficient in Na [3]. Therefore, both merrillite and plagioclase competed for limited supply of Na. This may have contributed to the high excess silica in mesosideritic plagioclase. A peculiar feature of mesosideritic plagioclase with high excess silica is the presence of fine silica particles. This is observed in NWA1878, Dong Ujimqin Qi and Bondoc. (A caveat on the reported excesses in these mesosiderites is that they could be due to hidden silica particles. Some of the data are likely to be affected by such hidden silica particles, but we believe many of the excesses are authentic.) Investigations of excess silica, exsolved silica particles, and the compositional relationship between plagioclase and merrillite would clarify the reheating history of mesosiderites.

References:

[1] D.W. Beaty and A.L. Albee, 1980, Silica solid solution and zoning in natural plagioclase. Am. Mineral.

©2021. Japan Geoscience Union. All Right Reserved.

65, 63-74.

[2] T.J. Tenner+, 2014, Silica excess in anorthitic plagioclase from type 3.00 chondrite chondrules: Evidence for retaining primary 26Al-26Mg systematics. 45th LPSC, 1187.pdf.

[3] N. Sugiura and T. Arai, 2020, Volatile loss from mesosiderites. 11th Symposium on Polar Science, OAp12_Sugiura_00260_01.pdf.

Keywords: mesosiderites, plagioclase, silica

©2021. Japan Geoscience Union. All Right Reserved.

The petrological and mineralogical descriptions of nakhlites NWA 6148 and NWA 10153

*Kakeru Kukihara[1], Masaaki Miyahara[1], Akira Yamaguchi[2], Yoshio Takahashi[3], Yasuo Takeichi[4], Naotaka Tomioka[5], Eiji Ohtani[6]

1. hiroshima university , 2. National Institute of Polar Research, 3. Tokyo university, 4. Institute of Materials Structure Science, High-Energy Accelerator Research Organization (KEK), 5. Kochi Institute for Core Sample Research, Japan Agency for Marine-Earth Science and Technology (JAMSTEC), 6. Tohoku university

We conducted a petrological and mineralogical study of nakhlites NWA 6148 and NWA 10153 to clarify an aqueous alteration in the nakhlites complex. NWA 6148 is suggested to have derived from the deeper part of the nakhlite complex [1]. NWA 10153 was hardly investigated and its position in the nakhlites complex is unknown. For the petrological and mineralogical descriptions, microtextural observations by an FE-SEM and chemical composition analysis by an EMPA were conducted. We used a FIB system to prepare the foils of alteration textures found in the samples. The chemical species of iron, oxygen, carbon, and sulfur in the foils were analyzed by XANES. The microtextures, chemical compositions, and crystal structures of minerals in the foils were analyzed using an FE-STEM-EDS.

NWA 6148 consists mainly of olivine, low-Ca pyroxene, plagioclase, K-feldspar, pyrrhotite, and Fe-Ti oxides. Plagioclase, K-feldspar, pyrrhotite, and Fe-Ti oxides occur in a mesostasis. NWA 6148 has a higher fraction of a mesostasis (55.2 vol.%) than other nakhlites (7–24 vol.%) [2]. The low-Ca pyroxene has normal compositional zoning. The Ca content increases toward the rim in some pyroxene grains. Alteration texture is not found in NWA 6148. NWA 10153 also has a high fraction of a mesostasis (36.3 vol.%), and its major constituents are low-Ca pyroxene, plagioclase, K-feldspar, pyrite, and Fe-Ti oxides. Only a small amount of olivine occurs as small grains ($< 100\ \mu m$) in the mesostasis. Alteration textures are found between low-Ca pyroxene grains and/or plagioclase grains. The alteration textures can be divided into four types: i) Fe-rich, ii) Si-Fe-rich, iii) Fe-S-rich, and iv) Carbonate-rich types. Based on Fe L-edge XANES, Fe^{3+} is dominant in the Fe-rich portion. Considering the SAED pattern and chemical compositions, the Fe-rich portion consists mainly of goethite. The absorption peaks both of Fe^{2+} and Fe^{3+} are observed in the Si-Fe rich portion. The Si-Fe-rich portion seems to consist mainly of smectite. Fe^{3+} is dominant and SO_4^{2-} is included in the Fe-S rich portion. Considering the SAED pattern and chemical compositions, the Fe-S rich portion consists mainly of Na/K-jarosite.

Cohen et al. (2017) [3] suggest that the nakhlite complex formed through several lava flows. The high proportions of mesostasis in NWA 6148 and NWA 10153 mean low crystallization degrees, suggesting that both of them were originated from lava flows that rapidly cooled and solidified near a surface. The Ca zoning in a pyroxene grain is observed in other nakhlites NWA 5790 and MIL 03346 along with NWA 6148 [1, 2]. The petrological similarities indicate that NWA 6148 and NWA 5790 might have formed by the same lava flow. However, more detailed investigations are necessary for the conclusion, because the proportion of a mesostasis in NWA 6148 (55.2 vol.%) is higher than NWA 5790 (36.3±3 Vol.%)[2]. NWA 6148 seems to be escaped from an aqueous alteration.

By contrast, NWA 10153 includes goethite, smectite, and carbonates as alteration minerals. Considering the formation conditions of the alteration mineral assemblage, two different aqueous alteration events likely occurred. In the first event, a hot neutral-basic fluid containing carbon dioxide gas formed smectite and carbonates. In the second event, a weak acidic fluid dissolved pyrite, which made the fluid to become

©2021. Japan Geoscience Union. All Right Reserved.

more acidic. Jarosite formed under very low-pH. With increasing the pH again due to the reaction between the surrounding minerals and the strongly acidic fluid, goethite precipitated from the fluid finally.

References:

[1] Jambon et al. (2016) Geochimica et Cosmochimica Acta 190, 191–212.

[2] Mikouchi et al. (2006) 37thLPSC, abstract no.1865.

[3] Cohen et al. (2017) Nature Communications 8, 1–8.

Keywords: Aqueous alteration, NWA 6148, NWA 10153, Chemical condition of the fluid

©2021. Japan Geoscience Union. All Right Reserved.

[E] Oral | P (Space and Planetary Sciences)：P-EM Solar-Terrestrial Sciences, Space Electromagnetism & Space Environment

Sat. Jun 5, 2021 9:00 AM - 10:30 AM JST | Sat. Jun 5, 2021 12:00 AM - 1:30 AM UTC | Ch.06 Zoom Room 06

[P-EM08] Space Weather and Space Climate

convener:Ryuho Kataoka(National Institute of Polar Research), A Antti Pulkkinen(NASA Goddard Space Flight Center), Kanya Kusano(Institute for Space-Earth Environmental Research, Nagoya University), Kaori Sakaguchi(National Institute of Information and Communications Technology), Chairperson:Kanya Kusano(Institute for Space-Earth Environmental Research, Nagoya University), Kaori Sakaguchi(National Institute of Information and Communications Technology)

We share the latest scientific papers to understand how the space environment changes in various time scales, and to discuss how we will react via international and interdisciplinary collaborations. More specifically, welcomed papers include space climate studies to reconstruct the long-term variations from radio isotopes; cutting-edge observational and modeling studies of the ionosphere, geospace, heliosphere and the sun; simulation and statistical studies to predict the future space weather and space climate; applied science such as operational space weather forecast and mitigation of the social impact due to extreme space hazards. Focused topics in 2021 include extreme events, theoretical maxima and benchmarks for hazard assessments, and space weather and deep space human spaceflight activities at Moon and at Mars.

9:00 AM - 9:15 AM JST | 12:00 AM - 12:15 AM UTC

[PEM08-13] Statistical analysis of variations of geoelectric field during magnetic storms/substorms in Japan

*Tian Zhang[1], Yusuke Ebihara[1] (1.Kyoto University)

9:15 AM - 9:30 AM JST | 12:15 AM - 12:30 AM UTC

[PEM08-14] How do auroral substorms depend on Earth's dipole magnetic moment?

*Yusuke Ebihara[1], Takashi Tanaka[2] (1.Research Institute for Sustainable Humanosphere, Kyoto University, 2.International Center for Space Weather Science and Education, Kyushu University)

9:30 AM - 9:45 AM JST | 12:30 AM - 12:45 AM UTC

[PEM08-15] Direct numerical simulation of the Alfvénic solar wind: a theoretical origin of magnetic switchback

★Invited Papers

*Munehito Shoda[1] (1.National Astronomical Observatory of Japan)

9:45 AM - 10:00 AM JST | 12:45 AM - 1:00 AM UTC

[PEM08-16] Simulation study on the deformation of magnetic field in interplanetary CMEs

*Minami Mori[1], Daikou Shiota[2], Kanya Kusano[1] (1.Institute for Space-Earth Environmental Research, Nagoya University , 2.National Institute of Information and Communications Technology (NICT))

10:00 AM - 10:15 AM JST | 1:00 AM - 1:15 AM UTC

[PEM08-17] Onset Mechanism of the Successive M-class Solar Flares in the Solar Active Region 12673 Based on a Nonlinear Force-Free Modeling

*Daiki Yamasaki[1], Satoshi Inoue[2], Takako T. Ishii[1], Ayumi Asai[1], Shin'ichi Nagata[1], Kiyoshi Ichimoto[1] (1.Astronomical Observatory, Kyoto University, 2.Institute for Space-Earth Environmental Research)

10:15 AM - 10:30 AM JST | 1:15 AM - 1:30 AM UTC

[PEM08-18] Data-driven MHD simulation of successive solar plasma eruptions

*Takafumi Kaneko[1], Sung-Hong Park[1], Kanya Kusano[1] (1.Institute for Space-Earth Environmental Research, Nagoya University)

Statistical analysis of variations of geoelectric field during magnetic storms/substorms in Japan

*Tian Zhang[1], Yusuke Ebihara[1]

1. Kyoto University

Since the GIC (geomagnetically induced current) of power grids is a global problem, to effectively prevent geomagnetic storm disaster is an important problem. Predicting the GIC is considered as a possible solution to this problem. Since GIC is directly generated by GIE (geomagnetically induced electric field), we used GIE measured at Kakioka Magnetic Observatory (geomagnetic latitude of 28 deg) as a proxy of GIC flowing in the Japanese power grid to acquire a statistical view of the response of GIC to magnetic storms and substorms, and to understand how the magnetospheric and ionospheric current systems affect GIC. The magnetic storms were sorted in accordance with the minimum value of the SYM-H index. The magnetic storms driven by coronal mass ejections (CMEs) and the corotating interaction regions (CIRs) were in particular focused on. A total of 38 intense storms associated with (during 1996-2004), 31 CME- and 69 CIR-associated moderate storms (during 1996-2008), as well as 17,273 substorms (during 1996-2004) are used to perform superposed epoch analyses. The east-west component of the electric field |Ey| dominates the north-south component |Ex| for all the three kinds of magnetic storms. For the CME-associated storms, Ey tends to show a negative excursion during the initial phase, a positive one during the main phase and a negative one during the recovery phase, which can be understood the contribution from the magnetopause current and the ring current. Ey responds largely to substorms with its polarity depending on magnetic local time. We discuss the possible current systems that can cause the large-amplitude GIE at geomagnetically low latitude by shown histograms of the maximum |Ey| during the magnetic storms and substorms.

Keywords: geoelectric field , magnetic storms, coronal mass ejections, corotating interaction regions

©2021. Japan Geoscience Union. All Right Reserved.

How do auroral substorms depend on Earth's dipole magnetic moment?

*Yusuke Ebihara[1], Takashi Tanaka[2]

1. Research Institute for Sustainable Humanosphere, Kyoto University, 2. International Center for Space Weather Science and Education, Kyushu University

The near-Earth space environment is suggested to depend on Earth's dipole magnetic moment *M*. The dependence on *M* is not straightforward since the solar wind-magnetosphere-ionosphere coupling system is complicated. Here, we show how the change in *M* affects the development of an auroral substorm by using global magnetohydrodynamics (MHD) simulation. We artificially increased *M* by a factor of 1.5 (corresponding to the Earth about 630 BC) and decreased *M* by a factor of 1.5 (corresponding to the Earth about 2850 AD) in the MHD simulation. The ionospheric conductivity decreases with increasing *M*, in accordance with the aid of empirical relations. An auroral substorm took place regardless of *M*, but its development depends largely on *M*. The major results can be summarized as follows. In the future (when *M* decreases monotonically), (1) the expansion onset of the substorm takes place later, (2) the auroral electrojet develops slowly, (3) the amount of energy coming into the magnetosphere decreases whereas the maximum auroral electrojet increases, and (4) the bright auroral region expands more equatorward. The first two consequences are probably associated with the slow magnetospheric convection. The third consequence is associated with the dependence the ionospheric conductivity on *M*. The fourth consequence is related to the weakness of the magnetic pressure force that impedes earthward penetration of hot plasma. It is shown that the evolution of substorms depends largely on the value of Earth's dipole moment.

Keywords: Auroral substorm, Strength of Earth's magnetic field, MHD simulation

©2021. Japan Geoscience Union. All Right Reserved.

Direct numerical simulation of the Alfvénic solar wind: a theoretical origin of magnetic switchback

*Munehito Shoda[1]

1. National Astronomical Observatory of Japan

One of the most important early findings from Parker Solar Probe is the ubiquitous presence of sudden reversals of magnetic polarity in the near-Sun solar wind. Such events are called "magnetic switchbacks". The presence of magnetic switchbacks in the near-Sun solar wind is not predicted from the standard solar wind model, in which the solar wind is heated and accelerated by Alfvén waves and turbulence. Our theoretical understanding of the solar wind acceleration is now challenged.
In this presentation, we propose the idea that the magnetic switchbacks emerge as a natural consequence of large-amplitude Alfvén waves, thus explaining the origin of magnetic switchbacks without disturbing the standard understanding. We have performed an unprecedentedly large simulation of the solar wind acceleration from the corona to the sufficiently distant region beyond the orbits (perihelions) of Parker Solar Probe. By imposing Alfvénic fluctuations from the bottom boundary, magnetic switchbacks that exhibit several observational properties are reproduced, meaning that the presence of magnetic switchback is not contradictory to the wave/turbulence-driven solar wind model. The appearance rate (filling factor) of switchback is, however, 100 times smaller than the observed value. We also directly compare our model with Parker Solar Probe observation. The simulated data show quite similar behavior to the observed data in the "quiet phase" in which the number of switchbacks is small. Our conclusion is that a part of magnetic switchbacks originates from large-amplitude Alfvén waves in the solar wind.

Keywords: solar wind, turbulence, Parker Solar Probe

©2021. Japan Geoscience Union. All Right Reserved.

Simulation study on the deformation of magnetic field in interplanetary CMEs

*Minami Mori[1], Daikou Shiota[2], Kanya Kusano[1]

1. Institute for Space-Earth Environmental Research, Nagoya University , 2. National Institute of Information and Communications Technology (NICT)

Coronal mass ejections (CMEs) are the largest eruption in the solar system. CMEs carry huge plasmas in the solar corona of 10^11 to 10^13 kg into interplanetary space at velocities of a few hundred - thousand km/s. CMEs can affect a variety of space weather conditions when they collide with the magnetosphere of the earth. In particular, the magnetic field of CMEs is a serious factor of space weather disturbance, because the southward component of the magnetic field in CMEs could cause the geomagnetic field storm. We developed a numerical simulation of CME propagation in the inner heliosphere using the magnetohydrodynamic (MHD) model, SUSANOO-CME (Shiota & Kataoka, 2016). In this model, the CME magnetic field is given by the distorted spheromak force-free field in which the orientation of the major axis and position of the spheromak is determined with free parameters. To make the simulation and its analysis simple, we assume that the major axis of the spheromak is on the equator plane of the Sun and direct westward. To clarify the interaction between the CME magnetic field and the solar wind motion, we assume that the background magnetic field of the solar wind is negligibly small, omitting the effect of the interplanetary magnetic field (IMF). We calculated the four different cases in which the toroidal and poloidal components of the spheromak magnetic field are respectively inverted. As the results of the simulations, we found that the toroidal and poloidal magnetic fluxes in the front torus of the spheromak shrink in the initial phase of the CME propagation when the CMEs keep fast speed. The results can be explained as the result that the magnetic fluxes in the front side of the spheromak are convected to the rear side of the CMEs by the interaction with the solar wind. It looks like the CME's internal magnetic structure is almost reversed along the propagation direction. After the initial phase, however, the magnetic structure of the interplanetary CMEs (ICMEs) is sustained during the propagation. The results suggest that the interaction with the solar wind may largely deform the ICME magnetic field mainly in the initial phase of propagation. Based on the simulations, we will discuss how the magnetic field of ICME can be deformed by the interactions with the solar wind and the IMF.

Keywords: MHD, CME, solar wind

©2021. Japan Geoscience Union. All Right Reserved.

Onset Mechanism of the Successive M-class Solar Flares in the Solar Active Region 12673 Based on a Nonlinear Force-Free Modeling

*Daiki Yamasaki[1], Satoshi Inoue[2], Takako T. Ishii[1], Ayumi Asai[1], Shin'ichi Nagata[1], Kiyoshi Ichimoto[1]

1. Astronomical Observatory, Kyoto University, 2. Institute for Space-Earth Environmental Research

Active region (AR) 12673 successively produced M5.5 and M4.2 flares, between 2017 September 4th 20:30UT and September 5th 01:30UT. On one hand, in both flares, the initial brightenings and the flare ribbons were observed in 1600 angstrom at the similar location. On the other hand, coronal mass ejection (CME) was only observed just after the peak time of the M5.5 flare. The purpose of this study is to answer the following questions; ” How the magnetic free energy of the M4.2 flare was build up in just 5 hours?”, ” Whether the onset mechanisms of these two flares were same or not?”, and ” Why only the M5.5 flare was accompanied with CME?”. According to the analyses of the photospheric magnetic field before the flares and the extreme-ultraviolet images during the flares, we found that the small-scale magnetic flux evolved at the polarity inversion line and the flare ribbons were observed outside of it. Thus, we suggest that the evolution of the small-scale magnetic flux played an important role in the rapid formation of the magnetic flux rope. We extrapolated the three-dimensional (3D) coronal magnetic field by using a nonlinear force-free field (NLFFF) extrapolation method before and after the time when the brightening on the small-scale magnetic flux was observed. As a result, we found that strongly twisted lines are formed compared to the NLFFF just after the M5.5 flare. Furthermore, we compared the 3D coronal magnetic field before the two flares. We found that, in both of the flares, the magnetic null point exists in the overlying field lines. We suggest that, in both cases, the null point reconnection would play an important role in the initiation of the flares. Eventually, we will discuss the generation mechanism of the CME in terms of a relationship between the flare-triggering process and global magnetic field covering the twisted magnetic field lines.

Keywords: Sun: flares, Sun: magnetic fields, Magnetohydrodynamics (MHD)

©2021. Japan Geoscience Union. All Right Reserved.

Data-driven MHD simulation of successive solar plasma eruptions

*Takafumi Kaneko[1], Sung-Hong Park[1], Kanya Kusano[1]

1. Institute for Space-Earth Environmental Research, Nagoya University

Solar flares and plasma eruptions are the origins of the strong space weather events. They are manifestations of sudden energy release in the solar magnetized atmosphere. To understand the physical mechanisms and predict their occurrences, three-dimensional magnetic fields from the photosphere up to the corona must be studied. The solar photospheric magnetic fields are observable, whereas the coronal magnetic fields cannot be measured. One method for inferring coronal magnetic fields is performing data-driven simulations, which involves time-series observational data of the photospheric magnetic fields with the bottom boundary of magnetohydrodynamic simulations. We developed a data-driven method in which temporal evolutions of the observational vector magnetic field can be reproduced at the bottom boundary in the simulation by introducing an inverted velocity field. This velocity field is obtained by inversely solving the induction equation and applying an appropriate gauge transformation. Using this method, we performed a data-driven simulation of successive small eruptions observed by the Solar Dynamics Observatory and the Solar Magnetic Activity Telescope in November 2017. The simulation well reproduced the converging motion between opposite-polarity magnetic patches, demonstrating successive formation and eruptions of helical flux ropes.

Keywords: solar filament/prominence, filament eruption, data-driven simulation

©2021. Japan Geoscience Union. All Right Reserved.

[E] Poster | P (Space and Planetary Sciences)：P-EM Solar-Terrestrial Sciences, Space Electromagnetism & Space Environment

Sat. Jun 5, 2021 5:15 PM - 6:30 PM JST | Sat. Jun 5, 2021 8:15 AM - 9:30 AM UTC | Ch.03_1

[P-EM08] Space Weather and Space Climate

convener:Ryuho Kataoka(National Institute of Polar Research), A Antti Pulkkinen(NASA Goddard Space Flight Center), Kanya Kusano(Institute for Space-Earth Environmental Research, Nagoya University), Kaori Sakaguchi(National Institute of Information and Communications Technology)

We share the latest scientific papers to understand how the space environment changes in various time scales, and to discuss how we will react via international and interdisciplinary collaborations. More specifically, welcomed papers include space climate studies to reconstruct the long-term variations from radio isotopes; cutting-edge observational and modeling studies of the ionosphere, geospace, heliosphere and the sun; simulation and statistical studies to predict the future space weather and space climate; applied science such as operational space weather forecast and mitigation of the social impact due to extreme space hazards. Focused topics in 2021 include extreme events, theoretical maxima and benchmarks for hazard assessments, and space weather and deep space human spaceflight activities at Moon and at Mars.

[PEM08-P01] NASA Goddard Space Flight Center Space Weather Activities

*Antti A Pulkkinen[1] (1.NASA Goddard Space Flight Center)

[PEM08-P02] Relationship between X-ray and EUV solar flare emissions and the Dellinger phenomenon

*Kyoko Watanabe[1], Munechika Arao[1], Shohei Nishimoto[1], Chihiro Tao[2], Michi Nishioka[2] (1.National Defense Academy of Japan, 2.National Institute of Information and Communications Technology)

[PEM08-P03] A comparative study of the empirical and physics-based methods for solar flare predictions

*Kaho Kondo[1], Kanya Kusano[1] (1.Institute for Space-Earth Environmental Research, Nagoya University)

[PEM08-P04] Data-driven MHD Simulation of Solar Active Region NOAA 11283

*Yeongmin Kang[1], Takafumi Kaneko[1], Kanya Kusano[1] (1.Institute for Space-Earth Environmental Research)

[PEM08-P05] Unusual enhancement of ~30 MeV proton flux in an ICME sheath region

*Takahiro Obara[1], Mitsuo Oka[2], Nariaki V Nitta[3], Seiji Yashiro[4], Daikou Shiota[5], Kiyoshi Ichimoto[6] (1.Planetary Plasma and Atmospheric Research Center,Tohoku University, 2.University of California Berkeley, 3.Lockheed Martin Solar and Astrophysics Laboratory, 4.The Catholic University of America, 5.National Institute of Information and Communications Technology, 6.Kyoto University)

[PEM08-P06] Development of spectral riometer for observation of energetic electron precipitation at Syowa Station, Antarctica

*Yoshimasa Tanaka[1,2,3], Masayuki Yamamoto[4], Koji Nishimura[1,2,3], Hisao Yamagishi[1], Antti Kero[5], Akira Kadokura[1,2,3], Akira Mizuno[6], Akira Sessai Yukimatu[1,3], Herbert Akihito Uchida[3], Ryuho Kataoka[1,3], Yasunobu Ogawa[1,2,3], Takanori Nishiyama[1,3], Masaki Tsutsumi[1,3], Mitsunori Ozaki[7], Yoshizumi Miyoshi[6], Shin-ichiro Oyama[6], Fuminori Tsuchiya[8] (1.National Institute of Polar Research, 2.Polar Environment Data Science Center, Joint Support-Center for Data Science Research, Research Organization of Information and Systems, 3.The Graduate University for Advanced Studies, SOKENDAI, 4.National Institute of Information and Communications Technology, 5.Sodankyla Geophysical Observatory, 6.Institute for Space-Earth Environmental Research, Nagoya University, 7.Faculty of Electrical and Computer Engineering, Institute of Science and Engineering, Kanazawa University, 8.Planetary Plasma and Atmospheric Research Center, Graduate School of Science, Tohoku University)

[PEM08-P07] Auroral oval in the last 3000 years and future

*Ryuho Kataoka[1], Shin ya Nakano[2] (1.National Institute of Polar Research, 2.The Institute of Statistical Mathmatics)

[PEM08-P08] Solar cycles around the onset of the Maunder Minimum

*Hiroko Miyahara[1], Fuyuki Tokanai[2], Toru Moriya[2], Mirei Takeyama[2], Hirohisa Sakurai[2], Kazuho Horiuchi[3], Hideyuki Hotta[4] (1.College of Art and Design, Musashino Art University, 2.Faculty of Science, Yamagata University, 3.Graduate School of Science and Technology, Hirosaki University, 4.Graduate School of Science, Chiba University)

[PEM08-P09] Simultaneous observation of cosmic rays with muon detector and neutron monitor at the Syowa station in the Antarctic

*Chihiro Kato[1], Kazuoki Munakata[1], Akira Kadokura[2], Ryuho Kataoka[2], Shoko Miyake[3], Paul Evenson[4], Shunta Asano[1] (1.Shinshu University, 2.National Institute of Polar Research, 3.National Institute of Technology, Ibaraki College, 4.University of Delaware)

[PEM08-P10] Measurement of cosmogenic 10Be in endogenic travertine deposits at Baishuitai

*Hiroko Miyahara[1], Hongyang Xu[2], Limin Zhou[2], Kazuho Horiuchi[3], Hiroyuki Matsuzaki[4] (1.College of Art and Design, Musashino Art University, 2.East China Normal University, 3.Hirosaki University, 4.The University Museum, The Univ. of Tokyo)

[PEM08-P11] **Be-7 in Japan, Iceland and Thailand during solar cycle 24 descent phase**

*Hirohisa Sakurai[1], Youmei Kawamura[1], Souichiro Suzuki[1], Fuyuki Tokanai[1], Emiko Inui[1], Mirei Takeyama[1], Toru Moriya[1], Satosi Kikuchi[1], Fusa Miyake[2], Akira Kadokura[3], Natsuo Sato[3], Naoko Sugihara[6], Bjornsson Gunnlaugur[4], David Ruffolo[5], Warit Mitthumsiri[5], Ronald Macatangay[7] (1.Yamagata University, 2.ISEE, Nagoya University, 3.National Institute of Polar Research, 4.Science Institute, Iceland University, 5.Department of Physics, Mahidol University, 6.Department of Chemical Oceanography Atmosphere and Ocean Research Institute,The University of Tokyo, 7.National Astronomical Research Institute of Thailand)

[PEM08-P12] Forecast of energetic electron flux variations of the outer belt using the machine learning

*Satoshi Fukuoka[1], Yoshizumi Miyoshi[1], Daikou Shiota[2], Shinji Saito[4], Takefumi Mitani[3], Tomoaki Hori[1], Nana Higashio[3], Shun Imajo[1], Iku Shinohara[3] (1.Institute for Space-Earth Environmental Research, Nagoya University, 2.National Institute of Information and Communications Technology (NICT), 3.Japan Aerospace Exploration Agency, Institute of Space and Astronautical Science, 4.National Institute of Information and Communications Technology)

[PEM08-P13] Spacecraft surface charging environment in the medium earth orbit

*Masao Nakamura[1], Kosei Nagasawa[1] (1.Osaka Prefecture University)

[PEM08-P14] Active Region Detection in the HMI magnetograms using the Mask R-CNN technique

*Akito Komatsu[1], Yusuke Iida[1] (1.Niigata University)

[PEM08-P15] Operations of Solar Flare Prediction Model Using Deep Neural Networks

*Naoto Nishizuka[1], Yuki Kubo[1], Komei Sugiura[2], Mitsue Den[1], Mamoru Ishii[1] (1.National Institute of Information and Communications Technology, 2.Keio University)

[PEM08-P16] Empirical/physical-based modeling of three-dimensional outer radiation belt for real-time operation

*Shinji Saito[1], Kaori Sakaguchi[1], Yuki kubo[1] (1.National Institute of Information and Communications Technology)

[PEM08-P17] **Mid-term Research Plan of NICT Space Weather Monitoring and Forecast**

*Mamoru Ishii[1] (1.National Institute of Information and Communications Technology)

[PEM08-P18] Development of a prediction system of the sporadic E layer occurrence: Current status and future prospects

*Hiroyuki Shinagawa[1], Chihiro Tao[1], Hidekatsu Jin[1], Yasunobu Miyoshi[2], Hitoshi Fujiwara[3] (1.National Institute of Information and Communications Technology, 2.Kyushu University, 3.Seikei University)

[PEM08-P19] Economic impacts of atmospheric radiation storm on aircraft operations and potential use of space weather information

*Susumu Saito[1], Navinda Kithmal Wickramasinghe[1], Tatsuhiko Sato[2], Daikou Shiota[3] (1.Electronic Navigation Research Institute, National Institute of Maritime, Port, and Aviation Technology, 2.Japan Atomic Energy Agency, 3.National Institute of Information and Communications Technology)

[PEM08-P20] Status of the GEO-X (Geospace X-ray imager) mission

*Yuichiro Ezoe[1], Ryu Funase[2,6], Harunori Nagata[3], Yoshizumi Miyoshi[4], Hiroshi Nakajima[5], Ikuyuki Mitsuishi[4], Kumi Ishikawa[1], Munetaka UENO[6], Atsushi Yamazaki[6], Hiroshi Hasegawa[6], Makoto Mita[6], Masaki Fujimoto[6], Yasuhiro Kawakatsu[6], Takahiro Iwata[6], Kazuhisa Mitsuda[7], Junko Hiraga[8], Satoshi Kasahara[6], Hironori Sahara[1], Yoshiaki Kanamori[9], Kohei Morishita[10], Takefumi Mitani[6], Masaki Numazawa[11] (1.Tokyo Metropolitan University, 2.University of Tokyo, 3.Hokkaido University, 4.Nagoya University, 5.Kanto Gakuin University, 6.ISAS/JAXA, 7.NAOJ, 8.Kwansei Gakuin University, 9.Tohoku University, 10.Kyushu University, 11.RIKEN)

[PEM08-P21] Soft-X ray emissions from Geospace: Possible science objectives of GEO-X

*Yoshizumi Miyoshi[1], Yosuke Matsumoto[2], Yuichiro Ezoe[3] (1.Institute for Space-Earth Environmental Research, Nagoya University, 2.Chiba University, 3.Tokyo Metropolitan University)

[PEM08-P22] Effects of Solar Proton Event on Global Lightning Activity

*Mitsuteru Sato[1], Ryuho Kataoka[2] (1.Department of Cosmoscience, Hokkaido University, 2.National Institute of Polar Research)

[PEM08-P23] Atmospheric electric field measurement for the study of space and atmospheric climate changes

*Masashi Kamogawa[1], Yasuhiro Minamoto[2], Akira Kadokura[3], Mitsuteru Sato[4] (1.Global Center for Asian and Regional Research, University of Shizuoka, 2.Laboratory for Environmental Research at Mount Fuji, 3.National Institute of Polar Research, 4.Hokkaido University)

[PEM08-P24] Current status of the new multi-frequency millimeter-wave spectrometer installed at Showa Station and initial results of multi-line observations

*Akira Mizuno[1], Daichi Tsutsumi[1], Takahiko Kosegaki[1], Hiroyuki Iwata[1], Kouki Satani[1], Taku Nakajima[1], Kohei Haratani[1], Tomoo Nagahama[1], Syoki Iriyama[1], Genma Mizoguchi[1], Shixun Fan[1], Naoto Sekiya[2], Takuma Hayashi[2], Masaki Tsutsumi[3], Yoshihiro Tomikawa[3], Mitsumu K. Ejiri[3], Kaoru Sato[4] (1.ISEE, Nagoya University, 2.University of Yamanashi, 3.National Institute of Polar Research, 4.University of Tokyo)

[PEM08-P25] Antarctica-based future space weather research project since 2022

*Ryuho Kataoka[1] (1.National Institute of Polar Research)

[PEM08-P26] Development of real-time prediction system of CME arrival and magnetic field with ensemble SUSANOO-CME simulation 2

*Daikou Shiota[1,4], Seiji Yashiro[2], Ryuho Kataoka[3], Kazumasa Iwai[4], Yusuke Ebihara[5], Kaori Sakaguchi[1], Yuki Kubo[1] (1.National Institute of Information and Communications Technology (NICT), 2.Catholic

University of America, 3.National Institute of Polar Research, 4.Institute for Space-Earth Environmental Research, Nagoya University, 5.Research Institute for Sustainable Humanosphere, Kyoto University)

[PEM08-P27] Ionospheric storms in GAIA under lower atmospheric and magnetospheric inputs

*Chihiro Tao[1], Hidekatsu Jin[1], Hiroyuki Shinagawa[1], Yasunobu Miyoshi[2], Hitoshi Fujiwara[3] (1.National Institute of Information and Communications Technology, 2.Kyushu University, 3.Seikei University)

[PEM08-P28] The relevance between cosmic ray and ozone depletion

*Kazuyoshi Yamashita[1] (1.The Open University of Japan)

[PEM08-P29] Geomagnetically induced currents observed around solar minimum of Cycle 24

*Shinichi Watari[1], Satoko Nakamura[2], Yusuke Ebihara[3], Aoi Nakamizo[1] (1.National Institute of Information and Communications Technology, 2.Institute for Space-Earth Environmental Research, Nagoya University, 3.Research Institute for Sustainable Humanosphere, Kyoto University)

NASA Goddard Space Flight Center Space Weather Activities

*Antti A Pulkkinen[1]

1. NASA Goddard Space Flight Center

The NASA Goddard Space Flight Center’ s Heliophysics Science Division (HSD) conducts research on the Sun, its extended solar-system environment (the heliosphere), and interactions of Earth, other planets, small bodies, and interstellar gas with the heliosphere. Division research also encompasses geospace -- Earth's uppermost atmosphere, the ionosphere, and the magnetosphere -- and the changing environmental conditions throughout the coupled heliosphere. Scientists in the HSD develop models, spacecraft missions and instruments, and systems to manage and disseminate heliophysical data. They interpret and evaluate data gathered from instruments, draw comparisons with computer simulations and theoretical models, and publish the results. The Division also conducts education and public outreach programs to communicate the excitement and social value of NASA heliophysics.

Space weather is a major part of HSD activities and the Division is the home for entities such as Community Coordinated Modeling Center and Space Physics Data Facility. HSD scientists work in close collaboration with federal partner organizations such as NOAA, USGS and Air Force to help transition the latest scientific information into space weather operations. HSD scientists are also supporting many of the National Space Weather Action Plan goals and play significant role in a variety of international space weather efforts. In this talk, we will provide a general introduction to HSD and its many activities that pertain to space weather. We also discuss our views for future directions of space weather and opportunities for enhanced collaborations.

Keywords: Space weather, Heliophysics

©2021. Japan Geoscience Union. All Right Reserved.

Relationship between X-ray and EUV solar flare emissions and the Dellinger phenomenon

*Kyoko Watanabe[1], Munechika Arao[1], Shohei Nishimoto[1], Chihiro Tao[2], Michi Nishioka[2]

1. National Defense Academy of Japan, 2. National Institute of Information and Communications Technology

The radiation from the sun is the most important ionization and heating energy source for the Earth’s upper atmosphere. When solar flares occur, the intensity of multi-wavelength electromagnetic emissions suddenly increases. Among these, the intensification of X-rays to extreme ultraviolet (EUV) emissions accelerates the ionization and molecular dissociation of atmospheric components in the ionosphere and thermosphere, and it may cause a sharp increase in electron density. It is generally considered that ultraviolet (UV) emissions with a long wavelength of 100 nm or more affect the lower atmosphere, whereas short-wavelength EUVs and X-rays may also affect the mesosphere (e.g. Woods et al., 2000). These short-wavelength UV radiation reaches the ionosphere D region at 60–90 km, thereby causing an increase in electron density in this region. The communication failure caused by the absorption of the short-wave due to the variations in electron density in the ionosphere D region is known as the Dellinger phenomenon (Dellinger 1937). Generally, the Dellinger phenomenon is considered to be caused by the occurrence of M-class or higher solar flares and predicted by using the magnitude of the solar flares. However, reportedly, the Dellinger phenomenon sometimes occurred even in during C-class flares; however, it did not occur even in during X-class flares (e.g. Tao et al., 2020). From these results, it is considered that the flare emissions contributing to the occurrence of the Dellinger phenomenon may also be affected by emissions that are not proportional to the X-ray intensity.

The occurrence of the Dellinger phenomenon can be known by using the minimum reflection frequency (fmin) from vertical incident ionograms. When a strong Dellinger phenomenon occurs, the reflected wave from ionosonde becomes invisible due to ionospheric absorption, and the fmin cannot be measured. However, in the case of the Dellinger phenomenon, which is not too strong, increases of fmin values are observed. Therefore, we checked the fmin observed in the ionosonde held by the National Institute of Information and Communications Technology (NICT) at Kokubunji. And then, we statistically compared with the solar flare emission (X-rays and EUVs). When the fluctuation of fmin (about 4,000 events) between 1996 and 2018 was compared with the GOES X-ray intensity, a relationship was seen that was almost in agreement with the results of previous studies (Sato, 1975; Tao et al., 2020).

In this paper, we will report the results of statistical comparison of the Dellinger phenomenon (fmin fluctuation) that occurred from 1996 to 2018 with X-ray data. We also report on the results of comparisons between fmin and EUV data which are observed by the Solar and Heliospheric Observatory (SOHO)/Solar EUV Monitor (SEM) and Project for On-Board Autonomy (PROBA)-2/LYman-alpha RAdiometer (LYRA), and discuss the effects of EUV emission on the Dellinger phenomenon.

Keywords: Dellinger phenomenon, Solar flare, EUV

©2021. Japan Geoscience Union. All Right Reserved.

A comparative study of the empirical and physics-based methods for solar flare predictions

*Kaho Kondo[1], Kanya Kusano[1]

1. Institute for Space-Earth Environmental Research, Nagoya University

Solar flares suddenly emit electromagnetic waves, plasma, and energetic particles into the interplanetary space, and cause space weather disturbances. Therefore, the prediction of solar flares is important to mitigate the space weather impact. For predicting solar flares, various types of empirical methods have been developed so far, and very recently the physics-based prediction of large solar flares, called the kappa-scheme, has been developed by Kusano et al. (2020). In this study, we conduct a comparative study of empirical and physics-based predictions of solar flares with the aim of developing a new type of solar flare prediction by combining empirical methods and the physics-based method. As the preliminary study, we focus on Schrijver’ s R-parameter (Schrijver 2007), which is given by the unsigned magnetic flux near the polarity inversion line (PIL) of the high magnetic gradient, as a typical empirical method. First, we use the vector magnetic field data of the active region NOAA 12673 observed by the Solar Dynamics Observatory before the onset time of the largest solar flare in the solar cycle 24 (11:48 UT on September 6, 2017), and calculated the unsigned magnetic flux (local magnetic flux) within a circle of radius 2 Mm centered at each point on the PILs. As a result, we found the following features. (1) The local magnetic flux correlates well with the magnetic gradient on PIL. (2) The local magnetic flux was also high at the flaring point predicted accurately by the kappa-scheme. (3) However, there were places where the local magnetic flux was high although flare did not occur. The results suggest that the local magnetic flux near PIL is only partially related to the predictors of the kappa-scheme. Second, we calculated the total unsigned magnetic flux within 2 Mm from all points on PILs for the two groups of active regions. Group 1 is seven active regions that produced flare larger than the GOES X2-class and group 2 is 199 active regions that did not produce any X-class flare for 20 hours after the observation. The comparison between the analyses of the unsigned total flux and the kappa-scheme suggests that the kappa-scheme can better discriminate the two groups than the unsigned total flux while the unsigned total flux has a moderate power to discriminate the flaring active regions. We consider a new scheme using these results.

Keywords: solar flare, prediction, space whether

©2021. Japan Geoscience Union. All Right Reserved.

Data-driven MHD Simulation of Solar Active Region NOAA 11283

*Yeongmin Kang[1], Takafumi Kaneko[1], Kanya Kusano[1]

1. Institute for Space-Earth Environmental Research

Solar eruptive events such as flares or prominence eruptions are caused by the release of magnetic energy accumulated in the solar atmosphere. They occur in the solar active regions (ARs) where the strong magnetic fields are present. Focusing on flare events, not all of the energy accumulated in AR is released with a single flare. It is still difficult to predict the exact value of released energy. Moreover, the physical mechanism to determine the ratio between the released energy and the stored magnetic energy is unclear because the coronal magnetic field cannot be observed directly. MHD simulation is a powerful method to investigate and understand the evolution of the coronal magnetic fields. In this study, we conducted an MHD simulation on AR11283 where multiple M and X class flares have occurred. The objective of this study is to know about the energy release rate of these two flares and the physical mechanism to determine the rate. We applied a newly developed data-driven simulation method in which the time series observational photospheric magnetic field data are introduced as the bottom boundary condition to the MHD simulation. The SDO/HMI vector magnetic data of AR11283 were used. As a result, the dynamic evolution of the coronal magnetic fields was reproduced. We investigated the energy build-up and evolution of trigger magnetic fields leading to the sudden energy releases.

Keywords: Sun, AR11283, MHD Simulation, Solar Flare

©2021. Japan Geoscience Union. All Right Reserved.

Unusual enhancement of ~30 MeV proton flux in an ICME sheath region

*Takahiro Obara[1], Mitsuo Oka[2], Nariaki V Nitta[3], Seiji Yashiro[4], Daikou Shiota[5], Kiyoshi Ichimoto[6]

1. Planetary Plasma and Atmospheric Research Center,Tohoku University, 2. University of California Berkeley, 3. Lockheed Martin Solar and Astrophysics Laboratory, 4. The Catholic University of America, 5. National Institute of Information and Communications Technology, 6. Kyoto University

In gradual Solar Energetic Particle (SEP) events, shock waves driven by coronal mass ejections (CMEs) play a major role in accelerating particles, and the energetic particle flux enhances substantially when the shock front passes by the observer. Such enhancements are historically referred to as Energetic Storm Particle (ESP) events, but it remains unclear why ESP time profiles vary significantly from event to event. In some cases, energetic protons are not even clearly associated with shocks. Here we report an unusual, short-duration proton event detected on 5 June 2011 in the compressed sheath region bounded by an interplanetary shock and the leading-edge of the interplanetary CME (or ICME) that was driving the shock. While <10 MeV protons were detected already at the shock front, the higher-energy (>30 MeV) protons were detected about four hours after the shock arrival, apparently correlated with a turbulent magnetic cavity embedded in the ICME sheath region.

Keywords: SEP, shock, acceleration

©2021. Japan Geoscience Union. All Right Reserved.

Development of spectral riometer for observation of energetic electron precipitation at Syowa Station, Antarctica

*Yoshimasa Tanaka[1,2,3], Masayuki Yamamoto[4], Koji Nishimura[1,2,3], Hisao Yamagishi[1], Antti Kero[5], Akira Kadokura[1,2,3], Akira Mizuno[6], Akira Sessai Yukimatu[1,3], Herbert Akihito Uchida[3], Ryuho Kataoka[1,3], Yasunobu Ogawa[1,2,3], Takanori Nishiyama[1,3], Masaki Tsutsumi[1,3], Mitsunori Ozaki[7], Yoshizumi Miyoshi[6], Shin-ichiro Oyama[6], Fuminori Tsuchiya[8]

1. National Institute of Polar Research, 2. Polar Environment Data Science Center, Joint Support-Center for Data Science Research, Research Organization of Information and Systems, 3. The Graduate University for Advanced Studies, SOKENDAI, 4. National Institute of Information and Communications Technology, 5. Sodankyla Geophysical Observatory, 6. Institute for Space-Earth Environmental Research, Nagoya University, 7. Faculty of Electrical and Computer Engineering, Institute of Science and Engineering, Kanazawa University, 8. Planetary Plasma and Atmospheric Research Center, Graduate School of Science, Tohoku University

Recently, from the viewpoint of the space weather research, much interest has been focused on the effect of energetic electron precipitation (EEP) from the magnetosphere on the atmosphere. The precipitation of the electrons with energies greater than several tens of keV can be detected by riometers from the ground. The riometer is an instrument that measures the ionospheric absorption of cosmic radio noise (CRN), which is caused by the electron density enhancement mainly in the ionospheric D region due to the auroral electron precipitation. However, the existing riometer which observes the CRN at a single frequency can detect the appearance of EEP only, but it cannot estimate the flux of the precipitating electrons quantitatively. In order to investigate the flux of precipitating electrons quantitatively, a wide-band riometer, so-called spectral riometer has recently been developed by the Sodankyla Geophysical Observatory (SGO) (Kero et al., 2014). We have developed the spectral riometer to conduct the wide-band-frequency riometer observation at Syowa Station, Antarctica, during the 63rd Japanese Antarctic Research Expedition (JARE-63, 2022-2023). The spectral riometer measures cosmic noise absorption (CNA) in the frequency range from 20 to 60 MHz and enables us to estimate the height profile of the electron density between about 50 and 120 km and the electron energy spectra in the energy range from several keV to about 1 MeV.

There is a problem to be solved in the spectral riometer observation at Syowa Station. At Syowa, a high-power atmosphere radar, PANSY, is being regularly operated at a frequency of 47 MHz, which is inside the frequency range of the spectral riometer. To solve this problem, we collect only the CRN signals when the PANSY radar is not transmitting pulses by using the software-defined radio (SDR) technique. The CRN signals and the transmission timing pulses from the radar are sampled by a sampler for SDR, and then the signals are transferred to the personal computer (PC). Using the transmission timing pulse, PC extracts CRN signals when the PANSY radar is not transmitting. The extracted CRN signals are then fast Fourier transformed and decimated in real-time, and the obtained power spectra are recorded every second. In the presentation, we will show the scientific goal of the spectral riometer observation, the observation system, and results of test observation.

References:

Kero, A., J. Vierinen, D. McKay-Bukowski, C.-F. Enell, M. Sinor, L. Roininen, and Y. Ogawa, Ionospheric electron density profiles inverted from a spectral riometer measurement, Geophys. Res. Lett., doi:10.1002/2014GL060986, 2014.

Keywords: aurora, energetic electron precipitation, riometer, Syowa Station, cosmic noise absorption, software-defined radio

©2021. Japan Geoscience Union. All Right Reserved.

©2021. Japan Geoscience Union. All Right Reserved.

Auroral oval in the last 3000 years and future

*Ryuho Kataoka[1], Shin ya Nakano[2]

1. National Institute of Polar Research, 2. The Institute of Statistical Mathmatics

We investigate the global shape of auroral oval based on the paleomagnetism models for the last 3000 years. Recent IGRF models are also used for future extraporation. Similar method as proposed by Oguti (1993, JGR) is adopted to draw the auroral oval. The method as well as the dependence on the geomagnetic activity etc. are examined by the >30 year data from DMSP satellites and the >70 year data from ground-based magnetometers located at high latitudes. It is confirmed that there is only a weak effect of the dipole moment to change the shape of the auroral oval, as theoretically expected.

Keywords: aurora, paleogeomagnetism

©2021. Japan Geoscience Union. All Right Reserved.

Solar cycles around the onset of the Maunder Minimum

*Hiroko Miyahara[1], Fuyuki Tokanai[2], Toru Moriya[2], Mirei Takeyama[2], Hirohisa Sakurai[2], Kazuho Horiuchi[3], Hideyuki Hotta[4]

1. College of Art and Design, Musashino Art University, 2. Faculty of Science, Yamagata University, 3. Graduate School of Science and Technology, Hirosaki University, 4. Graduate School of Science, Chiba University

The Sun indicates long-term activity variations at the time scales of a few hundred years to a few millenia, and sometimes experience grand minima when number of sunspots significantly decreases for more than several decades. In order to understand the physical mechanism of such grand minima, we conducted high-precision measurements of carbon-14 in tree rings with annal resolution and reconstructed the solar cycles around the onset of the Maunder Minimum (1645-1715 CE). In this presentation, we report the transition of cycle lengths indicated by the high-precision data.

Keywords: Solar cycle, Grand solar minimum, The Maunder Minimum, Carbon-14

©2021. Japan Geoscience Union. All Right Reserved.

Simultaneous observation of cosmic rays with muon detector and neutron monitor at the Syowa station in the Antarctic

*Chihiro Kato[1], Kazuoki Munakata[1], Akira Kadokura[2], Ryuho Kataoka[2], Shoko Miyake[3], Paul Evenson[4], Shunta Asano[1]

1. Shinshu University, 2. National Institute of Polar Research, 3. National Institute of Technology, Ibaraki College, 4. University of Delaware

Since 2018.2, simultaneous observation of cosmic ray muon and neutron is continued. The operation is quite stable and its duty cycle is higher than 94%. These detectors are showing their usefulness by responding to, for example, a peculiar CME event in August 2018. There is another interesting event in September 2019. A Sudden Stratospheric Warming (SSW) was observed and muon counts responded to the SSW. This response is caused by that muon counts on the ground are affected by high altitude temperature. Temperature effect on CR muon now can be corrected with high altitude temperature data. There is, however, some matter of research about how the method works. This event seems to be valuable to improve correction method. We describe a character of muon and neutron data accumulated during the last three years and discuss potential use in studying atmospheric effect on CR muon and neutron count rates.

Keywords: Cosmic Ray, Atmospheric Effect

©2021. Japan Geoscience Union. All Right Reserved.

Measurement of cosmogenic 10Be in endogenic travertine deposits at Baishuitai

*Hiroko Miyahara[1], Hongyang Xu[2], Limin Zhou[2], Kazuho Horiuchi[3], Hiroyuki Matsuzaki[4]

1. College of Art and Design, Musashino Art University, 2. East China Normal University, 3. Hirosaki University, 4. The University Museum, The Univ. of Tokyo

Past solar and cosmic ray variations are often reconstructed using the carbon-14 in tree rings and the beryllium-10 in ice cores. Previous studies have suggested that beryllium-10 in travertine deposits may also reflect the temporal variation of cosmic rays and thus can be used to trace the past solar activity variations. In this paper, we report our preliminary results obtained from the measurement of beryllium-10 in annual layers of travertine from Baishutai, China.

Keywords: Cosmogenic nuclide, solar activity, cosmic ray variations

©2021. Japan Geoscience Union. All Right Reserved.

Be-7 in Japan, Iceland and Thailand during solar cycle 24 descent phase

*Hirohisa Sakurai[1], Youmei Kawamura[1], Souichiro Suzuki[1], Fuyuki Tokanai[1], Emiko Inui[1], Mirei Takeyama[1], Toru Moriya[1], Satosi Kikuchi[1], Fusa Miyake[2], Akira Kadokura[3], Natsuo Sato[3], Naoko Sugihara[6], Bjornsson Gunnlaugur[4], David Ruffolo[5], Warit Mitthumsiri[5], Ronald Macatangay[7]

1. Yamagata University, 2. ISEE, Nagoya University, 3. National Institute of Polar Research, 4. Science Institute, Iceland University, 5. Department of Physics, Mahidol University, 6. Department of Chemical Oceanography Atmosphere and Ocean Research Institute,The University of Tokyo, 7. National Astronomical Research Institute of Thailand

Be-7 concentrations (BEC) in surface air should be correlated to cosmic rays, because Be-7 is produced by interactions between cosmic rays and nitrogen and/or oxygen in the atmosphere, and then it falls down with aerosols. Since cosmic rays which reach the earth are modulated by the solar activities when travelling the heliosphere, the variation in BEC involve some modulation profiles such as 27-day variation and 11-year solar cycle. Daily Be-7 concentrations in surface air have been continuously observed at Yamagata (38˚ N), Japan since 2000. To investigate the latitude effect of 11-year solar cycle, we set up a daily observation system of Be-7 concentration at Husafell in Iceland located (64˚ N) and have been continuously observed BEC since September 2003 as well as in Japan. Furthermore, we set up a daily observation system of Be-7 concentration at Bangkok in Thailand located (13.7˚ N) and have been continuously observed BEC since June 2014.

The BEC at Iceland, Japan, and Thailand were 2.0 mBq/m^3, 5.5 mBq/m^3, and 2.0 mBq/m^3 on average during 2015 and 2019, respectively, representing a kind of latitude effect. The increasing rates of BEC from 2019 to 2015 were 29.8%, 19.6%, and 43.5% at Iceland, Japan, and Thailand, respectively, while that of Oulu neutron monitor data was 8.8%. The larger increasing rates of BEC than the neutron monitor data is due to the much lower production threshold of Be-7 which is approximately 10MeV. Also, the latitude effects of BEC would indicate a response of cosmic ray spectral variation at lower energy band caused by solar modulation. However, as the increasing rates include a factor of air-mass advection in the atmosphere, the rates do not merely appear the solar modulation of cosmic rays. We describe the observed data of Be-7 concentrations taking account of latitudes effects of Be-7 production rates in the stratosphere and troposphere.

Keywords: Be-7, cosmogenic nuclide, solar modulation

©2021. Japan Geoscience Union. All Right Reserved.

Forecast of energetic electron flux variations of the outer belt using the machine learning

*Satoshi Fukuoka[1], Yoshizumi Miyoshi[1], Daikou Shiota[2], Shinji Saito[4], Takefumi Mitani[3], Tomoaki Hori[1], Nana Higashio[3], Shun Imajo[1], Iku Shinohara[3]

1. Institute for Space-Earth Environmental Research, Nagoya University, 2. National Institute of Information and Communications Technology (NICT), 3. Japan Aerospace Exploration Agency, Institute of Space and Astronautical Science, 4. National Institute of Information and Communications Technology

The relativistic/sub-relativistic electron flux variations of the outer radiation belt often cause serious damage on the satellite operations through the dielectric charging. In order to forecast flux variations of these electrons, various forecast methods based on the physics-based simulation and empirical modeling have been developed. For the physics-based simulation, we have operated the SUSANOO system that is simulating a code-coupling simulation of heliosphere and radiation belt provides MeV electron flux variations for the next couple of days. For the empirical modeling, the linear prediction filter and the auto-regressive moving average are popular methods, which have been used for the forecast of MeV electrons. Recently, the machine learning techniques have widely been used for the space weather forecast, for example, ionospheric variations, the flare prediction, etc. In this study, we have developed the forecast system of relativistic/sub-relativistic electron flux variations based on long short-term memory recurrent neural network (LSTM-RNN). As the training data, we use the solar wind data and energetic electron data observed by Arase/HEP, XEP instruments at different L-shells of the outer belt. Our developed network provides time variations of the energetic electron flux around L=4,5,6 using the solar wind data as an input parameter. In this presentation, we will report the forecast performance, focusing on how forecast skills depend on the lead-time and energy ranges.

Keywords: Forecast of energetic electron flux

©2021. Japan Geoscience Union. All Right Reserved.

Spacecraft surface charging environment in the medium earth orbit

*Masao Nakamura[1], Kosei Nagasawa[1]

1. Osaka Prefecture University

Analysis of spacecraft surface charging in the medium earth orbit (MEO) is important for spacecraft designs and operations, because the significant charging sometimes cause spacecraft anomalies due to discharging arcs. We study the surface charging environment using the Electric Field and Wave instruments (EFW) and the Helium Oxygen Proton Electron (HOPE) data of the Van Allen Probes. The charging events (< -50 V) are located about 25000 km further away from the center of the Earth and in the mid-night to dawn region. Among them, the significant charging (< -1 kV) events are only observed in eclipse. By using a charging analysis tool for the Van Allen Probes, we analyze the electron and ion energy flux spectrum observed in eclipse. The electrons usually have multi-temperature spectrum. For the onset of negative charging, the incoming hot electron (~ keV) current overcomes the outgoing secondary electron current emitted by warm electron (~hundreds eV) impacts. The analysis shows that the combination of critical temperature and threshold density of the hot electrons give the criterion for the onset of negative charging in the MEO eclipse. We will discuss the charging events in sunlight and the relationship between the charging events and space weather conditions.

Keywords: Spacecraft surface charging, Medium earth orbit, Space weather

©2021. Japan Geoscience Union. All Right Reserved.

Active Region Detection in the HMI magnetograms using the Mask R-CNN technique

*Akito Komatsu[1], Yusuke Iida[1]

1. Niigata University

For predicting solar flares, it is necessary and important to detect active regions accurately. Conventionally, active regions is detected using rule-based methods with the defined thresholds. In this study, we aimed to establish a noval prediction method that goes beyond the rule-based flare prediction method by using the Mask R-CNN technique.
We used the full-disk line-of-sight magnetograms taken by SDO/HMI from May 2010 to July 2011 for the inpbackground image, the SHARP dataset for annotation, and the SWAN dataset for labeling. We reduced the data cadence to 1 hour and used 80% for training and 20% for testing. Training is performed using Mask R-CNN, which is one of the methods of Instance Segmentation. Mask R-CNN takes the background image and the annotation for the object position in the image as input, and learns the features of the region representing the object in the image. The network can detect the bounding box and mask that indicate the location of the object in the image. The network of the Mask R-CNN is divided into a Region Proposal network (RPN), which detects the location of the object, and a recognition network that detects which object the detected region represents. Based on the feature map obtained from the Resnet51 pre-trained model, network reduce the loss functions of Class, BoundingBox, and Mask.
As a result of training, we achieved Average Precision[IoU=0.50] =0.940 with the constructed model. Since the maximum accuracy of training and detection in natural images using Mask R-CNN is about Average Precision[IoU=0.50] =0.600, we have shown that the Mask R-CNN is the very effective method even for solar magnetic images. In the future, we would like to construct a model that can predict whether the detected region actually causes a flare or not.

Keywords: Space weather, Deep learning, Image recognition, Big data

©2021. Japan Geoscience Union. All Right Reserved.

Operations of Solar Flare Prediction Model Using Deep Neural Networks

*Naoto Nishizuka[1], Yuki Kubo[1], Komei Sugiura[2], Mitsue Den[1], Mamoru Ishii[1]

1. National Institute of Information and Communications Technology, 2. Keio University

Solar flares are an origin of space weather phenomena, and it is important to predict solar flares more accurately. Especially, an automated prediction model in real-time operations, which can be used by even non-scientists and can give a better feedback from previous prediction experience, is expected. In our previous works, we developed an operational solar flare prediction model using deep neural networks, named Deep Flare Net (DeFN). DeFN can issue probabilistic forecasts of solar flares in two categories, such as >=M-class and <M-class events or >=C-class and <C-class events, occurring in the next 24 h after observations and the maximum class of flares occurring in the next 24 h. DeFN is set to run every 6 h and has been operated since January 2019.

The input database of solar observation images taken by the Solar Dynamic Observatory (SDO) is downloaded from the data archive operated by the Joint Science Operations Center (JSOC) of Stanford University. Active regions are automatically detected from magnetograms, and 79 features are extracted from each region nearly in real-time using multiwavelength observation data. Flare labels are attached to the feature database, then the database is standardized and input into DeFN for prediction. DeFN was pretrained using the datasets obtained from 2010 to 2015. The model was evaluated with the skill score of the true skill statistics (TSS) and achieved predictions with TSS = 0.80 for >=M-class flares and TSS = 0.63 for >=C-class flares.

For comparison, we evaluated the operationally forecast results from January 2019 to June 2020. We found that operational DeFN forecasts achieved TSS = 0.70 (0.84) for >=C-class flares with the probability threshold of 50 (40) %, although there were very few M-class flares during this period and we should continue monitoring the results for a longer time. Here, we adopted a chronological split to divide the database into two for training and testing. The chronological split appears suitable for evaluating operational models. Furthermore, we proposed the use of time-series cross-validation.

In this talk, we would like to introduce our solar flare prediction model, Deep Flare Net, and the operational prediction results. We also would like to discuss the standard evaluation methods for operational forecasting models, such as the preparation of observation, training, and testing datasets, and the selection of verification metrics.

Keywords: solar flares, space weather forecasting, operational model, deep neural networks, verification

©2021. Japan Geoscience Union. All Right Reserved.

Empirical/physical-based modeling of three-dimensional outer radiation belt for real-time operation

*Shinji Saito[1], Kaori Sakaguchi[1], Yuki kubo[1]

1. National Institute of Information and Communications Technology

Radiation belt electrons are controlled by various processes occurring in the earth's magnetosphere. Time and spatial scales of the processes are very broad, so it is difficult to demonstrate dynamics of electron radiation belts by only one physics-based model. Coupling of several models would be necessary to demonstrate radiation belt dynamics.
There are various empirical models to estimate the conditions of the earth's magnetosphere. If we can appropriately couple these empirical models, we might be able to reproduce the temporal variation of the geospace condition, and apply it to solve dynamics of radiation belt electrons using physics-based model. Based on this idea, we are developing the three dimensional radiation belt model coupling both empirical models for global dynamics, and physics-based models for electron kinetic dynamics, in order to forecast energetic electron environment at any location in magnetosphere.
In this talk we will introduce a provisional version of the three-dimensional (global) radiation belt model. This model couples two empirical models and one physics-based model to form the global radiation belt model. Empirical models used here calculate three-dimensional magnetic field configulation (Tsyganenko model TS04) and an energetic electron distribution j(L,E), where L is a L-value, E is an electron kinetic energy. Both models can be driven by real-time solar wind data set. As a physics-based model, we use a guiding-centered test-particle model, which calculates trajectories of energetic test-electrons in the three-dimensional magnetic field. The global radiation belt model imports real-time solar wind data, and calculates the magnetic field configuration and energetic electron flux distribution in L and E using empirical models. The test-particle model, which is the physics-based model, expands the electron flux distribution in L coordinate into that in the three dimensional GSM coordinate in earth's magnetosphere, by tracing adiabatic trajectories of test-electrons with energy E.
By tracing all of test-electrons distributed in outer radiation belt region, the model enables us to calculate phase space density in three-dimensional outer radiation belt. The model with higher-versions is expected to incorporate particle scattering processes corresponding to radial diffusion, pitch angle scattering, and nonlinear acceleration. The goal of this model is to demonstrate the temporal variation of three dimensional electron radiation belt governed by many kinds of electron scattering processes for real-time operation.

Keywords: electron radiation belt, numerical modeling, test-particle simulation

©2021. Japan Geoscience Union. All Right Reserved.

Mid-term Research Plan of NICT Space Weather Monitoring and Forecast

*Mamoru Ishii[1]

1. National Institute of Information and Communications Technology

National Institute of Information and Communications Technology, Japan (NICT) starts the fifth mid-term research plan since April 2021. Space Environment Laboratory, NICT is in charge of operational space weather monitoring and forecast in Japan, and the new research and development plan for space weather monitoring and forecast starts at the same time.

NICT has a long history to observe space weather phenomena with ground-based sensors, e.g., ionosondes, solar radio telescope, and GNSS receivers. In addition to the domestic observation, we have an international cooperative project for monitoring ionospheric disturbance in the equatorial region e.g., equatorial plasma bubbles (EPBs) in South-east Asia. We will try to extend the network under the cooperation. In addition, we will seek the opportunity of development of satellite-based sensors.

Prediction models are important to have precise space weather forecast. We have been developing numerical code for predicting the response of solar wind, magnetosphere and ionosphere with the solar activities. We will start operational forecast using data assimilation with these numerical codes.

For the dissemination of space weather information, we have been providing space weather forecast since 1988. We keep the communication with information users by establishing space weather users' committee for seeking the requirement of users. We will continue the activity and provide the necessary information for users.

We expect some specific targets of our activity is, high-precision satellite positioning with QZSS, support of deep space exploration for providing space weather information, and mitigation of space weather disaster by providing benchmark.

Keywords: space weather, ionosphere, magnetosphere, sun/solar wind

©2021. Japan Geoscience Union. All Right Reserved.

Development of a prediction system of the sporadic E layer occurrence: Current status and future prospects

*Hiroyuki Shinagawa[1], Chihiro Tao[1], Hidekatsu Jin[1], Yasunobu Miyoshi[2], Hitoshi Fujiwara[3]

1. National Institute of Information and Communications Technology, 2. Kyushu University, 3. Seikei University

Prediction of sporadic E (Es) layers is one of the most important issues in the space weather forecast. In our space weather forecasting, one-day prediction of the Es layer occurrence has been done, based on current observations of Es layers obtained by our ionosondes. However, Es layers occasionally show significant day-to-day variations, and present conditions may not last until one day later. In order to study a method of the Es layer occurrence prediction, we analyzed the simulation data of the whole atmosphere-ionosphere coupled model GAIA, and compared the data with foEs data. We found that the ion convergence at 120 km altitude agrees fairly well with the variation in the observed foEs. Based on this result, we have been investigating a prediction scheme of the Es layer occurrence. Our group has recently developed a real-time GAIA simulation system, which is capable of predicting ionospheric conditions for a few days ahead. Using data obtained from the real-time GAIA, we are developing a prediction system of the Es layer occurrence. We will report the status of development of the prediction system, preliminary results, problems, and future prospects.

Keywords: Sporadic E layer, Model, Prediction, Vertical ion convergence

©2021. Japan Geoscience Union. All Right Reserved.

Economic impacts of atmospheric radiation storm on aircraft operations and potential use of space weather information

*Susumu Saito[1], Navinda Kithmal Wickramasinghe[1], Tatsuhiko Sato[2], Daikou Shiota[3]

1. Electronic Navigation Research Institute, National Institute of Maritime, Port, and Aviation Technology, 2. Japan Atomic Energy Agency, 3. National Institute of Information and Communications Technology

Secondary particles generated by a solar energetic particle (SEP) event cause an atmospheric radiation storm (ARS) at aircraft cruising altitudes. Radiation storm is one of the advisories in the space weather information service for aircraft operations provided by the International Civil Aviation Organization (ICAO). However, it has not been defined well how aircraft operators shoud react when such advisories are issued.

In order to contribute to establishing effective reactions to space weather information, we estimate the economic impact which would be induced when certain means are taken to mitigate the radiation hazard. This would be an important information to establish effective reactions to space weather radiation advisories.
We used the Warning System for AVIation Exposure to Solar energetic particle (WASAVIES) to estimate the effective dose rate (EDR) along the aircraft trajectory. Flight path length, flight time, and fuel consumption for realistic flight routes are calculated by using a flight trajectory generation algorithm and the aircraft performance parameters from the Base of Aircraft Data (BADA) model developed by EUROCONTROL.

We used the conditions of the GLE-69 event as a reference. Two routes from Japan which go through high latitude regions, from New York JFK airport (JFK) to Tokyo Narita airport (NRT) and from NRT to London Heathrow airport (LHR), are chosen as examples. We set up flight scenarios based on several strategies of mitigation where constraints on the flight altitude and the latitude are imposed. For each scenarios, flight path length, flight time, and fuel consumption were estimated.

Our results show that the fuel consumption could be increased by 33-58% for JFK-NRT, if very conservative mitigation strategies are taken. Similar analysis has been performed for NRT-LHR.

This economic impact may be reduced, if the space weather nowcast for the ARS associated with the SEP and an optimal flight trajectory generation algorithm are used together. Setting more flexible constraints in the flight route and generating optimal flight trajectories with minimal economic impacts by fully utilizing the global EDR distribution would be effective, which is our next step. Furthermore, prediction of the progress of ARS associated with SEP events would be effective in reducing the economic impacts by adaptively modifying the flight path during the flight.

Keywords: Solar energetic particle event, Economic impact in aircraft operation, Radiation

©2021. Japan Geoscience Union. All Right Reserved.

Status of the GEO-X (Geospace X-ray imager) mission

*Yuichiro Ezoe[1], Ryu Funase[2,6], Harunori Nagata[3], Yoshizumi Miyoshi[4], Hiroshi Nakajima[5], Ikuyuki Mitsuishi[4], Kumi Ishikawa[1], Munetaka UENO[6], Atsushi Yamazaki[6], Hiroshi Hasegawa[6], Makoto Mita[6], Masaki Fujimoto[6], Yasuhiro Kawakatsu[6], Takahiro Iwata[6], Kazuhisa Mitsuda[7], Junko Hiraga[8], Satoshi Kasahara[6], Hironori Sahara[1], Yoshiaki Kanamori[9], Kohei Morishita[10], Takefumi Mitani[6], Masaki Numazawa[11]

1. Tokyo Metropolitan University, 2. University of Tokyo, 3. Hokkaido University, 4. Nagoya University, 5. Kanto Gakuin University, 6. ISAS/JAXA, 7. NAOJ, 8. Kwansei Gakuin University, 9. Tohoku University, 10. Kyushu University, 11. RIKEN

Understanding of geospace environment, especially response of the Earth's magnetosphere to solar wind, is crucial for planetary and space science, astrophysics and space weather. GEO-X (GEOspace X-ray imager) is a small satellite mission aiming global imaging of the Earth's magnetosphere in X-rays. It is proposed to be launched in 2023-25, around which solar cycle 25 is expected to peak. In this paper, we present its science objectives and development of spacecraft, proplusion system, and payload based on cutting edge technologies.

Keywords: Earth's magnetosphere, Global imaging, X-ray

©2021. Japan Geoscience Union. All Right Reserved.

Soft-X ray emissions from Geospace: Possible science objectives of GEO-X

*Yoshizumi Miyoshi[1], Yosuke Matsumoto[2], Yuichiro Ezoe[3]

1. Institute for Space-Earth Environmental Research, Nagoya University, 2. Chiba University, 3. Tokyo Metropolitan University

Recent studies have indicated that charge-exchange between geocorona and On+ ions of the solar wind causes the soft-X ray emission. The soft-X ray emission can be used as a tool to measure global topology of Geospace. In order to investigate how we can observe the soft-X ray emissions, we conduct a computer simulation by a code coupling of the global magnetospheric MHD simulation model (Matsumoto+, 2010) and empirical geocorona model. The simulation shows clear emissions from the dayside sheath region as well as the cusp region. The new satellite project GEO-X has been proposed to measure the soft-X ray emission through solar wind charge exchange (SWCX) from the dayside magnetosphere. In this presentation, we show the possible soft-X ray images by the computer simulation, by considering the GEO-X satellite orbit.

Keywords: solar wind-magnetosphere coupling, soft-Xray emissions

©2021. Japan Geoscience Union. All Right Reserved.

Effects of Solar Proton Event on Global Lightning Activity

*Mitsuteru Sato[1], Ryuho Kataoka[2]

1. Department of Cosmoscience, Hokkaido University, 2. National Institute of Polar Research

Lightning discharges tend to occur at active thunderclouds generated by the strong upward wind, which transports the moist air mass from the ground surface to the upper troposphere. In the global scale, lightning discharges mainly occur in tropical and subtropical land areas because the land surface can be easily heated by the solar radiation, which finally establishes the strong upward wind. Thus, it is the conventional theory that the lightning activities are purely determined by the tropospheric dynamics. However, recent studies show the observational evidences that the lightning activity and lightning-excited radio wave activity are modulated by the energetic solar event, such as solar-X-ray burst and solar proton event. For example, it was shown that the resonance frequency and amplitude of Schumann resonance waves radiated by lightning discharges are rapidly increased during the e energetic solar proton precipitation. It was also shown that the lightning occurrence number and thunder days over Europe were increased after the arrival of the high speed solar wind stream to the Earth and increase of the solar energetic proton flux. Despite these observational facts, it is still not clear whether these modulation was simply created by the rapid change of the Earth-ionosphere waveguide structure or by lightning activity. Even though these modulation was created by the change of lightning activity itself, it is not clear that such change occurs locally or globally. In order to clarify the relation between the energetic solar events and global lightning activity and to identify the effects of solar proton events on the global lightning occurrence number, we have analyzed lighting data derived from the global lightning detection network (WWLLN) and ELF magnetic field waveform data obtained at Syowa station, Antarctica in 2013-2015. We have conducted the superposed epoch analysis for the WWLLN lightning data and have calculated the time variation of the Schumann resonance amplitude and resonance frequency using Syowa ELF data. At the presentation, we will show the detailed results derived from these analysis and will report the effects of the energetic solar events on the global lighting activity.

Keywords: Lightning activity, Solar proton event

©2021. Japan Geoscience Union. All Right Reserved.

Atmospheric electric field measurement for the study of space and atmospheric climate changes

*Masashi Kamogawa[1], Yasuhiro Minamoto[2], Akira Kadokura[3], Mitsuteru Sato[4]

1. Global Center for Asian and Regional Research, University of Shizuoka, 2. Laboratory for Environmental Research at Mount Fuji, 3. National Institute of Polar Research, 4. Hokkaido University

The atmospheric electric field is an electric field perpendicular to the ground and has an average value of about 100 V/m in fair weather. This value varies daily, peaking around 2000 UTC, with a range of variation within tens of percent of the average. This diurnal variation is known to be similar throughout the globe in fair weather. This diurnal variation is called Carnegie Curve after the Carnegie research vessel that contributed to the discovery.

It has been pointed out since around the 1920s that the reason for understanding that the same diurnal variation globally occurs regardless of local time is that the entire earth consists of an electric circuit, called global electrical circuit. The electric circuit consists of a capacitor in which the ionosphere/mesosphere (Approximately 60 km altitude) and the conductive ground (including sea areas), both of which have high atmospheric conductivity, become spherical shell electrodes, and sandwich the atmosphere with low atmospheric conductivity. Although the conductivity of the atmosphere between these electrodes is low, it is slightly conductive due to the ionization of the atmosphere by cosmic rays and natural radionuclides. This yields electric current flows from the ionosphere to the earth in fair weather region due to the atmospheric electric field caused by the potential difference between the two electrodes. This means a discharge process. The atmosphere, therefore, plays a role of resistance in the global electrical circuit. On the other hand, since cloud-to-ground lightning and charged rainfall transport electric charges into the ionosphere and the ground during the thunderstorm activity which continuously and globally. Therefore, the capacitance is always charged in the thunderstorm region, and simultaneously discharged in the fair weather region. The ionospheric potential in the global electric circuit can be understood to some extent by observing the atmospheric electric field in the fair weather region.

Because the atmospheric electric field during fair weather varies greatly due to the presence of radioactive materials and transport of air pollution, many researchers point out that it is affected by global changes in radioactive materials (nuclear bomb tests, nuclear power plant accidents,) as well as climate change. In addition, the ionosphere/magnetosphere and the global electrical circuit are considered to be electrically coupled and not unrelated to space weather.

From the above history, it is considered that the measurement of atmospheric electric field on the ground surface can greatly contribute to the study of space weather and atmospheric climate change. We have conducted the measurement of the atmospheric electric field in Antarctica, where there is no air pollution. Although there is no air pollution in the polar regions, drifting snow is known to be a noise source for measurement. Therefore, we examined the atmospheric electric field generated by these drifting snow and developed a methodology to easily distinguish between drifting snow and fair weather. This made it possible to establish an environment for investigating the relationship between global electrical circuits and climate change and space weather.

©2021. Japan Geoscience Union. All Right Reserved.

©2021. Japan Geoscience Union. All Right Reserved.

Current status of the new multi-frequency millimeter-wave spectrometer installed at Showa Station and initial results of multi-line observations

*Akira Mizuno[1], Daichi Tsutsumi[1], Takahiko Kosegaki[1], Hiroyuki Iwata[1], Kouki Satani[1], Taku Nakajima[1], Kohei Haratani[1], Tomoo Nagahama[1], Syoki Iriyama[1], Genma Mizoguchi[1], Shixun Fan[1], Naoto Sekiya[2], Takuma Hayashi[2], Masaki Tsutsumi[3], Yoshihiro Tomikawa[3], Mitsumu K. Ejiri[3], Kaoru Sato[4]

1. ISEE, Nagoya University, 2. University of Yamanashi, 3. National Institute of Polar Research, 4. University of Tokyo

It is well-known that energetic particle precipitation (EPP) triggered by solar activity produces nitrogen oxides, which catalytically destroy ozone in the polar regions. We have been conducting steady measurements of millimeter-wave spectra of nitric oxide and ozone to monitor the temporal variation in the mesosphere and lower thermosphere above the Showa Station since 2012, in order to study the influences of the energetic particles on the atmospheric composition change. Simultaneous observations of several molecular species which are chemically and dynamically related with can provide useful information to understand the factors that cause temporal changes of atmospheric composition. However, due to the limitation of the instantaneous frequency bandwidth of the backend spectrometer, it is not possible to cover the line spectra of both molecules at the same time, so we had to switch the receiving frequency and observe nitric oxide and ozone alternately. To overcome this situation, we developed a new observing system for multi-frequency observations using a waveguide-type frequency multiplexer (Nakajima et al. 2020).

The new multi-frequency millimeter-wave spectrometer was installed at Showa Station by the 61st Antarctic Research Expedition, and the steady observation was started in November 2020. The new spectrometer enables simultaneous observations of NO, O_3, CO, and HO_2 spectral lines between 230 GHz and 250 GHz. In this spectrometer system, the radio waves are focused by a newly designed frequency-independent optical system using the quasi-optical approximation method (Gonzalez, 2016), and the signals in two frequency bands are extracted by two superconducting mixers cooled by a small power-saving refrigerator (Ulvac UR4K03) with a cooling power of 0.3W. Then, the signals of two frequency bands are recombined through the IF circuit into the 2 GHz band width of the final stage FFT processor to obtain the spectral signals of the multiple molecular species simultaneously.

In the presentation, we will explain the configuration of the new observation system in detail, and summarize the characteristics, problems, and issues of the actual system, and report the initial analysis results of the observation data acquired after November.

[References]
Nakajima et al., “Waveguide-Type Multiplexer for Multiline Observation of Atmospheric Molecules using Millimeter-Wave Spectroradiometer”, *J. Infrared Milli. Terahz Waves*, 41, 1530–1555, 2020.
Gonzalez, A. “Frequency Independent Design of Quasi-optical Systems”, *J. Infrared Milli. Terahz Waves*, 37, 147–159, 2016

Keywords: Millimeter-wave spectroscopy, Polar science, Energetic Particle Precipitation, Atmospheric minor constituents

©2021. Japan Geoscience Union. All Right Reserved.

©2021. Japan Geoscience Union. All Right Reserved.

Antarctica-based future space weather research project since 2022

*Ryuho Kataoka[1]

1. National Institute of Polar Research

We are planning a new Antarctic-based space weather research project, for coming 6 years from April 2022, which covers the solar-maximum active period of solar cycle 25. We will arrange the international collaboration to investigate the high-latitude polar cap, by multiple ground-based all-sky imagers. The low-cost and maintainance-free all-sky cameras with a new housing system are under development. Both polar cap auroral electronss and the direct impact of solar protons are of interest in the open magnetic field region, and possible wavelengths to be observed would be 630.0 nm and 391.4 nm, respectively. We discuss the science goals, and share the latest situation of the preparation to enhance international collaborations.

Keywords: polar cap, aurora, solar proton

©2021. Japan Geoscience Union. All Right Reserved.

Development of real-time prediction system of CME arrival and magnetic field with ensemble SUSANOO-CME simulation 2

*Daikou Shiota[1,4], Seiji Yashiro[2], Ryuho Kataoka[3], Kazumasa Iwai[4], Yusuke Ebihara[5], Kaori Sakaguchi[1], Yuki Kubo[1]

1. National Institute of Information and Communications Technology (NICT), 2. Catholic University of America, 3. National Institute of Polar Research, 4. Institute for Space-Earth Environmental Research, Nagoya University, 5. Research Institute for Sustainable Humanosphere, Kyoto University

The predictions of CME arrival to the Earth and the southward magnetic field brought by the CME flux ropes are one of crucial tasks for space weather forecast. We have developed an MHD simulation of the interplanetary propagation of multiple CMEs with their internal magnetic flux ropes, called as SUSANOO-CME (Shiota & Kataoka 2016). The simulation solves propagation of solar wind and CMEs in the inner heliosphere from 25 solar radii where all the balk flow exceeds fast mode speed. The information of solar wind and CME is specified at the inner boundary with empirical and analytical models using real-time observations of the Sun and the corona.
Recently, we have been constructing a prediction system of CME impacts (CME arrival and magnetic field) utilizing SUSANOO-CME with the real-time solar observations for the purpose of use in space weather forecast in NICT. The system is designed to be controlled through web-browser interfaces in all steps of the simulation: measuring CME speed, editing input parameters, submitting the ensemble jobs into supercomputer, seeing the ensemble results, and seeing aggregated results summarizing all or some of ensemble cases.
In this presentation, showing a demonstration prediction result on a CME occurred on December 7, 2020 associate with a C7.4 flare, we will report the current status of the development and discuss the remaining issues and the future development.

Keywords: CME, solar wind , space weather forecast

©2021. Japan Geoscience Union. All Right Reserved.

Ionospheric storms in GAIA under lower atmospheric and magnetospheric inputs

*Chihiro Tao[1], Hidekatsu Jin[1], Hiroyuki Shinagawa[1], Yasunobu Miyoshi[2], Hitoshi Fujiwara[3]

1. National Institute of Information and Communications Technology, 2. Kyushu University, 3. Seikei University

Upper atmosphere shows variations reflecting complex interactions under inputs from lower and upper regions. These interactions have been an important target of the upper atmosphere physics and space weather purpose. GAIA, Ground-to-Topside Model of Atmosphere and Ionosphere for Aeronomy, is the whole atmosphere model including interaction with ionized plasma under solar EUV variation and a various waves input using a meteorological reanalysis data. We input magnetospheric variation into GAIA via electric field deposition at polar region and auroral electron precipitation using empirical models. We input polar electric potential map based on Weimer model driven by solar wind and interplanetary magnetic field with saturation effect of cross-polar-cap potential for large potential case. Variable auroral precipitation driven by Kp index is considered. Enhancement of total electron content (TEC) up to mid-to-low latitude during the magnetospheric storm event is produced due to the consideration of penetration electric field.
Ionospheric storms, i.e., significant variations of ionospheric plasma, are detected using a scale called “I-scale”, which represents the relative levels of the ionospheric plasma deviations from their 27-day median among their statistical distribution over long-time. As a result, GAIA simulation over January 2019—March 2020 showed increased detection ability of ionospheric storms compared to the high latitude constant case.
We will discuss the effect of high latitude setting on the penetration of electric field and plasma distributions in this presentation.

Keywords: ionospheric storm, GAIA, simulation

©2021. Japan Geoscience Union. All Right Reserved.

The relevance between cosmic ray and ozone depletion

*Kazuyoshi Yamashita[1]

1. The Open University of Japan

In the upper atmosphere, ozone is thought to be destroyed by NOx produced by galactic cosmic rays and solar cosmic rays.In order to clarify the decrease in total ozone with increasing NOx, a correlation map between AEindex and total ozone was created. The results showed that total ozone increased with increasing AEindex at low latitudes in the Northern Hemisphere.This suggests that the decrease in total ozone due to the increase in NOx is due more to galactic cosmic rays than to solar cosmic rays.

Keywords: AEindex, cosmic ray, ozone

©2021. Japan Geoscience Union. All Right Reserved.

Geomagnetically induced currents observed around solar minimum of Cycle 24

*Shinichi Watari[1], Satoko Nakamura[2], Yusuke Ebihara[3], Aoi Nakamizo[1]

1. National Institute of Information and Communications Technology, 2. Institute for Space-Earth Environmental Research, Nagoya University, 3. Research Institute for Sustainable Humanosphere, Kyoto University

We started to install our equipment to substations around Kanto area and to measure geomagnetic induced currents (GICs) by the KAKENHI project (PSTEP) since the end of February 2017. Geomagnetic storms with Dst less than -100 nT occurred only three times during this periods because of solar minimum of Cycle 24. GICs were relatively often observed associated with bay disturbances, which were caused by aurora activities at high latitudes although GICs associated with SSCs or SIs were also observed. A GIC was observed associated with a geomagnetic disturbance by M4.4 flare on 1 April 2017. The geomagnetic disturbance caused by a solar flare is called Solar Flare Effect (SFE). This SFE was not an intense event. Kakioka magnetic observatory reported a SFE with a maximum variation of geomagnetic horizontal component of -67 nT on 15 November 1960. The maximum value of time derivative of this event was approximately -20 nT/min. We will report the analysis of these events using GIC observations of neighboring substations.

After solar minimum in December 2019, solar activities gradually increases and large flares and intense geomagnetic storms are expected. We will continue the GIC measurements and have a plan to utilize the result of the simulation of the Earth’s magnetosphere for the estimation of GICs.

Keywords: Geomagnetically Induced Current (GIC), geomagnetic storm, Sudden Storm Commencement (SSC), Sudden Impulse (SI), bay disturbance, Solar Flare Effect (SFE)

©2021. Japan Geoscience Union. All Right Reserved.

[E] Oral | P (Space and Planetary Sciences)：P-EM Solar-Terrestrial Sciences, Space Electromagnetism & Space Environment

Sat. Jun 5, 2021 9:00 AM - 10:30 AM JST | Sat. Jun 5, 2021 12:00 AM - 1:30 AM UTC | Ch.05 Zoom Room 05

[P-EM12] Dynamics of the Inner Magnetospheric System

convener:Kunihiro Keika(Department of Earth and Planetary Science, Graduate School of Science, The University of Tokyo), Yoshizumi Miyoshi(Institute for Space-Earth Environmental Research, Nagoya University), W Lauren Blum(University of Colorado Boulder), Yuri Shprits(Helmholtz Centre Potsdam GFZ German Research Centre for Geosciences), Chairperson:Lauren W Blum(University of Colorado Boulder), Kunihiro Keika(Department of Earth and Planetary Science, Graduate School of Science, The University of Tokyo)

The inner magnetosphere is highly variable because dynamical variations of incoming energy from the solar wind, magnetospheric tail, and the ionosphere. Cross-regional, cross-scale, and cross-energy couplings are the key processes for understanding this dynamical system. Coordinated observations by multi-satellites and ground-based observations are very essential to revealing these processes. In the 24th and 25th solar cycles, a number of satellites such as Van Allen Probes, MMS, THEMIS, DSX and Arase; coordinated ground-based observations (THEMIS-GBO, SuperDARN, EISCAT, magnetometers, riometer, etc); and numerical simulations (global kinetic model, MHD model, micro PIC, hybrid simulations) have successfully investigated the inner magnetosphere system. We invite papers on recent results of the inner magnetosphere and/or its coupling with the other regions including the ionosphere and the outer magnetosphere. Presentations on new projects such as sounding rocket experiments and data assimilation/machine learning are also welcome.

9:00 AM - 9:05 AM JST | 12:00 AM - 12:05 AM UTC

[PEM12-01] Introduction

9:05 AM - 9:30 AM JST | 12:05 AM - 12:30 AM UTC

[PEM12-02] Convection in the Inner Magnetosphere: Effects on Plasmasphere and Ring Current

★Invited Papers

*Jerry Goldstein[1,4], B. R. Sandel[2], D. J. McComas[3], P. W. Valek[1], J. Redfern[1] (1.Southwest Research Institute, 2.The University of Arizona, 3.Princeton University, 4.University of Texas at San Antonio)

9:30 AM - 9:55 AM JST | 12:30 AM - 12:55 AM UTC

[PEM12-03] Changing Composition of the Ring Current Source Region During Storm Main Phase

★Invited Papers

*Lynn M Kistler[1,2], Christopher G Mouikis[1], Kazushi Asamura[3], Satoshi Kasahara[4], Yoshizumi Miyoshi[2], Kunihiro Keika[4], Steven M Petrinec[5], Tomoaki Hori[2], Shoichiro Yokota[6], Iku Shinohara[3] (1.University of New Hampshire Main Campus, 2.Institute for Space-Earth Environmental Research, Nagoya University, 3.JAXA, 4.Graduate School of Science, University of Tokyo, 5.Lockheed-Palo Alto, 6.Graduate School of Science, Osaka University)

9:55 AM - 10:10 AM JST | 12:55 AM - 1:10 AM UTC

[PEM12-04] Multisatellite observations of field-aligned low-energy O^+ ion flux enhancements in the inner magnetosphere: September 22, 2018, Event

*Masahito Nose[1], Ayako Matsuoka[2], Yoshizumi Miyoshi[1], Kazushi Asamura[3], Mariko Teramoto[4], Iku Shinohara[3], Masafumi Hirahara[1], C. A. Kletzing[5], C. W. Smith[6], R. J. MacDowall[7], H. E. Spence[6], G. D. Reeves[8] (1.Institute for Space-Earth Environmental Research, Nagoya University, 2.Graduate School of Science, Kyoto University, 3.Institute of Space and Astronautical Science, Japan Aerospace Exploration Agency, 4.Department of Space Systems Engineering, Kyushu Institute of Technology, 5.Department of Physics and Astronomy, University of Iowa, 6.Institute for the Study of Earth, Oceans, and Space, University of New Hampshire, 7.Solar System Exploration Division, Goddard Space Flight Center, 8.Space Sciences and Applications Group, Los Alamos National Laboratory)

10:10 AM - 10:30 AM JST | 1:10 AM - 1:30 AM UTC

[PEM12-05] Deflection of upflowing ion beams by a converging electric field in the auroral flux tube: Alternative explanation for mass-dependent beam width

★Invited Papers

*Shun Imajo[1], Yoshizumi Miyoshi[1], Kazushi Asamura[2], Iku Shinohara[2], Masahito Nose[1], Yoshiya Kasahara[3], Yasumasa Kasaba[4], Ayako Matsuoka[5], Tomoaki Hori[1], Masafumi Shoji[1], Satoko Nakamura[1], Mariko Teramoto[6] (1.Nagoya University, 2.Institute of Space and Astronautical Science, 3.Kanazawa University, 4.Tohoku University, 5.Kyoto University, 6.Kyushu Institute of Technology)

[E] Oral | P (Space and Planetary Sciences) | P-EM Solar-Terrestrial Sciences, Space Electromagnetism & Space Environment

[P-EM12] Dynamics of the Inner Magnetospheric System

convener:Kunihiro Keika(Department of Earth and Planetary Science, Graduate School of Science, The University of Tokyo), Yoshizumi Miyoshi(Institute for Space-Earth Environmental Research, Nagoya University), W Lauren Blum(University of Colorado Boulder), Yuri Shprits(Helmholtz Centre Potsdam GFZ German Research Centre for Geosciences), Chairperson:Lauren W Blum(University of Colorado Boulder), Kunihiro Keika(Department of Earth and Planetary Science, Graduate School of Science, The University of Tokyo)

Sat. Jun 5, 2021 9:00 AM - 10:30 AM Ch.05 (Zoom Room 05)

The inner magnetosphere is highly variable because dynamical variations of incoming energy from the solar wind, magnetospheric tail, and the ionosphere. Cross-regional, cross-scale, and cross-energy couplings are the key processes for understanding this dynamical system. Coordinated observations by multi-satellites and ground-based observations are very essential to revealing these processes. In the 24th and 25th solar cycles, a number of satellites such as Van Allen Probes, MMS, THEMIS, DSX and Arase; coordinated ground-based observations (THEMIS-GBO, SuperDARN, EISCAT, magnetometers, riometer, etc); and numerical simulations (global kinetic model, MHD model, micro PIC, hybrid simulations) have successfully investigated the inner magnetosphere system. We invite papers on recent results of the inner magnetosphere and/or its coupling with the other regions including the ionosphere and the outer magnetosphere. Presentations on new projects such as sounding rocket experiments and data assimilation/machine learning are also welcome.

9:00 AM - 9:05 AM

[PEM12-01]Introduction

©Japan Geoscience Union

Convection in the Inner Magnetosphere: Effects on Plasmasphere and Ring Current

*Jerry Goldstein[1,4], B. R. Sandel[2], D. J. McComas[3], P. W. Valek[1], J. Redfern[1]

1. Southwest Research Institute, 2. The University of Arizona, 3. Princeton University, 4. University of Texas at San Antonio

We present two key elements of the effects of inner magnetospheric convection.

The first element is plasmaspheric erosion, a fundamental element of the dynamic magnetospheric response to solar wind driving. We use extreme ultraviolet (EUV) images from the Imager for Magnetopause-to-Aurora Global Exploration (IMAGE) mission to examine the relative timing of dayside and nightside plasmapause motion following southward interplanetary magnetic field turnings. For two case studies we find the delay between the dayside and nightside plasmapause response is less than the 10 min temporal resolution of IMAGE EUV, and the time-averaged plasmapause electric (E) field is 9% to 10% of the solar wind E-field. This first result yields important observational constraints on the day-to-night magnetospheric propagation of solar wind energy.

The second element of convection's effects is ring current intensification, widely considered a defining aspect of storms. We use a large database of energetic neutral atom (ENA) images from Two Wide-angle Imaging Neutral-atom Spectrometers (TWINS) to examine the statistical response of the ring current to solar wind driving. The database comprises 61 events, including 1838 maps of TWINS-derived equatorial ion flux. We find a strong correlation between solar wind E-field and ring current flux intensification: correlation coefficients are [0.95, 0.94, 0.88] at [1, 16, 30] keV. The strongest solar wind driven convection preferentially increases the least energetic ions. Lower-energy ions are increased farther eastward and higher-energy ions closer to midnight. Enhanced RC ion flux occurs or peaks (on average) at higher L-shells for strong solar wind pressure than for strong convection. This second result confirms and quantifies the high geoeffectiveness of convection.

Keywords: inner magnetosphere, convection, plasmasphere, ring current, erosion, storms

©2021. Japan Geoscience Union. All Right Reserved.

Changing Composition of the Ring Current Source Region During Storm Main Phase

*Lynn M Kistler[1,2], Christopher G Mouikis[1], Kazushi Asamura[3], Satoshi Kasahara[4], Yoshizumi Miyoshi[2], Kunihiro Keika[4], Steven M Petrinec[5], Tomoaki Hori[2], Shoichiro Yokota[6], Iku Shinohara[3]

1. University of New Hampshire Main Campus, 2. Institute for Space-Earth Environmental Research, Nagoya University, 3. JAXA, 4. Graduate School of Science, University of Tokyo, 5. Lockheed-Palo Alto, 6. Graduate School of Science, Osaka University

The ionospheric and solar wind contributions to the magnetosphere can be distinguished by their composition. While both sources contain significant H+, the heavy ion species from the ionospheric source are generally singly ionized, while the solar wind consists of highly ionized ions. Both the solar wind and the ionosphere contribute to the plasma sheet. It has been shown that with both enhanced geomagnetic activity and enhanced solar EUV, the ionospheric contribution, and particularly the ionospheric heavy ions contribution increases. However, the details of this transition from a solar wind dominated to more ionospheric dominated plasma sheet are not well understood. An initial study using AMPTE/CHEM data, a data set that includes the full charge state distributions of the major species, shows that the transition can occur quite sharply during storms, with the ionospheric contribution becoming dominant during the storm main phase. However, during the AMPTE time-period, there were no continuous measurements of the upstream solar wind, and so both the simultaneous solar wind composition and the driving solar wind and IMF parameters were not known. The HPCA instrument on MMS and both the LEPi and MEPi instruments on Arase are able to measure He++. With these data sets, the He++/H+ ratio can be compared to the simultaneous He++/H+ ratios in the solar wind to more definitively identify the solar wind contribution to the plasma sheet. This allows the ionospheric contribution to the H+ population to be determined, so that the full ionospheric population is known. We find that when the IMF turns southward during the storm main phase, the dominant source of the hot plasma sheet becomes ionospheric. This composition change explains why the storm time ring current also has a high ionospheric contribution.

Keywords: Ring Current, Ionospheric Source, Ion Composition, Plasma Sheet

©2021. Japan Geoscience Union. All Right Reserved.

Multisatellite observations of field-aligned low-energy O^+ ion flux enhancements in the inner magnetosphere: September 22, 2018, Event

*Masahito Nose[1], Ayako Matsuoka[2], Yoshizumi Miyoshi[1], Kazushi Asamura[3], Mariko Teramoto[4], Iku Shinohara[3], Masafumi Hirahara[1], C. A. Kletzing[5], C. W. Smith[6], R. J. MacDowall[7], H. E. Spence[6], G. D. Reeves[8]

1. Institute for Space-Earth Environmental Research, Nagoya University, 2. Graduate School of Science, Kyoto University, 3. Institute of Space and Astronautical Science, Japan Aerospace Exploration Agency, 4. Department of Space Systems Engineering, Kyushu Institute of Technology, 5. Department of Physics and Astronomy, University of Iowa, 6. Institute for the Study of Earth, Oceans, and Space, University of New Hampshire, 7. Solar System Exploration Division, Goddard Space Flight Center, 8. Space Sciences and Applications Group, Los Alamos National Laboratory

Recent studies employing the Arase and Van Allen Probes satellites [Chaston et al., 2015; Kistler et al., 2016; Nosé et al., 2016, 2018; Gkioulidou et al., 2019] have shown that unidirectional/bidirectional energy-dispersed O^+ flux appears a few minutes after substorms in the inner magnetosphere and lasts for ~10 min with a decrease in its energy from ~5 keV to 10–100 eV. Nosé et al. [2016] found that the unidirectional energy-dispersed O^+ flux is observed in 80% of the total events and that its direction is parallel (antiparallel) to the magnetic field when the satellites are located below (above) the geomagnetic equator. This strongly implies that these O^+ ions are extracted from the ionosphere at the onset of substorms and flow along the magnetic field toward the geomagnetic equator. Low-energy O^+ ions may be scattered near the geomagnetic equator and remain there, although the scattering mechanism is yet unknown. They may contribute to the O^+ content of the inner magnetospheric plasma such as the warm plasma cloak and the oxygen torus, and the resultant increase in the O^+ density may provide a precondition for the O^+-rich ring current.
In the present study, we examine the low-energy O^+ ion flux variations simultaneously observed by multiple satellites, Arase, Van Allen Probe A and B satellite, on September 22, 2018. The O^+ fluxes are enhanced after a substorm onset at 05:24 UT, at which three satellites are located in the nightside inner magnetosphere (Arase at MLT=0.3 hr, L=6.2, GMLAT=−9.6°; Probe A at MLT=0.7 hr, L=5.5, GMLAT=14.7°; Probe B at MLT=0.0 hr, L=5.3, GMLAT=10.6°). Arase observes O^+ flux enhancements only in the parallel direction to the magnetic field in the energy range from a few keV to 200 eV. Probe A and B, however, identify O^+ flux enhancements in both parallel and antiparallel directions at 1 keV to 10 eV. The antiparallel fluxes appear earlier than the parallel fluxes. Multiband flux enhancements are detected only by Probe A. We perform numerical calculation of O^+ ion trajectories to reproduce the observed E-t spectorgrams at three satellites. In the presentation, we will show results of data analysis and numerical simulation in more detail, and discuss the contribution of the low-energy O^+ ion flux enhancements to the O^+ content of the inner magnetospheric plasma.

Keywords: field-aligned low-energy O+ ion flux enhancements, inner magnetosphere, warm plasma cloak, oxygen torus

©2021. Japan Geoscience Union. All Right Reserved.

Deflection of upflowing ion beams by a converging electric field in the auroral flux tube: Alternative explanation for mass-dependent beam width

*Shun Imajo[1], Yoshizumi Miyoshi[1], Kazushi Asamura[2], Iku Shinohara[2], Masahito Nose[1], Yoshiya Kasahara[3], Yasumasa Kasaba[4], Ayako Matsuoka[5], Tomoaki Hori[1], Masafumi Shoji[1], Satoko Nakamura[1], Mariko Teramoto[6]

1. Nagoya University, 2. Institute of Space and Astronautical Science, 3. Kanazawa University, 4. Tohoku University, 5. Kyoto University, 6. Kyushu Institute of Technology

The pitch angle distribution of O^+ upflowing ion beams wider than that of H^+ beams has often been explained by mass-dependent perpendicular heating. Contrary to this conventional explanation, here we show that the mass-dependent pitch angle distribution of the ion beams can arise from a deflection of ion beams by a converging electric field in the auroral flux tube. On May 20, 2017, the Arase (ERG) satellite at ~32,000 km altitude and 1.1 h magnetic local time observed two consecutive ion beam events associated with an inverted-V shape spectrum in an energy range of ~1–8 keV. Magnetic and electric field variations during the ion beams corresponded to a relative equatorward motion of upward-field aligned current and converging perpendicular electric field, respectively, in the flux tube above the auroral acceleration region. Examining the gyro-phase distribution of the beam component, we found that the ion beams were significantly deflected in an east-west direction. The direction of ion flux was reversed from westward to eastward at the same time concurrently with the electric field reversal from outward to inward, indicating the ExB drift by the converging electric field causes this beam deflection. The difference of beam width between H^+ and O^+ tended to be large when the magnitude of the electric field was large. The field-aligned velocity of the H^+ beams is ~4 times higher than that of the O^+ beams, while the perpendicular beam velocity is consistent with the ExB drift. Because of the slower field-aligned velocity of O^+ beams, they are more easily deflected by the ExB drift compared with the light ions like H^+. This non-negligible perpendicular drift can result in an overestimation of beam width when it is estimated from a pitch angle distribution averaged over the entire gyro phase in a satellite-centered coordinate system.

Keywords: upflowing ion beam, auroral accelaration region, electric drift, mass-dependent characteristics

©2021. Japan Geoscience Union. All Right Reserved.

[E] Oral | P (Space and Planetary Sciences)：P-EM Solar-Terrestrial Sciences, Space Electromagnetism & Space Environment

Sat. Jun 5, 2021 10:45 AM - 12:10 PM JST | Sat. Jun 5, 2021 1:45 AM - 3:10 AM UTC | Ch.05 Zoom Room 05

[P-EM12] Dynamics of the Inner Magnetospheric System

convener:Kunihiro Keika(Department of Earth and Planetary Science, Graduate School of Science, The University of Tokyo), Yoshizumi Miyoshi(Institute for Space-Earth Environmental Research, Nagoya University), W Lauren Blum(University of Colorado Boulder), Yuri Shprits(Helmholtz Centre Potsdam GFZ German Research Centre for Geosciences), Chairperson:Kazuhiro Yamamoto(Graduate School of Science, The University of Tokyo)

The inner magnetosphere is highly variable because dynamical variations of incoming energy from the solar wind, magnetospheric tail, and the ionosphere. Cross-regional, cross-scale, and cross-energy couplings are the key processes for understanding this dynamical system. Coordinated observations by multi-satellites and ground-based observations are very essential to revealing these processes. In the 24th and 25th solar cycles, a number of satellites such as Van Allen Probes, MMS, THEMIS, DSX and Arase; coordinated ground-based observations (THEMIS-GBO, SuperDARN, EISCAT, magnetometers, riometer, etc); and numerical simulations (global kinetic model, MHD model, micro PIC, hybrid simulations) have successfully investigated the inner magnetosphere system. We invite papers on recent results of the inner magnetosphere and/or its coupling with the other regions including the ionosphere and the outer magnetosphere. Presentations on new projects such as sounding rocket experiments and data assimilation/machine learning are also welcome.

10:45 AM - 11:05 AM JST | 1:45 AM - 2:05 AM UTC

[PEM12-06] **Ion dynamics in the inner magnetosphere during Van Allen Probe Era**

★Invited Papers

*Chao Yue[1] (1.Peking University)

11:05 AM - 11:20 AM JST | 2:05 AM - 2:20 AM UTC

[PEM12-07] Multipoint measurements to understand the drivers and structure of EMIC waves in the inner magnetosphere

*Lauren W Blum[1] (1.University of Colorado Boulder)

11:20 AM - 11:35 AM JST | 2:20 AM - 2:35 AM UTC

[PEM12-08] Particles simulations of whistler-mode triggered emissions with subpacket structures

Takeshi Nogi[1], *Yoshiharu Omura[1] (1.Reserach Institute for Sustainable Humanosphere, Kyoto University)

11:35 AM - 11:55 AM JST | 2:35 AM - 2:55 AM UTC

[PEM12-09] Nonlinear wave-particles interaction in radiation belts: how can we include it to global models?

★Invited Papers

*Anton Artemyev[1,2], Anatoly Neishtadt[2,3], Alexei Vasiliev[2], Xiao-Jia Zhang[1], Didier Mourenas[4], Dmitri Vainchtein[5,2] (1.Institute of Geophysics and Planetary Physics, UCLA, Los Angeles, California 90095, USA, 2.Space Research Institute of the Russian Academy of Sciences (IKI), 84/32 Profsoyuznaya Str., Moscow 117997, Russia, 3.Department of Mathematical Sciences, Loughborough University, Loughborough LE11 3TU, United Kingdom, 4.Laboratoire Mati`ere sous Conditions Extremes, Paris-Saclay University, CEA, Bruy`eres-le-Chatel, France, 5.Nyheim Plasma Institute, Drexel University, Camden, NJ, USA)

11:55 AM - 12:10 PM JST | 2:55 AM - 3:10 AM UTC

[PEM12-10] Modeling of outer radiation belt electron dynamics associated with whistler mode chorus emissions via Green’s function method

*Yikai Hsieh[1], Yoshiharu Omura[1] (1.Reserach Institute for Sustainable Humanosphere, Kyoto University)

Ion dynamics in the inner magnetosphere during Van Allen Probe Era

*Chao Yue[1]

1. Peking University

Ion dynamics are controlled by the energy-dependent source, transport, energization, and loss processes. Systematic changes in the ion dynamics are essential to understand the ring current variations in the inner magnetosphere. The Van Allen Probes mission, which orbits near the equatorial plane inside the geosynchronous orbit, has a wide energy coverage with high energy resolution and state-of-the-art ion composition instrumentation. It provides a great opportunity to investigate the ion dynamics. In this talk, I will present some of our recent studies on the ion dynamics of different populations and species during geomagnetic quiet and active times.

Keywords: ion dynamics, ion composition , plasma waves

©2021. Japan Geoscience Union. All Right Reserved.

Multipoint measurements to understand the drivers and structure of EMIC waves in the inner magnetosphere

*Lauren W Blum[1]

1. University of Colorado Boulder

Wave-particle interactions provide a primary source of scattering and energization of energetic electrons in the Earth’ s radiation belts. Electromagnetic ion cyclotron (EMIC) waves are one intense wave mode observed in the inner magnetosphere that have been shown to contribute to scattering and loss of both energetic electrons and ions. Using multi-point measurements from the Heliospheric Systems Observatory, including NASA’ s Van Allen Probes, we examine the properties and source regions of EMIC waves in the inner magnetosphere, exploring the formation and evolution of plasma structures as they relate to observed wave growth. We also investigate the effects of this wave structure on energetic electrons in the outer radiation belt. These studies aid in the understanding of outer radiation belt dynamics and the relationship between electromagnetic waves, global magnetospheric conditions, and solar wind drivers.

Keywords: EMIC waves, inner magnetosphere, radiation belt

©2021. Japan Geoscience Union. All Right Reserved.

Particles simulations of whistler-mode triggered emissions with subpacket structures

Takeshi Nogi[1], *Yoshiharu Omura[1]

1. Reserach Institute for Sustainable Humanosphere, Kyoto University

We perform one-dimensional simulations[1] of whistler-mode triggered emissions to study nonlinear signatures of rising-tone emissions. We assume a parabolic magnetic field and energetic electrons with temperature anisotropy. We oscillate currents with a fixed frequency, 0.3 of electron cyclotron frequency, at the magnetic equator to inject finite amplitude whistler-mode waves. We observe rising-tone triggered emissions with sub-packet structures from 0.3 to 0.75 of electron cyclotron frequency. We find a clear separation of triggered emissions from the triggering waves. The first triggered wave packet is formed with growing wave amplitude and smooth rising-tone frequency over the frequency range 0.3-0.5 of electron cyclotron frequency. The electron hole initially formed at the equator expands spatially to the upstream region. The formation of electron holes takes place in the spatial range with the inhomogeneity factor |S| less than 1. When the frequency approaches to 0.5fce, we find some density modulation of the untrapped resonant particles around the electron holes. The modulation causes oscillations of resonant currents with a frequency of the same order of trapping frequencies, resulting in the generation of sub-packet structures.

[1] Nogi, T., Nakamura, S., & Omura, Y. (2020). Full particle simulation of whistler-mode triggered falling-tone emissions in the magnetosphere. Journal of Geophysical Research: Space Physics, 125, e2020JA027953, https://doi.org/10.1029/2020JA027953.

Keywords: wave-particle interaction, whistler-mode wave, nonlinear process

©2021. Japan Geoscience Union. All Right Reserved.

Nonlinear wave-particles interaction in radiation belts: how can we include it to global models?

*Anton Artemyev[1,2], Anatoly Neishtadt[2,3], Alexei Vasiliev[2], Xiao-Jia Zhang[1], Didier Mourenas[4], Dmitri Vainchtein[5,2]

1. Institute of Geophysics and Planetary Physics, UCLA, Los Angeles, California 90095, USA, 2. Space Research Institute of the Russian Academy of Sciences (IKI), 84/32 Profsoyuznaya Str., Moscow 117997, Russia, 3. Department of Mathematical Sciences, Loughborough University, Loughborough LE11 3TU, United Kingdom, 4. Laboratoire Mati`ere sous Conditions Extremes, Paris-Saclay University, CEA, Bruy`eres-le-Chatel, France, 5. Nyheim Plasma Institute, Drexel University, Camden, NJ, USA

The resonant wave-particle interaction is known to be one of the main drivers of dynamics of energetic electron fluxes in the Earth’ s radiation belts. The quasi-linear diffusion theory describes a sufficiently weak resonant scattering in energy/pitch-angle space and operates with a Fokker-Planck diffusion equation for the charged particle distribution function. In contrast to this description, the nonlinear resonant interact includes effects of phase trapping that assumes a fast transport in energy/pitch-angle space, when even a single resonant interaction changes significantly the electron's energy/pitch-angle. This essentially non-diffusive process cannot be directly included into the Fokker-Planck equation. This presentation reviews recent results for the mapping approach for a system with nonlinear resonant interaction. The main advances of this approach are the possibility to consider effects of many nonlinear resonances and to simulate the evolution of the resonant particle ensemble on long time ranges. For illustrative purposes we consider the system with resonant relativistic electrons and whistler-mode waves.

Keywords: radiation belts, wave-particle interaction, nonlinear resonances

©2021. Japan Geoscience Union. All Right Reserved.

Modeling of outer radiation belt electron dynamics associated with whistler mode chorus emissions via Green’ s function method

*Yikai Hsieh[1], Yoshiharu Omura[1]

1. Reserach Institute for Sustainable Humanosphere, Kyoto University

Energetic electron accelerations and precipitations in the Earth’ s outer radiation belt are highly associated with wave-particle interactions between whistler mode chorus waves and electrons. Two main processes take place in the whistler mode wave-particle interactions. One is the untrapped resonance process, which makes electron energy slightly smaller and lowers the equatorial pitch angle of the electron. The other is the nonlinear trapping process, which makes effective energy gain of the resonant electrons. We perform test particle simulation in a 3D dipole field to reproduce the interactions in the radiation belt and investigate the electron acceleration and precipitation interacting with both parallel and obliquely propagating chorus emissions. We build up a database of Green’ s functions, which are treated as results of the input electrons interacting with one emission, for a large number of electrons interacting with whistler mode chorus emissions. The formation processes and the loss processes of the outer radiation belt electron fluxes interacting with consecutive chorus emissions are traced by applying the convolution integrals for the Green’ s functions. In the acceleration parts, MeV electrons are generated promptly due to the combination of cyclotron resonance and Landau resonance of oblique chorus waves. We compare the precipitation phenomena between parallel waves and oblique waves, and the results show that oblique chorus emissions lead to more electron precipitation than that led by parallel chorus emissions. Since the precipitations by chorus emissions are much less than the accelerations, in this study we further take energetic electron precipitations by EMIC waves into account to simulate the overall acceleration and loss processes in the outer radiation belt.

Keywords: outer radiation belt, whistler mode chorus emissions, Green's function, energetic electron precipitation, Landau resonance, cyclotron resonance

©2021. Japan Geoscience Union. All Right Reserved.

[E] Oral | P (Space and Planetary Sciences)：P-EM Solar-Terrestrial Sciences, Space Electromagnetism & Space Environment

Sat. Jun 5, 2021 1:45 PM - 3:15 PM JST | Sat. Jun 5, 2021 4:45 AM - 6:15 AM UTC | Ch.05 Zoom Room 05

[P-EM12] Dynamics of the Inner Magnetospheric System

convener:Kunihiro Keika(Department of Earth and Planetary Science, Graduate School of Science, The University of Tokyo), Yoshizumi Miyoshi(Institute for Space-Earth Environmental Research, Nagoya University), W Lauren Blum(University of Colorado Boulder), Yuri Shprits(Helmholtz Centre Potsdam GFZ German Research Centre for Geosciences), Chairperson:Yikai Hsieh(Reserach Institute for Sustainable Humanosphere, Kyoto University)

The inner magnetosphere is highly variable because dynamical variations of incoming energy from the solar wind, magnetospheric tail, and the ionosphere. Cross-regional, cross-scale, and cross-energy couplings are the key processes for understanding this dynamical system. Coordinated observations by multi-satellites and ground-based observations are very essential to revealing these processes. In the 24th and 25th solar cycles, a number of satellites such as Van Allen Probes, MMS, THEMIS, DSX and Arase; coordinated ground-based observations (THEMIS-GBO, SuperDARN, EISCAT, magnetometers, riometer, etc); and numerical simulations (global kinetic model, MHD model, micro PIC, hybrid simulations) have successfully investigated the inner magnetosphere system. We invite papers on recent results of the inner magnetosphere and/or its coupling with the other regions including the ionosphere and the outer magnetosphere. Presentations on new projects such as sounding rocket experiments and data assimilation/machine learning are also welcome.

1:45 PM - 2:00 PM JST | 4:45 AM - 5:00 AM UTC

[PEM12-11] Statistical study on spatial distribution of plasma waves observed by PWE/OFA

*Yoshiya Kasahara[1], Kengo Nakashima[1], Shoya Matsuda[2], Yoshizumi Miyoshi[3], Ayako Matsuoka[4], Jean-Francois Rippol[5], David M. Malaspina[6] (1.Kanazawa University, 2.ISAS/JAXA, 3.Nagoya University, 4.Kyoto University, 5.CEA/DAM/DIF, 6.University of Colorado Boulder)

2:00 PM - 2:15 PM JST | 5:00 AM - 5:15 AM UTC

[PEM12-12] Long period modulations of pulsating aurora and chorus waves

*Yoshizumi Miyoshi[1], Keisuke Hosokawa[2], Yasunobu Ogawa[3], Satoshi Kurita[4], Shin-ichiro Oyama[1], Mariko Teramoto[5], Shinji Saito[6], Yoshiya Kasahara[7], Shoya Matsuda[8], Satoshi Kasahara[9], Shoichiro Yokota[10], Kunihiro Keika[9], Tomoaki Hori[1], Fuminori Tsuchiya[11], Atsushi Kumamoto[11], Satoko Nakamura[1], Masahiro Kitahara[1], Masafumi Shoji[1], Ayako Matsuoka[4], Shun Imajo[1], Iku Shinohara[8] (1.Institute for Space-Earth Environmental Research, Nagoya University, 2.The University of Electro-Communications, 3.NIPR, 4.Kyoto University, 5.Kyushu Inst. of Technology, 6.NICT, 7.Kanazawa University, 8.JAXA, 9.University of Tokyo, 10.Osaka University, 11.Tohoku University)

2:15 PM - 2:30 PM JST | 5:15 AM - 5:30 AM UTC

[PEM12-13] Whistler Driven Electron Precipitation Measured by ELFIN CubeSat and Arase Spacecraft

*Xiaojia Zhang[1], Vassilis Angelopoulos[1], Anton V. Artemyev[1], Satoshi Kasahara[2], Colin Wilkins[1], Ethan Tsai[1], Shoichiro Yokota[3], Kunihiro Keika[2], Tomoaki Hori[4], Yoshizumi Miyoshi[4], Yoshiya Kasahara[5], Shoya Matsuda[6], Ayako Matsuoka[7], Mariko Teramoto[8], Shun Imajo[4], Iku Shinohara[9] (1.University of California Los Angeles, 2.The Univ. of Tokyo, 3.Osaka Univ., 4.Nagoya Univ., 5.Kanazawa Univ., 6.ISAS, 7.Kyoto Univ., 8.Kyushu Institute of Technology, 9.ISAS, JAXA)

2:30 PM - 2:45 PM JST | 5:30 AM - 5:45 AM UTC

[PEM12-14] A case study to estimate energy spectra of pulsating auroral electrons from cosmic noise absorption and auroral brightness

*Shin-ichiro Oyama[1,2], Miyamoto Taishiro[1,6], Tero Raita[3], Keisuke Hosokawa[4], Yoshizumi Miyoshi[1], Yasunobu Ogawa[2], Satoshi Kurita[5] (1.Institute for Space-Earth Environmental Research, Nagoya

University, 2.National Institute of Polar Research, 3.Sodankyla Geophysical Observatory, University of Oulu, 4.University of Electro-Communications, 5.Research Institute for Sustainable Humanosphere, Kyoto University, 6.Nippon Steel Corporation Nagoya Works)

2:45 PM - 3:00 PM JST | 5:45 AM - 6:00 AM UTC

[PEM12-15] Statistical characteristics of the magnetic field variations observed by Arase

*Ayako Matsuoka[1], Masahito Nose[2], Yoshizumi Miyoshi[2], Mariko Teramoto[4], Reiko Nomura[3], Akiko Fujimoto[5], Yoshimasa Tanaka[6], Manabu Shinohara[7], Satoshi Kurita[8], Shun Imajo[2], Iku Shinohara[3] (1.Data Analysis Center for Geomagnetism and Space Magnetism, Graduate School of Science, Kyoto University, 2.Institute for Space-Earth Environmental Research, Nagoya University, 3.Institute of Space and Astronautical Science, JAXA, 4.Graduate School of Engineering, Kyushu Institute of Technology, 5.Graduate School of Computer Science and Systems Engineering, Kyushu Institute of Technology, 6.National Institute of Polar Research, 7.National Institute of Technology Kagoshima College, 8.Research Institute for Sustainable Humanosphere, Kyoto University)

3:00 PM - 3:15 PM JST | 6:00 AM - 6:15 AM UTC

[PEM12-16] Mode-coupling Pi2 pulsations on the off-equatorial plasmapause inferred from the Arase satellite observation

*Mariko Teramoto[1], Ayako Matsuoka[2], Yoshiya Kasahara[3], Yasumasa Kasaba[4], Atsushi Kumamoto[4], Fuminori Tsuchiya[4], Shoya Matsuda[6], Yoshizumi Miyoshi[5], Masahito Nose[5], Tomoko Nakagawa[7], Shun Imajo[5], Masafumi Shoji[5], Satoko Nakamura[5], Iku Shinohara[6] (1.Kyushu Institute of Technology, 2.Kyoto University, 3.Kanazawa University, 4.Tohoku University, 5.Nagoya University, 6.Japan Aerospace Exploration Agency, Institute of Space and Astronautical Science, 7.Tohoku Institute of Technology)

Statistical study on spatial distribution of plasma waves observed by PWE/OFA

*Yoshiya Kasahara[1], Kengo Nakashima[1], Shoya Matsuda[2], Yoshizumi Miyoshi[3], Ayako Matsuoka[4], Jean-Francois Rippol[5], David M. Malaspina[6]

1. Kanazawa University, 2. ISAS/JAXA, 3. Nagoya University, 4. Kyoto University, 5. CEA/DAM/DIF, 6. University of Colorado Boulder

In the present paper, we investigated the spatial distribution of the power spectrum measured by the PWE/OFA (Plasma Wave Experiment/Onboard Frequency Analyzer) on board the Arase.

The OFA (onboard frequency analyzer) measures electric and magnetic wave spectra in the frequency range below 20 kHz continuously with a time resolution of 1 second as a nominal operation mode. This frequency range is crucial for plasma wave observation because chorus waves, magnetospheric hiss, lightning whistlers and magnetosonic waves are detected.

First, we compared our results with the previous statistical work done using the spectral data recorded by the Van Allen Probes (e.g. Malaspina et al., 2017), and confirmed that the results are almost consistent with those derived from the observation by Van Allen Probes at low latitudes. Next we examined the spatial distribution of the wave activities in the off-equatorial region. Because the inclination of the Arase is 31 degrees, which is much larger than that of Van Allen Probes (~10 degrees), this orbital configuration provides the ability to explore not only the equatorial region but also the off-equatorial region in the inner magnetosphere.
In the presentation, we report the global distributions of various plasma waves as a function of magnetic latitude, magnetic local time and L-value.

Keywords: Arase, plasma wave, Inner magnetosphere

©2021. Japan Geoscience Union. All Right Reserved.

Long period modulations of pulsating aurora and chorus waves

*Yoshizumi Miyoshi[1], Keisuke Hosokawa[2], Yasunobu Ogawa[3], Satoshi Kurita[4], Shin-ichiro Oyama[1], Mariko Teramoto[5], Shinji Saito[6], Yoshiya Kasahara[7], Shoya Matsuda[8], Satoshi Kasahara[9], Shoichiro Yokota[10], Kunihiro Keika[9], Tomoaki Hori[1], Fuminori Tsuchiya[11], Atsushi Kumamoto[11], Satoko Nakamura[1], Masahiro Kitahara[1], Masafumi Shoji[1], Ayako Matsuoka[4], Shun Imajo[1], Iku Shinohara[8]

1. Institute for Space-Earth Environmental Research, Nagoya University, 2. The University of Electro-Communications, 3. NIPR, 4. Kyoto University, 5. Kyushu Inst. of Technology, 6. NICT, 7. Kanazawa University, 8. JAXA, 9. University of Tokyo, 10. Osaka University, 11. Tohoku University

Pulsating aurora (PsA) is primarily caused by intermittent precipitation of tens of keV electrons by the magnetospheric chorus waves. Variations of different time scales have been known to exist in the optical emission amplitude of PsA: the main pulsations of PsA with a few seconds are caused by chorus bursts and internal modulations of PsA within 1 second are caused by chorus short-lived elements composing the bursts. Here, we report chorus bundles that appear every a few tens of seconds as observed by Arase/PWE observations. Each chorus bundle includes several chorus bursts. In association with chorus bundles in the magnetosphere, we observed temporal variations in a series of the main pulsation of PsA using ground based EMCCD cameras. During the period of chorus bundles, continuous activities of main pulsations were observed. Concurrently, enhancements in the temperature anisotropy of tens of keV electrons as well as ULF pulsations were observed by Arase/MEPe and MGF, respectively. In this presentation, we report fundamental characteristics of chorus bundles and the corresponding signatures of PsA and discuss possible mechanisms to cause the long period modulations in order to fully understand the hierarchical temporal variation of PsA.

Keywords: Arase, chorus, pulsating aurora

©2021. Japan Geoscience Union. All Right Reserved.

Whistler Driven Electron Precipitation Measured by ELFIN CubeSat and Arase Spacecraft

*Xiaojia Zhang[1], Vassilis Angelopoulos[1], Anton V. Artemyev[1], Satoshi Kasahara[2], Colin Wilkins[1], Ethan Tsai[1], Shoichiro Yokota[3], Kunihiro Keika[2], Tomoaki Hori[4], Yoshizumi Miyoshi[4], Yoshiya Kasahara[5], Shoya Matsuda[6], Ayako Matsuoka[7], Mariko Teramoto[8], Shun Imajo[4], Iku Shinohara[9]

1. University of California Los Angeles, 2. The Univ. of Tokyo, 3. Osaka Univ., 4. Nagoya Univ., 5. Kanazawa Univ., 6. ISAS, 7. Kyoto Univ., 8. Kyushu Institute of Technology, 9. ISAS, JAXA

Resonant interaction with whistler mode waves is the primary driver for electron acceleration and precipitation in Earth’ s radiation belts. Although scattering rates and the resonant scattering process over long timescales can be well explained by quasi-linear theory, microphysics of electron resonant interaction with coherent, intense whistlers is still poorly understood. One important limitation is that most available observations lack direct measurements of electron fluxes within the loss cone, i.e., direct measurements of scattered electrons. High-energy (>50keV) electron flux measurements within the loss cone, as provided by the new low-altitude ELFIN CubeSats, can significantly advance our understanding of the scattering mechanism and their efficiency. In this presentation, we analyze ELFIN measurements in conjunction with near-equatorial Arase spacecraft. We focus on whistler-driven precipitation and discuss ELFIN measurements in different regimes of resonant electron scattering.

Keywords: Radiation Belts, Energetic Electron Precipitation, Whistler Mode Wave Scattering

©2021. Japan Geoscience Union. All Right Reserved.

A case study to estimate energy spectra of pulsating auroral electrons from cosmic noise absorption and auroral brightness

*Shin-ichiro Oyama[1,2], Miyamoto Taishiro[1,6], Tero Raita[3], Keisuke Hosokawa[4], Yoshizumi Miyoshi[1], Yasunobu Ogawa[2], Satoshi Kurita[5]

1. Institute for Space-Earth Environmental Research, Nagoya University, 2. National Institute of Polar Research, 3. Sodankyla Geophysical Observatory, University of Oulu, 4. University of Electro-Communications, 5. Research Institute for Sustainable Humanosphere, Kyoto University, 6. Nippon Steel Corporation Nagoya Works

This study focused on a pulsating aurora event associated with aurora morphological changes in Fennoscandia at early morning time on 7 March 2017. A high-speed sampling all-sky camera captured equatorward development of the pulsating auroral patch in association with a substorm centered at Greenland/North America region. Of particular interest of this event is interconnection between the auroral intensity and the cosmic noise absorption (CNA) derived from three riometers aligned meridionally in Finland (from north to south: Ivalo, Sodankylä and Rovaniemi). The analysis was made by dividing optical measurements into two oscillation components; longer and shorter than 40 s, that is, non-pulsating and pulsating auroral modulations. The interrelation showed linear correlation and change of the inclination would be interpreted as hardening or softening of the precipitating electron spectrum. In terms of the low-pass component, the inclination of the CNA-vs-intensity interrelation increased at the three riometer latitudes at the substorm recovery phase. On the other hand, in terms of the high-pass component, the inclination decreased at Rovaniemi (lower latitude) but stayed uniform at Sodankylä (higher latitude). These features suggest that the precipitating electron spectrum has softened in the low-pass or non-pulsating auroral component but the spectrum has hardened in the high-pass or pulsating auroral component at the lower side in latitudes of the auroral patch region. This study proposes a new application of the riometer-camera measurement to examination of the auroral particle precipitation.

Keywords: pulsating aurora, ionosphere, riometer

©2021. Japan Geoscience Union. All Right Reserved.

Statistical characteristics of the magnetic field variations observed by Arase

*Ayako Matsuoka[1], Masahito Nose[2], Yoshizumi Miyoshi[2], Mariko Teramoto[4], Reiko Nomura[3], Akiko Fujimoto[5], Yoshimasa Tanaka[6], Manabu Shinohara[7], Satoshi Kurita[8], Shun Imajo[2], Iku Shinohara[3]

1. Data Analysis Center for Geomagnetism and Space Magnetism, Graduate School of Science, Kyoto University, 2. Institute for Space-Earth Environmental Research, Nagoya University, 3. Institute of Space and Astronautical Science, JAXA, 4. Graduate School of Engineering, Kyushu Institute of Technology, 5. Graduate School of Computer Science and Systems Engineering, Kyushu Institute of Technology, 6. National Institute of Polar Research, 7. National Institute of Technology Kagoshima College, 8. Research Institute for Sustainable Humanosphere, Kyoto University

We are investigating the magnetic field variations in association with the relativistic electrons in the inner magnetosphere. The magnetospheric disturbance phenomena, e.g., dipolarization and bursty bulk flow from the night-side plasma sheet, are often accompanied by the broadband magnetic field variation. The variation between a few Hz and a few tens Hz has the potential for factor of the rapid increase of the relativistic electrons in the inner magnetosphere.
The magnetic field variations in those frequencies are measured by MGF, fluxgate magnetometer, onboard the Arase satellite. We have investigated the magnetic disturbance in the outer radiation belt; intensity, spatial distribution, occurrence probability and polarization are statistically analyzed. In the overview, large-amplitude magnetic variations often appear in accordance with the substorm and dipolarization phenomena in the pre-midnight sencor and the EMIC waves in the afternoon sector. The amplitude in the xy plane in the SM coordinate overwhelm and therefore indicate the transverse polarization characteristics. It should be examined in detail in the reference frame to the background field.
We are extending our study to the spectral characteristics associated with the local proton (and other ions) cyclotron frequency, dependence on the magnetic activity and solar-wind condition.

Keywords: magnetic field disturbance, radiation belt, inner magnetosphere

©2021. Japan Geoscience Union. All Right Reserved.

Mode-coupling Pi2 pulsations on the off-equatorial plasmapause inferred from the Arase satellite observation

*Mariko Teramoto[1], Ayako Matsuoka[2], Yoshiya Kasahara[3], Yasumasa Kasaba[4], Atsushi Kumamoto[4], Fuminori Tsuchiya[4], Shoya Matsuda[6], Yoshizumi Miyoshi[5], Masahito Nose[5], Tomoko Nakagawa[7], Shun Imajo[5], Masafumi Shoji[5], Satoko Nakamura[5], Iku Shinohara[6]

1. Kyushu Institute of Technology, 2. Kyoto University, 3. Kanazawa University, 4. Tohoku University, 5. Nagoya University, 6. Japan Aerospace Exploration Agency, Institute of Space and Astronautical Science, 7. Tohoku Institute of Technology

We investigated Pi2 pulsations in the electric and magnetic field and their relation to the ambient plasma density observed from the Arase satellite to explore the generation mechanism of low-latitude Pi2. At a geomagnetically quiet time, Pi2 pulsations were observed in all three components of the magnetic field and in the radial and azimuthal components of the electric field when the Arase satellite was located on the plasmapause off the equatorial plane (about 25 degrees Mlat) at midnight. The coherence and cross phase between the orthogonal electric and magnetic field components are high and approximately 90 degrees. The compressional component of the magnetic field has high coherence with the azimuthal component of the electric field. The cross phase properties indicate that the radial and field-aligned standing waves are excited on the plasmapause. These results confirm the mode coupling between the fast mode wave and Alfven waves in the plasmasphere, which was proposed by Takahashi et al. [2018].

We compared these Pi2 pulsations with those on the ground over a wide latitudinal and longitudinal range. Additionally, we discussed the generation mechanism of this event.

©2021. Japan Geoscience Union. All Right Reserved.

[E] Oral | P (Space and Planetary Sciences)：P-EM Solar-Terrestrial Sciences, Space Electromagnetism & Space Environment

Sat. Jun 5, 2021 3:30 PM - 5:00 PM JST | Sat. Jun 5, 2021 6:30 AM - 8:00 AM UTC | Ch.05 Zoom Room 05

[P-EM12] Dynamics of the Inner Magnetospheric System

convener:Kunihiro Keika(Department of Earth and Planetary Science, Graduate School of Science, The University of Tokyo), Yoshizumi Miyoshi(Institute for Space-Earth Environmental Research, Nagoya University), W Lauren Blum(University of Colorado Boulder), Yuri Shprits(Helmholtz Centre Potsdam GFZ German Research Centre for Geosciences), Chairperson:Kunihiro Keika(Department of Earth and Planetary Science, Graduate School of Science, The University of Tokyo)

The inner magnetosphere is highly variable because dynamical variations of incoming energy from the solar wind, magnetospheric tail, and the ionosphere. Cross-regional, cross-scale, and cross-energy couplings are the key processes for understanding this dynamical system. Coordinated observations by multi-satellites and ground-based observations are very essential to revealing these processes. In the 24th and 25th solar cycles, a number of satellites such as Van Allen Probes, MMS, THEMIS, DSX and Arase; coordinated ground-based observations (THEMIS-GBO, SuperDARN, EISCAT, magnetometers, riometer, etc); and numerical simulations (global kinetic model, MHD model, micro PIC, hybrid simulations) have successfully investigated the inner magnetosphere system. We invite papers on recent results of the inner magnetosphere and/or its coupling with the other regions including the ionosphere and the outer magnetosphere. Presentations on new projects such as sounding rocket experiments and data assimilation/machine learning are also welcome.

3:30 PM - 3:45 PM JST | 6:30 AM - 6:45 AM UTC

[PEM12-17] Controlling factors of the occurrence of multi-harmonic toroidal ULF waves: A statistical study of the Arase satellite observations

*Kazuhiro Yamamoto[1], Kanako Seki[1], Ayako Matsuoka[2], Shun Imajo[3], Mariko Teramoto[4], Yoshiya Kasahara[5], Atsushi Kumamoto[6], Fuminori Tsuchiya[6], Masafumi Shoji[3], Yoshizumi Miyoshi[3], Iku Shinohara[7] (1.Graduate School of Science, The University of Tokyo, 2.Graduate School of Science, Kyoto University, 3.Institute for Space-Earth Environmental Research, Nagoya University, 4.Kyushu Institute of Technology, 5.Graduate School of Natural Science and Technology, Kanazawa University, 6.Graduate School of Science, Tohoku University, 7.Japan Aerospace Exploration Agency)

3:45 PM - 4:08 PM JST | 6:45 AM - 7:08 AM UTC

[PEM12-18] Probing inner magnetosphere dynamics and radial transport via observations of electron flux oscillations

★Invited Papers

*Theodore E Sarris[1] (1.Democritus University of Thrace)

4:08 PM - 4:30 PM JST | 7:08 AM - 7:30 AM UTC

[PEM12-19] Radiation belt electron acceleration during periods of low plasma density

★Invited Papers

*Hayley J Allison[1], Yuri Y Shprits[1,2,3], Irina Zhelavskaya[1], Dedong Wang[1], Artem Smirnov[1,2] (1.Helmholtz Centre Potsdam GFZ German Research Centre for Geosciences, Potsdam, Germany, 2.University of Potsdam, Potsdam, Germany, 3.University of California, Los Angeles, CA, USA)

4:30 PM - 4:45 PM JST | 7:30 AM - 7:45 AM UTC

[PEM12-20] Parameterized Lifetime of Energetic Electrons due to Interactions with Chorus Waves

*Dedong Wang[1], Yuri Shprits[1,2,3] (1.Helmholtz Center Potsdam German Research Centre for Geosciences Potsdam, 2.University of Potsdam, 3.UCLA)

4:45 PM - 5:00 PM JST | 7:45 AM - 8:00 AM UTC

[PEM12-21] Statistical Comparisons of Spin-Averaged Electron Flux from ARASE and Van Allen Probes Instruments

*Matyas Szabo-Roberts[1,2], Yuri Shprits[1,2], Hayley J Allison[1], Artem Smirnov[1,2], Nikita Aseev[7], Ruggero Vasile[1], Yoshizumi Miyoshi[4], Takefumi Mitani[4,5,6], Nana Higashio[5], Satoshi Kasahara[3] (1.Helmholtz Centre Potsdam GFZ German Research Centre for Geosciences, 2.University of Potsdam, 3.Department of Earth and Planetary Science, School of Science, The University of Tokyo, 4.Nagoya University, 5.JAXA Japan Aerospace Exploration Agency, 6.ISAS Institute of Space and Aeronautical Science, 7.Huawei Technologies)

Controlling factors of the occurrence of multi-harmonic toroidal ULF waves: A statistical study of the Arase satellite observations

*Kazuhiro Yamamoto[1], Kanako Seki[1], Ayako Matsuoka[2], Shun Imajo[3], Mariko Teramoto[4], Yoshiya Kasahara[5], Atsushi Kumamoto[6], Fuminori Tsuchiya[6], Masafumi Shoji[3], Yoshizumi Miyoshi[3], Iku Shinohara[7]

1. Graduate School of Science, The University of Tokyo, 2. Graduate School of Science, Kyoto University, 3. Institute for Space-Earth Environmental Research, Nagoya University, 4. Kyushu Institute of Technology, 5. Graduate School of Natural Science and Technology, Kanazawa University, 6. Graduate School of Science, Tohoku University, 7. Japan Aerospace Exploration Agency

Ultralow frequency (ULF) waves can coherently or stochastically interact with charged particles through drift/drift-bounce resonance (e.g., Claudepierre et al., 2013; Schulz & Lanerotti, 1974). In the wave-particle interaction, wave frequency is one of the parameters which determine the energy where the interaction occurs. Because differences of frequency spectra may cause different results of wave-particle interaction, as numerically simulated by Sarris et al. (2017), ULF waves with a discrete frequency and those with broadband frequencies are investigated separately (e.g., Murphy et al., 2020). Therefore, classification of ULF waves according to their frequency spectra is important to accurately understand the wave-particle interaction.

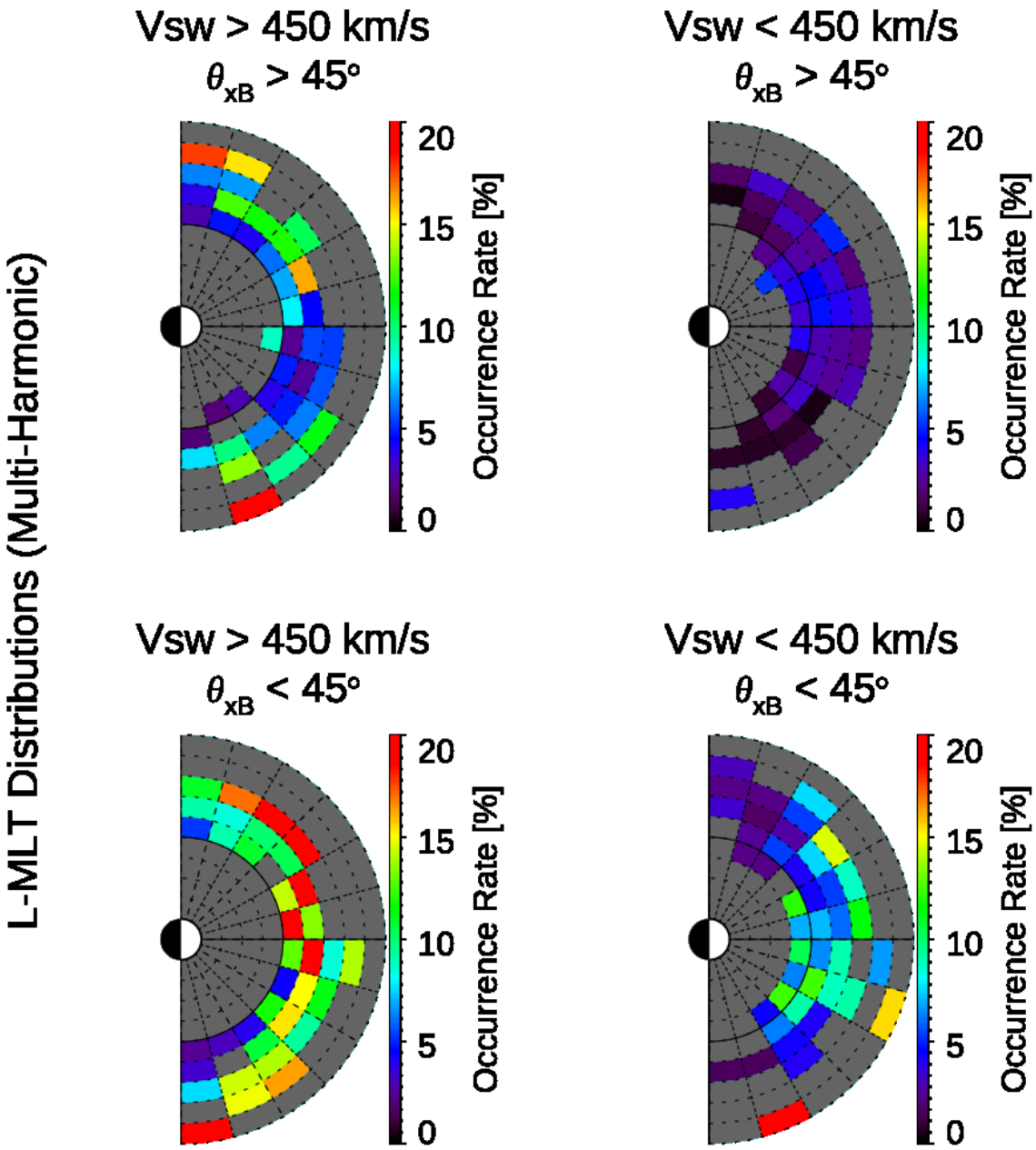
Toroidal ULF waves with multiple discrete frequencies were also reported in event studies (e.g., Takahashi & McPherron, 1984; Engebretson et al., 1986; Takahashi et al., 2020). It was suggested that multi-harmonic toroidal waves (hereinafter MTWs) occur when the cone angle (θ_{xB}) of the solar wind is small; however, controlling factors of MTWs are not fully investigated. One of the difficulties in investigation of the relation between ULF waves and the solar wind is that solar wind parameters are correlated with each other and it is difficult to determine which one controls wave excitation. To circumvent this difficulty, we conducted statistical analysis of the occurrence of MTWs under four conditions for the first time: high/low speed solar wind (V_{SW} greater/less than 450 km/s) and large/small cone angle (θ_{xB} greater/less than 45°).

From the ULF wave observations by the Arase/Magnetic Field Experiment (MGF) instrument, we found that not only θ_{xB} but also V_{SW} is correlated with the occurrence of MTWs. MTWs are frequently observed around noon sector when the cone angle is small, while the occurrence frequency and wave amplitude of MTWs on the flank side increase as V_{SW} increases. This result suggests that both the upstream waves excited in the ion foreshock region and the Kelvin-Helmholtz (KH) instability at the magnetopause can be the energy sources of MTWs at each sectors in the magnetosphere. We also examined the influence of the plasmasphere on the occurrence of MTWs. The occurrence frequency dramatically increases as the cold electron density (N_e) increases. This is probably because the interval of eigenfrequencies of wave harmonics decreases with the increase of N_e, and field line resonance (FLR) at multiple harmonic frequencies may be caused by disturbances with a finite frequency band. Outside the plasmasphere ($N_e <$ 50 cm^{-3}), the occurrence frequency of MTWs is relatively low, but the wave amplitudes are large on the flank side in the case of high speed solar wind. Thus, the plasmasphere has negative effect on the amplitudes of the waves driven by the KH instability. We further examined the relation between MTWs and fluctuation of the solar wind dynamic pressure (P_{dyn}), and revealed that P_{dyn} fluctuation can be the energy source of MTWs especially in the case of low speed solar wind. On the basis of our statistical analysis, V_{SW}, θ_{xB} and background plasma density are the principal controlling factors of the occurrence of MTWs, and

©2021. Japan Geoscience Union. All Right Reserved.

P_{dyn} fluctuation is categorized into the second group of the controlling factors.

Keywords: ULF waves, magnetosphere, solar wind, upstream waves, Kelvin-Helmholtz instability



©2021. Japan Geoscience Union. All Right Reserved.

Probing inner magnetosphere dynamics and radial transport via observations of electron flux oscillations

*Theodore E Sarris[1]

1. Democritus University of Thrace

Relativistic electrons in the inner magnetosphere undergo dynamical variations due to acceleration, transport, and loss processes under various physical mechanisms. One of the prevalent mechanisms is radial diffusion, caused by the resonant interaction between energetic electrons and ultra-low frequency (ULF) waves. We discuss how an indication of this resonant interaction is the appearance of periodic flux oscillations. These oscillations are observed in the form of drift-periodic flux fluctuations and have distinct characteristics from the more commonly observed drift echoes following storm- or substorm-related energetic particle injections. The amplitudes of such flux oscillations is dependent on a number of parameters, such as the local phase space density gradients, the amplitude of ULF waves and the width of electron energy channels. In particular, the latter is a critical parameter affecting the observed amplitude of flux oscillations, with narrower energy channel widths enabling the observation of higher-amplitude flux oscillations; this potentially explains why such features were not observed regularly before the Van Allen Probes era, as previous spacecraft generally had lower energy resolution. We present simulations and observations demonstrating the dependence of the observed flux oscillations on various parameters and we discuss how such flux oscillations could be used as indicators of radial transport rates.

Keywords: Radial transport, Electron flux oscillations, Phase space density, Radial diffusion

©2021. Japan Geoscience Union. All Right Reserved.

Radiation belt electron acceleration during periods of low plasma density

*Hayley J Allison[1], Yuri Y Shprits[1,2,3], Irina Zhelavskaya[1], Dedong Wang[1], Artem Smirnov[1,2]

1. Helmholtz Centre Potsdam GFZ German Research Centre for Geosciences, Potsdam, Germany, 2. University of Potsdam, Potsdam, Germany, 3. University of California, Los Angeles, CA, USA

Electrons in the Van Allen radiation belts can have energies in excess of 7 MeV. We present a unique way of analyzing phase space density data which demonstrates that local acceleration is capable of heating electrons up to 7 MeV. The Van Allen Probes mission not only provided unique measurements of ultra-relativistic radiation belt electrons, but also simultaneous observations of plasma waves that allowed for the routine inference of total plasma number density. Based on long-term observations, we show that the underlying plasma density has a controlling effect over local acceleration to ultra-relativistic energies, which occurs only when the plasma number density drops down to very low values (~10 cm^{-3}). The VERB-2D model is used to simulate ultra-relativistic electron acceleration during an event which exhibits an extreme cold plasma depletion. The results show that a reduced electron plasma density allows chorus waves to efficiently resonate with electrons up to ultra-relativistic energies, producing enhancements from 100s of keV up to >7 MeV via local diffusive acceleration. We analyse statistically the observed chorus wave power during ultra-relativistic enhancement events, considering the contribution from both upper and lower band chorus waves. The PINE density model allows for the investigation of global magnetospheric density changes. We analyze the how the global cold plasma density changes during ultra-relativistic enhancement events and compare to in-situ point measurements of the plasma density.

Keywords: chorus acceleration, Electron radiation belts, Plasma density, Ultra-relativistic electrons

©2021. Japan Geoscience Union. All Right Reserved.

Parameterized Lifetime of Energetic Electrons due to Interactions with Chorus Waves

*Dedong Wang[1], Yuri Shprits[1,2,3]

1. Helmholtz Center Potsdam German Research Centre for Geosciences Potsdam, 2. University of Potsdam, 3. UCLA

Chorus waves can cause the loss of energetic electrons in the Earth's radiation belts and ring current via pitch-angle diffusion. We calculated the bounce-averaged quasi-linear diffusion coefficients to quantify these processes. In this study, using these diffusion coefficients, we parameterize the lifetime of the electrons with energy range from 1 keV to 2 MeV. In each magnetic local time (MLT), we calculate the lifetime for each energy and L-shell using two different methods. By applying polynomial fits, we parameterize the electron life time as a function of L-shell and electron kinetic energy in each MLT. we derive the lifetime parameterization as a function of geomagnetic activity (Kp index), L, magnetic local time (MLT) and energy of electrons. The parameterized electron lifetimes show a strong functional dependence on Kp, L-shell and electron energy. During the storm time, the lifetimes for higher energy (> 100 keV) electrons range from hours to days in the heart of the radiation belts. In contrast, the lifetimes for electrons with lower energy (< 100 keV) range from minutes to hours. This parameterization of electron lifetime is convenient for inclusion in simulations in the inner magnetosphere.

Keywords: radiation belt electrons, lifetime, chorus waves

©2021. Japan Geoscience Union. All Right Reserved.

Statistical Comparisons of Spin-Averaged Electron Flux from ARASE and Van Allen Probes Instruments

*Matyas Szabo-Roberts[1,2], Yuri Shprits[1,2], Hayley J Allison[1], Artem Smirnov[1,2], Nikita Aseev[7], Ruggero Vasile[1], Yoshizumi Miyoshi[4], Takefumi Mitani[4,5,6], Nana Higashio[5], Satoshi Kasahara[3]

1. Helmholtz Centre Potsdam GFZ German Research Centre for Geosciences, 2. University of Potsdam, 3. Department of Earth and Planetary Science, School of Science, The University of Tokyo, 4. Nagoya University, 5. JAXA Japan Aerospace Exploration Agency, 6. ISAS Institute of Space and Aeronautical Science, 7. Huawei Technologies

Following the end of the Van Allen Probes mission, the ARASE satellite offers a unique opportunity to continue in-situ radiation belt particle measurements into the next solar cycle. In this study we compare spin-averaged flux measurements from the MEPe, HEP-L, HEP-H, and XEP-SSD instruments on ARASE with those from the MagEIS and REPT instruments on the Van Allen Probes, calculating Pearson R and the mean ratio of fluxes at L* conjunctions between the spacecraft. ARASE and Van Allen Probes measurements show a close agreement over a wide range of energies, observing a similar general evolution of electron flux, as well as average, peak, and minimum values. Measurements from the two missions agree especially well in the 3.5<L*<4.5 range where ARASE is at similar magnetic latitudes as the Van Allen Probes. ARASE tends to record higher flux <670 keV with longer decay times after flux enhancements, particularly for L*<3.5 . Conversely, for energies >1.4 MeV, ARASE flux measurements are generally lower than those of Van Allen Probes, especially for L*>4.5 . The Person R values show that the >1.4 MeV flux from both missions are well correlated and thus, although flux magnitudes differ, all spacecraft observe a similar general evolution. However, the correlation decreases as L* increases due to ARASE measuring at magnetic latitudes outside Van Allen Probes orbits for L*>4.5. We perform a preliminary intercalibration between the two missions using the mean ratio of the fluxes as an energy- and L*- dependent correction factor. The correction factor significantly improves agreement between the fluxes above 1.4 MeV.

©2021. Japan Geoscience Union. All Right Reserved.

[E] Poster | P (Space and Planetary Sciences)：P-EM Solar-Terrestrial Sciences, Space Electromagnetism & Space Environment

Sat. Jun 5, 2021 5:15 PM - 6:30 PM JST | Sat. Jun 5, 2021 8:15 AM - 9:30 AM UTC | Ch.04_1

[P-EM12] Dynamics of the Inner Magnetospheric System

convener:Kunihiro Keika(Department of Earth and Planetary Science, Graduate School of Science, The University of Tokyo), Yoshizumi Miyoshi(Institute for Space-Earth Environmental Research, Nagoya University), W Lauren Blum(University of Colorado Boulder), Yuri Shprits(Helmholtz Centre Potsdam GFZ German Research Centre for Geosciences)

The inner magnetosphere is highly variable because dynamical variations of incoming energy from the solar wind, magnetospheric tail, and the ionosphere. Cross-regional, cross-scale, and cross-energy couplings are the key processes for understanding this dynamical system. Coordinated observations by multi-satellites and ground-based observations are very essential to revealing these processes. In the 24th and 25th solar cycles, a number of satellites such as Van Allen Probes, MMS, THEMIS, DSX and Arase; coordinated ground-based observations (THEMIS-GBO, SuperDARN, EISCAT, magnetometers, riometer, etc); and numerical simulations (global kinetic model, MHD model, micro PIC, hybrid simulations) have successfully investigated the inner magnetosphere system. We invite papers on recent results of the inner magnetosphere and/or its coupling with the other regions including the ionosphere and the outer magnetosphere. Presentations on new projects such as sounding rocket experiments and data assimilation/machine learning are also welcome.

[PEM12-P01] Modulation of chorus intensity and UHR frequency in the off equatorial regions observed by the Arase satellite.

*Yuri Ampuku[1], Fuminori Tsuchiya[1], Yasumasa Kasaba[1], Satoshi Kurita[2], Yoshiya Kasahara[3], Shoya Matsuda[4], Atsushi Kumamoto[5], Ayako Matsuoka[6] (1.Planetary Plasma and Atmospheric Research Center, Graduate School of Science, Tohoku University, 2.Research Institute for Sustainable Humanosphere, Kyoto University, 3.Graduate School of Natural Science and Technology, Kanazawa University, 4.Institute of Space and Astronautical Science, JAXA, 5.Graduate School of Science, Tohoku University, 6.Graduate School of Science, Kyoto University)

[PEM12-P02] Spatio-temporal characteristics of the precipitating electron energy of pulsating aurora and comparison with the numerical simulation

*Kohei Toyama[1], Satoshi Kurita[2], Yoshizumi Miyoshi[1], Keisuke Hosokawa[3], Yasunobu Ogawa[4], Shin-ichiro Oyama[1], Satonori Nozawa[1], Tetsuya Kawabata[1], Shinji Saito[5], Yoshiki Ito[1] (1.Institute for Space-Earth Environmental Research, Nagoya University, 2.Research Institute for Sustainable Humanosphere, 3.University of Electro-Communications, 4.National Institute of Polar Research, 5.National Institute of Information and Communications Technology)

[PEM12-P03] An error estimation for energetic electron flux measured by the high-energy electron experiments (HEP) onboard the Arase satellite.

*Tomoaki Hori[1], Takefumi Mitani[2], Takeshi Takashima[2], Yoshizumi Miyoshi[1], Iku Shinohara[2] (1.Institute for Space-Earth Environmental Research, Nagoya University, 2.Japan Aerospace Exploration Agency)

[PEM12-P04] Relationship between polar cap potential and MLT distribution of ground delta H during geomagnetic storms using observations and RAM-SCB simulations

*Sandeep Kumar[1], Yoshizumi Miyoshi[1], Vania Jordanova[2] (1.Institute for Space Earth Environmental Research, Nagoya University, 2.Los Alamos National Laboratory, US)

[PEM12-P05] Global characteristics of cold protons in the near-Earth magnetotail: MMS/HPCA observations

*Kunihiro Keika[1], Masahiro Hoshino[1], Ryuta Asami[1] (1.Graduate School of Science, The University of Tokyo)

[PEM12-P06] Interaction between whistler waves and electrons at Earth's magnetotail: Test particle simulation and THEMIS observation

*Fumiko Otsuka[1], Kaiti Wang[2], Kirolosse Mina GIRGIS[1], Tohru Hada[1] (1.Earth System Science and Technology, 2.Tamkang University)

[PEM12-P07] Case analysis of SAPS wave structure events observed by ERG, DMSP, and SuperDARN

*Takehiro Fukami[1], Atsushi Kumamoto[1], Yuto Katoh[1], Nozomu Nishitani[2], Tomoaki Hori[2], Yasumasa Kasaba[3], Fuminori Tsuchiya[3], Mariko Teramoto[4], Tomoki Kimura[5], Yoshiya Kasahara[6], Masafumi Shoji[2], Satoko Nakamura[2], Masahiro Kitahara[2], Ayako Matsuoka[7], Shun Imajo[2], Satoshi Kasahara[8], Shoichiro Yokota[9], Kunihiro Keika[8], Yoichi Kazama[10], Shiang-Yu Wang Wang[10], Jun Chae-Woo[2], Kazushi Asamura[11], Yoshizumi Miyoshi[2], Iku Shinohara[11], Simon G. Shepherd[12] (1.Department of Geophysics, Graduate School of Science, Tohoku University, 2.Institute for Space-Earth Environmental Research, Nagoya University, 3.Planetary Plasma and Atmospheric Research Center, Tohoku University, 4.Kyushu Institute of Technology, 5.The Frontier Research Institute for Interdisciplinary Sciences, 6.Information Media Center, Kanazawa University, 7.Data analysis Center for Geomagnetism and Space Magnetism, Graduate School of Science, Kyoto University, 8.The university of Tokyo, 9.Graduate School of Science, Osaka University, 10.Academia Sinica Institute of Astronomy & Astrophysics, 11.Institute of Space and Astronautical Science, Japan Aerospace Exploration Agency, 12.Dartmouth College)

[PEM12-P08] Energetic electron precipitations showing ULF modulation observed by VLF/LF transmitter signals

*Tanaka Kentaro[1], Hiroyo Ohya[1], Fuminori Tsuchiya[2], Kazuo Shiokawa[3], Yoshizumi Miyoshi[3], Nozomu Nishitani[3], Tomoaki Hori[3], Mariko Teramoto[4], Martin G Connors[5], Simon G Shepherd[6], Hiroyuki Nakata[1] (1.Graduate School of Engineering, Chiba University, 2.Planetary Plasma and Atmospheric Research Center, Graduate School of Science, Tohoku University, 3.Institute for Space-Earth Environmental Research, Nagoya University, 4.Kyushu Institute of Technology, 5.Athabasca University, 6.Dartmouth College)

[PEM12-P09] A statistical study on the detachment of arc from the main auroral oval using all-sky imaging observations at Athabasca, Canada

*Sneha Yadav[1], Kazuo Shiokawa[1], Yuichi Otsuka[1], Martin G Connors[2,3] (1.Institute for Space-Earth Environmental Research, Nagoya University, Nagoya, Japan, 2.Athabasca University Observatories, Athabasca University, Athabasca, Alberta, Canada, 3.Department of Physics and Astronomy, University of Calgary, Calgary, Alberta, Canada)

[PEM12-P10] SAPS electric field and particle observations by the Arase satellite and SuperDARN

*Tomoya Takada[1], Nozomu Nishitani[1], Tomoaki Hori[1], Yasumasa Kasaba[2], Atsushi Kumamoto[2], Yuto Katoh[2], Yoshiya Kasahara[3], Masafumi Shoji[1], Satoko Nakamura[1], Masahiro Kitahara[1], Fuminori Tsuchiya[2], Kazushi Asamura[4], Yoshizumi Miyoshi[1], Yoichi Kazama[5], S Y Wang[5], Shoichiro Yokota[6], Satoshi Kasahara[7], Kunihiro Keika[7], Ayako Matsuoka[8], Shun Imajo[1], Iku Shinohara[4], Chae-Woo Jun[1], Simon G Shepherd[9] (1.Institute for Space-Earth Environmental Research, 2.Tohoku University, 3.Kanazawa University, 4.JAXA, 5.Academia Sinica, 6.Osaka University, 7.The University of Tokyo, 8.Kyoto University, 9.Thayer School of Engineering)

[PEM12-P11] Properties of EMIC waves observed by Van Allen Probes and ground-based magnetometers during relativistic electron precipitation

*Asuka Hirai[1], Fuminori Tsuchiya[1], Takahiro Obara[1], Yasumasa Kasaba[1], Yuto Katoh[2], Hiroaki Misawa[1], Kazuo Shiokawa[3], Yoshizumi Miyoshi[3], Chae-Woo Jun[3], Satoshi Kurita[4], Martin G Connors[5], Aaron Hendry[6] (1.Planetary Plasma and Atmospheric Research Center, Graduate School of Science, Tohoku Univ. , 2.Department of Geophysics, Graduate School of Science, Tohoku University, 3.Institute for Space-Earth

Environmental Research, Nagoya University, 4.Research Institute for Sustainable Humanosphere, Kyoto University, 5.Athabasca University, 6.Otago University)

[PEM12-P12] A Study on the Effect of the Number of Snapshots for Averaging and the Noise Level on the Estimation Accuracy in Direction Finding

*Yuji Tanaka[1], Yoshiya Kasahara[1] (1.Division of Electrical Engineering and Computer Science, Graduate School of Natural Science and Technology, Kanazawa University)

[PEM12-P13] Relative Contribution of ULF Waves and Whistler-mode Chorus to the Radiation Belt Variation during the May 2017 Storm

*Naoko Takahashi[1], Kanako Seki[1], Mei-Ching Fok[2], Yihua Zheng[2], Yoshizumi Miyoshi[3], Satoshi Kasahara[1], Kunihiro Keika[1], David Hartley[4], Yoshiya Kasahara[5], Yasumasa Kasaba[6], Nana Higashio[1,7], Ayako Matsuoka[8], Shoichiro Yokota[9], Tomoaki Hori[3], Masafumi Shoji[3], Satoko Nakamura[3], Shun Imajo[3], Iku Shinohara[10] (1.Graduate School of Science, The University of Tokyo, 2.NASA Goddard Space Flight Center, 3.Institute for Space-Earth Environmental Research, Nagoya University, 4.Department of Physics and Astronomy, University of Iowa, 5.Graduate School of Natural Science and Technology, Kanazawa University, 6.Graduate School of Science, Tohoku University, 7.Japan Aerospace Exploration Agency, 8. Data Analysis Center for Geomagnetism and Space Magnetism, Graduate School of Science, Kyoto University, 9.Graduate School of Science, Osaka University, 10.Institute of Space and Astronautical Science, Japan Aerospace Exploration Agency)

[PEM12-P14] Initial results on multi event analysis of the simultaneous observation of isolated proton auroras at subauroral latitudes by a highly sensitive all-sky camera and the Van Allen Probes satellites

*Kohki Nakamura[1], Kazuo Shiokawa[1], Masahito Nose[1], Tsutomu Nagatsuma[2], Kaori Sakaguchi[2], Harlan Spence[3], Geoff Reeves[4], Herbert Funsten[4], Craig Kletzing[5], Robert MacDowall[6], Charles Smith[3], John Wygant[7], John Bonnell[7] (1.Nagoya Univ., 2.National Institute of Information and Communications Technology, 3.New Hampshire Univ., 4.Los Alamos National Laboratory, 5.Iowa Univ., 6.Goddard Space Flight Center, 7.Minnesota Univ.)

[PEM12-P15] Study of the excitation mechanism of internally driven ULF waves by the drift-bounce resonance with ring current ions based on the Magnetosphere-Ionosphere coupled model

*Tomotsugu Yamakawa[1], Kanako Seki[1], Takanobu Amano[1], Naoko Takahashi[1], Yoshizumi Miyoshi[2], Aoi Nakamizo[3] (1.Department of Earth and Planetary Science, School of Science, The University of Tokyo, 2.Institute for Space-Earth Environmental Research, Nagoya University, 3.National Institute of Information and Communications Technology)

[PEM12-P16] Statistical Analysis of Latitudinal Electron Density Distribution in the Plasmasphere

*Ayano Hambara[1], Yuki Obana[2], Yukinaga Miyashita[3,4], Atsuki Shinbori[5], Yuichi Otsuka[5], Atsushi Kumamoto[6], Fuminori Tsuchiya[7], Shoya Matsuda[8], Ayako Matsuoka[9], Yoshiya Kasahara[10], Yoshizumi Miyoshi[5], Iku Shinohara[8], William S. Kurth[11], Craig A. Kletzing[11], Charles W. Smith[12], Robert J. MacDowall[13] (1.Advanced Science and Engineering Course, Graduate School of Engineering, Osaka Electro-Communication University, 2.Department of Engineering Science, Faculty of Engineering, Osaka Electro-Communication University, 3.Korea Astronomy and Space Science Institute, 4.Korea University of Science and Technology, 5.Institute for Space-Earth Environmental Research, Nagoya University, 6.Department of Geophysics, Graduate School of Science, Tohoku University, 7.Planetary Plasma and Atmospheric Research Center, Graduate School of Science, Tohoku University, 8.Institute of Space and Astronautical Science/Japan Aerospace Exploration Agency, 9.Data Analysis Center for Geomagnetism and Space Magnetism, Graduate School of Science, Kyoto University, 10.Information Media Center, Kanazawa University, 11.Department of Physics and Astronomy, University of Iowa, 12.Institute for the Study of

Earth, Oceans, and Space, University of New Hampshire, 13. Solar System Exploration Division, Goddard Space Flight Center)

[PEM12-P17] A statistical study of longitudinal extent of Pc1 pulsations using seven PWING ground stations at subauroral latitudes

*Jie Liu[1], Kazuo Shiokawa[1], Shin-ichiro Oyama[1], Yuichi Otsuka[1], Chae-Woo Jun[1], Masahito Nose[1], Tsutomu Nagatsuma[2], Kaori Sakaguchi[2], Akira Kadokura[3], Mitsunori Ozaki[4], Martin G Connors[5], Dmitry Baishev[6], Nozomu Nishitani[1], Alexey Oinats[7], Vladimir Kurkin[7], Tero Reita[8] (1.Institude for Space-Earth Environmental Research, Nagoya University, 2.National Institute of Information and Communications Technology, Japan, 3.National Institute of Polar Research, Tokyo, Japan, 4.Kanazawa University, Kanazawa, Japan, 5.Athabasca University, Athabasca, Canada, 6.Yu.G.Shafer Institute of Cosmophysical Research and Aeronomy of Siberian Branch of the Russian Academy of Sciences, Yakutsk, Russia, 7.Institute of Solar-Terrestrial Physics, Siberian Branch of the Russian Academy of Sciences, Irkutsk, Russia, 8.Sodankyla Geophysical Observatory, University of Oulu, Oulu, Finland)

[PEM12-P18] Altitude profile of isolated proton aurora as estimated from digital camera observations from International Space Station

*Kazuteru Takahashi[1], Sota Nanjo[2], Yuta Hozumi[2], Keisuke Hosokawa[2], Yoshizumi Miyoshi[1] (1.Institute for Space–Earth Environmental Research, 2.The University of Electro-Communications)

[PEM12-P19] Development of ISEE_Wave; Interactive Plasma Wave Analysis Tool

*Shoya Matsuda[1], Yoshizumi Miyoshi[2], Satoko Nakamura[2], Masahiro Kitahara[2], Masafumi Shoji[2], Tomoaki Hori[2], Shun Imajo[2], Chae-Woo Jun[2], Satoshi Kurita[3], Yoshiya Kasahara[4], Ayako Matsuoka[5], Iku Shinohara[1] (1.Institute of Space and Astronautical Science/Japan Aerospace Exploration Agency, 2.Institute for Space-Earth Environmental Laboratory, Nagoya University, 3.Research Institute for Sustainable Humanosphere, Kyoto University, 4.Kanazawa University, 5.kyoto University)

[PEM12-P20] Radiation characteristics of upper-band and lower-band chorus emissions in the generation region deduced from the Arase observation

*Seigo Hayashi[1], Satoshi Kurita[2], Hirotsugu Kojima[2], Yoshiya Kasahara[3], Shoya Matsuda[4], Ayako Matsuoka[5], Iku Shinohara[4], Yoshizumi Miyoshi[6] (1.Undergraduate School of Electrical and Electronic Engineering, Kyoto University, 2.Research Institute for Sustainable Humanosphere, Kyoto University, 3.Graduate School of Natural Science and Technology, Kanazawa University, 4.ISAS/JAXA, 5.Graduate School of Science, Kyoto University, 6.Institute for Space-Earth Environmental Research, Nagoya University)

[PEM12-P21] Isolated Electrostatic Potentials Observed by the Arase Satellite

*Tomoe Taki[1], Satoshi Kurita[1], Hirotsugu Kojima[1], Yoshiya Kasahara[2], Yoshizumi Miyoshi[3], Ayako Matsuoka[4], Shoya Matsuda[5] (1.Research Institute for Sustainable Humanosphere, Kyoto University, 2.Information Media Center, Kanazawa University, 3.Institute Space-Earth Environmental Research, Nagoya University, 4.Data Analysis Center for Geomagnetism and Space Magnetism Graduate School of Science, Kyoto University, 5.Institute of Space and Astronautical Science/Japan Aerospace Exploration Agency)

[PEM12-P22] Statistical study of drifting electron holes associated with substorms observed by the Arase satellite

*Taku Namekawa[1,2], Iku Shinohara[1], Takefumi Mitani[1], Kazushi Asamura[1], Nagai Tsugunobu[1], Satoshi Kasahara[2], Shoichiro Yokota[3], Tomoaki Hori[4], Ayako Matsuoka[5], Yoshizumi Miyoshi[4] (1.ISAS / JAXA, 2.The University of Tokyo, 3.Osaka University, 4.Nagoya University, 5.Kyoto University)

[PEM12-P23] **The influence of EMIC (ElectroMagnetic Ion Cyclotron) wave-interaction on energetic protons in the magnetosphere using Arase observations**

*Chae-Woo Jun[1], Yoshizumi Miyoshi[1], Satoko Nakamura[1], Shun Imajo[1], Masafumi Shoji[1], Chao Yue[2], Jacob Bortnik[3], Larry Lyons[3], Yoshiya Kasahara[4], Yasumasa Kasaba[5], Fuminori Tsuchiya[5], Atsushi Kumamoto[5], Shoya Matsuda[6], Kazushi Asamura[6], Iku Shinohara[6], Ayako Matsuoka[7] (1.Institute for Space-Earth Environmental Research, Nagoya University, 2.Peking University, Beijing, China , 3.Atmospheric and Oceanic Sciences, University of California Los Angeles, Los Angeles, USA, 4.Kanazawa University, Kanazawa, Japan, 5.Tohoku University, Sendai, Japan, 6.Institute of Space and Astronautical Science, Japan Aerospace Exploration Agency, Sagamihara, Japan, 7.Kyoto University, Kyoto, Japan)

[PEM12-P24] A statistical study on high-energy electron injection events observed by Arase (ERG)

*JINGXUAN YANG[1], Iku Shinohara[2], Taku Namekawa[1], Takefumi Mitani[2], Kazushi Asamura[2], Satoshi Kasahara[3], Nana Higashio[4], Ayako Matsuoka[5] (1.Department of Earth and Planetary Science, Graduate School of Science, The University of Tokyo, 2.Institute of Space and Astronautical Science, Japan Aerospace Exploration Agency, 3.The University of Tokyo, 4.Japan Aerospace Exploration Agency, 5.Data Analysis Center for Geomagnetism and Space Magnetism, Graduate School of Science, Kyoto University)

[PEM12-P25] Development of a high-energy electron analyzer onboard CubeSats

*Iku Shinohara[1], Takefumi Mitani[1], Mariko Teramoto[2], Kazushi Asamura[1], Ryota Onogi[1], Takeshi Takashima[1] (1.Japan Aerospace Exploration Agency/Institute of Space and Astronautical Science, 2.Kyushu Institute of Technology)

[PEM12-P26] **An observational study on possible excitation of storm-time Pc5 waves**

*Kento Otani[1], Iku Shinohara[2], Mariko Teramoto[3], Tomotsugu Yamakawa[1], Kanako Seki[4], Satoshi Kasahara[4], Shoichiro Yokota[5], Kunihiro Keika[1], Naoko Takahashi[4], Takefumi Mitani[2], Nana Higashio[2], Ayako Matsuoka[6], Kazuhiro Yamamoto[4] (1.Tokyo University/Graduate School of Science, 2.JAXA, 3.Kyushu Institute of Technology, 4.Tokyo University, 5.Graduate school of Science, Osaka University, 6.Graduate school of Science, Kyoto University)

[PEM12-P27] A Novel Calibration Method of Short Time Waveform Signals and its Approcation for the PWE/WFC Data

*Masahiro Kitahara[1], Shoya Matsuda[2], Yuto Katoh[3], Yoshiya Kasahara[4], Hirotsugu Kojima[5], Yoshizumi Miyoshi[1], Mitsuru Hikishima[2] (1.Institute for Space-Earth Environmental Research, Nagoya University, 2.Institute of Space and Astronautical Science/Japan Aerospace Exploration Agency, 3.Department of Geophysics, Graduate School of Science, Tohoku University, 4.Information Media Center, Kanazawa University, 5.Research Institute for Sustainable Humanosphere, Kyoto University)

[PEM12-P28] Nitrogen and oxygen ions from the Earth's ionosphere observed by the Arase satellite

*Shoichiro Yokota[1], Koichiro Tsuda[1], Satoshi Kasahara[2], Tomoaki Hori[3], Kunihiro Keika[2], Yoshizumi Miyoshi[3], Iku Shinohara[4] (1.Osaka University, 2.University of Tokyo, 3.ISEE, Nagoya University, 4.ISAS/JAXA)

[PEM12-P29] Electron Energization during Dipolarization Events: Test Particle Simulations

*Kirolosse Mina Girgis[1], Tohru Hada[1], Fumiko Otsuka[1], Kaiti Wang[2] (1.Department of Earth System Science and Technology, Interdisciplinary Graduate School of Engineering Sciences, Kyushu University, Japan , 2.Department of Aerospace Engineering, University of Tamkang, Taiwan)

[PEM12-P30] Computer simulations of electron scatterings through chorus-wave particle interactions

Yoshiki Ito[1], *Yoshizumi Miyoshi[1], Shinji Saito[2] (1.Institute for Space-Earth Environmental Research, Nagoya University, 2.NICT)

[PEM12-P31] Statistical analyses of low energy ion heating by electromagnetic ion cyclotron waves via wave-particle interaction analyses: Arase observations

*Masafumi Shoji[1], Yoshizumi Miyoshi[1], Lynn M Kistler[1,2], Kazushi Asamura[3], Yasumasa Kasaba[4], Ayako Matsuoka[5], Yoshiya Kasahara[6], Shoya Matsuda[3], Fuminori Tsuchiya[4], Atsushi Kumamoto[4], Satoko Nakamura[1], Masahiro Kitahara[1], Shun Imajo[1], Chae-Woo Jun[1], Iku Shinohara[3] (1.Institute for Space-Earth Environmental Research, Nagoya Univ., 2.University of New Hampshire, 3.ISAS/JAXA, 4.Tohoku Univ., 5.Kyoto Univ., 6.Kanazawa Univ.)

[PEM12-P32] Plasma waves causing 20 Hz intensity modulation of pulsating aurora: High-speed Tjörnes-Arase-Syowa conjugate observation

*Herbert Akihito Uchida[1], Ryuho Kataoka[2,1], Kiyoka Murase[1], Shoya Matsuda[3], Yoshiya Kasahara[4], Masafumi Shoji[5], Yoshizumi Miyoshi[5], Iku Shinohara[3], Ayako Matsuoka[6], Satoshi Kurita[7], Keisuke Hosokawa[8], Shun Imajo[5] (1.The Graduate University for Advanced Studies, 2.National Institute of Polar Research, 3.Institute of Space and Astronautical Science, Japan Aerospace Exploration Agency, 4.Kanazawa University, 5.Institute for Space–Earth Environmental Research, Nagoya University, 6.Kyoto University, 7.Research Institute for Sustainable Humanosphere, Kyoto University, 8.University of Electro-Communications)

Modulation of chorus intensity and UHR frequency in the off equatorial regions observed by the Arase satellite.

*Yuri Ampuku[1], Fuminori Tsuchiya[1], Yasumasa Kasaba[1], Satoshi Kurita[2], Yoshiya Kasahara[3], Shoya Matsuda[4], Atsushi Kumamoto[5], Ayako Matsuoka[6]

1. Planetary Plasma and Atmospheric Research Center, Graduate School of Science, Tohoku University, 2. Research Institute for Sustainable Humanosphere, Kyoto University, 3. Graduate School of Natural Science and Technology, Kanazawa University, 4. Institute of Space and Astronautical Science, JAXA, 5. Graduate School of Science, Tohoku University, 6. Graduate School of Science, Kyoto University

The whistler mode chorus is a type of plasma wave generated near the geomagnetic equator by the wave-particle interactions. The chorus waves scatter the pitch angle of electrons by the wave-particle interactions, and the scattered electrons precipitate into the polar region and cause diffuse aurora. In particular, chorus waves which propagate to high latitudes could scatter the relativistic electrons, thus its propagation is of great importance for loss of radiation belt electrons and impact on the middle atmosphere. The mechanism of the chorus propagation from the source region at the equator to higher latitudes has not been clarified. However, the leading theory is chorus propagation along the duct (a field-aligned increase of the plasma density).

Plasma wave experiment (PWE) / Onboard frequency analyzer (OFA) on board Arase satellite observed modulations of chorus intensity which were correlated with variations in the UHR frequency with a period of a dozen seconds at geomagnetic latitude ~17° and Mallwain parameter L~6.0 at 00:06-00:10 UT, March 29, 2017. Interpretations of the phenomenon are as follows: (1) chorus propagating along the duct structure, (2)overlapping of another wave whose frequency is close to the UHR frequency, (3)electron density modulation caused by chorus. The simulation study reported (1) chorus propagation with duct structure (Hanzelka and Santolik, 2019). However, there is no report on observation of duct structure and the chorus propagating along the duct at off-equator. The case of (3) electron density modulation caused by chorus was reported by Nishimura et al. (2015).

In this study, we analyzed this plasma wave data at off-equator to consider whether the corresponding modulation of chorus intensity and UHR frequency could be explained by duct propagation. We assumed that Arase satellite crossed through ducts. We estimated the duct structure (width and relative density increase) from changes in UHR frequency and orbit data of Arase satellite. We identified UHR frequency by fitting the Gaussian function in the frequency direction to narrow band continuous emission observed by OFA with 1 s time resolution and calculated electron density by using magnetic field intensity observed by Magnetic Field Experiment (MGF). We obtain 20 examples of the presumed duct structure which correlated with chorus intensity modulation. Full width at half maximum of the duct structures and relative density increase in the center of the ducts are 5.9 km and 1.3 % (minimum), 17 km and 1.8 % (maximum), 10 km and 1.4 % (average), respectively. Hanzelka and Santolik (2019) simulated ducting chorus with various scales of duct and reported limits of the spatial scale and the relative density increase which were needed for ducting. Comparing our result with their simulation, the scale of density changes observed by Arase satellite was that the chorus could propagate up to geomagnetic latitude 45° or more at their propagation angle 15 degrees or loss.

We will investigate another possibility of (2) overlapping of other waves by using polarization information of the waves and look for similar events from the observation of the Arase satellite.

©2021. Japan Geoscience Union. All Right Reserved.

Reference:
Hanzelka, M., and Santolik, O. 2019, Geophysical Research Letters, 46, 5735– 5745. doi:10.1029/2019GL083115
Nishimura, Y. et al. 2015, Geophys. Res. Space Physics, 120, 7433– 7446, doi:10.1002/2015JA021330.

Keywords: whistler mode chorus, electron density, Arase satellite

©2021. Japan Geoscience Union. All Right Reserved.

Spatio-temporal characteristics of the precipitating electron energy of pulsating aurora and comparison with the numerical simulation

*Kohei Toyama[1], Satoshi Kurita[2], Yoshizumi Miyoshi[1], Keisuke Hosokawa[3], Yasunobu Ogawa[4], Shin-ichiro Oyama[1], Satonori Nozawa[1], Tetsuya Kawabata[1], Shinji Saito[5], Yoshiki Ito[1]

1. Institute for Space-Earth Environmental Research, Nagoya University, 2. Research Institute for Sustainable Humanosphere, 3. University of Electro-Communications, 4. National Institute of Polar Research, 5. National Institute of Information and Communications Technology

Pulsating aurora (PsA) is characterized by quasi-periodic intensity modulations with a period of 2-20 s which is known as the main modulation. Electrostatic Cyclotron Harmonic waves and whistler-mode waves are known to cause the pitch angle scattering of energetic electrons in the magnetosphere. In particular, whistler-mode chorus waves play a crucial role in the pitch angle scattering of the electrons. The lower-band chorus causes precipitation of electrons whose energy is greater than several keV [Miyoshi et al., 2015]. The energy of precipitating electrons causing PsA has been estimated from ground-based optical observations. Ono [1993] observed the emission intensities of PsAs at wavelengths of 427.8 and 844.6 nm using a multi-channel photometer at Syowa Station in Antarctica, and estimated the energy of the precipitating electrons by combining the ratio of the two emission intensities and the model calculation. However, Ono [1993] conducted observations using the instrument with a narrow field-of-view, and the energy estimation using all-sky imagers has not yet been performed. In Tromsoe, Norway, several highly-sensitive EMCCD cameras have been operated, which have simultaneously observed all-sky images of the emission intensity at the two wavelengths (427.8 and 844.6 nm) with a sampling frequency of 10 Hz. In this study, we investigate the spatio-temporal variations of precipitating electron energy using these EMCCD cameras. We estimated the precipitating electron energy of PsA by comparing the intensity ratio of the two emission lines using the all-sky images and the emission intensity calculation results obtained by the GLOW model. We will compare the emission intensity ratio obtained from a code coupling simulation of GEMSIS-RBW that calculates wave-particle interactions and resultant precipitations and the GLOW model to estimate the optical emissions at different wavelength. In this presentation, we show the spatio-temporal characteristics of the precipitating electron energy of PsA and discuss energy spectrum of precipitating electrons by comparing with the code-coupling simulation.

Keywords: Pulsating aurora, wave-particle interactions, optical obserbation

©2021. Japan Geoscience Union. All Right Reserved.

An error estimation for energetic electron flux measured by the high-energy electron experiments (HEP) onboard the Arase satellite.

*Tomoaki Hori[1], Takefumi Mitani[2], Takeshi Takashima[2], Yoshizumi Miyoshi[1], Iku Shinohara[2]

1. Institute for Space-Earth Environmental Research, Nagoya University, 2. Japan Aerospace Exploration Agency

We have developed an error estimation method for energetic electron flux data obtained by the high-energy electron experiments (HEP) onboard the Arase satellite. The error estimation is based on the assumption of counting statistics in which the error of raw electron counts measured by the HEP instrument is provided as a square root of the counts. The error propagation from the count error to a differential electron flux value, however, is not as simple as other types of particle instruments, such as electrostatic analyzers. This is because observed electron counts in each energy channel are contributed by not only incident electrons of the designated energy range but also those with energies higher than it, being a convolution of all such electrons. For this reason, we derive differential electron fluxes by applying “deconvolution” matrices, which have been developed with a set of Geant4 simulations best reproducing the response characteristics of the instrument. Accordingly, the same deconvolution needs to be applied also to the error of raw electron counts in order to correctly process the error propagation. The derived flux errors show a rough proportionality to the square root of the corresponding flux values, as expected from the above method. In addition, we confirm that a given flux value can have a range of flux error depending on the power law index of the energy spectrum of electron flux; the harder an energy spectrum is, the relatively larger the resultant flux error is. After initial check and brief validation studies, the preprocessed flux error values are going to be stored in an updated version of level-2 data files and then delivered to data users.

©2021. Japan Geoscience Union. All Right Reserved.

Relationship between polar cap potential and MLT distribution of ground delta H during geomagnetic storms using observations and RAM-SCB simulations

*Sandeep Kumar[1], Yoshizumi Miyoshi[1], Vania Jordanova[2]

1. Institute for Space Earth Environmental Research, Nagoya University, 2. Los Alamos National Laboratory, US

The hourly Dst index and the equivalent 1-min SYM-H index values derived from low-latitude magnetic observations are considered to represent the intensity of the magnetospheric ring current. However, due to limited number of stations used in the calculation, these indices are not enough to capture the spatial/longitudinal variation of ring current. Therefore 30 low to mid latitude (9-45º CGM lat) magnetic stations are used to calculate **Delta** H_m. In addition to building the ring currents, the incoming solar wind energy is also used to influence further disturbance processes such as polar and auroral magnetic substorm activity. Polar Cap (PC) indices is a good proxy of the polar cap potential. Therefore, it is expected that ring current intensities have close relationship with polar cap indices. Some studies have shown relationship between Sym/Asym H with PC indices. However, the MLT distribution of ground Delta H_{asy} (Delta H_{asy} = Delta H - Delta H_m) that represent ring current asymmetry and its relation to the polar cap potential is not explored. In this study, we will examine the relationship between ground Delta H_{asy} and polar cap potential during selected geomagnetic storms. In order to see the magnetospheric origin, RAM-SCB simulations will be used to compare the ring current pressure distribution during these events.

©2021. Japan Geoscience Union. All Right Reserved.

Global characteristics of cold protons in the near-Earth magnetotail: MMS/HPCA observations

*Kunihiro Keika[1], Masahiro Hoshino[1], Ryuta Asami[1]

1. Graduate School of Science, The University of Tokyo

We conduct a statistical study of cold protons in the near-Earth magnetotail under quiet magnetotail conditions. Performing two-component Maxwellian fits to velocity distributions, we extract densities and temperatures of cold protons. Cold protons are separated into three distinct populations in the density-plasma b space. We interpret that Population I, characterized by a positive correlation of density to b, is solar-wind origin plasma transported over the polar regions. Population II, seen only in the high-b (>0.1) and tailward region (r > 20 Re) particularly on the dusk side, is solar-wind origin plasma entering through the flank magnetopauses and remains cold. Population III, clearly identified in the near-Earth region (r < 10 Re), is of ionospheric origin. The results also suggest that plasma supply to the plasma sheet is dominated by Population I and that cold plasma in the near-Earth magnetotail is mostly of ionospheric origin.

Keywords: plasma transport in the magnetosphere, origin of plasma sheet populations, two-component plasma

©2021. Japan Geoscience Union. All Right Reserved.

Interaction between whistler waves and electrons at Earth's magnetotail: Test particle simulation and THEMIS observation

*Fumiko Otsuka[1], Kaiti Wang[2], Kirolosse Mina GIRGIS[1], Tohru Hada[1]

1. Earth System Science and Technology, 2. Tamkang University

Whistler waves play important roles in electron scattering in a collisionless plasma. We have analyzed a dipolarization event detected by THEMIS satellite on 19 February 2008. The event shows emission of whistler waves that lasted for a few seconds at the dipolarization site near the nightside equator at ~10 Re. Two types of waves were observed: one type has a frequency below ~0.1 f_{ce} (electron gyrofrequency) with the wave propagation angle relative to the background magnetic field around 120 degrees. The other type has a higher frequency from ~0.25 to ~0.5 f_{ce} with the propagation angles at ~20 and 160 degrees. Simultaneous observation of the electron pitch-angle distribution (PAD) reveals that associated with these waves, electron flux for energies below 4 keV is decreased while that with higher energies remains almost constant. These observations may indicate that the whistler waves are excited by the lower energetic electrons, whereas the higher energetic electrons may be treated as test particles in the given electromagnetic field.

In this presentation, we discuss electron scattering by obliquely propagating whistler waves performing test particle simulations and apply the results to the dipolarization event. The whistler waves are given as a superposition of sinusoidal waves obeying a cold plasma dispersion relation, using parameters consistent with the observation. Stretched dipole magnetic field is used as the background field model, assuming a Harris-type current sheet. Variation of the electron PAD is evaluated as a function of the electron energy and is compared with the THEMIS data. We discuss how the pitch-angle scattering by the whistler waves affects the variation of the PADs.

Keywords: whistler waves, electron scattering, earth's magnetotail

©2021. Japan Geoscience Union. All Right Reserved.

Case analysis of SAPS wave structure events observed by ERG, DMSP, and SuperDARN

*Takehiro Fukami[1], Atsushi Kumamoto[1], Yuto Katoh[1], Nozomu Nishitani[2], Tomoaki Hori[2], Yasumasa Kasaba[3], Fuminori Tsuchiya[3], Mariko Teramoto[4], Tomoki Kimura[5], Yoshiya Kasahara[6], Masafumi Shoji[2], Satoko Nakamura[2], Masahiro Kitahara[2], Ayako Matsuoka[7], Shun Imajo[2], Satoshi Kasahara[8], Shoichiro Yokota[9], Kunihiro Keika[8], Yoichi Kazama[10], Shiang-Yu Wang Wang[10], Jun Chae-Woo[2], Kazushi Asamura[11], Yoshizumi Miyoshi[2], Iku Shinohara[11], Simon G. Shepherd[12]

1. Department of Geophysics, Graduate School of Science, Tohoku University, 2. Institute for Space-Earth Environmental Research, Nagoya University, 3. Planetary Plasma and Atmospheric Research Center, Tohoku University, 4. Kyushu Institute of Technology, 5. The Frontier Research Institute for Interdisciplinary Sciences, 6. Information Media Center, Kanazawa University, 7. Data analysis Center for Geomagnetism and Space Magnetism, Graduate School of Science, Kyoto University, 8. The university of Tokyo, 9. Graduate School of Science, Osaka University, 10. Academia Sinica Institute of Astronomy & Astrophysics, 11. Institute of Space and Astronautical Science, Japan Aerospace Exploration Agency, 12. Dartmouth College

Subauroral Polarization Stream (SAPS) and Subauroral Ion Drift (SAID) are ionospheric high-speed westward flows found in the subauroral region mainly on the dusk side, and are considered to be driven by a strong poleward electric field [Spiro et al., 1979; Anderson et al., 1993; Foster and Burke, 2002]. Ericson et al. (2002) reported that irregular substructures with a scale size of the order of tens of km presented within SAPS. These structures are called “SAPS wave Structure (SAPSWS)”. Based on CRESS satellite observation, Mishin and Burke (2005) showed that high-temperature ions were transported into the inner magnetosphere, and showed a spatial distribution with characteristic energy dispersion (ion nose structure) when the electromagnetic field fluctuations of SAPSWS were observed. Ebihara et al. (2009) performed a simulation of coupling processes between the inner magnetosphere and the subauroral ionosphere, and reported that hot plasma with complex pressure distribution was transported into the inner magnetosphere, and contributed to the temporal and spatial variations of SAPS. Further detailed comparisons among electromagnetic field fluctuations and hot ions in the magnetosphere and plasma flows in the ionosphere are important for understanding the mechanism of SAPSWS.

In this study, we used data from the ERG satellite [Miyoshi et al., 2018], which measures the electromagnetic fields and the flux of ring current particles in the magnetosphere. For 15 events of ion nose structures found from the observations of particle instruments (MEP-i, LEP-I, LEP-e), we examined electric field variations in the radial direction and hot ion isotropic pressure derived from the particle flux in an energy range of 10-180 keV (measured by MEP-i). In several of the 15 events, we also analyzed data measured at the ionospheric conjugated positions by DMSP satellites and SuperDARN radar. DMSP satellites measure the drift velocity of ions and magnetic field in the ionosphere. SuperDARN radar [Greenwald et al., 1995] observes two-dimensional distribution of ionospheric plasma flow velocity in the direction of the line of sight.

In 7 of the 15 ion nose structure events, the amplitude of the electric field was more than twice as large as 1 mV/m. In 6 of the 7 events, the hot ion pressure variations were more than twice as large as those of the rest 8 events with electric field variation smaller than 1 mV/m. In a conjugated event between ERG and SuperDARN Christmas Valley East (CVE) in a period from 2:30 to 3:00 UT on July 9, 2017, a small-scale structure with a flow velocity fluctuation of 200 m/s or larger was observed by CVE radar. In a conjugate event between ERG and DMSP F18 satellite in a period from 8:40 to 9:10 UT on August 31, 2017, small

©2021. Japan Geoscience Union. All Right Reserved.

substructures with 200 m/s ionospheric flow were observed. In both events, variations of the ionospheric poleward electric field derived from ionospheric flow observations are about 10 mV/m. The electric field measured by ERG can be mapped to the ionosphere by assuming a dipole magnetic field. ERG observed a strong electric field with an amplitude of 2 mV/m or more near 17-19 MLT and L = 4-5. From the electric field measured in the magnetosphere, the electric field in the ionosphere was estimated to be 30-40 mV /m. The Electric field in the ionosphere based on SuperDARN and DMSP is comparable but a little smaller than that based on ERG. For further detailed comparison, we should take it into consideration that SuperDARN and DMSP measured a flow speed in a little different direction from westward, and the actual magnetic field could be different from the dipole field model. In the conjugate event between ERG and SuperDARN, the scale of the structure in the magnetosphere was estimated to be 4,000 km from the SuperDARN observation in the ionosphere and 3,000-3,600 km from the ERG observation in the magnetosphere. Based on ERG observation, we also confirmed the correspondence between variations of hot ion pressure and magnetic field, which indicated the existence of the field-aligned currents in the magnetosphere.

From the observations of plasma flows in the ionosphere, electric field, and hot ions pressure variations in the magnetosphere presented in this study, it is suggested that hot ions moving toward the earth with small-scale pressure inhomogeneities in the inner magnetosphere generate field-aligned currents and thereby cause SAPSWS in the ionosphere.

Keywords: SAPS, ERG / Arase, SuperDARN

©2021. Japan Geoscience Union. All Right Reserved.

Energetic electron precipitations showing ULF modulation observed by VLF/LF transmitter signals

*Tanaka Kentaro[1], Hiroyo Ohya[1], Fuminori Tsuchiya[2], Kazuo Shiokawa[3], Yoshizumi Miyoshi[3], Nozomu Nishitani[3], Tomoaki Hori[3], Mariko Teramoto[4], Martin G Connors[5], Simon G Shepherd[6], Hiroyuki Nakata[1]

1. Graduate School of Engineering, Chiba University, 2. Planetary Plasma and Atmospheric Research Center, Graduate School of Science, Tohoku University, 3. Institute for Space-Earth Environmental Research, Nagoya University, 4. Kyushu Institute of Technology, 5. Athabasca University, 6. Dartmouth College

Energetic electron precipitation (EEP; >100 keV) from radiation belts to the D-region ionosphere during substorms has been studied since the 1960s using very low frequency (VLF; 3 kHz to 30 kHz)/low-frequency (LF;30 kHz to 300 kHz) radio transmitter signals and riometers (Thorne and Larsen, 1976). The VLF/LF technique is most sensitive to the ionization of the D-region ionosphere, which is caused by energetic electron precipitation with energies typically >100 keV (Rodger et al., 2012). The low-latitude limit of particle precipitation is $L \sim 4.0$ (Berkey et al., 1974). Several studies have reported ionospheric modulations due to ultra low frequency (ULF) Pc5 and Pi2 modulations (Asnes et al., 2004). Modulation of D-region due to ULF waves during a substorm was reported (Miyashita et al., 2020). However, there was only one report for the EEP associated with ULF modulation using VLF/LF transmitter signals. In this study, we investigate the energetic electron precipitations associated with the ULF modulation that occurred on May 5, 2011, using the VLF/LF transmitter signals observed in North America. The three transmitters were NDK (frequency: 25.2 kHz, 46.37°N, 261.47°E, L=3.0); WWVB (60.0 kHz, 40.67°N, 254.95°E, L=2.3); and NLK (24.8 kHz, 48.20°N, 238.08°E, L=2.9). One receiver at Athabasca (ATHA), Canada (54.6°N, 246.7°E, L=4.3) was used. During 05:00-05:30 UT on May 5, 2011(magnetically quiet time), oscillations in amplitude and phase of VLF/LF waves with a period of 4-6 minutes were observed on the NDK-ATHA and WWVB-ATHA paths. This suggests that the EEP occurred over the two paths. The ground-based H-component magnetic field variations and Doppler velocity observed by the SuperDARN HF radars showed the there were small regions where the Doppler velocity was large near the WWVB-ATHA and NDK-ATHA paths during the VLF-LF oscillations. It is possible that the EEP occurred over the two paths. Based on ground-based magnetic field data, the propagation direction of the ULF wave was eastward (83.5 km/s) from the pre-midnight sector. In this presentation, we will discuss the cause of these VLF/LF oscillations.

©2021. Japan Geoscience Union. All Right Reserved.

A statistical study on the detachment of arc from the main auroral oval using all-sky imaging observations at Athabasca, Canada

*Sneha Yadav[1], Kazuo Shiokawa[1], Yuichi Otsuka[1], Martin G Connors[2,3]

1. Institute for Space-Earth Environmental Research, Nagoya University, Nagoya, Japan, 2. Athabasca University Observatories, Athabasca University, Athabasca, Alberta, Canada, 3. Department of Physics and Astronomy, University of Calgary, Calgary, Alberta, Canada

The phenomenon of ‘detached arcs’ was first reported by Anger et al. (1978) to describe the arc-like auroral emissions equatorward of the auroral particle precipitation region. Recently, a common feature of detachment of arc from the main auroral oval has been brought to the attention for SAR (Stable Auroral Red) arcs (e.g., Shiokawa et al., AIP, 2009; EPS, 2017; Takagi et al., GRL, 2018) and STEVE (strong thermal emission velocity enhancement) (e.g., Gallardo-Lacourt et al., JGR, 2018; Yadav et al., JGR, 2021). Although the occurrence characteristics and geomagnetic conditions under which these arcs occur are known, studies comparing the occurrence characteristics and specific geomagnetic under which these detached arcs culminate as pure-red (SAR) arc, STEVE, and red+green arc (arc consisting of both red and green line emissions) are lacking. Based on 15-years (2006-2020) of all-sky imaging observations at Athabasca (magnetic latitude = 61.5˚N), Canada, here we present a comparative statistical analysis on the occurrence characteristics and geomagnetic conditions of detached SAR arcs, STEVE, and red+green arcs. Results show that the occurrence of pure red arcs peaks during low geomagnetic activity, which is in contrast to the occurrence of red+green arcs that peaks during active geomagnetic conditions. In order to access the substorm activity in the longitude zone of the Athabasca ASI, we have analysed the X-component magnetogram at Fort Smith (FSMI; magnetic latitude: 67.28˚N) which is located ~6˚ magnetic latitude poleward of Athabasca. In general, STEVE and SAR arcs tend to occur at the beginning of recovery phase, whereas red+green arcs occur towards the end of expansion phase of a substorm. The geomagnetic activity levels were found to be highest for STEVE and lowest for the SAR arcs. Prior to the STEVE event, the ASY-H index shows gradual increase and STEVE occurred when the ASY-H values maximized, indicating the magnetospheric linkage of STEVE. STEVE is associated with substorms that have abrupt expansion and recovery, whereas substorms exhibit gradual expansion and recovery phase for the SAR arcs. Further, STEVE is found to be associated with the sharp increase in the X-component of the geomagnetic field at FSMI.

Anger et al. (JGR, 1978) https://doi.org/10.1029/JA083iA06p02683

Shiokawa et al. (AIP Conf. Proc., 2009) https://doi.org/10.1063/1.3169292

Shiokawa et al. (EPS, 2017) https://doi.org/10.1186/s40623-017-0745-9

Takagi et al. (GRL, 2018) https://doi.org/10.1029/2018GL079615

Gallardo-Lacourt et al. (JGR, 2018) https://doi.org/10.1029/2018JA025368

Yadav et al. (JGR, 2021) https://doi.org/10.1029/2020JA028622

Keywords: Arc detachment, Auroral oval, Imaging observations

©2021. Japan Geoscience Union. All Right Reserved.

©2021. Japan Geoscience Union. All Right Reserved.

SAPS electric field and particle observations by the Arase satellite and SuperDARN

*Tomoya Takada[1], Nozomu Nishitani[1], Tomoaki Hori[1], Yasumasa Kasaba[2], Atsushi Kumamoto[2], Yuto Katoh[2], Yoshiya Kasahara[3], Masafumi Shoji[1], Satoko Nakamura[1], Masahiro Kitahara[1], Fuminori Tsuchiya[2], Kazushi Asamura[4], Yoshizumi Miyoshi[1], Yoichi Kazama[5], S Y Wang[5], Shoichiro Yokota[6], Satoshi Kasahara[7], Kunihiro Keika[7], Ayako Matsuoka[8], Shun Imajo[1], Iku Shinohara[4], Chae-Woo Jun[1], Simon G Shepherd[9]

1. Institute for Space-Earth Environmental Research, 2. Tohoku University, 3. Kanazawa University, 4. JAXA, 5. Academia Sinica, 6. Osaka University, 7. The University of Tokyo, 8. Kyoto University, 9. Thayer School of Engineering

The comparison between the ionospheric convection and magnetospheric electric field is important for understanding the magnetosphere-ionosphere coupling. However, there have been few studies making comparison between the SuperDARN convection and satellite electric field related to the Sub-Auroral Polarization Streams (SAPS). In this study, simultaneous observation of the SAPS electric field were carried out by SuperDARN radar and the Arase satellite. In 52 simultaneous observation events identified during the analyzed period from June 2017 to Dec. 2019, SAPS were observed by the SuperDARN radar near the calculated footprint of the Arase satellite and almost concurrently the satellite detected electric field enhancements. In association with the SAPS electric field, the satellite observed the plasmapause crossing and increase of low energy (< 1 keV) ions fluxes in most of the events. We performed a statistical analysis of these low energy ion enhancement events. The result is that the low energy ion enhancement appears mainly in the field-aligned directions and the intensity of flux enhancement has a weak positive correlation with the flow velocity of SAPS. On the other hand, the gap in timing of SAPS encounter often seen between the satellite and the ground also suggests that the actual ionospheric footprint of the Arase satellite would deviate from the foot-print calculated using the empirical magnetic field model. Details of the relationship between these low-energy ion characteristics and the electric field distribution, as well as the deviation of the ionospheric footprint of the satellite, will be discussed.

©2021. Japan Geoscience Union. All Right Reserved.

Properties of EMIC waves observed by Van Allen Probes and ground-based magnetometers during relativistic electron precipitation

*Asuka Hirai[1], Fuminori Tsuchiya[1], Takahiro Obara[1], Yasumasa Kasaba[1], Yuto Katoh[2], Hiroaki Misawa[1], Kazuo Shiokawa[3], Yoshizumi Miyoshi[3], Chae-Woo Jun[3], Satoshi Kurita[4], Martin G Connors[5], Aaron Hendry[6]

1. Planetary Plasma and Atmospheric Research Center, Graduate School of Science, Tohoku Univ. , 2. Department of Geophysics, Graduate School of Science, Tohoku University, 3. Institute for Space-Earth Environmental Research, Nagoya University, 4. Research Institute for Sustainable Humanosphere, Kyoto University, 5. Athabasca University, 6. Otago University

Electromagnetic ion cyclotron (EMIC) waves are observed as Pc1-2 pulsations in the Earth’s magnetosphere. They are excited due to the temperature anisotropy of ring current ions, and scatter the pitch angle of relativistic electrons through cyclotron resonance. This process is considered as one of the mechanisms to cause the loss of the outer radiation belt. There still remain questions about the amount of the contribution from the EMIC waves to the overall loss of radiation belt electrons. In order to estimate quantitatively the electron loss from the outer radiation belt, we need to estimate the spatial extent and temporal evolution of the source region of EMIC waves. We investigated EMIC waves observed by Van Allen Probes and ground magnetometers in North America in 02:30-06:05UT on 19 April 2017. This event occurred in a substorm during main and early recovery phase of small geomagnetic storm. Van Allen Probe A observed EMIC waves in hot proton populations inside plasmapause. The footprint of Van Allen Probe A was located in North America during the wave activity observed by Van Allen probes. Simultaneously, Pc1 pulsations were observed at some stations of induction magnetometers from “Study of dynamical variation of Particles and Waves in the Inner magnetosphere using Ground-based network observations (PWING)” project and the Canadian Array for Realtime Investigations of Magnetic Activity (CARISMA). Energetic electron precipitation was detected by subionospheric VLF radio waves received at Athabasca, Canada and POES satellites. The VLF radio waves propagate near the footprint of Van Allen Probe A and ground-based magnetometers during EMIC wave activity. This suggests that detected electron precipitation was driven by EMIC waves. From satellite and ground-based magnetometer data, we estimated the local time extent of source region of ~6.8 hour and L shell extent of ~2.2. Pc1 pulsations started to be observed by east side stations on the ground. The time lag and difference of longitude between stations suggest that the source region of EMIC waves move westward and to low latitude.

©2021. Japan Geoscience Union. All Right Reserved.

A Study on the Effect of the Number of Snapshots for Averaging and the Noise Level on the Estimation Accuracy in Direction Finding

*Yuji Tanaka[1], Yoshiya Kasahara[1]

1. Division of Electrical Engineering and Computer Science, Graduate School of Natural Science and Technology, Kanazawa University

The analysis of plasma waves obtained from in-situ observations by scientific satellites is an effective method to investigate the plasma environment in the inner magnetosphere. Direction finding of plasma waves provides important information for understanding not only local plasma environment but also the global features of the inner magnetosphere.

In the direction finding, information on the amplitude and phase difference of the electromagnetic field extracted from the correlation matrix called spectral matrix is used. The quality of the information from the spectral matrix depends on the number of snapshots for averaging, the noise level on the electromagnetic sensor, and so on. What is more, the accuracy and the robustness of the estimated result about direction finding depends on the a priori information such as the number of waves, propagation mode, plasma density and geomagnetic field intensity.

In this study, the effect of the number of snapshots for averaging and the level of noise on the electromagnetic field sensors on the estimation accuracy of the direction finding is verified.

Keywords: Direction Finding, Spectral Matrix

©2021. Japan Geoscience Union. All Right Reserved.

Relative Contribution of ULF Waves and Whistler-mode Chorus to the Radiation Belt Variation during the May 2017 Storm

*Naoko Takahashi[1], Kanako Seki[1], Mei-Ching Fok[2], Yihua Zheng[2], Yoshizumi Miyoshi[3], Satoshi Kasahara[1], Kunihiro Keika[1], David Hartley[4], Yoshiya Kasahara[5], Yasumasa Kasaba[6], Nana Higashio[1,7], Ayako Matsuoka[8], Shoichiro Yokota[9], Tomoaki Hori[3], Masafumi Shoji[3], Satoko Nakamura[3], Shun Imajo[3], Iku Shinohara[10]

1. Graduate School of Science, The University of Tokyo, 2. NASA Goddard Space Flight Center, 3. Institute for Space-Earth Environmental Research, Nagoya University, 4. Department of Physics and Astronomy, University of Iowa, 5. Graduate School of Natural Science and Technology, Kanazawa University, 6. Graduate School of Science, Tohoku University, 7. Japan Aerospace Exploration Agency, 8. Data Analysis Center for Geomagnetism and Space Magnetism, Graduate School of Science, Kyoto University, 9. Graduate School of Science, Osaka University, 10. Institute of Space and Astronautical Science, Japan Aerospace Exploration Agency

The Earth's radiation belt exhibits a dramatic variation during the active condition of the magnetosphere such as magnetic storms. The dynamic variation of the radiation belt is, in part, contributed by various wave-particle interactions, including: (1) the radial diffusion of electrons driven by ultra-low-frequency (ULF) waves in the Pc5 frequency range (2-7 mHz), and (2) the local acceleration caused by wave-particle interactions between whistler-mode chorus and radiation belt particles. Over the past decade, multi-point observations and numerical simulations have separately demonstrated evidence for the contribution of ULF waves and whistler-mode chorus to the relativistic electron flux enhancement. However, comparison of the contribution of ULF waves and whistler-mode chorus has not been extensively made yet. To the best of our knowledge, only few papers have demonstrated the global picture of the relative contribution of waves to the total radiation belt content.

In this study, we investigate when and where ultra-low-frequency (ULF) waves and whistler-mode chorus contribute to the net flux enhancement of relativistic electrons during the May 2017 storm. During the early recovery phase, ULF waves mainly contribute to the global enhancement of relativistic electron flux in the dusk sector. On the nightside, both waves are related to the flux variation. During the late recovery phase, both Van Allen Probe (RBSP)-B and Arase show that whistler-mode chorus contributes to the flux enhancement confined in L-value. The Comprehensive Ring Current Model (CRCM) coupled with Block-Adaptive-Tree Solar-Wind Roe-Type Upwind Scheme (BATS-R-US) simulation qualitatively reproduces the global evolution of ULF waves. Although the electron flux is underestimated by the simulation, we find the large anisotropy of hot electrons in the region where whistler-mode chorus waves were actually observed by satellites. In addition, the estimated magnetic field curvature on the dayside is small during the recovery phase.

We also investigate what controls the wave evolution. Both observations and simulation suggest that observed ULF waves in a frequency range of ~2-4 mHz are excited by the enhancement of the solar wind dynamic pressure. Observations also indicate that whistler-mode chorus on the nightside is predominantly excited by hot electrons with temperature anisotropy, whereas dayside chorus is enhanced by the change of the magnetic field line configuration. Estimated spatial distributions of electron anisotropy and magnetic field curvature give an explanation for observational results that enhanced whistler-mode chorus exists in the dusk sector, which is far from the ordinary location of wave generation.

©2021. Japan Geoscience Union. All Right Reserved.

©2021. Japan Geoscience Union. All Right Reserved.

Initial results on multi event analysis of the simultaneous observation of isolated proton auroras at subauroral latitudes by a highly sensitive all-sky camera and the Van Allen Probes satellites

*Kohki Nakamura[1], Kazuo Shiokawa[1], Masahito Nose[1], Tsutomu Nagatsuma[2], Kaori Sakaguchi[2], Harlan Spence[3], Geoff Reeves[4], Herbert Funsten[4], Craig Kletzing[5], Robert MacDowall[6], Charles Smith[3], John Wygant[7], John Bonnell[7]

1. Nagoya Univ., 2. National Institute of Information and Communications Technology, 3. New Hampshire Univ., 4. Los Alamos National Laboratory, 5. Iowa Univ., 6. Goddard Space Flight Center, 7. Minnesota Univ.

Isolated proton aurora (IPA) appears at subauroral latitudes with Pc1 geomagnetic pulsations. This aurora has a spot-like feature extending in the east-west direction. Proton aurora is caused by energetic proton precipitating from the magnetosphere through charge-exchange collisions with atmospheric particles in the ionosphere. Previous studies suggested that IPA is caused by electromagnetic ion cyclotron (EMIC) waves which scatter pitch angle of energetic protons into the loss cone in the magnetosphere and making their precipitation into the ionosphere. EMIC waves are considered to make rapid loss of the radiation belt electrons into the atmosphere through wave-particle interaction. The IPA is the projection of the wave-particle interaction region into the ionosphere. Thus, simultaneous observation of magnetospheric EMIC waves and IPA is important to understand the scale sizes of the wave-particle interaction region. There have been few observation of IPA and its magnetospheric source region except for Nishimura et al. [JGR, 2014; doi: 10.1002/2014JA020029] and Nakamura et al. [submitted to JGR, 2021]. In this study, we detected three events of simultaneous observation of IPAs and plasma and electromagnetic variations in the magnetospheric source region of IPAs by using an all-sky camera at Kapuskasing, Canada, and the Van Allen Probes satellites. As a result, when the footprints of the Van Allen Probes satellites passed over IPAs, isolated EMIC waves were observed by the satellites (March 22, April 22, and September 7, 2018). All events were observed during geomagnetically quiet times. The equatorward boundaries of the EMIC waves correspond to the increase of the proton flux at energies of ~10 keV, and the flux was predominantly perpendicular to the magnetic field lines. On the other hand, the poleward boundaries of the EMIC waves correspond to the region where the local plasma density began to decrease rapidly. These characteristics were common to all events. Based on these results, we will discuss possible cause of localization of IPA and EMIC waves in the magnetosphere.

Keywords: isolated proton aurora, EMIC wave

©2021. Japan Geoscience Union. All Right Reserved.

Study of the excitation mechanism of internally driven ULF waves by the drift-bounce resonance with ring current ions based on the Magnetosphere-Ionosphere coupled model

*Tomotsugu Yamakawa[1], Kanako Seki[1], Takanobu Amano[1], Naoko Takahashi[1], Yoshizumi Miyoshi[2], Aoi Nakamizo[3]

1. Department of Earth and Planetary Science, School of Science, The University of Tokyo, 2. Institute for Space-Earth Environmental Research, Nagoya University, 3. National Institute of Information and Communications Technology

Internally driven ULF waves can be generated by ring current ions associated with the injection from the magnetotail during substorms. The excitation mechanism and global distribution of ULF waves are keys to understand dynamic variation of the outer radiation belt, since Pc5 ULF waves (1.67-6.67 mHz) can drive radial diffusion of radiation belt electrons [e.g. Elkington et al., 2003]. The drift-bounce resonance [Southwood, 1976] has been considered to be a candidate excitation mechanism. Previous spacecraft observations suggest both drift resonance and drift-bounce resonance excitation of ULF waves [e.g. Dai et al., 2013; Oimatsu et al., 2018]. Recently, Yamakawa et al. [2019] confirmed the drift resonance excitation of Pc5 waves by an isotropic Maxwellian PSD ion injection based on the drift-kinetic model. We also found the drift-bounce resonance excitation of Pc3 waves under asymmetric butterfly type injection [Yamakawa et al., 2020]. However the amplitude of the excited ULF waves is too small compared to spacecraft observations. One possible reason is the damping of field fluctuations at the ionospheric boundary in the model.

In order to improve the ionospheric boundary condition, we have made Magnetosphere-Ionosphere coupling between GEMSIS-RC [Amano et al., 2011] and GEMSIS-POT model [Nakamizo et al., 2012]. We use GEMSIS-RC model in the inner magnetosphere, in which 5D drift-kinetic equation for the PSD of ions and Maxwell equations are solved self-consistently. GEMSIS-POT is an ionospheric model, which solves 2-D electric potential. We use FAC from GEMSIS-RC as an input to GEMSIS-POT for the Region 2 current. The resultant electric field potential is then used as inner boundary condition of GEMSIS-RC. The coupled model enables us to simulate the ion injection from the plasma sheet into the inner magnetosphere. Simulation results have shown the excitation of Pc5 waves in the dayside (drift resonance) and Pc4 waves in the duskside (drift-bounce resonance). We have found that the amplitude of the excited ULF waves are enhanced by improving the ionospheric boundary condition. We will also report on the details of the effects of the boundary condition and R2FAC related electric field on the excitation of ULF waves.

Keywords: ring current, ULF wave, substorm, drift-kinetic model, drift-bounce resonance

©2021. Japan Geoscience Union. All Right Reserved.

Statistical Analysis of Latitudinal Electron Density Distribution in the Plasmasphere

*Ayano Hambara[1], Yuki Obana[2], Yukinaga Miyashita[3,4], Atsuki Shinbori[5], Yuichi Otsuka[5], Atsushi Kumamoto[6], Fuminori Tsuchiya[7], Shoya Matsuda[8], Ayako Matsuoka[9], Yoshiya Kasahara[10], Yoshizumi Miyoshi[5], Iku Shinohara[8], William S. Kurth[11], Craig A. Kletzing[11], Charles W. Smith[12], Robert J. MacDowall[13]

1. Advanced Science and Engineering Course, Graduate School of Engineering, Osaka Electro-Communication University, 2. Department of Engineering Science, Faculty of Engineering, Osaka Electro-Communication University, 3. Korea Astronomy and Space Science Institute, 4. Korea University of Science and Technology, 5. Institute for Space-Earth Environmental Research, Nagoya University, 6. Department of Geophysics, Graduate School of Science, Tohoku University, 7. Planetary Plasma and Atmospheric Research Center, Graduate School of Science, Tohoku University, 8. Institute of Space and Astronautical Science/Japan Aerospace Exploration Agency, 9. Data Analysis Center for Geomagnetism and Space Magnetism, Graduate School of Science, Kyoto University, 10. Information Media Center, Kanazawa University, 11. Department of Physics and Astronomy, University of Iowa, 12. Institute for the Study of Earth, Oceans, and Space, University of New Hampshire, 13. Solar System Exploration Division, Goddard Space Flight Center

Plasma density distributions along magnetic field lines give important information on plasma supply mechanisms from the ionosphere.However, most observations so far are biased near the equatorial plane; there have been few observations which give information on the density along field lines.The geospace exploration satellites Arase and Van Allen Probes(RBSP) have orbital inclinations of about 31 and 10 degrees, respectively.These satellites sometimes fly at different latitudes on the same field line, simultaneously.Using such conjunction data, the field aligned profile of the electron density can be estimated.

The electron densities were calculated from the Upper Hybrid Resonance frequencies obtained by HFA / PWE onboard Arase or the EMFISIS Waves instrument onboard RBSP.In this study, we assumed a power-law density model in which the density decreases with the m_{th}-power of the geocentric distance by comparing electron densities at Arase and RBSP-A or B.

At this moment, the conjunction events on April 5, 2017 were analyzed, and the following results were obtained.For flux tubes of 3.20 The expected power-law index m depends on the plasma supply model. In the collisionless models, m is close to 4.On the other hand, in the diffusive equilibrium model, close to 0.5~1.So our results suggest that the plasmasphere is in diffusive equilibrium.

In this presentation, we will introduce further results and discuss the plasma supply mechanism.

Keywords: plasmasphere, magnetosphere-ionosphere coupling

©2021. Japan Geoscience Union. All Right Reserved.

A statistical study of longitudinal extent of Pc1 pulsations using seven PWING ground stations at subauroral latitudes

*Jie Liu[1], Kazuo Shiokawa[1], Shin-ichiro Oyama[1], Yuichi Otsuka[1], Chae-Woo Jun[1], Masahito Nose[1], Tsutomu Nagatsuma[2], Kaori Sakaguchi[2], Akira Kadokura[3], Mitsunori Ozaki[4], Martin G Connors[5], Dmitry Baishev[6], Nozomu Nishitani[1], Alexey Oinats[7], Vladimir Kurkin[7], Tero Reita[8]

1. Institude for Space-Earth Environmental Research, Nagoya University, 2. National Institute of Information and Communications Technology, Japan, 3. National Institute of Polar Research, Tokyo, Japan, 4. Kanazawa University, Kanazawa, Japan, 5. Athabasca University, Athabasca, Canada, 6. Yu.G.Shafer Institute of Cosmophysical Research and Aeronomy of Siberian Branch of the Russian Academy of Sciences, Yakutsk, Russia, 7. Institute of Solar-Terrestrial Physics, Siberian Branch of the Russian Academy of Sciences, Irkutsk, Russia, 8. Sodankyla Geophysical Observatory, University of Oulu, Oulu, Finland

Ultra-low-frequency (ULF) Pc1 geomagnetic pulsations correspond to the electromagnetic ion cyclotron (EMIC) waves in the magnetosphere, and are excited sporadically in the magnetospheric equatorial plane with a frequency range of 0.2-5 Hz. Pc1/EMIC waves occur as a result of the ion-cyclotron instability. These waves may contribute to loss of the radiation belt electrons in the inner magnetosphere through wave-particle interactions. Previous researches on the spatial extent of EMIC waves mainly used only a specific ground station or a few ground stations. There are also some researches on the global distribution of EMIC waves using statistical study of data obtained by single satellite rather than through ground stations. However, the instantaneous longitudinal extent of Pc1 waves has not been fully understood yet. In order to investigate this instantaneous longitudinal extent of Pc1 waves, in this study, we analyze the magnetic field data obtained at the seven ground stations at Athabasca (54.6N, 246.36E), Kapuskasing (49.39N, 277.81E), Gakona (62.39N, 214.78E), Husafell (64.67N, 338.97E), Zhigansk (66.78N, 123.37E), Istok (70.03N, 88.01E), and Oulu (65.08N, 25.90E) for one year from July 2018 to June 2019. The magnetometers at the 6 stations have been deployed and operated by “study of dynamical variation of Particles and Waves in the INner magnetosphere using Ground-based network observations (PWING)” project, while the magnetometer at Oulu has been operated by Sodankylä Geophysical Observatory. We will report local time variations of the occurrence rates and average frequencies of the Pc1/EMIC waves at these stations and discuss the characteristics of the wave appearance including their instantaneous longitudinal extent. We also make some model calculation about the possible longitudinal extent to explain the observed instantaneous occurrence rate distributions. The above analysis reveals that the average instantaneous longitudinal extent of the Pc1 waves is about 80 degrees in longitudes at subauroral latitudes. There was no clear difference in the longitudinal extent of Pc1 waves between two different geomagnetic activity levels defined by the Dst index less/more than -15 nT.

©2021. Japan Geoscience Union. All Right Reserved.

Altitude profile of isolated proton aurora as estimated from digital camera observations from International Space Station

*Kazuteru Takahashi[1], Sota Nanjo[2], Yuta Hozumi[2], Keisuke Hosokawa[2], Yoshizumi Miyoshi[1]

1. Institute for Space–Earth Environmental Research, 2. The University of Electro-Communications

Proton aurora, that appears as an isolated spot at sub-auroral latitudes well away from the electron auroral oval, is called as the “Isolated Proton Aurora” (IPA). It has been believed that proton precipitation responsible for IPA is caused by scattering of protons through interaction with Electromagnetic Ion Cyclotron (EMIC) waves in the magnetosphere. It is well known that IPA appears in a horizontally (i.e., latitudinal and longitudinal directions) localized region. However, its spatial structure in the vertical direction has not been well understood. Therefore, we employ the full-color aurora images captured by the digital camera onboard the “International Space Station” (ISS) for deriving the altitude profile of emission of IPA. The digital camera onboard ISS is able to carry out limb viewing observations of the upper atmosphere of the Earth which allows us to capture the vertical structure of aurora, especially IPA. Nanjo et al. (2020) showed that it is possible to map the horizontal structure of aurora with high spatial/temporal resolutions. Thus far, however, The vertical structure of auroras has not been derived with the photographs captured from the ISS; thus, the details of the height structure of IPA are still unknown. In this study, we developed a method for mapping the vertical profile of the emission of IPA using limb-viewing digital camera images from ISS. In this presentation, we will discuss how the altitude profiles of the red and green emissions of IPA are distributed based on the mapping results of the altitude structure of the IPA observed in the southern hemisphere on April 20, 2018.

Keywords: Isolated proton aurora, International Space Station

©2021. Japan Geoscience Union. All Right Reserved.

Development of ISEE_Wave; Interactive Plasma Wave Analysis Tool

*Shoya Matsuda[1], Yoshizumi Miyoshi[2], Satoko Nakamura[2], Masahiro Kitahara[2], Masafumi Shoji[2], Tomoaki Hori[2], Shun Imajo[2], Chae-Woo Jun[2], Satoshi Kurita[3], Yoshiya Kasahara[4], Ayako Matsuoka[5], Iku Shinohara[1]

1. Institute of Space and Astronautical Science/Japan Aerospace Exploration Agency, 2. Institute for Space-Earth Environmental Laboratory, Nagoya University, 3. Research Institute for Sustainable Humanosphere, Kyoto University, 4. Kanazawa University, 5. kyoto University

In this study, we developed ISEE_Wave, which is an interactive plasma wave analysis tool for electric and magnetic field waveforms observed by the plasma wave experiment aboard the Arase satellite. ISEE_Wave provides an end-to-end wave analysis environment on a graphical user interface, where users can visualize advanced wave properties, such as the electric and magnetic field wave power spectra, wave normal polar angle, polarization ellipse, planarity of polarization, and Poynting vector angle. Users can simply select a time interval, and ISEE_Wave automatically downloads the waveform data, ambient magnetic field data, and spacecraft attitude data from the ERG Science Center, and performs coordinate transformation and spectral matrix calculation. Singular value decomposition is used as the core technique for the wave property analysis of ISEE_Wave. Users can freely specify the parameters of the wave property analysis and as well as the plot styles using the graphical user interface of ISEE_Wave. The results can be saved as image files and/or a tplot save file. The proposed tool aids in the identification of fine-structures of observed plasma waves, wave mode identification, and wave propagation analysis. These properties can be used to understand plasma wave generation, propagation, and wave-particle interaction in the inner magnetosphere. ISEE_Wave can also be applied to waveform data observed by other spacecrafts by replacing the data loading procedures.

Keywords: Plasma waves, Direction finding, Arase satellite

©2021. Japan Geoscience Union. All Right Reserved.

Radiation characteristics of upper-band and lower-band chorus emissions in the generation region deduced from the Arase observation

*Seigo Hayashi[1], Satoshi Kurita[2], Hirotsugu Kojima[2], Yoshiya Kasahara[3], Shoya Matsuda[4], Ayako Matsuoka[5], Iku Shinohara[4], Yoshizumi Miyoshi[6]

1. Undergraduate School of Electrical and Electronic Engineering, Kyoto University, 2. Research Institute for Sustainable Humanosphere, Kyoto University, 3. Graduate School of Natural Science and Technology, Kanazawa University, 4. ISAS/JAXA, 5. Graduate School of Science, Kyoto University, 6. Institute for Space-Earth Environmental Research, Nagoya University

Chorus waves are plasma waves that propagate along the geomagnetic field line. The waves are observed at frequencies below the electron cyclotron frequency (fce), and they often have a minimum in wave power at 0.5fce. Those observed above 0.5fce are called upper-band chorus (UBC), while those observed below 0.5fce are called low-band chorus (LBC). Chorus waves are excited near the magnetic equator and propagate to the polar region. Previous studies show that LBC frequently change their radiation direction within the generation region. However, the radiation characteristics of UBC in the generation region and the differences between UBC and LBC have not yet been clarified. The purpose of this study is to clarify the radiation characteristics of UBC and LBC in the generation region by analyzing the data obtained by the Arase satellite.
The Arase satellite has nine instruments on board. In this study, we use the background magnetic field data acquired by the MGF(Magnetic field experiment) and the electromagnetic waveform data acquired by the WFC (Waveform capture) of the PWE (Plasma wave experiment). Using the data acquired by the Arase satellite, we focused on the power spectrum of the electric and magnetic fields and the Poynting vector along the direction of the background magnetic field. Our results show that the Poynting flux ratio of northward to southward waves of UBC and LBC varies with the distance between the magnetic equator and the Arase satellite. Comparing the radiation direction of UBC with that of LBC, in many cases, we find that the generation region of these waves is located at the different directions relative to the satellite location. The results revealed by this study suggest that the radiation timing and generation region of UBC and LBC are different. We propose that the collection of localized UBC and LBC generation points forms the entire generation region of Chorus waves.

Keywords: Arase satellite, whistler mode, chorus, inner magnetosphere

©2021. Japan Geoscience Union. All Right Reserved.

Isolated Electrostatic Potentials Observed by the Arase Satellite

*Tomoe Taki[1], Satoshi Kurita[1], Hirotsugu Kojima[1], Yoshiya Kasahara[2], Yoshizumi Miyoshi[3], Ayako Matsuoka[4], Shoya Matsuda[5]

1. Research Institute for Sustainable Humanosphere, Kyoto University, 2. Information Media Center, Kanazawa University, 3. Institute Space-Earth Environmental Research, Nagoya University, 4. Data Analysis Center for Geomagnetism and Space Magnetism Graduate School of Science, Kyoto University, 5. Institute of Space and Astronautical Science/Japan Aerospace Exploration Agency

The present paper discuss the estimation of the spatial structure of the isolated electrostatic potentials observed by the Arase satellite in the Earth’ s inner magnetosphere applying the interferometry technique.

Isolated electrostatic potentials in the Earth's magnetosphere have been observed as Electrostatic Solitary Waves (ESWs) by many satellites such as GEOTAIL, RBSP, Polar, and FAST. It has been suggested that the isolated potentials contribute to electron acceleration in the magnetosphere because they may lead to spatial steps in the potential. Therefore, the spatial scale and structure of the isolated potentials and their electric energy are important. In the magnetotail region, a sheet-like structure represented by one-dimensional Gaussian was proposed, based on the ESW features observed by the GEOTAIL satellite. On the other hand, no specific spatial structure has been proposed for the isolated potential observed in the Earth's inner magnetosphere.

The purpose of this study is to propose a spatial structure of the isolated potentials observed by the Arase satellite. For this purpose, we calculate the spatial scale and polarity of the ESW observed by the Arase satellite, and propose a spatial structure model of the isolated potential that can reproduce the ESWs.

Using the monopole observation of the Arase satellite, it is possible to determine the direction of passage of the isolated potential relative to the satellite and the time difference between the two observation points. This provides the spatial scale of the potential. It is also possible to determine the polarity of the isolated potentials by considering the direction of its passage and the antenna polarity. In addition, the structure of the isolated potentials is discussed. Assuming a two-dimensional model of the electrostatic potential, numerical experiments are conducted to reproduce the waveform observed by Arase.

The ESWs observed by the Arase satellite have two characteristics: pulse waveforms are observed not only parallel but also perpendicular to the background magnetic field, and various types of waveforms such as bipolar and asymmetric waveforms are irregularly observed. We analyzed the waveforms of the monopole observations, focusing on the bipolar waveforms. The spatial scales are estimated to be between 380m and 3 km. The potentials with both positive and negative polarities are present. A model with a small scale structure in the perpendicular direction to the background magnetic field was proposed, and the above features could be reproduced in two-dimensional Gaussian by numerical experiments.

By using the monopole observations of the Arase satellite, we have succeeded in calculating the spatial scale of the isolated potential and determining their polarity. It is suggested that the isolated potentials observed by the Arase satellite has a different structure from the previously proposed model.
It is also suggested that the proposed structure does not have potential step and does not contribute to the acceleration of electrons.

©2021. Japan Geoscience Union. All Right Reserved.

Keywords: Electrostatic Solitary Waves, Isolated Potentials, Interferometry observation, Arase satellite, Time domain structures

©2021. Japan Geoscience Union. All Right Reserved.

Statistical study of drifting electron holes associated with substorms observed by the Arase satellite

*Taku Namekawa[1,2], Iku Shinohara[1], Takefumi Mitani[1], Kazushi Asamura[1], Nagai Tsugunobu[1], Satoshi Kasahara[2], Shoichiro Yokota[3], Tomoaki Hori[4], Ayako Matsuoka[5], Yoshizumi Miyoshi[4]

1. ISAS / JAXA, 2. The University of Tokyo, 3. Osaka University, 4. Nagoya University, 5. Kyoto University

Drifting electron hole (DEH) is a dropout in the electron flux frequently observed in an energy range similar to that of electron injections in the Earth's magnetosphere [Sergeev et al., 1992]. The flux dropout is thought to be caused by the deformation of the electron drift shell due to a large-scale reconfiguration of the magnetic field associated with substorm onset.
Most of these substorm-related DEHs were observed near and outside the geosynchronous orbit [Cohen et al., 2019, Liu et al., 2019, Shukhtina et al., 1996]. DEHs were also observed in the region of L > 5 inside the geosynchronous orbit by the Arase satellite [Miyoshi et al., 2018]. However, there has been very limited discussion of these DEHs since the statistics cover only quiet conditions and a small number of events, and this electron dropout is not yet fully understood.
To investigate the characteristics of DEH, we conducted a statistical study by analyzing data obtained by the HEP and MEP-e instruments onboard the Arase satellite. We selected the DEH events that were observed simultaneously with the injection by inspecting the data during the periods when Arase observed the night side to the dawn side of the magnetosphere from 2017 to 2019. The resultant DEH events were mainly observed in the pre-midnight sector to the dawn side. We estimated the drift trajectories of electrons corresponding to energy-dispersed DEHs to identify their source region. The source region of DEHs extends over 3-4 hours around local magnetic midnight, which distribution is similar to that of the injections simultaneously observed. This result is consistent with the model presented by Sergeev et al. [1992].
On the other hand, there are some events in which the source sectors of DEH and injection are different, even though they were observed simultaneously. The existence of such events suggests that DEHs may not be explained by a simple model assuming a single source region.

Keywords: Drifting electron hole, Particle injection, Substorm, Arase satellite

©2021. Japan Geoscience Union. All Right Reserved.

The influence of EMIC (ElectroMagnetic Ion Cyclotron) wave-interaction on energetic protons in the magnetosphere using Arase observations

*Chae-Woo Jun[1], Yoshizumi Miyoshi[1], Satoko Nakamura[1], Shun Imajo[1], Masafumi Shoji[1], Chao Yue[2], Jacob Bortnik[3], Larry Lyons[3], Yoshiya Kasahara[4], Yasumasa Kasaba[5], Fuminori Tsuchiya[5], Atsushi Kumamoto[5], Shoya Matsuda[6], Kazushi Asamura[6], Iku Shinohara[6], Ayako Matsuoka[7]

1. Institute for Space-Earth Environmental Research, Nagoya University, 2. Peking University, Beijing, China , 3. Atmospheric and Oceanic Sciences, University of California Los Angeles, Los Angeles, USA, 4. Kanazawa University, Kanazawa, Japan, 5. Tohoku University, Sendai, Japan, 6. Institute of Space and Astronautical Science, Japan Aerospace Exploration Agency, Sagamihara, Japan, 7. Kyoto University, Kyoto, Japan

Electromagnetic ion cyclotron (EMIC) waves have been driven by temperature anisotropy of energetic ions near the magnetic equator. These waves constitute a significant loss process of energetic protons and sub-relativistic electrons through pitch-angle scattering by wave-particle interactions. In our previous study, we found that EMIC waves show significantly different characteristics at the different peak occurrence regions depending on geomagnetic environments. In this study, we performed a statistical study to demonstrate the influence of EMIC wave-particle interaction on energetic protons in the magnetosphere using in-situ observations by Exploration of energization and Radiation in Geospace (Arase) satellite. For this study, we identified EMIC waves by visual inspection and separated them into two wave-bands (H+ and He+ bands) in 2017-2020. We also measured energetic proton pitch angle distributions with an energy range of 30 eV to 25 keV. In this presentation, we show spatial distributions of EMIC waves in the magnetosphere and comparisons of energetic proton pitch angle distributions between with and without EMIC wave activities, discuss possible free energy sources causing EMIC waves at different regions. We will demonstrate the influence of different generation processes of EMIC waves on energetic proton distributions using in-situ satellite observations and theoretical model calculations.

Keywords: Electromagnetic ion cyclotron (EMIC) waves, Exploration of energization and Radiation in Geospace (Arase) satellite mission, EMIC wave-particle interaction

©2021. Japan Geoscience Union. All Right Reserved.

A statistical study on high-energy electron injection events observed by Arase (ERG)

*JINGXUAN YANG[1], Iku Shinohara[2], Taku Namekawa[1], Takefumi Mitani[2], Kazushi Asamura[2], Satoshi Kasahara[3], Nana Higashio[4], Ayako Matsuoka[5]

1. Department of Earth and Planetary Science, Graduate School of Science, The University of Tokyo, 2. Institute of Space and Astronautical Science, Japan Aerospace Exploration Agency, 3. The University of Tokyo, 4. Japan Aerospace Exploration Agency, 5. Data Analysis Center for Geomagnetism and Space Magnetism, Graduate School of Science, Kyoto University

The substorm injection is a critical phenomenon for supplying the free-energy necessary to generate relativistic electrons in the radiation belts. Numbers of studies on substorm injections have been demonstrated. However, how the injected electrons penetrate the inner magnetosphere and get their energy remains unclear. The energization of the particle injection is thought to be resulting from the transient enhancement of the electric field associated with the dipolarization, although there is no observational evidence such large electric fields accelerate injection particles.
Arase (ERG) often observes electron injections whose maximum energies reach hundreds of keV, while the typical maximum energy of injected electrons is about 100 keV or less. In this study, we would like to address how injected electrons are accelerated to such high energies. Collecting injection events during the period when the apogee of Arase is located in the nightside, we are examining the statistical properties of the high-energy injection events, e.g., the distribution of their estimated source regions, characteristics of energy spectra, pitch angle anisotropy, and other parameters in detail. We expect that finding dependence on the maximum energy is a key to limit the acceleration mechanisms of electron injections.
In the presentation, we will present preliminary results.

©2021. Japan Geoscience Union. All Right Reserved.

Development of a high-energy electron analyzer onboard CubeSats

*Iku Shinohara[1], Takefumi Mitani[1], Mariko Teramoto[2], Kazushi Asamura[1], Ryota Onogi[1], Takeshi Takashima[1]

1. Japan Aerospace Exploration Agency/Institute of Space and Astronautical Science, 2. Kyushu Institute of Technology

Nowadays, the use of CubeSats for space science researches is no longer unusual in the world. We expect that CubeSats become a more powerful platform for space environment observations, enabling ultra-multi-point 'in-situ' measurements. More chances to install scientific instruments onboard CubeSats are desired to realize future observations and test new technologies in space. Thanks to the JSPS KAKENHI support and the collaboration with Kyushu Institute of Technology, we have an opportunity to install a new high-energy electron analyzer onboard the BIRDS-5 satellite, which is the fifth satellite in Joint Global Multi-Nation Birds Satellite (BIRDS) Program of Kyushu Institute of Technology. BIRDS-5 will be released from the international space station (ISS) in Spring 2022, and its orbit is almost the same as ISS.
Our high-energy electron analyzer for BIRDS-5 is nicknamed "Particle Instrument for NanO-satellite (PINO)." The mission objectives of PINO are followings. 1) To demonstrate a compact high-energy electron detector onboard a CubeSat using the Si/CdTe semiconductor, and 2) To measure the high-energy electron flux precipitating along the geomagnetic fields from the radiation belts. The CdTe semiconductor is commonly used for recent gamma-ray detectors in high-energy astrophysics, but the application of the CdTe semiconductor to the high-energy electron sensor is the first trial. We expect that the CdTe sensor can efficiently measure higher energy electrons because of the higher stopping power of CdTe than that of Si. This characteristic of the CdTe sensor is the advantage of developing a more compact analyzer. We will turn on PINO for continuous 5 minutes in an orbital revolution since electric power resource limits the operation. PINO can observe the precipitating high-energy electron fluxes above 60 degrees of the geomagnetic latitude in the northern hemisphere under this operational condition. With the collaboration between BIRDS-5 and Arase (ERG), we will be able to conduct simultaneous observations of precipitating high-energy electrons from the outer radiation belt at both low and high altitudes.
In this presentation, we will present the outline of science and the PINO development's latest status.

Keywords: high energy electron, radiation belt, cubesat

©2021. Japan Geoscience Union. All Right Reserved.

An observational study on possible excitation of storm-time Pc5 waves

*Kento Otani[1], Iku Shinohara[2], Mariko Teramoto[3], Tomotsugu Yamakawa[1], Kanako Seki[4], Satoshi Kasahara[4], Shoichiro Yokota[5], Kunihiro Keika[1], Naoko Takahashi[4], Takefumi Mitani[2], Nana Higashio[2], Ayako Matsuoka[6], Kazuhiro Yamamoto[4]

1. Tokyo University/Graduate School of Science, 2. JAXA, 3. Kyushu Institute of Technology, 4. Tokyo University, 5. Graduate school of Science, Osaka University, 6. Graduate school of Science, Kyoto University

The adiabatic acceleration associated with the radial diffusion by the ULF wave is an important mechanism that generates relativistic electrons in the radiation belts. Among various ULF waves observed in the geospace, the storm-time Pc5 wave is a possible candidate to drive the radial diffusion during magnetic storms, although its excitation process and the relation between the observed waves and the radial diffusion have not been confirmed. Storm-time Pc5 wave is thought to be excited by injected ions from magnetotail to the ring current. Recently, Yamakawa et al. (2019) demonstrate that Pc5 waves can be excited by the injected ions via the drift resonance by a numerical simulation study.

This paper would like to address the Pc5 excitation process based on recent multi-satellite observation datasets obtained in the inner magnetosphere. According to the results of Yamakawa et al. (2019), Pc5 waves excited by the drift resonance have a characteristic of the frequency evolution. Using the magnetic field observation of Arase (ERG), we have collected Pc5 wave events that show the same frequency evolution as that observed in the numerical simulation. As a result, the occurrence probability of the Pc5 wave events depends on the geomagnetic activity, and the spatial distribution of the selected events is consistent with the simulation results.

Further, we pick up the examples of Pc5 events where the ion injections are observed just before and investigate if the observed injected ions can excite Pc5 waves through drift resonance. This presentation will discuss the relationship between ion injection events and Pc5 observations in the drift resonance context.

©2021. Japan Geoscience Union. All Right Reserved.

A Novel Calibration Method of Short Time Waveform Signals and its Approcation for the PWE/WFC Data

*Masahiro Kitahara[1], Shoya Matsuda[2], Yuto Katoh[3], Yoshiya Kasahara[4], Hirotsugu Kojima[5], Yoshizumi Miyoshi[1], Mitsuru Hikishima[2]

1. Institute for Space-Earth Environmental Research, Nagoya University, 2. Institute of Space and Astronautical Science/Japan Aerospace Exploration Agency, 3. Department of Geophysics, Graduate School of Science, Tohoku University, 4. Information Media Center, Kanazawa University, 5. Research Institute for Sustainable Humanosphere, Kyoto University

The Waveform Capture (WFC) is a receiver of the Plasma Wave Experiment (PWE) on board the Arase satellite. The WFC measures the electric and magnetic field waveform in the frequency range from a few Hz to 20 kHz and aims to detect plasma waves related to the electron acceleration, such as whistler mode chorus emissions. A new-type instrument named Software-type Wave-Particle Interaction Analyzer (S-WPIA) is also installed in the Arase satellite to measure energy and momentum exchange between plasma waves and particles directly and quantitatively. The S-WPIA requires the high-accuracy calibration of both amplitude and phase of waveform data detected by the WFC with a reasonable processing load so as to realize the onboard calibration. In a typical calibration process, raw data passed through a system comprising of antennas, amplifiers, and filters should be (1) tapered by a window function to reduce the side lobe effect, (2) Fourier-transformed into a spectrum, (3) divided by a transfer function of the system in the frequency domain, (4) inverse-transformed into a waveform, and (5) divided by the window function in the time domain. However, the calibrated waveform data are distorted in the time domain in the case of using a short-time window consisting of several hundred of data points.
In this study, we reveal that the main lobe expansion caused by a window function yields the phase shift of the window function in the process (3) and the process (5) dividing by an un-shifted window function results in the distortion of waveforms in the time domain. To perform accurate calibration with a short-time window, we suggest a novel calibration method to estimate the phase shifts of a window function from the gradient of a transfer function and remove the distortion by dividing the shifted window functions at each frequency in the time domain. We applied the proposed method to simple sinusoidal signals and evaluated the frequency response of the accuracy of the calibrated data. As a result, we conclude that the proposed method can reduce errors to less than one percent of the signals even in the short-time window cases of using several hundred of data points. The accuracy tends to decrease at the low frequency range close to the frequency of a window function and at the high frequency range close to the Nyquist frequency. We also applied the methods to actual electric field data of chorus emissions observed by the PWE/WFC. In consequence, although the proposed method requires longer calculation time as compared to other conventional methods, the proposed method can reproduce the seamless waveforms of chorus emissions with errors of one percent of the wave amplitude or less in the case of using a band pass filter at the frequency range of the typical chorus emissions. We need to take account of the relation between the frequency range of the electromagnetic waveform and the window function in interpreting observation results.

Keywords: the Arase satellite, Plasma waves, waveform calibration

©2021. Japan Geoscience Union. All Right Reserved.

Nitrogen and oxygen ions from the Earth's ionosphere observed by the Arase satellite

*Shoichiro Yokota[1], Koichiro Tsuda[1], Satoshi Kasahara[2], Tomoaki Hori[3], Kunihiro Keika[2], Yoshizumi Miyoshi[3], Iku Shinohara[4]

1. Osaka University, 2. University of Tokyo, 3. ISEE, Nagoya University, 4. ISAS/JAXA

Various ion species originating from the Earth's upper ionosphere have been observed by the ERG (Exploration of energization and Radiation in Geospace)/Arase satellite. Among them, heavy ions such as O+ are used as markers to monitor ionospheric ion outflow, and their correlation with solar activity and magnetic activity has been investigated. The Arase satellite has successfully observed not only O+ but also molecular ions (N2+, NO+, and O2+). However, there have been a few reports of observations of N+ due to its close mass number to that of O+. In this presentation, we report on the extraction of N+ from the Arase observation data, which has been rarely observed due to its close mass number.
We used the TOF (Time-of-flight) mode data obtained by the MEP-i onboard the Arase satellite. The two types of ions were separated from the TOF spectra at each energy by fitting the TOF profiles of N+ and O+. On the other hand, calibration curves of the TOF profile were also prepared from the data obtained in the pre-launch calibration experiments. This calibration curves were calculated from a comprehensive model calculation by incorporating the TOF dispersion caused by the passage of ultra-thin carbon in the TOF mass spectrometer and the energy resolution of the energy analyzer. It was confirmed that the TOF profiles used in the fitting of the observation data analysis and the calibration curves obtained from the calibration data were in good agreement. From the Arase MEP-i data, the counts necessary for the separation of N+ and O+ were obtained from about 30 minutes of data.
The N+/O+ ratio obtained from the Arase data is expected to provide information on the ionospheric region where the outflow originates and its mechanism. Here we report the details of the N+ extraction method and the results.

Keywords: Nitrogen, Arase, ERG, Geospace, Inner Magnetosphere

©2021. Japan Geoscience Union. All Right Reserved.

Electron Energization during Dipolarization Events: Test Particle Simulations

*Kirolosse Mina Girgis[1], Tohru Hada[1], Fumiko Otsuka[1], Kaiti Wang[2]

1. Department of Earth System Science and Technology, Interdisciplinary Graduate School of Engineering Sciences, Kyushu University, Japan , 2. Department of Aerospace Engineering, University of Tamkang, Taiwan

In this research, we have developed a test particle simulation code to examine the electron energization during multiple dipolarization events. The Tao-Chan-Brizard guiding center model was implemented to evaluate the trajectories of 0.1, 1, 10 keV electrons with different initial pitch angles and *L*-shells. The time-varying magnetic field model was evaluated by the Tsyganenko model TS05 with the corresponding inductive electric field. Dipolarization events are characterized by an enhancement in particle energy in the nighttime magnetosphere. The increase in the magnetic field and the corresponding induced electric field can energize and transport the particles earthward, which can explain the mechanism of the particle flux enhancement in the inner magnetosphere. Numerical results will be compared with THEMIS measurements.

Keywords: Dipolarization, Electron Energization, Test Particle Simulations, Tsyganenko Model, Inductive Electric Field

©2021. Japan Geoscience Union. All Right Reserved.

Computer simulations of electron scatterings through chorus-wave particle interactions

Yoshiki Ito[1], *Yoshizumi Miyoshi[1], Shinji Saito[2]

1. Institute for Space-Earth Environmental Research, Nagoya University, 2. NICT

Whistler mode chorus waves cause scattering and acceleration of energetic electrons in the inner magnetosphere, and recent studies identified that chorus waves cause the pulsating aurora. The interaction processes have been modeled as diffusions in the velocity space, and the scattering rate increases with increasing the wave amplitude. However, actual wave-particle interactions with chorus waves are non-linear process, so that it is expected that the scattering rate does not have a simple correlation with wave amplitude. In this study, we conduct a computer simulation to investigate electron scattering process through chorus-wave particle interactions with the GEMSIS-RBW code. The GEMSIS-RBW simulation calculates variations of local pitch angle and energy of each test particle by the imposed chorus wavesby calculating the Max well equations.

We calculate the trajectory of a number of electrons with various energy and pitch angles. We analyzed the electron motion in the phase space and try to discriminate the motion with the parameter ρ [Bortnick et al., 2008] that is a proxy of the ratio of the wave-induced and the background inhomogeneity effects for the momentum change of the resonant electron. We identified that the phase trapping effect decreases the precipitating flux and contribute to generation of the butterfly type pitch angle distributions. Moreover, we identified diffusion and dislocation contribute to the precipitations into the atmosphere. Multiple resonance changes the ρ of electrons from the phase trapping to dislocation, which causes rapid precipitations of electrons.

Keywords: wave-particle interactions, Computer simulation

©2021. Japan Geoscience Union. All Right Reserved.

Statistical analyses of low energy ion heating by electromagnetic ion cyclotron waves via wave-particle interaction analyses: Arase observations

*Masafumi Shoji[1], Yoshizumi Miyoshi[1], Lynn M Kistler[1,2], Kazushi Asamura[3], Yasumasa Kasaba[4], Ayako Matsuoka[5], Yoshiya Kasahara[6], Shoya Matsuda[3], Fuminori Tsuchiya[4], Atsushi Kumamoto[4], Satoko Nakamura[1], Masahiro Kitahara[1], Shun Imajo[1], Chae-Woo Jun[1], Iku Shinohara[3]

1. Institute for Space-Earth Environmental Research, Nagoya Univ., 2. University of New Hampshire, 3. ISAS/JAXA, 4. Tohoku Univ., 5. Kyoto Univ., 6. Kanazawa Univ.

Electromagnetic ion cyclotron (EMIC) waves are generated through the cyclotron wave-particle interaction, affecting the plasma environment in the magnetosphere. Heating of ions by EMIC waves in the inner magnetosphere has been investigated using spacecraft observations by comparing the pitch angle distribution of the ions and the wave emissions. We can directly detect the energy transfer between the plasma waves and the ions via the wave-particle interaction analysis (WPIA) method which calculates the inner product between the wave electric fields and the ion velocities. We adapt the WPIA method to the Arase spacecraft data and investigate the spatial distribution of the positive region in the inner magnetosphere. From March 21st 2017 to September 27th 2019, we select 60 EMIC wave events with associated proton flux enhancement between 10 eV to 100 eV which are a suitable dataset for the WPIA method observed by PWE/EFD, MGF, and LEP-i onboard the Arase satellite. The peak of the proton heating occurrence appears in the dayside and post noon regions. Typical EMIC waves inside the plasma plume contribute to the peak in the afternoon sector in both geomagnetically quiet and active times. On the other hand, in the dayside region, the proton heating takes place predominantly during quiet times. It suggests that the protons in the region are energized by the EMIC waves generated through compression of the ambient magnetic field. We also discuss the species dependence of the ion heating.

Keywords: Wave-particle interaction, Ion heating

©2021. Japan Geoscience Union. All Right Reserved.

Plasma waves causing 20 Hz intensity modulation of pulsating aurora: High-speed Tjörnes-Arase-Syowa conjugate observation

*Herbert Akihito Uchida[1], Ryuho Kataoka[2,1], Kiyoka Murase[1], Shoya Matsuda[3], Yoshiya Kasahara[4], Masafumi Shoji[5], Yoshizumi Miyoshi[5], Iku Shinohara[3], Ayako Matsuoka[6], Satoshi Kurita[7], Keisuke Hosokawa[8], Shun Imajo[5]

1. The Graduate University for Advanced Studies, 2. National Institute of Polar Research, 3. Institute of Space and Astronautical Science, Japan Aerospace Exploration Agency, 4. Kanazawa University, 5. Institute for Space–Earth Environmental Research, Nagoya University, 6. Kyoto University, 7. Research Institute for Sustainable Humanosphere, Kyoto University, 8. University of Electro-Communications

We show the evidence of the simultaneously observed ~20 Hz intensity modulation of the auroral luminosity and the chorus wave intensity, and the evolution of pulsating aurora in terms of the transition of on and off of the pulsating patch, patch size, and pulsating period in different timescales. Pulsating auroras were observed by ground-based high-speed imagers after an auroral breakup at Tjörnes in Iceland and at its magnetic conjugate station, Syowa Station in Antarctica simultaneously on 22 September 2018. Two identical all-sky imagers at both stations and a narrow field-of-view imager at Syowa station were used to elucidate the hierarchical structure of the modulation in the auroral luminosity and the evolution of pulsating patches at different time scales. A few minutes before the main pulsation start, a fast intensity modulation of ~20 Hz was identified by the narrow field-of-view imager with ~3 Hz modulation in a small aurora patch. The foot-print of the Arase satellite was located within the all-sky field of view at that time, and the Plasma Wave Experiment onboard the Arase satellite observed chorus emissions whose intensity was modulated at the same period of the auroral fast intensity modulation. The patch size and the pulsation period evolved in time at both hemispheres and the period settled in the period of main pulsation. The pulsating patches differ in its shape and period between both hemispheres although several synchronized patches were also observed when the pulsating aurora drifted away from the all-sky field-of-view.

Keywords: Pulsating aurora, Chorus waves, High-speed observation

©2021. Japan Geoscience Union. All Right Reserved.

[J] Oral | P (Space and Planetary Sciences)：P-EM Solar-Terrestrial Sciences, Space Electromagnetism & Space Environment

Sat. Jun 5, 2021 10:45 AM - 12:15 PM JST | Sat. Jun 5, 2021 1:45 AM - 3:15 AM UTC | Ch.06 Zoom Room 06

[P-EM14] Heliosphere and Interplanetary Space

convener:Kazumasa Iwai(Institute for Space–Earth Environmental Research (ISEE), Nagoya University), Yasuhiro Nariyuki(Faculty of Education, University of Toyama), Ken Tsubouchi(University of Electro-Communications), N Masaki Nishino(Japan Aerospace Exploration Agency, Institute of Space and Astronautical Science), Chairperson:Kazumasa Iwai(Institute for Space–Earth Environmental Research (ISEE), Nagoya University)

This session aims to secure comprehensive insights into physical processes of plasmas and fields in the heliosphere. Presentations of the recent studies from any approaches (integrated observation/theoretical modeling/massive numerical simulation) are welcomed. Topics are not restricted to any specific issues: phenomenological studies on solar flares/CME/solar wind, and related fundamental physics problems such as shocks/waves/turbulence/particle transport and acceleration can be the main target, including heliospheric high-energy phenomena and their impact on the Earth's environment.

10:45 AM - 11:00 AM JST | 1:45 AM - 2:00 AM UTC

[PEM14-01] Yearly variation of the Sun’s polar regions during Solar Cycle 24 observed with Hinode

*Daikou Shiota[1], Masumi Shimojo[2] (1.National Institute of Information and Communications Technology (NICT), 2.National Astronomical Observatory of Japan (NAOJ))

11:00 AM - 11:15 AM JST | 2:00 AM - 2:15 AM UTC

[PEM14-02] Improvement of the computer assisted tomography of interplanetary scintillation observations

*Munetoshi Tokumaru[1], Ken'ichi Fujiki[1], Masayoshi Kojima[1], Kazumasa Iwai[1] (1.Institute for Space-Earth Environmental Research, Nagoya University)

11:15 AM - 11:30 AM JST | 2:15 AM - 2:30 AM UTC

[PEM14-03] Physical properties of fast and slow solar wind studied by spacecraft radio scintillation

*Shota Chiba[1], Takeshi Imamura[1], Munetoshi Tokumaru[2], Daikou Shiota[3], Hiroki Ando[4] (1.Graduate School of Frontier Sciences, The University of Tokyo, 2.Institute for Space-Earth Environment Research, Nagoya University, 3.National Institute of Information and Communications Technology, 4.Kyoto Sangyo University)

11:30 AM - 11:45 AM JST | 2:30 AM - 2:45 AM UTC

[PEM14-04] Solar wind density distribution derived from DM measurements of Crab pulsar

*Maeda Ryuya[1], Munetoshi Tokumaru[1], Kaito Tawara[1], Toshio Terasawa[2] (1.Institute for Space-Earth Environmental Research, Nagoya University, 2.Institute for Cosmis Ray Research,The University of Tokyo)

11:45 AM - 12:00 PM JST | 2:45 AM - 3:00 AM UTC

[PEM14-05] Next generation solar wind observation system: science requirements and pathfinders.

*Kazumasa Iwai[1], Munetoshi Tokumaru[1], Ken'ichi Fujiki[1] (1.Institute for Space–Earth Environmental Research (ISEE), Nagoya University)

12:00 PM - 12:15 PM JST | 3:00 AM - 3:15 AM UTC

[PEM14-06] Discussion

Yearly variation of the Sun’s polar regions during Solar Cycle 24 observed with Hinode

*Daikou Shiota[1], Masumi Shimojo[2]

1. National Institute of Information and Communications Technology (NICT), 2. National Astronomical Observatory of Japan (NAOJ)

Observations of the magnetic fields in the Sun’s polar regions are of crucial importance to understand the long-term variation of solar magnetism. As a consequence of the magnetic variation the three-dimensional structure of global solar corona and solar wind also show a drastic long-term variation and, as a result, fast solar wind emanates from the polar regions around solar minima. The first Hinode observation of the polar region reveals the fine structure of photospheric vector magnetic fields of the polar areas: the existence of many patchy magnetic concentrations with intrinsic field strengths of over 1kG distributed across the entire polar region (Tsuneta et al. 2008) around the solar minimum. Following the first polar observation, the monitoring of the polar regions has been continued for 12 years. Since 2012, which was before the solar maximum of this cycle, the time variations in the distribution of the whole polar regions during the polarity reversal period have been monitored with periodic SP observations during a month at the proper timing (March for the south pole and September for the north pole). At September 2020, Solar Cycle 25 Prediction Panel, an international group of experts co-sponsored by NASA and NOAA, announced that solar minimum occurred in December 2019. This means that Hinode succeeded to observe the Sun’s polar regions during whole of Solar Cycle 24.
In this study, we investigated the yearly variation in magneitc field distribution of both Sun’s polar regions obtained in the monitoring during Solar Cycle 24. We also combined the polar magnetic field data with HMI/SDO synoptic map. Using the maps, we calculated the three-dimensional coronal magnetic field with potential field source surface model. We will report yearly variation in the coronal magnetic field structure associated with the variation in the polar magnetic field.

Keywords: solar cycles, photospheric magnetic field, coronal magnetic field

©2021. Japan Geoscience Union. All Right Reserved.

Improvement of the computer assisted tomography of interplanetary scintillation observations

*Munetoshi Tokumaru[1], Ken'ichi Fujiki[1], Masayoshi Kojima[1], Kazumasa Iwai[1]

1. Institute for Space-Earth Environmental Research, Nagoya University

The computer assisted tomography (CAT) of interplanetary scintillation (IPS) observations allows reconstruction of global distribution of the solar wind speed. Earlier studies demonstrated that the solar wind data derived from the CAT analysis are comparable to those from in situ measurements. However, comparison between the CAT analysis and in situ measurements at the Earth orbit for the period after 2009 showed that the solar wind speeds derived from IPS observations are systematically higher than those from in situ observations. In this study, we examined two effects as a cause for this discrepancy; one is the effect of the number of IPS data used for the CAT analysis, and the other is the effect of the empirical relation between solar wind speed V and density fluctuations ΔN_e; $V \propto \Delta N_e^{\alpha}$, which is assumed in the CAT analysis. As the result, we found that the latter can explain the observed discrepancy if α varies with time, whereas the former is unlikely. Instead, the effect of the number of IPS data can account for variations of rms deviations and correlations between IPS and in situ observations. The index of α=-0.5 is optimal to analyze IPS observations between 1985 and 2008, and a positive and larger value of alpha (i.e. α=+1.0) yields better agreement between IPS and in situ observations. By using these optimal values for α, the CAT analysis of IPS observations is improved, and this leads to better understanding of global heliosphere. The result obtained here also suggests that physical properties of solar wind micro-turbulence may evolve over long timescale. If the momentum flux is invariant among different solar wind flows, the result obtained here implies that fractional density fluctuations of the solar wind for the recent period depend on the speed more strongly than those for the past period.

Keywords: solar wind, interplanetary scintillation, turbulence, tomography

©2021. Japan Geoscience Union. All Right Reserved.

Physical properties of fast and slow solar wind studied by spacecraft radio scintillation

*Shota Chiba[1], Takeshi Imamura[1], Munetoshi Tokumaru[2], Daikou Shiota[3], Hiroki Ando[4]

1. Graduate School of Frontier Sciences, The University of Tokyo, 2. Institute for Space-Earth Environment Research, Nagoya University, 3. National Institute of Information and Communications Technology, 4. Kyoto Sangyo University

The solar wind is a supersonic plasma flow streamed from the solar corona. The solar wind is classified into the fast wind (typically ~750 km/s) and the slow wind (~300 km/s). The acceleration of the solar wind mainly occurs in the outer corona at heliocentric distances of about 5–10 R_S (= solar radii), where the coronal heating by magnetohydrodynamic waves and the wave-induced magnetic pressure are thought to play major roles in the acceleration. The mechanisms have not been fully confirmed by observations because the acceleration region is too close to the Sun to be observed by in-situ probes.
Key physical processes in the acceleration region can be observed with radio occultation. Coronal plasma traversing the ray path disturbs radio wave's amplitudes and frequency, from which we can derive physical parameters such as the flow speed and wave's amplitudes. In this research, we analyze data taken by radio occultation observations carried out using JAXA's Venus orbiter Akatuki's during the superior conjunction periods from May 30 to June 15, 2016 and June 6 to July 8, 2011. Solar offset distances of about 1.4–9.0 R_S were probed intermittently by 11 observations in the former period and about 1.5–20.6 R_S were probed by 16 observations in the latter.
The radial velocity and the turbulence characteristics (power-law exponent, axial ratio, and inner scale) were retrieved from the intensity scintillation time series taken in 2016 by fitting a theoretical spectrum to the observed power spectra. In the radial distribution of the derived solar wind velocity, fast winds originating from regions near a coronal hole and slow winds from other regions were identified. We also found that the inner scale increases with the heliocentric distance and that the fast solar wind has larger inner scales than the slow solar wind. These tendencies are consistent with the inertial length model proposed by Coles and Harmon (1989).
We also applied wavelet analysis to the frequency time series taken in 2011 to detect quasi-periodic fluctuations (QPC), which are thought to represent acoustic waves, and quantify the amplitude, the period, and the coherence time of each wave event. The density amplitude and the wave energy flux were estimated following the method of Miyamoto et al. (2014). We confirmed that the fractional density amplitude increases with distance up to ~6 R_S. The amplitude reaches tens of percent, suggesting a possibility of wave breaking. The energy fluxes increase with distance up to ~6 R_S, suggesting local generation of waves. It is probable that these radial distributions indicate that the Alfven waves propagating from the photosphere generate acoustic waves in the outer corona, and the generated acoustic waves dissipate to heat the corona, as suggested by numerical models. The wave energy fluxes in the fast solar wind were larger than those in the slow wind. The results suggest that the fast solar wind originating from the coronal hole is powered by a larger injection of wave energy than the slow wind originating from other regions. In this presentation, we will also report results from the data taken in 2016.

Keywords: solar wind, Remote sensing, Fast and slow solar wind

©2021. Japan Geoscience Union. All Right Reserved.

Solar wind density distribution derived from DM measurements of Crab pulsar

*Maeda Ryuya[1], Munetoshi Tokumaru[1], Kaito Tawara[1], Toshio Terasawa[2]

1. Institute for Space-Earth Environmental Research, Nagoya University, 2. Institute for Cosmis Ray Research,The University of Tokyo

The pulsed radio wave emitted by a pulsar undergoes a delay by intervening plasma through propagation in the interstellar medium and the solar wind (SW). This delay depends on frequency, and the pulsar emission observed at the Earth exhibits the frequency dispersion. The magnitude of frequency dispersion is called dispersion measures (DM), and provides information of the plasma density integrated along the LOS from the pulsar to the observer. We have made observation of Crab pulsar since 2018 using 327MHz radio telescope (SWIFT) at Toyokawa. The LOS of Crab pulsar approaches the sun by ~5R_s (R_s: solar radius) in every mid-June. This enables to investigate the plasma density near the sun by using the DM of Crab pulsar. We derived the DM from Crab pulsar observations at Toyokawa by optimizing intensity height of the giant radio pulses (GRP), and determined the SW density distribution near the sun from derived DM data. In our previous study, we used the GRPs with a signal-to-noise ratio (S/R)>15. However, the number of GRP with S/N>15 observed in both 2018 and 2019 decreased as Crab pulsar's LOS approached to the sun, and this decrease significantly worsened the accuracy of DM measurements. In order to improve decrease in accuracy, we used GRPs with S/N>10 to derive DM in this study. A lower threshold for GRP intensity results in an increase of the number of GRP, and leading to better statistics even for the period when the number of GRPs greatly reduces. We found that errors and outliers of DM measurements were significantly reduced in the analysis with S/N>10. We determined the increase in DM (ΔDM) due to the solar wind by subtracting the effect of the interstellar medium. The effects of the interstellar medium were estimated from observations made for the period of a large solar elongation. The solar wind density model was fit to observed ΔDM. While the density model obtained here was almost the same as the one from the previous study, the estimation error was reduced by about one-third, and the accuracy of model determination was greatly improved.

Keywords: Solar Wind, Pulsar

©2021. Japan Geoscience Union. All Right Reserved.

Next generation solar wind observation system: science requirements and pathfinders.

*Kazumasa Iwai[1], Munetoshi Tokumaru[1], Ken'ichi Fujiki[1]

1. Institute for Space–Earth Environmental Research (ISEE), Nagoya University

Interplanetary scintillation (IPS) is a radio scattering phenomenon caused by the disturbances in the solar wind. The IPS observation using ground-based radio telescopes has been an important technique to investigate the global structure of the heliosphere. Nagoya University have observed the solar wind velocity and density irregularities for several decades using large radio telescopes at 327 MHz. In this study, we investigated the science requirements and design of next generation IPS observation instruments, and developed their pathfinders.
The main scope of this research is to elucidate the acceleration mechanisms of the solar wind. To do that, the relationship between the accelerated solar wind velocity and the magnetic field structure of its source region should be derived. We can derive the global structure of the solar wind from the IPS data using the tomography method. However, the spatial resolution of the solar wind distribution projected on the solar surface is not enough to distinguish its source structures. Therefore, we consider a new solar wind observation system that can observe multiple directions simultaneously by constructing a 2D flat phased-array antenna system consisting of multiple dipole antennas, and installing digital phased-array devices. The multidirectional simultaneous radio scintillation observation using this system enables the solar wind observation 10 times as much as the conventional radio instruments have been done, which will give enough spatial resolution of the solar wind distribution.
We also developed a proto type of the digital phased array instrument. This instrument has 8 analog-digital converters (ADCs), field-programmable gate array (FPGA), and 10-Gbit Ethernet output. This system enables us to measure four beams simultaneously by processing four types of different beamforming in parallel. We also added an automated calibration sequence to the FPGA. This sequence makes a calibration table that compensates an amplitude and phase differences of the 8 signals. By Appling this table, we can quickly calibrate the amplitude and phase differences of antennas and receivers. In the laboratory experiments, we confirmed that the calibration system works as expected.

Keywords: solar wind, CME, radio observation

©2021. Japan Geoscience Union. All Right Reserved.

[J] Oral | P (Space and Planetary Sciences) | P-EM Solar-Terrestrial Sciences, Space Electromagnetism & Space Environment

[P-EM14] Heliosphere and Interplanetary Space

convener:Kazumasa Iwai(Institute for Space–Earth Environmental Research (ISEE), Nagoya University), Yasuhiro Nariyuki(Faculty of Education, University of Toyama), Ken Tsubouchi(University of Electro-Communications), N Masaki Nishino(Japan Aerospace Exploration Agency, Institute of Space and Astronautical Science), Chairperson:Kazumasa Iwai(Institute for Space–Earth Environmental Research (ISEE), Nagoya University)

Sat. Jun 5, 2021 10:45 AM - 12:15 PM Ch.06 (Zoom Room 06)

This session aims to secure comprehensive insights into physical processes of plasmas and fields in the heliosphere. Presentations of the recent studies from any approaches (integrated observation/theoretical modeling/massive numerical simulation) are welcomed. Topics are not restricted to any specific issues: phenomenological studies on solar flares/CME/solar wind, and related fundamental physics problems such as shocks/waves/turbulence/particle transport and acceleration can be the main target, including heliospheric high-energy phenomena and their impact on the Earth's environment.

12:00 PM - 12:15 PM

[PEM14-06]Discussion

©Japan Geoscience Union

[J] Oral | P (Space and Planetary Sciences)：P-EM Solar-Terrestrial Sciences, Space Electromagnetism & Space Environment

Sat. Jun 5, 2021 1:45 PM - 3:15 PM JST | Sat. Jun 5, 2021 4:45 AM - 6:15 AM UTC | Ch.06 Zoom Room 06

[P-EM14] Heliosphere and Interplanetary Space

convener:Kazumasa Iwai(Institute for Space–Earth Environmental Research (ISEE), Nagoya University), Yasuhiro Nariyuki(Faculty of Education, University of Toyama), Ken Tsubouchi(University of Electro-Communications), N Masaki Nishino(Japan Aerospace Exploration Agency, Institute of Space and Astronautical Science), Chairperson:Yasuhiro Nariyuki(Faculty of Education, University of Toyama), Masaki N Nishino(Japan Aerospace Exploration Agency, Institute of Space and Astronautical Science)

This session aims to secure comprehensive insights into physical processes of plasmas and fields in the heliosphere. Presentations of the recent studies from any approaches (integrated observation/theoretical modeling/massive numerical simulation) are welcomed. Topics are not restricted to any specific issues: phenomenological studies on solar flares/CME/solar wind, and related fundamental physics problems such as shocks/waves/turbulence/particle transport and acceleration can be the main target, including heliospheric high-energy phenomena and their impact on the Earth's environment.

1:45 PM - 2:00 PM JST | 4:45 AM - 5:00 AM UTC

[PEM14-07] Identification of solar wind regimes using the non-hierarchical cluster analysis

*Shinichi Watari[1] (1.National Institute of Information and Communications Technology)

2:00 PM - 2:15 PM JST | 5:00 AM - 5:15 AM UTC

[PEM14-08] Numerical simulation on invasion process of galactic cosmic rays into the heliosphere: Particle orbits and statistics

*Kotaro Yoshida[1], Shuichi Matsukiyo[2,3], Haruichi Washimi[3], Tohru Hada[2,3] (1.Department of Earth System Science and Technology, Interdisciplinary Graduate School of Engineering Sciences, Kyushu University, 2.Faculty of Engineering Sciences, Kyushu University, 3.International Center for Space Weather Science and Education, Kyushu University)

2:15 PM - 2:30 PM JST | 5:15 AM - 5:30 AM UTC

[PEM14-09] Kaguya Observations of Solar Wind Electron Modification by Electrostatic Waves Above the Lunar Day Side: Preliminary Results

*Yuki Harada[1], Yoshiya Kasahara[2], Masaki N Nishino[3], Satoshi Kurita[4], Yoshifumi Saito[3], Shoichiro Yokota[5], Futoshi Takahashi[6], Hisayoshi Shimizu[7] (1.Graduate School of Science, Kyoto University, 2.Information Media Center, Kanazawa University, 3.ISAS, JAXA, 4.Research Institute for Sustainable Humanosphere, Kyoto University, 5.Graduate School of Science, Osaka University, 6.Faculty of Sciences, Kyushu University, 7.Earthquake Research Institute, University of Tokyo)

2:30 PM - 2:45 PM JST | 5:30 AM - 5:45 AM UTC

[PEM14-10] Elliptically polarized 0.01-0.3 Hz magnetic field variation in the lunar wake

*Tomoko Nakagawa[1], Futoshi Takahashi[2], Hisayoshi Shimizu[3], Yoshifumi Saito[4] (1.Information and Communication Engineering, Tohoku Institute of Technology, 2.Department of Earth and Planetary Sciences, Faculty of Science, Kyushu University, 3.Earthquake Research Institute, University of Tokyo, 4.Institute of Space and Astronautical Science, Japan Aerospace Exploration Agency)

2:45 PM - 3:00 PM JST | 5:45 AM - 6:00 AM UTC

[PEM14-11] On the relationship between the cross-helicty and the residual energy in the solar wind MHD turbulence: A phenomenological approach

*Yasuhiro Nariyuki[1] (1.Faculty of Education, University of Toyama)

3:00 PM - 3:15 PM JST | 6:00 AM - 6:15 AM UTC

[PEM14-12] Discussion

Identification of solar wind regimes using the non-hierarchical cluster analysis

*Shinichi Watari[1]

1. National Institute of Information and Communications Technology

By identifying solar wind regimes, we can get information on their solar sources and situations. Experience is necessary for us to identify the solar wind regimes. We need an objective identification method for this. Richardson and Cane (2004) identified solar wind regimes using heavy ion charge states. However, heavy ion charge states are not always observed by satellites. A method using basic solar wind data (speed, density, temperature, density, and magnitude of magnetic field) is suitable as proposed by Xu and Borovsky (2015).

Here we report identification of the solar wind regimes using one of the non-hierarchical cluster analysis, the k-means method. Data are classified into given number of clusters optimizing the distances of data from the cluster centers by the k-means method. We used speed, temperature, density, and magnitude of magnetic field in the one-hour solar wind data from the OMNI data of the NASA/NSSDC. The data between 1998 and 2019 were applied for our analysis because almost continuous data are available during this period. We also used three parameters, entropy, Alfven speed, and ratio of expected temperature from speed to observed temperature, which were used by Xu and Borovsky (2015).

Keywords: non-hierarchical cluster analysis, k-means method, solar wind, identification of solar wind regimes

©2021. Japan Geoscience Union. All Right Reserved.

Numerical simulation on invasion process of galactic cosmic rays into the heliosphere: Particle orbits and statistics

*Kotaro Yoshida[1], Shuichi Matsukiyo[2,3], Haruichi Washimi[3], Tohru Hada[2,3]

1. Department of Earth System Science and Technology, Interdisciplinary Graduate School of Engineering Sciences, Kyushu University, 2. Faculty of Engineering Sciences, Kyushu University, 3. International Center for Space Weather Science and Education, Kyushu University

Galactic cosmic rays (GCRs) are produced in our galaxy. Some of them invade the heliosphere and reach the earth. The motion of GCRs in the heliosphere is very complicated because of the influence of solar wind flow and magnetic field. The transport processes of GCRs have been discussed by using convection-diffusion models. But the model does not tell us the information of GCRs trajectories. Our goal in this study is to understand the invading process of GCRs into the heliosphere in the level of particle trajectory.
We performed three-dimensional relativistic test particle simulations using electromagnetic fields reproduced by the global MHD simulation of the heliosphere ([1] Washimi et al. 2015). In the MHD simulation, the solar wind velocity, density, magnetic field strength and temperature at 1 AU are set to be 400 km/s, 5.0 /cc, 35 μG and 10^5 K, respectively. These quantities are assumed to be time stationary and simply extrapolated to the inner boundary of the simulation domain at 50 AU from the sun. For the outer boundary at 900AU, the corresponding parameters of the stationary interstellar plasma are 23 km/s, 0.1 /cc, 6,300 K, and 3 μG, respectively. In the test particle simulation, the motions of protons initially distributed outside the heliopause with Lorentz factor γ are solved. Their velocity distribution function is given by a mono-energetic shell distribution. We found various patterns of particle trajectories. They exhibit different characteristics depending on their initial energy. Some concrete trajectories will be discussed in detail. Furthermore, we will estimate some statistics of the particles reached at the inner boundary, such as distribution of arrival position, energy, momentum, etc.

Keywords: galactic cosmic rays, heliosphere

©2021. Japan Geoscience Union. All Right Reserved.

Kaguya Observations of Solar Wind Electron Modification by Electrostatic Waves Above the Lunar Day Side: Preliminary Results

*Yuki Harada[1], Yoshiya Kasahara[2], Masaki N Nishino[3], Satoshi Kurita[4], Yoshifumi Saito[3], Shoichiro Yokota[5], Futoshi Takahashi[6], Hisayoshi Shimizu[7]

1. Graduate School of Science, Kyoto University, 2. Information Media Center, Kanazawa University, 3. ISAS, JAXA, 4. Research Institute for Sustainable Humanosphere, Kyoto University, 5. Graduate School of Science, Osaka University, 6. Faculty of Sciences, Kyushu University, 7. Earthquake Research Institute, University of Tokyo

Despite the lack of a global intrinsic magnetic field and a dense atmosphere, the Moon drives many observable effects on the upstream solar wind plasma through absorption, scattering, reflection, and emission of charged particles by the surface and crustal magnetic fields. As a result, a variety of plasma waves are excited in the upstream solar wind in a similar manner to planetary foreshocks, though a global bow shock is absent at the Moon. Recently, Chu et al. (2020) reported two case studies of THEMIS-ARTEMIS observations above lunar crustal magnetic anomalies, thereby proposing two sources of electrostatic waves around the Moon: (i) counter-streaming electron beams consisting of incoming solar wind electrons and reflected electrons, and (ii) relative drift across the magnetic field between reflected ions and solar wind electrons. The former drives electron two stream instability generating electric field structures parallel to the background magnetic field, while the latter drives electron cyclotron drift instability leading to perpendicular electric field waves. They also proposed that these electrostatic instabilities cause substantial heating of solar wind electrons. However, the global nature of these electrostatic waves and resulting solar wind electron modification remains largely unexplored, partly because of the nearly equatorial orbits of the THEMIS-ARTEMIS probes.

In this study, we generate global selenographic maps of electric field waves and solar wind electron modification from Kaguya data obtained on the lunar dayside at ~100 km altitude polar orbits. The global maps clearly demonstrate the lunar crustal field control of electrostatic wave generation and incoming solar wind electron modification. Additionally, we identify IMF cone angle dependence of the waves and electron modification above strong magnetic anomalies. We discuss these preliminary results in the context of the proposed electrostatic instabilities.

Keywords: Moon, Solar Wind Electron, Electrostatic Waves

©2021. Japan Geoscience Union. All Right Reserved.

Elliptically polarized 0.01-0.3 Hz magnetic field variation in the lunar wake

*Tomoko Nakagawa[1], Futoshi Takahashi[2], Hisayoshi Shimizu[3], Yoshifumi Saito[4]

1. Information and Communication Engineering, Tohoku Institute of Technology, 2. Department of Earth and Planetary Sciences, Faculty of Science, Kyushu University, 3. Earthquake Research Institute, University of Tokyo, 4. Institute of Space and Astronautical Science, Japan Aerospace Exploration Agency

Elliptically polarized magnetic field variation in the frequency range of 0.01-0.3 Hz was detected by Kaguya MAP-LMAG in the lunar wake. The polarization was highly elliptic and the direction of rotation was consistent with the vortex behind an obstacle in a fast flow, but no clear vortex motion was found in ion velocity observed by MAP-PACE onboard Kaguya. The magnetic variation was compressional, and the wave number vector was nearly parallel or oblique to the background magnetic field. The waves persisted in the deepest wake, suggesting that they were not surface waves. High frequency components above the local ion cyclotron frequency exhibited circular polarization of right-handed or left-handed rotation with respect to the background magnetic field.

Keywords: moon, lunar wake, polarization, magnetic field variation, ion cyclotron frequency, Kaguya

©2021. Japan Geoscience Union. All Right Reserved.

On the relationship between the cross-helicty and the residual energy in the solar wind MHD turbulence: A phenomenological approach

*Yasuhiro Nariyuki[1]

1. Faculty of Education, University of Toyama

It is known that solar wind turbulence is well characterized by the cross-helicty and the residual energy[Tu+Marsch, Space Sci. Rev., 1995; Bruno+Carbone, Living Rev. Solar Phys., 2013]. A simple linear relation derived by a MHD turbulence model[Tu+Marsch, JGR, 1993] has been compared with the observational studies, while the observational data is usually scattered around the line [e.g., Bruno et al, Ann. Geophys., 2007; Perri+Balogh, GRL, 2010]. Recently, the Langevein equation is applied to model the Alfvenic fluctuations with non-equilibrium cross-helicty and residual energy. Although circularly polarized waves are used, the Langevin model can reproduce the linear relation mentioned above. In this talk, the extension of the previous Langevin model is discussed. Non-circularly polarized, multi-dimensional Alfven wave solution [Primavera et al, ApJ, 2019] is applied to consider deviation from the linear relation.

Keywords: solar wind turbulence, Langevin model

©2021. Japan Geoscience Union. All Right Reserved.

[J] Oral | P (Space and Planetary Sciences) | P-EM Solar-Terrestrial Sciences, Space Electromagnetism & Space Environment

[P-EM14] Heliosphere and Interplanetary Space

convener:Kazumasa Iwai(Institute for Space–Earth Environmental Research (ISEE), Nagoya University), Yasuhiro Nariyuki(Faculty of Education, University of Toyama), Ken Tsubouchi(University of Electro-Communications), N Masaki Nishino(Japan Aerospace Exploration Agency, Institute of Space and Astronautical Science), Chairperson:Yasuhiro Nariyuki(Faculty of Education, University of Toyama), Masaki N Nishino(Japan Aerospace Exploration Agency, Institute of Space and Astronautical Science)
Sat. Jun 5, 2021 1:45 PM - 3:15 PM Ch.06 (Zoom Room 06)

This session aims to secure comprehensive insights into physical processes of plasmas and fields in the heliosphere. Presentations of the recent studies from any approaches (integrated observation/theoretical modeling/massive numerical simulation) are welcomed. Topics are not restricted to any specific issues: phenomenological studies on solar flares/CME/solar wind, and related fundamental physics problems such as shocks/waves/turbulence/particle transport and acceleration can be the main target, including heliospheric high-energy phenomena and their impact on the Earth's environment.

3:00 PM - 3:15 PM

[PEM14-12]Discussion

©Japan Geoscience Union

[J] Poster | P (Space and Planetary Sciences)：P-EM Solar-Terrestrial Sciences, Space Electromagnetism & Space Environment

Sat. Jun 5, 2021 5:15 PM - 6:30 PM JST | Sat. Jun 5, 2021 8:15 AM - 9:30 AM UTC | Ch.03_2

[P-EM14] Heliosphere and Interplanetary Space

convener:Kazumasa Iwai(Institute for Space–Earth Environmental Research (ISEE), Nagoya University), Yasuhiro Nariyuki(Faculty of Education, University of Toyama), Ken Tsubouchi(University of Electro-Communications), N Masaki Nishino(Japan Aerospace Exploration Agency, Institute of Space and Astronautical Science)

This session aims to secure comprehensive insights into physical processes of plasmas and fields in the heliosphere. Presentations of the recent studies from any approaches (integrated observation/theoretical modeling/massive numerical simulation) are welcomed. Topics are not restricted to any specific issues: phenomenological studies on solar flares/CME/solar wind, and related fundamental physics problems such as shocks/waves/turbulence/particle transport and acceleration can be the main target, including heliospheric high-energy phenomena and their impact on the Earth's environment.

[PEM14-P01] Relationship between solar type III radio bursts and electron energy spectra in solar impulsive electron events

Tatsuya Fujimoto[1], *Hiroaki Misawa[1], Fuminori Tsuchiya[1], Takahiro Obara[1] (1.Planetary Plasma and Atmospheric Research Center, Graduate School of Science, Tohoku University)

[PEM14-P02] Occurrence dependence on solar activity cycle for ordinary type III bursts and micro-type III bursts

*Yuichiro Seki[1], Hiroaki Misawa[1], Takahiro Obara[1], Fuminori Tsuchiya[1] (1.Tohoku University)

[PEM14-P03] Simple Estimation of the Global Solar Wind Structure

*Ken'ichi Fujiki[1], Munetoshi Tokumaru[1], Kazumasa Iwai[1] (1.Institute for Space-Earth Environmental Research)

Relationship between solar type III radio bursts and electron energy spectra in solar impulsive electron events

Tatsuya Fujimoto[1], *Hiroaki Misawa[1], Fuminori Tsuchiya[1], Takahiro Obara[1]

1. Planetary Plasma and Atmospheric Research Center, Graduate School of Science, Tohoku University

Solar Energetic Particles (SEPs) are protons, electrons, and heavy ions of 10 keV to several tens GeV generated with flares and coronal mass emissions (CMEs), which are explosive phenomena near the solar surface. SEPs are classified into two types; i.e., impulsive and gradual types, based on the elemental abundances and the time profile of ion flux variations. Impulsive SEPs, also known as electron-based events. In particular, electron events, in which the electron flux increases for a short period, have been understood to be the result of electrons accelerated by flares propagating through interplanetary medium and observed near the Earth. It has been reported that spectral shapes of electrons observed in electron events are frequently show broken power laws at the break energy of several tens of keV. Reid & Kontar [2013] proposed an explanation for the generation of the break: low energy electrons lose their kinetic energy during their propagations due to wave-particle interaction, which converts their kinetic energy into Langmuir wave energy. They also reported that type III radio bursts, which are suddenly appearing emissions caused by flares, are almost always observed in electron events in the several tens meter to kilometer wave bands. Type III radio bursts are thought to be generated by non-thermal electrons accelerated by magnetic reconnections, which propagate along open magnetic field lines. That is, an injection of energetic electrons into interplanetary medium leads to excite Langmuir waves, and the waves are converted into radio waves as type III bursts where the radio wave frequency is as same as the local plasma frequency. Type III bursts are therefore interpreted as being excited by energetic electrons causing electron events, and their characteristics have information on properties of energetic electrons. However, precise relationship between energetic electrons and Type III bursts in solar impulsive electron events has not been clarified.
In order to reveal the relationship by a statistical approach, we have made analyses for characteristics of energetic electrons and Type III radio bursts using solar electron spectral data of the 3DP instrument and type III bursts of the WAVES instrument onboard the WIND spacecraft. Among the significant single-event electron events observed by the WIND satellite from 1994 to 2005, we identified 37 events that simultaneously showed both a bend in the electron energy spectrum and type III burst spectrum with simple spectral form. As the results, we confirmed that the power law indices of electrons below the spectral break energy show a positive correlation with radio wave intensities/energies and the electron beam velocity calculated from the frequency drift features of type III bursts. On the other hand, no correlation was found between the kinetic energy of the electrons, which is assumed to be converted to wave energy and lost during the propagation, and the radio wave energy. These results suggest that 1) the electrons on the lower side of the break energy are responsible for the excitation of the type III bursts, and the spectral shape of energetic electrons is an important factor to control intensity and energy of Type III radio waves, and 2) the spectrum shapes of electrons with the break energy cannot be explained only by the energy loss process in the wave-particle interaction generating Type III bursts.

Keywords: sun, solar energetic particle, electron event, type III burst

©2021. Japan Geoscience Union. All Right Reserved.

Occurrence dependence on solar activity cycle for ordinary type III bursts and micro-type III bursts

*Yuichiro Seki[1], Hiroaki Misawa[1], Takahiro Obara[1], Fuminori Tsuchiya[1]

1. Tohoku University

Type III bursts are one of intense solar radio emissions and show a large negative frequency drift. Some of them originate above solar active regions and appear with solar flares. These type III bursts are hereafter referred to as ordinary type III bursts. On the other hand, type III bursts sometimes appear as clusters which are characterized by thousands of short-lived type III bursts lasting for a few days or more than a week. Morioka et al. (2007) proposed the term ‘micro-type III bursts’, which are elements of type III storms. It is suggested that micro-type III bursts originate near the edge of coronal streamers and are not just weaker versions of the ordinary type III bursts because a distribution of emitted power flux is different from that of ordinary bursts.

Generation processes of both ordinary and micro type III bursts are thought that high energy electrons originally generated with magnetic reconnections excite Langmuir waves in the solar corona and/or interplanetary space, then the Langmuir waves are converted into electromagnetic waves observed as type III bursts. It is therefore generally assumed that the frequency of type III bursts reflects the plasma density in the solar corona and/or interplanetary space where the radio waves are generated, and their frequency drift reflects the plasma density distribution and the velocity of high-energy electrons.

It is well known that density distributions of the solar plasma differ depending on the activity of solar surface area (ex. Aschwanden and Acton, 2001). This implies that the plasma density distribution roughly varies with the solar activity cycle and therefore the frequency drift rates of type III bursts might show solar cycle dependence since the drift rates should reflect plasma density distributions. Although the occurrence rates of type III bursts are known to show a positive correlation with solar activity, our knowledge for solar cycle dependence of the drift rates has been still limited (ex. Zhang et al., 2018). Moreover, there has been no study that clearly classifies ordinary type III bursts and micro-type III bursts, and simultaneously analyzes the long-term variation of their drift rates.

In this study, we have investigated occurrence features of drift rates for ordinary type III bursts and micro-type III bursts to clarify their solar cycle dependences. For this purpose, we have tried to make statistical analyses of type III bursts using a database of solar radio spectra observed with the Nancay Decameter Array (NDA). We have analyzed the low-resolution data (175 kHz frequency resolution, 1 second time resolution) of the NDA. Although the observation frequency range of NDA is 10MHz-80MHz, we have used the spectra for 30-80MHz to avoid noises below 30MHz.

An automatic burst detection system was newly developed to make the statistical analyses. Threshold methods, Convolution Neural Network (CNN) methods, and least squares methods with curve fitting are applied to our detection system. From candidates of type III bursts detected by this system, we finally selected ordinary type bursts and micro-type III bursts through a visual check.

Using the developed automatic detection system, we have analyzed 7 years of solar activity cycle 24, 2012-2014(around solar maximum) and 2017-2020(around solar minimum) so far, and detected 1145 ordinary type III bursts and 1021 micro-type III bursts in total and a preliminary result shows for ordinary

©2021. Japan Geoscience Union. All Right Reserved.

type III bursts, drift rates (|df/dt|) in 2019 and 2020 are lower than those in other years, and for micro-type III bursts, lower solar activity is, higher drift rates are. In the presentation, we will show solar cycle dependence for the occurrence characteristics of both ordinary and micro type III bursts with the discussion of their background processes.

Acknowledgments: The solar radio spectrum data was provided by the Nancay Observatory, Observatoire de Paris, France. We would appreciate Dr. L. Lamy and the NDA operation group.

Keywords: Radio emission, Particle acceleration, Nancay decameter array, Type III bursts, Micro-type III bursts

©2021. Japan Geoscience Union. All Right Reserved.

Simple Estimation of the Global Solar Wind Structure

*Ken'ichi Fujiki[1], Munetoshi Tokumaru[1], Kazumasa Iwai[1]

1. Institute for Space-Earth Environmental Research

The solar wind is composed of a slow wind (~450 km/s) and a fast wind (~800 km/s), which is known as the bimodal signature of the solar-wind velocity. These slow and fast wind are the main components of the solar wind in the low-mid and high latitudes of the heliosphere, respectively. The solar wind structure is stratified by latitude. For example, the slow wind is confined in a narrow band around the solar equator (or heliospheric current sheet with a small tilt angle) during the solar minimum. The width of the narrow slow wind band increases in rising and declining phases then the tilt angle of HCS becomes larger. During solar maxima, the latitude structure is lost, and the heliosphere is dominated by slow solar wind and frequent CMEs.

In this study, we focus a variation of boundary latitudes of the slow-fast solar wind through three solar cycles by using the interplanetary scintillation (IPS) observation at the Institute for Space-Earth Environmental Research (ISEE). The latitudinal structure of the bimodal solar wind is derived from the solar wind synoptic map for each Carrington rotation and compared with the maximum tilt angle of the HCS derived from observations by the Wilcox Solar Observatory (WSO). The results show that the HCS tilt angle correlates well with the latitudinal average of the solar wind speed of 600 km/s (correlation coefficient of 0.8). The empirical results allow us to estimate the latitudinal structure of the solar wind by the bimodal solar wind velocity after the 1970s when continuous magnetic field observations of the Sun began.

Keywords: solar wind, long-term variation, magnetic field

©2021. Japan Geoscience Union. All Right Reserved.

[E] Oral | A (Atmospheric and Hydrospheric Sciences)：A-OS Ocean Sciences & Ocean Environment

Sat. Jun 5, 2021 9:00 AM - 10:30 AM JST | Sat. Jun 5, 2021 12:00 AM - 1:30 AM UTC | Ch.09 Zoom Room 09

[A-OS11] Ocean Mixing Frontiers

convener:Toshiyuki Hibiya(Department of Earth and Planetary Science, Graduate School of Science, University of Tokyo), Chairperson:Takashi Ijichi(The University of Tokyo)

Ocean mixing plays crucial roles both in the open and coastal ocean, affecting key physical, biological and chemical processes. Mixing in the upper ocean influences the sea surface temperature and hence air-sea interactions which impact global climate change, while mixing in the deep ocean maintains abyssal stratification of the world's oceans and impacts the global overturning circulation. In coastal oceans, mixing modulates the transport and dispersal of dissolved and suspended materials including pollutants and nutrients. Planktonic ecosystems are controlled by nutrient pumping associated with ocean mixing.

In this session, we encourage contributors to present recent findings of ocean mixing obtained through field observations as well as theoretical, numerical, and laboratory studies. Through the related detailed discussions, we would like to confirm how far has our understanding of the ocean mixing processes advanced, defining the new frontier of ocean mixing research to be tackled in the next decade. The session encompasses a wide variety of aspects of coastal and open ocean mixing processes; within the water column from the surface through the interior to the near boundary benthic mixing, including the roles of mixing in the biological processes and productivity of the ocean. Observational, theoretical, and numerical modeling studies are all encouraged.

9:00 AM - 9:15 AM JST | 12:00 AM - 12:15 AM UTC

[AOS11-01] Tide-topography interactions with a background sheared current: critical layers and asymmetric internal wave breaking

*Kevin Lamb[1] (1.University of Waterloo)

9:15 AM - 9:30 AM JST | 12:15 AM - 12:30 AM UTC

[AOS11-02] Small-scale topographic effects on the generation of along-shelf propagating internal solitary waves on the Amazon Shelf

*Xiaolin Bai[1], Kevin Lamb[1], Jose C. B. da Silva[2] (1.Department of Applied Mathematics, The University of Waterloo, Canada, 2.Department of Geosciences, Environment, and Spatial Planning, and Instituto Ciencias da Terra (ICT), Polo Porto, Porto, Portugal)

9:30 AM - 9:45 AM JST | 12:30 AM - 12:45 AM UTC

[AOS11-03] Energetic turbulence and internal waves in Tokara Strait

*Anne Takahashi[1], Ren-Chieh Lien[1], Eric Kunze[2] (1.Applied Physics Laboratory, University of Washington, 2.NorthWest Research Associates)

9:45 AM - 10:00 AM JST | 12:45 AM - 1:00 AM UTC

[AOS11-04] A parameterization of local and remote tidal mixing

*Casimir de Lavergne[1] (1.LOCEAN laboratory, Sorbonne University)

10:00 AM - 10:15 AM JST | 1:00 AM - 1:15 AM UTC

[AOS11-05] **A new parameterization of turbulent mixing enhanced over rough seafloor topography**

*Toshiyuki Hibiya[1] (1.Department of Earth and Planetary Science, Graduate School of Science, The University of Tokyo)

10:15 AM - 10:30 AM JST | 1:15 AM - 1:30 AM UTC

[AOS11-06] Turbulent mixing variability in an energetic standing meander of the Southern Ocean

*Ajitha Cyriac[1,2], Helen Phillips[1,3], Nathan Bindoff[1,3], Kurt Polzin[4] (1.IMAS, University of Tasmania, Hobart, Australia, 2.ARCCSS, Hobart, Australia, 3.AAPP, Hobart, Australia, 4.WHOI, Woods Hole, USA)

Tide-topography interactions with a background sheared current: critical layers and asymmetric internal wave breaking

*Kevin Lamb[1]

1. University of Waterloo

Internal wave generation by tide-topography interactions has been the subject of many studies in recent decades. Many of these studies have considered the generation of internal waves over a two-dimensional symmetric ridge in the absence of steady background currents. In this situation, waves propagating to the left and right of the ridge are the same. This symmetry is broken in the presence of steady background currents. In this talk, the effects of a uni-directional steady background current confined to lie above a ridge will be discussed. The background current introduces asymmetries in the characteristics of the leftward and rightward propagating waves. If the current is strong enough, then critical layers are present on one side of the ridge for low mode waves that further modify the wave field. The implications for wave breaking and mixing will be discussed.

Keywords: Internal waves, Tide-topography interactions, Critical layers, Wave-breaking

©2021. Japan Geoscience Union. All Right Reserved.

Small-scale topographic effects on the generation of along-shelf propagating internal solitary waves on the Amazon Shelf

*Xiaolin Bai[1], Kevin Lamb[1], Jose C. B. da Silva[2]

1. Department of Applied Mathematics, The University of Waterloo, Canada, 2. Department of Geosciences, Environment, and Spatial Planning, and Instituto Ciencias da Terra (ICT), Polo Porto, Porto, Portugal

In this talk, we consider the joint effects of tidal and steady currents to investigate internal wave generation and propagation on the Amazon shelf, a hotspot for internal solitary wave (ISW) generation. The Amazon Shelf is off the mouth of the Amazon River in the southwest tropical Atlantic Ocean, affected by strong tidal constituents over complex bottom bathymetry and a strong western boundary current, the North Brazilian Current (NBC). Satellite observations and numerical modelling are used in this study. Satellite observations provide a clear visualization of the wave characteristics, such as temporal and spatial distributions, propagating direction and its relation to background currents. These ISWs appear as streak-like patterns in satellite images along a narrow path within the NBC propagating against the current. Near-critical conditions (Froude number close to 1) created by the NBC and tide result in strong ISW generation, while the dominant subcritical conditions result in the upstream propagation of these ISWs. Their streak-like patterns are a result of the quasi-two-dimensional bathymetry below, suggesting the possibility of using sea surface imprints to detect the topographic features beneath. This study demonstrates that small-scale topographic features can result in a rich generation of ISWs, which are expected to significantly contribute to ocean mixing and, potentially, sediment resuspension. The ISW-induced current also contributes to sea surface wave breaking as observed by satellites.

Keywords: Internal solitary wave, Along-shelf propagation, Small-scale topography, ISW-induced mixing

©2021. Japan Geoscience Union. All Right Reserved.

Energetic turbulence and internal waves in Tokara Strait

*Anne Takahashi[1], Ren-Chieh Lien[1], Eric Kunze[2]

1. Applied Physics Laboratory, University of Washington, 2. NorthWest Research Associates

Internal lee waves generated by geostrophic flows interacting with small-scale topography are one leading energy sink for the 1-TW wind-forcing input to gyre-scale circulation and eddies. In this study, we examine the relationship between turbulence and finescale velocity variations above and downstream of where the Kuroshio interacts with a ~O(10-km) wide seamount in the Tokara Strait. Data were collected during November 2019 using Chi-augmented EM-APEX profiling floats which measured temperature, salinity, horizontal velocity (u, v) and microstructure temperature variance dissipation rate χ from the surface to bottom at vertical resolutions of $\Delta z \approx 5$ m. Finescale vertical velocity w is also estimated following Cusack et al. (2016).

Average turbulent kinetic energy dissipation rates ε and diapycnal diffusivities K_ρ, inferred from χ, are at least an order of magnitude greater than open ocean thermocline values with ε ~10^{-8} W/kg and K_ρ ~10^{-4} m^2/s. They are further enhanced above the seamount (ε ~10^{-7} W/kg and K_ρ ~10^{-2} m^2/s) and in a ~200-m layer below the surface mixed layer downstream of the seamount (ε ~10^{-6} W/kg and K_ρ ~10^{-2} m^2/s). The vertical wavenumber shear spectrum $\Phi_{Sh}(m)$ is an order of magnitude higher than the canonical GM level and resembles the saturated spectral slope −1 above a rolloff vertical wavenumber $m_c \approx 0.01$ cpm and shows no correlation with ε. The ratio of horizontal kinetic energy to vertical kinetic energy decreases from 100 at m = 0.01 cpm to 10 at m = 0.1 cpm, suggesting that the velocity field is more isotropic at small vertical scales. Dissipation rates ε are correlated within a factor of three with vertically-high-passed (m > 130 cpm) vertical velocity w and vertical divergence dw/dz, consistent with the large-eddy parameterization (e.g., Beaird et al. 2012). The internal-wave finescale parameterization scheme fails in this energetic regime.

Keywords: Turbulence, Internal waves, Kuroshio, Internal lee waves

©2021. Japan Geoscience Union. All Right Reserved.

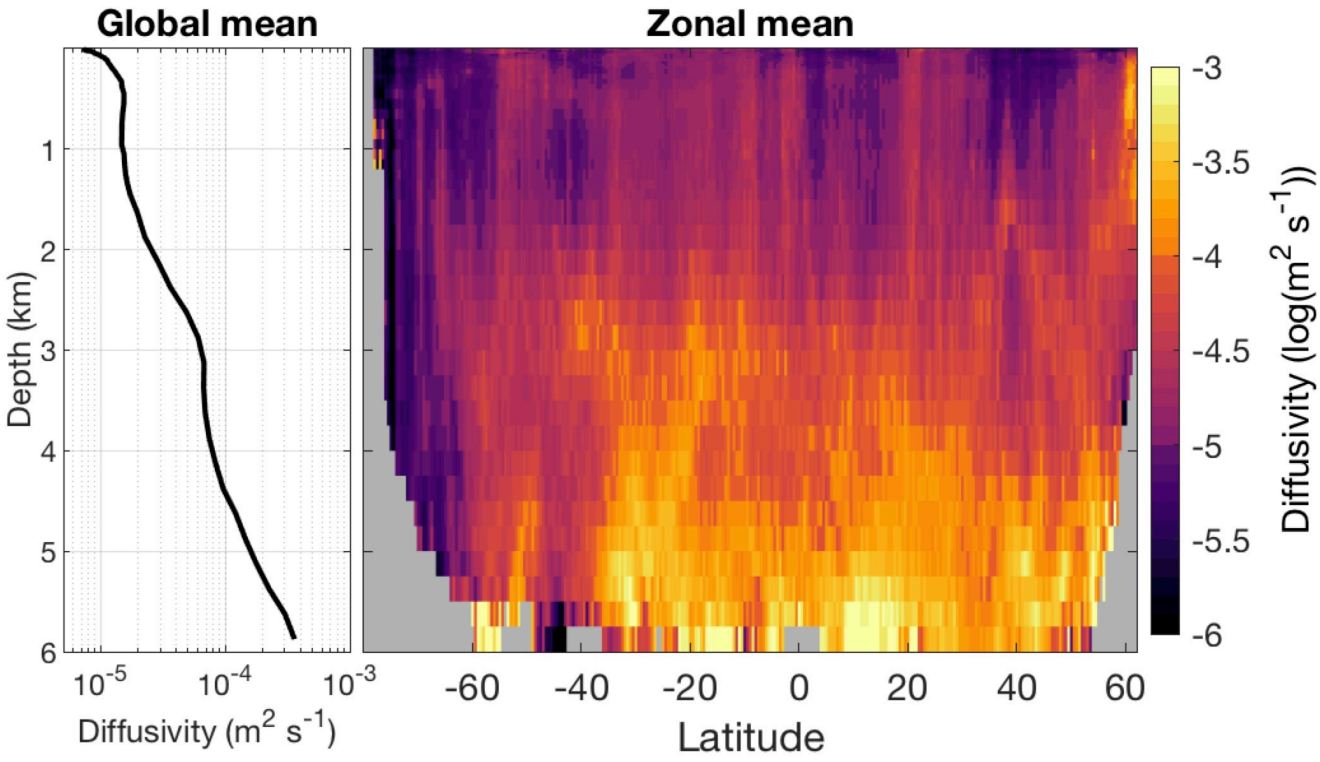
A parameterization of local and remote tidal mixing

*Casimir de Lavergne[1]

1. LOCEAN laboratory, Sorbonne University

Internal tides power much of the observed small-scale turbulence in the ocean interior. To represent mixing induced by this turbulence in climate-scale ocean models, energy routes from the generation to the dissipation of internal tides must be understood and mapped. Here we present a mixing scheme which accounts for the local breaking of high-mode internal tides and the distant dissipation of low-mode internal tides. The scheme relies on four static 2D maps of internal tide dissipation, constructed using mode-by-mode Lagrangian tracking of energy beams from sources to sinks. Each map is associated with a distinct dissipative process and a corresponding vertical structure. Applied to an observational climatology of stratification, the scheme produces a global 3D map of dissipation and mixing which compares well with available microstructure observations and with upper-ocean finestructure mixing estimates. Implemented in the NEMO global ocean model, the scheme improves the representation of deep water-mass transformation and obviates the need for a constant background diffusivity.

Keywords: ocean mixing, tides, turbulence, parameterization



©2021. Japan Geoscience Union. All Right Reserved.

A new parameterization of turbulent mixing enhanced over rough seafloor topography

*Toshiyuki Hibiya[1]

1. Department of Earth and Planetary Science, Graduate School of Science, The University of Tokyo

In the present study, I propose a new parameterization of tidal mixing enhanced over a rough seafloor with the revised formulation of its vertical decay scale. Of special importance is that internal waves emanating from the seafloor transform from internal tides to internal lee waves as tide-topography interaction strengthens. Taking into account this fact, I formulate the vertical decay scale of the energy dissipation rate off the seafloor assuming that it can be substituted by a “vertical mean free path” of the internal lee waves emanating from the seafloor and then resonantly interacting with the background Garrett-Munk internal wave field. The resulting formula predicts that the vertical extent of the mixing hotspot off the seafloor increases in proportion to U_0 squared, but independently of k_H, where U_0 is the amplitude of the barotropic tidal flow and k_H is the dominant horizontal wavenumber of the seafloor. Encouraged by the fact that this theoretical prediction is consistent with the results of the eikonal calculations by *Hibiya et al*. [2017], as well as the results of microstructure measurements in the Southern Ocean by *Sheen et al*. [2013], I propose a new parameterization of tidal mixing enhanced over the rough seafloor by incorporating the above formulated vertical decay scale of energy dissipation rates.

As is well known, tidal mixing in the global ocean is classified into the “far-field” mixing and the “near-field” mixing; it has long been believed that the far-field mixing is associated with nonlinear interactions between propagating low-mode internal tidal waves and the background internal wave field in the ocean interior, while the near-field mixing is associated with nonlinear interactions between high-mode internal tidal waves and the background internal wave field near the seafloor. However, even if tidal flow over the rough seafloor in the deep ocean is barely sufficient to generate internal tidal waves, it can be locally amplified, for example, over the rough seafloor at the top of the ocean ridge so that internal lee waves might occur. In such a case, we can expect that resulting tidal mixing region extends further upward from the seafloor, even possibly reaching the thermocline; thus compensating the shortfall of turbulent mixing required to sustain the global overturning circulation. The intensity and the vertical extent of the near-field tidal mixing employed in the current global ocean circulation models should therefore be reconsidered on the basis of the present study.

Keywords: Parameterization of turbulent mixing, Rough seafloor topography, Tidal flow, Geostrophic flow, Internal lee waves, Southern Ocean

©2021. Japan Geoscience Union. All Right Reserved.

Turbulent mixing variability in an energetic standing meander of the Southern Ocean

*Ajitha Cyriac[1,2], Helen Phillips[1,3], Nathan Bindoff[1,3], Kurt Polzin[4]

1. IMAS, University of Tasmania, Hobart, Australia, 2. ARCCSS, Hobart, Australia, 3. AAPP, Hobart, Australia, 4. WHOI, Woods Hole, USA

Turbulent mixing is a crucial mechanism that controls the distribution of heat, salt, sediments and organisms throughout the world oceans. It also plays an important role in driving large-scale oceanic processes such as watermass transformation, overturning circulation and stratification. Here we present mixing estimates from field observations of a standing meander near the Macquarie ridge, a major topographic obstacle for the Antarctic Circumpolar Current (ACC). It is a region of high eddy kinetic energy and interior upwelling. We collected more than 1400 profiles of temperature, salinity and velocity of the upper ocean using state of the art Electromagnetic Autonomous Profiling Explorer (EM-APEX) profiling floats in the upper 1600 m. By applying a finescale parameterization, we estimated the spatial and temporal variability of diapycnal mixing along the float tracks and investigated the sources. Elevated turbulent mixing is mostly associated with regions of subantarctic front and mesoscale eddies. In the upper layers, wind-generated downward propagating near-inertial waves dominate the enhanced mixing. The mixing is also high in cyclonic eddies associated with upward propagating internal waves. The dissipation rate estimates over rough and smooth topography has similar magnitudes suggesting that topography plays less role in mixing the upper 1600 m.

Keywords: Turbulent mixing, Internal waves

©2021. Japan Geoscience Union. All Right Reserved.

[E] Oral | A (Atmospheric and Hydrospheric Sciences)：A-OS Ocean Sciences & Ocean Environment

Sat. Jun 5, 2021 10:45 AM - 12:15 PM JST | Sat. Jun 5, 2021 1:45 AM - 3:15 AM UTC | Ch.09 Zoom Room 09

[A-OS11] Ocean Mixing Frontiers

convener:Toshiyuki Hibiya(Department of Earth and Planetary Science, Graduate School of Science, University of Tokyo), Chairperson:Toshiyuki Hibiya(Department of Earth and Planetary Science, Graduate School of Science, University of Tokyo)

Ocean mixing plays crucial roles both in the open and coastal ocean, affecting key physical, biological and chemical processes. Mixing in the upper ocean influences the sea surface temperature and hence air-sea interactions which impact global climate change, while mixing in the deep ocean maintains abyssal stratification of the world's oceans and impacts the global overturning circulation. In coastal oceans, mixing modulates the transport and dispersal of dissolved and suspended materials including pollutants and nutrients. Planktonic ecosystems are controlled by nutrient pumping associated with ocean mixing.

In this session, we encourage contributors to present recent findings of ocean mixing obtained through field observations as well as theoretical, numerical, and laboratory studies. Through the related detailed discussions, we would like to confirm how far has our understanding of the ocean mixing processes advanced, defining the new frontier of ocean mixing research to be tackled in the next decade. The session encompasses a wide variety of aspects of coastal and open ocean mixing processes; within the water column from the surface through the interior to the near boundary benthic mixing, including the roles of mixing in the biological processes and productivity of the ocean. Observational, theoretical, and numerical modeling studies are all encouraged.

10:45 AM - 11:00 AM JST | 1:45 AM - 2:00 AM UTC

[AOS11-07] Enhanced turbulent mixing in the equatorial thermocline

*Kelvin John Richards[1], Andrei Natarov[1], Yanli Jia[1] (1.International Pacific Research Center, School of Ocean and Earth Science Technology, University of Hawaii)

11:00 AM - 11:15 AM JST | 2:00 AM - 2:15 AM UTC

[AOS11-08] Convection enhances upper ocean mixing during a tropical cyclone

*Devang Falor[1], Bishakhdatta Gayen[1,2], Debasis Sengupta[1], Dipanjan Chaudhuri[3,1] (1.Indian Institute of Science, Bangalore, 2.University of Melbourne, Australia, 3.University of Washington, Seattle)

11:15 AM - 11:30 AM JST | 2:15 AM - 2:30 AM UTC

[AOS11-09] Near-inertial wave modulated turbulence in a Kuroshio anticyclonic eddy east of Japan

*Sebastian Essink[1], Ren-Chieh Lien[1], Eric Kunze[2] (1.UW/APL, 2.NWRA)

11:30 AM - 11:45 AM JST | 2:30 AM - 2:45 AM UTC

[AOS11-10] Upper ocean turbulence in the Icelandic Basin under strong forcing

*Harper L Simmons[1], Sophia Merrifield[2], Eric Skyllingstad[3], Louis St. Laurent[4] (1.University of Alaska Fairbanks, 2.Scripps Institution of Oceanography, University of California San Diego, 3.Oregon State University, 4.Applied Physics Laboratory, University of Washington)

11:45 AM - 12:00 PM JST | 2:45 AM - 3:00 AM UTC

[AOS11-11] Observed spectral distortion of temperature microstructure

*Takashi Ijichi[1], Louis St. Laurent[2] (1.Department of Earth and Planetary Science, Graduate School of Science, The University of Tokyo, 2.Applied Physics Laboratory, University of Washington)

12:00 PM - 12:15 PM JST | 3:00 AM - 3:15 AM UTC

[AOS11-12] 2D Horizontal-Vertical Wavenumber Spectra of Density Finestructure from a towed CTD chain

*Anda Vladoiu[1], Ren-Chieh Lien[1], Eric L Kunze[2] (1.Applied Physics Laboratory, University of Washington, Seattle, WA, USA, 2.NorthWest Research Associates, Redmond, WA, USA)

Enhanced turbulent mixing in the equatorial thermocline

*Kelvin John Richards[1], Andrei Natarov[1], Yanli Jia[1]

1. International Pacific Research Center, School of Ocean and Earth Science Technology, University of Hawaii

Enhanced mixing caused by small vertical scale features (SVSs) in the equatorial thermocline is known to impact the state of the ocean and its interaction with the atmosphere, in particular the sea temperature of the Pacific cold tongue and ENSO variability. The SVSs are produced by wind variability and instabilities. The good news is that with enough resolution these features can be captured in both observations and models. From observations we show that the vertical distribution of turbulent activity in the thermocline is very dependent on the turbulent length scale. From models we show that inertial and parametric subharmonic instability play a role and that wind driven inertia-gravity waves lead to an enhancement in mixing by a combination of three factors: a stronger super-inertial component of the wind forcing close to the equator, wave action convergence at turning latitudes for equatorially trapped waves, and nonlinear wave-wave interactions between equatorially trapped waves. Using a combination of ideal models and an OGCM we investigate the properties of SVS activity and its impact on mixing. Of particular interest is the dependency on stratification, the spatial and temporal variability of wind forcing and model resolution (both vertical and horizontal). The impact of the spatially and temporally varying mixing on the seasonal and inter-annual variability of the Pacific with be discussed. Such knowledge is invaluable in the planning of future observational studies and the design of the next generation climate models.

Keywords: Ocean turbulence, Ocean/atmosphere interaction

©2021. Japan Geoscience Union. All Right Reserved.

Convection enhances upper ocean mixing during a tropical cyclone

*Devang Falor[1], Bishakhdatta Gayen[1,2], Debasis Sengupta[1], Dipanjan Chaudhuri[3,1]

1. Indian Institute of Science, Bangalore, 2. University of Melbourne, Australia, 3. University of Washington, Seattle

Cyclones are extreme weather events accompanied by large wind shear and high latent heat loss on the ocean surface. Due to these large surface forcings, the ocean usually responds with enhanced upper ocean turbulence and a drop in the sea surface temperature (SST). This study investigates the upper ocean turbulent mixing in the Bay of Bengal from a category 5 tropical cyclone, Phailin, using both in-situ data and large-eddy simulations (LES). We show the presence of both diffusive convection and near-inertial shear in the upper ocean response. We are able to capture turbulent boundary layer dynamics and also quantify the associated turbulent mixing during the cyclone event for the first time. Our simulated mixed layer depth, SST, and other dynamical variables match the observed mooring data well. We estimate the mixing efficiency, η, which is defined as the energy sink ratio due to irreversible diapycnal mixing to the total mechanical energy sink. η was found to be close to 0.2 in the first half of the response, when the wind shear was picking up, while it increased to about 0.5 in the second half, as convection became dominant and the surface stress decreased. Our study further improves the mixing parametrization used by a large-scale ocean model to predict ocean response better during the cyclones.

Keywords: Turbulent Mixing, Cyclone, Convection

©2021. Japan Geoscience Union. All Right Reserved.

Near-inertial wave modulated turbulence in a Kuroshio anticyclonic eddy east of Japan

*Sebastian Essink[1], Ren-Chieh Lien[1], Eric Kunze[2]

1. UW/APL, 2. NWRA

Storm-generated near-inertial waves are a significant source for deep-ocean mixing. However, their energy pathways beyond wind generation and equatorward propagation as low modes are still elusive. Previous studies suggest that the bulk of inertial wind power is lost in the nearfield of storm forcing, but there is little observational evidence to confirm this.

Finescale horizontal velocity, temperature, salinity and microscale temperature profiles to 500-m depth were collected in the Kuroshio-Oyashio Confluence east of Japan during the storm-seasons of 2016 and 2017 with -augmented EM-APEX floats. Temporal sampling was at 1-h resolution during storms, sufficient to resolve near-inertial motions. Turbulent dissipation rates and diapycnal diffusivities K were inferred from microscale temperature-gradient spectra. Several floats were trapped near the velocity maximum of anticyclonic eddies. Mesoscale eddies are known to trap and amplify near-inertial waves and to modulate near-inertial wave distribution and dissipation.

Near-inertial energy-fluxes within the eddy are mostly inward and downward. Signatures of a critical layer, e.g., increasing vertical wavenumbers, shear, and turbulence are present at the depth where the eddy vorticity approaches the surface value, and strong vertical mean shears and vorticity-gradients occur. Turbulence is reduced by a factor of 10 above 180-m depth, despite elevated near-inertial energy, and enhanced between 200 and 255 m. Three mechanisms for the generation of enhanced turbulence are hypothesized: i) local and remotely forced near-inertial waves superimposing to create shear-unstable layers, ii) kinematic superposition of eddy and near-inertial shear that generates patches of turbulence at inertial periods, iii) a near-inertial critical layer due to dynamic wave/mean interaction. Ray tracing simulations will be performed to examine whether vertical vorticity gradients and/or Doppler shifting are responsible for the presence of a critical layer.

Keywords: Turbulence, Near-inertial waves, Mixing, Mesoscale eddy, Profiling float, Kuroshio

©2021. Japan Geoscience Union. All Right Reserved.

Upper ocean turbulence in the Icelandic Basin under strong forcing

*Harper L Simmons[1], Sophia Merrifield[2], Eric Skyllingstad[3], Louis St. Laurent[4]

1. University of Alaska Fairbanks, 2. Scripps Institution of Oceanography, University of California San Diego, 3. Oregon State University, 4. Applied Physics Laboratory, University of Washington

Concurrent near-surface measurements of turbulence and air-sea interactions can be difficult to obtain in the open ocean, and the challenges are exacerbated in high sea states. In May 2018 a field program in the Icelandic Basin made measurements of air-sea interactions, significant wave height, and upper ocean turbulence.

Winds were strong through most of the mission with a series of storms with significant wave heights from 5m to over 8m. The combination of nearby ship sampling, drifters and autonomous turbulence measurements from a Slocum Glider equipped with a Rockland Microrider turbulence package allowed comparisons of known shear and convective turbulence scalings to direct shear-probe estimates of turbulence in the upper 200m of the ocean. Mixed layers depths varied in space and time from 150 to 200m so that the measurements were predominantly in the upper ocean boundary layer.

Conventional near-surface dissipation scalings are based on competition between buoyancy and shear-driven production. Buoyancy forcing transitioned from cooling in the first week to warming however the turbulence was in a shear-dominated regime throughout the mission. Turbulence exceeded scaling predictions suggesting that the observations are in a strongly forced wind-wave range and highlight the need for improvements to boundary layer turbulence in extreme sea states.

Large-eddy simulations confirm that the addition of surface wave Stokes vortex forcing is essential for correctly modeling the measured mixed layer depth. Without the Stokes drift term, mixed layer depth was roughly 60% of the observations.

Keywords: Boundary layer turbulence, Large eddy simulation, Surface wave mixing

©2021. Japan Geoscience Union. All Right Reserved.

Observed spectral distortion of temperature microstructure

*Takashi Ijichi[1], Louis St. Laurent[2]

1. Department of Earth and Planetary Science, Graduate School of Science, The University of Tokyo, 2. Applied Physics Laboratory, University of Washington

Measurements of temperature microstructure from fast response thermistors are becoming more prevalent in the ocean-mixing community to estimate dissipation rates of both turbulent kinetic energy and thermal variance. This dissipation estimation method relies on the spectral shape of scalar microstructure prescribed in the high-Reynolds number turbulence theory. Using diverse datasets, we discuss some problematic cases where observed temperature spectra deviate from the corresponding theoretical one, leading to potential bias in dissipation estimates. From a technical viewpoint, the high-frequency thermistor response is suggested to depend on a vehicle flight condition. When temperature microstructure was measured on board autonomous underwater gliders, the thermistor response is found to be better corrected by a single-pole frequency function with a stronger vehicle speed dependence rather than the conventional double-pole function supported from free-falling vertical microstructure profiler data. From a physics viewpoint, the viscous-convective subrange is found to be greatly contaminated by thermohaline finestructure associated with salt finger convection. The Ozmidov wavenumber is suggested to be a threshold parameter that distinguishes turbulent microstructure from such finestructure contamination.

Keywords: temperature microstructure, finestructure contamination

©2021. Japan Geoscience Union. All Right Reserved.

2D Horizontal-Vertical Wavenumber Spectra of Density Finestructure from a towed CTD chain

*Anda Vladoiu[1], Ren-Chieh Lien[1], Eric L Kunze[2]

1. Applied Physics Laboratory, University of Washington, Seattle, WA, USA, 2. NorthWest Research Associates, Redmond, WA, USA

2D horizontal and vertical wavenumber spectra of isopycnal slope, vertical strain and isopycnal salinity-gradient were characterized on horizontal scales between 50 m and 250 km and on vertical scales between 2 and 48 m, using towed CTD chain measurements complemented by shipboard ADCP surveys and concurrent EM-APEX float profiles. 2D wavenumber spectra of isopycnal slope and vertical strain are similar to the Garrett-and-Munk internal-wave model spectrum at vertical wavenumbers below the 0.1-cpm rolloff. At vertical scales smaller than 10 m, the horizontal wavenumber spectrum of isopycnal slope has a +1/3 spectral slope and the vertical wavenumber spectrum of vertical strain has a -1 spectral slope, consistent with previous 1D measurements, numerical simulations and the predictions of anisotropic turbulence theory. Turbulent diapycnal diffusivities were estimated using a vertical strain-based finescale parameterization in the internal-wave subrange at vertical wavelengths of 10-48 m and horizontal wavelengths of 1-5 km, and using horizonal wavenumber spectra of isopycnal slope in the finescale subrange at vertical wavelengths of 2-10 m and horizontal wavelengths of 50-200 m. The two independent estimates from the internal-wave and finescale subranges show good agreement, suggesting that the energy cascade between weakly nonlinear internal waves and isotropic turbulence is connected by a distinct subrange between the rolloff and Ozmidov wavenumbers, consistent with anisotropic turbulence theory. At vertical wavenumbers below 0.1 cpm, horizontal wavenumber spectra for isopycnal salinity-gradient are approximately flat, analogous to most previous studies, while at vertical wavenumbers above 0.1 cpm, the spectra have slopes between +1/3 and +1, similar to passive tracer spectra in the isotropic turbulence subrange. Further investigation of dynamic variables might explain the disagreements between the observed spectra and theoretical predictions.

Keywords: 2D horizontal-vertical wavenumber spectra, isopycnal slope, vertical strain, isopycnal salinity-gradient, anisotropic turbulence, towed CTD chain -measured density finescale

©2021. Japan Geoscience Union. All Right Reserved.

[E] Oral | A (Atmospheric and Hydrospheric Sciences)：A-OS Ocean Sciences & Ocean Environment

Sat. Jun 5, 2021 1:45 PM - 3:15 PM JST | Sat. Jun 5, 2021 4:45 AM - 6:15 AM UTC | Ch.09 Zoom Room 09

[A-OS11] Ocean Mixing Frontiers

convener:Toshiyuki Hibiya(Department of Earth and Planetary Science, Graduate School of Science, University of Tokyo), Chairperson:Taira Nagai(Graduate School of Science, The University of Tokyo)

Ocean mixing plays crucial roles both in the open and coastal ocean, affecting key physical, biological and chemical processes. Mixing in the upper ocean influences the sea surface temperature and hence air-sea interactions which impact global climate change, while mixing in the deep ocean maintains abyssal stratification of the world's oceans and impacts the global overturning circulation. In coastal oceans, mixing modulates the transport and dispersal of dissolved and suspended materials including pollutants and nutrients. Planktonic ecosystems are controlled by nutrient pumping associated with ocean mixing.

In this session, we encourage contributors to present recent findings of ocean mixing obtained through field observations as well as theoretical, numerical, and laboratory studies. Through the related detailed discussions, we would like to confirm how far has our understanding of the ocean mixing processes advanced, defining the new frontier of ocean mixing research to be tackled in the next decade. The session encompasses a wide variety of aspects of coastal and open ocean mixing processes; within the water column from the surface through the interior to the near boundary benthic mixing, including the roles of mixing in the biological processes and productivity of the ocean. Observational, theoretical, and numerical modeling studies are all encouraged.

1:45 PM - 2:00 PM JST | 4:45 AM - 5:00 AM UTC

[AOS11-13] Internal tide radiation and intensified mixing in the Philippine Sea

*Zhenhua Xu[1], Jia You[1], Yang Wang[1], Qun Li[1], Toshiyuki Hibiya[2], Robin Robertson[3] (1.Institute of Oceanology, CAS, 2.Department of Earth and Planetary Science, Graduate School of Science, The University of Tokyo, Japan, 3.Xiamen University Malaysia, Malaysia)

2:00 PM - 2:15 PM JST | 5:00 AM - 5:15 AM UTC

[AOS11-14] Tidal and Wind Mixing in the Arafura Sea

*Robin Robertson[1] (1.Xiamen University Malaysia)

2:15 PM - 2:30 PM JST | 5:15 AM - 5:30 AM UTC

[AOS11-15] Verifying the parameterization of vertical eddy viscosity and diffusivity in the bottom boundary layer

*Takahiro Endoh[1], Takuya Hirooka[1] (1.RIAM Research Institute for Applied Mechanics)

2:30 PM - 2:45 PM JST | 5:30 AM - 5:45 AM UTC

[AOS11-16] The role of double-diffusive convection in basal melting and mixed layer under Antarctic ice shelves

*Bishakhdatta Gayen[1,2], Madi Rosevear [3,5], Ben Galton-Fenzi[4] (1.The University of Melbourne, 2. Indian Institute of Science, 3.University of Tasmania , 4.Australian Antarctic Division, 5.University of Western Australia)

2:45 PM - 3:00 PM JST | 5:45 AM - 6:00 AM UTC

[AOS11-17] The Kuroshio nutrient stream, where the diapycnal mixing matters

*Takeyoshi Nagai[1], Gloria Silvana Duran Gomez[1] (1.Department of Ocean Sciences, Tokyo University of Marine Science and Technology)

3:00 PM - 3:15 PM JST | 6:00 AM - 6:15 AM UTC

[AOS11-18] Turbulent mixing and its contribution to oxygen flux in the northwestern boundary current region of the Japan/East Sea, April-October 2015

*Dmitry Stepanov[1], Alexander Ostrovskii[2], Dmitry Kaplunenko[1], Jae-Hun Park[3], Young-Gyu Park[4], Pavel Tishchenko[1] (1.Pacific Oceanological Institute, Russia, 2.Shirshov Institute of Oceanology, Russia, 3.Department of Ocean Sciences, Inha University, Korea, 4.Korea Institute of Ocean Science and Technology, Korea)

Internal tide radiation and intensified mixing in the Philippine Sea

*Zhenhua Xu[1], Jia You[1], Yang Wang[1], Qun Li[1], Toshiyuki Hibiya[2], Robin Robertson[3]

1. Institute of Oceanology, CAS, 2. Department of Earth and Planetary Science, Graduate School of Science, The University of Tokyo, Japan, 3. Xiamen University Malaysia, Malaysia

The spatially inhomogeneous and seasonally variable diapycnal diffusivities in the upper Philippine Sea were estimated from ARGO float data using a strain-based finescale parameterization. We found that internal tides are the main driving process for diapycnal diffusivities. Based on a coordinated analysis of multi-source data, we provide evidence that the mesoscale environment in the Philippine Sea played a significant role in regulating the intensity and shaping the spatial inhomogeneity of the internal tidal mixing. The combined and relative contributions of various factors to the long-range radiation and dissipation map of internal tides were also clarified.

Keywords: Internal tides, Turbulent mixing

©2021. Japan Geoscience Union. All Right Reserved.

Tidal and Wind Mixing in the Arafura Sea

*Robin Robertson[1]

1. Xiamen University Malaysia

Time series of shipboard observations in the southern Arafura Sea near the Tiwi Islands indicated that the water column dynamics differed between the east and west sides of the islands. On the west side, the water column, defined as temperature, salinity, and velocity, was barotropic and tidal advection dominated. On the east side, the water column was baroclinic and internal tides were present along with tidal advection. These conditions affected the distribution of the turbidity and fluorescence in the water column with the fluorescence distributed throughout the water column on the western side, but concentrated in the lower layer on the eastern side. Likewise, the influence of the daily solar radiation cycle reached the bottom on the western side, but was limited to the upper layer above the thermocline on the eastern side. The fluorescence peaks also differed between the east and west sides, with the eastern side dominated by the semidiurnal tides and the western side by the daily solar cycle. Also on the eastern side, fluorescence was limited to the lower layer, while on the western side, it encompassed the entire water column at times and peaked below the warmer, higher oxygen water generated by solar radiation. These dynamics have distinct implications for biological productivity and also may affect a proposed tidal power system in the region.

Keywords: wind, Tides, Arafura Sea

©2021. Japan Geoscience Union. All Right Reserved.

Verifying the parameterization of vertical eddy viscosity and diffusivity in the bottom boundary layer

*Takahiro Endoh[1], Takuya Hirooka[1]

1. RIAM Research Institute for Applied Mechanics

By estimating the terms of the steady-state turbulent kinetic energy (TKE) budget from microstructure data obtained over the continental shelf of the East China Sea, we verify a recently proposed parameterization of vertical eddy viscosity and diffusivity in the bottom boundary layer (BBL), where mixing efficiency is expressed as a function of the gradient Richardson number (Ri). The dissipation term (ε) is calculated from the micro-scale vertical shear measured with a freely-falling microstructure profiler, whereas the production term (P) is calculated from Reynolds stress and the fine-scale vertical shear measured with an acoustic Doppler current profiler (ADCP) mounted on the seabed. If the proportional relationship between the flux Richardson number (Rf) and Ri holds, which is assumed in the proposed BBL parameterization, the buoyancy flux term (B) as well as the transport term (T) can be estimated from P, ε, and Ri. Therefore, we use the iterative procedure to find a constant of proportionality which is close to a slope of the regression line for Rf (=-B/(P+T)) and Ri. The resulting constant is within the range suggested by laboratory experiments, large eddy simulations, and observations of the atmospheric boundary layer. The parameterized eddy viscosity agrees remarkably well with the observed one, whereas the parameterization underestimates the observed eddy diffusivity by a factor of two to three presumably because of the uncertainty involved in the estimated values of B.

Keywords: Bottom boundary layer, Vertical eddy viscosity, Vertical eddy diffusivity, Flux Richardson number, Gradient Richardson number, Turbulent kinetic energy budget

©2021. Japan Geoscience Union. All Right Reserved.

The role of double-diffusive convection in basal melting and mixed layer under Antarctic ice shelves

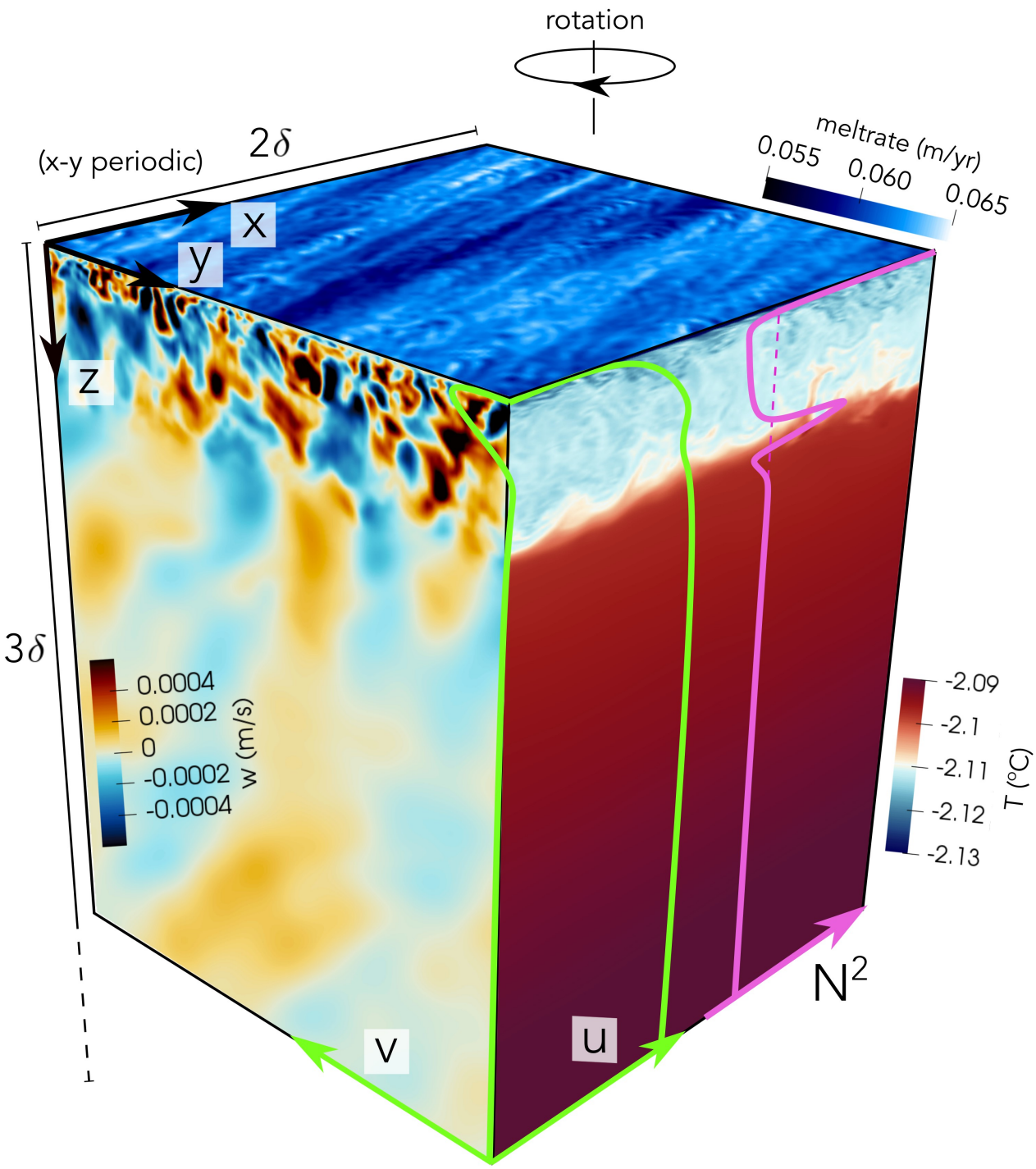
*Bishakhdatta Gayen[1,2], Madi Rosevear [3,5], Ben Galton-Fenzi[4]

1. The University of Melbourne, 2. Indian Institute of Science, 3. University of Tasmania , 4. Australian Antarctic Division, 5. University of Western Australia

The Antarctic Ice Sheet, which comprises the enormous ice volume on our planet, is losing mass at an alarming rate, contributing to a considerable global sea-level rise in the future. Ocean-driven melting is the largest cause of ice mass loss from the Antarctic continent. Therefore, accurate representation of ocean-driven melting is crucial for future sea-level predictions; however, the fine-scale ice shelf-ocean boundary layer (ISOBL) processes that control ocean melt rates are not well understood. Ocean-climate models cannot resolve the ISOBL and rely on parameterizations to predict melting. In this study, we use cutting-edge Large Eddy Simulation to examine the geostrophic boundary layer beneath an ice shelf for the first time. A small-scale mixing process (Diffusive Convection) is an emergent property of our simulations. It explains the water column structure and low melt rates observed beneath the Ross Ice Shelf under similar conditions. We show that Diffusive Convection is the primary control of basal melting and oceanic mixed layer formation and persists despite shear-generated turbulence. Thus, our finding has significant potential implications for ice-sheet models that rely on ocean melt rate parameterizations to predict ice sheet stability and evolution.

Keywords: Diffusive-convection, ocean interactions, large-eddy simulation, thermohaline staircases

©2021. Japan Geoscience Union. All Right Reserved.



©2021. Japan Geoscience Union. All Right Reserved.

The Kuroshio nutrient stream, where the diapycnal mixing matters

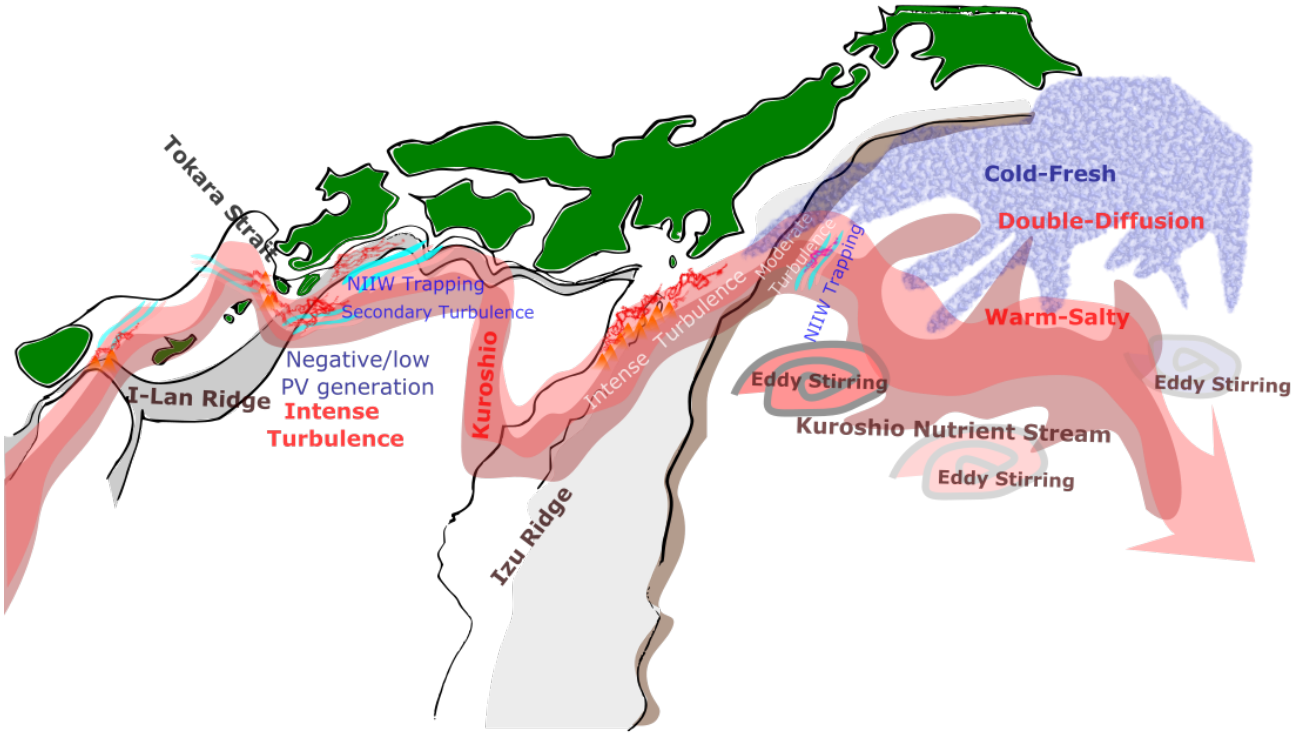
*Takeyoshi Nagai[1], Gloria Silvana Duran Gomez[1]

1. Department of Ocean Sciences, Tokyo University of Marine Science and Technology

While the Kuroshio and the Gulf Stream carry a large amount of nutrients in dark subsurface layers and supply them to the downstream subpolar regions, it has remained unclear how the elevated nutrient concentrations along these nutrient streams are formed and/or maintained. This is particularly important as these positive nutrient anomalies on the relatively less dense water along the nutrient streams can be injected more easily to the euphotic zone. In the North Pacific, the regions of anomalously high nitrate concentrations along the Kuroshio Extension coincide with one of the major net CO_2 sinks of the world oceans. Although the elevated nutrient concentrations on the density surface were attributed to diapycnal nutrient flux along the nutrient stream in the earlier studies, recent studies concluded that the horizontal advection carries this anomaly from the upstream tropical regions and that diapycnal mixing can be negligible in the Gulf Stream. However, because the Kuroshio flows over rough topography more frequently than the Gulf Stream, it still remains elusive whether the diapycnal mixing is really not playing a role at all to form the high nutrient concentration layer along the Kuroshio nutrient stream.
In this study, using a numerical model of the Kuroshio nutrient stream, and direct microscale turbulence measurements, the importance of the diapycnal mixing in the Kuroshio is examined.
The eddy flux analyses on the density surface in the simulation suggest that the eddies stir and dilute the elevated nitrate concentration, resulting in the decreasing trend of nitrate along the nutrient stream with the increasing trends on the both sides of the stream.
A series of the tow-yo microstructure observations in the Kuroshio flowing over the rough topography shows that the large nitrate diffusive diapycnal flux of 1-10 mmol $m^{-2}day^{-1}$ are frequently observed in the Tokara Strait, the Hyuganada Sea, and over the Izu Ridge. The time scale required for the diapycnal nitrate flux at 1 mmol $m^{-2}day^{-1}$ to generate the observed positive anomaly of nitrate concentrations, which is estimated to be 26 Gmol over 5000 km, is found to be as short as 50 days, assuming the area of nitrate injection of 1000 km^2. The observations suggest that the nitrate injection at 1 mmol $m^{-2}day^{-1}$ over the area of 1000 km^2 is plausible if the all the contributions in these mixing hot-spots along the Kuroshio are integrated.
This time scale of 50 days is comparable to or slightly less than the advection time scale, and therefore, unlike the Gulf Stream, the diapycnal turbulent diffusive flux is unlikely negligible in the Kuroshio nutrient stream. Furthermore, in the Kuroshio Extension, rich high vertical wavenumber thermohaline interleaving structures are found to induce a large double-diffusive nitrate flux at 1-10 mmol mmol $m^{-2}day^{-1}$ in the pycnostad of sigma_theta=26-27 kgm^{-3}. Because these relatively dense layers in this region are not outcropping even during winter, whether this nitrate diffused upward by double-diffusion can be supplied to the euphotic zone depends on further stirring processes such as the northward and upward eddy fluxes. In addition, although the detailed mechanisms still remain unclear, the Argo float data analyses show that these double-diffusive flux in the dense layers modulates interannually.

Keywords: Kuroshio, Nutrient sream, Diapycnal mixing

©2021. Japan Geoscience Union. All Right Reserved.



©2021. Japan Geoscience Union. All Right Reserved.

Turbulent mixing and its contribution to oxygen flux in the northwestern boundary current region of the Japan/East Sea, April-October 2015

*Dmitry Stepanov[1], Alexander Ostrovskii[2], Dmitry Kaplunenko[1], Jae-Hun Park[3], Young-Gyu Park[4], Pavel Tishchenko[1]

1. Pacific Oceanological Institute, Russia, 2. Shirshov Institute of Oceanology, Russia, 3. Department of Ocean Sciences, Inha University, Korea, 4. Korea Institute of Ocean Science and Technology, Korea

The Japan/East Sea is well ventilated and is the most oxygen-rich region in the Pacific. However, quantitative estimates of the turbulent fluxes are missing due to a lack of observational data. To assess turbulent mixing, we employ data from the moored profiler Aqualog survey of April - October 2015 near the northwestern boundary of this region. The survey allowed observation of collocated depth profiles of conductivity, temperature, ocean current, and dissolved oxygen 8 times per day. Based on the finescale parameterization framework, the dissipation rate, the eddy diffusivity, and the diapycnal fluxes of heat, salt and oxygen are estimated in the depth range from 130 to 350 m throughout the profiler deployment period.
The survey average diffusivity increased with depth from 0.5×10^{-5} to 4.0×10^{-5} m^2 s^{-1}. The month-to-month variability in the mixing is presented. It was shown that the turbulent mixing undergoes intraseasonal variability. Early in May 2015, a transition in mixing occurred from the winter regime with upward turbulent fluxes of both heat and salt to the summer regime with the downward mixing of heat. The turbulent mixing was elevated in June when large anticyclonic eddies passed the profiler mooring. The probability distributions of the ratios of the turbulent heat and oxygen fluxes to the observed local changes in heat and oxygen were rather stable, particularly in the warm season. The application of the MX Toolbox to the profiler mooring data yields an estimate of the downward oxygen flux of roughly 8.6×10^{3} μ mol m^{-2} $month^{-1}$.

The data analysis was partly performed in the framework of the assignment of FASO Russia (theme 0149-2019-0011) and supported in part by RFBR grant 19-05-00459. The contribution of Dmitry Stepanov in modifying the Mixing Oceanographic Toolbox was supported by RFBR grant 20-05-00083.

Keywords: diapycnal mixing, Japan/East Sea, fine-scale parameterization, diapycnal fluxes of heat and salt, downward oxygen flux

©2021. Japan Geoscience Union. All Right Reserved.

[E] Poster | A (Atmospheric and Hydrospheric Sciences)：A-OS Ocean Sciences & Ocean Environment

Sat. Jun 5, 2021 5:15 PM - 6:30 PM JST | Sat. Jun 5, 2021 8:15 AM - 9:30 AM UTC | Ch.05_1

[A-OS11] Ocean Mixing Frontiers

convener:Toshiyuki Hibiya(Department of Earth and Planetary Science, Graduate School of Science, University of Tokyo)

Ocean mixing plays crucial roles both in the open and coastal ocean, affecting key physical, biological and chemical processes. Mixing in the upper ocean influences the sea surface temperature and hence air-sea interactions which impact global climate change, while mixing in the deep ocean maintains abyssal stratification of the world's oceans and impacts the global overturning circulation. In coastal oceans, mixing modulates the transport and dispersal of dissolved and suspended materials including pollutants and nutrients. Planktonic ecosystems are controlled by nutrient pumping associated with ocean mixing.

In this session, we encourage contributors to present recent findings of ocean mixing obtained through field observations as well as theoretical, numerical, and laboratory studies. Through the related detailed discussions, we would like to confirm how far has our understanding of the ocean mixing processes advanced, defining the new frontier of ocean mixing research to be tackled in the next decade. The session encompasses a wide variety of aspects of coastal and open ocean mixing processes; within the water column from the surface through the interior to the near boundary benthic mixing, including the roles of mixing in the biological processes and productivity of the ocean. Observational, theoretical, and numerical modeling studies are all encouraged.

[AOS11-P01] Sensitivity of the ocean state estimation to the vertical distribution of tidally induced far-field mixing

*Satoshi Osafune[1], Shinya Kouketsu[1], Toshimasa Doi[1], Nozomi Sugiura[1], Shuhei Masuda[1] (1.Japan Agency for Marine-Earth Science and Technology)

[AOS11-P02] Tracer distribution produced by an optimized physical field with an improved vertical mixing

*Toshimasa Doi[1], Shinya Kouketsu[1], Satoshi Osafune[1], Shuhei Masuda[1], Nozomi Sugiura[1] (1.Japan Agency for Marine-Earth Science and Technology)

[AOS11-P03] Lagrangian Dispersion and Mixing in the Open-ocean convection

*Ankit Bhadouriya[1,2], Bishakhdatta Gayen[1,3] (1.The University of Melbourne, Australia, 2.Indian Institute of Technology Kanpur, India, 3.Indian Institute of Science, India)

[AOS11-P04] Assessing the role of deep ocean mixing on carbon and nutrients cycles using an Earth System Model

*Michio Watanabe[1], Akitomo Yamamoto[1], Tomohiro Hajima[1], Hiroaki Tatebe[1] (1.Research Center for Environmental Modeling and Application, Japan Agency for Marine-Earth Science and Technology (JAMSTEC))

[AOS11-P05] Performance of microstructure measurements using a deep float with a fast-response thermistor

*Shuo Zhai[1], Ichiro Yasuda[1] (1.Atmosphere and Ocean Research Institute, The University of Tokyo)

[AOS11-P06] Seasonal variations in salinity of the North Pacific Intermediate Water and vertical mixing intensity over the Okinawa Trough

*Hirohiko Nakamura[1], Ryuichiro Inoue[2], Ayako Nishina[1], Toshiya NAKANO[3] (1.Kagoshima University, Faculy of Fisheries, 2.Japan Agency for Marine-Earth Science and Technology, 3.Nagasaki Meteorological Office)

[AOS11-P07] **Elevated nutrient supply caused by the approaching Kuroshio to the southern coast of Japan**

*Gloria Silvana Duran Gomez[1], Takeyoshi Nagai[2] (1.Graduate School of Tokyo University of Marine Science and Technology, 2.Tokyo University of Marine Science and Technology)

[AOS11-P08] Direct estimates of turbulent mixing in the Indonesian Archipelago and its role in the transformation of the ITF waters

*Taira Nagai[1], Toshiyuki Hibiya[1] (1.Graduate School of Science, The University of Tokyo)

[AOS11-P09] **Double diffusion in the Arabian Sea during winter and spring**

*Ashin Kuriakose[1,2], Girishkumar M S -[1], Jofia Joseph -[1], Eric D'Asaro -[3], Sureshkumar N -[1], Sherin V R -[1], Murali B -[1], Thangaprakash V P -[1], E Pattabhi Ram Rao[1], S. S. C. Shenoi (1.Indian National Centre for Ocean Information Services, 2.School of Ocean Science and Technology, Kerala University of Fisheries and Ocean Studies, 3.Applied Physics Laboratory and School of Oceanography, University of Washington, Seattle, Washington, USA)

[AOS11-P10] On widespread intensified thermocline turbulence in the seasonally stratified Yellow Sea

*Wei Yang[1] (1.Tianjin University)

[AOS11-P11] Observation of energy transfer from traveling typhoons to turbulent mixing in the ocean

*Aiqi Zhang[1], Ichiro Yasuda[1], Daigo Yanagimoto[1], Shinzou Fujio[1], Yusuke Sasaki[1] (1.the University of Tokyo)

[AOS11-P12] Can tidal forcing alone generate a GM-like internal wave spectrum?

*Zhiwu Chen[1], Shaomin Chen[1], Zhiyu Liu[2], Jiexin Xu[1], Jieshuo Xie[1], Yinghui He[1], Shuqun Cai[1] (1.South China Sea Institute of Oceanology, Chinese Academy of Sciences, 2.Department of Physical Oceanography, College of Ocean and Earth Sciences, Xiamen University)

Sensitivity of the ocean state estimation to the vertical distribution of tidally induced far-field mixing

*Satoshi Osafune[1], Shinya Kouketsu[1], Toshimasa Doi[1], Nozomi Sugiura[1], Shuhei Masuda[1]

1. Japan Agency for Marine-Earth Science and Technology

Vertical mixing plays an important role in determining the large-scale ocean circulation including the meridional overturning and the distribution of water properties. The breaking of internal tide is a major source of interior vertical mixing below the surface mixed layer. Recent numerical studies have shown the importance of incorporating tidally induced far-field mixing in addition to the near-field mixing. In our previous study under the OMIX project, we conducted a linear optimization experiment to reproduce the climatological distribution of water properties with an ocean general circulation model using tidally induced near- and far-field mixing schemes with an assumption that diffusivity is vertically constant for far-field mixing. The optimized model performed reasonably well in reproducing the deep-water properties of the Pacific Ocean. However, the reproducibility of water mass distribution is degraded in some places, especially in the sub-surface-intermediate layers, when compared with the optimized state in the earlier version of our model using semi-empirical interior mixing schemes. This shortcoming may be overcome by improving model interior mixing. Our new model uses the far-field mixing scheme only related to the wave-wave interactions, but the far-field mixing is caused through various mechanisms, on which the vertical structure of diffusivity depends. In this study, we conducted numerical experiments using our new model but with different vertical distribution function for the far-field mixing on the basis of a previous semi-empirical scheme. We show the incorporation of a vertical structure into the far-field mixing representation can possibly resolve the upper layer issues in our state estimation. It can be a clue to uncover nature of vertical mixing in the real ocean. We will discuss the effectiveness of the proposed implementation in our experiments, referring the recent vertical mixing schemes suggested in the theoretical studies.

Keywords: tide, vertical mixing, thermohaline circulation

©2021. Japan Geoscience Union. All Right Reserved.

Tracer distribution produced by an optimized physical field with an improved vertical mixing

*Toshimasa Doi[1], Shinya Kouketsu[1], Satoshi Osafune[1], Shuhei Masuda[1], Nozomi Sugiura[1]

1. Japan Agency for Marine-Earth Science and Technology

Revealing the global oceanic tracer distribution is vital for climate research. To investigate how the circulation reproduced with the spatial changes in vertical mixing affects the biogeochemical cycles, in this study, the numerical experiment of advection/diffusion for chlorofluorocarbon (CFC) was conducted. An effect of spatial changes in vertical mixing was considered to an ocean general circulation model with near- and far-field vertical mixing schemes. The improved model was optimized with a four-dimensional variational data assimilation system, so that the temperature and salinity fields were consistent to a certain extent with the observations. It is known that the CFC is one of the anthropogenic substances, has no sink in the interior of the ocean, and the diffusion strongly influence on the transient behavior of CFC after being absorbed from the sea surface into the ocean. The time series of atmospheric CFCs concentration were given as the boundary condition of the model, and we show that transports by advection and diffusion of the absorbed CFCs in the ocean were calculated on the reanalysis circulation. Furthermore, we will discuss the effects of the spatial changes in the vertical field by comparing the result with the one with different vertical mixing schemes.

©2021. Japan Geoscience Union. All Right Reserved.

Lagrangian Dispersion and Mixing in the Open-ocean convection

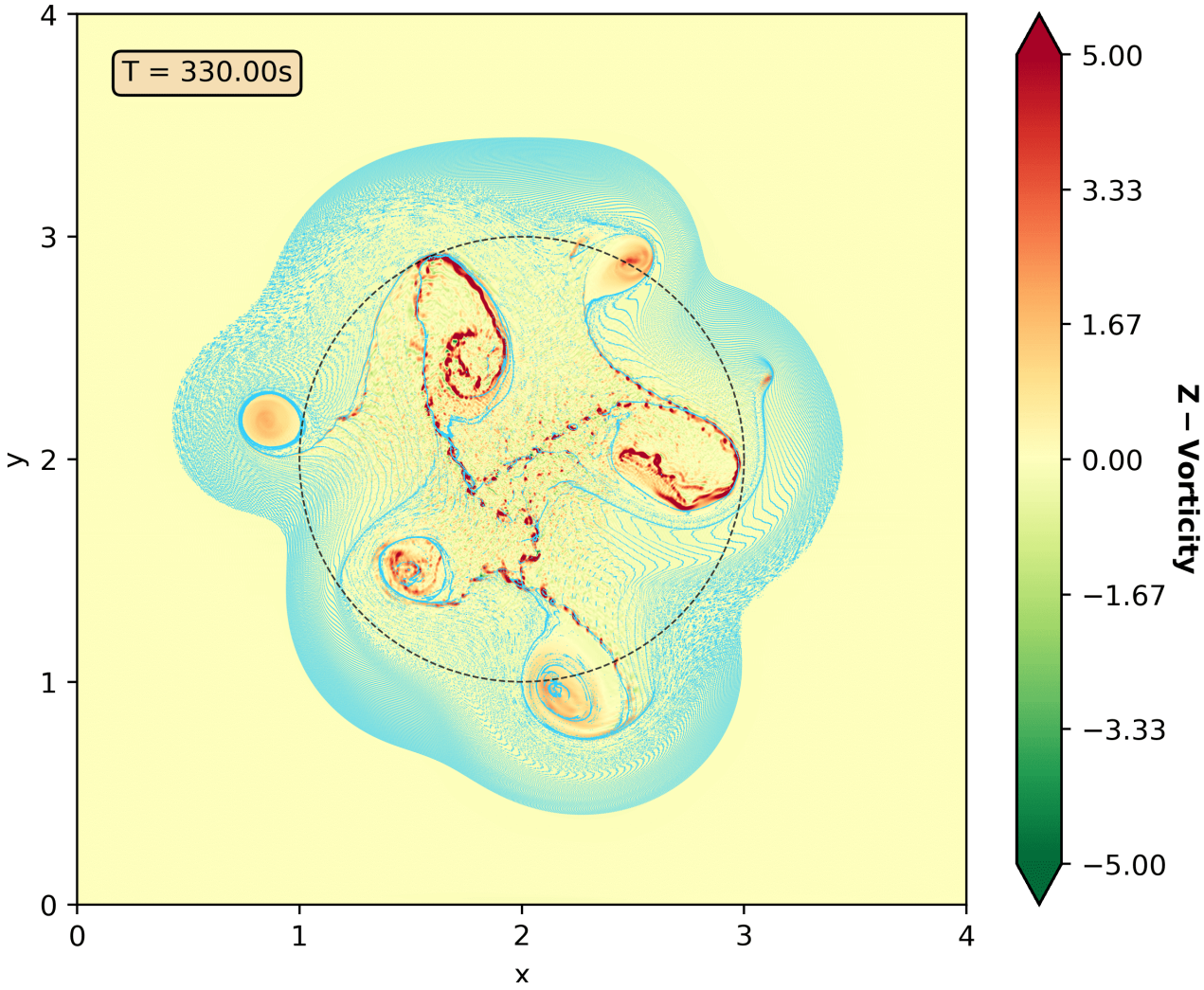
*Ankit Bhadouriya[1,2], Bishakhdatta Gayen[1,3]

1. The University of Melbourne, Australia, 2. Indian Institute of Technology Kanpur, India, 3. Indian Institute of Science, India

Open ocean convection (OOC) connects the surface ocean to the abyssal in high latitude regions, regulating heat, global marine biological activity, and carbon uptake. It creates destabilizing stratification by intense heat loss to the atmosphere, which results in turbulent convection and the mixing of surface water to greater depths. Large amounts of organic matter, including particulate and dissolved carbon, are often injected into the deep ocean by sinking dense water through convection. Therefore, convection has a significant pathway for the export of organic matter and fields of passive chemical tracers. However, the importance of the deep convection phenomenon on biogenic particle transport remains uncertain. Ocean climate models are limited to resolve all the spatial and temporal scales generated within the mixed layer during the development of convective plumes, which necessitated a study of OOC through turbulence resolving simulations. The dispersion and mixing of particles during convection events is thus required to assess the accumulation, mixing, redistribution of it and, in general, to understand better particulate or biogeological cycling. A three-dimensional velocity field computed from well-resolved DNS is used to make trajectory analysis of Lagrangian particles. This work aims to evaluate the dispersion and mixing of tracer and dynamic properties associated with Lagrangian particles to assess the transport and mixing mechanism.

Keywords: Deep convection, Lagrangian particles, Dispersion, Mixed layer

©2021. Japan Geoscience Union. All Right Reserved.



©2021. Japan Geoscience Union. All Right Reserved.

Assessing the role of deep ocean mixing on carbon and nutrients cycles using an Earth System Model

*Michio Watanabe[1], Akitomo Yamamoto[1], Tomohiro Hajima[1], Hiroaki Tatebe[1]

1. Research Center for Environmental Modeling and Application, Japan Agency for Marine-Earth Science and Technology (JAMSTEC)

Earth System Models (ESMs) that incorporate biogeochemical processes into General Circulation Models (GCMs) have been developed to project future climate. In the Earth system, the ocean redistributes heat, anthropogenic carbon dioxide absorbed from the atmosphere, and nutrients that control primary production, and the meridional circulation in the ocean plays a major role in this redistribution. The pattern and strength of this circulation is strongly controlled by microscale turbulent mixing due to tide-induced internal wave breaking in the deep ocean. However, the distribution of the intensity of deep-ocean mixing is not clear, and the effects of deep-ocean mixing on the global carbon and nutrient cycles have not been well discussed. In this study, two implementations of deep ocean mixing were used to execute an ESM under pre-industrial forcing and under increasing atmospheric CO2 concentration by 1% per year. The results will be discussed in terms of how the distribution of the intensity of deep ocean mixing affects the distribution of carbon and nutrients in the ocean.

Keywords: Deep ocean mixing, Earth System Model, Carbon cycle, Nutrient cycle

©2021. Japan Geoscience Union. All Right Reserved.

Performance of microstructure measurements using a deep float with a fast-response thermistor

*Shuo Zhai[1], Ichiro Yasuda[1]

1. Atmosphere and Ocean Research Institute, The University of Tokyo

Turbulence measurements are required to quantify diapycnal flux of heat and substances which controls general ocean circulation, nutrients supply and marine ecosystem. Whereas, since turbulence measurements are still scarce especially in the deep ocean or near the bottom, autonomous microstructure observations are strongly desired. In the present study, as a step to realize autonomous microstructure observations using profiling deep floats, vibration impacts by active motors to adjust buoyancy on the fast-response thermistor (FP07) measurements were examined by using field data obtained in the western North Pacific in the vicinity of Japan. Although the FP07 measurements are much less sensitive to instrument vibration than velocity shear measurements, overestimations were evident when the float ascending speed was small and the motor vibration was active for acceleration, and those were proportional to and to the magnitude of the instrument acceleration. These are explained by the vibrational noise generated by high-frequency motion of the instrument, and the noise was amplified in the slow speed as a function of . By subtracting the vibrational noise estimated from the measured acceleration, corrected turbulence data in abyssal ocean or near ocean bottom can be obtained. The present study is the first study which discusses the impact of vibration on the turbulence estimation using FP07, and contributes to improving deep ocean turbulence measurements by proposing the effective methods which can be applied to Argo floats, gliders, CTDs and moorings.

Keywords: turbulence, deep float

©2021. Japan Geoscience Union. All Right Reserved.

Seasonal variations in salinity of the North Pacific Intermediate Water and vertical mixing intensity over the Okinawa Trough

*Hirohiko Nakamura[1], Ryuichiro Inoue[2], Ayako Nishina[1], Toshiya NAKANO[3]

1. Kagoshima University, Faculy of Fisheries, 2. Japan Agency for Marine-Earth Science and Technology, 3. Nagasaki Meteorological Office

Seasonal variations in vertical mixing intensity in the intermediate layer of the northern Okinawa Trough were deduced using the seasonal variations in salinity in the North Pacific Intermediate Water (NPIW) using two distinct datasets: the World Ocean Atlas 2013 and historical conductivity, temperature, and depth data in the Okinawa Trough. Water mass analysis of the NPIW with a simple advection model showed that the vertical mixing intensity in the intermediate layer is enhanced in the winter at a rate of 20%–50% of the annual mean amplitude value. To determine the driving force behind the seasonal variations in vertical mixing, we examined moored current-meter data in the northern Okinawa Trough during 2004–2011 and showed that the near-inertial internal wave energy in the intermediate layer was enhanced around January beneath the Kuroshio on the continental slope; this was due to strong southwestward flows associated with deep cyclonic eddies developing in the winter. We used density and velocity data from a realistic high-resolution ocean general circulation model simulation to hypothesize that the large-amplitude Kuroshio meander and associated deep cyclonic eddies in the winter generate near-inertial internal waves through centrifugal/inertial instability in the area of negative potential vorticity that appears not only beneath the Kuroshio near the western slope but also near the eastern slope of the trough. In addition, the symmetric instability along the offshore Kuroshio front and the wind energy input in the winter are suggested as possible sources of winter-enhanced near-inertial internal wave energy in the intermediate layer.

Keywords: Seasonal variation, Vertical mixing, North Pacific Intermediate Water, Kuroshio, Near-inertial internal wave

©2021. Japan Geoscience Union. All Right Reserved.

Elevated nutrient supply caused by the approaching Kuroshio to the southern coast of Japan

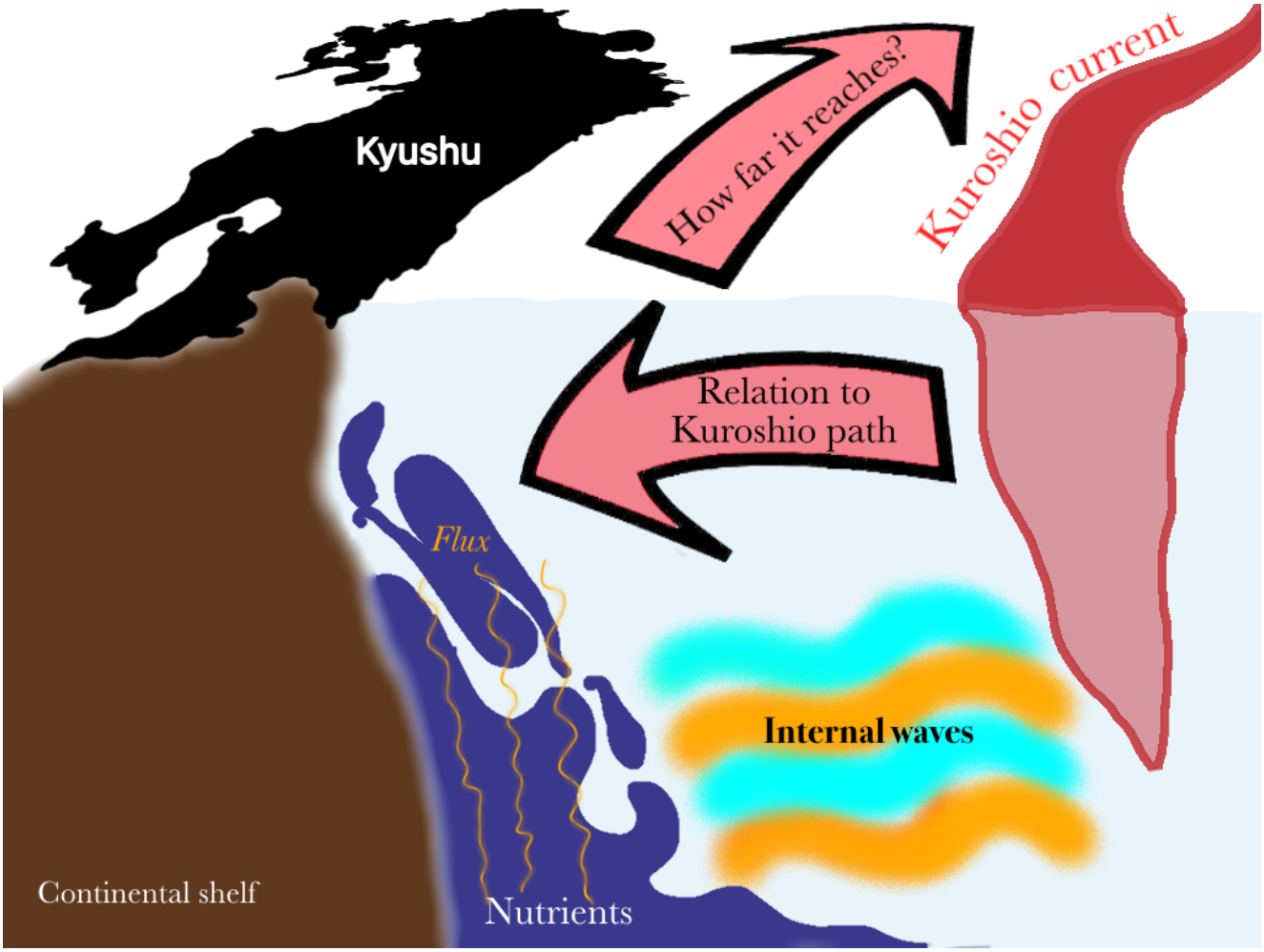
*Gloria Silvana Duran Gomez[1], Takeyoshi Nagai[2]

1. Graduate School of Tokyo University of Marine Science and Technology, 2. Tokyo University of Marine Science and Technology

Although the Kuroshio Current has been known for being nutrient poor in its upper layers, it supports a great fishery industry in Japan due to the great biodiversity it presents. Previous studies reported that the Kuroshio carries a large amount of nutrients in dark subsurface layers, but the mechanisms of how these nutrients from dark subsurface layers are brought to the sunlit layers are still unclear. In a previous observational study by the authors, it is showed that the Kuroshio flowing on the continental shelf can induce very strong turbulent dissipation rates O(10^{-7} W kg^{-1}) associated with trapped near-inertial internal waves in this region, leading to the generation of a large diffusive nitrate flux of >O(1 mmol N m^{-2} day^{-1}). Nevertheless, since this previous study was conducted for just one transect survey, questions remain of how long this enhanced turbulent diffusive nitrate flux extends further to the downstream and how the Kuroshio path modulations can influence on this nutrient injection.
In this study, using a high-resolution nested simulation coupled with a N_2PZD_2 ecosystem model, observed features were reproduced, showing that when the model Kuroshio flows closer to the coast, it hits the small bump in the upstream region of the Hyuganada Sea producing negative potential vorticity. At the same time, it is observed that near-inertial internal waves are trapped in the streak of lowered lowest internal wave frequencies, producing the strong turbulence and vertical mixing. As a result, the elevated mixing diffuses up the nitrate from dark subsurface layers to sunlit shallow layers. The results of this study can improve our understanding of the role of the Kuroshio in providing nutrients and enhancing biological productions including fish abundances, providing a better predicting of the ecosystem responses to the Kuroshio path modulations.

Keywords: Nutrient injection, Hyuganada Sea

©2021. Japan Geoscience Union. All Right Reserved.



©2021. Japan Geoscience Union. All Right Reserved.

Direct estimates of turbulent mixing in the Indonesian Archipelago and its role in the transformation of the ITF waters

*Taira Nagai[1], Toshiyuki Hibiya[1]

1. Graduate School of Science, The University of Tokyo

Turbulent mixing enhanced in the Indonesian Archipelago (IA) is thought to influence the coupled ocean-climate system through sea surface temperature cooling and water-mass transformation. The present study describes the first extensive microstructure measurements conducted in the IA in 2019. A total of 120 profiles of turbulent energy dissipation rates showed that strong turbulent mixing was extremely localized in a few narrow tidal straits, where large density overturns and high vertical diffusivity associated with downslope jets were found. Far away from mixing hotspots, in contrast, observed vertical diffusivities were similar to typical open ocean values. Microstructure measurements together with a high-resolution numerical simulation suggest that significant water-mass transformation occurred within very short distances, O(10 km), in these narrow tidal straits through not only vertical mixing but also horizontal mixing enhanced by submesoscale topographic eddies.

Keywords: Direct microstructure measurements, Indonesian Archipelago, Water-mass transformation

©2021. Japan Geoscience Union. All Right Reserved.

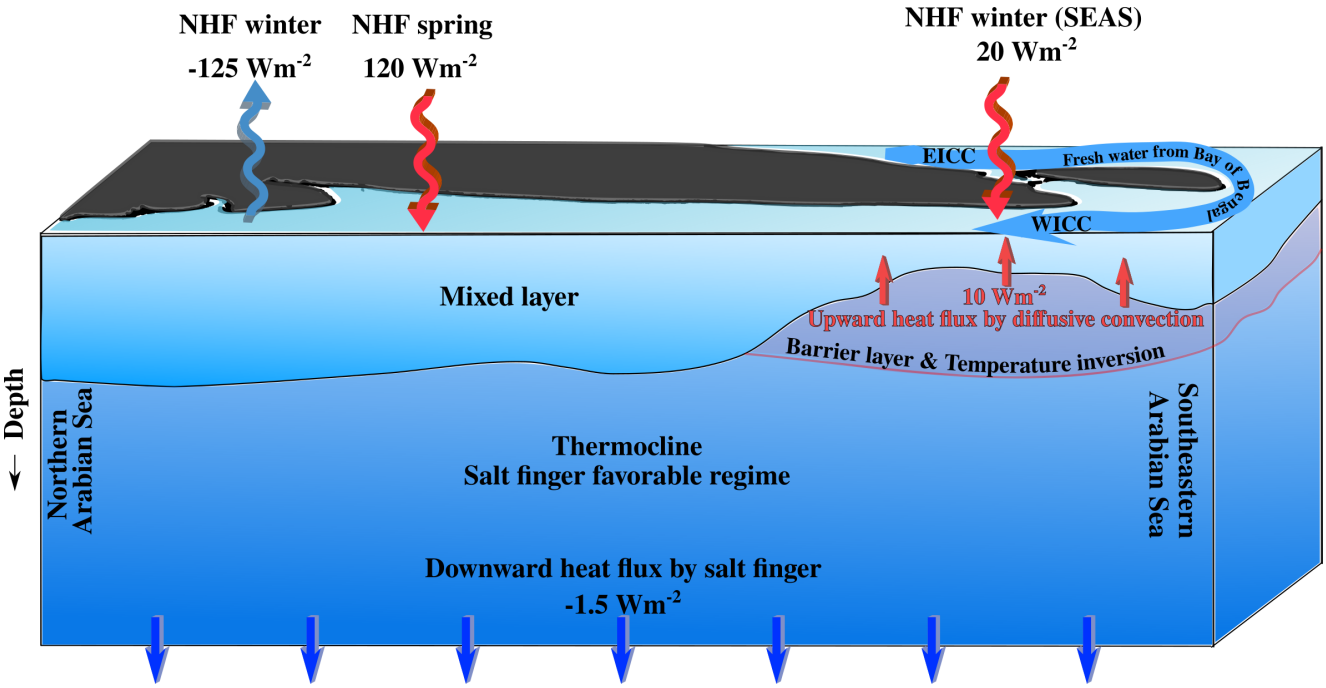
Double diffusion in the Arabian Sea during winter and spring

*Ashin Kuriakose[1,2], Girishkumar M S -[1], Jofia Joseph -[1], Eric D'Asaro -[3], Sureshkumar N -[1], Sherin V R -[1], Murali B -[1], Thangaprakash V P -[1], E Pattabhi Ram Rao[1], S. S. C. Shenoi

1. Indian National Centre for Ocean Information Services, 2. School of Ocean Science and Technology, Kerala University of Fisheries and Ocean Studies, 3. Applied Physics Laboratory and School of Oceanography, University of Washington, Seattle, Washington, USA

Microstructure measurements from two cruises during winter and spring 2019 documented the importance of double diffusion processes for small-scale mixing in the upper 400 m of the open ocean region of the eastern Arabian Sea (EAS). The data indicated that shear-driven mixing rates are weak, contributing diapycnal diffusivity (K_ρ) of not more than 5.2×10^{-6} m^2 s^{-1} in the EAS. Instead, signatures of double diffusion were strong, with the stratification favorable for salt fingers in 70% of the region and favorable for diffusive convection in 2-3% of the region. Well-defined thermohaline staircases were present in all the profiles in these regions that occupied 20% of the water column. Stratification favorable for strong diffusive convection occurred in ~ 45% of data in the barrier layer region of the south EAS (SEAS). The mean dissipation ratio ($\gamma_{\chi\varepsilon}$) in the salt fingering (0.8) and diffusive convection (19-39) regimes were much higher than the expected turbulence mixing efficiency (γ_{Rf}=0.2), again suggesting the importance of double-diffusive processes here. Validation of different parameterizations of double diffusion with the measurements of vertical heat diffusivity (K_T) found that the Radko and Smith (2012) salt fingering scheme and the Kelley (1984) diffusive convection scheme showed the best agreement with observations. The downward heat flux associated with salt fingering in the thermocline region of the EAS of approximately -1.5 Wm^{-2} and upward heat flux due to diffusive convection in the barrier layer region of the SEAS of ~10 Wm^{-2} combine to cool the thermocline.

Keywords: Double Diffusion in the Arabian Sea, Heat flux due to Double diffusion



©2021. Japan Geoscience Union. All Right Reserved.

On widespread intensified thermocline turbulence in the seasonally stratified Yellow Sea

*Wei Yang[1]

1. Tianjin University

Thermocline turbulent mixing lies at the heart of shelf sea systems, regulating the vertical exchange of momentum, mass, and biogeochemical constituents. Based on microstructure measurements conducted in the summer of 2013 and 2017, here we show for the first time that there is widespread intensified thermocline turbulence in the summer stratified Yellow Sea. Shipboard velocity measurements demonstrate that the wind-induced near-inertial waves have driven prevailing strong velocity shear across the thermocline. However, analysis shows that the shear is not always large enough to excite shear instability according to the Richardson number criterion (Ri < 1/4). Strikingly, we show that the elevated thermocline turbulent kinetic energy dissipation rates ε O(10^{-7} Wkg^{-1}) and microscale thermal dissipation rates χ O(10^{-6} K^2s^{-1}) are more related to the presence of low-salinity water layers (5 –15 m thick) adjacent to the main thermocline at isopycnals 24 –25 kgm^{-3}. Turner angle (Tu) analysis demonstrates the presence of salt-finger favorable conditions (Tu > 45˚) at the upper boundary of the intrusion. High values of ε and χ tend to occur in the salt-finger favorable layers suggesting the occurrence of double-diffusive convective instability. These results have important implications for nutrients cycling and the maintenance of primary productivity in seasonally stratified shelf seas.

Keywords: Thermocline turbulence, Salt fingers, Low-salinity water intrusion, Near-inertial waves, The Yellow Sea

©2021. Japan Geoscience Union. All Right Reserved.

Observation of energy transfer from traveling typhoons to turbulent mixing in the ocean

*Aiqi Zhang[1], Ichiro Yasuda[1], Daigo Yanagimoto[1], Shinzou Fujio[1], Yusuke Sasaki[1]

1. the University of Tokyo

Double-inertial internal waves are supposed to play an important role in transferring wind-induced energy from the surface layer to the deep ocean, thus sustaining the Meridional Overturning Circulation (MOC). However, the influence of double-inertial internal waves on the MOC is not fully understood due to the scarcity of observational data.

During the R/V Shinsei-maru cruise (KS-20-11) from August 4 through August 13, 2020, two typhoons passed the observation areas (in the Oyashio region) coincidentally, and the measurement of the oceanic response was carried out. Both near-inertial and double-inertial internal waves were detected with the moored ADCP. The vertical distribution of kinetic energy indicates that the internal waves at the surface are strengthened by the typhoons, and gradually propagate downward. The frequency spectra of kinetic energy suggests that double-inertial energy is enhanced down to ~600 m within the depth limitation of ADCP. Furthermore, we analyze wind energy input to each mode of internal waves, in order to examine the energy transfer process. Among them, much energy is fed into high-vertical-mode near-inertial waves below the mixed layer. The result suggests that traveling typhoons may contribute to turbulent mixing in the ocean interior through a nonlinear wave-wave interaction.

Keywords: near-inertial internal wave, double-inertial internal wave, typhoon, turbulent mixing

©2021. Japan Geoscience Union. All Right Reserved.

Can tidal forcing alone generate a GM-like internal wave spectrum?

*Zhiwu Chen[1], Shaomin Chen[1], Zhiyu Liu[2], Jiexin Xu[1], Jieshuo Xie[1], Yinghui He[1], Shuqun Cai[1]

1. South China Sea Institute of Oceanology, Chinese Academy of Sciences, 2. Department of Physical Oceanography, College of Ocean and Earth Sciences, Xiamen University

An idealized two-dimensional numerical model is utilized to study internal wave generation by tide-topography interaction and wind forcing. Previous studies suggest that the quasi-universal Garrett-Munk (GM) internal wave spectrum can be generated and maintained only when energy is supplied from both the wind and the tides, while the present study shows that M_2 tidal forcing alone is sufficient to generate a GM-like spectrum in a latitude band roughly between 17° and 29°, with the steepness parameter $\varepsilon > 1$, $N_0 h_0 / u_0 > 1$ (N_0 is buoyancy frequency, h_0 topographic height, and u_0 tidal amplitude), and a finite excursion parameter. The key lies in the generation of near-inertial waves (NIWs) by breaking internal tides and triadic resonant interactions around supercritical topography. Remarkably, in the northern South China Sea, tidal forcing can contribute a comparable amount of near-inertial energy as that contributed by the summer wind and thus is an important NIW generation mechanism.

Keywords: Internal waves, Garrett-Munk spectrum, Near-inertial waves, Parametruc Subharmonic Instability

©2021. Japan Geoscience Union. All Right Reserved.

[E] Oral | A (Atmospheric and Hydrospheric Sciences)：A-OS Ocean Sciences & Ocean Environment

Sat. Jun 5, 2021 3:30 PM - 5:00 PM JST | Sat. Jun 5, 2021 6:30 AM - 8:00 AM UTC | Ch.11 Zoom Room 11

[A-OS12] Physical, biogeochemical, and ecological processes and variability in the Indian Ocean

convener:Yukio Masumoto(Graduate School of Science, The University of Tokyo), Hiroaki Saito(Atmosphere and Ocean Research Institute, The University of Tokyo), Chairperson:Yukio Masumoto(Graduate School of Science, The University of Tokyo), Hiroaki Saito(Atmosphere and Ocean Research Institute, The University of Tokyo)

The Indian Ocean has been recognized to play important roles in regional and global climate systems, material circulations, ecosystems, and their variability, with linked biophysical phenomena that span a wide range of spatial and temporal scales. These phenomena include, for example, diurnal cycling, intraseasonal disturbances, seasonal variations, Indian Ocean dipole events, and decadal to multi-decadal variations as well as secular trends under the global warming stress. In situ and remotely-sensed physical and biogeochemical observations using the Indian Ocean Observing System (IndOOS) and other means are now accumulating high quality data, and research efforts with numerical models and analyses of comprehensive datasets are also being conducted under International Indian Ocean Expedition-2 (IIOE-2) and the Eastern/Western Indian Ocean Upwelling Research Initiative (EIOURI/WIOURI). To advance our understanding of such Indian Ocean phenomena, disciplinary studies are essential, as are interdisciplinary investigations that elucidate the linkages between the physical and biogeochemical/ecological researches realms.
The objective of this session is to share our knowledge on, and to advance our understanding of, all facets of Indian Ocean variability. We invite papers on physical, biogeochemical and ecological aspects of the variability, as well as those related to atmosphere-ocean interactions, over the full spectrum of temporal and spatial scales. Discussions to facilitate mutual interactions among different research communities would also be expected and encouraged.

3:30 PM - 3:45 PM JST | 6:30 AM - 6:45 AM UTC

[AOS12-01] Determination of nitrogen source for phytoplankton in the eastern Indian Ocean by $\delta^{15}N$ of chlorophyll *a* and divinylchlorophyll *a*

*Yuta Isaji[1], Chisato Yoshikawa[1], Nanako O. Ogawa[1], Kazuhiko Matsumoto[1], Naoto F. Ishikawa[1], Akiko Makabe[1], Hiroshi Ogawa[2], Hiroaki Saito[2], Makio Honda[1], Naohiko Ohkouchi[1] (1.Japan Agency for Marine-Earth Science and Technology, 2.Atmosphere and Ocean Research Institute, University of Tokyo)

3:45 PM - 4:00 PM JST | 6:45 AM - 7:00 AM UTC

[AOS12-02] **Temporary phytoplankton bloom induced by physical disturbances in the Eastern Indian Ocean**

*Siyu Jiang[1], Fuminori Hashihama[2], Hiroaki Saito[1] (1.Atmosphere and Ocean Research Institute, The University of Tokyo, 2.Tokyo University of Marine Science and Technology)

4:00 PM - 4:15 PM JST | 7:00 AM - 7:15 AM UTC

[AOS12-03] Intraseasonal variation of surface Chlorophyll-a associated with coastal upwelling along the southern coast of Java

*Takanori Horii[1], Eko Siswanto[2], Iskhaq Iskandar[3], Iwao Ueki[1] (1.Global Ocean Observation Research Center, Research Institute for Global Change, Japan Agency for Marine-Earth Science and Technology (JAMSTEC), 2.Earth Surface System Research Center, Research Institute for Global Change, Japan Agency for Marine-Earth Science and Technology (JAMSTEC), 3.Faculty of Mathematics and Natural Sciences, Sriwijaya University, Indonesia)

4:15 PM - 4:30 PM JST | 7:15 AM - 7:30 AM UTC

[AOS12-04] Interannual variability in sea surface temperature off Somalia in boreal summer
– Similarities and differences between “Warm year” and “Cold year” –

*Kusumi Takahiro[1], Yukio Masumoto[1] (1.the Unversity of Tokyo)

4:30 PM - 4:45 PM JST | 7:30 AM - 7:45 AM UTC

[AOS12-05] Seasonal and Interannual Variations of Indian Ocean Subtropical Mode Water Based on the Argo Data

*Hanani Adiwira[1], Toshio Suga[1] (1.Tohoku University)

4:45 PM - 5:00 PM JST | 7:45 AM - 8:00 AM UTC

[AOS12-06] Distribution and movement of microplastics in the Indian Ocean

*Yukio Masumoto[1] (1.Graduate School of Science, The University of Tokyo)

Determination of nitrogen source for phytoplankton in the eastern Indian Ocean by $\delta^{15}N$ of chlorophyll *a* and divinylchlorophyll *a*

*Yuta Isaji[1], Chisato Yoshikawa[1], Nanako O. Ogawa[1], Kazuhiko Matsumoto[1], Naoto F. Ishikawa[1], Akiko Makabe[1], Hiroshi Ogawa[2], Hiroaki Saito[2], Makio Honda[1], Naohiko Ohkouchi[1]

1. Japan Agency for Marine-Earth Science and Technology, 2. Atmosphere and Ocean Research Institute, University of Tokyo

The eastern Indian Ocean is unique for its meridional gradients in physical and chemical properties with distinct biogeochemical regimes. Constraining the biogeochemical parameters in each of these regions is critical as the Indian Ocean represents 15–20% of global ocean net primary production (Behrenfeld and Falkowski, 1997). The nitrogen source assimilated by phytoplankton is of particular importance, because new production is supported by nitrate supplied from the subsurface ocean or by N_2 fixation, and regenerated production by ammonium and other reduced nitrogen species remineralized within the photic zone. Here, we conducted compound-specific nitrogen isotope analysis of chloropigments in order to determine nitrogen source assimilated by phytoplankton, and to obtain detailed snapshot of primary production in the eastern Indian Ocean. Suspended particulate materials were collected on GF-75 glass-fiber filter on board at subsurface chlorophyll maximum along 88˚E transect in the eastern Indian Ocean (16˚N–20˚S) during the cruise KH-18-6 Leg 2. The depth of subsurface chlorophyll maximum was shallowest at the northernmost station and deepened southward, with chlorophyll *a* concentration showing decreasing trend toward southern stations. Compositions of chlorophylls (i.e., chlorophyll *a*, *b*, *c*, and divinylchlorophyll *a*) and carotenoids (i.e., fucoxanthin, 19’-hexanoyloxyfucoxanthin, 19’-butanoyloxyfucoxanthin, prasinoxanthin, zeaxanthin) indicated predominance of eukaryotic phytoplankton in the northern and equatorial stations. The proportion of *Prochlorococcus* increased in the southern stations in response to deepening of the nutricline. The $\delta^{15}N$ values of eukaryotic phytoplankton and *Prochlorococcus* were estimated by those of chlorophyll *a* and divinylchlorophyll *a*, respectively. We will present meridional variation in the nitrogen source assimilated by each group of phytoplankton, and discuss its possible causes as well as implications of our results.

Keywords: Indian Ocean, primary production, nitrogen isotope, Prochlorococcus, divinylchlorophyll

©2021. Japan Geoscience Union. All Right Reserved.

Temporary phytoplankton bloom induced by physical disturbances in the Eastern Indian Ocean

*Siyu Jiang[1], Fuminori Hashihama[2], Hiroaki Saito[1]

1. Atmosphere and Ocean Research Institute, The University of Tokyo, 2. Tokyo University of Marine Science and Technology

Phytoplankton growth and microzooplankton grazing are critical processes which support higher trophic levels in marine ecosystems. In oligotrophic marine ecosystems, these processes are generally coupled with each other and the balance between them keeps phytoplankton biomass consistently low. However, it has been reported the coupling was easily violated by physical disturbances. The Eastern Indian Ocean is an oligotrophic ecosystem with strong seasonal and intraseasonal variabilities induced by physical activities. However, phytoplankton growth and microzooplankton grazing mortality were rarely studied in this area, and their responses to physical disturbances remain unclear. In this study, we conducted a series of dilution experiments in the surface layer (10 m) in subtropical and tropical Eastern Indian Ocean (88˚E, 16.5 ˚N to 20 ˚S) to measure phytoplankton growth and microzooplankton grazing mortality rates. The study area was throughout oligotrophic (dissolved inorganic nitrogen concentration lower than 60 nM). The Chl *a* concentration was low (0.13 ±0.09 μg L^{-1}) except the equatorial stations (0.26 ±0.06 μg L^{-1}). However, the high biomass at the equator decreased to approximate 0.1 μg L^{-1} after the cruise, as demonstrated by satellite Chl *a* observations. Further, the phytoplankton growth at the equator was low or even negative (-0.07 and 0.28 d^{-1}) and was limited by nutrients availability, while at other stations growth rates were higher (0.68 ±0.33 d^{-1}) and the nutrient limitation was not serious. The significant response of phytoplankton growth to additional ammonium (by ~3.3 times high growth rate) and the higher phytoplankton Chl:C ratio at the equator indicated there was once relatively abundant nutrients. The equatorial Wyrtki Jet formed before the cruise possibly transported the nutrient-rich water to the Eastern Indian Ocean. The time-lag between the jet formation and the cruise might allow phytoplankton to exhaust the nutrients and accumulate the biomass. Our results indicated in the Eastern Indian Ocean, the balance between phytoplankton growth and grazing mortality could be violated by physical disturbances and the growth exceeded mortality could induce temporary phytoplankton blooms.

Keywords: Indian Ocean, Phytoplankton, Microzooplankton, Dilution technique, Physical disturbances, Wyrtki Jet

©2021. Japan Geoscience Union. All Right Reserved.

Intraseasonal variation of surface Chlorophyll-a associated with coastal upwelling along the southern coast of Java

*Takanori Horii[1], Eko Siswanto[2], Iskhaq Iskandar[3], Iwao Ueki[1]

1. Global Ocean Observation Research Center, Research Institute for Global Change, Japan Agency for Marine-Earth Science and Technology (JAMSTEC), 2. Earth Surface System Research Center, Research Institute for Global Change, Japan Agency for Marine-Earth Science and Technology (JAMSTEC), 3. Faculty of Mathematics and Natural Sciences, Sriwijaya University, Indonesia

Coastal upwelling along the southern coast of Java brings cold and nutrient-rich subsurface water upward and plays an important role in controlling ocean surface heat balance, biogeochemical balance, coastal ecosystem, and regional fisheries. To understand the coastal upwelling, we investigated satellite-based Chlorophyll-a data south of Java, with a focus on the seasonal and intraseasonal-scale variability. We first interpolated the data and produced daily timeseries. The spectrum analysis showed that annual, semi-annual, and intraseasonal (20-60-day) variations were significant in the Chlorophyll-a variations. The Chlorophyll-a peaks were accompanied with decreases in the local sea level and sea surface temperature, suggesting a coastal upwelling of cold and nutrient-rich subsurface water at the intraseasonal timescale. A relationship between the intraseasonal Chlorophyll-a variations and the Indian Ocean Dipole will be discussed.

Keywords: Surface Chlorophyll-a, Java island, Indian Ocean Dipole

©2021. Japan Geoscience Union. All Right Reserved.

Interannual variability in sea surface temperature off Somalia in boreal summer –Similarities and differences between “Warm year” and “Cold year” –

*Kusumi Takahiro[1], Yukio Masumoto[1]

1. the Unversity of Tokyo

Strong alongshore southwesterly winds in the western Arabian Sea (AS) associated with the Indian summer monsoon locally force coastal upwelling, northward western boundary current, known as the Somali Current, and two oceanic Gyres, called the Southern Gyre and the Great Whirl. Interannual modulations of all these phenomena are believed to affect sea surface temperature (SST) anomaly during boreal summer in the western AS. To investigate processes responsible for interannual variability in the SST anomaly there, a composite analysis is performed for years with positive (negative) SST anomaly in the western AS during summer, hereafter referred as “Warm year (Cold year)”, using outputs from a regional model based on the Regional Ocean Modeling System (ROMS).
While the overall evolutions of anomalous upper-ocean conditions are similar in the two cases, with the sign of anomalies reversed, there is a significant difference in the SST anomaly field. Two regions of filament-like SST anomaly appear around 4˚N and 10˚N near the coast of Somalia by mid-June both in Warm and Cold years. These two filament-like anomalies remain almost the same locations through the summer in Warm years. On the other hand, in Cold years, the cold SST anomaly and associated cyclonic circulation around 4˚N move northward along the coast of Somalia and eventually coalesces with another filament-like cold SST structure located around 10˚N. When this coalescence occurs, the SST around 10˚N near the Somali coast decreases rapidly and the cold SST anomaly around 4˚N disappears. This merger of two gyres does not occur every year but tends to occur in the Cold years. The merger between two filament-like cold SST anomalies may be related to the stronger alongshore southwesterly winds in the Cold years compared to that in the normal years. This discrepancy between the two cases may result in asymmetric responses in interannual variations of the Indian summer monsoon to the SST anomalies over the western AS.

Keywords: Western Arabian Sea, Interannual variation, Filament, Coalescence

©2021. Japan Geoscience Union. All Right Reserved.

Seasonal and Interannual Variations of Indian Ocean Subtropical Mode Water Based on the Argo Data

*Hanani Adiwira[1], Toshio Suga[1]

1. Tohoku University

Subtropical Mode Water (STMW) is a water mass that is formed during winter season and located in the western part of subtropical gyre. STMW covers a large area both in horizontal and vertical, and distinguished by the extreme uniformity of water properties. Extensive studies have been done for STMWs in the Pacific and Atlantic Oceans, meanwhile, there are only few studies that specifically discuss about Indian Ocean Subtropical Mode Water (IOSTMW). Sparseness of observational data was the obstacle for studying the Indian Ocean. However, this situation has been changing due to Argo program started in 1999, where numerous Argo floats were deployed to collect temperature and salinity data globally. Until now, the increasing Argo data in Subtropical Indian Ocean region has not been fully utilized. The seasonal and interannual variability of IOSTMW is still not clear yet. Therefore, by using the Argo data, this study investigates the interannual variability of IOSMTW in a longer time period and the mechanisms behind the variability. In Situ Analysis System (ISAS) gridded fields of temperature and salinity, which entirely based on in situ measurements, are used to examine the temporal variability of IOSTMW. Additionally, the turbulence heat flux data from OAFlux (Yu et al., 2018) and the radiative heat flux data from CERES (Kato et al., 2018) are used to see the relationship between winter atmospheric cooling and the formation of IOSTMW.

The definition of IOSTMW layer itself is not clearly defined yet. IOSTMW has been defined differently by each of the previous study. In this study, IOSTMW layer is defined by using the temperature gradient (dT/dz) and temperature range. Based on the previous studies, there are four IOSTMW definitions that are analyzed in this study: (1) dT/dz < 1.5˚C/100 m with temperature of 15-18˚C, (2) dT/dz < 1.5˚C/100 m with temperature of 16-18˚C, (3) dT/dz < 1˚C/100 m with temperature of 15-18˚C, (4) dT/dz < 1˚C/100 m with temperature of 16-18˚C.

The correlation coefficients between late-winter IOSTMW thickness and both winter (Jun-Aug) heat flux and ocean summer (Jan-Mar) stratification are examined. Significant correlation coefficients are found between winter heat flux and IOSTMW thickness for the definitions with dT/dz < 1˚C/100 m ($p < 0.01$), higher than the definitions with dT/dz < 1.5˚C/100 m. This implies IOSTMW defined as layer with dT/dz < 1.5˚C/100 m, or the older and more stratified mode water, is less sensitive to the atmospheric forcing in the same year. Moreover, the comparison between cumulative winter heat flux and the difference of ocean heat content at the beginning of the winter and the end of winter also indicates the strong connection between atmospheric forcing and the upper ocean stratification. On the other hand, low correlation coefficients are found between IOSTMW thickness of each definition and summer stratification (0-150 m).

Therefore, the atmospheric cooling is found more dominant in determining the formation of IOSTMW, while the summer stratification is less influential. Layer with dT/dz < 1˚C/100 m and temperature of 16-18˚C is chosen as the definition of IOSTMW in the further analysis because this layer is sensitive to air-sea interaction and correlates relatively well with the summer stratification among all definitions.

©2021. Japan Geoscience Union. All Right Reserved.

Keywords: Indian Ocean, Subtropical Mode Water, Argo Float, Air-Sea Interaction

©2021. Japan Geoscience Union. All Right Reserved.

Distribution and movement of microplastics in the Indian Ocean

*Yukio Masumoto[1]

1. Graduate School of Science, The University of Tokyo

Considering that one of the largest microplastic source regions is located in the maritime continent between the Pacific and Indian Oceans and that the Indonesian throughflow is passing through the maritime continent toward the Indian Ocean, much of microplastics injected in the region would be expected to flow into the Indian Ocean. However, details on their distributions and movements within the Indian Ocean have not been investigated. Using outputs of a high-resolution ocean general circulation model (OFES), particle tracking calculations are conducted to determine horizontal distribution of the microplastics in the Indian Ocean and to quantify how much of the microplastics flow into the Indian Ocean from the maritime continent. Most of the microplastics are accumulated within the subtropical gyre in the southern hemisphere. Although microplastics have been observed in the Southern Oceans near Antarctica, this study suggests that it is difficult to reach far south near Antarctica by the simple dispersion of the materials flowing at the sea surface. Further analysis on a role of three-dimensional circulations to transport microplastics farther south across the Antarctic Circumpolar Currents would be required.

©2021. Japan Geoscience Union. All Right Reserved.

[E] Poster | A (Atmospheric and Hydrospheric Sciences)：A-OS Ocean Sciences & Ocean Environment

Sat. Jun 5, 2021 5:15 PM - 6:30 PM JST | Sat. Jun 5, 2021 8:15 AM - 9:30 AM UTC | Ch.05_2

[A-OS12] Physical, biogeochemical, and ecological processes and variability in the Indian Ocean

convener:Yukio Masumoto(Graduate School of Science, The University of Tokyo), Hiroaki Saito(Atmosphere and Ocean Research Institute, The University of Tokyo)

The Indian Ocean has been recognized to play important roles in regional and global climate systems, material circulations, ecosystems, and their variability, with linked biophysical phenomena that span a wide range of spatial and temporal scales. These phenomena include, for example, diurnal cycling, intraseasonal disturbances, seasonal variations, Indian Ocean dipole events, and decadal to multi-decadal variations as well as secular trends under the global warming stress. In situ and remotely-sensed physical and biogeochemical observations using the Indian Ocean Observing System (IndOOS) and other means are now accumulating high quality data, and research efforts with numerical models and analyses of comprehensive datasets are also being conducted under International Indian Ocean Expedition-2 (IIOE-2) and the Eastern/Western Indian Ocean Upwelling Research Initiative (EIOURI/WIOURI). To advance our understanding of such Indian Ocean phenomena, disciplinary studies are essential, as are interdisciplinary investigations that elucidate the linkages between the physical and biogeochemical/ecological researches realms.
The objective of this session is to share our knowledge on, and to advance our understanding of, all facets of Indian Ocean variability. We invite papers on physical, biogeochemical and ecological aspects of the variability, as well as those related to atmosphere-ocean interactions, over the full spectrum of temporal and spatial scales. Discussions to facilitate mutual interactions among different research communities would also be expected and encouraged.

[AOS12-P01] **Nitrogen cycling in the primary nitrite maximum of the Indian Ocean**

*Shigenobu Takeda[1], Kunioki Hirata[1], Takuhei Shiozaki[2] (1.Nagasaki University, 2.The University of Tokyo)

[AOS12-P02] Coastal ecosystem study in the Indian Ocean and adjacent seas under international collaboration

*Hiroaki Saito[1], Yukio Masumoto[2], Zainal Arifin[3] (1.Atmosphere and Ocean Research Institute, The University of Tokyo, 2.Graduate School of Science, The University of Tokyo, 3.Research Centre for Oceanograph, Indonesian Institute of Sciences)

[AOS12-P03] Issues and future directions of the Indian Ocean researches

*Yukio Masumoto[1] (1.Graduate School of Science, The University of Tokyo)

Nitrogen cycling in the primary nitrite maximum of the Indian Ocean

*Shigenobu Takeda[1], Kunioki Hirata[1], Takuhei Shiozaki[2]

1. Nagasaki University, 2. The University of Tokyo

The mechanisms that maintains a peak in nitrite concentrations at the bottom of the euphotic zone (primary nitrite maximum, PNM) remains unclear, despite data supporting either microbial nitrification or phytoplankton release of nitrite. In this study, based on field observations and on board incubation experiments conducted at three stations in the Bay of Bengal (BB), Equatorial Region (ER), and Subtropical South Indian Ocean (SI) along 88 degree E in the Indian Ocean, we tested the hypothesis that iron limitation stimulates the release of nitrite from phytoplankton cells into ambient water near the subsurface chlorophyll maximum (SCM) by inhibiting the nitrite metabolic pathway.
In BB, the PNM layer was shallower than 1% light depth and appeared near the bottom of the subsurface chlorophyll maximum. In contrast, in ER and SI, the PNM layer was deeper than 1% light depth and was formed between the subsurface chlorophyll maximum and the upper part of the nitracline. Ammonia oxidation rates measured under dark conditions increased with depth within the euphotic layer in BB. However, in ER and SI, it was not detected within the euphotic layer and increased from layers deeper than 1% light depth. Among the ammonia-oxidizing archaea, Shallow Marine Clade (SMC) appeared in all subsurface layers and showed a tendency to increase in abundance with depth, while Deep Marine Clade (DMC) was detected only in layers deeper than around 1% light depth. The SMC accounted for more than 95% of the ammonia-oxidizing archaeal community detected near the PNM layer, suggesting a relationship with nitrite accumulation. The effects of Fe and light on the plankton community near the PNM suggested that a lack of light or iron in BB, a lack of light in ER, and a lack of both Fe and light in SI may be responsible for the release of nitrite. The changes in nitrite concentration during the incubation experiments indicated that the regulation of ammonia oxidation by light and nitrite oxidation by iron in ER. Based on these results, it is clear that the effects of light intensity and Fe availability on microbial nitrification and phytoplankton nitrogen metabolism near the PNM are different in the northern and southern Indian Ocean.

Keywords: Trace metal, Nitrogen cycle, Indian Ocean, Nitrite, Iron

©2021. Japan Geoscience Union. All Right Reserved.

Coastal ecosystem study in the Indian Ocean and adjacent seas under international collaboration

*Hiroaki Saito[1], Yukio Masumoto[2], Zainal Arifin[3]

1. Atmosphere and Ocean Research Institute, The University of Tokyo, 2. Graduate School of Science, The University of Tokyo, 3. Research Centre for Oceanograph, Indonesian Institute of Sciences

Coastal ecosystems in the eastern Indian Ocean and its adjacent seas are in the center of coral triangle, the hot spot of marine diversity. The society in this region receives various ecosystem services, such as food supply, water quality regulation, cultural and spiritual services. The region is also the center of changing ocean influenced by anthropogenic activities. With development of industry and increase in population, demands on ecosystem services are increasing. The users of marine ecosystem, or stakeholders, are increasing which makes it difficult to build consensus for wise and sustainable use of marine ecosystems. Since scientific knowledge forms the basis for consensus building between different stakeholders, scientists are expected from society to prepare the best scientific knowledge on the structure and dynamics of marine ecosystems in appropriate timing. The scientific issues are, however, too big to solve by one country, and need international collaboration with exchanging scientists and transfer of marine science technology. Recognizing the situation, the United Nation declared the Decade of Ocean Science for Sustainable Development (2021-2030). It is also pointed out that the importance of international collaboration since the marine ecosystems are connected each other and counter measures to prevent the destruction of marine ecosystems is to be driven under international collaboration scheme even each EEZ is under the control of national jurisdiction. In the presentation, we will discuss what issues are emerged in the coastal ecosystems in the eastern Indian Oceans and its adjacent seas and the direction of international collaboration as well as remaining issue to realize the collaboration.

©2021. Japan Geoscience Union. All Right Reserved.

Issues and future directions of the Indian Ocean researches

*Yukio Masumoto[1]

1. Graduate School of Science, The University of Tokyo

Based on presentations during the session, current issues and future directions of the Indian Ocean researches will be discussed.

©2021. Japan Geoscience Union. All Right Reserved.

[E] Oral | A (Atmospheric and Hydrospheric Sciences)：A-OS Ocean Sciences & Ocean Environment

Sat. Jun 5, 2021 9:00 AM - 10:30 AM JST | Sat. Jun 5, 2021 12:00 AM - 1:30 AM UTC | Ch.11 Zoom Room 11

[A-OS13] Marine ecosystems and biogeochemical cycles: theory, observation and modeling

convener:Takafumi Hirata(Arctic Research Center, Hokkaido University), Shin-ichi Ito(Atmosphere and Ocean Research Institute, The University of Tokyo), E Eileen Hofmann(Old Dominion University), N Enrique Curchitser(Rutgers University New Brunswick), Chairperson:Shin-ichi Ito(Atmosphere and Ocean Research Institute, The University of Tokyo), Takafumi Hirata(Arctic Research Center, Hokkaido University), Eileen E Hofmann(Old Dominion University), Enrique N Curchitser(Rutgers University New Brunswick)



The ocean accounts for about 50% of global net primary production. This production is significant for carbon cycling and ecosystem functioning, and is related directly or indirectly to a variety of climatic and ecological phenomena. The responses to natural and anthropogenic environmental stressors that influence marine production and diversity can cause perturbations to marine ecosystems that alter trophic dependencies and interactions among organisms at a range of space and time scales. Quantification of the principal mechanisms driving spatio-temporal variability of marine ecosystem remains to be done, especially in terms of evaluation of uncertainty in responses. As a result, evaluating vulnerability of marine ecosystems to environmental change requires systematic and holistic approaches that integrate physics to ecology and are based in observations and modelling. In addition, expectations to deliver these science to public society is raising. This session aims to provide a venue for not only discussing recent advances in understanding marine biogeochemical cycles, ecosystems and their interactions, but also networking with a variety of people to seed new ideas in marine ecological research. Observational, modeling and conceptual studies, including technological development and operational applications, that consider linkages among biogeochemical and ecosystem processes, biodiversity, and the effects of multiple stressors from molecular to planetary scales are encouraged.

9:00 AM - 9:05 AM JST | 12:00 AM - 12:05 AM UTC

[AOS13-01] Introduction

9:05 AM - 9:30 AM JST | 12:05 AM - 12:30 AM UTC

[AOS13-02] Understanding Marine Ecosystems – A View to the Future

★Invited Papers

*Eileen E Hofmann[1] (1.Old Dominion University)

9:30 AM - 9:45 AM JST | 12:30 AM - 12:45 AM UTC

[AOS13-03] Marine Ecosystem Variations Over the North Pacific and Their Linkage to Large-Scale Climate Variability and Change

*Emi Yati[1], Shoshiro Minobe[2,3], Nathan Mantua[4], Shin-ichi Ito[5], Emanuele Di Lorenzo[6] (1.Remote Sensing Application Center, Indonesian National Institute of Aeronautics and Space, Jakarta, Indonesia, 2.Department of Natural History Sciences, Graduate School of Science, Hokkaido University, Sapporo, Japan, 3.Department of Earth and Planetary Sciences, Faculty of Science, Hokkaido University, Sapporo, Japan, 4.Fish Ecology Division, Southwest Fisheries Science Center, National Marine Fisheries Service, National Oceanographic and Atmospheric Administration, Santa Cruz, CA, United States, 5.Atmosphere and Ocean Research Institute, University of Tokyo, Kashiwa, Japan, 6.School of Earth and Atmospheric Sciences, Georgia Institute of Technology, Atlanta, GA, United States)

9:45 AM - 10:00 AM JST | 12:45 AM - 1:00 AM UTC

[AOS13-04] **Future biogeographic shifts of marine biodiversity in the Pacific Arctic**

*Irene Alabia[1], Jorge Garcia Molinos[1], Sei-Ichi Saitoh[1], Takafumi Hirata[1], Toru Hirawake[1], Franz Mueter[2] (1.Hokkaido University, 2.University of Alaska Fairbanks)

10:00 AM - 10:15 AM JST | 1:00 AM - 1:15 AM UTC

[AOS13-05] Instantaneous Acclimation allows computationally efficient modelling of the biogeochemical impacts of plankton ecophysiology

*S. Lan Smith[1], Onur Kerimoglu[2], Prima Anugerahanti[1], Yoshio Masuda[3], Yasuhiro Yamanaka[3], Yoshikazu Sasai[1] (1.Marine Ecosystem Dynamics Research Group, Research Institute for Global Change, Japan Agency for Marine-Earth Science and Technology, 2.ICBM, University of Oldenburg, Germany, 3.Faculty of Environmental Earth Science, Hokkaido University)

10:15 AM - 10:30 AM JST | 1:15 AM - 1:30 AM UTC

[AOS13-06] Interannual Variability in contributions of the Equatorial Undercurrent (EUC) to Peruvian Upwelling

*Gandy Maria Rosales Quintana[1], Robert Marsh[2], Luis Alfredo Icochea Salas[3] (1.Course of Applied Marine Environmental Studies, Tokyo University of Marine Science and Technology, 2.University of Southampton, UK, 3.Universidad Nacional Agraria La Molina, Peru)

[E] Oral | A (Atmospheric and Hydrospheric Sciences) | A-OS Ocean Sciences & Ocean Environment

[A-OS13] Marine ecosystems and biogeochemical cycles: theory, observation and modeling

convener:Takafumi Hirata(Arctic Research Center, Hokkaido University), Shin-ichi Ito(Atmosphere and Ocean Research Institute, The University of Tokyo), E Eileen Hofmann(Old Dominion University), N Enrique Curchitser(Rutgers University New Brunswick), Chairperson:Shin-ichi Ito(Atmosphere and Ocean Research Institute, The University of Tokyo), Takafumi Hirata(Arctic Research Center, Hokkaido University), Eileen E Hofmann(Old Dominion University), Enrique N Curchitser(Rutgers University New Brunswick)

Sat. Jun 5, 2021 9:00 AM - 10:30 AM Ch.11 (Zoom Room 11)

The ocean accounts for about 50% of global net primary production. This production is significant for carbon cycling and ecosystem functioning, and is related directly or indirectly to a variety of climatic and ecological phenomena. The responses to natural and anthropogenic environmental stressors that influence marine production and diversity can cause perturbations to marine ecosystems that alter trophic dependencies and interactions among organisms at a range of space and time scales. Quantification of the principal mechanisms driving spatio-temporal variability of marine ecosystem remains to be done, especially in terms of evaluation of uncertainty in responses. As a result, evaluating vulnerability of marine ecosystems to environmental change requires systematic and holistic approaches that integrate physics to ecology and are based in observations and modelling. In addition, expectations to deliver these science to public society is raising. This session aims to provide a venue for not only discussing recent advances in understanding marine biogeochemical cycles, ecosystems and their interactions, but also networking with a variety of people to seed new ideas in marine ecological research. Observational, modeling and conceptual studies, including technological development and operational applications, that consider linkages among biogeochemical and ecosystem processes, biodiversity, and the effects of multiple stressors from molecular to planetary scales are encouraged.

9:00 AM - 9:05 AM

[AOS13-01]Introduction

©Japan Geoscience Union

Understanding Marine Ecosystems –A View to the Future

*Eileen E Hofmann[1]

1. Old Dominion University

Integrated ecosystem analyses provide an approach for understanding and projecting responses of marine ecosystems to changing climate conditions and direct human impacts such as fisheries. Complex interactions within food webs modify responses of individual species and influence the responses of entire ecosystems to change. Reliable projections of the impacts of past and future changes on marine ecosystems require fundamental understanding of the factors that determine the structure and function of the food webs at multiple scales, incorporation of this understanding into coupled modeling frameworks, and approaches for translating information so that it can be used for development of policies and regulations. Ecosystem adjustments resulting from exploitation of living resources and climate change are ongoing and significant changes are becoming apparent at all trophic levels. Management Strategy Evaluations (MSE), which are systems of linked models, allow the cascade of effects initiated by changes in climate, ocean or food webs to be identified using comprehensive mechanistic descriptions of ecosystem responses, which are then evaluated in terms of potential social and economic effects. The information from a MSE then provides inputs for evaluating and developing management and regulatory policies for a resource. This presentation overviews MSEs developed for marine ecosystems and implications for management and policy. The lessons learned from MSE implementation point to research needs that in turn will inform development of initiatives for the UN Decade of Ocean Science for Sustainable Development.

Keywords: Management Strategy Evaluation , IMBeR

©2021. Japan Geoscience Union. All Right Reserved.

Marine Ecosystem Variations Over the North Pacific and Their Linkage to Large-Scale Climate Variability and Change

*Emi Yati[1], Shoshiro Minobe[2,3], Nathan Mantua[4], Shin-ichi Ito[5], Emanuele Di Lorenzo[6]

1. Remote Sensing Application Center, Indonesian National Institute of Aeronautics and Space, Jakarta, Indonesia, 2. Department of Natural History Sciences, Graduate School of Science, Hokkaido University, Sapporo, Japan, 3. Department of Earth and Planetary Sciences, Faculty of Science, Hokkaido University, Sapporo, Japan, 4. Fish Ecology Division, Southwest Fisheries Science Center, National Marine Fisheries Service, National Oceanographic and Atmospheric Administration, Santa Cruz, CA, United States, 5. Atmosphere and Ocean Research Institute, University of Tokyo, Kashiwa, Japan, 6. School of Earth and Atmospheric Sciences, Georgia Institute of Technology, Atlanta, GA, United States

In order to understand how North Pacific (NP) marine ecosystems have varied, 120 marine biological time series for both the western (29 time series) and eastern (91 time series) NP were analyzed with a Principal Component Analysis (PCA) for the period 1965–2006. This is the first attempt to conduct a multivariate analysis for a large number of marine biological data in the western and eastern NP combined. We used Monte-Carlo simulation to evaluate confidence levels of correlations and explained variance ratio of PCA modes while accounting for auto-correlation within the analyzed time series. All first mode principal components (PC1s), which are the time coefficients of the first PCA modes, calculated for the data in the whole, western, and eastern NP exhibit a long-term trend. The PC1s were associated with an overall increase of Alaskan and Japanese/Russian salmon, and decreases of groundfish across the basin. This mode was closely related to the warming of sea-surface temperature over the NP and over the global oceans, thereby suggesting that the strongest mode of the NP marine ecosystem was already influenced by global warming. The eastern NP PC2, characterized by multi-decadal variability, was correlated positively with salmon and negatively with groundfish. On the other hand, the western NP PC2 exhibited slightly shorter timescale interdecadal variability than the eastern NP PC2 and was negatively correlated with zooplankton and two small pelagic fish time series around Japan. The eastern NP PC2 was most strongly related to the Pacific (inter-)Decadal Oscillation index, while the western NP PC2 was most closely related to the North Pacific Gyre Oscillation index. Consequently, the present analysis provides a new and unified view of climate change and marine ecosystem variations across the western and eastern NP. In particular, it is suggested that global warming has already substantially influenced the NP marine ecosystem, and that groundfish may suffer more than pelagic fish in response to future global warming.

This study has been published in Frontiers in Marine Science. 7:578165. doi: 10.3389/fmars.2020.578165

Keywords: marine ecosystem, decadal climate variability, global warming, North Pacific, regime shift

©2021. Japan Geoscience Union. All Right Reserved.

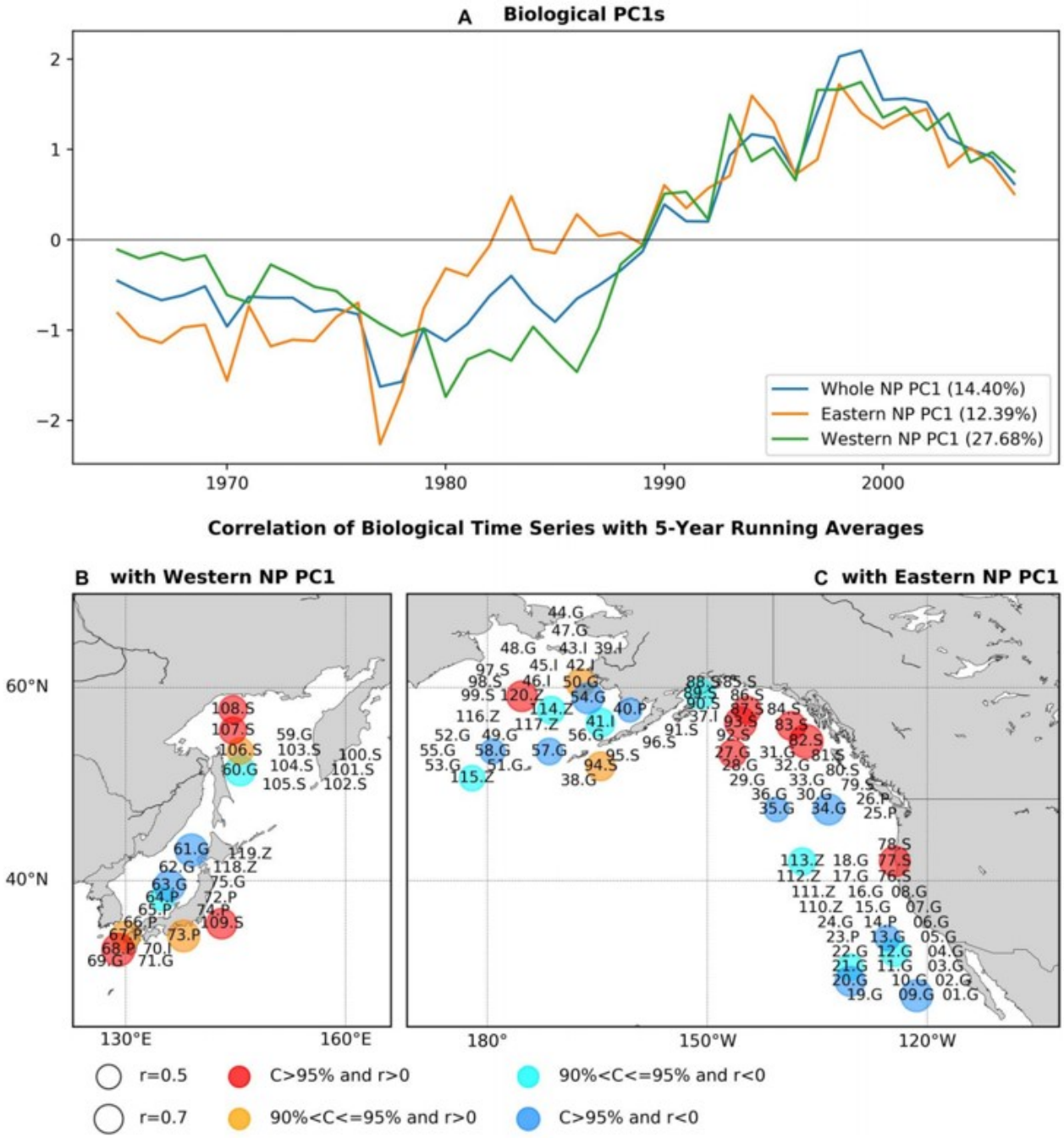


FIG 1. **(A)** PC1s for the whole NP, eastern NP, and western NP marine biological time series, and statistically significant correlations of marine biological time series **(B)** with the western NP PC1, **(C)** with the eastern NP PC1. Before calculating correlations 5-year running means are applied to PC1s and marine biological time series. In (B,C), numbers indicate species ID, while S, G, P, Z, and I indicate salmon, groundfish, small-pelagic, zooplankton, and invertebrate, respectively. Circle size indicates the absolute values of correlations and colors of the circles (red, orange, cyan, blue) indicate the sign of correlations and the corresponding confidence levels

©2021. Japan Geoscience Union. All Right Reserved.

Future biogeographic shifts of marine biodiversity in the Pacific Arctic

*Irene Alabia[1], Jorge Garcia Molinos[1], Sei-Ichi Saitoh[1], Takafumi Hirata[1], Toru Hirawake[1], Franz Mueter[2]

1. Hokkaido University, 2. University of Alaska Fairbanks

Climate change triggers a global reorganization of marine life. Biogeographical transition zones are redistribution hotspots that offer a unique opportunity to understand the mechanisms and consequences of climate-driven thermophilization processes in natural communities. Here, we examined the impacts of climate change projections in the 21st century (2026-2100) on marine biodiversity in the Eastern Bering and Chukchi seas, a climate-sensitive boreal-to-Arctic transition zone. Overall, projected changes in species distributions, resulted in poleward increases in species richness and functional redundancy, along with pronounced reductions in phylogenetic distances by century’ s end (2076-2100). Future poleward shifts of boreal species in response to warming and sea ice changes are projected to alter the biogeography of present-day Arctic communities as larger, longer-lived, and predatory taxa expand their leading distribution margins. Drawing from the existing evidence from other Arctic regions, these changes are anticipated to increase the future vulnerability of Arctic ecosystems, as trophic connectivity between biotic components increases. Our findings provided key insights into relationships between climate change, species composition, and ecosystem functioning across marine biogeographic regions.

Keywords: Biodiversity, climate change, biogeographic transition zones, Pacific arctic, species distribution

©2021. Japan Geoscience Union. All Right Reserved.

Instantaneous Acclimation allows computationally efficient modelling of the biogeochemical impacts of plankton ecophysiology

*S. Lan Smith[1], Onur Kerimoglu[2], Prima Anugerahanti[1], Yoshio Masuda[3], Yasuhiro Yamanaka[3], Yoshikazu Sasai[1]

1. Marine Ecosystem Dynamics Research Group, Research Institute for Global Change, Japan Agency for Marine-Earth Science and Technology, 2. ICBM, University of Oldenburg, Germany, 3. Faculty of Environmental Earth Science, Hokkaido University

Many coupled physical-biogeochemical models reproduce large-scale patterns of chlorophyll, primary production and biogeochemistry, but they often underestimate observed variability and gradients. One common reason is insufficient representation of systematic variations in the elemental composition and chlorophyll (Chl) content of phytoplankton. Chl is widely taken as a proxy for phytoplankton biomass, despite well known variations in Chl:biomass ratios as an acclimative response to changing environmental conditions. However, for the sake of simplicity and computational efficiency, many large scale biogeochemical models ignore this flexibility, compromising their ability to capture phytoplankton dynamics. Although some models account for the dynamics of phytoplankton composition by adding state variables (one for each element or pigment considered), that approach substantially increases computational requirements in spatially explicit (1-D and 3-D) setups. The Instantaneous Acclimation (IA) approach addresses these challenges by assuming that Chl:C:nutrient ratios are instantly optimized locally (within each modelled grid cell, at each timestep), such that they can be resolved as diagnostic variables.However, the IA approach was developed in a 0-D model and has not yet been rigorously tested in spatially explicit models. Here we present tests of IA in various spatially explicit models, including: an idealized, 1D vertical setup in the Framework for Aquatic Biogeochemical Models (FABM) coupled with the General Ocean Turbulence Model (GOTM), as well as a 3-D regional model and another 3-D global model. We show that the IA model and a fully dynamic, otherwise equivalently acclimative (DA) variant with an additional state variable behave similarly, and that both resolve chlorophyll

©2021. Japan Geoscience Union. All Right Reserved.

patterns and nutrient and growth dynamics not captured by the typical fixed-stoichiometry (FS) models [e.g., 1].

(1) Kerimoglu, O.; Anugerahanti, P.; Smith, S. Geosci. Model Dev. Discuss., in review 2021 , DOI: 10.5194/gmd-2020-396 .

Keywords: nutrients, photo-acclimation, phytoplankton, Earth System Modelling, marine ecosystems, biogeochemistry

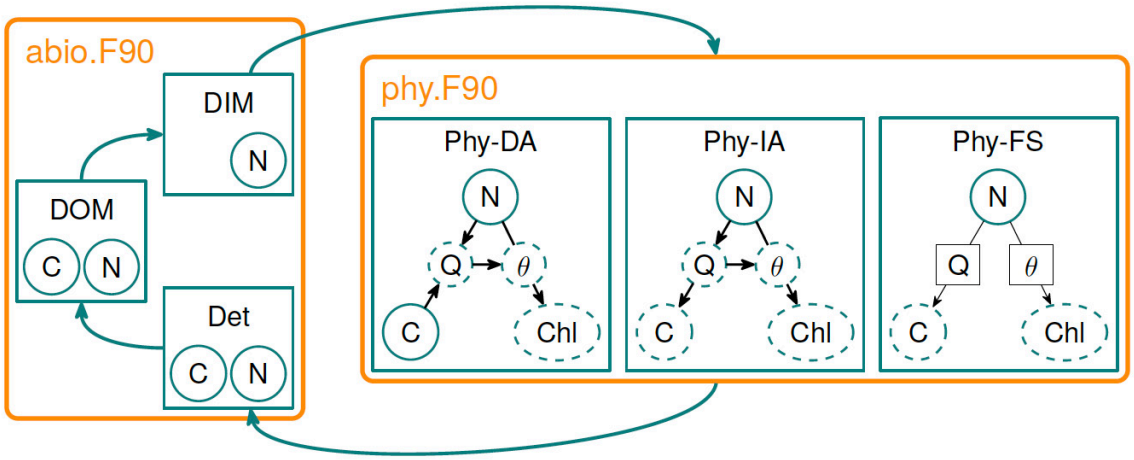


Figure 1: (Taken from [1]) Diagram of the FABM-NflexPD model. Abitoic components, DOM, DIM and Det are calculated by the module `abio.F90`, which are then coupled to the phytoplankton simulated by the module `phy.F90` that simulates the dynamics of Phy_N, Phy_C and Phy_{Chl} by the DA, IA and FS variants. Solid circles in the phytoplankton module represent state variables, dashed circles/ellipsoids represent diagnostically calculated variables and solid squares (for FS) represent prescribed values. The DA variant estimates the N, C and Chl content of phytoplankton based on a resource allocation scheme, whereas the FS variant estimates only N prognostically, while C and Chl are based on prescribed values of nitrogen quota (Q) and cellular Chl:C ratio (θ).

©2021. Japan Geoscience Union. All Right Reserved.

Interannual Variability in contributions of the Equatorial Undercurrent (EUC) to Peruvian Upwelling

*Gandy Maria Rosales Quintana[1], Robert Marsh[2], Luis Alfredo Icochea Salas[3]

1. Course of Applied Marine Environmental Studies, Tokyo University of Marine Science and Technology, 2. University of Southampton, UK, 3. Universidad Nacional Agraria La Molina, Peru

Time-varying sources of upwelling waters off the coast of northern Peruvian are analysed in a Lagrangian frame- work, tracking virtual particles backwards in time. Particle trajectories are calculated with temperature, salinity and velocity fields from a hindcast spanning 1988-2007, obtained with an eddy-resolving (1/12o) global configuration of the NEMO ocean model. At 30 and 100 m, where late-December coastal upwelling rates exceed 50 m per month, particles are seeded in proportion to the upwelling rate. Ensemble maps of particle concentration, age, depth, temperature, salinity and density reveal that a substantial but variable fraction of the particles upwelling off Peru arrive via the Equatorial Undercurrent (EUC). Particles follow the EUC core at around 250 m, characterized by temperatures of around 15-17oC, salinities in the range 34.9-35.2, and densities of = 25.5-26.5 . Additional inflows are via two slightly deeper branches further south from the main system, at around 3oS and 8o. The annual percentage of particles recruited by the EUC (17.5-47% and 16.5-54.6%, from 30 and 100 m respectively) reveal that more of the Peruvian upwelling can be tracked back to the EUC during El Niño and weak La Niña events. In contrast, upwelling waters are of more local origin during a strong La Niña,. Annually averaging EUC transport at specific longitudes, notable anomalies are evident during the major El Niño /La Niña transition of 1997-99. On short timescales, a degree of longitudinal coherence is evident in EUC transport, with transport anomalies at 160oW evident at the Galapagos Is- lands (92oW) around 30-35 days later. We conclude that the Peruvian upwelling system is subject to a variable EUC influence, on a wide range of timescales, most notably the interannual timescale of El Niño Southern Oscillation (ENSO).

Keywords: Peruvian Upwelling, Equatorial Undercurrent, Particle tracking

©2021. Japan Geoscience Union. All Right Reserved.

[E] Oral | A (Atmospheric and Hydrospheric Sciences)：A-OS Ocean Sciences & Ocean Environment

Sat. Jun 5, 2021 10:45 AM - 12:15 PM JST | Sat. Jun 5, 2021 1:45 AM - 3:15 AM UTC | Ch.11 Zoom Room 11

[A-OS13] Marine ecosystems and biogeochemical cycles: theory, observation and modeling

convener:Takafumi Hirata(Arctic Research Center, Hokkaido University), Shin-ichi Ito(Atmosphere and Ocean Research Institute, The University of Tokyo), E Eileen Hofmann(Old Dominion University), N Enrique Curchitser(Rutgers University New Brunswick), Chairperson:Takafumi Hirata(Arctic Research Center, Hokkaido University), Shin-ichi Ito(Atmosphere and Ocean Research Institute, The University of Tokyo), Eileen E Hofmann(Old Dominion University), Enrique N Curchitser(Rutgers University New Brunswick)



The ocean accounts for about 50% of global net primary production. This production is significant for carbon cycling and ecosystem functioning, and is related directly or indirectly to a variety of climatic and ecological phenomena. The responses to natural and anthropogenic environmental stressors that influence marine production and diversity can cause perturbations to marine ecosystems that alter trophic dependencies and interactions among organisms at a range of space and time scales. Quantification of the principal mechanisms driving spatio-temporal variability of marine ecosystem remains to be done, especially in terms of evaluation of uncertainty in responses. As a result, evaluating vulnerability of marine ecosystems to environmental change requires systematic and holistic approaches that integrate physics to ecology and are based in observations and modelling. In addition, expectations to deliver these science to public society is raising. This session aims to provide a venue for not only discussing recent advances in understanding marine biogeochemical cycles, ecosystems and their interactions, but also networking with a variety of people to seed new ideas in marine ecological research. Observational, modeling and conceptual studies, including technological development and operational applications, that consider linkages among biogeochemical and ecosystem processes, biodiversity, and the effects of multiple stressors from molecular to planetary scales are encouraged.

10:45 AM - 11:00 AM JST | 1:45 AM - 2:00 AM UTC

[AOS13-07] Influence of ENSO on surface chlorophyll-a in the Gulf of Thailand

*Dudsadee Leenawarat[1], Jutarak Luang-on[1], Anukul Buranapratheprat[2], Joji Ishizaka[3] (1.Graduate School of Environmental Studies, Nagoya University, 2.Department of Aquatic Science, Faculty of Science, Burapha University, Thailand, 3.Institute for Space-Earth Environmental Research, Nagoya University, Japan)

11:00 AM - 11:15 AM JST | 2:00 AM - 2:15 AM UTC

[AOS13-08] Nitrogen isotope mapping in the North Pacific using a marine nitrogen isotope model

*Chisato Yoshikawa[1], Masahito Shigemitsu[1], Akitomo Yamamoto[1], Akira Oka[2], Naohiko Ohkouchi[1] (1.JAMSTEC, 2.AORI)

11:15 AM - 11:30 AM JST | 2:15 AM - 2:30 AM UTC

[AOS13-09] **Interannual variations of the lower-trophic level ecosystem in the Harima-Nada, eastern Seto Inland Sea, Japan simulated by a plankton functional type model.**

*Naoki Yoshie[1], Ayaka Hiramine[1] (1.Center for Marine Environmental Studies, Ehime University)

11:30 AM - 11:45 AM JST | 2:30 AM - 2:45 AM UTC

[AOS13-10] **Occurrence of phytoplankton bloom as the Kuroshio passes an island**

*JIE GAO[1], Xinyu Guo[1] (1.Center for Marine Environmental Studies, Ehime University)

11:45 AM - 12:00 PM JST | 2:45 AM - 3:00 AM UTC

[AOS13-11] Long-term comparison between the Japanese sardine stock level and simulated zooplankton density around the Kuroshio axis

*Haruka Nishikawa[1], Hiroyuki Tsujino[2], Shiro Nishikawa[1], Hideyuki Nakano[2], Toru Sugiyama[1], Yoichi Ishikawa[1] (1.Japan Agency for Marine-Earth Science and Technology, 2.Meteorological Research Institute)

12:00 PM - 12:15 PM JST | 3:00 AM - 3:15 AM UTC

[AOS13-12] Changes in phytoplankton photophysiology during pre-bloom and bloom phases in the coastal Oyashio waters

*Tomonori Isada[1], Toru Hirawake[2], Koji Suzuki[3], Jun Nishioka[4], Hiromi Kasai[5] (1.Field Science Center for Northern Biosphere, Hokkaido University, 2.Faculty of Fisheries Sciences, Hokkaido University, 3.Faculty of Environmental Earth Science, Hokkaido University, 4.Institute of Low Temperature Science, Hokkaido University, 5.Japan fisheries research and education agency)

Influence of ENSO on surface chlorophyll-a in the Gulf of Thailand

*Dudsadee Leenawarat[1], Jutarak Luang-on[1], Anukul Buranapratheprat[2], Joji Ishizaka[3]

1. Graduate School of Environmental Studies, Nagoya University, 2. Department of Aquatic Science, Faculty of Science, Burapha University, Thailand, 3. Institute for Space-Earth Environmental Research, Nagoya University, Japan

The Gulf of Thailand (GoT) is a tropical and semi-enclosed sea. This area is surrounded by Vietnam, Cambodia, Thailand, and Malaysia, and connected to the South China Sea via southeastern part. The variation of surface chlorophyll-a (chl-a) in this region was controlled by monsoon system. The large-scale phenomena such as El Niño Southern Oscillation (ENSO) also caused the variation over the monsoon system. These environmental changes caused by ENSO may increase/decrease phytoplankton production. To investigate the impact of ENSO on surface chl-a in each season, monthly chl-a data from MODIS from 2002 to 2018 were used in this study. Environmental parameters including sea surface temperature (SST), wind, precipitation, and discharge were also considered to describe the variability. It was found that the influence of ENSO on chl-a was stronger during the northeast monsoon (NEM; November to February) to the non-monsoon (NON; March to May) than the southwest monsoon (SWM; June to October). In the coastal area, surface chl-a responded to abnormally low/high precipitation and river discharge during El Niño/La Niña in all seasons. In the offshore area, chl-a was affected by changes in wind and water mixing. Weak/strong wind and increased/decreased SST may reduce/enhance in mixing from deep layer water mass that contains higher nutrients. Under El Niño condition, weak/strong wind and increased SST were found during NEM/NON and the opposite condition was found during La Niña condition. Weak in mixing from the deep layer and strong mixing of warm water mass in the upper layer were expected to occur during NEM and NON under El Niño condition. In addition, wind anomaly seems to create the shifting in the high chl-a area near the GoT mouth.

Keywords: Gulf of Thailand , Chlorophyll-a, ENSO

©2021. Japan Geoscience Union. All Right Reserved.

Nitrogen isotope mapping in the North Pacific using a marine nitrogen isotope model

*Chisato Yoshikawa[1], Masahito Shigemitsu[1], Akitomo Yamamoto[1], Akira Oka[2], Naohiko Ohkouchi[1]

1. JAMSTEC, 2. AORI

Understanding the special distribution of nitrogen isotope composition ($\delta^{15}N$) of phytoplankton in the surface ocean is useful for uncovering the life histories of marine organisms including fish. The $\delta^{15}N$ of phenylalanine (one of the “source” amino acids) of fish tissues inherits the $\delta^{15}N$ of phytoplankton where the fish grew up. Recently, Vane et al. (2018) determined $\delta^{15}N$ of amino acids in otoliths and showed that otoliths preserved a record of the $\delta^{15}N$ of phytoplankton over the lifetime of individual fish. Moreover, Matsubayashi et al. (2020) determined time-series $\delta^{15}N$ of amino acids in vertebra centra and successfully tracked a migration of chum salmon. Thus, the reconstruction of the temporal variations of $\delta^{15}N$ of amino acids from various fish tissues has made remarkable progress. However, there is as yet no accurate $\delta^{15}N$ map of phytoplankton due to observational heterogeneity, and it prevents improvement in the accuracy of migratory route estimation. In this study, we made a $\delta^{15}N$ map of phytoplankton in the North Pacific by using a global ocean nitrogen isotope model. We installed a marine nitrogen isotope model (Yoshikawa et al., 2005) with denitrification (Shigemitsu et al., 2016) and N_2 fixation (Coles et al., 2007) schemes into an off-line biogeochemical model that is driven by climatological monthly mean physical fields obtained from the outputs of a preindustrial control simulation performed with MIROC 3.2 (K-1 Model Developers, 2004). The simulated phytoplankton was enriched in ^{15}N in the northern Bering and Chukchi Seas where sedimentary denitrification is significant. The simulated phytoplankton was depleted in ^{15}N in the Kuroshio extension region where N_2 fixation occurs, and in the subarctic North Pacific region where the phytoplankton never uses up nitrate in the surface water due to iron limitation. In this talk, we will report the validation result of the simulated $\delta^{15}N$ map with the various $\delta^{15}N$ data set obtained from the North Pacific.

Keywords: Nitrogen isotope ratio, Marine nitrogen cycle, Marine ecosystem model

©2021. Japan Geoscience Union. All Right Reserved.

Interannual variations of the lower-trophic level ecosystem in the Harima-Nada, eastern Seto Inland Sea, Japan simulated by a plankton functional type model.

*Naoki Yoshie[1], Ayaka Hiramine[1]

1. Center for Marine Environmental Studies, Ehime University

In recent years, the effects of considerable decline of nutrient concentration with the strong and long-term regulation of nutrient discharge on the lower-trophic level ecosystem have received a lot of attention in the Harima-nada, eastern Seto Inland Sea, Japan. To investigate these effects, we conducted the numerical simulations using a plankton functional type model from 2000 to 2013 with the several different boundary conditions, which included decreasing of nutrient concentration with the discharge regulation and increasing of water temperature with the climate change. The model successfully reproduced the observed quite strange interannual variations, which were almost constant biomass of total phytoplankton in spite of the considerable decline of nutrient concentration, and also reproduced significant decrease in biomass of meso-zooplankton such as copepod. This is because the decrease in large-sized phytoplankton such as diatom due to both the decline of nutrient and increase of water temperature was canceled out by the increase in small-sized phytoplankton associated with the increase of water temperature. The decrease of diatom with both the decline of nutrient and increase of water temperature caused the decrease of copepod, which was extremely important feed for anchovy and sand eel in this region. It might be a reason for significant reduce of fish resources in the Harima-Nada.

Keywords: nutrient, phytoplankton, zooplankton, ecosystem model, coastal ocean

©2021. Japan Geoscience Union. All Right Reserved.

Occurrence of phytoplankton bloom as the Kuroshio passes an island

*JIE GAO[1], Xinyu Guo[1]

1. Center for Marine Environmental Studies, Ehime University

When the Kuroshio flows over islands or seamounts, it causes irregular fluid motions in the wake, such as eddy generation and shedding (Von Karman Vortex Street), turbulence mixing, upwelling and downwelling, and even instability. Vertical perturbations such as mixing and upwelling, bring the nutrients from deep layer to the oligotrophic surface layer and therefore enhance biological activity in the euphotic layer. Biological enrichment forms in the vicinity of the island and extends downstream, which is known as ‘Island Mass Effect’ (IME).

To investigate the IME and its community variation in the Kuroshio region, we combine a hydrodynamic model (Princeton Ocean Model) and a lower-trophic-level ecosystem model (eNEMURO). The eNEMURO includes 4 nutrient compartments (NO_3, NH_4, $Si(OH)_4$, PO_4), 4 phytoplankton compartments (2 types of micro-phyt, nano-phyt, pic-phyt), 4 zooplankton compartments (macro-zoo, meso-zoo, micro-zoo, nano-zoo), 3 detritus compartments (POM, DOM, Opal). We apply the combined two models to a simulation of ideal baroclinic geostrophic current flowing over an island with an ambient biological condition similar to the situation at the PN section across the Kuroshio in the East China Sea.

The model produces the Von Karman Vortex Street in the case of a current with a speed of 1m/s passing over an island with a diameter of 10 km. The eddies form just behind the island and shed toward downstream with a period of 13 hours. The cold water in the cyclonic recirculation corresponds to local upwelling that supplies extra nutrient to the oligotrophic surface and induces the surface phytoplankton bloom and uplift of Subsurface Chl-a Maximum (SCM) in the downstream wake area. At the depth below SCM (50m), the concentration of DIN increases inside the cyclonic eddies, while the phytoplankton decreases in the same location in the vicinity of the island. The variation of biological components in Von Karmen Vortex Street is caused by a combination of physical processes and biochemical processes. From the island to the place 100 km behind the island, the variation is mainly controlled by physical processes. After that, with the eddies extending downstream, effects of biogeochemical process increase and gradually become important. The increase in the cyclonic eddy region caused by biogeochemical processes is mainly contributed by photosynthesis supported by extra nutrient supply. In the oligotrophic surface water, the supply of nitrate is more efficient to the photosynthesis of PS, which has the lowest half-saturation concentration of nitrate.

In the realistic ocean, the Kuroshio passes islands with a variety of diameter and with a variety of speed. The variation in current speed and island size can cause different hydrodynamic condition for the ecosystem. To understand the effect of such variation, we design a series of numerical simulations to obtain a general understanding of hydrodynamic condition and biological response at island wake in the Kuroshio region.

Keywords: biogeochemical model, kuroshio, island

©2021. Japan Geoscience Union. All Right Reserved.

Long-term comparison between the Japanese sardine stock level and simulated zooplankton density around the Kuroshio axis

*Haruka Nishikawa[1], Hiroyuki Tsujino[2], Shiro Nishikawa[1], Hideyuki Nakano[2], Toru Sugiyama[1], Yoichi Ishikawa[1]

1. Japan Agency for Marine-Earth Science and Technology, 2. Meteorological Research Institute

Food availability in the larval stage is thought to be one of the important control factors for the Japanese sardine (*Sardinops melanostictus*) stock fluctuation. However, it is hard to compare the stock level with food availability, because there are few long-term data set of zooplankton. In this study, we simulated the past zooplankton density in the Northwestern Pacific from 1930s by using an NPZD model to solve the problem. Following a previous study that suggested an importance of the Kuroshio axis region as a larval feeding grounds, we compared the modeled zooplankton density in that region with the logarithm of recruitment per spawner (LNRPS) from 1978 to 2017 and catch from 1938 to 2017. This is the first study that shows the timeseries of modeled zooplankton density in the Japanese sardine feeding grounds. We found that there is a significant positive correlation between the zooplankton density and the LNRPS. Also the zooplankton density variation is consistent with the catch variation. These results suggested that the zooplankton density variation in the Kuroshio axis region affected the stock fluctuation of the Japanese sardine over the past few decades.

Keywords: Japanese sardine, NPZD model, Kuroshio

©2021. Japan Geoscience Union. All Right Reserved.

Changes in phytoplankton photophysiology during pre-bloom and bloom phases in the coastal Oyashio waters

*Tomonori Isada[1], Toru Hirawake[2], Koji Suzuki[3], Jun Nishioka[4], Hiromi Kasai[5]

1. Field Science Center for Northern Biosphere, Hokkaido University, 2. Faculty of Fisheries Sciences, Hokkaido University, 3. Faculty of Environmental Earth Science, Hokkaido University, 4. Institute of Low Temperature Science, Hokkaido University, 5. Japan fisheries research and education agency

Measurement of phytoplankton biomass and productivity in the ocean serve fundamental information about marine biogeochemical cycles and the trophic status of marine ecosystems. Photosynthesis–irradiance (*PE*) curve experiment can provide a means of comparing the photosynthetic characteristics of phytoplankton across different natural populations. Here, we investigated changes over time in phytoplankton community structure and their photosynthetic properties in the coastal Oyashio region, NW Pacific, where massive spring phytoplankton blooms occur every year and the blooms contribute to the highest seasonal biological drawdown effect on seawater pCO_2 in the world’s oceans, from March 2015 to January 2016 through HPLC-CHEMTAX pigment analyses and the PE curve experiments with ^{13}C tracer technique. Our CHEMTAX outputs showed that diatoms were consistently predominant from the pre-bloom to bloom periods, although chlorophyll (Chl) *a* concentrations during bloom were significantly higher than those in pre-bloom. We found the E_k-independent variability associated with the parallel changes in the Chl *a* specific maximum photosynthetic rate (P^B_{max}) and the initial slope of the *PE* curve (α^B) in each phase, suggesting the different photoacclimation strategies of phytoplankton assemblages between pre-bloom and bloom phases. These results could be of help for the parameterization of primary production models using satellite ocean color data and of ecosystem models in the coastal Oyashio waters.

Keywords: phytoplankton, photosynthetic parameters, spring bloom, Coastal Oyashio

©2021. Japan Geoscience Union. All Right Reserved.

[E] Oral | A (Atmospheric and Hydrospheric Sciences)：A-OS Ocean Sciences & Ocean Environment

Sat. Jun 5, 2021 1:45 PM - 3:15 PM JST | Sat. Jun 5, 2021 4:45 AM - 6:15 AM UTC | Ch.11 Zoom Room 11

[A-OS13] Marine ecosystems and biogeochemical cycles: theory, observation and modeling

convener:Takafumi Hirata(Arctic Research Center, Hokkaido University), Shin-ichi Ito(Atmosphere and Ocean Research Institute, The University of Tokyo), E Eileen Hofmann(Old Dominion University), N Enrique Curchitser(Rutgers University New Brunswick), Chairperson:Shin-ichi Ito(Atmosphere and Ocean Research Institute, The University of Tokyo), Takafumi Hirata(Arctic Research Center, Hokkaido University), Eileen E Hofmann(Old Dominion University), Enrique N Curchitser(Rutgers University New Brunswick)



The ocean accounts for about 50% of global net primary production. This production is significant for carbon cycling and ecosystem functioning, and is related directly or indirectly to a variety of climatic and ecological phenomena. The responses to natural and anthropogenic environmental stressors that influence marine production and diversity can cause perturbations to marine ecosystems that alter trophic dependencies and interactions among organisms at a range of space and time scales. Quantification of the principal mechanisms driving spatio-temporal variability of marine ecosystem remains to be done, especially in terms of evaluation of uncertainty in responses. As a result, evaluating vulnerability of marine ecosystems to environmental change requires systematic and holistic approaches that integrate physics to ecology and are based in observations and modelling. In addition, expectations to deliver these science to public society is raising. This session aims to provide a venue for not only discussing recent advances in understanding marine biogeochemical cycles, ecosystems and their interactions, but also networking with a variety of people to seed new ideas in marine ecological research. Observational, modeling and conceptual studies, including technological development and operational applications, that consider linkages among biogeochemical and ecosystem processes, biodiversity, and the effects of multiple stressors from molecular to planetary scales are encouraged.

1:45 PM - 2:05 PM JST | 4:45 AM - 5:05 AM UTC

[AOS13-13] Biogeochemical fingerprints of ocean migration of Pacific salmon

★Invited Papers

*Jun Matsubayashi[1] (1.Chuo University)

2:05 PM - 2:20 PM JST | 5:05 AM - 5:20 AM UTC

[AOS13-14] Vertical habitat shifts of juvenile Japanese jack mackerel (*Trachurus japonicus*) estimated by otolith microchemistry

*Megumi Enomoto[1], Shin-ichi Ito[1], Motomitsu Takahashi[2], Chiyuki Sassa[2], Tomihiko Higuchi[1], Kotaro Shirai[1] (1.Atmosphere and Ocean Research Institute, The University of Tokyo, 2.Fisheries Resource Institute, Japan Fisheries Research and Education Agency)

2:20 PM - 2:35 PM JST | 5:20 AM - 5:35 AM UTC

[AOS13-15] Retrospective time-series nitrogen isotope analysis of fish otoliths

*Yota Harada[1], Chisato Yoshikawa[1], Nanako O. Ogawa[1], Saburo Sakai[1], Shin-ichi Ito[2], Naohiko Ohkouchi[1] (1.Biogeochemistry Research Center, Japan Agency for Marine-Earth Science and Technology, 2.Atmosphere and Ocean Research Institute, The University of Tokyo)

2:35 PM - 2:55 PM JST | 5:35 AM - 5:55 AM UTC

[AOS13-16] Fish specialize their metabolic performance to maximize bioenergetic efficiency in their local environment

★Invited Papers

*Chenying Guo[1], Shin-ichi Ito[1], Michio Yoneda[2], Hajime Kitano[2], Hitoshi Kaneko[3], Megumi Enomoto[1], Tomoya Aono[1], Masahiro Nakamura[2], Takashi Kitagawa[1], Nicolas C Wegner[4], Emmanis Dorval[5]
(1.Atmosphere and Ocean Research Institute, the University of Tokyo, 2.Japan Fisheries Research and Education Agency, 3.Japan Agency for Marine-Earth Science and Technology (JAMSTEC), 4.Southwest Fisheries Science Center, National Marine Fisheries Service, NOAA, 5.Lynker Technologies, LLC., under contract to Southwest Fisheries Science Center, NOAA)

2:55 PM - 3:10 PM JST | 5:55 AM - 6:10 AM UTC

[AOS13-17] Comparative study on environment experienced by jack mackerel in the East China Sea between 1960s and 2000s.

*Tomihiko Higuchi[1], Motomitsu Takahashi[2], Megumi Enomoto[1], Kotaro Shirai[1], Shin-ichi Ito[1]
(1.Atmosphere and Ocean Research Institute, The University of Tokyo, 2.Fisheries Resources Institute, Japan Fisheries Research and Education Agency, Nagasaki, Japan)

3:10 PM - 3:15 PM JST | 6:10 AM - 6:15 AM UTC

[AOS13-18] Discussion

Biogeochemical fingerprints of ocean migration of Pacific salmon

*Jun Matsubayashi[1]

1. Chuo University

Long-distance ocean migration by marine fish has long fascinated scientists, and a better understanding of such migrations may hold important keys to understanding the impacts of ongoing climate change as well as the evolutionary history and mechanisms of niche partitioning in these taxa. However, research into this topic has been hampered by the substantial investment of time and effort required to monitor fishes in the ocean using field surveys.

The migration history of a fish can be recorded as isotope ratios in tissues such as the otolith and vertebral centrum that undergo incremental growth. Specifically, by combining data on spatial patterns in isotope ratios (isoscapes) with retrospective isotope analysis of vertebral centra, it is possible to reconstruct potential individual migration routes.

In this study, I revealed chum salmon migration routes using the isoscape and retrospective isotope analysis of the salmon. Initially, the isoscape of stable nitrogen isotope ratios ($\delta^{15}N$) at the base of the food web ($\delta^{15}N_{Base}$) in the northern North Pacific was generated by conducting compound-specific isotope analysis of amino acids from copepods sampled across the region. Then, I performed retrospective stable nitrogen isotope analysis of mature chum salmon sampled from different streams in Japan. Finally, the migration routes of individual salmon were estimated by using a state-space model which can incorporate the isoscape and retrospective isotope shifts of salmon.

The isotope tracking successfully reproduced a known salmon migration route between the Okhotsk and Bering seas. In addition, the results suggested the presence of a new migration route to the continental shelf of the eastern Bering Sea during a later growth stage. The later stage of skeletal growth of salmon is corresponds to the timing of sexual maturation of this species. For this reason, this study strongly suggested that the Bering Sea Shelf is a destination of ocean migration of chum salmon, and the purpose of their journey should be fulfilling the nutritional demands of sexual maturation in this highly-productive region.

The results of this study suggested that Asian population of chum salmon strongly depend on the nutrient in the Bering Sea Shelf in the far distance from Japan. It anticipates that monitoring and management of the environment of their habitat while traveling in the ocean as well as their natal river and coastal area are important for sustainable use of salmon resources. The isoscape of stable nitrogen isotope ratios generated in this study can be applied for isotope tracking of various animals which migrate the North Pacific Ocean. Hence, the method of this study will strongly promote the future use of isoscape for migration study of marine animals.

Keywords: isoscape, salmon, migration, nitrogen stable isotope ratios

©2021. Japan Geoscience Union. All Right Reserved.

Vertical habitat shifts of juvenile Japanese jack mackerel (*Trachurus japonicus*) estimated by otolith microchemistry

*Megumi Enomoto[1], Shin-ichi Ito[1], Motomitsu Takahashi[2], Chiyuki Sassa[2], Tomihiko Higuchi[1], Kotaro Shirai[1]

1. Atmosphere and Ocean Research Institute, The University of Tokyo, 2. Fisheries Resource Institute, Japan Fisheries Research and Education Agency

Japanese jack mackerel (*Trachurus japonicus*) are distributed in the semi-demersal layer, while larvae are distributed in the surface layer in the East China Sea. Smooth vertical habitat layer shift (HLS) is important for their survival. However, details (start timing and duration) of HLS have been unclarified. To elucidate HLS, otolith oxygen stable isotope ratio ($\delta^{18}O_{oto}$), of which the value increases at lower temperature and higher salinity, was analyzed in high resolution by 5 days segment. From the history of $\delta^{18}O_{oto}$, HLS timing was estimated by two types of indices; HLS moment and HLS duration, which were identified by the largest $\delta^{18}O_{oto}$ gap signal and gradual $\delta^{18}O_{oto}$ change, respectively. In addition, daily ages and water temperature variances fish experienced were compared among three life history traits; the metamorphosis, the behavioral change from planktonic to self-swimming and the swimming ability increase. As a result, average HLS moment was estimated to be 42.2±18.2 daily age. HLS started at 28.0±11.0 daily age and average HLS duration was 27.9±16.2 days on average. The start of HLS duration corresponded to the start of metamorphosis, and development of swimming ability was happened simultaneously with HLS moment. From the $\delta^{18}O_{oto}$ value of edge, observed temperature and salinity in the layer fish caught and the relationship between salinity and $\delta^{18}O_{sw}$ ($\delta^{18}O$ of sea water) from the previous study, an equation between $\delta^{18}O$ ($\delta^{18}O_{oto} - \delta^{18}O_{sw}$) and temperature was estimated; Temperature(˚C) = −3.51 (±0.49) × $\delta^{18}O$ (‰) + 15.86 (±0.29). Temperature variance converted from $\delta^{18}O_{oto}$ suggested that juveniles gradually shift habitat layer as they experience early life history traits, not suddenly after specific trait.

Keywords: otolith, otolith oxygen stable isotope ratio, Japanese jack mackerel, vertical habitat layer shift, early life history, East China Sea

©2021. Japan Geoscience Union. All Right Reserved.

Retrospective time-series nitrogen isotope analysis of fish otoliths

*Yota Harada[1], Chisato Yoshikawa[1], Nanako O. Ogawa[1], Saburo Sakai[1], Shin-ichi Ito[2], Naohiko Ohkouchi[1]

1. Biogeochemistry Research Center, Japan Agency for Marine-Earth Science and Technology, 2. Atmosphere and Ocean Research Institute, The University of Tokyo

Fish otoliths that allow both age estimation and retrospective isotope analysis are a powerful tool for investigating life and movement histories of fish. Nitrogen isotopes that vary spatially in the ocean are useful for tracking fish migration, but fish otoliths that consist of calcium carbonate deposited within a proteinaceous matrix, generally do not contain enough nitrogen to allow retrospective δ^{15}N comparisons with the conventional elemental analyzer/isotope ratio mass spectrometry (EA IRMS) system. To achieve retrospective time-series nitrogen isotope analysis of otoliths from individual fish, an EA-IRMS system that was optimised for microscale isotope analysis was used. Otoliths from commercially important fish such as japanese sardine (*Sardinops melanostictus*), chub mackerel (*Scomber japonicus*), pacific saury (*Cololabis saira*), and jack mackerel (*Trachurus japonicus*) contained 0.31, 0.28, 0.26 and 0.18 % of nitrogen by weight, respectively. The weight of the otoliths were 2.7, 6.4, 0.7 and 22.9 mg, respectively. Although pacific saury had the smallest otolith, we were able to achieve retrospective bulk ^{15}N analysis with the δ^{15}N values ranging from 5.3 to 6.6‰ and recreated a known migration route of pacific saury in North west pacific. Retrospective time-series ^{15}N analysis of otoliths can be used with other isotopes, for example, oxygen isotopes that are used to estimate experienced water temperatures to improve the estimation of fish migration.

Keywords: isotope, nitrogen, fish, otolith

©2021. Japan Geoscience Union. All Right Reserved.

Fish specialize their metabolic performance to maximize bioenergetic efficiency in their local environment

*Chenying Guo[1], Shin-ichi Ito[1], Michio Yoneda[2], Hajime Kitano[2], Hitoshi Kaneko[3], Megumi Enomoto[1], Tomoya Aono[1], Masahiro Nakamura[2], Takashi Kitagawa[1], Nicolas C Wegner[4], Emmanis Dorval[5]

1. Atmosphere and Ocean Research Institute, the University of Tokyo, 2. Japan Fisheries Research and Education Agency, 3. Japan Agency for Marine-Earth Science and Technology (JAMSTEC), 4. Southwest Fisheries Science Center, National Marine Fisheries Service, NOAA, 5. Lynker Technologies, LLC., under contract to Southwest Fisheries Science Center, NOAA

Species-specific ecological traits in fishes are likely to vary between populations or stocks due to differences in regional oceanic conditions, such as latitudinal temperature. We examined potential intraspecific differences in the swimming performance and metabolism of chub mackerel (*Scomber japonicus*) from the Northwest and Northeast stocks, which are distributed on opposite sides of the North Pacific at similar latitudes, but where the temperature contrast is large. Swimming bioenergetics and metabolic data of Northwest stock were measured at 14˚C, 18˚C, and 24˚C using variable-speed swim-tunnel respirometers, and then the resulting bioenergetic parameters were compared with previous findings from the Northeast stock. At a given size, the maximum sustainable swimming speed (U_{max}) of the Northwest stock showed no significant difference compared to the Northeast stock at 18˚C and 24˚C, but was lower at 14˚C. In addition, the oxygen consumption rate (M_{O2}) of the Northwest stock showed lower mass dependence and different temperature dependence at a given swimming speed than in the Northeast stock. Combined with stock-specific data on growth and experienced temperatures in the wild, these bioenergetic differences indicate that the swimming performance and metabolism of the two stocks are specific to their local environment to maximize bioenergetic efficiency. This study has been already published on Frontiers in Marine Science (doi:10.3389/fmars.2021.613965).

Keywords: chub mackerel, Scomber japonicus, metabolism, oxygen consumption rate, temperature, swimming speed

©2021. Japan Geoscience Union. All Right Reserved.

Comparative study on environment experienced by jack mackerel in the East China Sea between 1960s and 2000s.

*Tomihiko Higuchi[1], Motomitsu Takahashi[2], Megumi Enomoto[1], Kotaro Shirai[1], Shin-ichi Ito[1]

1. Atmosphere and Ocean Research Institute, The University of Tokyo, 2. Fisheries Resources Institute, Japan Fisheries Research and Education Agency, Nagasaki, Japan

Jack mackerel *Trachurus japonicus* is distributed on the continental shelf waters along with the subtropical Kuroshio Current and the Tsushima Warm Current in the western North Pacific. The East China Sea (ECS) is one of the major spawning and nursery grounds for jack mackerel and understanding the recruitment processes of jack mackerel into the fishing grounds in the ECS is important. However, information on how jack mackerel respond to decadal temperature variability is limited. Also, it is known that jack mackerel change their habitat from the surface to the semi-demersal layer in early life stage in the ECS. This study aims to know the migration history including the vertical habitat layer change of jack mackerel in the ECS during the 1960s and the 2000s. To estimate their environment experienced during the larval and juvenile stages, oxygen ($\delta^{18}O$) stable isotope of jack mackerel otolith was analyzed by using isotope ratio mass spectrometer (n=422). Fish samples were taken at the ECS in 1960-70s and 2000-2010s (15 individuals, each period). The high-precision micro-milling system GEOMILL 326 was used for otolith subsampling. At every 10 daily rings (20-30 daily rings in section including core), a ring was tracked and used as the boundary of the micro-milling increment. As a result, there was no significant differences in temperature experienced by the larval-juvenile stages, which is estimated from $\delta^{18}O$, between the two survey periods. This indicate that both jack mackerel from different periods likely utilized a similar environment under a changing ocean state. By using assimilated ocean data (SODA2.2.4 for 1960s, 3.12.2 for 2000s), we estimated the distribution area of jack mackerel in each age. In the early life stage (~60 daily age), distribution areas were different between the periods and individuals in the 1960s migrated in the north compared with those in the 2000s. There was a significant positive relationship between habitat temperature and growth rates based on otolith increment width during the juvenile stage. This suggested that the effect of water temperature on the growth of jack mackerel in the early life stage. Thus, jack mackerel in ECS likely adapted to decadal climate variability and select the preferred environment.

Keywords: otolith isotope analysis, fish migration, temperature history

©2021. Japan Geoscience Union. All Right Reserved.

[E] Oral | A (Atmospheric and Hydrospheric Sciences) | A-OS Ocean Sciences & Ocean Environment

[A-OS13] Marine ecosystems and biogeochemical cycles: theory, observation and modeling

convener:Takafumi Hirata(Arctic Research Center, Hokkaido University), Shin-ichi Ito(Atmosphere and Ocean Research Institute, The University of Tokyo), E Eileen Hofmann(Old Dominion University), N Enrique Curchitser(Rutgers University New Brunswick), Chairperson:Shin-ichi Ito(Atmosphere and Ocean Research Institute, The University of Tokyo), Takafumi Hirata(Arctic Research Center, Hokkaido University), Eileen E Hofmann(Old Dominion University), Enrique N Curchitser(Rutgers University New Brunswick)

Sat. Jun 5, 2021 1:45 PM - 3:15 PM Ch.11 (Zoom Room 11)

The ocean accounts for about 50% of global net primary production. This production is significant for carbon cycling and ecosystem functioning, and is related directly or indirectly to a variety of climatic and ecological phenomena. The responses to natural and anthropogenic environmental stressors that influence marine production and diversity can cause perturbations to marine ecosystems that alter trophic dependencies and interactions among organisms at a range of space and time scales. Quantification of the principal mechanisms driving spatio-temporal variability of marine ecosystem remains to be done, especially in terms of evaluation of uncertainty in responses. As a result, evaluating vulnerability of marine ecosystems to environmental change requires systematic and holistic approaches that integrate physics to ecology and are based in observations and modelling. In addition, expectations to deliver these science to public society is raising. This session aims to provide a venue for not only discussing recent advances in understanding marine biogeochemical cycles, ecosystems and their interactions, but also networking with a variety of people to seed new ideas in marine ecological research. Observational, modeling and conceptual studies, including technological development and operational applications, that consider linkages among biogeochemical and ecosystem processes, biodiversity, and the effects of multiple stressors from molecular to planetary scales are encouraged.

3:10 PM - 3:15 PM

[AOS13-18]Discussion

©Japan Geoscience Union

[E] Poster | A (Atmospheric and Hydrospheric Sciences)：A-OS Ocean Sciences & Ocean Environment

Sat. Jun 5, 2021 5:15 PM - 6:30 PM JST | Sat. Jun 5, 2021 8:15 AM - 9:30 AM UTC | Ch.05_3

[A-OS13] Marine ecosystems and biogeochemical cycles: theory, observation and modeling

convener:Takafumi Hirata(Arctic Research Center, Hokkaido University), Shin-ichi Ito(Atmosphere and Ocean Research Institute, The University of Tokyo), E Eileen Hofmann(Old Dominion University), N Enrique Curchitser(Rutgers University New Brunswick)



The ocean accounts for about 50% of global net primary production. This production is significant for carbon cycling and ecosystem functioning, and is related directly or indirectly to a variety of climatic and ecological phenomena. The responses to natural and anthropogenic environmental stressors that influence marine production and diversity can cause perturbations to marine ecosystems that alter trophic dependencies and interactions among organisms at a range of space and time scales. Quantification of the principal mechanisms driving spatio-temporal variability of marine ecosystem remains to be done, especially in terms of evaluation of uncertainty in responses. As a result, evaluating vulnerability of marine ecosystems to environmental change requires systematic and holistic approaches that integrate physics to ecology and are based in observations and modelling. In addition, expectations to deliver these science to public society is raising. This session aims to provide a venue for not only discussing recent advances in understanding marine biogeochemical cycles, ecosystems and their interactions, but also networking with a variety of people to seed new ideas in marine ecological research. Observational, modeling and conceptual studies, including technological development and operational applications, that consider linkages among biogeochemical and ecosystem processes, biodiversity, and the effects of multiple stressors from molecular to planetary scales are encouraged.

[AOS13-P01] Marine fish distribution in the Kuroshio Extension area observed by OceanDNA

*ZESHU YU[1], Shin-ichi Ito[2], Marty Wong[2], Susumu Yoshizawa[2], Jun Inoue[2], Sachihiko Itoh[2], Susumu Hyodo[2] (1.Graduate School of Agricultural and Life Sciences, The University of Tokyo, 2. Atmosphere and Ocean Research Institute, The University of Tokyo)

[AOS13-P02] Introducing phytoplankton size structure in an ocean biogeochemical model OECO2

*Wenhui Sun[1], Ryota Shibano[1], Michio Watanabe[2], Sachihiko Itoh[1] (1.Atmosphere and Ocean Research Institute, The University of Tokyo, 2.Japan Agency for Marine-Earth Science and Technology)

[AOS13-P03] Origin of dissolved inorganic nitrogen in the Tsushima Strait and its seasonal and interannual variation

*Ryota Shibano[1], Akihiko Morimoto[2], Katsumi Takayama[3], Tetsutaro Takikawa[4], Joji Ishizaka[5], Xinyu Guo[2] (1.Atmosphere and Ocean Research Institute, The University of Tokyo, 2.Center for Marine Environmental Studies, Ehime University, 3.Research Institute for Applied Mechanics, Kyushu University, 4.Graduate School of Fisheries and Environmental Sciences, Nagasaki University, 5.Institute for Space-Earth Environmental Research, Nagoya University)

[AOS13-P04] Comparative study on respiration of Japanese anchovy (*Engraulis japonicus*) around Japan II.

*Shin-ichi Ito[1], Chenying Guo[1], Megumi Enomoto[1], Tomoya Aono[1], Michio Yoneda[2], Michiya Matsuyama[3], Takashi Kitagawa[1], Motomitsu Takahashi[2], Taketo Hashioka[4] (1.Atmosphere and Ocean Research Institute, The University of Tokyo, 2.Japan Fisheries Research and Education Agency, 3.Kyushu University, 4.Japan Agency for Marine-Earth Science and Technology)

[AOS13-P05] A state-space production model to analyze the impact of stock enhancement on population dynamics: a case study of Japanese flounder in the Seto Inland Sea

*LIN ZHEN[1], Toshihide Kitakado[2], Naoki Suzuki[2], Shin-ichi Ito[1] (1.Atmosphere and Ocean Research Institute, The University of Tokyo, 2.Tokyo University of Marine Science and Technology)

[AOS13-P06] Variability in phytoplankton Chlorophyll-a in the Kuroshio western boundary current: a result from 14-year observation by satellite remote sensing

*Takafumi Hirata[1], Keiko Sato[1], Satoshi Kitaoka (1.Arctic Research Center, Hokkaido University)

Marine fish distribution in the Kuroshio Extension area observed by OceanDNA

*ZESHU YU[1], Shin-ichi Ito[2], Marty Wong[2], Susumu Yoshizawa[2], Jun Inoue[2], Sachihiko Itoh[2], Susumu Hyodo[2]

1. Graduate School of Agricultural and Life Sciences, The University of Tokyo, 2. Atmosphere and Ocean Research Institute, The University of Tokyo

Due to huge volume of the ocean and the difficulty of observing in stormy weather, distribution patterns of marine fish species are still underdetermined. In recent years, a new survey technique using environmental DNA (eDNA) in water has been developed and actively conducted. However, the lower density of fish in the open ocean leaves questions about the effectiveness of ‘eDNA survey in the open ocean’ (hereafter OceanDNA). We have three purposes in this research: 1. comparing the fish distribution found by OceanDNA with the net-sampling result, 2. analyzing the difference between OceanDNA data from MiFish and from qPCR method, 3. comparing the OceanDNA data from Niskin bottle and from ship-bottom-intake seawater. During the KS-18-5 cruise by Shinsei-Maru, seawater samples were collected at several stations in the Kuroshio Extension area from different depth using two methods. One is water sampling by Niskin bottles from 5 to 300 m combined with Conductivity Temperature Depth (CTD) instrument, which measured water mass distribution, and by a bucket for 0 m (130 samples). The other is water sampling from intake seawater from the bottom of the ship (15 samples). Water samples were filtered by Sterivex DNA filter (0.45 μm) and the filters were stored at -20 ˚C, then DNA was extracted from filter after the cruise. To analyze the OceanDNA samples, we used the DNA metabarcoding method with universal MiFish primers targeting a hyper-variable region of fish mitochondrial 12S rRNA gene. The PCR results were compared to DNA library to identify the species. 60 marine fish species were identified and in terms of number of species, Myctophidae is the most dominating family that contains 15 species of all 60. The results showed spatial segregating distribution of 15 Myctophidae species, in which 4 groups were segregated by depth and 2 groups were segregated by sampling stations. On the other hand, two potential predator species of Myctophidae were found out from all 60 species, and both showed depth-segregating distribution with Myctophidae. The fish distribution pattern found here, especially the depth-segregating distribution in Myctophidae and in two prey/predator groups were consist with previous studies. We also used qPCR method to analyze the OceanDNA samples to detect 6 small pelagic fish species (*Sardinops melanostictus, Engraulis japonicus, Scomber japonicus, Scomber australasicus, Trachurus japonicus,* and *Cololabis saira*). We first compared the absence/presence of the 6 small pelagic species between MiFish and qPCR methods. When DNA of one species was found by either method, we admitted its existence. Two *Scomber* species and *Sardinops melanostictus* got high existence rate (higher than 40%) while *Engraulis japonicus* and *Cololabis saira* were found in less than 15% samples (*Trachurus japonicus* was found in only one sample). From the Niskin water samples, the positive significant correlations were found between data of qPCR and MiFish analyzing for the existence of two *Scomber* species and *Sardinops melanostictus*, but qPCR got more than three times discover rate compared with MiFish method. Same correlations were not found in data from ship-bottom-intake seawater. However, if pooling data of six species together, the positive significant correlation was found between data of qPCR and MiFish analyzing although qPCR got more discover rate than MiFish method in both two kinds of water. The result suggests that qPCR method we developed is a proper method to observe distribution of the small pelagic species. On the other hand, when looking at qPCR method data, discover rate from Niskin-bottles seawater and from ship-bottom-intake seawater were always similar in highly existed species. But for sparse distributed species *Engraulis japonicus*, it was discovered more from

©2021. Japan Geoscience Union. All Right Reserved.

ship-bottom-intake seawater rather than from Niskin-bottles seawater. When using MiFish data, the discover rates were often higher from ship-bottom-intake seawater than from Niskin-bottles seawater. The data was limited and the reason why the discover rates differ between the water sampling methods is still unclear. Further comparison is essential to clarify the mechanism in future.

Keywords: environmental DNA, fish distribution, Kuroshio Extension, small pelagics

©2021. Japan Geoscience Union. All Right Reserved.

Introducing phytoplankton size structure in an ocean biogeochemical model OECO2

*Wenhui Sun[1], Ryota Shibano[1], Michio Watanabe[2], Sachihiko Itoh[1]

1. Atmosphere and Ocean Research Institute, The University of Tokyo, 2. Japan Agency for Marine-Earth Science and Technology

The biodiversity ecosystem functioning (BEF) caused by biodiversity affects the ecosystem services that humans receive, through the enhancement of productivity, stability, resistivity against invasive species, nutrient dynamics, etc. Many previous studies for marine ecosystems suggested that biodiversity generally has positive impacts on the ecosystem functioning. For instance, increasing biodiversity enhances the productivity through selection effects and niche complementarity. The underlying mechanism, however, has yet to be revealed. Recently, trait-based marine ecosystem models are gaining increasing attention due to their ability to explore the ecological and biochemical mechanism of biodiversity, which can take the environmental variability into account and complement spatiotemporal sparseness of field observation. However, development of a trait-based model has mostly been separated from the achievements of classical non-trait-based plankton functional type models, which is widely used in the global scale modeling. Therefore, this study aim at introducing trait factors in the existing non-trait-based marine ecosystem model, and exploring the relationship between phytoplankton diversity and ecosystem functions. The biogeochemical component OECO-v2a for an earth system model MIROC-ES2L is used to do this extension, which is run with the physical environmental field driven by the average external forces during 1981–2000. To represent phytoplankton biodiversity and reduce the number of parameters in the model, we introduce the concept of relative volume and determine physiological parameters, such as the rate of nutrient uptake, using size-based power laws. Based on this BEF model, we will discuss the relationship between phytoplankton diversity and BEF such as primary production and export production in the North Pacific under changing environments.

Keywords: trait-based ecosystem modeling , size scaling, biodiversity ecosystem functioning

©2021. Japan Geoscience Union. All Right Reserved.

Origin of dissolved inorganic nitrogen in the Tsushima Strait and its seasonal and interannual variation

*Ryota Shibano[1], Akihiko Morimoto[2], Katsumi Takayama[3], Tetsutaro Takikawa[4], Joji Ishizaka[5], Xinyu Guo[2]

1. Atmosphere and Ocean Research Institute, The University of Tokyo, 2. Center for Marine Environmental Studies, Ehime University, 3. Research Institute for Applied Mechanics, Kyushu University, 4. Graduate School of Fisheries and Environmental Sciences, Nagasaki University, 5. Institute for Space-Earth Environmental Research, Nagoya University

Tsushima Strait is shallow and narrow straits connecting the East China Sea and the Japan Sea. Along the coast of Japan in the Japan Sea, a warm and saline water mass is supplied from the East China Sea (ECS) and the Pacific Ocean by the Tsushima Warm Current (TWC). This current transports water, heat, and nutrients from the southern regions to the Japan Sea. TWC is originated the transports from the six sources, the Pacific through the Kuroshio, the Taiwan Strait, the Changjiang and Yellow Rivers, the dust from the atmosphere, and the bottom layer in the East China and Yellow Seas. The transports by TWC have the large variations in the seasons and/or years according to the observations in the Tsushima Strait. To investigate the dynamics in the Tsushima Strait, the estimations on the nutrient cycles in ECS and the Yellow Sea.

We developed a physical and ecosystem coupled model for the East China, Yellow, and Japan Seas to investigate the origin of dissolved inorganic nitrogen (DIN) in the Tsushima Strait. Assuming the potential six sources of DIN in the Tsushima Strait, we calculated the contribution ratio of each source of DIN in the Tsushima Strait using the numerical model. The most dominant source of DIN in the strait was DIN from the Pacific Ocean, with a contribution ratio of 40–50%. The second most dominant source was that from the Taiwan Strait, with 10%. The contribution from the rivers was less than 5%. Although more than 70% of the freshwater discharged from the Changjiang River enters the Japan Sea through the Tsushima Strait, most of the DIN input from the river sinks to the bottom of the ECS. A small portion that is decomposed at the bottom of the sea is transported in subsurface and lower layers to the Tsushima Strait. Interannual variation in DIN concentration was caused by variation in the DIN flux across the continental shelf in the ECS, and the influence of DIN originating from the Changjiang River was small. However, a drastic increase in DIN concentration could possibly occur if the N/P ratio in the Changjiang River were to become much higher than the current ratio.

Keywords: East China Sea, nutrient cycle, river discharge

©2021. Japan Geoscience Union. All Right Reserved.

Comparative study on respiration of Japanese anchovy (*Engraulis japonicus*) around Japan II.

*Shin-ichi Ito[1], Chenying Guo[1], Megumi Enomoto[1], Tomoya Aono[1], Michio Yoneda[2], Michiya Matsuyama[3], Takashi Kitagawa[1], Motomitsu Takahashi[2], Taketo Hashioka[4]

1. Atmosphere and Ocean Research Institute, The University of Tokyo, 2. Japan Fisheries Research and Education Agency, 3. Kyushu University, 4. Japan Agency for Marine-Earth Science and Technology

Japanese anchovy (*Engraulis japonicus*) is an important species not only as an exploited species but also as prey for variety of predators including marine mammals, tunas, mackerels, flounders, etc. However, the biomass of Japanese anchovy has shown large fluctuation and is one of the main actors of the fish species alternation responding to basin scale climate variabilities. From the stock management views, three sub-populations are defined in Japan: Pacific stock, Tsushima stock (also called the East China Sea stock), and Seto-inland Sea stock. The three sub-population shows difference in weights-at-age and longevity. While the three sub-populations of anchovy share their spawning grounds, the migration route and nursery grounds are divided. In addition, while Seto-inland Sea sub-populations do not show a large migration, Pacific and Tsushima sub-populations make long distance ontogenetic migrations.

All anchovy sub-populations are plankton feeders and mainly conduct filter feeding. Therefore, we hypothesized that different respiration characteristics induce different behaviors and hence growth and migration routes between the anchovy sub-populations. To test the hypothesis, we conducted laboratory respiration experiments using a 5L swimming tunnel. Since anchovy is sensitive and difficult to stabilize by individual, two anchovies were putted in the sealed tank and were measured oxygen consumption rate with various temperatures and velocities. Based on the experiment data, oxygen consumption rate dependencies on temperature, swimming speed, and body weight were determined. In addition, basic oxygen consumption rate at 0 degC temperature without swimming was estimated. Those derived oxygen consumption characteristics showed similar dependency on swimming speed. However, the Pacific-stock showed lower dependency on temperature but higher dependency on body weight compared with those of the Seto-inland Sea stock. The oxygen consumption characteristics of the Pacific-stock were similar to those of Peruvian anchoveta (*Engraulis ringens*) and South African anchovy (*Engraulis capensis*).

Keywords: respiration, migration, Japanese anchovy

©2021. Japan Geoscience Union. All Right Reserved.

A state-space production model to analyze the impact of stock enhancement on population dynamics: a case study of Japanese flounder in the Seto Inland Sea

*LIN ZHEN[1], Toshihide Kitakado[2], Naoki Suzuki[2], Shin-ichi Ito[1]

1. Atmosphere and Ocean Research Institute, The University of Tokyo, 2. Tokyo University of Marine Science and Technology

More than 26 billion juveniles of 180 marine species have been released annually into the wild in over 20 countries. Because it is not easy to separate the wild fish and hatchery fish in the natural condition and clarify how released fish influence the biomass of the wild stock, the usefulness of stock enhancement remains unclear (Kitada, 2020). Recapture rate has been adopted as an important index to measure the success of the stock enhancement, and the corresponding cohort models were used to analyze the biomass of the hatchery stock separated by the recapture ratio. Lorenzen (2005) added the density-dependent parameters and depicted the growth of the hatchery cohort more rationally. However, those models require a huge amount of information, and generally, the dimensions and quality of data are not enough in the fishery. Thus, new models should be developed to cope with those situations. We developed state-space production models to answer the question about “Do hatcheries produce extra fish?”, and applied it in the fishery of Japanese flounder *Paralichthys olivaceus* in the Seto Inland Sea to shed some light on the effect of stock enhancement.

First, we developed the state-space production model (SSPM) to elucidate the fishery with stock enhancement. Considering the data with the large process and observation errors in the real fishery might vague the hidden information, maximum likelihood augmented with prior information (Maximum a posterior or MAP) was used in the parameter estimation. Time-trajectories of biomass and catch per unit effort (CPUE) data were simulated to test the reliability of MAP. Then, we used the SSPM to evaluate key parameter values that influence the biomass variation. The biomass increment by the stock enhancement can be extracted from the difference between the estimated current biomass and the hypothesized biomass trajectories without hatchery releasement. Furthermore, we used the Monte Calo Markov chain to calculate the distribution of process error, and projected future biomass under the different fishing pressures.

As a result, although the whole biomass resulting from the stock enhancement in the Seto Inland Sea has been increased until 2005, the extra biomass showed more moderate growth. It suggested the hatchery stock did not contribute to increasing much extra biomass, instead, it tended to “replace” the niche of the wild fish. In the future projections, the biomass increment by the stock enhancement was increased under higher fishing pressure, but the total biomass was reduced simultaneously. Therefore, the balance between the stock enhancement and the exploitation is important.

Keywords: Stock enhancement evaluation, State-space model, Japanese flounder

©2021. Japan Geoscience Union. All Right Reserved.

Variability in phytoplankton Chlorophyll-a in the Kuroshio western boundary current: a result from 14-year observation by satellite remote sensing

*Takafumi Hirata[1], Keiko Sato[1], Satoshi Kitaoka

1. Arctic Research Center, Hokkaido University

The Kuroshio western boundary current transports thermal energy and water mass from low latitudes to mid-latitudes in the Western Pacific and its water is characterized relatively oligotrophic by low Chlorophyll-a concentration (Chla). In spite of the oligotrophy, spawning and feeding grounds of fish are located along the Kuroshio, resulting in a higher fisheries production in the region. How the oligotrophic environment can support the high fishery production is unclear. To better understand the Kuroshio ecosystem, how a standing stock of primary producer varies and how higher trophic organisms follow it, spatio-temporal variability of Chla in and around the Kuroshio current between 125-140˚E is investigated using 14 years (2006-2020) of monthly satellite remote sensing data. The surface water in the region was classified according to seasonality of Chla, to find out that a dominant mode of seasonality on the Kuroshio is characterized by both spring bloom and winter increase. The spring and winter increases in Chla were approximately 8-month away from each other within a specific year. They showed no correlation with each other, implying that there is no “biological memory” kept from one to the other. Anomalously-High Seasonal Amplitudes (AHSA, defined as a peak Chla value exceeds 2 or 3 times its standard deviation at an observation point of interest) were also found in the Kuroshio, most evidently between Year 2010 and 2012. One-by-one seasonal peak analysis using satellite images showed that the AHSA were found either when the Kuroshio passes through a very high Chla water or when turbulent water patches with high Chla horizontally intrudes into the Kuroshio. The latter implies a possibility of intermittent supply of high Chla into the Kuroshio by local turbulences even at smaller temporal scales not resolved by our satellite data. Time series analysis showed that there is seemingly a periodic interannual variability. We suspect that the seemingly periodic inter-annual oscillation of Chla may result from random turbulences of water mass in local scale in and along the Kuroshio, which implied that the variability may merely reflect a seasonal modulation of Chla rather than an existence of interannual variability caused by a mechanism independent of the seasonal modulation. The estimation of a 14-year trend using two low-pass filtered Chla time series (> 1.5 years variability included, and >7 years variability included) and a regression analysis did not show a statistically significant difference. Thus, there was no significant effect of the interannual variability on the 14-year trend.

Keywords: phytoplankton, chlorophyll, Kuroshio, Remote Sensing

©2021. Japan Geoscience Union. All Right Reserved.

[J] Oral | A (Atmospheric and Hydrospheric Sciences)：A-OS Ocean Sciences & Ocean Environment

Sat. Jun 5, 2021 3:30 PM - 5:00 PM JST | Sat. Jun 5, 2021 6:30 AM - 8:00 AM UTC | Ch.09 Zoom Room 09

[A-OS14] Coastal physical processes associated with mixing, eddies, internal waves

convener:Eisuke Tsutsumi(Atmosphere and Ocean Research Institute, The University of Tokyo), Eiji Masunaga(Ibaraki University), Taira Nagai(Graduate School of Science, The University of Tokyo), Chairperson:Eisuke Tsutsumi(Atmosphere and Ocean Research Institute, The University of Tokyo), Eiji Masunaga(Ibaraki University), Taira Nagai(Graduate School of Science, The University of Tokyo)

Recently developed observational and numerical approaches have revealed details of physical processes in coastal regions, which are keys to understanding global ocean circulations and ecosystems. This session aims to provide discussions of mixing, eddies, nonlinear internal waves in coastal and marginal oceans, estuaries and lakes. Observations, numerical modeling and laboratory experiments associated with these phenomena are encouraged to submit an abstract to this session. In addition, studies that consider linkages between coastal physical processes and large scale open ocean processes, e.g., the Kuroshio, global ocean circulations.

3:30 PM - 3:45 PM JST | 6:30 AM - 6:45 AM UTC

[AOS14-01] Enhancement of turbulent mixing over tidal sandwaves and formation of front: an observational study in Seto Inland Sea

*Eisuke Tsutsumi[1], Xinyu Guo[2], Naoki Yoshie[2], Takahiro Endoh[3], Takeshi Matsuno[3], Sachihiko Itoh[1] (1.Atmosphere and Ocean Research Institute, The University of Tokyo, 2.Center for Marine Environmental Studies, Ehime University, 3.Research Institute for Applied Mechanics, Kyushu University)

3:45 PM - 4:00 PM JST | 6:45 AM - 7:00 AM UTC

[AOS14-02] Dynamics of the upwelling at the upstream of the East Sakhalin Current (ESC)

*Nan Yuan[1] (1.Hokkaido University, the Institute of Low Temperature Science)

4:00 PM - 4:15 PM JST | 7:00 AM - 7:15 AM UTC

[AOS14-03] Numerical study of tide-induced deep-ocean mixing near the head of Suruga Trough

*Taira Nagai[1], Toshiyuki Hibiya[1] (1.Graduate School of Science, The University of Tokyo)

4:15 PM - 4:30 PM JST | 7:15 AM - 7:30 AM UTC

[AOS14-04] **Amplitude modulation of currents at tidal and inertial bands at the Otsuchi Bay mouth**

*Tongjun Sun[3,1], Sachihiko Itoh[3], Eisuke Tsutsumi[3], Miho Ishizu[2], Kiyoshi Tanaka[3] (1.Graduate School of Agricultural and Life Sciences/Faculty of Agriculture,The University of Tokyo, 2.Japan Agency for Marine-Earth Science and Technology, 3.Atmosphere and Ocean Research Institute, The University of Tokyo)

4:30 PM - 4:45 PM JST | 7:30 AM - 7:45 AM UTC

[AOS14-05] Water mass classification off the east coast of Japan mainland using Regional Ocean Modeling System (ROMS)

*Masashi Ikeda[1], Eiji Masunaga[1], Yusuke Uchiyama[2], Yota Suzue[4], Sachihiko Itoh[3] (1.Ibaraki University , 2.Kobe University, 3.The University of Tokyo, 4.CTI Engineering)

4:45 PM - 5:00 PM JST | 7:45 AM - 8:00 AM UTC

[AOS14-06] Vertical mixing and mass transport in a shallow lake, Lake Kasumingaura, Japan

*Eiji Masunaga[1], Tatsumi Kitamura[2], Sachihiko Itoh[3] (1.Ibaraki University, 2.Ibaraki Kasumigaura Environmental Science Center, 3.The University of Tokyo)

Enhancement of turbulent mixing over tidal sandwaves and formation of front: an observational study in Seto Inland Sea

*Eisuke Tsutsumi[1], Xinyu Guo[2], Naoki Yoshie[2], Takahiro Endoh[3], Takeshi Matsuno[3], Sachihiko Itoh[1]

1. Atmosphere and Ocean Research Institute, The University of Tokyo, 2. Center for Marine Environmental Studies, Ehime University, 3. Research Institute for Applied Mechanics, Kyushu University

It is known that in Iyo-nada, Seto Inland Sea, Japan large sandwaves are formed in the southwest. The generation mechanism of large sandy bedforms has been intensively studied in rivers, estuaries, coastal and shelf seas. However, there has been less attention to how sandwaves affects ocean circulations and environments. In this study, we report on the significant enhancement of vertical mixing by sandwaves from a total of 24 field campaigns consisting of microstructure turbulence and current measurements in Iyo-nada conducted during 2012–2019. We document elevation of turbulence energy dissipation rate to $O(1\ \mathrm{W\ m^{-2}})$ over large sandwaves, flow separation at the sandwave crest, and the associated downstream turbulent wakes due to the form drag. This strong turbulence suggests that the turbulent buoyancy flux in the large sandwave region exceeds the surface buoyancy flux, creating a contrast in the vertical mixing regime to the region without sandwaves and promoting the formation of a front between the two regions.

Keywords: Flow-seabed interaction, Microstructure turbulence measurement, Tidal mixing front, Seto Inland Sea

©2021. Japan Geoscience Union. All Right Reserved.

Dynamics of the upwelling at the upstream of the East Sakhalin Current (ESC)

*Nan Yuan[1]

1. Hokkaido University, the Institute of Low Temperature Science

The resuspension of the sediments at the upstream of ESC was confirmed by ADCP high backscatter events *[Ito et al.,2017]*. Further observation discovered that the sediments resuspended was frozen into the frazil ice at the surface of the upstream of ESC and might be conveyed to the south to support the next spring broom when the ice melts *[Ito et al.,2017; Mustapha et al.,2008]*, which indicates the vertical mixing, whole depth upwelling typically, was at the upstream of ESC and corresponded with the strong wind event *[Ito et al.,2017]*. According to the dissolved oxygen distribution *[Ohshima et al.,2001 Figure 3(a)]*, there should be an upwelling at the southwest of the Sea of Okhotsk as well.

Downwelling-favorable wind from Siberia High in winter, buoyancy flux from Amur River carried by ATW, and the bottom friction are the main dynamic sources of the western coastal current of the Sea of Okhotsk, which might contribute to the coastal upwelling. There are many researches investigated the coast responses to different initial conditions. For a stratified coast with an alongshelf current, idealized simulation depicted an upwelling at the shelf break *[Benthuysen et al.,2015].* Benthuysen et al 2015 explained it with the well-known buoyancy shutdown process. The geostrophic current is modified by the tilted isopycnal via the thermal wind relation which induces the bottom Ekman transport convergence and the upwelling consequently. The shelf break is one of the main reasons for the isopycnal tilt in their research. A similar process might happen at the coast of the ESC, and the buoyancy instability is contributed to the downwelling favorable wind. In the idealized simulations by Allen and Newberger 1996, and Austin and Lentz 2002, the downwelling favorable wind remains a well-mixed water mass at the coast and a downwelling front shoulder by shoulder. With the freshwater discharge, the well-mixed water mass at the coast might be replaced by a stratified one, which could be the situation of the ESC.

We accomplished a simulation with the COCO, an Ocean General Circulation Model. The initial conditions are the same as the Matsuda et al [2015]. The grid size at the coast is finer to 3 km at the coast of the ESC. The reanalysis datasets ERA-Interim from 1980.01.01 to 2018.12.31 were adopted as the meteorological forces. The freshwater discharge is from Dai and Trenberth [2002]. Analyzing the output of the January mean, the upwelling is simulated at the upstream of the ESC. The buoyancy shutdown takes part in the formation of the upwelling according to the isopycnal distribution. Adjacent to the upwelling it is an anti-clockwise overturning, means the water is stratified with the surface onshore current and bottom offshore current. The eddy generated by the baroclinic instability attempts to maintain the coastal stratification, while the diffusion demolishes the stratification. We are figuring out how the mean current takes its responsibility in the coastal overturning. The reasonable hypothesis is the mean current just works inversely compared to the eddy.

Keywords: upwelling, baroclinic instability, eddy

©2021. Japan Geoscience Union. All Right Reserved.

©2021. Japan Geoscience Union. All Right Reserved.

Numerical study of tide-induced deep-ocean mixing near the head of Suruga Trough

*Taira Nagai[1], Toshiyuki Hibiya[1]

1. Graduate School of Science, The University of Tokyo

Coastal submarine canyons are widely expected to be sites of enhanced mixing which may offer a potential solution to the ‘missing mixing’ problem. In Suruga Bay, mooring observations along the steep submarine canyon (Suruga Trough) show the existence of strong semi-diurnal and diurnal internal tides near the ocean bottom. In this trough, therefore, enhanced turbulent mixing induced by breaking of these internal tides is expected, although details of physical processes that produce strong internal tides have not been discussed yet.

In order to investigate the excitation processes of internal tides in Suruga Trough, we carry out a couple of high-resolution ($\Delta x,\ \Delta y = 1/240^{o}$) non-hydrostatic three-dimensional numerical experiments incorporating realistic semi-diurnal (M_2) and diurnal (K_1) tidal forcing, respectively. We first investigate the energetics of M_2 internal-tide to show that (1) internal tides generated over Izu Ridge propagate towards Suruga Trough, (2) in which the incident waves interact with the reflected waves from the trough head, and finally (3) the internal tide energy together with its dissipation is intensified. The K_1 tidal frequency, on the other hand, is subinertial in this area, so that K_1 tidal flow mainly generates coastal trapped waves which propagate cyclonically along the coast of Suruga Bay. It is suggested that these coastal trapped waves induce strong velocity shear near the bottom of the trough causing bottom confined intense mixing.

Keywords: Suruga Trough, Internal tides, Coastal trapped waves

©2021. Japan Geoscience Union. All Right Reserved.

Amplitude modulation of currents at tidal and inertial bands at the Otsuchi Bay mouth

*Tongjun Sun[3,1], Sachihiko Itoh[3], Eisuke Tsutsumi[3], Miho Ishizu[2], Kiyoshi Tanaka[3]

1. Graduate School of Agricultural and Life Sciences/Faculty of Agriculture,The University of Tokyo, 2. Japan Agency for Marine-Earth Science and Technology, 3. Atmosphere and Ocean Research Institute, The University of Tokyo

In the Sanriku coastal areas, various current and waves vigorously interact on the narrow shelf and likely have major influences on the water exchanges between inshore and offshore areas. The inertial period dividing internal waves and coastal trapped waves is approximately 18.9 h at Otsuchi Bay in the middle of the Sanriku coast, and semidiurnal and diurnal frequencies become superinertial and subinertial, respectively. Consequently, both of these waves and their interactions are thought to have impacts on the inflow to and outflow from the bay. In this study, based on the mooring observations at the two stations at the north and south of the bay mouth during 2012–2016, we aim at showing the variability of internal waves forced by tidal flows and coastal trapped waves, and clarifying water exchange processes between the inshore and offshore areas. The mooring observation revealed that flow velocities were excited in summer at semidiurnal and diurnal bands, where the former was markedly strong. By contrast, the velocities of the semidiurnal and diurnal flows were comparable during winter, whereas their amplitude decreased down to ~1/5 of that during summer. Velocity data during July–October 2013 where both of the two stations are available showed that low-frequency background flow (period > 40 h) entered from the north and exited from the south of the bay mouth, respectively. Although the spring tide should appear approximately 2 times in one month due to its inherent fortnight period, semidiurnal and diurnal tidal flows had a shorter period and their amplitude showed irregular fluctuations. To investigate the cause of this fluctuation, harmonic analysis was applied to tide gauge records at the Kamaishi tide station, extracting semidiurnal and diurnal components, and were compared with the velocity fluctuations recorded at the mooring stations. The sea level fluctuations were dominated by the semidiurnal component during this period. The peaks of semidiurnal and diurnal tide almost coincided in the early July, but gradually separated after August, and then approached in the late October and finally coincided again. On the other hand, during February–May 2013, the sea level records showed spring/neap cycle and the fluctuation in the peak timing, but the velocity amplitude was very weak and the difference in the peak timing was hardly detected. As these phenomena cannot be explained solely by the local tides, interactions between semidiurnal and diurnal tides, wave propagations from remote areas, influences of low-frequency flows and changes in the stratification are thought to play some roles.

Keywords: Otsuchi Bay, tide, internal wave, coastal trapped wave, spring tide

©2021. Japan Geoscience Union. All Right Reserved.

Water mass classification off the east coast of Japan mainland using Regional Ocean Modeling System (ROMS)

*Masashi Ikeda[1], Eiji Masunaga[1], Yusuke Uchiyama[2], Yota Suzue[4], Sachihiko Itoh[3]

1. Ibaraki University , 2. Kobe University, 3. The University of Tokyo, 4. CTI Engineering

Marine environments off the Sanriku Coast are important for oceanic ecosystems and influence fishing grounds in the North Pacific Ocean. The T-S (Temperature - Salinity) combination has been frequently used for understanding water masses off the Sanriku Coast (e.g., Hanawa and Mitsudera., 1987). However, the water mass classification based on T-S diagram proposed by Hanawa and Mitsudera cannot explain seasonal variations of water masses in the surface layer. This study investigated the seasonal variation of water masses off the Sanriku coast using the Regional Ocean Modeling System (ROMS). The quality of the ROMS model was validated by comparing with the observed data obtained by the Iwate Prefectural Fisheries Laboratory. Model results well matches to the observed data. We have developed a method for the water mass classification for the three water masses of the Tsugaru Warm Current, Oyashio and Kuroshio using the normalized T-S combination. The normalized T-S diagram is computed from normalized temperature and salinity data with the standard deviation of unity. Three water masses (Tsugaru Warm Current, Oyashio, Kuroshio) were classified based on the distance between each T-S data and the three water masses on a normalized T-S diagram. Original T-S combinations of the Tsugaru Warm current, Oyashio, and Kuroshio were taken from averaged T-S values in Tsugaru Strait, Kuroshio Current Axis, and off Cape Erimo of Hokkaido, respectively. The three water masses were reasonably separated in the surface layer by this method and were not appropriately separated by a previously used conventional method. The water mass classification using this method is consistent with the velocity field of the surface layer. The area of the Oyashio water in the study area is majorly influenced by seasonal variations of the Tsugaru Warm Current.

Keywords: Water mass classification, Oyashio, Kuroshio

©2021. Japan Geoscience Union. All Right Reserved.

Vertical mixing and mass transport in a shallow lake, Lake Kasumingaura, Japan

*Eiji Masunaga[1], Tatsumi Kitamura[2], Sachihiko Itoh[3]

1. Ibaraki University, 2. Ibaraki Kasumigaura Environmental Science Center, 3. The University of Tokyo

This study presents vertical mixing and associated mass transport processes in a shallow lake, Kasumigaura, Japan. Field campaigns were carried out using a mooring system, microstructure profiler (VMP250) and high-resolution tow-yo instrument (YODA Profiler) in summer, 2020. The mooring system consisted of high and low frequency sampling thermistors (SBE56s and TidbiT v2s), and Aquadopp current profiler. Strong stratification and vertical mixing occurred with periods of several hours to several days. The Richardson number was less than 1/4 when complete vertical mixing occurred (temperature difference in the water column is less than 0.5 degrees). The rate of turbulent kinetic energy dissipation rate (e) and vertical eddy diffusivity (K_r) were 10^{-10}–10^{-9} W/kg and 10^{-7}–10^{-6} m^2/s, respectively, near the bottom boundary layer under weak wind stratified conditions.On the other hand, when vertical mixing occurred due to wind stress, e and K_r were 10^{-8}–10^{-5}W/kg and 10^{-5}–10^{-3} m^2/s, respectively. In addition to microstructure surveys, the eddy diffusivity was also estimated by two independent methods using high-frequency sampled temperature data: (1) $K_{rI18} = 0.09 L_E^2 S$, where L_E is the Ellison scale and S is the vertical velocity shear (Ivey et al., 2018); (2) a method with an assumption of $L_O \sim L_E$, where L_O is the Ozmidov length scale, *viz.*, $e = L_O^2 N^3 \sim L_E^2 N^3$, $K_{rLE} = G L_O^2 N \sim G L_E^2 N$, where G is the mixing efficiency 0.2. The relationship between L_O and L_E were estimated from the microstructure surveys and K_{rLE} was computed from high frequency sampled temperature. K_{rLE} showed reasonable agreements with K_r and K_{rI18}. We analyzed time series of the vertical mixing using K_{rLE}. Stratification and mixing were repeatedly generated by daily cycle shortwave radiation and sea-breeze, respectively. Surface stratification was increased by shortwave radiation from the sunrise to noon. The wind stress was enhanced by see breeze in the afternoon, which results in strong vertical mixing. Convective mixing due to night-time cooling was supposed to be weaker than wind-induced mixing. Vertical oxygen transport from the surface layer toward the bottom layer was generated by the wind-induced mixing in the afternoon. In addition, vertical mixing also contribute to nutrient supplies from sediments leading to eutrophication.

Keywords: Mixing, Heat flux, Coastal areas, Dissolved oxygen

©2021. Japan Geoscience Union. All Right Reserved.

[J] Poster | A (Atmospheric and Hydrospheric Sciences)：A-OS Ocean Sciences & Ocean Environment

Sat. Jun 5, 2021 5:15 PM - 6:30 PM JST | Sat. Jun 5, 2021 8:15 AM - 9:30 AM UTC | Ch.06_1

[A-OS14] Coastal physical processes associated with mixing, eddies, internal waves

convener:Eisuke Tsutsumi(Atmosphere and Ocean Research Institute, The University of Tokyo), Eiji Masunaga(Ibaraki University), Taira Nagai(Graduate School of Science, The University of Tokyo)

Recently developed observational and numerical approaches have revealed details of physical processes in coastal regions, which are keys to understanding global ocean circulations and ecosystems. This session aims to provide discussions of mixing, eddies, nonlinear internal waves in coastal and marginal oceans, estuaries and lakes. Observations, numerical modeling and laboratory experiments associated with these phenomena are encouraged to submit an abstract to this session. In addition, studies that consider linkages between coastal physical processes and large scale open ocean processes, e.g., the Kuroshio, global ocean circulations.

[AOS14-P01] Material transport and diffusion around Sagami Bay and Suruga Bay using a particle tracking model

*Takayoshi Inoue[1], Eiji Masunaga[1], Taichi Kosako[2], Yusuke Uchiyama[3] (1.Ibaraki University, 2.Port and Airport Research Institute, 3.Kobe University)

[AOS14-P02] Physical structure and mixing processes in the inner part of Tokyo Bay

*Haruki Itozu[1], Eiji Masunaga[1] (1.Ibaraki University)

[AOS14-P03] Secular variations of M_2 tide, its resonant amplification, and the associated energy dissipation in a semi-enclosed sea connected to the East China Sea (Ariake Sea, Japan), 1980–2019.

*Eisuke Tsutsumi[1], Matsuno Takeshi[2], Sachihiko Itoh[1] (1.Atmosphere and Ocean Research Institute, The University of Tokyo, 2.Research Institute for Applied Mechanics, Kyushu University)

Material transport and diffusion around Sagami Bay and Suruga Bay using a particle tracking model

*Takayoshi Inoue[1], Eiji Masunaga[1], Taichi Kosako[2], Yusuke Uchiyama[3]

1. Ibaraki University, 2. Port and Airport Research Institute, 3. Kobe University

In this study, material transport and diffusion processes in Sagami Bay and Suruga Bay were evaluated using the ROMS model with a 3-D Lagrangian particle tracking model. The model was run for the summer season performed with long term averaged climatological reanalyzed data. We also investigated effects of horizontal diffusion by a random walk model.

Particles that flowed out from Sagami Bay were mainly transported to the east (70%) caused by the Kuroshio Current. For Suruga Bay, particles were mainly outflowed on the west side of the bay mouth (75%). Most of the model cases showed that the particle outflow from the inner part of the bays was lower than the bay mouths. The Kuroshio current directly influences particle transport in Sagami Bay, which results in a small difference in the particle flow rate from the bay mouth and inner part of the bay. The semi-closed shape of Suruga Bay suppressed the particle outflow rate. Particle transport between the inner part of Suruga Bay and bay mouth requires more than six days. Particles in Suruga Bay mouth tended to move toward the inner part of the bay as the horizontal diffusion increased, and the particle outflow rate decreased. Except for Suruga Bay mouth case, the particle outflow rate from the bays to the open ocean increased with increasing in the horizontal diffusion. Particles that flowed out from Sagami Bay (Suruga Bay) increased by 12 % (15 %) caused by the random walk when the horizontal diffusion was set at 10^{-1} ~ 10^{1} m^2 /s.

Keywords: ROMS model, Particle tracking model, Sagami Bay, Suruga Bay, Diffusion, Random walk

©2021. Japan Geoscience Union. All Right Reserved.

Physical structure and mixing processes in the inner part of Tokyo Bay

*Haruki Itozu[1], Eiji Masunaga[1]

1. Ibaraki University

Numerous physical processes are involved in coastal regions of freshwater influence, e.g., river plume dynamics, tidal mixing, internal waves. In the inner part of Tokyo bay, one of the regions of freshwater influence, strong stratification often appeasers resulting in hypoxia and blue tide, which significantly influences ecosystems. Although there have been numerous studies on physical structures in Tokyo bay, few studies have focused on mixing process in the inner part of the bay. In this study, we analyzed data from long term observations at the Chiba light beacon located at the inner part of Tokyo Bay to understand physical structures associated with mixing process. The observational data showed that hypoxia events occurred with appearances of high density water in the bottom layer. The ratio of the vertical density gradient and vertical shear, namely the Richardson number, well explains appearance of hypoxia events. The wind stress largely influenced vertical mixing, rather than tidal currents. We calculated modified versions of the horizontal Richardson number (R_x^{wt}) developed by Burchard [2009]. Bottom hypoxia events occurred when R_x^{wt} were over 2.1×10^{-3} of critical value of stable stratification. The horizontal physical structure can be used to explain the vertical physical structure. By comparing R_x^{wt} with zonal winds, R_x^{wt} was over approximately 2.1×10^{-3} when east wind below 5 m/s. This suggests that weak offshore winds promote the upwelling of bottom hypoxia water mass from offshore rather than mixing. Weak winds less than 5 m/s enhance stratification in the inner part of Tokyo bay.

Keywords: Tokyo Bay, Stratification, Mixing

©2021. Japan Geoscience Union. All Right Reserved.

Secular variations of M_2 tide, its resonant amplification, and the associated energy dissipation in a semi-enclosed sea connected to the East China Sea (Ariake Sea, Japan), 1980–2019.

*Eisuke Tsutsumi[1], Matsuno Takeshi[2], Sachihiko Itoh[1]

1. Atmosphere and Ocean Research Institute, The University of Tokyo, 2. Research Institute for Applied Mechanics, Kyushu University

After 2000, decrease in M_2 tidal elevation amplitude have been obverved in and around a semi-enclosed shallow embayment connected to the eastern East China Sea, Ariake Sea. In this study, we present an updated analysis of the secular variation of M_2 tide in Ariake Sea by introducing the bottom friction and its nonlinearity, which have not been explicitly considered in the tidal studies of the Ariake Sea. Over the last five decades, M_2 tidal elevation amplitude has decreased at an average rate of ~−11 % century^{-1} both inside and outside of the sea. The result of the analysis indicated that linear bottom drag coefficient had decreased at ~−10 % century^{-1}, suggesting that if the quadratic bottom drag coefficient was unchanged, mean M_2 velocity in the sea also had decreased at the same rate. Comparing 1997 and 2015, when the lunar nodal factor for M_2 tide was nearly at its maximum, we found that the energy dissipation of M_2 tide decreased by ~11 % in 2015. The possible causes of these decreasing trends were changes in the frictional resonance properties of the sea and change in the incoming M_2 tide from the East China Sea.

Keywords: Changing tides, Ariake Sea, Bottom drag, Tidal energy dissipation

©2021. Japan Geoscience Union. All Right Reserved.

[J] Oral | A (Atmospheric and Hydrospheric Sciences)：A-OS Ocean Sciences & Ocean Environment

Sat. Jun 5, 2021 3:30 PM - 5:00 PM JST | Sat. Jun 5, 2021 6:30 AM - 8:00 AM UTC | Ch.07 Zoom Room 07

[A-OS16] Global ocean observing systems, their status, research results and future perspective

convener:Shigeki Hosoda(Japan Marine-Earth Science and Technology), Shuhei Masuda(Japan Agency for Marine-Earth Science and Technology), Yosuke Fujii(Meteorological Research Institute, Japan Meteorological Agency), Fujiki Tetsuichi(Japan Agency for Marine-Earth Science and Technology), Chairperson:Shuhei Masuda(Japan Agency for Marine-Earth Science and Technology), Yosuke Fujii(Meteorological Research Institute, Japan Meteorological Agency), Fujiki Tetsuichi(Japan Agency for Marine-Earth Science and Technology), Shigeki Hosoda(Japan Marine-Earth Science and Technology)

The global ocean is complementary covered by variable kinds of observing networks such as Argo, GO-SHIP, OceanSITES, earth observing satellite, then its observing network is crucial for research, monitoring and future predictions of climate changes and ocean environment. Besides, the ocean observing networks are also recognized as infrastructures for research, human societies, and industries in the SDGs and the UN Decade, which is suggested to achieve their goals and to develop the network within 10 years. In the session held previously, we discussed the status and future perspective on the ocean observing network, following themes in OceanObs19, etc., exchanging current information. After the previous session, the roadmap2020 for progress of the global ocean observation had been suggested, the GO BGC Argo project was accepted by the National Science Foundation in 2020, and the UN Decade starts from 2021. Under these circumstances, the target of this session is to host a meeting exchanging information on the recent status of the observing networks, and discussing for future perspectives regarding pilot studies of large-scale ocean observations, OSE and OSSE for the ocean observing networks, development of sensor and platform technologies. At the same time, we would like to share information of current research results regarding large-scale heat, freshwater, material transports, physical and biogeochemical mechanisms of water mass formation and modification, air-sea interaction, and developing measurement sensors and data quality controls contributing to those researches, overarching variable research fields.

3:30 PM - 3:35 PM JST | 6:30 AM - 6:35 AM UTC

[AOS16-01] Introduction

3:35 PM - 3:55 PM JST | 6:35 AM - 6:55 AM UTC

[AOS16-02] Biogeochemical Argo: Significances and Challenges

★Invited Papers

*Masao Ishii[1] (1.Meteorological Research Institute, Japan Meteorological Agency)

3:55 PM - 4:15 PM JST | 6:55 AM - 7:15 AM UTC

[AOS16-03] Global deployment of Deep Argo floats toward accurate prediction of future climate and ecosystem changes

★Invited Papers

*Toshiyuki Hibiya[1] (1.Department of Earth and Planetary Science, Graduate School of Science, University of Tokyo)

4:15 PM - 4:30 PM JST | 7:15 AM - 7:30 AM UTC

[AOS16-04] Two-year seismic observation by hydrophone floats

*Masayuki Obayashi[1], Hiroko Sugioka[2], Junko Yoshimitsu[1] (1.Japan Agency for Marine-Earth Science and Technology, 2. Department of Planetology, Kobe University)

4:30 PM - 5:00 PM JST | 7:30 AM - 8:00 AM UTC

[AOS16-05] Discussion toward a New Global Ocean Observing System

*Shuhei Masuda[1] (1.Japan Agency for Marine-Earth Science and Technology)

[J] Oral | A (Atmospheric and Hydrospheric Sciences) | A-OS Ocean Sciences & Ocean Environment

[A-OS16] Global ocean observing systems, their status, research results and future perspective

convener:Shigeki Hosoda(Japan Marine-Earth Science and Technology), Shuhei Masuda(Japan Agency for Marine-Earth Science and Technology), Yosuke Fujii(Meteorological Research Institute, Japan Meteorological Agency), Fujiki Tetsuichi(Japan Agency for Marine-Earth Science and Technology), Chairperson:Shuhei Masuda(Japan Agency for Marine-Earth Science and Technology), Yosuke Fujii(Meteorological Research Institute, Japan Meteorological Agency), Fujiki Tetsuichi(Japan Agency for Marine-Earth Science and Technology), Shigeki Hosoda(Japan Marine-Earth Science and Technology)

Sat. Jun 5, 2021 3:30 PM - 5:00 PM Ch.07 (Zoom Room 07)

The global ocean is complementary covered by variable kinds of observing networks such as Argo, GO-SHIP, OceanSITES, earth observing satellite, then its observing network is crucial for research, monitoring and future predictions of climate changes and ocean environment. Besides, the ocean observing networks are also recognized as infrastructures for research, human societies, and industries in the SDGs and the UN Decade, which is suggested to achieve their goals and to develop the network within 10 years. In the session held previously, we discussed the status and future perspective on the ocean observing network, following themes in OceanObs19, etc., exchanging current information. After the previous session, the roadmap2020 for progress of the global ocean observation had been suggested, the GO BGC Argo project was accepted by the National Science Foundation in 2020, and the UN Decade starts from 2021. Under these circumstances, the target of this session is to host a meeting exchanging information on the recent status of the observing networks, and discussing for future perspectives regarding pilot studies of large-scale ocean observations, OSE and OSSE for the ocean observing networks, development of sensor and platform technologies. At the same time, we would like to share information of current research results regarding large-scale heat, freshwater, material transports, physical and biogeochemical mechanisms of water mass formation and modification, air-sea interaction, and developing measurement sensors and data quality controls contributing to those researches, overarching variable research fields.

3:30 PM - 3:35 PM

[AOS16-01]Introduction

©Japan Geoscience Union

Biogeochemical Argo: Significances and Challenges

*Masao Ishii[1]

1. Meteorological Research Institute, Japan Meteorological Agency

Since 1980s, high-quality data of ocean carbon and biogeochemistry (BGC) have been acquired globally from the ocean interior in ship-based hydrographic programs such as WOCE/JGOFS and GO-SHIP and at time-series sites such as those at 137°E, station ALOHA near Hawaii and BATS near Bermuda. These datasets have been quality-controlled and are freely available from the database GLODAPv2, helping constrain the global budget of anthropogenic carbon and documenting the progress of ocean acidification and oxygen decline that are endangering the marine ecosystems worldwide and thus our societies. However, we still have large data gaps particularly in time for most of the ocean regions. The measurements with low time frequency in global oceans, typically once in several years to a decade in GO-SHIP, prevent from resolving seasonality in upper layers as well as distinguishing between the impact of human-induced forcing and that of ocean internal variability on ocean carbon and BGC.

On October 29, 2020, NSF announced a $53 million grant to build a global network of BGC-Argo (GO-BGC) (~500 floats). In Japan, several Argo floats installed with O_2 and pH sensors are to be deployed in the region of North Pacific Subtropical Mode Water in February 2021 as a part of Kakenhi project “Hybrid ocean observations” in “Hotspot 2”. A sustained observing network of BGC-Argo is expected to help fill in the large data gaps in the ocean carbon and BGC and greatly improve our understanding of their change and variability, thus understand and project impacts of climate change and variability as well as the changes in anthropogenic CO_2 emission on BGC and carbon-climate feedback. Massive data from BGC-Argo are also potentially to be critical in measuring the effectiveness of our policy and efforts to reduce CO_2 emission on the changes in ocean and its health on which our society depends.

However, collecting climate-quality data of BGC from sustained BGC-Argo network well enough to quantify the trends of, e.g., acidification and oxygen decline is still a challenge. It is required to establish a network of in-situ ocean observing networks which enables to provide high-quality reference data for calibration and validation of data from sensors, in addition to further improving the performance of sensors for BGC in terms of precision, stability, cost and so on.

Keywords: BGC Argo, GO-SHIP, ocean acidification, oxygen decline, ocean observing network

©2021. Japan Geoscience Union. All Right Reserved.

Global deployment of Deep Argo floats toward accurate prediction of future climate and ecosystem changes

*Toshiyuki Hibiya[1]

1. Department of Earth and Planetary Science, Graduate School of Science, University of Tokyo

Long-term assessment and conservation of marine bio-resources are crucial in securing the global food supply. Given the very rapid warming of global climate at present, however, marine environmental changes could be a very serious threat to human beings. Actually, acidification of surface seawater and decrease of dissolved oxygen in subsurface layers have been detected recently; if these trends are significant, an irreversible global/oceanic change in a longer time scale would be realistic. The deep oceanic circulation plays a key role in the marine environmental change. A recent numerical model suggests a global temperature change of more than 4°C and a decrease of marine biological production by 20% under a condition of weakened deep oceanic circulation. The actual feature and mechanism of the deep oceanic circulation are still largely unknown, and the comprehensive observation of deep sea would be also important in the assessment of oceanic ecosystem.

In association with the 17 academic societies in the Fisheries/Oceanography Research Liaison Council and the Paleontological Society of Japan, the Oceanographic Society of Japan submitted a research proposal to the "Master Plan 2020" designed by the Science Council of Japan. After document screening and hearing, this proposal was selected as one of the "High-Priority Large Research Projects 2020". The proposal aims to unveil the deep oceanic circulation, which is currently acting as the bottleneck in reproducing past and future climate variability and global environmental changes in numerical models. More specifically, the proposal focuses on observation of turbulence in the deep sea with a turbulence sensor attached to the deep-sea Argo float (target depth more than 4000 meters) or "Deep NINJA". More than 10 floats of this type with conventional temperature and salinity sensors are in actual operation in the Southern Ocean. By deploying approximately 1000 floats, observation of temperature, salinity and turbulence will be conducted globally from the ocean surface to seafloor. The obtained data will be incorporated into a coupled atmosphere-ocean global climate model, and the simulation conducted using the leading Japanese supercomputer facility would yield an accurate reproduction and prediction of the past and future climate. Responses of biological community to the reproduced paleo-environmental changes can be validated by paleontological data such as microfossil record in sediment core, and the validation further refine the model prediction. A far more accurate prediction of future climate, marine biological production and marine bio-resources will be achieved through the proposed research project.

Keywords: Deep Argo floats, Turbulence in the deep ocean, Deep oceanic circulation, Prediction of future climate changes, Prediction of future ecosystem changes

©2021. Japan Geoscience Union. All Right Reserved.

Two-year seismic observation by hydrophone floats

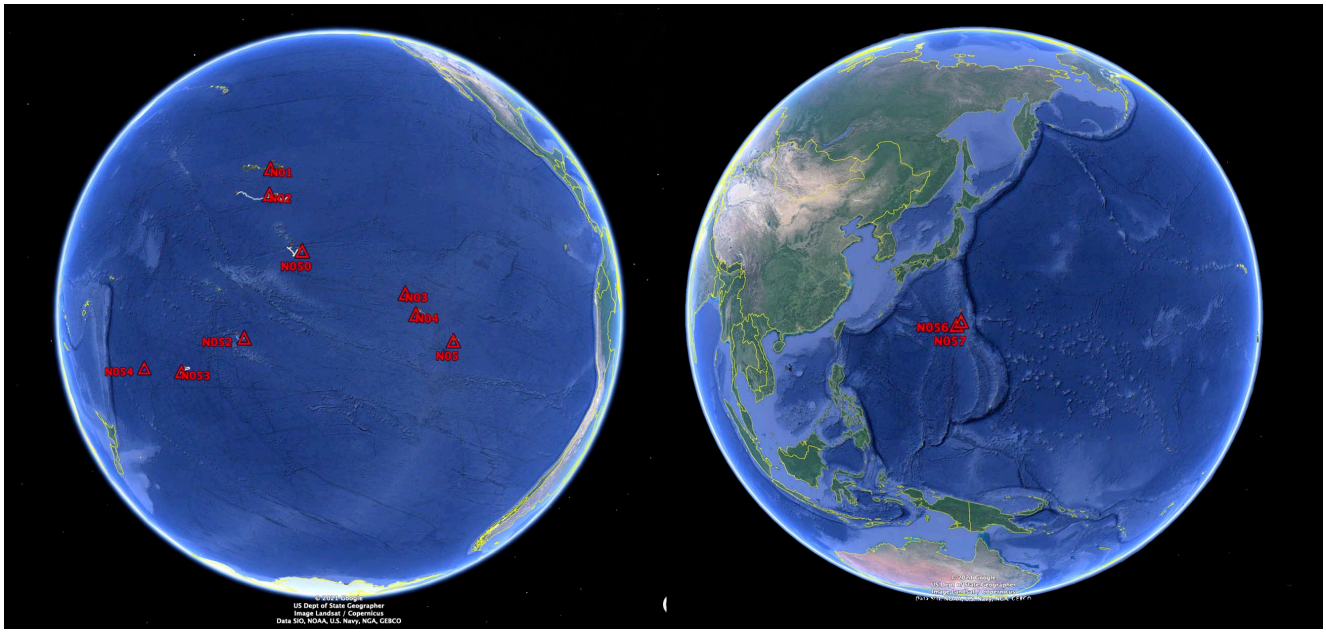
*Masayuki Obayashi[1], Hiroko Sugioka[2], Junko Yoshimitsu[1]

1. Japan Agency for Marine-Earth Science and Technology, 2. Department of Planetology, Kobe University

A new international joint seismic observation project using autonomous float instrument (MERMAID) started from 2018. More than 50 MERMAID instruments were deployed in the south Pacific to study the mantle beneath the South Pacific Superswell, broad seafloor anomalously elevated and concatenated by several volcanic island (hot spot) chain. The MERMAID is an autonomous robotic float equipped with a hydrophone and drifts passively at 1,500–2,000 m depth until an earthquake signal is detected. If this is identified as a strong P wave, the MERMAID ascends at speed of 10 cm/s for transmission of the recorded waveform within time window of a hundred seconds before and after the P wave arrival as well as its global positioning system coordinates at the surface. 9 Japanese MERMAIDs out of them were deployed in the winter and summer of 2019. So far, we obtained approximately 1700 P-wave records from about 480 earthquakes. One of the MEMRAID is recoding continuous pressure to search for a possibility to detect pressure changes due to tsunamis. Additionally, we launched two MERMAIDs to monitor the seismic activities of Nishinoshima volcano island that became active since 2013. We will introduce how we operate the Mermaid floats and what kind of data we obtained in the presentation.

Figure 1: Present locations of 11 Japanese MERMAIDs (9 in south Pacific and 2 near Nishinoshima volcano island)

Keywords: float, hydrophone, Pacific Plume, Nishinoshima, seismic observation



©2021. Japan Geoscience Union. All Right Reserved.

Discussion toward a New Global Ocean Observing System

*Shuhei Masuda[1]

1. Japan Agency for Marine-Earth Science and Technology

We will discuss a future vision of global ocean observation system based on presentations in this session.

©2021. Japan Geoscience Union. All Right Reserved.

[J] Poster | A (Atmospheric and Hydrospheric Sciences)：A-OS Ocean Sciences & Ocean Environment

Sat. Jun 5, 2021 5:15 PM - 6:30 PM JST | Sat. Jun 5, 2021 8:15 AM - 9:30 AM UTC | Ch.06_2

[A-OS16] Global ocean observing systems, their status, research results and future perspective

convener:Shigeki Hosoda(Japan Marine-Earth Science and Technology), Shuhei Masuda(Japan Agency for Marine-Earth Science and Technology), Yosuke Fujii(Meteorological Research Institute, Japan Meteorological Agency), Fujiki Tetsuichi(Japan Agency for Marine-Earth Science and Technology)

The global ocean is complementary covered by variable kinds of observing networks such as Argo, GO-SHIP, OceanSITES, earth observing satellite, then its observing network is crucial for research, monitoring and future predictions of climate changes and ocean environment. Besides, the ocean observing networks are also recognized as infrastructures for research, human societies, and industries in the SDGs and the UN Decade, which is suggested to achieve their goals and to develop the network within 10 years. In the session held previously, we discussed the status and future perspective on the ocean observing network, following themes in OceanObs19, etc., exchanging current information. After the previous session, the roadmap2020 for progress of the global ocean observation had been suggested, the GO BGC Argo project was accepted by the National Science Foundation in 2020, and the UN Decade starts from 2021. Under these circumstances, the target of this session is to host a meeting exchanging information on the recent status of the observing networks, and discussing for future perspectives regarding pilot studies of large-scale ocean observations, OSE and OSSE for the ocean observing networks, development of sensor and platform technologies. At the same time, we would like to share information of current research results regarding large-scale heat, freshwater, material transports, physical and biogeochemical mechanisms of water mass formation and modification, air-sea interaction, and developing measurement sensors and data quality controls contributing to those researches, overarching variable research fields.

[AOS16-P01] Spatiotemporal variability of vertical structures of temperature and salinity in the mid-latitude northwest Pacific Ocean based on unsupervised clustering

★Invited Papers

*Fumika Sambe[1], Toshio Suga[1,2] (1.Graduate School of Science, Tohoku University, 2.JAMSTEC)

[AOS16-P02] Temporal variations of Kuroshio transport based on a repeated hydrographic section along 137E

*Yuma Kawakami[1], Toshiya NAKANO[1], Atsushi Kojima[1], Kiyoshio Murakami[1], Shusaku Sugimoto[2] (1.Japan Meteorological Agency, 2.Tohoku University)

[AOS16-P03] Global distribution of 10-day differences of temperature and salinity around 2000 m depth observed with Argo floats

*Yoshimi Kawai[1] (1.Research Institute for Global Change, Japan Agency for Marine-Earth Science and Technology)

[AOS16-P04] GO-SHIP Easy Ocean: formatted and gridded ship-based hydrographic section data

*Katsuro Katsumata[1], Sarah Purkey[2], Rebecca Cowley[3], Bernadette Sloyan[3], Stephen Diggs[4], Thomas Moore, II[3], Lynne Talley[2], James Swift[4] (1.JAMSTEC, 2.Scripps Institution of Oceanography, 3.Oceans and Atmosphere, CSIRO, 4.CLIVAR and Carbon Hydrographic Data Office, Scripps Institution of Ocenaography)

[AOS16-P05] Salinity bias with negative pressure dependency caused by anisotropic deformation of CTD measuring cell under pressure examined with a dual-cylinder cell model

*Taiyo Kobayashi[1] (1.Japan Agency for Marine-Earth Science and Technology)

[AOS16-P06] pH measurement in the ocean

*Hajime Kayanne[1], Toshimasa Miyawaki[1], Nori Fujita[1], Kenta Suzuki[2], Hizuru Nakajima[2], Kazuhiro Morioka[3], Akihide Hemmi[4] (1.the University of Tokyo, 2.Tokyo Metropolitan Univ., 3.Tokyo Univ. Pharmacy Life Sci., 4.Möbius Advanced Tech.)

[AOS16-P07] Advances in the estimation of global surface net heat flux based on satellite observation: J-OFURO3 V1.1

*Hiroyuki Tomita[1], Kunio Kutsuwada[2], Masahisa Kubota[3], Tsutomu Hihara[4] (1.Institute for Space-Earth Environmental , Nagoya University, 2.School of Marine Science and Technology, Tokai University, 3.Institute of Ocean Research and Development, 4.Japan Fisheries Information Service Center)

[AOS16-P08] Keeping the PACE with the NASA Plankton, Aerosol, Cloud, ocean Ecosystem (PACE) mission

*Lachlan McKinna[1], Ivona Cetinić[2,3], Jeremy Werdell[3] (1.Go2Q Pty Ltd, 2.USRA, 3.NASA GSFC)

Spatiotemporal variability of vertical structures of temperature and salinity in the mid-latitude northwest Pacific Ocean based on unsupervised clustering

*Fumika Sambe[1], Toshio Suga[1,2]

1. Graduate School of Science, Tohoku University, 2. JAMSTEC

In the mid-latitude northwest Pacific Ocean, the transport, stirring and mixing of subtropical and subarctic water occur, resulting in multiple ocean domains characterized by a variety of unique oceanographic structures. Many studies were conducted on the characteristics and distribution of these ocean structures, and the boundaries of domains and characteristic water masses were defined. Most of subsequent studies on the ocean structure and water mass in this ocean region have been based on the existing definitions of the structure and water mass of interest based on spatiotemporally limited data. Even while a large amount of vertical profile data has become available evenly in space and time with the expansion of the Argo observing network, the basic research framework has not changed significantly. However, with the huge amount of data accumulated by Argo with a small spatiotemporal bias, it may be possible to objectively recapture the ocean structure by data-driven scientific methods, that is, machine learning. The Profile Classification Model (PCM) developed by Maze et al. (2017) is a machine learning method for vertical profile data in the ocean. The PCM classifies profiles by unsupervised clustering using Gaussian Mixture Model, and one of its main features is that it can perform analysis using a labeling metric that quantifies the certainty of the classification. Previous studies have shown that clustering with PCM represents the vertical structure and spatial distribution of each class representing a particular ocean structure and its main distribution area. In this study, PCM is applied for the first time to the temperature and salinity profiles by Argo floats in the mid-latitude northwest Pacific Ocean, and the results are compared with previous knowledge of ocean structure. In addition, we tried to understand the spatiotemporal variability of oceanographic structures from the results of PCM by grouping the results based on the Kuroshio Extension index (KE index), which is a measure of a stable and an unstable dynamic state of the KE, and discussing the characteristics of each group.
In this study, PCM clustering was performed on 57476 temperature and salinity profiles located between 30˚N and 60˚N and between 140˚E and 180˚E. Based on statistical criteria and the initial value dependence, the number of classes was set to five. The results showed that classes 1, 2, 3, 4, and 5 were distributed to form five regions: the subarctic region, the mixed water region, the subtropical subarctic intermediate region, the northwestern part of the subtropical gyre, and the downstream of the KE region. Each class has different oceanographic features. The relationship between the distribution area and the characteristics of each class corresponded to the relationship between the ocean structure and the area described in previous studies, which mainly focused on specific water masses and vertical structures. In addition, we investigated how the distribution of each class changed depending on the KE index. We found that the shape of the distribution area of class 4 and the degree to which classes other than class 5 coexist in the downstream of the KE region changed. This change in the distribution area was consistent with the results expected from the north-south shift of the KE position due to the dynamic state of the KE. The profiles with low labeling metrics were found to be concentrated near the boundaries of the main distribution areas of the classes. This may reflect “mixing” between different classes at the domain boundary. It was also confirmed that the proportion of profiles with low labeling metric to total profiles had a significant negative correlation with KE index, suggesting that the more unstable the KE dynamic state was, the more the interclass “mixing” became active.

©2021. Japan Geoscience Union. All Right Reserved.

Keywords: Mid-latitude Northwest Pacific Ocean, Kuroshio Extension, Argo float, Unsupervised Clustering, Data-driven Science, Oceanographic Structure

©2021. Japan Geoscience Union. All Right Reserved.

Temporal variations of Kuroshio transport based on a repeated hydrographic section along 137E

*Yuma Kawakami[1], Toshiya NAKANO[1], Atsushi Kojima[1], Kiyoshio Murakami[1], Shusaku Sugimoto[2]

1. Japan Meteorological Agency, 2. Tohoku University

Kuroshio is the western boundary current in the North Pacific subtropical gyre. It flows northeastward along the south coast of Japan. The Kuroshio has its origin in tropical region, and plays an important role for heat transport from low-latitude to mid-latitude North Pacific. Through its heat transport, the Kuroshio has a significant impact on basin-scale climate in the North Pacific. Therefore, in order to understand climate variability in the North Pacific, it is important to monitor and understand a temporal variation of the Kuroshio transport.

Past works reported that the Kuroshio transport fluctuates on decadal (about 10 years) and bi-decadal (about 20 years) timescales, responding to changes in the winter atmospheric field which reflects Aleutian Low activities. However, the length of Kuroshio transport time series used in the previous studies is about 35 years at most, and it cannot be said that low-frequency variations like decadal and bi-decadal timescale variations are detected robustly. The Japan Meteorological Agency has repeated ship-board observations along 137E across the Kuroshio since 1967 in winter and 1972 in summer. This long-term observational data is powerful tool to investigate the Kuroshio transport variation. In this study, we examine the Kuroshio transport variation based on the repeated hydrographic sections along 137E.

We estimate the Kuroshio transport by vertical and meridional integration of zonal geostrophic velocity. In this study, we focus on net eastward transport across the 137E section (hereafter, referred as net Kuroshio transport). The net Kuroshio transport is calculated by subtracting westward transports associated with the cold-core eddy and Kuroshio Counter current in the north and south of the Kuroshio from eastward Kuroshio transport.

The net Kuroshio transport fluctuates on inter-annual, decadal, and bi-decadal timescales. The inter-annual variation is detected before 1985 and after 2000, and the decadal variation is dominant before 2000. The bi-decadal timescale is detectable throughout the analysis period. As shown by previous studies, the net Kuroshio transport variation is caused by changes of the winter atmospheric forcing. We confirmed that the net Kuroshio transport responds to changes of winter wind stress curl (WSC) in the central North Pacific with a lag of two years.

To examine temporal variations of winter WSC field in the North Pacific subtropical gyre, we next performed an EOF analysis. As a result, the mode-1 is linked to a meridional movement of the Aleutian Low which has an inter-annual timescale before 1980 and after 1995, and the mode-2 reflects an Aleutian Low intensity fluctuation with a decadal timescale before 2000 and bi-decadal timescale throughout the analysis period. A correlation analysis shows that the winter WSC in the central North Pacific resulting in the net Kuroshio transport variation well reflects mode-2, especially before 2000 when the Aleutian Low intensity fluctuation has a decadal timescale. In addition, the winter WSC in the central North Pacific relatively well correlates to also mode-1 after 1985 and before 2000 when the meridional Aleutian Low movement has an inter-annual timescale. These results suggest that the winter WSC in the central North Pacific is determined by the Aleutian Low intensity fluctuation on decadal and bi-decadal timescales whereas influenced by the meridional movement of the Aleutian Low on an inter-annual

©2021. Japan Geoscience Union. All Right Reserved.

timescale.

From the above results, we concluded that the net Kuroshio transport variation on an inter-annual timescale is caused by the meridional Aleutian Low movement, and that on decadal and bi-decadal timescale results from the Aleutian Low intensity fluctuation. It can be also pointed out that temporal changes of timescales in the net Kuroshio transport derives from changes of timescales in the Aleutian Low activities.

Keywords: Kuroshio transport, Repeated hydrographic section along 137E, Aleutian Low

©2021. Japan Geoscience Union. All Right Reserved.

Global distribution of 10-day differences of temperature and salinity around 2000 m depth observed with Argo floats

*Yoshimi Kawai[1]

1. Research Institute for Global Change, Japan Agency for Marine-Earth Science and Technology

It has been indicated from repeat hydrographic observations up to the bottom that the warming of the oceans already spread to the global abyssal waters, not only near the surface. Investigating processes of energy and material transport and their variations is essentially important for global climate changes. It had been difficult to do that globally due to lack of observation, but now the observation system by the Argo floats covers almost the whole world. Previous studies have utilized the Argo data to investigate absolute geostrophic velocity, vertical diffusivity, warming trend, and intraseasonal oscillations globally around 1000-m depth or deeper, for example. Short-term variations induced by atmospheric cyclones and internal tides in the intermediate and deep layers are, however, not examined enough. In this study, the authors examines the variability of the layer around 2000 m depth, which is the “bottom” of the present, dense Argo observation system, using all of available Argo float data. In particular, this study focuses on the difference between two successive observations, that is, nearly 10-day variation, aiming to detect rapid changes, mainly due to developed cyclones or internal tides. Even 1-day sampling is too coarse to resolve the Ekman suction or near-inertial oscillations, but a large number of samples will highlight areas where the frequency of large changes in a short period is high.
All delayed quality controlled float data that were available as of 20 September 2020 were downloaded from the ftp site of Argo Global Data Assembly Center and analyzed only the measurements flagged as good. Each profile was vertically interpolated on a 10-dbar grid using the Akima spline. Then the author obtained differences in properties between two successive observations for each individual float at an isobaric or isopycnal surface. The differences with an observation interval of 9-12 days, $\Delta T_i=T_i-T_{i-1}$ for temperature, and $\Delta S_i=S_i-S_{i-1}$ for salinity, were selected and averaged on 2˚×2˚ grids. T and S are temperature and salinity, and subscript *i* denotes observation cycle. The average of the absolute value of ΔT or ΔS at 1000 dbar or 1950 dbar are mainly examined in this study.
Mean ΔT at 1000 dbar is large in the western boundary currents: the Gulf Stream, the North Atlantic Current, the Agulhas and Agulhas Return Currents, the East Australian Current, and the Kuroshio Extension. At 1950 dbar, ΔT is remarkable in the eastern North Atlantic Ocean west of Europe, the Argentine basin, and the northwestern Indian Ocean. Large ΔT is localized in some areas in the Southern Ocean: around 30ºE, 85ºE, 155ºE, 135ºW, and the Scotia Sea. For salinity, the spatial patterns are similar to those of temperature, but ΔS at 1000 dbar is also large in the east North Atlantic. There is no clear seasonality in the 10-day variations at 1000 dbar or deeper. The ΔT distribution at 1950 dbar shown by this simple procedure appears to reflect internal waves related with bottom topography, rather than atmospheric turbulence. The locally enhanced ΔT in the Southern Ocean are located over the ridges or leeward of the plateau, and may be caused by internal lee waves from geostrophic flows. On the other hand, the spatial distribution of ΔT in the North Atlantic Ocean is similar to that of the Mediterranean Outflow Water, which is a saline and warm water mass produced as a result of mixing the Mediterranean Sea Water and the ambient North Atlantic Central Water. The large ΔT in the North Atlantic Ocean would reflect the mixing and spreading processes of the saline water. The results of this study does not directly indicate the strength of ocean mixing, but is useful to infer where the mixing is vigorous in the intermediate layer, and will contribute to designing the observation system of the deep Argo float.

©2021. Japan Geoscience Union. All Right Reserved.

Keywords: Argo float, intermediate layer, 10-day change

©2021. Japan Geoscience Union. All Right Reserved.

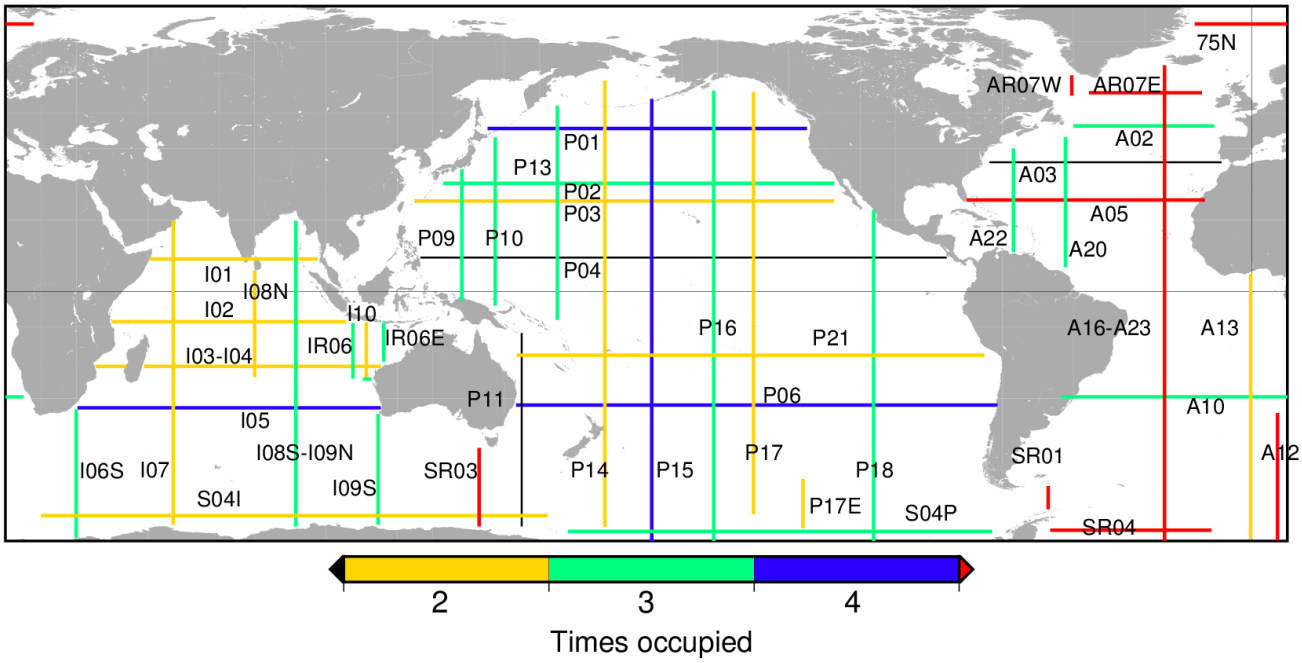
GO-SHIP Easy Ocean: formatted and gridded ship-based hydrographic section data

*Katsuro Katsumata[1], Sarah Purkey[2], Rebecca Cowley[3], Bernadette Sloyan[3], Stephen Diggs[4], Thomas Moore, II[3], Lynne Talley[2], James Swift[4]

1. JAMSTEC, 2. Scripps Institution of Oceanography, 3. Oceans and Atmosphere, CSIRO, 4. CLIVAR and Carbon Hydrographic Data Office, Scripps Institution of Ocenaography

Despite numerous technological advances over the last several decades, ship-based hydrography remains the only method for obtaining high-quality, high spatial and vertical resolution measurements of a suite of physical, chemical, and biological parameters over the full water column essential for physical, chemical, and biological oceanography and climate science. The Global Ocean Ship-based Hydrographic Investigations Program (GO-SHIP) coordinates a network of globally sustained hydrographic sections as part of the global ocean observing system, building on previous programs. These data provide a unique data set that spans four decades, comprised of more than 40 cross-ocean transects, many with multiple repeats. The section data are, however, difficult to use owing to inhomogeneous format. The purpose of this data product is to increase the value of these data by better combining, reformatting and gridding in order to facilitate their use with less effort by a wider audience. The product is machine readable and readily accessible by many existing visualisation and analysis software packages. The data processing can be repeated with modifications to suit various applications such as analysis of deep ocean , validation of numerical simulation output, and calibration of autonomous platforms. This initial release includes temperature, salinity, and dissolved oxygen data from Conductivity-Temperature-Depth profiles, but the product will include other properties such as nutrients and carbon items in future releases.

Keywords: hydrographic data, ship observation, global



©2021. Japan Geoscience Union. All Right Reserved.

Salinity bias with negative pressure dependency caused by anisotropic deformation of CTD measuring cell under pressure examined with a dual-cylinder cell model

*Taiyo Kobayashi[1]

1. Japan Agency for Marine-Earth Science and Technology

Measurements made by deep floats had a salinity bias with a negative pressure dependency. Salinity is affected by conductivity measurements via changes in the CTD measuring cell geometry under pressure. To remove the effect, a canceling factor for pressure CPcor is prepared theoretically by the manufacturer considering the isotropic deformation of a single-cylinder measuring cell under pressure; the observed negative pressure dependency, however, requires an even smaller CPcor. This study examined the causes of the inconsistency for salinity measurements with a dual-cylinder cell model, considering that the actual CTD measuring cell is a glass cell covered by a polyurethane jacket. The dual-cylinder cell model clarifies that the CTD measuring cell deforms anisotropically to yield a smaller CPcor; mainly because the inner glass cell deforms radially to a greater extent than the single-cylinder model due to the radial stress from the outer cylinder (jacket) being stronger than the hydrographic pressure. The observed fresh bias at the sea surface is attributed to a slight shrinkage of the outer jacket because of compression set of polyurethane in deep ocean. The shrunken polyurethane jacket is elongated over time due to a creep phenomenon, which causes less-freshening of the fresh bias found at the sea surface. The observed linear relationship between the smaller CPcor and the fresher bias at the sea surface is attributed to the variation of the wall thickness of the polyurethane jacket when it shrinks similarly. The study suggests another idea to improve the salinity accuracy of CTD sensors greatly: a change of the jacket material into an elastomer. The improvement makes the present setting of CPcor be more valid and reliable, because the elastomer jacket hardly affects the change of the measuring cell geometry under pressure, which in turn removes the pressure effects on salinity measurements.

Keywords: Deep Argo, Salinity measurement, CTD sensor

©2021. Japan Geoscience Union. All Right Reserved.

pH measurement in the ocean

*Hajime Kayanne[1], Toshimasa Miyawaki[1], Nori Fujita[1], Kenta Suzuki[2], Hizuru Nakajima[2], Kazuhiro Morioka[3], Akihide Hemmi[4]

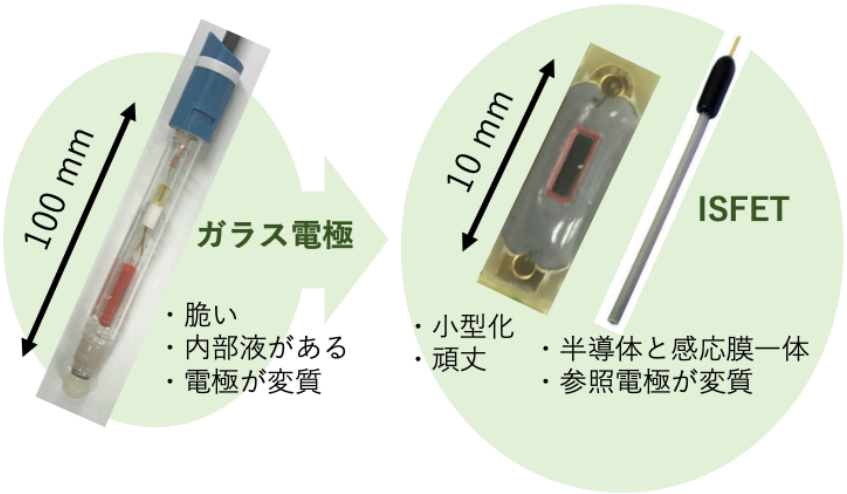
1. the University of Tokyo, 2. Tokyo Metropolitan Univ., 3. Tokyo Univ. Pharmacy Life Sci., 4. Möbius Advanced Tech.

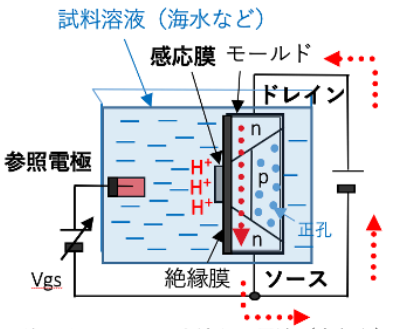
For a century since Cremer (1906) discovered glass membrane potential and Sørensen and Palitzsch (1910) measured ocean pH for the first time, glass electrodes have been used universally to measure ocean pH.
The ion sensitive membrane of the indicator electrode is a thin fragile glass film. The principle behind the selective response of the glass membrane electrode to hydrogen ions is unknown, and manufacturing process is a black boxes varying among manufacturers. Since Ag-AgCl electrodes are used for both the indicator and reference electrodes, they react with the sample solution and deteriorate. In addition, the reference electrode is constantly leaking internal solution to maintain conductivity with the indicator electrode through the sample as a salt bridge, and the solution needs to be replaced. Despite the vast amount of pH data accumulated by glass electrodes, the values are considered less reliable than those obtained by spectrophotometry due to drift and degradation of the electrodes without proper calibration (Dickson 1993, McLaughlin et al. 2017). The measurement of ocean pH by spectrophotometry was established by Clayton and Byrne (1993). Seidel et al. (2008) evaluated a in-situ measurement system as a precision of 0.0007 and accuracy of 0.0017. However, spectrophotometric measurement requires mixing of reagents for coloring the sample, which poses a limitation of in-situ measurement.
Since 1970, a pH sensor using a solid-state semiconductor was developed and put into practical use (Bergveld 1970). This is called an ISFET (Ion Sensitive Field Effect Transistor), which measure the potential of the ion-selective membrane (e.g. Ta_2O_5) by the transistor. The principle of ISFET is electrochemically clear and there is no black box. The semiconductor sensor is durable and can be reduced its size. ISFETs are also applied in Argo Float for pH measurement. The most commonly used Durafet sensor has a short time accuracy (repeatability) of 0.0005, a multi-year accuracy of 0.005, and an accuracy of 0.01 (Martz et al. 2010, Johnson et al. 2016).
However, since the semiconductor should be immersed in the solution united with the membrane, the semiconductor must be tightly molded. For deep-sea measurements, a pressure resistance of 10 MPa or higher is required. Pressure dependancy of the semiconductor must be taken into consideration for measurement in deep sea. Also, there is a limit for reduction in size of the semiconductor. In addition, Ag-AgCl is used as the reference electrode, which reacts with the chloride ions in the solution, causing the electrode to deteriorate. KCl gel is used as the internal solution of the reference electrode, and its replacement is also necessary.
The pH is the most fundamental chemical variable in the ocean. In particular, ocean acidification due to rising atmospheric CO_2 has been recognized as a new issue related to global environmental change, and pH measurement has become increasingly important. In addition to pH, the three other variables of the four measurable ones of the ocean carbonate system (pH, CO_2, total inorgnic carbon, and alkalinity) can be determined by adding acid to the seawater sample (total inorgnic carbon and alkalinity) or by extracting CO_2 through a gas permeable membrane into the solution (CO_2, total carbon dioxide) and measuring its pH. The development of a pH sensor that can maintain stability and accuracy even in seawater and high-pressure deep waters will greatly advance the monitoring of the ocean's carbonate system, based on which ocean acidification and the ocean's CO_2 sink capacity would be evaluated. The new pH sensor must be small, have low power consumption, be reagent-free, be stable over the long term, not be altered by seawater, be resistant to high pressure, and have little been dependent on pressure. The

©2021. Japan Geoscience Union. All Right Reserved.

precision and accuracy must be within 0.0002 and 0.001 considering the propagation of errors in calculating the carbonate system.

Keywords: pH, ocean, measuement, Ocean Acidification, ISFET





ドレインーソースを流れる電流（赤矢印）を一定にするゲート電位（Vgs）によって，感応膜の電荷（H^+: pH）を計測する．

ISFET の原理

©2021. Japan Geoscience Union. All Right Reserved.

Advances in the estimation of global surface net heat flux based on satellite observation: J-OFURO3 V1.1

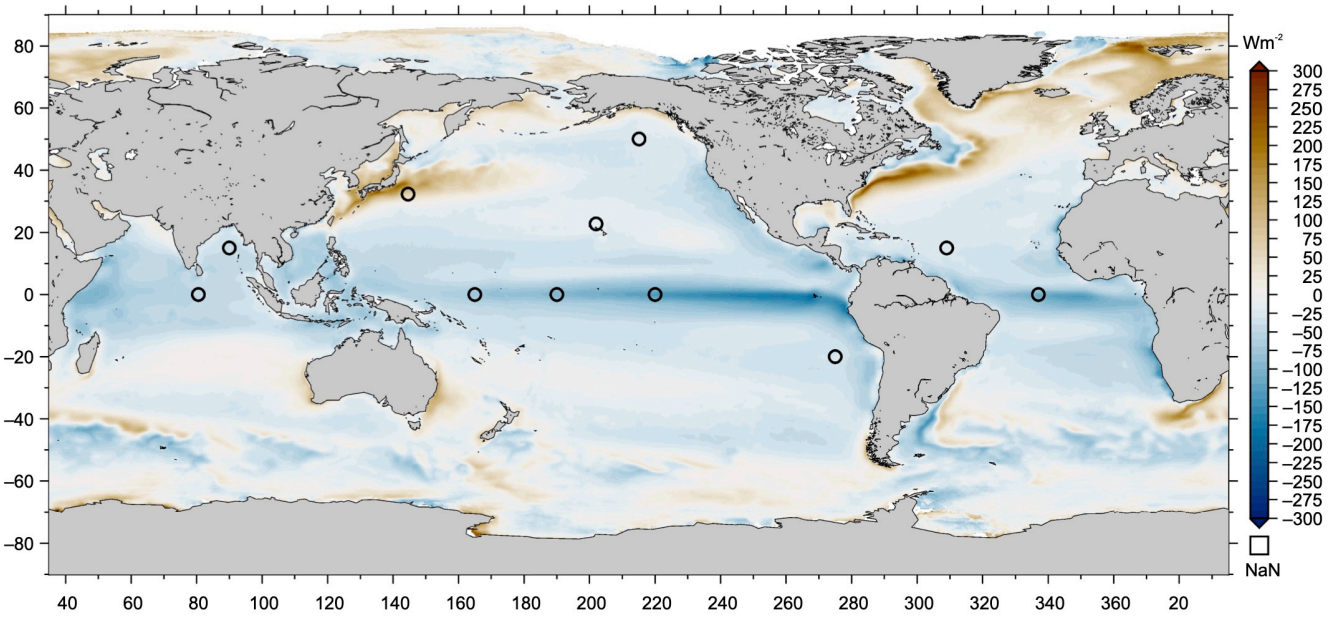
*Hiroyuki Tomita[1], Kunio Kutsuwada[2], Masahisa Kubota[3], Tsutomu Hihara[4]

1. Institute for Space-Earth Environmental , Nagoya University, 2. School of Marine Science and Technology, Tokai University, 3. Institute of Ocean Research and Development, 4. Japan Fisheries Information Service Center

Surface net heat flux, defined as the total heat exchange between the atmosphere and oceans, affects both atmospheric and oceanic processes. Global estimates based on observations are necessary to understand long-term climate change and related responses and to validating climate model results. Consequently, estimating and improving surface net heat flux using satellite observations are of vital importance. The reliability of surface net heat flux data obtained from the latest satellite-based estimation (the third-generation Japanese Ocean Flux Data Sets with Use of Remote Sensing Observations [J-OFURO3, V1.1]) was investigated. Three metrics were utilized: 1) the long-term (30 years) mean for 1988–2017, 2) the local accuracy evaluation based on comparison with observations recorded at buoys located at 11 global oceanic points with varying climatological characteristics, and 3) the physical consistency with the freshwater balance related to the global water cycle. The globally averaged value of the surface net heat flux of J-OFURO3 was −22.2 W m^{-2}, which is largely imbalanced to heat the ocean surface. This imbalance was due to the turbulent heat flux being smaller than the net downward surface radiation. On the other hand, compared with the local buoy observations, the average difference was −5.8 W m^{-2}, indicating good agreement. These results indicate a paradox of the global surface net heat flux. In relation to the global water cycle, the balance between surface latent heat flux (ocean evaporation) and precipitation was estimated to be almost 0 when river runoff from the land was taken into consideration. The reliability of the estimation of the latent heat flux was reconciled by two different methods. Systematic ocean heating biases by surface sensible heat flux (SHF) and longwave radiation were identified. The bias in the SHF was globally persistent and especially large in the mid- and high latitudes. The correction of the bias has an impact on improving the global mean net heat flux by +5.5 W m^{-2}. Furthermore, since J-OFURO3 SHF has low data coverage in high-latitudes areas containing sea ice, its impact on global net heat flux was assessed using the latest atmospheric reanalysis product. When including the sea ice region, the globally averaged value of SHF was approximately 1.4 times larger. In addition to the bias correction mentioned above, when assuming that the global ocean average of J3 SHF is 1.4 times larger, the net heat flux value changes to the improved value (-11.3 W m^{-2}), which is approximately half the original value (-22.2 W m^{-2}).

Keywords: surface flux, air-sea interaction, satellite remote sensing

©2021. Japan Geoscience Union. All Right Reserved.



©2021. Japan Geoscience Union. All Right Reserved.

Keeping the PACE with the NASA Plankton, Aerosol, Cloud, ocean Ecosystem (PACE) mission

*Lachlan McKinna[1], Ivona Cetinić[2,3], Jeremy Werdell[3]

1. Go2Q Pty Ltd, 2. USRA, 3. NASA GSFC

This presentation will showcase the current status of the NASA Plankton, Aerosol, Cloud, ocean Ecosystem (PACE) mission. PACE is a strategic climate continuity activity that will not only extend key heritage ocean color, cloud, and aerosol data records, but also enable new insight into oceanographic and atmospheric responses to Earth's changing climate. PACE’ s primary instrument is a global spectrometer that spans the ultraviolet to near-infrared region in 2.5 nm steps and also includes seven discrete shortwave infrared bands from 940 to 2260 nm. This leap in technology will enable improved understanding of aquatic ecosystems and biogeochemistry, as well as provide new information on phytoplankton community composition and improved detection of algal blooms. PACE's spectrometer will also continue many aerosol and cloud capabilities from MODIS and VIIRS, which in combination with its ocean measurements, will enable improved assessment of aerosol impacts on ocean biology and chemistry. The PACE payload will be complemented by two small multi-angle polarimeters with spectral ranges that span the visible to near infrared spectral region, both of which will significantly improve aerosol and hydrosol characterizations and provide opportunities for novel ocean color atmospheric correction. Scheduled for launch in late 2023/early 2024, this PACE instrument suite will revolutionize studies of global biogeochemistry, carbon cycles, and hydrosols / aerosols in the ocean-atmosphere system.

Keywords: Ocean color, Hyperspectral, Remote sensing, Polarimetry, Biogeochemistry



©2021. Japan Geoscience Union. All Right Reserved.

[J] Oral | A (Atmospheric and Hydrospheric Sciences)：A-OS Ocean Sciences & Ocean Environment

Sat. Jun 5, 2021 10:45 AM - 12:15 PM JST | Sat. Jun 5, 2021 1:45 AM - 3:15 AM UTC | Ch.10 Zoom Room 10

[A-OS19] Physical Oceanography (General)

convener:Yoshimi Kawai(Research Institute for Global Change, Japan Agency for Marine-Earth Science and Technology), Kitade Yujiro(Tokyo University of Marine Science and Technology), Chairperson:Yoshimi Kawai(Research Institute for Global Change, Japan Agency for Marine-Earth Science and Technology)

This session invites presentations on a wide variety of topics related to physical oceanography, including observation, theory, technology, and numerical modeling.

10:45 AM - 11:00 AM JST | 1:45 AM - 2:00 AM UTC

[AOS19-01] Frontal waves in the east of the Tsugaru Strait revealed by the high-frequency radar observation

*Hitoshi Kaneko[1], Takahiro Tanaka[2], Hiroto Abe[1,3], Masahide Wakita[1], Ken'ichi Sasaki[1], Daisuke Hasegawa[2], Takeshi Okunishi[2], Shuichi Watanabe[1], Shoko Tatamisashi[1], Yoshiaki Sato[1] (1.Japan Agency for Marine-Earth Science and Technology, 2.Japan Fisheries Research and Education Agency, 3.Graduate School/Faculty of Fisheries Sciences, Hokkaido University)

11:00 AM - 11:15 AM JST | 2:00 AM - 2:15 AM UTC

[AOS19-02] 17 year observation of bottom water current on deep seafloor offshore of Tokachi in Hokkaido: Recovery of acoustic Doppler current profiler (ADCP) data of cabled observatory

*Ryoichi Iwase[1] (1.National Research and Development Agency, Japan Agency for Marine-Earth Science and Technology)

11:15 AM - 11:30 AM JST | 2:15 AM - 2:30 AM UTC

[AOS19-03] Winter large-scale atmospheric circulation during La Niña events: A comparison between the first year and second year of events

*Gaku Nishihira[1], Shusaku Sugimoto[1] (1.Graduate School of Science, Tohoku University)

11:30 AM - 11:45 AM JST | 2:30 AM - 2:45 AM UTC

[AOS19-04] Decadal variation of the asymmetry of SSTA in the tropical Atlantic and its relations with midlatitude atmosphere circulation

*Yoshinobu Furukawa[1], Shusaku Sugimoto[1] (1.Graduate School of Science, Tohoku University)

11:45 AM - 12:00 PM JST | 2:45 AM - 3:00 AM UTC

[AOS19-05] Nearshore wave–current interaction effects on wave power density near Japan

*Adrean Webb[1], Takuji Waseda[2] (1.Kyoto University, Disaster Prevention Research Institute, Coastal Disaster Research, 2.The University of Tokyo, Graduate School of Frontier Sciences, Department of Ocean Technology Policy and Environment)

12:00 PM - 12:15 PM JST | 3:00 AM - 3:15 AM UTC

[AOS19-06] Medium-term oceanic transport of microplastics in and around the South China Sea analyzed with climatological and synoptic models

*Kosei Matsushita[1], Yusuke Uchiyama[1], Naru Takaura[1], Taichi Kosako[2] (1.Kobe University, 2.Port and Airport Research Institute)

Frontal waves in the east of the Tsugaru Strait revealed by the high-frequency radar observation

*Hitoshi Kaneko[1], Takahiro Tanaka[2], Hiroto Abe[1,3], Masahide Wakita[1], Ken'ichi Sasaki[1], Daisuke Hasegawa[2], Takeshi Okunishi[2], Shuichi Watanabe[1], Shoko Tatamisashi[1], Yoshiaki Sato[1]

1. Japan Agency for Marine-Earth Science and Technology, 2. Japan Fisheries Research and Education Agency, 3. Graduate School/Faculty of Fisheries Sciences, Hokkaido University

Surface velocity observations of the eastern part of the Tsugaru Strait made by the high-frequency radar revealed frequent occurrence of frontal waves along the axis of the Tsugaru Warm Current in 2017–2019. The current axis (zonal flow maximum in the meridional direction) disturbed in the north-south direction with period of about 14 days that is dominant timescale of tide modulation in the strait. In addition, another peak of the timescale of the modulation was also recognized around ~27 days. The amplitude of the axis fluctuation increased in the downstream direction, from the eastern neck of the channel (~141˚E) to the wider mouth adjacent to the Pacific Ocean (~141˚30’ E). The disturbance propagated downstream with far later speed than that of surface advection especially in the seasons when the stratification was developed. It took from a week to 10 days for propagation of about 100 km. The density and vertical velocity distribution obtained from repeated shipboard observations across the channel in each season were used for investigation for phase speed of the baroclinic instability waves. The propagation speed of the disturbance agreed well with that estimated from the theory based on the two-layer baroclinic instability model except for winter when the stratification was weak. The north–south modulation of the axis at the outlet of the strait (~141˚30˚E) could cause short-term (from 20 days to one month) clockwise rotation of the Tsugaru gyre that is developed in the east of the outlet during summer, as suggested by the previous studies. In addition, such frontal disturbance may contribute to the water mass exchange and modification between the water of the Tsugaru Warm Current and the Oyashio water across the front, and subsequent faster acidification in the strait than in the open ocean.

Keywords: Tsugaru Strait, Tsugaru Warm Current, High Frequency Radar, Frontal Wave

©2021. Japan Geoscience Union. All Right Reserved.

17 year observation of bottom water current on deep seafloor offshore of Tokachi in Hokkaido: Recovery of acoustic Doppler current profiler (ADCP) data of cabled observatory

*Ryoichi Iwase[1]

1. National Research and Development Agency, Japan Agency for Marine-Earth Science and Technology

In order to observe earthquakes and tsunamis in Kuril Trench region, the cabled observatory attached with three ocean bottom seismometers (OBSs) and two pressure gauges (PGs) along a 240km long submarine was deployed offshore of Kushiro-Tokachi in Hokkaido in 1999. The observatory is equipped not only with the OBSs and the PGs but also with various types of sensors, such as hydrophones, an acoustic Doppler current profiler (ADCP), an electro-magnetic current meter, a CTD (conductivity, temperature and depth) sensor, and a video camera. The ADCP is mounted on the cable-end station which is located at a depth of 2540 m offshore of Tokachi. The observation with the ADCP was continued until 2016 after the deployment. However, much of the data are left unanalyzed and moreover some might be dissipated. This time, the recovery of the ADCP data is carried out.

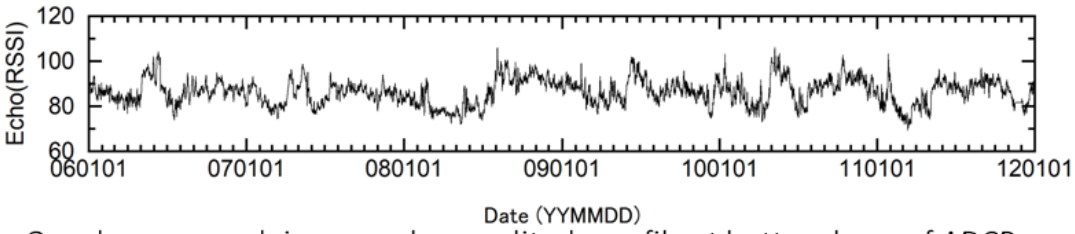
The raw data of the ADCP are usually converted to the ASCII data by using the software “WinADCP” which is supplied by Teledyne RDI Instruments. There are some problems with the raw ADCP data. Some of the data contain bit errors due to the communication error during data transmission. The raw data contain check sum bytes at each record obtained at one ping. The WinADCP converts each raw record to ASCII only when the corresponding check sum bytes are normal. In other words, if there is a single bit error in a record, the corresponding whole record including the other part without error cannot be converted. This time, we refer to the documentations produced by Teledyne RDI Instruments and decode the raw binary data directly. As a result, we can convert some raw data that cannot be done with the WinADCP.

The ADCP measures the vertical profile of the current velocities in 48 layers. The thickness of each layer is 8 meters and the height of the bottom layer is 12 meters from the seafloor. The sampling rate is usually 30 minutes. The ADCP measures not only current velocities but also acoustic backscatter (echo) intensity from each layer and the bottom water temperature. The echo intensity indicates the concentration of the suspended materials in each layer. The echo intensity tends to have a peak in late spring or early summer. Meanwhile visual observation of the seafloor was carried out with the video camera of the cable-end station from June 2006 to June 2008. JPEG format still images were acquired approximately every 10 seconds. Although significant turbidity has not been observed, moderate increase in benthic organisms tends to be observed in May or June. Those phenomena may relate to the spring bloom in sea surface.

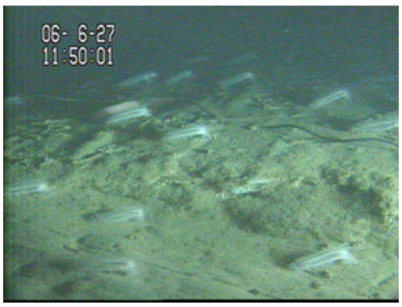
Including the above phenomena preliminary results obtained through the data recovery will be reported in the presentation.

Keywords: acoustic Doppler current profiler (ADCP), long term observation on deep seafloor offshore of Tokachi in Hokkaido, benthic organisms

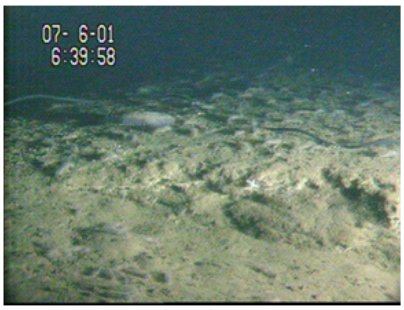
©2021. Japan Geoscience Union. All Right Reserved.



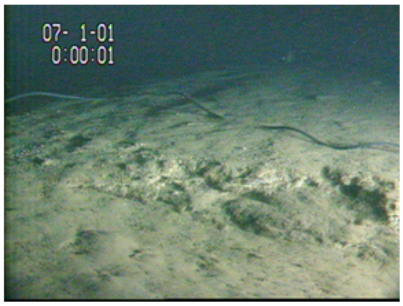
One day averaged six year echo amplitude profile at bottom layer of ADCP from 2006 to 2011.



2006/06/27 11:50:01



2007/06/01 06:39:58



2007/01/01 00:00:01

Seafloor images observed with the video camera

©2021. Japan Geoscience Union. All Right Reserved.

Winter large-scale atmospheric circulation during La Niña events: A comparison between the first year and second year of events

*Gaku Nishihira[1], Shusaku Sugimoto[1]

1. Graduate School of Science, Tohoku University

The sea surface temperature (SST) distribution associated with ENSO generates large-scale atmospheric teleconnection patterns, such as the PNA pattern characterized by a wave-train from the central North Pacific to North America, and results in affecting the global climate. Recent studies have reported that there is a temporal asymmetry between El Niño and La Niña, with La Niña tending to last for multiple years compared to El Niño. It is suggested that atmospheric response would differ between the first year and the following year of the La Niña. However, the understanding has not been obtained yet. In this study, we conducted statistical analysis using observational and reanalysis datasets since 1950 and numerical experiments using the linear baroclinic model (LBM) to investigate characteristics of winter large-scale atmospheric circulation associated with La Niña.

First, we conducted a composite analysis using observational and reanalysis datasets. As a result, in the first year of La Niña, we detected enhanced convective activity over the western equatorial Pacific and the South China Sea, and low-pressure anomalies were distributed over Japan. A wave-train in geopotential height fields was observed from Japan to North America. This atmospheric pattern was not consistent with existing teleconnection patterns. Surface air temperature showed significant cooling around Japan, as previously pointed out in past works. We investigated the cold air mass distribution and indicated that a large amount of cold air flowing into Japan from the continent was a cause of the cold winter in Japan. We conducted the same analysis for the second year of La Niña. Results represented that convection in the western equatorial Pacific was not as active as in the first year. The large-scale pressure pattern indicated the wave-train from the central North Pacific to North America, consistent with the negative PNA pattern. Negative surface air temperature anomalies around Japan were obtained, but its amplitude was smaller than that of the first year, and it was not significant.

This study revealed the atmospheric responses attributable to La Niña events differ between the first and second years. Also, the heating sensitivity experiments by the LBM showed almost identical atmospheric responses.

Keywords: multiyear La Niña, teleconnection, cold air mass

©2021. Japan Geoscience Union. All Right Reserved.

Decadal variation of the asymmetry of SSTA in the tropical Atlantic and its relations with midlatitude atmosphere circulation

*Yoshinobu Furukawa[1], Shusaku Sugimoto[1]

1. Graduate School of Science, Tohoku University

A north-south asymmetric pattern of SSTA, whose boundary lies along the equator in the Atlantic exists, and this has a decadal (about 10 years) timescale as pointed out by past work (Tanimoto and Xie, 2002). Past works denoted that this asymmetric pattern develops due to the Wind-Evaporation-SST (WES) feedback mechanism. On the other hand, it has been implied that the asymmetric pattern could be influenced by the mid-latitude large-scale atmospheric pattern such as NAO. In this study, we examine the dominant timescale of the asymmetric pattern by using the long-term SST dataset, and then investigate a relationship between the asymmetric pattern and the large-scale atmospheric pattern such as NAO and EA using atmospheric reanalysis data. Two data were used for the indicator of north-south asymmetric pattern of the Atlantic Equator region: ERA5 SST (January 1978 to August 2019) and HadISST (January 1870 to September 2019). The indicator was calculated as follows; (1) we calculate SSTA regional-mean values over the northern equator (5 ˚-15 ˚N, 20 ˚-60 ˚W) and the southern equator (5 ˚-15 ˚S, 0 ˚-40 ˚W), (2) we obtain the 37-month running mean values of the difference between northern equation and southern equation, and then (3) we regard the smoothed time series as the asymmetry index. In addition, the meridional wind speed and SLP of ERA5 were used. We calculate monthly climatology for 30 years from 1978 to 2007. The NAO and EA index produced by NOAA. The asymmetric index by ERA5 SST showed a marked decadal-scale variations as a result of a wavelet analysis,. Identical timescale features were obtained from HadISST; the decadal timescale can be traced back to 1870. To investigated whether the WES feedback worked on this asymmetric pattern, we performed correlation analyses of the asymmetric index versus the north-south wind speed and SLP of ERA5. Results indicated a strong positive correlation with the north-south wind over the equator, and negative SLP correlation coefficients in the North Atlantic Ocean and positive SLP coefficients in the South Atlantic Ocean. It can be concluded that the WES feedback works for this asymmetric pattern. We focused on the winter (December-February) and investigated the relationship between the asymmetric index and the NAO index / EA index. Resultantly, significant correlation coefficients were not obtained, and it is pointed out that the asymmetric pattern is almost independent of NAO / EA. In the presentation, we will also discuss results of CMIP6 under future climate.

Keywords: tropical Atlantic, atmospheric-ocean interaction, long period variability

©2021. Japan Geoscience Union. All Right Reserved.

Nearshore wave–current interaction effects on wave power density near Japan

*Adrean Webb[1], Takuji Waseda[2]

1. Kyoto University, Disaster Prevention Research Institute, Coastal Disaster Research, 2. The University of Tokyo, Graduate School of Frontier Sciences, Department of Ocean Technology Policy and Environment

For countries with extensive coastlines such as Japan, energy harvested from surface ocean waves has the potential to be a notable source of green energy. Along many southern parts of Japan however, a strong Kuroshio current flows near the coastline, with surface velocities routinely exceeding 1 m/s. Wave-current interactions (WCI) in such regions can significantly modify the wave resource both locally and remotely and is a source of epistemic uncertainty in many assessments.

In order to quantify these nearshore effects, comparisons are conducted here between long-term (21 years) and high-resolution (1 km) wave resource assessments of Japan with and without WCIs included (Webb et al., 2020). The wave resource assessment (named TodaiWW3) is based on NOAA WAVEWATCH III (version 4.18) simulations using NCEP and JAMSTEC forcings, and includes a new Doppler-shifted wave power density formulation.

In general, short-term differences in wave power due to changes in the wave field alone can be exceptional (over 80%), while longer-term differences are often offset by the Doppler-shift in the group velocity. In this study, the largest long-term differences occur in the nearshore Kuroshio region, with overall differences (and relative differences) between 21-year climatologies of wave power density reach 3 kW/m (and approximately 20%). Further details of the comparison will be discussed, including the underlying mechanisms of change and the role of the Doppler-shift in the wave power density equation.

References:
A. Webb, T. Waseda, and K. Kiyomatsu, 2020. A high-resolution, long-term wave resource assessment of Japan with wave–current effects. Renewable Energy, 161:1341–1358. doi:10.1016/j.renene.2020.05.030.

Keywords: Wave resource assessment, Wave–current interactions, Wave power density, Doppler-shift, NOAA WAVEWATCH III

©2021. Japan Geoscience Union. All Right Reserved.

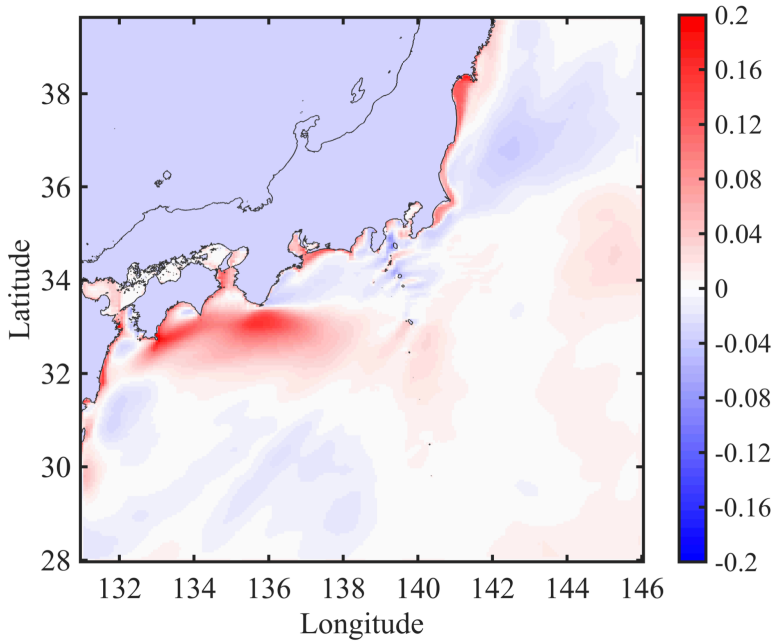


Figure 1. Relative difference between 21-year climatologies of wave power density with and without inclusion of WCI effects (using latter as reference).

©2021. Japan Geoscience Union. All Right Reserved.

Medium-term oceanic transport of microplastics in and around the South China Sea analyzed with climatological and synoptic models

*Kosei Matsushita[1], Yusuke Uchiyama[1], Naru Takaura[1], Taichi Kosako[2]

1. Kobe University, 2. Port and Airport Research Institute

Lagrangian particle tracking experiments were conducted to evaluate the transport of microplastics (MPs) derived from the four major rivers, i.e., Pearl , Han (China), Mekong (Vietnam), Pasig (Philippines) rivers, that have been known to discharge a huge amount of plastic wastes into the South China Sea (SCS). We carried out two types of the experiments: 1) 2D tracking of MP particles placed at surface to represent positively buoyant (light) MPs, and 2) 3D tracking of neutrally buoyant MP particles that are passively transported by ambient flow, using the pre-computed 3D current velocity field by the HYCOM-ROMS downscaling model at a lateral resolution of 5 km for the SCS. We released more than 1×10^5 particles continuously for the four-year period from 2012 to 2015 into the synoptic model and for one year into the climatological model. The MP particles are discharged at the mouths of the four major MP-source rivers located in the SCS. The comparative synoptic and climatological experiment enables us to analyze the seasonal and inter-annual variability of the river-derived MP transport. The seasonally varying monsoons in the SCS are found to provoke strong seasonal variability in the river-derived MP transport. We found that mesoscale eddies generated along the east coast of the Philippines promote westward transport and accumulation of the MPs from Pasig river. The comparative experiments also allow extracting medium-term climatological variability in the MP transport in the El Niño years (2014-2015).

Keywords: Microplastics, the South China Sea, Particle tracking model, monsoons, mesoscale eddies, El Niño

©2021. Japan Geoscience Union. All Right Reserved.

[J] Poster | A (Atmospheric and Hydrospheric Sciences)：A-OS Ocean Sciences & Ocean Environment

Sat. Jun 5, 2021 5:15 PM - 6:30 PM JST | Sat. Jun 5, 2021 8:15 AM - 9:30 AM UTC | Ch.06_3

[A-OS19] Physical Oceanography (General)

convener:Yoshimi Kawai(Research Institute for Global Change, Japan Agency for Marine-Earth Science and Technology), Kitade Yujiro(Tokyo University of Marine Science and Technology)

This session invites presentations on a wide variety of topics related to physical oceanography, including observation, theory, technology, and numerical modeling.

[AOS19-P01] Long-term variability of summertime convective activity over the tropical northwestern Pacific and its influence on large-scale atmospheric circulation

*Shota Sera[1], Shusaku Sugimoto[1] (1.Graduate School of Science, Tohoku University)

[AOS19-P02] **Temporal variation of heat content within surface mixed layer in the western Arctic from Iridium-based autonomous thermistor strings**

*EunYae Son[1], Yusuke Kawaguchi[1] (1.University of Tokyo)

[AOS19-P03] Data and Sample Management for Marine Observation Cruises: Complaint can be Awareness

*Takayuki Tomiyama[1], Takako Sato[1], Kazuyo Fukuda[1], Hajime Kawakami[1], Makoto Ito[1], Chizuru Saito[1] (1.Japan Agency for Marine-Earth Science and Technology)

[AOS19-P04] Meridional heat transport in the North Pacific subtropical gyre -Analysis by ARMOR 3D-

*Yukina Fukaumi[1], Kazuyuki Uehara[1] (1.The Graduate School of Marine Science and Technology of Tokai University)

Long-term variability of summertime convective activity over the tropical northwestern Pacific and its influence on large-scale atmospheric circulation

*Shota Sera[1], Shusaku Sugimoto[1]

1. Graduate School of Science, Tohoku University

It is known that convective activity over the tropical northwestern Pacific during boreal summer affects atmospheric circulation around East Asia. Nitta (1987) showed that convective activity around the Philippine Sea influences the pressure field around Japan, and this teleconnection pattern is called the Pacific-Japan (PJ) pattern. On the other hand, there are few studies on the impact of convective activity in the South China Sea on the large-scale atmospheric circulation. In this study, we focused on the convective activity in the South China Sea, in order to obtain new insights into the fluctuations of atmospheric circulation around Japan.

The main data used in this study are NOAA Interpolated OLR, ERA5 850 hPa geopotential height, and AMeDAS surface air temperature. We used monthly mean values of 1979–2018. The years which OLR averaged over the South China Sea (110˚E-120˚E, 7.5˚N-22.5˚N) exceeds plus one standard deviation were classified as South China Sea weak convection years, and minus one standard deviation were classified as strong convection years for the composite analysis. The PJ index was calculated based on Wakabayashi and Kawamura (2004).

First, we examined the spatial distribution and variability of OLR around tropical northwestern Pacific. Results indicate that both the convective activity and the amplitude of the variability around the South China Sea in July tend to be getting strong in recent years. Therefore, we focused on July. A correlation coefficient between the PJ index and OLR in the South China Sea was 0.44, which does not necessarily indicate a well agreement. Next, we conducted a composite analysis of OLR. As a result, it was found that the center of activity for the South China Sea OLR was located locally over the South China Sea, and significant signal is not extracted over the Philippine Sea. The composite map for 850 hPa height between the strong and weak convective years indicates a north-south dipole structure appears, showing a westward shift/movement of atmospheric circulation pattern compared to the PJ pattern. The South China Sea OLR variability affects a wide area of Japan, including southwest Japan, thought the PJ pattern influences surface air temperature mainly over eastern Japan. These suggest that convective activity in the South China Sea may have a different impact from the PJ pattern.

In the presentation, we also introduce results of the LBM experiment that simulated convective activity in the South China Sea and discuss convective activity in the South China Sea under the future climate of CMIP6 outputs.

Keywords: PJ pattern, South China Sea

©2021. Japan Geoscience Union. All Right Reserved.

Temporal variation of heat content within surface mixed layer in the western Arctic from Iridium-based autonomous thermistor strings

*EunYae Son[1], Yusuke Kawaguchi[1]

1. University of Tokyo

In recent years, the delayed sea ice onset has been detected from satellite observations. The suspended sea ice onset can generate the longer sea surface exposure, which can enhance the kinetic energy input to the ocean from atmosphere. The increased kinetic energy can be a direct source to deepen the bottom of surface mixed layer (SML). We deployed two drifting buoys, with 17 thermistors and 3 pressure sensors on a 60 m long wire to investigate the heat and SML variation in the upper part of the Canada Basin, Arctic. The buoy collects the temperature, pressure, and GPS data with an hour interval and send it via the Iridium satellite. The deployment was done during the Mirai Arctic cruises of 2019 and 2020. Each buoy was deployed in the outer edge of pack ice in mid-October when the sea ice started to freeze up. The buoy deployed in 2019 survived only for three weeks and continued to report the cold surface water near -1.5 ˚C at 2.5 m depth. The surface temperature at the depth in the same season of 2020 showed warmer water near -1.2˚C than that collected in 2019. Another noticeable point is that the signal of the near-surface temperature maximum (NSTM), a thin warm water layer near 20 m, is more well-defined with the temperature of -0.5˚C in 2020 than in 2019. The upper water temperature showed that the signal of NSTM was weakened by a strong wind event. The difference between temperatures from the two buoys can also be found in the Pacific Summer Water layer (PSW) that forms the upper pycnocline. The PSW was located about 50 m depth in October 2020 where it was about 10 m deeper in October 2019. We found the several cases of upwelling and downwelling, which were recognized from the isothermal fluctuation, and which were driven by gale winds. In the data collected in 2020, periodic motion of sea ice showed variation according to ice formation. In melting phase when sea surface temperature is higher than the local freezing point, inertial motion is dominant in sea ice drift. When the surface temperature becomes colder than the point, the inertial motion disappeared. The detailed interpretation on the surface heat budget and SML thickness variation will be given in presentation.

Keywords: Western Arctic, Sea ice onset, Upper heat variation

©2021. Japan Geoscience Union. All Right Reserved.

Data and Sample Management for Marine Observation Cruises: Complaint can be Awareness

*Takayuki Tomiyama[1], Takako Sato[1], Kazuyo Fukuda[1], Hajime Kawakami[1], Makoto Ito[1], Chizuru Saito[1]

1. Japan Agency for Marine-Earth Science and Technology

Japan Agency for Marine-Earth Science and Technology (JAMSTEC) manages archives of data, samples and their metadata that are obtained during research cruises and submersible dives, and publicly distributes them for additional uses with research or educational purposes. These information services are accessible online through DARWIN website [1] and a series of surrounding online databases [2].

This activity has experienced continuous modifications since when it was founded more than a decade ago. For operating data and samples, we need to deal with new frameworks for organization, research project selection and funding, with volumetric growths of data and samples, and with developments and maintenances of information systems and workflows. Meanwhile, we have to keep the workflows in line as well, for collecting, processing, and distributing of data and samples. For example, as recent progresses, we have got enrolled into the JURCAOS Cooperative Research Cruises [3], introduced Digital Object Identifier (DOI) to our data management [4], and established newly integrated sample information management database [5]. It was not easy to apply these modifications to our work, because we have had reducing budget and human strengths for these years.

In addition, exceptional conditions are sometimes applied to individual research projects, because of contracts for research cooperation, inter-institutional agreements and official permission applications for research and observation. For such projects, we have to pay special care for ownership and handling of data and samples. The chances of having exceptional conditions are not necessarily rare, and their influences are not always small. We have to prepare for identifiable problems, and for unidentifiable problems, we have to develop a robust working system to avoid getting into serious troubles.

In this presentation, we will overview flows of data and samples of research cruises and submersible dives, with describing information systems and workflows, cooperation efforts among researchers, management offices, and institutional organizations. Then we will discuss future plans. For the better operation of data and samples, we have to cultivate cooperative relationship with researchers, by providing services that meet with the researchers needs, and by maintaining operation structure simple.

[1] JAMSTEC DARWIN website: http://www.godac.jamstec.go.jp/darwin/
[2] JAMSTEC NUUNKUI website: http://www.godac.jamstec.go.jp/jmedia/portal/
[3] AORI Tokyo Univ. Cooperative Research System Website: https://www.aori.u-tokyo.ac.jp/coop/
[4] Fukuda et al. (2020) https://doi.org/10.1002/essoar.10503966.1
[5] Tomiyama et al. (2020) https://doi.org/10.1002/essoar.10504056.1

Keywords: marine geological samples, data curation service

©2021. Japan Geoscience Union. All Right Reserved.

Meridional heat transport in the North Pacific subtropical gyre -Analysis by ARMOR 3D-

*Yukina Fukaumi[1], Kazuyuki Uehara[1]

1. The Graduate School of Marine Science and Technology of Tokai University

To clarify heat transports of the ocean interior is very important to understand the climate variability, because thermal inertia in the Ocean is larger than that of the atmosphere. In this study, we report the north-south ocean heat transports using ARMOR3D which are ocean three dimensional dataset and are based by in situ observations. First of all, we computed relative geostrophic velocities setting the reference level as the deepest layer from 3D-temperature and salinity fields. We then computed the volume transports and heat transports from these relative velocities. And we also computed the same two transports using the absolute geostrophic velocities in ARMOR3D. The northward relative volume and heat transports across the 25N-latitude line as one-year average in 2018 were calculated to be 57.2 Sv and 1.8 PW, respectivey. The northward absolute transports were 126.3 Sv and 2.8 PW. At the time of our presentaion on the day, we will discuss time variabilities of each transports of each ocean basins.

Keywords: heat transport, Subtropical gyre

©2021. Japan Geoscience Union. All Right Reserved.

[E] Oral | A (Atmospheric and Hydrospheric Sciences)：A-HW Hydrology & Water Environment

Sat. Jun 5, 2021 9:00 AM - 10:30 AM JST | Sat. Jun 5, 2021 12:00 AM - 1:30 AM UTC | Ch.12 Zoom Room 12

[A-HW20] Hydrology & Water Environment

convener:Takeshi Hayashi(Faculty of Education and Human Studies, Akita University), Keisuke Fukushi(Institute of Nature & Environmental Technology, Kanazawa University), Koichi Sakakibara(Department of Environmental Sciences, Faculty of Science, Shinshu University), Dai Yamazaki(Institute of Industrial Sciences, The University of Tokyo), Chairperson:Takeshi Hayashi(Faculty of Education and Human Studies, Akita University), Keisuke Fukushi(Institute of Nature & Environmental Technology, Kanazawa University), Koichi Sakakibara(Department of Environmental Sciences, Faculty of Science, Shinshu University), Dai Yamazaki(Institute of Industrial Sciences, The University of Tokyo)

We focus on various issues of water cycle and environment and aim to answer questions of hydrological and earth system sciences; 1) surface, subsurface and their boundary hydrological processes of water cycle, 2) natural and anthropogenic hydrothermal systems, 3) environments issues and studies on a watershed or global scale, 4) water-related issues with ecological, environmental, and geochemical aspects, and 5) other issues in hydrological sciences. We welcome presentations regarding various kinds of approaches and techniques such as field survey, remote sensing, chemical and isotope tracers, numerical simulation, and theoretical analysis. This session is jointly hosted by societies of water-related geoscience (Geochemical Society of Japan, Japanese Association of Groundwater Hydrology, Japanese Association of Hydrological Sciences, and Japan Society of Hydrology and Water Resources), and accepts wide-range research topics related to water cycle and environment described above.

9:00 AM - 9:05 AM JST | 12:00 AM - 12:05 AM UTC

[AHW20-01] Introduction

9:05 AM - 9:20 AM JST | 12:05 AM - 12:20 AM UTC

[AHW20-02] Behavior of pore-air entrapment in unsaturated soil layer in two small headwater catchments with different soil depth

*Sho Iwagami[1], Shoji Noguchi[2], Takanori Shimizu[1], Tayoko Kubota[1], Shin'ichi Iida[1] (1.Forestry and Forest Products Research Institute, Forest Research and Management Organization, National Research and Development Agency, 2.Kansai Research Center, Forestry and Forest Products Research Institute, Forest Research and Management Organization, National Research and Development Agency)

9:20 AM - 9:35 AM JST | 12:20 AM - 12:35 AM UTC

[AHW20-03] Developement of a 2D Eulerian SPH shallow water model for dam break flows

*Kao-Hua Chang[1] (1.National Taiwan Ocean University)

9:35 AM - 9:50 AM JST | 12:35 AM - 12:50 AM UTC

[AHW20-04] Investigating the validity of a meso scale constitutive equation using micro scale water dynamics simulations for hillslope rainfall-runoff processes

*Yutaka Ichikawa[1], Yuusuke Mori[1], Yasuto Tachikawa[1] (1.Graduate School of Engineering, Kyoto University)

9:50 AM - 10:05 AM JST | 12:50 AM - 1:05 AM UTC

[AHW20-05] A review of ensemble flood forecasting for operational warning

*Megumi Watanabe[1], Shunsuke Ito[2], Wenchao Ma[1], Dai Yamazaki[1] (1.Institute of Industrial Science, The University of Tokyo, Japan, 2.School of Engineering, The University of Tokyo, Japan)

10:05 AM - 10:20 AM JST | 1:05 AM - 1:20 AM UTC

[AHW20-06] ***Toward Downscaling Storage-Discharge Dynamics: Training Long Short-Term Memory (LSTM) model for Simulating Nonlinear Storage-Discharge Relation in HUC-8 Rum***

River Watershed, MN

*Pai-Feng Victor Teng[1] (1.University of Minnesota)

10:20 AM - 10:30 AM JST | 1:20 AM - 1:30 AM UTC

[AHW20-07] Discussion

[E] Oral | A (Atmospheric and Hydrospheric Sciences) | A-HW Hydrology & Water Environment

[A-HW20] Hydrology &Water Environment

convener:Takeshi Hayashi(Faculty of Education and Human Studies, Akita University), Keisuke Fukushi(Institute of Nature &Environmental Technology, Kanazawa University), Koichi Sakakibara(Department of Environmental Sciences, Faculty of Science, Shinshu University), Dai Yamazaki(Institute of Industrial Sciences, The University of Tokyo), Chairperson:Takeshi Hayashi(Faculty of Education and Human Studies, Akita University), Keisuke Fukushi(Institute of Nature &Environmental Technology, Kanazawa University), Koichi Sakakibara(Department of Environmental Sciences, Faculty of Science, Shinshu University), Dai Yamazaki(Institute of Industrial Sciences, The University of Tokyo)

Sat. Jun 5, 2021 9:00 AM - 10:30 AM Ch.12 (Zoom Room 12)

We focus on various issues of water cycle and environment and aim to answer questions of hydrological and earth system sciences; 1) surface, subsurface and their boundary hydrological processes of water cycle, 2) natural and anthropogenic hydrothermal systems, 3) environments issues and studies on a watershed or global scale, 4) water-related issues with ecological, environmental, and geochemical aspects, and 5) other issues in hydrological sciences. We welcome presentations regarding various kinds of approaches and techniques such as field survey, remote sensing, chemical and isotope tracers, numerical simulation, and theoretical analysis. This session is jointly hosted by societies of water-related geoscience (Geochemical Society of Japan, Japanese Association of Groundwater Hydrology, Japanese Association of Hydrological Sciences, and Japan Society of Hydrology and Water Resources), and accepts wide-range research topics related to water cycle and environment described above.

9:00 AM - 9:05 AM

[AHW20-01]Introduction

©Japan Geoscience Union

Behavior of pore-air entrapment in unsaturated soil layer in two small headwater catchments with different soil depth

*Sho Iwagami[1], Shoji Noguchi[2], Takanori Shimizu[1], Tayoko Kubota[1], Shin'ichi Iida[1]

1. Forestry and Forest Products Research Institute, Forest Research and Management Organization, National Research and Development Agency, 2. Kansai Research Center, Forestry and Forest Products Research Institute, Forest Research and Management Organization, National Research and Development Agency

Many researches have been conducted to clarify the mechanism of rainfall-runoff process in a forested catchment in humid warm-temperate regions, however it remains only partially understood. Since the 1980’s, the important issue in rainfall-runoff process studies has been solving how pre-event old water stored in the slope discharge in rapid response during rainstorm event. To explain it, there has been a focus on preferential flows, such as flow in macro-pore, pipe flow, flow in the soil–bedrock interface, and subsurface flow in bedrock fractures. One of other possible explanations of the rapid outflow of pre-event old water is the effect of pore-air entrapment. Experimental studies have shown that pore-air entrapment in the unsaturated zone of soil by infiltrating rainwater and the underlying groundwater table will effect on discharge. Although there have been few reports of pore-air behavior in the field, entrapped pore-air may have an impact on stream discharge.
Despite the fact that the pore pressure measured using a tensiometer is the sum of the pore-water pressure and the pore-air pressure (P_{air}), P_{air} has been neglected. We observed the behavior of P_{air} in the soil layer in a mountainous slope using a simple handmade probe together with the atmospheric pressure (P_{atm}). Pore-air entrapment and its compression was considered to be detected by the positive pressure difference ($\Delta P = P_{air} - P_{atm}$). Also, we expected that entrapped pore-air develops more frequently in a thinner soil catchment because the space between the ground surface and the bedrock is smaller. Thus, two catchments with thin and thick soil were selected for this study: One was a sub-catchment of Hitachi-ohta Experimental Watershed (HA) and another was a sub-catchment of Tsukuba Experimental Watershed (TC), respectively. Both sites are located in Ibaraki Prefecture, Japan, and observations were conducted for about 1 year. As a result, the number of pore-air entrapment events detected were 21 at HA (thin soil catchment), while it was 6 at TC (thick soil catchment). The values of ΔP at the discharge peak were correlated with peak discharge at one of the nearby spring observation points in HA, suggesting the importance of the pore-air entrapment in the rainfall-runoff process, particularly for a headwater catchment with relatively thin soil.

Keywords: Rainfall-runoff process, Pore-air pressure, Pore-air entrapment, Soil layer, Headwater catchment

©2021. Japan Geoscience Union. All Right Reserved.

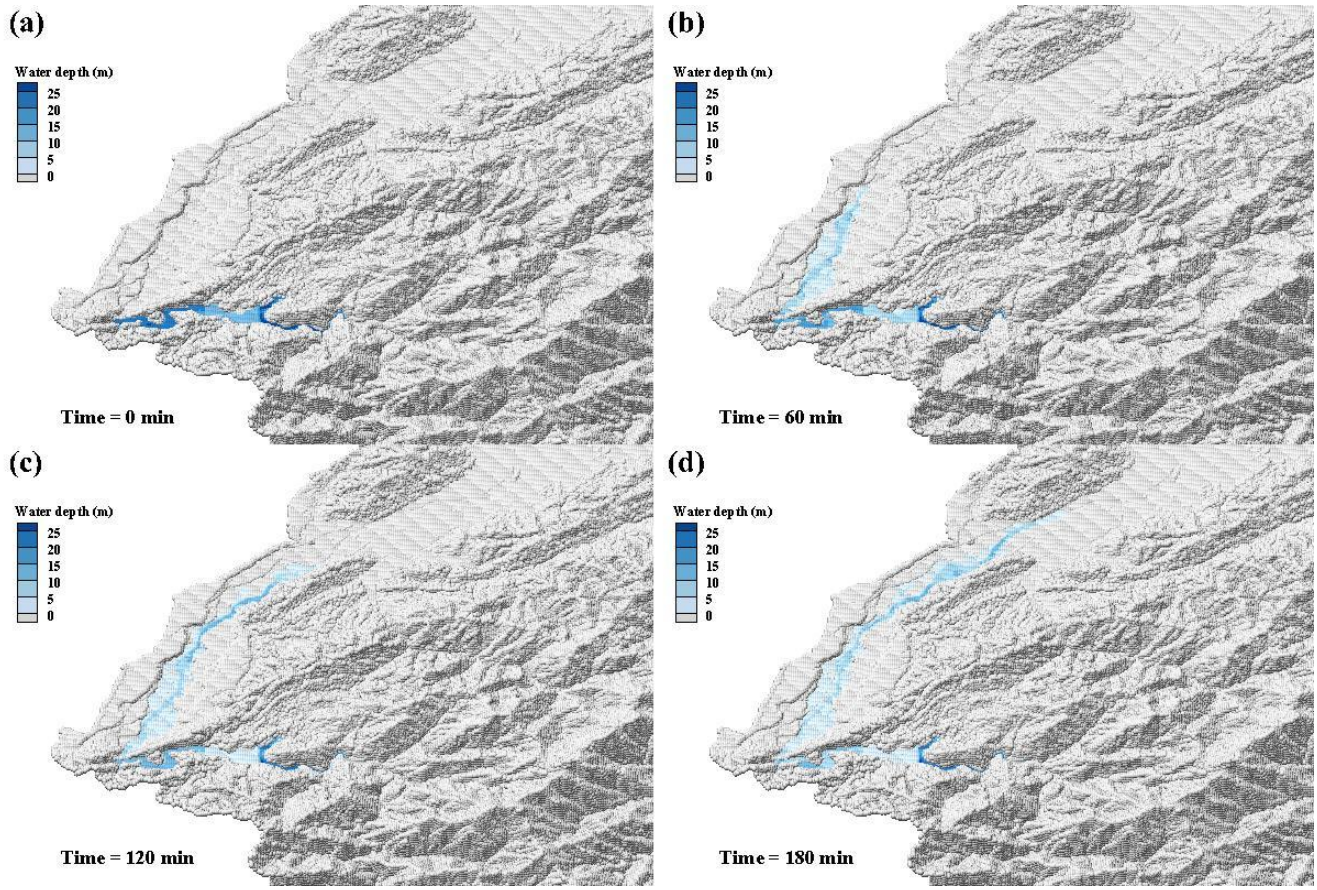
Developement of a 2D Eulerian SPH shallow water model for dam break flows

*Kao-Hua Chang[1]

1. National Taiwan Ocean University

In the study, we propose a two-dimensional (2D) Eulerian meshless shallow water model (SWM) using smoothed particle hydrodynamics (SPH) to simulate various dam break flows. The proposed Eulerian SPH-SWM can significantly improve the efficiency of the existing Lagrangian SPH-SWMs for handling real-world cases. To ensure the stability of the proposed model, an HLLC approximate Riemann solver and a hydrostatic reconstruction scheme are introduced to satisfy the well-balanced and positivity-preserving properties. Two study cases such as dam-break flows respectively on a dry flat bed and through a dry 45-degree bend channel are used to validate the proposed model against the exact and measured solutions. Finally, a scenario of the Shihmen dam in Taiwan broken is investigated to predict 3-hour-ahead flood extent to show the ability of the proposed model dealing with large-scale problems.

Keywords: smoothed particle hydrodynamics, meshless, shallow water equations, dam break flow



©2021. Japan Geoscience Union. All Right Reserved.

Investigating the validity of a meso scale constitutive equation using micro scale water dynamics simulations for hillslope rainfall-runoff processes

*Yutaka Ichikawa[1], Yuusuke Mori[1], Yasuto Tachikawa[1]

1. Graduate School of Engineering, Kyoto University

A number of rainfall-runoff models have been developed in the field of hydraulic and hydrologic engineering, with a special attention on simulating temporal patterns of river discharge in order to meet practical demands such as discharge predictions. Conceptual rainfall-runoff models were initially developed, followed by physical-based models. The physical-based models have achieved a certain level of success, which was partly due to the considerable advancement of computers and the increasing availability of a variety of datasets. It is pointed out, however, that recent important findings based on field studies are not incorporated into rainfall-runoff models, especially used for engineering purposes. To examine the raised issue, this study conducted detailed simulations coupling surface flow and saturated-unsaturated flow for hillslope rainfall-runoff dynamics, and investigated the validity of a constitutive equation used in a rainfall-runoff model. The results revealed that the constitutive equation was capable of describing depth-discharge relationships for hillslopes with relatively shallow soil layers but not for those with thick soil layers.

Keywords: rainfall-runoff, hillslope, depth-discharge relationship, constitutive equation

©2021. Japan Geoscience Union. All Right Reserved.

A review of ensemble flood forecasting for operational warning

*Megumi Watanabe[1], Shunsuke Ito[2], Wenchao Ma[1], Dai Yamazaki[1]

1. Institute of Industrial Science, The University of Tokyo, Japan, 2. School of Engineering, The University of Tokyo, Japan

There is growing international interest in the potential of ensemble flood forecast to improve operational warning. Ensemble flood forecasting systems promise two significant advantages over conventional deterministic forecasting techniques depending on water level observations of upstream rivers. First, ensemble flood forecasting systems have a long lead time for effective evacuation. Second, ensemble flood forecasting systems can also provide quantitative probability to estimate the uncertain forecasts. The introduction of an ensemble flood forecasting system has been under consideration in Japan. We need a comprehensive and integrated assessment based on multiple information from ensemble flood forecasting systems. This study surveyed ways to deliver detailed information in operational ensemble flood forecast systems outside of Japan. We summarized effective visualizations and improvements of the forecast systems by user feedbacks. We found that forecasts with multiple variables are delivered to public administration units with low spatial resolution while forecasts with fewer variables are delivered to each local point or each river segment with high spatial resolution. We also found that user feedbacks have improved the forecasts systems through discussions, although ensemble forecasts are complicated, and they have different characters from local forecasts. Communication with potential users concerning the forecasts is necessary for an effective operation.

Keywords: ensemble, flood, forecast, probabilistic, communication

©2021. Japan Geoscience Union. All Right Reserved.

Toward Downscaling Storage-Discharge Dynamics: Training Long Short-Term Memory (LSTM) model for Simulating Nonlinear Storage-Discharge Relation in HUC-8 Rum River Watershed, MN

*Pai-Feng Victor Teng[1]

1. University of Minnesota

Flooding is one of the most financially devastating natural hazards in the world. The current hydrological models have focused on rainfall-runoff models in flood forecasting, and studying storage-discharge relations has the potential to improve existing flood forecasting. This presentation will assess the relation between daily water storage (ΔS) and discharge (Q) with physical-based hydrological modeling, and storage-discharge dynamics with the machine-learning mechanism located at Rum River Watershed, a HUC8 watershed in Minnesota, between 1995-2015. Currently, linear regression models cannot adequately predict the relationship between the total ΔS and total Q at the HUC-8 watershed (R^2 = 0.3667). Since machine learning (ML) algorithms have already been used for predicting the outputs that represent arbitrary non-linear functions between predictors and predictands, this research will determine how ML algorithms will be used for improving the accuracy of the non-linear relation of the storage-discharge dynamics. Long Short-Term Memory (LSTM), the time-series deep learning neural network that has been used for predicting rainfall-runoff relations, will be used for simulating non-linear relations between ΔS and Q. It will compare two sets of storage-discharge relationships with the hydrological variables simulated by the semi-distributed Hydrological Simulated Program-Fortran (HSPF): dynamics between simulated discharge and input hydrological variables, including air temperature, cloud cover, dew point, potential evapotranspiration, precipitation, evapotranspiration, solar radiation, and wind speed, and the dynamics between simulated discharge and input variables that also includes total water storage at the HUC-8 watershed. 7670 samples are used. 90% of the inputs will be used for training the LSTM network and 10% will be used for testing the prediction. The result shows that the inclusion of total water storage can improve the prediction of total discharge at Rum River Watershed. Inputs of LSTM network can already adequately predict the discharge (NSE = 0.6147, R^2 = 0.8801, Bias Test = -0.4127) without including total water storage; inputting total water storage can significantly improve the prediction (NSE = 0.6977, R^2 = 0.9652, Bias Test = -0.4127). Yet, the main challenge is that both results underpredicted the discharge values in the spring of 2014. The result of the research lays the foundation for assessing the accuracy of downscaling storage-discharge dynamics by applying LSTM networks to evaluate storage-discharge dynamics at smaller, HUC-12 watershed simulated by hydrological models.

Keywords: Hydrological Modeling, Machine Learning , Long Short-Term Memory , Hydrology

©2021. Japan Geoscience Union. All Right Reserved.

[E] Oral | A (Atmospheric and Hydrospheric Sciences) | A-HW Hydrology & Water Environment

[A-HW20] Hydrology &Water Environment

convener:Takeshi Hayashi(Faculty of Education and Human Studies, Akita University), Keisuke Fukushi(Institute of Nature &Environmental Technology, Kanazawa University), Koichi Sakakibara(Department of Environmental Sciences, Faculty of Science, Shinshu University), Dai Yamazaki(Institute of Industrial Sciences, The University of Tokyo), Chairperson:Takeshi Hayashi(Faculty of Education and Human Studies, Akita University), Keisuke Fukushi(Institute of Nature &Environmental Technology, Kanazawa University), Koichi Sakakibara(Department of Environmental Sciences, Faculty of Science, Shinshu University), Dai Yamazaki(Institute of Industrial Sciences, The University of Tokyo)

Sat. Jun 5, 2021 9:00 AM - 10:30 AM Ch.12 (Zoom Room 12)

We focus on various issues of water cycle and environment and aim to answer questions of hydrological and earth system sciences; 1) surface, subsurface and their boundary hydrological processes of water cycle, 2) natural and anthropogenic hydrothermal systems, 3) environments issues and studies on a watershed or global scale, 4) water-related issues with ecological, environmental, and geochemical aspects, and 5) other issues in hydrological sciences. We welcome presentations regarding various kinds of approaches and techniques such as field survey, remote sensing, chemical and isotope tracers, numerical simulation, and theoretical analysis. This session is jointly hosted by societies of water-related geoscience (Geochemical Society of Japan, Japanese Association of Groundwater Hydrology, Japanese Association of Hydrological Sciences, and Japan Society of Hydrology and Water Resources), and accepts wide-range research topics related to water cycle and environment described above.

10:20 AM - 10:30 AM

[AHW20-07]Discussion

©Japan Geoscience Union

[E] Oral | A (Atmospheric and Hydrospheric Sciences)：A-HW Hydrology & Water Environment

Sat. Jun 5, 2021 10:45 AM - 12:15 PM JST | Sat. Jun 5, 2021 1:45 AM - 3:15 AM UTC | Ch.12 Zoom Room 12

[A-HW20] Hydrology & Water Environment

convener:Takeshi Hayashi(Faculty of Education and Human Studies, Akita University), Keisuke Fukushi(Institute of Nature & Environmental Technology, Kanazawa University), Koichi Sakakibara(Department of Environmental Sciences, Faculty of Science, Shinshu University), Dai Yamazaki(Institute of Industrial Sciences, The University of Tokyo), Chairperson:Takeshi Hayashi(Faculty of Education and Human Studies, Akita University), Koichi Sakakibara(Department of Environmental Sciences, Faculty of Science, Shinshu University), Dai Yamazaki(Institute of Industrial Sciences, The University of Tokyo), Shin'ichi Iida(Department of Disaster Prevention, Meteorology and Hydrology, Forestry and Forest Products Research Institute)

We focus on various issues of water cycle and environment and aim to answer questions of hydrological and earth system sciences; 1) surface, subsurface and their boundary hydrological processes of water cycle, 2) natural and anthropogenic hydrothermal systems, 3) environments issues and studies on a watershed or global scale, 4) water-related issues with ecological, environmental, and geochemical aspects, and 5) other issues in hydrological sciences. We welcome presentations regarding various kinds of approaches and techniques such as field survey, remote sensing, chemical and isotope tracers, numerical simulation, and theoretical analysis. This session is jointly hosted by societies of water-related geoscience (Geochemical Society of Japan, Japanese Association of Groundwater Hydrology, Japanese Association of Hydrological Sciences, and Japan Society of Hydrology and Water Resources), and accepts wide-range research topics related to water cycle and environment described above.

10:45 AM - 10:50 AM JST | 1:45 AM - 1:50 AM UTC

[AHW20-08] Introduction

10:50 AM - 11:05 AM JST | 1:50 AM - 2:05 AM UTC

[AHW20-09] Distribution of Uranium and Arsenic in Surface Water around Alkaline-Hyposaline Lake from Valley of Gobi Lakes in Mongolia

*Baasansuren Gankhurel[1], Keisuke Fukushi[1], Davaadorj Davaasuren[2], Eigo Imai[1], TAKUMA KITAJIMA[1], Tuvshin Gerelmaa[2], Yasuhito Sekine[3], Yoshio Takahashi[4], Noriko Hasebe[1] (1.Kanazawa University, 2.National University of Mongolia, 3.Tokyo Institute of Technology, 4.The University of Tokyo)

11:05 AM - 11:20 AM JST | 2:05 AM - 2:20 AM UTC

[AHW20-10] Differences in nitrogen biogeochemical cycles of a reservoir with a hydraulic retention time of several days, before and after the dam was built

*Qingqing Sun[1] (1.Tianjin University)

11:20 AM - 11:35 AM JST | 2:20 AM - 2:35 AM UTC

[AHW20-11] **Plastic debris as a carrier of inorganic contaminants in the urban river of Mongolia**

*Batdulam Battulga[1], Masayuki Kawahigashi[1], Bolormaa Oyuntsetseg[2] (1.Department of Geography, Tokyo Metropolitan University, Tokyo, 192-0397, Japan , 2.Department of Chemistry, National University of Mongolia, Ulaanbaatar, 210646, Mongolia)

11:35 AM - 11:50 AM JST | 2:35 AM - 2:50 AM UTC

[AHW20-12] Geochemisty and environmental impact on groundwater in Eastern Serbia

*Dragana Adamovic[1,2], Daizo Ishiyama[1], Hiroshi Kawaraya[1], Yasumasa Ogawa[1] (1.Akita University, Japan, 2.MMI Bor, Serbia)

11:50 AM - 12:05 PM JST | 2:50 AM - 3:05 AM UTC

[AHW20-13] **Measurement of reactive oxygen species (ROS) and fluorescent organic matter in selected rivers in Hiroshima Prefecture, Japan.**

*Taiwo Tolulope Ayeni[1], Takashi Umeda[1], Yoko Iwamoto[1], Kazuhiko Takeda[1], Hiroshi M. G. Sakugawa[1], Khan M. G. Mostofa[2] (1.Hiroshima University Japan, 2.Tianjin University, China)

12:05 PM - 12:15 PM JST | 3:05 AM - 3:15 AM UTC

[AHW20-14] Discussion

[E] Oral | A (Atmospheric and Hydrospheric Sciences) | A-HW Hydrology & Water Environment

[A-HW20] Hydrology &Water Environment

convener:Takeshi Hayashi(Faculty of Education and Human Studies, Akita University), Keisuke Fukushi(Institute of Nature &Environmental Technology, Kanazawa University), Koichi Sakakibara(Department of Environmental Sciences, Faculty of Science, Shinshu University), Dai Yamazaki(Institute of Industrial Sciences, The University of Tokyo), Chairperson:Takeshi Hayashi(Faculty of Education and Human Studies, Akita University), Koichi Sakakibara(Department of Environmental Sciences, Faculty of Science, Shinshu University), Dai Yamazaki(Institute of Industrial Sciences, The University of Tokyo), Shin'ichi Iida(Department of Disaster Prevention, Meteorology and Hydrology, Forestry and Forest Products Research Institute)

Sat. Jun 5, 2021 10:45 AM - 12:15 PM Ch.12 (Zoom Room 12)

We focus on various issues of water cycle and environment and aim to answer questions of hydrological and earth system sciences; 1) surface, subsurface and their boundary hydrological processes of water cycle, 2) natural and anthropogenic hydrothermal systems, 3) environments issues and studies on a watershed or global scale, 4) water-related issues with ecological, environmental, and geochemical aspects, and 5) other issues in hydrological sciences. We welcome presentations regarding various kinds of approaches and techniques such as field survey, remote sensing, chemical and isotope tracers, numerical simulation, and theoretical analysis. This session is jointly hosted by societies of water-related geoscience (Geochemical Society of Japan, Japanese Association of Groundwater Hydrology, Japanese Association of Hydrological Sciences, and Japan Society of Hydrology and Water Resources), and accepts wide-range research topics related to water cycle and environment described above.

10:45 AM - 10:50 AM

[AHW20-08]Introduction

©Japan Geoscience Union

Distribution of Uranium and Arsenic in Surface Water around Alkaline-Hyposaline Lake from Valley of Gobi Lakes in Mongolia

*Baasansuren Gankhurel[1], Keisuke Fukushi[1], Davaadorj Davaasuren[2], Eigo Imai[1], TAKUMA KITAJIMA[1], Tuvshin Gerelmaa[2], Yasuhito Sekine[3], Yoshio Takahashi[4], Noriko Hasebe[1]

1. Kanazawa University, 2. National University of Mongolia, 3. Tokyo Institute of Technology, 4. The University of Tokyo

Saline lakes represent 23% of the area of all lakes on Earth and located mostly in arid and semiarid climates.
Saline lakes are mainly fed by precipitation and surface flow. But also, water lost by evaporation has significant role in saline lakes. Evaporation of the lake water results the formation of contaminated lake water and salt deposits containing high levels of dissolved species including trace elements such as arsenic and uranium. The chemical speciation of trace elements in sediments and distribution between the sediments and lake water are essential for the understanding of formation process and the mobility of trace elements.
This study aims to clarify distribution and formation process of As and U in saline lake water based on their sediment and water chemistry analysis of surface waters (springs, rivers, wells) around the study area. The sediment and water chemistry samples of alkaline-hyposaline lake catchment area (Orog and Olgoy lakes) in semi-arid climates of the Valley of Gobi lakes in Mongolia were studied. We measured lakes, river and spring water samples in different seasons from 2015 to 2020. Also, well water samples around the study area in 2017 and 2018 were measured. Sediment samples were analyzed by using sequential extraction procedure (SEP), X-ray diffraction (XRD) and synchrotron-based X-ray absorption spectroscopy (XAFS).
Olgoy and Orog lakes exhibited pH exceeded 9 and salinity above 1300 mg/kg. The lake waters major cation and anion is Na^{+}, Cl^{-} and SO_4^{2-}. The high Na and Cl concentrations are result of evaporation of the lake waters. Also, our results showed that high concentrations of As (~3019ppb) and U (~590ppb) in lake water, respectively. Therefore, the concentration of arsenic and uranium differed in different months throughout the year which need more clarification to understand the process between lake-sediment interaction. The results of SEP of lake sediment showed that arsenic and uranium in sediments are distributed into calcium carbonates rather than amorphous iron oxide. XRD analysis results shows that sediment sample has authigenic minerals including calcite and Monohydrocalcite. The results of XAFS analysis shown As in Orog lake sediment was As (V) and primarily coprecipitated with calcite and secondarily adsorbed on ferrihydrite. As in Olgoi lake sediment was mainly As (V) and 20-30% was As (III) and coprecipitated with calcite. As and U possibly are removed by the authigenic carbonates. Carbonates are not “source” of these elements but “sink”. However, we need to clarify how much the carbonates play a role of “sink”. The springs, rivers, and well water have pH around 6.3-8.3 and low salinity. The major cation of surface water excluding lake water are Ca^{2+} and concentrations of Na^{+}, Cl^{-}, SO_4^{2-} were low. But we found in some well and spring point has high concentration of U(~39ppb) and As (~61ppb). The high concentrations of As and U in lake water might be related to the surface water around lake and the evaporation of river water.

Keywords: saline lake, water, uranium, arsenic

©2021. Japan Geoscience Union. All Right Reserved.

Differences in nitrogen biogeochemical cycles of a reservoir with a hydraulic retention time of several days, before and after the dam was built

*Qingqing Sun[1]

1. Tianjin University

Despite the fragmentation of rivers and irreparable damage to biodiversity, around the world, more and more DAMS are being built to alleviate energy, water, and food shortages. The retention time of these reservoirs varies from a few days to several years. Suofengying Reservoir ((26° 94’ N, 106° 35’ E, 70 m of depth) in Wujiang River Watershed of China was selected. The dam was built and put into use in 2004, mainly for power generation, with a hydraulic retention time of 0.012 years. It made the reservoir change a little vertically, which interacts with aquaculture. On the one hand, the proportion of fish prefers rapid water or still water. On the other hand, a large number of nutrients are input, etc.
In this abstract, I used environmental fluid dynamics code, ArcGIS, water balance model, mass balance model, and box model to build the reservoir hydrodynamic model, water quality model of nitrogen. I discussed 1) The dam's interdicting effect on the river is interpreted in combination with atmospheric nitrogen deposition, sediment-water interface release, and settlement. Because of the hydrodynamic defense, nitrogen cycle differences occur in the river, mixing zones, and still water zones. 2) The effects of other biogenic elements, especially P limitation, on nitrogen bioavailability. 3) Interaction of the whole system of atmosphere, surface water, groundwater, soil, sediment, and organisms.
Special thanks to China National Meteorological Data Center (https://data.cma.cn/), Watershed Biogeochemistry Team, School of Earth System Science, Tianjin University, School of Environment and Chemistry, Shanghai University, and State Key Laboratory of Environmental and Chemical Engineering, Institute of Geochemistry, Chinese Academy of Sciences, Guizhou Hydrological Resources Bureau and DSI LLC. for their foundation work.

Keywords: Nitrogen, Environmental fluid dynamics code, Suofengying Reservoir

©2021. Japan Geoscience Union. All Right Reserved.

Plastic debris as a carrier of inorganic contaminants in the urban river of Mongolia

*Batdulam Battulga[1], Masayuki Kawahigashi[1], Bolormaa Oyuntsetseg[2]

1. Department of Geography, Tokyo Metropolitan University, Tokyo, 192-0397, Japan , 2. Department of Chemistry, National University of Mongolia, Ulaanbaatar, 210646, Mongolia

Plastic pollution in the aquatic environment has become a social concern by their long life in the ecosystems. Although a global survey has mainly focused on the accumulation and distribution of plastic debris, interactions between plastic debris and inorganic pollutants and the behavior of those plastics aggregates are still unclear. In this study, we addressed plastics associated with inorganic pollutants in the urban river of Mongolia. The aims of the current study are i.) identification of inorganic pollutants on the surface of plastic debris, particularly on polystyrene foam (PSF), and ii.) evaluation of the elemental association and potential sources of inorganic pollutants with the PSFs in the river environment.

The PSF samples were collected from the 6 sampling locations of the urban river shores. The concentrations of major (Al and Na) and trace (B, Cr, Cu, Mn, Mo, Ni, Pb and Zn) elements were determined in the macro (20-100 mm), meso (5-20 mm), and micro (<5 mm) sized PSFs. The mixture of hydrogen peroxide (30%, H_2O_2) and iron (II) catalyst solution (0.05 M) was used to digest all organic substances and separate surface adhered inorganic pollutants from the PSF samples. The digested solution was applied to determine the concentrations of major and trace elements adhered on the PSFs using an Inductively Coupled Plasma Atomic Emission Spectrometer (ICP-AES).

The mean concentrations of Al, B, Cr, Cu, Mn, Mo, Na, Ni, Pb and Zn accumulated on the PSFs (n=57) were determined as 1967.0±270.5, 119.5±43.2, 16.1±7.5, 39.4±8.7, 174.2±20.7, 9.6±2.5, 1506.8± 476.8, 40.8±11.2, 17.7±9.2 and 283.0±100.8 $\mu g\ g^{-1}$ (mean content ±standard error), respectively. Comparing levels of elements among the different size fractions, rather higher values of elements were measured in the meso-sized PSFs except for Al and Mo, which were higher in micro-sized PSF particles. In addition, strong correlations among B, Na and Zn indicate the chemical association of those elements with the environmental PSFs. A wide range of the elemental concentrations illustrates the adsorption of the elements from the surrounding environment on the surface of PSFs which might be mediated by a biofilm. On the contrary, some elements (i.e., Zn) can be leached from additives of PSFs through degradation. The widespread plastic debris could be one of the carriers and sources of hazardous chemicals in the aquatic environment.
While the consequences of plastic debris on environmental health are poorly understood, the fate and behavior of hetero-aggregates of plastics in the aquatic environment should be continuously studied in future.

Keywords: Plastic debris, Inorganic pollutants, Polystyrene foam (PSF), Urban river, Aggregates

©2021. Japan Geoscience Union. All Right Reserved.

Geochemisty and environmental impact on groundwater in Eastern Serbia

*Dragana Adamovic[1,2], Daizo Ishiyama[1], Hiroshi Kawaraya[1], Yasumasa Ogawa[1]

1. Akita University, Japan, 2. MMI Bor, Serbia

Contamination of water bodies is a large problem in many mining areas in the world. Mining activities have been carried out for about 120 years in Eastern Serbia. Nowadays, there are four active copper mines in two mining areas, the Bor mining area and the Majdanpek mining area, in Eastern Serbia. The long history of mining in Eastern Serbia causes serious environmental problems, which are most pronounced on water pollution downstream of the mining sites. Many studies focused on river water pollution. However, there is no comprehensive research about groundwater in Eastern Serbia. Therefore, this research aims to clarify the geochemistry of groundwater and to know whether mining activities give an effect on groundwater quality or not.

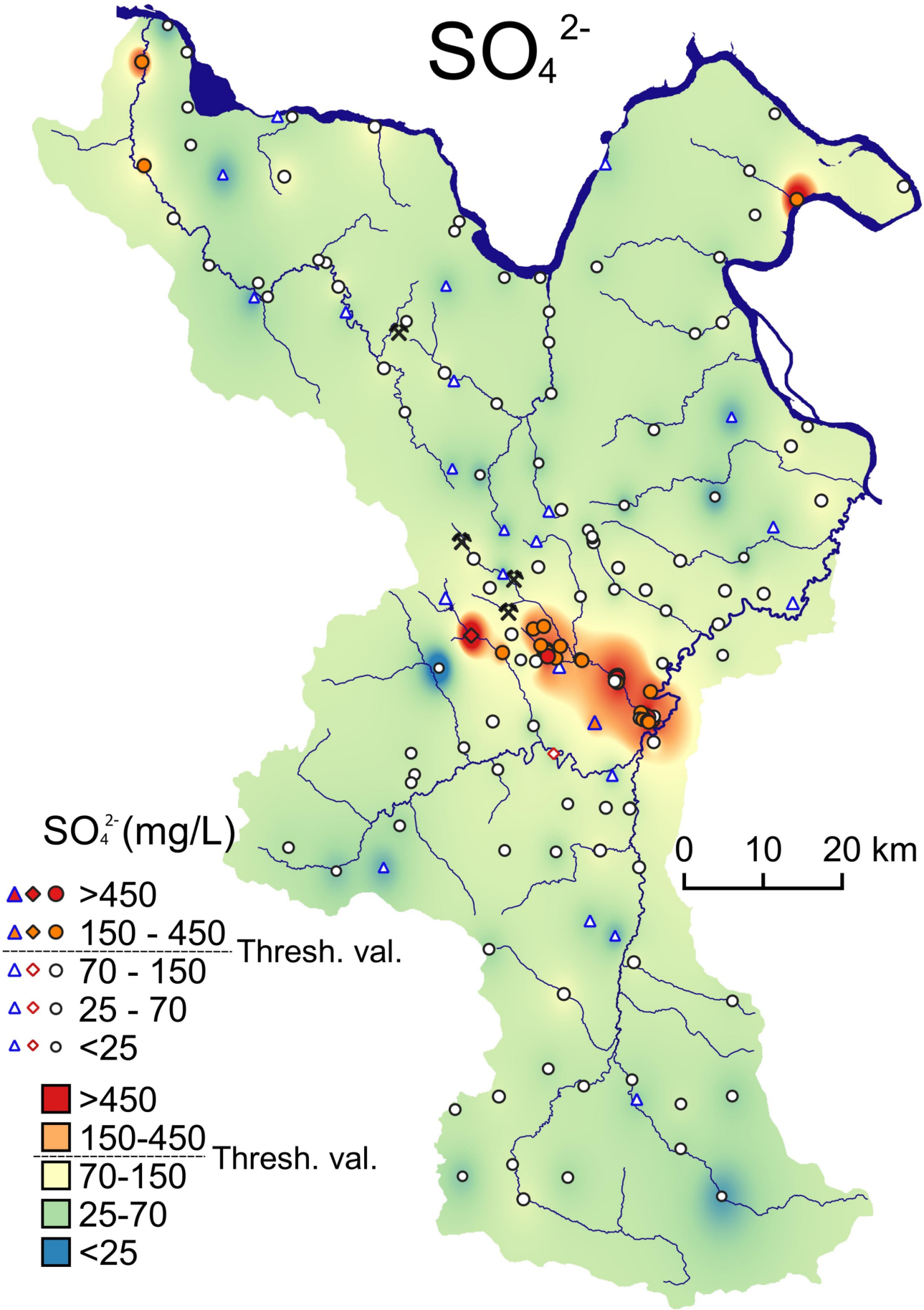
Sample collection was carried on in August and September 2019. The total number of groundwater samples was 172, including 144 samples collected from wells, 23 cold spring samples, 3 hot spring samples and 2 samples from boreholes. All water samples were filtrated through a 0.2 μm cellulose acetate hydrophilic filters. After filtration, two kinds of samples were prepared. They are non-acidified samples used for the determination of major elements and acidified samples (with ultrapure HNO_3) used for the determination of trace elements. In the field, coordinates of sampling points, pH and Eh values, water temperature and the concentration of HCO_3^- were also determined.

To understand the geochemical signature and environmental impact of groundwater in the study area, geochemical maps were created. Threshold values for discrimination of anomalous populations from background populations were also estimated for Ca^{2+}, SO_4^{2-}, Cu and As.

Groundwater in the study area is characterized by pH values from 6.4 to 8.8 and a high concentration of HCO_3^- (30 to 930 mg/L). In general, groundwater from the study area has good quality. However, anomalous concentrations of Ca^{2+}, SO_4^{2-}, Cu and As are recognized in groundwater around ore deposits of the Bor mine and along polluted rivers downstream of the Bor mine. Distributions of anomalous concentrations of major elements (Ca^{2+} and SO_4^{2-}) in groundwater are similar to the distributions of anomalous concentrations of these components in river water. Therefore, there is a possibility that groundwater along highly polluted river water in the Bor mining area is affected by acid mine drainage bearing-river water. Based on mass balance calculation between components in polluted river water and groundwater, polluted river water having high concentrations of Ca^{2+} and SO_4^{2-} in riverbed sediments flows into groundwater in the area where the water surface level of polluted river water is higher than the level of the groundwater table. On the other hand, the mixing was not observed based on the mass balance calculation based on the concentrations of Cu and As in river water and groundwater because of the precipitation of these elements as a result of the change of pH value from acidic to neutral. An appropriate component for groundwater monitoring in mining areas located in Eastern Serbia is SO_4^{2-}, which can be present as aqueous species without precipitation in groundwater from acidic to neutral pH.

Keywords: Bor, Groundwater pollution, Mining activities, Threshold value

©2021. Japan Geoscience Union. All Right Reserved.



©2021. Japan Geoscience Union. All Right Reserved.

Measurement of reactive oxygen species (ROS) and fluorescent organic matter in selected rivers in Hiroshima Prefecture, Japan.

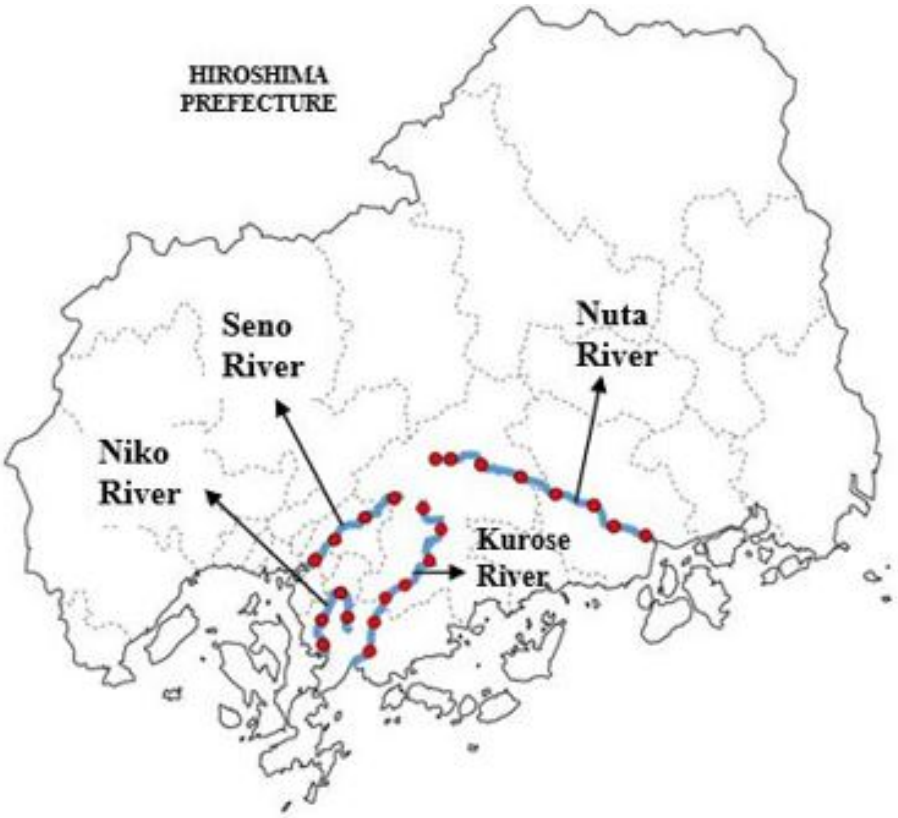
*Taiwo Tolulope Ayeni[1], Takashi Umeda[1], Yoko Iwamoto[1], Kazuhiko Takeda[1], Hiroshi M. G. Sakugawa[1], Khan M. G. Mostofa[2]

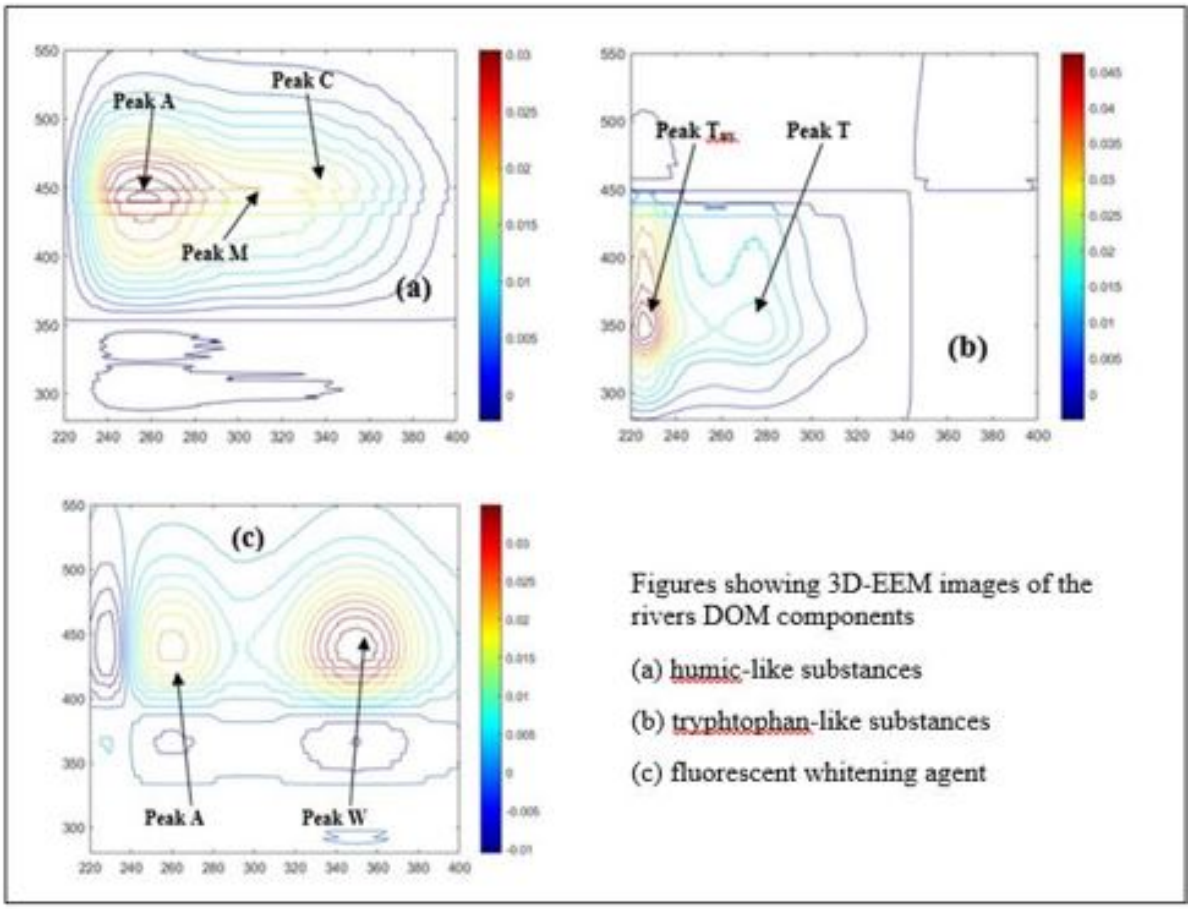
1. Hiroshima University Japan, 2. Tianjin University, China

The incidence of solar irradiation on natural water surfaces could excite their inorganic or organic components to produce some transitory species otherwise called reactive oxygen species (ROS) such as hydroxyl radical (•OH), nitric oxide radical (NO•) and singlet oxygen ($^1O_2$). These species could facilitate the photochemical degradation of natural organic matter or pollutants and also partake in some biological or redox reactions. Recent comprehensive study on Japanese rivers reveals that nitrite was the major source of •OH and NO• while $^1O_2$ was predominantly sourced from Chromophoric dissolved organic matter (CDOM). In the present study, the photogeneration of these three ROS and investigation of their dissolved organic components were carried out across 23 stations in four rivers (Niko, Seno, Kurose, and Nuta) located in the Hiroshima Prefecture of Japan during the winter of 2020. Analysis involving dissolved organic carbon (DOC), absorption properties, and ions were carried out using TOC-V_{CSH} analyzer, UV-Visible spectrophotometer, and Ion chromatography, respectively. Parallel factor analysis (PARAFAC) modelling was employed in identifying the DOM components of the rivers. The photogeneration rates of the ROS were determined by means of established HPLC methods. The DOC values across the rivers ranged from the low of 34.7 μM C in the Nuta river to the high of 259 μM C in the Kurose river. The absorption coefficient at 300 nm (a_{300}), which is a measure of CDOM abundance and the concentration of inorganic nitrite also followed the same pattern as that of the DOC and were within the ranges of (1.61 to 9.06) m^{-1} and (0.07 and 17.9) μM, respectively. The ROS values ranged from (12.4 –392) $\times 10^{-12}$ M s^{-1} for •OH, (4.17 –1050) $\times 10^{-12}$ M s^{-1} for NO• and (4.66 –32.4) $\times 10^{-9}$ M s^{-1} for $^1O_2$ and were also minimum in the Nuta river and maximum in the Kurose river. Humic-like and tryptophan-like components were the predominant organic matter across the rivers, however fluorescent whitening agent was observed in some stations of the rivers.

Keywords: hydroxyl radical, nitric oxide radical, singlet oxygen, dissolved organic matter, PARAFAC, river water

©2021. Japan Geoscience Union. All Right Reserved.





Figures showing 3D-EEM images of the rivers DOM components

(a) humic-like substances

(b) tryphtophan-like substances

(c) fluorescent whitening agent

©2021. Japan Geoscience Union. All Right Reserved.

[E] Oral | A (Atmospheric and Hydrospheric Sciences) | A-HW Hydrology & Water Environment

[A-HW20] Hydrology &Water Environment

convener:Takeshi Hayashi(Faculty of Education and Human Studies, Akita University), Keisuke Fukushi(Institute of Nature &Environmental Technology, Kanazawa University), Koichi Sakakibara(Department of Environmental Sciences, Faculty of Science, Shinshu University), Dai Yamazaki(Institute of Industrial Sciences, The University of Tokyo), Chairperson:Takeshi Hayashi(Faculty of Education and Human Studies, Akita University), Koichi Sakakibara(Department of Environmental Sciences, Faculty of Science, Shinshu University), Dai Yamazaki(Institute of Industrial Sciences, The University of Tokyo), Shin'ichi Iida(Department of Disaster Prevention, Meteorology and Hydrology, Forestry and Forest Products Research Institute)

Sat. Jun 5, 2021 10:45 AM - 12:15 PM Ch.12 (Zoom Room 12)

We focus on various issues of water cycle and environment and aim to answer questions of hydrological and earth system sciences; 1) surface, subsurface and their boundary hydrological processes of water cycle, 2) natural and anthropogenic hydrothermal systems, 3) environments issues and studies on a watershed or global scale, 4) water-related issues with ecological, environmental, and geochemical aspects, and 5) other issues in hydrological sciences. We welcome presentations regarding various kinds of approaches and techniques such as field survey, remote sensing, chemical and isotope tracers, numerical simulation, and theoretical analysis. This session is jointly hosted by societies of water-related geoscience (Geochemical Society of Japan, Japanese Association of Groundwater Hydrology, Japanese Association of Hydrological Sciences, and Japan Society of Hydrology and Water Resources), and accepts wide-range research topics related to water cycle and environment described above.

12:05 PM - 12:15 PM

[AHW20-14]Discussion

©Japan Geoscience Union

[E] Poster | A (Atmospheric and Hydrospheric Sciences)：A-HW Hydrology & Water Environment

Sat. Jun 5, 2021 5:15 PM - 6:30 PM JST | Sat. Jun 5, 2021 8:15 AM - 9:30 AM UTC | Ch.07_1

[A-HW20] Hydrology & Water Environment

convener:Takeshi Hayashi(Faculty of Education and Human Studies, Akita University), Keisuke Fukushi(Institute of Nature & Environmental Technology, Kanazawa University), Koichi Sakakibara(Department of Environmental Sciences, Faculty of Science, Shinshu University), Dai Yamazaki(Institute of Industrial Sciences, The University of Tokyo)

We focus on various issues of water cycle and environment and aim to answer questions of hydrological and earth system sciences; 1) surface, subsurface and their boundary hydrological processes of water cycle, 2) natural and anthropogenic hydrothermal systems, 3) environments issues and studies on a watershed or global scale, 4) water-related issues with ecological, environmental, and geochemical aspects, and 5) other issues in hydrological sciences. We welcome presentations regarding various kinds of approaches and techniques such as field survey, remote sensing, chemical and isotope tracers, numerical simulation, and theoretical analysis. This session is jointly hosted by societies of water-related geoscience (Geochemical Society of Japan, Japanese Association of Groundwater Hydrology, Japanese Association of Hydrological Sciences, and Japan Society of Hydrology and Water Resources), and accepts wide-range research topics related to water cycle and environment described above.

[AHW20-P01] Contribution of understory vegetation to evapotranspiration in a tropical dry forest, Cambodia

*Shin'ichi Iida[1], Takanori Shimizu[1], Koji Tamai[1], Naoki Kabeya[1], Akira Shimizu[1], Eriko Ito[1], Yasuhiro Ohnuki[1], Sophal Chann[2], Delphis F. Levia[3] (1.Forestry and Forest Products Research Institute, Japan, 2.Institute of Forest and Wildlife Research and Development, Cambodia, 3.University of Delaware, USA)

[AHW20-P02] Rainfall partitioning in two Japanese cedar stands with high stand densities as evidence of splash droplet evaporation hypothesis

*Shigeki Murakami[1], Kenzo Kitamura[1] (1.Kyushu Research Center, Forestry and Forest Products Research Institute)

[AHW20-P03] Vegetation response to soil moisture and groundwater in west-central Africa revealed by satellite observations

*Ryotaro Suzuki[1], Atsushi Higuchi[2] (1.Graduate School of Science and Engineering, Chiba University, Japan, 2.Center for Environmental Remote Sensing, Chiba University, Japan)

[AHW20-P04] An Efficient Surrogate Model for Extreme Hydrologic Predictions using Polynomial Chaos-Kriging

Vinh Ngoc Tran[1], *Jongho Kim[1] (1.University of Ulsan)

[AHW20-P05] Hydrological Hindcasts and Parameterizations for Flash Floods Real-Time Forecasting in the Chugoku Region of Japan

*Josko Troselj[1], Han Soo Lee[1] (1.Graduate School of Advanced Science and Engineering, Hiroshima University)

[AHW20-P06] Geochemical signature of trace elements in lake water at Lake Tazawa

*Arata Katamura[1], Daizo Ishiyama[1], Takeshi Hayashi[2], Yasumasa Ogawa[1] (1.Graduate School of International Resource Science, Akita University, 2.Faculty of Education and Human Studies, Akita University)

Contribution of understory vegetation to evapotranspiration in a tropical dry forest, Cambodia

*Shin'ichi Iida[1], Takanori Shimizu[1], Koji Tamai[1], Naoki Kabeya[1], Akira Shimizu[1], Eriko Ito[1], Yasuhiro Ohnuki[1], Sophal Chann[2], Delphis F. Levia[3]

1. Forestry and Forest Products Research Institute, Japan, 2. Institute of Forest and Wildlife Research and Development, Cambodia, 3. University of Delaware, USA

Tropical dry forests cover about 20% of the global forested area, and their annual amounts of evapotranspiration are equivalent to more than 70% of annual rainfall, suggesting significant enhancements of water-vapor circulation between the land surface and the atmosphere over this land cover type. For example, Kanae et al. (2001) reported a decrease of rainfall around the Indochina peninsula engendered by forest decline. Although previous studies investigated evapotranspirational processes on the Indochina peninsula, Tanaka et al. (2008) pointed out the lack of research on dry deciduous forests. A dense understory vegetation generally covers the ground of dry deciduous forests, however, its contribution to evapotranspirational processes has not been comprehensively estimated. Here, we measured whole ecosystem evapotranspiration (ET_W) and evapotranspiration from the understory vegetation (ET_U) separately, and analyzed the factors controlling the understory contribution to evapotranspiration (ET_U/ET_W).

We measured evapotranspiration components at the dry deciduous forest located in Kratie province, Cambodia. The forest consists of deciduous trees, comprised of *Dipterocarpus tuberculatus*, *Terminalia alata*, *Shorea obtusa* and *Xylia xylocarpa*, and understory vegetation (*Vietnamosasa pusilla*). Both ET_W and ET_U were estimated by the band-pass eddy covariance method, applying the instruments installed above the sparse overstory canopy (leaf area index, LAI = 1.05) and understory vegetation, respectively. The overstory transpiration (TR) was estimated by sap flow technique (Granier, 1985) for all trees within the measurement plot (n=12). Canopy interception loss was calculated as the difference between gross rainfall and the sum of throughfall and stemflow. The period of analysis was from June 2010 to June 2011 (total available days was 354).

The total amount of ET_W was 1064 mm corresponding to 74% of the annual rainfall. This percentage was typically similar with previous reports (e.g., Farrick and Branfireun, 2013). The dry season ET_W (424 mm) was larger than rainfall (353 mm) indicating that this ecosystem uses water resources recharged during the wet season. The understory contribution to evapotranspiration (ET_U/ET_W) was 35%, and we concluded that understory vegetation is one of the most important components of evapotranspiration in this ecosystem. Seasonal changes of ET_U/ET_W were negatively correlated with LAI. We reviewed annual ET_U/ET_W values among the tropics, temperate, subhumid and boreal forests. We found that the annual ET_U/ET_W showed a negative correlation with LAI when LAI < 4. Thus, it is concluded that both seasonality and magnitude of ET_U/ET_W were controlled by LAI. On the other hand, overstory transpiration (TR) estimated by the original calibration coefficient showed high and positive correlation with the difference between ET_W and the sum of ET_U and interception loss, but we found clear underestimations of TR. When we applied recently published sets of calibration coefficients (Fuchs et al., 2017; Ouyang et al., 2018), the

©2021. Japan Geoscience Union. All Right Reserved.

underestimation was improved. Applications of the coefficients of Ouyang et al. (2018) corrected almost all underestimations. We highly recommend the establishment of new calibration coefficients to evaluate TR precisely at dry deciduous forests in future studies.

This presentation is based on the following open access article: Iida, S., Shimizu, T., Tamai, K., Kabeya, N., Shimizu, A., Ito, E., Ohnuki, Y., Chann, S., Levia, D.F. (2020): Evapotranspiration from the understory of a tropical dry deciduous forest in Cambodia. Agricultural and Forest Meteorology, 295, 108170.

Cited papers:

Farrick and Branfireun (2013) Hydrol. Process. 27, 3254–3262.

Fuchs et al. (2017) Agric. For. Meteorol., 244, 151-161.

Granier (1985) Ann. Sci. For., 42, 193-200.

Kanae et al. (2001) J. Hydrometeorol., 2, 51-70.

Ouyang et al. (2018) Forests, 9, 162.

Tanaka et al. (2008) Agric. For. Meteorol., 148, 807-819.

Keywords: Tropical dry forest, Understory vegetation, Evapotranspiration, Leaf area index

©2021. Japan Geoscience Union. All Right Reserved.

Rainfall partitioning in two Japanese cedar stands with high stand densities as evidence of splash droplet evaporation hypothesis

*Shigeki Murakami[1], Kenzo Kitamura[1]

1. Kyushu Research Center, Forestry and Forest Products Research Institute

1. Introduction

Rainfall partitioning in two Japanese cedar stands with the stand densities of 5700 trees/ha (the stand A) and 9700 trees/ha (the stand B) was measured, which were the highest densities in measurements of rainfall partitioning in Japanese coniferous plantations (Jeong et al. 2019). Gross rainfall GR, throughfall TF, stemflow SF and canopy interception CI were analyzed. The results were discussed from the viewpoint of splash droplet evaporation hypothesis that claims splash droplets generated by raindrops impacting on the canopy surface evaporate that is a major mechanism of CI (Murakami, 2006).

2. Site and methods

Both stands were 7 years old and located at Kyushu Research Center, Forestry and Forest Products Research Institute, Kumamoto, Japan. Four tipping bucket type flowmeters were used to measure TF and SF of each stand for some 6 months. Data were recorded with an interval of 10 minutes, and analysis was conducted on a rain event basis. Hourly analysis was also made and the results will be shown at the time of the presentation.

3. Results

Total GR during the period was 1405.0 mm. The percentage of CI/GR, TF/GR and SF/GR in the stand A (B) was 18.2% (13.1%), 38.6% (24.7%) and 43.2% (62.2%), respectively. TF/GR and SF/GR in the stand B were, respectively, the smallest and the largest record in Japanese coniferous stands referring to Jeong et al. (2019).

As shown in Fig. 1 CI, TF and SF increase with GR in both stands on a rain event basis. However, in each stand data do not fit with a single linear regression line except for SF of the stand B in Fig. 1c. Instead, there are threshold values, over which data are not placed on the regression line. In Fig. 1a the increment in CI with respect to GR abruptly becomes large for GR > 107.0 mm (162.5 mm) in the stand A (B). Inversely, in Fig. 1b the increment in TF reduces for GR>107.0 mm (37.0 mm) in the stand A (B). In Fig. 1c SF has a single linear relationship with GR in the stand B, but the increment in SF declines for GR>139.5 mm in the stand A.

4. Discussion

©2021. Japan Geoscience Union. All Right Reserved.

High stand density restricts wider extension of branches because of limited canopy area per tree that forces the tree to grow branches upward with steeper angle. The branches collect rainwater effectively and produce much SF.

There exists a possible mechanism to reduce TF and SF for large rain events that are often accompanied by high rainfall intensity. Bassette and Bussière (2008) pointed out that the steeper the leaf angle was the smaller the production of splash became and that the proportion of splash increased with drop kinetic energy. Similar mechanism can work for branches. Upward branches collect rainwater efficiently like a funnel and generate SF without producing much splash for rainfall with low intensity. TF is also large for low-intensity rainfall because raindrops generate less splash with less splash droplet evaporation on upward branches. Nonetheless, when rainfall intensity becomes high the production rate of splash is boosted that reduces TF (Fig. 1b) and SF (Fig. 1c, the stand A) because of active splash droplet evaporation. As a consequence CI is augmented for heavy rainfall, though we have no idea why the threshold values exist.

References

Bassette and Bussière. 2008. Partitioning of splash and storage during raindrop impacts on banana leaves. Agricultural and Forest Meteorology. 97, 9-19. doi: 10.1016/j.agrformet.2008.01.016

Jeong, S. et al. 2019. Marked difference of rainfall partitioning in an unmanaged coniferous plantation with high stand density. Journal of Forest Research. 24, 107-114. doi: 10.1080/13416979.2018.1551116

Murakami, S. 2006. A proposal for a new forest canopy interception mechanism: Splash droplet evaporation. Journal of Hydrology, 319, 72–82. doi:10.1016/j.jhydrol.2005.07.002

Keywords: Canopy interception, Throughfall, Stemflow, Splash droplet evaporation

©2021. Japan Geoscience Union. All Right Reserved.

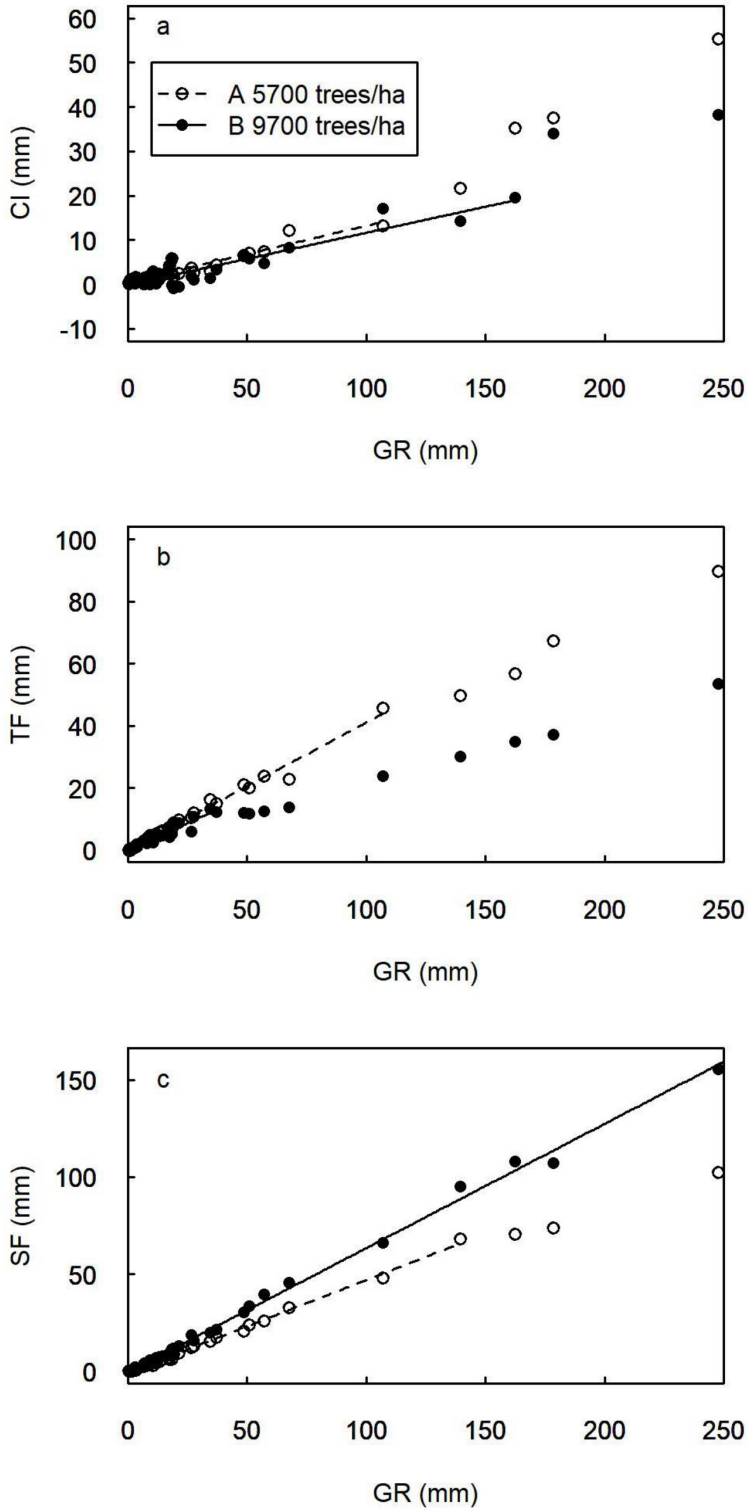


Fig. 1 Relationship between gross rainfall *GR* and (a) canopy interception *CI*, (b) throughfall *TF* and (c) stemflow *SF* on a rain event basis.

©2021. Japan Geoscience Union. All Right Reserved.

Vegetation response to soil moisture and groundwater in west-central Africa revealed by satellite observations

*Ryotaro Suzuki[1], Atsushi Higuchi[2]

1. Graduate School of Science and Engineering, Chiba University, Japan, 2. Center for Environmental Remote Sensing, Chiba University, Japan

Vegetation is always exposed to environmental changes, and vegetation green-up is mainly affected by water in arid lands. Root systems primarily carry out water intake by terrestrial plants. Therefore, it is vital to grasp soil water for the investigation of vegetation responses to water. However, in-situ data are generally limited and spatially sparse. We investigated the relationship between water availability and vegetation growth in west-central Africa, which contains dry regions south of the Sahara Desert and wet regions in the Equatorial region. Used satellite observation data including Advanced Microwave Scanning Radiometer for Earth Observing System (AMSR-E) Soil Moisture Content (SMC), i.e., reflecting soil moisture in the near-surface layer, and Gravity Recovery and Climate Experiment (GRACE) Terrestrial Water Storage (TWS), i.e., reflecting terrestrial water change.
We performed multiple regression analysis using Leaf Area Index (LAI) as the response variable and considering SMC and TWS as explanatory variables. The relationship between the SMC and LAI is vital in the region covered by annual plants, utilizing only near-surface soil water because of the shallow rooting system. The region’s relationship covered by perennial plants is relatively weak, caused by a more in-depth rooting system. TWS contains soil water that cannot be used by plants because of too deep. Therefore, the relationship between LAI and TWS is weak.
We found that TWS decline during the primary dry season becomes more pronounced toward the equatorial region. Thus, we assessed the relationship between TWS fluctuation and LAI in the preceding dry season. We confirmed the strong negative relationship between LAI and the inclination of TWS change in areas that receive very little rainfall during the considered period, which may be caused by clarifying vegetation activities’ difference by a scant supply of water.
The above findings suggest that it can be possible to investigate the relationship between soil water and vegetation using microwave signatures in the regions covered by annual plants and those in the regions covered by perennial plants by focusing on TWS decline.Following this, it is necessary to consider the water availability and investigate the relationship in the equatorial region and other regions during the rainy season to grasp vegetation’s water stress due to the effects of cloud cover.

Keywords: GRACE, Africa, AMSR-E, satellite observations, LAI

©2021. Japan Geoscience Union. All Right Reserved.

An Efficient Surrogate Model for Extreme Hydrologic Predictions using Polynomial Chaos-Kriging

Vinh Ngoc Tran[1], *Jongho Kim[1]

1. University of Ulsan

Due to their versatility and high-performance, surrogate models have become an attractive approach that yields the potency to break down the computational barrier of the expensive hydrological models that are often confronted with parameter uncertainties. However, the surrogate models are not qualified for accurately diagnosing extreme events that are not designed in the training data space. This study presents a state-of-the-art surrogate model, i.e., polynomial chaos-kriging (PCK), that enables us to fill the gap above effectively. The effectiveness of PCK was evidenced by comparing it with two well-known surrogate models of polynomial chaos expansion (PCE) and ordinary kriging (OK). Comprehensive analyses demonstrate that: (1) PCK outperforms others in mimicking the original model more precisely with a smaller number of design sites; (2) the extraordinary predictability of PCK is manifest by accurate predictions for extreme flood events with the flood peak about three times higher than those used to train itself, while PCE and OK failed; (3) results of sensitivity analysis verify that characteristics and behaviors of uncertain parameters in PCK are closer to those in the original model compared to PCE and OK; (4) based on a new efficient index that depicts for the robustness of the surrogate models in providing accurate predictions, PCK has shown superiority to both PCE and OK due to its accurate prognosis for extreme events, although all three surrogates speed up to about 500 times than the original model. Overall, our study reinforces a knowledge basis to perform a robust, efficient surrogate model for ensemble predictions of extreme flood events.

Acknowledgment:
This research was supported by the Water Management Research Program funded by Ministry of Environment of Korean government (127554) and by the National Research Foundation of Korea (NRF) grant funded by the Korea government (MSIT) (NRF-2019R1C1C1004833).

Keywords: Surrogate model, Hydrologic predictions, Extreme floods, Polynomial chaos-kriging, Uncertainty quantification

©2021. Japan Geoscience Union. All Right Reserved.

Hydrological Hindcasts and Parameterizations for Flash Floods Real-Time Forecasting in the Chugoku Region of Japan

*Josko Troselj[1], Han Soo Lee[1]

1. Graduate School of Advanced Science and Engineering, Hiroshima University

As a result of climate change, unprecedented heavy rainfall disasters are increasingly occurring worldwide. It is therefore important to develop Early Warning Systems for real-time forecasting of extreme river water levels and discharges. This study applies the Cell Distributed Runoff Model version 3.1.1 (CDRM) hydrological model calibrated by the Shuffled Complex Evolution optimization method developed at the University of Arizona (SCE-UA) for seven first-class river basins in the Chugoku region of Japan, to obtain hydrological parameterizations and hindcasts of river mouth discharge hydrographs during the Heavy Rainfall Event of in July 2018. This study evaluates hypothesis that calibrated river basin parameters from historical extreme rainfall-induced extreme river discharge events can be used to accurately forecast extreme river discharge hydrographs from future events of similar scales by introducing an innovative historical extreme rainfall event classification methodology based on similarities between the events on the way that the classification criterion is meaningful for future real-time forecasting application. Using this approach, this study produced cumulative ensemble mean validation results with very high reproducibility metrics for the two evaluated methods, using 5 and 7 calibrated parameters. This methodology can therefore be used for accurate real-time forecasting of future flash floods caused by extreme rainfall in the region and similarly also worldwide.

Keywords: extreme river discharge, 2018 Japanese flash floods, CDRM hydrological model, SCE-UA optimization method, real-time flood forecasting

©2021. Japan Geoscience Union. All Right Reserved.

Geochemical signature of trace elements in lake water at Lake Tazawa

*Arata Katamura[1], Daizo Ishiyama[1], Takeshi Hayashi[2], Yasumasa Ogawa[1]

1. Graduate School of International Resource Science, Akita University, 2. Faculty of Education and Human Studies, Akita University

Lake Tazawa is located at the eastern part of Akita Prefecture in Japan. The lake has the maximum depth of 423.4 m and is known as the deepest lake in Japan. Various kinds of fishes including endemic species had lived in the lake. However, an acidic river water of Tama River has been introduced to the lake for electricity and agriculture developments. As a result, numerous kinds of fishes and endemic species were died out because the lake water quality changed to acidic dramatically. The pH of the lake water decreased from 6.7 in 1920s to 4.6 in 1970s (Kato, 1989). Since 1991, a neutralization treatment of the acidic river water was started and the neutralized river water has been introduced to the lake. The pH of the lake surface water was 5.6 in August, 2020 (this study).

To investigate how the lake water quality be able to improve, understanding of details of the lake water quality and mechanism of lake water circulation are essential. Previous studies have pointed out that the lake water quality is homogeneous from shallow to deep parts and the circulation of the lake water occurs in a limited period (Boehrer et al., 2008; Ishiyama et al., 2013). In addition, Chikita et al. (2019) suggested that there are turnovers of the lake water in cold seasons around March. This study aims to clarify the geochemical signature of the lake water in Lake Tazawa from June to November.

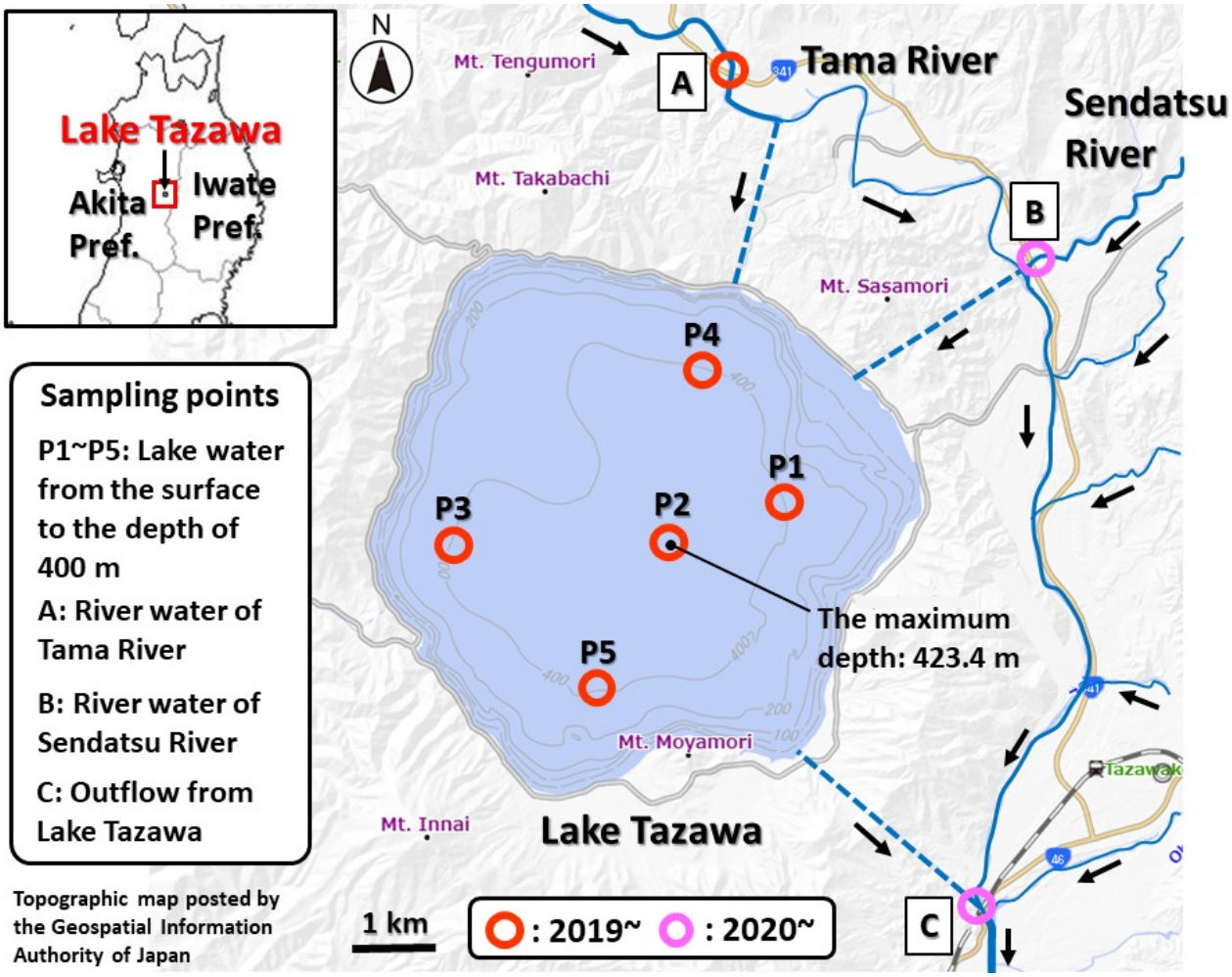
The samplings of the lake water were carried out from June to October in 2019 and from August to November in 2020. The lake water samples were collected from the depths of 400 m to the lake surface at five locations in the lake (P1 to P5 in the map). In addition, the river waters of Tama Rriver (A) and Sendatsu Rriver (B) that inflow into the lake and an outflow of the lake water to Tama River (C) were also collected. Water temperature, pH, Eh, EC, major dissolved ions and trace elements were measured. Trace elements were analyzed separately in dissolved and particulate fractions.

Concentrations of Na, Cl and Al in the lake water increase from the lake surface to the depth of 400 m in August, 2019 (Na: 4.7 ppm (0 m), 4.9 ppm (50 m), 5.1 ppm (400 m); Cl: 17.3 ppm (0 m), 18.8 ppm (50 m), 19.3 ppm (400 m); Total Al: 269 ppb (0 m), 437 ppb (50 m), 522 ppb (400 m)). On the other hand, the concentration of total Fe (T-Fe) in the lake water decreases from 14.5 ppb (0 m) to 8.5 ppb (100 m), then gradually increases to 25.8 ppb (400 m). The ratio of the amount of Al particulate fraction in the total amount of Al is 0.04. While, the ratio of the amount of Fe particulate fraction in the total amount of Fe is 0.42. Therefore, approximately half of Fe is present as particulate fraction in the lake water. There is a possibility that the Fe particulate fraction scavenges other metals by adsorption. Boron-normalized values (N_B), which defined as $N_B=(M/B)_{X(total)} / (M/B)_{Base\ point(total)}$, where $(M/B)_{X(total)}$ and $(M/B)_{Base\ point(total)}$ denote the ratio of total mobile amounts (the sum of dissolved and particulate fractions) of the target elements *M* and B at the certain point (X) and the base point, respectively. The base point is acidic river water of Tama River at the Kawasaki bridge immediately before inflow of the river water to Lake Tazawa (Point A in the map). The N_B of Al of the surface water is 0.6 and the value increases around 0.7 toward the depth of 400 m. While, the N_B of Fe of the surface water is around 0.5 and the value decrease to around 0.2 at the depth of 50 m. Then, the value increases to 0.5 towards at the depth of 400 m. These facts that the surface water has low N_B of Al and Fe between 0.5 and 0.6 suggests that there is a process of dilution of acidic river water of Tama River by the lake water having low Al/B and Fe/B ratios in the lake. In addition,

©2021. Japan Geoscience Union. All Right Reserved.

N_B of Al and Fe in the lake water from the depth of 50 m to 400 m range from 0.2 to 0.7. This fact suggests that Al and Fe in the lake water from the depth of 50 m to 400 m are precipitated on the lake bed. According to the profiles of chemical compositions of lake sediments (Ishiguro et al., 2017), the concentrations of Al and Fe in the sediments of Lake Tazawa increase from prior to posterior to the introduction of the acidic river water of Tama River. The estimation on Al and Fe based on the N_B is consistent with variations of Al and Fe contents in the sediments of the lake.

Keywords: Lake Tazawa, Water quality, Trace elements, Dilution, Precipitation



©2021. Japan Geoscience Union. All Right Reserved.

[E] Oral | A (Atmospheric and Hydrospheric Sciences)：A-HW Hydrology & Water Environment

Sat. Jun 5, 2021 9:00 AM - 10:30 AM JST | Sat. Jun 5, 2021 12:00 AM - 1:30 AM UTC | Ch.13 Zoom Room 13

[A-HW21] Interdisciplinary approach to support climate change adaptation measures in regional scale

convener:TEBAKARI TAICHI(Toyama Prefectural University), Sompratana Ritphring(Kasetsart University), Masashi Kiguchi(University of Tokyo), weerakaset Suanpaga(Associate professor in Civil Engineering,Kasetsart University), Chairperson:TEBAKARI TAICHI(Toyama Prefectural University), Masashi Kiguchi(University of Tokyo)

In Japan, the impact of climate change has already become apparent and may become even more serious in the future. For example, there are the following specific damages; crop damage such as mandarin orange edema and white immature grains of rice, health hazards such as the northward distribution of Aedes albopictus and heat stroke patients, meteorological disasters such as increased torrential rain and increased number of strong typhoons, and coral bleaching Ecosystem.
The climate change adaptation law, which was enacted in 2018, clarified the legal position of adaptation measures in Japan, and is a legal for the national, local governments, businesses and citizens to cooperate and cooperate to promote adaptation measures. Based on this law, the Climate Change Adaptation Information Platform (A-PLAT) was established to develop and provide tools to support information provision and adaptation actions, and to collect, organize and provide best practices. AP-PLAT and T -Overseas development such as -PLAT is also progressing. Overseas expansion such as AP-PLAT and T-PLAT are also progressing.
In each research field, it is necessary to promote effective adaptation measures based on reliable and detailed information, and measures based on scientific knowledge of future impacts and strengthening of adaptation in the region are urgently needed.
This proposed session would like to invite presentations on the latest achievements in interdisciplinary fields such as hydrology, agriculture, forestry, weather, and climate that support specific climate change adaptation measures, as well as on the development of new research.

9:00 AM - 9:15 AM JST | 12:00 AM - 12:15 AM UTC

[AHW21-01] ADAP-T for water-related adaptation to climate change and supporting its policy making

★Invited Papers

*Taikan Oki[1], Thanya Kiatiwat[2], Hiroaki Shirakawa[3], Weerakaset Suanpaga[2], Taichi Tebakari[4], Sompratana Ritphring[2], Masashi Kiguchi[5], Kyoko Matsumoto[4] (1.Graduate School of Engineering, The University of Tokyo, 2.Faculty of Engineering, Kasetsart University, 3.Granduate School of Environmental Studies, Nagoya University, 4.Department of Civil and Environmental Engineering, Toyama Prefectural University, 5.Institute of Industrial Science, The University of Tokyo)

9:15 AM - 9:30 AM JST | 12:15 AM - 12:30 AM UTC

[AHW21-02] The GEWEX Regional Hydroclimate Projects in High Mountainous Terrain in Asia

★Invited Papers

*Petrus J van Oevelen[1] (1.George Mason University)

9:30 AM - 9:45 AM JST | 12:30 AM - 12:45 AM UTC

[AHW21-03] **Effectiveness of Flood Diversion Canals and Retention Ponds as Adaptation Strategies in the Upper Chao Phraya River Basin**

*Saritha Padiyedath Gopalan[1], Naota Hanasaki[1] (1.National Institute for Environmental Studies)

9:45 AM - 10:00 AM JST | 12:45 AM - 1:00 AM UTC

[AHW21-04] **The impact of sensible heat and latent heat on monsoon onset over Indochina peninsula**

Tomohito Yamada[1], Ryosuke Kato[1], *Sourabh Shrivastava[1] (1.Hokkaido University)

10:00 AM - 10:15 AM JST | 1:00 AM - 1:15 AM UTC

[AHW21-05] S2S prediction challenge with deep learning in Thailand

*Kiyoharu Hasegawa[1], Shinjiro Kanae[1] (1.Toyko Institute of Technology)

10:15 AM - 10:30 AM JST | 1:15 AM - 1:30 AM UTC

[AHW21-06] Local knowledge: A comprehensive agricultural system and incremental drought adaptation strategy for Javanese society

*Muhamad Khoiru Zaki[1], Keigo Noda[1], Kengo Ito[1], Komariah Komariah[2], Sumani Sumani[2] (1.Gifu University, 2.Sebelas Maret University)

ADAP-T for water-related adaptation to climate change and supporting its policy making

*Taikan Oki[1], Thanya Kiatiwat[2], Hiroaki Shirakawa[3], Weerakaset Suanpaga[2], Taichi Tebakari[4], Sompratana Ritphring[2], Masashi Kiguchi[5], Kyoko Matsumoto[4]

1. Graduate School of Engineering, The University of Tokyo, 2. Faculty of Engineering, Kasetsart University, 3. Granduate School of Environmental Studies, Nagoya University, 4. Department of Civil and Environmental Engineering, Toyama Prefectural University, 5. Institute of Industrial Science, The University of Tokyo

The anthropogenic climate change is increasing water-related disaster risks such as flood and drought because most of the adverse impacts of climate change is delivered to society through water. Mitigation efforts to reduce the greenhouse gas, e.g., CO2, emission and to reduce the speed of climate change are essentially important, and at the same time, adaptation measures to reduce the vulnerability and exposure of human lives and properties from the risks exacerbated by climate change are also relevant. After the Paris Agreement of UNFCCC in 2015, all the member states are encouraged to set their National Adaptation Plans (NAPs).

The formulation of “Thailand’s National Adaptation Plan” is being led by the Office of Natural Resources and Environmental Policy and Planning (ONEP) under Ministry of Natural Resources and Environment as a plan for the implementation of adaptation measures by each ministry and agency. For supporting the NAP formulation and development of climate change measures that contribute to a resilient and sustainable society, a new research project entitled "Advancing co-design of integrated strategies with adaptation to climate change in Thailand (ADAP-T)" with international collaboration between Thailand and Japan was proposed, approved, and implemented since 2016, supported by JICA and JST under the framework of SATREPS.

ADAP-T has three piers of research, namely i) Knowledgebase of climate change, ii) Adaptation measures to climate change, and iii) Co-designing adaptation measures. Disciplines relevant for the major sectors prone to climate change, such as riverine hydrology, forest hydrology, sediment erosion, coastal erosion, urban hydrology, and agricultural hydrology are collaborating under ADAP-T, and Kasetsart University, Thai Meteorological Department, Royal Irrigation Department, and ONEP are managing the ADAP-T project in Thailand with close communication with The University of Tokyo and associated researchers in several universities in Japan.

The overall goal of ADAP-T is to support the development of a climate change adaptation strategy that can maximize the benefits of society by combining various countermeasures through dialogue with various stakeholders such as the government and citizens. These research results have been contributed to the formulation of NAP, which was compiled and published as ADAP-T Special Report 2018 and research and implementation of good practice of adaptation measures in each sector are expected to contribute to NAP guidelines which currently being developed by ONEP for policy makers. Moreover, these results and basic information on cost-benefit estimation of adaptation options in each sector based on future scenarios are integrated into a web-based adaptation simulator as a tool to assist the multilateral dialogue among citizens, policy makers, and researchers. Furthermore, it is expected that these outcomes will be expanded to neighboring Southeast Asian countries for adaptation to climate change, which is becoming increasingly necessary and important in developing countries.

©2021. Japan Geoscience Union. All Right Reserved.

Keywords: Thailand, National Adaptation Plan, water resources management

©2021. Japan Geoscience Union. All Right Reserved.

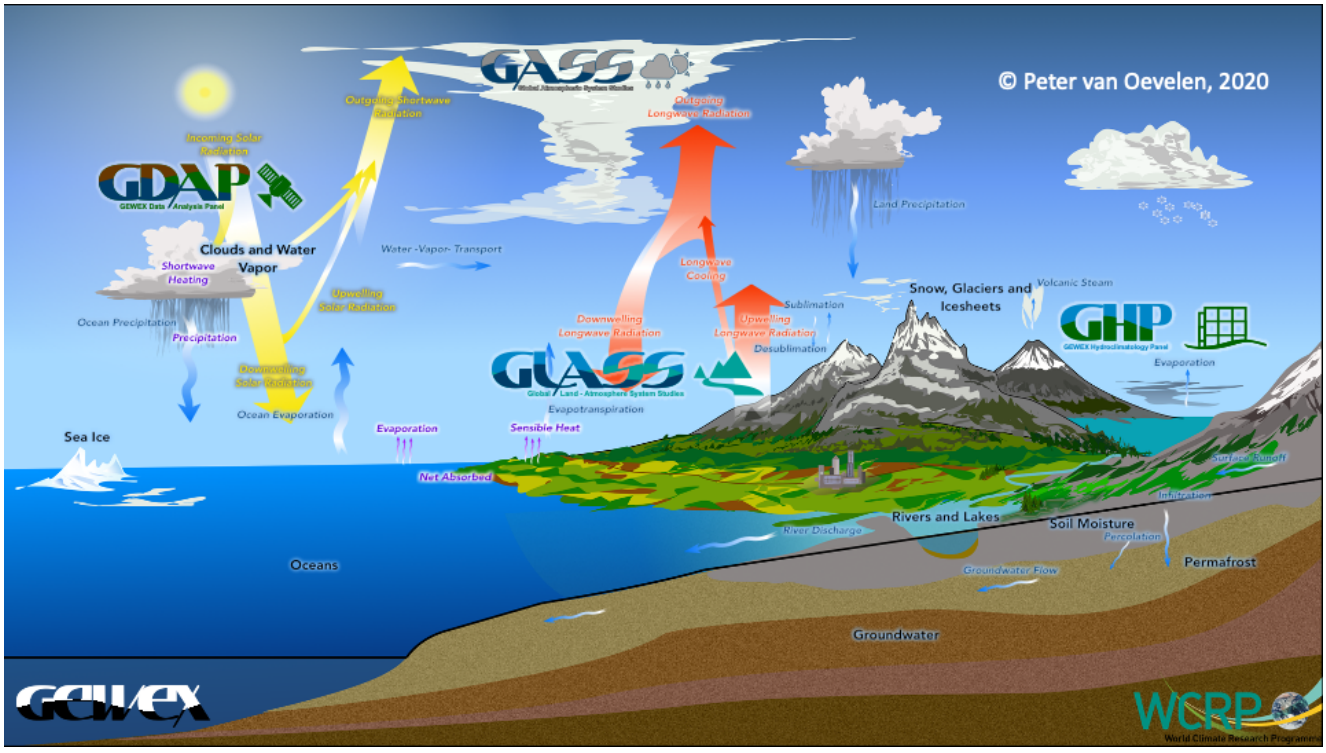
The GEWEX Regional Hydroclimate Projects in High Mountainous Terrain in Asia

*Petrus J van Oevelen[1]

1. George Mason University

The Global Energy and Water EXchanges Project (GEWEX) of the World Climate Research Programme focuses on in particular process understanding of how water and energy manifest themselves in the earth system. To address the science at a more regional level the Regional Hydroclimate Projects (RHPs) provide a unique opportunity to bring better the scientific community and rally around those issues that are specific and relevant to the region. High mountainous regions of the world and in particular those in Asia provide a unique challenge both in terms of observations as well as modeling. At the same time these regions are of crucial importance to our water resources for a major part of the global population. Better understanding of the processes in these regions under climate and environmental change is of the essence to provide for sustainable solutions. These mountainous regions act not only as physical barriers but also link communities as they provide the (water) resources they depend upon. At the same time these regions are also more vulnerable and strongly impacted by climate change. The GEWEX Regional Hydroclimate Projects in the Asian mountain regions can help bridge the knowledge gap and expertise and as such translate global environmental change to local change and impacts.

Keywords: Regional Climate, Water Resources, Global Science Collaboration



©2021. Japan Geoscience Union. All Right Reserved.

Effectiveness of Flood Diversion Canals and Retention Ponds as Adaptation Strategies in the Upper Chao Phraya River Basin

*Saritha Padiyedath Gopalan[1], Naota Hanasaki[1]

1. National Institute for Environmental Studies

The flood assessment in the upper Chao Phraya River basin (CPRB) is vital due to frequent flood occurrence in the past decades that has caused tremendous economic as well as agricultural losses. The upper CPRB is characterized by four major tributaries of Ping, Wang, Yom, and Nan. Among the tributaries, flooding is regular in the lower Yom Basin due to its gentle slope, lack of major flow regulation structures, and the low channel carrying capacity at various locations. The government has implemented flood mitigation measures such as Yom-Nan flood diversion canal system to divert water from Yom to Nan River and retention ponds since 2014. Hence, the objective of this study is to analyze the effect of this diversion canal system and retention ponds as adaptation strategies on reducing the daily discharge below the channel carrying capacity for the historic (1980-1999) as well as future (2080-2099) scenarios under representative concentration pathway (RCP) 4.5 and 8.5 emission scenarios using the H08 global hydrological model with the generalized scheme (GS; universal parameters) as well as the regionalized scheme (RS; regional parameters). The effect was mainly analyzed at three stations of Sukhothai, Bang Rakam, and Sam Ngam in Yom basin, where the channel carrying capacities are 550, 207, and 614 m^3/s, respectively.

The results of the historic simulation (Figure 1) show that the incorporated adaptation strategies can reduce the discharge below the channel carrying capacity at Sukhothai and Sam Ngam, while there was no significant reduction in the discharge at the Bang Rakam due to the low channel capacity. Although a similar pattern was observed in the future scenarios with adaptation strategies, the number of flooding days were still quite high in all the considered stations. Therefore, from this result, it can be envisaged that the canal system along with retention ponds alone cannot manage future floods in the basin. Regarding the effectiveness of the diversion schemes, the highest reduction in flooding days was exhibited by the RS simulation at both Sukhothai and Sam Nagam stations due to the regionalized parameters. On the contrary, the GS simulation has been found to be superior at Bang Rakam. This is because a part of the water diverted from the upstream of Yom River is returning to its lower reaches (at Bang Rakam station) through the canal system in RS simulation, whereas this return flow is absent in GS simulation due to universal parameters. The GS would be comparable with the RS by better parameterizations and can be implemented in hydrological models.

Keywords: Climate change, Thailand, H08 model

©2021. Japan Geoscience Union. All Right Reserved.

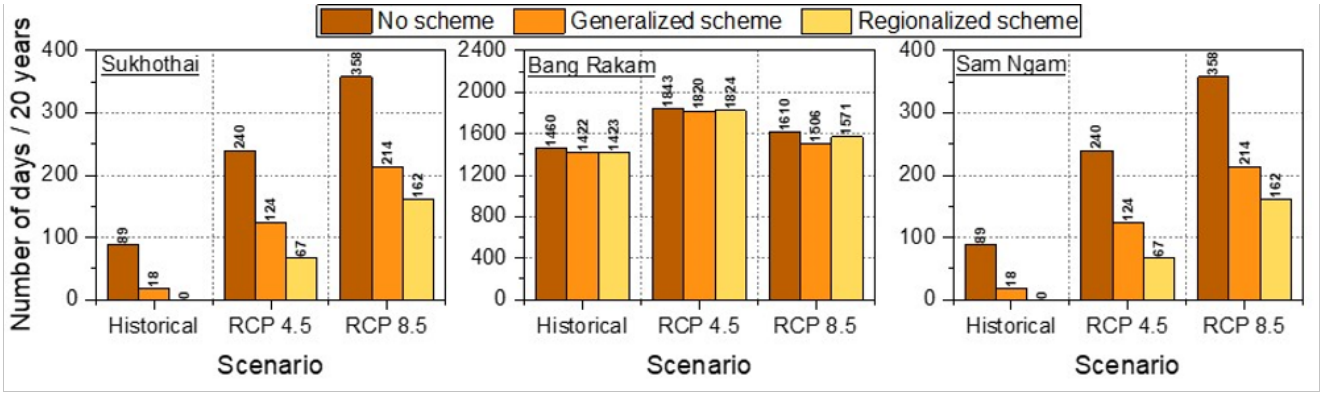


Figure 1. The number of days the daily discharge exceeded the channel carrying capacity at Sukhothai, Bang Rakam, and Sam Ngam stations in the historic as well as the future scenarios.

©2021. Japan Geoscience Union. All Right Reserved.

The impact of sensible heat and latent heat on monsoon onset over Indochina peninsula

Tomohito Yamada[1], Ryosuke Kato[1], *Sourabh Shrivastava[1]

1. Hokkaido University

In this study, interannual variations of the summer monsoon onset over the Indochina Peninsula were studied using the CPC Merged Analysis of Precipitation (CMAP) panted rainfall and NCEP reanalysis data from 1979 to 2016. For the climatological onset over Indochina Peninsula, 27th panted is considered. Equal numbers (9-9) of early and late monsoon onset years are identified during the last 3 decades. Sensible heat flux (Q1) and latent heat flux (Q2) influence the atmospheric circulation over the Indochina peninsula during monsoon onset. Composite analysis of Q1 and Q2 shows that the large change in Q1 and Q2 over the mainland of Indochina peninsula during early (late) monsoon years. The positive Q1 and Q2 anomalies suggest the strong convection in the early monsoon over the Indochina peninsula. It seems to be a dipole pattern over the mainland of the Indochina peninsula and the eastern Indian Ocean, where north-central Thailand have a positive (negative) anomaly and the eastern Indian Ocean have a negative (positive) anomaly during early (late) monsoon onset. Results also suggested the strong cyclonic flow at 850 hPa winds associated with the rainfall over the Indochina peninsula during early monsoon onset.

Keywords: Monsoon onset, Sensible Heat, latent heat

©2021. Japan Geoscience Union. All Right Reserved.

S2S prediction challenge with deep learning in Thailand

*Kiyoharu Hasegawa[1], Shinjiro Kanae[1]

1. Toyko Institute of Technology

Subseasonal to seasonal (S2S) prediction still remains as a challenge task even today. S2S prediction refers to a lead time ranging from one to several months, which is known to result in rapidly decreasing forecast accuracy. Deep learning (DL), one of the most powerful statistical models, is expected to overcome current difficulty of S2S prediction because of its spatio-temporal locality. In this study, one-month rainfall prediction is carried out for the Chao Phraya River basin in Thailand during the rainy season from May to October, where the introduction of long-term rainfall prediction to dam management is urgently required for flood mitigation. The DL model is constructed using global maps of sea surface temperature and heat content as input values. 17 climate models output from CMIP5 dataset is used to expand the training data from 65 existing observations to 2500, which enables us to train the DL model proper. The prediction accuracy of the DL model is compared with that of the physical model and the linear regression model. The results show that the DL model is slightly inferior to the physical model, but has higher prediction accuracy than the linear model. In addition, the deep learning model has the highest prediction accuracy when trained only on the CMIP5 dataset, indicating that the DL model has potential to outperform the physical model in the future.

Keywords: deep learning, 1 month rainfall prediction, Thailand, CMIP5, Sea surface temperature, ECMWF

©2021. Japan Geoscience Union. All Right Reserved.

Local knowledge: A comprehensive agricultural system and incremental drought adaptation strategy for Javanese society

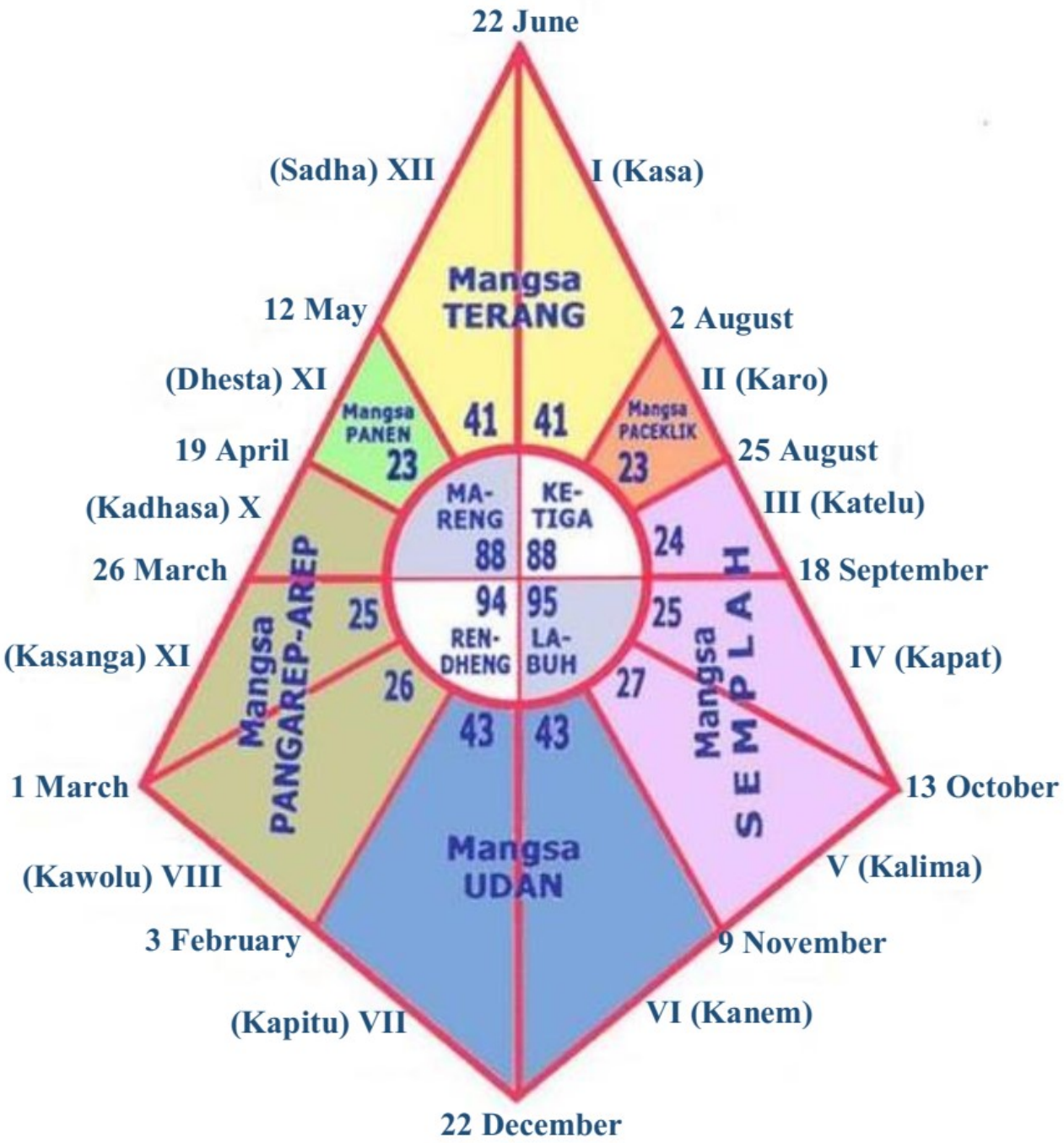
*Muhamad Khoiru Zaki[1], Keigo Noda[1], Kengo Ito[1], Komariah Komariah[2], Sumani Sumani[2]

1. Gifu University, 2. Sebelas Maret University

Local knowledge can be defined as a person’ s ability to use his/her understanding and senses to respond to an event, object, or situation in the local environment. We reevaluate *Pranata Mangsa* as a form of local knowledge that can aid in adapting to drought. *Pranata Mangsa* is used on the Indonesian islands of Java and Bali, particularly by farmers, for managing agricultural activities in fields and is based on *Titen*, i.e., the observation of natural signs. The relationships between natural signs and farming activities are arranged in four primary and twelve secondary *Mangsa*, or seasons. Each *Mangsa* is characterized by activities such as *Bero* (maintaining fallow land) and burning rice straw, which reduce the loss of crops from meteorological drought and soil moisture deficits caused by agricultural drought. These practices suggest the potential for applying local knowledge to drought adaptation and indicate that a revaluation of the local knowledge of *Pranata Mangsa* with its specific characteristics could provide an effective strategy for adapting to drought and meeting the 2030 Sustainable Development Goals. This study integrated local knowledge (Pranata Mangsa) in Jawa, Indonesia, with scientific data on diurnal rainfall, extreme precipitation events, using the Local and Indigenous Knowledge System (LINKS). The results showed that Pranata Mangsa has informed aspects of agriculture including crop calendars, crop patterns, and farming activities, for over 1000 years in Jawa. Pranata Mangsa also enhances community resilience by mitigating the effects of extreme droughts; this finding was validated using scientific data.

Keywords: Pranata Mangsa, Local and scientific knowledge, LINKS method, Community ressiliences

©2021. Japan Geoscience Union. All Right Reserved.



©2021. Japan Geoscience Union. All Right Reserved.

[E] Oral | A (Atmospheric and Hydrospheric Sciences)：A-HW Hydrology & Water Environment

Sat. Jun 5, 2021 10:45 AM - 12:15 PM JST | Sat. Jun 5, 2021 1:45 AM - 3:15 AM UTC | Ch.13 Zoom Room 13

[A-HW21] Interdisciplinary approach to support climate change adaptation measures in regional scale

convener:TEBAKARI TAICHI(Toyama Prefectural University), Sompratana Ritphring(Kasetsart University), Masashi Kiguchi(University of Tokyo), weerakaset Suanpaga(Associate professor in Civil Engineering,Kasetsart University), Chairperson:Masashi Kiguchi(University of Tokyo), TEBAKARI TAICHI(Toyama Prefectural University)

In Japan, the impact of climate change has already become apparent and may become even more serious in the future. For example, there are the following specific damages; crop damage such as mandarin orange edema and white immature grains of rice, health hazards such as the northward distribution of Aedes albopictus and heat stroke patients, meteorological disasters such as increased torrential rain and increased number of strong typhoons, and coral bleaching Ecosystem.
The climate change adaptation law, which was enacted in 2018, clarified the legal position of adaptation measures in Japan, and is a legal for the national, local governments, businesses and citizens to cooperate and cooperate to promote adaptation measures. Based on this law, the Climate Change Adaptation Information Platform (A-PLAT) was established to develop and provide tools to support information provision and adaptation actions, and to collect, organize and provide best practices. AP-PLAT and T -Overseas development such as -PLAT is also progressing. Overseas expansion such as AP-PLAT and T-PLAT are also progressing.
In each research field, it is necessary to promote effective adaptation measures based on reliable and detailed information, and measures based on scientific knowledge of future impacts and strengthening of adaptation in the region are urgently needed.
This proposed session would like to invite presentations on the latest achievements in interdisciplinary fields such as hydrology, agriculture, forestry, weather, and climate that support specific climate change adaptation measures, as well as on the development of new research.

10:45 AM - 11:00 AM JST | 1:45 AM - 2:00 AM UTC

[AHW21-07] Climate change effect the relationship between land-use and poverty in major cities of Thailand.

★Invited Papers

*weerakaset Suanpaga[1], Shirakawa Hiroaki[2], Nichanun Trakulphudphong [3], Wuthiporn Klinhom[3], Krittanut Thumsatsarn[3] (1.Associate professor in Civil Engineering,Kasetsart University,Thailand, 2.Associate professor in Graduate School of Engineering,Nagoya University,Japan, 3.Bachelor degree student in Civil Engineering,Kasetsart University,Thailand)

11:00 AM - 11:15 AM JST | 2:00 AM - 2:15 AM UTC

[AHW21-08] Local adaptation strategy to climate change considering local context in Thailand

★Invited Papers

*Kyoko Matsumoto[1], Sompratana Ritphring[2], Masashi Kiguchi[3], Taichi Tebakari[1], Taikan Oki[4] (1.Department of Civil and Environmental Engineering, Toyama Prefectural University, 2.Faculty of Engineering, Kasetsart University, 3.Institute of Industrial Science, The University of Tokyo, 4.School of Engineering, The University of Tokyo)

11:15 AM - 11:30 AM JST | 2:15 AM - 2:30 AM UTC

[AHW21-09] Beach Nourishment to Mitigate the Impact of Beach Erosion and Sea Level Rise, Thailand

*Sompratana Ritphring[1], Keiko Udo[2] (1.Department of Water Resources Engineering, Kasetsart University, 2.International Research Institute of Disaster Science, Tohoku University)

11:30 AM - 11:45 AM JST | 2:30 AM - 2:45 AM UTC

[AHW21-10] Valuation of Sandy Beach Tourism Benefit with Respect to Hotel Room Rates by Using a Spatial Hedonic Model in Thailand

*Chatuphorn Somphong[1], Keiko Udo[1], Sompratana Ritphring[2], Hiroaki Shirakawa[3] (1.International Research Institute of Disaster Science, Tohoku University, Japan, 2.Department of Water Resources Engineering, Kasetsart University, Thailand, 3.Graduate School of Environmental Studies, Nagoya University, Japan)

11:45 AM - 12:00 PM JST | 2:45 AM - 3:00 AM UTC

[AHW21-11] Impacts of urban flood and adapataion on traffic flow in Bangkok

*Shinichiro NAKAMURA[1], Horoyoshi Morita[4], Tsuyoshi Takano[4], Varameth Vichiensan[2], Sanit Wongsa[3], Napaporn Piamsa-nga[2] (1.Nagoya University, 2.Kasetsaet University, 3.King Mongkut's University of Technology Thonburi, 4.Nippon Engineering Consultants Co., Lld)

12:00 PM - 12:15 PM JST | 3:00 AM - 3:15 AM UTC

[AHW21-12] Effectiveness of crop calendar shift as an adaptation measure for climate change - Case study for rice production in Hokkaido, Japan

*Kenji Tanaka[1], Tomoki Yamada[2], Shigenobu Tanaka[1] (1.Disaster Prevention Research Institute, Kyoto University, 2.Faculty of Engineering, Kyoto University)

Climate change effect the relationship between land-use and poverty in major cities of Thailand.

*weerakaset Suanpaga[1], Shirakawa Hiroaki[2], Nichanun Trakulphudphong [3], Wuthiporn Klinhom[3], Krittanut Thumsatsarn[3]

1. Associate professor in Civil Engineering,Kasetsart University,Thailand, 2. Associate professor in Graduate School of Engineering,Nagoya University,Japan, 3. Bachelor degree student in Civil Engineering,Kasetsart University,Thailand

Nowadays, the effect of climate change in Thailand causes floods, storms, and drought that lead to land-use change. According to the report in 2015, the heavy rain caused floods in Khon Kaen province, Thailand. In 2019 the forest area in Khon Kaen has decreased by 0.67 percent. The urban and agricultural areas have been increasing. The objective of these studies was to determine the relationship between climate change and land-use change, also to determine the relationship of the land-use change effects on poverty which is one of the problem factors that influence the economy of Thailand.

The study areas were the four major cities (Chiang Mai, Khon Kaen, Chai Nat, and Songkla) of Thailand. The changes of monthly current income per capita and Gross Provincial Product (GPP) of each province were analyzed.

The land-use were classified into 4 categories, named agriculture area, built-up area, water, forest, and miscellaneous area.
The land-use were classified into 4 categories, named agriculture area, built-up area, water, forest, and miscellaneous area. These were analyzed the future trend of land use variation which related to climate change and disaster occurring in the future. The final adaptation measure or best practice tackle and conform were proposed to the National strategy plan.

Keywords: Climate change , Land-use change, poverty

©2021. Japan Geoscience Union. All Right Reserved.

The climate change effect the relationship between land-use and poverty in major cities of Thailand

Weerakaset suanpaga[1*], Hiroki Shirakawa[2], Nichanun Trakulphudphong [3], Wuthiporn Klinhom[4] and Krittanut Thumsatsarn[5]

Email: 1 weerakaset.s@ku.ac.th , Faculty of Engineering, Kasetsart University,Thailand * corresponding author.
2. sirakawa@urban.env.nagoya-u.ac.jp , Graduate School of Engineering, Nagoya University,Japan
3. nichanun.t@ku.th , Faculty of Engineering, Kasetsart University,Thailand
4. wuthiporn.k@ku.th , Faculty of Engineering, Kasetsart University,Thailand
5. Krittanut.t@ku.th , Faculty of Engineering, Kasetsart University,Thailand

Abstract

Nowadays, the effect of climate change in Thailand causes floods, storms, and drought that lead to land-use change. According to the report in 2015, the heavy rain caused floods in Khon Kaen province, Thailand. In 2019 the forest area in Khon Kaen has decreased by 0.67 percent. The urban and agricultural areas have been increasing. The objective of these studies was to determine the relationship between climate change and land-use change, also to determine the relationship of the land-use change effects on poverty which is one of the problem factors that influence the economy of Thailand.

The study areas were the four major cities (Chiang Mai, Khon Kaen, Chai Nat, and Songkla) of Thailand. The changing of monthly current income per capita and Gross Provincial Product (GPP) of each province were analyzed.

The land-use were classified into 4 categories, named agriculture area, built-up area, water, forest and miscellaneous area.

The land-use were classified into 4 categories, named agriculture area, built-up area, water, forest, and miscellaneous area. These were analysed the future trend of land use variation which related to climate change and disaster occurring in the future. The final the adaptation measure or best practice tackle and conform were proposed to National strategy plan.

©2021. Japan Geoscience Union. All Right Reserved.

Local adaptation strategy to climate change considering local context in Thailand

*Kyoko Matsumoto[1], Sompratana Ritphring[2], Masashi Kiguchi[3], Taichi Tebakari[1], Taikan Oki[4]

1. Department of Civil and Environmental Engineering, Toyama Prefectural University, 2. Faculty of Engineering, Kasetsart University, 3. Institute of Industrial Science, The University of Tokyo, 4. School of Engineering, The University of Tokyo

This presentation deal with the issue on building local adaptation strategy to climate change considering local context and how to deliver the scientific knowledge into local level to promote the implementation of adaptation in rural area in Thailand.

Thai government formulated the Climate Change Master Plan 2015-2050 in 2015. The plan outlines steps to achieve climate resilience and low carbon growth in accordance with a sustainable development agenda. The Master Plan includes three key strategies: adaptation, mitigation, and capacity building. Thailand has also adopted a National Adaptation Plan following The Master Plan, and the NAP guidelines for policy makers currently is developed. Although adaptation plans have been developed on the national level, there are still gaps in implementation at the local level. The content, scale of the climate change impact and those vulnerability vary depending on the local characteristics such as the climatic, geographical, and socio-economic conditions. Formulation of local adaptation strategies needs to be addressed among various stakeholders, especially the decision-making in facing the uncertainties in climate scenarios requires promoting a understanding of climate change among stakeholders. It is important to know the awareness and needs of each stakeholder in addition to information of scientific knowledge to formulate adaptation strategies.

Moreover, the current situation on people’ s perception to climate change based on our field survey in rural area in Thailand will be introduced. It was found that a high proportion of residents recognized climate change as causing changes to their daily lives, however, there is still a need to raise awareness concerning the implementation of climate change adaptation measures. It is necessary to promote adaptation measures with local community cohesion in accordance with an understanding of the way in which resident’ s perception of climate change and adaptation, as well as the impact to each stakeholder by climate change and accessibility to government support.

Keywords: Adaptation to climate change, Thailand, Local adaptation strategy

©2021. Japan Geoscience Union. All Right Reserved.

Beach Nourishment to Mitigate the Impact of Beach Erosion and Sea Level Rise, Thailand

*Sompratana Ritphring[1], Keiko Udo[2]

1. Department of Water Resources Engineering, Kasetsart University, 2. International Research Institute of Disaster Science, Tohoku University

In the twenty-first century, global sea level rise associated with climate change will affect beach areas, which contribute a number of benefits that include benefits to the recreational sector of the economy. In Thailand, the use of structural measures to slow beach erosion and mitigate the impact of sea level rise is commonly implemented. However, structural measures often bring about negative effects on adjacent coastal areas. For this reason, beach nourishment was adopted as a suitable solution to protect and reclaim beach areas and to preserve the Tourism Carrying Capacity of the beach. This research analysed historical shoreline changes using satellite images and assessed beach value with the hedonic pricing method. We used a benefit-cost ratio analysis to evaluate the economic valuation assessment of two beaches. The results indicated that the beach values of Pattaya Beach and Chalatat Beach were 1,072,250 and 92,092 USD, respectively. The benefit-cost ratio analysis proposes that it is worth implementing beach nourishment to cope with all climate change scenarios. In response to climate change, these findings could be applied to protect beach tourism.

Keywords: climate change, sea level rise, beach erosion, beach nourishment, Pattaya beach, Chalatat beach

©2021. Japan Geoscience Union. All Right Reserved.

Valuation of Sandy Beach Tourism Benefit with Respect to Hotel Room Rates by Using a Spatial Hedonic Model in Thailand

*Chatuphorn Somphong[1], Keiko Udo[1], Sompratana Ritphring[2], Hiroaki Shirakawa[3]

1. International Research Institute of Disaster Science, Tohoku University, Japan, 2. Department of Water Resources Engineering, Kasetsart University, Thailand, 3. Graduate School of Environmental Studies, Nagoya University, Japan

An economic assessment for a non-market resource like sandy beaches is always a challenge for Thailand's coastal policy planners due to the lack of data availability, especially on the national scale. While beach tourism in Thailand has been representing an essential part of the Thai economy, the sandy beaches are probably exposed to the future sea-level rise. Therefore, the need for tourism benefit of the beaches should be conducted. The research attempted to measure the effect of sandy beach characteristics and hotel location with respect to the hotel room rates. A sample of 3,331 hotel rooms across Thailand's coastal sub-districts, covering the entire sandy beaches in Thailand, was collected through a hotel-booking online database during the country peak season. The considered variables include hotel room attributes, sandy beach characteristics, hotel locations, and coastal infrastructures. Through a hedonic price model based on geographically weighted regression analysis, the relationship between the dependent variables (hotel room rate) and the independent variables (selected beach variable) was estimated to evaluate the marginal effect and its spatial variations. The tourism benefit was assumedly calculated from the marginal effect of the hotel's beachfront locations on hotel price. The study suggested the location in front of the beach raised the average hotel room rates by 15.0-36.5%. The results emphasized the significant spatial variability of the estimated *Beachfront* coefficient. In addition, the effect of beach protection structures (i.e. seawall, breakwaters, groins) on the hotel price was also investigated and implied a slight drop by 1.0-3.0% of the average price. The other sandy beach variables (such as beach length, width, slope) effects on hotel price were also investigated.

Keywords: Coastal tourism, Hedonic pricing method, Hotel Price, Geographically weighted regression analysis, climate change adaptation

©2021. Japan Geoscience Union. All Right Reserved.

Impacts of urban flood and adapataion on traffic flow in Bangkok

*Shinichiro NAKAMURA[1], Horoyoshi Morita[4], Tsuyoshi Takano[4], Varameth Vichiensan[2], Sanit Wongsa[3], Napaporn Piamsa-nga[2]

1. Nagoya University, 2. Kasetsaet University, 3. King Mongkut's University of Technology Thonburi, 4. Nippon Engineering Consultants Co., Lld

Traffic is an important economic and social activities in urban area, and its congestion tends to be a bottleneck for their activities and economic developments, especially in developing countries. Heavy rainfall and urban flood are factors which generate or enhance the traffic congestions in urban area. Bangkok, our target city, has been under a rapid economic growth in last decades and the traffic congestion have been one of important and urgent social issue through the increasing population and economic activities. This study aims to analyze the impacts of urban flood and effects of adaptation measures on the traffic flow in Bangkok with connecting rainfall/floods and probe data which obtained from a large number of vehicles in motion through communication networks. In addition, we evaluated the effectiveness of adaptation measures to reduce the impacts of urban flood on traffic by applying the connected flood and traffic models to several adaptation scenarios.

Keywords: Urban flood, Traffic, Bangkok, Adaptation

©2021. Japan Geoscience Union. All Right Reserved.

Effectiveness of crop calendar shift as an adaptation measure for climate change - Case study for rice production in Hokkaido, Japan

*Kenji Tanaka[1], Tomoki Yamada[2], Shigenobu Tanaka[1]

1. Disaster Prevention Research Institute, Kyoto University, 2. Faculty of Engineering, Kyoto University

In this study, effectiveness of the shifting crop calendar as an adaptation measure against climate change is assesssed for the rice production in Hokkaido, Japan. Future climate scenario was produced by dynamical downscalling from 6GCMs using WRF with 9km resolution. Rice growth model SIMRIW, land surface model SiBUC, distributed hydrological model CaMa-Flood were used to evaluate the suitable growing period, irrigation water demand, river discharge etc.
SIMRIW generally showed the higher potential yield under future climate conditon, and the optimal transplant date will be 2 weeks to 1 month earlier by the end of this century. Also, from the point of climate condition, the areas suitable for rice production will extend toward north and east, suggesting that Hokkaido will have higher potential for the rice production in future climate condition.
Irrigation water demand was evaluated by SiBUC considering the deep water irrigation, an additional water demand against cold damage. Even in the future warm climate condition, cold air temperature caused by summer time storms will still remain until 2070's. Also, due to the temperature rise, base irrigation water demand will continue to increase year by year.
River discharge was evaluated by the result of SiBUC and CaMa-Flood. Due to the earlier snowmelt under warmer climate will shift the timing of snowmelt flood in sprinf season. So shifting crop calendar earlier is reasonable from the point of hydrological condition. Deep water irrigation in future condition will tend to provide water stress as the river discharge in July will decrease in future.

Keywords: rice production, cropping calendar, irrigation water demand, climate change

©2021. Japan Geoscience Union. All Right Reserved.

[E] Poster | A (Atmospheric and Hydrospheric Sciences)：A-HW Hydrology & Water Environment

Sat. Jun 5, 2021 5:15 PM - 6:30 PM JST | Sat. Jun 5, 2021 8:15 AM - 9:30 AM UTC | Ch.07_2

[A-HW21] Interdisciplinary approach to support climate change adaptation measures in regional scale

convener:TEBAKARI TAICHI(Toyama Prefectural University), Sompratana Ritphring(Kasetsart University), Masashi Kiguchi(University of Tokyo), weerakaset Suanpaga(Associate professor in Civil Engineering,Kasetsart University)

In Japan, the impact of climate change has already become apparent and may become even more serious in the future. For example, there are the following specific damages; crop damage such as mandarin orange edema and white immature grains of rice, health hazards such as the northward distribution of Aedes albopictus and heat stroke patients, meteorological disasters such as increased torrential rain and increased number of strong typhoons, and coral bleaching Ecosystem.
The climate change adaptation law, which was enacted in 2018, clarified the legal position of adaptation measures in Japan, and is a legal for the national, local governments, businesses and citizens to cooperate and cooperate to promote adaptation measures. Based on this law, the Climate Change Adaptation Information Platform (A-PLAT) was established to develop and provide tools to support information provision and adaptation actions, and to collect, organize and provide best practices. AP-PLAT and T -Overseas development such as -PLAT is also progressing. Overseas expansion such as AP-PLAT and T-PLAT are also progressing.
In each research field, it is necessary to promote effective adaptation measures based on reliable and detailed information, and measures based on scientific knowledge of future impacts and strengthening of adaptation in the region are urgently needed.
This proposed session would like to invite presentations on the latest achievements in interdisciplinary fields such as hydrology, agriculture, forestry, weather, and climate that support specific climate change adaptation measures, as well as on the development of new research.

[AHW21-P01] Attempt to separate factors to reduce locality of precipitation-elevation dependence in Japan

*Mayu Otsuki[1], Atsushi Higuchi[2], Hitoshi Hirose[3] (1.Chiba University, 2.Center for Environmental Remote Sensing Chiba University, 3.Japan Aerospace Exploration Agency)

[AHW21-P02] Prediction process in the seasonal forecast model of monthly precipitation by global climate data using deep learning

*Shingo Zenkoji[1], TEBAKARI TAICHI[1], SAKAKIBARA KAZUTOSHI[1] (1.Toyama Prefecural University)

[AHW21-P03] Regional climate change impacts on groundwater level in the Kurobe River alluvial fan, Japan

*Takuya Matsuura[1], TEBAKARI TAICHI[1] (1.Toyama prefectural University)

[AHW21-P04] Atmosphericfronts of the rainy season in kyushu region using an objective method

*Maki Miyamoto[1], Tomohito Yamada[1] (1.Hokkaido University)

[AHW21-P05] Climate Change Impact on Salt Affected Soil in Northeast Thailand

*KOSHI YOSHIDA[1], Supranee SRITUMBOON[2], Mallika SRISUTHAM[3], KOKI HOMMA[4], MASAYASU MAKI[5], KAZUO OKI[6] (1.The University of Tokyo, 2.Land Development Department, Thailand, 3.Khon Kaen University, Thailand, 4.Tohoku University, 5.Fukushima University, 6.Kyoto University of Advanced Science)

[AHW21-P06] Development of a numerical model to simulate the salinity distribution in the tidal area of the lower Chao Phraya Basin, Thailand

*Ryota Tsuji[1], TAICHI TEBAKARI[1], Keisuke Nakayama[2] (1.Toyama Prefectural University, 2.Kobe University)

Attempt to separate factors to reduce locality of precipitation-elevation dependence in Japan

*Mayu Otsuki[1], Atsushi Higuchi[2], Hitoshi Hirose[3]

1. Chiba University, 2. Center for Environmental Remote Sensing Chiba University, 3. Japan Aerospace Exploration Agency

Japan is located in the northwest of the Pacific Ocean. There is the Sea of Japan between Japan and the Eurasian continent. Japan, which has such geographical characteristics, has a climate different from other regions in the mid-latitude. For example, the annual precipitation amount in the mid-latitude is approximately 800 mm, while 1700 mm in Japan. The orographic effect attributes such regional differences in annual precipitation in precipitation. Forced rise aloft the airmass by the mountain enhances the condensation; thus, the mass of precipitation varies with the elevation. It is well-known as elevation dependence. Previous studies have been conducted on the elevation dependence over various regions, but not many analyze Japan. Therefore, this study analyzed the elevation dependence of precipitation in Japan from 2016 to 2018 using radar AMeDAS analysis rainfall. Hokkaido and Nansei Islands are excluded due to different climatic zone with Japan's mainland. In addition, the areas over 1000 m in elevation are masked to take into account radar-beam shielding. Since the elevation dependence dramatically depends on the precipitation and topographical characteristics of the region, this study aimed to separate the factors that bring regionality to the elevation dependence and evaluate Japan's elevation dependence more universally. At this time, we hypothesized that the factors that cause regional differences in precipitation are "frontal precipitation," "typhoons," and "cold outbreak precipitation in winter." Not only do these precipitation systems bring large amounts of precipitation to some areas, but they also have different elevation dependence. Therefore we separated these factors. After removing these three factors, the regional difference in annual precipitation amount becomes more homogeneous. Its amount is approximately 800 mm, which close to the mid-latitude's value. Seasonal variability in separated precipitation was analyzed. There was a clear regionality in the season when precipitation was brought about.

Keywords: Elevation dependence, Orographic precipitation, Radar AMeDAS, Precipitation, Topography

©2021. Japan Geoscience Union. All Right Reserved.

Prediction process in the seasonal forecast model of monthly precipitation by global climate data using deep learning

*Shingo Zenkoji[1], TEBAKARI TAICHI[1], SAKAKIBARA KAZUTOSHI[1]

1. Toyama Prefecural University

Thailand, a country in Southeast Asia, has a clear distinction between the dry season (November-April) and the rainy season (May-October). As a result, many natural disasters such as droughts occur during the dry season and tropical storms and floods occur during the rainy season, and their frequency and intensity are increasing. The GCM model using physical equations is often used as a long-term prediction method for precipitation. However, the prediction by the GCM model is highly uncertain and cannot be quantitatively predicted. The purpose of this study is to develop a lunar precipitation prediction model after 2 months in the upper Chao Phraya River basin, Thailand, from global climate value data using deep learning.

The used data were five types of global monthly average climate values (surface temperature, atmospheric pressure, specific humidity, soil moisture content, precipitation), latitude, longitude, and land mask obtained from JRA55. The study period was 1958 / 1-1988 / 12, the verification period was 1989 / 1-2009 / 12, and the examination period was 2010 / 1-2020 / 9.

In this study, we developed a model for predicting monthly precipitation two months later using the Deep Convolutional Neural Network (DCNN), which is one of the deep learning algorithms. The input data is a total of 4 types of global climate data (surface temperature, pressure, specific humidity, soil moisture) and 3 types of geographic data (Lat, Lon, Land mask) 2 to 9 months before the forecast month. Output data is monthly precipitation after 2 months. For the purpose of reducing the calculation cost and suppressing overfitting, the input data was average pooled using a 3 ×3 window. The DCNN model consists of one convolutional layer and two fully connected layers. In the convolution layer, the global data at each point is compressed into one feature (neuron) by the filter. The hyperparameters of the deep learning method were optimized using Bayesian optimization.

Next, as a result of predicting the monthly precipitation after 2 months under the above-mentioned conditions, the MAE was 41 mm and the RMSE was 53 mm during the test period. When the amount of precipitation by JRA55 was large, the predicted precipitation was underestimated, and when the amount of precipitation by JRA55 was small, the predicted amount of precipitation was overestimated (threshold value of about 300 mm). However, from 2011 to 2016, the fluctuations in the predicted monthly precipitation in June and July showed the same behavior as the fluctuations in the monthly precipitation by JRA55. Therefore, it was suggested that this prediction model has prediction skills. We visualized the first fully connected layer of the developed monthly precipitation prediction model. The positive and negative values of neurons in this layer are related to the occurrence and suppression of precipitation phenomena. Looking at the distribution of the neuron values at each point output from the first fully connected layer of the DCNN model during the test period, the maximum neuron values in the continental regions are a large positive value was confirmed, and a large negative value was confirmed for the minimum neuron value in the waters.

Finally, as a result of developing a monthly precipitation prediction model in the upper reaches of the Chao Phraya River in Thailand from global climate value data using deep learning, the monthly

©2021. Japan Geoscience Union. All Right Reserved.

precipitation prediction model is difficult to predict quantitatively. It was confirmed that he had predictive skills. By visualizing this precipitation prediction model, it was found that this prediction model has the characteristic that the precipitation phenomenon is caused by the meteorological conditions of the continental area and the precipitation phenomenon is suppressed by the meteorological conditions of the sea area.

Keywords: Seasonal forecast, Deep learning, Monthly precipitation, Climate factor, Thailand

©2021. Japan Geoscience Union. All Right Reserved.

Regional climate change impacts on groundwater level in the Kurobe River alluvial fan, Japan

*Takuya Matsuura[1], TEBAKARI TAICHI[1]

1. Toyama prefectural University

The purpose of this study is to clarify the impact of climate change on the groundwater level in the Kurobe River Alluvial Fan. It has been pointed out that the temperature is on the rise due to climate change, and that the form of precipitation in the future will change from snowfall to rainfall. As a result, water supply from snow cover will decrease and the peak period of river flow will be earlier. Groundwater is also predicted to change its peak groundwater level in the same way as river flow. Increased rainfall is predicted to increase winter recharge and raise the groundwater level. This study evaluates the effects of climate change on the water balance and fan groundwater level in the Kurobe River basin using the RCP8.5 scenario.

The meteorological data used were precipitation, temperature, and solar radiation which used was the NIES statistical downscaled 1 km mesh data provided by the National Institute for Agro-Environmental Sciences. The analysis was conducted for the historical climate (1981-2000) and the end of the 21st century (2081-2100). This study was developing a model that combines a distributed water balance model and a groundwater analysis model (Dtransu), and conducted numerical experiments. The snowfall rate was calculated as 100% for temperatures below 0 ℃ and 0% for temperatures above 4.5 ℃. The snowfall rate between 0 and 4.5 ℃ was approximated by a linear line, and the amount of snowfall and rainfall was calculated by multiplying the amount of precipitation by the snowfall rate. The validity of the model was evaluated based on the river flow rate at the observation points where no water engineering facilities exist in the upstream area, 18 groundwater level stations located in the alluvial fan area, and the groundwater residence time calculated from the tritium analysis results. As a result, the flow rate of the river and the residence time of the groundwater were generally the same and could be reproduced. On the other hand, the groundwater level could not be reproduced at all stations, but the contour map of the groundwater level in the whole alluvial fan area could be reproduced.

As a result of the increase in temperature, it was found that at the end of the 21st century, the amount of snow water equivalent would decrease by 23 % (260 mm) compared to the historical climate, and the snow disappearance period would end one month earlier than the historical. As a result, the water balance of the Kurobe River basin showed that the peak of surface runoff and infiltration in the late 21st century was projected to be one month earlier than historical, and the surface runoff and infiltration increased from November to February. The groundwater level in the alluvial fan area increased during January to March and decreased during May to July. The results suggest that the current water system may not be able to provide sufficient water supply during the cultivation period, because climate change causes a decrease in surface runoff and groundwater level during the cultivation period from May to June.

©2021. Japan Geoscience Union. All Right Reserved.

Atmosphericfronts of the rainy season in kyushu region using an objective method

*Maki Miyamoto[1], Tomohito Yamada[1]

1. Hokkaido University

Torrential rainfall disasters induced by baiu fronts, which are stationary fronts appearing from May to July in Japan, occur frequently in kyushu region, western Japan. It is significant for society to examine variation of frontal rainfall associated with climate change. Atmospheric fronts depicted on a surface weather map published from Japan Meteorology Agency are estimated by forecasters[1]. We need to use an objective method for the detection of fronts in order to quantitative analysis.

Weather elements which defines atmospheric fronts are thermodynamical and dynamical variables[2]. The former is primary and used in TFP(Thermal Frontal Paramater)[2], which is common for an objective analysis[1][3]. The latter is secondary variables such as change of wind direction and employed for detection of fronts[4]. Another method using dimensionless number made of both variables is also proposed[5]. No method can detect all atmospheric fronts. We should investigate the feature of objective methods for frontal analysis and adopt an appropriate method.

In this research, we apply the method using thermodynamical and dynamical variables for analysis of atmospheric fronts, F diagnostic, subject to the rainy season in Japan. It is presented that fronts on surface weather chart exist succesively around the kyushu resion for many days in heavy rainfall events. In such a case, there are fronts detected by the objective method more frequently than usual.

[1] JMA, 2018, Quantitative Forecasting Technical Documents, **23**, 84-103.

[2] Renard and Clarke, 1965, Mon. Weather Rev., **93**, 547-556.

[3] Hewson, T. D., 1998, Meteorol. Appl., **5**, 37-65.

[4] Simmonds et al., 2012, J. Clim., **25**(6), 1945-1962

[5] Parfitt et al., 2017, Geophys. Res. Lett., **44**, 4351-4358.

Keywords: atmospheric fronts, surface weather chart, objective analysis

©2021. Japan Geoscience Union. All Right Reserved.

Climate Change Impact on Salt Affected Soil in Northeast Thailand

*KOSHI YOSHIDA[1], Supranee SRITUMBOON[2], Mallika SRISUTHAM[3], KOKI HOMMA[4], MASAYASU MAKI[5], KAZUO OKI[6]

1. The University of Tokyo, 2. Land Development Department, Thailand, 3. Khon Kaen University, Thailand, 4. Tohoku University, 5. Fukushima University, 6. Kyoto University of Advanced Science

In North East Thailand, annual rainfall is about 1200mm and average rice yield is only 2.1 t/ha (rain-fed). In addition, 50% of total agricultural land in this region are classified as salt affected area. Improvement of salt-affected soils in NE Thailand is a major concern of responsible agency Land Development Department(LDD) and other relevant institutions. Currently, numerous efforts have been carried out for this purpose, but existing knowledge is still insufficient. In future, climate change may cause negative impact on salt-affected soil problems. Therefore, in this study, we conducted the field survey to evaluate the seasonal changes of salt affected soil indicator such as ECe and SAR. Then, Hydrus1D was applied to predict how change the salinity level under climate change condition.
The study area was located in the salt-affected area in Ban Phai District, Khon Kaen Province, Northeast of Thailand. According to the LDD salt affected soil classification, agricultural land was classified into 4 classes including class 1 “very severely” (salt crust >50 %, ECe >16 dS/m), class 2 “severely” (salt crust 10-50%,ECe 8-16 dS/m), class 3 “moderately” (salt crust 1-10%,ECe 4-8 dS/m), and class 4 “slightly” (salt crust < 1%, ECe 2-4 dS/m). In this study, class 2 field was selected and 15 soil samples were collected in every 2 weeks from October 2016 to December 2018. Because farmers still can continue rice cultivation in class 2 field, although any crop can not grow in class 1 fields. To protect the class 2 fields is major concern for sustainable agriculture in this area. The electrical conductivity (ECe), Sodium Adsorption Ratio (SAR), soil moisture content SMC(%w/w), and soil textures were analyzed at Land Development Department Regional Office 5’s laboratory.
To predict the climate change impact, Hydrus1D model was employed in this study. Hydrus-1D is a one-dimensional finite element model for simulating the movement of water, heat, and multiple solutes in variably saturated media. The model is supported by an interactive graphics-based interface for data-preprocessing, discretization of the soil profile, and graphic presentation of the results. The soil parameters were calibrated. Calculated SMC, ECe were good agreement with observed data and SAR also simulated in sufficient. By using this Hydrus1D, future ECe and SAR were calculated by using the global circulation model (MIROC5) outputs of RCP8.5 scenario. Due to the temperature increase of 3 degree Celsius from 2006 to 2100, annual evapotranspiration increased 154 mm in 2100. And both ECe and SAR increased in the rate of 0.02dS/m/year and 0.04/year respectively. For the countermeasure, 20cm reduction of ground water level had significant effect to mitigate the salt accumulation.

Keywords: Soil Environment, Climate Change, Thailand

©2021. Japan Geoscience Union. All Right Reserved.

Development of a numerical model to simulate the salinity distribution in the tidal area of the lower Chao Phraya Basin, Thailand

*Ryota Tsuji[1], TAICHI TEBAKARI[1], Keisuke Nakayama[2]

1. Toyama Prefectural University, 2. Kobe University

The purpose of this study is to clarify the actual situation of saltwater intrusion in the lower Chao Phraya River in Thailand. In coastal flatlands, sea level rise due to climate change causes an increase in the extent of saltwater intrusion. As a result, there is a risk of tap water intake failure in areas where brackish area in river is used as water intake source.
Thailand has large seasonal variations in river flows due to its tropical monsoon climate. 75% of BMA tap water is taken from Chao Phraya River. The intake plant is located in a brackish area 95.1 km upstream from the river mouth, and is affected by water intake failure when the river flow is low. In this study, a numerical model was developed to estimate the salinity distribution in the lower Chao Phraya River in Thailand.
This study used a three-dimensional environmental hydrodynamic model, Fantom, which is based on a k-ε turbulence model. The structure of the longitudinal section was the riverbed elevation surveyed by the ultrasonic sounding (DT-X). The structure in the cross section was a constant upstream river width. The used data were the flow velocity observed by the acoustic Doppler current profiler(ADCP), the periodical water quality analysis data and the monitoring data of water quality observed by MWA. The boundary condition at the upstream end was the discharge (m^3/s) of Chao Phraya dam, 287.4 km upstream from the river mouth, and the boundary condition for water quality was 0.1 (‰) of the lowest observed salinity. The boundary condition at the downstream end was the water level (m MSL.) at the river mouth and the boundary condition for water quality was 30 (‰) of the average salinity of the Thailand Bay. The meteorological conditions were the hourly wind speed (m/s), temperature (˚C), relative humidity (‰), pressure (Pa), and rainfall (mm) at Bang Na, where a station of the Meteorological Department of Thailand is located.
As the result of the simulation, the peak salinity at the intake plant in the dry season and the fluid mixing near the bottom layer could be modeled. However, the study has not been able to simulate the peak salinity timing and quantitatively.
The numerical model in this study was able to model the qualitative seasonal variation of salinity. In the future, it is necessary to analyze the risk of water intake using the experimental results of climate change.

©2021. Japan Geoscience Union. All Right Reserved.

[J] Poster | A (Atmospheric and Hydrospheric Sciences)：A-HW Hydrology & Water Environment

Sat. Jun 5, 2021 5:15 PM - 6:30 PM JST | Sat. Jun 5, 2021 8:15 AM - 9:30 AM UTC | Ch.07_3

[A-HW24] Water Environment and Geology in Urban Areas

convener:Takeshi Hayashi(Faculty of Education and Human Studies, Akita University), Akinobu Miyakoshi(Geological Survey of Japan, AIST)

The scope of this session is to create an interdisciplinary forum on the most recent advances in water environment and environmental geology research in urban areas. Various kinds of studies concerning environmental issues on water and geology in urban areas (e.g. water balance, water cycle, water resource development and management, inundations, hydrogeology, pollution and remediation, geohazard, basic law on the water cycle) are welcome from academia, industry, and government as well as wider geographic diversity.

[AHW24-P01] Variability of land-use in the catchments of spring water in the western marginal area of Kanto Plain

*Takeshi Hayashi[1], Masaya Yasuhara[2], Takashi Nakamura[3] (1.Faculty of Education and Human Studies, Akita University, 2.Department of Environment Systems, Rissho University, 3.ICRE, University of Yamanashi)

[AHW24-P02] Evaluation of subsurface warming in the Tokyo metropolitan area, Japan: Effective application of groundwater observation wells for subsurface temperature monitoring

*Akinobu Miyakoshi[1], Takeshi Hayashi[2], Hideki Hamamoto[3], Shoichi Hachinohe[3] (1.Geological Survey of Japan, AIST, 2.Faculty of Education and Human Studies, Akita University, 3.Center for Environmental Science in Saitama)

[AHW24-P03] Demonstration of Ground Source Heat Pump systems and variations of the subsurface temperatures in Saitama Prefecture

*Hideki Hamamoto[1], Hidetaka Shiraishi[1], Masaki Nakayama[2], Shingo Uchiyama[2], Shuhei Ishiguro[3], Junya Takeshima[3] (1.Center for Environmental Science in Saitama, 2.Environmental Energy Division, Environment Department, Saitama Prefecture, 3.OYO Corporation)

[AHW24-P04] Examination of groundwater level measurement method by microtremor array exploration

*Yuji Miyashita[1], Hideki Hamamoto[2], Shigeki Senna[3] (1.Hot Springs Research Institute of Kanagawa Prefecture, 2.Center for Environmental Science in Saitama, 3.National Research Institute for Earth Science and Disaster Resilience)

Variability of land-use in the catchments of spring water in the western marginal area of Kanto Plain

*Takeshi Hayashi[1], Masaya Yasuhara[2], Takashi Nakamura[3]

1. Faculty of Education and Human Studies, Akita University, 2. Department of Environment Systems, Rissho University, 3. ICRE, University of Yamanashi

Marginal areas of the Kanto plain are composed of several topographical units such as alluvial fans (e.g. Arakawa alluvial fan), uplands (e.g. Iruma-Musashino upland), and hills (e.g. Tama hills). These units show both topographical and geological variations. From the hydrological viewpoint, these units have various spring water that had been used as water resources in each area. Although a number of the springs were disappeared in the process of urbanization, there are still many springs in these areas. These existing springs have a wide variety of land-use such as woodlands, agricultural areas, and residential areas in each catchment area.

This study aims to evaluate the effect of land-use change on the water environment of these springs that still remain or are already depleted. In this study, topographical maps that have been published since the Meiji Period and Google Maps have used for understanding the land-use change. As for details of topography surrounding each spring water, 5m DEM published by the Geospatial Information Authority of Japan has been used.
As a result, we found both the existing spring water of which land-use in the catchment area has been historically changed and the disappeared spring water of which land-use has not been changed clearly. We will discuss the effects of land-use change on the processes of the water cycle and the sources of water for these springs.

This study was supported by JSPS KAKENHI Grant Number 19K12293-00.

Keywords: Kanto Plain, spring water, land-use change

©2021. Japan Geoscience Union. All Right Reserved.

Evaluation of subsurface warming in the Tokyo metropolitan area, Japan: Effective application of groundwater observation wells for subsurface temperature monitoring

*Akinobu Miyakoshi[1], Takeshi Hayashi[2], Hideki Hamamoto[3], Shoichi Hachinohe[3]

1. Geological Survey of Japan, AIST, 2. Faculty of Education and Human Studies, Akita University, 3. Center for Environmental Science in Saitama

Effects of urbanization-related changes in the environment and regional groundwater flow, on the subsurface thermal environment of the Tokyo metropolitan area in Japan, were evaluated. This was conducted by examining subsurface temperatures and their three-dimensional distribution as well as long-term changes. For this purpose, multiple observations of temperature-depth profiles from the year 2000 and subsurface temperature monitoring in observation wells from 2007 in Saitama Prefecture and 2013 in Tokyo Metropolis were used.

Subsurface warming was found at shallow depths throughout the study area in our previous study (Miyakoshi et al., 2010). Subsurface temperatures beneath the city center, such as those in central Tokyo, were particularly high, not only in the shallow parts but also in the deep parts. In contrast, relatively low temperatures were found beneath suburban areas. A comparison of past subsurface temperature data (2003–2005) and present subsurface temperature data (2013–2020) shows that subsurface warming has occurred in the shallow parts in the last 10 to 15 years. The increases in subsurface temperatures in the city center were found to be larger than those in the suburban area. The temporal differences in temperatures indicate an increasing trend of subsurface temperatures in both the areas. Additionally, present data indicate that subsurface warming occurred in deeper parts. This result suggests that the distribution of subsurface warming is expanding toward the deeper parts.

Based on the results of subsurface temperature monitoring, subsurface warming was confirmed to have occurred continuously. The warming rate varied depending on the location and depth. An almost-constant warming rate of 0.01–0.02 K/year was found to occur at a depth of 30 m in the observation wells in the southeastern area of Saitama Prefecture and the eastern area of Tokyo Metropolis(Miyakoshi et al., 2017). These observations were from the alluvial lowland, and the warming was driven mainly by heat conduction due to warming of the surface from urbanization.

In the Musashino upland, the southwestern area of Saitama Prefecture, the western area of Tokyo Metropolises, and the Arakawa alluvial fan in the northwestern part of Saitama Prefecture, continuous subsurface warming, similar to that in lowland, was found. However, the warming rate fluctuated with time in some observation wells. Additionally, significant temperature changes were observed at depths greater than 100 m. Comparing the Musashino upland and the Arakawa alluvial fan, the period, magnitude, and depth of these changes were different. Complex subsurface temperature changes were observed around areas where significant changes in hydraulic heads had occurred. It is considered that artificially induced change in groundwater flow is one of the main reasons for long-term changes in subsurface temperatures. Furthermore, the differences in the magnitude of subsurface temperature changes in the two regions reflect the differences in hydrogeological conditions and groundwater development. The mechanism of subsurface warming is expected to be evaluated by a combined analysis of changes in geological conditions, groundwater flow, and subsurface temperatures.

©2021. Japan Geoscience Union. All Right Reserved.

The research in Saitama Prefecture was conducted as a part of AIST- Akita University -Saitama Prefecture joint research. The utilization of the observation wells in the Tokyo Metropolis was supported by Civil Engineering Support and Training Center, Tokyo Metropolitan Government. The part of this study was supported by JSPS KAKENHI Grant Number 19K12364.

Keywords: subsurface temperature, groundwater flow, subsurface warming, observation well, urbanization, Tokyo metropolitan area

©2021. Japan Geoscience Union. All Right Reserved.

Demonstration of Ground Source Heat Pump systems and variations of the subsurface temperatures in Saitama Prefecture

*Hideki Hamamoto[1], Hidetaka Shiraishi[1], Masaki Nakayama[2], Shingo Uchiyama[2], Shuhei Ishiguro[3], Junya Takeshima[3]

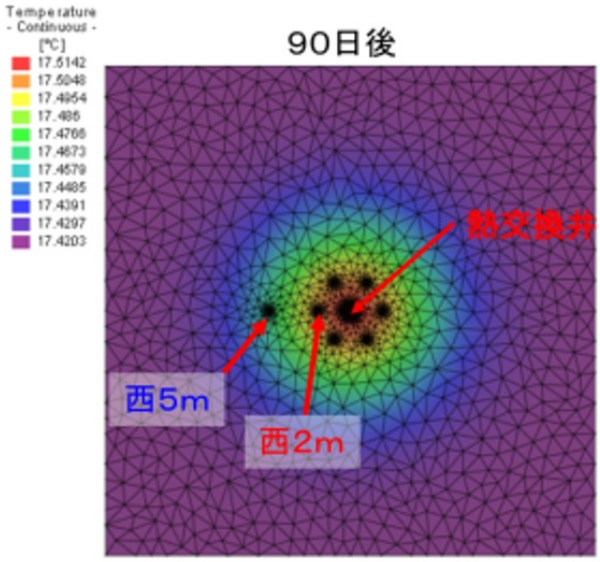
1. Center for Environmental Science in Saitama, 2. Environmental Energy Division, Environment Department, Saitama Prefecture, 3. OYO Corporation

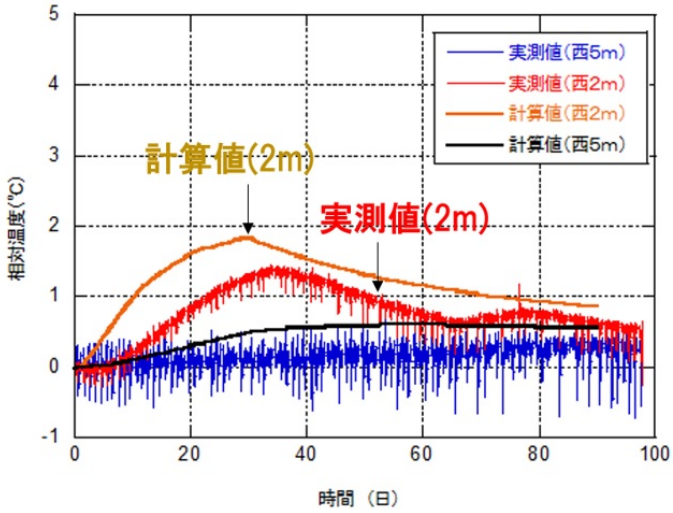
Geothermal energy systems are a type of renewable energy system. They are superior in energy conservation and are spreading in Japan and overseas. The ground-source heat-pump (GHP) system is widely used for room heating and cooling and hot water supply in large facilities and housings. It is important to quantitatively compare the operating efficiency, cost, and environmental effects of GHP and air source heat pumps (AHP) through experiments to promote the use of GHP in the future. The operating efficiency of both heat pumps varies with the weather conditions and heat loads at the installation sites and only the efficiency of GHP varies with the subsurface environmental conditions.
In 2018, the Local Government of Saitama Prefecture installed both GHP and AHP in five small-scale buildings in the prefecture. Among the five sites, four sites (Hanno City, Hanyu City, Miyashiro Town, and Kasukabe City) contain atmosphere-monitoring stations and the fifth (Kazo City) site is the Eco-Lodge of the Center for Environmental Science in Saitama. At the atmosphere-monitoring stations in four sites where the demonstration experiments were conducted, the continuous cooling and heating operation tests were conducted at the target room temperature (Cooling: 27˚C, Heating: 25˚C) of general housing to examine the operation efficiency of the GHP and AHP. Specifically, either of the HPs was operated alternately in summer and winter at 15-day intervals, and the SCOP was calculated by measuring the inlet/outlet temperatures, the circulating flow rate of the secondary circulating fluid, and power consumption. As a result, the average SCOP of the four sites in the cooling operation was 5.7 and 2.6 for the GHP and AHP, respectively, and 3.0 and 2.4 for GHP and AHP, respectively, in the heating operation. The efficiency of the GHP was higher than that of the AHP in all sites. The efficiency of the cooling operation was higher than that of the heating operation in the same site, and this tendency is consistent with the results of existing demonstration experiments.
In two sites (Kazo City and Miyashiro Town), observation wells (six wells at 2 m and one well at 5 m from the heat exchange well) were installed to investigate the temperature fluctuation in the vicinity of the heat exchange wells. In the eco-lodge, cooling and heating operations were conducted at the maximum load. The GHP was operated under a high load for 30 days to monitor the process of the rise and fall in subsurface temperature. The operation was halted for the next 60 days and the recovery process was monitored. This paper presents the results of the cooling operation. The temperature increased by 2˚C at the observation well, 2 m away from the heat exchange well (West 2 m well). And large temperature rise was not observed at the well 5 m away (West 5 m well). Next, assuming that the heat propagates from the heat exchange well to the surroundings by heat diffusion, the temperature variation was calculated using a numerical simulator (FEFLOW) and employing the finite element method. The attached figure shows the areal temperature distribution 90 days after starting the monitoring at a depth of 40 m. It was confirmed that heat spreads concentrically from the heat exchange well to the circumference. The measured and calculated values at the observation well 2 m west were compared and they are consistent. This could be well explained by assuming that the heat propagates by thermal diffusion. In more detail, however, the measured temperatures at the west 2 m observation well and the east 2 m well increased at the same rate during the heating process, whereas the temperatures differed by 0.5˚C in the recovery process (the east 2 m well was hotter than the west 2 m well). This suggests that variations in thermal properties and

©2021. Japan Geoscience Union. All Right Reserved.

groundwater flow influence the observed temperatures. These factors shall be considered in our future studies.

Keywords: ground source heat pump, subsurface temperature, groundwater flow





©2021. Japan Geoscience Union. All Right Reserved.

Examination of groundwater level measurement method by microtremor array exploration

*Yuji Miyashita[1], Hideki Hamamoto[2], Shigeki Senna[3]

1. Hot Springs Research Institute of Kanagawa Prefecture, 2. Center for Environmental Science in Saitama, 3. National Research Institute for Earth Science and Disaster Resilience

1. Introduction

One of the geophysical exploration methods is "microtremor exploration", which estimates the S wave velocity by constantly observing microtremors on the surface of the earth, and requires an S wave velocity structure in the vertical one-dimensional direction at the exploration point. Since the S wave velocity is determined by the physical properties of the ground, the geological structure such as the distribution of the aquifer and the basement can be grasped from the vertical distribution of the S wave velocity.

On the other hand, the ground is composed of three phases: a solid phase part such as soil and rock, a liquid phase part such as groundwater and soil water, and a gas phase part existing in the unsaturated zone near the ground surface. Therefore, if the ratio of the liquid phase portion in the ground (≈ groundwater level) changes, it is expected that the S wave velocity will change.

Takahashi (2019) reviewed and model-analyzed the relationship between S-wave velocity and saturation of rocks. From past experiments in the literature, in the case of sandstone and shale, the S wave velocity decreases with increasing water saturation, in limestone there is no change in S wave velocity due to water saturation, and in granite, S wave with increasing water saturation. It showed a tendency to increase in speed. On the other hand, although the experimental results for the unconsolidated sedimentary layer were not obtained, it is possible that the fluctuation of the water content has an effect on the S wave velocity from the large pore space in comparison with the consolidated layer.

Therefore, in this study, the relationship between the groundwater level change and the S wave velocity distribution was investigated by repeating the measurement of the groundwater level and the micro-array tremor exploration at the same point at the same time.

2. Method

Repeated tremor exploration at fixed points was conducted nine times from June to November 2014 and once each in August 2019 and January 2020 at two points (H54, R50) located in the alluvial fan area in the upper reaches of the Ashigara Plain. A total of 11 micro-array microtremor surveys were conducted. In addition, the groundwater level was continuously measured at the shallow groundwater observation wells attached to these points.

Microtremor observation was performed using JU210 and JU410 manufactured by Hakusan Kogyo with a sampling interval of 200 Hz. The results of microtremor exploration were analyzed according to the method of Senna et. al, (2014).

©2021. Japan Geoscience Union. All Right Reserved.

3. Results and discussion

As a result of 11 microtremor surveys, the maximum exploration depth was 68.9 m at H54 and 86.9 m at R50, and the S wave velocity at maximum depth was 965 m/s at H54 and 940 m/s at R50. It showed almost the same S wave velocity. The groundwater level during tremor exploration changed from -12.73 to -15.30 m at H54 and from -7.24 to -8.41 m at R50.

The S wave velocity near the groundwater table is 370 to 880 m/s at the H54 point and 230 to 370 m/s at the R50 point. The results show that the S wave velocity differs greatly depending on the exploration time. In addition, explorations in which the S wave velocity changed up and down across the vicinity of the water table were observed in 8 out of 11 explorations at H54 and 10 out of 11 at R50.

Factors that cause the S-wave velocity at the same depth to change significantly for each microtremor exploration include errors in exploration and analysis such as installation errors of microtremors for each microtremor exploration and waveform reading errors in analysis, as well as changes in soil temperature and inadequacy. Factors such as differences in soil moisture content in the saturated zone are possible. In the future, in addition to examining these error factors, we will also examine other geological and climatic conditions.

Keywords: Microtremor exploration, groundwater level, repeated measurements

©2021. Japan Geoscience Union. All Right Reserved.

[E] Oral | A (Atmospheric and Hydrospheric Sciences)：A-CG Complex & General

Sat. Jun 5, 2021 10:45 AM - 12:15 PM JST | Sat. Jun 5, 2021 1:45 AM - 3:15 AM UTC | Ch.07 Zoom Room 07

[A-CG30] Multi-scale ocean-atmosphere interaction in the tropics

convener:Hiroki Tokinaga(Research Institute for Applied Mechanics, Kyushu University), Yu Kosaka(Research Center for Advanced Science and Technology, University of Tokyo), Ayako Seiki(Japan Agency for Marine-Earth Science and Technology), Tomoki Tozuka(Department of Earth and Planetary Science, Graduate School of Science, The University of Tokyo), Chairperson:Yu Kosaka(Research Center for Advanced Science and Technology, University of Tokyo), Ayako Seiki(Japan Agency for Marine-Earth Science and Technology)

Tropical ocean-atmosphere interactions exert a significant impact on regional and global climate on a broad range of spatio-temporal scales. Since the 1980s, in-situ and satellite observations, reanalysis products, and advancements in climate modeling have led to depicting various aspects of intraseasonal (e.g., MJO), interannual (e.g., ENSO, IOD, and Atlantic Nino) and decadal (e.g., IPO) variability in the tropical ocean basins and their linkages with tropical (e.g., monsoons) and extratropical (e.g., storm track) climate. Newer studies find an active role of salinity in tropical ocean-atmosphere interaction, including tropical cyclone intensification. Other recent studies highlight the tropical inter-basin coupling among the Pacific, Indian Ocean, and Atlantic in seasonal prediction of the Asian summer monsoon and decadal redistribution of ocean heat content associated with the so-called "hiatus" of global warming. Long term change in the Pacific Walker circulation has been recapturing attention in terms of the pattern effect of warming on climate feedback and sensitivity against radiative forcing as well as ENSO modulations under a warmer climate. A variety of processes are mutually interrelated and shape the climate, its variability, and change. To examine these challenging issues from various perspectives and foster understanding of the role of tropical ocean-atmosphere interaction in the climate system, this session offers a forum to discuss recent progress in observational, modeling and theoretical studies of multi-scale ocean-atmosphere interaction in the tropics.

10:45 AM - 11:00 AM JST | 1:45 AM - 2:00 AM UTC

[ACG30-01] The impact of North Pacific climate variability on historical ENSO and its mechanisms

★Invited Papers

*Dillon J Amaya[1,2], Yu Kosaka[3], Wenyu Zhou[4], Yu Zhang[5], Shang-Ping Xie[6], Arthur J Miller[6] (1.Cooperative Institute for Research in Environmental Sciences, 2.University of Colorado Boulder, 3.University of Tokyo, 4.Pacific Northwest National Laboratory, 5.Ocean University of China, 6.Scripps Institution of Oceanography)

11:00 AM - 11:15 AM JST | 2:00 AM - 2:15 AM UTC

[ACG30-02] Radiative impacts of low clouds on the subtropical North Pacific climate

*Ayumu Miyamoto[1], Hisashi Nakamura[1], Takafumi Miyasaka[2], Yu Kosaka[1], Shang-Ping Xie[3] (1.Research Center for Advanced Science and Technology,The University of Tokyo, 2.Japan Meteorological Business Support Center, 3.Scripps Institution of Oceanography, University of California San Diego)

11:15 AM - 11:30 AM JST | 2:15 AM - 2:30 AM UTC

[ACG30-03] Disparate Midlatitude Responses to El Niño/Southern Oscillation

*Shiozaki Masahiro[1], Takeshi Enomoto[2,3], Takaya Koutarou[4] (1.Research Institute for applied mechanics, Kyushu University, 2.Disaster Prevention Research Institute, Kyoto University, 3.Application Laboratory, Japan Agency for Marine-Earth Science and Technology, 4.Kyoto Sangyo University)

11:30 AM - 11:45 AM JST | 2:30 AM - 2:45 AM UTC

[ACG30-04] Formation of Barrier Layers and Temperature Inversions in the Eastern Tropical Pacific Detected by Mooring Observation

*Shota Katsura[1], Janet Sprintall[1], Thomas Farrar[2], Dongxiao Zhang[3,4], Meghan Cronin[3] (1.Scripps Institution of Oceanography, University of California, San Diego, 2.Department of Physical Oceanography,

Woods Hole Oceanographic Institution, 3.NOAA Pacific Marine Environmental Laboratory, 4.Cooperative Institute for Climate, Ocean, and Ecosystem Studies, University of Washington)

11:45 AM - 12:00 PM JST | 2:45 AM - 3:00 AM UTC

[ACG30-05] The intraseasonal relationship between the boreal summer intraseasonal oscillation and the Pacific-Japan pattern

*Ayako Seiki[1], Yu Kosaka[2], Satoru Yokoi[1] (1.Japan Agency for Marine-Earth Science and Technology, 2.The University of Tokyo)

12:00 PM - 12:15 PM JST | 3:00 AM - 3:15 AM UTC

[ACG30-06] Why does convection weaken over Sumatra Island in an active phase of the MJO?

*Ning Zhao[1], Peiming Wu[1], Miki Hattori[1] (1.JAMSTEC Japan Agency for Marine-Earth Science and Technology)

The impact of North Pacific climate variability on historical ENSO and its mechanisms

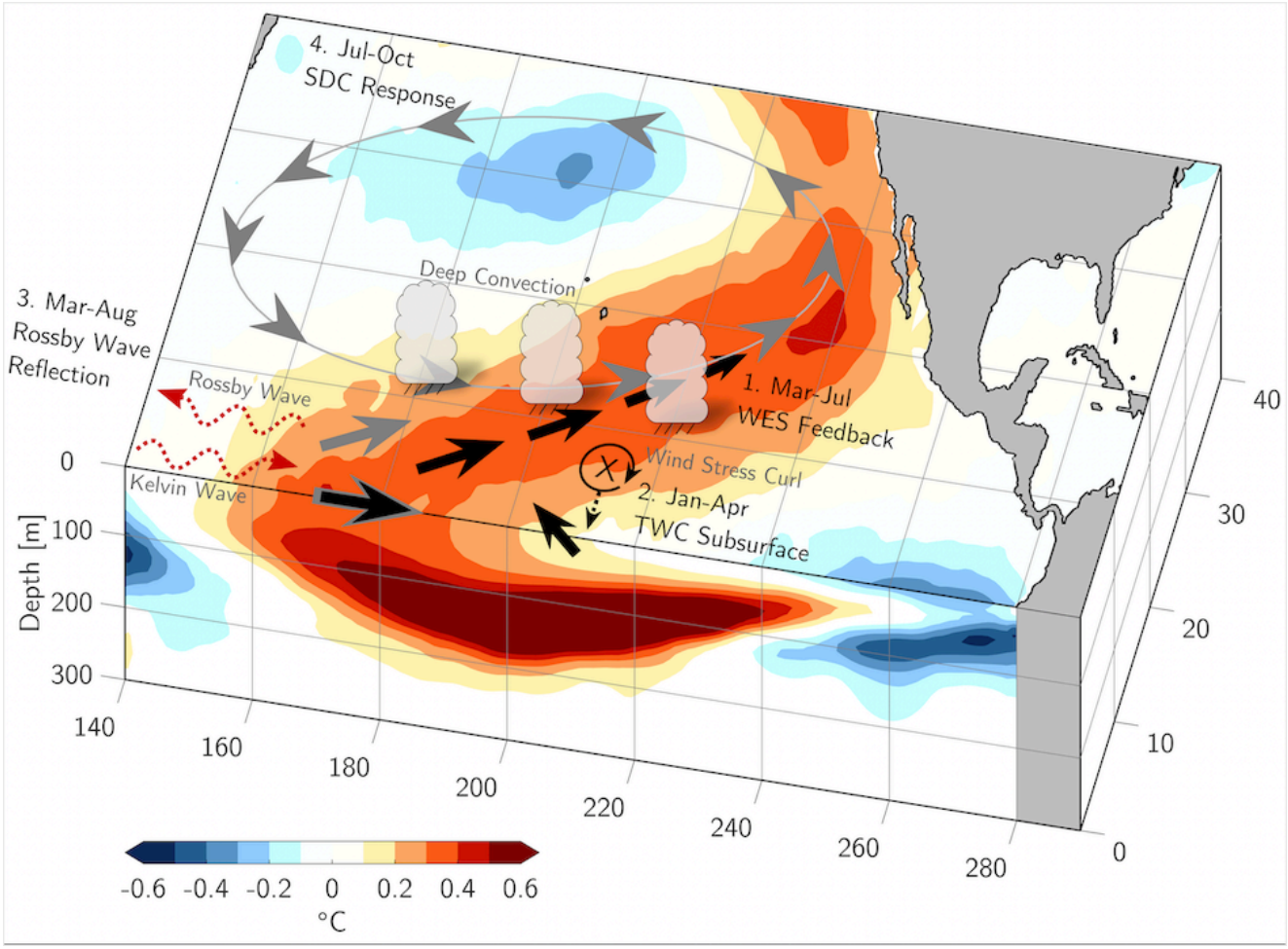
*Dillon J Amaya[1,2], Yu Kosaka[3], Wenyu Zhou[4], Yu Zhang[5], Shang-Ping Xie[6], Arthur J Miller[6]

1. Cooperative Institute for Research in Environmental Sciences, 2. University of Colorado Boulder, 3. University of Tokyo, 4. Pacific Northwest National Laboratory, 5. Ocean University of China, 6. Scripps Institution of Oceanography

Studies have indicated that North Pacific sea surface temperature (SST) variability can significantly modulate the El Nino–Southern Oscillation (ENSO), but there has been little effort to put these extratropical–tropical interactions into the context of historical events. To quantify the role of the North Pacific in pacing the timing and magnitude of observed ENSO, we use a fully coupled climate model to produce an ensemble of North Pacific Ocean–Global Atmosphere (nPOGA) SST pacemaker simulations. In nPOGA, SST anomalies are restored back to observations in the North Pacific (>15˚N) but are free to evolve throughout the rest of the globe. We find that North Pacific SST has significantly influenced observed ENSO variability, accounting for approximately 15% of the total variance in boreal fall and winter. The connection between the North and tropical Pacific arises from two physical pathways: 1) a wind–evaporation–SST (WES) propagating mechanism, and 2) a Gill-like atmospheric response associated with anomalous deep convection in boreal summer and fall, which we refer to as the summer deep convection (SDC) response. The SDC response accounts for 25% of the observed zonal wind variability around the equatorial date line. On an event-by-event basis, nPOGA most closely reproduces the 2014/15 and the 2015/16 El Ninos. In particular, we show that the 2015 Pacific Meridional Mode event increased wind forcing along the equator by 20%, potentially contributing to the extreme nature of the 2015/16 El Nino. Our results illustrate the significant role of extratropical noise in pacing the initiation and magnitude of ENSO events and may improve the predictability of ENSO on seasonal time scales.

Keywords: Climate Variability, ENSO, Teleconnection, Tropics, Air-Sea Interactions, Climate Model

©2021. Japan Geoscience Union. All Right Reserved.



©2021. Japan Geoscience Union. All Right Reserved.

Radiative impacts of low clouds on the subtropical North Pacific climate

*Ayumu Miyamoto[1], Hisashi Nakamura[1], Takafumi Miyasaka[2], Yu Kosaka[1], Shang-Ping Xie[3]

1. Research Center for Advanced Science and Technology,The University of Tokyo, 2. Japan Meteorological Business Support Center, 3. Scripps Institution of Oceanography, University of California San Diego

Low clouds that cool the Earth radiatively are extensive off California over the North Pacific. The present study assesses their radiative impacts on the subtropical North Pacific climate with coupled general circulation model experiments. Comparison of a freely coupled control experiment with a sensitivity experiment where low-cloud radiative effect off California is artificially switched off demonstrates that low clouds lower sea surface temperature (SST) and reinforce the subtropical anticyclone locally. These responses extend southwestward from off California, suggestive of wind-evaporation-SST feedback. Following enhanced albedo effect of low clouds in spring and summer, the responses become strongest in summer and autumn in association with suppressed deep convective precipitation. In these seasons, low clouds strengthen surface trade winds and upper-tropospheric subtropical westerly jet, explaining 25% of climatological vertical wind shear around Hawaii. Low clouds thus act to protect Hawaii from hurricanes by lowering SST and increasing vertical wind shear.

Keywords: Low clouds, North Pacific

©2021. Japan Geoscience Union. All Right Reserved.

Disparate Midlatitude Responses to El Niño/Southern Oscillation

*Shiozaki Masahiro[1], Takeshi Enomoto[2,3], Takaya Koutarou[4]

1. Research Institute for applied mechanics, Kyushu University, 2. Disaster Prevention Research Institute, Kyoto University, 3. Application Laboratory, Japan Agency for Marine-Earth Science and Technology, 4. Kyoto Sangyo University

To investigate the disparate influences of the eastern Pacific (EP) El Niño on the winter climate in the Far East, we conducted composite analyses using long-term reanalysis datasets.

Our analysis shows that the western Pacific (WP) pattern dominates in the warm winter (typical) composite and the Pacific–North American (PNA) pattern dominates in the non-warm winter (atypical) composite.

In the warm winter case, the amplitudes of the negative sea surface temperature (SST) anomalies in the western Pacific Ocean are large whereas in the non-warm winter case, these amplitudes are small. In addition, the Indian Ocean basin warming occurs following the Indian Ocean dipole mode, as seen in the warm winter composite.

We investigated the dynamical mechanisms responsible for the disparate midlatitude responses to the EP El Niño by focusing on Rossby wave sources and propagation. These SST anomalies modulate the Walker and Hadley circulations and the convective activity in the western Pacific Ocean. Upper-tropospheric divergences at the mid-latitudes due to the anomalous Hadley circulation result in different teleconnection patterns. In the warm winter composite, the anticyclonic anomaly in the southern part of the WP pattern is created by the upstream negative Rossby wave source, while the other cyclonic anomaly is reinforced by the northward Rossby wave propagation. The cyclonic second and fourth centers of action of the PNA pattern are created by the positive Rossby wave sources. Furthermore, the equatorial SST gradient near the date line is found be a good precursor of the winter climate in the Far East.

We will also discuss the cold and the non-cold winter cases in East Asia during La Niña.

Keywords: El Niño/Southern Oscillation, winter climate, teleconnection pattern

©2021. Japan Geoscience Union. All Right Reserved.

Formation of Barrier Layers and Temperature Inversions in the Eastern Tropical Pacific Detected by Mooring Observation

*Shota Katsura[1], Janet Sprintall[1], Thomas Farrar[2], Dongxiao Zhang[3,4], Meghan Cronin[3]

1. Scripps Institution of Oceanography, University of California, San Diego, 2. Department of Physical Oceanography, Woods Hole Oceanographic Institution, 3. NOAA Pacific Marine Environmental Laboratory, 4. Cooperative Institute for Climate, Ocean, and Ecosystem Studies, University of Washington

It is known that salinity plays a dominant role in determining the stratification of the upper ocean, especially where barrier layers (BLs) form between the bases of the mixed layer and the isothermal layer in some regions. The BL interferes with heat and momentum exchange between surface and subsurface layers and can affect sea surface temperature and air-sea interactions. In the eastern tropical Pacific, BLs are distributed along the SSS front south of the eastern Pacific fresh pool in boreal summer and autumn and tend to be associated with temperature inversions (TIs) in boreal autumn. A mixed layer salinity and temperature budget was constructed based on time-series from three mooring observations to investigate the formation of BLs and TIs in the eastern tropical Pacific. BLs and TIs observed at the moorings showed a clear seasonality in their formation and amplitude, which is consistent with the previous climatological studies. However, in contrast to previous studies in the region, the mixed layer salinity budget indicates that precipitation was dominant for the surface freshening in boreal summer and autumn and contributed to the BL formation. The mixed layer temperature budget found that the penetration of shortwave radiation through the mixed layer base had a dominant contribution to the surface cooling and hence the TI formation during the boreal summer and autumn. Geostrophic and Ekman advection also occasionally contributed to the BL and TI formation. The existence of BLs significantly reduced the entrainment cooling and detrainment warming. In addition, the entrainment warmed the mixed layer when BLs with TIs existed. The shallower mixed layers associated with BLs were more sensitive to surface heat and freshwater flux than when BLs were not observed in the water column.

Keywords: Barrier Layer, Temperature Inversion, Eastern Tropical Pacific

©2021. Japan Geoscience Union. All Right Reserved.

The intraseasonal relationship between the boreal summer intraseasonal oscillation and the Pacific-Japan pattern

*Ayako Seiki[1], Yu Kosaka[2], Satoru Yokoi[1]

1. Japan Agency for Marine-Earth Science and Technology, 2. The University of Tokyo

The influence of the dominant tropical intraseasonal variability during boreal summer, called the boreal summer intraseasonal oscillation (BSISO), on the tropical-midlatitudes teleconnection, called the Pacific-Japan (PJ) pattern, is investigated. A lag correlation analysis between the intraseasonal PJ index and phases of the BSISO index shows that the positive correlation between the BSISO and the PJ pattern peaks during the early stage of the BSISO phase 8 when the center of the BSISO enters the central north Pacific. Composite analysis based on the BSISO events shows that intraseasonal responses to the migration of the BSISO are apparent even in midlatitudes. During the phase 7-8, cyclonic wind anomalies with low pressure signals north of the Philippines are drastically intensified and easterly wind anomalies blow into the southern side of Japan. Apparent intraseasonal signals in surface pressure anomalies are also found over the central north Pacific around 40˚N. The migration of the BSISO might influence summer climate in East Asia through the PJ pattern at intraseasonal time scales.

Keywords: the boreal summer intraseasonal oscillation, the Pacific-Japan pattern

©2021. Japan Geoscience Union. All Right Reserved.

Why does convection weaken over Sumatra Island in an active phase of the MJO?

*Ning Zhao[1], Peiming Wu[1], Miki Hattori[1]

1. JAMSTEC Japan Agency for Marine-Earth Science and Technology

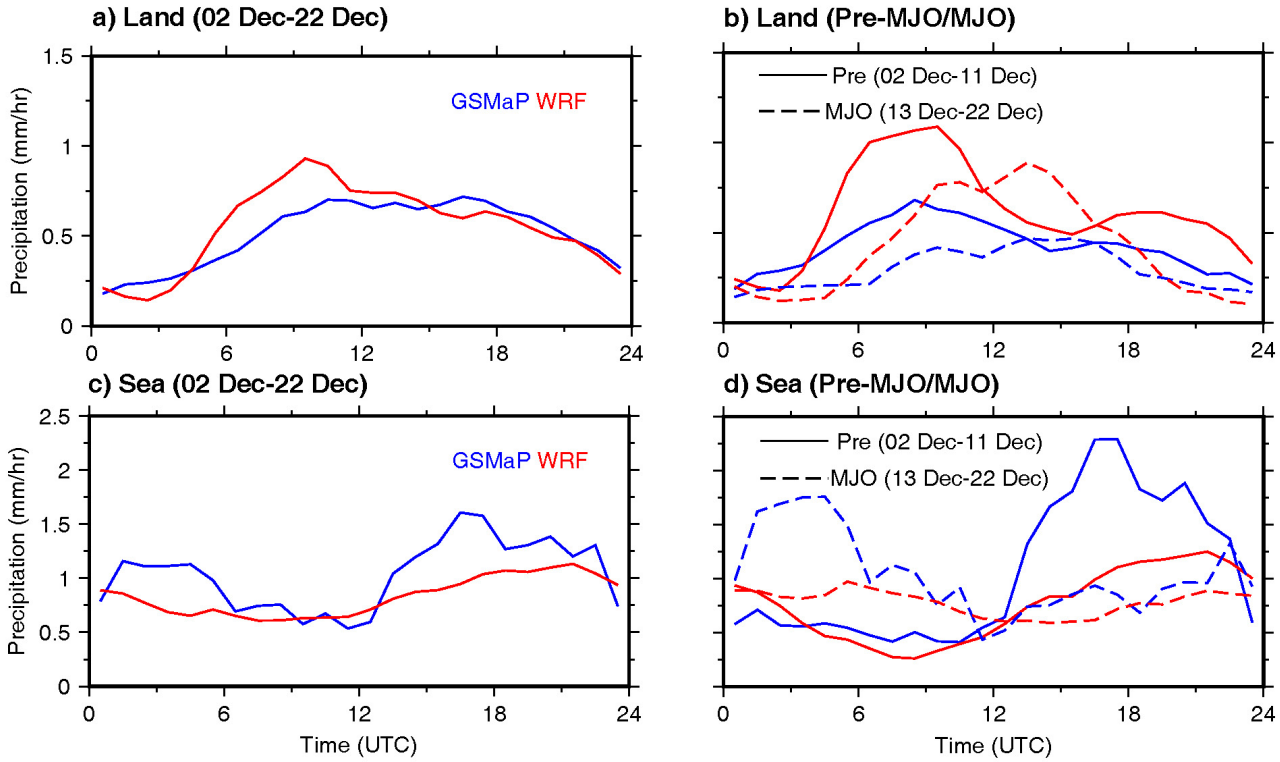
This study examined the diurnal cycle of convection over Sumatra Island in an active phase of the Madden-Julian Oscillation (MJO) during the pre-Years of the Maritime Continent (YMC) observation campaign in December 2015 based on observations and convection-permitting numerical model. Satellite observation indicates that, prior to an active phase of the MJO in early December, convection frequently occurred over the island in the afternoon. In contrast, during the active phase of the MJO in mid-December, afternoon convection over the island was suppressed, and a gap in convection aligned with the island was evident during the early morning hours. On the contrary, convective activities were observed over the offshore region within the whole day, especially during the daytime that was much weaker before.

Our numerical experiments successfully replicated the main features of the observed modulation of the diurnal convection. Results suggest that, during the active phase of the MJO, although the moisture was accumulated within the boundary layer over the mountainous areas as before, the afternoon convection was suppressed and delayed. Moisture budget analysis demonstrates that vertical moisture advection over the island, the dominating factor of diurnal convection, was weakened and delayed during the MJO active phase. It further became negative within the lower-to-mid troposphere from midnight to the next morning, indicating that the convection over the island was suppressed by the subsidence. Our results showed that such subsidence was highly related to the enhanced convective activities over the offshore region. On the other hand, our results also suggest that the strong westerlies played a secondary role in weakening and delaying the diurnal convection over the island, which induced the negative horizontal moisture advection within the mid-troposphere.

Overall, this study suggests that the modulated diurnal cycle over Sumatra Island was likely induced by the enhanced convective activities over the offshore region during the active phase of the MJO. Detailed results and further analyses would be shown in our presentation.

Keywords: Diurnal Convection, Land-sea Interaction, Madden–Julian Oscillation, Pre-YMC 2015

©2021. Japan Geoscience Union. All Right Reserved.



©2021. Japan Geoscience Union. All Right Reserved.

[E] Oral | A (Atmospheric and Hydrospheric Sciences)：A-CG Complex & General

Sat. Jun 5, 2021 1:45 PM - 3:15 PM JST | Sat. Jun 5, 2021 4:45 AM - 6:15 AM UTC | Ch.07 Zoom Room 07

[A-CG30] Multi-scale ocean-atmosphere interaction in the tropics

convener:Hiroki Tokinaga(Research Institute for Applied Mechanics, Kyushu University), Yu Kosaka(Research Center for Advanced Science and Technology, University of Tokyo), Ayako Seiki(Japan Agency for Marine-Earth Science and Technology), Tomoki Tozuka(Department of Earth and Planetary Science, Graduate School of Science, The University of Tokyo), Chairperson:Hiroki Tokinaga(Research Institute for Applied Mechanics, Kyushu University), Tomoki Tozuka(Department of Earth and Planetary Science, Graduate School of Science, The University of Tokyo)

Tropical ocean-atmosphere interactions exert a significant impact on regional and global climate on a broad range of spatio-temporal scales. Since the 1980s, in-situ and satellite observations, reanalysis products, and advancements in climate modeling have led to depicting various aspects of intraseasonal (e.g., MJO), interannual (e.g., ENSO, IOD, and Atlantic Nino) and decadal (e.g., IPO) variability in the tropical ocean basins and their linkages with tropical (e.g., monsoons) and extratropical (e.g., storm track) climate. Newer studies find an active role of salinity in tropical ocean-atmosphere interaction, including tropical cyclone intensification. Other recent studies highlight the tropical inter-basin coupling among the Pacific, Indian Ocean, and Atlantic in seasonal prediction of the Asian summer monsoon and decadal redistribution of ocean heat content associated with the so-called "hiatus" of global warming. Long term change in the Pacific Walker circulation has been recapturing attention in terms of the pattern effect of warming on climate feedback and sensitivity against radiative forcing as well as ENSO modulations under a warmer climate. A variety of processes are mutually interrelated and shape the climate, its variability, and change. To examine these challenging issues from various perspectives and foster understanding of the role of tropical ocean-atmosphere interaction in the climate system, this session offers a forum to discuss recent progress in observational, modeling and theoretical studies of multi-scale ocean-atmosphere interaction in the tropics.

1:45 PM - 2:00 PM JST | 4:45 AM - 5:00 AM UTC

[ACG30-07] Understanding tropical interbasin interaction using linear inverse modelling

*Shoichiro Kido[1], Ingo Richter[1], Tomoki Tozuka[2,1], Ping Chang[3] (1.JAMSTEC Application Lab, 2.Department of Earth and Planetary Science, University of Tokyo, 3.Texas A&M University)

2:00 PM - 2:15 PM JST | 5:00 AM - 5:15 AM UTC

[ACG30-08] **An assessment of the tropical Atlantic influence on El Niño-Southern Oscillation**

*Ingo Richter[1], Hiroki Tokinaga[2], Yu Kosaka[3], Takeshi Doi[1], Takahito Kataoka[1] (1.Japan Agency for Marine-Earth Science and Technology, Yokohama, Japan, 2.Kyushu University, Kasuga, Japan, 3.University of Tokyo, Tokyo, Japan)

2:15 PM - 2:30 PM JST | 5:15 AM - 5:30 AM UTC

[ACG30-09] **The roles of diabatic heating for the seasonality of the Atlantic Niño**

★Invited Papers

*Hyacinth C. Nnamchi[1], Mojib Latif[1], Noel S. Keenlyside[2,3], Joakim Kjellsson[1], Ingo Richter[4] (1.GEOMAR Helmholtz Centre for Ocean Research Kiel, 2.Geophysical Institute, University of Bergen, and Bjerknes Centre for Climate Research, Bergen, Norway, 3.Nansen Environmental and Remote Sensing Center, Bergen, Norway, 4.Application Laboratory, Research Institute for Value-Added-Information Generation, Japan Agency for Marine-Earth Science and Technology, Yokohama, Japan)

2:30 PM - 2:45 PM JST | 5:30 AM - 5:45 AM UTC

[ACG30-10] Simulated thermocline tilt over the tropical Indian Ocean and its influence on future sea surface temperature variability

★Invited Papers

*Guojian Wang[1,2], Wenju Cai[1,2], Agus Santoso[1,3] (1.Center for Southern Hemisphere Oceans Research (CSHOR), CSIRO Oceans and Atmosphere, 2.Key Laboratory of Physical Oceanography–Institute for

Advanced Ocean Studies, Ocean University of China and Qingdao National Laboratory for Marine Science and Technology, 3.The University of New South Wales)

2:45 PM - 3:00 PM JST | 5:45 AM - 6:00 AM UTC

[ACG30-11] Asymmetry in sea surface temperature anomalies and atmospheric teleconnection associated with the Indian Ocean Dipole

Mai Nakazato[1], Shoichiro Kido[2], *Tomoki Tozuka[1,2] (1.Department of Earth and Planetary Science, Graduate School of Science, The University of Tokyo, 2.Application Laboratory, Research Institute for Value-Added-Information Generation, Japan Agency for Marine-Earth Science and Technology)

3:00 PM - 3:15 PM JST | 6:00 AM - 6:15 AM UTC

[ACG30-12] Investigation of interannual variability in the tropical Indian Ocean based on the transfer routes of wave energy

*Zimeng Li[1], Hidenori AIKI[2] (1.Graduate school of environmental studies, Nagoya university, 2.Institute for Space-Earth Environmental Research)

Understanding tropical interbasin interaction using linear inverse modelling

*Shoichiro Kido[1], Ingo Richter[1], Tomoki Tozuka[2,1], Ping Chang[3]

1. JAMSTEC Application Lab, 2. Department of Earth and Planetary Science, University of Tokyo, 3. Texas A&M University

Many observational and modelling studies have recently underlined the importance of tropical interbasin coupling in understanding climate variability and predictability. The coupling among tropical basins can be separated into three components; the interaction between Pacific and Indian Oceans (the PO-IO interaction), that between Pacific and Atlantic Oceans (the PO-AO interaction), and that between the Atlantic and Indian Oceans (the AO-IO interaction). Though many previous studies have discussed the significance of individual components, the relative importance of these coupling components has not been carefully evaluated and fully understood. To address this issue, we have constructed a linear inverse model (LIM) based on observed sea surface temperature (SST) anomalies in the tropical Pacific, Atlantic, and Indian Oceans, and performed a series of prediction experiments using this LIM. We found that our LIM has a good skilll in forecasting tropical SST variability, including those associated with the El Niño and Southern Oscillation (ENSO). To assess the impact of interbasin interaction, we have removed individual coupling component by modifying off-diagonal elements of the linear operator. Using this “decoupled” operator, we have conducted several prediction experiments. We find that the decoupling leads to a substantial decrease in prediction skill of ENSO and related SST variability, especially at longer lead times. Partial decoupling experiments that nullify specific coupling components suggest that the PO-IO interaction has the largest impact on the prediction skill of ENSO-related variability, whereas the PO-AO interaction also has a nonnegligible contribution. On the other hand, the impacts of the AO-IO interaction seem to be smaller than those of the other two coupling components. Results from the LIM simulations with white noise forcing, as well as an analysis of optimum initial conditions will be also discussed. These are aimed to examine the underlying statistical relations and physical processes.

Keywords: Interbasin interaction, Linear inverse modeling

©2021. Japan Geoscience Union. All Right Reserved.

An assessment of the tropical Atlantic influence on El Niño-Southern Oscillation

*Ingo Richter[1], Hiroki Tokinaga[2], Yu Kosaka[3], Takeshi Doi[1], Takahito Kataoka[1]

1. Japan Agency for Marine-Earth Science and Technology, Yokohama, Japan, 2. Kyushu University, Kasuga, Japan, 3. University of Tokyo, Tokyo, Japan

The influence of the tropical Atlantic on El Niño-Southern Oscillation (ENSO) is examined using sensitivity experiments with the SINTEX-F general circulation model with prescribed sea surface temperature (SST) distributions based on observations for the period 1982-2018. In the control experiment (CTRL) observed SSTs are prescribed over the global oceans, whereas in the sensitivity experiment (OTA) observed SSTs are prescribed in the tropical Atlantic only while in other regions the climatological annual cycle is prescribed.

A composite analysis of the model output suggests that cold SST events in the northern tropical Atlantic (NTA) during boreal spring are associated with near-surface wind changes over the equatorial and subtropical Pacific that are conducive to the development of El Niño, consistent with previous studies. The amplitude of these changes, however, is at most 20% of those observed during typical El Niño events. Likewise, warm events in the equatorial Atlantic produce only about 10% of the wind changes seen in the western equatorial Pacific during the developing phase of typical La Niña events. Similar results are obtained from a partial regression analysis performed on an ensemble of atmosphere-only simulations from the Atmospheric Model Intercomparison Project (AMIP) Phase 6. Further analysis of the AMIP models indicates that model biases do not have a major impact on the Atlantic-to-Pacific influence. Overall, the results suggest that the tropical Atlantic has a weak influence on ENSO development, and that this influence mostly acts to modulate ongoing events rather than to initiate them.

Keywords: tropical Atlantic, ENSO, teleconnections

©2021. Japan Geoscience Union. All Right Reserved.

The roles of diabatic heating for the seasonality of the Atlantic Niño

*Hyacinth C. Nnamchi[1], Mojib Latif[1], Noel S. Keenlyside[2,3], Joakim Kjellsson[1], Ingo Richter[4]

1. GEOMAR Helmholtz Centre for Ocean Research Kiel, 2. Geophysical Institute, University of Bergen, and Bjerknes Centre for Climate Research, Bergen, Norway, 3. Nansen Environmental and Remote Sensing Center, Bergen, Norway, 4. Application Laboratory, Research Institute for Value-Added-Information Generation, Japan Agency for Marine-Earth Science and Technology, Yokohama, Japan

The physics underlying the Atlantic Niño remain under debate; however, the role of diabatic heating which represents the atmospheric component of the Bjerknes feedback loop is often overlooked. In this study, we use multiple observations to show that diabatic heating variability that is linked to the seasonal migration of the inter-tropical convergence zone controls the seasonality of the Atlantic Niño. The strongest diabatic heating variability in spring leads that in the SST in summer, whereas the atmospheric response to the SST variability is relatively weak. This can be linked to net surface heat flux tendencies which drive the mixed-layer temperature anomalies in spring, but is the major damping term in June-July when the SST variability peak, although observational uncertainty is quite large. Entrainment is the dominant heating term associated with the peak SST variability in June. Our findings point to the existence of a strong meridional variability in the atmosphere, which by terminating the Bjerknes feedback, controls the seasonality of the Atlantic Niño.

Keywords: Bjerknes feedback, Atlantic Niño, Diabatic heating, ITCZ

©2021. Japan Geoscience Union. All Right Reserved.

Simulated thermocline tilt over the tropical Indian Ocean and its influence on future sea surface temperature variability

*Guojian Wang[1,2], Wenju Cai[1,2], Agus Santoso[1,3]

1. Center for Southern Hemisphere Oceans Research (CSHOR), CSIRO Oceans and Atmosphere, 2. Key Laboratory of Physical Oceanography–Institute for Advanced Ocean Studies, Ocean University of China and Qingdao National Laboratory for Marine Science and Technology, 3. The University of New South Wales

Most coupled climate models simulate an overly shallow thermocline over the southeastern equatorial Indian Ocean (SEIO). Through the Bjerknes feedback loop, the associated unrealistic thermocline tilt leads to warmer sea surface temperature (SST) over the western equatorial Indian Ocean than the SEIO, which is conducive to equatorial easterly winds. Similar to phase 5 of the Coupled Model Intercomparison Project (CMIP), phase 6 of the CMIP continues to simulate such overly tilted thermocline. On the one hand, this leads to overly strong SST variability, and on the other hand, it provides an inherent limit for the thermocline to incline further under greenhouse warming. Consequently, models with a more realistic tilt in the present-day climate project a greater shoaling of the thermocline under global warming, which facilities upwelling of cool subsurface water, leading to stronger increase in SST variability over the SEIO, compared to models with an overly large thermocline tilt.

Keywords: Thermocline bias, Tropical Indian Ocean

©2021. Japan Geoscience Union. All Right Reserved.

Asymmetry in sea surface temperature anomalies and atmospheric teleconnection associated with the Indian Ocean Dipole

Mai Nakazato[1], Shoichiro Kido[2], *Tomoki Tozuka[1,2]

1. Department of Earth and Planetary Science, Graduate School of Science, The University of Tokyo, 2. Application Laboratory, Research Institute for Value-Added-Information Generation, Japan Agency for Marine-Earth Science and Technology

One of the important features of the Indian Ocean Dipole (IOD) is its asymmetry; negative sea surface temperature (SST) anomalies in the eastern pole during the positive IOD are stronger than positive SST anomalies during the negative IOD. Based on an online mixed layer heat budget analysis using the Regional Ocean Modeling System, it is shown that the vertical diffusion term plays an important role in generating this asymmetry in addition to the contributions from the nonlinear advection and the thermocline feedback proposed by some previous studies. To understand the origin of the asymmetry in the vertical diffusion term, a detailed decomposition is carried out. It is found that the asymmetry is primarily explained by differences in subsurface temperature anomalies; during positive IOD events, anomalous cooling below the mixed layer contributes to SST cooling via vertical mixing. However, such effects are weaker in the case of negative IOD events due to weaker subsurface temperature anomalies. Furthermore, analyses of the Rossby wave source and wave activity fluxes suggest that the SST asymmetry in the IOD indeed have asymmetric impacts on the mid-latitudes via atmospheric teleconnection.

Keywords: Indian Ocean Dipole, Mixed layer heat budget analysis, Atmospheric teleconnection, Tropical Indian Ocean

©2021. Japan Geoscience Union. All Right Reserved.

Investigation of interannual variability in the tropical Indian Ocean based on the transfer routes of wave energy

*Zimeng Li[1], Hidenori AIKI[2]

1. Graduate school of environmental studies, Nagoya university, 2. Institute for Space-Earth Environmental Research

We have performed a set of 61-year hindcast experiments of Indian Ocean using monthly wind forcing and provide a new perspective for the interannual variability in the tropical Indian Ocean based on the transfer routes of wave energy using a new diagnostic scheme. There are two sets of Rossby waves along the equator during 1994 IOD positive event. One is the same phase speed with theoretical phase speed of equatorial Rossby waves, the other is slightly slower than theoretical phase speed of equatorial Rossby waves. First set is the boundary-reflected equatorial Rossby waves at eastern boundary from the equatorial Kelvin waves. Second set is the off-equatorial Rossby waves generated by southeasterly winds from the southeastern Indian Ocean, which may account for the appearance of slightly slower phase speed of Rossby wave along the equator.

Keywords: Indian Ocean, interannual variability, wave energy, Kelvin wave, Rossby wave

©2021. Japan Geoscience Union. All Right Reserved.

[E] Poster | A (Atmospheric and Hydrospheric Sciences)：A-CG Complex & General

Sat. Jun 5, 2021 5:15 PM - 6:30 PM JST | Sat. Jun 5, 2021 8:15 AM - 9:30 AM UTC | Ch.08_1

[A-CG30] Multi-scale ocean-atmosphere interaction in the tropics

convener:Hiroki Tokinaga(Research Institute for Applied Mechanics, Kyushu University), Yu Kosaka(Research Center for Advanced Science and Technology, University of Tokyo), Ayako Seiki(Japan Agency for Marine-Earth Science and Technology), Tomoki Tozuka(Department of Earth and Planetary Science, Graduate School of Science, The University of Tokyo)

Tropical ocean-atmosphere interactions exert a significant impact on regional and global climate on a broad range of spatio-temporal scales. Since the 1980s, in-situ and satellite observations, reanalysis products, and advancements in climate modeling have led to depicting various aspects of intraseasonal (e.g., MJO), interannual (e.g., ENSO, IOD, and Atlantic Nino) and decadal (e.g., IPO) variability in the tropical ocean basins and their linkages with tropical (e.g., monsoons) and extratropical (e.g., storm track) climate. Newer studies find an active role of salinity in tropical ocean-atmosphere interaction, including tropical cyclone intensification. Other recent studies highlight the tropical inter-basin coupling among the Pacific, Indian Ocean, and Atlantic in seasonal prediction of the Asian summer monsoon and decadal redistribution of ocean heat content associated with the so-called "hiatus" of global warming. Long term change in the Pacific Walker circulation has been recapturing attention in terms of the pattern effect of warming on climate feedback and sensitivity against radiative forcing as well as ENSO modulations under a warmer climate. A variety of processes are mutually interrelated and shape the climate, its variability, and change. To examine these challenging issues from various perspectives and foster understanding of the role of tropical ocean-atmosphere interaction in the climate system, this session offers a forum to discuss recent progress in observational, modeling and theoretical studies of multi-scale ocean-atmosphere interaction in the tropics.

[ACG30-P01] Evaluation of externally forced component on interannual-scale SST anomalies over the tropical Indo-Pacific Ocean

*Takuya Hasegawa[1,2], Yuma Miyaji[1], Youichi Tanimoto[1,3] (1.Hokkaido University, 2.Tohoku University, 3.JAMSTEC)

[ACG30-P02] Potential predictability of regional extreme events associated with large-scale teleconnection from the tropical ocean

*Yukiko Imada[1], Hiroaki Kawase[1] (1.Meteorological Research Institute, Japan Meteorological Agency)

[ACG30-P03] External and Internal forcings of the Indian Ocean Dipole

*Lianyi Zhang[1,2], Yan Du[1,2], Tomoki Tozuka[3] (1.South China Sea Institute of Oceanology, Chinese Academy of Sciences, 2.Southern Marine Science and Engineering Guangdong Laboratory, 3.Dept. of Earth and Planetary Science Graduate School of Science, Univ. of Tokyo)

[ACG30-P04] Variations of sea surface temperature and salinity using coral Sr/Ca and $\delta^{18}O$ in the Java Sea and the Lombok Strait.

*Ai Genda[1], Ali Arman[2], Minoru Ikehara[3], Atsushi Suzuki[4], Mayuri Inoue[1] (1.Graduate School of National Science and Technology, Okayama University, 2.National Nuclear Energy Agency of Indonesia (BATAN), 3.Center of Advanced Marine Core Research, Kochi University, 4.Geological Survey of Japan, National Institute of Advanced Industrial Science and Technology)

Evaluation of externally forced component on interannual-scale SST anomalies over the tropical Indo-Pacific Ocean

*Takuya Hasegawa[1,2], Yuma Miyaji[1], Youichi Tanimoto[1,3]

1. Hokkaido University, 2. Tohoku University, 3. JAMSTEC

In order to investigate internal variability phenomena in the atmosphere-ocean climate system, it is necessary to remove the components generated by the external forcing such as anthropogenic global warming and volcanic eruptions (hereinafter referred to as externally forced component) from analyzed time series. In past studies, a method removing a linear trend at each grid point of the data has been widely used (hereinafter, LT method). On the other hand, in recent studies (e.g., Steinman et al. 2015; Dai et al. 2015), the new method of evaluating the externally forced component using the multi-model ensemble mean (MME) of the global mean surface temperature (GMST) anomaly using a large number of simulations in the Coupled Model Intercomparison Project Phase 5 (CMIP5) (hereinafter, GMST method) was applied to surface air temperature anomalies and sea surface temperature anomalies at each grid point by using the MME of GMST (GMSTmme). The purpose of this study is an inter-comparison between the LT and GMST methods when applying to interannual SST anomalies in the tropical Pacific and Indian Oceans.

In this study, we use the historical simulations with three ensemble members on a basis of the 12 CMIP5 models including MIROC5 (i.e., totally 36 historical experiments) to calculate the GMSTmme. After the linear regression coefficient (α) of the SST anomalies at each grid point onto the GMSTmme is calculated, the product of α and GMSTmme at each grid point is removed from the original SST anomalies. The remaining SST anomalies will be treated as the component of the natural internal variability.

We examined the different characteristics in the component of the natural internal variability in the Nino-3 index between the LT and the GMST methods on a basis of the observed SST of the COBE SST 2 (analysis period: 1850-2017). The monthly values of the Nino-3 index for the period 1960-1999 (2000-2017) tend to be 0.2℃ lower (higher) by the GMST method than by the LT method.

To quantify the different characteristics in the Nino-3 index between GMST and LT methods, the ratio of the root mean square deviation of externally forced components between the GMST and LT methods (RMSD) and the standard deviation of the internal variability component estimated by the GMST method (SD) was defined as R (R = RMSD/SD x 100). R of the Nino-3 index for a period of 1960-2017 is approximately 10%.

For the Indian Ocean Basin-wide warming (IOBW) index, the difference in amplitude between the GMST and LT methods was approximately 0.3˚C, i.e., approximately 50% lager than that of Nino-3 index. The amplitude of the internal variability of the IOBW index was a fraction of that of the Nino-3 index. Therefore, R of the IOBW (approximately 50%) was much larger than that of Nino-3 index (10%). On the other hand, Indian Ocean dipole mode index (DMI) shows little difference between the two methods. Because the externally forced component are mostly equal in the western and eastern tropical Indian Ocean, it is mostly canceled out by definition of the DMI.

To investigate the different characteristics in natural internal SST variability between the two methods, R is calculated in the whole ocean basin in two analysis periods such as a long term during 1850-2017 and

©2021. Japan Geoscience Union. All Right Reserved.

a short term during 1958-2017, respectively. R is 10 to 20% larger in the long-term analysis than in the short-term analysis for the whole ocean basin. When the GMSTmme by MIROC5 is employed for a longer period using the historical simulation and the RCP4.5 scenario simulation (1850-2100), R becomes much larger in all ocean basins. The results of this study indicate that the conventional LT method induces large estimation errors of the externally forced component by changing the calculation periods, suggesting usefulness of the GMST method.

Keywords: global warming, externally forced component, sea surface temperature, ENSO/IOD/IOBW, tropical Indo-Paicifc Ocean

©2021. Japan Geoscience Union. All Right Reserved.

Potential predictability of regional extreme events associated with large-scale teleconnection from the tropical ocean

*Yukiko Imada[1], Hiroaki Kawase[1]

1. Meteorological Research Institute, Japan Meteorological Agency

Compared to the high predictability of seasonal forecasts in the tropics, predictability in the mid- and high- latitudes is low due to the high atmospheric noise and low signal-to-noise ratio. Large ensemble prediction is one solution to reduce noise by taking the ensemble average. Despite the enormous computational cost issues, a large ensemble is also a powerful tool for capturing rare extreme weather and climate events.
Here, I will present our recent studies using high-resolution large ensemble simulations, focusing on the potential predictability of extreme event probability. The large ensemble simulations were carried out by the global atmospheric general circulation model with a horizontal resolution of 60 km and the regional climate model around Japan with a horizontal resolution of 20 km, which were prescribed by the observed SST. The dataset covers more than 6000 years (100 members from 1951 to the present). Using this dataset, we confirmed that a large ensemble improves temporal anomaly correlation skills over land at the mid-latitudes. Furthermore, the high-resolution 20-km runs can reproduce local heavy rainfall affected by fine topography and mesoscale rainfall systems. By combining global and regional simulations, we found that large-scale slow tropical ocean variability affects the frequency of local heavy rainfall, and local terrain sometimes helps to reduce atmospheric noises, resulting in higher potential predictability of rainfall in some areas of Japan.

Keywords: Potential Predictability, heavy rain events, large-ensemble simulation, teleconnection from the tropics

©2021. Japan Geoscience Union. All Right Reserved.

External and Internal forcings of the Indian Ocean Dipole

*Lianyi Zhang[1,2], Yan Du[1,2], Tomoki Tozuka[3]

1. South China Sea Institute of Oceanology, Chinese Academy of Sciences, 2. Southern Marine Science and Engineering Guangdong Laboratory, 3. Dept. of Earth and Planetary Science Graduate School of Science, Univ. of Tokyo

The Indian Ocean Dipole (IOD) is a climatic phenomenon occurring in the tropical Indian Ocean, which can cause anomalous weather and climate over the surrounding rims even the globe. This study investigates the remote impacts of the El Nino-Southern Oscillation (ENSO), and the internal forcing from the southern Indian Ocean on the IOD. The ENSO impacts on the IOD are revisited by a new statistical method namely the Combine Linear Regression (CLR). When the ENSO impacts are isolated, the IOD survives with same phase-locking to boreal fall season, while it weakens and peaks earlier by 1 month. After removing the ENSO impacts by the CLR, we propose a new triggering mechanism of IOD originating from the Southern Hemisphere, namely the Southern Hemisphere Mechanism (SHM). The SHM is independent from ENSO and cooperate with ENSO to affect the IOD in fall, leading to the IOD diversity such as the unseasonable IOD. The subtropical high in the southern Indian Ocean and high-latitude climate activities play important roles in the SHM. To consider these forcings would help to improve the IOD predictability.

Keywords: Indian Ocean Dipole , ENSO , Tropical-Extratropical Interaction

©2021. Japan Geoscience Union. All Right Reserved.

Variations of sea surface temperature and salinity using coral Sr/Ca and $\delta^{18}O$ in the Java Sea and the Lombok Strait.

*Ai Genda[1], Ali Arman[2], Minoru Ikehara[3], Atsushi Suzuki[4], Mayuri Inoue[1]

1. Graduate School of National Science and Technology, Okayama University, 2. National Nuclear Energy Agency of Indonesia (BATAN), 3. Center of Advanced Marine Core Research, Kochi University, 4. Geological Survey of Japan, National Institute of Advanced Industrial Science and Technology

The Indonesian Throughflow (ITF) runs from the Pacific into the Indian Ocean through the Indonesian archipelago. The ITF modulate heats and water budget between the Pacific and the Indian Ocean, and therefore the ITF plays an important role in climate change. In addition, during northwest monsoon, sea surface currents drive low salinity and buoyant water from the Java Sea to the southern Makassar Strait. This water caps surface flow through the Makassar Strait and called "freshwater plug". In contrast, during southeast monsoon, sea surface currents remove freshwater plug from the southern Makassar Strait. Thus, it is suggested that behavior of freshwater plug would affect variation of Asia monsoon and climate change. However, instrumental records have accumulated only for decades in the Indonesian Seas partially due to the complex topography. In this study, we reconstructed sea surface environments using Sr/Ca and oxygen isotopic ratios ($\delta^{18}O$) in coral skeleton collected from Seribu Islands and Bali Island. While both coral Sr/Ca and $\delta^{18}O$ depend on sea surface temperature (SST), coral $\delta^{18}O$ also depend on seawater $\delta^{18}O$ which mostly correspond to salinity. Therefore, both SST and salinity can be reconstructed from based on coral Sr/Ca and $\delta^{18}O$.
Coral samples used in this study were collected from two sites: one is the Seribu Islands located in the Java Sea where freshwater plug appears and the other is the southeast of Bali Island in the Lombok Strait, which is one of outlet of ITF connecting to the Indian Ocean. Seribu's and Bali's records covered about 70-year from 1931-2002 and 50-year from 1962-2012, respectively. In 1997 when positive Indian Ocean Dipole mode and El Niño occurred, Bali's record show large anomaly (cool SST and drought), whereas Seribu's record shows only a slightly change. Furthermore, it seems that a relatively big change of marine environments like a regime shift has occurred in the Lombok Strait around late 1990s with no clear change in the Java Sea. We will show and discuss the temporal and spatial change of the variation of SST and salinity based on coral Sr/Ca and $\delta^{18}O$ in both sites over the past decades.

©2021. Japan Geoscience Union. All Right Reserved.

[E] Oral | A (Atmospheric and Hydrospheric Sciences)：A-CG Complex & General

Sat. Jun 5, 2021 9:00 AM - 10:30 AM JST | Sat. Jun 5, 2021 12:00 AM - 1:30 AM UTC | Ch.08 Zoom Room 08

[A-CG34] Global Carbon Cycle Observation and Analysis

convener:Kazuhito Ichii(Chiba University), Prabir Patra(Research Institute for Global Change, JAMSTEC), Akihiko Ito(National Institute for Environmental Studies), Chairperson:Prabir Patra(Research Institute for Global Change, JAMSTEC), Kazuhito Ichii(Chiba University)

The Paris Agreement under the United Nations Framework Convention on Climate Change (UNFCCC) is a landmark agreement, which aims at reduction of greenhouse gases (GHGs) emission to keep the global warming below 2 deg C. The national commitments and progresses should be carefully monitored and verified by international bodies using different but complementary methodologies.

Many observation and technique to monitor GHGs budget have been improved in recent years. The improvements include observational platforms for monitoring atmospheric GHGs, national or regional emission inventories, top-down estimations (e.g. atmospheric inverse analysis), and bottom-up estimations (e.g. process-based models). However, due to uncertainties in sparse observation network and integration methods, large uncertainty remains in GHGs sources/sinks estimations at global and regional scales.

The purpose of the session is to discuss state-of-the-art techniques for estimations of GHGs (e.g. CO2, CH4, N2O) budget at global and regional scales. The topic includes natural and anthropogenic processes, various methodologies (e.g. in-situ observation, aircraft monitoring, remote sensing, modeling), and various targets (e.g. atmosphere, terrestrial, and ocean), various spatial and temporal coverage (e.g. regional to global scales and past-present-future). Improved estimates of emissions from land use change, forest fires, and other anthropogenic sources (urban developments and thermal power station etc.) are also of interest. We also welcome discussions for designs and plans for future studies targeting city and country scale emission estimations using sophisticated modeling tools and inventories.

9:00 AM - 9:15 AM JST | 12:00 AM - 12:15 AM UTC

[ACG34-01] Atmospheric inversions of greenhouse gas fluxes: A story of uneven development

★Invited Papers

*Peter J Rayner[1] (1.University of Melbourne)

9:15 AM - 9:30 AM JST | 12:15 AM - 12:30 AM UTC

[ACG34-02] **Decadal variability in land and ocean carbon fluxes by inverse modelling of atmospheric CO_2**

★Invited Papers

*Naveen Chandra[1,2], Prabir Patra[2] (1.National Institute for Environmental Studies, Japan, 2.Japan Agency for Marine-Earth Science and Technology)

9:30 AM - 9:45 AM JST | 12:30 AM - 12:45 AM UTC

[ACG34-03] **Changes in the atmospheric CO_2/CH_4 variability in the East Asian outflow region caused by plummet of fossil fuel-derived CO_2 in China due to COVID-19 outbreak**

*Yasunori Tohjima[1], Prabir Patra[2], Yosuke Niwa[1], Hitoshi Mukai[1], Motoki Sasakawa[1], Toshinobu Machida[1], Shin-ichiro Nakaoka[1] (1.National Institute for Environmental Studies, 2.Japan Agency for Marine-Earth Science and Technology)

9:45 AM - 10:00 AM JST | 12:45 AM - 1:00 AM UTC

[ACG34-04] Impact of anomalous high temperature anomaly in the 2020 spring-summer on terrestrial environment across Siberia

*Kazuhito Ichii[1], Riku Kawase[1], Yuhei Yamamoto[1], Shunji Kotsuki[1] (1.Chiba University)

10:00 AM - 10:15 AM JST | 1:00 AM - 1:15 AM UTC

[ACG34-05] CH_4 surface flux estimation based on local ensemble transform Kalman filter

*Jagat Bisht[1], Prabir Patra[1,2], Masayuki Takigawa[1], Takashi Sekiya[1], Yugo Kanaya[1], Naoko Saito[2] (1.Japan Agency for Marine-Earth Science and Technology , 2.Center for Environ. Remote Sensing, Chiba University)

10:15 AM - 10:30 AM JST | 1:15 AM - 1:30 AM UTC

[ACG34-06] Toward multi-scale greenhouse gas monitoring system for supporting global stock take

*Akihiko Ito[1,2], Yosuke Niwa[1], Tomohiro Hajima[2], Nobuko Saigusa[1] (1.National Institute for Environmental Studies, 2.Japan Agency for Marine-Earth Science and Technology)

Atmospheric inversions of greenhouse gas fluxes: A story of uneven development

*Peter J Rayner[1]

1. University of Melbourne

Atmospheric inversion is a technique for estimating the fluxes of tracers (here greenhouse gases) given observations and a model of atmospheric transport. The dominant methodology is Bayesian inference in which a model of atmospheric transport is combined with prior information and observations. Bayesian inference describes all input quantities as probability distributions. The methods differ in how they describe their inputs and the technique for constructing the posterior distribution. In this talk I will outline the current state of development of each of these inputs. I will argue that this development has proceeded unevenly. For much of their history inversions were limited by the sparsity of observations. The advent of increasingly accurate and dense satellite measurements has changed this so that the chief weakness is now the atmospheric models. I will sketch some possible remedies for this state of affairs.

©2021. Japan Geoscience Union. All Right Reserved.

Decadal variability in land and ocean carbon fluxes by inverse modelling of atmospheric CO_2

*Naveen Chandra[1,2], Prabir Patra[2]

1. National Institute for Environmental Studies, Japan, 2. Japan Agency for Marine-Earth Science and Technology

An improved understanding of the variabilities and trends in the CO_2 fluxes due to the land-biosphere and oceanic exchange is essential for the predictions of future climate feedback. Inverse modelling of atmospheric CO_2 provides estimation of spatio-temporal variation of the fluxes, allowing us to relate the CO2 flux variabilities with the modes of regional climate and with trends in socio-economic changes.

Monthly CO_2 fluxes for the period 1996-2019 are estimated by a time dependent inverse (TDI) model that uses measurements of CO_2 at 34 sites across the globe and MIROC4-ACTM forward model simulation. The inversion fluxes are evaluated in detail using the independent aircraft measurements of CO_2. The simulations of CO_2 concentrations using inverted fluxes agree within ±0.5 ppm at all the aircraft vertical profile sites. The long-term global land (ocean) fluxes are estimated to be -2.2±0.8 (-1.4±0.2) PgC yr^{-1} for the 2000s (2000-2009) and -2.7±0.7 (-1.6±0.2) PgC yr^{-1} for the 2010s (2010-2019. A large fraction of the interannual variability in global CO_2 flux anomaly originate over the tropical land regions, induced by El-Nio Southern oscillation. Sensitivity studies, based different prior flux uncertainty, different set of prior fluxes, and different data network including ship-based measurements and JAL/NIES CONTRAIL aircraft data, are conducted to get the uncertainty range in the estimated fluxes.

Keywords: Inverse modelling, CO2 flux, ENSO

©2021. Japan Geoscience Union. All Right Reserved.

Changes in the atmospheric CO_2/CH_4 variability in the East Asian outflow region caused by plummet of fossil fuel-derived CO_2 in China due to COVID-19 outbreak

*Yasunori Tohjima[1], Prabir Patra[2], Yosuke Niwa[1], Hitoshi Mukai[1], Motoki Sasakawa[1], Toshinobu Machida[1], Shin-ichiro Nakaoka[1]

1. National Institute for Environmental Studies, 2. Japan Agency for Marine-Earth Science and Technology

To prevent the spread of the new coronavirus (COVID-19) in China, the government of China imposed a nationwide lockdown and strict restrictions on the inter-city transport and socio-economic activity during the period from the end of January through March in 2020. Such restrictions were expected to significantly reduce the fossil-fuel-derived CO_2 ($FFCO_2$) emissions from China during the above period. Previous study revealed that the ratio of the synoptic-scale variability between CO_2 and CH_4 ($\Delta CO_2/\Delta CH_4$) observed in the downwind region of the East Asian continent reflected the emission ratio of the source region. Accordingly, since the restrictions would not cause any immediate effects on the CH4 emissions in China, the atmospheric observations in the downwind region would detect the significant reduction of $\Delta CO_2/\Delta CH_4$ ratio during the restriction period.

The National Institute of Environmental Studies (NIES) has been monitoring the atmospheric greenhouse gases including CO_2 and CH_4 mainly in the Asia Pacific region by using variety of platforms including ground sites, commercial cargo ships, and passenger airplane. The continental marginal region of the East Asia corresponds to the outflow region of the continental emissions during the period from late fall through early spring because of the East Asian monsoon. In this presentation, we examined the temporal or spatial variability ratio between the atmospheric CO_2 and CH_4 mole fractions obtained from continuous measurements at Hateruma Island (HAT; lat. 24.1˚N, long. 123.8˚E), in-situ measurements aboard cargo ships sailing between Japan and Southeast Asia, and airplane sampling over Shanghai. For example, the monthly mean ratio of the synoptic scale variations between CO_2 and CH_4 observed at HAT in February 2020 showed significant decrease in comparison with those observed in the previous decadal period (2010-2019). The decrease in the $\Delta CO_2/\Delta CH_4$ ratio was well reproduced by the model simulation based on an atmospheric transport model (NICAM-TM) and a set of corresponding CO_2 and CH_4 fluxes when the $FFCO_2$ emissions from China reduced by 30%. The relationship between the atmospheric CO_2 and CH_4 observed over Shanghai and in the South and East China sea in February 2020 agreed well with the simulated relationship with the similarly reduced $FFCO_2$ emissions from China. These results show the utility of high-precision measurements of CO_2 and CH_4 to detect signals from the emission change from specific regions.

Keywords: COVID-19 outbreak, lockdown, atmospheric CO2, atmospheric CH4, synoptic-scale variation

©2021. Japan Geoscience Union. All Right Reserved.

Impact of anomalous high temperature anomaly in the 2020 spring-summer on terrestrial environment across Siberia

*Kazuhito Ichii[1], Riku Kawase[1], Yuhei Yamamoto[1], Shunji Kotsuki[1]

1. Chiba University

Siberia has been experiences one of the most distinct warming trends across global, and this tendency will continue in future. Among the effects of global climate change, extreme climate anomaly is one of the important issues. Siberia experienced anomalous high temperature in 2020 spring to summer. However, the effects of the anomaly on terrestrial environment have not been studied so far. In this study, we analyzed multiple satellite remote sensing datasets/products and model outputs to understand the response of terrestrial environment to the warming. We detected clear positive anomaly in land surface temperature, and it exceeds over five degree above long-term (20 years) mean based on MODIS products. Snow cover duration also show much earlier snowmelt (e.g. one month) compared with the normal. NDVI and LAI also consistently shows positive anomalies in March to June seasons. Gross primary productivity (GPP) also shows 10-20% larger than those of normal years. We will report further progress on this analysis, including river outflow, whole carbon cycle (including resporation). Further analysis is expected to include greenhouse gas observing satellite data, such as GOSAT, to detect carbon atmospheric CO2 concentration signals.

Keywords: Siberia, extreme climate event, Terrestrial environment, Remote Sensing

©2021. Japan Geoscience Union. All Right Reserved.

CH_4 surface flux estimation based on local ensemble transform Kalman filter

*Jagat Bisht[1], Prabir Patra[1,2], Masayuki Takigawa[1], Takashi Sekiya[1], Yugo Kanaya[1], Naoko Saito[2]

1. Japan Agency for Marine-Earth Science and Technology , 2. Center for Environ. Remote Sensing, Chiba University

Methane (CH_4) is an important greenhouse gas which is substantially increased during last decade in the atmosphere, raising serious sustainability and climate change issues. With the advancement of satellite observations with global coverage, we aim to study the regional or country-wise contributions of CH_4 emissions to the global CH_4 increase. Present study attempts to estimate the CH_4 fluxes using Local Ensemble Transform Kalman Filter (LETKF) data assimilation technique. Since atmospheric CH_4 is primarily affected by surface fluxes, its variability should be large near the surface. We perform the sensitivity experiment on Observation System Simulation Experiment (OSSE) setting by updating observed changes only into the lower tropospheric CH_4. We also update the observed change into the full column my mimicking the GOSAT observations in the OSSE experiment. It has been found that LETKF is able to retrieve the true fluxes to a larger extent, from the perturbed emission intensities of 20 or 30% relative to the true flux over the East and South Asia regions. We have also found that longer assimilation window (at least 20 days long) is advantageous to CH_4 flux estimation.

©2021. Japan Geoscience Union. All Right Reserved.

Toward multi-scale greenhouse gas monitoring system for supporting global stock take

*Akihiko Ito[1,2], Yosuke Niwa[1], Tomohiro Hajima[2], Nobuko Saigusa[1]

1. National Institute for Environmental Studies, 2. Japan Agency for Marine-Earth Science and Technology

Achievement of the carbon-neutral society is one of the overarching tasks for the sustainability of humanity. Under the Paris Agreement of the United Nations Framework Convention of Climate Change, it becomes an important task for research community to establish a comprehensive, high-precision, and transparent system of greenhouse gas (GHG) budget estimation. In April 2021, a new task-force project will be launched in Japan to develop a GHG monitoring system, provisionally called the Comprehensive Observation and Modeling for Multi-scale Estimation of Greenhouse Gas budgetS (COMM-EGGS), funded by the Ministry of the Environment, Japan. This is a joint project of National Institute for Environmental Studies, Japan Agency for Marine-Earth Science and Technology, Chiba University, and Meteorological Research Institute. The project is composed of three research components: 1) observation and top-down estimation of GHG budget, 2) evaluation of GHG mitigation with an Earth system model, and 3) bottom-up estimation of GHG budget. These activities cover different spatial scales spanning from major city to national and global emissions, by using ground observatory, aircraft, and satellite observations and fine-mesh atmospheric and surface emission models. In the project, we put emphasis on the Asia-Pacific region, in which a comprehensive GHG monitoring system is deficient to date. Through mutual comparison and validation, we will make attempt to improve confidence of the estimation system for GHG budget verification. Finally, the system aims at contributing to the Global Stocktake of the Paris Agreement by providing scientific evidence for GHG emission reduction.

Keywords: Global Warming, Paris Agreement, Greenhouse Gas Budget

©2021. Japan Geoscience Union. All Right Reserved.

[E] Oral | A (Atmospheric and Hydrospheric Sciences)：A-CG Complex & General

Sat. Jun 5, 2021 10:45 AM - 12:15 PM JST | Sat. Jun 5, 2021 1:45 AM - 3:15 AM UTC | Ch.08 Zoom Room 08

[A-CG34] Global Carbon Cycle Observation and Analysis

convener:Kazuhito Ichii(Chiba University), Prabir Patra(Research Institute for Global Change, JAMSTEC), Akihiko Ito(National Institute for Environmental Studies), Chairperson:Kazuhito Ichii(Chiba University), Akihiko Ito(National Institute for Environmental Studies)

The Paris Agreement under the United Nations Framework Convention on Climate Change (UNFCCC) is a landmark agreement, which aims at reduction of greenhouse gases (GHGs) emission to keep the global warming below 2 deg C. The national commitments and progresses should be carefully monitored and verified by international bodies using different but complementary methodologies.

Many observation and technique to monitor GHGs budget have been improved in recent years. The improvements include observational platforms for monitoring atmospheric GHGs, national or regional emission inventories, top-down estimations (e.g. atmospheric inverse analysis), and bottom-up estimations (e.g. process-based models). However, due to uncertainties in sparse observation network and integration methods, large uncertainty remains in GHGs sources/sinks estimations at global and regional scales.

The purpose of the session is to discuss state-of-the-art techniques for estimations of GHGs (e.g. CO2, CH4, N2O) budget at global and regional scales. The topic includes natural and anthropogenic processes, various methodologies (e.g. in-situ observation, aircraft monitoring, remote sensing, modeling), and various targets (e.g. atmosphere, terrestrial, and ocean), various spatial and temporal coverage (e.g. regional to global scales and past-present-future). Improved estimates of emissions from land use change, forest fires, and other anthropogenic sources (urban developments and thermal power station etc.) are also of interest. We also welcome discussions for designs and plans for future studies targeting city and country scale emission estimations using sophisticated modeling tools and inventories.

10:45 AM - 11:00 AM JST | 1:45 AM - 2:00 AM UTC

[ACG34-07] Co-evolution of carbon cycle and air quality fluxes constrained by CMS-Flux and MOMO-Chem assimilation systems

★Invited Papers

*Kevin W Bowman[1], Kazuyuki Miyazaki[1], Junjie Liu[1], Anthony Bloom[1] (1.Jet Propulsion Laboratory)

11:00 AM - 11:15 AM JST | 2:00 AM - 2:15 AM UTC

[ACG34-08] Lower anthropogenic fossil CH_4 emissions inferred from multi-isotopic constraints on the global CH_4 budget

★Invited Papers

*Ryo Fujita[1,2], Heather Graven[2] (1.Meteorological Research Institute, 2.Imperial College London)

11:15 AM - 11:30 AM JST | 2:15 AM - 2:30 AM UTC

[ACG34-09] The burned area extracting in Chernobyl Exclusion Zone using random forest

*JUN HU[1], Shunji Kotsuki[1], Yasunori IGARASHI[2], Mykola TALERKO[3], Kazuhito Ichii[1] (1.Center for Environmental Remote Sensing, Chiba University, Chiba, Japan, 2.Institute of Environmental Radioactivity, Fukushima University, Fukushima, Japan, 3.Institute for Safety Problems of Nuclear Power Plants, National Academy of Sciences of Ukraine, Kyiv, Ukraine)

11:30 AM - 11:45 AM JST | 2:30 AM - 2:45 AM UTC

[ACG34-10] Monitoring and evaluation of carbon absorption in pasture areas near Ulaanbaatar and far from cities

*Qinxue Wang[1], Tomohiro OKADERA[1], Masataka WATANABE[2], Ochirbat Batkhishig[3] (1.National Institute for Environmental Studies, 2.Research and Development Initiative, 3.Institute of Geography and

Geoecology, Mongolian Academy of Sciences)

11:45 AM - 12:00 PM JST | 2:45 AM - 3:00 AM UTC

[ACG34-11] An observation-based reconstruction reveals progressive ocean acidification around Japan

*Yosuke Iida[1], Takashi Nakamura[1], Yoshikazu Fukuda[1], Masao Ishii[2] (1.Japan Meterological Agency, 2.Meteorological Research Institute)

12:00 PM - 12:15 PM JST | 3:00 AM - 3:15 AM UTC

[ACG34-12] Trend in Southern Ocean CO_2 sink – a review and outlook

*Prabir Patra[1], Naveen Chandra[2], Pedro S Monteiro[3], Masao Ishii[4] (1.Research Institute for Global Change, JAMSTEC, 2.National Institute for Environmental Studies, 3.CSIR-CHPC, South Africa, 4.Meteorological Research Institute)

Co-evolution of carbon cycle and air quality fluxes constrained by CMS-Flux and MOMO-Chem assimilation systems

*Kevin W Bowman[1], Kazuyuki Miyazaki[1], Junjie Liu[1], Anthony Bloom[1]

1. Jet Propulsion Laboratory

Rapid regional changes in anthropogenic emissions in response to the COVID-19 pandemic have underscored the contribution of fossil fuel (FF) emission uncertainty to regional carbon budgets. Typical methods for spatially-explicit FF emissions are dependent on national reporting, which can incur substantial latencies. However, the concomitant changes in short-lived pollutants from common emission sources point to opportunities to develop independent low-latency estimates of fossil fuel emissions and to better understand anthropogenic processes. Here we combine state-of-the-art Multiple Model Multi Constituent chemical data assimilation system (MOMO-Chem) with bottom-up FF emissions to repartition the net carbon fluxes from the NASA Carbon Monitoring System Flux (CMS-Flux) project. To that end, we implement a novel Kalman filtering algorithm that predicts emission ratio co-evolution of air quality (AQ) and carbon species. Based upon top-down estimates of AQ emissions, FF CO2 emissions and uncertainties can be rapidly determined. We show overall good agreement between predicted FF fluxes and the latest bottom-up inventories. These data are in turn used to interpret the decadal evolution of CMS-Flux net carbon exchange. This approach is an important step in quantifying both regional fossil fuel and natural carbon fluxes contributions to the atmospheric CO2 growth rate.

©2021. Japan Geoscience Union. All Right Reserved.

Lower anthropogenic fossil CH_4 emissions inferred from multi-isotopic constraints on the global CH_4 budget

*Ryo Fujita[1,2], Heather Graven[2]

1. Meteorological Research Institute, 2. Imperial College London

Stable isotope measurements of atmospheric CH_4 ($\delta^{13}C\text{-}CH_4$, $\delta D\text{-}CH_4$) have been utilized to resolve major three CH_4 sources (i.e., biogenic, fossil fuel, and biomass burning sources) in the global CH_4 budget. However, given the uncertainty of both the source isotope signatures and kinetic isotope effects, recent estimates of the global CH_4 budget using stable isotope observations are still inconclusive. Radiocarbon measurements ($\Delta^{14}C\text{-}CH_4$) could provide stronger additional constraint on the fossil-fuel CH_4 sources (i.e., ^{14}C-free), but the uncertainty of $^{14}CH_4$ emissions from nuclear power facilities and a lack of data have limited such utilization. Here we present a new approach to estimate plausible global CH_4 emissions and sinks scenarios over 1750–2015 using historical observations and Monte Carlo simulations of atmospheric CH_4, $\delta^{13}C\text{-}CH_4$, $\delta D\text{-}CH_4$, and $\Delta^{14}C\text{-}CH_4$. We utilize a particle filter (or Sequential Monte Carlo filter) approach to optimize the key 19 parameters of global CH_4 sources and sinks. The ensemble members of CH_4 source and sink scenarios, generated by the ensembles of 19 parameter combinations considering their uncertainties, were used to simulate atmospheric CH_4, $\delta^{13}C\text{-}CH_4$, $\delta D\text{-}CH_4$, and $\Delta^{14}C\text{-}CH_4$, and then retained when matching the historical observations. Our multi-isotopic model-data analysis suggests that current bottom-up estimates in natural and anthropogenic fossil and natural biogenic CH_4 emissions are too high, whereas those in anthropogenic biogenic and biomass burning emissions are too low. The estimated global total fossil emission is also lower than the recent $\Delta^{14}C\text{-}CH_4$ -derived top-down estimates, but an independent estimate of global nuclear $^{14}CH_4$ emissions would rather support our result. To obtain more robust estimates from multi-isotopic model-data analysis, many more global background observations of atmospheric $\delta^{13}C\text{-}CH_4$, $\delta D\text{-}CH_4$, and $\Delta^{14}C\text{-}CH_4$, with their inter-laboratory measurement differences reduced, are indispensable to characterize their global representatives.

Keywords: methane, isotope, GHGs, carbon cycle, atmospheric chemistry

©2021. Japan Geoscience Union. All Right Reserved.

The burned area extracting in Chernobyl Exclusion Zone using random forest

*JUN HU[1], Shunji Kotsuki[1], Yasunori IGARASHI[2], Mykola TALERKO[3], Kazuhito Ichii[1]

1. Center for Environmental Remote Sensing, Chiba University, Chiba, Japan, 2. Institute of Environmental Radioactivity, Fukushima University, Fukushima, Japan, 3. Institute for Safety Problems of Nuclear Power Plants, National Academy of Sciences of Ukraine, Kyiv, Ukraine

The Chernobyl Nuclear Power Plant (CNPP) accident that happened in 1986 is the largest source of anthropogenic radionuclides released into the environment in history. In recent 20 years, the climate and land-use changes have increased the frequency of large forest fires in and around the Chernobyl Exclusion Zone. It is critical to extract the burned areas accurately, because they are the basis to estimate the biomass burning emission and then analyze the second diffusion of radioactive residue released from the CNPP accident. In this study, we established a burned area extracting method based on the random forest (RF) algorithm using the Moderate Resolution Imaging Spectroradiometer (MODIS) MOD09GA / MYD09GA and LANDSAT -7 ETM+ /-8 OLI images. The field observation in 2015 and MODIS MOD14A1 (thermal anomaly data) product were adopted to generate sampling points for RF. The reflectance difference spectroscopy of near-infrared band and difference in vegetation indices (NDVI, NBR, NDWI) between pre- and post-fire imagery were used as input data for the RF classifier. Subsequently, the historical burned area in 2015 and 2020 were detected using the trained RF classifier. The preliminary results of the identified burned area show good consistency with the MODIS MCD64A1.006 product of NASA and FireCCI51product of ESA. It should be noted that our RF algorithm can even detect the relatively small fire scars compared to the two existing products due to the usage of high-resolution LANDSAT image.

Keywords: Wildfire, Chernobyl Exclusion Zone, Random forest, Satellite observation, Landsat, MODIS

©2021. Japan Geoscience Union. All Right Reserved.

Monitoring and evaluation of carbon absorption in pasture areas near Ulaanbaatar and far from cities

*Qinxue Wang[1], Tomohiro OKADERA[1], Masataka WATANABE[2], Ochirbat Batkhishig[3]

1. National Institute for Environmental Studies, 2. Research and Development Initiative, 3. Institute of Geography and Geoecology, Mongolian Academy of Sciences

To obtain the ground observation data to verify the data products derived from the greenhouse gas observation technology satellite (GOSAT) series, this study targets the carbon emission and absorption in Mongolia. For this purpose, we have established two flux towers to monitor the greenhouse gas CO2 in the pastures near Ulaanbaatar (Nalaikh site) and a vast grassland area far from cities (Hustai site), where the net ecosystem exchange (NEE) has been monitored by the eddy correlation method since 2015. To guarantee the accuracy of the measurement data, the accuracy of the CO2 analyzer was calibrated regularly by using standard gas.

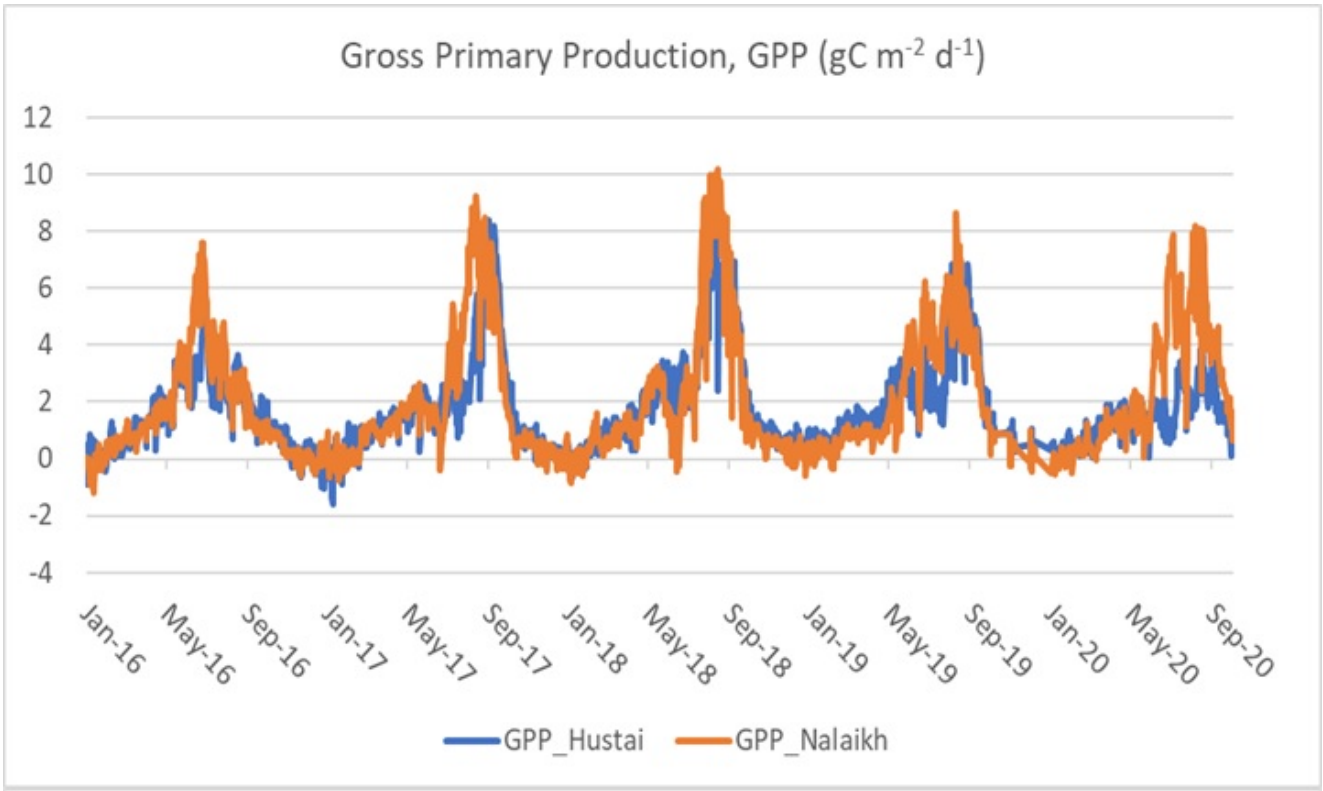
According to the meteorological data observed during 2016-2019, the daily average wind speeds at both sites are in the range of 1 to 10 m/s, but the annual averages are 2.4 m/s and 2.8 m/s at Hustai and Naliakh site, respectively. The temperature fluctuation range is -30 dgr. C to 30 dgr. C, and the annual fluctuation range is 60 dgr. C or more, but the annual average values are only 2.0 dgr. C and -1.6 dgr. C, respectively. Annual precipitation is 193.6 mm at the Hustai site and 165.7 mm at the Nalaikh site. Looking at the heat balance measured at both sites, we found that the net radiant flux (Rn) is in the range of -50 to 200 W m-2, and the annual average is 59.6 W m-2 at the Hustai site and 60.6 W m-2 at the Nalaikh site, which is almost the same. The soil heat flux is in the range of -30 to 30 W m-2, and the annual average values are 0.8 W m-2 and 1.9 W m-2, respectively. The annual averages of sensible heat are 28.1 W m-2 and 28.2 W m-2, respectively, which are almost the same, but the latent heat is 20.3 W m-2 and 25.6 W m-2, respectively.

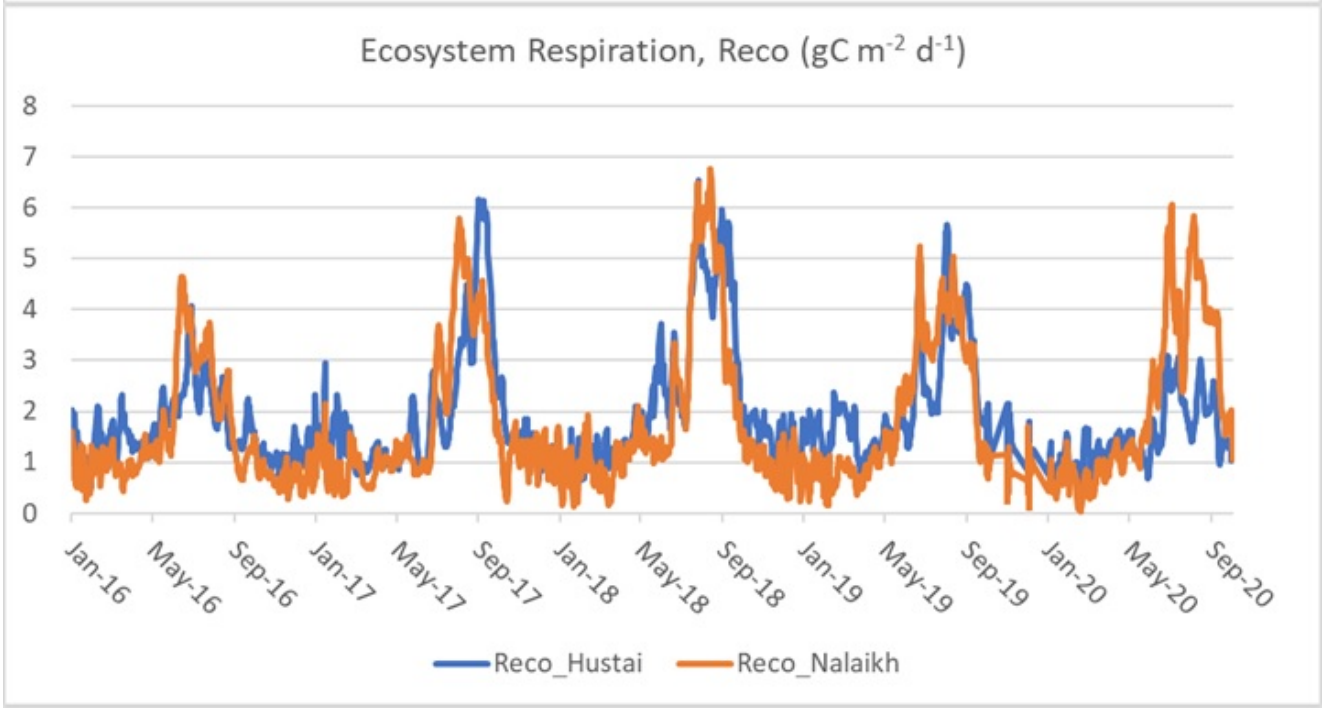
Finally, the net ecosystem exchanges (NEE) measured at both sites were analyzed using EddyPro 7 and ToviTM which were jointly developed by LI-COR in the United States and the related research communities. These tools are developed for analyzing carbon absorption, so-called gross primary production (GPP), respiration by ecosystems (RECO) as well as net absorption (NEP=GPP-RECO). The results of daily variation of GPP, RECO, and NEP are shown in Fig. 1. Further analysis shows that, first, only looking into the growing seasons of grassland, GPP at Hustai and Nalaikh site is 527.2 gC m-2 y-1 and 599.2 gC m-2 y-1, respectively, and RECO are 457.2 gC m-2 y-1 and 446.2 gC m-2 y-1, respectively. As a result, the NEP are 87.4 gC m-2 y-1 and 152.5 gC m-2 y-1, respectively, which means both sites are carbon sinks, and about 1.7 times larger at the Nalaikh site than the Hustai site. On the other hand, when we count together both the growing seasons and the non-growing seasons, the annual GPP at two sites are 686.0 gC m-2 y-1 and 654.9 gC m-2 y-1, respectively, and RECO are 700.1 gC m-2 y-1 and 611.8 gC m-2 y-1, respectively. As a result, the annual NEP are -45.2 gC m-2 y-1 and 74.3 gC m-2 y-1, respectively, which means the grassland at the Nalaikh site is a carbon sink, but it is a carbon source at the Hustai site throughout the year. Here, the large uncertainty in the non-growing seasons may be influenced not only by the error of equipment due to freezing but also by the influence of carbon emissions from cities and residents nearby.

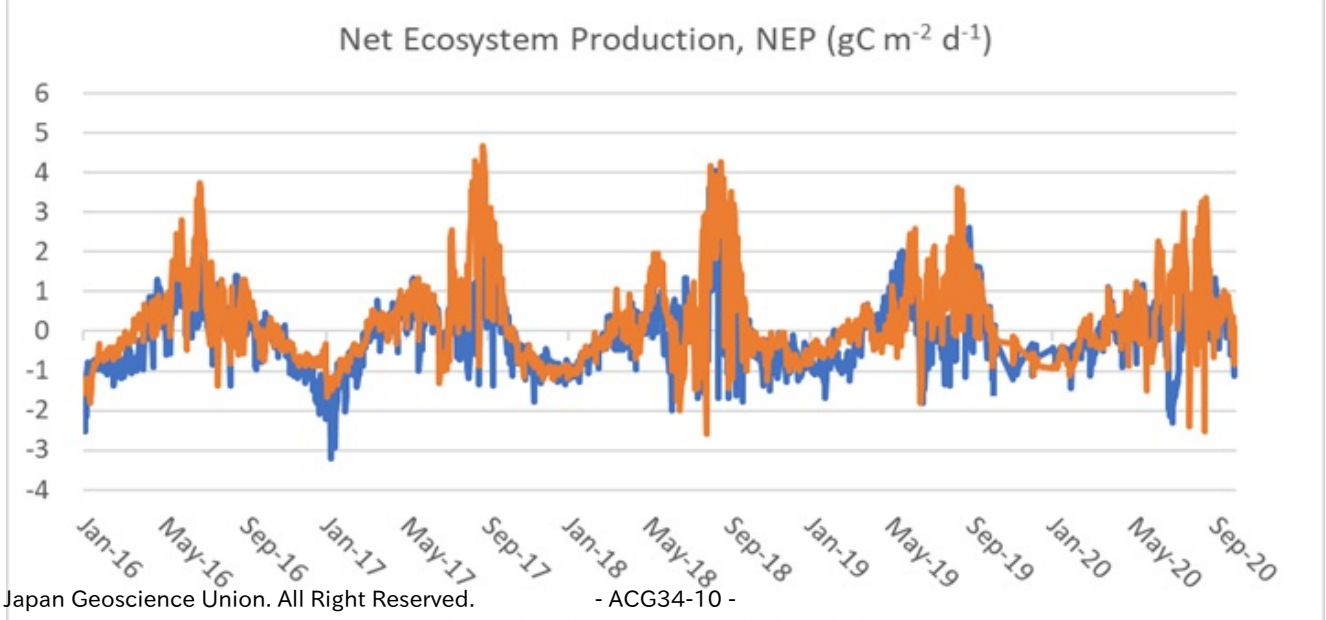
Keywords: carbon absorption, pasture area, Mongolia

©2021. Japan Geoscience Union. All Right Reserved.

©2021. Japan Geoscience Union. All Right Reserved.







©2021. Japan Geoscience Union. All Right Reserved.

©2021. Japan Geoscience Union. All Right Reserved.

An observation-based reconstruction reveals progressive ocean acidification around Japan

*Yosuke Iida[1], Takashi Nakamura[1], Yoshikazu Fukuda[1], Masao Ishii[2]

1. Japan Meterological Agency, 2. Meteorological Research Institute

Ocean acidification caused by anthropogenic carbon has reduced ecosystem service of our ocean through its adverse impacts on the chemistry and biology in the seawater. Recent studies have well revealed the increase of carbon in the surface seawaters in global open ocean to coastal zones (Bates et al. 2014, Landschützer et al. 2020), and also have clarified progress of coastal ocean acidification in Japan (Ishizu et al. 2019). The results of these studies imply that the ocean ecosystem service is ubiquitously under threat, of course in the seas around Japan. To frame comprehensive ocean policy that would address the threat, it is necessary for us to recognize how vulnerable our sea is. We investigated the rates of pH decrease in the seas around Japan based on surface ocean carbon measurements, which can provide information on a science basis of ocean vulnerability for progressive acidification. We reconstructed monthly pH fields around Japan by 0.25 degrees latitude and longitude by using a moving-window multiple linear regression method. The sea around Japan as a whole has decreased its pH value by −0.021/decade during the period 1998-2020 (Figure), similar to that for the global ocean (−0.016/decade CMEMS 2020; −0.018/decade MEXT and JMA 2020). Japan’ s global indicator of SDG 14.3, based on winter pH values observed along the 137°E meridian, is 8.096 in 2010 and 8.070 in 2020 (Japan SDGs Action Platform 2021). The pH value averaged over the sea around Japan of 8.103 in 2010 and 8.083 in 2020 estimated in this study, in which the regional and seasonal variability were considered, could provide information to support the indicator. The estimated rates of pH decreases have regional differences, −0.027/decade in the Sea of Japan whereas −0.019/decade in the seas around Kyushu and Okinawa, and what controls the variations is to be investigated. We can obtain the fields of seawater pCO_2 as well from the same method as used in reconstructing pH fields, which potentially be used for evaluating sea-air CO_2 flux and carbon sink in the seas around Japan in combination with a proper atmospheric CO_2 product.

References

Bates et al. 2014: Oceanography, 27, 126–141
CMEMS 2020: https://marine.copernicus.eu/science-learning/ocean-monitoring-indicators
Ishizu et al. 2019: Biogeosciences, 16, 4747–4763
Japan SDGs Action Platform 2021: https://www.mofa.go.jp/mofaj/gaiko/oda/sdgs/statistics/index.html
Landschützer et al. 2020: Earth Syst. Sci. Data, 12, 2537–2553
MEXT and JMA 2020: https://www.data.jma.go.jp/cpdinfo/ccj/index.html

Keywords: carbon cycle, ocean acidification, the seas around Japan, SDGs

©2021. Japan Geoscience Union. All Right Reserved.

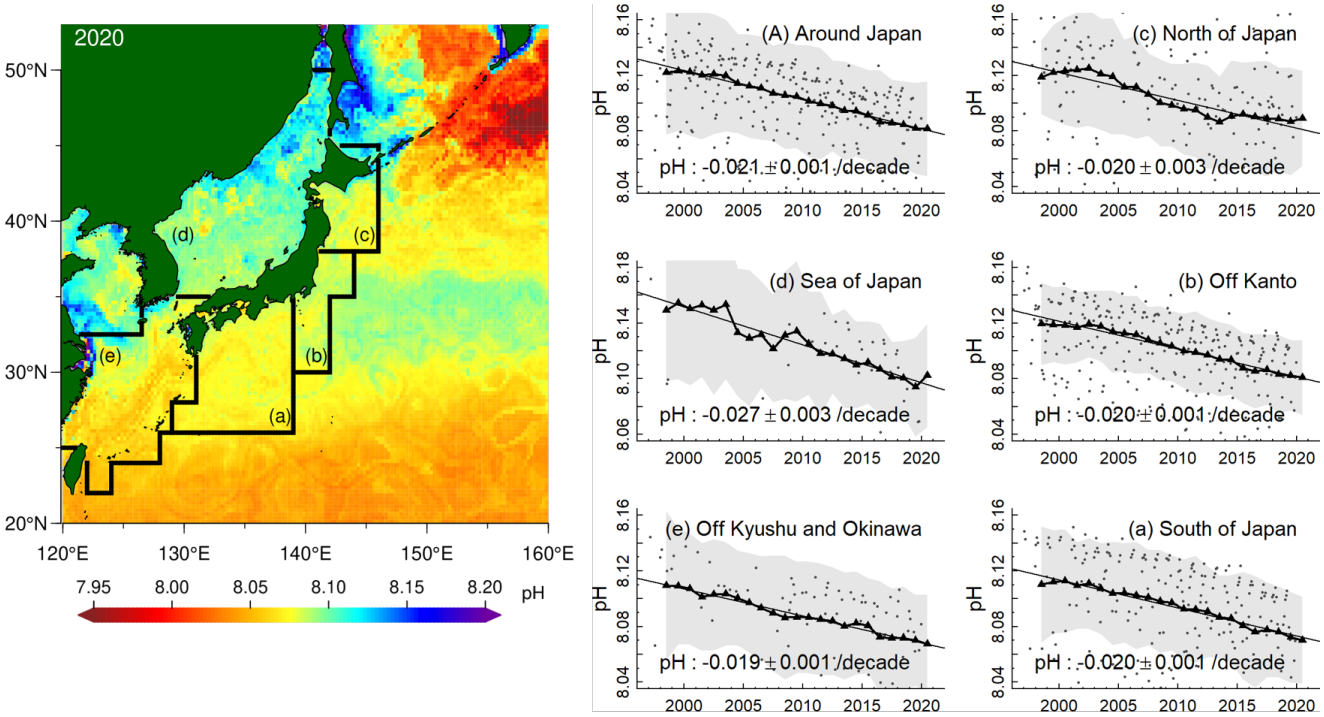


Figure The map left shows pH distribution around Japan averaged in 2020 and the time-series right shows the annual pH anomaly averaged over the area bordered by black lines in the left map (a-e). The triangles of the right indicate annual mean pH values and the color-shaded means spatial variance (1σ). The thin line indicates the long-term trend of the values and small plots show observed pH values.

©2021. Japan Geoscience Union. All Right Reserved.

Trend in Southern Ocean CO_2 sink –a review and outlook

*Prabir Patra[1], Naveen Chandra[2], Pedro S Monteiro[3], Masao Ishii[4]

1. Research Institute for Global Change, JAMSTEC, 2. National Institute for Environmental Studies, 3. CSIR-CHPC, South Africa, 4. Meteorological Research Institute

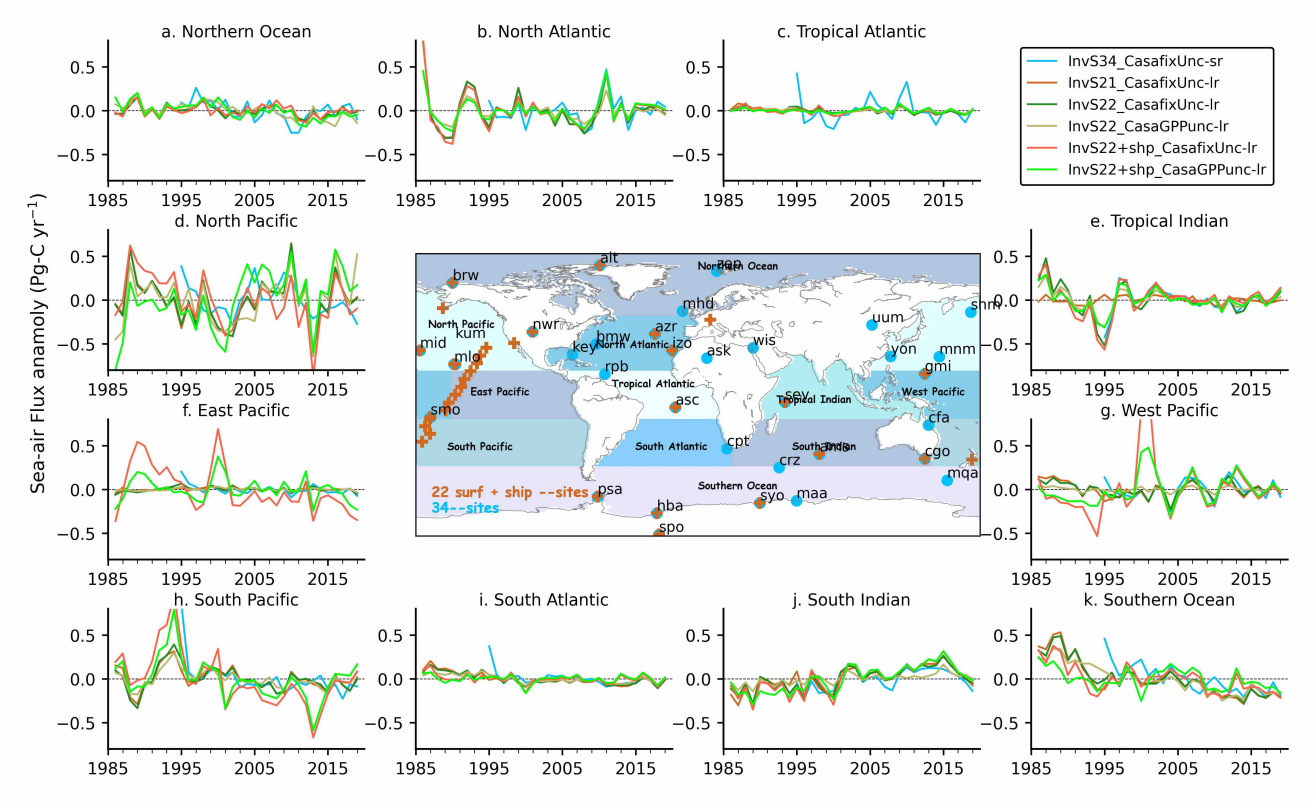
The Southern Ocean (south of 14°S) has played significant role in removing carbon dioxide (CO_2) from the atmosphere in the past decades. There several studies which discussed a slowing down of CO_2 uptake rate or even an opposite trend in CO_2 uptake since the late 1980s through the early 2000s, in contrast to that is expected from the pCO_2 increase in the atmosphere and the ocean biogeochemical models. The JAMSTEC' s inverse model, based on MIROC4-ACTM forward simulations, climatological sea-air CO_2 flux and atmospheric CO_2 observations, shows more or less systematic increase in sink uptake since the late 1980s to the present. We suspect there are issues with data coverage with time that is posing challenges in the pCO_2 observation based upscaling products; and for the global ocean biogeochemical models difficulty in the simulation of seasonal cycle of sea-air pCO_2 difference may inadvertently lead to a wrong climate sensitivity.

In this presentation, we will review some of these issues and possibly come up with a revised assessment of the trends in Southern Ocean CO_2 flux.

The figure below shows the CO_2 flux anomalies calculated by 6 cases of MIROC4-ACTM inversions, by varying the prior flux model (flxUnc vs GPPunc) or network of CO_2 observations (S34, S22, S22+ship). Although the magnitude of flux anomalies vary between the inversions, the long-term trends and phase of the variability are consistently derived for the overlapping inversion periods.

Keywords: Southern Ocean CO2 flux, Inverse modelling, Global ocean CO2 flux models

©2021. Japan Geoscience Union. All Right Reserved.



©2021. Japan Geoscience Union. All Right Reserved.

[E] Poster | A (Atmospheric and Hydrospheric Sciences)：A-CG Complex & General

Sat. Jun 5, 2021 5:15 PM - 6:30 PM JST | Sat. Jun 5, 2021 8:15 AM - 9:30 AM UTC | Ch.08_2

[A-CG34] Global Carbon Cycle Observation and Analysis

convener:Kazuhito Ichii(Chiba University), Prabir Patra(Research Institute for Global Change, JAMSTEC), Akihiko Ito(National Institute for Environmental Studies)

The Paris Agreement under the United Nations Framework Convention on Climate Change (UNFCCC) is a landmark agreement, which aims at reduction of greenhouse gases (GHGs) emission to keep the global warming below 2 deg C. The national commitments and progresses should be carefully monitored and verified by international bodies using different but complementary methodologies.

Many observation and technique to monitor GHGs budget have been improved in recent years. The improvements include observational platforms for monitoring atmospheric GHGs, national or regional emission inventories, top-down estimations (e.g. atmospheric inverse analysis), and bottom-up estimations (e.g. process-based models). However, due to uncertainties in sparse observation network and integration methods, large uncertainty remains in GHGs sources/sinks estimations at global and regional scales.

The purpose of the session is to discuss state-of-the-art techniques for estimations of GHGs (e.g. CO2, CH4, N2O) budget at global and regional scales. The topic includes natural and anthropogenic processes, various methodologies (e.g. in-situ observation, aircraft monitoring, remote sensing, modeling), and various targets (e.g. atmosphere, terrestrial, and ocean), various spatial and temporal coverage (e.g. regional to global scales and past-present-future). Improved estimates of emissions from land use change, forest fires, and other anthropogenic sources (urban developments and thermal power station etc.) are also of interest. We also welcome discussions for designs and plans for future studies targeting city and country scale emission estimations using sophisticated modeling tools and inventories.

[ACG34-P01] Asian methane outflow captured by the CONTRAIL flask air samplings

*Yosuke Niwa[1,2], Toshinobu Machida[1], Taku Umezawa[1], Kazuhiro Tsuboi[2], Kentaro Ishijima[2], Ryo Fujita[2], Hidekazu Matsueda[3], Takuya Saito[1] (1.National Institute for Environmental Studies, 2.Meteorological Research Institute, 3.Dokkyo University)

[ACG34-P02] High-resolution mapping of anthropogenic CO_2 emissions in Japan

*Makoto Saito[1], Hiroko Yamada[1] (1.National Institute for Environmental Studies)

[ACG34-P03] Estimating solar-induced chlorophyll fluorescence using process-based ecosystem model VISIT-SIF

*Tatsuya Miyauchi[1], Makoto Saito[1], Hibiki M. Noda[1], Yukio Yoshida[1], Haruki Oshio[1], Akihiko Ito[1], Tsuneo Matsunaga[1] (1.National Institute for Environmental Studies)

[ACG34-P04] Estimation of Aerosol Optical Characteristics of Wildfires in 2018 - 2020 with GCOM-C/SGLI

*Kazuhisa Tanada[1], Hiroshi Murakami[1] (1.Earth Observation Research Center, Japan Aerospace Exploration Agency)

[ACG34-P05] Satellite-data based monitoring of changes in the terrestrial carbon cycle in Mongolia: Synthesis analysis

*ZAYA MART[1], Ichii Kazuhito [1], Tsolmon Renchin[2] (1.Chiba University , 2.National University of Mongolia)

[ACG34-P06] Changes in terrestrial vegetation activities observed by satellite-based products across Eurasia

*Da WANG[1], Kazuhito Ichii[1] (1.Chiba University)

Asian methane outflow captured by the CONTRAIL flask air samplings

*Yosuke Niwa[1,2], Toshinobu Machida[1], Taku Umezawa[1], Kazuhiro Tsuboi[2], Kentaro Ishijima[2], Ryo Fujita[2], Hidekazu Matsueda[3], Takuya Saito[1]

1. National Institute for Environmental Studies, 2. Meteorological Research Institute, 3. Dokkyo University

Methane (CH_4) is one of important greenhouse gases. A large part of the global CH_4 emission exists in Asia with various kinds of sources such as fossil fuel exploitation, wetland, rice cultivation and biomass burning. Estimating and monitoring those Asian CH_4 emissions are imperative for better understanding of the growth of the atmospheric CH_4 and for developing a strategy to mitigate CH_4 emissions. Atmospheric observations over the western North Pacific, at the downwind side of Asia, have frequently captured CH_4 -rich outflows from the Asian continent. From those elevated CH_4 concentrations, we could obtain useful information of CH_4 emissions in Asia. Especially, sporadic high CH_4 concentrations observed in the upper troposphere during the summer monsoon season are noteworthy because they are largely contributed by biogenic sources that are increased in the summer. Biogenic CH_4 emissions have distinct seasonal variations in response to variations of temperatures and precipitations, and also have a significant role in interannual variations of the atmospheric CH_4. In fact, the commercial aircraft observation project named CONTRAIL has observed notably elevated CH_4 concentrations in the upper troposphere during summer by flask air sampling measurements along Japan-East/Southeast Asia routes. However, the transport mechanism of such a CH_4 outflow is still unclear. Furthermore, the fossil fuel exploitation and other sources that constantly emit CH_4 through a whole year could also contribute the summer CH_4 elevations, which complicates quantitative estimation of the biogenic sources. In this study, the atmospheric transport model NICAM-TM is used to elucidate transport pathways and origins of CH_4 outflows that reach the upper troposphere over the western North Pacific. Furthermore, using simultaneous observations of other chemical species such as ethane (C_2H_6) are used to separate contributions of biogenic sources of CH_4.

Keywords: methane, Asia, aircraft, atmospheric transport model

©2021. Japan Geoscience Union. All Right Reserved.

High-resolution mapping of anthropogenic CO_2 emissions in Japan

*Makoto Saito[1], Hiroko Yamada[1]

1. National Institute for Environmental Studies

Fossil fuel combustion is a main contributor of increasing atmospheric carbon dioxide (CO_2) concentration. Fossil fuel CO_2 ($FFCO_2$) emission inventories have been usually compiled for global and national scales. However, evaluation of local climate action for global warming necessitates quantifying the $FFCO_2$ emissions from cities, which are responsible for more than 70% of the global $FFCO_2$, with more detailed information on temporospatial distribution of the emission at sub-city levels. This study proposes a new $FFCO_2$ emission inventory using a bottom-up approach for whole area in Japan. The emission inventory consists of the emissions from 3 sources: point (electricity generation, waste incineration, civil aviation, and waterborne navigation sectors); line (road transport sector); and area (industrial and commercial, residential, and agricultural machinery sectors) sources with 1 km spatial resolution and monthly temporal resolution. The emissions for each sector were calculated based on the census data and the national statistical data. We will present the calculation methodology for our emission inventory and the results with comparison with other emission estimates.

Keywords: Anthropogenic CO2 emissions, Fossil fuel, Inventory

©2021. Japan Geoscience Union. All Right Reserved.

Estimating solar-induced chlorophyll fluorescence using process-based ecosystem model VISIT-SIF

*Tatsuya Miyauchi[1], Makoto Saito[1], Hibiki M. Noda[1], Yukio Yoshida[1], Haruki Oshio[1], Akihiko Ito[1], Tsuneo Matsunaga[1]

1. National Institute for Environmental Studies

Photosynthesis is a fundamental process of carbon fixation in terrestrial ecosystem and monitoring changes of photosynthetic activity is necessary to probe global carbon cycle. Solar-induced chlorophyll fluorescence (SIF) is known as a good index to monitor photosynthetic activity, and satellite-observed SIF is useful to improve global carbon cycle simulations by terrestrial ecosystem models. The forward model which can calculate SIF based on ecophysiological process is required for utilization of SIF for model parameter adjustment. Moreover model-simulated SIF needs to calculate the satellite observing proportion of total canopy SIF to compare satellite-observed SIF. We developed the process-based ecosystem model to estimate SIF based on VISIT model (VISIT-SIF). We incorporated biochemical process of SIF and geometric effect of observing direction to the model and assessed the reproducibility of SIF by comparing SIF simulated by VISIT-SIF with SIF observed by Greenhouse gases Observating SATellite (GOSAT). The annual mean global SIF by VISIT-SIF showed good agreement with one observed by GOSAT. The seasonal change of SIF in several regions by VISIT-SIF also showed good agreement with one by GOSAT. However, some region showed deference of phenological term. In our presentation, we will explain the model processes and results of comparing SIF by VISIT-SIF and GOSAT.

Keywords: Solar-induced chlorophyll fluorescence, Process based ecosystem model, Global carbon cycle, Satellite observation

©2021. Japan Geoscience Union. All Right Reserved.

Estimation of Aerosol Optical Characteristics of Wildfires in 2018 - 2020 with GCOM-C/SGLI

*Kazuhisa Tanada[1], Hiroshi Murakami[1]

1. Earth Observation Research Center, Japan Aerospace Exploration Agency

It is known that wildfires not only damage land ecosystems, but also have a great impact on the atmospheric environment due to the release of large amounts of CO2, aerosols and so on. Greenhouse gases such as CO2 are well known to have positive radiative forcing, however, aerosols from wildfires have both positive and negative radiation forcing potentials, which can perturb the global radiation balance. Therefore, it is important to investigate the aerosol optical characteristics of wildfires and estimate their radiative forcing in order to predict the future climatic impacts by wildfires.

GCOM-C (Global Change Observation Mission - Climate) called “SHIKISAI”, which is JAXA polar-orbit satellite, has been launched on 23 December 2017. In this work, we analyze the world’s wildfires that occurred after 2018 with the GCOM-C products. By comparing the characteristics of aerosols such as aerosol optical thickness (AOT), aerosol angstrom exponent (AE), and aerosol single scattering albedo (SSA), we visualize the difference between wildfire events. According to the results, we can suggest that the values of AE seem to depend on the latitude of the fire location. In addition, the values of SSA also slightly different for each event, which might be caused by the differences of the land cover and/or human activity and the like. In the future, we plan to estimate the radiative forcing for each event in order to understand the direct and indirect effects of wildfire aerosols.

Keywords: GCOM-C, SHIKISAI, SGLI, wildfire, aerosol, radiative forcing

©2021. Japan Geoscience Union. All Right Reserved.

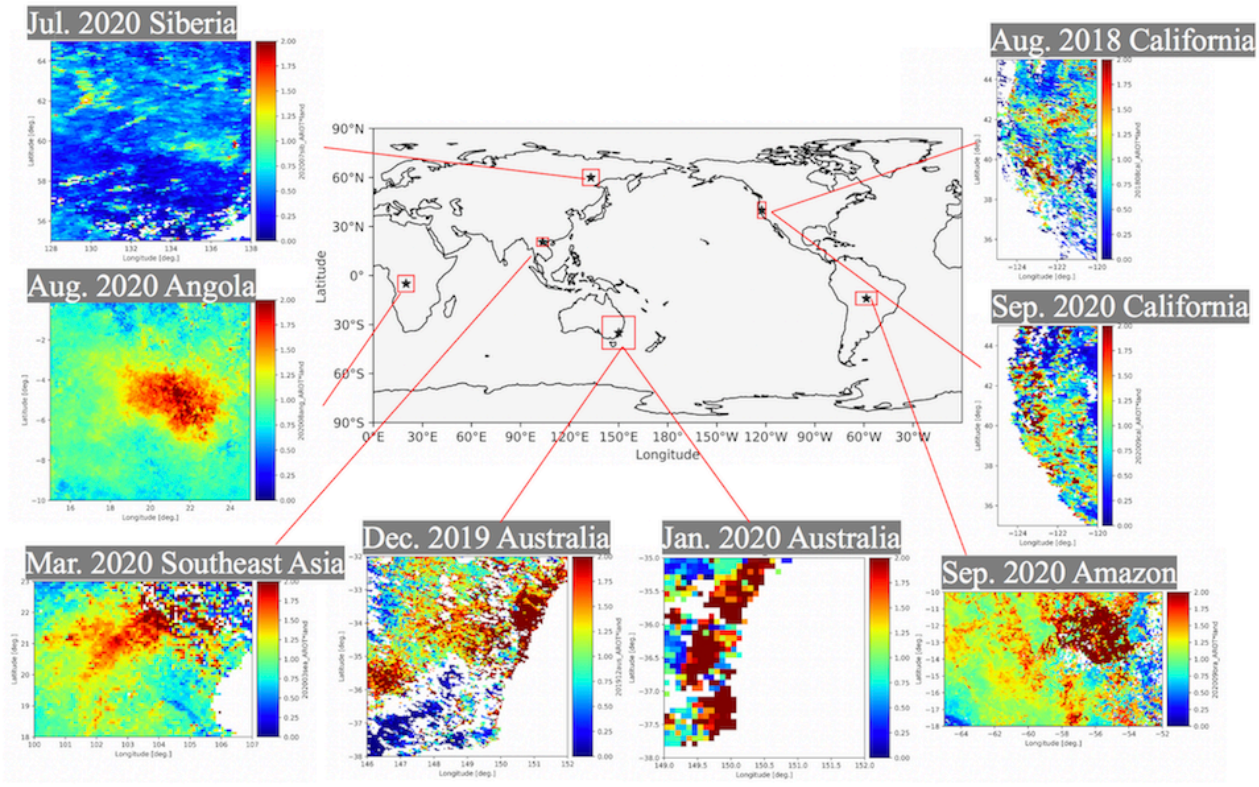


Fig. Estimated Aerosol Optical Thickness (AOT) over land for the world's wildfire events occurred after 2018. We use GCOM-C/SGLI's AOT products provided by JAXA.

©2021. Japan Geoscience Union. All Right Reserved.

Satellite-data based monitoring of changes in the terrestrial carbon cycle in Mongolia: Synthesis analysis

*ZAYA MART[1], Ichii Kazuhito [1], Tsolmon Renchin[2]

1. Chiba University , 2. National University of Mongolia

The terrestrial biosphere plays an important role in the global carbon cycle link with climate change, the main cause of global warming. Mongolian ecosystems are particularly vulnerable due to the relatively high altitude of the country and the continental semi-arid climate. Therefore, it is important to monitor environmental changes. So far, many studies have analyzed terrestrial vegetation changes in Mongolia using a single satellite-based vegetation index, datasets, such as MODIS and GIMMS datasets. However, synthesis analysis using ground observation, remote sensing, and ecosystem modeling is missing.

The purpose of this study is to show robust vegetation and terrestrial carbon cycle changes using multiple available datasets of climate, vegetation, and carbon cycles, covering ground observation, remote sensing datasets, and model outputs. This study covers periods from the 1980s to 2020.

Keywords: Carbon cycle, Remote sensing, Climate change

Satellite-data based monitoring of changes in terrestrial carbon cycle in Mongolia: Synthesis analysis

Mart Zaya[1], Kazuhito Ichii[1], Tsolmon Renchin[2]
1 "Center for Environmental Remote Sensing (CEReS), Chiba university, Chiba, Japan."
2 "NUM-ITC-UNESCO Space Science/Remote Sensing", National University of Mongolia, Ulaanbaatar, Mongolia

The terrestrial biosphere plays an important role in the global carbon cycle link with climate change, the main cause of global warming. Mongolian ecosystems are particularly vulnerable due to the relatively high altitude of the country and the continental semi-arid climate. Therefore, it is important to monitor environmental changes. So far, many studies have analyzed terrestrial vegetation changes in Mongolia using a single satellite-based vegetation index, datasets, such as MODIS and GIMMS datasets. However, synthesis analysis using ground observation, remote sensing, and ecosystem modeling is missing.
The purpose of this study is to show robust vegetation and terrestrial carbon cycle changes using multiple available datasets of climate, vegetation, and carbon cycles, covering ground observation, remote sensing datasets, and model outputs. This study covers periods from the 1980s to 2020.

©2021. Japan Geoscience Union. All Right Reserved.

Changes in terrestrial vegetation activities observed by satellite-based products across Eurasia

*Da WANG[1], Kazuhito Ichii[1]

1. Chiba University

Eurasia experienced significant temperature and precipitation changes, and these changes can affect terrestrial vegetation environments. So far, many studies analyzed satellite-based vegetation datasets using NOAA AVHRR and Terra and Aqua MODIS. Most studies focused on the years by 2015. Therefore, more updated analysis is required since more clear warning has been occurred. Therefore, in this study, we used multiple satellite datasets from 2000 to 2019 to understand the long-term trends of vegetation changes across Eurasia. We used multiple Terra and Aqua MODIS products and multiple climate datasets to understand changes in vegetation and potential causes of these vegetation changes.

Regions with increased NDVI are widely distributed in Eurasia. There is an increasing trend in 45.6% of the regions and a decreasing trend in 2.5% of the regions. NDVI increased significantly in Siberia, China, India, Turkey and western Russia. On the other hand, NDVI decreased in some parts of Central Asia such as the northwestern part of Kazakhstan. As a result of analyzing the rank correlation between NDVI and climate variables, the correlation between NDVI and temperature was high in Siberia, northeastern China and western Russia (NDVI-temperature: r = 0.66 (Siberia), r = 0.51 (northeast China), r = 0.55 (Western Russia)). On the other hand, there was a high correlation between NDVI and precipitation in southern China, India, Turkey and northwestern Kazakhstan (NDVI-precipitation: r = 0.35 (southern China), r = 0.48 (India), r = 0.52 (Turkey), r = 0.75 (northwestern Kazakhstan)). Thus, we clarified vegetation change trends and its potential mechanisms. As future plans, we will analyze the factors by adding parameters such as the amount of solar radiation, soil moisture, and human activities.

Keywords: remote sensing, NDVI, Eurasia

©2021. Japan Geoscience Union. All Right Reserved.

[J] Oral | A (Atmospheric and Hydrospheric Sciences)：A-CG Complex & General

Sat. Jun 5, 2021 1:45 PM - 3:15 PM JST | Sat. Jun 5, 2021 4:45 AM - 6:15 AM UTC | Ch.08 Zoom Room 08

[A-CG37] Biogeochemical cycles in Land Ecosystem

convener:Tomomichi Kato(Research Faculty of Agriculture, Hokkaido University), Kazuhito Ichii(Chiba University), Takeshi Ise(FSERC, Kyoto University), Munemasa Teramoto(Arid Land Research Center, Tottori University)

Terrestrial ecosystem influences global climate through cycles of water, carbon, and nitrogen between land surface and atmosphere. For better understanding of those behaviors, a great effort has been paid for developing varieties of approaches and techniques such as biometric survey, eddy and chamber methods, near and satellite remote sensing, biosphere modeling and so on.
In particular, the JapanFlux, founded in 2006 as a researchers network of CO2, H2O and other trace gas flux measurement, has promoted the multi-disciplinal studies not only for flux measurement community, but also for remote sensing and biosphere modeling communities. Moreover, the Research-Group-on-Integrated-Land-Processes, which was founded in 2006, also has contributed to build networks between Japanese researchers to better understanding of physical and biological processes on interactions between terrestrial surface and atmosphere.
This session unites those multi-disciplinal activities, and promotes the oral and poster presentations on the role of terrestrial ecosystem in material circulations of water, carbon, nitrogen, energy and other substances by any approaches and technics. This session takes over the former session in last year: A-CG54.

1:45 PM - 2:00 PM JST | 4:45 AM - 5:00 AM UTC

[ACG37-01] Temporal and spatial variation of soil CO_2/CH_4 fluxes in two cool-temperate forests in Japan

*Lifei Sun[1], Naishen Liang[1], Takashi Hirano[2], Yoshiyuki Takahashi [1], Munemasa Teramoto[3], Kentaro Takagi[2], Toshiaki Kondo[4], Jun Koarashi[5], Mariko Atarashi-Andoh[5], Reiko Ide[1], Xin Zhao[1], Sachinobu Ishida[6], Masahiro Takagi[7], Tomotsugu Yazaki[8] (1.National Institute for Environmental Studies Japan, 2.Hokkaido University, 3.Tottori University, 4.Japan International Research Center for Agricultural Sciences , 5.Japan Atomic Energy Agency , 6.Hirosaki University, 7.University of Miyazaki, 8.Meji University)

2:00 PM - 2:15 PM JST | 5:00 AM - 5:15 AM UTC

[ACG37-02] Decomposition of coarse woody debris produced through land conversion from a forest to an oil palm plantation

*Takashi Hirano[1], Shoko Murata[2], Guan Xhuan Wong[3], Joseph Wenceslaus Waili[3], Kim San Lo[3], Frankie Kiew[3], Edward Baran Aeries[3], Ryuichi Hirata[4], Tomohiro Shiraishi[4], Masato Hayashi[6], Masayuki Itoh[5], Lulie Melling[3] (1.Research Faculty of Agriculture, Hokkaido University, 2.Japan Science and Technology Agency, 3.Sarawak Tropical Peat Research Institute, 4.National Institute for Environmental Studies, 5.University of Hyogo, 6.Japan Aerospace Exploration Agency)

2:15 PM - 2:30 PM JST | 5:15 AM - 5:30 AM UTC

[ACG37-03] Anticipation of research development on the atmosphere-land interactions of the terrestrial nitrogen cycle

*Kentaro Hayashi[1] (1.Institute for Agro-Environmental Sciences, NARO)

2:30 PM - 2:45 PM JST | 5:30 AM - 5:45 AM UTC

[ACG37-04] Simulation of snow algal blooming in the global scale using a land surface model

*Yukihiko Onuma[1], Kei Yoshimura[1], Nozomu Takeuchi[2] (1.Institute of Industrial Science, The University of Tokyo, 2.Graduate School of Science, Chiba University)

2:45 PM - 3:00 PM JST | 5:45 AM - 6:00 AM UTC

[ACG37-05] Intercomparison of Data-Driven Estimation of Soil Respiration in Japan

*Hina Yamanuki[1], Kazuhito Ichii[1,2], Naishen Liang[2], Munemasa Teramoto[3], Yoshiyuki Takahashi[2], Jiye Zeng[2], Kentaro Takagi[4], Takashi Hirano[4], Sachinobu Ishida[5], Masahiro Takagi[6], Masaaki Naramoto[7], Kaneyuki Nakane[8], Toshiaki Kondo[9], Jun Koarashi[10], Mariko Atarashi-Andoh[10] (1.Center for Environmental Remote Sensing, Chiba University, 1-33 Yayoi-cho, Inage-ku, Chiba-shi, Chiba 263-8522, Japan, 2.Center for Global Environmental Research, National Institute for Environmental Studies, Tsukuba, Ibaraki 305- 8506, Japan, 3.Arid Land Research Center, Tottori University, 1390 Hamasaka, Tottori, Tottori 680-0001, Japan, 4.Hokkaido University, Kita 8, Nishi 5, Kita-ku, Sapporo, Hokkaido 060-0808, Japan, 5.Hirosaki University, 3 Bunkyo-cho, Hirosaki-shi, Aomori 036-8561, Japan, 6.University of Miyazaki, Gakuen-kibanadai-nishi-1-1, Miyazaki, Miyazaki 889-2192, Japan, 7.Shizuoka University, 836, Ohya, Suruga-ku, Shizuoka-Shi, Shizuoka 422-8529, Japan, 8.Hiroshima University, 1-3-2 Kagamiyama, Higashi-Hiroshima-Shi, Hiroshima 739-8511, Japan, 9.Japan International Research Center for Agricultural Sciences, 1-1 Ohwashi, Tsukuba, Ibaraki 305-8686, Japan, 10.Japan Atomic Energy Agency, 2-4 Shirakata, Tokai-mura, Naka-gun, Ibaraki 319-1195, Japan)

3:00 PM - 3:15 PM JST | 6:00 AM - 6:15 AM UTC

[ACG37-06] Overview of the Regional Carbon Budget Assessment and Processes (RECCAP2), and activities on Southeast Asia

*Masayuki Kondo[1] (1.Center for Global Environmental Research, National Institute for Environmental Studies)

Temporal and spatial variation of soil CO_2/CH_4 fluxes in two cool-temperate forests in Japan

*Lifei Sun[1], Naishen Liang[1], Takashi Hirano[2], Yoshiyuki Takahashi [1], Munemasa Teramoto[3], Kentaro Takagi[2], Toshiaki Kondo[4], Jun Koarashi[5], Mariko Atarashi-Andoh[5], Reiko Ide[1], Xin Zhao[1], Sachinobu Ishida[6], Masahiro Takagi[7], Tomotsugu Yazaki[8]

1. National Institute for Environmental Studies Japan, 2. Hokkaido University, 3. Tottori University, 4. Japan International Research Center for Agricultural Sciences , 5. Japan Atomic Energy Agency , 6. Hirosaki University, 7. University of Miyazaki, 8. Meji University

Forests cover about 30% of global land surface and the total forest carbon stocks (860 Pg) are responsible for about 45% of the carbon in the terrestrial biosphere. Forest soil carbon fluxes which include CO_2 and CH_4 play an important role in global climate change due to both high soil respiration and CH_4 absorption. Consequently, clarifying of mechanisms in forest soil carbon fluxes is critical for understanding the future global carbon cycle and climate change.
To investigate soil CO_2/CH_4 fluxes, we installed multi-channel automated chamber measurement systems in two cool-temperate forests of Tomakomai (natural recovered forest following the typhoon in 2004) of Hakkaido and Fuji-Hokuroku (65-year-old larch plantation) of central Japan. The chambers were separated into 3 groups each with control, trenching and covering understory treatment, respectively. Soil carbon fluxes were continuously measured at hourly and two-hour intervals during snow-free season.
In both forests, soil CO_2/CH_4 fluxes showed high seasonal variation. Soil respiration increased exponentially with changing in soil temperature, whereas soil CH_4 uptake was negatively correlated with soil moisture. Though both the soil temperature and moisture were not significant difference between two forests, we found significant larger soil respiration as well as CH4 absorption in Fuji-Hokuroku larch forest as compared with that of Tomakomai natural forest probably due to both the higher root biomass and soil organic carbon.

Keywords: Soil carbon fluxes, Chamber, Temporal variation, Spatial variation

©2021. Japan Geoscience Union. All Right Reserved.

Decomposition of coarse woody debris produced through land conversion from a forest to an oil palm plantation

*Takashi Hirano[1], Shoko Murata[2], Guan Xhuan Wong[3], Joseph Wenceslaus Waili[3], Kim San Lo[3], Frankie Kiew[3], Edward Baran Aeries[3], Ryuichi Hirata[4], Tomohiro Shiraishi[4], Masato Hayashi[6], Masayuki Itoh[5], Lulie Melling[3]

1. Research Faculty of Agriculture, Hokkaido University, 2. Japan Science and Technology Agency, 3. Sarawak Tropical Peat Research Institute, 4. National Institute for Environmental Studies, 5. University of Hyogo, 6. Japan Aerospace Exploration Agency

Tropical peatlands are widely distributed in Indonesia and Malaysia and have accumulated a huge amount of biomass and soil carbon as peat, coexisting with swamp forest. Recently, however, the huge carbon pool has been threatened by deforestation and peat decomposition through land conversion to oil palm plantations. The land conversion produces a large amount of coarse woody debris (CWD). The CWD is usually piled high in a row (stacking rows) in plantations and would become a large CO_2 source through decomposition, though quantitative information on CO_2 emission is still lacking. Thus, we conducted a field experiment to quantify how much CO_2 is emitted through CWD decomposition.

The study was conducted in a newly developed oil palm plantation from a tropical peat swamp forest in Sarawak, Malaysia. After land preparation, CWD was piled up at the center of each subrow (0.3 ha). We measured the effective volume of a 90-m-long stacking row four times between November 2011 and May 2020, assuming that the shape of a cross section is a triangle. In addition, we determined the moisture and carbon content of CWD samples taken from the stacking row.
The width and height of the stacking row had decreased gradually. The mean cross-sectional areas of the first three measurements were 4.9, 4.1 and 3.5 m^2, respectively. The total amount of carbon in the stacking row was estimated at 19.0 t in November 2018 and 9.0 t in May 2019 from the effective volume and carbon content. The carbon amount was converted to 56.8 and 30.1 t C ha^{-1}, respectively, which indicates that 26.7 t C ha^{-1} (= 16.1 g C m^{-2} d^{-1}) was lost between the two measurement dates for 166 days.

Keywords: Tropical peatlands, Coarse woody debris, Oil palm plantation, Decomposition, CO2 emissions

©2021. Japan Geoscience Union. All Right Reserved.

Anticipation of research development on the atmosphere-land interactions of the terrestrial nitrogen cycle

*Kentaro Hayashi[1]

1. Institute for Agro-Environmental Sciences, NARO

The Haber–Bosch process established in the early 20th century enables artificial creations of ammonia (NH_3) from dinitrogen (N_2). Artificially created reactive nitrogen (Nr: nitrogen species other than N_2) from NH_3 as the commencing material provides great benefits for human, ca. 80% of which is used for chemical fertilizer of crop production. The enhanced capacity of crop production has also increased livestock production providing feed crops, and then fed the global population growth since the 20th century. However, the nitrogen use efficiency of food production is low, that is, ca. 50% and 10% for crop and livestock production, respectively, as global mean. The remain is eventually lost to the environment as Nr and N_2. The Nr lost to the environment moves over the environmental media changing its physicochemical forms and provides a variety of effects according to its properties such as global warming, ozone destruction, air pollution, water pollution, eutrophication, and acidification until finally converted to N_2 again, which is known as the nitrogen cascade. Thus, the nitrogen use by human is a tradeoff between the benefit as fertilizer to earn food and the threat as various environmental impacts, which is called as the nitrogen issue. To cope with the nitrogen issue, quantitative information of Nr flows between human sector and environmental media and that within the environment is indispensable.
Hereafter the topic is narrowed into the Nr impacts on terrestrial ecosystems. There are various and active exchange processes of nitrogen between land and the atmosphere, even involving the inert N_2. For example, biological nitrogen fixation (BNF) and nitrogen deposition (wet and dry deposition of Nr) are key fluxes from the atmosphere to land, and gas emissions with denitrification (N_2 and nitrous oxide [N_2O]), NH_3 volatilization, and gas and particle emissions with wildfire are key fluxes from the land surface to the atmosphere. The N_2 flows with BNF and denitrification are large in quantity, and the Nr flows with nitrogen deposition, NH_3 volatilization, and N_2O emissions are particularly important in terms of environmental impact.
Numerical model and satellite remote sensing are advantageous to grasp the atmosphere–land exchanges of nitrogen in regional and global scales. Flux observation research at the ground surface has an important role that provides verification data to model and remote sensing research. The observation research is further indispensable for elucidating unknown mechanisms of nitrogen cycling in terrestrial ecosystems. Regular monitoring networks of atmospheric deposition are relatively common, whereas only accumulated respective studies are available for other processes. A wide-area expansion of nitrogen exchange observation research in collaboration with model and satellite sensing research has not been realized yet. In this presentation, cropland N_2O emissions are highlighted with particular interest. According to the Global N_2O Budgets (Tian et al., 2020), agricultural land is the biggest anthropogenic emitter of N_2O accounting for 52% from 2007 to 2016 on average, and its emissions have been increasing in contrast with the decreasing trends in other anthropogenic sources. Considering that the world population and food demand will continuously increase, it is required that effective measures to reduce the agricultural N_2O emissions are introduced and their effects are evaluated correctly. Furthermore, the effects of increased atmospheric CO_2 levels and climate change on the nitrogen cycle and N_2O emissions are unknown. Observational research is an important approach that brings flux data and elucidation of the mechanism. Therefore, in this presentation, the presenter will show an idea of efficiently developing observational research on N_2O. It is hoped that a chance for its realization will be created though discussion with participants.

©2021. Japan Geoscience Union. All Right Reserved.

Keywords: Nitrogen, N2O emissions, Denitrification, Biological nitrogen fixation, Atmospheric deposition, Flux observation

©2021. Japan Geoscience Union. All Right Reserved.

Simulation of snow algal blooming in the global scale using a land surface model

*Yukihiko Onuma[1], Kei Yoshimura[1], Nozomu Takeuchi[2]

1. Institute of Industrial Science, The University of Tokyo, 2. Graduate School of Science, Chiba University

Snow algae are cold-tolerant photosynthetic microbes growing on snow and ice during the melting season. The blooms of red snow algae (Sanguina nivaloides) changes the snow surface to red color due to carotenoid pigments in their cells, causing a reduction of the snow surface albedo and acceleration of the melting. Although the red snow phenomena have been reported on the snowfields and glaciers from the Arctic to the Antarctic by in-situ and satellite observations, it is still unclear how the species dispersed globally. Therefore, it is important for biegeosciences to reconstruct their blooming in the global scale. However, the snow algae model, which was proposed previously based on the in situ observations on a snowpack in Greenland, could not reproduce the timing of algal blooming in other areas worldwide, especially in the locations where the snow event frequently occurred or the day-night cycle is apparent during snow melting season. We incorporated the effect of snowfall and day-light length during the algal growth at the locations to the model. To evaluate the performance of the updated snow algae model, we conducted the model validation at fifteen sites from the Arctic to the Antarctic. The improvements enabled to reconstruct the snow algal blooming well reported previously in the various locations worldwide. Based on the model validation, we incorporated the updated snow algae model into a land surface model MATSIRO and performed a global simulation. The global snow algae model (Bio-MATSIRO) is useful to understand the global distribution of snow algal blooming, to evaluate their impact on the snow melting rate globally and to quantify carbon amount in the cryosphere.

Keywords: Snow algae, Numerical modeling, Land surface model

©2021. Japan Geoscience Union. All Right Reserved.

Intercomparison of Data-Driven Estimation of Soil Respiration in Japan

*Hina Yamanuki[1], Kazuhito Ichii[1,2], Naishen Liang[2], Munemasa Teramoto[3], Yoshiyuki Takahashi[2], Jiye Zeng[2], Kentaro Takagi[4], Takashi Hirano[4], Sachinobu Ishida[5], Masahiro Takagi[6], Masaaki Naramoto[7], Kaneyuki Nakane[8], Toshiaki Kondo[9], Jun Koarashi[10], Mariko Atarashi-Andoh[10]

1. Center for Environmental Remote Sensing, Chiba University, 1-33 Yayoi-cho, Inage-ku, Chiba-shi, Chiba 263-8522, Japan, 2. Center for Global Environmental Research, National Institute for Environmental Studies, Tsukuba, Ibaraki 305- 8506, Japan, 3. Arid Land Research Center, Tottori University, 1390 Hamasaka, Tottori, Tottori 680-0001, Japan, 4. Hokkaido University, Kita 8, Nishi 5, Kita-ku, Sapporo, Hokkaido 060-0808, Japan, 5. Hirosaki University, 3 Bunkyo-cho, Hirosaki-shi, Aomori 036-8561, Japan, 6. University of Miyazaki, Gakuen-kibanadai-nishi-1-1, Miyazaki, Miyazaki 889-2192, Japan, 7. Shizuoka University, 836, Ohya, Suruga-ku, Shizuoka-Shi, Shizuoka 422-8529, Japan, 8. Hiroshima University, 1-3-2 Kagamiyama, Higashi-Hiroshima-Shi, Hiroshima 739-8511, Japan, 9. Japan International Research Center for Agricultural Sciences, 1-1 Ohwashi, Tsukuba, Ibaraki 305-8686, Japan, 10. Japan Atomic Energy Agency, 2-4 Shirakata, Tokai-mura, Naka-gun, Ibaraki 319-1195, Japan

Soil Respiration (SR), the sum of root respiration and heterotrophic respiration, is one of the most essential components of soil carbon cycles. However, large uncertainties remain in its temporal and spatial variations. So far, various efforts have been conducted to understand SRs. Many observation stations directly measure SR using chambers. Using these observation data and literature survey, several studies estimated spatial and temporal patterns of SR at global and regional scales based on semi-empirical equations and machine-learning methods. However, the database (e.g. Soil Respiration Database; SRDB) used in these large-scale studies contains inconsistently observed datasets. These inconsistencies may produce additional uncertainties in estimated fluxes. The largest SR observation network across Asia developed and maintained by NIES, Japan can be a good candidate to estimate spatio-temporal variations in SR across Asia, since these observations have been conducted with a consistent observation protocol and quality controls.

In this study, we updated our data-driven estimation of SR across Japan with observation data (eight sites across Japan), remote sensing data (MODIS land products), and random forest regression. Our estimation shows a reasonable performance with R^2=0.87 for remote sensing only model and R^2=0.91 for remote sensing and in-situ combined model. Based on the established model, we also produced upscaled estimations of SR across Japan with 1km spatial resolution from 2000 to 2020.

Intercomparison of our estimation with other available datasets was also conducted to understand advantages of our estimation. Our results show spatially more explicit variations compared with other global products. In addition, our advantage is to capture temporal variations (e.g. 8days). We also confirmed that previous estimations do not reproduce our observation network datasets, indicating consistent observation approach is important to upscale soil respiration.

Keywords: Carbon Cycle, Soil Respiration, Remote Sensing, Machine Learning, Upscaling, CO2 Flux

©2021. Japan Geoscience Union. All Right Reserved.

Overview of the Regional Carbon Budget Assessment and Processes (RECCAP2), and activities on Southeast Asia

*Masayuki Kondo[1]

1. Center for Global Environmental Research, National Institute for Environmental Studies

Understanding the mitigation potential of the land and ocean against anthropogenic GHG emissions hinges upon accurate assessment of their net carbon fluxes. The net amount of carbon exchanged between the atmosphere and land, and the atmosphere and ocean comprises of multiple pathways of carbon fluxes, such as from atmosphere to terrestrial ecosystem, terrestrial ecosystem to inland water, inland water to atmosphere and to estuary, and estuary to ocean. Until today, our ability to diagnose carbon fluxes of terrestrial ecosystems (forests, grasslands, and crops), hydrosphere (rivers, lakes, and estuaries), and ocean have progressed by the development of observation networks and modelling in respective fields. Under the circumstances that anthropogenic emissions exacerbate climate change, a need for accurate assessment of the net land and ocean carbon budgets has been growing, which requires collective efforts of multiple fields towards integration of data, knowledge, and assessment of carbon fluxes.

Bringing together expert researchers from institutes and academia across the world for GHG budget assessment of the land and ocean, the REgional Carbon Cycle Assessment and Processes (RECCAP) was formed under an umbrella of the Global Carbon Project. Here I describe the overview of the second phase of RECCAP (RECCAP), including the objective and methodology, progress over the previous RECCAP1, current state of the project, etc. As an example among the 11 land, 4 ocean, and special interest regions (permafrost, semi-arid, coastal blue carbon, global synthesis) to be analyzed in RECCAP2, this presentation shares the research plan, aim, current state of GHG budget assessment for Southeast Asia.

Keywords: Carbon budget, RECCAP, Southeast Asia

©2021. Japan Geoscience Union. All Right Reserved.

[J] Oral | A (Atmospheric and Hydrospheric Sciences)：A-CG Complex & General

Sat. Jun 5, 2021 3:30 PM - 5:00 PM JST | Sat. Jun 5, 2021 6:30 AM - 8:00 AM UTC | Ch.08 Zoom Room 08

[A-CG37] Biogeochemical cycles in Land Ecosystem

convener:Tomomichi Kato(Research Faculty of Agriculture, Hokkaido University), Kazuhito Ichii(Chiba University), Takeshi Ise(FSERC, Kyoto University), Munemasa Teramoto(Arid Land Research Center, Tottori University)

Terrestrial ecosystem influences global climate through cycles of water, carbon, and nitrogen between land surface and atmosphere. For better understanding of those behaviors, a great effort has been paid for developing varieties of approaches and techniques such as biometric survey, eddy and chamber methods, near and satellite remote sensing, biosphere modeling and so on.
In particular, the JapanFlux, founded in 2006 as a researchers network of CO2, H2O and other trace gas flux measurement, has promoted the multi-disciplinal studies not only for flux measurement community, but also for remote sensing and biosphere modeling communities. Moreover, the Research-Group-on-Integrated-Land-Processes, which was founded in 2006, also has contributed to build networks between Japanese researchers to better understanding of physical and biological processes on interactions between terrestrial surface and atmosphere.
This session unites those multi-disciplinal activities, and promotes the oral and poster presentations on the role of terrestrial ecosystem in material circulations of water, carbon, nitrogen, energy and other substances by any approaches and technics. This session takes over the former session in last year: A-CG54.

3:30 PM - 3:45 PM JST | 6:30 AM - 6:45 AM UTC

[ACG37-07] Influence of fire and drainage on evapotranspiration in a tropical ex-peat swamp forest

*Shinjiro Ohkubo[1], Takashi Hirano[1], Kitso Kusin[2] (1.National University Corporation, Hokkaido University, 2.University of Palangkaraya)

3:45 PM - 4:00 PM JST | 6:45 AM - 7:00 AM UTC

[ACG37-08] Ground-Based Measurement of Solar-Induced Chlorophyll Fluorescence in Wetland by High-Spectral Resolution

*Kitpanuwat TANATARAKEREE[1], Tomomichi Kato[2,3], Tomoki Morozumi[3], KANOKRAT BUAREAL[2], Masahito Ueyama[4], Naohisa Nakashima[3], Hideki Ninomiya[2], Lan Wu[5] (1.Graduate School of Agriculture, Hokkaido University, 2.Graduate School of Global Food Resources, Hokkaido University, 3.Research Faculty of Agriculture, Hokkaido University , 4.Graduate School of Life and Environmental Science, Osaka Prefecture University, 5.Hainan University)

4:00 PM - 4:15 PM JST | 7:00 AM - 7:15 AM UTC

[ACG37-09] Accounting for the emissions of tree stems in the methane budget of forests: upscaling chamber measurements to the stand

*Daniel EPRON[1], Ayaka Sakabe[1], Kenshi Takahashi[1], Takeshi Ise[1] (1.Kyoto University)

4:15 PM - 4:30 PM JST | 7:15 AM - 7:30 AM UTC

[ACG37-10] Estimation of non-photosynthetic vegetation amount in the northern Gobi Desert using MODIS satellite data

*Jing Wu[1], Yasunori Kurosaki[1], Gantsetseg Batdelger[2], Batjargal Buyantogtoh[1], Ishizuka Masahide[3], Thomas Sekiyama[4], Jiaqi Liu[1] (1. Arid Land Research Center, Tottori University, 2.Information and Research Institute of Meteorology, Hydrology and Environment, 3.Kagawa University, 4.Meteorological Research Institute)

4:30 PM - 4:45 PM JST | 7:30 AM - 7:45 AM UTC

[ACG37-11] **Mapping Peatland Fires in Indonesia Using a Drone Equipped with an Infrared Camera**

*Taishin Kameoka[1], Osamu Kozan[2,3] (1.Educational Unit for Studies on Connectivity of Hills, Humans and Oceans, Kyoto University, 2.Center for Southeast Asian Studies, Kyoto University, 3.Research Institute for Humanity and Nature)

4:45 PM - 5:00 PM JST | 7:45 AM - 8:00 AM UTC

[ACG37-12] Incorporating non-structural carbon dynamics in individual-based vegetation model SEIB-DGVM

*Hideki Ninomiya[1], Tomomichi Kato[1] (1.Hokkaido University)

Influence of fire and drainage on evapotranspiration in a tropical ex-peat swamp forest

*Shinjiro Ohkubo[1], Takashi Hirano[1], Kitso Kusin[2]

1. National University Corporation, Hokkaido University, 2. University of Palangkaraya

Tropical peat swamp forests (PSFs) play a significant role in the exchange of water between land and the atmosphere. However, fire and drainage have been expanding in PSFs in recent decades. Although there is concern on the influence of fire and drainage on water circulation, their influence on evapotranspiration (ET) is insufficiently understood. Furthermore, repeated fire occurrences and their corresponding influence on the ET by recurrent burning and smoldering is unexplored. To elucidate these influences, we examined long-term variation of ET in an ex-peat swamp forest in Central Kalimantan, Indonesia that was affected by drainage and repeated fire. The continuous observation of energy fluxes was conducted for approximately 13 y between 2004 and 2016 by using the eddy covariance technique. The site burned in 2009 and 2014, and it was drained in 2014. Monthly ET was synchronized with net radiation (R_n) and thus decreased considerably under fire-induced dense haze during the El Niño drought. Troughs of ET were simultaneous with crests of vapor pressure deficit (VPD), and troughs of ground water level (GWL) and R_n. In the case of ET > precipitation (P), ET decreased when the GWL was lower than -0.5 m. Monthly ET had a strong correlation with R_n (R=0.87, p <0.01), and moderate correlation with VPD (R=−0.51, p <0.01), GWL (R=0.68, p <0.01), and P (R=0.38, p <0.01). ET had almost no correlation with the Enhanced Vegetation Index, which represents above ground biomass (R=0.01) for the entire observation period. Alternately, the results of path analysis showed that some environmental factors controlled ET differently depending on environmental conditions. Generally, VPD negatively affects ET due to stomatal regulation functions under dry atmospheric conditions. However, the effect was negligible during the water-logged periods. This is because atmospheric dryness facilitated evaporation from exposed water on the ground surface, which canceled out the negative effect of transpiration due to stomatal closure. After drainage by canal excavation, fluctuation of GWL did not significantly influence ET. Although, the absolute quantity of ET decreased. This may be due to the hydrophobic dried peat soil, which prevents rainwater infiltration, disconnection of capillary force, or disabled root water uptake as GWL is excessively lowered. Fire potentially decreased ET due to decreased transpiration by burning of vegetation. However, the decreasing effect was cancelled by increased evaporation from the waterlogged ground surface during the subsequent La Niña event. Drainage undoubtedly lowered the GWL, and ET severely decreased in cases with extremely low GWL.

Keywords: Groundwater level, Haze, Latent heat flux, Net radiation, Precipitation, Vapor pressure deficit

©2021. Japan Geoscience Union. All Right Reserved.

Ground-Based Measurement of Solar-Induced Chlorophyll Fluorescence in Wetland by High-Spectral Resolution

*Kitpanuwat TANATARAKEREE[1], Tomomichi Kato[2,3], Tomoki Morozumi[3], KANOKRAT BUAREAL[2], Masahito Ueyama[4], Naohisa Nakashima[3], Hideki Ninomiya[2], Lan Wu[5]

1. Graduate School of Agriculture, Hokkaido University, 2. Graduate School of Global Food Resources, Hokkaido University, 3. Research Faculty of Agriculture, Hokkaido University , 4. Graduate School of Life and Environmental Science, Osaka Prefecture University, 5. Hainan University

Solar-induced chlorophyll fluorescence (SIF) has been observed and discovered to relate linearly to gross primary production (GPP) in terrestrial ecosystem [Krause and Weis, 1991; Meroni et al., 2009; Frankenberg et al., 2011; Paul-Limoges et al., 2018]. However, SIF variations under different plant growth stages and sky conditions, and water table depth effects appear to limit the understandings about SIF-GPP relationship at the field-based measurement. It remains ambiguous linked to how this relationship is affected by varying changes of palnt growth stage, sky, and water table, especially for wetland where is a critical part of carbon sinks. We conducted the ground-base measurement of canopy-top SIF in wetland, Bibai Mire, northern Japan, Hokkaido (43º19'N, 141º48'E, 16 m above sea level) during the growing season (from March to November) in 2020, and examined its relationship to the eddy-covariance GPP [Ueyama et al., 2020]. QEPro spectroradiometer (range of wavelength 648-808 nm, the full width half maximum (FWHM) of 0.31 nm, Ocean Optics, Dunedin, FL, USA) and the spectral fitting method (SFM; Meroni and Colombo., 2006; Meroni et al., 2010; Mazzoni et al., 2012) were used for SIF retrievals at the oxygen absorption band (O_2-A, centered around 760 nm). SIF was captured by the spectra of downwelling and upwelling at the height of 2 meters above the ground by hemisphere spectroradiometer. The downward solar irradiance was estimated from cosine corrector fiber (CC fiber) from field of view (FOV) at 180º and the upward canopy-reflected radiance was received by bare fiber FOV 25º and CC fiber FOV 180º. The slope and correlation in positive linear regression between SIF and GPP were found to vary among the growth stages (slope = -2.99, 107.60, 62.57 and 47.97 (μmolmW^{-1}s^{-1} nm) and r^2 = 0.01, 0.41, 0.73 and 0.65 in Pre-Growing (DOY74-135), Growing (DOY144-179), Mature (DOY180-256) and Senescence (DOY260-295), respectively), suggesting that vegetation growth has a strong impact on the seasonal variations of canopy SIF and its realtion to GPP. In contrast, we found that sky conditions such as sunny (clearness index > 0.5) and cloudy (clearness index ≦ 0.5) have no clear influence on relationship of SIF and GPP (slope = 59.59 and 91.06 (μmolmW^{-1}s^{-1}nm) and r^2 =) and r^2 = 0.68 and 0.75 in sunny day and cloudy day, respectively).

Keywords: Solar-Induced Chlorophyll Fluorescence , Gross Primary Production, Ground-Based Measurement, Wetland, High-Spectral Resolution

©2021. Japan Geoscience Union. All Right Reserved.



©2021. Japan Geoscience Union. All Right Reserved.

Accounting for the emissions of tree stems in the methane budget of forests: upscaling chamber measurements to the stand

*Daniel EPRON[1], Ayaka Sakabe[1], Kenshi Takahashi[1], Takeshi Ise[1]

1. Kyoto University

Forests are a well-known carbon sink, which mitigate the rise in atmospheric CO_2 and hence global warming. However, methane emissions by stems of living trees become a major concern due to the increasing contribution of methane to global warming. Indeed, methane is the second most important anthropogenic greenhouse gas. Until now, global and regional methane budgets of forests, which cover one third of the land area (67% in Japan) have only considered the source and sink functions of soils, ignoring stem emissions. However, there are growing evidences that trees emit methane through their stem, and the role of trees, in addition to that of the soil, must be considered in the methane budget of forests.

Our objective was to evaluate how to upscale stem CH_4 emissions to the ecosystem level and a prerequisite was first to understand the variability of stem CH_4 emissions across individuals and species, and within individuals: does tree size influence stem CH_4 emission and how do these emissions vary spatially along the stem?

Measurements were carried out in the Ashiu experimental forest from August to December on two to three trees per species and two positions along the trunk. The trunk of five major species at this site emitted CH_4, with a large variability among species. While the temporal variation was low (both diurnal and day to day), CH_4 emission were higher for large trees than smaller ones for a given species and varied with the position along the trunk.

We have used these preliminary results to provide an estimate of the CH_4 emission from the whole trees and we present avenues for estimating these emissions at the stand level considering tree species diversity (contribution of the main species) and the stand structural attributes (tree diameter and height), using species-species allometric relations.

Keywords: Methane, Forest, Upscaling

©2021. Japan Geoscience Union. All Right Reserved.

Estimation of non-photosynthetic vegetation amount in the northern Gobi Desert using MODIS satellite data

*Jing Wu[1], Yasunori Kurosaki[1], Gantsetseg Batdelger[2], Batjargal Buyantogtoh[1], Ishizuka Masahide[3], Thomas Sekiyama[4], Jiaqi Liu[1]

1. Arid Land Research Center, Tottori University, 2. Information and Research Institute of Meteorology, Hydrology and Environment, 3. Kagawa University, 4. Meteorological Research Institute

The focus of monitoring vegetation amount has been mainly on green vegetation during the growing season. Comparatively less research has been done in estimations of non-photosynthetic vegetation (NPV) that includes litter and standing dead vegetation, although monitoring its coverage and mass is of great importance in various applications in arid and semi-arid regions, such as fire risk management, livestock forage assessment and wind erosion risk assessment. The present study intended to estimate the NPV amount based on MODIS vegetation indices and field observation data at one of the main source regions for Asia Dust, Tsogt-Ovoo (TsO) located in the northern Gobi Desert, Mongolia.

We compared the measured NPV coverage (fc_{NPV}) and mass (m_{NPV}) with NDVI and other six potential vegetation indices using the short wavelength infrared region (SWIR) bands. We found that the combination of band 6 (1.6 μm) and band 7 (2.1 μm), namely the Soil Tillage Index (STI) and Normalized Difference Tillage Index (NDTI), had a good performance in estimating fc_{NPV} and m_{NPV}.

We propose the roughness length z_0 and threshold friction velocity (u_{*t}) for sand saltation, which had been observed at non-stony and stony sites in TsO, as representative parameters for the vegetation amount. Using the parameters, we verified suitability of fc_{NPV} estimated from STI. At both sites, the observed z_0 and u_{*t} increased as the estimated fc_{NPV} increased. We established the relationship between the observed z_0 and the estimated fc_{NPV} at the sites. The predicted z_0 in the absence of NPV were 0.0010 cm and 0.0085 cm at non-stony and stony sites, respectively. These values are reasonable in accordance with those of other studies. We also established the relationship between the observed u_{*t} and the estimated fc_{NPV}. The predicted u_{*t} in the absence of NPV were 0.23 m s^{-1} and 0.30 m s^{-1} at non-stony and stony sites, respectively. The threshold wind speed at 10 m height (u_{10t0}) converted from u_{*t} were 5.3 and 6.7 m s^{-1}, close to the value of 6.5 m s^{-1} that commonly used in dust models.

Those verifications indicate that STI is suited to estimate the NPV amount at least at TsO in the Gobi Desert.

Keywords: non-photosynthetic vegetation , Soil Tillage Index, roughness length, threshold friction velocity, arid regions

©2021. Japan Geoscience Union. All Right Reserved.

Mapping Peatland Fires in Indonesia Using a Drone Equipped with an Infrared Camera

*Taishin Kameoka[1], Osamu Kozan[2,3]

1. Educational Unit for Studies on Connectivity of Hills, Humans and Oceans, Kyoto University, 2. Center for Southeast Asian Studies, Kyoto University, 3. Research Institute for Humanity and Nature

In this study, we created a peatland fire map using an infrared camera mounted on a drone to plot the position and scale of peatland fires to contribute to their prevention. We expect that this method offers a high potential for future activities and academic research on enhancing the detection and management of peatland fires. Fires occurring in peatlands, which store large amounts of organic matter, are of an especially serious concern. Indonesia has a substantial carbon stock, with an estimated 22.5 million hectares under peatlands and an estimated carbon storage capacity of 57.4 billion tons. Approximately 860,000 hectares of peatlands burned in 2015, resulting in the release of large amounts of soil carbon. Indonesia established the Peatland Restoration Agency in 2016 to conserve peatland areas. Large peatland fires had been difficult to occur since 2016 because of conservation activities and enough precipitation. However, it decreased the amount of rainfall in 2019 in Indonesia, frequent occurrences of peatland fires during 2019 indicate that the problem has not been solved. Peatland fires are difficult to detect visually since they persist underground. This characteristic causes serious problems in the field because it is not easy to extinguish them completely. In addition, certain fires remain undetected until they are large because they occur in remote areas that people cannot access. Therefore, drones equipped with infrared cameras can be a useful tool for detecting peatland fires.

Keywords: Carbon Dioxide, Drone, Indonesia, Infrared Camera, Petaland fire, Remote Sensing

©2021. Japan Geoscience Union. All Right Reserved.

Incorporating non-structural carbon dynamics in individual-based vegetation model SEIB-DGVM

*Hideki Ninomiya[1], Tomomichi Kato[1]

1. Hokkaido University

To understand the effect of climate change on the terrestrial ecosystem, the response of vegetation to atmospheric carbon is critical. As global warming is getting worse, it would contribute to widespread tree mortality related to drought, increased temperature, pest outbreak to name a few. Then, the tree mortality results in the negative impact on the earth; biological diversity, wild animal habitat, hydrological and carbon cycle, and vulnerability to invasion by unexpected exotic species (Adams et al, 2013). However, it is challenging to estimate the negative impact mainly because the mechanism of how plants are killed is poorly understood. To overcome these tree mortality, trees have grown to control their carbon resources and strategically allocate them to growth, respiration, storage, reproduction, and defense (Hoch et al, 2003; Henrik et al, 2018). The percentage of carbon allocation to each compartment is giving much attention today. Among carbon resources, non-structural carbon (NSC) is commonly considered a repository depending on the balance between the supply of assimilated carbon and carbon demand. Hence, the size of stored C pools can be considered an indicator of the carbon balance of the plant. Additionally, NSC could be the threshold of the conceptual “carbon starvation” as one of the mechanisms after drought (Hoch et al, 2003; McDowell et al., 2008). The objectives of the research are to apply the process representing NSC dynamics to the ecological model and expect the potential effect of NSC in the future.

The process-based Spatially Explicit Individual-Based Dynamic Global Vegetation Model (SEIB-DGVM; Sato et al., 2007), representing three-dimensional tree structure and individual tree growth, was used in this study. In a 30m×30m grid, each plant establishes and dies while sharing incoming solar photons with other plants. Here, we newly introduced a process of accumulating NSC in plants to SEIB-DGVM. Carbon from photosynthesis is mainly allocated to maintenance respiration and growth respiration of plant structure: leaf, stem, and root. In the research, I created a simple NSC pool. All carbon is not consumed but some of them are stored in three organs of plants each day. When photosynthesis rate declines, NSC compensates for maintenance respiration and gradually close to zero. We validated the NSC dynamics at a point and global scale. Firstly, we chose 4 sites representing different plant functional types for the validation: Austria, Swiss, Canada, and Panama, and used observation data as climate data. Secondly, we validated them depending on climate zones: tropical, temperate, and boreal. The climate data for global is Model for Interdisciplinary Research on Climate- Earth System Model (MIROC-ESM, Watanabe et al, 2011). The study contributes to improving the physiological leaf life cycle of the model. In addition, we can understand how NSC will affect the vegetation distribution, gross primary production (GPP), net primary production (NPP) in the future.

Keywords: Nonstructural carbon, Individual-based model, SEIB-DGVM, Carbon allocation, Vegetation dynamics

©2021. Japan Geoscience Union. All Right Reserved.

[J] Poster | A (Atmospheric and Hydrospheric Sciences)：A-CG Complex & General

Sat. Jun 5, 2021 5:15 PM - 6:30 PM JST | Sat. Jun 5, 2021 8:15 AM - 9:30 AM UTC | Ch.08_3

[A-CG37] Biogeochemical cycles in Land Ecosystem

convener:Tomomichi Kato(Research Faculty of Agriculture, Hokkaido University), Kazuhito Ichii(Chiba University), Takeshi Ise(FSERC, Kyoto University), Munemasa Teramoto(Arid Land Research Center, Tottori University)

Terrestrial ecosystem influences global climate through cycles of water, carbon, and nitrogen between land surface and atmosphere. For better understanding of those behaviors, a great effort has been paid for developing varieties of approaches and techniques such as biometric survey, eddy and chamber methods, near and satellite remote sensing, biosphere modeling and so on.
In particular, the JapanFlux, founded in 2006 as a researchers network of CO2, H2O and other trace gas flux measurement, has promoted the multi-disciplinal studies not only for flux measurement community, but also for remote sensing and biosphere modeling communities. Moreover, the Research-Group-on-Integrated-Land-Processes, which was founded in 2006, also has contributed to build networks between Japanese researchers to better understanding of physical and biological processes on interactions between terrestrial surface and atmosphere.
This session unites those multi-disciplinal activities, and promotes the oral and poster presentations on the role of terrestrial ecosystem in material circulations of water, carbon, nitrogen, energy and other substances by any approaches and technics. This session takes over the former session in last year: A-CG54.

[ACG37-P01] Change in soil respiration rate and soil organic matter for three years after clear-cutting in a *Cryptomeria japonica* plantation

*Yukiko Abe[1], Naishen Liang[2], Munemasa Teramoto[3], Takeshi Tange[1] (1.The University of Tokyo, 2.National Institute for Environmental Studies, 3.Tottori University)

[ACG37-P02] Continuous measurement of atmospheric methane mixing ratio at a cool-temperate deciduous forest site, Takayama, Japan

*Shohei Murayama[1], Shigeyuki Ishidoya[1], Tomoyuki Hori[1], Shinpei YOSHITAKE[2], Takahisa Maeda[1] (1.National Institute of Advanced Industrial Science and Technology, 2.Waseda University)

[ACG37-P03] Seasonal variation and controlling factors of stem methane emissions from *Alnus japonica* revealed by continuous measurements

*Ayaka Sakabe[1], Kenshi Takahashi[1], Wakana Azuma[2], Masayuki Itoh[3], Makiko Tateishi[1], Yoshiko Kosugi[1] (1.Kyoto University, 2.Kobe University, 3.University of Hyogo)

[ACG37-P04] **Spatio-temporal variation of soil respiration in coastal sand dunes and the mechanisms**

*Munemasa Teramoto[1], Toru Hamamoto[1], Naishen Liang[2], Takeshi Taniguchi[1], Takehiko Y. Ito[3], Richa Hu[4], Norikazu Yamanaka[1] (1.Arid Land Research Center, Tottori University, 2.Center for Global Environmental Research, National Institute for Environmental Studies, 3.International Platform for Dryland Research and Education, Tottori University, 4.The United Graduate School of Agricultural Sciences, Tottori University)

[ACG37-P05] Validation of Two Vegetation Indices: NDVI and PRI Derived from GCOM-C/SGLI

*Sasagawa Taiga[1], Tomoko Kawaguchi Akitsu[2], Kenlo Nishida Nasahara[2] (1.Graduate School of Science and Technology, University of Tsukuba, 2.Faculty of Life and Environmental Sciences, University of Tsukuba)

[ACG37-P06] **Seasonal variation in Solar Induced chlorophyll Fluorescence detected by multi-vertical layer spectroscopy in a canopy of cool-temperate deciduous broadleaf forest in Takayama, Gifu**

*Tomoki Morozumi[1], Tomomichi Kato[1], Katsuto Tsujimoto[2], KANOKRAT BUAREAL[3], Naohisa Nakashima[1], Yuma Sakai[4], Hideki Kobayashi[4], Kenlo Nasahara[5], Tomoko Akitsu[5], Shohei Murayama[6], Hibiki M Noda[7], Hiroyuki Muraoka[8] (1.Research Faculty of Agriculture, Hokkaido University, 2.Graduate School of Life Sciences, Tohoku University, 3.Graduate School of Global Food Resources, Hokkaido University, 4.Institute of Arctic Climate and Environment Research, Japan Agency for Marine-Earth Science and Technology, 5.Faculty of Life and Environmental Sciences, University of Tsukuba, 6.Environmental Management Research Institute, National Institute of Advanced Industrial Science and Technology, 7.Center for Global Environmental Research, National Institute for Environmental Studies, 8.River Basin Research Center, Gifu University)

[ACG37-P07] On the factors affecting reproducibility of GPP estimated by the Earth System Model MIROC-ES2L

*Akira Kurisu[1], Toru Nozawa[2], Manabu Abe[3], Tomohiro Hajima[3] (1.Faculty of Science, Okayama University, 2.Graduate School of Natural Science and Technology, Okayama University, 3.Japan Agency for Marine-Earth Science and Technology)

[ACG37-P08] Estimation of forest above ground biomass from PALSAR Data

*Hantao Li[1], Tomomichi Kato[2], Lan Wu[3], Masato Hayashi[4] (1.Graduate School of Agriculture, Hokkaido University, 2.Research Faculty of Agriculture, Hokkaido University, 3.College of Ecology and Environment, Hainan University, China, 4.Earth Observation Research Center, Japan Aerospace Exploration Agency)

[ACG37-P09] Development of process-based model for estimating wheat production MATCRO-Wheat

*Maki Nakaguki[1], Tomomichi Kato[2], Yuji Masutomi[3], Leilei Liu[4], Seiji Shimoda[5] (1.Hokkaido University, 2.Research Faculty of Agriculture, Hokkaido University, 3.National Institute for Environmental Studies, 4.National Engineering and Technology Center for Information Agriculture, Nanjing Agricultural University, 5.Hokkaido Agricultural Research Center, National Agriculture and Food Research Organization)

Change in soil respiration rate and soil organic matter for three years after clear-cutting in a *Cryptomeria japonica* plantation

*Yukiko Abe[1], Naishen Liang[2], Munemasa Teramoto[3], Takeshi Tange[1]

1. The University of Tokyo, 2. National Institute for Environmental Studies, 3. Tottori University

Clear-cutting of forests significantly alters the carbon dynamics in soil, with the large temporary supply of litter and dead roots, followed by significant decline. In this study, we measured soil respiration rates, amount of litter on soil surface, dead root, and soil carbon contents at 20 measurement points in a sugi (*Cryptomeria japonica*) plantation of Tokyo University of Agriculture Okutama Forest from May 2017 (just before clear-cutting) to August 2019. Litter and soil at 0-5 cm in depth were collected at soil respiration measurement points approximately every three months. After soil sampling, the measurement points were reestablished at new locations. Weeding had been done once a year in the study site, and the herbaceous vegetation that entered the measurement points was removed.
Soil respiration rate at 20 ˚C (R_{20}) was estimated using the exponential functions of soil respiration rate and soil temperature at 5 cm in depth. The mean R_{20}s of 20 measurement points in 2018 and 2019 were not significantly different from that of 2017. The dead root amount of sugi fine root in measurement points did not decreased until May 2018 compared to the fine root biomass before clear-cutting (0.33 ± 0.27 t ha^{-1}) significantly. After that, the dead root amount from September 2018 to August 2019 decreased significantly to 35.7-52.0% before clear-cutting. The amount of sugi leaf litter was 6.24±1.98 t ha^{-1} before clear-cutting, but decreased significantly to 2.03±1.74 t ha-^{1} three months after clear-cutting, which may have been affected by the ground preparation after clear-cutting. The amount of sugi leaf litter after March 2018 has decreased significantly compared to August 2017, and it was 20.9-54.9% in August 2017. The fact that the soil respiration rate in the third year after clear-cutting did not decrease compared to the first year after clear-cutting could be due to the continuous supply of organic matter to the soil by litter and dead roots.

Keywords: litter, dead root, soil carbon

©2021. Japan Geoscience Union. All Right Reserved.

Continuous measurement of atmospheric methane mixing ratio at a cool-temperate deciduous forest site, Takayama, Japan

*Shohei Murayama[1], Shigeyuki Ishidoya[1], Tomoyuki Hori[1], Shinpei YOSHITAKE[2], Takahisa Maeda[1]

1. National Institute of Advanced Industrial Science and Technology, 2. Waseda University

Methane (CH_4) is a greenhouse gas that contributes to global warming next to carbon dioxide (CO_2). Forest ecosystems other than wetlands are considered to be CH_4 sinks due to the oxidative activities by soil microbes while it has also been pointed out that CH_4 may be released from trees. However, the factors governing CH_4 budgets in the ecosystem are not fully understood. To examine the variations in the atmospheric mixing ration and the budgets of CH_4 in the forest ecosystem and the factors governing them, continuous measurement of the atmospheric CH_4 mixing ratio has initiated at a cool-temperate deciduous forest site in the central Japan, Takayama (TKY: 36°08'N, 137°25'E, 1420 m) since July 2020. TKY is the longest monitoring site in the AsiaFlux network.

The continuous CH_4 measurement was made using a laser spectroscopy analyzer (Ultra-Portable GGA, Los Gatos Research). Meteorological instruments and air intakes for the CH_4 mixing ratio measurement were mounted on a 27-m tower. Sample air was collected from six different heights (27, 18, 8.8, 5.8, 2.0 and 1.3 m); the top level was above the canopy, the second just above the canopy and the other four below the canopy. The air was drawn by a diaphragm pump and introduced into the analyzer after removing aerosol particles and water vapor. The sample flow rate and the pressure in the sample cell of the analyzer were stabilized, and the analyzer was placed in a temperature-controlled box to reduce output drift. The analyzer was calibrated using three air-based CO_2-CH_4 standards with different mixing ratios every three hours. The overall precision was estimated to be less than 0.8 ppb, and the measured CH_4 values were almost in agreement with those measured by a flask sampling method using an FID-GC.

The atmospheric CH_4 observed at all heights did not show clear diurnal variation but fluctuations with a period of several days while the atmospheric CO_2 showed clear diurnal variation from summer to early fall reflecting photosynthesis and respiratory activities. The variation patterns of the atmospheric CH_4 observed at all heights were very similar, but the mixing ratios were lower at 1.3 m than at 27 m during most of the observation period. The vertical CH_4 difference between 27 m and 1.3 m above the ground clearly showed positive correlation with soil temperature near the ground surface, which is consistent with the seasonal variation in intensity of soil CH_4 sink observed at TKY using a soil chamber. The vertical difference also showed negative correlation with soil moisture, which suggests that the oxidation of CH_4 is enhanced under dry conditions. Significant sources of CH_4 from the above-ground parts of trees were not detected from the observed vertical profiles.

On the other hand, it was found from backward trajectory analyses that the observed high and low CH_4 on the several-day scale described above were related to long-range atmospheric transport originated from the Asian Continent and the North Pacific Ocean, respectively. The results suggest that the high CH_4 reflects the CH_4 emissions originated from wetlands and anthropogenic activities on the continent.

We plan to further investigate the mechanism governing variations in the CH_4 mixing ratio and the CH_4 budgets in the forest ecosystem at TKY through data accumulation, genetic analyses of soil microbes, etc.

©2021. Japan Geoscience Union. All Right Reserved.

Acknowledgements

We would like to thank members of River Basin Research Center of Gifu University and AIST for their support for our observation. A. Kudo and C. Abe for their technical support for our measurements. This research was supported by JSPS KAKENHI Grant Numbers JP18H03365, JP19H03301 and JP19H01975.

Keywords: Methane, Forest ecosystems

©2021. Japan Geoscience Union. All Right Reserved.

Seasonal variation and controlling factors of stem methane emissions from *Alnus japonica* revealed by continuous measurements

*Ayaka Sakabe[1], Kenshi Takahashi[1], Wakana Azuma[2], Masayuki Itoh[3], Makiko Tateishi[1], Yoshiko Kosugi[1]

1. Kyoto University, 2. Kobe University, 3. University of Hyogo

Recent studies suggest that tree-mediated methane emissions have the potential to offset the soil methane sink and may convert the forest from a net sink to a net source. However, tree-mediated CH_4 emissions represent an uncertain pathway of the total CH_4 flux from forested ecosystems. We measured the stem CH_4 fluxes from *Alnus japonica* in a riparian wetland of a temperate forest for a year using automated chambers. Three mature *Alnus japonica* trees grown naturally in the riparian wetland were selected for this study. Dissolved CH_4 concentrations in groundwater at two depths beneath each tree were measured biweekly. The sap flux for each tree was measured with Granier-type sensors.

The stem CH_4 fluxes seasonally vary, showing summertime maxima and wintertime minima. The stem CH_4 fluxes positively correlate with dissolved CH_4 concentration in groundwater beneath the trees. In addition, stem CH_4 emissions were observed when the sap flux diminished during the defoliation period. These results indicate that CH_4 in the rhizosphere is transported in the gaseous form through intercellular space in trees. On the other hand, CH_4 transport by sap flux also likely exists based on our observations; stem CH_4 fluxes showed diurnal variation. We also observed that rainfall caused a clear increase in the stem CH_4 emissions. Temporal changes in the groundwater flow paths by rainfall would have affected the belowground CH_4 concentrations and the stem CH_4 flux. Dynamic changes in soil environmental conditions (soil temperature, groundwater flow) controlled dissolved CH_4 concentrations in groundwater, thus, stem CH_4 flux. Our findings highlight the need for continuous stem CH_4 flux measurements to better understand the controlling factors and future response of CH_4 dynamics in forests to climate change.

Keywords: Stem methane emission, Alnus japonica, closed chamber

©2021. Japan Geoscience Union. All Right Reserved.

Spatio-temporal variation of soil respiration in coastal sand dunes and the mechanisms

*Munemasa Teramoto[1], Toru Hamamoto[1], Naishen Liang[2], Takeshi Taniguchi[1], Takehiko Y. Ito[3], Richa Hu[4], Norikazu Yamanaka[1]

1. Arid Land Research Center, Tottori University, 2. Center for Global Environmental Research, National Institute for Environmental Studies, 3. International Platform for Dryland Research and Education, Tottori University, 4. The United Graduate School of Agricultural Sciences, Tottori University

Coastal sand dunes are unique ecosystems where zonal distribution of coastal vegetations is typically observed. Globally, costal sand dunes are decreasing the area because of development and climate change. On the other hand, coastal sand dunes are gathering attention as multipurpose green infrastructure for mitigation and adaptation against global climate change. Studies for carbon cycle in coastal sand dunes can contribute to add a new value for the unique ecosystems from the viewpoint of carbon sequestration and sustainable ecosystem management.

Soil respiration (R_s) is one of the largest carbon flux components in terrestrial carbon cycle. Many field observations were conducted until now, and those observation data have been used for global estimation of R_s. However, observations were mainly conducted in forests, croplands and grasslands, major terrestrial ecosystems. Observations for R_s in coastal sand dunes are totally limited, and there is no example of R_s measurement in coastal sand dunes with consideration for zonal distribution of coastal vegetation.

To examine the spatio-temporal variation of R_s and related mechanisms in coastal sand dunes, we conducted field observations for R_s and environmental parameters from June to December in 2020 in coastal sand dunes in Tottori, Japan. We set four measurement plots (n = 10 in each plot) in the study site representing bare sand (plot 1), clusters of *Vitex rotundifolia* (plot 2), Mixture of *V. rotundifolia* and *Artemisia capillaris* (plot 3) and boundary area between a pine forest (*Pinus thunbergii*) and coastal vegetation zone (plot 4). In those measurement plots, we conducted R_s measurement once in two weeks using portable automated chamber measurement system. At the same time, environmental parameters like air temperature, soil temperature and soil moisture were continuously measured using environmental measurement system that composed of car battery, data logger (CR1000, Campbell Scientific Inc.), solar panel, temperature (thermocouples) and soil moisture sensors (CS616, Campbell Scientific Inc.).

R_s was exponentially increased along with the temperature rise in plot 1 and 2. Such exponential increase was also confirmed in plot 3 and 4 if we excluded data in August (remarkably small R_s) under drought stress because of little rainfall. In addition, significant relationships between soil moisture and temperature-normalized R_s were also confirmed in plot 2, 3 and 4. Those results suggested that soil temperature is the primary environmental factor caused for seasonal variation of R_s, but soil moisture can also demonstrate strong influence on R_s as drought stress in summer period in this study site. In this presentation, mechanisms for spatio-temporal variation of R_s will be also discussed including the analysis for sand CN, root biomass and microbial community.

Keywords: Chamber, Drought stress, Zonal distribution, Coastal vegetation, Carbon cycle

©2021. Japan Geoscience Union. All Right Reserved.

Validation of Two Vegetation Indices: NDVI and PRI Derived from GCOM-C/SGLI

*Sasagawa Taiga[1], Tomoko Kawaguchi Akitsu[2], Kenlo Nishida Nasahara[2]

1. Graduate School of Science and Technology, University of Tsukuba, 2. Faculty of Life and Environmental Sciences, University of Tsukuba

Forests play a significant role in terrestrial ecosystems and greatly influence the material cycle in terrestrial ecosystems. Therefore, an accurate understanding of forest conditions is fundamental and indispensable for understanding terrestrial ecosystems. In order to accurately understand the state of forests, which cover a large area, local observations are often insufficient. An example of such a method that can cover a large area is satellite remote sensing.
One example of satellite that is used for observation of terrestrial ecosystems is GCOM-C (Global Change Observation Mission-Climate), which was recently launched by JAXA (Japan Aerospace Exploration Agency). GCOM-C is equipped with a sensor called the SGLI (Second-generation Global Imager). This sensor is capable of observing a larger number of spectral bands than the sensors on other earth observation satellites. This means that GCOM-C/SGLI has a higher wavelength resolution. In addition, GCOM-C/SGLI has a wide observation range, which means that the frequency of observations is high, and thus the temporal resolution is high. Therefore, it is expected that GCOM-C/SGLI can be used for more detailed and frequent observation of forest conditions.
Usually, various indices are calculated from satellites' data to understand the condition of vegetation, such as forests. From the GCOM-C/SGLI data, several indices can be calculated, and typical indices derived from the GCOM-C/SGLI data are NDVI (Normalized Difference Vegetation Index) and PRI (Photochemical Reflectance Index).
The NDVI is widely used in remote sensing of vegetation and can be calculated from many earth observation satellites, but the NDVI derived from GCOM-C/SGLI has a feature that multiple NDVI can be calculated.
That is, it is possible to calculate four NDVIs: two in the red region and two in the near-infrared region since GCOM-C/SGLI has two observation bands each. This is a major feature of GCOM-C/SGLI, and the use of these four NDVIs will enable more detailed remote sensing of forests.
PRI is an indicator that reflects the chemical changes of xanthophylls in chloroplasts (xanthophyll cycle). Xanthophylls are closely related to the heat dissipation of excess energy in photosynthesis, and by quantitatively evaluating the xanthophyll cycle and combining it with other vegetation indices, it is thought that the gross primary production of forests can be estimated. Therefore, PRI, which reflects the xanthophyll cycle, is one of the most important indices in remote sensing of forests. However, the PRI is calculated from the reflectance of very close wavelengths, 531 nm and 570 nm, which requires high wavelength resolution. Therefore, it is not easy to calculate PRI from satellite data. Nevertheless, the GCOM-C/SGLI is able to observe these wavelengths independently. So observing the PRI is a great advantage of the GCOM-C/SGLI.
As described above, although the GCOM-C/SGLI data can be used to calculate the NDVI (four types) and PRI, which are significant vegetation indices, the detailed validation of the accuracy of the data has not been done so far. In this study, we focused on two vegetation indices: NDVI and PRI, which can be calculated from GCOM-C/SGLI observation data, and aimed to validate their accuracy.
For the accuracy verification, we used the ground validation data for three years from 2018 to 2020 at several sites in Japan (Teshio, Tomakomai, Takayama, Mase, Fuji-yoshida, and Fuji-hokuroku). These ground validation data were acquired by spectroradiometers installed at each site. In addition, the

©2021. Japan Geoscience Union. All Right Reserved.

phenology change of the forest was detected by the photographs of the forest taken by the fisheye camera installed with the spectroradiometer. The relationship between the phenological changes and the changes in each index was investigated.
The results of ground-based verification suggested that NDVI and PRI can be obtained from GCOM-C/SGLI. However, the difference between the ground-based measurements and satellite data was sometimes large, especially for PRI. It was also found that each vegetation index had a unique relationship with changes in forest phenology.
In the future, it will be necessary to develop a method to detect and remove the outliers of NDVI and PRI obtained from GCOM-C/SGLI.

Keywords: Remote Sensing, Forest, GCOM-C/SGLI, NDVI, PRI

©2021. Japan Geoscience Union. All Right Reserved.

Seasonal variation in Solar Induced chlorophyll Fluorescence detected by multi-vertical layer spectroscopy in a canopy of cool-temperate deciduous broadleaf forest in Takayama, Gifu

*Tomoki Morozumi[1], Tomomichi Kato[1], Katsuto Tsujimoto[2], KANOKRAT BUAREAL[3], Naohisa Nakashima[1], Yuma Sakai[4], Hideki Kobayashi[4], Kenlo Nasahara[5], Tomoko Akitsu[5], Shohei Murayama[6], Hibiki M Noda[7], Hiroyuki Muraoka[8]

1. Research Faculty of Agriculture, Hokkaido University, 2. Graduate School of Life Sciences, Tohoku University, 3. Graduate School of Global Food Resources, Hokkaido University, 4. Institute of Arctic Climate and Environment Research, Japan Agency for Marine-Earth Science and Technology, 5. Faculty of Life and Environmental Sciences, University of Tsukuba, 6. Environmental Management Research Institute, National Institute of Advanced Industrial Science and Technology, 7. Center for Global Environmental Research, National Institute for Environmental Studies, 8. River Basin Research Center, Gifu University

Solar Induced chlorophyll Fluorescence (SIF) is a quantitative remote sensing signal relating to the photosynthetic activity including gross primary productivity (GPP) of terrestrial ecosystems. After excitation by solar photon, chlorophyll pigment emits a part of unusable excess energy as fluorescence, which equals to SIF. On the contrary to other remote sensing vegetation indices (VIs), SIF has an advantage to be able to explain both diurnal and seasonal GPP variations with relating to photosynthetic active radiation (PAR), leaf absorptance, and photochemical reaction. Previous studies in a deciduous broadleaf forest argued that decrease at the canopy top VIs had lagged after that in the photosynthetic capacity in senescence period, although understory photosynthesis could be activated after crown leaf-off. Recent heavy rainfall events also may affect photosynthetic activity. Therefore, rapidly responding SIF can be expected to be an aid of monitor real-time suppression of photosynthetic activity in the vertical layer of forest canopy. The purpose of this study is to examine whether the ground-based SIF could respond at an autumn-winter senescence period and rainfall events when GPP supposed to decline. We continuously observed ultra-fine (full width at half maximum < 0.4 nm) spectral radiation in a deciduous broadleaf forest ecosystem, at TKY flux site (36.15˚N, 137.42˚E), Takayama, Gifu since August 2019 to December 2020. A spectrometer (QEpro, Ocean Optics, Dunedin, FL, USA) was equipped of 7 optical fiber cables via optical fiber switch and captured the upward and downward spectral radiation at three heights: 8, 14, and 18m (canopy top) with field of view (FOV) of 180˚ and FOV of 25˚. SIF was retrieved using spectral fitting method for O_2-A absorption band (759-767 nm). Half-hourly SIF varied 1.5-0.5 to 0.1-0 (mW m^{-2} nm^{-1} sr^{-1}) from summer to winter. Decreasing SIF besides almost stable VIs variations were shown at heavy rainfall events in late September 2019 and in early July 2020. A timing of SIF decline was earlier at the canopy top, and SIF signal remained detectable from understory till the end of senescence period. The result also suggests that there is a potential contribution of evergreen understory (< 8 m) in snowless winter periods.

Keywords: Chlorophyll Fluorescence, Heavy Rain Event, Remote Sensing, Tower Observation

©2021. Japan Geoscience Union. All Right Reserved.

On the factors affecting reproducibility of GPP estimated by the Earth System Model MIROC-ES2L

*Akira Kurisu[1], Toru Nozawa[2], Manabu Abe[3], Tomohiro Hajima[3]

1. Faculty of Science, Okayama University, 2. Graduate School of Natural Science and Technology, Okayama University, 3. Japan Agency for Marine-Earth Science and Technology

Earth System Models (ESM) that include biogeochemical cycles in land and marine ecosystems have come to be used for global warming simulations. Reproducibility of the biogeochemical cycles in the ESM, however, does not seem to be sufficient. For example, the MIROC-ES2L, one of the ESM developing in Japan, has some problems on the reproducibility of the Gross Primary Production (GPP); the terrestrial GPP has very little seasonality over the tropics. In this study, focusing on the African continent, we investigated that biases (defined as differences between the MIROC-ES2L outputs and satellite observations) in what kind of variables are related to the biases in the GPP.

We analyzed datasets of historical runs done by the MIROC-ES2L and those obtained by satellite and in-situ observations. The MIROC-ES2L data has horizontal resolutions of 2.8 degrees in longitude times 2.8 degrees in latitude. The horizontal resolutions of the observation datasets are converted into the same ones of the MIROC-ES2L. We investigated relationships between biases in the GPP and those in Leaf Area Index (LAI), surface downward shortwave radiation, surface temperature, surface soil moisture content, and precipitation.

Latitude-time distributions of the GPP biases over the African continent show that they are larger in June-October on the south of the Equator whereas larger in December-March on the north of the Equator. Comparing geographical distributions of the GPP biases with those of the LAI ones, both biases have the same sign in June-October on the south of the Equator and in December-March on the north of the Equator. On the other hand, both biases have the opposite sign in June-October on the north of the Equator and in December-March on the south of the Equator. Therefore, the GPP biases seems to be largely explained by the LAI biases, especially in December-March. However, in June-October over the tropical area, the GPP biases cannot be explained by the LAI biases only. The GPP biases in that case might be largely related to the other climatic variables in addition to the LAI biases.

Keywords: Earth System Models, GPP

©2021. Japan Geoscience Union. All Right Reserved.

Estimation of forest above ground biomass from PALSAR Data

*Hantao Li[1], Tomomichi Kato[2], Lan Wu[3], Masato Hayashi[4]

1. Graduate School of Agriculture, Hokkaido University, 2. Research Faculty of Agriculture, Hokkaido University, 3. College of Ecology and Environment, Hainan University, China, 4. Earth Observation Research Center, Japan Aerospace Exploration Agency

Under climate change and increasingly prominent environmental issues, the estimation on forest carbon stock has become hot research topic. Huge volume and high carbon content of tree is the main carbon storage reservoir of the terrestrial biosphere and plays an important role in the global carbon cycle. Therefore, accurate estimation of forest biomass enables us to evaluate and track the status of forest carbon stocks, and to predict the role and feedback of forests in the regional and global carbon cycle, and to provide an important basis for specifying policies to response climate change.

Remote sensing approach offers considerable contribution to forest monitoring via long-term and repetitive observations over vast area (Mermoz et al 2015). Synthetic aperture radar (SAR) is one of the most promising remote detectors to map the global forest above ground biomass (AGB). Especially, the L-band SAR is widely used to retrieve forest biomass, primarily based on a positive correlation between SAR backscatter and in situ AGB. A few studies have successfully used SAR data to map AGB, such as in Madagascar by Minh et al (2018), in Matang Mangroves, Malaysia b Hamdan et al (2014), in Africa by Bouvet et al (2018). These proved that the L-band SAR had a significant relationship with forest biomass, however, many studies have also proved that when AGB reaches a certain level, the correlation between it and the signal will decrease, which is also called saturation phenomenon. Inevitably, SAR shows poor accuracy in high biomass. In addition, satellite attitudes will also bring considerable noise to the inversion results. Although these noises can be avoided by geometric correction and extraction of areas with better local incident angle conditions, a relatively high-precision inversion result can still be hard to achieve.

The purpose of this study is to try to improve the inversion accuracy through filtering calculations and machine learning methods.
This study takes Hokkaido as the research area, based on ALOS-PALSAR and optical remote sensing data, combined with field survey data of forest resources, extracts a variety of remote sensing data modeling variables, and uses random forest and support vector machine methods to target the forest biomass of different tree species. Noted that there are two sets of variables for modeling, which are optical remote sensing data and SAR data. The forest coverage rate in Hokkaido is over 70%, with abundant vegetation types and species. Naturally distributed species mainly include Pinus densiflora, Abies sachalinensis, Cryptomeria japonica, Picea jezoensis, Fagus crenata, oak, etc., covering broad-leaved forests, coniferous forests, Coniferous and broad-leaved mixed forest. In this study, the sample plot data we used are the forest resource survey data provided by the Japanese Forestry Agency. The field data collection time was from 2004 to 2008, a total of 2907 sample sites were collected, and the area of each sample site was 1 ha. The main investigation factors of the field data of the Japanese Forestry Agency include tree height, tree age, volume per ha, tree types, slope, aspect, etc. In this study, the forest aboveground biomass is calculated by the biomass-accumulation relationship equation (Xu et al, 2007). In order to match the acquisition time of the field sample location as much as possible in time, we selected PALSAR data from 2007 to 2008, with two polarization modes, HH and HV, with a resolution of 25 meters. The accuracy of forest biomass estimation by different modeling methods, different tomographic parameters and different forest types was compared. Finally mapping the forest aboveground biomass in Hokkaido.

©2021. Japan Geoscience Union. All Right Reserved.

Keywords: forest aboveground biomass, ALOS, random forest, support vector machine, Landsat-8 OLI

©2021. Japan Geoscience Union. All Right Reserved.

Development of process-based model for estimating wheat production MATCRO-Wheat

*Maki Nakaguki[1], Tomomichi Kato[2], Yuji Masutomi[3], Leilei Liu[4], Seiji Shimoda[5]

1. Hokkaido University, 2. Research Faculty of Agriculture, Hokkaido University, 3. National Institute for Environmental Studies, 4. National Engineering and Technology Center for Information Agriculture, Nanjing Agricultural University, 5. Hokkaido Agricultural Research Center, National Agriculture and Food Research Organization

Crop yield has been significantly influenced by climate change (Schindeler et al .2001). In recent years, there is a concern that crop yields will decline due to rising temperatures and extreme weather events caused by global warming. Under the assumption that rapid population growth could cause food shortages in near future, therefore, many crop models have been developed though most of them are statistical models or site-based models. Statistical model is generally not able to show each process in the interaction between climate change and crops because they do not take into account the material cycle based on plant physiology. On the other hand, though site-based model has the elaborate representation of crop growth, they rarely have been applied at global scales (Zhang et al .2017), probably due to lack of high precision input data and representative parameter sets. Therefore, this study aims to develop a process-based crop model, extended version of Minimal Advanced Treatment of Surface Interaction and Runoff (MATSIRO; Takata et al., 2003) for wheat yield estimation at a global scale, named here as MATCRO-Wheat.

To estimate the wheat yields, MATCRO-Rice model (Masutomi et al. 2016) for rice yield, was modified and added new function specialized for wheat. First, the model parameters were newly set for wheat and a vernalization process was newly introduced. Second, the model was validated with observational data in 5 field sites: Memuro, Hokkaido in Japan (Hokkaido Agricultural Research Center), Nanjing in China (Nanjing Agricultural University), Wongan Hills in Australia, Valcarce in Argentina, and Wanningen in Netherland (AgMIP wheat for last three sites; Benchmark data set for wheat growth models: field experiments and AgMIP multi-model simulations). Model parameters were adjusted to match the modeled biomass evolution and yield to the measured ones as much as possible. Finally, MATCRO-Wheat was run at global scale with adjusted parameter with vernalization process with the spatial resolution of 0.5 degree x 0.5 degree and with the simulation period from 2009 to 2010. Yield per unit land area was calculated by weighting rain-fed and irrigated yields according to the fraction of irrigated area which is drive from AQUASTAT (FAO. AQUASTAT –Global Map of Irrigation Areas), and were validated with the national yields survey according to the GDHY-aligned version v1.2+v1.3 dataset (Iizumi et al .2020).

Results showed that wheat yields were generally well represented of field observations. In the Netherland and Japan, the overestimation of crop growth was improved by introducing vernalization treatment during winter. The global simulation indicated that wheat yields were overestimated in higher latitudinal zones and in summer wet regions. These would be caused as much photosynthate was produced because MATCRO-Wheat does not consider vernalization and growth restriction due to high humidity. Therefore, further improvement of MATCRO-Wheat is required for accurate representation of wheat growth and yield.

©2021. Japan Geoscience Union. All Right Reserved.

Keywords: Process-based model, climate change, vernalization

©2021. Japan Geoscience Union. All Right Reserved.

[J] Oral | H (Human Geosciences)：H-QR Quaternary research

Sat. Jun 5, 2021 9:00 AM - 10:30 AM JST | Sat. Jun 5, 2021 12:00 AM - 1:30 AM UTC | Ch.16 Zoom Room 16

[H-QR04] Quaternary, Diachronic dynamics of human-environment interactions

convener:Mamoru Koarai(Earth Science course, College of Science, Ibaraki University), Yusuke Yokoyama(Atmosphere and Ocean Research Institute, University of Tokyo), Koji Okumura(Graduate School of Letters, Hiroshima University), Yasufumi Satoguchi(Lake Biwa Museum), Chairperson:Mamoru Koarai(Earth Science course, College of Science, Ibaraki University), Tsutomu Nakazawa(Geological Survey of Japan, AIST)

Humans have attained their specific development by indigenous cultures and evolved through environmental adaptation. The session raises issues of human-environmental interactions, views from diverse changes of climate, ocean, land and biota having made striking influence on humans. It welcomes various fields from human-environment change and their chronometric dating among Quaternary disciplines.

9:00 AM - 9:15 AM JST | 12:00 AM - 12:15 AM UTC

[HQR04-01] Distribution and classification of buried flat surfaces beneath the post-LGM deposits in central Tokyo

*Junko Komatsubara[1], Yoshinori Miyachi[1], Susumu Nonogaki[1], Toshio Nakayama[2] (1.National Institute of Advanced Industrial Science and Technology, 2.Civil Engineering Support and Training Center)

9:15 AM - 9:30 AM JST | 12:15 AM - 12:30 AM UTC

[HQR04-02] 240 ka Ata-Th tephra layer found in Tokyo and its geological significance

*Kunihiko Endo[1], Mari Sumita[2], Toshihiko Sugai[4], Hisashi Fujine[3], Masaaki Suzuki[5], Kyota Uemura[6], Yusuke Suginaka[7], Marie Noguchi[3], Shigeko Ishiwata[8], Reisuke Kondo[9], Takato Takemura[10] (1.Nihon University, 2.GEOMAR, 3.Paleo Labo, 4.Tokyo University , 5.Education Center of Bunkyo, 6.The Institute of Natural Sciences, College of Humanities and Sciences, Nihon University, 7.RCCM, 8.GaNT, 9.Atmosphere and Ocean Research Institute, The University of Tokyo, 10.Nihon University college of humanities and sciences)

9:30 AM - 9:45 AM JST | 12:30 AM - 12:45 AM UTC

[HQR04-03] Estimation of sedimentary condition in Kinu River and Kokai River lowland using micro tremor survey

*Mamoru Koarai[1], Kanaho Miki[1], Keiichi Takami[1], Shigeki Senna[2] (1.Earth Science course, College of Science, Ibaraki University, 2.National Research Insutitute of Earth Science and Disaster Resilience)

9:45 AM - 10:00 AM JST | 12:45 AM - 1:00 AM UTC

[HQR04-04] Ground-type classification based on Quaternary stratigraphy and sedimentary facies and the corresponding ground motion characteristics, with special reference to the 3D Urban Geological Map of Central Tokyo

★Invited Papers

*Tsutomu Nakazawa[1], Ikuo Cho[1], Junko Komatsubara[1], Tomonori Naya[1], Susumu Nonogaki[1], Yoshinori Miyachi[1], Masanori Ozaki[1], Kentaro Sakata[1], Hiroomi Nakazato[2], Takehiko Suzuki[3], Toshio Nakayama[4] (1.Geological Survey of Japan, AIST, 2.NIRE, NARO, 3.Tokyo Metropolitan University, 4.Civil Engineering Support and Training Center, Bureau of Construction, Tokyo Metropolitan Government)

10:00 AM - 10:15 AM JST | 1:00 AM - 1:15 AM UTC

[HQR04-05] Stratigraphic division, age and distribution pattern of the Middle to Upper Pleistocene Shimosa Group in central Tokyo area

*Tomonori Naya[1], Tsutomu Nakazawa[1], Susumu Nonogaki[1], Kentaro Sakata[1], Hiroomi Nakazato[2], Takehiko Suzuki[3], Toshio Nakayama[4] (1.Geological Survey of Japan, National Institute of Advanced Industrial Science and Technology, 2.Institute for Rural Engineering, NARO, 3.Tokyo Metropolitan

University , 4.Civil Engineering Support and Training Center, Bureau of Construction, Tokyo Metropolitan Government)

10:15 AM - 10:30 AM JST | 1:15 AM - 1:30 AM UTC

[HQR04-06] Paleoenvironmental change in Paleo-Tokyo Bay during MIS 5e inferred from ostracode assemblages of the Pleistocene Kioroshi Formation, Shimosa Group, northern Chiba Prefecture, central Japan.

*Mai Harashima[1], Tsutomu Nakazawa[2], Hirokazu Ozawa[3], Minoru Kaneko, Hiroyuki Ishikawa, Masahiro Nomura[4], Sachiko Agematsu[1] (1.University of Tsukuba, 2.Geological Survey of Japan, AIST, 3.Nihon University, 4.Surugadai University)

Distribution and classification of buried flat surfaces beneath the post-LGM deposits in central Tokyo

*Junko Komatsubara[1], Yoshinori Miyachi[1], Susumu Nonogaki[1], Toshio Nakayama[2]

1. National Institute of Advanced Industrial Science and Technology, 2. Civil Engineering Support and Training Center

The Tokyo Lowland in the eastern part of Tokyo metropolitan area is underlain by the thick post-Last Glacial Maximum (LGM) deposits. Many studies have been conducted on the post-LGM deposits in the Tokyo Lowland since the 1923 Kanto earthquake. Based on those previous works and borehole logs of the Civil Engineering Support and Training Center, Tokyo Metropolitan Government, the most detailed three-dimensional geological map, 3D Urban Geological Map of Central Tokyo has been published by Geological Survey of Japan, AIST. As a part of this achievement, we introduce a classification result of buried flat surfaces (BFSs) beneath the post-LGM deposits. In this study, a base of the post-LGM deposits is defined as the bottom of conglomerate around the incised valley areas and top of conglomerate in buried terraces areas.

BFSs are classified into one valley floor and four other higher flat surfaces. The valley floor is located along the axis of incised valley formed during LGM. It has an altitude of −50 to −80 m and is covered with thick conglomerate. BFSs 1–4 are 0 to −10 m, −18 to −36 m, −21 to −25 m, −45 to −54 m altitude, respectively. BFS 1 and BFS 3 lack conglomerate. BFS 2 and BFS 4 are accompanied by widely traceable conglomerate on them.

BFS 1 is interpreted mostly as Holocene wave-cut platform, partly as remains of MIS 5a marine terrace. BFS 2, known as Honjo buried terrace, is interpreted MIS 3 fluvial terrace and correlated with Tachikawa II surface in Tamagawa area, western Tokyo. The age and origin of BFS 3 remain unknown, and BFS 4 is interpreted as a fluvial terrace formed during MIS 3 or older age.

BFS 1 and BFS 2 have a potential to be subdivided due to their wide range of altitudes. Drilling core survey on those surfaces for volcanic ash soil and/or tephrostratigraphy may provide clues for subdivision.

Keywords: Tokyo Lowland, post-LGM deposits, buried flat surfaces, basal conglomerates, borehole logs, 3D geomodelling

©2021. Japan Geoscience Union. All Right Reserved.

240 ka Ata-Th tephra layer found in Tokyo and its geological significance

*Kunihiko Endo[1], Mari Sumita[2], Toshihiko Sugai[4], Hisashi Fujine[3], Masaaki Suzuki[5], Kyota Uemura[6], Yusuke Suginaka[7], Marie Noguchi[3], Shigeko Ishiwata[8], Reisuke Kondo[9], Takato Takemura[10]

1. Nihon University, 2. GEOMAR, 3. Paleo Labo, 4. Tokyo University , 5. Education Center of Bunkyo, 6. The Institute of Natural Sciences, College of Humanities and Sciences, Nihon University, 7. RCCM, 8. GaNT, 9. Atmosphere and Ocean Research Institute, The University of Tokyo, 10. Nihon University college of humanities and sciences

1. Introduction

Our recent study (Endo et al., 2020) shows that drilled cores and their geological information are extremely useful tools for understanding hidden underground, like densely populated Tokyo where almost no exposure exists nowadays. Here, we propose new geomorphic/geologic division of the Tokyo area together with the underground geology and geological history of Musashino Upland interpreted from the numerous drilled cores. Many of the cores included several tephra layers, and they provided the temporal geological evolution of the area very well. Also, we will discuss on the correlation of two major tephra layers that were found in the several cores, Ata-Torihama ash layer (Ata-Th ash) from Southern Kyushu and TCu-1 (Tm-2) sourced Hakone Caldera.

2. Tephra occurrence and correlation

Two clearly defined tephra layers were found in the NU-AKD-1 core, drilled site at Akabane-dai NE Musashino Upland, at 24 m below the surface, specifically from 24.15 m to 24.35 m. These two layers seem deposited almost no erosional interval, the upper (“24.2 m ash”) consist from very fine ash almost entirely of bubble-wall glass shards, and 15 cm thick lower unit (“24.3 m pumice”) consist from pale yellowish coarse-grained pumice lapillus. Similar ash and pumice were also found at Hongo and Kami-Nakazato site and probable correlation to Ata-Th ash and TCu-1(Tm-2) pumice by using mainly refractive index analyses of the glass shards and minerals (Suzuki et al., 2020).

3. Major element analyses of the tephra layers

According to the major elements chemical analyses of glass shards by EDS and EPMA, a) “24.2 m ash”, ash from Hongo and Kami-Nakazato site were similar to those of the matrix glass of Ata-Torihama pyroclastic flow deposits (240 ka; Machida and Arai, 2004) sourced Ata Caldera, southern Kyushu, b) “24.3 m pumice”, and pumice samples of Hongo and Kami-Nakazato site were similar to TCu-1 (Tm-2) pumice and pyroclastic flows in Oiso Hills, main Hakone tephra type locality 15 km away from Hakone volcano.

The other tephra lenses (pumice) were found southern Tokyo in the NU-SKG-1 core, from the basal gravel layer of the Tokyo Formation of MIS 5.5 transgression. These pumice were chemically similar to Tu-1, Tu-7 to -8 pumice fall layers from the Hakone volcano, however, it is possible to distinguish from TCu-1 (Tm-2) by SiO2 vs. K2O plot.

4. Geological significance

Ata-Th tephra correspond to Tm-4 in Oiso Hills, which is separated by two tephra units above the TCu-1 (Tm-2). As the interval between Tm-4 (= Ata-Th) and TCu-1 (Tm-2) decrease towards to the east, these

©2021. Japan Geoscience Union. All Right Reserved.

two units became thinner and more closely overlain each other farther east in Tokyo. This unique unit combination would help for define the broad stratigraphical correlations. Thus, Ata-Th and Tm-2 became one of the most useful marker horizons of 240 ka and/or MIS7 in the middle Pleistocene geological sequences in Musashino Upland areas in Tokyo and the surroundings.

References

Danhara, T. et al. (2010) The Quat. Res., 19, 101-119.
Endo, K. and Uesugi,Y. (1972) The Quat. Res., 11, 15-28.
Endo, K. et al. (2019) The Quat. Res., 58, 353-375.
Endo, K. et al. (2020) 2020 Annu. Meet. Japan Assoc. Quat. Res.
Machida, H. and Arai, F. (2004) Tokyo Univ. Press.
Nagahashi ,Y. et al. (2004) The Quat. Res., 43, 15-35.
Naya, T. et al. (2020) Jour. Geol. Soc. Japan, 126, 575-587.
Oka, S. (1991) Bull. Geol. Surv. Japan, 42, 553-653.
Suzuki M. et al. (2020) 2020 Annu. Meet. Japan Assoc. Quat. Res.
Uemura, K. et al. (2020) Proc. Inst. Nat. Sci., Nihon Univ. 55, 155-164.
Uesugi, Y. (1976) Bull.Assoc. Kanto Quat. Res., 3, 28-38.

Keywords: Ata-Th tephra, Drilled core of Akabane-dai, Stratigraphic sequence of Tokyo, Musashino upland, Middle Pleistocene

©2021. Japan Geoscience Union. All Right Reserved.

Estimation of sedimentary condition in Kinu River and Kokai River lowland using micro tremor survey

*Mamoru Koarai[1], Kanaho Miki[1], Keiichi Takami[1], Shigeki Senna[2]

1. Earth Science course, College of Science, Ibaraki University, 2. National Research Insutitute of Earth Science and Disaster Resilience

The Misaka-Shinden and Oki-Shinden districts are located in the back marsh environment in the central part of the Kinu River and Kokai River lowland in the southern part of Ibaraki prefecture. These districts are located in an environment extremely vulnerable to flood disasters, and are flooded even during the 2015 Kanto and Tohoku Heavy Rain.

The authors attempted to estimate the sedimentary environment in these areas as basic information for examining the historical reasons for the settlements located in such places. Micro tremor survey is performed around the Ken-oudo High Way where there is boring data, and the boring data are compared with the S wave velocity structure obtained by micro tremor survey. From the results, the underground ground structures are estimated using the micro tremor survey at the point where there is no boring data. We also performed boring excavation with a hand auger and particle size analysis of the collected samples.

The authors set an approximate S-wave velocity range with respect to the ground from the comparison between the boring data and the micro tremor survry results. S wave velocity of less than 100 m / s is mud, around 200 m / s is sand, and over 300 m / s is gravel. Using these data, the ground conditions of the Misaka-Shinden and Oki-Shinden Districts and the surrounding areas, where there is no boring data, were estimated, and the estimated columnar sections of these areas were created.

As a result, it was estimated that there was a thick sand layer at a depth of about 5 to 15 m just below Misaka-Shinden, and that the river channel of that era was flowing around it. According to the results of boring by hand auger, it is presumed that the southern part of Oki-Shinden was a back marsh environment where flood sediments were difficult to reach, as the surface layer was almost a soft mud layer up to about 5 m.

Keywords: sedimentary environment, Kinu River and Kokai River lowland, micro tremor, boring data, Misaka-Shinden and Oki-Shinden

©2021. Japan Geoscience Union. All Right Reserved.

Ground-type classification based on Quaternary stratigraphy and sedimentary facies and the corresponding ground motion characteristics, with special reference to the 3D Urban Geological Map of Central Tokyo

*Tsutomu Nakazawa[1], Ikuo Cho[1], Junko Komatsubara[1], Tomonori Naya[1], Susumu Nonogaki[1], Yoshinori Miyachi[1], Masanori Ozaki[1], Kentaro Sakata[1], Hiroomi Nakazato[2], Takehiko Suzuki[3], Toshio Nakayama[4]

1. Geological Survey of Japan, AIST, 2. NIRE, NARO, 3. Tokyo Metropolitan University, 4. Civil Engineering Support and Training Center, Bureau of Construction, Tokyo Metropolitan Government

Ground motion characteristics in an urbanized coastal plain are influenced by shallow subsurface geologic conditions. We classified ground types in central Tokyo based on stratigraphy and sedimentary facies in reference to the 3D Urban Geological Map of Central Tokyo published in April 2021 by our research group of GSJ, AIST, and conducted microtremor observations in each ground type to clarify the corresponding ground motion characteristics.

The Musashino Upland is composed of the Middle to Upper Pleistocene strata including the Yabu (MIS 9), Kamiizumi (MIS 7e), and Tokyo (MIS 5e) formations. Of them, the Tokyo Formation contains thick inner-bay soft muddy sediments as incised-valley fills. The detailed distribution of the incised-valley fills was demonstrated by 3D geomodelling. Microtremor observations reveal that the H/V spectra show a peak at 1–2 Hz at the areas of the incised-valley fills. Particularly, a remarkable peak at 1 Hz is observed in the H/V spectra of the Setagaya Valley fills with the high mud-content. On the other hand, the H/V spectra exhibit higher peak frequencies around 4 Hz at the areas outside the incised valleys because of the hard substrate composed mainly of marine sand beds of the Yabu and Kamiizumi formations.

The Tokyo Lowland is underlain by the post-LGM deposits composed generally of fluvial to inner-bay sand and mud. The 3D geomodelling based on the detailed stratigraphic correlation reveals that the buried geomorphology almost corresponding to the base of the post-LGM deposits comprises the deepest valley floor and four buried flat surfaces. We carried out microtremor observations along a line across the deepest valley floor and the flat surfaces 1 and 2 beneath the Tokyo Lowland. The H/V spectra at the areas both of the deepest valley floor and the flat surface 2 exhibit a peak at 1 Hz. The peaks of the flat surface 2 area are clearer than those of the valley floor area because of the high contrast of physical properties between the firm buried terrace gravelly sediments and the overlying soft post-LGM deposits. On the other hand, the H/V spectra at the flat surface 1 area show flat shapes in high frequency ranges due to relatively thin soft sediments above the Pleistocene hard substrate.

Thus, the ground-type classification based on the detailed stratigraphy and sedimentary facies using the 3D geomodelling enables the efficient and accurate assessment of the earthquake hazard risks.

Keywords: Quaternary stratigraphy, 3D geomodelling, borehole logs, microtremor observation, ground motion characteristics

©2021. Japan Geoscience Union. All Right Reserved.

Stratigraphic division, age and distribution pattern of the Middle to Upper Pleistocene Shimosa Group in central Tokyo area

*Tomonori Naya[1], Tsutomu Nakazawa[1], Susumu Nonogaki[1], Kentaro Sakata[1], Hiroomi Nakazato[2], Takehiko Suzuki[3], Toshio Nakayama[4]

1. Geological Survey of Japan, National Institute of Advanced Industrial Science and Technology, 2. Institute for Rural Engineering, NARO, 3. Tokyo Metropolitan University , 4. Civil Engineering Support and Training Center, Bureau of Construction, Tokyo Metropolitan Government

The Middle to Upper Pleistocene deposits, mainly composed of shallow marine and fluvial sediments, are distributed in the upper subsurface of the central Tokyo area. This Pleistocene deposit has been called “Tokyo Formation” for a long time, and especially “Tokyo Gravel Bed” at the basal part of “Tokyo Formation” has been paid attention from the viewpoint of applied geology because of its importance such as a bearing layer for a mid–high rise buildings, an important aquifer for groundwater utilization, and a key bed for active tectonics analysis. However, the detailed age of “Tokyo Formation” has remained undetermined for many decades.

We are preparing a 3D geological map of the central Tokyo area (Urban Geological Map: Central Tokyo Area), which is scheduled to be released in April 2021, as part of GSJ project to develop geological information on urban area. In order to develop the Urban Geological Map, we have re-examined the stratigraphy and age of “Tokyo Formation” based on reconstruction of depositional environments according to facies analysis, tephra analysis, and pollen assemblages of borehole cores (Nakazawa et al. 2019, 2020: Naya et al. 2020). The results indicate that the strata previously considered to be “Tokyo Formation” are a mixture of several depositional cycles formed under the influence of eustatic sea-level changes in different periods. In the Middle to Upper Pleistocene Shimosa Group of Boso Peninsula, a sedimentary cycle formed by a single transgression–regression event is defined as a single formation. In this study, the criteria of the Shimosa Group in Boso Peninsula are applied to the stratigraphic division of the central Tokyo area, and the previous “Tokyo Formation” is subdivided into three formations; the Yabu, Kamiizumi, and Tokyo formations. In addition, based on this stratigraphic division, a 3D geological model was created using a large amount of borehole data over a wide area, and the distribution pattern of each formation was also clarified. In this presentation, we introduce an overview of the newly applied stratigraphic division, age and distribution pattern of the Shimosa Group in the central Tokyo area.

Nakazawa et al. (2019) The Journal of the Geological Society of Japan, 125, 367–385.

Nakazawa et al. (2020) Bulletin of the Geological Survey of Japan, 71, 19–32.

Naya et al. (2020) The Journal of the Geological Society of Japan, 126, 575–587.

Keywords: Middle Pleistocene, Upper Pleistocene, Stratigraphy, 3D geological map, Tokyo Formation, Shimosa Group

©2021. Japan Geoscience Union. All Right Reserved.

Paleoenvironmental change in Paleo-Tokyo Bay during MIS 5e inferred from ostracode assemblages of the Pleistocene Kioroshi Formation, Shimosa Group, northern Chiba Prefecture, central Japan.

*Mai Harashima[1], Tsutomu Nakazawa[2], Hirokazu Ozawa[3], Minoru Kaneko, Hiroyuki Ishikawa, Masahiro Nomura[4], Sachiko Agematsu[1]

1. University of Tsukuba, 2. Geological Survey of Japan, AIST, 3. Nihon University, 4. Surugadai University

The Pleistocene Kioroshi Formation, Shimosa Group which is distributed beneath the Shimosa Upland in Chiba Prefecture, central Japan is composed mainly of shallow marine deposits accumulated in Paleo-Tokyo Bay during MIS 5e. The depositional sequence of the Kioroshi Formation comprises a lower incised valley system and an upper barrier island system. Ostracode assemblages have been reported from the Kioroshi Formation by Yajima (1978, 1982) and Okazaki et al. (2018), but the succession of ostracode assemblages throughout the Kioroshi Formation including both incised valley and barrier island systems has not been examined so far. We report ostracode assemblages from the lower and upper parts of the Kioroshi Formation in sediment cores and interpret paleoenvironmental change in Paleo-Tokyo Bay during MIS 5e.

Fossil ostracodes were collected from two sediment cores: GS-NT-1 (Narita City, Chiba; oceanward) and GS-NY-1 (Nagareyama City, Chiba; landward) recovered from the sites within a buried incised valley. We identified 81 ostracode species from GS-NT-1 and 77 species from GS-NY-1. Based on the ostracode assemblages, the examined intervals in cores GS-NT-1 and GS-NY-1 are divided into four zones, respectively; zones NT-I–IV and zones NY-I–IV in ascending order.

Zone NT-I is characterized by *Spinileberis quadriaculeata–Bicornucythere bisanensis* assemblage accompanied with *Cytheromorpha acupunctata*, indicating an enclosed inner-bay environment near a middle bay. Zone NT-II characterized by *S. quadriaculeata–B. bisanensis–C. acupunctata–Pontocythere miurensis* assemblage shows an inner bay environment with coastal currents. Zone NT-III is characterized by *Neomonoceratina delicata* assemblage accompanied with *S. quadriaculeata* and *C. acupunctata*, seems to represent an inner bay environment under the influence of a warm current. Zone NT-IV is characterized by *Aurila* spp.–*P. miurensis* assemblage accompanied with *Cythere omotenipponica*, indicating an open bay environment near seaweed beds influenced by open-ocean water. According to Nakazawa et al. (2017), zones NT-I–NT-II, zone NT-III and zone NT-IV correspond to the sand bar facies which is incised valley system, the sand bar facies–the central basin facies, and the central basin facies–the flood tidal facies which is barrier island system, respectively.

Zone NY-I is characterized by *S. quadriaculeata–C. acupunctata* assemblage, indicating an enclosed inner bay environment slightly near a middle bay. Zone NY-II is characterized by *C. acupunctata* assemblage accompanied with *N. delicata* and *S. quadriaculeata,* seems to represent an inner bay environment under the influence of a warm current. Zone NY-III is characterized by *Loxoconcha uranouchiensis* assemblage accompanied with *S. quadriaculeata* and *C. acupunctata*, indicating an inner bay environment near seaweed beds. Zone NY-IV characterized by *Aurila* spp.–*Loxoconcha optima* assemblage accompanied with *C. acupunctata* and *Xestoleberis hanaii* shows an open bay environment near seaweed beds influenced by open water. The boundary between zones NY-I–NY-III and zone NY-IV correspond with lithologic divisions respectively the lower incised valley system and the upper barrier system.

©2021. Japan Geoscience Union. All Right Reserved.

References:

Nakazawa, T., Sakata, K., Hongo, M. and Nakazato, H. (2017) Transition from incised valley to barrier island systems during MIS 5e in the northern Chiba area, Kanto Plain, central Japan. Quaternary International, 456, 85–101.

Okazaki, H., Ishii, A., Kaneko, M., Tamura, T., Chigaku Club of Gunma Prefectural Ota Girls' High School, Kato, H., Isaji, S. and Tanaka, G. (2018) An Excavation Report of a Baleen Whale, from the Pleistocene Kioroshi Formation, Shimosa Group - Sedimentary Facies, Microfossils, Ground Penetrating Radar Analysis. J. Nat. Hist. Mus. Inst. Chiba, 14(1), 19–28 (in Japanese with English abstract).

Yajima (1978) Quaternary Ostracoda from Kisarazu near Tokyo. Trans. Proc. Palaeontol. Soc. Japan, N. S., 112, 371–409.

Yajima (1982) Late Pleistocene Ostracoda from the Atsumi Peninsula, central Japan. Trans. Proc. Palaeontol. Soc. Japan, N. S., 146, 49–76.

Keywords: Ostracoda, Kioroshi Formation, MIS 5e, Paleo-Tokyo Bay

©2021. Japan Geoscience Union. All Right Reserved.

[J] Oral | H (Human Geosciences)：H-QR Quaternary research

Sat. Jun 5, 2021 10:45 AM - 12:15 PM JST | Sat. Jun 5, 2021 1:45 AM - 3:15 AM UTC | Ch.16 Zoom Room 16

[H-QR04] Quaternary, Diachronic dynamics of human-environment interactions

convener:Mamoru Koarai(Earth Science course, College of Science, Ibaraki University), Yusuke Yokoyama(Atmosphere and Ocean Research Institute, University of Tokyo), Koji Okumura(Graduate School of Letters, Hiroshima University), Yasufumi Satoguchi(Lake Biwa Museum), Chairperson:Koji Okumura(Graduate School of Letters, Hiroshima University), Yusuke Yokoyama(Atmosphere and Ocean Research Institute, University of Tokyo)

Humans have attained their specific development by indigenous cultures and evolved through environmental adaptation. The session raises issues of human-environmental interactions, views from diverse changes of climate, ocean, land and biota having made striking influence on humans. It welcomes various fields from human-environment change and their chronometric dating among Quaternary disciplines.

10:45 AM - 11:00 AM JST | 1:45 AM - 2:00 AM UTC

[HQR04-07] Middle Pleistocene terraces in the Chita Peninsula, near Nagoya, central Japan

*Taku Komatsubara[1], Misao Hongo[2], Yoshiki Sato[1] (1.Institute of Geology and Geoinformation, Advanced Industrial Science and Technology, 2.Alps Technical Research Laboratory Co., Ltd.)

11:00 AM - 11:15 AM JST | 2:00 AM - 2:15 AM UTC

[HQR04-08] **Unveiling the black box: monthly measurements on dissolved inorganic radiocarbon in Fuji Five lakes water to understand the lake specific reservoir ages**

*Ota Kosuke[1,2], Yusuke Yokoyama[1,2], Yosuke Miyairi[2], Shinya Yamamoto[3], Toshihiro Miyajima[2] (1.Earth and Planetary Science Department, Graduate school of Science, University of Tokyo, 2.Atmosphere and Ocean Research Institute, University of Tokyo, 3.Mount Fuji Research Institute, Yamanashi Prefectural Government)

11:15 AM - 11:30 AM JST | 2:15 AM - 2:30 AM UTC

[HQR04-09] Eventual sediments presumed in lake deposits of coastal lakes along the western coast of Kyushu Island, Japan

*Kaoru Kashima[1], Yu Fukumoto[2], Tsuyoshi Haraguchi[2] (1.Department of Earth and Planetary Sciences, Kyushu University, 2.Osaka City University)

11:30 AM - 11:45 AM JST | 2:30 AM - 2:45 AM UTC

[HQR04-10] Origin and evolution of a delta-margin mangrove in Can Gio, southern Vietnam

★Invited Papers

Daniel S Collins[1,6], Lap V Nguyen[2], Oanh TK Ta[2], Limi Mao[3], Yuji Ishii[1], Hiroyuki Kitagawa[4], Rei Nakashima[1], *Toru Tamura[1,5] (1.Geological Survey of Japan, AIST, 2.HCMC Institute of Resources Geography, Vietnamese Academy of Science and Technology, 3.Nanjing Institute of Geology and Palaeontology, Chinese Academy of Sciences, 4.Institute for Space-Earth Environmental Research, Nagoya University, 5.Graduate School of Frontier Science, The University of Tokyo, 6.Shell International Ltd)

11:45 AM - 12:15 PM JST | 2:45 AM - 3:15 AM UTC

[HQR04-11] Discussion

Middle Pleistocene terraces in the Chita Peninsula, near Nagoya, central Japan

*Taku Komatsubara[1], Misao Hongo[2], Yoshiki Sato[1]

1. Institute of Geology and Geoinformation, Advanced Industrial Science and Technology, 2. Alps Technical Research Laboratory Co., Ltd.

1. Introduction
The Middle Pleistocene terraces in the Chita Peninsula had been subdivided into two surfaces and formations since Matsuda (1969). The authors re-examined topographic features and stratigraphy of them and tried to date them by pollen analysis.

2. Field survey

A large outcrop (Fig. 1) in the central area of the peninsula shows that the highest terrace that named “Taketoyo terrace” is subdivided two terrace surfaces, and its deposits are also subdivided two units by an unconformity. The higher one (newly named “H 1 terrace”) is composed by gravelly deposits and distributed on the top of hills that constitute watershed between the Kinuura on the east of peninsula and the Ise bay on the west of peninsula.. The H 1 terrace deposits contain a lot of rhyolite gravels. The lower one (newly named “H 2 terrace” is composed by sand and mud with bioturbation. The other Middle Pleistocene terrace 1 step lower than H 2 terrace (newly named “H 3 terrace”) is composed with two marine mud and fluvial top gravels. Rhyolite gravels are common in the H 2 terrace and H 3 terrace deposits in the western coast, however, it is few in them in the eastern coast.
3. Pollen analysis
Results of the pollen analysis in each terrace deposits are shown in Table 1.

4. Dating
All of the H1 ~ H3 terraces are late Middle Pleistocene (Chibanian) interglacial ones, because of red (2.5 ~ 5 YR in the Munsell color index) surface soil, degree of weathering of gravels (intensely weathered to be soft and brittle) and warm temperate pollen assemblages. H I is thought to be dated to a warm climate stage around MIS 11 fluvial terrace, H2 is thought to be MIS 9 marine terrace, H 3 is thought to be MIS marine to river mouth terrace.

Keywords: Middle Pleistocene terrace, Pollen analysis, Dating, Chita peninsula, Chibanian

©2021. Japan Geoscience Union. All Right Reserved.

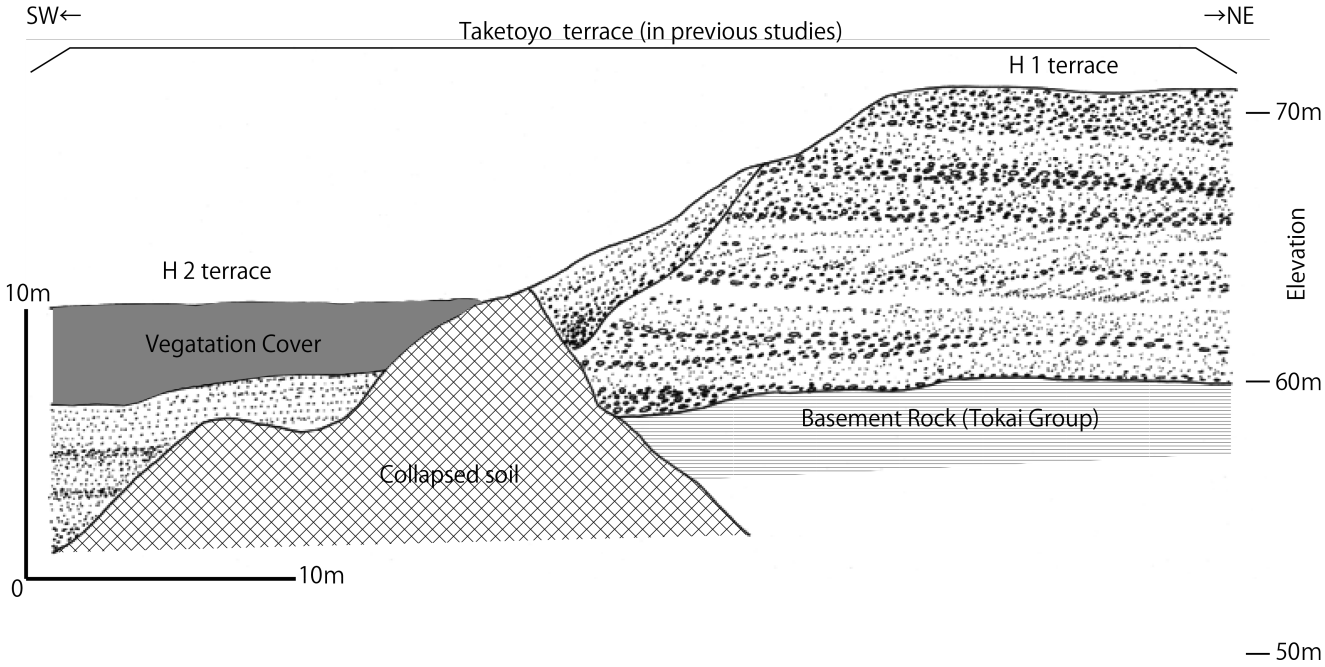


Fig. 1 Newly recovered outcrop in the central part of th Chita Paninsula (near Besso pond, Taketoyo town)

Table 1 Pollen assemblage in the Middle Pleistocene terrace deposits

Horizon	numver of tree pollen	Major taxon (Pollen assemblege)	Age
H3 Uppermost tidal deposit	211	Rhamnaceae, *Scidopitys*, *Quercus* (Subgen. *Lepidobalanus*)	MIS7 late subintergl acial age
H3 upper part debris flow deposits	221	*Pinus* > *Cryptomeria*, *Betula* > *Podocarpus*	
H3 lower marine layer ?	114	*Cryptomeria*, *Alnus* > *Quercus* (Subgen. *Cyclobalanopsis*), *Castanopsis* / *Pasania*, *Trema*, *Lagerstroemia*	MIS 7 early interglacia l age
H3 lower marine layer	99	*Cryptomeria* > *Quercus* (Subgen. *Lepidobalanus), Pinus*	
H3 lower marine layer	212	*Cryptomeria*, *Pinus* > *Quercus* (Subgen. *Cyclobalanopsis*), *Quercus* (Subgen. *Lepidobalanus*) > *Podocarpus*, *Betula,* Castanopsis / Pasania	
H3 lower marine layer	35	*Cryptomeria*, *Pinus*	
H3 lower marine layer	115	*Cryptomeria* > *Pinus*, *Betula*, *Camellia*	
H2 top of marine layer	40	*Cryptomeria, Pinus*, *Quercu* s (Subgen. *Cyclobalanopsis*), *Q*. (Subgen. *Lepidobalanus*),*Mallotus*, *Castanopsis* / *Pasania*, *Camellia*	MIS 9
H2 marine layer	224	*Pinus*, *Fagus* > *Quercus* (Subgen. *Lepidobalanus*) > *Abies*, *Tsuga*, *Sciadoptyis*, *Podocarpus*, *Sapium*	
H1upper part in fluvial layer	202	*Clethra* > *Quercus* (Subgen. *Lepidobalanus*), *Alnus, Cryptomeria* > *Quercus* (Subgen. *Cyclobalanopsis*), *Castanopsis* / *Pasania*	around MIS 11
H1 middle part in fluvial layer	11	*Pinus, Sciadopitys, Cryptomeria, Betula, Alnus, Quercus* (Snbgen. *Lepidobalanus*), *Fagus*	

©2021. Japan Geoscience Union. All Right Reserved.

Unveiling the black box: monthly measurements on dissolved inorganic radiocarbon in Fuji Five lakes water to understand the lake specific reservoir ages

*Ota Kosuke[1,2], Yusuke Yokoyama[1,2], Yosuke Miyairi[2], Shinya Yamamoto[3], Toshihiro Miyajima[2]

1. Earth and Planetary Science Department, Graduate school of Science, University of Tokyo, 2. Atmosphere and Ocean Research Institute, University of Tokyo, 3. Mount Fuji Research Institute, Yamanashi Prefectural Government

Lake sediments are important for paleoenvironmental studies, and it is important to estimate the radiocarbon reservoir effects within lake water with high accuracy. Although radiocarbon dating has a large range of uses, the radiocarbon reservoir effect causes water and sediment ages to appear older. This is due to the exchange of ^{14}C-depleted substances derived from biological remains and host rocks during the process of fixing, and from transporting modern carbon from the atmosphere. The radiocarbon reservoir effect from lake samples is known to be highly variable, showing a maximum of about 2200 years which can lead to problems for high-precision dating. Yet, there are few studies of radiocarbon reservoir effects on land due to complicated carbon transfer processes and lack of appropriate measurement techniques, and no studies have been performed on seasonal variations.

We study Fuji Five Lakes to unveil the mechanisms behind variability of their reservoir ages. Lakes Motosu, Shoji and Sai only have temporal inflow and outflow rivers, and the lake water is defined by precipitation and groundwater inflow. Therefore, the transportation pathway of water is simple and suitable for estimating the radiocarbon transport process around these lakes. By measuring the radiocarbon concentration ($\Delta^{14}C$) of precipitation, groundwater, and lake water, it is possible to clarify the effect of groundwater on the reservoir effect of lake water. In this study, for the first time, we measured lake water $\Delta^{14}C$, $\delta^{18}O$, and δD monthly at the Fuji Five Lakes, and compared results with groundwater $\Delta^{14}C$. The results show that Lake Kawaguchi had the lowest $\Delta^{14}C$ in August and Lake Motosu had the highest $\Delta^{14}C$ in January. In Lakes Motosu and Kawaguchi, $\Delta^{14}C$ was found to increase in winter. No clear seasonal changes were observed in Lake Sai and Lake Yamanaka. Regarding the relationship between the lake water and the sediment, the lake water $\Delta^{14}C$ coincided with surface sediment $\Delta^{14}C$ in the summer at Lakes Motosu and Kawaguchi. Sediment $\Delta^{14}C$ in both lakes may be defined by the fixation of lake water ^{14}C due to elevated biological production in the summer, and summer lake water $\Delta^{14}C$ can be used to estimate the reservoir effect of lake sediment. Therefore, at least seasonal measurements on lake water are recommended to better understand lake specific reservoir ages.

Keywords: Radiocarbon, Fuji Five Lakes, Lake water

©2021. Japan Geoscience Union. All Right Reserved.

Eventual sediments presumed in lake deposits of coastal lakes along the western coast of Kyushu Island, Japan

*Kaoru Kashima[1], Yu Fukumoto[2], Tsuyoshi Haraguchi[2]

1. Department of Earth and Planetary Sciences, Kyushu University, 2. Osaka City University

In coastal lake deposits often contained several disturbed layers by past tsunami, typhoons, high tide and natural hazard events. Those eventual layers were well preserved among lake sediments which deposited under stable water conditions, were identified easily by lithofacies of the sediments. In this paper, we presumed paleo-environmental histories of those eventual layers by diatom assemblages in the sediments. The compositions of diatom assemblages were shifted by characteristics and origins of natural disasters. Along the western coast of Kyushu Island where very huge typhoons often attacked by historic documents and meteorological records, we took undisturbed lake cores at coastal lakes to presume the frequencies and historic records of the disasters. Our research areas were **(a) Ikeda-ike (Daijya-ike) at Amakusa Peninsula, (b) Nakayama area at Shimokoshiki Island, (c) Nakakoshiki area at Nakakoshiki Island** and **(d) Namako-ike at Kamikoshiki Island.**

(a) Ikeda-ike (Daijya-ike) at Amakusa Peninsula: It was a small lake (WE200m, NS 150m), and has continued freshwater environment since 6700 yBP when the sand barrier closed the oceanic side of the lake. We presumed 11 eventual layers in the core sediments. Diatom assemblages presumed six of them were hazards with clear marine water invasions into the lake, two of them were with unclear marine invasions and last three were caused by huge flooding from surrounding mountains.

(b)Nakayama area at Shimokoshiki Island: It was a freshwater lake, however it changed to be a reclamation rice field about 50 years ago. The ancient lake had continued freshwater environment since 6500 yBP. Totally 16 eventually layers were presumed in the core. Diatom assemblages presumed seven of them were caused by marine invasions, and six of them were caused by inland flooding without marine invasions. Two of them were characterized by water level increasing (maybe artificially) and the last one was caused by the artificial land reclamation.

(c) Nakakoshiki area at Nakakoshiki Island: The top part of the core was disturbed by recent land flooding, the sediment during 2000-6000 yBP was kept. Four eventually layers were observed, and three of them were caused by marine invasions. The other one was caused by inland flooding without marine invasions.

(d) Namako-ike at Kamikoshiki Island: It is a brackish lake along north east coast of Kamikoshiki Island. We took the core until 6200 yBP layers, and 9 eventually layers were observed. Six of them were caused by caused by marine invasions, and three of them were characterized by freshwater flooding into the lake

(e) Correlation of the eventual layers in the cores: We found the strong correlation between the eventual layers at the research sites. The frequencies of the hazards surrounding 2.4ka, 2.8ka, 3.2ka, 3.7ka, 4.2ka, 4.7ka and 5.2ka were increased. They could be correlated to the hazard layers of Korean Peninsula**,** and were probably related to the global climatic processes in East Asia.

Keywords: The Holocene, Climatic Change, Hazard Deposits, Coastal lakes, Kyushu Island, Diatom

©2021. Japan Geoscience Union. All Right Reserved.

Origin and evolution of a delta-margin mangrove in Can Gio, southern Vietnam

Daniel S Collins[1,6], Lap V Nguyen[2], Oanh TK Ta[2], Limi Mao[3], Yuji Ishii[1], Hiroyuki Kitagawa[4], Rei Nakashima[1], *Toru Tamura[1,5]

1. Geological Survey of Japan, AIST, 2. HCMC Institute of Resources Geography, Vietnamese Academy of Science and Technology, 3. Nanjing Institute of Geology and Palaeontology, Chinese Academy of Sciences, 4. Institute for Space-Earth Environmental Research, Nagoya University, 5. Graduate School of Frontier Science, The University of Tokyo, 6. Shell International Ltd

Mangroves can deliver important socio-economic benefits and store significant volumes of carbon along tropical to temperate coastlines, but the distribution is controlled by complex geomorphologic, hydrodynamic and salinity conditions, as well as human-related pressures. In the Mekong delta, extensive mangroves presently occur along the northeastern delta margin (Can Gio, located 40 km southeast of Ho Chi Minh City), in an embayed, back-barrier environment subject to the highest tidal range (c. 4 m) and away from major fluvial distributary channels. However, the development of the Can Gio mangrove system during the Holocene evolution of the Mekong delta is not fully understood. This study aims to constrain the sedimentary evolution of the backbarrier mangrove in Can Gio based on stratigraphic, palynological and geochronological analyses of sediment cores. Two deep borehole cores (15 and 30 m deep) and four short auger cores (up to 4 m deep) were taken at the modern mangrove to characterize a 20-km-long shore-normal cross section dated with radiocarbon and optically stimulated luminescence (OSL) ages. The cores consist of a thick (> 20 m) subtidal mud from the base of the Holocene unit to the level of 3–4 m deep below the ground level, overlain by carbonaceous, intertidal mud. Chronological data reveal major episode of subtidal mud aggradation from 6 to 3.5 ka, forming the topography for mangrove development. Radiocarbon ages in the overlying intertidal mud range from 4 ka to modern and show some inconsistencies with the stratigraphy, suggesting mangrove root penetration and sediment mixing. The beach-ridge structure and OSL ages of the Can Gio barrier indicate that barrier formation initiated just before 3.2 ka. The transition from subtidal to intertidal mud aggradation and initiation of barrier formation, are broadly correlated with the onset of the subaqueous delta progradation and shift to a wave-dominated regime in the central delta. However, after 3.5 ka, the Can Gio shoreline had negligible sediment accretion while the central delta prograded up to 50 km seawards. Reduced sediment supply to Can Gio is consistent with more asymmetric, southwestward-dominated longshore drift after 3.5 ka. The negligible progradation at Can Gio also indicates minor sediment supply from the nearby Dong Nai River, which prevented upper intertidal accretion and translation of mangroves into a flood plain.

Keywords: mangrove, delta, coast, sea-level changes, sediment

©2021. Japan Geoscience Union. All Right Reserved.

[J] Oral | H (Human Geosciences) | H-QR Quaternary research

[H-QR04] Quaternary, Diachronic dynamics of human-environment interactions

convener:Mamoru Koarai(Earth Science course, College of Science, Ibaraki University), Yusuke Yokoyama(Atmosphere and Ocean Research Institute, University of Tokyo), Koji Okumura(Graduate School of Letters, Hiroshima University), Yasufumi Satoguchi(Lake Biwa Museum), Chairperson:Koji Okumura(Graduate School of Letters, Hiroshima University), Yusuke Yokoyama(Atmosphere and Ocean Research Institute, University of Tokyo)

Sat. Jun 5, 2021 10:45 AM - 12:15 PM Ch.16 (Zoom Room 16)

Humans have attained their specific development by indigenous cultures and evolved through environmental adaptation. The session raises issues of human-environmental interactions, views from diverse changes of climate, ocean, land and biota having made striking influence on humans. It welcomes various fields from human-environment change and their chronometric dating among Quaternary disciplines.

11:45 AM - 12:15 PM

[HQR04-11]Discussion

©Japan Geoscience Union

[J] Poster | H (Human Geosciences)：H-QR Quaternary research

Sat. Jun 5, 2021 5:15 PM - 6:30 PM JST | Sat. Jun 5, 2021 8:15 AM - 9:30 AM UTC | Ch.09_1

[H-QR04] Quaternary, Diachronic dynamics of human-environment interactions

convener:Mamoru Koarai(Earth Science course, College of Science, Ibaraki University), Yusuke Yokoyama(Atmosphere and Ocean Research Institute, University of Tokyo), Koji Okumura(Graduate School of Letters, Hiroshima University), Yasufumi Satoguchi(Lake Biwa Museum)

Humans have attained their specific development by indigenous cultures and evolved through environmental adaptation. The session raises issues of human-environmental interactions, views from diverse changes of climate, ocean, land and biota having made striking influence on humans. It welcomes various fields from human-environment change and their chronometric dating among Quaternary disciplines.

[HQR04-P01] Formation age of mire on marine terraces in Nemuro Peninsula, Hokkaido, Japan

*Reisuke Kondo[1], Minoru Yokochi[2], Takashi Inoue[5], Kazuhiro Kaneko[4], Hiroko Fujita[3], Mari Sumita[6], Yosuke Miyairi[1], Yusuke Yokoyama[1] (1.Atmosphere and Ocean Research Institute, The University of Tokyo, 2.Graduate School of Global Food Resources, Hokkaido University, 3.The Field Science Center for Northern Biosphere, Hokkaido University, 4.Graduate School of Agriculture, Hokkaido University, 5.Research Faculty of Agriculture, Hokkaido University, 6.GEOMAR Helmholtz Centre for Ocean Research Kiel)

[HQR04-P02] Changes in sedimentary environment during the Holocene in a wetland in Chanai area on Konsen plateau, eastern Hokkaido

*Ren Tsuneoka[1], Yusuke Yokoyama[1], Reisuke Kondo[1], Kosuke Ota[1], Minoru Yokochi[2], Kazuhiro Kaneko[3], Hiroko Fujita[4], Takashi Inoue[5], Norio Kito[6], Mari Sumita[7], Kyota Uemura[8], Yosuke Miyairi[1], Arata Momohara[9] (1.Atmosphere and Ocean Research Institute, The University of Tokyo, 2.Graduate School of Global Food Resources, Hokkaido University, 3.Graduate School of Agriculture, Hokkaido University, 4.The Field Science Center for Northern Biosphere, Hokkaido University, 5.Research Faculty of Agriculture, Hokkaido University, 6.International and Regional Studies, Hokkaido University of Education, 7.GEOMAR Helmholtz Centre for Ocean Research Kiel, 8.College of Humanities and Sciences, Nihon University, 9.Faculty of Horticulture, Chiba University)

[HQR04-P03] Holocene coastal evolution and vertical deformation in the Hachinohe plain, NE Japan, inferred from sedimentary analyses

*Yuichi Niwa[1], Toshihiko Sugai[2] (1.Faculty of Science and Engineering, Chuo University, 2.Department of Natural Environmental Studies, Graduate School of Frontier Sciences, The University of Tokyo)

[HQR04-P04] Landform evolution and estimation of crustal movement since MIS 12 in the central-northern part of the Kanto Plain

*Tatsuki Miyamoto[1], Toshihiko Sugai[1], Yuichi Niwa[2], Toshimichi Nakanishi[3], Tetsuya Komatsu[4], Yuki Hiura[4] (1.Department of Natural Environmental Studies, Institute of Environmental Studies,Graduate School of Frontier Science, The University of Tokyo, 2.Chuo Univ., 3.Museum of Natural and Environmental History, Shizuoka, 4.JAEA)

[HQR04-P05] Rock surface dating of granodiorite cobbles obtained from fluvial terrace deposits in the Chichibu Basin, central Japan

*Yuji Ishii[1], Takayuki Takahashi[2], Kazumi Ito[1] (1.National Institute of Advanced Industrial Science and Technology, 2.Tohoku Univ.)

[HQR04-P06] Identification of reworked volcaniclastic deposits composing the upper Alluvium along the Moto-arakawa River, east part of the Saitama Prefecture, Central Japan

*Masanori Murata[1], Takayuki Takahashi[2], Kaori Aoki[1], Fumikatsu NISHIZAWA[3], Makoto Kobayashi[4], Takehiko Suzuki[1,5] (1.Research Center for Volcanic Hazards and Their Mitigation, Tokyo Metropolitan

University, 2.International Research Institute of Disaster Science, Tohoku University, 3.Kanagawa Prefectural Museum of Natural History, 4.Mt. Fuji World Heritage Centre, Shizuoka, 5.Department of Geography, Tokyo Metropolitan University)

[HQR04-P07] Tephrostratigraphy during the past 30,000 years in the Jaishi Oike Moor, southern Izu Peninsula, Japan.

*Tatsuki Watanabe[1], Takehiko Suzuki[1], Daisuke Ishimura[1] (1.Department of Geography, Tokyo Metropolitan University)

[HQR04-P08] Landform evolution since the Middle Pleistocene estimated at the lower reaches of the Himekawa River, central Japan

*Jun Matsukaze[1], Masaaki Shirai[1] (1.Tokyo Metropolitan University)

[HQR04-P09] Radiocarbon dating using pollen fossils and its potential in Quaternary studies

*Keitaro Yamada[1], Takayuki Omori[2], Ikuko Kitaba[3], Takeshi Nakagawa[3] (1.Research Organization of Science and Technology, Ritsumeikan University, 2.The University Museum, The University of Tokyo, 3.Research Centre for Palaeoclimatology, Ritsumeikan University)

[HQR04-P10] Identification of middle to late Pleistocene marine sediments inferred from electric conductivity analysis of the Bando observation well core in Tokushima Plain, western Japan

*Yoshiki Sato[1], Kiyohide Mizuno[1], Yuki Haneda[1], Koretaka Nakatani[1], Rei Nakashima[1] (1.Advanced Industrial Science and Technology, Geological Survey of Japan)

Formation age of mire on marine terraces in Nemuro Peninsula, Hokkaido, Japan

*Reisuke Kondo[1], Minoru Yokochi[2], Takashi Inoue[5], Kazuhiro Kaneko[4], Hiroko Fujita[3], Mari Sumita[6], Yosuke Miyairi[1], Yusuke Yokoyama[1]

1. Atmosphere and Ocean Research Institute, The University of Tokyo, 2. Graduate School of Global Food Resources, Hokkaido University, 3. The Field Science Center for Northern Biosphere, Hokkaido University, 4. Graduate School of Agriculture, Hokkaido University, 5. Research Faculty of Agriculture, Hokkaido University, 6. GEOMAR Helmholtz Centre for Ocean Research Kiel

Large-scale mires are distributed on the marine terraces in Nemuro Peninsula, eastern Hokkaido. These mires are different in scale and morphology from mires / wetlands at the alluvial lowland of the floodplain in the valley and coastal lowland. The main part of the Habomai mire in the eastern part of the Nemuro Peninsula is located on several marine terraces at an altitude of about 20 to 40 m, and part of mire is hilly and sloping. There are no rivers in the Habomai mire, and erosional valleys are distributed the marginal area of the mire. In the Habomai mire, peat layers are known to be distributed on slopes, and historical botany has been studied (Igarashi et al., 2001; Momohara et al., 2009). However, the characteristics of peat covering on terraces and their relationship with the geomorphological development are unknown. The purpose of this study is to clarify the formation age and the geomorphological development of the Habomai mire.

Field surveys were conducted on the Habomai mire and the marine terraces of the Nemuro Peninsula. A cross-sectional surveys of the line transects were performed in the Habomai moor, and the sediments collected by the peat sampler, boring stick and borehole cores. And the marine terrace deposit were sampled at several outcrops around the Habomai mire. Tephrochronology, 14C dating and pIRIR dating were applied to date mire and terrace sediments.

In the Habomai mire, it was observed that the peat layer not only covers the gently sloping terrace surface, but also covers the buried depressions and terrace cliffs. In addition, the sedimentary environment often changes from wetland to peatland after the tephra deposition from Mashu volcano in the Middle Holocene (Ma-f~j). Around the locations where the buried depression and the terrace cliff, the peat layer above the Ma-f~j tephra is relatively thick, and the buried peat layer is intermittently deposited below. The Habomai mire is considered to be a blanket mire because the peat layer covers not only the sloped terrace surface but also the terrace cliffs. As a result of 14C dating, peat deposition started before the LGM. Since then, peatland environments have occurred intermittently at restrictive areas, such as buried depressions and terrace cliffs. From the results of pIRIR dating at the marine terraces around the Habomai mire, it is considered that the main part of marine terraces was formed during the Middle Pleistocene, and that periglacial environment contributed after the LGM. Therefore, it is considered that 1) the terrace surface became gentler due to solifluction during the last glacial period and the previous cold period, 2) subsequently, peat deposition began to accumulate locally at the base of terrace cliffs and buried depressions from an older age, 3) after that, peat deposition crawls up from the depression to the flat area, forming the present blanket mire.

Keywords: mire, marine terraces, 14C dating, pIRIR dating, tephra, Numuro peninsula

©2021. Japan Geoscience Union. All Right Reserved.

Changes in sedimentary environment during the Holocene in a wetland in Chanai area on Konsen plateau, eastern Hokkaido

*Ren Tsuneoka[1], Yusuke Yokoyama[1], Reisuke Kondo[1], Kosuke Ota[1], Minoru Yokochi[2], Kazuhiro Kaneko[3], Hiroko Fujita[4], Takashi Inoue[5], Norio Kito[6], Mari Sumita[7], Kyota Uemura[8], Yosuke Miyairi[1], Arata Momohara[9]

1. Atmosphere and Ocean Research Institute, The University of Tokyo, 2. Graduate School of Global Food Resources, Hokkaido University, 3. Graduate School of Agriculture, Hokkaido University, 4. The Field Science Center for Northern Biosphere, Hokkaido University, 5. Research Faculty of Agriculture, Hokkaido University, 6. International and Regional Studies, Hokkaido University of Education, 7. GEOMAR Helmholtz Centre for Ocean Research Kiel, 8. College of Humanities and Sciences, Nihon University, 9. Faculty of Horticulture, Chiba University

Widespread peatland and wetland distribution is common in eastern Hokkaido, Japan. However, few studies of paleoenvironmental transition history in small alluvial lowland marsh groups located on the Konsen plateau have been reported. A major obstacle is the reconstruction of a robust age model. Peat radiocarbon dating must be employed with caution due to the reservoir effect, since peat and wetland sediments contain not only plant remains at the time of sedimentation but also various organic materials such as roots that are mixed from the layer above after sedimentation (Shinozaki, 2013). If known tephra are identified in strata, accuracy of stratigraphically constrained ages increases. However, accurate ages from radiocarbon dating on macrofossils and marker tephra cannot always be found from wetland sediments.

In this study, we measured radiocarbon from pollen fossils contained in the sediments in a wetland of Chanai area in southern part of Konsen Plateau. This study marks the first use of large pollen on radiocarbon measurements using flow cytometry devices. To reconstruct paleoenvironments, we conducted high resolution elemental analysis on sediments to interpret the origin of the wetland sediments, in particular interpreting the origin of organic matter and its decomposition rate.

Tephra stratigraphy of the core sample indicate that the transition to a wetland setting at the study site occurred between about 7.5~2.5 ka. Results from elemental analysis showed that Total Organic Carbon (TOC) fluctuated between 20 and 40 % at depths of -90 to -60 cm, and between 40 and 50 % at -40 to -5 cm, with a peak of 53 % at -36 cm. Total Sulfur (TS) gradually rose from the bottom to the top, with 0.3~0.4 % at the base and 0.5~0.8 % at the top of the core. The resulted carbon and nitrogen (C/N) ratio was about 14~20 between -90 and -40 cm, and was about 25 in the upper 40 cm of the core, with a sharp rise around -40 cm. This suggests the changes in sedimentary preservation status occurred at around -40 cm, since the C/N ratio decreases with the decomposition of peat (Kondo et al., 1997).

From the C/N ratio, the degree of peat decomposition was highest at the core bottom and lower at the core top, suggesting a change in the decomposition rate or organic material depositional rate. We will further examine the transition of sedimentary environment in the wetland together with the results of radiocarbon dating.

Keywords: wetland, peat, radiocarbon dating, elemental analysis, wetland sedimentary environment, Chanai area on Konsen plateau

©2021. Japan Geoscience Union. All Right Reserved.

Holocene coastal evolution and vertical deformation in the Hachinohe plain, NE Japan, inferred from sedimentary analyses

*Yuichi Niwa[1], Toshihiko Sugai[2]

1. Faculty of Science and Engineering, Chuo University, 2. Department of Natural Environmental Studies, Graduate School of Frontier Sciences, The University of Tokyo

We report geomorphological and sedimentological analyses in the Hachinohe plain (northernmost Sanriku coast, NE Japan) that yield new insights into vertical deformation around the source region of the 2011 Tohoku-oki earthquake. Landform classification and analyses of seven sediment cores document the transgression and regression of the sandy barrier and back-barrier estuary during the Holocene.

Fluvial environment, which prevailed at lower part of the plain at 10,000 to 9,500 cal BP, changed to tidal river environment at 9,500 to 9,000 cal BP. Further transgression induced deeper bay environment at seaward site at 8,500 cal BP, whereas fluvial environments prevailed at upper part of the plain at that time. Because the Hachinohe plain is surrounded by Pleistocene marine terraces and the Mabechi River narrowly crosses them, we suggest that a wave-dominated estuary enclosed by a barrier formed in the present Hachinohe plain during the Middle Holocene. Transgressive lag sand and gravel layers and overlaying shoreface and foreshore sandy sediments imply that a barrier, which had been offshore during the Early Holocene, transgressed and truncated the back-barrier sediments. Consequently, the barrier has been located at present coastline after middle Holocene. The existence of barrier and upward-coarsening silt to sand layer, which filled in water area behind the barrier, indicates progradation of bay-head delta during the Middle Holocene. After progradation of the bay-head delta, fluvial environments again prevailed behind the barrier.
Comparison of height of a surface of the onset of tidal river environment (-22.76 m) at 9,460 cal BP, when sea-level was on or higher than the depositional surface, with hydro-isostatic sea-level prediction that do not account for tectonic deformation suggests maximum subsidence rate on a millennial scale in the Hachinohe plain is 0.7 mm/yr, if there is a millennial-scale subsidence trend at all. Similarly, comparison of a surface of onset of marsh environment (4.51 m) at 6,340 cal BP with hydro-isostatic sea-level predictions suggests that maximum uplift rate in the plain is 0.7 mm/yr. Therefore, the vertical deformation rate on a millennial scale in the Hachinohe plain ranges from -0.7 to 0.7 mm/yr (uplift positive). This vertical deformation is consistent with relative uplift in Kuji and Omoto, northern Sanriku coast and contrasts with subsidence along central to southern Sanriku coast. Our results also support a variation along the Sanriku coast in vertical deformation during the last 100 kyr; the southern part is subsidence while northern part has uplifted at least relative to southern part. Agreement of this trend with deformations during/before the 2011 Tohoku-oki earthquake that the amount/rate of subsidence decreased from south to north implies that effect of subduction and slip on megathrust for coastal deformation persist at least during 100 kyr around the source region of the 2011 earthquake.

Keywords: Sanriku coast, Holocene, millennial-scale crustal movements, sediment core, 2011 Tohoku-oki earthquake

©2021. Japan Geoscience Union. All Right Reserved.

Landform evolution and estimation of crustal movement since MIS 12 in the central-northern part of the Kanto Plain

*Tatsuki Miyamoto[1], Toshihiko Sugai[1], Yuichi Niwa[2], Toshimichi Nakanishi[3], Tetsuya Komatsu[4], Yuki Hiura[4]

1. Department of Natural Environmental Studies, Institute of Environmental Studies,Graduate School of Frontier Science, The University of Tokyo, 2. Chuo Univ., 3. Museum of Natural and Environmental History, Shizuoka, 4. JAEA

Kanto plain is one of the most studied tectonic basins in terms of landform evolution and crustal movement during the Late Quaternary in Japan, but the tectonic trends in the northern part of the plain, from Sashima to Takaragi terrace, have been little clarified. Miyamoto et al. (2020) and Nakanishi et al. (2020), based on the analysis of three all cores (GC-OY-1, OY-2 and NG-1), divided the cores into 19 sedimentary units, and compared Units 15-17 of GC-OY-2 and OY-1 to the Jizodo Formation, and Units 12-14 of GC-OY-2 and OY-1 are compared to the Yabu Formation. This presentation reports the outlines of landform evolution in this area since MIS 12 and the average crustal deformation rate during this period.

The upper surface elevation of the marine stratum in MIS 11 is -20.17 m above sea level for GC-OY-2 (foreshore) and -41.15 m above sea level for GC-OY-1 (delta front). Since the eustatic sea level in MIS 11 was about 6 m to 13 m higher than the present (Raymo and Mitrovica, 2012), the fluctuation amount since MIS 11 is estimated to be about -26 m to -33 m for GC-OY-2 (foreshore) and about -47 m to -54 m for GC-OY-1 (upper shoreface to foreshore). The water content ratio of the core does not decrease vertically downward, so the effect of consolidation is ignored. In addition, since the study area is located at the northern limit of the Paleo-Tokyo Bay expansion area and is heavily supplied by river sediments, it is assumed that the sea level at the time of the formation of the detached surface of the marine stratum approximates the highest sea level of the relevant evolution. From these results, the average rate of vertical change from MIS 11 to the present is estimated to be -0.08 mm/yr for GC-OY-2 and -0.13 mm/yr for GC-OY-1, indicating that the sediments have been settling at an average rate of about 0.1 mm/yr during this period.

The upper surface elevation of the marine stratum in MIS 9 is -9.74 m above sea level for GC-OY-2 and -24.13 m above sea level for GC-OY-1. Since the eustatic sea level in MIS 9 was about 9 m higher than the present (Spratt and Lisiecki, 2016), the fluctuation amount since MIS 9 is estimated to be about -19 m for GC-OY-2 and about -33 m for GC-OY-1. From these results, the average rate of vertical fluctuation during the period from MIS 9 to the present is calculated to be -0.06 mm/yr for GC-OY-2 and -0.11 mm/yr for GC-OY-1, indicating that the average rate of sedimentation during this period has been around 0.08 mm/yr.

The settling rate and the amount of settling are larger in the southern part of the region. This trend is in harmony with the fact that the center of settling is located around Kuki City, Saitama Prefecture in the southern part of the Sashima terrace (Kaizuka, 1987). The amount and rate of settling decrease with increasing age (MIS 11 and 9). This may reflect the shallowing and uplifting of the forearc basin throughout the Quaternary (Sugai et al., 2013).

©2021. Japan Geoscience Union. All Right Reserved.

Acknowledgements: This study used a part of the results of the research and developments funded by the Ministry of Economy, Trade and Industry (METI), Japan as part of its R&D supporting program titled “Establishment of Advanced Technology for Evaluating the Long-term Geosphere Stability on Geological Disposal Project of Radioactive Waste (Fiscal Years 2018 and 2019)

References: Miyamoto et al. 2020 AJG spring. Nakanishi et al. 2020 JpGU. Kaizuka 1987 Jour. of Geography. 96, 51-68. Sugai et al 2013 Jour. of Geography. 122(6), 921-948. Raymo and Mitrovica 2012 Nature 483, 453-456. Spratt and Lisiecki 2016 Climate of the Past 12, 1079-1092.

Keywords: Middle Pleistocene, crustal movement, Kanto plain

©2021. Japan Geoscience Union. All Right Reserved.

Rock surface dating of granodiorite cobbles obtained from fluvial terrace deposits in the Chichibu Basin, central Japan

*Yuji Ishii[1], Takayuki Takahashi[2], Kazumi Ito[1]

1. National Institute of Advanced Industrial Science and Technology, 2. Tohoku Univ.

Fluvial fill terraces are common in middle reach of Japanese rivers, and they were formed in the last glacial period. Ages of terraces have been investigated mainly based on the tephrochronology, but it may have some problems; abandonment ages of terraces may be underestimated because some part of the tephra deposits might have been eroded, or conversely, may be overestimated because tephra layers overlying terrace deposits only indicates the minimum age of the terraces. These problems should be overcome to correctly estimate the uplift rate in the middle reach of rivers as well as to understand the development of fluvial terraces. Optically-stimulated luminescence (OSL) dating could provide depositional ages of fluvial terraces, which may improve the chronology of fluvial terraces. We need to examine the validity of OSL dating of fluvial terrace deposits based on the comparison of tephra chronology.

Sand-sized grains or silt grains are usually used for OSL dating, but recently, cobble dating method have been developed and applied. Fluvial terrace deposits in the middle reach of Japanese rivers are mainly composed of gravels, and sand layers are sometimes difficult to find. Furthermore, cobbles might be better bleached compared to sand-sized grains because of long residence time in river channels. This study examines the luminescence dating of granodiorite cobbles obtained from the uppermost part of terrace deposits formed in the last glacial period in the Chichibu Basin, central Japan.

We obtained three granodiorite cobbles from an outcrop and treated them in a darkroom. We obtained three cores (with 10 mm diameters and 20–30 mm depths) for each cobble and sliced them using water-cooled, diamond-edged wafering blade, and rock slices of 1.2 or 0.65 mm thickness were produced. Measurements were conducted using Risø TL/OSL DA-20 and a post-IR $IRSL_{50/225}$ SAR protocol was used to estimate the depositional ages of cobbles. We also obtained samples from a silty sand layer and obtained post-IR $IRSL_{50/225}$ age of sand-sized K-rich feldspars (180–250 μm) and OSL age of fine-grained quartz grains (4–11 μm).

The OSL age of fine-grained quartz was ca. 9.4 ka, which is 5 ka younger than the UG tephra (16–15 ka) found in the lowest part of the loess deposits overlying the terrace. The decay curve of the quartz OSL signal suggests significant contribution of the medium component, which is thermally unstable, and led to age underestimate. The IR_{50} age of K-rich feldspars is ca. 46 ka and we infer that the luminescence signal was not completely bleached. Three cobbles yielded IR_{50} ages of 19–17 ka, which is consistent with the tephra age. The post-IR $IRSL_{50/225}$ ages of cobbles are considerably different between cobbles (125–34 ka). We introduce and discuss the calculation of dose rate and fading correction methods in the presentation.

Keywords: OSL dating, rock surface dating, fluvial terrace, Pleistocene

©2021. Japan Geoscience Union. All Right Reserved.

Identification of reworked volcaniclastic deposits composing the upper Alluvium along the Moto-arakawa River, east part of the Saitama Prefecture, Central Japan

*Masanori Murata[1], Takayuki Takahashi[2], Kaori Aoki[1], Fumikatsu NISHIZAWA[3], Makoto Kobayashi[4], Takehiko Suzuki[1,5]

1. Research Center for Volcanic Hazards and Their Mitigation, Tokyo Metropolitan University, 2. International Research Institute of Disaster Science, Tohoku University, 3. Kanagawa Prefectural Museum of Natural History, 4. Mt. Fuji World Heritage Centre, Shizuoka, 5. Department of Geography, Tokyo Metropolitan University

In order to study the impacts of the reworking of volcanic products of volcanoes in the northern Kanto region on the Nakagawa and Tokyo Lowlands, we investigated the secondary volcanic products in the alluvial deposit along the Moto-arakawa River. According to the "Borehole map using WebGIS" published by Center for Environmental Science in Saitama, many pumice clasts have been found in the sediments at a depth of less than 5 m from the ground surface. along the Moto-arakawa River. These pumice clasts are considered to have been transported by the Tone River, because the lowland along the Moto-arakawa River was the former channel of the Tone River for some time from the beginning of the 8th century. We carried out borehole investigations at two locations, Iwatsuki Bunka Park, Saitama City (Iwatsuki Bunka Park core) and Koshigaya, Koshigaya City (Koshigaya 2236 core). Based on the analysis of the volcanic products in the two cores, it was found that the upper Alluvium at the depths of 4-5 m in Iwatsuki Bunka Park, and 2-5 m in Koshigaya, Koshigaya City contains secondary volcanic products originated from Hr-FP and Asama tephras. This suggests that the reworking of volcanic products from the upper reaches of the Tone River had a significant impact on the development of the alluvial lowland in the central part of the Kanto Plain during the late Holocene. In the future, we plan to reconstruct the ages and paleoenvironments of the sediments using radiocarbon dating, and to assess the spatial and temporal impacts of the reworking of volcanic products in the Nakagawa and Tokyo Lowlands.

Keywords: alluvial lowland, volcanic hazard, Saitama Prefecture

©2021. Japan Geoscience Union. All Right Reserved.

Tephrostratigraphy during the past 30,000 years in the Jaishi Oike Moor, southern Izu Peninsula, Japan.

*Tatsuki Watanabe[1], Takehiko Suzuki[1], Daisuke Ishimura[1]

1. Department of Geography, Tokyo Metropolitan University

Recently, detailed tephrostratigraphic studies using lacustrine and moor sediment records have been conducted both in the Japanese Islands and overseas, providing more widespread distributions and eruption ages of tephras and contributing to studies of volcanic eruptive history (e.g., McLean et al. 2018; Albert et al. 2018, 2019). Such studies focusing on lacustrine sediment core records in the Japanese Islands are concentrated in the Kinki and Chubu regions. There are a limited number of lakes and moors suitable for the establishment of a detailed tephrostratigraphy in the Tokai and South Kanto coastal regions, where many tephras from Quaternary volcanoes in southwest Japan are expected to be distributed due to westerlies. In this study, we focused on the Jaishi Oike Moor in the southwestern part of the Izu Peninsula in order to establish the detailed tephrostratigraphy of the Jaishi Oike Moor, including cryptotephras (Lowe and Hunt 2001). We conducted particle size analysis, particle composition analysis, tephra analysis (measurement of refractive index of volcanic glass shards and amphiboles, and major element compositions of volcanic glass shards) using a JIS core (core length is 12 m) drilled in September 2020. In particular, the content of volcanic glass shards, amphiboles, and morphological classification of volcanic glass shards were used as indicators to identify the tephric particle concentration horizons.

The sediments of the JIS core are mostly composed of silt deposited under lake to moor environments. Additionally, we also identified tephra layers and coarse-grained sediments deposited by debris flows interbedded within silty sediments. Two visible tephra layers were identified based on tephra analysis: the Amagi-Kawagodaira tephra (Kg, 3,151-3,126 cal yrs BP: Tani et al. 2013) and Aira-Tn tephra (AT, 30,078± 96 cal yrs BP: Smith et al. 2013). In addition, nine cryptotephras were identified from seven layers of tephric particle concentration horizons. They are a widespread tephra of the Kikai-Akahoya tephra (K-Ah, 7,307-7,196 cal yrs BP: McLean et al. 2018), the newly discovered tephra in this site are shown from the top as follows: the Niijima-Miyatsukayama Nanbu tephra (Nj-Mts, 5.5 ka: Kobayashi et al. 2020), Niijima-Shikinejima tephra (Nj-Sk, 8 ka: Kobayashi et al. 2020), one tephra that may be correlated with Daisen Sasaganaru tephra (DSs, 29,837 ±96 cal yrs BP or 29,830 cal yrs BP: Albert et al. 2018) or Daisen Higashidaisen tephra (DHg, 28,895 ±72 cal yrs BP or 28,888 ±72 cal yrs BP: Albert et al. 2018), and one uncorrelated tephra from Izu Islands.

The distribution of Nj-Mts and Nj-Sk in the Honshu Island is identified for the first time. Therefore, JIS core can provide a type tephrostratigraphy in the Izu Peninsula for studying the distribution of tephras from the Izu Islands. On the other hand, the eastern end of the distribution of DSs and DHg in the previous studies is Lake Biwa (Takemura et al. 2010). Therefore, it is likely that the distribution area of either DSs or DHg is expanded to 250 km further east from Lake Biwa by this study and the main axis of them is east-southeast direction from the source volcano. In this study, we analyzed the moor sediments continuously and identified the tephric particle concentration horizons by several indicators, and showed the detailed tephrostratigraphy during the past 30,000 years in the southern part of the Izu Peninsula.

Keywords: Moor sediment, Cryptotephra, Jaishi Oike Moor

©2021. Japan Geoscience Union. All Right Reserved.

Landform evolution since the Middle Pleistocene estimated at the lower reaches of the Himekawa River, central Japan

*Jun Matsukaze[1], Masaaki Shirai[1]

1. Tokyo Metropolitan University

Studies on fluvial terrace have been conducted in many areas of the Japanese islands, and their relationship with climate changes and sea-level changes has been discussed. However, studies focusing on gravel shape (form and roundness) of fluvial terrace deposithave been seldom carried out. In addition to topographic classification and construction of chronology, the authors compared gravel shape of fluvial terraces in the lower reaches of the Himekawa River in the western Niigata Prefecture with gravel shape of the present Himekawa river bed.

Throughout the study, some results were obtained;
(1) The form of the pebbles on the present Himekawa River show that ratio of spherical (cubic) and disc shapes decrease and rod shape increases downstreamward. Local increase in ratio of spherical (cubic) and disc shapes in the middle reaches near by the confluence with the Urakawa River should be influenced by a giant slope-failure “Hieda-Yama-Kuzure” where lots of breccia and boulders were supplied AD1911. It suggests that the effects of giant slope-failure and debris flow may be detected from shape of fluvial gravels.
(2) Fluvial terrace in the studied area are divided as H1~3, M1~3, and L surface in descending order. Volcanic glass shards and minerals originated from AT, DKP, Aso-4, K-Tz, and Tt-D were detected from the tephric loess (so-called loam) in this area. Detection of K-Tz and Tt-D from the basal part of the loam layer on the M2 terrace means that the ages of the M1 and M2 terraces become older than the previous estimation.
(3) A buried valley was discovered on the eastern side of the present Himekawa River as a result of the field survey. The buried valley is estimated as the paleo-Himekawa River channel during the Middle Pleistocene.
(4) The H1~H3 terraces contain sub-angular cubic andesite pebbles just like as the middle reaches of the present Himekawa River, so it is considered that sub-angular cubic andesite pebbles were transported by debris flow from the Umikawa volcanic rocks area near the study area.

Consequently, landform evolution in the lower reaches of the Himekawa River is estimated as follow; Himekawa River flows eastern side of the present Himekawa River valley separated by the ridge of the basement rock during the Middle Pleistocene. The interglacial sea-level rise buries the basement ridge below the alluvial plain deposits. Then, downward valley erosion during the subsequent sea-level fall made the present Himekawa River valley due to tilting to north–northwest direction. During the middle Pleistocene, a large amount of andesite gravels derived from slope failures in the Umikawa volcanic rocks area.

Keywords: Fluvial terrace, Himekawa River

©2021. Japan Geoscience Union. All Right Reserved.

Radiocarbon dating using pollen fossils and its potential in Quaternary studies

*Keitaro Yamada[1], Takayuki Omori[2], Ikuko Kitaba[3], Takeshi Nakagawa[3]

1. Research Organization of Science and Technology, Ritsumeikan University, 2. The University Museum, The University of Tokyo, 3. Research Centre for Palaeoclimatology, Ritsumeikan University

Radiocarbon dating is one of the most widely used dating methods in Quaternary science, including paleoclimatology, archaeology, and hazard protection. Macrofossils (e.g., leaves, wood fragments, and shells) and bulk sediment samples have been used for dating in terrestrial studies. However, macrofossils are not always included in sediments. Moreover, depending on the sedimentary and post-depositional processes, these materials are often not suitable for dating. Therefore, the possibility of radiocarbon dating using small plant fragments and microfossils, which are generally expected to have better radiocarbon integrity, has been explored.

Fossil pollen grains are often found in terrestrial sediments and are one of such materials that have potential to yield more robust radiocarbon ages. Pollen membranes consists of sporopollenin, a physicochemically stable organic polymer. Sporopollenin contains ca. 60% of carbon and has been studied since the 1990s as a potential material for radiocarbon dating. While these studies have successfully shown that fossil pollen grains are potentially suitable for ^{14}C dating, their applications in actual researches have been very limited.

One of the limiting factors is the difficulty of extracting fossil pollen grains from sediment matrixes in high purity. We need to concentrate fossil pollen grains because they comprise very small part of the sediments. However, the characteristics of pollen fossils, such as size, specific gravity, and chemical tolerance do not differ significantly from those of other organic materials in sediments. Therefore, it is difficult to isolate pollen grains using only conventional physicochemical treatments. In this study, we established a novel method to extract fossil pollen grains using “cell sorter” in combination with new physicochemical treatments. Cell sorters can separate individual particles based on scattered light and fluorescence.

In this study, we used SG06 core obtained from Lake Suigetsu, Fukui prefecture, Japan, Radiocarbon ages of >800 terrestrial leaf fossils have been measured, making the core almost ideal target for comparison to assess robustness of the radiocarbon dates obtained on fossil pollen pellets.

The extracted pellets are composed almost exclusively of pollen grains, with almost no solid impurities. The size of the extracted pollen grains depends on the specs of the cell sorter. Therefore, the extracted pollen fossils consist of grains with diameters of 10-50 μm, such as *Cryptomeria* and *Alnus*, and do not retain the original percentage composition of fossil pollen assemblage.

The radiocarbon ages obtained on fossil pollen pellets prepared by cell-sorter precisely reproduced those from leaf macro fossils, regardless of the taxa percentage composition. These agreements were maintained even near the radiocarbon limit (ca.50 ka). The fossil pollen grains extracted by our method were useful as materials for radiocarbon dating, as is also the case with the terrestrial leaf fossils. Our method enables robust radiocarbon dating of the sediments that do not contain macro remains suitable for radiocarbon dating.

We also confirmed that fossil pollen grains could be extracted from not only lacustrine deposits, but also peat and volcanic soils. The extraction method can be applied to a range of terrestrial sediments deposited in various environments. Combined with Bayesian modeling, radiocarbon dating of strategically chosen horizons can provide much stronger age constraints to event deposits such as volcanic ash and tsunami deposits.

©2021. Japan Geoscience Union. All Right Reserved.

Keywords: radiocarbon, pollen

©2021. Japan Geoscience Union. All Right Reserved.

Identification of middle to late Pleistocene marine sediments inferred from electric conductivity analysis of the Bando observation well core in Tokushima Plain, western Japan

*Yoshiki Sato[1], Kiyohide Mizuno[1], Yuki Haneda[1], Koretaka Nakatani[1], Rei Nakashima[1]

1. Advanced Industrial Science and Technology, Geological Survey of Japan

Tokushima Plain is a coastal plain located on the western coast of the Kii Channel. Along the northern margin of the plain, the Median Tectonic Line Fault Zone is distributed, and displaces fans and Pleistocene terraces. The fault zone is a reverse fault with large right-lateral displacement and uplift of the northern side around the plain (Okada, 2020). This suggests and the plain can be regarded as a tectonic basin by the MTL fault zone. Since 1960s, many studies about the subsurface geology of the plain have been conducted (Kawamura & Nishiyama, 2019). The Quaternary subsurface geology can be roughly divided into two formations, the Tokushima and Kitajima Formations, which are related to Alluvium and the middle to late Pleistocene, respectively. However, detail sedimentary periods and environments have not been clarified.

We attempted to identify the marine sediments in the Kitajima Formation based on electrical conductivity [EC] analysis of the Bando observation well core, 502 m long core drilled in the plain in 1995 by GSJ. Matsumoto & Arai (2021) reported stratigraphic description and pollen fossil and paleomagnetic analyses of the core. These indicate that several glacial-interglacial cycles are preserved, and the Brunhes-Matsuyama [B-M] boundary may be located between 339 and 440 m depth. In this study, EC analysis was carried out on subsamples collected from lower than 90 m depth. Sample treatment and interpretation were based on Yokoyama & Sato (1987) and Niwa *et al.* (2009).

As the results, we found five marine sediments; M1, 93.4–102.45 m depth; M2, 228.08–237.00 m; M3, 258.83–263.98 m; M4, 2 88.06–288.60 m depth; M5, 305.50 m. Comparison with the pollen fossil stratigraphy of the Osaka Group (Hongo, 2009), the M1 layer probably deposited during the MIS5e because of the high abundance of *Lagerstoemia* (Matsumoto & Arai, 2021). High abundance of *Cyclobalanopsis* in the M3 layer (Matsumoto & Arai, 2021) suggests that this layer deposited during the MIS11. Assuming these interpretations are correct, M2 layer, located between the M1 and M3 layers, should be corresponding to the MIS 7 or 9 marine sediment. In addition, the M4 and M5 layers might deposit during the MIS 13, 15, or 17 because these are above the B-M boundary.

These insights suggest that glacial-interglacial cycles sediments after the middle Pleistocene had been recorded in the subsurface geology of the Tokushima Plain. The average subsidence rate is estimated to be ˜0.7 to ˜0.8 mm/yr. For clarifying detail stratigraphy of the subsurface geology in the plain, we will conduct volcanic ash, pollen fossils and paleomagnetic analyses of the core materials in future.

References

Hongo, M. (2009) Middle Pleistocene pollen biostratigraphy in the Osaka sedimentary basin, southwest Japan, with special reference to paleoenvironmental change. The Journal of the Geological Society of Japan, **115**, 64–79.
Kawamura, N. & Nishiyama, K. (2019) Correlation study of the late Pleistocene and Holocene deposits underlying the major coastal plains of Shikoku, Southwest Japan. The Journal of the Geological Society of

©2021. Japan Geoscience Union. All Right Reserved.

Japan, **125**, 87–105.
Matsumoto, N. & Arai, T. (2021) Report on construction of facilities and equipment for groundwater monitoring for earthquake prediction in 1995, No.2*. Open-File Report of the Geological Survey of Japan, AIST, no.713.
Niwa, Y. et al. (2009) Evidence for late Holocene coseismic subsidence identified in drilling cores along the Yoro fault system, western margin of the Nobi plain, central Japan. Daiyonki-Kenkyu, **48**, 339–349.
Okada, A. (2020) Median Tectonic Line Fault Zone. 368p. Kokon-Shoin, Tokyo.
Yokoyama, T. & Sato, M. (1987) Analysis of paleo-environments based on electric conductivity of stirred clayey sediments into water -On two drilled cores of Osaka Group in Senriyama Hills and Biwako Group at bottom of Lake Biwa, Japan-. The Journal of the Geological Society of Japan, **93**, 667–679.

Keywords: Tokushima Plain, subsurface geology, Kitajima Formation, Median Tectonic Line Fault Zone

©2021. Japan Geoscience Union. All Right Reserved.

[E] Poster | H (Human Geosciences)：H-DS Disaster geosciences

Sat. Jun 5, 2021 5:15 PM - 6:30 PM JST | Sat. Jun 5, 2021 8:15 AM - 9:30 AM UTC | Ch.10_1

[H-DS06] Natural hazard impacts on human society, economics, and technological systems

convener:ELENA PETROVA(Lomonosov Moscow State University, Faculty of Geography), Hajime Matsushima(Research Faculty of Agriculture, Hokkaido University)

The last decade set a record for the number and scale of natural disasters and demonstrates high vulnerability of human society, economics, and ecosystems to their impacts. The most serious consequences have the so-called natural-technological disasters in which natural hazards trigger accidents at technology and infrastructure such as nuclear power and chemical plants, oil refineries and pipelines, power supply systems, buildings, roads, and railways. A distinctive feature of natural-technological events, such as of the 2011 Tohoku earthquake, is their multi-hazard and synergistic nature, which creates cascading impacts, resulting in simultaneous occurrences of myriad catastrophes. The main goal of this multidisciplinary session is to summarize case studies of relationships between natural hazards and technological disasters, their social and economic consequences; and to encourage a discussion about tools and methods to prevent disasters and to minimize their consequences, disaster reconstruction, and tourism for reconstruction, Eco-DRR, and green infrastructure.

[HDS06-P01] Introduction

[HDS06-P02] Effects of abandoned paddy field use for the conservation of threatened hydrophyte after the 2011 Tohoku-oki tsunami

★Invited Papers

*Korehisa Kaneko[1], Hiroshi Jinguji[2] (1.Hokuso Creature Association, 2.Fukushima University)

[HDS06-P03] Citizens' Awareness of Transmitting Information about Earthquake Experiences in the Areas Affected by the Great East Japan Earthquake: A Focus on the Use of Earthquake Ruins

*Ryo Nishisaka[1], Katsunori Furuya[1] (1.Chiba University)

[HDS06-P04] Location of the Visitor Centers of National Parks of Japan and their Adapt to Climate Change

*Satoshi Sasaki[1], Kiyotatsu Yamamoto[1], Kazuhiko W. Nakamura[1] (1.The University of Tokyo)

[HDS06-P05] **The Activity of Kamchatka Volcanoes and theirs Danger to Human Society**

*Olga Girina[1], Evgenii Loupian[2], Alexei Ozerov[1], Dmitry Melnikov[1], Alexander Manevich[1], Elena Petrova[3] (1.Institute of Volcanology and Seismology, Far East Division, Russian Academy of Sciences, Russia, 2.Space Research Institute, Russian Academy of Sciences, Russia, 3.Lomonosov Moscow State University, Geography Faculty, Russia)

[HDS06-P06] The impact of the reduction of beach width by seawall construction on the distribution of ground prowling insects

*Hinata Okoshi[1], Hajime Matsushima[1], Junjiro Negishi[2], Masahiro Ohara[3] (1.Graduate School of Agriculture, Hokkaido University, 2.Faculty of Environmental Earth Science, Hokkaido University, 3.The Hokkaido University Museum, Hokkaido University)

[HDS06-P07] Discussion

[E] Poster | H (Human Geosciences) | H-DS Disaster geosciences

[H-DS06] Natural hazard impacts on human society, economics, and technological systems

convener:ELENA PETROVA(Lomonosov Moscow State University, Faculty of Geography), Hajime Matsushima(Research Faculty of Agriculture, Hokkaido University)

Sat. Jun 5, 2021 5:15 PM - 6:30 PM Ch.10

The last decade set a record for the number and scale of natural disasters and demonstrates high vulnerability of human society, economics, and ecosystems to their impacts. The most serious consequences have the so-called natural-technological disasters in which natural hazards trigger accidents at technology and infrastructure such as nuclear power and chemical plants, oil refineries and pipelines, power supply systems, buildings, roads, and railways. A distinctive feature of natural-technological events, such as of the 2011 Tohoku earthquake, is their multi-hazard and synergistic nature, which creates cascading impacts, resulting in simultaneous occurrences of myriad catastrophes. The main goal of this multidisciplinary session is to summarize case studies of relationships between natural hazards and technological disasters, their social and economic consequences; and to encourage a discussion about tools and methods to prevent disasters and to minimize their consequences, disaster reconstruction, and tourism for reconstruction, Eco-DRR, and green infrastructure.

5:15 PM - 6:30 PM

[HDS06-P01]Introduction

©Japan Geoscience Union

Effects of abandoned paddy field use for the conservation of threatened hydrophyte after the 2011 Tohoku-oki tsunami

*Korehisa Kaneko[1], Hiroshi Jinguji[2]

1. Hokuso Creature Association, 2. Fukushima University

1. Introduction

Threatened plant species, *Ottelia alismoides*, *Monochoria korsakowii*, *Najas graminea*, *Najas minor,* and *Chara braunii* were found in swampy paddy field after the 2011 Tohoku-oki tsunami Japan. These hydrophyte are classified as near-threatened or vulnerable species in the Red Data book of Ministry of environment, Japan. Hygrophyte communities were vanishing rapidly as reconstruction of road and agriculture proceeds. Therefore, surface soil of hygrophytes community was transplanted to abandoned paddy field 5km away from the original hygrophyte community.

In the present study, we transplanted soil seed to examine whether abandoned paddy field is effective for the hygrophytes species conservation. We investigated 1) whether hygrophytes including threatened species emerge and grow in the abandoned paddy field and 2) management methods of abandoned paddy field to conserve hygrophytes species.

2. Method

The sturdy site was located at Hadenya district in Miyagi prefecture Japan (lat.38°38¢37.9’’ N. and long.141°28¢10.5’’ E). The vegetation survey conducted on July and September during 2014-2016 in accordance with the methodology of Braun-Blanquet (1964). The surface soil of paddy field was puddled by human power on April 2014 and 2015, and was strongly puddled by agricultural tractor on April 2016. The water temperature was recorded using a thermo-logger (Tidbit, Onset, USA) at the center of each quadrate frame in transplantation sites and donor seed bank. The water temperature was measured from May to September during 2014-2016 in transplantation site. The water depth was measured with ruler in the center of each quadrate frame.

3. Results

Monochoria korsakowii were recoveried in transplantation site from 2014 to 2016. In particular, *Monochoria korsakowii* formed large community in 2016, and the volume of plant increased singnificantly hihger than that in 2014 and 2015. *Ottelia alismoides* and *Chara braunii* were found in 2014 and 2016. The intensity disturbance with a agricultural tractor suppressed the flourishing of the herbaceous plants of *Phragmites australis* and *Typhaceae* spp. in 2016. Consequently, *Ottelia alismoides* and *Chara braunii* regenerated again in taransplantation site. *Najas graminea* and *Najas minor* were not found during vegetation survey. *Salvinia natans* and *Alisma plantago-aquatica* were newly appeared in transplantion site. Our findings suggest that transplantation of surface soil including seed bank to abandoned paddy field is effective for the conservation of hygrophyte, *Monochoria korsakowii, Ottelia alismoides* and *Chara braunii*. The intensity disturbance for suppression of herbaceous perennial plant is needed to maitain the habitat of threatened plant species.

4. Conclusion

For the future, keeping the intensity disturbance with tractor is desirable on April. In addition, weeding of *Echinochloa spp* by human work is needed to conserve threatened plant species. Furthermore, we must develop the field at water depth 25 cm for the habitat of *Najas graminea* and *Najas minor* and re-transplantation. Long-term field monitoring is needed to elucidate frequency, intensity and period of

©2021. Japan Geoscience Union. All Right Reserved.

suitable disturbance and water depth to maintain threatened hygrophytes.

Keywords: Threatened plant, Seed bank, Soil disturbance, Abandoned paddy field, Tunami

©2021. Japan Geoscience Union. All Right Reserved.

Citizens' Awareness of Transmitting Information about Earthquake Experiences in the Areas Affected by the Great East Japan Earthquake: A Focus on the Use of Earthquake Ruins

*Ryo Nishisaka[1], Katsunori Furuya[1]

1. Chiba University

1. Background
Ten years have passed since the Great East Japan Earthquake. One of the important projects for recovery after the earthquake is to transmit the lessons learned from the experience.Buildings and structures damaged by the earthquake and tsunami are being preserved by municipalities as earthquake ruins. The municipalities have preserved these as public facilities in anticipation of their use in transmitting lessons learned from the disaster and as a means of disaster prevention education. Some people have opposed the ruins' preservation because it reminds people of the horror of the earthquake, or on account of preservation efforts' costs. However, after much consideration, it has been decided more than 30 locations will be preserved in the Iwate, Miyagi, and Fukushima prefectures.

2. Purpose
To transmit the lessons learned from the earthquake, affected citizens' participation is important. Therefore, this study first aims to grasp citizens' awareness of the importance of transmitting the lessons from the earthquakes and what messages they want to transmit. In addition, the earthquake ruins are expected to play a role in communicating about the disaster. This is one of the desirable methods for using them to transmit citizens' experiences of the earthquake. Therefore, the second purpose is to clarify how close the citizens feel to the earthquake ruins and citizens' awareness of their use.

3. Method
A web survey was conducted from March 10–22, 2020 for citizens living in the nine municipalities where the earthquake ruins are preserved. Participants were asked about the importance of communicating the experience of the disaster to others, about their awareness of the earthquake ruins, and so on.

4. Results
4-1. Respondents
Responses were received from a total of 1,080 people from the nine target municipalities. The genders of the respondents were 566 males (52.4%) and 514 females (47.6%), with an average age of 49.4.
4-2. Awareness of and participation in the transmission of the earthquake experience
In all, 89.2% of respondents said, "It is important to transmit information about the disaster," 62.0% said, "I have told other people about the disaster," and 8.8% answered, "I have participated in activities to transmit information about the disaster."
4-3. Contents of knowledge transmission
Of those surveyed, 39.3% responded, "I want to tell how our homes and towns were destroyed by the disaster," and 47.9% responded, "I want to tell about what was lost in the disaster (human life, daily life, and culture)." More than half (54.5%) responded, "I want to tell about our efforts to recover from the disaster."
4-4. Recognition of the earthquake ruins
Almost half (42.3%) of the respondents answered, "I knew whether earthquake ruins would be preserved

©2021. Japan Geoscience Union. All Right Reserved.

in my city," and 39.2% said, "I often see and talk about the earthquake ruins."
4-5. Willingness to use the earthquake ruins
About one quarter (24.6%) of respondents said, "I want to participate if there is a ceremony or event," while 23.7% answered, "I want to visit on a daily basis," and 18.9% replied, "I want to be involved in the ruins' management and use."
4-6. Awareness of earthquake ruins
Most respondents (61.9%) said the ruins were "a symbol of the disaster," and 49.9% answered, "They are a symbol of recovery." Although the earthquake ruins are comprised of buildings and structures damaged by the disaster, they also have a positive image as symbols of recovery.

5. Discussion
Citizens in the disaster areas are very conscious of the importance of transmitting their experiences, but it seems difficult to engage them in actual activities related to the ruins. The high level of awareness of the need to transmit information about lessons learned is noteworthy, but in the future, it may be necessary to take measures to support the shift of awareness from transmission to action.
We found that the earthquake ruins are recognized as symbols both of the disaster and the recovery, and they have a positive image. By contrast, about 40% knew that ruins would be preserved in their town, and about 40% see and talk about them on a daily basis, but only 20% intend to use them, so the ruins, by and large, are not familiar facilities. Before supporting the use of the earthquake ruins by the citizens, it is first necessary to inform them of their existence.
Future studies should examine how earthquake ruins can be devoted to the activities of transmitting information about the citizens' experiences of the earthquake.

Keywords: earthquake ruins, Great East Japan Earthquake, transmitting earthquake experiences

©2021. Japan Geoscience Union. All Right Reserved.

Location of the Visitor Centers of National Parks of Japan and their Adapt to Climate Change

*Satoshi Sasaki[1], Kiyotatsu Yamamoto[1], Kazuhiko W. Nakamura[1]

1. The University of Tokyo

1. Introduction

Global warming is not only increasing the number of climate-related disasters, but also triggering complex disasters that affect many people around the world (Mora et al. , 2018), and this has led to calls for action on climate change. The VCs of national parks, which serve as refuge shelter in times of disaster, are also required to adapt to climate change. When the Ministry of the Environment and prefectural governments select sites for VCs, they focus on whether the sites are in location that is not subject to natural disasters. However, there is no existing knowledge that clarifies the potential of location of VCs to fulfill the aforementioned function in the aftermath of disasters. In this study, we focused on the potential of VCs to serve as refuge shelter in a disaster, with the following two objectives: 1) to clarify the differences between each type by classifying VCs of national parks of Japan according to their location, 2) to examine the potential of VCs as refuge shelter.

2. Methods

A total of 101 VCs in national parks of Japan were adopted as case study facilities and the following indicators were selected for analysis: (1) shortest distance from the VCs (highway interchanges, restaurants, stores), (2) land use within a radius of 500 m around the VCs (rice fields, agricultural land other than rice fields, forests, river lands and lakes, sea areas, building sites). Then, in order to prevent the effect of outliers, the distance scale in indicator (1) was replaced by an ordinal one. Finally, The cluster analysis (Ward's method, squared Euclidean distance) using indicator (1) and (2), and the multiple comparison tests (Bonferroni method, $P<.05$) were employed.

3. Results and Discussion

VCs were classified into four types through cluster analysis. Type I (N=48) is close to restaurants and stores, and has many forests and building sites in its vicinity, suggesting that this type is located at densely built-up area in mountainous national park. Type II (N=13) is close to restaurants and stores, and has many sea areas and building sites in its vicinity, suggesting that this is located at densely built-up area in coastal national park. Type III (N=28) is far from highway interchanges, restaurants and stores, and has many forests in the vicinity, suggesting that this is located near core area of mountains national park. Type IV (N=12) is located far from the highway interchange and is surrounded by rivers, lakes and marshes, and agricultural land, suggesting that this is located in a national park of lakes and marshes.

Type I is assumed that people can procure food, beverages and fuel because restaurants, stores, many buildings, forests are located near VCs. Similar to Type I, Type II, is inferred that food and beverages can be secured since there are restaurants, stores and many buildings. This type has also seawater areas and the countermeasures is necessary in order that facilities should not be isolated from surrounding areas in the event of a tsunami disaster. Compared to Type I, II, Type III is far away from restaurants and stores, and the surrounding area is mostly forest. Although fuel can be secured, it is difficult to secure supplies such as food and beverages, so it is important to stockpile supplies in preparation for disasters. Type IV is easy to secure drinking water because there are many rivers and lakes. Taken into consideration that the distance from restaurants and stores, and the small number of building in the area, it is necessary to stockpile food in particular.

©2021. Japan Geoscience Union. All Right Reserved.

In Conclusion, more than half of the VCs were located within walking distance (500m) from restaurants and stores, suggesting that they have the potential to serve as refuge shelter in a disaster. The results indicated that the resilience and vulnerability of VC differs depending on the location type and the planning and management should be proposed by referring the potential of VCs as refuge shelter.

Keywords: climate change, national parks, visitor center, location



©2021. Japan Geoscience Union. All Right Reserved.

The Activity of Kamchatka Volcanoes and theirs Danger to Human Society

*Olga Girina[1], Evgenii Loupian[2], Alexei Ozerov[1], Dmitry Melnikov[1], Alexander Manevich[1], Elena Petrova[3]

1. Institute of Volcanology and Seismology, Far East Division, Russian Academy of Sciences, Russia, 2. Space Research Institute, Russian Academy of Sciences, Russia, 3. Lomonosov Moscow State University, Geography Faculty, Russia

There are 30 active volcanoes in the Kamchatka, and several of them are continuously active. In the XX-XXI centuries 17 volcanoes of Kamchatka erupted. During this time, 183 volcanic eruptions occurred, including three catastrophic eruptions (Ksudach, 1907; Bezymianny, 1956; Sheveluch, 1964). Strong explosive eruptions of volcanoes were the most dangerous for human society because they produce in a few hours or days to the atmosphere till 2-3 cubic kilometers of volcanic products. Ash plumes and the clouds, depending on the power of the eruptions, the strength and wind speed, to traveled thousands of kilometers from the volcanoes for several days. Any territory of the Kamchatka Peninsula has repeatedly been exposed to ash falls, the thickness of ash in settlements was from less than 1 mm to 4-5 cm. Strong explosive eruptions of volcanoes Sheveluch, Klyuchevskoy, Bezymianny, Kizimen, Karymsky, Zhupanovsky, Avachinsky, Kambalny were the most dangerous for air travel not only over Kamchatka, but also hundreds of kilometers away from the peninsula.

The strong explosive and effusive eruptions of Sheveluch, Klyuchevskoy, Bezymianny, Kizimen and the other were often accompanied by the formation of hot mud flows (lahars), which sometimes disrupted transport communications (roads, bridges) of nearby settlements.

Scientists of KVERT monitor Kamchatkan volcanoes since 1993. Thanks to satellite monitoring of volcanoes carried out by KVERT, several explosive eruptions were predicted in the XXI century, and early warnings were made to the population about possible ashfalls in settlements and about hazard to aviation.

Keywords: volcano, eruption, Kamchatka, danger, population

©2021. Japan Geoscience Union. All Right Reserved.

The impact of the reduction of beach width by seawall construction on the distribution of ground prowling insects

*Hinata Okoshi[1], Hajime Matsushima[1], Junjiro Negishi[2], Masahiro Ohara[3]

1. Graduate School of Agriculture, Hokkaido University, 2. Faculty of Environmental Earth Science, Hokkaido University, 3. The Hokkaido University Museum, Hokkaido University

Seawalls were constructed on sandy beaches in the Sendai coast, Miyagi prefecture after the Great East Japan Earthquake occurred on 11 March 2011. These structures narrowed the beaches and it is concerned that the coastal ecosystems are degraded due to the direct impacts of habitat loss and indirect impacts of the increased environmental pressures from the sea such as waves, sand transportations, salt sprays, etc. It has been suggested that such anthropogenic impacts on ecosystems may also affect the nutrient cycle in the ecotone between sea and land, and it is required to clarify the impacts quantitatively. The purpose of this study was investigated whether the distribution of ground prowling insects living on the beach is affected by the reduction of the beach width caused by seawall constructions.
The survey was conducted in the coastline of Miyagi prefecture at five sites: Arahama A and B (Sendai City), Ido (Sendai City), Yuriage (Natori City), Kitagama (Natori City). These sites were selected considering the width of the beach and the state of the vegetation. Ground prowling insects were sampled by pitfall traps. The traps were set from the seawall to the shoreline in a direction vertical to the seawall at 20 m intervals for approximately 40 hours. These samplings were undertaken from 26 to 28 August 2020.
The results suggested that the loss of vegetation caused by the reduction of beach width affects the distribution of ground prowling insects. The narrower beaches received more environmental impacts from the sea, and it also lead to the loss of habitat of them and vegetation. In addition, Gonocephalum (Gonocephalum) recticolle and Meristhus (Sulcimerus) niponensis were found only in the vicinity of the seawalls in Yuriage, the widest beach (about 200 m width) of all five sites. At other sites, their habitat may have been lost due to the construction of seawalls.

©2021. Japan Geoscience Union. All Right Reserved.

[E] Poster | H (Human Geosciences) | H-DS Disaster geosciences

[H-DS06] Natural hazard impacts on human society, economics, and technological systems

convener:ELENA PETROVA(Lomonosov Moscow State University, Faculty of Geography), Hajime Matsushima(Research Faculty of Agriculture, Hokkaido University)

Sat. Jun 5, 2021 5:15 PM - 6:30 PM Ch.10

The last decade set a record for the number and scale of natural disasters and demonstrates high vulnerability of human society, economics, and ecosystems to their impacts. The most serious consequences have the so-called natural-technological disasters in which natural hazards trigger accidents at technology and infrastructure such as nuclear power and chemical plants, oil refineries and pipelines, power supply systems, buildings, roads, and railways. A distinctive feature of natural-technological events, such as of the 2011 Tohoku earthquake, is their multi-hazard and synergistic nature, which creates cascading impacts, resulting in simultaneous occurrences of myriad catastrophes. The main goal of this multidisciplinary session is to summarize case studies of relationships between natural hazards and technological disasters, their social and economic consequences; and to encourage a discussion about tools and methods to prevent disasters and to minimize their consequences, disaster reconstruction, and tourism for reconstruction, Eco-DRR, and green infrastructure.

5:15 PM - 6:30 PM

[HDS06-P07]Discussion

©Japan Geoscience Union

[J] Poster | H (Human Geosciences)：H-DS Disaster geosciences

Sat. Jun 5, 2021 5:15 PM - 6:30 PM JST | Sat. Jun 5, 2021 8:15 AM - 9:30 AM UTC | Ch.10_2

[H-DS07] Seismic hazards on subduction earthquakes and active faults in the Central Japan

convener:Takashi Azuma(National Institute of Advanced Industrial Science and Technology), Yasuhiro Suzuki(Nagoya University)

This session focuses on seismo-tectonics and disasters prevention for large earthquakes in the Central Japan. We would like to discuss possible hazards with low probability, problems related to quantatitive evaluation, such as modellings and evaluation of uncertainties, utilization of hazard information, and so on.

[HDS07-P01] Issues for long-term evaluation of Byobu-yama/Ena-san fault zone

*Yasuhiro Suzuki[1] (1.Nagoya University)

[HDS07-P02] Paleoseismological trenching surveys on the Enasan-Sanageyamakita fault zone, Central Japan

*Takashi Azuma[1], Norio Shigematsu[1], Rei Nakashima[1], Ken-ichi Yasue[2], Ryo Tateishi[2], Daisuke Hirouchi[3] (1.National Institute of Advanced Industrial Science and Technology, 2.Toyama University, 3.Shinshu University)

[HDS07-P03] Questionnaire survey for experts on long-term evaluation of active faults and evaluation of ground motion (Part 1)

*Noa Mitsui[1], Takeshi Sagiya[1] (1.Disaster Mitigation Research Center, Nagoya University)

Issues for long-term evaluation of Byobu-yama/Ena-san fault zone

*Yasuhiro Suzuki[1]

1. Nagoya University

Introduction

The Headquarters for Earthquake Research Promotion selected the northern part of the " Byobuyama/Enasann Fault and Sanageyama Fault" as the target of intensive research (2020-2022). The purpose of this survey is to improve active fault evaluation and strong motion evaluation. The research group led by Nagoya University summarized the problems of the conventional evaluation of the fault and formulated a research plan to improve them.

Issues and research objectives

The "Byobuyama/Enasann Fault and Sanageyama Fault" is a long active fault zone with a total length of over 100 km from the Ena Mountains through the Okazaki Plain to the Chita Peninsula. The faults that make up the fault zone are close to each other, and it is difficult to decide a source fault scenario. Around the fault, there are densely populated areas such as Nagoya City and industrially concentrated areas such as Toyota City.

In Japan, the survey on this fault zone was once carried out from 1995 to 2000, however the activity history and fault structure data are scarce. Based on such data, in the previous long-term evaluation, the Enasan-Sanageyama north fault zone was ranked A *, the Byobuyama fault and the Kagiya fault were ranked A, the Sanage-Takahama fault was ranked Z, and the Akagawa fault was ranked X. "Fault near Nagoya City" was unknown.

The conventional active fault evaluation has the following problems.

1) Comparing the active fault map of the Geographical Survey Institute (1996-2016), the detailed digital map of the active fault (2002), and the active fault map of Gifu Prefecture (2010), there is a difference in trace identification.

2) It is assumed that the Enasan fault and the Sanageyama north fault, which have different geometrical characteristics, activate together.

3) There is no specific activity history for the Byobuyama fault. Since the earthquake occurrence probability is calculated by the Poisson process model, it cannot be compared with the probability of other faults based on the renewal process model.

4) The northern part of the Sanage-Takahama fault zone is evaluated as Z rank in calculation, while it is assumed that the activity confirmed at one point is regarded as the latest activity and that the total length of 51 km causes a 4 m displacement.

Keywords: active fault, earthquake, long-term evaluation

©2021. Japan Geoscience Union. All Right Reserved.

Paleoseismological trenching surveys on the Enasan-Sanageyamakita fault zone, Central Japan

*Takashi Azuma[1], Norio Shigematsu[1], Rei Nakashima[1], Ken-ichi Yasue[2], Ryo Tateishi[2], Daisuke Hirouchi[3]

1. National Institute of Advanced Industrial Science and Technology, 2. Toyama University, 3. Shinshu University

We conducted paleoseismological trench surveys at 2 sites on the Enasan-Sanageyamakita fault zone. This fault zone is consisted with the Enasan fault (38 km in length) and the Sanageyamakita fault (22 km). One site is Tomida on the Enasan fault, where is close to a previous trenching survey site by Gifu Prefecture in 2001. In our trench, 2 fault planes with high angle were recognized, whereas this fault is evaluated as a reverse fault.Another site is Higashi-shirasaka on the Sanageyama-kita fault, where is same site with a previous trenching survey by Aichi Prefecture in 1996. In the trench, low-angle fault planes were recognized, whereas this fault is evaluated as a high-angle right-lateral strike-slip fault. It cut sand-silt sediments and covered with gravels. We will discuss faulting histories these sites on this fault zone. This survey was a part of the Comprehensive Research Project for the Enasan-Sanageyama-Kita Fault Zone by MEXT.

Keywords: active fault, Central Japan, Paleoseismological trenching survey

©2021. Japan Geoscience Union. All Right Reserved.

Questionnaire survey for experts on long-term evaluation of active faults and evaluation of ground motion (Part 1)

*Noa Mitsui[1], Takeshi Sagiya[1]

1. Disaster Mitigation Research Center, Nagoya University

Regarding earthquakes occuring on active faults, the Headquarters for Earthquake Research Promotion has evaluated the long-term earthquake occurrence potentials based on surveys of active faults conducted nationwide since 1996. In addition, evaluations of strong ground motion is also published. Since the frequency of earthquakes on active faults is very low and the quantity and quality of information obtained from active fault surveys are limited, long-term evaluation of active faults has large uncertainty. Therefore, when disseminating long-term evaluations of active faults and evaluation of strong ground motion to the residents as earthquake risk information, it is necessary to consider the appropriate content and transmission method from various viewpoints. The viewpoints are such as scientific validity, understanding and utilization of information in disaster prevention administration, and understanding of local residents who receive the information.
Opinions of experts in active faults and earthquakes are reflected in the work process of long-term evaluation and evaluation of strong ground motion. In addition, surveys are conducted on the residents and local governments regarding the published results. On the other hand, regarding the published results, the degree of recognition and evaluation as a group of experts including non-committee members has not been clarified.
Therefore in this research, as part of the survey on the method of transmitting information of earthquake evaluation with uncertainty, we will first conduct a survey targeting experts in active faults and earthquakes. We conducted a questionnaire survey to member of the Japanese Society for Active Fault Studies and councillor of the Seismological Society of Japan to collect opinions based on the scientific validity about information that should be conveyed to residents and about the proper method regarding active faults and strong ground motion.

Keywords: active fault, long-term evaluation, evaluations of ground motion, risk

©2021. Japan Geoscience Union. All Right Reserved.

[J] Oral | H (Human Geosciences)：H-DS Disaster geosciences

Sat. Jun 5, 2021 1:45 PM - 3:15 PM JST | Sat. Jun 5, 2021 4:45 AM - 6:15 AM UTC | Ch.16 Zoom Room 16

[H-DS10] Geohazards in humid, tectonically active countries and their precursors

convener:Satoru Kojima(Department of Civil Engineering, Gifu University), Taro Uchida(University of Tsukuba), Yoshihiko Kariya(Department of Environmental Geography, Senshu University), Chairperson:Yoshihiko Kariya(Department of Environmental Geography, Senshu University), Satoru Kojima(Department of Civil Engineering, Gifu University)

This session covers mass movements of landslide, slope failure, debris flow, and gravitational slope deformation in tectonically active, humid countries, and aims to discuss on their mechanisms, characteristics of occurrence sites, the significance in geological time scale, and the methodology to mitigate their affects by researchers with various related research fields.

1:45 PM - 2:00 PM JST | 4:45 AM - 5:00 AM UTC

[HDS10-01] Weathering styles and landslide types of granite

*Masahiro Chigira[1], Yasuto Hirata[2] (1.Fukada Geological Institute, 2.Central Research Institute of Electric Power Industry)

2:00 PM - 2:15 PM JST | 5:00 AM - 5:15 AM UTC

[HDS10-02] Slope failures induced by the 2020 July heavy rain in the Chubu Region

*Hidehisa Nagata[1] (1.Fu-Sui-Do Company Limited)

2:15 PM - 2:30 PM JST | 5:15 AM - 5:30 AM UTC

[HDS10-03] **Landslides in humid-temperate mountainous areas in northwestern Vietnam perceived by satellite images**

*Takahisa Furuichi[1,2,3], Hiromu Daimaru[1], Wataru Murakami[1], Takashi Okamoto[1] (1.Forest and Forest Products Research Institute, 2.University of the Sunshine Coast, 3.Miyagi University of Education)

2:30 PM - 2:45 PM JST | 5:30 AM - 5:45 AM UTC

[HDS10-04] Estimation of subsurface structure in the linear depression spreading over the landslide crown

*Hikaru Osawa[1], Issei Doi[2], Noriyuki Arai[2], Yosuke Yamakawa[1], Takuma Watakabe[3] (1.Mountain Science Center, University of Tsukuba, 2.DPRI, Kyoto University, 3.Forestry and Forest Products Research Institute)

2:45 PM - 3:00 PM JST | 5:45 AM - 6:00 AM UTC

[HDS10-05] Study on the landslide mechanism of the Iya area where the deep-seated landslide occurred by Typhoon Talas in 2011 using Drone Airborne TEM

*Atsuhiko Kinoshita[1,2], Suguru Shibata[2], Takao Yamakoshi[1], Hiroaki Nakaya[1], Yasumasa Fujiwara[3], Hideki Nakano[3], Akira Jomori[4], Katsushi Kawato[5], Muneki Mitamura[6], Tamotsu Matsui[7] (1.National Institute for Land and Infrastructure Management, 2.Sediment Disaster Prevention Technology Center, 3.Eight-Japan Engineering Consultants Inc., 4.NEOSCIENCE CO.LTD., 5.NIPPON ENGINEERING CONSULTANTS CO.,LTD., 6.Osaka City University, 7.Osaka University)

3:00 PM - 3:15 PM JST | 6:00 AM - 6:15 AM UTC

[HDS10-06] Creating a Landslide risk map of the Nachi River basin

*Makoto Msatsuzawa[1], Tatsuya Ito[1], Chiyoshi Minami[1], Atsuhiko Kinoshita[2], Suguru Shibata[2], Taku Yamada[3], Toshiaki Kotake[3], Yasutaka Tanaka[4] (1.PACIFIC CONSULTANTS CO., LTD., 2. Sediment Disaster Prevention Technology Center, 3.Kiisankei sabo office, 4.HOKKAIDO UNIVERSITY)

Weathering styles and landslide types of granite

*Masahiro Chigira[1], Yasuto Hirata[2]

1. Fukada Geological Institute, 2. Central Research Institute of Electric Power Industry

Weathered granite areas have suffered from many landslides induced by rain storms: For example, Hiroshima rainstorm disasters in 1999, 2014, and 2018, and southern Miyagi rainstorm disaster induced by typhoon 19 in 2019. The basic causes of these landslides were in two types of weathering styles: micro-sheeting and spheroidal weathering. Micro-sheeting forms loosened soil layers on slope surfaces, which fail during rainstorms; and spheroidal weathering forms corestones, which are destabilized when the intervening gruss is eroded in the ground. These two types of weathering have been known, but the reasons why were not known. Topographically, granite forms characteristic features like tors and boulder fields, but the reasons why have not been known. We investigated granite with high angle joints using UAV and SfM and found that columnar joints develop in granite body in 10 places. Many of these areas have tors, which we found were surrounded by columnar joints. We also investigated the boulder field at Kui, Hiroshima prefecture, and found that many columnar prims are included in the field as well as rounded corestones, which suggests that the boulder field is made through the collapse of rock columns weathered in the ground. Columnar joints of granite are probably made in the upper marginal part of a granite body near the surrounding rocks and not in the depths, in which granite is massive rock and later experiences sheeting and micro-sheeting. Such a history suggests that the fate of granite body after being exposed to the ground surface is already determined when it is emplaced in the depths.

Keywords: Granite, Weatheirng, Landslide, Spheroidal weathering, Micro-sheeting

©2021. Japan Geoscience Union. All Right Reserved.

Slope failures induced by the 2020 July heavy rain in the Chubu Region

*Hidehisa Nagata[1]

1. Fu-Sui-Do Company Limited

A weather front stayed in July, 2020 brought much rainfall to the Japanese Islands. As well as the Kyusyu Region, the Chubu Region including Gifu, Nagano and Aichi Prefectures were also suffered from slope disasters in various localities. An overview of the landslides occurred in the Chubu Region from geological and geomorphological standpoints is mentioned. The following cases were observed as slope failures. 1) Shallow rapid landslides on the slopes consist of pulutonic rocks and welded tuff: At Nishibora, Takayama city, Gifu Prefecture, both Mesozoic medium-grained granodiorite and crystalline welded tuff ("Nohi Rhyolites") are strongly weathered into decomposed sandy saprolite (Masa). Many slopes collapsed at the surface no more than 1 m depth, maximum width is 20 m. 2) Deep-seated rapid landslides on the slope of Jurassic accretionary complex: Weathered sandstone of the Mino Belt were in failure at Okudabora, Gujo City, Gifu Prefecture, and Kamiya, Kiso Town, Nagano Prefecture. Weathered meta-chert with small amount of granite and diorite of the Ryoke Belt were collapsed at Toko, Tenryu Village, Nagano Prefecture. Depths of landslides reach about 20m in the Okudabora and Toko, and their volumes are 50,000 m^3 and 100,000 m^3, respectively. In the case of Kamiya landslide, only two surface failures are visible, but they are located at the toes of larger deep-seated landslide of which 400 m wide. Also, the Okudabora landslide occurred in the larger gravitational deformed area. 3) Artificial slope failures in suburban area: Cut slope for railroad were collapsed by flooding water flowed from a road above the slope at Oshikamo, Toyota City, Aichi Prefecture. Embankment for widening of dwelling site along a terrace scarp broke involving retaining wall at Okacho, Okazaki City, Aichi Prefecture.

Keywords: plutonic rocks, welded tuff, accretionary complex, artificial slopes

©2021. Japan Geoscience Union. All Right Reserved.

Landslides in humid-temperate mountainous areas in northwestern Vietnam perceived by satellite images

*Takahisa Furuichi[1,2,3], Hiromu Daimaru[1], Wataru Murakami[1], Takashi Okamoto[1]

1. Forest and Forest Products Research Institute, 2. University of the Sunshine Coast, 3. Miyagi University of Education

Introduction

Landscape in northern Vietnam is characterized by intensive land-use on relatively steep mountain slopes, on which landslides often occur, induced by heavy rainfall brought by typhoons (or tropical storms) and convergence zones. Landslides are a major process of the geomorphic evolution in northern Vietnam and various studies for better understanding of landslides along the biophysical contexts in northern Vietnam have been progressing. We report here initial reconnaissance, which was only remotely possible due to COVID-19, on recent landslides in northewestern Vietnam, i.e. the region to the west of the Hong River (Red River).

Topography, Geology and Land-use

Three major rivers in northwestern Vietnam, namely the Hong River, Da River and Ma River, parallelly flow in the direction of NW-SE, which are aligned parallel to the Red River Fault Zone that represents the regional tectonic structure. The Con Voi Mountains have built between the Hong and Da Rivers up to the elevation higher than 2500 m. Paleozoic and Mesozoic sedimentary rocks that commonly include limestone units extensively occur in the area, while Mesozoic volcanic and pyroclastic rocks and metamorphic rocks predominantly underlie specific areas. Mountain slopes are extensively used for cultivation and forestry and are often terraced up to the ridge. Bare lands are occasionally distributed due to deforestation or intensive land-use.

Rainfall

Northwestern Vietnam is under a humid-temperate climate and experiences heavy rainfall mostly during the rainy season from April to September, which is either brought by typhoons (or tropical storms) or due to a strong wind convergence developed by the tropical disturbance together with the persistent Asian monsoon. A statistical analysis indicated an increase of heavy rainfall in northern Vietnam during both La Nina and El Nino events, suggesting an effect of the ENSO cycles on heavy rainfall in northern Vietnam. A GSM-based simulation projected an increase of heavy rainfall in the middle and late 21st century compared to the late 20th century in northern Vietnam.

Areas, characteristics and occurrence of landslides

We used multiple-year satellite images available on Google Earth as well as multiple-year images taken by the Worldview-2 and Pleiades satellites. Landslide features have been identified in various areas in northwestern Vietnam and most critical ones can be picked up in Yen Bai and Lai Chau provinces. Landslides in those areas likely occurred during the 2018 rainy season when three tropical storms, namely Ewiniar in June, Son-Tinh in July and Bebinca in August, brought heavy rainfall in northwestern Vietnam. In the Yen Bai site, numerous shallow landslides appear on deforested mountain slopes underlain by plutonic rocks at the altitudes of 1500-2000 m. In the Lai Chau site, a massive, deep-seated landslide with a dimension of 100 m in width and 650 m in length is found on broadly deforested mountain slopes underlain by on basaltic bedrocks at the altitude approximately 600 m. A village located immediately above the landslide body was disappeared after the devastating landslide. Landslide debris were

©2021. Japan Geoscience Union. All Right Reserved.

deposited along an approximately 4-km section of the valley, which also caused damage.

Working progress

Geomorphic attributes, such as topography, bedrocks, soil layers, hydrology and land-use, will be investigated in the Yen Bai and Lai Chau sites to uncover conditions and mechanisms of the 2018 landslides. Results should provide key features for creating landslide risk maps in the areas and proposing a concept of disaster-preventive land-use planning that accords with regional or local biophysical (and social) contexts. Importantly, climate change adaptation should be considered in the map and concept as heavy rainfall is projected to increase through the 21st century in northern Vietnam.

Keywords: Landslide, Northwestern Vietnam, Satellite image, Geology, Land-use, Heavy rainfall

©2021. Japan Geoscience Union. All Right Reserved.

Estimation of subsurface structure in the linear depression spreading over the landslide crown

*Hikaru Osawa[1], Issei Doi[2], Noriyuki Arai[2], Yosuke Yamakawa[1], Takuma Watakabe[3]

1. Mountain Science Center, University of Tsukuba, 2. DPRI, Kyoto University, 3. Forestry and Forest Products Research Institute

In recent years, deep-seated catastrophic landslides caused by heavy rainfall have occurred one after another in Japan, and there is a need to clarify the relationship between landslides and depressions in slopes, which are known as precursors to collapses, in order to mitigate the damage. In the 2011 Kii Peninsula heavy rainfall disaster, linear depressions and small mountain- and valley-facing scarps remained characteristic of the upper region of the landslide, which can be closely related to the mechanism of landslide occurrence (Chigira et al. 2013; Arai and Chigira 2019). According to Yokoyama (2019), the subsurface structure within these linear depressions is prone to storing water, suggesting that a rise in the groundwater level within the depressions may affect landslide occurrence. However, there are very few studies that have empirically clarified the subsurface structure in the depressions (Nishii and Ikeda, 2013). In this study, we conducted a geological survey and a surface-wave exploration inside and outside the linear depressions in order to clarify the subsurface structure in the linear depressions adjacent to the landslide, which is considered to have a significant influence on the mechanism of deep-seated landslide.

The study area was the uppermost stream of the Kogouchi River along Kangyou-mine in northern Shizuoka Prefecture. This area is locally known as "Goshiki-gare", where green, red, and weathered brown rocks are conspicuous, and there spreading over clear linear depressions at the head of the landslide.

As a result of ortho-imaging from aerial photographs taken by UAV, the size of the leaf-shaped landslide was 200 m in length and 150 m in width. The geological survey revealed that the area in and around Goshiki-gare is dominated by greenstone with basaltic hyaloclastite, and red mudstone is partially incorporated. Blocked greenstone was present at the top of the landslide. In the middle to upper part of the area, fractured and clayed greenstone and red mudstone were observed. At the end of the slope in the sub-catchment including the landslide, slate toppled outcrops with a north-south orientation of 60° and eastward trending were observed, suggesting gravitational deformation. We also found a 20-30 m wide greenstone fracture zone on the landslide 150 m west of Goshiki-gare. This is considered to be a fault outcrop of the Sasayama Tectonic Line.

As a result of the surface wave exploration of two lines crossing the depression and one longitudinal line, the S-wave velocity was less than 160 m/s from the ground surface to a depth of about 3 m, 200-300 m/s at a depth of about 3-6 m, and 400 m/s at a depth of about 7 m or more. Comparing the results with the geological cross-section, it is inferred that they correspond to soil layers, weathered bedrock, and basement rock, respectively. The depth at which the S-wave velocity is 160 m/s for the concave and convex portions of the transverse measurement line was compared. As a result, the depth of the convex part was 1.6 m while that of the concave part was 2.8 m, indicating that the concave part was deeper. This trend was the same for the two measurement lines in the transverse direction. The depths at which the S-wave velocities in the concave longitudinal survey line were 160 m/s and 300 m/s were 1.4-2.5 m and 3.3-6.4 m, respectively, indicating that the velocities varied even in the concave area.

©2021. Japan Geoscience Union. All Right Reserved.

References: Chigira et al. (2013): *Geomorphology*, 201(1), 479-493. Arai and Chigira (2019): *Engineering Geology*, 260(3), 105236, Yokoyama (2019): *Geomorphology*, 352(1), 106977. Nishii and Ikeda (2013): *J. of Geography*, 122(4), 755-767.

Keywords: Gravitational slope defomation, Accretionary complex, Surface wave exploration

©2021. Japan Geoscience Union. All Right Reserved.

Study on the landslide mechanism of the Iya area where the deep-seated landslide occurred by Typhoon Talas in 2011 using Drone Airborne TEM

*Atsuhiko Kinoshita[1,2], Suguru Shibata[2], Takao Yamakoshi[1], Hiroaki Nakaya[1], Yasumasa Fujiwara[3], Hideki Nakano[3], Akira Jomori[4], Katsushi Kawato[5], Muneki Mitamura[6], Tamotsu Matsui[7]

1. National Institute for Land and Infrastructure Management, 2. Sediment Disaster Prevention Technology Center, 3. Eight-Japan Engineering Consultants Inc., 4. NEOSCIENCE CO.LTD., 5. NIPPON ENGINEERING CONSULTANTS CO.,LTD., 6. Osaka City University, 7. Osaka University

In 2011 Typhoon Talas, the total precipitation on the Kii Peninsula exceeded 1,000 mm in a wide area. As a result, deep-seated landslides occurred at 72 slopes around the Peninsula. Immediately after the disaster, researches on the mechanisms of the deep-seated landslides have been conducted from various viewpoints. In this study, taking the Iya district in Tanabe City, Wakayama Prefecture as an example, the mechanism of deep-seated landslides has been investigated from the viewpoint of guiding and blocking of the flow of groundwater by the fault crush zones that cross the slope. In particular, the behavior of groundwater around the fault crush zones caused by the heavy rain is clarified by using Drone Airborne Transient Electromagnetics (Drone Airborne TEM) technology that has rapidly become to be used in recent years.

For the purpose of the survey was grasping the rough geological characteristics, the distribution of the height of the groundwater and the distribution of the springs, and the presence of fault crush zones. We investigated the resistivity distributions of about 0-200 m underground was investigated. The date of the survey was two days after the total rainfall of 98.5 mm, and it is probable that the effects of the rainfall remained. Next, the electrical prospecting (about 700 m length) about 0-200 m underground was carried out (November 25-27, 2020) for the purpose of investigating the location of the fault crush zones and the underground crush structure in detail. The location of the electrical prospecting was located on the upper right side of the landslide slope viewed from the bottom of the landslide slope in which the results of the field survey reveal that fault crush zones are concentrated. At the start of the measurement, it was no rainfall for 4 days. And so, the resistivity distribution during the dry period was obtained. Drone Airborne TEM was conducted two times around the time of the electrical prospecting and at the same location as the electrical prospecting. The surveys were conducted in the days when was 3 days after the end of rainfall of 217 mm in total rainfall of Typhoon CHAN-HOM (October 13, 2020) and the day when was in the dry period and without rainfall for 11 days (December 2, 2020). In the Drone Airborne TEM, the resistivity distributions about 0-200 m underground and about 700 m length. Then, by taking these differences, the behavior of groundwater around the fault crush zone at the time of Typhoon CHAN-HOM in 2020 was clarified.

It was found that there are four fault crush zones around the landslide slope in the Iya area. In addition, it was found that three of these fault crush zones are of the type that blocks the flow of the groundwater. Also, it was found that the other one is a type that induces the groundwater from the surroundings. It is probable that at the time of the disaster in 2011, groundwater was induced by these faults, and the groundwater was blocked, causing the deep-seated landslide.

©2021. Japan Geoscience Union. All Right Reserved.

Keywords: Drone Airborne TEM, fault crush zone, groundwater

©2021. Japan Geoscience Union. All Right Reserved.

Creating a Landslide risk map of the Nachi River basin

*Makoto Msatsuzawa[1], Tatsuya Ito[1], Chiyoshi Minami[1], Atsuhiko Kinoshita[2], Suguru Shibata[2], Taku Yamada[3], Toshiaki Kotake[3], Yasutaka Tanaka[4]

1. PACIFIC CONSULTANTS CO., LTD., 2. Sediment Disaster Prevention Technology Center, 3. Kiisankei sabo office, 4. HOKKAIDO UNIVERSITY

Due to the 2011 Kii Peninsula flood, Landslides occurred frequently in the Nachi River basin in Wakayama Prefecture, and the debris flow that accompanied it caused 28 deaths, missing persons, and many casualties. Most of the slope failures were Shallow Landslides. In the Nachi River basin, private houses are concentrated along the Nachi River, and it has been reported that debris flows caused by Landslides have caused casualties in the past during heavy rains. Therefore, in this study, we attempted to create a Landslide risk map based on the relationship between the topographical and geological classification and the Landslide area ratio in 2011.

Keywords: Landslide risk map, Shallow Landslide, Degree of Mountain Denudation, Granodiorite, Mudstone, Geologic Boundary

©2021. Japan Geoscience Union. All Right Reserved.

[J] Oral | H (Human Geosciences)：H-DS Disaster geosciences

Sat. Jun 5, 2021 3:30 PM - 5:00 PM JST | Sat. Jun 5, 2021 6:30 AM - 8:00 AM UTC | Ch.16 Zoom Room 16

[H-DS10] Geohazards in humid, tectonically active countries and their precursors

convener:Satoru Kojima(Department of Civil Engineering, Gifu University), Taro Uchida(University of Tsukuba), Yoshihiko Kariya(Department of Environmental Geography, Senshu University), Chairperson:Taro Uchida(University of Tsukuba), Satoru Kojima(Department of Civil Engineering, Gifu University)

This session covers mass movements of landslide, slope failure, debris flow, and gravitational slope deformation in tectonically active, humid countries, and aims to discuss on their mechanisms, characteristics of occurrence sites, the significance in geological time scale, and the methodology to mitigate their affects by researchers with various related research fields.

3:30 PM - 3:50 PM JST | 6:30 AM - 6:50 AM UTC

[HDS10-07] Back analysis for landslide occurrence based on the relationship between the rain and the slope condition.

★Invited Papers

*Reiko AKIYAMA[1], Kuniaki MIYAMOTO[2] (1.Oriental Consultants Co., Ltd., 2.Nippon Koei Co., Ltd.)

3:50 PM - 4:05 PM JST | 6:50 AM - 7:05 AM UTC

[HDS10-08] Spatial Variability of Rainfall-runoff Characteristics in a Large-scale Landslide-prone Area Underlain by Accretionary Sedimentary Rocks

*Yosuke Yamakawa[1], Kouji Koshimizu[2], Taro Uchida[1] (1.Faculty of Life and Environmental Sciences, University of Tsukuba, 2.Graduate School of Science and Technology, University of Tsukuba)

4:05 PM - 4:20 PM JST | 7:05 AM - 7:20 AM UTC

[HDS10-09] Observation of an effect of interstitial water saturation and water quality on changes in formation resistivity

*Yamato SUZUKI[1], Hiroaki NAKAYA[1], Atsushi FUNAYAMA[2], Toshihiko SAKASHIMA[2], Koushiro TANAKA[2], Akira JOMORI[3], Tetsuya TOYAMA[3] (1.National Institute for Land and Infrastructure Management, 2.Pacific Consultants Co., Ltd., 3.Neo-science Co. Ltd.)

4:20 PM - 4:35 PM JST | 7:20 AM - 7:35 AM UTC

[HDS10-10] Valley floor environmental changes and disasters associated with glacial collapse of mountain glaciers
-A case study of the 2003, 04 and 2021 floods in the Himalayas -

*Jiro Komori[1] (1.Teikyo Heisei University)

4:35 PM - 4:50 PM JST | 7:35 AM - 7:50 AM UTC

[HDS10-11] Characteristics of slope disasters triggered by sudden topographic deformation in the Himalayan region

*Hiroshi YAGI[1], Daisuke Higaki[2], Ching-Ying Tsuo[3], Akihiko Wakai[4], Yusuke Yamamoto[5] (1.Faculty of Art, Science and Education, Yamagata University, 2.Nippon Koei Co.,Ltd., 3.Faculty of Agriculture and Life Science, Hirosaki University, 4.Graduate School of Polytechnics, Gunma University, 5.Geoscience Research Laboratory Co.,Ltd.)

4:50 PM - 5:00 PM JST | 7:50 AM - 8:00 AM UTC

[HDS10-12] Discussion

Back analysis for landslide occurrence based on the relationship between the rain and the slope condition.

*Reiko AKIYAMA[1], Kuniaki MIYAMOTO[2]

1. Oriental Consultants Co., Ltd., 2. Nippon Koei Co., Ltd.

Studies on the prediction of the location and time of landslide occurrence have been actively conducted. The method of dynamic prediction by the slope stability model from the slope conditions, and the groundwater depth generated has made possible for landslide simulation based on the digital elevation model.In this study, the landslide occurrence based on the infinite slope stability model is normalized by the slope gradient and the unit volume weight of the soil layer. Then the water conditions and slope conditions at the time of the landslide occurrence are reversed for the landslide cases. Application results by the method are introduced in this report. The infinite slope stability model is generally expressed by the ratio of shear stress to resistance in the surface soil layer (Eq-1). This was organized by Fc and Fw as described in Imaizumi *et al.*[2003].In this time, the normalization parameter F_{CC} composed of the slope conditions (including the soil cohesion) was introduced into the soil cohesion force term, and when the safety factor Fs equals 1.0, it was normalized by the internal friction angle of the soil. It is shown as the relationship between the slope gradient, and the groundwater depth term due to the groundwater depth normalized by the soil layer thickness (Eq-2).In this paper, examples of estimating the soil layer thickness, and soil cohesion by applying the method to shallow landslides caused in Izu Oshima in the 2013, as well as to the landslides in the Amehata River basin in 1960-1970 are introduced. In this report, the result of trying to back analysis the assumed soil depth from the slope angle where the landslide is distributed is explained.

Keywords: Landslide, infinite slope stability model, back analysis, soil depth

©2021. Japan Geoscience Union. All Right Reserved.

$$F_s = \frac{W}{G} = \frac{c + (\bar{\rho} g D - \rho g h)\cos I \tan\phi}{D \bar{\rho} g \sin I} < 1.0 \quad \cdots\cdots \text{Eq-1}$$

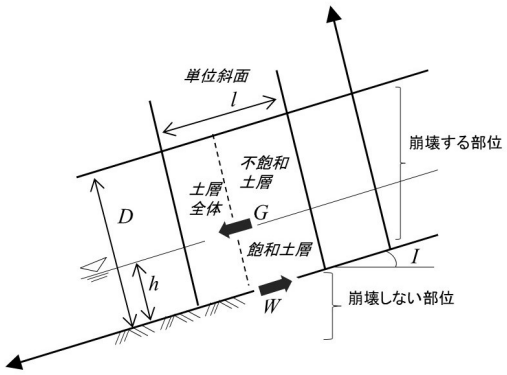
$$\bar{\rho} = \left\{ G_s(1-\lambda) + \lambda S_r + (1-S_r)\lambda \frac{h}{D} \right\} \rho$$

In case $F_s = 1.0$

$$F_{cc} = 1 - \frac{1 - F_w}{\frac{\tan I}{\tan\phi}} \quad \cdots\cdots \text{Eq-2}$$

$$F_w = \frac{\rho}{\bar{\rho}} \frac{h}{D}$$

$$F_c = F_{cc} \frac{\tan I}{\tan\phi} = \frac{1}{\bar{\rho}} \frac{c}{D g \sin I} \frac{\tan I}{\tan\phi}$$



c=Soil cohesion, ϕ = Internal friction angle, Gs=soil particle density
ρ=Water density, h= Water depth, g=Gravitational acceleration,
D=Soil depth, I=Slope angle, λ=Porosity, Sr= Degree of saturation

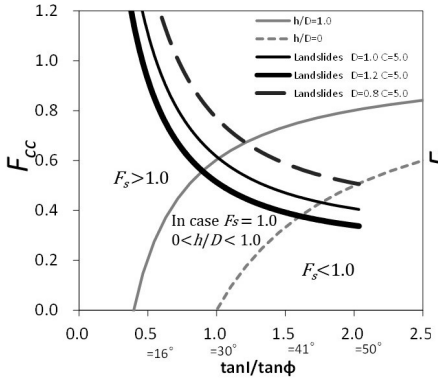


Fig.1 Okanesawa (c=5.0 kN/m²)

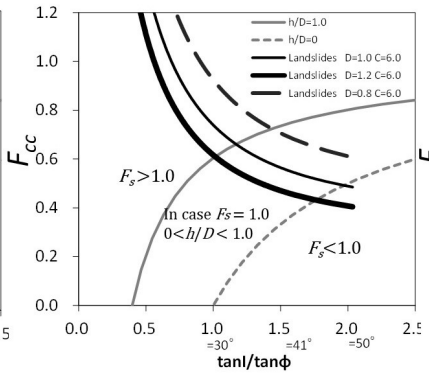


Fig.2 Okanesawa (c=6.0 kN/m²)

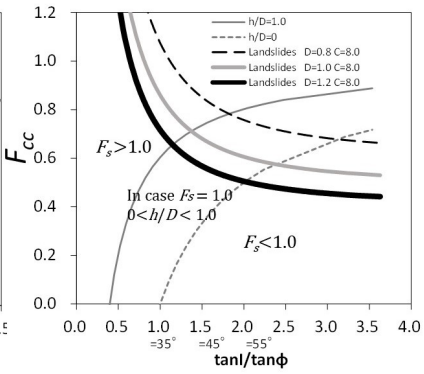


Fig.3 Inamatadani river(1982) (c=8.0 kN/m²)

©2021. Japan Geoscience Union. All Right Reserved.

Spatial Variability of Rainfall-runoff Characteristics in a Large-scale Landslide-prone Area Underlain by Accretionary Sedimentary Rocks

*Yosuke Yamakawa[1], Kouji Koshimizu[2], Taro Uchida[1]

1. Faculty of Life and Environmental Sciences, University of Tsukuba, 2. Graduate School of Science and Technology, University of Tsukuba

Understanding spatial variability of rainfall-runoff characteristics is essential for clarifying the mechanism that landslides due to rainfall occur selectively within a watershed. We investigated the relationship between antecedent precipitation conditions and runoff discharges for some tributary watersheds of the upper Ooi River, Shizuoka prefecture, central Japan, in consideration of their geographical conditions and geological structures. The upper Ooi River, underlain by Late Cretaceous accretionary complex, is a large-scale landslide-prone area. In this study, we especially focused on the hydro-geological structures related to the difference between dip and anti-dip slopes. As the results of in-situ measurement, specific discharge as base flow from the anti-dip slope dominated watersheds trended to be relatively high compared to dip slope dominated watersheds. Additionally, there were higher correlations between specific discharge and long-term antecedent precipitation on the anti-dip slope dominated watersheds rather than on dip slope dominated watersheds. These implied relatively long residence time of rainwater and gradual recession of discharge on the anti-dip slope dominated watersheds.
This work was supported by JSPS KAKENHI Grant Numbers JP19H02989, JP 20H00434.

Keywords: Rainfall-runoff, Accretionary sedimentary rocks, Dip/anti-dip slope, Large-scale landslide

©2021. Japan Geoscience Union. All Right Reserved.

Observation of an effect of interstitial water saturation and water quality on changes in formation resistivity

*Yamato SUZUKI[1], Hiroaki NAKAYA[1], Atsushi FUNAYAMA[2], Toshihiko SAKASHIMA[2], Koushiro TANAKA[2], Akira JOMORI[3], Tetsuya TOYAMA[3]

1. National Institute for Land and Infrastructure Management, 2. Pacific Consultants Co., Ltd., 3. Neo-science Co. Ltd.

In this observational study, effects of interstitial water saturation and water quality of pore water on formation resistivity were investigated, in order to estimate hydraulic geological structure from changes in formation resistivity. First, we compared formation resistivity under different conditions of antecedent precipitation rate. Relationships between the changes and ground permeability by geological reconnaissance were observed. Next, laboratory investigation of formation resistivity was carried out using samples taken at the study site. Effects of interstitial water saturation and water quality were measured for the adjusted test samples. The result showed a clear change in the formation resistivity around the depths with high permeability. After carefully considering possible influences such as measurement errors, the comparison of formation resistivity with different amounts of antecedent precipitation was regarded to show changes in the condition of pore water. Furthermore, another result of laboratory investigation indicated that interstitial water saturation and water quality have non-negligible impact on changes in formation resistivity. In particular, it was duly interpreted that a clear change can appear in response to the effects of precipitation recharge, since there was a large change between water quality of precipitation and mountain runoff water. The obtained relations among factors are useful for better estimation of hydraulic geological structure such as distribution of aquifers based on changes in formation resistivity.

Keywords: formation resistivity, pore water, antecedent precipitation rate, interstitial water saturation rate, water quality

©2021. Japan Geoscience Union. All Right Reserved.

Valley floor environmental changes and disasters associated with glacial collapse of mountain glaciers -A case study of the 2003, 04 and 2021 floods in the Himalayas -

*Jiro Komori[1]

1. Teikyo Heisei University

On the morning of February 7, 2021, the Rishi Ganga River (a tributary of the Burahi Ganga River in the Alaknanda system, which is the northeastern basin of the Ganges River basin) in the Chamoli district of Uttarakhand, India, flooded along Raini village and its downstream. As a result, more than 190 people were killed or missing (as of February 10), and major physical damage was caused to the Rishi Ganga hydroelectric power plant (13.2 MW; elevation of water intake: 2050 m; 12 km from the glacier-collapsed valley floor) and Tapovan Vishnugad hydroelectric power plant (520 MW; elevation of water intake: 1800 m; elevation of the valley floor) were washed away.

This event was initially suggested to be a glacial lake outburst flood, but the cause was attributed to glacier collapse from a 0.2 square kilometer of hanging glacier (Twitter, @Scott Watson https://bit.ly/3rHlPWu) and underlying slope bedrock collapse (Twitter, @Simon Gascoin https://bit.ly/3s4R3qM ; Higaki et al,(2021) Disaster Response Committee Web site, Association of Japanese Geographers https://bit.ly/3av8kTR). At the bottom of the valley (N 30.401, E 79.738. EL. 3800 m) on the slope of collapsed glacier (distribution elevation: about 6000-5500 m), sediments covered with rock debris are distributed in long and thin strips, and the existence of an ice body is expected from the sinking and cracking. It is known that this snowdrift-like ice body existed continuously along the valley floor as late as 2003 and continued to disappear until October 2017, the latest satellite images from Google Earth were available (Komori, (2021) Disaster Response Committee Web site, Association of Japanese Geographers https://bit.ly/3 dmH23Q). In particular, two periods, from 2013 to June 2014 and from May 2015 to October 2017, the distribution is more than 1 km longer than that of the earlier ice bodies. This indicates that there have been repeated collapses from the vicinity of the hanging glacier in the past, although on a smaller scale than the present collapse.

In this presentation, we will show an overview of this disaster and discuss the collapse history of the hanging glacier. In addition, we will compare glacier collapses and floods that occurred in 2003 and 2004 in the southeastern Annapurna massif, Nepal, and how similar glacier collapses (e.g., Kolka Glacier in the northern foothills of the Caucasus Mountains in 2002 and Gayari Glacier in the southern foothills of the Karakoram Range in Pakistan in 2012) have changed the valley floor.

Rescue work is continuing in the area. We sincerely pray for the safety of as many people as possible and the souls of the victims.

Keywords: hanging glacier, snow patch, Turkistan type glaciers, global warming, 2021 Uttarakhand flood, 2003 and 2004 Madi river flood

©2021. Japan Geoscience Union. All Right Reserved.

Characteristics of slope disasters triggered by sudden topographic deformation in the Himalayan region

*Hiroshi YAGI[1], Daisuke Higaki[2], Ching-Ying Tsuo[3], Akihiko Wakai[4], Yusuke Yamamoto[5]

1. Faculty of Art, Science and Education, Yamagata University, 2. Nippon Koei Co.,Ltd., 3. Faculty of Agriculture and Life Science, Hirosaki University, 4. Graduate School of Polytechnics, Gunma University, 5. Geoscience Research Laboratory Co.,Ltd.

Debris flow occurred in Chomoli district, the watershed of Alakananda river. It’ s source area is located on steep rock slope of high relief near Mt. Nanda Ghunti, it’ s altitude is ranging 5200-5600m a.s.l. It initiated as rock slide at first and then turned into rock avalanches and debris flow, considering from distribution of Rock Flour due to fracturing of the rock mass slid on steep slope over 35 degrees. Same phenomenon accompanying Rock Flour due to rock slide occurred in the Seti river watershed in 2012 and Langtang Himal area triggered by Nepal Earthquake 2015. Their source areas are located in high relief and high altitude areas in Nepal Himalayas and their mass-movement type are rock slide. Rock avalanches traveled very long distance over 50km.
There distributed many remnant of landslides and landslide dams in Manag area behind Annapurna Himal, Nepal, the upper reach of Marsyandhi river. And very thick debris deposit over 100m are distributed along the middle course of Marsyandhi river in the southern mount foot area of Annapurna Himal, forming higher terraces of the last glacial age. That implies debris flow deposits which were turned from rock slide and rock avalanches reached to the the Midland area traveled long distance across the Himalayan range in the last glacial age.

Keywords: Rock slide, rock avalanches, rock flour, debris flow

©2021. Japan Geoscience Union. All Right Reserved.

[J] Oral | H (Human Geosciences) | H-DS Disaster geosciences

[H-DS10] Geohazards in humid, tectonically active countries and their precursors

convener:Satoru Kojima(Department of Civil Engineering, Gifu University), Taro Uchida(University of Tsukuba), Yoshihiko Kariya(Department of Environmental Geography, Senshu University), Chairperson:Taro Uchida(University of Tsukuba), Satoru Kojima(Department of Civil Engineering, Gifu University)

Sat. Jun 5, 2021 3:30 PM - 5:00 PM Ch.16 (Zoom Room 16)

This session covers mass movements of landslide, slope failure, debris flow, and gravitational slope deformation in tectonically active, humid countries, and aims to discuss on their mechanisms, characteristics of occurrence sites, the significance in geological time scale, and the methodology to mitigate their affects by researchers with various related research fields.

4:50 PM - 5:00 PM

[HDS10-12]Discussion

©Japan Geoscience Union

[J] Poster | H (Human Geosciences)：H-DS Disaster geosciences

Sat. Jun 5, 2021 5:15 PM - 6:30 PM JST | Sat. Jun 5, 2021 8:15 AM - 9:30 AM UTC | Ch.10_3

[H-DS10] Geohazards in humid, tectonically active countries and their precursors

convener:Satoru Kojima(Department of Civil Engineering, Gifu University), Taro Uchida(University of Tsukuba), Yoshihiko Kariya(Department of Environmental Geography, Senshu University)

This session covers mass movements of landslide, slope failure, debris flow, and gravitational slope deformation in tectonically active, humid countries, and aims to discuss on their mechanisms, characteristics of occurrence sites, the significance in geological time scale, and the methodology to mitigate their affects by researchers with various related research fields.

[HDS10-P01] Large-scale collapse of permafrost waste dump at Kumtor gold mine in Kyrgyz republic

*Ayano Aoki[1], Chiyuki Narama[1], Tsutomu Yamanokuchi[2], Murataly Duishonakunov[3] (1.Niigata university, 2.Remote Sensing Technology Center of Japan, 3.Kyrgyz National University)

[HDS10-P02] Relationship between landslide distribution and topographic feature and subsurface structure for the case of the 2018 Hokkaido Eastern Iburi Earthquake

*Junichiro Furuyama[1], Issei Doi[1], Toshitaka Kamai[1], Yuki Matsushi[1] (1.Kyoto University)

[HDS10-P03] Sediment movement on landslide slopes and river channel after the 2018 Hokkaido Eastern Iburi Earthquake

*Takashi Koi[1], Yasutaka Tanaka[1], Shin'ya Katsura[2], Norifumi Hotta[3] (1.Center for Natural Hazards Research, Hokkaido University, 2.Research Faculty of Agriculture, Hokkaido University, 3.Graduate School of Agricultural and Life Sciences, The University of Tokyo)

[HDS10-P04] Surface changes of Ganpei landslide in Joetsu region

*Yutaka Inoue[1], Chiyuki Narama[2], Chunxiang WANG[3], Eiji Takita[3] (1.Graduate Student,Niigata University, 2.Niigata University, 3.KITAK Corporation)

[HDS10-P05] Surface changes of rock slopes in the Hakuba-Daisekkei Valley, northern Japanese Alps

*Hirotaka Sugiyama[1], Chiyuki Narama[1], Hiroshi Inoue[2] (1.Niigata University, 2.NIED)

[HDS10-P06] Revisiting stratigraphy and age of so-called Otsukigawa debris avalanche deposits in the upper Otsukigawa and Yukawa Rivers on the eastern side of Yatsugatake Volcano in central Japan

*Takahiro Kurimoto[1], Yoshihiko Kariya[2] (1.Graduate School of Humanities, Senshu Univ., 2.Senshu Univ.)

[HDS10-P07] Relationship between a natural dam at the Yomogisawa River in the headwater area of the Abe River and the Oya-Kuzure rockslide with reference to new chronological information

*Keiju Kimura[1], Yoshihiko Kariya[2] (1.Graduate, Senshu Univ., 2.Senshu Univ.)

[HDS10-P08] Activities of landslides and their precursors: Case studies in Okutabora, Gujo, Gifu Prefecture and in Kuchisakamoto, Shizuoka Prefecture, central Japan

*Satoru Kojima[1], Kazuhide Sawada[1], Mizuki Tatekawa[1] (1.Department of Civil Engineering, Gifu University)

Large-scale collapse of permafrost waste dump at Kumtor gold mine in Kyrgyz republic

*Ayano Aoki[1], Chiyuki Narama[1], Tsutomu Yamanokuchi[2], Murataly Duishonakunov[3]

1. Niigata university, 2. Remote Sensing Technology Center of Japan, 3. Kyrgyz National University

Large-scale collapse of mine waste dump occurred at the Kumtor gold mine in Kyrgyz Republic on 1 December 2019 and killed two mine workers. The Kumtor gold mine (4000m) is located in Ak-Shiyrak massif of inner Tien Shan. This area is permafrost and active glacier zone. In the Kumtor gold mine, mine dumps are composed of permafrost and glacier ice. The mine dumps are made on permafrost slope, moraine-complex including permafrost and glacier ice, and glacier. Before this collapse, unstable flows are reported in the terminus of the dump in 2013 (Jamieson et al.,2015). In this study, we investigated the collapse of the mine dump at the Kumtor gold mine using satellite image analysis. Furthermore, we compared three dumps in the Kumtor gold mine to consider the factor of the collapse.

Keywords: collapse, permafrost, satellite image

©2021. Japan Geoscience Union. All Right Reserved.

Relationship between landslide distribution and topographic feature and subsurface structure for the case of the 2018 Hokkaido Eastern Iburi Earthquake

*Junichiro Furuyama[1], Issei Doi[1], Toshitaka Kamai[1], Yuki Matsushi[1]

1. Kyoto University

The 2018 Hokkaido Eastern Iburi Earthquake caused numerous (> 6000) shallow tephra landslides with the regional differences in the number and density of their occurrences (Ito et al., 2020). Wang et al. (2019) suggested that the heterogeneous patterns of landslide distribution are attributed to base geology, while Tajika et al. (2020) pointed out that low landslide density is observed along anticline axes.
We estimated the ridge intervals and slope degree by topographic analysis based on Parron et al. (2008) as well as the S-wave velocity structure by microtremor array survey for the partitioned areas according to the base geology and/or the density of landslide distribution.
The ridge intervals were found to be different according to the landslide distribution and base geology. It was suggested that the topography was affected by base geology and also affected landslide generation. We also obtained S-wave velocity structure to the depths of 300 m. We will further estimate the S-wave velocity data in a wider area and discuss them in connection with the topographic feature as well as landslide distribution.

Acknowledgement: We used DEM data provided by Geospatial Information Authority of Japan.

Keywords: 2018 Hokkaido Eastern Iburi Earthquake, Coseismic landslide

©2021. Japan Geoscience Union. All Right Reserved.

Sediment movement on landslide slopes and river channel after the 2018 Hokkaido Eastern Iburi Earthquake

*Takashi Koi[1], Yasutaka Tanaka[1], Shin'ya Katsura[2], Norifumi Hotta[3]

1. Center for Natural Hazards Research, Hokkaido University, 2. Research Faculty of Agriculture, Hokkaido University, 3. Graduate School of Agricultural and Life Sciences, The University of Tokyo

The Hokkaido Eastern Iburi Earthquake that occurred before dawn on September 6, 2018 caused shallow landslides in more than 6,000 locations, mainly in Atsuma Town and Abira Town, Hokkaido, Japan. Most of the sediment and driftwood produced from the collapsed area remain in the basin, and it is thought that sediment movement occurs at the time of flooding, but the magnitude, frequency and spatial distribution of the movement is not clear. The surface soil in areas where many shallow landslides occur is mainly covered with volcanic ejecta, and the constituent materials of the produced sediment are relatively fine grains. Therefore, if the landslide sediment flows out to the downstream area, it may affect the turbidity of running water and changes in water quality. In this study, we focused on the surface erosion of the landslide slope and the landslides deposited on the river channel in the Habiu River catchment (0.38 km^2) of the Atsuma River system where shallow landslides occurred frequently due to the Hokkaido Eastern Iburi earthquake, and clarified the sediment movement for two years after the earthquake. The sediment movement of the catchment was grasped from the field survey and topographical analysis. Using the laser profiler data taken immediately after the earthquake (2018) and the elevation data acquired using the UAV in 2020, the amount of change in elevation values on the slope and in the river channel was calculated from the difference analysis between the two periods. From the field survey, it was confirmed that a large amount of landslide sediment and driftwood produced during the earthquake were deposited in the river channel. In addition, from the differential analysis of the elevation data of the two periods, the landslide slope was eroded as a whole, while the eroded area and the deposited area were mixed in the river channel within a range of several tens of centimeters. Even after the earthquake, the newly produced sediment from the landslide slope was supplied to the river channel, and it was considered that sediment movement occurred in the river channel at the time of flooding. On the other hand, as for the landslide slope, the south-facing slope was more eroded than the north-facing slope, and the gully was also well developed. The progress of such gully erosion could be confirmed from the field survey. The predominant erosion on the south-facing slopes may be due to the effects of freezing, thawing and snowmelt in winter season due to differences in the amount of solar radiation.

Keywords: the 2018 Hokkaido Eastern Iburi Earthquake, shallow landslide, sediment movement, slope-channel coupling, volcanic area

©2021. Japan Geoscience Union. All Right Reserved.

Surface changes of Ganpei landslide in Joetsu region

*Yutaka Inoue[1], Chiyuki Narama[2], Chunxiang WANG[3], Eiji Takita[3]

1. Graduate Student,Niigata University, 2. Niigata University, 3. KITAK Corporation

Unique topography and vegetation can be observed around the landslide. The surface changes reflect the internal structure and sliding morphology of landslides. However, there are few cases which the surface changes of landslides are observed spatially and many times.
In this study, we repeatedly conducted field surveys including UAV aerial photography and GNSS survey in the Ganpei area in the eastern part of the Takada Plain, Joetsu City, Niigata. We discussed the relationship between the surface change and motion of landslide based on our results.

Keywords: Landslide, GNSS, Surface change

©2021. Japan Geoscience Union. All Right Reserved.

Surface changes of rock slopes in the Hakuba-Daisekkei Valley, northern Japanese Alps

*Hirotaka Sugiyama[1], Chiyuki Narama[1], Hiroshi Inoue[2]

1. Niigata University, 2. NIED

Introduction

In the northern Japanese Alps, rock slope failure has caused mountaineering accidents frequently. In Hakuba-Daisekkei Valley, rock slope failure with victims occurred in 2005 (Kariya, 2006). However, the process and geomorphological characteristics of rock slope failure are unclear. As a reason, it is difficult to investigate the steep rock slope directly. The purpose of this study is to clarify the process of rock slope failure on different rock types in Hakuba-Daisekkei Valley using UAV and SfM methods.

Study area

Hakuba-Daisekkei is a perennial snow patch located at the bottom of the Hakuba-Daisekkei Valley. The valley is a popular mountaineering route to Mt. Hakuba-dake (2932 m asl). More than 10,000 people pass the route every year. Hakuba-Daisekkei Valley is surrounded by Mts. Shakushi-dake and Hakuba-dake. Mt. Hakuba consisted of felsic tuff and tuff breccia. Mt. Shakushi consisted of Felsite. Hakuba-Daisekkei Valley is high annual precipitation through summer and heavy snow climate in Japan.

Methods

We observed the retreat process of rock slopes using images of UAV, Cessna and aerial photography with SfM (Structure from Motion) technology.

Results

We confirmed the difference in the retreat process between Mt. Shakushi-dake and Mt. Hakuba-dake. On the rock slope of Mt. Shakushi-dake, we observed the discriminatory retreat that depended on rock joint density. On the other side, we observed the sudden retreat process with a tension crack opening on the rock slope of Mt. Hakuba-dake.

Keywords: rockfall, rock slope failure, SfM, UAV, freezing and thawing, ICP

©2021. Japan Geoscience Union. All Right Reserved.

Revisiting stratigraphy and age of so-called Otsukigawa debris avalanche deposits in the upper Otsukigawa and Yukawa Rivers on the eastern side of Yatsugatake Volcano in central Japan

*Takahiro Kurimoto[1], Yoshihiko Kariya[2]

1. Graduate School of Humanities, Senshu Univ., 2. Senshu Univ.

On the east side of Yatsugatake Volcano, large-scale landslide features with a long and clear head scarp and undulated emplacement bodies with hummocks exists. This spectacle landforms and their forming materials have been called "Otsukigawa debris avalanche (ODA)" and "Otsukigawa debris avalanche deposit (ODAD)", respectively (Kawachi 1983). The cause of ODA has been attributed to the AD887 Ninna mega-earthquake generated from the Suruga-Nankai submarine troughs based on conventional ^{14}C dates and interpretation of historical documents. However, the recent novel study by Yamada et al. (2021) using oxygen isotope dendrochronology of ODAD suggests that there is doubt about the age of ODA. Therefore, based on field investigations, we reexamined ODA and ODAD in the upper reaches of Otsukigawa and Yukawa Rivers on the east side of the volcano. We reconfirmed a previous study by Machida and Tamura (2010) that ODAD is distributed along the Otsukigawa River and its tributaries, from Midori-ike Pond immediately below the head scarp to the confluence point between Otsukigawa and Chikuma Rivers. ODAD consists of non-sorted breccias, dominantly bearing hornblende andesite, and yellowish white to dark brown fine-grained matrix with a hydrogen sulfide odor. We carried out new age determination of the upper part of ODA by ^{14}C, all wood samples gave the range from AD772 to 976. Additionally, an unreported mudflow deposit was newly found in the east of Inagoyu Spa, showing 42 to 48 ^{14}C ka. We name this "Inagoyu mudflow deposit (IMD)". The age of IMD coincides with the Last Glacial period around MIS4 and one of activated periods of Yatsugatake Volcano, suggesting that IMD would be derived from snowmelt or icemelt lahar. We also found another landslide deposit different from ODAD and IMD on the banks of Yukawa River near Honzawa Spa. We call this "Honzawa debris avalanche deposit (HDAD)". The fossil wood collected from HDAD shows 3.6 to 2.8 cal ka. From these results, it is considered that large to middle scale landslide phenomena have occurred repeatedly in the period from 48 ka to 1 ka on the eastern side of Yatsugatake Volcano. Our data suggest that the thick debris, which was conventionally called as ODAD, was not produced by single large-scale landslide event, and the ages of ODAD span widely from the late Pleistocene to the recent millennia. However, it should be emphasized that debris avalanche occurred in the period from AD772 to 976 in the upper Otsukigawa River. The latest event in AD772 to 976 may be caused by AD887 Ninna earthquake or AD762 Mino/Hida/Shinano earthquake, as well as AD841 Shinano earthquake. Aftershocks by these earthquakes were also possible triggers. More information on the stratigraphy and ages of "so-called" ODAD is required.

Keywords: Yatsugatake Volcano, Otsukigawa debris avalanche, AD887 Ninna earthquake, Paleoearthquake

©2021. Japan Geoscience Union. All Right Reserved.

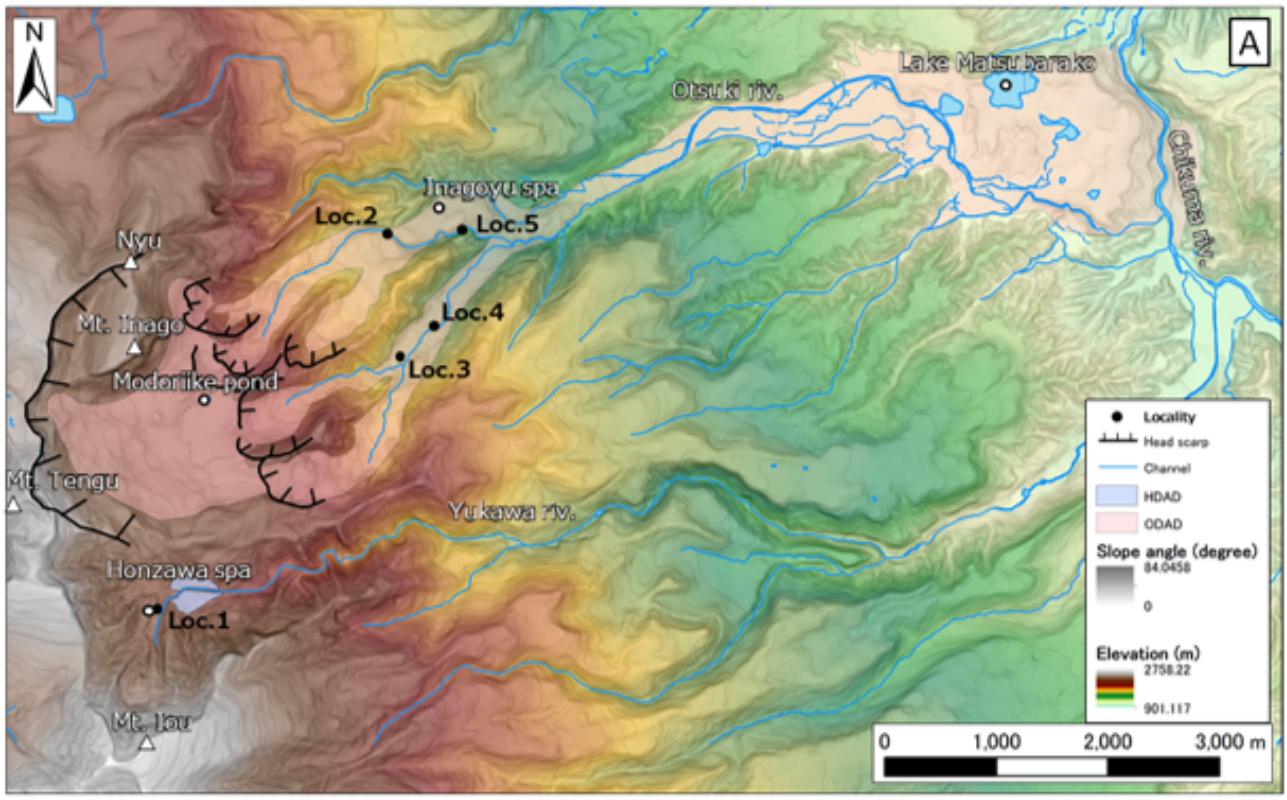






Figure and picture A to C ; A)Topography of the study area. Contour interval is 20 m. B)Picture of Outcrop(HDAD). C)Picture of Outcrop(ODAD).

©2021. Japan Geoscience Union. All Right Reserved.

Relationship between a natural dam at the Yomogisawa River in the headwater area of the Abe River and the Oya-Kuzure rockslide with reference to new chronological information

*Keiju Kimura[1], Yoshihiko Kariya[2]

1. Graduate, Senshu Univ., 2. Senshu Univ.

1. Introduction

The Oya-Kuzure is a huge landslide site located at the headwaters of the Abe River in Shizuoka Prefecture. This landslide is believed to be triggered by the CE1707 Hoei earthquake (est. M 8.6) (Shizuoka River Office, Ministry of Construction, 1988). There are, however, other arguments about the age of Oya-Kuzure, and all of them are based solely on historical documents without geological and chronological data. Machida (1959; Geogr. Rev. Jpn.) pointed out that lacustrine sediments are buried under the present riverbed near the confluence of the Oya and Mikochi Rivers upstream of the Abe River. He also showed that other lacustrine sediments are distributed along a few tributaries, whereas details were unknown.

In this presentation, we report landslide sediments originating from Oya-Kuzure and a resultant, natural dams, as well as the dammed lacustrine sediments found in Yomogisawa River, one of small tributaries of the Oya River, and show radiocarbon ages of those sediments. Then we will discuss the age of the Oya-Kuzure.

2. Landforms and geology

Oya-Kuzure has a following an area of 1.8 km^2, a headscarp width of 1.8 km, and a vertical difference of 800 m. The Oya River originates from the Oya-Kuzure, and the Mikochi River is combined to form the Abe River. As Oya-Kuzure has supplied a large number of debris, fill terrace is developed in this area.

The geology is mainly composed of alternating beds of sandstone and shale, but igneous rocks and serpentinite are limitedly distributed in the upper reaches of Yomogisawa River (Sugiyama and Matsuda, 2014).

3. Description of landslide and lacustrine sediments

An outcrop locality consisting of gravel layers and sandy silt layers is present on the left bank of Yomogisawa River, at which 1.1 km upstream from the confluence of Yomogisawa and Oya Rivers. The top surface (ground surface) of this outcrop corresponds to the terrace surface about 4 m high from the present riverbed of Yomogisawa River.

A paleosol layer S with a large amount of deformed wood fragments is confirmed at the bottom of outcrop. The paleosol S continues subsurface of outcrop and its thickness is estimated to 0.3 m or more. Above the paleosol S, an angular gravel layer A (max. thickness ca. 3 m) consisting of granule to boulder clast is observed. The gravel layer A becomes thinner in the upstream side. A sandy silt layer X (max. th. 0.6 m) and a sand layer Y (max. th. 0.5 m) are laid on the gravel layer A in this order, and both layers X and Y gradually become thinner in the downstream side contrary to the layer A. Layers X and Y abut on layer A and are finally disappear. Layers X and Y are covered by a gravel layer B (max. th. 1.5 m) with granule to boulder of debris flow origin.

Layers A and B can be distinguished by roundness and lithology of clastic materials. Layer A shows a lower degree of roundness than that of layer B, suggesting that layer A was caused by and moved by rock avalanche behavior. Layer B contains serpentinite and igneous rocks derived from the upper part of

©2021. Japan Geoscience Union. All Right Reserved.

Yomogisawa River, suggesting its source is restricted to the Yomogisawa River watershed.
Layer A is thought to be rock avalanche sediments supplied from the Oya-Kuzure and formed a natural dam obstructing the stream of Yomogisawa River. Layers X and Y are considered to be dammed lacustrine sediments by this natural dam. In addition, it is considered that the paleosol S is derived from disturbed soil at which layer A moved down and flowed into Yomogisawa River, or from a small-scale landslide occurred nearby the outcrop before formation of the natural dam.
Paleosol S, and layers A and X contain fossil wood fragments. We consequently measured ^{14}C age of those samples.

4. ^{14}C age

The wood samples showed the following ages. The calendar year was calculated by OxCal and INTCAL20 and shows a 2 σ error interval (1 σ for ^{14}C year). Paleosol layer S= cal CE1396-1441 (521±23 ^{14}C) BP, gravel layer A = cal CE1506-1596/1616-1655 (297±23 ^{14}C) BP, sandy silt layer X = cal CE1644-1680/1740-1753/1762-1800 (220±20 ^{14}C) BP.

5. Discussion

No stratigraphic reversal of ^{14}C ages are confirmed. Our age data can be considered as appropriate. Layer A may be up to 200 years older from CE1707, and it is probable that a landslide activity of Oya-Kuzure had preceded several hundred years before CE1707. On the other hand, the age of layer X includes CE1707, but it has a wide range and may have been deposited from the middle of CE1600’s to around CE1800. Therefore, in addition to 1707 Hoei earthquake, CE1498 Meio Tokai (est. M8.2-8.4), CE1605 Keicho Tokai (est. M7.9), and CE1703 Genroku (M7.9-8.2) earthquakes are candidate triggers of rock avalanche from the Oya-Kuzure site.

Keywords: Oya-Kuzure, lacustrine sediment, 14C age

©2021. Japan Geoscience Union. All Right Reserved.

Activities of landslides and their precursors: Case studies in Okutabora, Gujo, Gifu Prefecture and in Kuchisakamoto, Shizuoka Prefecture, central Japan

*Satoru Kojima[1], Kazuhide Sawada[1], Mizuki Tatekawa[1]

1. Department of Civil Engineering, Gifu University

Forecasting the slope movement is important for the mitigation of landslide disasters. After the landslide disaster in 2011 by the Typhoo Talas in Kii Peninsula, central Japan, the landforms formed by the process of deep-seated gravitational slope deformation (DSGSD) have been expected to be useful for the prediction of deep-seated landslides. We conducted researches on DSGSD in several regions of Japan, and in this session presented the results of two case studies analyzing the relationship between the DSGSD development and landslide activity. One of them is the landslide in the Okutabora Valley, Gifu Prefecture. About 20,000 m^3 debris slipped down along the valley in July 2018 by a rainstorm. In June 2020 a fissure, a type of DSGSD, was found above the main scarp of the landslide by the field survey after a strong rainstorm, and after that the LiDAR measurement was performed in order to grasp the total feature of the DSGSD. Another landslide occurred along the fissure in July 2020. Another case study examined three landslides named A-, B-, and No.2-landslides in the Kuchisakamoto area, Shizuoka Prefecture. Countermeasures against the A-landslide started in 1960, and the activity has calmed down recently. The B-landslide started the active in 1988, and has been active until now in spite of the extensive countermeasures for more than 30 years. The No.2-landslide started the activity in 2013. Double ridges, one of the typical DSGSD landforms, occur on the crests or slopes above the three landslides. Although the development histories of these DSGSD features are unknown, we estimate that they formed several thousand years ago on the basis of our research results on the similar double ridges located about 10 km north of this area. The double ridges above the A- and B-landslides have no signs of deformations, though the landslide scarps have reached just below the ridges. The ground extensometer installed on the uphill-facing scarplet, also one of the typical DSGSD landforms, of the No.2-landslide have recorded no movements during the last six years. These lines of evidence indicate that the DSGSD topographies stable for many years have not affected by the landslide activities below them. We need standardization of this model by more case studies. The data used in this study were provided by Gifu and Shizuoka Prefecture offices.

Keywords: landslide, deep-seated gravitational slope deformation (DSGSD)

©2021. Japan Geoscience Union. All Right Reserved.

[E] Poster | H (Human Geosciences)：H-TT Technology & Techniques

Sat. Jun 5, 2021 5:15 PM - 6:30 PM JST | Sat. Jun 5, 2021 8:15 AM - 9:30 AM UTC | Ch.11_1

[H-TT13] Environmental Remote Sensing

convener:Wei Yang(Chiba University), Akihiko Kondoh(Center for Environmental Remote Sensing, Chiba University)

Our planet Earth is encountering extensive environmental issues caused either by climate change or human activities. It is our urgent task to find out solutions for these issues based on all kinds of techniques, sciences, as well as transdisciplinary cooperation. Remote sensing is currently the only feasible technique to observe the Earth environment at regional/continental /global scales over long periods, and consequently detects the environmental changes occurred all over the world. Although remote sensing has been extensively applied to a number of environmental studies, there are still many challenges for data analysis and applications. Consequently, this session provides a communication platform on theory, science, technology, and applications of remote sensing to study the Earth environment from local, regional to global scales. Both oral and poster presentations are sincerely welcome.

[HTT13-P01] A study on the long-term dynamics and phenology of mangrove forests based on the narratives of inhabitants in western India using Landsat

*Kai Yamamoto[1], Nobuhito Ohte[1], Ranit Chatterjee[1], Kenlo Nasahara[2], Pankaj Joshi Sahjeevan[4], Lyla Mehta[3] (1.Graduate School of Informatics Kyoto University, 2.Faculty of Life and Environmental Sciences University of Tsukuba, 3. Institute of Development Studies, Brighton, United Kingdom, 4.Sahjeevan(NGO))

[HTT13-P02] **Mapping Paddy Rice Planting Areas on the Cloud: Is Spatio-Temporal Fusion Helpful or Not**

*Ziping Yang[1], Wei Yang[2], Akihiko Kondoh[2] (1.Graduate School of Science and Engineering, Chiba University, 2.Center of Environmental Remote Sensing, Chiba University)

[HTT13-P03] Removal of residual reflected skylight for accurate measurement of water-leaving reflectance

*Wei Yang[1], Bunkei Matsushita[2], Dalin Jiang[2] (1.Chiba University, 2.University of Tsukuba)

[HTT13-P04] Yield Estimation of Paddy Rice using High Spatial and Temporal Satellite Data in Indonesia

*Yuki Sofue[1], Chiharu Hongo[1], Naohiro Manago[1], Koki Homma[2], Gunardi Sigit[3], Budi Utoyo[4] (1.Chiba University, 2.Tohoku University, 3.West Java Food Crops and Horticultural Agency, 4.Bogor Agricultural University)

[HTT13-P05] **Random Forest for Estimating Soil Moisture Based on Remote Sensing Test**

*Jyun-Lin Chen[1], Hong-Ru Lin[1], Jet-Chau Wen[1] (1.National Yunlin University of Science and Technology)

A study on the long-term dynamics and phenology of mangrove forests based on the narratives of inhabitants in western India using Landsat

*Kai Yamamoto[1], Nobuhito Ohte[1], Ranit Chatterjee[1], Kenlo Nasahara[2], Pankaj Joshi Sahjeevan[4], Lyla Mehta[3]

1. Graduate School of Informatics Kyoto University, 2. Faculty of Life and Environmental Sciences University of Tsukuba, 3. Institute of Development Studies, Brighton, United Kingdom, 4. Sahjeevan(NGO)

Kutch, Gujarat, Western India (Kutch), is under an arid and semi-arid environment, and the terrestrial ecosystem is dominated by drought and salinity tolerant plants. Mangroves grow in the coastal areas of Kutch and have been continuously used by the local communities for timber, livestock feed, and as fishery resources. However, the ecosystem services of these mangrove forests have partly been lost due to the development of salt pans in coastal areas and disturbed by natural disasters such as cyclones and earthquakes. In order to use mangrove forests with maintaining the sustainability of ecosystem services, it is necessary to accumulate knowledge on the dynamics of these mangrove forests and their response to environmental changes.

In this study, the following three aspects were analyzed by using satellite images in order to understand the long-term and the phenology over the past 30 years. 1) The long-term changes in biomass of mangrove forests in the area. 2) How arid environment or droughts affects the biomass. 3) In the meantime, where have the mangrove forests expanded or shrunk due to development and other environmental alteration?

For 1), we used Landsat-5, 7&8 images, medium spatial resolution data, to investigate the long-term dynamics of mangrove forests by calculating NDVI, one of the vegetation indices that is considered to indicate the plant activity or biomass. For 2), the Standardized Precipitation Index (SPI), which is an index of the drought and dryness, was calculated from the precipitation data in the study area. For 3), the changes in mangrove coverage in the area were evaluated by pixel-based landcover maps for two years, 1988 and 2019.

The NDVI of mangrove forests in the area has basically increased from 1988 to the present, suggesting an increase in biomass. However, it decreased from the late 1990s to the early 2000s. The most possible reason was the increase in water stress due to the continuous occurrence of low precipitation period from the late 1990s to the early 2000s. The lack of significant changes in NDVI by single-year drought suggests that mangrove forests had the resilience against dryness and/or drought, and that continuous dryness affected mangrove vegetation. Several factors, such as relatively high precipitation from 2003, were considered to be responsible for the long-term increase in NDVI in mangrove forests over a 30-year period.

NDVI of mangrove forests in the area was found to be monotonically decreasing since the middle of the dry season (January) and started increasing with the onset of the rainy season. This was due to the leaf growth of mangroves was enhanced by the relief of water stress-related to salinity due to precipitation during the rainy season. On the other hand, during the dry season, the leaf area decreased by the leaf longevity and photosynthesis suppression caused by the increase in water stress.

The relief of water conditions for mangroves was due to the direct supply of freshwater to the soil by

©2021. Japan Geoscience Union. All Right Reserved.

rainfall and groundwater from inland. Considering the long-term relationship between NDVI changes, mangrove seasonality, and precipitation, it was possible that the amount of available water resources significantly affects mangrove leaf growth in these arid and semi-arid regions. It is important to evaluate the availability of water resources accurately in the future.

The comparison of the landcover maps of 1988 and 2019 showed that the main reasons for the decrease of mangrove forests were the erosion of sandy soil by tides and land-use conversion associated with the development of coastal areas. On the other hand, some mangrove forests expanded their area in areas that were not significantly affected by tides.

The information from this study will be provided to local communities, the government, and NGOs for use in formulating policies for the continuous usage of mangrove forests toward the future.

Keywords: remote sensing, NDVI, mangrove, phenology, landcover

©2021. Japan Geoscience Union. All Right Reserved.

Mapping Paddy Rice Planting Areas on the Cloud: Is Spatio-Temporal Fusion Helpful or Not

*Ziping Yang[1], Wei Yang[2], Akihiko Kondoh[2]

1. Graduate School of Science and Engineering, Chiba University, 2. Center of Environmental Remote Sensing, Chiba University

Mapping paddy rice planting area has great significance for calculating the paddy rice planting area, monitoring rice yield, monitoring global freshwater usage and monitoring methane emissions. If remote sensing satellite images can be used instead of manual visits to map paddy rice planting areas, it will greatly reduce the money and time. The basic principle of using remote sensing images to map paddy rice is to capture the characteristics of rice, that is, they are all transplanted in water. Different vegetation indices calculated from remote sensing images respond differently to water, so this characteristic of paddy rice can be used to distinguish it from other surface types. However, because Japan’ s farming modes mostly are family farming, the area of a single paddy field is small, and due to the existence of fallow or crop rotation, there are often multiple uses of land in a piece of farmland. Coarse spatial resolution remote sensing satellite images will not achieve good results. At the same time, due to the influence of climate and other factors, the transplantation period of rice generally occurs in the rainy season in Japan. Images with low temporal resolution will be affected by clouds and rain, and it is difficult for them to provide effective data. Unfortunately, due to technical limitations, no sensor can obtain images with high temporal resolution and high spatial resolution at the same time. One processing method is to use a fusion algorithm to fuse images with high temporal resolution and low spatial resolution (e.g. MODIS, MERIS) and images with high spatial resolution and low temporal resolution (e.g. Sentinel, Landsat) to obtain images have both high temporal resolution and high spatial resolution. However, the existing Spatio-temporal fusion algorithm does not have high accuracy for heterogeneous areas or areas where the type of landcover will change in one year (e.g. agricultural land). Therefore, this study will use Spatio-temporal fusion algorithm based on similar pixels (e.g. ESTARFM) and filtering based fusion algorithm (e.g. GF-SG) to fuse MODIS, Landsat and Sentinel images in different latitudes and regions. The vegetation index time series obtained after the fusion is used for searching for the flooding signal that can represent the rice transplantation period (that is, the time when the vegetation index LSWI is less than the NDVI before the start of the green up stage of paddy rice), and compare it with the real data published by the Ministry of Agriculture, Forestry and Fisheries. It is found that the fusion algorithm based on similar pixels retains the details of the time series better than the filtering-based fusion algorithm, and the time series fused by the filtering-based algorithm cannot reflect the mutation of LSWI or NDVI. But fusion algorithms based on similar pixels are more susceptible to cloud influence.

Keywords: mapping paddy rice, family farming, flooding signal, Spatio-temporal fusion

©2021. Japan Geoscience Union. All Right Reserved.



©2021. Japan Geoscience Union. All Right Reserved.

Removal of residual reflected skylight for accurate measurement of water-leaving reflectance

*Wei Yang[1], Bunkei Matsushita[2], Dalin Jiang[2]

1. Chiba University, 2. University of Tsukuba

Water-leaving reflectance (Rrs) is crucial for remote estimation of water quality parameters. However, Rrs measured using the above-water approach usually suffers from residual reflected skylight, and thus its applicability is limited. In this study, we proposed a simple method, which only required the in situ Rrs spectrum itself as input, to further remove this effect in the in situ Rrs spectrum. The performance of the proposed method was evaluated using both simulation data and in situ Rrs spectra measured using a radiance sensor with a black tube. The results showed that the proposed method outperformed other existing methods and can be applied to various types of waters. From a comparison analysis using skylight-free in situ Rrs data, the proposed method showed the best performance with the smallest MAPE of 45% (MAPE ranged from 52% to 260% for other existing methods). In addition, the proposed method can improve the quality of Rrs spectra collected under various sky conditions (clear, scattered clouds and overcast), with an increased proportion of higher quality assurance scores. Two showcases indicate that the skylight corrections should be carried out for all above water approach-measured Rrs spectra before they are applied to develop water quality estimation algorithms or to evaluate the performances of atmospheric correction algorithms.

Keywords: remote sensing, inland lakes, above-water method, water-leaving reflectance

©2021. Japan Geoscience Union. All Right Reserved.

Yield Estimation of Paddy Rice using High Spatial and Temporal Satellite Data in Indonesia

*Yuki Sofue[1], Chiharu Hongo[1], Naohiro Manago[1], Koki Homma[2], Gunardi Sigit[3], Budi Utoyo[4]

1. Chiba University, 2. Tohoku University, 3. West Java Food Crops and Horticultural Agency, 4. Bogor Agricultural University

Although Indonesia is one of the world's leading rice producers, it suffers from weather conditions such as precipitation, pest and disease. Therefore, it is important to conduct a quantitative damage assessment and utilize the agricultural insurance system. In quantitative damage assessment, it is essential to understand rice yield per field, however, the work to take yield data per field consume time and intensive labor. To solve this problem, we aim to reduce the time, labor, and cost in the field by estimating rice yield using remote sensing data.
In West Java, Indonesia, scale of paddy fields is small and paddy rice per field with different growth stages are mixed because transplanting date varies from field to field. Therefore, to better understand and estimate yield per field, time series data with high spatial and temporal resolution is required. In this study, an enhanced spatial and temporal adaptive reflectance fusion model (ESTARFM) was employed to combine 250-m Moderate Resolution Imaging Spectroradiometer (MODIS) and Sentinetl-2 data to generate a synthetic Sentinel-2 time series data for estimation of rice yield. The blue, green, red, near infrared and short wave infrared were chosen for this processing.
Normalized Different Vegetation Index (NDVI) was calculated, and defined heading stage at maximum NDVI of NDVI curve. It is clarified that the rice yield has a high relationship with some vegetation indices and reflectance at heading stage and after the stage in previous studies. These differences are considered to be due to environmental factors in the study area and differences in rice varieties. Based on these conclusions of previous studies, this analysis included the period from the heading period estimated by time-series NDVI to 40 days. For this period, synthetic Sentinel-2 time series data was used with original Sentinel-2 data to create time-series data of reflectance, NDVI, Green Normalized Difference Vegetation Index (GNDVI) and Normalized Different Water Index (NDWI). Then, yield estimation model was created based on these data every 5 days. Finally, the model which has GNDVI and NDWI as parameters was chosen based on AIC and RMSE.
The results showed that ESTARFM could be used to combine time series MODIS and Sentinel-2 data with a correlation coefficient from 0.77 to 0.92. The model could estimate yield per field with correlation coefficient of 0.6 and RMSE was about 1.30 t/ha. Therefore, it is considered that this methodology can be used for this study area to estimate rice yield.

Keywords: Data fusion, Sentinel-2, MODIS, Time-series

©2021. Japan Geoscience Union. All Right Reserved.

Random Forest for Estimating Soil Moisture Based on Remote Sensing Test

*Jyun-Lin Chen[1], Hong-Ru Lin[1], Jet-Chau Wen[1]

1. National Yunlin University of Science and Technology

This study used a remote sensing method to estimate surface soil moisture (SM) using images from the visible spectrum in the laboratory darkroom. The uniformity was analyzed in the ring light source from a hemispherical darkroom with a ring light source. The soil sample images were then taken and recorded with weight in a laboratory darkroom using a remote sensing test (RST) for five narrow-range soil particle sizes. Next, a comparison of the validation results for the five different narrow-range soil particle sizes using a Random Forest (RF) regression.

Results showed a uniformity test using the ring source set in the darkroom, and results have illumination uniformity without a hot spot existing. The best parameters for film speed, aperture, and shutter use Color Calibration Matrix (CCM) to reduce error for the digital image. SM analysis results showed that the mean value (red line) of SM versus time for five different narrow-range soil particle sizes is reproducible. Fine sand (0.149–0.250 mm) has the best regression and validation results, proving the feasibility and reference value of the previous regression models. The results of this research prove the feasibility of using the RF model for narrow-range soil particle size.

Keywords: Remote sensing, Soil moisture, Random Forest, Visible spectrum

©2021. Japan Geoscience Union. All Right Reserved.

[E] Oral | H (Human Geosciences)：H-TT Technology & Techniques

Sat. Jun 5, 2021 3:30 PM - 5:00 PM JST | Sat. Jun 5, 2021 6:30 AM - 8:00 AM UTC | Ch.15 Zoom Room 15

[H-TT15] Non-destructive techniques applied to stone cultural heritage

convener:Celine Thomachot-Schneider(University of Reims-Champagne-Ardenne), Chiaki T. Oguchi(Institute for Environmental Science and Technology, Graduate School of Science and Engineering, Saitama University), Patricia vazquez(University of Reims Champagne Ardenne), Chairperson:Celine Thomachot-Schneider(University of Reims-Champagne-Ardenne), Patricia vazquez(University of Reims Champagne Ardenne)

Non destructive and non invasive techniques applying to cultural heritage made of stones, soils and earthen materials have been significantly developed over past years, and thus, the interest in such techniques has greatly increased. Here, we focus the session on new devices, new protocols and new data treatments that allow better understanding of weathering mechanisms, decay states and response to treatments. A few topics would be listed as follows: 1) The development of new techniques and devices in cultural heritage and new protocols using non-destructive techniques; 2) The application of these techniques and protocols on indoor and outdoor case studies and laboratory studies; 3) The assessment of weathering mechanisms, weathering kinetics, decay state, and response to treatments and 4) The modeling and simulation of decay processes.

3:30 PM - 3:45 PM JST | 6:30 AM - 6:45 AM UTC

[HTT15-01] Comparison of classic aging and realistic tests: study of the compatibility between limestones and restoration mortar

*Emilie Huby[1], Celine Thomachot-Schneider[1], Patricia vazquez[1], Gilles Fronteau[1] (1.Groupe d'etude des environnements naturels, anthropiques et archeologiques - Universite de Reims-Champagne-Ardenne (France))

3:45 PM - 4:00 PM JST | 6:45 AM - 7:00 AM UTC

[HTT15-02] Measurement of anisotropy of liquid water diffusivity of brittle tuff stone of Takase stone buddhas using X-ray

*Masaru Abuku[1], Shuya Hiranuma[2], Takayuki Fumoto[1], Soichiro Wakiya[3], Daisuke Ogura[4] (1.Kindai University, 2.SEKISUI HOUSE. LTD., 3.Nara National Research Institute for Cultural Properties, National Institutes for Cultural Heritage, 4.Kyoto University)

4:00 PM - 4:15 PM JST | 7:00 AM - 7:15 AM UTC

[HTT15-03] Granite Characterisation of Three Asynchronous Quarries of the Archaeological Site of *Touças* (North of Portugal)

*David Martin Freire-Lista[1,2], Patricia Vazquez[3], Gerardo Vidal Gonçalves[4] (1.Universidade de Tras-os-Montes e Alto Douro. Quinta de Prados. 5001-801 Vila Real, Portugal., 2.Centro de Geociências da Universidade de Coimbra. Rua Silvino Lima. Universidade de Coimbra - Polo II. 3030-790 Coimbra, Portugal., 3.Université Reims-Champagne-Ardenne 2, esplanade Roland Garros 51100 Reims, France. , 4.Centro de Investigação e Desenvolvimento em Ciências Humanas e Sociais. Universidade de Évora, Portugal.)

4:15 PM - 4:30 PM JST | 7:15 AM - 7:30 AM UTC

[HTT15-04] Spatiotemporal evaluation of weathering-induced depressions in sandstone blocks by terrestrial laser scanning

*Yuichi S. Hayakawa[1], Hisashi Aoki[2] (1.Faculty of Environmental Earth Science, Hokkaido University, 2.Faculty of Education, Tokyo Gakugei University)

4:30 PM - 4:45 PM JST | 7:30 AM - 7:45 AM UTC

[HTT15-05] From photogrammetric modelling of the built heritage to the evaluation of the durability of stones via GIS

*Sebastien LARATTE[1,2], Celine Thomachot-Schneider[1,2], Gilles FRONTEAU[1,2], Alexandra GUILLANEUF[1,2]
(1.University of Reims-Champagne-Ardenne, 2.GEGENAA)

4:45 PM - 5:00 PM JST | 7:45 AM - 8:00 AM UTC

[HTT15-06] Discussion

Comparison of classic aging and realistic tests: study of the compatibility between limestones and restoration mortar

*Emilie Huby[1], Celine Thomachot-Schneider[1], Patricia vazquez[1], Gilles Fronteau[1]

1. Groupe d'etude des environnements naturels, anthropiques et archeologiques - Universite de Reims-Champagne-Ardenne (France)

Laboratory aging tests allow the study of stones' behaviors on the monument indirectly. **Classic aging tests** are designed to compare materials' resistance to different weathering mechanisms: they are **more intense than the on-site conditions** and do not reflect the real weathering intensity and kinetics. To study the **real weathering on a monument** and the **materials' behavior**, a **non-destructive experimental setup** using **realistic experimental conditions** was designed.

Materials of the Saint-Remi basilica of Rheims (France)were studied. In particular, the **compatibility of the restoration mortar Lithomex**, used in recent years, with the **Courville limestone** (original stone) and the **Savonnières limestone** (restoration stone) were compared.

The realistic experimental setup was designed to **reproduce the thermal and hydric strains experienced by a stone on a vertical façade** in a stone sample (10x5x4.5cm). The hybrid samples were constituted of a 1cm thick mortar layer applied on the limestones.

The temperature and humidity variations were based on **typical variations identified with an *in-situ* monitoring** of the basilica: **sunny days** with temperature cycles (20/35˚C), **rainy days** with a 1h imbibition followed by temperature variations (20/35˚C), and **frost days** with a 1h imbibition preceding low-temperature cycles (5/-10˚C). The mild conditions, similar to the on-site conditions, did not damage the samples.

Temperature and humidty variations were applied unidirectionally through one surface, defined as the exposed surface, placed against a heating/cooling plate or immersed in 5mm water for a 1h imbibition. The sample's behavior was monitored with thermocouples and strain gauges measuring **heat transfer** and **differential micro-dilatation**.

The stress **at the interface between the mortar and the limestones** was calculated from the deformation data. It appeared that higher stress was generated at the Lithomex-Savonnières interface. Unlike the Courville, the Savonnières limestone dilated very little compared to the mortar; the differential deformation generated higher stress. This indicated **a better compatibility between the Lithomex mortar and the Courville limestone.**

Accelerated aging tests were also applied on hybrid samples (Ø= 4.5cm and h=5cm) constituted of the limestones presenting a 1 or 3cm thick layer of mortar**. 29 thermal shock cycles** (10h at 70˚C followed by 2h immersion in 20˚C water) and **17 freeze/thaw cycles** (10h at -10˚C followed by 2h immersion in 10˚C water) were carried out and monitored with weight and ultrasound velocity measurements.

©2021. Japan Geoscience Union. All Right Reserved.

The harsh conditions and number of cycles **caused visible damage**. Some hybrids {Lithomex+Courville} were broken during the cycles, while the hybrids {Lithomex+Savonnières} did not present any measurable or visual damage. These results let us suppose, contrary to the realistic experiments, a **better compatibility between the restoration mortar Lithomex and the Savonnières limestone than between the Lithomex and the Courville limestone**.

The realistic setup allowed a **simulation of the temperature and water repartitions in the samples closer to reality**. The materials' properties, such as thermal conductivity and water transport properties, were taken into account. The water rarely attained the limestones underneath the mortar due to the low capillarity of the Lithomex. On the contrary, the accelerated aging tests with total sample's immersion led to both wet limestone and mortar, generating stress that does not normally occur on the monument.

These experiments highlighted the **need for realistic experimental conditions** to assess the durability of restoration mortars and stones on which it is applied. This experimental setup provides more **relevant information in this specific environment** and **more accurate description of the real behavior of materials without damaging the samples**.

Keywords: Aging test, Thermo-hydric strain, Limestone, Restoration mortar

©2021. Japan Geoscience Union. All Right Reserved.

Measurement of anisotropy of liquid water diffusivity of brittle tuff stone of Takase stone buddhas using X-ray

*Masaru Abuku[1], Shuya Hiranuma[2], Takayuki Fumoto[1], Soichiro Wakiya[3], Daisuke Ogura[4]

1. Kindai University, 2. SEKISUI HOUSE. LTD., 3. Nara National Research Institute for Cultural Properties, National Institutes for Cultural Heritage, 4. Kyoto University

Takase Stone Buddhas is one of the important old stone buddha sculptures curved into the inner wall of the caves in Oita, Japan. It is located in a cave curved into the cliff of a hill of volcanic tuff. In general, because the cave is currently protected from rain and direct solar radiation by the roof shelter and waterproof treatment, the Buddhas is well conserved and no currently ongoing weathering can be clearly observed. However, because of a high ground water level, there is a concern in the influence of water evaporation at and near the surface of the stone buddhas and the wall of the cave on their deterioration. In the past, we have been conducting our long-term field survey of the conservation environment and numerical analyses of heat and moisture transport in the cliff and stone buddhas. The field survey provided a yearly data set of the conservation environment that was used as input of the succesive numerical simulation of heat and water transport in the material, which strongly depends on the material properties of the tuff stone.

In this study, we have conducted a holistic study of the material properties of the tuff stone of Takase stone buddhas, with special attention to the anisotropy of liquid water diffusivity. Because the tuff stone of the Takase stone buddhas is rather brittle, X-ray was applied to enable non-destructive measurement of the anisotropy of the diffusivity so that the specimen neither deforms nor collapse. X-ray CT was used to understand the three dimensional characteristics of a specimen. The liquid water diffusivity of the specimen was measured for different directions using X-ray radiography. The results showed a strong anisotropy of the liquid water diffusivity. The measured data were taken into account the succesive numerical study to quantify the importance of the anisotropy of the liquid water diffusivity for the conservation of the stone buddhas.

Keywords: Stone Buddha, Boltzmann transformation, Material property

©2021. Japan Geoscience Union. All Right Reserved.

Granite Characterisation of Three Asynchronous Quarries of the Archaeological Site of *Touças* (North of Portugal)

*David Martin Freire-Lista[1,2], Patricia Vazquez[3], Gerardo Vidal Gonçalves[4]

1. Universidade de Tras-os-Montes e Alto Douro. Quinta de Prados. 5001-801 Vila Real, Portugal., 2. Centro de Geociências da Universidade de Coimbra. Rua Silvino Lima. Universidade de Coimbra - Polo II. 3030-790 Coimbra, Portugal., 3. Université Reims-Champagne-Ardenne 2, esplanade Roland Garros 51100 Reims, France. , 4. Centro de Investigação e Desenvolvimento em Ciências Humanas e Sociais. Universidade de Évora, Portugal.

Quarries deepen as extraction techniques evolve over time. Quarries were superficial in the Iron Age, and the granite extracted from them had more developed exfoliation microcracks than the one extracted from medieval quarries, when new techniques allowed to extract a sounder granite. Today's quarries can go tens of meters deep and produce sound granite, whose exfoliation microcracks are less developed.

Prehistoric, medieval and current quarries of the same granite exist near the archaeological site of *Touças* . It is located 500 meters to the northeast of *Garganta* village, in *São Martinho de Anta*, municipality of *Sabrosa* (North of Portugal). It consists of about 70 prehistoric standing stones of granite, several medieval granite sarcophagi, a twin carved grave in the outcropping granite and a granite landmark of Malta military order dated from 1776. In addition, *Madorras* dolmen has been excavated at approximately 700 meters from the archaeological site of *Touças*. These elements have been built with the same granite but with different degrees of alteration.

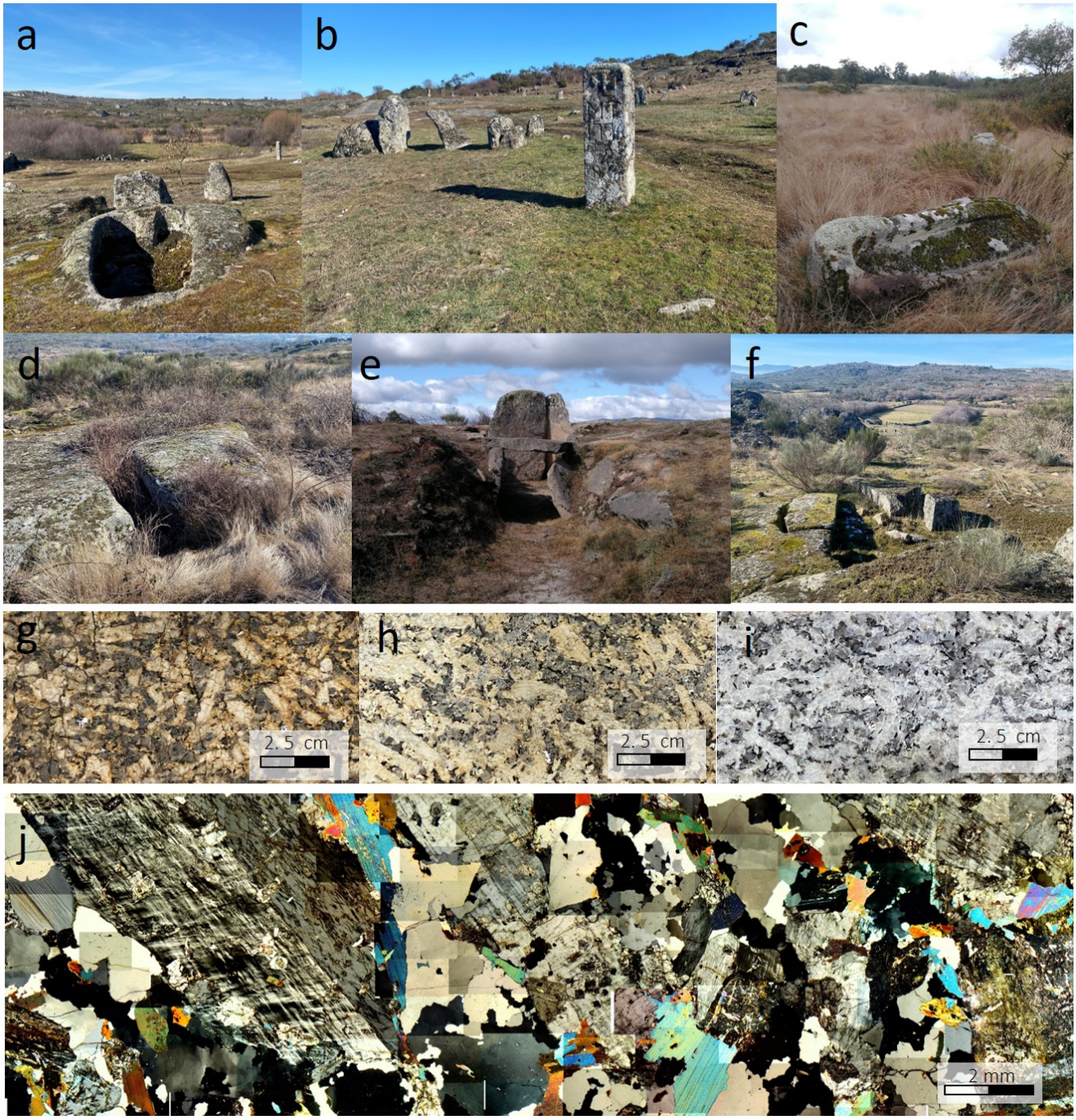
Granite from each quarry has been sampled for an in-depth analytical study. Eight cubic samples of each granite with dimensions of 5×5×5±0.5 cm were characterised. Effective porosity, water absorption and bulk density were obtained using the Natural Stone Test Method described in European standard UNE-EN 1936. Ultrasonic pulse velocity (wave propagation in??) of the granite cubes was measured with a CNS Electronics PUNDIT equipment following European standard UNE-EN 14579. The colour was assessed with an X-Rite colorimeter (model 964), using the three chromatic coordinates of CIE-L*a*b*system. Thin sections were prepared and analysed under a Leica DM-4500-P polarisation microscope equipped with a Leica DFC290-HD digital camera and LAS-4.9 software. Mercury intrusion porosimetry was conducted on single prismatic specimens (12±2 mm in diameter and 20±2 mm high) in a Micromeritics Autopore IV 9520 porosimeter. The capillary coefficient of each alteration grade of the granite was calculated based on the NF-EN 15801 standard. Infrared thermography monitoring was used to evaluate the alteration degree by means of the cooling rate index.

This archaeological site presents extremely relevant evidence for the understanding of the use of quarries throughout human occupation of *Trás-os-Montes e Alto Douro* territory. The main building granite of the archaeological site is a coarse-crystal-size granite with elongated pseudo-oriented feldspars. Granites mined in prehistoric times are much more susceptible to decay than those mined from deeper quarries. The alteration degree of the granite is directly related to the colour, number of microcracks, ultrasonic pulse velocity, hydric properties and thermal effect. Consequently, the conservation of granite must be adapted to its state of alteration.

Acknowledgements: Fundação para a Ciência e a Tecnologia (FCT) of Portugal. Stimulus of Scientific Employment, Individual Support 2017. CEECIND/03568/2017.

©2021. Japan Geoscience Union. All Right Reserved.

Keywords: Infrared thermography monitoring , Mercury intrusion porosimetry , Ultrasonic pulse velocity , Micrograph mosaic



©2021. Japan Geoscience Union. All Right Reserved.

Spatiotemporal evaluation of weathering-induced depressions in sandstone blocks by terrestrial laser scanning

*Yuichi S. Hayakawa[1], Hisashi Aoki[2]

1. Faculty of Environmental Earth Science, Hokkaido University, 2. Faculty of Education, Tokyo Gakugei University

For the quantitative evaluation of damages in stone-based cultural heritage by weathering, repeated measurements by terrestrial laser scanning (TLS) are an efficient way to monitor the surficial changes of the stone material. In particular, TLS enables quantifying the spatiotemporal changes in the morphology of rock surface by weathering at a high resolution. We apply TLS measurements to damaged masonry piers of a bridge (Yayoi Bridge at Aoshima, Miyazaki Prefecture, southwestern Japan; constructed in 1951) comprising vulnerable sandstone blocks in a coastal area, for which salt weathering is primarily responsible. The weathering-induced depressions in the sandstone block surface are quantified over six years and the weathering rates are assessed. The spatial distribution of the depression seems to correspond to the effectiveness of weathering conditions in the spray zone. The non-destructive assessment of the weathering conditions by TLS can thus provide basic information for the conservation of cultural heritage.

Keywords: salt weathering, TLS, change detection

©2021. Japan Geoscience Union. All Right Reserved.

From photogrammetric modelling of the built heritage to the evaluation of the durability of stones via GIS

*Sebastien LARATTE[1,2], Celine Thomachot-Schneider[1,2], Gilles FRONTEAU[1,2], Alexandra GUILLANEUF[1,2]

1. University of Reims-Champagne-Ardenne, 2. GEGENAA

The “Porte de Mars”, is one of the most emblematic ancient monuments of the city of Rheims. This three-bay roman arch rises at the northern end of former *Durocortorum,* capital of *Gallia Belgica* province. Its construction dates from the mid 2nd to early 3rd c. AD. It was then integrated into the Late Roman rampart of the city. Encased, from 1162 to 1856, in the medieval city wall and then in the castle of the city's archbishops, it was completely cleared and restored during the 19th century. During this period, it was barely saved from being dismantled after the ruin of the archbishops'castle and its complete dismantling by the town's population. It is considered the largest "arch" of the Roman Empire north of Roma. It is 32.35 m long, 6.45 m wide and 12 m high today. Since its rediscovery and until today, the “Porte de Mars” is located in the centre of Rheims.

Prior to restore the monument, a campaign to study the materials of the arch was achieved. For this purpose, a photogrammetric survey was carried out using a total of 370 high-resolution photos. Part of the photos were taken by fixing the camera on a pole and using a tablet as a means of preview, georeferencing and remote control. Pictures were processed with the Agisoft Metashape software which allows to carry out all the operations of the photogrammetry calculation chain (Close range photogrammetry - Structure From Motion method). This method allows the reconstruction of 3D objects from 2D data. The technique is based on an algorithm that automatically matches points in a set of photos. The model spatial coordinates were calculated by the software from the sets of photographs. Then the distances between 125 key points of the monument were measured using a laser rangefinder to scale the model. The software enabled orthophotographs to be extracted from the 3D mesh according to the chosen orientations.

The 3D data and derived orthophotos were injected into an interoperable geographic information system (QGis 3.4). Considered objects were then digitized in the form of polygons and a multifactor database was associated with them. This data included architectural information (typology, position, renovation phases) as well as petrographic and petrophysical information. Historical documents were also digitised in order to trace the recent evolution of the monument. Qualitative data (nature of the stone, petrography, presumed origin, restoration phase, etc.) were used to support the work of the monument's restoration teams, while quantitative data (chemical composition, mineralogy, porosity, capillarity, etc.) were used to produce durability assessment maps on the old parts of the building. The maps of alterations carried out in situ were also superimposed in order to relate their location to the characteristics of the building and the nature of the stones concerned. This approach could be supplemented by the projection of multiscalar data from other sensors such as thermal imaging data or the monitoring of parameters over time (magnetic, chemical or colorimetric for instance) and become a 4D tool.

Keywords: Building heritage, photogrammetry, GIS

©2021. Japan Geoscience Union. All Right Reserved.

[E] Oral | H (Human Geosciences) | H-TT Technology & Techniques

[H-TT15] Non-destructive techniques applied to stone cultural heritage

convener:Celine Thomachot-Schneider(University of Reims-Champagne-Ardenne), Chiaki T. Oguchi(Institute for Environmental Science and Technology, Graduate School of Science and Engineering, Saitama University), Patricia vazquez(University of Reims Champagne Ardenne), Chairperson:Celine Thomachot-Schneider(University of Reims-Champagne-Ardenne), Patricia vazquez(University of Reims Champagne Ardenne)

Sat. Jun 5, 2021 3:30 PM - 5:00 PM Ch.15 (Zoom Room 15)

Non destructive and non invasive techniques applying to cultural heritage made of stones, soils and earthen materials have been significantly developed over past years, and thus, the interest in such techniques has greatly increased. Here, we focus the session on new devices, new protocols and new data treatments that allow better understanding of weathering mechanisms, decay states and response to treatments. A few topics would be listed as follows: 1) The development of new techniques and devices in cultural heritage and new protocols using non-destructive techniques; 2) The application of these techniques and protocols on indoor and outdoor case studies and laboratory studies; 3) The assessment of weathering mechanisms, weathering kinetics, decay state, and response to treatments and 4) The modeling and simulation of decay processes.

4:45 PM - 5:00 PM

[HTT15-06]Discussion

©Japan Geoscience Union

[E] Poster | H (Human Geosciences)：H-TT Technology & Techniques

Sat. Jun 5, 2021 5:15 PM - 6:30 PM JST | Sat. Jun 5, 2021 8:15 AM - 9:30 AM UTC | Ch.11_2

[H-TT15] Non-destructive techniques applied to stone cultural heritage

convener:Celine Thomachot-Schneider(University of Reims-Champagne-Ardenne), Chiaki T. Oguchi(Institute for Environmental Science and Technology, Graduate School of Science and Engineering, Saitama University), Patricia vazquez(University of Reims Champagne Ardenne)

Non destructive and non invasive techniques applying to cultural heritage made of stones, soils and earthen materials have been significantly developed over past years, and thus, the interest in such techniques has greatly increased. Here, we focus the session on new devices, new protocols and new data treatments that allow better understanding of weathering mechanisms, decay states and response to treatments. A few topics would be listed as follows: 1) The development of new techniques and devices in cultural heritage and new protocols using non-destructive techniques; 2) The application of these techniques and protocols on indoor and outdoor case studies and laboratory studies; 3) The assessment of weathering mechanisms, weathering kinetics, decay state, and response to treatments and 4) The modeling and simulation of decay processes.

[HTT15-P01] Ultrasonic velocity attempted to the various rocks - laboratory experiment and field measurement -

*Chiaki T. Oguchi[1], Keishin Takahashi[2], Sota Noshiro[2], Yukina Ikeda[1] (1.Institute for Environmental Science and Technology, Graduate School of Science and Engineering, Saitama University, 2.Faculty of civil Engineering, Saitama University)

[HTT15-P02] Magnetic susceptibility of obsidian from Shirataki, Hokkaido, Japan, to identify the source of obsidian tools

*Kyohei Sano[1] (1.Graduate School of Regional Resource Management, University of Hyogo)

[HTT15-P03] Estimation of uniaxial compressive strength and water permeability from elastic waves measurements in sedimentary stones

*David Benavente[1], Juan Jose Galiana-Merino [2], Concepcion Pla[3], Marli De Jongh[4], Noe Garcia-Martinez[1], Javier Martinez-Martinez[5] (1.Department of Earth and Environmental Sciences, University of Alicante, 2.Department of Physics, Systems Engineering and Signal Theory, University of Alicante, 3.Department of Civil Engineering, University of Alicante, 4.University of Glasgow, School of Geographical & Earth Sciences, 5.Spanish Geological Survey)

[HTT15-P04] INFLUENCE OF POROSITY AND MINERALOGY ON INFRARED THERMOGRAPHY MEASUREMENTS

*Patricia vazquez[1], Thomas Junique[1], Sesil Can[1], Lena Ageorges[1], Dania Benkara[1] (1.University of Reims Champagne Ardenne)

Ultrasonic velocity attempted to the various rocks - laboratory experiment and field measurement -

*Chiaki T. Oguchi[1], Keishin Takahashi[2], Sota Noshiro[2], Yukina Ikeda[1]

1. Institute for Environmental Science and Technology, Graduate School of Science and Engineering, Saitama University, 2. Faculty of civil Engineering, Saitama University

The ultrasonic velocity test is one of the non-destructive and easy handling devices that allows the physical and mechanical properties of rocks to be investigated. Despite many research reports, there are still unclear in applying performed in the laboratory and the field as well. In this study, the correlation among porosity, hardness and the ultrasonic velocity was investigated by using soft rocks. First, for various tuffs (Oya tuff, Ashino tuff, Towada tuff, and Tatsuno tuff), the ultrasonic velocity of the rock sample in the air-dried state and the wet state was measured in the laboratory. As a result, the speed in the wet state was higher than the speed in the air-dried state in all cases except Towada tuff. On-site measurements were also performed at the Taya Cave (Sakae-Ku, Yokohama). The Taya Cave is composed of early to mid-Pleistocene deposits and is extremely low in strength. In the field, measurements were taken by the surface method at intervals of 20 cm. Although the sensitivity was low, the measured values converged and reproducible values were obtained.

Keywords: Ultrasonic velocity , Tuff, Taya Cave, Porosity

©2021. Japan Geoscience Union. All Right Reserved.

Magnetic susceptibility of obsidian from Shirataki, Hokkaido, Japan, to identify the source of obsidian tools

*Kyohei Sano[1]

1. Graduate School of Regional Resource Management, University of Hyogo

Magnetic susceptibility is often used to identify the source of tools and tombstones that are made from igneous rocks, such as obsidian and granite. This study reports on how the relationship between magnetic susceptibility and sample thickness of obsidian contributes to identifying the source of obsidian tools. Obsidian samples from Shirataki, Hokkaido, Japan, were analyzed, focusing on those from the lava flows of Tokachi-Ishizawa (TI), Akaishiyama (AK), and Horoka-Yubetsu (HY). The sample thickness ranges from 2.74 to 20.84 mm and the magnetic susceptibility ranges from 6.1 $\times 10^{-5}$ to 4.2 $\times 10^{-4}$ SI for the TI lava, from 2.52 to 13.78 mm and 3.3 $\times 10^{-5}$ to 2.1 $\times 10^{-4}$ SI for the AK lava, and from 2.05 to 23.28 mm and from 1.9 $\times 10^{-4}$ to 7.3 $\times 10^{-4}$ SI for the HY lava, depending on the thickness of the sample wafer. The results revealed that obsidian from the HY lava demonstrated the highest value of magnetic susceptibility among the analyzed samples; thus, obsidian from the HY lava could be identified by this characteristic. Concurrently, heterogeneity in the magnetic susceptibility within a single lava flow was observed in the AK lava. These results could contribute to the identification of the source of obsidian tools and development of nondestructive techniques for measurement of magnetic susceptibility.

Keywords: magnetic susceptibility, obsidian, nondestructive analysis, rock texture

©2021. Japan Geoscience Union. All Right Reserved.

Estimation of uniaxial compressive strength and water permeability from elastic waves measurements in sedimentary stones

*David Benavente[1], Juan Jose Galiana-Merino [2], Concepcion Pla[3], Marli De Jongh[4], Noe Garcia-Martinez[1], Javier Martinez-Martinez[5]

1. Department of Earth and Environmental Sciences, University of Alicante, 2. Department of Physics, Systems Engineering and Signal Theory, University of Alicante, 3. Department of Civil Engineering, University of Alicante, 4. University of Glasgow, School of Geographical & Earth Sciences, 5. Spanish Geological Survey

Uniaxial compressive strength (UCS) and water permeability (WP) are two of the most critical petrophysical parameters used in many fields of engineering and geosciences. Particularly, in stone conservation studies, these parameters are closely related to stone stability and durability in monuments. Although stone conservation studies can require large data sets, many have limited access to samples, and so require non-destructive on-site characterisation of UCS and WP.

Non-destructive methods (NDT) based on elastic wave measurements are commonly used in stone conservation studies and can be performed in both laboratory and field experiments. Experimentally, P-waves are easy to generate and acquire, whereas the generation and acquisition of pure S-waves in rocks can be difficult. Moreover, other ultrasonic parameters from the analysis of the recorded output waveform (mostly of the P-waves) can be extracted. These additional parameters provide complementary information from the same measurement performed for the calculation of P-wave velocity.

In this paper, we estimate USC and WP by combining connected porosity and ultrasonic parameters recorded from P- and S- waves for a wide range of carbonate sedimentary rock types. Fifteen rock samples were measured including calcarenites, sandstones, dolostones and travertines. These rock types are building stones quarried in Spain and were selected based on their different petrophysical and petrographic characteristics.

The ultrasonic measurements were carried out using the transmission method, which consists of two piezoelectric sensors (1 MHz Panametric transducers) coupled to the sample at constant pressure. We determine the onset of P- and S-waves considering signal pre-processing and the analysis of the recorded signals. We calculated P- and S-wave velocities, and the spatial attenuation and the wavelength of the first pulse of P-waves. Statistical analysis was applied to establish the structure of the variable dependence and their interrelationship using the code SPSS 22.0. Statistical analysis includes scattering diagrams and Pearson’s correlation coefficients, a principal component analysis, and a stepwise multiple regression analysis.

Mineralogical composition, porosity and particle size affect the wave velocity, attenuation, wavelength and waveform, which can be used as a selection criterion of parameters in the predictive functions. Results reveal that mineralogical composition significantly affects P-wave velocity values, especially for quartz-bearing rocks. Grain size is also reflected in the waveform. Thus, coarse-grained rocks have the highest wavelength and spatial attenuation. Spatial attenuation is a parameter sensitive to occasional rock defects such as the vuggy porosity observed in travertines. UCS and WP strongly depends on this type of vuggy porosity and how the vuggy porosity is connected.

Several simple and multiple predictive expressions for UCS and WP are fitted, which are quantified

©2021. Japan Geoscience Union. All Right Reserved.

through the Pearson correlation coefficient (R). Curve fitting improves as the number of petrophysical parameters increases in the multiple linear regressions. The best correlation is found when the predictive equation incorporates all the elastic wave parameters obtained non-destructively and connected porosity for UCS (R=0.921) and WP (R=0.903). Spatial attenuation is the most significant variable of the elastic wave parameters of the fitted regressions, and its addition into multiple linear equations causes an increase of goodness of fit. Connected porosity also improves R whereas wavelength and P-wave velocity have a lower statistical weight in the predictive expressions. The UCS and WC estimation from all NDT, without considering connected porosity, shows a good correlation (R=0.852 and 0.864, respectively). This study shows that UCS and WC can be obtained non-destructively using portable equipment and can provide large data sets at a relatively low cost.

Keywords: Ultrasounds, Hydraulic conductivity, Stone conservation, Petrophysics, Limestone

©2021. Japan Geoscience Union. All Right Reserved.

INFLUENCE OF POROSITY AND MINERALOGY ON INFRARED THERMOGRAPHY MEASUREMENTS

*Patricia vazquez[1], Thomas Junique[1], Sesil Can[1], Lena Ageorges[1], Dania Benkara[1]

1. University of Reims Champagne Ardenne

Infrared thermography (IRT) is a new tool in development in the field of cultural heritage, due mainly to the fact of being a non-destructive and non-invasive technique. Infrared thermography gives information about the apparent temperature of an object, related to its composition, shape, isolated defects and also decay state. However, within a building, sometimes the images show different values for the same material. Thus, a deep study on the consistency, the repeatability, and the establishment of key values is needed to better understand the reliability of this technique and to improve the accuracy in the stone characterization.

Three kinds of studies were carried out to determine the reliability and the influence of heterogeneity in the infrared thermographic signal:

- Detection threshold of small variations in porosity. For this study, ten cubes of 4 cm size of Fontainebleau sandstone were selected, with pure quartzitic composition, homogeneous grain size and sample color. Differents degrees of grain compaction were observed, which gave enough porosity and variability of physical properties for this study. Porosity was obtained following the standard EN-1936 and capillary water absorption as stated in EN-1925. Ultrasound measurements were measured with a Pundit-PL200 with transducers of 250KhZ. After this characterization, the cooling rate index (CRI) for each sample was obtained by infrared thermography as follows. The samples were dried at a temperature of 70˚C and then extracted at room temperature. The cooling from the time= 30 seconds up to 15 minutes and 30 seconds was monitored with an infrared thermographic camera FLIR A645 at a speed rate of 1 frame every 10 seconds. The data were analyzed with a software researchIR and the CRI calculated as:

T_f-T_o / t_f - t_o

Where To is the average temperature of the measured face at the beginning of the monitoring (to=30 sec after extraction of the oven), Tf is the average temperature of the measured face at a time tf.

A relationship between CRI and the porosity of each stone was studied, as well as the thermal response of each face with its vectorial properties (capillary coefficient and ultrasounds velocity).

-Influence of induced thermal fissuration on the thermosignal. Four granitoids with differences in mineralogy and grain size were tested. The samples were slabs of 7 x 3,5 x 2 cm. One sample of each type was submitted to one high- temperature heating, that is 200˚C, 400˚C, 600˚C, and 800˚C and compared to the intact rock. The heating rate was 6˚C/min to force the fissuration and the samples were kept at the set temperature for four hours, enough to get uniform temperature through the sample. The cooling down was carried out freely with a rate <1˚C/min, to ensure that the damage was only produced by the fast heating. Porosity, capillary water uptake and ultrasounds velocity was determined as in the previous study, as well as CRI calculation by IRT monitoring.

©2021. Japan Geoscience Union. All Right Reserved.

-Influence of mineralogy on the thermosignal. Each mineral has its own thermal properties. Thus, a rock behaves differently against temperature variations depending on its mineralogy and texture. Ten granitoids with differences in mineralogy and crystal size were heated at 70˚C and the CRI was measured by infrared thermography similarly to the other studies. A relationship between the mineral proportion, grain size and thermal properties of each stone were related to CRI results.

The results showed that only great variations of porosity are related to CRI values as occurred between the intact stone and the rocks heated at 600˚C or 800˚C. Lower temperatures as 200˚C or 400˚C produced a variation of the microstructural system, although the infrared thermography did not permit to differentiate it accurately. Mineralogy plays an important role in CRI values, although the grain size resulted more decisive than the mineral proportion.

Keywords: infrared thermography, porosity, mineralogy, cooling rate index

©2021. Japan Geoscience Union. All Right Reserved.

[J] Poster | H (Human Geosciences)：H-TT Technology & Techniques

Sat. Jun 5, 2021 5:15 PM - 6:30 PM JST | Sat. Jun 5, 2021 8:15 AM - 9:30 AM UTC | Ch.11_3

[H-TT18] Environmental Remote Sensing

convener:Naoko Saitoh(Center for Environmental Remote Sensing), Hitoshi Irie(Center for Environmental Remote Sensing, Chiba University), Hiroto Shimazaki(National Institute of Technology, Kisarazu College), Teppei Ishiuchi(Miyagi University)

Measuring environmental changes at various spatio-temporal scales is the key to improve our understanding of the relationship between human activities and environmental problems. Remote sensing is a powerful tool to acquire information on the earth's surface frequently and repeatedly over a broad spatial scale, enabling us to find the changes which might be related to the cause and consequence of environmental degradation. This session discusses the applications of remote sensing to the detection and monitoring of environmental changes in time and space, and aims to promote the knowledge-sharing for better management of the environmental problems and natural disaster in any place in the world.

[HTT18-P01] Feasibility of observations of middle and upper tropospheric and lower stratospheric ozone concentrations by GOSAT/TANSO-FTS

*Eito Seki[1], Naoko Saitoh[1] (1.Center for Environmental Remote Sensing, Chiba University)

[HTT18-P02] Data quality of GOSAT-2/TANSO-FTS-2 GHG profile data retrieved from the V102.102 radiance spectra

*Naoko Saitoh[1], Ryoichi Imasu[2], kei Shiomi[3] (1.Center for Environmental Remote Sensing, Chiba University, 2.Atmosphere and Ocean Research Institute, The University of Tokyo, 3.Japan Aerospace Exploration Agency)

[HTT18-P03] Land use and land cover change of illegal settlements by landless peasants in the Brazilian Amazon

*Sayaka Yoshikawa[1,3], Kanae Ishimaru[2] (1.Ibaraki university , 2.Fukui Prefectural University, 3.Tokyo institute of technology)

[HTT18-P04] Evaluation of heterogeneity in growth of black pines planted for artificial coastal forests in the Sendai Plain

*Takuto Kajiwara[1], Masayuki Kawahigashi[2] (1.Graduate Student of Tokyo Metropolitan University, 2.Tokyo Metropolitan University)

[HTT18-P05] Accounting for atmospheric factors to estimate photosynthetically active radiation from surface solar irradiance

*YAJIE DAI[1], Hitoshi Irie[1], Alessandro Damiani[1] (1.chiba university)

[HTT18-P06] Data-assimilation-based Estimation of Infectivity Parameter of COVID-19 Epidemic Model and its Relation to NO2 satellite observation.

*Osamu Kabayama[1], Okazaki Atsushi[2], Shunji Kotsuki[1] (1.Centre for Environment Remote Sensing, Chiba University, 2.The Pennsylvania State University)

[HTT18-P07] Changes in the NO2 weekly cycle under COVID-19 pandemic

*Alessandro Damiani[1], Hitoshi Irie[1], Saito Hikaru[1], Ying Cai[1], Dmitry Belikov[1], Raul R. Cordero[2] (1.CEReS, Chiba University, 2.Santiago de Chile University)

Feasibility of observations of middle and upper tropospheric and lower stratospheric ozone concentrations by GOSAT/TANSO-FTS

*Eito Seki[1], Naoko Saitoh[1]

1. Center for Environmental Remote Sensing, Chiba University

Ozone vertical profiles are simultaneously retrieved from thermal infrared (TIR) spectra observed with Thermal and Near infrared Sensor for Carbon Observation (TANSO)- Fourier Transform Spectrometer (FTS) on board Greenhouse Gases Observing Satellite (GOSAT) in the data processing of the Version 1 CO_2 product [Saitoh et al., 2016]. Focusing on polar regions where severe ozone depletions occur, we have analyzed characteristics of the TANSO-FTS ozone profiles and compared them with ozone data obtained with Atmospheric Chemistry Experiment (ACE)-FTS on board SciSat-1, which is a solar occultation sensor with higher vertical resolutions, for validating the TANSO-FTS ozone data.

First, we selected TANSO-FTS ozone data obtained in the latitude range of 70˚N–80˚N from 2009 to 2014 and calculated zonal means for each 10-day period for each month. We found that TANSO-FTS ozone concentrations in lower stratosphere (35–29 hPa) in February and March in 2011, when large-scale ozone destructions occurred, were significantly lower than ozone concentrations of a priori data used in the TANSO-FTS retrieval processing [McPeters et al., 2007] and lowest of the other years.

Next, we calculated averages of the TANSO-FTS ozone concentrations for each 15˚ longitude for shorter period in the northern high latitudes in 2011, and analyzed the ozone data by dividing them into the two regions: ozone-depleted region and no ozone-depleted region. The area of ozone depletion was determined from ozone column data of Ozone Monitoring Instrument (OMI) on board AURA; here, the region in the longitude of 0˚ to 30˚E from March 26 to 31, 2011 was selected as the “ozone-depleted region” because severe ozone depletions were continuously observed there. TANSO-FTS ozone concentrations were much lower than the a priori concentrations in the ozone-depleted region, while TANSO-FTS ozone concentrations were in contrast closer to the a priori data in the no ozone-depleted region. We then compared TANSO-FTS ozone data with SciSat-1/ACE-FTS ozone data in northern high latitudes (60˚N–70˚N) in 2011. Comparison results showed that the TANSO-FTS ozone concentrations were closer to the SciSat-1/ACE-FTS ozone concentrations than the a priori concentrations in the lower stratosphere (around 60-20 hPa) in the ozone-depleted region, which could demonstrate the possibility of capturing a detailed structure of ozone depletion in the polar lower stratosphere by the TIR band of GOSAT/TANSO-FTS.

Keywords: GOSAT, TANSO-FTS, ozone, Arctic ozone depletion

©2021. Japan Geoscience Union. All Right Reserved.

Data quality of GOSAT-2/TANSO-FTS-2 GHG profile data retrieved from the V102.102 radiance spectra

*Naoko Saitoh[1], Ryoichi Imasu[2], kei Shiomi[3]

1. Center for Environmental Remote Sensing, Chiba University, 2. Atmosphere and Ocean Research Institute, The University of Tokyo, 3. Japan Aerospace Exploration Agency

Greenhouse Gases Observing Satellite-2 (GOSAT-2), the successor of GOSAT launched in 2009, was successfully launched on 29th October, 2018 and started its regular operation on 1st February, 2019. Thermal infrared (TIR) bands of Thermal and Near Infrared Sensor for Carbon Observation-Fourier Transform Spectrometer-2 (TANSO-FTS-2) on board the GOSAT-2 can provide information on vertical structures of GHG concentrations and temperature in the atmosphere [Saitoh et al., 2009, 2016].

We have retrieved GHG concentrations and temperature in several atmospheric layers (up to 30 layers) from the TIR bands of GOSAT-2/TANSO-FTS-2 by adopting a non-linear maximum a posteriori (MAP) method with linear mapping. In the retrieval processing, we used the Level 1B V102.102 radiance spectra of TANSO-FTS-2. We have used 9, 10, and 15 μm bands for CO_2, O_3, and temperature retrieval and 7 and 8 μm bands for CH_4, N_2O, and H_2O retrieval, basically following the GOSAT/FTS TIR algorithm [Saitoh et al., 2009, 2016]. We have taken into account the EOF components of spectral residuals and simultaneously retrieved surface parameters. As the signal-to-noise ratio (SNR) values of the TIR bands of TANSO-FTS-2 are significantly larger than those of TANSO-FTS, we can expect TANSO-FTS-2 to observe greenhouse gases concentrations with higher accuracy and precision.

Retrieved CO_2, CH_4, and N_2O concentrations showed reasonable latitudinal gradients over the ocean. Over the land, the retrieved CH_4 and N_2O concentrations had larger variabilities than expected; they clearly had positive biases over the Sahara, which could be attributable to the inappropriate setting of surface emissivity there in the retrieval processing.

Keywords: satellite remote sensing, GHG, retrieval algorithm

©2021. Japan Geoscience Union. All Right Reserved.

Land use and land cover change of illegal settlements by landless peasants in the Brazilian Amazon

*Sayaka Yoshikawa[1,3], Kanae Ishimaru[2]

1. Ibaraki university , 2. Fukui Prefectural University, 3. Tokyo institute of technology

In Legal Amazon, land use and land cover changes have been reported to occur over large areas due to the introduction of large-scale mechanized agriculture, extensive cattle ranching and uncontrolled slash-and-burn cultivation since the 1980s. Around the same time, movements which landless peasants (or poor people) settle into abandoned land have been very active in Brazil. In many cases, these people lack agricultural experiences to yield sufficient production for livelihoods. Thus, it leads to abandon the land and repeat forest clearance. In this study, we specifically aimed at clarifying changes in land use and land cover using ground observation data, remote sensing (Geo-Eye-1) data and GIS techniques. We focus on two different settlements: established settlement (30 years) and productive settlement (14 years). These settlements were located at Santa Barbará province, about 40 km northeast from the center of Belé m, the Pará state capital, in the northern part of Brazil. This research is motivated by the following three questions: i) How much forest areas have disappeared due to the activities of landless peasants? ii) Can they get compliance with Brazilian Forest Code? iii) How much are agricultural lands developed? For the answering these questions, we clarified changes in land use and land cover under five approaches which employs original spectral data and lacunarity index.

Keywords: Amazon deforestation, Agrarian settlements by landless peasants, Lacunarity Index

©2021. Japan Geoscience Union. All Right Reserved.

Evaluation of heterogeneity in growth of black pines planted for artificial coastal forests in the Sendai Plain

*Takuto Kajiwara[1], Masayuki Kawahigashi[2]

1. Graduate Student of Tokyo Metropolitan University, 2. Tokyo Metropolitan University

1. Introduction
The 2011 tsunami caused by the Great East Japan Earthquake hit the coastal area, resulting in fatal damage to the black pine coastal forest in the Sendai Plain, which has been developed since the 17th century. Although the Forestry Agency immediately launched a coastal forest restoration project in the damaged area after the tsunami, there were many drawbacks to grow plants, such as high salinity due to seawater inundation and high groundwater level. The Forestry Agency constructed an embankment to raise basement for planting using excavated soil from the hilly areas surrounding the Sendai Plain. Seedlings of black pines planted on the basement showed uneven growth rates in the area after several years. Since the constant growth of trees has been required to function as embankment for alleviation of tsunami impact, negative factors should be urgently removed to promote their satisfactory growth. The present growth condition was evaluated by the normalized difference vegetation index (NDVI) calculated by satellite images.
2. Research method
The survey site was set in the Arabama Coastal Forest, Wakabayashi-Ku, Sendai City, Miyagi Prefecture. Totally 35 plots with different planting years were targeted to calculate NDVI. The NDVI value was calculated from satellite images taken by Sentinel-2 on 20 August, 2020. Distribution of NDVI values was mapped using ArcMap 10.5.1. The range of NDVI values in each planting plot was estimated by the kernel density estimation, which is an algorithm to estimate a probability density by extrapolating data of finite samples, based on the NDVI values of all pixels. Statistical significance for differences in normality, homoscedasticity, and mean values was evaluated to compare the non-uniformity of the growth status at each site.
3. Results and Discussion
There were statistically significant differences in NDVI values between planting plots established in the same year, indicating that different growth rate of black pines even under same growth condition. Again, the spatial distribution of NDVI differed depending on planting plots and the growth of the black pine varied even in the same plot with same planting year. Since there is no difference in the climatic conditions, such as sunshine and precipitation between planting plots, the differences in the growth of black pine could be growth factors in soil affected by microtopography and micro-scale variation in soil. Therefore, constant and detail surveys are necessary to elucidate the cause of the growth differences in black pines.

Keywords: satellite image, vegetation index, tree planting, embankment materials

©2021. Japan Geoscience Union. All Right Reserved.

Accounting for atmospheric factors to estimate photosynthetically active radiation from surface solar irradiance

*YAJIE DAI[1], Hitoshi Irie[1], Alessandro Damiani[1]

1. chiba university

Photosynthetically active radiation (PAR) is the energy source for organic matter production in plants. To analyze the long-term PAR changes where no proper PAR data are available, it has been proposed to build the long-term PAR data set using the ratio of PAR to surface solar irradiance (SSI) (PAR/SSI). However, the PAR/SSI is affected by local atmospheric factors. Particularly, the identification of weather conditions is necessary to estimate PAR, but accurate cloud segmentation is challenging. We propose a simple methodology to distinguish clear sky, overcast, and partial cloudy conditions. We exploited the broad range of meteorological instruments available at the SKYNET super site of Chiba University (Japan) to develop a reconstruction method accounting for the atmospheric factors more accurately than previous methods based on annual or monthly averages of PAR/SSI. Using high-temporal-resolution data, we optimized our PAR estimation under clear sky, overcast, and partial cloud conditions. Then, we achieved that the average deviation of the estimated PAR from the quantum sensor PAR-01D is less than 10% when the solar zenith angle is small. This study is expected to make more PAR data available, providing a basis for understanding the impact of microclimate changes on plant photosynthesis.

Keywords: Photosynthetically active radiation, the ratio of PAR to surface solar irradiance, atmospheric factors, identification of weather conditions

©2021. Japan Geoscience Union. All Right Reserved.

Data-assimilation-based Estimation of Infectivity Parameter of COVID-19 Epidemic Model and its Relation to NO2 satellite observation.

*Osamu Kabayama[1], Okazaki Atsushi[2], Shunji Kotsuki[1]

1. Centre for Environment Remote Sensing, Chiba University, 2. The Pennsylvania State University

With COVID-19 spreading around the world, it is necessary to understand the relationship between its infectivity and political decisions. This study uses data assimilation techniques and satellite observations to clarify the relevance. First, modified epidemiological model based on a commonly used compartment model is developed. The model assigns population into five compartments, Susceptible, Exposed, Infectious, Recovered, and Death (here after SEIRD model). In contrast to influenza epidemics, daily reports of deaths are issued by governments in COVID-19 outbreak. Therefore, Death compartment is explicitly separated to utilize the observation information. Ensemble data assimilation of SEIRD model revealed that the time series of infectivity of COVID-19 corresponded with political decisions such as the lockdowns, economic activity resume in the United States and economic restraints in Japan. In addition, satellite observations of NO2 also imply the economic restraint in Japan. We are now investigating the relationship between infectivity and political decisions based on estimated infectivity parameter of SEIRD and NO2 satellite observations. This presentation will include the most recent progress up to the time of the conference.

Keywords: COVID-19, NO2 satellite observation, mathematical epidemic model, Ensemble Data Assimilation, Data Assimilation

©2021. Japan Geoscience Union. All Right Reserved.

Changes in the NO2 weekly cycle under COVID-19 pandemic

*Alessandro Damiani[1], Hitoshi Irie[1], Saito Hikaru[1], Ying Cai[1], Dmitry Belikov[1], Raul R. Cordero[2]

1. CEReS, Chiba University, 2. Santiago de Chile University

Urban nitrogen dioxide (NO_2) concentrations arise from anthropogenic activities, mainly from traffic sources. In Chiba and Tsukuba cities, within the Great Tokyo Region (GTR, Japan), partial column MAX-DOAS (Multi-Axis Differential Optical Absorption Spectroscopy) NO_2 observations (at 0-1 km) usually show a reduction of about 45-50 %, compared with the business days, during the end of the year holiday season. Corresponding ozonesonde observations carried out in a close location showed enhanced ozone (O_3) concentrations during holiday peaking at the surface (+15 %) and decreasing with the altitude. This suggests that titration processes, under saturated NO_2 conditions, usually occur in the investigated urban region and affect the surface and the lowest atmospheric layers. Keeping this in mind, we examined the so-called weekend effect in MAX-DOAS NO_2. We noted that its extent is getting smaller over the last years, characterized by decreasing NO_2 trends. An evident exception occurred in 2020 when the strongest weekend effect on records has been recorded. This was confirmed by S5P/TROPOMI NO_2 observations showing a weekend effect in 2020 clearly larger than in 2019 over the GTR. In this talk, we will put such findings into context by analyzing the changes in other large urban areas both in Japan and abroad (e.g., US, Europe, South America). We will then examine the results in light of the different responses of the population to COVID-19 as view in mobility data, changes in meteorology, and recent results pointing to enhanced surface ozone during lockdowns.

Keywords: Remote sensing, Tropospheric gases, NO2, O3

©2021. Japan Geoscience Union. All Right Reserved.

[E] Poster | H (Human Geosciences)：H-CG Complex & General

Sat. Jun 5, 2021 5:15 PM - 6:30 PM JST | Sat. Jun 5, 2021 8:15 AM - 9:30 AM UTC | Ch.12_1

[H-CG22] Nuclear Geoscience in Developing Countries

convener:Mohammad Rajib(Bangladesh Atomic Energy Commission)

Application of nuclear techniques are being utilized in various fields of geoscience for many years. We would like to hear about the research outcomes of those studies, specially which are being conducted in developing countries. Peaceful application of nuclear energy is a very potential way of advanced researches and with the development of such techniques, many problems have been successfully solved in different countries. This session would like to accumulate the findings of such success stories and to gather various types of nuclear geoscience research at one place. Researches conducted in developed countries which can be implemented in any low or middle income countries with limited resources are also welcomed. Therefore, main objective of the session is to know various types of nuclear geoscientific researches which can be helpful in obtaining sustainable development.

[HCG22-P01] Radioactive waste disposal in Japan, especially focused on geological disposal of high-level radioactive waste

★Invited Papers

*Eiji Sasao[1] (1.Tono Geoscience Center, Japan Atomic Energy Agency)

[HCG22-P02] Effect of external radioactivity on the mineral grains from placer deposits of Bangladesh

*Mohammad Rajib[1,2,3], Mahmudul Hossain[1,4], Md. Fahad Hossain[1,5], Tumpa Saha[1,5] (1.Bangladesh Atomic Energy Commission, 2.Atomic Energy Research Establishment, 3.Institute of Nuclear Minerals, 4.Sterile Insect Technique Unit and INMAS, Cox's Bazar, 5.Beach Sand Minerals Exploitation Centre, Cox's Bazar)

Radioactive waste disposal in Japan, especially focused on geological disposal of high-level radioactive waste

*Eiji Sasao[1]

1. Tono Geoscience Center, Japan Atomic Energy Agency

Disposal of radioactive waste is one of the important issues for peaceful utilization of nuclear power. Trench and pit disposals have been performed for low- and intermediate-level radioactive waste in many countries: however, progress on geological disposal program varies from country to country.

In Japan, there are four principles of the treatment and disposal of radioactive waste: 1) the liability of generators, 2) minimization of radioactive waste, 3) rational treatment and disposal, and 4) implementation based on mutual understanding with the people. Under these principles, it is important to make appropriate classifications of the wastes and treat and dispose of them safely for each classification based on the recognition that the wastes may include materials with characteristics that take an extraordinary long time for the radioactivity to drop to insignificant levels (Japan Atomic Energy Commission, 2015).

Radioactive wastes generated by nuclear power are generally classified into low-level waste (LLW) and high-level waste (HLW), based on its origin and level of radioactivity in Japan. HLW is produced through the reprocessing spent fuel, and the others are classified as LLW. Disposal method is selected from the following four methods according to waste properties and radioactivity levels etc.; sub-surface trench, sub-surface pit, mid-depth underground and deep geological disposals.

A disposal business has already been established for most of the LLW generated at nuclear power plants. While the selection of a high-level waste repository site will be undertaken via a three-stage process based on the “Final Disposal Act”. The site selection procedure specified in the Final Disposal Act consists of three steps; literature survey, preliminary investigations and detailed investigations. Literature survey has actually been initiated in two municipalities of the northern part of Japan.

Geoscientifically, Japan is located on plate-boundary and affected by intense geological phenomena such as volcanic and fault activities, and erosion. A LLW disposal facility is regulated to locate in an area without influence of earthquake, tsunami and volcano (Sema, 2020). As for the mid-depth disposal, a repository should be located in an area without influence of volcanic activity, faulting and erosion for at least 100,000 years.

Since HLW will last higher radioactivity than natural uranium ore in the order of 100,000 years, it is necessary to consider longer time safety. In Japan, the Nationwide Map of “Scientific Features” relevant for Geological Disposal” was published. The map shows nation-wide distribution of unfavorable and preferable geoscientific features.

In this presentation, the speaker will introduce outline of radioactive waste disposal in Japan and geoscientific features preferable for HLW disposal.

©2021. Japan Geoscience Union. All Right Reserved.

Reference

Japan Atomic Energy Commission (2015) Framework for Nuclear Energy Policy

http://www.aec.go.jp/jicst/NC/tyoki/taikou/kettei/eng_ver.pdf

Sema (2020) Journal of Nuclear Fuel Cycle and Environment, vol.27, pp.40-42.

Keywords: Radioactive waste, Geological Disposal

©2021. Japan Geoscience Union. All Right Reserved.

Effect of external radioactivity on the mineral grains from placer deposits of Bangladesh

*Mohammad Rajib[1,2,3], Mahmudul Hossain[1,4], Md. Fahad Hossain[1,5], Tumpa Saha[1,5]

1. Bangladesh Atomic Energy Commission, 2. Atomic Energy Research Establishment, 3. Institute of Nuclear Minerals, 4. Sterile Insect Technique Unit and INMAS, Cox's Bazar, 5. Beach Sand Minerals Exploitation Centre, Cox's Bazar

Major beach placers of Bangladesh, such as ilmenite, magnetite, rutile, zircon, garnet along with potential monazite concentrated and silica were undergone irradiation. Co-60 gamma irradiator was utilized to irradiate the separated minerals. Objective of this research was to observe any effect of gamma irradiation to the morphology and composition and thereby obtaining information of possibility of synthesizing any mineral. The mentioned heavy minerals have variety of industrial uses. Among them, ilmenite has the largest quantity in beach placer deposits of Bangladesh. However, the chemical grade of Bangladesh ilmenite has lagging behind the international grade, with TiO_2 content of approximately 35% and Fe of 55%. Therefore, potential utilization of these ilmenites for Ti are still not possible. Moreover, zircon and monazite contains radioactive materials needs to be studied in details for the presence of radioactive and rare earth element. Placer garnet and silica could be a potential industrial mineral if characterized properly. As nuclear geoscientific research activity, the present study reports the characterization of those minerals with the artificially induced radiation.

Individual minerals were separated from beach sand and upgraded to best possible physical grade by density, magnetic and electric separators. Gamma dose of 0.01, 0.1 million Grey (mGy) was provided by the Co-60 source of initial activity of 12 KiloCurie, KCi (with present source activity of 9.511 KCi) and with 100% source efficiency. The samples were again irradiated at 1.0 mGy with similar source of approximate present activity of 90 KCi (from initial source activity of 350 KCi). Microscopic observation, X-ray diffraction analysis and elemental composition was attempted before and after irradiation, and radiation induced effects was analyzed. The study would provide the characterization of those minerals for various application. Besides, it would also contribute to the study of the minerals' property in the case of any radiation effect of geological materials in any potential host rock of geological repository for radioactive waste.

Keywords: Gamma irradiator, Radioactivity, Placer Mineral, Bangladesh

©2021. Japan Geoscience Union. All Right Reserved.

[J] Oral | H (Human Geosciences)：H-CG Complex & General

Sat. Jun 5, 2021 9:00 AM - 10:30 AM JST | Sat. Jun 5, 2021 12:00 AM - 1:30 AM UTC | Ch.17 Zoom Room 17

[H-CG23] Nuclear Energy and Geoscience

convener:Eiji Sasao(Tono Geoscience Center, Japan Atomic Energy Agency), Shinji Takeuchi(Department of Earth and Environmental Sciences, College of Humanities & Sciences, Nihon University), Takuma HASEGAWA(Central Research Institute of Electric Power Industry), Chairperson:Takuma HASEGAWA(Central Research Institute of Electric Power Industry)

Peaceful use of nuclear power is one of the most promising ways to solve energy problems and environmental problems. On the other hand, various problems are upcoming after nuclear disasters of Fukushima-Daiichi Nuclear Power Plant. The session provides a forum to deal with various aspects of scientific and engineering aspects of nuclear power. The session in this year focuses on radioactive waste disposal and covers not only scientific aspect such as characterization of geological environment but also engineering aspects such as microbe-nuclide, mineral-water, and cement-water interactions. In addition to this, themes on seismic hazards at nuclear facilities, environmental behavior of radionuclides emitted from nuclear power plants, and volume reduction and reuse of cesium contaminated soils are welcomed. Through these presentations, we promote intercultural communication and collaboration between science, engineering and social science.

9:00 AM - 9:15 AM JST | 12:00 AM - 12:15 AM UTC

[HCG23-01] Recent trends on long-term supply of uranium resources

*Eiji Sasao[1] (1.Tono Geoscience Center, Japan Atomic Energy Agency)

9:15 AM - 9:30 AM JST | 12:15 AM - 12:30 AM UTC

[HCG23-02] Geological Descriptive Model and AI Geo-Database of Coastal Area by Using Published data from National Public Research Institutes in Japan

*Atsunao Marui[1], Norikazu Imai[2], Teruhiko Suzuki[2], Akinari Honda[2] (1.Goelogical Survey of Japan, AIST, 2.GMLabo Co. LTD)

9:30 AM - 9:45 AM JST | 12:30 AM - 12:45 AM UTC

[HCG23-03] Attempt to identify the origin of deep-seated fluids in terms of hydrogeochemical characteristics

*Yuichi Tomioka[1], Hirofumi Kondo[1], Fumitake Kusuhara[1], Ayumi Sugiyama[1,2] (1.Central Research Institute of Electric Power Industry, 2.Asano Taiseikiso Engineering Co., Ltd.)

9:45 AM - 10:00 AM JST | 12:45 AM - 1:00 AM UTC

[HCG23-04] Characterization and Distribution of fractures in Granite, Ningyo-Toge, Okayama Pref., Japan

*Takesue Norito[1], Tsuyoshi Nohara[1] (1.Japan Atomic Energy Agency)

10:00 AM - 10:15 AM JST | 1:00 AM - 1:15 AM UTC

[HCG23-05] Study on the hydro-mechanical characterization of the calcareous concretion

*Shinji Takeuchi[1], Hidekazu Yoshida[2], Sachiko Nakamura[1] (1.Department of Earth and Environmental Sciences, College of Humanities & Sciences, Nihon University, 2.Nagoya University Museum)

10:15 AM - 10:30 AM JST | 1:15 AM - 1:30 AM UTC

[HCG23-06] Estimation of ^{137}Cs uptake from forest floor in Japanese cedar and Japanese konara oak stands of the Abukuma Mountains, Fukushima

*Tadafumi Niizato[1], Yoshito Sasaki[1], Satomi Ito[1], Takayoshi Watanabe[1], Hiroki Amamiya[2] (1.Japan Atomic Energy Agency, 2.QJ Science)

Recent trends on long-term supply of uranium resources

*Eiji Sasao[1]

1. Tono Geoscience Center, Japan Atomic Energy Agency

It is necessary to consider the long-term supply of uranium for the stable use of nuclear energy. Information on uranium resources is periodically reported by international and national organizations of various countries. For example, the OECD/NEA (Nuclear Energy Agency, The Organization for Economic Co-operation and Development) and IAEA (International Atomic Energy Agency) jointly prepare periodic report (currently every two years) called Uranium, which is updating on world uranium resources, production and demand. This report is commonly known as the “Red Book” and its latest update is the 2020 edition, published in December 2020 (OECD/NEA-IAEA, 2020). In this paper, supply and demand of uranium are reviewed mainly based on the Red Book, and future possibility on increase in uranium resources in Canada and Australia, the principal supplying countries, is discussed.

According to Red Book 2020 edition, total identified resources recoverable (reasonably assured and inferred) in the world as of 1 January 2019 amounted to about 8 million tonnes of uranium metal(tU) in the <USD 260/kgU (<USD 100/lb U_3O_8) cost category. Annual uranium requirements were 59,200tU as of 1 January 2019, that means identified resources are sufficient for about 135 years. Annual uranium requirements by the year 2040 are projected to increase to a total of between 56,640 tU and 100,225 tU, so that the number of years that uranium can be supplied by identified resources will vary (decrease) depending on the amount required.

Additionally, the COVID-19 pandemic affected uranium supply. In Canada, operation at the Cigar Lake mine were temporally suspended, and the McClean Lake mill was ceased accordingly. In Kazakhstan, Australia, Namibia, and other countries, the production volume decreased due to the furlough of workers.

One of the topics related to uranium mining is the termination of production at mine in which Japanese companies have participated. One of those, the Ranger mine in Australia ceased production on January 8, 2021. The Ranger Mine has remaining resources, and mining of the remaining resources was initially planned. However, the mine is located in an indigenous traditional land, and since the indigenous traditional land owners did not support the creation of a new Ranger Authority, which would provide the regulatory mechanism to enable mining after 2021, it was decided to close the mine. There is the Jabiluka deposit (approx.120,000tU) near the Ranger mine, but it cannot be mined either because the indigenous people have not given their permission. In Australia, there are five uranium projects awaiting better market conditions before proceeding with development: Honeymoon deposit in South Australia, Kintyre and Yeelirrie deposits, Wiluna and Mulga Rock deposits in Western Australia. Regarding the Mulga Rock deposit (approx. 29,000tU) was once discovered by the Power Reactor and Nuclear Fuel Development Corporation (PNC) but its concession was abandoned due to high mining costs, and was later obtained by an Australian company.

In Canada, a development plan of the Wheeler River project in the Athabasca region of Saskatchewan, the largest uranium deposit in the world, is underway. This project is expected to be the first application of in-situ recovery (ISR) mining method to an unconformity-related deposit at the Phoenix deposit (approx. 26,900tU). ISR method is generally used for sandstone-type uranium deposits. Since most deposits in the Athabasca Basin are considered hard rock mines, open-pit, and underground mining with explosives or

©2021. Japan Geoscience Union. All Right Reserved.

mechanical exploitations are required to mine uranium ore. The Phoenix deposit is located just above the unconformity between impermeable hard basement rock and relatively permeable soft Athabasca sandstone that lacks impermeable layer unlike sandstone-type deposits. Therefore a “freeze wall” will be constructed around the orebody and drilled approximately 300 boreholes for chemical injection and monitoring. And rock fracturing will be conducted as used for shale oil to increase the contact area between the chemical solution and the deposit. Furthermore, Phoenix has a higher grade (19.1% U_3O_8) than sandstone deposits, and thus the uranium is directly precipitated from the chemical solution and the chemical solution is reused (a circulation system is constructed), which results in relatively low cost and low environmental impact.

Reference

OECD/NEA-IAEA, 2020, Uranium 2020: Resources, Production and Demand.

Keywords: uranium resource

©2021. Japan Geoscience Union. All Right Reserved.

Geological Descriptive Model and AI Geo-Database of Coastal Area by Using Published data from National Public Research Institutes in Japan

*Atsunao Marui[1], Norikazu Imai[2], Teruhiko Suzuki[2], Akinari Honda[2]

1. Goelogical Survey of Japan, AIST, 2. GMLabo Co. LTD

A lot of public research institutions including Geological Survey of Japan, National Institute of Advanced Industrial Science and Technology release the geological and groundwater data of the whole country. However, there is problems as the notation methods, and there is a correspondence of land and the sea area, and it is difficult to understand the data of the coastal area continuously. Then, it was planned to make the database of documents and papers in addition to the published data from former research institutions, to make geological descriptive model which seemed to be probable one, moving ahead step by step. In this research, we will see the method of modelling by using the data of public institutions, first of all. And then, the 3D model has been continuously increase of more probable by the document data etc. for the lack part and no matching section. The finally, we evaluate and show the groundwater flow system and its long-term stable area in the 3D geological model of the coastal area. It is thought that the result of the study contributes to the groundwater profit use in the coastal area, and digging up of lack data for development and unused water resource.

Keywords: Coastal area, Geo-environment, Groundwater, Modeling, SDM

©2021. Japan Geoscience Union. All Right Reserved.

Attempt to identify the origin of deep-seated fluids in terms of hydrogeochemical characteristics

*Yuichi Tomioka[1], Hirofumi Kondo[1], Fumitake Kusuhara[1], Ayumi Sugiyama[1,2]

1. Central Research Institute of Electric Power Industry, 2. Asano Taiseikiso Engineering Co., Ltd.

For the safety assessment of the HLW geological disposal, it is necessary to evaluate the groundwater chemical and physical stability and inflowing of deep-seated fluids which is idiomatically classified as slab-derived fluid, fossil seawater, and oil-field brine. Among them, the slab-derived fluid, known as non-volcanogenic spring water, found in some areas in Japan which is recently elucidate their origin and behavior, they often have high temperature, high CO_2 gas, and high salinity sometimes over seawater. The features may have adverse impact for geological disposal systems. So, consolidation of the methodology for finding the fluid is required.
According to previous studies, typical features of slab-derived fluids show hydrothermal isotope shift of water, dissolved Li/Cl (w/w) tends to be exceeded 0.001, and isotope ratio of dissolved He gas is higher than the air. Fossil seawaters and oil-field brines have basically opposite features in slab-derived fluids, although some of them have high Li/Cl and hydrothermal shift of water isotopes. Identifying the origin of groundwaters is complicated problem. In this presentation, the authors show the results of sorting out the features of deep-seated fluids based on previous studies adding our field sampling results collected from over 40 of springs and boreholes to identify the origin of deep-seated fluids in terms of hydrogeochemical characteristics.

This study was funded by the Ministry of Economy, Trade and Industry, Japan as part of its R&D supporting program titled “Establishment of Advanced Technology for Evaluating the Long-term Geosphere Stability on Geological Disposal Project of Radioactive Waste (FY 2018-2020).

Keywords: deep-seated fluid, slab-derived fluid, fossil seawater, oil-field brine

©2021. Japan Geoscience Union. All Right Reserved.

Characterization and Distribution of fractures in Granite, Ningyo-Toge, Okayama Pref., Japan

*Takesue Norito[1], Tsuyoshi Nohara[1]

1. Japan Atomic Energy Agency

Ground-water flow in granitic rock is controlled by characterization and distribution of fractures and fault, have been analyzed using the distribution of fracture zone and the mean value of hydraulic conductivity. Modelling ground-water flow tend to be uncertainty by heterogeneous structures such as well-developed fractures and fault. Understanding heterogeneity and decreasing uncertainty is key to identify the ground-water flow.

We detected 2 sections (juxtaposing high-permeability and low-permeability) through boring research in granite around Ningyo-Toge. Upper high-permeability section is accompanied by distribution of parallel fractures. Fractures in lower low-permeability sections are poorly developed. These suggest that simplified structures are widely distributed around Ningyo-Toge.

Keywords: granite, fractures, ground-water flow

©2021. Japan Geoscience Union. All Right Reserved.

Study on the hydro-mechanical characterization of the calcareous concretion

*Shinji Takeuchi[1], Hidekazu Yoshida[2], Sachiko Nakamura[1]

1. Department of Earth and Environmental Sciences, College of Humanities & Sciences, Nihon University, 2. Nagoya University Museum

Porosity distribution, hydraulic conductivity, and hardness distribution of concretions were measured in the Neogene Hayama Group to clarify the hydraulic-mechanical properties of concretions. As a result, it has been confirmed that the concretion has been lower permeable and harder than the surrounding host rock.

Keywords: Concretion, Hydraulic property, Mechanical property, Sealing, Geological disposal

©2021. Japan Geoscience Union. All Right Reserved.

Estimation of ^{137}Cs uptake from forest floor in Japanese cedar and Japanese konara oak stands of the Abukuma Mountains, Fukushima

*Tadafumi Niizato[1], Yoshito Sasaki[1], Satomi Ito[1], Takayoshi Watanabe[1], Hiroki Amamiya[2]

1. Japan Atomic Energy Agency, 2. QJ Science

An understanding of long-term environmental dynamics of radiocesium in forested area, which is released by the TEPCO’s Fukushima Dai-ichi Nuclear Power Plant accident, is a key issue for predicting the future radiocesium distribution and forest products radioactivity, especially for ^{137}Cs (hereinafter, radiocesium) with long half-life of 30 years. In this paper we present the radiocesium uptake from forest floor in an evergreen Japanese cedar and a deciduous Japanese konara oak stands of the Abukuma Mountains, Fukushima.

An investigation was conducted in Oct. 2015 and Sept. 2017 at Japanese cedar stand and in Oct. 2018 and Oct. 2019 at Japanese konara oak stand near the living area. The average annual rainfall (1981–2010) is 1,221 mm and 1,465 mm in the konara oak and the cedar stands, and tree density is 791 trees ha^{-1} and 740 trees ha^{-1}, respectively. The breast height diameter has mode value of 10–14 cm and 25–30 cm in the konara oak and the cedar stands, respectively. Radioactive contamination in both stands is approximately 490–500 kBq m^{-2} via airborne monitoring results decay-corrected on April 1st, 2013. According to the procedure in International Biological Programme (IBP) for calculating of annual elemental uptake, annual radiocesium uptake from forest floor to the stand is defined as follows; annual radiocesium increment associated with tree growth plus annual loss through litterfall, stemflow, and throughfall [1].

The rate of annual radiocesium uptake associated with tree growth were estimated to be 0.1 and 0.06% of the total radiocesium inventory in Japanese konara oak and Japanese cedar stands, respectively. The sum of radiocesium uptake including the loss of radiocesium amount by litterfall, stemflow, and throughfall were 1.37 and 3.13% in the konara oak and the cedar stands, respectively.
The rate of radiocesium uptake estimated in this study are lower than the elemental uptake, such as nitrogen, phosphorus, potassium, in broad-leaved deciduous stand near Kyoto and Shimane Prefecture by IBP [2,3]. This indicate that the radiocesium uptake from forest floor to the konara oak and the cedar stands is restricted and no significant increase in radiocesium concentration of tree tissues is expected in the study stands.

[1] Cole et al. 1980, Inter.Biol.Prog. 23, 341-410.
[2] Katagiri & Tsutsumi, 1978, J.Jap.For.Soc., 60, 195-202.
[3] Katagiri, 1988, Jpn. J. Eloc., 38, 135-145.

Keywords: TEPCO’s Fukushima Dai-ichi Nuclear Power Plant accident, Japanese konara oak, Japanese cedar, radiocesium uptake

©2021. Japan Geoscience Union. All Right Reserved.

[J] Oral | H (Human Geosciences)：H-CG Complex & General

Sat. Jun 5, 2021 10:45 AM - 12:15 PM JST | Sat. Jun 5, 2021 1:45 AM - 3:15 AM UTC | Ch.17 Zoom Room 17

[H-CG23] Nuclear Energy and Geoscience

convener:Eiji Sasao(Tono Geoscience Center, Japan Atomic Energy Agency), Shinji Takeuchi(Department of Earth and Environmental Sciences, College of Humanities & Sciences, Nihon University), Takuma HASEGAWA(Central Research Institute of Electric Power Industry), Chairperson:Shinji Takeuchi(Department of Earth and Environmental Sciences, College of Humanities & Sciences, Nihon University)

Peaceful use of nuclear power is one of the most promising ways to solve energy problems and environmental problems. On the other hand, various problems are upcoming after nuclear disasters of Fukushima-Daiichi Nuclear Power Plant. The session provides a forum to deal with various aspects of scientific and engineering aspects of nuclear power. The session in this year focuses on radioactive waste disposal and covers not only scientific aspect such as characterization of geological environment but also engineering aspects such as microbe-nuclide, mineral-water, and cement-water interactions. In addition to this, themes on seismic hazards at nuclear facilities, environmental behavior of radionuclides emitted from nuclear power plants, and volume reduction and reuse of cesium contaminated soils are welcomed. Through these presentations, we promote intercultural communication and collaboration between science, engineering and social science.

10:45 AM - 11:00 AM JST | 1:45 AM - 2:00 AM UTC

[HCG23-07] Relationship between velocities in a single fracture and retardation effects by sorption investigated with laboratory tracer experiments

*Shunichi Okamoto[1], Kotaro Nakata[1], Takuma Hasegawa[1], Yasuharu Tanaka[1] (1.Central Research Institute of Electric Power Industry)

11:00 AM - 11:15 AM JST | 2:00 AM - 2:15 AM UTC

[HCG23-08] Evaluation on isotope and component separation by diffusion experiment

*Takuma HASEGAWA[1], Kotaro NAKATA[1], Rhys Gwynne[2] (1.Central Research Institute of Electric Power Industry, 2.University of Waterloo)

11:15 AM - 11:30 AM JST | 2:15 AM - 2:30 AM UTC

[HCG23-09] A study of U(VI) sorption on illite under carbonate-rich environments: Batch experiments, TRLFS and modeling

*Huiyang Mei[1], Noboru Aoyagi[1], Takumi Saito[2], Naofumi Kozai[1], Yukio Tachi[3] (1.Advanced Science Research Center, Nuclear Science Research Institute, Japan Atomic Energy Agency, Ibaraki, 2-4 Shirakata, Tokai-mura, Ibaraki 319-1195, Japan, 2.Nuclear Professional School, School of Engineering, The University of Tokyo, 2-22 Shirakata Shirane, Tokai-mura, Ibaraki 319-1188, Japan, 3.Nuclear Fuel Cycle Engineering Laboratories, Japan Atomic Energy Agency, 4-33 Muramatsu, Tokai-mura, Ibaraki 319-1194, Japan)

11:30 AM - 11:45 AM JST | 2:30 AM - 2:45 AM UTC

[HCG23-10] **Immobilization of Iodide and Iodate in Layered Double Hydroxide, Magnesium oxide and Silver embedded into Metakaolin-Based Alkali Activated Materials**

*CHAERUN Raudhatul Islam[1], Manami ISHIMURA[1], Kanako TODA[1], Tsubasa OTAKE[1], Ryosuke KIKUCHI[1], John PROVIS[2], Yogarajah ELAKNESWARAN[1], Tsutomu SATO[1] (1.Hokkaido University, 2.The University of Sheffield)

11:45 AM - 12:00 PM JST | 2:45 AM - 3:00 AM UTC

[HCG23-11] **Evolution of reaction and alteration of mudstone with cement leachate: Flow experiments and reactive-transport modelling**

*Keith Bateman[1], Yuki Amano[1], Yukio Tachi[1] (1.Radionuclide Migration Research Group, Japan Atomic Energy Agency, 4-33 Muramatsu, Tokai-Mura, IBARAKI, 319-1194 Japan)

12:00 PM - 12:15 PM JST | 3:00 AM - 3:15 AM UTC

[HCG23-12] Discussion

Relationship between velocities in a single fracture and retardation effects by sorption investigated with laboratory tracer experiments

*Shunichi Okamoto[1], Kotaro Nakata[1], Takuma Hasegawa[1], Yasuharu Tanaka[1]

1. Central Research Institute of Electric Power Industry

[Introduction]

On high-level waste disposal, it is important to evaluate retardation effects of solute transport in groundwater. Matrix diffusion, sorption on the fracture surface and bulk sorption in the matrix retard the transport of solute through fractured rock. In-situ tracer experiment that has been applied in many fractured rocks, is one of the methods for evaluating properties of the solute transport. Multi-rate tracer experiment is proposed to specify several parameters related to solute transport. However, previous study has clarified that sorption distribution coefficients (K_a and K_d) depend on pumping flow rate in the target fracture. Thus, the information about the relationships between a velocity in a fracture and K_a and K_d are important can be a key to improve the accuracy of estimating them. In this study, we conducted the laboratory tracer experiments and discuss relationship between velocities in a single fracture and the retardation effects by sorption. The two-dimensional numerical model composed of a fracture and a rock matrix was applied to simulate breakthrough curve (BTC) that was obtained by lab experiments.

[Methods]

Hirukawa granite rock was cut and shaped to be rectangular prism. Stainless spacers and an acrylic board were put on the granite rock and the 0.5mm of gap between the rock and the acrylic board was used as fracture in lab experiments. Sodium naphthionate (NAP) and Rb^+ were used as nonsorbing and sorbing tracer, respectively. The fracture aperture and the longitudinal dispersivity were calculated from BTCs of NAP and K_a and K_d were estimated from that of Rb^+. The parameters described above were obtained under 2 different flow rates (0.1 and 1.0 mL/min) and they were compared to understand the retardation effect of a velocity in the fracture. In these experiments, the setting fracture aperture is constant. Therefore, different flow-rate conditions are equivalent to different velocity conditions in the fracture.

[Results and discussions]

When the velocity in the fracture is 5.33×10^{-4} m/s, estimated K_a and K_d are 7.81×10^{-5} m and 4.50×10^{-3} m^3/kg, respectively. In the case of 5.95×10^{-5} m/s, the numerical fitting cannot reproduce the experimental BTC indicating that K_d and K_a are strongly dependent on the velocity in the fracture. Thus, revising curve-fitting method and/or construction of new model taking into account the effect of non-equilibrium sorption may be needed to deal with such cases.

This study was carried out under contracts awarded by the Japanese Ministry of Economy, Trade and Industry (METI).

Keywords: Fractured rock, Solute transport, Tracer experiment, Breakthrough curve, Sorption

©2021. Japan Geoscience Union. All Right Reserved.

Evaluation on isotope and component separation by diffusion experiment

*Takuma HASEGAWA[1], Kotaro NAKATA[1], Rhys Gwynne[2]

1. Central Research Institute of Electric Power Industry, 2. University of Waterloo

On safety assessment for radioactive waste disposal, it is important to show that groundwater flow is slow. Longer residence time makes lower radionuclide concentration because radionuclide decay with time. In a case the groundwater flow is very slow, diffusion will be the dominant transport mechanism (diffusion-dominant domain). It is a most promising condition for radioactive waste disposal. Indicating a diffusion-dominant domain, separation of component and fractionation of isotopes by diffusion will be useful index. Using rock core from Horonobe Underground Research Laboratory, diffusion experiments were conducted to confirm component separation and isotope fractionation.
The diffusion coefficients of water isotopes are three to four times higher than those of anions. The isotope fractionation factor of Cl and Br ranges 1.0017-1.0021 and 1.0007-1.0010, respectively. Moreover, effective porosity of diffusion was measured. The effective porosity for water isotope and anion is little bit different, but it will be small compared to the difference of diffusion coefficients. It is confirmed experimentally that component separation between water isotope and anion occur by diffusion. Therefore, it will be important index for the component separation of water isotope and anion, and isotope separation of Cl and Br to identify diffusion dominant domain.
This study entitled “FY2020 Research and development project on high-level radioactive waste disposal in geological formation (Development and Improvement on groundwater flow evaluation technique in rock)” supported by the Japanese Ministry of Economy, Trade and Industry. Some samples were provided from Japan Atomic Energy Agency.

Keywords: diffusion dominant domain, isotope fractionation, componetn separation

©2021. Japan Geoscience Union. All Right Reserved.

A study of U(VI) sorption on illite under carbonate-rich environments: Batch experiments, TRLFS and modeling

*Huiyang Mei[1], Noboru Aoyagi[1], Takumi Saito[2], Naofumi Kozai[1], Yukio Tachi[3]

1. Advanced Science Research Center, Nuclear Science Research Institute, Japan Atomic Energy Agency, Ibaraki, 2-4 Shirakata, Tokai-mura, Ibaraki 319-1195, Japan, 2. Nuclear Professional School, School of Engineering, The University of Tokyo, 2-22 Shirakata Shirane, Tokai-mura, Ibaraki 319-1188, Japan, 3. Nuclear Fuel Cycle Engineering Laboratories, Japan Atomic Energy Agency, 4-33 Muramatsu, Tokai-mura, Ibaraki 319-1194, Japan

The safety assessment for radioactive waste repositories largely relies on understanding the mechanisms involved in radionuclide retention by minerals in host rocks. Argillaceous rocks have been considered as one of the potential host-rock formations for geological repository in several countries. Carbonate ion is contained at relatively high concentrations in sedimentary groundwater in Japan (> 2,000 mg/L as HCO_3^- in some cases) and exerts a significant influence on the fate of radionuclides by formation of aqueous complexes. However, it is not clear whether the ternary surface complexes containing carbonate will be formed, which may affect the distribution of surface species and the subsequent construction of the predictive model. Thus, we investigate U(VI) sorption on illite (one of the main constituents of argillaceous rock) as functions of pH and HCO_3^- concentrations, by combining batch experiments, cryogenic time-resolved laser fluorescence spectroscopy (cryo-TRLFS), and surface complexation modeling using the 2 Site Protolysis Non-Electrostatic Surface Complexation and Cation Exchange sorption (2SPNE SC/CE) model. The cryo-TRLFS uses near liquid helium temperature to enhance the quality of fluorescence spectra (e.g., spectral intensity, resolution), which helps identify the surficial uranyl complexes in complicated environmental systems. In the talk, we will present the macroscopic and microscopic results of the (surface) speciation of U(VI) with illite in the presence of HCO_3^- and discuss the modeling of the sorption data, reflecting the speciation data.

*This work was part of “The project for validating near-field assessment methodology in geological disposal (FY2020)” supported by the Ministry of Economy, Trade and Industry of Japan.

Keywords: U(VI), illite, carbonate, surface complexation model, TRLFS

©2021. Japan Geoscience Union. All Right Reserved.

Immobilization of Iodide and Iodate in Layered Double Hydroxide, Magnesium oxide and Silver embedded into Metakaolin-Based Alkali Activated Materials

*CHAERUN Raudhatul Islam[1], Manami ISHIMURA[1], Kanako TODA[1], Tsubasa OTAKE[1], Ryosuke KIKUCHI[1], John PROVIS[2], Yogarajah ELAKNESWARAN[1], Tsutomu SATO[1]

1. Hokkaido University, 2. The University of Sheffield

In March 2011, an accident had occurred in Fukushima Daiichi Nuclear Power Station (FDNPS), which caused massive damage to the reactor and released I-131 and I-129 products. The radioactivity of I-131 and I-129 in the environment has a high impact on human health under a long exposure as observed from the Chernobyl incident. The concentration of these two isotopes varies in the environment. A large quantity of I-131 was initially released, which was hard to detect owing to its short half-life (8 days). On the other hand, I-129 was initially released with a low quantity. However, it has a longer half-life (1.57 x 10^7 years); thus, this isotope persists in the environment [1]. Hence, it is crucial to solidify and immobilize I-129 isotope to achieve safe disposal system.

Geopolymer is considered to be one of the best candidates as an encapsulation matrix for radionuclide immobilization (i.e., cesium (Cs^+) and strontium (Sr^{2+})) [2]. Similar to zeolite, geopolymer is an alkaline material, whose structure contains alumina-silicate tetrahedra in polymers. It is known for cation immobilization due to association with the negatively charged alumina tetrahedra.

Previous studies have been investigating the possible natural and synthetic adsorbent materials for removing iodine. In an aqueous environment, iodine mainly exists as iodide (I^-) and iodate (IO_3^-). They may have a possibility to be immobilized by a positively-charged adsorbent within the geopolymer matrix. Layered double hydroxide (LDH), magnesium oxide (MgO), and silver (Ag) are commonly used for anion immobilization, which are proven to exert high iodine retention due to their ability to offer positively charged structures [3,4,5]. However, I^- and IO_3^- could be repelled by the geopolymer structure. There are few studies of these adsorbents' stability with iodine under alkaline environments and no openly published study of I^- and IO_3^- immobilization within the geopolymer matrix. Therefore, in this study, the adsorbed iodine in the LDH, MgO, and Ag embedded within geopolymer matrix was investigated by evaluating the leaching behaviour of iodide and iodate and their adsorbents' stability.

After 19 days of leaching experiments, the iodine leaching levels of the materials were observed as follows: geopolymer matrix had leached out 89% I^- and 96% IO_3^-, LDH had 100% leached I^- and IO_3^-, MgO had leached 98% IO_3^-, and Ag had leached out 58% I^- and 2.4% IO_3^-. The stability of I^- and IO_3^- in the adsorbents embedded within geopolymer matrix was clarified by nano-micro analysis (i.e., SEM, TEM), and their mineral phases were characterized by XRD and calculated by thermodynamic calculations. Firstly, LDH after encapsulation (0 day) and after 19 days of leaching did not change into any phase. However, LDH preferred $H_{4-n}SiO_4^n$ adsorption over I^- and IO_3^- due to the high silica activity in the geopolymer matrix. Secondly, MgO changed its phase into magnesium silicate hydroxide (M-S-H) in the geopolymer matrix after 19 days of leaching. However, M-S-H did not have the capability for iodine retention. Finally, Ag^+ was precipitated with I^- to form iodyrite or iodargyrite, which were stable after 19 days of leaching. Therefore, Ag is an excellent adsorbent for immobilization of I^- and IO_3^- in the geopolymer matrix.

©2021. Japan Geoscience Union. All Right Reserved.

Keywords: Geopolymer, Fukushima Daiichi Nuclear Power Station, Layered double hydroxide, Magnesium oxide , Silver, Iodine retention

©2021. Japan Geoscience Union. All Right Reserved.

Evolution of reaction and alteration of mudstone with cement leachate: Flow experiments and reactive-transport modelling

*Keith Bateman[1], Yuki Amano[1], Yukio Tachi[1]

1. Radionuclide Migration Research Group, Japan Atomic Energy Agency, 4-33 Muramatsu, Tokai-Mura, IBARAKI, 319-1194 Japan

The construction of a repository for geological disposal of radioactive waste will include the use of cement-based materials. Following closure, groundwater will saturate the repository and the use of cement will result in the development of a highly alkaline porewater, pH >12.5 in the case of Ordinary Portland cement (OPC). The fluid will migrate into and react with the host rock. The chemistry of the migrating fluid will evolve over time, initially being high in Na and K, evolving to a Ca rich fluid and finally returning to the groundwater composition. This evolving fluid chemistry will affect the long-term performance of the repository altering the physical and chemical properties, including radionuclide behaviour. Understanding these changes forms the basis for modelling the long-term evolution of the repository. This study focused on the alteration due to OPC-type leachates on mudstone from the Horonobe URL, Hokkaido, Japan.

It was anticipated that the mudstone would react with the high pH fluids and that silicate minerals present would provide buffering together with the formation of secondary mineral phases which would evolve with time; this study was aimed at determining the specific nature and extent of these reactions. The flow experiments described here reacted in succession, fluids representing a 'young' OPC leachate, with high pH and high levels of Na and K. This was followed by an 'evolved' leachate (portlandite saturated) and finally Horonobe ground water (HGW). In addition, the experimental data were used as test cases for reactive transport geochemical modelling, to both assess and validate the predictive capability of the model.

The experiments were conducted using a small flow cell constructed from acrylic plastic, 10 mm long and 20 mm in diameter. The experiments used a dry density of 1 g/cm^3, with a typical volumetric flow rate ≈ 0.5 ml per hour. The evolution of the fluid chemistry was tracked by chemical analysis and mineralogy by characterisation of the reacted solids. A combination of PHREEQC and the 1-D reactive transport 'CABARET' geochemical codes were used to simulate the experiments.

Initially with the 'young' fluid, there was a reduction in [Na] and [K] due to ion exchange reactions with the clay mineral in the mudstone but these quickly returned to close to the initial concentrations. Si levels increased whilst Ca decreased. With the change to the 'evolved' leachate, [Ca] increased but remained below that of the 'evolved' fluid. Both [Na] and [K] decreased as did [Si]. The pH with both OPC leachates showed only a small decrease (≈ 0.2) from the initial values. With the change to the HGW, the pH returned to close to that of the HGW, as did both Na and K. Ca levels remained slightly lower than the HGW but Si levels increased.

The changes in Ca and Si with the OPC leachates were due to the formation of secondary C-S-H phases. This was confirmed by the mineralogical analysis, examination of the saturation indices (SI) for the reacted fluids and the output of the reactive transport modelling This showed continued dissolution of the primary minerals in the clay together with the saturation and hence precipitation of a variety of C-S-H phases. With the HGW, the secondary C-S-H phases re-dissolved releasing Si into solution and Ca levels were

©2021. Japan Geoscience Union. All Right Reserved.

controlled by the formation of calcite by reaction with bicarbonate in the HGW.

In summary, the reaction of the mudstone with the successive OPC leachates demonstrated its chemical buffering capacity, leading to a reduction in pH, the dissolution of primary minerals with Ca and Si concentrations being controlled by C-S-H phase precipitation. However, when the fluid returns to the natural background groundwater composition the C-S-H phases re-dissolve, which would potentially release any sorbed radionuclides. The experimental data has been used to help validate a 1-D reactive transport geochemical model generating increased confidence in its predictive capabilities.

Keywords: Radioactive waste, Mudstone, Geochemistry, Modelling, Flow experiments

©2021. Japan Geoscience Union. All Right Reserved.

[J] Oral | H (Human Geosciences) | H-CG Complex & General

[H-CG23] Nuclear Energy and Geoscience

convener:Eiji Sasao(Tono Geoscience Center, Japan Atomic Energy Agency), Shinji Takeuchi(Department of Earth and Environmental Sciences, College of Humanities &Sciences, Nihon University), Takuma HASEGAWA(Central Research Institute of Electric Power Industry), Chairperson:Shinji Takeuchi(Department of Earth and Environmental Sciences, College of Humanities &Sciences, Nihon University)

Sat. Jun 5, 2021 10:45 AM - 12:15 PM Ch.17 (Zoom Room 17)

Peaceful use of nuclear power is one of the most promising ways to solve energy problems and environmental problems. On the other hand, various problems are upcoming after nuclear disasters of Fukushima-Daiichi Nuclear Power Plant. The session provides a forum to deal with various aspects of scientific and engineering aspects of nuclear power. The session in this year focuses on radioactive waste disposal and covers not only scientific aspect such as characterization of geological environment but also engineering aspects such as microbe-nuclide, mineral-water, and cement-water interactions. In addition to this, themes on seismic hazards at nuclear facilities, environmental behavior of radionuclides emitted from nuclear power plants, and volume reduction and reuse of cesium contaminated soils are welcomed. Through these presentations, we promote intercultural communication and collaboration between science, engineering and social science.

12:00 PM - 12:15 PM

[HCG23-12]Discussion

©Japan Geoscience Union

[J] Poster | H (Human Geosciences)：H-CG Complex & General

Sat. Jun 5, 2021 5:15 PM - 6:30 PM JST | Sat. Jun 5, 2021 8:15 AM - 9:30 AM UTC | Ch.12_2

[H-CG23] Nuclear Energy and Geoscience

convener:Eiji Sasao(Tono Geoscience Center, Japan Atomic Energy Agency), Shinji Takeuchi(Department of Earth and Environmental Sciences, College of Humanities & Sciences, Nihon University), Takuma HASEGAWA(Central Research Institute of Electric Power Industry)

Peaceful use of nuclear power is one of the most promising ways to solve energy problems and environmental problems. On the other hand, various problems are upcoming after nuclear disasters of Fukushima-Daiichi Nuclear Power Plant. The session provides a forum to deal with various aspects of scientific and engineering aspects of nuclear power. The session in this year focuses on radioactive waste disposal and covers not only scientific aspect such as characterization of geological environment but also engineering aspects such as microbe-nuclide, mineral-water, and cement-water interactions. In addition to this, themes on seismic hazards at nuclear facilities, environmental behavior of radionuclides emitted from nuclear power plants, and volume reduction and reuse of cesium contaminated soils are welcomed. Through these presentations, we promote intercultural communication and collaboration between science, engineering and social science.

[HCG23-P01] Modeling of Radial Dikes by Topographical Analysis using GIS for Quaternary Volcanoes

Yuki Hiura[1], *Makoto Kawamura[1], Umeda Koji[2], Masakazu Niwa[1] (1.Japan Atomic Energy Agency, 2.Hirosaki Univ.)

[HCG23-P02] Three-dimensional resistivity distribution by magnetotelluric survey to evaluate the distribution of fossil seawater

*Naomi Satoh[1], Akira Hayano[1], Minoru Teshima[2], Tateyuki Negi[2], Terumasa Yamane[3], Shinji Kawasaki[3] (1.Japan Atomic Energy Agency, 2.Nittetsu Mining Consultants Co., Ltd., 3.JGI, Inc.)

[HCG23-P03] Microbial community analysis of deep-seated fluids: Do microbes live in slab-derived fluid?

*Ayumi Sugiyama[1,2], Yuichi Tomioka[1], Shin-ichi Hirano[1], Tokihiro Kurita[1] (1.Central Research Institute of Electric Power Industry, 2.Asano Taiseikiso Engineering Co., Ltd.)

[HCG23-P04] Constructions of hydrogeological structure and mass transport model around hydraulic conductive fractures

*Ai Hamada[1], Kimio Miyakawa[1], Yasuharu Tanaka[1] (1.Central Research Institute of Electric Power Industry)

[HCG23-P05] Development of multi-scale modeling for estimation of inflow volume into tunnels of the geological disposal facility

*Naoki Katsumata[1], Satoru Suzuki[1], Hiromitsu Saegusa[1], Tatsuya Tanaka[2], Yoshito Kitagawa[1] (1.Nuclear Waste Management Organization of Japan, 2.OBAYASHI CORPORATION)

[HCG23-P06] Introduction of the “KiNa” international project of natural analogue studies of the long-term stability of bentonite

*Satoru Suzuki[1], Tsutomu Sato[2], Tsubasa Otake[2], Kikuchi Ryosuke[2], Fujimura Tatsuya[2], Takahiro Goto[1], Yusuke Ogawa[1], Patrik Sellin[3], Daniel Svensson[3], Albert H. Gilg[4], Ulf B. Andersson[5], Elizaveta Klein[6], Olivier X. Leupin[6], Simon Norris[9], Russell W. Alexander[10], Mehran Behazin[7], Nicolas Michau[8] (1.Nuclear Waste Management Organization of Japan , 2.Hokkaido University, 3.SKB, 4.TU Munich, 5.Luossavaara-Kiirunavaara AB, 6.Nagra, 7.NWMO, 8.ANDRA, 9.RWM, 10.Bedrock Geosciences)

[HCG23-P07] Interaction at the interface between compacted bentonite and carbon steel plate in artificial seawater

*Tatsuya Fujimura [1], Tsutomu Sato[2], Tsubasa Otake[2], Kikuchi Ryosuke[2], Satoru Suzuki[3], Takahiro Goto[3]
(1.Graduate School of Engineering, Hokkaido University, 2.Faculty of Engineering, Hokkaido University, 3.Nuclear Waste Management Organization of Japan)

Modeling of Radial Dikes by Topographical Analysis using GIS for Quaternary Volcanoes

Yuki Hiura[1], *Makoto Kawamura[1], Umeda Koji[2], Masakazu Niwa[1]

1. Japan Atomic Energy Agency, 2. Hirosaki Univ.

One of the technical issues related to volcanic and igneous activities is the sophistication of technology for grasping the range of influence of magma. To address this issue, it is important to accumulate survey cases, especially when the dike develops over a radius of 15 km from the center of the Quaternary volcano, but it lies beneath the existing volcanic body. It is practically difficult to grasp the distribution of the conduits and the dikes derived from them. Therefore, the purpose of this study was to develop a method for estimating the distribution range of dikes distributed under the Quaternary volcanic body based on topographical data such as digital elevation models. In this study, we used digital maps and GIS software to target six volcanoes, such as stratovolcanoes and calderas. The parameters were measured, and modeling of the three-dimensional distribution range of radial dikes was examined from each parameter for each altitude. As a result, the transition of the center of gravity position for each altitude suggests the transition of the center of activity in the process of forming the volcanic body to some extent, and it is possible to extract not only the activity of the central crater but also the activity of lateral volcanoes. This suggests the possibility of quantitative evaluation of the transition and stability of the conduit even in volcanoes whose activity history is not clear by applying this method.

Keywords: Quaternary Volcanoes, Volcanic Conduit, Radial Dikes, Topographical Analysis, GIS

©2021. Japan Geoscience Union. All Right Reserved.

Three-dimensional resistivity distribution by magnetotelluric survey to evaluate the distribution of fossil seawater

*Naomi Satoh[1], Akira Hayano[1], Minoru Teshima[2], Tateyuki Negi[2], Terumasa Yamane[3], Shinji Kawasaki[3]

1. Japan Atomic Energy Agency, 2. Nittetsu Mining Consultants Co., Ltd., 3. JGI, Inc.

Introduction

The hydrological regime with “a slow groundwater movement that minimizes the transport of radioactive materials” is considered one of the most suitable geological conditions in the site selection of the geological disposal of high-level radioactive waste [1]. Fossil seawater is groundwater whose composition has been altered during the burial diagenetic process but has not been affected by the infiltration of meteoric fresh water [2]. Its presence indicates that the groundwater movement of the area is sufficiently slow. Thus, developing a workflow in the geological disposal project for investigating the distribution of fossil seawater is essential to determine where groundwater movement is sufficiently slow.
This study reports the preliminary results of the magnetotelluric (MT) survey aiming to evaluate the three-dimensional distribution of fossil seawater in the Horonobe area that is composed of the Neogene sedimentary rocks. Moreover, fossil seawater is characterized by high salinity. Consequently, the low resistive domain obtained by the MT survey can provide information about its distribution [3]. The audio-magnetotelluric (AMT) survey, where the depth of exploration is shallow, was applied in most of the previous electromagnetic surveys conducted in the Horonobe area. This study applied the MT survey, which can explore the deeper layers with high accuracy, to improve the resolution of fossil seawater distribution.

Materials and methods

The survey was conducted in a 9-km^2 area adjacent to the Horonobe Underground Research Laboratory of Japan Atomic Energy Agency. Moreover, 60 points were arranged in a grid pattern within the area to effectively estimate the three-dimensional distribution of fossil seawater. Consequently, the MT data were obtained at each point. In the three-dimensional inversion, 99 points including 39 existing points were used to estimate the resistivity distribution.

Results and future perspective

The overall distribution of resistivity was generally low, consistent with the geology of the Horonobe area, which consists mainly of mudstone and shale. However, resistivity appeared to vary following the geological structure. The resistivity was relatively high (>10 Ω-m) until 50 m in depth, while it was relatively lower (1–5 Ω-m) at a depth of 50–1,000 m. The area adjacent to the Omagari Fault showed higher resistivity compared to the surrounding area, suggesting the infiltration of meteoric fresh water preferentially along the Omagari Fault similar to the previous AMT survey [4]. The Yuchi Formation, an upper stratum distributed to the southwest part of the survey area, also showed high resistivity, which may be due to the groundwater recharge.
Examining a more optimal resistivity distribution considering the geological structure is necessary for future work. Furthermore, the integration of the MT survey with borehole investigations is a critical issue to estimate the three-dimensional distribution of fossil seawater.

This study was conducted as a part of the project on “FY2020 Development and Improvement on groundwater flow evaluation technic in rock” funded by the Japanese Ministry of Economy, Trade and

©2021. Japan Geoscience Union. All Right Reserved.

Industry.

[1] Nuclear Waste Management Organization of Japan, 2011, NUMO-TR-13-05.
[2] Muramatsue et al., 2016, J. Hot Spring Sci., 65, 216-233.
[3] Mizuno et al., 2017, 58, 178-187.
[4] Ishii et al., 2006, Jour. Geol. Soc. Japan, 112, 301-314.

Keywords: Fossil seawater, Magnetotelluric survey, Neogene sedimentary rock, Geological disposal

©2021. Japan Geoscience Union. All Right Reserved.

Microbial community analysis of deep-seated fluids: Do microbes live in slab-derived fluid?

*Ayumi Sugiyama[1,2], Yuichi Tomioka[1], Shin-ichi Hirano[1], Tokihiro Kurita[1]

1. Central Research Institute of Electric Power Industry, 2. Asano Taiseikiso Engineering Co., Ltd.

Microbes are present under various environments and their distribution in the subsurface environment extend for several kilometers. The distribution of microbes in the environment reflects environmental conditions such as temperature, pH, nutrients. Understanding the microbial community in the groundwater might be elucidated the origin of groundwater and difference in the groundwater flow paths. However, little is known the microbial communities in slab-derived fluid, which is characterized by high temperature, high salinity and high CO_2 concentration. In this study, we analyzed the microbial community in groundwater, which is considered to be contribution of slab-derived water, and examined whether the origin and mixing of groundwater could be estimated from microbial analysis.

The 11 groundwater samples were collected from hot and cold springs at different locations. The temperature measured at the outflows ranged from 7.4°C to 41.2°C. The value of pH and the electric conductivity ranged from 6.26 to 8.14, from 129 mS/m to 5050 mS/m, respectively. The density of microbes ranged from 2.2 x 10^3 cells/mL to 9.3 x 10^5 cells/mL. 16S rRNA gene sequencing, 110,000 to 390,000 reads were obtained, and they belonged to 44 to 56 phyla. The relative ratio of archaea, which mainly live in extreme environments, accounted for 0.2% to 17.4%. At all sites, *Methanomicrobia*, *Methanobacteria* and *Methanococci* dominated. In some samples, hyper-thermophilic archaea, *Archaeoglobi* and *Thermococci*, and highly halophilic archaea, *Halobacteria*, were detected. The detection of these hyper-thermophilic and highly halophilic microbes suggests that the examined groundwater experienced a high temperature and high salinity environment, and the contribution of slab-derived water as the origin of the groundwater could be considered. We will perform further analysis and examine the possibility of evaluating the origin and mixing of groundwater using microbes.

This study was funded by the Ministry of Economy, Trade and Industry, Japan as part of its R&D supporting program titled “Establishment of Advanced Technology for Evaluating the Long-term Geosphere Stability on Geological Disposal Project of Radioactive Waste (FY 2020).

Keywords: density of microbes, next generation sequencing, deep-seated fluids, slab-derived fluid

©2021. Japan Geoscience Union. All Right Reserved.

Constructions of hydrogeological structure and mass transport model around hydraulic conductive fractures

*Ai Hamada[1], Kimio Miyakawa[1], Yasuharu Tanaka[1]

1. Central Research Institute of Electric Power Industry

In geological disposal of high-level nuclear waste, hydraulic conductive fractures in crystalline rock such as granite have been considered as a main pathway for radionuclides. Diffusion and absorption of radionuclide through microstructure in rock matrix can make mass transport to retard. Because the change of the characteristics of microstructure in rock matrix by structural movement and hydrothermal alteration have an effect on mass transport, it is important to understand hydrogeological continuity of fractures as well as their porosity and mass transfer characterizations by field survey and laboratory test and moreover to construct hydrogeological structure and mass transport model around hydraulic conductive fractures by reflecting their parameter from physical property values. For the purposes of effectiveness evaluation of technological development for estimating the interstitial structure of hydraulic conductive fractures in Japan, we have conducted the advancement of hydraulic fracture investigation methods for Toki granite of Mizunami Underground Research Laboratory of JAEA. In this study, we focus on hydraulic fractures of the western part around GL −300 m Measurement Niche off Ventilation Shaft and suggest that hydraulic geological structure and mass transfer model and their parameters for groundwater flow / nuclide migration analysis taking into account for nuclide diffusion / sorption behavior based on in-situ resin infiltration tests and diffusion and sorption tests.

In the rock around GL −300 m Measurement Niche off Ventilation Shaft, on the west side, NW fractures with hydrogeological continuity form higher-permeability zone through low dip angle fractures (Hamada, 2019). The hydraulic conductive fractures across multiple boreholes to the west sides, which were recognized as resin infiltrated fractures, mainly show NW fracture. They are open along cataclastic vein texture which consists of fractured rock-forming minerals, with euhedral calcite crystals between the surfaces of fracture. From the composition analysis by EPMA, minerals consisting of cataclastic vein texture do not include secondary minerals. It is considered that NW strike fractures were formed by opening along weak lines of the surface of the cataclastic vein structures after crustal movement, which were granulated by the grinding action. Low dip fractures are universally distributed at this depth and euhedral calcite crystals developing between fracture surfaces were thought to be originated from freshwater because of C-axis developing (Folk, 1974). From these, low dip fractures were formed by uploading after granite ascending and filled with euhedral crystals of calcite formed after the intrusion of surface water.

Based on the characteristics of hydraulic fractures as described above, we suggest mass transport models for analyzing groundwater flow / nuclide migration through mainly single fracture model in crystalline rock as follows. From both macroscopic and polarizing microscope observation of core samples, we recognized the traces of past shear activity and hydrothermal alteration in the range from the fracture surface (0 mm) to 30 mm in depth. From the results of laboratory tests (diffusion test, sorption batch test focusing on mineral ratio), the porosity is generally larger near the fracture surface within this range, and the porosity becomes smaller as the distance from the fracture surface increases, resulting in an effective diffusion coefficient. The partition coefficient seemed to change according to the amount of secondary minerals, especially sericite, contained in each matrix around the fracture. In the conceptual model proposed from this, the mass transfer parameters obtained from the laboratory test are set for the range from the fracture surface to 30 mm for each width of 10 mm from the fracture surface. The region separated from the fracture surface by 30 mm or more is considered appropriate to introduce the value of non-alteration rock

©2021. Japan Geoscience Union. All Right Reserved.

as a reference value.
This study is commissioned by the Agency for Natural Resources and Energy in the Ministry of Economy, Trade and Industry. Core sampling were conducted as a part of a collaborative research with JAEA.

Keywords: geological disposal, hydrogeological structure, hydraulic conductive fracture, Toki granite, Mizunami Underground Research Laboratory, mass transport model

©2021. Japan Geoscience Union. All Right Reserved.

Development of multi-scale modeling for estimation of inflow volume into tunnels of the geological disposal facility

*Naoki Katsumata[1], Satoru Suzuki[1], Hiromitsu Saegusa[1], Tatsuya Tanaka[2], Yoshito Kitagawa[1]

1. Nuclear Waste Management Organization of Japan, 2. OBAYASHI CORPORATION

During the construction and operation of underground tunnels for geological disposal, groundwater inflow into the tunnels may occur. It is necessary to drain the inflow of groundwater to the ground surface. In case if inflow volume is large, the hydrochemical environment around the tunnel may be disturbed by up-corning the deeper water such as brine and/or drawing in the near surface water into the disposal depth. Therefore, it is important to estimate the inflow volume and to prepare measures to effectively reduce the inflow volume, prior to the construction of the underground tunnels. We therefore developed a method for estimation of inflow volume into the tunnels and effect of its decrease by applied countermeasures.

We developed the hydrogeological model for plutonic rocks, Neogene sedimentary rocks, and pre-Neogene sedimentary rocks, which are widely distributed in Japan and the modeled areas have suitable features for geological disposal. In this report, an application of our evaluation method of estimating inflow volume to the plutonic rocks model is reported.

In the case of Plutonic rocks, faults and fractures are to be characterized during site investigations since these may be the major pathway of groundwater flow. In order to develop a hydrogeological model, distribution of faults and fractures, and their transmissivity were stochastically generated using the discrete fracture network method. The hydrogeological model is composed of two different domains with different discretized mesh size; a repository scale (set to 5 km x 5 km x 1.5 km) including the underground tunnels, which is for modeling detail hydraulic heterogeneity, and a regional scale (set to 50 km x 50 km x 5 km) for setting hydraulic boundary conditions for the repository scale model.

Underground tunnels will be placed in an area where safety can be ensured during the construction, operation and after closure, taking into consideration of properties of the host rocks and distribution of the faults and fractures at the targeted depth. During construction and operation, disposal zones are divided into the ones for construction and the one for operation, and the works are carried out in parallel. It is thus important that the safety of workers is ensured in both zones. For example, there is a possibility of having abnormally large inflow when high conductive fault and tunnel are intersected each other. In order to lower the risk, the disposal zone in which many disposal tunnels are lined up in parallel should not be located where a water-conductive fault exists and the zones for construction and operation are not directly connected to avoid potential interactions, e.g. large amount of water flows in each other.

In this study, inflow volumes considering several types of tunnel layouts were estimated. As results, inflow volume into the access tunnels, which connects from surface to underground, was the largest and inflow volume into the disposal tunnels were relatively small. The reason of this result is analyzed that the disposal tunnels are located in parallel, thus local drawdown of the water table occurred around these tunnels, which result in the inflow volume is smaller than that evaluated for a single disposal tunnel. On the other hand, the access tunnel was open throughout the period of construction and operation, so the inflow volume was relatively large. The measures for reducing inflow volume such as grout at the access tunnel are effective.

©2021. Japan Geoscience Union. All Right Reserved.

The key-finding of this study was that the developed multi-scale modeling method is effective in estimating the groundwater inflow volume taking into account variation of tunnel layouts and application of measures of water inflow control. As further R&D, we are also trying to apply this method to estimate how the hydro-chemical environment changes with groundwater inflow during construction and operation of the repository.

©2021. Japan Geoscience Union. All Right Reserved.

Introduction of the “KiNa” international project of natural analogue studies of the long-term stability of bentonite

*Satoru Suzuki[1], Tsutomu Sato[2], Tsubasa Otake[2], Kikuchi Ryosuke[2], Fujimura Tatsuya[2], Takahiro Goto[1], Yusuke Ogawa[1], Patrik Sellin[3], Daniel Svensson[3], Albert H. Gilg[4], Ulf B. Andersson[5], Elizaveta Klein[6], Olivier X. Leupin[6], Simon Norris[9], Russell W. Alexander[10], Mehran Behazin[7], Nicolas Michau[8]

1. Nuclear Waste Management Organization of Japan , 2. Hokkaido University, 3. SKB, 4. TU Munich, 5. Luossavaara-Kiirunavaara AB, 6. Nagra, 7. NWMO, 8. ANDRA, 9. RWM, 10. Bedrock Geosciences

Disposal of high level radioactive waste is based on multi-barrier systems, where the barriers are supposed to retain their properties for hundreds of thousands of years. To demonstrate long term stability, experimental results can be complemented with the studies of natural systems (Natural Analogues). Bentonite is a common barrier material in many repository concepts and the aim of this natural analogue project is to assess the long-term behaviour of bentonite and its interaction with iron-minerals at the repository-like conditions.
Significant clay alteration zones have been encountered in the Kiruna (Lapland, Sweden) magnetite(-hematite)-apatite deposits, which are hosted in weakly to strongly metamorphosed intermediate to acid volcanic and subvolcanic rocks. These up to 50 m thick soft clay alteration zones occur within ores and within the country rocks along the ore contact of the southern parts of the Kiirunavaara ore body. They are found at various levels to depths of at least 1200 m below the surface, in zones further into the hanging wall and footwall lithologies of the deposit. The predominant clay mineral in the alteration zones of all deposits is a dioctahedral Fe-poor montmorillonite (Rieger 2017). K-Ar data of various Na-exchanged size fractions from two clay-altered gneiss samples from the nearby Johannes ore body, Malmberget, which are dominated by R3-ordered illite-smectite, yield age values ranging from 837 ±14 Ma to 941 ±15 Ma (Gilg et al. 2017, Rieger 2017).
In many respects, the clay layers in the Kiruna deposits resembles a bentonite barrier in a repository: the clay layers are in the meter scale, the surrounding is fractured rock under the water table and the magnetite could serve as an analogue for an iron corrosion product. A project has been initiated to further study the Kiruna clay with focus on:
geological site description and genesis of smectite-dating, mineralogical and chemical investigation understanding the very long-term behavior of bentonite under conditions of direct relevance to deep geological disposal; examination of long-term iron oxide minerals - bentonite interaction; the potential erosion properties of bentonite; and Microbiological investigation.
NUMO-Hokkaido University Joint Team is now responsible for mineralogical and geochemical investigations of iron oxide-bentonite interactions. So far, preliminary investigations have confirmed a high degree of montmorillonite, a substantial swelling pressure at high dry density, a low hydraulic conductivity and somewhat surprisingly low interaction with the magnetite.

References

Gilg HA, Rieger P, Wampler JM, Andersson UB (2017) Origin of clays in Kiruna-type iron ore deposits, Sweden. Living Clays: Clay Minerals Society Meeting, June 5th, 2017, NAIT, Edmonton, Alberta, Canada. Conference abstracts p. 22.
Rieger P (2017) Low-temperature alteration in the iron ore deposits of Norrbotten, Sweden. Master thesis. Ludwig-Maximilians University Munich, Germany, 100 pp.

©2021. Japan Geoscience Union. All Right Reserved.

Keywords: Benotnite, Iron ore, Natural Analogue

©2021. Japan Geoscience Union. All Right Reserved.

Interaction at the interface between compacted bentonite and carbon steel plate in artificial seawater

*Tatsuya Fujimura [1], Tsutomu Sato[2], Tsubasa Otake[2], Kikuchi Ryosuke[2], Satoru Suzuki[3], Takahiro Goto[3]

1. Graduate School of Engineering, Hokkaido University, 2. Faculty of Engineering, Hokkaido University, 3. Nuclear Waste Management Organization of Japan

Geological disposal of high-level radioactive waste is definitely based on multi-barrier system. The barrier system will be composed many kinds of materials such as borosilicate glass, stainless steel, carbon steel, bentonite, rock and so on. Whereas previous studies have aimed to understand respective longevity and alteration of materials, understanding of the interaction between the constituent materials in multi-barrier system is crucial for long-term safety assessments of the disposal. In this context, iron-bentonite interaction has been studied to understand alteration of bentonite by interaction with iron materials. According to some of the previous studies, montmorillonite, main constituent mineral of bentonite was changed to non-swelling clay minerals such as berthierine, iron-serpentine. Of course, this mineralogical change was clearly one of results due to the iron-bentonite interaction. However, it is not available to be assumed berthierinization for mineralogical evolution at the interface because this alteration was observed in the experiment in the system by using deionized water, powder bentonite and powder or fibrous iron to accelerate reaction, which is completely different from real situation at the interface in multi-barrier system.

This study focuses on interaction at the interface between compacted bentonite and carbon steel plate in artificial seawater to observe the alteration of minerals in the bentonite and the extent of alteration at the interface. Interface of the sample immersed in artificial seawater for three years at 80˚C under anaerobic condition was target for analyses by XRD, SEM-EDS, TEM-EDS and EPMA.

Color of the bentonite contacted with carbon steel plate was change from gray to black during the immersion in artificial seawater. Therefore, it can be easily recognized the area occurring some chemical reactions between two materials. In this area, migration of constituent element in the iron plate such as Fe and Mn into the bentonite was observed by SEM-EDS and EPMA. However, non-swelling clay minerals such as serpentine, kaolinite and chlorite were not observed based on XRD analysis. Montmorillonite was still survived in the altered area, even though small change of 060 reflection in the XRD pattern was observed, indicating change in octahedral chemistry of the montmorillonite. On the contrary, several metal carbonates such as siderite, calcite and rhodochrosite were observed in the altered area. From SEM-EDS analysis, dissolved iron reached 700 mm away from the carbon steel plate. According to iron depth profile from the line analysis, the apparent diffusion coefficient of Fe was estimated to be $3.59\times10^{-16}m^2/s$, which was clearly smaller than that obtained in previous studies for compacted bentonite (Arima et al., 2004 and Kozaki et al., 1995). Observations by electron microscopes showed formations of solid solution carbonate phases consisting Fe, Mn, Mg, Ca and Cr in the area around 100 mm away from the carbon steel plate and Fe-rich montmorillonite. The smaller apparent diffusion coefficient may be attributed to the secondary Fe-carbonate formations at the interface. Observations by electron microscopes also showed Cl ion concentrated area just at the interface. Thus, the reaction and mineralogical evolution at the interface between compacted bentonite and carbon steel plate in artificial sea water were completely different from the previous studies. Further studies including geochemical reaction and transport modeling are necessary to reproduce the above observed phenomena and to understand why there is difference in different experimental systems.

©2021. Japan Geoscience Union. All Right Reserved.

References
Arima, T., Idemitsu, K., Xia, X., Ishidera, T., & Iijima, K. (2004). Diffusion of Iron and Neptunium in Buffer Material. Evaluation.
Kozaki, T., Imamura, Y., Takada, J., Sato, S., & Ohashi, H. (1995). Corrosion of iron and migration of corrosion products in compacted bentonite.

Keywords: Iron-Bentonite interaction, Geological disposal, Engineering barrier

©2021. Japan Geoscience Union. All Right Reserved.

[J] Poster | H (Human Geosciences)：H-CG Complex & General

Sat. Jun 5, 2021 5:15 PM - 6:30 PM JST | Sat. Jun 5, 2021 8:15 AM - 9:30 AM UTC | Ch.12_3

[H-CG24] Coastal wetlands: geomorphologic, biologic and anthropogenic processes

convener:Kiyoshi Fujimoto(Nanzan University)

Coastal wetlands are very fragile environment against external environmental changes such as sea-level rise and anthropogenic impacts. On the other hand, coastal wetlands have a significant role as a place for carbon sequestration in the belowground as well as the aboveground. This session will discuss the geomorphologic, biologic and anthropogenic processes on the coastal wetlands in the various climate zones during the Holocene. For example, coastal wetlands in the tropics have evolved with the development of wetland forests such as mangrove forest, peat swamp forest and fresh water swamp forest. The most significant process for habitat formation and maintenance of the former two forests are peat production and decomposition, which are also significant processes on the coastal lowlands in the temperate and subarctic zones, though the mechanism of the processes might be different. Geomorphological processes such as sedimentation and erosion by fluvial and marine processes are also important for all of coastal wetlands. However, the environment of coastal wetlands has been destroyed by various human activities such as deforestation, agriculture land development, peat mining, and shrimp firming in and around mangrove forests in recent years. We would like to invite the wide discipline of research papers on not only the natural processes but also the anthropogenic processes in order to offer the scientific basis for creating sustainable management systems on the coastal wetlands in the future.

[HCG24-P01] Mapping of mangrove species and communities using UAV photography and high-resolution satellite data to evaluate surface erosion induced by sea-level rise on Pohnpei Island, Micronesia

*Kiyoshi Fujimoto[1], Takeki Yaguchi[1], Yasumasa HIrata[2], Shin Watanabe[3], Kodai Hasada[4], Kenji Ono[2], Shingo Taniguchi[3], Keita Furukawa[5], Saimon Lihpai[6] (1.Nanzan University, 2.Forestry and Forest Products Research Institute, 3.University of the Ryukyus, 4.Hosei University, 5.Association for Shore Environment Creation , 6.Pohnpei State Government, FSM)

[HCG24-P02] Consideration of sea level rise effect on sediment transport process in mangrove forest -preliminary attempt for long-term analysis-

*Keita Furukawa[1,2], Kiyoshi Fujimoto[3], Kenji Ono[4], Shin Watanabe[5], Shingo Taniguchi[5], Yasumasa Hirata[4], Kodai Hasada[6], Renpei Suwa[7], Saimon Lihpai[8] (1.Association for Shore Environment Creation, 2.Ocean Policy Research Institute, Sasakawa Peace Foundation, 3.Nanzan University, 4.Forestry and Forest Products Research Institute, 5.Ryukyu University, 6.Hosei University, 7.Japan International Research Center for Agricultural Sciences, 8.Pohnpei State Government)

[HCG24-P03] Comparison of Fine Root Production among Several Types of Tropical Mangrove Stands in the Federated States of Micronesia using the Continuous Inflow Estimation Method

*Kenji Ono[1], Kiyoshi Fujimoto[2], Yasumasa Hirata[3], Ryuuichi Tabuchi[3], Shingo Taniguchi[4], Shin Watanabe[4], Keita Furukawa[5], Rempei Suwa[6], Saimon Lihpai[7] (1.Tohoku research center, Forestry and Forest Products Research Institute, 2.Nanzan Univ., 3.Forestry and Forest Products Research Institute, 4.Univ. of Ryukyu, 5.Association for Shore Enviromnent Creation, 6.Japan International Research Center for Agricultural Science, 7.Phonpei State Gov. FSM)

Mapping of mangrove species and communities using UAV photography and high-resolution satellite data to evaluate surface erosion induced by sea-level rise on Pohnpei Island, Micronesia

*Kiyoshi Fujimoto[1], Takeki Yaguchi[1], Yasumasa HIrata[2], Shin Watanabe[3], Kodai Hasada[4], Kenji Ono[2], Shingo Taniguchi[3], Keita Furukawa[5], Saimon Lihpai[6]

1. Nanzan University, 2. Forestry and Forest Products Research Institute, 3. University of the Ryukyus, 4. Hosei University, 5. Association for Shore Environment Creation , 6. Pohnpei State Government, FSM

In the western Pacific low-latitude region between the Philippines and Micronesia, the sea level has been rising at over 10 mm/yr (IPCC 2013). In the mangrove habitat situated in the low sediment inflow environment, *Rhizophora* pure forest is generally formed as a pioneer community and mangrove peat is created. However, the mangrove peat accumulation rate is considered to decrease with the vegetation succession because of the decline of tree density of *Rhizophora* sp. The mangrove communities decreased mangrove peat accumulation rate is possibly affected by sea-level rise first. In Pohnpei Island, Micronesia, the surface erosion is not recognized in the *Rhizophora stylosa* and *Rhizophora apiculata* communities yet, while it is recognized in the communities dominated by other species.

In this study, we create canopy projections for existed permanent plots using UAV photography and ground data first. Secondly, we examine an auto-detect method for mangrove species using the high-resolution satellite data by reference to the canopy projections. Finally, we zone communities based on Mochida et al. (2006) using the mangrove species distribution maps.

UAV photography enable us to identify mangrove species from the size, shape and color of crown. *R. apiculata* has round and relatively small crown with green and brownish to yellowish green. *R. stylosa* has similar features, though their crown loose shape with more brownish color. The two species can be identified from the distribution pattern, i.e., the former widely distribute to the interior, while the latter develop along the seaward forest edge only. *Sonneratia alba* has large and irregular shape crown with yellowish green. *Bruguiera gymnorrhiza* has relatively roundish crown with blueish green and appear in the space among other species with relatively low tree height. *Xylocarpus granatum* has irregular shape crown with emerald green and appear among other species as with *B. gymnorrhiza*.

Pan sharpening using Panchromatic ortho image (ground resolution: 40 cm) and 8 bands multispectral ortho image (ground resolution: 1.6 m) by WorldView-3 (taken on October 17, 2018) enable us to identify some mangrove species automatically. ArcGIS Pro was used for the Pan sharpening and GIMP 2.10.22 was used for auto-detect of mangrove species. As the result, three groups, i.e., 1) *R. apiculata* or *R. stylos* a, 2) *S. alba* and 3) *B. gymnorrhiza* or *X. granatum* were identified automatically. We can create mangrove community map by considering the distribution pattern for *R. stylosa* and *X. granatum*, i.e., the former distributes along seaward edge only and the latter appears in a climax forest with low tree density. The mangrove community map will enable us to create an evaluation map of surface erosion induced by sea-level rise with consideration for tree density of *Rhizophora* species and distance from the seaward forest edge.

Keywords: Mangrove, Sea-level rise, UAV photography, High-resolution satellite data, Species distribution map, Vegetation community map

©2021. Japan Geoscience Union. All Right Reserved.

©2021. Japan Geoscience Union. All Right Reserved.

Consideration of sea level rise effect on sediment transport process in mangrove forest -preliminary attempt for long-term analysis-

*Keita Furukawa[1,2], Kiyoshi Fujimoto[3], Kenji Ono[4], Shin Watanabe[5], Shingo Taniguchi[5], Yasumasa Hirata[4], Kodai Hasada[6], Renpei Suwa[7], Saimon Lihpai[8]

1. Association for Shore Environment Creation, 2. Ocean Policy Research Institute, Sasakawa Peace Foundation, 3. Nanzan University, 4. Forestry and Forest Products Research Institute, 5. Ryukyu University, 6. Hosei University, 7. Japan International Research Center for Agricultural Sciences, 8. Pohnpei State Government

Preliminary measurement for detecting sea level rise (SLR) effects on mangrove forests has been observed at Iriomote Island, Japan and Ponpei Island, Federal States of Micronesia since 2018. The short term SLR effects were measured by surface erosion and sedimentation. If sedimentation rate on a mangrove forest floor is faster enough to catch up with SLR, the forest will adapt on the change (Fujimoto et.al. 1989). Nevertheless, if it is slower than SLR, or erosion rate becomes greater than sedimentation rate, the forest will NOT adapt on the change (Furukawa et.al. 2002).

According to the observations, existence of following sediment transport mechanisms was suggested i.e. the existence of a sheet-flow transport mechanism in a short period of time when seawater is flooded and drained, the occurrence of steady erosion due to tidal transports, and the temporally and spatially uneven transport mechanism (Furukawa et al. 2019). In particular, it is necessary to clarify the effects of sediment supply from the upstream and micro-topography (creeks) existing on the forest floor.

Therefore, we attempted to measure two-dimensional sedimentation rate and sediment transport in the plot with complex topography conditions in 2019 (Pompeii PK plot: Fujimoto et al. 2019). In particular, we attempted to measure the effects of sediment supply from the upstream side, microtopography (creeks) existing on the forest floor, two-dimensional deposition rate, and sediment transport. In order to examine the effects of tides and rainfall, we observed the spring tide period (during fine weather) and the low tide period (during rainfall) and conducted a short-term trend analysis (Furukawa et al. 2020).

We adapted the typified segment transport mode to the climate data in the area and examined the methodology for examining the long-term trend of change in the plot. It was shown that it is indispensable to carry out long-term continuous observations or use a so-called outflow model in the future.

This research has been done as a part of “Mangrove forests community situation understanding against SLR.”

Keywords: Sea Level Rise, Mangrove Forest, Sediment Transport

©2021. Japan Geoscience Union. All Right Reserved.

Comparison of Fine Root Production among Several Types of Tropical Mangrove Stands in the Federated States of Micronesia using the Continuous Inflow Estimation Method

*Kenji Ono[1], Kiyoshi Fujimoto[2], Yasumasa Hirata[3], Ryuuichi Tabuchi[3], Shingo Taniguchi[4], Shin Watanabe[4], Keita Furukawa[5], Rempei Suwa[6], Saimon Lihpai[7]

1. Tohoku research center, Forestry and Forest Products Research Institute, 2. Nanzan Univ., 3. Forestry and Forest Products Research Institute, 4. Univ. of Ryukyu, 5. Association for Shore Enviromnent Creation, 6. Japan International Research Center for Agricultural Science, 7. Phonpei State Gov. FSM

The dynamics of blue carbon (BC), that is sequestered and stored in the ocean ecosystems (IPCC 2009), has gained considerable attention due to recent alarming concern about global warming. The BC stocks are substantial in the ocean ecosystems and they play an important role in global climate change mitigation (Alongi 2018). Mangrove forests are major components of coastal ecosystems in the tropical and subtropical zones. They are highly productive ecosystems with mean sequestration rates of organic carbons in the earth as well as salt marsh and seagrass ecosystems (Alongi 2020). Donate et al. (2011) described mangrove ecosystems as “among the most carbon(C)-rich forests in the tropics.”
Previous studies suggest that the high ability of C accumulation and sequestration in submerged soils of mangrove ecosystems are ensured by the high productivity of biomasses above and below the ground, especially that of root production. However, our understanding about the contribution of fine root production in mangrove ecosystems due to C sequestration and its fluxes is that blue carbons are limited by difficulties and uncertainties associated with fine root dynamics, such as their stocks, fluxes, and longevity in the invisible belowground root systems (Majdi and Kangas 1997).
On the other hand, recent reports proposed new approaches for estimating fine root dynamics in terrestrial forest ecosystems (Osawa and Aizawa 2012, Do et al. 2016). These approaches include continuous inflow estimate methods, which can provide more accurate and comprehensive evaluations of the fine root dynamics estimated by a simple mass balance model with compartments (i.e., stocks of living and dead masses) and flow (production, mortality, and decomposition) of organic materials originating from fine roots.
In this study, we tried to clarify the contribution of fine root dynamics including the processes of production, mortality, and decomposition to net primary production in mangrove ecosystems and carbon sequestration in BC ecosystems. To achieve this purpose, we performed continuous inflow estimates of fine root dynamics at several types of mangrove stands in Pohnpei Is., Federated States of Micronesia (FSM), by using a simple mass balance model with a combination of an ingrowth core method and litterbag experiment according to a study by Osawa and Aizawa (2012). In this presentation, we will report our findings related to these topics.

Keywords: Mangrove, Sea level rise, Fine root production, Blue carbon

©2021. Japan Geoscience Union. All Right Reserved.

[J] Oral | H (Human Geosciences)：H-CG Complex & General

Sat. Jun 5, 2021 3:30 PM - 5:00 PM JST | Sat. Jun 5, 2021 6:30 AM - 8:00 AM UTC | Ch.17 Zoom Room 17

[H-CG27] Nuclear Power and Geoscience in Japan: 10 years after the 3.11 complex disaster

convener:Daisuke Suetsugu(institute for Marine Geodynamics, Japan Agency for Marine-Earth Science and Technology), Kohta Juraku(Department of Humanities, Social and Health Sciences, School of Engineering, Tokyo Denki University), Satoshi Kaneshima(Department of Earth and Planetary Sciences, Kyushu University), Takeshi Sagiya(Disaster Mitigation Research Center, Nagoya University), Chairperson:Daisuke Suetsugu(institute for Marine Geodynamics, Japan Agency for Marine-Earth Science and Technology), Takeshi Sagiya(Disaster Mitigation Research Center, Nagoya University)

Nuclear Power and Geoscience in Japan: 10 years after the 3.11 complex disaster
We have organized sessions in the JpGU meeting on the risk of nuclear power utilization in Japan mainly from the point of view of geoscience since 2013. It has shed new light on various aspects of the risk of nuclear power related to earthquakes, volcanic activities and tsunamis. The 2021 JpGU meeting will be held 10 years after the 3.11 complex disaster: the Great East Japan Earthquake with the Fukushima-Daiichi nuclear accident. On this occasion, we propose a reflexive session to review what we have discussed and understood through the past sessions or public debates: What should geoscience take the stance on the issue of scientific uncertainty and nuclear risk? How could scientists and engineers work together for public goods? We are also welcome to papers of other topics relevant to relationship of geoscience and nuclear utilization.

3:30 PM - 3:45 PM JST | 6:30 AM - 6:45 AM UTC

[HCG27-01] How was the long-term forecast of tsunami earthquake distorted?

★Invited Papers

*Kunihiko Shimazaki[1] (1.University of Tokyo)

3:45 PM - 4:00 PM JST | 6:45 AM - 7:00 AM UTC

[HCG27-02] Changes in the Treatment of Scientific Issues in Nuclear Power Plant Trials

★Invited Papers

*Kazuki Koketsu[1] (1.Earthquake Research Institute, University of Tokyo)

4:00 PM - 4:15 PM JST | 7:00 AM - 7:15 AM UTC

[HCG27-03] Human Capacity Building at The University of Tokyo towards Knowledge Base Development for Nuclear Risk Management

*Tatsuya Itoi[1], Naoto Sekimura[1], Tsuyoshi Takada[1,2], Takumi Saito[1], Kenji Satake[1] (1.The University of Tokyo, 2.Japan Atomic Energy Agency)

4:15 PM - 4:30 PM JST | 7:15 AM - 7:30 AM UTC

[HCG27-04] Scientific characteristics of high-level nuclear waste disposal site -Geological perspective at Suttsu and Kamoenai areas, Hokkaido -

★Invited Papers

*Satoshi Okamura[1] (1.Hokkaido Education University)

4:30 PM - 4:45 PM JST | 7:30 AM - 7:45 AM UTC

[HCG27-05] Selection of high-level radioactive waste disposal site in Japan

★Invited Papers

*Masahiro Chigira[1] (1.Fukada Geological Institute)

4:45 PM - 5:00 PM JST | 7:45 AM - 8:00 AM UTC

[HCG27-06] Discussion

*Daisuke Suetsugu[1] (1.institute for Marine Geodynamics, Japan Agency for Marine-Earth Science and Technology)

How was the long-term forecast of tsunami earthquake distorted?

*Kunihiko Shimazaki[1]

1. University of Tokyo

Tokyo Electric Power Co. (TEPCO) did not respond to the warning of huge tsunami publicized in 2002 by the governmental committee named Earthquake Research Committee (ERC). The 11th March 2011 tsunami and severe shakings attacked Fukushima Daiichi of TEPCO and caused level-7 severe nuclear accidents. This reports how TEPCO and related forces distorted the science. Relying on some authority they insist on one-sided argument on professional items. Several actual examples are shown. One is related to ‘Tsunami Assessment Method for Nuclear Power Plants in Japan’ by Tsunami Evaluation Subcommittee of the Japan Society of Civil Engineers, and another comes from poor Japanese seismological education on seismic hazard analysis.

Keywords: nuclear power plant, long-term forecast, March 11th tsunami

©2021. Japan Geoscience Union. All Right Reserved.

Changes in the Treatment of Scientific Issues in Nuclear Power Plant Trials

*Kazuki Koketsu[1]

1. Earthquake Research Institute, University of Tokyo

Since strong ground motions causing damage to nuclear power plants are rare phenomena, it is difficult to state with certainty whether or not they occur in several ten years, which is the operating period of nuclear power plants, and such scientific issues involve large incertitude. However, in order to make a serious conclusion to stop the operation of a nuclear power plant, it is necessary to carry out the reasoning which is deterministic to some extent, and in the judgments until now, there were many unreasonable things on the scientific issues. However, in the judgment of Osaka District Court on "request for an order to suspend operation of the Oi nuclear power plant" in December, 2020, unreasonable reasoning was not carried out for the scientific issues in Point 2 (Rationality of the formula of Irikura and Miyake and the formula of Dan et al.) and Point 3 (Rationality of using the seismic moment calculated based on the Irikura-Miyake formula as the seismic moment of a source model). Instead, the main issue was the failure of the defendant (the electric power company) to comply with "variation clause" ("When the earthquake scale is set using an empirical formula which relates the length or area of the source model or the fault displacement in a seismic cycle with the earthquake scale, it is necessary to also consider the variation of an empirical formula, because an empirical formula (. . .) gives the earthquake scale as an average value.") in the Seismic Ground Motion Review Guide. In other words, the incertitude in scientific issues was avoided by replacing it with a procedural problem.

Until then, it had been considered that the variation in the calculation of earthquake scale had been already taken into consideration by conservatively setting an earthquake source model (i.e., the model is set on the safe side), however, in the judgment, it is considered that the latter half of "variation clause" had to be taken into consideration explicitly and independently, because it was specially added in March 2012. Furthermore, one of the reasons why it is reasonable to use the Irikura-Miyake formula for the source fault as the result of active fault investigation from the ground surface is that the source model is set conservatively, so it is not appropriate to use it as a double reason.

Keywords: Nuclear Power Plant Trials, Scientific Issues, Changes in the Treatment

©2021. Japan Geoscience Union. All Right Reserved.

Human Capacity Building at The University of Tokyo towards Knowledge Base Development for Nuclear Risk Management

*Tatsuya Itoi[1], Naoto Sekimura[1], Tsuyoshi Takada[1,2], Takumi Saito[1], Kenji Satake[1]

1. The University of Tokyo, 2. Japan Atomic Energy Agency

For robust and effective nuclear regulation under uncertainties like the performance of safety-critical facilities like nuclear power plants exposed to natural hazards, the following items are required,
- a multi-diciplinary framework that bridges the gaps and integrates engineering, natural sciences and the social sciences,
- corporation with societies based on in-depth understanding of societies and diverse perspectives,
- human capacity building facilitating multi-diciplinary network,
- harmonization between compliance-based activities and proactive risk management including innovation.

The characteristics of decision makings under uncertainties like the performance of safety-critical facilities like nuclear power plants exposed to natural hazards that are considered important are integrating the following two aspects in a consistent manner:
- full utilization of wide range of scientific and engineering knowledge,
- impossibility to reach single decision (trans-scientific aspects).

It is considered important that higher education contributes to this field, especially for delivering experts who can discuss and make decisions on performance of safety-critical facilities considering regional characteristics and regional risk reduction including:
- holistic perspective,
- standardization,
- gap identification and change management

Based on this understanding, the University of Tokyo, collaboting with Japan Atomic Energy Agancy and supported from Japan Nuclear Regulation Authority (NRA), launched a human capacity building program towards development of knowledge base for nuclear risk management.

A proposed project comsists of:
A) Lecture for graduate students on "Disaster Risk Management of Engineering System" that provides a framework integrating engineering, natural science and the social sciences,
B) Special lectures from distinguised experts from international organizations etc.,
C) Site visit and discussion with nuclear experts,
D)
D-1) Excecises on risk-informed decitions, including treatment of updated knowledge under and management of conflicts,
D-2) Project based learning of nuclear safety research related to risk management,
E) Internships in international organization and/or research organizations,
F) Stakeholder workshops.

Keywords: Risk management, Nuclear safety, Natural hazard

©2021. Japan Geoscience Union. All Right Reserved.

©2021. Japan Geoscience Union. All Right Reserved.

Scientific characteristics of high-level nuclear waste disposal site -Geological perspective at Suttsu and Kamoenai areas, Hokkaido -

*Satoshi Okamura[1]

1. Hokkaido Education University

The “Scientific Characteristic Map” was published in 2017 to indicate selection site for high-level nuclear waste final repository in Japan. In 2020, based on the proposals from two municipalities, Suttsu and Kamoenai in Hokkaido, a literature search, which is the first stage of the selection of the disposal site survey, was started. The two municipalities have suitable sites for the final repository after the “Scientific Characteristic Map”. The geological characteristics of both areas, however, indicate definitely non suitability for the final depository. The two areas are characterized by Middle to Late Miocene volcanic rocks, such as pillow lava, hyaloclastite, feeder dyke, and reworked volcaniclastic rocks. The mode of occurrence has very heterogeneous and concealed cracks and fractures. The Suttsu area is situated at northern part of the active fault, the Kuromatsunai Lowland active faults. It may be impossible to judge the suitability as a disposal site in Japan from the recent scientific point of view.

Keywords: Scientific Characteristic Map, High-level nuclear waste, final repository, hyaloclastite

©2021. Japan Geoscience Union. All Right Reserved.

Selection of high-level radioactive waste disposal site in Japan

*Masahiro Chigira[1]

1. Fukada Geological Institute

I pointed out problems with the selection of high-level radioactive waste disposal site in Japan with a paper entitled “What is indispensable studies to achieve the disposal of high-level radioactive waste in Japan?” at this session of JpGU in 2018.. I said that we cannot avoid uncertainties in groundwater scenarios even though direct scenarios by fault movement, volcanic activity, uplift and erosion, and so on are cleared, so we need to find host rocks with fewer fractures as water pathways. We also need to select host rocks on which present nondestructive prospecting methods are applicable to find fractures or to develop new methods that could be used to difficult rocks. This view should have been reflected in the “Scientific Characteristic Map” published in July 2017, but this map is for the direct scenario and does not face the groundwater scenario head-on. Then, in 2020, based on the proposals from two municipalities in Hokkaido, a literature search, which is the first stage of the selection of the disposal site survey, was started. This started without any geological considerations for the groundwater scenario mentioned above, as far as I know. Although I have not directly observed the local geology, I would like to point out problems related to groundwater scenarios that would be encountered in the future from the geological literature of the area and my research experience of similar geology.

Geological sheets with a scale of 1:50000 of the two municipalities show that these areas are underlain by Miocene volcanics, such as lava and hyaloclastite intruded by volcanic dikes. The former two are generally very heterogeneous and their properties widely vary from place to place. They also have openings so that may be highly permeable. Volcanic dikes are generally permeable because of cooling joints, and their presence is not easy to detect with current nondestructive technology. These features provide conditions that make it very difficult to evaluate groundwater scenarios.

According to Japan's policy, the selection of high-level radioactive waste geological disposal sites will be carried out step by step. If the suitability as a disposal site is clearly lacking, it would be excluded from the suitable site during the investigation stage, but if it is unclear, the investigation would proceed to the next stage. If the survey is conducted on areas with complex geology and strong inhomogeneity, it is easy to assume that the suitability cannot be judged from the survey results at one stage and then proceed to the next stage. However, the local problems with the groundwater scenario mentioned above do not seem to be so easy to solve. In other words, it is necessary to keep in mind that no matter how far the investigation is conducted, it may not be possible to judge the suitability as a disposal site in a socially acceptable manner.

Keywords: High-level radioactive waste, Geological disposal, Site selection, Groundwater scenario, Volcanics, Uncertainty

©2021. Japan Geoscience Union. All Right Reserved.

Discussion

*Daisuke Suetsugu[1]

1. institute for Marine Geodynamics, Japan Agency for Marine-Earth Science and Technology

We would like to have a general discussion on broad issues as follows: What should geoscience take the stance on the issue of scientific uncertainty and nuclear risk? How could scientists and engineers work together for public goods?

Keywords: Nuclear power plants, Geoscience

©2021. Japan Geoscience Union. All Right Reserved.

[J] Poster | H (Human Geosciences)：H-CG Complex & General

Sat. Jun 5, 2021 5:15 PM - 6:30 PM JST | Sat. Jun 5, 2021 8:15 AM - 9:30 AM UTC | Ch.12_4

[H-CG27] Nuclear Power and Geoscience in Japan: 10 years after the 3.11 complex disaster

convener:Daisuke Suetsugu(institute for Marine Geodynamics, Japan Agency for Marine-Earth Science and Technology), Kohta Juraku(Department of Humanities, Social and Health Sciences, School of Engineering, Tokyo Denki University), Satoshi Kaneshima(Department of Earth and Planetary Sciences, Kyushu University), Takeshi Sagiya(Disaster Mitigation Research Center, Nagoya University)

Nuclear Power and Geoscience in Japan: 10 years after the 3.11 complex disaster
We have organized sessions in the JpGU meeting on the risk of nuclear power utilization in Japan mainly from the point of view of geoscience since 2013. It has shed new light on various aspects of the risk of nuclear power related to earthquakes, volcanic activities and tsunamis. The 2021 JpGU meeting will be held 10 years after the 3.11 complex disaster: the Great East Japan Earthquake with the Fukushima-Daiichi nuclear accident. On this occasion, we propose a reflexive session to review what we have discussed and understood through the past sessions or public debates: What should geoscience take the stance on the issue of scientific uncertainty and nuclear risk? How could scientists and engineers work together for public goods? We are also welcome to papers of other topics relevant to relationship of geoscience and nuclear utilization.

[HCG27-P01] Nuclear Power and Geoscience in Japan

*Daisuke Suetsugu[1], Satoshi Kaneshima[2], Takeshi Sagiya[4], Kohta Juraku[3] (1.institute for Marine Geodynamics, Japan Agency for Marine-Earth Science and Technology, 2.Department of Earth and Planetary Sciences, Kyushu University, 3.Department of Humanities, Social and Health Sciences, School of Engineering, Tokyo Denki University, 4.Disaster Mitigation Research Center, Nagoya University)

[HCG27-P02] Model and “Unexpected”

*Manabu Hashimoto[1] (1.Disaster Prevention Research Institute, Kyoto University)

[HCG27-P03] Does science give us THE answer? (2)
Issues centering on scientific advice

*Kohta Juraku[1] (1.Department of Humanities, Social and Health Sciences, School of Engineering, Tokyo Denki University)

[HCG27-P04] A personal summary of JPGU sessions about earth science and nuclear power plants in Japan

*Satoshi Kaneshima[1] (1.Department of Earth and Planetary Sciences, Kyushu University)

[HCG27-P05] Has the situation surrounding nuclear power generation and earth science changed during the last decade?

*Takeshi Sagiya[1] (1.Disaster Mitigation Research Center, Nagoya University)

Nuclear Power and Geoscience in Japan

*Daisuke Suetsugu[1], Satoshi Kaneshima[2], Takeshi Sagiya[4], Kohta Juraku[3]

1. institute for Marine Geodynamics, Japan Agency for Marine-Earth Science and Technology, 2. Department of Earth and Planetary Sciences, Kyushu University, 3. Department of Humanities, Social and Health Sciences, School of Engineering, Tokyo Denki University, 4. Disaster Mitigation Research Center, Nagoya University

Severe accident of the Fukushima-Daiichi nuclear power plant was caused by the 2011 Great East Japan earthquake and tsunami. Looking at the seriousness and broad extent of the accident, many geoscientists, including the authors, realized ourselves as those who have to consider the risk of nuclear power plants seriously, which motivated us to organize sessions in the JpGU meeting on the risk of nuclear power utilization in Japan mainly from the point of view of geoscience since 2013. It has shed new light on various aspects of the risk of nuclear power related to earthquakes, volcanic activities and tsunamis. The 2021 JpGU meeting will be held 10 years after the 3.11 complex disaster: the Great East Japan Earthquake with the Fukushima-Daiichi nuclear accident. On this occasion, we review what we have discussed and understood through the past sessions or public debates: What should geoscience bear geoscience hazard and risk of nuclear power plants to engineers, policy-makers, and Japanese people, with an emphasis on inevitably great uncertainty? Issues of the nuclear power plants in Japan are not only geoscientific risk, but including energy balance, economics and environment problems. How can we create a ‘public space’ consisting of all the stake-holders to discuss future of the nuclear power in Japan?

Keywords: Nuclear power plants, Geoscience

©2021. Japan Geoscience Union. All Right Reserved.

Model and “Unexpected”

*Manabu Hashimoto[1]

1. Disaster Prevention Research Institute, Kyoto University

Since the occurrence of the Great East Japan Earthquake Disaster, I have participated in several committees for the reexamination of earthquake countermeasures including the Nankai Trough earthquake. Under the banner of "No More Unexpected", model of the largest possible earthquake was asked to be discussed there, and various models were proposed. Ground motion and tsunami were calculated on the basis of these models, to estimate damages. As a result, the forecast of extremely large damage was announced, which shook the society. Since then, experts in surrounding fields and media have repeatedly used this estimate along with their arguments, which makes only these numbers prevalent. I guess some people are disgusted with the current situation.

By the way, what is a model on earth? In earth science, a wide variety of models are used, from conceptual qualitative models to precise numerical models with multiple degrees of freedom and analog models using actual materials. Just as the sand pile model, which is composed only of addition and subtraction calculations, creates a power law, even a highly abstracted model can show us the essence of the phenomenon. The analog model is constructed on a laboratory scale in order to understand the mechanism of phenomena that cannot be reproduced on a real scale. The model is extremely useful for understanding the phenomenon, because similar results can be obtained even if a third party executes them with the same settings.

On the other hand, the society counts on model’s predictability. Models of atmospheric phenomena have been used for future forecasts of weather and climate for many years, and information based on these forecasts are now a part of our lives. Following this success, models of generation of earthquakes and related disasters, such as long-term probabilistic forecast, strong ground motion prediction and tsunami forecast, are used. Based on these results, countermeasures are established, and building codes for important structures such as nuclear power plants and bridges are set.

However, the model is based on assumptions where complex factors are omitted. Therefore, the application of the model should be limited, but there are discussions that unconsciously go beyond, aren’t there? For example, the dislocation model, which is widely used in earthquake research, is also an approximate solution; the assumption of infinitesimal deformation is broken in the close vicinity of the fault. Long-term probability is calculated as a point process in which only earthquakes of a certain size or larger are extracted from the time series of earthquake occurrence. In the prediction of strong ground motion and tsunami, many assumptions such as homogeneous semi-infinite medium or stratified structure are made in the analysis, and the shape of the fault is an extremely simple rectangle. Real faults and structure are very complicated, but such complexities are stripped off. There is no assessment of the impact of the stripped elements and it is treated as an uncertainty that is difficult to quantify. Perhaps the "unexpected" is lurking there. We cannot rule the “unexpected” out.

Only researchers can criticize the validity of the model on which damage estimation is based from a professional viewpoint. Why not just make a statement, not just bitter?

©2021. Japan Geoscience Union. All Right Reserved.

Keywords: model, unexpected, earthquake science

©2021. Japan Geoscience Union. All Right Reserved.

Does science give us THE answer? (2) Issues centering on scientific advice

*Kohta Juraku[1]

1. Department of Humanities, Social and Health Sciences, School of Engineering, Tokyo Denki University

It has been discussed the relationship between the risk of nuclear utilization and geoscience, the role of scientist and engineer in the previous sessions. The author has analyzed those issues from the perspectives of interactions and gaps between science and engineering, their views on risk and safety behind the social mechanism and their senses of vocation, and pursued the better way to overcome the obstacles centering on them. This year, he would like to discuss the issues centering on so-called "scientific advice" in geo science field, in comparison with the case of the COVID-19 pandemic.

Before the 10th anniversary of the 3.11 complex disaster, the world faced the pandemic. The role, function and method of effective scientific advice to the policy has been attracted the public attention.

We have witnessed a wide-spread suspicion among the public that the relevant "experts" distort their scientific advice to government and society because of their own political and social interests, or politicians and bureaucrats cherry-pick or just neglect the expert's advices to protect themselves from public criticism. Very similar arguments were observed in the 3.11 disaster. We even saw the word *Goyo-gakusha* (lap-dog expert) again when people criticized the governmental public health advisors, exactly same to the Fukushima nuclear disaster case.

It was reasonable to use the word to criticize nuclear experts because they had a strong interest to trivialize the magnitude of the nuclear disaster to protect their nuclear technology, however, epidemiologist, virologist and pharmacologist could never share the interest with the COVID virus itself nor COVID-19 syndrome. Rather, it should even be advantageous to them to build a social consensus that the pandemic is more serious than the other people thought. Thus, it is questionable to use the same *Goyo-gakusha* rhetoric to critically analyze the problems behind the shortcomings of (Japanese) government's counter measures.

It must have a universal implication to answer this question for geoscientists who are involved in or interested in the relationship between the geoscience and the risks of nuclear technology. By touching upon the relevant frameworks on scientific advice in the field of STS, this paper try to answer the question.

Keywords: scientific advice, COVID-19, risk of nuclear technology, science and technology studies (STS)

©2021. Japan Geoscience Union. All Right Reserved.

A personal summary of JPGU sessions about earth science and nuclear power plants in Japan

*Satoshi Kaneshima[1]

1. Department of Earth and Planetary Sciences, Kyushu University

In this poster I discuss about the issues regarding the uncertainty of the scientific knowledge that earth scientists can provide for our society in order to help mitigate hazards associated with nuclear power plants. Through the series of our JPGU sessions held since 2013 about the relation between nuclear power plants and earth science, a consensus seems to have been reached among the participants. It is the recognition of substantial uncertainty inherent in the forecasts and/or evaluations on important issues such as the maximum size of earthquake at the trenches, the maximum ground motions anticipated at specific nuclear sites, and the long term safety of the nuclear waste deposition sites. Although this recognition seemingly is also shared by our society to some extent since the 2011 great Tohoku earthquake, the earth science community has to relentlessly keep announcing serious difficulties that any attempts to give reliable assessment must face. As long as the earth science issues mentioned above are concerned, the earth science community present day should not recommend a specific scientific model or evaluation for the society or policymakers to take, but rather should provide with the range of uncertainty in the models as clearly as possible. The community now needs to specifically develop an efficient system that can objectively and reasonably define the uncertainty ranges about those issues.

Keywords: nuclear power plants, earth scientific khowledge, uncertainty

©2021. Japan Geoscience Union. All Right Reserved.

Has the situation surrounding nuclear power generation and earth science changed during the last decade?

*Takeshi Sagiya[1]

1. Disaster Mitigation Research Center, Nagoya University

10 years have passed since the 2011 Great East Japan Earthquake and its disaster. After this disaster, The Seismological Society of Japan launched a special committee to discuss responses to this disaster and I served as the chair. We concluded with the following recommendation. "The seismological community should recognize the situation surrounding their research with sound criticism and we need to improve communication both inside and outside of the academic society" (Sagiya, 2012). After that, as a part of an attempt to put this recommendation in practice, we have been organizing a JpGU session where relationship between nuclear power generation and earth science is discussed. Looking back on these sessions, we can recognize various advances in earth science research and more interdisciplinary communication. On the other hand, the gap between the nuclear power generation side and general earth scientists sill exists. Scientists can mention possible future disasters, but such claim has a large uncertainty. The actual decision differs greatly depending on the treatment of the uncertainty. In order to make a proper decision, multidisciplinary discussion in a "public" space is indispensable, which has not been established yet. Considering such a situation, I would argue that the recommendation in 2012 is still valid.

Keywords: earth science, nuclear power generation, public space, social responsibility of scientists

©2021. Japan Geoscience Union. All Right Reserved.

[E] Poster | S (Solid Earth Sciences)：S-SS Seismology

Sat. Jun 5, 2021 5:15 PM - 6:30 PM JST | Sat. Jun 5, 2021 8:15 AM - 9:30 AM UTC | Ch.13_1

[S-SS03] New insights in Earthquake predictability: modelling and forecasting

convener:Hiroshi Tsuruoka(Earthquake Research Institute, Tokyo Univ.), Jiancang Zhuang(Institute of Statistical Mathematics), Danijel Schorlemmer(GFZ German Research Centre for Geosciences), Naoshi Hirata(National Research Institute for Earth Science and Disaster Resilience)

Probabilistic models have been developed for describing, analyzing, and forecasting seismicity, including recurrence and stress-release models for long-term earthquake hazard assessment, and short-term models describing earthquake clustering, e.g. the ETAS model. Some models have become standard tools in seismic hazard assessment. The Collaboratory for the Study of Earthquake Predictability and its Japan branch has provided the testing capabilities for rigorous and unbiased evaluation of forecasting models. This session invites contributions of model developments based on the increased understanding of the physical process of earthquakes, such as the preparation and rupture processes of the earthquake source and the interaction between earthquakes and tectonic environments. We also welcome development and implementation of improved statistical methods for forecasting seismicity

[SSS03-P01] A spherical version of the space-time ETAS model

*Jiancang Zhuang[1], Ziyao Xiong[1], Yosihiko Ogata[1] (1.Institute of Statistical Mathematics)

[SSS03-P02] Nonstationary Renewal Model for Forecasting Repeating Earthquakes under Aftershock-Triggering Effects

*Shunichi Nomura[1], Masayuki Tanaka[2] (1.The Institute of Statistical Mathematics, 2.Meteorological Research Institute)

[SSS03-P03] Machine Learning Models for Earthquake Number Forecasting in the Kanto Region

*Hanyuan Huang[1], Hiroe Miyake[1], Hiroshi Tsuruoka[1] (1.Earthquake Research Institute, University of Tokyo)

A spherical version of the space-time ETAS model

*Jiancang Zhuang[1], Ziyao Xiong[1], Yosihiko Ogata[1]

1. Institute of Statistical Mathematics

In this study, by modifying the spatial response function in the triggering term, we propose and implement a spherical version of the space-time ETAS model. At the small local scale, the new model is equivalent to the original 2D planar ETAS model. We analyze and forecast global seismicity with this new model, and test some interesting hypotheses related to global seismicity, such as antipolar triggering phenomena.

Keywords: ETAS model, Spherical, earthquake clustering, earthquake forecast

©2021. Japan Geoscience Union. All Right Reserved.

Nonstationary Renewal Model for Forecasting Repeating Earthquakes under Aftershock-Triggering Effects

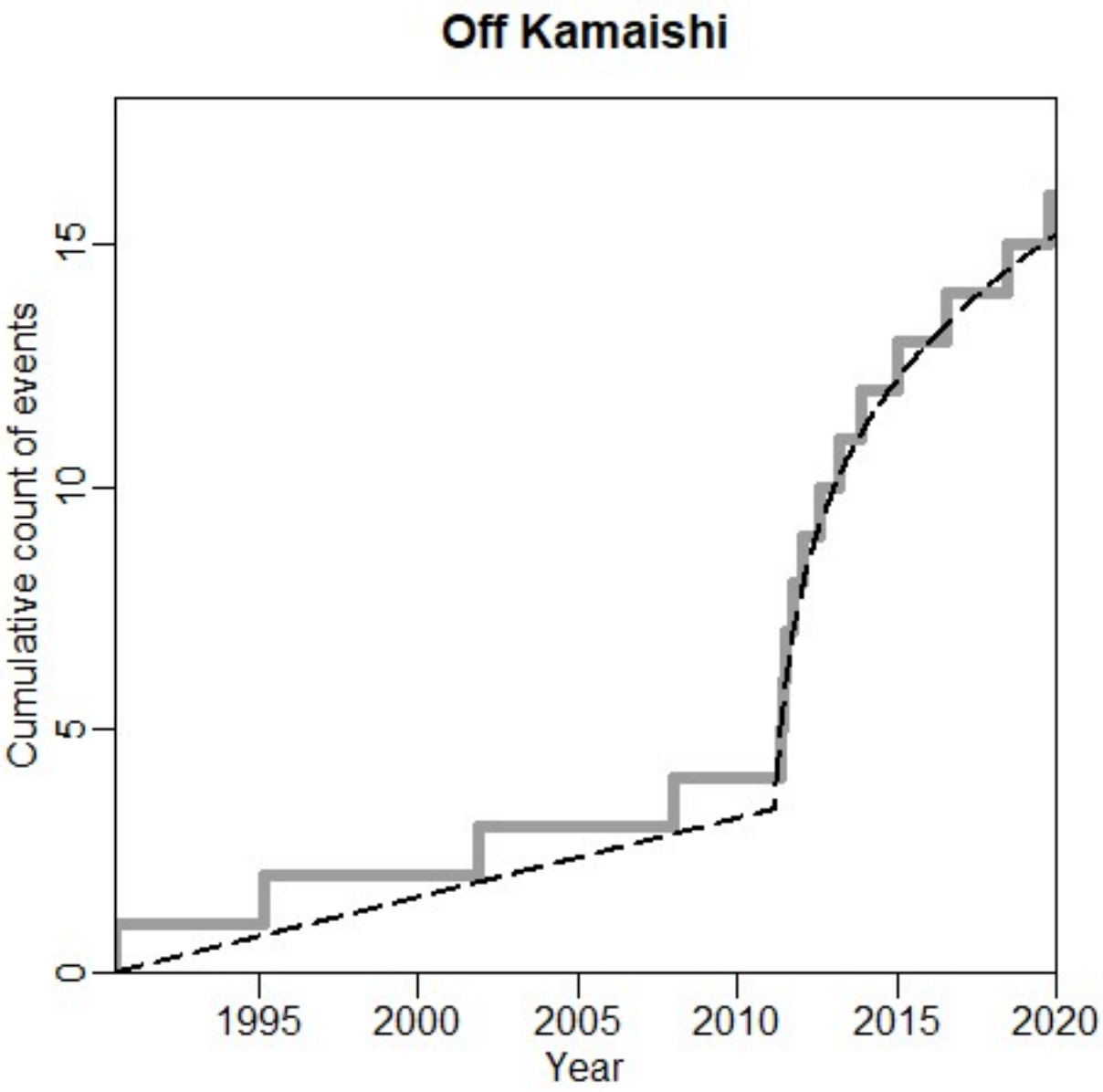
*Shunichi Nomura[1], Masayuki Tanaka[2]

1. The Institute of Statistical Mathematics, 2. Meteorological Research Institute

The point process models to predict earthquake occurrences are roughly classified into two types except for the simplest Poisson process; one is the renewal process for repeating earthquakes and the other is the ETAS (Epidemic-type aftershock sequence) model taking the aftershock-triggering effect of every earthquake into account. However, relatively small repeating earthquakes have the characteristics of both models such that they usually recur periodically but their recurrence intervals get much shorter after nearby large earthquakes. We propose a nonstationary renewal process model for such repeating earthquakes that incorporates the aftershock-triggering effect of nearby large earthquakes as a relative change in the loading rate. We apply the proposed model to the repeating earthquake catalog on Pacific Plate subduction zone in the northeastern Japan and evaluate probabilistic forecasts of the next repeating events considering the aftershock-triggering effect of the 2011 Tohoku earthquake.

Keywords: Recurrent earthquakes, Renewal processes, ETAS model

©2021. Japan Geoscience Union. All Right Reserved.



©2021. Japan Geoscience Union. All Right Reserved.

Machine Learning Models for Earthquake Number Forecasting in the Kanto Region

*Hanyuan Huang[1], Hiroe Miyake[1], Hiroshi Tsuruoka[1]

1. Earthquake Research Institute, University of Tokyo

Machine learning techniques are developing in seismology contributed by the increasing amount of observable information. Some researchers suggest the earthquake cannot be predicted while many others think it is a predictable phenomenon. Through years of research, some regularities and patterns are found in the spatial and temporal distribution of seismicity. This research focuses to forecast the earthquake number on a certain day by using machine learning techniques to analyze past earthquake catalog, which could be considered as a reference for future earthquake hazard evaluation. We obtained the earthquake catalog of the Kanto region (longitude from 34.5 to 37.0, latitude from 138.5 to 141.5) from the Japanese Meteorological Agency (JMA), from 1 January 1999 to 31 December 2019. And the earthquake catalog is converted to statistical data in the patterns of the summation, mean, median, and max value of earthquake magnitude and number in different time windows (1 day, 3 days, 5 days, 7 days, 1 month, 2 months, 3 months, and one year) before the targeted day. As the machine learning models, multiple linear regression (MLR), and a 9 layers recurrent neural network (RNN) containing full connected layers, convolution layers, and long short-term memory (LSTM) layers are applied. Considering that the different patterns may exist in different depth and magnitude, we built different datasets containing earthquakes whose JMA magnitude (M_J) are greater or equal to 2.0 (M_J 2.0 sets), 3.0 (M_J 3.0 sets), and 4.0 (M_J 4.0 sets), with depths in the range of 0–30 km, 0–100 km, and 30–100 km respectively. The ratio of training, validation, and test sets is 6:2:2, and each model is trained separately. In the sector of results, because the recorded catalog with magnitudes of 2.0 or larger in 0–100 km set is abundant almost linearly related to the time except at around December 2016 when a shallow M_J 6.3 earthquake occurred, both MLR and RNN models perform pretty well, but in 0–30 km set, the MLR model almost totally fail to fit the trending while the RNN model still yields good forecasting. Among all the test tests, the results yielded from the MLR model are unstable while the performance of the RNN model is always satisfactory. Compared the results from machine learning models with the epidemic type aftershock sequence (ETAS) model, in all tested sets (M_J 3.0 sets and M_J 4.0 sets), the RNN model yielded the best results in cumulative number forecasting ranging from 1 January 2016 to 31 December 2019 while each the ETAS model and the MLR model reaches the second tier at times. For instance, the observed number of earthquakes with magnitudes of M_J 3.0 or larger with depth 0–100 km is 1519, and the forecasted value from RNN, MLR, and ETAS model is 1408, 1166, 1967. Yet the RNN model’s performance right after a relatively large earthquake is worse than others, and the MLR model lacks stability prominently. To conclude, we applied a recurrent neural network to forecast the number of earthquakes in the Kanto region. Even though the large magnitude earthquake number forecasting in a short term time-window (one day) seems impossible, the RNN model can output more accurate results in a long term time-windows cumulative number forecasting compared with the ETAS model, and this result may indicate that the earthquake temporal distribution can be better described by deep layer machine learning models.

Keywords: earthquake number forecasting, machine learning, long short-term memory

©2021. Japan Geoscience Union. All Right Reserved.

[J] Oral | S (Solid Earth Sciences)：S-SS Seismology

Sat. Jun 5, 2021 9:00 AM - 10:30 AM JST | Sat. Jun 5, 2021 12:00 AM - 1:30 AM UTC | Ch.18 Zoom Room 18

[S-SS09] Seismic wave propagation: Theory and Application

convener:Kaoru Sawazaki(National Research Institute for Earth Science and Disaster Resilience), Kiwamu Nishida(Earthquake Research Institute, University of Tokyo), Takao Nibe(JAPEX), Kyosuke Okamoto(National Institute of Advanced Industrial Science and Technology), Chairperson:Kaoru Sawazaki(National Research Institute for Earth Science and Disaster Resilience), Kurama Okubo(National Research Institute for Earth Science and Disaster Resilience)

Seismic wave propagation provides rich information on earth's heterogeneities and the excitation sources. Understanding of this information requires various research fields: mathematical/numerical studies based on wave theory, physical experiments using rock samples, seismic data analysis, etc. With recent developments of observational techniques, various wave phenomena have been elucidated: seismic waves, acoustic waves, traveling ionospheric disturbances, and tsunamis. New frameworks will be crucial for comprehensive understanding of these phenomena. This session widely invites presentations about the theories and applications related to seismic and other geophysical waves.

9:00 AM - 9:15 AM JST | 12:00 AM - 12:15 AM UTC

[SSS09-01] Estimation of the elastic wave velocity in rock fractures revealed by the digital rock physics and energy approach

*Kazuki Sawayama[1], Osamu NISHIZAWA[2], Tatsunori Ikeda[3], Fei Jiang[4], Takeshi Tsuji[3], Yasuhiro Fujimitsu[3] (1.Department of Earth Resources Engineering, Graduate school of engineering, Kyushu University, 2.International Institute of Carbon Neutral Energy Research, Kyushu University, 3.Department of Earth Resources Engineering, Faculty of engineering, Kyushu University, 4.Department of Mechanical Engineering, Faculty of Engineering, Yamaguchi University)

9:15 AM - 9:30 AM JST | 12:15 AM - 12:30 AM UTC

[SSS09-02] SH-wave propagation through the random distribution of aligned line cracks

*Haruo Sato[1] (1.Tohoku Unvieristy)

9:30 AM - 9:45 AM JST | 12:30 AM - 12:45 AM UTC

[SSS09-03] Continuous monitoring of seismic velocity change at Parkfield towards identifying the strain accumulation

*Kurama Okubo[1,2], Brent Delbridge[2], Marine Denolle[3,2] (1.National Research Institute for Earth Science and Disaster Resilience, 2.Harvard University, 3.University of Washington)

9:45 AM - 10:00 AM JST | 12:45 AM - 1:00 AM UTC

[SSS09-04] Changes in attenuation and its anisotropy associated with seismic ground motion

*Shuhei Tsuji[1], Koshun Yamaoka[2], Ryoya Ikuta[3] (1.Graduate School of Environmental Studies, Nagoya University, 2.Earthquake and Volcano Research Center Graduate School of Environmental Studies, Nagoya University, 3.Department of Geosciences, Shizuoka University)

10:00 AM - 10:15 AM JST | 1:00 AM - 1:15 AM UTC

[SSS09-05] Seismic velocity response to ground water level revealed by ACROSS and seismic array

*hiromu oba[1], Ryoya Ikuta[1], Shuhei Tsuji[2], Chen Feng[2], Koshun Yamaoka[2], Toshiki Watanabe[2] (1.Shizuoka University, 2.Nagoya University)

10:15 AM - 10:30 AM JST | 1:15 AM - 1:30 AM UTC

[SSS09-06] On the relationship between the streamflow due to snowmelt flood and ambient seismic noise observed by Hi-net stations

*Kaoru Sawazaki[1], Shakti P.C.[1] (1.National Research Institute for Earth Science and Disaster Resilience)

Estimation of the elastic wave velocity in rock fractures revealed by the digital rock physics and energy approach

*Kazuki Sawayama[1], Osamu NISHIZAWA[2], Tatsunori Ikeda[3], Fei Jiang[4], Takeshi Tsuji[3], Yasuhiro Fujimitsu[3]

1. Department of Earth Resources Engineering, Graduate school of engineering, Kyushu University, 2. International Institute of Carbon Neutral Energy Research, Kyushu University, 3. Department of Earth Resources Engineering, Faculty of engineering, Kyushu University, 4. Department of Mechanical Engineering, Faculty of Engineering, Yamaguchi University

Recent advances in seismic velocity monitoring have enabled us to detect velocity changes not only in events with large stress changes (i.e., earthquakes), but also in geothermal reservoirs with smaller stress changes. Such velocity changes are generally interpreted by changes in porosity or crack density; however, velocity changes will also be triggered by the aperture in a fractured rock mass (e.g., seismogenic faults and geothermal reservoirs). Since the aperture will affect fluid flow behaviors in fractured rocks, velocity changes in fractures must have a correlation with hydraulic properties (e.g., fracture permeability). Although the relationship between the aperture and fracture permeability is well known, their relationships with elastic wave velocity are still unknown. It would be beneficial if changes in the aperture and fracture permeability are correlated with the seismic velocity that can be remotely monitored. In this study, we develop a method to estimate the elastic wave velocity in fractured rocks, and establish a model relating it to permeability changes. Since aperture changes are difficult to be measured in experiments, we employed an approach using digital data of real rock samples (i.e., digital rock physics).

We first analyzed the surface roughness characteristics of a single natural fracture (35 mm x 70 mm) retrieved from a geothermal area to create digital rock models. Based on the roughness characteristics, three synthetic fractures (24 mm, 48 mm, and 96 mm square) are generated by using fractional Brownian motion. We prepared digital rocks that have 10 mm thickness with 0.1 mm resolution, varying their mean aperture ranging between 0.05–0.2 mm. We then calculated the elastic moduli of the models by finite element analysis. In this analysis, the elastic energy was calculated under the isostrain condition, and the elastic moduli were calculated by the second-order derivative of the energy with respect to the strain. We also conducted fluid flow simulation using the lattice Boltzmann method on the same digital fracture model to investigate the relationship between permeability and velocity.

The numerical simulation of a single fracture shows that the P-wave velocity decreased up to 0.2 km/s and the S-wave velocity decreased up to 0.15 km/s as the aperture increases under our conditions. We also found that these velocity changes are less sensitive to the fracture size, and modeled the permeability-velocity relationship regardless of the fracture size. On the other hand, in the multi-fracture models, the velocity change depends on the fracture density, and it is necessary to estimate the fracture density in order to link it to the field observation data. In addition to elastic wave velocity direction perpendicular to the fracture plane, we also confirm the similar relationship between permeability and S-wave splitting.

Keywords: digital rock physics, elastic wave velocity, permeability, S-wave splitting, Lattice Boltzmann Method

©2021. Japan Geoscience Union. All Right Reserved.

SH-wave propagation through the random distribution of aligned line cracks

*Haruo Sato[1]

1. Tohoku Unvieristy

Recent seismological observations have revealed that random heterogeneities spread over the solid Earth for a wide range of scales. There are two possible candidates for the source of seismic wave scattering: one is a random fluctuation of velocity; the other is a random distribution of cracks or faults. This paper studies the propagation of SH waves through the random distribution of aligned line cracks as the simplest mathematical model.
The differential scattering cross-section of a single line crack is well described by using Mathieu functions. Note that the differential scattering cross-section is anisotropic and depends on both incident and scattering angles. The random distribution of cracks assures the mutual incoherence of scattered waves, which allows us to use the radiative transfer theory. The directional scattering power per unit area is given by the scattering coefficient, which is a product of the number density of cracks and the differential scattering cross-section. Stochastically interpreting the scattering coefficient, we synthesize the space-time distribution of the wave intensity for a unit isotropic radiation from a point source by the Monte Carlo simulation. This paper precisely studies the case that the wavenumber is larger than the reciprocal of the crack length. Syntheses show that direct wavelets around the direction normal to the aligned line cracks rapidly decrease with increasing distance because of strong scattering, but those around the direction parallel to the aligned line cracks decrease according to the geometrical decay only. At large lapse times, multiple scattering produces a swelling around the source location, which is prolonged to the crack line direction. Those characteristics well reflect the anisotropy of the line crack scattering.
Our next target is to solve more realistic cases, for example, the propagation of elastic-waves through the random distribution of penny shaped cracks in a 3-D elastic medium.

Keywords: seismic waves, cracks, scattering, wave theory, radiative transfer theory

©2021. Japan Geoscience Union. All Right Reserved.

Continuous monitoring of seismic velocity change at Parkfield towards identifying the strain accumulation

*Kurama Okubo[1,2], Brent Delbridge[2], Marine Denolle[3,2]

1. National Research Institute for Earth Science and Disaster Resilience, 2. Harvard University, 3. University of Washington

Fault zones are subject to the long-term loading of tectonic strains, to the short-term release of fault fast and slow earthquakes, and to hydrological and thermoelastic modulation from environmental forces. Each of these stresses are thought to impact the fault-zone material properties, such as elastic wave speed. In this work, we perform the continuous monitoring using nearly two decades (2002-2020) of ambient seismic noise recorded by 3-components seismometers from the Berkeley Seismological Laboratory's High Resolution Seismic Network (HRSN) to extract bulk properties, dv/v, near the rupture area of the 2004 Parkfield Earthquake on the San Andreas Fault.

Transient signals such as earthquakes and tremor are removed using a kurtosis and STA/LTA based algorithm, prior to computing the cross-correlation functions (CCFs). We compute the CCFs for all possible channel pairs and decompose them into narrow frequency bands using wavelet transform. During the stacking processes, we reject CCFs with low signal-to-noise ratio caused by the perturbation of noise sources and instrumental issues. The daily CCFs are stacked every 30 days with 15 days overlap. We explore the effects of various algorithms and waveform reference on our measurements.

This study aims to separate the potential tectonic and non-tectonic origins of the observed temporal variations in dv/v and to evaluate the effect of strain accumulation on its time history using geodetic measurements. The dv/v time history reveals the previously identified coseismic decrease in dv/v and the subsequent logarithmic recovery, as well as a newly observed long-term increase in dv/v. We show that the observed long-term increase exceeds the velocity healing model which is thought to explain the logarithmic postseimic behavior. We further show that this long-term increase cannot be explained by changes in ground water levels and does not follow the trend of decrease and recovery associated with the drought in California from 2011 to 2017. Instead, we discuss that the observed long-term increase in dv/v reflects strain change from quasi-static deformation at depth during the interseismic period.

Keywords: ambient seismic noise, velocity change, Parkfield

©2021. Japan Geoscience Union. All Right Reserved.

Changes in attenuation and its anisotropy associated with seismic ground motion

*Shuhei Tsuji[1], Koshun Yamaoka[2], Ryoya Ikuta[3]

1. Graduate School of Environmental Studies, Nagoya University, 2. Earthquake and Volcano Research Center Graduate School of Environmental Studies, Nagoya University, 3. Department of Geosciences, Shizuoka University

We found anisotropic change in attenuation associated with seismic ground motions in dataset obtained in the experiment using an artificial seismic source, ACROSS. A larger reduction in amplitude was observed in the direction with a larger delay in travel time. The dataset we analyzed was obtained by Ikuta et al. (2002) at Awaji ACROSS test site from 2000 to 2001. At this site, the ACROSS was installed on the surface and the signal was observed at two seismometers installed at the bottom of 800m and 1700m deep borehole near the source.

We calculated changes in amplitude using the ratio of power of the transfer functions to that of the reference transfer function as reported by Tsuji et al. (2020 JpGU). In this calculation, we removed power of noise that of the transfer functions to reduce effect of temporal change in noise level from the estimated change in amplitude.

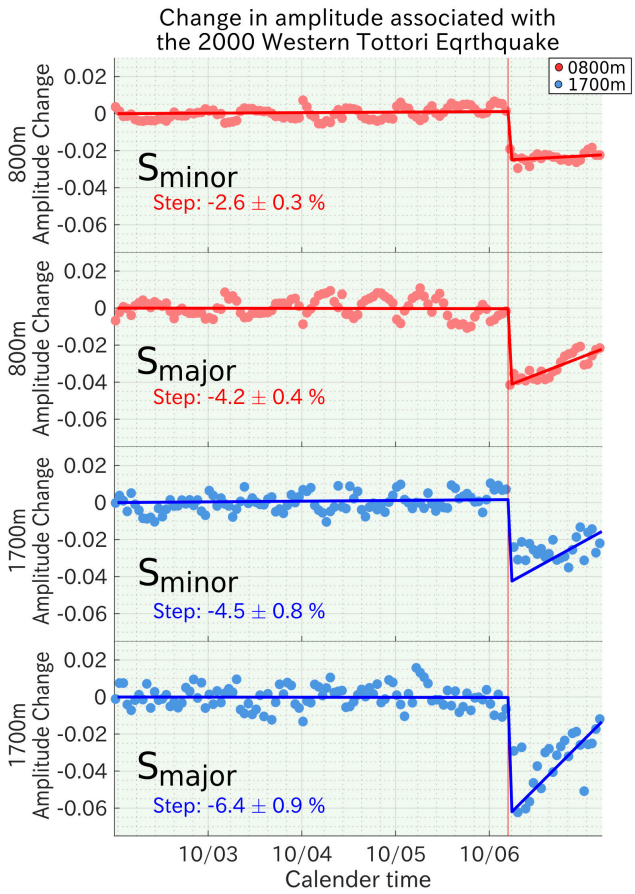
To analyze the anisotropic changes in amplitude, we reinvestigated the anisotropic change in S wave observed at the 2000 Western Tottori Earthquake (WT) and the 2001 Geiyo Earthquake (GY). We calculated the azimuthal variation of the coseismic delay of the S wave by rotating the sensor orientation with high resolution and found that the azimuthal pattern of coseismic delay cannot be approximated by an ellipse as Ikuta and Yamaoka (2004) did.

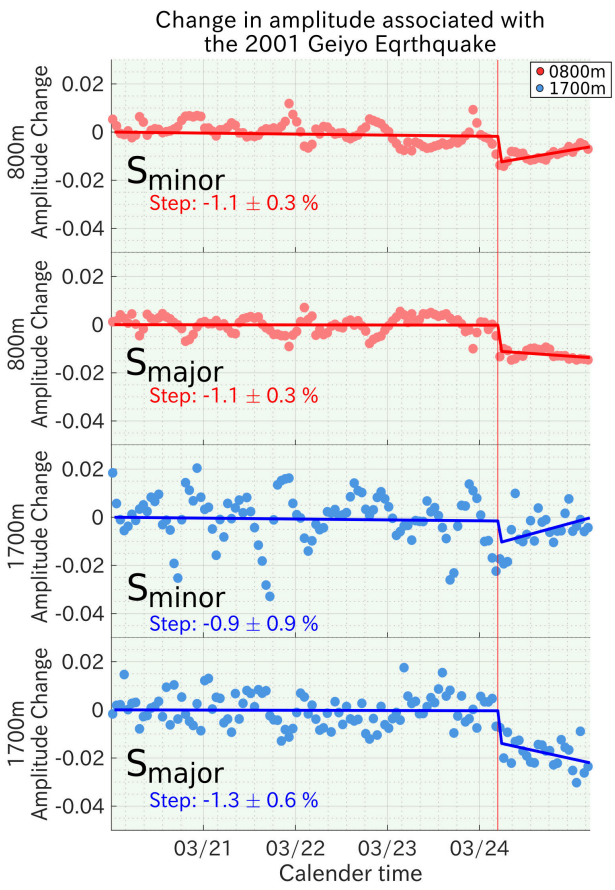
We modeled the azimuthal pattern with parameters that describe the anisotropy. By fitting the azimuthal pattern by the model on to the observation, we estimated directions of the principal axes. For WT, the directions of the major axis were N90˚E for both the 800 m and 1700 m borehole sensors. For GY, the directions were N85˚E and N95˚E for the 800 m and 1700 m borehole sensors, respectively. These directions coincide well with the results of Ikuta and Yamaoka (2004), in which the direction was N100˚E for WT and GY at the 800 m sensors.

We estimated the amplitude change in the direction of the principal axes. Changes in the amplitude and result of the model fitting in the principal axes are shown in the Figure. Dots and lines indicate amplitude changes and its fitting. The major and minor axes correspond to the axes of larger and smaller velocity change, respectively. For WT, a greater decrease in amplitude is obtained in the major axis of velocity anisotropy for both depths. For GY, no significant difference was observed for either depth. This result shows that the direction of greater attenuation corresponds to that of larger delay. That is consistent with laboratory experiments with cracked and saturated media.

Keywords: coseismic change, changes in anisotropy, changes in attenuation, artificial seismic source, ACROSS

©2021. Japan Geoscience Union. All Right Reserved.





©2021. Japan Geoscience Union. All Right Reserved.

Seismic velocity response to ground water level revealed by ACROSS and seismic array

*hiromu oba[1], Ryoya Ikuta[1], Shuhei Tsuji[2], Chen Feng[2], Koshun Yamaoka[2], Toshiki Watanabe[2]

1. Shizuoka University, 2. Nagoya University

Temporal variation in propagation property of seismic wave was monitored at the landslide area using Accurately Controlled Routinely Operated Signal System (ACROSS) and a seismic array. The ACROSS, which is a precisely-controlled seismic source, is deployed in Mori-machi, Shizuoka Prefecture, Japan, and used in this study.

Before this experiment, a preliminary observation was conducted for three weeks in each of 2017 and 2018. We set up two seismometers at a site which is 3 km away from the ACROSS source to investigate the response of seismic velocity to rainfalls by analyzing the transfer function obtained from the ACROSS signal. The temporal variation of the arrival time of the later phases showed a significant response to rainfalls. The rainfall is converted into the groundwater level to investigate the relation to the propagation property of seismic waves. We assumed a tank model in the conversion by the exponential decay function with a time constant of 20 days.

We found that there is a strong correlation between the arrival time variation of these waves and the groundwater level, and also found the sensitivity function of the two wave groups is different.

A small seismic array is deployed to identify the origin of the phases and to monitor the temporal variation. 14 seismometers were deployed following the typical array configuration of SPAC methods, which consists of a center and three triangles on concentric circles with radii of 4, 8, and 16 meters. Two additional seismometers on each of the south and north sides of the array to increase the wavenumber resolution in the source direction. The total size of the array is 70 m in NS and 30m in EW. This array arrangement is intended to estimate the shallow shear-velosity profiles by inversing the surface wave dispersion curve by SPAC method using ambient noises and analysis the ACROSS signal. The seismometers are Mark Products L-28-3D (sensitivity 120 V/m/s) of three-component velocity-type ones with a natural frequency of 4.5 Hz. The sampling frequency is 1 kHz, and the inter-channel skew of sampling is maintained within 15 μs.

The results of the array analysis of ACROSS signal showed that the phases arriving around 2.8 and 3.8 seconds, whose response to the rainfall was significant, had the same apparent velocity as the body waves (~2.5 km/s). This observation contradicts the result of the analysis of the 2017 and 2018 observations, in which the later phases are identified as Love and Raiyleigh waves based on their particle motions. The wave at 2.8 seconds had a dominant transverse component, which was regarded as a Love wave, and the wave at 3.8 seconds had retrograde motion in the vertical plane, which was regarded as Rayleigh wave.

The variation of the arrival time of the phase around 2.8 and 3.8 seconds were estimated by applying the cross-spectrum method to the transfer function during the observation period, and a strong correlation with rainfall was found in 2017 and 2018 experiments. For all observations from 2017 to 2020, there was a positive linear relationship between the change in the arrival time of the phase around 2.8 seconds and the groundwater level that is converted from the rainfalls. The sensitivity of the change in velocity [%] to the increase in groundwater level [m] was 1.04 [%/m]. In contrast, there was a third-order relationship

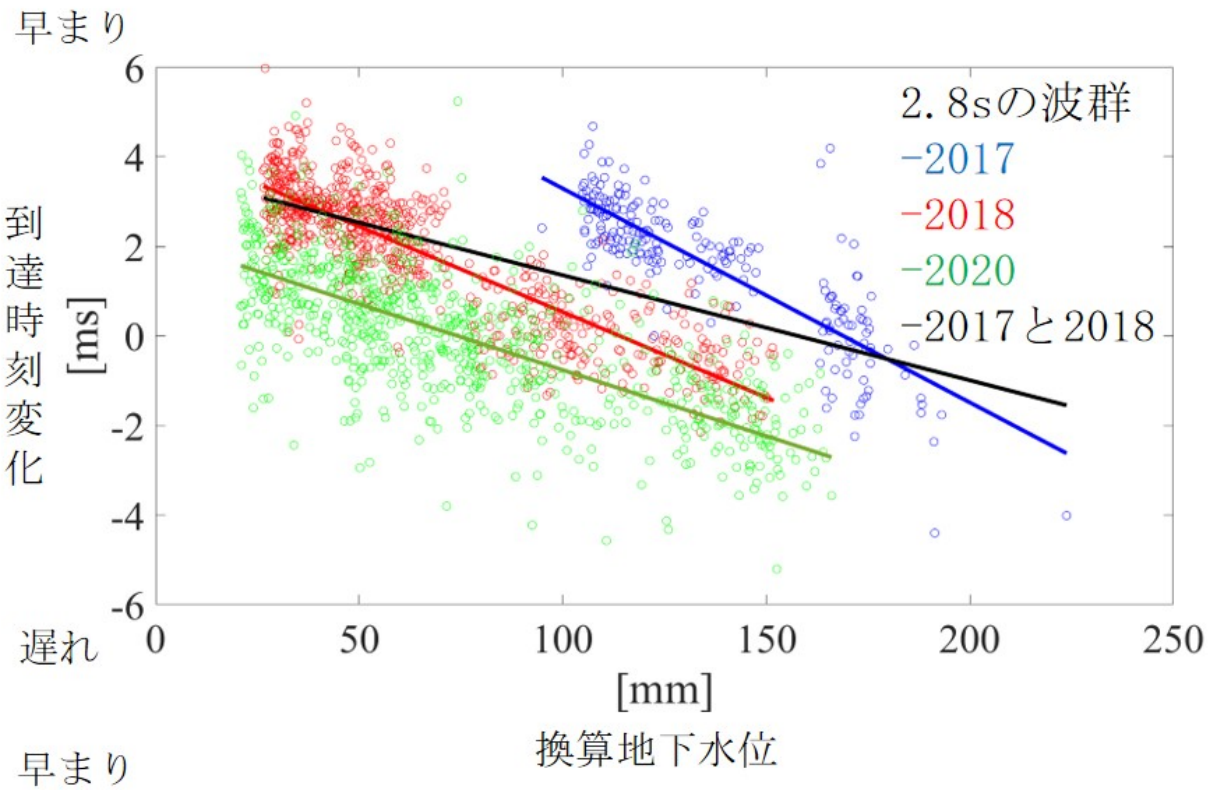
©2021. Japan Geoscience Union. All Right Reserved.

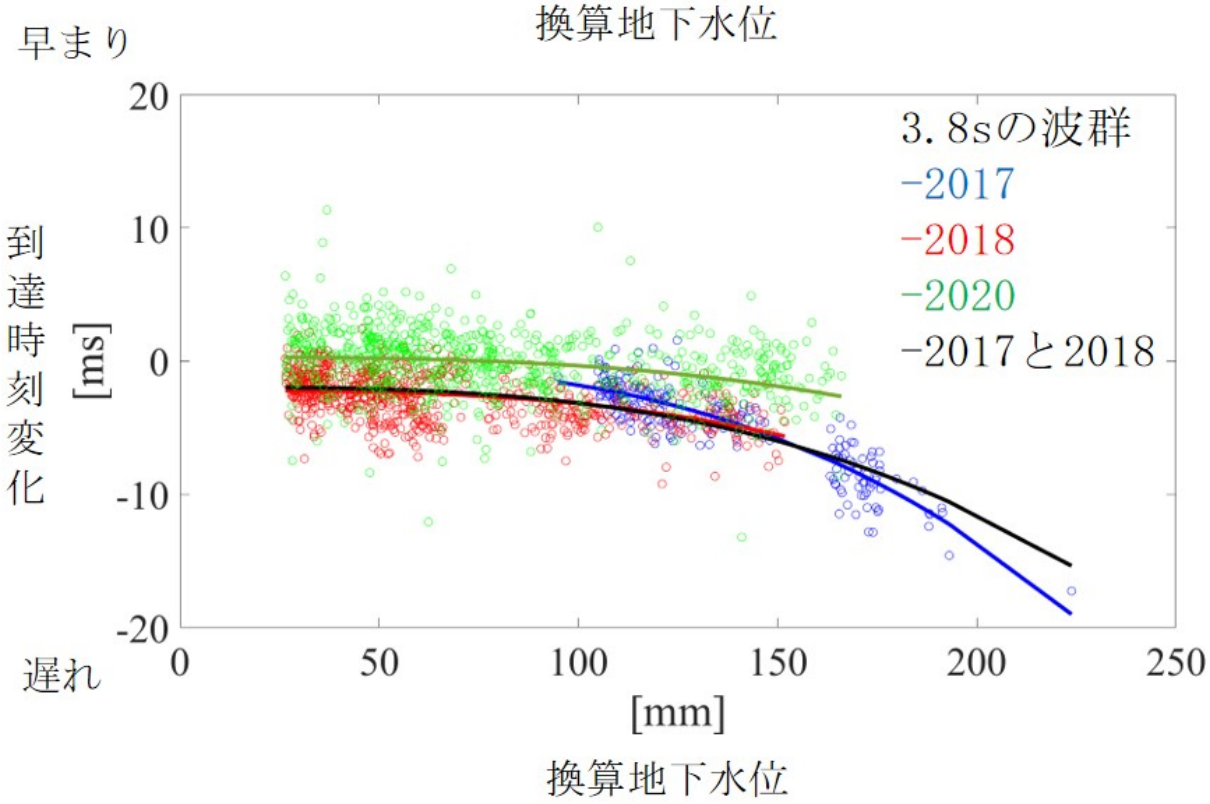
between the change in the arrival time of the phase arriving around 3.8 seconds and the groundwater level. The sensitivity of the velocity change became stronger when the groundwater level increased above a certain level.

The amount of precipitation during the observation period of 2020 was much less than the previous two years, and the relation cannot be extended outside the range of the previous two years' observation. We will continue the observation during the high precipitation season and pursue the mechanism of these variations.

Keywords: ACROSS, array, surface wave, groundwater level

©2021. Japan Geoscience Union. All Right Reserved.





©2021. Japan Geoscience Union. All Right Reserved.

On the relationship between the streamflow due to snowmelt flood and ambient seismic noise observed by Hi-net stations

*Kaoru Sawazaki[1], Shakti P.C.[1]

1. National Research Institute for Earth Science and Disaster Resilience

Seki River basin is located in Niigata and Nagano prefecture of Japan. Snowfall is common over the basin during the winter season. Such accumulated snow starts melting from the beginning of the spring season each year that increase the rate of streamflow in the Seki River. The variation of streamflow is synchronized by the ambient noise level of nearby Hi-net seismograph stations. In this study, we surveyed the relationship between the ambient noise power of Hi-net stations located in the basin and discharge of the Seki River, in the period from March to May in 2012.

The N.MKOH and N.MKGH Hi-net stations are located in the middle basin (elevation: 240 m asl) and upstream (elevation: 1305 m asl) of the Seki River, respectively. Ambient noise of N.MKOH station shows a clear one-day periodicity associated with social activity, whereas N.MKGH station contains much less social noise as it is located deep in the mountains. The Futagojima streamflow observation point is located about 10 km downstream from N.MKOH station (elevation: 65 m). We computed power spectra of UD component of each Hi-net station every one minute, and calculated power time series for six octave-bandwidths from 0.5 to 32 Hz. To remove transient signals like earthquakes, we selected the minimum one-minute power among every continuous 10 minutes records as the representative value of the 10-minutes ambient noise power. Then we averaged the obtained representative values every one hour. The discharge record of the Futagojima station is also measured every one hour.

Since noise power of N.MKOH exhibits one-day periodic social noise, we used only the records observed from 8PM to 12PM, within which social noise is relatively calm, for the comparison to the discharge record. As a result, clear correlations with the discharge record are observed especially at 2 - 16 Hz. More precisely, the noise power does not depend on the discharge when the discharge is less than a threshold value. It increases proportional to about the first power of the discharge above the threshold value, and proportional to 1 to 2 power as the discharge increased further. Through the target period, the ratio of the noise power with respect to the discharge did not change drastically.

On the other hand, N.MKGH does not show clear correlations with the discharge in March, but the correlations become distinctive after April. The ratio of noise power with respect to the streamflow increases as time lapses after April. According to the nearby temperature and snow depth records of AMeDAS, snowmelt may not have proceeded until April. This indicates that streamflow at upstream is very small in March and it gradually increased from April to May. Consequently, noise at N.MKGH station is excited only after April and this may be why correlations with the dicharge of Futagojima station become distinctive only after April.

Keywords: Snowmelt flood, Seismic ambient noise, Streamflow

©2021. Japan Geoscience Union. All Right Reserved.

[J] Oral | S (Solid Earth Sciences)：S-SS Seismology

Sat. Jun 5, 2021 10:45 AM - 12:15 PM JST | Sat. Jun 5, 2021 1:45 AM - 3:15 AM UTC | Ch.18 Zoom Room 18

[S-SS09] Seismic wave propagation: Theory and Application

convener:Kaoru Sawazaki(National Research Institute for Earth Science and Disaster Resilience), Kiwamu Nishida(Earthquake Research Institute, University of Tokyo), Takao Nibe(JAPEX), Kyosuke Okamoto(National Institute of Advanced Industrial Science and Technology), Chairperson:Kyosuke Okamoto(National Institute of Advanced Industrial Science and Technology), Shunsuke Takemura(Earthquake Research Institute, the University of Tokyo)

Seismic wave propagation provides rich information on earth's heterogeneities and the excitation sources. Understanding of this information requires various research fields: mathematical/numerical studies based on wave theory, physical experiments using rock samples, seismic data analysis, etc. With recent developments of observational techniques, various wave phenomena have been elucidated: seismic waves, acoustic waves, traveling ionospheric disturbances, and tsunamis. New frameworks will be crucial for comprehensive understanding of these phenomena. This session widely invites presentations about the theories and applications related to seismic and other geophysical waves.

10:45 AM - 11:00 AM JST | 1:45 AM - 2:00 AM UTC

[SSS09-07] Effects of subsurface heterogeneities and surface topography on long-period surface wave monitoring

*Shunsuke Takemura[1], Ryo Okuwaki[2], Takanori Matsuzawa[3] (1.Earthquake Research Institute, the University of Tokyo, 2.Moutain Science Center, Faculty of Life and Environmental Sciences, University of Tsukuba, 3.National Research Institute for Earth Science and Disaster Resilience)

11:00 AM - 11:30 AM JST | 2:00 AM - 2:30 AM UTC

[SSS09-08] Fracture detection and properties estimation using fiber optic sensors

★Invited Papers

*Keisuke Teranishi[1], Naoshi Aoki[1], Moeto Fujisawa[1], Hidehiko Shimizu[1], Shinya Onodera[2] (1.JGI, 2.JOGMEC)

11:30 AM - 11:45 AM JST | 2:30 AM - 2:45 AM UTC

[SSS09-09] Connection between the correlation of strain and rotation seismograms and Green's function: Surface-wave case

*Hisashi Nakahara[1] (1.Solid Earth Physics Laboratory, Department of Geophysics, Graduate School of Science, Tohoku University)

11:45 AM - 12:00 PM JST | 2:45 AM - 3:00 AM UTC

[SSS09-10] Ambient Noise Differential Adjoint Tomography Applied to a Linear Array in Los Angeles Basin

*Xin Liu[1,2], Gregory C Beroza[1] (1.Stanford Earth, 2.JAMSTEC)

12:00 PM - 12:15 PM JST | 3:00 AM - 3:15 AM UTC

[SSS09-11] Estimating finite fault slip distributions of large earthquakes based on time-reversal wave propagation simulation with data assimilation

*Yugo Shibata[1], Takashi Furumura[1], Takuto Maeda[2] (1.Earthquake Research Institute, the University of Tokyo, 2.Hirosaki University)

Effects of subsurface heterogeneities and surface topography on long-period surface wave monitoring

*Shunsuke Takemura[1], Ryo Okuwaki[2], Takanori Matsuzawa[3]

1. Earthquake Research Institute, the University of Tokyo, 2. Moutain Science Center, Faculty of Life and Environmental Sciences, University of Tsukuba, 3. National Research Institute for Earth Science and Disaster Resilience

Dense broadband seismic networks allow us to detect various phenomena, which radiate seismic waves. Especially because the effects of microseisms are weak in periods of 20-50s, this period band has been widely used in monitoring regular earthquakes, shallow very low frequency earthquakes, volcanic eruption, landslides, stormquakes…etc. (e.g., Tsuruoka et al., 2009; Matsuzawa et al., 2012; Fan et al., 2019; Takemura et al., 2019; Okuwaki et al., 2021). In this study, to achieve precise modeling of physical sources of these phenomena, we investigated the effects of subsurface heterogeneities and irregular surface topography on generation and propagation of long-period (20-50 s) surface waves using the numerical simulations via OpenSWPC (Maeda et al. 2017).
We simulated ground motions of a crustal earthquake that occurred at Awaji Island on 13 April 2013. The source parameters of this earthquake were referred from Takemura et al. (2020). We also simulated ground motions caused by a landslide that occurred at Shizuoka Prefecture. By using the estimated model parameters of Okuwaki et al. (2021), this source could be modeled by body forces on the surface. We used three heterogeneous models: (1) the Japan Integrated Velocity Structure Model (JIVSM; Koketsu et al. 2012) with ETOPO1 (Amante and Eakins, 2009), (2) the JIVSM with a flat surface, and (3) the F-net 1D crustal model (Kubo et al., 2002).

To evaluate quantities differences in simulation results, we calculated variance reductions (VRs) of simulated waveforms between the JIVSM with ETOPO1 and simplified models. In VR calculations, we did not permit any time shift, which adjusts travel time differences between synthetic and target waveforms. In the case of a crustal earthquake, high (> 90%) VRs in the F-net 1D model only appeared at distances shorter than 100 km due to non-time shift VR evaluation. In the JIVSM with a flat surface, VRs at almost all stations were greater than 90 %. This result indicates that the surface topography has limited effects on long-period surface waves from regular earthquakes. Similar characteristics were also found in the simulation results of the landslide source, but we found the directivity of VR decrease, especially in the transverse component. The VR decrease was localized around the Chugoku region. This directivity may be related to the topography around the landslide source. To achieve precise modeling of phenomena on the earth’s surface, Green’s functions, including effects of irregular topography, should be applied.

Acknowledgments: We used NIED Hi-net and F-net data https://doi.org/10.17598/NIED.0003 https://doi.org/10.17598/NIED.0005. Numerical simulations were conducted on the Fujitsu PRIMERGY CX600M1/CX1640M1 (Oakforest-PAC) in the Information Technology Center, University of Tokyo. This study was also supported by the ERI JURP 2020-S-04

Keywords: long-period surface wave, earthquake, landslides, ground motion simulation, topography, subsurface heterogeneity

©2021. Japan Geoscience Union. All Right Reserved.

Fracture detection and properties estimation using fiber optic sensors

*Keisuke Teranishi[1], Naoshi Aoki[1], Moeto Fujisawa[1], Hidehiko Shimizu[1], Shinya Onodera[2]

1. JGI, 2. JOGMEC

The knowledge of fracture locations and connections which are pathways for fluid and solute transport are crucial information for developing the geothermal field. This information contributes that plan to drill the sidetrack within the suspended well and detection the drilling target for a make-up production well. The development of Distributed Acoustic Sensing (DAS) technologies enables the operation under high temperature environment and dense spatial measurement. This could be particularly valuable for acquiring high spatial resolution images of seismic reflection survey and dipping faults in the vicinity of the well.

In the feasibility study, we acquired the overnight monitoring data and conducted SSP (surface seismic profiling) survey and DAS-VSP survey which was used the suspended well in the real geothermal field. We developed the fracture detection systems in the vicinity of the well described following and investigated their applicability for the real data set.
・acquire the seismic cross section with SSP and DAS
・FWI velocity model building which correspond with check shot
・extract the diffracted wave from overnight monitoring DAS data and evaluate the indicators that detect the fractures in the vicinity of the well.

The records of SSP and DAS provide seismic reflection section and represent the faults and fractures as the characteristics of each method. Fractures are represented as a gap in SSP section and as a fault plane in DAS-VSP section. It was confirmed the fracture locations in both reflection sections were consistent. Moreover, the result of joint FWI using SSP and VSP dataset showed a better agreement with the velocity along the well estimated by the zero-offset DAS-VSP analysis. This confirmed that accurate velocity information can be estimated from the DAS-VSP dataset.

The numerical studies were performed to simulate the DAS-VSP acquisition. In the synthetic experience, the presence of later phases including diffracted waves after direct P-wave and S-wave show the potential as seismic signatures that indicates the existence of fractures near wellbore.
These results stimulated us the development of diffraction enhancement workflow. We combine Plane Wave Destruction (Fomel, 2002) and Common Reflection Surface (Dell and Gajewski, 2011) to separate the diffractions from direct arrivals in the overnight monitoring data. Comparison with the wellbore information and the distribution of the extracted diffracted waves, it was confirmed that significant PS conversion waves after the direct P-wave which generated by the vicinity of the fracture zone were observed and significant amplification was also observed in the later phases which were identified as direct S-wave.

With the development of DAS sensing technology, its dense sampling could be possible to extract diffracted waves and to estimate accurate velocity model using FWI. In this presentation, the background and developed fracture detection systems will be explained and discussed these results and further works.

Acknowledgements:

©2021. Japan Geoscience Union. All Right Reserved.

We conducted this research as a part of Geothermal Borehole Exploration Techniques by JOGMEC. Nittetsu Mining Co., Ltd. and Kirishima Geothermal Co., Ltd. were kindly allowed us the use of their suspended well and fields. We want to thank these organizations.

Keywords: fiber optic sensors, DAS-VSP, diffraction, fracture detection

©2021. Japan Geoscience Union. All Right Reserved.

Connection between the correlation of strain and rotation seismograms and Green’ s function: Surface-wave case

*Hisashi Nakahara[1]

1. Solid Earth Physics Laboratory, Department of Geophysics, Graduate School of Science, Tohoku University

Dynamic strain (or strain rate) is recently measured by Distributed Acoustic Sensing (DAS) techniques along a fiber-optic cable with high spatial resolutions of 10m or less. Rotational ground motion is measured by rotational seismometers that are sometimes used in combination with translational seismometers (called the six-component (6C) observation) (e.g., Schmelzbach et al., 2018). Therefore, we need to accustom ourselves to using strain and rotation seismograms by adapting the methods used for traditional translational seismograms to these new kinds of seismograms. Nakahara et al. (2020, SSJ) formulated the SPAC method for DAS axial-strain seismograms. Nakahara et al. (2021) further extended the formulation to the other components of strain, rotation and tilt records. According to seismic interferometry, it is possible to connect SPAC to Green's function (e.g., Nakahara, 2006; Sanchez-Sesma and Campillo, 2006). In this study, we clarify the connection between cross-correlation functions of strain and rotation seismograms and Green's functions for the moment tensor under an assumption that surface waves only exist. Since the formulation is conducted in the frequency domain, the connection between the cross-spectral matrix of strain and rotation at two receivers and the Green's tensor is concerned. A general framework of seismic interferometry for strain and rotation was already provided by Paitz et al. (2019). However, the physical meanings of cross-correlation functions of strain and rotation are not yet fully understood.

We start from the strict expressions of surface-wave Green’ s tensors from moment-tensor sources in the Cartesian coordinate derived by Haney and Nakahara (2016). First, we convert the expression to the cylindrical coordinate and calculate the displacement gradients of Green's tensor. Then, we derive analytical expressions for strain and rotation Green's functions from moment-tensor sources. Finally, we compare these expressions with the SPAC expressions for strain and rotation derived by Nakahara et al. (2021). We obtain the following results for the isotropic incidence of random waves with a specific ratio between Rayleigh and Love wave energies. The (i, j)-component cross-spectral matrix of strain is found to be proportional to the strain Green's tensor at one receiver for the sum of (i,j)- and (j, i)-component moment tensor source at the other receiver. Regarding the rotational component, the (i, j)-component cross-spectral matrix is found to be proportional to the rotation of Green's tensor at one receiver for the difference of (i,j)- and (j, i)-component moment tensor source at the other receiver.

So far, we proved these relations for surface waves by the concrete calculation using the analytical expressions. Now we speculate that these relations hold for body waves as well. An extension of the proof to body waves will be the next target.

Keywords: cross correlation, Green's function, seismic interferometry, strain, rotation

©2021. Japan Geoscience Union. All Right Reserved.

Ambient Noise Differential Adjoint Tomography Applied to a Linear Array in Los Angeles Basin

*Xin Liu[1,2], Gregory C Beroza[1]

1. Stanford Earth, 2. JAMSTEC

The small time shifts that are used in ambient-field interferometric Green’ s function analysis may arise from either structural anomalies of interest, or spatio-temporal behavior of the noise source, which is usually not of interest. In seismic noise interferometry, the differential time kernel has been shown to be much less sensitive to variations in the spatio-temporal distributions of the noise source and more sensitive to the structural anomalies of interest, thus using differential measurements is an effective approach for reducing bias in tomographic images (Liu 2020). In this study, we generalize this technique by deriving the shear-wave velocity directly from differential time kernels for fundamental mode Love waves in noise cross-correlations along a linear array spanning ~37 km in the Los Angeles basin without the 1D depth conversion step that assumes a layered medium. The initial results show strong sensitivity to near-surface shear velocity structure in the uppermost 500 m. We then apply iterative inversion for shear velocity, and will present an updated near-surface shear velocity structure that should help to constrain future urban earthquake ground motion.

Keywords: ambient noise adjoint tomography, near surface shear velocity

©2021. Japan Geoscience Union. All Right Reserved.

Estimating finite fault slip distributions of large earthquakes based on time-reversal wave propagation simulation with data assimilation

*Yugo Shibata[1], Takashi Furumura[1], Takuto Maeda[2]

1. Earthquake Research Institute, the University of Tokyo, 2. Hirosaki University

Larmat et al. (2006) proposed Time-Reversal Imaging (TRI), which has shown great success in earthquake source estimation. This method is different from general source inversion; the source imaging is performed by back-propagating array observation waveform data to the hypocenter by time inversion calculation of the equations of motion. This feature enables us to estimate the source without the prior setting of a fault plane. In addition to the significant large earthquakes, the application of the TRI to long-lasting phenomena such as tremors is being considered. On the other hand, TRI generally requires dense observation to obtain high-resolution source images (e.g., Kawakatsu and Montagner, 2008; Fukahata et al., 2014; Nakahara and Haney, 2015). Recently Furumura and Maeda (2020) introduced a calculation and observation data assimilation mechanism into TRI (DA-TRI), and showed that the K-NET/KiK-net data whose interstation distance is 20 -25 km can be used for source imaging of small and medium earthquakes occurring around Japan. In this study, we apply the TRI to estimate slip distribution on the finite fault of large earthquakes.

We set the DA-TRI calculation area as 460.8 x 460.8 km in horizontal and 57.6 km depth directions, respectively, in central Japan. The subsurface structure model of the JIVSM (Koketsu et al., 2012) was used for sedimentary layer, crust, mantle structure, and Pacific/Philippine Sea plate. Waveform data recorded at 234 KiK-net borehole stations for a duration of 180 seconds of two earthquakes that occurred off Ibaraki prefecture in 2008 (Mw6.9) and 2011 (Mw7.9) were backpropagated to the hypocenters by the 3D finite-difference calculation to estimate slip distribution (or asperity) on the fault plane, respectively. The optimal interpolation method was used for the data assimilation. The assimilation parameter was set based on the assumption that the error distribution of the seismic wavefield follows the Gaussian distribution of the correlation distance 5 km, and that the error of calculation and observation data is equivalent.

First, we analyzed the 2008 off-Ibaraki earthquake. DA-TRI was used to find the time variation of elastic energy of all grids in the finite difference method calculation (Top of Figure 2a). The time before and after the peak was regarded as the fault rupture time. The maximum value of elastic energy at the upper surface of the Pacific plate at that time was displayed as a source image (Bottom of Figure 2a). The obtained source image showed a strong concentration of elastic energy in a range of 25 km x 35 km, on about 10 km northeast of the hypocenter after five seconds from the earthquake origin time based on the catalog of the Japan Meteorological Agency. This position coincides well with the position of the large source fault slip estimated by Yamanaka (2008) from the far-field body wave analysis.

For the larger 2011 earthquake, the temporal variation of elastic energy (Top of Figure 2b) obtained from DA-TRI had two peaks at 2 and 23 seconds from the catalog origin time, suggesting the existence of two large fault slips around each time. Thus, we obtained the slip distribution of this earthquake by superimposing wave amplitudes on the Pacific plate at the two time-steps. A concentration of strong elastic energy was obtained in an area of 30x20 km at about 20 km southeast of the hypocenter, while a concentration of weak elastic energy in 30 x 20 km at 40 km northwest. The locations of energy

©2021. Japan Geoscience Union. All Right Reserved.

concentration coincide with the asperity locations obtained from near-field strong motion records (Kubo et al., 2013), however, our results were unstable. This is because the calculation of the backpropagation of seismic waves continues to the past beyond the focal time, which we are tackling to improve.

©2021. Japan Geoscience Union. All Right Reserved.

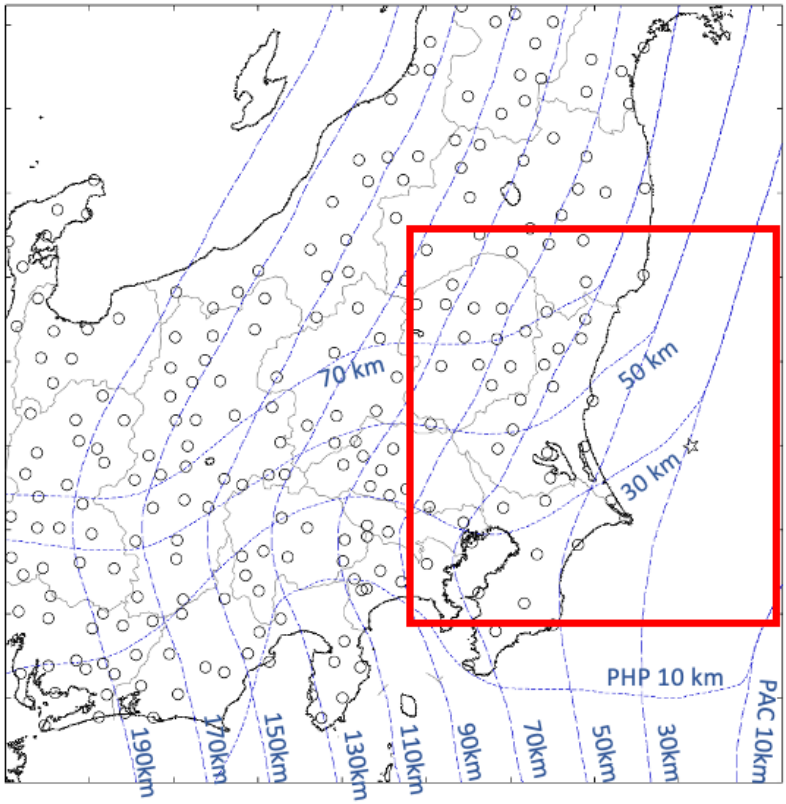


図1 この実験での計算領域と、KiK-net観測点の位置を示す。破線は、太平洋プレート（PAC）とフィリピン海プレート（PHP）の深さを示す。星印は、2011年茨城県沖地震の震央である。なお、赤枠は、図2の表示領域に対応する。

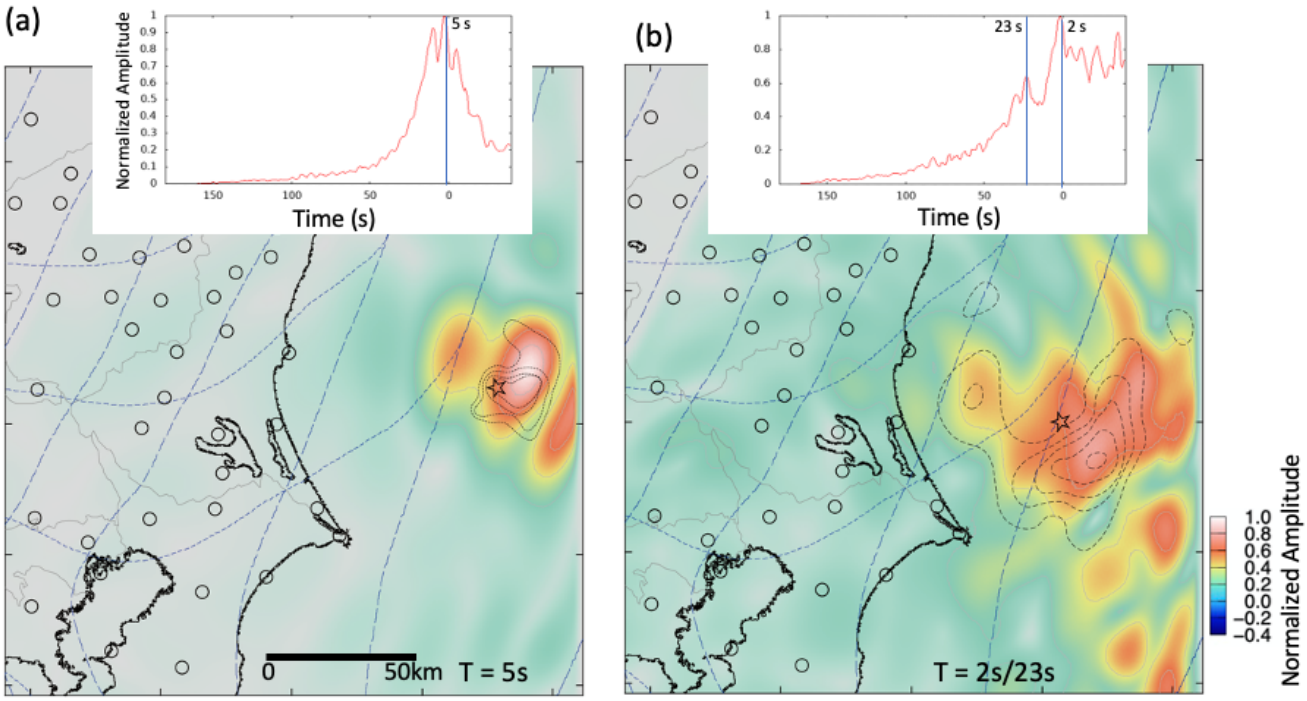


図2 DA-TRIにより求まった太平洋プレート上面での震源イメージ
(a) 2008年茨城県沖地震 （Mw 6.9）、コンターは山中 (2008)によるアスペリティの位置（0.3 m間隔）を表す。(b)2 011年茨城県沖地震 （Mw 7.9）、コンターはKubo et al. (2013) によるアスペリティの位置（1.26 m間隔）。星印は各地震の震央で、図中のグラフは、震源域全体のエネルギー振幅の時間変化 （時刻=0が発震時に対応）。

©2021. Japan Geoscience Union. All Right Reserved.

[J] Oral | S (Solid Earth Sciences)：S-SS Seismology

Sat. Jun 5, 2021 1:45 PM - 3:15 PM JST | Sat. Jun 5, 2021 4:45 AM - 6:15 AM UTC | Ch.18 Zoom Room 18

[S-SS09] Seismic wave propagation: Theory and Application

convener:Kaoru Sawazaki(National Research Institute for Earth Science and Disaster Resilience), Kiwamu Nishida(Earthquake Research Institute, University of Tokyo), Takao Nibe(JAPEX), Kyosuke Okamoto(National Institute of Advanced Industrial Science and Technology), Chairperson:Kiwamu Nishida(Earthquake Research Institute, University of Tokyo), Takashi Hirose(National Research Institute for Earth Science and Disaster Resilience)

Seismic wave propagation provides rich information on earth's heterogeneities and the excitation sources. Understanding of this information requires various research fields: mathematical/numerical studies based on wave theory, physical experiments using rock samples, seismic data analysis, etc. With recent developments of observational techniques, various wave phenomena have been elucidated: seismic waves, acoustic waves, traveling ionospheric disturbances, and tsunamis. New frameworks will be crucial for comprehensive understanding of these phenomena. This session widely invites presentations about the theories and applications related to seismic and other geophysical waves.

1:45 PM - 2:15 PM JST | 4:45 AM - 5:15 AM UTC

[SSS09-12] Imaging the solar interior using noise tomography

★Invited Papers

*Shravan Hanasoge[1] (1.Tata Institute of Fundamental Research)

2:15 PM - 2:30 PM JST | 5:15 AM - 5:30 AM UTC

[SSS09-13] Incorporating wind information in the inversion of co-located pressure and seismic data for shallow elastic structure

*Toshiro Tanimoto[1] (1.Department of Earth Science, University of California, Santa Barbara, CA93106, USA)

2:30 PM - 2:45 PM JST | 5:30 AM - 5:45 AM UTC

[SSS09-14] Study on Microseisms excited by Typhoons around Japan

*Hiroki Kawakami[1], Naoki Suda[1] (1.Hiroshima University)

2:45 PM - 3:00 PM JST | 5:45 AM - 6:00 AM UTC

[SSS09-15] Extraction of P-wave reflections of mantle discontinuities from ambient seismic noise beneath Japan

*Shota Kato[1], Kiwamu Nishida[1] (1.Earthquake Research Institute, the University of Tokyo)

3:00 PM - 3:15 PM JST | 6:00 AM - 6:15 AM UTC

[SSS09-16] A centroid catalog of P-wave microseisms

*Kiwamu Nishida[1], Ryota Takagi[2] (1.Earthquake Research Institute, University of Tokyo, 2.Research Center for Prediction of Earthquakes and Volcanic Eruptions, Graduate School of Science, Tohoku University)

Imaging the solar interior using noise tomography

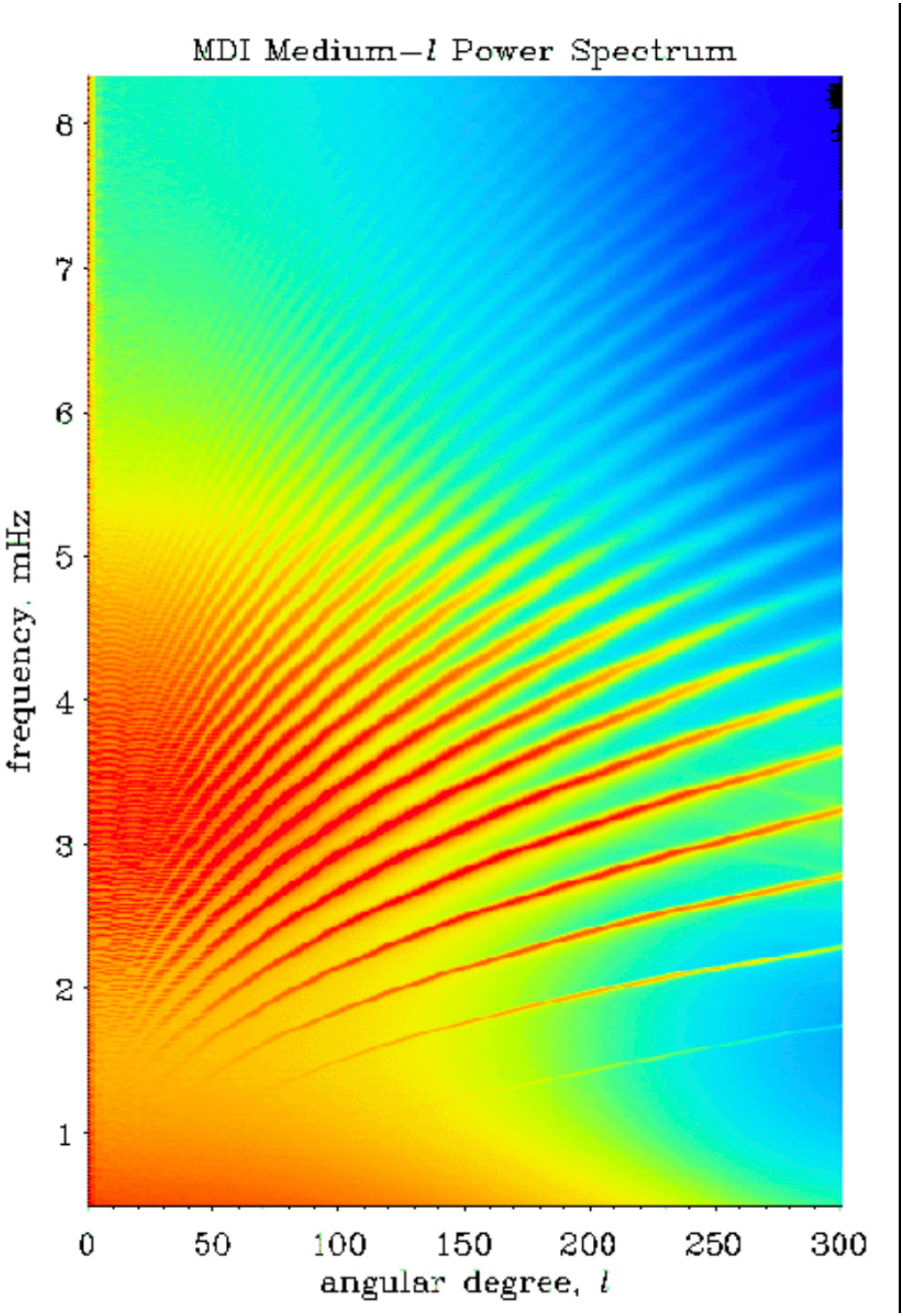
*Shravan Hanasoge[1]

1. Tata Institute of Fundamental Research

Helioseismology is the science of imaging the solar interior using observations of acoustic oscillations at the surface. These waves are stochastically excited by turbulence in the near-surface layers of the Sun, which then traverse the interior and re-emerge at the surface. Much as in terrestrial noise tomography, we measure cross-correlations of the surface wavefield to infer interior properties. Drawing parallels with noise tomography, I will describe the data, methods and the many successes of helioseismology in obtaining constraints on solar interior structure and dynamics.

Keywords: Noise tomography

©2021. Japan Geoscience Union. All Right Reserved.



©2021. Japan Geoscience Union. All Right Reserved.

Incorporating wind information in the inversion of co-located pressure and seismic data for shallow elastic structure

*Toshiro Tanimoto[1]

1. Department of Earth Science, University of California, Santa Barbara, CA93106, USA

When surface pressure is large, seismic noise between about 0.01 Hz and 0.05 Hz is mostly generated by wind-related surface pressure changes. By analyzing this phenomenon using co-located pressure and seismic data, we can derive shallow elastic structure in the uppermost 50-100 m.

However, there still remains a difficult question on seismic excitation by wind-related surface pressure because of complexity in wind behaviors. Roughly speaking, it consists of the mean shear flow part and the turbulent part. The mean flow part should act like a moving pressure source on the surface while the turbulent parts act like a stochastic source as the surface pressure field becomes heterogeneous.

We point out that this complexity may be reduced by selecting time intervals of stable wind directions. During such time intervals, pressure changes occur in the direction of winds, which justifies us to use a relatively simple, moving pressure source model. We quantify the stability of wind direction by the standard deviation of wind direction data.

For stations with co-located wind, pressure, and seismic data, we propose to select time intervals with stable wind directions first and apply our inversion method based on the moving pressure model. In the absence of wind data at a station with co-located pressure and seismic data, we propose to analyze the high-pressure end of data, as this selection partially satisfies the stable wind condition. Some representative results will be shown by using data from the EarthScope Transportable Array.

Keywords: Shallow elastic structure, Inversion of pressure and seismic data, Low-frequency seismic noise excited by winds

©2021. Japan Geoscience Union. All Right Reserved.

Study on Microseisms excited by Typhoons around Japan

*Hiroki Kawakami[1], Naoki Suda[1]

1. Hiroshima University

Seismograms include not only intermittent, high-amplitude oscillations due to earthquakes, but also continuous, low-amplitude ones due to atmospheric and oceanic disturbances. The oscillations at 0.05-0.5 Hz are generally called microseisms and have relatively large amplitudes. Microseisms are classified into weak primary microseism at 0.05-0.1 Hz and strong secondary microseism at 0.1-0.5 Hz. The former is thought to be excited by the ocean waves themselves, and the latter by the interaction of ocean waves. Microseisms are mainly composed of Rayleigh and Love waves, so that the energy of microseism efficiently propagates in the solid earth. Studies linking typhoons that excite large ocean waves and microseisms have been conducted so far, but the source and excitation mechanism of microseisms have not yet been fully understood. Locating the source area of microseism is important not only for understanding the interaction between atmosphere, ocean and solid earth, but also for estimating the Earth's internal structure using microseisms. In this study, we estimated the source areas of the primary microseism excited by typhoons approaching Japan.

We used seismic records from the F-net broadband seismograph network as the seismic wave data. We obtained 1st percentile power spectra for all the 72 F-net stations to select quiet 20 stations with the consideration of the station distribution. For typhoon information, we referred to the database of the Japan Meteorological Agency. In this study, we analyzed the seismic records in the periods of six large typhoons approaching Japan with the maximum wind speed of 33 m/s or more in 2019 and 2020, FRANCISCO (typhoon number 1908), KROSA (1910), FAXAI (1915), HAGIBIS (1919), HAISHEN (2010) and CHAN-HOM (2014).

Source areas were estimated using Rayleigh waves with a similar method to Park & Hong (2020) for locating the source areas of microseisms caused by the typhoon that passed through the South China Sea. This method utilizes the Rayleigh wave characteristic that the horizontal component is phase-shifted by $\pi/2$ in the negative direction of the time axis with respect to the vertical component. When the cross-correlation coefficient between the horizontal component rotated to a certain direction and the vertical component whose phase is shifted by $\pi/2$ in the negative direction of the time axis is maximum, the source is in that direction. In this study, we obtained the station averages of the cross-correlation coefficients computed for source grids with an interval of 0.1 degrees on the surface to estimate the source distribution of the primary microseism during the approach period of typhoon. We defined the area with high correlations as the source area of microseism.

The result has shown that the seismic energy of the primary microseism at 0.08-0.1 Hz is greatly excited with the approach of the typhoons, and the main source areas are almost the same as the typhoon storm areas. However, in the four typhoons HAGIBIS, FAXAI, HAISHEN and CHAN-HOM, it has been shown that the source areas stagnate after the passage of typhoon. There was a strong correlation between ocean-wave and microseism amplitudes during the stagnation. The stagnant source areas might be due to the seafloor sandwiched by topography highs, which efficiently excited the microseism even after the passage of typhoon.

©2021. Japan Geoscience Union. All Right Reserved.

Keywords: microseisms, typhoons, seismographs, ocean waves, storms

©2021. Japan Geoscience Union. All Right Reserved.

Extraction of P-wave reflections of mantle discontinuities from ambient seismic noise beneath Japan

*Shota Kato[1], Kiwamu Nishida[1]

1. Earthquake Research Institute, the University of Tokyo

Seismic interferometry (SI) is the technique that extracts the Green's function between a station pair by calculating the cross-correlation function (CCF) of the random seismic wavefield. Microseisms, which are excited by ocean swell activities, and earthquake coda, multiple scattered by the heterogeneous structure, are typical examples of a random seismic wavefield. Because surface waves dominate microseisms, the extracted surface waves are used to infer the S wave velocity structure of the crust and upper mantle (e.g., Shapiro et al., 2005). Recent studies also start to utilize information on the body waves as well as the surface waves extracted by SI. For example, some groups reported reflected P waves at the 410/660 km discontinuities (P410P/P660P) (Poli et al., 2012; Feng et al., 2017) using the continental stations. This study aims to extract the P410P/P660P by applying SI to microseisms and earthquake coda, recorded by Hi-sensitivity Seismograph Network Japan (Hi-net), and discuss the effect of the source distribution of wavefield on the retrievals.
The procedures of the CCF calculation of microseisms are as follows: The dataset in this study is the vertical components of 240 Hi-net stations in Southwest Japan and 168 stations in Northeast Japan (2007–2018). We down-sampled the original 100 Hz data to 2 Hz. The 1-day-length waveform was split into 1024-second-length segments and selected based on the mean square amplitude in 0.05-0.1 Hz and 0.1–0.2 Hz. We then calculated CCFs for every pair of stations by stacking over all the selected segments with spectral whitening from 0.1 to 0.2 Hz.
The method of the CCF calculation of earthquake coda is mostly the same as that of microseisms. The time-windows are the 1500-4800 s from the origin time of large earthquakes (Mw>6.5; 534 events). The running absolute mean method (Bensen et al., 2007) was applied to all earthquake coda waveforms.
In SW Japan, both CCFs of microseisms and CCFs of earthquake coda show P410P, but no or weak P660P. The lack of extraction of P660P despite CCFs calculated from independent wavefield suggests that the structure near 660 km discontinuity in SW Japan makes the extraction of P660P difficult. The CCFs of earthquake coda show P410P/P660P in NE Japan, partly because of the coincidence between the arrival direction of wavefield and the direction of stations, suggesting that many station pairs in NE Japan have incident waves with the adequate direction for the extraction. The extraction of P410P/P660P is limited by the distribution of wave sources and the geometry of stations, especially from microseisms.
As another analysis for obtaining the information of mantle discontinuities from microseisms, the receiver function analysis of microseismic P wave was performed. We focused on the P wave excited by the weather bomb in the Atlantic Ocean (Nishida and Takagi, 2016). For the estimation of the source time function, all the vertical components were stacked over all the stations after the back-propagations to the source. The deconvolution of the radial component with the source time function was calculated using 691 Hi-net stations. The preliminary result shows the extraction of converted S waves by 410 km discontinuity (P410s) beneath Japan. However, the result shows no or weak peak corresponding to P660s. The extraction of P410s and no or weak P660s is consistent with the result of SI, which shows the P410P and weak P660P.

Keywords: Seismic Interferometry

©2021. Japan Geoscience Union. All Right Reserved.

A centroid catalog of P-wave microseisms

*Kiwamu Nishida[1], Ryota Takagi[2]

1. Earthquake Research Institute, University of Tokyo, 2. Research Center for Prediction of Earthquakes and Volcanic Eruptions, Graduate School of Science, Tohoku University

Although observations of microseisms can date back to the early 1900s [e.g., Wiechert 1904], the excitation mechanisms are still in progress. The source distribution is a key for understanding the excitation mechanism.
When we observed teleseismic P-wave microseisms at a distant station, the source can be approximated by a centroid single force practically (e.g., Nishida and Takagi, 2016). The centroid location of P-wave microseisms is crucial for understanding the origins of microseisms. Backprojection method is feasible for locating the centroids of body-wave microseisms. The technique utilizes the information of both slowness and the curvature of the wavefront. It can also utilize information on multi-phases. However, the computational cost is still expensive for making a global catalog for over ten years. On the other hand, the computational cost of beamforming is inexpensive. However, the method cannot distinguish P from PP waves because it utilizes information only on slowness. In this study, we propose a new technique that can extract information, both slowness and the curvature of the wavefront, as a natural extension of beamforming.

In this method, we first infer the initial guess of the slowness vector at the center of the seismic array based on the conventional beamforming. We estimate the beam power according to an assumed curvature for the fixed slowness in the second step. By maximizing the beam power, we infer the initial guess of the curvature at the center. We update the values (slowness vector and the curvature at the center) iteratively based on the perturbation theory. The curvature gives us information on the epicentral distance between the center of the array and the source, although the accuracy is low in general. According to the distance information, we classify the detected slowness into the corresponding phase (e.g., P, or PP). Based on the classified phase, we infer the source location from the slowness value. The curvature information is also useful for reducing the false detection of the beamforming. To improve the accuracy of the centroid locations, we estimated corrections of the measured slowness vector for a global P-wave model (LLNL-G3Dv3: Simmons et al. 2012) using three-dimensional ray tracing (PMTI, Simmons, et al. 2011). To validate the technique, we applied this method for earthquakes with moment magnitudes larger than xx listed in the global CMT catalog (Ekström et al., 2012). The results with the corrections for the three-dimensional structure are consistent with the catalog.

We applied this method for vertical components of velocitymeters at about 800 Hi-net stations in Japan, operated by the National Research Institute for Earth Science and Disaster Prevention (NIED) from 2004 to 2018. The inferred centroid locations show seasonal variations, which are consistent with past studies. We will show a new preliminary catalog of source locations of global P-wave microseisms.

©2021. Japan Geoscience Union. All Right Reserved.

[J] Poster | S (Solid Earth Sciences)：S-SS Seismology

Sat. Jun 5, 2021 5:15 PM - 6:30 PM JST | Sat. Jun 5, 2021 8:15 AM - 9:30 AM UTC | Ch.13_2

[S-SS09] Seismic wave propagation: Theory and Application

convener:Kaoru Sawazaki(National Research Institute for Earth Science and Disaster Resilience), Kiwamu Nishida(Earthquake Research Institute, University of Tokyo), Takao Nibe(JAPEX), Kyosuke Okamoto(National Institute of Advanced Industrial Science and Technology)

Seismic wave propagation provides rich information on earth's heterogeneities and the excitation sources. Understanding of this information requires various research fields: mathematical/numerical studies based on wave theory, physical experiments using rock samples, seismic data analysis, etc. With recent developments of observational techniques, various wave phenomena have been elucidated: seismic waves, acoustic waves, traveling ionospheric disturbances, and tsunamis. New frameworks will be crucial for comprehensive understanding of these phenomena. This session widely invites presentations about the theories and applications related to seismic and other geophysical waves.

[SSS09-P01] Temporal variation in seismic velocity at the shallow part of the overriding plate in the Japan Trench

*Takashi Tonegawa[1], Ryota Takagi[2], Kaoru Sawazaki[3], Katsuhiko Shiomi[3] (1.Japan Agency for Marine-Earth Science and Technology, 2.Tohoku University, 3.National Research Institute for Earth Science and Disaster Resilience)

[SSS09-P02] Estimation of instrumental clock errors at 46 active volcanoes in Japan based on seismic interferometry

*Takashi Hirose[1] (1.National Research Institute for Earth Science and Disaster Resilience)

[SSS09-P03] On the factors influencing ambient-noise passive seismic imaging

*Xin Guo[1], Zhihui Zou[1,2], Yongjun Rui[3], Qinghui Cui[3], Xinmin Shang[3] (1.College of Marine Geosciences, Key Lab of Submarine Geosciences and Prospecting Techniques. MOE, Ocean University of China, Qingdao 266100, China, 2.Evaluation and Detection Technology Laboratory of Marine Mineral Resources, Qingdao National Laboratory for Marine Science and Technology, Qingdao 266061, China, 3.Geophysical Research Institute of Shengli Oilfield, Sinopec, Dongying, China 257022)

[SSS09-P04] Migration of fluid during oil recovery revealed by Reverse Time Imaging

*Runbi Yuan[1], Zhihui Zou[2,1], Cui Qinghui[3], Rui Yongjun[3], Shang Xinmin[3] (1.College of Marine Geosciences, Key Lab of Submarine Geosciences and Prospecting Techniques. MOE, Ocean University of China, Qingdao 266100, China, 2.Evaluation and Detection Technology Laboratory of Marine Mineral Resources, Qingdao National Laboratory for Marine Science and Technology, Qingdao 266061, China, 3.Geophysical Research Institute of Shengli Oilfield, Sinopec, Dongying, China 257022)

[SSS09-P05] Effects of fine-scale heterogeneity distribution in the Pacific slab on the generation of anomalously large intensities from deep-focus earthquakes

*Takashi Furumura[1], Brian LN Kennett[2] (1.Earthquake Research Institute The University of Tokyo, 2.Research School of Earth Sciences The Australian National University)

[SSS09-P06] Scattering properties in Japanese volcanoes as inferred from the peak ratio analysis of teleseismic P waves using the JMA seismometer network data

*Gugi Aucklandi Ganefianto[1], Hisashi Nakahara[1], Takeshi Nishimura[1] (1.Tohoku University)

[SSS09-P07] Crack source and volcanic structural heterogeneity inferred from oscillatory waveforms of long-period seismic events: Application at Kusatsu-Shirane Volcano

*Nakano Masayuki[1], Hiroyuki Kumagai[1] (1.Nagoya University)

[SSS09-P08] Applying the shortest path method to anisotropic media in order to calculate ray paths

*Shoji Sekiguchi[1] (1.National Research Institute for Earth Science and Disaster Resilience)

[SSS09-P09] Numerical simulations of weak localization of scalar waves based on the finite difference method (2)

*Jun Kawahara[1], Masanobu Sato[1] (1.Graduate School of Science and Engineering, Ibaraki University)

[SSS09-P10] Observability of seismic radial anisotropy parameters by the analysis of surface waves and receiver functions based on the MCMC analysis

*Jumpei Maruyama[1], Hitoshi Kawakatsu[1], Nozomu Takeuchi[1] (1.University of Tokyo, Earthquake Research Institute)

Temporal variation in seismic velocity at the shallow part of the overriding plate in the Japan Trench

*Takashi Tonegawa[1], Ryota Takagi[2], Kaoru Sawazaki[3], Katsuhiko Shiomi[3]

1. Japan Agency for Marine-Earth Science and Technology, 2. Tohoku University, 3. National Research Institute for Earth Science and Disaster Resilience

Ambient noise correlation technique is now a powerful tool for detecting temporal variation in seismic velocity. Because such studies require long-term continuous seismic records, they have been often used to land-based seismic records. However, permanent seismic observations have recently deployed offshore areas, particularly around Japan, this technique can be applied to temporal variation in seismic velocity structure at the subseafloor (e.g., Ikeda and Tsuji, 2018). In particular, Tonegawa et al. (2020, JpGU; AGU) has reported that seismic velocity and heterogeneity changes are induced by tectonic compression and fluid migration at the subseafloor structure in the Nankai subduction zone. In this study, we applied ambient noise correlation technique to the continuous records observed at S-net deployed around the Japan Trench, and investigated the relationships among temporal variation in seismic structure, seismic activities, and tectonic settings.

We calculated cross correlation functions (CCFs) at a frequency band of 0.5–1.0 Hz using ambient noise records in the vertical component. Here, the three-component seismograms were synthesized using a method of Takagi et al. (2019). The CCFs show ocean acoustically-coupled Rayleigh waves whose propagation velocity is slightly less than 1.5 km/s. The time length of the time series for calculating CCFs was 3600 s, but the time series was subtracted by those in the next 3600 s for removing instrumental noises, according to the method of Takagi et al. (2021). The calculated CCFs are stacked over 1 year for the reference CCF and 30 days for individual CCFs. We measured seismic velocity change (dv/v) by a stretching method (Wegler and Sens-Schönfelder 2007) and also seismic heterogeneity change (CC) by cross correlating the reference and individual CCFs (Obermann et al. 2013).

Our results show temporal changes in dv/v near the Japan Trench, while such changes cannot be observed in the region close to land. The maximum change of dv/v over 4 year was 0.3 % around the latitude of 39ºN. It is considered that the gradual change primarily corresponds to the recovery process of a velocity reduction associated with the 2011 Tohoku-oki earthquake. Another candidate is tectonic compression in the overriding plate near the trench at this region, which induces a seismic velocity increase due to fluid drainage at shallow depths to the sea water.

Our results also show abrupt reductions in CC, but the areas of the changes are wide compare with those observed in the Nankai area. Some of them correspond to the timing of relatively large earthquakes, indicating that seismic heterogeneity at shallow depths was varied with seafloor motion due to the earthquakes. However, it appears that other CC reductions do not correspond to the large earthquakes. It is necessary to investigate the CC reductions in more details.

Data citation

S-net: doi:10.17598/NIED.0007

©2021. Japan Geoscience Union. All Right Reserved.

Keywords: Seismic velocity, Temporal variation, Japan Trench

©2021. Japan Geoscience Union. All Right Reserved.

Estimation of instrumental clock errors at 46 active volcanoes in Japan based on seismic interferometry

*Takashi Hirose[1]

1. National Research Institute for Earth Science and Disaster Resilience

The correct absolute timing of seismograms is crucially required in many seismological analyses. In recent years, seismic interferometry [e.g., Curtis et al., 2006; Shapiro, 2004] has been widely used to detect structural changes related to large earthquakes and volcanic activities [e.g., Brenguier et al., 2008; Wang et al., 2019; Hirose et al., 2020; Nishida et al., 2020]. Some previous studies have investigated the use of seismic interferometry to correct seismometer clocks [e.g., Stehly et al., 2007; Sens-Schönfelder, 2008; Hable et al., 2018]. Estimating instrumental clock errors are also important for continuous seismic monitoring of active volcanoes. I develop an estimation method of instrumental clock errors based on seismic interferometry and apply this method to 46 active volcanoes in Japan.

I computed seismic ambient noise cross-correlation functions (CCFs) using continuous seismograms at V-net and JMA stations of 46 active volcanoes in Japan between Jan. 1, 2020, and Jan. 31, 2021. Continuous seismic records on vertical component were divided into 10-minutes-long segments and applied spectral whitening [e.g., Shapiro et al., 2006; Bensen et al., 2007] and one-bit normalization [Larose et al., 2004]. Daily CCFs (DCCFs) were obtained by stacking CCFs every 10 minutes. I measured delay times between a reference 3-days-stacked CCF and a current 3-days-stacked CCF for each station pair and lag time at a 0.2-4 Hz band using the windowed cross-correlation method [e.g., Snieder et al., 2012]. A clock error will cause the same delay times between the reference and current CCFs at all lag times. Therefore, I fitted a straight line to the delay times at each lag time and assumed the straight line's intercept as the clock difference for that station pair. On the straight-line fitting, I used L1 norm optimization to suppress the effect of outliers. Finally, I estimated clock errors at each seismic station by linear least-squares inversion with the estimated clock differences.

In this study, clock errors were estimated for the time period between Jan. 1, 2020, and Jan. 31, 2021. Significant clock errors were detected at some volcanoes: At Nasu volcano, the clock of station N.NSOV started to drift with about 0.009 s/day in early Jan. 2021. This drift was caused by a malfunction of the GPS antenna from Jan. 8, 2021. At Asama volcano, a clock jump of about 1.0 s occurred at station V.ASME during Apr.-Jun. 2020, and the clock of station V.ASMG had a drift of about 0.005 s/day during Aug.-Oct. 2020. At Miyakejima volcano, the clock of station V.MYKO repeatedly drifted with 0.002 to 0.006 s/day during May-Jul. 2020, Aug.-Nov. 2020, and Dec. 2020-Jan. 2021. Repeated clock drifts (0.003-0.096 s/day) also occurred at Kusatsu-Shirane volcano. Maximum clock errors of station V.KSHA at Kusatsu-Shirane were estimated to be 1.55 s in Aug. 2020 and 0.84 s in Nov. 2020. Estimated clock errors in this study could improve the results of various seismological analyses at the 46 volcanoes, for example, hypocenter determination of volcanic earthquakes and seismic interferometry analysis.

Acknowledgment: I used seismograms recorded by Japan Meteorological Agency (JMA).

©2021. Japan Geoscience Union. All Right Reserved.

Keywords: seismic interferometry, clock error, volcano monitoring

©2021. Japan Geoscience Union. All Right Reserved.

On the factors influencing ambient-noise passive seismic imaging

*Xin Guo[1], Zhihui Zou[1,2], Yongjun Rui[3], Qinghui Cui[3], Xinmin Shang[3]

1. College of Marine Geosciences, Key Lab of Submarine Geosciences and Prospecting Techniques. MOE, Ocean University of China, Qingdao 266100, China, 2. Evaluation and Detection Technology Laboratory of Marine Mineral Resources, Qingdao National Laboratory for Marine Science and Technology, Qingdao 266061, China, 3. Geophysical Research Institute of Shengli Oilfield, Sinopec, Dongying, China 257022

The passive seismic imaging method extracts the subsurface reflected signals using the cross-correlation of ambient noise. It has the advantages of low cost and little environmental damage, and can image the subsurface continuously. The passive seismic method has been applied in the fields of time-lapse monitoring the changes in petroleum reservoirs and mining processes. One of the effective passive seismic method is developed on the base of the seismic interferometry. The basic idea of seismic interference was proposed by Claerbout (1968) firstly, in which case the Green's function was estimated through the auto-correlation of seismic records generated by underground sources. In the exploration geophysics, Schuster et al. (2001) reconstructed the seismic wave field from the cross-correlation information using a generalized correlation of seismic data. Draganov et al. (2009) proposed a method based on cross-correlation to passively reconstruct the reflections using the seismic waveforms radiated from the underground sources. The workflow of passive seismic imaging is as follows: firstly, the seismic record is divided into a small time window for filtering analysis; secondly, select the panel dominated by body wave noise, and normalize each trace each panel; thirdly, select one trace as the position of virtual source shot to cross-correlate with other all traces; finally, stack them together to create one channel of the seismic record. A new seismic record is created by stacking the negative and positive parts. The main factors influencing the process of reflection extraction include: ①source distribution; ②wavelet type; ③ seismic recording time; ④wavelet coherence. These factors are essential for the successful extraction of reflected signals, but systematic studies in this area are still lacking.

To analyze the influencing factors of the quality of passive reflected signals, we conduct a series of numerical tests. The effects of various factors on the quality of the reflection waves are compared and analyzed by synthesizing the virtual source seismic records from the transmitted wave response of underground passive sources. The results show that the denser the distribution of the seismic sources, the longer the recording time, and the stronger the incoherence of the seismic source, the better the quality of the synthetic reflection wave recording. By analyzing the factors that influence the construction of reflection waves, the processing flow of passive seismic exploration can be optimized to improve the quality of passive seismic imaging.

©2021. Japan Geoscience Union. All Right Reserved.

Migration of fluid during oil recovery revealed by Reverse Time I maging

*Runbi Yuan[1], Zhihui Zou[2,1], Cui Qinghui[3], Rui Yongjun[3], Shang Xinmin[3]

1. College of Marine Geosciences, Key Lab of Submarine Geosciences and Prospecting Techniques. MOE, Ocean University of China, Qingdao 266100, China, 2. Evaluation and Detection Technology Laboratory of Marine Mineral Resources, Qingdao National Laboratory for Marine Science and Technology, Qingdao 266061, China, 3. Geophysical Research Institute of Shengli Oilfield, Sinopec, Dongying, China 257022

The goal of microseismic source location method is to determine the spatial location and time of origin of a seismic event (Thurber 2011), which has significant value in the study of active faults, earth's internal structure, and shale gas production. Traditional seismic source location method mainly depends on the first arrival time, which requires picking the first arrival time accurately. Such seismic event location methods have limitations, because it is difficult to pick up the first arrival time in the records of the microseismic events that has low signal-to-noise (S/N) ratio. Reverse Time Imaging (RTI) method is an alternative event location method that is based on reconstructing wavefront and constructive stacking of seismic waveforms. The RTI method does not need first-arrival time and is suitable for data with low S/N (Gajewski and Tessmer 2005).

After its invention, the RTI method was continuously developed and broadly used. Steiner et al. (2008) used low-frequency information to identify reservoirs locations and provides a possible method for reservoir localization. Zou et al. (2014) successfully identified a doublet of earthquakes in the TGR region. Zhu (2014) discussed the RTI using the acoustic wave equation in attenuation media and proposed a method to overcome the influence of attenuation on the result of event location. Ge et al. (2019) combined the travel time location and RIT methods, and proposed the reverse travel time imaging (RTTI) method. Zhu (2019) developed a hybrid multiplicative time-reversal imaging (HyM-TRI) algorithm, for automatically tracking the spatiotemporal distribution of microseismic events. For its applicability in low SNR situation, the RTI has potential to image the noise generated by the movement of fluid in petroleum reservoir.

In this paper, RTI is applied to study the dynamic evolution of subsurface fluid during the steam injection for petroleum production. The real data before and after steam injection are processed respectively, and then compared to show the changes beneath the oil field. Since the noise surrounding the petroleum reservoir generated by the injection process usually has a relatively stable energy in a period of several minutes, the data of the two parts are superimposed in the time domain to suppress the influence of the random noise. Two images that are before and during the injection are normalized into the same background, and then subtracted with each other to show the difference that reflects the microseismic information generated by fracturing in the steam injection process.

©2021. Japan Geoscience Union. All Right Reserved.

Effects of fine-scale heterogeneity distribution in the Pacific slab on the generation of anomalously large intensities from deep-focus earthquakes

*Takashi Furumura[1], Brian LN Kennett[2]

1. Earthquake Research Institute The University of Tokyo, 2. Research School of Earth Sciences The Australian National University

From the analysis of OBS records in northwest Pacific and 3-D FDM simulations of high-frequency oceanic *Pn/Sn* (*Po/So*) wave propagations, lateral variations in fine-scale heterogeneity in the oceanic lithosphere have been revealed in detail (Furumura & Kennett, SSJ2020 Fall meeting). The *Po/So* propagation variability can be explained with a von Karman distribution function for elastic properties in the lithosphere with a longer correlation distance of 20 km in the NE direction, and much shorter correlation distances in the perpendicular (0.5 and 2 km) direction and in depth (0.5 km), with standard deviation from the background wavespeed of 2%. Since the longer axis of the heterogeneity distribution aligns with the observed *Pn/Sn*-wavespeed anisotropy in the northwest Pacific, it is highly likely that it was also developed during the formation and growth of the oceanic plate. Such a structure is very effective to guide high-frequency *Po/So* with long codas by multiple forward scattering in the direction parallel to the elongated heterogeneity.

The complex heterogeneity in the Pacific plate is expected to be carried by subduction deep beneath Japan, and can then produce unusually large signals in certain directions from deep earthquakes within the subducted slab. For example, on 2007 July 16, a 378 km deep Mw 6.8 earthquake beneath the Sea of Japan, produced anomalously large shaking over central to northern Japan. The shaking intensity near the epicenter was less than 1 (JMA), but the maximum intensity of 4 occurred in Obihiro, Hokkaido (Fig.1a).

Usually, such a peculiar intensity pattern occurs from deep earthquakes, as high-frequency (>1-2 Hz) signals traverse the cold, high-*Q* slab. In addition, the waveguide effect is reinforced by multiple forward scattering of seismic waves in the heterogeneous slab that captures high-frequency signals (e.g., Furumura & Kennett, 2005, JGR; Kennett & Furumura, 2015, G3). For this earthquake the significantly extended PGA contours into Hokkaido, more than 1000 km away from the hypocenter, is rather anomalous compared to other deep-focus earthquakes, indicating that an additional directional waveguide effect is needed.

We have undertaken 3-D FDM simulations of high-frequency wave propagation (up to 4.6 Hz) using the heterogenous slab structure (Fig.1b) that was identified from the *Po/So* propagation variability in the northwest Pacific. The area of simulation was 1536 km by 768 km in horizontal direction and 665 km in depth (Fig.1c), discretized by a uniform grid of 0.875 km. The crust and mantle structure was based on Crust 1.0 (Laske et al., 2013) and deeper structure was *ak135* (Kennett et al., 1995) with earth flattening. The Pacific plate model was based on Yokota et al. (2017).

The simulation results show that the presence of an elongated fine-scale heterogeneity in N45^{o}E direction in the Pacific slab (Model A in Fig.2a) can reproduce the main pattern of larger PGA extending to Hokkaido, similar to the observations, though the level of simulated ground motion was about a half of observation due to high-frequency limitations in the FDM simulation. The importance of the orientation of

©2021. Japan Geoscience Union. All Right Reserved.

the heterogeneity distribution for enhanced waveguide effects is demonstrated by comparison with the results using another model (Model B) in which the longer correlation length is orthogonal (N135°E; Fig. 2b). The simulation for Model B displays large PGA contours from Tokyo to the offshore of Tohoku, but these do not extend to Hokkaido.

A further deep event beneath Sakhalin (2013 July 23; depth=487 km, Mw6.8) did not display large PGA over Japan. FDM simulation shows that this effect arises from the propagation of seismic waves to Japan perpendicular to the elongated heterogeneity in the Pacific slab.

Keywords: Deep earthquake, Fine-scale heterogeneity, Oceanic lithosphere

©2021. Japan Geoscience Union. All Right Reserved.

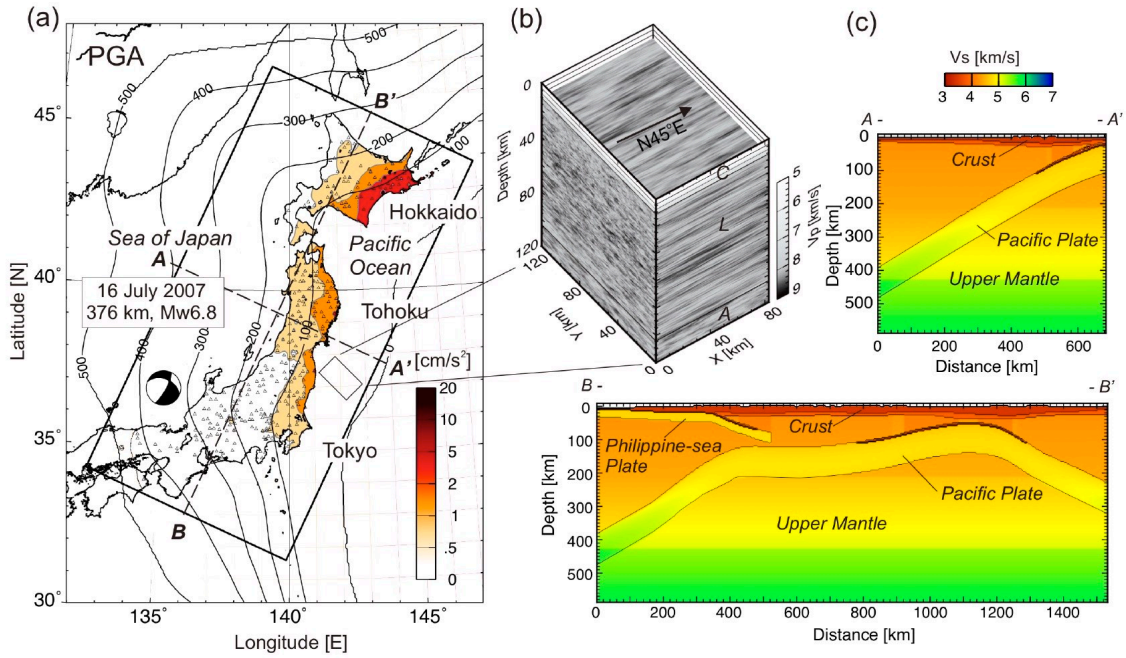


Figure 1. (a) Distribution of peak ground acceleration (PGA) for horizontal motions during the 376 km deep, Mw6.8 earthquake of 16 July 2007 that occurred in the subducting Pacific slab beneath the Sea of Japan. The black square outlines the area used for 3-D FDM simulation. (b) A 3-D view of a segment of *P*-wavespeed model of oceanic crust (*C*), lithosphere (*L*) and asthenosphere (*A*) with fine-scale heterogeneity is shown. (c) Vertical cross sections along A--A′ and B--B′, and *S*-wavespeed without fine-scale heterogeneity are shown.

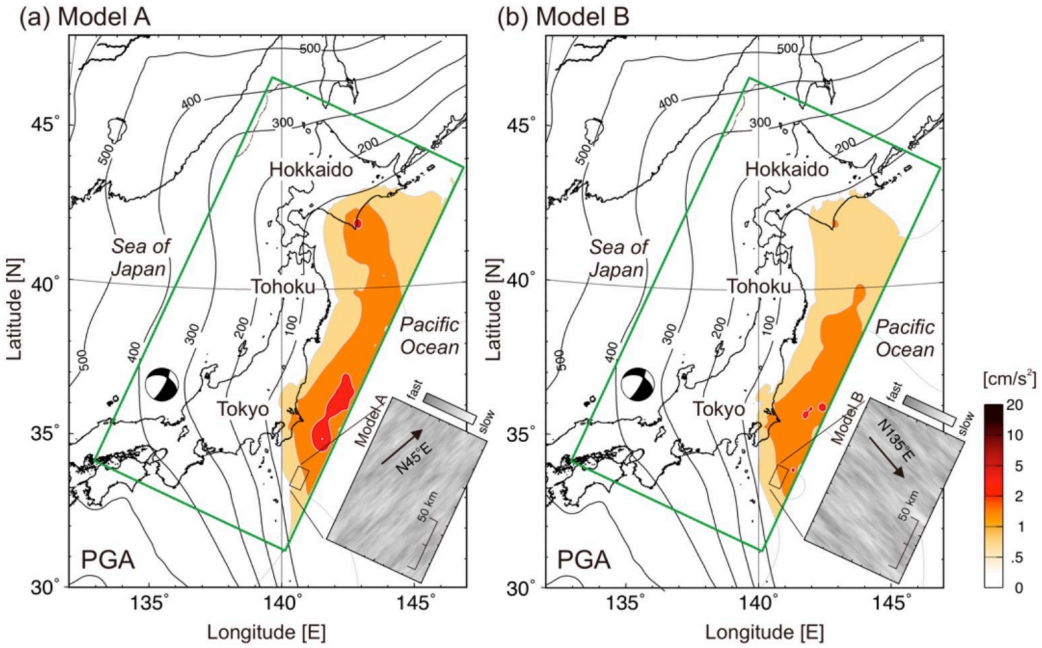


Figure 2. Comparison of the simulated PGA distribution for a deep earthquake beneath Sea of Japan obtained by simulation using different heterogeneity models; (a) Model A with a horizontally elongated heterogeneity in N45°E direction and (b) Model B in N135°E direction (illustrations of the velocity fluctuations at the crust-lithosphere boundary of the Pacific slab are shown to the right). The green rectangle indicates the area used for the 3-D FDM simulation and solid lines denote the iso-depth contours of the Pacific slab at 100 km interval.

©2021. Japan Geoscience Union. All Right Reserved.

Scattering properties in Japanese volcanoes as inferred from the peak ratio analysis of teleseismic P waves using the JMA seismometer network data

*Gugi Aucklandi Ganefianto[1], Hisashi Nakahara[1], Takeshi Nishimura[1]

1. Tohoku University

Stochastic approaches to study the small-scale medium heterogeneities are based on seismic scattered waves invoked by them. One approach is to use the partition of teleseismic P wave energy into the transverse component seismogram. The parameter used to measure the strength of this seismic wave scattering is the peak energy ratio, which is defined as the ratio of the maximum P wave energy in the transverse component seismogram envelope, to that of the sum of the transverse, radial, and vertical components. According to Sato (2006), the peak ratio can be approximated as $1.81 \varepsilon^2 h/a$ where ε, h, and a are fractional fluctuation in seismic velocity, thickness of the heterogeneous medium, and correlation distance respectively.

The quantification of the small-scale velocity heterogeneities through the computation of the peak ratio has been done by Kubanza et al., (2007) on a global scale. Nishimura (2012) estimated the peak ratio values at the Hi-net seismometer network in Japan. There are two significant observations that can be made from these two studies. One is that the peak ratio increases with increasing frequency. The second is that the more active regions, such as those in the proximity of quaternary volcanoes, yield higher peak ratios. The first observation has been explored by Ganefianto et al. (2020 SSJ meeting) through our estimation of the frequency gradient which characterises the power spectral density function of the small-scale heterogeneity. In this study, we would like to further examine the second observation, by calculating the peak ratios at JMA stations in many volcanoes of Japan. Through this approach, we would like to test the conjecture that the peak ratio gets higher at stations closer to a volcanic centre, in line with the increase in geological activity.

Data from 99 teleseismic events, recorded between 2010 and 2019 were considered. These earthquakes have depths of >300 km, magnitudes of roughly 5 to 6.5, and range between 0° to 60° epicentral distance from Japan. Analyses were performed under four separate frequency bands: 0.5-1, 1-2, 2-4, and 4-8 Hz. Source-receiver pairs with the signal-to-noise ratio of <10 were discarded. We computed seismogram envelopes of the remaining pairs. Finally, for individual stations that record >10 earthquakes, we stacked their envelopes together to obtain the mean-squared envelopes.

Our results show that the peak ratio of the JMA stations mostly range from roughly 0.16-0.44, 0.22-0.52, 0.24-0.54, and 0.30-0.60 for the 0.5-1, 1-2, 2-4, and 4-8 Hz band, respectively. The average and median value is increasing with the frequency as well. These ranges are on the high-end scale of what was found for the corresponding Hi-net peak ratios (e.g. Nishimura, 2012). As a result, on average, the peak ratio of the JMA network is larger than the Hi-net network in all frequency bands. This is also true when comparing only the Hi-net stations that are near quaternary volcanoes. We differentiate the JMA stations in our study according to the volcano they monitor. We see that most JMA stations indicate larger peak ratios than what was estimated for the quaternary volcano stations in the previous study. Furthermore, we differentiate the JMA stations into borehole and surface stations. And we observed that the peak ratios at the surface stations are higher than those at the borehole stations. All of these observations are verified to

©2021. Japan Geoscience Union. All Right Reserved.

be statistically significant from the t test. In other words, this suggests that it is highly unlikely that the patterns that we see are simply due to chances.

We speculate that there are two interdependent causes for such observations. One is because the JMA stations are positioned much closer to the volcanic centre which exposes them to richer heterogeneous elements created by volcanism. The second is due to the topography where it may convert P wave energies into surface waves, which can also excite the station’ s transverse component. This second cause seems to be much more prevalent at the surface stations compared to the borehole stations, owing to the penetration depth of surface waves.

Acknowledgement: We would like to thank the National Research Institute for Earth Science and Disaster Resilience (NIED) and the Japan Meteorological Agency (JMA) for the access to the data of the high sensitivity seismograph network (Hi-net) and the JMA volcanic seismometer network.

Keywords: Heterogeneity, Seismic scattering, Volcanoes, JMA seismometers, Hi-net, Surface wave conversion

©2021. Japan Geoscience Union. All Right Reserved.

Crack source and volcanic structural heterogeneity inferred from oscillatory waveforms of long-period seismic events: Application at Kusatsu-Shirane Volcano

*Nakano Masayuki[1], Hiroyuki Kumagai[1]

1. Nagoya University

Long-period (LP) events observed at active volcanoes are interpreted as oscillations of fluid-filled resonators in magma and hydrothermal systems. The fluid-filled crack model has been used to interpret LP waveforms. However, the crack source was estimated for only specific LP events due to technical difficulty in synthetic waveform calculations and poor understanding of volcano heterogeneity. To solve these problems, we developed a method to estimate crack sources of LP events and volcano heterogeneity easily by using multiple spectral peaks in LP events. We used peak-to-peak amplitudes of observed and synthetic waveforms to obtain stable inversion results. First, we performed numerical tests to verify the waveform inversion method using the analytical solution of Green's functions in an infinite homogeneous medium. We used OpenSWPC (Maeda et al., EPS, 2017) based on a finite difference method (FDM) accommodating topography and heterogeneity, and calculated synthetic waveforms for a horizontal crack, which were regarded as observed waveforms. By assuming the source mechanism as a crack, we conducted inversion using synthetic waveforms calculated with the analytical solution. As a result, the source depth was estimated to be shallower, but the crack inclination was estimated to be within errors of 10º. Thus, the analytical solution may be used to estimate LP sources, although there are some errors. Next, we applied our inversion method to an LP event observed on 26 April, 1992 at Kusatsu-Shirane volcano, Japan. Our result indicates that the estimated crack angles are similar to those of Nakano and Kumagai (GRL, 2005) which used synthetic waveforms calculated with a homogeneous half-space, although the source depth is slightly shallower than the previous estimate. Our application of the inversion method to other three LP events at this volcano, of which source mechanisms were not estimated before, indicates that the crack angles of the four LP events are similar, suggesting that these events were excited by the same crack. Taguchi et al. (JGR, 2018) considered that steam generated by degassing from magma entered into a crack repeatedly. Therefore, our results support this source model. By assuming that the source mechanism for multiple spectral peaks is same as the crack for the lowest frequency peak, we estimated normalized residuals by fitting observed waveforms at individual spectral peaks to synthetic waveforms calculated with the analytical solution. We found that the estimated residuals increased with increasing frequency. To evaluate this trend, we conducted FDM simulations using a von Kármán-type heterogeneity model characterized by the correlation distance (a) and heterogeneity fluctuation (ε). Volcano heterogeneity is characterized by smaller a and larger ε than those in the crust, and a = 50 m and ε = 0.2 were used by Morioka et al. (JGR, 2017). Wegler (JGR, 2004) and Kumagai et al. (JGR, 2018) indicated that strongly heterogeneous layers at volcanoes are limited to a depth of 1 km. Using a heterogeneous layer with a = 50 m and ε = 0.2 to a depth of 1 km from topography surface, we calculated synthetic waveforms with FDM for individual spectral peaks in 3–8 Hz, and fitted them to the synthetic waveforms calculated by the analytical solution. Their normalized residuals were, however, much smaller than those estimated for the observed LP events. The mean free path (l_0) for a = 50 m and ε = 0.2 around 5–10 Hz is about 1700 m, but l_0 at volcanoes around 5–10 Hz has been estimated to be about 100–200 m (Wegler, JGR, 2004; Kumagai et al., JGR, 2020). The heterogeneity used in our simulations may not be appropriate and weaker than the actual heterogeneity. We cannot use large values of ε because such FDM calculations are unstable. Monte Carlo simulations

©2021. Japan Geoscience Union. All Right Reserved.

(e.g., Yoshimoto, JGR, 2000) based on the radiative transfer theory may be required to estimate the heterogeneity.

©2021. Japan Geoscience Union. All Right Reserved.

Applying the shortest path method to anisotropic media in order to calculate ray paths

*Shoji Sekiguchi[1]

1. National Research Institute for Earth Science and Disaster Resilience

Calculating ray paths in anisotropic media in travel-time tomography is carried out in only a few studies. It is meaningful to apply the shortest path method to anisotropic media in order to calculating ray paths. Applying the shortest path method is easy, because nodes distributed in the media and ray paths between nodes are given and only the travel-time along the path need to be evaluated. However, it should be noted that it is important that ray (group) velocity in a given ray path direction can be easily evaluated in order to save calculation time. Generally, in ray tracing algorithms of anisotropic media, determinant of elastic parameter tensor in a given phase slowness direction is solved at first. The obtained phase slowness, etc. are substituted into the ray tracing equation. From the ray tracing equation, ray path and travel-time are calculated. Ray (group) velocity and its direction are also evaluated, but not input parameters. Here, in advance, we calculate ray (group) velocity in various phase slowness direction at each node by solving the determinant numerically, smooth them by Spline function and save them as linear function of two parameters: group velocity directions (colatitude, longitude). Using them when needed, we can easily obtain the ray (group) velocity of a given ray direction. The phase slowness is not needed anymore, but it is used in travel-time tomography. In such a case, three vector components of the phase slowness are saved as linear functions of the two parameters: group velocity directions. Next, to confirm that our way of the calculation is correct, we calculate ray (group) velocity in homogeneous transversely isotropic media, and compare our results with analytic solutions. We use elastic parameters of PREM at depth of 24.4km (at the top of LID layer). Our results are almost same as the analytic ones, which shows our calculation works fine. Anisotropic media produce two S phases (qS1 and qS2), but, only one travel-time as an S phase is picked in most observed data processing. To adjust to the actually available data, we assume the picked S data correspond to the first S arrivals, and adopt the faster group velocity of two S phases at each node to calculate the travel-time of the first S arrival.

Keywords: shortest path method, anisotropy, ray tracing

©2021. Japan Geoscience Union. All Right Reserved.

Numerical simulations of weak localization of scalar waves based on the finite difference method (2)

*Jun Kawahara[1], Masanobu Sato[1]

1. Graduate School of Science and Engineering, Ibaraki University

Short-wavelength random heterogeneities in the Earth’ s lithosphere scatter seismic waves propagating therein. In most cases, we can consider scattered waves to be incoherent. Nevertheless, there exists an interference phenomenon due to multiple scattering called weak localization (WL), if a wave source and a receiver are located at the same position. WL is caused because a pair of waves, which propagate along reciprocal paths via identical scatterers, have the same phase and hence constructively interfere. Margerin et al. (2001) theoretically investigated WL of scalar waves and concluded that the intensity at around the source is enhanced twice as large as that in a distant position, the diameter of the volume of intensity enhancement corresponds to the wavelength of the input wave, and the emergence time of this volume is governed by the scattering mean-free time (SMFT).

In our previous study (2019, SSJ fall meeting), we simulated WL of scalar waves in 2-D von Karman-type random media, using the finite difference method (FDM). We confirmed that the obtained intensities at the sources were nearly doubled as time passed. The peak widths of intensity were about half the dominant wavelength of the input waves. However, we found no systematic relationship between the peak emergence times and the SMFTs predicted based on the Born approximation (Sato et al., 2012). A possible reason may be the breakdown of the approximation under the present model setting.

In this study, we simulated WL of scalar waves in media with randomly distributed discrete scatterers, like cracks or inclusions. In contrast to random media, the total scattering cross section (TSCS) of a discrete scatterer can be defined without approximations. If scatterers with TSCS σ_0 are distributed with a number density n, then the SMFT is given as $(n\sigma_0 V_0)^{-1}$, where V_0 is the background wave velocity.

We adopted again a velocity-stress scheme FDM (Virieux, 1984). We modeled scatterers as small low-velocity squares with the side length of several grid intervals. These scatterers were distributed randomly, but without overlapping, in an area on the grid. We repeated simulations for many such areas with the same number density, and then calculated the ensemble average of intensity distributions from synthesized wavefields. We also estimated the TSCS of each scatterer after Suzuki et al. (2006). We repeatedly simulated plane waves propagating in areas with scatterers, and then evaluated scattering Q^{-1} as a function of wavenumber k from the spectra of the ensemble-averaged waves. We then obtained the TSCS $\sigma_0(k)$ via the relation $Q^{-1}=n\sigma_0/k$. Here we assumed the sparse distributions of scatterers and the wavelength much longer than the scatter size, which means nearly isotropic scattering.

Our simulations denoted again the intensity enhancement at the sources, with the relative peak heights of intensity being about two. The peak widths of the intensity were close to the dominant wavelength of the input waves. The peak emergence times were fairly smaller than the SMFT, but we found positive correlation between them. The peaks tended to emerge earlier for denser distribution of scatterers, that is, stronger scattering.

Keywords: weak localization, scalar waves, finite difference method, discrete scatterers

©2021. Japan Geoscience Union. All Right Reserved.

©2021. Japan Geoscience Union. All Right Reserved.

Observability of seismic radial anisotropy parameters by the analysis of surface waves and receiver functions based on the MCMC analysis

*Jumpei Maruyama[1], Hitoshi Kawakatsu[1], Nozomu Takeuchi[1]

1. University of Tokyo, Earthquake Research Institute

Although recent studies have reported the existence of strong radial anisotropy (RA) in the upper mantle/crust beneath the ocean and in the shallow crust directly under volcanos (e.g., Ekstrom & Dziewonski, 1998; Nettles & Dziewonski, 2008; Russell et al., 2019; Jaxybulatov. et al., 2014; Nagaoka, 2020), no constraint for its origin has been obtained from seismic observations. This is partly because the Rayleigh wave sensitivity kernels for vertical S wave velocity β_V and dimentionless parameter η_K, which is recently defined to represent the incident angle dependence of the bodywave phase velocity in RA, are similar, and thus, it is difficult to estimate each independently by surface wave analysis (Kawakatsu 2016). It should be also noted that the inaccuracy of η_K may mean β_V is not determined exactly.
In this study, we try to evaluate the observability of the new parameter η_K using Markov chain Monte Carlo (MCMC) method. In order to confirm the independence of estimations for multiple parameters, the Metropolis-Hastings method analysis is performed using surface wave dispersion data and receiver functions with multiple different incident angles. As a result of preliminary tests on a simple two-layer structure model with radial anisotropy, the trade-off between η_K and β_V can be resolved and both can be estimated accurately in the case that incident angles range between 20-30 [deg] for the S-wave and 20-50 [deg] for the P-wave receiver functions. This result may suggest that the RA parameters can be estimated by combining surface waves and receiver functions even in a more complicated structural model. In the presentation, we plan to clarify how the observability of radial anisotropy changes depending on data corresponding to various observation environments, which may further contribute to future analysis and/or observation.

Keywords: radial anisotropy, surface wave, receiver function , MCMC

©2021. Japan Geoscience Union. All Right Reserved.

[J] Oral | S (Solid Earth Sciences)：S-SS Seismology

Sat. Jun 5, 2021 3:30 PM - 5:00 PM JST | Sat. Jun 5, 2021 6:30 AM - 8:00 AM UTC | Ch.18 Zoom Room 18

[S-SS11] Strong Ground Motion and Earthquake Disaster

convener:Kazuhiro Somei(Geo-Research Institute), Yasuhiro Matsumoto(Kozo Keikaku Engineering), Chairperson:Tomohisa Okazaki(RIKEN Center for Advanced Intelligence Project), Kentaro Emoto(Graduate School of Science, Tohokuk University)

Strong ground motion has social impacts as it induces earthquake disasters. We solicit contribution on any seismological topics related to strong ground motion that includes, but are not limited to, source processes, wave propagation, and site effects. We also welcome contribution on earthquake related disaster mitigation.

3:30 PM - 3:45 PM JST | 6:30 AM - 6:45 AM UTC

[SSS11-01] High-density estimation of site amplification characteristics from DAS observation along Route 4

*Kentaro Emoto[1], Hisashi Nakahara[1], Takeshi Nishimura[1], Mare Yamamoto[1] (1.Graduate School of Science, Tohokuk University)

3:45 PM - 4:00 PM JST | 6:45 AM - 7:00 AM UTC

[SSS11-02] Long-term fluctuation of microtremor at a permanent observation site in Tottori University

*Takao Kagawa[1], Soma Nishigaki[1], Tatsuya Noguchi[1] (1.Tottori University, Faculty of Engineering)

4:00 PM - 4:15 PM JST | 7:00 AM - 7:15 AM UTC

[SSS11-03] Numerical elucidation of the Aso Caldera graben mechanism focusing on stratum irregularities, soft clay and two consecutive earthquakes

*Kentaro Nakai[1], Toshihiro Noda[2], Akira Asaoka[3], Shinya Fukuda[1] (1.Graduate School of Engineering, Nagoya University, 2.Disaster Mitigation Research Center, Nagoya University, 3.Association for The Development of Earthquake Prediction)

4:15 PM - 4:30 PM JST | 7:15 AM - 7:30 AM UTC

[SSS11-04] Estimation of site amplification and S-wave velocity structure in Kumamoto Prefecture based on spectral inversion analysis of strong motion records

*Tomomi IIDA[1], Hiroaki Yamanaka[1], Kosuke Chimoto[1], Daiki Shinoyama[2], Seiji Tsuno[3], Masahiro Korenaga[3], Nobuyuki Yamada[4], Hiroe Miyake[5], Tatsuo Kanno[6], Michiko Shigefuji[6], Masayuki Yoshimi[7], Shinichi Matsushima[8], Hiroshi Kawase[8], Kimiyuki Asano[8], Tomotaka Iwata[8] (1.Tokyo institute of Technology, 2.Central Research Institute of Electric Power Industry, 3.Railway Technical Research Institute, 4.Kochi University, 5.The University of Tokyo, 6. Kyushu University, 7.National Institute of Advanced Industrial Science and Technology, 8. Kyoto University)

4:30 PM - 4:45 PM JST | 7:30 AM - 7:45 AM UTC

[SSS11-05] Toward Development of Spectral Inversion Method Considering with Rupture Directivity

*Kazuhiro Somei[1,2], Kimiyuki Asano[3], Tomotaka Iwata[3] (1.Graduate School of Science, Kyoto University, 2.Geo-Research Institute, 3.Disaster Prevention Research Institute, Kyoto University)

4:45 PM - 5:00 PM JST | 7:45 AM - 8:00 AM UTC

[SSS11-06] Broadband Ground Motion Synthesis Using Wasserstein Interpolation of Acceleration Envelopes

*Tomohisa Okazaki[1], Hirotaka Hachiya[1,2], Asako Iwaki[3], Takahiro Maeda[3], Hiroyuki Fujiwara[3], Naonori Ueda[1] (1.RIKEN Center for Advanced Intelligence Project, 2.Wakayama University, 3.National Research Institute for Earth Science and Disaster Resilience)

High-density estimation of site amplification characteristics from DAS observation along Route 4

*Kentaro Emoto[1], Hisashi Nakahara[1], Takeshi Nishimura[1], Mare Yamamoto[1]

1. Graduate School of Science, Tohokuk University

In the past few years, dense seismic observations using the distributed acoustic sensing (DAS) and fiber optic cables have been used in seismology. Compared to the conventional observation using seismometers, the cost of the DAS observation is low. Only one DAS equipment and a pre-existing telecommunication cable are required for the DAS observation. DAS observations have been used for the shallow-structure estimations and the hypocenter determination by using the record obtained in a high spatial density. Site amplification characteristics estimated from dense DAS records at a volcano was found to be in good agreement with the geological structure [Nishimura et al., 2021]. In this study, we report the site amplification characteristics calculated from the DAS observation with the fiber optic cable deployed along Route 4.

We installed the DAS equipment at Furukawa Maintenance Branch Office of Ministry of Land, Infrastructure, Transport and Tourism. The fiber optic cable is lined to the south along Route 4. The axial strain rates along the 50 km long fiber with an interval of 5m are recorded with a sampling rate of 500 Hz. The observation period is 1 month from 10 January 2020. We analyze 9 earthquakes whose magnitudes range from 2.7 to 4.8. Their hypocenters are widely distributed from Ibaraki to Hokkaido. The effect of the traffic noise can be reduced by taking the average of the results from different earthquakes.

Bandpass filters of 0.5-1, 1-2, 2-4, 4-8 and 8-16 are applied to the strain rate at each channel. The RMS amplitude of the strain rate in a 10 s time window starting from 2 s before the arrival of S-wave is calculated at each frequency range. The RMS amplitude is normalized so that its average over the channels to be one and then the average RMS amplitude over the earthquakes is calculated. We apply similar processing to P-wave as well, but the available number of earthquakes is only one.

The difference in the spatial distribution of the RMS amplitude among the earthquakes is not significant. This means that the RMS amplitude reflects the effect of the heterogeneity near the site. The large RMS amplitudes are observed at channels 10 km from the southern end of the cable. This may be affected by the road construction and the low signal to noise ratio due to the large distance from the interrogator. The local variation in the RMS amplitude ranges from 1/3 to 3. The large-scale spatial distribution of the RMS amplitude coincides with that of the amplification factor between the engineering bedrock with Vs=400 m/s and the surface provided by NIED Japan Seismic Hazard Information Station (J-SHIS). The large RMS amplitude and the large amplification areas are located in Osaki city, Taiwa town and around Sendai city. However, small-scale differences exist between the RMS amplitude and the J-SHIS amplification factors are different and the variation scale of the RMS amplitude is smaller than that of the amplification factor. The result from P-wave shows the same characteristics as that of the S-wave. The spatial power spectrum

©2021. Japan Geoscience Union. All Right Reserved.

density of the RMS amplitude exhibits the power-law decay with the exponent of 3 at the high wavenumber range.

In this study, we have shown the possibility to estimate the site amplification characteristics in a very high spatial density from the DAS observation. We will investigate the small-scale variation of the site amplification in more detail by taking into account the effect of the coupling between the cable and the ground. The output of the DAS observation is the single component of the axial strain rate along the cable. Since the strain is the spatial derivative of the translational signal, the sensitivity to the small-scale heterogeneity of the structure can be strong. It is necessary to examine the effect of the small-scale heterogeneity on wave propagation in terms of the strain.

Acknowledgement:
DAS observation was supported by Ministry of Land, Infrastructure, Transport and Tourism, Tohoku Regional Development Bureau, Sendai Office of River and National Highway.

Keywords: DAS, Site Amplification, Dense Observation

©2021. Japan Geoscience Union. All Right Reserved.

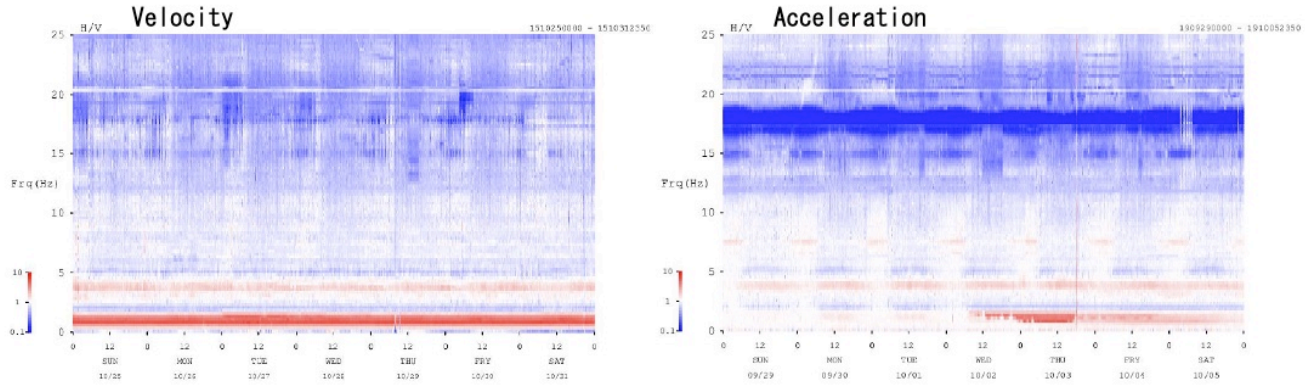
Long-term fluctuation of microtremor at a permanent observation site in Tottori University

*Takao Kagawa[1], Soma Nishigaki[1], Tatsuya Noguchi[1]

1. Tottori University, Faculty of Engineering

Long-term fluctuations of microtremors were analyzed using continuous seismic observation records installed on the premises of Tottori University. In recent years, systems that combine an accelerometer and a high-resolution recording system have become mainstream. It is important to verify the stability of the microtremor H/V spectrum ratio considering decrease in sensitivity of accelerometer especially at low frequencies. Therefore, it was verified by comparing with the records by a velocity type sensor. In low frequency band below 1 Hz, the velocity type sensor shows a stable peak for long-term, however the acceleration type sensor shows an unstable peak depending on the strength of the microtremor sources such as sea waves (see attached Figure). Due to the self-restraint of activities due to the COVID-19 from the spring of 2020, microtremor amplitude of horizontal components in the frequency band of 5 Hz or higher is smaller than the previous year on the premises of Tottori University. Microtremor amplitude also changed due to a shift in traffic flow caused by the opening of a new motorway near the observation site in May 2019. Since the stability of the peak of microtremor H/V spectral ratios captured by accelerometer in low frequency band is important for the study of ground motion characteristics, we would like to continue to analyze trends at other sites.

Keywords: Microtremor, Long-term fluctuation, H/V, Natural phenomenon, Human activity



©2021. Japan Geoscience Union. All Right Reserved.

Numerical elucidation of the Aso Caldera graben mechanism focusing on stratum irregularities, soft clay and two consecutive earthquakes

*Kentaro Nakai[1], Toshihiro Noda[2], Akira Asaoka[3], Shinya Fukuda[1]

1. Graduate School of Engineering, Nagoya University, 2. Disaster Mitigation Research Center, Nagoya University, 3. Association for The Development of Earthquake Prediction

In the 2016 Kumamoto earthquake, graben damage extending about 10 km occurred in the northwest part of Aso Caldera. Two strong motions measuring maximum seismic intensity of 7 (foreshock and main shock) occurred in rapid succession. It has been reported that the graben damage occurred not during the foreshock, but immediately after the main shock although the shocks had the similar degree of intensity. It was thought that the Futagawa fault zone that caused the Kumamoto earthquake did not reach to the Aso Caldera, and no causal relationship has been identified between the graben damage and the Hinagu fault zone. Therefore, various causes have been considered, such as collapse of underground cavities, surface seismic faults, liquefaction-induced horizontal movement of large-scale geological blocks in deeper ground, etc. However, the definite cause of graben has not been identified yet because no trace of fault movement or liquefaction has been found. On the other hand, Yasuda et al.[1)] and Ishikawa et al. [2)] revealed that most of the grabens appeared at the ground above the old lake which existed about 9,000 years ago. In addition, they have confirmed that the lake sedimentary layer has the property that the shear rigidity decreased sharply with strong repeated shear stress from the laboratory testing, and conducted a reproduction analysis of the graben damage. However, they have still not mentioned why localized and strong repeated shear was acted on the lake sedimentary layer.

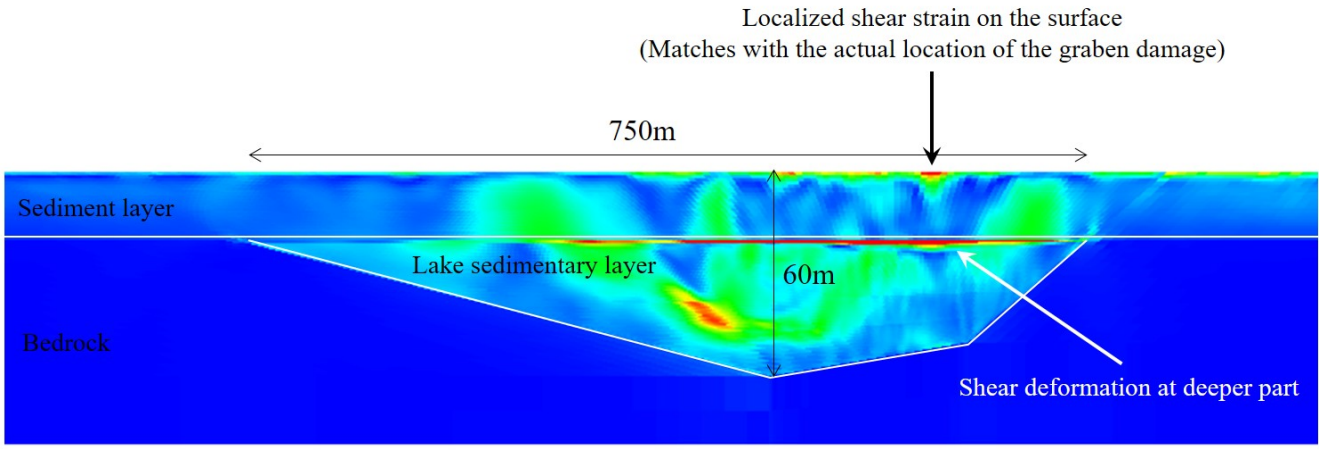
The aim of this study is to elucidate the mechanism of graben that occurred in the Aso Caldera in terms of "stratum irregularity" formed by the old lake basin in the Aso Caldera, the "presence of soft clayey soil" of the old lake deposit and the "two consecutive earthquakes" that characterize the Kumamoto earthquakes. Therefore, 2-dimensional seismic response analysis was conducted to elucidate these effects on the surface ground damage. The analysis code employed was the soil-water coupled finite deformation analysis[3)], which incorporates an elasto-plastic constitutive model that allows description of mechanical behavior of soils ranging from sand through intermediate soils to clay within the same theoretical framework[4)].

The following conclusions were obtained.
(1) By considering the effect of stratum irregularity, (a) the focal phenomena of the body waves, (b) the excitation of the surface waves and (c) the amplification interference of the body waves and surface waves ("edge effect") were numerically reproduced. Therefore, the wave propagation became complicated and the oscillation became larger at a specific point near the ground surface.
(2) The clayey lake deposit was in a soft condition. Therefore, the effective stress was easily decreased by seismic motions, which causes further increase in natural period of the ground.
(3) As mentioned in (2), natural period of the ground was increased by foreshock. The continuous occurrence of main shocks containing long-period components significantly amplified long-period oscillations. This long-period and large shaking caused graben damage at the ground surface.
It was analytically demonstrated that the graben damage of the Aso Caldera was caused by the combined effect of all of the above three characteristics (1), (2) and (3). In other words, if even one is missing, graben damage may not have occurred.

©2021. Japan Geoscience Union. All Right Reserved.

1) Yasuda, S. et al., Deformation survey of the Kario district in Aso city where caused graben damage during the Kumamoto earthquake, Proc. of 13th JAEE, 2-13, 2017.
2) Ishikawa, K. et al., Residual deformation analysis due to softening of the lacustrine sediment in the Aso caldera in the 2016 Kumamoto earthquake, Proc. of 54th JGS, 1925-1926, 2019.
3) Asaoka, A. et al., An elasto-plastic description of two distinct volume change mechanisms of soils, S&F, 42(5), 47-57, 2002.
4) Noda, T. et al., Soil-water coupled finite deformation analysis based on a rate-type equation of motion incorporating the SYS Cam-clay model, S&F, 48(6), 771-790, 2008.

Keywords: Kumamoto earthquake, Aso Caldera, Stratum irregularity, Soft clayey soil, Consecutive earthquakes, Seismic response analysis



Shear strain distribution immediately after the occurrence of main shock

©2021. Japan Geoscience Union. All Right Reserved.

Estimation of site amplification and S-wave velocity structure in Kumamoto Prefecture based on spectral inversion analysis of strong motion records

*Tomomi IIDA[1], Hiroaki Yamanaka[1], Kosuke Chimoto[1], Daiki Shinoyama[2], Seiji Tsuno[3], Masahiro Korenaga[3], Nobuyuki Yamada[4], Hiroe Miyake[5], Tatsuo Kanno[6], Michiko Shigefuji[6], Masayuki Yoshimi[7], Shinichi Matsushima[8], Hiroshi Kawase[8], Kimiyuki Asano[8], Tomotaka Iwata[8]

1. Tokyo institute of Technology, 2. Central Research Institute of Electric Power Industry, 3. Railway Technical Research Institute, 4. Kochi University, 5. The University of Tokyo, 6. Kyushu University, 7. National Institute of Advanced Industrial Science and Technology, 8. Kyoto University

In this study, we estimated site amplifications and S-wave velocity structures for shallow and deep soils using ground motion records in Kumamoto, Japan. We first apply a spectral inversion technique to the earthquake records to estimate the effects of source, path, and site amplification. And then these site amplifications are inverted to subsurface S-wave velocity. We used the data of 256 earthquakes obtained at strong motion stations of K-NET, KiK-net, seismic intensity-meters stations by local governments, and aftershock observation stations by Yamanaka et al. (2016). The estimated Q value of the propagation path is modeled as $72f^{0.83}$ and it is similar to that from previous studies (e.g. Somei et al. 2019). The source characteristics can be approximated with the omega-square model. The site effects in the plain area show large values in a frequency range of 0.5-2.0Hz. At a high frequency above 5Hz, the site amplifications in the mountain are larger than those in the plain area. The amplifications of 0.5-1Hz are larger in the central area of the Kumamoto plain than in the other area because of the large sediments. The amplifications in Mashiki show different characteristic features around 2Hz due to the various thickness of the shallow soils. The Q value of deep soils in the plain area tends to be larger than in the mountainous area.

Acknowledgements

We used the data from the aftershock observation conducted as a part of the Comprehensive Study on the Futagawa-Hinagu fault zone after the 2016 Kumamoto earthquake, MEXT.

Keywords: Spectral inversion, The 2016 Kumamoto Earthquake, Site amplification, S-wave velocity

©2021. Japan Geoscience Union. All Right Reserved.

Toward Development of Spectral Inversion Method Considering with Rupture Directivity

*Kazuhiro Somei[1,2], Kimiyuki Asano[3], Tomotaka Iwata[3]

1. Graduate School of Science, Kyoto University, 2. Geo-Research Institute, 3. Disaster Prevention Research Institute, Kyoto University

Source, propagation path, and site effects were separated from strong motion records observed during the 2016 Kumamoto earthquake sequence using the spectral inversion method (Somei et al., 2019). Somei et al. (2020) have obtained a source spectrum for a specific station from an observed Fourier amplitude spectrum by removing the propagation path and site effects, in order to clarify the factor of variation in residual of spectral inversion results. For several events (M_w: 3.6-5.3) in the 2016 Kumamoto earthquake sequence, the azimuthal dependence of both the corner frequencies and fall-off rate was found in the displacement source spectra at stations. They thought this azimuthal dependence was caused by rupture directivity. In this study, we estimated the rupture directivity coefficient based on the variation in source spectra among stations toward developing a new spectral inversion method considering with the rupture directivity.

The rupture directivity coefficient assuming the bilateral line source model (e.g., McGuire, 2004) was estimated from the variation in the fall-off rate of the displacement source spectra among stations. The S-wave velocity was assumed to be 3.4 km/s in the rupture directivity coefficient. The take-off angle between the source and station was calculated using the 1D velocity structure model of JMA2001 (Ueno et al., 2002). The model parameters in rupture directivity coefficient are horizontal and vertical rupture directions, rupture velocity, and directivity ratio (i.e., percentage of unilateral rupture). These parameters were determined by grid searching to minimize the misfit function (Boatwright, 2007). In this misfit function, Boatwright (2007) originally used the ratio of the peak ground motion (PGA and PGV) for each station to that expected from the ground motion prediction equation, in order to estimate the directivity coefficient. We used the ratio of the fall-off rate for each station to -2 (i.e., the fall-off rate of the ω^{-2} source spectral model).

For an example of an M_w5.3 event at 17:52 on 19 April 2016 (JST) occurring in southwest of aftershock area, the estimated rupture directivity coefficient showed that the horizontal and vertical rupture directions are N214° E and 135° from vertically down, respectively, with a rupture velocity of 2.4 km/s. The best directivity ratio was 1.0, which means the rupture propagates unilaterally. On the other hand, the strong motion generation area for this event modeled by simulating the observed ground motions using the empirical Green’ s function method showed the rupture propagated southwest and shallow direction from the hypocenter (Somei et al., 2020). These results indicate that rupture directivity coefficient estimated from the variation in the fall-off rate was reasonable though the rupture directivity coefficient was upon the assumption of the line source model. Based on the rupture directivity coefficient, we will develop a new spectral inversion method considering with the rupture directivity.

Acknowledgements: The strong motion data were provided from the K-NET, KiK-net, and F-net operated by the National Research Institute for Earth Science and Disaster Resilience (NIED), Japan Meteorological Agency (JMA), Kumamoto Prefectural Government, Kagoshima Prefectural Government, and Nagasaki

©2021. Japan Geoscience Union. All Right Reserved.

Prefectural Government. This study was supported by JSPS KAKENHI Grant Number JP20K05044. and by achievements of the collaborative research program (2020H-01) of the Disaster Prevention Research Institute of Kyoto University.

Keywords: Spectral inversion, Rupture directivity, Source spectrum

©2021. Japan Geoscience Union. All Right Reserved.

Broadband Ground Motion Synthesis Using Wasserstein Interpolation of Acceleration Envelopes

*Tomohisa Okazaki[1], Hirotaka Hachiya[1,2], Asako Iwaki[3], Takahiro Maeda[3], Hiroyuki Fujiwara[3], Naonori Ueda[1]

1. RIKEN Center for Advanced Intelligence Project, 2. Wakayama University, 3. National Research Institute for Earth Science and Disaster Resilience

Hybrid approaches to broadband (BB) ground motion synthesis combine long-period (LP) and short-period (SP) waveforms calculated by two methods suitable for each period range. They have been applied in research and practice, but it is disadvantageous that simulations are independently carried out under different assumptions, which can lead to incompatible time histories and frequency properties.

This study explores an approach for maintaining consistency between LP and SP components using an empirical relationship of past observation records. We propose a machine learning method that generate SP waveforms from LP waveforms obtained using physics-based simulations. Acceleration envelopes and Fourier amplitude spectra are transformed, and they are combined to produce a broadband waveform. To effectively obtain the relationship of envelopes from limited amount of data, we formulate the problem as the conversion of probability distributions to allow the introduction Wasserstein distance, and embed pairs of LP and SP envelopes into a common latent space to improve the consistency of the entire waveform. An experimental application to the 2008 M7 off Ibaraki earthquake demonstrates that the proposed method exhibits superior performance compared to existing methods and neural network approaches. In particular, the proposed method reproduces global properties in the time domain, which confirms the effectiveness of the embedding approach and the advantage of the Wasserstein distance as a dissimilarity measure of envelopes.

©2021. Japan Geoscience Union. All Right Reserved.

[E] Oral | S (Solid Earth Sciences)：S-IT Science of the Earth's Interior & Techtonophysics

Sat. Jun 5, 2021 3:30 PM - 5:00 PM JST | Sat. Jun 5, 2021 6:30 AM - 8:00 AM UTC | Ch.23 Zoom Room 23

[S-IT17] Property and role of liquids inside terrestrial planets

convener:Tatsuya Sakamaki(Department of Earth Science, Tohoku University), Yoichi Nakajima(Kumamoto University, Priority Organization for Innovation and Excellence), Chairperson:Tatsuya Sakamaki(Department of Earth Science, Tohoku University), Yoichi Nakajima(Kumamoto University, Priority Organization for Innovation and Excellence)

Liquids of silicates and metals inside terrestrial planets play important role in the physical, chemical, and thermal evolutions of planets. This session aims at understanding the physical and chemical properties of liquids from shallow to deep parts of terrestrial planets, which are strongly related to the long history of those planets from the planetary accretion to the present-day dynamics. In addition, we call for presentations by researchers from various backgrounds of geochemical, experimental, theoretical/computational, and seismic/geodynamical ones, who investigate the physical and chemical properties of liquids and the behaviors and roles inside of terrestrial planets. Relevant topics include, but are not limited to, partial melting and melt extraction, liquid-solid partitioning, high pressure experiments on melts, and seismic detections of mantle melts and outer core anomaly.

3:30 PM - 3:45 PM JST | 6:30 AM - 6:45 AM UTC

[SIT17-01] Pressure-induced structural change of basaltic glass up to 18 GPa

*Tomonori Ohashi[1], Tatsuya Sakamaki[1], Ken-ichi Funakoshi[2], Takanori Hattori[3], Naoki Hisano[1], Jun Abe[2], Akio Suzuki[1] (1.Department of Earth Science, Tohoku University, 2.Neutron Science and Technology Center, Comprehensive Research Organization for Science and Society (CROSS), 3.J-PARC Center, Japan Atomic Energy Agency)

3:45 PM - 4:00 PM JST | 6:45 AM - 7:00 AM UTC

[SIT17-02] Atomic structure of CO_2-bearing melts along the carbonatite-basalt join at high pressure and temperature

*Veronica Stopponi[1], Annalisa D'Arco[2,3], Rostislav Hrubiak[4], Yoshio Kono[5], Stefano Lupi[2,6], Craig E Manning[7], Manuela Nazzari[8], Brent T Poe[9], Claudia Romano[10], Vincenzo Stagno[1,8] (1.Department of Earth Sciences, Sapienza University of Rome, Rome, Italy, 2.INFN National Institute of Nuclear Physics, Rome, Italy, 3.SBAI Department of Basic and Applied Sciences for Engineering, Physics, Sapienza University of Rome, Rome, Italy, 4.High Pressure Collaborative Access Team (HPCAT), X-ray Science Division, Argonne National Laboratory, Argonne, IL, USA, 5.Geodynamic Research Center, Ehime University, Matsuyama, Japan, 6.Department of Physics, Sapienza University of Rome, Rome, Italy, 7.Department of Earth, Planetary and Space Sciences, University of California, Los Angeles, CA, USA, 8.Istituto Nazionale di Geofisica e Vulcanologia (INGV), Rome, Italy, 9.Department of Engineering and Geology, University of Chieti-Pescara, Chieti Scalo, Italy, 10.Department of Sciences, University of Studies Roma Tre, Rome, Italy)

4:00 PM - 4:15 PM JST | 7:00 AM - 7:15 AM UTC

[SIT17-03] *In situ X-ray study of liquid geomaterials under extreme conditions using Free-Electron Lasers*

★Invited Papers

*Guillaume Morard[1] (1.ISTerre, UGA, CNRS)

4:15 PM - 4:30 PM JST | 7:15 AM - 7:30 AM UTC

[SIT17-04] Density and thermal expansion of liquid and solid iron at 1 atm determined using high-temperature furnace

★Invited Papers

*Hidenori Terasaki[1], Asaka Kamiya[2], Tadashi Kondo[2] (1.Department of Earth science, Okayama University, 2.Department of Earth and Space science, Osaka University)

4:30 PM - 4:45 PM JST | 7:30 AM - 7:45 AM UTC

[SIT17-05] Sound velocity measurements of liquid Fe-N up to 100 GPa

Asaki Iwamoto[1], *Yoichi Nakajima[1,2], Daisuke Kinoshita[1], Yasuhiro Kuwayama[3], Kei Hirose[3,5], Daisuke Ishikawa[2,4], Alfred Q.R. Baron[2,4] (1.Kumamoto Univ., 2.RIKEN MDL, 3.Univ. Tokyo, 4.JASRI, 5.Tokyo Tech. ELSI)

4:45 PM - 5:00 PM JST | 7:45 AM - 8:00 AM UTC

[SIT17-06] Density and Sound Velocity of Liquid Fe and FeO at High Pressure

*Yasuhiro Kuwayama[1], Kei Hirose[1,2], Yoichi Nakajima[3,4], Yuki Adachi[3], Alfred Q.R. Baron[4], Guillaume Morard[5], Saori I. Kawaguchi[6], Daisuke Ishikawa[6,4], Naohisa Hirao[6], Yasuo Ohishi[6] (1.The University of Tokyo, 2.Tokyo Institute of Technology, 3.Kumamoto University, 4.RIKEN MDR, 5.Laboratoire ISTERRE, Université Grenoble Alpes, 6.JASRI)

Pressure-induced structural change of basaltic glass up to 18 GPa

*Tomonori Ohashi[1], Tatsuya Sakamaki[1], Ken-ichi Funakoshi[2], Takanori Hattori[3], Naoki Hisano[1], Jun Abe[2], Akio Suzuki[1]

1. Department of Earth Science, Tohoku University, 2. Neutron Science and Technology Center, Comprehensive Research Organization for Science and Society (CROSS), 3. J-PARC Center, Japan Atomic Energy Agency

The structures of cold-compressed basaltic glass were investigated at pressures of up to 18 GPa using in situ X-ray and neutron diffraction to acquire insights into the physicochemical properties of deep magmas. On compression, basaltic glass changes its compression behavior: the mean O-O coordination number (CN_{OO}) starts to rise with maintaining the mean O-O distance (r_{OO}) above about 2–4 GPa, and then CN_{OO} stops increasing and r_{OO} begins to shrink along with the increase in the mean coordination number of Al (CN_{AlO}) above ~9 GPa. The change around 9 GPa is interpreted by the change in the contraction mechanism from bending tetrahedral networks of glass to increasing oxygen packing ratio via the increase in CN_{AlO}. The analysis of the oxygen packing fraction (η_O) under high pressure revealed that η_O exceeds the value for dense random packing, suggesting that the oxygen-packing hypothesis recently proposed cannot account for the pressure-induced structural transformations of silica and silicate glasses. The rise of the CN_{OO} at 2–4 GPa reflects the elastic softening of fourfold-coordinated silicate glass, which may be the origin of anomalies of elastic moduli in basaltic glass at ~2 GPa previously reported by Liu and Lin (2014).
The widths of both the first sharp diffraction peak and the principal peak show contrastive compression behaviors between modified silicate and silica glasses. This result suggests that modified silicate glasses represent different pressure evolutions in the ranges of the intermediate- and the extended-range order structures from those of silica glass, likely due to the presence of modifier cations and the resultant formations of smaller rings and cavity volume.

Reference

Liu, J., and Lin, J.-F. (2014) Abnormal acoustic wave velocities in basaltic and (Fe,Al)-bearing silicate glasses at high pressures. Geophysical Research Letters, 41, 8832–8839.

Keywords: silicate glass, oxygen packing, X-ray diffraction, neutron diffraction

©2021. Japan Geoscience Union. All Right Reserved.

Atomic structure of CO_2-bearing melts along the carbonatite-basalt join at high pressure and temperature

*Veronica Stopponi[1], Annalisa D'Arco[2,3], Rostislav Hrubiak[4], Yoshio Kono[5], Stefano Lupi[2,6], Craig E Manning[7], Manuela Nazzari[8], Brent T Poe[9], Claudia Romano[10], Vincenzo Stagno[1,8]

1. Department of Earth Sciences, Sapienza University of Rome, Rome, Italy, 2. INFN National Institute of Nuclear Physics, Rome, Italy, 3. SBAI Department of Basic and Applied Sciences for Engineering, Physics, Sapienza University of Rome, Rome, Italy, 4. High Pressure Collaborative Access Team (HPCAT), X-ray Science Division, Argonne National Laboratory, Argonne, IL, USA, 5. Geodynamic Research Center, Ehime University, Matsuyama, Japan, 6. Department of Physics, Sapienza University of Rome, Rome, Italy, 7. Department of Earth, Planetary and Space Sciences, University of California, Los Angeles, CA, USA, 8. Istituto Nazionale di Geofisica e Vulcanologia (INGV), Rome, Italy, 9. Department of Engineering and Geology, University of Chieti-Pescara, Chieti Scalo, Italy, 10. Department of Sciences, University of Studies Roma Tre, Rome, Italy

Melting of carbonated peridotite rocks in the Earth’ s interior produces a variety of magmas the composition of which is controlled by pressure, temperature and oxygen fugacity (Gudfinnsson and Presnall 2015; Stagno 2019). Within a depth interval of 25 and 250 km, the continuum from carbonatitic, kimberlitic, melilititic, picritic and basaltic melts is characterized by CO_2 content that decreases gradually with increasing temperature and, therefore, melt fraction. As a consequence, the rheology of these magmas is expected to change dramatically with implications for their migration rate and the geodynamic transport of carbon.
The aim of this study was to investigate the atomic structure and vibrational properties of a variety of synthetic glasses representative of CO_2-bearing melts (i.e. carbonatite-kimberlite-melilitite-nephelinite-picrite-basalt) as a function of the increasing SiO_2 content, pressure and temperature.
The atomic structure of molten glasses was investigated at pressures of about 1-7 GPa and temperatures varying from about 1150 to 2000˚C using the Paris-Edinburgh press installed at beamline 16BM-B of the Advanced Photon Source (Argonne, IL, USA) combined with synchrotron radiation to perform in situ multi-angle energy dispersive X-ray diffraction measurements. The vibrational properties were studied on the recovered quenched glasses using both micro-Raman and micro-reflectance-FTIR.
Preliminary results shed light on different compressibility mechanisms upon increasing pressure both in the intermediate-range ordering and in the local structure of melts. The position of the first sharp diffraction peak in the structure factor S(q) shows that kimberlitic, melilititic and nephelinitic melts display a much less closely packed structure with respect to volatile-free depolymerized silicate melts. Bond lengths between tetrahedrally coordinated cations, such as Si^{4+}, Al^{3+}, and oxygen (T-O) increase for all the compositions investigated in the experimental pressure range, with the exception of T-O lengths of the basalt melt where a turnover at about 4.5 GPa is observed as in Sakamaki et al. (2013).
The vibrational spectroscopic investigation shows significant changes in the speciation of C-O molecular bonds that likely reflect a more complex C-dominated atomic environment than what is known so far.

Gudfinnsson and Presnall 2005, J Petrol 46, 8, 1645-1659.

©2021. Japan Geoscience Union. All Right Reserved.

Sakamaki et al. 2013, Nat Geosci 6, 1041-1044.
Stagno 2019, J Geol Soc London 176, 375-387.

Keywords: High pressure, Melt structure, Carbonate-bearing melts, Paris-Edinburgh press, Vibrational spectroscopy, Mantle melting

©2021. Japan Geoscience Union. All Right Reserved.

In situ X-ray study of liquid geomaterials under extreme conditions using Free-Electron Lasers

*Guillaume Morard[1]

1. ISTerre, UGA, CNRS

Study of liquids and partial melting under extreme conditions is of great interest for the geophysical community, to understand the Magma Ocean dynamics during Early Earth stage as well as to constrain the present day Earth’ s core dynamics and composition. However, probing geomaterials (e.g. silicates and iron alloys) in the liquid state under extreme conditions using Laser-Heated Diamond Anvil Cell could present several drawbacks, related to chemical contamination from the diamonds and chemical migration along temperature gradient. Studying the melting properties during transient state using the time-resolved capabilities of Free Electron Laser sources, under dynamic or static compression, can give access to physical properties of high quality for molten geomaterials.

Keywords: Liquid silicates, Liquid iron alloys, Planetary Interior

©2021. Japan Geoscience Union. All Right Reserved.

Density and thermal expansion of liquid and solid iron at 1 atm determined using high-temperature furnace

*Hidenori Terasaki[1], Asaka Kamiya[2], Tadashi Kondo[2]

1. Department of Earth science, Okayama University, 2. Department of Earth and Space science, Osaka University

To estimate the structure and composition of a planetary core, the equation of state of iron alloys is an important information, along with planetary exploration data. The density and thermal expansion coefficient is one of the most fundamental characteristics to describe the equation of state. In this study, we precisely measured the densities of solid and liquid iron at high temperatures and ambient pressure using a high-temperature furnace with optical windows. The sample volume was determined from the optical image measured at each temperature. The density error of solid Fe was estimated to 0.11–0.7% in the temperature range of 295–1803 K with increments of 1–10 K. The two discontinuous density jumps were observed at 1162 and 1666 K which were derived from phase transitions (alpha/gamma/delta phases). The density decreased linearly with increasing temperature in each phase. For liquid, the density of liquid Fe was determined with uncertainty of 0.4–0.7% in the range of 1818–1998 K with temperature increments of 5 K. The obtained thermal expansion coefficient of liquid iron was 2.42(1) x 10^{-4} K^{-1}.

Keywords: density, thermal expansion, iron, liquid

©2021. Japan Geoscience Union. All Right Reserved.

Sound velocity measurements of liquid Fe-N up to 100 GPa

Asaki Iwamoto[1], *Yoichi Nakajima[1,2], Daisuke Kinoshita[1], Yasuhiro Kuwayama[3], Kei Hirose[3,5], Daisuke Ishikawa[2,4], Alfred Q.R. Baron[2,4]

1. Kumamoto Univ., 2. RIKEN MDL, 3. Univ. Tokyo, 4. JASRI, 5. Tokyo Tech. ELSI

The Earth’s liquid outer core consists of iron alloy with ~5 wt.% nickel and ~10 wt.% lighter elements [1]. Nitrogen is one of the candidates for the core light elements. The Earth’s atmosphere and silicate mantle is depleted in nitrogen relative to carbonaceous chondrites, which indicates that a large portion of the nitrogen in bulk earth can be stored in the core [2,3]. To examine the possibility of nitrogen in the core, it is utilized to compare the sound velocity of liquid Fe-N alloy under high-pressure and –temperature conditions relevant to the core conditions with seismological observations. We have determined the longitudinal (P-wave) velocity of liquid Fe-N alloy up to 99 GPa and 2600 K based on the inelastic X-ray scattering (IXS) measurements in a laser-heated diamond-anvil cell (LH-DAC).

We carried out IXS measurements at the RIKEN Quantum NanoDynamics beamline BL43LXU of SPring-8 [4]. A $Fe_{80}N_{20}$ (Fe_4N) foil was used as the starting specimen and single-crystal Al_2O_3 discs were used as the thermal- and chemical-insulator. The liquid state of the sample was confirmed before and after each IXS measurement based on X-ray diffraction measurements. The IXS spectra were collected in a momentum transfer range of 3-5.7 nm^{-1} with an energy resolution of ~2.8 meV at 17.94 keV. The P-wave velocity of liquid $Fe_{80}N_{20}$ was determined from the dispersion relation of the longitudinal acoustic phonon mode of the liquid. We constructed an equation of state (EoS) for liquid $Fe_{80}N_{20}$ from the pressure and velocity data. Compared with pure Fe [5], the P-wave velocity of liquid $Fe_{80}N_{20}$ is faster by ~10% in the present experimental conditions. By extrapolating the present results to the Earth’s outer core conditions with the present EoS and then comparing with seismological observations, we found that the upper limit of nitrogen is ~3.8 wt% in the outer core.

References

[1] Stevenson, Science **214**, 611-619 (1981).
[2] Marty, Earth Planet. Sci. Lett. **313-314**, 56-66 (2012).
[3] Li et al., Earth Planet. Sci. Lett. **377-378**, 311-323 (2013).
[4] Baron, SPring-8 Inf. Newsl. **15**(1), 14-19 (2010).
[5] Kuwayama et al. Phys. Rev. Lett. **124**(16), 165701 (2020).

Keywords: Earth's core, Liquid Fe-N, Sound velocity, IXS, High pressure

©2021. Japan Geoscience Union. All Right Reserved.

Density and Sound Velocity of Liquid Fe and FeO at High Pressure

*Yasuhiro Kuwayama[1], Kei Hirose[1,2], Yoichi Nakajima[3,4], Yuki Adachi[3], Alfred Q.R. Baron[4], Guillaume Morard[5], Saori I. Kawaguchi[6], Daisuke Ishikawa[6,4], Naohisa Hirao[6], Yasuo Ohishi[6]

1. The University of Tokyo, 2. Tokyo Institute of Technology, 3. Kumamoto University, 4. RIKEN MDR, 5. Laboratoire ISTERRE, Université Grenoble Alpes, 6. JASRI

The Earth's core is almost molten. While the dominant component of the core is believed to be iron, a large amount of lighter impurities can be dissolved into the core. Oxygen is a possible candidate for the light impurity in the liquid outer core. Seismological observations exhibit the presence of a low-velocity layer (LVL) at the top of the Earth's core, which might be attributed to the enrichment of oxygen [1,2]. Furthermore, the enrichment of the FeO component and/or partial melting are considered to be the origin of the ultra-low velocity zone (ULVZ) at the base of the lower mantle (e.g. [3]). Therefore, the density (ρ) and longitudinal sound velocity (V_P) of Fe-O liquids under relevant high-pressure and -temperature conditions are of great importance to understand those seismological anomalies. Here we present those elastic properties of liquid Fe and FeO under high-pressure and -temperature (*P*-*T*) conditions.

We have determined the ρ of liquid Fe up to 116 GPa based on in-situ x-ray diffraction measurements at BL10XU, SPring-8, using a laser-heated diamond-anvil cell (LH-DAC) [4]. The V_P of liquid Fe was obtained up to 45 GPa by inelastic x-ray scattering (IXS) measurements in the LH-DAC at BL43LXU, SPring-8 [5]. From these results combined with previous shock-wave data, we obtained the P–T–ρ–V_P–γ relation for the Earth's entire outer core conditions [6]. Also, we determined the V_P of liquid FeO up to 82 GPa using the IXS technique. The present results show that the V_P of liquid FeO is faster than that of liquid Fe by ~15% at the condition of the Earth's core-mantle boundary (CMB). Since the FeO component increases the P-wave velocity of liquid iron alloy, the enrichment of FeO cannot be the origin of the low-velocity anomaly at the top of the outer core. On the other hand, the V_P of liquid FeO is slower by ~35% relative to lower mantle minerals at the base of the lower mantle, so that the ULVZ can be attributed to a tiny amount of liquid FeO component.

[1] G. Helffrich and S. Kaneshima, Nature **468**, 807 (2010).
[2] T. Komabayashi, J. Geophys. Res. Solid Earth **119**, 4164 (2014).
[3] S. Labrosse, J. W. Hernlund, and N. Coltice, Nature **450**, 866 (2007).
[4] N. Hirao, S. I. Kawaguchi, K. Hirose, K. Shimizu, E. Ohtani, and Y. Ohishi, Matter Radiat. Extrem. **5**, 018403 (2020).
[5] A. Q. R. Baron, SPring-8 Inf. Newsl. **15**, 14 (2010).
[6] Y. Kuwayama, G. Morard, Y. Nakajima, K. Hirose, A. Q. R. Baron, S. I. Kawaguchi, T. Tsuchiya, D. Ishikawa, N. Hirao, and Y. Ohishi, Phys. Rev. Lett. **124**, 165701 (2020).

Keywords: liquid, density, sound velocity, high-pressure, core

©2021. Japan Geoscience Union. All Right Reserved.

[E] Poster | S (Solid Earth Sciences)：S-IT Science of the Earth's Interior & Techtonophysics

Sat. Jun 5, 2021 5:15 PM - 6:30 PM JST | Sat. Jun 5, 2021 8:15 AM - 9:30 AM UTC | Ch.14_1

[S-IT17] Property and role of liquids inside terrestrial planets

convener:Tatsuya Sakamaki(Department of Earth Science, Tohoku University), Yoichi Nakajima(Kumamoto University, Priority Organization for Innovation and Excellence)

Liquids of silicates and metals inside terrestrial planets play important role in the physical, chemical, and thermal evolutions of planets. This session aims at understanding the physical and chemical properties of liquids from shallow to deep parts of terrestrial planets, which are strongly related to the long history of those planets from the planetary accretion to the present-day dynamics. In addition, we call for presentations by researchers from various backgrounds of geochemical, experimental, theoretical/computational, and seismic/geodynamical ones, who investigate the physical and chemical properties of liquids and the behaviors and roles inside of terrestrial planets. Relevant topics include, but are not limited to, partial melting and melt extraction, liquid-solid partitioning, high pressure experiments on melts, and seismic detections of mantle melts and outer core anomaly.

[SIT17-P01] Viscosity of silicate melts under high pressures

*Tatsuya Sakamaki[1] (1.Department of Earth Science, Tohoku University)

[SIT17-P02] Elastic wave velocity of silicate glasses at high pressure

*Tatsuya Sakamaki[1] (1.Department of Earth Science, Tohoku University)

[SIT17-P03] Density of Fe_2O_3–bearing magma under high pressure

*Rintaro Ban[1], Akio Suzuki[1], Tatsuya Sakamaki[1] (1.Department of Earth Science, Graduate School of Science, Tohoku University)

[SIT17-P04] **Melting phase equilibrium relations in the $MgSiO_3$-SiO_2 system at 13.5 GPa**

*Takuya Moriguti[1], Yusuke Yachi[1], Akira Yoneda[1], Eiji Ito[1] (1.Institute for Planetary Materials, Okayama University)

Viscosity of silicate melts under high pressures

*Tatsuya Sakamaki[1]

1. Department of Earth Science, Tohoku University

I would like to review the viscosity measurements of silicate melts at high pressure. The viscosity of silicate melts controls their mobility, and gives us important knowledge about the timescale of volcanic activities and eruption styles in the present Earth. In addition, viscosity plays a central role in the dynamics of a terrestrial magma ocean, core formation, and chemical differentiation of the mantle in the Earth’s early history. For silicate melts, viscosity measurements at high pressure have been performed by a falling sphere method using a large volume press. The falling sphere method has been significantly advanced by combination with synchrotron-based X-ray radiography, which enables us to determine the melt viscosity more accurately. Because the viscosity of silicate melts is considered to be closely related to the network structure, simultaneous measurements of viscosity and structure at high pressure and high temperature significantly have enhanced our understanding of the relationship between viscosity and structure.
The ratio between the number of non-bridging oxygen anions (NBO) and that of tetrahedrally coordinated cations (T), NBO/T, is widely used as an indicator of the network structure of silicate melts. The degree of polymerization, which increases with decreasing NBO/T, has long been recognized as a fundamental structural factor influencing physical properties. Also, the viscosity of silicate melts is characterized by the degree of polymerization. Polymerized melts show higher viscosity at ambient pressure due to their strong three-dimensional network featuring oxygen bridges between tetrahedral cations. Depolymerized melts have lower tetrahedral connectivity and lower viscosity. The contrasting behavior between polymerized and depolymerized melts is also shown in the pressure dependence of viscosity. Although free-volume theory predicts that viscosity increases with pressure, isothermal viscosity of polymerized melts decreases with pressure up to 3-5 GPa, above which it turns over to positive pressure dependence.

Keywords: Viscosity, Silicate melt, High pressure

©2021. Japan Geoscience Union. All Right Reserved.

Elastic wave velocity of silicate glasses at high pressure

*Tatsuya Sakamaki[1]

1. Department of Earth Science, Tohoku University

I would like to review the elastic wave velocity measurements of silicate glasses under high pressures. Knowledge of the elastic properties of silicate melts/glasses enables us to infer the magma behavior at high pressure. Elastic wave velocities have been reported for several silicate glasses. Sakamaki et al. (2014) have investigated sound velocities of polymerized (jadeite and albite composition: NBO/T=0 at 1 atm) and depolymerized (diopside composition: NBO/T=2 at 1 atm) glasses at pressures up to 10 GPa using an ultrasonic technique and synchrotron radiation in a Paris-Edinburgh press, and demonstrated the dichotomous trend of elastic wave velocity of silicate glasses. The pressure dependence of velocities also clearly falls into two groups, one for polymerized (jadeite, albite, and silica) glasses, and the other for depolymerized (diopside and enstatite) glasses. These results indicate that the degree of polymerization fundamentally affects the behavior of silicate glasses under compression. For fully polymerized glasses, sound velocities first decrease with pressure before increasing above a certain pressure, similarly to silica glass. The velocity softening is much more pronounced for V_S than V_P. In contrast, for partially depolymerized glasses such as diopside and enstatite glasses, both V_P and V_S change only slightly with increasing pressure, a behavior different from that of polymerized glasses. The cation substitution of Fe and Al into the enstatite composition glass reduces the velocities at ambient pressure. Glasses with higher SiO_2 content have lower sound velocities, while the higher MgO content promotes increases in velocities. Basaltic glasses, which have the most complex composition among all glasses and an NBO/T around 0.7, have an intermediate pressure dependence: V_P and V_S decrease slightly with increasing pressure.

Keywords: Elastic wave velocity, Silicate glass, High pressure

©2021. Japan Geoscience Union. All Right Reserved.

Density of Fe_2O_3–bearing magma under high pressure

*Rintaro Ban[1], Akio Suzuki[1], Tatsuya Sakamaki[1]

1. Department of Earth Science, Graduate School of Science, Tohoku University

Previous studies indicate the high concentration of Fe_2O_3 in the lower mantle. Even though the partial molar volume of Fe_2O_3 has become essential for discussing the magma in the deep mantle, there is no data of partial molar volume of Fe_2O_3 at high pressure and temperature. This study is aimed to obtain partial molar volume of Fe_2O_3 in silicate melts under high pressure. Fe_2O_3 -bearing starting material was compressed by a Kawai-type multi-anvil apparatus. We determined the density of silicate melts using sink-float method. By combining the density and the equation of state of silicate melts proposed in Wakabayashi and Funamori (2013), partial molar volumes were yielded.

Keywords: magma, lower mantle, sink-float method, partial molar volume

©2021. Japan Geoscience Union. All Right Reserved.

Melting phase equilibrium relations in the $MgSiO_3$-SiO_2 system at 13.5 GPa

*Takuya Moriguti[1], Yusuke Yachi[1], Akira Yoneda[1], Eiji Ito[1]

1. Institute for Planetary Materials, Okayama University

Melting relations in the system $MgSiO_3$-SiO_2 were investigated at 13.5 GPa and up to 2900 ºC using the Kawai-type of multi anvil apparatus (KMAA) in this study. The melting relations of the system MgO-SiO_2 as a representative of the mantle have been extensively studied since a pioneering work by Bowen and Anderson (1914). However, almost all of these works have been carried out on the compositions ranging from MgO to $MgSiO_3$ because the bulk mantle composition has been assumed to be peridotitic or close to that derived from CI chondrite. On the other hand, enstatite chondrite (E-chondrite) has been recommended as the source material of bulk Earth (e.g., Javoy et al., 2010) because the isotope compositions of the Earth, Moon and E-chondrite are indistinguishable over O, N, Mo, Ru, Os, Cr, and Ti. In order to understand the mantle differentiation in the E-chondrite model, it is indispensable to clarify the melting relations in the system $MgSiO_3$-SiO_2 at high pressures. Nevertheless, there have been limited works on the melting behavior of the system $MgSiO_3$-SiO_2 under high pressures. In this study, we aimed to determine the melting relations in the system $MgSiO_3$-SiO_2 at 13.5 GPa as precisely as possible using the KMAA. We found that the X_{Si} value (SiO_2/(SiO_2+MgO) (mol)) of the eutectic composition increases from 0.556 to 0.61 at a range from 1 to 13.5 GPa (down to ~400 km depth in mantle) (Hudon et al., 2005; Dalton and Presnall, 1997; Moriguti et al., under review), which are close to those of E-chondrites (0.533 - 0.577). This implies that if bulk Earth composition corresponds to E-chondrites, the upper mantle composition resulting from fractional crystallization of a terrestrial magma ocean would be around 0.6 in X_{Si}, significantly enriched in SiO_2 compared with estimates of the current upper mantle composition, 0.47. In addition, melting relations in the $MgSiO_3$ - SiO_2 system up to 13.5 GPa show that the liquidus phase is enstatite if E-chondrites melted in the magma ocean. Consequently, it is impossible to produce the present upper mantle composition through simple fractional crystallization processes without efficient Si partitioning out from a silicate mantle to molten iron (the core).

In the present study, the sample heating was conducted up to 2900 ˚C. In this presentation, the special endeavor to pressure calibration at such extreme temperature are also shown. In the multi anvil apparatus, the generated pressure is substantially altered on heating the specimen due to the increases of the thermal expansion and the fluidity of the pressure medium as shown in previous works conducted at high temperatures, > 1000 ˚C (e.g., Gasparik, 1989; Ito and Takahashi, 1989). However, the high temperature effect to the generated pressure under > 2000 ˚C has not been known well. Therefore, the temperature effect was also evaluated at 2500 and 2850 ˚C on the basis of phase transition between coesite and stishovite in SiO_2 determined by Zhang et al. (1996). Compared with the generated pressure at room temperature (10.5 GPa), the pressure increases by 2.1 and 3.0 GPa were recognized at 2500 ˚C against the press load of 2.25 MN and at 2850 ˚C against that of 2.4 MN, respectively.

References

Dalton, J.A. and Presnall, D.C. (1997) Geochim. Cosmochim. Acta 61, 2367-2373.
Gasparik, T. (1989) Contrib. Min. petrol., 102, 389-405.
Hudon P. et al. (2005) J. Petrol., 46, 1859-1880.
Ito, E. and Takahashi, E. (1989) J. Geophys. Res. 94, 10637-10646.
Javoy M. et al. (2010) Earth Planet. Sci. Let. 293, 259-268.

©2021. Japan Geoscience Union. All Right Reserved.

Moriguti, T. et al. (under review) Am. Min.
Zhang, J. et al. (1996) Phys. Chem. Minerals 23, 1-10.

Keywords: MgSiO3-SiO2 system, Enstatite chondrite model, Mantle, Multi anvil, High pressure and high temperature, Pressure calibration

©2021. Japan Geoscience Union. All Right Reserved.

[E] Oral | S (Solid Earth Sciences)：S-IT Science of the Earth's Interior & Techtonophysics

Sat. Jun 5, 2021 9:00 AM - 10:30 AM JST | Sat. Jun 5, 2021 12:00 AM - 1:30 AM UTC | Ch.23 Zoom Room 23

[S-IT20] MAGMA, FLUID TRANSPORT, AND SEISMICITY IN THE EARTH'S INTERIOR

convener:Eiji Ohtani(Department of Earth and Planetary Materials Science, Graduate School of Science, Tohoku University), Saeko Kita(International Institute of Seismology and Earthquake Engineering, BRI), Michihiko Nakamura(Division of Earth and Planetary Materials Science, Department of Earth Science, Graduate School of Science, Tohoku University), Bjorn Mysen(Geophysical Laboratory, Carnegie Inst. Washington), Chairperson:Bjorn Mysen(Geophysical Laboratory, Carnegie Inst. Washington), Michihiko Nakamura(Division of Earth and Planetary Materials Science, Department of Earth Science, Graduate School of Science, Tohoku University)

The mass transfer depends on properties of the Earth's materials and geodynamic processes including cold slab subduction and magmatism due to hot plume activity. The mass transfer processes are imaged by geophysical observations such as seismic tomography and electrical conductivity profiles. One of the most important processes to transport volatiles is the slab subduction. The degree of hydration and dehydration in the slab is essential to evaluate amounts of volatiles transported into the deep mantle. Hydration and dehydration in the slab directly related to slab earthquakes, deformation of the slabs, and the arc magmatism. The fate of the fluid dehydrated in the deep slab is also a debated issue since permeability at the depth may be small, and the fluid might be trapped in the slabs and transported in the deep earth's interior at that depths without escaping to the mantle wedge. Recent seismic tomographic studies of the slab revealed direct observations of hydration and dehydration sites in the slabs. There exists growing evidence for alteration and hydration of the old lithosphere due to fracturing and Putit spot volcanisms which affect the volatile transport into the deep mantle due to slab subduction. The mass transfer to the surface can also be observed as the volcanic eruption in which phase separation of magma and fluid, and crystallization during the magma ascent controls the type of eruptions. The proposed session will focus on those phenomena including laboratory experiments, numerical modeling, and geophysical and geochemical observations including physical and chemical properties of magma and fluid, and geophysical imaging of various scales including seismic tomography of the descending slabs, and monitoring of near surface processes of volcanic eruptions. Contributions to any of these subjects are encouraged. We also encourage papers stimulating an interdisciplinary collaboration relating to establishment of the SEDI-Japan community.

9:00 AM - 9:15 AM JST | 12:00 AM - 12:15 AM UTC

[SIT20-07] HDAC experiments on silica solubility and speciation in Na_2CO_3–H_2O fluids at high pressure and temperature

*Naoko Takahashi[1], Tatsuki Tsujimori[1,2], Seiji Kamada[1,3], Michihiko Nakamura[1] (1.Department of Earth Science, Graduate School of Science, Tohoku University, 2.Center for Northeast Asian Studies, Tohoku University, 3.Frontier Research Institute for Interdisciplinary Sciences, Tohoku University)

9:15 AM - 9:30 AM JST | 12:15 AM - 12:30 AM UTC

[SIT20-08] Permeability determination from multi-anvil experiments: Implications for the fluid flux in subduction zones

★Invited Papers

*Lisa Eberhard[1], Philipp Eichheimer[1], Marcel Thielmann[1], Michihiko Nakamura[2], Gregor Golabek[1], Dan Frost[1] (1.Bayerisches Geoinstitut, University of Bayreuth, Germany, 2.Departement of Earth Science, Tohoku University, Japan)

9:30 AM - 9:45 AM JST | 12:30 AM - 12:45 AM UTC

[SIT20-09] Fluid segregation and chemical compaction through efficient solute transport along wet grain boundaries

*Wakana Fujita[1], Michihiko Nakamura[1], Kentaro Uesugi[2] (1.Graduate School of Science, Tohoku University, 2.Synchrotron Radiation Research Institute (JASRI/SPring-8))

9:45 AM - 10:00 AM JST | 12:45 AM - 1:00 AM UTC

[SIT20-10] Coupling between fluid flux and dynamical permeability evolution in the middle-lower crust, an example from Sør Rondane Mountains (SRM), East Antarctica.

*Diana Mindaleva[1], Masaoki Uno[1], Atsushi Okamoto[1], Noriyoshi Tsuchiya[1] (1.Graduate school of environmental studies, Tohoku University)

10:00 AM - 10:15 AM JST | 1:00 AM - 1:15 AM UTC

[SIT20-11] Attenuation contrast in mantle wedge across the volcanic front of NE Japan that controls propagations of high-frequency S-wave later phases

*Takahiro Shiina[1], Kei Katsumata[2], Kiyoshi Yomogida[2], Aitaro Kato[3] (1.National Institute of Advanced Industrial Science and Technology (AIST), 2.Graduate School of Science, Hokkaido University, 3.Earthquake Research Institute, the University of Tokyo)

10:15 AM - 10:30 AM JST | 1:15 AM - 1:30 AM UTC

[SIT20-12] The effect of water on energy dispersion of olivine and its implications for the origin of the sharp contrast of seismic observation at the lithosphere-asthenosphere boundary

*Chao Liu[1], Takashi Yoshino[1] (1.Institute for Planetary Materials, Okayama University)

HDAC experiments on silica solubility and speciation in Na_2CO_3–H_2O fluids at high pressure and temperature

*Naoko Takahashi[1], Tatsuki Tsujimori[1,2], Seiji Kamada[1,3], Michihiko Nakamura[1]

1. Department of Earth Science, Graduate School of Science, Tohoku University, 2. Center for Northeast Asian Studies, Tohoku University, 3. Frontier Research Institute for Interdisciplinary Sciences, Tohoku University

Silica is the most dominant solute in subduction-zone fluids. Recent thermodynamic models predict the presence of deprotonated monomer, $SiO(OH)_3^-$(aq), the monomers, $Si(OH)_4$(aq), and the dimers, $Si_2O(OH)_6$(aq), as primary silica species in the alkaline fluids equilibrated with subducted silicate rocks [1]. However, the silica speciation in alkaline fluids at high *P*–*T* conditions remains unclear due to the complexities of equilibrium constants among silica species. Aranovich et al. [2] reported the higher silica solubility in Na_2CO_3 solutions at 500–700˚C and 0.4–0.5 GPa than that expected solely from the known species in the extended Deep Earth Water (DEW) model [3], suggesting the possible presence of deprotonated dimer, $Si_2O(OH)_6^-$(aq). To confirm the speciation of silica in Na_2CO_3 solutions at high *P*–*T* conditions, we conducted a Raman spectroscopic study on silica speciation in pure H_2O and Na_2CO_3 solutions (0.5 and 1.0 *m* [mol/kg H_2O]) up to 750˚C and 2 GPa using a hydrothermal diamond anvil cell. Moreover, we measured the solubility of quartz by direct observation of dissolving quartz grains.

The measured Raman spectra showed an asymmetric and broad band at ~770 cm^{-1}, which can be assigned to symmetric Si–OH stretching of the monomeric species $SiO(OH)_3^-$(aq) and $Si(OH)_4$(aq). Besides, we newly detected the intense broad bands at ~600 cm^{-1} consisting of at least three components, which represent the bending vibrations of bridging oxygen Si–O–Si of several oligomers. The lowest frequency component at ~530 cm^{-1} was interpreted as the asymmetric breathing mode of ring trimer. While the uncertainty remains in assigning the broad bands at ~1080 cm^{-1} to a single species, we presume the main contributions from deprotonated or oligomeric species. The ratio of the oligomer band area at ~600 cm^{-1} to the monomer band area at ~770 cm^{-1} of each experimental spectrum increases according to the increase pressure and temperature at quartz-saturated conditions.

The determined quartz solubility in pure H_2O at 718˚C and 1.0 GPa fell in the range of 0.62 to 0.82 *m*, which is almost consistent with the value of 0.72 *m* calculated by the DEW model. On the other hand, the silica solubility in the Na_2CO_3 solutions at experimental conditions increased to the range of 1.5 to 3.0 *m* with increasing Na_2CO_3concentration and temperature. A preliminary comparison among our experimental results and thermodynamic models has led the following conclusions. (1) the silica solubility in the Na_2CO_3 solutions of the present experiments was several times higher than the value calculated based on the thermodynamic properties of aqueous silica species in the DEW model. (2) Although the addition of thermodynamic parameters of deprotonated dimer $Si_2O(OH)_6^-$(aq) can readily explain the high solubility of silica in the Na_2CO_3 solutions, our Raman spectroscopic data suggest the presence of several other oligomeric species that contributed to the high silica solubility. Therefore, additional oligomeric silica species should be considered in the estimation of silica solubility in alkaline fluids at deep-crust and upper mantle conditions.

References: [1] Connolly and Galvez (2018) Earth Planet. Sci. Lett., 501, 90–102, [2] Aranovich et al. (2020) Chem. Geol., 550, 119699, [3] Huang and Sverjensky (2019) Geochim. Cosmochim. Acta, 254, 192–230.

©2021. Japan Geoscience Union. All Right Reserved.

Keywords: hydrothermal diamond anvil cell, Raman spectroscopy, silica species, solubility

©2021. Japan Geoscience Union. All Right Reserved.

Permeability determination from multi-anvil experiments: Implications for the fluid flux in subduction zones

*Lisa Eberhard[1], Philipp Eichheimer[1], Marcel Thielmann[1], Michihiko Nakamura[2], Gregor Golabek[1], Dan Frost[1]

1. Bayerisches Geoinstitut, University of Bayreuth, Germany, 2. Departement of Earth Science, Tohoku University, Japan

Dehydration of hydrous minerals and the subsequent transport of the released fluids are important for a number of subduction zone processes. The fluids carry dissolved element and are responsible for metasomatism of the overlying mantle wedge, which is an important stage in the geochemical cycle of many trace and volatile elements. Within the mantle wedge fluids raise the degree of melting. Furthermore, subduction zone fluids are often linked to the origin of deep focused earthquakes. These processes necessitate a significant fluid flux between serpentine layers, which are likely to be the main source of water in subduction zones, and the overlying mantle, which requires fluid permeability to be sufficiently high.

Shear deformation in subduction zones most likely causes strong foliation and preferred orientation of serpentine minerals. Previous experiments at low pressures (100 MPa) indicate the occurrence of permeability anisotropy in foliated serpentinites. Accordingly, fluids may preferentially migrate parallel to the foliation but then become channelized into deep-rooted fault zones.

However, so far permeability measurements were limited to low pressures (<0.5 GPa). Based on pressure-dependent changes in volumes of both solids and liquids it becomes questionable as to whether the results of such permeability measurements can be extrapolated to the significantly higher conditions of subduction zone dehydration.

We report a new experimental method, which allows the permeability in dehydrating mineral assemblages to be determined through the analysis of recovered samples. For this purpose, we performed high pressure multi-anvil experiments. Our assembly consists of an orientated serpentinite drill core embedded in an MgO sleeve. At 2 - 5 GPa antigorite dehydrates over a temperature interval of approximately 100 ˚C at temperatures <700 ˚C. The released fluid migrates into the MgO and reacts to form brucite. The fluid can leave the serpentine sample in a direction either parallel or perpendicular to the initial serpentine foliation. The analysis of the location and proportion of brucite formed allows the fluid discharge at the experimental conditions to be calculated over the experimental run time. We combined these results with numerical simulations and μCT-scans to estimate the porosity.

Our results show that serpentinites in subduction zones are expected to form an essentially impermeable layer prior to dehydration. As progressive dehydration occurs at temperatures exceeding 550 ˚C the permeability increases by 2 orders of magnitude. We also show that the dehydration reaction causes in a change in texture, so that fluid flow becomes isotropic. This should favour pervasive fluid flow rather than channelized flow.

Keywords: serpentinite, multi-anvil, permeability

©2021. Japan Geoscience Union. All Right Reserved.

Fluid segregation and chemical compaction through efficient solute transport along wet grain boundaries

*Wakana Fujita[1], Michihiko Nakamura[1], Kentaro Uesugi[2]

1. Graduate School of Science, Tohoku University, 2. Synchrotron Radiation Research Institute (JASRI/SPring-8)

Segregation of geological fluids such as supercritical aqueous fluids and silicate melts is an essential elementary process for volatile cycles in subduction zones. To explain the mechanism of fluid segregation, various processes have been examined including matrix deformation[1, 2], interfacial tension driven fluid redistribution[3, 4, 5] and melt rock reaction[6, 7]. A common feature in these processes is that fluid migrates through interconnected networks along the grain boundaries and channels. In this presentation, we will report a model of efficient fluid segregation which occurs without fluid interconnections.

The CHO fluid-bearing quartz aggregates were synthesized with nominal fluid fractions between 0 and 0.18 from powdered mixture of Arkansus quartz and amorphous silica prepared by sol-gel method. The mixture was hot-pressing in a piston–cylinder apparatus at 900℃ and 1.0 GPa for 24–382 hours for X_{CO2} = 0–0.44. The recovered run products were imaged with synchrotron X-ray microtomography and the porosity was measured. The quartzites with high initially added fluid fraction ($\phi_{add} > 0.056$) tend to consist of fluid rich section and fluid poor section, which irrelevantly locate to top and bottom of the run products. The fluid poor sections retained very small fluid fractions (< 0.01) regardless of the high added fluid fraction. Partially deformed platinum sleeves and nickel capsules demonstrate that fluids were squeezed out from this region at the initial stage of the segregation. This deformation-assisted fluid segregation would continue until the fluid interconnection was pinched off. The pinch-off fluid fractions of our samples were 0.031–0.037 for X_{CO2} = 0 and 0.044–0.048 for X_{CO2} = 0.28–0.44, implying the occurrence of the second stage fluid segregation to form the very dense section of quartzite after the deformation. We calculated diffusive flux of the dissolved SiO_2 driven by the difference in the fluid pressure between the fluid rich section and the fluid poor section that lacks fluid interconnection considering the matrix viscosity. We found that the silica flux from the fluid poor to rich sections was 10^5 times larger than that expected from the reported grain boundary diffusivity. Our results imply that efficiency of the fluid segregation through silica redistribution along the wet or transient grain boundaries is comparable to the fluid segregation along interconnected fluid networks driven by interfacial tension[8] and deformation[9] when the spatial scale is less than ~0.1 meter.

Reference:
1. Mckenzie, D. (1984). The generation and compaction of partially molten rock. *J. Petrol.*, 25, 713–765.
2. Holtzman, B. K., & Kohlstedt, D. I. (2007). Stress-driven melt segregation and strain partitioning in partially molten rocks: Effects of stress and strain. *J. Petrol.*, 48, 2379–2406.
3. Stevenson, D. J. (1986). On the role of surface tension in the migration of melts and fluids. *Geophys. Res. Lett.*, 13, 1149–1152.
4. Watson, E. B. (1982). Melt infiltration and magma evolution. *Geology*, 10, 236–240.
5. Nakamura, M., & Watson, E. B. (2001). Experimental study of aqueous fluid infiltration into quartzite: Implications for the kinetics of fluid redistribution and grain growth driven by interfacial energy reduction. Geofluids, 1, 73–89.
6. Daines, M. J., & Kohlstedt, D. L. (1994). The transition from porous to channelized flow due to melt / rock reaction during melt migration. Geophys. Res. Lett., 21, 145–148.
7. Pec, M., Holtzman, B. K., Zimmerman, M., & Kohlstedt, D. L. (2015). Reaction infiltration instabilities in

©2021. Japan Geoscience Union. All Right Reserved.

experiments on partially molten mantle
rocks. Geology, 43, 575–578.
8. Takei, Y., & Hier-Majumder, S. (2009). A generalized formulation of interfacial tension driven fluid migration with dissolution/precipitation. Earth. Planet. Sc. Lett., 288, 138–148.
9. Stevenson, D. J. (1989). Spontaneous small-scale melt segregation in partial melts in undergoing deformation. *Geophys. Res. Lett.*, 16, 1067–1070.

Keywords: fluid segregation, chemical compaction, quartzite

©2021. Japan Geoscience Union. All Right Reserved.

Coupling between fluid flux and dynamical permeability evolution in the middle-lower crust, an example from Sør Rondane Mountains (SRM), East Antarctica.

*Diana Mindaleva[1], Masaoki Uno[1], Atsushi Okamoto[1], Noriyoshi Tsuchiya[1]

1. Graduate school of environmental studies, Tohoku University

Fluid flow causes hydration reactions, which induce mass transport, and changes rheology of rocks. Permeability increases due to fluid pressure rise cause rock fracturing and provide fluid infiltration. Such fluid activity is related to earthquake generation, tremors, and slow slip events. It was suggested that H_2O released due to dehydration reactions increases fluid pressure, causes fracturing, and induce tremors (e.g., Abers et al., 2009; Katsumata and Kamaya, 2003; Obara et al., 2004). However, quantitative constraints on fluid fluxes and crustal permeability are limited, particularly with regards to its temporal evolution. Therefore, it is important to constrain amount of fluid fluxes to understand roles of fluids in seismic events, permeability evolution, and water-rock interaction in the crust. Here, based on metamorphic fluid-rock reaction zones, we constrain fluid fluxes through the fractured crust by thermodynamic modeling of fluid chemistry and observed fracture geometry, and discuss the relation of fluid flux, their duration, and size of fractures that possibly related to seismic events.

We investigated fluid-rock reaction zones in hydrated metamorphic rocks samples from the Mefjell and Brattnipene Sør Rondane Mountains (SRM), East Antarctica. Amphibolite-facies planar fractures and millimeter-scale hydration zones around them provide unique information on duration and hydraulic parameters of fluid infiltration. Based on reactive-transport analysis of trace elements, in our previous study (Mindaleva et al., 2020) we have investigated timescales of fluid infiltration and estimated permeability evolution. The timescales are constrained to tens of hours. The permeability of the wall rock and fractures were estimated to be 10^{-20}–10^{-22} and 10^{-8}–10^{-9} m^2, respectively. We used these estimations to calculate fluid fluxes in the reaction zones and through the fracture.

To understand amount of fluids transported through the single fracture, we estimated fluid fluxes through the fractures and through the reaction zones. Fluid fluxes through the reaction zone were estimated by two ways: total amount of H_2O added to reaction zone ($Q_{RZ}H_2O$) and modelled fluid flux required for chlorine transport ($Q_{RZ}Cl$). Fluid fluxes through the fracture were estimated by two different approaches. First method utilizes permeability of the fracture, pressure gradient, and timescales of the fluid infiltration, constrained for each sample ($Q_{FR}Hyd$). Second method is based on the advective reaction-transport equation applied to fluid speciation phase equilibrium modelling results ($Q_{FR}Si$). We also measured seismic moment and magnitude from the fluid flux volumes and provide insights about possible seismic events.

Fluid fluxes through the reaction zone log $Q_{RZ}H_2O$ range -4.2– -3.3 m, flux required for Cl transport log $Q_{RZ}Cl$ is same order, ranges -4.7– -3.5 m. Fluid flux through the fracture log $Q_{FR}Hyd$ ranges 1.6– 3.8 m, and fluid flux estimated by thermodynamic modeling of fluid chemistry log $Q_{FR}Si$ ranges 2.1– 2.9 m, respectively.
Magnitude of the possible seismic even estimated from the fluid fluxes by two different approaches ranges -1– 2.6. First method based on the McGarr,1976 equation suggesting relationship between seismic moment and fluid flux. Second method is based on the fault geometry, we used cross-section area as

©2021. Japan Geoscience Union. All Right Reserved.

5–30 ×5–30 m, and slip displacement ranges 1–0.1 mm. Magnitude estimated by McGarr’ s equation ranges 2.0– 2.6, while second approach provides ranges -1– 0. We compared our estimations to the results of fluid injection experiments (e.g., Baisch et al., 2006; Baisch et al., 2009; Häring et al., 2008; Deichmann et al., 2014). Moment magnitude estimated by first approach is the maximum magnitude observed in series of fluid injection experiments in the shallow crust. However, first approach is not tested for deep crustal conditions and at very low fluid fluxes. Second approach possibly provides more realistic results for our conditions, incorporating geological observations, low fluid fluxes and middle-lower crustal conditions.

Our results show that much amount of fluids are transported by fractures rather than to be stored in the reaction zones. Such fluid infiltration can possibly induce fracturing and low magnitude seismic events in the crust.

Keywords: Fluid flux , Hydration, Fluids activity, Permeability , Reaction zones, Timescales

©2021. Japan Geoscience Union. All Right Reserved.

Attenuation contrast in mantle wedge across the volcanic front of NE Japan that controls propagations of high-frequency S-wave later phases

*Takahiro Shiina[1], Kei Katsumata[2], Kiyoshi Yomogida[2], Aitaro Kato[3]

1. National Institute of Advanced Industrial Science and Technology (AIST), 2. Graduate School of Science, Hokkaido University, 3. Earthquake Research Institute, the University of Tokyo

Distinct later phases of waves containing high-frequency (>8 Hz) components were observed for intraslab earthquakes that occurred at intermediate depths, particularly at depths exceeding 100 km, in the NE Japan subduction zone. These high-frequency later phases showed anomalously large peak-amplitude delays, up to ~50 s after direct S-wave arrivals at stations in the backarc region. Using a source-scanning algorithm, we investigated the locations of passing points affecting the propagation of high-frequency later phases. The passing points were estimated to be in the forearc region in the entire NE Japan, indicating that high-frequency later phases are scattered waves that pass through the forearc region. The propagating high-frequency later phases seem to bypass the backarc mantle wedge, as a consequence of the distinct attenuation contrast in the mantle wedge across the volcanic front in NE Japan. These high-frequency later phase observations suggest that the high-attenuation zone in the backarc mantle wedge controls propagations of the high-frequency waves of intraslab earthquakes, in addition to the scatterers possibly locate in the forearc region.

Keywords: Later phase, Intraslab earthquake, S-wave attenuation, Scattering

©2021. Japan Geoscience Union. All Right Reserved.

The effect of water on energy dispersion of olivine and its implications for the origin of the sharp contrast of seismic observation at the lithosphere-asthenosphere boundary

*Chao Liu[1], Takashi Yoshino[1]

1. Institute for Planetary Materials, Okayama University

Seismic observations have shown a sharp drop of shear wave velocity at the lithosphere-asthenosphere boundary (LAB) (Kawakatsu et al., 2010) and strong attenuation in the asthenosphere. The temperature difference itself was difficult to explain such sharp change (Karato et al., 2015). Such as presence of partial melt, deduced grain size, or increased water content in asthenosphere have been considered as the possible origins for those anomalies (e.g., Anderson and Sammis, 1970; Hirth and Kohlstedt, 1996; Faul and Jackson, 2005; Yoshino et al., 2006; Jackson et al., 2010; Karato, 2012). Considering the thermal structure and sharp drop of velocity in the old oceanic upper mantle (100 Myr), those anomalies could not be explained by partial melting (Hirschmann, 2010) or reduced grain size (Karato, 2018). Seismic attenuation is a useful tool to figure out this origin. Although recently Cline et al. (2018) showed a small effect of water content on energy dispersion of olivine aggregates, they measured attenuated properties for Ti-related H defects, which is stable at the low pressure they conducted. Because the actual H substitution mechanism in the upper mantle is related to Mg or Si vacancies, thus we need to measure anelastic properties at relatively higher pressure at which these substitution mechanisms become dominant.

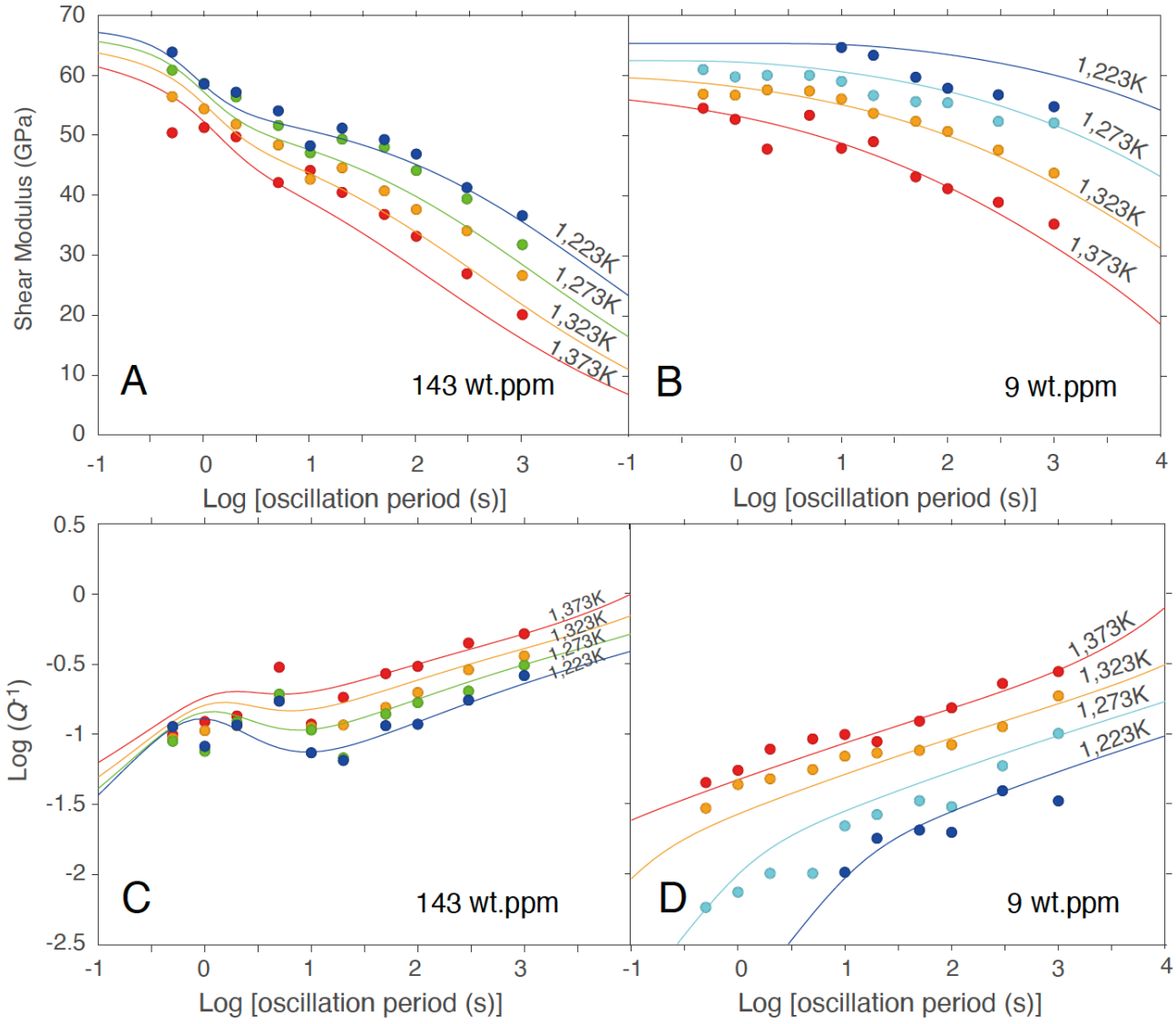
To investigate the effect of water on anelastic property of mantle materials, we measured the energy dispersion and Young's modulus of olivine aggregates, which is the most dominant mineral in the upper mantle, in various oscillation periods (0.5 -1000 s) at 1373 K and 3 GPa (70 km depth in the Earth). The newly built short-period cyclic loading system in situ X-ray observation was used in our experimental procedures (Yoshino et al., 2016).

The experimental results show that the energy dispersion increases with increasing period of oscillation, decreasing grain size, and increasing the water content of olivine, while the energy dispersion reduces its Young's modulus. When water content increases, an attenuation peak appears at the short period (5~10 s). The modified generalized Burger's model was used to acquire the effect of water content and grain size on attenuation and velocity of seismic wave quantitatively (Jackson et al., 2005). The fitting results show that there are two contributions from the high-temperature background (diffusion accommodated grain boundary sliding, DGBS) and attenuation peak to the energy dispersion. The characteristic relaxation time for DGBS showed a mild frequency dependence (0.33), which is consistent with the results of the previous study. The water could enhance the relaxation time with an exponent factor of 2.5(0.1) for DGBS. For the attenuation peak, water could enhance the peak height with an exponent factor of 1.2(1).

Takeuchi et al. (2017) found little frequency-dependent attenuation beneath the old oceanic floor, which is consistent with the attenuation behavior of hydrous samples showing an attenuation peak at a short period. The present results demonstrate that the old lithosphere with less than 1 wt.ppm H_2O overlying hydrous asthenosphere (100 wt. ppm H_2O) can produce the observed velocity drop (5-10 %). The difference of seismic properties between the asthenosphere and the old oceanic lithosphere can be explained by a remarkable difference in water content between them.

©2021. Japan Geoscience Union. All Right Reserved.

Keywords: energy dispersion, water, upper mantle, attenuation, velocity, lithosphere and asthenosphere boundary



©2021. Japan Geoscience Union. All Right Reserved.

[E] Poster | S (Solid Earth Sciences)：S-IT Science of the Earth's Interior & Techtonophysics

Sat. Jun 5, 2021 5:15 PM - 6:30 PM JST | Sat. Jun 5, 2021 8:15 AM - 9:30 AM UTC | Ch.14_2

[S-IT20] MAGMA, FLUID TRANSPORT, AND SEISMICITY IN THE EARTH'S INTERIOR

convener:Eiji Ohtani(Department of Earth and Planetary Materials Science, Graduate School of Science, Tohoku University), Saeko Kita(International Institute of Seismology and Earthquake Engineering, BRI), Michihiko Nakamura(Division of Earth and Planetary Materials Science, Department of Earth Science, Graduate School of Science, Tohoku University), Bjorn Mysen(Geophysical Laboratory, Carnegie Inst. Washington)

The mass transfer depends on properties of the Earth's materials and geodynamic processes including cold slab subduction and magmatism due to hot plume activity. The mass transfer processes are imaged by geophysical observations such as seismic tomography and electrical conductivity profiles. One of the most important processes to transport volatiles is the slab subduction. The degree of hydration and dehydration in the slab is essential to evaluate amounts of volatiles transported into the deep mantle. Hydration and dehydration in the slab directly related to slab earthquakes, deformation of the slabs, and the arc magmatism. The fate of the fluid dehydrated in the deep slab is also a debated issue since permeability at the depth may be small, and the fluid might be trapped in the slabs and transported in the deep earth's interior at that depths without escaping to the mantle wedge. Recent seismic tomographic studies of the slab revealed direct observations of hydration and dehydration sites in the slabs. There exists growing evidence for alteration and hydration of the old lithosphere due to fracturing and Putit spot volcanisms which affect the volatile transport into the deep mantle due to slab subduction. The mass transfer to the surface can also be observed as the volcanic eruption in which phase separation of magma and fluid, and crystallization during the magma ascent controls the type of eruptions. The proposed session will focus on those phenomena including laboratory experiments, numerical modeling, and geophysical and geochemical observations including physical and chemical properties of magma and fluid, and geophysical imaging of various scales including seismic tomography of the descending slabs, and monitoring of near surface processes of volcanic eruptions. Contributions to any of these subjects are encouraged. We also encourage papers stimulating an interdisciplinary collaboration relating to establishment of the SEDI-Japan community.

[SIT20-P01] Electrical conductivity in texturally equilibrated fluid-bearing forsterite aggregates at 800°C and 1 GPa: implications for the high electrical conductivity anomalies in mantle wedges

*Yongsheng HUANG[1], Haihao Guo[2], Takayuki Nakatani[1,4], Kentaro Uesugi[3], Michihiko Nakamura[1], Hans Keppler[2] (1.Graduate School of Science, Tohoku University, 2.Bayerisches Geoinstitut, University of Bayreuth, 3.Spring-8, Japan Synchrotron Radiation Research Institute (JASRI), 4.Geological Survey of Japan)

[SIT20-P02] Role of water in subducting slabs: dry phase transformation kinetics in wet slabs

*Eiji Ohtani[1], Takayuki Ishii[2,3] (1.Department of Earth and Planetary Materials Science, Graduate School of Science, Tohoku University, 2.Bayeriches Geoinstitut, University of Bayreuth, 3.Center for High Pressure Science and Technology Advanced Research)

[SIT20-P03] Melting phase relation of hydrous peridotite at the top of the lower mantle

*Kayan Lau[1], Takashi Yoshino[1], Hideharu Kuwahara[1] (1.Institute for Planetary Materials, Okayama University)

[SIT20-P04] Completeness magnitude of earthquakes and spatial variations of b-VALUE in Myanmar

Ngun Za Iang[1], *Saeko Kita[2] (1.Department of Meteorology and Hydrology (DMH), Ministry of Transport and Communications, Naypyitaw, Myanmar, 2.Building Research Institute)

Electrical conductivity in texturally equilibrated fluid-bearing forsterite aggregates at 800ºC and 1 GPa: implications for the high electrical conductivity anomalies in mantle wedges

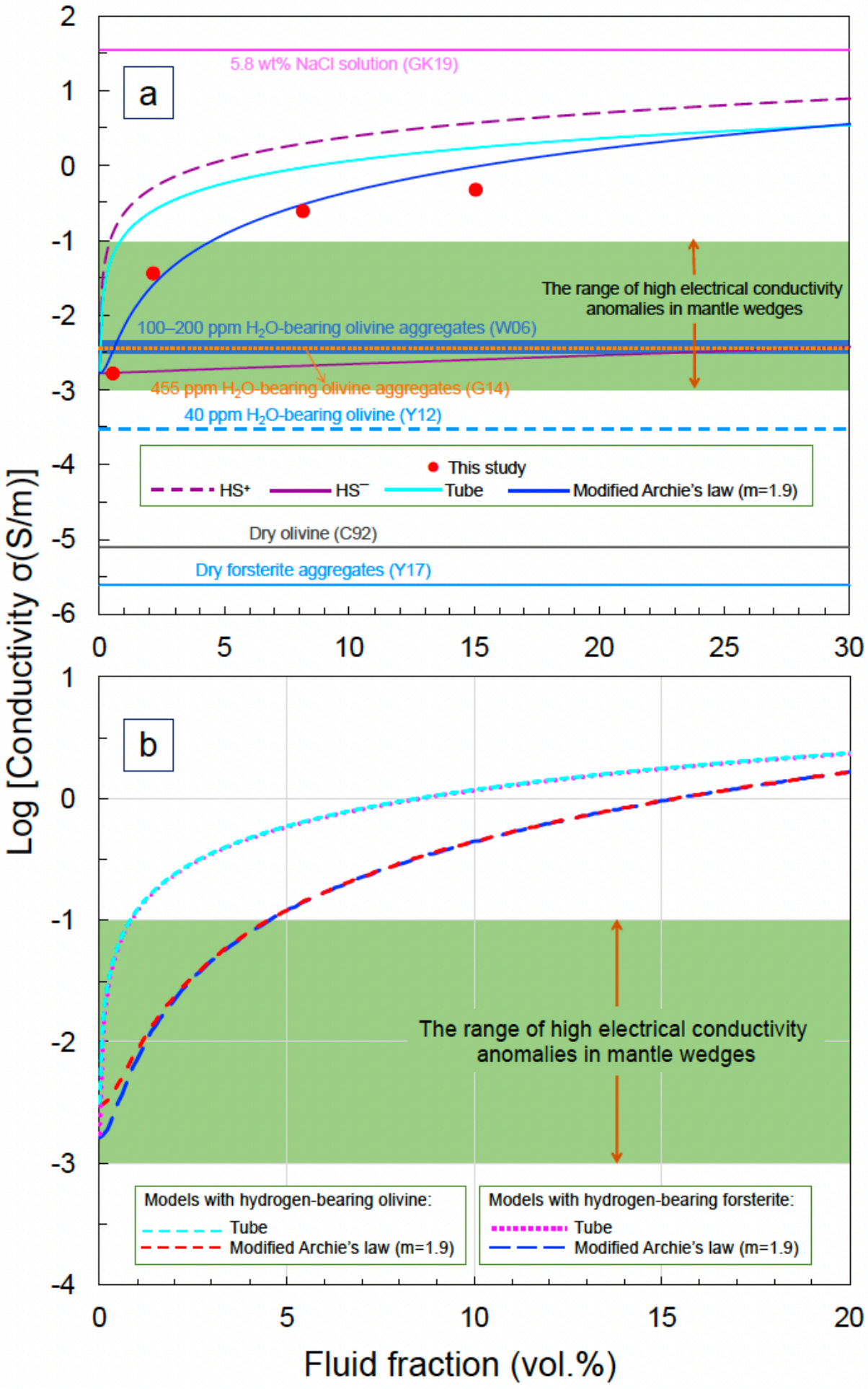
*Yongsheng HUANG[1], Haihao Guo[2], Takayuki Nakatani[1,4], Kentaro Uesugi[3], Michihiko Nakamura[1], Hans Keppler[2]

1. Graduate School of Science, Tohoku University, 2. Bayerisches Geoinstitut, University of Bayreuth, 3. Spring-8, Japan Synchrotron Radiation Research Institute (JASRI), 4. Geological Survey of Japan

In subduction zones, aqueous fluids released from the subducting slab percolate through the mantle wedge, controlling arc magma genesis and element recycling. Because the presence of fluid significantly enhances the bulk electrical conductivity of rocks, the distribution of fluids in subduction zones may be imaged by magnetotelluric (MT) observations. Recently, a growing number of MT observations have revealed high electrical conductivity anomalies (0.001–1 S/m) in the deep fore-arc crust and mantle wedge in some subduction zones. The precise determination of fluid fraction is essential to understand bulk physical-properties such as rheology and permeability, and the geophysical-state of the mantle. Laboratory-based electrical conductivity measurements are an effective method to estimate the fluid distribution and fraction in a fluid-bearing rock. In this study, the electrical conductivity of texturally equilibrated fluid-bearing forsterite aggregates was for the first time measured for various fluid fractions at a constant salinity of 5.0 wt.% NaCl at 1 GPa and 800 ˚C. We found that the electrical conductivity nonlinearly increases with increasing fluid fraction, and the data can be well reproduced by the modified Archie’s law model. Three-dimensional (3-D) microstructure of interstitial-pores visualized by the high-resolution synchrotron X-ray computed micro-tomography shows a change in fluid distribution from isolated pockets at fluid fraction of 0.51 vol.% to interconnected networks at fluid fractions of 2.14 vol.% and above due to grain anisotropy and grain size differences, accounting for the nonlinear-increase in the electrical conductivity. The rapid-enhancement of conductivity indicated that there is a threshold fluid fraction between 0.51 and 2.14 vol.% for forming interconnected fluid networks, which is consistent with the 3-D images. Our results provide direct evidence that > 1.0 vol.% aqueous fluid with 5.0 wt.% NaCl is required to explain the high conductivity anomalies above 0.01 S/m detected in deep fore-arc mantle wedges. This work was supported by JSPS Japanese–German Graduate Externship, International Joint Graduate Program in Earth and Environmental Sciences, Tohoku University (GP-EES).

Keywords: Electrical conductivity, Brine-bearing forsterite aggregates, Textural equilibrium, X-ray CT, Mantle wedge, Subduction zones

©2021. Japan Geoscience Union. All Right Reserved.



©2021. Japan Geoscience Union. All Right Reserved.

©2021. Japan Geoscience Union. All Right Reserved.

Role of water in subducting slabs: dry phase transformation kinetics in wet slabs

*Eiji Ohtani[1], Takayuki Ishii[2,3]

1. Department of Earth and Planetary Materials Science, Graduate School of Science, Tohoku University, 2. Bayeriches Geoinstitut, University of Bayreuth, 3. Center for High Pressure Science and Technology Advanced Research

We have investigated the water partitioning between nominally hydrous minerals and hydrous minerals under the water-undersaturated conditions. Our experiments on partitioning of water between olivine and hydrous phase A, wasleyite and hydrous phase A, bridgmanite and phase D/phase d revealed that water is strongly preferred to hydrous phases resulting in formation of nearly dry nominally anhydrous minerals such as olivine (<1 ppm), wadsleyite (<300ppm), and bridgmanite (<1ppm) under the water-undersaturated conditions.

Oceanic lithosphere generated at the ridge originally contains very small amount of water about 100-200 ppm [1]. However, after formation of the oceanic plates, various processes provided hydration of the oceanic plates such as ascending plumes across the lithosphere [2], Putit spot volcanisms recently discovered in the back-arc regions [3], fracturing of the plate bending at the shallow depths of the slab subduction estimated from the seismicity near the trenches [4, 5]. Seismic tomography studies in subducting slabs [6, 7] and distributions of the intermediate earthquakes such as double seismic zones reveal that wet regions in the slabs extend into exceeding 50 km inward from the slab surface [8, 9]. We estimated the average water contents in the slabs based on the analyses of geophysical observations and mineral physics data on hydrous and nominally hydrous minerals by Hacker et al. [10] to be in the range from 1600-3500 ppm. These water contents in the slabs together with our experiments reveal that water in the slabs is stored in hydrous minerals, i.e., the subducting slabs are under the wet conditions, whereas coexisting nominally anhydrous minerals contain very small amount of water, resulting in dry conditions.

Rheology and deformation of dry olivine and its phase transformation kinetics have been applied for the large deformation of subducting slabs in the mantle transition zone [11] and origin of the deep seismicity [12, 13]. Geophysical and mineral physics data together with our experiments revealed that subducting slabs are under the wet conditions, and water in the slabs is stored only in hydrous minerals, and coexisting nominally anhydrous minerals are essentially dry. Therefore, the dry transformation kinetics of olivine and its high-pressure polymorphs can be applied even for the wet slabs under water-undersaturated conditions. Our results also revealed that hydrous minerals with dry anhydrous minerals could exist in wet slabs at the top of the lower mantle. Therefore, some of the deep earthquakes occurred at the depths exceeding 660 km may be caused by dehydration of hydrous minerals such as superhydrous phase B or phase D which is stable at the top of the lower mantle [14].

References:

[1] Peslier, A. H. et al., Space Science Reviews, **212**, 743-810 (2017). [2] Seno, T. & Yamanaka, Geophys. Monogr. Ser., vol. 96, edited by G. E. Bebout et al., pp. 347–355, AGU, Washington, D.C. (1996). [3] Hirano et al. Science, 313, 1426-1428. [4] Peacock, S. M. Geology, **29**, 299-302 (2001). [5] Kanamori, H. Physics of the Earth and Planetary Interiors, **4**, 289-300 (1971). [6] Nakajima, J. et al., Gondwana Research, **16**, 470-481 (2009). [7] Bloch, W. et al., Geochemistry, Geophysics, Geosystems, **19**,

©2021. Japan Geoscience Union. All Right Reserved.

3189–3207 (2018). [8] Wei, S. S. et al., Science advances, **3**, e1601755(2017). [9] Kita, S. & Ferrand, T.P., Scientific reports, **8**, 1-11 (2018). [10] Hacker, B. R. et al., Journal of Geophysical Research: Solid Earth, **108**, 2030, (2003). [11] Mohiuddin, A. et al., Nature Geosci. **13**, 170–174 (2020). [12] Green II, H.W. & Houston, H. Annu. Rev. Earth Planet. Sci. **23**, 169–213 (1995). [13] Kirby, S.H. et al., Rev. Geophys. **34**, 261–306 (1996). [14] Zahradnik, J. et al., Sci. Rep., **7**, 1-11 (2017).

Keywords: Hydrous mineral, Nominally hydrous mineral, Subducting slab, Water content, Seismicity, Phase transforamation kinetics

©2021. Japan Geoscience Union. All Right Reserved.

Melting phase relation of hydrous peridotite at the top of the lower mantle

*Kayan Lau[1], Takashi Yoshino[1], Hideharu Kuwahara[1]

1. Institute for Planetary Materials, Okayama University

Previous seismic observations on the Earth’ s mantle have found the low-velocity anomaly around 750 km depth and proposed the existence of partial melting layer atop the lower mantle (e.g., Schmandt et al., 2014; Liu et al., 2018). This layer could be formed by dehydration melting upon the decomposition of hydrous ringwoodite to bridgmanite and ferropericlasein downward flow from the mantle transition zone into the lower mantle.According to the melting relation of hydrous KLB1 peridotite in this depth reported by Kawamoto (2004), at lower temperatures less than 1300C, dense hydrous Mg silicate (DHMS) phases should appear rather than dehydration of ringwoodite. In addition,the observed seismic low-velocity region is approximately 100 km deeper than the ringwoodite-bridgmanite phase transition depth (i.e., 660 km), suggesting that the major cause of partial melting at the top of the lower mantle has been poorly understood.
In order to constrain the melting phase relation of hydrous peridotite at the top of the lower mantle, we conducted high-pressure experiments using a Kawai-type multi-anvil apparatus. The starting material was a powder mixture of natural KLB1 peridotite and brucite + talc as a water source. High-pressure experiments were performed at various pressures from 22 GPa to 28GPa and temperatures from 1200C to 1400C. The recovered samples were observed by scanning electron microscope, and phases were identified by micro-focused X-ray diffractometer, and infrared spectroscopy. In the presentation, we will discuss the origin of the low velocity anomalyfrom the view point ofdehydration melting at the top of the lower mantlebased on the melting phase relation of hydrous peridotite.

Keywords: hydrous phase, melting, lower mantle, low-velocity anomaly

©2021. Japan Geoscience Union. All Right Reserved.

Completeness magnitude of earthquakes and spatial variations of b-VALUE in Myanmar

Ngun Za Iang[1], *Saeko Kita[2]

1. Department of Meteorology and Hydrology (DMH), Ministry of Transport and Communications, Naypyitaw, Myanmar, 2. Building Research Institute

In order to estimate completeness magnitude of earthquakes and b-value of events in Myanmar and surrounding areas, we examined 1,350 hypocenters in the NEDC (National Earthquake Data Center, Myanmar) hypocenter catalog from 2014 to 2018, which determined by a hypocenter determination code SEISAN (Havskov and Ottemoller, 2010) and 21 seismic stations. The completeness magnitude (Mc) was estimated as 2.8 with a b-value of 0.68±0.02 in the whole study area, and the b-values regionally varied from 0.52 to 1.0. The values of completeness magnitude became improved with increase of time. The tendency relation between b-value and faulting styles was found along the Sagaing Fault. The southern part with a smaller b-value indicates thrust type focal mechanism, whereas the northern part with a larger b-value shows strike-slip type focal mechanism. The b-value generally increases with the increase of depth in the whole study area. In the active fault region, the b-value decrease with the increase of depth at depths of less than 15 km. At a depth of more than 15 km, the b-value then increases with the increase of depth. In contrast, a significant decrease of b-value with depth was observed at depths of 75-85 km in the subduction zone of the study region, which could be related with the dehydration process in the subducting oceanic plate. The information of spatial variation of b-value could help to understand the seismotectonics beneath Myanmar and the methodology of this study might be fruitful for the evaluation of ability of detectivity of seismicity there.

Keywords: b-value, Myanmar, intraslab earthquake, the Sagaing Fault, seismicity

©2021. Japan Geoscience Union. All Right Reserved.

[J] Oral | S (Solid Earth Sciences)：S-GL Geology

Sat. Jun 5, 2021 9:00 AM - 10:30 AM JST | Sat. Jun 5, 2021 12:00 AM - 1:30 AM UTC | Ch.24 Zoom Room 24

[S-GL23] Geologic structure and tectonic history of East Asia and Japanese Islands

convener:Makoto Otsubo(Geological Survey of Japan, Research Institute of Earthquake and Volcano Geology), Jun Hosoi(Geological Survey of Japan, Institute of Geology and Geoinformation, AIST), Chairperson:Makoto Otsubo(Geological Survey of Japan, Research Institute of Earthquake and Volcano Geology)

The main aim of this session is to discuss geologic structure and tectonic history of East Asia, especially of Japanese Islands, on the basis of the recent results of geology and other earth sciences.

9:00 AM - 9:15 AM JST | 12:00 AM - 12:15 AM UTC

[SGL23-01] Age spectra of detrital zircons of Paleogene fore-arc sandstones in Japan and the irreversible major change in mid-Eocene relevant to the initiation of Median Tectonic Line.

*Yukio Isozaki[1], Yukiyasu Tsutsumi[2], Tomohito Nakano[1] (1.Department of Earth Science and Astronomy, Graduate School of Arts and Sciences, The University of Tokyo, 2.Deprtment of Geology and Paleontology, National Musem of Nature and Science)

9:15 AM - 9:30 AM JST | 12:15 AM - 12:30 AM UTC

[SGL23-02] Zircon U-Pb ages of Momonoki Subgroup in the Koma Mountains

*Takashi Hakomori[1], Kenichiro Tani[2], Junichiro Kuroda[1], Asuka Yamaguchi[1] (1.Atmosphere and Ocean Research Institute, The University of Tokyo, 2.National Museum of Nature and Science)

9:30 AM - 9:45 AM JST | 12:30 AM - 12:45 AM UTC

[SGL23-03] **Tectonostratigraphic characterization of Maizuru back-arc basin during its closure: geochemical and U-Pb detrital geochronological approaches.**

*Larissa NGOMBI MAVOUNGOU[1], Kaushik Das[1,2], Yasutaka Hayasaka[1,2], Haruna Kuriu[1], Kenta Kawaguchi[3] (1.Department of Earth and Planetary Systems Science, Graduate School of Science, Hiroshima University, 2.HiPeR, Hiroshima, 3.Chonbuk National University, Korea)

9:45 AM - 10:00 AM JST | 12:45 AM - 1:00 AM UTC

[SGL23-04] Southwest Japan rotated clockwise during opening of the Japan Sea: Evidence from Miocene sediments in the Outer Zone

*Hiroyuki Hoshi[1], Hideki Iwano[2], Tohru Danhara[2] (1.Department of Earth Sciences, Aichi University of Education, 2.Kyoto Fission-Track Co., Ltd.)

10:00 AM - 10:15 AM JST | 1:00 AM - 1:15 AM UTC

[SGL23-05] Provenance of sandstones from the Eocene Urahoro Group, Hokkaido, Northern Japan: Tectonic Implications

*Toru Takeshita[1], Hiromi Kaji[1,2] (1.Department of Natural History Sciences, Graduate School of Science, Hokkaido University, 2.Oyo Co. Ltd.)

10:15 AM - 10:30 AM JST | 1:15 AM - 1:30 AM UTC

[SGL23-06] Shallow structure and late Quaternary slip rate on the Osaka Bay Fault: Aspects of climate-tectonic interaction

*Mari Hamahashi[1], Hironori Otsuka[1], Yoshiaki Suzuki[2], Jun Arimoto[2], Tetsuo Matsuno[1,3], Nobukazu Seama[1,3], Satoshi Shimizu[1,4], Hikaru Iwamaru[1,4], Mamoru Sano[1,4], Keita Suzuki[1,4], Katsuya Kaneko[1,3], Kazuo Nakahigashi[5], Itsuko Hidaka[1], Yuzuru Yamamoto[1,3], Yoshiyuki Tatsumi[1] (1.Kobe University, Ocean-Bottom Exploration Center, 2.Geological Survey of Japan, National Institute of Advanced Industrial Science and Technology, 3.Department of Planetology, Graduate School of Science, Kobe University, 4.Nippon Marine Enterprises, Ltd. , 5.School of Marine Resources and Environment, Tokyo University of Marine Science and Technology)

Age spectra of detrital zircons of Paleogene fore-arc sandstones in Japan and the irreversible major change in mid-Eocene relevant to the initiation of Median Tectonic Line.

*Yukio Isozaki[1], Yukiyasu Tsutsumi[2], Tomohito Nakano[1]

1. Department of Earth Science and Astronomy, Graduate School of Arts and Sciences, The University of Tokyo, 2. Deprtment of Geology and Paleontology, National Musem of Nature and Science

The unique age spectra of detrital zircons in Paleogene fore-arc sandstones in Japan, and tectonic implications of their irreversible secular change are discussed. The tectono-sedimentary setting of the Palegene fore-arc in Japan can be divied into two distinct phases; i.e. Paleocene to Early Eocene and the Late Eocene to Oligocene. The major change occurred sometime in the mid-Eocene, most probably by the initiation of the Median Tectonic Line (MTL) as a low-angle fault of arc-contraction nature. Recent studies confirmed that the Paleocene sediments unconformably lying on the Ryoke Cretaceous granitoids regionally overthrust the coeval Sanbagawa schists on the south from Kyushu to Kanto (Hasegawa et al., 2020; Isozaki et al, 2020), constraining the tectonic timing to the post-Paleocene (< 56 Ma). U-Pb ages of detrital zircons were measured for Paleocene bench sandstones deposited on the Shimanto accretionary complexes (Domeki Formation) in SW Shikoku. The age spectrum of zircons in the Domeki Fm is almost identical to those of coeval sandstones in the Ryoke belt (Upper Kokawa Fm and Nate Fm of the Izumi Group in Kinki, Kanohara Conglomerate and Yorii Fm in Kanto), suggesting the ubiquitous supply of mootonous terrigenous clastics into the Paleocene fore-arc domain for more than 80 km across the arc from the southern margin of the Ryoke belt (northern margin of the main fore-arc basin) to the central Shimanto belt (bench on slope). This confirms that the stable and continous deposition on the fore-arc crust of SW Japan arc from the Late Cretaceous to Paleocene without any major tectonic disturbance. In contrast, younger Paleogene sandsotnes in Japan show remarkably different age spectra of detrital zircons (Isozaki et al., in prep.).

Keywords: fore-arc basin, Cretaceous, Plaeogene, Japan, MTL

©2021. Japan Geoscience Union. All Right Reserved.

Zircon U-Pb ages of Momonoki Subgroup in the Koma Mountains

*Takashi Hakomori[1], Kenichiro Tani[2], Junichiro Kuroda[1], Asuka Yamaguchi[1]

1. Atmosphere and Ocean Research Institute, The University of Tokyo, 2. National Museum of Nature and Science

Momonoki Subgroup distributed in the western part of Yamanashi Prefecture has been considered to be trough-fill sediments formed in a trough located between Honshu arc and Izu-Bonin-Mariana arc before their arc-arc type collision has started. Previous studies have classified Momonoki Subgroup into three formations; the Lower Formation (or Yunokawa Fm.) is composed of mudstone, conglomerates, and alternation of sandstone and mudstone, the Middle Formation (or Maruyama Fm.) is composed of mudstone and alternation of sandstone and mudstone, and the Upper Formation (or Senshirosawa Fm.) is mainly composed of conglomerates (Tamura et al., 1984; Aoike, 1999; Kuroda, 2000, B.S. thesis). Depositional age and provenance of Momonoki Subgroup will provide important constraint on the timing of the collision. Previous researches have indicated that it was formed 16-15 Ma (Koyama, 1993) or 15-13.5 Ma (Aoike, 1999) or 12 Ma (Amano, 1991) based on biostratigraphy and estimated cooling age of the Kaikomagatake pluton, and that its provenance was mainly Honshu arc (Okuzawa and Hisada, 2008). In this study, U-Pb dating of zircon were applied to reconsider the depositional age and provenance of Momonoki Subgroup.

U-Pb ages of zircon grains obtained from tuff and sandstones of Momonoki Subgroup were analyzed. The zircon crystals for analysis were handpicked from heavy fraction of constituent particles separated from samples by high voltage pulsed power selective fragmentation device (SELFRAG-Lab) and stamp mill. The measurement was carried out using LA-ICP-MS installed at the National Museum of Nature and Science. Tuff sandwiched in the Lower Formation shows concordant ages concentrated at 23.5 Ma. Sandstones in the Lower Formation show concordant ages ranging from 21 to 2364 Ma. Arkose sandstone in the Middle Formation show the concordant ages ranging from 13 to 2184 Ma and concentrated around 14.6 Ma. The U-Pb age spectrums of sandstones between 100 and ~250 Ma show similarity with those of samples from Shimanto Belt (Tokiwa *et al.*, 2018).

The depositional age of the Momonoki Subgroup has been previously estimated as 16-15 Ma (Koyama, 1993) or 15-13.5 Ma (Aoike, 1999) or 12 Ma (Amano, 1991), but our new zircon age revealed that the Lower Formation may be as old as 23.5 Ma since the tuff in the Lower Formation is considered to be air-fall volcanic ash because of the concentration of zircon U-Pb ages and the absence of other ages. Though the arkose sandstone in the Middle Formation was deposited at 14.6 Ma or later, it is not clear whether the zircons that give concentrated U-Pb age around 14.6 Ma were derived from air-fall volcanic ash or from granite in the hinterland. The 9 My difference in depositional age between tuff in the Lower Formation and the arkose sandstone in the Middle Formation suggests that there may be structural discontinuities in the Momonoki Subgroup, or that the geological setting of the Momonoki Subgroup may have been different from trough-fill sediments.

The similarity of the U-Pb age spectrums of detrital zircons between the Momonoki Subgroup and Shimanto Belt suggests that the provenance of the Momonoki Subgroup is considered to have been mainly the Shimanto Belt with some influence from the Jurassic accretionary complex, with minimum contribution from the Izu-Bonin arc. In addition to the results of zircon U-Pb dating, the sandstones and conglomerates of the studied Momonoki Subgroup contain very few igneous rock fragments and conglomerates, which further provide evidence that sediment supply from the Izu-Bonin arc was

©2021. Japan Geoscience Union. All Right Reserved.

volumetrically small. These results suggest that the collision between the Izu-Bonin arc and the Honshu arc may have started after 14.6 Ma, but further research is required for estimating the precise timing of the collision.

Keywords: zircon, U-Pb, Izu Collision Zone

©2021. Japan Geoscience Union. All Right Reserved.

Tectonostratigraphic characterization of Maizuru back-arc basin during its closure: geochemical and U-Pb detrital geochronological approaches.

*Larissa NGOMBI MAVOUNGOU[1], Kaushik Das[1,2], Yasutaka Hayasaka[1,2], Haruna Kuriu[1], Kenta Kawaguchi[3]

1. Department of Earth and Planetary Systems Science, Graduate School of Science, Hiroshima University, 2. HiPeR, Hiroshima, 3. Chonbuk National University, Korea

The rocks of the Maizuru terrane are considered to be related to a paleo back-arc basin that opened during early Permian and closed at the end of Permian. The deposits of this basin are exposed in the central zone of the present-day Maizuru terrane. They are mainly characterized by the Maizuru Group consisting dominantly of massive mudstone, and sandstone, with restricted occurrence of breccia that overly the Yakuno ophiolitic group considered as the basement of Maizuru back-arc basin. The breccia-dominated unit is a part of the Tonoshiki Formation with unclear stratigraphic position. The aim of this study is to understand the final stage of the evolution of Maizuru back-arc basin and for that, fixing the stratigraphic position of Tonoshiki Formation is of utmost importance. This may hold the key to defining the deformation style and mechanism of Maizuru back-arc basin rocks and the tectonic processes occurring prior to its closure. To address these issues, geochemical and geochronological studies have been conducted. Tonoshiki breccia is a collapse breccia with different sized extremely angular clasts. Clasts are made up of blocks of mafic and felsic rocks with minor but ubiquitously present mudstone. The mudstone clasts in Tonoshiki breccia and mudstone of Maizuru Group are both massive in nature and having similar mineral compositions (quartz and minor feldspar clasts in a pool of illite and chlorite-dominated matrix). Moreover, the bulk-rock chemical data indicate that those mudstones samples mostly sourced from felsic igneous rocks of the upper continental crust. The similar characteristics between the mudstone clasts in Tonoshiki breccia unit and the massive mudstone of Maizuru Group fix the stratigraphic position of the Tonoshiki Formation over the Maizuru Group. There is no known rock unit overlying this Permian sequence, making the Tonoshiki Formation as the topmost unit of Maizuru Group. The U-Pb detrital zircon geochronological studies conducted on two samples of Tonoshiki breccia show closed space probability peaks between ca. 285 Ma to 271 Ma for a sample with clasts from Yakuno ophiolites and one slightly younger single probability peak at 268 Ma for a sample with clasts of shallow crustal rocks. This indicates that there are two major possible sources for the Tonoshiki breccia. Its formation possibly occurred by debris flow during two episodes of tectonic activity that affected Maizuru back-arc basin at the end of Permian. The closure of the basin is characterized by multiple pulses of collapse breccia formation, probably induced by a faulting movement.

Keywords: Maizuru back-arc basin, Tonoshiki breccia, Maizuru Group, Timing of basin closure

©2021. Japan Geoscience Union. All Right Reserved.

Southwest Japan rotated clockwise during opening of the Japan Sea: Evidence from Miocene sediments in the Outer Zone

*Hiroyuki Hoshi[1], Hideki Iwano[2], Tohru Danhara[2]

1. Department of Earth Sciences, Aichi University of Education, 2. Kyoto Fission-Track Co., Ltd.

There are two end-member hypotheses for the mode of migration of Southwest Japan (the southwestern half of the Japanese island arc in front of the Japan Sea) during Miocene major back-arc opening of the Japan Sea. One is that Southwest Japan split and then migrated southward from the eastern margin of the Asian continent with clockwise rotation around a pivot located near its western end. In this hypothesis, Miocene and older remanent magnetization directions clockwise deflected from an expected direction, which were reported from the Inner Zone (the area to the north of an E-W-trending fault called the Median Tectonic Line; MTL), are interpreted to be the unequivocal evidence of the clockwise rotation of Southwest Japan. This has been incorporated into the famous double-door opening model of the Japan Sea. On the other hand, another hypothesis is that Southwest Japan split and then migrated southward from the continental margin without pivotal rotation; the clockwise deflection of remanent magnetization directions is interpreted to be due to block rotations in the Inner Zone. This has been accepted by the pull-apart opening model of the Japan Sea. To determine which of the two hypotheses is correct, an effective approach is to obtain paleomagnetic data from the Outer Zone (the area to the south of the MTL) because regional geologic structures suggest that the Outer Zone has not suffered block rotation. Here we will present geochronological and paleomagnetic results from Miocene sediments of the Tanabe Group in the Outer Zone. Our new U-Pb zircon dates indicate that the lower part of the group is of late early Miocene age. Samples for paleomagnetic study were collected at eight sites in the lower part, and site-mean directions of characteristic remanent magnetization (ChRM) were determined for five sites through detailed stepwise demagnetization experiments. Thermal or ‘hybrid’ demagnetization methods were effective to isolate ChRM. A positive tilting test demonstrates ChRM acquisition before tilting. Importantly, tilt-corrected directions are almost parallel to the directions of the same age reported from the Inner Zone, indicating no relative rotation between the Inner and Outer zones. Comparison of the tilt-corrected directions with an early Miocene reference direction suggests clockwise rotation in the study area with respect to the Asian continent. Therefore, our results are more compatible with the hypothesis of clockwise rotation of Southwest Japan and cast serious doubt on the drift migration hypothesis.

Keywords: paleomagnetism, Southwest Japan, Tanabe Group, tectonics, U-Pb dating

©2021. Japan Geoscience Union. All Right Reserved.

Provenance of sandstones from the Eocene Urahoro Group, Hokkaido, Northern Japan: Tectonic Implications

*Toru Takeshita[1], Hiromi Kaji[1,2]

1. Department of Natural History Sciences, Graduate School of Science, Hokkaido University, 2. Oyo Co. Ltd.

In the southeastern Hokkaido, the Late Cretaceous to Oligocene sediments are widely distributed, and the Eocene sediments distributed in the Shiranuka hill is called the Urahoro Group. We have recently been investigating the Shitakara and Shakubetsu Formations of the Urahoro Group distributed to the east of the Urahoro-town. We have found deformation bands in the Shakubetsu Formation constituting a flexure, and analyzed microstructures in them (Kaji and Takeshita, this meeting, session S-IT19). On the other hand, we noted that sandstones from the Urahoro Group are characteristically rich in biotite and K-feldspar detrital grains, and discussed the provenance based on the mineral mode analysis of these sandstones. In this presentation, we will discuss the location of the provenance and its composition together with recently acquired U-Pb ages of detrital zircon grains from the Urahoro Group, and their implications.

The Urahoro Group is widely distributed to the east of Kushiro-city and Shiranuka hill to the west, which is covered by the Kushiro marsh in the middle. While the Urahoro Group shows moderately dipping structures with E-W strike in the east, the one distributed in the Shiranuka hill constitutes a fold and thrust belt trending N-S (Suzuki, 1958). This structure is inferred to have been formed due to the collision of the proto-Kuril arc against Honshu arc (Kimura and Tamaki, 1985). The Urahoro Group, which yields coal beds, consists of the Beppo, Harutori, Tenneru, Yuubetsu, Shitakara, and Shakubetsu Formations in ascending order (Sasa, 1940). Although the age of the Urahoro Group has been considered as the Late Eocene based on the fossils of shell and plant (Sasa, 1940) and foraminifera (Kaiho, 1983), Katagiri obtained the U-Pb age of 39.06±0.23 Ma in zircons from tuff beds of the Tenneru Formation of the Kushiro district. Further, Katagiri et al. (2020) obtained the youngest U-Pb ages of 39.54 ±0.27 Ma and 40.8 ±1.1 Ma in zircons in two samples from the Harutori Formation of the Shiranuka hill district, and confirmed that the sedimentary age of the Urahoro Group is in the Middle Eocence. However, it remains unknown where the igneous activity at c. 40 Ma which provided detrital grains for the Urahoro Group occurred. On the other hand, it has been accepted that sediments of the latest Ctretaceous to earliest Paleogene Kushiro Group which is unconformably overlain by the Urahoro Group are provided from the proto-Kuril arc, which was perhaps situated at the distribution area of the Kushiro Group. If this is true, it might be considered that the igneous activity at c. 40 Ma also occurred in the proto-Kuril arc. However, not only there is no evidence for this hypothesis, but al so it contradicts the paleocurrent direction. To resolve this discrepancy, since it is important to clarify the composition of the provenance of the Urahoro Group, we have carried out the mineral mode analysis of sandstone from one for each sample of the Shitakara and Shakubetsu Formations. Although the analyses are underway, it is safely concluded that the sandstones are a typical arkosic sandstone, and the provenance mostly consists of granite sensu stricto. Further, since the sandstone contain lithic fragments of rhyolite, it is inferred that the provenance could consist of a plutonic-volcanic rock complex of granite-rhyolite. Furthermore, biotite and K-feldspar grains are extremely fresh, and also granite conglomerates occur in the Urahoro Group, the provenance was located not far from the site of sedimentation. In this respect, one important finding is that it has been inferred that the detrital grains could have been provided from the ESE direction based on paleocurrent analysis. Therefore, the continental shelf off the Kushiro-city is the possible provenance, where the magnetic anomaly belt called “the East Hokkaido belt” is widely distributed. Nanayama et al. (1994) inferred that this magnetic anomaly belt is an extension of the Nikoro Group ophiolite of the Tokoro belt,

©2021. Japan Geoscience Union. All Right Reserved.

based on the fact that chromian spinel was provided from it.

However, since the origin of magnetic anomaly could be equally considered as granitic rocks as the one in the “Ishikari-Kitakami magnetic anomaly belt” (Japanese nuclear fuel research, 2016), the detrital grains could have been provided from this belt mostly consisting of granitic rocks. Although the tectonics of large-scale felsic igneous activity in the continental shelf off the Kushiro city remains unknown, this problem could be argued in relation to c. 40 Ma granitic rocks (Maeda et al., 1986; Kawakami et al., 2006), and also recently found c. 40 Ma metamorphic ages (Takahashi, 2021, accepted) in the Hidaka belt.

Keywords: Eocene Urahoro Group, Provenance, Arkosic sandstone, Collision of the Proto-Kuril arc against Honshu arc, East Hokkaido magnetic anomaly belt, 40 Ma igneous activity in Hokkaido

©2021. Japan Geoscience Union. All Right Reserved.

Shallow structure and late Quaternary slip rate on the Osaka Bay Fault: Aspects of climate-tectonic interaction

*Mari Hamahashi[1], Hironori Otsuka[1], Yoshiaki Suzuki[2], Jun Arimoto[2], Tetsuo Matsuno[1,3], Nobukazu Seama[1,3], Satoshi Shimizu[1,4], Hikaru Iwamaru[1,4], Mamoru Sano[1,4], Keita Suzuki[1,4], Katsuya Kaneko[1,3], Kazuo Nakahigashi[5], Itsuko Hidaka[1], Yuzuru Yamamoto[1,3], Yoshiyuki Tatsumi[1]

1. Kobe University, Ocean-Bottom Exploration Center, 2. Geological Survey of Japan, National Institute of Advanced Industrial Science and Technology, 3. Department of Planetology, Graduate School of Science, Kobe University, 4. Nippon Marine Enterprises, Ltd. , 5. School of Marine Resources and Environment, Tokyo University of Marine Science and Technology

>100 km inboard from the subduction interface in western Japan, the crustal seismogenic zone exists at ~5–20 km depth, as inferred from cut-off depths of seismicity and heat flow gradient. Active faulting is manifested under the contemporary compressional regime formed by the oblique subduction of the Philippine Sea Plate under the Japan arc at a current velocity of ~4–6 cm/yr. At the latitude of 34°N from the Ise bay to the Osaka bay, patterns of geodetic strain accumulation infer that NW-SE shortening of ~1–2 cm/yr is nearly perpendicular to existing faults, posing a major seismic hazard potential to the densely-populated areas of the Kansai region. Previous seismic reflection surveys have revealed a fold-and-thrust belt consisting of ~40° west- and east dipping reverse faults beneath the Osaka basin, Ise basin, and the Suzuka mountains. Whereas, to the west, ~70–80° east dipping, high-angle reverse faults characterize the structures around the Awaji island and contribute to the subsidence in the Osaka bay, including the Nojima fault that ruptured in the devastating 1995 Mw6.9 Southern Hyogo Prefecture Earthquake, and the offshore Osaka bay fault, which did not rupture in the 1995 earthquake.

To study the recent deformation history on the Osaka bay fault, high-resolution seismic profile data were collected along 14 survey lines in the Osaka bay, using a Mini GI air gun (Sercel; 15/15 in^3) and Boomer (100–200 J) as active sources, together with multi-beam bathymetry data on the T/S Fukaemaru and R/V Onokoro. In this study, we characterize the shallow structures of the Osaka bay fault, and assess the fault slip rates, in comparison with deep structures imaged by previous seismic surveys that targeted greater depth. The Osaka bay is filled by ~3 km-thick sediments of the Plio-Pleistocene Osaka Group, which consists of fluvial, lacustrine, and marine sequences, as revealed by multiple boreholes around the bay. Within the sedimentary section, distinct marine clay layers that correlate with global eustatic sea-level highstands are present, marking key beds useful for tying the regional stratigraphy. In this study, we assign the ages in our seismic profiles based on the age-correlated reflectors by Inoue et al. (2003), at the intersection points between our survey lines and previously acquired lines.

Our seismic profiles show that the Osaka bay fault is blind and not surface emergent, and that the deformation along the thrust reaches near surface by fault-propagation folding, characterized by a >5 km-wide asymmetric anticline of which its forelimb becomes steeper with depth. In the footwall, a >2 km-wide syncline and associated thickening of sediments develop packages of growth strata. These strata are further buried by younger sediments, where distinct on-laps of sediments onto folded strata form a regional sequence boundary. We interpret these shallow sediments to represent the Holocene alluvial sequence, overlying the late Pleistocene Upper Osaka Group strata. From the seismic profiles, we observe along-strike variation of sediment thickness of the Holocene sediments (0–20 m thick) in the hanging wall and footwall, revealing horizons where the erosional surface of the fold is exposed at the seafloor, and horizons where the fold is buried by recent sediments.

©2021. Japan Geoscience Union. All Right Reserved.

To document the strain accommodated by the thrust, we use three approaches by measuring: 1) the sediment thickness variations between the hanging wall and footwall, 2) the offsets across the forelimb, and 3) the areas of uplift defined by the geometry of the hanging wall anticline and footwall syncline. The observed variations in shallow sediments on the thrust system indicate multiple changes in deposition, additionally affected by paleoclimate and tidal currents in the bay. We combine our observations with borehole data and regional sea-level records, and report on our assessments of fault slip rates and sediment responses through time, and their north-south variations on the Osaka bay fault.

Keywords: Osaka bay fault, Fold-and-thrust belt, Seismic reflection survey

©2021. Japan Geoscience Union. All Right Reserved.

[J] Poster | S (Solid Earth Sciences)：S-GL Geology

Sat. Jun 5, 2021 5:15 PM - 6:30 PM JST | Sat. Jun 5, 2021 8:15 AM - 9:30 AM UTC | Ch.15_1

[S-GL23] Geologic structure and tectonic history of East Asia and Japanese Islands

convener:Makoto Otsubo(Geological Survey of Japan, Research Institute of Earthquake and Volcano Geology), Jun Hosoi(Geological Survey of Japan, Institute of Geology and Geoinformation, AIST)

The main aim of this session is to discuss geologic structure and tectonic history of East Asia, especially of Japanese Islands, on the basis of the recent results of geology and other earth sciences.

[SGL23-P01] Estimation of fluid migration along the Out of Sequence Thrust from quartz vein geometric information
-Estuimation of permeability at Nobeoka Thrust in Kyushu, southwest Japan-

*Hinako Hosono[1], Takato Takemura[1], Makoto Otsubo[2] (1.Nihon University Colledge of Humanities and Sciences, 2.Geological Survey of Japan, Research Institute of Earthquake and Volcano Geology)

[SGL23-P02] Detrital zircon geochemistry in the Shimanto Accretionary Complex: Tectonic constraints on formations of the Jurassic to Cretaceous batholiths in the eastern Asian margin

*Shogo Aoki[1], Kazumasa Aoki[2], Mayuko Fukuyama[3], Masatsugu Ogasawara[4] (1.Graduate School of International Resource Sciences, Akita University, 2.Center For Fundamental Education, Okayama Univerisity of Science, 3.Graduate School of Engeneering Science, Akita University, 4.Institute of Geology and Geoinformation, Geological Survey of Japan, National Institute of Advanced Industrial Science and Technology)

[SGL23-P03] Itayama Nappe, meta-chert and gabbro in the Ryoke Belt of the Takato-Itayama area, central Japan

*Akira Ono

[SGL23-P04] Publication of the 1:50,000 geological map of the Ikeda District

*Atsushi Noda[1], Kazuhiro Miyazaki[1], Kiyohide Mizuno[1], Mitsuhiro Nagata[2] (1.National Institute of Advanced Industrial Science and Technology, 2.Japan Atomic Energy Agency)

[SGL23-P05] Tectonic slices at the Anko outcrop of Median Tectonic Line, Oshika Village, Nagano Prefecture, Japan

*RYOSUKE ISAJI[1], HIDEO TAKAGI[1] (1.Waseda University)

[SGL23-P06] Zircon U–Pb age of Paleoproterozoic granite gneiss from the Ogcheon Belt, Geumsan area and Paleoproterozoic leucogranite and quartzite from the Yeongnam Massif, Seolcheon area, South Korea

*Kenichiro Iwamizu[1,2], Yasutaka Hayasaka[1], Ji-Hoon Kang[3], Kosuke Kimura[1,4], Tomoyuki Shibata[1] (1.Hiroshima Univ., 2.The Univ. of Tokyo, 3.Andong National Univ., 4.National Inst. of Tech., Kure College)

Estimation of fluid migration along the Out of Sequence Thrust from quartz vein geometric information
-Estuimation of permeability at Nobeoka Thrust in Kyushu, southwest Japan-

*Hinako Hosono[1], Takato Takemura[1], Makoto Otsubo[2]

1. Nihon University Colledge of Humanities and Sciences, 2. Geological Survey of Japan, Research Institute of Earthquake and Volcano Geology

Slow slip earthquake has been attracting attention as a phenomenon that induces a megathrust earthquake along the plate boundary. The existence of fluid as well as the surrounding rock physical properties is an important factor for the slow slip earthquake. Geophysics studies demonstrated that the region storing the fluid and seismogenic zones are well overlapping, however, the heterogeneities of spatial fluid distribution and the processes of the increasing fluid pressure are poorly understood. In order to discuss the fluid migration and increasing fluid pressure along the out-of-sequence thrust based on permeability, numerical analysis was carried out using the geometric information of the quartz veins measured at the outcrop at Nobeoka, southwest Japan.
Footwall consisted of muddy melange with maximum paleo-temperature of 250 ˚C and hanging wall consisted of sand and mudstone with maximum paleo-temperature of 320 ˚C locate in the west and east part respectively of the Nobeoka thrust. The depth of the Nobeoka thrust fault is estimated to be 9.1 to 7.0 km from the geothermal gradient(Kondo et al., 2005). In this study, the following a) to c) were carried out at the Nobeoka thrust fault. a) observation of thin sections: The thin sections of the mineral veins took at the outcrop were observed, and the constituent minerals were identified and the mineral veins were classified. b) measuring veins: 8 square grids (A to G in the footwall, H in the hanging wall) with a side of 2.5m to the east-west direction across the Nobeoka thrust were generated and width, length, strike, and dip of the mineral veins in the grid were measured. c) Calculation of permeability by the numerical analysis: The permeability k_1, k_2, k_3 and flow direction are calculated from three-dimensional geometry information of veins measured in b) using the tensor analysis method proposed by Oda (1983).
As a result, the veins mainly consisted of quartz and calcite. The three-dimensional geometric distribution of the veins at the footwall could be classified into two groups, A to D and E to G. From the estimated permeability and its flow direction, it was found that the maximum permeability k_1 was almost perpendicular to the fault, and the fluid was easy to flow in this direction. The order of the maximum permeability k_1 was 10^{-9} to 10^{-10}. In the grid from E to G, it is difficult to flow in the direction orthogonal to the fault plane (k_3 is in the direction orthogonal to the fault plane), and the magnitude of the permeability was $k_1 = k_2 >> k_3$. On the other hand, in the A to D grids, permeabilities were almost $k_1 = k_2 = k_3$. These permeabilities estimated from outcrops are expected to enable us to consider the fluid behavior along the fault when considering the Fault valve model by Sibson (1992) using a specific permeability.

Keywords: Quartz vein, Permeability, Accretionary prism, Permeability tensor, Nankai Trough, Subduction zone

©2021. Japan Geoscience Union. All Right Reserved.

Detrital zircon geochemistry in the Shimanto Accretionary Complex: Tectonic constraints on formations of the Jurassic to Cretaceous batholiths in the eastern Asian margin

*Shogo Aoki[1], Kazumasa Aoki[2], Mayuko Fukuyama[3], Masatsugu Ogasawara[4]

1. Graduate School of International Resource Sciences, Akita University, 2. Center For Fundamental Education, Okayama Univerisity of Science, 3. Graduate School of Engeneering Science, Akita University, 4. Institute of Geology and Geoinformation, Geological Survey of Japan, National Institute of Advanced Industrial Science and Technology

Most of the Phanerozoic granite batholiths in the North and South China blocks have a tectonical-petrogenetical relation to the Pacific-type orogeny. In connection with this aspect, the major orogenic components including the batholiths of the Jurassic and Cretaceous are relatively well preserved especially in SW Japan. However, it is difficult to estimate the paleo-geologic structures even in the Jurassic and Cretaceous components, because they suffered from later disturbances such as tectonic and surface erosions. In this study, we compared the detrital zircon U–Pb ages and Hf isotopic ratios obtained from fifteen terrigenous clastic rocks in the Cretaceous Shimanto Accretionary Complex of the Shikoku, SW Japan. This comparison is a key to understand the Jurassic-to-Cretaceous spatial-temporal distributions of the batholiths connected with the inner structures of the subduction zone.
The zircon age spectra from the formations before ca. 100 Ma show two age clusters of Permian to middle Jurassic (from ca. 280 to 160 Ma) and early-to-middle Cretaceous (ca. 130 to 100 Ma). On the other hand, those from the formations after ca. 100 Ma show a single age peak of middle-to-late Cretaceous (< ca. 130 Ma). The major change in the age distributions suggests an oceanward migration of the magmatic front in the late Cretaceous (ca. 100 Ma), and the large batholiths formed after 100 Ma played a role in controlling terrigenous supply routes between coeval back-arc and fore-arc domains.
The Hf isotopic ratios ($\varepsilon_{Hf(t)}$) obtained from the analyzed zircons show characteristics values in corresponding to their crystallization ages; moderate juvenile to intermediate values (+6 to -4) for ca. 220 to 200 Ma, moderate juvenile to highly evolved values (+10 to -26) for ca. 200 to 180 Ma, moderate to highly evolved values (-4 to -30) for ca. 180 to 130 Ma, moderate juvenile to intermediate values (+10 to -4) for ca. 130 to 100 Ma, and intermediate to moderate evolved values (+4 to -10) for < ca. 100 Ma.
Integration of these results with the U–Pb age spectra leads to suggestion that the late Jurassic to early Cretaceous granites were generated from the older materials at the inland areas of the China blocks; on the other hand, the late Cretaceous granites were originated from the younger materials at the coastal areas. Moreover, subducting oceanic crusts and/or asthenospheric materials are also suggested to be involved in the early Cretaceous granites. Probably, the major change of source materials in relation to each granite was close to the transition in the position of magmatic front at the time in the North and South China blocks.

Keywords: zircon, U–Pb dating, Hf isotopic ratio

©2021. Japan Geoscience Union. All Right Reserved.

Itayama Nappe, meta-chert and gabbro in the Ryoke Belt of the Takato-Itayama area, central Japan

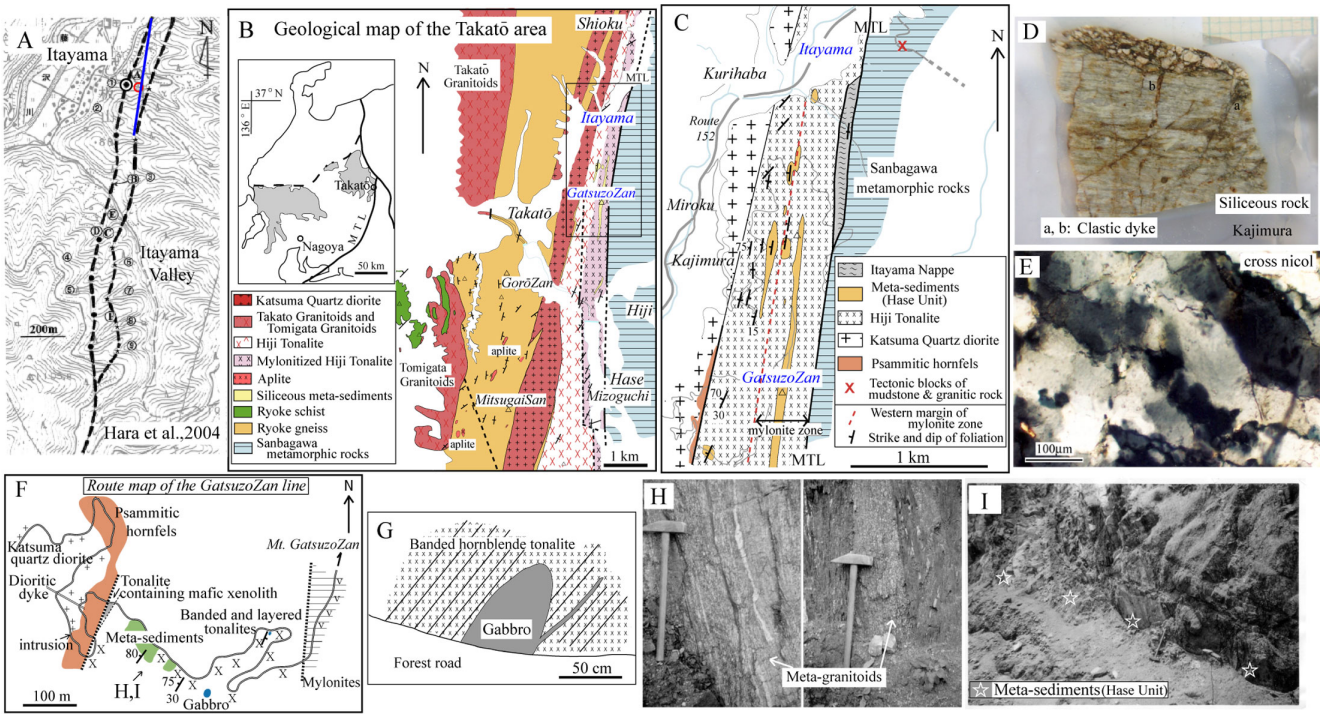
*Akira Ono

Itayama Nappe, meta-chert and gabbro are distributed near the Median Tectonic Line (MTL) of the Itayama area, Takato Town. Here, we introduce these geological bodies. Small Nappe occurs in the Itayama area [1]. Here, this is called Itayama Nappe. The Itayama Nappe is composed of various rocks derived from the Ryoke and Sanbagawa Belts. However, low-grade metamorphic rocks and sedimentary rocks in the Itayama Nappe are not exposed in the nearby Ryoke and Sanbagawa Belts. The Itayama Nappe is sandwiched between two faults, MTL-E and MTL-W (Figure A). However, there is a problem with the geology of the northern part of the Itayama Nappe. In this area an outcrop of MTL exists near the Miyadonosawa dam [2]. That is, the blue fault in Figure A is the MTL. The two MTLs do not exist in this area. Hence, the Itayama Nappe is a narrow geological body extending from north to south that has entered the Kashio mylonite zone (Figures B and C).
Narrow and long meta-chert is distributed in the vicinity of MTL [3]. To the west of the long meta-chert, mylonitized pelitic and siliceous rocks are exposed as xenoliths of Hiji tonalite. For example, various siliceous rocks are exposed almost continuously over about 120 m along a small valley to the east of the Kajimura village (Figure C). These mylonites are derived from the Hase Unit of the accretionary complex [4]. Sizes of quartz grains are about 100 μm for the quartz-rich portion of a siliceous mylonite (Figures D and E) near the red dotted line in Figure C. The red dotted line is the western margin of the Kashio mylonite zone for granitic rocks [3]. The psammitic hornfels in Figure C are not metamorphic rocks derived from the Hase Unit.
Small hornblende gabrro is exposed in two places along the forest road leading to Mt.Gatsuzozan (Figure F). The gabbro intrudes into banded tonalite (Figure G). The Hiji tonalite in the Itayama area has a relatively uniform lithology, but tonalites near the gabbro exhibit remarkably diverse lithologies (Figures H and I). The geological relationship between the Hiji tonalite and Katsuma quartz diorite is unknown, but in the Shioku to the north of Itayama, an outcrop was found in which these granitoids are almost vertically in contact with each other.
The Itayama Nappe is a geological body that has entered the Kashio mylonite zone. The existence of allochthonous geological body in the Kashio mylonite zone was first reported from the Kashio area. Watanabe & Kinugasa [5] reported the occurrence of metamorphic rocks which are thought to be the Sanbagawa metamorphic rocks. Next, microbreccia is found near the Bungui Pass of the Hase area [6]. Subsequently, Awasawa metamorphic rocks were reported which belong to neither Sanbagawa metamorphic rocks, Kashio mylonite nor microbreccia [7]. Microbreccia is a fractured Awasawa metamorphic rock. The Awasawa metamorphic rocks are mainly composed of garnet-biotite-muscovite schist. This pelitic schist is finer than the Sanbagawa schist containing garnet and biotite. Moreover, white mica is not phengite.The (FeO+MgO) content of muscovite is not high as compared with that of the Sanbagawa schist.

[1] Hara et al., 2004, Struc. Geol, No 48, 1. [2]Ono, 2013, GSJ Meeting, R5-P-13. [3]Makimoto et al, 1996, Geology of the Takato district, Geol.Surv.Jpn. [4] Ono, 2018, GSJ Meeting, R15-P-13.[5] Watanabe & Kinugasa, 1970, GSJ Meeting, p.286. [6] Takagi, 1984, Geol. Soc. Jpn, 81. [7] Ono, 2002, Geol. Soc. Jpn, 733.

©2021. Japan Geoscience Union. All Right Reserved.

Keywords: Ryoke belt, Takato-Itayama, Median Tectonic Line, Kashio mylonite, Hase unit



©2021. Japan Geoscience Union. All Right Reserved.

Publication of the 1:50,000 geological map of the Ikeda District

*Atsushi Noda[1], Kazuhiro Miyazaki[1], Kiyohide Mizuno[1], Mitsuhiro Nagata[2]

1. National Institute of Advanced Industrial Science and Technology, 2. Japan Atomic Energy Agency

Geological map of the Ikeda District, which is located in the northeastern part of Shikoku Island, has been published. The basement rocks are divided into the Inner and Outer zones of Southwest Japan by the Median Tectonic Line (MTL). The Inner Zone is composed of the Ryoke Complex, the Izumi Group (Upper Cretaceous), the Setouchi volcanic rocks (Miocene), and the Mitoyo Group (Lower Pleistocene). The Outer Zone comprises the Sanbagawa Complex (Upper Cretaceous–Paleogene) and the Dochu Formation (Lower Pleistocene). The southern margin of the Sanuki Mountain Range is bounded by active faults of the MTL, which include the Ikeda, Mino, and Hashikura faults, and they cut the lower terrace deposits (Upper Pleistocene) and the Holocene. The northern margin of the mountain range is bordered by Takenari, Ebata, and Kashihara faults; the Takenari Fault deformed the Mitoyo Group (Lower Pleistocene), and the Ebata Fault partly cut the lower terrace deposits (Upper Pleistocene). Landslide deposits are common in this district, especially in the southern part of the mountain range. Therefore, this district is an important area in terms of understanding of the basement geology as well as geohazards of earthquakes and landslides.

The Ryoke Complex comprises high-T/P metamorphic rocks, granitic rocks (Kan-onji Granite), and dikes. The protolith age of the metamorphic rocks is Late Permian based on the youngest peak age (258 Ma). The zircon U–Pb ages of granites and dikes range between 94 and 88 Ma. The Izumi Group unconformably overlies the Kan-onji Granite, which is composed of the northern marginal facies and the main facies. The northern marginal facies is characterized by conglomerate and massive mudstone, while the main facies is composed of alternating beds of sandstone and mudstone with felsic tuff beds. Ammonite fossils (*Metaplacenticeras subtilistriatum* zone) and zircon U–Pb ages (79–78 Ma) of felsic tuff beds indicate that the depositional age is the middle Campanian, Late Cretaceous. The Sanbagawa Complex is subdivided into the Itano, Minawa, and Koboke units from north to south. They are composed of mafic, pelitic, and psammitic schist. U–Pb ages of detrital zircons extracted from psammitic schists (93–81 Ma for Minawa unit and 76–74 Ma for Koboke unit) and K–Ar ages of phengite (74–72 Ma for Minawa unit and 65–62 Ma for Koboke unit). The Lower Pleistocene includes the Mitoyo Group (Saita, Koda, and Yakeo formations), Norouchi and Dochu formations. Formations of the Mitoyo Group are interfingered each other. Two widespread tephras constrain the depositional ages (2.4–2.3 Ma for the Yakeo and 1.75 Ma for the Saita). The *Metasequoia* sp. fossils also occur in the Mitoyo Group and the Dochu Formation.

Based on the above evidences, the geological history in this district can be summarized as follows. In the arc side, granitic magmas continuously provided to the lower crust that caused high-temperature and low-pressure metamorphism during the Late Cretaceous (94–88 Ma). At the same time (93–74 Ma), trench-fill deposits subducted beneath a forearc wedge to the depths of 20–35 km along the plate boundary, and then experienced low-temperature and high-pressure metamorphism at the later stage of subduction (74–62 Ma). In addition, the Kan-onji Granite was exposed on the seafloor and unconformably overlain by the Izumi Group (79–78 Ma). The simultaneous occurrences of magmatic, metamorphic, and depositional events recognized in this district imply an importance of flow/transport paths of materials in a forearc, which include supply of continuous magma to the lower crust, uplift and exhumation of the upper crust, sediment transport and deposition on the arc, subduction of trench-fill sediments beneath

©2021. Japan Geoscience Union. All Right Reserved.

the arc. Finally, in response to the regional stress change in Southwest Japan since early Pleistocene, the Sanuki Mountain Range began to uplift and the Mitoyo Group and Dochu Formation deposited at the both sides of the mountain range.

Keywords: Geological map, Ryoke Complex, Izumi Group, Sanbagawa Complex, Mitoyo Group, Median Tectonic Line

©2021. Japan Geoscience Union. All Right Reserved.

Tectonic slices at the Anko outcrop of Median Tectonic Line, Oshika Village, Nagano Prefecture, Japan

*RYOSUKE ISAJI[1], HIDEO TAKAGI[1]

1. Waseda University

The Median Tectonic Line (MTL) divides low-grade Sanbagawa schists and high-grade Ryoke metamorphic rocks with large amount of granitic rocks. The fault rocks along the MTL in the Anko outcrop in Oshika Village, Nagano Prefecture, is highly deformed and altered. Therefore, there was some ambiguity about the exact location of the MTL, it was determined by chemical analysis and microscopic observations conducted by Kawamoto et al. (2013). When the black gouge of the MTL is designated as G1, there are three black gouge on the Ryoke side of the MTL, which the authors call G2 (1.4 m thick), G3 (1.6 m thick), and G4 (Anko West outcrop in Takagi et al., 2015: 5.0 m thick) in order of northwestward direction. In this report, we determined the attribution of the gouge (G2, G3) using small rock fragments that had been randomly collected in the gouges, and conducting microscopic observations of the plagioclase fragments there. The plagioclase fragments derived from the Sanbagawa schist are rather fresh albite with inclusions, whereas those from the Ryoke rocks are highly altered because of original Ca content in the plagioclase.
As a result of above observations, albite with inclusions was observed in all five samples of the gouge G3, and in three samples in the gouge G2, but the attribution was uncertain for other two samples, because the fracturing and alteration were particularly severe. In addition, the cataclasite between G2 and G3, which is considered to belong to the Ryoke Belt, showed significant alteration of plagioclase porphyroclasts and was distinctly different from that from the Sanbagawa schist. From the observations mentioned above, it is clear that the black gouge in G2 and G3 is almost exclusively attributed to the Sanbagawa Belt. At G4 (Anko-west outcrop), located 40 m northwest from the MTL, rocks derived from the Sanbagawa schist have been recognized (Ishikawa et al., 2014), and at Anko-Sawa outcrop, about 24 m northwest from the MTL, rocks derived from the Sanbagawa belt are also recognized in the Ryoke belt.
In the Anko outcrop, at least three gouge zone derived from the Sanbagawa schist are intercalated in the Ryoke Belt near the MTL. In this outcrop, variations of strikes exist among the gouges including exact MTL gouge (G1: N25°E) and another gouges such as G4 (N10°E ; Takagi et al., 2015) which involves Quaternary activity history. The cataclasites and a slightly consolidated fault gouge shows sinistral shear sense, while the G4 gouge shows younger dextral slip sense. These lines of evidence suggest that the Sanbagawa schist were intercalated into the Ryoke Belt as tectonic slices due to the repeated strike-slip activities of the MTL in the study area.

References

Ishikawa, T., Hirono, T., Matsuta, N., Kawamoto, K., Fujimoto, K., Kameda, J., Nishio, Y., Maekawa, Y., Honda, G, 2014, *Planets and Space*, **66**: 36.
Kawamoto, K., Ishikawa, T., Matsuta, N., Hirono, T., 2013, *Natural history reports of Inadani*, **14**, 1-17.
Takagi, T., Sugiyama, K., Kawamoto, K., Kitazawa, N., 2015, Abstracts, *the 122nd Annual Meeting of the Geological Society of Japan,* R14-O12.

Keywords: Median Tectonic Line, fault gouge, Anko outcrop, tectonic slice

©2021. Japan Geoscience Union. All Right Reserved.

Zircon U–Pb age of Paleoproterozoic granite gneiss from the Ogcheon Belt, Geumsan area and Paleoproterozoic leucogranite and quartzite from the Yeongnam Massif, Seolcheon area, South Korea

*Kenichiro Iwamizu[1,2], Yasutaka Hayasaka[1], Ji-Hoon Kang[3], Kosuke Kimura[1,4], Tomoyuki Shibata[1]

1. Hiroshima Univ., 2. The Univ. of Tokyo, 3. Andong National Univ., 4. National Inst. of Tech., Kure College

Jurassic Daebo granite is widespread in the Geumsan area, Ogcheon Belt, South Korea, and Precambrian rocks are present on a small scale in it (Hong and Choi, 1978). Precambrian rocks are mainly composed of biotite gneiss and granite gneiss. Iwamizu et al. (2021, in press) reported that the granite gneiss (Gn) has an igneous age of ca. 2.5 Ga and two metamorphic ages of ca. 1.89 Ga and 174 ±74 Ma by LA-ICP-MS zircon U–Pb analysis. Gn is one of the second oldest rocks in south Korea, along with the granite gneisses which have the same igneous ages reported by Lee et al. (2016) in the southern Gyeonggi Massif.

The zircon U–Pb ages of Gn that Iwamizu et al. (2021, in press) reported are mostly the result of analysis of the zircon core and mantle data. The cores have various internal structures and show a wide range of ages of 2.5–1.9 Ga. The older the age, the higher the Th/U ratio and the smaller the discordance. Therefore, the igneous age is expected to be ca. 2.5 Ga. The 1.9–1.8 Ga mantle data show vague and round oscillatory zoning and all the Th/U ratios are lower than 0.04. A discordia line can be defined by 1.9–1.8 Ga mantle data in the Tera-Wasserburg concordia diagram. The upper intercept age and the lower intercept age are ca. 1.89 Ga and 174 ±74 Ma, respectively, which are interpreted to be metamorphic ages related to Paleoproterozoic and Jurassic magmatism, respectively. The upper intercept age is consistent with metamorphic ages of the Gyeonggi and Yeongnam Massif (Lee and Cho, 2012). The lower intercept age is consistent with surrounding Jurassic granite. All the zircon U–Pb data are discordant because of the Jurassic metamorphism. Since the detailed location of SKTL (South Korean Tectonic Line) in the Geumsan area is unknown, it is unknown whether the Gn is derived from the Gyeonggi or Yeongnam Massif.

In addition to the above, we newly report Paleoproterozoic leucogranite and quartzite in the Seolcheon area, Yeongnam Massif, which is about 25 km east of the Geumsan area.

The leucogranite looks white because it does not have biotite. It contains approximately 73 wt% SiO_2. It exhibits metaluminous whole rock chemical composition, which is different from the leucogranitoids that have peraluminous whole rock chemical composition reported by Lee et al. (2010) and Lee et al. (2019) in the Yeongnam Massif. Its zircons exhibit two layered structures, core and mantle. The cores (5 points) have homogeneous or banded zoning, concordant U–Pb ages of ca. 2.5–2.4 Ga and high Th/U ratios higher than 0.1. The mantle data (12 points) have oscillatory or banded zoning, concordant U–Pb ages concentrating near 2 Ga and Th/U ratios higher than 0.1. The mean age of the concordant mantle data concentrating near 2 Ga is 1997 ±10 Ma, which is interpreted to be an igneous age. This age is close to an igneous age of 1985 ±10 Ma of the leucogranite gneiss in the Muju area (Lee et al., 2019). The 2.5–2.4 Ga cores are considered to be inherited zircons. Metamorphic age has not been obtained.

The quartzite is mainly composed of coarse quartz and contains a small amount of muscovite. It contains approximately 98 wt% SiO_2. Its detrital zircons mainly show oscillatory zoning. The zircon U–Pb ages (63 points) show a wide range of ages of ca. 3.5–1.9 Ga. Most data are concordant, and all the discordances

©2021. Japan Geoscience Union. All Right Reserved.

are smaller than ca. 7.7 %. The oldest age is 3505 ±28 Ma. The youngest age is 1902 ±31 Ma, which is an upper limit of deposition. The detrital zircons of the quartzite have the biggest age peak at ca. 2.5 Ga, which is the same as the Paleoproterozoic Yuli Group, Yeongnam Massif (Lee et al., 2011) and the Cambrian Jangsan Formation, Taebaeksan zone (Kim et al., 2019).

From the above, ca. 2.5 Ga granite gneiss exists in the Geumsan area, Ogcheon Belt (Iwamizu et al., 2021, in press) and ca. 2.5 Ga inherited or detrital zircons are dominant in the Seolcheon area, Yeongnam Massif (this study). Therefore, extensive magmatism at ca. 2.5 Ga can be suggested in the Geumsan–Seolcheon area if Gn is located southeast of SKTL. If Gn is located northwest of SKTL, Gn can be correlated with the same age granite gneiss in the southern Gyeonggi Massif (Lee et al., 2016), which indicates ca. 2.5 Ga extensive magmatism there.

[References]
Hong, S.-H. and Choi, W.-C. (1978) Geumsan Sheet. Korea Research Inst. of Geoscience and Mineral Resources.
Iwamizu, K. et al. (2021) *J. Geol. Soc. Japan*, **127**, in press, doi: 10.5575/geosoc.2020.0057
Kim, H.-S. et al. (2019) *Int. J. Earth Sci.*, **108**, 1509–1526.
Lee, B.-C. et al. (2016) *Precambrian Res.*, **283**, 169–189.
Lee, B.-C. et al. (2019) *Gondwana Res.*, **72**, 34–53.
Lee, S.-G. et al. (2010) *Chem. Geol.*, **276**, 360–373.
Lee, S.-R. and Cho, K. (2012) *J. Petrol. Soc. Korea*, **21**, 89–112.
Lee, Y.-I. et al. (2011) *J. Geol. Soc. Korea*, **47**, 81–87.

Keywords: Korea, Ogcheon Belt, Yeongnam Massif, zircon, granite, quartzite

©2021. Japan Geoscience Union. All Right Reserved.

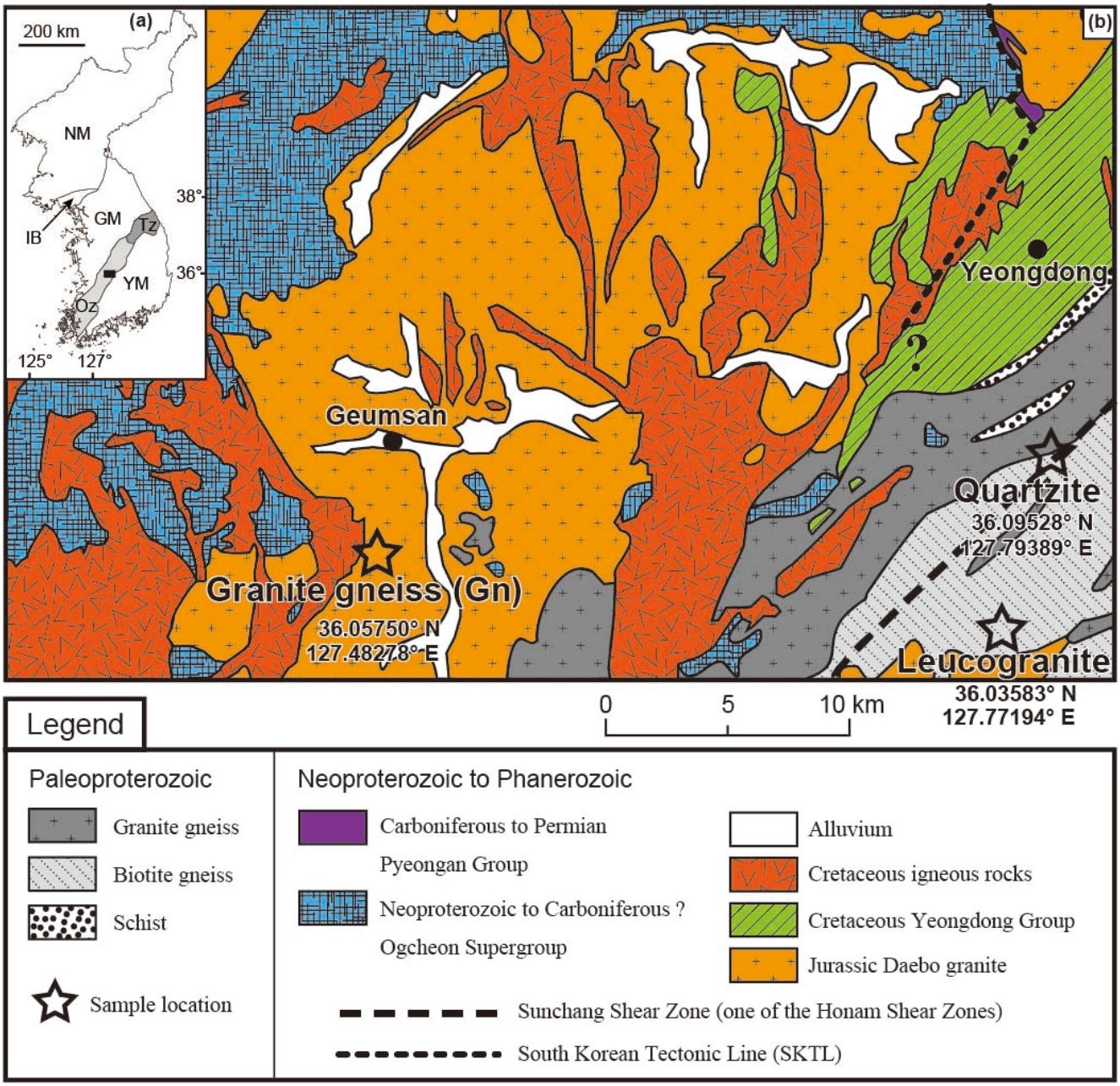


Fig. 1. based on Iwamizu et al. (2021, in press) and references therein.

(a) Tectonic province map of Korea. Black rectangle is study area (b). NM: Nangrim Massif, IB: Imjingang Belt, GM: Gyeonggi Massif, Oz: Ogcheon Metamorphic zone, Tz: Taebaeksan zone, YM: Yeongnam Massif.

(b) Geological map around the Geumsan–Seolcheon area, South Korea.

©2021. Japan Geoscience Union. All Right Reserved.

[E] Oral | S (Solid Earth Sciences)：S-MP Mineralogy & Petrology

Sat. Jun 5, 2021 1:45 PM - 3:15 PM JST | Sat. Jun 5, 2021 4:45 AM - 6:15 AM UTC | Ch.20 Zoom Room 20

[S-MP24] Supercontinents and Crustal Evolution

convener:Tomokazu Hokada(National Institute of Polar Research), Tetsuo Kawakami(Graduate School of Science, Kyoto University), Krishnan Sajeev(Centre for Earth Sciences, Indian Institute of Science), Madhusoodhan Satish-Kumar(Department of Geology, Faculty of Science, Niigata University), Chairperson:Tomokazu Hokada(National Institute of Polar Research), Madhusoodhan Satish-Kumar(Department of Geology, Faculty of Science, Niigata University)

Supercontinent formation and dispersion has been enigmatic in the Earth's history. Eurasia is one such current supercontinent and incredible progress in the understanding of its geological evolution has been achieved in the past decade. Earlier supercontinents in the Earth's history such as Gondwana (0.5 Ga), Rodinia (1.0 Ga), Columbia/Nuna (2.0 Ga), Kenorland (2.5 Ga) and Vaalbara (3.1 Ga), have been the focus of several studies, however limited information on older supercontinents has restricted an understanding their tectonic evolution. Several important unsolved issues remain, such as how, when and where these supercontinents formed and how long they remained as such before breaking apart. Additional questions arise on the processes that triggered the fragmentation and unification of continents. In this session, we invite authors around the world to present original new data as well as review results on the continental scale crustal processes and tectonic evolution that are associated with supercontinent formation events in Earth's history. The well-studied Eurasia and Gondwana supercontinents are of particular focus. Topics of interest include, but not restricted to, extremes in metamorphism, P-T-d-t evolution, magmatism, and the role of fluids. We hope to provide a platform for scientific discussions that will enlighten our understanding of the physical and chemical processes in the continental crust that records episodes of orogenesis that contributed to the formation and evolution of supercontinents.

1:45 PM - 2:00 PM JST | 4:45 AM - 5:00 AM UTC

[SMP24-01] Decompression *P-T* evolution recorded in a pelitic gneiss from Tangarden, Sør Rondane Mountains, East Antarctica

*Tetsuo Kawakami[1], Fumiko Higashino[2], Tatsuro ADACHI[3], Masaoki Uno[4] (1.Graduate School of Science, Kyoto University, 2.Okayama University of Science, 3.Advanced Asian Archaeological Research Center, Kyushu University, 4.Graduate School of Environmental Studies, Tohoku University)

2:00 PM - 2:15 PM JST | 5:00 AM - 5:15 AM UTC

[SMP24-02] Post-peak Cl- and CO_2-bearing fluids in a Grt-Sil-Bt gneiss from southern Perlebandet, Sør Rondane Mountains, East Antarctica

*Fumiko Higashino[1], Tetsuo Kawakami[2], Tatsuro ADACHI[3], Masaoki Uno[4] (1.Faculty of Science, Okayama University of Science, 2.Kyoto University, 3.Kyushu University, 4.Tohoku University)

2:15 PM - 2:30 PM JST | 5:15 AM - 5:30 AM UTC

[SMP24-03] Contrasting chemical reactions and fluid transport by melt and aqueous fluids during middle crustal fracturing (Sør Rondane Mountains, East Antarctica)

*Masaoki Uno[1], Tetsuo Kawakami[2], Tatsuro Adachi[3], Fumiko Higashino[4], Noriyoshi Tsuchiya[1] (1.Tohoku University, 2.Kyoto University, 3.Kyushu University, 4.Okayama University of Science)

2:30 PM - 2:45 PM JST | 5:30 AM - 5:45 AM UTC

[SMP24-04] Geochemical characterization of zircon for U-Pb age determination in Fyfe Hills of the Napier Complex, East Antarctica

*Mami Takehara[1], Kenji Horie[1,2], Tomokazu Hokada[1,2] (1.National Institute of Polar Research, 2.The Graduate University for Advanced Studies, SOKENDAI)

2:45 PM - 3:00 PM JST | 5:45 AM - 6:00 AM UTC

[SMP24-05] Petrology, metamorphic conditions, and monazite dating of metapelites of the Zambezi Belt supracrustal sequence, Zambia

*Kabangu Grace Sakuwaha[1], Toshiaki Tsunogae[1] (1.University of Tsukuba)

3:00 PM - 3:15 PM JST | 6:00 AM - 6:15 AM UTC

[SMP24-06] Petro-tectonic setting of the Karagwe–Ankole Belt (Rwanda) and implications for the amalgamation of Rodinia

*Claude Nambaje[1], Madhusoodhan Satish-Kumar[2], Ian S. Williams[3], Toshiro Takahashi[2], Krishnan Sajeev[1] (1.Indian Institute of Science, 2.Niigata University, 3.Australian National University)

Decompression *P-T* evolution recorded in a pelitic gneiss from Tangarden, Sør Rondane Mountains, East Antarctica

*Tetsuo Kawakami[1], Fumiko Higashino[2], Tatsuro ADACHI[3], Masaoki Uno[4]

1. Graduate School of Science, Kyoto University, 2. Okayama University of Science, 3. Advanced Asian Archaeological Research Center, Kyushu University, 4. Graduate School of Environmental Studies, Tohoku University

The Sør Rondane Mountains (SRM), East Antarctica exposes a collision zone lower to middle crust recording tectono- and plutono-metamorphic events at ca. 650-500 Ma that possibly correspond to the EAAO and Kuunga orogeny. The SRM is divided into the NE and SW terranes bounded by the Main Tectonic Boundary (MTB), along which the NE terrane is considered to have thrusted up onto the SW terrane (Osanai et al., 2013). This model was built on the observation that the metamorphic rocks of the NE terrane (with inherited zircons >1200 Ma present) record clockwise *P-T* paths whereas the SW terrane rocks (without inherited zircons >1200 Ma) record counter-clockwise *P-T* paths. However, this tectonic model is only build on small number of *P-T* path constraints and needs to be tested from more *P-T* path constraints from wide area of the SRM. This study aims to constrain the *P-T* path from Tangarden located in the SW terrane.

In Tangarden, intercalations of intermediate, mafic, calcsilicate and pelitic gneisses are dominated. Mylonite is developed parallel to the gneissose structure. Where mylonitization is weak, mafic and calcsilicate gneisses are boudinaged to form lenses within the host gneisses. The sample used in this study is a garnet-sillimanite-biotite gneiss (sample TK2020010101H) collected from the intercalation dominated by mafic, felsic and intermediate bulk compositions. Pelitic lithology is locally affected by retrograde hydration that replaced garnet with Ti-poor green biotite aggregate, but the sample TK2020010101H is only weakly affected by this hydration. In this sample, biotite (mostly $TiO_2 > 0.5$ wt%) and sillimanite are arranged along the gneissosity, which is overgrown by cordierite. Garnet (X_{Mg} = 0.21-0.38) commonly include biotite (mostly $TiO_2 > 1.0$ wt%) throughout the grain, and rarely includes sillimanite at the rim. Garnet is partly surrounded by cordierite (X_{Mg} = 0.76-0.81) and Ti-poor biotite (mostly $TiO_2 < 0.5$ wt%), and these minerals also form pressure shadows developed on garnet. Isolated cordierite in the matrix (X_{Mg} = 0.77-0.80) exhibit elongated shape with biotite inclusions arranged parallel to the gneissosity. Cordierite (X_{Mg} = 0.79) and hercynite (X_{Mg} = 0.28-0.31, ZnO = 3.5-3.7 wt%) are formed between garnet and sillimanite. This sillimanite grain is most likely a former inclusion enclosed in the garnet rim before the development of cordierite + spinel between garnet and the sillimanite grain. Cracks developed in garnet are filled with cordierite + biotite ±quartz. Anthophyllite (X_{Mg} = 0.60-0.68) is common in the cracks developed in garnet, and is intergrown with crack-filling cordierite. These pieces of observation suggest that following reactions took place:

(1) Bt + Sil + Qtz = Grt +Kfs + melt
(2) Bt + Sil + Qtz = Grt + Crd + Kfs + melt
(3) Grt+ Kfs + melt/H_2O = Crd + Bt
(4) Grt + Sil = Crd + Spl
(5) Grt + Qtz + H_2O = Ath + Crd

Based on petrogenetic grid for the NaKFMASH system (Spear et al., 1999), reaction sequence from (1) to (4) suggests nearly isothermal decompression *P-T* path from ~7 kbar, 800 °C to ~3 kbar, 750°C. This result is not consistent with the shape of counter-clockwise *P-T* paths reported from the SRM, and rather mimics to clockwise *P-T* paths. More examples of *P-T* paths from wide area of the SRM are needed to understand the tectonic history of the SRM.

©2021. Japan Geoscience Union. All Right Reserved.

Keywords: Continental collision zone, Metamorphism, Antarctica, Pressure-temperature path

©2021. Japan Geoscience Union. All Right Reserved.

Post-peak Cl- and CO_2-bearing fluids in a Grt-Sil-Bt gneiss from southern Perlebandet, Sør Rondane Mountains, East Antarctica

*Fumiko Higashino[1], Tetsuo Kawakami[2], Tatsuro ADACHI[3], Masaoki Uno[4]

1. Faculty of Science, Okayama University of Science, 2. Kyoto University, 3. Kyushu University, 4. Tohoku University

Low H_2O activity fluids (e.g., CO_2-, NaCl-, and KCl-bearing fluids) are often recognized in the middle to lower crust (e.g., Newton et al., 1998; Touret and Huizenga, 2011). CO_2-rich fluid in high-grade metamorphic rocks is usually observed as fluid inclusions, whereas Cl-bearing fluid is presumed by high-Cl concentration in hydrous minerals. In addition, some metamorphic minerals, such as cordierite, can incorporate molecular CO_2 and H_2O in the channel-cavities. In the H_2O-CO_2-NaCl ternary system, CO_2 - and NaCl-bearing fluids are extremely immiscible even at high-temperature (Shmulovich and Graham, 2004). In order to understand the metamorphic fluid evolution, therefore, it is important to examine whether both fluids coexisted simultaneously or not when both fluid compositions are presumed from a single sample.

In the Sør Rondane Mountains (SRM), East Antarctica, Late Proterozoic to Cambrian granulites are widely exposed (e.g., Jacobs and Thomas, 2004; Shiraishi et al., 2008; Osanai et al., 2013). Perlebandet is ~10 km long nunataks located at the westernmost part of the SRM. Perlebandet was categorized into NE-terrane which exhibits a clockwise *P-T* path, whereas SW-terrane exhibits a counter-clockwise *P-T* path (Osanai et al., 2013). However, Mieth et al. (2014) interpreted that Parlebandet is part of the SW-terrane on the basis of magnetic survey. The counter-clockwise *P-T* path estimated by Kawakami et al. (2017) supports this interpretation. So far, all previous studies in Perlebandet reporting the *P-T* conditions, zircon U-Pb ages, and CHIME ages in monazite dealt with samples from northern part of the nunataks (Asami et al., 2005; Shiraishi et al., 2008; Kawakami et al., 2017). This study deals with a Grt-Sil-Bt gneiss collected from the southern part of nunataks in Perlebandet.

The studied sample (sample FH19123001Q) mainly comprises garnet, sillimanite, biotite, cordierite, plagioclase, K-feldspar, and quartz. Black cracks filled by Cl-rich biotite (~0.5 wt% Cl) cut the gneissose structure. Cordierite is exclusively present as biotite-cordierite intergrowth around garnet porphyroblasts, suggesting the garnet breakdown reaction during retrograde metamorphism. Since sillimanite is included in cordierite within the intergrowth microstructure in rare cases, garnet breakdown reaction probably occurred under sillimanite stability field. Therefore, the reaction

Grt + Kfs + H_2O --> Bt + Crd (1)

is likely to have occurred. Within the biotite-cordierite intergrowth microstructure, biotite has ~0.2-0.3 wt% Cl, whereas the CO_2 and H_2O peaks were obtained from cordierite by Raman spectrometer. Since both minerals within the intergrowth were formed simultaneously, the H_2O-CO_2-Cl^- fluid infiltration is suggested to be triggered the reaction (1). The *P-T* conditions when the reaction (1) occurred are considered to be ~730 ºC, ~0.4 GPa in NaKFMASH system, because X_{Fe} value of garnet is ~0.8 (Spear et al., 1999). The dehydration reaction line and wet solidus shift to low-temperature and high-temperature side, respectively, due to the low H_2O activity fluid (cf. Johannes and Holtz, 1996). This means that the isopleth of reaction (1) possibly shifts to high-temperature side, although H_2O activity of the H_2O-CO_2-Cl^- fluid is not estimated.

Further information is needed to constrain whether the reaction (1) is a part of counter-clockwise *P-T* path or not. The undated granite bodies are mapped in the southern part of nunataks in Perlebandet. Post-peak granitic intrusion can be a heat source and then the reaction (1) can occur, even following the counter-clockwise *P-T* path. To constrain the *P-T* path helps understand the origin and evolution of the H_2O-CO_2-Cl^- fluid.

©2021. Japan Geoscience Union. All Right Reserved.

Keywords: metamorphic fluid, high-temperature metamorphic rock, Antarctica

©2021. Japan Geoscience Union. All Right Reserved.

Contrasting chemical reactions and fluid transport by melt and aqueous fluids during middle crustal fracturing (Sør Rondane Mountains, East Antarctica)

*Masaoki Uno[1], Tetsuo Kawakami[2], Tatsuro Adachi[3], Fumiko Higashino[4], Noriyoshi Tsuchiya[1]

1. Tohoku University, 2. Kyoto University, 3. Kyushu University, 4. Okayama University of Science

Fluids in the deep crust promote heat and mass transport, control rock rheology and fracturing, and play essential roles on the dynamics of plate boundaries. Although fluid activities are geophysically recognized as migrations of hypocenters and seismic velocity anomalies (e.g., Hasegawa et al., 2005; Yoshida et al., 2018), roles of melt and aqueous fluids in deep crustal fracturing are not always clear, due to limitations in distinguishing melt or aqueous fluids in geophysical observations. Exceptionally well-exposed crust-fluid reaction zones in the Sør Rondane Mountains (SRM), East Antarctica provides an ideal opportunity to evaluate the fluid flow in the deep crust from mm to km-scale (e.g., Adachi et al., 2010; Osanai, et al., 2013; Higashino et al., 2013, 2019; Kawakami et al., 2017; Uno et al., 2017; Mindaleva et al., 2020). Here we examine the amphibolite-facies melt–rock and aqueous fluid–rock reaction zones of hosted in felsic gneiss (so called “bleached” zones) that are widely distributed in the SRM, and discuss the contrasting modes of chemical transport between melt and aqueous fluids during crustal fracturing.

We have analyzed amphibolite-facies melt/aqueous fluid–rock reaction zones, Mefjell area, SRM. Orthopyroxene-bearing felsic gneiss are crosscut by numerous granitic veins and biotite veins (m to 100s m in length) and are associated with cm– to decimeter–scale whitish reaction zones composed of hornblende-biotite-bearing felsic gneiss, showing “bleached” zones. The bleached zones are characterized by complete hydration of orthopyroxene and clinopyroxene to grunerite, hornblende and biotite, representing fluid infiltration at 0.40–0.55 GPa, 600–670˚C (Uno et al., 2020). Mineralogy, mineral chemistry and temperature conditions of bleached zones around granitic veins and biotite veins are essentially identical, except for characteristic minor element profiles described below.

Bleached zones associated with granitic vein (“granitic vein-bleached zones”) are characterized by relatively high MnO contents at the vein wall (hornblende 2.0 wt%; biotite 0.6 wt%; ilmenite 6.0 wt%) and they gradually decrease towards the host rock within ~15 mm length (≅ bleached zone width). Similar gradual profiles are observed for Be, Ga, Zn, Sn, Rb, Cs and Pb in biotite and/or hornblende. TiO_2 in biotite are within the range of host rock (3.9–4.5 wt%). The Cl contents in biotite and hornblende are low (<0.08wt%). Contrarily, in bleached zones associated with biotite vein (“biotite vein-bleached zones”), the Cl contents in hornblende and biotite are relatively high and constant within the middle of the bleached zones (0.40–0.52 wt%; ~7 mm length from the vein wall) and sharply decrease towards the host rock (<0.04 wt%; ~15 mm length). MnO in biotite and hornblende are low (<0.4 wt%), and TiO_2 contents in biotite are depleted in bleached zone (~2 wt%) compared to those in the host rock (~4 wt%).

Reactive-transport analysis of MnO and Cl in the bleached zone show that transports from the vein wall to the host rock are diffusion-dominant (P_e = 0) in granitic vein-bleached zone, whereas those in biotite vein-bleached zone are advection dominant (P_e ~300). The MnO, TiO_2 enriched, Cl-depleted nature of the granitic vein-bleached zone is likely to be explained by infiltration of granitic melt, whereas Cl-enriched, MnO, TiO_2 depleted nature of the biotite vein-bleached zone is affected by infiltration of Cl-bearing aqueous fluids. Assuming near lithostatic fluid pressure of the veins, the differences of the modes of

©2021. Japan Geoscience Union. All Right Reserved.

chemical transport (diffusional vs. advectional) of the two bleached zones suggest contrasting viscosity of the granitic melt and aqueous fluids during infiltration from the veins to the host rock.

The results of this study indicate that both viscous granitic melt and Cl-bearing aqueous fluids contribute to fracturing at middle crustal conditions (0.40–0.55 GPa, 600–670˚C). Further reactive-transport analyses of these reaction zones would reveal timescales of fluids infiltration and associated hydraulic parameters operated during middle crustal fracturing.

References

Adachi, et al., 2010. Polar Sci. 3, 222–234.
Hasegawa et al., 2005. Tectonophysics 403, 59–75.
Higashino et al., 2013. Precambrian Res. 234, 229–246.
Higashino et al., 2019. J. Petrol. 60, 329–358.
Kawakami et al., 2017. Lithos 274–275, 73–92.
Mindaleva et al., 2020. Lithos 372–373, 105521.
Osanai et al., 2013. Precambrian Res. 234, 8–29.
Yoshida et al., 2018. Tectonophysics 733, 132–147.
Uno et al., 2017. Lithos 284–285, 625–641.
Uno et al., 2020. Abstract for the 11th Symposium on Polar Science, OGo02.

Keywords: Fluid-rock reactions, Reactive-transport model, Amphibolite- and granulite-facies, Sør Rondane Mountains, East Antarctica, Chlorine

©2021. Japan Geoscience Union. All Right Reserved.

Geochemical characterization of zircon for U-Pb age determination in Fyfe Hills of the Napier Complex, East Antarctica

*Mami Takehara[1], Kenji Horie[1,2], Tomokazu Hokada[1,2]

1. National Institute of Polar Research, 2. The Graduate University for Advanced Studies, SOKENDAI

Ultra-high temperature (UHT) metamorphism is critical to understanding the large-scale tectonic processes affecting the deep crust and lithosphere throughout Earth’ s history. The Napier Complex in East Antarctica is the location where the regional UHT metamorphism was first recognized (Dallwitz, 1968) and experienced extremely high temperatures (>1100 ˚C) based on the mineral assemblage of sapphirine + quartz (Harley, 2016 and reference therein). The thermal history of the Napier Complex is essential for unraveling the Earth’ s crustal evolution, including deep crust; however, geochronological constraints, such as the timing and duration of the metamorphic events, are still debated. Two hypotheses for the timing are proposed in previous studies: (i) the UHT metamorphism occurred no earlier than 2840 Ma and possibly from 2590 to 2550 Ma (e.g., Harley et al., 2001), (ii) it occurred from around 2500 to 2450 Ma (e.g., Carson et al., 2002).
In this study, U–Pb zircon geochronology integrated with rare earth element (REE) and oxygen isotope was applied to a garnet-bearing quartzo-feldspathic gneiss to confirm the timing of UHT metamorphism in Fyfe Hills in the western part of the Napier Complex. The quartzo-feldspathic gneiss is mainly composed of garnet + mesoperthite (ternary feldspar) + quartz, with small amounts of zircon and opaque minerals (Horie et al., 2012).
The zircons collected from the quartzo-feldspathic gneiss are observed in backscattered electron (BSE) and cathodoluminescence (CL) images obtained using the low-vacuum mode of a scanning electron microscope (JEOL JSM-5900LV) with a Gatan mini CL detector at National Institute of Polar Research, Japan (NIPR). The zircons were analyzed using a sensitive high-resolution ion microprobe (SHRIMP) at National Institute of Polar Research. After the all SHRIMP analysis, true color CL images of the grain mount were obtained using a Gatan ChromaCL2 system installed with a field emission SEM (FE-SEM; JEOL JSM-7100F) at the NIPR. The CL observation and U–Pb ages allowed us to classify the analytical domains into three types: inherited domains, metamorphic domains, and U–Pb system disturbed domains. The REE patterns of metamorphic domains are characterized by a weak fractionation between the middle REE and heavy REE, which reinforces the classification based on the CL observation and the U–Pb ages. The $^{207}Pb/^{206}Pb$ ages of metamorphic domains have an age peak at 2501 Ma, therefore, the gneiss experienced high-temperature metamorphism at 2501 Ma. The $\delta^{18}O$ of zircons are homogeneous among the three groups (5.53 ±0.11‰, 5.51 ±0.14‰, and 5.53 ±0.23‰), which suggests the oxygen isotope compositions in zircon were re-equilibrated after the metamorphism at ca. 2501Ma under dry UHT conditions.

Keywords: zircon, U-Pb age, Napier Complex

©2021. Japan Geoscience Union. All Right Reserved.

Petrology, metamorphic conditions, and monazite dating of metapelites of the Zambezi Belt supracrustal sequence, Zambia

*Kabangu Grace Sakuwaha[1], Toshiaki Tsunogae[1]

1. University of Tsukuba

The Zambezi Belt located in southern Zambia forms part of E-W trending late Pan-African Kuunga orogen associated with assembly of Gondwana supercontinent. Lithologic units of the belt include Neoarchean to Neoproterozoic granitic basement, unconformably overlain by supracrustal sequences, consisting of meta-pelites, psammites, calc-silicates, marbles, and magmatic rocks with NE-SW shortening. Several studies have been conducted to determine the metamorphic conditions of separate localities within this region but data on the textural context to directly link metamorphic paragenesis to geochronological data is limited. We present the first texture-based age determinations of the metamorphism of the metapelite sequence located between the Mpande and Ngoma basement terrains. The data presented includes petrology, metamorphic *P-T* conditions and geochronological data obtained by in-situ microprobe techniques on monazite to link metamorphic paragenesis to key tectonic events in the Pan-African orogeny. The studied rocks exhibit penetrative foliations with mineral assemblages consisting of garnet, biotite, quartz, kyanite, ±staurolite, muscovite, and chlorite or kyanite, biotite, muscovite, chlorite and quartz with accessory rutile, ilmenite, tourmaline, and monazite. Application of garnet-biotite geothermometers on appropriate samples yields peak metamorphic *P-T* conditions of 572 - 627˚C and 4 - 6.2 ±1.3 kbar. Application of CHIME age calculations on monazites identifies two age populations which potentially represent long-lived metamorphism from ca. 630 and 573 Ma. These ages are also nearly consistent with previously reported ages from other localities within the belt which have been interpreted to correspond to collisional orogenesis and closure of the Mozambique ocean, followed by burial metamorphism prior to exhumation and erosion.

Keywords: Zambezi Belt, Zambia, Metamorphic P-T, Monazite dating

©2021. Japan Geoscience Union. All Right Reserved.

Petro-tectonic setting of the Karagwe–Ankole Belt (Rwanda) and implications for the amalgamation of Rodinia

*Claude Nambaje[1], Madhusoodhan Satish-Kumar[2], Ian S. Williams[3], Toshiro Takahashi[2], Krishnan Sajeev[1]

1. Indian Institute of Science, 2. Niigata University, 3. Australian National University

Petrological, geochemical and geochronological studies of granitic rocks from the Karagwe–Ankole Belt (KAB) have helped to establish the tectonic setting of the orogenic belt and the implications for Rodinia assembly. Four categories of granitic rocks have been recognised, providing constraints on the geodynamic evolution of the KAB.
Anorogenic (A-type) garnet-biotite granite was emplaced at 1368 ±5 Ma. Its major, trace and rare earth element composition, Nd TDM model age of up to 2.33–1.96 Ga, high initial 87Sr/86Sr (0.7119–0.7216) and negative ε Nd (-1.9 to -4.0), indicates derivation from a much older mafic source, probably asthenospheric or lower continental lithospheric mantle contaminated by crustal material. Ascent of the magma was aided by a localised crustal-scale zone of weakness within Archean crust underlying both the Eastern and Western Domains of the KAB. The rest of the granites have S-type orogenic characteristics. Large batholiths of two-mica granite emplaced at 1369 ±5 Ma have major, trace and rare earth element compositions, high initial 87Sr/86Sr (0.7081–0.7329), strongly negative ε Nd (-9.4 to -10.1) and a Nd TDM model age of 2.82–2.40 Ga, consistent with derivation by partial melting of a pelitic source containing Paleoproterozoic and Archean components, possibly with a minor contribution from magma derived from the lower crust. The magmatism occurred in a convergent setting between the Congo and Tanzania cratons during an early stage of Rodinia amalgamation. Muscovite granite and leucogranite resulting from fluid-fluxed partial melting of metapelites were emplaced at ca. 1011–976 Ma in a late to post-collisional setting of Rodinia. Their high initial 87Sr/86Sr (0.7289–0.7446) and strongly negative ε Nd (-6.8 to -12.4) indicate a supracrustal source. One younger S-type leucogranite (614 ±9 Ma) was emplaced in a volcanic-arc setting, possibly during the West Gondwana Orogeny. The combined available evidence points to evolution of the Mesoproterozoic KAB during accretion-collisional tectonism.

©2021. Japan Geoscience Union. All Right Reserved.

[E] Oral | S (Solid Earth Sciences)：S-MP Mineralogy & Petrology

Sat. Jun 5, 2021 3:30 PM - 5:00 PM JST | Sat. Jun 5, 2021 6:30 AM - 8:00 AM UTC | Ch.20 Zoom Room 20

[S-MP24] Supercontinents and Crustal Evolution

convener:Tomokazu Hokada(National Institute of Polar Research), Tetsuo Kawakami(Graduate School of Science, Kyoto University), Krishnan Sajeev(Centre for Earth Sciences, Indian Institute of Science), Madhusoodhan Satish-Kumar(Department of Geology, Faculty of Science, Niigata University), Chairperson:Krishnan Sajeev(Centre for Earth Sciences, Indian Institute of Science), Tetsuo Kawakami(Graduate School of Science, Kyoto University)

Supercontinent formation and dispersion has been enigmatic in the Earth's history. Eurasia is one such current supercontinent and incredible progress in the understanding of its geological evolution has been achieved in the past decade. Earlier supercontinents in the Earth's history such as Gondwana (0.5 Ga), Rodinia (1.0 Ga), Columbia/Nuna (2.0 Ga), Kenorland (2.5 Ga) and Vaalbara (3.1 Ga), have been the focus of several studies, however limited information on older supercontinents has restricted an understanding their tectonic evolution. Several important unsolved issues remain, such as how, when and where these supercontinents formed and how long they remained as such before breaking apart. Additional questions arise on the processes that triggered the fragmentation and unification of continents. In this session, we invite authors around the world to present original new data as well as review results on the continental scale crustal processes and tectonic evolution that are associated with supercontinent formation events in Earth's history. The well-studied Eurasia and Gondwana supercontinents are of particular focus. Topics of interest include, but not restricted to, extremes in metamorphism, P-T-d-t evolution, magmatism, and the role of fluids. We hope to provide a platform for scientific discussions that will enlighten our understanding of the physical and chemical processes in the continental crust that records episodes of orogenesis that contributed to the formation and evolution of supercontinents.

3:30 PM - 3:45 PM JST | 6:30 AM - 6:45 AM UTC

[SMP24-07] **A comparison between carbon isotope thermometry and Raman spectra of carbonaceous material (RSCM) thermometry in low-medium grade carbonate rocks from the Chitradurga Schist Belt, Dharwar Craton**

*Kiran Sasidharan[1], Madhusoodhan Satish-Kumar[1], Yoshihiro Nakamura[2], Hiroaki Ohfuji[3] (1.Niigata University, 2.Geological Survey of Japan, AIST, 3.Tohoku University)

3:45 PM - 4:00 PM JST | 6:45 AM - 7:00 AM UTC

[SMP24-08] Insights into failed rift processes in the Archean, evidence from the Western Dharwar Craton, southern India.

*Sreehari Lakshmanan[1], Tsuyoshi Toyoshima[2], Madhusoodhan Satish-Kumar[2] (1.Graduate School of Science and Technology, Niigata University, Niigata, Japan, 2.Department of Geology, Niigata University, Niigata, Japan)

4:00 PM - 4:15 PM JST | 7:00 AM - 7:15 AM UTC

[SMP24-09] **Trace and rare earth element geochemistry of the clinopyroxene of dolerite dykes from Western Dharwar craton, southern India**

*Silpa Ammini Sasidharan[1], Madhusoodhan Satish-Kumar[1], Eiichi TAKAZAWA[1], Krishnan Sajeev[2] (1.Faculty of Science Niigata University, 2.Indian Institute of Science, Bangalore, India)

4:15 PM - 4:30 PM JST | 7:15 AM - 7:30 AM UTC

[SMP24-10] Evidence of carbonic crustal fluid during deep to shallow crustal evolution of the interior of Eastern Ghats Belt India: Grenvillian to Kuunga orogenies

*Kaushik Das[1,6], Sankar Bose[2,6], Junji Torimoto[3], Yasutaka Hayasaka[1,6], Daniel Dunkley[4,5] (1.Hiroshima University, 2.Presidency University, 3.JAMSTEC, Yokotsuka, 4.NIPR, Tokyo, 5.IG-PAS, Poland, 6.HiPeR, Japan)

4:30 PM - 4:45 PM JST | 7:30 AM - 7:45 AM UTC

[SMP24-11] **Metasomatic Corundum-Sapphirine-Spinel-Clinozoisite assemblage Indications for Ca-Al rich fluid**

*Krishnan Sajeev[1], S Veni[1] (1.Centre for Earth Sciences, Indian Institute of Science)

4:45 PM - 5:00 PM JST | 7:45 AM - 8:00 AM UTC

[SMP24-12] A geochemical perspective on tectonic setting and depositional environment of Precambrian metacarbonate rocks in collisional orogenic belts

*Madhusoodhan Satish-Kumar[1] (1.Department of Geology, Faculty of Science, Niigata University)

A comparison between carbon isotope thermometry and Raman spectra of carbonaceous material (RSCM) thermometry in low-medium grade carbonate rocks from the Chitradurga Schist Belt, Dharwar Craton

*Kiran Sasidharan[1], Madhusoodhan Satish-Kumar[1], Yoshihiro Nakamura[2], Hiroaki Ohfuji[3]

1. Niigata University, 2. Geological Survey of Japan, AIST, 3. Tohoku University

The Dharwar Craton (DC), southern India, is a much-discussed Archean terrain that encompasses rocks spanning from approximately Meso to Neoarchean. Generally, the DC is divided into the Western Dharwar Craton (WDC) and Eastern Dharwar Craton (EDC) based on the abundance of greenstone belts, volume of granitoids and grade of metamorphism (Swami Nath and Ramakrishnan, 1981; Chadwick et al., 2000). The major lithological units are the Basement Gneiss (Tonalite Tronjhemite Granodiorite gneiss), two set of volcano-sedimentary sequences and younger granitic intrusions (Jayananda et al., 2018). The oldest stratigraphic unit in the DC, the Sargur Group, occurs as enclaves in Basement Gneiss. The younger volcano-sedimentary sequence is the Dharwar Supergroup consists of lower Bababudan Group and upper Chitradurga Group. The Chitradurga Schist Belt (CSB) in the WDC is one of the granite-greenstone belts that preserves an almost complete stratigraphic section of the DC and undergone low to medium grade metamorphism. However, the metamorphic temperature within CSB using mineral thermometry (Hokada et al., 2013) is not well established due to low grade conditions. To resolve this issue, we attempted to estimate the regional-scale metamorphic temperature conditions of the CSB using carbon isotope thermometry and Raman spectra of carbonaceous material (RSCM) in the meta-carbonate rocks.

The weakly metamorphosed organic materials included in sedimentary rocks are termed as Carbonaceous Material (CM). The CM undergoes thermal maturation and subsequent recrystallisation during metamorphism is known as graphitization. The irreversible and progressive graphitization with increasing temperature forms the basis for metamorphic geothermometer such as carbon isotope thermometry in carbonate rocks and RSCM in metapelitic rocks (Beyssac et al., 2002). Exchange of isotopes between the lighter carbon (^{12}C) from CM and heavier carbon (^{13}C) from carbonate minerals during prograde metamorphism in equilibrium condition is the basis of carbon isotope thermometry (Satish-Kumar et al., 2002). Moreover, RSCM exhibits a systematic change in the crystallinity with metamorphic grade (Wopenka & Pasteris, 1993) and metamorphic temperature can be obtained using spectral features such as intensity (height) ratio R1, area (integrated intensity) ratio R2, and width (full width at half maximum; FWHM) between several prominent peaks (D1 and G peaks).

The CMs are found mainly in associated with carbonate minerals as well as in quartz as inclusions. The CM which are isolated by the silica phase were avoided for isotopic analysis, since they were not in isotopic equilibrium with the carbonate minerals. The carbon isotope thermometry results yield a metamorphic temperature of range from 340 - 560˚C estimated by using Wada and Suzuki (1983). Meanwhile, RSCM gave a temperature range from 400 - 570˚C estimated using R2 ratio (area ratio) following the calibration by Beyssac et al., (2002). Both thermometric results are corresponding to each other and observed a progression in the metamorphic temperature from upper green schist facies to lower amphibolite facies from north to south of CSB respectively. We compare the morphological, Raman spectral and carbon isotopic characteristics of CMs in low grade metamorphic rocks to evaluate the lower limit of temperature estimation using RSCM and carbon isotope thermometry. This study also provides the

©2021. Japan Geoscience Union. All Right Reserved.

first report of regional metamorphic temperature gradient in the Chitradurga Schist Belt, in the Western Dharwar Craton.

References:
Swami Nath & Ramakrishnan (1981) Geological Survey of India Memoir, 112, 23-38 Chadwick et al (2000) Precambrian Research, 99, 91-111 Jayananda et al (2018) Earth-Science Reviews, 181, 12-42 Hokada et al (2013) Precambrian Research, 227, 99-199 Beyssac et al (2002) Journal of Metamorphic Geology, 20, 859-871 Wopenka & Pasteris (1993) American Mineralogist, 78, 553-557 Satish-Kumar et al (2002) Journal of Metamorphic Geology, 20, 335-350. Wada & Suzuki (1983) Geochimica et Cosmochimica Acta, 47, 697-706

Keywords: Chitradurga Schist Belt, Carbon isotope thermometry, Raman Spectra of Carbonaceous Material thermometry

©2021. Japan Geoscience Union. All Right Reserved.

Insights into failed rift processes in the Archean, evidence from the Western Dharwar Craton, southern India.

*Sreehari Lakshmanan[1], Tsuyoshi Toyoshima[2], Madhusoodhan Satish-Kumar[2]

1. Graduate School of Science and Technology, Niigata University, Niigata, Japan, 2. Department of Geology, Niigata University, Niigata, Japan

Field and structural geological information from different schist belts within Western Dharwar Craton (WDC), Dharwar Craton (DC), southern India are collected. Volcanic and sedimentary rocks of the WDC show characteristics evolved in a shallow-marine, narrow basin identical to a failed rift zone developed by the fracturing of basement rocks. 'Rift debris' type poorly sorted conglomerates are preserved in the boundary between Basement Gneiss and schist belts. Folded sequences of volcanic, volcanoclastic, and sedimentary rocks squeezed in between thrust/reverse faults summarizes the major structural association in the study area. This association is identical to a neotectonic inverted failed rift structure. Regional-scale strike-slip faults are also identified from the study area which is either associated with sinistral transpression or independent tectonic activity.
Geochemical signatures preserved in volcanic and volcaniclastic rocks also point to an intracratonic mafic to intermediate volcanism. The variation in the geochemical pattern can be attributed to the degree of crustal contamination during volcanism.
Field relations, structural association, and geochemical characteristics of WDC are pointing to the presence of well-preserved aborted rifts in the Archean DC. Post-3.0 Ga crustal growth throughout the Western Dharwar Craton is therefore initiated by similar failed rifting events. Multiple events of failed rifting and later basin inversion events associated with regional-scale shortening resulted in the current fold-and-thrust belt architecture of WDC. This shortening probably connected to the collision between Western Dharwar Craton and Eastern Dharwar Craton.

Keywords: Archean, Failed rift, Basin tectonics

©2021. Japan Geoscience Union. All Right Reserved.

Trace and rare earth element geochemistry of the clinopyroxene of dolerite dykes from Western Dharwar craton, southern India

*Silpa Ammini Sasidharan[1], Madhusoodhan Satish-Kumar[1], Eiichi TAKAZAWA[1], Krishnan Sajeev[2]

1. Faculty of Science Niigata University, 2. Indian Institute of Science, Bangalore, India

The late Archean to early Proterozoic mafic dyke swarms of the Western Dharwar craton (WDC) are significant as they represent the nature and composition of Sub-continental Lithospheric Mantle (SCLM). They provide key information regarding the mantle dynamics during the Precambrian and helps to understand the tectonic evolution of the Dharwar craton. Major and trace element zoning of the minerals like clinopyroxenes from these mantle-derived rocks are indicators of magmatic processes like fractional crystallization or magma mixing, melt extraction and compositional evolution [1, 2]. Furthermore, the rare earth element concentrations help to identify the origin and evolution of the mafic igneous rocks.

The major and trace element characteristics of the clinopyroxene from two generations of dolerite and olivine dolerite dykes of Western Dharwar Craton have been investigated by using electron microprobe and LA-ICPMS. The clinopyroxene in dolerite dykes show compositional zoning that are considered to be primary in nature. The major element analysis of the dolerite shows significant differences in Cr concentrations within the clinopyroxene grain. The core is rich in Cr_2O_3 (0.538 wt%) and the rim is poor in Cr_2O_3 (0.007 wt%). There is also a concomitant decrease in Mg# from the core (85) to the rim (51) and Cr $_2O_3$ content decreases towards the rim. The trace and rare earth element pattern of the core shows a depleted pattern compared to the rim. The dolerites and olivine dolerites are formed from different source magmas and the dolerites have a different fractional crystallization history. The melt composition in equilibrium with clinopyroxene was estimated and they are consistent with the bulk rock geochemical characteristics reported previously [3]. The clinopyroxene in the olivine dolerites, although doesn’ t show any zoning, is compositionally more primitive than the dolerites as observed by the general trace element and REE concentrations. In the case of dolerites, the Cr-rich clinopyroxene cores preserve the original melt composition prior to fractional crystallization and the trace elements and rare earth element compositions indicate the influence of subducted materials on the mantle source.

References: Blundy, J., Wood, B., 2003. Earth Planet. Sci. Lett. 210, 383–397. [2] Natland J.H., Dick H.J.B., 2001. J. Volcanol. Geotherm. Res. 110 (3–4). 191–233. [3] Silpa, A.S., Satish-Kumar, M., Takahashi, T., 2021. Lithos (in press).

Keywords: LA-ICPMS,, Clinopyroxene, , Dolerite dykes , Western Dharwar craton

©2021. Japan Geoscience Union. All Right Reserved.

Evidence of carbonic crustal fluid during deep to shallow crustal evolution of the interior of Eastern Ghats Belt India: Grenvillian to Kuunga orogenies

*Kaushik Das[1,6], Sankar Bose[2,6], Junji Torimoto[3], Yasutaka Hayasaka[1,6], Daniel Dunkley[4,5]

1. Hiroshima University, 2. Presidency University, 3. JAMSTEC, Yokotsuka, 4. NIPR, Tokyo, 5. IG-PAS, Poland, 6. HiPeR, Japan

We report an occurrence of aluminous granulite and associated gneiss metamorphosed in ultra-high temperature conditions at the continental deep crust at the Eastern Ghats Belt (EGB), India. The detailed pressure-temperature-time-fluid history is retrieved from this suite of aluminous granulite and associated gneisses from a single exposure, which were injected by granitic aplite veins at a high angle at a ductile depth of the host gneissic rocks. The sapphirine-spinel-quartz-bearing aluminous granulite reveals a peak metamorphic condition of ~1000 ˚C at ~8 kbar at ~990 Ma (U-Pb zircon SHRIMP age). Porphyroblastic garnet and quartz in the peak assemblage have mono-phase, high-density, CO_2-rich primary fluid inclusions (~1 g/cm^3). Secondary fluid inclusions in quartz grains of the retrograde cooled and/or decompressed assemblages of the same aluminous granulite have the signature of bi-phase CO_2-H_2O fluids with a comparatively low estimated density (0.8 g/cm^3). The CO_2 isochore plots suggest a pressure drop from 7-8 kbar to 4-5 kbar (simultaneous or after the cooling from 1000 ºC to 800 ºC). While the late aplite dykes were emplaced at an high angle with asymmetrically bent foliation of the surrounding gneiss at 492±3 Ma (monazite U-Th-total Pb EPMA age). This aplite dyke also contain numerous primary and pseudosecondary fluid inclusions in the quartz grains (CO_2 monophase to biphase at room temperature). The calculated density is in the range of 0.71-0.82 g/cm^3, suggesting the entrapment of this stage at < 3 kbar. This is the only occurrence known so far from the "orogenic interior" of the EGB that preserves the evidence of carbonic fluid presence during the evolution of UHT metamorphosed deep crust till its exhumation to shallow crust in a period encompassing the Grenvillian orogeny and the Kuunga orogeny, the later one being the age of the final cratonization of the EGB.

Keywords: Eastern Ghats Province, UHT metamorphic rocks, Zircon and monazite age dating, C-O-H fluid

©2021. Japan Geoscience Union. All Right Reserved.

Metasomatic Corundum-Sapphirine-Spinel-Clinozoisite assemblage Indications for Ca-Al rich fluid

*Krishnan Sajeev[1], S Veni[1]

1. Centre for Earth Sciences, Indian Institute of Science

Sapphirine-spinel assemblage is typical in Mg-Al rich silica undersaturated ultrahigh temperature granulites. However, clinozoisite is an epidote series mineral with low to medium grade regional metamorphic or in contact metamorphic region. Corundum is usually present in silica undersaturated highly aluminous rocks. Hence it is difficult to form these minerals together unless in typical conditions or settings.
Here we report a Corundum-Sapphirine-Spinel-Clinozoisite vein with or without Ti-free högbomite from Manavadi near the Palghat-Cauvery-Shear zone in southern India. Sapphirine is identified as inclusions only within the spinel. Spinel grains are porphyroblasic and associated with clinozoisite-plagioclase assemblage along the fracture boundary associated with the host amphibolite. Högbomite is present as a later phase associated with spinel grain boundary. Spinel and clinozoisite form a partial rim around the corundum. In few other domains of the same rock consist of spinel corona over corundum and spinel growth along the amphibole grain boundaries associated with a calcite vein.
The spinel is Fe-Mg rich with slightly rich in Mg (XMg = 0.67) composition. Sapphirine is peraluminous with a composition near to 7:9:3 or even more aluminous. Sapphirine present in garnet-orthopyroxene or quartz-bearing Mg-Al rich granulite is more silica-rich. The host amphibolite is a calcium-rich sample with only clino-amphibole and plagioclase as mineral assemblage.
Based on the textural association, P-T estimates, and fluid composition, we demonstrate that sapphirine bearing assemblage formed through metasomatic reactions between a Ca-Al rich fluid and the host amphibolite. The corollary of our observation also indicates the immobile elements like aluminum can dissolve as salt in aqueous fluids and become mobile to form unique mineral assemblages. The present study also caution that many of the UHT assemblages may be resulted from metasomatic reactions that lead to misinterpretation.

Keywords: Metasomatism, Sapphirine, Al-Ca fluid

©2021. Japan Geoscience Union. All Right Reserved.

A geochemical perspective on tectonic setting and depositional environment of Precambrian metacarbonate rocks in collisional orogenic belts

*Madhusoodhan Satish-Kumar[1]

1. Department of Geology, Faculty of Science, Niigata University

Carbonate rocks are the remnants of chemically precipitated sediments that preserve important records of paleo-oceanic continental margins, especially in Precambrian time. Although vulnerable to post-depositional alterations, pure carbonate rocks preserve geochemical proxies for understanding the depositional age and environment, and tectonic setting. A review of geochemical and isotopic characteristics is presented here to prove the versatility of metamorphosed carbonate rocks in deducing the premetamorphic signatures. The examples considered here are from East Antarctica, Sri Lanka, India, Madagascar and Africa that formed the part of the East African-Antarctic Orogen.

A comprehensive screening procedure involving field relations, C–O isotopic compositions, trace element distribution, and REE + Y patterns helped in selecting samples that preserve pre-metamorphic information. Shale-normalized REE patterns in most metacarbonate layers have typical signatures of open ocean deposition in a passive continental margin with variable fluvial input. In comparison to Phanerozoic equivalents, the absence of a Ce anomaly is most significant, whereas other REE variables such as $(La/Sm)_{SN}$, $(Sm/Yb)_{SN}$ and $(La/Yn)_{SN}$ show positive and characteristic correlations with carbon and oxygen isotopes, Sri, epsilon Nd values and Nd model ages. Each depositional basin has distinctive geochemical parameters, especially those adjacent to preexisting continents and island arcs. From a compilation of the geochemical proxies of metacarbonate rocks from different terrains in the East Gondwana supercontinent, we can identify the paleogeographic distribution of carbonate rocks with respect to their apparent depositional age and their proximity to continents. The carbonate sedimentation progressed in a wide span across what is now the East African-Antarctic Orogenic Belt probably from the early Proterozoic to the Cryogenian. In summary, extracting trace and rare earth element characteristics and comparing them with carbon, oxygen, sulfur, strontium, neodymium and lead isotopes in carefully screened unaltered metacarbonate rocks in collisional orogenic belts can help in understanding the variations in the environment of deposition, age of deposition and the tectonic setting in which they were deposited, and in decoding the history of the lost oceans.

Keywords: Metacarbonate rocks, East African Antarctic Orogen, Trace and rare earth element geochemistry, C, O, S, Sr, Nd and Pb isotope geochemistry

©2021. Japan Geoscience Union. All Right Reserved.

[E] Poster | S (Solid Earth Sciences)：S-MP Mineralogy & Petrology

Sat. Jun 5, 2021 5:15 PM - 6:30 PM JST | Sat. Jun 5, 2021 8:15 AM - 9:30 AM UTC | Ch.15_2

[S-MP24] Supercontinents and Crustal Evolution

convener:Tomokazu Hokada(National Institute of Polar Research), Tetsuo Kawakami(Graduate School of Science, Kyoto University), Krishnan Sajeev(Centre for Earth Sciences, Indian Institute of Science), Madhusoodhan Satish-Kumar(Department of Geology, Faculty of Science, Niigata University)

Supercontinent formation and dispersion has been enigmatic in the Earth's history. Eurasia is one such current supercontinent and incredible progress in the understanding of its geological evolution has been achieved in the past decade. Earlier supercontinents in the Earth's history such as Gondwana (0.5 Ga), Rodinia (1.0 Ga), Columbia/Nuna (2.0 Ga), Kenorland (2.5 Ga) and Vaalbara (3.1 Ga), have been the focus of several studies, however limited information on older supercontinents has restricted an understanding their tectonic evolution. Several important unsolved issues remain, such as how, when and where these supercontinents formed and how long they remained as such before breaking apart. Additional questions arise on the processes that triggered the fragmentation and unification of continents. In this session, we invite authors around the world to present original new data as well as review results on the continental scale crustal processes and tectonic evolution that are associated with supercontinent formation events in Earth's history. The well-studied Eurasia and Gondwana supercontinents are of particular focus. Topics of interest include, but not restricted to, extremes in metamorphism, P-T-d-t evolution, magmatism, and the role of fluids. We hope to provide a platform for scientific discussions that will enlighten our understanding of the physical and chemical processes in the continental crust that records episodes of orogenesis that contributed to the formation and evolution of supercontinents.

[SMP24-P01] Geochronology of the metamorphic rocks at the Oyayubi ridge of Brattnipene, Sør Rondane Mountains, East Antarctica.

*Tatsuro ADACHI[1], Tetsuo Kawakami[2], Masaoki Uno[3], Fumiko Higashino[4] (1.Kyushu University, 2.Kyoto University, 3.Tohoku University, 4.Okayama University of Science)

[SMP24-P02] **Evidence of Paleoproterozoic rift-to-drift transition in eastern margin of Singhbhum Craton, India from U-Pb zircon, Sr-Nd isotopic and geochemical study of dismembered gabbro-wehrlite of Bangriposi**

*Tushar Mouli Chakraborti[1,2], Kosuke Kimura[1,2], Arijit Ray[3], Ramananda Chakrabarti[4], Gautam Kumar Deb[3] (1.Earth and Planetary System Science program, Graduate School of Advanced Science and Engineering, Hiroshima University, Japan, 2.Hiroshima Institute of Plate Convergence Region Research (HiPeR), Hiroshima University, Japan, 3.Department of Geology, Presidency University, Kolkata, India, 4.Centre for Earth Sciences, Indian Institute of Science, Bangalore, India)

[SMP24-P03] Sulfur isotope study of high-grade metamorphic rocks in Highland Complex, Sri Lanka

*Tokuya Mitsubori[1], Madhusoodhan Satish-Kumar[2], Sanjeewa P.K. Malaviarachchi[3] (1.Graduate School of Science and Technology, Niigata University, 2.Department of Geology, Faculty of Science, Niigata University, 3.Department of Geology, Faculty of Science, University of Peradeniya)

[SMP24-P04] **Sulfur isotope study of metacarbonate rocks from Highland Complex, Sri Lanka**

*Aoi Yoshioka[1], Madhusoodhan Satish-Kumar[1] (1.Department of Geology, Faculty of Science, Niigata University)

[SMP24-P05] Preliminary reports of U-Pb zircon age of charnockites in Aker Peaks of the Napier Complex, East Antarctica

*Kenji Horie[1,2], Mami Takehara[1], Tomokazu Hokada[1,2], Allen Nutman[3] (1.National Institute of Polar Research, 2.The Graduate University for Advanced Studies, SOKENDAI, 3.University of Wollongong)

[SMP24-P06] **Microtextural, fluid inclusion and C-O stable isotope studies of sparry magnesite of Deoban group of Kumaun Lesser Himalayas**

*Prakash Chandra Arya[1], Sajeev Krishnan[1], Kiran S[2,3], Satish Kumar[2], Claude Nambaje[1] (1.Centre for Earth Science, Indian Institute of Science, Bangalore, India, 2.Department of Geology, Faculty of Science, Niigata University, Niigata, Japan, 3.Graduate School of Science and Technology, Niigata University, Niigata, Japan)

[SMP24-P07] **Petrography and progressive metamorphism of Chitradurga Schist Belt, Dharwar Craton, southern India**

*Tomokazu Hokada[1,2], Madhusoodhan Satish-Kumar[3], Yuichiro Ueno[4], Tsuyoshi Toyoshima[3], Kaoru Mishima[4], Abdulla Nasheeth[4,5], Chiaki Ikawa[2] (1.National Institute of Polar Research, 2.The Graduate University for Advanced Studies (SOKENDAI), 3.Niigata University, 4.Tokyo Institute of Technology, 5.Osaka City University)

Geochronology of the metamorphic rocks at the Oyayubi ridge of Brattnipene, Sør Rondane Mountains, East Antarctica.

*Tatsuro ADACHI[1], Tetsuo Kawakami[2], Masaoki Uno[3], Fumiko Higashino[4]

1. Kyushu University, 2. Kyoto University, 3. Tohoku University, 4. Okayama University of Science

The Sør Rondane Mountains (SRM) comprise medium to high-grade metamorphic rocks with granitic, syenitic and minor mafic dikes (e.g. Shiraishi et al., 1997, *Antarctic Geological Map Series, Sheet 35*). The SRM is divided into the NE terrane and the SW terrane by the Main Tectonic Boundary (MTB), and each terrane is defined by shape of *P-T* path and age distribution of detrital zircon (Osanai et al., 2013, *Precambrian Research, 234*)). The SRM is considered to be formed by collision of both terranes at 600-650Ma during which the NE terrane have thrusted up over the SW terrane (Osanai et al., 2013). This model also suggests that whole of the SW terrane behaved as a single geological body during and after the 650-600 Ma collision event. However, this model is not sufficiently correlated with the *P-T* conditions and ages, so it requires to be tested by conducting more detailed analyses widely in the SRM. This study reports geochronological result (LA-ICP-MS zircon U-Pb dating and EPMA monazite U-Th-Pb dating) of rocks from Brattnipene area in the SW terrane.

At the eastern slope of the Oyayubi ridge of Brattnipene, pelitic gneisses (garnet-sillimanite-biotite gneiss and garnet-biotite gneiss) and felsic gneisses (hornblende-biotite gneiss and garnet-clinopyroxene gneiss) are in contact with each other by the low angle ductile shear zone. The pelitic gneisses are distributed structurally upper than the felsic gneisses. The *P-T* conditions of these gneisses examined in this study were reported by Adachi et al. (2020, *NIPR symposium abstract*).

The garnet-sillimanite-biotite gneiss (sample No. TA19120703C) shows several textures indicating retrograde hydration. The texture replacing garnet by kyanite, sillimanite and biotite is interpreted as retrograde products which are reported from several localities in the Brattnipene area (e.g. Adachi et al., 2013a, *Geological Society Special Publication,* 383). Peak-*T* condition is estimated as ca. 800 ˚C. The garnet in garnet-biotite gneiss (TA19120703F) is extensively replaced by biotite and plagioclase, suggesting intense retrograde hydration. These pelitic rocks are located a few tens of cm away from each other.

Zircon grains in TA19120703C shows oscillatory- or planer-zoned cores truncated by vaguely zoned rims. The grains were dated using LA-ICP-MS U-Pb method and the results from the inherited core are grouped at 1100-900 Ma and 800-700 Ma (Th/U: 1.00-0.02), and those from the rim range from 600 to 540 Ma (Th/U: 0.31-0.02), Similar date distribution is also obtained from monazite EPMA dating. Monazite grains in TA19120703F yield date distribution with a large peak centered at ca. 550 Ma and without older date than 700 Ma. These data suggest that these pelitic gneisses reached peak condition at ca. 600 Ma and suffered retrograde hydration at ca. 550 Ma, which is consistent with the result reported from the central SRM in the previous studies (e.g. Adachi et al., 2013b, *Precambrian Research, 234*).

In contrast, the hornblende-biotite gneiss (TA19120703A) and garnet-clinopyroxene gneiss (TA19120701B) preserve information acquired under the peak metamorphic conditions in the matrix minerals. Especially plagioclase in hornblende-biotite gneiss shows increase in calcium concentration rimward, suggesting prograde process. No clear hydration texture can be recognized in these rocks. Peak *P-T* condition is estmated as 700-750 ˚C and 5-9 kbar. Zircons are present in the matrix whereas

©2021. Japan Geoscience Union. All Right Reserved.

monazites are absent in these samples.

Zircon grains in TA19120701B shows oscillatory-zoned cores truncated by bright-CL mantles which are surrounded by dark-CL rims. Each domain yields different date cluster: the core at ca. 600 Ma (Th/U: 0.56-0.21, Ave. 0.43), the mantle at ca. 570 Ma (Th/U: 0.32-0.17, Ave. 0.23) and the rim at ca. 550 Ma (Th/U: 0.54-0.06, Ave. 0.16). Zircon grains in TA19120703A preserve oscillatory-zoned cores which are truncated and partially replaced by unzoned domains. The core dates cluster at ca. 600 Ma (Th/U: 0.75-0.12, Ave. 0.25), and the rim dates at ca. 550 Ma (Th/U: 0.20-0.06, Ave. 0.14). These data from the felsic gneisses indicate that igneous activity which formed the protolith of the felsic gneisses at ca. 600 Ma and the subsequent metamorphism which reached peak condition at ca. 550 Ma.

In summary, the pelitic gneisses experienced peak and subsequent retrograde metamorphism at around 600-540 Ma, whereas the felsic gneisses record prograde metamorphism after 600 Ma. This suggests that two distinct metamorphisms are recognized at the Oyayubi ridge of the Brattnipene in the SW terrane. If such a relationship can be observed widely in the SRM, the tectonic model for the SRM needs to be reconsidered.

Keywords: Sør Rondane Mountains, East Antarctica, metamorphic rocks, geochronology, zircon, monazite

©2021. Japan Geoscience Union. All Right Reserved.

Evidence of Paleoproterozoic rift-to-drift transition in eastern margin of Singhbhum Craton, India from U-Pb zircon, Sr-Nd isotopic and geochemical study of dismembered gabbro-wehrlite of Bangriposi

*Tushar Mouli Chakraborti[1,2], Kosuke Kimura[1,2], Arijit Ray[3], Ramananda Chakrabarti[4], Gautam Kumar Deb[3]

1. Earth and Planetary System Science program, Graduate School of Advanced Science and Engineering, Hiroshima University, Japan, 2. Hiroshima Institute of Plate Convergence Region Research (HiPeR), Hiroshima University, Japan, 3. Department of Geology, Presidency University, Kolkata, India, 4. Centre for Earth Sciences, Indian Institute of Science, Bangalore, India

Dismembered modally layered gabbro and serpentinized wehrlite are found emplaced within multiply deformed metapelites of the North Singhbhum Mobile Belt assemblage, Singhbhum Craton, India. Zircon grains from the gabbro unit analyzed by LA-ICP MS yields an average U-Pb crystallization age of 1881.1 ± 8.4 Ma. The undeformed, cumulate gabbroic body exhibits excellent modal and cryptic layering, generated by the interplay of ad cumulate and textural coarsening growth process. It is moderately evolved with Mg number (100Mg/Mg+Fe) 48-63, low Alkali and TiO_2, high Al_2O_3; enrichment of Pb, Ba, Rb with depletion of U, Th, Zr and unfractionated rare earth patterns with positive Eu anomaly. The serpentinized wehrlite shows evidence of cumulate nature of the protolith and extensive post-crystallization metasomatism. Mineral chemistry, whole-rock geochemistry and clinopyroxene trace elements reveals progressive fluid-rock interaction from very high-temperature to low-temperature regimes. Calculated melts in equilibrium with the gabbroic rocks display enrichment in lighter elements similar to EMORBs and resembles the estimated average composition of the metasomatic fluid of the wehrlite rocks. The gabbros have initial $^{87}Sr/^{86}Sr$ 0.70600-0.71099, initial $^{143}Nd/^{144}Nd$ 0.510130-0.510294, and E_{Nd} (t) 1.8 to -1.4. The serpentinized wehrlite displays extreme enrichment with initial $^{87}Sr/^{86}Sr$ 0.71045- 0.72640, initial $^{143}Nd/^{144}Nd$ 0.509120- 0.509706, and almost crust-like E_{Nd} (t) of -9.7 to -21.2. The cumulate nature of the mafic-ultramafic rocks with other petrographical evidences imply formation in a static magma chamber. Dismembered nature, occurrence within an orogenic belt assemblage and temporal considerations suggest emplacement by obduction and affinity towards oceanic magma chambers. This is also reflected in mineralogy, whole-rock geochemistry and trace element compositions of modeled equilibrium melts which resemble rift volcanics and are similar to mafic dykes of continental margin ophiolites. The isotopic character of the gabbros can be explained by 30%-40% mixing between a depleted and a subduction-influenced enriched domain in the Sub-Continental Lithospheric Mantle beneath Singhbhum Craton. The isotopic signature of the wehrlite has been perturbed by the metasomatic event and reflects the enriched nature of the fluid phase. The occurrence of the mafic-ultramafic rocks within the shallow-deep marine, intra-continental rift basinal assemblage of Chaibasa formation, shows that rift-to-drift transition took place during Paleoproterozoic and incipient oceanic crust was formed. A 1.86 Ga orogenic event marked by intrusion of anorogenic granites caused closure of this basin and obduction of these fragments onto the orogenic belt assemblage. This result represents the first such discovery in Singhbhum Craton and can be correlated Paleoproterozoic ophiolites of south India. The formation and emplacement of these oceanic crustal rocks fits with the rift-dominated tectonics of that era and the widespread continental amalgamation and ophiolite emplacement which took place in Columbia supercontinent during Paleoproterozoic.

Keywords: Layered gabbro, Wehrlite, Cumulate dunite, Rift-to-drift, Ophioplite, Columbia supercontinent

©2021. Japan Geoscience Union. All Right Reserved.

©2021. Japan Geoscience Union. All Right Reserved.

Sulfur isotope study of high-grade metamorphic rocks in Highland Complex, Sri Lanka

*Tokuya Mitsubori[1], Madhusoodhan Satish-Kumar[2], Sanjeewa P.K. Malaviarachchi[3]

1. Graduate School of Science and Technology, Niigata University, 2. Department of Geology, Faculty of Science, Niigata University, 3. Department of Geology, Faculty of Science, University of Peradeniya

Large deviations from mass independent fractionation in sulfur isotopes, termed as MIF-S, are characteristic of Archean sediments[1]. Although there are reports of Archean detrital zircon ages from 2400 to 3200 Ma in the Highland Complex (HC), Sri Lanka, it is not clear whether the sediments itself have detrital components other than zircon grains. Multiple sulfur isotope studies may provide some information in this aspect. Furthermore, the behavior of sulfur during high-grade metamorphism is not well understood, although sulfur isotope studies have been conducted in low-grade metamorphic rocks, previously[2]. In this study, we measured sulfur isotopes ratios for bulk rock samples from the HC, Sri Lanka, to verify whether the Archean MIF-S is preserved and try to discuss the behavior of sulfur during high-grade metamorphism.

Sulfide minerals in the metapelitic Grt-Sil gneiss are composed of pyrrhotite, chalcopyrite and pentlandite, that has a wide range of $\delta^{34}S_{V\text{-}CDT}$ from -1.7 ‰to 14.2 ‰. Charnockite contain various sulfide minerals such as pyrrhotite, chalcopyrite, pyrite, pentlandite and molybdenite, and their $\delta^{34}S_{V\text{-}CDT}$ values range between -1.0 ‰to 5.9 ‰. These values are consistent with an igneous origin for charnockites in the HC. However, there was no clear signature of MIF-S, although minor positive trend is observed in metapelitic rocks.

The with positive $\delta^{34}S_{V\text{-}CDT}$ values Grt-Sil gneiss are assumed to be sedimentary pyrite that are close to the sulfur isotopic composition of seawater sulfate, considering that the sulfate concentration in seawater was low at that time. When pyrite breakdown to pyrrhotite during metamorphism, $\delta^{34}S$ values increases at most 2-3 ‰[3]. Considering that the $\delta^{34}S_{V\text{-}CDT}$ values represent near seawater sulfate values, the bulk sulfur isotopic composition is preserved even after high grade metamorphism. Considering the minor spikes in MIF-S in metapelitic rocks, further detailed studies are in progress.

References

1. Kröner et al., 1987 The Journal of Geology 95, 775-791
2. Ono et al., 2006 South African of Journal of Geology 109, 97-108
3. Bucholz et al., 2020 Earth and Planetary Science Letters 549, 116494

Keywords: Sulfur isotopes, Archean, High-grade metamorphism, Highland Complex, Sri Lanka

©2021. Japan Geoscience Union. All Right Reserved.

Sulfur isotope study of metacarbonate rocks from Highland Complex, Sri Lanka

*Aoi Yoshioka[1], Madhusoodhan Satish-Kumar[1]

1. Department of Geology, Faculty of Science, Niigata University

Sulfur isotopes in carbonate rocks record variations in seawater sulfate reservoirs associated with global oxygenation as well as depositional environments. During the Proterozoic, several evolutionary and biogeochemical events have occurred, with particular attention being paid to the rise in oxygen (GOE and NOE) in the Earth's atmosphere and oceans. These events appear to be closely linked to global sulfur geochemistry by both the production of weathered sulphates on land and the oxidation of sulfides and the evolution of disproportionated bacteria in the marine environment (Bottrell and Newton, 2006). Here, we report sulfur isotopic compositions of pyrite in metacarbonate rocks in order to estimate the depositional environment and gain insight into the effects of metamorphism. Metamorphic carbonate rocks containing pyrite from the Highland Complex in Sri Lanka was investigated in this study, which is believed to have been deposited in the Precambrian period. The $\delta^{34}S_{V\text{-}CDT}$ values of pyrite ranges from +6 to +26‰, and $\Delta^{33}S$ was slightly negative, most of which falls in the same quadrant in a $\Delta^{33}S$ vs. $\delta^{34}S$ diagram. This reflects a closed system sulfur isotope behavior caused by microbial sulfate reduction (MSR) and high sulfate demand, among other factors. In addition, while comparing the results of this study with un-metamorphic carbonate rocks in Proterozoic, the $\Delta^{33}S/\delta^{34}S$ and $\Delta^{33}S/\Delta^{36}S$ tendency of sulfur isotopes were similar. Therefore, it is considered that the change of sulfur isotopes due to metamorphism is negligible and the carbonate rocks act as perfect time capsule for preserving Precambrian ocean signatures. In addition, comparison with sulfur isotopic composition of pyrite in carbonate rocks of various ages indicate that the sulfur isotopic composition in the metacarbonate rocks in the Highland Complex were higher than in Archean, and similar to those in other Proterozoic eras. Therefore, we believe that the carbonate rocks provide key information in support of the hypothesized global ocean.

Reference

Bottrell, S. H., and Newton, R. J., 2006. Reconstructionofchangesin global sulfur cycling from marine sulfate isotopes. *Earth science Reviews.*, 75, 59-83.

Keywords: sulfur isotopes, metamorphism, microbial sulfate reduction, Highland Complex Sri Lanka, metacarbonate rocks

©2021. Japan Geoscience Union. All Right Reserved.

Preliminary reports of U-Pb zircon age of charnockites in Aker Peaks of the Napier Complex, East Antarctica

*Kenji Horie[1,2], Mami Takehara[1], Tomokazu Hokada[1,2], Allen Nutman[3]

1. National Institute of Polar Research, 2. The Graduate University for Advanced Studies, SOKENDAI, 3. University of Wollongong

The Napier Complex in East Antarctica has attracted considerable interest on account of its long Archaean crustal history from 3800 Ma to 2500Ma as well as position in Precambrian supercontinents as well as its extremely high peak metamorphic temperature (UHT: ultra-high temperature), which exceeds 1100 ˚C. The discovery of extremely ancient crustal material of ca. 4000Ma obtained by Pb-Pb isochron in the Fyfe Hills (Sobotovich et al., 1976) generated intense interest in the Napier Complex. Similar evidences of ancient crustal materials were reported for the Mt. Sones and Gage Ridge region (Black et al., 1986; Harley and Black, 1997). Belyatsky et al. (2011) reported Eoarchean U-Pb zircon age of 3981 ± 8 Ma from charnockites in Aker Peaks. In this study, we report preliminary geochronological and geochemical data of zircons collected from two charnockite samples of Aker Peaks.

The sample #22a is phlogopite-bearing orthopyroxene-mesoperthite-charnockite and contains zircon, monazite and rutile as accessory mineral. Phlogopite replaces orthopyroxene forming symplectites with quartz. The sample #36a is phlogopite-bearing orthopyroxene-mesoperthite-cataclastic charnockite and contains zircon as accessory mineral. Plagioclase is replaced by mesoperthite which is corroded by quartz. The zircon garains separated from both samples were analyzed using a sensitive high-resolution ion microprobe (SHRIMP) at National Institute of Polar Research.

Both samples show Paleoarchean to Eoarchean evidence. The sample #22a yielded two age peaks centered at ca. 3600 Ma and ca. 3500 Ma. The former is the protolith age and the latter indicates the timing of recrystallization. On the other hand, some zircon grains in the sample #36a shows core-rim structure. The age data are scattered from >3700 Ma to 3300 Ma and major age peak is ca. 3630 Ma. The Pb-Pb age of rim is ca. 2500 Ma, whith corresponds to the timing of UHT metamorphism. The results are consistent with previous report that early high-temperature metamorphic event accompanied by the emplacement of granodiorite intrusions occurred in the vicinity of Aker Peaks at 3620-3630 Ma. Further geochemical information such as trace element concentrations including rare earth elements will be demonstrated.

Keywords: Napier Complex, U-Pb zircon, Antarctica, SHRIMP

©2021. Japan Geoscience Union. All Right Reserved.

Microtextural, fluid inclusion and C-O stable isotope studies of sparry magnesite of Deoban group of Kumaun Lesser Himalayas

*Prakash Chandra Arya[1], Sajeev Krishnan[1], Kiran S[2,3], Satish Kumar[2], Claude Nambaje[1]

1. Centre for Earth Science, Indian Institute of Science, Bangalore, India, 2. Department of Geology, Faculty of Science, Niigata University, Niigata, Japan, 3. Graduate School of Science and Technology, Niigata University, Niigata, Japan

Carbonate-hosted voluminous sparry magnesite (Pinolite) occurrence are known from Deoban group of Kumaun Lesser Himalayas. The origin of the sparry magnesite is still not fully understood and is still a matter of debate. Several models have been proposed for their origin such as evaporative, diagenetic, hydrothermal, metamorphic, metasomatic, and biogenic. In the Kumaun region, the field evidence suggests a close association of stromatolites with the magnesite-bearing beds (10-120 mts). The sparry magnesite's microtextural and fluid inclusion studies are investigated to understand the magnesite formation and trapping temperatures of fluids during magnesite crystallization. The color of the sparry magnesite of Kumaun Himalayas varies from yellow to white-off white, grey, and muck colored. The grain size of magnesite crystal varies from few millimeters to 2 to 3 cm, with deformed rhombohedral cleavage. Fluid inclusion results suggest, presence of low density bi-phase primary and bi-phase pseudo secondary fluids. Three fluids populations were classified based on the homogenization temperature (T_h) and final ice melting (T_f). The first category (T_f ~ -18 to -23 °C with T_h ~160 to 200 °C), the second (T_f ~ -7 to -12 °C with T_h ~150 to 320 °C), and the third (T_f ~ 0 to -5 °C with T_h ~160 to 280 °C). The maximum homogenization temperature of fluids ~320 °C. These observations suggest that the magnesites hosting in the Deoban group were subjected to a minimum temperature of 320 °C. Preliminary carbon and oxygen stable isotope results indicate that magnesite have a relatively constant carbon isotopic composition comparable to marine carbonates, however with large variations in oxygen isotopic composition. Further studies are ongoing and we present a comprehensive discussion on the origin of sparry magnesite.

Keywords: Microtexture, Fluid Inclusion, Sparry magnesite (Pinolite), Stable isotopes

©2021. Japan Geoscience Union. All Right Reserved.

Petrography and progressive metamorphism of Chitradurga Schist Belt, Dharwar Craton, southern India

*Tomokazu Hokada[1,2], Madhusoodhan Satish-Kumar[3], Yuichiro Ueno[4], Tsuyoshi Toyoshima[3], Kaoru Mishima[4], Abdulla Nasheeth[4,5], Chiaki Ikawa[2]

1. National Institute of Polar Research, 2. The Graduate University for Advanced Studies (SOKENDAI), 3. Niigata University, 4. Tokyo Institute of Technology, 5. Osaka City University

Dharwar Crton in southern India is typical Archaean granite-greenstone belt, and underwent regional metamorphism at about 2.5 Ga. The progressive change of the regional metamorphic conditions has been summarized by Raase et al. (1986), and they concluded the metamorphic grade increasing from greenschist-facies in the north to granulite-facies in the south. This is based on the change of the metamorphic minerals in mafic rocks either associated with felsic orthogneiss (granite-zone) or metasedimentary sequences (greenstone-zone).

We have investigated metamorphic mineral assemblages of pelitic and psammitic rocks within the greenstone belt of the Chitradurga Schist Belt that is one of well-studied area and located middle of the Dharwar Craton. The sedimentary sequences of this greenstone belt consist of four groups (Sargur, Bababudan, Chitradurga, Hiriyuru Groups from lower to upper structure; e.g., Sreehari and Toyoshima, 2020). Pelitic and psammitic rocks are charactreized by biotite-muscovite asssemblage with minor muscovite/muscovite-chlorite assemblages. Wihtin the schist belt, progressive change of the metamorphic grade is not clear, but muscovite-chlorite assemblage is observed sporadically in central to eastern part (relatively lower structural layer). These observation are not always consistent with the previously summarized south-north metamorphic variation (Raase et al., 1986) estimated from mafic rocks.

We will discuss in this presentation on the petrography and progressive metamorphism of this part of Dharwar Craton and implications on the regional metamorphism of the Archaean greenstone belt.

Keywords: Archaean, Dharwar Craton, India, Metamorphism

©2021. Japan Geoscience Union. All Right Reserved.

[J] Oral | S (Solid Earth Sciences)：S-VC Volcanology

Sat. Jun 5, 2021 9:00 AM - 10:30 AM JST | Sat. Jun 5, 2021 12:00 AM - 1:30 AM UTC | Ch.25 Zoom Room 25

[S-VC28] Active Volcanism

convener:Yuta Maeda(Nagoya University), Takahiro Miwa(National research institute for earth science and disaster prevention), Takeshi Matsushima(Institute of Seismology and Volcanology, Faculty of Science, Kyushu University), Chairperson:Taketo Shimano(Graduate School of Environment and Disaster Research, Tokoha University), Takahiro Miwa(National research institute for earth science and disaster prevention)

This session discusses various aspects of active volcanisms including, but not limited to, rec ent and historical eruptions, various phenomena associated with the volcanic activities, und erground structures of the volcanoes, and developments of new instruments based on geop hysical, geochemical, geological, and multidiscipline approaches. We also welcome studies o n understanding and predicting the transitions of the eruptive activities from observational, theoretical, and experimental approaches.

9:00 AM - 9:15 AM JST | 12:00 AM - 12:15 AM UTC

[SVC28-19] Temporal variation of conduit process during the 2018 eruptive activity at Shinmoedake volcano, Japan: Implications from a time series of ash characteristics

*Takahiro Miwa[1], Masashi NAGAI[1], Hideki Ueda[1], Taku Ozawa[1], Eisuke Fujita[1] (1.National research institute for earth science and disaster resilience)

9:15 AM - 9:30 AM JST | 12:15 AM - 12:30 AM UTC

[SVC28-20] An emplacement mechanism of submarine pyroclastic products: insight form the seismic studies on Kikai caldera

*Satoshi Shimizu[1,2], Nobukazu Seama[3,1], Reina Nakaoka[1], Keiko Suzuki-Kamata[1], Koji Kiyosugi[1], Katsuya Kaneko[3,1], Tetsuo Matsuno[1], Yoshiyuki Tatsumi[1] (1.Kobe Ocean-Bottom Exploration Center, Kobe University, 2.Nippon Marine Enterprises, Ltd., 3.Department of Planetology, Graduate School of Science, Kobe University)

9:30 AM - 9:45 AM JST | 12:30 AM - 12:45 AM UTC

[SVC28-21] Comparison of subaerial and submarine deposits from the Kikai Akahoya eruption

*Reina NAKAOKA[1], Keiko Suzuki-Kamata[1], Satoshi Shimizu[1], Katsuya Kaneko[2], Nobukazu Seama[2], Koji Kiyosugi[1], Takeshi Hanyu[3], Yoshiyuki Tatsumi[1], CK20-S01 Leg2 Cruise Scientists, KS19-17 Cruise Scientists, KR20-11 Cruise Scientists (1.Kobe Ocean-Bottom Exploration Center, Kobe University, 2.Department of Planetology, Kobe University, 3.Japan Agency for Marine-Earth Science and Technology)

9:45 AM - 10:00 AM JST | 12:45 AM - 1:00 AM UTC

[SVC28-22] Tephrostratigraphy of drilled core C9010E off the Boso Peninsula: Estimated source volcano for 9th century eruption events

*Kaori Aoki[1], Makoto Kobayashi[2,1], Masanori Murata[1], Takehiko Suzuki[1] (1.Research Center for Volcanic Hazards and Their Mitigation, Tokyo Metropolitan University, 2.Mt.Fuji World Heritage Centre, Shizuoka)

10:00 AM - 10:15 AM JST | 1:00 AM - 1:15 AM UTC

[SVC28-23] Caldera structure and formation at Atosanupuri and Akaigawa, Hokkaido, northern Japan: A comparison of analogue sandbox experiments and field data

*Ryuhei Sanjo[1] (1.Institute of Geography, Graduate School of Science, Tohoku University)

10:15 AM - 10:30 AM JST | 1:15 AM - 1:30 AM UTC

[SVC28-24] Current state evaluation and long-term prediction of volcanic activity based on historical tracking of volcanic ash deposits at Suwanosejima volcano

*Taketo Shimano[1], Atsushi Yasuda[2], Masato Iguchi[3] (1.Graduate School of Environment and Disaster Research, Tokoha University, 2.Earthquake Research Institute, University of Tokyo, 3.Sakurajima Volcano Research Center, Disaster Prevention Research Institute, Kyoto University)

Temporal variation of conduit process during the 2018 eruptive activity at Shinmoedake volcano, Japan: Implications from a time series of ash characteristics

*Takahiro Miwa[1], Masashi NAGAI[1], Hideki Ueda[1], Taku Ozawa[1], Eisuke Fujita[1]

1. National research institute for earth science and disaster resilience

We investigated a time series of characteristics of ash particles to discuss change of the conduit process during the 2018 eruptive activity at Shimoedake volcano, Kirishima, Japan. The 2018 eruptive activity exhibited following a transition of three stages of eruptive style: (1) Ash emission in March 1–5, (2) dome-forming with strombolian eruptions in March 6–8, and (3) discrete vulcanian eruptions after March 9. Along with the transition, magma supply rate from the chamber inferred from tiltmeter and GNSS data was constant in the ash emission stage, increases (March 6) and subsequent decreases (March 7–8) in the dome formation stage, and constant again in the vulcanian stage (Ueda, 2018). Also, the volume of lava dome linearly increases from morning of March 6 to March 8 in the dome stage, and almost constant in the vulcanian stage, as revealed by SAR observation (Ozawa, 2018).

We analyzed twenty ash samples during the 2018 eruptive activity: two from the ash emission stage, fifteen from the dome stage, and three from the vulcanian stage. The ash particles were divided into 9 type as VCF (vecicular colorless), DCFF (dense colorless with fine microlite), DCFC (dense colorless with coarse microlite), VBF (vecicular black), DBF (dense black), LITH, ALT, PL, and MM (mafic mineral), based on the observations by stereoscopic microscope and SEM. The glossy surfaces in the VCF, VBF, DCF, and DBF indicate these particles are juvenile particles. The component analysis of the ash samples reveals that (1) the ALT and LITH dominated in the ash emission stage, (2) the VCF and DCF are abundant in the dome-forming stage with high abundant of DCFC in March 6, and (3) the DCF is rich and VCF is poor in the vulcanian stage. The textural analysis suggests the characteristics of plagioclase microlite (crystallinity, number density (MND) and crystal size distribution) are similar among the VCF, VBF, DCFF and DBF, whereas the DCFC has high crystallinity with low MND. The co-existence of parts of DCFF with DCFC were often found in a single particle. The glossy surfaces, textural similarity in plagioclase microlite, and different vesicularity in the VCF, DCF, VBF, and DBFF suggest these particles originate fresh new magma undergoing similar decompression path with different degree of outgassing. In contrast, the DCFC is interpreted as a partially-consolidated magma that ascended prior to the dome eruption or as part of the 2011 lava dome from the high crystallinity with low MND. Also the co-existence of parts of DCFF and DCFC in a single particle implies an erosion of partially-consolidated magma in the shallow conduit (DCFC) by newly ascended magma (DCFF).

Temporal variation of the conduit process during the 2018 eruptive activity at Shinmoedake volcano is explained by the enlargement of the conduit associated with increase in magma supply rate and subsequent outgasssing and sealing of the lava dome with the decrease in magma supply. During the ash emission stage in March 1–5, volcanic gas was emitted, destructing the country rock consisting of hydrothermally altered materials. In the early dome-forming stage of March 6, the increase of magma supply rate caused the erosion of the partially-consolidated magma, resulting in the enlargement of the conduit region. In the later dome-forming stage of March 7, the magma supply rate decreases, which ceased the enlargement and gradually sealed the conduit. Consequently in the vulcanian stage after March 9, the sealing of pathway of outgassing in the shallow conduit due to decrease of magma supply

©2021. Japan Geoscience Union. All Right Reserved.

rate caused pressurization inside the dome, generating the vulcanian eruptions.

Keywords: Transition of eruptive style, Volcanic ash, Texture, Shinmoedake volcano, Kirishima

©2021. Japan Geoscience Union. All Right Reserved.

An emplacement mechanism of submarine pyroclastic products: insight form the seismic studies on Kikai caldera

*Satoshi Shimizu[1,2], Nobukazu Seama[3,1], Reina Nakaoka[1], Keiko Suzuki-Kamata[1], Koji Kiyosugi[1], Katsuya Kaneko[3,1], Tetsuo Matsuno[1], Yoshiyuki Tatsumi[1]

1. Kobe Ocean-Bottom Exploration Center, Kobe University, 2. Nippon Marine Enterprises, Ltd., 3. Department of Planetology, Graduate School of Science, Kobe University

Pyroclastic density current entering into water is not well understood on its emplacement mechanism. The emplacement mechanism in marine environment is subjects to location of vent, and temperature, velocity, density and angle of entrance of flow with water (Cas&Wright, 1991). When subaerial pyroclastic flow encounters water, it is subdivided into subaerial and subaqueous parts: subaerial flow interacts with water, making steam explosions, accelerating the flow, and generating co-ignimbrite ash cloud; subaqueous pyroclastics can be mixed with water, making ash plumes and seafloor hugging density current, or displace the water in shallow water. Many experimental studies and numerical modeling have documented for a variety of emplacement mechanisms (e.g., Freundt, 2003). However, a few attempts to explain the subaqueous emplacement with actual seafloor deposits on modern eruptions have been still controversial.

We have conducted high resolution seismic reflection studies around Kikai caldera located to the south of Kyusyu Island, Japan. Our seismic studies, together with chemical analyses of volcanic glasses, revealed that the uppermost unit distributed in an area of >4,500 km^2 with a volume of >71 km^3 is composed of pyroclastic deposits of 7.3 ka Akahoya eruption. This study is aiming to fill the gap between subaerial pyroclastic-flow deposits on proximal islands and distal islands where open water dominates the area surrounding the caldera in terms of volume and emplacement mechanism in the marine setting.

The distribution of the pyroclastic unit lying on the seafloor around Kikai caldera is confined by the basin topography. Although some areas of the unit were reworked by the mass movements observed as debris flow, slumping, and debris avalanche from the caldera rims to the basin, the east side of caldera has no evidence of such mass transports, possibly capturing the syn-eruptive deposition. This east area exhibits smooth seafloor on almost flat to slightly upward to the shelf of Tanegashima. The unit forms exponential thinning from the caldera wall to the shelf, filling the basin, depressions and fault steps. This deposition contrasts with shallow-marine deposits of Krakatau 1883 eruption that does not form systematic thinning but mottle-like thickening distribution, and bypass the annular moats, interpreted as that initially subaerial flow sank through the water column as increasing the density by gravity segregation (Mandeville et al. 1996; Legros&Druitt, 2000). Subaqueous fall-out deposition was also demonstrated by Freundt (2003); it occurs entirely in the water only on shallow-tank setting. In other deep-tank settings, either hot or cool-ash flow, generate seafloor-hugging currents, forming exponentially thinning extensive deposits. The exponential thinning of pyroclastic flow deposition was introduced by Wilson (1991), and the rate of the decay is decided by volume flux and settlement velocity of particles (Woods et al.,1998). This rate indicated in our pyroclastic unit is comparable to the values of on-land super-eruption ignimbrites that is much bigger than Kikai 7.3 ka eruption. This is possibly explained by not large mass flux as such super-eruptions generate, but slower settlement due to the subaqueous flow. The volume flux caused in the water is expected to be lower than that in the air because a large fraction of pyroclastics is elutriated from the flow into the subaerial flow over water and co-ignimbrite ash. On the other hand, the subaqueous settlement speed is supposed to be slower by reduced gravity than that in hot air entrained

©2021. Japan Geoscience Union. All Right Reserved.

in subaerial flow. On a given mass flux, the submarine pyroclastic current can make longer run-out deposition than that made by subaqueous current. From the distribution and morphology of the unit, we can conclude that the pyroclastic density current of 7.3 ka eruption made the submarine deposit predominantly emplaced by seafloor-hugging current characterized by long run-out distance.

Keywords: Caldera, Pyroclastic Flow, Seismic Survey, Emplacement Mechanism

©2021. Japan Geoscience Union. All Right Reserved.

Comparison of subaerial and submarine deposits from the Kikai Akahoya eruption

*Reina NAKAOKA[1], Keiko Suzuki-Kamata[1], Satoshi Shimizu[1], Katsuya Kaneko[2], Nobukazu Seama[2], Koji Kiyosugi[1], Takeshi Hanyu[3], Yoshiyuki Tatsumi[1], CK20-S01 Leg2 Cruise Scientists, KS19-17 Cruise Scientists, KR20-11 Cruise Scientists

1. Kobe Ocean-Bottom Exploration Center, Kobe University, 2. Department of Planetology, Kobe University, 3. Japan Agency for Marine-Earth Science and Technology

The 7.3 ka Kikai Akahoya (K-Ah) eruption is a large-scale eruption of the submarine Kikai caldera volcano. It started with a Plinian Funakura pumice fall followed by an intra-Plinian Funakura pyroclastic flow (PF). This was followed by large-scale Koya ignimbrite accompanied by the Akahoya co-ignimbrite ash. On land, Funakura PF is deposited only on proximal islands, which have caldera walls. Koya ignimbrite is thickly deposited on the caldera walls and thinly deposited ~1 m in distal areas tens of kilometers across the sea. The Multi-Channel seismic survey (MCS) around the caldera showed that the Unit S-1, which is estimated to be the K-Ah products, was deposited thickly over a wide area (Shimizu et al., 2020JpGU). Based on their distribution and internal structure, it is assumed that it was deposited by flowing over the seafloor rather than as a fall deposit. The purpose of this study is to clarify the flow and depositional process of pyroclastic materials by comparing the components, depositional structures, and chemical compositions of the volcanic glass of the K-Ah ejecta on both land and seafloor.

On-land investigation and sampling were conducted in the proximal and distal areas. Marine deposits were drilled by the CHIKYU SCORE program to a depth of about 100 m at a location 4.3 km northeast of Takeshima. Also, piston cores (lengths of 1 to 4 m) were conducted by the Shinseimaru and Kairei at 7 sites in the proximal area, including near the SCORE drilling site, and at 14 sites in the distal area. SCORE drilled intermittently from 10 - 100 m below the seafloor, and Unit S-1 is identified by MCS as two different units Lower S-1 (depth 17-22 m) and Upper S-1 (depth <17 m, but not sampled below 10 m). Lower S-1 is a poorly sorted, reddish-brown pumice lapilli tuff often with lamina; Upper S-1 is a poorly sorted massive lapilli tuff with pumice and lithic fragments. These boundaries are distinct because the components are different. In the piston core near the SCORE site, 2 m of sediment corresponding to the uppermost part of Upper S-1 was collected. The submarine deposit consists of pumice lapilli, volcanic ash, lithic fragments, and crystals, and the sedimentary structure is often massive, but at some sites, there are normal grading of the pumice and weak lamination.

The chemical composition of the volcanic ash glass in each deposit was measured by EPMA. The Funakura PF contains only high SiO_2 glass (SiO_2 = ~75 wt.%). In the lower part of the Koya ignimbrite, there is only high SiO2 glass as in the Funakura PF, but low SiO_2 (SiO_2= ~65 wt.%) is mixed into the upper part (Fujihara and Suzuki-Kamata, 2013). The SCORE samples, Lower S-1 and Upper S-1, both contain only high SiO_2 glass consistent with that of the on-land K-Ah products. The piston core samples, both near and far, including the area around the SCORE site, contain both high and low SiO_2 glasses consistent with the K-Ah eruption.

On land, the Funakura PF composed of high SiO_2 magma was deposited, and then the Koya ignimbrite is presumed to have erupted only high SiO_2 magma in the early stage and gradually deposited from the lower levels with the mixing of low SiO_2 magma as the eruption continued (Fujihara and Suzuki-Kamata, 2013). The submarine K-Ah products also contain only high SiO_2 glass in the Lower S-1 and lower part of Upper S-1, suggesting that the deposits were initially deposited by the Funakura PF and later by the early Koya ignimbrite. The uppermost Unit S-1 near the seafloor by piston cores contains both high and low SiO_2 glasses, suggesting that they were deposited during the late K-Ah eruption stage. On the other hand, the

©2021. Japan Geoscience Union. All Right Reserved.

sedimentary structure and grain size of marine deposits are different from those of on-land deposits, and they often show sedimentary structures suggestive of underwater sedimentation, suggesting that they were deposited in a different flow regime than large-scale pyroclastic flows on land.

©2021. Japan Geoscience Union. All Right Reserved.

Tephrostratigraphy of drilled core C9010E off the Boso Peninsula: Estimated source volcano for 9th century eruption events

*Kaori Aoki[1], Makoto Kobayashi[2,1], Masanori Murata[1], Takehiko Suzuki[1]

1. Research Center for Volcanic Hazards and Their Mitigation, Tokyo Metropolitan University, 2. Mt.Fuji World Heritage Centre, Shizuoka

We have been studying tephra correlations intervening in the sediment core off the Boso Peninsula, on the basis of the geologic, petrographic and geochemical characters of tephra samples collected at the reference sites on land. The sedimentary core C9010E was drilled at the site (34˚33.46'N, 139˚53.38'E, water depth: 2027.25 m) of about 40 km south of Boso Peninsula by the D/V Chikyu in 2009. The length of all core is 190.38 m. We collected 354 samples for tephra analysis from this core, including 161 tephra samples described (Tsuchiya et al., 2009). The major-element chemistry of volcanic glass shards in the fraction of 63-125 μm for all samples have been determined by EPMA of the Center for Advanced Marine Core Research, Kochi University. Aoki et al. (2019a) showed the core C9010E included tephras from Mukaiyama tephra (AD886) to Akasakimine tephra series at ca.15-20 ka of the Niijima Volcano origin (Aoki et al., 2019b). Furthermore, Aoki et al. (2020) presented that the tephra bed of the 22 cm thickness at 32.965-33.185 m was correlated to Iz-Tos2 tephra which was provided from unknown volcanic source (Takahashi et al., 2020) and the tephra spot at the 41.21-41.23 m was correlated to Asama Itahana Kasshoku (Brown) tephra group which provided during 26-28 ka (As-BP; Arai, 1962; Aramaki et al., 1998; Takahashi et al., 2003, Takahashi et al., 2018; Shitaoka et al., 2020).

Today, we present on a source volcano of a scoria patch between Niijima Mukaiyama tephra (AD886) and Kozushima Tenjyosan tephra (AD838) in the sedimentary core C9010E. The tephra bed at the depth of 1.15-1.17 m, which was correlated to Niijima Mukaiyama tephra, includes white pumice grains and black scoria grains of the maximum diameter 2 mm. Particles smaller than 250 μm consist of mostly white to clear colored volcanic glass shards which are various forms like as pumiceous, fibrous, bubble-wall, and chunky types. Biotite, orthopyroxene, hornblende, cummingtonite, plagioclase and quartz are observed.

The tephra bed at the depth of 1.63-1.66 m, which was correlated to Kozushima Tenjyosan tephra, includes white pumice grains and black scoria grains of the maximum diameter 1 mm. Particles smaller than 250 μm consists of mostly white to clear colored pumiceous and bubble-wall type volcanic glass shards, a small amount of black scoria grains and rarely brown colored glass shards. Observed minerals are mainly plagioclase and quartz, and rarely biotite.

Between above two tephra bed, tephra patch intervened at the depth of 1.51-1.53 m. Particles larger than 250 μm includes black and dark gray scoria grains of the maximum diameter 2.5 mm, white pumice grains of the maximum diameter 1.5 mm, quartz, beta-type quarts, plagioclase, and a small amount of orthopyroxene and cummingtonite/hornblende. Particles smaller than 250 μm consist of large amount of white to clear colored pumiceous and chunky type, rarely bubble-wall type volcanic glass shards, quartz, beta-type quarts, plagioclase, rarely orthopyroxene. Major-element composition of volcanic glass shards in tephra patch at the depth of 1.51-1.53 m is rhyolite which similar to geochemistry of Niijima Mukaiyama tephra and Kozushima Tenjyosan tephra. However, the contents of CaO and K_2O is different from them, rhyolite glass shards in tephra patch at the depth of 1.51-1.53 m would be correlated to a series of tephras provided from Niijima Kudamaki/Atsuchi event (Kobayashi et al., 2020). Furthermore, the contents of Na_2O and MgO of tephra patch at the depth of 1.51-1.53 m are different from N1, N2, N3 and N4 scoria layers from 6 cent. to 9 cent.(Kawanabe, 2012) at Izu-Oshima and Fuji Hoei scoria (AD1707). Therefore, the origin of scoria grains in tephra patch at the depth of 1.51-1.53 m is presumed as basaltic magma of Niijima volcano. According to Kobayashi et al. (2020), Niijima Kudamaki/Atsuchi

©2021. Japan Geoscience Union. All Right Reserved.

event started from eruptions of basaltic magma, and changed to eruption of rhyolitic magma. So, tephra patch at the depth of 1.51-1.53 m is likely correlated to tephra of Niijima Kudamaki/Atsuchi event.

References: Aoki et al. (2019a), JpGU2019, HQR05-05, Aoki et al. (2019b), JpGU2019, SVC38-P21, Aoki, K. (2020), Arai (1962), Aramaki et al., (1993), Kawanabe (2012), Kobayashi et al.(2020) , Takahashi, M., et al.(2003), Takahashi, M., et al. (2018), Takahashi, T., et al. (2020), Tsuchiya et al. (2009)

Keywords: tephrostratigraphy, Izu islands, marine sediment

©2021. Japan Geoscience Union. All Right Reserved.

Caldera structure and formation at Atosanupuri and Akaigawa, Hokkaido, northern Japan: A comparison of analogue sandbox experiments and field data

*Ryuhei Sanjo[1]

1. Institute of Geography, Graduate School of Science, Tohoku University

Calderas are volcanic depressions that are induced by inflation or deflation of magma chambers beneath volcanic edifices and are common features in volcanic areas. Various field data have been used to investigate caldera structure and to understand processes of its formation. Calderas are generally several km or more in diameter and the depth of magma chambers is often estimated over 10 km from the earth’s surface, whereas only a few caldera–forming eruptions have been observed scientifically because they are infrequent phenomena. Therefore, it is still controversial how the deeper structure of calderas is and how this is formed, because of these spatiotemporal problems. To overcome previously mentioned spatiotemporal obstacles, various analogue sandbox experiments have been carried out. The knowledge gained from sandbox experiments help us infer the inner structure of calderas and its processes of development. Analogue sandbox experiments generally attempt to simplify phenomena and structures in nature. Yet, natural calderas are under complex conditions (*e.g.*, topography, geological features, stress field). Hence, this study verifies whether sandbox experiments can simulate caldera structures and their development processes within different conditions or not, by comparing field data and results from sandbox experiments. Atosanupuri and Akaigawa that are under different condition each other are chosen as subject areas.

Atosanupuri Caldera is located in the center of Kutcharo Caldera, eastern Hokkaido, northern Japan. According to previous studies, Kutcharo Caldera was formed between 40 and 30 ka, whereas Atosanupuri Caldera was developed approximately 20 ka. Atosanupuri Caldera has L–shaped somma, and its diameter is about 3 km. Lacustrine terraces are developed around Kutcharo Lake, which is the caldera lake of Kutcharo, and remarkable uplift of these terraces is detected on the near part of Atosanupuri Caldera. On the other hand, the significant uplift of the basement and lacustrine deposits around Atosanupuri Caldera is also inferred by drilling surveys. Based on these field data, inflation of a magma chamber beneath Atosanupuri Caldera accompanied by uplift of earth’s surface is assumed. Accordingly, calderas induced by inflation of magma chambers are experimentally simulated in this section. The mixture of dry quartz sand and wheat flour is used as analogue upper crust, and columnar foamed polystyrene is employed as analogue magma chamber. The scale of models is 10^{-5}. When the initial depth of the magma chamber analogue is between 17.5 and 21 cm, a caldera whose diameters is about 3 cm is formed. Both the depth of magma chamber analogue and the size of experimental calderas and those of Atosanupuri Caldera are similar to each other. Thus Atosanupuri Caldera is quantitatively reproduced by sandbox experiments. In other words, analogue sandbox experiments are applicable to natural calderas within the conditions on Atosanupuri Caldera.

Akaigawa caldera is located at the southwestern Hokkaido, and is surrounded by the circular mountain range, which is called Yoichigawa Caldera. Akaigawa caldera is thought to have been formed between 2.0 and 1.6 Ma. The caldera is bounded by the subcircular lineament which is 4 km in diameter, and an uplift of basement is not confirmed by field data. They suggest that Akaigawa Caldera was induced by deflation of the magma chamber underlying the caldera. Thereupon a sandbox experiment that simulate deflation of magma chambers is carried out in this section. The scale, apparatus, and material are same as the previous section. Subcircular or circular calderas are reproduced by deflation of the magma chamber

©2021. Japan Geoscience Union. All Right Reserved.

analogue. However, all calderas reproduced in this section are smaller in diameter than scaled Akaigawa Caldera. The caldera may have been influenced by the pre–existing structure, namely, Yoichigawa Caldera. Further field data and analogue experiments are required to verify this hypothesis.

Keywords: Caldera, Analogue experiments, Atosanupuri Caldera, Akaigawa Caldera

©2021. Japan Geoscience Union. All Right Reserved.

Current state evaluation and long-term prediction of volcanic activity based on historical tracking of volcanic ash deposits at Suwanosejima volcano

*Taketo Shimano[1], Atsushi Yasuda[2], Masato Iguchi[3]

1. Graduate School of Environment and Disaster Research, Tokoha University, 2. Earthquake Research Institute, University of Tokyo, 3. Sakurajima Volcano Research Center, Disaster Prevention Research Institute, Kyoto University

It would be one of the largest interests for geologists engaged in eruption prediction whether or not the deposits of ancient eruption provide any informative sign or precursor for the next serious eruption. Suwanosejima volcano is one of the most active volcanoes in Japan, and continuously releases volcanic ash. Previous studies on the stratigraphy have revealed that this volcano has been active almost continuously for about 4000 years with thick ashy deposit. On the other hand, during this period, sub-Plinian-scale eruptions that settled thick scoria layers have occurred every several hundred to one thousand years (Shimano et al., 2013). Regarding the long-term activity transition and disaster mitigation, we should understand the cause of such bimodality in eruptive activity and the mechanism of transition toward vigorous eruption (eg. VEI >4). It is because similar transition is commonly reported in geological time scale from many active volcanoes that release volcanic ash for a long period of time. It thus would be worth accumulating time-sequence of such long-term record in detail by ancient activity, and comparing with that of current activity. Then, if any sign of larger scale eruption could be obtained in advance during ash eruption period, which is relatively less active, it would surely reduce disasters caused by larger eruptions.
In this study, we report the characteristics of the volcanic ash that erupted during an activation from the end of 2020 up to date, and compare with that of the ejecta over the past 20 years based on systematic petrological analysis of time-series samples. Then, we interpret this time sequence of eruptive products based on the comparison with ash layers leading up to the latest sub-Plinian eruption of the 1813 eruption. The matrix glass composition of the recent 20 years has been relatively similar, including the 2020-21 products, but minor changes are observed with crystallization at shallow depth, probably reflecting magma ascent rate leading to small temporal changes in eruption styles. On the contrary, the pattern of glass composition from the pre-1813 ash up to the climactic sub-plinian phase changes systematically with SiO2 decrease and MgO increase. In addition, MgO increases as a stepwise manner which is followed by K2O increase due to microlite crystallization at shallow depth. We interpret such temporal change in glass composition to reflect evolution of magmatic system as well as magma ascent. Current state of the volcanic activity of Suwanosejima is less active than that for urgent sub-Plinian activity, because there is no clear evidence of large or frequent input of mafic magma as a precursory sign.

Keywords: volcanic ash, magma plumbing system, Suwanosejima, mid- to long-term prediction

©2021. Japan Geoscience Union. All Right Reserved.

[J] Oral | S (Solid Earth Sciences)：S-VC Volcanology

Sat. Jun 5, 2021 10:45 AM - 11:30 AM JST | Sat. Jun 5, 2021 1:45 AM - 2:30 AM UTC | Ch.25 Zoom Room 25

[S-VC28] Active Volcanism

convener:Yuta Maeda(Nagoya University), Takahiro Miwa(National research institute for earth science and disaster prevention), Takeshi Matsushima(Institute of Seismology and Volcanology, Faculty of Science, Kyushu University), Chairperson:Urumu Tsunogai(Graduate School of Environmental Studies, Nagoya University), Takeshi Ohba(Department of chemistry, School of Science, Tokia University)

This session discusses various aspects of active volcanisms including, but not limited to, rec ent and historical eruptions, various phenomena associated with the volcanic activities, und erground structures of the volcanoes, and developments of new instruments based on geop hysical, geochemical, geological, and multidiscipline approaches. We also welcome studies o n understanding and predicting the transitions of the eruptive activities from observational, theoretical, and experimental approaches.

10:45 AM - 11:00 AM JST | 1:45 AM - 2:00 AM UTC

[SVC28-25] Behavior of magmatic components in fumarolic gases related to the 2018 phreatic eruption at Ebinokogen Ioyama volcano, Kirishima Volcanic Group, Kyushu, Japan

*Takeshi Ohba[1], Muga Yaguchi[2], Urumu Tsunogai[3], Masanori Ito[3], Ryo Shingubara[3] (1.Department of chemistry, School of Science, Tokia University, 2.Meteorol. Res. Inst., 3.Grad. School of Envir. Studies Nagoya University)

11:00 AM - 11:15 AM JST | 2:00 AM - 2:15 AM UTC

[SVC28-26] Time variation in the composition of volcanic gases at Mt Hakone (2018-2020)

*Seiya Toyoshima[1], Nozomi Numanami[1], Takeshi Ohba[1], Muga Yaguchi[2] (1.Tokai University, 2.Meteorological Research Institute, JMA)

11:15 AM - 11:30 AM JST | 2:15 AM - 2:30 AM UTC

[SVC28-27] **Development of an automatic volcanic plume sampler SelPS for UAS**

*Urumu Tsunogai[1], Ryo Shingubara[1], Masanori Ito[1], Yuhei Morishita[1], Fumiko Nakagawa[1], Shin Yoshikawa[2], Mitsuru Utsugi[2], Akihiko Yokoo[2] (1.Graduate School of Environmental Studies, Nagoya University, 2.Graduate School of Science, Kyoto University)

Behavior of magmatic components in fumarolic gases related to the 2018 phreatic eruption at Ebinokogen Ioyama volcano, Kirishima Volcanic Group, Kyushu, Japan

*Takeshi Ohba[1], Muga Yaguchi[2], Urumu Tsunogai[3], Masanori Ito[3], Ryo Shingubara[3]

1. Department of chemistry, School of Science, Tokia University, 2. Meteorol. Res. Inst., 3. Grad. School of Envir. Studies Nagoya University

Direct sampling and analysis of volcanic gas was conducted at three fumaroles on Ebinokogen Ioyama volcano, Japan, between December 2015 and July 2020. Notable changes in the chemical composition of gases related to volcanic activity included a sharp increase in SO2 and H2 concentrations in May 2017 and March 2018. The analyses in March 2018 immediately preceded the April 2018 eruption at Ioyama volcano. The isotopic ratios of H2O in fumarolic gas suggested the formation of fumarolic gas. Up to 49% high enthalpy magmatic vapor mixed with 51% of cold local meteoric water to generate coexisting vapor and liquid phases at 100-160C. Portions of the vapor and liquid phases were discharged as fumarolic gases and hot spring water. The CO2/SO2 ratio of the fumarolic gas was higher than that previously estimated for magmatic vapor due to SO2 hydrolysis during the formation of the vapor phase. When the flux of the magmatic vapor was high, effects of hydrolysis were small resulting in low CO2/SO2 ratios in fumarolic gases. The high apparent equilibrium temperature (AETS) defined for reactions involving SO2, H2S, H2 and H2O, together with low CO2/SO2 and H2S/SO2 ratios were regarded to be precursor signals of fumarolic gas prior to the phreatic eruption at Ioyama volcano. The apparent equilibrium temperature (AETD) obtained from the hydrogen isotope ratio of H2O and H2 also increased significantly in May 2017 and March 2018, but there were cases where the changes did not coordinate between the fumaroles. For example, AETD of one fumarole increased, but AETD of another fumarole decreased at the same time. The distance between fumaroles is at most 200 m, and it is estimated that AETD is influenced by the phenomenon occurring in the shallow underground. AETS increased rapidly in May 2017 and March 2018 suggesting an increased flux of magmatic vapor. Between September 2017 and January 2018, AETS was low suggesting the suppression of magmatic vapor flux. During this period, magmatic eruptions took place at Shinmoedake volcano 5 km away from Ioyama volcano. We conclude that magma sealing and transport to Shinmoedake volcano occurred simultaneously in the magma chamber beneath Ioyama volcano.

Keywords: Phreatic eruption, Volcanic gas, SO2

©2021. Japan Geoscience Union. All Right Reserved.

Time variation in the composition of volcanic gases at Mt Hakone (2018-2020)

*Seiya Toyoshima[1], Nozomi Numanami[1], Takeshi Ohba[1], Muga Yaguchi[2]

1. Tokai University, 2. Meteorological Research Institute, JMA

Mt. Hakone is an active volcano located in the western part of Kanagawa prefecture. Earthquake swarms began at the end of April 2015, and a small phreatic eruption occurred on June 29. After that, earthquake swarms occurred again in May 2019. Even now, volcanic gas is actively discharged from fumaroles in Owakudani geothermal area. In this study, we consider the volcanic activity of Mt. Hakone after 2018 based on the changes in the chemical composition of volcanic gas.

Volcanic gases were collected at three fumaroles in Owakudani (N, C) and Kamiyuba (S) once a month. The fumarole C was formed during a phreatic eruption in 2015. The chemical composition of C is similar to the steam composition of the adjacent No. 52 steam well with depth of 500 m, suggesting that the fumarole of C is representative of gas around 500 m beneath surface (Ohba et al, 2019). Titanium pipe was inserted into the fumarole to collect volcanic gas, and the interstice between the tube and the outlet of fumarole was closed with soil to prevent air contamination. Titanium pipe was connected to a rubber tube, and volcanic gas was collected by an absorption tube containing a mixed solution of potassium iodate and potassium iodide, and vacuum glass bottle containing potassium hydroxide. The composition of the collected volcanic gas was analyzed using gravimetric analysis for H2S and SO2, microdiffusion analysis for CO2, and gas chromatography for other components.

The CO2/H2S molar ratios at all points increased in harmony with the increase in the number of earthquakes observed by the Japan Meteorological Agency, peaking in August 2019. After that, it decreased at N and C, but the CO2/H2S molar ratio of S did not decrease, which increased slightly after the swarm earthquake. The SO2/H2S molar ratio increased at C to a peak in August 2019 and then decreased. In the SO2-CO2-H2S ternary diagram (Stix and de Moor, 2018), the positions of the three points were significantly different. N and S were distributed near the edge connecting the CO2 and H2S vertex because of the scarcity of SO2. Since C contains relatively high concentrations of SO2, it deviated from the edge connecting the CO2 and H2S vertices and was distributed on the line with CO2/SO2 molar ratio of about 5. N and S moved slightly toward the H2S vertex overall in 2018, but moved toward the CO2 vertex from January to August 2019, and then back toward the H2S vertex. C moved away from the H2S vertex along the line with CO2/SO2 molar ratio of about 5 from January to August 2019, and then back toward the H2S vertex.

From the variation of CO2/H2S and SO2/H2S molar ratios, it is estimated that the magmatic gas supply to the hydrothermal system of Mt. Hakone peaked in August 2019. This variation was in harmony with the increase and decrease in the number of earthquakes. After that, the activity was quieted down. Since the positions of N, S and C are significantly different in the ternary diagram, it is suggested that the process from the generation process of volcanic gas is significantly different. Fumarole C is considered to have a large magmatic contribution than other points because of the large variation in the CO2/H2S and SO2/H2S molar ratios and the high concentration of SO2. Fumarole S was distributed in the direction to the CO2 vertex compared to the other two points. The relatively small variation in the CO2/H2S ratio and the enrichment in CO2 suggest that the sulfur component of S was removed during its passage through the shallow aquifer and became relatively rich in CO2.

©2021. Japan Geoscience Union. All Right Reserved.

References

Ohba T, Yaguchi M, Nishino K, Numanami N, Daita Y, Sukigara C, Ito M, Tsunogai U (2019) Earth, Planets and Space, doi.org/10.1186/s40623-019-1027-5

Stix J, de Moor J M (2018) Earth Planets Space, doi.org/10.1186/s40623-018-0855-z

Keywords: Mt. Hakone, Volcanic gas, Phreatic eruption

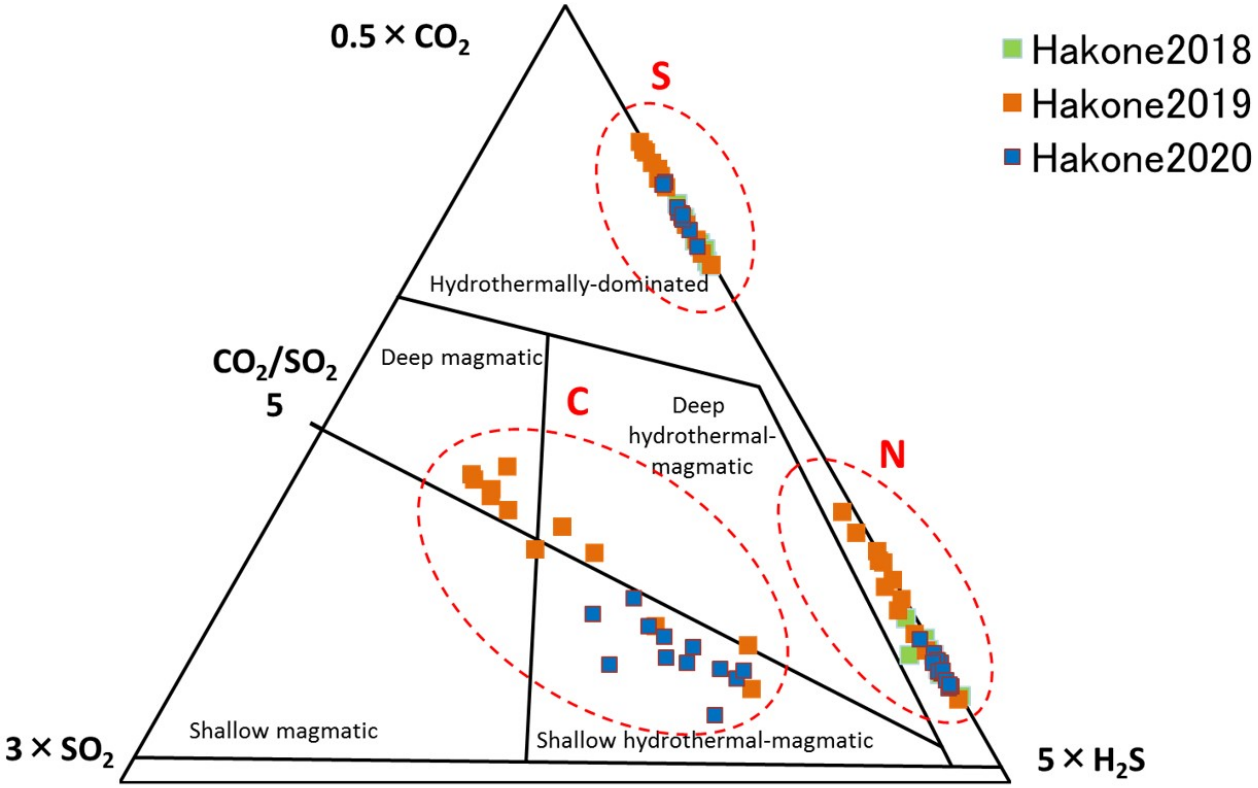


Fig.1
SO2-CO2-H2S ternary diagram for April 2018 to December 2020. Areas showing the origin of each volcanic gas component in the figure are based on Stix and de Moor (2018).

©2021. Japan Geoscience Union. All Right Reserved.

Development of an automatic volcanic plume sampler SelPS for UAS

*Urumu Tsunogai[1], Ryo Shingubara[1], Masanori Ito[1], Yuhei Morishita[1], Fumiko Nakagawa[1], Shin Yoshikawa[2], Mitsuru Utsugi[2], Akihiko Yokoo[2]

1. Graduate School of Environmental Studies, Nagoya University, 2. Graduate School of Science, Kyoto University

Both chemical and isotopic compositions of volcanic plumes are highly useful in evaluating the present status of active volcanoes. Monitoring their temporal changes can facilitate the forecasts of volcanic activity as well. In the present study, we developed a drone-borne automatic sampler for volcanic plumes in which an output signal from a sulfur dioxide (SO_2) sensor triggered a pump to collect samples when its SO_2 concentration exceeded a predefined threshold. We fitted the sampler on a drone at Nakadake central cone, Aso volcano, Japan, where only the crater rim was accessible.

In the sampling campaign done on October 2020, good consistency in isotope ratios ($^2H/^1H$) of molecular hydrogen (H_2) between samples collected by the automatic sampler and those collected directly into pre-evacuated flasks was obtained. Furthermore, by using the drone-borne sampler at Aso volcano, we obtained plume samples with much higher concentrations of H_2 and carbon dioxide (CO_2) than those taken directly into flasks at the crater rim. Our sampler can be utilized to collect volcanic plume samples for the determination of stable isotopic compositions in general by subsequent laboratory analysis and the remote establishment of fumarole outlet temperature based on the $^2H/^1H$ ratios of hydrogen, including their temporal changes. This study was supported by MEXT Integrated Program for Next Generation Volcano Research and Human Resource Development (Theme B).

Keywords: fumarolic gases, volcanic plume, carbon dioxide, Unoccupied Aerial Systems, automatic volcanic plume sampler

©2021. Japan Geoscience Union. All Right Reserved.

[J] Poster | S (Solid Earth Sciences)：S-VC Volcanology

Sat. Jun 5, 2021 5:15 PM - 6:30 PM JST | Sat. Jun 5, 2021 8:15 AM - 9:30 AM UTC | Ch.16_1

[S-VC28] Active Volcanism

convener:Yuta Maeda(Nagoya University), Takahiro Miwa(National research institute for earth science and disaster prevention), Takeshi Matsushima(Institute of Seismology and Volcanology, Faculty of Science, Kyushu University)

This session discusses various aspects of active volcanisms including, but not limited to, rec ent and historical eruptions, various phenomena associated with the volcanic activities, und erground structures of the volcanoes, and developments of new instruments based on geop hysical, geochemical, geological, and multidiscipline approaches. We also welcome studies o n understanding and predicting the transitions of the eruptive activities from observational, theoretical, and experimental approaches.

[SVC28-P01] Local deformation at Mt.Tokachi detected by TS-InSAR

*Satoshi Okuyama[1], Shinobu Ando[1] (1.Meteorological Research Institute)

[SVC28-P02] Volcanic tremor source location at Tokachidake volcano from cross-correlation analysis of 2018-2020 seismic data

*Theodorus Permana[1], Hiroshi Aoyama[1] (1.Institute of Seismology and Volcanology, Faculty of Science, Hokkaido University.)

[SVC28-P03] Time-series of crustal deformation on Azuma volcano revealed by PALSAR-2 data

*Yuji Himematsu[1], Taku Ozawa[1] (1.National Research Institute for Earth Science and Disaster Resilience)

[SVC28-P04] Existence of deep pressure sources and its behaviors during recent volcanic activity at Azumayama, NE Japan

*Jun Okada[1], Yu Nihara[2], Yuji Miyagawa[3], Susumu Seki[3], Takuya Yamamura[2], Shin Chikasawa[3] (1.Volcanology Research Department, Meteorological Research Institute - Japan Meteorological Agency, 2.Regional Volcanic Observation and Warning Center, Sendai Regional Headquarters - Japan Meteorological Agency, 3.Seismology and Volcanology Division, Sendai Regional Headquarters - Japan Meteorological Agency)

[SVC28-P05] Amorphous silica coating on flank deposits of the 1783 CE (Tenmei) eruption at Asama volcano

*Takayuki Nakatani[1], Sarina Sugaya[2], Maya Yasui[3], Satoshi Okumura[2], Michihiko Nakamura[2] (1.Geological Survey of Japan, National Institute of Advanced Industrial Science and Technology, 2.Department of Earth Science, Graduate School of Science, Tohoku University, 3.Department of Earth and Environmental Sciences, College of Humanities and Sciences, Nihon University,)

[SVC28-P06] **Monitoring of underground temperature in Jigokudani, Midagahara volcano using LPWA devices**

*Tohru Watanabe[1] (1.Faculty of Sustainable Design, University of Toyama)

[SVC28-P07] Formation of N_3 member from the younger Ō-shima group distributed around the Habu area, southeastern part of Izu-Ō-shima Island.

*Ryota Uchiyama[1], Izumi Sakamoto[1] (1.School of Marine and Technology, Tokai University)

[SVC28-P08] Banded Tremors Activity at Miyakejima Volcano

*Yoshihiro Otsuka[1], Shinya Nagato[1] (1.Japan Meteorological Agency)

[SVC28-P09] Estimating the underground pressure source of Miyakejima volcano by integrated processing of GNSS and leveling data

*Haruna Watanabe[1], Takeshi Matsushima[2], Miyo Fukui, Atsushi Watanabe[3], Jun Oikawa[3], Takashi OKUDA[4], Taku Ozawa[5], Yosuke Miyagi[5] (1.Department of Earth and Planetary Sciences, Graduate School of Science, Kyushu University, 2.Institute of Seismology and Volcanology, Faculty of Sciences, Kyushu University, 3.Earthquake Research Institute, University of Tokyo, 4.Earthquake and Volcanology Research Center, 5.National Research Institute for Earth Science and Disaster Resilience)

[SVC28-P10] Three-Dimensional Crustal Structure beneath Hachijojima Island using dense seismic observation data

*Shotaro Kanke[1], Hiroyuki Azuma[1], Yoshiya Oda[1] (1.Tokyo Metropolitan Univ.)

[SVC28-P11] Ground deformation between eruptions at Nishinoshima Island using InSAR time series analysis

*Shinobu Ando[1], Satoshi Okuyama[1] (1.Volcanology Research Department, Meteorological Research Institute)

[SVC28-P12] Abrupt change in eruption style during the 2019-2020 eruption of Nishinoshima, Ogasawara

*Fukashi Maeno[1], Takayuki Kaneko[1], Natsumi Hokanishi[1], ATSUSHI YASUDA[1], Yoshihiko Tamura[2] (1.Earthquake Research Institute, University of Tokyo, 2.Japan Agency for Marine-Earth Science and Technology)

[SVC28-P13] The depth of the air-magma interface and the sound velocity in the shallow conduit of Aso volcano inferred from seismic and infrasound signals

*Kyoka Ishii[1], Akihiko Yokoo[1] (1.Graduate School of Science, Kyoto University)

[SVC28-P14] Estimation of source location of high-frequency tremor at Aso volcano by array analysis

*hirotaka tanaka[1], Takahiro Ohkura[2], Hiroyuki Inoue[2], Shin Yoshikawa[2] (1.kyoto university, 2.Aso Volcanological Laboratory)

[SVC28-P15] Debris avalanche deposits and the stratigraphy on the outcrop to north east from Mt.Unzen

*Daisuke Nagai[1] (1.Mt.Unzen disaster memorial hall)

[SVC28-P16] Vault-housed extensometers and tiltmeters recorded continuous crustal movement during the eruption of Kirishima Shinmoe-dake in 2018

*Koki Yoshinaga[1], Takeshi Matsushima[2], Hiroshi Shimizu[2], Yusuke Yamashita[3], Shintaro Komatsu[3], Ken'ichi Yamazaki[3] (1.Department of Earth and Planetary Sciences, Graduate School of Science, Kyushu University, 2.Institute of Seismology and Volcanology, Faculty of Sciences, Kyushu University, 3.Miyazaki Observatory, Disaster Prevention Research Institute, Kyoto University)

[SVC28-P17] Two experiments using a small-aperture infrasonic array at Kirishima

*Kazuya Yamakawa[1], Mie Ichihara[1], Dan Muramatsu[2], Takeshi Matsushima[2], Ruka Wada[3], Hideki Takahashi[3], Isao Shimoyama[4] (1.Earthquake Research Institute, University of Tokyo, 2.Institute of Seismology and Volcanology, Faculty of Science, Kyushu University, 3.Department of Mechanical Engineering, Faculty of Science and Technology, Keio University, 4.Department of Intelligent Robotics, Toyama Prefectural University)

[SVC28-P18] Estimating the source of volcanic earthquakes during eruption events at Kirishima Volcanos, in 2018, using spatial distribution of earthquake amplitude.

*Daiki Goshima[1], Satoshi Matsumoto[2], Ayaho Mitsuoka[1], Yuhei Yuasa[4], Yuta Kawamura[1], Mie Ichihara[3] (1.Department of Earth and Planetary Sciences, Graduate School of Science, Kyushu University,

2.Institute of Seismology and Volcanology, Faculty of Sciences, Kyushu University, 3.Earthquake Research Institute, University of Tokyo, 4.Osaka Regional Headquarters, Japan Meteorological Agency)

[SVC28-P19] S-wave attenuation structure of Mt.Kirishima estimated using coda of S-wave

*Takuji Watanabe[1], Ayaho Mitsuoka[1], Yuhei Yuasa[1], Yuta Kawamura[1], Daiki Goshima[1], Satoshi Matsumoto[2], Mie Ichihara[3] (1.Department of Earth and Planetary Sciences, Graduate School of Science, Kyushu University, 2.Institute of seismology and Volcanology, Faculty of Sciences, Kyushu University, 3.Earthquake Research Institute, University of Tokyo)

[SVC28-P20] Estimate of magma supply beneath Aira caldera during the last 10 years based on ground deformation observation and amount of volcanic ejecta

*Daisuke Miki[1], Tomoki Tsutsui[1], Masato Iguchi[1] (1.Sakurajima Volcano Research Center, Disaster Prevention Research Institute, Kyoto University)

[SVC28-P21] Temporal changes of seismic velocities and scattering properties at Suwanosejima volcano inferred from seismic interferometry

*Takashi Hirose[1], Hideki Ueda[1], Eisuke Fujita[1] (1.National Research Institute for Earth Science and Disaster Resilience)

[SVC28-P22] Development of volcano deformation calculation system using boundary element method (2)

*Ryohei Kawaguchi[1] (1.Meteorological Research Institute)

[SVC28-P23] Estimation of seismic scattering coefficients at active volcanoes

*Mare Yamamoto[1] (1.Research Center for Prediction of Earthquakes and Volcanic Eruptions, Graduate School of Science, Tohoku University)

[SVC28-P24] Temporal Change in Coda-Q at the upper East Rift Zone of Kīlauea volcano, Island of Hawai‘i

*Takuji Yamada[1], Paul G Okubo[2] (1.Faculty of Science, Graduate School of Science and Technology, Ibaraki University, 2.University of Hawai‘i at Mānoa)

[SVC28-P25] A prototype of advanced Multi-GAS for unmanned aircraft systems

*Masaaki Morita[1], Toshiya Mori[2] (1.Geological Survey of Japan, AIST, 2.Graduate School of Science, The University of Tokyo)

Local deformation at Mt.Tokachi detected by TS-InSAR

*Satoshi Okuyama[1], Shinobu Ando[1]

1. Meteorological Research Institute

Introduction

Mt.Tokachi is one of the most active volcanoes in Hokkaido, Japan. Its notable eruptions took place around every 30 years; in 1926, 1962 and 1988-89 (4th edition of National Catalogue of the Active Volcanoes in Japan). 32 years have passed since the last eruption, which implies that Mt.Tokachi is at a preparation stage for the next eruption.

GNSS observation revealed the local inflation since 2006, and as much as 10cm of displacement is observed at Mae-Tokachi GNSS station established by Geological Survey of Hokkaido. After that, inflation slowdowned in 2017, then turned to deflation in 2018.

We have been monitoring the activity of Mt.Tokachi through SAR interferometry and reported about the deformation at western flank (Okuyama et al., 2019). In this presentation, we report the result of time-series analysis using GIAnT (Agram et al., 2012).

Data and Method

We composed 58 pairs of path 122 (Ascending, Right-looking), path 17 (Descending, Right-looking) and path 18 (Descending, Right-looking) observed by ALOS-2/PALSAR-2. We could not collect large number of SAR images due to low observation frequency and the fact that the target area is covered by snow for more than 6 months. Hence, to increase the number of pairs, we regard path 17 and 18, whose incidence angles differ by about 10 decimal degrees, as same path of which incidence angle is the average of those. We applied NSBAS method to those pairs to detect time evolution of the deformation, linearly interpolated between observation dates, then calculated two-dimensional displacement.

Result

The result timeseries show two main characteristics –upheaval around Furikozawa fumaroles and complex deformation at the slope located at the west of Mae-Tokachi. The former turns into subsidence in late 2017, then became stagnant after 2018. This trend is same as the displacement observed at Mae-Tokachi GNSS station. The latter, on the other hand, shows partial correspondence with the topography, which implies the effect of landslide. However, as we reported in Okuyama et al. (2019), the pattern includes local upheaval, which cannot be explained by the landslide. Unlike the deformation around Furikozawa fumaroles, these deformation progress at a uniform rate.

Acknowledgement

PALSAR-2 SLC data are shared among PIXEL (PALSAR Interferometry Consortium to Study our Evolving Land surface), and provided from JAXA under a cooperative research contract with ERI, Univ., Tokyo. The ownership of PALSAR-2 data belongs to JAXA. We used RINC (Ozawa et al., 2016) and Fundamental Geospatial Data (Elevation) published by GSI for interferogram processing. We used GSI tile for displaying displacement map.

©2021. Japan Geoscience Union. All Right Reserved.

Keywords: Mt.Tokachi, SAR Interferometry, Crustal Deformation

©2021. Japan Geoscience Union. All Right Reserved.

Volcanic tremor source location at Tokachidake volcano from cross-correlation analysis of 2018-2020 seismic data

*Theodorus Permana[1], Hiroshi Aoyama[1]

1. Institute of Seismology and Volcanology, Faculty of Science, Hokkaido University.

Volcanic tremors are known to be related to the processes that involve the movement of magma and gas within a volcano. During the 1988-1989 eruptive activity at Tokachidake volcano, Hokkaido, Japan, volcanic tremors were observed accompanying explosive eruptions. Volcanic tremors were sometimes associated with other phenomena such as low-frequency earthquakes and tilt changes. Considering that past major eruptive activities have occurred with an interval of a few tens of years, and the risk the volcano imposed on the surrounding inhabited areas, monitoring of volcanic tremors is important among other phenomena that could provide us with insights into the ongoing volcanic activity at Tokachidake. However, volcanic tremors are challenging to locate due to their complex seismic waveforms showing unclear onset of seismic phases. We use cross-correlation analysis of seismic data that measures the travel time differences between seismic stations and avoid picking the arrival time of seismic phases. We compute stacked cross-correlation functions and find the most probable source location using a grid-search scheme. We analyzed tremors that occurred during 2018-2020, mainly those who are reported by the Japan Meteorological Agency (JMA). Specifically, we determine the source location of every 1-minute seismic data in WIN format used in Japanese monitoring system and focus on 1-minute data that contain volcanic tremors. We find that tremor source locations are located beneath the northwest flank of Tokachidake and the 62-II and Taisho craters at shallow depths of about 0.5 km from the ground surface. The distribution area of volcanic tremor sources is generally consistent with that of the hypocenter of volcanic earthquakes. We also show the possibility to detect more tremors at Tokachidake by measuring the spatial coherency of seismic signals. Our results show that the seismic correlation-based volcanic tremor location method is applicable at Tokachidake and could be used together with other monitoring techniques to gain insights into volcanic activity.

Keywords: volcanic tremor, seismic data, cross-correlation, volcano monitoring, Tokachidake

©2021. Japan Geoscience Union. All Right Reserved.

Time-series of crustal deformation on Azuma volcano revealed by PALSAR-2 data

*Yuji Himematsu[1], Taku Ozawa[1]

1. National Research Institute for Earth Science and Disaster Resilience

Azuma volcano is an active volcanic complex in central Japan and comprises pyroclastic cones and/or volcanic craters aligning in the northwest-southeast direction. Several previous papers have reported increases of the volcanic earthquake and uplifts around Oana crater, one of the most active craters of the Azuma volcano in 2015 and 2018-2019, and sulfur combustion in 2020.

We applied multi-temporal InSAR analysis of ALOS-2/PALSAR-2 data observed in 2014-2020 for investigating the time-series of crustal deformation of the Azuma volcano. We report the spatiotemporal variety of line-of-sight (LOS) changes on Azuma volcano during 2014-2020 using PALSAR-2 data, which were acquired from both right-looking ascending and descending orbits.

Time-series of both ascending and descending LOS changes on Oana crater shows peaks of LOS shortening in 2015 and 2019, implying intermittent uplift. It takes about a year to reach the peak of LOS shortening, while about two years to reach zero for the 2015 LOS shortening. The northwest-southeast cross-section of the ascending LOS change revealed a peak of LOS shortening in 2015 on the northern rim of Oana crater and that in 2019 on the point of 200 m away from Oana crater for the northwest direction. We expect that the observed crustal deformation in Oana crater was driven by pressure change of the shallow hydrothermal system because the spatial extent of LOS changes is consistent with that of ground thermal activity and active fumaroles with steam/volcanic gas emission.
Acknowledgment: ALOS-2/PALSAR-2 data in this study are sharing among the PIXEL consortium, and are provided from JAXA under a cooperative research contract with ERI, the University of Tokyo.

Keywords: SAR, Crustal deformation, Azuma volcano

©2021. Japan Geoscience Union. All Right Reserved.

Existence of deep pressure sources and its behaviors during recent volcanic activity at Azumayama, NE Japan

*Jun Okada[1], Yu Nihara[2], Yuji Miyagawa[3], Susumu Seki[3], Takuya Yamamura[2], Shin Chikasawa[3]

1. Volcanology Research Department, Meteorological Research Institute - Japan Meteorological Agency, 2. Regional Volcanic Observation and Warning Center, Sendai Regional Headquarters - Japan Meteorological Agency, 3. Seismology and Volcanology Division, Sendai Regional Headquarters - Japan Meteorological Agency

Recent volcanic activity of Azuma volcano, NE Japan is characterized by the repetitive unrests where the shallow seismic activities coincide with ground deformation attributed to the various depths. In the volcanic activities of 2014-2015 and 2018-2019, there are two types of ground deformation such as (1) months-long inflation at both shallow and deep parts and (2) short-term shallow inflation and deep deflation during the volcanic tremors (Okada *et al*., 2019, JpGU). This indicates that both shallow and deep parts beneath the volcano are related each other. Regarding (2), the shallow inflation preceded the deep deflation at least for the 2018-2019. The recent studies of Tohoku University (2019) and Seki *et al*. (2020) pointed out long-period events with the frequency lower than 0.1 Hz exist during the above-mentioned short-term deformation. Their results show the shallow volcanic activities might have affected the deeper parts. The existence of deep inflation sources (BSL 3-4km and/or more) is suggested by Seki *et al*. (2020) in order to explain the entire activity of the 2018-2019. Similar deep inflation episode exists during 2003-2004, 2006-2007 and 2014-2015, and all these cases resulted in volcanic unrests with intense seismic activities beneath Oana crater. However, the volcanic episodes of the 2008-2012 and the March-October 2020 seem exceptional. The former episode misses a clear deep inflation but shows the significant thermal activity on the surface. The latter episode shows deep inflation but does not lead any clear volcanic unrests hitherto (February 2021). Different behaviors of deep pressure sources may address the feasibility of magma ascent/supply from the depth and provide important constraints on the changeable condition of the shallow hydrothermal system such as wet/dry environments or with/without sealing of the preexisting conduits/vents.

Reference:
1. Okada *et al*. (2019) Ground deformation associated with the 2014-2015 and the 2018-2019 volcanic activities at Azumayama. SVC38-P02, Japan Geoscience Union Meeting 2019.
2. Seki *et al*. (2020, accepted) Volcanic activity in 2018-2019 at Azumayama Volcano, Japan. Kenshin-Jiho, 35pp.
3. Tohoku University (2019) Seismic activity of Azumayama, Report of the 144th Coordinating Committee for Prediction of Volcanic Eruption (No. 5) additional material, 9-10.

Keywords: Azumayama, GNSS, deformation, deep pressure sources, magma resorvoirs

©2021. Japan Geoscience Union. All Right Reserved.

Amorphous silica coating on flank deposits of the 1783 CE (Tenmei) eruption at Asama volcano

*Takayuki Nakatani[1], Sarina Sugaya[2], Maya Yasui[3], Satoshi Okumura[2], Michihiko Nakamura[2]

1. Geological Survey of Japan, National Institute of Advanced Industrial Science and Technology, 2. Department of Earth Science, Graduate School of Science, Tohoku University, 3. Department of Earth and Environmental Sciences, College of Humanities and Sciences, Nihon University,

Recently, rock coatings have attracted attention in the broader field of geosciences because of their potential to record the changes in their immediate environment. Despite the potential for silica-rich rock coatings to evaluate past volcanic activity and its impacts on the surface environment, detailed reports on the silica-rich rock coatings at the proximal area are still rare, and its occurrence and formation processes are not fully understood. In this study, we report the amorphous silica-rich coating on the juvenile volcanic lapilli and blocks of the 1783 CE (Tenmei) pyroclastic flow deposits 1.9–3.6 km northeast of the Maekake crater of Asama volcano in Central Japan. These coatings are up to 660 μm in thickness and composed of fine-grained volcanic ash particles with silica-rich cement. Raman spectroscopic measurements showed that the interstitial silica-rich phase is hydrous amorphous silica and is considered to be a reaction product of ash particles with acidic volcanic rain and fog like volcanic smog (vog) as it has been recorded in Hawaii. The formation of amorphous silica without jarosite and the preferential alteration of plagioclase compared with pyroxene indicate that the reaction occurred with a sulfuric acid solution of pH < ~3. The dissolution of sintered volcanic ash and the resultant precipitation of amorphous silica would have been facilitated by the porous structure and large surface area of the ash layer. The thickness of the coating and degree of alteration in the plagioclase phenocrysts adjacent to the coating tend to decrease with an increase in distance from the volcanic crater, which is consistent with the absence of fumarolic areas in the flank. Since 1783 CE, the Asama-Maekake volcano has repeated Vulcanian and phreatic eruptions, especially in the first half of the 20th century. The amorphous silica coating recognized in this study is assumed to have formed mainly during this period, which can thus be an indicator of the acidity and distribution of past acidic volcanic rain and fog.

Keywords: Rock coating, Amorphous silica, Acid rain, Vog, Asama volcano

©2021. Japan Geoscience Union. All Right Reserved.

Monitoring of underground temperature in Jigokudani, Midagahara volcano using LPWA devices

*Tohru Watanabe[1]

1. Faculty of Sustainable Design, University of Toyama

Jigokudani is an active geothermal area in Midagahara volcano, Toyama prefecture, central Japan. It was formed as a result of repeated phreatic eruptions over 40,000 years. Increased volcanic activity in this area has been observed since 2011. In order to detect a precursory signal of a phreatic eruption, observations should be conducted on seismicity, ground deformation, geothermal activity, volcanic gas, etc. A monitoring system of underground temperature using LPWA (Low Power, Wide Area) devices has been tested since 2018. LPWA devices (netvox, R718CX2) for measuring underground temperature were deployed at 8 points in Jigokudani. One device has two thermocouples at the depths of 10 and 50 cm. Underground temperature is sent every 30 minutes to a gateway to the internet situated in Hotel Tateyama. Short-period (~10 hours) variations in temperature are remarkable at 10 cm, while quite weak at 50 cm. Short-period variations come from the temporal change in the surface temperature. The heat flux can be estimated from temperatures at different depths. Jigokudani has heavy snow fall in winter. The operation of this system has been tested since October 2020. Temperature data can still be received at least until February 2021.

Keywords: Midagahara volcano, Jigokudani, underground temperature

©2021. Japan Geoscience Union. All Right Reserved.

Formation of N_3 member from the younger Ōshima group distributed around the Habu area, southeastern part of Izu-Ōshima Island.

*Ryota Uchiyama[1], Izumi Sakamoto[1]

1. School of Marine and Technology, Tokai University

Izu-Ōshima island is an active volcano located at the northernmost point of the Izu-Bonin Arc. In Izu-Ō shima Island, outcrops of lava and volcanic sediments flowing from eruptions of mainly low-alkaline tholeiite series basalts can be seen in many places. In this study, we describe the outcrops and lithology of the area from Habu Port to Ryuozaki in the southeastern part of Izu-Ōshima Island, and examine the activity patterns that formed the Habu Port and Ryuozaki area.

The volcanic ejecta exposed on the sea cliffs distributed from the Ryuozaki to the Habu area can be classified into the Ryuozaki Lava, the Ryuozaki layer, the Suribachi layer, the M layer, the Habu lava and the Habu breccia layer.

Based on the stratigraphic sequence of each layer and the characteristics of the rock fragments collected, it is considered that the activities from the northern part of Habu Port to the Ryuozaki area occurred in the following order: 1) eruption of the Ryuozaki lava, which is the basement rock, 2) formation of the Ryuozaki layer by magmatic steam explosion off Ryuozaki, 3) activities of the Suribachi layer and the M layer, 4) eruption of the Habu lava, and 5) magmatic steam explosion (formation of the Habu Conglomerate layer) caused by the contact of the Habu lava with seawater. 5) magma generated by the contact of Habu lava with seawater, and steam explosion (formation of the Habu breccia layer).

©2021. Japan Geoscience Union. All Right Reserved.

Banded Tremors Activity at Miyakejima Volcano

*Yoshihiro Otsuka[1], Shinya Nagato[1]

1. Japan Meteorological Agency

Introduction

Since the 2000 eruption, volcanic tremors (banded tremors) that occur intermittently in 2000-2006, 2011 (September-October) and 2015 (October-December) have been observed on Miyakejima Volcano. Banded tremors are characterized by volcanic tremors with a maximum duration of about 20 minutes and a predominant cycle of about 0.2 seconds, which occur repeatedly at intervals of about 30 minutes (some events exceed 1 hour). The maximum amplitude (maximum during in the Oyamahokutou) was 16 μm / s from 2000 to 2006, 30 μm / s in 2011, and 62 μm / s in 2015. We considered the relationship between the changes in the location of banded tremors since 2000 and volcanic activity.

Discussion

Otsuka et al. (2012) estimate that the location of banded tremors from 2000 to 2011 is about 2 km near the crater. Similarly, when estimating the location of occurrence in 2015, the depth near the crater was about 1 km. It is possible that these occur in shallower areas than before 2011 (Fig.1). Slightly low-frequency earthquakes (BH-type earthquakes) tend to be shallower than 2 km in 2004, shallower than 1.5 km in 2011, and shallower than 1 km in 2015. Low-frequency earthquakes (BL-type earthquakes) have a small number of events, but are often found shallower than 1.5 km.

In order to consider the occurrence of banded tremors, we divided the transition of volcanic activity into three periods from seismic activity and crustal deformation after the 2000 eruption. The period (1) "2000-2007", the banded tremors that had been observed since the start of the eruption disappeared after April 2006 as the thermal activity decreased. However, from around this time, the pressure source in the deep part turned to inflation. The period (2) "2008-2012", eruptions accompanied by BH-type and BL-type earthquakes were repeated until July 2010. The inflation of the deep part has continued since around 2006, but the deflation of the shallow part has been stagnant since about October 2010, and banded tremors have been observed since then. The period (3) "2013-present", deep inflation continues. The stagnation in the shallow part changed to inflation from around September 2014, but banded tremors occurred during the temporary stagnation from around May 2015 (Report of Coordinating Comittee for Prediction of Volcanic Eruptions, 2018). After the banded tremors subsided in the first half of 2016, crustal deformation showing rapid inflation were observed. After that, volcanic gas ejection event with tilt change occurred in May 2016 (Nagato et al., 2017).

Since all banded tremors occur during the period when the temperature inside the crater and the volcanic fume index (Q) are high, it is considered to be related to thermal activity (Fig.2). The epicenter of the BH-type earthquakes became shallow from around 2013. The GNSS baseline associated with the shallow pressure source began to shift from deflation to stagnation and then inflation from around 2013. From these facts, it is possible that the location of thermal activity, which is the cause of banded tremors, has moved in the shallow direction due to seismic activity and movement of the pressure source. In addition, the period (1) is the period when volcanic activity such as deflation of the pressure source is low, the period (2) is the period when the deflation of the shallow part is temporarily stagnated, and the period (3) is the period when the gradual inflation of the shallow part is temporary. After stagnation, banded tremors occur. From these facts, it is possible that the supply balance of volcanic fluid underground changes. On the other hand, in the 1962 and 1983 eruptions, continuous tremors occurred for several days, but no records of volcanic tremors have been observed since then. From this, banded tremors are considered to be a peculiar phenomenon of the 2000 eruption.

©2021. Japan Geoscience Union. All Right Reserved.

Keywords: Miyakejima Volcano, Banded Tremors

Fig1

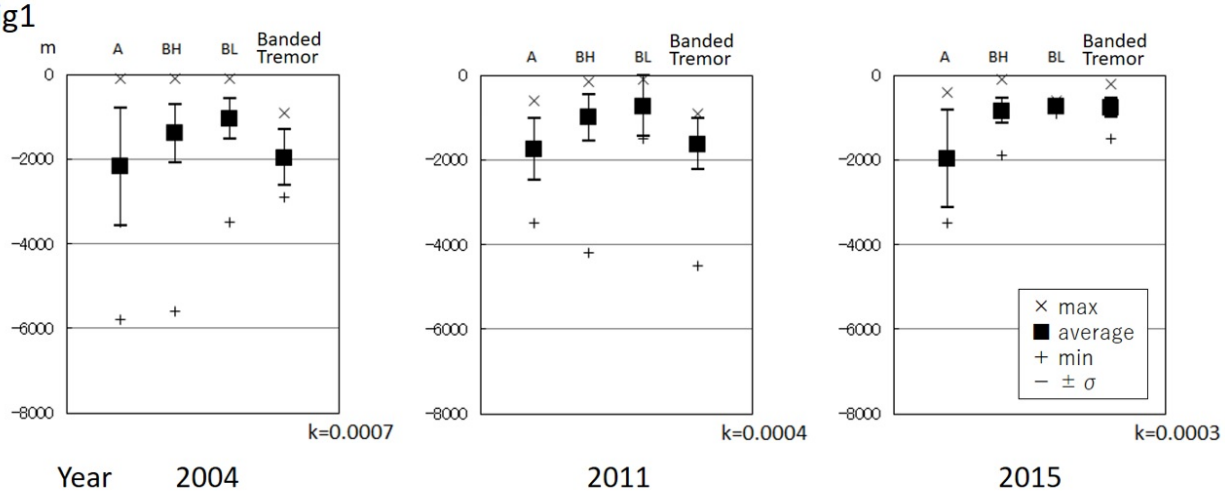
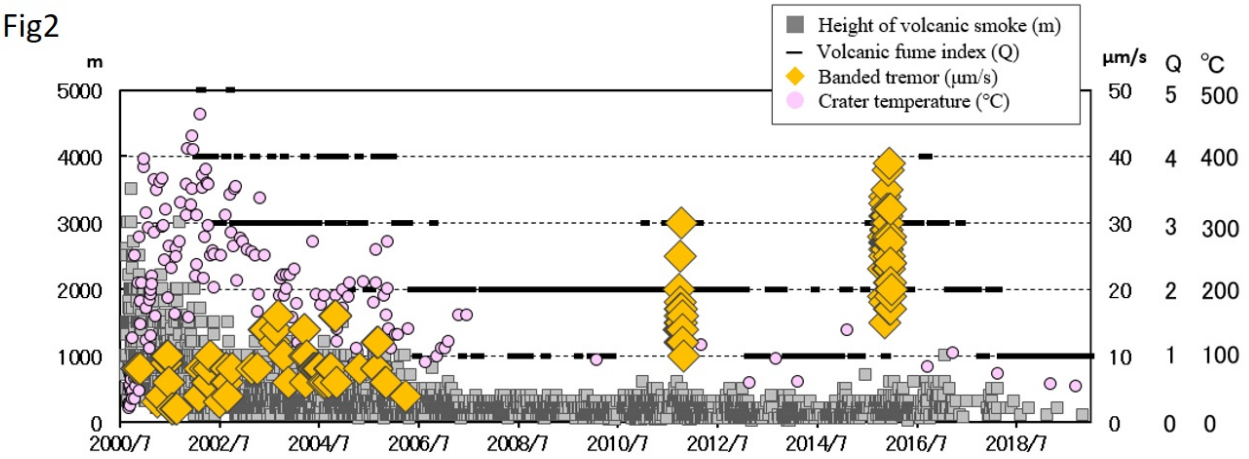


Fig2



©2021. Japan Geoscience Union. All Right Reserved.

Estimating the underground pressure source of Miyakejima volcano by integrated processing of GNSS and leveling data

*Haruna Watanabe[1], Takeshi Matsushima[2], Miyo Fukui, Atsushi Watanabe[3], Jun Oikawa[3], Takashi OKUDA[4], Taku Ozawa[5], Yosuke Miyagi[5]

1. Department of Earth and Planetary Sciences, Graduate School of Science, Kyushu University, 2. Institute of Seismology and Volcanology, Faculty of Sciences, Kyushu University, 3. Earthquake Research Institute, University of Tokyo, 4. Earthquake and Volcanology Research Center, 5. National Research Institute for Earth Science and Disaster Resilience

Miyakejima is an active volcano located about 180 km south of Tokyo, and since the 20th century it erupted at intervals of about 20 years (1940, 1962, 1983, and 2000). Although there are continuous GNSS stations on Miyakejima, the number is limited and detailed crustal movements have not been obtained. Therefore, we conducted dense GNSS campaign observations six times from 2011 to 2019. Fukui et al. (2015) estimate the position and volume change of the pressure source on Miyakejima based on the observation results from 2011 to 2013, but consider only the data of the horizontal component of GNSS observation. This study accurately grasps the crustal movement of Miyakejima by enhancing GNSS observations and using leveling data during the latest 2013-2019 period, and we estimated in detail the location and temporal changes of the pressure source under Miyakejima volcano.

In September 2013, 2015, 2016 and 2019, we conducted GNSS campaign observations at benchmark points (up to 30 points) arranged so as to be distributed almost evenly over Miyakejima. In this study, 12 points of continuous data obtained from this GNSS campaign observation and 10 points of data during the same period of continuous observation points set up by the Geospatial Information Authority of Japan, Japan Meteorological Agency, and National Research Institute for Earth Science and Disaster Resilience used. We also used the data from the Miyakejima leveling survey conducted by the Tokyo Metropolitan Government almost every two years, and used the vertical fluctuations during the same period.

We used RTKLIB ver.2.4.2 (Takasu et al., 2007) to analyze the GNSS data, and we obtained the coordinate values of the GNSS stations. The horizontal displacement of GNSS from 2013 to 2019 showed radial displacement centered on the southwestern part of Miyakejima during all periods. On the other hand, the vertical displacement of leveling survey from 2014 to 2019 showed sedimentation on the northeastern side of Miyakejima with respect to the southwestern side during all periods.

The pressure source was estimated based on the GNSS horizontal displacement from 2013 to 2019 and the vertical displacement of leveling survey from 2014 to 2019. The optimum values of the position and volume change of the pressure source were obtained by using MaGCAP-V software (Meteorological Research Institute, 2008) for analyzing crustal activity for volcano. As a result, two pressure sources with different depths were estimated. One is a horizontal plate-shaped sill just below the Miyakejima crater and 0.3 km below sea level, and the other is a spherical pressure source located about 2.5 km southwest of the Miyakejima crater and 9.0 km below sea level. The volume change of each volume was -3.3×10^5 m^3/yr for sill and $+1.2 \times 10^7$ m^3/yr for spherical pressure source. It is presumed that the sill in the shallow part contracts due to degassing from the crater, and the spherical pressure source in the deep part accumulates and expands due to the rise of magma from the deeper part.

In this study, the position of the pressure source in the island could be accurately determined by

©2021. Japan Geoscience Union. All Right Reserved.

analyzing the fluctuation of the vertical components by leveling survey. The deep spherical pressure source was estimated at almost the same position as the result of Nishimura et al. (2002). In the addition, Nishimura et al. (2002) estimated that the volume accumulation rate of magma chamber deep underground during the last eruption rest period (1983~2000) was 10.2×10^6 m^3/yr. On the other hand, the volume accumulation rate between 2000 and 2019 was estimated to be 12.6×10^6 m^3 / yr from the Geospatial Information Authority of Japan data (2011), Fukui et al. (2015), and this study. Therefore, in the 2000 eruption, a caldera crater was formed, which is very different from previous eruptions, but since then, the deep underground magma chamber have been in the same position as in the 1983-2000 period, and have been increasing at about the same rate.

This work is partly supported by MEXT under its The Second Earthquake and Volcano Hazards Observation and Research Program, and also supported by Earthquake Research Institute, The University of Tokyo under JURP (2016-B-09). Continuous GNSS data was provided by GSI and JMA. Leveling survey data was provided by the Bureau of General Affairs of the Tokyo Metropolitan Government. Many member of the Japanese University Consortium for GPS Research (JUNCO) cooperated in the GNSS campaign observation. We would like to express our gratitude to all.

Keywords: Miyakejima, GNSS observation, leveling survey

©2021. Japan Geoscience Union. All Right Reserved.

Three-Dimensional Crustal Structure beneath Hachijojima Island using dense seismic observation data

*Shotaro Kanke[1], Hiroyuki Azuma[1], Yoshiya Oda[1]

1. Tokyo Metropolitan Univ.

Hachijojima Island is a volcanic island belonging to the Izu Islands, and in 2002, a volcanic earthquake swarm and a crustal movement were observed. Because of these volcanic activity, Hachijojima Island has been monitored by JMA. In order to interpret volcanic activity correctly, it is effective to understand the underground structure of the volcano by means of geophysical method.

Hagiwara and Watanabe (2019) have estimated the underground structure beneath Hachijojima Island from earthquakes data observed by permanent stations. In this study, in order to estimate the underground structure of Hachijojima Island in more detail, we installed 46 stations of 1Hz velocity seismograph (LE-3Dlite) on Hachijojima Island and Hachijo-kojima Island and conducted temporary seismic observation from September 2019 to March 2020 (182 days). We have picked P-wave and S-wave first arrivals manually on the seismic waveform data processing system, WIN system (Urabe and Tsukada, 1992), and the hypocenter determination by hypocenter determination program hypomh (Hirata and Matsu'ura, 1987).

We used the tomography program, SIMULPS12 (Evans et. al., 1994) to estimate the underground velocity structure. As a result of 3D analysis, we found that the high Vp anomaly at the depth of 2-5km just beneath Nishiyama. In particular, P-wave velocity structure was estimated with high resolution up to the depth of 4km. We compared our results with previous studies and discussed the validity of the analysis results and the effect of dense seismic observation on the resolution.

Keywords: natural earthquake tomography, velocity structure, dense seismic observation, Hachijojima Island

©2021. Japan Geoscience Union. All Right Reserved.

Ground deformation between eruptions at Nishinoshima Island using InSAR time series analysis

*Shinobu Ando[1], Satoshi Okuyama[1]

1. Volcanology Research Department, Meteorological Research Institute

The eruptive activity of Nishinoshima Island in the Ogasawara Islands, which began erupting in November 2013, is largely classified into the following phases: Phase I: 2013.11-2015.12, Phase II: 2017.4-2017.8, Phase III: 2018.7-2018.8, and Phase IV: 2019.12-2020.8. In Phase III, the lava flow did not reach the coast, but in all other phases, the lava effused a large amount of lava and expanded the land area. The second half of Phase IV was the most active eruptive activity in the series of eruptions, with a large amount of ash fall (Ando et al. 2020, JPGU or Geodetic Society of Japan).

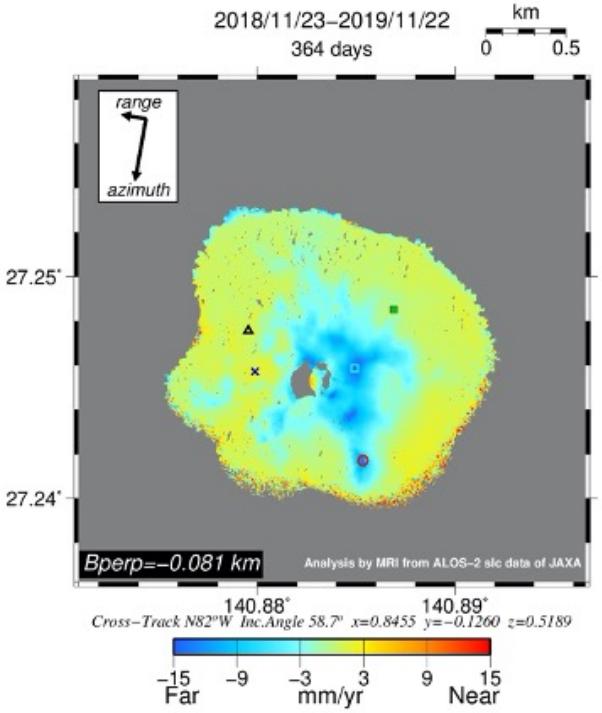
The Meteorological Research Institute (MRI) has been analyzing large-scale earthquakes and volcanic eruptions since August 2014, when the ALOS-2/PALSAR-2 data became available. In the area around Nishinoshima Island, we have been conducting analysis using spotlight mode (SPT: resolution 3m ×1m (Range ×Azimuth)) data, which is particularly frequently observed. In general, the interferometric SAR analysis becomes significantly worse with increasing the perpendicular baseline (Bperp) distance. However, in the case of ALOS-2, the Bperp is generally very well controlled (Bperp < 500m), and the interferometric analysis is possible for almost all pairs except for the degradation of temporal coherence.

In this paper, we report the results of InSAR time series analysis to investigate the fine ground deformation between eruption phases of Nishinoshima Island. For example, in the case of phase III-IV, we set a one-year period from the end of November 2018, when the most recent differential interferometric pair showed no significant phase change, to the end of November 2019, just before the start of phase IV eruption. There were 25 scenes imaged by PALSAR-2 in SPT mode during this period, and a total of 129 pairs of data were obtained by creating pairs of data within about three months. For the individual interferometry analyses, tropospheric and ionospheric delay corrections were not processed, except for the baseline re-estimation, because the land area of Nishinoshima Island is very small. Using these results, an InSAR time series analysis using the SBAS method was applied to detect temporal varies in local ground deformation. As a result, the phase difference of elongation in the constant line-of-sight direction of about 14 mm/year can be confirmed locally around the east side of the central pyroclastic cone, and the elongation deformation decreases exponentially at the south end of the lava flowed in Phase III. In this presentation, we also present the results of the analysis of Phases I-II and II-III.

The PALSAR-2 data were prepared by the Japan Aerospace Exploration Agency (JAXA) via Coordinating Committee for the Prediction of Volcanic Eruption as part of the project 'ALOS-2 Domestic Demonstration on Disaster Management Application' of the SAR analysis of volcano Working group. The PALSAR-2 data belongs to JAXA. PALSAR-2 was analyzed using Gamma, RINC (Ozawa et al., 2016), and LiCSBAS (Morishita et al., 2020). Topographic data generated from GSI Technical Document C1-No.463, 478, and 489 were used in the processing process.

Keywords: ALOS-2/PALSAR-2, spotlight mode, InSAR time analysis, Nishinoshima

©2021. Japan Geoscience Union. All Right Reserved.



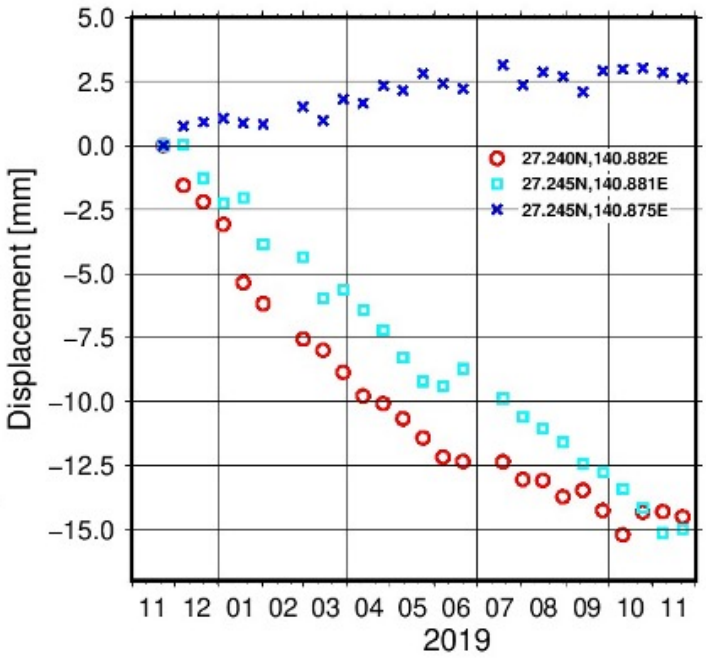


Fig. Time series of displacement

©2021. Japan Geoscience Union. All Right Reserved.

Abrupt change in eruption style during the 2019-2020 eruption of Nishinoshima, Ogasawara

*Fukashi Maeno[1], Takayuki Kaneko[1], Natsumi Hokanishi[1], ATSUSHI YASUDA[1], Yoshihiko Tamura[2]

1. Earthquake Research Institute, University of Tokyo, 2. Japan Agency for Marine-Earth Science and Technology

The style of volcanic eruption often changes significantly during a series of activity. Elucidation of the causes of such changes of eruption is important in prediction of eruption sequence. In the latest eruption of Nishinoshima, Ogasawara, magma discharge rate abruptly increased in June-July 2020, and the eruption style changed from lava flow-dominated to pyroclast-dominated one. In this presentation, we will report geological and geomorphological features and current state of volcanic activity of Nishinoshima, which was clarified by survey and observation on KR20-E06 cruise conducted in December 2020. Also we will discuss the eruption sequence and the causes of the change of volcanic activity based on the results of analysis of eruptive materials obtained by sample return with drone.

The most notable feature on the activity in 2019-2020 is that the entire island was covered with pyroclastic deposits due to the change in eruption style to explosive one. As a result of producing a DEM based on still images acquired by drone and estimating the amount of topographical change before and after the latest eruption, it was unveiled that the new pyroclastic cone accounts for ~60% of the increased volume of ~100 million m^3. This value is significantly larger than before the eruption, ~10%. Although lava flows were thickly covered with pyroclastic deposits, some parts are eroded, and lava interior is exposed. In such places, fumarolic activity and high temperature regions are recognized. This situation that even six months after the eruption high temperature regions are widely recognized on the entire surface of the island has not been observed in the previous activity of Nishinoshima. One of plausible reasons is that cooling of lava flows has been delayed due to low thermal conductivity of porous pyroclastic deposits.

Lapilli and ash were collected at multiple locations on the western side of the island by drone. Analysis of the whole rock chemical composition revealed that they are basaltic andesite with 54-55 wt.% in SiO_2. This result is almost the same as the value of bulk ash chemistry for samples collected by Meteorological Research Institute, JMA, in July 2020. Thus it is understood that the magma composition has changed significantly from andesite with 59-60 wt.% in SiO_2. There are also major changes in phenocrysts, such as increase in An# of plagioclase and the presence of olivine. In addition, changes of incompatible element concentration ratios such as Zr/Y in whole rock composition are identified. Such changes in eruption patterns and magma characteristics suggest that new undifferentiated magma was involved in the latest eruption, apart from the mafic magma that was steadily involved in the previous eruptions. Specifically, there are possibilities that undifferentiated magma rich in volatile components accidentally ascended from the deeper part, or the discharge of a large amount of magma from the shallow magma reservoir due to long-term eruptive activity triggered the movement, redistribution and ascent of deeper magma.

Keywords: Nishinoshima, Eruption, Drone, Basaltic andesite, Pyroclastic deposits, Lava flows

©2021. Japan Geoscience Union. All Right Reserved.

The depth of the air-magma interface and the sound velocity in the shallow conduit of Aso volcano inferred from seismic and infrasound signals

*Kyoka Ishii[1], Akihiko Yokoo[1]

1. Graduate School of Science, Kyoto University

The depth of the air-magma interface in the shallow conduit can be used as an indicator of the volcanic activity of open-vent volcanoes. Although there are many methods for the estimation of such depth, most of them are unable to constrain the depth into the narrow range due to multiple unknown parameters. In order to estimate the depth more accurately, we combine two methods; one is using the time delay (Δt) of arrivals between seismic and infrasound signals of explosions (Ishii et al., 2019), and another is using the resonant infrasound in the conduit observed as the peak frequency (f_0) (e.g., Johnson et al., 2018). The time delay of the signals is controlled by the depth of the air-magma interface (i.e., the depth of the explosive source) and the sound velocity in the conduit, and the peak frequency of infrasound is also controlled by the same two parameters. Therefore, this combined method provides both estimations of the depth and the sound velocity in the conduit simultaneously. The seismic and infrasound data were acquired at the vicinity of Nakadake 1st crater of Aso volcano, Japan in April 2015. A high-frequency seismic arrival is followed by an infrasound compressional phase accompanied by each Strombolian explosion at the vent. The infrasound signals are characterized by clear peaked frequency spectra (f_0, 0.5 Hz), which are derived from acoustic resonance in the gas-filled conduit (Yokoo et al., 2019). In this study, 318 events are used for analysis. Before combining the two methods, some effects have to be considered regarding the relationship between the infrasound peak frequency f_0 and the estimated depth, such as the conduit shape (cylinder or frustum), the sound velocity profile in the conduit, and the topography between a source and a station. Therefore, the estimation of the depth is performed by the following procedures. First, the conduit shape is determined by the infrasound frequency ratio of the fundamental resonant mode and overtone. The frequency ratio is theoretically related to the ratio of radii between open and closed ends of a pipe (Ayers et al., 1985). The observed frequency ratio of the peak frequency and overtone (2 Hz) suggests that the shape of the conduit wall is like a frustum of which the small end is open. Then, 3-D FDTD simulation is conducted to test how the sound velocity profile in the conduit and the topography of the propagation path affect the observed peak frequency of infrasound. High-resolution topographic data and 1-D profiles of sound velocity are assumed in the simulation. There is a transition zone from sound velocity in the conduit to that in the air at shallow depth within the 1-D profiles of sound velocity. The results of the 3-D simulation show the synthetic peak frequency of infrasound at a station is lower than the theoretical value (Ayers et al., 1985), especially in the case that sound velocity in the conduit is faster than that in the air. Based on this result, the calibrated relationship among the three parameters, the peak frequency of infrasound, the depth, and the sound velocity in the conduit, are acquired. Finally, two methods, using time delay of seismo-acoustic signals (Δt) and infrasound peak frequency (f_0), are combined. The depth and the sound velocity in the conduit estimated by the combined method are <100 m and 300-600 m/s, respectively. This estimated depth is constrained in the narrower range than the estimates by using only Δt (Ishii et al., 2019). However, only 10 % of all events are used for the estimation because the observed pair of Δt and f_0 of the other events are not explained by any realistic depths and sound velocities. This problem may be solved by considering the horizontal location of the explosive source.

©2021. Japan Geoscience Union. All Right Reserved.

Keywords: Shallow conduit, Infrasound, Aso volcano

©2021. Japan Geoscience Union. All Right Reserved.

Estimation of source location of high-frequency tremor at Aso volcano by array analysis

*hirotaka tanaka[1], Takahiro Ohkura[2], Hiroyuki Inoue[2], Shin Yoshikawa[2]

1. kyoto university, 2. Aso Volcanological Laboratory

1.Introduction
Volcanic microtremors are closely related to the movement of fluids such as magma, hydrothermal fluids and volcanic gases, and it is important to understand the generation process of volcanic microtremors in order to understand volcanic phenomena and predict eruptions. In Aso volcano, microtremors such as long-period tremor, isolated tremor, and continuous tremor have been observed. The new high-frequency tremor precedes the long-period tremor, suggesting that this tremor has a mechanism to excite the crack oscillation, which is the source of the long-period tremor. Furthermore, the amplitude of the high-frequency tremor and the time difference from the long-period tremor are time-varying and that is expected to be closely related to the changes in volcanic activity.
In this study, in order to investigate the source mechanism of the high-frequency tremor, we investigated the temporal variation of the tremor generation pattern and estimated the source location using the data from several seismometer arrays including a 3D array installed near the first crater of Nakadake and broadband seismographs from 23 February to 31 July 2020.

2.Observation and data analysis
In this study, several arrays were installed near the first crater of Nakadake to observe the high-frequency tremors. The arrays are located about 1 km away from the first crater and consist of four stations: South (SUN), Northwest (WES), North (UMA) and Southwest (HND). At SUN, WES and UMA, a 2D array consisting of six vertical seismometers with a spacing of 10-30 m and a natural frequency of 2 Hz was installed. At HND, a 3D array consisting of 13 three-component seismometers with a horizontal spacing of 10-15 m and a vertical spacing of about 30 m and a natural frequency of 2 Hz was installed above the ground and in an observation tunnel located about 30 m below the surface.
In this study, we first tried to extract the high-frequency tremors from the band-pass filtered waveforms of 2Hz to 6Hz by the correlation coefficient with the reference waveform. The amplitude of the extracted tremor and the time difference from the long-period tremors were investigated. We also analyzed the source location using the semblance method assuming plane waves, and estimated the epicenter using the 2D arrays at SUN, WES and UMA, and then estimated the epicenter depth using the 3D array at HND.

3.Result and consideration
The epicenters of the high-frequency tremors are estimated to be the west wall of the first crater of Nakadake and do not change with time estimated from the results of the apparent velocity and the direction of arrival of the tremors from the semblance analysis of 2D arrays. The depth of the source is estimated to be about 200 m to 500 m from the semblance analysis of the 3D array. Furthermore, it is found that the high-frequency tremors have the large amplitude when the time difference from the long-period tremors is short, and that the frequency of high-frequency tremors increase or decrease due to the temperature change at the source or the heavy rainfall.
The estimated region of the source of the high-frequency tremors coincides with a highly conductive region estimated from electromagnetics observations (Kanda et al., 2018). In this region, it is considered that continuous tremors are generated by the inflow of volcanic fluid from deep underground, which destroys the sulfide precipitated to seal the fractures (Kanda et al., 2018). The high-frequency tremors

©2021. Japan Geoscience Union. All Right Reserved.

analyzed in this study occur in the same region as the continuous tremors and the spectra of the high-frequency tremors are well correlated with the spectra of the continuous tremors, suggesting that they are generated by the same process. On the other hand, Yamamoto (2005) reported that volcanic fluid flows constantly into the cracks-like conduit from the deep underground, and that the inflow of volcanic fluid causes a disturbance near the top of the cracks, which in turn vibrates the cracks and generates long-period tremors. In addition, it was found that the inflow of volcanic fluid into the shallower part of the cracks cause cylindrical deformation at the upper end of the cracks, and isolated tremors is generated.
These suggest that the high-frequency tremors are caused by the breakdown of sulfides blocking the fluid path in the upper part of the crack-like conduit, which perturbs the outflow of volcanic fluid from the inside to the upper part of the crack, causing the crack to vibrate and generating long-period tremors.

Keywords: Aso volcano, volcanic tremor, array analysis

©2021. Japan Geoscience Union. All Right Reserved.

Debris avalanche deposits and the stratigraphy on the outcrop to north east from Mt.Unzen

*Daisuke Nagai[1]

1. Mt.Unzen disaster memorial hall

Unzen Volcano is a stratovolcano which repeatedly grew through the formation of lava dome, the generation of pyroclastic flow and the mountain collapse. Pyroclastic flow deposits originating from Mt. Fugen have been found in the northeastern foot of Mt. Fugen (Kobayashi and Kato,1985,Kobayashi and Nakada,1991, Watanabe and Hoshizumi,1995). It is important to investigate what kind of activity the Unzen Volcano is going to do in the future and the past ejecta to consider future disaster prevention measures. In Nagai (2019), this paper reports on the debris avalanche deposit which has never been seen before in the Tateno area which is located about 5km in the northeast foot of Mt. Fugen. This time, another debris avalanche deposit was newly found in Ide no Kawamachi (About 7 km from Mt. Fugen), Mie district, northeast foot of the same mountain. The stratigraphy of ejecta was compared with that of outcrops in the Tateno area. The newly discovered debris avalanche deposit is found to be a newer age debris avalanche different from the one reported in Nagai (2019). This debris avalanche is thought to have occurred during a series of eruptions of the Kureishibaru pyroclastic flow at about 19000 years ago. There are unclear points, such as the identification of the source of the mountain collapse, which has become a subject of future research. We hope the results will be useful for future disaster prevention measures.

Keywords: active volcano, Debris avalanche deposits, Unzen Volcano

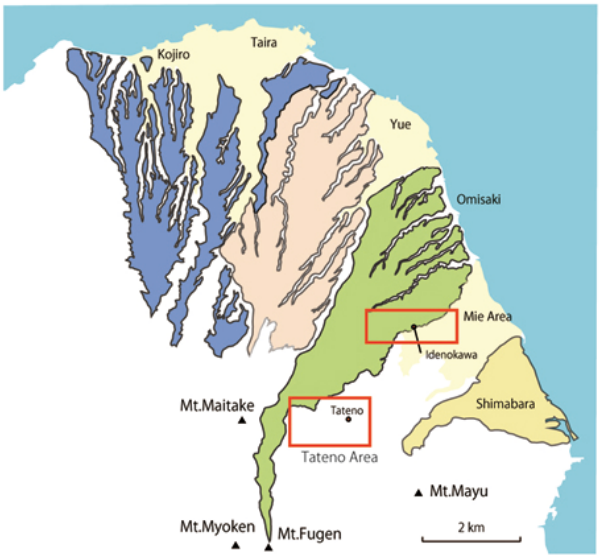


Fig.1 Location map of study area and alluvial fan related volcanic eruptions on the north-east flank of Mt.Unzen

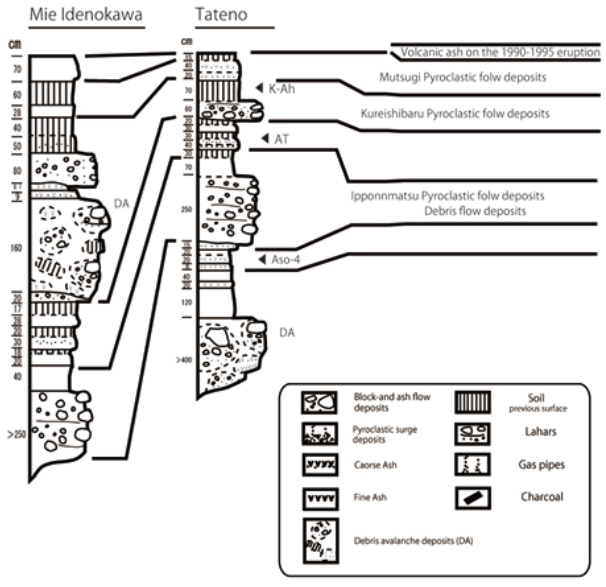


Fig.2 Columnar sections of pyroclastic deposits and stratigraphy

©2021. Japan Geoscience Union. All Right Reserved.

Vault-housed extensometers and tiltmeters recorded continuous crustal movement during the eruption of Kirishima Shinmoe-dake in 2018

*Koki Yoshinaga[1], Takeshi Matsushima[2], Hiroshi Shimizu[2], Yusuke Yamashita[3], Shintaro Komatsu[3], Ken'ichi Yamazaki[3]

1. Department of Earth and Planetary Sciences, Graduate School of Science, Kyushu University, 2. Institute of Seismology and Volcanology, Faculty of Sciences, Kyushu University, 3. Miyazaki Observatory, Disaster Prevention Research Institute, Kyoto University

Shinmoe-dake is one of the volcanoes constituting the Kirishima volcanic group in southern Kyushu, and it is an active volcano with major eruptions in 2011 and 2018 in recent years. In this study, we use vault-housed extensometer and tiltmeter data to analyze the ground deformation recorded during the Shinmoe-dake eruption in 2018. The purpose of this study is to clarify what occurred underground during the eruption with high spatial and temporal resolution.
We used the vault-housed extensometer data installed at the Isa Observatory (ISA), Kyoto University. The ISA consists of tunnels in three directions, E1, E2, and E3. Each extensometer made up of 30m lengths of super-invar rods. E1 extends in the direction of the presumed contraction source of the 2018 eruption, and E2 in the direction orthogonal to E1. The tiltmeter data were obtained from three stations: Takachihokawara (KITK) station of the Japan Meteorological Agency (JMA), Hinamoridai (KRHV) station and Manzen (KRMV) station of the National Research Institute for Earth Science and Disaster Resilience (NIED). We resampled the original data at 1 hour by simple averaging and removed tidal components from the original time series using the tidal analysis software BAYTAP-G (Ishiguro *et al.*, 1984). According to the Japan Meteorological Agency (JMA), the deep point source of the 2018 eruption contracted at the beginning of March, and we focused this period and compared each data and arranged its character.
The tilt at the KITK and the KRHV started to change around 9:00 a.m. on March 6, while the strain at Isa and the tilt at KRMV started to change in the morning of March 5. New lava was found in the crater on March 6, and the changes in Isa and KRMV were detected earlier than that. Strain variations in ISA were characterized by an extension in the E1 component and by contraction in the E2 component, which can be interpreted as the contraction of the pressure source estimated by the JMA to be located about 6 km northwest of Shinmoe-dake. In addition, the tilt in KRMV changed in the direction of subsidence from north to northeast until 9:00 a.m. on the 6th, and the strain rate in ISA also changed after 9:00 a.m. on the 6th.
In summary, we think that the first contraction occurred at depth on the morning of the March 5th, before new lava was found in the crater, and the second contraction occurred at a shallower depth on the northeast side during the 2018 eruption.

Keywords: Shinmoe-dake, Extensometers, Tiltmeter, Ground deformation

©2021. Japan Geoscience Union. All Right Reserved.

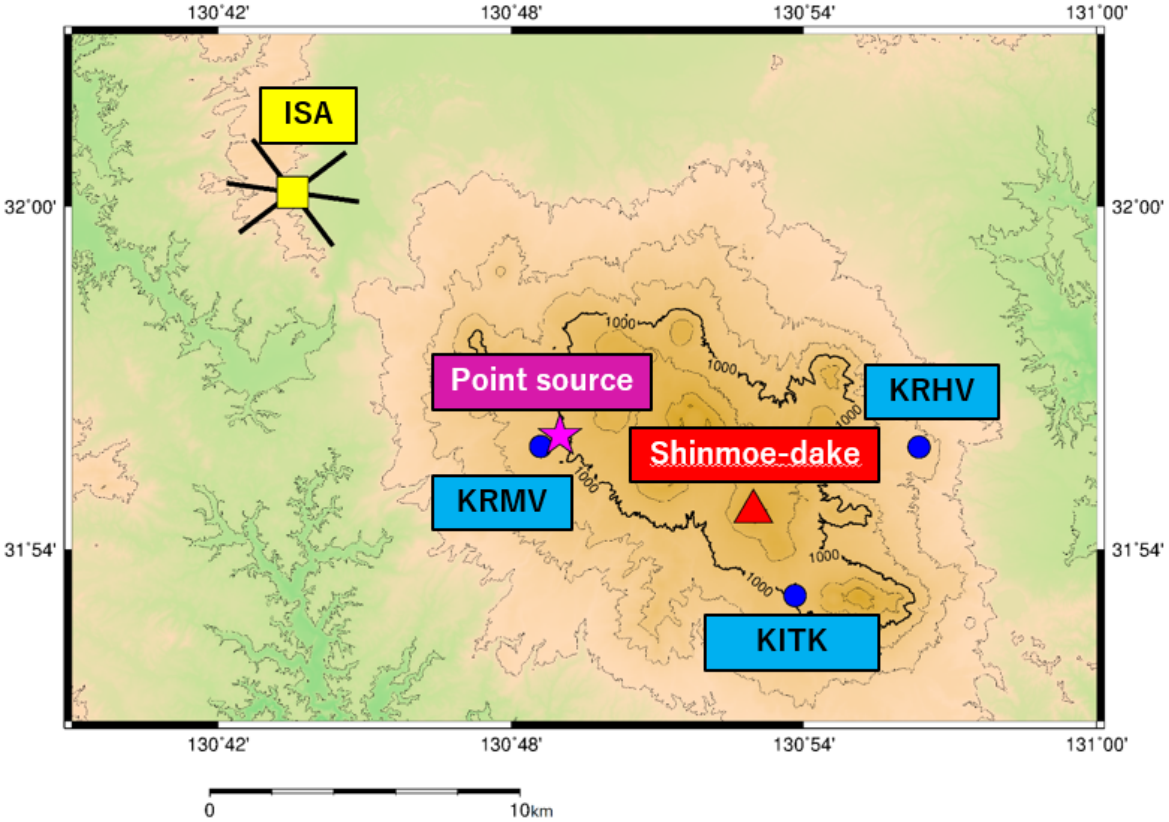


Fig.1 Map showing the location of Shinmoe-dake volcano crater and observation sites. The red triangle indicates the Shinmoe-dake volcano crater. The yellow square indicates the extensometers site (ISA), and the blue circle indicates the tiltmeter sites, respectively. The pink star represents the source location inferred from GNSS data (JMA., 2018).

©2021. Japan Geoscience Union. All Right Reserved.

Two experiments using a small-aperture infrasonic array at Kirishima

*Kazuya Yamakawa[1], Mie Ichihara[1], Dan Muramatsu[2], Takeshi Matsushima[2], Ruka Wada[3], Hideki Takahashi[3], Isao Shimoyama[4]

1. Earthquake Research Institute, University of Tokyo, 2. Institute of Seismology and Volcanology, Faculty of Science, Kyushu University, 3. Department of Mechanical Engineering, Faculty of Science and Technology, Keio University, 4. Department of Intelligent Robotics, Toyama Prefectural University

Infrasound, which is the air vibration with sub-audible frequency (< 20 Hz), is generated by various geophysical phenomena and is used for monitoring them. A small-aperture (10-30 m) infrasonic array with high-performance microphones is shown to have a practical resolution of the direction of arrival of an incident signal [Johnson & Palma, 2015; Yamakawa et al., 2018]. Also, a new infrasonic MEMS (Micro Electro Mechanical Systems) microphone is being developed, which is inexpensive and has a reasonably good performance [Wada and Takahashi, Japanese Journal of Applied Physics, 2020]. In this study, we conducted two experiments using a small aperture array at Kirishima volcano in 2020.

The first experiment examined the performance of the MEMS microphones [Wada and Takahashi, 2020]. It was conducted for 19 hours from 5 p.m. on 19 October 2020 at Kirishima Ioyama, where several fumaroles were active. The MEMS microphones were compared with the latest model of infrasound microphones (Type 7744N, ACO CO., LSD., hereafter referred to as ACO microphone) that had been used in several infrasonic studies. We installed two identical three-element infrasonic arrays with an aperture of 15 meters (Figure 1). The one consisted of the MEMS microphones and the other of the ACO microphones. At each array element, a MEMS microphone and an ACO microphone were put in the same box. There were two active fumaroles around the array. One was Iwo-yama West Craters, 150 m northeast of the array, and the other was Iwo-yama South Crater, 270 m northwest of the array [Tajima et al., 2020; Muramatsu et al., 2021]. Here we refer to the fumarole of Iwo-yama West Craters as NW fumarole and the fumarole of Iwo-yama South Crater as NE fumarole. We also placed a microphone (Type SI104, Hakusan Co., hereafter referred to as SI microphone) near the NW fumarole.
The recorded waveforms and the array processing results were excellently matched between the MEMS microphone array and the ACO microphone array, confirming that the MEMS microphones are practically useful.
The array processing showed that the infrasound from the NE fumarole was dominant at the arrays. We found that the NW fumarole also emanated infrasound by the combined analysis of the array data with the data from the SI microphone located close to the NW fumarole. The NW signals were weak compared to the NE signals: the cross-correlation coefficient between the array microphones and the SI microphone was 0.13 for the NE and 0.01 for the NW (Figure 2). With the monopole source assumption and the ratio of the correlation coefficient, the NW-to-NE amplitude ratio was approximately 0.06-0.1.

The second experiment was a mobile array survey for infrasound noise. It was conducted around Makizono-cho, Kirishima city, from 3 p.m. to 5 p.m. on 20 October 2020. While traveling by car, we stopped at an observation point, deployed the small-aperture (15 m) array for several minutes, retrieved them, and then moved to the next point. We used the ACO microphones that were used in the first experiment. We obtained the infrasonic array data at four locations in 2 hours.
The results indicated that the dominant infrasound noise was from the fumarolic area (Iodani Fumarolic Area Park) at the P1, P2, and P4 (Figure 3). At the P3, the estimated source direction was deviated. This deviation should have been brought by the topographical barrier of a hill between P3 and the fumarolic

©2021. Japan Geoscience Union. All Right Reserved.

area. Fumarolic noise is persistent and can disturb infrasonic monitoring of volcanoes. The array survey for background noise will be useful for designing infrasound observations for volcanoes.

Two experiments were successful. In the first experiment, new MEMS microphones was proven as practical. This new and inexpensive microphone will benefit the infrasonic studies. The first experiment also succeeded in detecting the existence of the infrasound signals that were masked by another signals. In the second experiment, we proved the movability of a small infrasonic array, and succeeded to identify the infrasonic noise source in a short time. These two experiments demonstrated the wide usage of a small infrasonic array.

Keywords: Infrasound, array, volcano

©2021. Japan Geoscience Union. All Right Reserved.

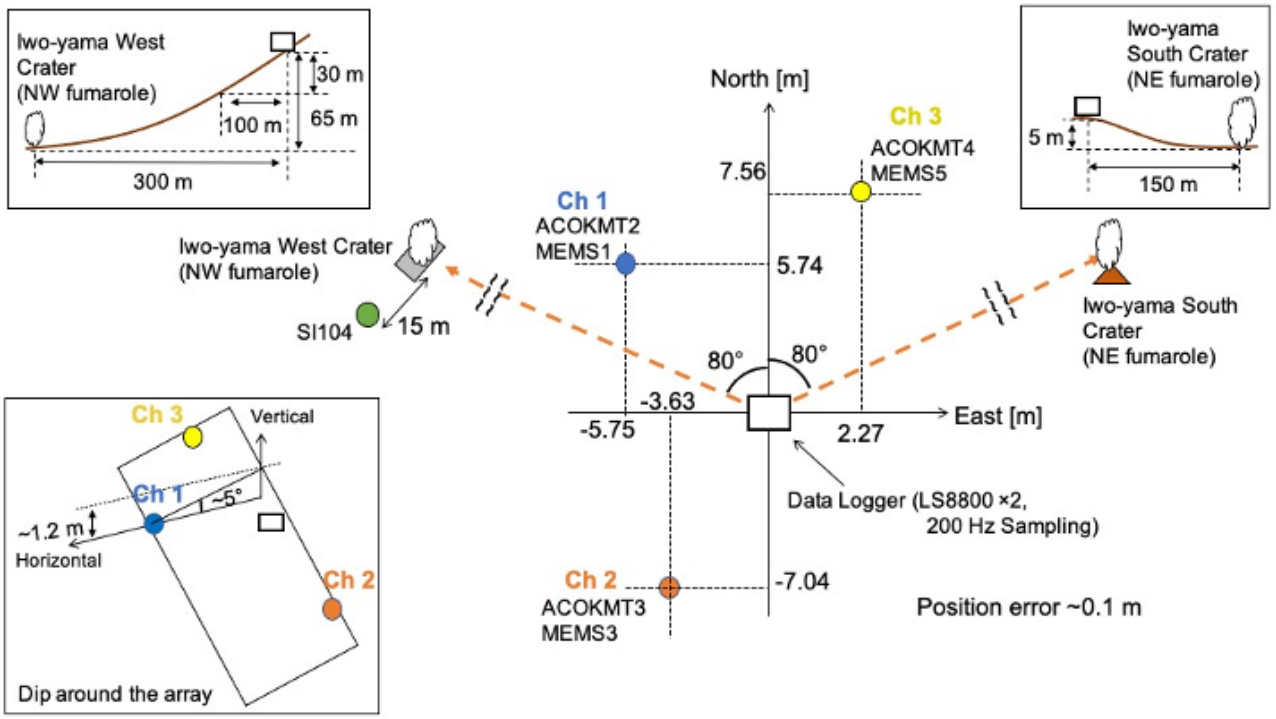


Figure 1. Experiment at Kirishima Ioyama. The colored circles show the positions of microphones.

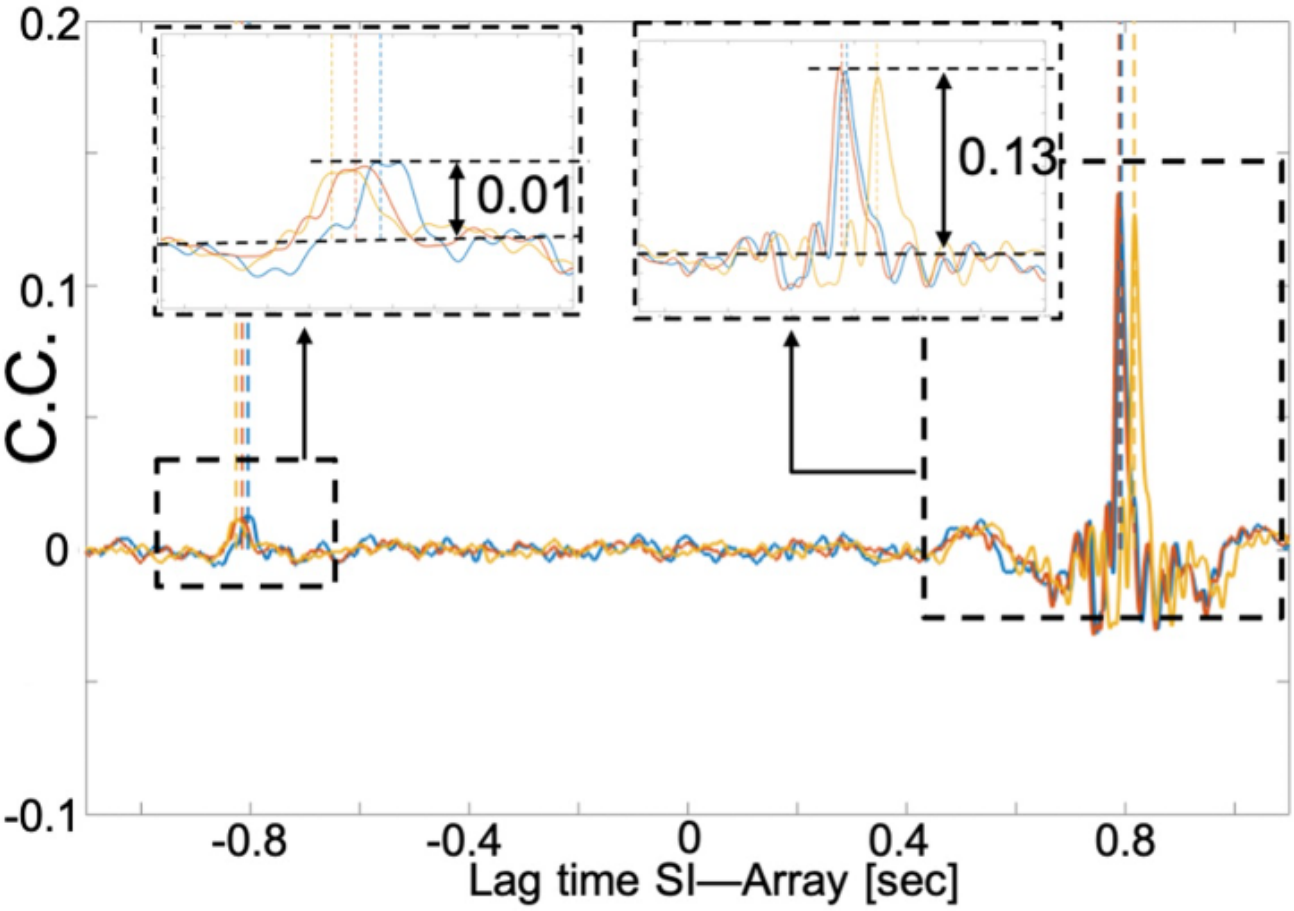


Figure 2. Correlation coefficient between the SI microphone and each array components (Figure 1). The solid lines show the correlation coefficient (blue: SI-Ch1, red: SI-Ch2, yellow: SI-Ch3). The dashed lines show the lag times corresponding to the northeast fumarole (right) and the northwest fumarole (left). In this figure, the ACO microphones' data were used. Note that the MEMS microphones' data also produced the similar result.

©2021. Japan Geoscience Union. All Right Reserved.

©2021. Japan Geoscience Union. All Right Reserved.

Estimating the source of volcanic earthquakes during eruption events at Kirishima Volcanos, in 2018, using spatial distribution of earthquake amplitude.

*Daiki Goshima[1], Satoshi Matsumoto[2], Ayaho Mitsuoka[1], Yuhei Yuasa[4], Yuta Kawamura[1], Mie Ichihara[3]

1. Department of Earth and Planetary Sciences, Graduate School of Science, Kyushu University, 2. Institute of Seismology and Volcanology, Faculty of Sciences, Kyushu University, 3. Earthquake Research Institute, University of Tokyo, 4. Osaka Regional Headquarters, Japan Meteorological Agency

Kirishima volcanic area consists of about 20 volcanoes and is located around the border of Kagoshima and Miyazaki prefectures. Ichihara et al (2017) analyzed the volcanic tremors associated with volcanic activity in 2011 eruption. They obtained tremor sources just below the crater and discussed its relationship with surface phenomena. However, source of tremor that might be associated with magma migration to the crater have not been determined and their relationships are not known well. The location of magma chamber of the Kirishima Volcanos was inferred from pressure source detected by GPS observations, which is located at 5 km northwest of Shinmoe-dake and depth of 8 km (Nakao et al., 2013). On the other hand, Aizawa et al (2014) discussed the location to be 5 km northeast of Iwo-yama. In this study, we attempt to detect magma behavior associated with the 2018 eruptions of Shinmoe-dake and Iwo-yama through detection of volcanic tremor.

In order to detect tremor and determine source location, we use seismic stations around the volcano. Tremor location is determined from amplitude distribution at the seismic stations. Generally, seismic signal is affected by source, path, and site factors. Then, we estimate the site amplification characteristics at the stations using the distant earthquake occurred in Shimane Prefecture on 9 April 2018, and remove the effect from amplitude data. After that, we estimate the source location of tremor. The location was determined by spatial amplitude distribution through grid-search processing for trial source locations.

Prior to tremor detection, we performed source determination for events at known location. At the same time, we estimated optimal attenuation factor to eliminate propagation path effect. We used two natural earthquakes and two volcanic eruptions for the checking. The result of the check showed that the processing could not determine the depth of the source well but the horizontal location of the source can be estimated by it. Undetermined depth might be attributed to the effect of radiation pattern from the natural earthquake source. Therefore, we confirmed the processing can be used for the determination of tremors.

Keywords: volcanic tremor, amplitude distribution

©2021. Japan Geoscience Union. All Right Reserved.

S-wave attenuation structure of Mt.Kirishima estimated using coda of S-wave

*Takuji Watanabe[1], Ayaho Mitsuoka[1], Yuhei Yuasa[1], Yuta Kawamura[1], Daiki Goshima[1], Satoshi Matsumoto[2], Mie Ichihara[3]

1. Department of Earth and Planetary Sciences, Graduate School of Science, Kyushu University, 2. Institute of seismology and Volcanology, Faculty of Sciences, Kyushu University, 3. Earthquake Research Institute, University of Tokyo

Mt.Kirishima is a volcanic group located on the border of Kagoshima prefecture and Miyazaki prefecture in Japan. Shinmoe-dake in the center of Mt.Kirishima has been active in 2011 and 2018. Therefore, it is important to estimate the underground structure of Mt.Kirishima in order to consider volcanic activities in the future.

When seismic waves go through the fluid such as a magma reservoir, the energy of waves is absorbed and scattered and the amplitude is attenuated. In this study, we estimated the underground structure of Mt.Kirishima by comparing the amplitudes of S-waves that normalized by coda-waves.

In this study, we used the data were obtained from 23 stations (Kyushu University, Tokyo University, JMA and NIED). We used seven earthquake events (M=1.3~2.3). These station and event were located around Mt.Kirishima. In the analysis, we used coda-normalization method which removes the source effect and site effect by amplitude of coda-wave. We used method (1) that image range of attenuation by comparing amplitude of S-wave and method (2) that estimate Q-value by ratio of root mean square amplitude of coda-wave (C_RMS) and root mean square amplitude of S-wave (S_RMS). In the method (1), we made amplitude of coda-wave recorded all station the same size that maximum amplitude of coda-wave for 3 seconds after the arrival time of coda-wave recorded at the station farthest from the hypocenter and we compared amplitude for 1 second after the arrival time of S-wave recorded at each station. In the method (2), we calculated C_RMS for 3 seconds after the arrival time of coda-waves (twice the travel time of S-wave) at each station and S_RMS for 1 second after the arrival time of S-waves at each station. We divided S_RMS calculated at each station by respective C_RMS and calculated the amplitude ratio. In the method (1), we connected hypocenter and station that amplitude of S-wave is smaller than standard on the map. We did the same procedure each events and imaged attenuation range where the lines overlapped. In the method (2), we divided the range where include hypocenters and stations into blocks in two dimensions and estimated Q-value in each blocks by least squares method.

In our results, attenuation range located south of Karakuni-dake in both methods. The hypocenters of volcanic earthquake distribute neighborhood of this attenuation range. Therefor we suggested there is heterogeneous structure related to volcanic activity at south of Karakuni-dake.

Keywords: Coda-wave, Attenuation structure

©2021. Japan Geoscience Union. All Right Reserved.

Estimate of magma supply beneath Aira caldera during the last 10 years based on ground deformation observation and amount of volcanic ejecta

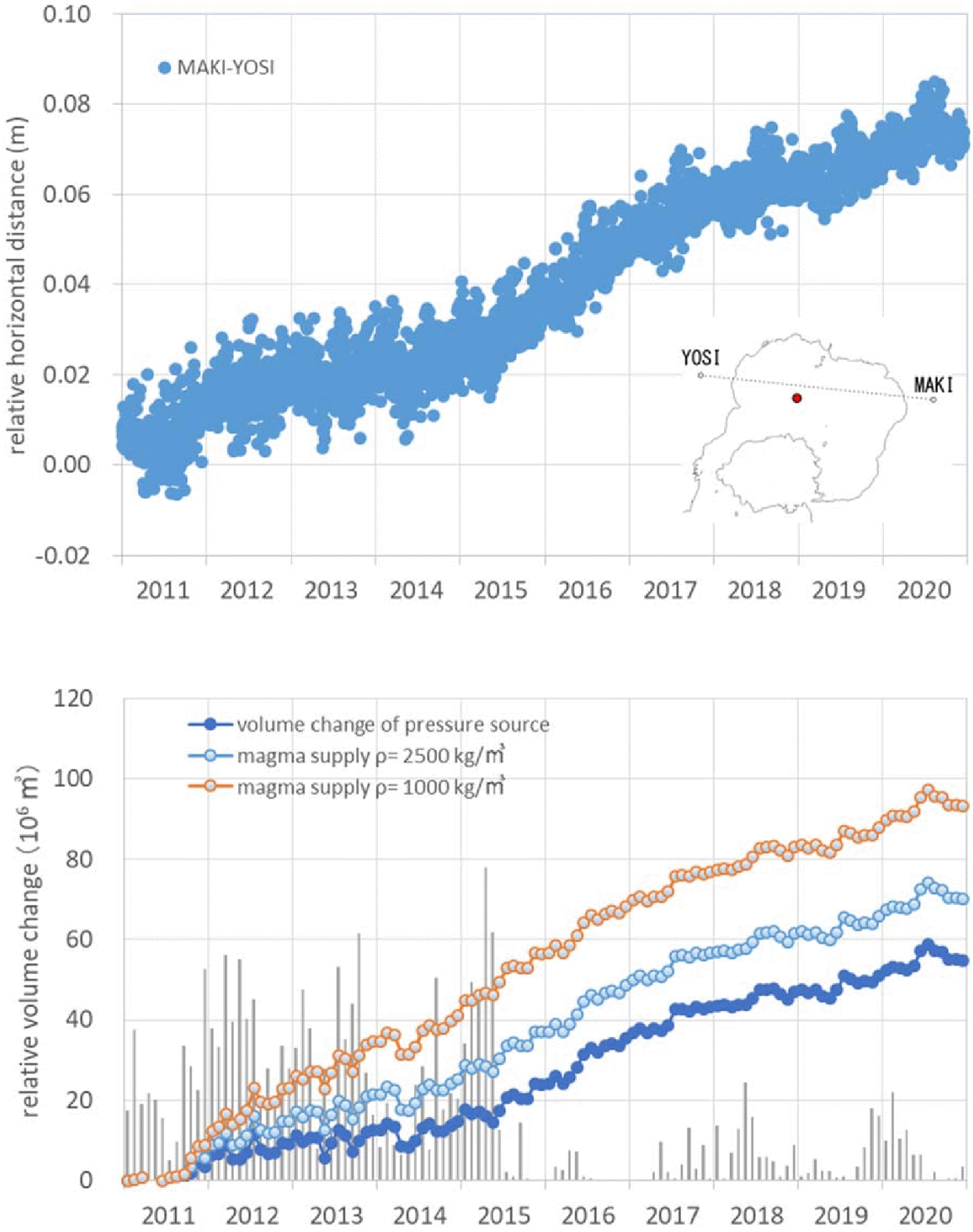
*Daisuke Miki[1], Tomoki Tsutsui[1], Masato Iguchi[1]

1. Sakurajima Volcano Research Center, Disaster Prevention Research Institute, Kyoto University

We applied a composite analysis of spherical pressure source at around Aira caldera, Kyushu Japan. Horizontal displacements obtained from GNSS observations and vertical displacements from leveling survey, during 2017 to 2019, were used for the analysis. A volume increase source of 15.2 $\times 10^6$ m^3 was estimated at a depth of 11.2 km near the central part of Aira Caldera. The volume change during the last 10 years was calculated based on the estimated location of the pressure source beneath Aira caldera and change in horizontal distance between MAKI and YOSI, which crosses the central part of Aira caldera from east to west. The amount of magma supplied to Aira caldera was estimated by adding the amount of volcanic ash ejected from Sakurajima volcano, to volume change of pressure source. Estimated magma supply during the last 10 years are 70 $\times 10^6$ m^3 and 93 $\times 10^6$ m^3, respectively, assuming equivalent densities of 2500 kg/m^3 and 1000 kg/m^3. The average magma supply rate is close to the 10 $\times 10^6$ m^3/yr obtained in previous studies.

Keywords: Aira caldera, ground deformation, magma supply

©2021. Japan Geoscience Union. All Right Reserved.



Daily change in horizontal distance between MAKI and YOSI (upper figure) and monthly variation of magma supply to Aira caldera (lower figure). The lower figure also shows the volume change at the pressure source and amount of volcanic ejecta.

©2021. Japan Geoscience Union. All Right Reserved.

Temporal changes of seismic velocities and scattering properties at Suwanosejima volcano inferred from seismic interferometry

*Takashi Hirose[1], Hideki Ueda[1], Eisuke Fujita[1]

1. National Research Institute for Earth Science and Disaster Resilience

In recent years, seismic interferometry [e.g., Curtis et al., 2006; Shapiro, 2004] has been widely used to detect seismic velocities and/or scattering properties related to large earthquakes and volcanic activities. Some previous studies succeeded in detecting precursory changes in volcanic regions 10 days - a few days before eruption/increase in activity [e.g., Budi-Santoso and Lesage, 2016; Obermann et al., 2013a; Olivier et al., 2018]. Increasing the number of applications will be important to improve volcano monitoring with seismic interferometry. In this study, we conduct seismic interferometry analyses at Suwanosejima volcano, where the number of eruptions increases in the last few months, and discuss temporal changes of seismic velocities and scattering properties.

We used seismic ambient noise data of three JMA stations during Jan. 2018 - Feb. 2021 at Suwanosejima volcano and estimated temporal changes of seismic velocities and scattering properties during that period. A reduction of waveform correlation (decorrelation) will indicate a seismic scattering property change. We firstly divided continuous seismic records on vertical component into 10-minutes-long segments and applied spectral whitening [e.g., Shapiro et al., 2006; Bensen et al., 2007] and one-bit normalization [Larose et al., 2004]. Daily CCFs (DCCFs) were obtained by stacking CCFs every 10 minutes. Finally, we measured relative velocity change and waveform correlation (CC) between a reference CCF and 3-days-stacked CCF at 0.5-1 Hz, 1-2 Hz, and 2-4 Hz bands by using stretching method [Lobkis and Weaver, 2003]. Where the reference CCF is computed by stacking DCCFs between Jun. 10, 2020, and Jan. 31, 2021.

At the 0.5-1 Hz band, seismic velocity decreased by 2.6-2.9 % from 12 days before the explosion on Dec. 28, and significant decorrelations were detected 5-15 days before this explosion. Seismic velocity decreased by 2.1 % at the maximum of 9 days before the eruption on Jan. 20. Significant decorrelations were detected from 7 days before to 3 days after this eruption. Estimated seismic velocity changes just before those eruptions have large errors caused by significant decorrelations. Therefore, it is difficult to discuss seismic velocity changes related to those explosions. Although the seismic velocity changes and the decorrelations were also detected at 1-2 Hz and 2-4 Hz bands, further investigation is required because CCs at these frequency bands show large fluctuations. To investigate temporal changes of CC values in more detail, we directly computed CCs between each DCCF. CC values between DCCFs around those eruptions have relatively high, suggesting that scattering properties at the shallow region of the volcano in those periods of time are similar to each other.

To discuss possible causes of significant decorrelations, we compared temporal changes of CC with other observations. No heavy precipitations were observed at AMeDAS station in Suwanosejima during Dec. 2020 - Feb. 2021, indicating the significant decorrelations should not have been caused by heavy rains. No geodetic data showed precursory changes related to the explosions. Finally, we checked temporal changes of SO_2 flux. Daily SO_2 flux increased to 2,500 tons on Dec. 26, 2020 [JMA, 2021], suggesting that volcanic gas moved to the shallow region of Suwanosejima. The inflow of volcanic gas to cracks at the shallow part of Suwanosejima might have caused significant decorrelations.

©2021. Japan Geoscience Union. All Right Reserved.

Acknowledgments: We used seismograms recorded by Japan Meteorological Agency (JMA) and AMeDAS data provided by JMA.

Keywords: seismic interferometry, scattering property change, Suwanosejima volcano

©2021. Japan Geoscience Union. All Right Reserved.

Development of volcano deformation calculation system using boundary element method (2)

*Ryohei Kawaguchi[1]

1. Meteorological Research Institute

Volcanic deformation data observed by tilt meter and/or GNSS stations were useful for monitoring and evaluating the volcanic activities. The Japan Meteorological Agency (JMA) has been constructing such observation stations around volcanoes, and these observed data were used for monitoring operation of volcanic activities. Because these observation stations around volcanoes were located on the steep topography of the volcano, the observed data were affected by the topography. It was important to consider the effect of the topography in the analysis of the observation data. To investigate the influence of topography on the analysis results of volcanic deformation data, we have developed a program for calculating volcanic deformation which considering the effect of topography by using the boundary element method (BEM). As a result, when the depth of the deformation source was about the same as the elevation of the observation station, the analysis result assuming an elastic half space was overestimated or underestimated the depth and the magnitude of the deformation source (Kawaguchi, 2020, JpGU). To utilize the developed program for the volcano monitoring operation by the JMA, we have developed functions for creating the mesh model of volcanic topography and converting the calculation results for data at observation station. In this study, we introduce the developing system and report the examples of its application.

The volcano deformation calculation system was consisted by the functions of creating a mesh model of the topography of volcano, calculating the volcanic deformation using the BEM, and converting of the calculation results into observational data. The mesh model of the topography of volcano and pressure sources was made by setting some parameters such as the name of the volcano and the location of the pressure source. The topography of the volcano was created using a 10-meter mesh digital elevation model (DEM) of the Geospatial Information Authority of Japan. A spherical or ellipsoidal pressure source can be set as the deformation source. The calculated results were output as displacement for each coordinate of the mesh model. These results were converted into the tilt change and displacement of each observation station for analysis. The converted tilt changes and displacements were output in the format of input files of MaGCAP-V developed by the Meteorological Research Institute, JMA. We have developed the program that can be applied to 20 volcanoes.
As an example of application of this system, we created the topographic model of Izu-Oshima volcano and calculate the volcanic deformation. Assuming a dike penetration, we set a pressure source below the summit area. The tilt changes and displacements at the observation stations at Izu-Oshima volcano were numerically calculated. As a result, when the depth of the pressure source was 1,000 m below sea level, the difference in calculated tilt changes and displacements were small compared to the those obtained by assuming the elastic half space. When the elevation of the pressure source was set to 0 m above sea level, the calculated tilt changes and displacements were more than twice as large as those obtained by assuming the elastic half space at some stations.

Keywords: volcano deformation, BEM

©2021. Japan Geoscience Union. All Right Reserved.

Estimation of seismic scattering coefficients at active volcanoes

*Mare Yamamoto[1]

1. Research Center for Prediction of Earthquakes and Volcanic Eruptions, Graduate School of Science, Tohoku University

Volcanoes are considered one of the most heterogeneous field in the Earth’ s crust, and the understanding of such small-scale inhomogeneities in volcanoes may provide us important information on the various volcanic processes including fluid transport related to past and present volcanic activities. In heterogeneous media, like shallow volcanic structure, the seismic wave propagation is strongly affected by the scattering, and the conversion scattering between P and S waves and their multiple scattering play an important role in wave propagation and energy transportation. Such mode conversion and multiple scattering are also important to consider the applicability of seismic interferometry and Green’ s function extraction which are often related to the requirement of equipartitioning. In our previous work, we estimated the total scattering coefficients including those of conversion scattering using the spatial distribution of propagating energy from an active seismic source at Asama volcano, Japan (Yamamoto and Sato, 2010). In this presentation, we report the results of systematic estimation of the scattering coefficients at several volcanoes and discuss the relation between the estimated scattering coefficients and the structure of each volcano.

In this study, we estimated the scattering coefficients at Aso, Bandai, Iwate, and other volcanoes using the data of active seismic experiments which were conducted as a part of the national project for the prediction of volcanic eruptions in 1990s and 2000s. The most remarkable characteristic of observed seismograms is the existence of long and dominant coda waves after the onset of P wave, and the spatial distribution of propagating energy at fixed time shows a clear pattern exhibiting two slopes which are indicative of multiple scattering P and S modes having different scattering coefficients. From the comparison between the observed energy distributions and those calculated by the radiative transfer model considering the mode conversions between P and S energies and the multiple isotropic scattering of these two modes in the full space, we found that the total scattering coefficients of P-S scattering at 4-8 Hz and 8-16 Hz bands are approximately 1.5 km at all volcanoes we examined. These estimated values of the total scattering coefficients were close to those estimated in our previous study at Asama and are also consistent with those estimated by an array observation at Sakurajima. In this study, we also verified the validity and reliability of the use of the radiative transfer model in the full space by analyzing the energy propagation in the half space and the layered models which are computed by numerical means (i.e., finite-difference and Monte Carlo methods). We found that the maximum error of the estimated total scattering coefficients is about 40%, and thus the wave scattering at shallow volcanic structure is still one or two order stronger than that in the ordinary crust.

These results suggest that the conversion scattering between P and S waves and significant multiple scattering of each mode have an indispensable effect in the modeling and analysis of seismic wave propagation in heterogeneous volcanic environments. Since we have been assuming the scattering caused by statistical random fluctuations, it is also necessary to consider the scattering by discrete cavities as pointed out by Sato (2019, GJI; 2020, JpGU) for a better understanding of wave scattering in the shallow volcanic structure in the future.

©2021. Japan Geoscience Union. All Right Reserved.

Keywords: Shallow volcanic structure, Seismic scattering, Active seismic experiments

©2021. Japan Geoscience Union. All Right Reserved.

Temporal Change in Coda-Q at the upper East Rift Zone of Kīlauea volcano, Island of Hawai ʻi

*Takuji Yamada[1], Paul G Okubo[2]

1. Faculty of Science, Graduate School of Science and Technology, Ibaraki University, 2. University of Hawai ʻi at Mā noa

1. Introduction

Quality factor coda-Q, or Qc, is measured from the decay rates of coda-wave amplitudes for local earthquakes. The decay of the coda amplitude is independent of the distance and path between source and receiver (Aki, 1969) and can be used as an indicator of subsurface complexity, such as the density of cracks and other wave scatterers. Lower suggests higher density of cracks and scatterers.

Elevated volcanic activity at Kīlauea volcano has persisted for decades, with essentially continuous eruption in its middle East Rift Zone from the Pu ʻu O ʻo vent from 1983 to mid-2018. A vent within Halema ʻuma ʻu Crater in the Kīlauea summit region was formed in 2008, and a lava lake occupied the vent also until mid-2018. In May 2018, magma intruded into and erupted from Kīlauea’s lower East Rift Zone for much of the summer of 2018. Punctuating Kīlauea’s sustained eruptions from the vents at its summit and East Rift Zone were intervals when the summit lava lake formed, a fissure eruption between the summit and Pu ʻu O ʻo, and two overflows of the lava lake within Halema ʻuma ʻu. During such intervals, we presume that magma rising toward the surface or migrating through the volcano will activate and fill cracks and fractures in the shallow crust. This suggests that changes in Qc could be detected prior to visible changes in the eruptions.

In this study, we focused on the upper East Rift Zone, now being referred to as the east rift connector between the summit and rift zone, where occasional elevation of seismicity has been detected. We analyzed waveforms of 462 earthquakes (M ≧ 2.0) that occurred at the upper East Rift Zone from 2009 to 2015 (Figures 1a and 1b) and investigated temporal change in Qc.

2. Methods

We first applied band-pass filters with five different frequency bands for S-coda waves, which were 1-2, 2-4, 4-8, 8-16, and 16-32 Hz. We then calculated the root-mean-square amplitude Ac of a S-coda wave in a moving time window with a duration of 4/fc, where fc is the center frequency of each frequency band. From the single backscattering model (Aki and Chouet, 1975), Ac and Qc will obey the following equation, $\ln Ac + \ln t = -\pi(fc/Qc)t + const.$, where t is the lapse time from the origin time of the earthquake. We finally estimated values of Qc for individual frequency bands and hypocenter-station pairs from waveforms of 462 earthquakes (M ≧ 2.0) and investigated temporal change in the values.

3. Results and Discussion

Figure 1c shows temporal change in Qc for the east-west component of the seismogram at a station (HV.PAU) for the five analyzed frequency bands. Figure 1d shows a temporally smoothed result in each

©2021. Japan Geoscience Union. All Right Reserved.

month for a frequency band of 2 to 4 Hz. We observed no clear change associated with elevated seismicity in 2009, 2011, and 2015. On the other hand, a long-term decrease in Qc was detected at some stations and frequency bands. We interpret this as suggesting an increasing density of cracks and scatterers associated with a raised volcanic activity at the upper East Rift Zone.

Keywords: Kīlauea volcano, Coda-Q, scatterer density

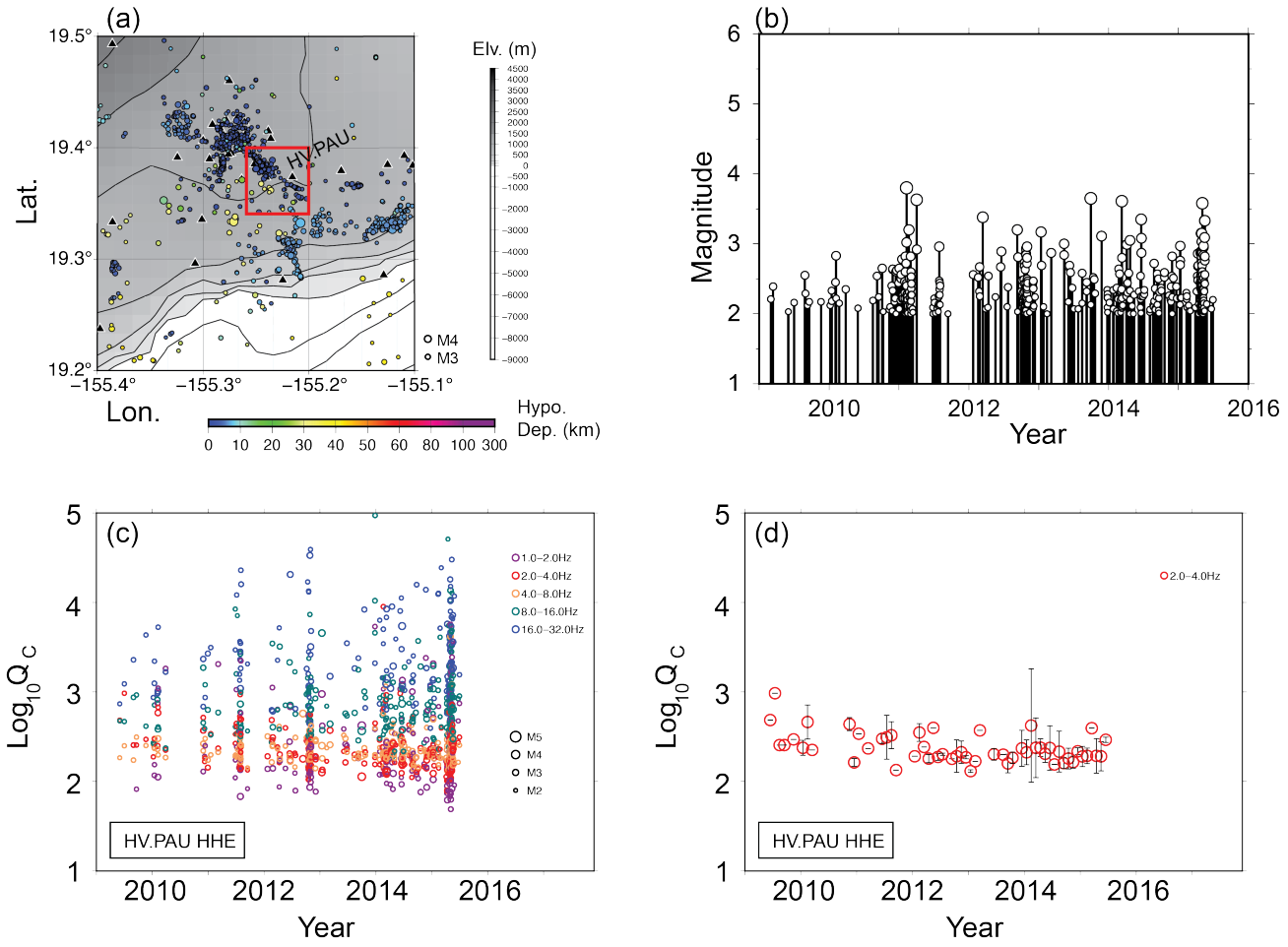


Figure 1. (a) Seismicity around Kīlauea volcano from 2009 to 2015 (Matoza et al., 2020). Circles and triangles indicate hypocenters and seismic stations, respectively. Earthquakes in the red square were used for the coda-Q analysis in this study. (b) Magnitudes of earthquakes as a function of time in the study area. (c) Estimated values of coda-Q for individual earthquakes at a station HV.PAU for the five analyzed frequency bands. (d) A temporally smoothed result in each month for a frequency band of 2 to 4 Hz. Vertical bars indicate standard errors.

©2021. Japan Geoscience Union. All Right Reserved.

A prototype of advanced Multi-GAS for unmanned aircraft systems

*Masaaki Morita[1], Toshiya Mori[2]

1. Geological Survey of Japan, AIST, 2. Graduate School of Science, The University of Tokyo

The composition of volcanic gases reflects the temperature and pressure where they exsolved from magma and the chemical equilibrium reactions during their ascent to the surface. A measurement of their composition is essential to understand the supply system of volcanic gases and their fluctuations during the volcanic unrest. In addition to a conventional method of the volcanic gas composition measurement (sampling and wet chemical analysis), in-situ measurement of plume composition using multiple gas sensors (Multi-GAS: Shinohara et al., 2005, JVGR; Aiuppa et al., 2005, GRL) has become possible. A smaller and lighter Multi-GAS has been recently made with minimal gas sensors, batteries, and data loggers. It has been installed on unmanned aircraft systems (UASs, drones) and has operated at volcanoes with limited access to the craters or volcanoes that are inaccessible due to eruptions (Mori et al., 2016, EPS; Rüdiger et al., 2018, AMT; Stix et al., 2018, JGR; Liu et al., 2018, G-cubed).

In Multi-GAS measurements, the sensor detects changes in the concentration of each component relative to the surrounding atmosphere, and the composition is calculated by the concentration ratio of each component based on the correlation of the concentration changes. It is currently necessary to balance the payload of the drone and the type and accuracy (signal-to-noise ratio) of the onboard gas sensors depending on the situation. At present, it is difficult to measure the main components of volcanic gases comprehensively and accurately with a small drone for general use, and on the other hand, even if a large drone for industrial use can mount high-quality sensors, it is difficult to carry the drone and its peripheral equipment, and the mobility of the drone must be sacrificed to some extent. Therefore, in this study, we have tried to create a lightweight and highly functional drone-borne Multi-GAS that can measure the major components of volcanic gases comprehensively and accurately.

The prototype of drone-borne Multi-GAS (size: L 16 cm ×W 21 cm ×H 14 cm) consisted of a non-dispersive infrared spectroscopic CO_2 sensor and a solid-state H_2O sensor (SBA-5, PP Systems, Amesbury, USA), controlled potential electrolysis SO_2 and H_2S sensors (KTS-512P and KHS 5TA, Komyo Rikagaku Kogyo, Kawasaki, Japan), and a semiconductor H_2 sensor (SB-19, Nissha FIS, Osaka, Japan). The analog output of each sensor was recorded to an SD card inside the Multi-GAS by using a microcomputer Lazurite Sub-GHz (LAPIS Technology, Yokohama, Japan; 12 bit AD converter) and a data logging shield for Arduino (Adafruit Industries, New York, USA). The data were also transferred to the pilot in real-time via specified low-power radio communication (920 MHz band). The weight of the Multi-GAS alone was about 600 g, and it is possible to fly safely within the allowable payload of a small industrial drone that can be carried by researchers at volcanoes (e.g., DJI's Matrice 200 V2, 4.69 kg weight with batteries, 1.45 kg maximum payload).

In the future, we will conduct a flight test at an actual volcano to evaluate the measurement accuracy of the new drone-borne Multi-GAS and the data transfer by radio communication. Also, it is necessary to conduct comparative observations with a conventional Multi-GAS to evaluate its performance.

Keywords: Multi-GAS, Volcanic gas, Volcanic plume, UAS, Drone

©2021. Japan Geoscience Union. All Right Reserved.

[J] Oral | S (Solid Earth Sciences)：S-VC Volcanology

Sat. Jun 5, 2021 1:45 PM - 3:15 PM JST | Sat. Jun 5, 2021 4:45 AM - 6:15 AM UTC | Ch.25 Zoom Room 25

[S-VC31] Dynamics of volcanic eruptions and their physical and chemical processes

convener:Yujiro Suzuki(Earthquake Research Institute, The University of Tokyo), Atsuko Namiki(Graduate School of Environmental Studies, Nagoya University), Masatoshi Ohashi(Earthquake Research Institute, the University of Tokyo), Chairperson:Yujiro Suzuki(Earthquake Research Institute, The University of Tokyo), Masatoshi Ohashi(Earthquake Research Institute, the University of Tokyo)

A Volcanic eruption is a hazardous phenomenon that results from a sequence of coupled processes, including storage in the subsurface and ascent to the surface. The volcanic gas exsolving from the ascending magma generates bubbles, which influence both the potential energy of the magma (density) and its resistance to flow (viscosity). Bubbles can sometimes deform and/or fragment the surrounding magma, leading up to explosive eruptions that develop volcanic plumes and/or pyroclastic flows. A broad range of approaches is required to tackle these processes and better understand the factors that govern the physics of explosive eruptions. We welcome contributions from interdisciplinary approaches, including, geophysical observations of active/quiet volcanoes, geochemical measurements of eruptive products, theoretical approaches, and numerical simulations, and laboratory experiments designed to explore the fundamental processes underlying explosive volcanism.

1:45 PM - 2:15 PM JST | 4:45 AM - 5:15 AM UTC

[SVC31-01] Experimental constraint on redox evolution of magma during decompression

★Invited Papers

*Satoshi Okumura[1], Hidemi Ishibashi[2], Shoichi Itoh[3], Akimasa Suzumura[3], Yoshihiro Furukawa[1], Takahiro Miwa[4], Hiroyuki Kagi[5] (1.Division of Earth and Planetary Materials Science, Department of Earth Science, Graduate School of Science, Tohoku University, 2.Department of Geosciences, Fuculty of Science, Shizuoka University, 3.Division of Earth and Planetary Sciences, Graduate School of Science, Kyoto University, 4.National Research Institute for Earth Science and Disaster Resilience, 5.Geochemical Research Center, Graduate School of Science, The University of Tokyo)

2:15 PM - 2:30 PM JST | 5:15 AM - 5:30 AM UTC

[SVC31-02] Factors affecting the sequence of Asama volcano 1783 eruption inferred from rock texture

*Tatsuki Mizuno[1], Fukashi Maeno[1], Atsushi Yasuda[1] (1.Earthquake Research Institute, Department of Earth and Planetary Science, University of Tokyo)

2:30 PM - 2:45 PM JST | 5:30 AM - 5:45 AM UTC

[SVC31-03] Genesis of vesiculation in dolerite sills of the Shimokawa ophiolite in the northern Hidaka belt, Hokkaido: Genesis of trachyte in the MORB

*Kato Satomi[1], Sumio Miyashita[2] (1.Graduate School of Science and Technology, Niigata University, 2.Hokkaido Research Center of Geology)

2:45 PM - 3:15 PM JST | 5:45 AM - 6:15 AM UTC

[SVC31-04] Discussion time

*Yujiro Suzuki[1] (1.Earthquake Research Institute, The University of Tokyo)

Experimental constraint on redox evolution of magma during decompression

*Satoshi Okumura[1], Hidemi Ishibashi[2], Shoichi Itoh[3], Akimasa Suzumura[3], Yoshihiro Furukawa[1], Takahiro Miwa[4], Hiroyuki Kagi[5]

1. Division of Earth and Planetary Materials Science, Department of Earth Science, Graduate School of Science, Tohoku University, 2. Department of Geosciences, Fuculty of Science, Shizuoka University, 3. Division of Earth and Planetary Sciences, Graduate School of Science, Kyoto University, 4. National Research Institute for Earth Science and Disaster Resilience, 5. Geochemical Research Center, Graduate School of Science, The University of Tokyo

Redox condition of magma controls stable mineral phases and coexisting chemical species of volcanic gases; hence, its information is essential to the understanding of magmatism in the crust and volcanic eruption. A recent petrological study (Waters and Lange, 2016) demonstrated that redox condition of hydrous rhyolite is not changed during magma ascent to the surface. However, this conflicts with laboratory experiments, that is, strongly oxidation of hydrous rhyolite during decompression was observed from decompression experiments (Humphreys et al. 2015). To resolve this problem, we focused on sulfur that is a major volatile component in magma but not considered in previous studies, and experimentally investigated redox evolution of sulfur-bearing hydrous rhyolite during decompression.

We performed decompression experiments for sulfur-bearing hydrous rhyolitic glasses. The glassy samples were sealed in a gold tube and heated at 800˚C under 100 MPa in a cold-seal pressure vessel. The continuous decompressions to 10, 30 and 50 MPa were isothermally carried out with rates of 10 and 100 MPa/h. The run products were observed under SEM. Bulk sulfur contents of the samples and water and sulfur contents in glass parts of the samples were measured using EA and SIMS, respectively. To investigate redox evolution, the Fe K-edge XANES spectra of the glass parts were measured and ferric to total iron ratio (Fe^{3+}/Fe_{total}) was determined based on the calibration using standard samples on loan from the National Museum of Natural History, Smithsonian Institution. The oxygen fugacity (fO_2) was calculated from the measured Fe^{3+}/Fe_{total} value and the empirical relationship between the Fe^{3+}/Fe_{total} ratio and fO_2 (Kress and Carmichael, 1991).

Our experimental results showed that the fO_2 slightly decreases with decompression. No clear effect of decompression rate was observed. The water contents decreased with decompression and were almost consistent with equilibrium solubility. In contrast, the sulfur contents showed a slight decrease during decompression from 100 to 50 MPa and then no clear increase and decrease during additional decompression.

The results obtained were compared with the redox evolution predicted from the thermodynamic model of Burgisser et al. (2015). The model shows that magma is reduced if the existence of a pre-exsolved fluid phase is assumed, while magma is oxidized when it contains only water or no pre-exsolved fluid phases. This is because sulfur buffers the oxidation of magma through a reaction with oxygen in the fluid phase. In our experiments, pre-exsolved fluid phase existed and the experimental and theoretical redox evolutions are qualitatively consistent. Based on these results, we inferred that the redox condition of sulfur-bearing hydrous magma is not oxidized during explosive volcanism with a pre-exsolved fluid phase and closed-system degassing. In contrast, if magma contains only water or sulfur-bearing hydrous magma experiences open-system degassing, it may be oxidized. Finally, we conclude that the effects of fluid composition, pre-exsolved fluid phases, and degassing processes on redox evolution must be evaluated to

©2021. Japan Geoscience Union. All Right Reserved.

understand redox evolution during decompression and thus to determine redox condition of magma reservoir.

Keywords: magma, redox condition, decompression, water, sulfur

©2021. Japan Geoscience Union. All Right Reserved.

Factors affecting the sequence of Asama volcano 1783 eruption inferred from rock texture

*Tatsuki Mizuno[1], Fukashi Maeno[1], Atsushi Yasuda[1]

1. Earthquake Research Institute, Department of Earth and Planetary Science, University of Tokyo

Plinian eruption is characterized by a large, sustained column, and often changes into pyroclastic flow eruptions. Determining how the eruptive style changes is important for predicting such volcanic activity. Processes during magma ascent such as crystallization, degassing, and vesiculation are reflected in rock texture, thus analyses of rock texture are important to constrain magma ascent process. In this study, we focus on the 1783 eruption of Asama Volcano, and discuss the mechanism of eruption transition through analysis of chemical composition and observation of rock texture. In the climactic phase of 1783 eruption, Plinian column was generated and pumice-fall deposits are formed at first, then eruptive style changed to pyroclastic flow later. Pumice-fall deposits are divided into 14 layers. Upper half of deposits were formed in climactic phase. In the middle level of deposits, there are some reddish-brown silt layer which might come from pyroclastic flows before climactic phase. Each layer in the middle level contain more than 10 wt.% of juvenile lava fragments.

The 14 layers of Pumice-fall deposits and two types of pyroclastic flow deposits are chosen for measurement of density, microscopy, and chemical analysis. The average apparent densities range 0.7-0.8 g/cm^3 for fall deposits, 0.8-0.9 g/cm^3 and >1.20 g/cm^3 for pyroclastic flow deposits. Groundmass glass is heterogeneous in some cases, and SiO_2 content shows bimodal distribution around 67 wt.% and 73 wt.%. Pyroclastic flow deposits have lower SiO2 glass than pumice-fall deposits. Magma temperature (T) and water content (Cw) are estimated based on the compositions of plagioclase and glass matrix (Putirka, 2008; Waters and Lange, 2015). For pyroclastic flow deposits (67 wt.% in SiO_2), T = 1030-1090℃ and Cw = 1.6-2.0 wt.%. For pyroclastic fall deposits (73 wt % in SiO_2), T = 960-1000℃ and Cw = 1.9-2.3 wt.%. Bubble size distribution is basically bimodal, which is characterized by bubbles smaller than 100 μm that were formed just before the eruption and bubbles larger than 100 μm that were strongly affected by coalescence or formed in the magma reservoir. Bubbles smaller than 5 μm are significantly included in pumices from the pyroclastic flow deposits. The bubble number density (BND) is about 10^{14}-10^{15} (bubbles/m^3). Using the method of Toramaru (2006) and BND, SiO_2 content, water content, and temperature, decompression rates were estimated to be 4.2-12 MPa/s for fall deposits, 16-21 MPa/s for fall deposit with reddish ash, and 15-36 MPa/s for pyroclastic flow deposits, respectively. These values are significantly larger than the decompression rate estimated in assumption of steady-state ascent, suggesting that the magma ascent for the 1783 eruption cannot be explained by steady state process.

Increase of juvenile lava fragments in the deposits of pyroclastic flow phases suggests that the lava-plug was formed onto the upper conduit. In this situation, when the lava-plug was ruptured, the rapid decompression may cause bubble nucleation effectively. In the pyroclastic flow deposit, small size bubbles less than 5 μm are remarkable and they show high number density. Such pyroclasts also have low vesicularity. In the pyroclastic flow phase, bubble growth and coalescence were not promoted. This suggests that the time between bubble nucleation and magma fragmentation might be shorter due to deeper fragmentation front. Based on the observation that amount of non-juvenile fragments are not significantly changed, a significant increase of the vent radius and decrease in the exit velocity are unlikely. If the time between decompression (thus bubble nucleation) and magma fragmentation was

©2021. Japan Geoscience Union. All Right Reserved.

shorter, the amount of gas precipitated into the gas phase will decrease and may not be easily separated from pyroclastic particles to outside without promoting coalescence of bubbles. This process will reduce the amount of gas supplied to the plume and is possible to contribute to generate pyroclastic flows.

Keywords: Asama Volcano, eruptive style, magma ascent process

©2021. Japan Geoscience Union. All Right Reserved.

Genesis of vesiculation in dolerite sills of the Shimokawa ophiolite in the northern Hidaka belt, Hokkaido: Genesis of trachyte in the MORB

*Kato Satomi[1], Sumio Miyashita[2]

1. Graduate School of Science and Technology, Niigata University, 2. Hokkaido Research Center of Geology

Highly vesiculated dolerite sills are found in three places in the Shimokawa ophiolite. Dolerites which intruded into soft sediments are considerably vesiculated up to 10 % (Miyashita, 1999). Highly vesiculated dolerite sill 1 has different texture and vesiculation texture between the margin part and inside part. There are few researches dealing with texture and vesiculation texture. In this presentation, we clarified texture and vesiculation texture and examined a process of vesiculation in the dolerite sill. We present new finding of Ab-Kfs veins and aggregates. Based of the geological and chemical features of the Ab-Kfs veins and aggregate, we examined the formation process.

The Shimokawa ophiolite is exposed in the northern part of central Hokkaido. Serpentinized harzburgite and gabbro occur at the lowest part. The lower part of the main body consists of alternation of dolerite and sediments, the upper part consists of pillow lava, and the middle part shows intermediate features between the upper and lower parts. Dolerites show MORB features (Miyashita and Watanabe, 1988).

Highly vesiculated dolerite sill 1 about 22 to 24 m thick occurs at the lowest horizon in the highly vesiculated dolerite sills. Dolerite is composed plagioclase, clinopyroxene and opaque minerals. The marginal part of the sill shows hyalo-ophitic textures, inside part show dolerite texture, and the most upper part shows fine-grained dolerite texture. Vesicles are irregular shape, about 1 mm^2 size, filled with chlorite and quartz. We measured vesicularities of 22 samples. The marginal part within 50 cm from the contact is not vesiculated. Vesicularities increase as much as 10 vol % upward until about 18 m from the lower contact. But dolerites containing Ab-Kfs veins show high vesicularity. Plagioclase number densities (PND) show a systematic variation. The margin shows a high value (40 number/mm^2) and inside shows low values (4-6 number/mm^2), implying that the margin is fine-grained and inside is coarse-grained. The PND of basalt containing the Ab-Kfs vein is higher than the surrounding rocks (15 number/mm^2), indicating fine-grained than the surrounding basalts. Above facts suggest that the Ab-Kfs veins were formed before the solidification of the sills.

The Ab-Kfs vein and aggregates are found from 8 locations in the highly vesiculated dolerite sill 1. In the marginal part of the sill the Ab-Kfs aggregates appearing intergranular crystals, show irregular shape and $<100\,\mu m^2$ size. The Ab-Kfs veins are >2 mm width and thicker than later calcite veins. The border of the Ab-Kfs vein is not straight and waves. It is noted that the Ab-Kfs veins do not cut primary igneous crystals. The Ab-Kfs veins and aggregates are mostly composed of albite and K-feldspar. The bulk composition of the veins estimated from averaged analyses from 44 spot measured by SEM-EDS exhibits a trachytic composition (IUGS igneous rock classification). The bulk compositions are also estimated from color mapping and mineral analyses by EPMA-WDS of the vein and shows again similar trachytic composition. The Ab-Kfs veins have irregular shaped vesicles of 3 mm^2 size which are filled with chlorite and quartz. It’s difficult that trachyte melts were produced by fractional crystallization of MORB magma. Trachyte melts are brought from outside the dolerite sill.

The Shimokawa ophiolite generally shows poor vesiculation. Dolerite sill 1 shows high vesiculation except for the chilled margin. PND analyses show a systematic variation. The margin shows a fine-grained and

©2021. Japan Geoscience Union. All Right Reserved.

inside shows coarse-grained. Texture made by crystallization after magma intrudes. The chilled margin is not vesiculated, but inside of the sill is vesiculated > 5 %. We found 2 type of Ab-Kfs aggregates one is vein in the inside parts, the other is aggregates in the chilled margin. Composition of the Ab-Kfs vein is trachytic. Here we show trachytic melts is interstitial melt brought from outside the MORB magma. Surrounding dolerites of the Ab-Kfs veins are highly vesiculated. Therefore, the Ab-Kfs veins release volatile components into magma. The factor of the high vesiculation in the dolerite sill 1 is multiple.

[1]Miyashita and Watanabe, 1988. [2]Miyashita, 1999.

Keywords: Hokkaito Hidaka belt, dorelite sill, Shimokawa ophiolite, vesiculation

©2021. Japan Geoscience Union. All Right Reserved.

Discussion time

*Yujiro Suzuki[1]

1. Earthquake Research Institute, The University of Tokyo

Poster presenters can give a flash talk within 3 minutes.

©2021. Japan Geoscience Union. All Right Reserved.

[J] Oral | S (Solid Earth Sciences)：S-VC Volcanology

Sat. Jun 5, 2021 3:30 PM - 5:00 PM JST | Sat. Jun 5, 2021 6:30 AM - 8:00 AM UTC | Ch.25 Zoom Room 25

[S-VC31] Dynamics of volcanic eruptions and their physical and chemical processes

convener:Yujiro Suzuki(Earthquake Research Institute, The University of Tokyo), Atsuko Namiki(Graduate School of Environmental Studies, Nagoya University), Masatoshi Ohashi(Earthquake Research Institute, the University of Tokyo), Chairperson:Atsuko Namiki(Graduate School of Environmental Studies, Nagoya University), Masatoshi Ohashi(Earthquake Research Institute, the University of Tokyo)

A Volcanic eruption is a hazardous phenomenon that results from a sequence of coupled processes, including storage in the subsurface and ascent to the surface. The volcanic gas exsolving from the ascending magma generates bubbles, which influence both the potential energy of the magma (density) and its resistance to flow (viscosity). Bubbles can sometimes deform and/or fragment the surrounding magma, leading up to explosive eruptions that develop volcanic plumes and/or pyroclastic flows. A broad range of approaches is required to tackle these processes and better understand the factors that govern the physics of explosive eruptions. We welcome contributions from interdisciplinary approaches, including, geophysical observations of active/quiet volcanoes, geochemical measurements of eruptive products, theoretical approaches, and numerical simulations, and laboratory experiments designed to explore the fundamental processes underlying explosive volcanism.

3:30 PM - 3:45 PM JST | 6:30 AM - 6:45 AM UTC

[SVC31-05] The run-out distance of large-scale pyroclastic density currents in magmatic and phreatomagmatic eruptions: Numerical simulations of a two-layer depth-averaged model

*Hiroyuki A. Shimizu[1], Takehiro Koyaguchi[2], Yujiro J. Suzuki[2] (1.National Research Institute for Earth Science and Disaster Resilience, 2.Earthquake Research Institute, The University of Tokyo)

3:45 PM - 4:00 PM JST | 6:45 AM - 7:00 AM UTC

[SVC31-06] Effects of the dynamics of conduit flow with a plug on pre-eruptive crustal deformation

*Tomofumi Kozono[1], Chihiro Matsuno[2] (1.Department of Geophysics, Graduate School of Science, Tohoku University, 2.IDAJ Co., LTD.)

4:00 PM - 4:15 PM JST | 7:00 AM - 7:15 AM UTC

[SVC31-07] Volcanic glow fluctuation prior to vulcanian eruptions at Showa Crater, Sakurajima volcano, Japan

*Dan Muramatsu[1], Koki Aizawa[2], Akihiko Yokoo[3], Masato Iguchi[4] (1.Department of Earth and Planetary Sciences, Graduate School of Science, Kyushu University, 2.Institute of Seismology and Volcanology, Faculty of Science, Kyushu University, 3.Aso Volcanological Laboratory, Institute for Geothermal Sciences, Kyoto University, 4.Sakurajima Volcano Research Center, Disaster Prevention Reserach Institute, Kyoto University)

4:15 PM - 4:45 PM JST | 7:15 AM - 7:45 AM UTC

[SVC31-08] Discussion time

*Atsuko Namiki[1] (1.Graduate School of Environmental Studies, Nagoya University)

4:45 PM - 5:00 PM JST | 7:45 AM - 8:00 AM UTC

[SVC31-09] Discussion

The run-out distance of large-scale pyroclastic density currents in magmatic and phreatomagmatic eruptions: Numerical simulations of a two-layer depth-averaged model

*Hiroyuki A. Shimizu[1], Takehiro Koyaguchi[2], Yujiro J. Suzuki[2]

1. National Research Institute for Earth Science and Disaster Resilience, 2. Earthquake Research Institute, The University of Tokyo

During large-scale explosive volcanic eruptions, a mixture of volcanic particles and gas is continuously ejected from the volcanic vent and can flow along the ground surface as a pyroclastic density current (PDC). Understanding the relationship between the run-out distance of PDCs (i.e., the extent of PDC deposits) and the eruption conditions (e.g., the magma discharge rate and the mass fraction of external surface water mixed with the magma) is desired to mitigate volcanic hazard associated with explosive eruptions. In particular, the effect of the surface-water mass fraction is a key issue, because it closely relates to the eruption style (i.e., magmatic and phreatomagmatic eruptions). This study aims to clarify the effect of surface water on the run-out distance of large-scale PDCs on the basis of numerical simulations of PDC dynamics.

PDC is a gravity current with strong stratification of particle concentrations; its run-out distance is determined by lift-off of the upper dilute current (particle concentrations <~1 vol.%) or deposition of the lower dense current (~10-50 vol.%). In order to reproduce this basic property, we have developed a two-layer depth-averaged model. This model can evaluate the effect of the temperature decrease due to surface water on the PDC dynamics through the suppression of the thermal expansion of the entrained air in the dilute current (e.g., Shimizu et al., 2019, JpGU Meeting, SVC37-09). In addition, this study considers the phase change between water vapor and liquid water and the latent heat associated with the phase change on the basis of the fact that the temperature of PDCs can become less than 100℃ by a large amount of surface water. We assume that a homogeneous mixture consisting of magma and surface water is steadily supplied during time >0 from the source vent and it spreads as a two-layer PDC radially from the source along the horizontal ground surface. We performed a parametric study for various mass fractions of surface water at the source (i.e., (mass of surface water)/(mass of magma and surface water)=0-0.5).

The numerical results show that as the dilute current spreads from the source, its flow density decreases through particle settling, air entrainment, and thermal expansion of the entrained air. When the frontal region of the dilute current becomes lighter than the ambient air to reverse buoyancy and lift off, the dilute current stops forward propagation and converges to a steady state (the distance between the front position and the source position is referred to as r_U). Particles settling from the base of the dilute current form a thin dense current, which also spreads radially. When the radial mass flux of the dense current at the front is balanced with the basal deposition rate, the dense current stops forward propagation and converges to a steady state (the distance between the front position and the source position is referred to as r_L). The results of the parametric study show that the relative magnitude between r_U and r_L depends on the surface-water mass fraction at the source; r_U is shorter than r_L when the surface-water mass fraction is small (<~0.2), whereas r_U is longer than r_L when the surface-water mass fraction is large (>~0.2). This variation comes from the fact that the lift-off distance of the dilute current (i.e., r_U) significantly increases as the surface-water mass fraction at the source increases. The increase in r_U results from the delay of

©2021. Japan Geoscience Union. All Right Reserved.

lift-off caused by two factors: (1) the suppression of the thermal expansion of the entrained air and (2) the increase in flow density due to the condensation of water vapor. The results for large surface-water mass fractions (i.e., $r_U > r_L$) explain the observation that stratified surge deposits originated from dilute PDCs are widely observed in the deposits of phreatomagmatic eruptions.

Keywords: Pyroclastic density current, Two-layer model, Run-out distance, Magmatic eruption, Phreatomagmatic eruption, Ignimbrite

©2021. Japan Geoscience Union. All Right Reserved.

Effects of the dynamics of conduit flow with a plug on pre-eruptive crustal deformation

*Tomofumi Kozono[1], Chihiro Matsuno[2]

1. Department of Geophysics, Graduate School of Science, Tohoku University, 2. IDAJ Co., LTD.

Pre-eruptive crustal deformation is one of the key observations for eruption precursors, and it is caused by complex magma dynamics in volcanic conduit and magma chamber. In particular, the magma flow in the conduit (i.e., the conduit flow) shows wide variations in pressure, velocity, and magma viscosity during magma ascent, which may lead to a drastic crustal deformation. Most previous studies for conduit flow modeling have mainly focused on eruption phases such as effusive and explosive eruptions and a transition process between them. In this study, for the sake of modeling a pre-eruptive process in the conduit, we developed a 1-dimensional conduit flow model in which a formation of a solid plug beneath the vent is considered. By combining this model with a model for an elastic deformation of crust surrounding the conduit-chamber system, we investigated how the conduit flow dynamics affect the pre-eruptive crustal deformation which can be geodetically measured such as by tiltmeters and strainmeters.

The conduit flow model is based on Kozono and Koyaguchi (2012) and Wong et al. (2017), in which the magma ascent velocity is described by the sum of the velocity of viscous flow and that of the solid plug. In the viscous flow, essential processes controlling magma dynamics such as equilibrium vesiculation, vertical and lateral gas escapes, crystallization kinetics, and magma viscosity change are considered. The solid plug frictionally slips on the conduit wall, following rate-dependent friction law. The transition from the viscous flow to the solid plug is assumed to occur when the frictional plug velocity is greater than the viscous flow velocity. In the crustal deformation model, the elastic modulus surrounding the conduit-chamber system is set in the 2-dimensional axisymmetric domain, and we calculate the surface displacement caused by the normal and shear stresses acting on the conduit wall and the normal stress on the chamber wall which are obtained from the conduit flow model.

In the analysis of the conduit flow, we found that the solid plug is formed beneath the vent for a low magma flow rate. When the magma influx to the magma chamber reaches a critical value, the conduit-chamber system becomes unstable, leading to abrupt transition of the conduit flow accompanied by drastic increases in the magma flow rate, the magma porosity, and the overpressure inside the conduit. During the transition, the thickness of the plug decreases, and finally, the plug diminishes. This transition can be treated as a pre-eruptive process in the conduit. The analysis of the crustal deformation revealed that the increases in the overpressure and the magma ascent velocity beneath the plug cause near-field displacements just before the eruption, leading to observable tilt and strain changes. We also found that our results qualitatively agree with tilt and strain changes observed before the Vulcanian eruptions at Sakurajima volcano, suggesting that the conduit flow-plug dynamics play a key role in excitation of the pre-eruptive crustal deformation.

Keywords: Conduit flow, Crustal deformation, Numerical model, Pre-eruptive process

©2021. Japan Geoscience Union. All Right Reserved.

Volcanic glow fluctuation prior to vulcanian eruptions at Showa Crater, Sakurajima volcano, Japan

*Dan Muramatsu[1], Koki Aizawa[2], Akihiko Yokoo[3], Masato Iguchi[4]

1. Department of Earth and Planetary Sciences, Graduate School of Science, Kyushu University, 2. Institute of Seismology and Volcanology, Faculty of Science, Kyushu University, 3. Aso Volcanological Laboratory, Institute for Geothermal Sciences, Kyoto University, 4. Sakurajima Volcano Research Center, Disaster Prevention Reserach Institute, Kyoto University

Introduction

A volcanic glow is occasionally observed at active volcanoes, which is interpreted that radiative visible light from red-hot bodies (e.g., magma) is reflected by fumarolic gas or clouds above the crater. At Showa Crater of Sakurajima volcano, the glow sometimes appears before vulcanian eruptions. Aizawa et al. (2013, JpGU) reported that the glow intensity increases from at ~1 s before the onset of the explosion and which synchronizes with the infrasound preceding phase (Yokoo et al., 2009). In this study, we re-analyze these glow events and discuss their implications for triggering processes of vulcanian eruptions.

Methods

We analyzed visible light video recordings (30 fps) and infrasound data observed at Kurokami station (Kyoto Univ.) for 36 events from 2011 to 2012. For video recordings, we calculated R-value averaged over a rectangular range (30×60 pixels) set above the crater for each frame to quantify glow intensity. For infrasound, we shifted the waveforms to their origin times based on the estimated travel times and then compared them with the time-series change of R-value.

Results

In addition to the correspondence of glow increase and infrasound preceding phase that reported by Aizawa et al. (2013, JpGU), we found 13 events in which a gradual increase in glow intensity began 2-33 seconds before the infrasound onset. The glow gradually intensifies from a few seconds to several tens of seconds before the eruption (we call stage Ⅰ), and then increases rapidly with the onset of infrasound preceding phase (stage Ⅱ), leading to an explosion.

Discussion

Since it is thought that the lava dome (caprock) caps the crater bottom before vulcanian eruptions, thermal radiations from the exposed high-temperature body (red-hot portion) due to crack formations on the dome surface may cause the glow. In this case, based on the theory of thermal radiation, there are two possible reasons for glow intensity increase: (a) temperature increase in the red-hot portion and (b) expansion of the red-hot portion without temperature increase. Thus, we calculated G/R ratio (green light / red light) based on a methodology of color ratio pyrometry as an indicator of temperature change. Consequently, we suggest that the glow intensity increased by the mechanism (b) in stage Ⅰ and (a) in stage Ⅱ. Therefore, stage Ⅰ may reflect, e.g., the widening of cracks due to the expansion of the lava dome and accompanying expansion of the red-hot portion, and stage Ⅱ correspond to a rapid temperature increase due to an opening of crack which reaches a gas pocket beneath the caprock.

Keywords: Vulcanian eruption, Volcanic glow, Sakurajima volcano

©2021. Japan Geoscience Union. All Right Reserved.

Discussion time

*Atsuko Namiki[1]

1. Graduate School of Environmental Studies, Nagoya University

Poster presenters can give a flash talk within 3 minutes.

©2021. Japan Geoscience Union. All Right Reserved.

[J] Oral | S (Solid Earth Sciences) | S-VC Volcanology

[S-VC31] Dynamics of volcanic eruptions and their physical and chemical processes

convener:Yujiro Suzuki(Earthquake Research Institute, The University of Tokyo), Atsuko Namiki(Graduate School of Environmental Studies, Nagoya University), Masatoshi Ohashi(Earthquake Research Institute, the University of Tokyo), Chairperson:Atsuko Namiki(Graduate School of Environmental Studies, Nagoya University), Masatoshi Ohashi(Earthquake Research Institute, the University of Tokyo)

Sat. Jun 5, 2021 3:30 PM - 5:00 PM Ch.25 (Zoom Room 25)

A Volcanic eruption is a hazardous phenomenon that results from a sequence of coupled processes, including storage in the subsurface and ascent to the surface. The volcanic gas exsolving from the ascending magma generates bubbles, which influence both the potential energy of the magma (density) and its resistance to flow (viscosity). Bubbles can sometimes deform and/or fragment the surrounding magma, leading up to explosive eruptions that develop volcanic plumes and/or pyroclastic flows. A broad range of approaches is required to tackle these processes and better understand the factors that govern the physics of explosive eruptions. We welcome contributions from interdisciplinary approaches, including, geophysical observations of active/quiet volcanoes, geochemical measurements of eruptive products, theoretical approaches, and numerical simulations, and laboratory experiments designed to explore the fundamental processes underlying explosive volcanism.

4:45 PM - 5:00 PM

[SVC31-09]Discussion

©Japan Geoscience Union

[J] Poster | S (Solid Earth Sciences)：S-VC Volcanology

Sat. Jun 5, 2021 5:15 PM - 6:30 PM JST | Sat. Jun 5, 2021 8:15 AM - 9:30 AM UTC | Ch.16_2

[S-VC31] Dynamics of volcanic eruptions and their physical and chemical processes

convener:Yujiro Suzuki(Earthquake Research Institute, The University of Tokyo), Atsuko Namiki(Graduate School of Environmental Studies, Nagoya University), Masatoshi Ohashi(Earthquake Research Institute, the University of Tokyo)

A Volcanic eruption is a hazardous phenomenon that results from a sequence of coupled processes, including storage in the subsurface and ascent to the surface. The volcanic gas exsolving from the ascending magma generates bubbles, which influence both the potential energy of the magma (density) and its resistance to flow (viscosity). Bubbles can sometimes deform and/or fragment the surrounding magma, leading up to explosive eruptions that develop volcanic plumes and/or pyroclastic flows. A broad range of approaches is required to tackle these processes and better understand the factors that govern the physics of explosive eruptions. We welcome contributions from interdisciplinary approaches, including, geophysical observations of active/quiet volcanoes, geochemical measurements of eruptive products, theoretical approaches, and numerical simulations, and laboratory experiments designed to explore the fundamental processes underlying explosive volcanism.

[SVC31-P01] PHENO-BUBBLE NUMBER DENSITY (PBND) AS INDICATOR OF OVERPRESSURE IN PRE-ERUPTIVE MAGMA CHAMBER

*Indranova Suhendro[1], Atsushi Toramaru[1] (1.Department of Earth and Planetary Sciences, Graduate School of Sciences, Kyushu University)

[SVC31-P02] Crystal Fracture in the Youngest Toba Tuff (74 ka) Pumices

*Gabriela Nogo Retnaningtyas Bunga Naen[1], Atsushi Toramaru[1], Haryo Edi Wibowo[2] (1.Department of Earth and Planetary Science, Kyushu University, Fukuoka, Japan, 2.Geological Engineering Department, Universitas Gadjah Mada, Yogyakarta, Indonesia)

[SVC31-P03] Textural study of the 7.3 ka caldera-forming eruption of Kikai Caldera: Correlating bulk density to bubble-size observations

*Selvia Novianty[1], Masatoshi Ohashi[1], Atsushi Toramaru[1] (1.Department of Earth and Planetary Sciences, Graduate School of Science, Kyushu University)

[SVC31-P04] Factors controlling bulk density of pumice in explosive eruption deposits

*Atsushi Toramaru[1], Miki Ogata[1], Haruka Ino[1], Indranova Suhendro[1], Gabriela Bunga Naen[1] (1.Department of Earth and Planetary Sciences, Faculty of Sciences, Kyushu University)

[SVC31-P05] Eruptive style and sequence of the 1235 eruption of Ohachi volcano, Kirishima, Japan -constraints from distribution, shape, and texture of pyroclasts-

*Sayaka Shohata[1], Fukashi Maeno[2], Natsumi Hokanishi[2], ATSUSHI YASUDA[2] (1.Department of Earth and Planetary Science, School of Science, The University of Tokyo, 2.Earthquake Research Institute, The University of Tokyo)

[SVC31-P06] Conduit ascent process of mafic subplinian eruption: Constraints from plagioclase microlites in the 1235 scoria of Kirishima-Ohachi volcano, Japan.

*Yoshiharu Iwaki[1], Hidemi Ishibashi[1], Natsumi Hokanishi[2], ATSUSHI YASUDA[2], Toru Ishikawa[3], Taketo Shimano[4] (1.Shizuoka University Graduate School of Integrated Science and Technology, 2.Earthquake Research Institute, University of Tokyo, 3.Kirishima Geopark Council, 4.Graduate School of Environment and Disaster Reserch, Tokoha University)

[SVC31-P07] Texture of ejecta of summit eruptions in Izu-Oshima

*Yuya Ikenaga[1], Fukashi Maeno[1], ATSUSHI YASUDA[1] (1.Earthquake Research Institute, The University of Tokyo)

[SVC31-P08] Shallow conduit process of Strombolian eruption: A case study of Izu-Omuroyama monogenetic volcano, Japan

*Hidemi Ishibashi[1], Risako Hatakeyama[1], Ryuta Sakamoto[1], Natsumi Hokanishi[2], ATSUSHI YASUDA[2] (1.Faculty of Science, Shizuoka University, 2.Earthquake Research Institute, The University of Tokyo)

[SVC31-P09] **Parameters to control bubble - crystal interaction styles**

*Kyoko Ikeda[1], Atsushi Toramaru[2] (1.Department of Earth and Planetary Sciences, Graduate School of Science, Kyushu University, 2.Department of Earth and Planetary Sciences, Faculty of Science, Kyushu University)

[SVC31-P10] 3D crystal size distributions of pyroxene nanolites plotted against short-axis length reflect magma ascent dynamics

*Shota Okumura[1], Mayumi Mujin[2], Akira Tsuchiyama[3,4], Akira Miyake[1] (1.Department of Geology and Mineralogy, Graduate School of Science, Kyoto University, 2.Division of Earth and Planetary Materials Science, Department of Earth Science, Tohoku University, 3.Research Organization of Science and Technology, Ritsumeikan University, 4.Guangzhou Institute of Geochemistry, Chinese Academy of Sciences)

[SVC31-P11] Petrological characteristics of the Kawago-daira rhyolite lava, Izu Peninsula, Japan

*Hiroshi Oka[1], Motohiro Tsuboi[1], Kuniyuki Furukawa[2] (1.Kwansei Gakuin University, 2.Aichi University)

[SVC31-P12] Determination of water solubility in the rhyolitic melt at 650°C and its interpretation by "hydrogen bonding model"

*Mizuki Nishiwaki[1], Takahiro Miwa[2] (1.Department of Earth and Planetary Sciences, Graduate School of Sciences, Kyushu University, 2.National Research Institute for Earth Science and Disaster Resilience)

[SVC31-P13] Flowage of the 1991 Unzen lava: Discussion to Goto et al.(2020) Rigid migration of Unzen lava rather than flow. JVGR

*Hiroaki Sato[1], Shigeru Suto[2], Tadahide Ui[3], Toshitsugu Fujii[4], Takahiro Yamamoto[2], Shinji Takarada[2], Keiichi Sakaguchi[2] (1.Kobe Univ., 2.Geological Survey of Japan, 3.Hokkaido Univ., 4.Mount Fuji Research Institute)

PHENO-BUBBLE NUMBER DENSITY (PBND) AS INDICATOR OF OVERPRESSURE IN PRE-ERUPTIVE MAGMA CHAMBER

*Indranova Suhendro[1], Atsushi Toramaru[1]

1. Department of Earth and Planetary Sciences, Graduate School of Sciences, Kyushu University

Magma chamber overpressure which caused by the oversaturation of preexisting bubbles (hereafter referred as “pheno-bubble” as a mimic of “phenocryst” in the common terminology of crystals in magma chamber) has been considered as one of the most important factors for triggering explosive volcanic eruptions. However, such qualitative and quantitative information of pheno-bubbles which are preserved in juvenile materials (e.g. pumice and scoria) is not yet provided. Therefore, in this study, we present the qualitative and quantitative study of pheno-bubble by examining natural samples which were obtained from 16 volcanoes, ranging from the VEI (volcanic explosivity index) 3 to 8 eruptions with various eruption style (subplinian to caldera forming eruptions) and various magma compositions (basaltic andesite to rhyolite). Based on our 2D-bubble size distributions (BSDs) data, we confirm that pheno-bubble can be defined as bubbles with diameter larger than approximately 0.1 mm, regardless to its compositions. We found that the number densities of pheno-bubble (PBND) in pre-eruptive magma chamber exhibit positive correlation with VEI. Particularly, VEI 3-5 eruptions have typically smaller PBNDs value (0.07 to 0.3x10^{11} m^{-3}) compared to VEI 6-8 eruptions (0.8 to 2x10^{11} m^{-3}). This suggest that the large and long-lived magma chambers experience with more intense heterogeneous nucleation of bubbles (or second boiling) thus results in more intense supersaturation of volatiles and provides larger amount of overpressure. In addition, we also found that bulk density has strong dependence on PBND value, as supported by the fact that juvenile materials from VEI 3-5 eruptions are typically denser than VEI 6-8 eruptions (avg. 0.6-1.4 gr/cm^3 and 0.3-0.8 gr/cm^3, respectively).

Keywords: Pheno-bubble, Pheno-bubble number density, Magma chamber, Overpressure, Explosive eruptions, Bulk density

©2021. Japan Geoscience Union. All Right Reserved.

Crystal Fracture in the Youngest Toba Tuff (74 ka) Pumices

*Gabriela Nogo Retnaningtyas Bunga Naen[1], Atsushi Toramaru[1], Haryo Edi Wibowo[2]

1. Department of Earth and Planetary Science, Kyushu University, Fukuoka, Japan, 2. Geological Engineering Department, Universitas Gadjah Mada, Yogyakarta, Indonesia

Pumice clasts from the enormous eruption of the Youngest Toba Tuff (YTT) contain crystals that are fragmented. That special texture is commonly seen as a product of large caldera-forming eruptions, thus understanding the origin of it can help to reveal the factors that lead to the eruptions. This study focuses on white pumices from non-welded YTT, especially feldspar (plagioclase and alkali feldspar) as the most abundant crystal and is expected to record the dynamic processes of YTT super eruption.

YTT white pumices consist of transparent (TWP: mainly containing larger vesicles, > 0.1 mm) and non-transparent pumices (NTWP: mainly containing smaller vesicles, < 0.1 mm). We studied 25 thin sections of pumice clasts with optical microscope. Textural analysis was carried out using microphotographs taken by SEM and further analysed using image processing software to extract the number of crystal fragments, pheno-bubble number density (PBND), and matrix-bubble number density (MBND). Chemical analysis for feldspar chemistry was conducted using EPMA.

First, we define a fragmented crystal (hereafter “crystal”) as a region containing broken pieces that preserve the initial form as one single crystal. We tentatively classify the size of feldspar into two groups based on crystal size namely microphenocryst (< 1mm), and phenocryst (> 1mm). In addition, we quantified fractured-crystals by classifying them into two classes in terms of number of fragments included in a “crystal”: type A includes 2 –9 fragments, and type B does more than 10 fragments. Then, we examined the correlation among the average number of fragments in one thin section with total individual crystals in the same thin section, MBND, PBND, and chemical composition (anorthite content).

YTT feldspar is mostly characterized by crystal fractures (58.6%), especially up to 85.8% in phenocryst. Broken melt inclusions and melt inclusions containing vapor bubbles are observed in some of the crystals, especially associated with type B crystals. TWP is dominated by crystal type A with low average of crystal fragments per one thin section (2 –10.5) and low MBND (10^4 mm^{-3}). On the other hand, NTWP is dominated by crystal type B, which shows various values of average crystal fragments per one thin section (2 –67) and has high MBND (10^5 mm^{-3} –10^7 mm^{-3}). However, the PBND is not so much different between the two types of pumices. Furthermore, crystal type B exhibits slightly higher anorthite content (An_{35-45}) compared to less fragmented crystal type A (An_{25-35}), and occasionally crystal type B occurs with some disequilibrium textures like patchy zoning, reverse zoning, and hollow texture.

Crystal fracture in YTT is thought to be formed by several mechanisms. YTT, as a crystal-rich magma system, experienced intensive collision of crystals. Phenocrysts, compared with microphenocrysts, are characterized by high number of crystal fragments. This could be explained by their longer times in magma chamber, which expose them to various dynamic processes as implied by the disequilibrium texture. These processes facilitate the formation of the cleavage planes that accommodate the crystals to be broken. From the correlation between MBND and the crystal fragmentation class, it is found that higher decompression rates make crystals fractured more, whereas lower decompression rates make less fractured crystals. In addition, magma decompression causes the volatile explosion of melt inclusions trapped in the crystals, which forces the crystal to be broken into many pieces, as was observed in crystal

©2021. Japan Geoscience Union. All Right Reserved.

type B. Moreover, crystals with high anorthite content are characterized by high average number of fragments, suggesting that the crystal composition influences the strength of crystals which affects the crystal fracture formation.

Keywords: YTT Pumices, Crystal fracture, Feldspar, Bubble, Textural study

©2021. Japan Geoscience Union. All Right Reserved.

Textural study of the 7.3 ka caldera-forming eruption of Kikai Caldera: Correlating bulk density to bubble-size observations

*Selvia Novianty[1], Masatoshi Ohashi[1], Atsushi Toramaru[1]

1. Department of Earth and Planetary Sciences, Graduate School of Science, Kyushu University

The 7.3 eruption of Kikai Caldera is one of the catastrophic events that cause devastating damage on southern Kyushu, Japan (Maeno et al., 2007). A comprehensive study on the detailed stratigraphy and transport-mechanism of its products has been carried out by Maeno et al. (2007). Regardless, the textural study of the 7.3 ka eruptive deposits of Kikai Caldera hasn't been conducted yet. In addition to the detailed description of the stratigraphic sequence of the eruptive deposits, the bubble size observation in the pumice is useful to characterize the vesicle texture and to gain insights into the eruption dynamics such as decompression rate in the conduit and overpressure condition in the magma chamber prior to the eruption. Integrating the bulk density data to the bubble-size observation for pumices is the aim of this study.

Samples were collected from all of the layers of Unit A, Unit C, and Unit D of the 7.3 ka caldera-forming eruption of Kikai Caldera at three localities, Southern Kyushu (Distal Locality), Takeshima Island (Proximal Locality), and Satsuma-Iojima Island (Proximal Locality). From all the localities, we had confirmed the stratigraphy which is coherent with the results by Maeno et al. (2007). Bulk density analyses were conducted for the pumice grains with the selected size range (2-16 mm) by 3D scanner (Medit Solutonix D700) and measuring software (Hira 3D viewer).

We selected 1131 pumice grains from all localities and measured the wide range (0.17 g/cm^3 –1.31 g/cm^3) of pumice bulk density from Unit A, Unit C, and Unit D. From the observation of pumice grains, we identified some physical characteristic such as bubble size, bubble shape, and crystal abundance. We compared each unit and analysed the different physical characteristics from its appearance qualitatively. Thus, from the measured bulk density, Unit A (0.17 g/cm^3 –1.14 g/cm^3) has a relatively lower bulk density compared to Unit C (0.27 g/cm^3 –1.31 g/cm^3) and Unit D (0.22 g/cm^3 –1.24 g/cm^3). We observed the dominant mode bulk of Unit A (0.45 g/cm^3) angular and spherical bubble shape, crystal poor, and relatively has smaller bubble size, sometimes has a foamy appearance. On the other hand, the dominant mode of Unit C (0.54 g/cm^3) and Unit D (0.50 g/cm^3) have similar physical characteristics such as have sub-angular and frequently stretched to elongated bubble shape, have a bigger bubble size, and have prismatic jointing appearance in some grains. The ranges of densities and physical characteristics in pumices may imply that each unit has a different vesiculation and fragmentation process such as different quenching. Thus, the difference fragmentation process affects measurable properties such as shape, vesicularity, permeability, bubble, and crystal size distribution (Rust et al., 2011). In this study, we attempt to reveal the eruption dynamic between each unit by connecting the bulk density with the bubble-size observation that comprises measurement of vesicularity, bubble size distribution (BSD), bubble number density (BND); and crystal contents.

Keywords: Kikai Caldera, Textural Analyses, Bulk Density, Bubble, Fieldwork

©2021. Japan Geoscience Union. All Right Reserved.

Factors controlling bulk density of pumice in explosive eruption deposits

*Atsushi Toramaru[1], Miki Ogata[1], Haruka Ino[1], Indranova Suhendro[1], Gabriela Bunga Naen[1]

1. Department of Earth and Planetary Sciences, Faculty of Sciences, Kyushu University

The bulk density of pumice clasts produced by explosive eruptions has thought to have the significant information on vesiculation processes that the magmas experience in the volcanic conduits and the magma chambers. As known well, there are the wide variations of bulk density even in the single eruption deposits. However, it is unclear that what causes the variation in bulk density, e.g., vesicularity or crystallinity. To reveal factors controlling the bulk density variations, we examine the correlation between the bulk density and other textural properties such as vesicularity, phenocryst-crystallinity, pheno-bubble abundance, and matrix bubble abundance for three eruptions; Aira caldera forming eruption, Japan, Mount St. Helens 1980 eruption, USA, and Manijau caldera-forming eruption, Indonesia. We determine the bulk density of pumice clasts (mainly 8 –16 mm) from the volume by 3D scanner and the weight by electric balance, and conduct the textural analysis for vesicularity (pheno-bubble (PB) (>0.1 mm) and matrix-bubble (MB) (< 0.1 mm)), phenocryst-crystallinity by the 2D image analysis for the SEM microphotographs. In the case of the Aira caldera-forming eruption, both PB and MB abundance have negative correlations with the bulk density and bulk vesicularity, the crystallinity has no correlation with bulk density. In the case of the Mount St. Helens 1980 plinian eruption, PB abundance has no correlation with bulk density, whereas MB abundance has a negative correlation and crystallinity has a positive correlation with bulk density. In the case of Maninjau caldera-forming eruption, both PB and MB abundance have negative correlations with bulk densities, whereas the crystallinity has no correlation with bulk density. Thus, in two large-volume caldera-forming eruptions among these three eruptions, only vesicularity controls the bulk density. In smaller plinian eruption of Mount St. Helens 1980 eruption, in addition to vesicularity, the crystallinity controls the bulk density. In the presentation, data for other eruptions such as Toba YTT caldera forming eruption will be shown to discuss the processes to make such PB, MB and crystallinity.

Keywords: pumice, bulk density, vesicularity, phenocryst, pheno-bubble, matrix-bubble

©2021. Japan Geoscience Union. All Right Reserved.

Eruptive style and sequence of the 1235 eruption of Ohachi volcano, Kirishima, Japan -constraints from distribution, shape, and texture of pyroclasts-

*Sayaka Shohata[1], Fukashi Maeno[2], Natsumi Hokanishi[2], ATSUSHI YASUDA[2]

1. Department of Earth and Planetary Science, School of Science, The University of Tokyo, 2. Earthquake Research Institute, The University of Tokyo

The diversity of the eruptive styles of basaltic magma is still poorly understood. In particular, it is necessary to understand the processes that determine eruptive events, such as explosive eruptions and pyroclastic flows. Ohachi volcano, Kirishima, is known to have had multiple explosive eruptions during the historical period due to the presence of tephra layers. Although the general framework of the time-series change of the eruptions have been described, the details of the style change and the factors of the change have not been fully understood. In this study, we investigate Takaharu tephra associated with the 1235 eruption in detail, and discuss the eruption transition and its driving process based on the re-examination of the eruption volume and changes in rock shape, density, and textural characteristics along the time series.

Takaharu tephra is divided into three units (A-B) based on the characteristics of the constituent pyroclasts. The total volume of the tephra is estimated to be 1.5 to 2 times larger than previously estimated, indicating that the 13th century eruption may have been larger than previously thought. Furthermore, field observations unveiled that each unit can be further divided into two or three layers. We collected samples of pyroclastic flow (PDC) deposits from the stage of Unit C and each subdivided layer, and measured the apparent density and grain density (density excluding connected voids). We also carried out quantitative evaluation of grain shape, textural observation by polarized light microscopy, and identification of phenocrysts.

The apparent density measurement results showed different peaks for below the lower of Unit C and for above the middle of unit C. The lower part showed low values (0.8-1.0 g/cm3) and the upper part showed high values (1.0-1.2 g/cm3). PDC clasts also showed high values. The results of grain density measurement showed low values (about 2.6 g/cm3) for unit B and below, and high values (about 2.9 g/cm3) for unit C and above, but PDC clasts showed low values as well as unit B and below. This suggests that the PDCs have smaller amount of connected porosity. The actual calculated connected porosity is 0.59 for PDCs compared to 0.62-0.69 for tephra layers.

The shape of scoria has different characteristics for each unit at the macroscopic observation level; A is flaky, B is relatively smooth, and C is intermediate. The three indices of circularity, roundness, and solidity (shape indices) were obtained from the projected images of the particle shapes, and were found to reflect the irregularities and other features in the observation.

There is no significant difference in the phenocrysts (plagioclase, pyroxene, and olivine) throughout the layers. However, the whole rock composition is slightly rich in SiO2 in the late stage of eruption (Unit C) (Miyamoto and Tsutsui, 1996). The groundmass crystallinity is high in the order PDC >B >C >A, and the lower the crystallinity, the larger the crystal size. Microscopic bubble texture shows that A is dominated by small isolated bubbles, B is dominated by large connected bubbles, C is dominated by large but

©2021. Japan Geoscience Union. All Right Reserved.

wall-separated bubbles, and PDC is dominated by small bubbles connected in a complex manner. The textures vary with stratigraphy.

A comparison of shape index and rock texture shows that there is a relationship between them, with the exception of pyroclastic density currents. For example, in Unit A, the low crystallinity and low connected pore fraction are seemingly reflected in the roughness of the particle surface. In this case, it can be interpreted that the low viscosity magma has a high ascent velocity and it was strecthed and broken apart by the explosion to form the specific shape. The relationship we have found between particle shape/density and rock texture may be an important constraint for understanding the origin of pyroclastic particles in different units and the eruptive sequence.

Keywords: eruptive style, scoria, Ohachi volcano

©2021. Japan Geoscience Union. All Right Reserved.

Conduit ascent process of mafic subplinian eruption: Constraints from plagioclase microlites in the 1235 scoria of Kirishima-Ohachi volcano, Japan.

*Yoshiharu Iwaki[1], Hidemi Ishibashi[1], Natsumi Hokanishi[2], ATSUSHI YASUDA[2], Toru Ishikawa[3], Taketo Shimano[4]

1. Shizuoka University Graduate School of Integrated Science and Technology, 2. Earthquake Research Institute, University of Tokyo, 3. Kirishima Geopark Council, 4. Graduate School of Environment and Disaster Reserch, Tokoha University

Mildly explosive eruption is common styles of high-temperature, less viscous mafic magma. However, many cases of Plinian eruptions of mafic magmas have been reported in this decade. Recent studies suggest that microlite crystallization at the shallow conduit depth significantly increases viscosity and causes the viscous-brittle transition of mafic magma, which induces sustained fragmentation and explosion. Therefore, it is important to clarify the processes of microlite crystallization during conduit ascent for understanding the eruption mechanism of mafic magmas. The 1235 subplinian eruption is the largest eruption of Ohachi volcano, which is one of the active volcanoes in Kirishima, Japan. During the eruption, basaltic andesite magma with bulk SiO_2 content ~51-55wt.% erupted and formed three thick fall scoria layers (ThT-a, ThT-b, and ThT-c) called Takaharu scoria (Tsutsui et al., 2007). Because the groundmass crystallization occurred at the shallow conduit depth, the groundmass texture is expected to have information about the conduit ascent process of the magma. In this study, we performed textural analyses of the plagioclase microlites in Takaharu scoria to clarify the conduit ascent process of mafic magma during a subplinian eruption.

In this study, we investigated glassy scoria grains (2-8 mm in size) in ThT-a, ThT-b, and ThT-c. FE-EPMA (JEOL JCXA-8530FPlus) at Earthquake Research Institute (ERI) of the University of Tokyo, Japan, was used to acquire backscatter electron (BSE) images of the groundmass of the samples. The BSE images were quantitatively analyzed to determine crystal volume fractions, crystal number densities, and crystal size distributions (CSDs) of plagioclase microlites.

Plagioclase, olivine, orthopyroxene, and clinopyroxene were found as phenocrysts in the Takaharu scoria, with a total phenocryst contents of ~19-22 vol.%. The groundmass is composed of plagioclase, mafic minerals and glass. Because olivine and pyroxene in the groundmass are difficult to distinguish on BSE images, we treated them together as mafic minerals. The microlite contents (Φ) of plagioclase are ~10-30 vol.% for ThT-a, ~10-37 vol.% for ThT-b, and ~6-33 vol.% for ThT-c, respectively. On the other hand, the microlite contents were less than 5 vol.% for mafic minerals.

Measured CSDs for plagioclase microlites are often inflected. Least-squares regression into the combination of two distinct log-linear CSD relations was done to determine the intercept, log $n_{0,}$ and the slope, $1/L_0$, of each CSD relation. The n_0 for the finer crystals ranges ~$10^{8.6\text{-}9.4}$ mm^{-4} for ThT-a, $10^{8.7\text{-}9.7}$ mm^{-4} for ThT-b, and $10^{9.1\text{-}10.2}$ mm^{-4} for ThT-c, respectively; it increases from ThT-A to C. On the other hand, the $1/L_0$ varies in the ranges of 78-169 mm^{-1} for ThT-a, 94-166 mm^{-1} for ThT-b, and 116-261 mm^{-1} for ThT-c, respectively; it also increases from ThT-A to C. The number densities of plagioclase microlite (N) were determined from the values of n_0 and $1/L_0$. The Ns of plagioclase microlites were ~3.8×10^{15}-$1.3\times10^{16}$$m^{-3}$ for ThT-a, ~7.6×10^{15}-$3.6\times10^{16}$$m^{-3}$ for ThT-b, and ~1.0×10^{16}-$6.8\times10^{16}$$m^{-3}$ for ThT-c, respectively. N

©2021. Japan Geoscience Union. All Right Reserved.

was almost constant regardless of Φfor ThT-a, whereas positive relations between Φand N are observed for ThT-B and C.

The microlite number density decompression-rate meter (Toramaru et al., 2008) was applied to the plagioclase microlites to estimate the conduit ascent rate of the magma. The decompression rates were estimated to be in the range of ~0.31-0.73 MPa/s for ThT-a, ~0.45-1.38 MPa/s for ThT-b, and ~0.34-1.24 MPa/s for ThT-c, respectively; these are comparable with those estimated for other mafic subplinian eruptions. The estimated decompression rate increases from ThT-a to ThT-b, and then decreases to ThT-c. These results are consistent with the relation of the dispersal areas between three scoria units (Tsutsui et al., 2007). Our results suggest that the eruption intensity is controlled by the conduit ascent rate of the mafic magma.

Keywords: plagioclase, mafic subplinian eruption, Kirishima, Ohachi volcano, shallow conduit process, microlite crystallization

©2021. Japan Geoscience Union. All Right Reserved.

Texture of ejecta of summit eruptions in Izu-Oshima

*Yuya Ikenaga[1], Fukashi Maeno[1], ATSUSHI YASUDA[1]

1. Earthquake Research Institute, The University of Tokyo

Izu-Oshima, which is an active volcano erupting basaltic magma, have caused many eruptions from both summit and flank craters. The eruptions which occurred in 1986 and 1950 are known as recent middle-scale eruptions. It is also known that large-scale eruptions have occurred every 150-200 years before recent middle-scale eruptions (Nakamura 1964, Isshiki 1984, Koyama and Hayakawa 1996, Endo et al. 1988). There are various kinds of geological and petrological research in Izu-Oshima, and the sequence and magma system of each eruption has gradually become revealed (Kawanabe 1991, Nakano and Yamamoto 1991, Hamada 2014, Ishizuka et al. 2015). On the other hand, there are few studies which analyze the textures of ejecta, and the relationship between eruption intensities and textures of ejecta is not clear. We focused on the summit eruptions in this study, and analyzed the bubble and microlite textures of scoriae of Strombolian eruption (1986 eruption) and sub-Plinian eruptions (Y1, Y2, Y4 and Y6 eruptions). In Y1 eruption, scoria deposits were divided into lower part (Unit A) and upper climax part (Unit C).

We measured scoria density of each eruption by glass beads, and selected one low-density, two middle-density and one high-density samples to create thin sections. Backscattered electron images of thin sections were obtained by FE-EPMA and analyzed by ImageJ.

Bubble textures changed according to the intensities of eruptions. In 1986 eruption, large bubbles were mainly observed. On the other hand, in the sub-Plinian (Y1, Y2, Y4 and Y6) eruptions, there were many small bubbles and the bubble number densities were higher than 1986 eruption. Bubble number density was especially high in Y1 Unit C. Scoria density was highest in Y1 Unit C. Microlites were observed in almost all eruptions, except Y1 Unit C.

From bubble textural analyses, there is a tendency that scoriae include many small bubbles in high-intensity eruptions. It is assumed that magma ascent rates were high and magma was supersaturated in volatiles and bubble nucleation progressed in high-intensity eruptions. In the low-intensity eruption such as 1986 eruption, there were many large bubbles and bubble number density was low as a result of growth, coalescence and degassing of bubbles. There were nearly no microlites in Y1 Unit C. Although it is estimated that magma was highly supersaturated in this Unit, there is possibility that liquidus temperature didn’t become lower sufficiently and crystallization of microlites didn’t occur because magma ascent rate was high and volatiles couldn’t precipitate enough as bubbles.

Keywords: Izu-Oshima, Bubble texture, Microlite

©2021. Japan Geoscience Union. All Right Reserved.

Shallow conduit process of Strombolian eruption: A case study of Izu-Omuroyama monogenetic volcano, Japan

*Hidemi Ishibashi[1], Risako Hatakeyama[1], Ryuta Sakamoto[1], Natsumi Hokanishi[2], ATSUSHI YASUDA[2]

1. Faculty of Science, Shizuoka University, 2. Earthquake Research Institute, The University of Tokyo

Izu-Omuroyama volcano is one of the monogenetic volcanoes in the Higashi-Izu monogenetic volcanic field (HIMVF) and was formed by the Strombolian eruption that occurred at 4ka. The eruption formed the largest scoria cone in HIMVF and simultaneously effused abundant lava flows. In this study, we performed quantitative textural analyses of minerals and chemical analyses of glasses in the groundmass of the Izu-Omuroyama scoria to clarify the shallow-conduit processes inducing the branch of the scoria-forming explosion and the lava effusion.

The scoria of the cone-forming stage was investigated. BSE images were acquired using FE-EPMA at ERI. We quantified volume fractions (Fs), number densities (NDs), and size distributions (CSDs) by image analyses for plagioclase (80 samples) and mafic minerals (40 samples), respectively. Because it is difficult to discriminate olivine and pyroxene in BSE images, we treated these minerals collectively as mafic minerals.

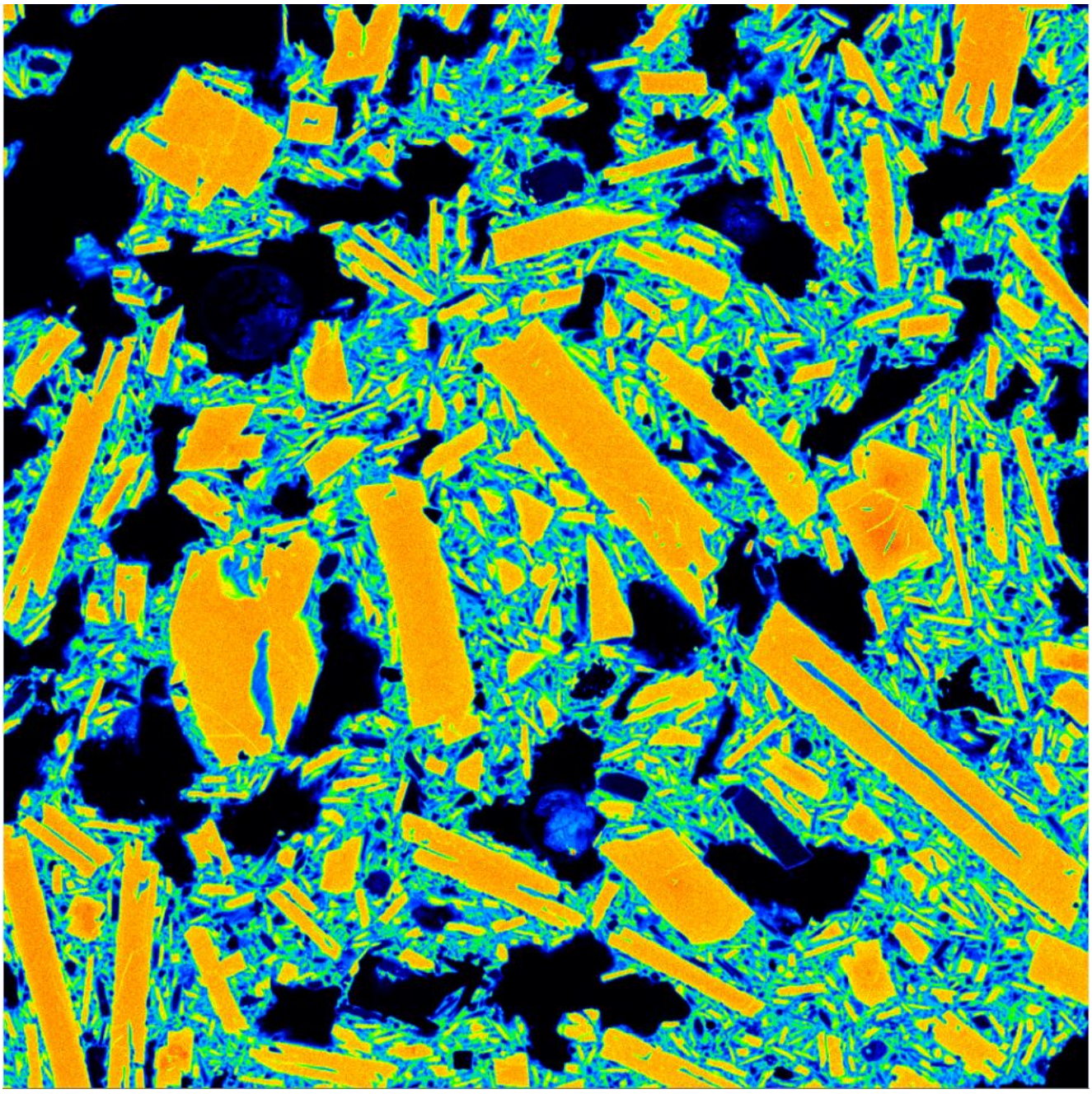
The groundmass of the scoria is composed of plagioclase, olivine, pyroxene, and glass. Fs of plagioclase and mafic minerals vary ~5-40 vol.% and ~3-20 vol.%, respectively. NDs are ~2000-20000 mm^{-1} for both minerals. An-rich, coarse and An-poor, fine plagioclase grains are found; the former and the latter are called microphenocryst and microlite, respectively. We discriminated against the microphenocrysts and the microlites based on CSDs. Inflected CSDs are found for both plagioclase and mafic minerals in the scoria; they are successfully explained by combinations of two linear CSD relations. The inflected sizes are determined for each sample. We regarded the mineral grains coarser and finer than the inflected size as microphenocrysts and microlites, respectively.

For microphenocrysts, Fs vary ~5-40 vol.% for plagioclase and ~0.4-20 vol.% for mafic minerals, respectively. NDs are 20-1000 mm^{-2} for both minerals. Positive relations are found between F and ND for both minerals. The ND of plagioclase microphenocryst increases from lower to higher units of the stratigraphy. The NDs of the higher units are similar to those of the lava flow, indicating that the groundmass texture of the lava flow can be explained by the crystal growth of microphenocryst without microlite crystallization. For microlites, Fs vary ~5-40 vol.% for plagioclase and ~2-20 vol.% for mafic minerals, respectively. The NDs are 1000-20000 mm^{-2} for both minerals. Contrary to the scoria case, the ND of plagioclase microphenocryst decreases from lower to higher units of stratigraphy. Fs of microphenocrysts are lower than ~40 vol.%, whereas those of all groundmass minerals are higher than ~40 vol.%. Previous experimental studies show that plagioclase-bearing magma behaves as solid when the F of suspended crystal is larger than ~40 vol.%, suggesting that the liquid-solid rheological transition was induced by microlite crystallization. The depth condition of microlite crystallization is constrained to be < 400m based on the chemical compositions of interstitial glasses and MELTS simulation.
Our results suggest that microlite crystallization at < 400m depth induced solidification of magma, which resulted in brittle fragmentation and explosion at the summit vent. On the other hand, the branch of the conduit to the flank vent occurred at a deeper depth than that of microlite crystallization, resulting in lava flow effusion. The increase and decrease of NDs of microphenocrysts and plagioclase microlite,

©2021. Japan Geoscience Union. All Right Reserved.

respectively, from the lower to the higher stratigraphic units can be attributed to the resupply of the deep-derived hot magma, which is consistent with the abundant lava effusion following the scoria cone formation.

Keywords: mafic magma, Strombolian eruption, microlite crystallization, Shallow conduit process, Higashi-Izu monogenetic volcano group, eruption style



©2021. Japan Geoscience Union. All Right Reserved.

Parameters to control bubble - crystal interaction styles

*Kyoko Ikeda[1], Atsushi Toramaru[2]

1. Department of Earth and Planetary Sciences, Graduate School of Science, Kyushu University, 2. Department of Earth and Planetary Sciences, Faculty of Science, Kyushu University

In the magma, the interaction between suspended crystals and the rising bubble due to buoyancy is important because their stratification through the rheological properties and bulk densities. Belien et al. (2010) showed that there are three interactionstyleswithchangingbubblediameter bylaboratoryexperimentsusingan analog material: a single plastic cube and a controlled single bubble in viscous liquid. However, the crystal - bubble interaction is still poorly understood because factors determining the interaction styles have not been revealed in terms of dimensionless parameters. In order to solve this problem, we try to find the dimensionless parameters by the analogue experiments with varying viscosity and size ratio of solid cube to bubble.

The experiments are performed in the tank filled with viscous liquid (analog material of silicate melt) and prepared six different viscosity(0.041 Pa・s –47.2 Pa・s). The plastic cube (analog material of crystal) with 10 mm is suspended in liquid by a rod. The bubble is injected into the liquid from 11cm below the plastic cube from a syringe connected to a motor controlled by the PC program by which we can change the initial bubble size. We examine the probability of occurrence of three styles of interaction: "stuck", "pass", and "split"; "stuck" in which a bubble stays below the solid cube, "pass" in which a bubble passes around the cube and "split" in which a bubble splits into two bubbles. To determine the probabilities, we did the repetition of 10 times for the same condition of initial bubble radii and viscosity.

In our experiments, we observed two styles of the interaction of "stuck" and "pass" and not "split". It is found that the smaller bubble tends to “stuck”, on the other hand, the probability of “pass” became higher as the bubble radii are larger. To reveal the boundary of “stuck” and “pass”, we estimated three parameters in my previous research (Ikeda and Toramaru, 2020 JpGU meeting) ; the size ratio of the crystal and the bubble, the Bond number(Bo), which represents the deformation scale of the bubble caused by buoyancy, and the Reynolds number(Re), which is the ratio of inertial to viscous forces. In high Re regime, the bubble bounces back after impacting the crystal because of inertia force. In this region, the bubble is easily deformed because the Bo is large. Because of the both effect of inertial force and the bubble deformation, “pass” occurs even if the size ratio of crystal and bubble is smaller than in other regions. On the other hand, in low Re regime, rebounding does not occur because the viscous force is larger than inertia force. In this region, Bo is also small, therefore, bubble deformation is difficlut to occur. This indicates that "pass" does not occur unless the size ratio of bubble and crystal is larger than in other regions.

In this presentation, we measured the rheology of analog liquid used in this experiments. Using the measured viscosity for Re, it was found that the boundary value of the size ratio of crystal and bubble is constant as the Re increased. This indicates that the viscosity does not affect the interaction-style boundary. To be more precise in measuring the size of bubble, we used the bubble radius calculated from the area measured from the images. From these results, we propose the new criterion dividing “stuck” and “pass” as the critical value of product of Bo and the size ratio: in one regime, “stuck “occurs when both of Bo and the size ratio of crystal and bubble were small. in the other regime, “pass” occurs when the Bo and the size ratio of crystal and bubble were large.

©2021. Japan Geoscience Union. All Right Reserved.

Keywords: analog experiment, bubble-crystal interaction

©2021. Japan Geoscience Union. All Right Reserved.

3D crystal size distributions of pyroxene nanolites plotted against short-axis length reflect magma ascent dynamics

*Shota Okumura[1], Mayumi Mujin[2], Akira Tsuchiyama[3,4], Akira Miyake[1]

1. Department of Geology and Mineralogy, Graduate School of Science, Kyoto University, 2. Division of Earth and Planetary Materials Science, Department of Earth Science, Tohoku University, 3. Research Organization of Science and Technology, Ritsumeikan University, 4. Guangzhou Institute of Geochemistry, Chinese Academy of Sciences

Groundmass crystals indicate syn-eruptive magmatic conditions and thus their crystal size distributions (CSDs) reflect magma ascent histories via their crystallizing balance between nucleation and growth (e.g., Marsh 1998; Mujin and Nakamura 2014). 3D CSDs are most commonly estimated from 2D observations and plotted against long-axis length, *L* (e.g., Higgins 2000). *L*-plot CSDs of phenocrysts estimated from 2D observations were confirmed to agree well with those measured directly in 3D (e.g., Mock and Jerram 2005; Jerram et al. 2009). However, Castro et al. (2003) pointed out the possibility that largely varied shapes of groundmass crystals cause inconsistency among the CSDs in 2D and 3D.

Because *L*-plot CSDs require additional stereological corrections compared to CSDs plotted against *S* or *I* when they are estimated from 2D observations, the estimated *L*-plot CSDs should include large errors associated with the stereological corrections. Nevertheless, it has not been discussed fully whether *L* is the most representative size for CSDs of groundmass crystals in order to infer magma ascent conditions in conduits. Therefore, it is necessary to evaluate the influences of size criteria on the CSDs.

Here, we observed groundmass pyroxene crystals in pumices from sub-Plinian and Vulcanian eruptive phases during the 2011 eruption of Shinmoedake (Kirishima volcano group, Japan) by both a JEOL JSM-7001F field-emission scanning electron microscope (FE-SEM) at Kyoto University and synchrotron radiation-based X-ray computed nanotomography (SR-XCT) at beamline BL47XU of the SPring-8 synchrotron facility (Hyogo, Japan; Uesugi et al. 2006; Takeuchi et al. 2009). The SR-XCT observations with effective spatial resolution of 200 nm provided detailed 3D morphologies, triaxial lengths (*S*, *I*, and *L*), and true 3D CSDs of pyroxene crystals ranging from a few hundred nanometers to a few micrometers in width. We compared 3D CSDs estimated from 2D SEM observations (SEM-CSDs) with those measured directly by SR-XCT (CT-CSDs) to investigate whether the prevalent *L*-plot SEM-CSDs are accurate for groundmass crystals of various shapes. We also compared 3D CSDs plotted as a function of *S*, *I*, and *L* to explore which plot types are most representative of eruptive style.

The slopes of *S*- and *I*-plot SEM-CSDs were similar to the slopes of the CT-CSDs compared to *L*-plot SEM-CSDs. This inconsistency of *L*-plot CSDs results from the difficulty in estimating a representative 3D aspect ratio for fairly elongated groundmass crystals ($L/S = 1–40$) from 2D observations, which is critical for the accuracy of stereological conversion into 3D CSDs. Moreover, the slopes of *S*- and *I*-plot CT-CSDs differed more markedly according to eruption style (by ~20%) than those of *L*-plot CT-CSDs.

For estimating magma ascent histories, we propose that the optimum method for acquiring SEM-CSDs is to measure the cross-sectional widths of crystals and convert the 2D dataset into *S*-plot CSDs. By calculating *S*-plot CSD slopes from previous studies reporting *L*-plot SEM-CSDs and 3D aspect ratios, we show that plotting CSDs against *S* preserves their actual slopes, which more reliably reflect magma ascent conditions than those plotted against *L*.

©2021. Japan Geoscience Union. All Right Reserved.

Keywords: crystal size distribution, X-ray CT, nanolite, morphology, magma ascent

©2021. Japan Geoscience Union. All Right Reserved.

Petrological characteristics of the Kawago-daira rhyolite lava, Izu Peninsula, Japan

*Hiroshi Oka[1], Motohiro Tsuboi[1], Kuniyuki Furukawa[2]

1. Kwansei Gakuin University, 2. Aichi University

The explosive and effusive rhyolitic eruptions were occurred in Kawago-daira in 3000 years ago[1)], which relates to the Amagi volcanic group in the Izu peninsula, Japan[2)]. The eruptions began with pyroclastic density currents, which were followed by the lava effusion. The Kawago-daira lava is composed of obsidian and pumiceous lithofacies.
In this study, the whole-rock chemical compositions and water contents of the Kawago-daira lava were provided to reveal the development process of the lithofacies. All samples were collected from the distal part of the lava. Major and trace elements were determined by wavelength dispersive X-ray fluorescence spectrometry (WDXRF), and rare earth elements (REE) were determined by inductively coupled plasma mass spectrometry (ICP-MS). Water contents were estimated using micro-Fourier-transformed infrared spectroscopy (m-FT-IR). Thickness of double polished thin sections for m-FT-IR analysis were 108-208 μm. The absorbance at 1630 cm^{-1} (bending vibration of H_2O molecule) and 3580 cm^{-1} (stretching vibration of OH group) was measured 25 times for groundmass of each sample. The water content was calculated from the absorbance, using the Lambert-Beer's law. Molar absorption coefficients used are 55 L/mol・cm and 67 L/mol・cm for 1630 cm^{-1} and 3580 cm^{-1}, respectively[3)].
The whole-rock SiO_2contents of both lithofacies show 70.18-71.41 wt.%. In Harker diagrams and chondrite-normalized REE patterns, the results of pumiceous and obsidian lithofacies were indistinguishable from each other. A total amount of H_2O molecules and OH groups ranges from 0.23 to 0.25 wt.% for pumiceous lithofacies and from 0.18 to 0.31 wt.% for obsidian lithofacies. While the water contents of both lithofacies appear to be consistent, it is needed to assess the amount of secondary water to evaluate the accurate water contents. We will discuss the development process of the lithofacies from the chemical characteristics and the textures in thin sections.

1) Shigeru Shimada, *The Quaternary Research*, **39**, (2000) 151-164.
2) Konosuke Sawamura, EXPLANATORY TEXT OF THE GEOLOGICAL MAP OF JAPAN Scale1:50,000 SHUZENJI, *Tokyo*, **100**, (1954) 34-37.
3) Yohei Yoshimura, Kazuhiko Kano, Daizo Ishiyama, *Bulletin of the Volcanological Society of Japan*, **57**, (2012) 159-176.

Keywords: rhyolite, obsidian, pumice, infrared microspectrometry, Izu Peninsula

©2021. Japan Geoscience Union. All Right Reserved.

Determination of water solubility in the rhyolitic melt at 650℃ and its interpretation by "hydrogen bonding model"

*Mizuki Nishiwaki[1], Takahiro Miwa[2]

1. Department of Earth and Planetary Sciences, Graduate School of Sciences, Kyushu University, 2. National Research Institute for Earth Science and Disaster Resilience

We experimentally determined the water solubility in the rhyolitic melt at 650˚C with pressures of 30, 90, and 150 MPa. First, we hydrated a clear rhyolitic obsidian glass pellet with water of ~10 wt%, at 800 or 900℃ with arbitrary pressures for 21-48h in a cold-seal pressure vessel. Subsequently, we lowered the temperature to 650℃ at the isobaric condition and kept it for 0-120h. Then, the system was instantaneously decompressed to the pressures of 30, 90, and 150 MPa, and put for 24-96h to induce vesiculation. The run products, which did not contain any microlite or nanolite, were sliced into several pieces and double-polished. The content and distribution of water species of the run products were measured by using the doubly-polished thin sections and Fourier transform infrared (FT-IR) micro-spectroscopy (JASCO FT/IR-660 Plus spectrometer and a JASCO IRT-30 microscope in ERI, University of Tokyo). The total water contents (H_2O_m + OH^-) and its gradients around the bubbles were determined by transmittance and reflectance spectra, respectively. H_2O_m means H_2O molecule.

As a result of the experiment, we found the obtained solubility (2.70 ±0.25 wt% at 30 MPa, 5.84 ±0.54 wt% at 90 MPa, and 6.84 ±0.63 wt% at 150 MPa) is significantly higher than that calculated by the “Burnham model” (Burnham, 1979). In the Burnham model, the whole water is dissolved into melt as OH^- groups through the hydrolysis of Si-O bondings, despite the contribution of H_2O_m cannot be neglected in low temperature. Therefore we developed a new solubility model accounting for the dissolution of H_2O_m into the rhyolitic melt by considering a hydrogen bonding between hydrogen of H_2O_m and oxygen of the Si-O network. We analytically derived the pressure-temperature dependence of H_2O_m solubility in melt and substituted the molar enthalpy of formation of hydrogen bonding in water-saturated aluminosilicate melt $\Delta H = 10$ kJ/mol (Mysen, 2012). The solubility of total water is evaluated from the sum of the solubilities of H_2O_m and OH^- which is calculated from the equilibrium constant between H_2O_m and OH^- ($K = [OH^-]^2/[\text{oxygen}][H_2O_m]$). This new “hydrogen bonding model” can explain our experimental data very well when $K \fallingdotseq 0.040$-0.10.

Our new theoretical model can calculate the water solubility in low-temperature melt below 700℃, in that region extrapolation of conventional theoretical equations has not yielded reliable values until now. A precise study of the physicochemical properties of low-temperature magma, including the water solubility determined in this study, may provide further insights into the cooling process near the walls of magma reservoirs and volcanic conduits, the formation process of dikes and sills, and the behavior of obsidian lava flows.

Keywords: water solubility, 650℃, rhyolitic melt, vesiculation, hydrogen bonding model

©2021. Japan Geoscience Union. All Right Reserved.

Flowage of the 1991 Unzen lava: Discussion to Goto et al.(2020) Rigid migration of Unzen lava rather than flow. JVGR

*Hiroaki Sato[1], Shigeru Suto[2], Tadahide Ui[3], Toshitsugu Fujii[4], Takahiro Yamamoto[2], Shinji Takarada[2], Keiichi Sakaguchi[2]

1. Kobe Univ., 2. Geological Survey of Japan, 3. Hokkaido Univ., 4. Mount Fuji Research Institute

Goto et al. (2020) presented new rheological data on the bulk rocks and a groundmass glass synthetic sample of the ejecta of the 1991 Unzen dacite, and together with the previous rheological data of groundmass glass, they suggested that bulk viscosity of Unzen dacite is more than 1 order of magnitude larger than those obtained by Jeffreys model calculated from the apparent velocity of the lava front, slope inclination, lava height and density of the lava by Suto et al.(1993) and Yamamoto et al. (1993). Although they suggested possible effect of water in the lower part of the lava where higher pressure (ca. 1.4 MPa) affords retaining of water in the matrix glass, they suggested rigid migration of the lava from the video image analyses. Our discussion is concerned with more fluidal aspect of the lava from the pictures at the time of eruption, suggesting that at least some part of the lava flowed as viscous fluid, and that shear zone at the base of the lava, which Goto et al.(2020) suggested, is not likely.

Figure 9 of Goto et al.(2020) vaguely show that apparent advance of the lava lobe front is accompanied by crack widening in the lava lobe, and they suggested that apparent advance of the lava lobe represents rotation of the frontal block. However, our sequential pictures show that upstream area also advance nearly parallel to the frontal area, which indicate the deformation of the lava lobe. Other evidence of flowage of the lava lobe includes thickening of the lava lobe in the downstream area, protrusions of the front of the lava lobe, crease structure of the lava lobe near the site of upwelling, and wrinkle structure on the surface of the lava block. Thickening of lava lobe in the downstream area has been illustrated in Figure 7 of Nakada and Fujii (1993)jvgr and our pictures. Protrusive front is also described in Nakada and Fujii (1993) jvgr, Ohta (1992) and our photographs taken from helicopter of the Ground Self-Defence Force in August and November, 1991. Crease structure show viscous deformation of the upwelling lava from the source vent, and are often observed in the 1991 Unzen eruption. Wrinkle texture is sometimes observed on the surface of lava blocks of the Unzen lava lobes including the supplementary movie of Goto et al.(2020). Interval of wrinkles is generally 2-5 meters, and indicate much less viscous interior than the surface of the lava block (Fink and Fletcher, 1978 jvgr).

Several shear zones are observed in the section of lava lobe such as Figure 3 of Suto et al.(1993) and lava lobe-11. The presence of shear zones within the lava lobe together with protrusive front of the lava lobes suggest that basal boundary of the lava lobe is resistant to slide.

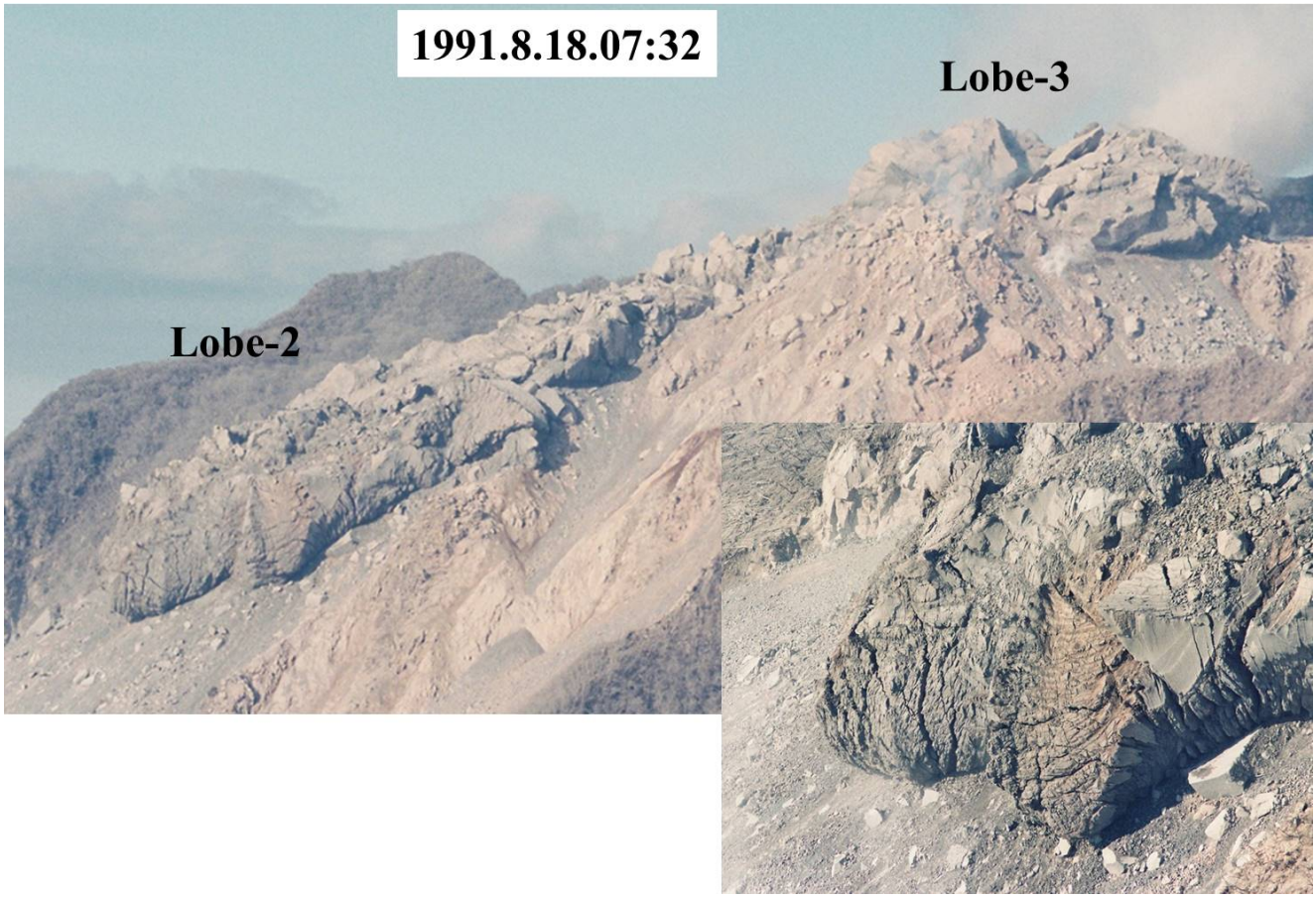
The discrepancy of the idea may be caused by slight difference in temperature and glass composition of the lavas: temperature Goto et al.(2020) used was ca. 850˚C, whereas experimentally duplicated temperature of Venezky and Rutherford (1999) gave 900±30˚C, and glass composition of Nakada and Motomura (1999) gave 1-2wt% lower SiO_2 and 0.3-0.4 wt% higher Na_2O, which result in the estimated viscosity difference of more than 1 log unit.

The experimental work of Goto et al.(2020) together with those of Cordonnier et al. (2009) and Coats et al. (2018) showed fairly large variation of viscosity on the bulk rock of Unzen lava samples (more than 2 orders of magnitude at 900˚C), which may correspond to wide variations of fluidity/rigidity as pictures of

©2021. Japan Geoscience Union. All Right Reserved.

the 1991 Unzen lava lobes show. Viscosity of effusing lava is delicately influenced by dewatering, cooling, and crystallization during effusive action, and application of the rheological experimental results to natural lava behavior should be carried out with much more caution.

Keywords: Unzen volcano, Lava lobe, Viscosity, Flowage of lava, Magma temperature, Groundmass glass composition



©2021. Japan Geoscience Union. All Right Reserved.

[E] Oral | S (Solid Earth Sciences)：S-GC Geochemistry

Sat. Jun 5, 2021 10:45 AM - 12:15 PM JST | Sat. Jun 5, 2021 1:45 AM - 3:15 AM UTC | Ch.23 Zoom Room 23

[S-GC32] Volatiles in the Earth - from Surface to Deep Mantle

convener:Takeshi Hanyu(Japan Agency for Marine-Earth Science and Technology, Research Institute for Marine Geodynamics), E Gray Bebout(Lehigh University), Yuji Sano(Division of Ocean and Earth Systems, Atmosphere and Ocean Research Institute, University of Tokyo), Hirochika Sumino(Department of General Systems Studies, Graduate School of Arts and Sciences, The University of Tokyo), Chairperson:Gray E Bebout(Lehigh University), Hirochika Sumino(Department of General Systems Studies, Graduate School of Arts and Sciences, The University of Tokyo)

Volatiles play an important role in the dynamical and chemical processes in the Earth. The presence of volatiles drastically changes mineral stability and rheological behavior of the rocks. Chemical fractionation, such as partial melting, hydration, and dehydration are controlled by volatiles in the rocks. Volatiles enhance the production of magmas and drive their ascent and volcanic eruption. The atmosphere and hydrosphere have been generated by variety of degassing events from the mantle through volcanism. Some volatiles in the Earth's surface have been suggested to be recycled back into the mantle beyond subduction zones. Although the significance of volatiles in the Earth's evolution has been recognized, each of these processes is poorly constrained. We therefore welcome contributions from experimental, observational, and modeling studies that help shed light on the behavior, chemical/physical characteristic, and flux/budget of volatiles, such as hydrogen, carbon, nitrogen, noble gases, halogens, and sulfur. We encourage studies linking the behavior of multiple volatile elements and their isotopic compositions. Studies investigating the linkage between volatile and solid geochemical tracers, the phase equilibria of volatile-bearing mantle assemblages, and the effect of volatiles on the physical properties of the mantle are also welcome.

10:45 AM - 11:00 AM JST | 1:45 AM - 2:00 AM UTC

[SGC32-01] Helium isotope analyses of volcanic gases and HESJ standard gas using a multi-turn time-of-flight mass spectrometer

*Yuki Hattori[1], Yoshihide Akiyama[1], Hirochika Sumino[1] (1.Graduate School of Arts and Science, The University of Tokyo)

11:00 AM - 11:15 AM JST | 2:00 AM - 2:15 AM UTC

[SGC32-02] Systematic depth variation of water in the lithosphere-asthenosphere boundary beneath Ichinomegata, NE Japan

*Yuto Sato[1], Eiichi Takahashi[1], Kazuhito Ozawa[2] (1.State Key Labolatory of Isotope Geochemistry, Guangzhou Institute of Geochemistry, CAS, 2.Department of Earth and Planetary Science, Graduate School of Science, The University of Tokyo)

11:15 AM - 11:45 AM JST | 2:15 AM - 2:45 AM UTC

[SGC32-03] Impact of mantle hydration on the global carbon cycle

★Invited Papers

*Ikuo Katayama[1] (1.Department of Earth and Planetary Systems Science, Hiroshima University)

11:45 AM - 12:15 PM JST | 2:45 AM - 3:15 AM UTC

[SGC32-04] The story of Earth’s volatile accretion and evolution

★Invited Papers

*Sujoy Mukhopadhyay[1], Sandrine Peron[1] (1.Department of Earth and Planetary Sciences, University of California Davis, Davis, CA, USA)

Helium isotope analyses of volcanic gases and HESJ standard gas using a multi-turn time-of-flight mass spectrometer

*Yuki Hattori[1], Yoshihide Akiyama[1], Hirochika Sumino[1]

1. Graduate School of Arts and Science, The University of Tokyo

Helium isotope ratio ($^3He/^4He$ ratio) shows different values in geochemical reservoirs such as the atmosphere, crust, and mantle, depending on relative contributions of primordial and radiogenic helium. $^3He/^4He$ ratios of volcanic gases vary between magmatic (up to 1.1×10^{-5} or lower) and crustal (less than 1×10^{-7}) values. When magma becomes active, $^3He/^4He$ ratio of volcanic gas may increase due to the increased contribution of magmatic helium. Therefore, $^3He/^4He$ ratio of volcanic gas has the potential as a monitoring tool of volcanic activity. Such $^3He/^4He$ ratio increases preceding volcanic eruptions have been reported for El Hierro, Canary Islands[1], Mt. Etna, Italy[2], and Ontake, Japan[3].

Although continuous analysis of volcanic gas is necessary to monitor volcanic activity, it is difficult because a magnet-sector type mass spectrometer equipped with a massive electromagnet is currently used to analyze helium isotopes. There are two reasons why a magnet-sector type mass spectrometer is necessary. One is that adequate mass resolution is required to distinguish $^3He^+$ from HD^+, and the other is that high sensitivity is required to detect trace amounts of ^3He. For these reasons, helium isotope analysis is limited to suitable laboratory and on-site, real-time measurement of $^3He/^4He$ ratio around a volcano is almost impossible.

We have been developing a new technique of noble gas analysis using the “infiTOF” (MSI TOKYO, Inc.), which is a portable mass spectrometer derived from the multi-turn time-of-flight mass spectrometer MULTUM-S II[4, 5]. The high mass resolution achieved by an infiTOF is more than enough to distinguish $^3He^+$ from HD^+. However, the sensitivity of a normal infiTOF was far lower than the requirement to analyze noble gases in volcanic gas because most of noble gas molecules admitted to the spectrometer were pumped out by vacuum pumps directly connected to the spectrometer before ionized by an electron ionization source. Therefore, we installed valves between the spectrometer and the vacuum pumps to operate the mass spectrometer while it is isolated from the pumps. Getter pumps, which absorb active gases but not noble gases, were also installed to keep high vacuum in the spectrometer during the operation. In addition, we introduced the ion counting method for signal processing of the secondary electron multiplier to detect weak signals of ^3He ions.

As a result, it has become possible to detect a significant number of ^3He ions during analyses of volcanic gas samples. The $^3He/^4He$ ratios of samples were calibrated by comparing with the analysis of the helium standard gas (HESJ) with a known $^3He/^4He$ ratio[6]. Besides, we investigated the pressure conditions, which enable accurate measurement of $^3He/^4He$ ratios, from the stability of observed $^3He/^4He$ ratios versus the pressure of sample gas admitted to the spectrometer. It was finally demonstrated that $^3He/^4He$ ratios of volcanic gas samples, which were measured under optimized conditions and calibrated with HESJ, were consistent with those measured with a magnet-sector type mass spectrometer within analytical errors.

[1] E. Padrón *et al.*, *Geology*, 41(5), 539–542 (2013).
[2] A. Paonita *et al.*, *Geology*, 44(7), 499–502 (2016).
[3] Y. Sano *et al.*, *Sci. Rep.*, 5:13069 (2015).

©2021. Japan Geoscience Union. All Right Reserved.

[4] M. Toyoda *et al.*, *J. Mass Spectrom.*, 38(11), 1125–1142 (2003).
[5] S. Shimma *et al.*, *Anal. Chem.*, 82(20), 8456–8463 (2010).
[6] J. Matsuda *et al.*, *Geochem. J.*, 36(2), 191–195 (2002).

Keywords: mass spectrometry, isotope ratio, helium isotope, volcanic gas, ion counting

©2021. Japan Geoscience Union. All Right Reserved.

Systematic depth variation of water in the lithosphere-asthenosphere boundary beneath Ichinomegata, NE Japan

*Yuto Sato[1], Eiichi Takahashi[1], Kazuhito Ozawa[2]

1. State Key Labolatory of Isotope Geochemistry, Guangzhou Institute of Geochemistry, CAS, 2. Department of Earth and Planetary Science, Graduate School of Science, The University of Tokyo

Mantle xenoliths are fragments of mantle materials rapidly brought by alkali-basalt and kimberlite magmas. They are source of information for better understanding dynamics operated in the lithosphere, asthenosphere, and their boundary. Water is one of the most important components because it significantly affects the solidus temperature (e.g., Kushiro et al, 1968) and rheological properties such as viscosity (e.g., Mei & Kohlstedt, 2000) and deformation mechanism (e.g., Jun et al., 2006). For instance, the chemical stratification of water has been considered as one of the key factors for defining lithosphere-asthenosphere boundary (LAB) (e.g., Hirth and Kohlstedt, 1996; Lee et al., 2005). In this study, we examined the role of water in defining LAB in the arc settings by analysis of water contents of minerals in mantle xenoliths from Ichinomegata maar in NE Japan, where thermal and petrologic structures of the upper mantle are constrained by our geothermobarometry (Sato & Ozawa, 2019). The mantle beneath Ichinomegata is granular, amphibole- and plagioclase-bearing, and subsolidus at the depth of 28-32 km and porphyroclastic, amphibole- and plagioclase-free, and partially molten in the depth range of 41-55 km. They correlated the former to the lithospheric mantle and the latter to the LAB-zone.

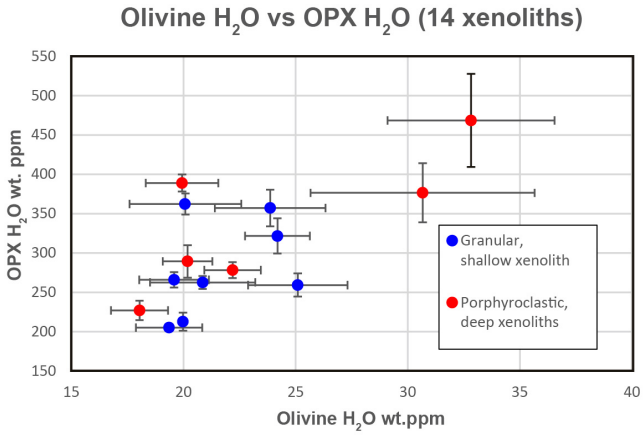
We analyzed water contents of 57 olivine, 71 orthopyroxene, and 33 clinopyroxene grains hand-picked from 14 peridotite xenoliths (2-7 grains for each mineral in each xenolith). IR spectra of three random but orthogonal sections of each grain were measured using polarized light to determine total absorbance (Libowitzky & Rossman, 1996) with a Jasco FTIR-6100 spectrometer with a Jasco IRT-5000 microscope in GIGCAS. The calibration factors determined by Bell et al., (1995; 2003) were used. The obtained water contents of olivine, orthopyroxene, and clinopyroxene range 16.8-37.0, 198-547, 477-886 wt. ppm, respectively. The error (1SD) for each grain is ~3% and that for each mineral in each xenolith is ~8%. Satsukawa et al. (2017) measured water contents of olivine and pyroxenes in peridotite xenoliths from the shallow depths. Their water contents are consistently lower than our results probably due to the selection of samples or underestimation caused by the methods. The water contents of olivine are higher than those reported from spinel peridotites (Demouchy & Bolfan-Casanova, 2016). The range of clinopyroxene is comparable to the reported range, but the highest water content of orthopyroxene exceeds the reported highest values from the world xenolith localities. These water contents in the Ichinomegata xenoliths reflect high water contents in the wedge mantle above subducting slab.

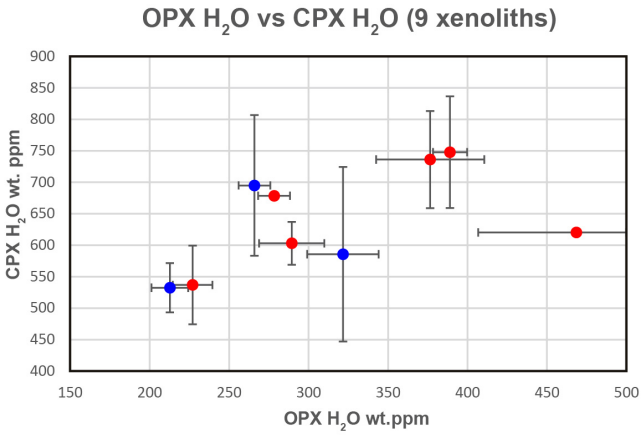
We conducted chemical analysis of olivine using EPMA (JEOL JXA-8230 in GIGCAS) to estimate the derivation depths and temperatures by combining pyroxene geothermobarometry. The CaO contents in olivine range 297-937 wt. ppm, which split into two clusters corresponding to the 8 granular samples (297-398 ppm) and 6 porphyroclastic samples (634-937 ppm). Their estimated depths range 25-48 km and temperature of 820-1055 ˚C. There are depth variations in the water contents. The water contents of olivine and pyroxenes in the granular samples are quite variable and high in the maximum and mean water contents. By contrast, those in the shallow samples are less variable and low in the maximum and mean water contents. The xenolith registering the highest water contents underwent partial melting and the deformation featuring porphyroclastic texture when it stayed at 45 km and 1024 ˚C. The estimated

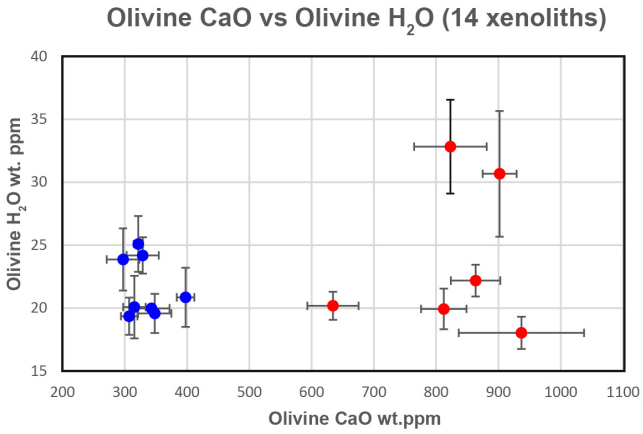
©2021. Japan Geoscience Union. All Right Reserved.

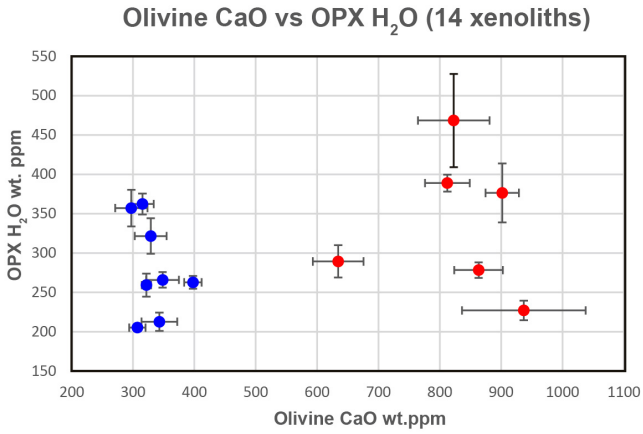
water contents in minerals are consistent with experimentally determined water solubility of minerals coexisting with basaltic melts containing ~5 wt.% of H_2O at 1.2 GPa and 1200 ˚C (Hauri et al., 2006). These suggest that water was supplied into the deeper levels corresponding to the LAB zone beneath Ichinomegata from underlying asthenospheric mantle through heterogenous paths.

Keywords: Water in Nominally Anhydrous Minerals, Subduction zone, Lithosphere-Asthenosphere Boundary, Fourier-transform infrared spectroscopy, Geothermobarometry









©2021. Japan Geoscience Union. All Right Reserved.

Impact of mantle hydration on the global carbon cycle

*Ikuo Katayama[1]

1. Department of Earth and Planetary Systems Science, Hiroshima University

The long-term stabilization of the Earth's surface environment is likely controlled by the global carbon cycle through the negative feedback system. The oceanic plate can capture carbon dioxide from seawater through water-rock interactions in the crust and mantle, in addition to carbonates and organic matter deposited on the seafloor, which is responsible for carbon transport to the Earth's interior. In the uppermost part of the oceanic crust, carbonates are precipitated in the volcanic rocks, filling the fractures and voids, and the carbon content tends to increase with the age of oceanic plates (e.g., Alt and Teagle 1999). On the other hand, although the amount of carbon uptake in the deep crust and mantle is not well known, if seawater penetrates along faults, carbonates are likely to be precipitated by water-rock interactions. In particular, alteration of mantle rocks can promote carbonate precipitation via increasing pH of the aqueous fluids. Extensive carbonation of peridotites is evident in the Oman ophiolite; for example, listvenite is widespread in the lower part of the ophiolite, where serpentine is completely replaced by carbonate due to metamorphic sole-derived fluids (Kelemen et al. 2013). Mantle hydration has recently been suggested along the outer-rise faults that develop in the relatively old plate subduction, such as the Japan Trench, where seawater infiltrates to mantle and extensive serpentinization is expected to occur (e.g., Fujie et al. 2013). In such case, carbonation process may have occurred during the mantle hydration, and the amount of carbon uptake in the oceanic lithosphere may have increased significantly. Although the negative feedback system of carbon cycle has contributed to the stabilization of the surface environment throughout the geological history, the extensive mantle carbonation may break the feedback system and result in global cooling. We hope that the upcoming deep drilling project at off Hawaii (Umino et al. 2020) provides a clue to understand the carbon uptake process in the deep crust and mantle.

Keywords: Carbon cycle, Mantle hydration

©2021. Japan Geoscience Union. All Right Reserved.

The story of Earth’s volatile accretion and evolution

*Sujoy Mukhopadhyay[1], Sandrine Peron[1]

1. Department of Earth and Planetary Sciences, University of California Davis, Davis, CA, USA

The geochemistry of mantle-derived lavas requires long-term differences to be preserved between different regions of the Earth’s mantle, and between the mantle and the atmosphere. Reading this history has required developing higher precision measurement techniques, which has provided a wealth of information regarding volatile accretion. Often this information has come from mantle noble gases that have recorded events during Earth’s earliest history. Being chemically inert, the evolution of noble gas isotopic and elemental ratios trace physical processes during accretion, such as magma ocean degassing, early mantle degassing and atmospheric loss. Furthermore, there are large differences in the primordial isotopic ratios of noble gases between different volatile sources, allowing one to infer the sources that contributed volatiles to Earth during accretion.

The primordial neon isotopic ratio ($^{20}Ne/^{22}Ne$) of mantle plumes, which sample material from near the core-mantle boundary and separated from the mid-ocean ridge basalt source within the first 90 Ma, is dramatically different from the atmospheric and chondritic values, but close to values of the nebular gas [1]. This observation requires early acquisition of solar neon and likely reveals the growth of the proto-Earth in the presence of a gas disk [1]. These same deep mantle materials, however, also carry the fingerprint of chondritic krypton [2,3]. This surprising observation requires concomitant acquisition of solar as well as chondritic volatiles during the early phase of Earth’s formation; chondritic volatiles, including water, were therefore added not just late in Earth’s formation.

A careful characterization of the solid Earth’s noble gas fingerprint reveals that the atmospheric noble gases cannot be related to the solid Earth noble gases through any combination of mantle outgassing and atmospheric escape. The distinct signature of the atmospheric noble gases requires their derivation from sources different from those that contributed to solid Earth after the last major interior-atmosphere equilibration –the Moon forming giant impact. While the nature of these volatile sources to the atmosphere is not entirely clear, they include comets [4.5]. Additionally, the distinct noble gas signatures of the atmosphere and mantle place constraints on the rate of volatile exchange between the interior and the surface over 4.5 Ga. In particular, the Xe isotopic composition of modern day lavas and the observation of increasing Xe isotopic mass fractionation in the Archean atmosphere indicates efficient Xe subduction into the mantle occurred after 3.0-2.5 Ga [6,7].

[1] Williams and Mukhopadhyay, Nature 565, 2018 [2] Broadley M. et al. PNAS 117, 2020. [3] Peron et al. in review. [4] Marty B. et al Science 356, 2017. [5] Bekaert D. et al., Scientific Reports 10, 2020. [6] Parai and Mukhopadhyay, Nature 560, 2018. [7] Peron and Moreira GPL 9, 2018.

Keywords: volatiles, accretion, atmosphere, giant impacts, early Earth, subduction

©2021. Japan Geoscience Union. All Right Reserved.

[E] Oral | S (Solid Earth Sciences)：S-GC Geochemistry

Sat. Jun 5, 2021 1:45 PM - 3:15 PM JST | Sat. Jun 5, 2021 4:45 AM - 6:15 AM UTC | Ch.23 Zoom Room 23

[S-GC32] Volatiles in the Earth - from Surface to Deep Mantle

convener:Takeshi Hanyu(Japan Agency for Marine-Earth Science and Technology, Research Institute for Marine Geodynamics), E Gray Bebout(Lehigh University), Yuji Sano(Division of Ocean and Earth Systems, Atmosphere and Ocean Research Institute, University of Tokyo), Hirochika Sumino(Department of General Systems Studies, Graduate School of Arts and Sciences, The University of Tokyo), Chairperson:Yuji Sano(Center for Advanced Marine Core Research, Kochi University), Takeshi Hanyu(Japan Agency for Marine-Earth Science and Technology, Research Institute for Marine Geodynamics)

Volatiles play an important role in the dynamical and chemical processes in the Earth. The presence of volatiles drastically changes mineral stability and rheological behavior of the rocks. Chemical fractionation, such as partial melting, hydration, and dehydration are controlled by volatiles in the rocks. Volatiles enhance the production of magmas and drive their ascent and volcanic eruption. The atmosphere and hydrosphere have been generated by variety of degassing events from the mantle through volcanism. Some volatiles in the Earth's surface have been suggested to be recycled back into the mantle beyond subduction zones. Although the significance of volatiles in the Earth's evolution has been recognized, each of these processes is poorly constrained. We therefore welcome contributions from experimental, observational, and modeling studies that help shed light on the behavior, chemical/physical characteristic, and flux/budget of volatiles, such as hydrogen, carbon, nitrogen, noble gases, halogens, and sulfur. We encourage studies linking the behavior of multiple volatile elements and their isotopic compositions. Studies investigating the linkage between volatile and solid geochemical tracers, the phase equilibria of volatile-bearing mantle assemblages, and the effect of volatiles on the physical properties of the mantle are also welcome.

1:45 PM - 2:15 PM JST | 4:45 AM - 5:15 AM UTC

[SGC32-05] H/D partitioning between forsterite, wadsleyite and ringwoodite : ab initio free energy calculation

★Invited Papers

*Jun Tsuchiya[1], Taku Tsuchiya[1] (1.Geodynamics Research Center, Ehime University)

2:15 PM - 2:45 PM JST | 5:15 AM - 5:45 AM UTC

[SGC32-06] **Volatile characteristics of Central American geothermal fluids**8.6.0

★Invited Papers

*Peter H Barry[1], David V Bekaert[1], J M de Moor[2], Jabrane Labidi[3], Esteban Gazel[4], M Nakagawa[5], Donato Giovannelli[6], Matt Schrenk[7], Karen G Lloyd[8] (1.Woods Hole Oceanographic Institution, 2.Observatorio Volcanológico y Sismológico de Costa Rica (OVSICORI), Universidad Nacional, Costa Rica, 3.Université de Paris, Institut de physique du globe de Paris, CNRS, Paris, France, 4.Department of Earth and Atmospheric Sciences, Cornell University, Ithaca, New York 14853, USA, 5.Earth-Life Science Institute, Tokyo Institute for Technology, Tokyo, Japan, 6.Department of Biology, University of Naples “Federico II”, Naples, Italy, 7.Department of Earth and Environmental Sciences, Michigan State University, MI, USA, 8.Department of Microbiology, University of Tennessee, TN, USA)

2:45 PM - 3:00 PM JST | 5:45 AM - 6:00 AM UTC

[SGC32-07] Halogen and noble gas compositions of mantle wedge and subducted sediment, recorded in metamorphic rocks from the Sanbagawa belt

*JIE REN[1], Hirochika Sumino[1], Yui Kouketsu[2], Simon Richard Wallis[3] (1.Graduate School of Arts and Sciences, The University of Tokyo , 2.Graduate School of Environmental Studies, Nagoya University, 3.Graduate School Sciences, The University of Tokyo)

3:00 PM - 3:15 PM JST | 6:00 AM - 6:15 AM UTC

[SGC32-08] Discussion

H/D partitioning between forsterite, wadsleyite and ringwoodite : ab initio free energy calculation

*Jun Tsuchiya[1], Taku Tsuchiya[1]

1. Geodynamics Research Center, Ehime University

Deuterium is the heavy stable isotope of hydrogen. The D/H ratio shows large variation in various astronomical bodies such as protosolar nebula ($2x10^{-5}$), Earth (SMOW= 1.5×10^{-4}, average seawater), Venus ($1.6x10^{-2}$) and carbonaceous chondrites (~$2x10^{-4}$) (e.g. Saal et al. 2013). Many studies are conducted to determine the D/H ratio in various rocks with different origins of the Earth, since this may be the key to understand the evolutional history and the origin of water of the Earth.
Many studies suggest that hydrous minerals in subducting cold slabs can transport water into deep Earth’ s interiors. There is a possibility that several times of sea water exist in the transition zone at depth between 410km and 660 km if the constituent minerals are largely hydrated (e.g. Smyth 1994). Recently, hydrous ringwoodite with 1 wt%H_2O has been found in natural diamond, suggesting that the transition zone is at least locally hydrated (Pearson et al. 2014). Therefore, the D/H ratio may be changed by the partitioning behaviors of D and H among these mantle minerals by the circulation of water in deep interiors.
In this study, we determined the free energy of D and H bearing forsterite, wadsleyite and ringwoodite by ab initio calculation in order to determine the equilibrium constants of D and H isotopic exchange reactions between them. First, we determined the stable structures of hydrous forsterite, wadsleyite and ringwoodite with Mg vacancy with two hydrogen atoms or Si vacancy with four hydrogen atoms by first principles calculation based on density functional theory. Then, the phonon frequencies are calculated based on density functional perturbation theory (Baroni et al. 2001) and also by the finite displacement method (Parlinski et al. 1997, Togo and Tanaka 2015). Then, we used quasi-harmonic approximation to calculate the Gibbs free energy of H and D baring phases. In this presentation, we report the Gibbs free energy of isotopic exchange reaction between forsterite and wadsleyite, and also between wadsleyite and ringwoodite.

Keywords: ab initio calculation, high pressure, H/D partitioning

©2021. Japan Geoscience Union. All Right Reserved.

Volatile characteristics of Central American geothermal fluids8.6.0

*Peter H Barry[1], David V Bekaert[1], J M de Moor[2], Jabrane Labidi[3], Esteban Gazel[4], M Nakagawa[5], Donato Giovannelli[6], Matt Schrenk[7], Karen G Lloyd[8]

1. Woods Hole Oceanographic Institution, 2. Observatorio Volcanológico y Sismológico de Costa Rica (OVSICORI), Universidad Nacional, Costa Rica, 3. Université de Paris, Institut de physique du globe de Paris, CNRS, Paris, France, 4. Department of Earth and Atmospheric Sciences, Cornell University, Ithaca, New York 14853, USA, 5. Earth-Life Science Institute, Tokyo Institute for Technology, Tokyo, Japan, 6. Department of Biology, University of Naples "Federico II", Naples, Italy, 7. Department of Earth and Environmental Sciences, Michigan State University, MI, USA, 8. Department of Microbiology, University of Tennessee, TN, USA

Earth's various mantle reservoirs (e.g., depleted mid ocean ridge basalt (MORB) mantle, plume mantle source) retain distinct volatile geochemical features that inform our understanding of planetary accretion, mantle convection and mixing, as well as subduction-driven recycling processes. At subduction zones, volatile elements (e.g., helium, carbon, nitrogen) are actively cycled between terrestrial reservoirs by plate tectonics. The efficiency of volatile transfers between Earth's interior (crust and mantle) and exterior (atmosphere and oceans) controls Earth's redox conditions, mantle heterogeneities and atmospheric evolution. The distribution of terrestrial volatiles, which is controlled by the long-term balance between volcanism and recycling, has enabled conditions favorable for life on Earth. Despite the importance of volatile elements on a global scale, their fluxes and sources (slab vs. mantle), and sinks however remain under-constrained, particularly in subduction-related fluids.

The Central America Volcanic Arc (CAVA), is one of the best studied[1,2,3] arc segments globally. However, relatively few studies have focused on constraining volatile fluxes throughout the southern segment of the CAVA due to the lack of active volcanism in the region. This area is tectonically unique, as the border between Costa Rica and Panama represents the transition between the orthogonal subduction of the Cocos Plate and the oblique subduction of the Nazca Plate relative to the Caribbean Plate. Here, we present unpublished He, CO_2 and N_2 isotope and relative abundance data from geothermal fluids in southern Costa Rica and western Panama. In total, isotope data are reported for 65 deeply sourced wells, seeps and springs, as well as gas samples. These data reveal a clear southeastward increase in $^3He/^4He$, from typical volcanic arc values (about 7 times the atmospheric ratio, R_A) in Costa Rica, up to MORB-like values (8 plus/minus1 R_A) in the volcanically-dormant region of western Panama. Remarkably, "cold" seeps in Panama display $^3He/^4He$ up to 8.9 R_A, equivalent to the highest values ever reported for active volcanic arc settings worldwide. These data suggest contribution from a ^3He-rich mantle source under western Panama, potentially associated with the Galapagos plume. $d^{13}C$ vary from −29.7‰ to +6.7‰ vs. PDVB, suggesting CO_2 loss due to calcite precipitation, as it has been recently shown in Costa Rica's Nicoya Peninsula[4]. N isotopes and clumped N isotopologues[5] in CAVA samples cluster around +5‰ vs. air, suggesting N is mainly derived from sediments. Flux considerations suggest that subducting N may be quantitatively recycled into the arc, although uncertainties on fluxes allow up to 63% of slab-N to be transported into the mantle past the arc melting region, which is consistent with previous studies[6,7]. In summary, we show evidence for 1) the existence of a pervasive (plume) mantle component in southern CAVA samples, and 2) extensive CO2 fractionation during low temperature C sequestration as calcite in the forearc region and 3) strong N sediment signatures in arc fluids.

By combining these findings with other geochemical tracers (clumped N-isotopes, Pb isotopes, Ce/Pb[8]) and high-resolution simulations of global mantle flow around the Galapagos plume[9], we conclude that there may be an asthenospheric "pipeline" connecting the Galapagos plume to a slab window that

©2021. Japan Geoscience Union. All Right Reserved.

formed via subduction of a spreading ridge under western Panama[10,11]. This finding is globally significant, as the lateral entrainment and dispersal of plume material by large-scale asthenospheric mantle winds provides a straightforward explanation for the worldwide observation of OIB-like geochemical signatures in mantle domains that are remote from plume sources.

[1] Shaw et al., 2003.

[2] De Leeuw et al., 2007.

[3] de Moor et al., 2017.

[4] Barry et al., 2019.

[5] Labidi et al., 2021 (In Review - EPSL).

[6] Busigny et al. (2019)

[7] Bekaert et al., 2021.

[8] Gazel et al. 2011.

[9] Conrad and Behn 2010.

[10] Herrstrom et al. 1995.

[11] Abratis and Wörner 2001. 8.6.0

Keywords: Carbon, Helium, Nitrogen, Central America, Costa Rica, Panama

©2021. Japan Geoscience Union. All Right Reserved.

Halogen and noble gas compositions of mantle wedge and subducted sediment, recorded in metamorphic rocks from the Sanbagawa belt

*JIE REN[1], Hirochika Sumino[1], Yui Kouketsu[2], Simon Richard Wallis[3]

1. Graduate School of Arts and Sciences, The University of Tokyo , 2. Graduate School of Environmental Studies, Nagoya University, 3. Graduate School Sciences, The University of Tokyo

Subduction of crustal rocks results in transportation of volatiles into the mantle, which can have a major effect on the chemical and physical properties of constituent rocks. Volatile transport also plays an important role in arc volcanism and seismicity. However, the details of volatile cycling process remain debated. The distinct elemental and/or isotopic compositions of halogens and noble gases in different reservoirs (e.g. MORB-source mantle, seawater, subducted sediments and igneous rocks) make them good tracers for fluid origin in subduction zones. We analyzed the halogen and noble gas compositions in a series of metamorphic rocks that recorded a paleo slab-mantle wedge boundary *(Kawahara et al, 2016)*. Analyzed samples are ultramafic serpentinite (derive from the mantle wedge) and schist (derive from subducted sediment) located in the Mt. Shiraga region of the Sanbagawa belt in central Shikoku.

In order to determine the trace amounts of halogens, especially those contained in fluid inclusions, a portion of each sample was neutron-irradiated in the Kyoto University Research Reactor to convert halogens (^{37}Cl, ^{79}Br and ^{127}I) to noble gas isotopes (^{38}Ar, ^{80}Kr,^{128}Xe), which have lower detection limits than direct analyses of halogens with other methods. Stepwise crushing and heating processes were conducted in order to extract volatiles contained in different sites of the rocks. The irradiated and un-irradiated portions were analyzed by noble gas mass spectrometry at the University of Tokyo, to determine halogen and noble gas compositions respectively.

The halogen compositions of fluids obtained by crush extraction show relatively high I/Cl ratios with stable Br/Cl ratios compared with halogens in MORB-mantle or seawater. These features are similar to the data for the nearby Higashi-akaishi mantle wedge peridotite exhumed from ~100 km depth *(Sumino et al, 2010)*, which are considered to partially preserve the signals of sedimentary pore fluids. In addition, the serpentinite body shows overall decreasing I/Cl ratios with increasing distance from the subduction boundary. This supports the idea that the original high I/Cl fluids were transported along the subduction interface and penetrated upward into the mantle wedge.

The isotopic data of the noble gases are complex. Neon and Argon isotopic compositions are almost overwhelmed by the seawater/atmosphere component. Helium shows distinct and diverse ^{3}He/^{4}He ratios, which is likely to be strongly influenced by the cosmic ray, producing ^{3}He preferentially. Nevertheless, a radiogenic ^{3}He/^{4}He component possibly derived from subducted crust/sediment was identified in the fluids extracted from the serpentinite body, which is similar to slab-derived fluids preserved in the Higashi-akaishi peridotite *(Sumino et al, 2010)*. This adds support to the idea that the shallow part of mantle wedge has been influenced by addition of volatiles from the subducted slab.

Keywords: Mantle wedge, Sanbagawa belt, Halogen, Noble gas

©2021. Japan Geoscience Union. All Right Reserved.

[E] Oral | S (Solid Earth Sciences) | S-GC Geochemistry

[S-GC32] Volatiles in the Earth - from Surface to Deep Mantle

convener:Takeshi Hanyu(Japan Agency for Marine-Earth Science and Technology, Research Institute for Marine Geodynamics), E Gray Bebout(Lehigh University), Yuji Sano(Division of Ocean and Earth Systems, Atmosphere and Ocean Research Institute, University of Tokyo), Hirochika Sumino(Department of General Systems Studies, Graduate School of Arts and Sciences, The University of Tokyo), Chairperson:Yuji Sano(Center for Advanced Marine Core Research, Kochi University), Takeshi Hanyu(Japan Agency for Marine-Earth Science and Technology, Research Institute for Marine Geodynamics)

Sat. Jun 5, 2021 1:45 PM - 3:15 PM Ch.23 (Zoom Room 23)

Volatiles play an important role in the dynamical and chemical processes in the Earth. The presence of volatiles drastically changes mineral stability and rheological behavior of the rocks. Chemical fractionation, such as partial melting, hydration, and dehydration are controlled by volatiles in the rocks. Volatiles enhance the production of magmas and drive their ascent and volcanic eruption. The atmosphere and hydrosphere have been generated by variety of degassing events from the mantle through volcanism. Some volatiles in the Earth's surface have been suggested to be recycled back into the mantle beyond subduction zones. Although the significance of volatiles in the Earth's evolution has been recognized, each of these processes is poorly constrained. We therefore welcome contributions from experimental, observational, and modeling studies that help shed light on the behavior, chemical/physical characteristic, and flux/budget of volatiles, such as hydrogen, carbon, nitrogen, noble gases, halogens, and sulfur. We encourage studies linking the behavior of multiple volatile elements and their isotopic compositions. Studies investigating the linkage between volatile and solid geochemical tracers, the phase equilibria of volatile-bearing mantle assemblages, and the effect of volatiles on the physical properties of the mantle are also welcome.

3:00 PM - 3:15 PM

[SGC32-08]Discussion

©Japan Geoscience Union

[E] Poster | S (Solid Earth Sciences)：S-GC Geochemistry

Sat. Jun 5, 2021 5:15 PM - 6:30 PM JST | Sat. Jun 5, 2021 8:15 AM - 9:30 AM UTC | Ch.17_1

[S-GC32] Volatiles in the Earth - from Surface to Deep Mantle

convener:Takeshi Hanyu(Japan Agency for Marine-Earth Science and Technology, Research Institute for Marine Geodynamics), E Gray Bebout(Lehigh University), Yuji Sano(Division of Ocean and Earth Systems, Atmosphere and Ocean Research Institute, University of Tokyo), Hirochika Sumino(Department of General Systems Studies, Graduate School of Arts and Sciences, The University of Tokyo)

Volatiles play an important role in the dynamical and chemical processes in the Earth. The presence of volatiles drastically changes mineral stability and rheological behavior of the rocks. Chemical fractionation, such as partial melting, hydration, and dehydration are controlled by volatiles in the rocks. Volatiles enhance the production of magmas and drive their ascent and volcanic eruption. The atmosphere and hydrosphere have been generated by variety of degassing events from the mantle through volcanism. Some volatiles in the Earth's surface have been suggested to be recycled back into the mantle beyond subduction zones. Although the significance of volatiles in the Earth's evolution has been recognized, each of these processes is poorly constrained. We therefore welcome contributions from experimental, observational, and modeling studies that help shed light on the behavior, chemical/physical characteristic, and flux/budget of volatiles, such as hydrogen, carbon, nitrogen, noble gases, halogens, and sulfur. We encourage studies linking the behavior of multiple volatile elements and their isotopic compositions. Studies investigating the linkage between volatile and solid geochemical tracers, the phase equilibria of volatile-bearing mantle assemblages, and the effect of volatiles on the physical properties of the mantle are also welcome.

[SGC32-P01] Secular variation of helium isotope ratios in Izu Oshima: What will be observed in the next eruption?

*Hirochika Sumino[1], Kei Ikehata[2], Aya Shimizu[3], Kotaro Toyama[4], Tomoya Obase[1], Kenji Notsu[5] (1.Department of General Systems Studies, Graduate School of Arts and Sciences, The University of Tokyo, 2.Faculty of Life and Environmental Sciences, University of Tsukuba, 3.Tokyo Metropolitan Industrial Technology Research Institute, 4.Atmosphere and Ocean Research Institute, The University of Tokyo, 5.Geochemical Research Center, Graduate School of Science, University of Tokyo)

[SGC32-P02] Noble gas analysis and microstructure observation of the Finero phlogopite peridotite in Northern Italy to constrain the origin of deformation process of mantle wedge peridotite

*Nanae Fukushima[1], Hirochika Sumino[1], Jun-ichi Ando[2], DAS KAUSHIK[2], Masahiro Kobayashi[3], Hiroyuki Kagi[4], Takafumi Yamamoto[2] (1.Graduate School of Arts and Sciences, the University of Tokyo, 2.Graduate School of Advanced Science and Engineering, Hiroshima University, 3.Metropolitan Industrial Technology Research Institute, 4.Graduate School of Science, the University of Tokyo)

[SGC32-P03] Noble gas isotopic composition of directly ascending petit-spot from the northwest Pacific Ocean

*Kaishi Nakao[1], Naoto Hirano[2], Hirochika Sumino[3] (1.Department of Earth Science, Graduate School of Science, Tohoku University, 2.Center for Northeast Asian Studies, Tohoku University, 3.Graduate School of Arts and Sciences, The University of Tokyo)

[SGC32-P04] Fate of Subducting Organic Carbon: Evidence from HP/UHP Metasedimentary Suites and Implications for Isotopic Compositions of Arc Volcanic Gases

*Gray E Bebout[1], Kaylee H. Kraft[1], Jennie Pinho[2], Gabe S. Epstein[1] (1.Lehigh University, Dept. Earth and Environmental Sciences, Bethlehem, Pennsylvania, USA, 2.Lafayette College, Dept. Chemistry, Easton, Pennsylvania, USA)

[SGC32-P05] Monitoring the magmatic activity and volatile fluxes of Wakamiko caldera in southern Japan

*Ma. Teresa Escobar[1], Naoto Takahata[1], Kotaro Shirai[1], Takanori Kagoshima[1,2], Kentaro Tanaka[1], Hajime Obata[1], Yuji Sano[1] (1.Atmosphere and Ocean Research Institute University of Tokyo, 2.University of Toyama)

[SGC32-P06] Heterogeneous accretion of Earth's volatiles as constrained by nitrogen isotopes

*Lanlan Shi[2,1,3], Takanori Kagoshima[2], Yuji Sano[2] (1.State Key Laboratory of Isotope Geochemistry, Guangzhou Institute of 7 Geochemistry, Chinese Academy of Sciences, Guangzhou 510640, China, 2.Division of Ocean-Earth System Science, Atmosphere and Ocean Research Institute, University of Tokyo, Kashiwa, Chiba 277-8564, Japan, 3.University of Chinese Academy of Sciences, Beijing 100049, China)

[SGC32-P07] **Hydrogen isotope of the mantle source in Pitcairn Island**

*Takahiro Ozawa[1], Akira Ishikawa[1], Takeshi Hanyu[2], Kenji Shimizu[3], Takayuki Ushikubo[3], Morihisa Hamada[2], Hikaru Iwamori[4] (1.Department of Earth and Planetary Sciences, Tokyo Institute of Technology, 2.Japan Agency for Marine-Earth Science and Technology, 3.Kochi Core Center, Japan Agency for Marine-Earth Science and Technology, 4.Earthquake Research Institute, the University of Tokyo)

[SGC32-P08] Helium isotope heterogeneity recorded in different phenocrysts in Samoan lavas

*Takeshi Hanyu[1] (1.Japan Agency for Marine-Earth Science and Technology, Research Institute for Marine Geodynamics)

Secular variation of helium isotope ratios in Izu Oshima: What will be observed in the next eruption?

*Hirochika Sumino[1], Kei Ikehata[2], Aya Shimizu[3], Kotaro Toyama[4], Tomoya Obase[1], Kenji Notsu[5]

1. Department of General Systems Studies, Graduate School of Arts and Sciences, The University of Tokyo, 2. Faculty of Life and Environmental Sciences, University of Tsukuba, 3. Tokyo Metropolitan Industrial Technology Research Institute, 4. Atmosphere and Ocean Research Institute, The University of Tokyo, 5. Geochemical Research Center, Graduate School of Science, University of Tokyo

The helium isotope ratio ($^3He/^4He$ ratio) differs significantly in geochemical reservoirs ($^3He/^4He$ in air and meteoric water: 1 Ra = 1.4×10^{-6}, crust: 0.02 Ra, MORB source mantle: 8±1 Ra), and because helium is chemically inert, the $^3He/^4He$ ratio does not change by degassing from magma or by dissolution/degassing in water. Therefore, helium in volcanic gases, hot spring water, and hot spring gases can be used as a sensitive tracer of magma activity, and in fact, it has been reported that the $^3He/^4He$ ratio increased or decreased before and after eruptions at several volcanoes (Padrón et al., Geology 2013; Sano et al., Sci. Rep. 2015; Paonita et al., Geology 2016). Izu-Oshima volcano, an active volcanic island located around 100 km SSW of Tokyo, regularly erupted with 30 to 40 years intervals, but no eruption has occurred since the last activity in 1986-1990. In this presentation, we report the $^3He/^4He$ ratios of volcanic gases and olivines in pyroclastic materials collected in Izu Oshima, and discuss the long-term secular variation of $^3He/^4He$ ratios combining the reports of previous studies (Sano et al., EPSL 1991; Shimoike and Notsu, JVGR 2000).

The $^3He/^4He$ ratio of the observation steam well located in the north of the caldera in the center of Izu Oshima increased sharply immediately after the 1986 eruption from a low value of 1.7 Ra, peaked in 1988 at 5.5 Ra, and has been decreasing until now. The present $^3He/^4He$ ratio is around 1.5 Ra, which is lower than that before the last eruptive activity. The $^3He/^4He$ ratio corrected for atmospheric contamination using $^4He/^{20}Ne$ ratio was about 6.2 Ra throughout the last active period from 1986 to 1990. On the other hand, air-corrected $^3He/^4He$ ratios of hot spring gas collected from a well 500 m away from the steam well have been constant at 6.2 Ra since 2001. These results suggest that the mixing ratio of magma-derived and atmospheric helium in the steam well has changed in response to the decrease of supply of magma-derived helium, and the magmatic contribution has now almost completely decayed, while the $^3He/^4He$ ratio of magmatic gas itself has been constant over the past 30 years.

The observation that the helium released from the present magma is significantly lower than the value of 8 Ra, which is considered to be the value of the mantle wedge in subduction zone, suggests the significant contribution crustal helium in the magma reservoir. On the other hand, the $^3He/^4He$ ratio of olivines separated from lava flows of the Senzu Group, which erupted 20,000-40,000 years ago, and that from scoria in the lowest part (O95) of pyroclastic layers of the Older Oshima group, which was active after 20,000 years ago, are 7.4±0.4 Ra and 7.1±0.7 Ra, respectively, suggesting that $^3He/^4He$ ratios of the magma at these stages were almost equal to that of the mantle. However, the $^3He/^4He$ ratio of olivines in the N4 scoria erupted about 1300 years ago is 4.6±0.2 Ra, indicating that crustal helium was significantly contaminated into the magma.

Based on these results, two possible changes in the $^3He/^4He$ ratios of the steam and hot-spring wells can be expected: first, if the magma reservoir erupted in 1986 is reactivated, the $^3He/^4He$ ratio of hot spring gas will remain unchanged at about 6 Ra, and only the contribution of magma-derived helium observed in

©2021. Japan Geoscience Union. All Right Reserved.

the steam well will increase. This means that the change in the $^{3}He/^{4}He$ ratio observed during the previous activity in 1986-1990 will be reproduced. The second scenario, in which the reactivation of the magma reservoir is caused by the supply of primitive magma with a high $^{3}He/^{4}He$ ratio derived from the mantle, is that not only the contribution of magmatic helium in the steam well increases, but also the air-corrected $^{3}He/^{4}He$ ratio of the steam and hot-spring wells themselves become higher than 6 Ra. In other words, it is expected that the $^{3}He/^{4}He$ ratio can be used to clarify whether the next eruption results from new magma supply from greater depths or just reactivation of the old magma.

Keywords: helium isotopes, Izu-Oshima volcano, eruption

©2021. Japan Geoscience Union. All Right Reserved.

Noble gas analysis and microstructure observation of the Finero phlogopite peridotite in Northern Italy to constrain the origin of deformation process of mantle wedge peridotite

*Nanae Fukushima[1], Hirochika Sumino[1], Jun-ichi Ando[2], DAS KAUSHIK[2], Masahiro Kobayashi[3], Hiroyuki Kagi[4], Takafumi Yamamoto[2]

1. Graduate School of Arts and Sciences, the University of Tokyo, 2. Graduate School of Advanced Science and Engineering, Hiroshima University, 3. Metropolitan Industrial Technology Research Institute, 4. Graduate School of Science, the University of Tokyo

Since the rheology of mantle control the behavior of deep earthquakes and orogenic activity, it is important to understand the elementary processes of deformation of the mantle rocks. Alpine-type peridotites are rock bodies formed by the solid penetration of upper mantle fragments along large faults at convergent plate boundaries, and are likely to preserve deformation structures in the brittle-ductile regime during the ascending process. We focus on the effect of water in mantle region on the deformation characteristics preserved in Finero phlogopite peridotite in Northern Italy, which is an alpine-type peridotite and had been metasomatized by slab dehydration in the mantle wedge during the Paleozoic and Mesozoic (Selverstone & Sharp, EPSL 2011; Hartmann & Wedepohl, GCA 1993; [3] Zanetti et al., Contrib. Mineral. Petrol. 1999).

In order to clarify the water-rock interaction and deformation history of the peridotite, we performed: (1) microstructural observations using a scanning electron microscope and a transmission electron microscope, and (2) noble gases analysis of the fluid/melt inclusions in mineral grains, which provide information of the origin of fluids/melts. In the noble gas analysis, the crushing method was adopted to selectively extract noble gases from fluid/melt inclusions.

In the field survey, we found a strain localization zone about 80 m wide in the peridotite, and collected rocks in the strain localization zone and 750 m away from the strain localization zone, respectively. A comparison of the two rocks by thin-section observation shows that the rock of the strain localization zone may have been deformed with forming microcracks under hydrous condition and subsequently may have trapped the fluid/melt inclusions. On the other hand, no such characteristic was observed in the samples away from the strain localization zone. The results of the olivine slip system observation suggest that fluid may have penetrated the rock of the strain localization zone during brittle-ductile deformation.

Noble gas analyses of fluid/melt inclusions show that the He, Ne, and Ar isotope ratios of all samples can be accounted for by three-component mixing of atmosphere/seawater, radiogenic/nucleogenic and mantle components. Similar mixing relation has been observed in very fine-grained apatite and orthopyroxene separated from the Finero peridotite (Matsumoto et al., EPSL 2005). On the other hand, the Ne-Ar-Xe elemental ratios of the samples show that a seawater-derived component is dominant. In addition, while the $^{3}He/^{4}He$ ratios are uniform, the $^{40}Ar/^{36}Ar$ ratios become lower with increasing deformation of the sample rock. This suggests that the seawater-derived component may have added to the mantle + radiogenic/nucleogenic component, and that the metasomatism by slab-derived, water-rich fluids may have promoted plastic deformation of peridotite in the mantle region. The observation that the mantle + radiogenic/nucleogenic end members behave as a single component cannot be explained by an addition of fluid released from surrounding metamorphic rocks, in which abundant

©2021. Japan Geoscience Union. All Right Reserved.

radiogenic/nucleogenic noble gases had accumulated, during exhumation of the Finero peridotite body. Alternatively, the radiogenic/nucleogenic component would result from accumulation of radiogenic/nucleogenic noble gases in the mantle wedge previously metasomatized by slab-derived fluids enriched in U, Th, and K.

Keywords: peridotite, mantle, noble gas, metasomatism

©2021. Japan Geoscience Union. All Right Reserved.

Noble gas isotopic composition of directly ascending petit-spot from the northwest Pacific Ocean

*Kaishi Nakao[1], Naoto Hirano[2], Hirochika Sumino[3]

1. Department of Earth Science, Graduate School of Science, Tohoku University, 2. Center for Northeast Asian Studies, Tohoku University, 3. Graduate School of Arts and Sciences, The University of Tokyo

The petit-spot magmatism provides us with information about the mantle beneath old part of oceanic lithosphere prior to subduction where we have never seen besides the underlying mantle below hotspot volcanoes and mid-ocean ridges. The asthenospheric $^{3}He/^{4}He$ ratios are recognized only using the mid-ocean ridge basalts (MORBs) as shown by uniform values of 8.75 ±2.14 Ra in the world MORBs (Graham, 2002). The petit-spot volcanoes on the northwestern Pacific Plate are classified into two types based on magmatic compositions and the difference in stress fields associated with plate flexure. One is erupted at the eastern slope of the outer rise (regular petit-spot). In this case, the differentiated melt without phenocrystic olivine does not ascend rectilinearly due to the compressional stress field of upper lithosphere, which may cause the metasomatic interaction with lithospheric mantle. The other is the directly ascending petit-spot (DAP) erupted at the top of outer rise where the tectonic stress-field is totally tensile in lithosphere. The DAP melt directly ascends to the surface without magma-stagnations in lithospheric mantle, uniquely including phenocrystic olivines. Therefore, DAPs likely have more primordial composition than regular petit-spots.

In this study, we measured the noble gas isotopic compositions of quenched glasses and phenocrystic olivines separated from DAP lavas using stepwise heating methods. The samples were both regular petit-spot and DAP, located at the Japan Trench axis and at the top of the outer-rise, respectively.

The $^{3}He/^{4}He$ ratios of phenocrystic olivines of DAPs, relatively young in eruption age, are similar to those of MORB (7.5- 9.7 Ra), and the $^{40}Ar/^{36}Ar$ ratios are 337- 3284 at 600℃ and 1800℃. The $^{3}He/^{4}He$ ratio of the quenched glasses of regular petit-spot is 3.1 Ra, and the $^{40}Ar/^{36}Ar$ ratio is as high as 7000 at 1500℃. The Ne isotope ratios of all the samples are similar to the MORB trend although the values are close to atmosphere. The data of regular petit-spots are explained by the three components of MORB source, crust or sediment (radiogenic) and atmospheric components. Most of DAPs, on the other hand, simply show the mixing of atmospheric components and MORB sources, designating more primary composition than those of regular petit-spots. An exceptional data of high $^{3}He/^{4}He$ ratio (13.5 Ra) of the DAP quenched glasses is enigmatic. As the phenocrystic olivines of same sample, initially crystallized from primary melts, show MORB value, it might be due to the influence of shallower lithosphere or marine sediments, in which cosmic dusts with high $^{3}He/^{4}He$ ratios and high He concentrations are contained.

Keywords: petit-spot, noble gas, olivine, quenched glass

©2021. Japan Geoscience Union. All Right Reserved.

Fate of Subducting Organic Carbon: Evidence from HP/UHP Metasedimentary Suites and Implications for Isotopic Compositions of Arc Volcanic Gases

*Gray E Bebout[1], Kaylee H. Kraft[1], Jennie Pinho[2], Gabe S. Epstein[1]

1. Lehigh University, Dept. Earth and Environmental Sciences, Bethlehem, Pennsylvania, USA, 2. Lafayette College, Dept. Chemistry, Easton, Pennsylvania, USA

Western Alps high-pressure and ultrahigh-pressure (HP/UHP) metasedimentary rocks record transit of organic (reduced) C through forearcs (40-70 km) to depths approaching those beneath volcanic fronts. The Schistes Lustrés, exposed in the Italian and French Alps, represents subduction of sediment to depths of up to ~70km, where they were underplated, along an extremely low-P/T trajectory of 7-8ºC/km. Across the range of grade in this suite (peak temperatures of ~350-550ºC), reduced C shows little evidence of loss (based on normalization to concentrations of Al_2O_3, TiO_2, and Zr) but considerable increase in $\delta^{13}C_{VPDB}$ to near mantle values of -6‰ related to isotopic exchange with coexisting carbonate. In Schistes Lustrés metashales lacking carbonate, reduced C preserves protolith $\delta^{13}C$ of -24 to -21‰ independent of grade and degrees of devolatilization. Reduced C occurs as amorphous carbonaceous matter at low grades and its transformation to graphite at higher grades presumably enhances isotopic exchange with carbonate. For comparison, in carbonate-poor lower-grade units of the Catalina Schist (in California), and Franciscan Complex (California) and Western Baja Terrane (Mexico) blueschist-facies rocks, together representing subduction to 10-40 km depths, reduced C concentrations and $\delta^{13}C$, C/N, and $\delta^{15}N$ are similar to those of sediment protoliths (see Sadofsky and Bebout, 2003; G-cubed), as in the lowest-grade unit of the Schistes Lustrés (regardless of carbonate content; for the N isotope data see Bebout et al., 2013; Chem. Geol.). In Catalina Schist units that experienced warmer prograde P-T paths, reduced C is shifted in $\delta^{13}C$ from -25 to -19‰ related to minor loss of C as CH_4 during devolatilization.

Our work implies that much of the reduced C reservoir is retained in rocks subducting to depths approaching those beneath volcanic fronts and could be available for transfer into the sub-arc mantle wedge, perhaps via partial melting. Yet unknown is whether reduced and oxidized C reservoirs, and their isotopic compositions, are fractionated during sub-arc mobilization and delivery into the mantle wedge. Such fractionation, and any isotopic exchange between the two reservoirs (in addition to accretion and underplating; see House et al., 2019, Geology), could have implications for application of the $CO_2/^3He$-$\delta^{13}C$ approach used in studies of arc volcanic gases to calculate contributions from mantle and disparate sediment sources.

Keywords: carbon cycling, subduction, metamorphism

©2021. Japan Geoscience Union. All Right Reserved.

Monitoring the magmatic activity and volatile fluxes of Wakamiko caldera in southern Japan

*Ma. Teresa Escobar[1], Naoto Takahata[1], Kotaro Shirai[1], Takanori Kagoshima[1,2], Kentaro Tanaka[1], Hajime Obata[1], Yuji Sano[1]

1. Atmosphere and Ocean Research Institute University of Tokyo, 2. University of Toyama

Volatiles from subduction zones, submerged calderas in particular, are poorly quantified. Unlike subaerial volcanoes, underwater volcanic activity is difficult to observe. Wakamiko, a submerged caldera in southern Japan shares a magma source with the active subaerial volcano, Mt. Sakurajima . Following years of inactivity, the volcanic eruptions in Mt. Sakurajima became more frequent in 2009; however, it is undetermined how the neighboring Wakamiko caldera has behaved in relation to this upsurge in activity. In this study, we assess the state of hydrothermal venting inside Wakamiko following recent disturbances in Mt. Sakurajima. Based on gas bubbles, seawater and sediment pore water measurements of samples obtained in 2015, it appears that acidic fluids enriched in ^{3}He continue to be discharged to the seafloor. Excess ^{3}He in the water column shows no apparent change since 2010; however, the helium isotopic ratio of the magmatic source continues to be elevated at ~7.2 Ra. This ratio for the magmatic component is higher than previously observed in 1986 (~6 Ra). The difference could be related to changes in the degassing activity as well as the mantle composition of the magmatic source. Using the new data from sediment pore water, we estimate the diffusive fluxes of ^{3}He and ^{4}He through the seafloor at 16.05 atoms $cm^{-2}s^{-1}$ and 1.52 x 10^{6} atoms $cm^{-2}s^{-1}$, respectively. We also calculated the vent ^{3}He flux at 3.38 x10^{4} atoms $cm^{-2}s^{-1}$. With the use of the ^{3}He flux, we calculated the diffusive CO_2 flux from Wakamiko at 1.41 x 10^{6} mol yr^{-1} and the vent flux at 3.72 x 10^{8} mol yr^{-1}. The available data that we have are still limited and a more frequent and longer observation is necessary to deduce the temporal changes in Wakamiko and its relation to the volcanic activity of Mt. Sakurajima.

Keywords: submarine caldera, helium isotopes, magmatic volatiles

©2021. Japan Geoscience Union. All Right Reserved.

Heterogeneous accretion of Earth’s volatiles as constrained by nitrogen isotopes

*Lanlan Shi[2,1,3], Takanori Kagoshima[2], Yuji Sano[2]

1. State Key Laboratory of Isotope Geochemistry, Guangzhou Institute of 7 Geochemistry, Chinese Academy of Sciences, Guangzhou 510640, China, 2. Division of Ocean-Earth System Science, Atmosphere and Ocean Research Institute, University of Tokyo, Kashiwa, Chiba 277-8564, Japan, 3. University of Chinese Academy of Sciences, Beijing 100049, China

The origin of planetary volatiles such as nitrogen is critical for understanding planetary accretion, differentiation, and habitability. However, the detailed processes for the origin of Earth’s volatiles remain unresolved. Nitrogen shows large isotopic fractionations among geochemical and cosmochemical reservoirs, which places tight constraints on Earth’s volatile accretion process. Here we experimentally determine N-partitioning and -isotopic fractionations between planetary cores and silicate mantles at 1–8 GPa and 1700–2200 ˚C. We show that the core/mantle N-isotopic fractionations increase from −4‰ to +10‰, as oxygen fugacity decreases from 0.3 to 4.7 log units below the iron-wüstite buffer. The core/mantle nitrogen partition coefficients, ranging from 0.03 to 80, are a multifunction of oxygen fugacity, temperature, pressure, and the compositions of core and mantle. We apply N partition coefficients and isotopic fractionations in in a state-of-the-art model of planetary accretion and core-mantle differentiation. We find that the N-budget and -isotopic composition of Earth’s atmosphere plus crust, silicate mantle, and the source region of oceanic island basalts are best explained by Earth’s early accretions of enstatite chondrite-like reduced impactors, followed by late accretions of increasingly oxidized impactors and minimal CI chondrite-like material shortly before and during the Moon-forming giant impact. Earth may thus have acquired its nitrogen and other major volatiles heterogeneously, and its volatile budget may have been established during the main accretion stages.

Keywords: nitrogen, isotope fractionation, core formation, oxygen fugacity, volatiles

©2021. Japan Geoscience Union. All Right Reserved.

Hydrogen isotope of the mantle source in Pitcairn Island

*Takahiro Ozawa[1], Akira Ishikawa[1], Takeshi Hanyu[2], Kenji Shimizu[3], Takayuki Ushikubo[3], Morihisa Hamada[2], Hikaru Iwamori[4]

1. Department of Earth and Planetary Sciences, Tokyo Institute of Technology, 2. Japan Agency for Marine-Earth Science and Technology, 3. Kochi Core Center, Japan Agency for Marine-Earth Science and Technology, 4. Earthquake Research Institute, the University of Tokyo

The origin of Earth’s water has long been debated based on the hydrogen isotope [deuterium/hydrogen (D/H)] ratio of the Earth. However, the D/H ratio of the bulk Earth estimate remains controversial since substantial amounts of water could be present inside the Earth. The relatively uniform D/H ratio for the upper mantle (δ D of -60 ±5 ‰relative to VSMOW) is established by the analysis of submarine glass from mid-oceanic ridge basalts (Clog et al., 2013). Recently, Hallis et al. (2015) reported much lower D/H ratios from olivine-hosted melt inclusions in Baffin Island and Icelandic lavas, and suggested that the Earth’s deep mantle has much lower D/H ratio (δ D < -218 ‰). They attributed such low- δ D signature to a protosolar nebula origin which is derived from an isolated reservoir resided in the Earth’s deep interior. However, another possibility that such low- δ D signature was created via dehydration of subducting slab (Shaw et al., 2008) needs to be evaluated.

The oceanic island basalt (OIB) of Pitcairn Island is typical of containing recycled material such as subducted slab (Eisele et al., 2002; Garapic et al., 2015). We found rapidly-quenched hyaloclastite containing abundant automorphic fresh olivine crystals and volcanic glass shards. Since the olivine crystals contain many crystal-free glassy inclusions, we analyzed concentration of volatiles (CO_2, H_2O, F, S and Cl) and P_2O_5, and hydrogen isotope ratio (δ D) with SIMS, and major elements with EPMA for melt inclusions and glass shards, and compared them with the aim to evaluate the D/H fractionation during magma evolution and to constrain the D/H ratio of recycled components stored in the deep mantle.

Our results demonstrate that olivine-hosted melt inclusions have much higher H_2O and CO_2 contents than matrix-derived glass shards, consistent with that magma degassing is responsible for their volatile element abundances. Their δ D values positively correlate with H_2O contents, also indicative of vapor-melt D/H fractionation during final stage of degassing. Since most measured melt inclusions were high in CO_2, such degassing of H_2O and D/H fractionation could be minor. With the exception of some inclusions depleted in volatiles, we obtained an average water content of 1.06 ±0.16 wt.% and an average δ D value of -89 ± 12‰ (2 SD) as the composition of primitive melt, which is significantly lower than the upper mantle value. This suggests that Pitcairn mantle plume tapped the material with a low D/H ratio, which could be derived from recycled slab components.

Keywords: hydrogen isotope ratio, hotspot, Pitcairn Island

©2021. Japan Geoscience Union. All Right Reserved.

Helium isotope heterogeneity recorded in different phenocrysts in Samoan lavas

*Takeshi Hanyu[1]

1. Japan Agency for Marine-Earth Science and Technology, Research Institute for Marine Geodynamics

Ocean island basalts (OIBs) are generally considered to be fed by upwelling mantle plumes sourced from deep mantle domain. Geochemical variation observed in OIBs should reflect heterogeneous deep mantle materials including subducted slabs. Isotopically enriched signature of Samoan OIBs have been recognized to be the manifestation of subducted sedimentary materials. Samoan OIBs also show depleted and primordial isotopic signature, suggesting that variety of source materials are involved in the magma sources as demonstrated by geochemical heterogeneity in the inter-island scale to phenocryst scale. For example, lavas on Ofu Island show large $^{3}He/^{4}He$ range (19-34 Ra) despite limited Sr and Nd isotopic variation. Lavas with very high $^{87}Sr/^{86}Sr$ show Sr isotopic difference between clinopyroxene and whole rock. Moreover, variation in $^{87}Sr/^{86}Sr$ has been found in melt inclusions in olivine. In this study, we show $^{3}He/^{4}He$ isotopic difference between olivine and clinopyroxene in a single lava from Tutuila Island. Radiogenic isotope data from the literatures and this study indicate the presence of at least four mixing components; EM2 (enriched mantle-2), HIMU (high-mu), FOZO (focal zone mantle), and depleted mantle. Olivine and clinopyroxene in lavas with FOZO-like compositions show similar $^{3}He/^{4}He$. In contrast, olivine show higher $^{3}He/^{4}He$ than clinopyroxene in lavas with radiogenic $^{87}Sr/^{86}Sr$. Some lavas with radiogenic $^{87}Sr/^{86}Sr$ also have $^{87}Sr/^{86}Sr$ that is different from clinopyroxene hosted in them. The 3-D isotopic plot (e.g., Sr-Pb-He) of Samoan OIBs displays a cone-shape distribution with the FOZO component at the top (high $^{3}He/^{4}He$) and EM2, HIMU and depleted component at the bottom (low $^{3}He/^{4}He$). Tutuila lavas plot on a steep slope of the cone. I suggest that small difference in mixing proportion of the components is responsible for relatively large isotopic difference. Such isotopic difference may not be caused by the coupled effect of temporal change in magma composition and mineral crystallization, as Mg# of olivine and clinopyroxene overlaps with each other. I infer that compositional variation existed in a magma chamber where olivine and clinopyroxene crystallized, and thereby geochemical heterogeneity in a deep-rooted mantle plume was preserved to the shallow depth.

Keywords: Helium, Ocean island basalt, Samoa

©2021. Japan Geoscience Union. All Right Reserved.

[J] Oral | S (Solid Earth Sciences)：S-GC Geochemistry

Sat. Jun 5, 2021 1:45 PM - 3:15 PM JST | Sat. Jun 5, 2021 4:45 AM - 6:15 AM UTC | Ch.24 Zoom Room 24

[S-GC33] Solid Earth Geochemistry, Cosmochemistry

convener:Gen Shimoda(Geological Survey of Japan, AIST), Katsuhiko Suzuki(Submarine Resources Research Center, Japan Agency for Marine-Earth Science and Technology), Katsuyuki Yamashita(Graduate School of Natural Science and Technology, Okayama University), Akira Ishikawa(Department of Earth and Planetary Sciences, Tokyo Institute of Technology), Chairperson:Katsuhiko Suzuki(Submarine Resources Research Center, Japan Agency for Marine-Earth Science and Technology), Katsuyuki Yamashita(Graduate School of Natural Science and Technology, Okayama University), Akira Ishikawa(Department of Earth and Planetary Sciences, Tokyo Institute of Technology), Gen Shimoda(Geological Survey of Japan, AIST)

Solid Earth Geochemistry, Cosmochemistry" session aims at evaluating processes during the 4.6 billion years of the solar system and the Earth. Any approaches to this issue is welcomed, including, geochemistry, geophysics, geology, mineralogy and petrology.

1:45 PM - 2:00 PM JST | 4:45 AM - 5:00 AM UTC

[SGC33-01] Highly siderophile elements in Earth's oldest rocks from Acasta Gniess Complex, Canada: an impact melt origin or not?

*Akira Ishikawa[1,2], Keiko Koshida, Katsuhiko Suzuki[2], Tetsuya Yokoyama[1], Tsuyoshi Komiya[3] (1.Department of Earth and Planetary Sciences, Tokyo Institute of Technology, 2.Submarine Resources Research Center, Japan Agency for Marine-Earth Science and Technology, 3.Graduate School of Arts and Sciences, The University of Tokyo)

2:00 PM - 2:15 PM JST | 5:00 AM - 5:15 AM UTC

[SGC33-02] Estimation of highly siderophile element abundances in the primitive mantle from the perspective of the pyrolite model

*Tetsu Kogiso[1], Akira Ishikawa[2], Norikatsu Akizawa[3] (1.Kyoto University, 2.Tokyo Institute of Technology, 3.The University of Tokyo)

2:15 PM - 2:30 PM JST | 5:15 AM - 5:30 AM UTC

[SGC33-03] Chromium and titanium stable isotope measurements for volcanic rocks derived from deep mantle

*Yuki Hibiya[1], Tsuyoshi Iizuka[2], Katsuhiko Suzuki[1], Shigekazu Yoneda[3] (1.Submarine Resources Research Center, Japan Agency for Marine-Earth Science and Technology, 2.The University of Tokyo, 3.National Museum of Nature and Science)

2:30 PM - 2:45 PM JST | 5:30 AM - 5:45 AM UTC

[SGC33-04] $^{182}W/^{184}W$ of the komatiites from Dharwar and Singhbhum cratons, India: implications for the early evolution of the mantle

*Katsuhiko Suzuki[1,5], Madhusoodhan Satish-Kumar[2], Trisrota Chaudhuri[3], M. Jayananda[4] (1.Submarine Resources Research Center, Japan Agency for Marine-Earth Science and Technology, 2.Department of Geology, Faculty of Science, Niigata University, 3.Department of Geology, University of Calcutta, 4.Centre Earth and Space Sciences, University of Hyderabad, 5.Department of Earth Sciences, Graduate School of Science, Tohoku University)

2:45 PM - 3:00 PM JST | 5:45 AM - 6:00 AM UTC

[SGC33-05] The magma generation process of the North Sredinny Range, Kamchatka – Insights from highly siderophile elements and Re-Os isotope system

Yuri Mitsude[1], *Tatsuji Nishizawa[2], Hitomi Nakamura[3], Tatiana Churikova[4], Boris Gordeychik[5], Akira Ishikawa[6], Hikaru Iwamori[1] (1.Earthquake Research Institute, The University of Tokyo, 2.Volcanic Fluid Research Center, School of Science, Tokyo Institute of Technology, 3.Institute of Earthquake and Volcano

Geology, Geological Survey of Japan, AIST, 4.Institute of Volcanology and Seismology, Far East Branch, RAS, 5.Institute of Experimental Mineralogy, RAS, 6.Department of Earth and Planetary Sciences, School of Science, Tokyo Institute of Technology)

3:00 PM - 3:15 PM JST | 6:00 AM - 6:15 AM UTC

[SGC33-06] The characteristics of highly siderophile elements in the high-Mg andesite and basalts and its implications for the origin of the Quaternary arc magmatism in the forearc region, Kamchatka

*Tatsuji Nishizawa[1], Yuri Mitsude[2], Hitomi Nakamura[3], Tatiana Churikova[4], Boris Gordeychik[5], Akira Ishikawa[6], Hikaru Iwamori[2] (1.Volcanic Fluid Research Center, School of Science, Tokyo Institute of Technology, 2.Earthquake Research Institute, The University of Tokyo, 3.Institute of Earthquake and Volcano Geology, Geological Survey of Japan, AIST, 4.Institute of Volcanology and Seismology, Far East Branch, RAS, 5.Institute of Experimental Mineralogy, RAS, 6.Department of Earth and Planetary Sciences, School of Science, Tokyo Institute of Technology)

Highly siderophile elements in Earth's oldest rocks from Acasta Gniess Complex, Canada: an impact melt origin or not?

*Akira Ishikawa[1,2], Keiko Koshida, Katsuhiko Suzuki[2], Tetsuya Yokoyama[1], Tsuyoshi Komiya[3]

1. Department of Earth and Planetary Sciences, Tokyo Institute of Technology, 2. Submarine Resources Research Center, Japan Agency for Marine-Earth Science and Technology, 3. Graduate School of Arts and Sciences, The University of Tokyo

The first billion years' history of the Earth is veiled in mystery due to the dearth of Hadean and earliest Archean rocks. Although this might be a natural outcome given the high efficiency of overprinting and reworking processes caused by plate tectonics, an important question of when plate subduction started on Earth still remains obscure. Alternatively, it has been proposed that the crust preservation was delayed by a barrage of asteroid impacts that caused global-scale melting and continuous resurfacing of Earth after a period referred to as "late heavy bombardment" on the Moon (~4.1-3.9 Ga).
A recent petrogenetic modelling suggests that the Earth's oldest evolved rocks, the 4.02 Ga Idiwhaa tonalitic gneisses of the Acasta Gneiss Complex [1], represent the predominant felsic crust at that time, which has been generated by impact melting of Hadean mafic crust [2]. We test this hypothesis by investigating abundances of highly siderophile elements (HSEs) and Re-Os isotope systematics for the Idiwhaa tonalitic gneisses collected from previously located outcrops and a newly identified exposure as a southern extension of the same unit. These tracers are considered to be sensitive for involvement of extraterrestrial components and relatively immune to secondary alteration.
Although quadruplicate measurements for each sample showed significant variations indicative of isotope and elemental heterogeneity inherent in studied samples, the preservation of Hadean HSE signatures in the Idiwhaa tonalites are supported by whole-rock Re-Os isotope data; extremely radiogenic ^{187}Os (>94% of total Os) provides a weighted mean ^{187}Re-^{187}Os model age ~4.0 Ga consistent with the U-Pb ages of zircon. Regarding HSE abundances, the Idiwhaa tonalites display strongly fractionated HSE patterns. Concentrations of common Os, Ir and Ru are low with chondrite-normalizing values ranging from 10^{-5} to 10^{-6} level. These data show no contribution of the meteoritic components to the generation of Idiwhaa tonalites, and lend no support to the hypothesis of impact melt origin.
[1] J. R. Reimink et al., Earth's earliest evolved crust generated in an Iceland-like setting. *Nature Geosci.* 7, 529–533 (2014).
[2] T. E. Johnson et al., An impact melt origin for Earth's oldest known evolved rocks. *Nature Geosci. 11*, 795–799 (2018).

Keywords: Highly siderophile elements, Re-Os isotopes, Acasta Gneiss Complex

©2021. Japan Geoscience Union. All Right Reserved.

Estimation of highly siderophile element abundances in the primitive mantle from the perspective of the pyrolite model

*Tetsu Kogiso[1], Akira Ishikawa[2], Norikatsu Akizawa[3]

1. Kyoto University, 2. Tokyo Institute of Technology, 3. The University of Tokyo

Highly siderophile elements (HSE: Ru, Rh, Pd, Re, Os, Ir, Pt and Au) are strongly concentrated in the metallic core in the Earth, and therefore their abundances in the silicate mantle are quite low (~ μg/g). Just because of the low abundances, HSE in the mantle are the key index for deciphering chemical processes involving metallic phases, such as the core-mantle segregation and subsequent core-mantle chemical interactions during the Earth's history. In particular, HSE abundances in the mantle at the time of core-mantle segregation, that is, the HSE abundances in the primitive mantle (PM), are one of the crucial constraints to know the initial condition of the chemical evolution of the mantle.
The HSE abundances in the primitive mantle (HSE_{PM} hereafter) have been estimated based on HSE concentrations of fertile peridotites, which are rich in "melt components" such as Al_2O_3, because fertile peridotites are thought to retain their pristine compositions. However, recent studies (e.g., [1]) have revealed that most of the fertile peridotites were formed by addition of basaltic melt to refractory peridotites (= refertilization). Therefore, more precise estimation of the HSE_{PM} can be done by calculation of supposed mixture of refractory peridotites (harzburgites) and refertilizing agents with basaltic composition. This calculation is just identical to the "pyrolite model" of Ringwood (e.g., [2]), which was proposed for estimating the major element composition of the primitive mantle. In fact, the major element composition of the pyrolite has widely been accepted as the representative of the Earth's mantle. This would be due to the facts that compositions of natural harzburgites are rather homogeneous and that major element compositions of the refertilizing agents (coincidentally?) resemble those of supposed melts extracted from the primitive mantle. On the other hand, HSE compositions of natural harzburgites are very variable (up to 2 orders of magnitude), which makes it difficult to select the composition of harzburgite to be used for the "pyrolitic" estimation of HSE_{PM}. Despite such difficulty, we can estimate the pyrolitic HSE abundances using compositions of the harzburgites that were not remarkably affected by secondary processes if we can properly select suitable harzburgite samples based on detailed petrography. Our preliminary estimation of the pyrolitic HSE abundances demonstrates non-chondritic relative ratios with significant depletion of Pd and Pt. This is contrary to the conventional view that the HSE_{PM} is chondritic.
[1] Le Roux V., Bodinier J.-L., Tommasi A., Alard O., Dautria J.-M., Vauchez A., Riches A.J.V. 2007. The Lherz spinel lherzolite: Refertilized rather than pristine mantle. *Earth Planet. Sci. Lett.*, 259, 599-612.
[2] Ringwood T.E. 1962. A model for the upper mantle. *J. Geophys. Res.* 67, 57-866.

Keywords: primitive mantle, highly siderophile element, platinum group element, early Earth

©2021. Japan Geoscience Union. All Right Reserved.

Chromium and titanium stable isotope measurements for volcanic rocks derived from deep mantle

*Yuki Hibiya[1], Tsuyoshi Iizuka[2], Katsuhiko Suzuki[1], Shigekazu Yoneda[3]

1. Submarine Resources Research Center, Japan Agency for Marine-Earth Science and Technology, 2. The University of Tokyo, 3. National Museum of Nature and Science

Introduction: Recent studies have shown that the primordial signatures (e.g., those characterized by nebular $^{20}Ne/^{22}Ne$ and D/H ratio; [1, 2]) of the Earth-forming materials are preserved in the deep mantle and that they are chemically and isotopically distinct from those of the ambient upper mantle. However, it is still unclear exactly which type of planetary materials those primordial signatures correspond to, and when those materials were accreted to proto-Earth. To address these issues, we use the nucleosynthetic ^{54}Cr and ^{50}Ti anomalies, which provide information about the genetic relationship between the planetary materials especially when the two systems are combined [3]. In addition, we use the stable ^{53}Cr, a decay product of a short-lived radionuclide ^{53}Mn, which provides chronological information about the first ~20 Ma of solar system history. Attention is focused on the basalts from the Ontong Java plateau (OJP) and Samoan ocean islands (OIBs), and komatiites from the Singhbhum Craton, because these are suggested to record the Archean to modern plume-dominated environments [4-6].

Results & Discussion: We prepared OJP drill core samples provided by the Ocean Drilling Program (ODP Leg 192), basalts from the Samoan Island of Tutuila, and komatiites from the Singhbhum Craton, Eastern India. The chemical separation and purification of Cr and Ti from the samples were made following the procedure described by [7]. The recovery rates of both Cr and Ti were 90–100% for all samples. We have measured Cr and Ti stable isotope compositions of the purified samples using Thermo Fisher Scientific TRITON Plus TIMS and Neptune Plus MC-ICP-MS, respectively. The Ti isotope analyses yielded no resolvable $^{46, 48, 50}Ti$ excesses or deficits for all samples. On the other hand, the Cr isotope analyses yielded $\varepsilon^{53}Cr = 0.02 \pm 0.10$ ~ 0.12 ± 0.07 (2σ), $\varepsilon^{54}Cr = 0.10 \pm 0.12$ ~ 0.25 ± 0.07 (2σ) for the OJP basalts, $\varepsilon^{53}Cr = 0.01 \pm 0.02$ ~ 0.03 ± 0.09, $\varepsilon^{54}Cr = -0.02 \pm 0.08$ ~ 0.16 ± 0.16 for the Samoan basalts, $\varepsilon^{53}Cr = -0.04 \pm 0.08$ ~ 0.13 ± 0.10, $\varepsilon^{54}Cr = 0.02 \pm 0.07$ ~ 0.21 ± 0.05 for the Singhbhum komatiites. The resolved ^{53}Cr and ^{54}Cr excesses in some sources potentially reflect the survival of carbonaceous chondrite-like (characterized by ^{53}Cr and ^{54}Cr excesses) materials from mixing by mantle convection over geological history. However, the exponential-law corrected $\varepsilon^{53}Cr$ and $\varepsilon^{54}Cr$ of respective samples are slightly correlated with a slope of ~1–4.8. Similarly, we found the residual correlation between $\varepsilon^{53}Cr$ and $\varepsilon^{54}Cr$ for the Cr standards calculated relative to the mean of all 463 measurements over a period of two years, yielding a slope of ~1.3 (R ~ 0.84). Although the slope ~1.3 is significantly shallower than that of the residual linear mass fractionation correlation line (slope ~2) in [8-10], it is indistinguishable from the slope obtained recently for the terrestrial basalts and peridotites by [11]. We are in the process of exploring the reason for the positive correlation observed between ^{53}Cr and ^{54}Cr.

[1] Williams and Mukhopadhyay (2019) *Nature* **565** 78–81, [2] Hallis et al. (2015) *Science* **350** 795–797, [3] Warren (2011) *EPSL* **311** 93–100, [4] Rizo et al. (2016) *Science* **352** 809–812, [5] Jackson et al. (2014) *Nature* **514** 355–358, [6] Chaudhuri et al. (2017) *Precambrian Res.* **298** 385–402, [7] Hibiya et al. (2019) *GGR* **43** 133–145, [8] Lugmair and Shukolyukov (1998) *GCA* **62** 2863–2886, [9] Trinquier et al. (2006) *EPSL* **241** 780–788, [10] Qin et al. (2010) *GCA* **74**1122–1145, [11] Mougel et al. (2018) *EPSL* **481** 1–8.

©2021. Japan Geoscience Union. All Right Reserved.

Keywords: chromium, titanium, komatiites, LIPs, OIBs, deep mantle

©2021. Japan Geoscience Union. All Right Reserved.

$^{182}W/^{184}W$ of the komatiites from Dharwar and Singhbhum cratons, India: implications for the early evolution of the mantle

*Katsuhiko Suzuki[1,5], Madhusoodhan Satish-Kumar[2], Trisrota Chaudhuri[3], M. Jayananda[4]

1. Submarine Resources Research Center, Japan Agency for Marine-Earth Science and Technology, 2. Department of Geology, Faculty of Science, Niigata University, 3. Department of Geology, University of Calcutta, 4. Centre Earth and Space Sciences, University of Hyderabad, 5. Department of Earth Sciences, Graduate School of Science, Tohoku University

Since Hf and W are lithophile and siderophile elements, Hf is likely to have remained in the silicate melt phase and W was preferentially partitioned to the metallic melt phase during the formation of the Earth's core. Such Hf-W fractionation is thought to have occurred before the disappearance of currently distinct ^{182}Hf, and the values of $\mu^{182}W$ (deviations from W standard in ppm) have been reported to show negative deviations from the present-day mantle value ($\mu^{182}W$ =0) in ocean island basalts such as Hawaii and Samoa (e.g., Mundl et al., 2017; Takamasa et al., 2020). In contrast, most rocks originated at depths and older than 2.5 Ga show relatively uniform $\mu^{182}W$ values of +10 to +20 (e.g., Willbold et al., 2011, Touboul et al., 2014, Liu et al., 2016, Mundl et al., 2018, Tusch et al., 2019). On the other hand, some komatiites, such as Schapenburg and Komati (both formed at 3.5 Ga), yield negative or have values near 0, respectively (Touboul et al., 2012, Puchtel et al., 2018). In addition, Mei et al. (2019) reported $\mu^{182}W$ values near 0 for 3.0 Ga Anshan komatiite. Therefore, it is still highly debated on when and how the mantle has reached the present state.

In this study, we analyzed the W isotopes of 3.3 Ga Singhbhum and Dharwar komatiites from India to determine the W isotopic variations in the mantle during the period from 3.5 Ga to 3.0 Ga. The chemical separation of W was carried out using a method modified from Takamasa et al. (2020), and isotope analysis was performed by MC-ICP-MS (Thermofisher Scientific, NEPUTUNE Plus). The $\mu^{182}W$ values ranged from -0.5 to +5.6 (n=3) and from -1.4 to +5.0 (n=4) for komatiites from the Singhbhum and Dharwar cratons, respectively. These values are also much smaller than the range of uniform $\mu^{182}W$ values (from +10 to +15) for older rocks above 2.5 Ga, as discussed above. This result suggests that between 3.5 and 3.0 Ga, the primitive mantle with positive $\mu^{182}W$ values may have been already sufficiently mixed with extraterrestrial materials such as Late Veneer with negative $\mu^{182}W$ values that some domains of the mantle had the $\mu^{182}W$ values of the present-day mantle. In other words, mantle convection may have been active as early as 3.5 Ga.

Keywords: early evolution of mantle, W isotope, komatiite

©2021. Japan Geoscience Union. All Right Reserved.

The magma generation process of the North Sredinny Range, Kamchatka –Insights from highly siderophile elements and Re-Os isotope system

Yuri Mitsude[1], *Tatsuji Nishizawa[2], Hitomi Nakamura[3], Tatiana Churikova[4], Boris Gordeychik[5], Akira Ishikawa[6], Hikaru Iwamori[1]

1. Earthquake Research Institute, The University of Tokyo, 2. Volcanic Fluid Research Center, School of Science, Tokyo Institute of Technology, 3. Institute of Earthquake and Volcano Geology, Geological Survey of Japan, AIST, 4. Institute of Volcanology and Seismology, Far East Branch, RAS, 5. Institute of Experimental Mineralogy, RAS, 6. Department of Earth and Planetary Sciences, School of Science, Tokyo Institute of Technology

The subduction zone is a relatively "cold place" on Earth. Observational and experimental studies in petrology, geochemistry, and geophysics suggest that magma is generated associated with the circulation of H_2O-rich fluids. A standard quantitative model has also been proposed that incorporates the following processes; generation and migration of the fluid released from the subducted plate, transportation into the mantle wedge, the melting point depression of rock, and melting to supply magma to the volcanoes. Within this framework, the structure and processes of the subducted side (i.e., arc side), such as the composition and temperature of the mantle wedge, have been extensively studied to understand the formation of arc lava. In addition to these studies, researches on the ocean area have progressed in recent years, and are being developed from the viewpoint that the material and thermal structure of the subducting ocean plate, that is, the condition of the "subducting side" has a great influence on geological processes on the arc.

For studying such a subduction zone-scale material cycle, the elemental concentrations and isotopic ratios of the island arc lava are useful as a tracer of the subducted material. In this study, we focused on highly siderophile elements (HSE) and Re-Os isotope systems, which are considered to be indicators of subduction substances and melting degree owing to the large variation in elemental partitioning of the HSE between melt/fluid and solid.

Kamchatka is one of the largest volcanic arcs in the world that has unique tectonic settings such as being adjacent to the triple junction of the plates, the significant along-arc variation of both arc magmatism and the subducting plate, and subduction of the prominent seamount chain. It is a suitable place for studying how the variable subduction conditions affects the arc magmatism. We studied North Sredinny Range (N-SR) area, which is located at the northernmost part of the long volcanic chain on the backarc side of Kamchatka and is located further north of the subducted Pacific Plate. We analyzed 30 Quaternary lava samples from the N-SR region for HSE and Re-Os isotopic ratios and discuss the volcanic processes in this region.

The Os concentrations in the N-SR lavas range from 0.0001 to 0.0814 ppb and $^{187}Os/^{188}Os$ ratios range from 0.1276 to 0.8421. The FeO*/MgO of N-SR lavas suggests fractional crystallization from a relatively undifferentiated lava. A positive correlation between Os, Ir, Ru concentrations and FeO*/MgO, and a model calculation of fractional crystallization show that the fractional crystallization of phenocryst minerals such as olivine has removed highly compatible elements including Os from the lavas. The correlation between 1/Os and $^{187}Os/^{188}Os$ ratio shows a linear relationship with different slopes for the individual sub-areas within the studied area, suggesting that each sub-area has undergone a different amount of crustal assimilation during the AFC process in the N-SR area. In addition, the Os concentration and $^{187}Os/^{188}Os$ in the mantle source were estimated from element and isotope correlations, and the fluid contribution to the source mantle estimated independently from other trace element data show that a seamount subducted in the past could exist under the N-SR area and may contribute to the generation of

©2021. Japan Geoscience Union. All Right Reserved.

magma.

Keywords: Kamchatka, Highly Siderophile Elements (HSE), Os isotope, Assimilation and Fractional Crystallization (AFC), Arc magmatism

©2021. Japan Geoscience Union. All Right Reserved.

The characteristics of highly siderophile elements in the high-Mg andesite and basalts and its implications for the origin of the Quaternary arc magmatism in the forearc region, Kamchatka

*Tatsuji Nishizawa[1], Yuri Mitsude[2], Hitomi Nakamura[3], Tatiana Churikova[4], Boris Gordeychik[5], Akira Ishikawa[6], Hikaru Iwamori[2]

1. Volcanic Fluid Research Center, School of Science, Tokyo Institute of Technology, 2. Earthquake Research Institute, The University of Tokyo, 3. Institute of Earthquake and Volcano Geology, Geological Survey of Japan, AIST, 4. Institute of Volcanology and Seismology, Far East Branch, RAS, 5. Institute of Experimental Mineralogy, RAS, 6. Department of Earth and Planetary Sciences, School of Science, Tokyo Institute of Technology

Kamchatka is a massive volcanic arc that corresponds to the subduction of the northern part of the Pacific Plate (PAP), which forms three sub-parallel volcanic belts; the Eastern Volcanic Front (EVF), the Central Kamchatka Depression (CKD), and the Sredinny Range. The Emperor Seamount Chain connected to the Hawaiian hot spot is subducting along with the PAP beneath the central part of Kamchatka. The subducting dip decreases sharply from 50˚ to 35˚ at the northern edge of the PAP slab, which causes the volcanic front from to bend from the EVF to the CKD at 55.5˚N. On the other hand, in the northestern extension of the EVF corresponding to the forearc region, there are Quaternary monogenetic cones dated at <1 Ma, the East Cone volcanic group (EC). The 16 fresh EC lavas sampled from 8 cones could be categorized into 5 rock types, including high-Mg andesite (HMA) and basalt (B). The EC lavas are primitive with low FeO*/MgO (<~1) and show typical arc-signatures such as positive Pb spikes. Based on the petrological and geochemical characteristics of EC lavas, the previous study suggests that the thermal and geochemical contributions from the subducted seamount chain have caused the temporal evolution of local arc magmatism in EC with a wide compositional range in the forearc region. For example, HMA including ultra-high-Ni olivine was derived from pyroxenite veins formed by the metasomatism of the mantle peridotite caused by silica-enriched fluids derived from the subducted seamount. On the other hand, the primitive B was generated by flux melting of the mantle peridotite source caused by silica-depleted slab fluids due to the previous metasomatism (Nishizawa et al., 2017).
In order to further elucidate the genesis of EC lavas, we focused on the highly siderophile elements (HSE) that are strongly partitioned into metal or sulfide phases. Therefore, HSE concentration in lavas could provide important information about melting and fractional processes. In this study, we analyzed the bulk-rock concentrations of Re and the platinum-group elements (PGE) including Ru, Pd, Os, Ir, and Pt. As results, the depleted mantle (DM; Salters & Stracke, 2004)-normalized HSE spidergram for EC lavas are different in each rock-type or cone, but all EC lavas are relatively depleted in iridium-PGE (I-PGE; Os, Ir, and Ru) compared to the platinum-PGE (P-PGE; Pt, Pd) and Re, which are common in volcanic rocks such as MORB and arc lavas (e.g. Gannoun, 2016). Especially, HMA and the primitive B show almost the same pattern and concentration of P-PGE and Re, but the concentration of I-PGE is in contrast. In the I-PGE concentration of EC lavas, HMA shows the lowest concentration, while the primitive B shows the highest concentration. HMA seems to have been generated by I-PGE “nugget” fractionation from the primitive B melt. In other words, the factors that determine P-PGE and Re concentration of the melts are the almost same while the factors that determine I-PGE concentration in the melts are different between HMA and the primitive B, which is an important feature of the genesis of EC lavas.
To elucidate the factors that determined the HSE concentration in the EC lavas, we performed forward calculations of primitive melt assuming the four different melting conditions: 1. bulk rock batch melting model, 2. sulfide melt entrainment model, 3. sulfide melt partitioning model, 4. sulfide melting model. These results suggest that the differences in HSE concentration between HMA and the primitive B cannot

©2021. Japan Geoscience Union. All Right Reserved.

be explained by a simple difference in the degree of partial melting. In addition, in any case, it is difficult to reproduce the HSE concentration of the EC lavas without assuming the sulfide phase that is the main host of HSE in the mantle rocks.

Keywords: Kamchatka, Highly Siderophile Elements (HSE), Arc magmatism, High-Mg andesite, Seamount

©2021. Japan Geoscience Union. All Right Reserved.

[J] Poster | S (Solid Earth Sciences)：S-GC Geochemistry

Sat. Jun 5, 2021 5:15 PM - 6:30 PM JST | Sat. Jun 5, 2021 8:15 AM - 9:30 AM UTC | Ch.17_2

[S-GC33] Solid Earth Geochemistry, Cosmochemistry

convener:Gen Shimoda(Geological Survey of Japan, AIST), Katsuhiko Suzuki(Submarine Resources Research Center, Japan Agency for Marine-Earth Science and Technology), Katsuyuki Yamashita(Graduate School of Natural Science and Technology, Okayama University), Akira Ishikawa(Department of Earth and Planetary Sciences, Tokyo Institute of Technology)

Solid Earth Geochemistry, Cosmochemistry" session aims at evaluating processes during the 4.6 billion years of the solar system and the Earth. Any approaches to this issue is welcomed, including, geochemistry, geophysics, geology, mineralogy and petrology.

[SGC33-P01] Origin of intra-plate magmatism in Kamchatka constrained by noble gas isotopes

*Masao Fukagawa[1], Hirochika Sumino[2], Anna O Volynets[3], Yuri Taran[3] (1.Department of Integrated Science, College of Arts and Science, the University of Tokyo, 2.Department of General Systems Studies Graduate School of Arts and Sciences, The University of Tokyo, 3.Russian Academy of Sciences)

[SGC33-P02] Rare earth elements composition of carbonate concretion in the Miocene Morozaki Group, southwestern Japan

*Ryosuke Kitanaka[1], Motohiro Tsuboi[1] (1.Kwansei Gakuin University)

[SGC33-P03] Investigation of Validity for Evaluation Particle numbers on Characterization of Soil Particle Morphology Using Automated Particle Image Analysis and Computed Simulations.

*Daisuke Sasakura[1] (1.Malvern Japan ,Div of Spectris Co.Ltd,.)

[SGC33-P04] Role of fluid rock reaction for the production of FOZO isotopic composition

*Gen Shimoda[1], Tetsu Kogiso[2], Katsuhiko Suzuki[3], Akira Ishikawa[4], Norikatsu Akizawa[5] (1.Geological Survey of Japan, AIST, 2.Kyoto University, 3.Japan Agency for Marine-Earth Science and Technology, 4.Tokyo Institute of Technology, 5.University of Tokyo)

Origin of intra-plate magmatism in Kamchatka constrained by noble gas isotopes

*Masao Fukagawa[1], Hirochika Sumino[2], Anna O Volynets[3], Yuri Taran[3]

1. Department of Integrated Science, College of Arts and Science, the University of Tokyo, 2. Department of General Systems Studies Graduate School of Arts and Sciences, The University of Tokyo, 3. Russian Academy of Sciences

Introduction: In Kamchatka, three volcanic chains (the first is volcanic front, the second is back-arc chain and the third is Sredinny Range, SR) are identified, and the former two are considered to result from the subduction of Pacific plate. On the other hand, several origins have been proposed for intra-plate magmatism in SR: ascent of deep mantle plumes, back-arc spreading in response to trench rollback, etc. The purpose of this study is to constrain the origin of magmatism in SR by using noble gas isotopes, which have different features in different geochemical reservoirs, such as convecting MORB-source mantle, deep-mantle-derived plume, and crust.

Samples and analysis: We extracted noble gases (He, Ne, Ar, Kr, and Xe) from fluid/melt inclusions in olivines and pyroxenes separated from basalts and andesites collected from SR by crushing in vacuum, and analyzed their abundances and noble isotope ratios. After that we heated in vacuum the recovered powders after crushing to melt the sample for complete noble gas extraction, and then analyzed in the same way.

Results and discussion: Helium isotope ratios ($^3He/^4He$ ratios) obtained with the crushing of olivines were in general around 8 Ra, where Ra denotes atmospheric $^3He/^4He$ ratio. The values are in the range of MORB-source mantle (8±1 Ra), which is similar to He in mantle-derived xenoliths from Avacha volcano in the volcanic front [1]. On the other hand, crush-released $^3He/^4He$ ratios of pyroxenes were systematically lower than those of olivines in the same host rocks. Because pyroxene crystallization is generally later than that of olivine in magma, the lower $^3He/^4He$ ratios of pyroxenes than olivines would have resulted from interaction of magma with surrounding crustal rocks, which have low $^3He/^4He$ ratios, between olivine and pyroxene crystallization. A few olivines showed lower $^3He/^4He$ ratios than MORB value during the crushing experiment, which would be trace of the slab fluids enriched in U and Th. Higher $^3He/^4He$ ratios than the MORB value were also observed during crushing of another fer olivines samples Because He extracted by heating of crushed powder yielded much higher $^3He/^4He$ ratio (>100 Ra), the high $^3He/^4He$ ratios obtained with crushing would be due to a small release of cosmic-ray produced He having accumulated in the sample after the eruption.

Based on the above observations, we conclude that the origin of magma erupted in SR is the convecting mantle, and the possibility of plume’ s involvement is low. We also conclude that there are significant traces of slab fluids in some regions in SR.

Reference: [1] Kobayashi et al., EPSL, 2017.

Keywords: Noble gasses, kamchatka

©2021. Japan Geoscience Union. All Right Reserved.

Rare earth elements composition of carbonate concretion in the Miocene Morozaki Group, southwestern Japan

*Ryosuke Kitanaka[1], Motohiro Tsuboi[1]

1. Kwansei Gakuin University

Carbonate concretions are observed in marine sedimentary rocks from all over the world, and are generally spherical in shape. They are mainly composed of calcium carbonate, and resistant to weathering. The formation of carbonate concretions may be related to the organic matters of marine life and formed rapidly in the pores of sediments (1). It sometimes contains well-preserved ammonite or other fossils. In this study, we measured rare earth elements (REE) composition of carbonate concretions and investigate the formation processes of concretion. The studied concretion samples are approximately 1.5 m in scale and the matrix is tuffaceous fine sandstones and mudstones of the Miocene Morozaki Group (15–18 Ma), Chita Peninsula, Aichi Prefecture, Japan. REE are measured by inductively coupled plasma mass spectrometry (ICP-MS). The core, mantle and front part of concretion and, matrix sedimentary rocks were analyzed. REE concentrations were normalized by CI chondrite, deep seawater and matrix sedimentary rocks. The REE patterns normalized by CI chondrite shows negative Eu anomaly and abundant light rare earth elements (LREE) in all samples. It shows negative Ce anomaly in the matrix. REE patterns of concretion, except for core, normalized by the matrix show flat curve. At the core part, LREE show higher value, while heavy rare earth elements (HREE) show lower value in all REE patterns. This may be due to the elemental mobility process or the original organism matters.

(1) Yoshida, H., Ujihara, A., Minami, M., Asahara, Y., Katsuta, N., Yamamoto, K., Sirono, S., Maruyama, I., Nishimoto, S. and Metcalfe, R., 2015, Early post-mortem formation of car-bonate concretions around tusk-shells over week-month timescales. Scientific Reports **5**, 14123.

Keywords: carbonate concretion, rare earth elements (REE)

©2021. Japan Geoscience Union. All Right Reserved.

Investigation of Validity for Evaluation Particle numbers on Characterization of Soil Particle Morphology Using Automated Particle Image Analysis and Computed Simulations.

*Daisuke Sasakura[1]

1. Malvern Japan ,Div of Spectris Co.Ltd,.

[Introduction]

Particle morphology, such as particle size and shape aspects are well known that to give affect to various bulk characteristics on mechanics aspect of grounds. Hence, to characterize particle morphology, an Image Analysis (IA) using a manually microscopic technic is commonly used to investigate particle morphology.
However, one of the major challenges of a conventional IA is the near impossible of measuring a statistically significant number of particles. Typically, realistic particle morphology in natural field should has aspects as broadly distribution. Indeed, ISO and JIS statements suggested to measuring over than tens of thousands of particles. Furthermore, reason of importance to concern of a deviation matter is as well as supported from that typical model of particle size distribution should follow with a lognormal distribution. Recent advances in computer technology have allowed for the development of a new automated particle image analysis (APIA) approach that uses digital imaging technology. This technology is based on allowed acquisition of a calculation of binarized (2D) particle projection images on each individual particle from on over than ten thousand particles within at least few hours. Hence, these approaches are allowed for the calculation of the various morphological parameters using graphical comparison, such as various distribution graph, such as frequency curve and cumulant curve. However, even if recently progress as mentioned above, it is still only limited suggestion for enough particles to determine distribution on realistic particles which has various aspects. This study will suggest and discussion for a practical investigation of relationship of particle number and distribution on soil particle by APIA combined with using statistically modeling and simulation.

[Method]

Tohoku Keisya and Milled Silica sand were used as model samples. APIA analyses were conducted on a Morphologi G3SE as automated image analysis system (Malvern Instruments, Worcestershire, UK). Sample was subsequently dispersed with an SDU using a short duration pulse of compressed air. Measurements were collected automatically using standard operating procedures (SOPs), which clearly define the software and hardware settings used during the measurement process. The measurement sample was dispersed on a glass plate, which was used as a sample carrier to minimize environmental exposure within the enclosed sample chamber unit.
A computer simulation was carried out mainly Scilab platform with implemented own programming to calculate various numerical model, MS Excel used as supportive.

[Simulation Design]

Regarding size distributions, determined any statistical numbers from over than 10,000 particle images were calculated by distribution graph and mean analysis. It was compared that statistical specific numbers from experiment and simulated results based on lognormal random distribution due to step-upped number. Regarding shape matters were not only used as statistical number approach and also fitting approach were carried out.

©2021. Japan Geoscience Union. All Right Reserved.

Keywords: Particle Size, Particle Shape, Image Analysis

©2021. Japan Geoscience Union. All Right Reserved.

Role of fluid rock reaction for the production of FOZO isotopic composition

*Gen Shimoda[1], Tetsu Kogiso[2], Katsuhiko Suzuki[3], Akira Ishikawa[4], Norikatsu Akizawa[5]

1. Geological Survey of Japan, AIST, 2. Kyoto University, 3. Japan Agency for Marine-Earth Science and Technology, 4. Tokyo Institute of Technology, 5. University of Tokyo

It has been noted that Pb-Nd-Sr isotopic compositions of OIB converge on a small space. Definitions of the convergent space were proposed by several groups, such as the Focus Zone (FOZO; Hart et al., 1992), the Common component (C; Hanan and Graham, 1996), Prevalent Mantle (PREMA; Zindler and Hart, 1986), *etc*. The convergent space has relatively small Nd and Sr isotopic variation but relatively large Pb isotopic range, resulting in vertical trend in 3D isotopic plot with $^{143}Nd/^{144}Nd$ (x axis), $^{87}Sr/^{86}Sr$ (y axis) and $^{206}Pb/^{204}Pb$ (z axis). A recent geochemical study proposed cause of isotopic convergence, in which reaction between subducted oceanic crust and fluid released by serpentinite dehydration can produced chemical composition that is suitable for the production of FOZO isotopic compositions when the recycling age of oceanic crust was about 1.0 Ga (Shimoda & Kogiso, 2019).
In this presentation, we estimated isotopic range of recycled oceanic crusts modified by subduction process, including dehydration and fluid-rock reaction. Isotopic variation was estimated with wide variety of geochemical conditions, such as chemical variation of oceanic crust, variable degree of dehydration, fluid rock ratios, recycling ages and different subduction conditions. We calculated isotopic compositions of recycled oceanic crust about a million sets of Pb-Sd-Sr-Hf isotopic compositions. The calculated isotopic compositions distributed near FOZO and PREMA. Although the tested subduction conditions were varied widely, isotopic compositions of recycled oceanic crust show small isotopic variation, indicating that isotopic composition of FOZO simply reflect isotopic variation of subduction modified oceanic crust. It may follow that focusing isotopic distribution of OIB simply express isotopic variation of recycled oceanic crust with variable subduction conditions and recycling ages.

Keywords: FOZO, mantle, isotopic composition

©2021. Japan Geoscience Union. All Right Reserved.

[J] Oral | S (Solid Earth Sciences)：S-TT Technology & Techniques

Sat. Jun 5, 2021 9:00 AM - 10:30 AM JST | Sat. Jun 5, 2021 12:00 AM - 1:30 AM UTC | Ch.22 Zoom Room 22

[S-TT36] Synthetic Aperture Radar and its application

convener:Yohei Kinoshita(University of Tsukuba), Takahiro Abe(Graduate School of Bioresources, Mie University), Shoko Kobayashi(Tamagawa University), Yuji Himematsu(National Research Institute for Earth Science and Disaster Resilience), Chairperson:Takahiro Abe(Graduate School of Bioresources, Mie University), Yohei Kinoshita(University of Tsukuba)

ALOS-2 and Sentinel-1, which have highly enhanced capacity compared to previous SAR satellites, were launched in 2014, and their utilization has been widely expanding as data have accumulated for approximately six years. Other long-operating SAR satellites like TerraSAR-X and Cosmo-SkyMed also contribute to expanding the SAR utilization. Now we are facing a new and abundant era of the satellite SAR, along with a worldwide trend to an open and free data policy of satellite data, under the situation of next-generation advanced and/or constellated SAR satellite plans by both public agencies (e.g. ALOS-4 and NISAR) and private sectors. In addition, SAR technologies with other platforms, such as ground-based SAR with high temporal resolution and UAV (Unmanned Aerial Vehicle) SAR with flexible operability, have also been developed and used for various targets. These facts indicate that the SAR utilization has become widespread in both basic researches (e.g., earth science) and diverse applications (e.g., disaster prevention and forest monitoring). In this session, we would like to invite various kinds of research and application results with regard to SAR, sharing our knowledge and having a discussion for the advancement of the SAR utilization.

9:00 AM - 9:15 AM JST | 12:00 AM - 12:15 AM UTC

[STT36-01] Automatic error-term estimation approach for improving the accuracy of InSAR time-series analysis - Example on the Arima-Takatsuki Fault Zone, Japan

*Yo Fukushima[1] (1.International Research Institute of Disaster Science, Tohoku University)

9:15 AM - 9:30 AM JST | 12:15 AM - 12:30 AM UTC

[STT36-02] Correlation between surface displacement and groundwater level displacement in the periods before and after the 2018 Northern Osaka earthquake

*Yutaro Shigemitsu[1], Kazuya Ishitsuka[1], Weiren Lin[1] (1.Kyoto University Graduate School of Engineering)

9:30 AM - 9:45 AM JST | 12:30 AM - 12:45 AM UTC

[STT36-03] Landslide and its displacement along the Marsyangdi River, Nepal detected by differential interferometric SAR

*Seiya Usami[1], Hiroshi, P. Sato[2], Hiroshi YAGI[3] (1.Grad student, Graduate School of Science and Technology, Nihon University, 2.College of Humanities and Science, Nihon University, 3.Faculty of Art, Science and Education, Yamagata University)

9:45 AM - 10:00 AM JST | 12:45 AM - 1:00 AM UTC

[STT36-04] Road blockage detection due to landslides using Sentinel-1 intensity images

*Keisho Ito[1], Yohei Kinoshita[1] (1.Tsukuba University)

10:00 AM - 10:15 AM JST | 1:00 AM - 1:15 AM UTC

[STT36-05] Short-term glacier velocity changes in the Southern Patagonian Ice Field detected by the Sentinel-1 satellite

*Yuya Ito[1], Masato Furuya[2] (1.Graduate School of Science, Hokkaido University, 2.Department of Earth and Planetary Hokkaido University)

10:15 AM - 10:30 AM JST | 1:15 AM - 1:30 AM UTC

[STT36-06] Discussion of the colour map for SAR interferograms

*Morishita Yu[1] (1.Geospatial Information Authority of Japan)

Automatic error-term estimation approach for improving the accuracy of InSAR time-series analysis - Example on the Arima-Takatsuki Fault Zone, Japan

*Yo Fukushima[1]

1. International Research Institute of Disaster Science, Tohoku University

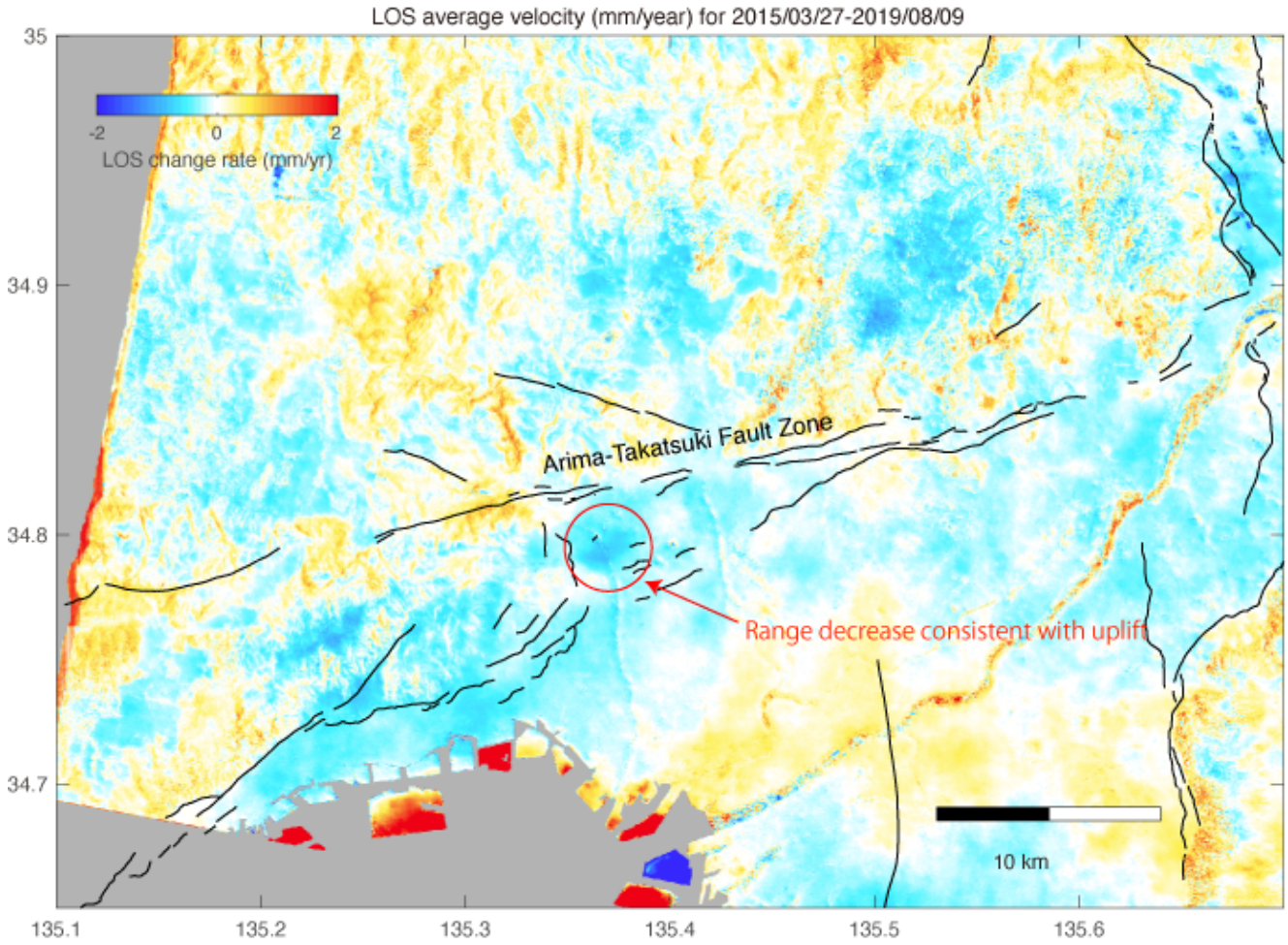
InSAR time-series (InSAR-TS) analysis enables us to obtain the time-series of line-of-sight (LOS) displacements over a wide area by using a number of SAR images repeatedly acquired on the area. Among the factors affecting the accuracy of the InSAR-TS analysis, I focus on three factors that may severely limit the detection of small signals. Firstly, it is often the case that the selection of the reference point (determining the offset in each interferogram) is problematic. Wrong selection largely deteriorates the accuracy of the displacement time-series, and there are cases where the whole scene cannot be assumed to be stable. Secondly, interferograms often contain ramp-type artifact that originate from inaccuracy in the orbit data or ionospheric disturbance. Correction for this type of noise is often difficult, especially when one attempts to obtain the displacements of long wavelengths. Thirdly, the altitude-correlated phase delay in the troposphere is often the most significant noise source in interferograms. Although many studies using weather models have been conducted to mitigate this kind of noise, simple regression of the phase change with respect to the altitude is often the most effective method. This kind of regression approach, however, can sometimes over-correct the true deformation signals.

Fukushima et al. (2019, Earth, Planets and Space) proposed an InSAR-TS analysis method to simultaneously solve for the displacement time-series and the error terms mentioned above (plus the error in the digital elevation model), and succeeded in obtaining clear signals caused by fault creep. In the proposed method, the unwrapped phase in interferograms is assumed to be composed of a linear combination of the LOS displacement, offset, planar ramp, altitude-correlated phase, and error in the used digital elevation model. A set of unwrapped small-baseline interferograms is then inverted to simultaneously obtain the displacement time-series and the parameters describing the error terms under the minimum norm condition on the displacement time-series.

In this study, the method was applied to the ALOS-2 data acquired around the Arima-Takatsuki Fault Zone located on the margin of the Osaka Plain in western Honshu, Japan. The data consisted of 26 images acquired between March 2015 and August 2019 from a descending orbit along Path 21 and Frame 2910. Some of the original interferograms contained severe noise such as a phase ramp equivalent to approximately 25 cm of LOS displacements. The average velocity field obtained by applying the method captured the relative range decrease (negative LOS change rate) of the southern side with respect to the northern side of the fault zone with a localized signal of up to approximately 1 mm/year around (latitude, longitude) = (34.79, 135.38), which are consistent with the results of an InSAR-TS analysis of Sentinel-1 data (Morishita, 2021, PEPS). Given the fact that the Sentinel-1 dataset had much favorable conditions (much larger number of data (133 images for the descending dataset) and much smaller ionospheric noise), the consistency in the average velocity field suggests the effectiveness of the noise correction method.

Keywords: InSAR, Arima-Takatsuki Fault Zone

©2021. Japan Geoscience Union. All Right Reserved.



©2021. Japan Geoscience Union. All Right Reserved.

Correlation between surface displacement and groundwater level displacement in the periods before and after the 2018 Northern Osaka earthquake

*Yutaro Shigemitsu[1], Kazuya Ishitsuka[1], Weiren Lin[1]

1. Kyoto University Graduate School of Engineering

It is known that displacement of groundwater level sometimes occurs around an epicenter or in a wide area immediately after an earthquake. For example, in the Kumamoto earthquake in 2016, some areas of the groundwater level increased due to the inflow of groundwater stored at the foot of the mountain. On the other hand, other area of the groundwater level decreased due to the groundwater flowing into the fracture area in the deep underground. It is widely known that displacement of ground surface is caused by such displacement of groundwater level. Land subsidence due to the lowering of the groundwater level is generally recognized and a model for it has been developed. However, in some areas, rising ground surface due to rising groundwater level has been observed as a phenomenon, but its model is not fully understood. It is important to examine which parameters contribute to rising ground surface when the groundwater level rises, such as speed and acceleration of the groundwater level.
In the periods before and after the Osaka Northern earthquake on June 18, 2018, the rises of the groundwater level have been observed at several groundwater wells in the Hanshin area, Japan. Therefore, the ground uplift due to the rise of the groundwater level may have occurred. In this study, we first estimated the amount of long-term change in ground surface displacement in the Hanshin area in the periods before and after the 2018 Osaka Northern Earthquake, and then discussed the correlation between surface displacements and groundwater levels. Finally, we discuss a simple model for uplift of the ground surface due to rising groundwater levels. PSInSAR analysis was used to estimate surface displacements because it can calculate displacements over a wide area. By combining the surface displacement from the PSInSAR analysis with the groundwater level displacement data, It will be possible to discuss changes in displacement of groundwater level and ground surface due to earthquakes, the magnitude of seasonal displacement of groundwater level and ground surface, and changes in two-dimensional displacement of groundwater level. The satellite data was obtained from the European Space Agency's Sentinel-1 northward orbit for the period April 2015 to April 25, 2019. For the groundwater level data, we used the groundwater level stations of the hydrological water quality database operated by the Ministry of Land, Infrastructure, Transport and Tourism, the groundwater level stations operated by the National Institute of Advanced Industrial Science and Technology, and the groundwater level stations operated by Osaka City.
As results of PSInSAR analysis, surface displacements in the direction of satellite line-of-sight shortening were observed in the vicinity of Takarazuka City and the eastern part of the Osaka Plain in the period before and after the earthquake. The direction of these displacements is westward or uplift direction in terms of actual displacements. These results are consistent with the groundwater level displacement at the groundwater level point near Takarazuka City because the groundwater level rose in the periods before and after the earthquake. On the other hand, in each observation point of groundwater level in the eastern part of the Osaka Plain, the displacement trend of groundwater level depends on the location. Specifically, some observation points showed seasonal changes in groundwater level due to increases and decreases in precipitation, while others showed no seasonal changes. This indicates that displacement of groundwater level and ground surface cannot be modeled simply, and that it is necessary to study the geological structure and aquifer characteristics of each site.

©2021. Japan Geoscience Union. All Right Reserved.

Acknowledgments:The groundwater level data for Osaka City was provided by the Environmental Management Division, Environmental Management Department, Osaka City Environment Bureau. We would like to express our gratitude to them.

Keywords: the 2018 Northern Osaka earthquake, groundwater level displacement, surface displacement, PSInSAR analysis, satellite Sentinel-1, Osaka Plane

©2021. Japan Geoscience Union. All Right Reserved.

Landslide and its displacement along the Marsyangdi River, Nepal detected by differential interferometric SAR

*Seiya Usami[1], Hiroshi, P. Sato[2], Hiroshi YAGI[3]

1. Grad student, Graduate School of Science and Technology, Nihon University, 2. College of Humanities and Science, Nihon University, 3. Faculty of Art, Science and Education, Yamagata University

Nepal has the areas prone to be affected by landslides in the world due to the steep topography and complex geological structure caused by plate collision. However, due to the highly undulating topography, on-site monitoring of landslide displacement is difficult, and the number of observation cases is limited. In this study, we attempted to monitor landslide displacement using D-InSAR and to elucidate the characteristics of landslide displacement along the Marsyangdi River, which was considered to be a high risk area of landslides in the previous studies.
A total of 17 ALOS-2 data observed from November 20, 2014 to August 6, 2020 was used in this study, and RINC0.41 software developed by Ozawa et al. (2016) was used for D-InSAR analysis. The D-InSAR images were projected onto a map using ArcGISpro for topographic interpretation and displacement analysis (Fig. 1).
Two landslides were interpreted on the right bank of the Marsyangdi River (28˚21'56 "N, 84˚23'25 "E; 28˚21'4 "N, 84˚23'17 "E). These sites (Fig. 2) are located about 1.5 km north of the Main Central Thrust (MCT), where a large landslide feature are identified and gneiss is distributed. The resulting displacement analysis using multi-temporal D-InSAR images showed that the displacement continued from September 15, 2015 to December 26, 2019 at the shortest. The maximum displacement was calculated from the D-InSAR image of October 18, 2018 - March 21, 2019 and it was compared with the precipitation. The results showed that the rate of displacement did not increase during the rainy season, but rather accelerated immediately after the rainy season (Fig. 3). In addition, we confirmed that top of the landslide body is located on the knick line on the slope, and that the lower part of the landslide body was displaced just after the displacement of the upper part (Fig. 1).
It is inferred that the geology fractured by the MCT is involved in this movement. The relationship with precipitation suggests that there is a temporal gap between landslide displacement and high precipitation. Since the top of the landslide body is located on the knick line, the topography associated with the down cutting after the last glacial period may contribute to the landslide behavior, and this point will be discussed in detail in the future.

Acknowledgement
This study was supported by KAKEN 19H01368, and data used in this study were provided by PIXEL (PALSAR Interferometry Consortium to Study our Evolving Land surface) under a cooperative research (2021-B-03) contract with ERI, Univ. of Tokyo. AW3D data (https://www.aw3d.jp/) were used for producing shaded relief map.

References:
Ozawa, T., Fujita, E., and Ueda, H. (2016): Crustal deformation associated with the 2016 Kumamoto Earthquake and its effect on the magma system of Aso volcano. Earth, Planets and Spase, 68: 16.
Yagi H, Sato G, Sato HP, Higaki D, Dangol V, Amatya SC, Slope deformation caused Jure landslide 2014 along Sun Koshi in lesser Himalaya and effect of Gorkha earthquake 2015, In Vilímek V, Wang F, Strom A, Sassa K, Bobrowsky PT, Takara K (eds.), Understanding and Reducing Landslide Disaster Risk, 5, 65-72, Springer, 2020.

©2021. Japan Geoscience Union. All Right Reserved.

Keywords: D-InSAR, ALOS-2, Landslide

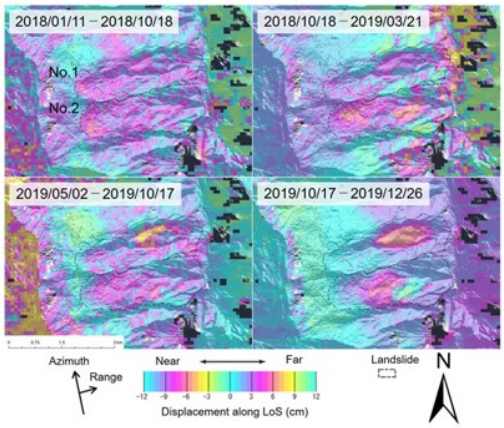


Fig.1 ALOS-2 D-InSAR along Marsyangdi river.
The dashed delineate Landslide areas.



Fig. 2 Local photo of Marsyangdi river.
Orange arrow shows the direction of flow.
(Photographed by Yagi, H.)

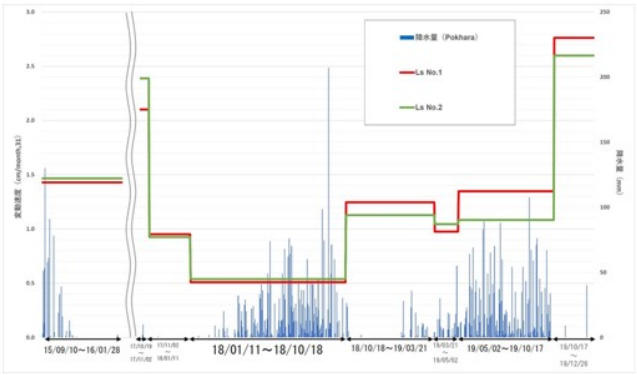


Fig. 3 Comparison of precipitation and displacement velocity.
The red and green line shows displacement velocity of No.1 and No.2 site, respectively.
The blue bars indicate precipitation of Pokhara.

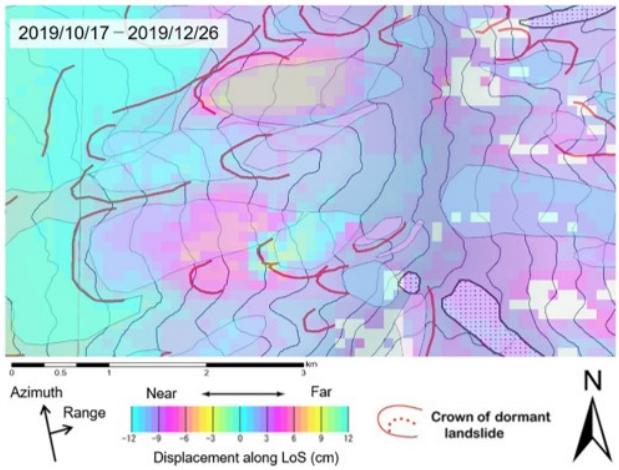


Fig. 4 Overlaying of landslide map and ALOS-2 D-InSAR.
Landslide map is based on Yagi et al.(2020)

©2021. Japan Geoscience Union. All Right Reserved.

Road blockage detection due to landslides using Sentinel-1 intensity images

*Keisho Ito[1], Yohei Kinoshita[1]

1. Tsukuba University

When natural disasters such as earthquakes and heavy rains occur, roads may be blocked due to rapid landslides. These road blockages can cause isolation of the community and delay of rescue and evacuation, leading to serious damage in both human and economics. Therefore, it is necessary to detect disaster-affected areas quickly after the disaster occurrence. The satellite synthetic aperture radar (SAR) has the ability to get information about affected areas by observing the ground surface over wide area regardless of time of day and the existence of clouds. This study proposed a new method to detect landslides and road blockages using Sentinel-1 intensity images.

This study used backscatter intensity difference between the time-averaged images in the pre-disaster stage and a single intensity image immediately after the disaster occurrence to detect anomalous signals associated with landslides. We analyzed several past landslides and found that these landslides caused large increase of backscatter intensity after the sediment collapse. Based on the above analysis, we set the threshold of the anomaly detection as 4dB intensity increase and created a landslide detection method using the decision tree technique composed of several kinds of thresholds with regard to radar intensity and topographical information such as the hill slope. The landslide detection in our proposed method was performed for square areas with several hundred meters on a side, because there were a lot of small noises in the raw-resolution image and the detailed shape and size of each landslides is not so important in practical use for administrations and municipalities. Then, we detected road blockage areas based on the information of detected landslides and an empirical model to estimate the mass flow length due to landslides. The detection accuracy of the proposed method was evaluated on two cases, the 2018 Hokkaido Eastern Iburi Earthquake and the 2017 heavy rain event in Northern Kyushu.
In the case of 2018 Hokkaido Eastern Iburi Earthquake, our proposed method could detect part of landslides, most of which were relatively large-size landslides. The accuracy of landslide detection for square areas of 400 meters on a side was 2.7% for the false detection rate and 85.2% for the undetected rate. Similarly, nearly half of the roadblock areas were detected by the proposed method. On the other hand, there were many false landslide detections in 2017 heavy rain event in Northern Kyushu, possibly due to sudden surface change of scatter characteristics due to the strong rainfall. The failure of the landslide detection also led to many failures in the road blockage detection. However, the proposed method might capture the areal concentration of landslides, which may showed a potential to roughly detect the damaged area under a heavy rainfall situation.

Keywords: SAR, Landslide, Road blockage, Sentinel-1, Intensity image

©2021. Japan Geoscience Union. All Right Reserved.

Short-term glacier velocity changes in the Southern Patagonian Ice Field detected by the Sentinel-1 satellite

*Yuya Ito[1], Masato Furuya[2]

1. Graduate School of Science, Hokkaido University, 2. Department of Earth and Planetary Hokkaido University

The glaciers of the Southern Patagonian Ice Field are the second largest group of glaciers in the Southern Hemisphere after Antarctica. Like the glaciers and ice sheet in Northern Hemisphere, they are retreating and losing their mass. Although the flow rate of glaciers in the Southern Patagonian Ice Field is known to change on a semi-annual to multi-year time-scale, their changes in flow rate within a year are uncertain. In order to investigate the detailed changes in the flow velocity, we obtained radar images acquired by the Sentinel-1B satellite with a recurrent period of 12 days between 2019 and 2020, and estimated the flow velocity at the relatively larger six glaciers using the pixel offset method on the assumption of parallel flow approximation. Of the six glaciers (Occidental Glacier, Pio XI Glacier, Asia Glacier, Tyndall Glacier, Viedma Glacier, O'Higgins Glacier), four (Pio XI Glacier, Asia Glacier, Viedma Glacier, O'Higgins Glacier) exhibit winter speed-up signals (Abe and Furuya, 2015), accelerating in winter and decelerating in summer. Pio XI Glacier, Asia Glacier, and Viedma Glacier showed significant changes in their downstream areas and accelerated by about 450%, 20%, and 30%, respectively, in winter. O'Higgins Glacier showed significant changes in the upstream, accelerating by 30% in winter. However, unlike the winter speed-up glaciers reported by Abe and Furuya (2015), the four glaciers except Pio XI glacier have not been known as surge-type glaciers. Moreover, it is not clear if any portion of those glaciers indicate so-called spring/summer speed-up signals like a number of mountain glaciers in Northern Hemisphere. We will extend the analysis period to confirm if the inferred short-term velocity changes are persistent every year.

Keywords: The Southern Patagonian Ice Field, Flow rate

©2021. Japan Geoscience Union. All Right Reserved.

Discussion of the colour map for SAR interferograms

*Morishita Yu[1]

1. Geospatial Information Authority of Japan

The accurate visualization of numerical data is essential in science communication. Crameri et al. (2020) reported that unscientific colour maps which have uneven colour gradients visually distort data and can lead to misinterpretation and that scientifically derived colour maps should be used to accurately represent data. Rainbow-like colour maps, including widely used jet, is one of the unscientific colour maps. Perceptual uniformity can be quantitatively evaluated by metrics such as L (lightness), a (red-green correlative), b (yellow-blue correlative), and ΔE (incremental lightness difference) (Figure). The Scientific Colour Maps (Crameri, 2018) based on these metrics are perceptually uniform and do not visually distort data.

SAR interferometry is a technique to measure surface deformation by calculating phase differences between two or more SAR images acquired at different times at the same location. Since the phase is measured only modulo 2π, the phase difference in a SAR interferogram becomes also wrapped, cyclic data. A cyclic colour map is suitable to visualize the interferogram containing wrapped phase differences because a non-cyclic colour map generates false boundaries between $-\pi$ and π. A rainbow colour map that GAMMA software developed by the GAMMA REMOTE SENSING normally uses has been the most commonly used so far (Figure). Other software packages such as GSISAR developed by GSI and ISCE developed by NASA have also used the GAMMA-style rainbow colour map. The Headquarters for Earthquake Research Promotion (2011) introduced the GAMMA-style as the standard colour map for the wrapped SAR interferogram. The GAMMA-style has been a de facto standard for more than 20 years.

However, the GAMMA-style is not a scientific colour map based on the metrics above. I present the theoretical background of the scientific colour maps and discuss the issues in the GAMMA-style rainbow colour map and potentially alternative colour maps.

References

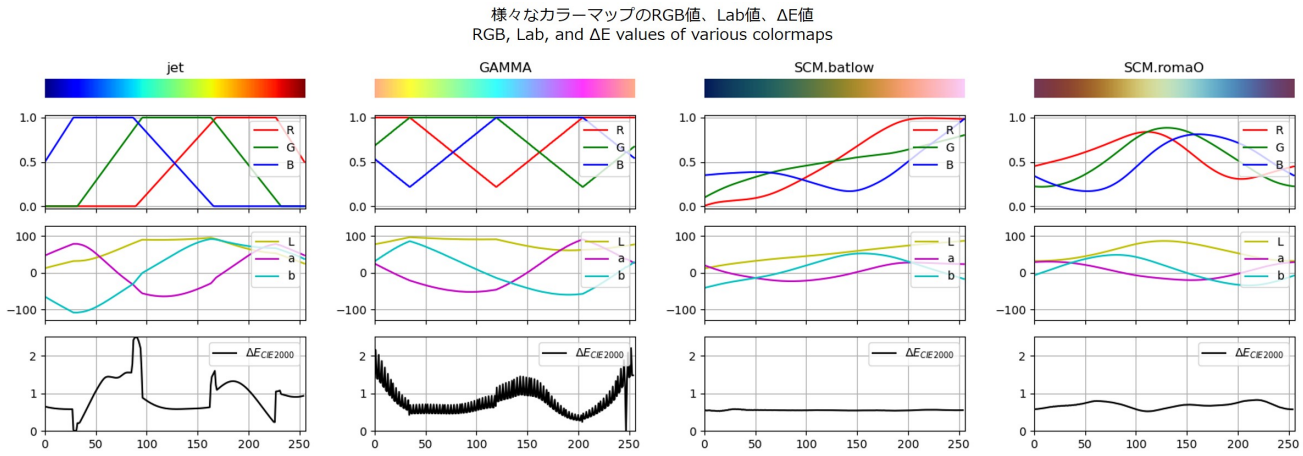
Crameri, F. (2018). Scientific colour maps. Zenodo. http://doi.org/10.5281/zenodo.1243862

Crameri, F., Shephard, G.E. & Heron, P.J. (2020). The misuse of colour in science communication. Nat Commun 11, 5444. https://doi.org/10.1038/s41467-020-19160-7

The Headquarters for Earthquake Research Promotion (2011). The observation technique of crustal deformation associated with seismic activities by Synthetic Aperture Radar (Appendix). https://www.jishin.go.jp/main/eisei/eisei_furoku.pdf

©2021. Japan Geoscience Union. All Right Reserved.

Keywords: InSAR, color map, scientific visualization



©2021. Japan Geoscience Union. All Right Reserved.

[J] Oral | S (Solid Earth Sciences)：S-TT Technology & Techniques

Sat. Jun 5, 2021 10:45 AM - 12:15 PM JST | Sat. Jun 5, 2021 1:45 AM - 3:15 AM UTC | Ch.22 Zoom Room 22

[S-TT36] Synthetic Aperture Radar and its application

convener:Yohei Kinoshita(University of Tsukuba), Takahiro Abe(Graduate School of Bioresources, Mie University), Shoko Kobayashi(Tamagawa University), Yuji Himematsu(National Research Institute for Earth Science and Disaster Resilience), Chairperson:Masatsugu otsuki(Institute of Space and Astronautical Science, Japan Aerospace Exploration Agency), Yuji Himematsu(National Research Institute for Earth Science and Disaster Resilience)

ALOS-2 and Sentinel-1, which have highly enhanced capacity compared to previous SAR satellites, were launched in 2014, and their utilization has been widely expanding as data have accumulated for approximately six years. Other long-operating SAR satellites like TerraSAR-X and Cosmo-SkyMed also contribute to expanding the SAR utilization. Now we are facing a new and abundant era of the satellite SAR, along with a worldwide trend to an open and free data policy of satellite data, under the situation of next-generation advanced and/or constellated SAR satellite plans by both public agencies (e.g. ALOS-4 and NISAR) and private sectors. In addition, SAR technologies with other platforms, such as ground-based SAR with high temporal resolution and UAV (Unmanned Aerial Vehicle) SAR with flexible operability, have also been developed and used for various targets. These facts indicate that the SAR utilization has become widespread in both basic researches (e.g., earth science) and diverse applications (e.g., disaster prevention and forest monitoring). In this session, we would like to invite various kinds of research and application results with regard to SAR, sharing our knowledge and having a discussion for the advancement of the SAR utilization.

10:45 AM - 11:00 AM JST | 1:45 AM - 2:00 AM UTC

[STT36-07] Examination of extraction method of topographical change due to eruption of Nishinoshima using time series SAR

*Daiki Inano[1], Masanobu Shimada[2] (1.Tokyo Denki University, graduate school of science and engineering ,division of architectural, civil and environmental engineering, 2.Tokyo Denki University, division of architectural, civil and environmental engineering)

11:00 AM - 11:15 AM JST | 2:00 AM - 2:15 AM UTC

[STT36-08] Tropospheric Dispersive Phase Anomalies during Heavy Rain Detected by L-band InSAR and Their Interpretation

Naufal Setiawan[1], *Masato Furuya[1] (1.Department of Earth and Planetary Sciences Hokkaido University)

11:15 AM - 11:30 AM JST | 2:15 AM - 2:30 AM UTC

[STT36-09] Error level evaluation of L-Band InSAR Water Vapor Observation by Comparison with GNSS Observations

*Keita Matsuzawa[1], Yohei Kinoshita[1] (1.University of Tsukuba)

11:30 AM - 11:45 AM JST | 2:30 AM - 2:45 AM UTC

[STT36-10] **Comparison of atmospheric delay correction methods in InSAR: Case study in Japan**

*Sardila Nurulhikmah Sailellah[1], Yo Fukushima[2] (1.Geophysics Department, Graduate School of Science Tohoku University, 2.International Research Institute of Disaster Science, Tohoku University)

11:45 AM - 12:00 PM JST | 2:45 AM - 3:00 AM UTC

[STT36-11] Development of ground-based radar interferometer for volcano deformation monitoring

*Taku Ozawa[1], Yuji Himematsu[1] (1.National Research Institute for Earth Science and Disaster Resilience)

12:00 PM - 12:15 PM JST | 3:00 AM - 3:15 AM UTC

[STT36-12] Small SAR satellite development and solution services
★Invited Papers

*Shuji Fujimaru[1] (1.Synspective Inc.)

Examination of extraction method of topographical change due to eruption of Nishinoshima using time series SAR

*Daiki Inano[1], Masanobu Shimada[2]

1. Tokyo Denki University, graduate school of science and engineering ,division of architectural, civil and environmental engineering, 2. Tokyo Denki University, division of architectural, civil and environmental engineering

The SAR image is subjected to two processes, synthetic aperture technology and pulse compression technology, to form a grid-like mesh on the ground surface, and the intensity of reflected waves is measured for each pixel. The reflected wave also differs greatly depending on the object. Therefore, in order to classify the land area and the sea area from the images observed by SAR, we consider the definition of the land area and the sea area. The land area is a place where the altitude is 0 m or more, and the backscattered signal in the land area is generally larger than that in the sea area. On the other hand, the sea area is an altitude of 0 m, and the reflected signal is generally small. Since the signal in the land area is larger than that in the sea area, it looks bright in the amplitude image.

In this study, we study Nishinoshima, an uninhabited volcanic island in the Ogasawara Islands of Japan, using time-series SAR data, focusing on temporal changes and area changes in topography associated with eruptions.In addition, the accuracy of the results obtained by these methods will be evaluated. Among the topographical changes, three methods were implemented for the area. The data used is time-series data of 23 scenes observed by JAXA's ALOS-2 / PALSAR-2 for 6 years from September 29, 2014.

The first is the threshold method. Determine one optimal threshold as a whole. The area is calculated by counting the number of pixels above the threshold value as the number of pixels on land. On the other hand, as the island expands, the brightness changes depending on the location due to the effects of ash fall. Therefore, the image is divided into four parts, threshold values are set in each area, and the land area is calculated. Therefore, the image is divided into four parts, threshold values are set in each area, and the land area is calculated. All of them are added together to calculate the total land area.

The second is the automation method. This method uses image analysis software called ImageJ to automatically determine the threshold. As a result, an image in which the land is white and the sea is black is created, and the area is calculated.

The third is the edge detection method. By multiplying the original image by the convolution matrix in the vertical and horizontal directions and adding the obtained pixel values, a differential weighted image with emphasized boundaries is created. By multiplying the original image by the convolution matrix in the vertical and horizontal directions and adding the obtained pixel values, a differential emphasis image with emphasized boundaries is created. This is an image with an increased backscattering coefficient on land. Therefore, even in the image where the backscattering coefficient of a part of the land is lowered due to the accumulation of volcanic ash, the backscattering coefficient of the sea is larger than the backscattering coefficient of the land as a whole, and the backscattering coefficient of the coastal area changes slightly can be extracted.

As a result, with respect to the local data of the Japan Coast Guard and the Japan Meteorological Agency, the relative error of each method is -2.79% for the threshold method, -12.63% for the threshold method

©2021. Japan Geoscience Union. All Right Reserved.

when the island is divided into four, and -10.94% for the automation method,the edge detection method resulted in -5.56%. At this point, the threshold method is considered to be the most effective for extracting the area of the island, and the edge detection method may also be an effective means depending on the treatment of sea noise.

Keywords: time series SAR, Nishinoshima

©2021. Japan Geoscience Union. All Right Reserved.

Tropospheric Dispersive Phase Anomalies during Heavy Rain Detected by L-band InSAR and Their Interpretation

Naufal Setiawan[1], *Masato Furuya[1]

1. Department of Earth and Planetary Sciences Hokkaido University

The split-spectrum method (SSM) can largely isolate and correct for the ionospheric contribution in the L-band interferometric synthetic aperture radar (InSAR). The standard SSM is performed on the assumption of only the first-order ionospheric dispersive effect, which is proportional to the total electron content (TEC). It is also known that during extreme atmospheric events, either originated from the ionosphere or in the troposphere, other dispersive effects do exist and potentially provide new insights into the dynamics of the atmosphere, but there have been few detection reports of such signals by InSAR. We apply L-band InSAR into heavy rain cases and examine the applicability and limitation of the standard SSM. Since no events such as earthquakes to cause surface deformation took place, the non-dispersive component is apparently attributable to the large amount of water vapor associated with heavy rain, whereas there are spotty anomalies in the dispersive component that are closely correlated with the heavy rain area. The ionosonde and Global Navigation Satellite System (GNSS) rate of total electron content index (ROTI) map both show little anomalies during the heavy rain, which suggests few ionospheric disturbances. Therefore, we interpret that the spotty anomalies in the dispersive component of the standard SSM during heavy rain are originated not in the ionosphere but the troposphere. While we can consider two physical mechanisms, one is runaway electron avalanche and the other is the dispersive effect due to rain, comparison with the observations from the ground-based lightning detection network and rain gauge data, we conclude that the rain dispersive effect is spatiotemporally favorable. We further propose a formulation to examine if another dispersive phase than the first-order TEC effect is present and apply it to the heavy rain cases as well as two extreme ionospheric sporadic-E events. Our formulation successfully isolates the presence of another dispersive phase during heavy rain that is in positive correlation with the local rain rate. In comparison with other dispersive phases during Sporadic-E episodes, the dispersive heavy rain phases seem to have the same order of magnitude with the ionospheric higher-order effects.

Keywords: heavy rain, non-dispersive medium, dispersive medium, interferometric synthetic aperture radar, split-spectrum method

©2021. Japan Geoscience Union. All Right Reserved.

Error level evaluation of L-Band InSAR Water Vapor Observation by Comparison with GNSS Observations

*Keita Matsuzawa[1], Yohei Kinoshita[1]

1. University of Tsukuba

Interferometric synthetic aperture radar (InSAR) can measure not only the surface deformation, but also the information of troposphere at the high spatial resolution This is caused by the propagation delay effect similar to the GNSS (Global Navigation Satellite System), which is approximately proportional to the zenith total delay (ZTD) or the precipitable water vapor (PWV). Previous researches have evaluated the precision of InSAR PWV observation using C-band SAR by comparing with GNSS (Tang et al. 2016, Mateus et al. 2020). In general, each satellite SAR sensor has a single frequency band. Most of all SAR satellites mainly use three types of frequency bands such as X-band, C-band, and L-band. The precision of meteorological observation data is necessary to calculate more accurate initial condition when observations are assimilated in weather forecasting. It is necessary to evaluate the precision of water vapor observation using InSAR data in each frequency band because each band has different characteristics in coherence and sensitivity to the ionosphere.

In this work, we evaluated the error level of water vapor observation by L-band InSAR. At first, we calculated the distribution of the zenith total delay difference (ΔZTD) from the InSAR data by the projection from the slant path delay using the simple trigonometric function. The overall offset of InSAR ΔZTD was corrected by the ΔZTD obtained from GNSS observations in the scene. Then, we computed the standard deviation of the residuals between the InSAR ΔZTD and the GNSS ΔZTD. The ΔZTD was then converted to the ΔPWV with a constant coefficient. Finally, we calculated the standard deviation of InSAR-derived PWV at a single epoch using the law of error propagation. Here we assumed that the noise level of water vapor observations on each SAR acquisition was at the same level, and the absolute error level of the GNSS ZTD was set to 16.1 mm that was obtained by a previous research (Boccolari et al. 2002). We used the GNSS Earth Observation Network System (GEONET) data processed with the 5-minutes PPP analysis by the Nevada Geodetic Laboratory at University of Nevada, Reno.

In the InSAR processing, we adopted the Split-Spectrum Method for compensating the differential ionospheric path delay in L-band interferograms. SAR data used were observed by the ALOS-2/PALSAR-2 stripmap mode. The data were collected over four areas in Japan: southern Ibaraki, western Tokyo and Kanagawa, Osaka, and southern Kyushu, spanning from 2014 to 2020. The multilook processing resulted in reduction of the decorrelation noise with sacrificing the spatial resolution to 100×100 m.

Our results showed that the overall distribution of residuals was unbiased and the standard deviation were 8.64 mm in ΔZTD. Estimated standard deviations from the residuals were different in each region, and tended to be larger for the data observed during the rainy season (from June to September). We evaluated the precision of the PWV measurement by L-band InSAR as 2.83 mm, indicating the precision of the L-band InSAR PWV observation is as good as other PWV measurements like C-band InSAR, GNSS, radiometer and weather satellites. By the time of the presentation, we will perform the time series analysis to evaluate the precision of the InSAR PWV measurement for each SAR acquisition days.

Keywords: InSAR, ALOS2, water vapor, error propagation

©2021. Japan Geoscience Union. All Right Reserved.

©2021. Japan Geoscience Union. All Right Reserved.

Comparison of atmospheric delay correction methods in InSAR: Case study in Japan

*Sardila Nurulhikmah Sailellah[1], Yo Fukushima[2]

1. Geophysics Department, Graduate School of Science Tohoku University, 2. International Research Institute of Disaster Science, Tohoku University

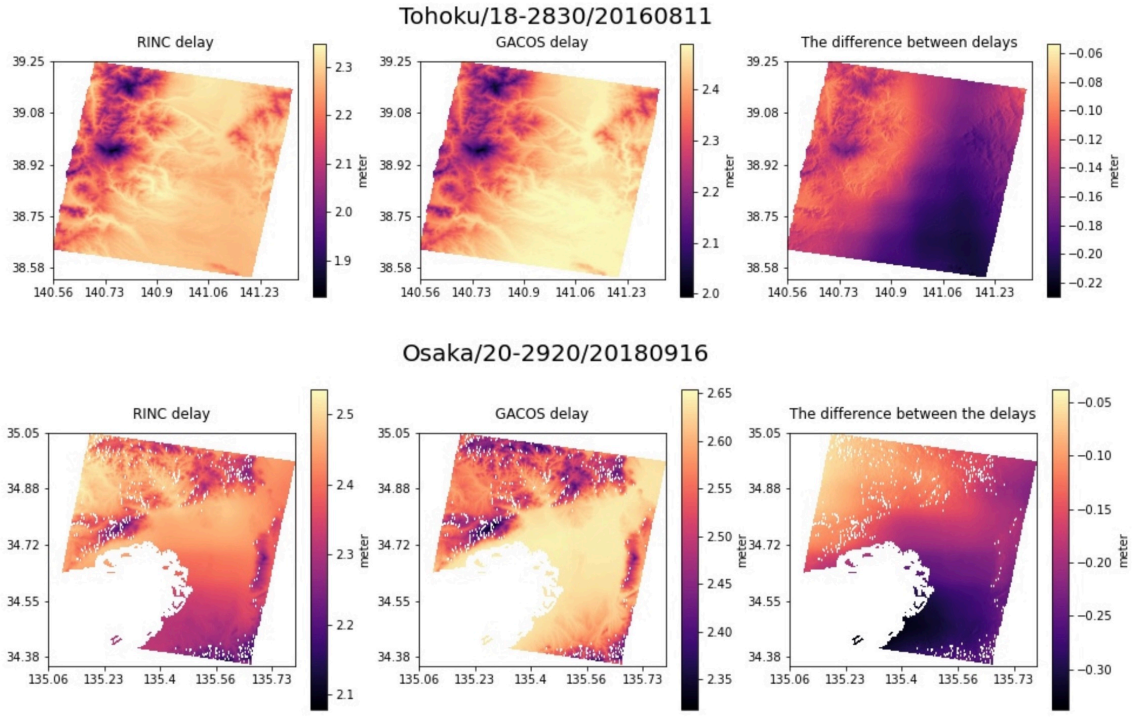
Interferometric synthetic aperture radar (InSAR) is widely used to measure surface displacements using the phase differences of two acquisition dates. Various Earth phenomena have been studied using InSAR such as volcanic activity, landslides, earthquakes and variations in groundwater levels. The delay of the microwave in the atmosphere is a major source of error in InSAR measurements. In the tropospheric layer, temperature, pressure, and relative humidity vary spatially and temporally, creating tropospheric delay masking out the surface displacement signals. Previous studies suggested methods to reduce the atmospheric noise by calculating the delay using atmospheric data and models. In this study, we compared the results of atmospheric delay calculation obtained by the RINC software (Ozawa et al., 2016) and GACOS (Yu, et al., 2017). The former directly integrates the delay along the propagation path using the atmospheric refractivity model of Thayer (1974) and the Meso-Scale Model (MSM) of Japan Meteorological Agency. The latter uses the atmospheric refractivity model of Berrada-Baby et al. (1988) combined with a decomposition model of the stratified and turbulent components, applied on the European Centre for Medium-Range Weather Forecasts (ECMWF) model and optionally the delay obtained from GNSS.

We calculated the delay on the timing of nine ALOS-2 acquisitions in the Tohoku region and fifteen ALOS-2 acquisitions in the Osaka region in Japan. We found that the amount of tropospheric delay tended to be larger for GACOS compared to RINC (Fig.1). To investigate the reason, we calculated the delay by applying the two refractivity models of Berrada-Baby et al. (1988) and Thayer (1974) on identical MSM data sets, and confirmed that the former systematically gives larger delay compared to the latter. For the topography-correlated stratified delay, some differences between the RINC and GACOS results were observed in the Tohoku region, whereas the topography-correlated delay was consistent in the Osaka region. As for the turbulent (topography-uncorrelated) component, the difference between the RINC and GACOS results was larger than 20 cm for half of the cases (12 out of 24), suggesting the difficulty in accurately estimating the turbulent contributions.

We applied the delay correction calculated by the both methods on the ALOS-2 interferograms processed for the two regions. The mean standard deviation of the LOS displacements did not reduce after applying the correction of RINC and GACOS, suggesting that the ionospheric delay contribution is dominated and thus indicating the importance of the ionospheric correction.

Keywords: InSAR, Atmospheric delay, Tropospheric delay

©2021. Japan Geoscience Union. All Right Reserved.



©2021. Japan Geoscience Union. All Right Reserved.

Development of ground-based radar interferometer for volcano deformation monitoring

*Taku Ozawa[1], Yuji Himematsu[1]

1. National Research Institute for Earth Science and Disaster Resilience

SAR interferometry using spaceborne SAR has been used as one of the general tools for detecting volcanic deformation. It is effective because spatially detailed deformation is obtained without ground observations. If volcano deformation can be detected with higher temporal resolution during active volcanic activity, it is expected to lead to a more detailed understanding of the volcanic activity mechanism. However, it has a disadvantage that the temporal resolution is limited to the satellite recurrence period. Therefore, we are researching on the use of ground-based radar interferometers that can illuminate radar wave from the ground and investigate crustal movements frequently for volcanic observation.

We have installed LiSA mobile k09 (synthetic aperture radar type) and GAMMA GPRI2 (real aperture radar type) using Ku-band radar waves at the Asama volcano and are continuing their operations for 5 years. After the start of operation, a very small eruption occurred at the Asama volcano, but no significant crustal movement was detected. On the other hand, atmospheric disturbances are prominent, and phase changes that exceed one cycle in a few minutes are often detected by real aperture radar. In such situation, processing of the synthetic aperture radar often fails. Its solution is difficult and this problem is one of the disadvantages of ground-based synthetic aperture radar.

We are also developing a portable synthetic aperture radar which can be used in a campaign observation during the time that volcanic activity increases. This synthetic aperture radar can select observation methods moving the antenna on the rail (GBSAR type), by vehicle-mounted (Car-borne type), and by hand (Man-borne type). Regarding the GBSAR and the Car-borne types, it has been confirmed that appropriate coherence can be obtained by repeat-pass observations. In the future, we will improve this sensor through experiment measurements in volcanoes and attempt to detect crustal deformation.

Keywords: SAR, crustal deformation, voilcano

©2021. Japan Geoscience Union. All Right Reserved.

Small SAR satellite development and solution services

*Shuji Fujimaru[1]

1. Synspective Inc.

1. Company Introduction

Synspective is world’ s only company having capability both development of own small SAR satellite constellation and providing solutions with its data and analytics. We create the Learning World where people can expand their capabilities and make tangible progress with new data and technologies.

We believe that there are three important pillars: the creation of new data by satellites, the analysis of data by data science and machine learning, and the development of human resources who will lead the learning world.

2. Small SAR Satellite

2-1. About SAR satellites

Synspective has developed and is operating a small SAR satellite that weighs 100 kg class.SAR (Synthetic Aperture Radar) satellites use microwaves to observe the shape of terrain and structures. Microwaves have a long wavelength and can transmit through clouds, making it possible to observe the earth's surface beneath clouds. Also, microwave observation is possible both during the day and at night because it actively emits radio waves. Particularly in Asia, where the rainy season is long and cloudy, it is often difficult to observe with optical satellites, and the demand for SAR satellites that can observe.

2-2. Differences from conventional satellite

The weight of our small SAR satellite "StriX" is 100 kg, which is about 1/10 of a conventional large SAR satellite. In terms of cost, the total cost of development and launch is about 1/20 of that of a conventional large SAR satellite.It will be possible to produce a number of SAR satellites at a lower cost by reducing their size and weight while maintaining performance similar to that of conventional large SAR satellites.

2-3. Results

On December 15, 2020, our first demonstration vehicle "StriX-α" was launched by Rocket Lab's Electron rocket from the launch site in Mahia Peninsula, New Zealand. It was successfully injected into its scheduled orbit (sun-synchronous orbit, 500 km altitude).
On February 16, 2021, we successfully acquired images from the first small SAR satellite (100kg class) in Japan.

2-4. Future development

In 2021, we plan to launch the second demonstration satellite, StriX-β, with the goal of demonstrating in orbit InSAR (Interferometric SAR), an analysis technology unique to SAR that detects millimeter-scale variations in the earth's surface. We aim to build a constellation of 6 satellites by 2023 and 30 satellites by the late 2020s.

3. SAR data utilization

As an example of the use of SAR data, we will observe an area that is in the midst of being damaged by a typhoon. It is possible to know where areas are submerged, which roads are blocked due to flooding, and the overall extent of damage after the typhoon passes. The data can be expected to be utilized by the

©2021. Japan Geoscience Union. All Right Reserved.

insurance and financial industries, as well as the government, which need to quickly assess the damage situation based on primary information when a flood occurs.

Another example is the use of SAR satellite data for infrastructure development and urban development, taking advantage of its wide area. At the planning stage of infrastructure and urban development, it is possible to obtain information on topography and land use, which can be used to determine where to install infrastructure. At the construction stage, the data can be used to obtain objective information on the progress of construction and the condition of materials at the site. Also, as the satellite orbits the earth, it is possible to observe construction sites in thousands of locations around the world. For subsequent maintenance, the satellite can also be used for time-series observation and analysis of ground deformation, which can be used for early detection of unexpected stresses and deformations in dams and distortions in large-scale structures such as ports and runways.

Recently, on February 13, a magnitude 7.1 earthquake occurred in Fukushima and Miyagi. Many people may have remembered the Tohoku earthquake and tsunami, however, there is a possibility that our solutions can be effectively used for disaster response in the occasion of such a disaster.

Synspective has already released the "Flood Damage Assessment" solution for assessing flood damage (flooded area, flooded depth, damaged roads, damaged buildings) for disaster response as a solution service. Also, we provide the "Land Displacement Monitoring" solution that detects and displays a time series of changes in the land surface in millimeters over a wide area.

Keywords: SAR, Small satellite

©2021. Japan Geoscience Union. All Right Reserved.

[J] Poster | S (Solid Earth Sciences)：S-TT Technology & Techniques

Sat. Jun 5, 2021 5:15 PM - 6:30 PM JST | Sat. Jun 5, 2021 8:15 AM - 9:30 AM UTC | Ch.18_1

[S-TT36] Synthetic Aperture Radar and its application

convener:Yohei Kinoshita(University of Tsukuba), Takahiro Abe(Graduate School of Bioresources, Mie University), Shoko Kobayashi(Tamagawa University), Yuji Himematsu(National Research Institute for Earth Science and Disaster Resilience)

ALOS-2 and Sentinel-1, which have highly enhanced capacity compared to previous SAR satellites, were launched in 2014, and their utilization has been widely expanding as data have accumulated for approximately six years. Other long-operating SAR satellites like TerraSAR-X and Cosmo-SkyMed also contribute to expanding the SAR utilization. Now we are facing a new and abundant era of the satellite SAR, along with a worldwide trend to an open and free data policy of satellite data, under the situation of next-generation advanced and/or constellated SAR satellite plans by both public agencies (e.g. ALOS-4 and NISAR) and private sectors. In addition, SAR technologies with other platforms, such as ground-based SAR with high temporal resolution and UAV (Unmanned Aerial Vehicle) SAR with flexible operability, have also been developed and used for various targets. These facts indicate that the SAR utilization has become widespread in both basic researches (e.g., earth science) and diverse applications (e.g., disaster prevention and forest monitoring). In this session, we would like to invite various kinds of research and application results with regard to SAR, sharing our knowledge and having a discussion for the advancement of the SAR utilization.

[STT36-P01] Long-term crustal deformation of domestic volcanoes detected by InSAR time series analysis

*Kano Mikihara[1], Takaaki Inukai[1], Nobuhiro Ishikura[1], Kumi Shimazaki[1], Masayoshi Ishimoto[1], Tomokazu Kobayashi[1] (1.GSI of Japan)

[STT36-P02] Surface displacement in Hachijojima Island since 2014 by InSAR analysis and GNSS

*yusei Hamamura[1], HIROYUKI AZUMA[1], Yoshiya Oda[1] (1.Tokyo Metropolitan University)

[STT36-P03] Observing Crustal Deformation Using Interferometric Synthesis Aperture Rader and Estimating Magma Chamber Associating with the 2018 Eruption of Shinmoedake of Kirishima Volcanoes, Japan.

*Takahisa Tashiro[1], Koichi Suzuki[2] (1.Cooperative Program for Resources Engineering, Graduate School of Engineering, Hokkaido University, 2.Research Group of Geoenvironmental Engineering, Division of Sustainable Resource Engineering, Faculty of Engineering, Hokkaido University)

[STT36-P04] **Using InSAR for evaluating the accuracy of earthquake location determination, Comparison of Iranian and Japanese cases**

*Nematollah Ghayournajarkar[1], Yo Fukushima[2] (1.Graduate School of Science, Tohoku University, 2.International Research Institute of Disaster Science, Tohuku University)

[STT36-P05] Progress on developing a GNSS-based InSAR atmospheric delay correction model

*Yohei Kinoshita[1] (1.University of Tsukuba)

[STT36-P06] **Ship Detection Using Synthetic Aperture Radar**

*Kengo Iwata[1], Masanobu Shimada[1] (1.Tokyo Denki University)

Long-term crustal deformation of domestic volcanoes detected by InSAR time series analysis

*Kano Mikihara[1], Takaaki Inukai[1], Nobuhiro Ishikura[1], Kumi Shimazaki[1], Masayoshi Ishimoto[1], Tomokazu Kobayashi[1]

1. GSI of Japan

GSI (Geospatial Information Authority of Japan) has been monitoring crustal and ground deformation all over Japan with ALOS-2 data by applying two-pass synthetic aperture radar Interferometry (InSAR) method. But, it is difficult to detect small deformations, because InSAR results often have errors due to tropospheric disturbances and ionospheric disturbances.
To overcome the flaw, in recent years, InSAR time series analysis that is statistically processing a number of images has been conducted. This is because InSAR time series analysis can effectively reduce errors contained in image and resultantly improves the measurement accuracy. Persistent Scatter Interferometry method (PSI method) and Small Baseline Subset algorithm method (SBAS method) are typical examples of InSAR time series analysis. GSI has developed the InSAR time series analysis system (GSITSA) which includes both PSI method and SBAS method (Kobayashi et al., 2018). Hayashi et al., (2019) conducted InSAR time series analysis using GSITSA for domestic volcanic areas and land subsidence areas. They confirmed that the SBAS method using ALOS-2 data is an effective analysis method for crustal deformation monitoring even in mountainous areas, in which they demonstrated that it could detect temporal changes on small ground deformations. In addition, with Advanced Land Observing Satellite-4 (ALOS-4), which is scheduled to be launched in 2022, the observation frequency will be increased five times more than ALOS-2. ALOS-4 is expected to enable more accurate measurement of deformations by applying InSAR time series analysis.
With the background, for the effective utilization of ALOS-4 data, we conducted InSAR time series analysis for the domestic volcanic area using ALOS-2 data accumulated since 2014. In this presentation, we will show the results of InSAR time series analysis of Mt. Kusatsushirane, Mt. Yakedake and Kuchino-Erabujima Is.. As a result of the analysis, we detected ground displacement away from the satellite in and around Kagamiike. We found that the deformation occurred slowly before an eruption that occurred in January 2018, and that the deformation speed changed after the eruption and continued to deform until around the summer of 2019. Around the summit of Mt. Shindake on Kuchino-Eerabujima Is., deformations away from the satellite were detected during the two periods from the eruption in May 2015 to around January 2018 and from the eruption in January 2019 to around August 2019. In addition, we found that near the summit of Mt. Yakedake, there was a deformation approaching the satellite at a speed of about 2 cm per year from 2016 to 2020. By applying InSAR time series analysis, we were able to significantly detect the temporal changes in small crustal deformations that have not been detected with sufficient accuracy by the conventional InSAR method.

Acknowledgments
ALOS-2 data were provided based on the joint research agreement with JAXA (Japan Aerospace Exploration Agency). The ownership of ALOS-2 data belongs to JAXA.

Keywords: “DAICHI-2” (ALOS-2), SAR, Volcanic activity, Crustal deformation

©2021. Japan Geoscience Union. All Right Reserved.

Surface displacement in Hachijojima Island since 2014 by InSAR analysis and GNSS

*yusei Hamamura[1], HIROYUKI AZUMA[1], Yoshiya Oda[1]

1. Tokyo Metropolitan University

In this study, as a volcanic disaster prevention study, the surface displacement of Hachijojima Island, a volcanic island belonging to Tokyo Metropolitan, has been estimated by InSAR time series analysis, ALOS-2 PALSAR-2 data observed during the period from August 2014 to August 2020 are used for InSAR analysis. In this study, we employed SBAS(Small Baseline Subset) method, which in one of the methods for InSAR time series analysis. 83 pairs for Descending, and 26 pairs for Ascending are used for SBAS analysis. In addition, we analyzed GNSS data observed at JMA “South mountainside of Nishiyama” station to verify the results.
The results of InSAR analysis, it is not possible to confirm significant displacement above noise level. In addition, it was not possible to find the long-term sueface displacement trend.
The results obtained by InSAR time series analysis are described. On Hachijojima Island, no regions with surface displacement of 4 cm or more was observed in 6 years. But it was confirmed that analysis results of both Descending and Ascending showed uplifting surface displacement in the flat area between Nishiyama and Higashiyama and near the summit of Nishiyama. Specifically, a displacement of about 4 cm was confirmed on the flat land, and a displacement of about 2 cm was confirmed near the summit of Nishiyama. Those area correspond to the area of the lavas of the Senjojiki stage and Okoshigahana Scoria fall.

©2021. Japan Geoscience Union. All Right Reserved.

Observing Crustal Deformation Using Interferometric Synthesis Aperture Rader and Estimating Magma Chamber Associating with the 2018 Eruption of Shinmoedake of Kirishima Volcanoes, Japan.

*Takahisa Tashiro[1], Koichi Suzuki[2]

1. Cooperative Program for Resources Engineering, Graduate School of Engineering, Hokkaido University, 2. Research Group of Geoenvironmental Engineering, Division of Sustainable Resource Engineering, Faculty of Engineering, Hokkaido University

Shinmoedake of Kirishima Volcanoes in Southern Kyushu, Japan is reported to be eruptive around March 2018. We investigated crustal deformations before (17th Oct. 2017 –8th Feb. 2018), while (8th Feb. 2018 –8th Mar. 2018) and after (8th Mar. 2018 –7th Feb. 2019) of this eruption using Interferometric Synthetic Aperture Rader (InSAR). We also applied a spherical source deposited in a half-space model, called Mogi Model (Mogi, 1958), to presume the pressure source that caused eruptions as well as its latitude, longitude, depth and volume changes. To obtain fitting parameters, we considered Pearson's X^2 test and assumed the smallest magnitude would be valid. We used grid searching as hyperparameter optimisation when finding them.

The InSAR observations revealed that LOS were 2.41 [cm] in pre-eruptive, -3.75 [cm] in syn-eruptive and 3.93 [cm] in post-eruptive periods. These results were harmonic to baseline estimations of GNSS performed by JMA (2019) and GSI (2019).

Estimated volume changes were 0.37 [m^3] in charging, -0.69 [m^3] in discharging and 0.79 [m^3] in re-charging process. We assumed the magma chamber that caused crustal deformations was located at the depth of 7.5 km at approximately 6 km away from the summit of Shinmoedake. These values are equivalent to JMA (2019), who obtained -0.66×10^7 [m^3] (1st Mar. –10th Mar. 2018), which applied Mogi Model to GNSS dataset. Since Shinmoedake is characteristic of its relatively spacious crater, NIED (2018) carried out SAR observations from 6th Mar. to 9th Mar. 2018 and determined the volume of accumulated ejecta was 1.32×10^7 [m^3]. All the values were on the same order (10^7 [m^3]).

Based on our analysis, we conclude that the 2011 events' magma chamber (*e.g.* Kobayashi *et al.*, 2011; Miyagi, Ozawa, and Kohno, 2013) could be attributed to 2018 events.

Acknowledgement

PALSAR level 1.0 data are shared amongst PIXEL and provided by JAXA under a cooperative research contract with ERI, Univ. of Tokyo. The ownership of PALSAR belongs to METI and JAXA.

References

GSI, *Rep. Coordinating Comm. Prediction Volcan. Erupt.*, **132**, 338-351, 2019. (in Japanese)
JMA, *Doc. Coordinating Comm. Prediction Volcan. Erupt.*, **144**, 89-101, 2019. (in Japanese)
Kobayashi, T. *et al.*, *Bull. GSI*, **121**, 195-201, 2011. (in Japanese)
Miyagi, Y., Ozawa, T. and Kohno, Y., *Kazan* (*Bull. Volcanol. Soc. Japan*), **58**(2),341-351, 2013. (in Japanese)
Mogi, K., *Bull. Earthq. Res. Inst. Univ. Tokyo*, **36**, 99-134, 1958.

©2021. Japan Geoscience Union. All Right Reserved.

NIED, https://www.bosai.go.jp/info/saigai/2017/pdf/20180309_01.pdf, 2018. (in Japanese)

Keywords: Shinmoedake of Kirishima Volcanoes, InSAR, Mogi Model

©2021. Japan Geoscience Union. All Right Reserved.

Using InSAR for evaluating the accuracy of earthquake location determination, Comparison of Iranian and Japanese cases

*Nematollah Ghayournajarkar[1], Yo Fukushima[2]

1. Graduate School of Science, Tohoku University, 2. International Research Institute of Disaster Science, Tohuku University

Accurate location and extent of the earthquake rupture provide fundamental information for seismic hazard evaluation. Interferometric Synthetic Aperture Radar (InSAR) is a promising technique to constrain fault parameters because it has high spatial resolution in the epicentral area for shallow earthquakes, and the fault model derived from InSAR can be taken as the ground truth. In this study, we compared the fault location derived from InSAR to the epicenters determined by local and global seismic networks. We focused on shallow earthquakes that occurred in Iran and Japan, where the station density of the local seismic networks differs significantly, in order to evaluate how the station density and azimuthal coverage influence the accuracy of the earthquake location determination. On each of the five Iranian and five Japanese earthquakes, we obtained the coseismic interferograms, applied a Particle Swarm Optimization (PSO) method assuming a rectangular finite fault with uniform slip to obtain the optimal rupture location, and then calculated the distance between seismic-derived epicenters and InSAR-derived surface-projected fault plane for each earthquake. The results for the Iranian earthquakes showed that the distance between IRSC (Iranian Seismological Center)-derived epicenter and the fault plane was larger than that between the USGS-derived epicenter and the fault plane. Since the spatial density of the IRSC network is better than the USGS network, we can attribute the higher accuracy of the USGS epicenters to the better azimuthal coverage of the USGS network. For the case of the Japanese earthquakes, the epicenter determined by JMA (Japan Meteorological Agency), which has good azimuthal coverage and much denser spatial coverage than the USGS network, was closer to the InSAR-derived fault plane compared to the USGS epicenter. These results indicate that 1) good azimuthal coverage of the seismic network is fundamentally important in obtaining accurate epicenters, and 2) the dense station coverage leads to improving the accuracy.

Keywords: InSAR, Finite rectangular fault, Earthquake location accuracy

©2021. Japan Geoscience Union. All Right Reserved.

Using InSAR for evaluating the accuracy of earthquake location determination, Comparison of Iranian and Japanese cases

Nematollah Ghayournajarkar[1], Yo Fukushima[2]

1: Department of Geophysics, Graduate School of Science, Tohoku University;

2: International Research Institute of Disaster Science, Tohoku University

Accurate location and extent of the earthquake rupture provide fundamental information for seismic hazard evaluation. Interferometric Synthetic Aperture Radar (InSAR) is a promising technique to constrain fault parameters because it has high spatial resolution in the epicentral area for shallow earthquakes, and the fault model derived from InSAR can be taken as the ground truth. In this study, we compared the fault location derived from InSAR to the epicenters determined by local and global seismic networks. We focused on shallow earthquakes that occurred in Iran and Japan, where the station density of the local seismic networks differs significantly, in order to evaluate how the station density and azimuthal coverage influence the accuracy of the earthquake location determination. On each of the five Iranian and five Japanese earthquakes, we obtained the coseismic interferograms, applied a Particle Swarm Optimization (PSO) method assuming a rectangular finite fault with uniform slip to obtain the optimal rupture location, and then calculated the distance between seismic-derived epicenters and InSAR-derived surface-projected fault plane for each earthquake. The results for the Iranian earthquakes showed that the distance between IRSC (Iranian Seismological Center)-derived epicenter and the fault plane was larger than that between the USGS-derived epicenter and the fault plane. Since the spatial density of the IRSC network is better than the USGS network, we can attribute the higher accuracy of the USGS epicenters to the better azimuthal coverage of the USGS network. For the case of the Japanese earthquakes, the epicenter determined by JMA (Japan Meteorological Agency), which has good azimuthal coverage and much denser spatial coverage than the USGS network, was closer to the InSAR-derived fault plane compared to the USGS epicenter. These results indicate that 1) good azimuthal coverage of the seismic network is fundamentally important in obtaining accurate epicenters, and 2) the dense station coverage leads to improving the accuracy.

©2021. Japan Geoscience Union. All Right Reserved.

Progress on developing a GNSS-based InSAR atmospheric delay correction model

*Yohei Kinoshita[1]

1. University of Tsukuba

Correcting the InSAR atmospheric delay noise is one of the problem for InSAR researches. In teh last year, Kinoshita (2020, GSJ) proposed a new InSAR atmospheric delay model by use of the GNSS zenith total delay (ZTD) and its horizontal gradient data, in which we referred the method proposed by Arief and Heki (2020). The preliminary result of our proposed model showed a better performance compared with a traditional correction approaches such as the GACOS global mode and the JMA's MSM based model. Here we investigated parameter sensitivities of our model in terms of the grid spacing and the use of the delay gradient.

We at first investigated the model sensitivity in the grid spacing. As a default, we have set it to 5 km spacing, although this setting may not be the best value. In this experiment, we changed the grid spacing ranging from 2 km to 30km while other parameters were fixed. The result showed that the InSAR phase reduction was most significant with the 4 km grid spacing. Even if the grid spacing were set to be finer such as 2 km and 3 km, the delay correction effectiveness slightly worsened. This would indicate the limitation of the resolvable ability of using the GNSS ZTD and gradient.

We next investigated the sensitivity to the GNSS station density. In this experiment, we performed model simulations under conditions that reduced the number of GNSS stations. Other parameters were fixed as a default and the grid spacing was set to 5 km as being the same as the original model run. The result showed the monotonical decrease of the phase reduction ability with decreasing the number of GNSS stations as expected. An interesting feature was that the decreasing ratio of the model correction ability done not worsened significantly until the GNSS station density was reduced to 20 % of the original number (average distance between stations was aproximately 50km). This result indicated that our proposed model would have an applicability for regions where only small numbers of GNSS stations are installed like south-eastern Asia and Africa.

In addition, we compared the model's correction ability with that of the model without using delay gradients. Contrary to our expectation, the InSAR phase reduction was slightly better in the model without using gradients (corrected phase standard deviation was 25.62 mm) than the model with using gradients (25.75 mm). This difference may be not significant statistically, but the cause of this may be 1) an overfitting to the observed gradients for the small scale (an order of kilometers) in the inversion, 2) an inadequacy of the smoothing hyper-parameter value that was set manually, or 3) inappropriate value of the scale height that we used the scale height value of 2.5 km which is for atmospheric water vapor.

In the presentation, we will discuss our model characteristics shown above.

Keywords: InSAR, delay correction, GNSS

©2021. Japan Geoscience Union. All Right Reserved.

Ship Detection Using Synthetic Aperture Radar

*Kengo Iwata[1], Masanobu Shimada[1]

1. Tokyo Denki University

Synthetic aperture radar image includes waves, internal waves, vessel detection, and tides. With regard to the ship detection, the synthetic aperture radar PALSAR-2 mounted on ALOS-2 and AIS (Automatic Identification System), which transmits and receives identification codes, ship names, positions, speeds, etc., will cooperate. Surveillance is being conducted to identify suspicious vessels.

In last year's study, we measured the average ($\sigma^0_{Avg.}$) of the backscatter coefficient (σ_0) in a small area and determined the area with a coefficient above a threshold (σ_{th}) as a vessel. As a result, the threshold of the directional scattering coefficient was set to -8.0 dB, and the number of detected vessels with AIS (Automatic Identification System) location information was 27/29 (95%) and 25/25 (100%), and many other points that were considered to be vessels were detected. In addition, we found problems related to the determination of the threshold value and the appearance of false detection points mainly in coastal areas. In this study, we compared the two methods in order to improve the detection accuracy.

The first is the fixed threshold method. We improved the threshold calculation method compared to the algorithm used in last year's study. We cut out a 500 x 500 pixel area (1) that shows one large ship and a 1000 x 1000 pixel area (2) that shows five small ships as samples from the image, and determined the threshold value based on the histograms of the sea surface and ships in areas (1) and (2). We applied this threshold to the entire image and detected pixels with a value greater than the threshold, which we considered to be ships.

The second method is the adaptive threshold method (ATM). In this method, a small region is set in the image and the threshold is calculated within this region. By scanning the entire image with this small region: the moving window, a threshold value is calculated for each region and the vessel is detected. In this study, we created an algorithm by referring to the formula for deriving the moving window and threshold used in the study by Mizukoshi, Ouchi, and Watanabe (2019).

We used one scene of November 18, 2019 in the waters from the Pacific Ocean in Wakayama Prefecture to the Kii Suido and Osaka Bay, taking into account the number of vessels traveling and the expected speed of navigation. At the same time, AIS information of the same area was used to compare ship detection .

We determined the threshold for the fixed threshold method to be DN=5000 based on the histograms of regions (1) and (2).The results of AIS and visual detection of the vessels were 33/33 (100%). The processing time of the algorithm was about 2 seconds.We set the ATM moving window as background window 81×81 and buffer window 41×41. The detection result was 33/33 ships (100%). The processing time of the algorithm was about 3 hours. The advantages of the fixed threshold method were the small number of false positives on the sea surface and the short processing time. In contrast, the advantages of ATM were clearer detection of small vessels and fewer false positives in coastal areas.

Keywords: Synthetic aperture radar, Ship Detection, Adaptive threshold method

©2021. Japan Geoscience Union. All Right Reserved.

©2021. Japan Geoscience Union. All Right Reserved.

[J] Oral | S (Solid Earth Sciences)：S-TT Technology & Techniques

Sat. Jun 5, 2021 9:00 AM - 10:30 AM JST | Sat. Jun 5, 2021 12:00 AM - 1:30 AM UTC | Ch.21 Zoom Room 21

[S-TT38] Creating future of solid Earth science with high performance computing (HPC)

convener:Takane Hori(R&D Center for Earthquake and Tsunami, Japan Agency for Marine-Earth Science and Technology), Yuji Yagi(Graduate School of Life and Environmental Sciences, University of Tsukuba, Tsukuba), Katsuhiko Shiomi(National Research Institute for Earth Science and Disaster Resilience), Ryoichiro Agata(Japan Agency for Marine-Earth Science and Technology), Chairperson:Takane Hori(R&D Center for Earthquake and Tsunami, Japan Agency for Marine-Earth Science and Technology), Ryoichiro Agata(Japan Agency for Marine-Earth Science and Technology)

Due to the development in computer science and computational science, large-scale or many times forward simulations and/or inversion analyses have become available recently. In solid Earth science, large-scale seismic wave propagation and crustal deformation with high fidelity models based on high resolution observation data have been demonstrated; uncertainty in crustal deformation caused by material properties and structures can be investigated based on many-time calculations for different material properties and structures; fault slip inversion analyses for non-Gaussian error distribution, etc. Thus, we will invite researchers who are applying HPC technology in forward simulations and inversion analyses and discuss how to improve more the collaboration between computer & computational sciences and solid Earth science. We are welcome submission by the researchers who are interested in this scope, especially students and young researchers.

9:00 AM - 9:15 AM JST | 12:00 AM - 12:15 AM UTC

[STT38-01] On large-scale numerical simulation of earthquake generation, wave propagation and soil amplification aiming for comprehensive earthquake damage estimation

Takane Hori[1], Tsuyoshi Ichimura[2,3,4], Kohei Fujita[2,3], *Ryoichiro Agata[1] (1.Japan Agency for Marine-Earth Science and Technology, 2.Earthquake Research Institute, 3.Riken Center for Computational Science, 4.Riken Center for Advance Intelligence Project)

9:15 AM - 9:30 AM JST | 12:15 AM - 12:30 AM UTC

[STT38-02] Large-scale earthquake simulation with supercomputing and data-learning

★Invited Papers

*Tsuyoshi Ichimura[1] (1.the University of Tokyo)

9:30 AM - 9:45 AM JST | 12:30 AM - 12:45 AM UTC

[STT38-03] Comparison of E-wave FEM and GMS in Calculation of Long-Period Ground Motion in 3D Heterogeneous Underground Structures

*Ryoichiro Agata[1], Yoshihisa Hiyoshi[1], Sayako Hirobe[1], Takahiro Maeda[2], Asako Iwaki[2], Kohei Fujita[3,4], Hiroyuki Fujiwara[2], Tsuyoshi Ichimura[3,4,5], Takane Hori[1] (1.Japan Agency for Marine-Earth Science and Technology, 2.National Research Institute for Earth Science and Disaster Resilience, 3.Earthquake Research Institute, 4.Riken Center for Computational Science, 5.Riken Center for Advance Intelligence Project)

9:45 AM - 10:00 AM JST | 12:45 AM - 1:00 AM UTC

[STT38-04] Three-dimensional thermal structure modeling in the Alaska subduction zone

*Kaya Iwamoto[1], Nobuaki Suenaga[2], Shoichi Yoshioka[2,1] (1.Department of Planetology, Graduate School of Science, Kobe University, 2. Research Center for Urban Safety and Security, Kobe University,)

10:00 AM - 10:15 AM JST | 1:00 AM - 1:15 AM UTC

[STT38-05] Sensitivity analysis with large-scale 3D finite element crust structure model for seafloor geodetic constraints on coseismic slip and interseismic slip-deficit distributions

*Sota Murakami[1], Tsuyoshi Ichimura[1], Kohei Fujita[1], Takane Hori[2], Yusaku Ohta[3] (1.Earthquake Research Institute, The University of Tokyo, 2.R&D Center for Earthquake and Tsunami, Japan Agency for Marine-

Earth Science and Technology, 3.Research Center for Prediction of Earthquakes and Volcanic Eruptions, Graduate School of Science, Tohoku University)

10:15 AM - 10:30 AM JST | 1:15 AM - 1:30 AM UTC

[STT38-06] Discussion

On large-scale numerical simulation of earthquake generation, wave propagation and soil amplification aiming for comprehensive earthquake damage estimation

Takane Hori[1], Tsuyoshi Ichimura[2,3,4], Kohei Fujita[2,3], *Ryoichiro Agata[1]

1. Japan Agency for Marine-Earth Science and Technology, 2. Earthquake Research Institute, 3. Riken Center for Computational Science, 4. Riken Center for Advance Intelligence Project

The operation of the supercomputer "Fugaku" has started in FY2020. The Ministry of Education, Culture, Sports, Science and Technology of Japan (MEXT) has established “Program for Promoting Researches on the Supercomputer Fugaku” (FY2020-2022). "Large-scale numerical simulation of earthquake generation, wave propagation and soil amplification," which the authors have applied for the project, has been adopted as one of the subjects. In this task, we have been developing finite element (FE) analysis methods targeting earthquake generation, wave propagation and soil amplification, which can make the most of the computational performance of “Fugaku”. “E-wave FEM” and “STRIKE” are programs for seismic wave propagation and soil amplification analysis that combine an implicit time integration scheme, unstructured tetrahedral quadratic elements, and an iterative solver using a high-performance preconditioner. By using these applications, seismic wave propagation and soil amplification analysis in complex ground can be performed accurately, stably, and rapidly.

In this project, we aim to lay a foundation for using numerical simulations with computational applications that utilize high-performance computation in policy making and practice uses. First, there is a need for more sophisticated methods in the evaluation of long-period ground motions in the national damage estimation. E-wave FEM, which meets this need, has been included in the committee's investigation for application to the national damage estimation. This project aims for ensuring the accuracy of the method based on calculations that can only be done at “Fugaku”, and then to actually use the method in the national damage estimation. Using “Fugaku”, we improved the program by using the most advanced technology of computational science and computer science to bring out the performance of “Fugaku” in the FE analyses (Ichimura et al., SC20, 2020). In addition, by comparing the numerical solutions of E-wave FEM and a finite difference method conventionally used in the national damage estimation through benchmark tests, we summarized the merits of adopting E-wave FEM as a tool for damage estimation. Then, preparations are made for the implementation of seismic wave propagation analysis using E-wave FEM in the national damage estimation. We also developed a platform for constructions and civil engineering companies to use a system that can perform calculations equivalent to those applied in the government. In order to provide the tools that is easy to use, we developed a computing environment, including manuals, pre-post processing computers, and tools. In addition, tutorials on calculations using E-wave FEM were held for companies participating in this project. We have already received feedback on the functions implemented in the tool set, and we will improve the environment based on the feedback. As for STRIKE, we are preparing for conducting soil amplification analyses at “Fugaku” based on the needs of each company, aiming for application to more practically relevant problems.

In this project, we have developed a large-scale simulation program for elastic and viscoelastic crustal deformation, E-cycle FEM, using a FE analysis solver that is essentially the same as E-wave FEM. Main applications of this program is to estimate the initial water level of tsunamis and the spatio-temporal evolution of fault slips in the Nankai Trough. In this project we mainly target to obtaining reference

©2021. Japan Geoscience Union. All Right Reserved.

solutions based on elastic and viscoelastic crustal deformation calculations that can only be done at Fugaku, such as those in 3D heterogeneous structures in a large area or very detailed structures in a limited area. Such a reference solution will be important for creating Green's functions with high accuracy, which can be provided to those applications mentioned above.

Keywords: High-performance computing, Finite element method, Supercomputer "Fugaku", Seismic wave propagation analysis, Nonlinear soil amplification, Crustal deformation

©2021. Japan Geoscience Union. All Right Reserved.

Large-scale earthquake simulation with supercomputing and data-learning

*Tsuyoshi Ichimura[1]

1. the University of Tokyo

Advanced observations have been carried out and various observation data have been accumulated. In order to make the best use of such valuable observation data, technological innovation is required to improve the analysis capability. Although seismic phenomena are diverse and have different length scales and resolutions, from the viewpoint of mathematical problems, many behaviors of seismic phenomena can be modeled as static/dynamic, nonlinear/linear responses of solids. Although the "constitutive laws" and "senses" differ depending on the target phenomenon, many phenomena can be attributed to these forward and inverse analysis problems, and the advancement of analysis methods that can solve such problems will play a major role in improving analysis capabilities. Since the above is a mathematical problem in which stress-free boundary conditions and geometry have a strong influence on the solution, the finite element method based on unstructured elements is one of the suitable methods, but it will be a large-scale problem due to the large size of the target problem and the high resolution required to ensure the reliability (convergence) of the solution. Therefore, it is necessary to develop a new method to solve the problem by efficiently synchronizing a large number of computer nodes, while solving the bottleneck caused by the fact that the core kernel of the finite element method is the random memory access dominant type, which is incompatible with modern computer architecture. In this talk, we present a large-scale earthquake simulation method that combines supercomputing and data-learning and show application examples on a supercomputer (e.g., Fugaku), which demonstrate the effectiveness of approaches of combining supercomputing and data-learning.

Keywords: large-scale simulation , supercomputing and data-learning, finite element method

©2021. Japan Geoscience Union. All Right Reserved.

Comparison of E-wave FEM and GMS in Calculation of Long-Period Ground Motion in 3D Heterogeneous Underground Structures

*Ryoichiro Agata[1], Yoshihisa Hiyoshi[1], Sayako Hirobe[1], Takahiro Maeda[2], Asako Iwaki[2], Kohei Fujita[3,4], Hiroyuki Fujiwara[2], Tsuyoshi Ichimura[3,4,5], Takane Hori[1]

1. Japan Agency for Marine-Earth Science and Technology, 2. National Research Institute for Earth Science and Disaster Resilience, 3. Earthquake Research Institute, 4. Riken Center for Computational Science, 5. Riken Center for Advance Intelligence Project

Estimation of long-period seismic motions and strong ground motions caused by large subduction zone earthquakes, which are anticipated to occur in the future, is important for advancing measures for earthquake damage in urban areas. For this purpose, it is necessary to calculate seismic ground motions in complex subsurface structures for appropriately set source fault models using numerical methods such as the finite difference method (FDM) and the finite element method (FEM). The advantage of using FDM in such calculations is that discretization using structural grids makes it relatively easy to generate a computational model, to decompose the model domain for parallel computation, and to achieve high computation performance due to efficient memory access. GMS (Aoi & Fujiwara 1999, Aoi & Fujiwara 1998, Aoi et al. 2004), a 3D FDM calculation program using a discontinuous grid, has been packaged and is widely used. Since FEM can handle computation models with unstructured elements, it is suitable for handling complex topography, seismic wave velocity structure, and various source fault models flexibly in seismic ground motion analyses. In combination with an implicit time integration scheme, it is easy to achieve more stable numerical calculations. On the other hand, it has been considered difficult to solve large-scale problems at high speed because of the inefficient memory access when dealing with unstructured elements, and the necessity of solving a large linear equation at every time step when using an implicit time integration scheme. On the other hand, recent development in the field of high-performance computing has led to the development of E-wave FEM (e.g., Ichimura et al. 2014), an implicit FEM simulation program that overcomes the above problems. Seismic ground motion analyses using supercomputers can be performed rapidly for large-scale problems of 10^{10} degrees of freedom or larger. Preparations are now underway to apply E-wave FEM to damage estimations conducted by the government (Agata et al., JpGU-AGU Joint Meeting, 2020). Although comparisons between FEM and FDM in seismic ground motion analyses have been performed already (e.g., Yoshimura et al. 2011, 2012, 2013), it is important to clarify how to use E-wave FEM and widely-used FDM programs such as GMS properly in damage estimations in national agencies, summarizing the differences in the basic features, calculation accuracy, calculation cost, and so on. In this study, long-period earthquake ground motions in 3D heterogeneous velocity structures are calculated using E-wave FEM and GMS, and the results and computational costs are compared and discussed.

We simulated the earthquake near Awaji Island (Mj 6.3) that occurred on April 13, 2013 by using E-wave FEM. Targeting seismic ground motions up to 0.35 Hz, we set up a 3D heterogeneous velocity structure without topography consisting of 33 layers with uniform seismic wave velocity in the region of 900 km, 748 km, and 50 km in the east-west, north-south, and vertical direction, respectively, based on J-SHIS database of NIED. The computational models for the velocity structure were constructed to satisfy the discretization conditions usually used in each program, i.e., at least five elements for E-wave FEM per wavelength for S-wave velocity, respectively. Seismic ground motions for 60 seconds were calculated with a time step size of 0.01 seconds. The resources required to obtain the numerical solution were about 22 minutes using 128 computation nodes of the Oakforest-PACS at The University of Tokyo for the E-wave

©2021. Japan Geoscience Union. All Right Reserved.

FEM. In the conference, we will compare the results and those obtained by using GMS and also show the results of the numerical solution by changing the mesh size, grid size and other settings. In addition, calculations for a larger target domain will be also discussed.

Keywords: High-performance computing, Seismic ground motion analysis, Finite element method, Finite difference method, Long-period ground motion

©2021. Japan Geoscience Union. All Right Reserved.

Three-dimensional thermal structure modeling in the Alaska subduction zone

*Kaya Iwamoto[1], Nobuaki Suenaga[2], Shoichi Yoshioka[2,1]

1. Department of Planetology, Graduate School of Science, Kobe University, 2. Research Center for Urban Safety and Security, Kobe University,

In the Alaska subduction zone, megathrust earthquakes such as the 1964 Alaska earthquake (Mw 9.2), and slow earthquakes such as slow slip events and tectonic tremors have occurred near the plate boundary.
In this region, the Pacific plate is subducting beneath the North American plate, and recent studies have revealed that the Yakutat terrane is subducting at the eastern edge of the Pacific plate. The Yakutat terrane has a significantly different tectonic setting from that of the Pacific plate, and is characterized by the occurrence of tectonic tremors, the absence of volcanoes, and the remarkable thicknesses of the marine sedimentary layer and the oceanic crust.

In this study, we constructed a three-dimensional thermomechanical model associated with the simultaneous subduction of the Yakutat terrane and the Pacific plate to identify the thermal conditions of the region where such interplate seismic events take place in the Alaska subduction zone.
In this numerical simulation, the subduction history of the plate was considered, referring to the plate rotation model, and the subduction velocities were given independently for the Yakutat terrane and the Pacific plate. We also assigned the thicknesses of the marine sedimentary layer and the oceanic crust separately for both regions. In addition, we introduced a low-viscosity layer at the plate boundary below the mantle wedge, which allows for lower temperatures in the forearc region.
Under these conditions, we solved the time-dependent problem of the temperature and mantle flow velocity fields from millions of years ago to the present, using the finite-difference method.
The present temperature field obtained from the numerical simulation was compared with the Curie-point depth distribution and heat flow observations, and we attempted to construct a model in which the residuals between the observed and calculated values can be minimized.

In the future, based on the thermal structure obtained from the numerical simulations, we plan to investigate the relationship between interplate seismic events and dehydration, using phase diagrams of hydrous minerals in the marine sedimentary layer and the oceanic crust.

Keywords: temperature, three-dimensional modeling, numerical simulation, Alaska, subduction zone

©2021. Japan Geoscience Union. All Right Reserved.

Sensitivity analysis with large-scale 3D finite element crust structure model for seafloor geodetic constraints on coseismic slip and interseismic slip-deficit distributions

*Sota Murakami[1], Tsuyoshi Ichimura[1], Kohei Fujita[1], Takane Hori[2], Yusaku Ohta[3]

1. Earthquake Research Institute, The University of Tokyo, 2. R&D Center for Earthquake and Tsunami, Japan Agency for Marine-Earth Science and Technology, 3. Research Center for Prediction of Earthquakes and Volcanic Eruptions, Graduate School of Science, Tohoku University

Estimating the coseismic slip distribution and interseismic slip-deficit distribution play an important role in understanding the mechanism of massive earthquakes and predicting the resulting damage. It is useful to observe the crustal deformation not only in the land area, but also directly above the seismogenic zone. Therefore, improvements in terms of measurement precision and increase in the number of observation points have been proposed in various forms of seafloor observation. However, there is a room for developing a quantitative evaluation method of the estimation accuracy in cases where new crustal deformation observation points are available or when the precision of the observation methods have been improved. In this study, we proposed a method for quantitatively evaluating the improvement in the estimation accuracy of the coseismic slip distribution and the interseismic slip-deficit distribution in cases where new crustal deformation observation points are available or where the precision of the observation methods have been improved. We will present application examples based on large-scale finite element analysis using high-fidelity 3D crust structure and show the usefulness of the proposed method.

Keywords: seafloor observation, inversion of fault slip, sensitivity analysis, crustal deformation, finite element analysis

©2021. Japan Geoscience Union. All Right Reserved.

[J] Oral | S (Solid Earth Sciences) | S-TT Technology & Techniques

[S-TT38] Creating future of solid Earth science with high performance computing (HPC)

convener:Takane Hori(R&D Center for Earthquake and Tsunami, Japan Agency for Marine-Earth Science and Technology), Yuji Yagi(Graduate School of Life and Environmental Sciences, University of Tsukuba, Tsukuba), Katsuhiko Shiomi(National Research Institute for Earth Science and Disaster Resilience), Ryoichiro Agata(Japan Agency for Marine-Earth Science and Technology), Chairperson:Takane Hori(R&D Center for Earthquake and Tsunami, Japan Agency for Marine-Earth Science and Technology), Ryoichiro Agata(Japan Agency for Marine-Earth Science and Technology)

Sat. Jun 5, 2021 9:00 AM - 10:30 AM Ch.21 (Zoom Room 21)

Due to the development in computer science and computational science, large-scale or many times forward simulations and/or inversion analyses have become available recently. In solid Earth science, large-scale seismic wave propagation and crustal deformation with high fidelity models based on high resolution observation data have been demonstrated; uncertainty in crustal deformation caused by material properties and structures can be investigated based on many-time calculations for different material properties and structures; fault slip inversion analyses for non-Gaussian error distribution, etc. Thus, we will invite researchers who are applying HPC technology in forward simulations and inversion analyses and discuss how to improve more the collaboration between computer &computational sciences and solid Earth science. We are welcome submission by the researchers who are interested in this scope, especially students and young researchers.

10:15 AM - 10:30 AM

[STT38-06]Discussion

©Japan Geoscience Union

[J] Poster | S (Solid Earth Sciences)：S-TT Technology & Techniques

Sat. Jun 5, 2021 5:15 PM - 6:30 PM JST | Sat. Jun 5, 2021 8:15 AM - 9:30 AM UTC | Ch.13_3

[S-TT38] Creating future of solid Earth science with high performance computing (HPC)

convener:Takane Hori(R&D Center for Earthquake and Tsunami, Japan Agency for Marine-Earth Science and Technology), Yuji Yagi(Graduate School of Life and Environmental Sciences, University of Tsukuba, Tsukuba), Katsuhiko Shiomi(National Research Institute for Earth Science and Disaster Resilience), Ryoichiro Agata(Japan Agency for Marine-Earth Science and Technology)

Due to the development in computer science and computational science, large-scale or many times forward simulations and/or inversion analyses have become available recently. In solid Earth science, large-scale seismic wave propagation and crustal deformation with high fidelity models based on high resolution observation data have been demonstrated; uncertainty in crustal deformation caused by material properties and structures can be investigated based on many-time calculations for different material properties and structures; fault slip inversion analyses for non-Gaussian error distribution, etc. Thus, we will invite researchers who are applying HPC technology in forward simulations and inversion analyses and discuss how to improve more the collaboration between computer & computational sciences and solid Earth science. We are welcome submission by the researchers who are interested in this scope, especially students and young researchers.

[STT38-P01] CMT catalog based on a local 3D structure model for simulations of long-period ground motions in the Kanto region, Japan

*Kazuo Yoshimoto[1], Kosuke Minamihama[1], Shunsuke Takemura[2], Katsuhiko Shiomi[3] (1.Yokohama City University, 2.Earthquake Research Institute, The University of Tokyo, 3.NIED)

[STT38-P02] Coordinate Independent Visualization Method for Stress Tensor Field by Using Principal Axis Line

*Sayako Hirobe[1], Kenji Oguni[1], Muneo Hori[1] (1.Japan Agency for Marine-Earth Science and Technology)

CMT catalog based on a local 3D structure model for simulations of long-period ground motions in the Kanto region, Japan

*Kazuo Yoshimoto[1], Kosuke Minamihama[1], Shunsuke Takemura[2], Katsuhiko Shiomi[3]

1. Yokohama City University, 2. Earthquake Research Institute, The University of Tokyo, 3. NIED

Long-period ground motions associated with shallow local and/or regional earthquakes have been observed in the Kanto region due to the excitation and amplification of the Kanto sedimentary basin structure. To improve the evaluation of the characteristics of long-period ground motions, it is necessary to have an accurate information on focal mechanisms of earthquakes. However, moment tensor inversion using a 1D velocity structure model had been commonly used to construct a focal mechanism catalog in Japan. In this study, we conducted centroid moment tensor inversion using a 3D velocity structure model (the Japan Integrated Velocity Structure Model version 1 (JIVSM) [Koketsu et al. 2012]) to estimate the focal mechanism solutions of earthquakes in and around the Kanto region more accurately. Then, we compared our focal mechanism solutions with the MT solutions of F-net.

For the 3D CMT inversion, we analyzed 82 earthquakes of magnitude 5.5 or greater occurred between January 2004 and June 2020 (Lat.: 34°N~38°N, Lon.: 138°E~142°E, Depth: 40 km or shallower). The broadband seismic waveforms recorded by F-net were used for our 3D CMT inversion, and the displacement waveforms in the period band of 25~100 seconds were used for waveform fitting. The Green's functions of the seismic motion for the 3D velocity structure model were evaluated by the reciprocal calculations via the OpenSWPC [Maeda et al., 2017]. In this calculation, source grids were uniformly distributed at a horizontal interval of 0.1° and vertical interval of 2 km from depth 6 km to 60 km. The Küpper wavelet with a duration of 1 s was employed as a source time function. The reproducibility of the observed waveforms was evaluated by the variance reduction (VRs), and the moment tensor, centroid location, and time of occurrence of the earthquake were estimated by searching for the solution with the maximum VRs. Other details are described in Takemura et al. (2021).

We compared our 3D CMT solution with the F-net MT solution, and found that the two solutions are highly consistent over the land area. The Kagan angle, which was calculated as an index value for comparison, is generally less than 30° for all earthquakes. However, the difference between the 3D CMT solution and the F-net MT solution is larger for earthquakes that occurred in the offshore region such as off the coast of Ibaraki Prefecture and near the triple junction off the Boso Peninsula. This result suggests that the use of an appropriate seismic velocity structure model is important in the estimation of focal mechanisms for offshore earthquakes, which occur in a more complex structure than the land area. Other than that, as pointed out by Takemura et al. (2021), our study confirmed that the seismic moments estimated using JIVSM are systematically slightly smaller than those estimated by using F-net 1D velocity structure model. The details of our results and ground motion simulations will be presented in the conference presentation.

Acknowledgements
We used F-net waveform data and the F-net MT catalog. The FDM simulations of seismic wave propagation were conducted using the computer system of the Earthquake and Volcano Information Center at the Earthquake Research Institute, the University of Tokyo, and Fujitsu PRIMERGY CX600M1/CX1640M1 (Oakforest-PAC) at the Information Technology Center, the University of Tokyo.

©2021. Japan Geoscience Union. All Right Reserved.

Keywords: CMT inversion, Focal mechanism solution, Kanto region, Long-period ground motion

©2021. Japan Geoscience Union. All Right Reserved.

Coordinate Independent Visualization Method for Stress Tensor Field by Using Principal Axis Line

*Sayako Hirobe[1], Kenji Oguni[1], Muneo Hori[1]

1. Japan Agency for Marine-Earth Science and Technology

The physical quantities in the physics problems are written in tensor. The scalar field written in the zeroth-order tensor and the vector field written in the first-order tensor are easily visualized and are implemented on various visualization tools.
On the other hand, in the three-dimensional space, the fields of physical quantities written in the symmetric second-order tensor (e.g., strain or stress in continuum) have the six independent components. For instance, in the conventional visualization method of the stress field, we need the set of six contour maps color-coded by the three normal stresses and the three shear stresses, or the set of the three contour maps color-coded by the three principal stresses (i.e., major, medium, and minor principal stress) and the three line segment maps showing the directions of three principal axes. Therefore, it is almost impossible to intuitively understand the whole second-order tensor field by comparing these several images.
To solve this problem, some topological-based visualization method have been proposed. In these method, a ellipsoid is defined at every point in the analysis domain. The axes of this ellipsoid are parallel to the three principal axes and the length of the axes are scaled by the absolute value of the principal value. Then, these ellipsoids or the tube obtained by connecting glyphs in the longitudinal axis direction are displayed in the analysis domain. However, these method is only effective as long as the all principal values are positive (e.g., diffusion tensor used in a tractography of MRI images). In the case of the stress or strain tensor, since the principal value becomes the negative under compression, these visualization methods cannot show the second-order tensor field correctly.
In this research, we propose the new visualization method and the algorithm to help the correct and intuitive understanding of the second-order symmetric tensor field in three-dimensional space. Here, for the sake of simplicity, we use the stress tensor for the explanation of the outline of the proposed method. In the proposed method, the visualization domain are divided into small domains arranged so as not to overlap with each other. If the constant stress tensor field is given in each small domain, the line segment tangent to the principal axis can be defined in each small domain. When this line segment passes through the boundary of the small domain, we select the line segment direction from the three principal axes direction in the next domain. Here, we select the direction so that the two line segments are connected with each other most smoothly. Then, we draw the next line segment tangent to the selected principal axis. It should be noted here that the selection of the line segment direction is not carried out to connect between the major (medium, minor) principal axes. The line segment is colored according to the principal value associated with the line segment direction. Performing the series of these drawing operations from several start points (called ‘seed’) placed in arbitrary position to three orthogonal principal axis direction, we can draw multiple lines (called ‘principal axis line’) in the visualization domain. These principal axis lines enable to show the six independent components of the second-order symmetric tensor in one figure.
According to these principal axis lines, we can understand the flow and magnitude of the second-order symmetric tensor field. Also, while the contour maps showing the components of the second-order symmetric tensor are completely changed by the rotation of the coordinate system, the principal axis lines given by the proposed method are independent from the rotation of the coordinate system.
In the conference, we will show some examples and will discuss about the application to the dynamic

©2021. Japan Geoscience Union. All Right Reserved.

wave field.

Keywords: Visualization, Tensor Field, Stress

©2021. Japan Geoscience Union. All Right Reserved.

[E] Oral | S (Solid Earth Sciences)：S-CG Complex & General

Sat. Jun 5, 2021 10:45 AM - 12:15 PM JST | Sat. Jun 5, 2021 1:45 AM - 3:15 AM UTC | Ch.21 Zoom Room 21

[S-CG39] Science of slow earthquakes: Toward unified understandings of whole earthquake process

convener:Satoshi Ide(Department of Earth an Planetary Science, University of Tokyo), Hitoshi Hirose(Research Center for Urban Safety and Security, Kobe University), Kohtaro Ujiie(Faculty of Life and Environmental Sciences, University of Tsukuba), Takahiro Hatano(Department of Earth and Space Science, Osaka University), Chairperson:Kohtaro Ujiie(Faculty of Life and Environmental Sciences, University of Tsukuba)

Accumulating observational studies on various types of slow deformation events, such as tectonic tremors, very low frequency events, and slow slip events, portrays some universal characteristics in generally complex behavior, including interaction among events and influence by various outer loading. Some of these phenomena seem to have causal relation with the occurrence of very large earthquakes. A unified understanding of these slow and fast earthquake processes requires an approach integrating geophysics, seismology, geodesy, geology, and non-equilibrium statistical physics. We welcome presentations based on, but not limited to, geophysical observation, data analysis, analytical theory, numerical simulation, field study, and laboratory experiments.

10:45 AM - 11:00 AM JST | 1:45 AM - 2:00 AM UTC

[SCG39-01] The stabilizing effect of pore-fluid pressure along subduction megathrust faults: Evidence from experiments on Nankai Trough sediments

*John D Bedford[1,2], Daniel R Faulkner[2], Michael J Allen[2], Takehiro Hirose[1] (1.JAMSTEC, 2.Univ. of Liverpool)

11:00 AM - 11:15 AM JST | 2:00 AM - 2:15 AM UTC

[SCG39-02] **Depth-dependent deep-slow earthquakes controlled by temperature dependence of brittle-ductile transitional rheology**

*Ryosuke Ando[1], Kohtaro Ujiie[2], Naoki Nishiyama[2], Yasushi Mori[3] (1.Graduate School of Science, University of Tokyo, 2.Graduate School of Life and Environmental Sciences, University of Tsukuba, 3.Kitakyushu Museum of Natural History and Human History)

11:15 AM - 11:30 AM JST | 2:15 AM - 2:30 AM UTC

[SCG39-03] **Localized megathrust slip controlled by chemical reactions in subduction mélanges**

*Kohtaro Ujiie[1], Kazuya Noro[2], Norio Shigematsu[3], Ake Fagereng[4], Naoki Nishiyama[1], Christopher Tulley[4], Haruna Masuyama[2], Yasushi Mori[5] (1.Faculty of Life and Environmental Sciences, University of Tsukuba, 2.Graduate School of Life and Environmental Sciences, University of Tsukuba, 3.Geological Survey of Japan, National Institute of Advanced Industrial Science and Technology, 4.School of Earth and Environmental Sciences, Cardiff University, 5.Kitakyushu Museum of Natural History and Human Histor)

11:30 AM - 11:45 AM JST | 2:30 AM - 2:45 AM UTC

[SCG39-04] Lithological heterogeneity and fluid flow related to seamount subduction: an exhumed example from Amami-Oshima Island

*Madison Frank[1], Ginta Motohashi[1], Kohtaro Ujiie[2] (1.Graduate School of Life and Environmental Sciences, University of Tsukuba, 2.Faculty of Life and Environmental Sciences, University of Tsukuba)

11:45 AM - 12:00 PM JST | 2:45 AM - 3:00 AM UTC

[SCG39-05] Constraints on silica transport along subduction boundaries based on volume change estimates of metamorphic rocks

*Shogo Soejima[1], Simon Richard Wallis[1] (1.Department of Earth and Planetary Science, Graduate School of Science, The University of Tokyo)

12:00 PM - 12:15 PM JST | 3:00 AM - 3:15 AM UTC

[SCG39-06] Discussion

The stabilizing effect of pore-fluid pressure along subduction megathrust faults: Evidence from experiments on Nankai Trough sediments

*John D Bedford[1,2], Daniel R Faulkner[2], Michael J Allen[2], Takehiro Hirose[1]

1. JAMSTEC, 2. Univ. of Liverpool

Pore-fluid pressure is an important parameter in controlling fault mechanics as it lowers the effective normal stress allowing fault slip at lower shear stress. It is also thought to influence the nature of fault slip, particularly in subduction zones where the occurrence of slow-slip has been linked to areas of elevated pore-fluid pressure. Despite the importance of pore-fluid pressure on fault mechanics, its role on controlling fault stability, which is determined by the friction rate parameter (a-b), is poorly constrained, particularly for fault materials from subduction zones. In the winter of 2018-19 the accretionary complex overlying Nankai Trough subduction zone (SW Japan) was drilled as part of Integrated Ocean Drilling Program (IODP) Expedition 358. Here we test the frictional stability of the accretionary sediments recovered during the expedition by performing a series of velocity-stepping experiments on simulated fault gouges while systematically varying the pore-fluid pressure and effective normal stress conditions. The Nankai gouges are strongly rate-strengthening and exhibit negative values for the rate-and-state parameter b. We find that for experiments where the effective normal stress is held constant and the pore-fluid pressure is varied the Nankai gouges become more rate-strengthening, and thus more stable, at higher pore-fluid pressures. In contrast, when the pore-fluid pressure is held constant and the effective normal stress is varied, there is minimal effect on the frictional stability of the gouge. The increase in frictional stability of the gouge at elevated pore-fluid pressure is caused by an evolution in the rate-and-state parameter b, which becomes more negative at high pore-fluid pressure. These results have important implications for understanding the nature of slip in subduction zones and suggest the stabilizing effect of pore-fluid pressure could promote slow-slip or aseismic creep on areas of the subduction interface that might otherwise experience earthquake rupture.

Keywords: Slow slip, Pore-fluid pressure, Nankai Trough, Fault friction

©2021. Japan Geoscience Union. All Right Reserved.

Depth-dependent deep-slow earthquakes controlled by temperature dependence of brittle-ductile transitional rheology

*Ryosuke Ando[1], Kohtaro Ujiie[2], Naoki Nishiyama[2], Yasushi Mori[3]

1. Graduate School of Science, University of Tokyo, 2. Graduate School of Life and Environmental Sciences, University of Tsukuba, 3. Kitakyushu Museum of Natural History and Human History

Recent geophysical observations have classified the deep-slow earthquakes, down-dip the seismogenic zone, into Long-term Slow Slip Events (L-SSEs), Short-term Slow Slip Events (S-SSEs), and Low-frequency earthquakes (LFEs) and tremor in the order from slow to fast. The same ordering has also become recognized as converted from the shallow to the deep in the source depths, apparently contradicting the well-established transitional behavior from the shallower brittle/fast regime to the deeper ductile/slow regime, as described by the “seismogenic inversion layer”. Here we propose a new mechanical model that can consistently explain these two, only by considering the competitive temperature-dependent effects on the fraction of the brittle material, *Rb*, and the viscosity of the ductile material, η, in fault zones. Our model is geologically motivated and is an extension of the previous physical model with the brittle-ductile heterogeneity on faults. The key to understanding the enigmatic depth dependencies is that the reduction of η is more significant than the reduction of *Rb* as increasing temperature. Our results highlight the importance of rock plasticity, rather than friction, and rheological heterogeneity as universal mechanisms of deep-slow earthquakes independent of tectonic environments.

Keywords: Rheology, Fault rocks, Mathematical model, SSEs, LFEs, Heterogeneity

©2021. Japan Geoscience Union. All Right Reserved.

Localized megathrust slip controlled by chemical reactions in subduction mélanges

*Kohtaro Ujiie[1], Kazuya Noro[2], Norio Shigematsu[3], Ake Fagereng[4], Naoki Nishiyama[1], Christopher Tulley[4], Haruna Masuyama[2], Yasushi Mori[5]

1. Faculty of Life and Environmental Sciences, University of Tsukuba, 2. Graduate School of Life and Environmental Sciences, University of Tsukuba, 3. Geological Survey of Japan, National Institute of Advanced Industrial Science and Technology, 4. School of Earth and Environmental Sciences, Cardiff University, 5. Kitakyushu Museum of Natural History and Human Histor

Megathrust slip down-dip of the seismogenic zone is accommodated by either steady creep or episodic slow slip events (SSEs). However, the geological conditions defining the rheology of megathrust slip remain elusive. Field observation and laboratory analyses show that subduction mélanges deformed at ~370–500 ˚C in warm-slab environments record fluid release and viscous shear localization associated with chemical reactions between juxtaposed metapelitic and metabasaltic rocks. In the mélange deformed near the base of the seismogenic zone, very fine-grained reaction products facilitated grain boundary diffusion creep at lower shear stresses than surroundings, whereas in the mélange deformed near the mantle wedge corner, chemical reactions led to viscous shear at two orders of magnitude faster strain rate than surroundings. We suggest that chemical reactions facilitate localized changes in megathrust slip mode with depth, potentially providing a mechanism for change from viscous creep to SSEs.

©2021. Japan Geoscience Union. All Right Reserved.

Lithological heterogeneity and fluid flow related to seamount subduction: an exhumed example from Amami-Oshima Island

*Madison Frank[1], Ginta Motohashi[1], Kohtaro Ujiie[2]

1. Graduate School of Life and Environmental Sciences, University of Tsukuba, 2. Faculty of Life and Environmental Sciences, University of Tsukuba

Recent geophysical surveys and deep ocean drilling revealed that shallow slow earthquakes have been spatially and temporally correlated to lithological heterogeneity associated with the subduction of seamounts. Furthermore, it has been proposed that the rise in fluid pressure and fluid flow on the leading edge of the seamount during subduction results in tectonic tremor. However, geological perspective of shallow slow earthquakes related to seamount subduction remains elusive. Our preliminary geologic investigations conducted on an exhumed accretionary complex exposed in Amami-Oshima Island, Ryukyu Arc reveal a section containing mélange sequences related to subduction of a seamount. Outcrops include altered basalt, a sequence of variable limestone and low grade basaltic sediments, and a mudstone dominated sequence showing a block-in-matrix fabric. A complex quartz vein network is present in the mudstone dominated mélange where extensional fractures have formed in competent blocks. Viscous shear was accommodated along the mixed rocks composed of limestone and basaltic materials, which is consistent with lithological heterogeneity inferred for the shallow slow slip source region. The quartz-filled fracture network in the mudstone dominated mélange may represent tremorgenic fluid flow along brittle fractures that occurred near the subducting seamount. We suggest that the exhumed section at Amami-Oshima Island is representative of the source conditions under which shallow slow earthquakes occur during seamount subduction.

Keywords: seamount, subduction, slow earthquakes, mélange, lithological heterogeneity, Amami-Oshima Island

©2021. Japan Geoscience Union. All Right Reserved.

Constraints on silica transport along subduction boundaries based on volume change estimates of metamorphic rocks

*Shogo Soejima[1], Simon Richard Wallis[1]

1. Department of Earth and Planetary Science, Graduate School of Science, The University of Tokyo

Transport of significant quantities of SiO2 along subduction boundaries has been highlighted as important in processes such as silicification of the lower crust that may influence the time scales of slow earthquakes and the formation of a broad antigorite-rich domain along the base of the wedge mantle. The source of such silica is thought to be subducted quartz-rich sediments and water-rich fluids transported along the subduction boundary have the potential to transport silica over large distances. However, there are few studies that can help place bounds of the amount of silica that has been transported in subducted rocks. The removal of silica from one domain and its redeposition in another should be related to large changes in rock volume. The changes in volume that are important are those that take place at depth where the metamorphic temperature is the greatest and where the rocks are influenced by deep-sourced fluids. Previously proposed methods to estimate the volume change of rocks can be broadly classified into two categories: geometric methods based on strain estimates including absolute stretching, and chemical methods based on the bulk chemical compositions. However, application of the geometric methods to slate belts generally indicates large volume decreases not recognized by chemical methods. Possible reasons for this discrepancy are: uncertainties associated with assumptions about the original composition and the nature of immobile elements may and lack of good methods to assess the contribution of grain boundary sliding to bulk rock deformation. This study examines how orientations and deformation types of deformed mineral vein sets can be used to estimate volume change. This possibility of using this approach has been previously recognized but its practical application has been little studied. The deformed vein set analysis method is potentially more reliable than other geometric approaches because veins develop on scales much larger than individual grains and should record the otherwise hidden contribution to deformation by grain boundary sliding. In this study we developed a new approach that incorporates a statistical analysis to evaluate appropriate uncertainties. The newly developed approach was applied to analyze deformed metagreywacke in the Del Puerto canyon of the Franciscan belt. The analysis allows constraints to be placed on all three components of finite deformation: strain, mean vorticity number and volume change. The results are compatible with negligible volume change but also allow for significant volume increase. The results are not compatible with previously estimated significant amounts of volume reduction in the same region based on grain-scale analysis. The lack of prominent overgrowths around individual grains suggests that any volume increase is limited. Strain analysis using the Rf / ϕ method applied to individual grains showed maximum shortening was about 50%, implying that about 10% of strain was provided by grain boundary sliding. Furthermore, comparing the results of the Rf / ϕ method with those of the deformed vein sets method, it is suggested that the deformation during subduction is negligible compared to that developed during exhumation. The lack of volume change implies a lack of large-scale silica transport in the region either due to a limited fluid flux and/or silica saturation. This implies that there is not sufficient silica to form antigorite domains with kilometer-scale thicknesses or forming major silicification of the lower crust. Our data suggest that zones of antigorite-rich domains along the base of the mantle wedge will be more limited than generally thought and processes other than silica deposition may control time scales of slow earthquakes.

Keywords: Volume change, Deformed vein, Slow earthquakes, Silica transport

©2021. Japan Geoscience Union. All Right Reserved.

©2021. Japan Geoscience Union. All Right Reserved.

[E] Oral | S (Solid Earth Sciences) | S-CG Complex & General

[S-CG39] Science of slow earthquakes: Toward unified understandings of whole earthquake process

convener:Satoshi Ide(Department of Earth an Planetary Science, University of Tokyo), Hitoshi Hirose(Research Center for Urban Safety and Security, Kobe University), Kohtaro Ujiie(Faculty of Life and Environmental Sciences, University of Tsukuba), Takahiro Hatano(Department of Earth and Space Science, Osaka University), Chairperson:Kohtaro Ujiie(Faculty of Life and Environmental Sciences, University of Tsukuba)

Sat. Jun 5, 2021 10:45 AM - 12:15 PM Ch.21 (Zoom Room 21)

Accumulating observational studies on various types of slow deformation events, such as tectonic tremors, very low frequency events, and slow slip events, portrays some universal characteristics in generally complex behavior, including interaction among events and influence by various outer loading. Some of these phenomena seem to have causal relation with the occurrence of very large earthquakes. A unified understanding of these slow and fast earthquake processes requires an approach integrating geophysics, seismology, geodesy, geology, and non-equilibrium statistical physics. We welcome presentations based on, but not limited to, geophysical observation, data analysis, analytical theory, numerical simulation, field study, and laboratory experiments.

12:00 PM - 12:15 PM

[SCG39-06]Discussion

©Japan Geoscience Union

[E] Oral | S (Solid Earth Sciences)：S-CG Complex & General

Sat. Jun 5, 2021 1:45 PM - 3:15 PM JST | Sat. Jun 5, 2021 4:45 AM - 6:15 AM UTC | Ch.21 Zoom Room 21

[S-CG39] Science of slow earthquakes: Toward unified understandings of whole earthquake process

convener:Satoshi Ide(Department of Earth an Planetary Science, University of Tokyo), Hitoshi Hirose(Research Center for Urban Safety and Security, Kobe University), Kohtaro Ujiie(Faculty of Life and Environmental Sciences, University of Tsukuba), Takahiro Hatano(Department of Earth and Space Science, Osaka University), Chairperson:Takahiro Hatano(Department of Earth and Space Science, Osaka University)

Accumulating observational studies on various types of slow deformation events, such as tectonic tremors, very low frequency events, and slow slip events, portrays some universal characteristics in generally complex behavior, including interaction among events and influence by various outer loading. Some of these phenomena seem to have causal relation with the occurrence of very large earthquakes. A unified understanding of these slow and fast earthquake processes requires an approach integrating geophysics, seismology, geodesy, geology, and non-equilibrium statistical physics. We welcome presentations based on, but not limited to, geophysical observation, data analysis, analytical theory, numerical simulation, field study, and laboratory experiments.

1:45 PM - 2:00 PM JST | 4:45 AM - 5:00 AM UTC

[SCG39-07] Systematic understanding of the slip-front-propagation velocity in terms of Linear Marginal Stability Hypothesis

*Takehito Suzuki[1] (1.Department of Physics and Mathematics, Aoyama Gakuin University)

2:00 PM - 2:15 PM JST | 5:00 AM - 5:15 AM UTC

[SCG39-08] Effects of periodic stress perturbations on earthquake nucleation

*Takuya Saito[1], Takahiro Hatano[2] (1.Aoyama Gakuin University, 2.Osaka University)

2:15 PM - 2:30 PM JST | 5:15 AM - 5:30 AM UTC

[SCG39-09] Feasibility of periodic solution in Rate-State friction Law

*Ryo Mizushima[1], Takahiro Hatano[1] (1.Department of Earth and Space Science, Osaka University)

2:30 PM - 2:45 PM JST | 5:30 AM - 5:45 AM UTC

[SCG39-10] **Slow earthquake signatures in the ratio between acoustic and internal gravity wave amplitudes in coseismic ionospheric disturbances**

*Kosuke Heki[1], Yuki Takasaka [1] (1.Department of Earth and Planetary Sciences, Faculty of Science, Hokkaido University)

2:45 PM - 3:00 PM JST | 5:45 AM - 6:00 AM UTC

[SCG39-11] Observation of shallow slow slip event propagating updip to the trough in the Nankai Trough.

*Eiichiro Araki[1], Takeshi Iinuma[1], Yojiro Yamamoto[1], Toshinori Kimura[1], Yuya Machida[1], Ryoichiro Agata[1], Keisuke Ariyoshi[1], Tsuyoshi Ichimura[2], Takane Hori[1], Shuichi Kodaira[1] (1.Japan Agency for Marine-Earth Science and Technology, 2.Earthquake Research Insitute, the University of Tokyo)

3:00 PM - 3:15 PM JST | 6:00 AM - 6:15 AM UTC

[SCG39-12] Discussion

Systematic understanding of the slip-front-propagation velocity in terms of Linear Marginal Stability Hypothesis

*Takehito Suzuki[1]

1. Department of Physics and Mathematics, Aoyama Gakuin University

Slip-front-propagation on an interface between two media has attracted interests of many researchers in scientific and industrial fields. In particular, the slip-front-propagation velocity has been obtained using some friction laws such as the slip-velocity-dependent law. Notably, to obtain the propagation velocity, Linear Marginal Stability Hypothesis (LMSH) has been widely employed. First, LMSH assumes the plane wave solution for the slip profile near the slip front, i.e., u~exp(i (k x-omega t)), where u is the slip and k and omega are the complex wave number and frequency, respectively. The imaginary parts of k and omega are written as k_i and $omega_i$, respectively, and the slip-front-propagation velocity is given by $v=omega_i/k_i$. We consider the friction law depending on both the slip and slip velocity, leading to two model parameters in the governing equation. We therefore assume that the terms C_1 u and C_2 \dot{u}, where C_1 and C_2 are the constants, emerge in the governing equation for u. We have obtained the cubic equation for $omega_i$ using LMSH, and found that the numbers of the solutions for $omega_i$ can be categorized into 12 regions on the C_1-C_2 phase space. Here, we aim to categorize the slip-front-propagation velocity on the C_1-C_2 phase space, and give some implications associated with slow earthquakes.

We should emphasize that the slip front has two forms: the intruding and extruding fronts (see details in Suzuki and Matsukawa, 2019). Actually, we have obtained the analytical solutions for $omega_i$, and they are called $omega^{in}_1$, $omega^{in}_2$, and $omega^{in}_3$ for the intruding front, and $omega^{ex}_1$, $omega^{ex}_2$, and $omega^{ex}_3$ for the extruding front. Using these values and the relationship between k_i and $omega_i$, we have also obtained the analytical forms of k_i, which are called k^{in}_1, k^{in}_2, and k^{in}_3 for the intruding front, and k^{ex}_1, k^{ex}_2, and k^{ex}_3 for the extruding front. Therefore, we can write analytical forms for the intruding and extruding slip-front-propagation velocities, $v^{in}_j=omega^{in}_j/k^{in}_j$ and $v^{ex}_j=omega^{ex}_j/k^{ex}_j$ (j=1,2,3), respectively.

In terms of the solutions of v^{in}_j and v^{ex}_j, the C_1-C_2 phase space is divided into 7 regions. They are the regions with (A) v^{in}_1, (B) v^{ex}_1, (C) v^{in}_1 and v^{ex}_2, (D) v^{ex}_1 and v^{ex}_3, (E) v^{in}_1, v^{ex}_2, and v^{in}_3, (F) v^{in}_1, v^{ex}_2, and v^{ex}_3, and (G) no propagation velocity. In particular, we emphasize that there exists the region where v^{in}_j or v^{ex}_j does not exist. This region cannot generate the steady slip-front-propagation, and may imply the generation of slow earthquakes from seismological viewpoint.

Keywords: slip-front-propagation velocity, friction law, Linear Marginal Stability Hypothesis

©2021. Japan Geoscience Union. All Right Reserved.

Effects of periodic stress perturbations on earthquake nucleation

*Takuya Saito[1], Takahiro Hatano[2]

1. Aoyama Gakuin University, 2. Osaka University

One of the crucial methods to discover underlying physics is to investigate a mechanical response. This idea is inherent not only in laboratory scale, but applicable to a kilometer-scale fault [1]. Recent studies have been showing a high susceptibility of tremors in slow earthquake [2], which may be sorted into an issue of the mechanical response. This study numerically investigates effects on earthquake nucleation growths of periodic stress perturbations like ocean tides. By assuming the rate- and state-dependent friction law on a flat fault embedded in an elastic continuum, we compute the earthquake occurrence rate as a function of the stress or the phase of stress perturbation.

The remarkable points in the results are as follows:
(1) The phase distributions do not show a large phase shift.
(2) The earthquake occurrence is defined as the moment when the slip velocity exceeds a given threshold value. The occurrence rate is one-to-one mapped onto the shear or the normal stress at the moment of occurrence. This implies an instantaneous response.
(3) The dependences of occurrence rate on the shear or the normal stress appear to be exponential. This indicates existence of a characteristic stress.
(4) Variation of the normal stress additionally alters a frictional state on the interface according to the rock experiments performed by Linker and Dieterich [3], but this Linker-Dietrich effect on the stress response has not been well understood yet. As a result of numerical simulation, the Linker-Dieterich effect is found to suppress a difference in value of the phase distributions. Eventually, if the effect is very large, we observe even antiphase distribution (see fig. 1).

[1] T. J. Ader, N. Lapusta, J.-P. Avouac, and J.-P. Ampuero, Geophys. J. Int. 198, 385 (2014).
[2] S. Ide and Y. Tanaka, Geophys. Res. Lett. 41, 3842 (2014); S. Ide, S. Yabe, H.-J. Tai, and K. H. Chen, Geophys. Res. Lett., 42, 3248 (2015).
[3] M. F. Linker, J. H. Dieterich, J. Geophys. Res. 97 4923 (1992).

Keywords: slow earthquake, nonequilibrium statistical physics, nucleation, stress perturbation

©2021. Japan Geoscience Union. All Right Reserved.

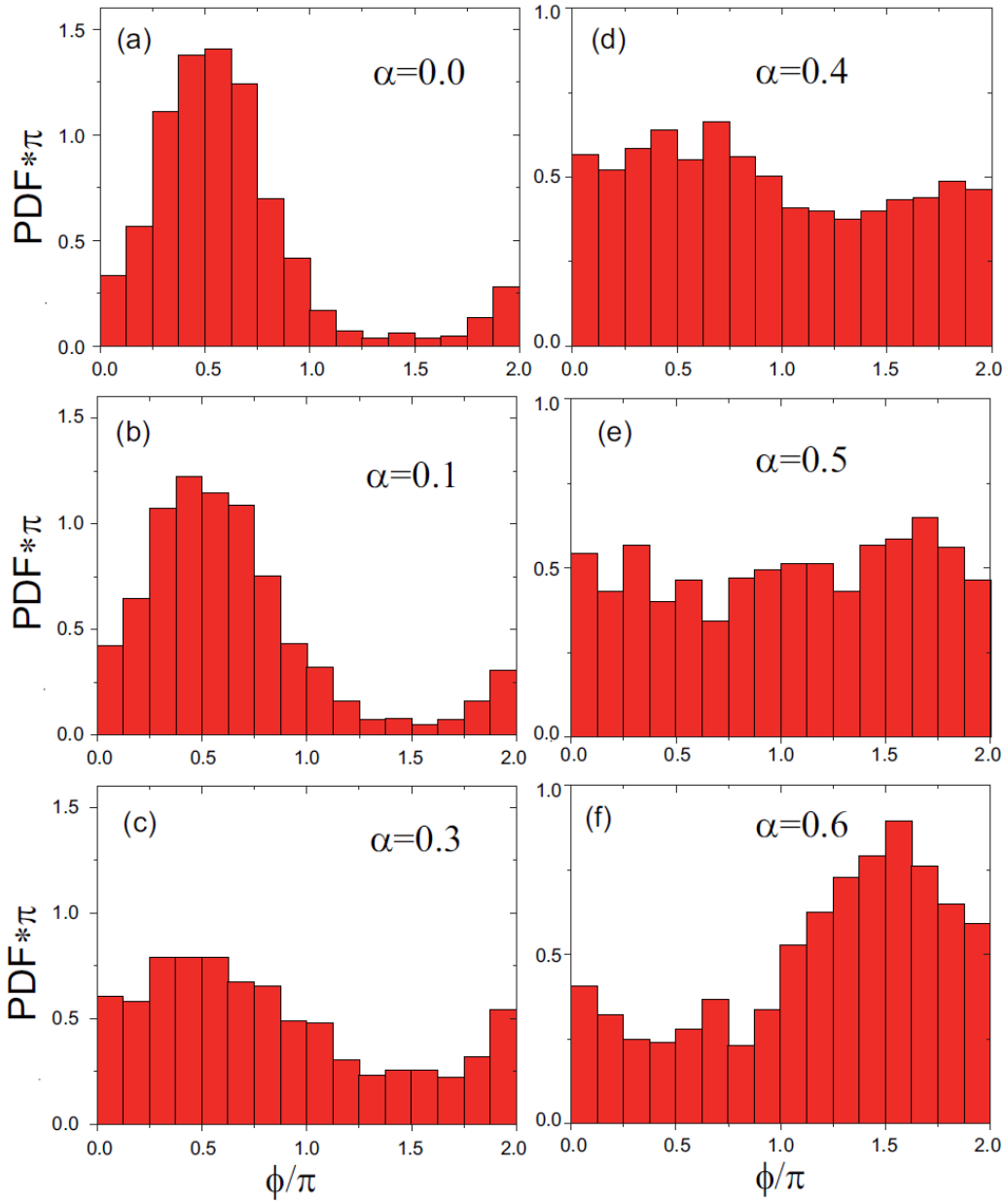


FIG. 1: Distributions of the normal-stress phase at the earthquake occurrence. As an increase of the Linker-Dieterich parameter α, a difference in value of the phase distribution becomes small, and eventually the phase distribution is inverted.

©2021. Japan Geoscience Union. All Right Reserved.

Feasibility of periodic solution in Rate-State friction Law

*Ryo Mizushima[1], Takahiro Hatano[1]

1. Department of Earth and Space Science, Osaka University

Slow earthquakes are phenomena with a wide range of time scales and a variety of characteristics. Among them, slow slip event (SSE) has a remarkable feature of periodic motion. For example, off the coast of Tohoku, the subduction rate fluctuates with a period of about three years. In addition to that, interestingly, relatively large earthquakes have occurred at the timing of accelerated slip (Uchida et al., 2016).

Since the mechanism of periodic occurrence of SSE is not clear, various models have been proposed. As a quasi-static model, the "fault patch model" has been used in many studies. In this model, a patchy sliding region is considered to exist on the fault plane. The sliding behavior is determined by considering the balance between elastic forces and friction (determined by the Rate-State friction law) on the patch region. However, there is a problem with this model. When the sliding behavior is examined numerically, the solution diverges. To prevent divergence, the effect of elastic wave radiation (radiation damping) is conventionally used (Rice 1993). However, since this model is quasi-static, elastic waves are not generated. Also, if elastic waves do occur, the model cannot be used as an SSE. Therefore, radiation damping is not a solution to the problem.

First, in this study, we reconsider what kind of behavior appears after the slip becomes unstable without radiation damping. For this calculation, we use a nonlinear analysis method called Dulac's criterion. Using this method, the nonlinearity of friction is rigorously taken into account to determine the feasibility of the periodic solutions. As a result, it is shown that there are no periodic solutions and the solution diverges when the aging law, slip law, and Nagata's law (Nagata et al., 2012) is used.

In this study, we further devise a new evolution law that avoids divergence. Considering the wear effect, we create a new evolution law. By applying this law to the model, we show that it is possible to realize periodic solutions without divergence. We also confirm that the velocity dependence of the friction coefficient in steady-state is similar in the granite experiment (Kilgore et al., 1993). Finally, the period of the sliding behavior derived from the new law is discussed. Then, we consider what values of the parameters are suitable for SSE.

Keywords: Rate-State friction law, Nonlinear analysis

©2021. Japan Geoscience Union. All Right Reserved.

Slow earthquake signatures in the ratio between acoustic and internal gravity wave amplitudes in coseismic ionospheric disturbances

*Kosuke Heki[1], Yuki Takasaka [1]

1. Department of Earth and Planetary Sciences, Faculty of Science, Hokkaido University

Frequency spectra of seismic waves from a fault rupture reflects the size of the faults, i.e. larger amplitudes of long period waves are excited by larger magnitude earthquakes. Anomalies in rise times of the fault movements would also influence the spectra. For example, earthquakes characterized by slow faulting, known as tsunami earthquakes, excite large tsunamis for the amplitudes of short-period seismic waves. In this study, we compare amplitudes of long- and short-period atmospheric waves excited by vertical crustal movements associated with earthquake faulting. Such atmospheric waves often reach the ionospheric F region and cause coseismic ionospheric disturbances (CID) observed as oscillations in ionospheric total electron content (TEC), with ground Global Navigation Satellite System (GNSS) receivers. CID often includes long-period internal gravity wave (IGW) components in addition to short period acoustic wave (AW) components. The latter has a period of ~4 minutes and propagate by 0.8-1.0 km/s, while the former has a period of ~12 minutes and propagate as fast as 0.2-0.3 km/s. Here we compare amplitudes of these two different waves for five earthquakes, 2011 Tohoku-oki (Mw9.0), 2010 Maule (Mw8.8), 1994 Hokkaido-Toho-Oki (Mw8.3), 2003 Tokachi-oki (Mw8.0), and the 2010 Mentawai (Mw7.9) earthquakes, using data from regional dense GNSS networks. We found two important features, i.e. (1) larger earthquakes show larger IGW/AW amplitude ratios, and (2) the Mentawai earthquake, a typical tsunami earthquake, exhibits abnormally large IGW amplitudes relative to AW amplitudes. These findings demonstrate that earthquakes with longer durations for faulting, take longer times for vertical crustal movements, and excite longer period atmospheric waves such as IGW more efficiently.

Keywords: slow earthquake, ionospheric disturbance, GNSS-TEC

©2021. Japan Geoscience Union. All Right Reserved.

Observation of shallow slow slip event propagating updip to the trough in the Nankai Trough.

*Eiichiro Araki[1], Takeshi Iinuma[1], Yojiro Yamamoto[1], Toshinori Kimura[1], Yuya Machida[1], Ryoichiro Agata[1], Keisuke Ariyoshi[1], Tsuyoshi Ichimura[2], Takane Hori[1], Shuichi Kodaira[1]

1. Japan Agency for Marine-Earth Science and Technology, 2. Earthquake Research Insitute, the University of Tokyo

We report observation of shallow slow slip in Kumano-nada, the Nankai Trough, south of Japan in December 2020 to January 2021 period from nearby seafloor and seafloor borehole observations. We investigated long-term pore-fluid pressure, and tilt data at three seafloor borehole stations (IODP C0002, C0010, C0006), a seafloor tilt station data (BMS1), as well as 13 DONET seafloor pressure station data, to identify slow crustal deformation. Seafloor broadband seismic data were also analyzed to identify low frequency earthquakes (LFT) and very low frequency earthquakes (VLFE) activity.

The observed episodic slow event is hereby reported in several stages (Stage A-D).

Stage A (Dec. 3-13): The slow event was first observed at Dec. 3, 2020 by the seafloor tilt station (BMS1) in DONET1-B Node with no accompanied LFT and VLFE activity, with firstly southward tilting and then turned to northward tilting, through stagnant period in Dec. 6-11 when active burst of LFT and VLFE activity started.

Stage B (Dec. 13-29): After two days in Dec. 13, slow change also started at borehole stations in the south-western side. Observed pore-fluid pressure change were trending continuously negative for C0002 (-8.7 kPa) and C0010 (-9.2kPa) and positive for C0006 (nearest to the trough in Node C, 15.4kPa). These changes were much larger than past episodes reported (Araki et al., 2017 and Ariyoshi et al., 2021). The seafloor and borehole tilt data also responded with large tilt change as large as 1.9 (BMS1) ~9 (C0010) and ~90 microradians (C0006) respectively. Seafloor pressure data between nearby stations in Nodes B, C and D also showed significant relative differences with slow transition, such as +1hPa (KMD06 and KMD07-KMD05), +2hPa (KMC11 and KMC12-KMC09). Pressure KMC12-KMC09 went through notable negative polarity change of ~ -1 hPa in +2 hPa change in overall, suggesting crustal deformation migrated beneath KMC09 site during the period. LFT and VLFE activity during the stage was active.

Stage C (Dec. 29-Jan. 10, 2021): While C0002 and C0010 pore-fluid pressure data continues to trend negatively, C0006 changed its trend from positive to negative after Dec. 29, suggesting the source of observed crustal deformation migrated from north to south beyond C0006 located within 10 km from the trough. Seafloor pressure between KMC11(at the trough axis)-KMC09 exhibited significant change of −1.3 hPa during the period, also suggests crustal deformation migration reached to the trough.

Stage D (Jan. 10-29): Intermittent slow changes in pore-fluid pressure were observed in C0010 and C0006 accompanying local LFT activity.

We performed slip fault modeling to account observed tilt and pore-fluid pressure change in the stages to understand what caused observed crustal deformation, using grid search of best fit Okada models for fault geometry and slip. Modeling was performed in time segments in these stages, first assuming the fault on the subducting plate boundary, and model with higher fault dipping angle to check validity of the assumption. In Dec. 16-21 period in the stage B, the best fit model was Mw 6.1 slip located in south of

©2021. Japan Geoscience Union. All Right Reserved.

DONET1-B node, where LFT activity was concentrated. Mechanisms of VLFE events during the period was also analyzed to give pronounced low angle reverse fault solutions. Therefore, we consider the observed event in the period was slow slip in the shallow subducting plate interface, probably initiated downdip in Kumano Basin, propagating updip on the subducting Philippine Sea plate interface toward the trough.

The borehole pore-fluid trend polarity change observed at C0006 (< 10km from the trough axis) in the stage C to D as well as seafloor pressure change at KMC11, strongly suggests crustal deformation took place very close to the trough axis where the plate subduction interface originated. From these direct observations in the seafloor above the plate interface, we argue that the slow slip event reached to the trough.

Keywords: Slow slip event, the Nankai Trough, seafloor observation, slow earthquakes, seafloor borehole observation

©2021. Japan Geoscience Union. All Right Reserved.

[E] Oral | S (Solid Earth Sciences) | S-CG Complex & General

[S-CG39] Science of slow earthquakes: Toward unified understandings of whole earthquake process

convener:Satoshi Ide(Department of Earth an Planetary Science, University of Tokyo), Hitoshi Hirose(Research Center for Urban Safety and Security, Kobe University), Kohtaro Ujiie(Faculty of Life and Environmental Sciences, University of Tsukuba), Takahiro Hatano(Department of Earth and Space Science, Osaka University), Chairperson:Takahiro Hatano(Department of Earth and Space Science, Osaka University)

Sat. Jun 5, 2021 1:45 PM - 3:15 PM Ch.21 (Zoom Room 21)

Accumulating observational studies on various types of slow deformation events, such as tectonic tremors, very low frequency events, and slow slip events, portrays some universal characteristics in generally complex behavior, including interaction among events and influence by various outer loading. Some of these phenomena seem to have causal relation with the occurrence of very large earthquakes. A unified understanding of these slow and fast earthquake processes requires an approach integrating geophysics, seismology, geodesy, geology, and non-equilibrium statistical physics. We welcome presentations based on, but not limited to, geophysical observation, data analysis, analytical theory, numerical simulation, field study, and laboratory experiments.

3:00 PM - 3:15 PM

[SCG39-12]Discussion

©Japan Geoscience Union

[E] Oral | S (Solid Earth Sciences)：S-CG Complex & General

Sat. Jun 5, 2021 3:30 PM - 5:00 PM JST | Sat. Jun 5, 2021 6:30 AM - 8:00 AM UTC | Ch.21 Zoom Room 21

[S-CG39] Science of slow earthquakes: Toward unified understandings of whole earthquake process

convener:Satoshi Ide(Department of Earth an Planetary Science, University of Tokyo), Hitoshi Hirose(Research Center for Urban Safety and Security, Kobe University), Kohtaro Ujiie(Faculty of Life and Environmental Sciences, University of Tsukuba), Takahiro Hatano(Department of Earth and Space Science, Osaka University), Chairperson:Hitoshi Hirose(Research Center for Urban Safety and Security, Kobe University)

Accumulating observational studies on various types of slow deformation events, such as tectonic tremors, very low frequency events, and slow slip events, portrays some universal characteristics in generally complex behavior, including interaction among events and influence by various outer loading. Some of these phenomena seem to have causal relation with the occurrence of very large earthquakes. A unified understanding of these slow and fast earthquake processes requires an approach integrating geophysics, seismology, geodesy, geology, and non-equilibrium statistical physics. We welcome presentations based on, but not limited to, geophysical observation, data analysis, analytical theory, numerical simulation, field study, and laboratory experiments.

3:30 PM - 3:45 PM JST | 6:30 AM - 6:45 AM UTC

[SCG39-13] Development of the detection method for short-term slow slip events using GNSS data and its application to the Nankai subduction zone

*Yutaro Okada[1], Takuya Nishimura[2], Takao Tabei[3], Takeshi Matsushima[4], Hitoshi Hirose[5] (1.Graduate School of Science, Kyoto University, 2.Disaster Prevention Research Institute, Kyoto University, 3.Faculty of Science and Technology, Kochi University, 4.Faculty of Science, Kyushu University, 5.Research Center for Urban Safety and Security, Kobe University)

3:45 PM - 4:00 PM JST | 6:45 AM - 7:00 AM UTC

[SCG39-14] Spatiotemporal slip distributions of the 2018-2019 Bungo Channel long-term slow slip event

*Yukinari Seshimo[1], Shoichi Yoshioka[2,1] (1.Department of Planetology, Graduate School of Science, Kobe University, 2.Research Center for Urban Safety and Security, Kobe University)

4:00 PM - 4:15 PM JST | 7:00 AM - 7:15 AM UTC

[SCG39-15] What controls along-strike variations in Long term SSE recurrence intervals in the Western Nankaui Subduction Zone?

*Takanari Ohata[1], SHINICHI MIYAZAKI[1], Kazuro Hirahara[2] (1.KYOTO UNIVERSITY, 2.KAGAWA UNIVERSITY)

4:15 PM - 4:30 PM JST | 7:15 AM - 7:30 AM UTC

[SCG39-16] Post-seismic to Co-seismic Moment Ratio: a Case Study of the 2016 Moderate Earthquakes along Chaman Fault Inferred from Sentinel-1 InSAR Time-Series

*Masato Furuya[1], Fumiko Matsumoto[2] (1.Department of Earth and Planetary Sciences Hokkaido University, 2.PASCO)

4:30 PM - 4:45 PM JST | 7:30 AM - 7:45 AM UTC

[SCG39-17] The moment release rate of short-term slow slip events in the northern Kii Peninsula from 2002 to 2015 based on NIED Hi-net tilt data

*Naoya Chujo[1], Hitoshi Hirose[2,1,3], Takeshi Kimura[3] (1.Department of Planetology, Graduate School of Science, Kobe University, 2.Research Center for Urban Safety and Security, Kobe University, 3.National Research Institute for Earth Science and Disaster Resilience)

4:45 PM - 5:00 PM JST | 7:45 AM - 8:00 AM UTC

[SCG39-18] Discussion

Development of the detection method for short-term slow slip events using GNSS data and its application to the Nankai subduction zone

*Yutaro Okada[1], Takuya Nishimura[2], Takao Tabei[3], Takeshi Matsushima[4], Hitoshi Hirose[5]

1. Graduate School of Science, Kyoto University, 2. Disaster Prevention Research Institute, Kyoto University, 3. Faculty of Science and Technology, Kochi University, 4. Faculty of Science, Kyushu University, 5. Research Center for Urban Safety and Security, Kobe University

Slow slip events (SSEs), which are kinds of slow earthquakes, are observed in a geodetic time domain and are categorized by their duration into long-term SSEs lasting several months to years and short-term SSEs (S-SSEs) lasting several days to weeks. S-SSEs east of the Bungo Channel have been systematically detected by using tiltmeters [Sekine et al., 2010] and GNSS [Nishimura et al., 2013] and their duration has been determined by tiltmeters based on corresponding low-frequency tremors [e.g., Sekine et al., 2010]. However, it is important to estimate the duration of S-SSEs by using only geodetic measurements because S-SSEs do not always accompany tremors. On the other hand, S-SSEs in the Kyushu region have been detected by only using GNSS data [Nishimura, 2014] and their duration has never been estimated objectively. Therefore, we developed a new S-SSE detection method which can estimate their source parameters including duration and applied it to 23-year-long GNSS data in the whole Nankai subduction zone from the Kyushu to the Tokai regions.

In this study, we use 734 GNSS stations in the period from February 1, 1997, to January 31, 2020. These coordinates were estimated using GIPSY/OASIS version 6.4 software with a strategy of precise point positioning-ambiguity resolution. As preprocessing of GNSS data, we remove post-seismic deformation, co-seismic displacements, long-terms trend including seasonal oscillation, and common-mode error. Firstly, we compute correlation coefficients between a synthetic template representing a time evolution of an S-SSE and 121-day-coordinates of GNSS data for each horizontal component at all stations. Secondly, we average the correlation coefficients weighted by the synthetic displacements predicted from the sub-faults. In this study, we assumed 429 sub-faults on the Philippine Sea plate interface [Iwasaki et al., 2015] and computed synthetic displacements with an elastic half-space dislocation model [Okada, 1992]. We then detected dates and locations of the candidate events by applying thresholds to the weighted average of correlation coefficients. Thirdly, we estimate a rectangular fault model of the events [Matsu’ura and Hasegawa, 1987] by using observed displacements of the candidate event. Fourthly, we stack 121-day-long GNSS coordinates weighted by the displacements predicted from the estimated fault model. Then, we estimate a duration of the candidate event by extracting a maximum correlation coefficient between stacked coordinates and a synthetic template. Finally, we detect S-SSEs by applying the criteria to the fault model and duration estimation result of the candidate events.

In our preliminary result, we detected 280 S-SSEs in the Nankai subduction zone during the analyzed period. Their typical moment magnitude is approximately 6.0, and their duration mainly distributes from 1 to 10 days. Some of S-SSEs detected in offshore Kyushu roughly correspond to repeating earthquakes [Uchida et al., 2020] and very low-frequency earthquakes [Baba et al., 2020]. This is the first geodetic evidence of the synchronization between S-SSEs and other phenomena in offshore Kyushu.

Estimation of slip amount and duration in the developed method enables us to clarify the spatial variation of slip rates of S-SSEs in the Nankai subduction zone. The average slip rate of S-SSEs, which is computed by dividing the cumulative slip by the cumulative duration, shows some regional characteristics (Figure 1). The average slip rate in western Shikoku is about twice larger than that of eastern Shikoku, and the average slip rate in Kyushu is the smallest among the Nankai subduction zone. These differences are statistically significant and possibly relate to the geometry of the subducting Philippine Sea plate.

©2021. Japan Geoscience Union. All Right Reserved.

Acknowledgments
We thank the Geospatial Information Authority of Japan, Japan Coast Guard, Japan Crustal Activity Science Consortium, and International GNSS Service for providing GNSS RINEX data. This research was supported by JSPS KAKENHI Grant Number JP16H06474 in Scientific Research on Innovative Areas “Science of Slow Earthquakes”, the MEXT of Japan under its "The Second Earthquake and Volcano Hazards Observation and Research Program", and ERI under its "Joint Usage/Research Program 2020-A-03".

Keywords: Slow slip event, Nankai subduction zone, GNSS

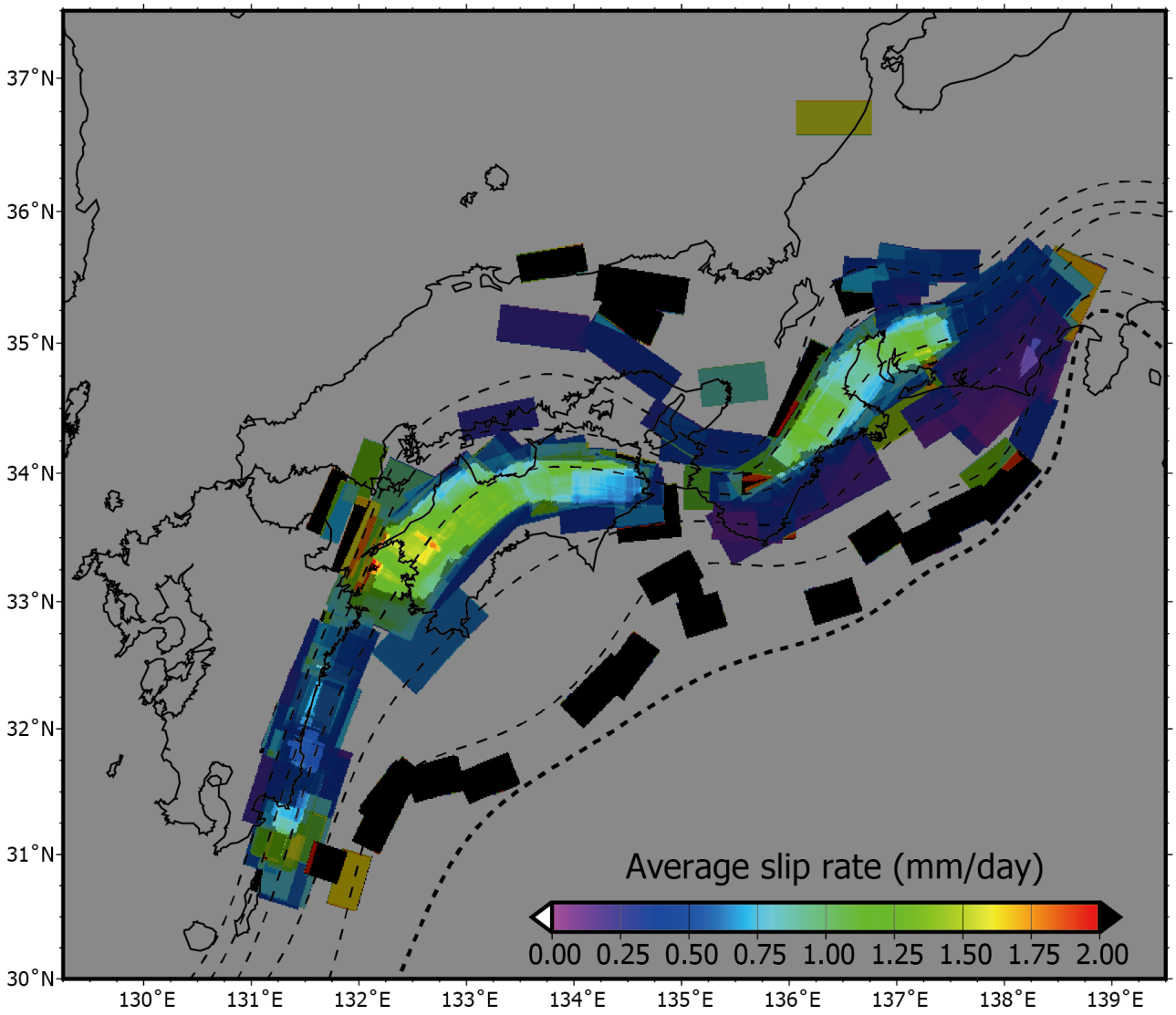


Figure 1. Average slip rates of S-SSE for 23 years. Note that the grid points that underwent less than 10 SSEs are shaded.

©2021. Japan Geoscience Union. All Right Reserved.

Spatiotemporal slip distributions of the 2018-2019 Bungo Channel long-term slow slip event

*Yukinari Seshimo[1], Shoichi Yoshioka[2,1]

1. Department of Planetology, Graduate School of Science, Kobe University, 2. Research Center for Urban Safety and Security, Kobe University

We estimated the spatiotemporal slip distributions of the long-term slow slip event (L-SSE) that occurred beneath the Bungo Channel from 2018 to 2019, by using the GNSS time series data operated by Geospatial Information Authority of Japan.
In this region, the Philippine Sea plate is subducting beneath the Amurian plate in the northwest direction at a rate of about 6.5 cm/yr. At the plate boundary beneath the Bungo Channel, aseismic interplate long-term slow slip events, which are hereafter referred to as L-SSEs, have occurred repeatedly with durations of several months to a couple of years. From previous studies, L-SSEs beneath the Bungo Channel have been identified to take place at intervals of about 6 years such as the events that occurred during the periods from 1997 to 1998, from 2002 to 2004, and from 2009 to 2011.
We used the daily coordinate values (F3 solutions) of GEONET and 114 GNSS observation stations in western Shikoku and eastern Kyushu for the period between January 1, 2016 and June 30, 2020. We set six stations as reference stations located in the northern Chugoku district, which were not affected by crustal deformations associated with the L-SSE. The GNSS time series data include coseismic steps, steps caused by antenna exchange, common-mode errors, and annual and semi-annual components. We removed these components to investigate crustal deformation associated with the L-SSE. We approximated tectonic deformation associated with plate motion as a liner function and removed its trend. The data period used for its calculation was taken from January 1, 2016 to December 31, 2017. After that, we employed an inversion method with three prior constraints: the spatial slip distribution was smooth to some extent, the slip directions were mostly oriented in the direction of plate convergence, and the temporal change in slip was smooth to some extent (Yoshioka et al., 2015). The data period used for the inversion analysis was taken from January 1, 2018 to December 31, 2019. We divided the time series into an equal time span of 0.1 yr.
As a result of the inversion analysis, the maximum slip of about 27 cm, the moment release of 3.7×10^{19} Nm, and equivalent moment magnitude of 7.0 were estimated. The slips can be divided into two slip stages. The first slip occurred on the southwest side of the Bungo Channel from 2018.3 to 2018.7. The maximum slip, moment release and equivalent moment magnitude were estimated to be about 10 cm, 8.9×10^{18} Nm, and 6.6, respectively. The maximum slip velocity was estimated to be about 36 cm/yr during the period from 2018.5 to 2018.6. The second slip took place beneath the Bungo Channel from 2018.8 to 2019.4. The maximum slip, moment release and equivalent moment magnitude were estimated to be about 19 cm, 2.0×10^{19} Nm, and 6.8, respectively. The maximum slip velocity was estimated to be about 53 cm/yr during the period from 2019.1 to 2019.2. After the second slip, slight slip occurred beneath the Bungo Channel from 2019. 5 to 2019.7.
Tectonic tremors appear to have been activated on the downdip side of the L-SSE occurrence region when large slow slips occurred beneath the Bungo Channel.
As described above, the first slip occurred on the southwest side of the Bungo Channel, and the second slip took place near the center of the Bungo Channel. Compared to the L-SSEs that occurred beneath the Bungo Channel in the past, this spatiotemporal slip pattern was similar to that of the L-SSE that occurred from 2002 to 2004. However, the difference is that the interval between the first slip and the second slip was shorter, and that the slip expanded in the northeast-southwest direction in the latter half of the

©2021. Japan Geoscience Union. All Right Reserved.

second slip. The moment release was almost the same, but the maximum slip and the maximum slip velocity were larger. This may be related to a slight increase in the interval from the last L-SSE occurrence.

Keywords: Bungo Channel, 2018-2019, long-term slow slip event, spatiotemporal slip distribution

©2021. Japan Geoscience Union. All Right Reserved.

What controls along-strike variations in Long term SSE recurrence intervals in the Western Nankaui Subduction Zone?

*Takanari Ohata[1], SHINICHI MIYAZAKI[1], Kazuro Hirahara[2]

1. KYOTO UNIVERSITY, 2. KAGAWA UNIVERSITY

There have been observed a variety of slow earthquakes. Recent simulation studies based on rate and state friction (RSF) laws have showed that these activities can be changed before occurrence of megaquakes (e.g., Matsuzawa et al., 2010). In this respect, it is important to understand frictional properties controlling slip evolution of these slow earthquakes in relation to megaquake forecasting. Here we focus on Long-term Slow Slip Events (L-SSEs) among these slow earthquakes. SSE simulations have so far been executed by trial-and-error assignments of RSF parameters. In these situations, Hirahara and Nishikiori (2019) executed numerical twin experiments of a simple Bungo channel L-SSE patch with Ensemble Kalman Filter (EnKF) to show a potential of determining frictional parameters from synthetic GNSS data. Further, Fujita (2020) showed a capability of short-term forecasting L-SSE activity using the slip rate data on the SSE fault inverted from actual GNSS data. However, it was also found that we need quite good pairs of initial parameters to obtain converged parameters even with EnKF.

Recent study revealed along-strike variations of recurrence interval (Tr) of L-SSE in the Western Nankai Subduction Zone; in the Southern Hyuga-nada, 2-3 years, the Bungo channel, 3 years, and the Northern Hyuga-nada and Western Shikoku, 5-6 years. Takagi et al. (2019) proposed that the up-dip locked region controls these variations. That is, at the down-dip of the locked region, Tr of L-SSE tends to be longer because of the low accumulation of the stress. To confirm this idea, we make a numerical model with the actual 3-D geometry of PHS slab to simulate such L-SSE behaviors. In our model, we set kinematically slip deficiency rate in the locked zone, and RSF parameters in the depth-dependent SSE zone and creep zone where slip evolution is quasi-dynamically simulated. We found that along-strike Tr variations cannot be fully explained only by the along-strike difference of slip deficiency rate. Thus, we need to consider another model.

In our RSF model without cut-off velocities, slip instability of a L-SSE zone with velocity weakening frictional property is basically controlled by the ratio of the width of the L-SSE zone and the critical nucleation size (W/h*) (e.g., Liu and Rice, 2007). Other parameters, however, possibly control SSE slip behaviors (e.g., Ampuero, 2019). Therefore, it is necessary to understand which parameters control the observed along-strike Tr variations and the physical meanings. First, we make a simple dipping plain model composing three zones of locked, SSE and creep in the down-dip direction, each of which has uniform parameters. Then, we execute experiments by changing parameters to examine produced Tr, maximum SSE velocity (Vmx) and duration (Td). These simulations showed that almost all parameters, such as frictional parameters, effective normal stress, width of the L-SSE zone, and slip deficiency of the locked region, make effects on Tr by roughly the same weight. Especially, we note that simulations with a constant W/h* produce considerable different slip behaviors. Second, we construct a plane model including several SSE zones with different parameters to reveal the along-strike interactions. We found that the heterogeneous distribution of parameters, such as width of the SSE zone and effective normal stress, can produce along-strike variations of Tr, Vmx and Td. It was also recognized that the boundary conditions assigned in the both sides of SSE zones affect slip behaviors such as along-strike slip propagations.

©2021. Japan Geoscience Union. All Right Reserved.

Keywords: SSE, Rate and State Friction Law, Recurrence interval, Nankai Subduction Zone

©2021. Japan Geoscience Union. All Right Reserved.

Post-seismic to Co-seismic Moment Ratio: a Case Study of the 2016 Moderate Earthquakes along Chaman Fault Inferred from Sentinel-1 InSAR Time-Series

*Masato Furuya[1], Fumiko Matsumoto[2]

1. Department of Earth and Planetary Sciences Hokkaido University, 2. PASCO

Postseismic-to-co-seismic moment ratios for large earthquakes greater than M7 are roughly around 0.3 or less, but those for moderate to even smaller earthquakes could be greater than 1 or more (Chen and Lapsta, 2009; Alwahedi and Hawthorne, 2018). However, there have been limited estimates on those ratios for moderate earthquakes. Of those limited estimates on postseismic-to-co-seismic moment ratio, the one reported by Furuya and Satyabala (2008) is exceptionally large, reaching nearly 6, in which a long-lasting afterslip due to an M5.0 earthquake in 2005 along Chaman Fault was detected. Chaman Fault is the western transform plate boundary between Indian and Eurasian plates and is well known for its low seismicity, which was interpreted as either a long-recurrent interval of large earthquakes or steady creep. Meanwhile, on May 13 and July 10, 2016, moderate earthquakes occurred along the Chaman fault, and are the largest earthquakes since the 2005 M5.0 event but located ~150 km further to the south. The USGS reports that the 1st event on May 13 consists of the triplet at almost the same hypocenter with Mw 5.2, 4.7, and 5.5 and that the 2nd event ~20 km to the north-east was mb 4.7 (body-wave magnitude). Our goals are to check if the Chaman Fault is anomalous in terms of its frictional properties and/or if the post-seismic to co-seismic moment ratio for moderate earthquakes will always get larger, compared to those for larger earthquakes. To estimate the post- to co-seismic moment ratios for these events, we examine the surface deformation associated with these moderate earthquakes, using 75 Sentinel-1A SAR images from October 2014 to August 2018 to generate 428 interferograms. We perform InSAR time-series analysis, using the LiCSBAS package by Morishita et al (2020). Below are our findings so far:

- The post-seismic to co-seismic moment ratio for the smaller mb 4.7 earthquake was ~10, whereas that for the larger Mw5-class events to the south was ~2.

- Slips on the fault for the mb4.7 earthquake reached the surface, whereas those for the Mw5 events did not.

-The apparent seasonality for the post-seismic moment release for the larger Mw5 earthquakes is probably caused because the areas are ~20 km distant from the reference area.

- No clear secular creep signals were detected before the earthquakes. Although we could notice possible triggered slip signals before the mb4.7 earthquake, their LOS changes are at most 5 mm and the estimated slip-patches for the mb4.7 earthquake were clearly distant from those for the possible triggered slip.

- Significant gap in the slip patches between the M5-class events and the mb4.7 event is located in the fault-bending zone that also coincides with the ruptured area by the 1892 M6.6 earthquake.

- Slip velocities and stress drops estimated for the mb4.7 event are smaller than those of the M5-class events.

©2021. Japan Geoscience Union. All Right Reserved.

Keywords: Chaman Fault, Afterslip, moderate earthquake, InSAR

©2021. Japan Geoscience Union. All Right Reserved.

The moment release rate of short-term slow slip events in the northern Kii Peninsula from 2002 to 2015 based on NIED Hi-net tilt data

*Naoya Chujo[1], Hitoshi Hirose[2,1,3], Takeshi Kimura[3]

1. Department of Planetology, Graduate School of Science, Kobe University, 2. Research Center for Urban Safety and Security, Kobe University, 3. National Research Institute for Earth Science and Disaster Resilience

In the southwest Japan subduction zone, short-term slow slip events (S-SSEs) with nonvolcanic tremor (Episodic Tremor and Slip: ETS, Rogers and Dragert, 2003) which last for several days to weeks occur repeatedly (e.g., Obara et al., 2004). Because the S-SSEs occur at the downdip extension of a megathrust earthquake rupture zone, the SSEs are one of the key factors for stress buildup processes of the megathrust earthquakes (e.g., Obara and Kato, 2016). Therefore, detailed slip distributions of S-SSEs are important for understanding the strain accumulation and release at the ETS zone. In the northern Kii Peninsula, S-SSEs have been detected (e.g., Hirose and Obara, 2006). In addition, previous studies examine the moment release rate by S-SSEs in this area (Sekine et al., 2010; Nishimura et al., 2013). For example, Nishimura et al. (2013) show the long-term moment release rate is roughly constant for nearly 16 years (1996-2012). Since we obtained more recent data, it is important to explore longer-term moment release history as S-SSEs.

Here we apply an inversion method (Hirose and Kimura, 2020) which can express a spatial slip distribution to tilt offset measurements in the northern Kii Peninsula and estimate detailed slip distributions of 52 S-SSEs from March 2002 to October 2015. We also calculate the long-term moment release rate of S-SSEs over a more recent period than the previous studies, and discuss regional differences of S-SSEs activity in the northern Kii Peninsula.

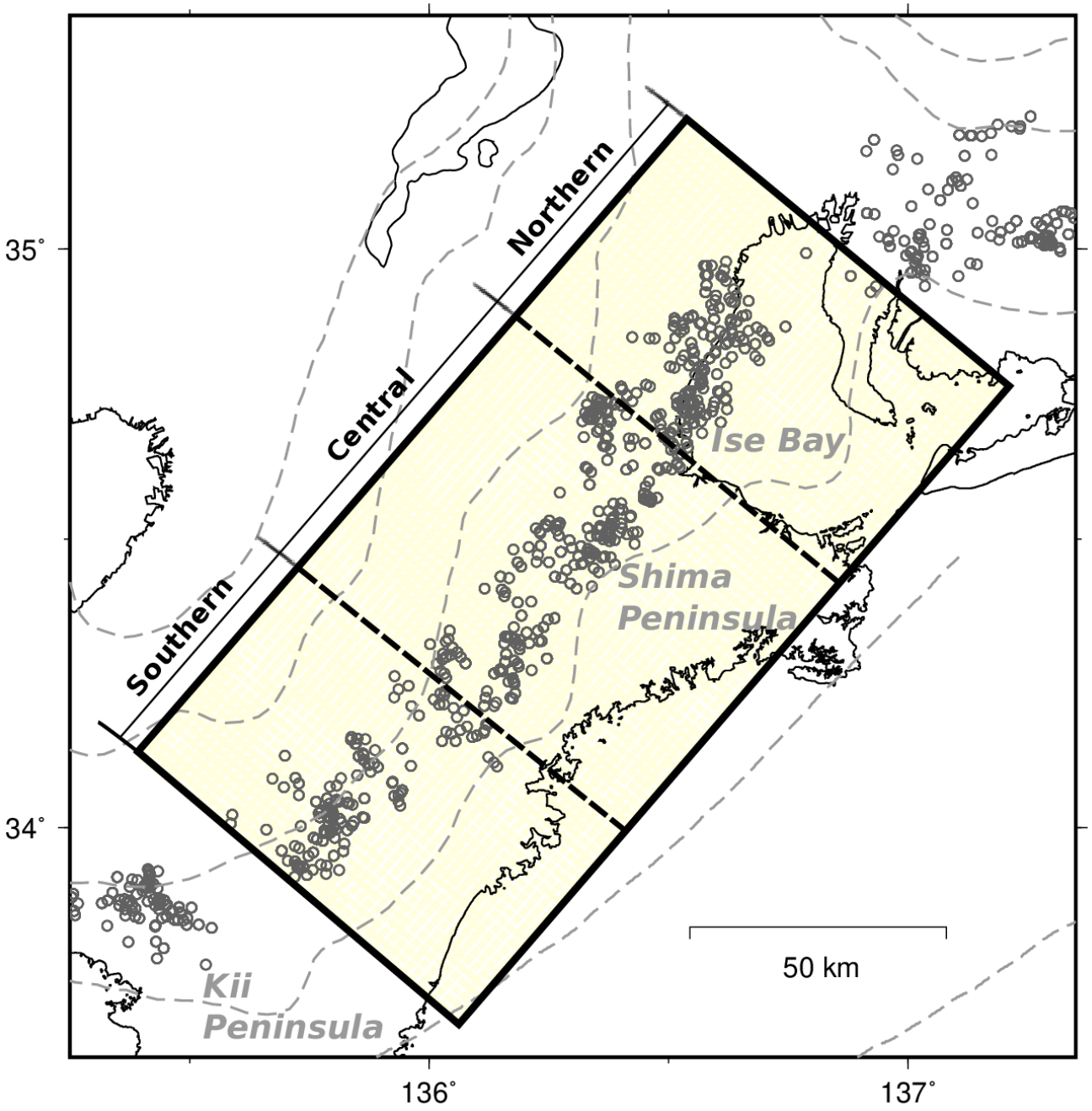
We used time-series records of a high-sensitivity accelerometer (tiltmeter) installed at NIED Hi-net stations located in the Kii Peninsula and Tokai areas. We applied the BAYTAP-G (Tamura et al., 1991) program together with atmospheric pressure records observed at the Tsu Local Meteorological Observatory to the tilt records in order to remove tidal components and an atmospheric pressure response. First, we checked the tremor activity in the northern Kii Peninsula based on the NIED tremor catalog (Maeda and Obara, 2009; Obara et al., 2010) to find out “active episodes”. Next, We try to identify a corresponding tilt transient to an active episode of tremor, then we define the event duration of the SSE from the tilt transient if it is identified. We measured a tilt offset due to an SSE from a detrended tilt record as a difference in tilt just before and after the SSE. We estimated a slip distribution that explains the tilt offset dataset for an SSE by a conventional inversion method by Hirose and Kimura (2020).

We successfully identified and estimated 52 S-SSEs in the study area in 13 years. The estimated moment magnitudes of the 52 SSEs range from 5.4 to 6.2. The cumulative seismic moment in the entire modeled region (the rectangle with the solid line in Fig.) indicates the moment release rate is mostly constant (~ 4E+18 Nm/year) through the study period. Then, we divide the modeled region into three segments (southern, central, northern; separated by dashed lines in Fig.) based on the slip distributions of S-SSEs. We find that the long-term moment release rate in the central and northern segments (corresponding to the Shima Peninsula and Ise Bay part of the ETS zone) is higher than that in the southern segment (corresponding to the southern Nara Prefecture in the ETS zone), indicating the regionality of S-SSEs activity in the northern Kii Peninsula. In addition, in the central and northern segments, the moment release rate decreases around 2011, suggesting a possible effect of the crustal deformations caused by the 2011 Tohoku earthquake.

Acknowledgments: This work was supported by JSPS KAKENHI Grant Number JP16H06474.

©2021. Japan Geoscience Union. All Right Reserved.

Meteorological data were provided by Japan Meteorological Agency.



©2021. Japan Geoscience Union. All Right Reserved.

[E] Oral | S (Solid Earth Sciences) | S-CG Complex & General

[S-CG39] Science of slow earthquakes: Toward unified understandings of whole earthquake process

convener:Satoshi Ide(Department of Earth an Planetary Science, University of Tokyo), Hitoshi Hirose(Research Center for Urban Safety and Security, Kobe University), Kohtaro Ujiie(Faculty of Life and Environmental Sciences, University of Tsukuba), Takahiro Hatano(Department of Earth and Space Science, Osaka University), Chairperson:Hitoshi Hirose(Research Center for Urban Safety and Security, Kobe University)

Sat. Jun 5, 2021 3:30 PM - 5:00 PM Ch.21 (Zoom Room 21)

Accumulating observational studies on various types of slow deformation events, such as tectonic tremors, very low frequency events, and slow slip events, portrays some universal characteristics in generally complex behavior, including interaction among events and influence by various outer loading. Some of these phenomena seem to have causal relation with the occurrence of very large earthquakes. A unified understanding of these slow and fast earthquake processes requires an approach integrating geophysics, seismology, geodesy, geology, and non-equilibrium statistical physics. We welcome presentations based on, but not limited to, geophysical observation, data analysis, analytical theory, numerical simulation, field study, and laboratory experiments.

4:45 PM - 5:00 PM

[SCG39-18]Discussion

©Japan Geoscience Union

[J] Oral | S (Solid Earth Sciences)：S-CG Complex & General

Sat. Jun 5, 2021 9:00 AM - 10:30 AM JST | Sat. Jun 5, 2021 12:00 AM - 1:30 AM UTC | Ch.19 Zoom Room 19

[S-CG45] Ocean Floor Geoscience

convener:Kyoko Okino(Atmosphere and Ocean Research Institute, The University of Tokyo), Chairperson:Yukari Kido(Japan Agency for Marine-Earth Science and Technology), Asuka Yamaguchi(Atomosphere and Ocean Research Institute, The University of Tokyo)

Most of Earth's volcanism and much of its tectonic activity occur on and beneath the s eafloor. Various phenomena on the seafloor are closely linked to plate tectonics, Earth s tructure and dynamics, and also related to Earth's environments through the hydrosphe re and atmosphere. Seafloor rocks and sediments record Earth's evolution and heat an d material fluxes on the Earth. Ocean Floor Geoscience session covers a broad range of research on seafloor such as mid-ocean ridge process, subduction dynamics, arc magm atism, hot spot and LIPs, crustal movement and structure etc. Every field of researches and every approaches are welcomed.The session aims to encourage discussion among scientists from different study fields and to integrate our understanding of ocean floor. The session is co-chaired by K. Tadokoro (Nagoya Univ.), O. Ishizuka (AIST), T. Toki (Univ . Ryukyus), and N. Takahashi (JAMSTEC).

9:00 AM - 9:15 AM JST | 12:00 AM - 12:15 AM UTC

[SCG45-01] JAMSTEC Contribution to the NIPPON FOUNDATION-GEBCO SEABED2030 Project

*Yukari Kido[1], Mitsuko Hidaka[1], Daisuke Matsuoka[1], Tatsu Kuwatani[1], Junji Kaneko[1], Takafumi Kasaya[1], Yoichi Ishikawa[1], Eiichi Kikawa[1] (1.Japan Agency for Marine-Earth Science and Technology)

9:15 AM - 9:30 AM JST | 12:15 AM - 12:30 AM UTC

[SCG45-02] The new tectonic model between the Madagascar Ridge and the Del Cano Rise in the southern Indian Ocean

*Taichi Sato[1], Yoshifumi Nogi[2], Hiroshi Sato[3], Masakazu Fujii[2] (1.National Institute of Advanced Industrial Science and Technology, 2.National Institute of Polar Research, 3.Senshu University)

9:30 AM - 9:45 AM JST | 12:30 AM - 12:45 AM UTC

[SCG45-03] Sedimentation process at the South Shetland Trench in the Antarctic Ocean

*Asuka Yamaguchi[1] (1.Atomosphere and Ocean Research Institute, The University of Tokyo)

9:45 AM - 10:00 AM JST | 12:45 AM - 1:00 AM UTC

[SCG45-04] Highly refractory dunite formation in Gibbs Island and Bruce Bank, and its role in the evolution of the circum-Antarctic continent

*Norikatsu Akizawa[1], Asuka Yamaguchi[1], Chihiro Ohshima[1], Kenichiro Tani[2], Akira Ishikawa[3], Ryo Fujita[3], SUNG HI CHOI[4] (1.Atmosphere and Ocean Research Institute, The University of Tokyo, 2.National Museum of Nature and Science, 3.Tokyo Institute of Technology, 4.Chungnam National University)

10:00 AM - 10:15 AM JST | 1:00 AM - 1:15 AM UTC

[SCG45-05] Magmatic evolutions erupted on the Cretaceous seamount province, western Pacific Plate

*Naoto Hirano[1], Hirochika Sumino[2], Taisei Morishita[3] (1.Center for Northeast Asian Studies, Tohoku University, 2.Graduate School of Arts and Sciences, The University of Tokyo, 3.Hydrographic and Oceanographic Department, Japan Coast Guard)

10:15 AM - 10:30 AM JST | 1:15 AM - 1:30 AM UTC

[SCG45-06] Pre-stack depth imaging and pore-fluid pressure estimation along the Nankai Trough subduction zone off the Kii Peninsula, SW Japan

*YU FAN[1], Ehsan Jamali Hondori[1], Jin-Oh Park[1] (1.The University of Tokyo)

JAMSTEC Contribution to the NIPPON FOUNDATION-GEBCO SEABED2030 Project

*Yukari Kido[1], Mitsuko Hidaka[1], Daisuke Matsuoka[1], Tatsu Kuwatani[1], Junji Kaneko[1], Takafumi Kasaya[1], Yoichi Ishikawa[1], Eiichi Kikawa[1]

1. Japan Agency for Marine-Earth Science and Technology

In October 2019, a new research program called “Mathematical Seafloor Geomorphology” was launched in the Japan Agency for Marine-Earth Science and Technology (JAMSTEC) to establish collaborations between various research fields. One of the major objectives of this program is to contribute to the “Nippon Foundation - General Bathymetric Chart of the Oceans (GEBCO) Seabed 2030 Project.” Efforts are also ongoing to establish a new method for creating high-resolution seafloor bathymetry using machine learning technology.
This is a joint enterprise, being led by an oceanography committee formed by the International Hydrographic Organization (IHO), GEBCO, and the United Nations Educational, Scientific and Cultural Organization Intergovernmental Oceanographic Commission (UNESCO-IOC). GEBCO standardizes the creation of bathymetry maps to fill bathymetric gaps in the world’s oceans. Funded by the Nippon Foundation, the Nippon Foundation - GEBCO Seabed2030 Project started in 2017. In January 2021, UNESCO also started the “UN Decade of Ocean Science for Sustainable Development (2021-2030, hereafter the UN Decade),” and has since collaborated with and supported the “Seabed2030” project. The Hydrographic and Oceanographic Department of the Japan Coast Guard is a formal desk for a coordination engine of Japanese seabed bathymetry data. JAMSTEC is sharing information with the Japan Oceanographic Data Center (JODC), is collecting bathymetry data using six research vessels, and is cooperating with GEBCO’s grid making process. A database site, called “DARWIN,” is being used to display the collected data and provide the bathymetry data obtained so far. Due to the different projection mappings being used by DARWIN and the National Oceanic and Atmospheric Administration (NOAA)/IHO Data Center for Digital Bathymetry (DCDB), this program was corrected and revised in July. The displays of the NOAA/IHO DCDB and DARWIN are jointly integrated and provide bathymetry data globally. A method for generating super-high-resolution topographic data and analyzing gaps where no investigations have yet been conducted has also successfully been developed using mechanical learning. Herein, we would like to outline the current state of bathymetry data collection, introduce a timeline for 2030, and highlight the crowd-sourced development achieved by outreach activities discussions that were held during the GEBCO week Map the Gaps symposium that was performed in January, 2021. We would like to hold your attention to collaborate for data collection, and to ensure complete seafloor mapping.

Keywords: GEBCO project, Seabed2030 project, seafloor bathymetry

©2021. Japan Geoscience Union. All Right Reserved.

The new tectonic model between the Madagascar Ridge and the Del Cano Rise in the southern Indian Ocean

*Taichi Sato[1], Yoshifumi Nogi[2], Hiroshi Sato[3], Masakazu Fujii[2]

1. National Institute of Advanced Industrial Science and Technology, 2. National Institute of Polar Research, 3. Senshu University

The Indian Ocean is among the best locations worldwide to understand the supercontinent fragmentation process because the seafloor spreading history following the breakup of Gondwana has mostly remained. Focusing on the south Indian Ocean, the seafloor is dominated by the Southwest Indian Ridge (SWIR), and several aseismic ridges and hotspots are emplaced. Several aseismic ridges have been recognized as oceanic large igneous provinces. Many studies have already presented seafloor-spreading models of the Indian Ocean; however, previously reported magnetic survey lines are sparse and not adequately aligned to detect the seafloor spreading direction. Therefore, the detailed spreading history, including these aseismic ridges, is still an open question.

Based on our newly obtained magnetic data (total and vector magnetic field data) as well as using an open dataset of magnetic data, we re-interpreted seafloor ages in the SWIR segments between the Discovery II and Gallieni fracture zones. The Madagascar Ridge, Del Cano Rise, Crozet plateau, and Conrad rise are emplaced on both off-axis areas. The identified oldest isochron was Chron 31o (71.4 Ma). Before Chron 21y (45.7 Ma), the spreading rate was ultraslow (18–19 km/Ma). Following Chron 21y, the spreading rate was changed to slow (~25 km/Ma). The spreading direction was changed from N10°W to N05°E around Chron 21. The segmentation pattern at Chron 30 (66.5 ~ 68.4 Ma) differs from the present SWIR. The reorganization had occurred around Chron 24 (52.6 ~ 57.1 Ma) and then changed into the present pattern around Chron 21. Revised seafloor ages suggest that the southern Madagascar Ridge and the Del Cano Rise had once formed a single bathymetric high at least before Chron 30. These two rises have thick crusts and have been recognized as formed by excess volcanism on or near the spreading axis of SWIR, or Marion hotspot-SWIR interaction; however, isochrons and linear magnetic anomalies implying the seafloor spreading process do not observe on the two rises. Therefore, we propose that excess volcanism related to seafloor spreading is not the only factor for their gravity anomaly and thick crust, the other factor, such as continental fragments, most likely contributes to the formation of the rises.

©2021. Japan Geoscience Union. All Right Reserved.

Sedimentation process at the South Shetland Trench in the Antarctic Ocean

*Asuka Yamaguchi[1]

1. Atomosphere and Ocean Research Institute, The University of Tokyo

Sediments incoming subduction zones affect mechanics of plate boundary fault and mass balance in subduction zones. The nature and distribution of sediments incoming trenches such as Nankai Trough, Japan Trench, Cascade, Costa Rica, Barbados, Hikurangi, Sumatra, etc. were elucidated by ocean drilling. On the other hand, the nature of sediments in trenches around the Arctic and Antarctic region are not well-understood, though the existence of abundant Iceberg-Rafted Debris (IBRD) and biogenic opal derived from diatom is speculated. In this study we report preliminary result of characteristics of surface sediments sampled from the South Shetland Trench in the Antarctic Ocean to reveal sedimentation process in a trench in the polar regions.
The South Shetland Trench in the northwest of Antarctic Peninsula is the boundary between the former Phoenix Plate and Antarctic Plate. Although active back-arc spreading is on-going at the Bransfield Strait located in between the South Shetland Islands and the Antarctic Peninsula, forearc seismicity is inactive. 9 piston cores were sampled from the Antarctic and Atlantic Ocean during R/V Hakuho-maru KH-19-6 cruise (Dec. 2019-Jan. 2020), and 4 cores (PC02, PC03, PC04, PC5) were sampled from around the South Shetland Trench. Sample localities include bottom of the trench (PC02 and PC04), landward trench slope (PC03) and seaward trench slope (PC05). All the cores were shipped to Kochi Core Center and X-CT analysis was conducted prior to splitting. Visual core description, MSCL and ITRAX analyses were performed by using split core.
PC02 and PC04 are characterized by turbidite layers which contain fine sands at the bottom. At least 28 and 10 turbidite layers were found in PC02 and PC04, respectively. Sand layers are enriched in Ca and Sr. Mud layers sandwiched in between sand layers show gradual color change, from brown at the lower part to olive gray at the upper part, which would correspond to turbidite mud and hemipelagic mud, respectively. ^{14}C ages of total organic carbon (TOC) in hemipelagic mud of PC02 range from 19076-18826 to 9684-9531 cal BP, suggesting ~0.4 m/1 ky of hemipelagic sedimentation rate and ~300 years of turbidite recurrence interval. PC03 includes poorly sorted subangular gravel, and is interpreted as diamicton or channel deposit. PC05 contains inclined and disrupted sand and silt layers in bluish gray mud matrix, which are characteristic in slump deposit. IBRD are rare in all the cores.
Preliminary analyses of four cores suggest sediments were transported to the South Shetland Trench by gravity flow from both landward and seaward sides. On the other hand, IBRD are not common in the bottom of the trench, reflecting that icebergs mainly drift towards eastern side of the Antarctic Peninsula.

Keywords: the Antarctic Ocean, the South Shetland Trench, Hakuho-maru

©2021. Japan Geoscience Union. All Right Reserved.

Highly refractory dunite formation in Gibbs Island and Bruce Bank, and its role in the evolution of the circum-Antarctic continent

*Norikatsu Akizawa[1], Asuka Yamaguchi[1], Chihiro Ohshima[1], Kenichiro Tani[2], Akira Ishikawa[3], Ryo Fujita[3], SUNG HI CHOI[4]

1. Atmosphere and Ocean Research Institute, The University of Tokyo, 2. National Museum of Nature and Science, 3. Tokyo Institute of Technology, 4. Chungnam National University

The continental margin is of profound importance as it records continental growth by steady-state accretion of orogenic magmas and following rifting. Intense mantle melting due to hydrous fluid input is expected to simultaneously stimulate the continental growth and lower intrinsic density of the mantle than more fertile mantle, which in turn isolate the continental lithosphere from the convective mantle. Gibbs Island (South Shetland Islands) and Bruce Bank located between South America and the Antarctic Peninsula, are tectonic windows into the Earth’ s interior in the circum-Antarctic region. To investigate the continental growth of Antarctica, we present geochemical data of 8 dunites from Gibbs Island and 1 dunite from Bruce Bank, including Re-Os isotope and highly siderophile element compositions.

The dunites are severely suffered from serpentinization of antigorite + brucite or lizardite (loss on ignition = LOI ranging from 3 to 34 wt%), but contain primary euhedral to subhedral chromian spinels with or without spherical olivine inclusions. The chromian spinels rarely form lens-shaped aggregates. A dunite from Gibbs Island contains fresh olivine grains filling a fracture of chromian spinel with low LOI (3 wt%), indicating a deserpentinization origin from serpentinized dunite. The dunites show highly depleted bulk major-element composition: Mg/Si = 1.4–1.6 and Al/Si = 0.004–0.01 for the dunites from Gibbs Island, and Mg/Si = 0.66 and Al/Si = 0.008 for the dunite from Bruce Bank. The positive correlation in Re/Ir and LOI space corroborates Re input during latest serpentinization process. The $^{187}Os/^{188}Os$ of the dunites vary significantly (0.1188–0.1445).

Phanerozoic Re-depletion (melt-depletion) ages of ca. <470 Ma are recorded in the dunites, except for a dunite from Gibbs Island with Proterozoic Re-depletion age of ca. 1.2 Ga. Since there exists serpentinization-related perturbation of Re, they provide minimum time estimates for melt depletion events. The early Paleozoic magmatism is inferred to have occurred during Ross orogeny in response to plate convergence along the margin of the eastern Gondwana, whereas the Mesoproterozoic Re-depletion age is consistent with the Re-depletion ages of mantle xenoliths and Nd model ages of granites and orthogneisses in Marie Byrd Land, West Antarctica. The petrographic characteristics of the chromian spinels with highly depleted nature of the dunites corroborate peridotite-melt reaction and subsequent melt mixing in a subduction setting. Thus, a simple interpretation of the Re-depletion ages of the dunites is that “residual” lithospheric mantle of Antarctica that experienced multiple fluid-assisted melting was incorporated into the continental outskirts during continental break-up. Widespread existence of the dunites in Gibbs Island and Bruce Bank may be attributed to pervasive removal of the continental lithospheric mantle at continental margin and possible incorporation into the oceanic convection system. This process reconciles with the existence of refractory mantle domains in the oceanic mantle lithosphere.

Keywords: highly siderophile element, subduction zone, peridotite

©2021. Japan Geoscience Union. All Right Reserved.

Magmatic evolutions erupted on the Cretaceous seamount province, western Pacific Plate

*Naoto Hirano[1], Hirochika Sumino[2], Taisei Morishita[3]

1. Center for Northeast Asian Studies, Tohoku University, 2. Graduate School of Arts and Sciences, The University of Tokyo, 3. Hydrographic and Oceanographic Department, Japan Coast Guard

Numerous seamounts on the western part of Pacific Plate, occur within a region called the western Pacific seamount province (WPSP) that occurred during the Early to Late Cretaceous, where a group of short-lived hotspot seamount chains has formed over the present southern Pacific superplume (Koppers et al., 2003). The majority of Early Cretaceous guyots on the northern part of WPSP were instantaneously submerged as a result of a contemporaneous eustatic sea level rise during the middle Cretaceous time (e.g., Larson, 1991).

Some of the seamount chains cannot be explained using a classical hotspot hypothesis, such as that outlined for the Hawaii–Emperor seamount chain. The seamount chains do not exhibit linear age progression due to, for example, overlapping a younger hotspot (Koppers et al., 1998), coeval volcanism along pre-existing lithospheric fractures (Davis et al., 2002), or the presence of recycled material within the upper mantle immediately after a continental breakup event (Taneja et al., 2016). Moreover, it should be theoretically impossible to identify the age of seamount formation using a single radiometric age because the evolutions of seamount take a long duration of time, exemplified by present Hawaiian shield volcano (a few m.y.; Macdonald and Katsura, 1964), the Aitutaki Island along the Cook–Austral hotspot (7-8 m.y.; Jackson et al., 2020), and the Early Cretaceous Quesada seamount at Mariana Trench oceanward slope (over 10 m.y.; Hirano et al., 2002).

Newly provided Ar-Ar ages for basaltic rocks from seamount, knoll, plateau, ridge, spur, and the Minamitorishima (Marcus) Island outline the evolution of hotspot and petit-spot volcanisms in the northern part of WPSP (Hirano et al., 2019; 2021). This study first reports the Eocene ages for basaltic rocks within the WPSP, an area that has only previously yielded Cretaceous ages. The Eocene basalts from the Chuo Seamount (Ogasawara Plateau) and Minamitorishima Island are thought to reflect volcanic events that overprinted the Cretaceous volcanic edifices in this region. Although some examples of rejuvenated seamounts were previously identified during Ocean Drilling Program Leg 144, no research has yet identified rejuvenating post-Cretaceous volcanic events on pre-existing Cretaceous seamounts within the WPSP. The Minamitorishima Island, moreover, records two stages of Eocene submarine volcanic eruption that generated older pillow lavas (~40 Ma) and younger hyaloclastites of highly vesicular lava (~37 Ma), implying shield-building and rejuvenated volcanoes, respectively. The Eocene volcanic overprints of Minamitorishima mean the island represents a unique part of the northern WPSP as the majority of the Early to middle Cretaceous seamounts within this province became submerged as a result of latest Early to Late Cretaceous sea-level rise. Finally, a petit-spot volcano (younger than 3 Ma) in this region erupted at the greater distance from the trench axis which could be equally explained by a wider outer rise than that at other subduction systems.

References:
Davis et al. (2002) G-cubed, 3. DOI: 10.1029/2001GC000190
Hirano et al. (2002) Marine Geology, 189, 371-379.
Hirano et al. (2019) Deep-Sea Research Part I, 154, 103142.

©2021. Japan Geoscience Union. All Right Reserved.

Hirano et al. (2021) Island Arc, in press. DOI: 10.1111/iar.12386
Jackson et al. (2020) Journal of Petrology, 61, egaa037.
Koppers et al. (1998) Journal of Geophysical Research, 94, 10501-10523.
Koppers et al. (2003) G-cubed, 4. DOI: 10.1029/2003GC000533
Larson (1991) Geology, 19, 963-966.
Macdonald & Katsura (1964) Journal of Petrology, 5, 82-133.
Taneja et al. (2016) Lithos, 262, 561-575.

Keywords: seamount, Pacific, alkali-basalt, petit-spot, hotspot

©2021. Japan Geoscience Union. All Right Reserved.

Pre-stack depth imaging and pore-fluid pressure estimation along the Nankai Trough subduction zone off the Kii Peninsula, SW Japan

*YU FAN[1], Ehsan Jamali Hondori[1], Jin-Oh Park[1]

1. The University of Tokyo

Introduction

At the Nankai Trough margin, the Philippine Sea Plate is being subducted beneath the Eurasian Plate to the northwest at a convergence rate of ~4 cm/yr [Seno et al., 1993]. Historic, great megathrust earthquakes with a recurrence interval of 100-200 years [Ando, 1975] have generated strong motion and large tsunamis along the Nankai Trough subduction zone. The plate-boundary fault (i.e., decollement) is a source fault of the devastating Nankai megathrust earthquakes. While there were lots of seismic reflection studies across the Nankai Trough axis to reveal the mechanism of the Nankai megathrust earthquakes, only a few studies on pore-fluid pressure estimation were conducted. In order to figure out detailed crustal structure of the Nankai Trough subduction zone off the Kii Peninsula, southwest Japan, we carry out 2D pre-stack depth migration (PSDM) imaging by using multi-channel seismic (MCS) reflection data that were acquired by JAMSTEC. Moreover, we estimate pore-fluid pressure of the shallow underthrust sediments using the PSDM velocities and ODP/IODP drilling data.

MCS data acquisition and processing

The 2D MCS reflection data were acquired along line KI01 by R/V Kairei of the JAMSTEC in 2011. For deep-penetration seismic imaging, a large volume (~130 liters) tuned air gun array and air pressure (2000 psi) was used as the controlled sound source with 50 m shot interval and about 10 m towing depth standard. The MCS data were recorded by a 444-channel streamer with 12.5 m group spacing (~6 km maximum offset) and about 12 m towing depth standard. We tried to do pre-conditioning including air-gun bubble suppression, ghost suppression, FX deconvolution, demultiple filtering by surface-related multiple attenuation (SRMA) and parabolic radon transform (PRT). Then, we performed CDP sorting and generated seismic time sections by stacking and post-stack time migration.

Results and future work

We performed layer stripping for interval velocity model building in the depth domain by using Kirchhoff pre-stack depth migration (KPSDM), and semblance analysis for velocity QC. Currently we are improving the velocity model to obtain a model with an uncertainty of less than 5%. We will then estimate pore-fluid pressure of the shallow underthrust sediments using the PSDM velocities and drilling data.

Acknowledgments: The authors would like to thank JAMSTEC for providing the seismic reflection data. We also thank Paradigm/Emerson (http://www.pdgm.com) for providing seismic data processing software.

Keywords: Nankai Trough, Pore-fluid pressure, Multi-channel seismic

©2021. Japan Geoscience Union. All Right Reserved.

[J] Oral | S (Solid Earth Sciences)：S-CG Complex & General

Sat. Jun 5, 2021 10:45 AM - 12:15 PM JST | Sat. Jun 5, 2021 1:45 AM - 3:15 AM UTC | Ch.19 Zoom Room 19

[S-CG45] Ocean Floor Geoscience

convener:Kyoko Okino(Atmosphere and Ocean Research Institute, The University of Tokyo), Chairperson:Ryuta Arai(Japan Agency for Marine-Earth Science and Technology), Masakazu Fujii(National Institute of Polar Research and SOKENDAI)

Most of Earth's volcanism and much of its tectonic activity occur on and beneath the s eafloor. Various phenomena on the seafloor are closely linked to plate tectonics, Earth s tructure and dynamics, and also related to Earth's environments through the hydrosphe re and atmosphere. Seafloor rocks and sediments record Earth's evolution and heat an d material fluxes on the Earth. Ocean Floor Geoscience session covers a broad range of research on seafloor such as mid-ocean ridge process, subduction dynamics, arc magm atism, hot spot and LIPs, crustal movement and structure etc. Every field of researches and every approaches are welcomed.The session aims to encourage discussion among scientists from different study fields and to integrate our understanding of ocean floor. The session is co-chaired by K. Tadokoro (Nagoya Univ.), O. Ishizuka (AIST), T. Toki (Univ . Ryukyus), and N. Takahashi (JAMSTEC).

10:45 AM - 11:00 AM JST | 1:45 AM - 2:00 AM UTC

[SCG45-07] Marine and earth science surveys in the Okinawa Trough for the IODP Scientific Drilling: Hakuhomaru KH-21-3 cruise preliminary reports

*Makoto Otsubo[1], Yoshimi Kubota[2], Ayanori Misawa[1], Ken Ikehara[1], Saki Ishino[1], Masataka Kinoshita[3], Kenji Matsuzaki[4], Katsura Kameo[4], Chiori Tamura[4], Ryuta Arai[5], Tomohiro Toki[6], Yuki Mitsudome[6], Zhirong Cai[7], Keiko Takehara[8], Kodai Kato[8], Daisuke Kuwano[9], Koshiro Matsuo[10], Keita Suzuki[11], Misaki Horiuchi[11], Yohei Katayama[12], Satoshi Okumura[13] (1.Geological Survey of Japan, AIST, 2.National Museum of Nature and Science, 3.The University of Tokyo, ERI, 4.The University of Tokyo, AORI, 5.JAMSTEC, 6.University of Ryukyus, 7.Kyoto University, 8.Kochi University, 9.Chiba University, 10.Kyushu University, 11.Nippon Marine Enterprises, Ltd., 12.Marine Works Japan, Ltd., 13.MOL Marine Co., Ltd.)

11:00 AM - 11:15 AM JST | 2:00 AM - 2:15 AM UTC

[SCG45-08] Structure and seismicity in the southern part of the Okinawa Trough and their implications for rifting and volcanic processes

*Ryuta Arai[1], Ayanori Misawa[2], Makoto Otsubo[2], Saki Ishino[2], Masataka Kinoshita[3], KH-21-3 Shipboard Scientists (1.Japan Agency for Marine-Earth Science and Technology, 2.Geological Survey of Japan, National Institute of Advanced Industrial Science and Technology, 3.Earthquake Research Institute, The University of Tokyo)

11:15 AM - 11:30 AM JST | 2:15 AM - 2:30 AM UTC

[SCG45-09] Heat flow anomaly in the southern part of Okinawa Trough – A preliminary result from the KH-21-3 cruise-

*Masataka Kinoshita[1], Ryuta Arai[2], Chiori Tamura[3], Ayanori Misawa[4], Saki Ishino[4], Makoto Otsubo[4], Shipboard Scientists KH-21-3 (1.Earthquake Research Institute, The University of Tokyo, 2.Japan Agency for Marine-Earth Science and Technology, 3.Atmospheric and Ocean Research Institute, the University of Tokyo, 4.National Institute of Advanced Industrial Science and Technology)

11:30 AM - 11:45 AM JST | 2:30 AM - 2:45 AM UTC

[SCG45-10] GNSS/Acoustic geodetic measurement at the southern end of Ryukyu Trench 2014-2020

*Akihiro Nagaya[1], Ryoya Ikuta[2], Mamoru Nakamura[3], Masataka Ando[4] (1.Undergraduate school of department of Geoscience, Shizuoka University, 2.Faculty of Science, Shizuoka University, 3.Faculty of Science, University of the Ryukyu, 4.Center for Natural Hazards of Integrated Education and Research, Shizuoka University)

11:45 AM - 12:00 PM JST | 2:45 AM - 3:00 AM UTC

[SCG45-11] Fluid-flow simulation for clarifying ore generation processes in the Izena Hole hydrothermal field, Okinawa Trough

*Shohei Albert Tomita[1], Katsuaki Koike[1], Tada-nori Goto[2], Katsuhiko Suzuki[3], Takafumi Kasaya[3] (1.Graduate School of Engineering, Kyoto University, 2.Graduate School of Life Science, University of Hyogo, 3.Research and Development Center for Submarine Resources, Japan Agency for Marine-Earth Science and Technology (JAMSTEC))

12:00 PM - 12:15 PM JST | 3:00 AM - 3:15 AM UTC

[SCG45-12] Examining the origin and depositional process of turbidites in the southern part of Okinawa Trough based on cores from Expedition KH-21-3

*Cai Zhirong[1], Hajime Naruse[1], Ken Ikehara[2], KH-21-3 Shipboard Scientists - (1.Department of Geology and Mineralogy, Graduate School of Science, Kyoto University, 2.Institute of Geology and Geoinformation, National Institute of Advanced Industrial Science and Technology)

Marine and earth science surveys in the Okinawa Trough for the IODP Scientific Drilling: Hakuhomaru KH-21-3 cruise preliminary reports

*Makoto Otsubo[1], Yoshimi Kubota[2], Ayanori Misawa[1], Ken Ikehara[1], Saki Ishino[1], Masataka Kinoshita[3], Kenji Matsuzaki[4], Katsura Kameo[4], Chiori Tamura[4], Ryuta Arai[5], Tomohiro Toki[6], Yuki Mitsudome[6], Zhirong Cai[7], Keiko Takehara[8], Kodai Kato[8], Daisuke Kuwano[9], Koshiro Matsuo[10], Keita Suzuki[11], Misaki Horiuchi[11], Yohei Katayama[12], Satoshi Okumura[13]

1. Geological Survey of Japan, AIST, 2. National Museum of Nature and Science, 3. The University of Tokyo, ERI, 4. The University of Tokyo, AORI, 5. JAMSTEC, 6. University of Ryukyus, 7. Kyoto University, 8. Kochi University, 9. Chiba University, 10. Kyushu University, 11. Nippon Marine Enterprises, Ltd., 12. Marine Works Japan, Ltd., 13. MOL Marine Co., Ltd.

We conducted a research cruise (KH-21-3 cruise) on the Okinawa Trough by R/V Hakuhomaru. In this presentation, we report the outline and preliminary results on the cruise. Two legs (Leg 1 and Leg 2) were carried out on this cruise for the IODP Scientific Drilling.

[KH-21-3 cruise Leg 1] The Okinawa Trough is a back-arc basin located on the Eurasian plate, and has been undergoing rifting since 2 Ma. Especially, the rifting in the southern part of the Okinawa Trough started about 0.1 Ma, but there are still no reports of basaltic oceanic crust. In the KH-21-3 cruise Leg 1, we find the detailed normal faults that construct the graben, the lithology and age of sediments that filled the graben, the heat flow and rocks in the knoll to understand the geohistory from Quaternary to present on the Okinawa Trough. In KH-21-3 cruise Leg 1, we conducted the seismic survey, SBP, swath bathymetry, gravity, magnetic and XCTD observations, piston coring, rock sampling by dredge, heat flow measurements and plankton sampling in the southern part of the Okinawa Trough.

[KH-21-3 cruise Leg 2] The northern part of the East China Sea has large salt fluctuations in summer, and the IODP site U1429 (Danjo Basin) is an important site for elucidating the history of changes in the Asian monsoon. However, the coring at U1429 in 2013 was blocked by a sand layer (thickness unknown) at a depth of 200 m below seafloor. Therefore, in the KH-21-3 cruise Leg 2, in order to extract the effective drilling sites, we investigate the geological structures in the southeastern part of the U1429 site. In KH-21-3 cruise Leg 2, we conducted the seismic survey, sediment sampling by piston coring, seafloor surface sediment sampling using multiple coring, SBP, swath bathymetry, gravity, magnetic and XCTD observations and plankton sampling in the Danjo Basin.

Keywords: Okinawa Trough, Scientific Drilling, Normal fault, Backarc basin, Monsoon, Paleoenvironment

©2021. Japan Geoscience Union. All Right Reserved.

Structure and seismicity in the southern part of the Okinawa Trough and their implications for rifting and volcanic processes

*Ryuta Arai[1], Ayanori Misawa[2], Makoto Otsubo[2], Saki Ishino[2], Masataka Kinoshita[3], KH-21-3 Shipboard Scientists

1. Japan Agency for Marine-Earth Science and Technology, 2. Geological Survey of Japan, National Institute of Advanced Industrial Science and Technology, 3. Earthquake Research Institute, The University of Tokyo

The Okinawa Trough is an active rift zone behind the Ryukyu subduction zone and provides a great research field to study the deformation and evolution of the lithosphere in a back-arc setting. The southern part of the Okinawa Trough exhibits the highest rifting rate and the deepest seafloor depth (>2,000 m) in the basin. Consistently, recent seismic surveys show that significant crustal stretching occurs beneath the rift axis marked by the linear bathymetric depression (Yaeyama Rift) and suggest that the southern part of the Okinawa Trough is thought to be at a transitional stage from continental rifting to seafloor spreading (e.g., Arai et al., 2017). Another important feature here is that off-axis volcanic features are in close proximity to on-axis magmatic intrusions. From the viewpoint of seismicity, large earthquakes (with a magnitude greater than 5) frequently occur around the rift axes. These earthquakes mostly accompany rapid increase in seismicity rate (swarm activity), implying sudden changes in stress regime probably induced by large-scale dike intrusion. Although these tectonic and volcanic processes are expected to closely interact each other, their relative roles in controlling the overall back-arc rifting process are poorly understood.
Aiming at better understanding the tectonic and volcanic processes associated with the continental back-arc rifting, we conducted integrated marine geophysical and geological surveys in the southern part of the Okinawa Trough using the research vessel *Hakuhomaru* in January 2021 (KH-21-3). During the cruise, we acquired high-resolution multichannel seismic reflection data along the 5 rift-parallel (SW-NE direction) lines and 4 rift-perpendicular (NW-SE direction lines using two GI guns with a total volume of 710 cu.in. and a 1200-m-long, 48-channel streamer cable. The study area covers the Yaeyama Rift and the potential submarine volcano located further south, providing three-dimensional structural constraints on both on-axis and off-axis magmatic intrusions at shallow depths. In this presentation, we discuss the structure and rifting processes in the southern part of the Okinawa Trough based on the newly obtained seismic reflection images and seismic activity.

Keywords: Okinawa Trough, Back-arc rifting, Submarine volcano

©2021. Japan Geoscience Union. All Right Reserved.

Heat flow anomaly in the southern part of Okinawa Trough –A preliminary result from the KH-21-3 cruise-

*Masataka Kinoshita[1], Ryuta Arai[2], Chiori Tamura[3], Ayanori Misawa[4], Saki Ishino[4], Makoto Otsubo[4], Shipboard Scientists KH-21-3

1. Earthquake Research Institute, The University of Tokyo, 2. Japan Agency for Marine-Earth Science and Technology, 3. Atmospheric and Ocean Research Institute, the University of Tokyo, 4. National Institute of Advanced Industrial Science and Technology

The southern part of Okinawa Trough, located between Ryukyu Islands and the East China Sea, has been extending since ~10 Ma. In its middle is a central graben, called the Yaeyama Rift (YR), bounded by a series of E-W trending normal faults. Previous seismic refraction surveys reveal a thick (~15 km) crust, indicating that the southern Okinawa Trough is in a continental rifting stage having extension/subsidence.

One of the key observations to test this hypothesis is the heat flow. However, so far very little data exist here, except for some very low heat low within YR. During the KH-21-3 cruise Leg 1, 17 new heat flow data were obtained as well as seismic reflection survey, piston coring, bathymetry and dredge sampling in the southern part of Okinawa Trough (Figure).

Obtained temperature vs. depth profiles are all linear, supporting a thermal conduction dominant near the surface. Thermal conductivity values, measured on piston core samples, are generally close to 1 $Wm^{-1}K^{-1}$, typical of surface marine sediments.

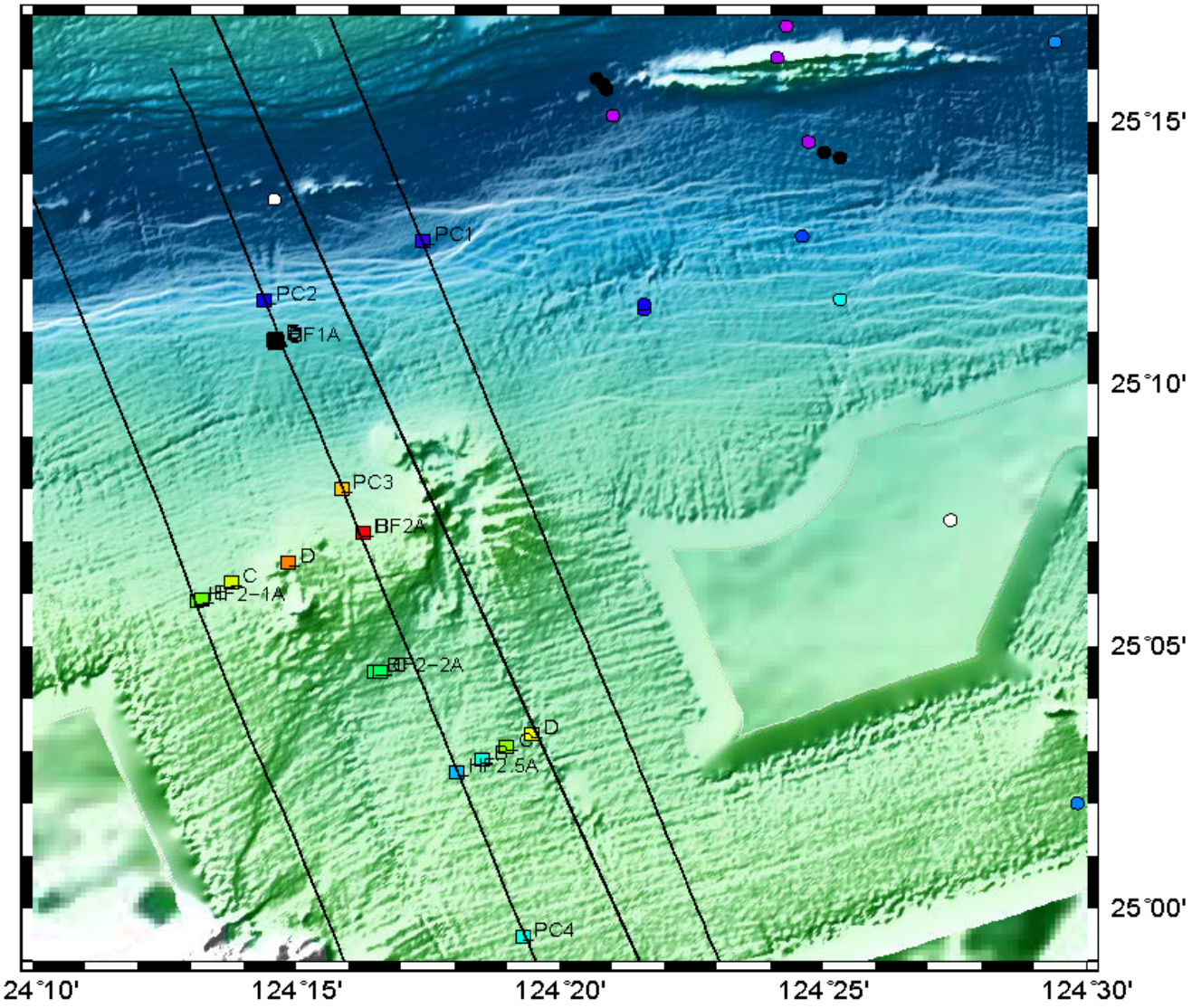
Preliminary heat flow values vary greatly from < 40 mWm-2 to 120mWm-2, suggesting local-scale excursions ongoing at the sites. Low heat flow in the southern slope of YR can either be due to rapid sedimentation or to the recharge od seawater in the hydrothermal system.

At site HF2, we conducted 8 measurements. It is located between the Ishigaki Knoll and the Yaeyama Knoll, where a bathymetric swell and subseafloor ‘melt lens’ are identified by Arai et al. (2016 JGR), called the ‘magmatic uplift’. Through the multi-narrow bathymetric survey we identified two seamount aligned E-W with their height ~100 m. HF2 measurements were made along E-W line running in the northern rim of the western seamount. Surprisingly the heat flow increases eastward. The eastern most point is located between two seamounts, and has the highest value 120 mWm^{-2}. The seismic reflection profiles show anomalous reflection beneath the seamounts, implying the relation with the magmatic uplift by Arai et al.

The purpose of this leg is to get new data for the IODP drilling proposal. As such, it is necessary to show the regional heat flow in the south Okinawa Trough. Because of large scatter in heat flow, so far we cannot show the regional heat flow in this area. The southern most site shows 70mWm-2 (PC4), but this site may also be disturbed by the turbidites supplied from south. However, the finding of twin seamounts and heat flow anomaly should give us a new insight on the evolution of Okinawa Trough.

Keywords: Okinawa Trough, Heat flow, IODP

©2021. Japan Geoscience Union. All Right Reserved.



©2021. Japan Geoscience Union. All Right Reserved.

GNSS/Acoustic geodetic measurement at the southern end of Ryukyu Trench 2014-2020

*Akihiro Nagaya[1], Ryoya Ikuta[2], Mamoru Nakamura[3], Masataka Ando[4]

1. Undergraduate school of department of Geoscience, Shizuoka University, 2. Faculty of Science, Shizuoka University, 3. Faculty of Science, University of the Ryukyu, 4. Center for Natural Hazards of Integrated Education and Research, Shizuoka University

We present the results of six years of GNSS/acoustic measurement conducted from October 2014 to September 2020 in the forearc basin of the Yaeyama Islands, the southernmost part of the Ryukyu Trench.

To the south of the Yaeyama Islands, the Philippine Sea Plate is subducting under the Eurasian Plate (Yangtze Plate) at a rate of about 8 cm/yr along the Ryukyu Trench. Behind the Yaeyama Islands, the Okinawa Trough back arc basin is opening at a rate of about 4-5 cm/yr. As a result, the convergence rate between the Yaeyama Islands and the Philippine Sea Plate is fast at about 12-13 cm/yr. The Ryukyu subduction zone beneath the Yaeyama Islands is an extensional plate boundary where back-arc opening occurs, and it has been thought that the interplate coupling is weak and does not capable of huge earthquakes (Scholz and Campos, 2012, JGR).

However, there are several old legends of tsunamis in Miyakojima and Ishigakijima islands, and it is known that the Yaeyama earthquake of April 24, 1771 caused a devastating tsunami in these islands (Nakamura, 2009, GRL).

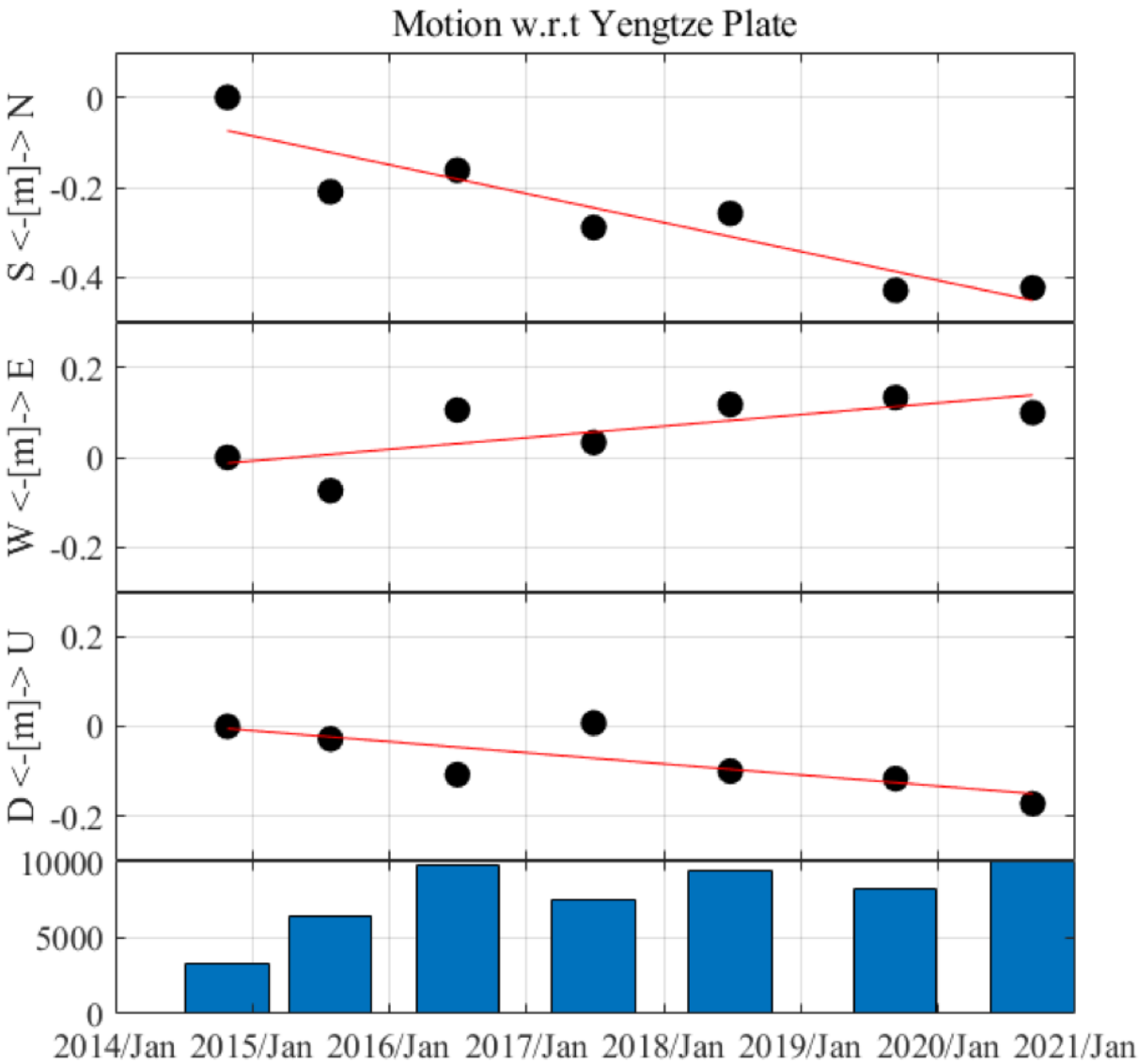
Nakamura (2009, GRL) conducted a numerical simulation of the tsunami based on the Tsunami inundation data by Nakata and Kawana (1995), and estimated the Yaeyama earthquake as a tsunamigenic earthquake of Mw 8.0 that occurred in the Ryukyu Trench. In addition, trenching of tsunami deposits in Ishigaki Island estimated that the Yaeyama earthquake was a massive earthquake with severe strong ground motion, and that tsunamis of approximately the same size as the 1771 earthquake occurred four times in the past 2000 years at intervals of about 600 years (Ando et al., 2018, Tectonophysics). In order to estimate the presence or absence of the inter-plate coupling around the tsunami fault area estimated by Nakamura (2009, GRL), seafloor transponders were deployed in the forearc region at a depth of about 3300 m, about 40 km off the south coast of Hateruma Island, by Shizuoka University and the University of the Ryukyus in October 2014. In this study, we estimated the motion of the transponders over a period of six years from the observation data taken seven times in total from October 2014 to September 2020.

The position of the transponders was estimated using the method of Ikuta et al. (2008, JGR) using kinematic GPS, ship attitude, two-way travel time of acoustic ranging, and XCTD data. To estimate the kinematic GPS positions, we used Interferometry Trajectory (IT), a long baseline analysis software developed by NASA/GSFC in six of the seven campaigns expect for the campaign in 2014. In 2014 campaign, the results of the IT analysis showed a large discrepancy between the astronomical tide and the GPS antenna height change. We reanalyzed the kinematic GPS for the 2014 campaign only using RTKLIB (Takasu, 2006). For the estimation of the three transponders positions, we introduced the assumption that the sound velocity structure changes smoothly with time and that the geometries of them do not change through all campaigns. And we estimated the positions of the three transponders for all campaigns simultaneously by penalized least squares method.

©2021. Japan Geoscience Union. All Right Reserved.

As a result, the average velocity vectors calculated from the positions of the transponders for all campaigns were estimated to be 64.2±11.2 mm/yr in the south direction, 25.8±9.8 mm/yr in the east direction, and 24.8±8.0 mm/yr in the subsidence direction relative to the Eurasian plate. The rms of the residuals between the predicted and actual transponders positions for each campaign at the calculated velocities were 54.3 mm north-south, 47.8 mm east-west, and 39.0 mm up-down; before the reanalysis of the 2014 GNSS data by RTKLIB, these were 61.0 mm, 66.4 mm, and 40.7 mm, respectively. It can be seen that the improvement of GNSS data in 2014 affected the analysis results.
In this presentation, based on the above results, we discuss the extent of inter-plate coupling at this southernmost tip of the Ryukyu Trench.

Keywords: Yaeyama Tsunami, Ryukyu Trench, GNSS/Acoustic measurement, Seafloor crustal deformation, Inter-plate coupling



©2021. Japan Geoscience Union. All Right Reserved.

Fluid-flow simulation for clarifying ore generation processes in the Izena Hole hydrothermal field, Okinawa Trough

*Shohei Albert Tomita[1], Katsuaki Koike[1], Tada-nori Goto[2], Katsuhiko Suzuki[3], Takafumi Kasaya[3]

1. Graduate School of Engineering, Kyoto University, 2. Graduate School of Life Science, University of Hyogo, 3. Research and Development Center for Submarine Resources, Japan Agency for Marine-Earth Science and Technology (JAMSTEC)

Seafloor hydrothermal deposits have a high potentiality for new metal resources. An understanding of the genesis of the deposits is indispensable to exploring the deposits. In the previous study, we conducted a hydrothermal flow simulation for the Iheya North hydrothermal field, Okinawa Trough and clarified that a formation of the cap layer induced the lateral flow and boiling of the hydrothermal fluids, which caused the metallic mineral deposition below the seafloor (Tomita et al., 2020). In this study, we aim to verify the applicability of the Iheya North mineral precipitation model to other seafloor hydrothermal deposits by selecting the Izena Hole hydrothermal field, Okinawa Trough as a case study field and a hydrothermal flow simulation using TOUGH2.

The field observations such as the drilling data, seismic survey, and heat flux measurement were used to construct a proper three-dimensional numerical model that contains two hydrothermal sites, Jade and Hakurei sites. In the simulation, the seafloor was set as the top boundary where the temperature and pressure were fixed at 4 ℃ and hydrostatic conditions, respectively. The physical properties of rocks were set by the data of seafloor drillings, and the permeabilities (hereinafter, *k*) of the five elements were adjusted with trial-and-error approaches so that the heat flux and temperature differences would be acceptably small with consideration of heat balance. To clarify the general fluid flow pattern and the temperature and pressure distributions, the model domain was simply divided into five geologic elements, conduit (high *k*), fault (high *k*), volcanic basement (medium *k*), cap layer (low *k*), and sediment (low *k*), by excluding geological and hydrological heterogeneities. The conduits were set vertically from the bottom to seafloor at the middle area common to Jade and Hakurei sites. The hydrothermal fluid of 360 ˚C was injected from the conduit bottoms, and the hydrothermal fluid was set to discharge from the conduit surfaces.

As a result of the simulation, the hydrothermal fluid ascending along the conduit was trapped by the cap layer near the surface and flowed laterally in addition to the outflow from the seafloor. The calculated heat fluxes generally corresponded with the measured values. The hydrothermal fluids that ascended along the conduit boiled under the seafloor at both the Jade and Hakurei sites due to the pressure decrease.

In the Hakurei site, a two-layer structure of exposed ore bodies on the seafloor and lower ore bodies below the seafloor were found in the northern mound around the C9027 drilling hole. We considered the origin of this two-layer structure in three stages through the simulation results and observations. In the early stage, hydrothermal fluids discharging from black smokers formed the upper seafloor massive sulfide (SMS) deposits on the seafloor. In the middle stage, cap layers (anhydrite and clay minerals) formed below the seafloor, which induced the lateral flow and boiling under the cap layers. The presence of cap layer below the seafloor was confirmed by the drilling data. After formation of the cap layers, liquid-dominated hydrothermal fluids rich in metals flow laterally below the cap layers, forming the lower SMS deposits at tens of meters depth below the seafloor. In the late stage, the center of hydrothermal activity shifted from

©2021. Japan Geoscience Union. All Right Reserved.

the northern mound to the Dragon chimney, because the pore spaces were filled with mineral precipitation and then *k* was largely decreased at the mound.

In conclusion, this study clarified that the Iheya North mineralization model could be applied to the Izena Hole.

Reference
Tomita, S. A., Koike, K., Goto, T., & Suzuki, K. (2020). Numerical simulation-based clarification of a fluid-flow system in a seafloor hydrothermal vent area in the middle Okinawa Trough. Geophysical Research Letters, 47, e2020GL088681. https://doi.org/10.1029/2020GL088681

Keywords: hydrothermal flow simulation, TOUGH2, temperature, boiling, seafloor massive sulfide deposit, cap layer

©2021. Japan Geoscience Union. All Right Reserved.

Examining the origin and depositional process of turbidites in the southern part of Okinawa Trough based on cores from Expedition KH-21-3

*Cai Zhirong[1], Hajime Naruse[1], Ken Ikehara[2], KH-21-3 Shipboard Scientists -

1. Department of Geology and Mineralogy, Graduate School of Science, Kyoto University, 2. Institute of Geology and Geoinformation, National Institute of Advanced Industrial Science and Technology

Okinawa Trough is an actively rifting back-arc basin and an important area for examining the tectonic history of the Ryukyu subduction zone. Past studies showed that the main sources of sediment deposition in the southern part of Okinawa Trough were Taiwan and the East China Sea continental shelf. The main process of sediment transportation to the Okinawa Trough was turbidity currents in addition to hemipelagic sediment transport. Estimating sediment flux from Taiwan as well as local sediment input from volcanic arcs into this region is important for understanding the development of the Okinawa Trough and the temporal changes in orogenic activity in Taiwan. However, the scale and source of turbidity current events related to the depositional process within the region is still unclear.

The KH-21-3 expedition surveyed the southern part of Okinawa Trough and four piston cores were obtained. Each core contained more than one turbidite unit. In order to better understand the origin and scale of turbidity current events that resulted in turbidites in the southern part of Okinawa Trough, we conducted a 2D numerical experiment of turbidity current events using a shallow water equation model that reproduced turbidites in borehole cores. This presentation will also contain a preliminary report of the characteristics of turbidites within the cores obtained from KH-21-3 and an overview of the numerical model used for simulation.

Keywords: Numerical Simulation, Turbidity Currents, Back-arc Basin

©2021. Japan Geoscience Union. All Right Reserved.

[J] Oral | S (Solid Earth Sciences)：S-CG Complex & General

Sat. Jun 5, 2021 1:45 PM - 3:15 PM JST | Sat. Jun 5, 2021 4:45 AM - 6:15 AM UTC | Ch.19 Zoom Room 19

[S-CG45] Ocean Floor Geoscience

convener:Kyoko Okino(Atmosphere and Ocean Research Institute, The University of Tokyo), Chairperson:Motoyuki Kido(International Research Institute for Disaster Science, Tohoku University), Fumiaki Tomita(Japan Agency for Marine-Earth Science and Technology)

Most of Earth's volcanism and much of its tectonic activity occur on and beneath the s eafloor. Various phenomena on the seafloor are closely linked to plate tectonics, Earth s tructure and dynamics, and also related to Earth's environments through the hydrosphe re and atmosphere. Seafloor rocks and sediments record Earth's evolution and heat an d material fluxes on the Earth. Ocean Floor Geoscience session covers a broad range of research on seafloor such as mid-ocean ridge process, subduction dynamics, arc magm atism, hot spot and LIPs, crustal movement and structure etc. Every field of researches and every approaches are welcomed.The session aims to encourage discussion among scientists from different study fields and to integrate our understanding of ocean floor. The session is co-chaired by K. Tadokoro (Nagoya Univ.), O. Ishizuka (AIST), T. Toki (Univ . Ryukyus), and N. Takahashi (JAMSTEC).

1:45 PM - 2:00 PM JST | 4:45 AM - 5:00 AM UTC

[SCG45-13] Preliminary results of ocean bottom pressure observation around Kikai submarine caldera, SW Japan

Yuko Asai[1], *Nobukazu Seama[1,2], Tomoko Hanyu[2], Tetsuo Matsuno[2,1], Hitoshi Hirose[3,1], Takuto Minami[1], Hiroko Sugioka[2,1] (1.Department of Planetology, Graduate School of Science, Kobe University, 2.Kobe Ocean Bottom Exploration Center, Kobe University, 3.Research Center for Urban Safety and Security, Kobe University)

2:00 PM - 2:15 PM JST | 5:00 AM - 5:15 AM UTC

[SCG45-14] Characteristic of depth dependence and annual variation of OBP time series in DONET

*Hideto Otsuka[1], Yusaku Ohta[1], Ryota Hino[1], Tatsuya Kubota[2], Daisuke Inazu[3] (1.Department of Geophysics, Graduate School of Science, Tohoku University, 2.National Research Institute for Earth Science and Disaster Resilience, 3.Department of Marine Resources and Energy, Tokyo University of Marine Science and Technology)

2:15 PM - 2:30 PM JST | 5:15 AM - 5:30 AM UTC

[SCG45-15] GNSS-Acoustic observations using a Wave Glider and their results

*Fumiaki Tomita[1], Takeshi Iinuma[1], Motoyuki Kido[2], Yusaku Ohta[3], Chie Honsho[3], Tatsuya Fukuda[1], Takane Hori[1] (1.Japan Agency for Marine-Earth Science and Technology, 2.International Research Institute of Disaster Science, Tohoku University, 3.Graduate School of Science, Tohoku University)

2:30 PM - 2:45 PM JST | 5:30 AM - 5:45 AM UTC

[SCG45-16] Semi-realtime transmission of GNSS-A data using a Wave Glider

*Motoyuki Kido[1], Tatsuya Fukuda[2], Yusaku Ohta[3], Fumiaki Tomita[2], Chie Honsho[3], Takeshi Iinuma[2] (1.IRIDeS, Tohoku University, 2.JAMSTEC, 3.Sci. Division, Tohoku University)

2:45 PM - 3:00 PM JST | 5:45 AM - 6:00 AM UTC

[SCG45-17] Operation experiment of the system for seafloor crustal deformation observation system using a buoy

*Keiichi Tadokoro[1], Natsuki Kinugasa[1], Teruyuki Kato[2], Yukihiro Terada[3], Kenjiro Matsuhiro[4], Haruno Koike[4] (1.Research Center for Seismology, Volcanology and Earthquake and Volcano Research Center, Nagoya University, 2.Hot Springs Research Institute of Kanagawa Prefectural Government, 3.National Institute of Technology, Kochi College, 4.Technical Center, Nagoya University)

3:00 PM - 3:15 PM JST | 6:00 AM - 6:15 AM UTC

[SCG45-18] Initial results of sea trials on bathymetric survey performance of “AUV-NEXT”: aiming to acquire higher-quality bathymetric data

*MASANAO SUMIYOSHI[1], Ryosuke Nagasawa[1], Takashi Hashimoto[1], Kenji Nagahashi[2], Takao Sawa[2], Tadahiro Hyakudome[2], Takeshi Nakatani[2], Tatsuya Aso[2], Yusuke Yokota[3] (1.Hydrographic and Oceanographic Department, Japan Coast Guard, 2.JAMSTEC, 3.Institute of Industrial Science, University of Tokyo)

Preliminary results of ocean bottom pressure observation around Kikai submarine caldera, SW Japan

Yuko Asai[1], *Nobukazu Seama[1,2], Tomoko Hanyu[2], Tetsuo Matsuno[2,1], Hitoshi Hirose[3,1], Takuto Minami[1], Hiroko Sugioka[2,1]

1. Department of Planetology, Graduate School of Science, Kobe University, 2. Kobe Ocean Bottom Exploration Center, Kobe University, 3. Research Center for Urban Safety and Security, Kobe University

We perform tidal analysis of ocean bottom pressure variation, which were measured by 4 'OBEMP (Ocean Bottom Electro-Magnetometer with absolute Pressure gauge)' instruments at observation sites around Kikai submarine caldera, SW Japan. These measurements were made during periods of April/2018-Oct./2018, Nov./2018-Sept./2019, Nov./2018-March/2019, and Nov./2019-March/2020, with their water depths of 392m, 312m, 206m, and 196m, respectively. Tidal analysis of these data is performed using BAYTAP-G program (Tamura et al., 1991) to derive tidal amplitudes, factors, and phases of 14 diurnal and semidiurnal tidal groups, and these data are decomposed into three parts: 1) a tidal part, 2) a part that is correlated with the ocean bottom temperature measurement data, and 3) a nontidal part. The tidal factors are estimated at ~2 and ~ 3.5 for diurnal and semidiurnal tidal groups, respectively. Some tidal factors and phases that are well estimated with small errors indicate slight difference among the observation sites. Comparison of tidal factors and phases between our results and a global ocean tide model, NAO.99b (Matsumoto et al., 2000), also shows slight differences. These differences could be due to local loading effect on crust with relation to the existence of Kikai submarine caldera. We will perform further analysis with respect to site location difference, period dependence, and time variation to investigate possible local loading effect on crust. The result from the nontidal part indicates two characteristic features. One is a sudden increase of pressure values (~30 hPa) with in 6 hours, which occurred on August 22, 2018 at one observation site. We will investigate possible causes of the sudden pressure increase. The second one is pressure variation of 20 hPa with its period longer than a week. This variation was observed at two observation sites during Nov./2018-March/2019, which was the only duration that we made simultaneous observation at two observation sites. The similar pressure variations at two sites that are separated by 45 km in distance suggest that these variations are due to a same cause. Since pressure variation at ocean bottom corresponds to the sum of air pressure and pressure due to total mass of ocean water above observation site, we compare our pressure variation with air pressure variations observed at three Japan Meteorological Agency observation sites (Makurasaki, Tanegashima, and Yakushima) far around Kikai submarine caldera, whose data were provided by Japan Meteorological Agency. The overall air pressure variations at three sites are the same with a very small difference within ~2 hPa, suggesting air pressure variations at our ocean bottom observation sites would be the same. The comparison indicates no correlation for the period longer than a week, suggesting two things. The air pressure variations are well compensated by change in total mass of ocean water (change in ocean height level), and leads no effective variation on pressure at ocean bottom. Thus, the pressure variation of 20 hPa with its period longer than a week should be due to pressure due to total mass of ocean water above two observation sites that is probably caused by ocean current variation. We will analyze period dependence of correlation between ocean bottom pressure variations and air pressure variations. We will present all these results and possible implications from them.

Keywords: Ocean bottom pressure variation, Ocean tide, Loading effect on crust

©2021. Japan Geoscience Union. All Right Reserved.

Characteristic of depth dependence and annual variation of OBP time series in DONET

*Hideto Otsuka[1], Yusaku Ohta[1], Ryota Hino[1], Tatsuya Kubota[2], Daisuke Inazu[3]

1. Department of Geophysics, Graduate School of Science, Tohoku University, 2. National Research Institute for Earth Science and Disaster Resilience, 3. Department of Marine Resources and Energy, Tokyo University of Marine Science and Technology

Ocean Bottom Pressure-gauge (OBP) is extremely important sensor to observe the continuous seafloor vertical deformation. The observed OBP data, however, contain not only the signal of crustal deformation but also the other components such as tidal-component, non-tidal oceanographic fluctuation, and sensor specific drift. Therefore, appropriate assessment of these contributions are essentially important to extract the signal of crustal deformation. Especially, the non-tidal oceanographic fluctuation is the largest noise because of its similarity in time constant to the crustal deformation. The non-tidal oceanographic model (e.g., Inazu et al., 2012) is one of the candidate to estimate its contribution. Dobashi and Inazu (2021) compared the time series of observed data with non-tidal oceanographic models in short-term time series (3-90 days) to evaluate the contribution of the non-tidal fluctuation on OBP data. In contrast, almost all previous studies did not assess the characteristics of non-tidal oceanographic component in long-term data more than several years. In this study, we investigate the long-term spatio-temporal characteristic of non-tidal oceanographic fluctuation based on the data of DONET OBP time series.

In this study, we used the 8-year continuous data between 2012 to 2019 for analyses. DONET observation network extends 200km east-west, 100km north-south, and 1-4km sea depth. Ocean tide components were removed by tide-killer filter (Hanawa and Mitsudera, 1985), and instrumental drift were approximated and removed by linear and exponential functions.

Firstly, the similarity of OBP time series of each stations was evaluated using distance and difference of sea depth between stations as indicators. We assumed a reference site, which locates in the most north-eastern part of the network, and the sea depth of the site is 2039m. We subtracted the time series of the reference site from all of the DONET sites. The standard deviation of the relative pressure time series was calculated and their dependence on station distance and sea depth difference was evaluated. The correlation coefficient with the station distance was quite small (0.15). In contrast, the correlation coefficient with the sea depth difference was 0.69. It may indicate that effective removal of the non-tidal oceanographic fluctuation is possible by selecting the reference site considering the sea depth difference rather than the distance. Secondly, we estimated the amplitude and phase of the annual component of OBP time series to evaluate the annual fluctuation based on 8-year data. Estimated amplitude and phase of the annual component also clearly show the dependency with difference of sea depth. These results suggest that the annual component is a main factor in the sea depth dependence of the non-tidal component. In the presentation, we also evaluate the temporal variation of the characteristic of the annual component.

Keywords: Marine geodesy, Ocean Bottom Pressure gauge, DONET

©2021. Japan Geoscience Union. All Right Reserved.

GNSS-Acoustic observations using a Wave Glider and their results

*Fumiaki Tomita[1], Takeshi Iinuma[1], Motoyuki Kido[2], Yusaku Ohta[3], Chie Honsho[3], Tatsuya Fukuda[1], Takane Hori[1]

1. Japan Agency for Marine-Earth Science and Technology, 2. International Research Institute of Disaster Science, Tohoku University, 3. Graduate School of Science, Tohoku University

Using the GNSS-Acoustic (GNSS-A) observation technique, seafloor crustal deformation associated with an earthquake cycle has been measured [e.g., Honsho et al., 2019, JGR]. A sea-surface platform, which conducts GNSS measurement and acoustic ranging between the sea-surface and the seafloor, is essential for the GNSS-A observation; in general, a research vessel has been used. However, employment of a research vessel requires high financial and human resources, which makes frequent GNSS-A observations for many sites difficult. Then, JAMSTEC and Tohoku University have developed system for GNSS-A observations using a Wave Glider (WG) as the sea-surface platform. The WG is an unmanned surface vehicle which can move by sea-surface wave energy. We conducted a trial short-term observation using the WG at single site in July 2019, and we showed that precision of the GNSS-A measurements using the WG was comparable with that using research vessels [Iinuma et al., 2021, Frontiers in Earth Science]. Moreover, we successfully operated the WG in June–July 2020 and conducted GNSS-A observations at 14 sites [Tomita et al., 2020, GSJ Meeting]. In this study, we report outline of the GNSS-A observation using the Wave Glider in Oct. 2020 and its results. Although we also simply report the results of the observation in Nov.–Dec. 2020, this observation was conducted as urgent survey associated with activation of seismicity off northern Sanriku from early Nov. 2020; thus, its outline is reported by Hori et al. [this meeting], and its technical issues are reported by Kido et al. [this meeting].

The WG equipped GNSS-A observation instruments and Thuraya satellite communication instruments for confirming state of the obtained data. The equipped GNSS-A instruments are following: two GNSS antennas for position and attitude (heading and pitch) of the sea-surface platform, an acoustic ranging unit, an acoustic transducer, and a MEMS gyro. The Wave Glider was deployed at G24 site on Oct. 8 during the KS-20-16 cruise. After the observation for 25 days, it was recovered by a charter vessel at G13 site on Nov. 1. Although GNSS data was unavailable because of the logging system error at one site, we successfully obtained the observational data in the other sites.

We estimated horizontal displacement of the seafloor transponder array for each acoustic ping by the means of Kido et al. [2006, EPS]. The initial geometry of the transponder array was calculated by Honsho et al. [2019] using the past observational data. We then calculated average and standard deviation of the horizontal displacement during the survey for each site. We found that the temporal variations of the horizontal array position for each ping were generally large, which suggested that spatial variation in the underwater sound speed structure was complex during the observation in Oct. 2020. Although precision of the horizontal displacements in Oct. 2020 was relatively larger than the past cruises, we successfully obtained the analysis results.

Although we had conducted at least one GNSS-A observation cruise for each site per a year in the off-Tohoku region before 2016, we have hardly conducted the cruises after 2016 due to the operating cost of vessels. However, we conducted the surveys for most GNSS-A sites off Miyagi–Aomori in 2020 using the WG. Off Iwate and Aomori, the displacement rates had been small in the previous studies, and this characteristic was also confirmed in the latest results. Meanwhile, off Miyagi, large landward motions

©2021. Japan Geoscience Union. All Right Reserved.

had been observed due to the viscoelastic relaxation of the 2011 Tohoku-oki earthquake; we found that the landward motions were still continued from the latest results, but their displacement rates were little smaller than the previous studies.

In the presentation, we will introduce outline of the observations using the WG, and we will discuss the present postseismic deformation associated with the 2011 Tohoku-oki earthquake for the horizontal components. Note that vertical motions in the whole off-Tohoku region will be discussed by Honsho et al. [this meeting].

Keywords: GNSS-Acoustic observation, Wave Glider, Seafloor geodetic observation, Crustal deformation, The 2011 Tohoku-oki earthquake

©2021. Japan Geoscience Union. All Right Reserved.

Semi-realtime transmission of GNSS-A data using a Wave Glider

*Motoyuki Kido[1], Tatsuya Fukuda[2], Yusaku Ohta[3], Fumiaki Tomita[2], Chie Honsho[3], Takeshi Iinuma[2]

1. IRIDeS, Tohoku University, 2. JAMSTEC, 3. Sci. Division, Tohoku University

Seafloor crustal deformation obtained by GNSS-Acoustic observation is now essential to evaluate the long-term risk for huge subduction earthquakes and to estimate the fault extent of a huge event. A network of GNSS-A sites was rapidly constructed since the 2011 Tohoku earthquake. However, the increase in the number of sites prevents frequent shipboard surveys since it takes nearly a day for a single site. To get over the situation, JAMSTEC and Tohoku Univ. jointly started automatic GNSS-A surveys using a Wave Glider (WG) capable of long-period and autonomous navigation (Iinuma et al., 2021, Frontiers in Earth Science). Obtaining data of an equivalent quality to usual postprocessing during the automatic survey, we can immediately assess a devastating earthquake, and even in an inter-seismic period, we can flexibly modify the subsequent survey plan according to the realtime data. We report the improvement in our WG system regarding the on-demand data transmission as well as automatic observation sequence.

WG to onshore communication is via Iridium Satellite system for WG navigation and Thuraya Satellite system for the payload including the GNSS-A part. When the WG arrived around a particular site and the main power is turned on from onshore, GNSS positioning is started. If the WG is found close enough to the site, GNSS and attitude data recording are automatically started. Simultaneously the acoustic unit sends wake-up and other commands to individual transponders until the commands certainly functioned. After that, it started simultaneous periodic acoustic ranging to the transponders and storing acoustic signal with a 1-minute interval. When the WG leaves the site, measurement and data recording are stopped and then the system is halted.

The GNSS-A essential data consists of GNSS antenna position, attitude of the WG, and traveltimes of acoustic signals. GNSS receiver outputs adequate precision at 10 Hz rate through realtime processing of kinematic Precise Point Positioning using the Trimble CenterPoint RTX service. Attitude is obtained 9-DOF MEMS device at 20 Hz as well as GNSS dual antenna system at 10 Hz rate. An acoustic signal is recorded for 10 sec. for every shot, in which the reply signals from all the transponder are included.

Antenna positions and attitude data at a time of transmission and predicted times of reception of acoustic signals are read from stored data for every shot. These data at arbitrary timings are interpolated with neighboring three epochs. Phase Only Correlation (POC: Honsho et al., 2021, Frontiers in Earth Science) of the acoustic signal with five wavelengths before and after the main peak is to be sent to onshore rather than traveltime, because complicated processing to detect true peak is needed due to the distortion of a signal. The introduction of the POC significantly reduces the scatter in traveltime detection. All the relevant data above are archived each time of ranging in a file of 570 bytes with gzip-compression, ready to transmit upon request, which only amounts to 34 KB per hour. Further data reduction is possible by transmitting only transducer position, however, including raw attitude data would help to recognize in case of a possible problem in the data.

In the urgent WG survey off Aomori in December 2020, we analyzed the data immediately after the transmission, which found to perform comparable quality of result with postprocessing of full data set or even shipboard survey data. We are now working on the further refinement of the WG operation

©2021. Japan Geoscience Union. All Right Reserved.

algorithm, especially in the intelligent automatic handling against a case for unexpected behavior of seafloor transponder and in the fully automatic onshore processing immediately after reception of the WG data. In the presentation, we also introduce the detail of the system and observed data quality in individual processing steps.

Keywords: GNSS-A, Wave Glider, Realtime, Autonomous survey, Marine Geodesy

©2021. Japan Geoscience Union. All Right Reserved.

Operation experiment of the system for seafloor crustal deformation observation system using a buoy

*Keiichi Tadokoro[1], Natsuki Kinugasa[1], Teruyuki Kato[2], Yukihiro Terada[3], Kenjiro Matsuhiro[4], Haruno Koike[4]

1. Research Center for Seismology, Volcanology and Earthquake and Volcano Research Center, Nagoya University, 2. Hot Springs Research Institute of Kanagawa Prefectural Government, 3. National Institute of Technology, Kochi College, 4. Technical Center, Nagoya University

The observation of seafloor crustal deformation, which combines GNSS positioning and acoustic ranging, is an indispensable tool for investigating large subduction-zone earthquakes such as the Nankai Trough earthquake. However, at present, observations are carried out using ships, and the problem is that the frequency of observations is low.

Our research group has been developed a system using buoys in order to perform continuous observation of seafloor crustal deformation. This system has been installed on a fishery buoy of Kochi Prefecture, which is moored immediately above the submarine station located 32 km off Cape Ashizuri, and has been tested for continuous observation. Observation of seafloor crustal deformation using this system started on March 28, 2018. The acoustic ranging could be carried out continuously for about 6 months, but due to power outages occurring three times, especially in winter, the power supply capacity was improved from December 2019 to March 2020 by increasing the solar panels from 5 to 8, and the amount of storage batteries was doubled; also the power supply system was separated into two systems for a 12V system and a 24V system, respectively. The acoustic ranging has been continued for about 10 months or more since March 12, 2020 after improving the power supply capacity. Therefore, it was confirmed that our system can perform the acoustic ranging measurement continuously as long as power is continuously supplied. However, the satellite communication part is insufficient quality, and acoustic ranging data transmitted to land base stations accounts for only about 60 % of the total. The GNSS positioning and attitude measurement data using a gyro are required for seafloor crustal deformation observation, as well as the acoustic ranging data, but these measurements also had problems, and the period when all data are available was only from August 2020 and January 2021. The accuracy of the seafloor positioning was about several centimeters when we used the data during this period.

Keywords: seafloor crustal deformation, moored buoy

©2021. Japan Geoscience Union. All Right Reserved.

Initial results of sea trials on bathymetric survey performance of “AUV-NEXT”: aiming to acquire higher-quality bathymetric data

*MASANAO SUMIYOSHI[1], Ryosuke Nagasawa[1], Takashi Hashimoto[1], Kenji Nagahashi[2], Takao Sawa[2], Tadahiro Hyakudome[2], Takeshi Nakatani[2], Tatsuya Aso[2], Yusuke Yokota[3]

1. Hydrographic and Oceanographic Department, Japan Coast Guard, 2. JAMSTEC, 3. Institute of Industrial Science, University of Tokyo

In AUV bathymetric survey, since AUV can approach the seafloor for ocean mapping, it is possible to acquire bathymetric data with higher resolution and less noise even at the deep waters. However, in order to acquire higher-quality bathymetric data in an actual AUV bathymetric survey, it is required to establish a method for acquiring bathymetric data with sufficiently high reproducibility within the range of the bathymetric data precision. To aim at such a standardization of AUV bathymetric survey technology for acquiring high-quality bathymetric data, the JAMSTEC and JHOD conducted sea trials to verify an actual bathymetric data performance using the "AUV-NEXT".
In these sea trials, in March and November 2020, the "AUV-NEXT" dived around the Nankai Trough area (at depths of 2500-2800 m) offshore the Kii Peninsula and the Suruga Bay, and bathymetry was surveyed by using a bathymetric side scan sonar (Bathy-SSS: EdgeTech 2205AUV) installed on the AUV. After sufficient preliminary tests such as DVL calibration, which is important for AUV navigation, and patch test for correcting the mounting angle of the sonar, bathymetric data were acquired, and by confirming the reproducibility of bathymetric data to which various necessary corrections were applied, we were able to find out some important points in AUV bathymetric survey technology. As a result, higher quality bathymetric data can be acquired by using the “AUV-NEXT”. In this paper, we report the initial results of these sea trials.

Keywords: Autonomous Underwater Vehicle (AUV), “AUV-NEXT”, Bathymetric survey, Bathymetric side scan sonar (Bathy-SSS), Multibeam echosounder (MBES), Sea trials on bathymetric survey performance

©2021. Japan Geoscience Union. All Right Reserved.

[J] Poster | S (Solid Earth Sciences)：S-CG Complex & General

Sat. Jun 5, 2021 5:15 PM - 6:30 PM JST | Sat. Jun 5, 2021 8:15 AM - 9:30 AM UTC | Ch.19_1

[S-CG45] Ocean Floor Geoscience

convener:Kyoko Okino(Atmosphere and Ocean Research Institute, The University of Tokyo)

Most of Earth's volcanism and much of its tectonic activity occur on and beneath the s eafloor. Various phenomena on the seafloor are closely linked to plate tectonics, Earth s tructure and dynamics, and also related to Earth's environments through the hydrosphe re and atmosphere. Seafloor rocks and sediments record Earth's evolution and heat an d material fluxes on the Earth. Ocean Floor Geoscience session covers a broad range of research on seafloor such as mid-ocean ridge process, subduction dynamics, arc magm atism, hot spot and LIPs, crustal movement and structure etc. Every field of researches and every approaches are welcomed.The session aims to encourage discussion among scientists from different study fields and to integrate our understanding of ocean floor. The session is co-chaired by K. Tadokoro (Nagoya Univ.), O. Ishizuka (AIST), T. Toki (Univ . Ryukyus), and N. Takahashi (JAMSTEC).

[SCG45-P01] **Temporal variation of crustal accretion along the Vulcan Transform, the Southern Ocean: Preliminary results of KH-19-6 cruise**

*Kyoko Okino[1], Kenichiro Tani[2], Osamu Ishizuka[3], Hiroaki Koge[3], JINYU ZHOU[1] (1.Atmosphere and Ocean Research Institute, The University of Tokyo, 2.National Museum of Nature and Science, 3.National Institute of Advanced Industrial Science and Technology)

[SCG45-P02] S wave velocity structure at the Kairei Hydrothermal Vent Field near the Rodriguez Triple Junction in the Indian Ocean

*Ayato Morii[1], Toshinori Sato[1], Hiroyoshi Takata[1], Tomoaki Yamada[2], Masanao Shinohara[3] (1.Chiba Unv., 2.JMA, 3.ERI, Unv. Tokyo)

[SCG45-P03] **Deep-tow magnetics for 29–33 Myr seafloor of the Southeast Indian Ridge**

*Masakazu Fujii[1,2], Kyoko Okino[3], Chiori Tamura[3] (1.National Institute of Polar Research, 2.SOKENDAI (The Graduate University for Advanced Studies), 3.AORI, UTokyo)

[SCG45-P04] **Magnetic and gravity constraints on crustal structure of the Nosappu Fracture Zone, Northwestern Pacific**

*Mai Kintsu[1], Nobukazu Seama[1], Masakazu Fujii[2,3], Tomoko Hanyu[4] (1.Department of Planetology, Graduate School of Science, Kobe University, 2.National Institute of Polar Research, 3.SOKENDAI (The Graduate University for Advanced Studies), 4.Kobe Ocean-Bottom Exploration Center)

[SCG45-P05] Multibeam bathymetric and single-channel seismic surveys of the Mid-Slope Terrace off Sanriku in the northern Japan Trench

*Toshiya Fujiwara[1], Toshiya Kanamatsu[1], KanHsi Hsiung[1] (1.Research Institute for Marine Geodynamics, Japan Agency for Marine-Earth Science and Technology)

[SCG45-P06] Deformation of the upper plate within the Tohoku Region Pacific Coast analyzed by the top surface structure

*Hiroaki Koge[1], Ayanori Misawa[1], Toshiya Fujiwara[2], Yoshiaki Suzuki[1], Yusuke Sato[3], Ryosuke Komatsu[5], Chiori Tamura[4], Katsura Kameo[4] (1.AIST, 2.JAMSTEC, 3.Tokai Univ., 4.AORI. UTokyo, 5.MOL Marine Co., Ltd)

[SCG45-P07] Classification and estimation of petit-spot volcanos by multibeam backscatter data

*Matamura Yuki[1], Naoto Hirano[2], Masakazu Fujii[3,4] (1.Tohoku University, 2.Center for Northeast Asian Studies, Tohoku University, 3.National Institute of Polar Research, 4.SOKENDAI)

[SCG45-P08] Origin of Philippine Sea basins -Tectonic setting leading to subduction initiation of Izu-Bonin-Mariana arc-

*Osamu Ishizuka[1,2], Kenichiro Tani[3], Gen Shimoda[1], Yumiko Harigane[1], Taichi Sato[1], Rex Taylor[4], Susumu Umino[5], Tian Yu Ping[5], Izumi Sakamoto[6], Yuka Yokoyama[6], Sho Yatsuka[6], Ryota Uchiyama[6], Tomoaki Wakayama[6], Aimi Suzuki[6], Kana Narita[7], Chinatsu Ogawa[7], Yasuhiko Ohara[8,2,9], Chris Conway[1] (1.Geological Survey of Japan, AIST, 2.JAMSTEC, 3.NMNS, 4.University of Southampton, 5.Kanazawa University, 6.Tokai University, 7.Ehime University, 8.Japan Coast Guard, 9.Nagoya University)

[SCG45-P09] What happened to the seafloor around Nishinoshima volcano during deployment of OBEMs between September 2018 and December 2020?

*Noriko Tada[1], Kiyoshi Baba[2], Toshiya Fujiwara[1], Yoshihiko Tamura[1], Toshiya Kanamatsu[1], Kenta Yoshida[1], Akimichi Takagi[3], Fukashi Maeno[2] (1.Research Institute for Marine Geodynamics, Japan Agency for Marine-Earth Science and Technology, 2.Earthquake Research Institute, The University of Tokyo, 3.Japan Meteorological Agency)

[SCG45-P10] Estimation of the Active Faults from BSR-derived heat flow by Automated Velocity Analysis in the Nankai Trough, Japan

*Shuto Takenouchi[1], Kota Mukumoto[1], Takeshi Tsuji[1], Shuichi Kodaira[2], Gou Fujie[2], Yasuyuki Nakamura[2], Kazuya Shiraishi[2] (1.Kyushu-university, 2.Japan Agency for Marine-Earth Science and Technology)

[SCG45-P11] Precipitation process and early diagenesis after deposition of iron hydroxide in Nagahama Bay, Satsuma Iwo-Jima Island, Kagoshima, Japan.

*Koki Hori[1], Shoichi Kiyokawa[2], Minoru Ikehara[3] (1.Department of Earth and Planetary Sciences, Graduate School of Sciences, Kyushu University, 2.Department of Earth and Planetary Sciences Faculty of sciences, Kyuushu University, 3.Center for Advanced Marine Core Research, Kochi University)

[SCG45-P12] Geological structures in the southern part of the Okinawa Trough north off Ishigaki Island: Preliminary results of the KH-21-3 cruise

*Ayanori Misawa[1], Ryuta Arai[2], Masahiko Sato[3], Saki Ishino[1], Misaki Horiuchi[4], Keita Suzuki[4], Chiori Tamura[5], Katsura Kameo[5], Satoshi Okumura[6], Makoto Otsubo[1], KH-21-3 Shipboard Scientists (1.Geological Survey of Japan, National Institute of Advanced Industrial Science and Technology(AIST), 2.Research Institute for Marine Geodynamics, Japan Agency for Marine-Earth Science and Technology (JAMSTEC), 3.Department of Earth and Planetary Science, The University of Tokyo, 4.Nippon Marine Enterprises, Ltd., 5.Atmosphere and Ocean Research Institute, The University of Tokyo, 6.MOL Marine Co. Ltd.)

[SCG45-P13] **The link between volcanism and tectonics at back-arc rifting stage: analysis of three volcanic areas in the southern Okinawa Trough**

*JINYU ZHOU[1], Kyoko Okino[1], Masakazu Fujii[2,3] (1. Atmosphere and Ocean Research Institute, The University of Tokyo, 2.National Institute of Polar Research, 3.The Graduate University for Advanced Studies)

[SCG45-P14] Mineralogical and geochemical study of sediment cores collected from the Ieyama hydrothermal field in the Okinawa Trough

*Jun-ichiro Ishibashi[1], Takashi Miyamoto[1,3], Shuhei Totsuka[1,2], Kazuhiko Shimada[1], Toru Yamasaki[2], Ken Ikehara[2], Toshiro Nagase[4], Yutaro Takaya[5], Hideaki Machiyama[6], Koichi Iijima[6], Hirofumi Yamamoto[6], Hidenori Kumagai[6] (1.Department of Earth and Planetary Sciences, School of Science, Kyushu University, 2.National Institute of Advanced Industrial Science and Technology, 3.School of science, University of Tokyo, 4.Tohoku University Museum, 5.Waseda Research Institute for Science and Engineering, 6.Japan Agency for Marine-Earth Science and Technology)

[SCG45-P15] Geochemical and geochronological study of barite in sediment cores obtained from Higashi Izena hydrothermal field, Okinawa Trough

Yushi Itatani[1], *Jun-ichiro Ishibashi[1], Makiko Tomita[2], Shin Toyoda[2], Ryuichi Shinjo[3], Kazuno Arai[4], Taisei Fujiwara[5] (1.Department of Earth and Planetary Sciences, Graduate School of Science, Kyushu University, 2.Okayama University of Science, 3.Faculty of Science, University of Ryukyus, 4.Center for Advanced Marine Core Research, Kochi University, 5.Institute for Geology and Geochronology)

[SCG45-P16] Fin whale signals recorded by S-net

*Masashi Mochizuki[1], Takeshi Nakamura[2], Ryoichi Iwase[3], Kenji Uehira[1] (1.National Research Institute for Earth Science and Disaster Resilience, 2.Central Research Institute of Electric Power Industry, 3.Japan Agency for Marine-Earth Science and Technology)

[SCG45-P17] Effective removal of oceanic variation from ocean bottom pressure gauge data using the MSSA

*Kenta Shimizu[1], Toshinori Sato[1], Koichi Murata[1], Norihisa Usui[2], Hajime Shiobara[3], Tomoaki Yamada[4], Masanao Shinohara[3] (1.Chiba Univ., 2.MRI, 3.ERI. Univ. Tokyo, 4.JMA)

[SCG45-P18] Sampling process of seafloor sediments as a source of information on their rheology

*Nikita Dubinya[1,2], Sergey Tikhotskiy[1,2], Victor Nachev[1,3] (1.Moscow Institute of Physics and Technology, 2.Schmidt Institute of Physics of the Earth of the Russian Academy of Sciences, 3.Sadovsky Institute of Geosphere Dynamics of the Russian Academy of Sciences)

[SCG45-P19] Technical protocol for deep-sea environmental monitoring by the portable seafloor observation platform Edokko Mark 1

*Hiroyuki Yamamoto[1], Tetsuya Miwa[1], Shinsuke Kawagucci[1], Sangkyun Lee[2], Atsuo Oono[3], Kousuke Tsutsumi[3], Hideki Sugishima[3] (1.Japan Agency for Marine-Earth Science and Technology, 2.J-MARES/JGI, 3.J-MARES/idea)

Temporal variation of crustal accretion along the Vulcan Transform, the Southern Ocean: Preliminary results of KH-19-6 cruise

*Kyoko Okino[1], Kenichiro Tani[2], Osamu Ishizuka[3], Hiroaki Koge[3], JINYU ZHOU[1]

1. Atmosphere and Ocean Research Institute, The University of Tokyo, 2. National Museum of Nature and Science, 3. National Institute of Advanced Industrial Science and Technology

The Vulcan transform is a 120 km long, east-west trending strike-slip boundary between the Antarctic and Sur plates. The ridge axis offsets right-stepped, and the Sur plate moves westward at 15-16 mm/yr. relative to the Antarctic plate (MORVEL, DeMets et al., 2010). R/V Hakuho-maru KH-19-6 cruise conducted geophysical mapping along with this transform and conducted five dredge hauls along Antarctic side of transform wall from the present-day ridge axis to 120 km off-axis, that roughly corresponds 15 Ma crust assuming global plate motion model. As part of the project MOWALL (Moho Observation along transform fault WALLs), we try to investigate the temporal variation of the mid-ocean ridge process and the relationship with mantle heterogeneity by systematic rock sampling along with long oceanic transform, where the whole crustal section is exposed in chronological order. In this presentation, we present the preliminary analysis of geophysical data collected during the cruise.

The axial valley of the southern ridge segment shows an asymmetric structure. In the western part of the axial valley, ridge-parallel, inward-facing fault scarps develop to the ridge flank. In the eastern part, contrary, relatively smooth, doomed high forms the deeper part of the axial wall, and a large volcanic peak continues eastward. The doomed high is likely a detachment surface suggesting magma-starved spreading. A steep and oblique lineament develops about 20 km east of the axis. The abyssal hills are well-ordered east of 17˚W, showing typical magmatic seafloor.
The magnetic profiles along the TF were also collected, to obtain the exact history of the spreading rate. Our forward modeling (2D, assuming constant thickness magnetization layer draped the observed bathymetry) provides two possible scenarios of spreading. The preliminary result of age dating of dredged rock samples possibly supports one of these two models, assuming the change of spreading rate at 2~3 Ma. We also calculate mantle Bouguer anomaly (MBA) using newly collected multibeam bathymetry. Anomalous high positive MBA appears around the eastern axial wall, suggesting the exposure of high-density material. The variation of crustal thickness is also estimated from gravity anomalies. The result indicates that the thickness of crust shows a million-year order fluctuation, reflecting the temporal variation of melt supply at this ridge segment.

Keywords: mid-ocean ridge process, transform fault, oceanic crust

©2021. Japan Geoscience Union. All Right Reserved.

S wave velocity structure at the Kairei Hydrothermal Vent Field near the Rodriguez Triple Junction in the Indian Ocean

*Ayato Morii[1], Toshinori Sato[1], Hiroyoshi Takata[1], Tomoaki Yamada[2], Masanao Shinohara[3]

1. Chiba Unv., 2. JMA, 3. ERI, Unv. Tokyo

1. Introduction

The Kairei Hydrothermal Vent Field (KHF) is located at eastern area of the first segment of the Central Indian Ridge which is extended from the Rodriguez Triple Junction. The KHF extrudes fluid with rich H_2 content. Although the KHF itself exists above a basaltic rock massif (Hakuho Knoll), gabbro and mafic rocks such as peridotite were discovered on the seafloor around the KHF. These deep rocks may move upward, may be serpentinized by sea water, and may contribute to the high H_2 concentration of the Kairei vent fluid. To investigate seismic structure, we conducted a seismic survey with ocean bottom seismometers and an air-gun in 2013. Takata et al. (JpGU, 2015) reported the P wave velocity structure. They revealed high velocity areas with more than 6.0 km/s of the P wave velocity under 1-2 km from the seafloor at the Hakuho Knoll and the Yokoniwa Rise which is located north of the Hakuho Knoll. This result indicated uplift of deep rocks. To investigate these rock’ s properties, we determine the S wave structure using the air-gun.

2. Data acquisition and analysis methods

We conducted a seismic refraction/reflection survey from January 27 to March 19 in 2013 using S/V Yokosuka of Jamstec. In the experiment, we used 19 OBSs, an air-gun (G.I. gun) and a single channel steamer cable.

To make the S phase easer to see, we rotate the horizontal components of seismic sensors to the radial and transverse directions. We estimate horizontal direction of the sensors from trajectories of water waves. Using picking data of the S phase, we construct a 3D S wave velocity structure by the FAST program (Zelt and Barton, 1998).

3. Results

A provisional result is that the high P wave velocity areas under the Hakuho Knoll and the Yokoniwa Rise have high Vp/Vs ratio with about 2.0. This ratio is higher than those for gabbro (about 1.9) and peridotite (about 1.7). Since the Vp/Vs ratio of serpentine is about 1.8-2.2, this result may indicate serpentinization of these areas.

Acknowledgment

We thank the captain and crew of S/V Yokosuka of JAMSTEC for their support. This work was supported by Grant-in-Aid for Scientific Research on Innovative Areas of the Ministry of Education, Culture, Sports, Science and Technology (Grant Number 20109002, TAIGA project).

©2021. Japan Geoscience Union. All Right Reserved.

Keywords: S wave velocity structure, Vp/Vs ratio, Kairei hydrothermal vent field, serpentinization

©2021. Japan Geoscience Union. All Right Reserved.

Deep-tow magnetics for 29–33 Myr seafloor of the Southeast Indian Ridge

*Masakazu Fujii[1,2], Kyoko Okino[3], Chiori Tamura[3]

1. National Institute of Polar Research, 2. SOKENDAI (The Graduate University for Advanced Studies), 3. AORI, UTokyo

Knowledge of the Earth's magnetic field intensity variations provides an essential constraint on the age benchmark and geodynamo model. A record of absolute palaeointensity has been compiled from archaeomagnetic and volcanic materials, and long-term relative palaeointensity has been obtained from sedimentary sequences. Although geomagnetic intensity signal recorded as the oceanic crust's thermoremanence should provide a higher-time-resolution record of crustal accretion at mid-ocean ridges (e.g., Gee et al., 2000), available data is essentially limited due to observation difficulty. Here, we present new observation data of near-seafloor magnetic anomalies of 29–33 Myr seafloor at the Southeast Indian Ridge.

We conducted a deep-tow operation during the R/V Hakuho-maru cruise of KH-20-1 (Cape Town to Fremantle, January –February 2020). Underway geophysical data (e.g., multibeam bathymetry and total magnetic field) of the target area has been obtained during the KH-07-4 and KH-16-1 cruises. The deep-sea total magnetic fields were measured using the deep-tow cesium magnetometer developed by the Atmosphere and Ocean Research Institute, The University of Tokyo. The towed proton magnetometer data was simultaneously observed at the sea-surface. The deep-tow sensor was kept 30 m away from the mainframe using the electric cable. The stainless mainframe consists of the magnetometer body, a pressure sensor, a motion sensor, and a transponder for acoustic positioning. The mainframe is 100 m away from the 600kg-weight tied to the ship No.1 wire. Another transponder was also set to the ship No.1 wire 20 m above the weight. The data of total magnetic field, depth, and attitude are merged and recorded at 2Hz. This observation covers the signal from the northern off-axis area of the Southeast Indian Ridge on 13–14 February. The sensor reached ~4,500m deep. The total length of obtained data at >3,000m deep is up to 40 miles.

Obtained near-seafloor magnetic anomalies ranges 60,700 to 62,300 nT. This variation is three times larger than the total intensity variation observed at sea-surface. Long-wavelength signatures are well correlated with each other. Comparing with geomagnetic polarity chrons (Gee and Kent, 2015), previously obtained surface data (Quesnel et al., 2009), and globally picked isochrons (Seton et al., 2014), we individually picked magnetic isochrons of C11n12n, C11r, C12n, and C12r from obtained near-seafloor magnetic anomalies. The corresponding age is 29.401 to 33.058 Myr. Several tiny wiggles with an amplitude of up to 300 nT are remarkably observed in C12r. This result is generally consistent with summarized cryptochrons (Cande and Kent, 1992; Cande and Kent, 1995). A few tiny wiggles with an amplitude of up to 200 nT were also observed in C12n, which have never been reported. We consider that this result can be a new finding of short-term fluctuations in the geomagnetic field, but careful examination considering crustal processes is needed. In this presentation, we aim to discuss these observed tiny wiggles' origin by comparing our results with sea-surface anomaly data of faster spreading seafloor segments (western slopes of the East Pacific Rise 22–33°S and Pacific Antarctic Ridge 33–40°S). Besides, Oligocene sediment record from IODP Sites U1331, U1332, and U1333 (140°W Pacific equatorial high-productivity zone; Yamazaki et al., 2013; Yamamoto et al., 2013), and DSDP Site 522 (Walvis Ridge, South Atlantic Ocean; Hartl et al., 1993; Tauxe and Hartl, 1997) are utilized to discuss palaeointensity variation. We will also compare our results with 30Myr lava flow data from the Lima Limo

©2021. Japan Geoscience Union. All Right Reserved.

section of the Ethiopian trap (Ahn et al., 2021; Yoshimura et al., 2020).

Keywords: Near-seafloor magnetic anomaly, C11n12n, C11r, C12n, & C12r, Southeast Indian Ridge

©2021. Japan Geoscience Union. All Right Reserved.

Magnetic and gravity constraints on crustal structure of the Nosappu Fracture Zone, Northwestern Pacific

*Mai Kintsu[1], Nobukazu Seama[1], Masakazu Fujii[2,3], Tomoko Hanyu[4]

1. Department of Planetology, Graduate School of Science, Kobe University, 2. National Institute of Polar Research, 3. SOKENDAI (The Graduate University for Advanced Studies), 4. Kobe Ocean-Bottom Exploration Center

The structure and lithology of fracture zones (FZ) are essential for understanding long-term tectonic evolution of the seafloor as well as Earth water and material cycles. Widely obtained marine geophysical dataset such as magnetic anomalies can provide strong constraint on crustal structures, in which several historical information such as magnetic field variations, crustal accretion processes, and temporal change of lithology should be reserved. Here,we present analyses of magnetic dataset obtained along and across the Nosappu Fracture Zone (NFZ). The NFZ is located on the old Pacific lithosphere just before subducting into the Kuril trench. It extends over 1000 km NNE-SSW direction from around 33˚N,154˚E; the Shatsky Rise, to around 42˚ N,148˚E; the Kuril Trench. The horizontal distance of offset is about 350 km based on the magnetic isochron M5r, which is 6 Myr or more converted to age (Nakanishi, 1993). The purpose of this study is to understand the geophysical properties of the magnetic, as well as gravity and topography, in the NFZ for providing constraints on the crustal structure.

Multibeam bathymetry, total and vector magnetic fields, and gravity data were acquired along and across the NFZ during two research cruises; the KR06-03 with R/V Kairei and YK14-09 with R/V Yokosuka. The magnetic anomaly was calculated by subtracting the International Geomagnetic Reference Field (IGRF12; e.g., Thébault et al., 2015) from each magnetic field data point. The amplitude of the magnetic anomaly ranged from -500 to +600 nT for the east side of the NFZ, and from -200 to +400 nT for the west side. The clear magnetic stripes appeared in the magnetic anomaly map and were divided into the east and west sequences, which corresponds to each formation age of the crust in contact with the NFZ. The crustal magnetization structure was estimated from the calculated magnetic anomaly based on the well-established inversion methods (e.g., Macdonald et al., 1980; Parker & Huestis, 1974). The inversion calculation was carried out with a focus on the area where dense data were obtained, assuming a 1.0 km thick magnetized source layer without vertical variation of magnetization. No annihilator was added. For estimating paleo-latitude when the oceanic crust was formed, we examined various magnetization directions to determine the optimal one by comparing them with the results of the topography and gravity analysis. To determine the FZ area semi-objectively, slope angle was calculated from the multibeam bathymetric data using the Generic Mapping Tools (GMT; Wessel & Smith, 1991). Slope azimuth was also calculated to detect the strike of abyssal hills using GMT. We determined the east and west boundaries of the FZ area between normal oceanic crust by using the maximum value of the slope angle. The strike of abyssal hills around the NFZ was also detected by using the results of slope azimuth. In addition, mantle bouguer anomaly (MBA) was calculated from the satellite-derived free-air gravity anomaly (Sandwell et al., 2014) by subtracting the predicted gravity for the gridded multibeam bathymetry data and a constant thickness crust using the method of Parker (1973).

The low intensity of the crustal magnetization was observed along the FZ area. Two magnetic boundaries parallel to the NFZ were identified by the vector magnetic anomaly and the crustal magnetization. Assuming the magnetization inclination was -30˚, the magnetic boundaries almost coincided with the east and west boundaries of the FZ area based on the bathymetric results. The region where low MBA value appeared also corresponded to the FZ area. Inside the FZ area, several local areas with high

©2021. Japan Geoscience Union. All Right Reserved.

magnetization intensity were observed at the areas with local low value of the MBA. In this presentation, we aim to discuss geophysical insights to the formation background of crustal structure at regional scales.

Keywords: fracture zone, magnetic anomaly, marine geophysics

©2021. Japan Geoscience Union. All Right Reserved.

Multibeam bathymetric and single-channel seismic surveys of the Mid-Slope Terrace off Sanriku in the northern Japan Trench

*Toshiya Fujiwara[1], Toshiya Kanamatsu[1], KanHsi Hsiung[1]

1. Research Institute for Marine Geodynamics, Japan Agency for Marine-Earth Science and Technology

We conducted JAMSTEC R/V Kaimei KM19-03 cruise in 2019. During the research cruise, we carried out mulibeam bathymetry and single-channel seismic reflection surveys in the Mid-Slope Terrace (MST) off Sanriku in the northern Japan Trench (39-40˚N).

The Mid-Slope Terrace (MST) is a flat to gentle slope with an average slope angle of about 0-2˚. The MST is situated at a depth of 4000-6000 m and is a slope break between the steep upper and the lower trench landward slopes. The MST has the regional variation in the depth and width of the terrace from south to north along the trench. It may reflect regional differences in the dynamics of the upper plate in the subduction zone exerting on the landward slope, or differences in the stage of the tectonic evolution. Our study area is located at a depth of 4600-4800 m and has one of the largest east-west (trench to landward) widths of the MST, about 20 km, and is a region where the MST is well developed.

The Kaimei bathymetric data were obtained using a KM122 multibeam echo sounder. And also, cross-track bathymetric data were collected using a KM122 echo sounder by the German R/V Sonne SO251A cruise and using a SeaBeam 3012 echo sounder by the JAMSTEC R/V Mirai MR16-09 Leg 4 cruise, respectively. These bathymetric data have higher resolution compared with previous data, because the data were measured using recent echo sounders. Therefore, the complex topography of co-existing slope failures, steep scarps, minor ridges, and small sedimentary basins covering the MST (e.g., Sasaki, 2003) were mapped more clearly.

The slope failures suggest erosion and landslides, the steep scarps suggest faulting, the minor ridges suggest uplift, and the small sedimentary basins suggest subsidence. The single-channel reflection record shows that the thickness of sediment basin is about 75 m even in the thickest deposits. Considering the sedimentation rate of about 36-109 cm/kyr estimated from sediment cores obtained by piston coring in the sedimentary sub-basin in the study area, the sedimentary sub-basin on the MST has been formed within about 70-200 ka. The sedimentary layers located on the western and landward sides of the MST are inclined toward the landward in the lower part of the layer, suggesting that the western side of the MST has been tilted toward the landward while subsiding.

In this paper, we will describe features and relations of the seafloor and the sub-surface structures, and discuss the tectonic evolution of the upper plate in the Japan Trench.

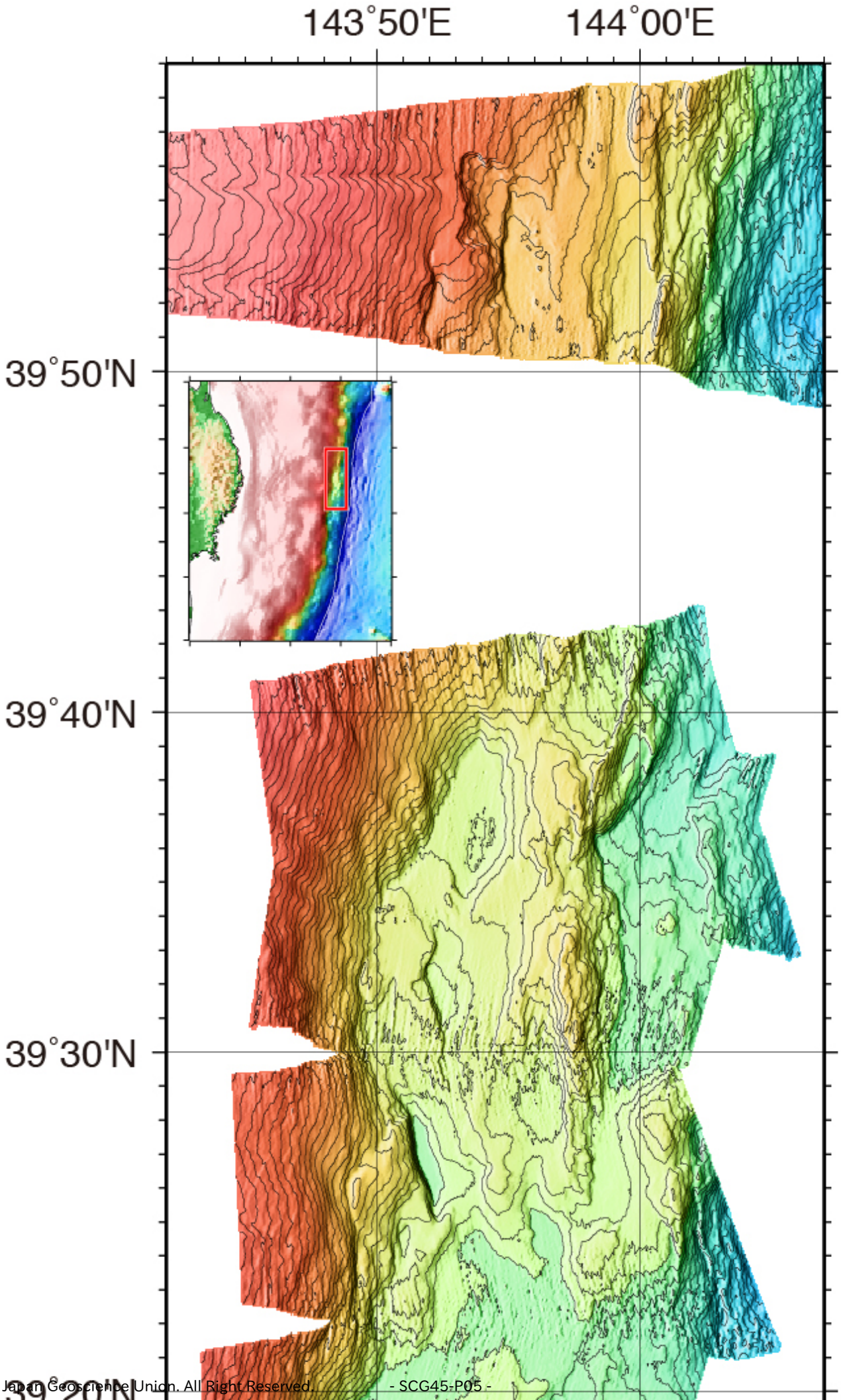
We thank the officers and crew of R/V Kaimei for outstanding professionalism and dedication that made the cruise successful. We are indebted to marine technicians from Nippon Marine Enterprises, M. Takaesu, Y. Ohwatari, H. Iwamaru, and M. Morioka for their invaluable help to acquire data at sea.

Figure: Bathymetry of the Mid-Slope Terrace off Sanriku in the northern Japan Trench. Contour interval is 50 m.

©2021. Japan Geoscience Union. All Right Reserved.

Keywords: Japan Trench, Mid-Slope Terrace, Multibeam Bathymetric Survey, Single-Channel Seismic Reflection Survey

©2021. Japan Geoscience Union. All Right Reserved.



©2021. Japan Geoscience Union. All Right Reserved.

©2021. Japan Geoscience Union. All Right Reserved.

Deformation of the upper plate within the Tohoku Region Pacific Coast analyzed by the top surface structure

*Hiroaki Koge[1], Ayanori Misawa[1], Toshiya Fujiwara[2], Yoshiaki Suzuki[1], Yusuke Sato[3], Ryosuke Komatsu[5], Chiori Tamura[4], Katsura Kameo[4]

1. AIST, 2. JAMSTEC, 3. Tokai Univ., 4. AORI. UTokyo, 5. MOL Marine Co., Ltd

Large earthquakes and tsunamis have repeatedly occurred along the Japan Trench. In the 2011 Tohoku-Oki earthquake (Mw 9.0), the fault rupture extended to the shallow portion of the Japan Trench. These large slips on shallow decollement resulted in the huge tsunami that devastated much of the east coast of Japan. Therefore, it is key to understand the deformation of forearc for disaster prevention. Geodetic observations have provided insights into the deformation in the landward plate after the 2011earthquake. However, there are few kinds of research that throughout the direct observation of bathymetry or the shallow structure below the seafloor. Therefore, to discuss the following two purposes, we have conducted the shipboard geophysical observation in the KH-20-10 cruise; a multi-narrow beam echo sounder (MBES); proton precession magnetometer (PPM), shipboard three-component magnetometers (STCM), shipboard gravimeter, and sub-bottom profiler (SBP). 1)Subsidence in the forearc slope from the surface structure of the hollow-shaped sedimentary basin. To consider the development of normal faults on the sedimentary basin, we obtained the SBP cross-sections in sedimentary basins scattered in the forearc slope. 2) Revisit postseismic deformation in the forearc slope, The survey lines obtained from the seafloor topography cross-section of Fujiwara et al. (2011) were re-obtained in this cruise. We compare the three seafloor topography data before the 2011 earthquake, immediately after the 2011 earthquake, and approximately 10 years after the earthquake, and examine the presence or absence of postseismic deformation.
We were able to carry out all the planned observations on the KH-20-10 voyage, because of the good conditions of the sea and the equipment. In this presentation, we will introduce the preliminary results while the KH-20-10 voyage. In particular, our presentation will focus on the results related to the topic 2).

Keywords: japan trench, subduction zone, sub-bottom profiler, bahtymetry

©2021. Japan Geoscience Union. All Right Reserved.

Classification and estimation of petit-spot volcanos by multibeam backscatter data

*Matamura Yuki[1], Naoto Hirano[2], Masakazu Fujii[3,4]

1. Tohoku University, 2. Center for Northeast Asian Studies, Tohoku University, 3. National Institute of Polar Research, 4. SOKENDAI

Petit-spots are small monogenetic volcano generated on the outer rise system prior to subduction of oceanic plate. It shows several important features of the Earth (e.g. the composition of asthenosphere: Hirano et al., 2006). Although the geochemical composition of petit-spot basalts recently provides new insights both into lithospheric and asthenospheric mantle prior to subduction (e.g. Yamamoto et al., 2014; Machida et al., 2015; Pilet et al., 2016), the surface structure of volcanic distributions and lava-flowing patterns are not enough discussed in their tectonic regime. For example, the detail distribution of petit-spot volcano generally follows the tectonic lines of surface environment. Petit-spot volcanic province after the subduction plausibly controls the occurrence of interplate earthquake, contrasting the pelagic sediment of the surface of subducting plate. However, we have found only a few locations of petit-spot volcanic field. Previously, the acoustic backscatter images have been macroscopically checked to discover a petit-spot on the KR04-08 cruise in 2004 (Hirano et al., 2006). In this research, we aim to establish a method to find new petit-spots by acoustic measurement data and to classify petit-spots by topographic features such as their distributions and lava-flowing patterns.

As the petit-spot volcanic edifices are small and monogenetic of less than 1 km^3 and few hundred meters in height (Hirano et al., 2008), it is difficult to find them using onboard bathymetry for deep ocean floor. The acoustic backscatter image, on the other hand, is a powerful tool to visualize submarine lava flow. In this research, we picked up data from a petit-spot volcanic field Site C, off the Fukushima and Miyagi Prefecture, as a target area, where tens of strong backscatter zones has been recognized as the presence of petit-spot sites (up to 80 sites; Hirano et al., 2008). We conducted geophysical mapping of multibeam echo sounder in this area during three cruises (KR04-08, YK14-05 and KS18-09). The CARIS HIPS and SIPS software (Teledyne CARIS Inc., Ltd., Fredericton, Canada) was used for raw data processing. In this cleaning process, both CUBE algorism and manual editing were applied. The sound velocity was corrected by real-time data of the surface water velocity meter, and observations of XCTD (expendable conductivity, temperature, and depth) probe profiles.

Backscatter image shows many of high intensity locations that are similar to some locations of petit-spot that were already sampled. There is a variation of intensity. It is considered that sediments signature or measurement conditions (e.g., track direction, horizontal distance from the ship) can affect observed beam-pattern and scattering. Additionally, highly intensity zones have a variation of the area. Comparing with topography, small areas (approximately 1 km in diameter) are located flat field. In contrast, large areas (approximately 5 km in diameter) are located topographical height (approximately 500 m in height). Therefore, it is suggested that intensity variations are also caused by scattering on the slope or existing relatively large petit-spot. Furthermore, some of large areas show some peaks on topography. It suggests an eruption by multiple petit-spot activities.

In following analytical steps, we are applying clustering of gray level co-occurrence matrix (GLCM), in which the probability of neighboring some target pixel value with any neighbor pixel value can be estimated. It is calculated by each texel of any size subarea cut from image, then calculating some values

©2021. Japan Geoscience Union. All Right Reserved.

to explain textual feature (e.g. regularly pattern area, strong signal area). The features of backscatter image provide an effective means to compile topography before the clustering features by k-means clustering (e.g. Honsho et al., 2015; Fakiris et al., 2019). Based on results of the textural feature classes that describe rough surface, and intensity of backscatter image, we aim to discuss the correlation between our classified groups and the geochemical and physical variation of petit-spot lavas.

Keywords: petit-spot, GLCM, acoustic backscatter image, classification

©2021. Japan Geoscience Union. All Right Reserved.

Origin of Philippine Sea basins -Tectonic setting leading to subduction initiation of Izu-Bonin-Mariana arc-

*Osamu Ishizuka[1,2], Kenichiro Tani[3], Gen Shimoda[1], Yumiko Harigane[1], Taichi Sato[1], Rex Taylor[4], Susumu Umino[5], Tian Yu Ping[5], Izumi Sakamoto[6], Yuka Yokoyama[6], Sho Yatsuka[6], Ryota Uchiyama[6], Tomoaki Wakayama[6], Aimi Suzuki[6], Kana Narita[7], Chinatsu Ogawa[7], Yasuhiko Ohara[8,2,9], Chris Conway[1]

1. Geological Survey of Japan, AIST, 2. JAMSTEC, 3. NMNS, 4. University of Southampton, 5. Kanazawa University, 6. Tokai University, 7. Ehime University, 8. Japan Coast Guard, 9. Nagoya University

Robust tectonic reconstruction of the evolving Philippine Sea Plate for the period immediately before and after subduction initiation at ~52 Ma to form the Izu-Bonin-Mariana (IBM) arc is prerequisite to understand cause of subduction initiation (SI) and test competing hypotheses for SI such as spontaneous or induced nucleation. Understanding of nature and origin of overriding and subducting plates is especially important because plate density is a key parameter controlling SI based on numerical modeling (e.g., Leng and Gurnis 2015). There is increasing evidence that multiple geological events related to changing stress fields took place in and around Philippine Sea plate about the time of SI ~52 Ma (Ishizuka et al., 2011). For our understanding of the early IBM arc system to increase, it is important to understand the pattern and tempo of these geological events, particularly the duration and extent of seafloor spreading in the proto arc associated with SI, and its temporal relationship with spreading in the West Philippine Basin (WPB) and structural development of the Daito Ridge Group.

Recent cruises (KS-17-15 and YK19-07S cruises) in the Philippine Sea basins investigated origin and age of formation of ocean basins in and around the Daito Ridge group. The data are still preliminary, but some fresh basalt samples returned well-defined $^{40}Ar/^{39}Ar$ ages older than the age of onset of subduction along the IBM arc at c. 52 Ma. Combined with interpretation of seafloor magnetic anomaly data, this strongly implies that some part of the Philippine Sea basins such as the West Philippine Basin existed prior to the IBM arc, and this basin could be a part of overriding plate at subduction initiation.

Temporal variation of geochemical characteristics of basalts in the Philippine Sea basins appears to indicate that major compositional variation occurred in sub-Philippine Sea mantle subsequent to subduction initiation. This might imply that sinking of large volume of Pacific Plate along the entire IBM arc margin triggered counterflow of asthenospheric mantle and reorganization of sub-Philippine Sea mantle.

The Kita-Daito Basin separates the Amami Plateau and the Daito Ridge. No rock sampling has been reported from this basin to constrain its age and origin of this basin. The Vp model of the Kita-Daito Basin suggests the presence of a 4 –6 km thick crust, similar to the backarc basin oceanic crust in the Shikoku and Parece Vela Basins, as revealed by Nishizawa et al. (2011, 2013). These features seem to imply that rifting and seafloor spreading occurred between the Amami Plateau and Daito Ridge to form the Kita-Daito Basin. Dredge sampling and Shinkai 6500 submersible survey observed and recovered samples from the crustal sections exposed in the deepest part of the basin. Collected samples are mostly composed of volcanic rocks, porphyries and trace amount of sedimentary rock and conglomerate. The volcanic rocks are basalt to andesite clasts. These samples show geochemical characteristics implying influence of material released from subducting slab. This implies that these rocks are not part of ocean crust composed of MORB. These volcanic rocks gave ages of middle Eocene, which indicates that these

©2021. Japan Geoscience Union. All Right Reserved.

volcanic rocks formed after the period of subduction initiation of Izu-Bonin-Mariana arc. These observations seem to imply that the Kita-Daito Basin did not exist at the subduction initiation, and formed by rifting in middle Eocene accompanied by basaltic to andesitic volcanism.

Keywords: subduction initiation, Izu-Bonin-Mariana arc, Philippine Sea Plate

©2021. Japan Geoscience Union. All Right Reserved.

What happened to the seafloor around Nishinoshima volcano during deployment of OBEMs between September 2018 and December 2020?

*Noriko Tada[1], Kiyoshi Baba[2], Toshiya Fujiwara[1], Yoshihiko Tamura[1], Toshiya Kanamatsu[1], Kenta Yoshida[1], Akimichi Takagi[3], Fukashi Maeno[2]

1. Research Institute for Marine Geodynamics, Japan Agency for Marine-Earth Science and Technology, 2. Earthquake Research Institute, The University of Tokyo, 3. Japan Meteorological Agency

We have conducted geomagnetic and electric fields observation using OBEMs and VTMs (hereafter “OBEM” is used to express both instruments) on the seafloor around Nishinoshima volcano belonging to Bonin Islands since 2016 in order to find magma reservoirs and estimate an electrical conductivity structure beneath Nishinoshima. We totally deployed 22 instruments by January 2021, but five OBEMs, two of six OBEMs deployed in September 2018 and three of five OBEMs deployed in July 2019, were not able to be recovered.

Two OBEMs deployed in September 2018 were first tried to recover by self-pop-up in July 2019. Although they normally received the release commands of weights through underwater acoustic communication, they could not float up to the sea surface. We determined the position of the OBEMs both in September 2018 and in July 2019, which indicates both OBEMs shifted a few tens meters in about ten months. It might be possible that the OBEMs were partially buried in sediments by sector collapse or something like that. Two OBEMs were deployed in July 2019 and were safely recovered by self-pop-up in December 2020. Both of them were moved about 3 km in a direction away from Nishinoshima island. We tried to search and rescue three of five OBEMs which would be still on the seafloor by using KM-ROV (KM20-11 cruise in December 2020) and HPD (KS-21-2 cruise in January 2021), but could not find.

According to videos during the dives of KM-ROV and HPD, volcanic activities of Nishinoshima, especially violent Strombolian eruptions after December 2019 (Yanagisawa et al., 2020) might have some influence on the displacements and disappearances of OBEMs. We are analyzing bathymetric data obtained before May 2019 and since December 2020 to evaluate the effect of changing of bathymetric feature on the OBEMs quantitatively.

Keywords: Nishinoshima volcano, OBEM, VTM, bathymetric feature change

©2021. Japan Geoscience Union. All Right Reserved.

Estimation of the Active Faults from BSR-derived heat flow by Automated Velocity Analysis in the Nankai Trough, Japan

*Shuto Takenouchi[1], Kota Mukumoto[1], Takeshi Tsuji[1], Shuichi Kodaira[2], Gou Fujie[2], Yasuyuki Nakamura[2], Kazuya Shiraishi[2]

1. Kyushu-university, 2. Japan Agency for Marine-Earth Science and Technology

Along the Nankai Trough southwest Japan, the recurrence of great earthquakes with an interval of approximately 100 years have been identified from historical literature (Satake, 2015). Therefore, it is important to characterize the active faults for causing great earthquakes and tsunami in the Nankai Trough.

Previously, geophysical surveys have observed many faults in the Nankai Trough (e.g., Ashi et al., 2002). A seismic survey is one of the most effective methods to characterize the faults (e.g. Tsuji et al., 2014). Moreover, the joint interpretation of seismic reflection images and heat flow value estimated from the bottom-simulating reflector (BSR) makes it possible to identify the active faults (Yamano et al., 1982). In the Nankai subduction zone, the active faults cutting through accretionary prisms may act as permeable paths for pore fluid flow, and such localized fluid flow transports heat in an advective manner (Yamano et al., 2014). Especially, the active faults that have recently ruptured include open fractures and thus have higher permeability and higher heat flow. Therefore, if we identify the heat flow anomalies, we can infer the active faults there.

Some methods have evaluated heat flow in the Nankai Trough (e.g., heat flow probe (Christoffel et al., 1969); piston core samples (Kinoshita et al., 2008)). One of them is using the information of BSR (e.g., Yamano et al., 1982). On seismic profiles, BSR appears as the high-amplitude reverse-polarity waveforms parallel to the seafloor reflection: BSR indicates CH4 phase boundary between free gas and hydrate (Markl et al., 1970). The heat flow estimation method using BSR uses the depth of BSR from a seismic profile. Then from the depth information, we determine the temperature and the pressure of BSR. The temperature and depth finally estimate the spatial heat flow distribution. However, inaccurate depth information cannot lead us to accurate heat flow values. To obtain an accurate depth model and infer BSR, we have applied automated velocity analysis (Fomel et al., 2013; Chhun et al., 2018). This analysis yielded a high-resolution P-wave velocity structure (Mukumoto et al., 2019). In this analysis, P-wave velocity can be determined to all CMP gathers, and we could obtain accurate depth model for heat flow estimation.
When we applied this method to the seismic data in the Nankai Trough off Kii-suido, the heat flow mapping value was estimated approximately 40-80 (mW/m2). This result is consistent with previous studies (Ohde et al., 2018). Moreover, we interpreted the location of the active faults from the area based on high heat value. The inferred active fault is located in outer ridge region where the strike-slip faults are developed. The presence of such faults supports the interpretation of heat flow anomalies estimated by our approach.

Keywords: Heat Flow, Velocity Analysis, Nankai Trough, Seismic Reflection, Bottom-Simulating Reflector

©2021. Japan Geoscience Union. All Right Reserved.

Precipitation process and early diagenesis after deposition of iron hydroxide in Nagahama Bay, Satsuma Iwo-Jima Island, Kagoshima, Japan.

*Koki Hori[1], Shoichi Kiyokawa[2], Minoru Ikehara[3]

1. Department of Earth and Planetary Sciences, Graduate School of Sciences, Kyushu University, 2. Department of Earth and Planetary Sciences Faculty of sciences, Kyuushu University, 3. Center for Advanced Marine Core Research, Kochi University

Satsuma Iwo-Jima is a volcanic island located about 50 km south of Makurazaki City, Kagoshima Prefecture, on the northwestern edge of the Kikai caldera, and the size is about 6 km east to west and 3 km north to south. In Nagahama Bay on Satsuma Iwo-jima, iron hydroxide deposition is caused by the supply of acidic hot water rich in dissolved iron and free CO_2 (Shikaura and Tasaki, 2001; Sakamoto, 2015). However, there has never been a clear explanation for the oxidation-precipitation process in the bay, and mineral species after deposition. Therefore, in this study, we measured physicochemical properties of seawater, and observed and analyzed sediment samples or sediment porewater. And finally, we summarized a series of morphological changes from iron oxidation to the earliest diagenesis phase.

As a result of infrared thermography drone exploration in the bay, hydrothermal sources were identified at multiple locations, and we could observe that hot water spreads to the sea surface. The results of water quality measurement showed relatively low pH, ORP, EC values and high turbidity values near the water surface, and toward the deep part of the water mass, the former increased and the latter decreased. In particular, the pH and turbidity values showed a strong negative correlation, with the pH being the lowest and the turbidity being the highest near the sea surface. Correspondingly, it was confirmed from the captured water mass image that the sea surface layer was strongly turbid, and that the precipitation progressed toward the deep part (pH ≈8) and the turbidity became weaker. Furthermore, DO was higher than the metabolizable concentration of marine microaerobic iron-oxidizing bacteria (*zetaproteobacteria*) reported in previous studies (Krepski et al., 2013).
As a result of pH and dissolved element measurement of porewater from the sediment surface core sample with a length of about 40 cm collected from Nagahama Bay in 2020, the pH value changed from 7.5(near sea bottom) to 5.8(deepest part of core), and at that time concentrations of elements such as Fe, Mn, and Si increased. As a result of XRD of samples collected from another core sample collected in 2020 with a length of 1m, a peak of goethite was obtained from the upper part of the sediment (10 to 20 cmbsf) and a peak of siderite was obtained from the more deeper part. This siderite represented a rhombic euhedral shape in SEM observation. In addition, as a result of comparing the XRD peaks of the samples (5 sites) from same stratigraphy between above core and the core sample obtained in 2010, a clear siderite peak was identified at the shallowest sample from the new core, but not at the same stratigraphy sample from the past core.

Summarizing these above results, the following precipitation model can be considered in Nagahama Bay. It is suggested that abiotic oxidation of Fe (II) occurs near the surface of the water mass, and that it precipitates as ferrihydrite, which is a precursor of goethite. Also, the increase in pH toward deeper part caused by mixing with seawater is thought to strongly control the aggregation of iron hydroxide during precipitation. In addition, after deposition, parts of sediments are transformed into goethite near the sea bottom (a few cmbsf). In more deep part, dissolved iron derived from the reduction of iron hydroxide deposits and the supply of hydrothermal fluid from more deep part is contained in the pore water and it is

©2021. Japan Geoscience Union. All Right Reserved.

thought to be used for the precipitation of siderite.Especially, siderite crystals detected in shallow part are suggested to have grown in sediments over the last decade.

Keywords: Satsuma Iwo-Jima, iron hydroxide, siderite

©2021. Japan Geoscience Union. All Right Reserved.

Geological structures in the southern part of the Okinawa Trough north off Ishigaki Island: Preliminary results of the KH-21-3 cruise

*Ayanori Misawa[1], Ryuta Arai[2], Masahiko Sato[3], Saki Ishino[1], Misaki Horiuchi[4], Keita Suzuki[4], Chiori Tamura[5], Katsura Kameo[5], Satoshi Okumura[6], Makoto Otsubo[1], KH-21-3 Shipboard Scientists

1. Geological Survey of Japan, National Institute of Advanced Industrial Science and Technology(AIST), 2. Research Institute for Marine Geodynamics, Japan Agency for Marine-Earth Science and Technology (JAMSTEC), 3. Department of Earth and Planetary Science, The University of Tokyo, 4. Nippon Marine Enterprises, Ltd., 5. Atmosphere and Ocean Research Institute, The University of Tokyo, 6. MOL Marine Co. Ltd.

Backarc basins on continental margins are important constituents of the plate tectonic paradigm, and knowledge of their evolution is key to understanding the lithosphere’s development. Since the backarc basins in the rifting state at the continental margin are limited to the Okinawa Trough and the Bransfield Strait, they are not well understood due to the current rarity of such deformations. In the Okinawa Trough, intermittent rifting has been occurring since 2 Ma. Based on seismic profiles from the Yaeyama Rift, Arai et al. (2017) and Nishizawa et al. (2019) reported normal faults bounding the Yaeyama Rift and the stratigraphy of well-stratified trough-fill sediments. Arai et al. (2017) reported a magma intrusion directly beneath the narrow rift valley of the Yaeyama Rift. Arai et al. (2017) also identified a less reflective zone and a low-velocity zone in the trough-fill sediments and suggested an off-axis magma chamber in the Okinawa Trough. However, the spatial distribution of the normal faults around the Yaeyama Rift and the intrusive structure beneath the Yaeyama Rift has not yet been clarified.

To clarify the detailed geological structure of the southern part of the Okinawa Trough, an integrated marine geological and geophysical survey was conducted using *R/V Hakuho-maru* of JAMSTEC (KH-21-3 cruise) in January 2021. In this cruise, we conducted the following survey: swath bathymetric survey, multi-channel seismic (MCS) reflection survey, subbottom profiler survey, geomagnetic measurements (proton precession magnetometer and shipboard three-component magnetometers), and gravity measurement. The MCS survey used two 355 cubic inch GI guns (total volume of 710 cubic inches) and a 1,200 m 48ch streamer cable. In the MCS profiles, we could obtain clear images down to approximately 1.6 sec (Two-Way Travel Time: TWT) below the seafloor in the trough-fill sediments of the Okinawa Trough. In the Yaeyama Rift, the graben formed by innumerable normal faults were clarified. Moreover, total magnetic field data were acquired with a surface-towed proton magnetometer. The proton magnetometer sensor was towed approximately 290 m behind the ship to minimize magnetization effects from the ship. In this presentation, we will show the preliminary results of the KH-21-3 cruise in the southern part of the Okinawa Trough.

Keywords: Okinawa Trough, Backarc Basin, Yaeyama Graben, Normal fault

©2021. Japan Geoscience Union. All Right Reserved.

The link between volcanism and tectonics at back-arc rifting stage: analysis of three volcanic areas in the southern Okinawa Trough

*JINYU ZHOU[1], Kyoko Okino[1], Masakazu Fujii[2,3]

1. Atmosphere and Ocean Research Institute, The University of Tokyo, 2. National Institute of Polar Research, 3. The Graduate University for Advanced Studies

Back-arc basins are semi-closed seas developed under extensional stress field along subduction zones. Though the origin of the extensional field is still debating, the evolution generally follows the common process; arc or continental crust thinning, development of normal faults (=rifting), breaking off the pre-existed crust, and finally continuous oceanic crust formation. The initial rifting stage is sometimes accompanied by sporadic volcanism, but the link between arc/back-arc volcanism and rifting has not been well-understood. The Okinawa Trough was a back-arc basin at the rifting stage, where the Philippine Sea Plate subducts beneath the Yangtze Plate. The previous studies on the back-arc rifting mainly dealt with rifting in oceanic island arcs. Since the southern Okinawa Trough (OT) is one of few places where we can observe the back-arc rifting on the continental crust, it provides us a valuable opportunity to understand the details of the continental rifting process and its relationship with volcanism.

In our research, geophysical data of the Yonaguni Knolls, the Irabu Knolls, and the Tarama Knolls - three volcanic areas near the rifting axis locating in the southern Okinawa Trough are analyzed. These three volcanic areas are located in different tectonic settings. Through the bathymetry, gravity anomaly, magnetic anomaly, and other compiled data, I tried to elucidate the character of these knolls and the adjacent areas and then to discuss the relationship with their tectonic background.

The axial rift valley generally extends the E-W direction and segmented. The rift valley is 18 km-wide and is accompanied by a high Bouguer anomaly in the eastern Yonaguni area. Both the widths and the Bouguer anomalies of the rift valleys surrounding the Irabu and Tarama Knolls decrease eastward. These observations suggest that the rifting stage is more progressed in the western end of the Okinawa Trough. High magnetic anomalies are observed at minor ridge and knolls within the rift valley and along the rift walls, indicating magma injection. Three volcanic areas show different geophysical features, reflecting their tectonic settings.

The Yonaguni Knolls, located at the western end of the Okinawa Trough, forms an en echelon arrangement of the E-W trending knoll chain (row), likely controlled by the rift faults.

Irabu Knolls locates at the intersection of two differently trending segments of the Okinawa Trough. It may form many faults that enhance the magma intrusion.

Tarama Knolls is located on the arc side flat seafloor. Two types of volcanic eruption are presumed here; fissure-eruption with higher magnetic anomaly and explosive eruption with a large volume of pumice causing low gravity anomaly and no magnetic anomaly.

As the result of the forward modeling of magnetic anomalies, I estimated the magnetization of Yonaguni, Tarama, and Irabu Knolls as 14, 10, and 2 A/m, respectively. This result is consistent with previously collected rock samples.

©2021. Japan Geoscience Union. All Right Reserved.

Keywords: Gravity and magnetic anomalies, Back-arc basin, Okinawa Trough

©2021. Japan Geoscience Union. All Right Reserved.

Mineralogical and geochemical study of sediment cores collected from the Ieyama hydrothermal field in the Okinawa Trough

*Jun-ichiro Ishibashi[1], Takashi Miyamoto[1,3], Shuhei Totsuka[1,2], Kazuhiko Shimada[1], Toru Yamasaki[2], Ken Ikehara[2], Toshiro Nagase[4], Yutaro Takaya[5], Hideaki Machiyama[6], Koichi Iijima[6], Hirofumi Yamamoto[6], Hidenori Kumagai[6]

1. Department of Earth and Planetary Sciences, School of Science, Kyushu University, 2. National Institute of Advanced Industrial Science and Technology, 3. School of science, University of Tokyo, 4. Tohoku University Museum, 5. Waseda Research Institute for Science and Engineering, 6. Japan Agency for Marine-Earth Science and Technology

Ieyama hydrothermal field is located at the seafloor around a water depth of 1050-1100 mbsl (meters below the sea level) in the mid-Okinawa Trough. Semi-detailed exploration survey during YK17-18C cruise using AUV (Autonomous underwater vehicle) identified negative self-potential anomalies probably related to mineralization on and beneath the seafloor in this area (Kasaya et al., 2020). Moreover, ROV (Remotely operated vehicle) surveys conducted in the same and later durations observed and accessed present hydrothermal activities represented by high temperature fluid venting from mound structure consisted of sulfide and sulfate mineral deposits. Scientific drilling was performed by J-MARES during the SIP Integrated Ocean Resource Surveying System JM18-04 Cruise in September 2018. Sediment cores were obtained from 3 sites in the Ieyama field, employing BMS (Boring Machine System) installed on *Shincho-maru*. Lithology and mineralogy of the obtained sediment cores were studied based on VCD (Visual Core Description), measurements of physical properties, XRD (X-ray diffractometer) analysis, and electron probe microanalyzer (EPMA) analysis.

Sulfide mineralization was recognized in the layer from 50 to 65 mbsf (meters below the seafloor) of the sediment core collected from a bottom of circular depression of about 100 m diameter. This layer was overlaid by thick pile of pumice and pumiceous tuff, and underlaid by tuffaceous breccia. Mineralogical and chemical studies of sulfide minerals revealed several similarities to sulfide minerals collected from chimney and mound structures found in the vicinity of the drilled site.

Acknowledgements:

This study was conducted under the framework of the Next-Generation Technology for Ocean Resources Exploration Project, Cross-ministerial Strategic Innovation Promotion Program (SIP) funded by CSTI, Cabinet Office, Government of Japan. We are thankful to J-MARES (Research and Development Partnership for Next Generation Technology of Marine Resources Survey) for providing samples used in this study.

Keywords: seafloor massive sulfide deposits, sulfide and sulfate mineralization, subseafloor of hydrothermal field, scientific drilling using BMS(Boring Machine System)

©2021. Japan Geoscience Union. All Right Reserved.

Geochemical and geochronological study of barite in sediment cores obtained from Higashi Izena hydrothermal field, Okinawa Trough

Yushi Itatani[1], *Jun-ichiro Ishibashi[1], Makiko Tomita[2], Shin Toyoda[2], Ryuichi Shinjo[3], Kazuno Arai[4], Taisei Fujiwara[5]

1. Department of Earth and Planetary Sciences, Graduate School of Science, Kyushu University, 2. Okayama University of Science, 3. Faculty of Science, University of Ryukyus, 4. Center for Advanced Marine Core Research, Kochi University, 5. Institute for Geology and Geochronology

Ieyama hydrothermal field is located at the seafloor around a water depth of 1050-1100 mbsl (meters below the sea level) in the mid-Okinawa Trough. Scientific drilling performed by J-MARES during JM18-04 Cruise in September 2018 confirmed sulfide and sulfate mineralization in the layer from 50 to 65 mbsf (meters below the seafloor) of the sediment core collected from a bottom of circular depression of about 100 m diameter (Ishibashi et al., this meeting). We focused on barite in the sediment core and conducted measurement of strontium isotope ratio, gamma ray measurement to determine radium content, and geochronological studies employing ESR dating and 226Ra-210Pb radioactive disequilibrium dating. Vertical profile of radium content in barite showed monotonic change along the depth, as well as variation of strontium isotope ratio. These results suggest barite formation within the sediment layer by mixing of radium-rich hydrothermal fluid and seawater penetrated through a volcaniclastic sediment layer of high porosity. Results of radioactive disequilibrium dating barite within the sediment core showed similar age to barite obtained from hydrothermal mound on the seafloor where high temperature fluid venting. These results imply barite within the sediment layer is formed by present hydrothermal activity.

Keywords: seafloor massive sulfide deposits, strontium isotopic composition, radioactive disequilibrium dating, electron spin resonance dating

©2021. Japan Geoscience Union. All Right Reserved.

Fin whale signals recorded by S-net

*Masashi Mochizuki[1], Takeshi Nakamura[2], Ryoichi Iwase[3], Kenji Uehira[1]

1. National Research Institute for Earth Science and Disaster Resilience, 2. Central Research Institute of Electric Power Industry, 3. Japan Agency for Marine-Earth Science and Technology

S-net (Seafloor observation network for earthquakes and tsunamis along the Japan trench) is the online and real-time seafloor observation network of 150 observatories for earthquakes and tsunamis along the Japan Trench. It covers the focal region of the 2011 off the Pacific coast of Tohoku earthquake and its vicinity regions. All the data from 150 seafloor observatories are being transferred to the data center and being automatically processed for monitoring of earthquake activities in these regions.

We have investigated noise sources that contaminate seismic signals recorded by S-net and cause deteriorating of automatic earthquake detection capability. One of such noise sources is fin whale signal. Waveforms of fin whale signals have characteristic spectral peaks in narrow frequency bands of 14-25 Hz. They have a short duration of about one second and are repeated at regular intervals of several tens of seconds.

Nakamura and Iwase (2020) developed a method that automatically detect and count fin whale signals from continuous seismic records. This method was applied to the seismic data caught by the 150 observatories of S-net from 2017 to 2019. They found that the observatories, located at area off Kushiro and Aomori, recorded the fin whale signals frequently from early autumn to spring. The migration of the signals among the observatories from northeast to southwest direction in winter was also recognized.

Monitoring and counting the fin whale signals within S-net area with the method by Nakamura and Iwase (2020) have continued, in order to understand characteristics of observation environment at each of S-net observatories. We report spatiotemporal distributions of fin whale signals recorded by S-net observatories in the year of 2020 in this presentation.

Keywords: ocean bottom observation, S-net, fin whale

©2021. Japan Geoscience Union. All Right Reserved.

Effective removal of oceanic variation from ocean bottom pressure gauge data using the MSSA

*Kenta Shimizu[1], Toshinori Sato[1], Koichi Murata[1], Norihisa Usui[2], Hajime Shiobara[3], Tomoaki Yamada[4], Masanao Shinohara[3]

1. Chiba Univ., 2. MRI, 3. ERI. Univ. Tokyo, 4. JMA

1. Introduction

Ocean bottom pressure gauges (OBPs) can observe vertical movement of the seafloor continuously, and are useful to detect slow movement due to slow slip events. The OBP data include components such as oceanic tide, oceanic variation, and instrumental drift. To detect crustal movement, these components must be removed. To remove the oceanic variation, several methods were proposed in the previous studies such as average subtraction using neighboring OBPs (e.g. Suzuki et al. 2016), fitting of a parametric model (Sato et al. 2017), and subtraction of a data-assimilated oceanic model (e.g. Inazu et al. 2012). This study conducts the Multi-channel Singular Spectrum Analysis (MSSA) for the observed data and an oceanic model, and divides into components. Then, we remove only good correlation components of the oceanic model from the observed data. This method can extract vertical movement better, because this method may remove incompleteness of the oceanic model.

2. Method

As an oceanic model, we use a four-dimensional variational ocean reanalysis
for the Western North Pacific over 30 years (FORA-WNP30) (Usui et al. 2017). The OBP data are obtained at off Boso Peninsula from 2013-2015, which include the 2014 Boso slow slip event.
From the observed data, we remove the oceanic tide using Baytap08 (Tamura et al. 1991), and the drift using a linear fitting. We conduct the MSSA for the removed data and the FORA-WNP30 data, and calculate correlation between them for each component. We reconstruct oceanic model data using only good correlation components, then remove them from the removed data.

3. Results

The residual between the removed data and the reconstructed oceanic model has standard deviation of about 1.0 hPa. On the other hand, the residual between the removed data and the original oceanic model has about 1.6 hPa. This suggests that the present method can remove oceanic variation better than the previous methods.
We fit a parametric model to the residual between the removed data and the reconstructed oceanic model, and obtain standard deviation of about 0.8 hPa.

Acknowledgments

We thank the captains and crew of R/V Hakuho-maru and R/V Natsushima of JAMSTEC for their support. This work was supported by the Earthquake and Volcano Hazards Observation and Research Program authorized by the Ministry of Education, Culture, Sports, Science and Technology. This work was supported by JSPS (25287109).

Keywords: Multi-channel Singular Spectrum Analysis, ocean bottom pressure gauge, oceanic model

©2021. Japan Geoscience Union. All Right Reserved.

Sampling process of seafloor sediments as a source of information on their rheology

*Nikita Dubinya[1,2], Sergey Tikhotskiy[1,2], Victor Nachev[1,3]

1. Moscow Institute of Physics and Technology, 2. Schmidt Institute of Physics of the Earth of the Russian Academy of Sciences, 3. Sadovsky Institute of Geosphere Dynamics of the Russian Academy of Sciences

The study is related to the problem of offshore infrastructure construction with an especial focus on development of offshore hydrocarbon fields from the perspective of geomechanics. It is essential to have a model of mechanical properties of seafloor sediments for effective construction of safe infrastructure. The problem of creating such model is rather complicated as the rheological properties of seafloor sediments are nonlinear –mechanical behavior of sediments appears to be described by nonlinear visco-elasto-plastic models. At the same time there are limited opportunities to estimate these properties as engineering drilling –a valid source of information on mechanical properties –may be very expensive and complicated at offshore conditions.

Sediment sampling with various corers provides one of the most valuable sources of information regarding mechanical properties of seafloor sediments. The collected samples may be analyzed in laboratory conditions using various techniques. One of the problems with this procedure is related to difficulties in recreating mechanical conditions of the sample before coring procedure: any sample could have been significantly altered before arriving to the laboratory. There are various ways to deal with this problem –in the current study we focus on one of them.

In the current study we analyze the sampling process itself as a source of information regarding rheological properties of seafloor sediments. From the perspective of continuum mechanics the interaction between corer and seafloor may be considered as a contact problem –a rigid body (corer) penetrates into a visco-elasto-plastic medium (seafloor). It is clear that the dynamics of penetration is governed by a set of conditions, including initial conditions, setting distance, geometry and mechanical properties of the seafloor at the vicinity of the contact point. As rheological properties of the seafloor are included into this set of factors, one may postulate and try to solve the inverse problem: can mechanical properties of the seafloor sediments be estimated if all other factors mentioned above are known alongside with the changes of measurable corer acceleration with time?

In the current paper we analyze this question using numerical modeling. A numerical finite-element model has been constructed for the mentioned contact problem in the case of gravity tubular corer penetrating into plastic medium without hardening. A set of numerical experiments has been carried out to obtain the dependencies between changes in acceleration of the corer and mechanical properties of seafloor sediments: density, elastic moduli, and strength properties. The obtained dependencies revealed that it is possible to deal with the inverse problem mentioned above. There are nonlinear relationships between the corer penetration dynamics and mechanical properties of the seafloor. It appears that the postulated inverse problem may have more than one solution even without viscosity taken into account. Nevertheless, the obtained results prove that sampling process itself may provide information regarding the type of rheological model properly describing the mechanical behavior of seafloor sediments.

Keywords: Seafloor sampling, Indentation, Rheology, Geomechanics

©2021. Japan Geoscience Union. All Right Reserved.

©2021. Japan Geoscience Union. All Right Reserved.

Technical protocol for deep-sea environmental monitoring by the portable seafloor observation platform Edokko Mark 1

*Hiroyuki Yamamoto[1], Tetsuya Miwa[1], Shinsuke Kawagucci[1], Sangkyun Lee[2], Atsuo Oono[3], Kousuke Tsutsumi[3], Hideki Sugishima[3]

1. Japan Agency for Marine-Earth Science and Technology, 2. J-MARES/JGI, 3. J-MARES/idea

The mooring, lander, and cable connected station are conventional methods for deep-sea monitoring. Recently, increasing interest for seabed mining, requirement of environmental management, and demand for marine biodiversity raises the issue of seafloor monitoring techniques, especially for deep-sea environments. The portable seafloor observation platforms with standalone operation mechanisms have been developed. In Japan, the joint project of private companies and academia developed the portable seafloor observation platform Edokko Mark 1, consisting of grass spheres with a built-in HD video cameras system and an acoustic release mechanism (1). The Edokko Mark 1 has four types with unique abilities to adopt monitoring targets; HSG for anti-corrosion, 365 for long-term observation, COEDO for simple operation by human power. These products are commercially available from Okamoto Glass Co. Ltd. (https://ogc-jp.com/productinfo/glassball/).

The system of Edokko Mark 1 has been improved in the Japan projects for technology development on seabed mining. Since the trial to 8000m depth of Japan trench in 2013, the Edokko Mark 1 has been deployed on the seafloor of Okinawa Trough from 2014 to18 and off Minami Torishima from 2018 to 2021. The video image is commonly used for biological and ecological survey in deep-sea expedition, although the observation area is limited within lighting power. The hydrophone is an optional sensor of Edokko Mark 1, can record biological sound as well as anthropogenic and geological sources. The soundscape is complementary to image data, and enables the expand observation area for deep-sea communites. Electromagnetic current meter and acoustic current meter could be installed on Edokko Mark 1 at 1.5m position from the seafloor and measured bottom current. Another observation of 2019 in the Suruga Bay recorded deep-sea turbidity current triggered by heavy precipitation of the Super Typhoon Hagibis (2). In this case, a deep-water displacement phenomenon was determined and drastic turbidity change was quantified from video images.

The projects of marine environmental assessment anticipate the transportability and quick deployment capability of the portable seafloor observation platform such as Edokko Mark 1. The guidance for environmental impact assessment on seabed mining (ISBA/25/LTC/6/Rev.1) published by the International Seabed Authority recommends the Edokko Mark 1 as a suitable system adopted deep-sea observation protocol (https://www.isa.org.jm/). These knowledge on video observation strongly supported establishing the technical protocol and making the International Standard (ISO /DIS23730, 23731).
In this presentation we will explain the observation techniques and results from deep-seafloor surveys.

References:

1) Miwa, T., et al. 2016. Underwater Observatory Lander for the Seafloor Ecosystem Monitoring using a Video System. Pages 333-336 in Techno-Ocean. IEEE, Kobe.
2) Kawagucci, S., et al. 2020. Deep-sea water displacement from a turbidity current induced by the Super Typhoon Hagibis. PeerJ 8:e10429.

©2021. Japan Geoscience Union. All Right Reserved.

Keywords: seafloor monitoring, deep-sea environments, environmental impact assessment

©2021. Japan Geoscience Union. All Right Reserved.

[J] Oral | S (Solid Earth Sciences)：S-CG Complex & General

Sat. Jun 5, 2021 9:00 AM - 10:30 AM JST | Sat. Jun 5, 2021 12:00 AM - 1:30 AM UTC | Ch.20 Zoom Room 20

[S-CG46] Rheology, fracture and friction in Earth and planetary sciences

convener:Shintaro Azuma(Department of Earth and Planetary Sciences, School of Science, Tokyo Institute of Technology), Ichiko Shimizu(Division of Earth and Planetary Sciences, Graduate School of Science, Kyoto University), Osamu Kuwano(Japan Agency for Marine-Earth Science and Technology), Miki Tasaka(Shizuoka University), Chairperson:Shintaro Azuma(Department of Earth and Planetary Sciences, School of Science, Tokyo Institute of Technology), Miki Tasaka(Shizuoka University)

The aim of this session is to join people from various research area in the earth and planetary sciences and to stimulate discussion beyond the boundaries of each research area. Our goal is to deepen our understanding of dynamics in geosciences by looking over whole areas in the earth and planetary sciences from the viewpoint of PHYSICS OF DEFORMATION, FLOW, AND FRACTURE. We welcome any field (e.g., earthquake, volcano, earth surface, crust, mantle and the core, and other planets and satellites) and any approach (e.g., laboratory experiments, numerical simulations, field observations, and theories).

9:00 AM - 9:15 AM JST | 12:00 AM - 12:15 AM UTC

[SCG46-01] Low stress power-law creep of olivine

★Invited Papers

*Kosuke Yabe[1], Kenta Sueyoshi[1], Takehiko Hiraga[1] (1.Earthquake Research Institute, the University of Tokyo)

9:15 AM - 9:30 AM JST | 12:15 AM - 12:30 AM UTC

[SCG46-02] Vickers indentation tests on olivine: grain size and indentation size effects

*Sanae Koizumi[1], Takehiko Hiraga[1] (1.Earthquake Research Institute,The University of Tokyo)

9:30 AM - 9:45 AM JST | 12:30 AM - 12:45 AM UTC

[SCG46-03] Extremely slow grain growth of albitic feldspar

*Norio Shigematsu[1], Masanori Kido[1], You Zhou[2], Hideki Hyuga[2], Yuichi Yoshizawa[2] (1.Research Institute of Earthquake and Volcano Geology, Geological Survey of Japan, National Institute of Advanced Industrial Science and Technology, 2.Multi-material Research Institute, National Institute of Advanced Industrial Science and Technology)

9:45 AM - 10:00 AM JST | 12:45 AM - 1:00 AM UTC

[SCG46-04] The effect of grain size and porosity on compaction localisation in high-porosity sandstones

*Elliot Rice-Birchall[1], Daniel R Faulkner[1], John D Bedford[1,2] (1.University of Liverpool, 2.Kochi Institute for Core Sample Research, Japan Agency for Marine-Earth Science and Technology (JAMSTEC))

10:00 AM - 10:15 AM JST | 1:00 AM - 1:15 AM UTC

[SCG46-05] Deformation of simulated quartz-feldspar faults at the brittle-ductile transition zone

*Miho Furukawa[1], Berend A. Verberne[2], Jun Muto[1], Miki Takahashi[2], Hiroyuki Nagahama[1] (1.Department of Earth Sciences, Tohoku University, 2.Geological Survey of Japan, The National Institute of Advanced Industrial Science and Technology (AIST))

10:15 AM - 10:30 AM JST | 1:15 AM - 1:30 AM UTC

[SCG46-06] Initial results on high Pc-Pp-T rock deformation experiments under drained conditions

★Invited Papers

*Keishi Okazaki[1], Jun Muto[2] (1.Japan Agency for Marine-Earth Science and Technology, 2.Department of Earth Sciences, Tohoku University)

Low stress power-law creep of olivine

*Kosuke Yabe[1], Kenta Sueyoshi[1], Takehiko Hiraga[1]

1. Earthquake Research Institute, the University of Tokyo

Strain localization plays a critical role in mantle shear zone. Some studies attributed it to grain-size-sensitive creep (i.e., diffusion creep) through grain-size reduction by dislocation creep (e.g., Warren & Hirth, 2006). Some friction experiments suggest a superplastic deformation mechanism accommodated by diffusion to play an important role even during seismic faulting (De Paola et al., 2015). Conventionally, it has widely assumed that Newtonian diffusion creep overwhelms dislocation creep at the condition of the lower stress and/or the smaller grain size. However, it is well known in material science community that power-law interface creep dominates at the lower stress and the smaller grain size than diffusion creep, which could potentially be important for the rheology of the Earth interior. We conducted one-atmosphere uniaxial compression experiments on fine-grained (~1 μm) Fe-bearing olivine ($Mg_{1.8}Fe_{0.2}SiO_4$) aggregates that were variably doped with CaO $\pm Al_2O_3$. We identified power-law interface-controlled creep at low stresses and grain-boundary diffusion creep at high stresses, which operate as mutually coupled, i.e., sequential processes. We established constitutive equations for interface-controlled creep and diffusion creep of undoped olivine and used the combined rate equation as a reference to examine the effect of doping on creep rates. Ca and Al were found to enhance rates of both interface-controlled creep and diffusion creep above certain temperatures, and this effect becomes significant with increasing temperature. We attribute the rate enhancements to grain-boundary-disordering promoted by grain boundary segregation of the dopants at near-solidus conditions. The enhancements are well described in relation to the sample solidus temperature and an additional activation energy relative to that of the reference creep state. Based on our established flow laws of diffusion and interface-controlled creep, we constructed deformation mechanism map and found that grain-boundary diffusion creep dominates in most of the upper mantle, while interface-controlled creep can be effective during seismic faulting in the mantle at a shallow depth.

Keywords: olivine aggregates, power law creep

©2021. Japan Geoscience Union. All Right Reserved.

Vickers indentation tests on olivine: grain size and indentation size effects

*Sanae Koizumi[1], Takehiko Hiraga[1]

1. Earthquake Research Institute,The University of Tokyo

Vickers indentation tests on Fe-free (Mg_2SiO_4) and Fe-bearing ($Mg_{1.8}Fe_{0.2}SiO_4$) olivine single crystals and highly dense polycrystalline material with average grain sizes ranging from 170 to 890 nm were conducted. The Vickers microhardness (H_v) of the Fe-free polycrystalline material with the finest grain size is 17 GPa at a load of 0.1 N, while that of the Fe-bearing single crystal is 8 GPa at the largest load applied. Overall, H_v decreases with increasing grain size, load (indentation depth), and the presence of Fe. For each grain size, H_v is well characterized by a power law of the form $H_v/H_{0v} \propto l^{-x}$, where H_{0v} is the depth-independent value of H_v, l represents either grain size or indentation depth, and x is 0.09. Despite the small exponent value for each size effect, the nonlinear interaction of the two size effects results in large variations of H_v in our samples.
We show that our semi-empirically derived relationship as a function of grain size and indentation depth explains the H_v of both polycrystalline and single-crystal olivine at any indentation conditions. Indentation fracture toughness of the finest grained material is 0.8 MPa $m^{1/2}$, which increases slightly to 1.1 MPa $m^{1/2}$ with increasing grain size, while the toughness of the single crystals varies from 0.5 to 0.8 MPa $m^{1/2}$ depending on the crystallographic orientation of the fracture planes.

Keywords: Olivine, Vickers hardness, fracture toughness, Grain size

©2021. Japan Geoscience Union. All Right Reserved.

Extremely slow grain growth of albitic feldspar

*Norio Shigematsu[1], Masanori Kido[1], You Zhou[2], Hideki Hyuga[2], Yuichi Yoshizawa[2]

1. Research Institute of Earthquake and Volcano Geology, Geological Survey of Japan, National Institute of Advanced Industrial Science and Technology, 2. Multi-material Research Institute, National Institute of Advanced Industrial Science and Technology

Feldspar is one of the main constituent minerals of the Earth's crust. The grain growth and the mechanical behavior of plastic deformation of feldspar have well been studied for anorthite ($CaAl_2Si_2O_8$), because it is considered that this mineral controls the strength of the lower crust. However, the grain growth of albite ($NaAlSi_3O_8$) has not been studied previously. Grain growth follows the grain growth law and the rate constant was determined in the experiments.
The starting materials were prepared as follows. Albite powders for industrial use were pulverized using a HERZOG HP-MS60 automatic pulverizer at the GSJ Laboratory (GSJ-Lab.) of Geological Survey of Japan, National Institute of Advanced Industrial Science and Technology (GSJ, AIST), and fine-grained fractions less than a few hundred nm were separated by decantation. The fine-grained powders were hot pressed using a multi-purpose high temperature furnace (Fuji Dempa High Multi 10000 at AIST Chubu) at temperature of 1080 ºC and pressure of 120 MPa for 16 hours. Then the sample were cut into small pieces to perform the grain growth experiments at different conditions. Surfaces of samples were mirror polished using 1 mm diamond paste before the experiments to observe the grain boundaries by thermal or chemical etching. The grain growth experiments were performed by annealing the sample in a tube furnace (Carbolite 14/450 at AIST Tsukuba Central 7) at the atmospheric pressure and temperatures of 1030, 1050, 1065 ºC. The grain size was determined by linear intercept method after chemical etching for the initial grain size. The sample surfaces were observed in the HITACHI SU-3500 scanning electron microscope (SEM) installed at the GSJ-Lab. of GSJ, AIST.
The initial grain size is 172.9 nm. The grains grow to the grain sizes of about 282 nm after 156 hours, about 378 nm after 190 hours and about 329 nm after 64 hours at the temperatures of 1030 ºC, 1050 ºC and 1065 ºC, respectively. When the growth exponent is assumed to be 2.6, the regressions of the results yield the rate constants of 1.26×10^{-23} $m^{2.6}s^{-1}$, 2.58×10^{-23} $m^{2.6}s^{-1}$ and 5.07×10^{-23} $m^{2.6}s^{-1}$ at 1030 ºC, 1050 ºC and 1065 ºC, respectively. The Arrhenius plot for the results of the annealing experiments of albite yield the activation energy of Q=580 kJ/mol and the pre-exponent of the rate constant k_0=1.83 $m^{2.6}s^{-1}$.
The extrapolation of the grain growth curves to geological time scale indicates that it takes almost 1 century for grains to grow from 1 μm to 10 μm even at the temperature of 1050 ºC, the grain growth is extremely slow. The experiments in this study can be considered to have been under anhydrous conditions and may be different from the natural hydrous conditions. An experiment of reaction rim of albite that were formed from nepheline ($NaAlSiO_4$) and quartz (SiO_2) suggests that grain growth rate under hydrous and anhydrous conditions are not significantly different at the temperature of 1100 ºC.
The results in this study and above discussion suggest that once fine-grained feldspar with composition close to albite is formed, these feldspar grains will never grow and affect the mechanical behavior for long time. This process enables the grain-size sensitive creep of plagioclase to be important in the wide range of crustal conditions.

Keywords: Albite, Grain Growth, Crustal Rheology

©2021. Japan Geoscience Union. All Right Reserved.

The effect of grain size and porosity on compaction localisation in high-porosity sandstones

*Elliot Rice-Birchall[1], Daniel R Faulkner[1], John D Bedford[1,2]

1. University of Liverpool, 2. Kochi Institute for Core Sample Research, Japan Agency for Marine-Earth Science and Technology (JAMSTEC)

As sandstone reservoirs are depleted, the pore pressure reduction can sometimes result in pore collapse and the formation of compaction bands. These localised features can significantly reduce the bulk permeability of the reservoir and are therefore problematic in the hydrocarbon, groundwater, geothermal, and CO_2 sequestration industries. However, the influence that grain size, grain shape and sorting have on compaction band formation in sandstone is still poorly understood, due to the fact that finding natural sandstones with specific properties is challenging. Consequently, a method of forming synthetic sandstones has been developed, in order to produce a suite of sandstone specimens with controlled grain size and porosity characteristics. During production of the synthetic sandstones, amorphous quartz cement and sodium chloride are precipitated between sand grains as a product of the reaction between sodium silicate and hydrochloric acid. The salt can then be dissolved, resulting in synthetic sandstones that have very comparable physical properties to their natural counterparts. In this study, triaxial experiments were performed on synthetic sandstone cores with four different grain size ranges of 250-300, 425-500, 600-710 and 850-1000 microns, at three different starting porosities of 27%, 32% and 37%. The samples were each axially loaded from a point along their hydrostat corresponding to 85% of their hydrostatic yield point (P*) values. These conditions mean that yielding will occur within the shear-enhanced compaction regime, which is also where localised compaction structures typically form. All samples were taken to 5% axial strain. The microstructural results indicate that localisation of deformation within the samples did occur and was favoured by low starting porosity and small grain size. Localisation of deformation was most easily recognised by grain size reduction as a result of grain crushing. This was weakly correlated to a change in porosity but recognition of localisation was difficult to make using variations in porosity alone. Porosity reduction was not necessarily associated with a reduction in grain size. With increasing grain size and starting porosity, the deformation becomes more distributed in the samples with the highest starting porosity samples (37%) exhibiting more widely distributed grain crushing which was less intense overall. The results indicate a significant grain size and porosity influence on localisation, but also that compaction can occur via two mechanisms; one involving mostly grain rearrangement and the other primarily by grain fracturing. Consequently, the localisation of deformation is most evident in grain size reduction and is only weakly shown by porosity reduction.

Keywords: Porous rock, Sandstones, Compaction bands, Grain size, Localisation, Grain crushing

©2021. Japan Geoscience Union. All Right Reserved.

Deformation of simulated quartz-feldspar faults at the brittle-ductile transition zone

*Miho Furukawa[1], Berend A. Verberne[2], Jun Muto[1], Miki Takahashi[2], Hiroyuki Nagahama[1]

1. Department of Earth Sciences, Tohoku University, 2. Geological Survey of Japan, The National Institute of Advanced Industrial Science and Technology (AIST)

Continental earthquakes frequently nucleate in the brittle-ductile transition zone. Recently, experimental studies revealed that nano- or microscale deformation processes, such as amorphization (Peč et al., 2016) or intergranular dilatation (Verberne et al., 2017), may lead to nucleation of unstable slip hence runaway fault rupture. Since the continental upper crust is dominantly composed of granitoids, studying the rheological behaviors of fault rocks composed of quartz and feldspar is key for better understanding upper-crustal fault mechanics. Aiming to improve insight into the microphysical processes controlling fault slip in the continental crust, we conducted Griggs shear experiments on ~1 mm thick simulated faults composed of 50:50 wt% quartz-albite gouges. Temperatures and pressures in each experiment were varied to simulate conditions at 7, 8, 10, 13, and 18 km depths in the crust, assuming geothermal and lithostatic gradients of respectively 30℃/km and 2700 kg/m^3. The bulk shear strain rate was sequentially stepped between ~10^{-3} and ~10^{-4} /s, achieving total bulk shear strains of up to 3.5 to 5.0. Recovered sheared samples were investigated using an optical and a scanning electron microscope (SEM), energy dispersive X-ray spectroscopy (EDS) analyses in an SEM.
In general, when frictional regime dominates, shear resistance increases with increasing normal stress, whereas when flow regime dominates, shear resistance decreases with increasing temperature. Unlike this tendency, shear stresses obtained from the experiments showed positive dependences on both pressure and temperature. Since the shear resistances increased even with the increase in temperature, the mechanical data may suggest frictional regime was dominant in all experiments.
However, microstructural observations of recovered samples indicate a change in deformation style from brittle to partially plastic as the simulated depth condition increases. Specifically, backscattered electron micrographs showed that microcrack distribution changes as pressure and temperature increases. At the shallower conditions, large numbers of short cracks are observed in various directions, while at the deeper conditions, the cracks are less, and are seen to coalesce to constitute R_1- and Y- shears. Using image analysis, we characterized the deformation properties of individual grains. At the shallower conditions, the long axes of K-feldspar marker grains, present in minor amounts, are distributed randomly, whereas at the deeper conditions these are aligned along the direction of maximum tensile strain. Our interpretation is that brittle crushing and rotation are dominant under shallow conditions, with a progressively more important role for plastic flow takes towards deeper conditions. This transition is consistent with a change in autocorrelation function (ACF) of K-feldspar grains with increasing temperature and pressure.
Our results indicate that even within the range of frictional behavior, plastic deformation gradually emerges on the scale of microstructure as increasing temperature and pressure.

References

- Peč, M., H. Stünitz, R. Heilbronner, and M. Drury (2016), Semi-brittle flow of granitoid fault rocks in experiments, *J. Geophys. Res. Solid Earth*, 121, 1677-1705, doi:10.1002/2015JB012513.
- Verberne, B. A., Chen, J., Niemeijer, A. R., de Bresser, J. H., Pennock, G. M., Drury, M. R., and Spiers, C. J. (2017), Microscale cavitation as a mechanism for nucleating earthquakes at the base of the seismogenic zone, *Nat. Commun.*, 8, 1-8, doi: 10.1038/s41467-017-01843-3.

©2021. Japan Geoscience Union. All Right Reserved.

Keywords: quartz, feldspar, gouge, Griggs shear experiment, microstructure

©2021. Japan Geoscience Union. All Right Reserved.

Initial results on high Pc-Pp-T rock deformation experiments under drained conditions

*Keishi Okazaki[1], Jun Muto[2]

1. Japan Agency for Marine-Earth Science and Technology, 2. Department of Earth Sciences, Tohoku University

At subduction plate boundaries and inland active faults, most of large earthquakes (Mw >7) occur at the base of the seismogenic zone with a depth of about 10–25 km. The PT conditions of these areas corresponds to lithostatic pressures ranging 300–800 MPa and temperatures ranging 200–400 degC. In addition, seismological observations indicate that the pore fluid pressure is nearly lithostatic, meaning 300–800 MPa. The presence of high pore fluid pressure plays a key role in controlling the rock rheology, because the frictional strength of the fault is a function of the effective pressure and physico-chemical properties of fluids changes exponentially under high pressure. However, most of rock friction experiments have been conducted under pressures lower than 200 MPa. Therefore, understanding of fault rheology at the base of the seismogenic zone is limited by the extrapolations of low PT experiments and experiments using analog materials. We recently built two new solid pressure medium apparatuses at KCC/JAMSTEC and Tohoku University. They are capable of increasing the confining pressure, the pore pressure and the temperature up to 2 GPa, 1 GPa and 1200 degC, respectively. These apparatuses can reproduce the in-situ or even deeper P-Pp-T conditions of the seismogenic zone. Our preliminary experiment on San Carlos olivine deformed under the confining pressure of 1 GPa, the pore pressure of 480 MPa at the temperature of 462 degC indicates that the nominal friction coefficient was 0.42 with assuming fully undrained condition. The recovered sample showed the formation of chlorite-rich shear zone along the piston-sample boundary probably due to reaction among the sample, water and alumina piston. Serpentine and Fe-oxide were also observed in the sample matrix. This presentation will also report basic performances, calibration data of the apparatuses and further experimental results.

Keywords: Rheology, Fault, Subduction zone

©2021. Japan Geoscience Union. All Right Reserved.

[J] Oral | S (Solid Earth Sciences)：S-CG Complex & General

Sat. Jun 5, 2021 10:45 AM - 12:15 PM JST | Sat. Jun 5, 2021 1:45 AM - 3:15 AM UTC | Ch.20 Zoom Room 20

[S-CG46] Rheology, fracture and friction in Earth and planetary sciences

convener:Shintaro Azuma(Department of Earth and Planetary Sciences, School of Science, Tokyo Institute of Technology), Ichiko Shimizu(Division of Earth and Planetary Sciences, Graduate School of Science, Kyoto University), Osamu Kuwano(Japan Agency for Marine-Earth Science and Technology), Miki Tasaka(Shizuoka University), Chairperson:Ichiko Shimizu(Division of Earth and Planetary Sciences, Graduate School of Science, Kyoto University), Osamu Kuwano(Japan Agency for Marine-Earth Science and Technology)

The aim of this session is to join people from various research area in the earth and planetary sciences and to stimulate discussion beyond the boundaries of each research area. Our goal is to deepen our understanding of dynamics in geosciences by looking over whole areas in the earth and planetary sciences from the viewpoint of PHYSICS OF DEFORMATION, FLOW, AND FRACTURE. We welcome any field (e.g., earthquake, volcano, earth surface, crust, mantle and the core, and other planets and satellites) and any approach (e.g., laboratory experiments, numerical simulations, field observations, and theories).

10:45 AM - 11:00 AM JST | 1:45 AM - 2:00 AM UTC

[SCG46-07] Dehydration experiments of antigorite serpentinite under slab-mantle conditions

Sakurako Okude[1], *Ichiko Shimizu[1] (1.Division of Earth and Planetary Sciences, Graduate School of Science, Kyoto University)

11:00 AM - 11:15 AM JST | 2:00 AM - 2:15 AM UTC

[SCG46-08] Variation of stick-slip behaviors controlled by dehydration kinetics of simulated gypsum gouges

*Mikihiro Kawabata[1], Rei Shiraishi[1], Jun Muto[1], Hiroyuki Nagahama[1], Yuto Sasaki[2] (1.Department of Earth Science, Graduate School of Science and Faculty of Science, Tohoku University, 2.Earthquake Research Institute, The University of Tokyo)

11:15 AM - 11:30 AM JST | 2:15 AM - 2:30 AM UTC

[SCG46-09] Experimental study on drainage process of liquid film between bubbles during bubble growth

★Invited Papers

*Masatoshi Ohashi[1], Atsushi Toramaru[1], Atsuko Namiki[2] (1.Department of Earth and Planetary Sciences, Graduate School of Science, Kyushu University, 2.Graduate School of Environmental Studies Department of Earth and Environmental Sciences)

11:30 AM - 11:45 AM JST | 2:30 AM - 2:45 AM UTC

[SCG46-10] Transition from viscous to inertial regime in dense frictional suspensions

*Franco Antonio Tapia[1], Olivier Pouliquen[3], Elisabeth Guazzelli[2] (1.Department of Mechanical Systems Engineering, Tokyo University of Agriculture and Technology, 2.Université de Paris, CNRS, Matière et Systèmes Complexes (MSC) UMR 7057, Paris, France, 3.Aix-Marseille Université, CNRS, IUSTI, Marseille, France)

11:45 AM - 12:00 PM JST | 2:45 AM - 3:00 AM UTC

[SCG46-11] Peridodic fluctation in a compressed dust-aggregate layer

*Hiroaki Katsuragi[1], Felipe Pacheco Vazquez[2], Tomomi Omura[3] (1.Department of Earth and Space Science, Osaka University, 2.BUAP, Mexico, 3.Osaka Sangyo University)

12:00 PM - 12:15 PM JST | 3:00 AM - 3:15 AM UTC

[SCG46-12] Elasto-plastic behavior of carbonate rocks under high strain rate deformation

★Invited Papers

*Kosuke Kurosawa[1], Hidenori Genda[2], Shintaro Azuma[3], Keishi Okazaki[4], Haruka Oono[1], Takafumi Niihara[5], Takashi Mikouchi[6], Naotaka Tomioka[4], Tatsuhiro Sakaiya[7], Tadashi Kondo[7], Masahiro KAYAMA[8], Mizuho Koike[9], Yuji Sano[10], Takuya Matsuzaki[11], Masafumi MURAYAMA[11], wataru Satake[1], Takafumi Matsui[1,12] (1.Planetary Exploration Research Center, Chiba Institute of Technology, 2.Earth–Life Science Institute, Tokyo Institute of Technology, 3.Department of Earth and Planetary Sciences, Tokyo Institute of Technology, 4.Kochi Institute for Core Sample Research, Japan Agency for Marine-Earth Science and Technology, 5.Department of Systems Innovation, School of Engineering, The University of Tokyo, 6.The University Museum, The University of Tokyo, 7.Department of Earth and Space Science, Graduate School of Science, Osaka University, 8.Department of General Systems Studies, Graduate School of Arts and Sciences, The Univ. of Tokyo, 9.Department of Earth and Planetary Systems Science, Graduate School of Science, Hiroshima University, 10.Atmosphere and Ocean Research Institute, The University of Tokyo, 11.Center for Advanced Marine Core Research, Kochi University, 12.Institute of Geo-Cosmology, Chiba Institute of Technology)

Dehydration experiments of antigorite serpentinite under slab-mantle conditions

Sakurako Okude[1], *Ichiko Shimizu[1]

1. Division of Earth and Planetary Sciences, Graduate School of Science, Kyoto University

A popular hypothesis for the occurrence of double seismic zones in subducting slabs is "dehydration embrittlement" of serpentinized mantle. In the classical deformation experiments of antigorite-serpentinites conducted by Raleigh & Paterson (1965), brittle failure was observed at the temperature beyound the stability field of antigorite (> 650 °C) at the confining pressures up to 0.5 GPa. However, it is questionable if the same mechanism could be effective in subducting slabs at the depth. Here we report the results of deformation and dehydration experiments of antigorite-serpentinite, taken from the Nagasaki Metamorphic Belt, at comfining pressures up to 1.7 GPa. Using a modified Kumazawa-type solid-medium apparatus, intact serpentinite samples were axially compressed at a constant strain rate of 3.3 x 10^{-5} sec^{-1}, while laterally confined by talc assembly.

In the experimental run at 500 °C and 1.2 GPa confining pressure, the serpentinite wample was strong and show strain-hardening behavior. The final differential stress exceeded 1.8 GPa. The sample was deformed in a brittle mannar with conjugate faults. The samples deformed at 700 °C exhibited "dehydration softening" and stable creep behaviors and showed semi-brittle deformation. Forsterite and enstatite were formed along the fault zones, suggesting enhancement of dehydration reaction by fracturing and shearing. Implication of the present results to the mechanism of intermediate-depth earthquakes well be discussed.

Keywords: serpentinite, dehydration reaction, deformation experiments, intermediate-depth earthquakes

©2021. Japan Geoscience Union. All Right Reserved.

Variation of stick-slip behaviors controlled by dehydration kinetics of simulated gypsum gouges

*Mikihiro Kawabata[1], Rei Shiraishi[1], Jun Muto[1], Hiroyuki Nagahama[1], Yuto Sasaki[2]

1. Department of Earth Science, Graduate School of Science and Faculty of Science, Tohoku University, 2. Earthquake Research Institute, The University of Tokyo

In the subduction zone, the increase in pore fluid pressure causes slow slip (Katayama, 2016), slow slip accumulates stress in the asperities and accumulation of stress eventually leads to the occurrence of large earthquakes (Hasegawa et al., 2015). Because gypsum undergoes phase transition and dehydration at relatively low temperatures and pressures, it can easily reproduce the dehydration instability of hydrous minerals in the laboratory (Brantut et al., 2011). Therefore, there have been many studies on the effect of pore fluid pressure on slip events using gypsum (e.g., Leclère et al., 2016). There are also many studies on the dehydration reaction of hydrous minerals from the viewpoint of reaction kinetics (e.g., Liu et al., 2015). In order to illuminate how the dehydration kinetics controls the frictional behavior, Sasaki et al. (2016) conducted friction experiments of simulated gypsum gouges under various temperature and pressure conditions, and found the change in recurrence intervals of repeated stick-slip events with time in an experiment conducted under dehydration condition. Later by analyzing the data of Sasaki et al. (2016), Iwasaki et al. (2017) derived the time function of pore fluid pressure causing the change in the recurrence intervals assuming that gypsum underwent phase transition and dehydration during the friction experiment. However, both studies did not confirm the presence of a dehydration product (anhydrite) after experiments. In this study, we first discussed the possibility of dehydration of gypsum in the experimental conditions and then evaluated the time function of pore fluid pressure.
Sasaki et al. (2016) conducted friction experiments using gypsum gouge under the conditions of confining pressures of 10 - 200 MPa and temperatures of room temperature - 180 ˚C by gas apparatus. The data showed that the stress drops and recurrence periods of stick-slip events increased with increasing confining pressure at room temperature and 70 ˚C, while the stress drop and recurrence period decreased with time at 200 MPa and 110 ˚C (Iwasaki et al., 2017). This is presumably because the phase transition and dehydration of the gypsum created pore fluid pressure that reduced the apparent mechanical strength. Iwasaki et al. (2017) obtained a time function of pore fluid pressure by fitting the reaction kinetics using ‘Avrami's equation’ (Avrami, 1940) to temporal variation of pore fluid pressure. As for the dehydration potential of gypsum, under the condition where the stress drop varied with time, the frictional coefficient decreased with time when the pore fluid pressure was not taken into account. However, taking the pore fluid pressure into account, the frictional coefficient remained almost constant, which is consistent with the previous studies reporting the similar frictional coefficients of gypsum and anhydrate. In addition, the microstructure under the presumed dehydration condition did not show much Riedel shear planes, which may be due to the decrease in shear stress caused by the occurrence of pore fluid pressure (Leclère et al., 2016). Furthermore, we calculated the porosity of the gypsum gouge on the assumption that pore fluid pressure was generated, and the value was slightly smaller than the value known from previous studies, but it was considered that dehydration reaction occurred. This suggests that the gypsum may have undergone phase transition and dehydration during the shear deformation experiment, and then we evaluated the time function of the pore fluid pressure. The Avrami equation used for the temporal variation of pore fluid pressure includes the reaction rate k and the exponent n, which is related to the formation and growth mechanism of the material. The reaction rate k depends on the conditions of temperature, pressure, etc., and is generally harmonic when compared with the conditions of previous studies (Liu et al., 2015; Ballirano and Melis, 2009; Carbone et al., 2008). The exponent n

©2021. Japan Geoscience Union. All Right Reserved.

indicates the formation and growth mechanism of the material. Therefore, the obtained time function of pore fluid pressure is considered to be reasonable. If the time function of the pore fluid pressure obtained from the friction experiment using gypsum can be used to estimate the time until slow slip occurs, it will contribute to the estimation of the period of stress accumulation in the asperities and to the study of the occurrence of large earthquakes caused by slow slip.

Keywords: stick-slip, subduction zone, dehydration instability, pore fluid pressure, kinetics

©2021. Japan Geoscience Union. All Right Reserved.

Experimental study on drainage process of liquid film between bubbles during bubble growth

*Masatoshi Ohashi[1], Atsushi Toramaru[1], Atsuko Namiki[2]

1. Department of Earth and Planetary Sciences, Graduate School of Science, Kyushu University, 2. Graduate School of Environmental Studies Department of Earth and Environmental Sciences

Bubble coalescence has attracted attention in volcanology in recent decades because it can control volcanic eruption styles. Pre- and syn-eruptive magmas involve compressive bubbles, which reduce the effective density of magma and can be a driving force of the explosion. Thus, the explosivity of dry eruptions depends on the amount of gas in magma that exists as bubbles. The interconnected bubbles formed by coalescence can help to release the gas and prevent the magma from an explosive eruption. Bubble coalescence is divided into two stages: (1) approach stage in which the distance between bubbles shorten due to bubbles growth with maintaining the round shape, and (2) drainage stage in which the liquid film between bubbles drains out until a critical thickness. Here, we focus on the drainage stage. Previous studies investigated the timescale of drainage theoretically and experimentally under gravitational and capillary force effects (e.g., Proussevitch et al., 1993; Nguyen et al., 2013). However, the drainage by bubble growth associated with decompression is poorly understood, which must be a dominant process in a conduit. Therefore, we perform laboratory experiments and investigate if the rapid growth of bubbles accelerates or decelerates the drainage of the liquid film.

We used a Hele-Shaw cell made from two glass plates separated by 0.1 mm thick spacers. We filled the cell with silicone oil of 10 Pa・s viscosity and injected a mm-size bubble by microsyringe. By penetrating the bubble with a needle, we divided it into two nearly equal-size bubbles. We then placed the cell in a transparent acrylic container sealed by O-ring. The interior of the container was decompressed with a vacuum pump from the atmospheric pressure to 5 kPa. The decompression rate was varied by a vacuum regulator. The two bubbles gradually approached each other as the bubbles grow, and drained out the liquid film between them. The drainage process was recorded with an optical microscope and analyzed using Matlab.

The experimental results show that the growth rate of a bubble during decompression is faster than that expected from the ideal gas law. This difference can be attributed to the diffusional influx of dissolved air into bubbles. As the decompression rate increases, the bubble growth rate increases, which shortens the film rupture timescale. In the rapid decompression regime, a linear plateau border forms between two adjacent bubbles. The most striking finding in our experiments is that, under the higher decompression rate, the bubbles grow larger just before the onset of film rupture than in the case under the smaller decompression rate. The large growth rate enhances the viscous resistance in the plateau border, so that the bubble growth continues until the film thickness reaches a critical value. This finding significantly suggests that the formation of the permeable network in an eruption depends not only on the void fraction but also on the decompression rate.

Keywords: bubble coalescence, magma, laboratory experiment

©2021. Japan Geoscience Union. All Right Reserved.

Transition from viscous to inertial regime in dense frictional suspensions

*Franco Antonio Tapia[1], Olivier Pouliquen[3], Elisabeth Guazzelli[2]

1. Department of Mechanical Systems Engineering, Tokyo University of Agriculture and Technology, 2. Université de Paris, CNRS, Matière et Systèmes Complexes (MSC) UMR 7057, Paris, France, 3. Aix-Marseille Université, CNRS, IUSTI, Marseille, France

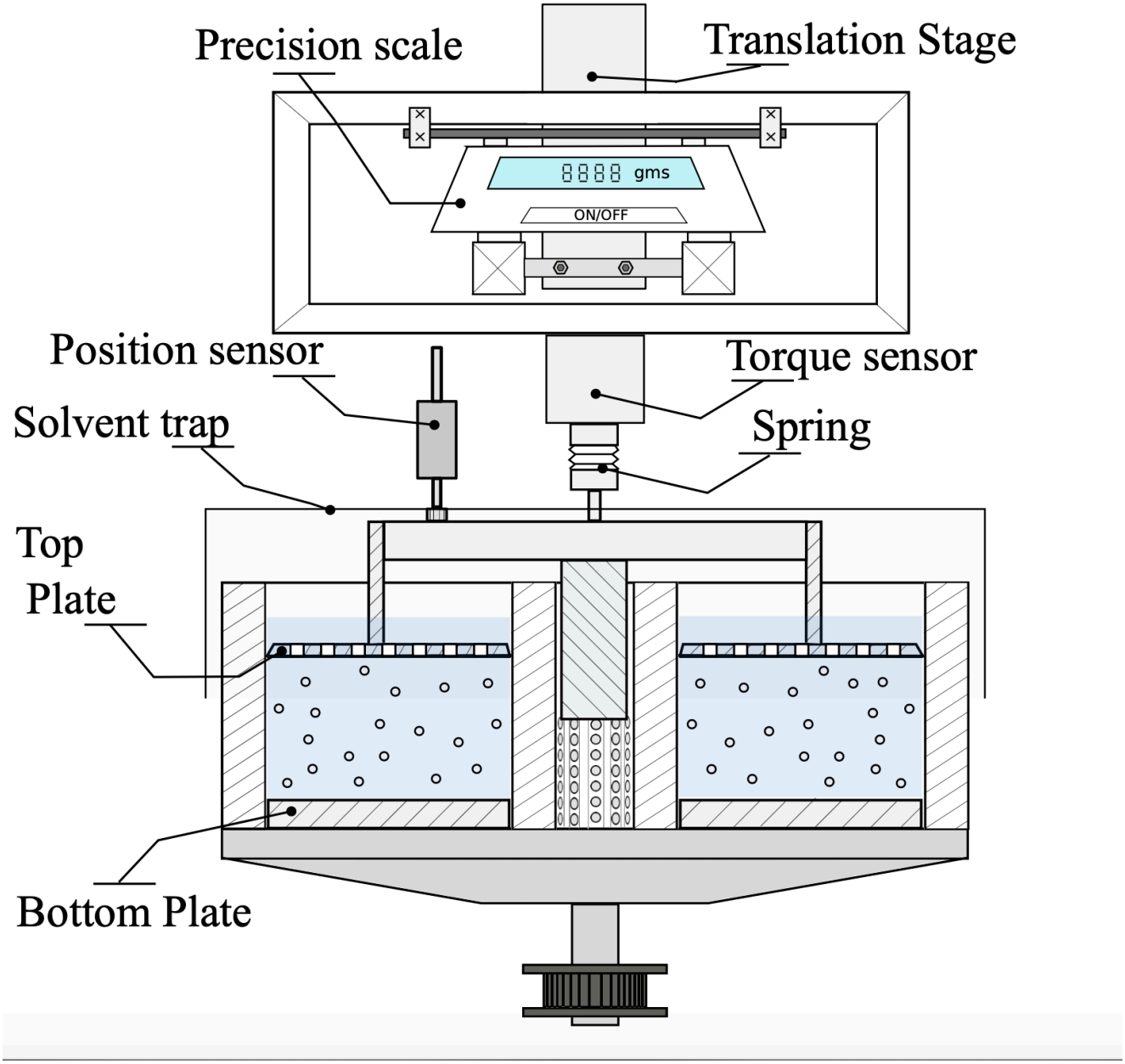
Failure and flow of granular materials are involved in many natural disasters and industrial processes. Several peculiar phenomena such as shear rate dependence behaviour, yield stress onset, normal stress difference, etc., distinguish them dramatically from classical newtonian flows. One of the most intriguing questions, which still remain a big challenge, are jamming-unjamming process and dissipation energy rate in a dense regime. Both of them seems to be strongly ruled by microscopic nature of inter-particle interaction forces and particle coupling with interstitial fluid. While hydrodynamic interactions or lubrication forces between the particles are important in the dilute regime, they become of lesser significance when the concentration is increased, and direct particle contacts become dominant in the rheological response. Despite its have been studied extensively, none of which is clearly understood so far.

Depending on boundary condition and stress distribution, dense granular flows can shows two different regimes : (i) rate-independent quasi-static flow, for moderate shear rate deformation, partially well described by continuous viscous-plastic models, inspired by soils mechanics, and (ii) rate-dependent behaviour, in which shear a normal stresses shows a power law function of the shear rate deformation in volume imposed rheology. In this frame of work, jamming transition is presented in a classical viscous approach as a shear viscosity divergence. In order to unifies theses two regimes, a non-classical rheology is suggested, wherein normal pressure, P, is imposed on the sample instead of the volume. Thus, a non-classical-frictional approach is suggested, in which the effective friction coefficient, defined by the ratio of macroscopic shear and normal stresses, and the flowable global solid-volume fraction are meanly controlled by an empirical power-law function of the ratio of macroscopic shear rate deformation and the normal pressure (perpendicular to the gradient direction). Moreover, particle-fluid coupling rules on the algebraical effective rheological properties of granular suspension; while for low viscosity interstitial fluid, the rheology has a high influence of inertial effect, newtonian rheology become important for high viscosity regime.

We present here an experimental study of viscous-inertial transition for a dense suspension of non-colloidal rigid PMMA particles by varying systematically the interstitial fluid viscosity for a both : Pressure and Volume-imposed rheology. The effect of inter-particle interaction is also explored by changing the elastic properties of solid particles by manufacturing soft hydrogel particles suspended in a water solution of UCON oil.

Keywords: Granular, Rheology, Suspensions, Jamming, Friction

©2021. Japan Geoscience Union. All Right Reserved.



©2021. Japan Geoscience Union. All Right Reserved.

Peridodic fluctation in a compressed dust-aggregate layer

*Hiroaki Katsuragi[1], Felipe Pacheco Vazquez[2], Tomomi Omura[3]

1. Department of Earth and Space Science, Osaka University, 2. BUAP, Mexico, 3. Osaka Sangyo University

Granules formed by tiny powder can be found in various situations even in our everyday lives. For example, dust aggregates are considered the candidate for materials forming planetesimals. Granules of flour, sugar, salt can be easily found in a kitchen. Although the fundamental understanding on behaviors of dust aggregates is crucial to properly understand/handle them, systematic physical investigation has not been sufficiently carried out so far. Therefore, we performed a set of simple experiments. In specific, uniaxial compression test of a hierarchical granular matter was performed. The hierarchical granular matter consists of a collection of dust aggregates. Dust aggregates were formed by mixing tiny glass beads (5 micro-meter in diameter) and small amount of water. Diameter of aggregate is approximately 1 mm. Dust aggregates were poured in a cylindrical cell and uniaxially compressed by a universal testing machine (Shimadzu AGX) with a constant speed. The compression speed was varied from 0.17 to 2000 micro-meter per second (over four orders of magnitude). During the compression, the compression force was measured. The compression force gradually increased as the compression proceeds. At the same time, periodic fluctuation of the compression force was observed on the increasing compression force. To characterize the nature of periodic fluctuation, we analyzed the experimental data (fluctuation amplitude, wavelenght, etc.) and obtained an empirical form. In addition, we performed the same experiment with glass beads and compared that result with the dust-aggregate case. In this presentation, details on the analyzed result will be presented.

Keywords: dust aggregate, uniaxial compression, periodic fluctuaion

©2021. Japan Geoscience Union. All Right Reserved.

Elasto-plastic behavior of carbonate rocks under high strain rate deformation

*Kosuke Kurosawa[1], Hidenori Genda[2], Shintaro Azuma[3], Keishi Okazaki[4], Haruka Oono[1], Takafumi Niihara[5], Takashi Mikouchi[6], Naotaka Tomioka[4], Tatsuhiro Sakaiya[7], Tadashi Kondo[7], Masahiro KAYAMA[8], Mizuho Koike[9], Yuji Sano[10], Takuya Matsuzaki[11], Masafumi MURAYAMA[11], wataru Satake[1], Takafumi Matsui[1,12]

1. Planetary Exploration Research Center, Chiba Institute of Technology, 2. Earth–Life Science Institute, Tokyo Institute of Technology, 3. Department of Earth and Planetary Sciences, Tokyo Institute of Technology, 4. Kochi Institute for Core Sample Research, Japan Agency for Marine-Earth Science and Technology, 5. Department of Systems Innovation, School of Engineering, The University of Tokyo, 6. The University Museum, The University of Tokyo, 7. Department of Earth and Space Science, Graduate School of Science, Osaka University, 8. Department of General Systems Studies, Graduate School of Arts and Sciences, The Univ. of Tokyo, 9. Department of Earth and Planetary Systems Science, Graduate School of Science, Hiroshima University, 10. Atmosphere and Ocean Research Institute, The University of Tokyo, 11. Center for Advanced Marine Core Research, Kochi University, 12. Institute of Geo-Cosmology, Chiba Institute of Technology

Impact craters dominate the surface topography of planets/satellites/asteroids with solid surfaces and without atmospheres and hydrospheres. Most of the meteorites found on the Earth contain unique metamorphic features caused by deformation under high stress conditions. These facts are evidence that mutual collisions between planetary bodies are one of the fundamental geological processes in the solar system. In hypervelocity collisions, materials are fluidized and deformed by induced shock waves. The characteristic strain rate of celestial collisions is expressed as the ratio of the impact velocity to the projectile diameter, and it typically exceeds 1 s^-1. In the case of an impact at >10 km/s, shock pressure exceeds 100 GPa, and a temperature rise due to irreversible compression leads to the perfect fluid approximation being valid. Our understanding of impact phenomena has often been based on the perfect fluid approximation. However, the typical impact velocity in the asteroid belt where meteorite parent bodies existed is ~5 km/s, which is comparable to the sound speed of rocky materials, and the elasto-plastic response of shocked rocks during impact events could not be ignored. Recently, Kurosawa and Genda (2018), GRL, 45, 620-626, numerically showed that the degree of impact heating due to plastic deformation during low-velocity impacts (<10 km/s) can be larger than that due to irreversible compression during shock wave propagation. The accurate understanding of the rock rheology is becoming more important in planetary sciences than previously thought.

We have started multifaceted studies to explore the responses of carbonate rocks under deformation with high strain rates. The advantages of the use of carbonate rocks are: (1) the temperature and pressure dependence of yield strength can be expressed by the same empirical law pertaining to igneous rocks, (2) the volatile component (CO2) is released at a relatively low temperature, and the degree of impact heating in the shocked sample can be quantitatively evaluated by measuring the amount of CO2 generated, and (3) homogeneous samples can be obtained at low cost. In this study, Carrara marble from Italy was used as a reference material. The marble constitutes crystallographically randomly-oriented calcite crystals having 100–300 um in diameter without gaps between grains.
In this presentation, we show the importance of the flow law to accurately estimate the amount of CO2 generated from shocked marbles based on the results of numerical impact calculations incorporating a simple rheology model for Calcite [Kurosawa, Genda, Azuma, and Okazaki, Revised]. We also present the results of an on-going shock-recovery experiment with the marble. In our experiments, shocked marbles,

©2021. Japan Geoscience Union. All Right Reserved.

which have experienced pressures of 1 - 10 GPa and strain rates of 10^5 –10^6 s-1, could be recovered for in-depth analyses.

Keywords: Celestial collisions, calcite, plastic deformation

©2021. Japan Geoscience Union. All Right Reserved.

[J] Poster | S (Solid Earth Sciences)：S-CG Complex & General

Sat. Jun 5, 2021 5:15 PM - 6:30 PM JST | Sat. Jun 5, 2021 8:15 AM - 9:30 AM UTC | Ch.18_2

[S-CG46] Rheology, fracture and friction in Earth and planetary sciences

convener:Shintaro Azuma(Department of Earth and Planetary Sciences, School of Science, Tokyo Institute of Technology), Ichiko Shimizu(Division of Earth and Planetary Sciences, Graduate School of Science, Kyoto University), Osamu Kuwano(Japan Agency for Marine-Earth Science and Technology), Miki Tasaka(Shizuoka University)

The aim of this session is to join people from various research area in the earth and planetary sciences and to stimulate discussion beyond the boundaries of each research area. Our goal is to deepen our understanding of dynamics in geosciences by looking over whole areas in the earth and planetary sciences from the viewpoint of PHYSICS OF DEFORMATION, FLOW, AND FRACTURE. We welcome any field (e.g., earthquake, volcano, earth surface, crust, mantle and the core, and other planets and satellites) and any approach (e.g., laboratory experiments, numerical simulations, field observations, and theories).

[SCG46-P01] Experimental investigation of the pyroxene-garnet and olivine-spinel transformations under shear deformation using synchrotron radiation and acoustic emission techniques

*Yuki Mori[1], Tomoaki Kubo[1], Rikuto Honda[1], Takuya Iwasato[2], Yuji Higo[3], Yoshinori Tange[3] (1.Kyushu Univ., 2.Shin-Nippon Nondestructive Inspection Co.,Ltd., 3.JASRI)

[SCG46-P02] Creep behavior during the post-spinel transformation in $(Mg, Fe)_2SiO_4$

*Yuta Goto[1], Tomoaki Kubo[1], Rikuto Honda[1], Yumiko Tsubokawa[1], Yuichiro Mori[2] (1.Kyushu Univ., 2.The University of Tokyo)

[SCG46-P03] SOR and AE study on the olivine-spinel transformation in $(Mg,Fe)_2SiO_4$ under uniaxial deformation with D111-type apparatus

*Rikuto Honda[1], Tomoaki Kubo[1], Yuichiro Mori[2], Goto Yuta[1], Yumiko Tsubokawa[1], Takuya Iwasato[3], Yuji Higo[4] (1.Kyushu University, 2.The University of Tokyo, 3.Shin-Nippon Nondestructive Inspection Co., Ltd., 4.JASRI)

[SCG46-P04] Frequency characteristics of acoustic emission in the fracture process of thermally cracked granite

*Sueyoshi Kazumasa[1], Manami Kitamura[2], Xinglin Lei[2], Ikuo Katayama[1] (1.Department of Earth and Planetary Systems Science, Hiroshima University, 2.National Institute of Advanced Industrial Science and Technology)

[SCG46-P05] Flow-to-fracture transition of linear Maxwell-type fluid by air injection

*Claudia Sanchez[1], Osamu Kuwano[2], Mie Ichihara[1] (1.Earthquake Research Institute, Tokyo University , 2.JAMSTEC)

[SCG46-P06] Role of lithology in deformation mechanisms of shallow-crustal active faults: Evidence from the Nahan thrust of Himalayas

*Dyuti Prakash Sarkar[1], Jun-ichi Ando[1], Kaushik Das[1], Gautam Ghosh[2], Prabir Dasgupta[3] (1.Hiroshima University, 2.Presidency University, 3.Durgapur Govt. College)

[SCG46-P07] Study of the mobile granular layer in bedload transport by laminar shearing flow in a tilted channel

*Chong-Wei Hong[1], Franco Tapia[2], Pascale Aussillous[3], Élisabeth Guazzelli[4], Chi-Yao Hung[1] (1.Department of Soil and Water Conservation, National Chung Hsing University, Taichung, Taiwan, 2.Department of Mechanical Engineering, Tokyo University of Agriculture and Technology, Tokyo, Japan, 3.Aix-Marseille

Université, CNRS, IUSTI, Marseille, France, 4.Université de Paris, CNRS, Matière et Systèmes Complexes (MSC) UMR 7057, Paris, France)

[SCG46-P08] Fracture behavior of silicate network phase-separating from aqueous fluid

*Takehito Koyama[1] (1.Institute of Industrial Science, the University of Tokyo)

[SCG46-P09] Evolution of patterns of hydraulically conductive natural fractures during inelastic deformation of rocks

*Nikita Dubinya[1,2] (1.Moscow Institute of Physics and Technology, 2.Schmidt Institute of Physics of the Earth of the Russian Academy of Sciences)

[SCG46-P10] Theoretical study on rock anelasticity;
Extension of a grain-boundary sliding model to two dimensions

*Mitsuyoshi Kunugihara[1], Yasuko Takei[1] (1.Earthquake Research Institute,The University of Tokyo)

[SCG46-P11] A DEM model of uniaxial and triaxial compression test of rocks

*Mikito Furuichi[1], Daisuke Nishiura[1], Yuzuru Yamamoto[2] (1.Japan Agency for Marine-Earth Science and Technology, 2.Kobe University)

[SCG46-P12] Relaxation of the frictional force in a statistical mechanical model of magnetic friction

*Komatsu Hisato[1] (1.National Institute for Materials Science)

Experimental investigation of the pyroxene-garnet and olivine-spinel transformations under shear deformation using synchrotron radiation and acoustic emission techniques

*Yuki Mori[1], Tomoaki Kubo[1], Rikuto Honda[1], Takuya Iwasato[2], Yuji Higo[3], Yoshinori Tange[3]

1. Kyushu Univ., 2. Shin-Nippon Nondestructive Inspection Co.,Ltd., 3. JASRI

Detection of acoustic emission (AE) has been recently performed combined with high-pressure deformation apparatus and synchrotron radiation to study the mechanisms of deep-focus earthquakes. To understand effects of large strains on shear localization and instability, deformation experiments in shear is more effective than uniaxial compression. However, the sample volume in shear deformation experiment is generally much smaller than that in uniaxial deformation experiment, which may make it difficult to conduct AE study with required accuracy. In this study, we carried out the pyroxene-garnet and olivine-spinel transformation experiments under shear deformation using AE techniques combined with deformation-DIA (D-DIA) apparatus and synchrotron radiation. Both pyroxene and olivine are major constituent minerals in subducting slabs, but their transformation processes are different. Here we report preliminary results on AE activities induced by these high-pressure transformations in shear.

The high-pressure shear deformation experiments were conducted using a uniaxial press (SPEED Mk. II) with a D-DIA type guide block installed at beamline BL04B1 in SPring-8, Japan. The 60 keV monochromatic X-ray was used to obtain 2D X-ray diffraction pattern and radiograph every 5 min during the experiments. We used MA 6-6 type AE measurement system attached with D-DIA guide block (Iwasato et al., 2020). Three kinds of starting materials of synthesized Al-rich clinopyroxene (Al-rich cpx), natural Al-poor clinopyroxene (Al-poor cpx), and synthesized fayalite were prepared for our study. They were sintered and cut to form polycrystalline disks (300 μm in thick and 1.3 mm in diameter). Each disk was assembled together with strain marker of gold foil between two 45˚-cut alumina pistons. The samples were first deformed to shear strains of ~30% at ~10 GPa and 650˚C for clinopyroxene and 475˚C for fayalite (stage 1), and then heated with a constant rate of 0.05 ℃/sec to cause the phase transformations (stage 2). The shear strain rates and the final shear strains were 1–5 x 10^{-4} /s and ~70-160%, respectively.

The pyroxene-garnet transformation already started during the deformation at 650˚C in Al-rich cpx and proceeded with increasing temperature. In contrast, no transformation was observed in Al-poor cpx up to ~850˚C. This is possibly originated from the difference in the Al content. We detected many AEs from the sample region at the stage 2 in the Al-rich cpx run, but no AEs at the stage 2 in the Al-poor cpx run, implying that AEs were induced by the pyroxene-garnet transformation in shear. FE-SEM observations of the recovered sample in the Al-rich cpx run revealed that garnet formed along grain boundary of clinopyroxene, and the shear deformation was localized in some regions. We also detected large AEs from the sample region in the fayalite run during the stage 2 associated with the olivine-spinel transformation. Thus, both the pyroxene-garnet and olivine-spinel transformations caused AE activity in our shear deformation experiments. We recognized two types of waveform of AE: AE with rapid increase in amplitude to the maximum (type 1), and AE with gradual increase in amplitude to the maximum (type 2). The type 2 is dominant in the Al-rich cpx run, whereas AEs in the fayalite run were type 1 only. The estimated locations of AE source were concentrated within the sample region in the case of type 1 AE, whereas those of type 2 AE were widely scattered from the sample to pressure medium. This is probably because the AIC pick is difficult in the type 2 AE. Our study demonstrated that both the pyroxene-garnet

©2021. Japan Geoscience Union. All Right Reserved.

and olivine-spinel transformations caused AE activity under shear deformation at ~10 GPa, however further investigations are necessary to understand why the waveform of AEs are rather different between theses transformations.

Keywords: Acoustic emission, In situ X-ray observation, Deep-focus earthquake, Pyroxene, Olivine

©2021. Japan Geoscience Union. All Right Reserved.

Creep behavior during the post-spinel transformation in $(Mg, Fe)_2SiO_4$

*Yuta Goto[1], Tomoaki Kubo[1], Rikuto Honda[1], Yumiko Tsubokawa[1], Yuichiro Mori[2]

1. Kyushu Univ., 2. The University of Tokyo

Seismological studies have shown large deformation and no deep earthquakes in the lower mantle slabs, which may be attributed to the post-spinel transformation (the decomposition reaction of $(Mg,Fe)_2SiO_4$ ringwoodite into $(Mg,Fe)SiO_3$ bridgmanite and (Mg,Fe)O ferropericlase). *Poirier et al.* (1986) reported that the post-spinel transformation is a eutectoid reaction with alternating fine lamellar structure in the colony texture. Based on microstructural observations, *Ito and Sato* (1991) suggested that aseismicity in the lower mantle is caused by superplastic flow of the fine-grained post-spinel assemblage. The weakening of the lower mantle slab has also been suggested from the degree of the grain-size reduction and diffusion creep viscosity (e.g., *Kubo et al.*, 2009). Syn-deformational reaction experiments using analog materials have shown that eutectoid reaction does not directly weaken the material, but the degeneration of eutectoid colony is an important process for rheological weakening (e.g., *Doi et al.* 2014; *Zhao et al.* 2012). However, there have been no direct experimental studies to understand effects of the post-spinel transformation on creep behavior.

In this study, syn-deformational post-spinel transformation experiments in $(Mg, Fe)_2 SiO_4$ were conducted by in-situ X-ray observation method using a D-111 type deformation apparatus (MAX-III) at PF-AR NE-7 beamline. The starting material is polycrystalline ringwoodite (grain size ~a few to 10 μm) that was synthesized from single crystalline San Carlos olivine. The ringwoodite sample was first uniaxailly deformed at ~27 GPa and 600˚C to ~3% strain, and then heated to around 1000˚C at a constant rate of 0.06˚C/s to cause the post-spinel transformation. 2D-XRD patterns and radiography images were taken every ~5 min to obtain stress-strain and transformation-time curves. Deformation and transformation microstructures in recovered samples were examined by FE-SEM.

We conducted two runs at the similar P, T, and strain rate conditions. The strain rates changed from 1.3-1.5e-5 s^{-1} to 4.9-5.6e-5 s^{-1} at the timing of the initiation of the transformation. The final strains and transformed fraction were ~27-37% and ~50-80%, respectively. Creep behaviors in ringwoodite suggested that it reached steady state at the strain of ~5% and the stress of ~4 GPa, and then exhibited weakening with the increase in temperature. The decrease in the flow stress of ringwoodite became more rapidly at higher than ~800-850˚C, which may be linked to the initiation of the transformation. However, the stress of bridgmanite newly transformed is larger than that of ringwoodite. FE-SEM observation revealed that many eutectoid colonies with the size of ~1 μm in diameter are present at grain boundaries of ringwoodite. The lamellar spacing in the colony is ~50 nm. It is noteworthy that the eutectoid colonies themselves are not deformed and degenerated after the deformation with nearly 30% strain. Both the colony size and lamellar spacing are much smaller than those observed in transformation experiments with similar overpressures but no deformation (e.g., *Kubo et al.*, 2011).

Each phase (bridgmanite and ferropericlase) in a eutectoid colony is thought to be an interconnected single crystal. No deformation in the eutectoid colonies implies that the stiffer bridgmanite supports the colony (i.e., isostrain in the two phase of the colony), which means that the transformed post-spinel colony is stiffer than the parental ringwoodite. Thus, it is unlikely that the reaction-induced weakening occurs in our experiments. The weakening of ringwoodite observed at higher than ~800-850˚C may be originated by the change of the dominant deformation mechanism from low-temperature plasticity to

©2021. Japan Geoscience Union. All Right Reserved.

dislocation creep (e.g., *Imamura*, 2018). Our study demonstrates that rheological weakening due to the post-spinel transformation is difficult at low temperatures ~1000°C and larger strains are required to degenerate the post-spinel colony.

Keywords: post-spinel transformation, eutectoid reaction, deformation experiment, in situ X-ray observation, deep slab deformation, rheological weakening

©2021. Japan Geoscience Union. All Right Reserved.

SOR and AE study on the olivine-spinel transformation in $(Mg,Fe)_2SiO_4$ under uniaxial deformation with D111-type apparatus

*Rikuto Honda[1], Tomoaki Kubo[1], Yuichiro Mori[2], Goto Yuta[1], Yumiko Tsubokawa[1], Takuya Iwasato[3], Yuji Higo[4]

1. Kyushu University, 2. The University of Tokyo, 3. Shin-Nippon Nondestructive Inspection Co., Ltd., 4. JASRI

In cold subducting slabs, it has been pointed out that olivine remains in metastable phase beyond the equilibrium boundary. The metastable olivine transforms into its high-pressure phases, such as wadsleyite or ringwoodite under non-equilibrium conditions. It has been suggested that this phenomenon leads to rheological weakening and shear instability causing large deformation and deep-focus earthquakes in subducting slabs. For example, Schubnel et al. (2013) reported AE activity following the olivine-spinel transformation with in-situ X-ray observation using D-DIA apparatus. However, they used olivine analogue, Mg_2GeO_4, which transformed to spinel phase at low pressures (~2 GPa). In the present study, we conducted deformation experiments with San Carlos olivine polycrystal under the mantle transition zone (MTZ) conditions using D111-type apparatus combined with synchrotron radiation to observe creep behavior during the phase transformation. In addition, we developed 8-channel Kawai-type AE measurement system attached with D111-type apparatus to observe shear instability at MTZ pressures. Here we report some preliminary results on these experimental studies.

We carried out deformation and transformation experiments with synchrotron X-ray using a D111-type apparatus (MAX-III) installed at PF-AR NE7 beamline. The starting material was polycrystalline San Carlos olivine sintered at 1323 K (grain size of ~100 μm, Run oldt11) and 1223 K (grain size of ~30 μm, Run oldt12). The sample was first uniaxially deformed to ~1-3 % strain with a constant anvil displacement rate of 300 μm/h at ~20 GPa and 773 K / 873 K, and then heated with a constant rate of 0.09 K/s to cause transformation during deformation. We obtained 2D-XRD patterns and radiography image every 5 minutes using a 60 keV monochromatic X-ray to measure stress-strain curves and reaction kinetics.

Transition to ringwoodite started at ~20 GPa and ~1000K with ~5% strain, and finally proceeded more than 90% transformation at 1273K with the final strain of ~20-35%. The strain rate was 0.4-7.5e-5 s^{-1}. The stress of olivine reached to ~5 GPa at most before the transition and gradually decreased to ~2-3 GPa with the increase in temperature and transformed fraction. In contrast, the stress of ringwoodite newly appeared was very small less than 1 GPa and subtly increased. The similar results have been reported in the RDA study (Mohiuddin et al., 2020), however, the strength of ringwoodite kept small in our experiments. The temperature dependence of the olivine stress was almost consistent with the flow law of Peierls mechanism constructed by Mei et al. (2010) at the initial stage, and the olivine got more weakened as the transformation proceeded especially in Run oldt11. These creep behaviors suggest that reaction-induced weakening occur, but not significant. It is unlikely that the interconnected weak layer was formed at the initial stage of the transformation. In the recovered samples, intracrystalline lamellae filled with fine ringwoodite grains were widely observed. Similar textures have been reported in shocked meteorite (Chen et al., 2004) and the syn-deformational olivine-spinel transition of fayalite (Mori et al., 2020).

We also have set up 8-channel Kawai-type AE measurement system attached with another D111-type apparatus (QDES2) newly installed at Kyushu University. This is almost similar to 6-channel MA6-6 type AE measurement system with D-DIA apparatus (Iwasato et al., 2020) for lower-pressure experiments. After the

©2021. Japan Geoscience Union. All Right Reserved.

verification of the performance by conducting cold compression runs using grass beads and single crystalline San Carlos olivine, we have started syn-deformational transformation experiment in San Carlos olivine under the MTZ conditions with the AE system. We have recorded AE from the sample during transformation, however no distinct faulting structure was observed so far except for lenses and thin lamellae filled with fine-grained ringwoodite.

Keywords: high-pressure deformation experiments, in-situ X-ray observation, acoustic emission, slab weakening , deep earthquakes, olivine-spinel transformation

©2021. Japan Geoscience Union. All Right Reserved.

Frequency characteristics of acoustic emission in the fracture process of thermally cracked granite

*Sueyoshi Kazumasa[1], Manami Kitamura[2], Xinglin Lei[2], Ikuo Katayama[1]

1. Department of Earth and Planetary Systems Science, Hiroshima University, 2. National Institute of Advanced Industrial Science and Technology

Fluid flow-induced seismicity has been observed in various engineering fields such as enhanced geothermal system (EGS). Especially, in the Pohang EGS project, the Mw 5.4 earthquake was likely induced by fluid injection after the events in the entire period of stimulations (Kim et al., 2018). To understand the processes of induced earthquakes due to fluid injection, it is necessary to research the propagation process of pre-existing cracks in thermally damaged granites. The acoustic emission (AE) is defined as elastic waves released by rapid cracking, which is a useful tool for investigating generation and propagation of rock fractures. The frequency of AE signals from fracturing provides information about internal structure of rock. In this study, we measure AE and P-wave velocity of thermally cracked granite during triaxial deformation under dry and fluid-saturated conditions.

We conduct triaxial compression tests at confining pressure of 22.5 MPa and strain rate of ~10^{-6} s^{-1} under dry and wet conditions using the loading system at AIST. Permeability is measured by a fluid flow method using water as a pore fluid, in which a constant upstream pore pressure was maintained at 4 MPa. Cylindrical coarse-grained Inada granite (50 mm in diameter and 125 mm in length), which are intact and thermally damaged at 550 ℃, are used as samples. We measure AEs with 28 piezoelectric transducers (PZTs) with variable resonance frequencies of 0.25 - 2 MHz. In the frequency spectrum obtained from the fast Fourier transform, the peak amplitude is defined as the largest amplitude in the spectrum, and the peak frequency is defined as the frequency at the peak amplitude.
Our result shows that wet samples behave elastically until the onset of dilatancy ranging from 27.1 to 32.7 % of the peak stress, and then shows inelastic behavior. After the peak stress of 357-413 MPa, post-yield behavior of the sample indicates brittle failure with drastic stress drop. AE activity was initiated at the crack damage stress ranging from 51.8 to 62.6 % of the peak stress. Frequency analysis based on the fast Fourier transform shows that the peak frequency was mainly distributed in the range of 0 to 0.6 MHz. Chen et al. (2020) has shown that low peak frequency signal with high peak amplitude normalized by the maximum value in the test (LH signal) reflected the formation of macrocracks. In our results of PZTs with resonant frequency of 1 and 0.5 MHz, LH signals were only recorded after 99 % of the peak stress for the thermally cracked sample, while LH signal began to appear after approximately 80 % of the peak stress for the intact sample. A comparison of the results indicates that stress-induced crack growth in the thermally cracked sample was not detected due to the large scale of thermal cracks.

Keywords: acoustic emission, frequency, triaxial compression

©2021. Japan Geoscience Union. All Right Reserved.

Flow-to-fracture transition of linear Maxwell-type fluid by air injection

*Claudia Sanchez[1], Osamu Kuwano[2], Mie Ichihara[1]

1. Earthquake Research Institute, Tokyo University , 2. JAMSTEC

Due to decompression during magma ascent, bubbles grow, rise, and burst. These behaviors are coupled with the rheology of the magma. The complex nature of magma and the conditions under which the bubbles develop may control the eruption styles, whether explosive or effusive. Among the complexity, the viscoelasiticy is considered essential for the flow and fracture transition. The linear Maxwell model is the simplest model to represent the magma viscoelasticity. It has a single relaxation time. Brittle fracture of magma is considered to occur when the deformation time scale is shorter than the relaxation time. Although this concept has been used in many eruption models, the ductile-to-brittle transition of flowing fluid has not been sufficiently investigated in the laboratory. We report the experimental study of using an aqueous solution of cetyltrimethylammonium bromide and sodium salicylate (CTAB/NaSal), which forms wormlike micelles known to have a simple Maxwell-type viscoelasticity. We inject air through the fluid and observe the elastic and viscous deformation of the fluid around the bubble. The brittleness of the bubble burst on the fluid surface is characterized by visualizing the elastic strain by the birefringence technic and by measuring the bursting sounds.

Keywords: Viscoelasticity, magma, bubble

©2021. Japan Geoscience Union. All Right Reserved.

Role of lithology in deformation mechanisms of shallow-crustal active faults: Evidence from the Nahan thrust of Himalayas

*Dyuti Prakash Sarkar[1], Jun-ichi Ando[1], Kaushik Das[1], Gautam Ghosh[2], Prabir Dasgupta[3]

1. Hiroshima University, 2. Presidency University, 3. Durgapur Govt. College

Research on deformation nature and fault rock geochemistry of shallow-crustal active faults has been widely studied for elucidating the stress accommodation mechanisms and response to the fault movement in terms of stress localizations, fault weakening, and earthquake nucleation. The heterogeneous nature of the fault in response to tectonic stresses is also reported by few researchers. The current study is focused on Nahan Thrust (NT), a shallow-crustal thrust fault within the Main Frontal Thrust (MFT) sheet of the Himalayan Fold Thrust belt. In the present study, we have attempted to elucidate the nature of deformation mechanisms inferred from detailed field mapping of the fault zone, microstructural observation, and characterization of deformation mechanisms. In the studied area, NT has developed within the alternation of quartz-rich and phyllosilicate-rich siltstone of the Paleogene Dagshai Formation. It forms a wide brittle fault zone with a damage zone of 110 m and a fault core of 40 m. The damage zone of NT shows dominantly brittle deformation with an increasing degree of brecciation toward the fault core. The fault core shows several layers of chaotic breccia-grey gouge and foliated red gouge with a single layer of black gouge ~1 m (forming black gouge). Calcite vein fragments present with the damage zone rocks and fault core show the development of deformation twins, which suggests a deformation temperature of ~170 ℃. The modal mineral analysis of the intact and gouge rocks, determined in conjunction with SEM-BSE, EPMA, and image processing by ImageJ software, as well as the obtained XRD patterns from intact and gouge rocks indicate that the formation of different gouges within the fault core is dependent on the intact rocks. Based on the microstructural observations, the quartz-rich intact rock has dominantly deformed by fracturing and cataclasis with minimum effects of fluid alteration (if any) during the fault activity. The phyllosilicate-rich layer, however, has exhibited pervasive alteration and generation of finer phyllosilicates, with deformation dominantly by pressure solution mechanisms. The phyllosilicate-rich layers also act as sealing zones, localizing stress and subsequent stress buildup within the quartz-rich layers, thereby narrowing the active zone of the fault during subsequent fault activity. Additionally, grain size analysis of the gouge rocks by ImageJ, and their XRD patterns indicate the presence of amorphous material in the black gouge. The presence of amorphous materials is also evident from Transmission Electron Microscopy (TEM) analysis of the black gouge. The black gouge in the studied area is, therefore a product of co-seismic frictional heating, indicated by the presence of amorphous materials, gas escape structures, and clay clast aggregates.

Keywords: NT, Fault gouge, CCA, Calcite e-twins

©2021. Japan Geoscience Union. All Right Reserved.

Study of the mobile granular layer in bedload transport by laminar shearing flow in a tilted channel

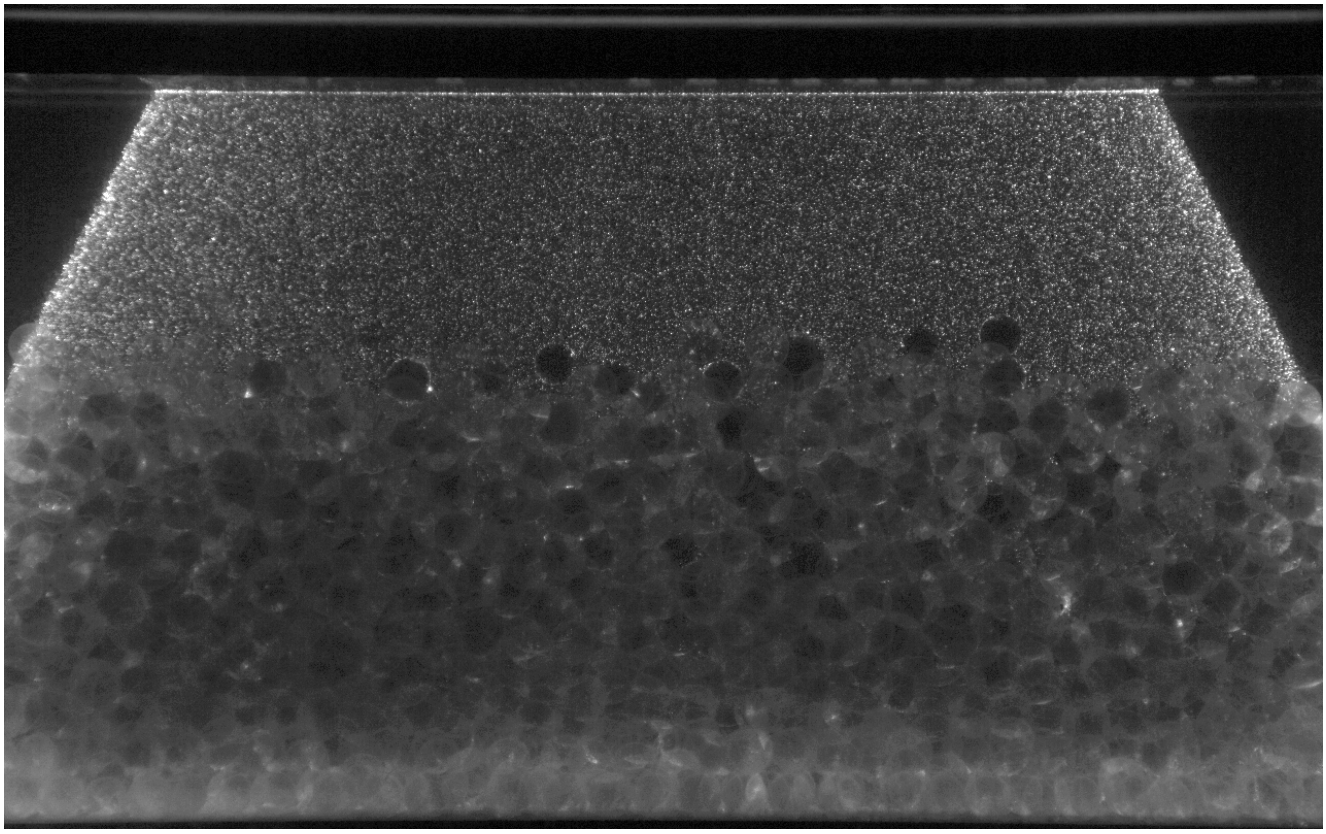
*Chong-Wei Hong[1], Franco Tapia[2], Pascale Aussillous[3], Élisabeth Guazzelli[4], Chi-Yao Hung[1]

1. Department of Soil and Water Conservation, National Chung Hsing University, Taichung, Taiwan, 2. Department of Mechanical Engineering, Tokyo University of Agriculture and Technology, Tokyo, Japan, 3. Aix-Marseille Université, CNRS, IUSTI, Marseille, France, 4. Université de Paris, CNRS, Matière et Systèmes Complexes (MSC) UMR 7057, Paris, France

Erosion is a natural phenomenon which moves materials from the earth's surface thanks to a shearing fluid, and has a significant effect on the morphodynamics of river beds. When sands and rocks are transported, this process is hard to clarify since we can only observe the surface motion. Following previous work to investigate experimentally the mobile layer of a granular bed due to a shearing fluid flow we use a refractive index matching technique. The experimental setup consists of a rectangular channel partially filled with particles as shown in the figure. We use index-matched combinations of spherical hydrogel particles and a mixture of water, citric acid, and ucon oil to control the hydrogel particles diameter (which have swelled in the fluid) and the fluid viscosity. The tube is tilted, between 20 deg and 40 deg, and we impose an upward fluid flow thanks to a pump, which ensures a stationary regime. Indeed, the upper layers of particles are transported upstream due to the fluid shearing flow whereas the granular bed tends to slide down due to gravity. Both particle and fluid velocity profiles are obtained using particle image velocimetry. The experimental results are compared with a two-phase continuum model having frictional rheology to describe particle-particle interactions. By varying the viscosity of the fluid, we study the influence of inertia while staying in a laminar regime. We also focus on the role of the elasticity of the particles on the frictional rheology.

Keywords: granular media, particle/fluid flow, sediment transport

©2021. Japan Geoscience Union. All Right Reserved.



©2021. Japan Geoscience Union. All Right Reserved.

Fracture behavior of silicate network phase-separating from aqueous fluid

*Takehito Koyama[1]

1. Institute of Industrial Science, the University of Tokyo

Assuming the crustal structure with “actively-shrinking” lower crust of silicate network phase-separating from aqueous fluid below “passively-deformed” upper crust of usual rocks, I tried to explain the crustal activities including the intra-crustal seismicity in the short time scale and the crustal stabilization from its compaction in the long time scale (Koyama, JpGU 2019, JpGU-AGU2020, JPS2020, AGU2020). One of the important problems in the deformation of the “active” lower beneath the “passive” upper is the strength of the lower-crustal network solid filled with the fluid, because the fluid pressurized into cracks in rocks can weaken the rocks through inducing the fracture, which is a known fact (Hubbert and Rubey, 1959; Michaelske, 1982).
This fluid effect promotes mechanically and chemically fracture of crustal rocks: In the case of aqueous fluids, H_2O can slide the cracks through opening the impermeable crack walls with the pressure (Hubbert and Rubey, 1959) and can propagate the crack tips through disconnecting the bonds of the rock materials around there with the chemical reactions (Michaelske, 1982). These must result from the contact between the two materials originating from their different thermodynamic states, which create their impermeable interface for their counter pressures and their chemical potential gradient for their mutual dissolution around the interface.
Then, how do the fluid effect arises in the fluid-solid coexistence in the same single thermodynamic state? Phase separation between shrinking amorphous network solid and diffusing fluid realizes this situation (Tanaka, 2000, 2017; Koyama, 2009, 2018); In phase separation between shrinking silicate network and diffusing aqueous fluid, the question is whether the fluid effect on the network fracture are the same with the case of the contact between fluid and rock from different origin or not. I expect to be not, because thermodynamic relation between H_2O and SiO_2 in the phase separation is the opposite from that in the above fluid-rock contact: In the two coexisting phases from the same origin the pressure is common between them and the fluid can diffuse through the network, and chemical potential gradient demixing them in the phase separation, on the other hand, must prevent the reactions for network dissociation. Thus, the counter pressure and the crack tip propagation by the fluid must be difficult to arise on the coexisting network: The fluid must be difficult to weaken the network.
If these are true, the network coexisting with the fluid in the lower crust can keep its strength under the fluid-filled situation. On the other hand, the fluid diffusing from the shrinking lower-crustal network can weaken the usual upper-crustal rocks as a result of its permeation from the crustal lower to the upper. Thus, we can consider the possibility that the lower-crustal network is stronger than the upper-crustal rocks, and that the “actively-shrinking” former deform the latter one-sidedly.

Keywords: Fracture, Silicate netowrk, Aqueous fluid, Phase separation or phase demixing

©2021. Japan Geoscience Union. All Right Reserved.

Evolution of patterns of hydraulically conductive natural fractures during inelastic deformation of rocks

*Nikita Dubinya[1,2]

1. Moscow Institute of Physics and Technology, 2. Schmidt Institute of Physics of the Earth of the Russian Academy of Sciences

The study is focused on spatial orientations of hydraulically conductive natural fractures existing in rock masses subjected to varied stresses. Fluid conductivity of natural fractures is a serious issue in various fields as the opportunity to predict it is essential for such problems as assessing risks in underground infrastructure engineering or unconventional hydrocarbon reservoirs development. This problem is complicated as the inner structure of rock masses is often unknown with limited sources of information regarding it.

The current study is focused on establishing the relationship between deformation of naturally fractured rock samples and spatial orientations of hydraulically conductive fractures existing in them. Only geomechanical aspect of the problem is taken into account in the current study with other factors being outside of its scope.

The study is based on the results of series of laboratory experiments. A series of triaxial tests have been carried out using cylindrical samples of naturally fractured rocks. These samples were saturated and subjected to external stresses. Typical deformation curves –interrelationships between components of stress and strain tensors –were obtained for varied conditions. These dependencies proved to be nonlinear, so the results have been consequently analyzed through the concept of non-associated plastic flow law: a mathematical model to establish stress-strain relationship has been constructed. Plastic hardening resulting into varied elastic moduli and friction angle was taken into account within this model. The constructed model made it possible to estimate the preferable directions of natural fractures propagation during inelastic stage of rock deformation as the planes of optimally oriented fractures evolve alongside with friction angle. As a result, the constructed model made it possible to predict the statistics on spatial orientations of developed natural fractures in a rock sample subjected to inelastic deformation.

Nevertheless, this statistics itself is not enough to predict fluid conductivity of the developed natural fractures. Critically stressed fractures concept was used to analyze, which of the fractures existing in the rock are hydraulically conductive, and which are not. According to this concept, hydraulic conductivity of a natural fracture is governed by the relationship between normal and shear stress acting on its surface. There is an analytical solution providing spatial orientations of all fractures that are hydraulically conductive for a given arbitrary stress tensor. This solution is valid if critically stressed fractures concept is true and hydraulic conductivity of natural fractures is governed solely by relationship between stresses. Other cases are not within the scope of the current study. Application of the mentioned solution to the obtained statistics on spatial orientations of natural fractures existing in the rock sample may provide insights regarding the changes in hydraulically conductive natural fractures patterns caused by evolution of stress-strain state of naturally fractured rock mass. Laboratory experiments were analyzed with this technique: each stage of deformation process was characterized by such factors as current spatial orientations of all developed natural fractures alongside with spatial orientations of hydraulically conductive fractures; changes in relative number and total free surface of all developed fractures and hydraulically conductive fractures and so on.

©2021. Japan Geoscience Union. All Right Reserved.

The proposed approach of treating naturally fractured rock masses may be used for solving various problems. In the current study an example of such application is considered from the perspective of hydrocarbon reservoir development: the proposed approach made it possible to predict changes in fluid conductivity of natural fractures existing in oil reservoirs during various operations related to reservoir development.

Keywords: Plastic hardening, Critically stressed fractures, Non-associated flow rule

©2021. Japan Geoscience Union. All Right Reserved.

Theoretical study on rock anelasticity; Extension of a grain-boundary sliding model to two dimensions

*Mitsuyoshi Kunugihara[1], Yasuko Takei[1]

1. Earthquake Research Institute,The University of Tokyo

Rock anelasticity has a significant effect on seismic velocity and attenuation structure in the upper mantle. However, experiments are difficult and data are limited. Therefore, theoretical approaches to rock anelasticity are important. Existing experimental data indicate that grain boundary sliding is one of the major mechanisms of rock anelasticity under upper mantle conditions (e.g., Jackson & Faul, 2010; Takei et al., 2014). A model of grain boundary sliding was developed by Raj & Ashby (1971). Their model is a quasi-one-dimensional model that deals with the sliding between two elastic blocks with interlocking nonplanar boundary. When the amplitude of the nonplanarity is small, they analytically obtained the effective shear modulus and attenuation as functions of frequency. Their model successfully reproduced the seamless transition of a polycrystalline material from elastic, through anelastic, to viscous body with decreasing frequency. Morris & Jackson (2009) introduced a minute quantity ε to represent the amplitude of the nonplanarity, and reformulated the model of Raj & Ashby (1971) more rigorously using the perturbation method. In these previous quasi-one-dimensional models, the base state only represents the relaxation of shear stress applied to a single planar grain boundary, and does not represent the real grain boundary in a polycrystalline material where both normal and shear stresses act. In addition, the previous models predict the existence of a large peak on the high-frequency side, but experimental results using polycrystalline olivine (Jackson & Faul, 2010) and rock analogs (Takei et al., 2014) do not show such a peak. In this study, we develop a two-dimensional model for grain boundary sliding in a polycrystalline material. By modeling with a more realistic geometry, the base state reflects self-locking at the mineral grain scale, and hence we can consider atomic-scale steps along the grain boundary in the first order perturbation. For a quantitative prediction of the peak amplitude, it is important to consider a granular aggregate interlocked both at mineral grain scale and atomic scale.

In this study, we obtain the shear modulus and attenuation of a two-dimensional polycrystalline material with arbitrary grain shape as functions of frequency. Using the perturbation method proposed by Morris & Jackson (2009), we first solve for the case where the grain shape is a perfect circle as the base state. The general solution of the elastic displacement field and stress field of a circle was obtained by Love (1927). By adding boundary conditions for grain boundary diffusion and grain boundary viscosity, we can obtain the displacement and stress fields of a grain in the presence of matter diffusion and grain boundary sliding. For a grain of arbitrary shape deviating from the circle, the approximate solution depending on the detailed grain shape can be obtained analytically by using the perturbation method. So far, we have obtained the base state solution and found that it has the viscoelastic properties of the Burgers model. In the next step, we plan to obtain solutions up to the first order perturbation.

Keywords: anelasticity, grain-boundary sliding, seismic attenuation

©2021. Japan Geoscience Union. All Right Reserved.

A DEM model of uniaxial and triaxial compression test of rocks

*Mikito Furuichi[1], Daisuke Nishiura[1], Yuzuru Yamamoto[2]

1. Japan Agency for Marine-Earth Science and Technology, 2. Kobe University

The Discrete Element Method (DEM) is a fundamental simulation method to investigate solid earth dynamics. A simple friction model between the contacting particles is known to simulate the behavior of the sand layer which is the scaled analog model of accretionary prism formation. However, to simulate the mechanical behavior of rocks in such DEM-based geoscience simulation, we have to extend the model to support the bonding model between the particles. Here, we present the parametric study and technique to reproduce the uniaxial and triaxial compression test of rocks sampled in the Hota accretionary complex. Our model based on the ratios of tensile to compressive strength can reproduce essential behaviors of non-linear failure envelopes. We will discuss the role of bonding parameters in the normal and tangential direction in the pre-and post- failure processes.

Keywords: DEM, Compression test of rocks, Accretionary prism

©2021. Japan Geoscience Union. All Right Reserved.

Relaxation of the frictional force in a statistical mechanical model of magnetic friction

*Komatsu Hisato[1]

1. National Institute for Materials Science

Magnetic friction, the frictional force caused by the magnetic interaction between materials, is studied in recent years to investigate the microscopic mechanism of the friction. As part of these studies, we previously proposed a statistical mechanical model of magnetic friction obeying the Dieterich-Ruina law in the steady state with sufficiently weak external force(Komatsu 2019). This law is a well-known empirical law observed in the usual solid surfaces, so our previous study implies that the analogy between the magnetic and usual frictions exists.
In this presentation, we investigate the behavior of the magnetic friction in the non-steady state using a model similar to our previous one. Specifically, we consider a chain moving on the edge of a two-dimensional lattice, and let each lattice point of them have one spin variable interacting with each other. The chain is combined with a spring, and the other edge of the spring moves with a constant veocity v.
We investigate the responce of the frictional force to the sudden change of v by the numerical simulation. If the time scale of the spin relaxation is slower than that of the chain motion, the relaxation of the frictional force is divided into two processes: the sudden change accompanied by that of v called direct process, and the slow relaxation after that called indirect process. This behavior resembles that observed in the usual solid surfaces. In the case of the usual solid surfaces, it is said that these two processes result from the creep motion of the materials. In the case of our model, on the other hand, this behavior is caused by the slow relaxation of the magnetic structure. Hence, the change of the magnetic structure of our model has a similar role to the creep motion of usual solid surfaces.

Keywords: friction, magnetic materials, statistical mechanics

©2021. Japan Geoscience Union. All Right Reserved.

[E] Poster | M (Multidisciplinary and Interdisciplinary)：M-IS Intersection

Sat. Jun 5, 2021 5:15 PM - 6:30 PM JST | Sat. Jun 5, 2021 8:15 AM - 9:30 AM UTC | Ch.20_1

[M-IS06] Human-environment Nexus from Pre-Historic to Modern Times

convener:F Harry Lee(The Chinese University of Hong Kong)

We sincerely invite researchers to present their works pertaining to the socio-economic and demographic impacts of climate change in pre-historic, historical, and modern times, which is a topic focusing on human-environment interactions. The related knowledge may have important implications for global and regional sustainability. This session is going to serve as an interdisciplinary platform for collecting different views and facilitating a constructive debate about the ways in which human-environment interactions can be generalized, contextualized, or even denied - - - a philosophical issue pertinent to the theoretical underpinnings of environmental humanities. To further facilitate the debate about global and regional sustainability from different perspectives, scholars who agree on the significant impact of climate change on human societies, or who are skeptical about this relationship, are welcome to present their related works in this session. Topics of interest include, but are not limited to, the following:

A. How and to what extent human societies are (or are not) affected by climate change or climatic extremes;

B. The use of empirical archaeological/historical data in investigating human-environment interactions;

C. Case studies in illustrating human-environment interactions;

D. The influence of spatio-temporal scale, study period, and study area on human-environment interactions; and

E. Philosophical discussion about human-environment interactions.

[MIS06-P01] The socio-hydrological interactions in modern China: a case study based on flood events in Yangtze River Basin

*CHANG LIU[1], Akiyuki Kawasaki[1], Tomoko Shiroyama[2] (1.Department of Civil Engineering, the University of Tokyo, 2.Graduate School of Economics, the University of Tokyo)

[MIS06-P02] Historical climate-war nexus in the eyes of geographers

*Harry F Lee[1] (1.The Chinese University of Hong Kong)

The socio-hydrological interactions in modern China: a case study based on flood events in Yangtze River Basin

*CHANG LIU[1], Akiyuki Kawasaki[1], Tomoko Shiroyama[2]

1. Department of Civil Engineering, the University of Tokyo, 2. Graduate School of Economics, the University of Tokyo

As the longest river in Asia, the Yangtze River has shown its impact on human societies with floods recorded since 12th century. In 1931, the Yangtze River has manifested its force again with one of the deadliest floods ever recorded in Chinese history, causing 422,499 deaths, damages to more than 25.2 million people and 58.7 billion m^2 farmland. Similar flood occurred again in 1954, resulting in 31,762 deaths, damages to 18.9 million people and 31.7 billion m^2 farmland. Researches have shown 1954 flood being larger and higher compared to 1931 flood. However, it is still unclear for what reason that a more severe flood leading to fewer casualties, especially when there being no significant progress in the countermeasure technique. To answer this question, here we propose a conceptual socio-hydrological framework within which the mutual influence between society and water system is analyzed. We found that before and after 1931 flood, a change of social structure of villages aggravated the vulnerability of agricultural production towards natural hazards, and hydrological extremes speeded-up such structure change afterwards. As for 1954 flood, remolding of village structure strengthened the resilient ability to a certain degree, while the damage was controlled at the cost of rural settlements. Our results demonstrate how the conceptual framework is likely to help comprehend the inner correlation of a pre-industrial society like the early 20th century of China. We anticipate our study to be a starting point for more sophisticated socio-hydrological models, which will likely to be applicable to many other regions and times.

Keywords: socio-hydrology, Yangtze River Basin, flood

©2021. Japan Geoscience Union. All Right Reserved.

Historical climate-war nexus in the eyes of geographers

*Harry F Lee[1]

1. The Chinese University of Hong Kong

Did climate change cause wars in history? While a growing number of quantitative studies (particularly in the field of geography) illustrate the climate-war nexus in pre-industrial societies, there are opposing opinions on the subject. Such conflicting views invite us to reconsider whether the climate-war nexus can be conceptualized as a yes/no dichotomy. This paper seeks to address this issue. I will first recapitulate the key findings of those quantitative studies of geographers that substantiate the significant role of climate deterioration in causing wars. Then I will pinpoint those issues that complicate the conceptualization of the climate-war nexus, indicating that the nexus cannot be taken as a simple yes/no question. Finally, I will propose a research approach that may facilitate a productive interdisciplinary collaboration, perhaps between geographers and historians, to conduct research on the interconnection between climate change and wars in history. I hope that the interpretation of the climate-war nexus can move away from a dichotomy of yes/no, and the multiple dimensions of wars and social resilience to climate change will be thoroughly considered. Also, the advantages of geography and history could be integrated to enrich understanding of the climate-war nexus in history.

Keywords: Climate change, War, Geography, History, Preindustrial era

©2021. Japan Geoscience Union. All Right Reserved.

[E] Oral | M (Multidisciplinary and Interdisciplinary)：M-IS Intersection

Sat. Jun 5, 2021 10:45 AM - 12:15 PM JST | Sat. Jun 5, 2021 1:45 AM - 3:15 AM UTC | Ch.03 Zoom Room 03

[M-IS07] Effects of lightning, severe weather and tropical storms

convener:Mitsuteru Sato(Department of Cosmoscience, Hokkaido University), Hisayuki Kubota(Hokkaido University), C. Glenn Vincent Lopez(- - -), Purwadi Purwadi(Department of Cosmosciences, Hokkaido University, Sapporo 0600810, Japan), Chairperson:Mitsuteru Sato(Department of Cosmoscience, Hokkaido University), Hisayuki Kubota(Hokkaido University)

Thunderstorms are markers of deep convection and severe weather, producing heavy precipitation, hail and strong winds that lead to significant natural hazards, especially in coastal and urban areas. Huge economic damages and loss of human lives often result from such events. As the intensity and frequency of thunderstorms is projected to increase in the future - when the atmosphere and oceans become warmer - the need for detecting and nowcasting thunderstorms and lightning on local and regional scales becomes crucial.
We invite contributions dealing with thunderstorms and lightning and their atmospheric effects. We seek contributions focusing on convective storm evolution, forecasting of thunderstorms and lightning using local, regional and global detection networks as well as other sensors. Also, works on global lightning patterns in an era of climate change, satellite-based studies of thunderstorms and other remote-sensing technologies, as well as urban effects on lightning and public safety from lightning danger.

10:45 AM - 11:00 AM JST | 1:45 AM - 2:00 AM UTC

[MIS07-01] Current status and prospects of ULAT/SATREPS

*Yukihiro Takahashi[1,2], Mitsuteru Sato[1,2], Hisayuki Kubota[1,2], Tetsuro Ishida[1,2], Ellison Castro[3], Loren Jay Estrebillo[3], Purwadi Purwadi[4], Meryl Algodon[1], Gay Perez[3], Joel Marciano[5], Jun Matsumoto[6], Jun-Ichi Hamada[6] (1.Department of Cosmosciences, Graduate School of Science, Hokkaido University, 2.Department of Earth and Planetary Sciences, Faculty of Science, Hokkaido University, 3.University of the Philippines, Diliman, 4.BPPT, Indonesia, 5.PhilSA, Phlippines, 6.Tokyo Metropolitan University)

11:00 AM - 11:15 AM JST | 2:00 AM - 2:15 AM UTC

[MIS07-02] **The relationship between CG lightning detected by AVON V-POTEKA and thunderstorm parameters**

*Purwadi Purwadi[1], Yukihiro Takahashi[2], Mitsuteru Sato[2], Hisayuki Kubota[2], Kozo Yamashita[3] (1.Agency for Assessment and Application for Technology, Jakarta 10340, Indonesia, 2.Faculty of Science, Hokkaido University, Sapporo 0600810, Japan, 3.Department of Electrical Engineering, Salesian Polytechnic, Tokyo, Japan)

11:15 AM - 11:30 AM JST | 2:15 AM - 2:30 AM UTC

[MIS07-03] Machine Learning Prediction of Precipitation in Metro Manila, Philippines

★Invited Papers

*Akira Noda[1], Yukihiro Takahashi[2], Hisayuki Kubota[2], Ken-ichi Fukui[3], Mitsuteru Sato[2] (1.Department of Earth and Planetary Sciences, School of Science, Hokkaido University., 2.Department of Cosmosciences, Graduate School of Science, Hokkaido University, 3.The Institute of Scientific and Industrial Research, Osaka University)

11:30 AM - 11:45 AM JST | 2:30 AM - 2:45 AM UTC

[MIS07-04] **3D Reconstruction of Typhoon Trami Eye Using Airborne Camera**

★Invited Papers

*Meryl Regine Llenaresas Algodon[1], Yukihiro Takahashi[2], Mitsuteru Sato[2], Hisayuki Kubota[3], Tetsuro Ishida[3], Kozo Yamashita[4], Ellison Caparas Castro[5], Gay Jane Perez[6], Joel Joseph Marciano[7], Jun Matsumoto[8], Jun-Ichi Hamada[9], Kazuhisa Tsuboki[10], Hiroyuki Yamada[11] (1.Hokkaido University, Graduate School of Science, 2.Hokkaido University, 3.Hokkaido University, Faculty of Science, 4.Ashikaga University, 5.University of the Philippines Quezon City (Philippines), 6.NASA Goddard Space Flight Center

Earth Science Division Greenbelt MD 20771-0000 (United States), 7.Advanced Science and Technology Institute Quezon City (Philippines), 8.Tokyo Metropolitan University Tokyo 192, 9.Tokyo Metropolitan University Hachioji, 10.Nagoya University, Institute for Space–Earth Environmental Research Nagoya 464, 11.University of the Ryukyus Nishihara)

11:45 AM - 12:00 PM JST | 2:45 AM - 3:00 AM UTC

[MIS07-05] Successive observation of atmospheric electric observation at Kakioka Geomagnetic Observatory

*Masashi Kamogawa[1], Tomoyuki Suzuki[1], Toshiyasu Nagao[3], Yasuhiro Minamoto[2] (1.Global Center for Asian and Regional Research, University of Shizuoka, 2.Laboratory for Environmental Research at Mount Fuji, 3.Institute of Oceanic Research and Development, Tokai University)

12:00 PM - 12:15 PM JST | 3:00 AM - 3:15 AM UTC

[MIS07-06] Observation of Elves and Transient Luminous Events from the International Space Station with the Mini-EUSO telescope

*Marco Casolino[1], Toshikazu Ebisuzaki[1], Yoshiyuki Takizawa[1], Naoto Sakaki[1], Satoshi Wada[1] (1.Riken)

Current status and prospects of ULAT/SATREPS

*Yukihiro Takahashi[1,2], Mitsuteru Sato[1,2], Hisayuki Kubota[1,2], Tetsuro Ishida[1,2], Ellison Castro[3], Loren Jay Estrebillo[3], Purwadi Purwadi[4], Meryl Algodon[1], Gay Perez[3], Joel Marciano[5], Jun Matsumoto[6], Jun-Ichi Hamada[6]

1. Department of Cosmosciences, Graduate School of Science, Hokkaido University, 2. Department of Earth and Planetary Sciences, Faculty of Science, Hokkaido University, 3. University of the Philippines, Diliman, 4. BPPT, Indonesia, 5. PhilSA, Phlippines, 6. Tokyo Metropolitan University

Our projects of a SATREPS “ULAT” is to realize precise real-time monitoring and issuing alert for extreme weather, such as torrential rainfall or typhoon. We have been developing a ground observation network with lightning sensors and trying to establish semi real-time operation of micro-satellites to capture the typhoon and thunderstorms. In these projects, we apply two new technologies, that is, the lightning activity estimated by the ground-based lightning networks with 12 sites for VLF radio wave measurement in nation-wide of Philippines and with 50 sites for electrostatic field measurement in Metro Manila together with infrasound sensor and automated weather station, and the 3 dimensional capturing of thunderstorms by the on-demand operation of 50-kg micro-satellites, including the Philippine-developed satellites. We started ULAT project in 2017 and completed the installation of the ground lightning observation station with automated weather station about 70 percent of the original plan and started continuous recording of the data. Although, due to COVID-19, now the installation of ground station is stopping, we plan to carry out the work remotely making use of the latest IT devices. As for the satellite observation, we succeeded in reconstructing detailed 3-D cloud structure near the center of typhoon Maysak 2020 with camera onboard DIWATA-1. In this presentation we update the recent progress of the projects.
This research was supported by Science and Technology Research Partnership for Sustainable Development (SATREPS), Japan Science and Technology Agency (JST) / Japan International Cooperation Agency (JICA).

Keywords: ULAT, SATREPS, microsatellite, lightning, extreme weather, monitoring

©2021. Japan Geoscience Union. All Right Reserved.

The relationship between CG lightning detected by AVON V-POTEKA and thunderstorm parameters

*Purwadi Purwadi[1], Yukihiro Takahashi[2], Mitsuteru Sato[2], Hisayuki Kubota[2], Kozo Yamashita[3]

1. Agency for Assessment and Application for Technology, Jakarta 10340, Indonesia, 2. Faculty of Science, Hokkaido University, Sapporo 0600810, Japan, 3. Department of Electrical Engineering, Salesian Polytechnic, Tokyo, Japan

Cloud to ground (CG) lightning observation networks, namely AVON V-POTEKA, have been established using a 1-40 kHz very low frequency (VLF) receiver. It has been deployed and operated to cover East and South East Asia since 2017. In this study, the CG lightning geolocation estimation of AVON V-POTEKA data is estimated using the time of arrival method and found the best accuracy of ~30 km. The relationship between lightning and thunderstorm cloud parameters over the maritime continent (MC) can be conducted with additional data of the Himawari 8 band 15 (12.4 μm) to provide cloud top temperature (CTT), radiosonde archived data, and the Global Satellite Mapping of Precipitation with gauge adjusted (GSMaP_Gauge) standard V7. Using the statistical method and grid size 0.5˚ x 0.5º, the relationship between CG lightning and thunderstorm clouds parameters is found in this study. Moreover, the CTT of thunderstorm clouds is found to be less than -30ºC to produce at least 1 CG lightning, which can be detected by AVON V-POTEKA. Both CTT and cloud top height (CTH) shows a logarithmic relationship with the CG lightning with R^2=0.95. On the other hand, the relationship between CG lightning and rainfall shows a power relationship with R^2=0.92. The relationship between CG lightning and precipitation water area is estimated to be a power relationship.

Keywords: cloud to ground lightning, cloud top temperature, cloud top height, rainfall

©2021. Japan Geoscience Union. All Right Reserved.

Machine Learning Prediction of Precipitation in Metro Manila, Philippines

*Akira Noda[1], Yukihiro Takahashi[2], Hisayuki Kubota[2], Ken-ichi Fukui[3], Mitsuteru Sato[2]

1. Department of Earth and Planetary Sciences, School of Science, Hokkaido University., 2. Department of Cosmosciences, Graduate School of Science, Hokkaido University, 3. The Institute of Scientific and Industrial Research, Osaka University

It is difficult to accurately predict the occurrence and rain volume of torrential rains such as guerrilla rain, rain band with typhoon and linear precipitation zones even in Japan, where meteorological observations from the ground and space and weather forecasts using numerical models are well established. One of the reasons for this is that the spatial narrowness of the rainfall area and the rapid development of these extreme weather events exceed the temporal and spatial resolution of conventional weather observation networks. Furthermore, in Southeast Asia, where the meteorological observation infrastructure is relatively weak, many disasters such as heavy rains and floods caused by monsoons and typhoons occur every year. There is an urgent need to establish the cost-effective weather forecasting technology. In recent years, the development of machine learning technology has been remarkable owing to the increased processing speed of computers and big data. In addition, in the field of meteorology, the researches on the forecasting method development using machine learning have been actively conducted. Our research group has developed an automatic weather and lightning observation system called as P-POTEKA since 2017, and has been deploying it in Metro Manila, Philippines, which is frequently affected by heavy rains and associated flooding. To date, 35 P-POTEKA units have been installed in Metro Manila and continue the acquisition of meteorological data (precipitation, temperature, pressure, humidity, wind speed, wind direction and solar irradiance every minutes). While AMeDAS (The Automated Meteorological Data Acquisition System) in Japan is deployed with the average interval of 17km, P-POTEKA in Metro Manila is deployed with the average interval of 2-3km, making the observation network with the world’s highest spatial and temporal resolution suitable for capturing extreme weather events. Using the P-POTEKA rainfall data, RGB image data corresponding to the spatial distribution of rainfall in Metro Manila was created by interpolating the data using the ordinary kriging method. By training these time-series rainfall image data on a machine learning model called ConvLSTM (Convolutional Long-Short Term Memory), we predicted the distribution and rainfall amount from the present to 1-hour later with the 10-minutes intervals using the observation data of the past 1-hour. The root mean squared error (RMSE) of the RGB values of pixels corresponding to the predicted and actual observed precipitation distributions were calculated for untrained rainfalls (40 patterns) to evaluate the performance of our machine learning method. As a result, it was found that the prediction using ConvLSTM is relatively accurate up to 30 minutes from the present, but the prediction accuracy of the spatio-temporal change of prediction becomes significantly worse after 40-60 minutes from the present. In this presentation, the details of the machine learning method model using ConvLSTM and the prediction results of precipitation and precipitation distribution predictions will be explained more in detail.

Keywords: torrential rainfalls, machine learning, mesoscale meteorology

©2021. Japan Geoscience Union. All Right Reserved.

3D Reconstruction of Typhoon Trami Eye Using Airborne Camera

*Meryl Regine Llenaresas Algodon[1], Yukihiro Takahashi[2], Mitsuteru Sato[2], Hisayuki Kubota[3], Tetsuro Ishida[3], Kozo Yamashita[4], Ellison Caparas Castro[5], Gay Jane Perez[6], Joel Joseph Marciano[7], Jun Matsumoto[8], Jun-Ichi Hamada[9], Kazuhisa Tsuboki[10], Hiroyuki Yamada[11]

1. Hokkaido University, Graduate School of Science, 2. Hokkaido University, 3. Hokkaido University, Faculty of Science, 4. Ashikaga University, 5. University of the Philippines Quezon City (Philippines), 6. NASA Goddard Space Flight Center Earth Science Division Greenbelt MD 20771-0000 (United States), 7. Advanced Science and Technology Institute Quezon City (Philippines), 8. Tokyo Metropolitan University Tokyo 192, 9. Tokyo Metropolitan University Hachioji, 10. Nagoya University, Institute for Space–Earth Environmental Research Nagoya 464, 11. University of the Ryukyus Nishihara

Typhoons are extreme weather phenomena that inflict damages and casualties around the globe. These phenomena are difficult to study because of their chaotic behaviour but the capacity to measure their intensity can help mitigate the hazards that they bring. In the past, several attempts have been done to relate typhoon's intensity with the structural evolution of its eye. This suggests the possible relation between the typhoon intensity with typhoon eye altitude. In this research, we visualize Typhoon Trami’s structure by reconstructing the three-dimensional model inside its eye and integrating the information of its cloud top altitude. An experiment was conducted under the SATREPS/ULAT project (SATREPS: Science and Technology Research Partnership for Sustainable Development, ULAT: Understanding Lightning and Thunderstorm) where images of Typhoon Trami were taken from an aircraft last September 26, 2018. Aircraft images were used to reconstruct the 3D model inside the typhoon eye because they provide closer views of the typhoon than that of geostationary satellite images making it easier to reconstruct a 3D model. The 3D reconstruction generated covers approximately 50 km distance from the typhoon eye at 24.3 m/pixel spatial resolution. Three cross-sections of the 3D model were analyzed, and the resulting altitude distribution was compared with the cloud-top altitude estimated by mapping the brightness temperature of the Himawari Thermal Infrared Band 13 with cloud-top height as measured by NOAA sonde data. From the 3D model, the altitude distribution ranges from 5.3 km to 14.3 km while the altitude estimated from the brightness temperature ranges from 5.2 km to 14.6 km. However, regions of altitude difference can also be observed between the two methods. This study shows that a three-dimensional model could be a good mode of typhoon visualization as it shows a more detailed typhoon structure such as the stairstep structures that was detected at some regions within the typhoon eye. This research was supported by SATREPS, funded by Japan Science and Technology Agency (JST) / Japan International Cooperation Agency (JICA).

Keywords: 3D Reconstruction, Typhoon Monitoring

©2021. Japan Geoscience Union. All Right Reserved.

Successive observation of atmospheric electric observation at Kakioka Geomagnetic Observatory

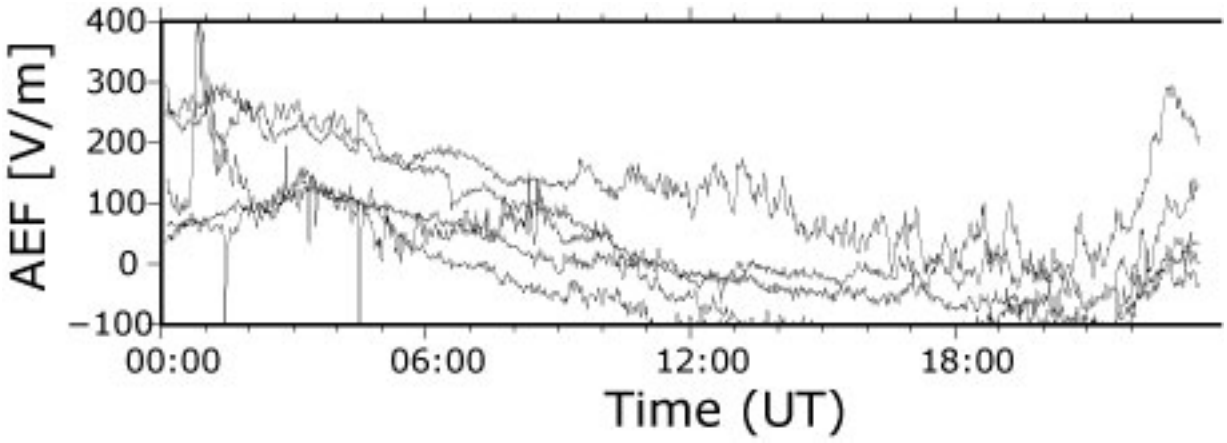
*Masashi Kamogawa[1], Tomoyuki Suzuki[1], Toshiyasu Nagao[3], Yasuhiro Minamoto[2]

1. Global Center for Asian and Regional Research, University of Shizuoka, 2. Laboratory for Environmental Research at Mount Fuji, 3. Institute of Oceanic Research and Development, Tokai University

The atmospheric electric field (AEF) measurement has been carried out by the Japan Meteorological Agency (JMA) at Kakioka geomagnetic observatory since 1929. The JMA decided that the AEF measurement would terminate at the end of February 2021. Since many researchers have used the AEF data at Kakioka, several research groups such as universities examined whether or not successive observations could be conducted at Kakioka. In our grope, we installed one field mill with board range of intensity developed by Otowa Co. Ltd., sensitive and insensitive field mills developed by Boltek and two all-sky cameras at 18 of Feb., 2021. This observation was available on not only traditional fair-weather study but also the study of severe weather accompanying heavy lightning activities. The sampling of field mills are 20 Hz (Otowa) and 10 Hz (Boltek). The time stamp was synchronized by GPS.

This paper is a preliminary report of the AEF measurement in the vicinity of the current AEF observation operated by our group. This figure shows that the time-series of AEF records (Otowa) from 19 to 23 of Feb. of 2021 in UT.

Keywords: Atmospheric electric field, Potential gradient, Kakioka



©2021. Japan Geoscience Union. All Right Reserved.

Observation of Elves and Transient Luminous Events from the International Space Station with the Mini-EUSO telescope

*Marco Casolino[1], Toshikazu Ebisuzaki[1], Yoshiyuki Takizawa[1], Naoto Sakaki[1], Satoshi Wada[1]

1. Riken

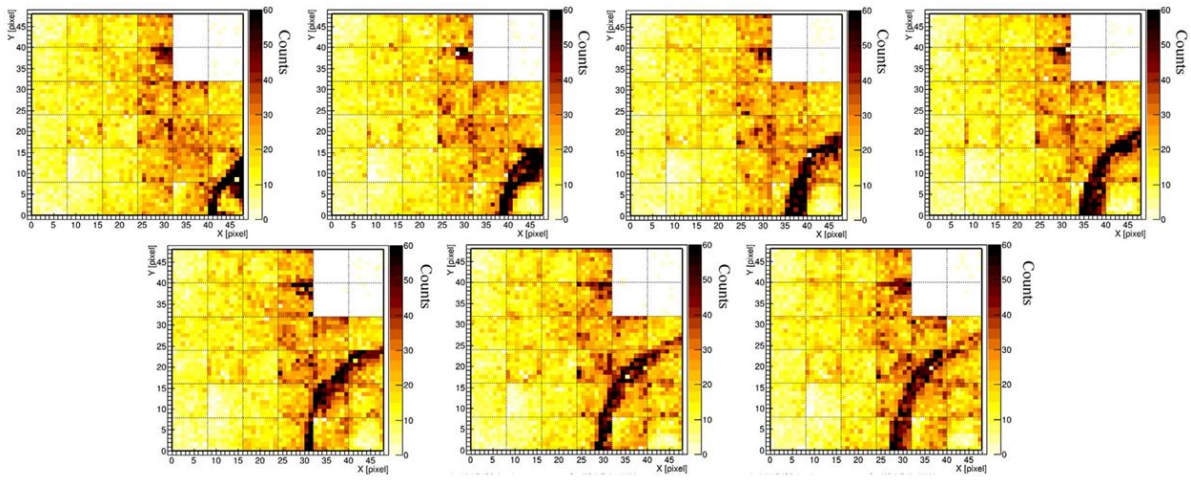
Mini-EUSO is a telescope observing the Earth in the ultraviolet band from a nadir-facing, UV transparent window of the International space station.

The instrument - launched in 2019 - has a field of view of 44degrees, a spatial resolution on the ionosphere of 4.7 km and a sampling rate of 2.5 microseconds. The telescope consists in an optical system with two Fresnel lenses and a focal surface composed of an array of 36 Hamamatsu multi-anode photomultiplier tubes, for a total of 2304 pixels. The telescope also contains two ancillary cameras, in the near infrared and visible ranges, to complement measurements in these bandwidths.

The telescope detects UV emissions of cosmic, atmospheric and terrestrial origin on different time scales, from 2.5 microseconds and above. At the fastest sampling rate, Mini-EUSO is able to observe atmospheric phenomena such as ELVES and other Transient Luminous Events with the imaging camera, allowing to study in detail the expansion and propagation.

In this work we will present the ELVES observations done by Mini-EUSO, discussing their rate of occurrence, location and structure (ring size, speed, shape), in particular the multi-ringed events.

Keywords: TLE, ELVES, International Space Station



©2021. Japan Geoscience Union. All Right Reserved.

[E] Poster | M (Multidisciplinary and Interdisciplinary) : M-IS Intersection

Sat. Jun 5, 2021 5:15 PM - 6:30 PM JST | Sat. Jun 5, 2021 8:15 AM - 9:30 AM UTC | Ch.21_1

[M-IS07] Effects of lightning, severe weather and tropical storms

convener:Mitsuteru Sato(Department of Cosmoscience, Hokkaido University), Hisayuki Kubota(Hokkaido University), C. Glenn Vincent Lopez(- - -), Purwadi Purwadi(Department of Cosmosciences, Hokkaido University, Sapporo 0600810, Japan)

Thunderstorms are markers of deep convection and severe weather, producing heavy precipitation, hail and strong winds that lead to significant natural hazards, especially in coastal and urban areas. Huge economic damages and loss of human lives often result from such events. As the intensity and frequency of thunderstorms is projected to increase in the future - when the atmosphere and oceans become warmer - the need for detecting and nowcasting thunderstorms and lightning on local and regional scales becomes crucial.
We invite contributions dealing with thunderstorms and lightning and their atmospheric effects. We seek contributions focusing on convective storm evolution, forecasting of thunderstorms and lightning using local, regional and global detection networks as well as other sensors. Also, works on global lightning patterns in an era of climate change, satellite-based studies of thunderstorms and other remote-sensing technologies, as well as urban effects on lightning and public safety from lightning danger.

[MIS07-P01] Lightning bursts observed during the tropical cyclone genesis over the Philippine Sea

*Hisayuki Kubota[1], Yukihiro Takahashi[1], Mitsuteru Sato[1] (1.Hokkaido University)

[MIS07-P02] Spatial and temporal variations of heavy rainfall in the Metro Manila, Philippines in the dry-wet transitional season based on a dense surface meteorological observation network

*Jun-Ichi Hamada[1], Jun Matsumoto[1], Hisayuki Kubota[2], Mitsuteru Sato[2], Yukihiro Takahashi[2], Glenn Vincent[3] (1.Tokyo Metropolitan University, 2.Hokkaido University, 3.Advanced Science and Technology Institute, Philippines)

[MIS07-P03] Estimation of the relation between electrical properties of lightning and tropical cyclone intensity in the western north Pacific.

*Shunsuke Niwa[1], Mitsuteru Sato[1], Yukihiro Takahashi[1], Hisayuki Kubota[1] (1.Department of Cosmoscience, Hokkaido University)

[MIS07-P04] Lightning Activity in Western North Pacific Measured by the V-POTEKA Network and Its Relation to Typhoon Intensity

*Mitsuteru Sato[1], Yukihiro Takahashi[1], Hisayuki Kubota[1], Glenn Vincent C. Lopez[2] (1.Faculty of Science, Hokkaido University, 2.ASTI, DOST)

Lightning bursts observed during the tropical cyclone genesis over the Philippine Sea

*Hisayuki Kubota[1], Yukihiro Takahashi[1], Mitsuteru Sato[1]

1. Hokkaido University

The accuracy of tropical cyclone (TC) track forecast has been improved year by years, on the other hand, the forecast of tropical cyclone intensity still has a difficulty of improvement. Recently the relationship between lightning activity and tropical cyclone intensity has been investigated. Lightning tends to increase during the rapid intensification of the TC. Therefore, monitoring the lightning activity becomes important for a TC intensity forecast. Lightning observation network are deployed over the western north Pacific by five very long frequency events trigger measurements called V-POTEKA at Palau, Guam, Manila Philippines, Okinawa Japan and Serpong Indonesia under the ULAT (Understanding Lightning and Thunderstorm) of SATREPS (Science and Technology Research Partnership for Sustainable Development) in the Philippines.

Lightning activity was drastically increased around the TC during the TC genesis stage of tropical storm Maysak on 28 August 2020. Numbers of lightning reached the maximum during the life cycle of the TC. Location of lightnings were concentrated near the center of TC in about 100 to 200 km radius. Convective clouds reached less than 190K of blackbody temperature near the center of the TC. We called this phenomenon as “lightning burst”. It seems that lightning burst is associated with the convective burst which tends to occur during the TC genesis stage. About half of TCs observed lightning bursts during the TC genesis stage over the Philippine Sea in 2020. We will investigate further what kind of structure occurred during the lightning burst and what kind of mechanism responsible for the lightning burst.

Keywords: Tropical cyclone, Lightning, Philippine Sea

©2021. Japan Geoscience Union. All Right Reserved.

Spatial and temporal variations of heavy rainfall in the Metro Manila, Philippines in the dry-wet transitional season based on a dense surface meteorological observation network

*Jun-Ichi Hamada[1], Jun Matsumoto[1], Hisayuki Kubota[2], Mitsuteru Sato[2], Yukihiro Takahashi[2], Glenn Vincent[3]

1. Tokyo Metropolitan University, 2. Hokkaido University, 3. Advanced Science and Technology Institute, Philippines

To monitor heavy rainfall and thunder cloud in the Metro Manila, Philippines, an observational network of the automatic weather station with lightning detection sensors (P-POTEKA) has been established since 2018. As of June 2020, 35 P-POTEKA stations were installed in the area. In this study, we aimed to investigate spatial and temporal distributions of heavy rainfall in the Metro Manila during the dry-wet transitional season (May-June) of 2019 and 2020 using the P-POTEKA observational data.

The wet season (westerly monsoon season) started in the middle of June in the both of 2019 and 2020. Two tropical cyclones landed in the Philippines in the transitional season of 2020, whereas no tropical cyclone approached in the 2019. The area average total rainfall amounts were larger in 2019 (484.5 mm) than 2020 (309.5 mm). Total numbers (hours) of heavy rainfall events (equal or more than 20.0 mm/h) for all the P-POTEKA stations were also larger in 2019 (131 hours) than 2020 (82 hours). These obtained results may imply that local convection was predominant in 2019. We will introduce the spatial distributions of the heavy rainfall events in the Metro Manila and their diurnal variations at the meeting.

This work was supported by Japan Science and Technology Agency (JST) and Japan International Cooperation Agency (JICA) under the Science and Technology Research Partnership for Sustainable Development (SATREPS) Project.

Keywords: Heavy rainfall, Monsoon, Local convection, Metro Manila

©2021. Japan Geoscience Union. All Right Reserved.

Estimation of the relation between electrical properties of lightning and tropical cyclone intensity in the western north Pacific.

*Shunsuke Niwa[1], Mitsuteru Sato[1], Yukihiro Takahashi[1], Hisayuki Kubota[1]

1. Department of Cosmoscience, Hokkaido University

Although the track prediction of tropical cyclones (TC) is improved year by year, the prediction of the TC intensities such as the minimum sea level pressure and the maximum wind speed is getting worse year by year and is an big issue to be solved. Previous studies indicate that the lightning activities in TCs can be a good proxy of the TC intensity development. In the previous studies, the relation between the lightning occurrence number and the TC intensity development were investigated. However, the relation of the electrical properties (EPs) of lightning discharges with the TC intensity development is poorly investigated. As there are some reports showing close relation between the lightning EPs and the thunderstorm activities causing severe weather, it’ s important to clarify the relation between the lightning occurrence number, lightning EPs and the TC intensity development.
The purpose of this study is to clarify the relation between the lightning EPs and the TC intensity development and to verify whether the lightning EPs or the lightning occurrence number is a better proxy to predict the TC intensity development. For this purpose, we have (1) estimated the lightning occurrence number in the inner core and the rainband of TCs using the ground-based lightning detection network data, (2) identified the transient ELF waves detected by the ground-based ELF observation network and related to lightning discharge in the TC region, and (3) estimated the lightning EPs and analyzed relation between the lightning EPs and the TC intensity development. We used the best track data of TCs provided by Joint Typhoon Warning Center (JTWC), lightning data containing both time and location data provided by World Wide Lightning Location Network (WWLLN) and ELF magnetic field waveform data obtained at Syowa station in Antarctica and Kuju station in Japan, that are the two stations of Global ELF Observation Network (GEON). As the collection window of lightning discharges in TCs, we defined (i) the inner core as the region within the 100 km (200 km) distance from the TC center for normal (large) TCs, (ii) the rainband as the region of 100-500 km (200-1000 km) from the center for normal (large) TCs. Using ELF waveform data, we estimated the peak current (Ip), charge moment change (Qdl), and charge amount (Q) as the lightning EPs. Ip and Qdl were estimated from ELF data obtained at Syowa, while Q was estimated from ELF data obtained at Kuju. Using above methods and the estimated parameters, we conducted the cross-correlation analyses between the TC intensity development and the lightning EPs for 40 TCs occurred in the western north Pacific in 2013 and 2014.
First, we found that the median value of the lightning EPs in positive cloud-to-ground (+CG) discharges peaked at the generation stage in the 29 TCs. When multiple cumulonimbus are merged in the TC region, the cloud top of these cumulonimbus reaches near the tropopause, and the upper clouds will horizontally spread. Then +CG with long discharge length occur from the upper positive charge region overhanging or the developing stratiform region. Second, we found that total value and median value of the EPs of -CGs peaked during the development stage in the 11 super TCs (very strong typhoons and violent typhoons) out of the 12 super TCs analyzed. This is probably caused by the updraft intensification in the eyewall which tends to reduce the electrical breakdown voltage and transfer the negative charge to upper layer. As the EPs of -CG discharges during the development stage in the super TCs peaked 1-2 days before the TC intensity maximum, the EPs of -CG discharges as well as lightning occurrence number can be a good predictor of the TC intensity development.

©2021. Japan Geoscience Union. All Right Reserved.

Keywords: lightning , typhoon, ELF, charge moment change

©2021. Japan Geoscience Union. All Right Reserved.

Lightning Activity in Western North Pacific Measured by the V-POTEKA Network and Its Relation to Typhoon Intensity

*Mitsuteru Sato[1], Yukihiro Takahashi[1], Hisayuki Kubota[1], Glenn Vincent C. Lopez[2]

1. Faculty of Science, Hokkaido University, 2. ASTI, DOST

Lightning activity is the good proxy representing precipitations and the updraft intensities in thunderclouds. Recent studies revealed that the lightning occurrence number in tropical cyclones (TCs) shows clear relation to the intensity development of TCs, whereas the prediction of the typhoon intensity development is very hard even though the recent meteorological model is used. Many countries in the western north Pacific suffer from the attack of TCs (typhoons) and have a strong demand to predict the intensity development of typhoons by a cost-effective methods. Thus, we have developed a new automatic weather and lightning observation system (V-POTEKA) and installed this system in the Philippines, Guam, Palau, Jakarta, Okinawa since September 2017. Using the V-POTEKA data, lightning locations are estimated by using the time-of-arrival geolocation algorithm. We have compared the relation between the lightning activities measured by the V-POTEKA network and the intensity change of the western north Pacific typhoons in the period of 2018-2020. In this 3 years, a total of 81 typhoons occurred. As for the 2018 typhoons, we selected 11 of 29 typhoons and conducted cross-correlation analysis between lightning activities and typhoon intensity development. We confirmed that the time variations of the detected lightning event numbers and typhoon intensities (maximum wind speed and center pressure) are highly correlated. Especially, there is clear time lag (~1.5 days) between lightning activities and typhoon intensities in the category 1-3 typhoons, that is, the peak of lightning activity comes first, then the peak of the typhoon intensity comes next. However, as for the super typhoons (category 5 typhoons), this relation is not always clear. At the presentation, we will also show the detailed results derived from this cross-correlation analysis between lightning activities and intensity development of the 2019, 2020 typhoons.

Keywords: Lightning activity, Typhoon, Intensity prediction

©2021. Japan Geoscience Union. All Right Reserved.

[E] Oral | M (Multidisciplinary and Interdisciplinary)：M-IS Intersection

Sat. Jun 5, 2021 1:45 PM - 3:15 PM JST | Sat. Jun 5, 2021 4:45 AM - 6:15 AM UTC | Ch.15 Zoom Room 15

[M-IS09] Weathering and conservation of cultural heritage and geosites

convener:Luigi Germinario(University of Padova, Italy), Chiaki T. Oguchi(Institute for Environmental Science and Technology, Graduate School of Science and Engineering, Saitama University), Akos Torok(Budapest University of Technology and Economics), Tetsuya Waragai(Graduate School of Science and Engineering, Nihon University), Chairperson:Luigi Germinario(University of Padova, Italy), Chiaki T. Oguchi(Institute for Environmental Science and Technology, Graduate School of Science and Engineering, Saitama University)

Cultural heritage (World Heritage Sites, historical structures, archaeological artifacts, etc.) and geoheritage (geosites, geoparks, etc.) are exposed to weathering in the geological and human time scale. The resulting deterioration of the rocks and other geological materials in cultural and natural contexts can be often severe and demands the prompt adoption of conservation measures. The relevant research involves a range of disciplines: mineralogy, geomorphology, geoarchaeology, environmental science, engineering geology, materials science, analytical chemistry, etc. However, our knowledge on many aspects is still limited. This session welcomes contributions presenting original research, case studies, and discussions on damage assessment, experimental techniques, monitoring, predictive models, conservation procedures, documentation, etc. related to geological materials in cultural heritage and geosites.

1:45 PM - 2:00 PM JST | 4:45 AM - 5:00 AM UTC

[MIS09-01] Evaluation of the degradation state of dinosaur footprint based on 3D measurement.

*Nobuaki Kuchitsu[1], Shuji SAKAI[2], Masato FUJITA[3] (1.Tokyo National Research Institute for Cultural Properties, 2.Toppan Printing Co., Ltd., 3.Toyama Science Museum)

2:00 PM - 2:15 PM JST | 5:00 AM - 5:15 AM UTC

[MIS09-02] Study on relations between deterioration of tuff stone used as exteriors of a historical building and microenvironment factors

*Uno Tomoko[1], Chiemi Iba[2], Masaru Abuku[3] (1.Mukogawa Womens University, 2.Kyouto University, 3.Kinki University)

2:15 PM - 2:30 PM JST | 5:15 AM - 5:30 AM UTC

[MIS09-03] Changes in pore-size distribution of rocks induced by thermal cycles of low temperature

*Tetsuya Waragai[1] (1.Graduate School of Science and Engineering, Nihon University)

2:30 PM - 2:45 PM JST | 5:30 AM - 5:45 AM UTC

[MIS09-04] **Non-destructive strength tests of heritage buildings: an overview of Schmidt hammer and Duroskop tests**

*Akos Torok[1] (1.Budapest University of Technology and Economics)

2:45 PM - 3:00 PM JST | 5:45 AM - 6:00 AM UTC

[MIS09-05] Numerical analysis of heat, moisture, and salt transfer and deformation in porous materials under atmospheric conditions

*Masaru Abuku[1], Koichi Ishii[2] (1.Kindai University, 2.Research Center of Computational Mechanics, Inc.)

3:00 PM - 3:15 PM JST | 6:00 AM - 6:15 AM UTC

[MIS09-06] HYPERION: understanding and quantifying the effects of climate change on cultural heritage

*Chiara Coletti[1], Luigi Germinario[1], Fabrizio Antonelli[2], Renzo Bertoncello[3], Antonio Galgaro[1], Lara Maritan[1], Matteo Massironi[1], Jacopo Nava[1], Rebecca Piovesan[2], Raffaele Sassi[1], Elena Tesser[2], Claudio Mazzoli[1] (1.Department of Geosciences, University of Padova, Via Gradenigo 6, 35131 Padova, Italy, 2.LAMA - Laboratory for Analysing Materials of Ancient origin, University Iuav of Venice, San Polo 2468/B, 30125 Venice, Italy, 3.Department of Chemical Sciences, University of Padova, Via Marzolo 1, 35131 Padova, Italy)

Evaluation of the degradation state of dinosaur footprint based on 3D measurement.

*Nobuaki Kuchitsu[1], Shuji SAKAI[2], Masato FUJITA[3]

1. Tokyo National Research Institute for Cultural Properties, 2. Toppan Printing Co., Ltd., 3. Toyama Science Museum

Past degradation of footprint fossils of dinosaurs at Oyama Area in Toyama City is discussed through constructing and comparing the past 3D shapes of the fossil. The 3D shapes of the fossil as of the plural in the past were estimated based on the replicas made by taking a mold in the past as well as old photographs taken from various directions as of the plural in the past. The change in the degradation rate in the past was argued by comparing the established 3D shapes in the past. As a result, degradation was detected just after the discovery of a sauropd footprint located in the original outcrop caused by a road construction, but the rate is getting smaller as time passes. On the other hand, the degradation of the ornithopoda footprint, newly found on the one-step lower out crop due to the additional excavation, seems to be getting larger. It will contribute to the discussion of how to conserve such fossils to understand the tendency of the degradation fluctuation in the past.

Keywords: three-dimensional measurement, replica, weathering rate, past shape, Oyama area of Toyama City

©2021. Japan Geoscience Union. All Right Reserved.

Study on relations between deterioration of tuff stone used as exteriors of a historical building and microenvironment factors

*Uno Tomoko[1], Chiemi Iba[2], Masaru Abuku[3]

1. Mukogawa Womens University, 2. Kyouto University, 3. Kinki University

Two types of tuff stone (Nichika Seki, produced in Ishikawa prefecture, and Tatsuyama Ishi produced in Hyogo prefecture) are used as exterior in the former Koshien Hotel, which was built in 1930 and used as the campus building at Mukogawa Women’ s University. According to the condition survey of the stone, we found that the deterioration types in the two stones are different. In addition, even if the stone is in a similar environment, one side is damaged, while the other side is not damaged.

To investigate these factors of the deterioration, we grasped the material properties of these stones; stone structure, pore size distribution of the stones, thermal and moisture conductivity. We also investigated the deterioration condition of the stone and the surrounding microenvironment.

As a result, it was expected that the area and degrees of the stone getting a wetting by rain, the surface temperature changes of the stone exposed by solar and nocturnal radiation were affecting the deterioration. Based on the results of the condition survey, thermal and moisture properties, and boundary conditions, we are planning to analysis the temperature and water content inside the stone.

Keywords: Deterioration Condition, Microenvironment, Conservation of Historical Building

©2021. Japan Geoscience Union. All Right Reserved.

Changes in pore-size distribution of rocks induced by thermal cycles of low temperature

*Tetsuya Waragai[1]

1. Graduate School of Science and Engineering, Nihon University

Many case studies have analyzed the relationship between thermo–mechanical fracture and temperature change induced by the insolation of rocks. However, extracting only thermal effects and discussing fracture in field observations are difficult. Therefore, laboratory experiments in which thermal cycles are applied to rocks are considered to be effective methods for simplifying and analyzing the relationship between fracture and thermal cycles. In particular, this approach is considered effective in measuring the generation of the acoustic emission (AE) and changes in pores to capture the initial stage of microscopic phenomena such as thermal fatigue fracture. Therefore, we experimentally investigated the fracture of rock specimens based on changes in pore-size distribution, ultrasonic propagation velocity, and the occurrence of AE. For the experiment, we used three rock types—granite and marble with a porosity of 2% or less and sandstone with a porosity of approximately 14%, which are often used as stone materials. Thereafter, we repeatedly subjected the prepared specimens from the rock types to temperature changes from 4℃ to 84℃ using a temperature-controlled chamber at a temperature change rate of ±2℃/min, which is the threshold for thermal shock fracture. Consequently, the P-wave velocity decreased by approximately 25%, 7.2%, and 2.5% for the granite, marble, and sandstone, respectively. Furthermore, for granite, the pore-size distribution decreased by approximately 6% in the diameter range of 0.8–0.5 μm and increased by approximately 5% in the diameter range of 0.4–0.1 μm. For the marble, the pore-size distribution decreased by approximately 16% in the diameter range of 0.5–0.1 μm and increased by approximately 16% in the diameter range of 6–0.65 μm. For the sandstone, the variation in pore size was negligible. Moreover, the occurrence of AE was detected in all rock types, but we found that its magnitude for the granite was the largest, followed by the marble and sandstone, respectively. Therefore, a low-temperature thermal cycle causes thermo–mechanical fracture inside rocks.

Keywords: Thermal weathering, Thermo–mechanical fracture, Acoustic emission, Microcrack, Pore size distribution

©2021. Japan Geoscience Union. All Right Reserved.

Non-destructive strength tests of heritage buildings: an overview of Schmidt hammer and Duroskop tests

*Akos Torok[1]

1. Budapest University of Technology and Economics

Strength tests of heritage structures require special care since in most cases, only non-destructive tests are possible to detect the surface strength of materials. The most widely used tool is Schmidt hammer. It has been applied for a few decades to assess the strength of building stones. Another less widely used tool is Duroskop, a non-destructive test device with lower impact strength, and it can detect smaller surface strength than Schimdt hammer. In this paper, the non-destructive strength test results of the faç ades of several buildings are presented. The aim is to assess Schmidt hammer rebound and Duroskop rebound variations representing various states of weathering. The studied buildings were constructed from porous limestone, travertine, non-porous crystalline limestone and sandstone. The Schmidt hammer rebound values and Duroskop rebound values of ashlars were recorded representing various weathering conditions. The large data set of measurements was evaluated using geostatistical methods. The results indicate that besides the lithology, the differences in exposure and air quality alos influences surface strength. The data sets help to outline the weathering-related changes in Schmidt hammer and Duroskop rebound.

Keywords: weathering, surface strenght, Schmidt hammer, Duroskop, non-destructive testing

©2021. Japan Geoscience Union. All Right Reserved.

Numerical analysis of heat, moisture, and salt transfer and deformation in porous materials under atmospheric conditions

*Masaru Abuku[1], Koichi Ishii[2]

1. Kindai University, 2. Research Center of Computational Mechanics, Inc.

Salt weathering of porous materials such as stone, brick, etc. is a phenomenon composed of heat, moisture and salt transfer in porous materials, crystallization and phase change of salt, deformation of porous materials, and so on. Thus far, several numerical models have been developed by researchers for studying such phenomena, in addition to the efforts of measuring physical and chemical data of porous materials, ions, and salt crystals. When a numerical simulation obtained using one of these models is applied to different real-world objects, such as a building wall, stone cultural property, or masonry systems, one has to often deal with complex geometries comprising various materials and boundary conditions. To render such an application of the salt weathering prediction feasible, we have developed a generic finite element method code, namely: PMSolver. This code analyzes non-steady heat, moisture, and salt transfer in porous materials, while examining the deformation of materials from the temperature, salt solution content, and salt crystal content. Further, this code is equipped with a GUI that works on a pre- and postprocessor Femap, and incorporates the input data of geometries, material properties, and initial and boundary conditions into the solver. Furthermore, the transport, phase change, and crystallization/dissolution of a mixture, which is obtained by dissolving two different salts in water, are elucidated in this model while maintaining electrical neutrality. The code includes the data on sodium chloride and sodium sulfate. During the mechanical analysis, the pore liquid pressure, crystallization pressure, and thermal stress are considered, in addition to the stress obtained from a static mechanical analysis; this is aimed at determining the strain field at each time step. The code can also consider different types of atmospheric boundary conditions such as temporally and spatially distributed wind-driven rain with ions, sea spray, atmospheric salt deposition, and seepage water. When the seepage flow is analyzed, two iteration steps are considered.

Keywords: Poromechanics, Finite Element Method, Salt weathering, Salt crystallization, Moisture transfer

©2021. Japan Geoscience Union. All Right Reserved.

HYPERION: understanding and quantifying the effects of climate change on cultural heritage

*Chiara Coletti[1], Luigi Germinario[1], Fabrizio Antonelli[2], Renzo Bertoncello[3], Antonio Galgaro[1], Lara Maritan[1], Matteo Massironi[1], Jacopo Nava[1], Rebecca Piovesan[2], Raffaele Sassi[1], Elena Tesser[2], Claudio Mazzoli[1]

1. Department of Geosciences, University of Padova, Via Gradenigo 6, 35131 Padova, Italy, 2. LAMA - Laboratory for Analysing Materials of Ancient origin, University Iuav of Venice, San Polo 2468/B, 30125 Venice, Italy, 3. Department of Chemical Sciences, University of Padova, Via Marzolo 1, 35131 Padova, Italy

Climate change is one of the most critical global challenges of our time. During the last century, the anthropic activity had a great impact not only on the environment, affecting even the conservation of cultural heritage. This is becoming a mandatory issue to be tackled by international and local administrations and heritage stakeholders.

Stone is the natural materials most utilized in historical monuments. Although stone decay phenomena have been broadly investigated in the past, only few studies are moving towards the understanding and quantification of the short- and long-term effects of climate change. This research direction, however, is essential for supporting sustainable mitigation plans and the city’ s resilience management.

The HYPERION project aims to fill this gap, improving the knowledge of measurable material- and climate-based parameters that influence stone decay rate. The project includes simulations of future scenarios and potential effects of changing climate patterns and air quality, extreme climate events, and multi-hazard circumstances in the historical urban context.

In this contribution, we present the preliminary results of the study of selected building stones used in four European demonstration sites, in Italy (Venice), Greece (Rhodes), Spain (Granada), and Norway (Tø nsberg). The basic petrographic and physical-mechanical investigation of the stone materials is combined with accelerated ageing tests under different environmental stresses (cycles of salt crystallization and freeze-thaw and interaction with rainwaters with different compositions) and field-exposure tests. The expected results will help refining adequate material-specific models of stone surface recession and support structural and hygrothermal simulations about the future decay of cultural heritage. Data recorded will also be exploited for hypothesize in advance the best conservative treatments of the building stones investigated.

Keywords: Stones, Decay, Salt weathering, Freeze-thaw, Surface recession, Climate change

©2021. Japan Geoscience Union. All Right Reserved.

[E] Poster | M (Multidisciplinary and Interdisciplinary)：M-IS Intersection

Sat. Jun 5, 2021 5:15 PM - 6:30 PM JST | Sat. Jun 5, 2021 8:15 AM - 9:30 AM UTC | Ch.20_2

[M-IS09] Weathering and conservation of cultural heritage and geosites

convener:Luigi Germinario(University of Padova, Italy), Chiaki T. Oguchi(Institute for Environmental Science and Technology, Graduate School of Science and Engineering, Saitama University), Akos Torok(Budapest University of Technology and Economics), Tetsuya Waragai(Graduate School of Science and Engineering, Nihon University)



Cultural heritage (World Heritage Sites, historical structures, archaeological artifacts, etc.) and geoheritage (geosites, geoparks, etc.) are exposed to weathering in the geological and human time scale. The resulting deterioration of the rocks and other geological materials in cultural and natural contexts can be often severe and demands the prompt adoption of conservation measures. The relevant research involves a range of disciplines: mineralogy, geomorphology, geoarchaeology, environmental science, engineering geology, materials science, analytical chemistry, etc. However, our knowledge on many aspects is still limited. This session welcomes contributions presenting original research, case studies, and discussions on damage assessment, experimental techniques, monitoring, predictive models, conservation procedures, documentation, etc. related to geological materials in cultural heritage and geosites.

[MIS09-P01] Mineralogical and microclimatic control on the salt weathering of Oya stone

*Luigi Germinario[1,2], Chiaki T. Oguchi[2] (1.University of Padova, Italy, 2.Saitama University, Japan)

[MIS09-P02] Relationship between carbon dioxide concentration and temperature in the Taya cave

*Chiaki T. Oguchi[1], Rina Matsumoto[2], Yasuhiko TAMURA[3] (1.Institute for Environmental Science and Technology, Graduate School of Science and Engineering, Saitama University, 2.Faculty of civil Engineering, Saitama University, 3.Executive Committee for the Preservation of TAYA CAVERN)

[MIS09-P03] Material properties and durability of stone in a medieval fortress; lessons to learn: an example from Hungary

*Akos Torok[1], Benedek Lógó[1] (1.Budapest University of Technology and Economics)

Mineralogical and microclimatic control on the salt weathering of Oya stone

*Luigi Germinario[1,2], Chiaki T. Oguchi[2]

1. University of Padova, Italy, 2. Saitama University, Japan

Oya tuff is one of the most renowned building stones in Japan. It has been used historically in vernacular architecture, construction, rock-cut and relief sculpture, but its extensive exploitation began only in the Edo period (17th century). The extraction has been conducted mostly underground in over 200 quarries in Tochigi prefecture, with few being still active, many others abandoned or transformed into sites of geoheritage and touristic value. This study deals with the salt weathering of Oya stone, one of the most common decay patterns in underground cultural heritage and geosites, following a mineralogical and environmental approach. The experimental outline included field explorations, mineralogical and geochemical analyses of the rock and its efflorescences, a microclimate monitoring, and the chemical analysis of groundwater and rainwater. The efflorescences turn out to be composed of mixed sulfates, including gypsum, mirabilite, and thenardite. Their formation and stability is strictly dependent on the weathering of accessory phases, in particular pyrite and zeolites, reflected on the groundwater composition; and the subterranean microclimate, especially the variations of relative humidity in time and space, controlling the seasonality and principal composition of the salt mixtures and the occurrence of crystallization/dissolution cycles.

Keywords: Tuff, Underground geoheritage, Efflorescences, Sulfates

©2021. Japan Geoscience Union. All Right Reserved.

Relationship between carbon dioxide concentration and temperature in the Taya cave

*Chiaki T. Oguchi[1], Rina Matsumoto[2], Yasuhiko TAMURA[3]

1. Institute for Environmental Science and Technology, Graduate School of Science and Engineering, Saitama University, 2. Faculty of civil Engineering, Saitama University, 3. Executive Committee for the Preservation of TAYA CAVERN

The Taya Caves, an artificial hand-dug cave in the Josenji Temple in Yokohama City, originated in the Kamakura period as one of the worship places of Shingon Esoteric Buddhism. Many people are still visiting the cave. There remains still questions about how 800m of tunnels were manually dug in the dark and narrow spaces of the ground when there were no large tools. A torch should have been lit in the dark, however, there must be a ventilation pit to prevent oxygen deficiency. No such pit is found. Further, it is known that CO2 concentration also increases due to bacterial activities in the underground environment.In this study, we will examine the causes of the increase in CO2 concentration due to the continuation of temperature and humidity monitoring inside and outside the cave, daily changes in the number of visitors, and changes in CO2 concentration. From the correlation between the daily maximum temperature and the CO2 concentration, and the correlation between the temperature at each site and the CO2 concentration, it is expected that the increase in temperature may cause the increase in the CO2 concentration.

Keywords: Taya Cave, CO2 concentration, Temperature

©2021. Japan Geoscience Union. All Right Reserved.

Material properties and durability of stone in a medieval fortress; lessons to learn: an example from Hungary

*Akos Torok[1], Benedek Lógó[1]

1. Budapest University of Technology and Economics

The material use of Medieval structures justifies the local knowledge and experience of the builders. Studying material properties and construction technology helps to understand medieval skills and expertise. In this study, the stone and renders of a 14th to the 15th-century fortress is presented. The fortress is located at Balaton Highland at Nagyvázsony (Hungary). It has an emblematic 25 m high tower, which was used as a living quarter. The fortress is surrounded by a system of external walls, while the tower is in the courtyard. The structure was mostly built from stone but rammed earth was also used for the interior parts of the wall. Stone, render were studied on-site using various non-destructive techniques. Surface strength of materials was tested by Schmidt hammer and Duroskop while moisture content was measured on-site with a portable device. Petrology of lithotypes was identified on site using a portable microscope. Samples were also taken for laboratory testing. Physical and mechanical properties such as density, ultrasonic pulse wave propagation, uniaxial compressive strength (UCS) and indirect tensile strength (Brasilian) test were measured in laboratory conditions according to EN and ASTM standards. Samples were measured in dry and water-saturated conditions. According to lithological description and laboratory tests, the prevailing lithotypes are basaltic tuffs, well-cemented limestone and travertine. A few ashlars of Miocene porous limestone, travertine and sandstone were also identified. The condition assessment of stone elements and laboratory tests suggest that basaltic tuffs suffered the most for weathering while other stone types seem to be more durable. This current study provides new hints to understand the medieval construction techniques and the material selection of medieval fortresses of Central Europe.

Keywords: basaltic tuff, physical properties, condition assessment, medieval

©2021. Japan Geoscience Union. All Right Reserved.



©2021. Japan Geoscience Union. All Right Reserved.

[E] Poster | M (Multidisciplinary and Interdisciplinary)：M-IS Intersection

Sat. Jun 5, 2021 5:15 PM - 6:30 PM JST | Sat. Jun 5, 2021 8:15 AM - 9:30 AM UTC | Ch.21_2

[M-IS10] Exploring Origin of Space, Galaxies, Earth, Moon, Solar System, Plate Tectonics, and Life

convener:Akira Taneko(SEED SCIENCE Lab.)

The purpose of SCIENCE is to explain the mystery of the universe.
Traditional methods include analytical inquiry followed by integration, and qualitative and quantitative inquiry. In nature, there are periodic phenomena and one-way evolution and differentiation phenomena. Periodic phenomena are easy to reproduce, the laws of physics are elucidated, and elucidation is easy, but the mystery of evolution is difficult to elucidate because the time axis is particularly long and the mechanism is unknown.
Is there anyone who challenges the origin of the solar system or the origin of the galaxy or the universe?
Creative reasoning (hypothesis reasoning) that verifies using the results of evolution can be verified that a hypothesis that can uniformly explain the results (characteristics) of evolution that has occurred only once and surely is correct.
Please challenge the search for the origin as well.

[MIS10-P01] **Investigating Origin and how to verify it-** Verification goes back to the past -make Hypothesis and explain of Evolution Resules ***in a unified manner***,MIH as a sanple

★Invited Papers

*Akira Taneko[1] (1.SEED SCIENCE Lab.)

[MIS10-P02] Most Scientists **do not deny the existence of Plate Tectonics**, but ***cannot explain why Plate Tectonics happened.*** **"Multi-Impact Hypothesis"** ***can explain Origin of Plate Tectonics*** and also ***verify Origin of Moon and Solar System.***

★Invited Papers

*Akira Taneko[1] (1.SEED SCIENCE Lab.)

[MIS10-P03] Liquid Crystal Peptide/DNA Coacervates in the Context of Prebiotic Molecular Evolution

★Invited Papers

*Tony Z Jia[1,2], Tommaso P Fraccia[3] (1.Earth-Life Science Institute, Tokyo Institute of Technology, 2.Blue Marble Space Institute of Technology, 3.Institut Pierre-Gilles de Gennes, CBI, ESPCI Paris, Université PSL, CNRS)

Investigating Origin and how to verify it- Verification goes back to the past -make Hypothesis and explain of Evolution Resules *in a unified manner* ,MIH as a sanple

*Akira Taneko[1]

1. SEED SCIENCE Lab.

When I learned of ***Simulation Paper*** called **Giant Impact Theory**,it was correct(?) because ***a Mars-Sized Model collided with*** **Earth Model**, and Moon with only Mantle was created, was Reasoning.It is unclear whether or not it will **hit Earth**, but even if Luna finally arrives to **Potential Energy as *1/20*** by ***Specifying Speed-Angle***, **so it is *strange* Lunar not to accelerate.**

Search for Origin is *more True as there are more Items* that *can make Hypotheses* and ***explain*** **Evolutionary Results (Characteristics and Current Situation)** ***in a unified manner.***
If even one Item cannot be explained, it is False.It is the Mistake of Hhypothetical Model that even one Item of the Feature cannot be completely explained by the Simulation. If Hypothetical Model is correct, **it can be verified by Creative Reasoning (Abduction with Evolution)**, and even unexpected Results can be verified at Same Time.

Comparing with **Lunar Origin Hypothesis**.
Multi-Impact Hypothesis / Giant-Impact Hypothesis,
with Model of Collision body.
Only Moon-Sized Mantle / Differentiated Mars-Sized Mantle with Core,
with Verification Methods.
Inevitable Collision of Creative Reasoning /Selection by Calculation Comparison of Collision Conditions in Simulation.

Comparing with Conclusion of Lunar origin hypothesis

In M-IH,
> M1. As an explanation of **Origin of Moon** M1-1.**Inevitable Collision**,M1-2.Origin of **Mantle Impactor**, M1-3.Collision **Velocity12.4km/s and Angle36˚**, M1-4.**Orbital Energy** of Ejected Moon, 1-5.**Eccentricity** of Moon and Cause of always **facing Earth**, M1-6.Origin of **Moon's Sea**, M1-7.**Backside Legoris** of Moon,
>M2. As an explanation of **Origin of Earth**, M2-1.Origin of **Deep Ocean Floor of Earth**, M2-2.Origin of **Plate Tectonics**, M2-3.Origin of Plate Bundary, M2-4. Origin of **Driving Force**, M2-5.Ocean Reasons for No Wrinkles or Buckling of Plates, M2-6.Mechanism of Transform Faults, M2-7.Origin of Arc-shaped archipelago, dorsal arc concave basin and seafloor, M2-8.Mechanism of **Plate Overlap**, M2 -9.Mechanism of **Sudden Change in Plate Movement Direction**, M2-10.Source of geomagnetic reversal, M2-11.Cause of van allen zone eccentricity, M2-12.Cause of **Non-Movement of Antarctic continent**,M2-13.Himalayan mountains Causes of arcs, M2-14.Origin of Titis Sea, M2-15.Origin of **Kimberlite pipes**, M2-16.Origin of Tilt of Earth's axis,
>M3. Explanation of **Origin of Solar system** M3-1.Origin of **Jupiter's Great Red Spot**, M3-2.Origin of Pluto(first flyby), M3-3.Cause of **Mercury core rich**, M3-4.Origin of **asteroid belt**, M3-5.Causes of Earth meteorite **differentiation**, M3-6.Causes of **asteroids as mantle aggregates.**

©2021. Japan Geoscience Union. All Right Reserved.

In G-IH. As an explanation of **Origin of Moon**,
>G1-1.Prediction of results **for Each Initial Condition** by Simulation, G1-2.×Prediction and Comparative Evaluation with Current Situation, G1-3.Evaluation of **Core Ratio of Lunar** Component, G1-4.×Assuming Collision **at Time of Magma Ocean**, G1-5. Visualization of Collision,
>G2.As Explanation of **Origin of Earth**, G2-1.**×No Origin of Earth's Ocean**, G2-2.**×No Origin of Plate Tectonics,**
>G3. As Explanation of **Origin of Solar System**, G3-1. Completely Ignored, G3-2.**×Ignoring** Planet **Formation Mechanism assuming Accidental Collision,** G3-3. **Same Orbit or Planetary Migration Hypothesis,** *Need for proof.*

Hypothetical Model is Moon Size of MIH **Mantle only** and Size of Mars of GIH **Differentiated Core** + **Mantle**, which are Different Collision Models. **Evaluation Method** is *different* from **Creative Reasoning** and ***Simulation***, and ***MIH****Evaluation is 7 + 16 + 6 = 29*, and Selection of lunar of Collision Condition of **Moon only in Mantle** and Explanation of Visualization 1 ***question Truth?****, and Difference is like this.* **It will come out.**

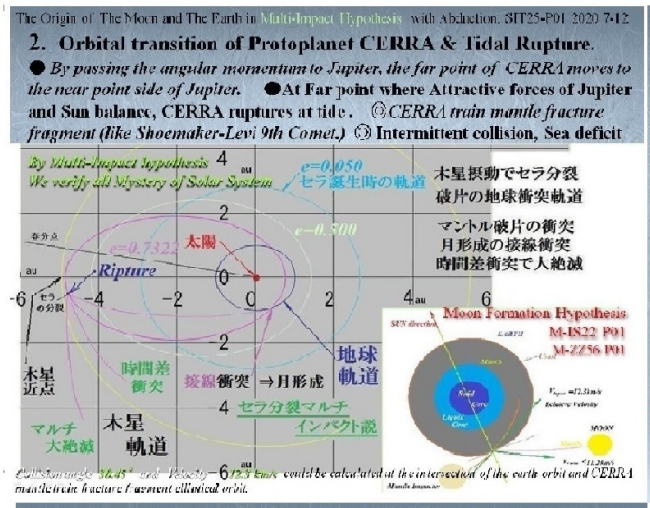
It is **Important** to ***select*** **First Model** and **Evaluation Method.**

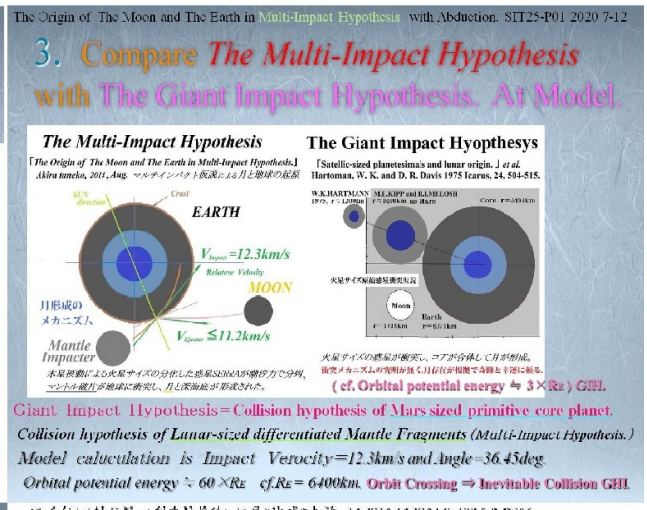
So, let's Discuss here Tips on **how to make Model** *for Creative Reasoning.*
>First, **Don't be overconfident.**
>Considering **all Possibilities**, **Natural Nature** is used as Evaluation Standard.
>Listen to **Laws of Universe**. believe. There is, but Ephemeral. **Listen to Truth**.
>Discover Law, not make it,**thank Nature.**
>Models that violate Law are free from **Nature.**
>**Do not explain with Result, explain Result.** How to research**, why to explore.**
>Path to **Truth is Narrow**, but I believe to be always One.
Life is born in Galaxy in Corner of Vast Universe, **we explore Origin of Life, Earth, Solar System, and Galaxy, is Miracle.**

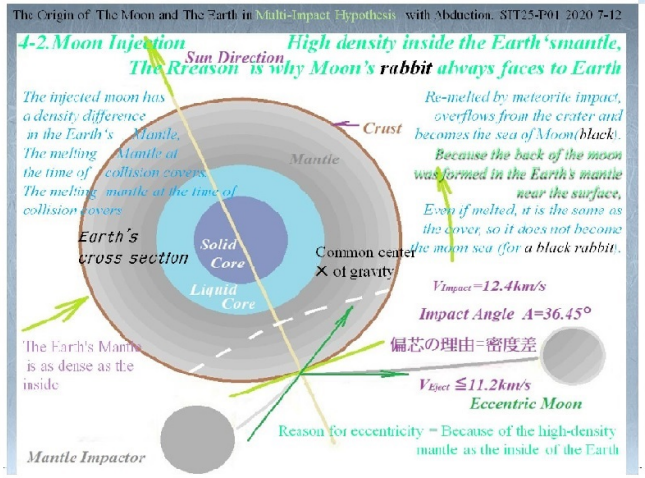
Assuming Collision Body **with only Mantle**, and **considering Inevitable** Collision **Mechanism**, Orbits of Moon matched and Mysteries of Solar system and Earth could be explained together, and Simple Unified Story was created. Excel was sufficient for Calculation, and *Collision* ***Speed and Angle*** *could be derived from Model.*

Keywords: Search for Origin and Verification Method, verification that goes back to Past-Make Hypothesis and explain All Results (Characteristics) of Evolution in a Unified Manner, Multi-Impact Hypothesis verifies Origin of Moon, Plate Tectonics, and Mercury, Multi-Impact Hypothesis verifies Origin of Asteroid Belt, Great Red Spot of Jupiter, Origin of Pluto, Multi-Impact Hypothesis verifies Origin of Deep Ocean Floor, Pacific Rim Arc Archipelago and Back-Arc Basin, Multi-Impact Hypothesis explains Origin of Plate Boundaries, Plate Driving Forces, and Sudden Changes in Direction of Movement, Explain Orbit of Moon, Origin of Lunar Mare, and Mystery that Moon always faces Earth with Multi-Impact Hypothesis

©2021. Japan Geoscience Union. All Right Reserved.









©2021. Japan Geoscience Union. All Right Reserved.

Most Scientists **do not deny the existence of Plate Tectonics**, but ***cannot explain why Plate Tectonics happened.*** **"Multi-Impact Hypothesis"** ***can explain Origin of Plate Tectonics*** and also ***verify Origin of Moon and Solar System.***

*Akira Taneko[1]

1. SEED SCIENCE Lab.

Most Scientists do not deny Existence of **Plate Tectonics**, but cannot explain *why Plate Tectonics happened.*
It has been 100 years since Wegener proposed **Theory of Continental Drift**, but No one could explore Mechanism that forms Plate Tectonics and *why Plate moves*.
Wegener's **Theory of Continental Drift** was denied that Driving Force could not be explained, but Name was changed to ***Plate Tectonics***, and although Driving Force could not be explained, it behaved as if **Most Scientists** had discovere ***the Pate Tectonics.*** Therefore, Scientists leave "Why Plate moves?" to **Thermal Convection Hypothesis** and work only on "how it moves".

1. Planetary accumulation mechanism (Bode's law and supply range, coalescence law)
(1).As Law of coalescence in Solar System, all but Sun draw an Elliptical Orbit with Central Star as **one Unifocal Focus.**
(2).As a Coalescence Condition, when **Speed Difference is small and a Collision occ**urs, Potential Energy decreases b**y Amount of Thermal Energy** and becomes **an Inner Orbit.**
(3). When passing near Central Star, it is captured by Central Star.
(4). Circular Orbits and Elliptical Orbits **with Same Orbital Energy** have **Same Period and Semimajor Axis**.
(5). Bode's Law was **an Empirical Law** between Planetary Orbits in Solar System. <**Feeding zone**>
[My discovery] **Law of orbital degeneracy.**
An EllipticalOrbit that has Same Orbital Energy as **Earth's Orbit** and tangent to **Forbidden Band** is inscribed in Orbit of Mars. Similarly, ***an Elliptical Orbit*** that has Same Orbital Energy as Venus Orbit and is tangent to **Forbidden Band** is approximately inscribed in Earth's Orbit.
This means that Planetesimals with a Substantially Elliptical Orbit that **accumulate on Earth** have **an Accumulation Range** of Earth's Orbit Range inside Mars orbit (according to 1-(3)).

2. "Multi-impact hypothesis" and moon formation cf. MIS10-1,PPS06-xx.
He explained Origin of Moon, Mechanism of moon formation only in Mantle, Feature that Sea of Moon always faces Earth due to Eccentricity, and Feature only in regolith on Back side in Earth collision of Mantle impactor. (By Abduction using the result of evolution)

3.Origin of deep ocean floor, Formation of Plate Boundary Cracks and Origin of **Plate Tectonics**, Driving Force.
Intermittent Collisions of **Multiple Train Mantle Fragments** with Earth showed Formation Mechanism of Deep Seafloors spreading with an Average Depth of 4 km and Origin of Species Extinction, due to Detachment of Earth's Mantle and Uplift caused by Isostasy. Origin of Land Plate due to Formation Mantle Crack of Sea, which Occupies 70% of Earth's Surface Area by Connecting Multiple Seas, was also shown.
In Collision of Mantle Impactor with Earth,Mantle was craked and an Eccentric Moon was formed like a Newton cradle. Furthermore, Semi-molten Structure of Asthenosphere gave Plate Fluidity, and it was

©2021. Japan Geoscience Union. All Right Reserved.

driven until Plate was balanced by a Couple that minimized an Eccentric Moment of Inertia due to Earth's Rotation and Plate Imbalance.

4. Origin of **Pacific Rim arc arch archipelago and back-arc basin**, reason for Plate overlap, origin of obliquity, origin of sudden change in plate movement direction, origin of Van Allen belt eccentricity, Origin of geomagnetic reversal, Origin of kimberlite pipe

Considering Van Allen Belt Eccentricity in Cross-Sectional View of Earth passing through Pacific Ocean and Rio, Core Eccentricity of about 500 km is about 10% (500/6400), so it is a Mantle Defect due to **Lunar Ejection** and a Darwin Uplift due to **Isostasy**. Pacific Rim Arc Basin are Back-Arc Basin are **surrounding Depressions** due to Uplift of Darwin, and Japanese Archipelago and Sea of Japan are Result.

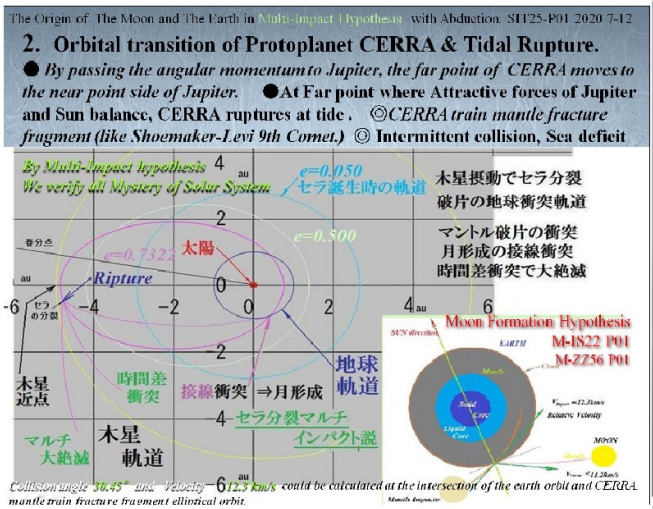
5. Explain Origin of about **30 Items of Universe**, such as Origin of Great Red Spot of Jupiter, Origin of Asteroid belt, Origin of Pluto, Origin of Mercury Corerich, Origin of Differentiated Rocks of Ryugu and Itokawa, and Origin of Planet. I think MIH has been completely Verified.

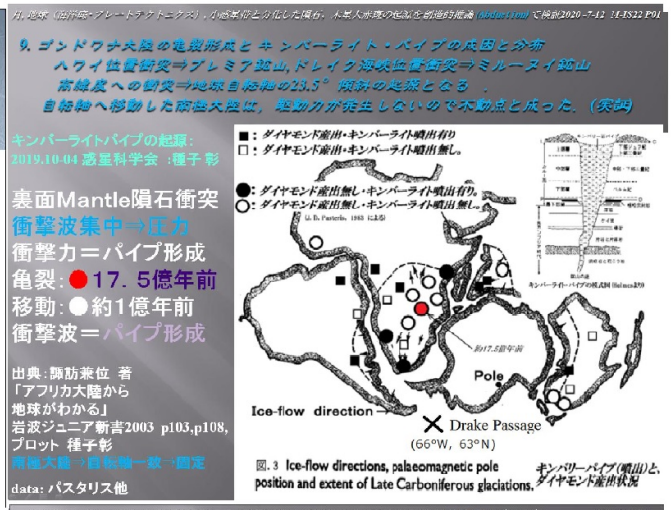
"Multi-Impact Hypothesis" can explain **Origin of Plate Tectonics** and also verify **Origin of Moon and Solar System.**

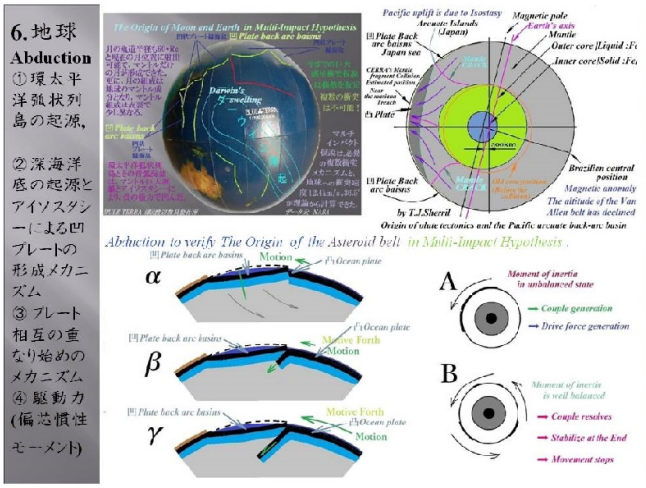
This time, it was announced on P-PS06 (3 Thu J). S-IT16 (4 Fri E), M-IS10 (5 Sat E), M-IS24 (6 Sun J). General and high school students can also participate on Sundays.WHY?

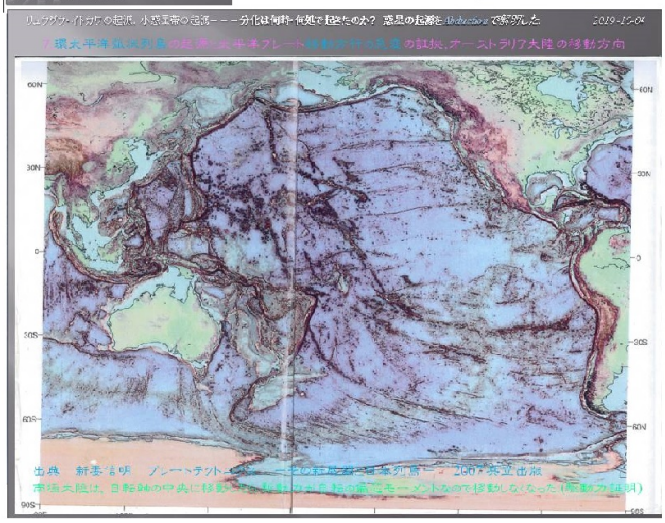
Keywords: Plate Tectonics Origin, Multi-Impact Hypothesis Evolution , Moon Earth Solar System Origin Space Life, Diamond mine kimber lite pipe collision , Jupiter Great Red Spot Pluto Mercury Origin , Lunar mare front side, always facing the earth, eccentric Pacific Rim arc-shaped archipelago

©2021. Japan Geoscience Union. All Right Reserved.









©2021. Japan Geoscience Union. All Right Reserved.

Liquid Crystal Peptide/DNA Coacervates in the Context of Prebiotic Molecular Evolution

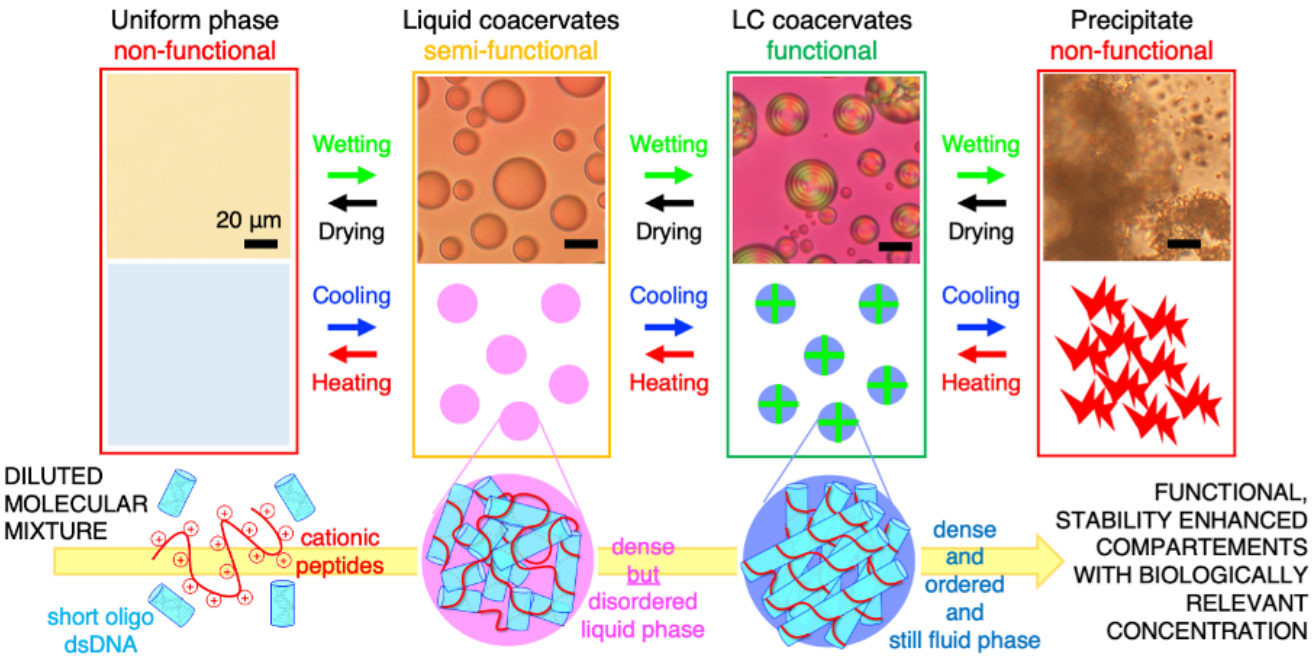
*Tony Z Jia[1,2], Tommaso P Fraccia[3]

1. Earth-Life Science Institute, Tokyo Institute of Technology, 2. Blue Marble Space Institute of Technology, 3. Institut Pierre-Gilles de Gennes, CBI, ESPCI Paris, Université PSL, CNRS

Liquid–liquid phase separation (LLPS) phenomena are ubiquitous in biological systems, as various cellular LLPS structures control important biological processes. Due to their ease of in vitro assembly into membraneless compartments and their presence within modern cells, LLPS systems have been postulated to be one potential form that the first cells on Earth took on. Recently, liquid crystal (LC)-coacervate droplets assembled from aqueous solutions of short double-stranded DNA (s-dsDNA) and poly-L-lysine (PLL) have been reported. Such LC-coacervates conjugate the advantages of an associative LLPS with the relevant long-range ordering and fluidity properties typical of LC, which reflect and propagate the physico-chemical properties of their molecular constituents. Here, we investigate the structure, assembly, and function of DNA LC-coacervates in the context of prebiotic molecular evolution and the emergence of functional protocells on early Earth. We observe through polarization microscopy that LC-coacervate systems can be dynamically assembled and disassembled based on prebiotically available environmental factors including temperature, salinity, and dehydration/rehydration cycles. Based on these observations, we discuss how LC-coacervates can in principle provide selective pressures effecting and sustaining chemical evolution within partially ordered compartments. Finally, we speculate about the potential for LC-coacervates to perform various biologically relevant properties, such as segregation and concentration of biomolecules, catalysis, and scaffolding, potentially providing additional structural complexity, such as linearization of nucleic acids and peptides within the LC ordered matrix, that could have promoted more efficient polymerization. While there are still a number of remaining open questions regarding coacervates, as protocell models, including how modern biologies acquired such membraneless organelles, further elucidation of the structure and function of different LLPS systems in the context of origins of life and prebiotic chemistry could provide new insights for understanding new pathways of molecular evolution possibly leading to the emergence of the first cells on Earth.

Keywords: Origin of Life, Origin of the Cell, Protocell, Prebiotic Chemistry, Astrobiology

©2021. Japan Geoscience Union. All Right Reserved.



©2021. Japan Geoscience Union. All Right Reserved.

[J] Oral | M (Multidisciplinary and Interdisciplinary)：M-IS Intersection

Sat. Jun 5, 2021 9:00 AM - 10:30 AM JST | Sat. Jun 5, 2021 12:00 AM - 1:30 AM UTC | Ch.02 Zoom Room 02

[M-IS12] Planetary Volcanology

convener:Rina Noguchi(Faculty of Science, Niigata University), Nobuo Geshi(Geological Survey of Japan, The National Institute of Advanced Industrial Science and Technology), Tomokatsu Morota(Department of Earth and Planetary Science, The University of Tokyo), Chairperson:Rina Noguchi(Faculty of Science, Niigata University), Nobuo Geshi(Geological Survey of Japan, The National Institute of Advanced Industrial Science and Technology), Tomokatsu Morota(Department of Earth and Planetary Science, The University of Tokyo)

Volcanoes exist on solid planetary surface across the solar system. They tell insight into the interior, and the surface environment when they were formed and subsequent evolution. Recent high-resolution remote sensing data on extraterrestrial body allows us to analyze on outcrop scales. Now we are on the stage to share the research targets beyond fields of general volcanology and planetary science. Because some geomorphological and geological environments in other planets are similar to those on Earth, research on volcanic geomorphology and geology on Earth will provide good terrestrial analogues to understand planetary volcanology. The aim of this session is to discuss formation history and mechanism of volcanoes across the solar system.

9:00 AM - 9:15 AM JST | 12:00 AM - 12:15 AM UTC

[MIS12-01] Structures and formation age of lunar linear gravity anomalies constrained by impact simulations

*Gaku Nishiyama[1], Noriyuki Namiki[2], Seiji Sugita[1] (1.University of Tokyo, 2.National Astronomical Observatory of Japan)

9:15 AM - 9:30 AM JST | 12:15 AM - 12:30 AM UTC

[MIS12-02] Laboratory investigations of salt precipitation upon decompression and degassing of volatile-containing brines: Implication for carbonate mineral formations on Solar system icy bodies

*Masahiro Yoda[1,2], Yasuhito Sekine[2,3] (1.Department of Earth and Planetary Science, The University of Tokyo, 2.Earth-Life Science Institute of Tokyo Tech, 3.Institute of Nature and Environmental Technology, Kanazawa University)

9:30 AM - 9:45 AM JST | 12:30 AM - 12:45 AM UTC

[MIS12-03] Rootless cones in the southwest of Emuruangogolak Volcano, Kenya

*Rina Noguchi[1] (1.Institute of Space and Astronautical Science, Japan Aerospace Exploration Agency)

9:45 AM - 10:00 AM JST | 12:45 AM - 1:00 AM UTC

[MIS12-04] Conditions for the formation of rootless cones on Mars and Earth

*Kei Kurita, Rina Noguchi[1] (1.ISAS/JAXA)

10:00 AM - 10:15 AM JST | 1:00 AM - 1:15 AM UTC

[MIS12-05] Development of an efficient geological survey method for volcanoes on extraterrestrial bodies

★Invited Papers

*Junichi Haruyama[1], Rina Noguchi[1], Nobuo Geshi[2], Motomaro Shirao[3], Keiichiro Fujimoto[1], Daigo Shoji[1] (1.Japan Aerospace Exploration Agency, 2.National Institute of Advanced Industrial Science and Technology, 3.Institute of Planetary Geology)

10:15 AM - 10:30 AM JST | 1:15 AM - 1:30 AM UTC

[MIS12-06] Discussion

Structures and formation age of lunar linear gravity anomalies constrained by impact simulations

*Gaku Nishiyama[1], Noriyuki Namiki[2], Seiji Sugita[1]

1. University of Tokyo, 2. National Astronomical Observatory of Japan

High-resolution lunar gravity data were acquired by NASA's GRAIL gravity mission, and positive linear gravity anomalies sometimes extending over 100 km were discovered. These gravity anomalies are interpreted as intrusions denser than the crust and indicate that the lunar surface was subject to tensile stress in the past. Since such a stress field is likely to occur during the time of lunar expansion and to affect the mechanism of intrusion formation, estimation of the formation age and shapes of the intrusions possibly constrain the ancient thermal history of the Moon. Although the depths of the intrusions have been estimated from the inversion of gravity anomalies, those depths are possibly overestimated in the conventional calculation method. On the other hand, the formation ages have been determined from the crosscutting relationship with giant basins. However, a qualitative discussion has been made only for the linear gravity anomalies near Crisium basin, and other linear gravity anomalies remain without quantitative discussion. So, we investigate two examples, Roche and Rowland craters, in this study.

In this study, we estimate the effect of crater formation directly above the underlying linear gravity anomaly using the iSALE hydrocode and attempt to constrain the depth and age of the intrusive body. First, we assume the depth and width of the intrusions that match the Bouguer gravity anomalies for various densities. Then we calculate the meteoroid collision numerically with iSALE and trace the movement of the subsurface intrusion. By comparing the simulated gravity anomalies after the crater formation with the observation, we can constrain the depth and age.

Roche crater is an example of craters above linear gravity anomalies. The linear gravity anomalies cut Roche crater in a northwest-southeast direction, and the Bouguer gravity anomalies are about 40 mGal lower inside of the crater than outside. This decrease of gravity anomalies is likely due to impact excavation, indicating that the top depth of intrusive rock is shallower than 10 km below the surface. This depth is shallower than the previous estimate of 20 km. Also, because Roche crater modified the structure of preexisting intrusion, the age of the gravity anomaly is older than the formation of Roche crater and is before Nectarian. The second example is Rowland crater. The linear gravity anomaly does not extend into the crater but stops at the rim. Our numerical simulation shows that the excavation depth of Rowland crater is too shallow to erase the linear gravity anomaly completely. Thus, this gravity anomaly is likely to have formed after Rowland crater and is younger than Nectarian. Based on the comparison between the numerical calculation and the Bouguer gravity anomaly data, we will discuss the formation age and possible structure of the linear gravity anomaly in this presentation.

Keywords: moon, gravity anomaly, impact

©2021. Japan Geoscience Union. All Right Reserved.

Laboratory investigations of salt precipitation upon decompression and degassing of volatile-containing brines: Implication for carbonate mineral formations on Solar system icy bodies

*Masahiro Yoda[1,2], Yasuhito Sekine[2,3]

1. Department of Earth and Planetary Science, The University of Tokyo, 2. Earth-Life Science Institute of Tokyo Tech, 3. Institute of Nature and Environmental Technology, Kanazawa University

Chemical compositions of subsurface oceans on Europa, Ceres, Enceladus and other icy bodies can be constrained based on observations of non-ice materials on the surfaces. Carbonate mineral (i.e., sodium carbonate (Na_2CO_3)) is indeed found on bright spots of Ceres (*De Sanctis et al.*, 2016), suggesting the presence of carbonate-rich subsurface brine reservoirs and precipitations of the carbonate salts upon cryovolcanic activities. The mineralogical and chemical compositions of the salts would reflect not only the water chemistry of liquid reservoirs, but also eruption dynamics and degassing processes. For instance, the previous experimental studies showed that rapid freezing of brine results in formation of Na_2CO_3, compared with $NaHCO_3$ precipitation in slow freezing (e.g., *Vu et al.,* 2017; *Thomas et al.,* 2018). In addition to rapid freezing, decompression upon cryovolcanic activities could affect salt precipitations through degassing of dissolved volatiles from brine. However, no experimental studies have been conducted to investigate the effects of rapid decompression and degassing of volatile on salt precipitation.

Here, we perform laboratory experiments to investigate the effect of decompression on salt mineralization. To this end, we newly constructed an experimental system, which can simulate rapid decompression and degassing of volatile from brine. Through evacuation of gas in a vacuum chamber, volatile-containing brine evaporates and subsequently freezes. We collected salt residues after the experiments and analyzed their size and structure using SEM and mineralogical and chemical compositions using both of SEM and micro XRD. We also observed dynamics of eruption using a high-speed camera as a function of dissolved CO_2 gas in starting brines.

In the experiments, we find a clear dependence of precipitated mineralogical compositions on speed of decompression. Precipitations of Na_2CO_3 tend to be suppressed in slow decompression and ineffective degassing, resulting in precipitation of $NaHCO_3$. To form more Na_2CO_3, rapid decompression and effective degassing are favored. Together with the results of the previous studies (*Vu et al.*, 2017; *Thomas et al.*, 2018), the occurrence of Na_2CO_3 on the bright spots of Ceres implies that occurrence of explosive eruption of cryomagma with degassing and rapid freezing, rather than effusive eruption.

Keywords: Cryovolcanic activities, Salts mineralization on the icy bodies, Degassing upon decompression

©2021. Japan Geoscience Union. All Right Reserved.

Rootless cones in the southwest of Emuruangogolak Volcano, Kenya

*Rina Noguchi[1]

1. Institute of Space and Astronautical Science, Japan Aerospace Exploration Agency

The formation condition of rootless cones (pseudocraters) is still in an enigma. In simple, they are formed by continuous explosive interactions of molten hot lava and external water. Therefore, possible rootless cones on Mars have been thought to be evidence of not only volcanic activity but also subsurface water-ice in the last 100 Ma (e.g., Greeley and Fagents, 2001). The explosive interaction (hereafter rootless eruption) does not always occur where lava meets water. For example, in the 2014-2015 Holuhraun eruption, effused lava flowed into a glacial river, but rootless eruptions that form conical mounds did not occur (Dundas et al., 2020). To constrain occurrence conditions of rootless eruptions, we have to survey the environment of rootless cone fields in detail.

Here I report a rootless cone field in the southwest of Emuruangogolak Volcano, Kenya. Emuruangogolak Volcano is a shield volcano with ~40 km extent and locates in the Great Rift Valley. This volcano is characterized by a 5 x 3.5 km summit caldera, trachytic and basaltic lava flows emanated from NNE and SSW flanks and inside of the caldera, and lateral cones/maars in the NNE-SSW trend. In the west of the volcano, a seasonal river, Suguta is located. Tiny ponds are distributed in the southwest of the volcano. In the previous report, rootless cones have been identified but never described in detail (Dunkley et al., 1993). Therefore, I described spatial distribution, bottom/crater diameters of rootless cones using high-resolution (~1 m/pixel) satellite images on Google Earth Pro.

In the Emuruangogolak rootless cone fields, 919 rootless cones were identified. They can be divided into three major localities: north, east, and west. They are split by subsequent lava flows. The lava that rootless cones are located on has been described as “Upper Basaltic Lavas” emplaced during the upper Pleistocene to recent (Dunkley et al., 1993). Since several cones are destroyed and buried by subsequent lava flows and fluvial deposits, the original amount of rootless cones in this field considered being larger than today. The bottom diameter of rootless cones in this field ranges from 3.9 m to 164.4 m, and its average is 28.2 m. For the crater diameter, it ranges from 1.4 m to 98.0 m, and 14.2 m on average. The bottom diameter to crater diameter ratio (Dcr/Dco) ranges from 0.15 to 0.75 and has 0.50 on average. In the presentation, I describe regional differences of these geomorphometry and compare them with the other rootless cone fields on Earth and Mars.

Keywords: rootless cone, Kenya, Mars, Emuruangogolak Volcano

©2021. Japan Geoscience Union. All Right Reserved.



©2021. Japan Geoscience Union. All Right Reserved.

Conditions for the formation of rootless cones on Mars and Earth

*Kei Kurita, Rina Noguchi[1]

1. ISAS/JAXA

The rootless cone is one of the most popular and representative surface features on Mars. It has been widely recognized as a marker of lava field as well as an indicator of aqueous environment. Both are critical characteristics in the evolution of martian surface. This ubiquitus nature throws a deep enigma. RC has been considered as the product of magma-water interaction in terrestrial volcanology. Although water is ubiquitus on the Earth and a lot of occasions for lava flow to meet water are witnessed the formation of RC seems quite rare. On the other hand free water does not exist at least in the Amazonian period of Mars whereas a lot of RC were formed. This enigma indicates existence of unknown factors in the formation of RC. What is the specific condition on Mars? Motivated by this question we have conducted comparative study on microstructure of vesiculated samples between RC eruption and SC eruption. This is a second report to the precedent one,JPGU2020. This report focuses on inspection of microstructures by XCT.
Microstructural Characteristics Investigated pyroclasts were collected at Myvatn,Iceland(Noguchi et al 2016) and Miyakejima. 3D microstructure is reconstructed by the images of microfocus XCT. The spatial resolution is 5 to 8 microns. In addition we complimentarily used SEM-BI images with higher resolution. Overall characteristics of bubble size and morphology seems almost similar for pyroclasts of RC(Myvatn) and SC(Myvatn,Miyakejima) down to the scale of 50 microns. The resemblance in bubble size and morphology of RC samples at remote place(Hagi RC at Myvatn,over 40km away from the source)to those of SC is surprising. This means the external water is well mixed into the magma down to 50 micron scale.
Requirements for the formation of RC on the Earth and Mars Our microstructural investigations suggest simple water magma interaction could not explain the high degree vesiculation of rootless eruption. If free water meets high temperature magma rapid expansion of the volume induces explosion, where magma should be fragmented at the interface. This suppress further mixing of water intomagma. Well-vesiculated structure of RC samples indicates a different style of water-magma interaction. Furthermore the formation of cone of the scale of over hundreds meters requires duration of quasi-steady eruption for certain time. To maintain the eruption suppressing process to the vesiculation is necessary. In Myvatn we have proposed involvement of lake sedeiment(mud) plays an important role. If magma meets water-saturated mud this should be easily entrained into magma in small scale. Then vesiculation occurs subsequently.This scenario is consistent with the field observations. In Myvatn Rittmann(1938) describes existence of mud materials in the pyroclasts of RC. The spatial distribution of RC also semms that RC prefers the area of with deep mud sediments. We consider the viscous nature of mud delays water supply to the magma, which works as a suppressive role in vesiculation. If this scenario can explain the formation of terrestrial RC how about on Mars? In the recent period mud with free water might not be present on the surface. Recent observations by Curiosity(Ehlmann et al 2017) reports aeolian fine dust has size at the order of several tens microns and contained volatiles. This surface layer is composed with mixture of fine aeolian dust and ice particle. This should work similarly as the mud in the terrestrial RC formation.
Ehlmann et al,2017 JGR-E 122(12) 2510-43
Noguchi et al,2016 JVGR313,89-102

Keywords: rootless cone, water-magma interaction, planetary volcanology, Mars

©2021. Japan Geoscience Union. All Right Reserved.

Development of an efficient geological survey method for volcanoes on extraterrestrial bodies

*Junichi Haruyama[1], Rina Noguchi[1], Nobuo Geshi[2], Motomaro Shirao[3], Keiichiro Fujimoto[1], Daigo Shoji[1]

1. Japan Aerospace Exploration Agency, 2. National Institute of Advanced Industrial Science and Technology, 3. Institute of Planetary Geology

Conventional outcrop surveys such as volcanic fieldwork have mainly been conducted by the expertized researchers based on tacit knowledge. Such conventional surveys have significant time limitations due to the weather changes and the accessibility limitation due to the rugged terrain, which is resulting in many problems such as losing the chance to obtain valuable data. With the remarkable advancement of unmanned aerial vehicles and autonomous robots in recent years, a large amount of data can be obtained quickly even in the outcrops where researchers' reconnaissance is usually difficult. To exploit the benefit of these advanced technologies, the establishment of new survey methods is important in terms of the scientific research fields and the industrial fields. An efficient geological survey method based on the extraction of the in-situ geological information by computational image processing has been investigated in this study. While research efforts have been made on the image segmentation and texture classification to extract the geological information, little research efforts have been made to establish the algorithm to evaluate the scientific importance metrics based on the segmentation and texture classification results to achieve a new practical geological survey method. Development of the efficient geological survey method based on such scientific importance metrics is underway in this study. It will contribute to improving the efficiency and effectiveness of the geological surveys for outcrops of volcano regions, even for extraterrestrial ones. Advantages and the features of the proposed method and the research status are presented and discussed.

Keywords: planetary volcanism, geological survey , improving efficiency, image analysis, robotics, outcrop

©2021. Japan Geoscience Union. All Right Reserved.

[J] Oral | M (Multidisciplinary and Interdisciplinary) | M-IS Intersection

[M-IS12] Planetary Volcanology

convener:Rina Noguchi(Faculty of Science, Niigata University), Nobuo Geshi(Geological Survey of Japan, The National Institute of Advanced Industrial Science and Technology), Tomokatsu Morota(Department of Earth and Planetary Science, The University of Tokyo), Chairperson:Rina Noguchi(Faculty of Science, Niigata University), Nobuo Geshi(Geological Survey of Japan, The National Institute of Advanced Industrial Science and Technology), Tomokatsu Morota(Department of Earth and Planetary Science, The University of Tokyo)

Sat. Jun 5, 2021 9:00 AM - 10:30 AM Ch.02 (Zoom Room 02)

Volcanoes exist on solid planetary surface across the solar system. They tell insight into the interior, and the surface environment when they were formed and subsequent evolution. Recent high-resolution remote sensing data on extraterrestrial body allows us to analyze on outcrop scales. Now we are on the stage to share the research targets beyond fields of general volcanology and planetary science. Because some geomorphological and geological environments in other planets are similar to those on Earth, research on volcanic geomorphology and geology on Earth will provide good terrestrial analogues to understand planetary volcanology. The aim of this session is to discuss formation history and mechanism of volcanoes across the solar system.

10:15 AM - 10:30 AM

[MIS12-06]Discussion

©Japan Geoscience Union

[J] Poster | M (Multidisciplinary and Interdisciplinary)：M-IS Intersection

Sat. Jun 5, 2021 5:15 PM - 6:30 PM JST | Sat. Jun 5, 2021 8:15 AM - 9:30 AM UTC | Ch.21_3

[M-IS12] Planetary Volcanology

convener:Rina Noguchi(Faculty of Science, Niigata University), Nobuo Geshi(Geological Survey of Japan, The National Institute of Advanced Industrial Science and Technology), Tomokatsu Morota(Department of Earth and Planetary Science, The University of Tokyo)

Volcanoes exist on solid planetary surface across the solar system. They tell insight into the interior, and the surface environment when they were formed and subsequent evolution. Recent high-resolution remote sensing data on extraterrestrial body allows us to analyze on outcrop scales. Now we are on the stage to share the research targets beyond fields of general volcanology and planetary science. Because some geomorphological and geological environments in other planets are similar to those on Earth, research on volcanic geomorphology and geology on Earth will provide good terrestrial analogues to understand planetary volcanology. The aim of this session is to discuss formation history and mechanism of volcanoes across the solar system.

[MIS12-P01] Review of duration and spatial heterogeneity of mare volcanism on the Moon

*Tomokatsu Morota[1] (1.Department of Earth and Planetary Science, The University of Tokyo)

[MIS12-P02] **Possible existence of lava tube cave and pit/fissure cave in the Moon and Mars**

*Tsutomu Honda[1] (1.Vulcano-speleological Society)

[MIS12-P03] Geomorphological and geological study of the summit caldera of Olympus Mons on Mars.

*Mayuko Nakamura[1], Tomohiro Tsuji[1] (1.Division of Earth Science The Graduate School of Sciences and Technology for Innovation , Yamaguchi University)

[MIS12-P04] The extent of shallow underground water-ice in the Amazonian period on Mars inferred from the distribution of rootless cones

*Rina Noguchi[1] (1.Institute of Space and Astronautical Science, Japan Aerospace Exploration Agency)

Review of duration and spatial heterogeneity of mare volcanism on the Moon

*Tomokatsu Morota[1]

1. Department of Earth and Planetary Science, The University of Tokyo

Unraveling the duration and spatial activity of mare volcanism on the Moon is fundamental to understand the thermal evolution of small terrestrial planets. Lunar mare basalts, which are the most common volcanic features on the Moon, cover 17% of its total surface area. We have investigated the eruption ages and volumes of mare basalts and the relationship between mare distribution and crustal thickness using geological and geophysical data obtained by the SELENE (Kaguya) and recent lunar missions. In this talk, we will review the results and discuss the thermal evolution of the Moon.

Keywords: Moon, Mare volcanism, Lunar dichotomy

©2021. Japan Geoscience Union. All Right Reserved.

Possible existence of lava tube cave and pit/fissure cave in the Moon and Mars

*Tsutomu Honda[1]

1. Vulcano-speleological Society

[Introduction]

There is a large number of lava tube caves(~150) on the foot of Mt. Fuji, though there are also some fissure/pit crater caves(~4)[1,2]. It is also thought that the lava tube cave is preponderant because of the vast lava flow on the Moon and the Mars, but the possibility of the existence of the fissure/pit crater cave cannot be denied. We compared the lava tube cave such as Banba ana cave and fissure/pit crater cave such as Kaminari ana cave on Mt.Fuji, then, examined the possible existence of fissure/pit crater caves on the Moon and Mars.

[Comparison of lava tube cave/Banba ana cave and fissure cave/Kaminari ana cave]

As shown in Fig. 1 and 2, horizontal cavities communicate with the vertical hole for both caves.
Banba ana cave has,under the32m-deep vertical hole. a tubular cavity of length of 1 km. Banba ana cave is formed in Futagoyama/Anmoyama lava flow erupted from the fissure vent of Futagoyama. Banba ana cave has lava shelves, ropy lava flow, and lava stalactite inside of the tubular cavity, indicating the characteristics of a typical lava tube cave(Photo 1). The obtained lava yield strength $f_B=H(\rho g \sin\alpha)/4$ of $3.4x10^3$ to $6.8x10^3$Pa for the slope angle:4.8˚and for the tube height 5m to 10m,is a reasonable value as a basalt.
Kaminari ana cave was formed in Kansuyama lava flow under with the vertical hole depth of 10 m. Kaminari ana cave has a horizontal fissure cavity of height of 3m to 6m with a width of 7m. it is a part of the fissure/pit vent. In the fissure/pit cavity of Kaminari ana cave, a scoria layer can be seen behind the collapsed side wall of the fissure cavity at the bottom (Photo 2). This cavity can be regarded as a fissure cave created by draining back of magma.

[Possibility of pit/fissure vent cave on the Moon/Mars]

The cavity height($H=4f_B/(\rho g \sin\alpha)$) as a lava tube cave is estimated for the vertical holes of the Moon and Mars[3,4,5]. For Lacus Mortis Pit in the Moon, the estimated tube height as the lava tube cave deviates greatly in comparison to the vertical hole depth (estimated tube height 2.5 m~9.8 m for a vertical hole depth of 112 m), so the cavity could be a pit/fissure cave where magma is drained back[3]. As for Arsia Mons on the Mars[4], the estimated value for the vertical hole on the steep slope of Arsia Mons (slope angle 1.0˚~3.5˚) has a large deviation from the vertical hole depth, so that there is a possibility to be a pit/fissure cave. On the other hand, the vertical holes on the gentle slope on the foot of Arsia Mons (slope angle 0.12˚ to 0.54˚) show almost the same value as the estimated tube height, suggesting that a lava tube cave is likely to exist. Regarding Elysium Mons[5], for the vertical holes on the steep slope of Elysium Mons (slope angle ~6˚), the difference between the vertical hole depth and the estimated tube cavity height is large, so it may be a pit/fissure cave.

[Conclusion]

Exploration of the internal structure of the vertical hole in order to clarify how the cavity under the vertical hole of the Moon and Mars is necessary at first for understanding the igneous activity and for possible future use as human base. It is expected that the fissure/pit cave and the lava tube cave will clarify the eruption mechanism and the behaver of lava flow after the eruption. In any case, both the lava tube cave and fissure/pit cave will be possible as underground bases of the Moon and Mars in the future.

References:

[1]Takanori Ogawa (1991): Volcanic cave of Fujimiya, Fujimiya City Folk Museum, Fujimiya City Board of

©2021. Japan Geoscience Union. All Right Reserved.

Education, [2]Takanori Ogawa (1991): Volcanic cave at the southern foot of Fuji, Susono city Education Committee,
[3]Tsutomu Honda(2019): PPS08-P0 Cave height of lava tube cave under the vertical hole estimated from the surface topography of the Moon, Japan Geoscience Union 2019 Meeting, [4]Tsutomu Honda(2017): P117 Mars Possibility of Lava Tube Cave in Vertical Hole of Asia Mons, Japan Volcanic Society Autumn Meeting,[5]Tsutomu Honda(2018): SVC43-P02 Lava yield strength and possibility of lava tube cave below the vertical hole of Mars Elysium volcano, Japan Geoscience Union 2018 Meeting

Keywords: Lava flow, Lava tube cave, Pit cave, Moon, Mars

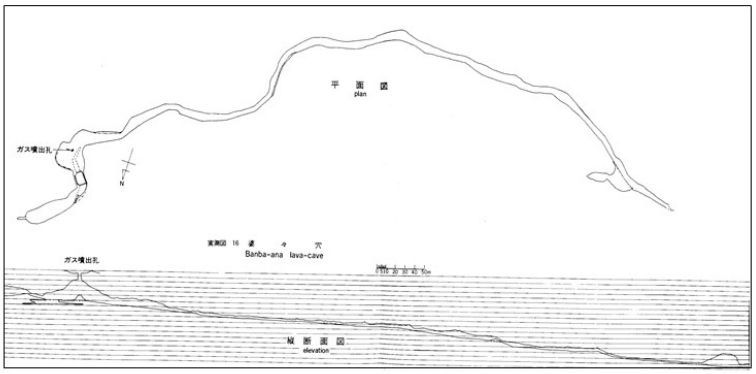


図1 婆々穴測量図(長さ621.2m部分,現在長さが1101.1mに更新)



写真1 婆々穴のチューブ状空洞の内部
©NPO法人火山洞窟学会

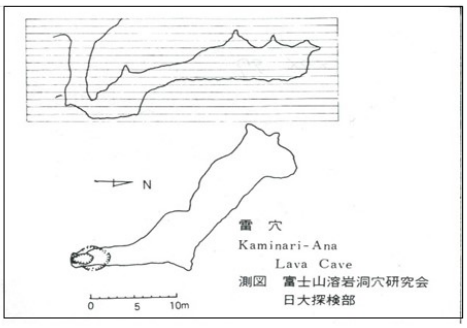


図2 雷穴測量図



写真2 雷穴の割れ目状空洞の内部©NPO法人火山洞窟学会

©2021. Japan Geoscience Union. All Right Reserved.

Geomorphological and geological study of the summit caldera of Olympus Mons on Mars.

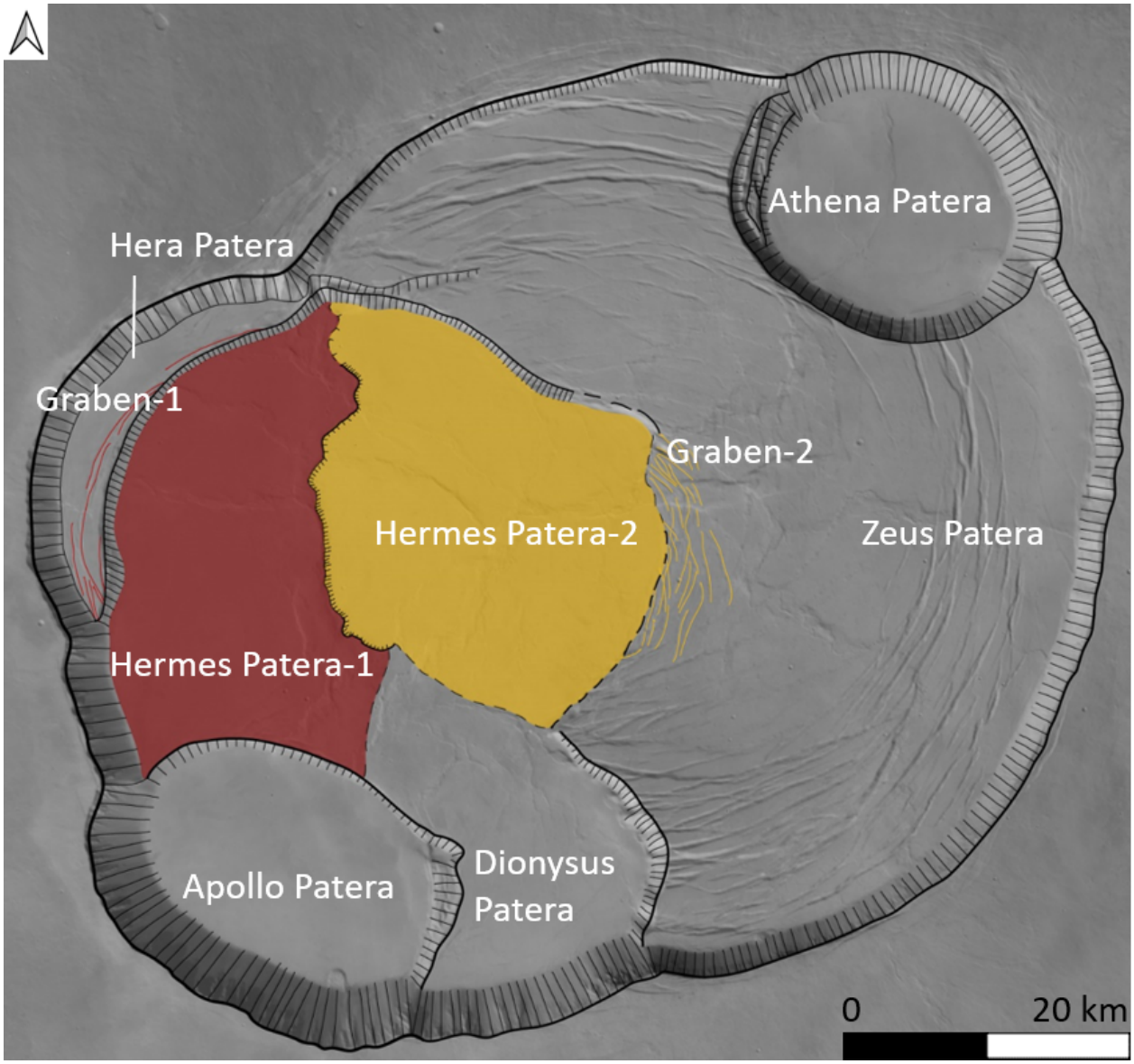
*Mayuko Nakamura[1], Tomohiro Tsuji[1]

1. Division of Earth Science The Graduate School of Sciences and Technology for Innovation , Yamaguchi University

The Olympus Mons, located in the northwestern part of the Tharsis Highlands on Mars, is the largest volcano in the Solar System. It has a basal width of 840 ×640 km (Plescia, 2004), and an elevation of 21,241 m (MOLA DEM data). Olympus Paterae are located in the northern part of the summit and are divided into six calderas (Mouginis-Mark, 2019). In this research, we reconsider the formation of Hames Patera based on the geological and morphological study. The Hermes Patera, located in the center of the western part of Olympus Paterae, has diameters of ~40 km. It could be divided into the western (Hermes Patera-1) and the eastern patera (Hermes Patera-2)(Fig. 1. Hermes Patera-1 and 2).
The floor of Hermes-Patera-2 is ~ 200 m deeper than that of Hermes Patera-1. The boundary of them is a north-south-strike cliff in the central area of the Patera recognized by a 10 m-interval topographic map that has been recognized as a wide ridge by Mouginis-Mark (2018). The elevation of the east side of the cliff is ~200 m lower than that of the west side. This landform constitutes a cliff topography with a dense concentration of contour lines on the 10 m interval contour map. The cliff shows an arc shape that curves northeast-trend at the north and southeast-trend at the south end of the cliff. The entire floor of the western part slopes toward the east. In contrast, the eastern floor is circular and slopes toward the northeast. The eastern shows a circularly enclosed topography, it is necessary to consider the different landforms of the western and eastern parts. Consequently, it is necessary to consider different collapses in Hermes Patera-1 and 2. The cliffs deserve the Hermes Patera-2 caldera rim. In addition, circumferential graben (Zuber and Mouginis-Mark, 1992) are distributed in Olympus Patera. Above all, we Focus on the west of Zeus patera and the graben of Hera patera. This graben surrounding Hermes Patera-is divided in Graben-1 and 2 based on its circumferential curvature. The Graben-1 restricted to the floors of the Hera Patera (Fig. 1. Graben-1). It has a curvature that is subparallel to the western rim of the Hermes Patera-1. The Graben-2 exists along the eastern margin of Hermes Patera-2 (Fig. 1. Graben-2). It has a smaller curvature than Graben-1, and each one is smaller in size. These graben were cut by Hermes Patera-1 and 2, and don't extend to the subsequent collapse of Patera.
Patera and graben are considered to have been formed in the following formation order. Hermes Patera-2 shows a lower elevation than Hermes Patera-1, and thus Hermes Patera-1 considered to have subsidence before Hermes Patera-2. The first, Graben-1 formed on the floors of Hera Patera, which is the subsidence of Hermes Patera-1. Subsequently, Hermes Patera-2 did subsidence of the caldera floors. Graben-2 formed on the floors of Zeus Patera, which is the subsidence of Hermes Patera-2. It can be estimated that these graben were formed at the same time as Hermes Patera-1 and 2 on the geological time scale. Therefore, we need to reconsider Hermes Patera-1n the present proposed formation sequence of the Olympus Patera.

Keywords: Mars , Caldera, Planetary Volcano

©2021. Japan Geoscience Union. All Right Reserved.



©2021. Japan Geoscience Union. All Right Reserved.

The extent of shallow underground water-ice in the Amazonian period on Mars inferred from the distribution of rootless cones

*Rina Noguchi[1]

1. Institute of Space and Astronautical Science, Japan Aerospace Exploration Agency

On Mars, volcanism in the Amazonian period is characterized by the emplacement of flood lava, contrasting to that of Noachian and Hesperian that built large shield volcanoes (e.g., Keszthelyi et al., 2006). Previous studies have found conical mounds on Amazonian lava flows which have been considered to be possible rootless cones (e.g., Greeley and Fagents, 2001; Fagents and Thordarson, 2007; Keszthelyi et al., 2010). Rootless cones are formed by intermittent explosions that occurred by the interaction of lava and water (ice)-logged sediments (Thorarinsson, 1953). Thus, the existence of rootless cones suggests not only volcanic activity but also the presence of water-ice in the shallow subsurface. Possible rootless cone fields have been described in several places. According to Fagents and Thordarson, 2007, candidates of rootless cone fields are mapped in Amazonis Planitia, Olympus Mons aureole, Acidalia Planitia, S. Utopia Planitia, Isidis Planitia, Hephaestus Fossae, Elysium Planitia, Cerberus, Marte Valles, and Arrhenius. Most of the fields are located in low-mid latitudes of the northern lowland plains. Since this mapping was based on studies before 2000 with low-resolution images, those rootless cone fields are uncertain and should be revised with higher resolution images. In the presentation, I update and summarize possible rootless cone fields on Mars, and discuss the extent of groundwater-ice in Amazonian.

Keywords: Mars, rootless cone, ground water-ice

©2021. Japan Geoscience Union. All Right Reserved.

[J] Oral | M (Multidisciplinary and Interdisciplinary)：M-IS Intersection

Sat. Jun 5, 2021 10:45 AM - 12:15 PM JST | Sat. Jun 5, 2021 1:45 AM - 3:15 AM UTC | Ch.02 Zoom Room 02

[M-IS14] Aqua planetology

convener:Yasuhito Sekine(Earth-Life Science Insitute, Tokyo Institute of Technology), Takazo Shibuya(Japan Agency for Marine-Earth Science and Technology), Hidenori Genda(Earth-Life Science Institute, Tokyo Institute of Technology), Keisuke Fukushi(Institute of Nature & Environmental Technology, Kanazawa University), Chairperson:Takazo Shibuya(Japan Agency for Marine-Earth Science and Technology), Yasuhito Sekine(Earth-Life Science Insitute, Tokyo Institute of Technology), Keisuke Fukushi(Institute of Nature & Environmental Technology, Kanazawa University), Tomohiro Usui(Japan Aerospace Exploration Agency), Hidenori Genda(Earth-Life Science Institute, Tokyo Institute of Technology)

This proposed session covers a wide range of topics related to aqua planetology, including chemical reactions involving water on planetary bodies, water-rock reactions within planetesimals, distribution of water in the early Solar system and the origin of water on terrestrial planets, hydrological and biogeochemical processes on Earth, geochemical cycles and habitability on Mars and icy moons, exploration of water in the solar system, and theory to understand how to build a habitable aqua planet.

10:45 AM - 11:00 AM JST | 1:45 AM - 2:00 AM UTC

[MIS14-01] Internal heating of icy ocean worlds

*Shunichi Kamata[1], Kento Nakanishi[1], Kiyoshi Kuramoto[1] (1.Faculty of Science, Hokkaido University)

11:00 AM - 11:15 AM JST | 2:00 AM - 2:15 AM UTC

[MIS14-02] Field investigations on salt partitioning in frozen closed-basin lakes in Mongolia as terrestrial analogues of subsurface brine reservoirs on Solar System icy bodies

*Masahiro Yoda[1,2], Yasuhito Sekine[2,3], Keisuke Fukushi[3], Takuma Kitajima[4], Baasansuren Gankhurel[4], Davaadorj Davaasuren[5], Tuvshin Gerelmaa[5], Shuukhaaz Ganbat[4], Daigo Shoji[6], Yoshio Takahashi[1] (1.Department of Earth and Planetary Science, The University of Tokyo, 2.Earth-Life Science Institute of Tokyo Tech, 3.Institute of Nature and Environmental Technology, Kanazawa University, 4.Division of Earth and Environmental Sciences, Graduate School of Natural Science and Technology, 5.Department of Geography, The National University of Mongolia, 6.Institute of Space and Astronautical Science, Japan Astronautical Exploration Agency)

11:15 AM - 11:30 AM JST | 2:15 AM - 2:30 AM UTC

[MIS14-03] In-situ observation of gas hydrate formation as a simulation of the bottom of ice crust in icy bodies

*Atsushi Tani[1], Kenshiro Moriyama[1] (1.Department of Human Environmental Science, Graduate School of Human Development and Environment, Kobe University)

11:30 AM - 11:45 AM JST | 2:30 AM - 2:45 AM UTC

[MIS14-04] Evolution processes of asteroid Ryugu inferred from orbit and spin dynamics

*Masanori Kanamaru[1], Ryuki Hyodo[1], Tomohiro Usui[1], Tatsuaki Okada[1] (1.Japan Aerospace Exploration Agency)

11:45 AM - 12:00 PM JST | 2:45 AM - 3:00 AM UTC

[MIS14-05] Oxygen isotopic systematics of chondrules in Tagish Lake (C2) and implications of volatiles in the protoplanetary disk

*Takayuki Ushikubo[1], Makoto Kimura[2] (1.Kochi Institute for Core Sample Research, Japan Agency for Marine-Earth Science and Technology, 2.National Institute of Polar Research)

12:00 PM - 12:15 PM JST | 3:00 AM - 3:15 AM UTC

[MIS14-06] Development of a technique for a multi-isotopic analyses of asteroid materials (small amount samples ~ 30 mg) returned by the Hayabusa2 mission

*Tetsuya Yokoyama[1], Ikshu Gautam[1], Yusuke Ohkuma[1], Tsuyoshi Iizuka[2], The Hayabusa2 initial analysis team “Isotopes and Chemistry” (1.Department of Earth and Planetary Sciences, School of Science, Tokyo Institute of Technology, 2.Department of Earth and Planetary Science, School of Science, The University of Tokyo)

Internal heating of icy ocean worlds

*Shunichi Kamata[1], Kento Nakanishi[1], Kiyoshi Kuramoto[1]

1. Faculty of Science, Hokkaido University

Surface temperatures of outer solar system bodies are very low (i.e., ~100 K), and the surface of the most solid bodies are covered by ice mainly composed of water. Despite its low temperature, some of such icy bodies are “aqua planets”; they possess subsurface oceans. It can be said that one of the major research subjects in Aqua planetology is to understand how such oceans are maintained.
In addition to the decay of radiogenic isotopes only slightly contained in rocks, tidal heating is considered as an important heat source maintaining subsurface ocean in satellites of giant planets. Recent theoretical studies quantifying the amount of heat produced in internal solid and liquid layers enable us to calculate the total amount as well as the spatial pattern of heating for a given internal structural model and orbital property. Nevertheless, little is known about the total amount and the spatial pattern of heating on actual satellites because of large uncertainties in their interior structures.
In this study, we calculate the total amount and the spatial pattern of tidal heating in several icy satellites, such as the Jovial icy satellite Europa, the Saturnian icy satellite Enceladus, the Neptunian satellite Triton, under a wide variety of parameter conditions using previously-reported theoretical models. We confirm that Europa and Enceladus are mainly heated by eccentricity-type, while Triton is heated by inclination-type tides, and that the total amount of heat due to the former increases while the latter decreases with increasing ocean thickness. We find that a large increase in the heating rate due to tidal resonance is unlikely to occur for Enceladus. We also find that the spatial pattern of solid tides is not sensitive to the interior structure while that of liquid tides is; the latter relatively strongly depends on the ocean thickness and the drag coefficient. This result implies that the main heating mechanism and/or the mean ocean thickness can be constrained based on the shape of the ice shell.

Keywords: Icy satellites, Tidal heating

©2021. Japan Geoscience Union. All Right Reserved.

Field investigations on salt partitioning in frozen closed-basin lakes in Mongolia as terrestrial analogues of subsurface brine reservoirs on Solar System icy bodies

*Masahiro Yoda[1,2], Yasuhito Sekine[2,3], Keisuke Fukushi[3], Takuma Kitajima[4], Baasansuren Gankhurel[4], Davaadorj Davaasuren[5], Tuvshin Gerelmaa[5], Shuukhaaz Ganbat[4], Daigo Shoji[6], Yoshio Takahashi[1]

1. Department of Earth and Planetary Science, The University of Tokyo, 2. Earth-Life Science Institute of Tokyo Tech, 3. Institute of Nature and Environmental Technology, Kanazawa University, 4. Division of Earth and Environmental Sciences, Graduate School of Natural Science and Technology, 5. Department of Geography, The National University of Mongolia, 6. Institute of Space and Astronautical Science, Japan Astronautical Exploration Agency

Geologically-active icy bodies, e.g., Europa and Ceres, would have possessed near-surface brine reservoirs, which may be a source of salts on the surfaces (e.g., Europa’s chaos terrains and Ceres’ bright spots). Previous studies hypothesized a few processes, in which an overlying ice layer can capture salinity from a subsurface brine reservoir; however, few field investigations have been conducted for inferring the salt partitioning between ice layers and subsurface reservoirs on the icy bodies.
Here, we report results of field surveys to ice-covered, closed-basin saline lakes of Orog and Olgoy lakes in Mongolia in February 2019 and January 2020. The surface ice exhibited complex geomorphology with pressurized ridges formed by compressive force and wet cracks formed by extensional force. We collected the ice samples, including both of the contraction and wet cracks, as well as underlying lake water samples at the lakes. The salinity of ices collected from field surveys suggest that wet cracks could provide salinity to the ice layer and surface. In addition, concentrated bottom lake water, together with suspended authigenic carbonates, would be captured within the ice layer during freezing. We evaluate both of the salts partitioning and lake water chemistry in the frozen lakes using a coupled model of mass balance and low-temperature aqueous chemistry. Our model results can reproduce both the salinity in ice and major dissolved species, e.g., Na^{+}, Cl^{-}, and SO_4^{2-}, in the bottom lake water. To explain the Mg^{2+} and Ca^{2+} concentrations of in the bottom lake water metastable carbonates of amorphous magnesium carbonate and monohydrocalcite should be taken into account. We discuss the implications of the salts partitioning and water chemistry to subsurface liquid reservoirs of the icy bodies.

Keywords: Freezing brine within icy bodies, Water chemistry of frozen saline lakes, Ice-mineralization

©2021. Japan Geoscience Union. All Right Reserved.

In-situ observation of gas hydrate formation as a simulation of the bottom of ice crust in icy bodies

*Atsushi Tani[1], Kenshiro Moriyama[1]

1. Department of Human Environmental Science, Graduate School of Human Development and Environment, Kobe University

Gas hydrates are clathrate compounds where hydrogen-bonded water cages include a guest gas molecule. Methane hydrate is one of famous gas hydrates because it is naturally found in deep-sea and permafrost sediments on the Earth. Gas hydrates would exist in icy bodies as well. One of the candidates is Pluto where the presence of subsurface ocean is suggested. Gas hydrates may exist between the ice shell and subsurface ocean and play an important role as insulator to keep warm inside. The presence of subsurface ocean is also suggested in some icy satellites like Enceladus. INMS (Ion and Neutral Mass Spectrometer) aboard the Cassini orbiter has investigated composition of the plumes there that includes H_2O (< 90 %), CH_4, CO_2, NH_3, and other various organic materials. These results could reflect the composition of the subsurface ocean and imply the presence of clathrate hydrates in the ocean.
Density of gas hydrates depends on guest gas molecules. For example, methane hydrate is lighter than the water, whereas CO_2 hydrate is heavier. If CO_2 hydrate forms at the bottom of the icy shell, the average density may become large and the ice (water ice + CO_2 hydrate) may start to sink locally. If the size of each gas hydrate become small and granular gas hydrates exist in the upper part of the subsurface ocean, heat can be transferred by not only thermal conduction but also convection. This means that icy bodies may be cooled faster. To elucidate how gas hydrates form in the subsurface ocean in icy bodies, we developed the in-situ observation system of gas hydrate formation and dissociation below the ice sheet and observed gas hydrate formation.

The observation system was filled with water and set in thermostatic cooling bath. After temperature in the cell degreased enough, water ice was formed in the lower part of the cell. In this study, CF_4 gas was supplied to the cell up to 7 MPa to form CF_4 hydrate. The reason why we chose CF_4 instead of CH_4 is that CF_4 hydrate is heavier than water and should sink in the water cell even if the hydrate forms in the water.

Long period observation revealed that 1) at first, tiny hydrate particles formed in the water and drifted in the water after shaking the cell, 2) then, a few mm size of hydrate crystals formed and stuck on the ice sheet, 3) hydrate particles were embedded in the ice if formation rate of ice was faster than that of the hydrate. We expect that gas hydrate layer beneath the ice sheet in icy bodies may form after the growth of the ice sheet becomes slow and ice and gas hydrate mixed layer may be formed above the gas hydrate layer.

Keywords: icy bodies, ice crust, subsurface ocean, gas hydrate

©2021. Japan Geoscience Union. All Right Reserved.

Evolution processes of asteroid Ryugu inferred from orbit and spin dynamics

*Masanori Kanamaru[1], Ryuki Hyodo[1], Tomohiro Usui[1], Tatsuaki Okada[1]

1. Japan Aerospace Exploration Agency

Orbital evolution of small solar system bodies supplies near-Earth asteroids from the main asteroid belt. The inward migration of small bodies is also an important source of supply of meteorites to the Earth and transport of volatile materials in the solar system. In order to interpret the results of the coming analysis of Hayabusa2's sample, it is essential to understand the dynamical evolution processes of the target asteroid, 162173 Ryugu, in terms of its orbit and spin.

As well as the gravitational effect of the major planets, the thermal recoil force also affects the dynamics of an asteroid. The thermal recoil force and torque that secularly changes its orbit and spin are known as the Yarkovsky effect and Yarkovsky-O'Keefe-Radzievskii-Paddack (YORP) effect, respectively. The direction of the Yarkovsky drift, i. e., a change of the orbital semi-major axis depends on the direction of rotation. It is required to simulate the combined effect of Yarkovsky and YORP for understanding the evolutional path of Ryugu's orbit from the source region in the inner main belt.

First, we conducted a numerical simulation of Ryugu's spin alteration caused by the YORP effect (Kanamaru et al., submitted to JGR-Planets). Given the current near-Earth orbit and three-dimensional shape of Ryugu observed by Hayabusa2, it is estimated that the rotation of the asteroid is decreasing at a rate of (-0.42 to -6.3) $\times 10^{-6}$ deg/day^2. The corresponding time scale of the spin-down is 0.58 to 8.7 million years. This "recent" spin-down is considered to be caused by a major resurfacing event on Ryugu such as the formation of the western bulge or the largest crater, Urashima. Our YORP simulation also indicates that the thermal torque has maintained the spin pole upright with respect to the orbital plane. The spin-pole stability with the retrograde rotation results in the inward migration of Ryugu by the Yarkovsky effect.

Second, we developed a N-body simulator for orbital evolution of small bodies, which incorporates the combined effect of the gravitational perturbation and above thermal force. We will present some possible paths of Ryugu's orbital evolution and its time scale from the source region in the main belt to the near-Earth orbit.

Keywords: Asteroid, 162173 Ryugu, Yarkovsky effect, YORP effect, Orbital evolution, N-body calculation

©2021. Japan Geoscience Union. All Right Reserved.

Oxygen isotopic systematics of chondrules in Tagish Lake (C2) and implications of volatiles in the protoplanetary disk

*Takayuki Ushikubo[1], Makoto Kimura[2]

1. Kochi Institute for Core Sample Research, Japan Agency for Marine-Earth Science and Technology, 2. National Institute of Polar Research

Previous studies on oxygen isotope systematics of chondrules show that individual chondrules preserve information of oxygen isotopic composition and redox state of chondrule-forming environments in the protoplanetary disk [e.g., 1, 2]. Highly MgO-rich (Mg# ≧ 96; Mg# ≡mol.% of MgO/(MgO + FeO)) and ^{16}O-rich ($\Delta^{17}O$ ~ −5‰; $\Delta^{17}O \equiv \delta^{17}O_{VSMOW} - 0.52 \times \delta^{18}O_{VSMOW}$) chondrules are abundant in CM, CO, and CV chondrites. Minor ^{16}O-poor ($\Delta^{17}O$ ~ −2‰) and FeO-rich (Mg# < 90) chondrules are also found in them. Increase of $\Delta^{17}O$ values of FeO-rich chondrules indicates that oxidizing environment to form ferroan chondrules was caused by enrichment of an ^{16}O-poor oxidizing agent (most likely ^{16}O-poor H_2O ice) [2]. Assuming that CM, CO, and CV chondrites are derived from C- or K-type asteroids, reducing environment was common and enrichment of ^{16}O-poor H_2O ice occurred in middle to outer asteroid main belt region of the protoplanetary disk.

In addition to these two types chondrules, FeO-rich chondrules with higher $\Delta^{17}O$ values ($\Delta^{17}O$ ≧ 0‰) were found in Tagish Lake meteorite [3]. Such chondrules have been found in Tagish Lake-like meteorites [4], CR chondrites [2 and references therein] and the comet Wild 2 returned samples [e.g., 5, 6]. Since comet Wild 2 is originally a Kuiper belt object and Tagish Lake meteorite is possibly derived from a D-type asteroid [7], the occurrence of FeO-rich chondrules with higher $\Delta^{17}O$ values in Tagish Lake and comet Wild 2 suggests existence of a more ^{16}O-depleted oxidizing agent further out than the outer main belt. Recently, Fujiya et al. [8] found the evidence for accretion of CO_2 ice as well as H_2O ice into the parent body of Tagish Lake meteorite. Higher $\Delta^{17}O$ values of FeO-rich chondrules in Tagish Lake and comet Wild 2 may represent higher $\Delta^{17}O$ values of the chemically distinct icy components existed in the outermost part of chondrule-forming environment.

The ^{26}Al-^{26}Mg systematics of chondrules show that the initial $^{26}Al/^{27}Al$ values of FeO-rich chondrules from comet Wild 2 and CR chondrites (< 3×10^{-6}) are significantly lower than those of typical chondrules in CO and CV chondrites (~5×10^{-6}) [e.g., 9, 10], suggesting that the former group of chondrules formed more than one million years later than the formation of the latter group of chondrules. The occurrence of more ^{16}O-depleted oxidizing agent can be results of temporal isotopic evolution of icy components in the protoplanetary disk.

Although we cannot tell either spatial heterogeneity or temporal change of the oxygen isotopic composition of the oxidizing agents formed distinct FeO-rich chondrule groups ($\Delta^{17}O$ ~ −2‰ or ≧ 0‰), we suggest that oxygen isotopic compositions of chondrules would be important constrains for better understanding of volatile components in the protoplanetary disk.

References:
[1] Ushikubo T. et al. (2012) GCA, 90, 242-240.
[2] Tenner T. J. et al. (2018) Chapter 8 in Chondrules (Cambridge Univ. press).
[3] Ushikubo T. and Kimura M. (2021) GCA, 293, 328-343.
[4] Yamanobe M. et al. (2018) Polar Science, 15, 29-38.
[5] Nakamura T. et al. (2008) Science, 321, 1664-1667.
[6] Nakashima D. et al. (2012) EPSL, 358, 355-365.
[7] Hiroi T. et al. (2001) Science, 293, 2234-2236.

©2021. Japan Geoscience Union. All Right Reserved.

[8] Fujiya W. et al. (2019) Nature Astornomy, 3, 910-915.
[9] Ogliore R. C. et al. (2012) Astrophys. J. Lett., 745, L19.
[10] Tenner T. J. et al. (2019) GCA, 260, 133-160.

Keywords: Tagish Lake meteorite, Chondrule, Oxygen isotope, SIMS

©2021. Japan Geoscience Union. All Right Reserved.

Development of a technique for a multi-isotopic analyses of asteroid materials (small amount samples ~ 30 mg) returned by the Hayabusa2 mission

*Tetsuya Yokoyama[1], Ikshu Gautam[1], Yusuke Ohkuma[1], Tsuyoshi Iizuka[2], The Hayabusa2 initial analysis team "Isotopes and Chemistry"

1. Department of Earth and Planetary Sciences, School of Science, Tokyo Institute of Technology, 2. Department of Earth and Planetary Science, School of Science, The University of Tokyo

The sample-return mission Hayabusa2 conducted two sampling sequences that collected the surface and sub-surface materials from a C-type asteroid, Ryugu in 2019. The Sample Return Capsule (SRC) containing the collected materials was brought back to the Earth on Dec 6th of 2020. The curation team opened the SRC in a clean chamber at the curation facility of JAXA at Sagamihara, and found black chunks of rocks and dust from Ryugu, of which the total weight reached >5 g. Although the retrieved sample mass was far more than that was expected at the planning stage (0.1–1 g), each of the initial analysis team can use only limited amount of the samples (< 0.1 g) to obtain scientific data that characterize the asteroidal materials. We have developed a technique for a multi-isotopic analysis that uses ~ 30 mg of the Ryugu sample. Two terrestrial basalts (BCR-2, BHVO-2) and two CM chondrites (Murchison, Jbilet Winselwan) were chosen as the analog samples to evaluate the performance of the developed technique. The powdered sample was decomposed by a mixture of HF + HNO_3 in a Teflon vessel. The sample was conditioned with HBr for the separation of Pb by anion exchange chromatography (Column-1; AG1-X8). The major element fraction of the Column-1 was dried and conditioned with 0.4 M HCl-0.5 M HF for the separation of Ti+Zr+Hf, W, and Mo (Column-2; AG1-X8). The major element fraction of the Column-2 was dried and conditioned with 6 M HCl for the separation of Fe and U (Column-3; AG1-X8), followed by the separation of Sr and Ba (Column-4; Sr-Resin), REEs (Column-5; RE-Resin), Ca (Column-6; DGA-n Resin), and Cr (Column-7; 1:1 mixture of AG50W-X8 and AG50W-X12). Finally, Mg and Ni were separated using Ni Resin (Column-8). The recovery yields of individual target elements are generally >90% during each step of the chromatography. However, these loss are not unique to our method and is always associated during any chemical separation procedures. Although extreme care was taken for handling samples but a certain loss are unavoidable such as during sample drying, pipetting and sample sticking to the Teflon beaker. The isotopic compositions of these analog samples, especially for Cr and Ti, will be reported in the presentation.

Keywords: Hayabusa2, Ryugu, initial analysis, multi-isotope analysis

©2021. Japan Geoscience Union. All Right Reserved.

[J] Oral | M (Multidisciplinary and Interdisciplinary)：M-IS Intersection

Sat. Jun 5, 2021 1:45 PM - 3:15 PM JST | Sat. Jun 5, 2021 4:45 AM - 6:15 AM UTC | Ch.02 Zoom Room 02

[M-IS14] Aqua planetology

convener:Yasuhito Sekine(Earth-Life Science Insitute, Tokyo Institute of Technology), Takazo Shibuya(Japan Agency for Marine-Earth Science and Technology), Hidenori Genda(Earth-Life Science Institute, Tokyo Institute of Technology), Keisuke Fukushi(Institute of Nature & Environmental Technology, Kanazawa University), Chairperson:Yasuhito Sekine(Earth-Life Science Insitute, Tokyo Institute of Technology), Takazo Shibuya(Japan Agency for Marine-Earth Science and Technology), Keisuke Fukushi(Institute of Nature & Environmental Technology, Kanazawa University), Tomohiro Usui(Japan Aerospace Exploration Agency), Hidenori Genda(Earth-Life Science Institute, Tokyo Institute of Technology)

This proposed session covers a wide range of topics related to aqua planetology, including chemical reactions involving water on planetary bodies, water-rock reactions within planetesimals, distribution of water in the early Solar system and the origin of water on terrestrial planets, hydrological and biogeochemical processes on Earth, geochemical cycles and habitability on Mars and icy moons, exploration of water in the solar system, and theory to understand how to build a habitable aqua planet.

1:45 PM - 2:00 PM JST | 4:45 AM - 5:00 AM UTC

[MIS14-07] Comparative metagenomic studies of diverse serpentinized ecosystems

★Invited Papers

*Shino Suzuki[1], Shunichi Ishii[2], Nealson H. Kenneth[3] (1.JAXA, 2.JAMSTEC, 3.USC)

2:00 PM - 2:15 PM JST | 5:00 AM - 5:15 AM UTC

[MIS14-08] Thioester synthesis through geoelectrochemical CO2 fixation on Ni and Mo sulfides.

*Norio Kitadai[1] (1.Japan Agency for Marine-Earth Science and Technology)

2:15 PM - 2:30 PM JST | 5:15 AM - 5:30 AM UTC

[MIS14-09] Effects of pH on the ribose synthesis in the formose reaction: implication for abiotic synthesis on ancient Mars

*Chinatsu Ono[1], Takeshi Kakegawa[1], Yoshihiro Furukawa[1] (1.Graduate School of Science, Tohoku University)

2:30 PM - 2:45 PM JST | 5:30 AM - 5:45 AM UTC

[MIS14-10] Elucidation of the mechanism of organic matter synthesis process by reducing reaction of clay minerals on the surface of the planet by STXM

*Takahiro Kawai[1], Hiroki Suga[2], Yasuo Takeichi[3], Yoshio Takahashi[1,3] (1.University of Tokyo, 2.JASRI, 3.KEK-PF)

2:45 PM - 3:00 PM JST | 5:45 AM - 6:00 AM UTC

[MIS14-11] Solubility of amorphous magnesium carbonate: rarity of Mg-carbonate on surface of closed-basin lakes that existed on early Mars

*TAKUMA KITAJIMA[1], Keisuke Fukushi[2], Yasuhito Sekine[2,3], Masahiro Yoda[3,4], Baasansuren Gankhurel[1], Davaadorj Davaasuren[5] (1.Kanazawa university, 2.The Institute of Nature and Environmental Technology, Kanazawa University, 3.Earth-Life Science Institute, Tokyo Institute of Technology, 4.Department of Earth and Planetary Science, The University of Tokyo, 5.Department of Environment and Forest Engineering, The National University of Mongolia)

3:00 PM - 3:15 PM JST | 6:00 AM - 6:15 AM UTC

[MIS14-12] **Parent body processes reproduce soluble organics in carbonaceous chondrites via geo-electrochemistry**

★Invited Papers

*LI Yamei[1], Yasuhito Sekine[1], Norio Kitadai[1,2] (1.Earth-Life science Institute, Tokyo Institute of Technology, 2.Japan Agency for Marine-Earth Science and Technology)

Comparative metagenomic studies of diverse serpentinized ecosystems

*Shino Suzuki[1], Shunichi Ishii[2], Nealson H. Kenneth[3]

1. JAXA, 2. JAMSTEC, 3. USC

Serpentinization is a process whereby water interacts with reduced mantle rock called peridotite to produce a new suite of minerals (e.g., serpentine), a highly alkaline fluid, and hydrogen. The hydrogen and carbon dioxide present in the system are thought to react under the highly reducing and alkaline conditions, leading to the formation of methane and hydrocarbons and the concomitant production of carbon monoxide, formate, formaldehyde and methanol. Given that the reduced compounds delivered from the water-rock reaction can support microbial energy metabolisms, such serpentinization systems have been viewed as potential habitats for early life or the other planetary bodies.

Studies of serpentinizing environments to date have shown that these ecosystems host extremely low-abundance microbial communities, which is presumably attributed to the multiple extremes: 1) the highly-alkaline condition of the fluid; 2) the extremely low concentrations of oxidants (electron acceptors); and, 3) the low levels of and nutrients (available carbon and phosphate). Although it is known that the serpentinization reaction results in unique geochemical conditions overall, terrestrial ophiolite The Cedars (USA), Voltri Massif (Italy), Santa Elena Ophiolite (Costa Rica), terrestrial intrusive body Cabeç o de Vide (Portugal), shallow-water hydrothermal deposit Prony Bay (New Caledonia), deep-sea Mariana serpentine have different geochemical properties due to the reacting waters (natural and seawater) and the depths. Here, we present the microbial genomes from serpentinizing springs in different sites and discuss how diverse chemical characteristics define the microbial communities and metabolisms in this system.

Keywords: serpentinization, early Earth, Enceladus, Microbial genomics

©2021. Japan Geoscience Union. All Right Reserved.

Thioester synthesis through geoelectrochemical CO2 fixation on Ni and Mo sulfides.

*Norio Kitadai[1]

1. Japan Agency for Marine-Earth Science and Technology

A prevailing scenario of the origin of life postulates thioesters as key intermediates in protometabolism, but there is no experimental support for the prebiotic CO_2 fixation routes to thioesters. Here we introduce a two-steps thioester synthesis pathway starting from CO2 and H2S. First, we show MoS2-catalyzed efficient methanethiol production from CO2 and H2S in seawater in the presence of supercritical CO2. Then, simulating a geoelectrochemical condition in primordial ocean hydrothermal systems (−0.6 to −1.0 V versus the standard hydrogen electrode), we show that nickel sulfide (NiS) gradually reduces to Ni^0 with the surface bound by carbon monoxide (CO) formed through CO_2 electroreduction. The resultant partially reduced NiS realizes thioester (S-methyl thioacetate) formation from CO and methanethiol even at room temperature and neutral pH with the yield up to 35% based on CO. This thioester formation is not inhibited, or even improved, by 50:50 coprecipitation of NiS with FeS or CoS (the maximum yields; 27 or 56%, respectively). Such a simple thioester synthesis likely occurred in Hadean deep-sea vent environments, setting a stage for the autotrophic origin of life.

Keywords: protometabolism

©2021. Japan Geoscience Union. All Right Reserved.

Effects of pH on the ribose synthesis in the formose reaction: implication for abiotic synthesis on ancient Mars

*Chinatsu Ono[1], Takeshi Kakegawa[1], Yoshihiro Furukawa[1]

1. Graduate School of Science, Tohoku University

DNA, RNA, and proteins work together to support the essential system of the present life. RNAs catalyze biological reactions as well as have nucleotide sequence transcribed from DNA. Therefore, abiotic RNA formation has been regarded as an essential step of the origin of life. Ribose is an essential constituent of RNA and is known to form in the formose reaction in which a series of condensation and polymerization of formaldehyde forms many sugar molecules. Ribose synthesis by the formose reaction is known to proceed under alkaline conditions, but the effects of pH on the ribose synthesis have not been clear. The effects of pH on the formose reaction is important to constrain the possibility of ribose synthesis on prebiotic Earth and on ancient Mars. Therefore, this study investigates the effects of pH on the formose reaction and evaluated potential ribose synthesis on ancient Mars. Ancient Mars is shown to have liquid water on the surface and/or subsurface and had CO_2-rich atmosphere. Thus, photochemical formaldehyde formation would have been possible. Moreover, it is estimated that pH of surface water acidified from mildly alkaline to acidic from Noachian to Hesperian based on the mineral composition found by some of Mars surface explorations.
The formose reaction experiments were conducted with formaldehyde and glycolaldehyde in phosphate buffer solutions of different pH. Ribose was formed even in neutral solutions. The yields decreased one orders of magnitude by the decrease of pH by 1. Ribose formation was below our detection limit in acidic solution, pH < 4, although tetroses were formed.
These results suggest that ribose was spontaneously formed from formaldehyde and glycolaldehyde even in near neutral aquatic environments implying that environments existed on Noachian Mars could promote spontaneous ribose formation.

Keywords: ribose, formose reaction, ancient Mars

©2021. Japan Geoscience Union. All Right Reserved.

Elucidation of the mechanism of organic matter synthesis process by reducing reaction of clay minerals on the surface of the planet by STXM

*Takahiro Kawai[1], Hiroki Suga[2], Yasuo Takeichi[3], Yoshio Takahashi[1,3]

1. University of Tokyo, 2. JASRI, 3. KEK-PF

[Background]

Many studies have been conducted to elucidate the evolutionary process of organic matter in extraterrestrial materials, which related to the formation of organic matter as a material for life. Elucidation of the process by which organic matter is synthesized from inorganic carbon (CO_2) in the natural environment is important in considering primordial organic matter and its evolution. There is an evolutionary process in which several organic substances change to polycyclic aromatic hydrocarbons (PAHs) due to thermal stability, but the process of aliphatic carbon compounds formation, which cannot be explained by this process, requires further investigation. On the other hand, on Earth, it has been proposed that hydrogen and aliphatic carbon compounds may be produced near minerals containing Fe2+ such as serpentine and iron saponite (Sforma et al., 2018). However, in these studies, local chemical species analysis may be necessary to investigate the interaction between minerals and organic matter in detail, but its application is not yet sufficient.

The scanning transmission X-ray microscopy (STXM) is a method that enables chemical species analysis of carbon (C), nitrogen (N), and iron (Fe) with a spatial resolution of up to 30 nm, and it is important to apply this technique to meteorite and earth geological samples for the above purposes. In this study we analyzed the local chemical species of C and Fe in the Aguas Zarcas and Tagish Lake meteorites, which are expected to show water-mineral-organic interactions using STXM.

[Experiment]

Elemental mapping of C and Fe in thin FIB samples of meteorites were done using STXM at BL19A in KEK-PF. The experimental data were analyzed with aXis2000 (analysis of X-ray microscopy Images and Spectra), and the species mapping was performed using the absorption near edge structure (XANES) of each chemical element. Similarly, the XANES of magnesium (Mg) and aluminum (Al) were used to estimate the type of mineral around the organic matter.

[Results/Discussion]

In this study, based on the hypothesis that when Fe (II) in clay minerals is oxidized to Fe (III), organic matter is reduced to produce aliphatic carbon, the distinction between Fe(II) and Fe(III) and the distribution of carbon species (carbonic acid, aliphatic carbon, carboxylic acid, etc.) were investigated intensively in STXM analysis.

In the Aguas Zarcas meteorite, there was a concentration of aliphatic caron coexisting with carbonate near Fe (II).
In the Tagish Lake meteorite, the distribution of Fe (II) coincided with that of carbonate, suggesting the

©2021. Japan Geoscience Union. All Right Reserved.

formation of siderite in some parts of the meteorite. In areas with low Fe (II), there was little carbonate, suggesting that carbonate was reduced during the oxidation of Fe (II) to Fe (III). Other peaks derived from carboxylic acids and carbon chains were also observed, but the peak intensities were not sufficient for mapping.
In the future, we plan to investigate how these materials were formed by preparing more appropriate samples, analyzing them by STXM, and conducting isotope analysis of the organic materials found in this study. As related materials, we will search for organic matter around secondary minerals in the dunite layer in the Oman ophiolite boring core samples and analyze the local speciation of carbon and iron.

Keywords: Organic matter, Origin of life, STXM, meteorite

©2021. Japan Geoscience Union. All Right Reserved.

Solubility of amorphous magnesium carbonate: rarity of Mg-carbonate on surface of closed-basin lakes that existed on early Mars

*TAKUMA KITAJIMA[1], Keisuke Fukushi[2], Yasuhito Sekine[2,3], Masahiro Yoda[3,4], Baasansuren Gankhurel[1], Davaadorj Davaasuren[5]

1. Kanazawa university, 2. The Institute of Nature and Environmental Technology, Kanazawa University, 3. Earth-Life Science Institute, Tokyo Institute of Technology, 4. Department of Earth and Planetary Science, The University of Tokyo, 5. Department of Environment and Forest Engineering, The National University of Mongolia

Recent advances in in-situ chemical and mineralogical analyses by exploration rovers and high-resolution remote-sensing data by orbiters have revealed the existence of aqueous environments and geochemical cycle on early Mars. Early Mars would have possessed liquid water on the surface in semiarid climates (Ehlmann et al., 2014), evidenced by the widespread presence of valley networks, lake deposits, and clay minerals. The presence of liquid water on early Mars is thought to have been maintained by warmer climates than today’ s, possibly due to a denser CO_2 atmosphere in addition to effective greenhouse effect gas, such as H_2 and CH_4 (David et al., 2017; Wordsworth et al., 2017).

On present-day Earth, authigenic carbonates are, in general, generated in closed-basin lakes developed in semiarid climates as monohydrocalcite and amorphous magnesium carbonate (AMC) (Fukushi and Matsumiya, 2018). Closed-basin lakes as saline, alkaline lakes have a role of fixing CO_2 in the atmosphere through generating carbonates on Earth. On early Mars, saline, circumneutral-to-alkaline lakes, if present, should have also generated authigenic carbonates in a dense CO_2 atmosphere, playing a role of a carbon sink in carbon cycles. Recent studies suggested that such saline, circumneutral-to-alkaline lakes developed within Gale Crater (Fukushi et al., 2019), where the Curiosity rover landed. Formation of authigenic Mg-carbonates is expected on early Mars given both the widespread occurrence of mafic/ultramafic basement rocks on Mars and the facts that Mg-/Fe-carbonates are found by remote-sensing data. However, in-situ mineralogical analyses performed by the Curiosity rover have found little carbonates, including Mg-carbonates, in lacustrine sediments of Gale Crater. from surface of Gale crater. Since AMC is the precursor of authigenic deposition of Mg-carbonates, such as hydromagnesite and magnesite, the lack of Mg-carbonates in early Gale lakes implies the possibility that no effective AMC deposition occurred despite of the presence of a dense CO_2 atmosphere.

In this study, we perform field surveys for closed-basin lakes developed in cold and semiarid climates in Mongolia, which are promising terrestrial analogues of early Martian lakes. In addition to the field surveys, we conduct laboratory experiments on solubility of AMC at low temperatures to understand condition formation of AMC in saline lakes in cold environments.

Keywords: solubility, amorphous magnesium carbonate

©2021. Japan Geoscience Union. All Right Reserved.

Parent body processes reproduce soluble organics in carbonaceous chondrites via geo-electrochemistry

*LI Yamei[1], Yasuhito Sekine[1], Norio Kitadai[1,2]

1. Earth-Life science Institute, Tokyo Institute of Technology, 2. Japan Agency for Marine-Earth Science and Technology

Organics in carbonaceous chondrites (CCs) and other extraterrestrial bodies recorded the history of solar system chemistry and/or parent body processes. Biologically relevant organics, particularly amino acids, have been intensively investigated owing to their ubiquitous presence and plausible contribution to the prebiotic chemical evolution towards the origin of life on the Earth. Organics in CCs showed substantial heterogeneity in molecular abundance, isomer/homolog, and isotopic features, providing unique chemical signatures. To account for such chemical heterogeneity, the nature of the underlying driving force needs to be clarified in the context of interstellar and/or parent body processes. This will be also important for constraining the geochemical parameters including redox and energetic conditions.
In solvent-extractable fractions of CCs, amino acids typically coexist with a complex suite of other soluble, low molecular weight organics, including α-hydroxy acids, monocarboxylic acids, and monoamines. These organics show associated structures and similar isomer distributions with amino acids, which suggests a strong mechanistic relation in their genesis or conversion. Notably, these soluble organics are biologically significant, because of their participation in various organic syntheses for the chemical evolution or roles as essential nutrients for the primordial life.
Here we attempted to test whether geo-electrochemical processes in icy planetesimals can facilitate the decomposition of amino acids to generate meteoritic organics (e.g., amines, carboxylic and hydroxy acids). Four types of amino acids with aliphatic side chains, including glycine, alanine, valine, and 2-aminobutyric acid (ABA) were tested, which are among the most common and pervasive amino acids in CCs. Our results show that geo-electrochemical decomposition of these amino acids simultaneously generates monoamines, monocarboxylic and α-hydroxy acids under a wide range of redox conditions. The generated amines exhibited a similar homolog tendency as reported in CM2 Murchison meteorites, showing the validity of this model. Based on the quantitative results obtained, the water-rock interaction conditions were constrained for the parent icy planetesimals of Murchison meteorite. The implications on the geochemistry of icy bodies were addressed.

Keywords: Carbonaceous chondrites, Soluble organics, Geo-electrochemistry, Icy planetesimals

©2021. Japan Geoscience Union. All Right Reserved.



©2021. Japan Geoscience Union. All Right Reserved.

[J] Oral | M (Multidisciplinary and Interdisciplinary)：M-IS Intersection

Sat. Jun 5, 2021 3:30 PM - 5:00 PM JST | Sat. Jun 5, 2021 6:30 AM - 8:00 AM UTC | Ch.02 Zoom Room 02

[M-IS14] Aqua planetology

convener:Yasuhito Sekine(Earth-Life Science Insitute, Tokyo Institute of Technology), Takazo Shibuya(Japan Agency for Marine-Earth Science and Technology), Hidenori Genda(Earth-Life Science Institute, Tokyo Institute of Technology), Keisuke Fukushi(Institute of Nature & Environmental Technology, Kanazawa University), Chairperson:Hidenori Genda(Earth-Life Science Institute, Tokyo Institute of Technology), Yasuhito Sekine(Earth-Life Science Insitute, Tokyo Institute of Technology), Tomohiro Usui(Japan Aerospace Exploration Agency), Keisuke Fukushi(Institute of Nature & Environmental Technology, Kanazawa University), Takazo Shibuya(Japan Agency for Marine-Earth Science and Technology)

This proposed session covers a wide range of topics related to aqua planetology, including chemical reactions involving water on planetary bodies, water-rock reactions within planetesimals, distribution of water in the early Solar system and the origin of water on terrestrial planets, hydrological and biogeochemical processes on Earth, geochemical cycles and habitability on Mars and icy moons, exploration of water in the solar system, and theory to understand how to build a habitable aqua planet.

3:30 PM - 3:45 PM JST | 6:30 AM - 6:45 AM UTC

[MIS14-13] Degassing history and the structural evolution of Martian mantle

★Invited Papers

*Masaki Ogawa[1] (1.Division of General Systems Studies, Graduate School of Arts and Sciences, University of Tokyo)

3:45 PM - 4:00 PM JST | 6:45 AM - 7:00 AM UTC

[MIS14-14] Effect of photo-oxidation reactions of ferrous iron on geochemical conditions required for redox stratification on early Gale lake

*Haruhisa Tabata[1,2], Yasuhito Sekine[2], Kazumi Ozaki[3] (1.Department of Earth and Planetary Science, University of Tokyo, 2.Earth-Life Science Institute, Tokyo Institute of Technology, 3.Department of Environmental Science, Toho University)

4:00 PM - 4:15 PM JST | 7:00 AM - 7:15 AM UTC

[MIS14-15] Water vapor vertical distributions on Mars: Results from three years of TGO/NOMAD science operations

*Shohei Aoki[1,2], Ann Carine Vandaele[2], Frank Daerden [2], Geronimo L. Villanueva [3], Giuliano Liuzzi [3], Ian R, Thomas [2], Justin T. Erwin [2], Loic Trompet [2], Lori Neary [2], Severine Robert [2,9], Sebastien Viscardy [2], Arianna Piccialli [2], R. Todd Clancy [4], Michael Smith[3], Matteo Crismani [5], Bojan Ristic [2], Miguel A. Lopez-Valverde[6], Adrian Brines [6], Manish R. Patel [7], James A. Holmes [7], Giancarlo Bellucci[8], Jose J. Lopez-Moreno[6] (1.Université de Liège, 2.Royal Belgian Institute for Space Aeronomy, 3.NASA Goddard Space Flight Center, 4.Space Science Institute, 5.California State University, 6.Instituto de Astrofísica de Andalucía, 7.Open University, 8.Istituto di Astrofisica e Planetologia, 9.Université catholique de Louvain)

4:15 PM - 4:30 PM JST | 7:15 AM - 7:30 AM UTC

[MIS14-16] Theoretic study of atmosphere and hydrological cycle with groundwater transportation on land planets

*Taniguchi Keigo[1,2], Yasuhito Sekine[1], Takanori Kodama[3], Natsumi Noda[4], Hidenori Genda[1], Ayako Abe-Ouchi[5] (1.Earth-Life Science Institute, Tokyo Institute of Technology, 2.Department of Earth & Planetary Sciences, Tokyo Institute of Technology, 3.The university of Tokyo, 4.Department of Earth and Planetary Science, Graduate School of Science, The University of Tokyo, 5.Atmosphere and Ocean Research Institute, The University of Tokyo)

4:30 PM - 4:45 PM JST | 7:30 AM - 7:45 AM UTC

[MIS14-17] Possibility of formation of local reductive environment by cometary impact on the early Earth

*Ryo Miyazaki[1], Hidenori Genda[1] (1.Earth Life Science Institute, Tokyo Institute of Technology)

4:45 PM - 5:00 PM JST | 7:45 AM - 8:00 AM UTC

[MIS14-18] Oceanic retention of ammonia and thermal stability of the atmosphere-ocean system on the primitive earth

*Kirara Arima[1], Kiyoshi Kuramoto[1] (1.Hokkaido university)

Degassing history and the structural evolution of Martian mantle

*Masaki Ogawa[1]

1. Division of General Systems Studies, Graduate School of Arts and Sciences, University of Tokyo

The surface environment of Mars was clement in the early Hesperian, about 3.7 Gyr ago, when active magmatism took place in the Tharsis and the surrounding area. The earlier less clement surface environment suggested in the literatures is, however, difficult to explain with the traditional thermal history models of Mars where its magmatic activity is suggested to have been maximum at 4.5 Ga and have monotonously declined with time since then. To resolve this difficulty, I propose a four-stage evolution model of Mars caused by the structural evolution of the mantle based on a numerical model of coupled magmatism-mantle convection system: at 4.5 Ga, extensive magmatism formed the crust and compositionally stratified the mantle (Stage I); the stratification suppressed mantle convection and magmatism for the next several hundred million years (Stage II); then, hot plumes grew from the deep mantle to cause episodic magmatism and degassing to make the surface environment clement (Stage III); eventually, magmatism waned, as heat producing elements are extracted from the deep mantle (Stage IV). The plume magmatism of Stage III is caused by a positive feedback called the magmatism-mantle upwelling feedback, where mantle upwelling flow generates magma whose buoyancy boosts the upwelling flow itself (the MMUb feedback). I extensively carried out numerical experiments at various parameter values to see how robust the four-stage evolution model is. I found that the four stages arise, when the permeability of magma through the coexisting matrix is moderate. When the permeability is too high, the MMUb feedback does not operate, the mantle stratification formed on Stage I suppresses magmatism throughout the 4.5 Gyr history, and Stage III does not arise. When the permeability is too low, the MMUb feedback strongly stirs the mantle on Stage I to suppress mantle stratification, the mantle remains homogeneous throughout the 4.5 Gyr history, and the mantle evolves as traditional thermal history models predict. The permeability is probably “moderate” for Mars, and Mars is likely to have evolved in the four stages.

Keywords: Mars, mantle evolution, degassing

©2021. Japan Geoscience Union. All Right Reserved.

Effect of photo-oxidation reactions of ferrous iron on geochemical conditions required for redox stratification on early Gale lake

*Haruhisa Tabata[1,2], Yasuhito Sekine[2], Kazumi Ozaki[3]

1. Department of Earth and Planetary Science, University of Tokyo, 2. Earth-Life Science Institute, Tokyo Institute of Technology, 3. Department of Environmental Science, Toho University

Recent observations on iron mineralogy and geochemical data by NASA's Curiosity rover suggested that Gale Crater had sustained closed-basin, redox-stratified lakes at around Hesperian (~3.5–3.3 Ga) (Hurowitz et al., 2017). On Earth, redox stratification in closed-basin lakes is largely maintained by biological processes, e.g., photosynthesis. For Martian lakes without photosynthetic life to be redox stratified, photo-oxidation of ferrous iron could have been a source of oxidants at shallow lakes; whereas, upwelling of reducing ferrous iron is hypothesized to have occurred from the bottom (Hurowitz et al., 2017). However, no quantitative evaluations have been conducted to investigate conditions that can achieve redox stratification on early Mars.

In the present study, we investigate geohydrological and atmospheric conditions (e.g., Fe^{2+} fluxes from rivers and groundwater, advection rate and pH of lake water, and UV flux) to achieve redox stratification on early Gale lakes using a one-dimensional reaction-transport model. We took into account pH-dependent, photo-oxidation of Fe^{2+} into the model using our experimental data (Tabata et al., 2021). Attenuation of UV light due to atmospheric gas species and dissolved species was considered in the model; accordingly, the effeciency of oxidant production is highly sensitive to atmospheric and water compositions.

Our results suggest that when Fe^{2+} is supplied from the top of a lake, acidic pH of 4–5, high Fe^{2+} influx (0.1–100 mol m^{-2} yr^{-1}), and thick atmosphere (~1 bar CO_2) are required for redox stratification. In the case of Fe^{2+} input from the top, Fe^{2+} needs to be transported to the deep before being fully photo-oxidized for redox stratification. The required conditions can achieve low efficiency of Fe^{2+} photo-oxidation near the surface sufficient to transport to the deep. When Fe^{2+} is supplied only from the bottom of a lake, required conditions for redox stratification are circum-neutral pH (6–7) and moderate Fe^{2+} influx (0.01–1 mol m^{-2} yr^{-1}). At acidic pH, water became ferruginous throughout a lake due to inefficient photo-oxidation and low levels of Fe^{2+} near the surface. High input flux of Fe^{2+} results in abundance of carbonate formation, which is inconsistent with the finding of little carbonates in Gale's lacustrine sediments. Considering the recent estimate of circum-neutral pH of early Gale lake (Fukushi et al., 2019), our results prefer groundwater upwelling as the major source of Fe^{2+} on the lakes. In addition, low CO_2 in the atmosphere would be prefered to avoid Fe-carbonate formation and to promote efficient Fe^{2+} photo-oxidation for redox stratification, which implies the need of abundance of other efficient greenhouse effect gases to warm the surface on early Mars.

Keywords: Mars, Geochemistry, Photochemistry, Iron oxidation, Redox stratification

©2021. Japan Geoscience Union. All Right Reserved.

Water vapor vertical distributions on Mars: Results from three years of TGO/NOMAD science operations

*Shohei Aoki[1,2], Ann Carine Vandaele[2], Frank Daerden [2], Geronimo L. Villanueva [3], Giuliano Liuzzi [3], Ian R, Thomas [2], Justin T. Erwin [2], Loic Trompet [2], Lori Neary [2], Severine Robert [2,9], Sebastien Viscardy [2], Arianna Piccialli [2], R. Todd Clancy [4], Michael Smith[3], Matteo Crismani [5], Bojan Ristic [2], Miguel A. Lopez-Valverde[6], Adrian Brines [6], Manish R. Patel [7], James A. Holmes [7], Giancarlo Bellucci[8], Jose J. Lopez-Moreno[6]

1. Université de Liège, 2. Royal Belgian Institute for Space Aeronomy, 3. NASA Goddard Space Flight Center, 4. Space Science Institute, 5. California State University, 6. Instituto de Astrofísica de Andalucía, 7. Open University, 8. Istituto di Astrofisica e Planetologia, 9. Université catholique de Louvain

Nadir and Occultation for Mars Discovery (NOMAD) onboard ExoMars Trace Gas Orbiter (TGO) started science measurements on 21 April, 2018. Here, we present results on the retrievals of water vapor vertical distributions in the Martian atmosphere from three years of TGO/NOMAD science operations.

NOMAD is a spectrometer operating in the spectral ranges between 0.2 and 4.3 μm onboard ExoMars TGO. NOMAD has 3 spectral channels: a solar occultation channel (SO –Solar Occultation; 2.3–4.3 μm), a second infrared channel capable of nadir, solar occultation, and limb sounding (LNO –Limb Nadir and solar Occultation; 2.3–3.8 μm), and an ultraviolet/visible channel (UVIS –Ultraviolet and Visible Spectrometer, 200–650 nm). The infrared channels (SO and LNO) have high spectral resolution (λ/dλ ~10,000–20,000) provided by an echelle grating used in combination with an Acousto Optic Tunable Filter (AOTF) which selects diffraction orders. The sampling rate for the solar occultation measurement is 1 second, which provides a good vertical sampling step (~1 km) with higher resolution (~2 km) from the surface to 200 km. Thanks to the instantaneous change of the observing diffraction orders achieved by the AOTF, the SO channel is able to measure five or six different diffraction orders per second in solar occultation mode. In this study, we analyze the solar occultation measurements at diffraction order 134 (3011-3035 cm^{-1}), order 136 (3056-3080 cm^{-1}), order 168 (3775-3805 cm^{-1}), and order 169 (3798-3828 cm^{-1}) acquired by the SO channel in order to investigate water vapor vertical distributions.
Knowledge of the water vapor vertical profile is important to understand the water cycle and its escape process. Solar occultation measurements by two new spectrometers onboard TGO - NOMAD and Atmospheric Chemistry Suite (ACS) - allows us to daily monitor the water vapor vertical distributions through the whole Martian Year and obtain a good latitudinal coverage for every ~20° of Ls. In 2018, for the first time after 2007, a global dust storm occurred on Mars. It lasted for more than two months (from June to August). Moreover, following the global dust storm, a regional dust storm occurred in January 2019. The NOMAD and ACS observations therefore fully cover the majority of the global and regional dust storms and offer a unique opportunity to study the trace gases distributions during the dust storms. We analyzed those datasets and found a significant increase of water vapor abundances in the middle atmosphere (40-100 km) during the global dust storm from June to mid-September 2018 and the regional dust storm in January 2019. In particular, water vapor reaches very high altitude, at least 100 km, during the global dust storm (Aoki et al., 2019). A GCM simulation explained that dust storm related increases of atmospheric temperatures suppress the hygropause, hence reducing ice cloud formation and so allowing water vapor to extend into the middle atmosphere (Neary et al., 2019). This study presents the results with the extended dataset, which covers a full Mars year. The extended dataset newly includes aphelion season that involves interesting phenomena such as sublimation of water vapor from the northern polar cap and formation of the equatorial cloud belt, which are known as key periods to understand the large

©2021. Japan Geoscience Union. All Right Reserved.

north-south hemispheric asymmetries of Mars water vapor. Yet, only a few papers report the water vapor vertical distributions in the aphelion season. The extended dataset also includes the southern summer season (dusty season) in MY 35, which will allow us to compare the water vapor distributions in the global dust storm year with those in the non-global dust storm year. In the presentation, we will discuss the water vapor vertical profiles as well as the aerosols vertical distributions retrieved from the three-year measurements of the TGO/NOMAD.

Keywords: Mars, Water, Atmosphere

©2021. Japan Geoscience Union. All Right Reserved.

Theoretic study of atmosphere and hydrological cycle with groundwater transportation on land planets

*Taniguchi Keigo[1,2], Yasuhito Sekine[1], Takanori Kodama[3], Natsumi Noda[4], Hidenori Genda[1], Ayako Abe-Ouchi[5]

1. Earth-Life Science Institute, Tokyo Institute of Technology, 2. Department of Earth & Planetary Sciences, Tokyo Institute of Technology, 3. The university of Tokyo, 4. Department of Earth and Planetary Science, Graduate School of Science, The University of Tokyo, 5. Atmosphere and Ocean Research Institute, The University of Tokyo

The presence of liquid water is essential for planetary habitability. Knowledge of a variety of hydrological cycles and climate systems developed on terrestrial planets is important to understand a diversity of habitable planets. According to the previous theoretical studies using general circulation models (GCM) (Abe et al., 2011; Kodama et al., 2018), there are two major planetary climate systems depending on the amount of water on the surface. One is an aqua planet with wet climates and global oceans, and the other is a land planet with arid climates and polar ice caps. Although the previous studies showed that water distributed predominantly in polar regions as ice caps on a land planet, groundwater circulation could transport liquid water formed at the basement of ice caps to middle to low latitudes. Global-scale groundwater circulations would have occurred in reality on land planets in the Solar System, i.e., early Mars and Titan (e. g., Carr et al., 2003; Faulk et al., 2020). Here, we numerically investigate the roles of groundwater circulations in a diversity of planetary climate systems and hydrological cycles on land planets.

In the numerical simulations, we used two models: One is the general circulation model (GCM) of agcm5.4g (Kodama et al., 2018), which calculates atmospheric dynamics, precipitations, and radiation processes in three dimensions, and the other is the commercially-available groundwater circulation simulator of GETFLOWS (Tosaka et al., 2000), which calculates groundwater transport in three dimensions. To achieve a consistency between the models, we performed calculations in the following 3 steps. In Step 0, spatial distribution of ice caps and precipitation/evaporation on land planets are calculated for given atmospheric CO_2 levels and orbital setting using the GCM. We obtain snow-line latitudes, until which ice caps can exist. In Step 1, we calculated the transport dynamics and distribution of groundwater generated at the basement of the ice caps using the groundwater circulation model. In the calculations, we find that groundwater beneath the ice caps is transported to the middle and low latitudes as the permeability of crustal rocks increases. In particular, if the permeability is higher than 10^5~10^6 md, which corresponds to the permeability of gravels and sands on Earth, efficient groundwater transport extends water-existing areas to low latitudes. In Step 2, we investigated the atmospheric circulations and climatic conditions using the GCM for the surface water distributions derived from the groundwater circulation model. We find that when the permeability is high (higher than 10^5~10^6 md), the water-existing areas reach the edge of Hadley Cell at ~30 degrees in latitude. This leads to wetting of air in low latitudes due to water vapor transport by the Hadley circulation, and the climate state shifts from an extremely dry land planet to a wet aqua planet.

Our results of a combination of the numerical simulations show that planetary climate systems are largely affected by surface and shallow-subsurface geological conditions (i.e., permeability of rocks), which have not been considered previously. In particular, the present study suggests the possible existence of a planetary climate state, which has the characteristics of a land planet in terms of surface water distribution (ice caps at high latitudes) and the characteristics of an aqua planet in terms of climate (wet low latitudes). Given the fact that air in low latitudes becomes wet for high permeabilities, we suggest that land planets do not necessary have a wide habitable zone, depending on geological conditions of the

©2021. Japan Geoscience Union. All Right Reserved.

surface and shallow subsurface.

Keywords: land planets, atmosphere, groundwater

©2021. Japan Geoscience Union. All Right Reserved.

Possibility of formation of local reductive environment by cometary impact on the early Earth

*Ryo Miyazaki[1], Hidenori Genda[1]

1. Earth Life Science Institute, Tokyo Institute of Technology

When an impact of asteroids or comets in high velocity occurs, they evaporates due to shock heating, forming an impact vapor plume. Chemical reaction in the impact vapor plume is one of the processes that locally bring a reduced environment on the early Earth. Impact experiments show that some organic materials related to life building blocks are formed via chemical reactions in the impact vapor plume. On the other hand, because it is difficult to reproduce planetary-scale collisions in collision experiments, and it is difficult to achieve collision velocities exceeding 10 km/s , theoretical methods are also important.

Ishimaru et al. (2010), which is one of the theoretical methods estimated the quenched composition of impact vapor plume using numerical model that solves the motion of the plume and the chemical reactions simultaneously. However, this model simplifies the motion of vapor plumes based on a few assumptions.

In this study, we investigated the quench composition generated by cometary impacts on the ocean on the early Earth. Specifically, we first performed impact calculations using the impact code iSALE-2D(cylindrical coordinate system) to precisely follow the physical processes of the vapor plume, and to explore the temperature and pressure changes of the plume. Then, the chemical reaction of the HCNO system was calculated under the obtained temperature and pressure changes to estimate quenched composition.

The impact calculations showed the peak temperature and pressure of the plume are found to be consistent with Ishimaru et al. (2010) for the pressure, but about 1/2~1/3 for the temperature. Tis because the previous study estimated the peak temperature based on the planar impact assumption and did not consider the temperature dependence of the specific heat ratio and evaporation heat of ice. In addition, it was thought that the change in comet size did not affect the peak temperature and pressure of the plume, but it was found that if the comet size is larger than the thickness of the ocean, penetration into the oceanic crust occurs and the peak temperature and pressure increases due to the difference in shock wave characteristics with the ocean.

As a result of chemical reaction calculations, it is found that the quenched composition obtained by cometary impact on the early Earth is rich in H_2, H_2O, CO. Moreover, even at the same collision velocity (15 km/s), the compositions of strongly reducing species (CH_4, NH_3) and life building blocks (HCN) are 10 to 1000 times richer than those in Ishimaru et al.(2010). This is because Ishimaru et al.(2010) overestimated the entropy of the plume.

Considering the formation of vapor plume, which is a mixture of comets and oceans during the impact process, we calculated the chemical reaction when H_2O is mixed in. The result shows, as the mixing ratio of the target ocean(H_2O) in vapor plume increased, the molar fractions of reductive nitrogen and carbon compounds in the quench composition became smaller, while oxidative nitrogen, carbon compounds, and H_2 became larger. This is considered to be due to the fact that the mixed target(H_2O) was used to oxidize the reductive nitrogen and carbon.

©2021. Japan Geoscience Union. All Right Reserved.

It was found that a strongly reducing quench composition can be obtained at an impact velocity of ~15 km/s, which is favorable for the formation of life building blocks on the early Earth. On the other hand, since cometary impact velocities to the Earth are often much higher, it is difficult to create a strongly reducing environment on the early Earth by simple HCNO system reactions. However, by the use of metallic elements in the comet as catalysts (e.g., Sekine et al., 2006).it is possible that even a high-velocity cometary impact could have brought a strongly reducing environment.

Keywords: early Earth, impact vapor plume, life building block

©2021. Japan Geoscience Union. All Right Reserved.

Oceanic retention of ammonia and thermal stability of the atmosphere-ocean system on the primitive earth

*Kirara Arima[1], Kiyoshi Kuramoto[1]

1. Hokkaido university

One of the hypotheses solving the faint young Sun paradox on the ancient earth is the greenhouse effect of NH_3 that has strong infrared absorptions (Sagan and Mullen, 1972). NH_3 might be important for the synthesis of prebiotic organic compounds like amino acids on primitive earth (Bada and Miller, 1968). Although NH_3 tends to be removed from the atmosphere rapidly due to photochemical conversion to N_2 (Kasting, 1982), Sagan and Chyba (1997) estimate that the lifetime of NH_3 (10^{-5} bar) with the amount required for enough greenhouse effect may be as long as 50 million years as organic haze photochemically derived from CH_4 shields NH_3 from UV. They also argue that it might extend to 500 million years if NH_3 was supplied continuously to the atmosphere from a reservoir initially containing NH_3 with the amount equivalent to the total of current atmospheric N_2. However, it has been little discussed what could be the possible reservoirs of NH_3.

NH_3 has high solubility to water; it dissolves 200 mol/kg in pure water under standard temperature and 1 bar of NH_3. Its solubility increases when CO_2 dissolved in water because H^+ and therefore NH_4^+ concentrations increase in water associated with the ionization of CO_2. Therefore, a large amount of NH_3 might be dissolved in the primitive ocean if NH_3 was present in the primitive earth atmosphere. On the other hand, NH_3 solubility has strong temperature dependence which releases NH_3 from water to gas under high temperatures. Thus, the greenhouse effect of NH_3 and the release of NH_3 from oceans might have a positive feedback relationship. Here we assess whether thermal stability could be established in the NH_3-bearing atmosphere-ocean system and the possible strength of greenhouse effect and the NH_3 partitioning between atmosphere and ocean at stable states if exist. Based on those analyses, we clarify whether or not the primitive ocean could function as a long-term reservoir for NH_3. We used a one-dimensional radiative-convective equilibrium atmospheric model for the atmosphere and the solution equilibria model for the isothermal, uniform ocean taking NH_3 and CO_2 as solvents.

We take N_2, NH_3, CO_2, and CH_4 as atmospheric composition and apply 75% of the present solar constant. The vertical NH_3 profile in the atmosphere is given taking into account the effect of rainout. The outgoing planetary radiation to space is calculated by using a line-by-line model and the surface temperature balanced with the absorption of solar radiation is obtained as a function of atmospheric composition, especially NH_3 partial pressure. Here the planetary albedo is fixed at 0.3. The solution equilibria model shows the amount of NH_3 dissolution to the ocean with the present oceanic mass as a function of NH_3 and CO_2 partial pressures. For simplicity, other dissolved components are ignored. The thermal stability of the atmosphere-ocean system can be judged by comparing the temperature dependence of NH_3 partial pressure at solution equilibria under a fixed total amount of NH_3 in the system and the dependence of surface temperature on NH_3 partial pressure in the radiative-convective equilibrium atmosphere.

As the reference case, we suppose 1 bar of N_2 atmosphere with 0.1 vol% of CO_2 and CH_4, respectively, and 1.0×10^{19} mol (equivalent to 3% of N_2 in the present atmosphere) for the total amount of NH_3. In this case, a thermally stable solution is uniquely obtained. At this solution, NH_3 is partitioned 5.8×10^{16} mol (2.0×10^{-4} bar) to the atmosphere and the surface temperature is 330 K which exhibits a strong NH_3 greenhouse. Thermally stable solutions are found when the total amount of NH_3 and partial pressures of N

©2021. Japan Geoscience Union. All Right Reserved.

$_2$, CO_2, CH_4 are varied. Surface temperatures at thermally stable solutions little depend on the CH_4 volume fraction. We obtained single stable solutions with surface temperatures from 273 K to 373 K when the CO_2 volume fraction is smaller than to 10^{-5}. On the other hand, two stable solutions with high and low surface temperatures appear under larger CO_2 volume fractions. The surface temperature at thermally stable solution increases with increasing the total amount of NH_3 and N_2 partial pressure. Our result suggests that thermally stable states with surface temperatures above 273 K were possibly established when NH_3 existed in the ancient atmosphere in solution equilibrium with the ocean. If NH_3 loss from the atmosphere-ocean system is mostly caused by photolysis, a sufficient greenhouse effect by NH_3 might have lasted 500 million years because the ocean could store a large amount of NH_3 with replenishing NH_3 into NH_3 into the atmosphere.

Keywords: primitive earth, ammonia, atmosphere-ocean system, reduced atmosphere, faint young Sun paradox

©2021. Japan Geoscience Union. All Right Reserved.

[J] Poster | M (Multidisciplinary and Interdisciplinary)：M-IS Intersection

Sat. Jun 5, 2021 5:15 PM - 6:30 PM JST | Sat. Jun 5, 2021 8:15 AM - 9:30 AM UTC | Ch.22_1

[M-IS14] Aqua planetology

convener:Yasuhito Sekine(Earth-Life Science Insitute, Tokyo Institute of Technology), Takazo Shibuya(Japan Agency for Marine-Earth Science and Technology), Hidenori Genda(Earth-Life Science Institute, Tokyo Institute of Technology), Keisuke Fukushi(Institute of Nature & Environmental Technology, Kanazawa University)

This proposed session covers a wide range of topics related to aqua planetology, including chemical reactions involving water on planetary bodies, water-rock reactions within planetesimals, distribution of water in the early Solar system and the origin of water on terrestrial planets, hydrological and biogeochemical processes on Earth, geochemical cycles and habitability on Mars and icy moons, exploration of water in the solar system, and theory to understand how to build a habitable aqua planet.

[MIS14-P01] Experimental study of hypervelocity impact penetration of asteroids into the Ocean and benthic cratering

*Manabu Nishizawa[1] (1.Japan Agency for Marine-Earth Science and Technology)

[MIS14-P02] Experimental study on the growth process of iron rind in Fe-oxide concretions

*Hiroyuki Okamura[1], Sin-iti Sirono[1] (1.Department of Earth and Planetary Sciences, Nagoya University)

[MIS14-P03] Redox change by coseismic water-rock reactions in the interior of planets

*Takehiro Hirose[1], Ryoichi Nakada[1], Keishi Okazaki[1], Takazo Shibuya[1] (1.Japan Agency for Marine-Earth Science and Technology)

[MIS14-P04] Characterizations of mineralogy and infrared spectra of serpentinized samples in Oman ophiolite along with redox gradients in subsurface: Toward identification of redox gradients in Martian subsurface

*Takumi Sato[1], Yasuhito Sekine[1], Ikuo Katayama[2] (1.Tokyo Institute of Technology , 2.Hiroshima University)

[MIS14-P05] Experimental study of element dissolution to liquid CO_2 from artificial seawater and hydrothermal vent chimney

*Kaito Seo[1,2], Takazo Shibuya[2], Kosuke Fujishima[3], Ken Takai[2], Masaru Tomita[1,4] (1.Graduate School of Media and Governance, Keio Univ., 2.JAMSTEC, 3.ELSI, 4.IAB, Keio Univ.)

[MIS14-P06] Rocognition and classification of Martian chaos terrains using imagery marchine learning: Implications for groundwater distribution and hydrological cycles

Hiroki Shozaki[2], *Yasuhito Sekine[1], Nicholas Guttenberg[1] (1.Earth-Life Science Insitute, Tokyo Institute of Technology, 2.Dept. Earth Planetary Sci., Tokyo Institute of Technology)

[MIS14-P07] No effective oxychloride formations on Europa's surface inferred from UV/electron irradiation experiments onto salt-ice mixtures

*Shuya Tan[1], Yasuhito Sekine[1], Takashi Kikuchi[2], Hisayuki Suematsu[2], Tetsuya Hama[3], Yoshio Takahashi[4] (1.Earth-Life Science Institute, Tokyo Institute of Technology, 2.Nagaoka University of Technology, 3.Komaba Institute for Science, The University of Tokyo, 4.Department of Earth and Planetary Science, Graduate School of Science, The University of Tokyo)

[MIS14-P08] An experimental study on evaporite formation around the north pole of Titan

*Eito Hirai[1,2], Yasuhito Sekine[2], ZHANG NAIZHONG[2] (1.Department of Earth and Planetary Sciences, School of Science, Tokyo Institute of Technology, 2.Earth-Life Science Institute, Tokyo Institute of Technology)

[MIS14-P09] **Prediction of the composition of the primordial ocean just after its formation**

*Hisahiro Ueda[1], Takazo Shibuya[1] (1.JAMSTEC)

[MIS14-P10] **Formation conditions of magnetite and hematite in Sheepbed mudstone and bioavailable energies in lake water-groundwater mixing zone in Gale crater, Mars**

*Sakiko Kikuchi[1], Takazo Shibuya[1] (1.Japan Agency for Marine-Earth Science and Technology)

[MIS14-P11] Measurements of elastic wave velocity of mafic and ultramafic rocks below the freezing point: Consideration about reflectivity due to ice-water phase transition in Mars

*Haruna Wakabayashi[1], Ikuo Katayama[1] (1.Hiroshima University)

[MIS14-P12] Viscosity of aqueous MgSO4 solutions at high-pressure and low-temperature: implications for icy satellites

*Shunsuke Nozaki[1], Seiji Kamada[2,3], Akio Suzuki[2] (1.Division of Earth and Planetary Materials Science, Faculty of Science, Tohoku University , 2.Department of Earth Science, Graduate School of Science, Tohoku University, 3.Frontier Research Institute for Interdisciplinary Sciences, Tohoku University)

[MIS14-P13] Formation mechanism of spherical concretions in Tatsukushi area: Possible analogy with spherical nodule in Gale crater, Mars

*Saki Asai[1], Hitoshi Hasegawa[1], Hidekazu Yoshida[2], Minoru Ikehara[1], Nagayoshi Katsuta[3], Masakazu Nara[1], Yui Tomonao[1], Satoru Imai[4] (1.Kochi University, 2.Nagoya University, 3.Gifu University, 4.Tosashimizu GeoPark)

[MIS14-P14] Synthesis and reversible redox properties of iron-saponite

*Hiroshi Sakuma[1], Koki Morida[2], Keisuke Fukushi[2], Yoshio Takahashi[3], Natsumi Noda[3,4], Yasuhito Sekine[4], Kenji Tamura[1] (1.National Institute for Materials Science, 2.Kanazawa University, 3.University of Tokyo, 4.Tokyo Institute of Technology)

[MIS14-P15] Physical dependence of stable carbon and hydrogen isotopic ratio of methane gas in gas hydrate

*Kushi Kudo[1], Atsushi Tani[1], Keita Yamada[2], Naohiro Yoshida[3] (1.Graduate School of Human Development and Environment, Kobe University, 2.Department of Chemical Science and Engineering, School of Materials and Chemical Technology, Tokyo Institute of Technology, 3.Earth–Life Science Institute)

[MIS14-P16] **Clumped isotope signatures of abiotic methane formed via Fischer-Tropsch catalysis and their implications**

*ZHANG NAIZHONG[1], Yasuhito Sekine[1], Mayuko Nakagawa[1], Naohiro Yoshida[1] (1.Tokyo Institute of Technology)

[MIS14-P17] Possibilities of the rubidium stable isotope ratio as geochemical tools

*Rimi Konagaya[1], Hiroyuki Tsuboi[1], Takaaki Itai[1], Yoshio Takahashi[1] (1.The University of Tokyo)

[MIS14-P18] **Determination method of ^{13}C-labeled isotopomer ratio of dissolved organic acids by GC-MS analysis**

*Konomi Suda[1] (1.National Institute of Advanced Industrial Science and Technology)

[MIS14-P19] **Selectivity coefficient of Na^+-NH_4^+ exchange in saponite interlayer: Reconstruction of ammonium concentration in early ocean on Ceres**

*Hiroto Tokumon[1], Keisuke Fukushi[2], Yasuhito Sekine[3], Kosuke Inoue[1], Koki Morida[1] (1.Kanazawa University , 2.Institute of Nature and Environmental Technology Kanazawa University, 3.Tokyo institute of

technology)

Experimental study of hypervelocity impact penetration of asteroids into the Ocean and benthic cratering

*Manabu Nishizawa[1]

1. Japan Agency for Marine-Earth Science and Technology

The hypervelocity (measured in km/s) impact of extraterrestrial bodies in the marine environment is more common than that on land because ~70% of the Earth's surface is covered by oceans. Seafloor cratering is important for recording Earth's impact history, driving environmental, biotic, and climatic perturbations by ejecting crustal materials into the atmosphere (e.g., the K–T boundary event); impactors can also affect the fate of extraterrestrial organic matter and may have been key components of primitive life on early Earth (the so-called panspermia hypothesis). Herein, we simulated the oceanic hypervelocity impacts of asteroids in a laboratory to derive a scaling relationship for benthic cratering. The results are reported for experimental hypervelocity impacts of chondrite and other projectiles (olivine, stainless-steel, polycarbonate) on a water-covered iron target. In situ observations of 5-km/s impacts quantify the deceleration of projectiles in the water column by shock-induced deformation and fragmentation. The minimum water depths at which multiple craters appeared on the benthic target were two and four times the projectile diameter for chondrite and stainless steel, respectively. Based on the observed deceleration of projectiles in water, the cratering efficiency of a benthic target for a given impact velocity is predicted to follow an exponential decay law in terms of water depth normalized by projectile diameter (H/d), given by $\pi v \propto \exp(-(H/d)/\kappa)$, when a projectile of original mass collides with the target. Comparing the volume of the largest crater in the experiments and that derived from the scaling relation, mass ratios of the largest projectile fragment to original projectile in the 5-km/s impact were calculated to be 0.1–0.3 (H/d = 2–6) and 1.0 ±0.3 (H/d = 5.5) for chondrite and stainless steel, respectively. Using the scaling relationship, the volume of the transient crater on oceanic crust by an asteroid impact is estimated to be smaller than previously predicted by hydrocode simulation when the asteroid fragmentation in the water column controls seafloor cratering. Our results suggest that deformation and fragmentation of asteroid impactor control the water depth conditions that enable benthic cratering.

Keywords: Oceanic impact, scaling relation, chondrite

©2021. Japan Geoscience Union. All Right Reserved.

Experimental study on the growth process of iron rind in Fe-oxide concretions

*Hiroyuki Okamura[1], Sin-iti Sirono[1]

1. Department of Earth and Planetary Sciences, Nagoya University

Introduction

The Navajo Sandstone in Utah, U.S.A. and the Gobi Desert in Mongolia have geological formations containing Fe-oxide concretions. They are several mm to cm in size and have spherical shape. The surface is covered with a rind of iron and the interior is filled with sandgrain. An analog of Fe-oxide concretion was discovered on Mars by NASA's Opportunity rover. Fe-oxide concretions form only under limited conditions. Therefore, identification of the formation process of Fe-oxide concretions on Earth will lead to clarification of the ancient environment of Mars. In 2018, a research group at Nagoya University proposed a new model for the formation of Fe-oxide concretions on the Earth. The hypothesis is that Fe-oxide concretions were originally $CaCO_3$ concretions. They were replaced by iron through processes including (1) dissolution and (2) precipitation due to neutralization reactions with iron rich acidic groundwater (Yoshida et al., 2018). However, the growth rate and width of the iron rind have not been clarified in this model.

Objectives

The purpose of this study is to generate artificial Fe-oxide concretions and to measure the (1) growth rate (infiltration, precipitation, and dissolution rate) and (2) width of the iron rind.
Based on geological evidence, the formation process of Fe-oxide concretions on Earth can be applied to one on Mars. Thus, this study will provide clues to the ancient environment of Mars.

Methods

We used artificial $CaCO_3$ concretions that made by kneading $CaCO_3$ powder, glass beads with the same particle size as desert sand (150-180 μm), and distilled water. Also, groundwater was simulated with $FeCl_2$ solution (Molarity=1.07 [mol/l]). We fixed an artificial $CaCO_3$ concretion in a Petri dish and simulated the environment where groundwater with iron ion reacts with the $CaCO_3$ concretion. We set a sample on a fixed-point imaging system that we made ourselves.

Results and Discussion

We investigated the relationship between width of rind and time. We analyzed width of a rind on 300 images. The results showed that the solution rapidly penetrated the $CaCO_3$ concretion (about 5.2×10^{-4} [mm/s]) in five minutes, and the width slowly grew (about 3.4×10^{-7}[mm/s])(Fig.1). This indicates that the iron rind grows through the processes of (1) penetration, (2) dissolution, and (3) precipitation. We describe the relationship between natural $CaCO_3$ concretions and artificial $CaCO_3$ concretion. We performed the same experiment with the moisture content of the concretion set to 0[%] in another preliminary experiment. A thicker iron rind was formed than in this experiment. From the above, It is expected that the porosity (in artificial $CaCO_3$ concretions, moisture content) determines the penetration rate and width of rind. Porosity of natural $CaCO_3$ concretions is about 10.2[%]. It is technically difficult to reproduce this porosity in artificial $CaCO_3$ concretions. We will create an artificial $CaCO_3$ concretion with a feasible porosity about 15-25 [%] and calibrate the porosity, penetration velocity and width of rind. We use this as a basis for correcting the results of this experiment and can derive the penetration rate and width of rind for a porosity of 10.2 [%]. This mean that it is possible to estimate the reaction of natural $CaCO_3$ concretions. Also, The existence of a penetration process means that we need to consider a "dissolution from the part where the solution has finished penetration " model, rather than the traditional "dissolution from the surface" model.

©2021. Japan Geoscience Union. All Right Reserved.

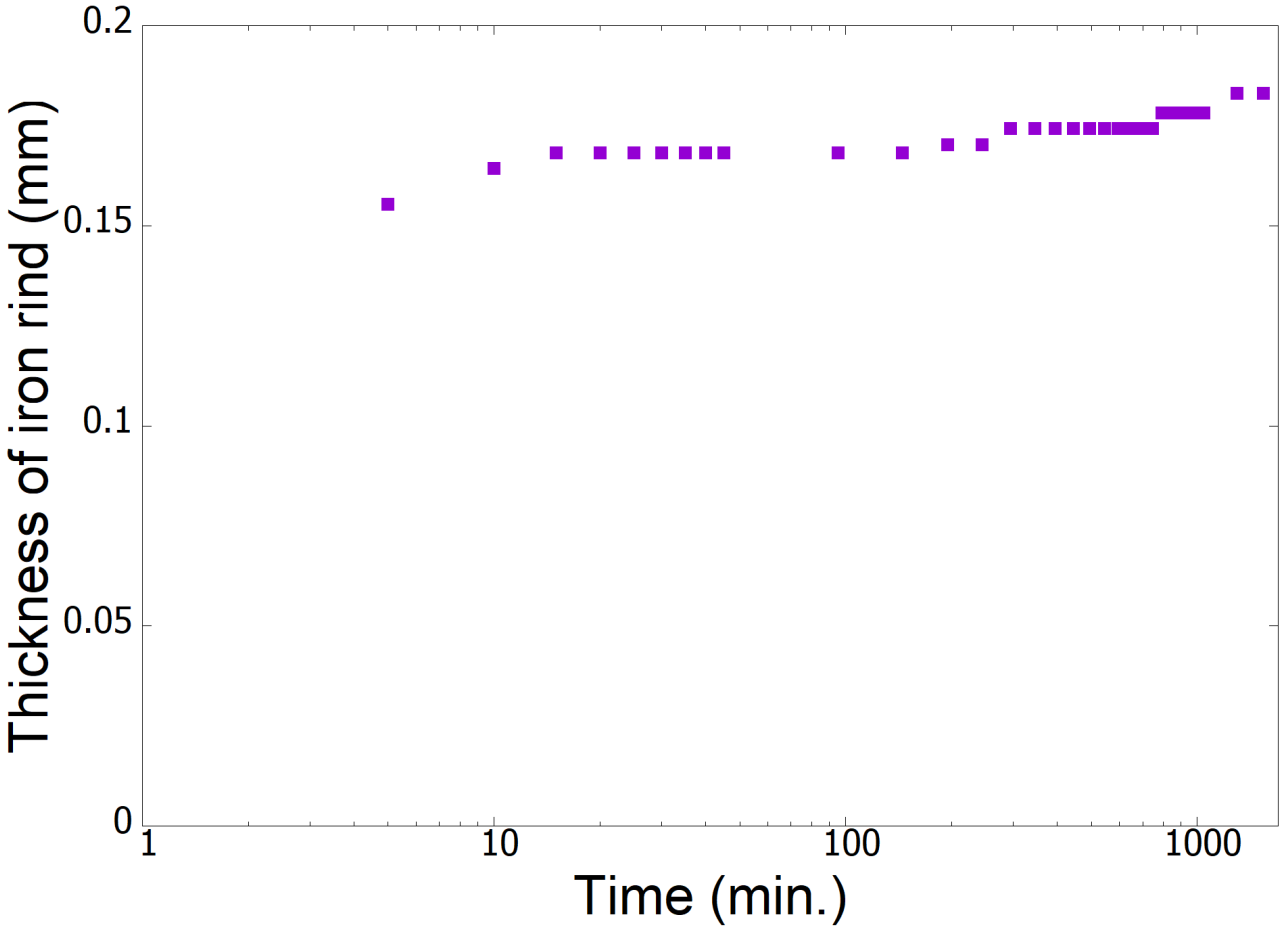
Conclusion

We have succeeded in experimentally photographing the growth of the iron rind over time. As a result, we discovered a new process, " penetration " that was not previously hypothesized. We propose to incorporate the effects of penetration into numerical calculations and formation processes. In the future, we will conduct similar experiments by varying the soil concentration and moisture content. In addition, elemental mapping will be created using SXAM.

References

Yoshida et al., (2018) Fe-oxide concretions formed by interacting with carbonate-acidic waters on Earth and Mars. Sci. Adv. 4:eaau0872. doi:10.1126/sciadv.aau0872

Keywords: Fe-oxide concretion, CaCO3 concretion



©2021. Japan Geoscience Union. All Right Reserved.

Redox change by coseismic water-rock reactions in the interior of planets

*Takehiro Hirose[1], Ryoichi Nakada[1], Keishi Okazaki[1], Takazo Shibuya[1]

1. Japan Agency for Marine-Earth Science and Technology

An earthquake releases elastic energy stored in the planets. The stored energy is dissipated mostly as a heat, which facilitates coseismic water-rock reactions along a fault and eventually changes in redox conditions in the planets. In this study we have reproduced earthquake faulting by laboratory friction experiments and determined redox change within a simulated fault by X-ray absorption near edge structure (XANES) analysis, in order to explore a hypothesis that the coseismic water-rock reactions could provide a potential metabolic energy for life on the planets.

Friction experiments have performed on San Carlos olivine powder with grain sizes of 100~180 μm and on clay-rich décollement materials from the Nankai Trough plate boundary using a rotary shear apparatus at Kochi/JAMSTEC. Earthquake faulting was reproduced at slip velocity of 1.0 m/s with different displacements of 2.6~18 m under normal stress and fluid pressure conditions of 30 and 25 MPa, respectively. After the experiments, the specimens were thin-sectioned to observe microstructures under FE-SEM and to determine how the ($Fe^{2+}/\Sigma Fe$) and ($S^0/\Sigma S$) ratios change with input shear energy by the XANES analyses using the BL27SU at SPring-8.

On the olivine specimen the mean value of $Fe^{2+}/\Sigma Fe$ in the fault zone decreases from 0.68 to 0.59 (i.e. oxidization) as increasing shear energy from 0 to ~34 MJ/m^2. In contrast, on the décollement specimen the $Fe^{2+}/\Sigma Fe$ ratio tends to increase with shear energy from 0.48 at 0 MJ/m^2 (starting material) to 0.51 at ~3.2 MJ/m^2 (i.e. reduction). However, the décollement specimen contains sulfide minerals (S^{-2}) in which the $S^0/\Sigma S$ increases from ~0.3 to 0.09 as increasing shear energy to ~3.2 MJ/m^2 (i.e. oxidization). Thus, both specimens oxidized during rapid coseismic faulting in several seconds. This is likely attributed to the reactions between minerals and water, that is enhanced by the formation of tens-nanometer-size minerals with fresh reactive surfaces by rapid faulting. Particularly in the olivine experiments with high shear energy inputs, frictional heat transforms liquid water into supercritical state, promoting the oxidization reactions. If seismicity in the planets could be monitored, the proposed correlation between the shear energy (equivalent to earthquake magnitude) and the oxidation progress enables us to estimate the quake-induced redox change in the interior of planets.

Keywords: earthquake, redox change, water-rock interaction

©2021. Japan Geoscience Union. All Right Reserved.

Characterizations of mineralogy and infrared spectra of serpentinized samples in Oman ophiolite along with redox gradients in subsurface: Toward identification of redox gradients in Martian subsurface

*Takumi Sato[1], Yasuhito Sekine[1], Ikuo Katayama[2]

1. Tokyo Institute of Technology , 2. Hiroshima University

Mars would have possessed liquid water on the surface, at least temporally, in late Noachian to early Hesperian in a dense CO2 atmosphere. In addition to surface water, groundwater is highly likely to have been abundant and interacted with mafic rocks that consisted of Martian crust. Hydrological cycles between these endmember waters would have generated redox and pH gradients in the subsurface, through vertical mixing of acidic, oxidizing surface water with alkaline, reducing groundwater. On Earth, chemoautotrophic life can live in the redox and pH gradients generated in subsurface. Thus, identifications of redox states of (sub)surface rocks on Mars through remote sensing is critical to select landing sites and to collect promising samples for microbial life in future missions to Mars. In this study, we aim to characterize mineralogical compositions and infrared spectra of serpentinized Semail Ophiolite, Oman, along with redox and pH gradients in the subsurface. Semail Ophiolite consists of basalt, gabbro, and upper mantle ophiolite, which are exposed on the surface. Oxidizing surface water infiltrates into the subsurface where in-situ serpentinization proceeds, generating steep redox and pH gradients. This geohydrological setting allows this area as a promising terrestrial analog of aqueous alterations in particular areas on Mars where ultramafic, olivine-rich rocks are exposed (e.g., Nili Fossae). We used core samples (Hole BA1B) from an area of active serpentinization of the Semail Ophiolite, drilled during the ICDP Expedition 5057 and stored at Hiroshima Univ. SEM-EPMA, XRD, and FTIR analyses were performed for the core samples. Based on mineralogical and chemical compositions of the samples, we classified core samples based on alteration stages. In the stage 1 (160–350 m in depth), samples contain unaltered minerals, e.g., olivine and diopside, and, thus, serpentinization was proceeding. The samples also contain secondary minerals of serpentine and brucite. Water chemistry of pore water at these depth were measured on site previously and reported as alkaline and reducing. The samples in the stage 1 exhibit characteristic steep slopes at 0.8–1.5 μm in infrared reflectance spectra. In the stage 2 (30–100 m in depth), serpentinization has completed without unaltered olivine or diopside. The samples are predominantly composed of serpentine and brucite. According to previous study, water chemistry of pore water was reported as alkaline and moderately oxidizing. The infrared spectra of the stage-2 samples have moderate slopes at 0.8–1.5 μm. In the stage 3 (10–30 m in depth), the samples are composed mainly of serpentine with trace Mg/Fe smectite. Fe(III) oxides appear in veins in the samples. These suggest alterations with high water-to-rock ratio with oxidizing surface water. Pore water was reported as highly oxidizing. The infrared spectra of the stage-3 samples have moderate slopes at 0.8–1.5 μm with absorption features at 1.4 and 1.9 μm owing to smectite. In the stage 4 (< 10 m in depth), the samples contain serpentine together with Mg/Fe smectite, Fe(III) oxides, and carbonate. Owing to the secondary minerals other than serpentine, the color of the samples was whitish red. The infrared spectra of the stage-4 samples have gentle slopes at 0.8–1.5 μm with clear absorption features at 1.4 and 1.9 μm. Our results show that we can distinguish the alteration stages of core samples solely based on infrared features (namely, slope gradient at 0.8–1.5 μm and absorptions at 1.4 and 1.9 μm). According to a previous microbiological study at the Semail Ophiolite site, methanogens and acetogens were found in depth of the stage 1 (and 2). Reflectance spectra features resembling to those of the stage 1 can be found in Nili Fossae regions on Mars, suggesting the importance of this area as a future landing site.

©2021. Japan Geoscience Union. All Right Reserved.

Keywords: Serpentine, Mars, Redox gradients

©2021. Japan Geoscience Union. All Right Reserved.

Experimental study of element dissolution to liquid CO_2 from artificial seawater and hydrothermal vent chimney

*Kaito Seo[1,2], Takazo Shibuya[2], Kosuke Fujishima[3], Ken Takai[2], Masaru Tomita[1,4]

1. Graduate School of Media and Governance, Keio Univ., 2. JAMSTEC, 3. ELSI, 4. IAB, Keio Univ.

Pools of carbon dioxide (CO_2) fluid have been found under the ocean floor in the vicinity of a few hydrothermal vent sites (Sakai et al., 1990; Konno et al., 2006; Lupton et al., 2006; Pedersen et al., 2010; Zhang et al., 2020). CO_2 fluid acts as hydrophobic solvent under a certain range of temperature and pressure due to its non-polar property (Hyatt, 1984). Because various hydrophobic compounds such as organometallic complex, amides, alcohols, carboxylic acids and phenols can dissolve into CO_2 fluid (Š kerget et al., 2011; Knez et al., 2018), the pools of CO2 fluid have the potential to behave as a distribution and condensation field for those compounds. Indeed, Stensland et al., (2019) suggested that heavy metals are transported to shallower part of a water column by upwelling of CO_2 hydrate released from CO_2 pools and hydrothermal vents.

Even in the Hadean ocean, liquid/supercritical CO_2 is presumed to have acted as a solvent for hydrophobic molecules and elements related to origin of life and as a reaction field providing condensation, and as reaction field (Shibuya and Takai, 2017, Zhang et al., 2020). Despite utilization in industrial technologies such as extraction, dry cleaning, and homogenization, particularly in the form of supercritical CO_2 (Beckman, 2004), geochemical roles of CO_2 fluid in natural environments are poorly understood.

In this study, we developed a corrosion-resistant high-pressure reactor and extraction/analytical methods of CO_2 fluid. Then, we experimentally simulated distribution of major elements in artificial seawater and heavy metals included in hydrothermal vent chimney samples to liquid CO_2. As a result, dissolution of major elements; Na, Mg and heavy metals; Cu, Mg, Zn, and etc., were observed from artificial seawater and hydrothermal vent chimneys, respectively. The results suggest that transition metals and the elements in boron group (Al, Ga, In, Tl) form complexes with CO_2. We will further discuss about implications of modern and Hadean hydrothermal systems.

Keywords: liquid CO2, elemental distribution, hydrothermal vent, origin of life, Hadean eon

©2021. Japan Geoscience Union. All Right Reserved.

Rocognition and classification of Martian chaos terrains using imagery marchine learning: Implications for groundwater distribution and hydrological cycles

Hiroki Shozaki[2], *Yasuhito Sekine[1], Nicholas Guttenberg[1]

1. Earth-Life Science Insitute, Tokyo Institute of Technology, 2. Dept. Earth Planetary Sci., Tokyo Institute of Technology

Water activities have played central roles in the environmental evolution on Mars, through creating landforms and secondary minerals, driving geochemical cycles, and possibly supporting life. Knowledge on the distribution and activities of groundwater is critical in the hydrology, the habitability, and in-situ resource utilization for future manned missions. Chaos are fractured depressions that consist of broken blocks and locate on sources of outflow channels. Some of chaos are interpreted to have been formed through outbursts of groundwater triggered by melting of ground ice; thus, they can be clues to understand the distribution and activities of groundwater. On the other hand, other chaos may have been formed through an inflation-deflation of a magma chamber without water activities. A large number of chaos and chaos-like features have been found on Mars. However, the formation mechanisms of these chaos remained uninvestigated.

Here, we perform recognition and classification of chaos based on the formation mechanisms using imagery machine learning. We developed neural network models (i.e., classifiers) to classify chaos formed by water activities (called as water-related chaos), chaos formed by volcano-tectonic activities (called as volcano-tectonic chaos), and non-chaos surface features (e.g., valleys, plains, and craters) using remote-sensing data of chaos previously investigated. Our developed classifiers can recognize chaos and non-chaos surface features with ~97% of test accuracy and can classify water-related chaos and volcano-tectonic chaos with ~95% of test accuracy.
By applying our classifiers to a large number of unclassified chaos, we found two types of chaos terrains on Mars. One is hybrid chaos terrains, in which water-related chaos and volcano-tectonic chaos coexist in one terrain, and the other is water-dominant chaos terrains, in which water-related chaos are predominant. Hybrid chaos terrains are mainly found in the circum-Chryse outflow channels region. Based on our geomorphic analyses, hybrid chaos terrains would have formed through a combination of upwelling of magma and consequent melting of ground ice. The groundwater from the hybrid chaos terrains formed outflow channels and supplied water to water-dominant chaos terrains in the downstream. Water-dominant chaos terrains are mainly located near the dichotomy boundary. The locations of water-dominant chaos terrains coincide with the proposed regions of upwelling of groundwater on ancient Mars. The locations of water-dominant chaos terrains can be potential landing sites for future missions, where frozen ancient groundwater may be available near surface.

Keywords: Mars, hydrological cycles, machine learning

©2021. Japan Geoscience Union. All Right Reserved.

No effective oxychloride formations on Europa's surface inferred from UV/electron irradiation experiments onto salt-ice mixtures

*Shuya Tan[1], Yasuhito Sekine[1], Takashi Kikuchi[2], Hisayuki Suematsu[2], Tetsuya Hama[3], Yoshio Takahashi[4]

1. Earth-Life Science Institute, Tokyo Institute of Technology, 2. Nagaoka University of Technology, 3. Komaba Institute for Science, The University of Tokyo, 4. Department of Earth and Planetary Science, Graduate School of Science, The University of Tokyo

Recent observations of Europa's surface suggest that chlorides (e.g., NaCl, $MgCl_2 \cdot nH_2O$) exist on Europa's geologically active chaos regions (Fischer et al., 2015; Ligier et al. 2016). Europa's surface is irradiated by high-energy particles, such as electrons, and solar UV light. These irradiations would cause the oxidation of surface materials due to dissociation of H_2O ice and subsequent escape of H_2 into space. Through the irradiation, chlorides on the surface could be oxidized to form oxychlorides, such as chlorates (e.g., $Mg(ClO_3)_2 \cdot 6H_2O$) or perchlorates (e.g., $NaClO_4$, $Mg(ClO_4)_2 \cdot 6H_2O$) (e.g., Johnson et al., 2019). However, the oxidation reactions have been poorly investigated based on laboratory experiments.
Here, we perform laboratory experiments to investigate formation of oxychlorides on Europa. We irradiated ~10-keV electron or UV light onto mixtures of H_2O ice and chlorides at temperatures of ~120 K using a newly-developed irradiation experimental system. In addition, we irradiated MeV electron onto mixture of H_2O ice and chlorides using an electron-beam accelerator, ETIGO-III (Tokuchi et al., 1998). Our results show no significant formations of ClO_4 and ClO_3 from chlorides regardless of the experimental conditions. The upper limits of conversion efficiency from NaCl to $NaClO_4$ are estimated in our experiments. The estimated upper limits of conversion efficiency are 10^{-19}–10^{-20} /electron. Considering the upper limits of conversion efficiency, together with the fluxes of electrons or photons on Europa (Paranicas et al., 2009; Clare et al., 2012), an upper limit abundance of $NaClO_4$ are estimated as less than ~2 mol% relative to H_2O ice over Europa's surface age (30–100 Myr). Our experimental results and estimations suggest that oxychlorides are minor components as salts and oxidants on Europa's surface.

Keywords: Europa, Irradiation experiment, Perchlorate

©2021. Japan Geoscience Union. All Right Reserved.

An experimental study on evaporite formation around the north pole of Titan

*Eito Hirai[1,2], Yasuhito Sekine[2], ZHANG NAIZHONG[2]

1. Department of Earth and Planetary Sciences, School of Science, Tokyo Institute of Technology, 2. Earth-Life Science Institute, Tokyo Institute of Technology

Through the Cassini-Huygens mission, 5 μm-bright deposits are found at dried lakebeds and along paleo-shorelines of the north pole regions of Titan, which are inferred as organic evaporites (Barnes et al. 2009, 2011).

Evaporites on Titan can be formed when dissolved organic matter in liquid methane lakes is concentrated and precipitated upon drying (Barnes et al. 2009, 2011). Thus, they could be a proxy indicator of arid climates through effective evaporation of liquid methane. In addition, evaporative condensation promotes syntheses of complex organic molecules on Titan.

The previous study (Cordier et al. 2013) suggested that the main components of evaporites would be acetylene and butane solids based on results of photochemical calculation of precipitation rates of organic solids in Titan atmosphere (Lavvas et al. 2008).

However, spectral features of evaporites resembles to benzene and cyanoacetylene solids, rather than acetylene and butane solids (Clark et al. 2010).

Given that organic aerosols may be composed of PAHs, such as benzene, and nitriles, such as cyanoacetylene, dissolution of benzene and nitriles from organic aerosols by liquid methane could explain the enrichments of these molecules in evaporates on Titan. Nevertheless, there is no experimental study that investigates the solubility of organic aerosol analogs by liquid methane.

Here, we construct laboratory experimental system that can investigate interactions between organic aerosol analogues, called Titan tholin, and liquid methane. We developed a stainless-steel liquid methane generator that can keep liquid methane through controlling temperature inside the chamber. After immersing Titan tholin into liquid methane in the generator, dissolved species in liquid methane are analyzed with a gas chromatograph.

Keywords: Titan, Liquid methane, Evaporites, Organic aerosols, Tholin

©2021. Japan Geoscience Union. All Right Reserved.

Prediction of the composition of the primordial ocean just after its formation

*Hisahiro Ueda[1], Takazo Shibuya[1]

1. JAMSTEC

Hadean is an enigmatic period in the Earth's history when ocean formation and the emergence of life occurred. However, minimal geological evidence is left from this period. Regarding the ocean in the early Earth, previous research indicates that seawater had weak acidity (pH 4–7) because the carbon dioxide concentration in the atmosphere was high compared to that today (e.g., Walker, 1985; Grotzinger and Kasting, 1993; Macleod et al., 1994), or it was strongly acidic (pH 1–2) because a large amount of halogen substance in the high-temperature vapor atmosphere eventually dissolved into seawater (Maruyama et al., 2013). Previously, pH, CO_2 concentrations, and other elements were considered (Morse and Mackenzie, 1988) but these estimations did not provide information about the quantitative chemical compositions of seawater. To understand the primordial ocean's composition, we focused on the ocean's formation processes from CO_2- and HCl-bearing water vapor in the high-temperature atmosphere. When the temperature of the lower atmosphere fell below the critical point, high-temperature rain reached the ground surface. Then, hydrothermal reactions between the subcritical fluid and primordial crust started. Eventually, a liquid ocean emerged on the completely altered crust as the temperature decreased to approximately 25 ˚C until the ocean's temperature stabilized. Here, we conducted two experiments and modeling simulating the reactions between hypothetical primordial crustal rock (basalt or komatiite). The results indicate that the primordial ocean was mildly acidic and rich in CO_2, Mg, and Ca relative to Na, irrespective of the rock type, which is different from the modern equivalents. Therefore, unlike the present seawater, the primordial seawater could have been carbonic, bitter, and harsh rather than salty. The ocean's composition started to evolve once plate tectonics began on Earth.

Keywords: primordial ocean composition, ocean formation, water-rock reactions, Hadean, experiment

©2021. Japan Geoscience Union. All Right Reserved.

Formation conditions of magnetite and hematite in Sheepbed mudstone and bioavailable energies in lake water-groundwater mixing zone in Gale crater, Mars

*Sakiko Kikuchi[1], Takazo Shibuya[1]

1. Japan Agency for Marine-Earth Science and Technology

The Sheepbed mudstone of Yellowknife Bay, Gale crater was interpreted as an ancient habitable environment, based on its detailed mineralogical and geochemical composition analyses. However, the energetic availability for metabolic reactions is poorly constrained. Here, we propose the possible mixing of surface water and groundwater that (i) explains the formation of magnetite and hematite detected in Sheepbed mudstone and (ii) works as a potential habitable zone for aerobic Fe^{2+}-oxidizing microbes. Our thermodynamic modeling of water–rock reactions revealed that the formation of abundant Fe-rich saponite in Sheepbed mudstone may occur under various conditions of water-to-rock mass ratios, temperatures (5–300ºC) and initial fluid compositions (O_2/H_2+CO_2-bearing and gas-free fluids). In contrast, the formation of magnetite and hematite in the mudstone can be explained only by the mixing of Fe^{2+}-rich groundwater and oxygenated surface water, where the Fe^{2+}-rich groundwater can be generated by the low-temperature water–rock reactions with a CO_2-bearing initial fluid. The calculated free energy yield of aerobic Fe^{2+} oxidation in the fluid-mixing zone on Mars is similar to that estimated for a fluid-mixing zone on Earth actually inhabited by aerobic Fe^{2+}-oxidizing microbes. The findings will contribute to a better understanding of potential habitability on Mars.

Keywords: early Mars, saponite, bioavailable energy, water-rock reactions

©2021. Japan Geoscience Union. All Right Reserved.

Measurements of elastic wave velocity of mafic and ultramafic rocks below the freezing point: Consideration about reflectivity due to ice-water phase transition in Mars

*Haruna Wakabayashi[1], Ikuo Katayama[1]

1. Hiroshima University

It has been pointed out that a large amount of water existed on the surface of Mars in the past, and it is expected that life may have existed there. However, Mars is currently dry, with an average surface temperature of about -50 degrees Celsius, so water exists mainly as ice in the ice sheets and the deep underground cryosphere. On the other hand, the gravity of Mars is lower than that of the Earth, and rocks are less compressible. Therefore, Mars retains high porosity deep underground, and a phase transition from ice to water is predicted to occur underground from the heat flow rate. Therefore, in this study, we will measure the elastic wave velocity in the phase transition from ice to water in rocks, and verify whether water in the subsurface can be detected by seismic reflection surveys such as the InSight mission on Mars. Diabase, peridotite, and serpentinite which are considered to be the basement rocks of Mars, were used as samples to measure the elastic wave velocity. Elastic wave measurements were performed under dry, wet, and frozen conditions (-55˚C). In the measurements, the effect of porosity on elastic waves was examined. In order to examine the effect of porosity on elastic waves, thermal cracks were introduced into the samples. The porosity of the diabase was 0.14% at Intact, 0.55% at 600˚C and 1.17% at 800˚C. The porosity of the peridotite was 0.32% at Intact, 1.32% at 600˚C and 1.70% at 800˚C. Elastic wave velocities were calculated using the pulse transmission method by crimping a piezoelectric element with a resonant frequency of 2MHz to the sample. The elastic wave velocities of all rock samples decreased with increasing porosity, and increased as the pores were filled with water, with the highest velocities observed under frozen conditions. The Vp/Vs ratio was also calculated and showed a decreasing trend with increasing porosity in the dry condition, an increasing trend in the wet condition, and constant in the frozen condition. Using these results, the aspect ratio (short axis/major axis) of the voids was estimated from the effective medium theory (Kuster and Toksoz 1974), and the crack with aspect ratio of 0.01 is consistent with the experimental data. Using the results of this velocity measurement, we calculated the acoustic impedance and calculated the reflectivity at 5 km underground, where the ice-water phase transition is predicted to occur in the Martian subsurface. As a result, the reflectivity at the ice-water phase transition was 0.269 for diabase and 0.319 for peridotite. Thus, when the phase transition from ice to water occurs, high seismic wave reflectance is expected, and future seismic surveys on Mars may reveal the existence of water.

Keywords: Mars, Elastic wave velocity, Aspect ratio

©2021. Japan Geoscience Union. All Right Reserved.

Viscosity of aqueous MgSO4 solutions at high-pressure and low-temperature: implications for icy satellites

*Shunsuke Nozaki[1], Seiji Kamada[2,3], Akio Suzuki[2]

1. Division of Earth and Planetary Materials Science, Faculty of Science, Tohoku University , 2. Department of Earth Science, Graduate School of Science, Tohoku University, 3. Frontier Research Institute for Interdisciplinary Sciences, Tohoku University

Some icy satellites, such as Europa, Ganymede, Enceladus, and Titan, have a subsurface ocean under the thick crusts. Though transport properties are essential to discuss the fluid behavior in these subsurface oceans, there are few viscosity data within P-T conditions corresponding to the ocean. Because fluid viscosity is dependent on temperature, pressure, and concentration, understanding these relationships leads to a more accurate view of the subsurface ocean.

The viscosity data of 10 wt% aqueous magnesium sulfate solutions were measured using a diamond anvil cell (DAC). The solutions' viscosity was determined up to 1100 MPa in the temperature range from −10 to 40˚C from the falling sphere measurements with DAC by constructing apparatus with a rotating stage, microscope, and camera. The pressure was measured using the ruby fluorescence method (Piermarini et al., 1975), while the temperature was controlled by flowing cooling or warming water through the DAC. The obtained viscosity was in the range of 1−10 mPa s and showed high pressure dependence of viscosity as well as temperature-dependence. Assuming that the subsurface ocean is composed of 10 wt% magnesium sulfate and satisfies the high-pressure and low-temperature conditions of the ocean, the ocean's dynamic viscosity would be in the range from 1 to 10 mPa s in the pressure condition below 700 MPa, which is higher than the viscosity of Earth's seawater. Because viscosity affects convection, diffusion rate, chemical reaction rate, and flowing velocity through the seafloor, this property might change the predicted habitability and oceanic composition.

Keywords: Icy satellites, Subsurface ocean, Viscosity, Aqueous magnesium sulfate solution, Diamond anvil cell

©2021. Japan Geoscience Union. All Right Reserved.

Formation mechanism of spherical concretions in Tatsukushi area: Possible analogy with spherical nodule in Gale crater, Mars

*Saki Asai[1], Hitoshi Hasegawa[1], Hidekazu Yoshida[2], Minoru Ikehara[1], Nagayoshi Katsuta[3], Masakazu Nara[1], Yui Tomonao[1], Satoru Imai[4]

1. Kochi University, 2. Nagoya University, 3. Gifu University, 4. Tosashimizu GeoPark

On Earth, spherical carbonate ($CaCO_3$) concretions are widely recognized. Many of these concretions are centered on fossils, and thought to be formed by decaying of soft body organic matter as carbon source. On the other hand, carbonate concretions are also formed by inorganic precipitation of calcite-saturated groundwater in arid environment. In addition, Fe-oxide encrusted concretions are found both on Earth (Utah and Mongolia) and Mars (Meridiani Planum). Yoshida et al. (2018) proposed that Martian Fe-oxide concretions are formed by dissolution of pre-existing carbonate concretions. They further suggested that spherical-shaped nodules in Gale crater can also formed by similar process, although shape and size of the Gale nodules are more variable. Here we report that spherical and variable-shaped concretions in Tatsukushi area, western Kochi, whose shapes are resembling to Gale nodules. In order to understand formation mechanisms of concretions in Tatsukushi area, we performed analyses of X-ray CT scan, elemental mapping, and stable carbon and oxygen isotope on samples of variable shapes of concretion. The results reveal that large-sized spherical-shaped concretion can be formed by organic matter origin. In this presentation, we will discuss the similarity of both concretions in Tatuskushi area and Gale crater.

Reference

Yoshida, H., Hasegawa, H., et al. (2018). Fe-oxide concretions formed by interacting carbonate and acidic waters on Earth and Mars. *Science advances*, *4*(12), eaau0872.

Keywords: spherical concretion, organic matter origin, carbon isotope, Mars, Gale crater

©2021. Japan Geoscience Union. All Right Reserved.

Synthesis and reversible redox properties of iron-saponite

*Hiroshi Sakuma[1], Koki Morida[2], Keisuke Fukushi[2], Yoshio Takahashi[3], Natsumi Noda[3,4], Yasuhito Sekine[4], Kenji Tamura[1]

1. National Institute for Materials Science, 2. Kanazawa University, 3. University of Tokyo, 4. Tokyo Institute of Technology

Clay minerals widely distribute on the surface of Mars. In these clay minerals, (Fe,Mg)-smectites were commonly discovered and useful for understanding the history of Mars. The valence state of iron in smectite is one of the key properties to reveal the redox state at the smectite formation. It has been believed that the redox state can be revealed from the crystal structures of iron-rich smectite. In the smectite, ferrous (Fe^{2+}) ions fully occupy the octahedral sites, while the ferric (Fe^{3+}) can occupy only two third of the sites due to the charge balance. This difference should be identified from the X-ray diffraction (XRD) profile. From the XRD analysis, ferrous saponite can be an analogue of smectites discovered at Yellowknife Bay in Gale Crater [Chemtob *et al.*, 2015]. However, the natural iron saponite on the Earth can also explain the XRD pattern and surprisingly the most iron was characterized by ferric (Fe^{3+}) state [Treiman *et al.*, 2014]. A central question is whether the XRD analysis can provide the oxidation state on formation of smectite.

A hypothesis was proposed for the crystal structure of ferric iron-rich saponite [Treiman *et al.*, 2014]. The saponite was initially synthesized under reduced conditions and oxidized later. The oxidation may occur by the deprotonation from structural OH groups. If this is correct, the oxidation and reduction can occur reversibly without large deformation in the crystal structure. In this study, the reduction and oxidation of ferrian (ferric iron-rich) saponite were investigated to study the hypothesis.

Ferrian saponite was synthesized by the hydrothermal method similar to the method proposed for the synthesis of ferrous saponite [Baldermann *et al.*, 2014]. The precipitates were dispersed in ultrapure water for one to five days. These samples were analyzed by inductively coupled plasma optical emission spectrometry (ICP-OES), humidity-controlled X-ray diffraction (XRD), transmission electron microscopy (TEM), X-ray absorption fine structure (XAFS), and infrared spectroscopy.

The chemical composition of precipitates and their swelling behavior indicate that the precipitates are smectite. The crystal structure of synthesized samples is categorized to trioctahedral smectite which is characteristic to ferrous saponite, but the XANES and TEM-electron energy loss spectroscopy (EELS) analysis indicates that most iron is present as ferric iron. These results indicate that the smectite is ferrian saponite. The reduction treatment was conducted for the ferrian saponite for one hour. There is no difference in the XRD profile before and after the treatment, but about 40% of ferric ion was reduced to ferrous ion in the saponite. This reduction may be interpreted by the exchange of hydrogen in the crystal as proposed for the formation mechanism of natural ferrian saponite [Treiman *et al.*, 2014].

Our results indicate that the ferrian saponite preserves the oxidation state on formation in the crystal structure, and the redox state of iron ions can be changed without deformation in the structure.

References

©2021. Japan Geoscience Union. All Right Reserved.

A. Baldermann, R. Dohrmann, S. Kaufhold, C. Nickel, I. Leftofsky-Papst, M. Dietzel, *Clay Minerals*, (2014) **49**, 391-415.

S. M. Chemtob, R. D. Nickerson, R. V. Morris, D. G. Agresti, J. G. Gatalano, *J. Geophys. Res. Planets*, (2015) **120**, 1119-1140.

A. H. Treiman *et al.*, *Am. Mineral.*, (2014) **99**, 2234-2250.

Keywords: Smectite, Mars, Iron, Redox

©2021. Japan Geoscience Union. All Right Reserved.

Physical dependence of stable carbon and hydrogen isotopic ratio of methane gas in gas hydrate

*Kushi Kudo[1], Atsushi Tani[1], Keita Yamada[2], Naohiro Yoshida[3]

1. Graduate School of Human Development and Environment, Kobe University, 2. Department of Chemical Science and Engineering, School of Materials and Chemical Technology, Tokyo Institute of Technology, 3. Earth–Life Science Institute

Icy satellites have capability of having extra biota due to eruption of plume, which is consisted by sea ice particles including organic matter. The observation using Cassini clarified that this plume included hydrogen molecule (H_2), CO_2, methane (CH_4) and organic matter (e.g. Porco et al. 2006; Waite et al. 2006, 2009, 2017). Especially in plume gas species, methane (CH_4) is regarded as one of the candidate of signature of biological activity due to CH_4 formation reaction by methanogen. However, CH_4 gas in plume is consisted of not only microbial origin but also primitive and/or hydrothermal origin and this fact does not let CH_4 detection is sufficient for conclusion for existence of biological activity by microbe. Therefore, we consider that evaluation of the elementary process of CH_4 isotopic fractionation ($\delta^{13}C$ and δD of CH_4) via room experiment is important for isotopic observation of icy satellite in nearly future.

In this study, we focus on CH_4 hydrate which is reservoir to produce the plume (Kieffer et al. 2006; Kamata et al. 2019) and plan to evaluate isotopic fractionation with its formation. Isotopic fractionation with hydrate formation has been found at only δD of CH_4(liquid_water+CH_4: ~5‰; ice+CH_4: ~10‰) (P: 0–6 MPa) (Hachikubo et al. 2007; Lapham et al. 2012). In the case of condition of icy satellites, the pressure range is wider than of the Earth, and therefore we need to estimate isotopic fractionation.

We formed clathrate hydrate samples using hydrate formation equipment under the extreme environments, which can hold until 50 MPa. We lowered cell temperature from room temperature to 276 K, and then stirred CH_4 gas and pure water at 85 or 400 RPM stirring rotation speed to form hydrate sample. We inserted CH_4 gas at slightly higher pressure than the previous studies (4.4–9.7 MPa). We collected gas samples of primitive gas from CH_4 gas cylinder and remained gas samples from the high pressure cell after hydrate formation, and then we measured stable isotopic ratio ($\delta^{13}C$ and δD of CH_4) using GC-IRMS equipment. We used the working standard with $\delta^{13}C$ = –48.17‰ and δD = –178‰ for isotopic measurement. Precision of $\delta^{13}C$ and δD value were estimated as 0.3‰ (n = 6, 1 σ) and 0.7‰ (n = 4, 1 σ), respectively, which were based on repeated analyses of the standards.

Results in isotopic measurements showed that the $\delta^{13}C$ value of remained gas phase was slight lower than of primitive gas phases ($|\varepsilon|$ ~1‰, which was almost same as a few previous studies) and became lower at higher pressure. This suggested that 1) $^{13}CH_4$ and $^{12}CH_4$ easily condensed into gas phase in hydrate and remained gas phase with clathrate hydrate formation, respectively, and 2) this condensation became stronger at higher pressure. On the other hand, results in the δD value of remained gas phase maximized at around 6–7 [MPa] (theoretical value). Hachikubo et al. (2007) reported that δD value of hydrate phase became lower than those of remained and primitive gas, and host–guest interaction did not cause the isotopic fractionation of δD. Furthermore, Casco et al. 2015 reported that CH_4 adsorption ratio and hydrate formation speed rapidly increased from 6 to 8 [MPa]. Above results and previous studies might suggest that isotopic fractionation of δD with hydrate formation was not caused by water molecule of host cage and CH_4 molecule, which had only H atom, was most easily taken at 6–7 [MPa]. Furthermore, results of remained gas phase showed that the $\delta^{13}C$ value and pressure of theoretical δD maxima

©2021. Japan Geoscience Union. All Right Reserved.

became lower at faster stirring rotation speed ($\delta^{13}C$ value at 85 and 400 [RPM]: $p < 0.05$, $n = 8$; pressure of theoretical δD maxima: 7.1 and 5.7 [MPa] at 85 and 400 [RPM], respectively). Since Wijayanti (2018) reported that stability and storage capacity of hydrate became higher at higher stirring rotation speed. Thus, above tendencies and previous study might suggest that faster stirring rotation speed caused stronger hydrate stability due to easiness of ^{13}C adsorption, and most easiness statement of only H atom having CH_4molecule adsorption easily occurred at lower pressure.

Therefore, we found that physical condition such as pressure and stirring rotation speed, which was concerned to flow velocity of internal ocean, might become important factor of effect of gas hydrate formation at icy satellites condition on transportation and release processes of CH_4 gas.

Keywords: gas hydrate, methane gas, icy satellite, stable isotope, isotopic fractionation, physical dependence

©2021. Japan Geoscience Union. All Right Reserved.

Clumped isotope signatures of abiotic methane formed via Fischer-Tropsch catalysis and their implications

*ZHANG NAIZHONG[1], Yasuhito Sekine[1], Mayuko Nakagawa[1], Naohiro Yoshida[1]

1. Tokyo Institute of Technology

Abiotic CH_4 has been widely observed in nature, such as in hydrothermal vents, springs and so on. However, our knowledge on pathways of their formation remains pool. The bulk isotopic compositions of CH_4, such as $\delta^{13}C$ and δD, are widely used as tracers for identifying the CH_4 formation processes. However, obvious defects are existent, such as partly overlapping of isotopic signatures for different CH_4 sources, difficulty in constraining CH_4 generated from two or more sources, suffering from post-processes and so on (Douglas et al., 2017). Very recently, CH_4 clumped isotope signatures have been regarded as helpful constraints to provide additional information on origins of natural CH_4 (e.g. Douglas et al., 2017; Young et al., 2017).

The clumped isotope refers to molecules substituted by two or more rare stable isotopes, e.g. $^{13}CH_3D$ and $^{12}CH_2D_2$, whose abundance relative to a random distribution is temperature dependent (Stolper et al., 2014). Therefore, the formation or bond reordering temperatures of CH_4 can be obtained if the clumped isotope signatures are presented at intra-species equilibrium. On the other hand, kinetic effect and secondary processes like mixing and diffusion, will introduce disequilibrium values, which can be used in identifying specific process/mechanism (Stolper et al., 2015; Young et al., 2017). Limited data derived from abiotic CH_4 synthesized by ruthenium (Ru) so far presented strongly depleted signals in both $\Delta^{13}CH_3D$ and $\Delta^{12}CH_2D_2$, and the mechanism has been explained by quantum tunneling effect, combinatory effect and/or kinetic effect (Young et al., 2017; Cao et al., 2019; Young, 2019). Nonetheless, a recent study on abiotic CH_4 samples from hydrothermal systems suggested near-equilibrium clumped signals, being attributed to bond reordering at local fluid temperatures (Labidi et al, 2020).

In this study, we will present the clumped isotopic signatures of laboratory produced abiotic CH_4 via series of gaseous FTT reactions, applying various experimental parameters and catalysts, such as Ni, Fe, Ru and Co. Both $\Delta^{13}CH_3D$ and $\Delta^{12}CH_2D_2$ values are analyzed by a 253 Ultra High Resolution Isotope Ratio Mass Spectrometer established in Earth-Life Science Institute (ELSI), Tokyo Institute of Technology, following the similar procedures described in Eldridge et al. (2019). Preliminary data presented similar depleted signal in $\Delta^{12}CH_2D_2$, both for Ni and Ru catalyzing reactions at 300-400 ˚C. The mechanism causing depleted clumped values in laboratory produced abiotic methane will be discussed based on our new results, as well as its implication in the natural abiotic CH_4 samples.

References: Douglas et al., 2017, Organic Chemistry; Eldridge et al., 2019, ACS Earth Space Chem.; Stolper et al., 2014, Geochim. Cosmochim. Acta.; Stolper et al., 2015, Geochim. Cosmochim. Acta.; Wang et al., 2018, Geochim. Cosmochim. Acta.; Young et al., 2017, Geochim. Cosmochim. Acta.; Cao et al., 2019, Geochim. Cosmochim. Acta; Young, 2019, Deep Carbon; Past to Present; Labidi et al., 2020, Geochim. Cosmochim. Acta

Keywords: Methane, Isotope, Clumped isotope

©2021. Japan Geoscience Union. All Right Reserved.

Possibilities of the rubidium stable isotope ratio as geochemical tools

*Rimi Konagaya[1], Hiroyuki Tsuboi[1], Takaaki Itai[1], Yoshio Takahashi[1]

1. The University of Tokyo

One of important aspects of molecular geochemistry is to develop new isotope tools of various processes by focusing on physico-chemical properties of elements from their atomic scales. There have been no studies so far on the isotope fractionation of rubidium (Rb) caused by Rb behavior during water-rock interaction, possibly due to general knowledge that the reactivity of Rb^+, or alkaline metal ion, is very low. This is not the case, however, if we think about its interaction with phyllosilicates. It has been clarified that cesium (Cs) is adsorbed on 2:1 type phyllosilicates as inner-sphere (IS) complex by analyzing extended X-ray absorption fine structure (EXAFS). It is considered that the specific adsorption structure is caused by the ionic radius of Cs. Therefore, it was predicted that Rb which is close to Cs in terms of ionic radius also forms IS complex on phyllosilicates. Therefore, in this study, it was aimed to clarify whether the concentration and isotopic ratio of Rb change by the formation of IS complex to phyllosilicate. Rb^+ was adsorbed on vermiculite, montmorillonite, and illite under various pH and ionic strength conditions, and the adsorption structure was analyzed by EXAFS. For comparison, the same experiment was carried out for the strongly acidic cation-exchange resin (SCR). After these adsorption experiments, Rb stable isotope ratios ($^{87}Rb/^{85}Rb$) in liquid and solid phases were measured with a multi-collector type inductively coupled plasma mass spectrometry (MC-ICP-MS) and the degree of the isotope fractionations were analyzed. The host phase of Rb^+ in marine sediment in the Pacific Ocean and the standard rock samples were also analyzed with EXAFS and their Rb stable isotope ratios were measured with MC-ICP-MS. In addition, dissolved Rb^+ and Rb^+ in suspended particles in river water samples collected in the Tone River were also analyzed with EXAFS and their Rb stable isotope ratios were measured with MC-ICP-MS. In this study, it was verified experimentally that Rb forms IS complexes in specific phyllosilicates (vermiculite and illite) and Rb stable isotope fractionation occurs during its adsorption. The lighter isotope (^{85}Rb) was concentrated in the solid phases in this isotope fractionation. On the other hand, Rb was mainly adsorbed as outer-sphere complexes in montmorillonite and strongly acidic cation-exchange resin, and the isotope fractionations were small. These results showed that the fractionation was clearly observed for the adsorption system with formation of IS complex (vermiculate and illite). EXAFS analysis also revealed that Rb in sedimentary rocks is also dominated by IS complexes with phyllosilicates. In the ocean system, it was revealed that the fractionation has occurred between marine sediment and seawater. The lighter isotope was concentrated in the solid phases in these systems. Hence, the Rb isotope fractionation observed in the laboratory experiments was also found in the marine environment. However, the mean Rb isotope ratio of seawater-marine sediments is significantly higher than the crustal average, suggesting that the Rb isotope ratio is higher in rivers before its inflow into the ocean. Actually, $\delta^{87}Rb$ of the Tone River water was fractionated between dissolved and suspended particle phases and this fractionation was consistent with the fractionation observed in the laboratory experiments for illite and vermiculite. Finally, $\delta^{87}Rb$ of seawater and marine sediment can be explained by considering adsorption reaction on phyllosilicates in both rivers and oceans in this study. Also, Illite and smectite are typical clay minerals in pelagic sediments, and these minerals are also ubiquitous in planetary materials such as meteorites. Therefore, I proposed that possible geochemical applications of the $^{87}Rb/^{85}Rb$ isotope ratio can be estimation of the record of sea water fluctuation and water-rock ratio. It has now been widely recognized that various planets had initially water, and the water-rock ratio is important for the study on the evolution of planets and asteroids within the solar system. Measurement of Rb isotope in clay minerals in meteorites and halite, which represents Rb remaining aqueous phase, may provide constraints on the water-rock

©2021. Japan Geoscience Union. All Right Reserved.

ratios in the parent body of the meteorites. If this method can be applied to the “Ryugu” return sample provided by the spacecraft “Hayabusa2”, it can be used to estimate the water-rock ratio of the parent body.

Keywords: rubidium, stable isotope, clay mineral, geochemistry

©2021. Japan Geoscience Union. All Right Reserved.

Determination method of ^{13}C-labeled isotopomer ratio of dissolved organic acids by GC-MS analysis

*Konomi Suda[1]

1. National Institute of Advanced Industrial Science and Technology

Organic acids, especially formic acid and acetic acid, have been predicted to form abiotically from inorganic precursors under certain aqueous conditions (e.g., McCollom, 2013, *Reviews in Mineralogy & Geochemistry* 75: pp. 467-494; Preiner et al., 2020, *Nature ecology & evolution* 4.4: pp. 534-542). Stable isotope tracers are powerful tool for visualizing a specific reaction pathway and distinguishing between experimental products and contamination. Laboratory experiments with stable-isotopically labeled starting materials require the determination of isotope enrichment of product materials. Gas chromatography-Mass spectrometry (GC-MS) technique with direct injection of aqueous sample has been a simple and rapid method for determining the isotope enrichment of underivatized acetic acid (Mulat and Feilberg, 2015, *Talanta* 143: pp. 56-63). However, the applicability of ^{13}C-tracer analysis by GC-MS to formic acid has still not been investigated adequately. Furthermore, the previous calculation method which estimates the ^{13}C-labeled mass isotopomer ratio of acetic acid by using ion intensities of m/z 60, 61 and 62 (Mulat and Feilberg, 2015) cannot distinguish between two kinds of singly labeled isotopomers, i.e., $CH_3{}^{13}COOH$ and $^{13}CH_3COOH$. In this study, I investigate a determination method for ^{13}C-labeled isotopomer ratio of formic acid and acetic acid in aqueous solution by using GC-MS data. Standard solutions were prepared from sodium formate and sodium acetate reagents. The unlabeled sodium salts with natural isotope abundance were purchased from Sigma-Aldrich. The ^{13}C-labeled sodium salts, which were artificially enriched in ^{13}C atom in some specific position with isotopic purity of 99%, were purchased from Cambridge Isotope Laboratories, Inc. Pure standard solutions (50 to 1000 μmol/L) were individually prepared; unlabeled formic acid (HCOOH), labeled formic acid ($H^{13}COOH$), unlabeled acetic acid (CH_3COOH), singly labeled acetic acids ($CH_3{}^{13}COOH$ and $^{13}CH_3COOH$) and doubly labeled acetic acid ($^{13}CH_3{}^{13}COOH$). Then, mixture solutions in which two or more isotopomers presented were prepared by mixing of these pure standards. The aqueous samples were analyzed by GC-MS (7890B gas chromatograph and 5977B mass spectrometer, Agilent Technologies) which was placed at the dedicated analysis laboratory for samples labeled with heavy stable isotopes such as ^{2}H, ^{13}C and ^{15}N…etc. in the Geomicrobiology Research Group (Geological Survey of Japan, AIST). Prior to direct injection of aqueous sample into the GC-MS system, sample was acidified to about pH 2 with phosphoric acid to improve peak sharpness and reduce ghost peaks (Pind et al., 2003, *Biotechnology and Bioengineering* 82: pp. 791-801; Mulat and Feilberg, 2015). Dissolved formic acid and acetic acid were detected with good peak sharpness at minimum concentration of 50 μmol/L and 4 μmol/L, respectively.
In this presentation, I will report the following results and discussions.
- Comparison of results from different data acquisition modes to assess the optimal GC-MS configuration; Profile mode vs. Selected Ion Monitoring (SIM) mode.
- Effectiveness assessment of new calculation approach by least-square method with GC-MS data for determining each mixing ratio of ^{13}C isotopomeric tracers of formic acid and acetic acid.

Keywords: GC-MS, Stable isotope tracer, 13C-label, Acetic acid, Formic acid

©2021. Japan Geoscience Union. All Right Reserved.

Selectivity coefficient of Na^+-NH_4^+ exchange in saponite interlayer: Reconstruction of ammonium concentration in early ocean on Ceres

*Hiroto Tokumon[1], Keisuke Fukushi[2], Yasuhito Sekine[3], Kosuke Inoue[1], Koki Morida[1]

1. Kanazawa University , 2. Institute of Nature and Environmental Technology Kanazawa University, 3. Tokyo institute of technology

Recent space explorations have revealed the existence of a subsurface ocean in early Ceres due to the melting of ice components by the decay heat of short-lived radionuclides. NASA's Dawn survey has also revealed the existence of ammonium-type saponite containing ammonium ions in the interlayer on Ceres. Recent theories of solar system formation as known as the Grand Tuck Model (Walsh et al., 2011) suggest that during the planet-forming period when protoplanets existed, large-scale mass transfer may have occurred as the orbits of gas giant planets such as Jupiter and Saturn evolved. Ceres may have been transported from a distant location to its present position by the migration of these gas giants. If we can estimate the ammonium concentration in the early ocean on Ceres, we can determine whether the location of early Ceres was outside of the ammonia snow line or not. Currently, a geochemical model has been developed that can reconstruct the chemical properties of water with the clay mineral smectite. The model can estimate the cation concentrations in ancient liquid water from the cation composition in smectite via selectivity coefficients of relevant cation. However, the Na^+-NH_4^+ selection coefficient of saponite, which is essential to reconstruct the water quality of the early Ceres' ocean, has not yet been estimated. In this study, we aim to quantitatively estimate the Na^+-NH_4^+ selection coefficient of saponite. Furthermore, from the obtained selection coefficients, we re-examine the water quality of the early Ceres' ocean as reported by De Sanctis et al. (2020).

Keywords: Saponite, Selectivity coefficient, Ceres

©2021. Japan Geoscience Union. All Right Reserved.

[J] Oral | M (Multidisciplinary and Interdisciplinary)：M-IS Intersection

Sat. Jun 5, 2021 9:00 AM - 10:30 AM JST | Sat. Jun 5, 2021 12:00 AM - 1:30 AM UTC | Ch.26 Zoom Room 26

[M-IS16] Paleoclimatology and paleoceanography

convener:Yusuke Okazaki(Department of Earth and Planetary Sciences, Graduate School of Science, Kyushu University), Hitoshi Hasegawa(Faculty of Science and Technology, Kochi University), Atsuko Yamazaki(Faculty of Science, Kyushu University), Akitomo Yamamoto(Japan Agency for Marine-Earth Science and TechnologyAtmosphere and Ocean Research Institute), Chairperson:Akitomo Yamamoto(Japan Agency for Marine-Earth Science and TechnologyAtmosphere and Ocean Research Institute)

Past environmental changes and events at interannual to tectonic timescale toward an understanding of Earth climate system by an integration of terrestrial and marine proxy studies and numerical modeling will be discussed. At JpGU2021, a series of presentations on "high-resolution" paleo data and model studies will be held. We welcome a variety of paleo-environmental studies from a wide range of background. We hope that this session will provide an opportunity to promote communication between participants from multidisciplinary field.

9:00 AM - 9:15 AM JST | 12:00 AM - 12:15 AM UTC

[MIS16-11] **Reconstruction of the ice sheet history since the Last Glacial Maximum based on field-based geomorphological observations and surface exposure ages along the southern Soya Coast, Lützow-Holm Bay, East Antarctica**

*Moto Kawamata[1], Yusuke Suganuma[2,1], Koichiro Doi[2,1], Keiji Misawa[2,1], Motohiro Hirabayashi[2], Akihisa Hattori[1], Takanobu Sawagaki[3] (1.Department of Polar Science, School of Multidisciplinary Science, SOKENDAI (The Graduate Unversity for Advanced Studies), 2.National Institute of Polar Research, 3.Hosei University)

9:15 AM - 9:30 AM JST | 12:15 AM - 12:30 AM UTC

[MIS16-12] Characteristic of radiocarbon dates in response to sea-level changes in the Bonaparte Gulf, Northwestern Australia

*Takeshige Ishiwa[1,2,3], Yusuke Yokoyama[2,3,4], Stephen Obrochta[5], Katsuto Uehara[6], Jun'ichi Okuno[1,7], Minoru Ikehara[8], Yosuke Miyairi[2] (1.National Institute of Polar Research, 2.Atmosphere and Ocean Research Institute, The University of Tokyo, 3.Department of Earth and Planetary Science, Graduate School of Science, The University of Tokyo, 4.Japan Agency for Marine-Earth Science and Technology, 5.Graduate School of International Resource Science, Akita University, 6.Research Institute for Applied Mechanics, Kyushu University, 7.Department of Polar Research Science, School of Multidisciplinary Science, The Graduate University for Advanced Studies (SOKENDAI), 8.Center for Advanced Marine Core Research, Kochi University)

9:30 AM - 9:45 AM JST | 12:30 AM - 12:45 AM UTC

[MIS16-13] Wind-wave changes in Tokyo Bay during the Holocene: impact of sea-level change and land configuration

*Katsuto Uehara[1] (1.Kyushu University)

9:45 AM - 10:00 AM JST | 12:45 AM - 1:00 AM UTC

[MIS16-14] Reconstruction of organic matter inflow fluctuations from the Bolling-Allerod interstadial to Late Holocene using Lake Baikal sediments

*Keiko Takehara[1], Masatoshi Nakakuni[2], Shuichi Yamamoto[3] (1.Kochi university Graduate School of Integrated Arts and Sciences, 2.Faculty of Agriculture, Kagawa University, 3.Department of Environmental Engineering for Symbiosis, Graduate School of Engineering, Soka University)

10:00 AM - 10:15 AM JST | 1:00 AM - 1:15 AM UTC

[MIS16-15] Reconstruction of Early Pleistocene sea-surface temperature in the Northwestern Pacific Ocean based on calcareous microfossils

*Daisuke Kuwano[1], Yuki Tsuchiya[2], Yuma Oura[1], Hiroki Hayashi[3], Yoshimi Kubota[4], Kanako Mantoku[5], Koji Kameo[1] (1.Chiba University, 2.Nagoya University, 3.Shimane University, 4.National Museum of Nature and Science, 5.National Institute for Environmental Studies)

10:15 AM - 10:30 AM JST | 1:15 AM - 1:30 AM UTC

[MIS16-16] Variation of the North Pacific Ocean circulation during the Late Pleistocene glacial-interglacial cycles

*Furukawa Keisuke[1], Osamu Seki[1], Masanobu Yamamoto[1], Tomohisa Irino[1] (1.Hokkaido University)

Reconstruction of the ice sheet history since the Last Glacial Maximum based on field-based geomorphological observations and surface exposure ages along the southern Soya Coast, Lützow-Holm Bay, East Antarctica

*Moto Kawamata[1], Yusuke Suganuma[2,1], Koichiro Doi[2,1], Keiji Misawa[2,1], Motohiro Hirabayashi[2], Akihisa Hattori[1], Takanobu Sawagaki[3]

1. Department of Polar Science, School of Multidisciplinary Science, SOKENDAI (The Graduate Unversity for Advanced Studies), 2. National Institute of Polar Research, 3. Hosei University

The thinning and retreat history of the East Antarctic Ice Sheet (EAIS) since the Last Glacial Maximum (LGM) is essential for understanding the mechanisms and drivers of the large-scale and potentially non-linear (abrupt) response of the ice sheet melting. Such information is needed to assess and capture the key process enacting of abrupt deglaciation over this century and beyond for the future prediction. However, a detailed reconstruction of the history of the EAIS involving changes in its thickness and lateral extent since the LGM remains sparse. Here, we show a new detailed ice sheet history from the southern Soya Coast, Lützow-Holm Bay, East Antarctica, based on field-based geomorphological observations and surface exposure ages. Our results demonstrate that the ice sheet completely covered the highest peak of Skarvsnes (400 m a.s.l.) prior to ~9 ka and retreated eastward by at least 10 km during the Early to Mid-Holocene (ca. 9 to 6 ka). The timing of the abrupt ice-sheet thinning and retreat is consistent with the intrusion of modified Circumpolar Deep Water into deep submarine valleys in Lützow-Holm Bay, as inferred from fossil foraminifera records of marine sediment cores. Thus, we propose that the process of marine ice-sheet instability and ocean-driven melting most likely cause the abrupt thinning and retreat of the EAIS along the southern Soya Coast since the LGM. Such abrupt ice-sheet thinning and retreat with similar magnitude and timing have also been reported from an outlet glacier from Enderby Land, East Antarctica. This geological evidence emphasizes the importance of understanding paleo ice-sheet changes based on geological and geomorphological study not only in West Antarctica but also in East Antarctica to predict potential ice mass loss areas associated with the ocean–ice-sheet interactions in the future.

Keywords: East Antarctic Ice Sheet, Glacial geomorphology, Surface exposure dating, Marine ice-sheet instability, Ice sheet history

©2021. Japan Geoscience Union. All Right Reserved.

Characteristic of radiocarbon dates in response to sea-level changes in the Bonaparte Gulf, Northwestern Australia

*Takeshige Ishiwa[1,2,3], Yusuke Yokoyama[2,3,4], Stephen Obrochta[5], Katsuto Uehara[6], Jun'ichi Okuno[1,7], Minoru Ikehara[8], Yosuke Miyairi[2]

1. National Institute of Polar Research, 2. Atmosphere and Ocean Research Institute, The University of Tokyo, 3. Department of Earth and Planetary Science, Graduate School of Science, The University of Tokyo, 4. Japan Agency for Marine-Earth Science and Technology, 5. Graduate School of International Resource Science, Akita University, 6. Research Institute for Applied Mechanics, Kyushu University, 7. Department of Polar Research Science, School of Multidisciplinary Science, The Graduate University for Advanced Studies (SOKENDAI), 8. Center for Advanced Marine Core Research, Kochi University

Radiocarbon dating is an essential method for constraining Late Quaternary age models and applied to carbon-containing materials. Past climate and sea-level changes influence depositional process so that paleoenvironmental reconstruction is needed to select an appropriate dating material. We present radiocarbon dates variation performed on macrofossils, foraminifers, and acid-insoluble carbon (AIC), as well as paleo-tidal modeling results from the Bonaparte Gulf in northwestern Australia. The varied topography and large tidal range of this gulf are the dominant factors of the past depositional process in response to sea-level change. We will reveal the variation of radiocarbon dates in response to sea-level changes, which appear as changes in paleowater depth and paleotide. Carbonate fossil material reveals a more reliable depositional age than acid insoluble carbon at sea level below -70 m because of little lateral transport caused by reduced tidal activity. On the other hand, acid insoluble carbon ages are more reliable at sea level above −70 m because redeposition of old fossil influences carbonate fossils ages due to enhanced tidal activity. Our results indicate that the age models' reliability has changed over time, especially on the continental shelf, where environmental changes due to sea-level fluctuations are significant.

Keywords: Radiocarbon dating, Sea-level change, Paleotidal modeling

©2021. Japan Geoscience Union. All Right Reserved.

Wind-wave changes in Tokyo Bay during the Holocene: impact of sea-level change and land configuration

*Katsuto Uehara[1]

1. Kyushu University

A paleowave simulation has been carried out to reconstruct changes in the wind-wave field in Tokyo Bay during the Holocene, when the bay configuration altered greatly due to the inundation of a drawn valley associated with a rapid sea-level rise and subsequent infilling of the valley by fluvial sediments. The numerical run was conducted by combining a third-generation wave model SWAN and paleobathymetries reconstructed by the author for every 1kyr from 10ka to 4ka. A preliminary experiment made by applying uniform sea-surface winds indicated an increase of the significant wave height by 10-20% compared to the present-day state.

Keywords: paleowave reconstruction, numerical modeling, Holocene, estuary

©2021. Japan Geoscience Union. All Right Reserved.

Reconstruction of organic matter inflow fluctuations from the Bolling-Allerod interstadial to Late Holocene using Lake Baikal sediments

*Keiko Takehara[1], Masatoshi Nakakuni[2], Shuichi Yamamoto[3]

1. Kochi university Graduate School of Integrated Arts and Sciences, 2. Faculty of Agriculture, Kagawa University, 3. Department of Environmental Engineering for Symbiosis, Graduate School of Engineering, Soka University

Stable oxygen isotope ($d^{18}O$) records in ice cores obtained by the North Greenland Ice Core Project show climate change due to periodic temperature changes from 130,000 to 20,000 years ago. Whereas, the records show a more stable warm period during Holocene (present to 11,700 years ago) when comparing to the previous temperature changes. However, Bond et al. (1997) have reported that rapid climate change (RCC; Mayewski et al., 2004) has occurred in the Holocene. Most of such reports are discovered from marine area including the North Atlantic Ocean and the Indian Ocean regions, but the elucidation of the actual situation on continental regions has been delayed because it is difficult to secure samples for restoration of the paleoenvironment.

Lake Baikal is located in the area that receives the most significant solar radiation fluctuations on the earth (Short et al., 1991). Therefore, it is recognized that the lake records continental climate changes relating the solar radiation fluctuations in detail, and therefore many studies have been conducted using various paleo-environmental proxies. However, most of such papers were focused on glacial to interglacial cycles due to the limitation on sedimental time resolution (> 1 kyr sample^{-1}). Thus, in previous studies, elucidating short-term and rapid climate changes such as the Bolling-Allerod, the Younger Dryas, and Holocene was difficult to (Horiuchi et al., 2000). Therefore, using high time resolution sediment samples obtained from Lake Baikal, the purpose of this study is to reconstruction climate changes from the last glacial termination to Holocene and the accompanying changes in the inflow of organic matter into the lake.

A 1.9 m-long gravity core (VER98-1 St.5GC) was collected from the Academician Ridge, Lake Baikal central basin in 1998. We selected on the upper 0.8 m sediment to study focused on the Pleistocene–Holocene interval including the Bolling-Allerod warming period and the Younger Dryas period. At two intervals of 70–63 cm (the Bolling-Allerod) and 60–20 cm (pre-boreal to sub-boreal in Holocene), TOC ranged from 1–2%, slightly higher than before and after of the depths, the C/N ratios (terrestrial input proxy) ranged from 8.4–11.3 and the ratios of Va to Vh ((Ad/Al)v) were showed maximum 5.6, and these records suggesting high degraded terrestrial material inputs to the lake during these intervals (the Bolling-Allerod and the pre-boreal to sub-boreal period). At the same intervals, $\delta^{13}C$ values showed lighter values of −26 to −29 ‰, which is within the values of C3 plants (C3 plants: −20 to −37 ‰; Kohn, 2010), and ratios of syringyl to vanillyl phenols (S/V) and cinnamyl to vanillyl phenols (C/V) was shown that sediments OM was derived from the non-woody angiosperms (grasses and leaves). The vegetation around Lake Baikal from the last glacial period to about 6,000 years ago was composed of tundra (herbs) characteristic of the permafrost zone (Demske et al., 2005). Additionally, at the present, $\delta^{13}C$ values in DOM of Siberian permafrost melting water showing −25 to −27.6 ‰(Tesi et al., 2016) and Canadian high arctic permafrost spring flush (Ad/Al)v in DOM implying maximum at 3.6 (Woods et al., 2011) were reported. From these results and investigations, it is considered that the inflow of high decomposition products from the pre-boreal period to the late Holocene is caused by the inflow of

©2021. Japan Geoscience Union. All Right Reserved.

permafrost melting water containing herbaceous plants into the lake. Such a Siberian permafrost melting during the Bolling-Allerod and pre-boreal periods has also been reported in lake Baikal southern basin and lake Hovsgol (Katsuta et al., 2019). In addition, in this study, Siberian permafrost melting during the sub-boreal period was inferred because similar organic records were observed during this interval as well as the previous one. However, the organic records probably also be influenced by increasing amount of vegetation by warmer climates.

Keywords: Lake Baikal, TMAH method, Holocene

©2021. Japan Geoscience Union. All Right Reserved.

Reconstruction of Early Pleistocene sea-surface temperature in the Northwestern Pacific Ocean based on calcareous microfossils

*Daisuke Kuwano[1], Yuki Tsuchiya[2], Yuma Oura[1], Hiroki Hayashi[3], Yoshimi Kubota[4], Kanako Mantoku[5], Koji Kameo[1]

1. Chiba University, 2. Nagoya University, 3. Shimane University, 4. National Museum of Nature and Science, 5. National Institute for Environmental Studies

Planktonic foraminifera and calcareous nannofossils have been used to clarify past marine environments based on relationships between distributions of living taxa and sea-water conditions (e.g., Takemoto and Oda, 1997; Aizawa et al., 2004). In this study, we reconstruct the sea surface temperature (SST) based on the Modern Analog Technique (MAT) of calcareous microfossil assemblages. The MAT is a useful method for reconstructing SST by comparing the similarity between fossil and modern assemblages (e.g., Pflaumann et al., 1996). Around the Pacific coast of Japanese islands, many surface sediments have been obtained by grab sampler and piston corer, and the modern microfossil assemblages of those have been studied (e.g., Tanaka, 1991). We apply the MAT to 27 samples of the upper part of the Kiwada Formation, Kazusa Group, obtained by Kuwano et al. (in press). We estimated the SST by calculating the squared chord distance (SCD) between fossil and modern assemblages, subsequently taking the weighted temperature average of the top five samples with the highest similarity. The modern foraminiferal and nannofossil assemblage dataset were obtained from Takemoto and Oda (1997) and Tanaka (1991), respectively. The modern SST dataset was used in July from the Japan Oceanographic Data Center (2004).
The reconstructed SST tends to be high during interglacial, and the summer SST ranged between 23.4 and 27.7 ℃. On the other hand, during the glacial Marine Isotope Stage (MIS) 38, the SSTs temporarily dropped by 1–2 ℃. This sea-surface variation is similar to that of planktonic foraminiferal $\delta^{18}O$ change although the nannofossil SSTs were sharp declines rather than planktonic $\delta^{18}O$ changes in some horizons.

[Reference]
Aizawa et al., 2004, *Marine Micropaleontology*, 52, 277–297.
Japan Oceanographic Data Center, 2004, https://jdoss1.jodc.go.jp/vpage/bts_j.html
Kuwano et al., in press, *Stratigraphy*.
Pflaumann et al., 1996, *Paleoceanography*, 11, 15–35.
Takemoto and Oda, 1997, *Paleontological research*, 1, 291–310.
Tanaka, 1991, *Sci. Rep., Tohoku Univ., 2nd ser. (Geol.)*, 61, 127-198.

Keywords: Calcareous nannofossils, Planktonic foraminifera, Modern Analog Technique, Paleoceanography, Pleistocene, Kazusa Group

©2021. Japan Geoscience Union. All Right Reserved.

Variation of the North Pacific Ocean circulation during the Late Pleistocene glacial-interglacial cycles

*Furukawa Keisuke[1], Osamu Seki[1], Masanobu Yamamoto[1], Tomohisa Irino[1]

1. Hokkaido University

The Late Pleistocene glacial-interglacial (G-IG) cycle, characterized by 100 kyr variations in global ice volume and atmospheric CO_2 concentration, governs the global climate (e.g., global mean surface temperature). Reported long-term SST records in the Equatorial and North Pacific show a unique response to the orbital forcing, despite their overall patterns reflecting the G-IG cycle. This suggests the reorganization of the ocean-atmosphere circulation in the region associated with the G-IG cycle. However, available SST records in the subarctic region of the North Pacific are limited to the Last Glacial Maxima. Therefore, the whole picture of the North Pacific response to global climate change remains unclear.

In this study, we reconstructed changes in sea surface temperature (SST) at the western and eastern margins of the North Pacific subarctic region for the past 470 kyrs based on TEX_{86}^{L} and U^{K}_{37}' analyses in Ocean Drilling Program (ODP) Sites ODP 882 and 887. The SST records in Sites 882 and 887 during the last glacial cycle show a typical G-IG pattern. This correspondence confirms the robustness of our reconstruction. However, extended SST records back to 470 ka revealed a unique response to the orbital forcing with relatively low SSTs during the super interglacials compared to the Holocene. The subarctic region's unique response appears to be linked climate variation in the low latitude Pacific, implying large-scale reorganization of the ocean-atmosphere circulation associated with the global climate change.

Keywords: North Pacific, glacial-interglacial cycle, SST reconstruction

©2021. Japan Geoscience Union. All Right Reserved.

[J] Oral | M (Multidisciplinary and Interdisciplinary)：M-IS Intersection

Sat. Jun 5, 2021 10:45 AM - 12:15 PM JST | Sat. Jun 5, 2021 1:45 AM - 3:15 AM UTC | Ch.26 Zoom Room 26

[M-IS16] Paleoclimatology and paleoceanography

convener:Yusuke Okazaki(Department of Earth and Planetary Sciences, Graduate School of Science, Kyushu University), Hitoshi Hasegawa(Faculty of Science and Technology, Kochi University), Atsuko Yamazaki(Faculty of Science, Kyushu University), Akitomo Yamamoto(Japan Agency for Marine-Earth Science and TechnologyAtmosphere and Ocean Research Institute), Chairperson:Hitoshi Hasegawa(Faculty of Science and Technology, Kochi University)

Past environmental changes and events at interannual to tectonic timescale toward an understanding of Earth climate system by an integration of terrestrial and marine proxy studies and numerical modeling will be discussed. At JpGU2021, a series of presentations on "high-resolution" paleo data and model studies will be held. We welcome a variety of paleo-environmental studies from a wide range of background. We hope that this session will provide an opportunity to promote communication between participants from multidisciplinary field.

10:45 AM - 11:00 AM JST | 1:45 AM - 2:00 AM UTC

[MIS16-17] Reconstruction of the Mediterranean sulfur cycle during the Messinian salinity crisis using evaporites

*Takeru Kochi[1], Junichiro Kuroda[1], Nanako O. Ogawa[2], Toshihiro Yoshimura[2], Takashi Miyazaki[2], Bogdan Stefanov Vaglarov[2], Naohiko Ohkouchi[2] (1.the University of Tokyo, 2.Japan Agency for Marine–Earth Science and Technology)

11:00 AM - 11:15 AM JST | 2:00 AM - 2:15 AM UTC

[MIS16-18] Increased eolian dust in the Pacific since around the Eocene-Oligocene boundary estimated from a rock-magnetic study of red clay

*Toshitsugu Yamazaki[1], Wei Fu[1], Takaya Shimono[2], Yoichi Usui[3] (1.Atmosphere and Ocean Research Institute, The University of Tokyo, 2.Geological Survey of Japan, AIST, 3.Japan Agency for Marine-Earth Science and Technology)

11:15 AM - 11:30 AM JST | 2:15 AM - 2:30 AM UTC

[MIS16-19] **Authigenic and detrital Mg and Li isotopes as a tracer of Antarctic chemical silicate weathering across the EOT**

*Adam David Sproson[1,2,3], Toshihiro Yoshimura[1], Yusuke Yokoyama[1,3], Takahiro AZE[3], Tsuyoshi Ishikawa[4], Shigeyuki Wakaki[4], Naohiko Ohkouchi[1] (1.Department of Biogeochemistry, Japan Agency for Marine-Earth Science and Technology, 2-15 Natsushima, Yokosuka, Kanagawa 237-0061, Japan, 2.Submarine Resources Research Center, Japan Agency for Marine-Earth Science and Technology, 2-15 Natsushima, Yokosuka, Kanagawa 237-0061, Japan, 3.Atmosphere and Ocean Research Institute, University of Tokyo, 5-1-5 Kashiwanoha, Kashiwa, Chiba 277-8564, Japan, 4.Kochi Institute for Core Sample Research, Japan Agency for Marine-Earth Science and Technology 200 Monobe Otsu, Nankoku City, Kochi 783-8502, Japan)

11:30 AM - 11:45 AM JST | 2:30 AM - 2:45 AM UTC

[MIS16-20] Terrestrial environmental response to the global climate change during the early to middle Eocene (52.7-43.8 Ma): evidence from lacustrine deposits of the Green River Formation, Utah, USA

*Ryusei Kuma[1], Hitoshi Hasegawa[2], Koshi Yamamoto[1], Jessica H. Whiteside[3], Amy L. Elson[3], Hidekazu Yoshida[1], Koichi Mimura[1] (1.Nagoya University, 2.Kochi University, 3.University of Southampton)

11:45 AM - 12:00 PM JST | 2:45 AM - 3:00 AM UTC

[MIS16-21] C40-alkenone unsaturation index from the Cretaceous and paleothermometry in southern high latitude of Proto-Indian Ocean

*Takashi Hasegawa[1], Akiko S. Goto[2,1], Hiromichi Komiya[3], Shota Morikawa[3] (1.Faculty of Geoscience and Engineering, Institute of Science and Engineering, Kanazawa University, 2.Center of Ecological Research, Kyoto University, 3.Graduate School of Natural Science and Engineering, Kanazawa University)

12:00 PM - 12:15 PM JST | 3:00 AM - 3:15 AM UTC

[MIS16-22] Opposing responses in the hydrological cycle of the East Asia to climate warming related with the Tibetan Plateau

*Taro Higuchi[1], Ayako Abe-Ouchi[1], Wing-Le Chan[1] (1.Atmospheric and Ocean Research Institute, the University of Tokyo)

Reconstruction of the Mediterranean sulfur cycle during the Messinian salinity crisis using evaporites<gdiv></gdiv>

*Takeru Kochi[1], Junichiro Kuroda[1], Nanako O. Ogawa[2], Toshihiro Yoshimura[2], Takashi Miyazaki[2], Bogdan Stefanov Vaglarov[2], Naohiko Ohkouchi[2]

1. the University of Tokyo, 2. Japan Agency for Marine-Earth Science and Technology

Evaporite is a group of rocks composed of minerals precipitated from a saturated brine through solar evaporation. Halite (NaCl) and gypsum ($CaSO_4 \cdot 2H_2O$) are representative evaporite-forming minerals in the natural environment. During the Phanerozoic, voluminous evaporite bodies, so-called “salt giant”, have been formed repeatedly. The Messinian Salinity Crisis (MSC: 5.97-5.33 Ma) occurred in the Mediterranean Sea during the later stage of Messinian (7.246-5.333 Ma) represents one of the largest and the youngest salt giants in the Phanerozoic. This event is subdivided into three stages (Stages 1 to 3) based on the lithological features of evaporites. It has been proposed that the MSC was caused by tectonic uplift around the Atlantic spillway and global sea level drop, both of which could have limited the connection between the Mediterranean Sea and the Atlantic Ocean. During the MSC, a huge amount of gypsum was deposited in marginal and central deep basins of the Mediterranean Sea. The sulfate removed from seawater could have affected the sulfur isotopic composition ($\delta^{34}S$) in the Mediterranean Sea. Previous studies have already demonstrated that, gypsum samples deposited during the MSC have sulfur isotopic compositions slightly heavier than that of the contemporaneous global seawater sulfate. However, there are few studies on the detailed spatiotemporal variation of sulfur isotopic composition within the Mediterranean basins through the MSC, which is necessary to quantitatively reconstruct the sulfur cycles in the Mediterranean Sea during the MSC.
In this study, we assessed how sulfur cycles in the Mediterranean Sea changed during the MSC based on sulfur isotopic composition of sulfate minerals deposited on six sites all around the Mediterranean Sea (three on land sites and three offshore borehole sites). The sulfur isotopic compositions were measured using an Elemental Analyzer-Isotope Ratio Mass Spectrometer (EA-IRMS) at Japan Agency for Marine-Earth Science and Technology (JAMSTEC). Sulfur isotopic compositions of evaporite samples deposited during the MSC are summarized as follows: gypsum deposited during Stage 1 ranges from 22.37 to 23.75 ‰, gypsum and halite deposited during Stage 2 ranges from 22.61 to 23.60 ‰, and gypsum deposited during Stage 3 is from 21.20 to 22.82 ‰. Based on these values, we reconstructed the sulfur isotopic composition of the brine water of the Mediterranean Sea with applying sulfur isotopic fractionation associated with the precipitation of evaporitic minerals from brine water estimated by our evaporation experiments (i.e., $\varepsilon^{34}S = \delta^{34}S_{mineral} - \delta^{34}S_{brine} = 1.4$ ‰for gypsum and $\varepsilon^{34}S = 0$ ‰for halite). This reconstruction showed that the sulfur isotopic compositions were constant during Stage 1 throughout the Mediterranean Sea, but they decreased by 1-1.5 ‰from Stage 2 to Stage 3. To explain the decreasing sulfur isotopic composition, we estimated seawater exchange rate and gypsum deposition volume using a box model. The calculation results suggest that the variation of sulfur isotopic compositions could be explained by combined effects of (1) a decrease in the relative contribution of seawater influx from the Atlantic Ocean (or increased riverine flux), (2) voluminous deposition of gypsum with ^{34}S-enriched sulfur, and (3) additional local effects by biological sulfate reduction that may account for the local heterogeneity in sulfur isotopic compositions.<gdiv></gdiv>

Keywords: sulfur isotope, evaporite, the Messinian Salinity Crisis

©2021. Japan Geoscience Union. All Right Reserved.

Increased eolian dust in the Pacific since around the Eocene-Oligocene boundary estimated from a rock-magnetic study of red clay

*Toshitsugu Yamazaki[1], Wei Fu[1], Takaya Shimono[2], Yoichi Usui[3]

1. Atmosphere and Ocean Research Institute, The University of Tokyo, 2. Geological Survey of Japan, AIST, 3. Japan Agency for Marine-Earth Science and Technology

Red clay widely occupies the seafloor of pelagic environments in middle latitudes, and potentially preserves long paleoceanographic records. We conducted a rock-magnetic study of Pacific Ocean red clay to elucidate paleoenvironmental changes. Three piston cores from the western North Pacific Ocean and IODP Hole U1365A cores in the South Pacific Ocean were studied here. Principal component analyses applied to first-order reversal curve diagrams (FORC-PCA) reveal three magnetic components (endmembers EM1 through EM3) in a core of the western North Pacific. EM1, which represents the features of interacting single-domain (SD) and vortex states, is interpreted to be of terrigenous origin. EM2 and EM3 are carried by non-interacting SD grains with different coercivity distributions, which are interpreted to be of biogenic origin. The EM1 contribution suddenly increases upcore at a depth of ~2.7 m, which indicates increased eolian dust input. The age of this event is estimated to be around the Eocene-Oligocene (E/O) boundary. Transmission electron microscopy reveals that EM2 is dominated by magnetofossils with equant octahedral morphology, while EM3 has a higher proportion of bullet-shaped magnetofossils. An increased EM3 contribution from ~6.7 to 8.2 m suggests that the sediments were in the oxic-anoxic transition zone (OATZ), although the core is oxidized in its entire depths now. The chemical conditions of OATZ may have been caused by higher biogenic productivity near the equator. FORC-PCA of Hole U1365A cores identified two EMs, terrigenous (EM1) and biogenic (EM2). The coercivity distribution of the biogenic component at Hole U1365A is similar to that of the lower coercivity biogenic component in the western North Pacific. A sudden upcore terrigenous-component increase is also evident at Hole U1365A with estimated age around the E/O boundary. The eolian increase may have been coeval in both hemispheres and associated with the global cooling at the E/O boundary.

Keywords: eolian dust, biogenic magnetite, red clay, Eocene-Oligocene boundary

©2021. Japan Geoscience Union. All Right Reserved.

Authigenic and detrital Mg and Li isotopes as a tracer of Antarctic chemical silicate weathering across the EOT

*Adam David Sproson[1,2,3], Toshihiro Yoshimura[1], Yusuke Yokoyama[1,3], Takahiro AZE[3], Tsuyoshi Ishikawa[4], Shigeyuki Wakaki[4], Naohiko Ohkouchi[1]

1. Department of Biogeochemistry, Japan Agency for Marine-Earth Science and Technology, 2-15 Natsushima, Yokosuka, Kanagawa 237-0061, Japan, 2. Submarine Resources Research Center, Japan Agency for Marine-Earth Science and Technology, 2-15 Natsushima, Yokosuka, Kanagawa 237-0061, Japan, 3. Atmosphere and Ocean Research Institute, University of Tokyo, 5-1-5 Kashiwanoha, Kashiwa, Chiba 277-8564, Japan, 4. Kochi Institute for Core Sample Research, Japan Agency for Marine-Earth Science and Technology 200 Monobe Otsu, Nankoku City, Kochi 783-8502, Japan

Future warming beyond 2C could lead to the crossing of a threshold beyond which positive feedbacks within the Earth System, such as permafrost thawing, increased bacterial respiration and forest dieback, would create a “Hothouse Earth” [1]. Understanding the interplay of feedback mechanisms is therefore of utmost importance to predicting future climate change. On million-year timescales, the hydrolysis of silicate minerals and subsequent precipitation of carbonate minerals in the ocean acts as a negative feedback within the carbon-cycle [2]. On shorter, more relevant, timescales, the production of fine-grained material and associated subglacial chemical weathering during expansion and contraction of glaciers may influence atm. CO_2 and temperature [3].

The Eocene-Oligocene Transition (EOT; ca. 34 Ma) marks the sudden appearance of large ice sheets on Antarctica which caused a surge in erosion recorded by Nd isotopes, Pb isotopes and clay mineralogy [4, 5]. However, the response of chemical silicate weathering is not well understood. Here, we present Mg and Li isotope and rare-earth element (REE) data for the authigenic and detrital phases of marine sediments from ODP Site 738 on the Kerguelen Plateau. Magnesium and Li isotopes fractionate significantly during chemical weathering, with the retention of the heavier ^{26}Mg and ^{7}Li in weathering residues [6, 7]. During secondary mineral formation, the heavier (lighter) isotopes of Mg (Li) become preferentially incorporated, driving the $\delta^{26}Mg$ ($\delta^{7}Li$) to higher (lower) values.

The $\delta^{26}Mg$ and $\delta^{7}Li$ records of the authigenic and silicate phases from Site 738 display similar variation to previous Pb and Nd isotope records, revealing a dramatic intensification of silicate weathering across the EOT. This intensification is well correlated to oxygen isotopes suggesting continental ice sheet expansion over Antarctica led to increased silicate weathering, atm. CO_2 drawdown and further cooling. Such feedbacks may help reverse future warming as ice sheets begin to retreat.

[1] Steffen et al. (2018) *PNAS* **115**, 8252-8259. [2] Berner (2006) *GCA* **70**, 5653-5664. [3] Kump & Alley (1994) 46-60. [4] Basak & Martin (2013) *Nature Geoscience* **6**, 121-124. [5] Scher et al. (2011) *Geology* **39**, 383-386. [6] Wimpenny et al. (2011) *EPSL* **304**, 260-269. [7] Huh et al. (1998) *GCA* **62**, 2039-2051.

Keywords: Chemical weathering, Eocene-Oligocene Transition, Mg & Li isotopes

©2021. Japan Geoscience Union. All Right Reserved.

Terrestrial environmental response to the global climate change during the early to middle Eocene (52.7-43.8 Ma): evidence from lacustrine deposits of the Green River Formation, Utah, USA

*Ryusei Kuma[1], Hitoshi Hasegawa[2], Koshi Yamamoto[1], Jessica H. Whiteside[3], Amy L. Elson[3], Hidekazu Yoshida[1], Koichi Mimura[1]

1. Nagoya University, 2. Kochi University, 3. University of Southampton

The evolution of early Eocene climate and oceans has been the focus of significant study due to the elevated atmospheric CO_2 levels (>1,000 ppm) of this warmest interval of the Cenozoic. In contrast, the terrestrial response during this period is less understood. This study focused on the Early Eocene Climatic Optimum (EECO) recorded in the Uinta Basin’ s lower to middle Green River Formation, western United States, ca. 52.7-43.8Ma This section (ca. 1000 m in thickness) affords a high temporal resolution of 1-2 m (10-20 kyrs resolution).
In this study, detailed lithofacies descriptions of lake level change, as well as elemental and mineralogical analyses, were used to quantitatively reconstruct the terrestrial environment. Alterations in lithofacies allow us to subdivide the succession into the following nine paleoenvironmental stages: the fluvio-lacustrine stage; the deep-lake stage; the fluvio-lacustrine stage; the deep-lake stage; the shallow lake stage; the evaporative lake stage; the shallow lake stage; fluctuating lake stage; and the fluvio-lacustrine stage, in ascending order. By comparing the lithofacies and the composition of major elements, Ca/Al can be utilised as a proxy of lake level, Mn/Fe as an indicator of lake bottom redox conditions, and K/Al as a proxy for chemical weathering rates. Each paleoclimatic proxy suggests that the Green River Formation had high lake levels, an anoxic lake bottom environment, and high chemical weathering during the EECO. Mineral composition changes reflect variation in the degree of chemical weathering during and after the EECO. In concert, these results suggest abundant precipitation during the EECO in the mid-latitudes of North America. In addition, our results correspond to the positive $\delta^{13}C$ trend in deep-sea benthic foraminifera and insolation phase change during the early to middle Eocene, indicating that the mid-latitudes of the Northern Hemisphere may have become wetter during the "hothouse" period of EECO which probably correspond to the northward expansion of the intertropical convergence zone due to global warming.

Keywords: lake sediment, Eocene, greenhouse, paleoclimate, carbon cycle, Milankovitch cycle

©2021. Japan Geoscience Union. All Right Reserved.

C40-alkenone unsaturation index from the Cretaceous and paleothermometry in southern high latitude of Proto-Indian Ocean

*Takashi Hasegawa[1], Akiko S. Goto[2,1], Hiromichi Komiya[3], Shota Morikawa[3]

1. Faculty of Geoscience and Engineering, Institute of Science and Engineering, Kanazawa University, 2. Center of Ecological Research, Kyoto University, 3. Graduate School of Natural Science and Engineering, Kanazawa University

What would happen on regional environments on the Earth with the worst scenario of global warming? Geologic archives memorized the results of “grand experiments of global warming” during greenhouse period of the past, like Cretaceous. As greenhouse periods are deep past older than 4000 Myr, geochemical signals are lost or seriously affected by diagenesis. In addition, because such periods are much warmer than the Quaternary, some paleoceanographic proxies cannot be applied with the same manner.

Sea surface temperature (SST) and its fluctuation (cyclicity, magnitude and their rate of changes etc.) is the most important environmental information. Only collecting SST information of greenhouse periods as same resolution as Quaternary can answer the question that we mentioned at the start.

Alkenones (strait chain alkyl ketone) are potential tool for this purpose. Alkenone molecules from marine sediments are known to be products of haptophyte algae and are often employed for paleothermometry for Quaternary and Neogene. Di- and Tri-unsaturated alkenones with 37 carbon atoms (C37 alkenones) are the target molecules for this purpose. On the other hand, only di-unsaturated one has been reported from Paleocene or Cretaceous. Thus alkenone paleothermometry cannot be applied as same manner for the greenhouse periods.

This study detected alkenones with 37-40 carbon atoms in the late Cretaceous sediments from southern margin of proto-Indian Ocean (IODP Exp. 369 Site U1516). Di-unsaturated C40 alkenone ($C_{40:2}$Et) was the most dominant species among the alkenones. In addition to $C_{40:2}$Et, tri-unsaturated C40 alkenone ($C_{40:3}$ Et) was observed by this study for the first time. Then we calculated C40 alkenones unsaturation index ($U^{K'}_{40}$) and discussed its stratigraphic characteristics through the Albian to uppermost Cenomanian up to OAE2 interval.

Content of $C_{40:2}$Et was highest at the top of black clay layer (BCL: sediment associated with OAE2). It is relatively low through the interval below BCL. It decreased above BCL and reach to substantially zero at 30 cm above the top of BCL, then no detection above.

$U^{K'}_{40}$ showed characteristic fluctuation in the Upper Cenomanian. Maximum value near 1.0 were detected from the lowest sample of BCL, as well as from samples of Albian/Cenomanian boundary interval. In the BCL, it showed dramatic decrease toward 0.85 within the interval of 15 cm. Not only C37 alkenones, C38, C41 and C42 alkenones also show their temperature-dependent nature of the unsaturation ratio based on *in vitro* experients (Araie et al., 2019). This fact strongly suggests that C40 alkenones produced during Cretaceous also had similar temperature dependence. If it is accepted, then following interpretation is possible for interval near the OAE2: (1) on the half way of the 1st build-up of the carbon isotope excursion (CIE), SST reached maximum. It is as same SST as that of Albian/Cenomanian boundary; (2) through the later phase of 1st build-up of CIE, SST dropped considerably and reached minimum just above the 1st peak of CIE. It could be comparable event with

©2021. Japan Geoscience Union. All Right Reserved.

“Plenus Cold Event”.

$U^{K'}_{40}$ cannot be converted into SST value so far, however, some approaches are possible to improve $U^{K'}_{40}$ as a proxy of SST for Cretaceous. Oxygen isotope study on individual planktonic foraminifera with excellent preservation from identical sample with C40 alkenones can provide SST information comparable with $U^{K'}_{40}$. Collecting haptophyte strain that produce C40 alkenones from present saline lake and cultural experiments using them could help discussion on temperature dependence of $U^{K'}_{40}$. Thus $U^{K'}_{40}$ is a promising proxy for quantitative paleothermometry for high temperature regime (>28 C).
Citation: Araie et al. (2018) Org. Geochem. 121, 89-103

Keywords: alkenone, Cretaceous, biomarkers, paleothermometry, OAE

©2021. Japan Geoscience Union. All Right Reserved.

Opposing responses in the hydrological cycle of the East Asia to climate warming related with the Tibetan Plateau

*Taro Higuchi[1], Ayako Abe-Ouchi[1], Wing-Le Chan[1]

1. Atmospheric and Ocean Research Institute, the University of Tokyo

The water cycle is closely linked to human lives, the ecosystem, ocean circulation and the carbon cycle, and its change due to increased atmospheric CO2 concentration is one of the major concerns in the field of global warming research. Numerical modelling studies using GCMs suggested that, in East Asia, the mean precipitation increases with future global warming, leading to more humid conditions. On the other hand, Cretaceous proxy data showed that aridification in the low latitudes of East Asia proceeded the mid-Cretaceous which was the warmest time during the Cretaceous Period, with an especially high CO2 concentration, compared to the relatively cold early and late Cretaceous. However, it remains unclear why the response of the water cycle in East Asia to increased CO2 differs during the present day and the Cretaceous and how the response in the Cretaceous compares with other periods. The aim of this study is to investigate the response of the climate and water cycle to increased atmospheric CO2 for a Cretaceous paleogeography and to compare results with the proxy data and warming experiments using the present-day, Pliocene, and Eocene conditions. In this study, simulations of the present-day, Pliocene, Eocene, and Cretaceous climate with different CO2 levels are carried out using the atmosphere-ocean general circulation model, MIROC4m. For all the experiments, the global hydrological sensitivity ranges from 1.98 to 2.14 %/K, which is fairly small. The "rich gets richer" mechanism can be seen zonally in all cases. On the other hand, there are two opposing responses in the local hydrological cycle in East Asia to climate warming. One response is that annual precipitation in East Asia increases as the climate warms, provided there is an elevated Tibetan Plateau (Present day, Pliocene), similar to global warming prediction. The other is that annual precipitation decreases without a Tibetan Plateau (Eocene, Cretaceous), consistent with the change in the hydrological cycle during the mid-Cretaceous as shown in proxy data. These opposing responses in the hydrological cycle may be attributed to the different basic climate fields and atmospheric circulation responses in Asia which, in turn, is associated with the presence or absence of the Tibetan Plateau. Furthermore, from the idealized sensitivity experiments of the Tibetan Plateau, it is found that the changes in the annual precipitation of East Asia due to increasing atmospheric CO2 are reversed by around 60% on the Tibetan Plateau.

Keywords: Hydrological cycle, East Asia, Global warming, Cretaceous, Tibetan plateau

©2021. Japan Geoscience Union. All Right Reserved.

[J] Poster | M (Multidisciplinary and Interdisciplinary)：M-IS Intersection

Sat. Jun 5, 2021 5:15 PM - 6:30 PM JST | Sat. Jun 5, 2021 8:15 AM - 9:30 AM UTC | Ch.23

[M-IS16] Paleoclimatology and paleoceanography

convener:Yusuke Okazaki(Department of Earth and Planetary Sciences, Graduate School of Science, Kyushu University), Hitoshi Hasegawa(Faculty of Science and Technology, Kochi University), Atsuko Yamazaki(Faculty of Science, Kyushu University), Akitomo Yamamoto(Japan Agency for Marine-Earth Science and TechnologyAtmosphere and Ocean Research Institute)

Past environmental changes and events at interannual to tectonic timescale toward an understanding of Earth climate system by an integration of terrestrial and marine proxy studies and numerical modeling will be discussed. At JpGU2021, a series of presentations on "high-resolution" paleo data and model studies will be held. We welcome a variety of paleo-environmental studies from a wide range of background. We hope that this session will provide an opportunity to promote communication between participants from multidisciplinary field.

[MIS16-P01] Temperature effect on Japanese stalagmite $\delta^{18}O$ records from Hiroshima and Gifu

*Hirokazu Kato[1], Taiki Mori[2], Shota Amekawa[1], Akihiro Kano[1] (1.Department of Earth and Planetary Science, The University of Tokyo, 2.Chuo Kaihatsu Corporation)

[MIS16-P02] **Oxygen isotope equilibrium of the shallow-water benthic foraminifer *Hanzawaia nipponica* (Asano) in Tosa Bay, southwest Japan**

*Minoru Ikehara[1,2], Shigetaka Kita[2], SHUNGO KAWAGATA[3] (1.Center for Advanced Marine Core Research, Kochi University, 2.Graduate School of Integrated Arts and Sciences, Kochi University, 3.Faculty of Education, Yokohama National University)

[MIS16-P03] **Variations in shell morphology of the planktonic foraminifer *Globigerina bulloides* in the sediment off Kashima**

*Yuya Hashimoto[1], Takuya Sagawa[2] (1.Kanazawa University College of Science and Engineering, 2.Institute of Science and Engineering, Kanazawa University)

[MIS16-P04] Climate characteristics of Amami , Kagoshima , Japan over the past 200 years inferred from tree-ring cellulose oxygen isotope ratio data

*Akihiro Masuoka[1], Kenjiro Sho[1], Masafumi Ohata[2], Zhen Li[3], Takeshi Nakatsuka[3] (1.Nagoya Institute of Technology, 2.Taisei Corporation, 3.Nagoya University)

[MIS16-P05] Coral skeletal records reveal the relationship between Kuroshio variability and North Pacific climate

*Atsuko Yamazaki[1,2], Tsuyoshi Watanabe[2,3] (1.Kyushu University, 2.KIKAI institute for Coral Reef Sciences, 3.Hokkaido University)

[MIS16-P06] Reconstruction of environmental and flooding histories since AD1250 at Lake Kortta, an annually laminated lake at the Central Finland presumed by Diatom and Chrysophyceae assemblages

*Kaoru Kashima[1], Yu Fukumoto[2], Timo Saarinen[3] (1.Department of Earth and Planetary Sciences, Kyushu University, 2.Osaka City University, 3.University of Turku)

[MIS16-P07] **Sphagnum and grass cellulose oxygen isotopes in peat cores reveal climate changes in northern Japan over the past 4400 years and close relationship with human histories**

*Masanobu Yamamoto[1], Osamu Seki[2] (1.Faculty of Environmental Earth Science, Hokkaido University, 2.Insititute of Low Temperature Science)

[MIS16-P08] Can Sedimentary fish DNA track decadal to centennial scale fish abundance?

*Michinobu Kuwae[1], Hiromichi Tamai[1], Hideyuki Doi[2], Masayuki Sakata[3], Toshifumi Minamoto[3], Yoshiaki Suzuki[4] (1.Center for Marine Environmental Studies, 2.Graduate School of Simulation Studies, University of Hyogo, 3.Graduate School of Human Development and Environment, Kobe University, 4.Research Institute of Geology and Geoinformation, Geological Survey of Japan, National Institute of Advanced Industrial Science and Technology)

[MIS16-P09] Paleoenvironmental variations reconstructed by algal biomarker analysis of a sediment core from Lake Nakaumi, Japan

*Akiko Taneichi[1], Yuki Hattori[1], Ken Sawada[1], Takuto Ando[2], Hideto Nakamura[3], Kotaro Hirose[4] (1.Hokkaido Univ., 2.Shimane Univ., 3.Osaka City Univ., 4.Waseda Univ.)

[MIS16-P10] Paleoceanographic changes in the western part of the Arctic Sea based on ostracods

*Katsura Yamada[1], Kosuke Yamaguchi[1], Masao Uchida[2], Takuya Itaki[3], Kanako Mantoku[2] (1.Department of Geology, Faculty of Science, 2.National Institute for Environmental Studies, 3.National Institute of Advanced Industrial Science and Technology)

[MIS16-P11] **Mid- to late Holocene variability of the Aleutian Low Atmospheric Pressure Cell: Forcing by the Western Jet**

*Kana Nagashima[1], Jason Addison[2], Tomohisa Irino[3], Takayuki Omori[4], Kei Yoshimura[5], Naomi Harada[1] (1.Research Institute for Global Change, Japan Agency for Marine-Earth Science and Technology, 2.U.S. Geological Survey, 3.Faculty of Environmental Earth Science, Hokkaido University, 4.The University Museum, The University of Tokyo, 5.Institute of Industrial Science, The University of Tokyo)

[MIS16-P12] Sedimentary characteristics, age and event of a marine core collected from Uranouchi Bay, Kochi, Japan

*Masafumi MURAYAMA[1,3], Wataru Tanikawa[2], Akira Ijiri[2], Tatsuhiko Hoshino[2], Takehiro Hirose[2], Katsuya Nejigaki[3], Kazuno Arai[3], Go-Ichiro Uramoto[3], Kondo Yasuo[4], Hiromasa Ozaki[5], Minoru Yoneda[5] (1.Faculty of Agriculture and Marine Science, Kochi University, 2. Institute for Extra-cutting-edge Science and Technology Avant-garde Research, Kochi Institute for Core Sample Research, JAMSTEC, 3.Center for Advanced Marine Core Research, Kochi University, 4.Faculty of Science and Technology, Kochi University, 5.The University Museum,The University of Tokyo)

[MIS16-P13] Estimation of amount of meltwater discharge from the Laurentide to the Arctic Ocean during the MWP1a event

★Invited Papers

*Kenta Suzuki[1], Masanobu Yamamoto[1], Leonid Polyak[2], Tomohisa Irino[1] (1.Faculty of Environmental Earth Science, Hokkaido Univ., 2.Byrd Polar and Climate Research Center, The Ohio State Univ.)

[MIS16-P14] Millennial variability in precipitation in Papua New Guinea during the last deglaciation

*Gaku Sudo[1], Masanobu Yamamoto[1], Samantha Bova[2], Yair Rosenthal[2] (1.Faculty of Environmental Earth Science, Hokkaido Univ., 2.Rutgers Univ.)

[MIS16-P15] A paleoclimatic reconstruction of the southeastern Pacific last deglacial using geochemical proxies obtained from offshore Chile

*Karin Nemoto[1,2], Yusuke Yokoyama[1,2], Adam David Sproson[2], Yosuke Miyairi[2], Takahiro AZE[2], Hiroyuki Matsuzaki[3,4], Yair Rosentha[5], Samantha Bova[5] (1.Department of Earth and Planetary Science, The University of Tokyo, 2.Atmosphere and Ocean Research Institute, The University of Tokyo, 3.The University Museum,The University of Tokyo, 4.School of Engineering, The University of Tokyo, 5.Department of Marine and Coastal Sciences, School of Environmental and Biological Sciences, Rutgers University)

[MIS16-P16] Paleovegetation changes in the northern Mongolia since the last glacial

*Ryosuke Imaoka[1], Koji Shichi[2], Hitoshi Hasegawa[1], Niiden Ichinnorov[3], Nagayoshi Katsuta[4], Davaasuren Davaadorj[5], Masafumi MURAYAMA[1], Masao Iwai[1], masami izuho[6] (1.Kochi University, 2.Forestry and Forest Products Research Institute, 3.Paleontological Center of Mongolia, 4.Gifu University, 5.National University of Mongolia, 6.Tokyo Metropolitan University)

[MIS16-P17] Glacial–interglacial variations in the Leeuwin Current for the last 50,000 years based on Nd isotope records of benthic foraminifers

*Ryota Wako[1], Hideko Takayanagi[1], Shigeyuki Wakaki[2], Takeshige Ishiwa[4], Yusuke Yokoyama[5], Hitomi Uchimura Wakaki[3], Tsuyoshi Ishikawa[2], Yasufumi Iryu[1] (1.Department of earth science, Tohoku university , 2.Kochi Institute for Core Sample Research, JAMSTEC, 3.Center for Advanced Marine Core Research, Kochi University, 4.National Institute of Polar Research, 5.Atmosphere and Ocean Research Institute, University of Tokyo)

[MIS16-P18] Changes in carbonate dissolution and preservation in Southern Ocean sediment off Chilean margin during the last 140 kyrs based on fragmentation and size-normalized weight of planktic foraminiferal tests.

*Takuto Kasuya[1], Yusuke Okazaki[2], Shinya Iwasaki[3], IODP Expedition 383 Scientific Party (1.Department of Earth and Planetary Sciences, School of Science, Kyushu University , 2.Department of Earth and Planetary Sciences, Faculty of Science, Kyushu University, 3.MARUM Center for Marine Environmental Sciences and Department of Geosciences, University of Bremen)

[MIS16-P19] Examining MIS 5e Sea-Levels around Japan: 60+ Years of Sea-Level Proxy Analysis and Applied Dating Techniques

*Evan Tam[1,2], Yusuke Yokoyama[1,2] (1.University of Tokyo, Atmosphere and Ocean Research Institute, 2.University of Tokyo, Graduate Program on Environmental Science)

[MIS16-P20] Integrated stratigraphy of the sediment core retrieved from the Manihiki Plateau in the central Pacific and the paleotemperature change for the last 800 kyr

*MISAKI URAKAMI[1], Takuya Sagawa[2], Yoshimi Kubota[3] (1.College of Science and Engineering, Kanazawa University, 2.Institute of Science and Engineering, Kanazawa University, 3.National Museum of Nature and Science)

[MIS16-P21] Preliminary results of oxygen isotopic, paleomagnetic, and pollen analyses from a mid-Piacenzian marine succession in the Boso Peninsula, central Japan.

*Yuki Haneda[1] (1.Geological Survey of Japan, AIST)

[MIS16-P22] The mid-Pliocene Warm Period: climate sensitivity to atmospheric CO_2 levels and inclusion of dynamic vegetation in the MIROC4m model

*Wing-Le Chan[1], Ayako Abe-Ouchi[1,2] (1.Atmosphere and Ocean Research Institute, The University of Tokyo, 2.National Institute of Polar Research)

[MIS16-P23] Chemical weathering feedback during the early Paleogene hyperthermals based on osmium isotope analysis

*Kakeru Ikegami[1], Kazutaka Yasukawa[1,2], Erika Tanaka[1], Junichiro Ohta[1,2], Yusuke Kuwahara[1], Moei Yano[2,1], Koichiro Fujinaga[2,1], Yasuhiro Kato[1,2] (1.School of Engineering, The University of Tokyo, 2.ORCeNG, Chiba Institute of Technology)

[MIS16-P24] High latitude paleoenvironments in Southern Hemisphere during mid-Cretaceous

*Hiromichi Komiya[1], Takashi Hasegawa[1] (1.Kanazawa University)

[MIS16-P25] A study on the responses of the climate field in the Cretaceous to orbital parameter changes

★Invited Papers

*Taro Higuchi[1], Ayako Abe-Ouchi[1], Wing-Le Chan[1] (1.Atmospheric and Ocean Research Institute, the University of Tokyo)

[MIS16-P26] **Eccentricity paced increase in the continental weathering in the latest Hauterivian, Early Cretaceous**

★Invited Papers

*Hironao Matsumoto[1], Rodolfo Coccioni[2], Fabrizio Frontalini[2], Kotaro Shirai[1], Junichiro Kuroda[1] (1.Atmosphere and Ocean Research Institute, the University of Tokyo, 2.University of Urbino)

[MIS16-P27] Millennial-scale cyclicities recorded in the Cretaceous lacustrine core using Monte Carlo approach

*Hitoshi Hasegawa[1], Hirofumi Asahi[2] (1.Faculty of Science and Technology, Kochi University, 2.Center for Advanced Marine Core Research, Kochi University)

Temperature effect on Japanese stalagmite $\delta^{18}O$ records from Hiroshima and Gifu

*Hirokazu Kato[1], Taiki Mori[2], Shota Amekawa[1], Akihiro Kano[1]

1. Department of Earth and Planetary Science, The University of Tokyo, 2. Chuo Kaihatsu Corporation

Stalagmites from caves are excellent archives of terrestrial paleoclimate information. Stalagmite $\delta^{18}O$ values are basically controlled by two major factors, temperature of calcite formation and cave drip water $\delta^{18}O$ derived from the local precipitation. The latter factor involves the changes in climatic factors including the monsoon intensity, moisture trajectory, and seasonality of precipitation. It is, however, not easy to determine relative importance of two fundamental controls, by conventional isotopic compositions alone. Carbonate clumped isotope thermometry is a resolution to this problem, which can directly reconstruct paleo-temperature regardless of drip water $\delta^{18}O$.
Recently, stalagmite studies focusing on temperature signals were reported for the late Pleistocene to middle Holocene stalagmites from Japan (e.g., Mori et al., 2018). We recently measured carbonate clumped isotope (Δ_{47}) from 50 layers of Hiro-1 stalagmite (18–4 ka) from Hiroshima Prefecture and successfully separated signals of temperature changes and drip water $\delta^{18}O$ in the Hiro-1 $\delta^{18}O$ values (Kato et al., 2021) using equations of temperature-dependencies of $\delta^{18}O$ and Δ_{47} (Tremaine et al., 2011; Kato et al., 2019). An important finding in Kato et al. (2021) was that meteoric water $\delta^{18}O$ (drip water $\delta^{18}O$) per se changes depending on temperature.
In this study, the authors newly analyzed Δ_{47} values from more than 60 layers of OT-02 stalagmite (63–35, 8–3 ka) collected from Ohtaki cave, Gifu prefecture, of which U-Th ages and $\delta^{18}O$ values had been already analyzed by Mori et al. (2018). The Δ_{47} measurements were performed using a dual inlet mass spectrometer (Finnigan MAT-253) at Kyushu University.
In the relevant interval of mid-Holocene (8 to 4 ka), OT-02 stalagmite shows a similar Δ_{47} profile with Hiro-1, the peak of warming around the Hypsithermal (6–5 ka) after a slight cooling around 7 ka. This agreement suggests that Δ_{47} values of the two Japanese stalagmites are reliable proxies of terrestrial temperature. In the period of 63–35 ka, Δ_{47} values of OT-02 exhibit periodic fluctuation relating Dansgaard-Oeschger cycles with 3–5 ºC cooling in Heinrich events 4–6. As considered by Mori et al. (2018), temperature variation is likely a major controlling factor of OT-02 $\delta^{18}O$. Reconstructed paleo drip water $\delta^{18}O$ by subtracting temperature effect from OT-02 $\delta^{18}O$ shows a correlation with the reconstructed temperature, which was also recognized in Hiro-1 stalagmite in Hiroshima. However, the correlation in OT-02 is even stronger than that of Hiro-1. It can be assumed that the drip water $\delta^{18}O$ in Gifu reflect the precipitation ratio of summer rainfall with higher $\delta^{18}O$ and winter snow/rainfall with lower $\delta^{18}O$, which differs depending on climatic periods.

References

Kato, H. et al (2019) Seasonal temperature changes obtained from carbonate clumped isotopes of annually laminated tufas from Japan: discrepancy between natural and synthetic calcites. GCA 244, 548–564.
Kato, H. et al (2021) Influences of temperature and the meteoric water $\delta^{18}O$ value on a stalagmite record in the last deglacial to middle Holocene period from southwestern Japan. QSR 253.
Mori, T. et al (2018) Temperature and seawater isotopic controls on two stalagmite records since 83 ka from maritime Japan. QSR 192, 47–58.

©2021. Japan Geoscience Union. All Right Reserved.

Keywords: stalagmite, paleo climate, stable oxygen isotope , carbonate clumped isotope, terrestrial temperature

©2021. Japan Geoscience Union. All Right Reserved.

Oxygen isotope equilibrium of the shallow-water benthic foraminifer *Hanzawaia nipponica* (Asano) in Tosa Bay, southwest Japan

*Minoru Ikehara[1,2], Shigetaka Kita[2], SHUNGO KAWAGATA[3]

1. Center for Advanced Marine Core Research, Kochi University, 2. Graduate School of Integrated Arts and Sciences, Kochi University, 3. Faculty of Education, Yokohama National University

Oxygen isotopic compositions ($\delta^{18}O$) of benthic foraminifer tests are widely used for reconstructing paleoceanographic changes, such as global ice volumes during glacial–interglacial cycles. Although deep-sea benthic foraminifers have been well characterized and are considered reliable indicators, little attention has been paid to the geochemistry of shallow-water benthic foraminifers. In this study we evaluated $\delta^{18}O$ in the shallow-water benthic foraminifer *Hanzawaia nipponica* (Asano), which lives in surface sediments on continental shelves and upper slopes under the influence of two warm currents, the Kuroshio and Tsushima currents, in the East China Sea, northwest Pacific, and southwestern Japan Sea. To evaluate oxygen isotope equilibrium, we analyzed $\delta^{18}O$ of *H. nipponica* and ambient seawater on the continental shelf in Tosa Bay, southwest Japan. Seawater $\delta^{18}O$ and salinity in Tosa Bay are similar to those of surface and subsurface waters in the Kuroshio region in the Okinawa Trough and the northwest Pacific. Vertical profiles of seawater $\delta^{18}O$ show no variation with water depth (0–200 m) in Tosa Bay. However, tests of living *H. nipponica* (as determined by staining with Rose Bengal) and fossil (non-stained) *H. nipponica*, picked from samples of the top centimeter of seafloor sediment, yielded carbonate $\delta^{18}O$ values that clearly increase with water depth, suggesting a temperature-dependent relationship. A comparison of carbonate $\delta^{18}O$ values in living *H. nipponica* and those predicted on the basis of seawater $\delta^{18}O$ and annual mean bottom temperature shows that *H. nipponica* tests are in oxygen isotopic equilibrium with ambient seawater. This result additionally suggests that the life cycle of this species is longer than one year. Thus, we propose that the carbonate $\delta^{18}O$ of *H. nipponica* are useful proxies to reconstruct shallow-water paleoenvironmental changes in the northwest Pacific and its marginal seas.

Keywords: benthic foraminifer, oxygen isotope equilibrium, Tosa Bay, Kuroshio

©2021. Japan Geoscience Union. All Right Reserved.

Variations in shell morphology of the planktonic foraminifer *Globigerina bulloides* in the sediment off Kashima

*Yuya Hashimoto[1], Takuya Sagawa[2]

1. Kanazawa University College of Science and Engineering, 2. Institute of Science and Engineering, Kanazawa University

Planktonic foraminifer *Globigerina bulloides* inhabits a wide range of latitudes, especially in the mid-latitudes. Domitsu and Oda. (2005) focused on such shell morphology and reported that it can be divided into two major types, corresponding to warm and cold water masses in Japan Sea. However, there is no such comprehensive study on water masses and shell morphology in the Pacific Ocean. In this study, we focused on the waters off Kashima, where the temperature gradient in the latitudinal direction increases due to the mixing of the warm and cold water masses and examined the diversity of shell morphology of *G. bulloides* in response to such water mass mixing by observing and quantitatively measuring the shells. We used *G. bulloides* which is 180-250 μm size from 120 individuals each from Holocene, glacial, and last glacial samples. Measurements were made on images taken with a digital microscope. The following parameters were measured: short diameter [maximum distance between the first chamber from the last (F-1) and the third chamber from the last (F-3)], long diameter [maximum distance between the second chamber from the last (F-2) and the last chamber (F)], foraminiferal area (FA), the area of each foraminiferal chamber and the coiling direction of the shell. Cross-sectional observation by SEM was also conducted to see the difference in shell thickness. The ratio of short to long diameters (short diameter/long diameter) and the ratio of the area of F to the area of F-3 (F/F-3) were taken as quantitative indices to reflect the differences in shell morphology using the data obtained from the measurements. Histograms were made for each sample, and the values and shell morphology were compared among samples of different ages. As for F/F-3, there was an inverse correlation between the two indices, reflecting the difference in shell morphology. Although there was no significant difference in the shell morphology of the representative individuals of the populations located at both ends of the value range, observations showed that the shell thickness of the individuals from the warm period samples was thinner than that of the individuals from the cold period samples. This is consistent with Domitsu and Oda. (2005), who reported that thin-shelled individuals predominate in warm water masses and thick-shelled individuals predominate in cold water masses. It could not be adapted to the classification of Kashima. The mean values of short/long diameters were compared for each coiling direction, but no significant differences were found. So, we conclude quantitative data on thickness are also needed to classify *G. bulloides* with different water masses, and it is necessary to consider those with intermediate morphology off Kashima.

Keywords: Planktonic foraminifera, morphology, Kashima

©2021. Japan Geoscience Union. All Right Reserved.

Climate characteristics of Amami , Kagoshima , Japan over the past 200 years inferred from tree-ring cellulose oxygen isotope ratio data

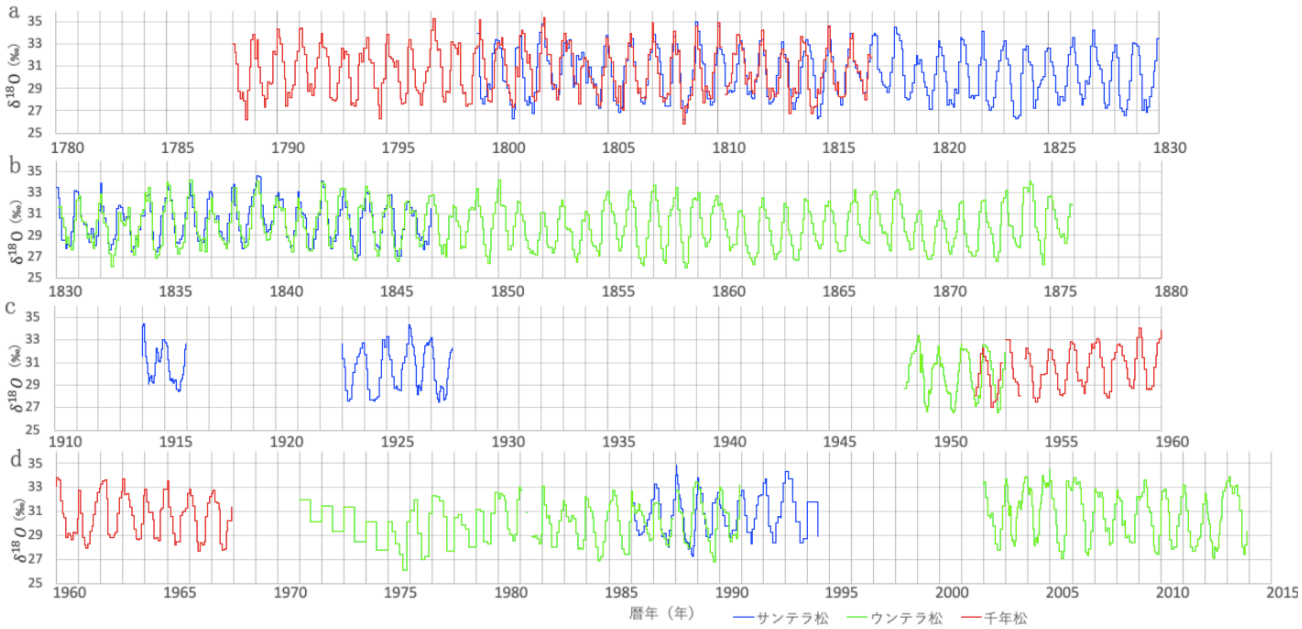
*Akihiro Masuoka[1], Kenjiro Sho[1], Masafumi Ohata[2], Zhen Li[3], Takeshi Nakatsuka[3]

1. Nagoya Institute of Technology, 2. Taisei Corporation, 3. Nagoya University

It has become clear that the oxygen isotope ratios contained in tree-ring cellulose reflect oxygen isotope ratios in precipitation and relative humidity , regardless of physiological factors of the tree. It is a useful tool to reconstruct past climate. In this study, we investigate climate characteristics over the past 200 years in Amami Oshima Island(28˚22’ N 129˚29’ E), southwestern Japan, by measuring the oxygen isotope ratio contained in tree-ring cellulose.
We collected disk samples from three Ryukyu pine (*pinus luchuensis*) trees (namely, “Sennen”, ”Santera”, “Untera”). The disk samples were cut into transverse thin plates with a thickness of 2 mm using a diamond wheel saw to extract cellulose. The prepared cellulose specimen was divided into 12 segments for each ring along the growth direction using a binocular stereomicroscope and an ophthalmic knife. We used an online system of a pyrolysis elemental analyzer and an isotope ratio mass spectrometer (TCEA-Delta V Advantage) installed at the Graduate School of Environmental Studies, Nagoya University for isotope measurement. The measured period is Santera pine: 1799 to 1847,1951 to 1967, Sennen pine: 1951 to 1967,1914,1915,1923 to 1927, 1986 to 1994 and Untera pine: 1830 to 1975,1948 to 1952, 1971 to 1990, 2002 to 2013.
To determine the seasonal growth pattern of the three sample trees, we analyzed correlation between intra-ring $\delta^{18}O$ variation and 10-day rative humidity data at Naze Meteorological Station (28˚22’ N 129˚29’ E) using 37 rings within 1961-2012. As a result, it was estimated that the first segment, corresponding to the earliest stage of tree-ring formation, is formed from early March to mid-April, and the 12th segment, corresponding to the end of tree-ring formation, is formed from late November to late December.
Old document "Oshima Daikanki" (document of prefectural office at Amami Oshima Island) states that there was a long rain from late February to April in 1833, and our oxygen isotope ratio data indicate anomalous wet condition (low δ^{18}) for the first and second segments of the 1833 ring. Similar resalt was found for the 1804 and 1819 rings, implying about 15-year periodical occurrence of long rain in spring.

Keywords: Tree-ring cellulose, Oxygen isotope ratio, Relative humidity, Amami Oshima Island, Ryukyu pines

©2021. Japan Geoscience Union. All Right Reserved.



a.1780 年～1829 年，b.1830 年～1879 年，c.1910 年～1959 年，d.1960 年～2014 年における酸素同位体比データ
測定期間　千年松(赤線):1788 年～1816 年，1951 年～1967 年
サンテラ松(青線):1799 年～1847 年，1914，1915，1923 年～1927 年，1986～1994 年
ウンテラ松(緑線):1830 年～1975 年，1948 年～1952 年，1971 年～1990 年，2002 年～2013 年

©2021. Japan Geoscience Union. All Right Reserved.

Coral skeletal records reveal the relationship between Kuroshio variability and North Pacific climate

*Atsuko Yamazaki[1,2], Tsuyoshi Watanabe[2,3]

1. Kyushu University, 2. KIKAI institute for Coral Reef Sciences, 3. Hokkaido University

The Kuroshio Current is a western boundary current in the North Pacific Ocean. The variations of its transport and migration under the global warming condition have been debated because they have a high impact on the climate, ecosystem, and fishery in the northwestern Pacific. Here, we reconstructed the Kuroshio transport variability and its migration over 70 years using coral skeletal records. Coral cores were collected from Tatsukushi Bay in 2008 on the Pacific coast of Japan, located on the northern front of the Kuroshio Current. Another coral cores were drilled at Cape Shionomisaki is located on the Kuroshio meander site.
The nitrogen isotope proxy in coral skeletons was used as a proxy to record the nitrogen isotope of nitrate controlled by the upwelling of subtropical subsurface water (+2−+3 permil), and coral nitrogen isotope was negatively correlated with observations of the Kuroshio transport ($R = -0.69$, $P < 0.001$) and the two years lagged PDO index ($R = -0.63$, $P < 0.005$) from 1972 to 2007. The 150-year record of coral nitrogen isotopes suggested that the Kuroshio transport varied with ~25-year cycle, and the amplitude became stable, and the volume was intensified through the twentieth century.
The Kuroshio transport was intensified with the La Nina state in the early 1900s and with the El Nino-PDO state after the 1920s. Our results suggested that the Kuroshio transport was influenced by the combined climate modes of ENSO and PDO during the last century. To detect the migration of Kuroshio, we used oxygen isotopes in dual coral cores at Cape Shionomisaki and Tatsukushi Bay. During 1930-2007, the maxima of the oxygen isotopes in the CS core correlated with the winter East China Sea temperature. However, the minima and maxima of the TB core's oxygen isotopes varied with salinity and temperature at the sea surface along the subtropical gyre. The oxygen isotope anomaly in the CS core from the TB core highlights cool and dry conditions with Kuroshio meander events. It correlated with Kuroshio meander's observational proxy, the tide level differences from Kushimoto to Urakami ($R=+0.56$, $P<0.01$).
The reconstructed Kuroshio migration suggested that Kuroshio migration is positively correlated with Kuroshio transport in an 8-12 year cycle. The axis of Kuroshio leaves Cape Shionomisaki with large transport. The Kuroshio meander events are not related to ENSO, but they have positive PDO mode. The coral skeletal archives in the northwestern Pacific can detect the transport and migration of Kuroshio currents.

Keywords: Coral skeletons, Kuroshio, nitrogen isotope, oxygen isotope

©2021. Japan Geoscience Union. All Right Reserved.

Reconstruction of environmental and flooding histories since AD1250 at Lake Kortta, an annually laminated lake at the Central Finland presumed by Diatom and Chrysophyceae assemblages

*Kaoru Kashima[1], Yu Fukumoto[2], Timo Saarinen[3]

1. Department of Earth and Planetary Sciences, Kyushu University, 2. Osaka City University, 3. University of Turku

Lake Kortta, located at the central part of Finland, is a small freshwater lake with 1000m length and 400 width. It has continued more than 3000 years for the sedimentation of laminated lake deposits. The average sedimentation rate was about 4mm/year (after AD1950) and 0.8-1.0mm/year (before AD1950). In this paper, we used the 80cm sedimentary core which was taken in 2010. The age of the base of the core was presumed as AD1250.

The annually laminations of Lake Kortta was related to melting flooding at early spring. The flooding layers were composed of whitish gray sands and were contrast to dark gray clay at other seasons. Among the fine laminated layers, we recognized the several thick whitish flooding layers, dated AD1260, AD1460, AD1780, AD1914-1918, AD1967 and AD1986 respectively. AD1260, AD1460 and AD1780 were presumed to be cold winter in North Europa by historic records, and AD1967 and AD1986 were recorded as lowering of winter temperatures by Meteorological observation in Finland. AD1914-1918 was the period of WWI, and the huge deforestation occurred.

Diatom assemblages were dominated by freshwater planktonic diatoms as Aulacoseira ambigua, A. valida, Stauroneis spp., those presumed the freshwater lake environment has continued since AD1250 to the present. In addition to those lake living diatoms, *Eunotia* spp., *Pinnuralia* spp., peat living diatoms, were observed abundantly. They presumed to be enter into the lake from the surrounding peat lands during the flooding Early Spring season.
Cists of Chrysophyceae increased at cold climatic years as AD1260, AD1460, AD1780, and AD1986. In addition to them, the ratio of Cists of Chrysophyceae increased during the Little Ice Age, about AD1780-1900. Chrysophyceae made cists when lake water conditions became unsuitable for growing, and the ratio of cists was presumed to be related to the climatic and flooding histories at the lake for these 750 years.

Keywords: Annually laminated sediment, Finland, Climatic Change, Flooding sediments, Diatom, Chrysophyceae cists

©2021. Japan Geoscience Union. All Right Reserved.

Sphagnum and grass cellulose oxygen isotopes in peat cores reveal climate changes in northern Japan over the past 4400 years and close relationship with human histories

*Masanobu Yamamoto[1], Osamu Seki[2]

1. Faculty of Environmental Earth Science, Hokkaido University, 2. Insititute of Low Temperature Science

The cellulose $\delta^{18}O$ of plant tissues in peat is a potential climatic proxy to understand the atmospheric dynamics of the past. In this study, we analyzed the $\delta^{18}O$ values of sphagnum and vascular plant cellulose in 4.6- and 4-m long peat cores from the Minamihama moor in Rishiri Island, Japan, to understand paleoclimate changes in northern Japan over the past 4400 years. Cellulose $\delta^{18}O$ of sphagnum showed multi-centennial and millennial variation with higher values in 4500–3400, 2800–2300, and after 700 year BP, and lower values around 3000, and 2200–1000 year BP. The difference of $\delta^{18}O$ between vascular plants and sphagnum ($\Delta\delta^{18}O_{vp-sp}$), a proxy of relative humidity, was reversely correlated with $\delta^{18}O$, indicating humid climate in the periods with higher sphagnum $\delta^{18}O$. The factors controlling the climate in Rishiri Island changed between 2800 and 1300 years BP. In the older period, the development of the North Pacific High determined the climate of entire Hokkaido area *via* changes in the position of the westerly jet and the East Asian summer monsoon rainfall. In the younger period, this mechanism continued to determine the climate of eastern Hokkaido facing the Pacific Ocean, while the intensity of the Tsushima Warm Current determined the climate in Rishri Island. The weakening of the North Pacific High shifted the westerly jet south of Rishiri Island so that the position of the westerly jet did not influence the precipitated water $\delta^{18}O$ in the Rishiri Island. The climate changes in Rishiri Island corresponded to the evolution of human culture in Hokkaido Island.

Keywords: cellulose oxygen isotopes, Holocene, Climate

©2021. Japan Geoscience Union. All Right Reserved.

Can Sedimentary fish DNA track decadal to centennial scale fish abundance?

*Michinobu Kuwae[1], Hiromichi Tamai[1], Hideyuki Doi[2], Masayuki Sakata[3], Toshifumi Minamoto[3], Yoshiaki Suzuki[4]

1. Center for Marine Environmental Studies, 2. Graduate School of Simulation Studies, University of Hyogo, 3. Graduate School of Human Development and Environment, Kobe University, 4. Research Institute of Geology and Geoinformation, Geological Survey of Japan, National Institute of Advanced Industrial Science and Technology

Far too little is known about the long-term dynamics of the abundance of most macro-organism species. We used sedimentary DNA technology to quantify marine fish DNA abundance in sediment sequences spanning the last 300 years. This study first shows the existence of fish DNA in the sequences and proves that fish abundance can be tracked using sedimentary DNA, highlighting the utility of sedimentary DNA for researchers to acquire lengthy records of macro-organism species abundance.

Reference
Kuwae, M., Tamai, H., Doi, H., Sakata, M.K., Minamoto, T., and Suzuki, Y. (2020) Sedimentary DNA tracks decadal-centennial changes in fish species abundance. Communications Biology, 3, 558, https://doi.org/10.1038/s42003-020-01282-9

Keywords: sedimentary DNA, fish abundance, Beppu bay

©2021. Japan Geoscience Union. All Right Reserved.

Paleoenvironmental variations reconstructed by algal biomarker analysis of a sediment core from Lake Nakaumi, Japan

*Akiko Taneichi[1], Yuki Hattori[1], Ken Sawada[1], Takuto Ando[2], Hideto Nakamura[3], Kotaro Hirose[4]

1. Hokkaido Univ., 2. Shimane Univ., 3. Osaka City Univ., 4. Waseda Univ.

Diverse microalgae species inhabit brackish and lacustrine environments, and sensitively change their assemblages and compounds they produce in response to environmental changes. Algal biomarkers have been used to reconstruct the paleoenvironment in aquatic system: aquatic ecology and environmental factors such as temperature and salinity. In particular, long-chain alkenones, haptophyte-produced biomarker, have been widely used for temperature reconstruction in ocean, but there are few examples of their discovery in Japanese lakes such as Lakes Toyoni (Hokkaido), Ichinomegata (Akita), and Nakaumi - Shinji (Tottori-Shimane). Long-chain (C_{28}-C_{32}) alkyl diols are widely distributed in marine and lacustrine sediments and recently used as paleoenvironmental indicators. In particular, C_{32} 1,15-diol is considered to originate from freshwater eustigmatophytes and has been proposed as indicator of freshwater input in coastal area (Lattaud et al., 2016). In the present study, we conducted a biomarker analysis of a sediment core from the Lake Nakaumi to evaluate how the algal biomarkers long-chain alkenones and alkyl diols record the changes in algal assemblages and environments in the brackish lake.
The sediment core was collected from central area of the lake (Nk3C) during May 2017. The ages were determined by Cs and Pb isotopes, and the lowermost horizon was estimated to be about 600 years ago. Biomarker analysis was performed as follows; freeze-dried sediments were extracted by solvents and then separated into fractions by silica-gel column chromatography. Resulted ketone-containing and alcohol-containing fractions were analyzed by GC-MS and GC-FID. The Lake Nakaumi, has been strongly affected by anthropogenic rearrangements during the high economic growth in Japan. Perticularly, the land reclamation and desalination projects in the 1960s to 1980s are known to have had a significant impact on the ecosystem.
The long-chain alkenones and alkyl diols were detected in all the samples from the Nk3C core. The alkenone compositions were clearly different between the samples above and below the horizons affected by the reclamation and desalination project during 1960s. Below the horizons, $C_{37:2}$ alkenones were dominant and C_{40} homologues was absent. On the other hand, $C_{37:4}$ alkenones and C_{40} alkenones were relatively abundant above the horizons. We presume that the main alkenone-producers in sediments below and above the horizons in 1960s were typical marine (Group III) and lacustrine species (Group II), respectively. The compositions of long-chain alkyl diols are also different between the sediments above and below the horizons in 1960s; C_{30} 1,15-diol, common alkyl diol produced by marine eustigmatophyte, was predominant below the horizons, while C_{32} 1,15-diol, biomarker for freshwater eustigmatophyte, was dominant above the horizons in 1960s. From these results, it is suggested that typical marine species of haptophyte and eustigmatophyte inhabit shallow marine environment in the Lake Nakaumi by the middle 20th century, and subsequently, the freshwater species flourished as the dominant producers under brackish environment in the lake after the anthropogenic rearrangements during 1960s. Furthermore, the paleo-temperature (T) calculated by using lacustrine-specific alkenone unsaturation index ($U^{K'}_{37}$; Zheng et al., 2016) gradually increased through the horizon that alkenone-producing species were converted, whereas the common index (U^{K}_{37})-based T showed unexpected change (sudden 5ºC inclease). Although the resolution of the biomarker data is still low, the variations in $U^{K'}_{37}$-based T appear to be broadly consistent with historical record of climate-related events such as the four great famines during the Edo Period and the long-term divisions of climatic periods after 17th century. Thus, the algal biomarker proxies can be expected to apply to reconstructing paleoenvironmental, moreover paleoclimatic

©2021. Japan Geoscience Union. All Right Reserved.

variations in lacustrine sediments.

Keywords: Brackish lake, Lake Nakaumi, Algae biomaker, Alkenone, Alkyl diol, Paleoenvironmental Reconstruction

©2021. Japan Geoscience Union. All Right Reserved.

Paleoceanographic changes in the western part of the Arctic Sea based on ostracods

*Katsura Yamada[1], Kosuke Yamaguchi[1], Masao Uchida[2], Takuya Itaki[3], Kanako Mantoku[2]

1. Department of Geology, Faculty of Science, 2. National Institute for Environmental Studies, 3. National Institute of Advanced Industrial Science and Technology

Abrupt climate changes for a few thousand years are identified between Late Pleistocene and Holocene. Some of them are found in the Arctic Sea and northwestern Atlantic Ocean, suggesting that importance to understand paleoceanographic shifts accurately in the Arctic Ocean. However, oceanographic changes during the Holocene are ambiguous yet there. Thus, our aim is to clarify the Holocene oceanographic shifts in the area shallower than 200 m water depth in the western part of the Arctic Ocean. The study area is influenced by waters from the Pacific, Atlantic Oceans and river input. We used two cores; One was taken from the bottom at a water depth of 65 m in the Mackenzie trough located in river mouth of the Mackenzie river. Another was taken from the bottom in the northern part of the Chukchi shelf at a water depth of 197 m. This water depth is close to the depth bounding waters from the Atlantic and Pacific Oceans. Fossil ostracod assemblages and chemical compositions of the ostracod shells are investigated taken from the core sediments. Shallow marine ostracod taxa were dominated in the Mackenzie trough, and it is considered that the assemblage shifts related to water salinity changes. Conversely, samples from the Chukchi Sea contained ostracod taxa inhabiting in the Pacific and Atlantic Ocean waters. Mg/Ca of ostracod shells were measured by using ICP-AES. First, past water temperatures by using regression lines between Mg/Ca of the genus *Krithe* and water temperature in the previous study was calculated. Then, past water temperatures were reconstructed by relationships between Mg/Ca of *Semicytherura complanate* and the calculated water temperatures in both areas. The bottom water temperatures in the Chukchi shelf showed relative high values during 7000 and 2000 cal year BP. Dominance of ostracod taxa inhabiting in the Atlantic Ocean waters was identified in the two periods inferring intensification of the Atlantic Ocean water influence. Bottom water temperatures in the Mackenzie trough showed high value between 5500-4900 cal year BP and was stable after 4900 cal year BP. Salinity generally had increased from 7700 cal year BP to the present based on ostracod assemblage changes in the Mackenzie trough. Further, relative high salinity was recognized in 2600, 600, and 200 cal year BP. The long-term increase and temporal high values in salinity coincide with the timing of ice sheet expansions since the 5000 cal year BP in the Northern Hemisphere, implying that the salinity was affected by the glacier expansion in the trough.

Keywords: Holocene, Paleoceanography, ostracod

©2021. Japan Geoscience Union. All Right Reserved.

Mid- to late Holocene variability of the Aleutian Low Atmospheric Pressure Cell: Forcing by the Western Jet

*Kana Nagashima[1], Jason Addison[2], Tomohisa Irino[3], Takayuki Omori[4], Kei Yoshimura[5], Naomi Harada[1]

1. Research Institute for Global Change, Japan Agency for Marine-Earth Science and Technology, 2. U.S. Geological Survey, 3. Faculty of Environmental Earth Science, Hokkaido University, 4. The University Museum, The University of Tokyo, 5. Institute of Industrial Science, The University of Tokyo

The North Pacific Ocean is the largest geographic feature in the Northern Hemisphere and its interactions with the overlying atmosphere drives critical components of the global climate system. The Aleutian Low (AL) is one of the major atmospheric systems that determines environmental conditions during winter in the North Pacific Ocean, with impacts that affect the climates of both Asia and North America. However, the multi-centennial and longer scale dynamics of the AL during the Holocene is not fully understood.

The climate mechanism(s) that are responsible for generating AL intensity and position changes over recent instrumental timescales are also poorly understood. One important component is the Westerly Jet (WJ), which is closely associated with the AL through its alternations on cyclogenesis, monsoon development, and storm tracks (e.g., White and Barnett, 1972; Lau, 1988; Dole and Black, 1990; Nakamura et al., 2002; Yang et al., 2002; Athanasiadis et al., 2010; Park and An, 2014). However, at timescales that exceed the recent instrumental record, the interactions between the AL and the WJ are virtually unknown. Therefore, it is critical to reconstruct paleoclimatic history of the AL and examine its interactions with other components of the climate system.

Here we conducted principal component analysis (PCA) using published $\delta^{18}O$ records from Alaska, northwestern Canada, and the western United States, thus eliminating local environmental effects on each record. The analysis was used to 1) identify common pattern(s) of $\delta^{18}O$ anomalies across the study area since 7.5 ka in order to trace multi-centennial and longer AL variations; 2) compare the reconstructed AL variations with proxy reconstructions of the WJ in East Asia and the western North Pacific Ocean to determine linkages; and 3) use these combined AL and WJ datasets to better clarify dynamic changes in North Pacific atmospheric circulation and elucidate the potential triggers of Holocene climate variability (after Nagashima et al., 2021).

The extracted Principal Component 1 (PC1) represents a dramatic change from the mid- to late Holocene, and appears to reflect long-term intensified AL related to interactions between orbitally-driven southward shift of the Westerly Jet (WJ) over East Asia and the northwestern Pacific, and intensification of the El Niño–Southern Oscillation. In contrast, PC2 is characterized by multi-centennial to millennial-scale oscillations, with a spatial loading pattern that suggests PC2 reflects AL intensity and position shifts; AL intensification with a westward shift during 7.5–5.1, 2.4–1.2 and 0.7–0.4 ka. These oscillations are contemporaneous with both WJ latitude and/or the meandering path shifts over East Asia and solar activity change, suggesting that a decrease/increase in solar irradiance is related to AL variability via interactions with the WJ (Nagashima et al., 2021).

Keywords: Aleutian Low, Holocene, oxygen isotope, Westerly Jet

©2021. Japan Geoscience Union. All Right Reserved.

Sedimentary characteristics, age and event of a marine core collected from Uranouchi Bay, Kochi, Japan

*Masafumi MURAYAMA[1,3], Wataru Tanikawa[2], Akira Ijiri[2], Tatsuhiko Hoshino[2], Takehiro Hirose[2], Katsuya Nejigaki[3], Kazuno Arai[3], Go-Ichiro Uramoto[3], Kondo Yasuo[4], Hiromasa Ozaki[5], Minoru Yoneda[5]

1. Faculty of Agriculture and Marine Science, Kochi University, 2. Institute for Extra-cutting-edge Science and Technology Avant-garde Research, Kochi Institute for Core Sample Research, JAMSTEC, 3. Center for Advanced Marine Core Research, Kochi University, 4. Faculty of Science and Technology, Kochi University, 5. The University Museum,The University of Tokyo

Sediment cores collected from the inner part (10m depth) of Uranouchi Bay, Kochi Prefecture, have been analyzed to investigate the history of changes in the marine environment. Uranouchi Bay that extends in the east-west direction with 12 km is located in the central part of Tosa Bay, Kochi Prefecture facing to the north side of the Yokonami Peninsula. This is well known as a sinking bay caused by subduction-zone earthquakes. Two 4 m sediment cores were collected by vibro coring using the university research vessel "Neptune". These core samples are considered to have recorded detailed environmental changes in the bay having no affecting the surrounding river. These core samples were carried out X-ray CT and visual observation, physical properties, identification and ^{14}C dating of fossil shells. The lithology of the sediments was olive to gray colored silty clay with a lot of shell fragments. The most upper part of these cores was providing dark colored and had a strong hydrogen sulfide odor. In addition, a well-laminated sedimentary layer with a thickness of 8 cm was observed in the lower part of the core (around 306 m from the core top). This sedimentary layer was confirmed in a similar depth collected at a nearby water depth of 8 M, but no lamination was developed. Radiocarbon dating (AMS 14C age) of shell fragments from the 8 layer of sediment was performed. At the bottom of the core, showing about 3800 years ago, the estimated average deposition rate was 102 cm / kyr. In this presentation, we will introduce these results.

Keywords: Uranouchi Inlet Bay, Marine Core, Event sediment, 14C age

©2021. Japan Geoscience Union. All Right Reserved.

Estimation of amount of meltwater discharge from the Laurentide to the Arctic Ocean during the MWP1a event

*Kenta Suzuki[1], Masanobu Yamamoto[1], Leonid Polyak[2], Tomohisa Irino[1]

1. Faculty of Environmental Earth Science, Hokkaido Univ., 2. Byrd Polar and Climate Research Center, The Ohio State Univ.

The significant sea-level rise events are recognized during the last deglaciation period. The global sea-level rose by 12-18 m in ~340 years at the MWP1a event. However, the sources of meltwater during the MWP1a event are uncertain. In this study, we identified the event layers deposited by MWP1a event from the western Arctic Ocean sediment cores and estimated the amount of meltwater discharged into the Arctic Ocean during this period based on the extent and thickness of sediments.

In this study, we used seven sediment cores collected in the western Arctic Ocean. Event layers by meltwater pulse were identified based on the amount of IRD, mineral composition, sedimentary structure, grain size distribution, and organic matter composition. The amount of suspended matter discharged during this period was calculated from the thickness range of the layer in MWP1a event, and the amount of meltwater that transported this sediment was estimated.

An event layer with sharp boundaries with the upper and lower layers, containing IRD, coarse grained, kaolinite-rich and terrestrial organic matter was identified around 14.7 ka in several sediment cores from the western Arctic Ocean. The characteristics of this layers suggest that those sediments were transported by meltwater discharge during MWP1a event. Rough-estimation indicates the meltwater discharge rate during the MWP1a event was 2 ~ 4 times higher than that of today. The amount of meltwater calculated from the amount of sediment discharged during MWP1a event was equivalent to ~30 % of the relative sea level change at that time.

Keywords: Arctic Ocean, MWP1a

©2021. Japan Geoscience Union. All Right Reserved.

Millennial variability in precipitation in Papua New Guinea during the last deglaciation

*Gaku Sudo[1], Masanobu Yamamoto[1], Samantha Bova[2], Yair Rosenthal[2]

1. Faculty of Environmental Earth Science, Hokkaido Univ., 2. Rutgers Univ.

Millennial climate changes during the last deglaciation is attributed to changes in the Atlantic Meridional Overturning Circulation (AMOC). Although the millennial climate changes have been observed worldwide, the mechanism by which the AMOC change is transmitted is not clear. One plausible hypothesis is that the AMOC variability changes the heat balance in the northern and southern hemispheres, which in turn changes the mean position of the Intertropical Convergence Zone (ITCZ), which in turn changes global temperature and precipitation. Indeed, it has been reported that when the AMOC weakened the ITCZ shifted southward in the Atlantic and eastern Pacific regions. However, there is no conclusive evidence in the regions away from the Atlantic Ocean.

In this study, to test this hypothesis, we reconstructed the variability of the ITCZ in the western Pacific Ocean over the past 25,000 years by analyzing GDGT and long-chain fatty acid isotopes in marine sediments from IODP site U1485 in the Bismarck Sea off the northern coast of Papua New Guinea (PNG). In PNG, orogenic precipitation caused by the northwest monsoon increase when the ITCZ is located south of PNG. The detrital matter is delivered via the Sepik and Ramu rivers to the study site. Thus, the study site is ideal to capture ITCZ variability.

The CBT and BIT, which reflect river discharge, were higher during Bølling-Allerød (BA) period and lower in the Younger-dryas (YD) period. Stable hydrogen isotope ratios (δ D) of long-chain fatty acid, which reflect atmospheric convective activity (and thus precipitation), were lower in the BA period and higher in the YD period. These results indicate that precipitation in PNG was higher in the BA period and lower in the YD period. This is contrary to the results predicted by the above hypothesis, and suggests that the AMOC weakening did not cause the ITCZ to move southward in the western Pacific.

Keywords: ITCZ, Bismarck Sea, Last deglaciation

©2021. Japan Geoscience Union. All Right Reserved.

A paleoclimatic reconstruction of the southeastern Pacific last deglacial using geochemical proxies obtained from offshore Chile

*Karin Nemoto[1,2], Yusuke Yokoyama[1,2], Adam David Sproson[2], Yosuke Miyairi[2], Takahiro AZE[2], Hiroyuki Matsuzaki[3,4], Yair Rosentha[5], Samantha Bova[5]

1. Department of Earth and Planetary Science, The University of Tokyo, 2. Atmosphere and Ocean Research Institute, The University of Tokyo, 3. The University Museum,The University of Tokyo, 4. School of Engineering, The University of Tokyo, 5. Department of Marine and Coastal Sciences, School of Environmental and Biological Sciences, Rutgers University

The southeastern Pacific is a key location to understand the relationship between global climate change and Southern Ocean condition. The coast of Chile is ideally located to clarify the mechanisms behind local climate change. The Southern Westerly Wind belt (SWW) blows over central Chile and interacts with the Southern Annular Mode, the El Niño-Southern Oscillation (ENSO) and the Atlantic Meridional Overturning Circulation (AMOC). The Antarctic Circumpolar Current (ACC) diverts to the north and the south, causing steep latitudinal gradients off the coast of Chile.

A marine sediment core recovered from offshore Chile (44˚S, 75˚W) was used in this study. The age model of this core is based on 14C Accelerator Mass Spectrometry (AMS) dates. The 10Be and 9Be abundances were measured by AMS and High Resolution Inductively Coupled Plasma Mass Spectrometry, respectively. The organic elemental analyzer was used to measure organic C, N and S.

The variation in 10Be may reflect atmospheric conditions such as the location of the SWW and associated precipitation since 10Be is produced in the atmosphere. The amount of 10Be and 9Be are affected not only by the source but also by delivery. When 10Be is normalized by 9Be, the latter effect can be offset (Simon et al., 2016). The 10Be/9Be may reflect atmospheric processes since the ratio is highly controlled by 10Be. The results of 10Be/9Be and 10Be indicates the intensity of the SWW became stronger and the amount of precipitation was increased from 12 ka to 3 ka, which is antiphase to those in the core zone of the SWW (Lamy et al., 2010).

Most of the records from both this and previous research fluctuate around 12 ka, 8 ka and 3 ka. Climatic changes off the coast of Chile are associated with changes in the ACC and the SWW. The changes observed in this study clearly suggests close relationship with global climate indicating importance of coupling between atmosphere and ocean in this region.

References

Lamy F. et al. Modulation of the bipolar seesaw in the Southeast Pacific during Termination 1. Earth Planet. Sci. Lett. 259, 400-413 (2007).

Pike J., Swann G.E.A., Leng M.J. & Snelling A.M. Glacial discharge along the west Antarctic Peninsula during the Holocene. Nat. Geosci. 6, 199-202 (2013).

Simon Q. etal. Authigenic $^{10}Be/^{9}Be$ ratios and ^{10}Be-fluxes ($^{230}Th_{xs}$-normalized) in central Baffin Bay sediments during the last glacial cycle: Paleoenvironmental implications. Quat. Sci. Rev. 140, 142-162 (2016).

©2021. Japan Geoscience Union. All Right Reserved.

Keywords: paleoclimate, westerly, beryllium

©2021. Japan Geoscience Union. All Right Reserved.

Paleovegetation changes in the northern Mongolia since the last glacial

*Ryosuke Imaoka[1], Koji Shichi[2], Hitoshi Hasegawa[1], Niiden Ichinnorov[3], Nagayoshi Katsuta[4], Davaasuren Davaadorj[5], Masafumi MURAYAMA[1], Masao Iwai[1], masami izuho[6]

1. Kochi University, 2. Forestry and Forest Products Research Institute, 3. Paleontological Center of Mongolia, 4. Gifu University, 5. National University of Mongolia, 6. Tokyo Metropolitan University

Northern Mongolia is located at the boundary between northern permafrost and southern desert belts and is sensitive to climate change such as permafrost thawing. In this study, we aimed to reconstruct changes in paleoenvironment and paleovegetation in northern Mongolia since the last glacial based on the analysis for lake sediment record of Sangiin Dalai lake. We took lake bottom sediment by gravity core in August 2016 (16SD02; 84 cm length), and five boring cores in March 2019 (19SD01~05; ca. 13 m length). Using these sediment cores, we performed palynological analysis at Forestry and Forest Products Research Institute and elemental composition analysis using XRF core scanner at Center for Advanced Marine Core Research, Kochi University.
Based on palynological analysis and biome reconstruction (Tarasov *et al*., 2000), paleovegetation changes from steppe-desert biome dominated by *Artemisia* and Chenopodiaceae in the last glacial to steppe-taiga biome composed of mixture of *Artemisia* and *Pinus* in the Holocene were reconstructed. Elemental composition analysis reveals that higher Si/Ti ratio in sand layer and higher Mn/Fe ratio (oxic environment) and Ca/Ti ratio (saline lake) in silt layer during the last glacial, and low Ca/Ti ratio (less saline lake) during the Holocene. Thus, marked paleoenvironmental change from shallow lake and alluvial plain during the last glacial to high lake-level during the Holocene are reconstructed. These result, in conjunction with palynological data-sets in surrounding area (Kotokel lake in southern Siberia: Shichi *et al*., 2009; and Orog lake in southern Mongolia: Yu *et al*., 2019) suggests that predominance of steppe-desert vegetation in southern Siberia and northern/southern Mongolia during the last glacial, and turned to Forest vegetation in southern Siberia, steppe-taiga vegetation in northern Mongolia, and desert vegetation in southern Mongolia during the Holocene, which likely caused by permafrost thawing by insolation change and climatic warming in deglaciation period.

References

Shichi, K., *et al*. (2009). Late Pleistocene and Holocene vegetation and climate records from Lake Kotokel, central Baikal region. *Quaternary International*, *205*, 98-110.

Tarasov, P. E., *et al*. (2000). Last glacial maximum biomes reconstructed from pollen and plant macrofossil data from northern Eurasia. *Journal of Biogeography*, *27*, 609-620.

Yu, K., *et al*. (2019). Late Quaternary environments in the Gobi Desert of Mongolia: Vegetation, hydrological, and palaeoclimate evolution. *Palaeogeography, Palaeoclimatology, Palaeoecology*, *514*, 77-91.

Keywords: Pollen analysis, Vegetation reconstruction, Last glacial period, Permanent frost, Global warming

©2021. Japan Geoscience Union. All Right Reserved.

©2021. Japan Geoscience Union. All Right Reserved.

Glacial–interglacial variations in the Leeuwin Current for the last 50,000 years based on Nd isotope records of benthic foraminifers

*Ryota Wako[1], Hideko Takayanagi[1], Shigeyuki Wakaki[2], Takeshige Ishiwa[4], Yusuke Yokoyama[5], Hitomi Uchimura Wakaki[3], Tsuyoshi Ishikawa[2], Yasufumi Iryu[1]

1. Department of earth science, Tohoku university , 2. Kochi Institute for Core Sample Research, JAMSTEC, 3. Center for Advanced Marine Core Research, Kochi University, 4. National Institute of Polar Research, 5. Atmosphere and Ocean Research Institute, University of Tokyo

The Leeuwin Current (LC) is a major warm current flowing poleward from the equatorial region along the west coast of Australia. Variations in the air-sea interaction in its surrounding area (e.g., ENSO and wind strength) and the intensity of the Australian monsoon are known to have a strong influence on the strength and pathway of the LC at the seasonal to interannual time scales. However, it is still controversial how the LC responded to paleoclimate and paleoceanographic conditions at the millennial or longer time scales, such as glacial-interglacial climate changes. In this study, we analyzed neodymium (Nd) isotope composition (ε Nd) of bulk benthic foraminifers from shallow-water to hemipelagic carbonate sediment cores (IODP Exp. 356 sites U1460, U1461, and U1463 from south to north) collected off West Australia to understand water mass exchanges and variations in the strength and pathway of the LC for the last 50,000 years.

Nd isotope results indicate that the coastal current, which flows the surface between the LC and Australian continent, became predominant at least in coastal areas around U1461 in the latest Pleistocene. This may indicate that the pathway of the LC moved slightly offshore at northwestern Australia due to the stronger Australian monsoon and/or thickening of surface to sub-surface water masses during the postglacial period. While, during the last glacial maximum (MIS2), the ε Nd composition of all sites exhibited more radiogenic values than those of the postglacial period. Our results suggest that, although the ε Nd values of the studied cores were affected by sea-level changes, the LC region was predominantly influenced by Pacific-origin waters flowing into the Indian Ocean from the northern and southern Pacific Ocean through the Indonesian Through Flow even during the last glacial period.

Keywords: Neodymium isotope composition, Leeuwin Current, Benthic foraminifera, Glacial-interglacial, Paleoenvironment, IODP

©2021. Japan Geoscience Union. All Right Reserved.

Changes in carbonate dissolution and preservation in Southern Ocean sediment off Chilean margin during the last 140 kyrs based on fragmentation and size-normalized weight of planktic foraminiferal tests.

*Takuto Kasuya[1], Yusuke Okazaki[2], Shinya Iwasaki[3], IODP Expedition 383 Scientific Party

1. Department of Earth and Planetary Sciences, School of Science, Kyushu University , 2. Department of Earth and Planetary Sciences, Faculty of Science, Kyushu University, 3. MARUM Center for Marine Environmental Sciences and Department of Geosciences, University of Bremen

The Southern Ocean plays an important role in global climate change as a reservoir of heat and carbon. Glacial atmospheric carbon dioxide concentrations were 80-100 ppm lower than the interglacial level. Changes in $CaCO_3$ dissolution and preservation in the deep-sea particularly for the Southern Ocean is thought to be a key factor for glacial carbon reservoir. In this study, we investigated change in dissolution and carbonate preservation in Southern Ocean sediment for the last 140 kyrs based on two proxies, fragmentation index and size-normalized weight of planktic foraminiferal tests. Fragmentation index represents a ratio of the number of fragments to the intact planktic foraminiferal tests. Two planktic foraminiferal species, *Neogloboquadrina pachyderma* and *Globigerina bulloides* were employed. For size-normalized weight of planktic foraminiferal tests, *Globigerina bulloides* tests were picked up from the 212-250 μm, 250-300 μm, and 300-355 μm sieve fractions. Sediment core samples used in this study were obtained at Site U1543 (54°35.06’ S; 76°40.58’ W; 3864 m water depth) in the eastern South Pacific west of the Chile Trench during the International Ocean Discovery Program (IODP) Expedition 383 in 2019. At U1543, foraminiferal tests in the sediment have been preserved only during glacial terminations to early interglacials during the last 140 kyrs, which is consistent with expected deep-sea carbonate ion response to atmospheric CO_2 elevations during the glacial terminations. During the last interglacial period (marine isotope stage 5e), both fragmentation ratio and size-normalized weight of planktic foraminiferal tests suggested two carbonate dissolution events at millennial time-scale.

Keywords: Carbonate preservation / dissolution, Southern Ocean, MIS 5, Planktonic foraminifera

©2021. Japan Geoscience Union. All Right Reserved.

Examining MIS 5e Sea-Levels around Japan: 60+ Years of Sea-Level Proxy Analysis and Applied Dating Techniques

*Evan Tam[1,2], Yusuke Yokoyama[1,2]

1. University of Tokyo, Atmosphere and Ocean Research Institute, 2. University of Tokyo, Graduate Program on Environmental Science

Sea-level proxies chronicling Marine Isotope Stage 5e (MIS 5e, ca. 124 ka) have been examined in Japanese geologic literature for over at least the last 60 years. Formed during sea-level highstands and preserved predominantly by tectonic uplift processes, sea-level proxies in Japan are commonly identified as marine terraces and are chronologically constrained by their relation to identified tephra layers or other dated strata. Stratigraphic correlations are used in conjunction to numerous dating techniques such as paleontological analysis, tectonic uplift rates, tephra (volcanic ash), Uranium-Thorium (U/Th), Carbon 14 (^{14}C), and Optically Stimulated Luminesce (OSL) dating techniques, linking these landforms to MIS 5e and a broader global history. Commissioned by the World Atlas of Last Interglacial Shorelines (WALIS), this study standardized data from over 70 studies, assembling data points for over 300 locations to create an updated overview of MIS 5e proxy sea-levels throughout Japan.

Keywords: Paleosea-level, MIS 5e, Last Interglacial

©2021. Japan Geoscience Union. All Right Reserved.

Integrated stratigraphy of the sediment core retrieved from the Manihiki Plateau in the central Pacific and the paleotemperature change for the last 800 kyr

*MISAKI URAKAMI[1], Takuya Sagawa[2], Yoshimi Kubota[3]

1. College of Science and Engineering, Kanazawa University, 2. Institute of Science and Engineering, Kanazawa University, 3. National Museum of Nature and Science

East-west sea surface temperature (SST) difference in the tropical Pacific like today developed after about 1.7 million years ago. Although many previous studies have investigated the evolution of the tropical Pacific SST using sediment cores in the east and west tropical Pacific, the central tropical Pacific SST is not well understood mainly due to the lack of long and continuous Pliocene/Pleistocene proxy record. The Manihiki Plateau is located at the southeastern edge of WPWP and is ideally situated to discuss the central tropical Pacific temperature changes. Here, we constructed an age model of the piston cores collected from the Manihiki Plateau (KR99-12 PC05) based on the magnetostratigraphy, the planktonic foraminiferal biostratigraphy, and the oxygen isotope stratigraphy. We obtained a total of 11 age constraints including four planktonic foraminiferal biohorizons and seven oxygen isotopic stratigraphic horizons in addition to five paleomagnetic polarity reversals reported by previous research. The results indicate that the core PC05 is continuously accumulated for the last 2.2 Ma with sedimentation rate of ~0.8 cm/kyr. We will also discuss the central Pacific SST change for the last 800 kyr reconstructed by Mg/Ca-paleothermometry of planktonic foraminifera.

©2021. Japan Geoscience Union. All Right Reserved.

Preliminary results of oxygen isotopic, paleomagnetic, and pollen analyses from a mid-Piacenzian marine succession in the Boso Peninsula, central Japan.

*Yuki Haneda[1]

1. Geological Survey of Japan, AIST

The Pliocene climate is one of the best analogs for the climate of a globally warmer future. In this presentation I show preliminary results of oxygen isotopic, paleomagnetic, and pollen analyses from the uppermost part of the Anno Formation, which is a forearc basin-fill deposit distributing in the Boso Peninsula. Lithological observations were conducted along the Minato River and its branch stream in Futtsu city, Chiba. The examined interval consists of silty stone, and pumice, scoria, and fine volcanic ash beds. Fifty-five samples for oxygen isotopic, paleomagnetic, and pollen analyses were collected from silty beds.
Progressive alternating field and thermal demagnetizations were conducted for each specimen to remove secondary remanence. Paleomagnetic results show a directional change from a reversed polarity to a normal polarity with transitional directions in the uppermost part of the examined interval. Oxygen isotope analyses were conducted for benthic foraminifera *Melonis pompiloides*, and *Bolivinita quadrilatera*. Resultant oxygen isotope record shows a glacial period in the lowermost part of the examined interval ($\delta^{18}O$ = ca. 3.70 ‰), and subsequent warm periods with a minor fluctuation of $\delta^{18}O$ between 3.07 ‰and 3.24 ‰in the upper interval. When comparing the oxygen isotope and paleomagnetic records of this study to the chronostratigraphy of the Anno Formation (Haneda & Okada, 2019), the examined interval ranges from Marine Isotope Stage (MIS) M2 to KM5 in the Mammoth Reversed Polarity Subchron.
A preliminary analysis of pollen fossil was conducted for 6 samples. All samples well preserve pollen fossils, and predominantly yield Taxodiaceae with *Cathaya* and *Quercus* (subgen. *Cyclobalanopsis*) as minor components. This flora indicates a warmer climate than present. Two samples from the MIS M2 interval yield genus *Picea*, *Tsuga*, and *Alnus*, likely indicating cooler climate condition relative to other 4 samples, consistent with the benthic oxygen isotope record. The oxygen isotope, paleomagnetic, and pollen records in this study indicate that the uppermost part of the Anno Formation is a potentially remarkable archive, recording paleoclimatic–paleoceanographic variations in the East Asian margin during the mid-Piacenzian warm period.

Keywords: oxygen isotope stratigraphy, magnetostratigraphy, pollen fossil, mid-Piacenzian Warm Period, Boso Peninsula, Anno Formation

©2021. Japan Geoscience Union. All Right Reserved.

The mid-Pliocene Warm Period: climate sensitivity to atmospheric CO_2 levels and inclusion of dynamic vegetation in the MIROC4m model

*Wing-Le Chan[1], Ayako Abe-Ouchi[1,2]

1. Atmosphere and Ocean Research Institute, The University of Tokyo, 2. National Institute of Polar Research

The mid-Pliocene Warm Period (mPWP), 3.3-3 million years ago, was a period of sustained warmth before global cooling occurred and a shift to glacial cycles. It was also the most recent time in the history of Earth when atmospheric CO_2 levels were similar to those of present day. The study of this period is thus of much importance, given the growing concerns over future climate change associated with anthropogenic emissions of greenhouse gases. A number of climate models have been used to investigate the mPWP climate, contributing to the Pliocene Model Intercomparison Project (PlioMIP), while a large collection of proxy data from both terrestrial and marine sources have become available. Reconciling model results and proxy data remains an important issue.

In our study, we use the mid-resolution MIROC4m coupled atmosphere-ocean general circulation model and apply ice sheet configuration, land-sea mask, orography and biome distribution based on PRISM data sets, as specified in the second phase of PlioMIP, one of the working groups of PMIP4. We conduct a series of experiments which include a range of atmospheric CO_2 levels given the spread in values suggested by different sources of proxy data and show how various aspects of the climate respond. While sea surface temperatures (SST) for all CO_2 levels show much less warming in the northern high latitudes as suggested by previous proxy data, there is improved agreement with more recent data in the tropical Pacific for 400ppm CO_2. We will show these and other results. Additional experiments were carried out with MIROC4m coupled to a dynamic global vegetation model. Compared to the prescribed Pliocene vegetation, temperate forests expand at mid-latitudes across Asia and North America. Across North Africa, shrubs and bare ground expand, replacing regions of savanna. Global surface temperatures are slightly lower with the inclusion of dynamic vegetation.

Keywords: Pliocene, climate modeling, dynamic vegetation, data-model comparison

©2021. Japan Geoscience Union. All Right Reserved.

Chemical weathering feedback during the early Paleogene hyperthermals based on osmium isotope analysis

*Kakeru Ikegami[1], Kazutaka Yasukawa[1,2], Erika Tanaka[1], Junichiro Ohta[1,2], Yusuke Kuwahara[1], Moei Yano[2,1], Koichiro Fujinaga[2,1], Yasuhiro Kato[1,2]

1. School of Engineering, The University of Tokyo, 2. ORCeNG, Chiba Institute of Technology

During the early Paleogene, multiple rapid global warming events called ‘hyperthermals’ occurred in a geologically short time scale (10^4–10^5 yr) [1]. These events coincided with distinct negative carbon isotope ($\delta^{13}C$) excursions, which indicates that the cause of hyperthermals was massive injection of ^{13}C-depleted greenhouse gases [2].

Chemical weathering of continental silicate rocks is known as one of the recovery processes from such warming events. Some previous studies have shown an intensification of the chemical weathering during the Paleocene-Eocene Thermal Maximum (PETM), using an osmium isotope ratio ($^{187}Os/^{188}Os$) in the ocean, which can constrain the changes in chemical weathering associated with short-term warming [3,4]. However, the marine Os isotope record during the early Eocene hyperthermals, including the PETM, has not been reported from the pelagic area of the Pacific Ocean.

In the presentation, we will report the results of $^{187}Os/^{188}Os$ measurement of deep-sea sediment samples collected from Ocean Drilling Program Site 1215 Hole A in the central North Pacific Ocean, which record multiple hyperthermal events including the PETM, Eocene Thermal Maximum (ETM) 2 and ETM3 [5]. Based on the analytical results, we will discuss the changes in the intensity of chemical weathering of continental silicate rocks during each hyperthermal event.

[1] Zachos et al. (2008) *Nature* **451**, 279-283. [2] Lunt et al. (2011) *Nature Geoscience* **4**, 775-778. [3] Ravizza et al. (2001) *Paleoceanography* **16**, 155-163. [4] Dickson et al. (2015) *Palaeogeography, Palaeoclimatology, Palaeoecology* **438**, 300-307. [5] Leon-Rodriquez and Dickens (2010) *Palaeogeography, Palaeoclimatology, Palaeoecology* **298**, 409-420.

Keywords: osmium isotopes, Paleogene, hyperthermals, chemical weathering, Earth system feedback

©2021. Japan Geoscience Union. All Right Reserved.

High latitude paleoenvironments in Southern Hemisphere during mid-Cretaceous

*Hiromichi Komiya[1], Takashi Hasegawa[1]

1. Kanazawa University

Cretaceous is known as a period of warm climate with higher sea levels and higher carbon dioxide concentrations than the present, as well as with active oceanic crust formation and volcanic activity. They were especially prominent during Mid-Cretaceous Cenomanian (100.5-93.9 Ma). Paleoenvironmental studies of the mid-Cretaceous have been conducted mainly in Europe and North America. In those areas, where global environmental changes such as oceanic anoxic events (OAEs) associated with isotope events and cyclic environmental changes derived from orbital forcing of Milankovitch cycle were recognized. In contrast, few studies have been reported in the high latitudes in the southern hemisphere. In high latitudes environmental changes more sensitive to global warming could be recorded. Can they be recognized actually? If yes, how can they be recorded, and can the magnitude and cyclicity be deciphered? This study analyzed the Cenomanian samples from the high latitudes in the Southern Hemisphere. It is a stage that typical Cretaceous greenhouse paleoenvironment developed, under ice-free condition.

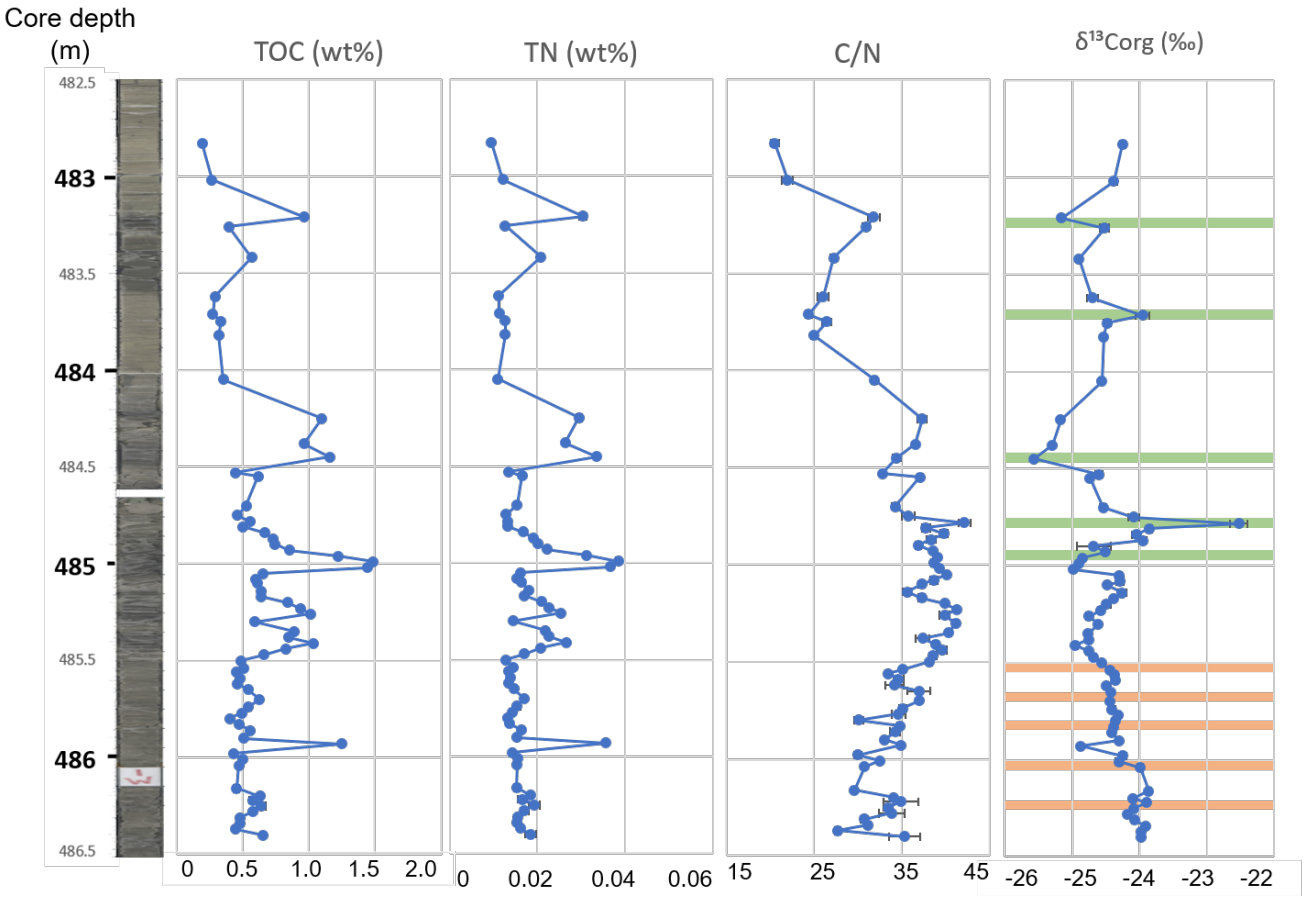
This study used core samples from IODP Exp,369 Site U1516C Cores 34R and 35R, which are estimated to be deposited during mid-Cenomanian based on biostratigraphy. For high-resolution analysis, organic carbon isotope ratio (d13Corg), total organic carbon (TOC), total nitrogen (TN) and C/N ratio were obtained and discussed. Biomarker analysis, focused on specific markers such as alkenones that were interpreted to be related to surface productivity. The following were discussed and concluded.

(1) The d18O variations in sea surface temperature as large as 4˚C found by previous study did not have concordant fluctuation with the terrestrial and seafloor environmental changes shown by TOC and d13Corg variations. Land and seafloor were controlled by separate factors.

(2) The variations in d13Corg can be interpreted to be partly related to the redox conditions of the seafloor, rather than being controlled by the mixing ratio of terrestrial and marine in origin.

(3) C37 alkenones derived from haptophytes were recognized. The detection of C37 alkenone with two-unsaturation sites and the absence of that with three-unsaturation sites. These facts suggest that the sea surface temperature at that time may have been higher than the current equatorial water temperature (>28˚C) even in the high latitude. Negative correlation of C40 alkenones with d18O of carbonate indicates its potential significance for paleothermometry.

©2021. Japan Geoscience Union. All Right Reserved.



©2021. Japan Geoscience Union. All Right Reserved.

A study on the responses of the climate field in the Cretaceous to orbital parameter changes

*Taro Higuchi[1], Ayako Abe-Ouchi[1], Wing-Le Chan[1]

1. Atmospheric and Ocean Research Institute, the University of Tokyo

Insolation changes to the orbital parameters, such as the eccentricity, obliquity, and precession, have a great impact on the climate. In particular, it is well-known that there have been periodic changes in ice sheets and climatic fields in the past hundreds of thousands of years, related to changes in orbital parameters. The physical mechanism of these changes has been investigated by using numerical simulations. The Cretaceous is known as one of the warmest periods in the Phanerozoic due to increased levels of greenhouse gases, and the proxies indicate the striking temperature amplifications in the high-latitude and polar regions, resulting in a smaller equator-to-pole temperature difference. Also, the Cretaceous cyclic sediments recording signals related to changes in the orbital parameters have been found in many parts of the world. In this study, we investigated the response of the Cretaceous climate field to changes in the orbital parameters using an atmospheric-ocean vegetation coupling model, MIROC4m-LPJ and also compared it with the proxy data and orbital parameter sensitivity experiments using the present-day configuration.
In the high latitude regions, the change in temperature with respect to the change in the orbital parameters is noticeable in the Cretaceous experiment. In particular, in conditions where the northern hemisphere summer is at perihelion and the obliquity is higher than the present-day value, polar amplification as shown by Cretaceous proxy data is obtained. By comparing the hydrological cycle responses in the present day and the Cretaceous, it was found that the fluctuation of the precipitation in East Asia due to orbital parameter changes is larger in the Cretaceous. This is attributed to the major structural changes in the East Asian summer monsoon in the Cretaceous. Furthermore, as a result, the variety of vegetation across East Asia in the Cretaceous has increased.

Keywords: Cretaceous, Orbital parameters, Polar amplification, Asian monsoon

©2021. Japan Geoscience Union. All Right Reserved.

Eccentricity paced increase in the continental weathering in the latest Hauterivian, Early Cretaceous

*Hironao Matsumoto[1], Rodolfo Coccioni[2], Fabrizio Frontalini[2], Kotaro Shirai[1], Junichiro Kuroda[1]

1. Atmosphere and Ocean Research Institute, the University of Tokyo, 2. University of Urbino

The 405-kyr eccentricity is a constant orbital parameter throughout the Phanerozoic and is commonly associated with long-term variations in the global continental weathering mechanism. However, the lack of reliable geological evidence has hampered the understanding of the role of the orbital-parameter on continental weathering during the Cretaceous. Os isotopic ratio ($^{187}Os/^{188}Os$) of sedimentary record reflects the balance between the radiogenic Os derived from continental weathering and unradiogenic Os derived from the unradiogenic sources (e.g., hydrothermal activity, the weathering of mafic rocks, and extraterrestrial sources), and can be therefore regarded as the best proxy for estimation of the global continental weathering. To trace the orbital-paced continental weathering, this study reconstructs the marine Os isotopic records across the Upper Hauterivian to the Lower Barremian (Lower Cretaceous) where previous studies already reported that variation in the clay-mineral composition is paced by the 405-kyr cycle. Our new Os isotopic record shows periodic oscillation of $^{187}Os/^{188}Os$ between 0.7 and 0.9, which corresponds to the 405-kyr Earth’ s eccentricity cycle. Since the sedimentary interval with the radiogenic $^{187}Os/^{188}Os$ values (~0.9) corresponds to an interval characterized by intensive humidity in areas surrounding the Tethys, a variation of $^{187}Os/^{188}O$ likely reflects the cyclic changes in the continental weathering caused by the eccentricity-paced intensification of monsoonal activity at low latitude. This variation could have been further amplified by the increase in the radiogenic Os input from higher latitude Paleozoic shale and Pre-Cambrian crust that was caused by the latitudinal shift of the intertropical convergence zone.

Keywords: osmium, Cretaceous

©2021. Japan Geoscience Union. All Right Reserved.

Millennial-scale cyclicities recorded in the Cretaceous lacustrine core using Monte Carlo approach

*Hitoshi Hasegawa[1], Hirofumi Asahi[2]

1. Faculty of Science and Technology, Kochi University, 2. Center for Advanced Marine Core Research, Kochi University

Detail paleoclimatic records under exceptionally warm “hothouse” condition provide crucial insights toward future climate predictions. However, climatic variations in millennial-scale at such deep-time archives commonly faces difficulties owing to the large uncertainties of absolute age at more than hundred kyr-scale. Annually laminated lacustrine deposits of Early Aptian (ca. 123–119 Ma) in southeast Mongolia firstly enable to obtain millennial- and shorter time-scale climate variability at such immemorial period. By combining μm-scale analysis of fluorescence microscopy images (seasonal resolution) and ultra-high-resolution elemental XRF scanning techniques (~1–5 year resolution), we were able to generate a continental climate record of unrivalled temporal resolution. Age model of the subject core was established at annual- to decadal time-scale, taking account a casual relation of ITRAX elemental composition and (annually formed) varve thickness. FFT power spectrum of high temporal resolution and long duration ITRAX record, with consideration of maximum age uncertainties (Monte-Carlo approach), exhibit partial presences of millennial-scale extreme drought events during the mid-Cretaceous ‘hothouse’ periods.

Keywords: Varve, Millennial-scale cyclicity, Age uncertainty, Monte Carlo approach

©2021. Japan Geoscience Union. All Right Reserved.

[J] Oral | M (Multidisciplinary and Interdisciplinary) : M-IS Intersection

Sat. Jun 5, 2021 1:45 PM - 3:15 PM JST | Sat. Jun 5, 2021 4:45 AM - 6:15 AM UTC | Ch.03 Zoom Room 03

[M-IS17] Interface- and nano-phenomena on crystal growth and dissolution

convener:Yuki Kimura(Institute of Low Temperature Science, Hokkaido University), Hitoshi Miura(Graduate School of Science, Department of Information and Basic Science, Nagoya City University), Hisao Satoh(Low-Level Radioactive Waste Disposal Center, Japan Nuclear Fuel Limited), Chairperson:Yuki Kimura(Institute of Low Temperature Science, Hokkaido University)

Recent developments of observations in nano-scale opened a detail discussion concerning mechanisms of crystal growth and dissolution based on interface phenomena including dynamics. In this session, growth and dissolution mechanisms of crystals will be discussed focusing on interface phenomena of minerals in the fields of biological origin, global environment, planets and space in addition to general minerals.

1:45 PM - 2:00 PM JST | 4:45 AM - 5:00 AM UTC

[MIS17-01] Nucleation of water particles in the mesosphere

*Kyoko Kitakami Tanaka[1,2], Yuki Kimura[3], Ingrid Mann[4] (1.Tohoku University, 2.Nihon University, 3.ILTS, Hokkaido University, 4.UiT the Arctic University of Norway)

2:00 PM - 2:15 PM JST | 5:00 AM - 5:15 AM UTC

[MIS17-02] Possible new water on an ice III crystal in water

*Hiromasa Niinomi[1], Tomoya Yamazaki[2], Hiroki Nada[3], Tetsuya Hama[4], Akira Kouchi[2], Junpei Okada[1], Nozawa Jun[1], Satoshi Uda[1], Yuki Kimura[2] (1.Institute for Materials Research, Tohoku University, 2.Institute of Low Temperature Science, Hokkaido University, 3.National Institute of Advanced Industrial Science and Technology, 4.Komaba Institute for Science, The University of Tokyo)

2:15 PM - 2:30 PM JST | 5:15 AM - 5:30 AM UTC

[MIS17-03] HCl droplets induced bunched steps on ice crystal surfaces under atmospheric-concentration HCl gas

*Ken Nagashima[1], Ken-ichiro Murata[1], Gen Sazaki[1] (1.The Institute of Low Temperature Science, Hokkaido University)

2:30 PM - 2:45 PM JST | 5:30 AM - 5:45 AM UTC

[MIS17-04] Adsorption of nucleotides on clay induced by change in hydration structure by magnesium ion

*Yuki Araki[1], Yoshihiro Furukawa[2] (1.Ritsumeikan University, 2.Tohoku University)

2:45 PM - 3:15 PM JST | 5:45 AM - 6:15 AM UTC

[MIS17-05] Surface-Selective Vibrational Micro-Spectroscopy Unveils Physicochemical States and the History of Crystals

★Invited Papers

*Hiroharu Yui[1] (1.Tokyo University of Science)

Nucleation of water particles in the mesosphere

*Kyoko Kitakami Tanaka[1,2], Yuki Kimura[3], Ingrid Mann[4]

1. Tohoku University, 2. Nihon University, 3. ILTS, Hokkaido University, 4. UiT the Arctic University of Norway

In the summer polar mesosphere at the altitude of 80-90 km, which is the coldest part of the earth’s atmosphere, small ice particles can form. They are observed from satellites, they form radar echoes observed from ground and they can form a dawn cloud from mid latitudes to the North, referred as a nuctilucent cloud (NLC) [1]. Although the condensed ice particles are known to exist in the high altitude mesosphere, the mechanism of condensation remains uncertain. In this study, we investigate a process of non-equilibrium condensation from dilute water vapor in relation to the origin of the NLCs. The previous study showed that amorphous solid water particles can nucleate homogeneously under conditions in the mesosphere using classical nucleation theory (CNT) [2]. However, it is known that rate predictions of water in the CNT disagree with experimental measurements by several order of magnitude [3]. In this study, we focus on the nucleation process and consider two possibilities of the homogeneous and heterogeneous nucleations. We adopt a semi-phenomenological model for nucleation process which corrects the evaluation of the formation energy of a molecular cluster with the use of the second virial coefficient and agrees with the results of both experiments and molecular dynamics simulations [3-5]. The condensation process depends on the atmospheric conditions such as temperature, pressure, number density of dust grains, and cooling rate. We find that the homogeneous nucleation of water is extremely difficult to occur in the mesosphere. The results show that the number density of dust grains necessary for heterogeneous nucleation is much lower than the observed value for the cooling rate smaller than 0.1 K/s. Our results imply that the heterogeneous nucleation occurs effectively in the upper mesosphere and the dust particles from meteoroids would work as nuclei of heterogeneous nucleation because meteoroids ablate at the high upper altitude in the mesosphere.

[1] T. Antonsen , O. Havnes , and I. Mann, Journal of Geophysical Research: Atmospheres, 122, 12,353, 2017

[2] B. J. Murray and E. J. Jensen, Journal of Atmospheric and Solar-Terrestrial Physics 72, 51, 2010

[3] A.Dillmann and G.E.A.Meier, Journal of Chemical Physics, 94, 3872, 1991

[4] K.K. Tanaka, A. Kawano, and H. Tanaka, Journal of Chemical Physics, 140, 114302, 2014

[5] R. Angelil, J. Diemand, K. K. Tanaka, and H. Tanaka, Journal of Chemical Physics, 143, 064507, 2015

Keywords: water, condensation, nucleation, mesosphere, ice

©2021. Japan Geoscience Union. All Right Reserved.

Possible new water on an ice III crystal in water

*Hiromasa Niinomi[1], Tomoya Yamazaki[2], Hiroki Nada[3], Tetsuya Hama[4], Akira Kouchi[2], Junpei Okada[1], Nozawa Jun[1], Satoshi Uda[1], Yuki Kimura[2]

1. Institute for Materials Research, Tohoku University, 2. Institute of Low Temperature Science, Hokkaido University, 3. National Institute of Advanced Industrial Science and Technology, 4. Komaba Institute for Science, The University of Tokyo

Ice is an abundant material on the Earth, and its surface plays a crucial role in controlling and catalyzing key chemical reactions governing the environment on the Earth. It is well-known that a wide variety of chemical reactions are governed by the structure and dynamics of interfacial layers on ice surfaces. The nature of the interface between water vapor and ice Ih has been actively debated in the context of a quasi-liquid layer as predicted by Michael Faraday in 1842. These active debates have highlighted the fact that ice surfaces are rich, not only in undiscovered phenomena governing key but obscure chemical processes but also in their underlying physics important for materials science. It is indisputable, therefore, that the elucidation of surface phenomena on ice is highly desirable for a broad range of scientific fields. However, other interfaces between liquid water and ice that are abundant on the Earth and on icy extraterrestrial bodies remain relatively underexplored, despite having an importance comparable with that of the water vapor-ice interface. Here, we investigated the interface between water and high pressure ice III growing/melting in water by in-situ optical microscopic observation. We show that a macroscopic thin layer of “unknown” liquid, separated from bulk water by a clear interface, forms on the water/ice III interface.

Ice III was crystallized from ultrapure water by attaining high pressure condition (~248 MPa) using a symmetric-type sapphire anvil cell (SEED; Syntek Co. Ltd, Yokohama) in a low-temperature room kept at −20°C (Figure 1B). Growth and melting of the ice III crystal in the cell were controlled by compression and decompression of anvil cell, respectively. The dynamics of crystallization/melting of water in the cell was observed in situ by using a polarized-light microscope in the low-temperature room. The microscopic images were recorded in situ by using a CCD camera.

Figure 1 shows the time-lapse micrographs of the faceted ice III crystal grown/melted in compressed water. The surface morphology of one of the faceted crystal face fluctuated in a wave-like manner during the crystal growth, suggesting fluidity of the surface (Figure 1 A ii). On the other hand, slight depressurization caused the formation of numerous partially wetting liquid droplets on the crystal surface (Figure 1 A i). The contrast difference between the wave-like liquid film and droplets on the crystal surface suggests that the wave-like liquid thin layer is thin layer with concave holes. These observation shows that an unknown liquid distinguishable from surrounding bulk water by a clear interface existed on the interface between bulk water and ice III crystal. Moreover, we found that the liquid thin layer exhibited bicontinuous pattern when the compression was stopped (Figure 1B). Bicontinous pattern can be often seen in spinodal-type liquid-liquid phase separation (LLPS) of two kinds of immiscible liquid in two component system, suggesting the unknown liquid is immiscible with water. This immiscibility should originate from the difference of density and liquid structure because of one-component system.

So far, the hypothesis that there exists the liquid-liquid critical point (LLCP) in which water separates into two kinds of liquid –high density liquid (HDL) and low density liquid (LDL)- via LLPS under a low-temperature and high pressure condition has been considered to explain the abnormal thermodynamic properties of water. However, direct observation and confirmation of the LLPS of water has never been achieved because the hypothesized LLCP lies on an experimentally inaccessible condition due to the limit of supercooling. Our observation of the separation of two kinds of immiscible liquid water

©2021. Japan Geoscience Union. All Right Reserved.

at water-ice III interface may have implications for the long-standing mystery of abnormal properties in water governing the environment on the Earth.

Keywords: Water, High-Pressure Ice, Liquid immiscibility , Interface, In-situ Microscopic Observation

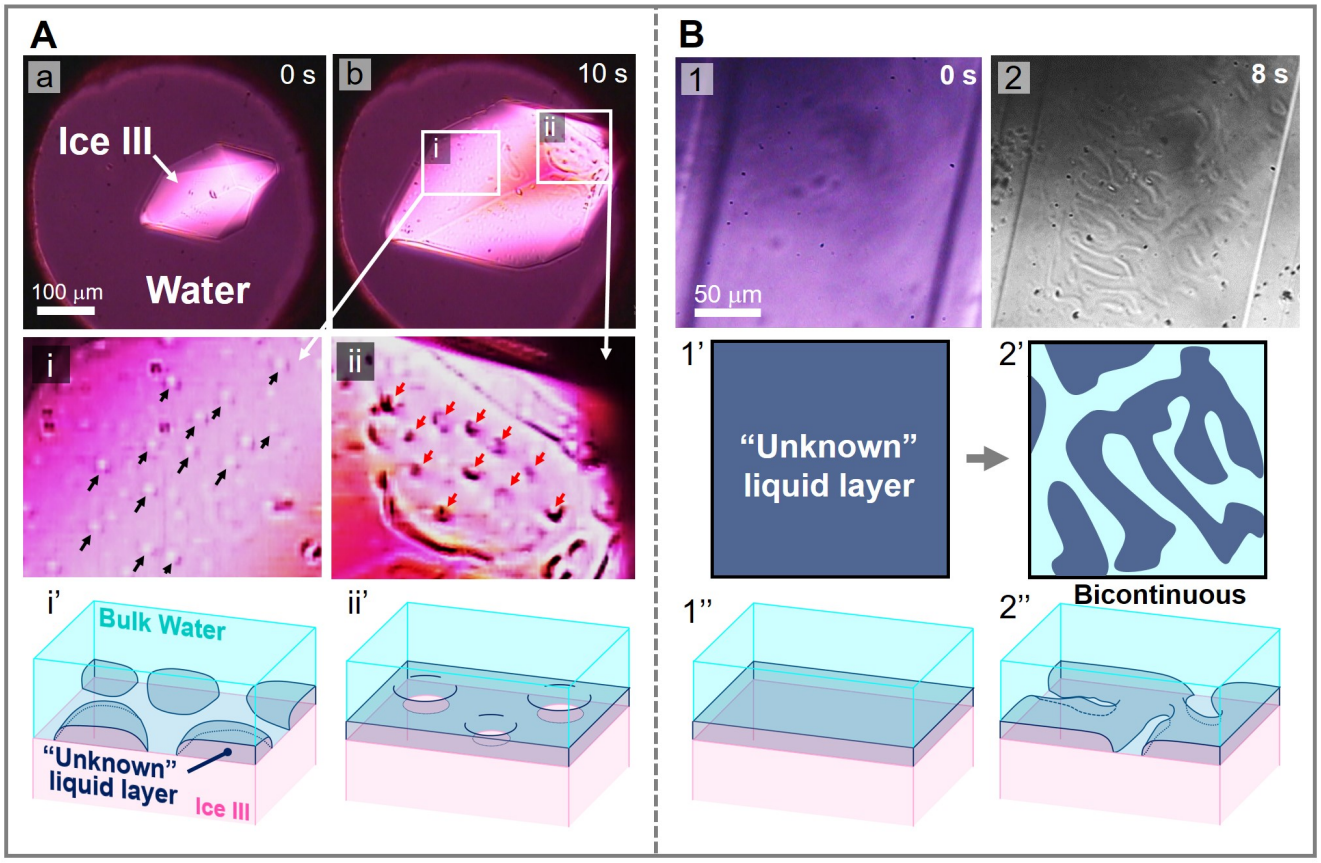


Figure 1 Time-lapse micrographs of in-situ microscopic observation on ice III crystallization from water. (A) the formation of liquid droplet and thin liquid layer of the unknown liquid. (B) the formation of bicontinous pattern of the liquid thin layer. Adopted with modification with permission from {Niinomi, H.; Yamazaki, T.; Nada, H.; Hama, T.; Kouchi, A.; Okada, J. T.; Nozawa, J.; Uda, S.; Kimura, Y. High-Density Liquid Water at a Water–Ice Interface. *J. Phys. Chem. Lett.* **2020**, 11, 6779−6784.} Copyright {2020} American Chemical Society.

©2021. Japan Geoscience Union. All Right Reserved.

HCl droplets induced bunched steps on ice crystal surfaces under atmospheric-concentration HCl gas

*Ken Nagashima[1], Ken-ichiro Murata[1], Gen Sazaki[1]

1. The Institute of Low Temperature Science, Hokkaido University

Ice is one of the most abundant crystals on the earth, and hence the molecular-level understanding of ice crystal surfaces holds the key to unlocking the secrets of a number of fields. In addition, surfaces of ice act as sites of various chemical reactions of atmospheric acidic gases, which cause serious environmental issues, such as the catalytic ozone depletion by hydrogen chloride (HCl) gas. As a means of direct observation of QLLs on ice surfaces, we and Olympus Engineering Co. Ltd., have developed laser confocal microscopy combined with differential interference contrast microscopy (LCM-DIM), which can directly visualize 0.37-nm-thick elementary steps [1] and QLLs on ice crystal surfaces [2].
Recently, we studied effects of HCl gas (10^2 Pa) on the behavior of QLLs on ice basal faces by LCM-DIM [3-4]. Then we found that the QLLs were not pure water but an HCl aqueous solution, whose HCl concentration was very close to that of a liquidus line of a binary phase diagram of water and HCl. Therefore, the HCl droplets did not disappear and were embedded in ice crystals stably without freezing [4]. However, in our previous studies, we used the HCl gas of 10^2 Pa HCl partial pressure, which is extremely higher than ordinary atmospheric partial pressure of HCl. Here, we show direct observations of ice basal faces by advanced optical microscopy under atmospheric-concentration HCl gases of from 10^{-4} to 10^{-2} Pa. Then, we investigated the appearance/disappearance of liquid water on ice surfaces and their effects on the growth of ice crystals [5].
Under atmospheric-concentration HCl gas, we found that liquid droplets and thin layers appeared/disappeared on the ice basal faces at about -1 ˚C with increasing/decreasing temperatures. These behaviors were similar to those in the absence of the HCl gases. In contrast, at temperatures below -10 ˚C, surprisingly we found that with decreasing temperature, the HCl gases induced the appearance of droplets of an HCl aqueous solution on the basal faces. In addition, the HCl droplets pinned the lateral advancement of spiral steps, resulting in the formation of bunched steps. The HCl droplets were finally embedded in the ice crystals by further growth of the bunched steps. In contrast, with increasing temperatures, the HCl droplets and the bunched steps disappeared at -10 ˚C.
These results indicate that a bulk of an ice crystal plays an important role in the uptake of HCl. So far, it has been believed that the contribution of a bulk of an ice crystal to the HCl uptake is less important than that of an ice surface, because of the small solubility of HCl and the slow diffusion of chloride ions in an ice crystal. Hence, the results found in this study suggest that the uptake of HCl in an ice crystal can be promoted via the bunching and embedding mechanism at temperatures below -10 ˚C. Our findings will give significant insights into various environmental issues caused by acidic gases in polar regions. However, it is crucially important to study whether the similar phenomena occur at -70 ˚C, at which temperature HCl on ice crystals plays an important role in the ozone depletion by the heterogeneous photochemical reactions in polar stratospheric clouds.

[1] Sazaki et al. (2010) PNAS 107, 19702.
[2] Sazaki et al. (2012) PNAS 109, 1052.
[3] Nagashima et al. (2016) Cryst. Growth Des. 16, 2225.
[4] Nagashima et al. (2018) Cryst. Growth Des. 18, 4117.
[5] Nagashima et al., Cryst. Growth Des. submitted.

©2021. Japan Geoscience Union. All Right Reserved.

We will present this study from other viewpoints in "A-AS05 Atmospheric Chemistry".

Keywords: ice crystal, air-snow interaction, atmospheric-concentration HCl gas, bunched step, HCl uptake, advanced optical microscopy

©2021. Japan Geoscience Union. All Right Reserved.

Adsorption of nucleotides on clay induced by change in hydration structure by magnesium ion

*Yuki Araki[1], Yoshihiro Furukawa[2]

1. Ritsumeikan University, 2. Tohoku University

Polymerization of nucleotide is an early stage of origin of life on the Earth. It is a dehydration reaction, so there are very few investigations which have succeeded to reproduce the polymerization in liquid environment. However, formation of long-chain oligomers in an aqueous solution in the presence of cations (transition metals, magnesium ion) and clay minerals have been reported [Ferris and Ertem (1992) Science 257, 1387-1389]. We have investigated the effects of impurities on the crystal growth in solution and the hydration structure by frequency modulation atomic force microscopy (FM-AFM). FM-AFM enables us to observe the atomic-scale phenomena and the three-dimensional water distribution at the solid surface *in situ*. So far, we have found that magnesium ions have the effect of disturbing the hydration structure at the calcite surface. This finding provided us an idea that hydrophilic ions such as magnesium instantly and locally induce dehydration of the molecular surface even in the polymerization reaction of nucleotide on the clay surface.

In this study, we carried out *in situ* observation of adsorption of nucleotide oligomers on mica by FM-AFM. All solution were prepared by using RNase free water. A solution of 30 oligomer (1 μg/mL) designed to have a characteristic ring shape as shown in the figure 1 was dropped onto a mica substrate and observed in RNase free water. No adsorbents were found on the mica surface (Fig.2a). Then, a magnesium chloride solution was added so as to be 100 mM. The adsorbate gradually increased on the mica (Fig.2b), and after 1 hour, the surface was almost covered with the adsorbates (Fig.2c). Such changes were not observed with the addition of KCl. These results indicate remarkable effect of magnesium ions on adsorption of oligomers. In the presentation, we will discuss the relation of hydration structure and the oligomer adsorption rate showing the results of changes the adsorption rate by the other cations and the change in hydration structure of mica.

Keywords: Clay, Hydration, Origin of Earth

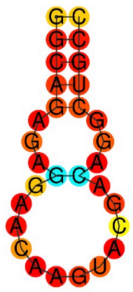


Fig.1 Designed nucleotide oligomer

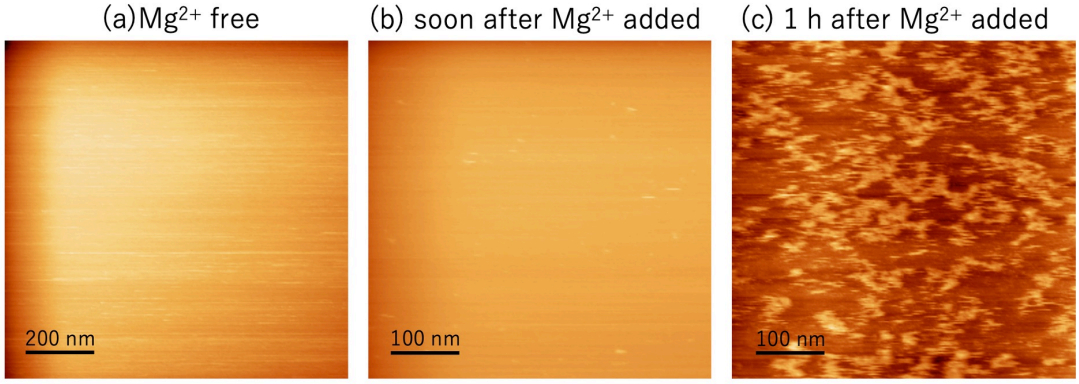


Fig.2 Topographic images of Mica surface in oligonucleotide solution.

©2021. Japan Geoscience Union. All Right Reserved.

Surface-Selective Vibrational Micro-Spectroscopy Unveils Physicochemical States and the History of Crystals

*Hiroharu Yui[1]

1. Tokyo University of Science

Vibrational spectroscopies, such as infrared (IR) absorption and Raman scattering ones, provide detailed information on the structures, orientations, and environments of the molecules and crystals that we focus on. The merits of these spectroscopies are that they do not require vacuum system and are easy to combine with optical microscopes. These properties provide us an advantage for investigating buried water / material interfaces as well as inhomogeneous material surfaces including water molecules at optional points. Here I introduce some examples of our researches on the surface analyses of crystals utilizing vibrational spectroscopies with combining surface-selective techniques and optical microscopes.

The first example is detecting surface hydroxyl (OH) groups on titanium dioxide (TiO_2) on single crystals. By combining polarization-modulation technique to external reflection IR spectroscopy (PM-ER-IR), we realized surface-selective measurements of OH groups buried under adsorbed water layers in atmospheric condition. We discriminated the surface OH groups from adsorbed water molecules by real-time cancellation of the signals derived from isotopically oriented water molecules. We discuss their binding site on TiO_2 surfaces and the origin of the super-wettability emerged under UV light irradiation.[1)]

The second example is probing the nanoscopic wetting phenomena of water molecules adsorbed on silica (SiO_2) surfaces by combining heterodyne detection technique with surface-selective vibrational sum frequency generation spectroscopy (HD-VSFG).[2)] The heterodyne detection allows us to extract “phase” information of the SFG signals and to obtain “true” absorption spectra with the molecular orientation information. With changing relative humidity (RH%) of the environments and comparing the spectra with those obtained by ATR-IR technique, we clarified inhomogeneous growth of the wetting site on the SiO_2 surfaces, especially under 50 RH %. [2)] We have also applied IR spectroscopic techniques to in-situ & real-time monitoring for the crystallization and the melting of the ice nanocrystals confined in reversed micelles, and the melt structures of triacylglycerol self-assemblies. [3,4)]

The final one is polymorphism discrimination of microcrystals embedded on the surfaces of carbonaceous chondrite meteorites utilizing Raman microscopy. Carbon materials and water molecules in phyllosilicate such as serpentinite are abundantly embedded in carbonaceous chondrites. They are believed to be one of the important origins of carbon atoms and water molecules to the early Earth. By probing the physical and/or chemical states of carbon materials and discriminating the polymorphism of the minerals that bring water molecules, we discussed the origin and the history of various types of carbonaceous chondrites. However, abundant amorphous carbons on them generally emit strong fluorescence, hindering us from discussing slight changes of Raman shift. Now we are considering another type of Raman microscopy utilizing near-infrared (NIR) excitation and/or non-linear Raman scattering techniques to avoid strong backgrounds of the fluorescence and enhance the ability to discriminate slight changes in crystal structures that should carry important information on the origin of the organic carbons and water molecules at the initial stage of the Earth and the solar system.

Acknowledgements
I would like to express my sincere thanks to the research collaborators: Dr. Shu-hei Urashima, Dr.

©2021. Japan Geoscience Union. All Right Reserved.

Toshinori Morisaku, Mr. Taku Uchida, and Mr. Aruto Kashima (Tokyo University of Science), Dr. Akira Yamaguchi and Dr. Naoya Imae (National Institute of Polar Research), and Dr. Yuki Araki (Ritsumeikan University).

References

1) K. Takahashi & H. Yui, *J. Phys. Chem. C*, **113**, 20322 (2011).
2) S. Urashima, T. Uchida, & H. Yui, *Phys. Chem. Chem. Phys.*, **22**, 27031 (2020).
3) A. Suzuki & H. Yui, *Langmuir*, **30**, 7274 (2014).
4) H. Yui, Y. Isozaki, & T. Morisaku, *Anal. Sci.*, **33**, 75 (2017).

Keywords: vibrational spectroscopy, titanium dioxide, silica, carbonaceous chondrite, surface, water

©2021. Japan Geoscience Union. All Right Reserved.

[J] Oral | M (Multidisciplinary and Interdisciplinary)：M-IS Intersection

Sat. Jun 5, 2021 3:30 PM - 5:00 PM JST | Sat. Jun 5, 2021 6:30 AM - 8:00 AM UTC | Ch.03 Zoom Room 03

[M-IS17] Interface- and nano-phenomena on crystal growth and dissolution

convener:Yuki Kimura(Institute of Low Temperature Science, Hokkaido University), Hitoshi Miura(Graduate School of Science, Department of Information and Basic Science, Nagoya City University), Hisao Satoh(Low-Level Radioactive Waste Disposal Center, Japan Nuclear Fuel Limited), Chairperson:Hitoshi Miura(Graduate School of Science, Department of Information and Basic Science, Nagoya City University)

Recent developments of observations in nano-scale opened a detail discussion concerning mechanisms of crystal growth and dissolution based on interface phenomena including dynamics. In this session, growth and dissolution mechanisms of crystals will be discussed focusing on interface phenomena of minerals in the fields of biological origin, global environment, planets and space in addition to general minerals.

3:30 PM - 3:45 PM JST | 6:30 AM - 6:45 AM UTC

[MIS17-06] Control of particles by electric field and its applicability in LC-TEM for observing crystallization and dissolution processes

*Tomoya Yamazaki[1], Hiromasa Niinomi[2], Yuki Kimura[1] (1.Institute of Low Temperature Science Hokkkaido University, 2.Institute for Materials Research, Tohoku University)

3:45 PM - 4:00 PM JST | 6:45 AM - 7:00 AM UTC

[MIS17-07] Time lapse imaging of pH/ionic concentration distribution for understanding the dissolution/formation process of minerals in aqueous solution

*Jun Kawano[1], Makoto Yazaki[2], Shinji Matsumoto[2], Takashi Toyofuku[3,4], Yukiko Nagai[3,5], Kazuya Ohno[2], Takaya Nagai[1] (1.Faculty of Science, Hokkaido Univ., 2.Graduate School of Science, Hokkaido Univ., 3.JAMSTEC, 4.TUMSAT, 5.NMNS)

4:00 PM - 4:15 PM JST | 7:00 AM - 7:15 AM UTC

[MIS17-08] Pore space property of clayey materials in the forms of gelled to compacted: a strategy for designing buffer materials

*Hisao Satoh[1], Yuki Araki[2] (1.Japan Nuclear Fuel Limited, 2.Ritsumeikan University)

4:15 PM - 4:30 PM JST | 7:15 AM - 7:30 AM UTC

[MIS17-09] Hidden stability of norsethite revealed by phase diagram

*Harutoshi Asakawa[1], Kaoru Isobe[1], Hiroshi Uneda[1], Itaru Echigo[1], Ryuichi Komatsu[1] (1.Graduate School of Sciences and Technology for Innovation Yamaguchi University)

4:30 PM - 5:00 PM JST | 7:30 AM - 8:00 AM UTC

[MIS17-10] Control of defect structure in functional bulk crystals

★Invited Papers

*Harada Shunta[1,2] (1.Nagoya University, 2.PRESTO JST)

Control of particles by electric field and its applicability in LC-TEM for observing crystallization and dissolution processes

*Tomoya Yamazaki[1], Hiromasa Niinomi[2], Yuki Kimura[1]

1. Institute of Low Temperature Science Hokkkaido University, 2. Institute for Materials Research, Tohoku University

Crystallization and dissolution in a solution are quite important not only for generation of new functional materials and protein crystallization, but also for understanding geochemical processes of ubiquitous phenomena on the Earth. Recent advances in microfabrication techniques have made it possible to fabricate liquid cells for observing liquid samples in electron microscopy. This combined technique is called liquid-cell transmission electron microscopy (LC-TEM) and allows us to visualize crystallization and dissolution processes in spatial and temporal resolution of TEM. However, this method is still struggling at observing these processes because decreasing temperature and concentration of sample, which are crucial parameters for crystallization, at observing area is still difficult. To solve this problem, here we focus on the technique of particle manipulation by applying electric field using electrodes in a liquid sample. We expect this technique to increase local concentration (number density) of particles, such as nanoparticles and colloidal particles, in a liquid sample. To introduce this technique into LC-TEM, it is required to develop liquid cells with adequate design for the particle manipulation by electric field. Firstly, we performed experiments using a existing liquid cell with electrodes and optical microscopy to confirm the effectiveness of the manipulation technique for increasing local concentration of nanoparticles in the cells. We used colloids to observe the electromechanics of each particle under electric field by an optical microscopy. In addition, we considered that the efficiency of electric field to control crystallization and dissolution processes of colloidal crystals.

Acknowledgement
This work was supported partly by the GIMRT Program of the Institute for Materials Research, Tohoku University (Proposal No. 20K0038) and JSPS KAKENHI Grant Numbers JP18J01470 and 20H02580.

Keywords: crystallization, electric field, colloid, dissolution, liquid-cell transmission electron microscopy, particle manipulation

©2021. Japan Geoscience Union. All Right Reserved.

Time lapse imaging of pH/ionic concentration distribution for understanding the dissolution/formation process of minerals in aqueous solution

*Jun Kawano[1], Makoto Yazaki[2], Shinji Matsumoto[2], Takashi Toyofuku[3,4], Yukiko Nagai[3,5], Kazuya Ohno[2], Takaya Nagai[1]

1. Faculty of Science, Hokkaido Univ., 2. Graduate School of Science, Hokkaido Univ., 3. JAMSTEC, 4. TUMSAT, 5. NMNS

Recent works have revealed that growth or dissolution mechanism of minerals in aqueous solution is more complicated than we had imagined. To understand these mechanisms, analyzing the local conditions of the solution around the dissolving or forming minerals is important. Recently, we succeeded in visualizing the distribution of pH around a calcium carbonate crystal dissolving in aqueous solution using a fluorescent probe. However, the ionic concentration is another important factor to describe the formation/dissolution reaction of calcium carbonate. In this study, we attempted to visualize the distribution of Ca^{2+} concentration along with the pH around a dissolving calcium carbonate crystal in aqueous solution.

By simultaneously using HPTS (8-hydroxypyrene-1,3,6-trisulfonic acid) and Rhod-FF as fluorescent probes, pH and Ca^{2+} could be measured independently and their distributions around the dissolving calcium carbonate in an aqueous solution were successfully visualized. Tendencies of their distributions were basically similar, but the pH was found to increase and saturate rapidly just above the surfaces, while the Ca^{2+} concentration changed more slowly and its 2D features seemed to be different from those of pH. Rough estimation of the solution composition just above the surface showed that concentration of bicarbonate ions was comparable with Ca^{2+} concentration, which suggest that bicarbonate ions play an important role in the surface reaction.

Here we will also report the result of pH/ionic concentration imaging for the calcium carbonate formation process in gel media. These results could provide new insights into the knowledge of the dissolution/formation reaction of minerals in aqueous solutions.

Keywords: imaging, calcium carbonate, pH, dissolution

©2021. Japan Geoscience Union. All Right Reserved.

Pore space property of clayey materials in the forms of gelled to compacted: a strategy for designing buffer materials

*Hisao Satoh[1], Yuki Araki[2]

1. Japan Nuclear Fuel Limited, 2. Ritsumeikan University

Context: Rock and clay are still used as major constructive materials in the modern ages, even for the underground facilities such as radioactive waste repository due to their long-term stability. The chemical and mineralogical robustness of these materials is promised by their low reactivity. Until recently, there are many studies developing the geochemical models to validate the safety of waste disposal, because the repository uses buffer clay barrier and dissolution information of clay is top priority. Direct measurement revealed that dissolution rate of clay is lowered by suppressed surface area as a function of compaction density [1]. Recently, we have successfully formulated the effective ESA as the function of density involving isotropic-nematic transition [2]. Step-interaction also affects the dissolution kinetics [1, 3] by the step-dynamic law [4, 1]. Very recently, we have developed an atomistic scale method to evaluate the surface property of hydration structure on clay in groundwater [5]. These knowledges need to be confirmed for the actual bentonite system.

Methods: Direct comparison between observation and measurement is the most persuasive approach. We used FESEM to observe pores in a clay rock from Tsukinuno mine (Kunimine Industries Co.). The tomographic observation was also made on this clay with micro focus X-ray CT (Fig. 1). Direct dissolution measurement with interferometer and AFM was carried out on a purified separate from same clay rock (Kunipia P) under compaction [4]. We newly applied FM-AFM to visualize electric double layer (EDL) above Stern layer. [6].

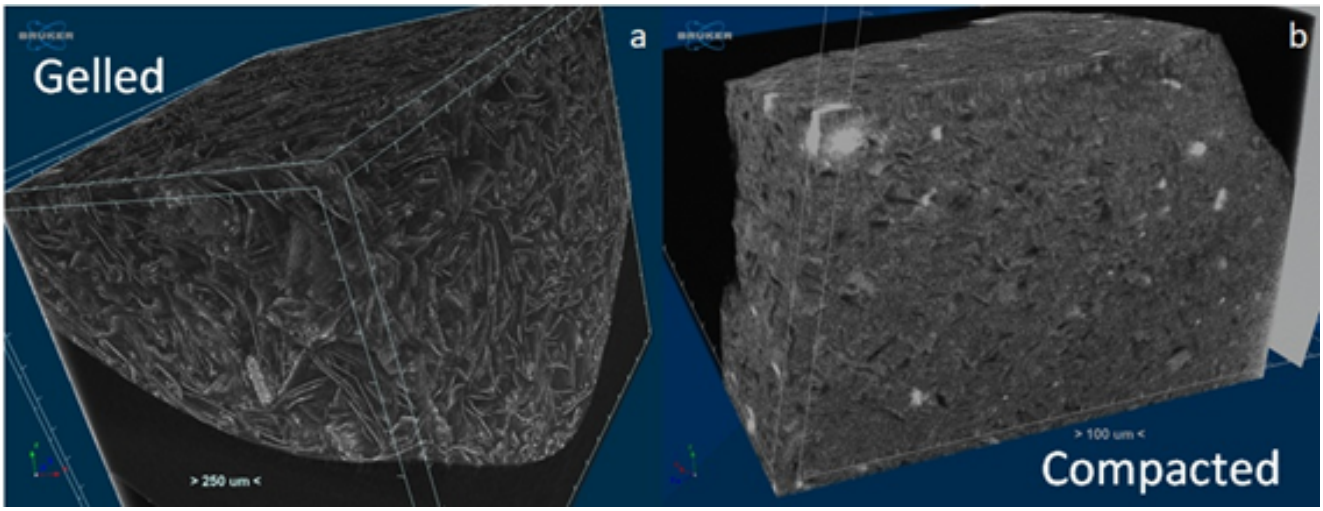
Results and Discussion: When we consider that groundwater passes though these pores of the clay-rock underlain at the mine, the pore spaces between clay grains are not only the flow-path but also hydration volume with swelling pressure. The actual space can be simply regarded as restricted by the EDL as well as clay density. Generally, it is understood that the hydraulic conductivity varies as the function of clay density. Recent FM-AFM exhibits that the water-path in the compacted clay is prepared by free space excluded from the EDL [5]. This approach realized that dissolution of clay mineral at the pore space filled with equilibrium groundwater (pH 8) is restricted by the pore size that affects the curvature made of elemental steps, unless the pore size is below ~20 nm. Based on the step-dynamics and hydration structure with EDL, we can give a constraint on evolution of actual pore size during alteration [5]. Clay density can affect not only the exposed area of the grain edge at which dissolution mainly occurs [2], but also the hydraulic property by the variety of EDL in the compacted clay. If the clay contains other secondary minerals such as zeolite or silica (see Fig. 1a), the pore structure can be developed as mixture of inter and intra-grains. Furthermore, from the scope of elemental migration by groundwater like pollution, hydration of the minerals changes their sorption property appeared as partition coefficient, Kd (ml/g) that suppresses contamination.
Consequently, in order to design the clayey buffer materials, (1) grain structure from gel to compacted states, (2) electrochemical property as the EDL, (3) diffusion and dissolution, (4) alteration by nucleation of secondary zeolite, and (5) elemental migration by Kd need to be focused to evaluate water-stopping behavior and elemental retardation in case of damage of the barrier. Such a bottom-up approach with focusing pore space science is necessary for repository safety.

©2021. Japan Geoscience Union. All Right Reserved.

References: [1] Satoh et al. (2013) Clay Min., 48, 285-294.; [2] Terada et al. (2017) Mat. Res. Exp. 6 (3) 035514.; [3] Satoh et al. (2007) Am. Min., 92, 503-509.; [4] Burton et al. (1951) Phil. Trans. Royal Soc. London, 243, 299; [5] Satoh et al. (2019), Abst. Migration 2019; [6] Araki et al. (2017) Surf. Sci, 665 32-36.

Figure 1. Micro XCT images of gelled (a) and compacted (b) montmorillonite clay-stone.

Keywords: clay, pore space, electric double layer: EDL, frequency mopdulation atomic force microscope: FM-AFM, microfocus X-ray computed tomography: micro XCT



©2021. Japan Geoscience Union. All Right Reserved.

Hidden stability of norsethite revealed by phase diagram

*Harutoshi Asakawa[1], Kaoru Isobe[1], Hiroshi Uneda[1], Itaru Echigo[1], Ryuichi Komatsu[1]

1. Graduate School of Sciences and Technology for Innovation Yamaguchi University

Since the norsethite $BaMg(CO_3)_2$ can be relatively easily synthesized at atmospheric pressure, the utilization of the norsethite is promising as a model crystal for solving the dolomite problem, which is the longstanding mineralogical problems. It is known that the norsethite is formed by the solution-mediated transformation from the $BaCO_3$. Hence, the driving force of the norsethite crystallization corresponds to the difference of solubility between the norsethite and $BaCO_3$. In contrast, our preliminary study has shown a two-step pH change during the dissolution process. When the dissolution of the norsethite started, pH steeply increased owing to the appearance of HCO_3^- at first. Then, pH remained constant. In 20 minutes, pH gradually decreased owing to the appearance of $BaCO_3$, pH, finally, remained constant in 20000 min again. When comparing between the solution-mediated transformation and the two-step dissolution, the inferences based on these results are thermodynamically difficult. This incoherence is resulting in the difficulty of understanding on the formation of the norsethite. Then, we expect that the ratio of Ba^{2+} and Mg^{2+} in an aqueous solution plays an important role in the norsethite crystallization from the difference of cations between the noresethite and $BaCO_3$ from the viewpoint of thermodynamics. In this study, we examined the relationship between the stability of the norsethite and the ratio of Ba^{2+} and Mg^{2+}.

The 100mg norsethite powder was added into 50 ml pure water heated at growth temperature T=40~90^{O}C, and the solution was kept stirring with measuring pH for one month. After the elution, the concentration of Ba^{2+}, Mg^{2+}, and CO_3^{2-} in the solution was evaluated by inductivity coupled plasma optical emission spectrometer and total organic carbon measurement. To confirm the stability of the norsethite, the sample was measured by XRD measurement.
Consequently, a small amount of the $BaCO_3$ appeared from the norsethite powder after the dissolution of the norsethite at more than 60 ^{O}C. In addition, the ratio of Ba^{2+} and Mg^{2+} in the solution became Mg^{2+} rich at less than 70 ^{O}C and Ba^{2+} rich at more than 70 ^{O}C. In contrast, the $BaCO_3$ became undersaturated in the saturated solution of the norsethite at more than 70 ^{O}C. These results demonstrate that the aqueous solution with the norsethite exhibits the saddle point composition, which is more stable than the stoichiometric composition.

Keywords: Norsethite, phase diagram, solution-mediated transformation

©2021. Japan Geoscience Union. All Right Reserved.

Control of defect structure in functional bulk crystals

*Harada Shunta[1,2]

1. Nagoya University, 2. PRESTO JST

Defects in crystalline materials often govern their physical properties. Therefore, control of defects in crystalline materials, especially in semiconductor materials, is very important. For example, the present electronics is largely depending on silicon as a semiconductor material because dislocation-free silicon crystal is possible to produce by necking technique established by Dash about 60 years ago[1]. In the field of electronics, defects in semiconductor materials are often harmful for electric device and should be eliminated. However, from a different point of view, defects can be regarded as local nanostructure in a perfect crystal, which would express novel new function. For both purpose, it is necessary to understand the structural principle and control the defect structures. In this talk, I will introduce the defect control for functional bulk crystals including ordered arrangement of vacancies in thermoelectric silicide[2,3], reduction of dislocation in silicon carbide for power electronic[4,5] and ordered arrangement of planar faults in titanium oxide natural superlattice for control of thermal phonons toward advanced heat control[6].

References
[1]W. C. Dash, J. Appl. Phys. **30** (1959) 459.
[2]S. Harada et al., Appl. Phys. Express **5** (2012) 035203.
[3]S. Harada et al., Phil. Mag. **91** (2011) 3108.
[4]S. Harada et al., APL Mater. **1** (2013) 022109.
[5]S. Harada et al., Acta Mater. **91** (2014) 284.
[6]S. Harada et al., J. Appl. Phys. **108** (2011) 083703.

Keywords: crystalline defect, dislocation, planr fault, power device, phonon

©2021. Japan Geoscience Union. All Right Reserved.

[J] Poster | M (Multidisciplinary and Interdisciplinary)：M-IS Intersection

Sat. Jun 5, 2021 5:15 PM - 6:30 PM JST | Sat. Jun 5, 2021 8:15 AM - 9:30 AM UTC | Ch.21_4

[M-IS17] Interface- and nano-phenomena on crystal growth and dissolution

convener:Yuki Kimura(Institute of Low Temperature Science, Hokkaido University), Hitoshi Miura(Graduate School of Science, Department of Information and Basic Science, Nagoya City University), Hisao Satoh(Low-Level Radioactive Waste Disposal Center, Japan Nuclear Fuel Limited)

Recent developments of observations in nano-scale opened a detail discussion concerning mechanisms of crystal growth and dissolution based on interface phenomena including dynamics. In this session, growth and dissolution mechanisms of crystals will be discussed focusing on interface phenomena of minerals in the fields of biological origin, global environment, planets and space in addition to general minerals.

[MIS17-P01] Toward for the developing the thermal storage materials utilizing the Electrostatic Levitation Furnace in "Kibo" in space

*Hidekazu Kobatake[1], Kazuki Tonooka[2], Shumpei Ozawa[2], Ken'ichi Sugioka[3], Suguru Shiratori[4], Ken Nagashima[5], Hirohisa Oda[6], Hideki Saruwatari [6], Chihiro Koyama[6], Takehiko Ishikawa[6] (1.Hirosaki University, 2.Chiba Institute of Technology, 3.Toyama Prefectural University, 4.Tokyo City University, 5.Hokkaido University, 6.JAXA)

[MIS17-P02] Heteroepitaxial growth mechanism in colloidal crystallization

*Jun Nozawa[1], Hiromasa Niinomi[1], Junpei Okada[1], Satoshi uda[1] (1.Tohoku University)

[MIS17-P03] Fabrication of evaluation model for adgesion mechanism between bone mineral and soft tissue

*Yuki Sugiura[1], Masahiro Okada[2], Ken Hirano[1], Takuya Matsumoto[2] (1.National Institute of Advanced Industrial Science and Technology, 2.Okayama University)

[MIS17-P04] Conversion from a stable crystal to a metastable crystal by grinding

*Hiroyasu Katsuno[1], Makio Uwaha[2] (1.Institute of Low Temperature Science, Hokkaido University, 2.Center for General Education, Aichi Institute of Technology)

[MIS17-P05] Improvement of transmission electron microscope images by neural network model

*Hiroyasu Katsuno[1], Shizuka Hirakawa[1], Tomoya Yamazaki[1], Ichigaku Takigawa[2], Yuki Kimura[1] (1.Institute of Low Temperature Science, Hokkaido University, 2.RIKEN, Center for Advanced Intelligence Project)

[MIS17-P06] Development of an early detection method of nucleation in in-situ liquid-cell TEM observation

*Yuki Kimura[1], Hiroyasu Katsuno[1], Tomoya Yamazaki[1], Ichigaku Takigawa[2,3] (1.Institute of Low Temperature Science, Hokkaido University, 2.AIP, RIKEN, 3.ICReDD, Hokkaido University)

[MIS17-P07] In-situ observation at the moments of bubble nucleation using a liquid-cell transmission electron microscope

*Yuki Kimura[1], Tomoya Yamazaki[1], Hiroyasu Katsuno[1], Shizuka Hirakawa[1] (1.Institute of Low Temperature Science, Hokkaido University)

Toward for the developing the thermal storage materials utilizing the Electrostatic Levitation Furnace in "Kibo" in space

*Hidekazu Kobatake[1], Kazuki Tonooka[2], Shumpei Ozawa[2], Ken'ichi Sugioka[3], Suguru Shiratori[4], Ken Nagashima[5], Hirohisa Oda[6], Hideki Saruwatari [6], Chihiro Koyama[6], Takehiko Ishikawa[6]

1. Hirosaki University, 2. Chiba Institute of Technology, 3. Toyama Prefectural University, 4. Tokyo City University, 5. Hokkaido University, 6. JAXA

Thermal storage has attracted attention for stabilizing the supply of renewable energy or for the utilization of the heat, which is emitted from the industry. Thermal storage technology has the potential to efficiently store and stabilize thermal energy in relatively compact equipment, but it is necessary to increase the heat exchange efficiency and durability. A phase-separated alloy has predictably effective for that purpose as thermal storage materials. Thermophysical properties of the phase-separated alloy of molten state are required to control the microstructure of the alloys. Despite the importance, it is difficult to measure the thermophysical properties of molten alloys on the ground.
In this project, we focus on phase-separated alloys such as Fe-Cu, Al-Si, and Cu-Si, measure their thermophysical properties and nucleation rate in outer space, and aim to design highly efficient energy storage materials.

Keywords: Thermophysical property, Electro Static Levitation

©2021. Japan Geoscience Union. All Right Reserved.

Heteroepitaxial growth mechanism in colloidal crystallization

*Jun Nozawa[1], Hiromasa Niinomi[1], Junpei Okada[1], Satoshi uda[1]

1. Tohoku University

Colloidal crystals, periodic arrays of colloidal particles, have been attracting great attention due to their versatile applications such as novel optical devices. Besides, the colloidal crystals have been regarded as a useful model of various phenomena as it displays similar phase transition to the atomic system. Among variable methods to control growth and structure of the colloidal crystals, a colloidal epitaxy that utilizes a patterned substrate is an effective technique. However, the technique has been limited to homoepitaxial growth, where structure and lattice spacing of the substrate and epitaxial phase are similar. In this thesis, colloidal crystals are fabricated with the heteroepitaxial growth, where lattice constant of the substrate and epitaxial layer is different. The mechanism is discussed for the heteroepitaxial growth in colloidal crystallization.

Polystyrene particles of 700 nm was used to grow the epitaxial layers. The particle size of the substrates is ranged from 400 to 1300 nm. The sodium polyacrylate is added to induce depletion attractive interaction, by which colloidal crystallization is achieved. The lattice misfit ratio is defined as the $(d_{eq} - d_{subst})/ d_{eq}$, where d_{eq} is equilibrium particle distance as the particle distance of colloidal crystals formed without the substrate (on cover glass), and d_{subst} is lattice spacing of the substrate. The heteroepitaxial growth was performed in various lattice misfit ratios.

Three growth modes are recognized in the experiment: Layer-by layer, Layer-plus-island, and Island, which is denoted as FM, SK, and VW mode, respectively, as is the heteroepitaxial growth of atomic system. This has been firstly recognized in the growth of the colloidal crystals. Importantly, SK mode in some growth conditions is transitioned into VW by decomposition of the formed layers, the process of which is uncovered by the in-situ observation.

Contrary to the expectation, growth modes do not show clear correlation with the lattice misfit ratio. We inferred that interaction between epitaxial layer and the substrate influences the epaxial growth. Relative particle interaction between substrate and the epitaxial layer is estimated by the strength of the depletion interaction. Consequently, three growth modes are suitably categorized by using two parameters; the interaction between substrate and epitaxial layers as well as the lattice misfit ratio. The findings in the study will well contribute to rational control of the structure and phase of the colloidal crystals.

Keywords: Colloidal crystals, Epitaxial growth

©2021. Japan Geoscience Union. All Right Reserved.

Fabrication of evaluation model for adgesion mechanism between bone mineral and soft tissue

*Yuki Sugiura[1], Masahiro Okada[2], Ken Hirano[1], Takuya Matsumoto[2]

1. National Institute of Advanced Industrial Science and Technology, 2. Okayama University

The disadvantages of surgical sutures, such as secondary tissue damage, surgical site infection, and liquid leaking, can be reduced by biological softtissue adhesives. Although non-bioresorbable bone substitute materials sufficiently adhere to soft tissues, enabling immobilization of implantable devices, their non-bioresorbable property limits their clinical use. This study reports the excellent adhesion properties of octacalcium phosphate (OCP), a bioresorbable mineral analogue of immature bone. Blocks of OCP strongly adhere to mouse dermal tissues, enhancing their protein adsorption capacity as demonstrated in ex vivo shear adhesion tests. When soaked in antibacterial solution, the OCP blocks easily adsorb the antibacterial agents in their internal nano-pores and on their surfaces, imbuing them with antibacterial ability. Therefore, the OCP blocks are a solid-state material with strong adherence to biological soft tissues and, are especially promising for detachable body-implantable and/or external devices.

Keywords: bone mineral, calcium phosphate, bone formation, biological adhesive

©2021. Japan Geoscience Union. All Right Reserved.

Conversion from a stable crystal to a metastable crystal by grinding

*Hiroyasu Katsuno[1], Makio Uwaha[2]

1. Institute of Low Temperature Science, Hokkaido University, 2. Center for General Education, Aichi Institute of Technology

Materials have some crystal structures. In general cases, the crystal structure of the ground state is unique. Other structures with higher free energy are thermodynamically metastable. When stable and metastable crystals coexist in a system, the stable crystal grows and the metastable one shrinks. Although temporal appearance of metastable crystal is well known as the Ostwald’ s step rule, eventually large stable crystals form in the system in equilibrium.

In the case of a chiral crystal, the chiral pair of crystal structures are realized with the same probability since the pair of structures are energetically equal. In 2005, Viedma discovered the conversion from racemic mixture of chiral sodium chlorate crystals to crystals with single chirality in a saturated solution by stirring with glass beads. In this system, the racemic mixture of crystals is the equilibrium state, and the single chirality state is the one of metastable states. This phenomenon is distinguished from the ordinary Ostwald ripening and called Viedma ripening. One of the hypotheses, which explain Viedma ripening, is the acceleration of crystal growth by the cluster incorporation. If the mechanism of Viedma ripening works effectively, it might be possible to convert from crystals of a stable structure to crystals of a metastable structure.

We demonstrate the conversion from crystals of a stable structure to crystals of a metastable structure using the theoretical idea of Viedma ripening. We introduce the generalized Becker-Döring model, which includes the cluster incorporation to the crystal of the same structure. When the amount of metastable crystals is large enough for that of stable crystals, metastable crystals grow and stable ones disappear at the steady state. If the cluster incorporation mechanism does not work, the amount of the metastable crystal is not amplified from any initial state. The system only reaches the equilibrium as well as the case without crystal grinding. Grinding effectively breaks crystals, and supplies small clusters, and then, the metastable crystals completely consumes the stable crystals by the acceleration of crystal growth due to the small cluster incorporation.

Keywords: phase conversion, cluster incoporation, crystal grinding

©2021. Japan Geoscience Union. All Right Reserved.

Improvement of transmission electron microscope images by neural network model

*Hiroyasu Katsuno[1], Shizuka Hirakawa[1], Tomoya Yamazaki[1], Ichigaku Takigawa[2], Yuki Kimura[1]

1. Institute of Low Temperature Science, Hokkaido University, 2. RIKEN, Center for Advanced Intelligence Project

Transmission electron microscopy (TEM) is a powerful tool in the field of material science and provides structural information by visualizing at the atomic level. In order to obtain a clear image, improvements of hardware and software are proceeded. Despite of its benefits, the application is limited due to the electron beam damage and the time resolution. One of the important techniques in the high resolution TEM imaging is dictionary learning method, which is called sparse coding [A. Stevens *et al.*, Microscopy **63**, 41 (2014)]. This method provides a denoised image from a noisy image by using a linear combination of basic elements. Sparse coding is succeeded in the field of scanning TEM imaging and electron holography [S. Anda *et al.*, Ultramicroscopy **206** 112818 (2019)].

Recently, the image improvement by machine learning is evolved remarkably. To support the improvement for low-light image processing, a dataset, including short-exposure low-light images and corresponding long-exposure reference images, are introduced [C. Chen *et al.*, arXiv:1805.091934 (2018)]. In this paper, we apply this idea to the TEM imaging and demonstrate the improvement of TEM image by a convolutional neural network (CNN) model.
For the training of CNN, we prepare the training dataset of TEM images, which is a pair of low-exposure images and corresponding long-exposure reference images. The exposure time is about 1—10 ms and 1 s for low-exposure and long-exposure images, respectively. The images were observed using a CMOS camera (Flash, EM-Z15327TCMOS; JEOL Ltd.). Before the training, the dataset is preprocessed: adjusting the position and equalizing/rescaling the brightness of each image. The network architecture of our model is UNet with ResNet encoder. During training, we minimize the L_1 loss between the image predicted from low-exposure image and the long-exposure image. Using about 100 images for training, the noise is removed, and the edges become clear on the verification images. We will show the condition of our model in detail and examples for some materials.

Keywords: Machine learning, Transmission electron microscopy, Convolutional neural network

©2021. Japan Geoscience Union. All Right Reserved.

Development of an early detection method of nucleation in in-situ liquid-cell TEM observation

*Yuki Kimura[1], Hiroyasu Katsuno[1], Tomoya Yamazaki[1], Ichigaku Takigawa[2,3]

1. Institute of Low Temperature Science, Hokkaido University, 2. AIP, RIKEN, 3. ICReDD, Hokkaido University

One of our goal is direct observation at the moments of nucleation in atomic scale. Nucleation process seems easy: Growth units agglomerate and form a particle by overcoming a nucleation barrier, which depends on a difference of the chemical potentials of two phases. However, recent investigations using a liquid-cell transmission electron microscope (LC-TEM) have reported more complex processes in the actual case. For instance, oriented-attachment growth of nano-crystallites [1] and the two-step nucleation of calcium carbonate [2] are reported. We found that two types of amorphous particles with different roles and properties promote protein crystallization [3]. It is easy to observe a nucleation by our naked eye or under optical microscope because of lower magnifications, i.e., large solution volume. However, it is not easy to observe a nucleation process in atomic scale under TEM, because even if the nucleation rate is controlled to be very high, the solution volume in the field of view is much smaller and, therefore, expected number of nuclei becomes much lower. In addition, it is also difficult to increase nucleation rate dramatically after starting the observation. Recent achievements have been based on great efforts such as a bunch of experimental runs and long-term observations. Therefore, to observe whole a process of nucleation with higher magnification, we are trying to develop an early detection method of a nucleation event in a stochastic nature using a neural network model.

Acknowledgement

This work was supported by Grant-in-Aid for Scientific Research (S) of JSPS KAKENHI Grant Number 20H05657.

References

[1] D. Li et al., Science 336 1014 (2012).
[2] M. H. Nielsen et al., Science 345 1158 (2014).
[3] T. Yamazaki et al. PNAS 114 2154 (2017).

Keywords: Nucleation, Machine learning, Transmission electron microscopy

©2021. Japan Geoscience Union. All Right Reserved.

In-situ observation at the moments of bubble nucleation using a liquid-cell transmission electron microscope

*Yuki Kimura[1], Tomoya Yamazaki[1], Hiroyasu Katsuno[1], Shizuka Hirakawa[1]

1. Institute of Low Temperature Science, Hokkaido University

Recently, the development of solution cells sandwiched between graphene or silicon plates has made it possible to overcome the high vacuum environment unless the spatial limitation of a TEM sample chamber. As a result, the "in-situ" observation of phenomena in solution using TEM is being actively conducted [e.g., Nielsen et al. *Science* 345 (2014) 1158]. We have been working on this method since its early days and have succeeded in directly observing nucleation processes. For instance, we found multistep nucleation in the crystallization process of lysozyme protein crystal, which crystallized via dense liquid [Yamazaki, Kimura et al. *PNAS* 114 (2017) 2154]. Since dehydration is a largest barrier for crystallization in an aqueous solution, it seems that lysozyme molecules agglomerate together with their hydrated layers at first and then gradually dehydrate to be a crystal. In addition, the crystallinity gradually becomes higher due to mobile defects and occasionally undergoes a phase transition to a more stable crystal [Yamazaki, Van Driessche, Kimura *Soft Matter*, 16 (2020) 1955]. In these in-situ TEM observations, the effects of the electron beam are largest concern and must be considered to discuss an observed process.

When observing an aqueous solution by TEM, water radiolysis due to electron beam irradiation is inevitable. Electrons generate protons, ions, and radicals in the aqueous solution. Then, solution environment varies and, therefore, it makes difficult to discuss crystal growth and conduct experiments that simulate environments such as living organisms. Furthermore, bubbles may be generated depending on the conditions and, in case, the experimental run cannot be continuing anymore. Therefore, estimation of the solution environment, such as temperature, pH, and concentrations of ion, hydrogen, and oxygen, has been attempted in response to electron beam intensity by solving many equations of possible chemical reactions [Schneider et al, *J. Phys. Chem. C*. 118 (2014) 22373; Ambrožič et al. *Chem. Sci.* 10 (2019) 8735]. Generally, electron beam irradiates only on an area of the window on a liquid cell, and there are abundant aqueous solutions around it that are not directly irradiated by the electron beam. Even if we predict the relationship between the amount of generated hydrogen and oxygen and their equilibrium concentrations, we cannot expect a bubble formation, because bubbles are generated through a nucleation after supersaturation. Therefore, observed conditions such as the magnification and the brightness (electron dose rate) of the field of view are adjusted based on experience. To overcome these difficulties, in this study, we conducted an experiment to observe the moments of nucleation of bubbles in situ while accurately measuring the electron dose rate using a Faraday cup. We will show the detail experimental results and imprecations on the bubble formation for future in-situ observation.

Keywords: nucleation, liquid-cell TEM, TEM, water, radiolysis

©2021. Japan Geoscience Union. All Right Reserved.

[J] Oral | M (Multidisciplinary and Interdisciplinary)：M-IS Intersection

Sat. Jun 5, 2021 1:45 PM - 3:15 PM JST | Sat. Jun 5, 2021 4:45 AM - 6:15 AM UTC | Ch.10 Zoom Room 10

[M-IS20] Ocean Plastics, an earth science perspective

convener:Atsuhiko Isobe(Research Institute for Applied Mechanics, Kyushu University), Kiichiro Kawamura(Yamaguchi University), Yusuke Okazaki(Department of Earth and Planetary Sciences, Graduate School of Science, Kyushu University), Masashi Tsuchiya(Research Institute for Global Change, Japan Agency for Marine-Earth Science and Technology), Chairperson:Atsuhiko Isobe(Research Institute for Applied Mechanics, Kyushu University)

Mismanaged plastic wastes accounting for 70% of marine debris remain persistently in the marine environment, even if they are degraded and fragmentized to tiny microplastics. To date, it has been unknown how this anthropogenic, buoyant, and persistent matter which was first appeared in the earth history, contaminates (or is incorporated into) the earth system. The ocean plastic study requires the insight and methodology of a variety of earth sciences such as the oceanography, geology, and palaeontology. Studies on the plastic circulation loaded from the land/atmosphere to upper oceans and bottom sediments, studies on microplastics as a proxy of the 'Anthropocene', and studies to establish procedures in monitoring and analyzing macro/microplastics are welcomed.

1:45 PM - 2:00 PM JST | 4:45 AM - 5:00 AM UTC

[MIS20-01] Numerical model approach on the fate of pelagic plastics in the world's ocean

*Atsuhiko Isobe[1] (1.Research Institute for Applied Mechanics, Kyushu University)

2:00 PM - 2:15 PM JST | 5:00 AM - 5:15 AM UTC

[MIS20-02] Estimating vertical distribution of microplastic particles under wind-driven and Langmuir turbulence by Large Eddy Simulation

*Yoshimasa Matsumura[1], Shin-ichi Ito[1], Chiharu Sasaki[1] (1.Atmosphere and Ocean Research Institute, University of Tokyo)

2:15 PM - 2:30 PM JST | 5:15 AM - 5:30 AM UTC

[MIS20-03] Numerical experiment on vertical motion of microplastics with biological processes

*Miho Yoshitake[1], Atsuhiko Isobe[1] (1.Kyushu university)

2:30 PM - 2:45 PM JST | 5:30 AM - 5:45 AM UTC

[MIS20-04] Numerical model approach of macroplastic transport to find microplastic sources around the Indonesian archipelago

*Ryohei Kono[1], Atsuhiko Isobe[1] (1.Research Institute for Applied Mechanics, Kyushu University)

2:45 PM - 3:00 PM JST | 5:45 AM - 6:00 AM UTC

[MIS20-05] Quantifying the degree of pollution of beaches using an AI technique

*Mitsuko Hidaka[1], Daisuke Sugiyama[1], Daisuke Matsuoka[1], Fumiaki Araki[1], Masafumi Kamachi[1], Yoichi Ishikawa[1] (1.Japan Agency for Marine-Earth Science and Technology)

3:00 PM - 3:15 PM JST | 6:00 AM - 6:15 AM UTC

[MIS20-06] Estimation of plastic litter abundance in cities using big data associated with citizen science and deep learning

*Shinichiro Kako[1], Shintaro Kanno[2], Atsuhiko Isobe[3], Masato Kuki[4], Kotaro Yamamoto[4], Fujio Kojima[4] (1.Graduate School of Science and Engineering, Kagoshima University, 2.Faculty of engineering, Kagoshima University, 3.Research Institute for Applied Mechanics, Kyushu University, 4.Pirika, Inc. / Prika association)

Numerical model approach on the fate of pelagic plastics in the world's ocean

*Atsuhiko Isobe[1]

1. Research Institute for Applied Mechanics, Kyushu University

A particle tracking model (PTM) computing behavior of both plastic debris and microplastics in the upper ocean was established. These particles were carried by surface ocean currents provided by an ocean reanalysis product, Stokes drift computed using a wave model driven by satellite-derived winds, and windage. The generating plastic debris was given from river mouths and fisheries worldwide based on the observed data. The PTM includes the processes of beaching/re-drifting, fragmentation from plastic debris to microplastics on beaches, and removal of microplastics from the model domain. These processes proceed on timescales specified in the model. The timescales for beaching/re-drifting were determined by the field experiments, while other two timescales were chosen through trial and error to be consistent with the actual abundance of oceanic microplastics worldwide. To obtain the actual abundance of oceanic microplastics, a total of 8156 pelagic microplastics samples from the world’ s oceans were synthesized to create a dataset composed of raw, calibrated, and processed data. The raw microplastic abundance data were obtained by different research projects using surface net tows or continuous seawater intake. Fibrous microplastics were removed from the calibrated dataset. Microplastic abundance, which fluctuates of microplastic abundance owing to vertical mixing under different oceanic conditions, was standardized in the processed data.
On the basis of the modeled results validated by the observed data, quantities of floating plastic debris, plastic debris washed ashore on beaches, floating microplastics, microplastics on beaches, and removing microplastics from the model domain were computed by reducing the PTM results to a linearized model.

©2021. Japan Geoscience Union. All Right Reserved.

Estimating vertical distribution of microplastic particles under wind-driven and Langmuir turbulence by Large Eddy Simulation

*Yoshimasa Matsumura[1], Shin-ichi Ito[1], Chiharu Sasaki[1]

1. Atmosphere and Ocean Research Institute, University of Tokyo

While microplastic particles consist of buoyant materials such as polypropylene (PP) and polyethylene (PE) are supposed to be suspended at the sea surface, these can be vertically dispersed in a water column under turbulent condition due to stormy weather and/or severe waves. The vertical distribution of microplastic particles in the open ocean may have strong effect on the frequency of biological removal processes (e.g., aggregation by detritus or ingestion by zooplankton), but is poorly understood particularly under severe condition due to difficulty of direct measurement. In the present study the vertical distribution of microplastic particles in an open ocean surface mixed layer was investigated using an idealized large eddy simulation (LES) model coupled with on-line Lagrangian particle tracking system under various wind and wave forcing.

The numerical code used in the present study is kinaco, a non-hydrostatic ocean model developed in AORI, University of Tokyo. We adopted the filtered structure function (FSF) model for the LES subgrid scheme and the effect of waves was introduced by the vortex-force term. The computational domain is horizontally 128 m x 128 m and vertically 80 m with periodic boundaries. We introduced two categories of plastic particles consist of PP and PE, whose density is set as 910 kg/m^3 and 965 kg/m^3, respectively. The diameter of particles is classified into 10 bins from 10 μm to 5.12 mm, and the buoyant terminal velocity for each size and material is estimated from the empirical formula derived by Kaiser et al. (2019).

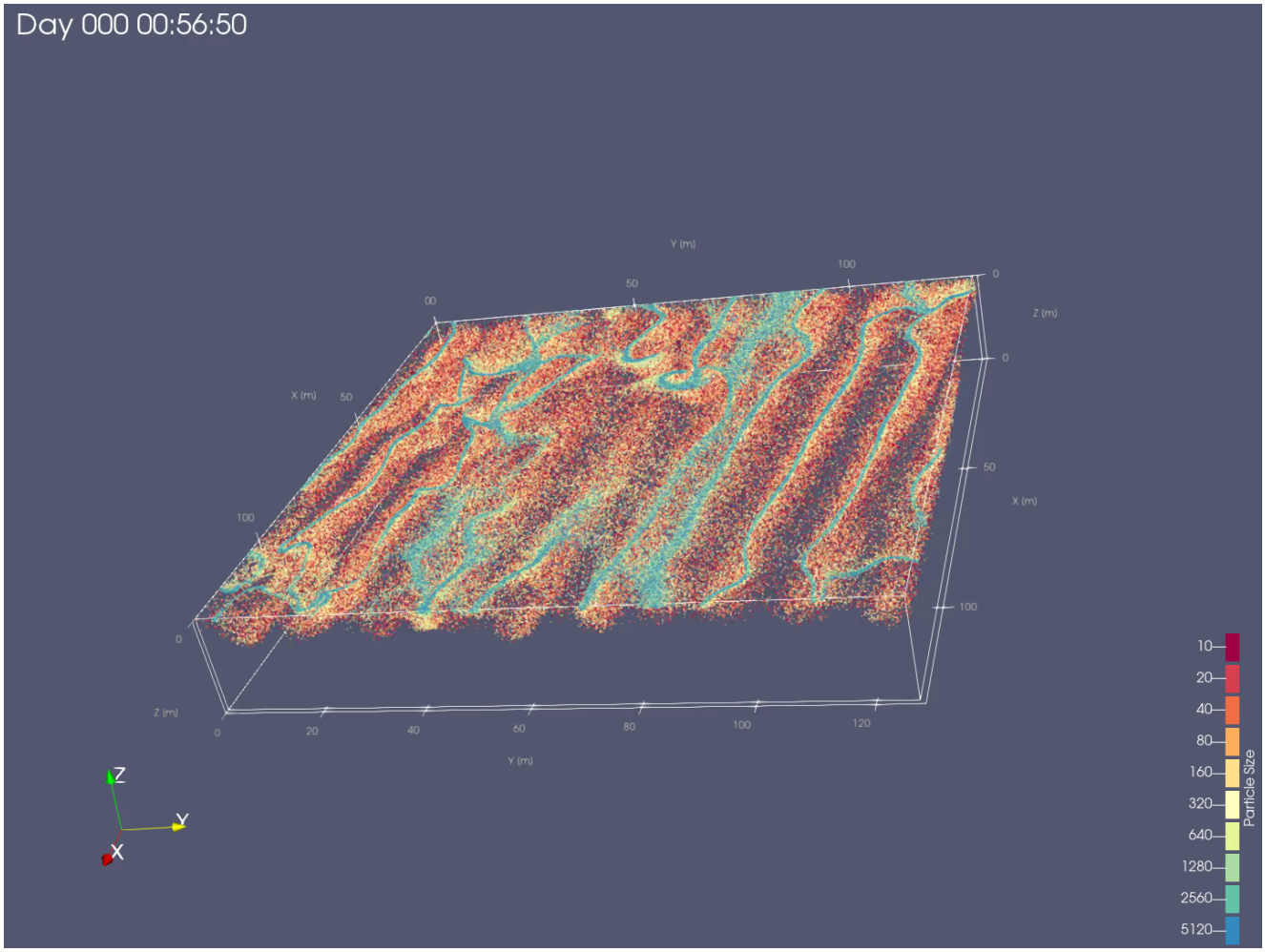
The initial stratification is based on the CTD observation carried out around the Tsushima Island in August 2020. The model was forced by surface wind of 0, 5, 10, 20 m/s and wave amplitude of 0, 0.316, 1.0, 3.16 m (total 15 cases), and integrated for 48 hours. The result of each case shows strong dependency of vertical distribution on the particle size but less dependency on the material difference. While almost all particles of greater than 1.28 mm diameter floated at the surface, certain amount of smaller particles were dispersed in the mixed layer. However, no particle was transported below pycnocline even in the severest case with 20 m/s wind and 3.16 m wave amplitude.

To investigate the seasonal variation, we also performed experiments with using monthly stratification of the same location simulated by DREAMS-D ocean forecast system operated by RIAM, Kyushu university. As expected, the vertical distribution of particles has strong dependency on the stratification. In particular, substantial number of particles less than 320 μm diameter reached the domain bottom in the winter season. The result suggests the possibility of physical removal of fine microplastic particles of buoyant material under severe weather condition in winter seasons over continental shelves.

The present simulations also recorded ultraviolet (UV) radiation exposure for each particle. It is suggested that floating plastic debris will be decomposed into finer particles by UV exposure, but finer particles tend to stay underwater for relatively longer period and be protected from UV radiation. The quantitative data provided by the present study may contribute to the estimation of decomposition process of plastic debris in the open ocean.

©2021. Japan Geoscience Union. All Right Reserved.

Keywords: Large Eddy Simulation, Langmuir turbulence, microplastic particles



©2021. Japan Geoscience Union. All Right Reserved.

Numerical experiment on vertical motion of microplastics with biological processes

*Miho Yoshitake[1], Atsuhiko Isobe[1]

1. Kyushu university

Plastic waste has flowed out into the world’s ocean through various routes, and gradually changes to microplastics with sizes are smaller than 5 mm. The relatively large plastics are degraded due to ultraviolet radiation and hydrolysis and are thereafter fragmentized by physical stimuli received from waves and sand on beach. Very small microplastics are easily intruded into various marine organisms, which may be damaged by these plastic debris. To investigate the influences of microplastics on the natural environment, field observations have been conducted worldwide. Although these observations adopted surface net towing to sample microplastics with a density lower than seawater, previous studies suggested that some process actually occurred to transport microplastics vertically downward from the sea surface to deeper layers. One of them is the inclusion into aggregation of phytoplankton, however, there have been not yet quantitative studies showing how the transport by aggregates affects the distribution of microplastics. Therefore, the purpose of this study was to verify the effect of biological processes on the vertical distribution of microplastics by reproducing the horizontal and vertical transport of microplastics with a numerical model with both physical and biological processes. Specifically, the model results were compared with the vertical distribution of microplastics reported by Song et al., (2018), where they collected very small microplastics > 20 micrometers from the sea surface to 1 m above the ocean floor in coastal waters.

Before modeling to reproduce both physical and biological processes, we started with a transport model based only on the physical processes: wind speed, significant wave height and buoyancy of microplastics were given to the model reproducing the oceanic turbulence. From this model, the physical process was sufficient to reproduce the size distribution of microplastics with a particle size range 0.2 to 5 mm at a depth of 5 m from the sea surface as that expected by a theoretical model given by Kukulka et al., (2012). However, particles < 100 μm disappeared from the water column in the observed results of Song et al., (2018), while the disappearance was not revealed in the numerical model which reproduce the vertical distribution in line with a physical mixing. Therefore, it was suggested that this inconsistency with the physical processes is caused by biological processes.

In the model considering both physical and biological processes, we added the aggregation of phytoplankton as a biological process to the above physical model. In this model, the particles representing phytoplankton move by oceanic turbulence, and aggregate to a single particle if they exist within the aggregation radius: aggregation occurs within this distance. Meanwhile, particles representing microplastics will be involved in the aggregated particle when they exist within the aggregation radius, and when the particle size is less than or equal to the aggregates. This model was able to reproduce the vertical distribution of Song et al., (2018), in which microplastics were transported to the seafloor together with heavy aggregates generated by biological processes, and their particle number reached the maximum in the subsurface layer. This indicates that if phytoplankton is present to some extent, the vertical distribution of microplastics will not show the maximum at sea surface, thus biological processes are more important than physical processes to determine the vertical distribution of microplastics. To support this, it was also suggested that these aggregates may have a sinking rate sufficiently large for the vertical velocity typically in the actual ocean. It is noted that the phytoplankton concentration given to this model occurs during spring or autumn bloom and red tide in the actual oceans.

©2021. Japan Geoscience Union. All Right Reserved.

Keywords: Microplastic, Numerical model, Aggregation

©2021. Japan Geoscience Union. All Right Reserved.

Numerical model approach of macroplastic transport to find microplastic sources around the Indonesian archipelago

*Ryohei Kono[1], Atsuhiko Isobe[1]

1. Research Institute for Applied Mechanics, Kyushu University

Accordingly to the increase of plastic materials' demand around the world, the amount of plastic garbage has been correspondingly enlarging. This plastic garbage is degraded and thereafter fragmentized to microplastics with size <5mm under the natural conditions such as ultra-violet radiation and waves. However, the areas where microplastics intensely generate are still undiscovered. Additionally, there is a concern that the absorption of toxic substances on microplastic surface is potentially harmful to living marine organisms after ingestion. Therefore, it is urgent to understand how macroplastics from the land sources changes to microplastics in the ocean, and how microplastics thereafter move from these oceanic sources to the marine ecosystem.
In this study, using a particle tracking model, macroplastic releases were given to river mouths around the Asian seas. Thereafter the beaches on which these macroplastics were washed ashore were recognized as potential sources of microplastics under the assumption that the inflow of plastic garbage to the ocean is all converted into microplastics at these potential sources.

Keywords: Microplastic, Particle tracking model, Numerical simulation

©2021. Japan Geoscience Union. All Right Reserved.

Quantifying the degree of pollution of beaches using an AI technique

*Mitsuko Hidaka[1], Daisuke Sugiyama[1], Daisuke Matsuoka[1], Fumiaki Araki[1], Masafumi Kamachi[1], Yoichi Ishikawa[1]

1. Japan Agency for Marine-Earth Science and Technology

Beached marine litter is harmful to both humans and nature. Monitoring litter on beaches solely through human effort is limiting in terms of both time and expenditure constraints. Establishing technologies that can quantify beached marine litter automatically will contribute to mitigation strategies and scientific understanding of litter. Therefore, we have attempted to develop an AI (Artificial Intelligence) system that can automatically estimate the degree of pollution of beaches using a deep-learning method. The core technology is “semantic segmentation”, which gives pixel-wise classification on images. For the training dataset, pairs of the original image and corresponding labels (ground truth) were prepared. We received monitoring data from the local government (Yamagata prefecture) and prepared the training dataset for the deep-learning model based on these images. For the labels, each region of an image is categorised into eight classes: sky, sea, sand beach, artificial litter, natural litter, installed object, and natural object. Using this dataset, we trained a deep-learning model that can classify an image into the eight classes. The mean IoU (Intersection over Union) between predicted results and ground truth was 76% for all classes. We will present preliminary results from the model, and would also like to discuss the detection of plastic litter.

Keywords: Artificial litter, Beach, Litter monitoring , Artificial Intelligence , Deep-learning , Object detection

©2021. Japan Geoscience Union. All Right Reserved.

Estimation of plastic litter abundance in cities using big data associated with citizen science and deep learning

*Shinichiro Kako[1], Shintaro Kanno[2], Atsuhiko Isobe[3], Masato Kuki[4], Kotaro Yamamoto[4], Fujio Kojima[4]

1. Graduate School of Science and Engineering, Kagoshima University, 2. Faculty of engineering, Kagoshima University, 3. Research Institute for Applied Mechanics, Kyushu University, 4. Pirika, Inc. / Prika association

In this study, we constructed a deep learning model using training data consisting of litter images in cities collected by citizen science using a smartphone application “Pirika.” Our deep learning model can classify and quantify the amount of litter in cities into various categories (plastic bags, plastic bottles, cans, and others). The model’s accuracies of object detection and classification were 83.0% and 82.9%, respectively. However, these accuracies of the model are guaranteed only under limited conditions and must be improved for practical use. The results of the learning curve shows that there is a limit to learning with the current training data and raises a concern that the model overfits the training data (validation accuracy of 70% and training accuracy of 99%). In future studies, the versatility of the model must be improved by increasing the size of the learning dataset by including various patterns for detection and classification. The smartphone app “Pirika” must also be updated with a function that disallows taking images that might lower the accuracy of our model.

Keywords: citizen science, deep learning, smartphone app “Pirika”, big data, plastic litter abundance in cities

©2021. Japan Geoscience Union. All Right Reserved.

[J] Oral | M (Multidisciplinary and Interdisciplinary)：M-IS Intersection

Sat. Jun 5, 2021 3:30 PM - 5:00 PM JST | Sat. Jun 5, 2021 6:30 AM - 8:00 AM UTC | Ch.10 Zoom Room 10

[M-IS20] Ocean Plastics, an earth science perspective

convener:Atsuhiko Isobe(Research Institute for Applied Mechanics, Kyushu University), Kiichiro Kawamura(Yamaguchi University), Yusuke Okazaki(Department of Earth and Planetary Sciences, Graduate School of Science, Kyushu University), Masashi Tsuchiya(Research Institute for Global Change, Japan Agency for Marine-Earth Science and Technology), Chairperson:Kiichiro Kawamura(Yamaguchi University)

Mismanaged plastic wastes accounting for 70% of marine debris remain persistently in the marine environment, even if they are degraded and fragmentized to tiny microplastics. To date, it has been unknown how this anthropogenic, buoyant, and persistent matter which was first appeared in the earth history, contaminates (or is incorporated into) the earth system. The ocean plastic study requires the insight and methodology of a variety of earth sciences such as the oceanography, geology, and palaeontology. Studies on the plastic circulation loaded from the land/atmosphere to upper oceans and bottom sediments, studies on microplastics as a proxy of the 'Anthropocene', and studies to establish procedures in monitoring and analyzing macro/microplastics are welcomed.

3:30 PM - 3:45 PM JST | 6:30 AM - 6:45 AM UTC

[MIS20-07] Large-scale distribution and composition of floating plastic debris in the transition region of the North Pacific

*Kentaro Miyazono[1], Rei Yamashita[2], Hiroomi Miyamoto[3], Kazuaki Tadokoro[4], Yugo Shimizu[5], Kazutaka Takahashi[1] (1.Graduate school of agricultural and life science, The University of Tokyo , 2.Atmosphere and Ocean Research Institute, The University of Tokyo , 3.Fisheries Research Agency, Hachinohe, 4.Fisheries Research Agency, Shiogama, 5.Fisheries Agency)

3:45 PM - 4:00 PM JST | 6:45 AM - 7:00 AM UTC

[MIS20-08] TARA-JAMBIO Microplastic Mission : Distributions of microplastics in water surface and sediment of Japanese coastal waters

*Kugako Sugimoto[1], JAMBIO Consortium[3], Tara Japan[2], Sylvain Agostini[1] (1.Shimoda Marine Research Center, University of Tsukuba, 2.Tara Océan Fondation, 3.Japanese Association for Marine Biology)

4:00 PM - 4:15 PM JST | 7:00 AM - 7:15 AM UTC

[MIS20-09] Distribution of Microplastics in the Deep-sea Sediments

*Tomo Kitahashi[1], Masashi Tsuchiya[1], Ryota Nakajima[1], Rie Matsui[1], Kazumasa Oguri[1,2], Kiichiro Kawamura[3], Yosaku Maeda[1], Sanae Chiba[1], Katsunori FUJIKURA[1] (1.Japan Agency for Marine-Earth Science and Technology, 2.University of Southern Denmark, 3.Yamaguchi University)

4:15 PM - 4:30 PM JST | 7:15 AM - 7:30 AM UTC

[MIS20-10] Chemical properties of film coatings developed on microplastics distributed on the urban river shore in Mongolia

*Masayuki Kawahigashi[1], Batdulam Battulga[1] (1.Tokyo Metropolitan University)

4:30 PM - 4:45 PM JST | 7:30 AM - 7:45 AM UTC

[MIS20-11] A trial of small microplastics collection by Neuston net

*Haodong XU[1], Haruka NAKANO[1], Tadashi TOKAI[1], Hisayuki ARAKAWA[1] (1.Tokyo University of Marine Science and Technology)

4:45 PM - 5:00 PM JST | 7:45 AM - 8:00 AM UTC

[MIS20-12] Non-contact real-time identification of microplastics in flow by combining holography and Raman spectroscopy

*Tomoko Takahashi[1,2,3], Zonghua Liu[2], Thangavel Thevar[4], Nicholas Burns[4], Dhugal Lindsay[1], John Watson[4], Sumeet Mahajan[3], Blair Thornton[2,3] (1.Japan Agency for Marine-Earth Science and Technology, 2.Institute of Industrial Science, The University of Tokyo, 3.University of Southampton, 4.University of Aberdeen)

Large-scale distribution and composition of floating plastic debris in the transition region of the North Pacific

*Kentaro Miyazono[1], Rei Yamashita[2], Hiroomi Miyamoto[3], Kazuaki Tadokoro[4], Yugo Shimizu[5], Kazutaka Takahashi[1]

1. Graduate school of agricultural and life science, The University of Tokyo , 2. Atmosphere and Ocean Research Institute, The University of Tokyo , 3. Fisheries Research Agency, Hachinohe, 4. Fisheries Research Agency, Shiogama, 5. Fisheries Agency

Distribution and composition of the floating plastic debris in the transition region across 4600 km between 141ºE to 165ºW in the North Pacific was investigated to obtain the information of its transportation process from coastal area of Asian continent to central/eastern subtropical Pacific based on the samples collected by a neuston-net for pre-season survey of Pacific saury. The concentration and composition in terms of size, colour, shape and polymer type (determined with a Fourier transform infrared spectrophotometer) were determined for 77 stations and those data were analyzed in relations to the oceanographic parameters including water temperature, salinity, and current flow pattern on sea surface. In the study area, on average, 152,762 ±459,807 pieces km^{-2} of floating plastic debris was found, with a maximum of 3,914,195 pieces km^{-2} and distribution was primarily influenced by the current system but the process to generate the high concentration area seemed to be different between western and eastern area of the transition region. In the west of 180º, floating plastic debris largely accumulated around convergent in the nearshore area and transported by eddies and quasi-stationary jet to the subarctic region. Furthermore, in addition to the effect of Stokes drift, floating plastic debris retained by the anti-cyclonic eddies (warm core rings) may be kept remained within the coastal area due to its westward migration. Meanwhile some plastics like styrene foam and lines seems to be selectively eliminated from water column and decrease towards offshore. The average of the western area (68,575 ± 74,734 pieces km^{-2}) was 15 % higher than previously reported value in 1989, suggesting the possible increase of plastic debris during this 30 year. In the east of 180º, floating plastic debris accumulated in the calm water area corresponds to the downstream of the Kuroshio Bifurcation, a northern branch of the Kuroshio Extension. The concentration (505,032±991,989 pieces km^{-2}) was considerably higher than in the western area, implying that the heavily polluted area of floating plastic debris in the central subtropical North Pacific is larger than our prediction. The high concentration seemed to be related with intensification of surface accumulation of small-sized transparent film caused by calm weather condition in this area, suggesting the importance of further investigation focusing on small-sized plastic (< 1mm) including film type in the subsurface depth in the subtropical central/eastern Pacific.

Keywords: Microplastics, the North Pacific Ocean, Kuroshio/Kuroshio Extension

©2021. Japan Geoscience Union. All Right Reserved.

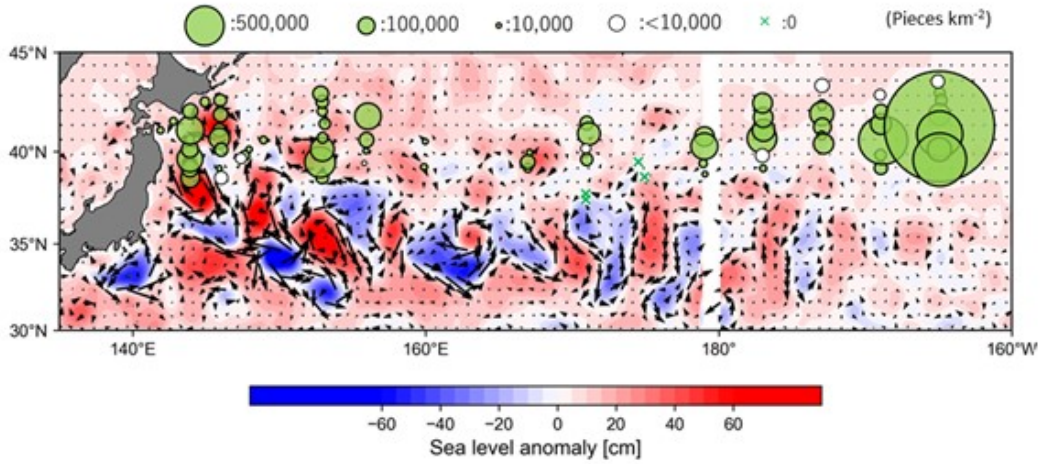


Fig.1. Sea level anomaly and current with plastic debris distribution

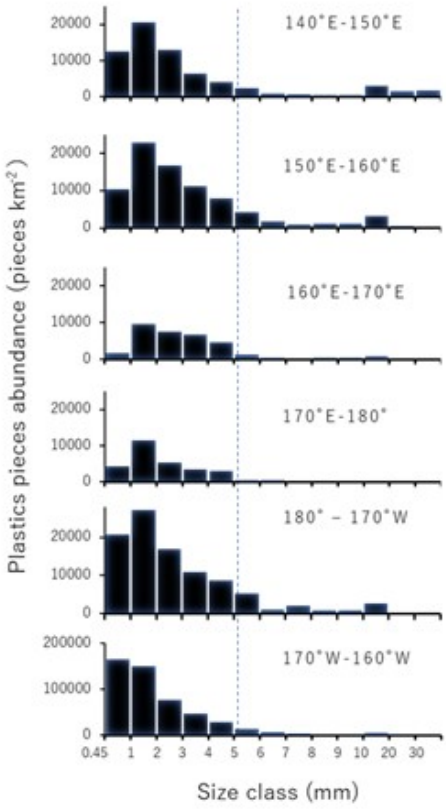


Fig. 2. Longitudinal variation of size distribution of plastic debris in the transitional zone of North Pacific in June, 2016. Note that scale unit of y-axis of 170° W-160° W is 10-fold higher than others.

©2021. Japan Geoscience Union. All Right Reserved.

TARA-JAMBIO Microplastic Mission : Distributions of microplastics in water surface and sediment of Japanese coastal waters

*Kugako Sugimoto[1], JAMBIO Consortium[3], Tara Japan[2], Sylvain Agostini[1]

1. Shimoda Marine Research Center, University of Tsukuba, 2. Tara Océan Fondation, 3. Japanese Association for Marine Biology

The Tara Océan Fondation is deidcated to the world’ s ocean and collaborates with scientific partners to organise scientific expeditions, raise awareness and educate, mobilize policy makers at the highest level, and enable emerging and developing countries to access the latest knowledge about the ocean. From 2020, the fondation partnered with the JAMBIO, the network of japanese marine stations to start a joint mission on microplastic pollution in japanese coastal waters. Due to their small size, microplastics cannot be fully retrieved from the ocean once they enter it and may cause damage to marine ecosystems and the organisms that ingest them. However there is still an important lack in the knowledge on the quantity, the sources and fluxes of microplastic in the ocean. The mission has two aims: 1) to assess the microplastic pollution in surface waters and sediment of Japanese coasts, the fluxes of microplastics from rivers and bays, and the microbial communities on the plastic fragments, the “plastisphere”; 2) to raise awareness of plastic pollution, promote a reduction in the use of plastic and generally inform on the threats that the ocean is facing due to human activities. A first sampling and outreach mission was conducted at six marine stations in West Japan. Namely sampling were performed at the Ushimado Marine Institute (Okayama University), the Takehara station (Hiroshima University), the Oki Marine station (Shimane University), the Amakusa Marine Station (Kyushyu University) and the Sugashima Marine Biological Laboratory (Nagoya University). Surface water were sampled using a Neuston net and sediment using a Smith McIntyre Sediment Grab. Microplastics were (300 –5000 μm) extracted using density separation following the degradation of organic materials by peroxide oxidation. For the plastisphere study, microplastic fragments were sampled under the microscope immediately after the sampling. Sampling was conducted in each station at a river mouth, within a bay and outside a bay, in order to assess the horizontal fluxes. Samples are now being analyzed but all surface waters visibly contained microplastic fragments. Outreach activities were also conducted at each location. Moreover a local artist also participated to the sampling and each artists produced a piece of art. Collaboration with artists has been an outreach approach used in all Tara expeditions and allow to reach a new public. The next sampling mission in East Japan is being organized for 2021.

©2021. Japan Geoscience Union. All Right Reserved.

Distribution of Microplastics in the Deep-sea Sediments

*Tomo Kitahashi[1], Masashi Tsuchiya[1], Ryota Nakajima[1], Rie Matsui[1], Kazumasa Oguri[1,2], Kiichiro Kawamura[3], Yosaku Maeda[1], Sanae Chiba[1], Katsunori FUJIKURA[1]

1. Japan Agency for Marine-Earth Science and Technology, 2. University of Southern Denmark, 3. Yamaguchi University

Marine plastic pollution is of global concern, and one of the Sustainable Development Goals (SDGs) set by the United Nations includes the reduction of marine pollution, including plastic, as one of its targets. Plastics are miniaturized by ultraviolet light and waves, and especially those particles smaller than 5 mm are called microplastics (MPs), and there are concerns about their adverse effects on marine organisms. It is an urgent issue to understand the actual status of MP pollution in the ocean, and it is essential to identify the sources and routes of plastic spills in order to properly regulate plastics and take measures against marine outflow.

MPs exist not only in the sea surface and water column, but also in sediments Especially, they are accumulated at the bottom of ocean trenches. In this study, we focused on the possibility of MPs transport from Sagami Bay, which has the largest population density in Japan in its hinterland, to the plate triple junction. We compared the number of MPs in the sediments of Sagami Bay and the triple junction to examine the transport process of MPs from the bathyal to the hadal zone.

Sediment samples at two stations of Sagami Bay (St. 1: off Hatsushima, 855 m water depth; St. 2: center of the bay, 1,387 m water depth) and at two stations of triple junction (St. 4, 9,218 m water depth; St. 5, 9,232 m water depth) were collected with push corers manipulated by the HOV *Shinkai 6500* and a free-fall camera system, respectively, during the research cruise of R/V *Yokosuka* YK19-11. Sediment samples were subjected to specific gravity separation using sodium iodide (NaI), dissolution of calcium carbonate using hydrochloric acid, and dissolution of organic matter using Fenton treatment to separate MPs from the sediment. The separated MPs were stained with Nile Red and observed and counted under a fluorescence microscope.

The results shows that the number of MPs per dry weight of sediment at the sediment surface (0-1 cm) was 25.5±19.3 MPs/g at St. 1, 67.5±14.7 MPs/g at St. 2, 26.6±0.05 MPs/g at St. 4, and 48.8 MPs/g at St. 5, respectively. The highest number of MPs was detected in the center of Sagami Bay, while the same level of MPs as those in Sagami Bay was detected at the two stations at the plate triple junction, which are far from human activities. In addition, no particles larger than 250 μm in diameter were detected at the two stations of the plate triple junction, and the average diameter tended to be smaller than that of the two stations in Sagami Bay. These results suggest that the MPs at the plate triple junction are transported through the submarine canyons, and that size fractionation of MPs occurs during the transport process. In the future, we plan to analyze the accumulation and depositional processes of MPs in more detail by using micro-Fourier Transform Infrared Spectroscopy (μ-FT-IR) to identify the types of plastics and by dating of the sediments.

Keywords: Microplastic, Deep-sea floor, Trench

©2021. Japan Geoscience Union. All Right Reserved.

Chemical properties of film coatings developed on microplastics distributed on the urban river shore in Mongolia

*Masayuki Kawahigashi[1], Batdulam Battulga[1]

1. Tokyo Metropolitan University

Plastics released into environment are deteriorated by solar radiation, physical impacts and freeze-thaw cycles, resulting in increase in surface areas of microplastics accompanied by reaction with pollutants. The reactivity of plastics can also be altered by organic matter coating which mainly mediated by microbial activity. Plant residues and minerals participated to the surface coating can induce various reaction on the surface. Environmental conditions where plastics reside also characterize the surface coating of plastics. Composition of plastic coatings can record the fate of plastics after release into environment. This study targets the surface coating of plastics by spectral analyses.

Samples of microplastics were polystyrene foams collected on a river shore along the Tuul River in Ulaanbaatar, Mongolia. Polystyrene foams, which were dominant plastics in the study area, distribute widely from the upper to lower stream. Those polystyrene foams have reached to the present positions through various processes, resulting that some are broken into numerous pieces with different color and others are probably well aged. Components consisting of the coating on the polystyrene surface were evaluated by a micro-FTIR spectroscopy. The differences in spectra between intact and digested surfaces of polystyrene were considered as spectra from the surface coating of polystyrene. IR absorptions at specific wavenumbers were statistically analyzed by the principal component analysis for classification of types of coatings.

Most of absorption peaks were assigned as characteristic organic functional groups mainly consisting of microorganisms, fragments of arthropods and plant debris derived from ligno-cellulose. Contribution of the assigned organic constituents were diverse in various coatings on polystyrenes which distributed in different environments. The nitrogen containing functional groups such as amino residues and peptides coupling with carbonyl groups strongly contributed to PC1 and classified polystyrene foams well. Polystyrene foams coated with living or dead microorganisms can be separated by PC1. The second principal component was characterized by lignin moieties consisting of aromatic rings with carbonyl stretching vibration, indicating that positive scores mean participation of plant residues into the surface coating developed on polystyrene distributed a dry shore region covered with vascular plants. The collected information from organic coatings explained the status of polystyrene foams under several different environmental conditions.

Keywords: biofilm, polystyrene foam, composition of organic substances, N containing functional groups, micro-FTIR

©2021. Japan Geoscience Union. All Right Reserved.

A trial of small microplastics collection by Neuston net

*Haodong XU[1], Haruka NAKANO[1], Tadashi TOKAI[1], Hisayuki ARAKAWA[1]

1. Tokyo University of Marine Science and Technology

Introduction:

The most efficiently as well as widely used sampling method for microplastics is neuston net due to its easy maneuverability, which normally has mesh size around 350μm. Therefore, researchers could be able to estimate the abundance and distribution of microplastics of the sea area. However, the contamination of small microplastics (less than 350μm) in the ocean cannot be researched and known because small microplastics escape from mesh. It is considered that the small microplastics perhaps cause more harm to the ecosystem and marine organism. Thus, we need to research on small microplastics urgently and systematically.

In this study, double neuston net (interior mesh size: 350μm; exterior mesh size: 50μm; 2 cod ends, Rigo Co. Ltd) and normal neuston net (mesh size: 350μm, Rigo Co. Ltd) were used to sample both the large microplastics (>350μm) and the small microplastics (50μm-350μm). Further, the aims of this study examined collecting method of the small microplastics and revealing the pollution of small microplastics in the sea area.

Materials and Methods:

Two observations were accomplished on 2020, in which, the fist observation containing 2 stations (Station 1, Station 2) was complemented from Nov. 9-Nov.11 in Tokai off the sea area, Japan, by T/V Shinyo Maru (986t, 64.6m) of Tokyo University of Marine Science and Technology (TUMSAT), the second observation containing 2 stations (Station 3, Station 4) was conducted on Dec. 12 in Tokyo Bay by T/V Seiyo Maru (170t, 35.5m) of TUMSAT.

Both neuston nets were equipped with flow meter. Moreover, tow speed, tow time were set to 1 knot of log speed, 10 minutes, respectively. Additionally, 2 samples can be obtained by double neuston net at one time. After sampling, samples were kept at refrigerator on cruise then transferred to laboratory. As to samples from 350μm-mesh neuston net, they were processed in a sequence of wet peroxide oxidation (WPO), density separation, picking up, microscope-based morphology recording, FTIR-based (Fourier-Transform infrared spectroscopy) spectrum measuring. On the other hand, the procedures of samples from 50μm-mesh neuston net were as same as 350μm-mesh neuston net samples until density separation, and the samples were filtrated by PTFE filters and the filters were scanned by μFTIR.

Results:

The concentrations of normal neuston net are 0.28 pieces/m^3 in Station 1, 0.11 pieces/m^3 in Station 2. Comparatively, double neuston net with 350μm mesh has the concentrations of 0.38 pieces/m^3 in Station 1, 0.10 pieces/m^3 in Station 2. No significant difference was found between these two neuston net. Yet, double neuston net with 50μm mesh has definitely higher concentration than those with 350μm, with the values of 15205±1288 pieces/m^3 in Station 1, 3389±1315 pieces/m^3 in Station 2.

As to the categories, PE (25.9%), PP (7.1%), PA (4.5%), PS (23.2%), PET (8.0%) have high percentage of large microplastics, while ‘others’ only account for 8.9%. By comparison, PE (5.4%), PP (1.5%), PA (1.5%), PS (0.2%), PET (1.9%) are all the minorities while ‘others’, including PolyHexadeculethylene, PolyOctadecylacrylamide, plastics additives etc., take a large proportion (74.2%) of small microplastics.

Particles within 50μm~60μm have the peak concentration in the particle size distribution. Besides, the particle concentrations decrease with increasing size. Therefore, it could be concluded that particles below 50μm have the higher concentration compared to particles above 50μm.

©2021. Japan Geoscience Union. All Right Reserved.

Keywords: Small Microplastics, Neuston Net

©2021. Japan Geoscience Union. All Right Reserved.

Non-contact real-time identification of microplastics in flow by combining holography and Raman spectroscopy

*Tomoko Takahashi[1,2,3], Zonghua Liu[2], Thangavel Thevar[4], Nicholas Burns[4], Dhugal Lindsay[1], John Watson[4], Sumeet Mahajan[3], Blair Thornton[2,3]

1. Japan Agency for Marine-Earth Science and Technology, 2. Institute of Industrial Science, The University of Tokyo, 3. University of Southampton, 4. University of Aberdeen

Hundreds of millions of tons of plastic waste are generated, and millions of tons enter the ocean every year [1]. “Microplastics”, with the size of less than 5 mm, become coated with biofilms, get attached to other particles, or ingested by microorganisms while floating in the ocean, and transported to all parts of the oceans. The global awareness of pollution in marine and other aquatic environments by microplastics has risen recently [2]. While spectroscopic techniques such as Fourier transformed infrared and Raman spectroscopy have been widely used for identification of plastics collected from aquatic environments, these are time-consuming due to the need for separation from other organic and inorganic particles, filtration, and long measurement time [3]. In this work, a novel method for non-contact fast identification of microplastics suspended in water was investigated.

An integrated method of holography and Raman spectroscopy for *in situ* real-time monitoring of microplastics is reported. Polystyrene (PS) and poly(methyl methacrylate) (PMMA) pellets with a size of 3 mm located in a 20 cm water channel were illuminated using a collimated continuous wave laser beam with a diameter of 4 mm and wavelength of 785 nm. The same laser beam was used to take a holograms for size and shape information, and produce a Raman spectrum for composition information of the suspended material. By the proposed method, PS and PMMA beads in a large water volume were successfully identified using a compact setup [4]. We have also demonstrated classification of particle types by this combined morphological and chemical analysis. While particles with distinctive shapes, such as plankton, can be easily identified by holography, chemical analysis by Raman measurements is necessary for some particles as shown in the Figure. Corresponding Raman peaks of the materials are observed in the Raman spectra of plastic pellets of PS and PMMA. Inorganic matter (Foraminifera) shows a $CaCO_3$ peak and other peaks that match Raman peaks taken for the same sample in air as a ground truth. While no obvious Raman peak is observed in the spectrum of organic matter (paste of replicated marine snow), a broad fluorescence peak is seen.

The proposed method demonstrates the potential for non-contact continuous *in situ* monitoring of marine particles, including microplastics, suspended in water without the need for collection/extraction. It is particularly promising for long-term measurements in deep-water columns, where the particle density is extremely low. The concept of the measurement process using the system is the following: holographic images are continuously captured in an open measurement chamber with a high frame rate to detect a particle. When a particle is detected, the chamber is closed to trap the particle and a Raman measurement is initiated (which takes several tens of seconds, but can be faster using higher power lasers). After the Raman measurement, the chamber is opened again and onset of holographic imaging waits for the next particle. The whole measurement process can be fully automated, which makes it possible to deploy the system on an autonomous platform such as autonomous underwater vehicles and buoys. This could be game-changing for current sampling-based analysis and will contribute to the understanding of global-scale microplastic pollution in aquatic environments.

©2021. Japan Geoscience Union. All Right Reserved.

References:

[1] J. Jambeck, R. Geyer, C. Wilcox, et al., Science (2015); **347**, 768–771.

[2]T. Galloway, C. Lewis, Curr. Biol. (2017); **27**, R445-R446.

[3] W. J. Shim, S. H. Hong, S. E. Eo, Anal. Methods (2017); **9**, 1384-1391.

[4] T. Takahashi, Z. Liu, T. Thevar, et al., Appl. Optics (2020); **59**, 5073-5078.

Keywords: Microplastics, Monitoring , Holography, Raman spectroscopy

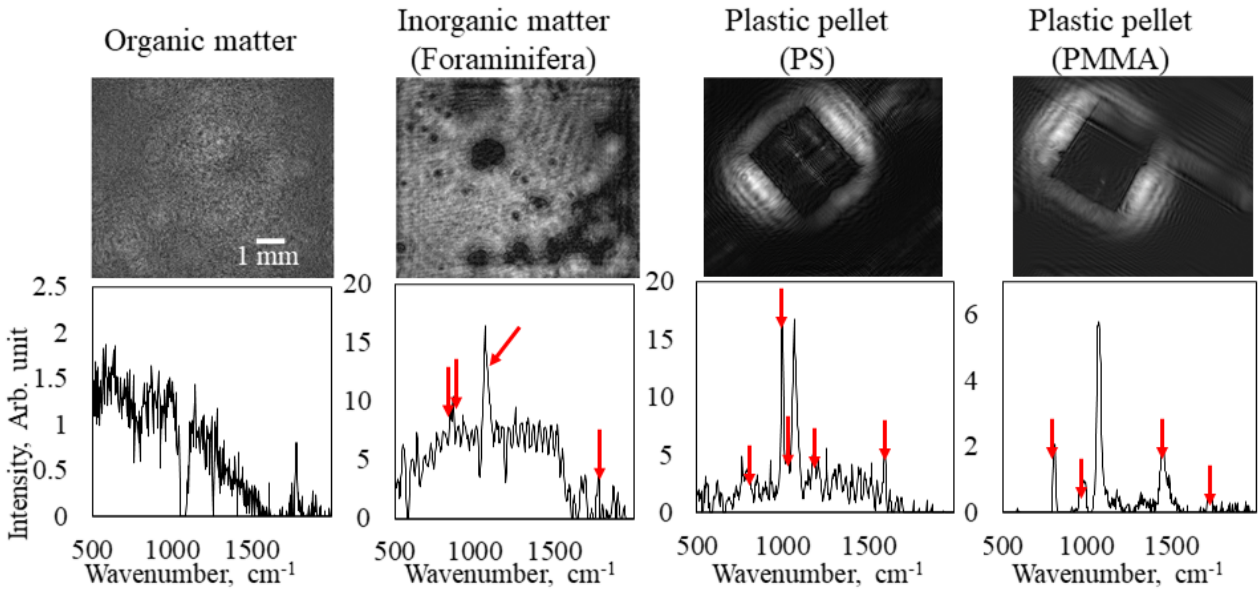


Figure: Holographic images and Raman spectra obtained for organic matter, inorganic matter, and two different types of plastic pellets. The red arrows indicate corresponding peaks of the materials.

©2021. Japan Geoscience Union. All Right Reserved.

[J] Poster | M (Multidisciplinary and Interdisciplinary)：M-IS Intersection

Sat. Jun 5, 2021 5:15 PM - 6:30 PM JST | Sat. Jun 5, 2021 8:15 AM - 9:30 AM UTC | Ch.20_3

[M-IS20] Ocean Plastics, an earth science perspective

convener:Atsuhiko Isobe(Research Institute for Applied Mechanics, Kyushu University), Kiichiro Kawamura(Yamaguchi University), Yusuke Okazaki(Department of Earth and Planetary Sciences, Graduate School of Science, Kyushu University), Masashi Tsuchiya(Research Institute for Global Change, Japan Agency for Marine-Earth Science and Technology)

Mismanaged plastic wastes accounting for 70% of marine debris remain persistently in the marine environment, even if they are degraded and fragmentized to tiny microplastics. To date, it has been unknown how this anthropogenic, buoyant, and persistent matter which was first appeared in the earth history, contaminates (or is incorporated into) the earth system. The ocean plastic study requires the insight and methodology of a variety of earth sciences such as the oceanography, geology, and palaeontology. Studies on the plastic circulation loaded from the land/atmosphere to upper oceans and bottom sediments, studies on microplastics as a proxy of the 'Anthropocene', and studies to establish procedures in monitoring and analyzing macro/microplastics are welcomed.

[MIS20-P01] Automatic detection for Nile Red-stained microplastic particles

*Masashi Tsuchiya[1], Tomo Kitahashi[1], Yosuke Taira[2], Hitoshi Saito[2], Kazumasa Oguri[1,3], Ryota Nakajima[1], Dhugal J. Lindsay[4], Katsunori FUJIKURA[1], Tomohiko Fukushima[1,5] (1.Research Institute for Global Change, Japan Agency for Marine-Earth Science and Technology, 2.NEC Corporation, 3.Danish Center for Hadal Research, University of Southern Denmark, 4.Institute for Extra-cutting-edge Science and Technology Avant-garde Research, Japan Agency for Marine-Earth Science and Technology, 5.Deep Ocean Resources Development Co., Ltd.)

[MIS20-P02] Deep sea Macro plastics in the Northwestern Pacific Ocean

*Tomoaki Kitayama[1], Takashi Hosono[1], Hideaki Saito[1] (1.Japan Agency for Marine-Earth Science and Technology)

Automatic detection for Nile Red-stained microplastic particles

*Masashi Tsuchiya[1], Tomo Kitahashi[1], Yosuke Taira[2], Hitoshi Saito[2], Kazumasa Oguri[1,3], Ryota Nakajima[1], Dhugal J. Lindsay[4], Katsunori FUJIKURA[1], Tomohiko Fukushima[1,5]

1. Research Institute for Global Change, Japan Agency for Marine-Earth Science and Technology, 2. NEC Corporation, 3. Danish Center for Hadal Research, University of Southern Denmark, 4. Institute for Extra-cutting-edge Science and Technology Avant-garde Research, Japan Agency for Marine-Earth Science and Technology, 5. Deep Ocean Resources Development Co., Ltd.

Marine microplastics (MPs) pollution has become a major social problem. MPs have been found to be widespread not only in coastal areas but also in the open ocean, including in the polar regions and in the Mariana Trench. Due to the effects of waves, UV and physical weathering, plastics become finer during and after discharged into the ocean. However, transporting processes into the deep sea have not yet been clarified. Although seafloor is considered to be one of the sinks of MP, there is less information about them than about the floating MPs at the surface of the ocean. In this study, we developed a flow system (flow cell) in which NR-stained MPs were continuously monitored, and the fluorescent particles that passed through the flow cell were visualized under a fluorescent stereomicroscope. In addition, we constructed an automatic detection system, with machine learning, to measure the shape and number of MPs from the captured images. As a result of image acquisition and automatic discrimination using this system, we were able to discriminate MPs consisting of particles and fibers smaller than 330 μm. This system enables discrimination at more than 60 MPs per minute.

Keywords: Microplastics, Nile-Red staining, machine learning, automatic detection

©2021. Japan Geoscience Union. All Right Reserved.

Deep sea Macro plastics in the Northwestern Pacific Ocean

*Tomoaki Kitayama[1], Takashi Hosono[1], Hideaki Saito[1]

1. Japan Agency for Marine-Earth Science and Technology

Enhancement of marine litter knowledge is essential to address the challenges of SDG14 such as marine pollution and conservation of sea and marine resources including biodiversity. However, information on seafloor litter is limited in marine litter studies. This is because it is not easy to approach the seafloor, and in order to clarify the life cycle of marine litter and the so-called Missing Plastics (99% out of all plastics that has entered into the ocean are missing), it is necessary to accumulate knowledge and information on seafloor litter. The Global Oceanographic Data Center (GODAC) of the Japan Agency for Marine-Earth Science and Technology (JAMSTEC) has published a “deep-sea debris dataset” using videos and photos taken during deep sea research in 2017, which data on categories, condition (accumulation point and drifting, etc.), and environments (sea bottom sediments and activities of organisms near the litters) of deep sea litter. A scientific paper based on this dataset has reported on distribution of plastic waste in the deep sea over 6000-m deep (Chiba et al., 2018). We also have been accumulating knowledge and information on seafloor litter of the northwestern Pacific Ocean, which has one of the most complex topographical characteristics in the world, with the triple junction and the world’s deepest seafloor, the Mariana Trench.
In this presentation, we will present a re-analysis of the spatial distribution and characteristics of seafloor litter of the northwestern Pacific Ocean using the “deep-sea debris dataset” with additional data from 2017 to 2021. Moreover, we will discuss how these data should be accumulated and provided to contribute to marine litter researches.

S. Chiba, H. Saito, R. Fletcher, T. Yogi, M. Kayo, S. Miyagi, M. Ogido, K. Fujikura,
Human footprint in the abyss: 30 year records of deep-sea plastic debris
Marine Policy (2018), 10.1016/j.marpol.2018.03.022

Keywords: Deep-sea debris, Marine litter, Seafloor litter, Macro plastics, Northwestern Pacific Ocean

©2021. Japan Geoscience Union. All Right Reserved.

[J] Oral | M (Multidisciplinary and Interdisciplinary) : M-IS Intersection

Sat. Jun 5, 2021 1:45 PM - 3:15 PM JST | Sat. Jun 5, 2021 4:45 AM - 6:15 AM UTC | Ch.26 Zoom Room 26

[M-IS28] Evolution of Pelagic Realm

convener:Atsushi Matsuoka(Department of Geology, Faculty of Science, Niigata University), Toshiyuki Kurihara(Graduate School of Science and Technology, Niigata University), Junichiro Kuroda(Department of Ocean Floor Geoscience, Atmosphere and Ocean Research Institute, the University of Tokyo), XIN LI(State Key Laboratory of Palaeobiology and Stratigraphy, Nanjing Institute of Geology and Palaeontology, Chinese Academy of Sciences), Chairperson:Atsushi Matsuoka(Department of Geology, Faculty of Science, Niigata University), Junichiro Kuroda(Department of Ocean Floor Geoscience, Atmosphere and Ocean Research Institute, the University of Tokyo)

This session focuses on the evolution of ecosystem and physical-chemical environments in the pelagic realm, including discussions on all aspects of pelagic biota covering evolution, biostratigraphy, biochronology, and biogeography, which are important to the reconstruction of the spatiotemporal framework in the pelagic realm. Reconstructions of plate configuration through time are included in the scope of this session. Biological, geochemical, and sedimentological approaches to the pelagic environments are welcomed. Science on form encompasses everything from plankton to outer space. We will discuss the evolution of the Panthalassa-Pacific Ocean since the scientific research vessel JOIDES Resolution comes back to the Pacific in 2023-2024.

1:45 PM - 2:00 PM JST | 4:45 AM - 5:00 AM UTC

[MIS28-01] Toward a global correlation of the Jurassic–Cretaceous boundary among pelagic, neritic and terrestrial sequences in the Pacific and Asia

*Atsushi Matsuoka[1] (1.Department of Geology, Faculty of Science, Niigata University)

2:00 PM - 2:15 PM JST | 5:00 AM - 5:15 AM UTC

[MIS28-02] **Early Cretaceous anti-tropical radiolarians of from Tibet at the breakup timing of Gondwana**

*XIN LI[1], Noritoshi Suzuki[2], Peter Baumgartner[4], Atsushi Matsuoka[3] (1.State Key Laboratory of Palaeobiology and Stratigraphy, Nanjing Institute of Geology and Palaeontology, Chinese Academy of Sciences, 2.Institute of Geology and Paleontology, Gradute School of Science, Tohoku University, 3.Department of Geology, Faculty of Science, Niigata University, 4.Institut des sciences de la Terre, Université de Lausanne)

2:15 PM - 2:30 PM JST | 5:15 AM - 5:30 AM UTC

[MIS28-03] Repeated organic-rich deposition in Early Triassic pelagic deep Panthalassa and its relationship with global seafloor anoxia

*Shun Muto[1] (1.Geological Survey of Japan, National Institute of Advanced Industrial Science and Technology)

2:30 PM - 2:45 PM JST | 5:30 AM - 5:45 AM UTC

[MIS28-04] Marine Os isotope record from the uppermost Barremian to the lowest Turonian

*Hironao Matsumoto[1], Rodolfo Coccioni[2], Fabrizio Frontalini[2], Kotaro Shirai[1], Junichiro Kuroda[1] (1.Atmosphere and Ocean Research Institute, the University of Tokyo, 2.University of Urbino)

2:45 PM - 3:00 PM JST | 5:45 AM - 6:00 AM UTC

[MIS28-05] Depositional ages of multiple REY peaks in deep-sea sediments around Minamitorishima Island based on osmium isotope stratigraphy

*Yuta Oda[1], Junichiro Ohta[1,2], Erika Tanaka[1], Kazutaka Yasukawa[1,2], Yusuke Kuwahara[1], Moei Yano[2,1], Koichiro Fujinaga[2,1], Kentaro Nakamura[1], Yasuhiro Kato[1,2] (1.School of Engineering, The University of Tokyo, 2.ORCeNG, Chiba Institute of Technology)

3:00 PM - 3:15 PM JST | 6:00 AM - 6:15 AM UTC

[MIS28-06] Depositional environments of the Late Cretaceous REY-rich mud in the western North Pacific Ocean inferred from deep-water agglutinated foraminifers

*Kondo Yuta[1], Junichiro Ohta[1,2], Kazutaka Yasukawa[1,2], Kentaro Nakamura[1], Koichiro Fujinaga[2,1], Yasuhiro Kato[1,2] (1.School of Engineering, The University of Tokyo, 2.ORCeNG, Chiba Institute of Technology)

Toward a global correlation of the Jurassic–Cretaceous boundary among pelagic, neritic and terrestrial sequences in the Pacific and Asia

*Atsushi Matsuoka[1]

1. Department of Geology, Faculty of Science, Niigata University

The decision of the Global Boundary Stratotype Section and Point (GSSP) of the Jurassic–Cretaceous boundary (JKB) is one of urgent tasks because the JKB is the last system boundary without stratotype in the Phanerozoic. The previous Berriasian Working Group (BWG) in the International Subcommission on Cretaceous Stratigraphy (ISCS) decided to use the base of the *Calpionella alpina* Subzone as the primary marker and proposed the Tre Maroua section in south France as the candidate for the GSSP of the Berriasian Stage in 2019. However, the ISCS did not support this proposal as the result of ballot by the voting members. Upon this situation, a new working group was organized in December 2020. The new chairperson is Jacek Grabowski in the Polish Geological Institute. The author (AM) is one of the BWG members (20 in total) and is expected to review radiolarian biostratigraphy and to provide new data from the pelagic sequences especially in the Pacific and Asian regions. Aims of the current BWG are to choose the primary marker and to propose the GSSP candidate for the base of the Berriasian Stage. Continuous sequences in the pelagic realm have a great potential for clarifying tie points among biostratigraphy, chemostratigraphy, magnetostratigraphy and any stratigraphies. This presentation introduces ongoing activities of the BWG including a global correlation among pelagic, neritic and terrestrial sequences in the Pacific and Asian regions around the JKB. A new proposal for deep-sea drilling in the western Pacific is also presented.

Keywords: Jurassic-Cretaceous boundary, International Subcommission on Cretaceous Stratigraphy, Berriasian Working Group, Global Boundary Stratotype Section and Point , deep-sea drilling, radiolaria

©2021. Japan Geoscience Union. All Right Reserved.

Early Cretaceous anti-tropical radiolarians of from Tibet at the breakup timing of Gondwana

*XIN LI[1], Noritoshi Suzuki[2], Peter Baumgartner[4], Atsushi Matsuoka[3]

1. State Key Laboratory of Palaeobiology and Stratigraphy, Nanjing Institute of Geology and Palaeontology, Chinese Academy of Sciences, 2. Institute of Geology and Paleontology, Gradute School of Science, Tohoku University, 3. Department of Geology, Faculty of Science, Niigata University, 4. Institut des sciences de la Terre, Université de Lausanne

The Yarlung–Tsangpo suture zone, which contains remnants of the ancient Neotethys Ocean, marks the tectonic boundary between Eurasia and India. South of the suture lies the Tethyan Himalaya, composed of sedimentary and volcanic rocks. Early Cretaceous marine sediments preserved in the northernmost Indian passive margin contain abundant radiolarians. Coeval radiolarian faunas and their paleobiogeographical affinities from the southern Tibet and Argo Basin have the potential to elucidate the northern extent of Greater India and the breakup of East Gondwana.

Parvicingulids, which are useful indicator of mid- to high-latitude deposition during the Jurassic to the Early Cretaceous, are common from radiolarians in southern Tibet and Argo Basin. However, the antitropical distribution of Parvicingulids have not been systematically analysed and their paleobiogeographical implications are still unclear. The locations, sedimentary setting, age assignment of species belong to Parvicingulidae are summarized to elucidating the time of their origin and, accordingly, outline how their antitropical distribution developed.

Tethyan species dominant in Gyangze during the Berriasian to Valanginian (145–132 Ma) indicate the deposition position of paleobiogeographical Tethyan Province. The change of radiolarian assemblages in Gyangze from Tethyan species dominant to Parvicingulids dominant occurred around Valanginian (140–130 Ma). The occurrence and dominance of Parvicingulids at Gyangze around 140–130 Ma indicate a later influx of southern paleolatitude origin circumantarctic current to the west. The influx of circumantarctic current transported to Zhongba around 130–125 Ma and the influence became weaker according to the dominance of Tethyan species with low abundance and diversity of Parvicingulids. Wide distribution of Parvicingulids in West Timor (Munasri and Sashida, 2017), Gyangze, Kangma, and Zhongba around 130 Ma corresponds to the breakup at 130 Ma and the Greater India’ s anticlockwise rotation from 136 to 120 Ma.

References:

Munasri and Sashida (2017) Earth Evolution Sciences, **12**, pp. 3-12

Keywords: Early Cretaceous, Parvicingulids, antitropical distribution, Gandwana

©2021. Japan Geoscience Union. All Right Reserved.

Repeated organic-rich deposition in Early Triassic pelagic deep Panthalassa and its relationship with global seafloor anoxia

*Shun Muto[1]

1. Geological Survey of Japan, National Institute of Advanced Industrial Science and Technology

Deep-sea sedimentary rocks deposited in pelagic Panthalassa during the Early Triassic are characterised by the presence of black organic-rich claystone and the general absence of radiolarian chert. This was considered to be a result of one of the most extensive episodes of oceanic oxygen depletion in the Phanerozoic. However, while oceanic anoxia repeatedly occurred throughout the Early Triassic according to studies on peri-continental sections, black claystone deposition in pelagic Panthalassa was thought to be restricted to earliest Triassic times.

In this study, the lithostratigraphy, conodont biostratigraphy and chemical composition are investigated for the Lower Triassic sedimentary sequence deposited in pelagic deep-water areas of Panthalassa with some new data for the upper part (upper Olenekian). Sedimentation rates and major element compositions of upper Olenekian to lower Anisian strata support published findings that the absence of chert is a consequence of increased clastic input while there is no apparent evidence of radiolarian extinction due to oceanic anoxia. Correlation of several sections from the Jurassic accretionary complex of Japan based on conodont biozonation reveals that the deposition of extensive black claystone occurred in the Induan, early Spathian (early late Olenekian) and across the Olenekian–Anisian boundary. Though a complete assessment is pending, sedimentary and geochemical evidence of anoxia in the water column and bottom waters have been obtained from the black claystone lithofacies. Conodont biozonation and stable carbon isotope curves allowed the correlation of the lithostratigraphy of pelagic deep Panthalassa and uranium (U) isotope records from shallow-marine carbonate, the latter of which is used as a proxy of the areal extent of anoxic seafloor on the global scale. Results showed that organic-rich deposition in pelagic Panthalassa was generally coeval with episodes of expanded anoxic seafloor, although the two phenomena are decoupled in Smithian (early Olenekian) times. This implies that the deposition of black organic-rich claystone in pelagic deep Panthalassa reflects global trends in the spatial extent of bottom water anoxia during the Early Triassic, probably controlled mainly by nutrient input to the oceans. Black claystone lithofacies straddling the Olenekian–Anisian boundary is particularly important, because it represents the first finding of a laterally extensive deposit associated with oceanic anoxia during this time interval.

Keywords: Black claystone, chert gap, siliceous claystone, total organic carbon, stable carbon isotope, conodont

©2021. Japan Geoscience Union. All Right Reserved.

Marine Os isotope record from the uppermost Barremian to the lowest Turonian

*Hironao Matsumoto[1], Rodolfo Coccioni[2], Fabrizio Frontalini[2], Kotaro Shirai[1], Junichiro Kuroda[1]

1. Atmosphere and Ocean Research Institute, the University of Tokyo, 2. University of Urbino

Mid-Cretaceous is characterized by repeated episodic phases of organic-carbon burial in various oceanographic settings (oceanic anoxic events: OAEs) and following marine biotic crises. Since the radiometric ages of huge basaltic plateaus called large igneous provinces (LIPs) roughly correspond to these environmental perturbations, the massive volcanic eruptions associated with the emplacement of LIPs have been proposed as the trigger of the mid-Cretaceous environmental perturbations. Indeed, the volcanic gases released from these LIPs eruptions could have played an important role to sustain the warm, high-pCO_2 mid-Cretaceous climate. Recent studies on sedimentary Os isotopic records have provided evidence suggesting their linkages. Marine Os isotopic ratios ($^{187}Os/^{188}Os$) reflect the balance between radiogenic Os from the continental crust and unradiogenic Os sources (e.g., hydrothermal activity, weathering of the basaltic plateau, and meteorite impact). During Early Aptian OAE1a and end-Cenomanian OAE2, $^{187}Os/^{188}Os$ of the sedimentary rocks show rapid shifts to unradiogenic values (~0.2). Since radiometric ages of Ontong Java Plateau and Caribbean Plateau correspond to the sedimentary ages of OAE1a and OAE2, respectively, these Os isotopic declines have been interpreted as the massive input of mantle-derived unradiogenic Os through submarine volcanism forming these basaltic plateaus. However, the Os isotopic data during the mid-Cretaceous are limited to the short interval around major Cretaceous OAEs (e.g., OAE1a, OAE1b, and OAE2), which have hampered a long-term reconstruction of the hydrothermal activity. Here, we reconstruct the continuous marine Os isotopic record during the mid-Cretaceous using Tethyan sedimentary records in order to reveal the long-term variation of hydrothermal activity and the unknown massive volcanic activity associated with the formation of LIPs.

Keywords: osmium, Cretaceous

©2021. Japan Geoscience Union. All Right Reserved.

Depositional ages of multiple REY peaks in deep-sea sediments around Minamitorishima Island based on osmium isotope stratigraphy

*Yuta Oda[1], Junichiro Ohta[1,2], Erika Tanaka[1], Kazutaka Yasukawa[1,2], Yusuke Kuwahara[1], Moei Yano[2,1], Koichiro Fujinaga[2,1], Kentaro Nakamura[1], Yasuhiro Kato[1,2]

1. School of Engineering, The University of Tokyo, 2. ORCeNG, Chiba Institute of Technology

Deep-sea sediments highly enriched in rare-earth elements and yttrium (REY), lying in the Japanese exclusive economic zone around Minamitorishima Island, are expected as a promising new resource for the industrially critical metals [1-4]. Multi-elemental chemostratigraphic correlation revealed that the deep-sea sediments around Minamitorishima Island have three distinct layers with >2000 ppm of total REY concentrations. These layers were named as the 1st, 2nd, and 3rd REY peaks from shallow to deep [4]. Using marine osmium isotope ratio ($^{187}Os/^{188}Os$), a previous study [5] revealed that the 1st REY peak was formed at 34.4 Ma and proposed that an enhanced northward flow of bottom water associated with the late Eocene event, a temporal expansion of Antarctic ice sheet, caused the upwelling of deep-ocean nutrients along with topographic highs, such as large seamounts. This upwelling could have stimulated the biological productivity and resulted in an increased fish productivity, leading to the substantial deposition of fish debris that accumulate REY on the seafloor [5].

In contrast to the detailed investigation of the 1st REY peak from a paleoceanographic perspective, the depositional ages and causes of the 2nd and 3rd REY peaks still remain uncertain. Here, we will report new results of the Os isotope analysis on the sediment samples from MR15-E01 PC07 core that clearly contains three REY peaks. The depositional ages of the REY peak of MR15-E01 PC07 core were estimated based on the osmium isotope stratigraphy. In the presentation, we will discuss the possible causes of the REY peaks based on their depositional ages.

[1] Kato et al. (2011) *Nature Geoscience* **4**, 535-539. [2] Iijima et al. (2016) *Geochemical Journal* **50**, 557-573. [3] Takaya et al. (2018) *Scientific Reports* **8**, 5763. [4] Tanaka et al. (2020) *Ore Geology Reviews* **119**, 103392. [5] Ohta et al. (2020) *Scientific Reports* **10**, 9896.

Keywords: deep-sea sediment, rare-earth elements, REY-rich mud, Minamitorishima Island, age determination, osmium isotopes

©2021. Japan Geoscience Union. All Right Reserved.

Depositional environments of the Late Cretaceous REY-rich mud in the western North Pacific Ocean inferred from deep-water agglutinated foraminifers

*Kondo Yuta[1], Junichiro Ohta[1,2], Kazutaka Yasukawa[1,2], Kentaro Nakamura[1], Koichiro Fujinaga[2,1], Yasuhiro Kato[1,2]

1. School of Engineering, The University of Tokyo, 2. ORCeNG, Chiba Institute of Technology

Deep-sea sediments highly enriched in rare-earth elements and yttrium (REY), called REY-rich mud, are widely distributed in the Pacific Ocean [1]. Notably, very high-grade REY-rich mud lies around Minamitorishima Island in the western North Pacific Ocean, and it is expected to be a promising new resource for REY [2]. Some radiolarian fossils in the uppermost part of the chert imply that the REY-rich mud around Minamitorishima Island started to deposit in the Late Cretaceous [3,4].

Pelagic clay including REY-rich mud has deposited very slowly over a long period of time, and thus, are expected to have recorded the history of pelagic environment. However, the water depth greater than the carbonate compensation depth (CCD) and generally low surface productivity hampered preserving calcareous and siliceous fossils, making it difficult to decipher the environmental changes in the pelagic realm.

Here, we focused on a certain type of benthic foraminifers called deep-water agglutinated foraminifers (DWAF). DWAF have agglutinative shells of aluminosilicates that do not dissolve even at depths below the CCD [4] and consist of various species such as those highly dependent on biological production or tolerant of oligotrophic environments [5]. Therefore, it is expected that investigation of DWAF assemblage will provide a new insight into the depositional environments of REY-rich mud. In the presentation, based on the production and species composition of DWAF, we will discuss the environmental conditions during the time of deposition of REY-rich mud around Minamitorishima Island in the Late Cretaceous.

[1] Kato et al. (2011) *Nature Geoscience* **4**, 535-539. [2] Takaya et al. (2018) *Scientific Reports* **8**, 5763. [3] Wightman and Kuhnt (1992) *Proc. ODP, Scientific Results* **129**, 247-264. [4] Nakamura et al. (2016) *Geochemical Journal* **50**, 605-619. [5] Kaminski and Gradstein (2005) *Grzybowski Foundation Special Publication* **10**, 547

Keywords: deep-water agglutinated foraminifers, pelagic clay, REY-rich mud, microfossils, Pacific Ocean, Cretaceous

©2021. Japan Geoscience Union. All Right Reserved.

[E] Poster | M (Multidisciplinary and Interdisciplinary)：M-GI General Geosciences, Information Geosciences & Simulations

Sat. Jun 5, 2021 5:15 PM - 6:30 PM JST | Sat. Jun 5, 2021 8:15 AM - 9:30 AM UTC | Ch.20_4

[M-GI32] Integration of Earth Observations and Multiple use for Earth Science and Benefits to Societies - GEO

convener:Kentaro Ando(Japan Agency for Marine and Earth Science and Technology), Hiroyuki Muraoka(River Basin Research Center), Osamu Ochiai(Japan Aerospace Exploration Agency), Shinichi Sobue(Japan Aerospace Exploration Agency)

Floods and drought, environment deterioration and pollution, global warming and island losing, and ecosystem degradation endanger the security of water, food, energy, health and ecosystem services. To confront these challenges, there is a demand to foster its application capacity and to develop an integrated, sharable, and sustained observation systems. Group on Earth Observations (GEO) as an intergovernmental body is a partnership of more than 100 national governments including Japan and in excess of 100 Participating Organizations that envisions a future where decisions and actions for the benefit of humankind are informed by coordinated, comprehensive and sustained Earth observations. To promote a regional cooperation on earth observation with broad engagement of various communities of earth observations, earth system modeling, environmental assessment and society, AOGEO as one of regional initiatives is established to foster regional application activities focusing on the emerging issues in the region.

The purpose of this session is 1) to exchange the current status of data integration efforts in global GEO and regional AOGEO, 2) to welcome any contributions of similar activities from outside of GEO and AOGEO, and 3) to foster GEO and AOGEO activities and its related activities via any submissions and contributions of analysis of earth observations both from integrated data and single unique data on the earth science and societal applications. Therefore, we seek submissions which include a) scientific researches by use of earth observation data both from various platforms including satellite and in-situ, b) development of new data sets for national, regional and global analyses, and c) development of data integration and management platforms and its broad application to our society including a concept of knowledge hubs.

[MGI32-P01] Developments of a new ocean data networking system for coastal ocean data sharing, and satellite data management system for Integrated Priority Study in AOGEO

*Kentaro Ando[1], Fumihiko Akazawa[1] (1.Japan Agency for Marine and Earth Science and Technology)

[MGI32-P02] Asia Pacific Biodiversity Observation Network (APBON) Strategic Plan 2030

*Hiroyuki Muraoka[1], Yayoi Takeuchi[2], Takehisa Yamakita[3], Yuichi Kano[4], Shin Nagai[3], Masahiro Nakaoka[5], Yongyut Trisurat[6], Runi Sylvester Pungga[7] (1.Gifu University, 2.National Institute for Environmental Studies, 3.Japan Agency for Marin-Earth Science and Technology, 4.Kyusyu University, 5.Hokkaido University, 6.Kasetsart University, 7.Forest Department Sarawak)

[MGI32-P03] Status of Global Forest Observation Initiative (GFOI) and its contribution to climate change monitoring

*Osamu Ochiai[1] (1.Japan Aerospace Exploration Agency)

Developments of a new ocean data networking system for coastal ocean data sharing, and satellite data management system for Integrated Priority Study in AOGEO

*Kentaro Ando[1], Fumihiko Akazawa[1]

1. Japan Agency for Marine and Earth Science and Technology

For contributing to the Asia-Oceania Group on Earth Observation (AOGEO) activities from the Ocean, Coasts and Islands (OCI) Task, new ocean data networking system for coastal ocean data sharing has been developing by using Geonetworks (open source, https://geonetwork-opensource.org/). This system allows all users visiting one site to jump to other sites by using the data-portal based on Geonetworks. The demonstration system was developed in 2019 by JAMSTEC and CSIRO, and it has been expanding to few Asian countries after the technology exchange session of OCI Task in February 2021. This new approach will bring us a new opportunity to use coastal data, which are not well accessed from a third party.

For contributing the Integrated Priority Study (IPS) of the AOGEO regional activity, we also have developed the demonstration system of Open Data Cube (ODC) to manage the satellite data (ALOS and ALOS-2) and satellite-based products. In the framework of IPS, Japan as well as Australia, China and Korea will develop own ODC system to be able to distribute each own satellite and satellite-based products. As the ODC will be able to provide Python Notebook/Hub for users to run demonstration codes and to develop own codes of python by using datasets from products provided by each country. We will report the update of preparations of ODC system in Japan and will show the preliminary plots and demonstration.

From the two presentations, any comments on these developments are welcomed.

Keywords: GEO, AOGEO, data utilization

©2021. Japan Geoscience Union. All Right Reserved.

Asia Pacific Biodiversity Observation Network (APBON) Strategic Plan 2030

*Hiroyuki Muraoka[1], Yayoi Takeuchi[2], Takehisa Yamakita[3], Yuichi Kano[4], Shin Nagai[3], Masahiro Nakaoka[5], Yongyut Trisurat[6], Runi Sylvester Pungga[7]

1. Gifu University, 2. National Institute for Environmental Studies, 3. Japan Agency for Marin-Earth Science and Technology, 4. Kyusyu University, 5. Hokkaido University, 6. Kasetsart University, 7. Forest Department Sarawak

Asia Pacific Biodiversity Observation Network (APBON) was established in 2009 and it is contributing to Asia Oceania Group on Earth Observations (AOGEO) as well as GEO Biodiversity Observation Network (GEO BON). We are now moving to the next steps to address challenges in biodiversity observations and assessments in our region, based on our 10-year achievements (Takeuchi et al. 2021, Ecological Research DOI: 10.1111/1440-1703.12212).

The societal demands for the Earth observation have been increasing because of emerging environmental issues such as climate change and species extinction in both global and local scale. Our ecosystem and biodiversity monitoring activities as “Earth observation” and subsequent scientific analyses provide an essential data to understand the status, trends, and projection of the future earth system including under climate and societal change. Through the high-quality observation of biodiversity change, APBON will strive to provide scientific evidence to develop sound assessments and facilitate policy-making.

Regional networks, such as APBON, play an essential role in taking an initiative to gather, explore, and prioritize local issues and practices and link these over regions, scientific communities, and stakeholders. We cherish the bottom-up approaches and/or landscape-level approaches, which our members have used, as it matches with the scale of the biodiversity-issues and the goal setting to maximize the benefits to local people, regional ecosystems, and biodiversity. It also offers more opportunities to work with scientists and local stakeholders and facilitate problem-solving corporation using the available knowledge. Another target is to promote data sharing and data accessibility through and by strengthening the networking of the observation networks in local to AP regional scale and deliver our information and knowledge to global platform. APBON plays a role as a “hub” to link the local, national, regional, and global needs of biodiversity observations, customizing observation designs and tools, and matching science-policy interface.
In this presentation we are willing to share our implementation plans with the Earth observation communities to respond to the following new needs to the biodiversity observations: (1) Developing national BONs and networking them in the region to contribute to CBD Aichi Biodiversity Targets and post 2020 Global Biodiversity Framework, (2) Filling observational and knowledge gaps for biodiversity status and trends to contribute to IPBES assessments, (3) Producing data and knowledge to address the issues particularly related to biodiversity and ecosystem sustainability by coordinated activities with GEO and AOGEO, (4) Contributing to achievements of SDGs by providing adequate and defensible biodiversity data that help developing policy for conservation and sustainable use of biodiversity, and (5) Learning the challenges of biodiversity issues under COVID-19 pandemic and on-going climate change.

Keywords: biodiversity, ecosystems, ecosystem services, forest, freshwater, marine

©2021. Japan Geoscience Union. All Right Reserved.

Status of Global Forest Observation Initiative (GFOI) and its contribution to climate change monitoring

*Osamu Ochiai[1]

1. Japan Aerospace Exploration Agency

Group on Earth Observation (GEO) coordinates multiple Earth observation activities around the world. The coordination is essential towards converging similar activities in many countries and making synegy for achievement various global challenges. As one of GEO Flagships, Global Forest Observation Initiative (GFOI) has been initiated in 2011. GFOI provides international coordination machanism in order to support implementing National Forest Monitoring System by using Earth observation data. GFOI provides method and guidance to use Earth observation data, research and development of new science and technologies, data and information provision support and capacity development for those who are not familiar to use Earth observation data. Recently, GFOI has initiated discussion on how to contribute GFOI activities to Paris agreement. It would be expected significant contributions by GFOI to the stakeholders in the Climate Change agenda.

Keywords: Earth obaservation, GFOI, data

©2021. Japan Geoscience Union. All Right Reserved.

[J] Oral | EVENT：EVENT

Sat. Jun 5, 2021 12:20 PM - 1:00 PM JST | Sat. Jun 5, 2021 3:20 AM - 4:00 AM UTC | Ch.01 Zoom Room 01

[EV-22] Lunchtime Special Lecture

12:20 PM - 1:00 PM JST | 3:20 AM - 4:00 AM UTC

[E-11-24] Uncover the cryptic nitrogen flows in the terrestrial ecosystems

[J] Oral | EVENT | EVENT

[EV-22] Lunchtime Special Lecture

Sat. Jun 5, 2021 12:20 PM - 1:00 PM Ch.01 (Zoom Room 01)

12:20 PM - 1:00 PM

[E-11-24]Uncover the cryptic nitrogen flows in the terrestrial ecosystems

Nitrogen fluxes in the natural ecosystems are difficult to study partly due to the high variety of the nitrogen compounds and to their low concentrations maintained by the biological nitrogen use. In this lecture, I introduce some case studies elucidating the cryptic nitrogen flows driven by the microbes and plants in the terrestrial ecosystems with the help of stable isotope techniques.

©Japan Geoscience Union

[E] Oral | EVENT：EVENT

Sat. Jun 5, 2021 9:00 AM - 9:45 AM JST | Sat. Jun 5, 2021 12:00 AM - 12:45 AM UTC | Ch.07 Zoom Room 07

[EV-23] Exhibitors' Seminar

昨年と同じく、出展者様にセミナーを開催していただきます。
地球惑星科学関連の、有用な情報を発信してくださいますので是非ご参加ください。

9:00 AM - 9:45 AM JST | 12:00 AM - 12:45 AM UTC

[E-11-23] Latest Application Developments from Picarro

[E] Oral | EVENT | EVENT

[EV-23] Exhibitors' Seminar

Sat. Jun 5, 2021 9:00 AM - 9:45 AM Ch.07 (Zoom Room 07)

昨年と同じく、出展者様にセミナーを開催していただきます。
地球惑星科学関連の、有用な情報を発信してくださいますので是非ご参加ください。

9:00 AM - 9:45 AM

[E-11-23]Latest Application Developments from Picarro

Latest Application Developments from Picarro

©Japan Geoscience Union

[J] Oral | EVENT：EVENT

Sat. Jun 5, 2021 1:45 PM - 2:30 PM JST | Sat. Jun 5, 2021 4:45 AM - 5:30 AM UTC | Ch.12 Zoom Room 12

[EV-24] Exhibitors' Seminar

昨年と同じく、出展者様にセミナーを開催していただきます。
地球惑星科学関連の、有用な情報を発信してくださいますので是非ご参加ください。

1:45 PM - 2:30 PM JST | 4:45 AM - 5:30 AM UTC

[E-11-25] An introduction to Research Institute for Humanity Nature (RIHN)'s interdisciplinary researches on global environmental issues. Earth Scientists, join our Research Projects!

[J] Oral | EVENT | EVENT

[EV-24] Exhibitors' Seminar

Sat. Jun 5, 2021 1:45 PM - 2:30 PM Ch.12 (Zoom Room 12)

昨年と同じく、出展者様にセミナーを開催していただきます。
地球惑星科学関連の、有用な情報を発信してくださいますので是非ご参加ください。

1:45 PM - 2:30 PM

[E-11-25]An introduction to Research Institute for Humanity Nature (RIHN)'s interdisciplinary researches on global environmental issues. Earth Scientists, join our Research Projects!

An introduction to Research Institute for Humanity Nature (RIHN)'s interdisciplinary researches on global environmental issues. Earth Scientists, join our Research Projects!

©Japan Geoscience Union